Scientific and Technical Aerospace Reports

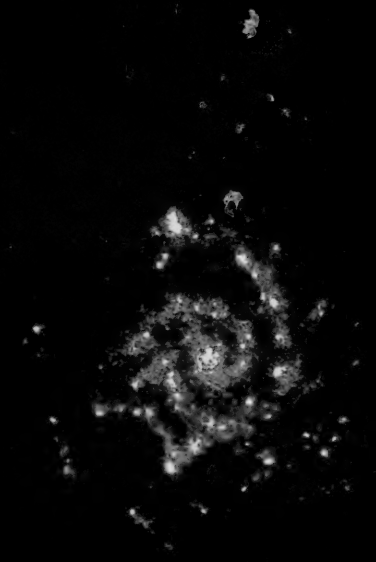

An Abstract Journal

Volume 31, Number 9
September 1993
N93-24659 to N93-26604

The NASA STI Program...in Profile

Since its founding, NASA has been dedicated to ensuring U.S. leadership in aeronautics and space science. The NASA Scientific and Technical Information (STI) Program plays an important part in helping NASA maintain its leadership role.

The NASA STI Program provides access to the NASA STI Database, the largest collection of aeronautical and space science STI in the world. The Program is also NASA's institutional mechanism for disseminating the results of its research and development activities.

A number of specialized services help round out the Program's diverse offerings, including creating custom thesauri, translating material to or from 34 foreign languages, building customized databases, organizing and publishing research results.

For more information about the NASA STI Program, you can:

- **Phone** the NASA Access Help Desk at (301) 621-0390
- **Fax** your question to NASA Access Help Desk at (301) 621-0134
- Send us your question via the **Internet** to help@sti.nasa.gov
- **Write to:**
  NASA Access Help Desk
  NASA Center for AeroSpace Information
  800 Elkridge Landing Road
  Linthicum Heights, MD 21090-2934

Scientific and Technical Aerospace Reports

Scientific and Technical Aerospace Reports (STAR), is published each month as a major product of the International Aerospace Database, managed by the NASA Scientific and Technical Information (STI) Program.

Inside this issue you will find:

Front Matter
A typical citation and abstract sample explaining the standard format, which includes codes for ordering reports.

An Abstract Section
Citations and abstracts of reports and publications that provide comprehensive coverage of worldwide aerospace-related topics including aeronautics and space science technology. *STAR* lists published and publicly available reports entered into the NASA STI Database during the four weeks preceding publication of this issue. These citations and abstracts are listed by subject categories.

An Index Section
- Subject
- Personal author
- Corporate source
- Contract number
- Report number.

Appendix
A guide for ordering cited reports, registering with the NASA STI Program, and using the available products and services. Additionally, price schedules, phone numbers, and addresses are included in this information packed section.

NASA also sponsors companion journals, *International Aerospace Abstracts (IAA)*, and *NASA Open Volumes on Aerospace (NOVA)*. They list abstracts of the open literature on aerospace subjects available worldwide. IAA is available from the American Institute of Aeronautics and Astronautics (AIAA), and *NOVA* is for internal NASA use only, available from the NASA Center for AeroSpace Information (CASI).

Reports found in *STAR* are also available through the NASA online retrieval service, RECON, and the Aerospace Database through DIALOG.

The NASA STI Program gathers information through national and international agreements and exchanges and makes this information available to the NASA community and to the public in many forms through various outlets.

For additional information on the NASA STI Program, call the NASA Access Help Desk at (301) 621-0390, or write to:

NASA Center for AeroSpace Information
800 Elkridge Landing Road
Linthicum Heights, Maryland 21090-2934

US ISSN 0036-8741

This publication was prepared by the NASA Center for AeroSpace Information,
800 Elkridge Landing Road, Linthicum Heights, MD 21090-2934, (301) 621-0390.

Volume 31 Number 9 / September 1993

TABLE OF CONTENTS

AERONAUTICS For related information see also *Astronautics.*

01 AERONAUTICS (GENERAL) **2573**

02 AERODYNAMICS **2574**
Includes aerodynamics of bodies, combinations, wings, rotors, and control surfaces; and internal flow in ducts and turbomachinery. For related information see also *34 Fluid Mechanics and Heat Transfer.*

03 AIR TRANSPORTATION AND SAFETY **2582**
Includes passenger and cargo air transport operations; and aircraft accidents. For related information see also *16 Space Transportation* and *85 Urban Technology and Transportation.*

04 AIRCRAFT COMMUNICATIONS AND NAVIGATION **2584**
Includes digital and voice communication with aircraft; air navigation systems (satellite and ground based); and air traffic control. For related information see also *17 Space Communications, Spacecraft Communications, Command and Tracking* and *32 Communications and Radar.*

05 AIRCRAFT DESIGN, TESTING AND PERFORMANCE **2586**
Includes aircraft simulation technology. For related information see also *18 Spacecraft Design, Testing and Performance* and *39 Structural Mechanics.* For land transportation vehicles see *85 Urban Technology and Transportation.*

06 AIRCRAFT INSTRUMENTATION **2591**
Includes cockpit and cabin display devices; and flight instruments. For related information see also *19 Spacecraft Instrumentation* and *35 Instrumentation and Photography.*

07 AIRCRAFT PROPULSION AND POWER **2592**
Includes prime propulsion systems and systems components, e.g., gas turbine engines and compressors; and onboard auxiliary power plants for aircraft. For related information see also *20 Spacecraft Propulsion and Power, 28 Propellants and Fuels,* and *44 Energy Production and Conversion.*

08 AIRCRAFT STABILITY AND CONTROL **2595**
Includes aircraft handling qualities; piloting; flight controls; and autopilots. For related information see also *05 Aircraft Design, Testing and Performance.*

09 RESEARCH AND SUPPORT FACILITIES (AIR) **2597**
Includes airports, hangars and runways; aircraft repair and overhaul facilities; wind tunnels; shock tubes; and aircraft engine test stands. For related information see also *14 Ground Support Systems and Facilities (Space).*

ASTRONAUTICS For related information see also *Aeronautics.*

12 ASTRONAUTICS (GENERAL) **2598**
For extraterrestrial exploration see *91 Lunar and Planetary Exploration.*

13 ASTRODYNAMICS **2599**
Includes powered and free-flight trajectories; and orbital and launching dynamics.

14 GROUND SUPPORT SYSTEMS AND FACILITIES (SPACE) **2608**
Includes launch complexes, research and production facilities; ground support equipment, e.g., mobile transporters; and simulators. For related information see also *09 Research and Support Facilities (Air).*

15 LAUNCH VEHICLES AND SPACE VEHICLES **2609**
Includes boosters; operating problems of launch/space vehicle systems; and reusable vehicles. For related information see also *20 Spacecraft Propulsion and Power.*

16 SPACE TRANSPORTATION **2610**
Includes passenger and cargo space transportation, e.g., shuttle operations; and space rescue techniques. For related information see also *03 Air Transportation and Safety* and *18 Spacecraft Design, Testing and Performance.* For space suits see *54 Man/System Technology and Life Support.*

17 SPACE COMMUNICATIONS, SPACECRAFT COMMUNICATIONS, COMMAND AND TRACKING . **2614**
Includes telemetry; space communications networks; astronavigation and guidance; and radio blackout. For related information see also *04 Aircraft Communications and Navigation* and *32 Communications and Radar.*

N.A.—no abstracts were assigned to this category for this issue.

18 SPACECRAFT DESIGN, TESTING AND PERFORMANCE **2614**
Includes satellites; space platforms; space stations; spacecraft systems and components such as thermal and environmental controls; and attitude controls. For life support systems see *54 Man/System Technology and Life Support.* For related information see also *05 Aircraft Design, Testing and Performance, 39 Structural Mechanics,* and *16 Space Transportation.*

19 SPACECRAFT INSTRUMENTATION **2620**
For related information see also *06 Aircraft Instrumentation* and *35 Instrumentation and Photography.*

20 SPACECRAFT PROPULSION AND POWER **2621**
Includes main propulsion systems and components, e.g., rocket engines; and spacecraft auxiliary power sources. For related information see also *07 Aircraft Propulsion and Power, 28 Propellants and Fuels, 44 Energy Production and Conversion,* and *15 Launch Vehicles and Space Vehicles.*

CHEMISTRY AND MATERIALS

23 CHEMISTRY AND MATERIALS (GENERAL) **2633**

24 COMPOSITE MATERIALS **2634**
Includes physical, chemical, and mechanical properties of laminates and other composite materials. For ceramic materials see *27 Nonmetallic Materials.*

25 INORGANIC AND PHYSICAL CHEMISTRY **2642**
Includes chemical analysis, e.g., chromatography; combustion theory; electrochemistry; and photochemistry. For related information see also *77 Thermodynamics and Statistical Physics.*

26 METALLIC MATERIALS **2649**
Includes physical, chemical, and mechanical properties of metals, e.g., corrosion; and metallurgy.

27 NONMETALLIC MATERIALS **2653**
Includes physical, chemical, and mechanical properties of plastics, elastomers, lubricants, polymers, textiles, adhesives, and ceramic materials. For composite materials see *24 Composite Materials.*

28 PROPELLANTS AND FUELS **2659**
Includes rocket propellants, igniters and oxidizers; their storage and handling procedures; and aircraft fuels. For related information see also *07 Aircraft Propulsion and Power, 20 Spacecraft Propulsion and Power,* and *44 Energy Production and Conversion.*

29 MATERIALS PROCESSING **2663**
Includes space-based development of products and processes for commercial application. For biological materials see *55 Space Biology.*

ENGINEERING For related information see also *Physics.*

31 ENGINEERING (GENERAL) **2665**
Includes vacuum technology; control engineering; display engineering; cryogenics; and fire prevention.

32 COMMUNICATIONS AND RADAR **2671**
Includes radar; land and global communications; communications theory; and optical communications. For related information see also *04 Aircraft Communications and Navigation* and *17 Space Communications, Spacecraft Communications, Command and Tracking.* For search and rescue see *03 Air Transportation and Safety,* and *16 Space Transportation.*

33 ELECTRONICS AND ELECTRICAL ENGINEERING **2687**
Includes test equipment and maintainability; components, e.g., tunnel diodes and transistors; microminiaturization; and integrated circuitry. For related information see also *60 Computer Operations and Hardware* and *76 Solid-State Physics.*

34 FLUID MECHANICS AND HEAT TRANSFER **2694**
Includes boundary layers; hydrodynamics; fluidics; mass transfer and ablation cooling. For related information see also *02 Aerodynamics* and *77 Thermodynamics and Statistical Physics.*

35 INSTRUMENTATION AND PHOTOGRAPHY **2708**
Includes remote sensors; measuring instruments and gauges; detectors; cameras and photographic supplies; and holography. For aerial photography see *43 Earth Resources and Remote Sensing.* For related information see also *06 Aircraft Instrumentation* and *19 Spacecraft Instrumentation.*

36 LASERS AND MASERS **2711**
Includes parametric amplifiers. For related information see also *76 Solid-State Physics.*

37 MECHANICAL ENGINEERING **2716**
Includes auxiliary systems (nonpower); machine elements and processes; and mechanical equipment.

38 QUALITY ASSURANCE AND RELIABILITY **2721**
Includes product sampling procedures and techniques; and quality control.

39 STRUCTURAL MECHANICS **2723**
Includes structural element design and weight analysis; fatigue; and thermal stress. For applications see *05 Aircraft Design, Testing and Performance* and *18 Spacecraft Design, Testing and Performance.*

GEOSCIENCES For related information see also *Space Sciences.*

42 GEOSCIENCES (GENERAL) **2732**

43 EARTH RESOURCES AND REMOTE SENSING **2737**
Includes remote sensing of earth resources by aircraft and spacecraft; photogrammetry; and aerial photography. For instrumentation see *35 Instrumentation and Photography.*

44 ENERGY PRODUCTION AND CONVERSION **2758**
Includes specific energy conversion systems, e.g., fuel cells; global sources of energy; geophysical conversion; and windpower. For related information see also *07 Aircraft Propulsion and Power, 20 Spacecraft Propulsion and Power,* and *28 Propellants and Fuels.*

45 ENVIRONMENT POLLUTION **2760**
Includes atmospheric, noise, thermal, and water pollution.

46 GEOPHYSICS **2769**
Includes aeronomy; upper and lower atmosphere studies; ionospheric and magnetospheric physics; and geomagnetism. For space radiation see *93 Space Radiation.*

47 METEOROLOGY AND CLIMATOLOGY **2777**
Includes weather forecasting and modification.

48 OCEANOGRAPHY **2788**
Includes biological, dynamic, and physical oceanography; and marine resources. For related information see also *43 Earth Resources and Remote Sensing.*

LIFE SCIENCES

51 LIFE SCIENCES (GENERAL) **2792**

52 AEROSPACE MEDICINE **2794**
Includes physiological factors; biological effects of radiation; and effects of weightlessness on man and animals.

53 BEHAVIORAL SCIENCES **2796**
Includes psychological factors; individual and group behavior; crew training and evaluation; and psychiatric research.

54 MAN/SYSTEM TECHNOLOGY AND LIFE SUPPORT **2799**
Includes human engineering; biotechnology; and space suits and protective clothing. For related information see also *16 Space Transportation.*

55 SPACE BIOLOGY **2803**
Includes exobiology; planetary biology; and extraterrestrial life.

MATHEMATICAL AND COMPUTER SCIENCES

59 MATHEMATICAL AND COMPUTER SCIENCES (GENERAL) **2803**

60 COMPUTER OPERATIONS AND HARDWARE **2805**
Includes hardware for computer graphics, firmware, and data processing. For components see *33 Electronics and Electrical Engineering.*

61 COMPUTER PROGRAMMING AND SOFTWARE **2808**
Includes computer programs, routines, algorithms, and specific applications, e.g., CAD/CAM.

62 COMPUTER SYSTEMS **2815**
Includes computer networks and special application computer systems.

63 CYBERNETICS **2817**
Includes feedback and control theory, artificial intelligence, robotics and expert systems. For related information see also *54 Man/System Technology and Life Support.*

64 NUMERICAL ANALYSIS **2827**
Includes iteration, difference equations, and numerical approximation.

65 STATISTICS AND PROBABILITY **2830**
Includes data sampling and smoothing; Monte Carlo method; and stochastic processes.

66 SYSTEMS ANALYSIS **2831**
Includes mathematical modeling; network analysis; and operations research.

67 THEORETICAL MATHEMATICS ..... **N.A.**
Includes topology and number theory.

PHYSICS For related information see also *Engineering.*

70 PHYSICS (GENERAL) **2831**
For precision time and time interval (PTTI) see *35 Instrumentation and Photography;* for geophysics, astrophysics or solar physics see *46 Geophysics, 90 Astrophysics,* or *92 Solar Physics.*

71 ACOUSTICS **2844**
Includes sound generation, transmission, and attenuation. For noise pollution see *45 Environment Pollution.*

72 ATOMIC AND MOLECULAR PHYSICS **2846**
Includes atomic structure, electron properties, and molecular spectra.

73 NUCLEAR AND HIGH-ENERGY PHYSICS **2851**
Includes elementary and nuclear particles; and reactor theory. For space radiation see *93 Space Radiation.*

74 OPTICS **2852**
Includes light phenomena and optical devices. For lasers see *36 Lasers and Masers.*

75 PLASMA PHYSICS **2857**
Includes magnetohydrodynamics and plasma fusion. For ionospheric plasmas see *46 Geophysics.* For space plasmas see *90 Astrophysics.*

76 SOLID-STATE PHYSICS **2862**
Includes superconductivity. For related information see also *33 Electronics and Electrical Engineering* and *36 Lasers and Masers.*

77 THERMODYNAMICS AND STATISTICAL PHYSICS **2871**
Includes quantum mechanics; theoretical physics; and Bose and Fermi statistics. For related information see also *25 Inorganic and Physical Chemistry* and *34 Fluid Mechanics and Heat Transfer.*

SOCIAL SCIENCES

80 SOCIAL SCIENCES (GENERAL) **2872**
Includes educational matters.

81 ADMINISTRATION AND MANAGEMENT **2872**
Includes management planning and research.

82 DOCUMENTATION AND INFORMATION SCIENCE **2873**
Includes information management; information storage and retrieval technology; technical writing; graphic arts; and micrography. For computer documentation see *61 Computer Programming and Software.*

83 ECONOMICS AND COST ANALYSIS **2886**
Includes cost effectiveness studies.

84 LAW, POLITICAL SCIENCE AND SPACE POLICY **2886**
Includes NASA appropriation hearings; aviation law; space law and policy; international law; international cooperation; and patent policy.

85 URBAN TECHNOLOGY AND TRANSPORTATION **2887**
Includes applications of space technology to urban problems; technology transfer; technology assessment; and surface and mass transportation. For related information see *03 Air Transportation and Safety, 16 Space Transportation,* and *44 Energy Production and Conversion.*

SPACE SCIENCES For related information see also *Geosciences.*

88 SPACE SCIENCES (GENERAL) **2887**

89 ASTRONOMY **2888**
Includes radio, gamma-ray, and infrared astronomy; and astrometry.

90 ASTROPHYSICS **2891**
Includes cosmology; celestial mechanics; space plasmas; and interstellar and interplanetary gases and dust. For related information see also *75 Plasma Physics.*

91 LUNAR AND PLANETARY EXPLORATION **2896**
Includes planetology; and manned and unmanned flights. For spacecraft design or space stations see *18 Spacecraft Design, Testing and Performance.*

92 SOLAR PHYSICS **2898**
Includes solar activity, solar flares, solar radiation and sunspots. For related information see *93 Space Radiation.*

93 SPACE RADIATION **2899**
Includes cosmic radiation; and inner and outer earth's radiation belts. For biological effects of radiation see *52 Aerospace Medicine.* For theory see *73 Nuclear and High-Energy Physics.*

GENERAL

Includes aeronautical, astronautical, and space science related histories, biographies, and pertinent reports too broad for categorization; histories or broad overviews of NASA programs.

99 GENERAL **2901**

SUBJECT INDEX **I-1**

PERSONAL AUTHOR INDEX **I-129**

CORPORATE SOURCE INDEX **I-145**

CONTRACT NUMBER INDEX **I-167**

REPORT NUMBER INDEX **I-171**

APPENDIX **A-1**

TYPICAL CITATION AND ABSTRACT

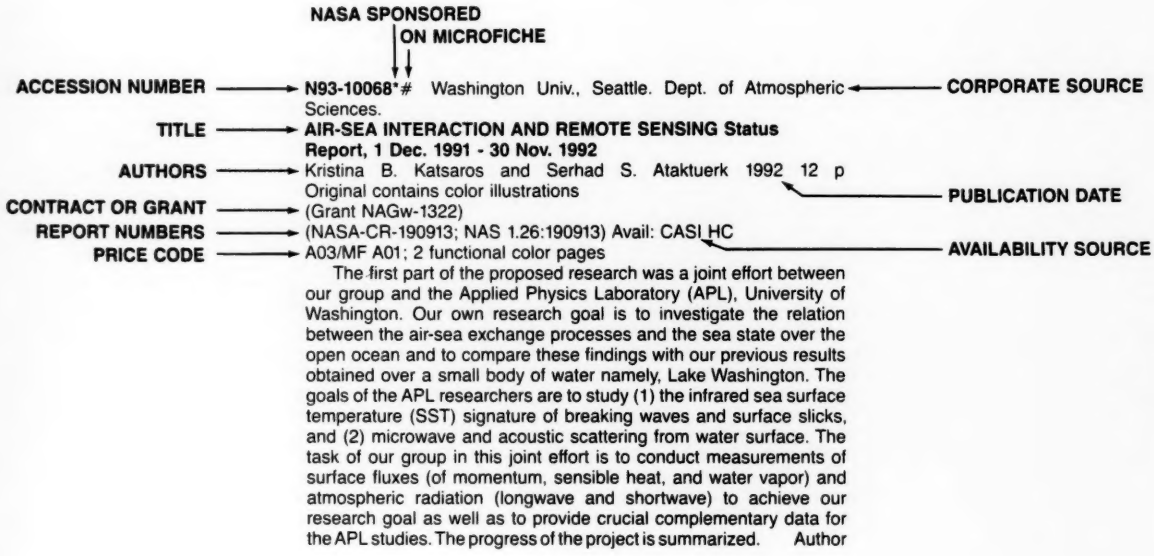
NASA SPONSORED
ON MICROFICHE
ACCESSION NUMBER
N93-10068*# Washington Univ., Seattle. Dept. of Atmospheric Sciences.
CORPORATE SOURCE
TITLE
AIR-SEA INTERACTION AND REMOTE SENSING Status Report, 1 Dec. 1991 - 30 Nov. 1992
AUTHORS
Kristina B. Katsaros and Serhad S. Ataktuerk 1992 12 p
Original contains color illustrations
PUBLICATION DATE
CONTRACT OR GRANT
(Grant NAGw-1322)
REPORT NUMBERS
(NASA-CR-190913; NAS 1.26:190913) Avail: CASI HC
AVAILABILITY SOURCE
PRICE CODE
A03/MF A01; 2 functional color pages
The first part of the proposed research was a joint effort between our group and the Applied Physics Laboratory (APL), University of Washington. Our own research goal is to investigate the relation between the air-sea exchange processes and the sea state over the open ocean and to compare these findings with our previous results obtained over a small body of water namely, Lake Washington. The goals of the APL researchers are to study (1) the infrared sea surface temperature (SST) signature of breaking waves and surface slicks, and (2) microwave and acoustic scattering from water surface. The task of our group in this joint effort is to conduct measurements of surface fluxes (of momentum, sensible heat, and water vapor) and atmospheric radiation (longwave and shortwave) to achieve our research goal as well as to provide crucial complementary data for the APL studies. The progress of the project is summarized. Author

VOLUME 31 NUMBER 9 / SEPTEMBER 1993

Scientific and Technical Aerospace Reports

A Monthly Publication of the National Aeronautics and Space Administration

01 AERONAUTICS (GENERAL)

N93-24760*# Purdue Univ., West Lafayette, IN.
THE WINCOF-I CODE: DETAILED DESCRIPTION
S. N. B. Murthy and A. Mullican Apr. 1993 119 p Sponsored in part by US DOT, Atlantic City International Airport, NJ
(Contract NAG3-481; RTOP 505-62-21; DTFA03-83-A-00328)
(NASA-CR-190779; E-7719; NAS 1.26:190779; DOT/FAA/CT-TN92-10)
Avail: CASI HC A06/MF A02

The performance of an axial-flow fan-compressor unit is basically unsteady when there is ingestion of water along with the gas phase. The gas phase is a mixture of air and water vapor in the case of a bypass fan engine that provides thrust power to an aircraft. The liquid water may be in the form of droplets and film at entry to the fan. The unsteadiness is then associated with the relative motion between the gas phase and water, at entry and within the machine, while the water undergoes impact on material surfaces, centrifuging, heat and mass transfer processes, and reingestion in blade wakes, following peal off from blade surfaces. The unsteadiness may be caused by changes in atmospheric conditions and at entry into and exit from rain storms while the aircraft is in flight. In a multi-stage machine, with an uneven distribution of blade tip clearance, the combined effect of various processes in the presence of steady or time-dependent ingestion is such as to make the performance of a fan and a compressor unit time-dependent from the start of ingestion up to a short time following termination of ingestion. The original WINCOF code was developed without accounting for the relative motion between gas and liquid phases in the ingested fluid. A modification of the WINCOF code was developed and named WINCOF-1. The WINCOF-1 code can provide the transient performance of a fan-compressor unit under a variety of input conditions. Author (revised)

N93-25077*# Michigan Univ., Ann Arbor. Space Physics Research Lab.
FEASIBILITY STUDY OF A LONG DURATION BALLOON FLIGHT WITH NASA/GSFC AND SOVIET SPACE AGENCY GAMMA RAY SPECTROMETERS
William E. Sharp and Glenn Knoll 18 Dec. 1989 23 p
(Grant NAG5-1158)
(NASA-CR-192934; NAS 1.26:192934) Avail: CASI HC A03/MF A01

A feasibility study of conducting a joint NASA/GSFC and Soviet Space Agency long duration balloon flight at the Antarctic in Jan. 1993 is reported. The objective of the mission is the verification and calibration of gamma ray and neutron remote sensing instruments which can be used to obtain geochemical maps of the surface of planetary bodies. The gamma ray instruments in question are the GRAD and the Soviet Phobos prototype. The neutron detectors are supplied by Los Alamos National Laboratory and the Soviet Phobos prototype. These are to be carried aboard a gondola that supplies the data and supplies the power for the period of up to two weeks. Author (revised)

N93-25134*# Purdue Univ., West Lafayette, IN. School of Mechanical Engineering.
TRANSIENT PERFORMANCE OF FAN ENGINE WITH WATER INGESTION Interim Report
S. N. B. Murthy (Purdue Univ., West Lafayette, IN.) and A. Mullican (Purdue Univ., West Lafayette, IN.) Apr. 1993 254 p
(Contracts NAG3-481; DTFA03-83-A-00328; RTOP 505-62-21)
(NASA-CR-190778; E-7709; NAS 1.26:190778; DOT/FAA/CT-TN92/11)
Avail: CASI HC A12/MF A03

In a continuing investigation on developing and applying codes for prediction of performance of a turbine jet engine and its components with water ingestion during flight operation, including power settings, and flight altitudes and speed changes, an attempt was made to establish the effects of water ingestion through simulation of a generic high bypass ratio engine with a generic control. In view of the large effects arising in the air compression system and the prediffuser-combustor unit during water ingestion, attention was focused on those effects and the resulting changes in engine performance. Under all conditions of operation, whether ingestion is steady or not, it became evident that water ingestion causes a fan-compressor unit to operate in a time-dependent fashion with periodic features, particularly with respect to the state of water in the span and the film in the casing clearance space, at the exit of the machine. On the other hand, the aerodynamic performance of the unit may be considered as quasi-steady once the distribution of water has attained an equilibrium state with respect to its distribution and motion. For purposes of engine simulation, the performance maps for the generic fan-compressor unit were generated based on the attainment of a quasi-steady state (meaning steady except for long-period variations in performance) during ingestion and operation over a wide enough range of rotational speeds.
Author (revised)

N93-26136*# National Aeronautics and Space Administration. Lewis Research Center, Cleveland, OH.
BIBLIOGRAPHY ON PROPULSION AIRFRAME INTEGRATION TECHNOLOGIES FOR HIGH-SPEED CIVIL TRANSPORT APPLICATIONS, 1980-1991
David J. Anderson and Masashi Mizukami Mar. 1993 343 p
(RTOP 537-02-23)
(NASA-TM-105602; E-6938; NAS 1.15:105602) Avail: CASI HC A15/MF A03

NASA has initiated the High Speed Research (HSR) program with the goal to develop technologies for a new generation, economically viable, environmentally acceptable, supersonic transport (SST) called the High Speed Civil Transport (HSCT). A significant part of this effort is expected to be in multidisciplinary systems integration, such as in propulsion airframe integration (PAI). In order to assimilate the knowledge database on PAI for SST type aircraft, a bibliography on this subject was compiled. The bibliography with over 1200 entries, full abstracts, and indexes. Related topics are also covered, such as the following: engine inlets, engine cycles, nozzles, existing supersonic cruise aircraft, noise issues, computational fluid dynamics, aerodynamics, and external interference. All identified documents from 1980 through early 1991 are included; this covers the latter part of the NASA Supersonic Cruise Research (SCR) program and the beginnings of the HSR program. In addition, some pre-1980 documents of significant merit or reference value are also included. The references were retrieved via a computerized literature search using the NASA RECON database system. Author (revised)

N93-26168# Naval Postgraduate School, Monterey, CA.
SPECIAL TOOLING DISPOSITION FOR AIRCRAFT ENTERING POST PRODUCTION SUPPORT M.S. Thesis
Lee G. Ebert Dec. 1992 53 p
(AD-A261614) Avail: CASI HC A04/MF A01

This thesis identifies and analyzes an important element of Department of Defense (DoD) Post Production Support (PPS) for plan execution: the

disposition of special tooling used to support future manufacturing of aircraft components. As a first step, PPS and its goals are described. Next, the DoD policies for special tooling management are described. Finally, the effects of special tooling disposition are analyzed and a decision process for disposition is presented which incorporates these effects. Further research is recommended to measure the effects tooling disposition decisions have on lead times and manufacturing costs when considering conventional, Rapid Acquisition of Manufactured Parts (RAMP) or Flexible Manufacturing System (FMS) manufacturing methods. DTIC

N93-26238# Air Force Inst. of Tech., Wright-Patterson AFB, OH. Foreign Aerospace Science and Technology Center.
AN ANALYSIS OF THE RELIABILITY AND MAINTAINABILITY OF THE JIAN 6 AND JIAN 7 AIRCRAFT AND WAYS TO IMPROVE THEM
Li Zishang and Mao Jingli 27 Jan. 1993 14 p Transl. into ENGLISH from unidentified Chinese document p 2-6
(Contract F33657-88-D-2188)
(AD-A261060; FASTC-ID(RS)T-0628-92) Avail: CASI HC A03/MF A01

Reliability and maintainability are major standards for measuring the superiority of an aircraft. They are major factors in the combat capabilities of the Air Force. Striving to improve and enhance the reliability and maintainability of the aircraft with which the Naval Air Forces are currently primarily equipped, the Jian 6 and the Jian 7, are urgent tasks of Air Force maintenance operations. This article presents a thorough and wide ranging survey of aircraft manufacturing facilities and Naval Air Force Unit plants, and by combining, analyzing and studying this survey, it presents methods and means of improving the reliability and maintainability of the Jian 6 and Jian 7 aircraft. DTIC

N93-26325# Joint Publications Research Service, Washington, DC.
JPRS REPORT: CENTRAL EURASIA. AVIATION AND COSMONAUTICS, NO. 9, SEPTEMBER 1992
26 Apr. 1993 33 p
(JPRS-UAC-93-003) Avail: CASI HC A03/MF A01

Translated articles cover the following topics: independent body to protect professional interests of pilots sought; future use of artificial intelligence on fighters considered; theoretical refinement to Zhukovskiy aerodynamic theorem proposed; comprehensive approach to seeking causes of air accidents urged; consideration of psychological factors in training and performance; new edition of aviation engineering support manual; a description of the plight of CIS strategic fliers outside Russia; more history of failed N1-L3 Lunar Launch-Vehicle Project; a plan to counter ozone layer destruction with space-based mirrors; Soviet air advisor recalls Vietnam tactics against B-52 Bombers; and comparison of ZMS2 and KC-135A tanker aircraft data. CASI

N93-26422*# National Aeronautics and Space Administration, Washington, DC.
AERONAUTICS IN NACA AND NASA
[1991] 81 p Original contains color illustrations
(NASA-NP-156; NAS 1.83:156) Avail: CASI HC A05/MF A01; 13 functional color pages

Initiated in 1915, the National Advisory Committee for Aeronautics/National Aeronautics and Space Administration (NACA/NASA) aeronautical programs have been the keystone of a sustained U.S. Government, industry, and university research effort which has been a primary factor in the development of our remarkable air transportation systems, the country's largest positive trade balance component, and the world's finest military Air Force. This overview summarizes the flow of events, and the major trends, that have led from the NACA origins to the present NASA Aeronautics program, and indicates some important directions for the years ahead. Derived from text

02 AERODYNAMICS

Includes aerodynamics of bodies, combinations, wings, rotors, and control surfaces; and internal flow in ducts and turbomachinery.

For related information see also *34 Fluid Mechanics and Heat Transfer.*

N93-24736*# Eloret Corp., Sunnyvale, CA.
DEVELOPMENT AND APPLICATION OF COMPUTATIONAL AEROTHERMODYNAMICS FLOWFIELD COMPUTER CODES Progress Report, 1 Apr. 1992 - 31 Jan. 1993
Ethiraj Venkatapathy 23 Apr. 1993 157 p
(Contract NCC2-420)
(NASA-CR-192940; NAS 1.26:192940) Avail: CASI HC A08/MF A02

Computations are presented for one-dimensional, strong shock waves that are typical of those that form in front of a reentering spacecraft. The fluid mechanics and thermochemistry are modeled using two different approaches. The first employs traditional continuum techniques in solving the Navier-Stokes equations. The second-approach employs a particle simulation technique (the direct simulation Monte Carlo method, DSMC). The thermochemical models employed in these two techniques are quite different. The present investigation presents an evaluation of thermochemical models for nitrogen under hypersonic flow conditions. Four separate cases are considered. The cases are governed, respectively, by the following: vibrational relaxation; weak dissociation; strong dissociation; and weak ionization. In near-continuum, hypersonic flow, the nonequilibrium thermochemical models employed in continuum and particle simulations produce nearly identical solutions. Further, the two approaches are evaluated successfully against available experimental data for weakly and strongly dissociating flows. Author (revised)

N93-24756 Georgia Inst. of Tech., Atlanta.
AN AEROELASTIC MODEL STRUCTURE INVESTIGATION FOR A MANNED REAL-TIME ROTORCRAFT SIMULATION Ph.D. Thesis
William Dean Lewis 1992 295 p
Avail: Univ. Microfilms Order No. DA9303126

Historically, rotorcraft simulations have assumed a model structure incorporating rigid blades and uniform inflow. Advances in computational techniques and rotorcraft theory have enabled the inclusion of higher order model elements into the real-time simulation. This research addresses a model structure assessment of a flexible rotary wing manned flight simulation. The model is a UH-60 blade element simulation. The model possesses a unique capability to provide a variable model structure with consistent matching between structural and aerodynamic theory. The structural model is a representation of the flexible blade based on apriori data. The dynamic inflow model is an adaptation of the Peters and He theory. The investigation methodology consisted of a piloted assessment, frequency domain, and time domain criteria evaluations. Real-time operation permitted a piloted evaluation with rapid alterations to the model structure in question. Frequency response testing permitted an evaluation of the mid to high frequency range. The Comprehensive Identification from Frequency Response (CIFER) program was used for determining the frequency responses. Time domain response was obtained by driving the simulator controls, recording the resultant response, and comparing it to flight test data. This testing methodology was a comprehensive approach which investigated the full range of operation including objective and perceptual fidelity. The CIFER program was invaluable as a frequency response tool. Results indicated that an increase in dynamic wake complexity increased the damping of the heave, pitch and roll channels. Inclusion of blade elasticity reduced the control sensitivity and increased the excitation of existing system modes. The real-time, coupled, simultaneous solution methodology for rotorcraft modeling was superior to previous techniques for off-axis and modal predictions. The previous used model assumptions of rigid blades and uniform inflow resulted in dramatic errors in off-axis response and predictability. The inclusion of second harmonic blade dynamics and dynamic wake is essential for a simulation used in analysis, design, flight test training, and modal prediction. Dissert. Abstr.

N93-24772 Stanford Univ., CA.
COMPUTATIONAL STUDY OF THE AERODYNAMICS AND CONTROL BY BLOWING OF ASYMMETRIC VORTICAL FLOWS OVER DELTA

WINGS Ph.D. Thesis
Kenneth John Craig 1992 126 p
Avail: Univ. Microfilms Order No. DA9302194

The flowfield produced by tangential leading-edge blowing on a rounded leading-edge 60-degree delta wing is investigated computationally by solving the Thin-Layer Navier-Stokes equations. Steady-state flowfields are calculated for various angles of attack and yaw, with and without the presence of tangential leading-edge blowing. The numerical grid is generated using algebraic generation and various interpolation and blending techniques. The jet emanates from a slot with linearly-varying thickness and is introduced into the flowfield using the concept of an actuator plane, thereby not requiring resolution of the jet slot geometry. The Baldwin-Lomax algebraic turbulence model is used to provide turbulent closure. The computational results are compared with those of experiments. The effectiveness of blowing as a rolling moment control mechanism to extend the envelope of controllability is illustrated at different angles of attack. The saturation effect of increased blowing is captured well in the computations. Control reversal noted in similar experimental studies is also observed in the computations. The results are combined in a model by observing the variation of forces and moments with the parameters angle of attack, sideslip angle and blowing momentum coefficient. The model attempts to explain the physical behavior and provides a structured way to study flows of this type. Dissert. Abstr.

N93-24911*# National Aeronautics and Space Administration. Lewis Research Center, Cleveland, OH.
SURFACE AND FLOW FIELD MEASUREMENTS IN A SYMMETRIC CROSSING SHOCK WAVE/TURBULENT BOUNDARY-LAYER INTERACTION
D. O. Davis and W. R. Hingst Jun. 1992 20 p Presented at the 10th AIAA Applied Aerodynamics Conference, Palo Alto, CA, 22-24 Jun. 1992; sponsored by AIAA Previously announced in IAA as A92-45574
(RTOP 505-62-52)
(NASA-TM-106086; E-7716; NAS 1.15:106086; AIAA Paper 92-2634)
Avail: CASI HC A03/MF A01

Results of an experimental investigation of a symmetric crossing shock/turbulent boundary layer interaction are presented for a Mach number of 3.44 and deflection angles of 2, 6, 8, and 9 degrees. The interaction strengths vary from weak to strong enough to cause a large region of separated flow. Measured quantities include surface static pressure (both steady and unsteady) and flowfield Pitot pressures. Pitot profiles in the plane of symmetry through the interaction region are shown for various deflection angles. Oil flow visualization and the results of a trace gas streamline tracking technique are also presented. Author

N93-25074*# National Aeronautics and Space Administration. Langley Research Center, Hampton, VA.
HIGH-ORDER CYCLO-DIFFERENCE TECHNIQUES: AN ALTERNATIVE TO FINITE DIFFERENCES
Mark H. Carpenter and John C. Otto Mar. 1993 29 p
(RTOP 505-70-62-06)
(NASA-TM-107745; NAS 1.15:107745) Avail: CASI HC A03/MF A01

The summation-by-parts energy norm is used to establish a new class of high-order finite-difference techniques referred to here as 'cyclo-difference' techniques. These techniques are constructed cyclically from stable subelements, and require no numerical boundary conditions; when coupled with the simultaneous approximation term (SAT) boundary treatment, they are time asymptotically stable for an arbitrary hyperbolic system. These techniques are similar to spectral element techniques and are ideally suited for parallel implementation, but do not require special collocation points or orthogonal basis functions. The principal focus is on methods of sixth-order formal accuracy or less; however, these methods could be extended in principle to any arbitrary order of accuracy. Author

N93-25075*# Continuum Dynamics, Inc., Princeton, NJ.
ROTOR DESIGN OPTIMIZATION USING A FREE WAKE ANALYSIS
Todd R. Quackenbush, Alexander H. Boschitsch, Daniel A. Wachspress, and Kiat Chua Apr. 1993 133 p
(Contract NAS2-13092; RTOP 505-59-36)
(NASA-CR-177612; A-93050; NAS 1.26:177612) Avail: CASI HC A07/MF A02

The aim of this effort was to develop a comprehensive performance optimization capability for tiltrotor and helicopter blades. The analysis incorporates the validated EHPIC (Evaluation of Hover Performance using Influence Coefficients) model of helicopter rotor aerodynamics within a general linear/quadratic programming algorithm that allows optimization using a variety of objective functions involving the performance. The resulting computer code, EHPIC/HERO (HElicopter Rotor Optimization), improves upon several features of the previous EHPIC performance model and allows optimization utilizing a wide spectrum of design variables, including twist, chord, anhedral, and sweep. The new analysis supports optimization of a variety of objective functions, including weighted measures of rotor thrust, power, and propulsive efficiency. The fundamental strength of the approach is that an efficient search for improved versions of the baseline design can be carried out while retaining the demonstrated accuracy inherent in the EHPIC free wake/vortex lattice performance analysis. Sample problems are described that demonstrate the success of this approach for several representative rotor configurations in hover and axial flight. Features that were introduced to convert earlier demonstration versions of this analysis into a generally applicable tool for researchers and designers is also discussed. Author (revised)

N93-25083*# Institute for Computer Applications in Science and Engineering, Hampton, VA.
A CONTRIBUTION TO THE GREAT RIEMANN SOLVER DEBATE
James J. Quirk Washington Nov. 1992 34 p Submitted for publication to the International Journal for Numerical Methods in Fluids
(Contracts NAS1-18605; NAS1-19480; RTOP 505-90-52-01)
(NASA-CR-191409; NAS 1.26:191409; ICASE-92-64; AD-A2599994) Avail: CASI HC A03/MF A01

The aims of this paper are threefold: to increase the level of awareness within the shock capturing community to the fact that many Godunov-type methods contain subtle flaws that can cause spurious solutions to be computed; to identify one mechanism that might thwart attempts to produce very high resolution simulations; and to proffer a simple strategy for overcoming the specific failings of individual Riemann solvers. Author

N93-25091*# National Aeronautics and Space Administration. Ames Research Center, Moffett Field, CA.
APPLIED AERODYNAMICS: CHALLENGES AND EXPECTATIONS
Victor L. Peterson and Charles A. Smith Feb. 1993 20 p Presented at the AIAA 10th Applied Aerodynamics Conference, Palo Alto, CA, 22-24 Jun. 1992 Original contains color illustrations
(RTOP 505-90-00)
(NASA-TM-103963; A-92160; NAS 1.15:103963) Avail: CASI HC A03/MF A01; 1 functional color page

Aerospace is the leading positive contributor to this country's balance of trade, derived largely from the sale of U.S. commercial aircraft around the world. This powerfully favorable economic situation is being threatened in two ways: (1) the U.S. portion of the commercial transport market is decreasing, even though the worldwide market is projected to increase substantially; and (2) expenditures are decreasing for military aircraft, which often serve as proving grounds for advanced aircraft technology. To retain a major share of the world market for commercial aircraft and continue to provide military aircraft with unsurpassed performance, the U.S. aerospace industry faces many technological challenges. The field of applied aerodynamics is necessarily a major contributor to efforts aimed at meeting these technological challenges. A number of emerging research results that will provide new opportunities for applied aerodynamicists are discussed. Some of these have great potential for maintaining the high value of contributions from applied aerodynamics in the relatively near future. Over time, however, the value of these contributions will diminish greatly unless substantial investments continue to be made in basic and applied research efforts. The focus: to increase understanding of fluid dynamic phenomena, identify new aerodynamic concepts, and provide validated advanced technology for future aircraft. Author (revised)

N93-25117*# Old Dominion Univ., Norfolk, VA. Dept. of Mechanical Engineering and Mechanics.
GRID SENSITIVITY FOR AERODYNAMIC OPTIMIZATION AND FLOW ANALYSIS Progress report, period ending Dec. 1992
I. Sadrehaghighi and S. N. Tiwari Apr. 1993 120 p
(Contract NCC1-68)
(NASA-CR-192980; NAS 1.26:192980) Avail: CASI HC A06/MF A02

After reviewing relevant literature, it is apparent that one aspect of aerodynamic sensitivity analysis, namely grid sensitivity, has not been investigated extensively. The grid sensitivity algorithms in most of these studies are based on structural design models. Such models, although sufficient for preliminary or conceptional design, are not acceptable for detailed design analysis. Careless grid sensitivity evaluations, would introduce gradient errors within the sensitivity module, therefore, infecting the overall optimization process. Development of an efficient and reliable grid sensitivity module with special emphasis on aerodynamic applications appear essential. The organization of this study is as follows. The physical and geometric representations of a typical model are derived in chapter 2. The grid generation algorithm and boundary grid distribution are developed in chapter 3. Chapter 4 discusses the theoretical formulation and aerodynamic sensitivity equation. The method of solution is provided in chapter 5. The results are presented and discussed in chapter 6. Finally, some concluding remarks are provided in chapter 7. Author

N93-25121# Sandia National Labs., Albuquerque, NM.
A SIMPLE, APPROXIMATE MODEL OF PARACHUTE INFLATION
J. M. Macha 1992 10 p Presented at the 12th Royal Aeronautical Society/American Institute of Aeronautics and Astronautics (RAS/AIAA) Aerodynamic Decelerator Systems Technical Conference, London, England, 10 May 1993
(Contract DE-AC04-76DP-00789)
(DE93-002465; SAND-92-2282C; CONF-930580-1) Avail: CASI HC A02/MF A01

A simple approximate model of parachute inflation is described. The model is based on the traditional, practical treatment of the fluid resistance of rigid bodies in nonsteady flow, with appropriate extensions to accommodate the change in canopy inflated shape. Correlations for the steady drag and steady radial force as functions of the inflated radius are required as input to the dynamic model. In this approach, the radial force is expressed in terms of easily obtainable drag and reefing fine tension measurements. A series of wind tunnel experiments provides the needed correlations. Coefficients associated with the added mass of fluid are evaluated by calibrating the model against an extensive and reliable set of flight data. A parameter is introduced which appears to universally govern the strong dependence of the axial added mass coefficient on motion history. Through comparisons with flight data, the model is shown to realistically predict inflation forces for ribbon and ringslot canopies over a wide range of sizes and deployment conditions. DOE

N93-25153*# Institute for Computer Applications in Science and Engineering, Hampton, VA.
INSTABILITY OF FLOW IN A STREAMWISE CORNER Final Report
Manhar R. Dhanak (Florida Atlantic Univ., Boca Raton.) Washington Dec. 1992 18 p Submitted for publication Sponsored by NASA. Langley Research Center
(Contract NAS1-19480; RTOP 505-90-52-01)
(NASA-CR-191410; NAS 1.26:191410; ICASE-92-70) Avail: CASI HC A03/MF A01

The linear stability of an incompressible laminar flow in the blending boundary layer between the boundary layer in a 90 deg streamwise corner and a Blasius boundary layer well away from the corner is examined using a locally parallel flow approximation. It is shown that the influence of the outer boundary conditions associated with oblique modes of disturbances which are anti-symmetric about the bisector plane have a profound effect on the stability of the flow. As a result, in good agreement with observation, the critical streamwise Reynolds number, associated with a spanwise location is significantly reduced as the corner is approached, being R(sub Cr) = 60 approximately for spanwise distance of $z^* = 6x^*R(\text{sup } -1)$ from the corner compared with R(sub Cr) = 322 approximately for $z^* = 20x^*R(\text{sup } -1)$, where x^* measures downstream distance from the leading edges. At R = 600, the growth rate of the most amplified mode of disturbance at the former location is over six times greater than that at the latter; the corresponding wave angle at the two locations is respectively 44 deg and 5 deg, approximately. Author (revised)

N93-25249*# Pennsylvania State Univ., University Park. Gas Dynamics Lab.
SUPERSONIC SHOCK WAVE/VORTEX INTERACTION Final Technical Report, 1 Apr. 1989 - 30 Sep. 1992
G. S. Settles and L. Cattafesta Apr. 1993 43 p
(Grant NAG2-575)
(NASA-CR-192917; NAS 1.26:192917) Avail: CASI HC A03/MF A01

Although shock wave/vortex interaction is a basic and important fluid dynamics problem, very little research has been conducted on this topic. Therefore, a detailed experimental study of the interaction between a supersonic streamwise turbulent vortex and a shock wave was carried out at the Penn State Gas Dynamics Laboratory. A vortex is produced by replaceable swirl vanes located upstream of the throat of various converging-diverging nozzles. The supersonic vortex is then injected into either a coflowing supersonic stream or ambient air. The structure of the isolated vortex is investigated in a supersonic wind tunnel using miniature, fast-response, five-hole and total temperature probes and in a free jet using laser Doppler velocimetry. The cases tested have unit Reynolds numbers in excess of 25 million per meter, axial Mach numbers ranging from 2.5 to 4.0, and peak tangential Mach numbers from 0 (i.e., a pure jet) to about 0.7. The results show that the typical supersonic wake-like vortex consists of a non-isentropic, rotational core, where the reduced circulation distribution is self similar, and an outer isentropic, irrotational region. The vortex core is also a region of significant turbulent fluctuations. Radial profiles of turbulent kinetic energy and axial-tangential Reynolds stress are presented. The interactions between the vortex and both oblique and normal shock waves are investigated using nonintrusive optical diagnostics (i.e. schlieren, planar laser scattering, and laser Doppler velocimetry). Of the various types, two Mach 2.5 overexpanded-nozzle Mach disc interactions are examined in detail. Below a certain vortex strength, a 'weak' interaction exists in which the normal shock is perturbed locally into an unsteady 'bubble' shock near the vortex axis, but vortex breakdown (i.e., a stagnation point) does not occur. For stronger vortices, a random unsteady 'strong' interaction results that causes vortex breakdown. The vortex core reforms downstream of the rear stagnation point, and the reduced circulation distribution once again becomes self-similar in this region. A new model of this interaction is proposed. Finally, a curve defining the approximate limits of supersonic vortex breakdown is presented.
Author (revised)

N93-25269 Virginia Polytechnic Inst. and State Univ., Blacksburg.
THE TRANSIENT DEVELOPMENT OF VORTICES OVER DELTA WINGS Ph.D. Thesis
Othon Kons Rediniotis 1992 359 p
Avail: Univ. Microfilms Order No. DA9304624

An experimental investigation was carried out on the flow over a 75 deg-sweep delta wing. The flowfield over a stationary delta wing at high angles of attack was studied, particularly focusing on breakdown behavior and natural unsteadiness. Static surface pressure measurements on the leeward side of the model were obtained for different Reynolds numbers and angles of attack. Detailed velocity fields, mapped out by a seven-hole probe and two different laser-Doppler velocimetry (LDV) systems, were studied to provide information on the structure of the leading-edge vortices. Comparisons were made of the results obtained using intrusive and non-intrusive techniques. Through surface pressure and velocity power spectra, organized periodic activity in the broken down vortex was detected and studied. The flowfield over a delta wing performing dynamic pitch-up motions was also investigated. Unsteady surface pressures were measured and compared with the steady case pressure distributions. The unsteady velocity field on different planes was mapped out using a specially manufactured and calibrated fast-response seven-hole probe as well as a 3-D and a 3-D laser-Doppler velocimeter. The transient development of the leading-edge vortices in terms of velocity and vorticity distribution was carefully studied. The flowfield in the wake of the delta wing was also examined at angles of attack as high as alpha = 90 deg, using hot-wire anemometry and flow visualization. Periodic vortex shedding was detected and its characteristics, such as Strouhal number variation and modes of shedding, were studied. Dissert. Abstr.

N93-25274 Colorado Univ., Boulder.
AERODYNAMIC FOUNDATIONS FOR USE OF UNSTEADY AERODYNAMIC EFFECTS IN FLIGHT CONTROL Ph.D. Thesis
Thomas Eugene McLaughlin 1992 177 p
Avail: Univ. Microfilms Order No. DA9304582

Unsteady aerodynamic effects have long been postulated as a means to enhance low speed performance of aircraft. Lift coefficients as high as

four to five times greater than the steady state values are possible. However, before the phenomenon can be exploited, the temporal nature of these forces must be quantified and predicted over the widest possible range of forcing conditions. Unsteady aerodynamic force generation collected from numerous experimental efforts was examined over a wide range of non-dimensional pitch rates, Reynolds numbers, mach numbers, and sinusoidal and constant rate motion histories. Airfoils tested included those of varying camber and with two- and three-dimensional geometries. Unsteady aerodynamic forces were found to change linearly with non-dimensional time. The duration of the unsteady event was found to be a function only of non-dimensional pitch rate or frequency, and of the initial state of the airfoil. Force magnitudes generated at any given time in the event were found to depend simply on the same parameters and on airfoil static characteristics. Sinusoidal and constant rate pitch motions were found to produce very similar force histories. Increasing airfoil sweep improved the duration of the unsteady event. In all cases, the unsteady forces produced were found highly predictable and well-correlated across the range of forcing parameters. These findings offer a basis on which flight control algorithms may be developed to increase aircraft low speed turn performance.

Dissert. Abstr.

N93-25339 Minnesota Univ., Minneapolis.
A NUMERICAL AND EXPERIMENTAL STUDIES OF FLOW CHARACTERISTICS IN CENTRIFUGAL FANS Ph.D. Thesis
Linxi Xia 1992 282 p
Avail: Univ. Microfilms Order No. DA9234032

Flow characteristics, performances, and noises of centrifugal fans were studied. The work can be grouped as: (1) experimentally examining the flow structure downstream of the impeller and its relationship with noise characteristics; (2) numerically simulating the flow field in impeller and fan housings, and establishing their aerodynamic design criteria; and (3) exploring new and more accurate sound rating and low-frequency fluctuation simulation methods. The objective is to increase understanding of fan aerodynamic noise generation mechanism, to advance engineering analysis and design tools, and to improve the efficiency and acoustic performances of the current centrifugal fans. The test results showed that the fan components designed with the proposed aerodynamic design method have 5 percent efficiency improvement and 3-15 dB noise reduction over the current designs. Also, the design effectiveness was increased significantly compared with the traditional fan design methods. Dissert. Abstr.

N93-25388 Arizona State Univ., Tempe.
NUMERICAL SIMULATION OF LEADING-EDGE RECEPTIVITY TO FREESTREAM VORTICITY Ph.D. Thesis
Thomas Alan Buter 1992 199 p
Avail: Univ. Microfilms Order No. DA9237239

The receptivity to freestream vorticity of the boundary layer over a flat plate with an elliptic leading edge is investigated numerically. The flow is simulated by solving the incompressible Navier-Stokes system in general curvilinear coordinates with the vorticity and stream function as dependent variables. A finite-difference scheme which is second-order accurate in both space and time is used. As a first step, the steady basic-state solution is computed. Then a small-amplitude vortical disturbance is introduced at the upstream boundary and the governing equations solved time accurately to evaluate the spatial and temporal growth of the perturbations leading to instability waves (Tollmien-Schlichting waves) in the boundary layer. Disturbance amplitude, orientation, the effect of the leading edge and of juncture curvature are investigated for the case of spanwise vorticity. Simulations reveal, for the conditions considered, a linear variation in the TS response with forcing amplitude for a perturbation of the freestream velocity which is either symmetrical or asymmetrical with respect to the basic-state stagnation streamline. The presence of a large transverse component of velocity along the basic-state stagnation streamline for the case of an asymmetrical perturbation of velocity results in the appearance of a superharmonic component near the nose. This superharmonic decays rapidly along the nose for the flow conditions considered. In all cases considered, the first clear appearance of the TS mode occurs aft of the surface pressure-gradient maximum in the juncture region. Changes to the geometry which increase the maximum the basic-state pressure gradient near the juncture are found to increase receptivity.

Dissert. Abstr.

N93-25409 Colorado Univ., Boulder.
COMPUTATION OF TRANSONIC FLOW OVER A POROUS SURFACE PROJECTILE Ph.D. Thesis
Jih-Lan Hsiung 1992 144 p
Avail: Univ. Microfilms Order No. DA9304565

A numerical tool is constructed to predict the aerodynamic performance of a projectile, and to examine the effects of making a part of the projectile surface porous on its performance in the transonic regime, 0.9 less than M less than 1.2. The code developed in this study, POROUS, includes the Darcy's law describing the flow through a porous surface and a turbulence model taking the transpiration effect into consideration. The computed results for transonic flow over a solid secant-ogive-cylinder-boattail (SOCBT) projectile show good agreements with experimental data in both pressure coefficient distribution and shock wave location. For the Mach numbers and angles of attack that have been examined so far for the solid SOCBT, the surface pressure predicted by our POROUS code is found to be more accurate than those by other numerical and semi-empirical codes. The passive control technique by using porous surface to reduce the total drag of a projectile has been investigated here for Mach numbers from 0.90 to 1.2 and angles of attack 0 to 4 degrees. The porous surface works very well in drag reduction at subsonic Mach numbers 0.94-0.98 when there are strong shocks on the boattail. At Mach 0.96, a total drag reduction as high as 28.43 percent has been achieved with properly selected porous surfaces. With an angle of attack, the efficiency of drag reduction can be improved if splitters are placed in the cavity, and the lift may also be increased. According to the present analysis, having porous surfaces of uniform porosity on both cylinder and boattail is found to be the most efficient arrangement. The total drag decreases with increasing maximum porosity factor, whose limiting value has been determined. The porosity is more effective if the original shock on the solid projectile is near the rear of the porous region on the cylinder; otherwise, efficiency increases with the length of the porous surface. Dissert. Abstr.

N93-25467 Oxford Univ. (England).
AN EXPERIMENTAL STUDY OF UNDER-EXPANDED JETS Ph.D. Thesis
Terrence M. Cain 1991 156 p
Avail: Univ. Microfilms Order No. BRD-98281

Experiments were conducted on turbulent under-expanded jets of nitrogen and carbon dioxide exhausted into still air from Mach 3 and Mach 5 conical nozzles. The ratio of the stagnation pressure in the nozzle to the static pressure in the receiving tank was of the order 10(exp 3) which is a condition representative of rocket exhaust plumes generated at altitudes near 20 km. The Oxford gun tunnel was adapted for the project by attaching a small nozzle to its barrel. Jets were generated in the tunnel's test section, photographed with a schlieren system and traversed by a Pitot probe. The traverse mechanisms developed for this work allow 100 mm travel during the period of 20 ms over which the tunnel stagnation pressure is constant. Methods of increasing this steady period (the test time) by modification of the tunnel's driver tube are suggested after a detailed investigation of the tunnel's operation. Pitot pressure surveys which reveal the plume structure and provide information about the turbulent mixing downstream of the first shock cell are presented. The measurements in plumes at various pressure ratios are correlated by normalizing the probe position with the size of the first shock cell and normalizing the Pitot pressure by the pressure in the receiver. The characteristics of under-expanded jets are summarized and available experimental data is reviewed and classified using recently published plume similarity parameters. The asymmetrical nature of plumes is discussed and a physical explanation for plume shock layer instability is given. Condensation of the plume gas is investigated by reference to previous experiments and theoretical models. It is shown that it is unlikely that condensation occurred anywhere within the nitrogen plumes as drop growth rates are negligible at high entropy. Method of characteristics (MOC) calculations of the initial plume expansion were compared with the Pitot measurements in the plume core. Variation of the nozzle exit conditions used for the boundary conditions of the MOC predictions is used to demonstrate that viscous and two-dimensional effects within the nozzle were not very significant. Dissert. Abstr.

N93-25487# Virginia Polytechnic Inst. and State Univ., Blacksburg.
EXPERIMENTAL AND COMPUTATIONAL INVESTIGATION OF HELIUM INJECTION INTO AIR AT SUPERSONIC AND HYPERSONIC SPEEDS

Ph.D. Thesis
Eric James Fuller 1992 187 p
Avail: Univ. Microfilms Order No. DA9233626

Experiments were performed to determine the mixing rate and core penetration of the injectant and the flow field total pressure losses when gaseous injection occurs into a supersonic freestream. Tested in a freestream Mach number of 3.0 and a freestream Reynolds number of 5.0 x 10(exp 7)/m, was a single, sonic 5x underexpanded helium jet with a transverse angle of 30 degrees, and rotated from 0 to -28 degrees to test injector yaw effects. Tested at Mach 6.0 with a freestream Reynolds number of 5.4 x 10(exp 7)/m, was an array of three supersonic, 5x underexpanded helium injectors with an exit Mach number of 1.7 and a transverse angle of 15 degrees. This injector array was tested at yaw angles of 0 and -15 degrees. Surface flow visualization showed that significant flow asymmetries were produced by injector yaw. Nanosecond exposure shadowgraph pictures showed the injection plume to be unsteady, and further studies demonstrated this unsteadiness to be related to observed shock waves orthogonal to the injectant bow shock, generated at a frequency of 30 kHz. The primary data technique was a concentration probe which measured the flow field molar concentration of helium. Concentration and meanflow data were taken at several downstream stations and yielded contours of helium concentration, total pressure, Mach number, as well as other flow field properties. The injectant mixing rates, expressed as the maximum concentration decay rates, and mixing distances were found to be unaffected by injector yaw, in the Mach 3.0 experiments, but adversely affected by injector yaw in the Mach 6.0 experiments. One promising aspect of injector yaw was that as the yaw angle was increased, lateral motion of the injectant plume became significant, and the turbulent mixing region increased by approximately 34 percent. Comparisons of the 15 degree injection into a Mach 6.0 flow to previous experiments with 15 degree injection into a Mach 3.0 freestream, demonstrated that there was a significant decrease in initial mixing, at Mach 6.0, resulting in a much longer mixing distance. From a parametric computational study of the Mach 6.0 experiments, the effects of adjacent injectors was found to decrease lateral spreading while increasing the vertical penetration of the injectant plume, and marginally increasing the injectant core decay rate. Dissert. Abstr.

N93-25542 Stanford Univ., CA.
NAVIER-STOKES SIMULATIONS OF UNSTEADY TRANSONIC FLOW PHENOMENA Ph.D. Thesis
Christopher Alexande Atwood 1992 131 p
Avail: Univ. Microfilms Order No. DA9234053

Numerical simulation of two classes of unsteady flows are obtained via the Navier-Stokes equation: a blast-wave/target interaction problem class and a transonic cavity flow problem class. The method developed for the viscous blast-wave/target interaction problem assumes a laminar, perfect gas implemented in a structured finite-volume framework. The approximately factored implicit scheme uses Newton subiterations to obtain the spatially and temporally second-order accurate time history of the interaction of blast-waves with stationary targets. The inviscid flux is evaluated using either of two upwind techniques, while the full viscous terms are computed by central differencing. Comparisons of unsteady numerical, analytical, and experimental results are made in two- and three-dimensions for Couette flows, a starting shock-tunnel, and a shock-tube blocking study. The results show accurate wave speed resolution and nonoscillatory discontinuity capturing of the predominantly inviscid flows. Viscous effects were increasingly significant at large post-interaction times. While the blast-wave/target interaction problem benefits from high resolution methods applied to the Euler terms, the transonic cavity flow problem requires the use of an efficient scheme implemented in a geometrically flexible overset mesh environment. Hence, the Reynolds averaged Navier-Stokes equations implemented in a diagonal form are applied to the cavity flow class of problems. Comparisons between numerical and experimental results are made in two-dimensions for free shear layers and both rectangular and quieted cavities, and in three-dimensions for Stratospheric Observatory For Infrared Astronomy (SOFIA) geometries. The acoustic behavior of the rectangular and three-dimensional cavity flows compare well with experiment in terms of frequency, magnitude, and quieting trends. However, there is a more rapid decrease in computed, acoustic energy with frequency than observed experimentally owing to numerical dissipation. In addition, optical phase distortion due to the time-varying density field is modelled using geometrical constructs. The computed optical distortion trends compare with the experimentally inferred result, but underpredicts the fluctuating phase difference magnitude. Dissert. Abstr.

N93-25545 Stanford Univ., CA.
TANGENTIAL FUSELAGE BLOWING ON AN OGIVE CYLINDER Ph.D. Thesis
Gabriel Ivan Font 1992 193 p
Avail: Univ. Microfilms Order No. DA9234095

The nose vortices of aircraft or missiles tend to become asymmetric at high angles of attack producing a side force which is destabilizing to the body. A jet located near the nose and blown tangentially to the fuselage has the ability to alter the flow field and diminish the unwanted side force. Alternatively, it can produce a large side force which can be used for improving the maneuverability of the vehicle. This work explores the effects of tangential blowing on the vortical structures that develop about the fuselage of a missile or aircraft at a high angle of attack. A tangent-ogive cylinder configuration was used to allow comparison with experiments. The study was carried out numerically by solving the Thin-Layer, Reynolds-Averaged, compressible Navier-Stokes equations. A zonal method was used to solve the equations. The jet was implemented with an actuator plane. Computations were conducted in a fully laminar and a fully turbulent manner. Appropriate algebraic turbulence models were used for the jet and the boundary layers in the turbulent computations. The study was conducted at a Reynolds number, based on diameter, of 52000, and Mach number of 0.2. The angles of attack used were 10, 30 and 45 deg. The influence of slot location were also explored. This study confirmed that large side forces could be generated from tangential blowing even at low angles of attack. Several conclusions were made concerning the physical mechanisms by which the jet interacts with the ambient flow field to produce a side force: (1) A pressure gradient normal to the surface is created near the wall due to the momentum of the jet being forced to follow the curvature of the surface. (2) A large amount of vorticity is added to the flow field by the jet. In the region of the slot, the vorticity has the effect of inducing circulation around the body. Downstream of the slot, the vorticity alters the strength of the nose vortices. And (3), the position of the nose vortices can be altered by the actions of the jet.
Dissert. Abstr.

N93-25664 Georgia Inst. of Tech., Atlanta.
AN INVESTIGATION ON PLANAR VELOCIMETRY BY SPATIAL CROSS-CORRELATION Ph.D. Thesis
Philip Andrew Fawcett 1992 213 p
Avail: Univ. Microfilms Order No. DA9303118

Advances in rotorcraft aerodynamics require the ability to measure instantaneous velocity fields with high temporal resolution over large areas. Existing measurement techniques are not adequate for such flows. This thesis explores planar velocimetry by spatial cross correlation. The spatial cross correlation is determined between two flowfield images separated by a known time delay. Unlike existing particle image velocimetry (PIV) techniques, there is no need to resolve individual particles. Instead, patterns of scattered light intensity are used to determine statistical correlations. With this process, the time required to measure velocity fields is vastly reduced. The post-processing is reduced to a completely computational procedure which takes advantage of the rapid advances in computer technology. This technique is seen to be a superset of PIV and laser speckle techniques. Numerical simulations were used to prove that the technique gives correct results with deterministic and random data, and it performs accurately despite the presence of high levels of noise. Initial experimental validation was performed using a moving solid surface with a random, fine grained pattern. The technique was next extended to the measurement of steady and unsteady flows in a water table with a standard video camera and ambient lighting. Low-speed and then high-speed air flows were measured using light sources ranging from a high-powered, pulsed, copper vapor laser to a 9 volt flashlight. A variety of imaging and computer equipment investigated during the development of SCV is described in the thesis along with the chronology of the experiments. The final form of the system is described in detail and consists of a dual camera imaging system coupled with an MS-DOS based computer and video digitizing board. Three advanced applications were used successfully to study the capabilities of the technique. The first was the flow around a wing of high aspect ratio executing plunging motion of large amplitude and high-rate in

a wind tunnel. The second was the quantification of the time history of velocity around a canard-wing configuration during continuous changes in canard position. The final application was the study of the highly three dimensional unsteady wake of a rotor in forward flight. Iterative computational algorithms for enhancing the statistical accuracy and spatial resolution are described. Dissert. Abstr.

N93-25706 Stanford Univ., CA.
ANALYSIS OF WING WAKE ROLL-UP USING A VORTEX-IN-CELL METHOD Ph.D. Thesis
Renato Silva Ribeiro 1992 213 p
Avail: Univ. Microfilms Order No. Da9234153

A wing producing lift generates a thin vorticity sheet behind it, called a vortex wake. This wake is convected downstream, adjusting its shape in order to remain force-free, and can interact with other surfaces and wakes as it does so. The determination of wake geometries and effects are of great interest in several aircraft design problems, including analysis of canard-wing interference, rotors and propeller-wing interference. This work applies a vortex-in-cell method to a singularity model for wings and wakes in steady, incompressible flow. Wings are represented by a vortex-lattice model, while wakes are formed by line vortices. The vorticity contained in the singularities is spread onto a rectangular grid, using quadratic splines based on the grid-cell dimensions. Velocities are computed from the vorticity field by an infinite boundary Fast Poisson Solver, which employs fast Sine and Cosine transforms and a boundary convolution scheme. Although the grid boundaries are placed close to the singularities, the solution is consistent with the condition of vanishing perturbations at infinity. Provisions are made to take into account portions of the wakes downstream of the grid box. Velocities at points inside the grid are obtained by interpolation. The result is the removal of infinite velocities, as if a infinite vortex-core model were introduced. The velocities computed with the vortex-in-cell method are used to relax the wake and to correct the singularity strengths on the wing, in a mixed iterative procedure. Several problems are studied to evaluate the performance of the method: velocity induced by single infinite and semi-infinite vortices, lift of rectangular and swept-back wings, roll-up of single wing wakes and interaction between wings and wakes in various arrangements. Solutions for these problems were compared with results from experiments and other methods. Detailed descriptions for wake geometry and accurate load distributions were obtained, even for cases where wakes intercepted wings directly. The method provides velocity values throughout the grid as part of the solution. The computational time required is controlled by the number of grid cells, not the number of singularities.
Dissert. Abstr.

N93-25720 Stanford Univ., CA.
AN INVESTIGATION OF PHOTOTHERMAL VELOCIMETRY FOR APPLICATION TO TRANSIENT, HIGH-SPEED GAS FLOWS Ph.D. Thesis
Theodore Philip Delianides 1992 144 p
Avail. Univ. Microfilms Order No. DA9234084

The measurement of velocity is fundamental to the study of fluid mechanics. Though much can be learned from flow visualization, a better understanding of a flow phenomenon requires the measurement of velocity and thermodynamic properties. In the modern gas-dynamics laboratory, bulky physical probes such as hot-wire anemometers and pitot tubes that were for many years the only means of measuring velocity have been supplemented by optical diagnostic techniques which are nonintrusive, have high spatial and temporal resolutions, and are capable of rapid data acquisition rates. From a flow-diagnostician's viewpoint, perhaps the most challenging flows are transient ones, that is, those exhibiting large-scale flow-structure variations with time. Unfortunately, the existing optical diagnostic techniques for velocity measurement are not well-suited for studying high-speed, transient flows. They are either too intrusive by nature or limited in their applicability because the various optical phenomena on which they are based are adversely affected by flow conditions. A new and potentially powerful velocimetry technique has been developed that is based on the heating that accompanies intermolecular quenching collisions. It uses a pulsed laser tuned to an absorption band of a seed species to create a thermally-tagged line in a flow. The line is tracked spatially and temporally using a refractive-index-sensitive imaging system. In the current work, thermal tags are created with a pulsed carbon dioxide laser in flows of nitrogen gas seeded with a small fraction of sulfur hexafluoride and are tracked either with a schlieren or shadowgraph imaging system. An initial investigation of the quasi-steady flow from an axisymmetric nozzle yield velocity measurements that compare well to pitot tube measurements at the same positions. The flow induced by a propagating normal shock wave is also studied, and measurements are reported of the velocity directly behind a shock wave as it exits a shock tube. The first application of the new technique is to the study of a 100 percent-duty-cycle-pulsed, high-speed axisymmetric jet. Axial velocity profiles at various times and spatial positions are presented, with peak velocities exceeding 300m/sec. For a mechanically-valve-actuated pulse jet, this is the highest output flow velocity ever investigated. Dissert. Abstr.

N93-25752 Houston Univ., TX.
INITIAL STREAMWISE VORTICITY FORMATION IN A TWO-STREAM MIXING LAYER Ph.D. Thesis
Chao-Hung Steve Tung 1992 240 p
Avail. Univ. Microfilms Order No. DA9235931

The formation and evolution of streamwise vortices in a two-stream mixing layer were experimentally investigated. The formation and pairing of the spanwise coherent structures were stabilized by acoustic excitation so that they occurred at fixed streamwise locations. The forcing signal consisted of two frequency components: the initial instability frequency and its first subharmonic. The latter also served as the triggering signal and phase reference for A/D sampling. No artificial spanwise forcing was applied but small disturbances originating from the splitter plate were allowed to develop with the mixing layer. Time traces of three velocity components on a two-dimensional grid of locations were recorded by hot-wire anemometry with an x-wire probe at successive streamwise stations. From these, three-dimensional distributions of ensemble-average spanwise and streamwise vorticities were computed and analyzed. The spanwise coherent structures remained quasi-two-dimensional from the initial roll-up to the end of the first structure amalgamation. During this process, the structure spacing changed from the initial instability wavelength to the first subharmonic wavelength. Concentrated streamwise vortices were first observed at the start of the first spanwise structure pairing. They appeared on the peripheries and between the amalgamating spanwise structures at isolated spanwise locations. Downstream, additional vortices were generated at spanwise locations adjacent to the original vortices, which remained at the same spanwise locations. These structures formed counter-rotating pairs located alternately along the spanwise direction. Their three-dimensional vorticity distributions agree with the interwinding-vortex-line model previously proposed by others. The upstream spacing between streamwise vortices of the same sign was about 2/3 of the initial instability wavelength of the spanwise structures. Near the end of the spanwise structure amalgamation, pairing between streamwise vortices of the same sign occurred. However, this phenomenon did not take place uniformly over the entire span of measurement. As a result, global doubling in spanwise wavelength did not occur when the streamwise wavelength doubled. Turbulent bursts were first observed in the regions occupied by the spanwise structures near the completion of the first amalgamation. Results from the present study were inconclusive in relating these bursts to the presence of streamwise structures in those regions. Dissert. Abstr.

N93-25759 North Carolina State Univ., Raleigh.
A NEW LU-SGS FLOW SOLVER FOR CALCULATING REENTRY FLOWS Ph.D. Thesis
David Ramos Olynick 1992 192 p
Avail: Univ. Microfilms Order No. DA9303674

An LU-SGS flow solver is developed and evaluated. The LU-SGS method of Yoon is adapted to calculate axisymmetric, chemically reacting, and weakly ionized flowfields characteristic of reentry vehicles. Modifications are presented that improve the numerical efficiency and stability of the LU-SGS scheme for the calculation of nonequilibrium reacting flows. A parallel effort is made to improve the physical modeling of the flowfield. A new two-temperature dissociation model is derived from kinetic theory to account for the coupled vibration-dissociation process. The model minimizes uncertainties associated with the Park two-temperature model. The effects of the model on AOTV type flowfields are examined. The accuracy of the continuum equations employed are examined by comparing with numerical flow solutions generated using the Direct Simulation Monte Carlo (DSMC) method. For this comparison, a four temperature thermal model is employed that allows the calculation of separate translational, rotational, vibrational, and electron-electronic temperatures. Calculations were made for flows

with and without ionization over the Project Fire 2 vehicle. For the Project Fire 2 conditions considered (76 km and above), assuming the translational temperature equal to rotational temperature and the vibrational temperature equal to the electron-electronic temperature were found to be poor approximations. Surface convective heat transfer for a number of Fire 2 flow calculations are compared. The trends of the Fire 2 experimental data were predicted and the present numerical results compared well with solutions from other Computational Fluid Dynamic (CFD) codes and the DSMC method. The effects of a number of flow phenomena on the convective surface heating are examined. For the Fire 2 conditions considered, the flow was almost fully dissociated. As a result, the recombination of nitrogen was found to have the most influence on the surface heating rates. Other phenomena such as changing the thermal model, transport model, number of species, and chemical rates had little effect on the surface convective heat transfer rates. Finally, the computational efficiency of the present method is compared to the Gauss-Siedel line relaxation method of Candler. CPU costs for each method are calculated for inviscid and viscous flows in thermal and chemical nonequilibrium over a cylinder. Total CPU costs for the methods were found to be comparable for the inviscid calculation. However, the Gauss-Siedel method was found to be much faster than the present LU-SGS scheme for viscous flow calculations. Dissert. Abstr.

N93-25865 Arizona State Univ., Tempe.
STATIONARY CROSSFLOW INSTABILITY ON AN INFINITE SWEPT WING Ph.D. Thesis
Ray-Sing Lin 1992 220 p
Avail: Univ. Microfilms Order No. DA9237268

The Swept Laminar Flow Wing has long been a goal for aerodynamic scientists and engineers. Here the ideas of Laminar Flow Control (LFC) are applied to delay transition and maintain laminar flow over a much larger fraction of a wing surface. When applied to a swept wing, a configuration adopted by current-generation civil-transport aircraft, a significant reduction in drag and substantial increase in energy efficiency could result. To successfully apply this technology, a thorough knowledge and understanding of the transition process on the swept wing is necessary. Because the boundary-layer flow over a swept wing is highly three-dimensional (3-D), streamwise co-rotating crossflow vortices exist, which strongly affect the transition of laminar flow to turbulent. In this work, the stability of the flow over a 70 degree swept, infinite-span wing is examined both by quasi-parallel linear stability theory and by numerically solving the 3-D unsteady incompressible Navier-Stokes (N-S) equations in primitive-variable form. Near the leading edge, steady blowing and suction of chosen wavelength in the spanwise direction is introduced on the wall surface to simulate surface irregularity and generate an instability. The linear stability problems are solved by a Chebyshev-collocation method, while the 3-D full N-S simulation is accomplished by a Fourier-spectral/finite-difference/multiple-grid scheme (developed by the author), which is shown to be accurate and robust. Results of the linear stability analysis indicate that the convex wall curvature has a stabilizing effect while the streamline curvature has a destabilizing effect on the stationary crossflow vortices. The results of direct N-S simulation support the so-called crossflow/crossflow structure which is a consequence of nonlinear interaction near the wall. Strong spanwise modulation of the streamwise-velocity profiles results in the appearance of multiple inflection points. A detailed comparison of the N-S calculation with linear theory and experimental results is provided. Dissert. Abstr.

N93-25881 Purdue Univ., West Lafayette, IN.
SIMULATION OF VORTEX BURSTING Ph.D. Thesis
Jiak-Kwang Tan 1992 164 p
Avail: Univ. Microfilms Order No. DA9301391

The 3-D, incompressible, time-dependent Navier-Stokes equations in primitive variables are used to simulate bursting of a line vortex embedded in a unbounded uniform flow. The entire study is divided into three parts. First, the steady axisymmetric vortex behavior with various swirl level is studied. At low swirl level, the vortex flow remains parallel and can be described by the quasi parallel equations. At higher swirl levels, the flow develops large amplitude waves. When the amplitude of these waves is large enough, recirculation bubbles will occur on the vortex axis. The flow within the recirculation bubbles is found to nearly obey the Prandtl-Batchelor's conditions. Secondly, the spatial and temporal evolution of axisymmetric vortex breakdown is investigated. When the swirl and Reynolds number are small, asymptotically steady flows develop, with steady recirculation bubbles at the higher swirl. When the swirl and Reynolds number are high enough, ring vortices are shed periodically from the primary (mostly steady) bubble, much as would happen from a bluff body. A steady/unsteady boundary dividing asymptotically steady and unsteady flow is constructed in the swirl parameter vs Reynolds number plane. It appears that the high Reynolds number limit of the boundary is at the swirl level corresponding to Benjamin's vortex criticality condition. As Reynolds number decreases, the swirl level required to induce unsteady flow increases. The Strouhal number of the shed vortices is about .2, independent to both the swirl parameter and Reynolds number. Lastly, 3-D stability of the steady and unsteady axisymmetric flows at some selected swirl parameter and at a constant Reynolds number, is examined. A small, but finite, first harmonic perturbation is introduced and the behavior of the flow is simulated by solving the full 3-D Navier-Stokes equations. At low swirl level, where quasi parallel is valid, the flow is found to be stable to 3-D perturbations. At higher swirl, where the quasi parallel approximation fails and the axisymmetric flow is wavy but has no bubble, the flow evolves into a spiral type of vortex breakdown. At even higher swirl, where recirculation bubbles occur, the first recirculation bubble is found to be stable to 3-D perturbations, but not the second one. Asymmetric amplification is concentrated at the second bubble. Hence, the flow has the appearance of bubble breakdown upstream and a downstream spiral breakdown. When the axisymmetric solution exhibits regular vortex shedding behavior, the shed ring vortices are found to be stretched and spiraling around an almost axisymmetric core. The flow appears to have a front end axisymmetric bubble, followed by a spiraling tail. When spiraling occurs, the first harmonic component dominates the asymmetric motion. Dissert. Abstr.

N93-25883*# Toledo Univ., OH.
ESTIMATING TURBINE LIMIT LOAD Final Report
Arthur J. Glassman Apr. 1993 10 p
(Grant NAG3-1165; RTOP 505-69-50)
(NASA-CR-191105; E-7705; NAS 1.26:191105) Avail: CASI HC A02/MF A01

A method for estimating turbine limit-load pressure ratio from turbine map information is presented and demonstrated. It is based on a mean line analysis at the last-rotor exit. The required map information includes choke flow rate at all speeds as well as pressure ratio and efficiency at the onset of choke at design speed. One- and two-stage turbines are analyzed to compare the results with those from a more rigorous off-design flow analysis and to show the sensitivities of the computed limit-load pressure ratios to changes in the key assumptions. Author

N93-25894# RAND Corp., Santa Monica, CA.
NUMERICAL SIMULATION OF HYPERSONIC AERODYNAMICS AND THE COMPUTATIONAL NEEDS FOR THE DESIGN OF AN AEROSPACE PLANE
S. K. Liu 1992 147 p
(Contract F49620-91-C-0003)
(AD-A260681; RAND/N-3253-AF) Avail: CASI HC A07/MF A02

This Note records the results of a review and analysis of the status of the computational fluid dynamic (CFD) modeling techniques related to the National Aerospace Plane (NASP) operation. It was undertaken as a task in the study, The National Aerospace Plane (NASP): Development Issues for Follow-on Systems, performed within the Technology Applications Program of Project AIR FORCE. The research sought to evaluate independently the degree of uncertainty and the technical risk involved in predicting the NASP performance using numerical simulation of aerothermal and chemical/combustion processes. This Note covers the technical review portion and identifies the areas for research emphasis so that the predictive reliability of the NASP's potential performance parameters can be improved. This study should interest those concerned with the aerospace plane development in general, and hypersonic CFD modeling in particular. DTIC

N93-26049*# Pennsylvania State Univ., University Park.
REDUCTION IN SIZE AND UNSTEADINESS OF A VTOL GROUND VORTEX BY GROUND FENCES
John M. Cimbala, Michael L. Billet, and Todd B. Harman 15 Apr. 1993 23 p

(Grant NAG2-484)
(NASA-CR-192997; NAS 1.26:192997) Avail: CASI HC A03/MF A01

A ground vortex, produced when a jet impinges on the ground in the presence of cross flow, is encountered by V/STOL aircraft hovering near the ground and is known to be hazardous to the aircraft. The objective of this research was to identify a ground-based technique by which both the mean size and fluctuation in size of the ground vortex could be reduced. A simple passive method was identified and examined in the laboratory. Specifically, one or two fine wire mesh screens (ground fences) bent in a horseshoe shape and located on the ground in front of the jet impingement point proved to be very effective. The ground fences work by decreasing the momentum of the upstream-traveling wall jet, effectively causing a higher freestream-to-jet velocity ratio (V(sub infinity)/V(sub j)) and thus, a ground vortex smaller in size and unsteadiness. At(V(sub infinity)/V(sub j)) = 0.15, the addition of a single ground fence resulted in a 70 percent reduction in mean size of the ground vortex. With two ground fences, the mean size decreased by about 85 percent. Fluctuations in size decreased nearly in proportion to the mean size, for both the single and double fence configurations. These results were consistent over a wide range of jet Reynolds number (10(exp 4) less than Re(sub jet) less than 10(exp 5)); further development and full-scale Reynolds number testing are required, however, to determine if this technique can be made practical for the case of actual VTOL aircraft. Author (revised)

N93-26085*# National Aeronautics and Space Administration. Langley Research Center, Hampton, VA.
EXPERIMENTAL EFFECTS OF WING LOCATION ON WING-BODY PRESSURES AT SUPERSONIC SPEEDS
Jerry M. Allen and Carolyn B. Watson Apr. 1993 198 p
(RTOP 505-59-30-01)
(NASA-TM-4434; L-17148; NAS 1.15:4434) Avail: CASI HC A09/MF A03

An experimental study was performed at supersonic speeds to measure wing and body spanwise pressure distributions on an axisymmetric-body delta wing model on which the wing vertical location on the body was systematically varied from low- to high-mounted positions. In addition, for two of these positions both horizontal and radial wing angular orientations relative to the body were tested, and roll angle effects were investigated for one of the positions. Seven different wing-body configurations and a body-alone configuration were studied. The test was conducted at Mach numbers from 1.70 to 2.86 at angles of attack from about -4 deg to 24 deg. Pressure orifices were located at three longitudinal stations on each wing-body model, and at each station the orifices were located completely around the body, along the lower surface of the right wing (looking upstream), and along the upper surface of the left wing. All pressure coefficient data are tabulated and selected samples are shown graphically to illustrate the effects of the test variables. The effects of angle of attack, roll angle, Mach number, longitudinal station, wing vertical location, wing angular orientation, and wing-body juncture are analyzed. The vertical location of the wing on the body had a very strong effect on the body pressures. For a given angle of attack at a roll angle of 0 deg, the pressures were virtually constant in the spanwise direction across the windward surfaces of the wing-body combination. Pressure-relieving, channeling, and vortex effects were noted in the data. Author (revised)

N93-26099*# National Aeronautics and Space Administration. Ames Research Center, Moffett Field, CA.
JET-INDUCED GROUND EFFECTS ON A PARAMETRIC FLAT-PLATE MODEL IN HOVER
Douglas A. Wardwell, Craig E. Hange, Richard E. Kuhn (KSA Technology, Columbus, OH.), and Vearl R. Stewart (KSA Technology, Columbus, OH.) Mar. 1993 306 p
(RTOP 505-68-32)
(NASA-TM-104001; A-93040; NAS 1.15:104001) Avail: CASI HC A14/MF A03

The jet-induced forces generated on short takeoff and vertical landing (STOVL) aircraft when in close proximity to the ground can have a significant effect on aircraft performance. Therefore, accurate predictions of these aerodynamic characteristics are highly desirable. Empirical procedures for estimating jet-induced forces during the vertical/short takeoff and landing (V/STOL) portions of the flight envelope are currently limited in accuracy. The jet-induced force data presented significantly add to the current STOVL configurations data base. Further development of empirical prediction methods for jet-induced forces, to provide more configuration diversity and improved overall accuracy, depends on the viability of this STOVL data base. The data base may also be used to validate computational fluid dynamics (CFD) analysis codes. The hover data obtained at the NASA Ames Jet Calibration and Hover Test (JCAHT) facility for a parametric flat-plate model is presented. The model tested was designed to allow variations in the planform aspect ratio, number of jets, nozzle shape, and jet location. There were 31 different planform/nozzle configurations tested. Each configuration had numerous pressure taps installed to measure the pressures on the undersurface of the model. All pressure data along with the balance jet-induced lift and pitching-moment increments are tabulated. For selected runs, pressure data are presented in the form of contour plots that show lines of constant pressure coefficient on the model undersurface. Nozzle-thrust calibrations and jet flow-pressure survey information are also provided. Author (revised)

N93-26134*# National Aeronautics and Space Administration. Langley Research Center, Hampton, VA.
CONICAL EULER ANALYSIS AND ACTIVE ROLL SUPPRESSION FOR UNSTEADY VORTICAL FLOWS ABOUT ROLLING DELTA WINGS
Elizabeth M. Lee-Rausch and John T. Batina Mar. 1993 30 p Original contains color illustrations
(RTOP 505-63-50-12)
(NASA-TP-3259; L-17059; NAS 1.60:3259) Avail: CASI HC A03/MF A01; 3 functional color pages

A conical Euler code was developed to study unsteady vortex-dominated flows about rolling, highly swept delta wings undergoing either forced motions or free-to-roll motions that include active roll suppression. The flow solver of the code involves a multistage, Runge-Kutta time-stepping scheme that uses a cell-centered, finite-volume, spatial discretization of the Euler equations on an unstructured grid of triangles. The code allows for the additional analysis of the free to-roll case by simultaneously integrating in time the rigid-body equation of motion with the governing flow equations. Results are presented for a delta wing with a 75 deg swept, sharp leading edge at a free-stream Mach number of 1.2 and at 10 deg, 20 deg, and 30 deg angle of attack alpha. At the lower angles of attack (10 and 20 deg), forced-harmonic analyses indicate that the rolling-moment coefficients provide a positive damping, which is verified by free-to-roll calculations. In contrast, at the higher angle of attack (30 deg), a forced-harmonic analysis indicates that the rolling-moment coefficient provides negative damping at the small roll amplitudes. A free-to-roll calculation for this case produces an initially divergent response, but as the amplitude of motion grows with time, the response transitions to a wing-rock type of limit cycle oscillation, which is characteristic of highly swept delta wings. This limit cycle oscillation may be actively suppressed through the use of a rate-feedback control law and antisymmetrically deflected leading-edge flaps. Descriptions of the conical Euler flow solver and the free-to roll analysis are included in this report. Results are presented that demonstrate how the systematic analysis of the forced response of the delta wing can be used to predict the stable, neutrally stable, and unstable free response of the delta wing. These results also give insight into the flow physics associated with unsteady vortical flows about delta wings undergoing forced motions and free-to-roll motions, including the active suppression of the wing-rock type phenomenon. The conical Euler methodology developed is directly extend able to three-dimensional calculations. Author (revised)

N93-26195# Naval Postgraduate School, Monterey, CA.
TRAILING VORTEX/FREE-SURFACE INTERACTION M.S. Thesis
Donald E. Neubert, Jr. Dec. 1992 81 p
(AD-A261654) Avail: CASI HC A05/MF A01

An investigation of the interaction of a trailing vortex with a free surface has been undertaken for the purpose of understanding the origin of scars and striations. Velocity and turbulence measurements have been carried out through the use of a Laser-Doppler-Velocimeter (LDV) for various positions of the vortex relative to the free surface. The results have shown that the vortex motion affects the free surface and is affected by it. This mutual interaction leads to the development of surface scars comprised primarily of heterostrophic vortices normal to the free surface. Furthermore, the velocity and turbulence characteristics are affected such that the vertical components of turbulence decay rapidly, and the horizontal components

stretch in the horizontal plane. The experiments have provided sufficient understanding of the physics of the phenomenon for the subsequent undertaking of the development of a predictive numerical model. DTIC

N93-26198# Naval Postgraduate School, Monterey, CA.
UNSTEADY AIRFOIL FLOW SOLUTIONS ON MOVING ZONAL GRIDS M.S. Thesis
Antonio M. Cricelli 17 Dec. 1992 146 p
(AD-A261925) Avail: CASI HC A07/MF A02

Investigation of subsonic and transonic steady and unsteady flowfields over airfoils is an active area of current computational and experimental research. The performance of rotary wing and fixed wing aircraft can be enhanced by taking advantage of unsteady phenomena such as dynamic lift. However, several undesirable effects have prevented designers from taking advantage of these concepts. In the past few years many advances have been made in algorithm development for the numerical solution of the Euler and the Navier Stokes equations. In this study, these new techniques are applied to the body fixed zonal grid approach. This zonal approach is more computationally efficient in solving the governing equations than previous approaches and has certain advantages over the standard single moving grid approach. The zonal grids consists of two grids: one being the inner grid which is fixed to the airfoil, and the other being the outer grid which extends to the far field or to a specified outer boundary. The inner grid is allowed to rotate with the body, while the outer grid remains fixed. The thin-layer Navier-Stokes equations are solved for the inner grid, and the Euler equations are solved for the outer grid. Communication between the two grids is accomplished by interpolating the flow quantities at the zonal interface. Solutions are obtained for flows at fixed angles of incidence, and for unsteady flows over pitching and oscillating airfoils. The computed results are in good agreement with available experimental data. DTIC

N93-26007 Wright Lab., Wright-Patterson AFB, OH.
STUDIES IN AIR/AIR SUPERSONIC MIXING LAYERS
D. J. Risha and B. Sekar *In* JHU, 29th JANNAF Combustion Subcommittee Meeting, Volume 2 Oct. 1992 p 9-18 (For primary document see N93-26005 09-20)
Avail: CPIA, 10630 Little Patuxent Pkwy., Suite 202, Columbia, MD 21044-3200 HC

N93-26078*# Houston Univ., TX. Dept. of Mathematics.
A HYBRID MULTIGRID TECHNIQUE FOR COMPUTING STEADY-STATE SOLUTIONS TO SUPERSONIC FLOWS Final Report
Richard Sanders *In* NASA. Johnson Space Center, National Aeronautics and Space Administration (NASA)/American Society for Engineering Education (ASEE) Summer Faculty Fellowship Program, 1992, Volume 2 Dec. 1992 p 16 (For primary document see N93-26070 09-99)
(Grant NGT-44-001-800)
Avail: CASI HC A03/MF A02

03 AIR TRANSPORTATION AND SAFETY

Includes passenger and cargo air transport operations; and aircraft accidents.

For related information see also *16 Space Transportation* and *85 Urban Technology and Transportation.*

N93-24773 Cranfield Inst. of Tech., Bedford (England).
CRASHWORTHINESS OF COMPOSITE SEATS FOR CIVIL AIRCRAFT Ph.D. Thesis
V. M. Stephens 1992 283 p
Avail: Univ. Microfilms Order No. BRDX98009

Within these terms of reference, the response of the seat restraint occupant system (SROS) to impact loading was analyzed using physical (dynamic testing) and analytical (computer simulation) modeling techniques. With the increasing use of fiber-reinforced polymer composites in aircraft for weight efficiency, and the consequent appearance of composite seats, attention must be given to the crash performance of these structures. Composite structures are characterized by brittle failure with low impact energy absorption, in comparison to the collapse of metal structures which may exhibit plastic deformation prior to failure. However, using the developing technology of composite sub-structures with high specific energy absorption capability, seat structures were modified to incorporate composite load-limiting elements. The redesign process involved the compatibility of energy absorber loads with occupant dynamics to minimize injury potential, together with the alleviation of forces in the structural load path to reduce damage and preclude failure to the seat, floor track, and other components. Shortcomings of existing seat designs were assessed, and the dynamics of lap-belted occupants analyzed, including secondary head impact with the forward seat structure. The computer model created was validated against the results of dynamic tests, and then used in a parametric study of occupant dynamics. Conclusions and recommendations include guidelines relating to the future design of both metal and composite seats.
Dissert. Abstr.

N93-25110# Sandia National Labs., Albuquerque, NM.
RELIABILITY ASSESSMENT AT AIRLINE INSPECTION FACILITIES. VOLUME 1: A GENERIC PROTOCOL FOR INSPECTION RELIABILITY EXPERIMENTS Final Report
Floyd Spencer, Giancarlo Borgonovi (Science Applications, Inc., Albuquerque, NM.), Dennis Roach, Don Schurman (Science Applications, Inc., Albuquerque, NM.), and Ron Smith (AEA Technology, London, England.) Mar. 1993 34 p
(DOT/FAA/CT-92/12-Vol-1) Avail: CASI HC A03/MF A01

The Aging Aircraft Nondestructive Inspection (NDI) Development and Demonstration Center (AANC) at Sandia National Laboratories is charged by the FAA to support technology transfer, technology assessment, and technology validation. A key task facing the center is to establish a consistent and systematic methodology to assess the reliability of inspections through field experiments. This task is divided into three major areas: reliability of eddy current lap splice inspections at transport aircraft maintenance facilities, reliability of inspection at commuter aircraft maintenance facilities, and reliability of inspection associated with visual inspection of aircraft structural parts. Volume 1 is the first document in a series of three describing the planning, execution, and results of an eddy current inspection field experiment. A generic protocol for inspection reliability experiments is defined. It contains an introduction to the currently accepted forms of data analysis and presentation (Probability of Detection and Receiver Operating Characteristic curves) and a discussion of the factors that may affect inspection reliability. Author (revised)

N93-25205# Federal Aviation Administration, Oklahoma City, OK. Civil Aeromedical Inst.
INWARD CONTAMINANT LEAKAGE TESTS OF THE S-TRON CORPORATION EMERGENCY ESCAPE BREATHING DEVICE. PHASE 1: TESTS OF THE ORIGINAL DESIGN. PHASE 2: TESTS WITH THE REDESIGNED NECK SEAL
Bruce C. Wilcox, Jr., Harvey M. England, Jr., and Garnet A. McLean Apr. 1992 28 p
(FAA Proj. AM-B-93-PHY-152)
(DOT/FAA/AM-92/18) Avail: CASI HC A03/MF A01

At the request of S-Tron Corporation, to support their contract with the U.S. Navy, performance tests of the Emergency Escape Breathing Device (EEBD) were conducted in the Environmental Physiology Research Section contaminant leakage chamber. Sulfur hexafluoride (SF6) challenge was used to determine contaminant leakage; oxygen and carbon dioxide levels, as well as temperature readings, were also obtained. Eight successful tests were conducted with the original neck seal design first used by Scott Aviation in their Crewmember Protective Breathing Equipment, four additional tests were conducted with a proprietary new neck seal designed by S-Tron. The EEBD all performed within test limits. Author

N93-25224# Federal Aviation Administration, Atlantic City, NJ.
NARROW-BODY AIRCRAFT WATER SPRAY OPTIMIZATION STUDY
Timothy R. Marker Feb. 1993 39 p Original contains color illustrations
(DOT/FAA/CT-TN93/3) Avail: CASI HC A03/MF A01

Twenty-five full-scale tests were conducted in a modified 707 narrow-body fuselage as part of an aircraft cabin water spray optimization study. The purpose was to test several spray configurations by varying the amount of water sprayed, the flow rate, and orientation of the nozzles, while keeping the fire conditions constant, in an attempt to minimize the quantity of water required to effectively suppress a postcrash aircraft fire

and improve occupant survivability. The original Safety Aircraft and Vehicles Equipment (SAVE) system was configured in the narrow-body cabin using 120 nozzles. Initially, three tests were conducted using 72, 48, and 24 gallons of water for 3-, 2-, and 1-minute spray durations, respectively. In the following series of tests, one-third of the SAVE system (40 nozzles) was configured in the area of the fire using 24, 16, and 8 gallons of water for 3-, 2-, and 1-minute spray durations, respectively. During the final series of tests, the spray system was configured in five separate sections for 'zones' with each zone carrying eight nozzles. A thermocouple was mounted at ceiling height in each zone, allowing for the activation of a particular zone when the temperature reached a predetermined value. The flow rate of the nozzles was varied as was the amount of water available during the tests. For comparison, a test was conducted without spraying water in order to establish a 'baseline.' Temperature, heat flux, smoke levels, gas concentrations, and video were continuously monitored at various locations throughout the fuselage. The optimal zoned system was more effective than the SAVE system and used only 11 percent of the water.

Author (revised)

N93-25827# National Transportation Safety Board, Washington, DC.

AIRCRAFT ACCIDENT REPORT: TOMY INTERNATIONAL, INC., D/B/A SCENIC AIR TOURS FLIGHT 22, BEECH MODEL E18S, N342E IN-FLIGHT COLLISION WITH TERRAIN, MOUNT HALEAKALA, MAUI, HAWAII, 22 APRIL 1992

2 Feb. 1993 67 p

(PB93-910401; NTSB/AAR-93/01) Avail: CASI HC A04/MF A01

This report explains Scenic Air Tours flight 22's collision with mountainous terrain on the Island of Maui, Hawaii, while the Beech E18S airplane was on an air tour flight from Hilo, Hawaii, to Honolulu, Hawaii, on 22 Apr. 1992. The safety issues discussed in the report include visual flight in instrument meteorological conditions, navigational errors, pilot preemployment qualifications and background checks, and the overall safety of the air tour industry. Recommendations concerning these issues were addressed to the Federal Aviation Administration and to Tomy International, Inc., d/b/a Scenic Air Tours. Author (revised)

N93-25896# Civil Aeromedical Inst., Oklahoma City, OK.

A REVIEW OF CIVIL AVIATION PROPELLER-TO-PERSON ACCIDENTS: 1980-1989 Final Report

William E. Collins Jan. 1993 10 p

(AD-A260695; DOT/FAA/AM-93/2) Avail: CASI HC A02/MF A01

Various types of paint schemes on aircraft propeller and rotor blades are used to improve the visual conspicuity and attention-getting value of those blades when they are rotating. The improved conspicuity resulting from the paint schemes has the purpose of reducing the number of injuries and fatalities that might occur due to accidental contact with a rotating blade by pilots, passengers, or ground crew. The present study was undertaken to provide information regarding the circumstances surrounding such accidents in recent years and to compare those findings with the frequency and circumstances of propeller accidents during the 1965-1979 period. Computer retrievals of brief reports of all propeller accidents during the period from 1980 through 1989 were provided by the National Transportation Safety Board. Those reports were examined and analyzed in terms of type of accident, degree of injury, actions of pilots, action of passengers and ground crew, night or day, and other conditions. The computer search yielded a total of 104 reports of propeller-to-person accidents involving 106 persons. Prop-to-person accident frequency for the 1980-1989 period was notably lower than that previously reported for the 1960's and 1970's. Recent declines appear due to a combination of FAA educational efforts, economic conditions, and changes in the types of aircraft used by present aviation pilots. Irrespective of the decade under study, persons at most risk for a propeller-to-person accident are deplaning passengers and passengers attempting to assist the pilot prior to takeoff and after landing. DTIC

N93-26263# Army Aviation Applied Technology Directorate, Fort Eustis, VA.

PROAV CABLE WARNING SYSTEM (CWS) - U.S. ARMY AIRCRAFT INTEGRATION ASSESSMENT AND OCONUS FIELD EVALUATION Technical Report

Kent F. Smith and Eric C. Littleton Feb. 1993 125 p

(AD-A261233; USAATCOM-TR-93-D-1) Avail: CASI HC A06/MF A02

The PROAV Cable Warning System (CWS) is a commercially available system designed to detect the electromagnetic field generated by current-carrying wires operating at frequencies of either 50 or 60 Hz. The system is designed to alert helicopter crewmen to the presence of these wires to help prevent wire strike mishaps. As directed by the U.S. Army Aviation and Troop Command, the Aviation Applied Technology Directorate performed an aircraft integration assessment of the CWS followed by field evaluations in Germany and Korea. These field evaluations were not operational tests, since no standard or specification exists by which to judge this system. The CWS was successfully integrated on the AH-64A, AH-1F, and UH-1H aircraft. During the field evaluations, the CWS was flown a total of 207 hours by 40 different pilots. The conclusions were that the CWS was not consistent in its ability to detect wires and provide sufficient reaction time and that pilot confidence in the capabilities of the CWS was marginal to low. Also, significant aircraft integration issues remain unresolved for several U.S. Army fleet aircraft. DTIC

N93-24879# Aerospatiale, Suresnes (France). Centre Commun de Recherches.

NUMERICAL MODELLING OF INDUCED EFFECTS OF LIGHTNING STRIKE ON AN ALL COMPOSITE HELICOPTER

Pascal Gondot, G. Donnet (Nucletudes, Montreuil, France.), and Patrick Trochet (Nucletudes, Montreuil, France.) *In* FAA, The 1992 International Aerospace and Ground Conference on Lightning and Static Electricity: Addendum Nov. 1992 11 p (For primary document see N93-24875 09-47)

Avail: CASI HC A03/MF A03

N93-24880# Rockwell International Corp., Downey, CA. Space Systems Div.

ZONING OF AIRCRAFT: A REVIEW OF THE DEFINITIONS

Nathaniel G. Bankston *In* FAA, The 1992 International Aerospace and Ground Conference on Lightning and Static Electricity: Addendum Nov. 1992 16 p (For primary document see N93-24875 09-47)

Avail: CASI HC A03/MF A03

N93-24885# Northrop Corp., Pico Rivera, CA.

A PROCEDURE FOR DEFINING LIGHTNING RISK TO AIR VEHICLES

David Beeman and Naomi Morita *In* FAA, The 1992 International Aerospace and Ground Conference on Lightning and Static Electricity: Addendum Nov. 1992 18 p (For primary document see N93-24875 09-47)

Avail: CASI HC A03/MF A03

N93-24886# United Kingdom Atomic Energy Authority, Abingdon (England). Lightning Test and Technology.

PARAMETERS INFLUENCING THE HOT-SPOT IGNITION OF AVIATION FUEL/AIR AND ETHYLENE/AIR MIXTURES

Stephen J. Haigh and C. John Hardwick *In* FAA, The 1992 International Aerospace and Ground Conference on Lightning and Static Electricity: Addendum Nov. 1992 9 p Sponsored by British Aerospace Aircraft Group; Civil Aviation Authority; Construcciones Aeronauticas S.A.; Dept. of Trade and Industry; Rolls-Royce Ltd.; Saab-Scania; and Short Bros. and Harland Ltd. (For primary document see N93-24875 09-47)

Avail: CASI HC A02/MF A03

N93-24887# SRI International Corp., Menlo Park, CA.

COMPARISON OF THE ELECTRICAL CHARGING AND DISCHARGING ENVIRONMENTS OF MULTIPLE AIRCRAFT-BORNE ELECTRIC-FIELD MEASUREMENT SYSTEMS

Kathy L. Giori and J. E. Nanevicz *In* FAA, The 1992 International Aerospace and Ground Conference on Lightning and Static Electricity: Addendum Nov. 1992 10 p (For primary document see N93-24875 09-47)

Avail: CASI HC A02/MF A03

N93-24894# United Kingdom Atomic Energy Authority, Abingdon (England). Lightning Test and Technology.

ZONING OF AIRCRAFT BY ELECTRIC FIELD MODELLING

C. John Hardwick and V. K. Thompson *In* FAA, The 1992 International Aerospace and Ground Conference on Lightning and Static Electricity: Addendum Nov. 1992 10 p Sponsored by British Aerospace Aircraft

Group; Construcciones Aeronauticas S.A.; Rolls-Royce Ltd.; Saab-Scania; Short Bros. and Harland Ltd.; Westland Helicopters Ltd.; Civil Aviation Authority; and Dept. of Trade and Industry (For primary document see N93-24875 09-47)
Avail: CASI HC A02/MF A03

N93-24898# Naval Air Warfare Center, Patuxent River, MD. Aircraft Div.
APPLICATIONS OF STRESS ENVELOPE CONCEPTS TO AIRCRAFT EMP AND LIGHTNING SURVIVABILITY
Sam Frazier *In* FAA, The 1992 International Aerospace and Ground Conference on Lightning and Static Electricity: Addendum Nov. 1992 6 p (For primary document see N93-24875 09-47)
Avail: CASI HC A02/MF A03

04 AIRCRAFT COMMUNICATIONS AND NAVIGATION

Includes digital and voice communication with aircraft; air navigation systems (satellite and ground based); and air traffic control.

For related information see also *17 Space Communications, Spacecraft Communications, Command and Tracking* and *Communications and Radar.*

N93-24741# Federal Aviation Administration, Atlanta, GA.
ILS MATHEMATICAL MODELING STUDY OF AN ILS GLIDE SLOPE PROPOSED FOR RUNWAY 19L AT THE MERIDIAN NAVAL AIR STATION, MISSISSIPPI Technical Report, Feb. 1993
James D. Rambone Apr. 1993 19 p
(Contract FAA-T0603-S)
(DOT/FAA/CT-TN93/8) Avail: CASI HC A03/MF A01

This Technical Note describes the Instrument Landing System (ILS) math modeling performed by the Federal Aviation Administration (FAA) Technical Center at the request of the Naval Command, Control, and Ocean Surveillance Center In-Service Engineering (NISE). Data are presented showing the computed performance for a glide slope proposed for runway 19L at the Meridian Naval Air Station (NAS). As requested, capture effect and null reference systems were modeled at the proposed glide slope site. The proposed site is located 783 feet back from the runway threshold and 400 feet left offset of centerline. NISE is concerned that severe terrain gradients in front of the site may adversely affect glide slope performance. Glide slope modeling was conducted using physical optics computations in the Geometric Theory of Diffraction 3D (GTD-3D) model. The GTD computations in the GTD-3D model could not accommodate a triple diffraction occurrence caused by sharp terrain gradients in front of the glide slope site. Glide slope modeling computed only the effect of the proposed terrain on glide slope performance. Preliminary modeling results for both the capture effect and null reference antennas with the proposed terrain grade indicated an out-of-tolerance excursion occurring approximately 3,000 feet in front of threshold. The first 1,000 foot section of proposed terrain grade in front of the antenna was modified slightly to eliminate this excursion in the final modeling runs. Modeled path structure and level run plots are provided for the proposed capture effect and null reference systems. Results indicate that the capture effect and null reference systems modeled with the modified proposed terrain grade should meet Category 1 path structure, linearity, and symmetry tolerances. Author (revised)

N93-24914*# National Aeronautics and Space Administration. Ames Research Center, Moffett Field, CA.
DISCRETE RANGE CLUSTERING USING MONTE CARLO METHODS
G. B. Chatterji and B. Sridhar Mar. 1993 16 p
(RTOP 505-64-36)
(NASA-TM-104004; A-93044; NAS 1.15:104004) Avail: CASI HC A03/MF A01

For automatic obstacle avoidance guidance during rotorcraft low altitude flight, a reliable model of the nearby environment is needed. Such a model may be constructed by applying surface fitting techniques to the dense range map obtained by active sensing using radars. However, for covertness, passive sensing techniques using electro-optic sensors are desirable. As opposed to the dense range map obtained via active sensing, passive sensing algorithms produce reliable range at sparse locations, and therefore, surface fitting techniques to fill the gaps in the range measurement are not directly applicable. Both for automatic guidance and as a display for aiding the pilot, these discrete ranges need to be grouped into sets which correspond to objects in the nearby environment. The focus of this paper is on using Monte Carlo methods for clustering range points into meaningful groups. One of the aims of the paper is to explore whether simulated annealing methods offer significant advantage over the basic Monte Carlo method for this class of problems. We compare three different approaches and present application results of these algorithms to a laboratory image sequence and a helicopter flight sequence. Author

N93-24948# Federal Aviation Administration, Atlantic City, NJ.
VISUAL APPROACH DATA COLLECTION AT ST. LOUIS LAMBERT FIELD (STL) Final Report, 2 Aug. - 23 Oct. 1990
James Thomas, Dominic Timoteo, and Amy E. Transue Jan. 1993 58 p
(Contract FAA-F2006-G)
(DOT/FAA/CT-TN93/2) Avail: CASI HC A04/MF A01

Data on aircraft executing simultaneous visual approaches to closely spaced parallel and intersecting runways were collected at Lambert - St. Louis International Airport (STL) between August 2 and October 23, 1990. The purpose of the data collection was to provide an accurate data base of the navigational characteristics of aircraft flying the 'fly visual' segment of the approach. Aircraft position data were collected using the in-place STL surveillance primary and secondary radars. The data were reduced and a limited analysis was performed at the Federal Aviation Administration (FAA) Technical Center by ATC Technology (ACD-340) personnel. The discussion in the Final Report concerns the accuracy of the collected position data and possible sources of error in the data collection. The reduced data were sent to the Standards Development Branch (AVN-540) for further analysis. AVN-540 will report on their findings and recommendations. Author (revised)

N93-25120# Oak Ridge National Lab., TN.
USING FUZZY BEHAVIORS FOR THE OUTDOOR NAVIGATION OF A CAR WITH LOW-RESOLUTION SENSORS
F. G. Pin and Y. Watanabe 1993 7 p Presented at the Institute of Electrical and Electronics Engineers International Conference on Robotics and Automation, Atlanta, GA, 2-7 May 1993
(Contract DE-AC05-84OR-21400)
(DE93-002428; CONF-930519-5) Avail: CASI HC A02/MF A01

Vehicle control in a priori unknown, unpredictable, and dynamic environments requires many calculational and reasoning schemes to operate on the basis of very imprecise, incomplete, or unreliable data. For such systems, in which all the uncertainties can not be engineered away, approximate reasoning may provide an alternative to the complexity and computational requirements of conventional uncertainty analysis and propagation techniques. A proposed approach using superposition of elemental fuzzy behaviors to emulate human-like qualitative reasoning schemes is first discussed. A previously developed navigation scheme implemented on custom-designed very large scale integration (VLSI) fuzzy inferencing boards for indoor navigation of a small laboratory-type robot was progressively enhanced to investigate two control modes for driving a car in a priori unknown environments on the basis of sparse and imprecise sensor data. In the first mode, the car navigates fully autonomously, while in the second mode, the system acts as a driver's aid providing the driver with linguistic (fuzzy) commands to turn left or right and speed up or slow down depending on the obstacles perceived by the sensors. Experiments with both modes of control are described in which the system uses only three acoustic range (sonar) sensor channels to perceive the environment. Simulation results as well as indoors and outdoors experiments are presented and discussed to illustrate the feasibility of outdoor navigation using fuzzy behaviors operating on possibly very inaccurate sensor data. DOE

N93-25243# Federal Aviation Administration, Atlantic City, NJ.
RUNWAY VISUAL RANGE (RVR) OPERATIONAL TEST AND EVALUATION (OT&E) INTEGRATION AND OT&E OPERATIONAL TEST REPORT
William E. Brenner, Thomas C. Carty, and Joseph J. Goslin Apr. 1993 94 p
(DOT/FAA/CT-TN93/37) Avail: CASI HC A05/MF A01

The Operational Test and Evaluation (OT&E) Integration and OT&E

Operational testing of the Runway Visual Range (RVR) was conducted at the Kansas City International (MCI) Airport Traffic Control Tower (ATCT) in Kansas City, MO, and at the Kansas City (ZKC) Air Route Traffic Control Center (ARTCC) in Olathe, KA. The purpose of this test was to verify National Airspace System (NAS) integration requirements of the subsystems and the operational effectiveness of the RVR within the NAS environment. The results of OT&E testing and the results of integration and operational testing of the RVR/Maintenance Data Terminal (MDT) and RVR/Maintenance Processing System (MPS) interface requirements are addressed. Testing of the Tower Control Computer Complex (TCCC) and the Automated Surface Observation System (ASOS) NAS subsystems was deferred. It was concluded that the New Generation RVR requires corrections and/or notifications to satisfactorily meet integration and operational requirements. The New Generation RVR should not be deployed until the deployment-critical issues detailed are resolved and successfully retested. The principal concerns pertain to (1) personnel safety, (2) product integrity during an equipment failure, and (3) accuracy of the visibility product. It is further recommended that all regression testing take place using the RVR and MPS operational baseline software. Author (revised)

N93-25261*# Ohio State Univ., Columbus. Cognitive Systems Engineering Lab.

DESIGN CONCEPTS FOR THE DEVELOPMENT OF COOPERATIVE PROBLEM-SOLVING SYSTEMS

Philip J. Smith, Elaine McCoy (Nebraska Univ., Omaha.), Chuck Layton (Galaxy Scientific Corp., Atlanta, GA.), and Tom Bihari (Adaptive Machine Technologies, Inc., Columbia, OH.) [1992] 34 p

(Contract NCC2-615)

(NASA-CR-192708; NAS 1.26:192708) Avail: CASI HC A03/MF A01

There are many problem-solving tasks that are too complex to fully automate given the current state of technology. Nevertheless, significant improvements in overall system performance could result from the introduction of well-designed computer aids. We have been studying the development of cognitive tools for one such problem-solving task, enroute flight path planning for commercial airlines. Our goal was two-fold. First, we were developing specific systems designs to help with this important practical problem. Second, we are using this context to explore general design concepts to guide in the development of cooperative problem-solving systems. These designs concepts are described. Author (revised)

N93-25330*# Ohio State Univ., Columbus. Cognitive Systems Engineering Lab.

DESIGN OF A COOPERATIVE PROBLEM-SOLVING SYSTEM FOR ENROUTE FLIGHT PLANNING: AN EMPIRICAL STUDY OF ITS USE BY AIRLINE DISPATCHERS Final Report

Philip J. Smith, C. Elaine McCoy (Nebraska Univ., Omaha.), Charles Layton (Galaxy Scientific Corp., Atlanta, GA.), Judith Orasanu, Sherry Chappel, Ev Palmer, and Kevin Corker (National Aeronautics and Space Administration. Ames Research Center, Moffett Field, CA.) 1993 69 p

(Contract NCC2-615)

(NASA-CR-192709; NAS 1.26:192709) Avail: CASI HC A04/MF A01

In a previous report, an empirical study of 30 pilots using the Flight Planning Testbed was reported. An identical experiment using the Flight Planning Testbed (FPT), except that 27 airline dispatchers were studied, is described. Five general questions were addressed in this study: (1) under what circumstances do the introduction of computer-generated suggestions (flight plans) influence the planning behavior of dispatchers (either in a beneficial or adverse manner); (2) what is the nature of such influences (i.e., how are the person's cognitive processes changed); (3) how beneficial are the general design concepts underlying FPT (use of a graphical interface, embedding graphics in a spreadsheet, etc.); (4) how effective are the specific implementation decisions made in realizing these general design concepts; and (5) how effectively do dispatchers evaluate situations requiring replanning, and how effectively do they identify appropriate solutions to these situations. Author (revised)

N93-25456# Mitre Corp., McLean, VA. Center for Advanced Aviation System Development.

THE DEPENDENT CONVERGING INSTRUMENT APPROACH PROCEDURE: AN ANALYSIS OF ITS SAFETY AND APPLICABILITY Final Report

Arthur P. Smith, III, Anand D. Mundra, David R. Barker, and Gerald A. Dorfman Nov. 1992 197 p

(Contract DTFA01-89-C-00001)

(DOE/FAA/RD-93/6) Avail: CASI HC A09/MF A03

When an airport experiences low ceiling or visibility conditions the arrival capacity is significantly reduced. This is particularly true at airports that use both their main runway and their crosswind runway in Visual Meteorological Conditions (VMC). The consequence of this is an increase in delays. A concept for continuing to conduct approaches in Instrument Meteorological Conditions (IMC) to converging runways has been proposed which calls for coordinating the approaches to the two runways such that a stagger between the aircraft is maintained. This procedure is known as Dependent Converging Instrument Approaches (DCIA). This paper develops a DCIA procedure applicable to any runway geometry. The procedure is defined and modeled to capture its safety critical aspects. From this analysis recommendations are made concerning the stagger values and other factors relevant to applying this procedure safely. Author

N93-26052*# University of Central Florida, Orlando. Dept. of Industrial Engineering and Management Systems.

DESIGN OF AN AIR TRAFFIC COMPUTER SIMULATION SYSTEM TO SUPPORT INVESTIGATION OF CIVIL TILTROTOR AIRCRAFT OPERATIONS Final Report

Ralph V. Rogers 15 Mar. 1993 180 p

(Grant NAG2-625)

(NASA-CR-192920; NAS 1.26:192920) Avail: CASI HC A09/MF A02

The TATSS Project's goal was to develop a design for computer software that would support the attainment of the following objectives for the air traffic simulation model: (1) Full freedom of movement for each aircraft object in the simulation model. Each aircraft object may follow any designated flight plan or flight path necessary as required by the experiment under consideration. (2) Object position precision up to +/- 3 meters vertically and +/- 15 meters horizontally. (3) Aircraft maneuvering in three space with the object position precision identified above. (4) Air traffic control operations and procedures. (5) Radar, communication, navaid, and landing aid performance. (6) Weather. (7) Ground obstructions and terrain. (8) Detection and recording of separation violations. (9) Measures of performance including deviations from flight plans, air space violations, air traffic control messages per aircraft, and traditional temporal based measures. Author

N93-26087*# National Aeronautics and Space Administration. Langley Research Center, Hampton, VA.

PILOTED SIMULATION OF AN AIR-GROUND PROFILE NEGOTIATION PROCESS IN A TIME-BASED AIR TRAFFIC CONTROL ENVIRONMENT

David H. Williams and Steven M. Green (National Aeronautics and Space Administration. Ames Research Center, Moffett Field, CA.) Apr. 1993 45 p

(RTOP 505-64-13-01)

(NASA-TM-107748; NAS 1.15:107748) Avail: CASI HC A03/MF A01

Historically, development of airborne flight management systems (FMS) and ground-based air traffic control (ATC) systems has tended to focus on different objectives with little consideration for operational integration. A joint program, between NASA's Ames Research Center (Ames) and Langley Research Center (Langley), is underway to investigate the issues of, and develop systems for, the integration of ATC and airborne automation systems. A simulation study was conducted to evaluate a profile negotiation process (PNP) between the Center/TRACON Automation System (CTAS) and an aircraft equipped with a four-dimensional flight management system (4D FMS). Prototype procedures were developed to support the functional implementation of this process. The PNP was designed to provide an arrival trajectory solution which satisfies the separation requirements of ATC while remaining as close as possible to the aircraft's preferred trajectory. Results from the experiment indicate the potential for successful incorporation of aircraft-preferred arrival trajectories in the CTAS automation environment. Fuel savings on the order of 2 percent to 8 percent, compared to fuel required for the baseline CTAS arrival speed strategy, were achieved in the test scenarios. The data link procedures and clearances developed for this experiment, while providing the necessary functionality, were found to be operationally unacceptable to the pilots. In particular, additional pilot control and understanding of the proposed aircraft-preferred trajectory, and a simplified clearance procedure were cited as necessary for operational implementation of the concept. Author (revised)

N93-26093 Department of the Navy, Washington, DC.
SYSTEM FOR CALIBRATING A GYRO NAVIGATOR Patent
John S. Stambaugh, inventor (to Navy) 24 Nov. 1992 4 p Filed 31 Mar. 1989
(AD-D015668; US-Patent-5,166,882; US-Patent-Appl-SN-349381; US-Patent-Class-364-453) Avail: US Patent and Trademark Office

The present invention relates to a system for calibrating translation equations of a gyro navigator of a submarine. A value of velocity and a value of position of the submarine are produced by using values of acceleration sensed by accelerometers in the navigation gyro. The value of velocity and position are produced with the aid of the translation equations. This value of velocity and value of position are compared with a value of velocity and a value position as produced by a more accurate and independent source. A comparison is made with the aid of Kalman filter. Any difference obtained during a comparison is used in order to calibrate the translation equations of the gyro navigator. DTIC

N93-26237# Army Aviation Technical Test Center, Fort Rucker, AL.
METHODOLOGY INVESTIGATION: GLOBAL POSITIONING SYSTEM INTEGRATION (GPS) Final Report, Oct. 1991 - Oct. 1992
Larry K. Martin Jan. 1993 16 p
(AD-A261054) Avail: CASI HC A03/MF A01

Testing at U.S. Army Aviation Technical Test Center (ATTC), Fort Rucker, Alabama, requires nap-of-the-earth time space position information (TSPI) of rotary-wing aircraft integrated with other aircraft parameters. The Global Positioning System (GPS), integrated with other sensors, is expected to meet the TSPI requirements. This methodology investigation explored the requirements and the problems encountered in using the GPS for this purpose. DTIC

N93-26274# Army Topographic Engineering Center, Fort Belvoir, VA.
REPAIR, EVALUATION, MAINTENANCE, AND REHABILITATION RESEARCH PROGRAM. CONTINUOUS DEFORMATION MONITORING SYSTEM (CDMS) Final Report
Carl A. Lanigan Dec. 1992 52 p
(AD-A261833; WES/TR/SL-REMR-CS-39) Avail: CASI HC A04/MF A01

The US Army Topographic Engineering Center (TEC) has developed an automated deformation monitoring technology known as the Continuous Deformation Monitoring System (CDMS). The CDMS is capable of computing structural deformation using the Global Positioning System (GPS) survey technology while operating in a continuous fashion over time. A network of two personal computers control GPS survey equipment and process the satellite data gathered to compute apparent structural deformation up to 24 times a day without the presence of an operator. Structural monitoring can take place at the project site or at a distant office. Performance testing by TEC has determined deformation measurement precision in the subcentimeter range. The CDMS was installed at Dworshak Dam in northern Idaho and tracked the upstream movement of the dam while undergoing reservoir drawdown. DTIC

N93-26447# Federal Aviation Administration, Oklahoma City, OK. Civil Aeromedical Inst.
CONVERSION OF THE CTA, INC., EN ROUTE OPERATIONS CONCEPTS DATABASE INTO A FORMAL SENTENCE OUTLINE JOB TASK TAXONOMY Final Report
Mark D. Rodgers and Gena K. Drechsler Jan. 1993 77 p
(AD-A261410; DOT/FAA/AM-93/1) Avail: CASI HC A05/MF A01

FAA Air Traffic Control Operations Concepts Volume VI: ARTCC-Host En Route Controllers (1990) developed by CTA, Inc., a technical description of the duties of an En Route air traffic control specialist (ATCS), formatted in User Interface Language, was restructured into a hierarchical formal sentence outline. To ensure that none of the meaning associated with a task or task element was lost during the conversion, the revised document was reviewed by subject matter experts (SME's) consisting of five groups of six En Route controllers and a quality assurance subject matter expert. SME's looked for words, phrases, or acronyms not commonly used by En Route controllers, and illogical sequencing of duties described in the document. Appropriate suggestions for change were implemented into the document before the next review. Five-hundred seventy-five changes were made to the document, with only two of these changes made during the final review, confirming that an improved document resulted from the research. The restructured document is intended to assist in the identification of tasks not performed or performed incorrectly during the commission of an operational error. However, an easily understood, detailed description of duties performed by an En Route ATCS has potential not only for use by researchers interested in En Route ATCS tasks, but also by quality assurance investigation teams and training personnel. DTIC

N93-26549*# Georgia Inst. of Tech., Atlanta. School of Aerospace Engineering.
IMAGE-BASED RANGING AND GUIDANCE FOR ROTORCRAFT
P. K. A. Menon Dec. 1991 80 p
(Contract NCC2-575)
(NASA-CR-177608; A-93061; NAS 1.26:177608) Avail: CASI HC A05/MF A01

This report documents the research carried out under NASA Cooperative Agreement No. NCC2-575 during the period Oct. 1988 - Dec. 1991. Primary emphasis of this effort was on the development of vision based navigation methods for rotorcraft nap-of-the-earth flight regime. A family of field-based ranging algorithms were developed during this research period. These ranging schemes are capable of handling both stereo and motion image sequences, and permits both translational and rotational camera motion. The algorithms require minimal computational effort and appear to be implementable in real time. A series of papers were presented on these ranging schemes, some of which are included in this report. A small part of the research effort was expended on synthesizing a rotorcraft guidance law that directly uses the vision-based ranging data. This work is discussed in the last section. Author

N93-25018# Kayser Threde G.m.b.H., Munich (Germany).
AN EXPERIMENTAL HEALTH MONITORING UNIT FOR GPS AND GLONASS
B. Eissfeller, M. Haunschild (Maschinenfabrik Augsburg-Nuernberg A.G., Munich, Germany.), A. Jansche, and N. Niklasch (Maschinenfabrik Augsburg-Nuernberg A.G., Munich, Germany.) *In* ESA, Frequency and Time Forum Jun. 1992 p 253-257 (For primary document see N93-24978 09-70)
(Contract ESA-9281/91/F/RD(SC))
Copyright Avail: CASI HC A01/MF A04

05 AIRCRAFT DESIGN, TESTING AND PERFORMANCE

Includes aircraft simulation technology.

For related information see also *18 Spacecraft Design, Testing and Performance* and *39 Structural Mechanics*.For land transportation vehicles see *85 Urban Technology and Transportation*.

N93-24739# Kansas Univ., Lawrence. Flight Research Lab.
GENERAL AVIATION AIRCRAFT: NORMAL ACCELERATION DATA ANALYSIS AND COLLECTION PROJECT Final Report
James E. Locke, Howard W. Smith, Edward A. Gabriel, and Thomas DeFlore Feb. 1993 341 p Prepared in cooperation with Wichita State Univ., KS
(DOT/FAA/CT-91/20; KU-FRL-926-1) Avail: CASI HC A15/MF A03

This report contains the analysis and condensation of repeated flight loads obtained from 77 airplanes that participated in the NASA Velocity Gravity Height (VGH) General Aviation Program. In addition, the load spectra for 98 airplanes in the NASA VGH data base are presented as plotted and tabulated data. Curve fit equations are listed for the original data and for extrapolation, which was used in the statistical analysis. Airspeed, normal load factor, and altitude were recorded continuously during flight. The load factor data were separated into gust and maneuver normal accelerations. The reduced data are presented as cumulative number of occurrences per nautical mile versus acceleration fraction (incremental normal acceleration divided by incremental limit load factor). For statistical analysis, the airplanes were grouped into seven single and twin-engine operational usage groups. The mean (weighted by flight time), weighted mean--plus one, two, and three standard deviation spectra, and the 90 percent probability/95 percent confidence spectra were determined for each operational usage group and for several of the groups combined. An estimate of the scatter associated

with groups having small sample size was determined by computing a pooled variance and pooled standard deviation. The resulting load spectra are to be used for wing fatigue test or safe-life estimation. The Federal Aviation Administration's plans for further study using the results of this report are discussed. The final objective of this effort is to produce a revised fatigue evaluation report for small and commuter airplane certification under Part 23 of the Federal Aviation Regulations. Author (revised)

N93-24768 Stanford Univ., CA.
AERODYNAMIC DESIGN AND SYNTHESIS OF THE OBLIQUE FLYING WING SUPERSONIC TRANSPORT Ph.D. Thesis
Alexander Jacobus M. VanderVelden 1992 310 p
Avail: Univ. Microfilms Order No. DA9234183

The performance of an oblique flying wing supersonic transport was investigated in this study and its economics were compared with those of conventional transports. Aerodynamics, structures, propulsion, environmental impact, (sonic boom, ozone, noise) and economy were analyzed for a given mission, subject to environmental constraints from Mach 0.8 to Mach 2.0. Twenty variables represented the aircraft geometry, engine characteristics, and mission. These variables were optimized simultaneously for the aircraft families as a function of Mach number, payload, and range. The globally optimized oblique flying wing was designed in detail with a new design method and analyzed with CFD codes. The wing did not only achieve the low drag predicted by the synthesis method but was trimmable over its entire flight envelope. Results showed oblique flying wings with payloads over 400 passengers to be superior for all missions considered. At supersonic speeds operating costs half that of delta-wing transports were achieved. The improvements were attributable to the higher lift-to-drag ratios as well as the beneficial effect of span loading on the structural weight. Dissert. Abstr.

N93-25162*# Arizona State Univ., Tempe. Coll. of Engineering and Applied Sciences.
GENERIC HYPERSONIC VEHICLE PERFORMANCE MODEL Interim Task Report
Frank R. Chavez and David K. Schmidt Apr. 1993 32 p
(Grant NAG1-1341)
(NASA-CR-192953; NAS 1.26:192953; ARC-93-3) Avail: CASI HC A03/MF A01

An integrated computational model of a generic hypersonic vehicle was developed for the purpose of determining the vehicle's performance characteristics, which include the lift, drag, thrust, and moment acting on the vehicle at specified altitude, flight condition, and vehicular configuration. The lift, drag, thrust, and moment are developed for the body fixed coordinate system. These forces and moments arise from both aerodynamic and propulsive sources. SCRAMjet engine performance characteristics, such as fuel flow rate, can also be determined. The vehicle is assumed to be a lifting body with a single aerodynamic control surface. The body shape and control surface location are arbitrary and must be defined. The aerodynamics are calculated using either 2-dimensional Newtonian or modified Newtonian theory and approximate high-Mach-number Prandtl-Meyer expansion theory. Skin-friction drag was also accounted for. The skin-friction drag coefficient is a function of the freestream Mach number. The data for the skin-friction drag coefficient values were taken from NASA Technical Memorandum 102610. The modeling of the vehicle's SCRAMjet engine is based on quasi 1-dimensional gas dynamics for the engine diffuser, nozzle, and the combustor with heat addition. The engine has three variable inputs for control: the engine inlet diffuser area ratio, the total temperature rise through the combustor due to combustion of the fuel, and the engine internal expansion nozzle area ratio. The pressure distribution over the vehicle's lower aft body surface, which acts as an external nozzle, is calculated using a combination of quasi 1-dimensional gas dynamic theory and Newtonian or modified Newtonian theory. The exhaust plume shape is determined by matching the pressure inside the plume, calculated from the gas dynamic equations, with the freestream pressure, calculated from Newtonian or Modified Newtonian theory. In this manner, the pressure distribution along the vehicle after body expansion surface is then determined. The aerodynamic modeling, the engine modeling, and the exhaust plume analysis are described in more detail. A description of the computer code used to perform the above calculations is given and an input/output example is then given. The computer code is available on a Macintosh floppy disk. Author (revised)

N93-25279 Virginia Polytechnic Inst. and State Univ., Blacksburg.
INTEGRATED AERODYNAMIC-STRUCTURAL WING DESIGN OPTIMIZATION Ph.D. Thesis
Eric Robert Unger 1992 101 p
Avail: Univ. Microfilms Order No. DA9220650

Several procedures for the simultaneous aerodynamic-structural design optimization of aircraft wings are investigated. These procedures include efficient methods for optimization and sensitivity calculations that are applied to two specific design examples. The first is a subsonic transport aircraft with a composite forward-swept wing. The aerodynamic modeling for this case is provided by vortex-lattice theory and the structural model initially utilizes finite-element analyses. Even with efficient sensitivity methods, the approximate optimization problem still requires a large computational effort. To reduce this cost, a variable-complexity model for the structural analyses is introduced. First, an algebraic equation model for wing weight is used in the optimization procedure to obtain an aerodynamic design that approximately accounts for the effects of wing geometry on wing weight. Then this design is refined by simultaneous aerodynamic-structural optimization based on the finite-element analysis. The net effect of this dual structural model is a substantial reduction in optimization costs. The second example is the wing design of a supersonic High-Speed Civil Transport (HSCT). For this case, the simple wing-weight equations for structures are retained. For the aerodynamics, a variable-complexity model was introduced with the complex models provided by volumetric wave drag analysis and panel methods. In addition, simple algebraic models for wave and drag use to lift provide inexpensive approximations during most of the optimization cycles. With the minimization of the costly complex sensitivity calculations, a reduction in optimization costs is realized. Dissert. Abstr.

N93-25408 Cranfield Inst. of Tech., Bedford (England).
A PRELIMINARY SIZING METHOD FOR UNMANNED AIRCRAFT USING MULTI-VARIATE OPTIMISATION Ph.D. Thesis
A. Turnbull 1990 383 p
Avail: Univ. Microfilms Order No. BRDX98006

The project was carried out, initially, under sponsorship from RAE Farnborough, the object being to obtain a design 'tool' to aid the initial project design work done on turbojet propelled unmanned aircraft. Hence, a sizing method for any unmanned air vehicle configuration with turbojet propulsion, using methods compatible with RAE multi-variate optimization techniques, evolved. The scope of the research was extended to include both turbojet and piston propulsion systems. The range of vehicle configuration is wide, with a choice of internally or externally mounted turbojet engines, forward tractor type or rear pusher type piston engines; conventional flying surfaces or twin boom, twin fin type configurations. The internal fuselage layout is user-defined and has numerous possibilities. The aircraft synthesis uses standard mass and drag estimations, where applicable, for the airframe and vehicle systems, such as fuselage, wing, propulsion, electrics, and recovery systems. The synthesized vehicle is assumed to fly a user-specified mission profile with the performance and fuel requirements for each leg of the sortie being calculated. The mission profile can consist of a maximum of seven legs: climb, cruise, loiter, acceleration, high speed dash, maneuver, and return. The total fuel consumption, along with the fuel reserves are calculated to give the total overall vehicle mass. The design synthesis can be used as a stand-alone program or with the optimization package, RQPMIN. During the latter the vehicle mass is optimized with respect to specified configuration parameters while having to satisfy user-specified constraints (both geometric and performance related). A detailed output is produced, giving the initial and final vehicle configurations; including component masses, total geometric values and mission performance details. The optimization program details, such as constraint and independent variable values are also given. Dissert. Abstr.

N93-25486 Georgia Inst. of Tech., Atlanta.
APPLICATION OF FINITE-STATE INFLOW TO FLAP-LAG-TORSION DAMPING IN HOVER Ph.D. Thesis
Donizeti deAndrade 1992 204 p
Avail: Univ. Microfilms Order No. DA9303157

The aeroelastic stability of helicopter rotors in hovering flight is investigated by a coupled set of generalized dynamic wake equations and hybrid equations of motion for an elastic blade cantilevered in bending and having a torsional root spring to model pitch-link flexibility. The

generalized dynamic wake model employed is based on an induced flow distribution expanded in a set of harmonic and radial shape functions, including undetermined time dependent coefficients as aerodynamic states. The flow is described by a system of first-order, ordinary differential equations in time, for which the pressure distribution at the rotor disk is expressed as a summation of the discrete loadings on each blade, accounting simultaneously for a finite number of blades and overall rotor effects. The nonlinear blade equations are simplified by the assumption of uniform blade mass and stiffness; and then they are reduced to nonlinear differential equations by Galerkin's method. Inflow and blade equations are matched in a way to establish a standard eigen-analysis for the stability of small motions about blade equilibrium and steady-state inflow. The coefficient matrices in the eigenproblem depend on the numerical solution of blade equilibrium and steady-state inflow nonlinear algebraic equations. The model has been applied to a two-bladed, untwisted, stiff inplane hingeless small scale rotor with torsionally soft blades, including a blade root offset, and hub designed to permit variation in precone, blade droop, pitch control stiffness, and blade pitch angle. Numerical results show that three-dimensional tip relief effects within the nonuniform steady-state inflow are significant to predict steady-state aerodynamic loads and blade deflections. The eigenvalue results confirmed the importance of unsteady, three-dimensional aerodynamics in predicting lead-lag damping, by means of correlations with unsteady three-dimensional panel theory and with experiments. Eigenvector analysis correlations reinforced qualitative and quantitative shortcomings associated with quasi-steady two-dimensional aerodynamic theory for aeroelastic applications in hover. Overall results from this research set the present finite-state methodology as a suitable tool to handle helicopter integrated dynamics. This is chiefly due to elimination of time-marching and moving block analysis inherent to previous approaches to the same problem, implying in substantial savings in computer memory and time, with no essential loss of accuracy. Dissert. Abstr.

N93-25526 Stanford Univ., CA.
STRUCTURAL AND AERODYNAMIC OPTIMIZATION OF JOINED-WING AIRCRAFT Ph.D. Thesis
John Waldemar Gallman 1992 258 p
Avail: Univ. Microfilms Order No. DA9234097

The joined wing is an innovative aircraft configuration with a rear wing that is attached near the top of the vertical tail and sweeps forward to join the trailing edge of the forward wing. This study evaluates the performance of joined-wing aircraft and demonstrates the use of numerical optimization in aircraft design. Initially, a parametric design study that considered a single cruise condition indicated an 11 percent savings in trimmed drag for a joined-wing with the same lifting surface area and 23 percent longer wing span than a conventional configuration. These results encouraged further study of the joined-wing concept and motivated the development of a computer program that uses numerical optimization to design both joined-wing and conventional configurations. This design program uses a vortex-lattice model of all aircraft components to calculate aerodynamic forces and a beam model of the lifting-surface structure to calculate wing and tail weight. Weight estimation depends on a fully-stressed design algorithm that includes a constraint on buckling and a correlation with a statistically based method for total lifting-surface weight. This fully-stressed sizing routine produced joined-wing structures that are nearly identical to minimum-weight structures designed using numerical optimization. A variety of 'optimum' joined-wing and conventional aircraft designs were compared on the basis of direct operating cost, gross weight, and cruise drag. Maximum lift and tail buckling were identified as critical joined-wing design issues. The addition of a buckling constraint was shown to decrease the optimum joined-wing space by 8 percent and increase direct operating cost by 4 percent. Although aeroelasticity and dynamic stability were neglected during the design study, separate analyses showed that the optimum configurations have sufficient damping for good handling qualities and flutter speeds that are well above the design dive speed. The most promising joined-wing designs have a joint location at about 70 percent of the wing semispan, a fuel tank in the tail to trim, and a flap spanning 70 percent of the wing. These designs are shown to cost 3 percent more to operate than a conventional configuration designed for the same medium-range mission. Dissert. Abstr.

N93-25530 Maryland Univ., College Park.
AEROELASTIC RESPONSE AND AEROMECHANICAL STABILITY OF HELICOPTERS WITH ELASTICALLY COUPLED COMPOSITE ROTOR BLADES Ph.D. Thesis
Edward C. Smith 1992 453 p
Avail: Univ. Microfilms Order No. DA9304398

A comprehensive formulation was developed to study the effects of elastically coupled composite helicopter rotor blades on aeroelastic response, blade and hub loads, rotor aeroelastic stability, and rotor-fuselage aeromechanical stability. Both hover and forward flight conditions are addressed, and the aeromechanical stability analysis includes both air and ground resonance phenomenon. A new analysis was formulated to model the laminated composite box-beam blade spar. The box-beam analysis includes the nonclassical structural effects of transverse shear, torsion-related out-of-plane warping, and two-dimensional ply elasticity. Elastic couplings are introduced through the anisotropy of the plies in the composite spar. For the aeroelastic and aeromechanical analysis, the blade is idealized as an elastic beam undergoing moderate deflections in flap and lag bending, elastic torsion, elastic axial deformation, and flap and lag transverse shear. A nineteen d.o.f. shear flexible beam element is introduced for the composite rotor blades. The structural model is validated by correlation with experimental data and finite element solutions for static deflections of elastically coupled graphite-epoxy composite box-beams. The quantitative importance of the nonclassical structural effects is also investigated. The free vibration analysis is validated by correlation with experimental data and finite element results for the in vacuo rotating natural frequencies of the composite box-beams. The aeromechanical stability analysis is correlated against experimental data for a model hingeless rotor-body configuration. Results indicate that elastic couplings introduced through the composite blade spar have a powerful effect on both shaft-fixed blade stability and rotor-body aeromechanical stability. The torsional response is also significantly affected by the composite couplings. Influence of composite couplings on blade and hub loads was measurable, but less pronounced. Dissert. Abstr.

N93-25538 Georgia Inst. of Tech., Atlanta.
AN INTEGRATED FINITE-STATE MODEL FOR ROTOR DEFORMATION, NONLINEAR AIRLOADS, INFLOW, AND TRIM Ph.D. Thesis
Walter Martin Stumpf 1992 236 p
Avail: Univ. Microfilms Order No. DA9303147

Existing models for forward flight rotor aeroelastic loads suffer from a number of deficiencies. These models often use crude aerodynamics coupled with sophisticated blade equations, require excessive computation, contain modules that must be solved sequentially rather than simultaneously, or contain hidden states or a large number of states. The aeroelastic model described here addresses these deficiencies. It is a time-domain, state-space aeroelastic model of a rotor in forward flight. The model computes trim, airloads, rotor shaft loads and the instantaneous inflow distribution. All components of the model are expressed as ordinary differential equations, which are solved by integrating the system in time until a periodic solution is reached. The states have physical significance and, since there are a finite number of them, Floquet theory may be applied. The aerodynamic and structural models are of a comparable level of sophistication and are strongly coupled. The section airloads are described by a classical thin airfoil theory, which treats the wake contribution as a external forcing function. The airloads are modified to reflect the presence of dynamic stall using the semi-empirical ONERA dynamic stall model. The wake contribution is computed using the Peters generalized dynamic inflow theory, which is based on a series solution of the potential-flow equation. The Hodges and Dowell elastic blade equations are approximated using the Galerkin-Ritz method. Trim is found using an automatic controller, also written as a set of ordinary-differential equations. When the number of shape functions and aerodynamic control points are chosen to include dynamics up to a frequency of four per rev., the model including inflow, stall, blade deformations and trim, is defined by about 50 state variables. A trimmed solution requires between 10 and 40 revolutions to trim, and costing about four minutes of CPU time per ten revolutions (on a VAX 6440). The model response has been validated using flight test data from the SA349 helicopter. The blade motions and aerodynamic normal forces predicted by the model agreed fairly well with the measured values, but the pitching moment predictions were less successful. Dissert. Abstr.

N93-25552# Old Dominion Univ., Norfolk, VA.
A COMPUTATIONAL AERODYNAMIC DESIGN OPTIMIZATION METHOD USING SENSITIVITY ANALYSIS Ph.D. Thesis
Mohamed El-Amin Eleshaky 1992 235 p
Avail: Univ. Microfilms Order No. DA9230207

A new and efficient procedure for aerodynamic shape optimization is presented. The salient lineaments of this procedure are: (1) using a discrete sensitivity analysis approach to determine analytically the aerodynamic sensitivity coefficients; (2) obtaining the flowfield solution either by a computational fluid dynamics (CFD) analysis or, alternatively, by a flowfield extrapolation method which is based on a truncated Taylor's series; (3) defining the aerodynamic shape in such a way that it is not restricted to any class of surfaces and the optimizer automatically shapes the aerodynamic configuration to any arbitrary geometry; and (4) requiring no expertise other than that needed for formulating the optimization problem in question. This procedure is successfully demonstrated on different aerodynamic optimization problems. In one of the optimization problems, the ramp shape of a scram jet nozzle-afterbody configuration is optimized to yield a maximum thrust force coefficient. However, prior to its design optimization, a CFD capability for the mixing of two-dimensional, viscous, multispecies flows has been developed in order to gain a detailed understanding of the complex flowfield features of the scram jet nozzle-afterbody configuration. It is shown that heavier exhaust mixture (simulated by a Freon-Argon mixture) undergoes gas dynamic expansion at a smaller rate than does lighter 'air' exhaust flow. In the sensitivity analysis approach, both Euler and thin-layer Navier-Stokes equations are used. Their discretized equations are solved using an implicit, upwind-biased, finite-volume scheme. The van Leer flux-vector splitting is used in the discretization of the pressure and convective terms. The direct and iterative solution methods, which are deemed most applicable to the large linear systems of algebraic equations arising in the sensitivity approach, are investigated with regards to their accuracies, computational time, and computer memory requirements. These methods are shown to be feasible only for small two-dimensional problems. Due to the prohibitively high memory requirements, they become impractical for large two-dimensional problems and inapplicable for any of the three-dimensional problems. To alleviate this limitation, a new scheme based on domain decomposition principles has been developed and is called the Sensitivity Analysis Domain-Decomposition (SADD) scheme. Dissert. Abstr.

N93-25670*# Iowa State Univ. of Science and Technology, Ames. Dept. of Aerospace Engineering and Engineering Mechanics.
TRAJECTORY OPTIMIZATION FOR THE NATIONAL AEROSPACE PLANE Semiannual Report, 13 Jun. - 12 Dec. 1992
Ping Lu Jan. 1993 10 p
(Grant NAG1-1255)
(NASA-CR-192954; NAS 1.26:192954) Avail: CASI HC A02/MF A01

While continuing the application of the inverse dynamics approach in obtaining the optimal numerical solutions, the research during the past six months has been focused on the formulation and derivation of closed-form solutions for constrained hypersonic flight trajectories. Since it was found in the research of the first year that a dominant portion of the optimal ascent trajectory of the aerospace plane is constrained by dynamic pressure and heating constraints, the application of the analytical solutions significantly enhances the efficiency in trajectory optimization, provides a better insight to understanding of the trajectory and conceivably has great potential in guidance of the vehicle. Work of this period has been reported in four technical papers. Two of the papers were presented in the AIAA Guidance, Navigation, and Control Conference (Hilton Head, SC, August, 1992) and Fourth International Aerospace Planes Conference (Orlando, FL, December, 1992). The other two papers have been accepted for publication by Journal of Guidance, Control, and Dynamics, and will appear in 1993. This report briefly summarizes the work done in the past six months and work currently underway. Derived from text

N93-25692 Cranfield Inst. of Tech., Bedford (England).
AN APPROACH TO CONFIGURATION DESIGN SYNTHESIS OF SUBSONIC TRANSPORT AIRCRAFT USING ARTIFICIAL INTELLIGENCE TECHNIQUES Ph.D. Thesis
H. M. Pasaribu 1991 272 p
Avail: Univ. Microfilms Order No. BRDX97987

This thesis outlines a computer system developed to tackle the configuration design synthesis of subsonic transport aircraft. The system provides an interactive design environment which combines the reasoning process of the aircraft configuration definition and the numerical analyses that lie behind the reasoning. The system applies artificial intelligence (AI) techniques to the configuration analysis. This gives the system the capability to reason with the configuration choices. The system is built in modules, with each module being clearly separated to deal with a complete analysis in a specific aspect of design. The integration of the modules is done through an intelligent interface and a common database. The interface also incorporates AI techniques in deciding the sequence of execution of the modules and the processing of the input/output data for a particular module. The interface permits the sharing of information among the modules and supports modularity and flexibility of the system for future development. Since each module is independent, it can be easily modified or replaced without disturbing the balance of the system. An extensive library of application programs is included in the engineering analysis module which enable detailed analysis to be performed. The system is equipped with a simplified database management and a special purpose graphics module which is extensively used for the presentation of the output. The system has been validated and tested. It can handle both propeller driven and jet engined aircraft. An example of the case studies is presented. The improvement of the system for future development is also considered. These include the extension of the knowledge base for dealing with problems in other modules, the enhancement of the application programs in the engineering module, and a possible interface with an established Computer Aided Drafting (CAD) system. Dissert. Abstr.

N93-25701 Rensselaer Polytechnic Inst., Troy, NY.
DESIGN AND ANALYSIS OF CURVED COMPOSITE COMPONENTS FOR ROTORCRAFT FUSELAGE FRAMES Ph.D. Thesis
Ann W. Peck 1992 238 p
Avail: Univ. Microfilms Order No. DA9302698

An investigation in the design and analysis of curved composite components for rotorcraft fuselage frames was conducted. Using a strength of material based approach, analytical expressions were developed to predict the flange and web stress resultants in curved beams made of anisotropic materials. Two parameters, which include flange and web geometric and material stiffness effects, have been identified that characterize the flange stress redistributions due to curling. After validation of the analytical solutions using a finite element model, a parameter study was performed to examine the effects material anisotropy and cross-sectional configuration have on the flange curving behavior. It has been found that the flange and web laminates have a significant effect on the internal stress distributions. Reducing flange curling reduces the amount of flange axial load redistribution but increases the maximum curling moment. An increase of the web bending stiffness increases the overall bending stiffness and flange efficiency, but also increases the flange root curling moment and the web bending moment in the C- and box cross-sectonal configurations. At some point, an increase in the web bending stiffness diminishes the overall load carrying capability as the web becomes the critical element. It appears to be difficult to utilize material anisotropy to improve the overall load carrying capability. Formal optimization techniques were used to investigate the maximum load carrying capability of curved composite beams. The overall driving design factor was found to be flange curling. To maximize overall load carrying capability in curved composite beams with fixed-length flanges, the overall bending stiffness is maximized by minimizing web thicknesses and moving structural material out towards the flanges and flange curling minimized by minimizing flange lengths, increasing flange thicknesses, minimizing web thicknesses in the C- and box beams, placing predominantly 0 degree and 90 degree fibers in the flange laminates with 0 degree fibers on the interior and 90 degree fibers on the outside, and placing predominantly 0 degree fibers in the web laminates of the C- and box configurations. The optimum cross-sectional configuration is dependent on chosen quantities, such as flange lengths, beam mass. For fixed-length flanges, no clear optimum cross-section was found. Dissert. Abstr.

N93-25704 Cranfield Inst. of Tech., Bedford (England).
ASTOVL COMBAT AIRCRAFT DESIGN SYNTHESIS AND OPTIMIZATION Ph.D. Thesis
N. Kehayas 1992 293 p
Avail: Univ. Microfilms Order No. BRDX98001

This thesis presents the development of a Baseline Configuration for

an Advanced Short Take-Off and Vertical Landing (ASTOVL) Combat Aircraft, the Design Synthesis and coding of this Baseline Configuration (Code VERTI), the interfacing of the Design Synthesis Code VERTI with the Optimizer code RQPMIN and the optimization of the Baseline Configuration. The background and the objectives of this Research Program are initially examined. The evaluation of the ASTOVL Combat Aircraft Baseline Configuration is then described, including all the problems, assumptions, choices and compromises that led to the specific configuration. The development of the Design Synthesis and the Code VERTI then follow, where the methodology used, the techniques adopted and the code operation are explained. A full description of the Design Synthesis is included as an appendix. Finally, the interfacing of Code VERTI with the optimizer RQPMIN and the optimization of the Baseline Configuration are presented. The problems and difficulties of the RQPMIN operation are thoroughly discussed. The RQPMIN-VERTI Code is used to optimize the initial Baseline Configuration and an optimization example is provided in appendix form. The optimized Baseline Configuration is partly validated against two ASTOVL combat aircraft designs. In addition to the optimization with the aircraft empty mass as objective function, a search for a better objective function is attempted. Dissert. Abstr.

N93-25719 Rensselaer Polytechnic Inst., Troy, NY.
STRUCTURAL DYNAMIC ANALYSIS OF BEARINGLESS ROTOR BLADE Ph.D. Thesis
Wuying Chiang 1992 261 p
Avail: Univ. Microfilms Order No. DA9236209

Conventional articulated helicopter rotor systems typically have mechanical hinges, dampers and bearings in the hub to relieve high blade root moments and to ensure dynamic stability. This hardware operates in a high stress field and experiences large cyclic and centrifugal loads. These devices require continuous inspection and frequent maintenance. In addition, they can significantly degrade the reliability of the rotor system. In order to improve helicopter reliability, reduce maintenance, and potentially improve rotor hub aerodynamic characteristics, the helicopter researchers have developed the hingeless and bearingless rotor by taking advantage of recent advancements in materials technology. The unique structural features of bearingless rotors calls for the development of design and modeling methodologies for laminated composite flex-structures. Indeed, the flex-structure should be flexible enough to replace the flap, lead-lag, and feathering bearings, while maintaining high strength and stiffness in the axial direction. Laminated composite materials are a material of choice for such an application. Chordwise deformations, transitional zones between different cross-sections and localized compressive stresses are all likely to be present in the flex-structure, rendering the validity of a beam model questionable. In this research an anisotropic shallow shell model is developed that accommodates transverse shearing deformations and arbitrarily large displacements and rotations. However, strains are assumed to remain small. Two kinematic models are developed in this research: the first model uses two rotation parameters to locate the direction of the normal to the shell's mid-plane while the second one uses a rotation tensor which is composed of three parameters. The latter model, which has an in-plane rotation degree-of-freedom, allows for an automatic compatibility of the shell model with other three-dimensional structural models. A shell model is validated by comparing its predictions with several benchmark problems which include static and dynamic, linear and nonlinear, as well as isotropic and anisotropic conditions. The performance of the in-plane rotation degree-of-freedom of the shell model is tested also by solving some special configurations. In actual helicopter rotor blade problems, the shell model of the flex-structure is shown to give very different results when compared to beam models. The lead-lag and torsion modes are strongly affected, whereas flapping modes seem to be less affected. A study was also carried out to simulate a tail rotor system; the pitch actuator force is found to vary significantly when shell or beam models are used. Dissert. Abstr.

N93-25733# Air Force Occupational Measurement Center, Randolph AFB, TX.
AIRCRAFT ELECTRICAL AND ENVIRONMENTAL SYSTEMS, AFSCs 452X5, 454X5, AND 454X6
Jan. 1993 71 p
(AD-A261213) Avail: CASI HC A04/MF A01

This is a report of an occupational survey of the Electrical and Environmental Systems career ladders conducted by the Occupational Analysis Flight, USAFOMS. The Headquarters Air Training Command (ATC) Aircraft/ Munitions maintenance Training Division requested this survey to project, plan, and develop Career Development Courses (CDC), STS's, and training for these career ladders due to the Rivet Workforce restructing of AFSC 423X0--Aircraft Electrical Systems and AFSC 423X1--Aircraft Environmental Systems. The last surveys pertaining to these career ladders were published in Feb. 1984 (AFSC 423X1) and Feb. 1985 (AFSC 423X0). The merger of the Electrical and Environmental, Strategic Electrical and Environmental, and Airlift Electrical and Environmental. Members of all these career ladders participated in this survey. In Jun. 1992, a U and TW decided to merge the three ladders into a single Aircraft Electrical and Environmental Systems career ladder (AFSC 452X5), effective Apr. 1993. DTIC

N93-25933# Naval Aerospace Medical Research Lab., Pensacola, FL.
PERFORMANCE-BASED TESTING AND SUCCESS IN NAVAL ADVANCED FLIGHT TRAINING Interim Report
David J. Blower Nov. 1992 35 p
(NR Proj. M00-96)
(AD-A260838; NAMRL-1378) Avail: CASI HC A03/MF A01

Roughly 5 percent of student naval aviators fail the advanced phase of flight training. At this stage of training, the Navy has spent between $300,000 and $1,000,000 per student. Any reduction in this attrition rate through prior screening would be of great economic benefit to the Navy. Computer-based performance tests developed at the Naval Aerospace Medical Research Laboratory were assessed to determine whether they could augment the present medical screening standards and thereby help identify potential failures in advanced flight training. A weak statistical relationship exists between a dual-task performance test, accession source, college major, an aptitude test, and success in advanced flight training. Discriminant analysis was employed to find a linear composite score of these variables that could be used to classify a student as a probable pass or fail in advanced flight training. For example, the model presented in this report reduced failures by 50 percent at the cost of rejecting roughly 20 percent of those students who eventually passed. A Bayesian analysis of the success rate parameter showed that this particular model significantly improved the present selection system. DTIC

N93-25949# Aerospace Medical Research Labs., Wright-Patterson AFB, OH. Human Engineering Div.
INFORMATION REQUIREMENTS ANALYSES FOR TRANSATMOSPHERIC VEHICLES Final Report, Jul. 1991 - Jun. 1992
Gilbert G. Kuperman Jun. 1992 218 p
(Contract F33615-89-C-0532)
(AD-A261189; AL-TR-1992-0082) Avail: CASI HC A10/MF A03

An information requirements analysis was performed as the initial step in the design of crew system concept for future transatmospheric vehicles (TAVs). A knowledge acquisition, synthesis, and representation process was conducted. A baseline system description was prepared. Concept Maps were generated. A mission event sequence was developed. System architecture depictions were generated. Measures of effectiveness and performance were documented. DTIC

N93-26444# Naval Postgraduate School, Monterey, CA.
AEW AIRCRAFT DESIGN M.S. Thesis
Michael J. Wagner Dec. 1992 114 p
(AD-A261800) Avail: CASI HC A06/MF A02

The aging E-2C fleet is expected to be retired by the year 2015. In order to provide Airborne Early Warning (AEW) for the battle group during the transitional years and beyond, the design of a replacement aircraft must begin soon. In order to conform with present day economic realities, one possible configuration is a new airframe using the radar system and rotodome which currently operates on the E-2C. Other likely requirements for a new AEW aircraft includes a high-speed dash (M=0.7-0.85) capability, an extended mission time (up to 7.5 hours), turbofan engines, and an aircrew ejection system. The results of this design effort includes an investigation of a possible configuration and the aerodynamics involved. Performance, stability and control characteristics are also discussed briefly. Finally, a qualitative analysis of the use of the E-2C's radar system on a new airframe will be presented. DTIC

N93-26462# Dayton Univ., OH.
EFFECT OF IMAGE UPDATE RATE ON MOVING-TARGET IDENTIFICATION RANGE Final Report, Jan. 1991 - Jun. 1992
Julie M. Lindholm and Elizabeth L. Martin Jan. 1993 24 p
(Contract F33615-90-C-0005)
(AD-A261562; AL-TR-1992-0172) Avail: CASI HC A03/MF A01

In prior research, moving-form perception tended to be nonveridical when the update rate of an image generator (IG) was less than the refresh rate of the display device. In this experiment, the effect of update rate on the range at which pilots could identify computer-generated representations of moving aircraft was examined. For a 60-Hz interlaced display, identification range was greater for a 60-Hz image update rate than for a 30-Hz update rate. This effect held for two views of three pairs of aircraft moving at two different velocities. These results suggest that image update rate is an important design parameter for simulators intended to support air-to-air combat training. To maximize the range at which a moving target can be identified, the update rate of the IG should equal the refresh rate of the display device. DTIC

N93-26553*# National Aeronautics and Space Administration. Langley Research Center, Hampton, VA.
SUPERSONIC AEROELASTIC INSTABILITY RESULTS FOR A NASP-LIKE WING MODEL
Stanley R. Cole, James R. Florance, Lee B. Thomason, Charles V. Spain (Lockheed Engineering and Sciences Co., Hampton, VA.), and Ellen P. Bullock (Lockheed Engineering and Sciences Co., Hampton, VA.) Apr. 1993 12 p Presented at the AIAA 34th SDM Conference, Hampton, VA, 19-23 Apr. 1993
(RTOP 763-23-41)
(NASA-TM-107739; NAS 1.15:107739) Avail: CASI HC A03/MF A01

An experimental study and an analytical study have been conducted to examine static divergence for hypersonic-vehicle wing models at supersonic conditions. A supersonic test in the Langley Unitary Plan Wind Tunnel facility was conducted for two wind-tunnel models. These models were nearly identical with the exception of airfoil shape. One model had a four-percent maximum thickness airfoil and the other model had an eight-percent maximum thickness airfoil. The wing models had low-aspect ratios and highly swept leading edges. The all-movable wing models were supported by a single-pivot mechanism along the wing root. For both of the wind-tunnel models, configuration changes could be made in the wing-pivot location along the wing root and in the wing-pivot pitch stiffness. Three divergence conditions were measured for the four-percent thick airfoil model in the Mach number range of 2.6 to 3.6 and one divergence condition was measured for the eight-percent thick airfoil model at a Mach number of 2.9. Analytical divergence calculations were made for comparison with experimental results and to evaluate the parametric effects of wing-pivot stiffness, wing-pivot location, and airfoil thickness variations. These analyses showed that decreasing airfoil thickness, moving the wing-pivot location upstream, or increasing the pitch-pivot stiffness have the beneficial effect of increasing the divergence dynamic pressures. The calculations predicted the trend of experimental divergence dynamic pressure with Mach number accurately; however, the calculations were approximately 25 percent conservative with respect to dynamic pressure. Author

06 AIRCRAFT INSTRUMENTATION

Includes cockpit and cabin display devices; and flight instruments.

For related information see also *19 Spacecraft Instrumentation* and *35 Instrumentation and Photography.*

N93-24764*# National Aeronautics and Space Administration. Langley Research Center, Hampton, VA.
EVALUATION OF ADVANCED DISPLAYS FOR ENGINE MONITORING AND CONTROL Final Report
L. G. Summers (McDonnell-Douglas Automation Co., Long Beach, CA.) Mar. 1993 71 p
(Contract NAS1-18028; RTOP 505-64-13-12)
(NASA-CR-191418; NAS 1.26:191418; MDC-92K0374) Avail: CASI HC A04/MF A01

The relative effectiveness of two advanced display concepts for monitoring engine performance for commercial transport aircraft was studied. The concepts were the Engine Monitoring and Control System (EMACS) display developed by NASA Langley and a display by exception design. Both of these concepts were based on the philosophy of providing information that is directly related to the pilot's task. Both concepts used a normalized thrust display. In addition, EMACS used column deviation indicators; i.e., the difference between the actual parameter value and the value predicted by an engine model, for engine health monitoring; while the Display by Exception displayed the engine parameters if the automated system detected a difference between the actual and the predicted values. The results showed that the advanced display concepts had shorter detection and response times. There were no differences in any of the results between manual and auto throttles. There were no effects upon perceived workload or performance on the primary flight task. The majority of pilots preferred the advanced displays and thought they were operationally acceptable. Certification of these concepts depends on the validation of the engine model. Recommendations are made to improve both the EMACS and the display by exception display formats. Author (revised)

N93-25783# MacAulay-Brown, Inc., Fairborn, OH.
DEVELOPMENT OF A FLIGHT INSTRUMENT PACKAGE Final Report, 16 Nov. 1987 - 30 Apr. 1991
Dan D. Fulgham, John L. Orr, and Brian Mikiten Dec. 1992 606 p Prepared in cooperation with Southeastern Center for Electrical Engineering Education (SCEEE)
(Contracts F33615-87-C-0534; F33615-87-D-0609)
(AD-A260830; AL/BROOKS-TR-1992-0155) Avail: CASI HC A99/MF A06

Subcontractor (Southwest Research Institute) describes the hardware and software comprising the Flight Instrument Package (FIP), a collection of transducers and electronic components that measure primary flight motion and position parameters and generate digital data representing those parameters. Pitch angle, bank angle, altitude, vertical velocity, airspeed, heading, and angle of attack are the main quantities digitized and relayed to a data port for processing into various displays of aircraft state. The FIP developed as part of this task was used in a Beech Queen Air aircraft to drive the Acoustic Orientation Instrument, which provides the pilot with an auditory display of aircraft bank, airspeed, vertical velocity, and other parameters as necessary. DTIC

N93-25909# MacAulay-Brown, Inc., Dayton, OH.
INFLIGHT EVALUATION OF AN ACOUSTIC ORIENTATION INSTRUMENT Interim Technical Report, 16 Nov. 1987 - 30 Apr. 1991
Dan D. Fulgham, John L. Orr, and Brian Mikiten Dec. 1992 434 p Prepared in cooperation with MacAulay Brown, Inc., Dayton, OH
(Contracts F33615-87-C-0534; F33615-87-D-0609; SwRI Proj. 12-2301)
(AD-A260752; AL-TR-1992-0160) Avail: CASI HC A19/MF A04

Subcontractor (Southwest Research Institute) provides engineering data and system software description for the Acoustic Orientation Instrument (AOI), which they developed for inflight testing. The overall scheme of operation of the system involves inputting a frame of scaled flight data (airspeed, bank angle, vertical velocity, etc.) from the Flight Instrument Package (FIP) over an RS232 serial link to the AOI, conversion of the flight data to corresponding output voltage waveforms by the AOI, and delivery of those outputs to stereo headphones to generate an auditory display of the flight parameters of interest. This report constitutes an operation and maintenance manual for the AOI, including system programming in the FORTH computer language. DTIC

N93-26572# TRW, Inc., Warner Robins, GA. Electronic Systems Group.
TECHNICAL OPERATING REPORT ON THE DATA INTEGRATION AND COLLECTION ENVIRONMENT (DICE) INSTRUMENTATION SYSTEM DESIGN Interim Report
Sep. 1992 68 p
(Contract F44606-89-D-0040)
(AD-A261105; WL-TR-93-1001) Avail: CASI HC A04/MF A01

This Technical Operating Report (TOR) provides the top level and intermediate level hardware design of the Data Integration and Collection Environment (DICE) system. The design objectives are: (1) provide the capability to configure and control the collection of specific APG-63 radar and weapons system data; (2) provide for the collection of any and all D-bus, PMUX, CCMUX, and PACS communication data; (3) provide a data

storage capability which exceeds two hours; (4) provide a mechanism for replaying the recorded data to the laboratory instrumentation data reduction and analysis system (IDRAS) in a time phased manner; (5) identify sources for dual compatible militarized and commercial off-the-shelf components; (6) provide prototype road map for the system's production; and (7) provide for filtered data capture processing. A brief description of the overall objectives of this system is presented. The applicable documents, both Government and non-Government, for the DICE system are identified. The instrumentation system design is described. DTIC

07 AIRCRAFT PROPULSION AND POWER

Includes prime propulsion systems and systems components, e.g., gas turbine engines and compressors; and onboard auxilliary power plants for aircraft.

For related information see also *20 Spacecraft Propulsion and Power, 28 Propellants and Fuels,* and *44 Energy Production and Conversion.*

N93-24754*# National Aeronautics and Space Administration. Lewis Research Center, Cleveland, OH.

FUEL INJECTOR: AIR SWIRL CHARACTERIZATION AEROTHERMAL MODELING, PHASE 2, VOLUME 1 Final Report

M. Nikjooy (General Motors Corp., Indianapolis, IN.), H. C. Mongia (General Motors Corp., Indianapolis, IN.), V. G. McDonell (California Univ., Irvine.), and G. S. Samuelsen (California Univ., Irvine.) Mar. 1993 407 p

(Contract NAS3-24350; RTOP 505-62-52)

(NASA-CR-189193; E-7593; NAS 1.26:189193) Avail: CASI HC A18/MF A04

A well integrated experimental/analytical investigation was conducted to provide benchmark quality relevant to a prefilming type airblast fuel nozzle and its interaction with the combustor dome air swirler. The experimental investigation included a systematic study of both single-phase flows that involved single and twin co-axial jets with and without swirl. A two-component Phase Doppler Particle Analyzer (PDPA) was used to document the interaction of single and co-axial air jets with glass beads that simulate nonevaporating spray and simultaneously avoid the complexities associated with fuel atomization processes and attendant issues about the specification of relevant boundary conditions. The interaction of jets with methanol spray produced by practical airblast nozzle was also documented in the spatial domain of practical interest. Model assessment activities included the use of three turbulence models (k-epsilon, algebraic second moment (ASM), and differential second moment (DSM)) for the carrier phase, deterministic or stochastic Lagrangian treatment of the dispersed phase, and advanced numerical schemes. Although qualitatively good comparison with data was obtained for most of the cases investigated, the model deficiencies in regard to modeled dissipation rate transport equation, single length scale, pressure-strain correlation, and other critical closure issues need to be resolved before one can achieve the degree of accuracy required to analytically design combustion systems. Author (revised)

N93-25079*# National Aeronautics and Space Administration. Lewis Research Center, Cleveland, OH.

SCREENING STUDIES OF ADVANCED CONTROL CONCEPTS FOR AIRBREATHING ENGINES

Peter J. Ouzts, Carl F. Lorenzo, and Walter C. Merrill Mar. 1993 22 p Presented at the 28th Joint Propulsion Conference and Exhibit, Nashville, TN, 6-8 Jul. 1992; sponsored by AIAA, SAE, ASME, and ASEE

(RTOP 505-62-50)

(NASA-TM-106042; E-7620; NAS 1.15:106042) Avail: CASI HC A03/MF A01

The application of advanced control concepts to airbreathing engines may yield significant improvements in aircraft/engine performance and operability. Accordingly, the NASA Lewis Research Center has conducted screening studies of advanced control concepts for airbreathing engines to determine their potential impact on turbine engine performance and operability. The purpose of the studies was to identify concepts which offered high potential yet may incur high research and development risk. A target suite of proposed concepts was formulated by NASA and industry. These concepts were evaluated in a two phase study to quantify each concept's impact on desired engine characteristics. To aid in the evaluation, three target aircraft/engine combinations were considered: a military high performance fighter mission, a high speed civil transport mission, and a civil tiltrotor mission. Each of the advanced control concepts considered in the study were defined and described. The concept's potential impact on engine performance was determined. Relevant figures of merit on which to evaluate the concepts were also determined. Finally, the concepts were ranked with respect to the target aircraft/engine missions. Author

N93-25106*# General Motors Corp., Indianapolis, IN. Allison Gas Turbine Div.

FUEL INJECTOR: AIR SWIRL CHARACTERIZATION AEROTHERMAL MODELING, PHASE 2, VOLUME 2 Final Report

M. Nikjooy, H. C. Mongia, V. G. McDonell (California Univ., Irvine.), and G. S. Samuelson (California Univ., Irvine.) Mar. 1993 294 p

(Contract NAS3-24350; RTOP 505-62-52)

(NASA-CR-189193; E-7593; NAS 1.26:189193) Avail: CASI HC A13/MF A03

A well integrated experimental/analytical investigation was conducted to provide benchmark quality data relevant to prefilming type airblast fuel nozzle and its interaction with combustor dome air swirler. The experimental investigation included a systematic study of both single-phase flows that involved single and twin co-axial jets with and without swirl. A two-component Phase Doppler Particle Analyzer (PDPA) equipment was used to document the interaction of single and co-axial air jets with glass beads that simulate nonevaporating spray and simultaneously avoid the complexities associated with fuel atomization processes and attendant issues about the specification of relevant boundary conditions. The interaction of jets with methanol spray produced by practical airblast nozzle was also documented in the spatial domain of practical interest. Model assessment activities included the use of three turbulence models (k-epsilon, algebraic second moment (ASM) and differential second moment (DSM)) for the carrier phase, deterministic or stochastic Lagrangian treatment of the dispersed phase, and advanced numerical schemes. Although qualitatively good comparison with data was obtained for most of the cases investigated, the model deficiencies in regard to modeled dissipation rate transport equation, single length scale, pressure-strain correlation, and other critical closure issues need to be resolved before one can achieve the degree of accuracy required to analytically design combustion systems. Author

N93-25129*# National Aeronautics and Space Administration. Lewis Research Center, Cleveland, OH.

EXPERIMENTAL PERFORMANCE OF A VENTRAL NOZZLE WITH PITCH AND YAW VECTORING CAPABILITY FOR SSTOVL AIRCRAFT

Barbara S. Esker and Jack G. McArdle Apr. 1993 12 p Presented at the Aerospace Atlantic Conference, Dayton, OH, 20-23 Apr. 1993; sponsored by SAE

(RTOP 505-68-32)

(NASA-TM-106054; E-7648; NAS 1.15:106054) Avail: CASI HC A03/MF A01

Aircraft with supersonic, short takeoff, and vertical landing capability were proposed to replace some of the current high-performance aircraft. Several of these configurations use a ventral nozzle in the lower fuselage, aft of the center of gravity, for lift or pitch control. Internal vanes canted at 20 deg were added to a swivel-type ventral nozzle and tested at tailpipe-to-ambient pressure ratios up to 5.0 on the Powered Lift Facility at NASA LeRC. The addition of sets of four and seven vanes decreased the discharge coefficient by at least 6 percent and did not affect the thrust coefficient. Side force produced by the nozzle with vanes was 14 percent or more of the vertical force. In addition, this side force caused only a small loss in vertical force in comparison to the nozzle without vanes. The net thrust force was 8 deg from the vertical for four vanes and 10.5 deg for seven. Author (revised)

N93-25455# Royal Aircraft Establishment, Farnborough (England). Aerospace Div.

MEASUREMENTS AND COMPUTATIONS OF EXTERNAL HEAT TRANSFER AND FILM COOKING IN TURBINES

S. P. Harasgama, C. D. Burton, and K. S. Chana 24 Feb. 1992 14 p Presented at the 10th International Symposium on Air Breathing Engines, Nottingham, England, 1-6 Sep. 1991 Previously announced in IAA as A91-56238

(RAE-TM-P-1223; BR310269) Copyright Avail: CASI HC A03/MF A01

A review of recent work on turbine heat transfer performed at the RAE (Pyestock) is presented. The work covers the effects of secondary flows on turbine nozzle guide vane heat transfer with and without film cooling. It is shown that the heat load to the platforms (end walls) are significantly affected by the secondary flow action. The platform film cooling data has been well correlated with flat plate single row film cooling data to within +11 percent. A three-dimensional Navier-Stokes computational study of the effects of turbine inlet temperature distortion on the thermo-fluid mechanics within a rotating blade passage is given. It is shown that the temperature distortion is modified within the rotor blade and can lead to increased pressure side and over tip heat transfer. Author

N93-25471 Council for National Academic Awards (England).
DESIGN AND PERFORMANCE OF NOZZLE-LESS VOLUTE CASINGS FOR INWARD FLOW RADIAL TURBINES Ph.D. Thesis
Hassam O. Owarish 1989 148 p
Avail: Univ. Microfilms Order No. BRDX97192

Inward Flow Radial Turbines are widely used in industry, particularly in turbochargers, small gas turbine engines, and aircraft starters and air conditioning systems. The turbine stage comprises essentially a stator or casing and a rotor. In feeding the flow into the turbine rotor, a well designed casing should achieve the following objectives: (1) acceleration of the working fluid and direct it at a specific angle in to the rotor; (2) production of congruent velocity triangles around the inlet periphery of the rotor; and (3) achieve (1) and (2) with a minimum loss of total pressure. The efficiency of Inward Flow Radial Turbines fitted with vaneless casings is lower than that of similar turbines fitted with the more expensive casings using guide vanes or nozzles. The difference is attributed to the more controlled flow occurring in the vaned casing. It is believed that such a flow can be achieved in the vaneless casing if the state of the art related to design methods is improved. In the past, all design methods have been based on the assumption of one-dimensional free vortex flow. The author's contribution has been in the development of a novel method of flow analysis and design of single-entry vaneless casing. This method is based on two-dimensional flow which takes the shape of the cross-section into account. In this method, the casing is divided into a number of segments which are sub-divided into a number of control volumes. By considering the changes in momenta in the tangential and radial directions across each control volume, together with the equations of energy, state, and continuity of mass, the changes in flow properties are computed. The flow model and the design method were constructed as FORTRAN computer programs that require only the operating conditions, that is mass flow rate, total pressure, and total temperature of entry as input, and make use of numerical methods to solve the equations. The relationships between geometrical dimensions at a fixed set of operating conditions, and the relationships between geometrical dimensions and operating conditions given by this design method have also been studied. Dissert. Abstr.

N93-25480 Maryland Univ., College Park.
OPTIMIZED SCRAMJET ENGINE INTEGRATION ON A WAVERIDER AIRFRAME Ph.D. Thesis
Mary Kae Lockwood ONeill 1992 205 p
Avail: Univ. Microfilms Order No. DA9304373

One of the keys to the success of air breathing hypersonic vehicles is the effective integration of the air breathing engine with the airframe. The practicality of integrating waveriders with hydrogen fueled scramjet engines is investigated. This is the first study to develop waveriders specifically for the purpose of scramjet integration. A method was developed, and a corresponding computer code was written, to optimize the waverider and scramjet together to take full advantage of the benefits of the waverider while providing the scramjet with the properties required for effective combustion. Two classes of air breathing hypersonic vehicle concepts, one for primarily cruise missions and the other for accelerator type missions, are presented. Cruise configurations are optimized for the product of specific impulse and lift-to-drag ratio while matching lift to weight, corrected for centrifugal force, and thrust to drag at some equivalence ratio. Accelerator configurations are optimized for effective specific impulse while matching lift to weight, corrected for centrifugal force, at an equivalence ratio of one. Waveriders are derived from conical flow-fields, the combustor is modeled with quasi 1-D flow and the inlet and nozzle are modeled with 2-D planar flow. The results of an optimization include the fore body shape, inlet shape, engine location along the length of the vehicle, engine span, vehicle volume, and the approximate values for effective specific impulse, L/D, specific impulse, and center of pressure for the optimized configuration. The results indicate that waveriders are promising configurations for hypersonic vehicles. A 60 m Mach 8 vehicle flying at 50.3 km altitude, optimized for cruise, has an L/D of 4.7, an Isp of 2786 sec, and a 2258 cu m volume. A 60 m Mach 10 cruise vehicle, flying at an altitude of 55.1 km has an L/D of 3.5, an Isp of 2417 sec, and a volume of 2686 cu m. A 60 m Mach 14 accelerator, flying at an altitude of 36.9 km has an Isp(sub eff) of 531 sec and a 3902 cu m volume. A 60 m Mach 10 accelerator, flying at an altitude of 31.8 m has an Isp(sup eff) of 1512 sec and a 4155 cu m volume. Dissert. Abstr.

N93-25668*# Massachusetts Inst. of Tech., Cambridge. Gas Turbine Lab.
THREE-DIMENSIONAL FLOW IN RADIAL TURBOMACHINERY AND ITS IMPACT ON DESIGN Final Report, Sep. 1985 - Oct. 1992
Choon S. Tan and William Hawthorne May 1993 15 p
(Grant NAG3-772)
(NASA-CR-192957; NAS 1.26:192957) Avail: CASI HC A03/MF A01

In the two papers on the 'Theory of Blade Design for Large Deflections' published in 1984, a new inverse design technique was presented for designing the shape of turbomachinery blades in three-dimensional flow. The technique involves the determination of the blade profile from the specification of a distribution of the product of the radius and the pitched averaged tangential velocity (i.e., r bar-V(sub theta), the mean swirl schedule) within the bladed region. This is in contrast to the conventional inverse design technique for turbomachinery blading in two dimensional flow in which the blade surface pressure or velocity distribution is specified and the blade profile determined as a result; this is feasible in two-dimensional flow because the streamlines along the blade surfaces are known a priori. However, in three-dimensional flow, the stream surface is free to deform within the blade passage so that the streamlines on the blade surfaces are not known a priori; thus it is difficult and not so useful to prescribe the blade surface pressure or velocity distribution and determine the resulting blade profile. It therefore seems logical to prescribe the swirl schedule within the bladed region for designing a turbomachinery blade profile in three-dimensional flow. Furthermore, specifying r bar-V(sub theta) has the following advantages: (1) it is related to the circulation around the blade (i.e., it is an aerodynamic quantity); (2) the work done or extracted is approximately proportional to the overall change in r bar-V(sub theta) across a given blade row (Euler turbine equation); and (3) the rate of change of r bar-V(sub theta) along the mean streamline at the blade is related to the pressure jump across the blade and therefore the blade loading. Since the publications of those two papers, the technique has been applied to the design of a low speed as well as a high speed radial inflow turbine (for turbocharger applications) both of which showed definite improvements in performance over that of wheels of conventional designs, the design study of a high pressure ratio radial inflow turbine with and without splitter blades. Derived from text

N93-25673*# National Aeronautics and Space Administration. Lewis Research Center, Cleveland, OH.
GAS TURBINE SYSTEM SIMULATION: AN OBJECT-ORIENTED APPROACH
Colin K. Drummond, Gregory J. Follen, and Charles W. Putt Apr. 1993 14 p Presented at the 23rd Annual Pittsburgh Conference on Modeling and Simulation, Pittsburgh, PA, 30 Apr. - 1 May 1992; sponsored by the Univ. of Pittsburgh, IEEE, ISA, and SCS
(RTOP 505-62-51)
(NASA-TM-106044; E-7632; NAS 1.15:106044) Avail: CASI HC A03/MF A01

A prototype gas turbine engine simulation has been developed that offers a generalized framework for the simulation of engines subject to steady-state and transient operating conditions. The prototype is in preliminary form, but it successfully demonstrates the viability of an object-oriented approach for generalized simulation applications. Although object oriented programming languages are-relative to FORTRAN-somewhat austere, it is proposed that gas turbine simulations of an interdisciplinary nature will benefit significantly in terms of code reliability, maintainability, and manageability. This report elucidates specific gas turbine simulation obstacles that an object-oriented framework can overcome and describes

the opportunity for interdisciplinary simulation that the approach offers.
Author

N93-25702 Cranfield Inst. of Tech., Bedford (England).
NUMERICAL MODELLING OF VISCOUS TURBOMACHINERY FLOWS WITH A PRESSURE CORRECTION METHOD Ph.D. Thesis
A. Tourlidakis 1992 369 p
Avail: Univ. Microfilms Order No. BRDX97988

A fully elliptic computational method for the analysis of steady viscous flow in high speed subsonic centrifugal compressor impellers with tip leakage, is presented. A generalized curvilinear, non-orthogonal grid is utilized and the time-averaged Navier-Stokes equations are transformed and expressed in a fully conservative form. The discretization of the governing equations is performed through finite volume integration. The solution procedure employs a non-staggered variable arrangement and a SIMPLE based method for coupling the velocity and pressure fields. The turbulence effects are simulated with the use of the k-epsilon model, modified to account for rotation and streamline curvature, and the near-wall viscous phenomena are modeled through the wall function method. The numerical model is implemented for the flow prediction in a series of two and three dimensional test cases. Incompressible flow predictions in two-dimensional cascades and three-dimensional ducting systems with different geometrical features and inlet conditions are initially performed and the numerical results are compared against available experimental data. The final objective of the present study is achieved through the comparative study of the predictions obtained against the results of Eckardt's experimental investigation of the viscous compressible flow in a high speed radial impeller operating at design condition and in a backswept impeller at design and off-design conditions. In addition, the flow is simulated in the passages of the Rolls Royce GEM impeller which was tested at Cranfield at design and off-design flow rates. A jet/wake pattern was discerned in all the simulated centrifugal compressor cases and a good overall agreement was achieved with the measured wake formation and development; and, encouraging results were obtained on the evolution of the secondary flows. The tip leakage effects influenced the loss distribution, the size and the location of the wake flow pattern at the rotor exit. The effects of the flow mass rate on the detailed flow pattern and on the compressor performance have been well represented. In certain cases, the quality of the present predictions is an improvement over that obtained by other state-of-the-art Navier-Stokes solvers. In conclusion, the developed finite volume flow model has captured a large number of complex flow phenomena encountered in the tested impellers and is expected to provide a useful aerodynamic analysis tool for stationary or rotating, axial or radial turbomachinery components.
Dissert. Abstr.

N93-25751 Council for National Academic Awards (England).
SIMULATION OF AIRCRAFT GAS TURBINE ENGINE Ph.D. Thesis
Ibrahim H. Ismail 1991 260 p
Avail: Univ. Microfilms Order No. BRDX97196

This thesis describes GTES (gas turbine engine simulation) a digital computer program that simulates the design and off-design performance of aircraft gas turbine engines. The program can also perform test analysis for the individual components of these engines. A general description of gas turbine engines and their applications is described in Chapter 1. A review of the previous work (papers and reports) related to this area is covered in Chapter 2. A theoretical background of aerothermodynamics and gas dynamics of gas turbine engines, also the components performance characteristics and performance of the complete engine is discussed in Chapter 3. A general description of the program philosophy and the modules control procedure is explained in Chapter 4. The modelling procedure for each component and for the complete engine is introduced in Chapter 5. A validity of the simulation program results in comparing with available engine test data and the discussion of the simulation result is shown in Chapter 6. The concluding remarks which are derived from this research and the recommendations for further work are included in Chapter 7. The main parts of this program are, data entry, components performance and complete engine run. The main features of this program are that, it has been written for IBM compatible micro computers and is modular in its approach, at the same time losses in the stationary components have been considered in this work. In author's view this approach is novel and it should make a significant contribution to the simulation work.
Dissert. Abstr.

N93-25882# Cranfield Inst. of Tech., Bedford (England).
THE EFFECTS OF REACTION ON AXIAL COMPRESSOR PERFORMANCE Ph.D. Thesis
C. D. Farmakalides 1992 312 p
Avail: Univ. Microfilms Order No. BRDX97979

The present study examined the effects of design point choice of degree of reaction on axial flow compressor performance. The study, which has been partly sponsored by a market leader in industrial compressors, has been born from the need to improve on the compressor's stable operating range preferably at no loss of efficiency. Two kinds of blading, one of 100 percent and one of 80 percent reaction, were designed for mass flow and work coefficients of .6 and .4 respectively. The 80 percent reaction blading was manufactured and together with an existing 50 percent reaction blading has been tested on CIT's three stage axial flow research facility. Tests carried out, using the 50 percent and 80 percent reaction blading, involved measurements of performance over the stable range of operation and included traverse investigation carried out at two flow conditions. Three builds were tested using each blading with stator stagger settings of design, design +10 degrees and design -10 degrees. For the six builds tested, performance measurements were carried out with particular attention given to the operating range and maximum efficiency. Mid pitch radial and mid span circumferential traverse investigation, carried out for flow conditions near optimum and stall, examined the variation of aerodynamic parameters with flow rate and helped to validate methods used for compressor blading design and performance analysis. Analysis of the experimental data was conducted using three performance prediction methods: (1) a simple method based on generalized correlations; (2) a through-flow method STRCUR based on Denton's stream-line curvature calculation technique and applied only to the two builds with design stator stagger settings and for flow conditions near optimum point; and (3) a stream-line curvature method AXCHAR which is based on the solution of a simplified radial equilibrium equation. The experimental findings of this study indicated that high reaction blading can result in some stall margin and stable operating range improvement at no loss of maximum efficiency. Such trends were indicated even when the level of reaction was increased by a stator restaggering process. The analysis carried out indicated that: (1) a simple methods for obtaining the stage characteristic curves are suitable for preliminary analysis; (2) the through-flow code STRCUR can predict the internal flow field provided secondary flow losses are accounted for; and (3) the code AXCHAR is a useful tool for the prediction of stage characteristics and also provides valuable information regarding radial distributions of aerodynamic parameters at flow conditions varying from choke to stall. The analysis identified areas for improvement in the correlations used for stall point and off-design deviation angle prediction.
Dissert. Abstr.

N93-25917# Cranfield Inst. of Tech., Bedford (England). Dept. of Turbomachinery and Engineering Mechanics.
RADIAL INFLOW TURBINE STUDY Final Report, 1 Mar. - 30 Jun. 1992
S. Hamid and R. L. Elder Jul. 1992 120 p
(Contract DAJA45-89-C-0006)
(AD-A260767; CIT/REF-06-769(E); RTD-5824-AN-01) Avail: CASI HC A06/MF A02

Small radial inflow turbines have various applications in industry and are successfully being used as a major component of gas turbines and turbochargers. The performance of the turbine is of great importance for the success of these systems. Although the design of radial inflow turbines has improved in the last few years, the detailed aerodynamic study of these components still needs considerable attention. Better understanding of the flow processes involved in these machines will provide a good basis for the design of improved components and for this purpose a joint research program has been undertaken by Cranfield, the U.S. Army Research Office and Turbomach (San Diego). The main objective of the study was to investigate the flow processes involved in the radial inflow turbine using experimental methods. The work presented in this report describes the various steps undertaken to perform these studies together with results. The project involved two phases, the first measurements downstream of the rotor and the second measurements between the nozzle guide vanes and rotor inlet. The scope of the study was limited to two man years during which considerable success was achieved in obtaining the desired measurement but more time to further reduce this data and to compare

with computational results, which was outside the scope of the present study, would have been advantageous. The studies using laser anemometry undertaken downstream of the turbine rotor indicated a swirling flow with a region of counter-rotating flow in the centre. A cobra probe was used to compare with the laser anemometry results. Both measuring techniques show similar trends of flow velocity and flow angle at various running conditions. DTIC

N93-26161*# National Aeronautics and Space Administration. Lewis Research Center, Cleveland, OH.

ROTATING RAKE DESIGN FOR UNIQUE MEASUREMENT OF FAN-GENERATED SPINNING ACOUSTIC MODES

Kevin E. Konno and Clifford R. Hausmann Apr. 1993 23 p

(RTOP 535-03-01)

(NASA-TM-105946; E-7814; NAS 1.15:105946) Avail: CASI HC A03/MF A01

In light of the current emphasis on noise reduction in subsonic aircraft design, NASA has been actively studying the source of and propagation of noise generated by subsonic fan engines. NASA/LeRC has developed and tested a unique method of accurately measuring these spinning acoustic modes generated by an experimental fan. This mode measuring method is based on the use of a rotating microphone rake. Testing was conducted in the 9 x 15 Low-speed Wind Tunnel. The rotating rake was tested with the Advanced Ducted Propeller (ADP) model. This memorandum discusses the design and performance of the motor/drive system for the fan-synchronized rotating acoustic rake. This novel motor/drive design approach is now being adapted for additional acoustic mode studies in new test rigs as baseline data for the future design of active noise control for subsonic fan engines. Included in this memorandum are the research requirements, motor/drive specifications, test performance results, and a description of the controls and software involved. Author (revised)

N93-26219# Massachusetts Inst. of Tech., Cambridge. Gas Turbine Lab.

FLOW CONTROL OF LOW HEAT LOAD TURBINE AIRFOILS Final Report, Jul. 1987 - Feb. 1991

A. H. Epstein, G. R. Guenette, T. D. Stone, and W. J. Stentoe 28 Feb. 1992 312 p

(Contract F33615-87-C-2729)

(AD-A260941; WL-TR-91-2079) Avail: CASI HC A14/MF A03

The goal of this work was to examine how the heat load to turbines may be reduced by aerodynamic design. The effort consisted of three separate investigations: (1) determination of the effect of small grooves in the flow direction (riblets) on heat transfer, (2) an investigation of the role of inviscid flow aerodynamics on heat load, and (3) examination of the measurement technology required to assess heat transfer and aerodynamic performance in a short duration turbine test facility. For the first effort, a low turbulence, constant wall temperature wind tunnel was constructed with one wall containing riblets. Measurements indicated a maximum of 5 percent reduction in heat transfer and 7 percent in skin friction drag. In the second effort, an integral technique was developed to predict laminar flow heat transfer and drag losses for a two-dimensional airfoil. The integral method was incorporated into the ISES inverse design code and comparisons were made to existing calculational methods and experimental data. For the third effort, errors associated with heat transfer and aerodynamic performance measurements in short duration (isothermal) test facilities were found to be small but not negligible. It is shown that these errors can be estimated to sufficient accuracy so that data from short duration facilities will have equal or better accuracy than that from conventional turbine rigs. DTIC

N93-26239# Air Force Inst. of Tech., Wright-Patterson AFB, OH. Foreign Aerospace Science and Technology Center.

THE BLADE CURVING EFFECTS IN A TURBINE STATOR CASCADE WITH LOW ASPECT RATIO

Wang Zhongqi and Han Wanjin 21 Jan. 1993 16 p Transl. into ENGLISH from Jnl. of Engineering Thermophysics (China), v. 11, no. 3, Aug. 1990 p 255-262

(Contract F33657-84-D-0165)

(AD-A261063; FASTC-ID(RS)T-0312-92) Avail: CASI HC A03/MF A01

In a low speed plane cascade tunnel, the experiments for the cascades equipped with conventional straight blades, linear inclined blades and curvilinear blades were carried out. Through the comparisons of the experimental results, the improving effects of blade curving on the flow fields are discussed. The experimental results show that using curvilinear blades in the rectangular turbine stator cascades with low aspect ratio can reduce the overall flow loss by 30-40%. DTIC

N93-26335# Massachusetts Inst. of Tech., Cambridge. Dept. of Aeronautics and Astronautics.

ACTIVE STABILIZATION OF AEROMECHANICAL SYSTEMS Final Technical Report, 1 Nov. 1989 - 31 Oct. 1992

Alan H. Epstein, Edward M. Greitzer, John Dugundji, Vincent H. Garnier, and Daniel L. Gysling 5 Jan. 1993 161 p

(Grant AF-AFOSR-0059-90)

(AD-A261366; AFOSR-93-0142TR) Avail: CASI HC A08/MF A02

This report details the work on the active control of surge and stall in gas turbine engines. The use of small amplitude waves predicted by theory as stall precursors were tested with experimental data. The nonlinear behavior of such waves was shown to explain much of the data in the literature. This theory was used to design an active stabilization system for rotating stall which was tested on both a single-stage and a three-stage axial compressor, increasing the stable operating range of the single-stage compressor by 25%. The dynamics of the three-stage compressor were shown to match closely with theory. The open-loop forced response characteristics of the compressors were measured and methodology developed in which this data was used to design the compressor control system. The models then developed were used to evaluate alternate control strategies. Engineering of the structural dynamics of the compression system was also shown to be successful in damping rotating stall and surge. DTIC

N93-26339# Naval Air Rework Facility, North Island, CA. Aircraft Environmental Support Office.

PARTICULATE EMISSIONS FROM GAS TURBINE ENGINES

1 Feb. 1992 150 p Revised

(AD-A261374; AESO-2-90-REV) Avail: CASI HC A07/MF A02

The Aircraft Environmental Support Office is one of four specialty offices within the Naval Environmental Protection Support Service which offers technical support to the naval community. The Aircraft Environmental Support Office is primarily responsible for the management and distribution of emissions data for gaseous and particulate air pollutants from aircraft engines. This handbook, Particulate Emissions From Aircraft Engines, is a summary of particulate emissions data collected by the Aircraft Environmental Support Office since 1981. This handbook is intended for environmental personnel at military installations who must provide regulatory agencies with information about particulate matter emitted from their engine test facilities. Most users will find that the sections on visible emissions and particulate emission rates and concentrations contain all the information normally required to make permit applications, emission inventories and related regulatory documents. Also, the section on particle size distributions is appropriate to design applications. Together these sections provide a comprehensive treatment of particulate emissions from aircraft engines. DTIC

08 AIRCRAFT STABILITY AND CONTROL

Includes aircraft handling qualities; piloting; flight controls; and autopilots.

For related information see also *05 Aircraft Design, Testing and Performance.*

N93-24762*# Pennsylvania State Univ., University Park. Dept. of Aerospace Engineering.

PREDICTION OF FORCES AND MOMENTS FOR HYPERSONIC FLIGHT VEHICLE CONTROL EFFECTORS Final Report

Mark D. Maughmer, Lyle N. Long, Neal Guilmette, and Peter Pagano 3 May 1993 70 p

(Grant NAG1-849)

(NASA-CR-193033; NAS 1.26:193033) Avail: CASI HC A04/MF A01

This research project includes three distinct phases. For completeness, all three phases of the work are briefly described in this report. The goal was to develop methods of predicting flight control forces and moments

for hypersonic vehicles which could be used in a preliminary design environment. The first phase included a preliminary assessment of subsonic/supersonic panel methods and hypersonic local flow inclination methods for such predictions. While these findings clearly indicated the usefulness of such methods for conceptual design activities, deficiencies exist in some areas. Thus, a second phase of research was conducted in which a better understanding was sought for the reasons behind the successes and failures of the methods considered, particularly for the cases at hypersonic Mach numbers. This second phase involved using computational fluid dynamics methods to examine the flow fields in detail. Through these detailed predictions, the deficiencies in the simple surface inclination methods were determined. In the third phase of this work, an improvement to the surface inclination methods was developed. This used a novel method for including viscous effects by modifying the geometry to include the viscous/shock layer. Author (revised)

N93-25199*# California Inst. of Tech., Pasadena.
ROBUST NONLINEAR CONTROL OF VECTORED THRUST AIRCRAFT
John C. Doyle, Richard Murray, and John Morris 31 May 1993 44 p
(Grant NAG2-792)
(NASA-CR-192727; NAS 1.26:192727) Avail: CASI HC A03/MF A01

An interdisciplinary program in robust control for nonlinear systems with applications to a variety of engineering problems is outlined. Major emphasis will be placed on flight control, with both experimental and analytical studies. This program builds on recent new results in control theory for stability, stabilization, robust stability, robust performance, synthesis, and model reduction in a unified framework using Linear Fractional Transformations (LFT's), Linear Matrix Inequalities (LMI's), and the structured singular value micron. Most of these new advances have been accomplished by the Caltech controls group independently or in collaboration with researchers in other institutions. These recent results offer a new and remarkably unified framework for all aspects of robust control, but what is particularly important for this program is that they also have important implications for system identification and control of nonlinear systems. This combines well with Caltech's expertise in nonlinear control theory, both in geometric methods and methods for systems with constraints and saturations. Author

N93-25292 Purdue Univ., West Lafayette, IN.
AEROSPACE VEHICLE MODEL SIMPLIFICATION FOR FEEDBACK CONTROL Ph.D. Thesis
Brett Alan Newman 1992 214 p
Avail: Univ. Microfilms Order No. DA9301354

This dissertation addresses three distinct topics within the broader scope of aerospace vehicle model simplification for feedback control. These topics include order reduction criteria for feedback control, frequency weighted internally balanced order reduction, and symbolic factoring of transfer function polynomials. Before ever reducing the dynamic order of a model located within a feedback system, it is critical to understand which dynamic characteristics are crucial to preserve so that the reduced order closed-loop system will exhibit those key characteristics similar to the higher order closed-loop system. Based upon closed-loop stability and stability robustness requirements, order reduction criteria are derived, specifically for sequential loop closure settings. The weighted, internally balanced truncation technique delivers a reduced model that is accurate in a frequency range specified by the user. As yet, however, no existing a priori error bound has been obtained for the technique. Building upon a previous attempt, an error analysis is presented which gives support to the technique. Also, a new reduction technique, which combines weighted, balanced coordinates with residualization, is presented. The functional dependence of linear system poles and zeros upon the basic system parameters appearing in the governing differential equations offers insight into the causes for key dynamic characteristics. A Taylor series based approach is offered to generate approximate symbolic expressions for the poles and zeros in terms of the basic system parameters. Dissert. Abstr.

N93-25353 California Univ., Berkeley.
CONTROL OF NONLINEAR SYSTEMS UNDER INPUT CONSTRAINTS WITH APPLICATIONS TO FLIGHT CONTROL Ph.D. Thesis
Albert W. Lee 1992 137 p
Avail: Univ. Microfilms Order No. DA9304980

In this dissertation, stability and performance enhancement of systems under input constraints are examined. A simultaneous Lyapunov stability problem is solved to examine sufficient conditions for global asymptotic stability of linear plants with input constraints. The sufficient conditions are then extended to systems whose nonlinearities are globally Lipschitz. For performance enhancement, a new design method is introduced to minimize performance degradation resulting from control saturation. Although the theories for input-output linearization and sliding control are well developed, they are not particularly well suited for systems with input constraints. An approximate input-output linearization method is presented to enhance performance of the closed loop systems under input constraints. This method is demonstrated on a longitudinal flight control problem to significantly improve the closed-loop performance. Dissert. Abstr.

N93-25543 Council for National Academic Awards (England).
CONTROL AND OPTIMIZATION OF AIRCRAFT TRAJECTORIES Ph.D. Thesis
Younis Sharif Daoud 1991 207 p
Avail: Univ. Microfilms Order No. BRDX97200

The thesis describes a multi-disciplinary program of research which covers three fields of study, namely: control systems engineering; flight dynamics; and numerical optimization. However the main thrust of the research is in the area of control system engineering. A real time computer algorithm has been developed to control and optimize the trajectory of an aircraft during a maneuver along a path in the vertical plane. The equations of motion of a craft represented by a point mass model moving in the vertical plane are known from flight dynamics. These equations are used to define the trajectory and an optimization routine is used to minimize the time of flight along this trajectory. The real time control algorithm controls the movement of the point mass along this trajectory with path and terminal constraints. The optimization utilizes an adjoint control transformation algorithm for solving the two point boundary value problem that describes the optimal control. The initial values of the adjoint multipliers are related non-linearly to the initial values of the controls by which the system is operated. Since the system is practical and initial values are chosen by an iterative optimization scheme, the optimization is solved without the sensitivity problems of the classical method. The optimization yields a reference family of optimal controls; a near optimal guidance law that transfers the aircraft to the vicinity of the reference family is then described. The control commands are fed to the auto-pilot consisting of the reference optimal controls plus correction terms that are linear combinations of the state deviations from reference values, weighted by a set of pre-calculated gains. In contrast to the neighboring optimal guidance scheme, the reference control and state variables as well as the feedback gains are stored as functions of velocity and path angle in the present approach. Numerical results comparing open loop optimal and approximate feedback solutions are presented. These results demonstrate close agreement between the feedback and optimal trajectories for flight in the vertical plane.
Dissert. Abstr.

N93-25729 Michigan Univ., Ann Arbor.
CONTROL AND STABILIZATION OF NONHOLONOMIC DYNAMIC SYSTEMS Ph.D. Thesis
Mahmut Reyhanoglu 1992 109 p
Avail: Univ. Microfilms Order No. DA9303808

A theoretical framework is established for the control of nonholonomic dynamic systems, i.e., dynamic systems with nonintegrable constraints. In particular, we emphasize control properties for nonholonomic systems that have no counterpart in holonomic systems. A model for nonholonomic dynamic systems is first presented in terms of differential-algebraic equations defined on a phase space. A reduction procedure is carried out to obtain reduced order state equations. Feedback is then used to obtain a control system in a normal form. The assumptions guarantee that the resulting normal form equations necessarily contain a nontrivial drift vector field. Conditions for smooth (C infinity) asymptotic stabilization to an m-dimensional equilibrium manifold are presented; we also demonstrate that a single equilibrium solution cannot be asymptotically stabilized using continuous static or dynamic state feedback. However, any equilibrium is shown to be strongly accessible and small time locally controllable. An approach using geometric phases is developed as a basis for the control of Caplygin dynamical systems, i.e., nonholonomic systems with certain symmetry properties which can be expressed by the fact that the constraints are cyclic in certain variables. The theoretical development is applied to physical

examples of systems that we have studied in detail elsewhere; the control of a knife edge moving on a plane surface and the control of a wheel rolling without slipping on a plane surface. The results are also applied to the reorientation of planar multi body systems using joint torque inputs and to the reorientation of a rigid spacecraft using momentum wheel actuators, since in these examples conservation of angular momentum gives rise to nonintegrable motion invariants. Dissert. Abstr.

N93-25998*# National Aeronautics and Space Administration. Langley Research Center, Hampton, VA.
HELICOPTER LOW-SPEED YAW CONTROL Patent
John C. Wilson, inventor (to NASA), Henry L. Kelley, inventor (to NASA), and Cynthia A. Crowell, inventor (to NASA) 11 May 1993 6 p Filed 7 Nov. 1991 Supersedes N92-30025 (30 - 20, p 3406)
(NASA-Case-LAR-14219-1; US-Patent-5,209,430; US-Patent-Appl-SN-788908; US-Patent-Class-244-17.19; US-Patent-Class-244-17.11; US-Patent-Class-244-75R; Int-Patent-Class-B64C-27/00) Avail: US Patent and Trademark Office

A system for improving yaw control at low speeds consists of one strake placed on the upper portion of the fuselage facing the retreating rotor blade and another strake placed on the lower portion of the fuselage facing the advancing rotor blade. These strakes spoil the airflow on the helicopter tail boom during hover, low speed flight, and right or left sidewards flight so that less side thrust is required from the tail rotor.
Official Gazette of the U.S. Patent and Trademark Office

N93-26046*# Maryland Univ., College Park. Dept. of Electrical and Aeronautical Engineering.
TECHNIQUES FOR DESIGNING ROTORCRAFT CONTROL SYSTEMS Annual Report, 1 Apr. 1992 - 31 Mar. 1993
William S. Levine and Jewel Barlow 5 Apr. 1993 48 p
(Grant NAG2-794)
(NASA-CR-192960; NAS 1.26:192960) Avail: CASI HC A03/MF A01

This report summarizes the work that was done on the project from 1 Apr. 1992 to 31 Mar. 1993. The main goal of this research is to develop a practical tool for rotorcraft control system design based on interactive optimization tools (CONSOL-OPTCAD) and classical rotorcraft design considerations (ADOCS). This approach enables the designer to combine engineering intuition and experience with parametric optimization. The combination should make it possible to produce a better design faster than would be possible using either pure optimization or pure intuition and experience. We emphasize that the goal of this project is not to develop an algorithm. It is to develop a tool. We want to keep the human designer in the design process to take advantage of his or her experience and creativity. The role of the computer is to perform the calculation necessary to improve and to display the performance of the nominal design. Briefly, during the first year we have connected CONSOL-OPTCAD, an existing software package for optimizing parameters with respect to multiple performance criteria, to a simplified nonlinear simulation of the UH-60 rotorcraft. We have also created mathematical approximations to the Mil-specs for rotorcraft handling qualities and input them into CONSOL-OPTCAD. Finally, we have developed the additional software necessary to use CONSOL-OPTCAD for the design of rotorcraft controllers. Author (revised)

N93-26196# Naval Postgraduate School, Monterey, CA.
DEVELOPMENT AND TESTING OF THE DIGITAL CONTROL SYSTEM FOR THE ARCHYTAS UNMANNED AIR VEHICLE M.S. Thesis
Paul V. Merz Dec. 1992 100 p
(AD-A261656) Avail: CASI HC A05/MF A02

The purpose of this study was to develop the digital sampling and control system for an Unmanned Air Vehicle (UAV) designed to takeoff and land vertically and to transition to forward flight. The system is designed to operate from a personal computer through an umbilical cable tethered to the platform for hover tests. The computer controls the sampling and digital conversion of onboard analog sensor signals and sends control-surface commands for pitch, roll, and yaw motions. The thesis effort includes the following four parts: (1) design of a controllable Pulse-Width-Modulated signal to command the servos which operate the various aerodynamic surfaces; (2) sampling and conversion of the signals to the sensors through the programming of an analog-to-digital card installed in the computer; (3) sensor Power-up and parameter verification of onboard devices; and (4) development of various power networks to allow operation of onboard systems prior to engine start with the ability to be self-sustaining once the engine is running. The system was fully tested during ground runs on a thrust/torque test stand. Integration of the system with the robust controller designed in a concurrent thesis will provide for the stability necessary for the innovative unmanned vehicle. DTIC

N93-26260# Army Research Lab., Aberdeen Proving Ground, MD.
HELICOPTER FORCED RESPONSE VIBRATION ANALYSIS METHOD RTVIB20 Final Report, Jan. 1990 - Jun. 1992
Joseph Fries Feb. 1993 33 p
(DA Proj. 1L1-62618-AH-80)
(AD-A261809; ARL-TR-75) Avail: CASI HC A03/MF A01

This report describes a helicopter vibration analysis method. In the method the rotor forcing for a single main rotor is calculated by integrating the forces and moments at the rotor center and then applying them to a rigid helicopter airframe. The vibrations (any place in the airframe) are calculated as the response to the applied hub center forces and moments. The method of analysis allows for dissimilar blades in the main rotor to simulate various types of blade damage and the resulting increase in vibrations transmitted into the airframe. The analysis method is generic and can be used to analyze any single main rotor helicopter. An application is made for the UH-60A helicopter, resulting from the loss of outboard sections of one blade of the rotor, and the resulting vibrations in the cockpit are calculated. DTIC

09 RESEARCH AND SUPPORT FACILITIES (AIR)

Includes airports, hangars and runways; aircraft repair and overhaul facilities; wind tunnels; shock tubes; and aircraft engine test stands.

For related information see also *14 Ground Support Systems and Facilities (Space).*

N93-25080*# National Aeronautics and Space Administration. Lewis Research Center, Cleveland, OH.
NASA LEWIS 8- BY 6-FOOT SUPERSONIC WIND TUNNEL USER MANUAL
Ronald H. Soeder Feb. 1993 55 p
(RTOP 505-62-84)
(NASA-TM-105771; E-7196; NAS 1.15:105771) Avail: CASI HC A04/MF A01

The 8- by 6-Foot Supersonic Wind Tunnel (SWT) at Lewis Research Center is available for use by qualified researchers. This manual contains tunnel performance maps which show the range of total temperature, total pressure, static pressure, dynamic pressure, altitude, Reynolds number, and mass flow as a function of test section Mach number. These maps are applicable for both the aerodynamic and propulsion cycle. The 8- by 6-Foot Supersonic Wind Tunnel is an atmospheric facility with a test section Mach number range from 0.36 to 2.0. General support systems (air systems, hydraulic system, hydrogen system, infrared system, laser system, laser sheet system, and schlieren system are also described as are instrumentation and data processing and acquisition systems. Pretest meeting formats are outlined. Tunnel user responsibility and personal safety requirements are also stated. Author

N93-25178 Tana-Jyra, Ky (Finland).
TRANSMISSION SYSTEM FOR A TRANSFER DEVICE GRIPPING A DOUBLE WHEEL Patent Application
Matti Sinkkonen, inventor (to Tana-Jyra) 5 Mar. 1992 14 p
(CA-Patent-Appl-SN-2024585; Int-Patent-Class-B64F-1/10; CTN-93-60683)
Copyright Avail: Micromedia Ltd., Technical Information Centre, 165 Hotel de Ville, Place du Portage, Phase 2, Hull, Quebec J8X 3X2, Canada HC

A transmission system is provided for a transfer device gripping a double wheel, intended to move an aircraft or other wheeled device over a base. The transfer device includes at least two friction rollers and motors to drive them, namely one for each ground wheel of the device to be moved. Compression devices are provided to create the compression to press the friction rollers against the ground wheel. The transmission system includes a power device and transmission devices to feed the operating power to the motors. The intention of the invention is to create a transmission

for a transfer device that creates a steady push irrespective of a poor location of the pushing point, which is the main undercarriage. The system according to the invention includes devices to feed the operating power separately and independently of each other to each of the motors driving the ground wheel. Author (CISTI)

N93-25656# Texas Univ., Austin.
EXPEDIENT REPAIR OF STRUCTURAL FACILITIES Final Report, 1 Jul. 1987 - 1 Jun. 1989
J. O. Jirsa, A. Teran, and P. T. Nash May 1992 148 p
(AF Proj. 2104)
(AD-A260727; AFESC/ESL-TR-88-79) Avail: CASI HC A07/MF A02

Damaged airbase facilities critical to restoring aircraft operations must be repaired quickly after an attack to provide the needed support. Repair technologies have been developed in earthquake damage research which have potential application to bomb damage repair. This report describes the repair techniques developed for earthquake damage and their potential application to bomb damage repair. Although the damage mechanisms from earthquake loads are quite different from damage mechanisms of blast loads, the damage resulting to structural elements can be quite similar. Typical damages and failure mechanisms are categorized and compared for earthquake and conventional weapon loadings. Typical structures are selected based upon design guidelines. Damages expected to the typical structures from conventional weapon attack are described. Functional damages are defined and methods for accomplishing facility repairs are then recommended depending upon the facility function and the degree of damage. Materials, equipment, and procedures developed for repairing earthquake damage are described along with their potential use in repairing bomb damages. DTIC

N93-25996* National Aeronautics and Space Administration. Langley Research Center, Hampton, VA.
NOZZLE DIFFUSER FOR USE WITH AN OPEN TEST SECTION OF A WIND TUNNEL Patent
P. Stephen Barna, inventor (to NASA) 18 May 1993 9 p Filed 8 Aug. 1991 Supersedes N91-32149 (29 - 24, p 3963)
(NASA-Case-LAR-14424-1-SB; US-Patent-5,211,057;
US-Patent-Appl-SN-743468; US-Patent-Class-73-147;
Int-Patent-Class-G01M-9/00) Avail: US Patent and Trademark Office

The nozzle diffuser has an inlet in fluid communication with the narrowed inlet of an open test chamber in a conventional wind tunnel. The nozzle diffuser has a passageway extending from its inlet to an outlet in communication with the open test section. The passageway has an internal cross sectional area which increases from its inlet to its outlet and which may be defined by top and bottom isosceles trapezoid walls of a particular flare angle and by isosceles trapezoid side walls of a different flare angle. In addition, a collector having a decreasing internal cross sectional area from inlet to outlet may be provided at the opposite end of the test chamber such that its outlet is in communication with a diffuser located at this outlet. Official Gazette of the U.S. Patent and Trademark Office

N93-26214*# National Aeronautics and Space Administration. Lewis Research Center, Cleveland, OH.
DEVELOPMENT AND USE OF HYDROGEN-AIR TORCHES IN AN ALTITUDE FACILITY
Roy A. Lottig and Gary T. Huber (Sverdrup Technology, Inc., Brook Park, OH.) Jun. 1993 15 p Prepared for presentation at the 29th Joint Propulsion Conference and Exhibit, Monterey, CA, 28-30 Jun. 1993; sponsored by AIAA, SAE, ASME, and ASEE
(RTOP 505-62-84)
(NASA-TM-106047; E-7633; NAS 1.15:106047; AIAA Paper 93-2176)
Avail: CASI HC A03/MF A01

A hydrogen-air ignition torch concept that had been used successfully in two rocket engine test facilities to consume excess hydrogen in their exhausters at atmospheric conditions was experimentally evaluated and developed in an altitude test facility at NASA Lewis Research Center. The idea was to use several of these torches in conjunction with hydrogen detectors and dilution air to prevent excess accumulation of unburned hydrogen or mixtures of hydrogen and air exceeding the sea-level lower flammability limit in the altitude facility exhaust system during hydrogen-fueled propulsion system tests. The torches were evaluated for a range of fuel-to-air ratios from 0.09 to 0.39 and for a range of exit diameters from 19/64 to 49/64 in. From the results of these tests a torch geometry and a fuel-to-air ratio were selected that produced a reasonably sized torch exhaust flame for consumption of unburned hydrogen at altitude pressures from sea level to 4 psia. Author

N93-26498# Argonne National Lab., IL. Advanced Photon Source Div.
POSTER SESSION: FIFTH USERS MEETING FOR THE ADVANCED PHOTON SOURCE
Nov. 1992 225 p Meeting held in Argonne, IL, 14-15 Oct. 1992
(Contract W-31-109-eng-38)
(DE93-006019; ANL/APS/TM-11; CONF-9210290-Summ) Avail: CASI HC A10/MF A03

The Advanced Photon Source (APS), which is currently under construction as a national user facility at Argonne National Laboratory is a third-generation synchrotron x-ray source, one of only three in the world. It is expected to produce x-rays that are 10,000 times brighter than any currently produced elsewhere for use in research in a wide range of scientific areas. Users from industry, national laboratories, universities, and business will be able to come to the APS to conduct research either as members of Collaborative Access Teams (CAT's) or as Independent Investigators. Principal users will be members of CAT's, which will be building and operating all of the beamlines present in the first phase of APS beamline development. The first set of CAT's has been selected through a competitive proposal process involving peer scientific review, thorough technical evaluation, and significant management oversight by the APS. This document is a compilation of posters presented at the Fifth Users Meeting for the Advanced Photon Source, held at Argonne National Laboratory on October 14-15, 1992. All CAT's whose scientific cases were approved by the APS Proposal Evaluation Board are included. In addition, this document contains a poster from the Center for Synchrotron Radiation and Research and Instrumentation at the Illinois Institute of Technology. DOE

N93-25574*# National Aeronautics and Space Administration. Langley Research Center, Hampton, VA.
USE OF HIGH PERFORMANCE NETWORKS AND SUPERCOMPUTERS FOR REAL-TIME FLIGHT SIMULATION
Jeff I. Cleveland, II *In* NASA, Washington, Technology 2002: The Third National Technology Transfer Conference and Exposition, Volume 1 Feb. 1993 p 129-138 (For primary document see N93-25561 09-99)
Avail: CASI HC A02/MF A04

N93-26006* National Aeronautics and Space Administration. Langley Research Center, Hampton, VA.
VISUALIZATION OF A MACH 2 REACTING FLOW USING PLANAR LASER-INDUCED FLUORESCENCE (PLIF)
R. Jeffrey Balla *In* JHU, 29th JANNAF Combustion Subcommittee Meeting, Volume 2 Oct. 1992 p 1-7 (For primary document see N93-26005 09-20)
Avail: CPIA, 10630 Little Patuxent Pkwy., Suite 202, Columbia, MD 21044-3200 HC

12 ASTRONAUTICS (GENERAL)

For extraterrestrial exploration see *91 Lunar and Planetary Exploration.*

N93-25322# Los Alamos National Lab., NM.
FORMER SOVIET REPUBLIC CAPABILITIES IN SPACE AND SCIENCE
G. H. Canavan Feb. 1993 145 p
(Contract W-7405-eng-36)
(DE93-007613; LA-12449-MS) Avail: CASI HC A07/MF A02

Recent Department of Commerce, US Space Council, and Strategic Defense Initiative Organization missions to the Former Soviet Republics (FSR's) provided an opportunity to view FSR capabilities in space and science and explore possibilities for cooperation in developing the dual-use capabilities of distributed remote sensing. The trips are summarized and promising areas for cooperation are suggested. DOE

N93-25400# Joint Publications Research Service, Arlington, VA.
JPRS REPORT: SCIENCE AND TECHNOLOGY. CENTRAL EURASIA: EARTH SCIENCES
26 Feb. 1993 25 p Transl. into ENGLiSH from various Russian articles (JPRS-UES-93-001) Avail: CASI HC A03/MF A01

Translated articles cover the following topics: geology; oceanography; physics of atmosphere; and ecology. CASI

N93-25693# Howard Univ., Washington, DC. Dept. of Mechanical Engineering.
DYNAMICS AND ROBUST CONTROL OF A SAMPLED DATA SYSTEM FOR LARGE SPACE STRUCTURES. VOLUME 2: THE LQG/LTR METHODOLOGY FOR THE DISCRETE-TIME SYSTEM AND THE DESIGN OF REDUCED ORDER ROBUST DIGITAL CONTROLLER FOR ORBITING FLEXIBLE SHALLOW SPHERICAL SHELL SYSTEM Final Report, Sep. 1989 - Sep. 1991
Peter M. Bainum, Xing Guangqian, and Aprille J. Ericsson Nov. 1992 66 p
(Contract F33615-89-C-3225)
(AD-A260793; WL-TR-92-3089-Vol-2) Avail: CASI HC A04/MF A01

The analysis and design of robust controllers for multivariable discrete-time feedback systems in the frequency domain are studied. The robustness stability conditions for discrete-time systems with additive alteration, and with multiplicative alteration are developed. The robust LQG/LTR method has been extended from the continuous-time system to the discrete-time system. It has been proven that the LQG/LTR method is also valid for the LQG control of the discrete-time system with the filtering observer. As an application of the LQG/LTR technique for discrete-time systems, the design of reduced order optimal digital LQG controllers for the orbiting flexible shallow spherical shell system is considered. The comparison between the digital optimal LQG controller with the filtering observer and with the predicting observer for the orbiting flexible shallow spherical shell has been made. DTIC

N93-26095*# ISX Corp., Westlake Village, CA. Intelligent Systems Engineering.
KNOWLEDGE-BASED DECISION SUPPORT FOR SPACE STATION ASSEMBLY SEQUENCE PLANNING Final Report
12 Apr. 1991 142 p
(Contract NAS2-13296)
(NASA-CR-193048; NAS 1.26:193048) Avail: CASI HC A07/MF A02

A complete Personal Analysis Assistant (PAA) for Space Station Freedom (SSF) assembly sequence planning consists of three software components: the system infrastructure, intra-flight value added, and inter-flight value added. The system infrastructure is the substrate on which software elements providing inter-flight and intra-flight value-added functionality are built. It provides the capability for building representations of assembly sequence plans and specification of constraints and analysis options. Intra-flight value-added provides functionality that will, given the manifest for each flight, define cargo elements, place them in the National Space Transportation System (NSTS) cargo bay, compute performance measure values, and identify violated constraints. Inter-flight value-added provides functionality that will, given major milestone dates and capability requirements, determine the number and dates of required flights and develop a manifest for each flight. The current project is Phase 1 of a projected two phase program and delivers the system infrastructure. Intra- and inter-flight value-added were to be developed in Phase 2, which has not been funded. Based on experience derived from hundreds of projects conducted over the past seven years, ISX developed an Intelligent Systems Engineering (ISE) methodology that combines the methods of systems engineering and knowledge engineering to meet the special systems development requirements posed by intelligent systems, systems that blend artificial intelligence and other advanced technologies with more conventional computing technologies. The ISE methodology defines a phased program process that begins with an application assessment designed to provide a preliminary determination of the relative technical risks and payoffs associated with a potential application, and then moves through requirements analysis, system design, and development. Author

N93-26146*# Boeing Defense and Space Group, Huntsville, AL. Advanced Civil Space Systems.
SPACE TRANSFER CONCEPTS AND ANALYSES FOR EXPLORATION MISSIONS. TECHNICAL DIRECTIVE 12: BEAMED POWER SYSTEMS STUDY Final Report
D. Eder Dec. 1992 71 p
(Contract NAS8-37857)
(NASA-CR-192532; NAS 1.26:192532; D615-10050) Avail: CASI HC A04/MF A01

Parametric models were constructed for Earth-based laser powered electric orbit transfer from low Earth orbit to geosynchronous orbit. These models were used to carry out performance, cost/benefit, and sensitivity analyses of laser-powered transfer systems including end-to-end life cycle cost analyses for complete systems. Comparisons with conventional orbit transfer systems were made indicating large potential cost savings for laser-powered transfer. Approximate optimization was done to determine best parameter values for the systems. Orbit transfer flights simulations were conducted to explore effects of parameters not practical to model with a spreadsheet. The simulations considered view factors that determine when power can be transferred from ground stations to an orbit transfer vehicle and conducted sensitivity analyses for numbers of ground stations, Isp including dual-Isp transfers, and plane change profiles. Optimal steering laws were used for simultaneous altitude and plane change. Viewing geometry and low-thrust orbit raising were simultaneously simulated. A very preliminary investigation of relay mirrors was made. Author (revised)

N93-25835*# Massachusetts Inst. of Tech., Cambridge.
THE MODE FAMILY OF ON-ORBIT EXPERIMENTS: THE MIDDECK ACTIVE CONTROL EXPERIMENT (MACE)
Edward F. Crawley, David W. Miller, Javier deLuis (Payload Systems, Inc., Cambridge, MA.), Mel Waldman (Lockheed Missiles and Space Co., Greenbelt, MD.), and Andy Bicos (McDonnell-Douglas Space Systems Co., Washington, DC.) *In its* MIT Space Engineering Research Center Dec. 1990 45 p (For primary document see N93-25833 09-63)
Avail: CASI HC A03/MF A02

N93-26125*# Jet Propulsion Lab., California Inst. of Tech., Pasadena.
GALILEO EARLY CRUISE, INCLUDING VENUS, FIRST EARTH, AND GASPRA ENCOUNTERS
P. E. Beyer, R. C. OConnor, and D. J. Mudgway (Mudgway, D. J., Pasadena, CA.) *In its* The Telecommunications and Data Acquisition Report 15 May 1992 p 265-281 (For primary document see N93-26105 09-32)
(RTOP 314-40-22-37-01)
Avail: CASI HC A03/MF A04

13 ASTRODYNAMICS

Includes powered and free-flight trajectories; and orbital and launching dynamics.

N93-24694*# National Aeronautics and Space Administration. Goddard Space Flight Center, Greenbelt, MD.
FLIGHT MECHANICS/ESTIMATION THEORY SYMPOSIUM, 1992
Thomas H. Stengle, ed. Washington Feb. 1993 575 p Symposium held in Greenbelt, MD, 5-7 May 1992
(RTOP 550-00-00)
(NASA-CP-3186; Rept-93B00012; NAS 1.55:3186) Copyright Avail: CASI HC A24/MF A04

This conference publication includes 40 papers and abstracts presented at the Flight Mechanics/Estimation Theory Symposium on May 5-7, 1992. Sponsored by the Flight Dynamics Division of Goddard Space Flight Center, this symposium featured technical papers on a wide range of issues related to orbit-attitude prediction, determination, and control; attitude sensor calibration; attitude determination error analysis; attitude dynamics; and orbit decay and maneuver strategy. Government, industry, and the academic community participated in the preparation and presentation of these papers. For individual titles, see N93-24695 through N93-24735.

N93-24695*# Rockwell International Corp., Seal Beach, CA. Guidance, Control, and Navigation Group.

MOMENTUM ACCUMULATION DUE TO SOLAR RADIATION TORQUE, AND REACTION WHEEL SIZING, WITH CONFIGURATION OPTIMIZATION **c18**

Hari B. Hablani *In* NASA. Goddard Space Flight Center, Flight Mechanics/Estimation Theory Symposium, 1992 Feb. 1993 p 3-22 (For primary document see N93-24694 09-13)

Copyright Avail: CASI HC A03/MF A04

This paper has a two-fold objective: determination of yearly momentum accumulation due to solar radiation pressure, and optimum reaction wheel sizing. The first objective is confronted while determining propellant consumption by the attitude control system over a spacecraft's lifetime. This, however, cannot be obtained from the daily momentum accumulation and treating that constant throughout the year, because the orientation of the solar arrays relative to the spacecraft changes over a wide range in a year, particularly if the spacecraft has two arrays, one normal and the other off-normal to different extent at different times to the sun rays. The paper first develops commands for the arrays for tracking the sun, the arrays articulated to earth-pointing spacecraft with two rotational degrees of freedom, and spacecraft in an arbitrary circular orbit. After developing expressions for solar radiation torque due to one or both arrays, arranged symmetrically or asymmetrically relative to the spacecraft bus, momentum accumulation over an orbit and then over a year are determined. The remainder of the paper is concerned with designing reaction wheel configurations. Four-, six-, and three-wheel configurations are considered, and for given torque and momentum requirements, their cant angles with the roll/yaw plane are optimized for minimum power consumption. Finally, their momentum and torque capacities are determined for one-wheel failure scenario, and six configurations are compared and contrasted. Author

N93-24696*# Florida Univ., Gainesville. Dept. of Aerospace Engineering, Mechanics, and Engineering Science.

SPACECRAFT DETUMBLING THROUGH ENERGY DISSIPATION **c18**

Norman Fitz-Coy and Anindya Chatterjee *In* NASA. Goddard Space Flight Center, Flight Mechanics/Estimation Theory Symposium, 1992 Feb. 1993 p 23-37 (For primary document see N93-24694 09-13)

Copyright Avail: CASI HC A03/MF A04

The attitude motion of a tumbling, rigid, axisymmetric spacecraft is considered. A methodology for detumbling the spacecraft through energy dissipation is presented. The differential equations governing this motion are stiff, and therefore an approximate solution, based on the variation of constants method, is developed and utilized in the analysis of the detumbling strategy. Stability of the detumbling process is also addressed. Author

N93-24697*# National Aeronautics and Space Administration. Goddard Space Flight Center, Greenbelt, MD.

THE RESULTS OF THE IN-FLIGHT ATTITUDE SENSOR CALIBRATION FOR THE ARTHUR HOLLY COMPTON GAMMA RAY OBSERVATORY **c19**

W. S. Davis (Computer Sciences Corp., Silver Spring, MD.), A. H. Eudell (Computer Sciences Corp., Silver Spring, MD.), L. S. Kulp (Computer Sciences Corp., Silver Spring, MD.), L. A. Lindrose (Computer Sciences Corp., Silver Spring, MD.), and R. R. Harman *In its* Flight Mechanics/Estimation Theory Symposium, 1992 Feb. 1993 p 39-54 (For primary document see N93-24694 09-13)

(Contract NAS5-31500)

Copyright Avail: CASI HC A03/MF A04

The Arthur Holly Compton Gamma Ray Observatory (GRO) was launched by the shuttle Atlantis in April 1991. This paper presents the results of the attitude sensor calibration that was performed during the early mission. The GSFC Flight Dynamics Facility (FDF) performed an alignment calibration of the two fixed-head star trackers (FHST's) and two fine Sun sensors (FSS's) on board Compton GRO. The results show a 27-arcsecond shift between the bore sights of the FHST's with respect to prelaunch measurements. The alignments of the two FSS's shifted by 0.20 and 0.05 degree. During the same time period, the Compton GRO science teams performed an alignment calibration of the science instruments with respect to the attitude reported by the on board computer (OBC). In order to preserve these science alignments, FDF adjusted the overall alignments of the FHST's and FSS's, obtained by the FDF calibration, such that when up linked to the OBC, the shift in the OBC-determined attitude is minimized. FDF also calibrated the inertial reference unit (IRU), which consists of three dual-axis gyroscopes. The observed gyro bias matched the bias that was solved for by the OBC. This bias drifted during the first 6 days after release. The results of the FDF calibration of scale factor and alignment shifts showed changes that were of the same order as their uncertainties. Author

N93-24698*# National Aeronautics and Space Administration. Goddard Space Flight Center, Greenbelt, MD.

TESTING OF THE ON-BOARD ATTITUDE DETERMINATION AND CONTROL ALGORITHMS FOR SAMPEX **c19**

Jon D. McCullough, Thomas W. Flatley, Debra A. Henretty, F. Landis Markley, and Josephine K. San *In its* Flight Mechanics/Estimation Theory Symposium, 1992 Feb. 1993 p 55-68 (For primary document see N93-24694 09-13)

Copyright Avail: CASI HC A03/MF A04

Algorithms for on-board attitude determination and control of the Solar, Anomalous, and Magnetospheric Particle Explorer (SAMPEX) have been expanded to include a constant gain Kalman filter for the spacecraft angular momentum, pulse width modulation for the reaction wheel command, an algorithm to avoid pointing the Heavy Ion Large Telescope (HILT) instrument boresight along the spacecraft velocity vector, and the addition of digital sun sensor (DSS) failure detection logic. These improved algorithms were tested in a closed-loop environment for three orbit geometries, one with the sun perpendicular to the orbit plane, and two with the sun near the orbit plane - at Autumnal Equinox and at Winter Solstice. The closed-loop simulator was enhanced and used as a truth model for the control systems' performance evaluation and sensor/actuator contingency analysis. The simulations were performed on a VAX 8830 using a prototype version of the on-board software. Author

N93-24699*# Hughes Danbury Optical Systems, Inc., CT.

STAR TRACKER OPERATION IN A HIGH DENSITY PROTON FIELD **c19**

Kenneth J. Miklus, Frank Kissh, and David J. Flynn *In* NASA. Goddard Space Flight Center, Flight Mechanics/Estimation Theory Symposium, 1992 Feb. 1993 p 69-81 (For primary document see N93-24694 09-13)

(Contract JPL-957849)

Copyright Avail: CASI HC A03/MF A04

Algorithms that reject transient signals due to proton effects on charge coupled device (CCD) sensors have been implemented in the HDOS ASTRA-I Star Trackers to be flown on the TOPEX mission scheduled for launch in July 1992. A unique technique for simulating a proton-rich environment to test trackers is described, as well as the test results obtained. Solar flares or an orbit that passes through the South Atlantic Anomaly can subject the vehicle to very high proton flux levels. There are three ways in which spurious proton generated signals can impact tracker performance: the many false signals can prevent or extend the time to acquire a star; a proton-generated signal can compromise the accuracy of the star's reported magnitude and position; and the tracked star can be lost, requiring reacquisition. Tests simulating a proton-rich environment were performed on two ASTRA-1 Star Trackers utilizing these new algorithms. There were no false acquisitions, no lost stars, and a significant reduction in reported position errors due to these improvements. Author

N93-24700*# Computer Sciences Corp., El Segundo, CA.

RESOLUTION OF THE COBE EARTH SENSOR ANOMALY **c19**

J. Sedler *In* NASA. Goddard Space Flight Center, Flight Mechanics/Estimation Theory Symposium, 1992 Feb. 1993 p 83-99 (For primary document see N93-24694 09-13)

Copyright Avail: CASI HC A03/MF A04

Since its launch on November 18, 1989, the Earth sensors on the Cosmic Background Explorer (COBE) have shown much greater noise than expected. The problem was traced to an error in Earth horizon acquisition-of-signal (AOS) times. Due to this error, the AOS timing correction was ignored, causing Earth sensor split-to-index (SI) angles to be incorrectly time-tagged to minor frame synchronization times. Resulting Earth sensor residuals, based on gyro-propagated fine attitude solutions, were as large as plus or minus 0.45 deg (much greater than plus or minus 0.10 deg from scanner specifications (Reference 1)). Also, discontinuities in single-frame coarse attitude pitch and roll angles (as large as 0.80 and

0.30 deg, respectively) were noted several times during each orbit. However, over the course of the mission, each Earth sensor was observed to independently and unexpectedly reset and then reactivate into a new configuration. Although the telemetered AOS timing corrections are still in error, a procedure has been developed to approximate and apply these corrections. This paper describes the approach, analysis, and results of approximating and applying AOS timing adjustments to correct Earth scanner data. Furthermore, due to the continuing degradation of COBE's gyroscopes, gyro-propagated fine attitude solutions may soon become unavailable, requiring an alternative method for attitude determination. By correcting Earth scanner AOS telemetry, as described in this paper, more accurate single-frame attitude solutions are obtained. All aforementioned pitch and roll discontinuities are removed. When proper AOS corrections are applied, the standard deviation of pitch residuals between coarse attitude and gyro-propagated fine attitude solutions decrease by a factor of 3. Also, the overall standard deviation of SI residuals from fine attitude solutions decrease by a factor of 4 (meeting sensor specifications) when AOS corrections are applied. Author

N93-24701*# Jet Propulsion Lab., California Inst. of Tech., Pasadena.
TDRSS ORBIT DETERMINATION USING SHORT BASELINE DIFFERENCED CARRIER PHASE
S. Nandi, C. D. Edwards, and S. C. Wu *In* NASA. Goddard Space Flight Center, Flight Mechanics/Estimation Theory Symposium, 1992 Feb. 1993 p 103-115 (For primary document see N93-24694 09-13)
Copyright Avail: CASI HC A03/MF A04

This paper discusses a covariance study on the feasibility of using station-differenced carrier phase on short baselines to track the TDRSS satellites. Orbit accuracies for the TDRSS using station-differenced carrier phase data and range data collected from White Sands, NM are given for various configurations of ground stations and range data precision. A one-sigma-position position accuracy of 25 meters can be achieved using two orthogonal baselines of 100 km for the station-differenced phase data and range data with 1 m accuracy. Relevant configuration parameters for the tracking system and important sources of error are examined. The ability of these data to redetermine the position after a station keeping maneuver is addressed. The BRTS system, which is currently used for TDRSS orbit determination, is briefly described and its errors are given for comparison. Author

N93-24702*# Jet Propulsion Lab., California Inst. of Tech., Pasadena.
APPLICATION OF GPS TRACKING TECHNIQUES TO ORBIT DETERMINATION FOR TDRS
B. J. Haines, S. M. Lichten, R. P. Malla, and S. C. Wu *In* NASA. Goddard Space Flight Center, Flight Mechanics/Estimation Theory Symposium, 1992 Feb. 1993 p 117-127 (For primary document see N93-24694 09-13)
Copyright Avail: CASI HC A03/MF A04

In this paper, we evaluate two fundamentally different approaches to TDRS orbit determination utilizing Global Positioning System (GPS) technology and GPS-related techniques. In the first, a GPS flight receiver is deployed on the TDRSS spacecraft. The TDRS ephemerides are determined using direct ranging to the GPS spacecraft, and no ground network is required. In the second approach, the TDRSS spacecraft broadcast a suitable beacon signal, permitting the simultaneous tracking of GPS and TDRSS satellites from a small ground network. Both strategies can be designed to meet future operational requirements for TDRS-2 orbit determination. Author

N93-24703*# National Aeronautics and Space Administration. Goddard Space Flight Center, Greenbelt, MD.
TDRSS-USER ORBIT DETERMINATION USING BATCH LEAST-SQUARES AND SEQUENTIAL METHODS
D. H. Oza (Computer Sciences Corp., Lanham, MD.), T. L. Jones (Computer Sciences Corp., Lanham, MD.), M. Hakimi (Computer Sciences Corp., Lanham, MD.), Mina V. Samii (Computer Sciences Corp., Lanham, MD.), C. E. Doll, G. D. Mistretta, and R. C. Hart *In its* Flight Mechanics/Estimation Theory Symposium, 1992 Feb. 1993 p 129-144 (For primary document see N93-24694 09-13)
(Contract NAS5-31500)
Copyright Avail: CASI HC A03/MF A04

The Goddard Space Flight Center (GSFC) Flight Dynamics Division (FDD) commissioned Applied Technology Associates, Incorporated, to develop the Real-Time Orbit Determination/Enhanced (RTOD/E) system on a Disk Operating System (DOS)-based personal computer (PC) as a prototype system for sequential orbit determination of spacecraft. This paper presents the results of a study to compare the orbit determination accuracy for a Tracking and Data Relay Satellite System (TDRSS) user spacecraft, Landsat-4, obtained using RTOD/E, operating on a PC, with the accuracy of an established batch least-squares system, the Goddard Trajectory Determination System (GTDS), and operating on a mainframe computer. The results of Landsat-4 orbit determination will provide useful experience for the Earth Observing System (EOS) series of satellites. The Landsat-4 ephemerides were estimated for the January 17-23, 1991, timeframe, during which intensive TDRSS tracking data for Landsat-4 were available. Independent assessments were made of the consistencies (overlap comparisons for the batch case and covariances and the first measurement residuals for the sequential case) of solutions produced by the batch and sequential methods. The forward-filtered RTOD/E orbit solutions were compared with the definitive GTDS orbit solutions for Landsat-4; the solution differences were less than 40 meters after the filter had reached steady state. Author

N93-24704*# National Aeronautics and Space Administration. Goddard Space Flight Center, Greenbelt, MD.
ORBIT DETERMINATION SUPPORT OF THE OCEAN TOPOGRAPHY EXPERIMENT (TOPEX)/POSEIDON OPERATIONAL ORBIT
A. F. Schanzle (Computer Sciences Corp., Greenbelt, MD.), J. E. Rovnak (Computer Sciences Corp., Greenbelt, MD.), D. T. Bolvin (Computer Sciences Corp., Greenbelt, MD.), and C. E. Doll *In its* Flight Mechanics/Estimation Theory Symposium, 1992 Feb. 1993 p 145-158 (For primary document see N93-24694 09-13)
(Contract NAS5-31500)
Copyright Avail: CASI HC A03/MF A04

The Ocean Topography Experiment (TOPEX/Poseidon) mission is designed to determine the topography of the Earth's sea surface over a 3-year period, beginning shortly after launch in July 1992. TOPEX/Poseidon is a joint venture between the United States National Aeronautics and Space Administration (NASA) and the French Centre Nationale d'Etudes Spatiales. The Jet Propulsion Laboratory is NASA's TOPEX/Poseidon project center. The Tracking and Data Relay Satellite System (TDRSS) will nominally be used to support the day-to-day orbit determination aspects of the mission. Due to its extensive experience with TDRSS tracking data, the NASA Goddard Space Flight Center (GSFC) Flight Dynamics Facility (FDF) will receive and process TDRSS observational data. To fulfill the scientific goals of the mission, it is necessary to achieve and maintain a very precise orbit. The most stringent accuracy requirements are associated with planning and evaluating orbit maneuvers, which will place the spacecraft in its mission orbit and maintain the required ground track. To determine if the FDF can meet the TOPEX/Poseidon maneuver accuracy requirements, covariance analysis was undertaken with the Orbit Determination Error Analysis System (ODEAS). The covariance analysis addressed many aspects of TOPEX/Poseidon orbit determination, including arc length, force models, and other processing options. The most recent analysis has focused on determining the size of the geopotential field necessary to meet the maneuver support requirements. Analysis was undertaken with the full 50 x 50 Goddard Earth Model (GEM) T3 field as well as smaller representations of this model. Author

N93-24705*# National Aeronautics and Space Administration. Goddard Space Flight Center, Greenbelt, MD.
ORBIT DETERMINATION AND ORBIT CONTROL FOR THE EARTH OBSERVING SYSTEM (EOS) AM SPACECRAFT
Joseph R. Herberg (General Electric Co., Fairfield, CT.) and David C. Folta *In its* Flight Mechanics/Estimation Theory Symposium, 1992 Feb. 1993 p 159-176 (For primary document see N93-24694 09-13)
(Contract NAS5-32500)
Copyright Avail: CASI HC A03/MF A04

Future NASA Earth Observing System (EOS) Spacecraft will make measurements of the earth's clouds, oceans, atmosphere, land and radiation balance. These EOS Spacecraft will be part of the NASA Mission to Planet Earth. This paper specifically addresses the EOS AM Spacecraft, referred to as 'AM' because it has a sun-synchronous orbit with a 10:30 AM descending node. This paper describes the EOS AM Spacecraft mission

orbit requirements, orbit determination, orbit control, and navigation system impact on earth based pointing. The EOS AM Spacecraft will be the first spacecraft to use the TDRSS Onboard Navigation System (TONS) as the primary means of navigation. TONS flight software will process one-way forward Doppler measurements taken during scheduled TDRSS contacts. An extended Kalman filter will estimate spacecraft position, velocity, drag coefficient correction, and ultrastable master oscillator frequency bias and drift. The TONS baseline algorithms, software, and hardware implementation are described in this paper. TONS integration into the EOS AM Spacecraft Guidance, Navigation, and Control (GN&C) System; TONS assisted onboard time maintenance; and the TONS Ground Support System (TGSS) are also addressed. Author

N93-24706*# National Aeronautics and Space Administration. Goddard Space Flight Center, Greenbelt, MD.

ANALYSIS OF THE EFFECTS OF MEAN LOCAL NODE-CROSSING TIME ON THE EVOLUTION OF SUN-SYNCHRONOUS ORBITS

P. Jordan (Computer Sciences Corp., Lanham, MD.), V. Blaes (Computer Sciences Corp., Lanham, MD.), L. Roszman (Computer Sciences Corp., Lanham, MD.), and J. Cooley *In its* Flight Mechanics/Estimation Theory Symposium, 1992 Feb. 1993 p 177-190 (For primary document see N93-24694 09-13)

(Contract NAS5-31500)

Copyright Avail: CASI HC A03/MF A04

An investigation of the effect of mean local node-crossing time on the evolution of Sun-synchronous orbits was undertaken during Phase-A orbit analysis for the National Oceanic and Atmospheric Administration (NOAA) O,P,Q environmental spacecraft. That analysis added to the growing body of evidence that individual Sun-synchronous missions, at differing node-crossing times, experience nodal drift rates that can differ in both magnitude and direction. A Sun-synchronous orbit is obtained by means of a nodal drift rate approximating the 0.9856-degree-per-day apparent precession of the position of the mean Sun. This drift rate is achieved through the interaction of the orbital semimajor axis and inclination in Earth's geopotential field. Influencing perturbations include atmospheric drag and, most important, the effects of solar gravitation on inclination. The present analysis examines a series of Sun-synchronous orbits with mean local node-crossing times at 1-hour intervals from 6 a.m. to 6 p.m. It considers the fixed geometry of each orbital plane with respect to both the Sun and the diurnal atmospheric bulge, then analyzes the influence of these features upon the evolution of the semimajor axix and inclination and thus upon the rate of the nodal drift in the course of 1 year. Author

N93-24707*# National Aeronautics and Space Administration. Goddard Space Flight Center, Greenbelt, MD.

A GROUND TRACK CONTROL ALGORITHM FOR THE TOPOGRAPHIC MAPPING LASER ALTIMETER (TMLA)

V. Blaes (Computer Sciences Corp., Lanham, MD.), R. McIntosh (Computer Sciences Corp., Lanham, MD.), L. Roszman (Computer Sciences Corp., Lanham, MD.), and J. Cooley *In its* Flight Mechanics/Estimation Theory Symposium, 1992 Feb. 1993 p 191-203 (For primary document see N93-24694 09-13)

(Contract NAS5-31500)

Copyright Avail: CASI HC A03/MF A04

The results of an analysis of an algorithm that will provide autonomous onboard orbit control using orbits determined with Global Positioning System (GPS) data. The algorithm uses the GPS data to (1) compute the ground track error relative to a fixed longitude grid, and (2) determine the altitude adjustment required to correct the longitude error. A program was written on a personal computer (PC) to test the concept for numerous altitudes and values of solar flux using a simplified orbit model including only the J sub 2 zonal harmonic and simple orbit decay computations. The algorithm was then implemented in a precision orbit propagation program having a full range of perturbations. The analysis showed that, even with all perturbations (including actual time histories of solar flux variation), the algorithm could effectively control the spacecraft ground track and yield more than 99 percent Earth coverage in the time required to complete one coverage cycle on the fixed grid (220 to 230 days depending on altitude and overlap allowance). Author

N93-24708*# Computer Sciences Corp., Lanham, MD.

REAL-TIME ATTITUDE DETERMINATION AND GYRO CALIBRATION

M. Challa, O. Filla, J. Sedlak, and D. Chu *In* NASA. Goddard Space Flight Center, Flight Mechanics/Estimation Theory Symposium, 1992 Feb. 1993 p 205-216 (For primary document see N93-24694 09-13)

(Contract NAS5-31500)

Copyright Avail: CASI HC A03/MF A04

We present results for two real-time filters prototyped for the Compton Gamma Ray Observatory (GRO), the Extreme Ultraviolet Explorer (EUVE), the Cosmic Background Explorer (COBE), and the next generation of Geostationary Operational Environmental Satellites (GOES). Both real and simulated data were used to solve for attitude and gyro biases. These filters promise advantages over single-frame and batch methods for missions like GOES, where startup and transfer-orbit operations require quick knowledge of attitude and gyro biases. Author

N93-24709*# McDonnell-Douglas Space Systems Co., Huntington Beach, CA.

COMPUTATIONALLY EFFICIENT ALGORITHMS FOR REAL-TIME ATTITUDE ESTIMATION **c61**

Steven R. Pringle *In* NASA. Goddard Space Flight Center, Flight Mechanics/Estimation Theory Symposium, 1992 Feb. 1993 p 217-225 (For primary document see N93-24694 09-13)

Copyright Avail: CASI HC A02/MF A04

For many practical spacecraft applications, algorithms for determining spacecraft attitude must combine inputs from diverse sensors and provide redundancy in the event of sensor failure. A Kalman filter is suitable for this task, however, it may impose a computational burden which may be avoided by sub optimal methods. A suboptimal estimator is presented which was implemented successfully on the Delta Star spacecraft which performed a 9 month SDI flight experiment in 1989. This design sought to minimize algorithm complexity to accommodate the limitations of an 8K guidance computer. The algorithm used is interpreted in the framework of Kalman filtering and a derivation is given for the computation. Author

N93-24710*# Computer Sciences Corp., Lanham, MD.

IMPROVEMENTS IN ERBS ATTITUDE DETERMINATION WITHOUT GYROS **c19**

D. Chu, J. Glickman, and E. Harvie *In* NASA. Goddard Space Flight Center, Flight Mechanics/Estimation Theory Symposium, 1992 Feb. 1993 p 227-242 (For primary document see N93-24694 09-13)

(Contract NAS5-31500)

Copyright Avail: CASI HC A03/MF A04

Previous papers have described the modification of the Earth Radiation Budget Satellite (ERBS) Attitude Determination System (ADS) to overcome the impact of on board gyro degradation and failure on attitude ground support of the mission. Two approaches were taken: implementing a Kalman filter in place of the batch-least-squares attitude estimator to account for the propagation error produced by high-noise gyro data, and modeling the ERBS attitude dynamics to restore rate information in the case of gyro failure. Both of these methods had shortcomings. In practice, the filter attitude diverged without complete sensor observability, and accurate dynamics modeling required knowledge of disturbance torque parameters that had to be determined manually. These difficulties have been overcome by improved tuning of the filter and by incorporating dynamics parameter estimation into the ERBS ADS. Author

N93-24711*# National Aeronautics and Space Administration. Goddard Space Flight Center, Greenbelt, MD.

POLAR DECOMPOSITION FOR ATTITUDE DETERMINATION FROM VECTOR OBSERVATIONS **c61**

Itzhack Y. Bar-Itzhack (Technion - Israel Inst. of Tech., Haifa.) *In its* Flight Mechanics/Estimation Theory Symposium, 1992 Feb. 1993 p 243-257 (For primary document see N93-24694 09-13)

Copyright Avail: CASI HC A03/MF A04

This work treats the problem of weighted least squares fitting of a 3D Euclidean-coordinate transformation matrix to a set of unit vectors measured in the reference and transformed coordinates. A closed-form analytic solution to the problem is re-derived. The fact that the solution is the closest orthogonal matrix to some matrix defined on the measured vectors and their weights is clearly demonstrated. Several known algorithms for computing the analytic closed form solution are considered. An algorithm is discussed which is based on the polar decomposition of matrices into the closest unitary matrix to the decomposed matrix and a Hermitian matrix. A somewhat

longer improved algorithm is suggested too. A comparison of several algorithms is carried out using simulated data as well as real data from the Upper Atmosphere Research Satellite. The comparison is based on accuracy and time consumption. It is concluded that the algorithms based on polar decomposition yield a simple although somewhat less accurate solution. The precision of the latter algorithms increase with the number of the measured vectors and with the accuracy of their measurement.
Author

N93-24712*# Johns Hopkins Univ., Laurel, MD. Applied Physics Lab.
ATTITUDE ANALYSIS IN FLATLAND: THE PLANE TRUTH
Malcolm D. Shuster *In* NASA. Goddard Space Flight Center, Flight Mechanics/Estimation Theory Symposium, 1992 Feb. 1993 p 259-274
(For primary document see N93-24694 09-13)
Copyright Avail: CASI HC A03/MF A04

Many results in attitude analysis are still meaningful when the attitude is restricted to rotations about a single axis. Such a picture corresponds to attitude analysis in the Euclidean plane. The present report formalizes the representation of attitude in the plane and applies it to some well-known problems. In particular, we study the connection of the 'additive' and 'multiplicative' formulations of the differential corrector for the quaternion in its two-dimensional setting.
Author

N93-24713*# Ball Corp., Boulder, CO. Space Systems Div.
RATE DETERMINATION FROM VECTOR OBSERVATIONS
Jerold L. Weiss *In* NASA. Goddard Space Flight Center, Flight Mechanics/Estimation Theory Symposium, 1992 Feb. 1993 p 275-284
(For primary document see N93-24694 09-13)
Copyright Avail: CASI HC A02/MF A04

Vector observations are a common class of attitude data provided by a wide variety of attitude sensors. Attitude determination from vector observations is a well-understood process and numerous algorithms such as the TRIAD algorithm exist. These algorithms require measurement of the line of site (LOS) vector to reference objects and knowledge of the LOS directions in some predetermined reference frame. Once attitude is determined, it is a simple matter to synthesize vehicle rate using some form of lead-lag filter, and then, use it for vehicle stabilization. Many situations arise, however, in which rate knowledge is required but knowledge of the nominal LOS directions are not available. This paper presents two methods for determining spacecraft angular rates from vector observations without a priori knowledge of the vector directions. The first approach uses an extended Kalman filter with a spacecraft dynamic model and a kinematic model representing the motion of the observed LOS vectors. The second approach uses a 'differential' TRIAD algorithm to compute the incremental direction cosine matrix, from which vehicle rate is then derived.
Author

N93-24714*# Computer Sciences Corp., Lanham, MD.
A MULTIMISSION THREE-AXIS STABILIZED SPACECRAFT FLIGHT DYNAMICS GROUND SUPPORT SYSTEM **c14**
J. Langston, K. Krack, and W. Reupke *In* NASA. Goddard Space Flight Center, Flight Mechanics/Estimation Theory Symposium, 1992 Feb. 1993 p 285-296 (For primary document see N93-24694 09-13)
(Contract NAS5-31500)
Copyright Avail: CASI HC A03/MF A04

The Multimission Three-Axis Stabilized Spacecraft (MTASS) Flight Dynamics Support System (FDSS) has been developed in an effort to minimize the costs of ground support systems. Unlike single-purpose ground support systems, which attempt to reduce costs by reusing software specifically developed for previous missions, the multimission support system is an intermediate step in the progression to a fully generalized mission support system in which numerous missions may be served by one general system. The benefits of multimission attitude ground support systems extend not only to the software design and coding process, but to the entire system environment, from specification through testing, simulation, operations, and maintenance. This paper reports the application of an MTASS FDSS to multiple scientific satellite missions. The satellites are the Upper Atmosphere Research Satellite (UARS), the Extreme Ultraviolet Explorer (EUVE), and the Solar Anomalous Magnetospheric Particle Explorer (SAMPEX). Both UARS and EUVE use the multimission modular spacecraft (MMS) concept. SAMPEX is part of the Small Explorer (SMEX) series and uses a much simpler set of attitude sensors. This paper centers on algorithm and design concepts for a multimission system and discusses flight experience from UARS.
Author

N93-24715*# Thomas Jefferson High School, Falls Church, VA.
WHAT IS THE RELATIONSHIP BETWEEN ALTITUDE AND WEIGHT IN A MODEL ROCKET? **c20**
Jonathan Betz *In* NASA. Goddard Space Flight Center, Flight Mechanics/Estimation Theory Symposium, 1992 Feb. 1993 p 299-318
(For primary document see N93-24694 09-13)
Copyright Avail: CASI HC A03/MF A04

This experiment was designed to find a function of payload weight for altitude. The same rocket was launched a repeated number of times with the same engine and varying amounts of weight. After performing experimentation, it was calculated that the altitude in meters could be predicted with the equation A = (2.8(W exp 2)) - (70.6W + 310.3), with weight expressed in the unit ounces.
Author

N93-24716*# National Aeronautics and Space Administration. Goddard Space Flight Center, Greenbelt, MD.
NONLINEAR TECHNIQUES FOR FORECASTING SOLAR ACTIVITY DIRECTLY FROM ITS TIME SERIES **c92**
S. Ashrafi (Computer Sciences Corp., Lanham, MD.), L. Roszman (Computer Sciences Corp., Lanham, MD.), and J. Cooley *In its* Flight Mechanics/Estimation Theory Symposium, 1992 Feb. 1993 p 319-335
Previously announced as N92-28870 (For primary document see N93-24694 09-13)
(Contract NAS5-31500)
Copyright Avail: CASI HC A03/MF A04

This paper presents numerical techniques for constructing nonlinear predictive models to forecast solar flux directly from its time series. This approach makes it possible to extract dynamical in variants of our system without reference to any underlying solar physics. We consider the dynamical evolution of solar activity in a reconstructed phase space that captures the attractor (strange), give a procedure for constructing a predictor of future solar activity, and discuss extraction of dynamical invariants such as Lyapunov exponents and attractor dimension.
Author

N93-24717*# National Aeronautics and Space Administration. Goddard Space Flight Center, Greenbelt, MD.
ANALYSIS OF REENTRY INTO THE WHITE SANDS MISSILE RANGE (WSMR) FOR THE LIFESAT MISSION **c18**
M. Hametz (Computer Sciences Corp., Lanham, MD.), L. Roszman (Computer Sciences Corp., Lanham, MD.), F. Snow, and J. Cooley *In its* Flight Mechanics/Estimation Theory Symposium, 1992 Feb. 1993 p 337-350
(For primary document see N93-24694 09-13)
(Contract NAS5-31500)
Copyright Avail: CASI HC A03/MF A04

This study investigates the reentry of the LifeSat vehicles into the WSMR. The LifeSat mission consists of two reusable reentry satellites, each carrying a removable payload module, which scientists will use to study long-term effects of microgravity, Van Allen belt radiation, and galactic cosmic rays on living organisms. A series of missions is planned for both low-Earth circular orbits and highly elliptic orbits. To recover the payload module with the specimens intact, a soft parachute landing and recovery at the WSMR is planned. This analysis examines operational issues surrounding the reentry scenario to assess the feasibility of the reentry.
Author

N93-24718*# Defense Intelligence Agency, Washington, DC.
TSIEN'S METHOD FOR GENERATING NON-KEPLERIAN TRAJECTORIES. PART 2: THE QUESTION OF THRUST TO ORBIT A SPHERE AND THE RESTRICTED THREE-BODY PROBLEM
P. A. Murad *In* NASA. Goddard Space Flight Center, Flight Mechanics/Estimation Theory Symposium, 1992 Feb. 1993 p 351-368
(For primary document see N93-24694 09-13)
Copyright Avail: CASI HC A03/MF A04

Tsien's method is extended to treat the orbital motion of a body undergoing accelerations and decelerations. A generalized solution is discussed for the generalized case where a body undergoes azimuthal and radial thrust and the problem is further simplified for azimuthal thrust alone. Judicious selection of thrust could generate either an elliptic or hyperbolic

trajectory. This is unexpected especially when the body has only enough energy for a lower state trajectory. The methodology is extended treating the problem of vehicle thrust for orbiting a sphere and vehicle thrust within the classical restricted three-body problem. Results for the latter situation can produce hyperbolic trajectories through eigen value decomposition. Since eigen values for no-thrust can be imaginary, thrust can generate real eigen values to describe hyperbolic trajectories. Keplerian dynamics appears to represent but a small subset of a much larger non-Keplerian domain especially when thrust effects are considered. The need for high thrust long duration space-based propulsion systems for changing a trajectory's canonical form is clearly demonstrated. Author

N93-24719*# Ball Corp., Boulder, CO. Space Systems Div.
PRACTICAL ASPECTS OF TRANSFER FROM GTO TO LUNAR ORBIT
Chauncey Uphoff *In* NASA. Goddard Space Flight Center, Flight Mechanics/Estimation Theory Symposium, 1992 Feb. 1993 p 369-380 Sponsored in part by LunCorp., Inc. (For primary document see N93-24694 09-13)
Copyright Avail: CASI HC A03/MF A04

This paper is a presentation of some practical aspects of orbital transfer from Geosynchronous Transfer Orbit (GTO) to close, near-circular orbits of the Moon. The intent is to identify the important parameters affecting the problem and to bound (approximately) the range of required delta V for a spacecraft that has been placed in GTO. The basic geometric relationships are described and the dynamics are simulated by use of the Zero-Sphere-of Influence Patched Conic method. It is found that the inclination of the transfer orbit to the Earth-Moon plane is relatively unimportant while the position of the line of apsides with respect to the Moon's orbit is the main geometric parameter of interest. It is shown that this parameter can be controlled by selecting the time of day for launch and that two launch windows of approximately 45 minutes duration are available each day of the year if use is made of the recommended phasing orbit transfer. The phasing orbit transfer not only provides twice-daily launch windows, but also provides a mechanism for efficacious correction of GTO injection errors. Delta V penalties for out-of-plane transfer and for late launch are evaluated and the method is recommended for use as an affordable means of achieving lunar orbit. Author

N93-24720*# McDonnell-Douglas Space Systems Co., Houston, TX.
AN APPROACH FOR FINDING LONG PERIOD ELLIPTICAL ORBITS FOR PRECURSOR SEI MISSIONS
Michael F. Fraietta and Victor R. Bond *In* NASA. Goddard Space Flight Center, Flight Mechanics/Estimation Theory Symposium, 1992 Feb. 1993 p 381-394 (For primary document see N93-24694 09-13)
Copyright Avail: CASI HC A03/MF A04

Precursors for Solar System Exploration Initiative (SEI) missions may require long period elliptical orbits about a planet. These orbits will typically have periods on the order of tens to hundreds of days. Some potential uses for these orbits may include the following: studying the effects of galactic cosmic radiation, parking orbits for engineering and operational test of systems, and ferrying orbits between libration points and low altitude orbits. This report presents an approach that can be used to find these orbits. The approach consists of three major steps. First, it uses a restricted three-body targeting algorithm to determine the initial conditions which satisfy certain desired final conditions in a system of two massive primaries. Then the initial conditions are transformed to an inertial coordinate system for use by a special perturbation method. Finally, using the special perturbation method, other perturbations (e.g., sun third body and solar radiation pressure) can be easily incorporated to determine their effects on the nominal trajectory. An algorithm potentially suitable for on-board guidance will also be discussed. This algorithm uses an analytic method relying on Chebyshev polynomials to compute the desired position and velocity of the satellite as a function of time. Together with navigation updates, this algorithm can be implemented to predict the size and timing for AV corrections. Author

N93-24721*# Air Force Academy, CO. Dept. of Math Sciences.
ORBIT DETERMINATION ERROR ANALYSIS AND COMPARISON OF STATION-KEEPING COSTS FOR LISSAJOUS AND HALO-TYPE LIBRATION POINT ORBITS AND SENSITIVITY ANALYSIS USING EXPERIMENTAL DESIGN TECHNIQUES
Steven C. Gordon *In* NASA. Goddard Space Flight Center, Flight Mechanics/Estimation Theory Symposium, 1992 Feb. 1993 p 395-409 Sponsored in part by Frank J. Seiler Research Lab. (For primary document see N93-24694 09-13)
Copyright Avail: CASI HC A03/MF A04

Spacecraft in orbit near libration point L1 in the Sun-Earth system are excellent platforms for research concerning solar effects on the terrestrial environment. One spacecraft mission launched in 1978 used an L1 orbit for nearly 4 years, and future L1 orbital missions are also being planned. Orbit determination and station-keeping are, however, required for these orbits. In particular, orbit determination error analysis may be used to compute the state uncertainty after a predetermined tracking period; the predicted state uncertainty levels then will impact the control costs computed in station-keeping simulations. Error sources, such as solar radiation pressure and planetary mass uncertainties, are also incorporated. For future missions, there may be some flexibility in the type and size of the spacecraft's nominal trajectory, but different orbits may produce varying error analysis and station-keeping results. The nominal path, for instance, can be (nearly) periodic or distinctly quasi-periodic. A periodic 'halo' orbit may be constructed to be significantly larger than a quasi-periodic 'Lissajous' path; both may meet mission requirements, but perhaps the required control costs for these orbits are probably different. Also for this spacecraft tracking and control simulation problem, experimental design methods can be used to determine the most significant uncertainties. That is, these methods can determine the error sources in the tracking and control problem that most impact the control cost (output); it also produces an equation that gives the approximate functional relationship between the error inputs and the output. Author

N93-24722*# Lockheed Technical Operations Co., Crofton, MD.
ANALYSIS OF THE COMMAND AND CONTROL SEGMENT (CCS) ATTITUDE ESTIMATION ALGORITHM **c61**
Catherine Stockwell *In* NASA. Goddard Space Flight Center, Flight Mechanics/Estimation Theory Symposium, 1992 Feb. 1993 p 413-421 Prepared for Consolidated Space Test Center, Onizuka AFB, CA (For primary document see N93-24694 09-13)
Copyright Avail: CASI HC A02/MF A04

This paper categorizes the qualitative behavior of the Command and Control Segment (CCS) differential correction algorithm as applied to attitude estimation using simultaneous spin axis sun angle and Earth cord length measurements. The categories of interest are the domains of convergence, divergence, and their boundaries. Three series of plots are discussed that show the dependence of the estimation algorithm on the vehicle radius, the sun/Earth angle, and the spacecraft attitude. Common qualitative dynamics to all three series are tabulated and discussed. Out-of-limits conditions for the estimation algorithm are identified and discussed. Author

N93-24723*# Hughes Danbury Optical Systems, Inc., CT.
OPTIMIZING THE FINE LOCK PERFORMANCE OF THE HUBBLE SPACE TELESCOPE FINE GUIDANCE SENSORS **c89**
David J. Eaton, Richard Whittlesey, Linda Abramowicz-Reed, and Robert Zarba *In* NASA. Goddard Space Flight Center, Flight Mechanics/Estimation Theory Symposium, 1992 Feb. 1993 p 423-437 (For primary document see N93-24694 09-13)
(Contracts NAS8-32700; NAS8-38494)
Copyright Avail: CASI HC A03/MF A04

This paper summarizes the on-orbit performance to date of the three Hubble Space Telescope Fine Guidance Sensors (FGS's) in Fine Lock mode, with respect to acquisition success rate, ability to maintain lock, and star brightness range. The process of optimizing Fine Lock performance, including the reasoning underlying the adjustment of uplink parameters, and the effects of optimization are described. The Fine Lock optimization process has combined theoretical and experimental approaches. Computer models of the FGS have improved understanding of the effects of uplink parameters and fine error averaging on the ability of the FGS to acquire stars and maintain lock. Empirical data have determined the variation of the interferometric error characteristics (so-called 's-curves') between FGS's and over each FGS field of view, identified binary stars, and quantified the systematic error in Coarse Track (the mode preceding Fine Lock). On the basis of these empirical data, the values of the uplink parameters can be selected more precisely. Since launch, optimization efforts have improved FGS Fine Lock performance, particularly acquisition, which now enjoys a nearly 100 percent success rate. More recent work has been directed

towards improving FGS tolerance of two conditions that exceed its original design requirements. First, large amplitude spacecraft jitter is induced by solar panel vibrations following day/night transitions. This jitter is generally much greater than the FGS's were designed to track, and while the tracking ability of the FGS's has been shown to exceed design requirements, losses of Fine Lock after day/night transitions are frequent. Computer simulations have demonstrated a potential improvement in Fine Lock tracking of vehicle jitter near terminator crossings. Second, telescope spherical aberration degrades the interferometric error signal in Fine Lock, but use of the FGS two-thirds aperture stop restores the transfer function with a corresponding loss of throughput. This loss requires the minimum brightness of acquired stars to be about one magnitude brighter than originally planned. Author

N93-24724*# Hughes Danbury Optical Systems, Inc., CT.
THE HUBBLE SPACE TELESCOPE FINE GUIDANCE SYSTEM OPERATING IN THE COARSE TRACK POINTING CONTROL MODE **c89**

Richard Whittlesey *In* NASA. Goddard Space Flight Center, Flight Mechanics/Estimation Theory Symposium, 1992 Feb. 1993 p 439-452 (For primary document see N93-24694 09-13)
(Contract NAS5-38494)
Copyright Avail: CASI HC A03/MF A04

The Hubble Space Telescope (HST) Fine Guidance System has set new standards in pointing control capability for earth orbiting spacecraft. Two precision pointing control modes are implemented in the Fine Guidance System; one being a Coarse Track Mode which employs a pseudo-quadrature detector approach and the second being a Fine Mode which uses a two axis interferometer implementation. The Coarse Track Mode was designed to maintain FGS pointing error to within 20 milli-arc seconds (rms) when guiding on a 14.5 Mv star. The Fine Mode was designed to maintain FGS pointing error to less than 3 milli-arc seconds (rms). This paper addresses the HST FGS operating in the Coarse Track Mode. An overview of the implementation, the operation, and both the predicted and observed on orbit performance is presented. The discussion includes a review of the Fine Guidance System hardware which uses two beam steering Star Selector servos, four photon counting photomultiplier tube detectors, as well as a 24 bit microprocessor, which executes the control system firmware. Unanticipated spacecraft operational characteristics are discussed as they impact pointing performance. These include the influence of spherically aberrated star images as well as the mechanical shocks induced in the spacecraft during and following orbital day/night terminator crossings. Computer modeling of the Coarse Track Mode verifies the observed on orbit performance trends in the presence of these optical and mechanical disturbances. It is concluded that the coarse track pointing control function is performing as designed and is providing a robust pointing control capability for the Hubble Space Telescope. Author

N93-24725*# Lockheed Technical Operations Co., Crofton, MD.
SCATHA MISSION TERMINATION REPORT **c18**

Kjell Stakkestad and Richard Fennessey *In* NASA. Goddard Space Flight Center, Flight Mechanics/Estimation Theory Symposium, 1992 Feb. 1993 p 453-469 Prepared for Consolidated Space Test Center, Onizuka AFB, CA (For primary document see N93-24694 09-13)
Copyright Avail: CASI HC A03/MF A04

The SCATHA (Spacecraft Charging at High Altitudes) satellite was operated from the Consolidated Space Test Center in Sunnyvale, California from February 1979 to May 1991. It was a spin stabilized vehicle in a highly eccentric orbit that collected data on spacecraft charging. The purpose of such data gathering was to predict and/or model the effects of the Earth's magnetic field on synchronous and near synchronous satellites. During the majority of its lifetime, attitude precession maneuvers were done every 10-15 days to maintain solar panel orientation. Maneuver planning was difficult due to the structural characteristics of SCATHA. It is cylindrically shaped and has seven booms ranging in length from 2 to 50 meters. These precession maneuvers induced predictable nutation that damped out after a few days. Eventually fuel began running low due to these frequent maneuvers. Experiments that had required the spin axis be in the orbit plane had already been turned off or had collected all their data. To increase the vehicle lifetime, the spin axis was moved to ecliptic normal. While this stopped the need for frequent attitude maneuvering (only two per year required now), this movement of the spin axis caused nutation that would not damp out for the remainder of the mission. This phase of the mission, with the ecliptic normal orientation, lasted for approximately three years. Although nutation never damped, data gathering was uninterrupted. In late 1990, when SCATHA's transmitter became seriously degraded, the Air Force decided to turn SCATHA off. This would only be done after the satellite was made 'safe'. The most difficult part of making the vehicle safe was quickly purging the fuel. Several plans were considered. The selected plan was to perform a series of 20 degree attitude precession maneuvers (3 days apart to allow for the worst nutation to damp) until the fuel was depleted. Although this sounded simple, the actual execution proved difficult. This was due to a nearly complete lack of available telemetry data, large undamped motion of the long booms, inadequacies in attitude determination software, and an error in the fuel level calculation software. This paper discusses the various proposed termination plans and execution of the selected one. Attitude determination methodologies, nutation from maneuvers, and effects of the flexible booms on the termination mission are presented and analyzed from a satellite analyst point of view. Author

N93-24726*# Barrios Technology, Inc., Houston, TX.
ACCURATE ATTITUDE DETERMINATION OF THE LACE SATELLITE

M. F. Miglin, R. E. Campion (Bendix Field Engineering Corp., Greenbelt, MD.), P. J. Lemos (Bendix Field Engineering Corp., Greenbelt, MD.), and T. Tran (Bendix Field Engineering Corp., Greenbelt, MD.) *In* NASA. Goddard Space Flight Center, Flight Mechanics/Estimation Theory Symposium, 1992 Feb. 1993 p 471-484 (For primary document see N93-24694 09-13)
Copyright Avail: CASI HC A03/MF A04

The Low-power Atmospheric Compensation Experiment (LACE) satellite, launched in February 1990 by the Naval Research Laboratory, uses a magnetic damper on a gravity gradient boom and a momentum wheel with its axis perpendicular to the plane of the orbit to stabilize and maintain its attitude. Satellite attitude is determined using three types of sensors: a conical Earth scanner, a set of sun sensors, and a magnetometer. The Ultraviolet Plume Instrument (UVPI), on board LACE, consists of two intensified CCD cameras and a gimbal led pointing mirror. The primary purpose of the UVPI is to image rocket plumes from space in the ultraviolet and visible wavelengths. Secondary objectives include imaging stars, atmospheric phenomena, and ground targets. The problem facing the UVPI experimenters is that the sensitivity of the LACF satellite attitude sensors is not always adequate to correctly point the UVPI cameras. Our solution is to point the UVPI cameras at known targets and use the information thus gained to improve attitude measurements. This paper describes the three methods developed to determine improved attitude values using the UVPI for both real-time operations and post observation analysis. Author

N93-24727*# Research Support Instruments, Inc., Alexandria, VA.
ATTITUDE CONTROL OF THE LACE SATELLITE: A GRAVITY GRADIENT STABILIZED SPACECRAFT

J. E. Ivory, R. E. Campion (Bendix Field Engineering Corp., Alexandria, VA.), and D. F. Bakeris (Bendix Field Engineering Corp., Alexandria, VA.) *In* NASA. Goddard Space Flight Center, Flight Mechanics/Estimation Theory Symposium, 1992 Feb. 1993 p 485-498 (For primary document see N93-24694 09-13)
(Contracts N00014-89-C-2011; N00014-91-C-2316)
Copyright Avail: CASI HC A03/MF A04

The Low-power Atmospheric Compensation Experiment (LACE) satellite was launched in February 1990 by the Naval Research Laboratory. The spacecraft's pitch and roll are maintained with a gravity gradient boom and a magnetic damper. There are two other booms with much smaller tip masses, one in the velocity direction (lead boom) of variable length and the other in the opposite direction (balance boom) also of variable length. In addition, the system uses a momentum wheel with its axis perpendicular to the plane of the orbit to control yaw and keep these booms in the orbital plane. The primary LACE experiment requires that the lead boom be moved to lengths varying from 4.6 m to 45.7 m. This and other onboard experiments require that the spacecraft attitude remain within tight constraints while operating. The problem confronting the satellite operators was to move the lead boom without inducing a net spacecraft attitude disturbance. A description of a method used to change the length of the lead boom while minimizing the disturbance to the attitude of the spacecraft is given. Deadbeating to dampen pitch oscillations has also been accomplished by maneuvering either the lead or balance boom and is discussed. Author

N93-24728*# Wright Lab., Eglin AFB, FL.
MINIATURE OPTICAL WIDE-ANGLE-LENS STARTRACKER (MINI-OWLS) **c19**
Rick Miller, Joe E. Coulter (Northrop Corp., Hawthorne, CA.), and Seymour Levine (Northrop Corp., Hawthorne, CA.) *In* NASA. Goddard Space Flight Center, Flight Mechanics/Estimation Theory Symposium, 1992 Feb. 1993 p 499-504 (For primary document see N93-24694 09-13)
Copyright Avail: CASI HC A02/MF A04

This paper provides a brief overview of the design considerations and the current status of the Miniature Optical Wide-Angle Lens Startracker Program. Mini-OWLS offers a revolutionary alternative to the conventional startracker. It is a small, lightweight, low cost, high performance startracker that can be used in a variety of applications including calibration and alignment of Inertial Measurement Units (IMU's) Mini-OWLS makes use of a strap down design incorporating Holographic Optical Elements (HOES) in place of conventional optics. HOES can be multiplexed so that the same aperture can be used for multiple separate optical paths looking in several directions simultaneously without startracker rotation. Additionally, separate Schmidt corrector plates are not required to compensate for spherical aberration. The optical assembly, or what would normally be considered as the telescope, is less than 20 cc in volume, weighs less than 55 grams, and contains the equivalent of three individual telescopes. Each one has a 4 deg Field of View (FOV) with a field of regard of 48 square degrees. Mini-OWLS has a bandwidth of approximately 300 nm in or near the visible wavelength. The projected resolution of the startracker is 5 to 10 arcseconds, depending on the centroiding algorithm used. The Mini-OWLS program was initiated last year and represents a miniaturized version of a similar design for aeronautical applications. The contract is managed by Wright Laboratory, Air Force Systems Command, Wright-Patterson AFB, Ohio, with funding from the Strategic Defense Initiative Organization through Eglin AFB. The initial phase of the program is to build and test a development unit. The second phase is to integrate the startracker with the Charles Stark Draper Laboratory Micromechanical Inertial Guidance System (MIGS) and the Signal Processing Packaging Design (SPPD) being developed by Texas Instruments. The preliminary design review was conducted in November 1991. Three-axes prototype telescope assemblies have been built and design evaluation tests initiated. Author

N93-24729*# State Univ. of New York, Buffalo. Dept. of Mechanical and Aerospace Engineering.
SCALAR GAIN INTERPRETATION OF LARGE ORDER FILTERS **c64**
Paul A. C. Mason and D. Joseph Mook *In* NASA. Goddard Space Flight Center, Flight Mechanics/Estimation Theory Symposium, 1992 Feb. 1993 p 507-521 Sponsored by NASA. Langley Research Center (For primary document see N93-24694 09-13)
Copyright Avail: CASI HC A03/MF A04

A technique is developed which demonstrates how to interpret a large fully-populated filter gain matrix as a set of scalar gains. The inverse problem is also solved, namely, how to develop a large-order filter gain matrix from a specified set of scalar gains. Examples are given to illustrate the method. Author

N93-24730*# National Aeronautics and Space Administration. Goddard Space Flight Center, Greenbelt, MD.
QUATERNION NORMALIZATION IN SPACECRAFT ATTITUDE DETERMINATION
J. Deutschmann, F. L. Markley, and Itzhack Y. Bar-Itzhack (Technion - Israel Inst. of Tech., Haifa.) *In its* Flight Mechanics/Estimation Theory Symposium, 1992 Feb. 1993 p 523-536 (For primary document see N93-24694 09-13)
Copyright Avail: CASI HC A03/MF A04

Attitude determination of spacecraft usually utilizes vector measurements such as Sun, center of Earth, star, and magnetic field direction to update the quaternion which determines the spacecraft orientation with respect to some reference coordinates in the three dimensional space. These measurements are usually processed by an extended Kalman filter (EKF) which yields an estimate of the attitude quaternion. Two EKF versions for quaternion estimation were presented in the literature; namely, the multiplicative EKF (MEKF) and the additive EKF (AEKF). In the multiplicative EKF, it is assumed that the error between the correct quaternion and its a-priori estimate is, by itself, a quaternion that represents the rotation necessary to bring the attitude which corresponds to the a-priori estimate of the quaternion into coincidence with the correct attitude. The EKF basically estimates this quotient quaternion and then the updated quaternion estimate is obtained by the product of the a-priori quaternion estimate and the estimate of the difference quaternion. In the additive EKF, it is assumed that the error between the a-priori quaternion estimate and the correct one is an algebraic difference between two four-tuple elements and thus the EKF is set to estimate this difference. The updated quaternion is then computed by adding the estimate of the difference to the a-priori quaternion estimate. If the quaternion estimate converges to the correct quaternion, then, naturally, the quaternion estimate has unity norm. This fact was utilized in the past to obtain superior filter performance by applying normalization to the filter measurement update of the quaternion. It was observed for the AEKF that when the attitude changed very slowly between measurements, normalization merely resulted in a faster convergence; however, when the attitude changed considerably between measurements, without filter tuning or normalization, the quaternion estimate diverged. However, when the quaternion estimate was normalized, the estimate converged faster and to a lower error than with tuning only. In last years, symposium we presented three new AEKF normalization techniques and we compared them to the brute force method presented in the literature. The present paper presents the issue of normalization of the MEKF and examines several MEKF normalization techniques. Author

N93-24731*# National Aeronautics and Space Administration. Goddard Space Flight Center, Greenbelt, MD.
ATTITUDE DETERMINATION USING VECTOR OBSERVATIONS: A FAST OPTIMAL MATRIX ALGORITHM **c61**
F. Landis Markley *In its* Flight Mechanics/Estimation Theory Symposium, 1992 Feb. 1993 p 537-551 (For primary document see N93-24694 09-13)
Copyright Avail: CASI HC A03/MF A04

The attitude matrix minimizing Wahba's loss function is computed directly by a method that is competitive with the fastest known algorithm for finding this optimal estimate. The method also provides an estimate of the attitude error covariance matrix. Analysis of the special case of two vector observations identifies those cases for which the TRIAD or algebraic method minimizes Wahba's loss function. Author

N93-24732*# National Aeronautics and Space Administration. Goddard Space Flight Center, Greenbelt, MD.
UPPER ATMOSPHERE RESEARCH SATELLITE (UARS) ONBOARD ATTITUDE DETERMINATION USING A KALMAN FILTER
Joseph Garrick *In its* Flight Mechanics/Estimation Theory Symposium, 1992 Feb. 1993 p 553-563 (For primary document see N93-24694 09-13)
Copyright Avail: CASI HC A03/MF A04

The Upper Atmospheric Research Satellite (UARS) requires a highly accurate knowledge of its attitude to accomplish its mission. Propagation of the attitude state using gyro measurements is not sufficient to meet the accuracy requirements, and must be supplemented by a observer/compensation process to correct for dynamics and observation anomalies. The process of amending the attitude state utilizes a well known method, the discrete Kalman Filter. This study is a sensitivity analysis of the discrete Kalman Filter as implemented in the UARS Onboard Computer (OBC). The stability of the Kalman Filter used in the normal on-orbit control mode within the OBC, is investigated for the effects of corrupted observations and nonlinear errors. Also, a statistical analysis on the residuals of the Kalman Filter is performed. These analysis is based on simulations using the UARS Dynamics Simulator (UARSDSIM) and compared against attitude requirements as defined by General Electric (GE). An independent verification of expected accuracies is performed using the Attitude Determination Error Analysis System (ADEAS). Author

N93-24733*# National Aeronautics and Space Administration. Goddard Space Flight Center, Greenbelt, MD.
GODDARD SPACE FLIGHT CENTER (GSFC) FLIGHT DYNAMICS FACILITY (FDF) CALIBRATION OF THE UPPER ATMOSPHERE RESEARCH SATELLITE (UARS) SENSORS **c19**
J. Hashmall (Computer Sciences Corp., Lanham, MD.) and J. Garrick *In its* Flight Mechanics/Estimation Theory Symposium, 1992 Feb. 1993 p 565-573 (For primary document see N93-24694 09-13)

(Contract NAS5-31500)
Copyright Avail: CASI HC A02/MF A04

Flight Dynamics Facility (FDF) responsibilities for calibration of Upper Atmosphere Research Satellite (UARS) sensors included alignment calibration of the fixed-head star trackers (FHST's) and the fine Sun sensor (FSS), determination of misalignments and scale factors for the inertial reference units (IRU's), determination of biases for the three-axis magnetometers (TAM's) and Earth sensor assemblies (ESA's), determination of gimbal misalignments of the Solar/Stellar Pointing Platform (SSPP), and field-of-view calibration for the FSS's mounted both on the Modular Attitude Control System (MACS) and on the SSPP. The calibrations, which used a combination of new and established algorithms, gave excellent results. Alignment calibration results markedly improved the accuracy of both ground and onboard Computer (OBC) attitude determination. SSPP calibration results allowed UARS to identify stars in the period immediately after yaw maneuvers, removing the delay required for the OBC to reacquire its fine pointing attitude mode. SSPP calibration considerably improved the pointing accuracy of the attached science instrument package. This paper presents a summary of the methods used and the results of all FDF UARS sensor calibration. Author

N93-24734*# National Aeronautics and Space Administration. Goddard Space Flight Center, Greenbelt, MD.
SOLAR ARRAY THERMAL SNAP AND THE CHARACTERISTICS OF ITS EFFECT ON UARS c18
M. Lambertson (Computer Sciences Corp., Silver Spring, MD.), D. Rohrbaugh (Computer Sciences Corp., Silver Spring, MD.), and J. Garrick *In its* Flight Mechanics/Estimation Theory Symposium, 1992 Feb. 1993 p 575-588 (For primary document see N93-24694 09-13)
(Contract NAS5-31500)
Copyright Avail: CASI HC A03/MF A04

The single solar array on the Upper Atmosphere Research Satellite (UARS) is subjected to a thermal distortion when the spacecraft enters and exits the Earth's shadow. The distortion results in a torque that alters the spacecraft attitude. Due to the sudden nature of the attitude discontinuity, the effect has been termed 'thermal snap'. Thermal snap has also been experienced by Landsats 4 and 5. Analyses by the spacecraft builder addressed the impact of the resultant torque on the onboard control system. This paper discusses the results of comparisons between the predicted effects of thermal snap on UARS and actual attitude solutions from UARS telemetry data. In addition, this paper describes the characteristics of the thermal snap on UARS in terms of maximum displacement, solar beta angle, and solar array drive angle. Comparisons are made between the actual times of thermal snaps and the predicted spacecraft sunrise and sunset times. The effects of the UARS thermal snap are summarized and a general comment is made relating possible effects of thermal snap on other satellites. Also, an analysis of UARS attitude solutions that span periods of thermal snap was performed to determine whether the gyro sampling time of 1/8 second is sufficient to properly model the resulting spacecraft attitude without compromising the accuracy requirements. The results of this analysis are discussed. Author

N93-24735*# National Aeronautics and Space Administration. Goddard Space Flight Center, Greenbelt, MD.
UPPER ATMOSPHERE RESEARCH SATELLITE (UARS) ATTITUDE ACCURACY USING COARSE ATTITUDE SENSORS Abstract Only c19
K. Krack (Computer Sciences Corp., Silver Spring, MD.), D. Foch (Computer Sciences Corp., Silver Spring, MD.), M. Lambertson (Computer Sciences Corp., Silver Spring, MD.), C. Woolsey (Computer Sciences Corp., Silver Spring, MD.), S. Underwood (Computer Sciences Corp., Silver Spring, MD.), C. Woodruff (Computer Sciences Corp., Silver Spring, MD.), and J. Garrick *In its* Flight Mechanics/Estimation Theory Symposium, 1992 Feb. 1993 p 589 (For primary document see N93-24694 09-13)
Copyright Avail: CASI HC A01/MF A04

The Upper Atmosphere Research Satellite (UARS) uses fixed-head star trackers (FHST's) and inertial reference units (IRU's) to determine and control its attitude. This combination of fine sensors results in attitude knowledge accuracies to better than 10 arc-seconds (1 sigma). UARS also has a variety of coarse attitude sensors on board: the three-axis magnetometer (TAM), the coarse Sun sensor (CSS), the fine Sun sensor (FSS), and the Earth sensor assembly (ESA). By comparing attitude solutions using coarse sensors with FHST-determined attitude solutions, estimates can be made of the accuracy of the coarse sensors. This paper presents the results of an analysis that compares attitude solutions using various combinations of UARS coarse attitude sensor data with FHST attitude solutions. Author

N93-24904 Illinois Univ. at Urbana-Champaign, Savoy.
OPTIMAL COOPERATIVE POWER-LIMITED RENDEZVOUS Ph.D. Thesis
Victoria Lynn Coverstone-Carroll 1992 229 p
Avail: Univ. Microfilms Order No. DA9236436

Minimum-fuel rendezvous of two power-limited low-thrust spacecraft is investigated. Both vehicles are active and provide thrust to complete the rendezvous. Total propellant consumption is minimized. Two gravitational field models are investigated: the Clohessy-Wiltshire linearized field and the inverse-square field. Analytical solutions are obtained for the linearized gravity field. A direct method using direct collocation with nonlinear programming is used for the nonlinear problem. Solutions obtained are checked against the primer vector necessary conditions for optimality. The optimal solutions depend in a complicated way on the power-to-mass ratios of the two spacecraft, the initial conditions, and the specified transfer time. Propellant and terminal orbit constraints are also discussed.
Dissert. Abstr.

N93-25272 Illinois Univ. at Urbana-Champaign, Savoy.
OPTIMAL FINITE-THRUST TIME-BOUNDED DIRECT-ASCENT INTERCEPTION Ph.D. Thesis
James Reagle Downey 1992 178 p
Avail: Univ. Microfilms Order No. DA9305510

Minimum-time and maximum final mass solutions are obtained for the problem of direct-ascent interception, from an arbitrary launch point on the surface of the Earth, of a target in a circular orbit. The intercepting rocket is assumed to have finite, bounded thrust and is subject to aerodynamic forces including lift and drag. The effect of Earth rotation is included and an initial waiting period or coast arc prior to launch is allowed. The problem is formulated as an optimal control problem with the objective of determining the thrust magnitude, aerodynamic pointing angle (pitch and yaw), and thrust vectoring angle histories to accomplish the interception. The continuous optimal control problem is converted to a discrete nonlinear programming problem and direct collocation is used to find numerical solutions. Solutions are found for both time-open and time-fixed problems. Optimal solutions include both postgrade and retrograde intercept trajectories. Solutions are obtained for a range of target orbit radii, inclinations, launch points, and initial target locations relative to the launch points. Problems which may include a singular arc as part of the optimal trajectory are also considered, and a method is demonstrated which allows such problems to be solved using direct collocation. Dissert. Abstr.

N93-25396 Florida Univ., Gainesville.
PROGRADE ANOMALOUS ORBITS IN TRIAXIAL GRAVITATIONAL POTENTIALS THAT ROTATE ABOUT THE LONG AXIS: VLA NEUTRAL HYDROGEN OBSERVATIONS AND MODELING OF THE INCLINED RINGS AROUND THE GALAXIES NGC 2685 AND NGC 660 Ph.D. Thesis
Mary Elaine Mahon 1992 201 p
Avail: Univ. Microfilms Order No.DA9304024

This dissertation presents the results of a systematic study of the inclined family of prograde anomalous orbits in rotating, triaxial gravitational potentials. In particular, for the case where the long axis of the potential is the rotation axis, the bifurcation sequence of orbits containing the prograde anomalous family is explored as a function of the rotation speed of the potential. Neutral hydrogen observations of the galaxies NGC 2685 and NGC 660 obtained with the Very Large Array Radio Telescope (VLA) are also presented. Maps derived from these observations show that both galaxies contain two kinematically distinct systems of gas, one in a nearly polar orientation, and the other approximately in the plane of the central stellar disk. If the underlying gravitational potential of the galaxy is triaxial and rotating, such configurations can be stable. It is shown that a model constructed from an ensemble of orbits, which contains the stable anomalous and prograde elliptical families, yields velocity and surface density maps similar to those derived from the VLA neutral hydrogen observations of NGC 2685 and NGC 660. The real interest of such a treatment is that, unlike the case for rotation about the short axis of the potential, it allows for the stars and gas in the disk of the central galaxy to rotate in the

same sense. These models indicate that for both NGC 2685 and NGC 660, the underlying gravitational potential is mildly triaxial and slowly rotating. An understanding of the shape of gravitational potential for these peculiar galaxies ultimately may lead to a better understanding of the three-dimensional distribution of matter in normal elliptical and spiral galaxies. Dissert. Abstr.

N93-25636# Naval Postgraduate School, Monterey, CA.
ORBITAL PARAMETER ESTIMATION USING AN EXTENDED KALMAN FILTER Ph.D. Thesis
Daniel J. Brett Dec. 1992 108 p
(AD-A260618) Avail: CASI HC A06/MF A02

The problem of orbital parameter estimation using angles only observations is examined. Direction cosine measurements, obtained from satellite passage of an earth-based stationary planar radar beam, are assimilated by an extended Kalman filter to improve estimates of a classical orbital element set. Several progressively comprehensive orbital motion models are considered and compared. The relative effectiveness of these models is illustrated by applying them to actual satellite data. DTIC

N93-25684 Princeton Univ., NJ.
MINIMUM-FUEL POWER-LIMITED TRANSFERS BETWEEN COPLANAR ELLIPTIC ORBITS Ph.D. Thesis
Christine Marie Haissig 1992 265 p
Avail: Univ. Microfilms Order No. DA9235255

Researchers have studied transfers for spacecraft using electric propulsion systems for many years. Previous work can be put into two categories--approximate results for restricted cases and numerical optimization results for specific missions or simple geometries. Approximate results exist for two limiting cases: many-revolution transfers with slowly changing orbit elements for which averaging applies and short duration transfers with small changes in the orbit elements for which linearization applies. Mission results are limited to transfers between circular orbits, as for the earth-Mars and earth-Venus missions, and escape problems. This research focuses on (1) the development of a systematic and accurate procedure for solving minimum-fuel, power limited transfers, and (2) the application of this procedure to characterize multiple revolution, minimum-fuel, power-limited transfers. The solution procedure is based on averaging. The adjoint from the average solution, referred to as the average adjoint, is the basis for two approximate solutions. In the first approximate solution the initial average adjoint serves as an estimate of the unknown initial adjoint. In the second approximation, the average adjoint is substituted into the minimum-fuel control law to provide an approximate optimal control. A canonical transformation is developed to transform the average adjoint from orbit element coordinates, which are used for averaging, to trajectory variable coordinates, which are used for numerical integration. These approximations are accurate for multiple revolution transfers. Their accuracy is inversely proportional to the transfer time, and transfers with extremely low or extremely high eccentricity are less accurate than those with moderate eccentricity for a given transfer time. The transformed adjoint from the average solution is used to generate the locally minimizing trajectories that are used in the characterization. Illustrative transfers are presented for many transfer times and transfer geometries. This characterization finds that (1) averaging qualitatively predicts the secular behavior of the semimajor axis and quantitatively predicts the eccentricity and argument of periapse for transfers with at least three revolutions; and (2) the linear theory qualitatively predicts the thrust magnitude and direction for an individual revolution given the secular predictions in the orbit elements.
Dissert. Abstr.

N93-25758 Purdue Univ., West Lafayette, IN.
OPTIMAL TRANSFERS BETWEEN LIBRATION-POINT ORBITS IN THE ELLIPTIC RESTRICTED THREE-BODY PROBLEM Ph.D. Thesis
Lisa Ann Hiday 1992 248 p
Avail: Univ. Microfilms Order No. DA9301310

A strategy is formulated to design optimal impulsive transfers between three-dimensional libration-point orbits in the vicinity of the interior L(1) libration point of the Sun-Earth/Moon barycenter system. Two methods of constructing nominal transfers, for which the fuel cost is to be minimized, are developed; both inferior and superior transfers between two halo orbits are considered. The necessary conditions for an optimal transfer trajectory are stated in terms of the primer vector. The adjoint equation relating reference and perturbed trajectories in this formulation of the elliptic restricted three-body problem is shown to be distinctly different from that obtained in the analysis of trajectories in the two-body problem. Criteria are established whereby the cost on a nominal transfer can be improved by the addition of an interior impulse or by the implementation of coastal arcs in the initial and final orbits. The necessary conditions for the local optimality of a time-fixed transfer trajectory possessing additional impulses are satisfied by requiring continuity of the Hamiltonian and the derivative of the primer vector at all interior impulses. The optimality of a time-free transfer containing coastal arcs is surmised by examination of the slopes at the endpoints of a plot of the magnitude of the primer vector over the duration of the transfer path. If the initial and final slopes of the primer magnitude are zero, the transfer trajectory is optimal; otherwise, the execution of coasts is warranted. The position and timing of each interior impulse applied to a time-fixed transfer as well as the direction and length of coastal periods implemented on a time-free transfer are specified by the unconstrained minimization of the appropriate variation in cost utilizing a multivariable search technique. Although optimal solutions in some instances are elusive, the time-fixed and time-free optimization algorithms prove to be very successful in diminishing costs on nominal transfer trajectories. The inclusion of coastal arcs on time-free superior and inferior transfers results in significant modification of the transfer time of flight caused by shifts in departure and arrival locations on the halo orbits. Dissert. Abstr.

N93-24986# European Space Agency. European Space Research and Technology Center, ESTEC, Noordwijk (Netherlands).
RELATIVISTIC EFFECTS FOR LOW EARTH ORBIT SATELLITES USING GPS
A. Spallicci, C. Jimenez (Zaragoza Univ., Spain.), G. Prisco, and N. Ashby (Colorado Univ., Boulder.) *In its* Frequency and Time Forum Jun. 1992 p 61-65 (For primary document see N93-24978 09-70)
Copyright Avail: CASI HC A01/MF A04

N93-24997# Centre National d'Etudes Spatiales, Toulouse (France).
DORIS PRECISE ORBIT DETERMINATION AND LOCATION SYSTEM PERFORMANCES OF ULTRA STABLE OSCILLATORS
M. Brunet *In* ESA, Frequency and Time Forum Jun. 1992 p 125-136 (For primary document see N93-24978 09-70)
Copyright Avail: CASI HC A03/MF A04

N93-24998# Consiglio Nazionale delle Ricerche, Bologna (Italy). Ist. di Radioastronomia.
PRECISE DOPPLER TRACKING FROM THE MEDICINA VLBI STATION
R. Ambrosini, G. Comoretto (Osservatorio Astrofisico di Arcetri, Florence, Italy.), L. less (Consiglio Nazionale delle Ricerche, Frascati, Italy.), and A. Messeri (Consiglio Nazionale delle Ricerche, Frascati, Italy.) *In* ESA, Frequency and Time Forum Jun. 1992 p 137-142 (For primary document see N93-24978 09-70)
Copyright Avail: CASI HC A02/MF A04

14 GROUND SUPPORT SYSTEMS AND FACILITIES (SPACE)

Includes launch complexes, research and production facilities; ground support equipment, e.g., mobile transporters; and simulators.

For related information see also *09 Research and Support Facilities (Air).*

N93-24714*# Computer Sciences Corp., Lanham, MD.
A MULTIMISSION THREE-AXIS STABILIZED SPACECRAFT FLIGHT DYNAMICS GROUND SUPPORT SYSTEM
J. Langston, K. Krack, and W. Reupke *In* NASA. Goddard Space Flight Center, Flight Mechanics/Estimation Theory Symposium, 1992 Feb. 1993 p 285-296 (For primary document see N93-24694 09-13)
(Contract NAS5-31500)
Copyright Avail: CASI HC A03/MF A04

N93-24876*# National Aeronautics and Space Administration. John F. Kennedy Space Center, Cocoa Beach, FL.
LAUNCH PAD LIGHTNING PROTECTION ENHANCEMENT BY INDUCED STREAMERS
James R. Stahmann (Boeing Aerospace Co., Cocoa Beach, FL.) and E. Ron Bentti *In* FAA, The 1992 International Aerospace and Ground Conference on Lightning and Static Electricity: Addendum Nov. 1992 17 p (For primary document see N93-24875 09-47)
Avail: CASI HC A03/MF A03

N93-25836*# Massachusetts Inst. of Tech., Cambridge.
MIT'S INTERFEROMETER CST TESTBED
Tupper Hyde, Ed Kim, Eric Anderson, Gary Blackwood, and Leonard Lublin *In its* MIT Space Engineering Research Center Dec. 1990 20 p (For primary document see N93-25833 09-63)
(Grant NAGw-1335)
Avail: CASI HC A03/MF A02

15 LAUNCH VEHICLES AND SPACE VEHICLES

Includes boosters; operating problems of launch/space vehicle systems; and reusable vehicles.

For related information see also *20 Spacecraft Propulsion and Power.*

N93-25770# California Univ., Los Angeles. Dept. of Electrical Engineering.
THEORETICAL AND EXPERIMENTAL INVESTIGATION OF ELECTRON BEAM ACCELERATION AND SUB-MILLIMETER WAVE GENERATION Final Report, 25 Jun. 1991 - 24 Jun. 1992
N. C. Luhmann, Jr. and D. B. McDermott Oct. 1992 76 p
(Contract DAAL03-91-G-0190)
(AD-A261117; ARO-28396.1-PH) Avail: CASI HC A05/MF A01

The overall objective of our research for ARO is to develop devices that have the potential for being compact generators of submillimeter-wave radiation. (1) The high-harmonic gyro-frequency multiplier, which is an efficient generator of high frequency RF, will be tested at the tenth-harmonic in our rebuilt test-stand. (2) High-power harmonic gyro-TWTs can be designed to operate in high order modes in large size waveguide by using the marginal stability design criterion. (3) Our high power, second-harmonic TE2 1 gyro-TWT, which is predicted to generate an order of magnitude higher power than state-of-the-art fundamental frequency gyrotrons, has been fully designed and construction is well underway. (4) The interaction strength in our high-harmonic CARM increases as the electron Larmor radius moves closer to the wall radius as the magnetic field is lowered towards a grazing intersection. (5) A high performance amplifier is predicted to result from our initial gyro-klystron experiment. DTIC

N93-25985# Army Chemical Research and Development Center, Aberdeen Proving Ground, MD.
MODIFIED POINT MASS TRAJECTORY SIMULATION FOR BASE-BURN PROJECTILES Final Report, Sep. 1990 - Dec. 1991
R. F. Lieske and J. E. Danberg Mar. 1992 40 p
(DA Proj. 1L1-62618-AH-80)
(BRL-TR-3321) Avail: CASI HC A03/MF A01

An addition to the Modified Point Mass Trajectory Model for Rocket-Assisted Projectiles is presented for the exterior ballistic simulation of base-burn projectiles. The addition models the change in aerodynamic base-drag based on the change in base pressure due to the base-burn motor's ejection of hot gas into the wake of the projectile. The mass flow rate of the remaining fuel of the base-burn motor is modeled as a function of the instantaneous projectile spin rate and atmospheric air pressure. HAWK Doppler radar data collected at Yuma Proving Ground, Arizona, for the 155mm, M1864 base-burn projectile were used to verify the modeling approach for a variety of test conditions. Author (revised)

N93-26098# Martin Marietta Corp., Denver, CO. Astronautics Group.
NATIONAL LAUNCH SYSTEM. TASK 4: SYSTEM ARCHITECTURE OPTIONS ANALYSIS Final Technical Report
A. C. Palen 25 Aug. 1992 357 p
(Contract F04701-88-C-0109)
(MCR-92-5011; CDRL-103A-10) Avail: CASI HC A16/MF A03

Task 4 was defined to fulfill the requirements of the NLS contract Statement of Work (SOW) 3.2.2 - System Level Trades. The objective, approach, subtasks, and schedule outlined for Task 4 System Architecture Options Analysis are given. This Final Report provides the documentation for Task 4. The objective is to establish the system approach (mission and ground capability requirements) for using a modular family of vehicles and associated operations and information infrastructure to satisfy the range of mission requirements commensurate with non-recurring and recurring cost goals, commonality, operability needs, and the requirements for growth potential. Using Level 3 concept definition and outputs from other tasks, candidate concepts for the vehicle family and operations concepts are developed. Concepts developed versus requirements and constraints are assessed to develop a system architecture. Tasks performed include obtaining input data and output needs from Level 3; conducting architecture analysis versus traffic model, design constraints, ground rules and break points; assessing architecture sensitivities to uncertain parameters; and documenting results. Derived from text

N93-26175# Martin Marietta Aerospace, Denver, CO. Launch Systems Co.
NLS OPERATIONS CONCEPTS: FAILURE MODES SCENARIO SIMULATION MODEL ANALYSIS Supplemental Report
Kevin Brughelli and Jerry Andersen 30 Nov. 1992 17 p
(Contract F04701-88-C-0109)
(MCR-92-5013; CDRL-103A10) Avail: CASI HC A03/MF A01

As part of the NLS contract termination activity, a task to determine failure modes impacts on the NLS operations concepts and time line process flows was recommended and approved. This report summarizes that activity. This is a final report and no further analyses are planned. To date, most NLS operations studies and analyses have examined 'normal' process activity, without any granular analysis of failures and their impacts on the NLS mission. 'Maintenance loops' have been identified as logical places in the flow where a failure is likely to occur and generic ('vanilla') times have been allocated to these loops. The purpose of this top level analysis was to examine in some detail the disruption to the flow caused by failures, the impact of these failures on the process and the mission model, and various scenarios for returning the system to operational status following a failure. Derived from text

N93-26176# Martin Marietta Aerospace, Denver, CO. Launch Systems Co.
TASK 5: ARCHITECTURE SENSITIVITY TO STME PERFORMANCE Final Report
J. A. Schnackel 7 Sep. 1992 61 p
(Contract F04701-88-C-0109)
(MCR-92-5010; CDRL-103A10) Avail: CASI HC A04/MF A01

This document was prepared for Task 5: Architecture Sensitivity to Space Transportation Main Engine (STME) Performance. Information provided in this report documents the architecture sensitivities with respect to STME performance parameters. Suggested STME thrust level was driven by Task 5 sensitivities and Task 4 vehicle configurations. Recommendations on STME thrust level are presented in this report. Sensitivities to STME parameters and vehicle system parameters were evaluated. Design of Experiment (DOE) approaches were used to understand the relative importance of each parameter. Suggested sensitivity parameters and their respective ranges were provided to the Task 5 lead. Our recommendation on analysis approach for the sensitivities was a central composite faced design. Task 5 sensitivities should be updated following final Task 4 architecture recommendations. A suggested analysis approach is provided in the analysis section of this report (Part C, Appendix I, Analysis). This analysis approach was used on Advanced Launch System (ALS) Phase 2 to improve the evaluation of alternate engine designs and vehicle subsystem evaluations. It is suggested that the analysis approach outlined in Part C be utilized to update Task when final Task 4 architecture information is available. Contents of this submittal include: Part A, Narrative Summary; Part B, View Graphs with facing page text; Part C, Appendix I, Analysis Part C, Appendix II, Data. Author

N93-26180# Martin Marietta Aerospace, Denver, CO. National Launch System.
TASK 2A: UNIS REQUIREMENTS AND CONCEPTS Final Report
W. J. Anderson 29 May 1992 139 p
(Contract F04701-88-C-0109)
(MCR-92-5006-Pt-A; CDRL-103A10) Avail: CASI HC A07/MF A02

This document was prepared as Task 2a: UNIS Requirements/Concept for the NLS Launch Management Control System (LMCS) Cross Functional Team (CFT). Data provided in this report is supplemented by the UNIS Information Model, copies of which are maintained and provided in a separate file and format with this submittal. This report reflects a compilation of inputs from LMCS CFT members who responded to our request for data. Where feasible, these inputs have been incorporated directly and/or conceptually. Reviewers are requested to consider the following: The results of this report may require additional analysis as NLS concepts mature or change. Terms and definitions used are frequently context sensitive and should be applied in the broadest sense, consistent with development of top level requirements and concepts. Transition to the next phase of NLS acquisition will generate more detailed and updated information system requirements analysis. Data contained in this report should be used for concept development and as input to the next phase of overall NLS system requirements analysis. Derived from text

N93-26181# Martin Marietta Aerospace, Denver, CO. Advanced Launch Vehicle Development and Applications Program.
ADVANCED LAUNCH SYSTEM (ALS) TEST REQUIREMENTS Final Report
D. E. Ernst 12 Jul. 1991 190 p
(Contract F04701-88-C-0109)
(MCR-91-5004; CDRL-103A10) Avail: CASI HC A09/MF A02

The objective of this task was to identify test requirements that drive new or modified test facilities and major test articles for the development and verification of the Advanced Launch System (ALS). The task identified major system/subsystem tests, test articles, test facility requirements, and potential government and contractor test facilities to perform these tests. Derived from text

N93-26182# Martin Marietta Aerospace, Denver, CO.
DEVELOP MARGIN PHILOSOPHY TO ATTAIN ROBUSTNESS
D. G. Herbener 15 May 1992 27 p
(Contract F04701-88-C-0109)
(MCR-92-5005; CDRL-103A10) Avail: CASI HC A03/MF A01

This report is submitted to document the results of the study and evaluations associated with the task delineated as Margin Philosophy to Attain Robustness in Annex A to Attachment 9 of the National Launch Development Program Statement of Work dated September 30, 1991. Task no. 31, as defined in the SOW, is shown on Figure 1. In the process of conducting Sub Task 1, as defined on Figure 1, it became apparent that Robustness was not obtained by the management and/or control of margins but is the result of appropriate design philosophy used in the design and development of the total launch system. This total system must include all ground operations facilities, processes and support equipment as well as the launch vehicle and the processes and equipment associated with the production, handling and launch of the vehicle. The developed design philosophy must reflect a thorough understanding of design parameters, their potential interactions and how they are addressed during the design and analysis process. This task attempts to develop an approach, 'Design Philosophy to Attain Robustness', that may be applied to any launch vehicle system resulting in a Robust total system design. As a result of the above, the Objective, Approach and Sub Tasks for Task no. 31 have been changed to the following. Identify the launch system attributes required to develop a robust system. Identify the analyses and/or trade studies required to define the design philosophy necessary to attain the desired system Robustness. Derived from text

N93-26591# Martin Marietta Aerospace, Denver, CO. Space Launch Systems Business Development and Advanced Programs.
TASK TYPE E REPORT FOR NATIONAL LAUNCH DEMONSTRATION CENTER (NLDC) (TASK 32)
G. E. Elliot 13 Dec. 1991 69 p
(Contract F04701-88-C-0109)
(MCR-91-5010; CDRL-103A10) Avail: CASI HC A04/MF A01

The objective of this task was to define National Launch Demonstration Center (NLDC) requirements in support of National Launch System (NLS) Joint Program Office (JPO) Level 11 Task #32, NLDC Requirement Definition. The following document provided the basis for the study: Task authorization - Contract FO4701-88-C-0109, Modification P00025, SOW 3.2.11, Define NLDC Requirements. The Task was structured into the following series of activities: (1) identify NLS vehicle, operations, or information system requirements which could be demonstrated, integrated, validated, or verified using the NLDC; (2) establish groundrules and constraints for the NLDC; (3) develop a time phased approach for implementing the NLDC to match the NLS need dates and Spaceport Florida Authority/JPO funding availability; (4) support development of NLS JPO NLDC Plan; and (5) support development of NLS JPO NLDC Coordination Briefing. Derived from text

N93-24899# Electro Magnetic Applications, Inc., Lakewood, CO.
DEVELOPMENT OF MODELS FOR PREDICTING THE TRIGGERING OF LIGHTNING BY LAUNCH VEHICLES
Rodney A. Perala, Terence H. Rudolph, and Calvin C. Easterbrook *In* FAA, The 1992 International Aerospace and Ground Conference on Lightning and Static Electricity: Addendum Nov. 1992 11 p (For primary document see N93-24875 09-47)
Avail: CASI HC A03/MF A03

16 SPACE TRANSPORTATION

Includes passenger and cargo space transportation, e.g., shuttle operations; and space rescue techniques.

For related information see also *03 Air Transportation and Safety* and *18 Spacecraft Design, Testing and Performance.* For space suits see *54 Man/System Technology and Life Support.*

N93-25479*# Boeing Aerospace and Electronics Co., Seattle, WA.
SPACE TRANSFER VEHICLE CONCEPTS AND REQUIREMENTS STUDY. VOLUME 1: EXECUTIVE SUMMARY Final Report, Aug. 1989 - Apr. 1991
Gary A. Weber Apr. 1991 101 p
(Contract NAS8-37855)
(NASA-CR-192524; NAS 1.26:192524; D180-32040-1-Vol-1) Avail: CASI HC A06/MF A02

A description of the study in terms of background, objectives, and issues is provided. NASA is currently studying new initiatives of space exploration involving both piloted and unpiloted missions to destinations throughout the solar system. Many of these missions require substantial improvements in launch vehicle and upper stage capabilities. This study provides a focused examination of the Space Transfer Vehicles (STV) required to perform these missions using the emerging national launch vehicle definition, the Space Station Freedom (SSF) definition, and the latest mission scenario requirements. The study objectives are to define preferred STV concepts capable of accommodating future exploration missions in a cost-effective manner, determine the technology development (if any) required to perform these missions, and develop a decision database of various programmatic approaches for the development of the STV family of vehicles. Special emphasis was given to examining space basing (stationing reusable vehicles at a space station), examining the piloted lunar mission as a primary design mission, and restricting trade studies to the high-performance, near-term cryogenics (LO2/LH2) as vehicle propellant. The study progressed through three distinct 6-month phases. The first phase concentrated on supporting a NASA 3 month definition of exploration requirements (the '90-day study') and during this phase developed and optimized the space-based point-of-departure (POD) 2.5-stage lunar vehicle. The second phase developed a broad decision database of 95 different vehicle options and transportation architectures. The final phase chose the three most cost-effective architectures and developed point designs to carry to the end of the study. These reference vehicle designs are mutually exclusive and correspond to different national choices about launch vehicles and in-space reusability. There is, however, potential for evolution between concepts. Author (revised)

N93-25510*# Boeing Aerospace and Electronics Co., Seattle, WA.
SPACE TRANSFER VEHICLE CONCEPTS AND REQUIREMENTS STUDY. VOLUME 2, BOOK 1: STV CONCEPT DEFINITION AND EVALUATION Final Report, 1 Aug. 1989 - 1 Apr. 1991
Gary A. Weber 1 Apr. 1991 552 p
(Contract NAS8-37855)
(NASA-CR-192525; NAS 1.26:192525; D180-32040-2-Vol-2-Bk-1) Avail: CASI HC A24/MF A04

The topics covered include the following: mission analysis; initial and evolutionary space transfer vehicle (STV) concept definition; configuration and subsystem trade studies; and operations and logistics. Author

N93-25511*# Boeing Aerospace and Electronics Co., Seattle, WA.
SPACE TRANSFER VEHICLE CONCEPTS AND REQUIREMENTS STUDY. VOLUME 2, BOOK 2: SYSTEM AND PROGRAM REQUIREMENTS TRADE STUDIES Final Report, 1 Aug. 1989 - 1 Apr. 1991
Gary A. Weber, Bill Richards, Greg Paddock, Peter Maricich, Bruce Bouton, Jim Hagen, Richard Kolesar, Craig Hosking, George Dishman, and Mike Furlong et al 1 Apr. 1991 194 p
(Contract NAS8-37855)
(NASA-CR-192526; NAS 1.26:192526; D180-32040-2-Vol-2-Bk-2) Avail: CASI HC A09/MF A03

During the 90-day study, support was provided to NASA in defining a point-of-departure space transfer vehicle (STV). The resulting STV concept was performance optimized with a two-stage LTV/LEV configuration. Appendix A reports on the effort during this period of the study. From the end of the 90-day study until the March Interim Review, effort was placed on optimizing the two-stage vehicle approach identified in the 90-day effort. After the March Interim Review, the effort was expanded to perform a full architectural trade study with the intent of developing a decision database to support STV system decisions in response to changing SEI infrastructure concepts. Several of the architecture trade studies were combined in a System Architecture Trade Study. In addition to this trade, system optimization/definition trades and analyses were completed and some special topics were addressed. Program- and system-level trade study and analyses methodologies and results are presented in this section. Trades and analyses covered in this section are: (1) a system architecture trade study; (2) evolution; (3) safety and abort considerations; (4) STV as a launch vehicle upper stage; and (5) optimum crew and cargo split. Author

N93-25512*# Boeing Aerospace and Electronics Co., Seattle, WA.
SPACE TRANSFER VEHICLE CONCEPTS AND REQUIREMENTS STUDY. VOLUME 2, BOOK 4: INTEGRATED ADVANCED TECHNOLOGY DEVELOPMENT Final Report, 1 Aug. 1989 - 1 Apr. 1991
Gary A. Weber 1 Apr. 1991 80 p
(Contract NAS8-37855)
(NASA-CR-192528; NAS 1.26:192528; D180-32040-2-Vol-2-Bk-4) Avail: CASI HC A05/MF A01

The Space Transfer Vehicle (STV) program provides both an opportunity and a requirement to increase our upper stage capabilities with the development and applications of new technologies. Issues such as man rating, space basing, reusability, and long lunar surface storage times drive the need for new technology developments and applications. In addition, satisfaction of mission requirements such as lunar cargo delivery capability and lunar landing either require new technology development or can be achieved in a more cost-effective manner with judicious applications of advanced technology. During the STV study, advanced technology development requirements and plans have been addressed by the Technology/Advanced Development Working Group composed of NASA and contractor representatives. This report discusses the results to date of this working group. The first section gives an overview of the technologies that have potential or required applications for the STV and identifies those technologies baselined for the STV. Figures are provided that list the technology categories and show the priority placed on those technology categories for either the space-based or ground-based options. The second section covers the plans and schedules for incorporating the technologies into the STV program. Author

N93-25513*# Boeing Aerospace and Electronics Co., Seattle, WA.
SPACE TRANSFER VEHICLE CONCEPTS AND REQUIREMENTS STUDY. VOLUME 2, BOOK 3: STV SYSTEM INTERFACES Final Report, 1 Aug. 1989 - 1 Apr. 1991
Gary A. Weber 1 Apr. 1991 18 p
(Contract NAS8-37855)
(NASA-CR-192527; NAS 1.26:192527; D180-32040-2-Vol-2-Bk-3) Avail: CASI HC A03/MF A01

This report presents the results of systems analyses and conceptual design of space transfer vehicles (STV). The missions examined included piloted and unpiloted lunar outpost support and spacecraft servicing, and unpiloted payload delivery to various earth and solar orbits. The study goal was to examine the mission requirements and provide a decision data base for future programmatic development plans. The final lunar transfer vehicles provided a wide range of capabilities and interface requirements while maintaining a constant payload mission model. Launch vehicle and space station sensitivity was examined, with the final vehicles as point design covering the range of possible options. Development programs were defined and technology readiness levels for different options were determined. Volume 1 presents the executive summary, volume 2 provides the study results, and volume 3 the cost and WBS data. Author

N93-25514*# Boeing Aerospace and Electronics Co., Seattle, WA.
SPACE TRANSFER VEHICLE CONCEPTS AND REQUIREMENTS STUDY. VOLUME 3, BOOK 1: PROGRAM COST ESTIMATES Final Report, 1 Aug. 1989 - 1 Apr. 1991
Al F. Peffley 1 Apr. 1991 154 p
(Contract NAS8-37855)
(NASA-CR-192529; NAS 1.26:192529; D180-32040-3-Vol-3-Bk-1) Avail: CASI HC A08/MF A02

The Space Transfer Vehicle (STV) Concepts and Requirements Study cost estimate and program planning analysis is presented. The cost estimating technique used to support STV system, subsystem, and component cost analysis is a mixture of parametric cost estimating and selective cost analogy approaches. The parametric cost analysis is aimed at developing cost-effective aerobrake, crew module, tank module, and lander designs with the parametric cost estimates data. This is accomplished using cost as a design parameter in an iterative process with conceptual design input information. The parametric estimating approach segregates costs by major program life cycle phase (development, production, integration, and launch support). These phases are further broken out into major hardware subsystems, software functions, and tasks according to the STV preliminary program work breakdown structure (WBS). The WBS is defined to a low enough level of detail by the study team to highlight STV system cost drivers. This level of cost visibility provided the basis for cost sensitivity analysis against various design approaches aimed at achieving a cost-effective design. The cost approach, methodology, and rationale are described. A chronological record of the interim review material relating to cost analysis is included along with a brief summary of the study contract tasks accomplished during that period of review and the key conclusions or observations identified that relate to STV program cost estimates. The STV life cycle costs are estimated on the proprietary parametric cost model (PCM) with inputs organized by a project WBS. Preliminary life cycle schedules are also included. CASI

N93-25955*# Lockheed Engineering and Sciences Co., Houston, TX. Flight Requirements Section.
STS-39 SPACE SHUTTLE MISSION REPORT
Robert W. Fricke Jun. 1991 34 p Sponsored by NASA. Lyndon B. Johnson Space Center
(NASA-CR-193063; NAS 1.26:193063; JSC-08250) Avail: CASI HC A03/MF A01

The STS-39 Space Shuttle Program Mission Report contains a summary of the vehicle subsystem operations during the fortieth flight of the Space Shuttle and the twelfth flight of the Orbiter Vehicle Discovery (OV-103). In addition to the Discovery vehicle, the flight vehicle consisted of the following: an External Tank (ET) (designated as ET-46 (LWT-39); three Space Shuttle main engines (SSME's) (serial numbers 2026, 2030, and 2029 in positions 1, 2, and 3, respectively); and two Solid Rocket Boosters (SRB's) designated as BI-043. The primary objective of this flight was to successfully perform the planned operations of the Infrared Background Signature Survey (IBSS),

Air Force Payload (AFP)-675, Space Test Payload (STP)-1, and the Multipurpose Experiment Canister (MPEC) payloads. Author (revised)

N93-25956*# Lockheed Engineering and Sciences Co., Houston, TX. Flight Requirements Section.

STS-37 SPACE SHUTTLE MISSION REPORT

Robert W. Fricke May 1991 32 p Sponsored by NASA. Lyndon B. Johnson Space Center

(NASA-CR-193062; NAS 1.26:193062; JSC-08249) Avail: CASI HC A03/MF A01

The STS-37 Space Shuttle Program Mission Report contains a summary of the vehicle subsystem activities during this thirty-ninth flight of the Space Shuttle and the eighth flight of the Orbiter Vehicle Atlantis (OV-104). In addition to the Atlantis vehicle, the flight vehicle consisted of the following: an External Tank (ET) (designated as ET-37/LWT-30); three Space Shuttle main engines (SSME's) (serial numbers 2019, 2031, and 2107 in positions 1, 2, and 3, respectively); and two Solid Rocket Boosters (SRB's) designated as BI-042. The primary objective of this flight was to successfully deploy the Gamma Ray Observatory (GRO) payload. The secondary objectives were to successfully perform all operations necessary to support the requirements of the Protein Crystal Growth (PCG) Block 2 version, Radiation Monitoring Experiment-3 (RME-3), Ascent Particle Monitor (APM), Shuttle Amateur Radio Experiment-2 (SAREX-2), Air Force Maui Optical Site Calibration Test (AMOS), Bioserve Instrumentation Technology Associates Materials Dispersion Apparatus (BIMDA), and the Crew and Equipment Transfer Aids (CETA) payloads. Author (revised)

N93-25957*# Lockheed Engineering and Sciences Co., Houston, TX. Flight Data Section.

STS-43 SPACE SHUTTLE MISSION REPORT

Robert W. Fricke Sep. 1991 34 p Sponsored by NASA. Lyndon B. Johnson Space Center

(NASA-CR-193064; NAS 1.26:193064; NSTS-08252) Avail: CASI HC A03/MF A01

The STS-43 Space Shuttle Program Mission Report contains a summary of the vehicle subsystem operations during the forty-second flight of the Space Shuttle Program and the ninth flight of the Orbiter Vehicle Atlantis (OV-104). In addition to the Atlantis vehicle, the flight vehicle consisted of the following: an External Tank (ET) designated as ET-47 (LWT-40); three Space Shuttle main engines (SSME's) (serial numbers 2024, 2012, and 2028 in positions 1, 2, and 3, respectively); and two Solid Rocket Boosters (SRB's) designated as BI-045. The primary objective of the STS-43 mission was to successfully deploy the Tracking and Data Relay Satellite-E/Inertial Upper Stage (TDRS-E/IUS) satellite and to perform all operations necessary to support the requirements of the Shuttle Solar Backscatter Ultraviolet (SSBUV) payload and the Space Station Heat Pipe Advanced Radiator Element (SHARE-2). Author (revised)

N93-25958*# Lockheed Engineering and Sciences Co., Houston, TX. Flight Requirements Section.

STS-40 SPACE SHUTTLE MISSION REPORT

Robert W. Fricke Jul. 1991 34 p Sponsored by NASA. Lyndon B. Johnson Space Center

(NASA-TM-108737; NAS 1.15:108737; NSTS-08251) Avail: CASI HC A03/MF A01

The STS-40 Space Shuttle Program Mission Report contains a summary of the vehicle subsystem operations during the forty-first flight of the Space Shuttle and the eleventh flight of the Orbiter Vehicle Columbia (OV-102). In addition to the Columbia vehicle, the flight vehicle consisted of an External Tank (ET) designated as ET-41 (LWT-34), three Space Shuttle main engines (SSME's) (serial numbers 2015, 2022, and 2027 in positions 1, 2, and 3, respectively), and two Solid Rocket Boosters (SRB's) designated as BI-044. The primary objective of the STS-40 flight was to successfully perform the planned operations of the Spacelab Life Sciences-1 (SLS-1) payload. The secondary objectives of this flight were to perform the operations required by the Getaway Special (GAS) payloads and the Middeck O-Gravity Dynamics Experiment (MODE) payload. Author (revised)

N93-25959*# Lockheed Engineering and Sciences Co., Houston, TX. Flight Data Section.

STS-45 SPACE SHUTTLE MISSION REPORT

Robert W. Fricke May 1992 34 p Sponsored by NASA. Lyndon B. Johnson Space Center

(NASA-CR-193054; NAS 1.26:193054; NSTS-08275) Avail: CASI HC A03/MF A01

The STS-45 Space Shuttle Program Mission Report contains a summary of the vehicle subsystem operations during the forty-sixth flight of the Space Shuttle Program and the eleventh flight of the Orbiter Vehicle Atlantis (OV-104). In addition to the Atlantis vehicle, the flight vehicle consisted of the following: an External Tank (ET) designated as ET-44 (LWT-37); three Space Shuttle main engines (SSME's), which were serial numbers 2024, 2012, and 2028 in positions 1, 2, and 3, respectively; and two Solid Rocket Boosters (SRB's) designated as BI-049. The lightweight redesigned Solid Rocket Motors (RSRM's) installed in each of the SRB's were designated as 360L021A for the left SRM and 360W021B for the right SRM. The primary objective of this mission was to successfully perform the planned operations of the Atmospheric Laboratory for Applications and Science-1 (ATLAS-1) and the Shuttle Solar Backscatter Ultraviolet Instrument (SSBUV) payloads. The secondary objectives were to successfully perform all operations necessary to support the requirements of the following: the Space Tissue Loss-01 (STL-01) experiment; the Radiation Monitoring Equipment-3 (RME-3) experiment; the Visual Function Tester-2 (VFT-2) experiment; the Cloud Logic to Optimize use of Defense System (CLOUDS-1A) experiment; the Shuttle Amateur Radio Experiment 2 (SAREX-2) Configuration B; the Investigation into Polymer Membranes Processing experiment; and the Get-Away Special (GAS) payload G-229. The Ultraviolet Plume Instrument (UVPI) was a payload of opportunity that required no special maneuvers. In addition to the primary and secondary objectives, the crew was tasked to perform as many as 10 Development Test Objectives (DTO'S) and 14 Detailed Supplementary Objectives (DSO's). Author (revised)

N93-25960*# Lockheed Engineering and Sciences Co., Houston, TX. Flight Evaluation and Engineering Office.

STS-47 SPACE SHUTTLE MISSION REPORT

Robert W. Fricke, Jr. Oct. 1992 38 p Sponsored by NASA. Lyndon B. Johnson Space Center

(NASA-CR-193056; NAS 1.26:193056; NSTS-08279) Avail: CASI HC A03/MF A01

The STS-47 Space Shuttle Program Mission Report provides a summary of the Orbiter, External Tank (ET), Solid Rocket Booster/Redesigned Solid Rocket Motor (SRB/RSRM), and the Space Shuttle main engine (SSME) subsystem performance during the fiftieth Space Shuttle Program flight and the second flight of the Orbiter Vehicle Endeavour (OV-105). In addition to the Endeavour vehicle, the flight vehicle consisted of the following: an ET which was designated ET-45 (LWT-38); three SSME's which were serial numbers 2026, 2022, and 2029 and were located in positions 1, 2, and 3, respectively; and two SRB's which were designated BI-053. The lightweight/redesigned RSRM that was installed in the left SRB was designated 360L026A, and the RSRM that was installed in the right SRB was 360W026B. The primary objective of the STS-47 flight was to successfully perform the planned operations of the Spacelab-J (SL-J) payload (containing 43 experiments--of which 34 were provided by the Japanese National Space Development Agency (NASDA)). The secondary objectives of this flight were to perform the operations of the Israeli Space Agency Investigation About Hornets (ISAIAH) payload, the Solid Surface Combustion Experiment (SSCE), the Shuttle Amateur Radio Experiment-2 (SAREX-2), and the Get-Away Special (GAS) payloads. The Ultraviolet Plume Instrument (UVPI) was flown as a payload of opportunity. Author (revised)

N93-25988*# Lockheed Engineering and Sciences Co., Houston, TX. Flight Evaluation Section.

STS-44 SPACE SHUTTLE MISSION REPORT

Robert W. Fricke Jan. 1992 32 p Sponsored by NASA. Lyndon B. Johnson Space Center

(NASA-TM-108735; NAS 1.15:108735; NSTS-08273) Avail: CASI HC A03/MF A01

The STS-44 Space Shuttle Program Mission Report is a summary of the vehicle subsystem operations during the forty-fourth flight of the Space Shuttle Program and the tenth flight of the Orbiter vehicle Atlantis (OV-104). In addition to the Atlantis vehicle, the flight vehicle consisted of the following: an External Tank (ET) designated as ET-53 (LWT-46); three Space Shuttle main engines (SSME's) (serial numbers 2015, 2030, and 2029 in positions 1, 2, and 3, respectively); and two Solid Rocket Boosters (SRB's) designated

as BI-047. The lightweight redesigned Solid Rocket Motors (RSRM's) installed in each one of the SRB's were designated as 360L019A for the left SRB and 360W019B for the right SRB. The primary objective of the STS-44 mission was to successfully deploy the Department of Defense (DOD) Defense Support Program (DSP) satellite/inertial upper stage (IUS) into a 195 nmi. earth orbit at an inclination of 28.45 deg. Secondary objectives of this flight were to perform all operations necessary to support the requirements of the following: Terra Scout, Military Man in Space (M88-1), Air Force Maui Optical System Calibration Test (AMOS), Cosmic Radiation Effects and Activation Monitor (CREAM), Shuttle Activation Monitor (SAM), Radiation Monitoring Equipment-3 (RME-3), Visual Function Tester-1 (VFT-1), and the Interim Operational Contamination Monitor (IOCM) secondary payloads/experiments. Author (revised)

N93-25989*# Lockheed Engineering and Sciences Co., Houston, TX. Flight Evaluation Section.

STS-42 SPACE SHUTTLE MISSION REPORT

Robert W. Fricke Feb. 1992 32 p Sponsored by NASA. Lyndon B. Johnson Space Center

(NASA-CR-193059; NAS 1.26:193059; NSTS-08274) Avail: CASI HC A03/MF A01

The STS-42 Space Shuttle Program Mission Report contains a summary of the vehicle subsystem operations during the forty-fifth flight of the Space Shuttle Program and the fourteenth flight of the Orbiter vehicle Discovery (OV-103). In addition to the Discovery vehicle, the flight vehicle consisted of the following: an External Tank (ET) designated as ET-52 (LWT-45); three Space Shuttle main engines (SSME's), which were serial numbers 2026, 2022, and 2027 in positions 1, 2, and 3, respectively; and two Solid Rocket Boosters (SRB's) designated as BI-048. The lightweight redesigned Solid Rocket Motors (RSRM's) installed in each one of the SRB's were designated as 360L020A for the left SRM and 360Q020B for the right SRM. The primary objective of the STS-42 mission was to complete the objectives of the first International Microgravity Laboratory (IML-1). Secondary objectives were to perform all operations necessary to support the requirements of the following: Gelation of Sols: Applied Microgravity Research (GOSAMR); Student Experiment 81-09 (Convection in Zero Gravity); Student Experiment 83-02 (Capillary Rise of Liquid Through Granular Porous Media); the Investigation into Polymer Membrane Processing (IPMP); the Radiation Monitoring Equipment-3 (RME-3); and Get-Away Special (GAS) payloads carried on the GAS Beam Assembly. Author (revised)

N93-25990*# Lockheed Engineering and Sciences Co., Houston, TX. Flight Data Section.

STS-48 SPACE SHUTTLE MISSION REPORT

Robert W. Fricke Oct. 1991 30 p Sponsored by NASA. Lyndon B. Johnson Space Center

(NASA-CR-193060; NAS 1.26:193060; NSTS-08254) Avail: CASI HC A03/MF A01

The STS-48 Space Shuttle Program Mission Report is a summary of the vehicle subsystem operations during the forty-third flight of the Space Shuttle Program and the thirteenth flight of the Orbiter vehicle Discovery (OV-103). In addition to the Discovery vehicle, the flight vehicle consisted of the following: an External Tank (ET) designated as ET-42 (LUT-35); three Space Shuttle main engines (SSME's) (serial numbers 2019, 2031, and 2107 in positions 1, 2, and 3, respectively); and two Solid Rocket Boosters (SRB's) designated as BI-046. The lightweight redesigned Solid Rocket Motors (RSRM's) installed in each one of the SRB's were designated as 360L018A for the left SRB and 360L018B for the right SRB. The primary objective of the flight was to successfully deploy the Upper Atmospheric Research Satellite (UARS) payload. Author (revised)

N93-25991*# Lockheed Engineering and Sciences Co., Houston, TX. Flight Data Section.

STS-46 SPACE SHUTTLE MISSION REPORT

Robert W. Fricke Oct. 1992 34 p Sponsored by NASA. Lyndon B. Johnson Space Center

(NASA-CR-193058; NAS 1.26:193058; NSTS-08278) Avail: CASI HC A03/MF A01

The STS-46 Space Shuttle Program Mission Report contains a summary of the Orbiter, External Tank (ET), Solid Rocket Booster/Redesigned Solid Rocket Motor (SRB/RSRM), and the Space Shuttle main engine (SSME) subsystem performance during the forty-ninth flight of the Space Shuttle Program, and the twelfth flight of the Orbiter vehicle Atlantis (OV-104). In addition to the Atlantis vehicle, the flight vehicle consisted of the following: an ET, designated ET-48 (LWT-41); three SSME's, which were serial numbers 2032, 2033, and 2027 in positions 1, 2, and 3, respectively; and two SRB's which were designated BI-052. The lightweight/redesigned SRM's that were installed in each SRB were designated 360W025A for the left RSRM and 360L025B for the right RSRM. The primary objective of this flight was to successfully deploy the European Retrievable Carrier (EURECA) payload and perform the operations of the Tethered Satellite System-1 (TSS-1) and the Evaluation of Oxygen Interaction with Material 3/Thermal Energy Management Processes 2A-3 (EOIM-3/TEMP 2A-3). The secondary objectives of this flight were to perform the operations of the IMAX Cargo Bay Camera (ICBC), Consortium for Material Development in Space Complex Autonomous Payload-2 and 3 (CONCAP-2 and CONCAP-3), Limited Duration Space Environment Candidate Materials Exposure (LDCE), Pituitary Growth Hormone Cell Function (PHCF), and Ultraviolet Plume Instrumentation (UVPI). In addition to summarizing subsystem performance, this report also discusses each Orbiter, ET, SSME, SRB, and RSRM in-flight anomaly in the applicable section of the report. Also included in the discussion is a reference to the assigned tracking number as published on the Problem Tracking List. All times are given in Greenwich mean time (G.m.t.) as well as mission elapsed time (MET). Author (revised)

N93-25992*# Lockheed Engineering and Sciences Co., Houston, TX. Flight Data Section.

STS-50 SPACE SHUTTLE MISSION REPORT

Robert W. Fricke Aug. 1992 43 p Sponsored by NASA. Lyndon B. Johnson Space Center

(NASA-CR-193057; NAS 1.26:193057; NSTS-08277) Avail: CASI HC A03/MF A01

The STS-50 Space Shuttle Program Mission Report contains a summary of the Orbiter, External Tank (ET), Solid Rocket Booster/Redesigned Solid Rocket Motor (SRB/RSRM), and the Space Shuttle main engine (SSME) subsystem performance during the forty-eighth flight of the Space Shuttle Program, and the twelfth flight of the Orbiter vehicle Columbia (OV-102). In addition to the Columbia vehicle, the flight vehicle consisted of the following: an ET which was designated ET-50 (LUT-43); three SSME's which were serial numbers 2019, 2031, and 2011 in positions 1, 2, and 3, respectively; and two SRB's which were designated BI-051. The lightweight/redesigned RSRM's installed in each SRB were designated 360L024A for the left RSRM and 360M024B for the right RSRM. The primary objective of the STS-50 flight was to successfully perform the planned operations of the United States Microgravity Laboratory (USML-1) payload. The secondary objectives of this flight were to perform the operations required by the Investigations into Polymer Membrane Processing (IPMP), and the Shuttle Amateur Radio Experiment 2 (SAREX-2) payloads. An additional secondary objective was to meet the requirements of the Ultraviolet Plume Instrument (UVPI), which was flown as a payload of opportunity. Author (revised)

N93-25993*# Lockheed Engineering and Sciences Co., Houston, TX. Flight Evaluation and Engineering Office.

STS-52 SPACE SHUTTLE MISSION REPORT

Robert W. Fricke, Jr. Dec. 1992 44 p Sponsored by NASA. Lyndon B. Johnson Space Center

(NASA-CR-193061; NAS 1.26:193061; NSTS-08280) Avail: CASI HC A03/MF A01

The STS-52 Space Shuttle Program Mission Report provides a summary of the Orbiter, External Tank (ET), Solid Rocket Booster/Redesigned Solid Rocket Motor (SRB/RSRM), and the Space Shuttle main engine (SSME) subsystem performance during the fifty-first flight of the Space Shuttle Program, and the thirteenth flight of the Orbiter vehicle Columbia (OV-102). In addition to the Orbiter, the flight vehicle consisted of the following: an ET (designated as ET-55/LWT-48); three SSME's, which were serial numbers 2030, 2015, and 2034 in positions 1, 2, and 3, respectively; and two SRB's, which were designated BI-054. The lightweight RSRM's that were installed in each SRB were designated 360L027A for the left SRB and 360Q027B for the right SRB. The primary objectives of this flight were to successfully deploy the Laser Geodynamic Satellite (LAGEOS-2) and to perform operations of the United States Microgravity Payload-1 (USMP-1). The secondary objectives of this flight were to perform the operations of the Attitude Sensor Package (ASP), the Canadian Experiments-2 (CANEX-2),

the Crystals by Vapor Transport Experiment (CVTE), the Heat Pipe Performance Experiment (HPP), the Commercial Materials Dispersion Apparatus Instrumentation Technology Associates Experiments (CMIX), the Physiological System Experiment (PSE), the Commercial Protein Crystal Growth (CPCG-Block 2), the Shuttle Plume Impingement Experiment (SPIE), and the Tank Pressure Control Experiment (TPCE) payloads.
Author (revised)

N93-26152*# Martin Marietta Corp., New Orleans, LA. Manned Space Systems.
LIQUID ROCKET BOOSTER (LRB) FOR THE SPACE TRANSPORTATION SYSTEM (STS) SYSTEMS STUDY. AMENDMENT 13: ORIENTATION MEETING
Sep. 1990 17 p Meeting held in Huntsville, AL
(Contract NAS8-37136)
(NASA-CR-192515; NAS 1.26:192515) Avail: CASI HC A03/MF A01

The topics are presented in viewgraph form and include the following: LRB study results summary -- Feb. 1989; LRB study results -- Jan. 1990; Shuttle configuration with booster options; LRB study results -- Sept. 1990; LRB statement of work tasks; ground rules and assumptions; study flow of design, manufacturing/production, and test program/certification; study products; study schedule; and candidate 1.5 stage engine arrangements.
Author

N93-26329*# Lockheed Engineering and Sciences Co., Houston, TX. Human Factors Engineering Dept.
ASSURED CREW RETURN VEHICLE MAN-SYSTEMS INTEGRATION STANDARDS
Jul. 1991 323 p
(NASA-CR-193065; NAS 1.26:193065; NASA-STD-3000-Vol-6) Avail: CASI HC A14/MF A03

This is Volume 6 of the Man-Systems Integration Standards (MSIS) family of documents, which is contained in several volumes and a relational database. Each volume has a specific purpose, and each has been assembled from the data contained in the relational database. Volume 6 serves as the Assured Crew Return Vehicle project man-systems integration design requirements. The data in this document is a subset of the data found in Volume 1 and defines the requirements which are pertinent to the Assured Crew Return Vehicle as defined in the SPRD. Additional data and guidelines are provided to assist in the design.
Author

17 SPACE COMM., SPACECRAFT COMM., COMMAND & TRACKING

Includes telemetry; space communications networks; astronavigation and guidance; and radio blackout.

For related information see also *04 Aircraft Communications and Navigation* and *32 Communications and Radar.*

N93-25952*# National Aeronautics and Space Administration. Lyndon B. Johnson Space Center, Houston, TX.
RENDEZVOUS, PROXIMITY OPERATIONS AND CAPTURE QUALITY FUNCTION DEPLOYMENT REPORT
Stephen L. Lamkin, ed. Dec. 1991 66 p
(RTOP 593-14-00)
(NASA-TM-108752; NAS 1.15:108752; JSC-25458) Avail: CASI HC A04/MF A01

Rendezvous, Proximity Operations, and Capture (RPOC) is a missions operations area which is extremely important to present and future space initiatives and must be well planned and coordinated. To support this, a study team was formed to identify a specific plan of action using the Quality Function Deployment (QFD) process. This team was composed of members from a wide spectrum of engineering and operations organizations which are involved in the RPOC technology area. The key to this study's success is an understanding of the needs of potential programmatic customers and the technology base available for system implementation. To this end, the study team conducted interviews with a variety of near term and future programmatic customers and technology development sponsors. The QFD activity led to a thorough understanding of the needs of these customers in the RPOC area, as well as the relative importance of these needs.
Author (revised)

N93-24667*# Jet Propulsion Lab., California Inst. of Tech., Pasadena.
A FUNCTIONAL DESCRIPTION OF THE BUFFERED TELEMETRY DEMODULATOR (BTD)
H. Tsou, B. Shah, R. Lee, and S. Hinedi *In its* The Telecommunications and Data Acquisition Report 15 Feb. 1993 p 50-73 (For primary document see N93-24659 09-32)
(RTOP 314-30-61-02-02)
Avail: CASI HC A03/MF A02

N93-25000# Alcatel Bell Telephone, Antwerp (Belgium). Space Ground Systems.
SYNCHRONISATION, ACQUISITION AND TRACKING FOR TELEMETRY AND DATA RECEPTION
A. VanDoninck *In* ESA, Frequency and Time Forum Jun. 1992 p 149-155 (For primary document see N93-24978 09-70)
Copyright Avail: CASI HC A02/MF A04

N93-26109*# Jet Propulsion Lab., California Inst. of Tech., Pasadena.
DEEP-SPACE NAVIGATION WITH DIFFERENCED DATA TYPES. PART 3: AN EXPANDED INFORMATION CONTENT AND SENSITIVITY ANALYSIS
J. A. Estefan and S. W. Thurman *In its* The Telecommunications and Data Acquisition Report 15 May 1992 p 56-73 (For primary document see N93-26105 09-32)
(RTOP 310-10-63-50-00)
Avail: CASI HC A03/MF A04

N93-26124*# Jet Propulsion Lab., California Inst. of Tech., Pasadena.
DSN ACQUISITION OF MAGELLAN HIGH-RATE TELEMETRY DATA
A. L. Berman and P. A. Au *In its* The Telecommunications and Data Acquisition Report 15 May 1992 p 253-264 (For primary document see N93-26105 09-32)
(RTOP 314-40-22-35-01)
Avail: CASI HC A03/MF A04

18 SPACECRAFT DESIGN, TESTING AND PERFORMANCE

Includes satellites; space platforms; space stations; spacecraft systems and components such as thermal and environmental controls; and attitude controls.

For life support systems see *54 Man/System Technology and Life Support.* For related information see also *05 Aircraft Design, Testing and Performance, 39 Structural Mechanics,* and *16 Space Transportation.*

N93-24755*# National Aeronautics and Space Administration. Lewis Research Center, Cleveland, OH.
CONTRIBUTIONS OF MICROGRAVITY TEST RESULTS TO THE DESIGN OF SPACECRAFT FIRE SAFETY SYSTEMS
Robert Friedman and David L. Urban (Sverdrup Technology, Inc., Brook Park, OH.) Mar. 1993 13 p Presented at the AHS/ASEE Second Aerospace Design Conference, Irvine, CA, 16-19 Feb. 1993; sponsored by AIAA
(RTOP 323-53-62)
(NASA-TM-106093; E-7445; NAS 1.15:106093; AIAA Paper 93-1152)
Copyright Avail: CASI HC A03/MF A01

Experiments conducted in spacecraft and drop towers show that thin-sheet materials have reduced flammability ranges and flame-spread rates under quiescent low-gravity environments (microgravity) as compared to normal gravity. Furthermore, low-gravity flames may be suppressed more easily by atmospheric dilution or decreasing atmospheric total pressure than their normal-gravity counterparts. The addition of a ventilating air flow to the low-gravity flame zone, however, can greatly enhance the flammability range and flame spread. These results, along with observations of flame and smoke characteristics useful for microgravity fire-detection 'signatures', promise to be of considerable value to spacecraft fire-safety designs. The

paper summarizes the fire detection and suppression techniques proposed for the Space Station Freedom and discusses both the application of low-gravity combustion knowledge to improve fire protection and the critical needs for further research. Author (revised)

N93-24767 Auburn Univ., AL.
DYNAMICS AND CONTROL OF MANEUVERABLE TETHERED FLIGHT VEHICLES Ph.D. Thesis
Tae Soo No 1992 171 p
Avail: Univ. Microfilms Order No. DA9237200

Problems concerning the dynamics and control of tethered flight vehicles (TFV) are addressed. These tethered systems include towed vehicle systems (TVS), tethered satellite systems (TSS) and tethered hypervelocity vehicles (THV). Rather general equations of motion are obtained. These are valid for three operational modes: deployment, station-keeping and retrieval. A computer simulation program based on the general equations of motion is used to investigate the dynamics and control of these types of systems. Stability characteristics of various TFV's are extensively investigated both numerically and analytically. It is found that the addition of attitude dynamics of an end body causes significant differences in the stability characteristics of both the THV and the TSS. It is also shown, via nonlinear simulation, that the perturbed motion of a TVS about an unstable equilibrium state approaches a stable limit cycle. The use of a simple physical model of a TFV in the design of a feedback control system is justified. Linear optimal control theory is used to synthesize control laws for station-keeping and maneuvers of the tethered vehicle. The rotational motion of the end body is well controlled during station-keeping and maneuvers. It is shown that under appropriate circumstances, aerodynamic control is a viable alternative to reaction (thruster) control. Dissert. Abstr.

N93-25090*# National Aeronautics and Space Administration. Lewis Research Center, Cleveland, OH.
PLASMA SHEATH EFFECTS ON ION COLLECTION BY A PINHOLE
Joel L. Herr (Sverdrup Technology, Inc., Brook Park, OH.) and David B. Snyder Apr. 1993 12 p Presented at the 31st AIAA Aerospace Sciences Meeting and Exhibit, Reno, NV, 11-14 Jan. 1993; sponsored by AIAA Previously announced in IAA as A93-24243
(RTOP 506-41-41)
(NASA-TM-106098; E-7740; NAS 1.15:106098) Avail: CASI HC A03/MF A01

This work presents tables to assist in the evaluation of pinhole collection effects on spacecraft. These tables summarize results of a computer model which tracks particle trajectories through a simplified electric field in the plasma sheath. A technique is proposed to account for plasma sheath effects in the application of these results and scaling rules are proposed to apply the calculations to specific situations. This model is compared to ion current measurements obtained by another worker, and the agreement is very good. Author

N93-25133*# General Electric Co., Princeton, NJ. Astro Space.
UARS IN-FLIGHT JITTER STUDY FOR EOS Final Report
John Molnar and Mike Garnek Jan. 1993 199 p
(Contract NAS5-32500; RTOP 585-03-11-01)
(NASA-CR-191419; NAS 1.26:191419) Avail: CASI HC A09/MF A03

Response data collected from gyroscopes on board the Upper Atmosphere Research Satellite (UARS) provided a unique opportunity to analyze actual flight pointing jitter data. Flight modal frequencies and damping values are derived from the measured data using an Eigensystem Realization Algorithm (ERA). Flight frequencies at various solar array positions are compared to analytical predictions obtained with a Finite Element Model. The solar array modal frequencies change with position due to the modes acting about different spacecraft inertial axes. Higher order modes were difficult to identify due to the limited instrumentation. Future flight jitter studies on other spacecraft would be significantly aided by additional instrumentation. Spacecraft jitter due to continuous disturbance sources such as the 1.6 meter scanning microwave antenna, the solar array drive, and reaction wheels is presented. The solar array drive disturbance dominates the spacecraft response during normal operation. Author

N93-25174*# National Aeronautics and Space Administration. Langley Research Center, Hampton, VA.
SPACE STATION FREEDOM ASSEMBLY AND OPERATION AT A 51.6 DEGREE INCLINATION ORBIT
Patrick A. Troutman, Laura M. Brewer (Analytical Mechanics Associates, Inc., Hampton, VA.), Michael L. Heck (Analytical Mechanics Associates, Inc., Hampton, VA.), and Renjith R. Kumar (Analytical Mechanics Associates, Inc., Hampton, VA.) Jan. 1993 34 p
(RTOP 476-14-15-01)
(NASA-TM-107731; NAS 1.15:107731) Avail: CASI HC A03/MF A01

This study examines the implications of assembling and operating Space Station Freedom at a 51.6 degree inclination orbit utilizing an enhanced lift Space Shuttle. Freedom assembly is currently baselined at a 220 nautical mile high, 28.5 degree inclination orbit. Some of the reasons for increasing the orbital inclination are (1) increased ground coverage for Earth observations, (2) greater accessibility from Russian and other international launch sites, and (3) increased number of Assured Crew Return Vehicle (ACRV) landing sites. Previous studies have looked at assembling Freedom at a higher inclination using both medium and heavy lift expendable launch vehicles (such as Shuttle-C and Energia). The study assumes that the shuttle is used exclusively for delivering the station to orbit and that it can gain additional payload capability from design changes such as a lighter external tank that somewhat offsets the performance decrease that occurs when the shuttle is launched to a 51.6 degree inclination orbit. Author

N93-25207 Maryland Univ., College Park.
MANEUVERING A REENTRY BODY VIA MAGNETO-GASDYNAMIC FORCES Ph.D. Thesis
Leo Patrick OHare 1992 171 p
Avail: Univ. Microfilms Order No. DA9304370

Some of the characteristics of the interaction of an electrically conducting fluid with a non-uniform applied magnetic field and a potential magnetogasdynamic control system which may be used on future aerospace vehicles are presented. The flow through a two dimensional channel is predicted by numerically solving the magnetogasdynamic equations using a time marching technique. The fluid was modeled as a compressible, inviscid, supersonic gas with finite electrical conductivity. Development of the algorithm provided a means to predict and analyze phenomena associated with magnetogasdynamic flows which had not been previously explored using numerical methods. One such phenomena was the prediction of oblique waves resulting from the interaction of an electrically conducting fluid with a non-uniform applied magnetic field. Development of this tool provided a means to explore an application which might have potential use for future aerospace vehicle missions. In order to appreciate the significance of this technology, predictions were made of the pitching moment about a slender blunted cone, generated by a system relying on the fluid-magnetic interaction. These moments were compared to predictions of a pitching moment generated by a deflecting control surface on the same vehicle. It was shown that the proposed magnetogasdynamic system could produce moments which were on the same order as the moments produced by the flap systems at low deflection angles. Dissert. Abstr.

N93-25217*# Committee on Earth Observations Satellites, London (England).
CEOS COMMITTEE ON EARTH OBSERVATIONS SATELLITES CONSOLIDATED REPORT, 1992
1992 68 p Presented at the 6th CEOS Plenary, London, England, 9-11 Dec. 1992
(NASA-TM-108776; NAS 1.15:108776) Avail: CASI HC A04/MF A01

A concise overview of the committee on Earth Observations Satellites (CEOS) and its Working Groups, covering the history and purpose of the Committee and its accomplishments to date are provided. The report will be updated annually before each Plenary meeting, and as developments in the Working Groups warrant. The committee on Earth Observations Satellites (originally named the International Earth Observations Satellite committee, IEOS) was treated in 1984, in response to a recommendation from the Economic Summit of Industrialized Nations Working Group on Growth, Technology, and Employment's Panel of Experts on Satellite Remote Sensing. This group recognized the multidisciplinary nature of satellite Earth observations, and the value of coordinating across all proposed missions. Thus, CEOS combined the previously existing groups for coordination on Ocean Remote-Sensing Satellites (CORSS) and coordination on Land

Remote-Sensing Satellites (CLRSS), and established a broad framework for coordination across all spaceborne Earth observations missions. The first three LEOS Plenary meetings focused on treating and guiding the Working Groups deemed necessary to carry out the objectives of the CEOS members. After the third meeting, it was agreed that a more active orientation was required by the Plenary, and additional issues were brought before the group at the fourth meeting. At the fifth Plenary, international scientific programs and relevant intergovernmental organizations accepted invitations and participated as affiliate members of CEOS. This enabled progress toward integrating satellite data users' requirements into the CEOS process. Data exchange principles for global change research were also adopted. An interim CEOS Plenary meeting was held in April 1992, in preparation for the United Nations Conference on Environment and Development (UNCED). Brief encapsulations of the Plenary sessions immediately follow the Terms of Reference that govern the activities of CEOS as a whole; Terms of Reference for the individual Working Groups are included as Appendix A. A complete listing of CEOS members is offered as Appendix B. Author (revised)

N93-25231*# National Aeronautics and Space Administration, Washington, DC.

TETHERED SATELLITE SYSTEM CONTINGENCY INVESTIGATION BOARD Final Report

6 Nov. 1992 51 p

(NASA-TM-108704; NAS 1.15:108704) Avail: CASI HC A04/MF A01

The Tethered Satellite System (TSS-1) was launched aboard the Space Shuttle Atlantis (STS-46) on July 31, 1992. During the attempted on-orbit operations, the Tethered Satellite System failed to deploy successfully beyond 256 meters. The satellite was retrieved successfully and was returned on August 6, 1992. The National Aeronautics and Space Administration (NASA) Associate Administrator for Space Flight formed the Tethered Satellite System (TSS-1) Contingency Investigation Board on August 12, 1992. The TSS-1 Contingency Investigation Board was asked to review the anomalies which occurred, to determine the probable cause, and to recommend corrective measures to prevent recurrence. The board was supported by the TSS Systems Working group as identified in MSFC-TSS-11-90, 'Tethered Satellite System (TSS) Contingency Plan'. The board identified five anomalies for investigation: initial failure to retract the U2 umbilical; initial failure to flyaway; unplanned tether deployment stop at 179 meters; unplanned tether deployment stop at 256 meters; and failure to move tether in either direction at 224 meters. Initial observations of the returned flight hardware revealed evidence of mechanical interference by a bolt with the level wind mechanism travel as well as a helical shaped wrap of tether which indicated that the tether had been unwound from the reel beyond the travel by the level wind mechanism. Examination of the detailed mission events from flight data and mission logs related to the initial failure to flyaway and the failure to move in either direction at 224 meters, together with known preflight concerns regarding slack tether, focused the assessment of these anomalies on the upper tether control mechanism. After the second meeting, the board requested the working group to complete and validate a detailed integrated mission sequence to focus the fault tree analysis on a stuck U2 umbilical, level wind mechanical interference, and slack tether in upper tether control mechanism and to prepare a detailed plan for hardware inspection, test, and analysis including any appropriate hardware disassembly. Author

N93-25351 Virginia Polytechnic Inst. and State Univ., Blacksburg.

IDENTIFICATION AND CONTROL OF LIGHTLY DAMPED, LARGE SPACE STRUCTURES: AN EXPERIMENTAL EVALUATION Ph.D. Thesis

Joel Lea Berg 1992 292 p

Avail: Univ. Microfilms Order No. DA9237137

This dissertation concentrates on the three principal problems facing experimentalists during their attempts to identify and control lightly damped, large space structures (LSS). The problems are low damping, high modal density, and low natural frequencies of oscillation. They present a blend of difficulties which lead the experimentalist to turn to multiple-input multiple-output (MIMO) identification techniques and high performance compensators. Presented here are two MIMO modal identification techniques: Polyreference, and the Eigensystem Realization Algorithm, as well as two types of compensator-based controllers: Linear Quadratic Gaussian, and Independent Modal Space Control. The various techniques are described in the context of controlling lightly damped LSS. Because the research in this dissertation is primarily applications oriented, problems which experimentalists encounter in the laboratory are addressed as well as the performance of the different identification and control techniques on the test articles. Polyreference and ERA are both shown to perform very well in identifying modal frequencies while overestimating model damping ratios. Simulations show that high modal density combined with noisy data results in standard deviations that increase linearly with respect to mode separation. Pseudo-Inverse IMSC is shown to be robust with respect to system uncertainties. Block Independent Control is shown to possess minor coupling between blocks and provides a powerful control approach to overcome actuator bandwidth limitations. Dissert. Abstr.

N93-25463 Surrey Univ., Guildford (England).

NUMERICAL AND EXPERIMENTAL ANALYSES OF LARGE COMPOSITE SKELETAL SATELLITE SYSTEMS Ph.D. Thesis

D. A. C. Sparry 1992 287 p

Avail: Univ. Microfilms Order No. BRDX98135

The world's ever increasing demand for communication capacity has been the catalyst for the development of a range of next generation satellite reflectors. This new generation of satellites is significantly larger than those currently in orbit. Their dimensions prohibit transportation into space in their operational configuration. The use of deployable tetrahedral trusses for the reflecting surface support structures of a 50 m diameter Land Mobile Communication System is investigated. A deployable structural system was selected ahead of other possible forms, as it satisfied the majority of the criteria of low part count, quick assembly times, and an economical packaging volume thereby minimizing transportation and on-orbit fabrication costs. The composite material examined is formed from a polyethersulphone thermoplastic matrix reinforced with high strength, low modulus carbon fibers, C-PES. The modal characteristics of a series of scaled sub-units of the proposed structure were examined. These units, manufactured from the two types of material considered, C-PES and Perspex, were subjected to a range of excitation functions. The C-PES units were thermally cycled under high vacuum to simulate the space environment. The accelerated thermal cycling of the composite structural units revealed that a shift in resonant frequency occurred, together with some surface cracking which could affect the long term stability of the material. The effects of surface pigmentation on the thermal response were also considered. An algorithm was developed which allows low cost materials to be used to predict the behavior of geometrically similar units manufactured from the composite material. The interaction between the predicted dynamic structural behavior and the electrical performance of the satellite is also addressed and suggests that some form of active control system will be required if the maximum defocus parameter is not to be violated.

Dissert. Abstr.

N93-25470 Stanford Univ., CA.

AN ALTERNATE APPROACH TO SPACE MISSIONS INVOLVING A LONG TETHER Ph.D. Thesis

Ehud Netzer 1992 226 p

Avail: Univ. Microfilms Order No. DA9234138

Uses of tethers for a variety of purposes in space have been investigated extensively for many years. Currently, interest is focused on two NASA missions, TSS-1 and TSS-2, in which, a satellite is to be deployed, by means of a tether, from the Shuttle, and performs a series of experiments. The tethers to be used in TSS-1 and TSS-2 are very long, namely 20 km and 100 km, respectively. Hence, significant problems of dynamics and control arise in connection with all mission phases, and it is not yet clear that all of these problems possess satisfactory solutions. This must be a source of concern, given the fact that TSS-1 and TSS-2 are manned missions involving the very valuable Shuttle. It is the purpose of this dissertation to propose alternative means to accomplish the goals of missions such as those of TSS-1 and TSS-2, a way that involves the Shuttle and astronauts either minimally or not at all. Stated most simply, the proposal is this: replace the Shuttle with an unmanned spacecraft. Although this idea was mentioned in early papers on tethered systems, its feasibility remained to be investigated. A comprehensive study of such a system is the topic of the present dissertation. The system is composed of a primary satellite, a tether, and a secondary satellite. The primary satellite carries scientific instruments, whereas the secondary one is equipped with a set of thrusters for purposes of control. First, a 3D model, in which the tether is represented by two segments, is analyzed. Thereafter, multi-segment

models for the tether are considered; only part of the system states are measured, and the other states are estimated by means of a reduced order estimator. To optimize the deployment and retrieval phases, a multi-controller, MATLAB based algorithm, is employed. The result is improved performance and a significant reduction in fuel consumption. Finally, to use electrodynamic forces for orbit transfer without exciting tether bending motions, the notion of synchronized impulses, that is, running electric current through the tether at pre-calculated instants and amplitudes, is presented. Dissert. Abstr.

N93-25494# Lawrence Livermore National Lab., CA.
EXPERIMENTAL MODAL SURVEY OF THE PROBE MASS MOCK-UP
P. A. Manning and T. G. Woehrle Jul. 1992 42 p
(Contract W-7405-eng-48)
(DE93-008846; UCRL-ID-112191) Avail: CASI HC A03/MF A01

The Lawrence Livermore National Laboratory is engaged in a technology development project which includes designing a lightweight, autonomous, highly maneuverable space vehicle, commonly referred to as a probe. The current probe design includes a guidance and control system that requires complete information on the dynamic response of the probe during operation. A finite element model of the probe was constructed to provide analytical information on the dynamic response to specific operational inputs. In order to verify the assumptions made in the model, a mass mock-up of the probe was constructed at LLNL and an experimental modal survey was performed to determine the frequencies, damping values and deflection shapes for each natural mode of the mock-up. The experimental modal parameters were compared with the parameters obtained through modal analysis of the finite element model to provide a measure of the correlation between the model and the actual structure. This report describes the experimental modal testing and analysis of the mass mock-up and compares the experimental results with the finite element results. DOE

N93-25525 Cranfield Inst. of Tech., Bedford (England).
THE DYNAMICS AND CONTROL OF LARGE FLEXIBLE ASYMMETRIC SPACECRAFT Ph.D. Thesis
T. T. Humphries 1991 273 p
Avail: Univ. Microfilms Order No. BRDX97972

This thesis develops the equations of motion for a large flexible asymmetric Earth observation satellite and finds the characteristics of its motion under the influence of control forces. The mathematical model of the structure is produced using analytical methods. The equations of motion are formed using an expanded momentum technique which accounts for translational motion of the spacecraft hub and employs orthogonality relations between appendage and vehicle modes. The controllability and observability conditions of the full spacecraft motions using force and torque actuators are defined. A three axis reaction wheel control system is implemented for both slewing the spacecraft and controlling its resulting motions. From minor slew results it is shown that the lowest frequency elastic mode of the spacecraft is more important than higher frequency modes, when considering the effects of elastic motion on instrument pointing from the hub. Minor slews of the spacecraft configurations considered produce elastic deflections resulting in rotational attitude motions large enough to contravene pointing accuracy requirements of instruments aboard the spacecraft hub. Active vibration damping is required to reduce these hub motions to acceptable bounds in sufficiently small time. A comparison between hub mounted collocated and hub/appendage mounted non-collocated control systems verifies that provided the non-collocated system is stable, it can more effectively damp elastic modes whilst maintaining adequate damping of rigid modes. Analysis undertaken shows that the reaction wheel controller could be replaced by a thruster control system which decouples the modes of the spacecraft motion, enabling them to be individually damped.
Dissert. Abstr.

N93-25527 Auburn Univ., AL.
NONLINEAR STABILITY ANALYSIS OF THE ATTITUDE MOTION OF SPIN-STABILIZED THRUSTING SPACECRAFT Ph.D. Thesis
Ja Young Kang 1992 154 p
Avail: Univ. Microfilms Order No. DA9237189

The attitude dynamics of a class of spin-stabilized, thrusting, upperstage spacecraft is examined. Certain spacecraft in the class has been observed to develop oscillations about their transverse axes which increase exponentially in magnitude by the time the solid propellant motor burns out. After burnout, the oscillations stabilize with approximately constant amplitudes. The basic model for examination consists of a rigid body, representing the spacecraft main body; and a point-mass spherical pendulum, representing a deposit of 'slag' formed as a by-product of the combustion of the solid propellant. Exact nonlinear equations of motion for the model are derived. Approximate nonlinear equations are obtained from these, by assuming that the mass of the slag deposit is much less than the total mass of the system. By applying certain additional restrictions, the coupled, approximate nonlinear equations are further simplified, and approximate near-resonant solutions are obtained by using the method of multiple scales. The results show that the slosh resonances caused by parametric and external type excitations due to the main body may occur. However, since the present system is a time-varying, nonstationary, nonlinear system, this study emphasizes the use of numerical methods based on using the exact nonlinear equations and real flight parameters of the WESTAR 4 spacecraft. Various slag disturbance models are used in the basic model. These include models of the effects of slag mass discharge, solidification, and viscosity. Attitude motions that result from numerical experiments performed using these slag models are very similar to observed motions of typical spin-stabilized upper stages. The best results are obtained by using the model in which a part of the slag mass is discharged through the nozzle near burnout time. Dissert. Abstr.

N93-25630# Logistics Management Inst., Bethesda, MD.
ESTIMATING SPARES REQUIREMENTS FOR SPACE STATION FREEDOM USING THE M-SPARE MODEL Final Report
Robert C. Kline and Craig C. Sherbrooke Aug. 1992 138 p
(Contract MDA903-90-C-0006)
(AD-A260878; LMI-NS101R1) Avail: CASI HC A07/MF A02

The Logistics Management Institute developed a methodology that estimates the optimal orbital replaceable unit (ORU) spares inventory for NASA's Space Station Freedom. NASA is using this methodology to select a spares inventory that will maximize station availability, i.e., the probability that no critical system is inoperative for lack of an ORU spare over the resupply cycle. It is based upon a marginal analysis approach. Spares are ranked in order of decreasing benefit per cost (the improvement provided to station availability per dollar) and added, in that order, to the inventory until a target resource expenditure or availability is reached. The methodology also develops optimal spares inventories constrained by the spares weight the shuttle can carry, the spares volume the station can store, or a combination of resources. To implement our methodology, we developed the Multiple Spares Prioritization and Availability to Resource Evaluation (M-SPARE) model that operates on a personal computer. M-SPARE presents the maximum availability for an entire range of resource expenditures. The model also converts annual spares requirements over any period of the station's life into funding estimates for the next 9 years. In this guide, we describe the M-SPARE methodology, operation, and analytical capabilities.
DTIC

N93-25726 Drexel Univ., Philadelphia, PA.
NONLINEAR DYNAMICS AND ATTITUDE CONTROL OF ARTICULATED FLEXIBLE SPACE STRUCTURES Ph.D. Thesis
Myung-Jin Baek 1992 177 p
Avail: Univ. Microfilms Order No. DA9305290

The present study is concerned with the development of a unified approach to the modeling and the design of an effective feedback linearizing and stabilizing nonlinear controller for multibody flexible and articulated systems. Modeling and control system design for such systems is of current interest. The principal objectives are to investigate the attitude regulation of rigid and/or flexible articulated multibody structures and to demonstrate how interacting nonlinear behaviors of flexible and articulated systems affect the stability and robustness properties of the controlled system. A systematic method for the formulation of the equations of motion for the nonlinear dynamics of flexible and articulated systems is employed based on a unified serial chain body algorithm, and this algorithm is integrated into Poincare's form of Lagrange's equations to formulate an innovative new approach to modeling of the system. The closed form solution of partial feedback linearization is derived using simple mathematical techniques and PFL compensation is applied as a general approach for the attitude decoupling and stabilization of the system having perfect knowledge of model uncertainties. The performance of a linear stabilizer, constructed on the same decoupling principle of the PFL stabilizer, is compared to that of

PFL stabilizer with respect to attitude decoupling and stabilization. In the presence of model uncertainties, parameter adaptive control method is combined with PFL to enhance stability and robustness properties. Throughout these analyses, it is shown that (1) the developed modeling procedure is an effective tool in constructing feedback linearizing control laws, (2) with the perfect knowledge of parametric uncertainties, PFL controller yields excellent performance with respect to attitude decoupling and stabilization, (3) the domain of attraction of the linear controller applied to nonlinear systems is critically small, and the boundary of stability is explained as a subcritical Hopf bifurcation, and (4) the equilibrium point of the closed-loop adaptive control system is asymptotically stable, but the domain of attraction of adaptive PFL is limited due to nonlinear effects between flexible and articulated bodies. Dissert. Abstr.

N93-26055* Remtech, Inc., Huntsville, AL.
EXTERNAL TANK AEROTHERMAL DESIGN CRITERIA VERIFICATION Final Report
Sarat C. Praharaj and Anthony J. Saladino 31 Jul. 1991 80 p
(Contract NAS8-38185)
(NASA-CR-192514; NAS 1.26:192514; RTR-227-01) Avail: CASI HC A05/MF A01

If a Space Shuttle Main Engine (SSME) fails during the initial 160 seconds of the Shuttle flight, a return-to-launch-site maneuver will be implemented. The period of concern for this task is the pitch-around maneuver when the vehicle is flying backward. The intent of this report is to identify and define the flowfield at the most critical locations from an environment perspective. The solution procedure used to predict the plume heating rates involves both computational analysis and engineering modeling. Author

N93-26148*# National Aeronautics and Space Administration. Lewis Research Center, Cleveland, OH.
THE INTERACTION OF HIGH VOLTAGE SYSTEMS WITH THE ENVIRONMENTS OF THE MOON AND MARS
G. Barry Hillard and Joseph C. Kolecki Jan. 1993 6 p Presented at the 31st Aerospace Sciences Meeting and Exhibit, Reno, NV, 11-14 Jan. 1993; sponsored by AIAA Previously announced in IAA as A93-24800
(RTOP 506-41-41)
(NASA-TM-106107; E-7756; NAS 1.15:106107; AIAA Paper 93-0704)
Avail: CASI HC A02/MF A01

High voltage systems designed for use on the lunar and Martian surfaces or in orbit will interact with environmental components such as electrically charged dust, low pressure atmospheres, ionospheric plasmas and neutrals, and chemically reactive species. As the Space Exploration Initiative (SEI) advances from the realm of feasibility study to that of conceptual design, guidelines will be required to ensure that these effects are properly accounted for. A first step in providing such guidelines is the prioritization of interactions for each of the space or surface environments that will be encountered. For those issues that are identified as high priority, the state of environmental knowledge, emphasizing essential data, must be determined. This report describes possible means of obtaining such information, including ground tests, modeling and analysis, and flight experiments. The development of computational tools which will enable engineers to simulate and thereby quantify the interactions will be especially considered. Our analysis is drawn from various study and workshop activities undertaken within the last two years. Author

N93-26209*# National Aeronautics and Space Administration. Lewis Research Center, Cleveland, OH.
CONCEPTUAL DESIGN FOR THE SPACE STATION FREEDOM FLUID PHYSICS/DYNAMICS FACILITY
Robert L. Thompson, Ronald J. Chucksa, Terence F. OMalley, and Richard C. Oeftering Apr. 1993 83 p Workshop held in Cleveland, OH, 24-25 Jan. 1990; sponsored by NASA Headquarters OSSA/MSAD Code SN
(RTOP 694-03-03)
(NASA-TM-103663; E-5868; NAS 1.15:103663) Avail: CASI HC A05/MF A01

A study team at NASA's Lewis Research Center has been working on a definition study and conceptual design for a fluid physics and dynamics science facility that will be located in the Space Station Freedom's baseline U.S. Laboratory module. This modular, user-friendly facility, called the Fluid Physics/Dynamics Facility, will be available for use by industry, academic, and government research communities in the late 1990's. The Facility will support research experiments dealing with the study of fluid physics and dynamics phenomena. Because of the lack of gravity-induced convection, research into the mechanisms of fluids in the absence of gravity will help to provide a better understanding of the fundamentals of fluid processes. This document has been prepared as a final version of the handout for reviewers at the Fluid Physics/Dynamics Facility Assessment Workshop held at Lewis on January 24 and 25, 1990. It covers the background, current status, and future activities of the Lewis Project Study Team effort. It is a revised and updated version of a document entitled 'Status Report on the Conceptual Design for the Space Station Fluid Physics/Dynamics Facility', dated January 1990. Author

N93-26215*# National Aeronautics and Space Administration. Lewis Research Center, Cleveland, OH.
PLASMA CURRENT COLLECTION OF Z-93 THERMAL CONTROL PAINT AS MEASURED IN THE LEWIS RESEARCH CENTER'S PLASMA INTERACTION FACILITY
G. Barry Hillard Apr. 1993 14 p
(RTOP 506-41-41)
(NASA-TM-106132; E-7804; NAS 1.15:106132) Avail: CASI HC A03/MF A01

A sample of Z-93 thermal control paint was exposed to a simulated space environment in a plasma chamber. The sample was biased through a series of voltages ranging from -100 volts to +300 volts and electron and ion currents were measured. Currents were found to be in the micro-ampere range indicating that the material remains a reasonably good insulator under plasma conditions. As a second step, the sample was left in the chamber for six days and retested. Collected currents were reduced by from two to five times from the previous values indicating a substantial loss of conductivity. As a final test, the sample was removed, exposed to room conditions for two days, and returned to the chamber. Current measurements showed that the sample had partially recovered the lost conductivity. In addition to presenting these results, this report documents all of the experimental data as well as the statistical analyses performed. Author

N93-26232# Systems Science and Software, La Jolla, CA.
DATA ANALYSIS SUPPORT FOR THE SHUTTLE POTENTIAL AND RETURN ELECTRON EXPERIMENT (SPREE) ON THE TETHERED SATELLITE SYSTEM 1 (TSS-1) FLIGHT
M. J. Mandell, I. Katz, V. A. Davis, and G. A. Jongeward 29 Jun. 1992 94 p
(Contract F19628-90-C-0133)
(AD-A261646; SSS-DTR-92-13437; PL-TR-92-2215; AD-E201419; SR-2)
Avail: CASI HC A05/MF A01

This report describes the second year of a scientific study of the interactions between the first flight of the Tethered Satellite System (TSS-1) and the ionosphere to increase understanding of the structure and current characteristics of high-voltage sheaths in the ionosphere. The investigations described here include an examination of electron collection and presheath structure by a positively biased, conducting sphere in the ionosphere moving at orbital velocity, including the effects of the earth's magnetic field and the current collection capabilities of the TSS-1 subsatellite considering the revised conductivity measurements. DTIC

N93-26295# Naval Postgraduate School, Monterey, CA.
A BIPHASE SHIFT KEYING (BPSK), DIRECT SEQUENCE, SPREAD SPECTRUM MODEM FOR PETITE AMATEUR NAVY SATELLITE (PANSAT) M.S. Thesis
Thomas M. Fritz Dec. 1992 80 p
(AD-A261301) Avail: CASI HC A05/MF A01

The development of a biphase shift keying (BPSK), direct sequence, spread spectrum modem is conducted for the purpose of developing a prototype design to be implemented in Petite Amateur navy Satellite (PANSAT). The design discussion includes the hardware used in the functional realization of a working design. The design itself, encompasses selection of components, and demonstrates through circuit diagrams and waveforms produced that the preliminary operational characteristics of a spread spectrum BPSK modulation scheme for PANSAT have been achieved. Limited performance analysis is conducted through IF loop-back testing

and analyzes the demodulator output waveforms providing the proof of concept for the design. The development of the final version operating at the specified radio frequency (RF) is not conducted. DTIC

N93-26438# Iowa State Univ. of Science and Technology, Ames. Dept. of Mechanical Engineering.
INVESTIGATION OF LIQUID SLOSHING IN SPIN-STABILIZED SATELLITES Final Report, 1 Jul. 1989 - 30 Nov. 1992
Joseph R. Baumgarten, Donald R. Flugrad, and Richard H. Pletcher 31 Jan. 1993 212 p
(Grant AF-AFOSR-0403-89)
(AD-A261671; ISU-ERI-AMES-93113; AFOSR-93-0077TR) Avail: CASI HC A10/MF A03

Several spin-stabilized communication satellites with liquid stores onboard have exhibited unstable nutational motion. Liquid sloshing is suspected as the cause of this undesirable behavior. During an initial three year grant period, a test rig was built and instrumented, a rigid body computer model was developed using a pendulum analogy to simulate the sloshing liquid, and computational fluid dynamics (CFD) methods were used to develop a primitive variable numerical algorithm to describe two and three dimensional liquid sloshing. During the current three year grant period, the test rig and rigid body computer model have been used to study the effect of various physical parameter values on the motion, and stability conditions have been determined. The structural mathematical model has been improved by introduction of finite element techniques to account for elastic deformation of the test rig, and an implicit-explicit numerical approach has been implemented to solve the coupled, nonlinear equations of motion. DTIC

N93-26456# Texas A&M Univ., College Station. Dept. of Aerospace Engineering.
MECHANICS AND CONTROL OF MULTIBODY STRUCTURAL SYSTEMS Final Report, 31 Jul. 1990 - 31 Oct. 1992
John L. Junkins and Andrew J. Kurdila 11 Jan. 1993 282 p
(Contract F49620-89-C-0084)
(AD-A261576; AFOSR-93-0080TR) Avail: CASI HC A13/MF A03

Research into methods for structural dynamical simulations control of large nonlinear notions of multi-body systems is summarized. A new Order N method is introduced which is shown to be a significant advancement for computing motions of nonlinear multi-body systems. A method is introduced for establishing globally stable maneuvers of flexible structures; both analytical and experimental results are presented. A new integration process is established which used the work/energy equation to stabilize the numerical integration of structural system differential equations. DTIC

N93-24692*# National Aeronautics and Space Administration, Washington, DC.
THE INITIAL FLIGHT ANOMALIES OF SKYLAB 1
In its Readings in Systems Engineering 1993 p 181-199 (For primary document see N93-24678 09-31)
Avail: CASI HC A03/MF A03

N93-24693*# National Aeronautics and Space Administration, Washington, DC.
REPORT OF THE SEASAT FAILURE REVIEW BOARD
In its Readings in Systems Engineering 1993 p 201-215 (For primary document see N93-24678 09-31)
Avail: CASI HC A03/MF A03

N93-24695*# Rockwell International Corp., Seal Beach, CA. Guidance, Control, and Navigation Group.
MOMENTUM ACCUMULATION DUE TO SOLAR RADIATION TORQUE, AND REACTION WHEEL SIZING, WITH CONFIGURATION OPTIMIZATION
Hari B. Hablani *In* NASA. Goddard Space Flight Center, Flight Mechanics/Estimation Theory Symposium, 1992 Feb. 1993 p 3-22 (For primary document see N93-24694 09-13)
Copyright Avail: CASI HC A03/MF A04

N93-24696*# Florida Univ., Gainesville. Dept. of Aerospace Engineering, Mechanics, and Engineering Science.
SPACECRAFT DETUMBLING THROUGH ENERGY DISSIPATION
Norman Fitz-Coy and Anindya Chatterjee *In* NASA. Goddard Space Flight Center, Flight Mechanics/Estimation Theory Symposium, 1992 Feb. 1993 p 23-37 (For primary document see N93-24694 09-13)
Copyright Avail: CASI HC A03/MF A04

N93-24717*# National Aeronautics and Space Administration. Goddard Space Flight Center, Greenbelt, MD.
ANALYSIS OF REENTRY INTO THE WHITE SANDS MISSILE RANGE (WSMR) FOR THE LIFESAT MISSION
M. Hametz (Computer Sciences Corp., Lanham, MD.), L. Roszman (Computer Sciences Corp., Lanham, MD.), F. Snow, and J. Cooley *In its* Flight Mechanics/Estimation Theory Symposium, 1992 Feb. 1993 p 337-350 (For primary document see N93-24694 09-13)
(Contract NAS5-31500)
Copyright Avail: CASI HC A03/MF A04

N93-24725*# Lockheed Technical Operations Co., Crofton, MD.
SCATHA MISSION TERMINATION REPORT
Kjell Stakkestad and Richard Fennessey *In* NASA. Goddard Space Flight Center, Flight Mechanics/Estimation Theory Symposium, 1992 Feb. 1993 p 453-469 Prepared for Consolidated Space Test Center, Onizuka AFB, CA (For primary document see N93-24694 09-13)
Copyright Avail: CASI HC A03/MF A04

N93-24734*# National Aeronautics and Space Administration. Goddard Space Flight Center, Greenbelt, MD.
SOLAR ARRAY THERMAL SNAP AND THE CHARACTERISTICS OF ITS EFFECT ON UARS
M. Lambertson (Computer Sciences Corp., Silver Spring, MD.), D. Rohrbaugh (Computer Sciences Corp., Silver Spring, MD.), and J. Garrick *In its* Flight Mechanics/Estimation Theory Symposium, 1992 Feb. 1993 p 575-588 (For primary document see N93-24694 09-13)
(Contract NAS5-31500)
Copyright Avail: CASI HC A03/MF A04

N93-24878*# National Aeronautics and Space Administration. John F. Kennedy Space Center, Cocoa Beach, FL.
APPLICATIONS OF TRIGGERED LIGHTNING TO SPACE VEHICLE OPERATIONS Abstract Only
William Jafferis, Rocco Sanicandro (Boeing Aerospace Co., Cocoa Beach, FL.), John Rompalla (Wisconsin-Stout Univ., Menomonie.), and Richard Wohlman (University of Western Carolina, Cullowhee, NC.) *In* FAA, The 1992 International Aerospace and Ground Conference on Lightning and Static Electricity: Addendum Nov. 1992 1 p (For primary document see N93-24875 09-47)
Copyright Avail: CASI HC A01/MF A03

N93-25971*# National Oceanic and Atmospheric Administration, Camp Springs, MD.
ANOMALOUS EVENT DIAGNOSIS FOR ENVIRONMENTAL SATELLITE SYSTEMS
Bruce H. Ramsay *In* NASA. Goddard Space Flight Center, The 1993 Goddard Conference on Space Applicati ons of Artificial Intelligence 1993 p 107-116 (For primary document see N93-25961 09-63)
Avail: CASI HC A02/MF A03

N93-26064*# Texas Technological Univ., Lubbock. Dept. of Mechanical Engineering.
STUDY OF PLATE-FIN HEAT EXCHANGER AND COLD PLATE FOR THE ACTIVE THERMAL CONTROL SYSTEM OF SPACE STATION Final Report
Ming-C. Chyu *In* NASA. Johnson Space Center, National Aeronautics and Space Administration (NASA)/American Society for Engineering Education (ASEE) Summer Faculty Fellowship Program, 1992, Volume 1 Dec. 1992 15 p (For primary document see N93-26058 09-99)
(Grant NGT-44-005-803)
Avail: CASI HC A03/MF A02

N93-26065*# City Univ. of New York, Bronx. Dept. of Physics.
A PROTOTYPE FOR SIMULATION OF THE SPACE-TO-GROUND ASSEMBLY/CONTINGENCY SYSTEM OF SPACE STATION FREEDOM Final Report
Louis A. DeAcetis *In* NASA. Johnson Space Center, National Aeronautics

and Space Administration (NASA)/American Society for Engineering Education (ASEE) Summer Faculty Fellowship Program, 1992, Volume 1 Dec. 1992 7 p (For primary document see N93-26058 09-99)
(Grant NGT-44-005-803)
Avail: CASI HC A02/MF A02

N93-26080*# Memphis State Univ., TN. Dept. of Electrical Engineering.
SPACELAB, SPACEHAB, AND SPACE STATION FREEDOM PAYLOAD INTERFACE PROJECTS Final Report
Dean Lance Smith *In* NASA. Johnson Space Center, National Aeronautics and Space Administration (NASA)/American Society for Engineering Education (ASEE) Summer Faculty Fellowship Program, 1992, Volume 2 Dec. 1992 5 p (For primary document see N93-26070 09-99)
(Grant NGT-44-005-803)
Avail: CASI HC A01/MF A02

N93-26081*# Cincinnati Univ., OH. Dept. of Aerospace Engineering.
MODEL REDUCTION FOR SPACE STATION FREEDOM Final Report
Trevor Williams *In* NASA. Johnson Space Center, National Aeronautics and Space Administration (NASA)/American Society for Engineering Education (ASEE) Summer Faculty Fellowship Program, 1992, Volume 2 Dec. 1992 p 15 (For primary document see N93-26070 09-99)
(Grant NGT-44-005-803)
Avail: CASI HC A03/MF A02

N93-26408*# Colorado Univ., Boulder. Center for Space Construction.
CONTROLS FOR ORBITAL ASSEMBLY OF LARGE SPACE STRUCTURES
Mark J. Balas, Roger Davidson, Ali A. Gooyabadi, Ralph Quan, Brian Reisenauer, L. Robertson, James Mohl (Ball Aerospace Systems Div., Boulder, CO.), Philip Good (Martin Marietta Corp., Denver, CO.), Loren Vredevoogd, and Jose Galvez et al *In its* Center for Space Construction Third Annual Symposium 1991 36 p (For primary document see N93-26405 09-31)
Avail: CASI HC A03/MF A03

19 SPACECRAFT INSTRUMENTATION

For related information see also *06 Aircraft Instrumentation* and *35 Instrumentation and Photography.*

N93-25317*# Lawrence Livermore National Lab., CA.
HANDBOOK OF ACTUATORS AND EDGE ALIGNMENT SENSORS
D. A. Krulewich Nov. 1992 77 p Sponsored in part by NASA. Marshall Space Flight Center
(Contract W-7405-eng-48)
(NASA-CR-193203; NAS 1.26:193203; UCRL-ID-112606; DE93-007387)
Avail: CASI HC A05/MF A01

This actuator and sensor handbook was developed during a cooperative project between the NASA-Marshall Space Flight Center, the SDI-Directed Energy Program, and Lawrence Livermore National Laboratory (LLNL). The common purpose of the joint effort was to develop precision actuators and sensors for the NASA initiated SpacE Laser ENE-rgy Program (SELENE). The purpose of the SELENE Program is to develop a highly cost effective segmented adaptive optics system for beaming laser power directly to spacecraft in earth orbit. DOE

N93-25474 Oxford Univ. (England).
ASPECTS OF THE DESIGN OF A SATELLITE BORNE INFRA-RED RADIOMETER Ph.D. Thesis
Stephen T. R. Werrett 1991 255 p
Avail: Univ. Microfilms Order No. BRD-97323

In an attempt to address some of the current concerns about changes in the composition of the upper atmosphere, the Upper Atmosphere Research Satellite (UARS) program was undertaken by NASA. The program is outlined and the satellite itself described. The Improved Stratospheric And Mesospheric Sounder (ISAMS) measures, from the UARS, infra-red radiation emitted by the atmosphere with the intention that temperature and the concentrations of important trace gases may be deduced. In order to improve the quality of the measurements it is necessary that the infra-red detectors and some optical components be cooled. At the time when the instrument development started no method of long term cooling to the required temperature of 80 K was available. Stirling cycle coolers were developed and the instrument designed to use them in conjunction with a 200 K radiative cooler. A cooling and support system for the detectors was developed. Low conductivity, all metal, supports are combined with a co-axial thermal conductor arrangement. Measurements were carried out to determine the performance of the detector support and cooling system. Excellent agreement between design calculations and measured performance was demonstrated. Measurements of the behavior of the gas in the Stirling cycle coolers was compared with predictions from mathematical models and this led to improved and repeatable performance. An electronic servo control system was developed for the cooler mechanisms. Performance of the coolers was measured in a thermal vacuum chamber in order to plan for the proper operation of them in the instrument and to be able to predict their performance. Tests were carried out in order to establish confidence in their suitability for a spacecraft installation. The ISAMS instrument requires an on board computer for its interaction with the spacecraft and ultimately its ground controllers. In addition, this system must support the loading and running of measurement sequence control programs. The system is microprocessor based and features data bus based control and data collection. Software for the microprocessor performs the basic data collection and command response tasks and allows for the running of the sequence control programs. A combination of a compiler in a ground computer and an interpreter in the microprocessor permit programs to be written in a high level language designed for this purpose.
Dissert. Abstr.

N93-26248# Amptek, Inc., Bedford, MA.
DETAILED COMPONENT DESIGN FOR A COMPACT ENVIRONMENTAL ANOMALY SENSOR (CEASE)
Alan C. Huber, John O. McGarity, Paul Okun, John A. Pantazis, David Sperry, Hugh Anderson (Science Applications International Corp., Bellevue, WA.), and Douglas Potter (Science Applications International Corp., Bellevue, WA.) 16 Nov. 1992 56 p
(Contract F19628-90-C-0159)
(AD-A261729; PL-TR-92-2307; AD-E201423) Avail: CASI HC A04/MF A01

As the size and sophistication of spacecraft have increased, anomalies in operational performance caused by the interaction of the energetic-particle population and the spacecraft have likewise increased. The Compact Environmental Anomaly Sensor (CEASE) is being developed as a small, low-power device to monitor space weather and provide autonomous warning of conditions that could cause operational anomalies. Based on the sensor-design and trade-off studies for CEASE, a dosimeter set consisting of solid-state detectors behind aluminum absorbers (of several thicknesses) has been chosen. The outputs of the detectors are fed into algorithms that warn of certain anomalies: (1) surface dielectric charging, (2) deep dielectric charging, (3) total radiation dose behind 0.035 g/cm to the 2nd power, (4) total dose behind 0.41 g/cm to the 2nd power, and (5) single event upsets. From seven quantities derived by algorithm processing, eight warning levels (1, 3, 100...3000 x base) are obtained for each of the five anomalies. Level flags can then be selected for a particular application. For such a CEASE instrument, we estimate a volume of 64 in.to the 3rd power (4-inch cube), a weight of 2 pounds, and power dissipation of 2 watts. DTIC

N93-24697*# National Aeronautics and Space Administration. Goddard Space Flight Center, Greenbelt, MD.
THE RESULTS OF THE IN-FLIGHT ATTITUDE SENSOR CALIBRATION FOR THE ARTHUR HOLLY COMPTON GAMMA RAY OBSERVATORY
W. S. Davis (Computer Sciences Corp., Silver Spring, MD.), A. H. Eudell (Computer Sciences Corp., Silver Spring, MD.), L. S. Kulp (Computer Sciences Corp., Silver Spring, MD.), L. A. Lindrose (Computer Sciences Corp., Silver Spring, MD.), and R. R. Harman *In its* Flight Mechanics/Estimation Theory Symposium, 1992 Feb. 1993 p 39-54 (For primary document see N93-24694 09-13)
(Contract NAS5-31500)
Copyright Avail: CASI HC A03/MF A04

N93-24698*# National Aeronautics and Space Administration. Goddard Space Flight Center, Greenbelt, MD.
TESTING OF THE ON-BOARD ATTITUDE DETERMINATION AND CONTROL ALGORITHMS FOR SAMPEX
Jon D. McCullough, Thomas W. Flatley, Debra A. Henretty, F. Landis Markley, and Josephine K. San *In its* Flight Mechanics/Estimation Theory Symposium, 1992 Feb. 1993 p 55-68 (For primary document see N93-24694 09-13)
Copyright Avail: CASI HC A03/MF A04

N93-24699*# Hughes Danbury Optical Systems, Inc., CT.
STAR TRACKER OPERATION IN A HIGH DENSITY PROTON FIELD
Kenneth J. Miklus, Frank Kissh, and David J. Flynn *In* NASA. Goddard Space Flight Center, Flight Mechanics/Estimation Theory Symposium, 1992 Feb. 1993 p 69-81 (For primary document see N93-24694 09-13)
(Contract JPL-957849)
Copyright Avail: CASI HC A03/MF A04

N93-24700*# Computer Sciences Corp., El Segundo, CA.
RESOLUTION OF THE COBE EARTH SENSOR ANOMALY
J. Sedler *In* NASA. Goddard Space Flight Center, Flight Mechanics/Estimation Theory Symposium, 1992 Feb. 1993 p 83-99 (For primary document see N93-24694 09-13)
Copyright Avail: CASI HC A03/MF A04

N93-24710*# Computer Sciences Corp., Lanham, MD.
IMPROVEMENTS IN ERBS ATTITUDE DETERMINATION WITHOUT GYROS
D. Chu, J. Glickman, and E. Harvie *In* NASA. Goddard Space Flight Center, Flight Mechanics/Estimation Theory Symposium, 1992 Feb. 1993 p 227-242 (For primary document see N93-24694 09-13)
(Contract NAS5-31500)
Copyright Avail: CASI HC A03/MF A04

N93-24728*# Wright Lab., Eglin AFB, FL.
MINIATURE OPTICAL WIDE-ANGLE-LENS STARTRACKER (MINI-OWLS)
Rick Miller, Joe E. Coulter (Northrop Corp., Hawthorne, CA.), and Seymour Levine (Northrop Corp., Hawthorne, CA.) *In* NASA. Goddard Space Flight Center, Flight Mechanics/Estimation Theory Symposium, 1992 Feb. 1993 p 499-504 (For primary document see N93-24694 09-13)
Copyright Avail: CASI HC A02/MF A04

N93-24733*# National Aeronautics and Space Administration. Goddard Space Flight Center, Greenbelt, MD.
GODDARD SPACE FLIGHT CENTER (GSFC) FLIGHT DYNAMICS FACILITY (FDF) CALIBRATION OF THE UPPER ATMOSPHERE RESEARCH SATELLITE (UARS) SENSORS
J. Hashmall (Computer Sciences Corp., Lanham, MD.) and J. Garrick *In its* Flight Mechanics/Estimation Theory Symposium, 1992 Feb. 1993 p 565-573 (For primary document see N93-24694 09-13)
(Contract NAS5-31500)
Copyright Avail: CASI HC A02/MF A04

N93-24735*# National Aeronautics and Space Administration. Goddard Space Flight Center, Greenbelt, MD.
UPPER ATMOSPHERE RESEARCH SATELLITE (UARS) ATTITUDE ACCURACY USING COARSE ATTITUDE SENSORS Abstract Only
K. Krack (Computer Sciences Corp., Silver Spring, MD.), D. Foch (Computer Sciences Corp., Silver Spring, MD.), M. Lambertson (Computer Sciences Corp., Silver Spring, MD.), C. Woolsey (Computer Sciences Corp., Silver Spring, MD.), S. Underwood (Computer Sciences Corp., Silver Spring, MD.), C. Woodruff (Computer Sciences Corp., Silver Spring, MD.), and J. Garrick *In its* Flight Mechanics/Estimation Theory Symposium, 1992 Feb. 1993 p 589 (For primary document see N93-24694 09-13)
Copyright Avail: CASI HC A01/MF A04

N93-25027# Frequency Electronics, Inc., Mitchel AFB, NY.
ULTRA STABLE OSCILLATORS FOR SATELLITE APPLICATIONS
John C. Ho *In* ESA, Frequency and Time Forum Jun. 1992 p 297-300 (For primary document see N93-24978 09-70)
Copyright Avail: CASI HC A01/MF A04

N93-25028# Compagnie d'Electronique et de Piezo-Electricite, Argenteuil (France).
PRELIMINARY RESULTS OF A NEWLY DESIGNED MINI-OCXO OSCILLATOR ESPECIALLY DEDICATED TO SPACE APPLICATIONS
Evelyne Gerard and Gerard Wagner *In* ESA, Frequency and Time Forum Jun. 1992 p 301-307 (For primary document see N93-24978 09-70)
Copyright Avail: CASI HC A02/MF A04

N93-26111*# Jet Propulsion Lab., California Inst. of Tech., Pasadena.
GEOMETRIC DISTORTION ANALYSIS OF A WIDE-FIELD ASTROGRAPH
W. M. Owen, Jr. and S. B. Shaklan *In its* The Telecommunications and Data Acquisition Report 15 May 1992 p 87-93 (For primary document see N93-26105 09-32)
(RTOP 310-10-63-92-01)
Avail: CASI HC A02/MF A04

N93-26112*# Jet Propulsion Lab., California Inst. of Tech., Pasadena.
APPLICATIONS OF INERTIAL-SENSOR HIGH-INHERITANCE INSTRUMENTS TO DSN PRECISION ANTENNA POINTING
R. E. Goddard *In its* The Telecommunications and Data Acquisition Report 15 May 1992 p 94-104 (For primary document see N93-26105 09-32)
(RTOP 310-20-65-67-00)
Avail: CASI HC A03/MF A04

20 SPACECRAFT PROPULSION AND POWER

Includes main propulsion systems and components, e.g., rocket engines; and spacecraft auxilliary power sources.

For related information see also *07 Aircraft Propulsion and Power, 28 Propellants and Fuels, 44 Energy Production and Conversion,* and *15 Launch Vehicles and Space Vehicles.*

N93-24740*# National Aeronautics and Space Administration. Lewis Research Center, Cleveland, OH.
NUCLEAR THERMAL PROPULSION TECHNOLOGY: RESULTS OF AN INTERAGENCY PANEL IN FY 1991
John S. Clark, Patrick McDaniel (Phillips Lab., Kirtland AFB, NM.), Steven Howe (Los Alamos National Lab., NM.), Ira Helms (Nuclear Utility Services, Inc., Damascus, MD.), and Marland Stanley (EI International, Inc., Idaho Falls, ID.) Apr. 1993 137 p
(RTOP 593-71-00)
(NASA-TM-105711; E-7099; NAS 1.15:105711) Avail: CASI HC A07/MF A02

NASA LeRC was selected to lead nuclear propulsion technology development for NASA. Also participating in the project are NASA MSFC and JPL. The U.S. Department of Energy will develop nuclear technology and will conduct nuclear component, subsystem, and system testing at appropriate DOE test facilities. NASA program management is the responsibility of NASA/RP. The project includes both nuclear electric propulsion (NEP) and nuclear thermal propulsion (NTP) technology development. This report summarizes the efforts of an interagency panel that evaluated NTP technology in 1991. Other panels were also at work in 1991 on other aspects of nuclear propulsion, and the six panels worked closely together. The charters for the other panels and some of their results are also discussed. Important collaborative efforts with other panels are highlighted. The interagency (NASA/DOE/DOD) NTP Technology Panel worked in 1991 to evaluate nuclear thermal propulsion concepts on a consistent basis. Additionally, the panel worked to continue technology development project planning for a joint project in nuclear propulsion for the Space Exploration Initiative (SEI). Five meetings of the panel were held in 1991 to continue the planning for technology development of nuclear thermal propulsion systems. The state-of-the-art of the NTP technologies was reviewed in some detail. The major technologies identified were as follows: fuels, coatings, and other reactor technologies; materials;

instrumentation, controls, health monitoring and management, and associated technologies; nozzles; and feed system technology, including turbopump assemblies. Author (revised)

N93-24744*# National Aeronautics and Space Administration. Lewis Research Center, Cleveland, OH.

SUMMARY AND RECOMMENDATIONS ON NUCLEAR ELECTRIC PROPULSION TECHNOLOGY FOR THE SPACE EXPLORATION INITIATIVE

Michael P. Doherty and Robert S. Holcomb (Oak Ridge National Lab., TN.) Apr. 1993 120 p

(RTOP 593-72-00)

(NASA-TM-105707; E-7783; NAS 1.15:105707) Avail: CASI HC A06/MF A02

A project in Nuclear Electric Propulsion (NEP) technology is being established to develop the NEP technologies needed for advanced propulsion systems. A paced approach has been suggested which calls for progressive development of NEP component and subsystem level technologies. This approach will lead to major facility testing to achieve TRL-5 for megawatt NEP for SEI mission applications. This approach is designed to validate NEP power and propulsion technologies from kilowatt class to megawatt class ratings. Such a paced approach would have the benefit of achieving the development, testing, and flight of NEP systems in an evolutionary manner. This approach may also have the additional benefit of synergistic application with SEI extraterrestrial surface nuclear power applications. Author (revised)

N93-24753*# National Aeronautics and Space Administration. Lewis Research Center, Cleveland, OH.

SPACE EXPLORATION INITIATIVE CANDIDATE NUCLEAR PROPULSION TEST FACILITIES

Darrell Baldwin (Sverdrup Technology, Inc., Brook Park, OH.) and John S. Clark Apr. 1993 259 p

(RTOP 593-71-00)

(NASA-TM-105710; E-7759; NAS 1.15:105710) Avail: CASI HC A12/MF A03

One-page descriptions for approximately 200 existing government, university, and industry facilities which may be available in the future to support SEI nuclear propulsion technology development and test program requirements are provided. To facilitate use of the information, the candidate facilities are listed both by location (Index L) and by Facility Type (Index FT). The included one-page descriptions provide a brief narrative description of facility capability, suggest potential uses for each facility, and designate a point of contact for additional information that may be needed in the future. The Nuclear Propulsion Office at NASA Lewis presently plans to maintain, expand, and update this information periodically for use by NASA, DOE, and DOD personnel involved in planning various phases of the SEI Nuclear Propulsion Project. Author (revised)

N93-24758*# National Aeronautics and Space Administration. Lewis Research Center, Cleveland, OH.

EXPERIMENTATION IN THE LOW-DENSITY PLUME OF A SIMULATED ELECTROTHERMAL THRUSTER FOR COMPUTER CODE VALIDATION Final Report

Dana L. Meissner (Toledo Univ., OH.) Apr. 1993 86 p

(Grant NAG3-577; RTOP 506-42-31)

(NASA-CR-191112; E-7728; NAS 1.26:191112) Avail: CASI HC A05/MF A01

Pressures and flow angles are measured in the plume of a 20 deg half-angle, conical nozzle in vacuum with Pitot tubes and conical probes. The area of measurement in the plume ranges from the nozzle exit plane to 480 mm axially downstream and from the plume centerline to 60 mm radially. The nozzle has an exit-to-throat area ratio of 100:1 and a throat diameter of 3.2 mm. The nozzle flow exhausts to a vacuum of order 10(exp -2) Pa to simulate a resistojet (an electrothermal rocket of less than 1 N of thrust) operating in space. Experimental data are given for flows of nitrogen at 55 and 68 mg/s, stagnation temperatures between 695 and 921 K, and stagnation pressures ranging from 5600 to 7100 Pa. Data are also given for argon at a rate of 68 mg/s, a stagnation temperature of 648 K, and stagnation pressures of 4500, 4750, and 4770 Pa. Measurements in the nitrogen plume are compared with computational results from a direct-simulation Monte Carlo method. Author (revised)

N93-24943*# Pennsylvania State Univ., University Park. Propulsion Engineering Research Center.

[VIEWGRAPH DESCRIPTION OF PENN STATE'S PROPULSION ENGINEERING RESEARCH CENTER: ACTIVITY HIGHLIGHTS AND FUTURE PLANS] Annual Report

Charles L. Merkle Jan. 1991 75 p Presented at the Annual Review Meeting of the University Space Engineering Research Program, Washington, DC, 22-23 Jan. 1991

(Grant NAGw-1356)

(NASA-CR-192317; NAS 1.26:192317) Avail: CASI HC A04/MF A01

Viewgraphs are presented that describe the progress and status of Penn State's Propulsion Engineering Research Center. The Center was established in Jul. 1988 by a grant from NASA's University Space Engineering Research Centers Program. After two and one-half years of operation, some 16 faculty are participating, and the Center is supporting 39 graduate students plus 18 undergraduates. In reviewing the Center's status, long-term plans and goals are reviewed and then the present status of the Center and the highlights and accomplishments of the past year are summarized. An overview of plans for the upcoming year are presented. Author (revised)

N93-25089*# National Aeronautics and Space Administration. Lewis Research Center, Cleveland, OH.

A NEURAL NETWORK-BASED ESTIMATOR FOR THE MIXTURE RATIO OF THE SPACE SHUTTLE MAIN ENGINE

T. H. Guo and J. Musgrave Nov. 1992 12 p Presented at the Fourth Annual Health Monitoring Conference for Space Propulsion Systems, Cincinnati, OH, 17-18 Nov. 1992; sponsored by Univ. of Cincinnati

(RTOP 582-01-11)

(NASA-TM-106070; E-7675; NAS 1.15:106070) Avail: CASI HC A03/MF A01

In order to properly utilize the available fuel and oxidizer of a liquid propellant rocket engine, the mixture ratio is closed loop controlled during main stage (65 percent - 109 percent power) operation. However, because of the lack of flight-capable instrumentation for measuring mixture ratio, the value of mixture ratio in the control loop is estimated using available sensor measurements such as the combustion chamber pressure and the volumetric flow, and the temperature and pressure at the exit duct on the low pressure fuel pump. This estimation scheme has two limitations. First, the estimation formula is based on an empirical curve fitting which is accurate only within a narrow operating range. Second, the mixture ratio estimate relies on a few sensor measurements and loss of any of these measurements will make the estimate invalid. In this paper, we propose a neural network-based estimator for the mixture ratio of the Space Shuttle Main Engine. The estimator is an extension of a previously developed neural network based sensor failure detection and recovery algorithm (sensor validation). This neural network uses an auto associative structure which utilizes the redundant information of dissimilar sensors to detect inconsistent measurements. Two approaches have been identified for synthesizing mixture ratio from measurement data using a neural network. The first approach uses an auto associative neural network for sensor validation which is modified to include the mixture ratio as an additional output. The second uses a new network for the mixture ratio estimation in addition to the sensor validation network. Although mixture ratio is not directly measured in flight, it is generally available in simulation and in test bed firing data from facility measurements of fuel and oxidizer volumetric flows. The pros and cons of these two approaches will be discussed in terms of robustness to sensor failures and accuracy of the estimate during typical transients using simulation data. Author (revised)

N93-25105*# National Aeronautics and Space Administration. Lewis Research Center, Cleveland, OH.

SPACE NUCLEAR THERMAL PROPULSION TEST FACILITIES SUBPANEL Final Report

George C. Allen (Sandia National Labs., Albuquerque, NM.), John W. Warren (Department of Energy, Washington, DC.), John Martinell (Idaho National Engineering Lab., Idaho Falls.), John S. Clark, and David Perkins (Phillips Lab., Edwards AFB, CA.) Apr. 1993 178 p

(RTOP 593-71-00)

(NASA-TM-105708; E-7781; NAS 1.15:105708) Avail: CASI HC A09/MF A02

On 20 Jul. 1989, in commemoration of the 20th anniversary of the

Apollo 11 lunar landing, President George Bush proclaimed his vision for manned space exploration. He stated, 'First for the coming decade, for the 1990's, Space Station Freedom, the next critical step in our space endeavors. And next, for the new century, back to the Moon. Back to the future. And this time, back to stay. And then, a journey into tomorrow, a journey to another planet, a manned mission to Mars.' On 2 Nov. 1989, the President approved a national space policy reaffirming the long range goal of the civil space program: to 'expand human presence and activity beyond Earth orbit into the solar system.' And on 11 May 1990, he specified the goal of landing Astronauts on Mars by 2019, the 50th anniversary of man's first steps on the Moon. To safely and ever permanently venture beyond near Earth environment as charged by the President, mankind must bring to bear extensive new technologies. These include heavy lift launch capability from Earth to low-Earth orbit, automated space rendezvous and docking of large masses, zero gravity countermeasures, and closed loop life support systems. One technology enhancing, and perhaps enabling, the piloted Mars missions is nuclear propulsion, with great benefits over chemical propulsion. Asserting the potential benefits of nuclear propulsion, NASA has sponsored workshops in Nuclear Electric Propulsion and Nuclear Thermal Propulsion and has initiated a tri-agency planning process to ensure that appropriate resources are engaged to meet this exciting technical challenge. At the core of this planning process, NASA, DOE, and DOD established six Nuclear Propulsion Technical Panels in 1991 to provide groundwork for a possible tri-agency Nuclear Propulsion Program and to address the President's vision by advocating an aggressive program in nuclear propulsion. To this end the Nuclear Electric Propulsion Technology Panel has focused it energies; this final report summarizes its endeavor and conclusions. Author (revised)

N93-25132*# Sverdrup Technology, Inc., Brook Park, OH. Research Center Group.

LASER BEAMED POWER: SATELLITE DEMONSTRATION APPLICATIONS Final Report

Geoffrey A. Landis and Larry H. Westerlund (Satellite Communications Consultants, Rockville, MD.) Aug. 1992 19 p Presented at the 43rd Congress of the International Astronautical Federation, Washington, DC, 28 Aug. - 3 Sep. 1992; sponsored by International Astronautical Federation Previously announced in IAA as A92-57056

(Contract NAS3-25266; RTOP 506-41-11)

(NASA-CR-190793; E-7629; NAS 1.26:190793; IAF-92-0600) Avail: CASI HC A03/MF A01

It is possible to use a ground-based laser to beam light to the solar arrays of orbiting satellites, to a level sufficient to provide all or some of the operating power required. Near-term applications of this technology for providing supplemental power to existing satellites are discussed. Two missions with significant commercial pay-off are supplementing solar power for radiation-degraded arrays and providing satellite power during eclipse for satellites with failed batteries. Author (revised)

N93-25236*# National Aeronautics and Space Administration. Lewis Research Center, Cleveland, OH.

CALCULATIONS OF COMBUSTION RESPONSE PROFILES AND OSCILLATIONS

Richard J. Priem (Priem Consultants, Inc., Cleveland, OH.) and Kevin J. Breisacher Apr. 1993 28 p Presented at the 1st International Symposium on Liquid Rocket Combustion Instability, University Park, PA, 18-20 Jan. 1993; sponsored by Pennsylvania State Univ. Original contains color illustrations

(RTOP 590-21-11)

(NASA-TM-106135; E-7775; NAS 1.15:106135) Avail: CASI HC A03/MF A01; 1 functional color page

The theory and procedures for determining the characteristics of pressure oscillations in rocket engines with prescribed burning rate oscillations are presented. Pressure and velocity oscillations calculated using this procedure are presented for the Space Shuttle Main Engine (SSME) to show the influence of baffles and absorbers on the burning rate oscillations required to achieve neutral stability. Results of calculations to determine local combustion responses using detailed physical models for injection, atomization, and vaporization with gas phase oscillations in baffled and unbaffled SSME combustors are presented. The contributions of the various physical phenomena occurring in a combustor to oscillations in combustion response were determined. Author

N93-25539 Stanford Univ., CA.

THE DESIGN OF A PROPULSION SYSTEM USING VENT GAS FROM A LIQUID HELIUM CRYOGENIC SYSTEM Ph.D. Thesis

Peter J. Wiktor 1992 244 p

Avail: Univ. Microfilms Order No. DA9302338

Two spacecraft, Gravity Probe B (GP-B) and the Satellite Test of the Equivalence Principle (STEP), incorporating on-board liquid helium cryogenic systems are scheduled to fly around the turn of the century. Effective propulsion systems can be implemented for these spacecraft by directing the helium gas which boils off from the cryogenic systems in specific directions through a set of thrusters. Due to extensive development and testing work at Stanford and elsewhere, the ultra low flow rate helium thrusters for such a propulsion system are now considered proven technology. This thesis is concerned with implementing these thrusters into an effective overall propulsion system. Our primary concern is maximizing the forcing capability or control authority of the propulsion system. A worst case analysis of the thruster system is performed. Various techniques are derived to calculate the worst case output or minimum control authority of the thruster system. The techniques are general and apply to any parallel configuration of actuators. They are used in this thesis to design a propulsion system for GP-B which maximizes the minimum control authority and to study redundancy of the GP-B thruster system under a worst case thruster failure. A general thruster controller is derived for a liquid helium propulsion system which can generate desired output forces and at the same time vent the required helium gas needed to cool the cryogenic system. We show how the helium gas vent rate can be controlled to maintain a stable liquid helium supply temperature and pressure. An on-orbit thruster calibration scheme is developed to make sure the correct output force is generated. Using a nonlinear simulation of the spacecraft dynamics, the calibration scheme is shown to calibrate the 108 parameters needed to describe the outputs of a set of 18 thrusters to better than 1 percent accuracy. Finally an on-orbit mass trim control system is derived to reduce the centrifugal force and moment disturbances on the propulsion system due to mass property offsets. Dissert. Abstr.

N93-25665 Princeton Univ., NJ.

ANODE POWER DEPOSITION IN COAXIAL MPD THRUSTERS Ph.D. Thesis

Alec Damian Gallimore 1992 225 p

Avail: Univ. Microfilms Order No. DA9302051

An array of diagnostic techniques was used to study anode phenomena in quasi-steady self-field MPD thrusters operated at power levels between 150 kW and 7 MW with argon and helium propellants. Spatially resolved anode heat flux measurements were made by embedding thermocouples to the inner surface of a hollowed section of the anode. These measurements indicate that at a thruster power level of 1 MW over 40 percent of the input power was deposited into the anode while at 7 MW this fraction decreased to less than 20 percent. The peak measured anode heat flux was approximately 10 kW/sq cm. Electron temperature and anode current densities were measured via Langmuir and magnetic probes, respectively, which with heat flux measurements permitted an estimate of the anode fall to be made. In addition, floating probes, which were used to measure the anode fall, served as a second means of estimating the anode heat flux. Comparison of anode fall data acquired through either method showed excellent agreement. Anode falls varied between 4 and 50 V for both argon and helium propellants. Furthermore, the anode fall was found to correlate well with electron Hall parameters calculated from triple Langmuir and magnetic probe data collected near the anode. Two possible explanations for this result are proposed: the establishment of large electric fields at the anode to maintain current conduction across the strong magnetic fields; anomalous resistivity resulting from the onset of microturbulence in the plasma. To investigate the latter hypothesis, electric field, magnetic field, and current density profiles measured in the vicinity of the anode were incorporated into Ohm's law to estimate electrical conductivity. Results of this analysis show a substantial deviation of the measured conductivity from that calculated with classical formulae. These results imply that anomalous effects are present in the plasma near the anode. In an attempt at reducing the anode fall by decreasing the local electron Hall parameter, a proof-of-concept test was conducted in which thirty six permanent magnets were embedded within an anode to counteract the ambient magnetic field.

The results of this experiment were promising with a reduction of the anode fall of up to 15 V (37 percent) with argon and 20 V (50 percent) with helium. Dissert. Abstr.

N93-25671*# National Aeronautics and Space Administration. Marshall Space Flight Center, Huntsville, AL.

AN IN-DEPTH PROBABILISTIC STUDY OF EXTERNAL TANK ATTACH RING

Frank Pizzano and C. S. Putcha (California State Coll., Fullerton.) Apr. 1993 65 p

(NASA-TM-108403; NAS 1.15:108403) Avail: CASI HC A04/MF A01

This report deals with conducting a probabilistic study of the external tank attach ring (ETA) used as an interface between the external tank attach struts and the solid rocket booster. The ideas were to use probabilistic distributions for material, geometric, and load properties; to calculate probabilistic margins of safety; and then to compare results against the deterministic factors of safety that were used in the actual design process. The report describes how this was done and discusses some of the road blocks and data problems that were encountered during the study and provides some conclusions. A further refinement of this study is being considered for future work which would make more direct use of finite element analysis data coupled with Monte Carlo simulation. The basic conclusion herein indicates that the probabilistic margins of safety for the cases analyzed (by use of existing data) appear to support deterministic results and actually indicate higher reliabilities. Author

N93-25913# Naval Postgraduate School, Monterey, CA.

PARTICLE BEHAVIOR IN SOLID PROPELLANT ROCKET MOTORS AND PLUMES M.S. Thesis

John D. McCrorie, II Dec. 1992 56 p

(AD-A260900) Avail: CASI HC A04/MF A01

The particle size distribution inside the combustion chamber and the changes that occurred across the exhaust nozzle were measured in a subscale solid propellant rocket motor with a 2 percent aluminized end-burning propellant grain and a highly underexpanded nozzle. A combination of diagnostic techniques were used. Size distributions in the exhaust plume were determined by a Single Particle Counter, a Malvern 2600 ensemble particle sizer, and by Scanning Electron Microscope (SEM) examinations of particles collected on a timed exposure impact probe. Size distributions inside the combustion chamber were determined by Malvern 2600 measurements through windows at the nozzle entrance, SEM examinations of particles collected from the nozzle entrance wall, and exhaust plume measurements of a helium quenched motor. It was determined that agglomeration processes dominated in the flow from the center of the combustion chamber up to the nozzle entrance. Particle breakup processes dominated particle behavior from the nozzle entrance, through the nozzle, and into the exhaust. DTIC

N93-26005 Johns Hopkins Univ., Columbia, MD. Chemical Propulsion Information Agency.

THE 29TH JANNAF COMBUSTION SUBCOMMITTEE MEETING, VOLUME 2

Mary T. Gannaway, ed. Oct. 1992 421 p Meeting held in Hampton, VA, 19-23 Oct. 1992; sponsored by the Joint NASA, Army, Navy, Air Force Interagency Propulsion Committee

(Contract N00014-91-C-0001)

(CPIA-Publ-593-Vol-2) Avail: CPIA, 10630 Little Patuxent Pkwy., Suite 202, Columbia, MD 21044-3200 HC

This volume, the second of five volumes, is a collection of 38 unclassified/unlimited papers which were presented at the 29th Joint Army-Navy-NASA-Air Force (JANNAF) Combustion Subcommittee Meeting, 19-23 October 1992, at NASA Langley Research Center, Hampton, Virginia. Specific subjects discussed include combustion phenomena in air breathing, liquid and solid systems, energetic materials in solids, and combustion instability in solid rocket motors. For individual titles, see N93-26006 through N93-26043.

N93-26006* National Aeronautics and Space Administration. Langley Research Center, Hampton, VA.

VISUALIZATION OF A MACH 2 REACTING FLOW USING PLANAR LASER-INDUCED FLUORESCENCE (PLIF) **c09**

R. Jeffrey Balla *In* JHU, 29th JANNAF Combustion Subcommittee Meeting, Volume 2 Oct. 1992 p 1-7 (For primary document see N93-26005 09-20)

Avail: CPIA, 10630 Little Patuxent Pkwy., Suite 202, Columbia, MD 21044-3200 HC

Planar laser-induced fluorescence (PLIF) has been used to study the mixing and combustion processes in a coaxial hydrogen/vitiated air turbulent reacting flow. Objectives of this study include providing qualitative information about: (1) the location of flow constituents; (2) the size, location, and orientation of instantaneous and average flow structures; and (3) the unsteadiness of the flow field. The flow facility consists of an inner fuel jet (I.D.= 2.36 mm) which injects hydrogen (Mach = 1 at 550K) and an outer jet (I.D. = 17.8 mm) which injects vitiated air (Mach = 2 at 1250K). This coaxial arrangement generates a turbulent diffusion flame. The flow field is visualized using a tunable excimer laser operating with XeCl and having a pulse length of 20 nanoseconds. The laser beam is formed into a sheet approximately 12.7 cm high and 0.3 mm thick. Laser-induced fluorescence (LIF) is generated by tuning the laser to 32,441.85 cm(exp -1) which excites the Q1(3) transition in the (0-0) band of the A 2Sigma(+) - X 2Pai system of OH. The fluorescence from all emission lines of the (0-0) band is imaged on an intensified CCD array detector, digitized, and stored for later analysis. Instantaneous images provide insight into the flow field which the average data cannot. Preliminary results indicate the presence of both large and small scale flow features in the instantaneous laser snapshots generated from the OH PLIF. In approximately 5-10 percent of the instantaneous images, the PLIF signal is minimal over a significant fraction of the flow field. Finally, it is observed that OH is present in the vitiated air and is transported over a significant fraction of the flow field. Author

N93-26007 Wright Lab., Wright-Patterson AFB, OH.

STUDIES IN AIR/AIR SUPERSONIC MIXING LAYERS **c02**

D. J. Risha and B. Sekar *In* JHU, 29th JANNAF Combustion Subcommittee Meeting, Volume 2 Oct. 1992 p 9-18 (For primary document see N93-26005 09-20)

Avail: CPIA, 10630 Little Patuxent Pkwy., Suite 202, Columbia, MD 21044-3200 HC

Results for the numerical simulation of a two-dimensional, supersonic, air-to-air shear layer with convective Mach numbers of 0.1 and 0.46 are presented. A two-dimensional Navier-Stokes code (SPARK2D), using a 4th order, cross MacCormack, time-accurate integration scheme is used to numerically solve the flow equations. Two versions of the code are used: (1) direct numerical simulations (DNS), and a two-equation k-epsilon turbulence model. Comparison of the DNS solutions with experimental results shows similar trends in the shear layer growth rate and the statistical parameters (stream wise turbulent intensity, transverse turbulent intensity, kinematic Reynolds stress) but at reduced magnitudes. Comparison of the k-epsilon simulated solutions with experimental results also showed similar trends in the shear layer growth rate and statistical parameters and are moderately comparable in magnitudes. However, all simulated results degrade with increasing convective Mach number. The validity and requirements of the DNS towards simulating a realistic laboratory test is argued in light of the available lessons learned and weighed against the engineering approaches. Author

N93-26008* National Aeronautics and Space Administration. Langley Research Center, Hampton, VA.

WORKSHOP REPORT: A VALIDATION STUDY OF NAVIER-STOKES CODES FOR TRANSVERSE INJECTION INTO A MACH 2 FLOW **c34**

Dean R. Eklund (Analytical Services and Materials, Inc., Hampton, VA.), G. Burton Northam, J. C. McDaniel (Virginia Univ., Charlottesville.), and Cliff Smith (CFD Research Corp., Huntsville, AL.) *In* JHU, 29th JANNAF Combustion Subcommittee Meeting, Volume 2 Oct. 1992 p 19-34 Previously announced as A93-21330 (For primary document see N93-26005 09-20)

Avail: CPIA, 10630 Little Patuxent Pkwy., Suite 202, Columbia, MD 21044-3200 HC

A CFD (Computational Fluid Dynamics) competition was held at the Third Scramjet Combustor Modeling Workshop to assess the current state-of-the-art in CFD codes for the analysis of scram jet combustors. Solutions from six three-dimensional Navier-Stokes codes were compared for the case of staged injection of air behind a step into a Mach 2 flow. This case was investigated experimentally at the University of Virginia and

extensive in-stream data was obtained. Code-to-code comparisons have been made with regard to both accuracy and efficiency. The turbulence models employed in the solutions are believed to be a major source of discrepancy between the six solutions. Author

N93-26009* National Aeronautics and Space Administration. Langley Research Center, Hampton, VA.
THE EFFECT OF ENTRANCE RADIUS AND FILM INJECTION ON WALL HEATING IN SCRAMJET NOZZLES
N. R. Baker (Lockheed Engineering and Sciences Co., Hampton, VA.), G. B. Northam, D. P. Capriotti (Analytical Services and Materials, Inc., Hampton, VA.), and S. D. Stouffer (Virginia Polytechnic Inst. and State Univ., Blacksburg.) *In* JHU, 29th JANNAF Combustion Subcommittee Meeting, Volume 2 Oct. 1992 p 35-46 Previously announced as A93-22505 (For primary document see N93-26005 09-20)
Avail: CPIA, 10630 Little Patuxent Pkwy., Suite 202, Columbia, MD 21044-3200 HC

An experimental study has been performed with a scramjet combustor and nozzle model to determine the effect of nozzle radii on relaminarization, and the effectiveness of film injection in reducing wall heat flux. The nozzle model was installed downstream of a swept-ramp scram jet combustor model, operated at Mach 2.7 with vitiated air, simulating Mach 6-7 flight enthalpies. Results from tests conducted with three nozzle radii, varying in curvature from a sharp Prandtl-Meyer expansion to a radius of two scramjet combustor exit heights, showed little or no effect on the downstream wall heat flux, which is not in agreement with both subsonic and supersonic relaminarization correlations in the available literature. In contrast, film injection upstream of all three radii produced reductions of 70 percent the entire nozzle model heating rate, for the nominal film-to-free stream pressure matched condition. Results from film injection, with and without pressure gradient, but without wall curvature, show that the gradients appear to stabilize the film, with the resulting reductions in wall heat transfer rates apparent far downstream of the point of injection. Author

N93-26010 Naval Postgraduate School, Monterey, CA.
SOLID FUEL SUPERSONIC COMBUSTION **c25**
W. J. Angus, M. A. Witt, D. Laredo, and D. W. Netzer *In* JHU, 29th JANNAF Combustion Subcommittee Meeting, Volume 2 Oct. 1992 p 47-57 (For primary document see N93-26005 09-20)
Avail: CPIA, 10630 Little Patuxent Pkwy., Suite 202, Columbia, MD 21044-3200 HC

A solid fuel scramjet which utilized a combustor made of Plexiglas has been successfully demonstrated. Hot air entered the Plexiglas combustor with a Mach number of 1.5. A small amount of hydrogen gas was injected into a mixed supersonic-subsonic flame stabilization zone at the head-end of the combustor to help sustain combustion. The combustor consisted of a short, constant area section followed by a diverging section. Combustor exit Mach numbers were typically 1.1-1.4 and combustion efficiencies as high as 87 percent have been attained with equivalence ratios between 0.49-0.65. Nozzle exit temperature rake measurements indicated that the rough surface generated in the near thermally choked constant diameter region generated enough mixing to provide high centerline temperatures. However, to date the heat addition and wall friction induced losses have resulted in 50-70 percent losses in stagnation pressure across the combustor. Author

N93-26011 Wright Lab., Wright-Patterson AFB, OH. Special Projects Office.
GASP 1.3 RESULTS FOR THE TRANSVERSE HYDROGEN REACTING JET **c25**
Balu Sekar *In* JHU, 29th JANNAF Combustion Subcommittee Meeting, Volume 2 Oct. 1992 p 59-76 (For primary document see N93-26005 09-20)
Avail: CPIA, 10630 Little Patuxent Pkwy., Suite 202, Columbia, MD 21044-3200 HC

The three-dimensional Navier-Stokes Code, GASP 1.3, was used to predict the air-to-air mixing for a twin jet configuration in a step-type of combustor with transverse injection, air-to-air mixing for an axial injection from a swept-ramp base, and air-H2 mixing and reaction for flow in a step-type of combustor. Turbulence was modeled with an algebraic eddy viscosity model. Chemically reacting flow was modeled with seven species with a seven-reaction mechanism. For the air-to-air mixing, effect of Turbulent Schmidt Number on the predicted mixing revealed that predictions with a Turbulent Schmidt Number of 0.5 compare well with the data. Numerical study of the axial injection from the swept-ramp base also supports this fact. The air-H2 mixing and reacting study included two expansion angles of two degrees and eight degrees at a total temperature of 1500K. The calculations revealed that mixing efficiency is not greatly affected by the increase in the expansion angle, but combustion efficiencies seem to depend on the expansion angle and decreased with the increased expansion angle. For the same mass flow rate of the fuel (for the same phi) and for the same fuel jet area, jet shapes with increased blockage like a square, and a circle in the crosswise plane, appear to yield higher combustion efficiencies, higher temperature and pressure at the end of the studied combustor configuration. Author

N93-26012 Alabama Univ., Huntsville. Dept. of Mechanical Engineering.
TURBULENCE INTERACTING WITH CHEMICAL KINETICS IN AIRBREATHING COMBUSTION OF DUCTED ROCKETS
T. J. Chung and W. S. Yoon *In* JHU, 29th JANNAF Combustion Subcommittee Meeting, Volume 2 Oct. 1992 p 77-90 (For primary document see N93-26005 09-20)
Avail: CPIA, 10630 Little Patuxent Pkwy., Suite 202, Columbia, MD 21044-3200 HC

Physical interactions between turbulence and shock waves are very complex phenomena. If these interactions take place in chemically reacting flows the degree of complexity increases dramatically. Examples of applications may be cited in the area of supersonic combustion, in which the controlled generation of turbulence and/or large scale vortices in the mixing and flame holding zones is crucial for efficient combustion. Equally important, shock waves interacting with turbulence and chemical reactions affect the combustor flowfield resulting in enhanced relaxation and chemical reaction rates. Chemical reactions in turn contribute to dispersion of shock waves and reduction of turbulent kinetic energies. Computational schemes to address these physical phenomena must be capable of resolving various length and time scales. These scales are widely disparate and the most optimum approach is found in explicit/ implicit adjustable schemes for the Navier-Stokes solver. This is accomplished by means of the generalized Taylor-Galerkin (GTG) finite element formulations. Adaptive meshes are used in order to assure efficiency and accuracy of solutions. Various benchmark problems are presented for illustration of the theory and applications. Geometries of ducted rockets, supersonic diffusers, flame holders, and hypersonic inlets are included. Merits of proposed schemes are demonstrated through these example problems. Author

N93-26013 University of Southern California, Los Angeles. Dept. of Mechanical Engineering.
PARTICLE SIZE AS A FACTOR IN AGGLOMERATION IN SLURRY FUELS **c28**
P. Roy Choudhury *In* JHU, 29th JANNAF Combustion Subcommittee Meeting, Volume 2 Oct. 1992 p 91-99 (For primary document see N93-26005 09-20)
Avail: CPIA, 10630 Little Patuxent Pkwy., Suite 202, Columbia, MD 21044-3200 HC

A series of experiments with JP-10 slurries, prepared with inert particles ranging in size from 0.3 to 22 micron, has been performed to study the influence of particle size on particle agglomeration in a slurry fuel. Inert SiC and Al2O3 particles were chosen to avoid the complexities associated with reacting solids. Similarly, slurries were prepared without any chemical additives which could decompose. The choice of non-stabilized slurry with inert particles was made in order not to cloud the issue of particle agglomeration due to secondary reactions. Scanning Electron Microscopic (SEM) studies of the residues from burning and also evaporating droplets suggest that instead of using very small particles (1 micron or smaller), intermediate size particles (approximately 3 microns) should be used in preparing the slurries. Intermediate size particles are affected neither by any interacting forces nor by chemical cementation caused by fuel decomposition at the particle surface. Therefore, the intermediate size particles are expected to minimize particle agglomeration. Author

N93-26014 United Technologies Research Center, East Hartford, CT.
A SUMMARY OF THE JANNAF WORKSHOP ON LIQUID ROCKET ATOMIZATION
D. J. Hautman *In* JHU, 29th JANNAF Combustion Subcommittee Meeting,

Volume 2 Oct. 1992 p 101-107 (For primary document see N93-26005 09-20)
Avail: CPIA, 10630 Little Patuxent Pkwy., Suite 202, Columbia, MD 21044-3200 HC

A JANNAF sponsored workshop, entitled 'Assessment of the Liquid Rocket Atomization Research Activities' was held after the 28th JANNAF Combustion Meeting in San Antonio, Texas. The objective of the workshop was to review current programs in the area of liquid rocket atomization and to identify research areas not being investigated by these programs. As a result of presentations during the JANNAF Combustion Meeting and during the workshop, current programs were reviewed and discussed. Recommendations for additional programs were then made with a level of importance being assigned to each program. The workshop also established a committee to summarize in a single document typical ranges of actual liquid rocket injector operating parameters, non-dimensional parameters, and liquid propellant/simulation properties. Finally, the workshop recommended that a committee be formed to investigate what procedures should be instituted for droplet size/velocity measurement technique calibration. Author

N93-26015 United Technologies Research Center, East Hartford, CT.
MEASUREMENT OF DROPLET VAPORIZATION RATE ENHANCEMENT CAUSED BY ACOUSTIC DISTURBANCES
T. J. Anderson and M. Winter *In* JHU, 29th JANNAF Combustion Subcommittee Meeting, Volume 2 Oct. 1992 p 109-117 (For primary document see N93-26005 09-20)
Avail: CPIA, 10630 Little Patuxent Pkwy., Suite 202, Columbia, MD 21044-3200 HC

Advanced laser diagnostics are being applied to quantify droplet vaporization enhancement in the presence of acoustic fields which can lead to instability in liquid-fueled rockets. While models have been developed to describe the interactions between subcritical droplet vaporization and acoustic fields in the surrounding gases, they have not been verified experimentally. In the super critical environment of a rocket engine combustor, little is understood about how the injected fluid is distributed. Experiments in these areas have been limited because of the lack of diagnostic techniques capable of providing quantitative results. Recently, however, extremely accurate vaporization rate measurements have been performed on droplets in a subcritical environment using morphology-dependent resonances (MDR's) in which fluorescence from an individual droplet provides information about its diameter. Initial measurements on methanol droplets behind a pressure pulse with a pressure ratio of 1.2 indicated that the evaporation rate in the first few microsec after wave passage was extremely high. Subsequent measurements have been made to validate these results using MDR's acquired from similarly-sized droplets using a pulse with a 1.1 pressure ratio. A baseline measurement was also made using a non evaporative fluid under similar Weber and Reynolds number conditions. The MDR technique employed for these measurements is explained and the facilities are described. The evaporation measurement results are shown and the rates observed from different droplet materials and different wave strengths are compared.
Author

N93-26016 Rockwell International Corp., Canoga Park, CA. Rocketdyne Div.
DEVELOPMENT OF A SECOND GENERATION SPRAY COMBUSTION CODE **c25**
Pak-Yan Liang *In* JHU, 29th JANNAF Combustion Subcommittee Meeting, Volume 2 Oct. 1992 p 119-129 (For primary document see N93-26005 09-20)
Avail: CPIA, 10630 Little Patuxent Pkwy., Suite 202, Columbia, MD 21044-3200 HC

Development has been initiated for a new family of multiphase, multispecies rocket spray combustion codes aimed at improving turnaround time over the first generation codes by up to one order of magnitude. Early versions integrate a proven, robust numerical platform with existing physical submodels, but with provision for continuous assimilation of future advanced performance enhancing features carefully designed into the code framework. The basic numerical extensions necessarily are described. Trial runs with one partially completed code version seem to indicate that a five times speed up is readily achievable at least for steady state flow.
Author

N93-26017* National Aeronautics and Space Administration. Marshall Space Flight Center, Huntsville, AL.
EULERIAN-EULERIAN TREATMENT OF TURBULENT DENSE SPRAY COMBUSTION IN A BIPROPELLANT LIQUID ROCKET ENGINE
H. K. Navaz (Physical Research, Inc., Torrance, CA.), A. L. Dang (Physical Research, Inc., Torrance, CA.), and K. W. Gross *In* JHU, 29th JANNAF Combustion Subcommittee Meeting, Volume 2 Oct. 1992 p 131-141 (For primary document see N93-26005 09-20)
Avail: CPIA, 10630 Little Patuxent Pkwy., Suite 202, Columbia, MD 21044-3200 HC

The Liquid Thrust Chamber Performance (LTCP) code is used to analyze the two-phase flow, evaporation and combustion processes in the F-1 engine. This engine uses LOX/RP-I as propellants. Multi-phase flow equations are solved in an Eulerian-Eulerian (E2) framework, and multi-step finite rate chemistry is used for combustion analysis. The discretization scheme is fully implicit and is based on the Total Variation Diminishing (TVD) scheme, which is accurate, robust, very efficient and capable of handling steep gradients and stiff chemistry. Results obtained from the LTCP program have been compared with available performance data.
Author

N93-26018 GenCorp Aerojet, Sacramento, CA. Aerojet Propulsion Div.
A NEW APPROACH TO COOLED COMBUSTION CHAMBERS: THE 40K FORMED PLATELET CHAMBER
David E. Janke and William A. Hayes *In* JHU, 29th JANNAF Combustion Subcommittee Meeting, Volume 2 Oct. 1992 p 143-148 (For primary document see N93-26005 09-20)
Avail: CPIA, 10630 Little Patuxent Pkwy., Suite 202, Columbia, MD 21044-3200 HC

Regeneratively cooled combustion chambers constructed with formed platelet liners have many benefits over chambers with conventionally machined liners. The formed platelet liner offers increased heat transfer efficiency, which can increase cycle life and enhance wall compatibility. A combustion chamber of the 40,000 lb thrust size has been fabricated and tested with a formed platelet liner to demonstrate this superior heat transfer capability. Chamber and liner design and fabrication process are presented in this paper. Author

N93-26019 Jet Propulsion Lab., California Inst. of Tech., Pasadena.
HYBRID ROCKET FUEL COMBUSTION STUDY **c25**
L. D. Strand and N. S. Cohen (Cohen, Norman S. Professional Services, Inc., Redlands, CA.) *In* JHU, 29th JANNAF Combustion Subcommittee Meeting, Volume 2 Oct. 1992 p 149-154 (For primary document see N93-26005 09-20)
Avail: CPIA, 10630 Little Patuxent Pkwy., Suite 202, Columbia, MD 21044-3200 HC

The objectives of this hybrid rocket study are to extend our understanding of the nature of the boundary layer combustion process and the critical engineering parameters that define this process. Tests were carried out with a hybrid slab window motor, using several diagnostic techniques, over a range of motor pressure and oxidizer mass flux using both single and double (opposed) fuel slabs. The results, detailed in the paper, basically confirmed turbulent boundary layer heat and mass transfer as the rate limiting process for hybrid fuel decomposition and combustion. Author

N93-26020 Illinois Univ., Urbana. Dept. of Mechanical and Industrial Engineering.
THERMAL RADIATION IN NON-METALIZED SOLID ROCKET MOTORS: EFFECT ON BURNING RATE AND TEMPERATURE SENSITIVITY
M. Q. Brewster and S. F. Son *In* JHU, 29th JANNAF Combustion Subcommittee Meeting, Volume 2 Oct. 1992 p 155-163 (For primary document see N93-26005 09-20)
Avail: CPIA, 10630 Little Patuxent Pkwy., Suite 202, Columbia, MD 21044-3200 HC

Thermal radiation from combustion gases in non-metalized solid rocket motors is examined using band model calculations. These calculations show that even pure molecular gas radiation (no particles) can reach near black body levels for realistic motor conditions. The effects of thermal radiation on burning rate and temperature sensitivity are also examined. It is shown that differences in burning rate and temperature sensitivity between motors and propellant strands which in the past have primarily been attributed to erosive burning, could in some instances be due to thermal gas radiation.

The implications of gas radiation on combustion stability are also discussed. It is shown that radiative feedback may have either a stabilizing or de-stabilizing effect, according to the temperature dependence of the temperature sensitivity sigma(sub p)(T(sub 0)). Author

N93-26021* Aerojet-General Corp., Iuka, MS.
IMPROVED BURN RATE DETERMINATION TECHNIQUES **c25**
T. J. Watson, F. W. Jordan, L. W. Stockham, and N. Leontsinis *In* JHU, 29th JANNAF Combustion Subcommittee Meeting, Volume 2 Oct. 1992 p 165-174 Sponsored by NASA. Marshall Space Flight Center (For primary document see N93-26005 09-20)
(Contract WE10E3640N)
Avail: CPIA, 10630 Little Patuxent Pkwy., Suite 202, Columbia, MD 21044-3200 HC

This paper reviews historical and industry standard methods of determining solid propellant burn rate. It identifies the advantages and disadvantages of the several methods and points out characteristics which lead to inaccuracy. The paper addresses ways to overcome the shortcomings of the various methods and presents AAD's technique for obtaining burn rate data having coefficients of variations under 0.25 percent, from 5C3-9 motor firings. This value is two to four times smaller than industry standard values. Author

N93-26022* Aerojet-General Corp., Iuka, MS.
ASRM DESIGN PHILOSOPHY AND MODELLING CHALLENGES
M. A. Eagar, F. W. Jordan, and L. W. Stockham *In* JHU, 29th JANNAF Combustion Subcommittee Meeting, Volume 2 Oct. 1992 p 175-183 Sponsored by NASA. Marshall Space Flight Center (For primary document see N93-26005 09-20)
(Contract WE10E3640N)
Avail: CPIA, 10630 Little Patuxent Pkwy., Suite 202, Columbia, MD 21044-3200 HC

The advanced solid rocket motor (ASRM) for the Space Shuttle presents an unusual set of modelling challenges because of its high length to diameter ratio and segmented motor design. In addition, the size of the motor limits the number of development motor firings and demands high confidence in the first time motor prediction to avoid costly motor and tooling re-design. For these reasons a design philosophy has been pursued for the ASRM that minimizes program risk and enhances ballistic confidence. This is accomplished by utilizing state of the art ballistic prediction methodology which incorporates deformed grain modelling, spatial burn rate mapping, erosive burning response, and ballistic/structural/CFD flow-grain interactions. These modelling methods are currently being validated using measured data from other motor programs, where available. Coupling these modelling methods with an aggressive prediction uncertainty assessment also allows early development of contingency plans to minimize risk and provide rapid recovery after the first demonstration motor firing (DM-1) should this become necessary. Application of these methods to the ASRM should produce increased confidence in the DM-1 motor prediction, rapid recovery potential after DM-1, and enhanced potential for program success. Author

N93-26023* Aerojet-General Corp., Iuka, MS.
DETERMINATION OF BURN RATE REQUIREMENTS FROM ASRM PERFORMANCE SPECIFICATIONS **c25**
S. S. Schlueter, F. W. Jordan, and L. W. Stockham *In* JHU, 29th JANNAF Combustion Subcommittee Meeting, Volume 2 Oct. 1992 p 185-191 Sponsored by NASA. Marshall Space Flight Center (For primary document see N93-26005 09-20)
(Contract WE10E3640N)
Avail: CPIA, 10630 Little Patuxent Pkwy., Suite 202, Columbia, MD 21044-3200 HC

There are many performance specifications on a large solid rocket motor which could potentially drive burn rate accuracy requirements. This paper shows the methods used to quantify the allowable burn rate variability for the Advanced Solid Rocket Motor (ASRM). It covers the impact of flight set thrust imbalance on burn rate requirements as well as normal ballistic variability limits. The thrust imbalance restraints are evaluated in terms of both average motor burn rate variations and localized longitudinal burn rate variations. Based on this work, it is recommended that the target value for the allowable mean motor burn rate difference between motors in a flight set be 0.62 percent, and that the localized motor burn rate variability target be a three sigma value of 2 percent. Author

N93-26024 Sandia National Labs., Albuquerque, NM.
HERO RESISTANT SEMICONDUCTOR BRIDGE IGNITER **c35**
R. W. Bickes, Jr., D. Greenway, M. C. Grubelich, W. J. Meyer, J. K. Hartman (SCB Technologies, Inc., Albuquerque, NM.), and C. B. McCampbell (SCB Technologies, Inc., Albuquerque, NM.) *In* JHU, 29th JANNAF Combustion Subcommittee Meeting, Volume 2 Oct. 1992 p 193-196 (For primary document see N93-26005 09-20)
(Contract DE-AC04-76DP-00789)
Avail: CPIA, 10630 Little Patuxent Pkwy., Suite 202, Columbia, MD 21044-3200 HC

The problem of accidental ignition of explosive components when exposed to radio frequency (RF) environments or radiation from other electromagnetic sources is commonly referred to as Hazards of Electromagnetic Radiation to Ordnance (HERO). One illustration of such a HERO problem is the MK 149 Phalanx ammunition, which is sensitive to RF energy over a broad range of frequencies. We have demonstrated that a potential solution to the Phalanx HERO problem consists of a semiconductor bridge (SCB) igniter that incorporates microcircuitry to protect the SCB from the RF environment. Direct RF injection and ground plane tests have demonstrated the resistance of our designs to severe RF environments. Author

N93-26025 Army Research Lab., Aberdeen Proving Ground, MD.
FLAME STRUCTURE STUDIES OF A LEAN, 20 TORR H2/N2O/AR FLAME EMPLOYING MOLECULAR BEAM MASS SPECTROMETRY **c25**
D. C. Dayton, R. C. Sausa, and A. W. Miziolek *In* JHU, 29th JANNAF Combustion Subcommittee Meeting, Volume 2 Oct. 1992 p 197-203 (For primary document see N93-26005 09-20)
Avail: CPIA, 10630 Little Patuxent Pkwy., Suite 202, Columbia, MD 21044-3200 HC

In this paper we report on our continued experimental efforts to investigate the structure of low pressure, burner stabilized H2/N2O/Ar flames. Coated Pt/Pt-Rh(10 percent) thermocouples and molecular beam sampling followed by quadrupole mass spectrometric detection (MB/MS) were employed to obtain temperature and species mole fraction profiles, respectively, in a fuel lean (Phi = 0.64), 20 torr H2/N2O/Ar flame. Species profiles of H2, N2O, N2, H2O, NO, O2, H, O, and OH are compared to profiles generated using a detailed flame kinetic model. The results provide a more stringent test of the detailed chemical flame model and chemical mechanism for the H2/N2O/Ar system which is presently being developed in our laboratory and will be described in a companion paper. Author

N93-26026 Army Research Lab., Aberdeen Proving Ground, MD.
MODELING OF H2/N2O FLAMES **c25**
W. R. Anderson and C. M. Faust *In* JHU, 29th JANNAF Combustion Subcommittee Meeting, Volume 2 Oct. 1992 p 205-213 (For primary document see N93-26005 09-20)
Avail: CPIA, 10630 Little Patuxent Pkwy., Suite 202, Columbia, MD 21044-3200 HC

Efforts have continued in our laboratory to study the detailed chemical structure of gas phase flames related to solid propellant combustion. Our recent research has focused on flames of H2/N2O. The oxidizer in this flame is known to be an important intermediate in the combustion of nitramine and double-base propellants. In a previous study, the reaction mechanism to describe H2/N2O chemistry has been critically reviewed and has been tested for a stoichiometric, low pressure H2/N2O/Ar flame. Agreement between model and experiment is good. However, in order to fully test the mechanism, it must be able to model other flame conditions, as well as other experiments. In this paper this mechanism will be subjected to modeling other literature flame studies at both low and atmospheric pressures of varying stoichiometries. Species profiles as well as flame speed calculations will be presented. Preliminary conclusions regarding the formation of NO and the importance of the reaction N2O + OH = HO2 + N2 are presented. Author

N93-26027 Princeton Univ., NJ. Dept. of Mechanical and Aerospace Engineering.

KINETIC STUDIES IN GAS-PHASE REACTION MECHANISMS IMPORTANT TO THE COMBUSTION PROCESS OF HIGH ENERGY DENSITY MATERIALS: THE H2/NO2 REACTION **c25**

R. A. Yetter, N. Ilincic, F. L. Dryer, M. Allen, and J. Gatto *In* JHU, 29th JANNAF Combustion Subcommittee Meeting, Volume 2 Oct. 1992 p 215-223 (For primary document see N93-26005 09-20)

Avail: CPIA, 10630 Little Patuxent Pkwy., Suite 202, Columbia, MD 21044-3200 HC

Kinetic experiments on mixtures of H2/NO2/N2 were performed in a variable temperature, variable pressure flow reactor over temperature, pressure, and residence time ranges of 694-944K, 1-12 atm, and 20-2000ms, respectively. Initial fuel to oxidizer ratios were varied from 0.4 to 80. Model predictions for the profiles of H2, H2O, NO2, NO, and temperature, obtained from solving the time-dependent kinetics of a detailed reaction mechanism were compared with the experimentally measured profiles. The predicted overall reaction rate was observed to be approximately 2-3 times too fast based on literature rate parameters. Reaction flux and sensitivity analyses were used to identify the rate controlling reactions. Among these reactions, the rate of H2 + NO2 = HONO + H had the largest uncertainty. Adjustment of this rate nearly within its uncertainty limits was found to yield generally good agreement between model and experiment. Author

N93-26028 Army Research Lab., Aberdeen Proving Ground, MD.

DARK ZONE MODELING OF SOLID PROPELLANT FLAMES **c25**

J. A. Vanderhoff, W. R. Anderson, and A. J. Kotlar *In* JHU, 29th JANNAF Combustion Subcommittee Meeting, Volume 2 Oct. 1992 p 225-237 (For primary document see N93-26005 09-20)

Avail: CPIA, 10630 Little Patuxent Pkwy., Suite 202, Columbia, MD 21044-3200 HC

Modeling of the dark zone and onset of the second reaction zone (luminous flame) has been attempted for solid propellant combustion. The model is a homogeneous thermal ignition model (SENKIN) which incorporates detailed chemistry. The chemistry comes from the Miller - Bowman mechanism with other additions and modifications. Sensitivity analyses have been performed on this reaction set and the two most sensitive reactions are not well characterized. This model and reaction set has been tested on experimental data from double base and nitramine propellants. The model can predict times to the onset of a luminous flame that encompass the experimental data for double base propellants. For nitamine propellants the model predicts times slower than what is observed experimentally. However, the experimental data base for the nitramine propellants much less complete than for double base propellants and this may be a dominant factor. Nonetheless, it is clear that more work on both reaction rate measurements and dark zone diagnostics needs to be done in order to develop a fuller understanding of this combustion region. Author

N93-26029 Army Research Lab., Aberdeen Proving Ground, MD.

DETECTION OF ATOMIC OXYGEN AND HYDROGEN IN SOLID PROPELLANT FLAMES AND PYROLYSIS GASES USING MULTIPHOTON LASER-INDUCED FLUORESCENCE **c25**

B. E. Forch *In* JHU, 29th JANNAF Combustion Subcommittee Meeting, Volume 2 Oct. 1992 p 239-248 (For primary document see N93-26005 09-20)

Avail: CPIA, 10630 Little Patuxent Pkwy., Suite 202, Columbia, MD 21044-3200 HC

Atomic oxygen and atomic hydrogen have been detected in solid propellant combustion (JA2) using two-photon laser-induced fluorescence near 225.6 nm and three-photon laser-induced fluorescence near 292 nm respectively. These atoms were also detected in pyrolysis gases generated at the propellant surface from a long-pulse Nd:YAG laser during ignition. Oxygen atom two-photon laser-induced fluorescence has been used as a probe of the ground electronic spin-orbit-split state distributions for temperature measurement. The experimentally determined distributions were fit using computer-generated synthetic spectra to yield a thermodynamic temperature of 600 +/- 70 K in laser-produced pyrolysis gases at the propellant surface and 2600 +/- 320 K in steady-state combustion at atmospheric pressure. Normalized relative intensity profiles for O and H atoms are shown in these environments and laser power dependencies for the processes are reported. Author

N93-26030 Army Research Lab., Aberdeen Proving Ground, MD.

TOMOGRAPHIC ANALYSIS OF SIGHT INFRARED SPECTRA OF LOW PRESSURE FLAMES **c25**

Kevin L. McNesby and Robert A. Fifer *In* JHU, 29th JANNAF Combustion Subcommittee Meeting, Volume 2 Oct. 1992 p 249-262 (For primary document see N93-26005 09-20)

Avail: CPIA, 10630 Little Patuxent Pkwy., Suite 202, Columbia, MD 21044-3200 HC

Line of sight Fourier transform infrared absorption spectra through a 17 torr methane/nitrous oxide flame have been tomographically analyzed using Abel's equations. Relative absorbances for N2O, CH4, CO2, NO, and CO have been mapped for various 'slices' of the flame at different heights in the flame. Results indicate that the region of maximum NO and CO formation occurs prior to the luminous region of the flame. The technique is shown to be useful in obtaining data from systems for which line of sight data may be unusable. Author

N93-26031 Aerodyne Research, Inc., Billerica, MA.

INFRARED FIBER OPTIC DIAGNOSTIC FOR SOLID PROPELLANT COMBUSTION **c25**

J. Wormhoudt and P. L. Kebabian *In* JHU, 29th JANNAF Combustion Subcommittee Meeting, Volume 2 Oct. 1992 p 263-268 (For primary document see N93-26005 09-20)

Avail: CPIA, 10630 Little Patuxent Pkwy., Suite 202, Columbia, MD 21044-3200 HC

We report on a program to develop and demonstrate a diagnostic technique using infrared fiber optics to probe the decomposition processes in burning gun propellant strands. The present experimental configuration involves measuring the absorption through a small gap between two embedded fibers. The gap can be filled with propellant, or left open to fill with gaseous decomposition products. Spectroscopic detection is presently achieved using pairs of band pass filters. The absorption record can be correlated with readings from an embedded thermocouple and with a high resolution video recording of the burn. The goal of this program is to develop a fast-response probe of solid phase processes which can support the development of a predictive modeling capability for gun propellant combustion. Examples of the data for atmospheric pressure burns the experiment is now producing are discussed. A full assessment of the usefulness of this technique will require further observations and analysis. Author

N93-26032 Army Research Lab., Aberdeen Proving Ground, MD.

CONDENSED-PHASE PROCESSES DURING SOLID PROPELLANT COMBUSTION. PART 4: CHEMICAL AND MICROSCOPIC EXAMINATION OF LASER-IRRADIATED PROPELLANT SAMPLES **c25**

M. A. Schroeder, R. A. Beyer, A. Cohen, R. A. Fifer, and R. A. Pesce-Rodriquez *In* JHU, 29th JANNAF Combustion Subcommittee Meeting, Volume 2 Oct. 1992 p 269-281 (For primary document see N93-26005 09-20)

Avail: CPIA, 10630 Little Patuxent Pkwy., Suite 202, Columbia, MD 21044-3200 HC

The surfaces of laser-irradiated gun propellants have been examined by Scanning Electron Microscopic (SEM) and Fourier Transform Infrared (FTIR) microscopy; the results suggest that the laser-irradiated surfaces exhibit chemical and physical changes similar to those exhibited by the burned surfaces of extinguished propellant samples. This is consistent with the idea that the main effect of the laser beam is thermal in nature. Some possible implications of these results for combustion and for the modeling of laser ignition are discussed. Author

N93-26033 Sandia National Labs., Livermore, CA. Combustion Research Facility.

THERMAL DECOMPOSITION OF HMX, MONONITROSO-RDX, TNCHP AND K6 IN THE LIQUID PHASE: RESULTS FROM SIMULTANEOUS THERMOGRAVIMETRY MODULATED BEAM MASS SPECTROMETRY MEASUREMENTS **c28**

Richard Behrens, Jr. and Suryanarayana Bulusu (Army Armament Research and Development Command, Dover, NJ.) *In* JHU, 29th JANNAF Combustion Subcommittee Meeting, Volume 2 Oct. 1992 p 283-293 Supported by U.S. Army Research Office (For primary document see N93-26005 09-20)

Avail: CPIA, 10630 Little Patuxent Pkwy., Suite 202, Columbia, MD 21044-3200 HC

The effects of physical properties and molecular conformation on the thermal decomposition kinetics of several cyclic nitramines are examined and compared to the relatively well characterized decomposition of RDX. The compounds used in the study are: octahydro-1,3,5,7-tetranitro-1,3,5,7-tetrazocine (HMX), hexahydro-1-nitroso-3,5 dinitro-s-triazine (ONDNTA), 1,3,5-trinitro-1,3,5-triazacycloheptane (TNCHP), and 2-oxo-1,3,5-trinitro-1,3,5-triazacyclohexane (K6). The comparisons are based on differences in the identities and temporal behaviors of the products formed during the thermal decomposition of these materials. The decomposition pathways of HMX in the liquid phase are similar to the four parallel decomposition pathways that control the decomposition of RDX in the liquid phase. Similarities and differences between HMX and RDX decomposition are discussed. The products formed during the thermal decomposition of ONDNTA arise from multiple reaction pathways. The mass spectrum of ONDNTA at 20 eV is presented. The identities and temporal behaviors of the ONDNTA decomposition products are discussed. TNCHP is thermally stable in the liquid phase. The decomposition products from TNCHP are formed via multiple reaction pathways. Decomposition through an intermediate that is the mononitroso analogue of TNCHP is observed for TNCHP. However, TNCHP does not form a stable product that is analogous to oxy-s-triazine (OST) formed in RDX or the smaller ring fragments formed in the liquid-phase decomposition of HMX. K6 is less thermally stable and the decomposition mechanism is much simpler than that of RDX, HMX and TNCHP. The thermal decomposition of K6 occurs between 150 and 180 C. The products formed during the decomposition of K6 are mainly CH2O and N2O with minor amounts or HCN, CO, NO, and NO2. Author

N93-26034 Sandia National Labs., Albuquerque, NM.
DEVELOPMENT OF RATE EXPRESSIONS FOR THE THERMAL DECOMPOSITION OF RDX **c28**

K. L. Erickson, R. Behrens, Jr. (Sandia National Labs., Livermore, CA.), and S. Bulusu (Army Armament Research and Development Command, Dover, NJ.) *In* JHU, e 2 Oct. 1992 p 295-305 e 2 p 295-311 Previously announced as N93-22502 (For primary document see N93-26005 09-20)

(Contract DE-AC04-76DP-00789)

Avail: CPIA, 10630 Little Patuxent Pkwy., Suite 202, Columbia, MD 21044-3200 HC

Decomposition and combustion of energetic materials involve processes in both condensed and gas phases. Development of reliable models for design, performance, stability, and hazard analyses requires detailed understanding of the mechanisms for both the initial condensed phase decomposition of the energetic material and the subsequent reaction of the decomposition species to form the ultimate reaction products. Those mechanisms must be described in terms of constitutive rate expressions that can be incorporated into mathematical models. The thermal decomposition of RDX has been studied by Behrens and Bulusu using Simultaneous Thermogravimetric Modulated Beam Mass Spectrometry (STMBMS). Their work provides a basis for developing some of the constitutive rate expressions that are needed in models for design, performance, stability and hazard analyses involving RDX. Behrens and Bulusu have identified four primary reaction pathways that control the liquid-phase decomposition of RDX at temperatures between 200 and 215 C, and one that controls solid-phase decomposition at temperatures below 200 C. Two of the liquid-phase pathways appear to be first order in RDX. Arrhenius parameters for the first-order rate constants were evaluated from data reported by Behrens and Bulusu. Reaction rates extrapolated to temperatures between 370 and 450 C are in good agreement with global reaction rates observed by Trott et al. using high-speed photography and laser-heated thin-film samples. Furthermore, the STMBMS results of Behrens and Bulusu appear to be consistent with condensed-phase infrared results reported by Trott et al. and Erickson et al. Author

N93-26035 Los Alamos National Lab., NM.
CHEMISTRY DURING THE INDUCTION TIME IN HEATED NITRAMINES **c28**

M. M. Stinecipher *In* JHU, 29th JANNAF Combustion Subcommittee Meeting, Volume 2 Oct. 1992 p 307-311 (For primary document see N93-26005 09-20)

(Contract W-7405-eng-36)

Avail: CPIA, 10630 Little Patuxent Pkwy., Suite 202, Columbia, MD 21044-3200 HC

What happens to an energetic material after it is heated, but before it begins to generate energy? Does the mechanism of the rate-limiting reaction of thermal decomposition of an energetic material affect the combustion mechanism? To find answers to such questions, RDX, as a model nitramine and an energetic material of interest to the propellant community, was heated in the isothermal-age mode of the accelerating-rate calorimeter (ARCTM) at a temperature about 20 C lower than its normal decomposition temperature. At the end of a long induction time, the chemical products formed were identified by GC-mass spectrometry. One of the well-known products and catalysts of RDX decomposition is formaldehyde. The purpose of this research was to increase the thermal stability of RDX by lengthening the induction time. The approach was to identify a chemical that would scavenge the formaldehyde formed during the induction time. The scavenger chemical and the new compound formed can not react with RDX, and the formaldehyde must be the only decomposition product that is the catalyst for this approach to work. Chemicals selected from the analytical procedures for analyzing formaldehyde were added to the cell containing RDX. Many of the chemicals chosen reacted with the RDX to shorten the induction time, but one, 2,4-dinitro-phenylhydrazine (DNPH), in small amounts lengthened the induction time by a few hours; however, crash precipitated mixtures gave short induction times. DNPH is under further investigation. A group of ammonium salts were also tested. They gave different results depending on their decomposition temperatures and products. Ammonium sulfate did not shorten the induction time but shortened the acceleratory period between the end of induction time and maximum heating rate. A possible explanation is the formation of hexamine, a product formed from ammonia and formaldehyde. Addition of hexamine to RDX gave rapid decomposition. Author

N93-26036 Naval Air Warfare Center, China Lake, CA. Weapons Div.
ADN PROPELLANT DIFFUSION FLAME STRUCTURE **c25**

Tim Parr and Donna Hanson-Parr *In* JHU, 29th JANNAF Combustion Subcommittee Meeting, Volume 2 Oct. 1992 p 313-327 (For primary document see N93-26005 09-20)

Avail: CPIA, 10630 Little Patuxent Pkwy., Suite 202, Columbia, MD 21044-3200 HC

The diffusion flame structure of sandwich geometry propellants made from ADN with a variety of binders including wax, HTPB, and GAP was studied using Planar Laser Induced Fluorescence (PLIF), emission, and Mie scatter imaging, and emission and LIF spectroscopy. Flame species imaged included CN, NH, CH, NO2, NO (v=0 and v=1), and OH. Diffusion flames between ADN and all binders were clearly evident. Various lamina thicknesses were studied down to a binder layer thickness of 80 micron. Diffusion flame heights were always taller than for comparable AP sandwiches under comparable conditions, sometimes by as much as an order of magnitude. Total flame height decreased with decreasing binder lamina thickness but the dark zone height stayed relatively constant. Ignition delays decreased significantly with increasing binder energy. In comparison to neat HMX flames, ADN/binder sandwich flames were found to be taller, and to contain much less CN radicals, less NO2, more CH, and a different distribution of NO (less towards the surface but significant amounts in the burnt gas region where HMX has essentially none). The dependence of the flame structure on CO2 laser flux was investigated and the flame height did not appear to vary significantly with decreased laser flux. LIF emission spectra were monitored concurrently with PLIF using an Optical Multichannel Analyzer (OMA) which also measured flame chemiluminescence. Mie scatter images showed large apparently liquid droplets directly above the ADN laminae but little or no smoke formation in the combusting regions. Large quantities of smoke were formed only when the ADN smoldered after a test. Author

N93-26037 Pennsylvania State Univ., University Park.
PHYSICAL AND CHEMICAL PROCESSES GOVERNING THE CO2 LASER-INDUCED DEFLAGRATION OF AMMONIUM DINITRAMIDE (ADN) **c28**

B. L. Fetherolf and T. A. Litzinger *In* JHU, 29th JANNAF Combustion Subcommittee Meeting, Volume 2 Oct. 1992 p 329-338 (For primary document see N93-26005 09-20)

(Contract N00014-89-J-1238)
Avail: CPIA, 10630 Little Patuxent Pkwy., Suite 202, Columbia, MD 21044-3200 HC

Experimental studies of the physical and chemical processes governing the CO2 laser-induced deflagration of ammonium dinitramide (ADN) are discussed. Results are presented as a function of pressure (0.1-3.0 atmospheres of argon) and incident laser heat flux (20-300 W/sq cm). Quantitative gaseous species measurements obtained by microprobe sampling and mass spectrometer analysis are presented in the form of spatial and temporal profiles. Both gas-phase temperature profiles and surface temperatures measured with fine-wire thermocouples are given. Visual observations of the laser heating event recorded with a high-magnification video recording system are described in detail. A surface melt layer was observed with tiny gas bubbles in the layer evident at pressures of one atmosphere or lower. A luminous flame was only observed when the pressure was raised to three atmospheres where a quasi-stable name was established. A significant amount of fine pale-white particles, believed to be ammonium nitrate (AN), were evolved from the melt layer when no flame existed but were not observed when a name was established. The pre-flame species measured with the microprobe/mass spectrometer (MPMS) system were, in order of descending mole fraction, H2O, N2O, N2, NO2, NH3, and NO. The flame reactions consumed N2O, NO2, and NH3, generating significant amounts of NO and H2O and smaller amounts of N2 and O2. Several temperature traces are also presented as a function of pressure and incident heat flux. The pre-flame zone temperature increased about 100 K when the pressure was raised from one atmosphere to three atmospheres. A surface temperature of 570-580 K was measured for laser heating at one atmosphere. Sporadic temperature measurements of the quasi-stable name indicated flame temperatures of 1250-1330 K. An enthalpy balance calculation using the measured name products predicted a name temperature of 1275 K. Chemical reactions governing the observed energetic behavior are proposed in an effort to interpret the experimental results in terms of possible mechanisms that depend on specific test conditions.
Author

N93-26038 Naval Surface Warfare Center, Silver Spring, MD.
THERMAL DECOMPOSITION AND STABILIZATION OF AMMONIUM DINITRAMIDE **c28**
T. P. Russell, A. G. Stern, W. M. Koppes, and C. D. Bedford *In* JHU, 29th JANNAF Combustion Subcommittee Meeting, Volume 2 Oct. 1992 p 339-345 (For primary document see N93-26005 09-20)
Avail: CPIA, 10630 Little Patuxent Pkwy., Suite 202, Columbia, MD 21044-3200 HC

This paper describes the thermal properties of ammonium dinitramide (ADN). The investigation of polymorphic phases as a function of temperature, a preliminary ammonium nitrate (AN)/ADN eutectic phase diagram, thermal decomposition, and thermal aging and stabilization of the ADN yield AN (ammonium nitrate) conversion are described.
Author

N93-26039 Pennsylvania State Univ., University Park. Dept. of Mechanical Engineering.
INTERACTIONS OF ACOUSTIC WAVES AND COMBUSTION OF HOMOGENEOUS SOLID PROPELLANTS IN ROCKET MOTORS **c28**
V. Yang and I. S. Tseng *In* JHU, 29th JANNAF Combustion Subcommittee Meeting, Volume 2 Oct. 1992 p 347-358 (For primary document see N93-26005 09-20)
Avail: CPIA, 10630 Little Patuxent Pkwy., Suite 202, Columbia, MD 21044-3200 HC

A comprehensive numerical analysis has been conducted to study the effect of propellant combustion on the acoustic waves in a solid rocket motor. The theoretical model is based on the full conservation equations of mass momentum, energy, and species concentration, with consideration of variable properties and finite-rate chemical kinetics. Turbulence closure is achieved rising a modified k-epsilon two-equation model which takes into account the wall injection effect arising from surface combustion of the propellant. Results indicate that the strong temperature gradient near the propellant surface has a significant effect on the behavior of the acoustic field. The unsteady flow motions may interact intimately with gas-phase chemical reactions when the characteristic time scales of these two mechanisms are closely matched, as evidenced by the large amplitude of temperature fluctuations within the flame zone.
Author

N93-26040 Georgia Inst. of Tech., Atlanta.
EXPERIMENTAL INVESTIGATION OF FLOW TURNING LOSSES IN UNSTABLE ROCKET MOTORS
B. T. Zinn and L. M. Matta *In* JHU, 29th JANNAF Combustion Subcommittee Meeting, Volume 2 Oct. 1992 p 359-368 (For primary document see N93-26005 09-20)
(Grant AF-AFOSR-0160-91)
Avail: CPIA, 10630 Little Patuxent Pkwy., Suite 202, Columbia, MD 21044-3200 HC

This paper describes an experimental investigation of the flow turning loss in solid propellant rocket motors experiencing an axial instability. It is caused by the interaction of the radially directed flow of combustion products that leaves the burning propellant surface with the axial acoustic field. This study utilized an experimental setup designed to simulate the flow conditions near the burning surface of a solid propellant motor in an unstable rocket motor. It consisted of a rectangular duct with a wall mounted injector that supplied a flow into the duct to simulate the flow of combustion products leaving the propellant surface. Acoustic drivers were used to excite acoustic oscillations that simulated an axial instability in the duct. The mean and acoustic velocities as well as the acoustic pressure oscillations were measured throughout a control volume encompassing a region where the flow turning loss was expected to occur. The measured data were then used to evaluate the various terms that appear in an acoustic stability equation, developed earlier under this program, that contains the various loss and gain terms including the flow turning loss. Experiments were performed to determine the effects of the injection and mean flow Mach numbers, the amplitude of the oscillation, and the location of the burner relative to the standing axial acoustic wave upon the magnitude of the flow turning loss in the investigated control volume. The measurements show that the magnitude of the flow turning loss is strongly dependent upon the injection velocity and the location of the injection point relative to the standing acoustic wave, which is in agreement with the predictions of relevant models. Finally, measured data were used to specify the boundary conditions in a previously developed numerical simulation of the experimental setup. The simulation's predictions were found to be in good agreement with the measured flow turning loss.
Author

N93-26041 Naval Air Warfare Center, China Lake, CA. Weapons Div.
FLAME RESPONSE IN OSCILLATORY SOLID PROPELLANT COMBUSTION **c25**
Tim Parr, Donna Hanson-Parr, and Jerry Finlinson *In* JHU, 29th JANNAF Combustion Subcommittee Meeting, Volume 2 Oct. 1992 p 369-374 (For primary document see N93-26005 09-20)
(Contract N00149-0-WX-24043)
Avail: CPiA, 10630 Little Patuxent Pkwy., Suite 202, Columbia, MD 21044-3200 HC

Flame structure for nitramines deflagrating under an oscillatory heat flux were measured as a function of forcing frequency and phase angle in an attempt to validate the quasi-steady state assumption for the gas phase response. For HMX deflagration the flame height response function was found to closely track the burn rate response function so the quasi-steady state assumption appears valid, at least for nitramines.
Author

N93-26042 Illinois Univ., Urbana-Champaign. Department of Mechanical and Industrial Engineering.
AN EXPERIMENTAL AND ANALYTICAL STUDY OF THE UNSTEADY COMBUSTION OF HOMOGENEOUS ENERGETIC SOLIDS USING THE LASER-RECOIL METHOD **c25**
S. F. Son, M. H. Hites, and M. Q. Brewster *In* JHU, 29th JANNAF Combustion Subcommittee Meeting, Volume 2 Oct. 1992 p 375-385 (For primary document see N93-26005 09-20)
(Contract N00014-91-J-1977)
Avail: CPIA, 10630 Little Patuxent Pkwy., Suite 202, Columbia, MD 21044-3200 HC

A theoretical and experimental investigation is being conducted on the unsteady combustion of homogeneous energetic materials under dynamic radiant heating conditions. A newly developed pulsed laser-recoil technique was used to study a fine oxidizer AP-HTPB composite and an M10 propellant. The linear stability analysis of steady burning in the presence of a constant radiant flux is also presented. Steady burning rate and temperature measurements are reported and are used to interpret the unsteady results. Large differences were observed between 5 micron and 25 micron

thermocouple traces. The larger thermocouples were unable to resolve the surface reaction zone. The frequency response of the fine oxidizer AP-HTPB composite exhibited two resonance peaks that are attributed to the thermal layer and the reaction zone for the low and high frequency peaks, respectively. This was verified by the measured time scales of the thermal layer and the surface reaction layer using the 5 micron thermocouples. The location of the surface on the temperature trace was confirmed by using an additional wire of the propellant to measure the current between it and the thermocouple. For this fine oxidizer AP-HTPB composite, at these conditions, the assumption of a quasi-steady surface reaction zone is clearly violated at frequencies as low as 50 Hz. These results illustrate that detailed information can be obtained using the laser recoil method that clarify the important structure of burning solids. These results further suggest that more detailed models that relax the quasi-steady assumption should be developed. Author

N93-26043 Illinois Univ., Urbana-Champaign. Department of Mechanical and Industrial Engineering.

DYNAMIC BURNING RATE MEASUREMENTS OF METALIZED COMPOSITE PROPELLANTS USING THE LASER-RECOIL TECHNIQUE **c25**

M. Q. Brewster, M. H. Hites, and S. F. Son *In* JHU, 29th JANNAF Combustion Subcommittee Meeting, Volume 2 Oct. 1992 p 387-397 Sponsored by Thiokol Corporation (For primary document see N93-26005 09-20)

Avail: CPIA, 10630 Little Patuxent Pkwy., Suite 202, Columbia, MD 21044-3200 HC

The combustion mechanisms of metalized AP/HTPB/Al composite propellants have been investigated using a newly developed pulsed laser-recoil technique to measure dynamic propellant burning rate. The results demonstrate that aluminum has a stronger influence on the combustion of AP/HTPB propellants than is indicated by the small changes observed in the macroscopically steady burning rate or the mean burning rate during macroscopically unsteady combustion. The addition of 18 percent Al in AP/HTPB propellant causes only a 10 percent increase in the mean burning rate at 1 atm pressure but a 300 percent increase in the amplitude of the laser-perturbed fluctuating component of the burning rate at 40 Hz. The prominent resonance observed at 40 Hz does not correspond to the classical thermal conduction-relaxation mechanism but appears to be related to the processes of unsteady accumulation, agglomeration, ignition, and departure of aluminum at the burning surface of the propellant. It was also found that a small quantity (1 percent) of chopped Kevlar fibers effectively damped the 40 Hz resonance and increased the steady burning rate at pressures below 5.4 MPa (800 psia). These observations are attributed to a flame-holding effect of the Kevlar fibers which protrude through the surface of the propellant and anchor the partially premixed, leading edge flame near the propellant surface. Author

N93-26053*# Remtech, Inc., Huntsville, AL.

SRB ENVIRONMENT EVALUATION AND ANALYSIS. VOLUME 1: REDESIGNED SRB FLIGHT HEATING EVALUATION Final Report

William K. Crain Sep. 1991 379 p

(Contract NAS8-37891)

(NASA-CR-192517; NAS 1.26:192517; RTR-213-01-Vol-1) Avail: CASI HC A17/MF A03

Following the Space Shuttle STS-51L disaster on January 28, 1986, a considerable redesign effort was launched on the Solid Rocket Booster. This effort culminated in three instrumented flights, STS-26R, 27R, and 29R, beginning in September of 1989. Aeroheating data were obtained on these flights in the form of pressure, heat flux, and gas temperature probe measurements. These data were analyzed from an ascent and reentry heating point of view. The flight data were verified, compared with historic and theoretical results, and scaled to design. Impact of these results on the current design environment set was assessed and recommendations made. This report documents this effort. Author

N93-26054*# Remtech, Inc., Huntsville, AL.

SRB ENVIRONMENT EVALUATION AND ANALYSIS. VOLUME 3: ASRB PLUME INDUCED ENVIRONMENTS Final Report

R. L. Bender, J. R. Brown, J. E. Reardon, J. Everson, L. W. Coons, C. I. Stuckey, and M. S. Fulton Sep. 1991 31 p

(Contract NAS8-37891)

(NASA-CR-192519; NAS 1.26:192519; RTR-213-01-Vol-3) Avail: CASI HC A03/MF A01

Contract NAS8-37891 was expanded in late 1989 to initiate analysis of Shuttle plume induced environments as a result of the substitution of the Advanced Solid Rocket Booster (ASRB) for the Redesigned Solid Rocket Booster (RSRB). To support this analysis, REMTECH became involved in subscale and full-scale solid rocket motor test programs which further expanded the scope of work. Later contract modifications included additional tasks to produce initial design cycle environments and to specify development flight instrumentation. Volume 3 of the final report describes these analyses and contains a summary of reports resulting from various studies. Author

N93-26056*# Remtech, Inc., Huntsville, AL.

REMTECH SSME NOZZLE DESIGN TPS Final Report

Steven A. Bancroft, Carl D. Engel, and John E. Pond Sep. 1990 114 p

(Contract NAS8-36151)

(NASA-CR-192516; NAS 1.26:192516; RTR-113-03) Avail: CASI HC A06/MF A02

Thermal damage to the Space Shuttle Main Engine (SSME) aft manifold Thermal Protection System (TPS) has been observed for flights STS-8 through STS-13. This damaged area is located on the ME2 and ME3 and extends over a region of approximately one square foot. Total failure or burn-through of the TPS could lead to severe thermal damage of the SSME manifold and loss of an engine nozzle necessitating nozzle replacement causing significant schedule delays and cost increases. Thermal damage to the manifold can be defined as a situation where the manifold temperature becomes greater than 1300 F; thereby causing loss of heat treatment in the nozzle. Results of Orbiter/nozzle wind tunnel tests and Hot Gas Facility tests of the TPS are presented. Aerothermal and thermal analysis models for the SSME aft manifold are discussed along with the flight predictions, design trajectory and design environment. Finally, the TPS design concept and TPS thermal response are addressed. Author

N93-26057*# Remtech, Inc., Huntsville, AL.

SRB ENVIRONMENT EVALUATION AND ANALYSIS. VOLUME 2: RSRB JOINT FILLING TEST/ANALYSIS IMPROVEMENTS Final Report, Sep. 1989 - Sep. 1991

E. C. Knox and G. Hamilton Woods Sep. 1991 81 p

(Contract NAS8-37891)

(NASA-CR-192518; NAS 1.26:192518; RTR-213-01-Vol-2) Avail: CASI HC A05/MF A01

Following the Challenger accident a very comprehensive solid rocket booster (SRB) redesign program was initiated. One objective of the program was to develop expertise at NASA/MSFC in the techniques for analyzing the flow of hot gases in the SRB joints. Several test programs were undertaken to provide a data base of joint performance with manufactured defects in the joints to allow hot gases to fill the joints. This data base was used also to develop the analytical techniques. Some of the test programs were Joint Environment Simulator (JES), Nozzle Joint Environment Simulator (NJES), Transient Pressure Test Article (TPTA), and Seventy-Pound Charge (SPC). In 1988 the TPTA test hardware was moved from the Utah site to MSFC and several RSRM tests were scheduled, to be followed by tests for the ASRM program. REMTECH Inc. supported these activities with pretest estimates of the flow conditions in the test joints, and post-test analysis and evaluation of the measurements. During this support REMTECH identified deficiencies in the gas-measurement instrumentation that existed in the TPTA hardware, made recommendations for its replacement, and identified improvements to the analytical tools used in the test support. Only one test was completed under the TPTA RSRM test program, and those scheduled for the ASRM were rescheduled to a time after the expiration of this contract. The attention of this effort was directed toward improvements in the analytical techniques in preparation for when the ASRM program begins. Author

N93-26149*# National Aeronautics and Space Administration. Lewis Research Center, Cleveland, OH.

PULSED LASER RAYLEIGH SCATTERING DIAGNOSTIC FOR HYDROGEN/OXYGEN ROCKET EXIT PLANE FLOWFIELD VELOCIMETRY

Frank J. Zupanc Jan. 1993 11 p Presented at the 31st Aerospace Sciences Meeting and Exhibit, Reno, NV, 11-14 Jan. 1993; sponsored by

AIAA Previously announced in IAA as A93-25552
(RTOP 506-42-31)
(NASA-TM-106098; E-7739; NAS 1.15:106098; AIAA Paper 93-0805)
Avail: CASI HC A03/MF A01

A Doppler-resolved, pulsed laser Rayleigh scattering diagnostic has been developed to obtain local flowfield velocity measurements at the exit plane of a low thrust hydrogen/oxygen rocket engine operating in a high-altitude test facility. Fiber optic signal collection was employed to obtain the forescatter and backscatter Doppler shifts necessary to resolve the axial and radial velocity components. A radial profile was obtained by traversing the collection probes along the beam path at the nozzle exit. The results are compared with theoretical predictions from a full Navier Stokes model (RK/RPLUS). Significant discrepancies between the measured and predicted axial velocity profiles are observed, in terms of both magnitude and character. Radial velocity measurements exhibit excellent agreement with predictions near the centerline but show some departure off-axis. The discrepancies between theory and experiment are potentially the result of enhanced mixing between the core and fuel-film region beyond that predicted, and/or flow stratification between the hydrogen and oxygen injected into the central core region. Author

N93-26174# Phillips Lab., Edwards AFB, CA.
APPLICATION OF THE SAHA EQUATION TO HIGH TEMPERATURE (GREATER THAN OR EQUAL TO) ROCKET EXHAUST Final Report, period ending Aug. 1992
Robert T. Nachtrieb Nov. 1992 148 p
(AD-A261648; PL-TR-92-3042) Avail: CASI HC A07/MF A02

Using the Saha equations and spectroscopic constants, the computer program in this report calculates the species populations of diatomic molecules, neutrals, ions, and electrons in a plasma. The code considers the equilibrium of a two-element, chemically reacting plasma, by calculating the partition function for each species. By rederiving theoretically, as the JANAF tables do, the thermodynamic properties of a rocket propellant, but using extended excitation levels, the program can estimate (above 6000 K) performance of advanced propulsion concepts. DTIC

N93-26200*# National Aeronautics and Space Administration. Lewis Research Center, Cleveland, OH.
NUCLEAR SAFETY POLICY WORKING GROUP RECOMMENDATIONS ON NUCLEAR PROPULSION SAFETY FOR THE SPACE EXPLORATION INITIATIVE
Albert C. Marshall (Sandia National Labs., Albuquerque, NM.), James H. Lee (Sandia National Labs., Albuquerque, NM.), William H. McCulloch (Sandia National Labs., Albuquerque, NM.), J. Charles Sawyer, Jr., Robert A. Bari (Brookhaven National Lab., Upton, NY.), Hatice S. Cullingford (National Aeronautics and Space Administration. John F. Kennedy Space Center, Cocoa Beach, FL.), Alva C. Hardy (National Aeronautics and Space Administration. John F. Kennedy Space Center, Cocoa Beach, FL.), George F. Niederauer (Los Alamos National Lab., NM.), Kerry Remp, and John W. Rice (Idaho National Engineering Lab., Idaho Falls.) et al Apr. 1993 63 p
(RTOP 593-71-00)
(NASA-TM-105705; E-7782; NAS 1.15:105705) Avail: CASI HC A04/MF A01

An interagency Nuclear Safety Working Group (NSPWG) was chartered to recommend nuclear safety policy, requirements, and guidelines for the Space Exploration Initiative (SEI) nuclear propulsion program. These recommendations, which are contained in this report, should facilitate the implementation of mission planning and conceptual design studies. The NSPWG has recommended a top-level policy to provide the guiding principles for the development and implementation of the SEI nuclear propulsion safety program. In addition, the NSPWG has reviewed safety issues for nuclear propulsion and recommended top-level safety requirements and guidelines to address these issues. These recommendations should be useful for the development of the program's top-level requirements for safety functions (referred to as Safety Functional Requirements). The safety requirements and guidelines address the following topics: reactor start-up, inadvertent criticality, radiological release and exposure, disposal, entry, safeguards, risk/reliability, operational safety, ground testing, and other considerations. Author

N93-26210*# National Aeronautics and Space Administration. Lewis Research Center, Cleveland, OH.
NUCLEAR ELECTRIC PROPULSION FOR PLANETARY SCIENCE MISSIONS: NASA TECHNOLOGY PROGRAM PLANNING
Michael P. Doherty May 1993 8 p Presented at the Tenth Symposium on Space Nuclear Power and Propulsion, Albuquerque, NM, 10-14 Jan. 1993; sponsored by the Univ. of New Mexico and the American Inst. of Physics
(RTOP 593-72-00)
(NASA-TM-106139; E-7820; NAS 1.15:106139) Avail: CASI HC A02/MF A01

This paper presents the status of technology program planning to develop those Nuclear Electric Propulsion technologies needed to meet the advanced propulsion system requirements for planetary science missions in the next century. The technology program planning is based upon technologies with significant development heritage: ion electric propulsion and the SP-100 space nuclear power technologies. Detailed plans are presented for the required ion electric propulsion technology development and demonstration. Closer coordination between space nuclear power and space electric propulsion technology programs is a necessity as technology plans are being further refined in light of NEP concept definition and possible early NEP flight activities. Author

N93-26211*# National Aeronautics and Space Administration. Lewis Research Center, Cleveland, OH.
ON-LINE IMPLEMENTATION OF NONLINEAR PARAMETER ESTIMATION FOR THE SPACE SHUTTLE MAIN ENGINE
Julia H. Buckland (Cincinnati Univ., OH.), Jeffrey L. Musgrave, and Bruce K. Walker (Cincinnati Univ., OH.) Nov. 1992 14 p Presented at the Fourth Annual Health Monitoring Conference for Space Propulsion Systems, Cincinnati, OH, 17-18 Nov. 1992; sponsored by the Space Engineering Center for Health Management Technology
(RTOP 584-03-11)
(NASA-TM-106097; E-7738; NAS 1.15:106097) Avail: CASI HC A03/MF A01

We investigate the performance of a nonlinear estimation scheme applied to the estimation of several parameters in a performance model of the Space Shuttle Main Engine. The nonlinear estimator is based upon the extended Kalman filter which has been augmented to provide estimates of several key performance variables. The estimated parameters are directly related to the efficiency of both the low pressure and high pressure fuel turbopumps. Decreases in the parameter estimates may be interpreted as degradations in turbine and/or pump efficiencies which can be useful measures for an online health monitoring algorithm. This paper extends previous work which has focused on off-line parameter estimation by investigating the filter's on-line potential from a computational standpoint. In addition, we examine the robustness of the algorithm to unmodeled dynamics. The filter uses a reduced-order model of the engine that includes only fuel-side dynamics. The on-line results produced during this study are comparable to off-line results generated previously. The results show that the parameter estimates are sensitive to dynamics not included in the filter model. Off-line results using an extended Kalman filter with a full order engine model to address the robustness problems of the reduced-order model are also presented. Author

N93-26216# Wisconsin Univ., Madison. Engine Research Center.
CENTER FOR ADVANCED PROPULSION SYSTEMS (FELLOWSHIP) Final Report, 1 Sep. 1986 - 30 Nov. 1992
G. L. Borman 31 Aug. 1992 43 p
(Contract DAAL03-86-G-0200)
(AD-A260571; ARO-24625.1-EG-UIF) Avail: CASI HC A03/MF A01

A brief description is given for sixteen fellows that studied at the ERC with the support of this grant. The individual research summaries are followed by a listing of the Ph.D. theses and publications for each fellow. DTIC

N93-26373# Photometrics, Inc., Woburn, MA.
ANALYSIS OF THE IBSS SPECTRA OF SPACE SHUTTLE CONTROL ENGINE EXHAUST
David L. Rall and Irving L. Kofsky 31 May 1992 30 p
(Contract F19628-91-C-0061)

(AD-A261749; PL-TR-92-2174; AD-E201418; SR-1) Avail: CASI HC A03/MF A01

Infrared Background Signature Survey spectra of exhaust gases from attitude controlling liquid-bipropellant thrusters, taken from onboard space shuttle on mission STS-39 in connection with the Orbiter Environment Experiment, are analyzed. The high-resolution multichannel sensor viewed both the expanding combustion products near the engine and through the volume where these high kinetic energy molecules react with atmospheric species. Its segments of data over about half the spectrum range between 2.5 and 17.5 microns showed primarily H2O and CO2 vibrational and rotational radiation, with no other emission features unambiguously identifiable. A comparison with synthetic spectra compiled from HITRAN gave a reasonably close fit to excited-state temperatures, 800-1200K, while the absolute radiances were in some cases below those that would result from the column-concentrations of exhaust species predicted by CONTAM because of collision limiting. These spectral radiances quantify the optical contamination resulting from Shuttle Orbiter's routine reaction control engine firings. DTIC

N93-26425*# Texas A&M Univ., College Station. Space Research Center.

DC-DC POWER CONVERTER RESEARCH FOR ORBITER/STATION POWER EXCHANGE

M. Ehsani May 1993 56 p

(Grant NAG9-431)

(NASA-CR-192939; NAS 1.26:192939) Avail: CASI HC A04/MF A01

This project was to produce innovative DC-DC power converter concepts which are appropriate for the power exchange between the Orbiter and the Space Station Freedom (SSF). The new converters must interface three regulated power buses on SSF, which are at different voltages, with three fuel cell power buses on the Orbiter which can be at different voltages and should be tracked independently. Power exchange is to be bi-directional between the SSF and the Orbiter. The new converters must satisfy the above operational requirements with better weight, volume, efficiency, and reliability than is available from the present conventional technology. Two families of zero current DC-DC converters were developed and successfully adapted to this application. Most of the converters developed are new and are presented. Derived from text

N93-26555*# Los Alamos National Lab., NM.

PRELIMINARY INVESTIGATION OF POWER FLOW AND ELECTRODE PHENOMENA IN A MULTI-MEGAWATT COAXIAL PLASMA THRUSTER Final Report

Kurt Schoenberg (Los Alamos National Lab., NM.), Richard Gerwin (Los Alamos National Lab., NM.), Ivars Henins (Los Alamos National Lab., NM.), Robert Mayo (North Carolina State Univ., Raleigh.), Jay Scheuer (Los Alamos National Lab., NM.), and Glen Nurden (Los Alamos National Lab., NM.) Mar. 1993 59 p

(Contract NAS3-30065; RTOP 506-42-31)

(NASA-CR-191084; E-7628; NAS 1.26:191084) Avail: CASI HC A04/MF A01

This paper summarizes preliminary experimental and theoretical research that was directed towards the study of quasisteady-state power flow in a large, un-optimized, multi-megawatt coaxial plasma thruster. The report addresses large coaxial thruster operation and includes evaluation and interpretation of the experimental results with a view to the development of efficient, steady-state megawatt-class magnetoplasmadynamic (MPD) thrusters. Author (revised)

N93-26557*# GenCorp Aerojet, Sacramento, CA. Propulsion Div.

SPACE TRANSPORTATION BOOSTER ENGINE THRUST CHAMBER TECHNOLOGY, LARGE SCALE INJECTOR Final Report

J. A. Schneider Feb. 1993 456 p Original contains color illustrations

(Contract NAS8-37470)

(NASA-CR-192531; NAS 1.26:192531) Avail: CASI HC A20/MF A04; 1 functional color page

The objective of the Large Scale Injector (LSI) program was to deliver a 21 inch diameter, 600,000 lbf thrust class injector to NASA/MSFC for hot fire testing. The hot fire test program would demonstrate the feasibility and integrity of the full scale injector, including combustion stability, chamber wall compatibility (thermal management), and injector performance. The 21 inch diameter injector was delivered in September of 1991. Author

N93-26561*# National Aeronautics and Space Administration. Lewis Research Center, Cleveland, OH.

MEASUREMENT AND ANALYSIS OF A SMALL NOZZLE PLUME IN VACUUM

P. F. Penko, I. D. Boyd (Eloret Corp., Moffett Field, CA.), D. L. Meissner (Toledo Univ., OH.), and K. J. DeWitt (Toledo Univ., OH.) Apr. 1993 18 p Presented at the 28th Joint Propulsion Conference and Exhibit, Nashville, TN, 6-8 Jul. 1992; sponsored by AIAA, SAE, ASME, and ASEE Previously announced in IAA as A92-48748

(RTOP 506-42-31)

(NASA-TM-106066; E-7383; NAS 1.26:106066; AIAA Paper 92-3108)

Avail: CASI HC A03/MF A01

Pitot pressures and flow angles are measured in the plume of a nozzle flowing nitrogen and exhausting to a vacuum. Total pressures are measured with Pitot tubes sized for specific regions of the plume and flow angles measured with a conical probe. The measurement area for total pressure extends 480 mm (16 exit diameters) downstream of the nozzle exit plane and radially to 60 mm (1.9 exit diameters) off the plume axis. The measurement area for flow angle extends to 160 mm (5 exit diameters) downstream and radially to 60 mm. The measurements are compared to results from a numerical simulation of the flow that is based on kinetic theory and uses the direct-simulation Monte Carlo (DSMC) method. Comparisons of computed results from the DSMC method with measurements of flow angle display good agreement in the far-field of the plume and improve with increasing distance from the exit plane. Pitot pressures computed from the DSMC method are in reasonably good agreement with experimental results over the entire measurement area. Author

N93-24715*# Thomas Jefferson High School, Falls Church, VA.

WHAT IS THE RELATIONSHIP BETWEEN ALTITUDE AND WEIGHT IN A MODEL ROCKET?

Jonathan Betz *In* NASA. Goddard Space Flight Center, Flight Mechanics/Estimation Theory Symposium, 1992 Feb. 1993 p 299-318

(For primary document see N93-24694 09-13)

Copyright Avail: CASI HC A03/MF A04

23 CHEMISTRY AND MATERIALS (GENERAL)

N93-26204*# National Aeronautics and Space Administration. Lewis Research Center, Cleveland, OH.

VICKERS INDENTATION HARDNESS OF STOICHIOMETRIC AND REDUCED SINGLE CRYSTAL TiO2 (RUTILE) FROM 25 TO 800 C

Christopher DellaCorte and Daniel L. Deadmore Apr. 1993 10 p

(RTOP 505-63-1A)

(NASA-TM-105959; E-7464; NAS 1.15:105959) Avail: CASI HC A02/MF A01

The indentation microhardness of stoichiometric and reduced single crystal rutile (TiO2) from 25 to 800 C is presented in this paper. The results serve two main purposes. One is to assess the effect of rutile's stoichiometry on its hardness. The other is to test recently suggested theory on solid lubrication with sub Stoichiometric rutile in an effort to better understand shear controlled phenomenon. Microhardness was measured using a Vickers diamond indentor on both vacuum and hydrogen reduced single crystal rutile from 25 to 800 C. The results indicate that stoichiometry and temperature have a pronounced effect on rutile's hardness. The measured effects lend support to theory on solid lubrication by enhanced crystallographic slip and suggest that solid lubricant materials may be produced by careful atomic level tailoring (stoichiometry control). Author

24 COMPOSITE MATERIALS

Includes physical, chemical, and mechanical properties of laminates and other composite materials.

For ceramic materials see *27 Nonmetallic Materials.*

N93-25071*# National Aeronautics and Space Administration. Lewis Research Center, Cleveland, OH.

STRESS DISTRIBUTION IN COMPOSITE FLATWISE TENSION TEST SPECIMENS

Curtis A. Scott (Ohio Aerospace Inst., Brook Park.) and J. Michael Pereira Mar. 1993 12 p

(RTOP 505-63-1B)

(NASA-TM-106074; E-7683; NAS 1.15:106074) Avail: CASI HC A03/MF A01

A finite element analysis was conducted to determine the stress distribution in typical graphite/epoxy composite flat wise tension (FWT) specimens under normal loading conditions. The purpose of the analysis was to determine the relationship between the applied load and the stress in the sample to evaluate the validity of the test as a means of measuring the out-of-plane strength of a composite laminate. Three different test geometries and three different material lay ups were modeled. In all cases, the out-of-plane component of stress in the test section was found to be uniform, with no stress concentrations, and very close to the nominal applied stress. The stress in the sample was found to be three-dimensional, and the magnitude of in-plane normal and shear stresses varied with the anisotropy of the test specimen. However, in the cases considered here, these components of stress were much smaller than the out-of-plane normal stress. The geometry of the test specimen had little influence on the results. It was concluded that the flat wise tension test provides a good measure of the out-of-plane strength for the representative materials that were studied. Author

N93-25072*# National Aeronautics and Space Administration. Langley Research Center, Hampton, VA.

MONITORING DAMAGE GROWTH IN TITANIUM MATRIX COMPOSITES USING ACOUSTIC EMISSION

J. G. Bakuckas, Jr., W. H. Prosser, and W. S. Johnson Mar. 1993 46 p

(RTOP 763-23-45-85)

(NASA-TM-107742; NAS 1.15:107742) Avail: CASI HC A03/MF A01

The application of the acoustic emission (AE) technique to locate and monitor damage growth in titanium matrix composites (TMC) was investigated. Damage growth was studied using several optical techniques including a long focal length, high magnification microscope system with image acquisition capabilities. Fracture surface examinations were conducted using a scanning electron microscope (SEM). The AE technique was used to locate damage based on the arrival times of AE events between two sensors. Using model specimens exhibiting a dominant failure mechanism, correlations were established between the observed damage growth mechanisms and the AE results in terms of the events amplitude. These correlations were used to monitor the damage growth process in laminates exhibiting multiple modes of damage. Results revealed that the AE technique is a viable and effective tool to monitor damage growth in TMC.

Author (revised)

N93-25234 California Univ., San Diego.

DYNAMIC DEFORMATIONS AND ANALYSIS OF A METAL MATRIX COMPOSITE Ph.D. Thesis

Brad Stewart Altman 1992 174 p

Avail: Univ. Microfilms Order No. DA9303231

Deformation of a model particulate reinforced metal-matrix composite is studied over strain rates ranging from 10(exp -3) to 10(exp 3)/s in compression and 10(exp -3) to 10(exp 2)/s in tension. The material is 2014 aluminum alloy with alumina particulate reinforcement of 10 and 20 volume percent. Tests are also performed on 2014 aluminum to provide a baseline for comparison. Micromechanical models are used to predict material response. All tested specimens are examined via scanning and transmission electron microscopy to characterize the differences in microstructural evolution and failure modes. Dissert. Abstr.

N93-25283 Department of the Navy, Washington, DC.

METHOD FOR PROVIDING EMI/EMP HARDENING AND BREAKDOWN PROTECTION IN COMPOSITE MATERIALS Patent

David S. Dixon, inventor (to Navy) and James V. Masi, inventor (to Navy) 22 Dec. 1992 6 p Filed 20 Jun. 1990

(AD-D015638; US-Patent-5,173,871; US-Patent-Appl-SN-544298) Avail: US Patent and Trademark Office

A method of forming a composite material for EMI/EMP hardening protection that has a predictable EM shielding performance in terms of penetration depth is provided. A base material is doped with a predetermined volume fraction of filler particles such that the base material forms a separating contact region between each pair of adjacent filler particles. An electrical equivalent circuit for a filler particle pair and separating contact region is used to represent electrical properties associated with the filler particle pair and separating contact region. A network equivalent impedance of the base material doped with the filler particles is generated using the electrical equivalent circuit. The network equivalent impedance, dielectric constants of the base material and the filler particles, and the predetermined volume fraction of filler particles are used to predict the EM shielding performance of the base material doped with the filler particles in terms of penetration depth. DTIC

N93-25333 Delaware Univ., Newark.

FRACTURE OF AN ELLIPTICAL INCLUSION AND ITS IMPLICATIONS FOR THE PROPERTIES OF SHORT FIBER COMPOSITES Ph.D. Thesis

Gunay Anlas 1992 147 p

Avail: Univ. Microfilms Order No. DA9301772

A model is developed to analyze the effect of fiber fracture on the elastic properties of short fiber composites. Tensile test specimens were prepared from 26.6 percent, 12.9 percent fiber V(f) samples. The specimens were tested in tension to failure. Fractography and optical metallography performed in the plane of the reinforcement showed fragmentation of fibers which eventually led to overall material failure. To model the fiber failure in an infinite matrix, the problem of crack and elliptical inclusion interaction is solved. The crack in the inclusion is formulated in terms of a distribution of dislocations. The dislocation solution is used as a Green's function and resulting singular integral equations are solved numerically. Stress intensity factors are tabulated for both a crack inside and outside the elastic elliptical inclusion. The specific case of a completely cracked inclusion is solved. The solution of a completely cracked inclusion is then used in a micromechanics model of the damaged composite. The energy dissipated through the opening of the crack in the inclusion is calculated and used in a self consistent method to find the overall effective moduli of the composite. The results are given for the prediction of the effective moduli, E and mu, of the 2-D composite containing cracked fibers which are randomly distributed and oriented. Dissert. Abstr.

N93-25338 Missouri Univ., Rolla.

ANALYSIS OF MATRIX DAMAGE IN UNIDIRECTIONAL COMPOSITES Ph.D. Thesis

V. G. Mukunda 1992 107 p

Avail: Univ. Microfilms Order No. DA9224675

The fracture behavior of composites in the presence of a flaw needs to be studied in order to exploit their vast structural potential. Thus analytical models were developed using shear lag concepts to determine the displacement and stress field in a fiber-reinforced unidirectional composite with various damage configurations. The effect of friction on the initiation and growth of longitudinal matrix damage is studied for center-noticed specimens. A consistent shear lag constitutive relationship is employed to take into account the load carrying capacity of the matrix. The results show that the introduction of friction within the matrix split in the form of a closed crack retards the split growth. Further, this model is employed to study the splitting mechanism in edge-noticed unidirectional composite specimens. The model predictions are shown to agree with the experimental results. Finally, a comparison is made between the classical shear lag model and a consistent shear lag model for different damage configurations. This comparison shows that the classical shear lag model predicts acceptable results if the ratio of Young's modulus of the fiber to the Young's modulus of the matrix is large. However, for composites in which fiber and matrix are comparable, the consistent shear lag formulations yields better results, especially in predicting some of the matrix-dominant failure modes. Dissert. Abstr.

N93-25383# Lawrence Livermore National Lab., CA.
PROCESSING AND MECHANICAL PROPERTIES OF LAMINATED METAL COMPOSITES OF Al/Al-25 VOL. PERCENT SiC AND ULTRAHIGH CARBON STEEL/BRASS
C. K. Syn, D. R. Lesuer, and O. D. Sherby (Stanford Univ., CA.) Jul. 1992 24 p Presented at the First International Conference on the Advanced Synthesis of Engineered Structural Materials, San Francisco, CA, 31 Aug. - 2 Sep. 1992
(Contract W-7405-eng-48)
(DE93-007504; UCRL-JC-111215; CONF-920890-1) Avail: CASI HC A03/MF A01

Al 5182/Al 6061-25 vol. percent SiCp and ultrahigh carbon (1.8 percent C) steel/brass (70 percent Cu-30 percent Zn type) laminates were prepared by press-bonding stacks of alternating layers of the component materials. Press bonding of these materials required consideration of the flow stresses of the component materials and the interlayer friction. Tensile properties and fracture toughness were measured for different processing conditions of surface oxide descaling, layer thickness, and heat treatment. Descaling of the surface oxide prior to the press-bonding was found to eliminate premature delamination along interfaces resulting in an increased yield strength and tensile ductility. Reduction in the layer thickness brought an increase in the tensile ductility for both laminates and a decrease in yield strength and fracture toughness for the Al laminate. The T6 heat treatment on the Al laminate induced a substantial increase in the yield and tensile strength but a decrease in tensile ductility. Fracture surface morphology indicated evidences of local delamination, crack blunting and bridging. Fracture toughness measured in the crack arrester and crack divider orientation showed a substantial enhancement over that of the Al 6061-SiCp or UHCS components. DOE

N93-25501# Arizona State Univ., Tempe.
HIGH RESOLUTION INTERFACE NANOCHEMISTRY AND STRUCTURE
1993 8 p
(Contract DE-FG02-87ER-45305)
(DE93-009750; DOE/ER-45305/T2) Avail: CASI HC A02/MF A01

A summary is given of results on nanospectroscopy etc. during the previous three years, divided into the following subsections: development of methods and instrumentation for interface/boundary chemical analysis, interface and boundary structure in ceramic matrix composites, quantitative composition measurements of thin films and inclusions, theoretical calculations for electron energy loss near edge fine structure and grain boundary structure, and small probe radiation effects in ceramics. Materials studied include SiC whisker-reinforced Si3N4, SiC, Si oxides, Si, Si oxynitride, other ceramics. Methods mentioned include field emission, EELS (electron energy loss spectroscopy), nanospectroscopy, and electron nanoprobe.
DOE

N93-25532 Michigan Univ., Ann Arbor.
THE DAMAGE, REPAIR AND DESIGN OF FIBER COMPOSITE STRUCTURAL MATERIALS Ph.D. Thesis
Fa-De Jack Chu 1992 210 p
Avail: Univ. Microfilms Order No. DA9303716

Three aspects of the repair of fiber reinforced composite materials were examined in this study. First, the in-plane compression damage of four typical fiber composite materials was studied, and different repair strategies were explored. Second, an optimum composite sheet design for least damaged by buckling and easiest to repair was studied. Third, the curing and resulting properties of the inter facial region between an anhydride-cured epoxy adhesive and E-glass fibers/vinyl ester matrix, which is critical to the quality of the repair, was investigated. For none of the four typical fiber composite materials subjected to in-plane compression do all of the load carrying fibers break, and those that do are usually in easily removable layers. Moreover, the behavior of each material was relatively consistent. As a result, a new repair strategy is proposed in which no more of the load-carrying fibers are removed from the damage zone than are broken. For the two laminated materials, a transition in failure mode from tensile to shear was found as the effective gage length of the specimen decreased. This suggests that the composite structure can be designed to relieve the applied load in desired locations and with benign failure modes. In the second part, ten composite materials with different fiber stacking sequences were subjected to in-plane compression. Three failure modes were dominant: shear, delamination buckling, and flexural failure. The volume of damage occurring in the 0 deg - fiber plies decreased and the repair efficiency increased in the sequence: shear, flexural, delamination buckling failure. With respect to the amount of damage and repair strength recovery, it is best to have the composite structure designed to fail in delamination buckling when failure is inevitable. In the third part, model systems were used to simulate the interfacial region between adhesive and adherent. These involved curing the adhesive against a FTIR-ATR plate and against adherent material ground to a fine powder to greatly increase its surface area. The increase in reaction heat and To suggest that there is no interfacial problem for an anhydride-cured epoxy adhesive used with E-glass/vinyl ester composite materials.
Dissert. Abstr.

N93-25541 Michigan State Univ., East Lansing.
DESIGN AND VALIDATION OF OPTIMAL EXPERIMENTS FOR ESTIMATING THERMAL PROPERTIES OF COMPOSITE MATERIALS Ph.D. Thesis
Ramsis Taktak 1992 156 p
Avail: Univ. Microfilms Order No. DA9303056

Composite materials have gained an unprecedented interest in the last twenty years. Their superior strength-to-weight ratios have made them very popular with aerospace, automotive, boat, biomedical, and even the sporting goods industry. The radar-absorbing quality of composite materials, together with their strength-to-weight ratios, make these attractive for military applications. When used in air and space vehicles, composite materials are exposed to harsh thermal loads. An understanding of the thermal behavior of these materials became necessary. The thrust of this work is the estimation of two thermal parameters: thermal conductivity and volumetric heat capacity. There are three main parts to the current research; each part describes a different aspect of estimating these thermal properties. The first part compares two experimental research paradigms pertaining to the effect of the temperature rise on the estimated parameters during transient parameter estimation experiments. The second part of this research relates to optimal experiments. Two one-dimensional experiments for finite and semi-infinite geometries are shown to be superior to some previously published ones. The two experimental parameters of heating time and cooling time are especially of interest for these experiments. An optimal value is obtained for each parameter using a selected optimality criterion. A two-dimensional case is studied following the same methodology. Design curves relating the optimality criterion to the geometry and directional properties of the material of interest are obtained. The analytical results of the optimal experiments pertaining to the finite one-dimensional geometry are verified using an experimental technique developed by Garnier and Beck. In the third part of this research, the thermocouple-induced errors, which are usually small quantities, are quantified using an analytical approach. Finite difference and finite element methods are supplemented because of their limitations in calculating small differences. Some experiments are then designed and implemented in order to verify these analytical results. The results of the three different parts of this research have great potential for improving the estimation of composite material thermal properties.
Dissert. Abstr.

N93-25544 Cornell Univ., Ithaca, NY.
DETERMINATION OF THE ELASTIC CONSTANTS OF COMPOSITE MATERIALS FROM ULTRASONIC GROUP VELOCITY MEASUREMENTS
Lin Niu 1992 180 p
Avail: Univ. Microfilms Order No. DA9236006

A nondestructive test procedure based on the ultrasonic point-source-receiver (PS/PR) technique is described in this thesis. In the procedure group velocity data determined from the signals detected in an anisotropic composite specimen is processed to recover the matrix of elastic constants of the material. The composites are modeled as homogeneous, elastically anisotropic materials, whose elastic constants or stiffness are related to the speeds of the elastic waves propagating in them. It is shown that the wave arrivals in the PS/PR waveforms detected in the far field from the source correspond closely to the group velocities of plane waves propagating in the associated directions. Since there is no explicit equation relating the group velocities and the material stiffness, the inverse problem of recovering the elastic constants from the wavespeed data is solved by an algorithm consisting of an inner minimization loop to determine the wave normals and an outer optimization loop to recover the elastic constants. The solution to the forward problem is used to identify

the arrivals of specific wave modes in the signals detected for a particular source/receiver geometry. A procedure for processing the arrivals of quasi-transverse waves propagating along directions through cuspidal regions of the wave surface is also developed. To evaluate the operation of the procedure, the sensitivity of the algorithm for recovering the elastic constants from perturbed wavespeed data was determined. Also considered was the use of only quasi-longitudinal wavespeed data to recover a subset of the material's elastic constants. Experiments were carried out using the PS/PR measurement configuration. The point source was a monopolar force with a step-unloading time-function which was obtained from the fracture of a small-diameter glass capillary on the surface of a specimen. Such a source generates ultrasonic signals that exhibit a broad angular spectrum in the material. The point-receiver was a small-aperture capacitive transducer whose output is proportional to the local vertical displacement of the medium over a broad bandwidth. The processing algorithm was first evaluated using wavespeed data obtained in a single crystal specimen of zinc, a material whose matrix of elastic constants is known. Then a number of composite specimens, including several uni-directional fiber-reinforced and cross-ply laminate composite plates, were tested. For transversely isotropic materials, the full set of elastic constants were recovered. For the orthotropic materials, a partial set of the elastic constants was recovered. The results were compared with those obtained using conventional ultrasonic measurement procedures. Dissert. Abstr.

N93-25631# Texas Univ., Arlington.
DAMAGE-SURVIVABLE AND DAMAGE-TOLERANT LAMINATED COMPOSITES WITH OPTIMALLY PLACED PIEZOELECTRIC LAYERS Final Report, Aug. 1989 - Dec. 1992
S. P. Joshi and W. S. Chan 13 Nov. 1992 151 p
(Contract DAAL03-89-G-0090)
(AD-A260879; ARO-27167.3-EG-SM) Avail: CASI HC A08/MF A02

The main objective of the research is to assure that the embedded sensors/actuators in a smart laminated composite structure are damage-survivable and damage-tolerant. The research requires development of analytical and computational techniques and tools together with the experimental evaluation of smart composite structural elements. An understanding of electroelastic constitutive behavior is critical to predicting the response of a structure with embedded piezoelectric material. Our research efforts in this area have produced a concise formulation of linear constitutive relations that have been extended to the nonlinear case. The CDA (Composite Delamination Analysis) and SDACLP (Static and Dynamic Analysis for Composite Laminated Plates) packages have been modified to incorporate piezoelectric coupling in a quasi-3D and plane stress analysis. DTIC

N93-25652# Naval Surface Warfare Center, Bethesda, MD. Ship Materials Engineering Dept.
EFFECT OF WATER IMMERSION ON FIBER/MATRIX ADHESION
Thomas Juska Jan. 1993 19 p
(Contract F33615-89-C-0532)
(AD-A260704; CDNSWC/SME-92/38) Avail: CASI HC A03/MF A01

A study was made on the effect of water immersion on fiber/matrix adhesion in composites. Representatives of the four main classes of continuous fiber composites were tested: glass/thermoset, carbon/thermoset, glass/thermoplastic, and carbon/thermoplastic. Water conditioning was done by immersion in 50 C distilled water. The only class of composites degraded by water was glass-reinforced thermoplastics. However, carbon-reinforced vinyl esters, a subset of the carbon/thermoset class, appear to have weak fiber/matrix bonds when dry, and these bonds are further degraded by water. In both cases, immersion in water hydrolyzed the interfacial bonds and caused large, irrecoverable property reductions. DTIC

N93-25661 Virginia Polytechnic Inst. and State Univ., Blacksburg.
NUMERICAL SIMULATION OF DAMAGE AND PROGRESSIVE FAILURES IN COMPOSITE LAMINATES USING THE LAYERWISE PLATE THEORY Ph.D. Thesis
Yeruva Satyanarayana Reddy 1992 148 p
Avail: Univ. Microfilms Order No. DA9237155

The failure behavior of composite laminates is modeled numerically using the Generalized Layerwise Plate Theory (GLPT) of Reddy and a progressive failure algorithm. The Layerwise Theory of Reddy assumes a piecewise continuous displacement field through the thickness of the laminate and therefore has the ability to capture the interlaminar stress fields near the free edges and cut outs more accurately. The progressive failure algorithm is based on the assumption that the material behaves like a stable progressively fracturing solid. A three-dimensional stiffness reduction scheme is developed and implemented to study progressive failures in composite laminates. The effect of various parameters such as out-of-plane material properties, boundary conditions, and stiffness reduction methods on the failure stresses and strains of a quasi-isotropic composite laminate with free edges subjected to tensile loading is studied. The ultimate stresses and strains predicted by the Generalized Layerwise Plate Theory (GLPT) and the more widely used First Order Shear Deformation Theory (FSDT) are compared with experimental results. The predictions of the GLPT are found to be in good agreement with the experimental results both qualitatively and quantitatively, while the predictions of FSDT are found to be different from experimental results both qualitatively and quantitatively. The predictive ability of various phenomenological failure criteria is evaluated with reference to the experimental results available in the literature. The effect of geometry of the test specimen and the displacement boundary conditions at the grips on the ultimate stresses and strains of a composite laminate under compressive loading is studied. The ultimate stresses and strains are found to be quite sensitive to the geometry of the test specimen and the displacement boundary conditions at the grips. The degree of sensitivity is observed to depend strongly on the lamination sequence. The predictions of the progressive failure algorithm are in agreement with the experimental trends. Finally, the effect of geometric nonlinearity on the first-ply and ultimate failure loads of a composite laminate subjected to bending load is studied. The geometric nonlinearity is taken in to account in the von Karman sense. It is demonstrated that the nonlinear failure loads are quite different from the linear failure loads, depending on the lamination sequence, boundary conditions, and span-to-depth ratio of the test specimen. Further, it is shown that the First order Shear Deformation Theory (FSDT) and the Generalized Layerwise Plate Theory (GLPT) predict qualitatively different results. Dissert. Abstr.

N93-25674 Purdue Univ., West Lafayette, IN.
INELASTIC BEHAVIOR OF THERMOPLASTIC COMPOSITES Ph.D. Thesis
Ilsup Chung 1992 123 p
Avail: Univ. Microfilms Order No. DA9301279

The mechanical behaviors of AS4 reinforced PEKK-based composites were studied. These new thermoplastic composite system developed by Du Pont exhibit pronounced nonlinear and time dependent behaviors. To characterize the inelastic behavior, classical plasticity and creep theory have been adopted and modified for the orthotropic case by using a one-parameter potential function. The elastic-plastic behavior of LDF(TM) AS-4/PEKK system employing aligned, long discontinuous fiber reinforced composites has been studied in comparison with the continuous fiber reinforced counterpart. A dual mode plastic potential action was employed to model the plastic behaviors of these composites at room and elevated temperatures up to 177 C. A one-parameter failure criterion was also applied to predict the failure strength. Off-axis coupon specimens were used to measure the failure strength and generate stress-strain curves from which the elastic-plastic properties were extracted. It was observed that the elastic-plastic performance and strength of LDF(TM) are as good as those of the continuous fiber system. A creep model for orthotropic material has been developed based on the same one-parameter potential function. The material constants were determined by using uniaxial creep tests of off-axis coupon specimens. In terms of effective stress and effective creep strain, the anisotropic creep behavior was described by a stress dependent master creep curve irrespective of loading direction relative to fiber orientation. This model was implemented into classical laminate theory to predict the creep behavior of composite laminate, and compared with experimental data of (+/- 45)4s laminate specimens. The influence of thermal stress was included. The micromechanical approach also was tried to model the inelastic behavior of continuous fiber reinforced composites. The fiber was assumed to be orthotropically elastic, and the matrix to conform to the classical elastic-plasticity and creep theories. For the so called mechanics of material type of approach, a representative volume element assuming simplified distribution of stress and strain was employed,

and numerical prediction was compared with other existing models or experiments. Dissert. Abstr.

N93-25675 Purdue Univ., West Lafayette, IN.
INVESTIGATION AND MODELING OF PENETRATION PROCESS FOR COMPOSITE LAMINATES IMPACTED BY A BLUNT-ENDED PROJECTILE Ph.D. Thesis
Shi-Wei Ricky Lee 1992 143 p
Avail: Univ. Microfilms Order No. DA9301336

The objectives of the present research are to investigate the penetration process and to develop a corresponding computational model for composite laminates subjected to the impact of a blunt-ended projectile. Three specimen configurations were arranged to study the effect in dimensions. A series of static punch tests were conducted to characterize the load-displacement relation. The progressive damage mechanisms were identified by terminating the tests at various check points along the static punch curve. X-ray radiography, optical microscopy, and acoustic microscopy were used to inspect the tested specimens. Delamination and plugging were found to be the two major damage modes in the penetration process. It was further observed that the delamination is initiated by some matrix cracks. However, the plugging appears to be a localized behavior, and the experimental data reveal that the load for plug formation is independent of the span of the specimen. High velocity impact experiments were also performed for dynamic penetration. In general, the major damage modes resemble those observed in the static punch tests. Besides the striking velocity, the residual velocity of the projectile was measured as well for specimens subjected to complete penetration. The ballistic limit of composite laminates can be calculated from the difference between the initial and the residual kinetic energy of the projectile. An axisymmetric finite element analysis was employed to model the penetration process of composite laminates. An apparent modulus scheme together with the fracture mechanics concept was adopted to simulate the major damage events during penetration. The static punch curve was incorporated into the present analysis as a penetration criterion so that the ballistic limit of composite laminates can be estimated. The validity of the proposed model is verified by the agreement between experimental data and computational results. It is concluded that the ballistic limit can be predicted by the present model without performing dynamic impact tests. Dissert. Abstr.

N93-25680 Virginia Polytechnic Inst. and State Univ., Blacksburg.
FINITE ELEMENT MICROMECHANICS MODELING OF INELASTIC DEFORMATION OF UNIDIRECTIONALLY FIBER-REINFORCED COMPOSITES Ph.D. Thesis
Su-Yen Hsu 1992 190 p
Avail: Univ. Microfilms Order No. DA9306156

A convenient and efficient algorithmic tangent matrix approach has been developed for 3-D finite element (FE) analysis using the endochronic theory without a yield surface. The underlying algorithm for integrating the endochronic constitutive equation was derived by piecewise linearization of the plastic strain path. The approach was employed to solve a micromechanics boundary value problem of a cyclically loaded unidirectional boron / 6061 aluminum composite. All the FE results consistently demonstrate superior numerical stability and efficiency of the proposed method. Extensions of the method to endochronic plasticity with a yield surface and to the plane stress case are also presented. A simple and unified weak formulation and its convenient FE implementation have been proposed. The weak formulation is valid for any doubly periodic model under uniform 3-D macro-stress, and serves as a common rational foundation of different FE approaches. The algorithmic tangent matrix approach for the endochronic theory has been incorporated into the FE formulation to model isothermal, rate-independent plastic macro-deformation of unidirectional fibrous composites with idealized two-phase microstructure and backed-out inelastic matrix properties. Methods for determining inelastic material parameters of the matrix have been established. Numerical results for a B/6061 Al composite subjected to on-axis and off-axis monotonic tensile loadings are in good agreement with experimental data. The micromechanics model also shows the potential for quantitative characterization of complicated cyclic behavior. Finally, some effects of model geometry on overall plastic response of the B/6061 Al composite are discussed from the viewpoint of theoretical experimental correlation. Dissert. Abstr.

N93-25691 Wisconsin Univ., Madison.
QUANTIFYING DISTRIBUTED DAMAGE IN COMPOSITES VIA THE THERMOELASTIC EFFECT Ph.D. Thesis
Brian Joseph Mahoney 1992 215 p
Avail: Univ. Microfilms Order No. DA9231211

A new approach toward quantifying transverse matrix cracking in composite laminates using the thermoelastic effect is developed. The thermoelastic effect refers to the small temperature changes that are generated in components under dynamic loading. Two models are derived, and the theoretical predictions are experimentally verified for three types of laminates. Both models include damage-induced changes in the lamina stress state and lamina coefficients of thermal expansion conduction effects, and epoxy thickness. The first model relates changes in the laminate TSA signal to changes in longitudinal laminate stiffness and Poisson's ratio. This model is based on gross simplifying assumptions and can be used on any composite laminate layup undergoing transverse matrix cracking. The second model relates TSA signal changes to longitudinal laminate stiffness, Poisson's ratio, and microcrack density for (0 sub p/90 sub q)sub s and (90 sub q/0 sub p)sub s cross-ply laminates. Both models yield virtually identical results for the cross-ply laminates considered. A sensitivity analysis is performed on both models to quantify the effects of reasonable property variations on the normalized stiffness vs. normalized TSA signal results for the three laminates under consideration. The results for the cross-ply laminates are very insensitive, while the (+/- 45)sub 5s are particularly sensitive to epoxy thickness and longitudinal lamina coefficient of thermal expansion. Experiments are conducted on (0 sub 3/90 sub 3)sub s and (90 sub 3/0 sub 3)sub s Gl/Ep laminates and (+/- 45)sub 5s Gr/Ep laminates to confirm the theoretical developments of the thesis. There is a very good correlation between the theoretical predictions and experimental results for the Gl/Ep laminates. There is also a good correlation for the (+/- 45)sub 5s Gr/Ep laminates; however, additional testing must be done to confirm the acceptability of the assumption that the epoxy thickness is equal to zero. Dissert. Abstr.

N93-25695 Purdue Univ., West Lafayette, IN.
LOW-VELOCITY IMPACT OF COMPOSITE SANDWICH PLATE Ph.D. Thesis
Chung-Lin Wu 1992 172 p
Avail: Univ. Microfilms Order No. DA9301415

Much work has been done on impact resistance and impact tolerance of composite sandwich panel. However, there is no research that predicts the impact force history of a composite sandwich plate and the corresponding stress distribution. Thus, the objectives of this research are to establish a model to analyze force response during the impact, application of a suitable failure criterion to explain the damage mechanism on the face sheets, and use the linear fracture mechanics to predict the propagation of delamination. Through the understanding of failure processing, a new type of core material and sandwich structure are designed to improve the damage resistance of core and face sheets. A finite element procedure was performed to predict the impact force history. Two types of impactors are used on this study. For the spherical impactor, plate finite element is adopted. For cylindrical impactor, Plane strain finite element was employed. For plate finite element, a new model treated facing as two independent Mindlin plates, core material resisted transverse normal strain and transverse shear deformation, and Impactor was assumed as a rigid body. The impact force history is determined experimentally and compared with the predicted values for foam core and honeycomb core sandwich plate. Damage mechanisms are observed by X-ray radiograph and cross-sectional optic microscopic photographs. Maximum principle stress criterion is chosen to predict the onset of matrix cracking. Fracture mechanics combined with nodal release technique is used to predict the propagation of interface delamination. Design of new core construction and the introduction of film adhesive between the 0/90 interfaces are utilized to improve the damage inside the face laminate and core section. Basic material properties tests and impact tests are performed on both tradition and new core construction. A nonlinear materials behavior for film adhesive is employed to study the effect of this tough layer on outset loading of matrix cracking and growth of interface delamination. Dissert. Abstr.

N93-25716 Case Western Reserve Univ., Cleveland, OH.
DAMAGE AND FAILURE ANALYSIS ON CONTINUOUS

FIBER-REINFORCED POLYMER COMPOSITES Ph.D. Thesis
Fuh-Sheng Chen 1992 178 p
Avail: Univ. Microfilms Order No. DA9306102

In chapter one, the damage that accompanies flexural deformation of a unidirectional glass fiber reinforced polyphenylene sulfide composite was examined by acoustic emission (AE) and scanning electron microscopy (SEM). The flexural stress-strain curve was nominally linear to about 1.0 percent strain, but the onset of damage detectable by AE occurred at 0.3 percent strain. Two peaks in the AE amplitude distribution were observed at 35dB and 60dB. Low amplitude events were detected along the entire length of the specimen. SEM observations suggested that these events arose from matrix cracking and fiber debonding. High amplitude events occurred primarily in the region of highest flexural stress between the inner loading points, they were attributed to fracture of glass fibers on the tension side and surface damage on the compressive side. In chapters two and three, the effects of the matrix modulus on the compressive failure mechanisms in flexure of unidirectional glass fiber reinforced thermoplastic Hytrel composites has been studied. An increase in the matrix Young's modulus leads to a change in the failure mode from cooperative fiber microbuckling to delamination splitting microbuckling. Cooperative fiber microbuckling is a catastrophic phenomenon without significant damage occurring in the composite system prior to the abrupt failure. Fibers are buckled both in the plane and normal to the plane of the compression surface. Delamination splitting microbuckling is associated with matrix splitting and consists of gradual accumulation of localized surface delaminations followed by buckling of fiber bundles. The transition in the mechanisms of flexural failure is semi-quantitatively explained by considering the criterion for each of the failure modes. The failure strength for cooperative fiber microbuckling is controlled by the shear modulus of the composite which is linear related to the Young's modulus of the matrix, while the failure strength for delamination splitting microbuckling is controlled by the composite shear strength which is not strongly affected on the Young's modulus of the matrix. Because the critical failure stresses have different dependencies on the matrix modulus, a transition from cooperative fiber microbuckling to delamination splitting microbuckling occurs as the matrix modulus increases. Dissert. Abstr.

N93-25723 Bath Univ. (England).
THE CORROSION OF METAL MATRIX COMPOSITES Ph.D. Thesis
Sarah L. Coleman 1991 243 p
Avail: Univ. Microfilms Order No. BRDX97176

The corrosion characteristics of aluminium alloys containing a number of ceramic reinforcements has been investigated. The reinforcements included continuous carbon and Nicalon fibers, short alumina (Saffil) fibers and silicon carbide particulate. The matrix metals consisted of aluminium, an Al-7Si-0.5Mg casting alloy and an Al-4Cu-1.5Mg precipitation hardening alloy. The composites were fabricated either by liquid metal infiltration (LMI), squeeze casting or powder metallurgy. The corrosion studies have been carried out using natural immersion and accelerated corrosion methods such as the cyclic polarization test. Special attention has been focused on a double cyclic polarization technique. This has proved to be invaluable for predicting the susceptibility of MMC to pitting attack, good correlation having been found between pitting and protection potentials derived from this method and those from open circuit potential measurements made under natural immersion conditions. The electrochemical studies have been combined with detailed microstructural analysis. Examination of the corroded surfaces and sections through the corroded material has been carried out using optical, scanning electron microscopy (SEM), transmission electron microscopy (TEM) and energy dispersive spectroscopy (EDS). These have enabled the sites of corrosion attack to be identified, such as fiber/matrix interfaces, secondary and intermetallic phases and pores and crevices caused by poor infiltration during fabrication. The MMC containing the most electrically conducting fiber, carbon, appeared to suffer the greatest degrees of attack at fiber/matrix interfaces. The effect was not wholly due to a galvanic action, but to the presence of a reaction product, aluminium carbide, Al4C3, which reacted strongly with water. The geometry of the reinforcement was found to effect the propagation of corrosion pits. Continuous fibers tended to act as barriers and channel the corrosion along the fibers, whereas the Saffil short fibers and SiC particulate allowed lateral growth of corrosion pits. The chemical composition of the metal matrix was found to play an important role regarding corrosion sites. In particular intermetallics containing iron, present largely as an impurity, proved detrimental to the corrosion resistance and caused enhanced attack of the surrounding metal due to a microgalvanic action. The method of composite manufacture also affected the corrosion process and was related to pores caused by poor infiltration in regions of densely-packed fibers. Dissert. Abstr.

N93-25760 Michigan Univ., Ann Arbor.
TRANSFORMATION PLASTICITY AND FRACTURE BEHAVIOR OF CERIA-TZP/ALUMINA COMPOSITES Ph.D. Thesis
Jyh-Shiarn Cherng 1992 226 p
Avail: Univ. Microfilms Order No DA9303712

A systematic study of transformation plasticity, R-curve behavior, and the strength characteristics in Ce-TZP/Al2O3 composites was conducted to explore the microstructural effects on the mechanical properties of transformation-toughened ceramics. Microstructures with different degrees of tetragonal phase connectivity and grain sizes were obtained by various amounts of alumina addition and different sintering temperatures. The test range, in terms of stress space for transformation plasticity and strength characteristics, was extended beyond those found in the literature. Four point bending and compression tests with a superimposed hydrostatic pressure constituted the experimental methods for that purpose. R-curves were measured by cycled loading-unloading in four point bending of fatigue-precracked specimens. Results from such a study indicate that a Mohr-Coulomb type of yield criterion can be used to describe the deformation behavior of the Ce-TZP/Al2O3 composites. Both alumina addition and grain refinement expand the yield surface outward. The evolution of the transformation curve from one with distinct two stages to one with continuously gradual transformation is facilitated by alumina addition or applied pressure. On the other hand, grain refinement favors perfectly plastic deformation but suppresses the burst-like transformation during cooling. Both the height and shape of the R-curve depend on the microstructure. The addition of alumina decreases K(sub 0) (slightly), K(sub m), and delta-K, while grain refinement increases K(sub 0) (slightly), but decreases Km, and delta-K. Above a certain alumina content, the R-curve exhibits a peak followed by extensive crack growth due to subcritical crack growth. The increase of crack resistance, delta-K, can be attributed to transformation toughening as the data fit well with a model proposed by Chen. An analysis of the bend strengths of the Ce-TZP/Al2O3 composites reveals a ductile-brittle-ductile-brittle transition map which serves as a framework to guide future materials development of transformation toughened zirconia. A simple model was also developed to correlate strength with the R-curves in these materials. Dissert. Abstr.

N93-25768# Aeronautical Research Labs., Melbourne (Australia).
IN-SITU ULTRASONIC C-SCANNER
S. C. Galea and D. S. Saunders Nov. 1992 20 p
(AD-A261113; ARL-TR-4; DODA-AR-006-634) Avail: CASI HC A03/MF A01

Monitoring damage growth in composite materials during axial fatigue tests, without removing the specimen from the loading machine, is normally achieved using techniques such as shadow moire fringe, X-radiography, thermography, or residual stiffness measurements. All except the last method provide an indication of the extent of damage. However, none of these techniques provide information on the through-the-thickness location of the damage. For detailed inspection, the specimen would normally be removed from the testing machine and C-scanned using an immersion scanning system. This Technical Report describes an in-situ C-scanning apparatus, based on the time-of-flight C-scanning technique developed at DSTO-ARL, for monitoring damage growth while the specimen is still located in the testing machine. This system uses a semi-impervious membrane and water couplant which allows the specimen to be scanned without full immersion of the specimen and the probe. Set-up procedures and operational details are also described. Comparisons of in-situ C-scans with immersion tank C-scans and optical macrographs of cross-sectioned specimens were undertaken, in order to validate the new system. DTIC

N93-25780# Catholic Univ. of America, Washington, DC. Dept. of Mechanical Engineering.
ACTIVE CONTROL OF NITINOL-REINFORCED STRUCTURAL COMPOSITES Final Report, 15 Aug. 1989 - 14 Aug. 1992
A. Baz 12 Oct. 1992 170 p LIMITED REPRODUCIBILITY: More than

20% of this document may be affected by microfiche quality
(Contract DAAL03-89-G-0084)
(AD-A261062; ARO-27216.6-EG-SM) Avail: Issuing Activity (Defense Technical Information Center (DTIC))

The rapidly growing technology of the shape memory nickel-titanium alloy (NITINOL) is utilized to develop SMART composite materials that are capable of adapting intelligently to internal and external excitations. The NITINOL fibers are embedded into the composite matrix, at optimal locations and orientations, to sense and control the static and dynamic characteristics of the resulting SMART composite. With such built-in self-inspecting and controlling capabilities, the performance of the SMART composite can be optimized and tailored, in real time, to match changes in the operating conditions. Emphasis has been placed on controlling the static, dynamic, and thermal characteristics of anisotropic NITINOL-reinforced beams. Furthermore, the sensing capabilities of the NITINOL fibers are investigated by using them as distributed strain gages to monitor the physical and modal displacements of NITINOL-reinforced composites. Finite element models are developed to predict structural stability and the static, dynamic, and thermal behavior of NITINOL-reinforced composite beams. The theoretical predictions of these models are validated experimentally. DTIC

N93-25862# Colorado Univ., Boulder. Dept. of Physics.
COMPOSITE NANOSTRUCTURED MATERIAL FABRICATION BY ELECTROCHEMICAL SCANNING PROBE MICROSCOPY Final Report, 1 Mar. 1992 - 31 Aug. 1992
Kenneth Douglas 31 Oct. 1992 4 p
(Contract DAAL03-92-G-0085)
(AD-A261017; ARO-30408.1-PH) Avail: CASI HC A01/MF A01

Progress has been made in characterizing the parameters needed to achieve selective electrodeposition onto a nanostructured surface and in techniques and procedures needed to create a nanoheterostructure, a class of composite solid-state/solid-state and biomolecular/solid-state materials with nanometer-scale structure. A newly created device called a minicell, a minielectrochemical cell, proved to be very successful in terms of dealing with the small substrate size (usually less than 20 mm squared) on which our nanostructures are formed. We found that a properly designed electrochemical cell for these experiments should have the working-reference and working-counter electrode distances the same. It should also use a counter electrode with a large surface area exposed to the electrolyte, and one which is located over the whole working electrode, so that deposition occurs smoothly and uniformly across the entire substrate surface. DTIC

N93-25908# Sydney Univ. (Australia). Centre for Advanced Materials Technology.
INTERNATIONAL WORKSHOP ON ADVANCES IN INORGANIC FIBRE TECHNOLOGY Final Report
Yiu-Wing Mai 14 Aug. 1992 102 p Workshop held in Melbourne, Australia, 13-14 Aug. 1992
(Contract DAAL03-92-G-0371)
(AD-A260719; ARO-30744.1-MS-CF) Avail: CASI HC A06/MF A02

Topics include the following: Recent development of SiC fibers 'NICALON' and their composites including properties of SiC fibers 'HI-NICALON' for ultrahigh temperature; Fine diameter polycrystalline SiC fibers; Pyrolytic behavior of polymer-derived SiC fibers; Polymer-derived SiC fibers with improved thermomechanical stability; New curing method for polycarbosilane with unsaturated hydrocarbons and application to thermally stable SiC fiber; Fiber-matrix interface micromechanics and ceramic matrix composites; Interfacial control and macroscopic failure in inorganic composites; and The role of fiber/matrix interface in the first matrix cracking of fiber-reinforced brittle matrix composites. DTIC

N93-25918# Wright Lab., Wright-Patterson AFB, OH.
CHARACTERIZATION OF AEROSPACE GRADE RESINS AND COMPOSITES THROUGH PRESSURIZED VOLUMETRIC DILATOMETRY Final Report, Dec. 1990 - Jul. 1992
J. D. Russell and D. B. Curliss Jul. 1992 91 p
(AD-A260794; WL-TR-92-4062) Avail: CASI HC A05/MF A01

The technique of Pressurized Volumetric Dilatometry has been used to characterize the specific volume changes over pressure and temperature of several state-of-the-art aerospace thermoplastic and thermoset resins and composites and several pitch precursors for carbon-carbon composites. The materials studied were poly(etheretherketone) PEEK; HTA; HTX; PBO/PEEK; 3501-6 epoxy; AS4/3501-6 prepreg; IM7/8551-7A prepreg; IM7/5250-2 prepreg; Ashland Oil pitches A-240, A-60, A-70, and A-80; Reilly Coal Tar; and Mitsubishi's AR Synthetic Mesophase Pitch. Accurate and reproducible Pressure-Volume-Temperature (PVT) data have been yielded by this technique. Important processing information such as Tg(P), CTE(TP), T-(P), Tc(P), cure shrinkage, and other phase changes which give rise to volume changes can be extracted from the PVT data. DTIC

N93-25919# Rensselaer Polytechnic Inst., Troy, NY. Dept. of Civil Engineering.
THERMOMECHANICAL RESPONSE OF SHAPE MEMORY COMPOSITES Technical Report
James G. Boyd and Dimitris C. Lagoudas 18 Jan. 1993 18 p LIMITED REPRODUCIBILITY: Availability: Document partially illegible
(Contract DAAL03-92-G-0123)
(AD-A260828; ARO-30378.4-EG-URI) Avail: CASI HC A03/MF A01

The Mori-Tanaka micromechanics method is used to predict the effective properties of composite materials consisting of a polymer matrix reinforced by a fiber made of a transformation shape memory effect (SME) material. The composite response is plotted for combinations of the following scenarios: (1) isothermal longitudinal and transverse stress input, (2) stress-free thermal loading, (3) constant fiber thermoelastic properties, and (4) thermoelastic fiber properties that vary with the martensite volume fraction. For the case of an isothermal stress input, the composite transformation stress, the maximum transformation strain, and the hysteresis are all reduced vis-a-vis the monolithic SME material. In contrast to a monolithic SME material, stress-free thermal loading of a SME composite can produce a transformation strain. It is shown that closed form solutions for the effective martensite and austenite start temperatures can be derived, that they are sensitive to the stress-free reference temperature of the fiber, and that the stress-free austenite and martensite start temperatures are higher than those of the monolithic SME material. DTIC

N93-25936# Fairfax Materials Research, Inc., Alexandria, VA.
COMPUTER MODELLING OF CYCLIC DEFORMATION OF HIGH-TEMPERATURE MATERIALS Technical Progress Report, 16 Nov. 1992 - 15 Feb. 1993
M. S. Duesbery 26 Feb. 1993 27 p
(Contract N00014-91-C-0067)
(AD-A260978) Avail: CASI HC A03/MF A01

This program aims at improving current methods of lifetime assessment by building in the characteristics of the micro-mechanisms known to be responsible for damage and failure. The broad approach entails the integration and, where necessary, augmentation of the micro-scale research results currently available in the literature into a macro-scale model with predictive capability. In more detail, the program will develop a set of hierarchically structured models at different length scales, from atomic to macroscopic, at each level taking as parametric input the results of the model at the next smaller scale. In this way the known microscopic properties can be transported by systematic procedures to the unknown macro-scale region. It may not be possible to eliminate empiricism completely, because some of the quantities involved cannot yet be estimated to the required degree of precision. In this case the aim will be at least to eliminate functional empiricism. DTIC

N93-25945# Rensselaer Polytechnic Inst., Troy, NY. Dept. of Mechanical Engineering, Aeronautical Engineering and Mechanics.
DAMAGE DETECTION AND MITIGATION OF COMPOSITE STRUCTURES USING SMART MATERIALS
Abu S. Islam and Kevin Craig 18 Jan. 1993 12 p
(Contract DAALO3-92-G-0123)
(AD-A261121; ARO-30378.7-EG-URI) Avail: CASI HC A03/MF A01

This paper reports the results of an ongoing experimental program for damage assessment and mitigation of composite structures using smart materials. One consequence of all damage to a composite structure is a change in its stiffness. This change in stiffness is measured by modal analysis which can be carried out using piezoelectric films as both sensor and actuator on the structure member. It is shown that the presence of damage can be detected by the change in natural frequencies and the location of the damage can be detected from the ratio of changes in frequencies between two successive modes. Experiments are now being

carried out using healthy and damaged composite beams of rectangular cross section with piezoceramic sensors and actuators. In this paper experimental results of damage detection will be described in detail.
DTIC

N93-25954# Army Materials Technology Lab., Watertown, MA.
THERMAL EXPANSION MEASUREMENTS OF POLYMER MATRIX COMPOSITES AND SYNTACTICS Final Report
Louise C. Sengupta and William A. Spurgeon Apr. 1992 15 p
(MTL-TR-92-27) Avail: CASI HC A03/MF A01

The coefficients of thermal expansion (CTE) of various polymer matrix materials were measured using a thermal mechanical analyzer. The measurements include a set of standard materials used as calibration materials for the instrument. The data for the base polymers, syntactics, and E and S-2 glass-reinforced polyester matrix composites were obtained in the temperature range from -77 to 120 C. The results for all of the polymeric materials, especially for the epoxy and epoxy syntactic (above 65 C), are nonlinear. The CTE of the syntactics were reduced by a factor of approximately 2 for the base resins. The data taken for the glass-reinforced composites show peaks and/or humps in the thermal expansion. These features are believed to be from the formation of voids within the plies of the composite laminate. The irregular behavior of the thermal expansion was minimized by thermal annealing under load conditions, whereas annealing in free-space does not significantly dampen this behavior. The thermal expansion of the material appears to be directly related to the fiber loading.
Author (revised)

N93-26100* National Aeronautics and Space Administration. Lewis Research Center, Clevelanu, OH.
CERAMIC FIBER REINFORCED GLASS-CERAMIC MATRIX COMPOSITE Patent
Narottam P. Bansal, inventor (to NASA) 25 May 1993 4 p Filed 4 Jun. 1992
(NASA-Case-LEW-15262-1; US-Patent-5,214,004;
US-Patent-Appl-SN-892055; US-Patent-Class-501-8;
US-Patent-Class-501-32; US-Patent-Class-501-89; US-Patent-Class-501-95;
US-Patent-Class-428-428; US-Patent-Class-428-698;
US-Patent-Class-264-58) Avail: US Patent and Trademark Office

A slurry of BSAS glass powders is cast into tapes which are cut to predetermined sizes. Mats of continuous chemical vapor deposition (CVD)-SiC fibers are alternately stacked with these matrix tapes. This tape-mat stack is warm-pressed to produce a 'green' composite which is heated to burn out organic constituents. The remaining interim material is then hot-pressed to form a BSAS glass-ceramic fiber-reinforced composite.
Official Gazette of the U.S. Patent and Trademark Office

N93-26143# Department of the Navy, Washington, DC.
ELECTROSTATIC FIBER SPREADER Patent Application
Jonathan M. Peritt, inventor (to Navy), Richard Everett, inventor (to Navy), and Alan Edelstein, inventor (to Navy) 5 Nov. 1992 14 p
(AD-D015677; US-Patent-Appl-SN-788018) Avail: CASI HC A03/MF A01

A fiber spreader is discussed. The spreader is designed to reduce the fiber damage that occurs during spreading. The fiber spreader includes a thin electrically grounded support sheet for supporting a layer of fibers on one surface. The fibers supported on the support sheet are guided by guide rollers past at least one corona discharge region at which the fibers are spread. A motor driven spool advances the support sheet past the corona discharge region. The fibers are attached to the support sheet by an electrostatic attraction. The guide rollers are positioned so as to provide at least one region in which the sheet and the fibers are physically separated to allow for the uniform spreading of the fibers. After the fibers are spread the fibers and the support sheet are united again and collected on a motor-driven spool.
DTIC

N93-26145# Department of the Navy, Washington, DC.
IMPROVED COMPOSITE FABRICATION PROCESS Patent Application
Benoit Gauthier, inventor (to Navy) 23 Jul. 1992 9 p
(AD-D015679; US-Patent-Appl-SN-917652) Avail: CASI HC A02/MF A01

In a filament winding machine for fabricating a composite product on a rotating mandrel, the dry tow of filaments is electrically charged prior to entry in the resin bath. The bath is oppositely charged to the mutually repelled filaments in the bath with the result that improved resin to filament adherence is achieved. The resulting product is stronger due to the absence of resin voids in the product.
DTIC

N93-26225# Nebraska Univ., Lincoln. Dept. of Mechanical Engineering.
SMART STRUCTURAL COMPOSITES WITH PIEZOELECTRIC MICRO-CONSTITUENTS Final Report, Sep. 1989 - Dec. 1992
Nisar Shaikh Dec. 1992 16 p
(Contract DAAL03-89-G-0086)
(AD-A260970; ARO-27198.1-MS-SM) Avail: CASI HC A03/MF A01

The research culminated into the feasibility of smart structural composite materials, in which the microstructure is modified with the introduction of a piezoelectric constituent. Greater success was achieved in the sensing aspect of smart properties, enabling the material to have an inherent property of health monitoring. By sensing and quantifying elastic strain, the material can monitor its dynamic state (vibration), degradation and damage. In actuation, the material is readily suitable for active vibration control and manipulative damping. One out-growth of the results was an active fibrous sensor, which offers a readily viable alternative to a passive fiber-optic sensor as it is marred with breakage problems. A new concept of piezoelectric emission, analogous to acoustic emission, emerged which imparts the material ability to sense stress waves. This ability can be used to locate the regions of delamination and local fractures through fabrication to operational life of structure. Techniques were developed for deposition of thin piezoelectric (ZnO) film on carbon and metal fibers. Sensing and actuation properties were imparted into carbon fiber composites. The results demonstrated self-sensing of strain and damage measurement in beam and shell elements. The concept is ready for technological advancement and application.
DTIC

N93-26236# Massachusetts Inst. of Tech., Cambridge. Materials Processing Center.
PROCESSING AND PROPERTIES OF SILICON CARBIDE REINFORCED REACTION BONDED SILICON NITRIDE COMPOSITES Final Report, 1 Sep. 1988 - 30 Sep. 1992
John S. Haggerty and Shanti Nair 30 Nov. 1992 49 p
(Contract DAAL03-88-K-0099)
(AD-A260570; ARO-25202.1-MS) Avail: CASI HC A03/MF A01

Reaction formed ceramic materials have not approached potential levels of utilization because of historically poor properties and the lack of familiarity by potential users. Research with reaction bonded silicon nitride (RBSN) has shown that reduced processing temperatures and times, high purities, net-shape fabrication, and improved properties can be achieved simultaneously with this class of materials if they are processed carefully by rather conventional techniques. Distinct from conventional high performance ceramics, reaction formed ceramics typically contain relatively high levels of residual porosity. As is true of conventional ceramics, superior properties are feasible with porous ceramics only if the microstructural characteristics of all final phases are precisely controlled; the major difference for the porous ceramics is that the pore structure must be as carefully controlled as is required for the solid phases in a high quality conventional ceramic material.
DTIC

N93-26301# Missouri Univ., Rolla. Dept. of Chemistry.
EFFECTS OF MOISTURE AND OTHER CONTAMINANTS IN FRICTION COMPOSITES Interim Report, Dec. 1991 - Dec. 1993
N. Subramamaniam, Frank D. Blum, and L. D. Dharani 30 Jan. 1993 36 p
(Contract N00014-91-J-1274)
(AD-A261226; UMR-FDB-28) Avail: CASI HC A03/MF A01

The role of water and other contaminants like salt water, isooctane, and ethylene glycol on neat resin, composites, and friction materials have been investigated. The maximum solvent uptake and the diffusion coefficient of the solvent in these systems were determined and the experimental data was fitted to a Fickian model. The nature of the diffusion process was determined in each case and deviations from Fickian behavior were accounted for. For the neat resin and the composites, the diffusion coefficients of the liquids were of the order of 10(exp -10) sq cm/sec. After exposure to these contaminants, mechanical properties of all the systems were determined and a general degradation in properties were

found. The flexural strength and fracture toughness showed reduction in values while the flexural modulus was not affected. DTIC

N93-26355# Massachusetts Inst. of Tech., Cambridge. Dept. of Mechanical Engineering.
THREE-DIMENSIONAL ANALYSIS AND VERIFICATION OF FRACTURE GROWTH MECHANISMS IN FIBER-REINFORCED CERAMIC COMPOSITES Final Report, 1 Apr. - 31 Dec. 1992
M. P. Cleary, W. D. Keat, M. C. Larson, and F. T. Patterson 31 Dec. 1992 33 p
(Contract F49620-92-J-0220)
(AD-A261483; AFOSR-93-0082TR) Avail: CASI HC A03/MF A01

This final report documents a 3-D computational and experimental investigation into the mechanics of roughening a brittle matrix by incorporating long brittle fibers. Computationally, small scale failure mechanisms ahead of a crack are explicitly modeled and merged with a continuum representation of the farfield outside the process zone. Particular attention is given to the interfacial decohesion and frictional slipping near the tip of a matrix crack which is impinging upon an inclusion. The surface integral and finite element (SIFEH) method, which employs the principle of superposition to combine the best features of two powerful numerical techniques, provides an extremely flexible and efficient computational platform for modeling linear elastic fractures near material inhomogeneities. Applications to general 3-D fracture growth in multimaterial media demonstrate the capabilities of the computational technique and are also described. The computational simulation is being guided by laboratory experiments. Crack growth observations made on a model (micro-) structure comprising a glass rod embedded in a cement matrix show the toughening mechanisms of crack pinning and crack bridging in operation. In a second experiment, interfacial slip evolution was modeled experimentally for planar bimaterial interfaces. This combined experimental and numerical program has provided insight into optimal combinations of the key parameters (e.g. residual stresses at interface, friction coefficient, strength of fibers) to maximize toughness. DTIC

N93-26371# Naval Postgraduate School, Monterey, CA.
THERMALLY INDUCED STRESSES IN A COMPOSITE EXPOSED TO FIRE M.S. Thesis
Edward A. Faxlanger, Jr. Dec. 1992 98 p
(AD-A261714) Avail: CASI HC A05/MF A02

This thesis investigates the behavior of graphite/epoxy composites subjected to fire as may occur on the decks of naval aircraft carriers. The analytical model consists of two parts: one for the determination of the temperature field within the composite due to a fire, and the other for determining the stresses within the composite due to the temperature field. Both problems are provided one-dimensional finite element models. Appropriate failure criteria are incorporated to predict the survivability of composites in various fire environments. Parametric studies were performed and the results are presented in both graphical and tabular form. DTIC

N93-26382# Utah Univ., Salt Lake City. Dept. of Mathematics.
FAILURE CONSIDERATIONS IN COMPOSITE SYSTEMS BASED ON 3D MICROMECHANICAL STRESS FIELDS, PART A Final Technical Report
E. S. Folias Dec. 1992 326 p
(Grant AF-AFOSR-0351-90)
(AD-A261698; AFOSR-93-0076TR-Pt-A) Avail: CASI HC A15/MF A03

In this investigation, a systematic 3D micromechanics approach is used to model a composite. The fibers are assumed to be cylindrical inclusions which are periodically embedded into a matrix plate. A three dimensional analysis is used in order to capture any edge effects which may be present. A set of fundamental key problems has been identified and their respective solutions for the displacement and stress fields are then used in order to provide us with some answers to the following fundamental questions: transverse strength, longitudinal strength, residual stresses due to thermal expansion mismatch, modeling of fiber matrix interface, edge effects. The 3D results are then used to first identify critical locations where failure, due to fracture, is most likely to initiate and second to derive fracture criteria for crack initiation at the local level. The criteria reveal the dependence of the composite strength on the material properties, the local cell geometry, the ratio of the fiber volume fraction, the ratio of fiber radius to fiber length and finally the applied mechanical and/or thermal loads. DTIC

N93-26552*# National Aeronautics and Space Administration. Lewis Research Center, Cleveland, OH.
METAL MATRIX COMPOSITE ANALYZER (METCAN): THEORETICAL MANUAL
P. L. N. Murthy and C. C. Chamis Feb. 1993 36 p
(RTOP 510-01-50)
(NASA-TM-106025; E-7588; NAS 1.15:106025) Avail: CASI HC A03/MF A01

This manuscript is intended to be a companion volume to the 'METCAN User's Manual' and the 'METAN Demonstration Manual.' The primary purpose of the manual is to give details pertaining to micromechanics and macromechanics equations of high temperature metal matrix composites that are programmed in the METCAN computer code. The subroutines which contain the programmed equations are also mentioned in order to facilitate any future changes or modifications that the user may intend to incorporate in the code. Assumptions and derivations leading to the micromechanics equations are briefly mentioned. Author (revised)

N93-26579# New Mexico Inst. of Mining and Technology, Socorro. Dept. of Materials and Metallurgical Engineering.
INTERFACE ENGINEERING IN OXIDE FIBER/OXIDE MATRIX COMPOSITES Annual Report, 1 Mar. 1992 - 28 Feb. 1993
K. K. Chawla 28 Feb. 1993 45 p
(Contract N00014-89-J-1459)
(AD-A261705) Avail: CASI HC A03/MF A01

In earlier work it was shown that fiber roughness is a very important parameter along with the thermal mismatch between the components. PRD-166 fiber, used so far, is a very rough fiber. Saphikon, single crystal alpha-alumina, is a relatively smooth fiber, but very expensive due to its processing cost. A new polycrystalline alumina fiber, Nextel 610, has recently become available. Due to its smoother surface than that of PRD-166 fiber, this fiber can be a good reinforcement candidate in oxide/oxide composites. Microstructural and mechanical characterization of Nextel 610 fiber was performed. The tensile strength of Nextel 610, after exposure to 900 C, 1100 C, and 1300 C was determined using a two-parameter Weibull distribution. It was observed that the primary reason for the loss of the fiber strength was the grain growth. DTIC

N93-26580# Connecticut Univ., Storrs. Inst. of Materials Science.
IN-PROCESS CURE MONITORING OF COMPOSITES VIA FIBER-OPTIC FLUORESCENCE Final Report, Apr. 1989 - Jul. 1992
C. S. Sung and N. H. Sung 23 Oct. 1992 3 p Prepared in cooperation with Tufts Univ., Medford, MA
(Contract DAAL03-89-K-0081)
(AD-A261712; ARO-26571.4-MS) Avail: CASI HC A01/MF A01

The objective of the research was to develop in-situ cure monitoring technique based on intrinsic and extrinsic chemical sensors using fiber optic fluorescence method for epoxy and polyimide and to use such a fiber-optic method to investigate fiber surface effects on epoxy structure and cure kinetics. As an extrinsic cure sensor, p,p'-diamino azobenzene (DAA) shows sensitive fluorescence intensity enhancement as a result of reaction with epoxide. It was implemented for in-situ cure monitoring of bulk epoxy cured with diaminodiphenyl sulfone (DDS) at high cure temperatures (140-180 C) using fiber optic fluorescence instrument, using an internal standard dye to calibrate the intensity. The intrinsic fluorescence excitation spectra of DDS was found to show sensitive spectral shifts with cure. This result was also implemented with real composites (carbon or glass fiber reinforced prepregs) in actual cure environment by fiber optic fluorescence instrument, by taking into account the effect of temperature on the spectral position. DTIC

N93-26589# Loyola Coll., Baltimore, MD. Japanese Technology Evaluation Center.
JAPANESE TECHNOLOGY EVALUATION CENTER WORKSHOP ON ADVANCED MANUFACTURING TECHNOLOGY FOR POLYMER COMPOSITE STRUCTURES IN JAPAN
18 Feb. 1993 255 p Conference held in Arlington, VA, 18 Feb. 1993 Sponsored by NSF; DOE; ARO; and AFOSR
(PB93-165249) Avail: CASI HC A12/MF A03

The report contains the viewgraphs used in the workshop on advanced manufacturing for polymer composite structures in Japan. The areas

represented are aerospace; sporting goods; automotive; industrial; civil engineering; manufacturing science; and product and process development methods. NTIS

N93-24890# British Aerospace Public Ltd. Co., Bristol (England). Research Centre.
A COMPUTATIONAL APPROACH TO PREDICTING THE EXTENT OF ARC ROOT DAMAGE IN CFC PANELS
Nicholas Jennings and C. John Hardwick (United Kingdom Atomic Energy Authority, Abingdon, England.) *In* FAA, The 1992 International Aerospace and Ground Conference on Lightning and Static Electricity: Addendum Nov. 1992 8 p Sponsored in part by Rolls-Royce Ltd.; Construcciones Aeronauticas S.A.; Saab-Scania; Civil Aviation Authority; Dept. of Trade and Industry; and Short Bros. and Harland Ltd. (For primary document see N93-24875 09-47)
Avail: CASI HC A02/MF A03

N93-24891# Dornier Luftfahrt G.m.b.H., Friedrichshafen (Germany).
COMPARISON OF THE DAMAGE FOR VARIOUS TYPES OF FIBRE REINFORCED COMPOSITES DUE TO DIFFERENT LIGHTNING TEST STANDARDS (MIL-STD-1757A, GERMAN MILITARY VG-STANDARD 96903)
Juergen Wiedmann, Jan-Uwe Roth, and Alexander W. Kern (Universitaet der Bundeswehr Muenchen, Neubiberg, Germany.) *In* FAA, The 1992 International Aerospace and Ground Conference on Lightning and Static Electricity: Addendum Nov. 1992 16 p Sponsored by Ministry of Defence (For primary document see N93-24875 09-47)
Avail: CASI HC A03/MF A03

N93-25586*# Naval Surface Warfare Center, Silver Spring, MD.
MULLITE WHISKERS AND MULLITE-WHISKER FELT
Inna G. Talmy and Deborah A. Haught *In* NASA, Washington, Technology 2002: The Third National Technology Transfer Conference and Exposition, Volume 1 Feb. 1993 p 241-249 Sponsored in part by Office of Naval Technology (For primary document see N93-25561 09-99)
Avail: CASI HC A02/MF A04

N93-25587*# National Aeronautics and Space Administration. Lewis Research Center, Cleveland, OH.
GRAPHITE/EPOXY COMPOSITE LAMINATES WITH CO-CURED INTERLAMINAR DAMPING LAYERS
J. Michael Pereira *In* NASA, Washington, Technology 2002: The Third National Technology Transfer Conference and Exposition, Volume 1 Feb. 1993 p 250-255 (For primary document see N93-25561 09-99)
Avail: CASI HC A02/MF A04

N93-26060*# Rice Univ., Houston, TX. Dept. of Mechanical Engineering and Materials Science.
COMPOSITE MATERIALS FOR THE EXTRAVEHICULAR MOBILITY UNIT Final Report
Enrique V. Barrera and Hector M. Tello *In* NASA. Johnson Space Center, National Aeronautics and Space Administration (NASA)/American Society for Engineering Education (ASEE) Summer Faculty Fellowship Program, 1992, Volume 1 Dec. 1992 15 p (For primary document see N93-26058 09-99)
(Grant NGT-44-005-803)
Avail: CASI HC A03/MF A02

25 INORGANIC AND PHYSICAL CHEMISTRY

Includes chemical analysis, e.g., chromatography; combustion theory; electrochemistry; and photochemistry.

For related information see also *77 Thermodynamics and Statistical Physics.*.

N93-24771 Michigan Univ., Ann Arbor.
A PREMIXED LAMINAR FLAME INTERACTING WITH A VORTEX RESULTING IN FLAME STRETCH AND QUENCHING Ph.D. Thesis
William Lafayette Roberts 1992 185 p
Avail: Univ. Microfilms Order No. DA9303811

A laminar axisymmetric vortex is interacted with laminar premixed flame in order to gain insight into the fundamentals of turbulent combustion. The interaction is visualized with Mie scattering tomography and planar laser induced fluorescence to determine the effect of the vortex on the flame. The vortex can have no effect, it can wrinkle the flame, it can cause a pocket of reactants to be formed, or the vortex can stretch the flame and cause local flame quenching. Disappearance of the reaction zone, as evidenced by the absence of superequilibrium OH fluorescence, was an excellent indicator of flamelet quenching. The size and strength of the vortex is varied to allow a combustion diagram to be constructed, which shows the borders between the above four regimes as a function of nondimensional vortex size and strength. The fuel was also varied to study thermodiffusive effects, as characterized by the Lewis number. The results show that flame quenching depends strongly on the temperature of the burnt gas. The Karlovitz number at the onset of quenching for a lean methane-air flame is defined as the nondimensional vortex strength divided by the nondimensional size of the vortex and was found to be as low as 0.1 for the larger diameter vortices and increased with decreasing vortex size. This is an order of magnitude lower than generally assumed. Lewis number effects are also quantified by considering the correlation between regions of high curvature and OH fluorescence intensity. Dissert. Abstr.

N93-24972# Sandia National Labs., Albuquerque, NM. Advanced Materials Physics Div.
COARSENING OF A QUIESCENT ELECTRORHEOLOGICAL FLUID I: EXPERIMENT
James E. Martin, Judy Odinek, and Thomas C. Halsey (Chicago Univ., IL.) 1992 9 p Presented at the 16th Material Research Society International Symposium on the Scientific Basis for Nuclear Waste Management, Boston, MA, 30 Nov. - 5 Dec. 1992
(Contract DE-AC04-76DP-00789)
(DE93-006776; SAND-92-2639C; CONF-921101-87) Avail: CASI HC A02/MF A01

A real-time, two-dimensional light scattering study of the evolution of structure in a concentrated electrorheological fluid during the 'liquid-solid' phase transition is reported. After particle chaining along the electric field lines, strong light scattering lobes appear at a finite scattering wavevector q orthogonal to the field lines, and then brighten as they move to $q = 0$. This indicates the existence of an unstable concentration fluctuation that signifies the segregation of chains into columns. In fact, the observed growth kinetics of the characteristic length, as well as the form of the structure factor, are qualitatively similar to two-dimensional spinodal decomposition in a system with a conserved order parameter. DOE

N93-25115# Massachusetts Univ., Amherst. Dept. of Chemical Engineering.
DESIGN AND SYNTHESIS OF REACTIVE SEPARATION SYSTEMS
M. F. Doherty 1992 28 p
(Contract DE-FG02-88ER-13946)
(DE93-008764; DOE/ER-13946/2) Avail: CASI HC A03/MF A01

During the last decade there has been a rapid upturn in interest in reactive distillation. The chemical process industry recognizes the favorable economics of carrying out reaction simultaneously with distillation for certain classes of reacting systems, and many new processes have been built based on this technology. Interest is also increasing by academics and software vendors. Systematic design methods for reactive distillation systems have only recently begun to emerge. In this report we survey the available design techniques and point out the contributions made by our group at the University of Massachusetts. DOE

N93-25116*# Purdue Univ., West Lafayette, IN.
MEASUREMENTS OF SOOT FORMATION AND HYDROXYL CONCENTRATION IN NEAR CRITICAL EQUIVALENCE RATIO PREMIXED ETHYLENE FLAME
Michael Andrew Inbody Mar. 1993 497 p
(Grant NAG3-1038; RTOP 537-02-20)
(NASA-CR-191099; E-7696; NAS 1.26:191099) Avail: CASI HC A21/MF A04

The testing and development of existing global and detailed chemical kinetic models for soot formation requires measurements of soot and radical concentrations in flames. A clearer understanding of soot particle inception relies upon the evaluation and refinement of these models in comparison with such measurements. We present measurements of soot formation

and hydroxyl (OH) concentration in sequences of flat premixed atmospheric-pressure C2H4/O2/N2 flames and 80-torr C2H4/O2 flames for a unique range of equivalence ratios bracketting the critical equivalence ratio (phi(sub c)) and extending to more heavily sooting conditions. Soot volume fraction and number density profiles are measured using a laser scattering-extinction apparatus capable of resolving a 0.1 percent absorption. Hydroxyl number density profiles are measured using laser-induced fluorescence (LIF) with broadband detection. Temperature profiles are obtained from Rayleigh scattering measurements. The relative volume fraction and number density profiles of the richer sooting flames exhibit the expected trends in soot formation. In near-phi(sub c) visibility sooting flames, particle scattering and extinction are not detected, but an LIF signal due to polycyclic aromatic hydrocarbons (PAH's) can be detected upon excitation with an argon-ion laser. A linear correlation between the argon-ion LIF and the soot volume fraction implies a common mechanistic source for the growth of PAH's and soot particles. The peak OH number density in both the atmospheric and 80-torr flames declines with increasing equivalence ratio, but the profile shape remains unchanged in the transition to sooting, implying that the primary reaction pathways for OH remain unchanged over this transition. Chemical kinetic modeling is demonstrated by comparing predictions using two current reaction mechanisms with the atmospheric flame data. The measured and predicted OH number density profiles show good agreement. The predicted benzene number density profiles correlate with the measured trends in soot formation, although anomalies in the benzene profiles for the richer and cooler sooting flames suggest a need for the inclusion of benzene oxidation reactions. Author

N93-25123# Brookhaven National Lab., Upton, NY.
FEMTOSECOND DYNAMICS IN HYDROGEN-BONDING SOLVENTS: FORMAMIDES
Yong Joon Chang and E. W. Castner, Jr. 1992 5 p Presented at the Quantum Electronics and Laser Science Conference, Baltimore, MD, 2-7 May 1993
(Contract DE-AC02-76CH-00016)
(DE93-003476; BNL-48196; CONF-930586-1) Avail: CASI HC A01/MF A01

We report the results of temperature-dependent optical Kerr effect experiments for formamide (FA) and N-methylformamide (NMF). Binary solutions of FA and NMF were also studied with water, acetonitrile, and N,N-dimethylformamide as cosolvents. DOE

N93-25229*# California Univ., San Diego, La Jolla. Dept. of Applied Mechanics and Engineering Sciences.
THE STRUCTURE OF PARTICLE CLOUD PREMIXED FLAMES Final Report, 14 Sep. 1991 - 13 Sep. 1992
K. Seshadri and A. L. Berlad 13 Sep. 1992 11 p
(Grant NAG3-1297)
(NASA-CR-192827; NAS 1.26:192827) Avail: CASI HC A03/MF A01

The structure of premixed flames propagating in combustible systems containing uniformly distributed volatile fuel particles in an oxidizing gas mixture is analyzed. This analysis is motivated by experiments conducted at NASA Lewis Research Center on the structure of flames propagating in combustible mixtures of lycopodium particles and air. Several interesting modes of flame propagation were observed in these experiments depending on the number density and the initial size of the fuel particle. The experimental results show that steady flame propagation occurs even if the initial equivalence ratio of the combustible mixture based on the gaseous fuel available in the particles, phi sub u, is substantially larger than unity. A model is developed to explain these experimental observations. In the model, it is presumed that the fuel particles vaporize first to yield a gaseous fuel of known chemical composition which then reacts with oxygen in a one-step overall process. The activation energy of the chemical reaction is presumed to be large. The activation energy characterizing the kinetics of vaporization is also presumed to be large. The equations governing the structure of the flame were integrated numerically. It is shown that the interplay of vaporization kinetics and oxidation process can result in steady flame propagation in combustible mixtures where the value of phi sub u is substantially larger than unity. This prediction is in agreement with experimental observations. Author

N93-25240*# San Jose State Univ., CA. Dept. of Materials Engineering.
THE PROPERTIES OF AND ANALYTICAL METHODS FOR DETECTION OF LiOH AND Li2CO3
Guna Selvaduray 8 Feb. 1991 58 p
(Contract NCC2-640)
(NASA-CR-192771; NAS 1.26:192771) Avail: CASI HC A04/MF A01

Lithium hydroxide (LiOH) is used as a CO2 absorbent in the Shuttle Extravehicular Mobility Unit (EMU) Portable Life Support System (PLSS). The first objective was to survey parameters that may be used to indicate conversion of LiOH to Li2CO3, and compile a list of all possible properties, including physical, chemical, structural, and electrical, that may serve to indicate the occurrence of reaction. These properties were compiled for the reactant (LiOH), the intermediate monohydrate compound (LiOH.H2O), and the final product (Li2CO3). The second objective was to survey measurement and analytical techniques which may be used in conjunction with each of the properties identified above, to determine the extent of conversion of LiOH to Li2CO3. Both real-time and post-run techniques were of interest. The techniques were also evaluated in terms of complexity, technology readiness, materials/equipment availability, and cost, where possible. Author (revised)

N93-25284 Department of the Navy, Washington, DC.
DYNAMIC TEST APPARATUS FOR ELECTRO-RHEOLOGICAL FLUIDS Patent
Wendell C. Maciejewski, inventor (to Navy) 12 Jan. 1993 5 p Filed 16 Sep. 1991
(AD-D015632; US-Patent-5,177,997; US-Patent-Appl-SN-762818) Avail: US Patent and Trademark Office

A device is disclosed for determining the dynamic mechanical properties, specifically, G*, G', G , and Tan Delta, of an electrorheological (ER) fluid as a function of frequency, voltage and temperature. This is accomplished by using the device in conjunction with a suitable driving and environmental control apparatus. An inner tubular electrode, coaxial with an outer tubular electrode, is oscillated along their common longitudinal axis at frequencies in a range of approximately 5 Hz to approximately 1,000 Hz while the spacing between the electrodes is maintained substantially constant at all opposed portions thereof. A power source provides an electrical field encompassing the inner and outer electrodes and the gap therebetween, and the associated driving and environmental control apparatus is operated for measuring the effort required to move the second electrode relative to said first electrode when the ER fluid is received between said inner and outer electrodes. Such measured effort is a function, respectively, of the characteristics of the ER fluid, the rate of oscillation of said second electrode, the strength of the electrical field, and the temperature of the ER fluid. DTIC

N93-25305# Manufacturing and Technolgy Conversion International, Inc., Columbia, MD.
PRODUCTION OF LOW-COST HYDROGEN Quarterly Technical Progress Report No. 11, 1 Apr. - 30 Jun. 1992
1992 7 p
(Contract DE-AC21-89MC-26367)
(DE93-008070; DOE/MC-26367/3235; MTCI-10039-11) Avail: CASI HC A02/MF A01

This eleventh Quarterly Technical Progress Report presents the results of work accomplished during the period 1 Apr. 1992 - 30 Jun. 1992 on production of low-cost hydrogen. The overall objective of this program is to verify the ability of the Manufacturing and Technology Conversion International (MTCI) indirectly heated fluid-bed gasifier to produce a hydrogen-rich product gas from liquefaction by-product streams and from char produced in mild gasification processes. The characterization unit was renovated and another burner/exhaust designed to replace the one that has been in use for several years. Initial shakedown tests for bed calcination indicated that the gasifier should be changed with fresh limestone and kept at temperature, with whatever make-up was required to maintain bed height until calcination was completed as determined by the CO concentration. Char gasification was then initiated and two relatively long-term tests (15.5 and 10.5 hours) were completed at two different temperatures. DOE

N93-25311# Delaware Univ., Newark. Dept. of Chemistry.
STUDIES OF THE ANALYTE-CARRIER INTERFACE IN FLOW INJECTION ANALYSIS Final Report, 1 Jun. 1987 - 31 Jan. 1992
S. D. Brown 1992 35 p
(Contract DE-FG02-86ER-13542)
(DE93-008374; DOE/ER-13542/5) Avail: CASI HC A03/MF A01

Chemical analysis in flowing solution is popular for automation of classical methods. However, most of the classical methods are not specific enough for direct multicomponent analysis of simple mixtures. This research project has the goals of study of rapid multicomponent analysis of transient species in flowing media, and investigations of chemical reactions at interfaces and of effects of competition on distribution of products from interfacial reaction. Work done over the past 4.5 years is summarized; support was terminated. DOE

N93-25312# Sandia National Labs., Albuquerque, NM.
MECHANISTIC STUDIES OF THE CVD OF SILICON NITRIDE FROM SiF4 AND NH3
R. J. Buss and P. Ho 1992 5 p Presented at the 183rd Electrochemical Society Meeting, Honolulu, HI, 16-21 May 1993
(Contract DE-AC04-76DP-00789)
(DE93-004500; SAND-92-2441C; CONF-930571-3) Avail: CASI HC A01/MF A01

An industrial process for the chemical vapor deposition (CVD) of silicon nitride from SiF4 and NH3 was studied with a wide variety of techniques, ranging from numerical models of the coupled chemistry and fluid mechanics to experimental studies of chemical reactions. The latter includes a set of molecular beam experiments that probed the temperature and flux dependencies of the reaction of SiF4 and NH3 at the surface. These experiments showed that the CVD reactor chemistry was dominated by surface kinetics rather than gas-phase decomposition. DOE

N93-25495# Purdue Univ., West Lafayette, IN. Heat Transfer Lab.
FLOW AND MORPHOLOGICAL CONDITIONS ASSOCIATED WITH THE DIRECTIONAL SOLIDIFICATION OF AQUEOUS AMMONIUM CHLORIDE
C. S. Magirl and F. P. Incropera Jan. 1993 229 p
(Contract DE-FG02-87ER-13759)
(DE93-008886; DOE/ER-13759/6) Avail: CASI HC A11/MF A03

Using 27 percent aq. NH4Cl solutions as transparent analog, shadowgraphy and dye injection were used to observe flow and morphology in unidirectional solidification (UDS) from below. Dendritic crystals that form at the cold surface reject lighter, solute-deficient fluid, and instability is shown by finger-type double-diffusive convection. As the mushy two-phase region grows, perturbations at the liquidus interface cause localized remelting and downward development of channels. Solutal plumes emanate from the channels, and in time, double-diffusive convection layers also form in the melt. When the solution is chilled at the sides as well as at the bottom, conditions are influenced by detachment and settling of crystals from the sidewall and by plumes from slanted channels. When a slow, oscillatory rocking motion is imposed on UDS, the freckle-type segregates in the final cast is suppressed. Within the melt, plumes and double-diffusive convection are eliminated. Inertially induced convection mixes the melt and produces a dense slurry. Although channels are eliminated from the bottom mushy region, overall heat transfer and macrosegregation in the cavity are unaffected by the slow rocking. Numerical simulations qualitatively predict trends in the field variables and provide insights on interdendritic flows and macrosegregation (freckle- and A-type segregates), although its quantitative predictions are hampered by simplifying assumptions. DOE

N93-25499# Sun Refining and Marketing Co., Marcus Hook, PA.
CATALYTIC CONVERSION OF LIGHT ALKANES
J. E. Lyons 30 Sep. 1992 21 p
(Contract DE-FC21-90MC-26029)
(DE93-009646; DOE/MC-26029/3273) Avail: CASI HC A03/MF A01

The third and last quarterly report of 1992 on the Catalytic Conversion of Light Alkanes reviews the work done between July, 1992 and September 30, 1992 on the Cooperative Agreement. The mission of this work is to devise a new catalyst which can be used in a simple economic process to convert the light alkanes in natural gas to oxygenate products which can either be used as clean-burning, high octane liquid fuels, as fuel components or as precursors to liquid hydrocarbon transportation fuel. During the past quarter we have continued to design, prepare, characterize and test novel catalysts for the mild selective reaction of light hydrocarbons with air or oxygen to produce alcohols directly. These catalysts are designed to form active metal oxo (MO) species and to be uniquely active for the homolytic cleavage of the carbon-hydrogen bonds in light alkanes producing intermediates which can form alcohols. We continue to investigate three molecular environments for the active catalytic species that we are trying to generate: electron-deficient macrocycles (PHASE I), polyoxometallates (PHASE II) and framework-substituted zeolites (PHASE III). DOE

N93-25500# Massachusetts Inst. of Tech., Cambridge.
CONVERSION OF LIGHT HYDROCARBON GASES TO METAL CARBIDES FOR PRODUCTION OF LIQUID FUELS AND CHEMICALS
A. F. Diaz, A. J. Modestino, J. B. Howard, and W. A. Peters Feb. 1993 5 p
(Contract DE-AC22-92PC-92111)
(DE93-009707; DOE/PC-92111/T1; FE-MIT-92111-1) Avail: CASI HC A01/MF A01

Light hydrocarbon gases could be reacted with low cost alkaline earth metal oxide (CaO, MgO) in high-temperature plasma reactor to achieve very high (less than 100 percent) gas conversion to H2, CO, and the corresponding metal carbides. These carbides could be stored, transported, and hydrolyzed to acetylene or methyl acetylene, which in turn could be upgraded to a wide range of chemicals and premium liquid hydrocarbon fuels. An electric arc discharge reactor was built for converting methane. Literature reviews were made. DOE

N93-25817# Texas A&M Univ., College Station. Dept. of Chemistry.
ACTIVATION OF METHANE BY CLEAN AND CHEMICALLY MODIFIED SINGLE CRYSTAL OXIDE SURFACES Annual Report, Oct. 1991 - Sep. 1992
D. W. Goodman Oct. 1992 37 p
(Contract GRI-5091-260-2182)
(PB93-157295; RF-6888; GRI-92/0486) Avail: CASI HC A03/MF A01

The oxidative coupling of methane to ethane over model MgO catalysts prepared under well-controlled, ultrahigh vacuum conditions was studied using a combination of surface science techniques and reaction kinetic measurements. The utilization of electron energy loss spectroscopy has allowed the characterization of a variety of defects in the catalysts and the identification of the active sites which are responsible for the methane coupling reaction. A quantitative correlation between the density of specific defects and the ethane formation rate indicates that (Li(+1)O(-)) centers are not likely directly involved in the methane activation step as previously proposed. The (Li(+1)O(-)) centers, rather, promote the formation in the near surface region of F-type centers which are responsible for the primary carbon-hydrogen bond scission reaction step. These results suggest new procedures to enhance the active site densities on Li/MgO catalysts and thus offer a potential new approach to enhanced activities and selectivities for this class of materials. Author (DTIC)

N93-25819# Michigan Univ., Ann Arbor. Gas Dynamics Labs.
A BASIC RESEARCH MODEL OF NATURAL GAS COMBUSTION IN TURBULENT FLOW, PHASE 2 Annual Report, 1 Aug. 1991 - 31 Jul. 1992
Werner J. A. Dahm, Gretar Tryggvason, and Robert Krasny 30 Sep. 1992 83 p
(Contract GRI-5088-260-1692)
(PB93-158509; GRI-92/0421-Phase-2) Avail: CASI HC A05/MF A01

This report describes progress made in the past twelve months in developing a local integral methods (LIM) model for numerically simulating natural gas mixing and combustion in complex flames. The LIM model is fundamentally different from conventional approaches for numerically simulating combustion in turbulent flames. It is based on the experimental observation that the strain-diffusion balance which establishes the mixing and reaction scales in turbulent flames leads to a self-similar internal structure in the diffusion-reaction layers which does not need to be continually recomputed. Instead, these diffusion and reaction scales are represented by a set of self-similar profile shapes whose moments are allowed to evolve freely to satisfy the governing equations. The resulting LIM computations thus need only follow the evolution of material surface in the flow and then solve ODE's (ordinary differential equations) on the surface, rather than PDE's (partial differential equations), throughout the whole flame. Results obtained to date show that the model is capable of correctly

predicting even highly sensitive non-linear characteristics associated with the combustion processes in turbulent natural gas flames, including the local flame extinction phenomenon in large Zeldovich number Arrhenius kinetics. The simplicity of the LIM technique allows large reductions in computation time in comparison with traditional computational approaches, thus allowing far more complex reaction chemistry to be addressed, as well as ranges of Reynolds, Schmidt, and Damkohler numbers which are otherwise completely inaccessible to simulation. Author (DTIC)

N93-25879# Connecticut Univ., Storrs.
ELECTRORHEOLOGICAL FLUIDS: A STRUCTURAL APPROACH TO MECHANISMS Final Report, 1 Aug. 1989 - 31 Jul. 1992
Montgomery T. Shaw 2 Nov. 1992 42 p
(Contract DAAL03-89-G-0080)
(AD-A260563; ARO-27210.4-MS-SM) Avail: CASI HC A03/MF A01

Fibrillation of the particulate phase has been widely observed in electrorheological (ER) fluids and has been suggested as a viable mechanism for the ER phenomena. In this work, the author has investigated the roles of particulate properties such as size and shape anisotropy, dielectric constant and dielectric anisotropy, and conductivity in the structural mechanism of ER fluids. Anhydrous ER fluids based on highly conjugated aromatic polymers were also developed. DTIC

N93-25916# Colorado State Univ., Fort Collins. Dept. of Chemistry.
LUMINESCENCE PROBE STUDIES OF IONOMERS. 3: DISTRIBUTION OF DECAY RATE CONSTANTS FOR TRIS BIPYRIDYL RUTHENIUM(2) IN NAFION MEMBRANES Interim Report
Jorge L. Colon and Charles R. Martin 9 Feb. 1993 25 p
(Contract N00014-82-K-0612)
(AD-A260764; TR-80; ONR-TR-80) Avail: CASI HC A03/MF A01

Measurements of the luminescence lifetime of Ru(bpy) sub 3(2+) (bpy = 2,2'-bipyridine) in Nafion were used to probe the heterogeneity of -SO3H(3) sites in the Nafion membrane. The decay kinetics of the probe ion are shown to depart from simple first-order behavior. Alber's model of a continuous distribution of rate constants is used to explain the decay kinetics. The results of these and related investigations indicate that the probe ions reside in sites with different local water activities. DTIC

N93-25920# Emory Univ., Atlanta, GA. Dept. of Chemistry.
THE INTERACTION OF HCN/DCN WITH Si(100)-2x1 Technical Report
Y. Bu, L. Ma, and M. C. Lin 1992 33 p
(Contract N00014-89-J-1235)
(AD-A260837; TR-14) Avail: CASI HC A03/MF A01

We have investigated the spectroscopy and reaction of HCN (DCN) adsorbed on Si(100)-2x1 at T(sub s) greater than or equal to 100 K using high resolution electron energy loss spectroscopy (HREELS), X-ray photoelectron spectroscopy (XPS), and ultraviolet photoelectron spectroscopy (UPS). HCN (DCN) formed dimers and/or polymers on the surface at 100 K and higher dosages (D greater than 4 L). The HREEL spectrum obtained after warming a 4.5 L HCN dosed surface to 200 K resembles that obtained with a lower HCN dosage (D less than 0.6 L). Two major species, HCNH and CN, could be identified from this spectrum. The former species showed peaks at 160, 368, and approx. 400 meV for HC=NH, CH, and NH stretching vibrations, respectively, while the latter showed a peak at 263 meV due to the C triple bonds N stretching vibration. In the corresponding DCN experiment, the DC=ND stretching mode was observed at 124 meV. Annealing the sample at 560 K appeared to cause the reorientation of the CN radical from an 'end-on' to a 'side-on' adsorption geometry as evidenced by HREELS, UPS, and XPS analyses. At 600-800 K, the breaking of CH, NH and CN bond occurred on the surface. Above 1000 K, only C and N species remained on the surface following the complete dissociation of CH, NH, and CN bonds and the desorption of H species. DTIC

N93-26045# Cornell Univ., Ithaca, NY. Dept. of Chemistry.
MECHANISMS OF DECOMPOSITION AND OXIDATION OF BORANE COMPOUNDS
S. H. Bauer 28 Dec. 1992 3 p
(Contract DAAL03-88-K-0187)
(AD-A261137; ARO-25523.2-CH) Avail: CASI HC A01/MF A01

The rates of gas phase reactions between boranes (B2H6, B5H9, B1OH14) and oxygen atoms ((sup 3)P state) were studied (at approximately 350 K) in a flow-tube reactor by determining time dependent levels of OH species, as functions of reactant concentrations. Quantitative fitting of these data for B2H6 and B5H9 led to mechanisms, and estimated rate constants, for the direct attack on the boranes, and for reactions of O((sub 3)P) with fragmentation products (in particular, HBO and HBOH). A degradation sequence was established for each. Measurements (via LIF) of (OH) from B1OH14 were not completed; our data show that under comparable conditions the deca produces approximately 60 fold higher (OH) than does penta. Our QPMS diagnostic of a newly designed flow-tube system and revitalized mass spectrometer permitted evaluation of a rate constant for the net destruction of B5H9, and qualitative estimates of relative concentrations of B5H9 fragmentation products. DTIC

N93-26220# Pennsylvania State Univ., University Park. Dept. of Mechanical Engineering.
FLAME-TURBULENCE INTERACTIONS Final Technical Report, 1 Nov. 1989 - 1 Oct. 1992
Domenic A. Santavicca 20 Jan. 1993 116 p
(Grant AF-AFOSR-0025-90)
(AD-A260957; AFOSR-93-0138TR) Avail: CASI HC A06/MF A02

The interaction between individual vortices and a premixed laminar flame was investigated in order to characterize the underlying dynamics of flame-turbulence interactions and thereby gain an improved understanding of premixed turbulent flames. In addition, previous two-dimensional flame structure measurements made in turbulent premixed flames were re-analyzed in order to obtain flame curvature and orientation statistics. DTIC

N93-26251# Aerospace Corp., El Segundo, CA. Technology Operations.
INTERACTION OF O2 WITH THE Fe(.84)Cr(.16) (001) SURFACE STUDIED BY PHOTOELECTRON SPECTROSCOPY
Jeffrey R. Lince, Stephen V. Didziulis, D. K. Shuh, T. D. Durbin, and J. A. Yarmoff 15 Jul. 1992 41 p
(Contract F04701-88-C-0089)
(AD-A261065; TR-92(2935)-10; SMC-TR-93-02) Avail: CASI HC A03/MF A01

The surface oxidation of a steel-like alloy was investigated to help determine how the efficiency of lubricant additives such as lead naphthenate might be affected by the chemical state of a high-Cr steel bearing surface. Soft X-ray photoelectron spectroscopy (SXPS; hv = 130 - 600 eV) employing synchrotron radiation and X-ray photoelectron spectroscopy (XPS; hv = 1486.6 eV) employing Al-K alpha X rays were used to study the effect of molecular oxygen adsorption (1 to 10(exp 4) L, where 1L triple bonds 10(exp-6) Torr-sec) on the (001) surface of Fe(.84)Cr(.16) at room temperature. The use of multiple photon energies allowed a qualitative determination of the distribution of species in the oxide film perpendicular to the surface. Prior to oxidation, Fe(.84)Cr(.16) samples were annealed to different temperatures to produce varying concentrations of Cr in the top few monolayers of the (001) surface. The differences between the oxide films produced on these different surfaces were determined with SXPS using primarily the Fe 3p, Cr 3p, and valence levels. Small amounts of carbidic carbon (less than or equal to 1 monolayer) that had segregated to the (001) surface of the Fe(.84)Cr(.16) alloy during initial sputter/anneal treatments were removed during the first approx. 5 L 02 exposure. In general, the resistance of the Fe(.84)Cr(.16) (001) surface to oxidation was directly related to the initial Cr concentration at the surface. The oxide films were richer in Cr compared to the bulk concentration for the lowest 02 exposures, and became increasingly enriched in Fe for increasing exposures, in agreement with studies by other groups. The resulting mixed Fe-Cr-O film contained Cr in the form of Cr(3+) for all exposures. DTIC

N93-26300# Missouri Univ., Rolla. Dept. of Chemistry.
STRUCTURE OF SODIUM 4-(1'-HEPTYLNONYL) BENZENESULFONATE ADSORBED ON ALUMINA USING H-2 NMR Interim Technical Report
E. Soederlind and Frank D. Blum 28 Feb. 1993 28 p
(Contract N00014-91-J-1274)
(AD-A261224; UMR-FDB-29) Avail: CASI HC A03/MF A01

Deuterium NMR was used to probe the molecular dynamics and structure of the surfactant sodium 4-(1'-heptylnonyl) benzenesulfonate (SHBS) adsorbed from water solution onto alumina. In order to investigate the dynamics of the headgroup, the phenyl ring of the surfactant was specifically deuterated. Two different surface coverages were studied in the temperature range of -30 to 80 C. At the adsorption plateau, evidence for the presence

of two distinct surfactant domains of approximately equal intensities, on the alumina surface, was found. One domain, the inner layer next to the solid surface, gave rise to a quadrupole splitting in the 2H NMR spectrum similar to that found for the surfactant in lamellar liquid crystals; whereas the second domain, the outer layer, gave rise to a broad unsplit resonance indicating a more isotropic environment. The chemical exchange between the two domains was found to be slow on the NMR timescale. At a lower coverage, a broad unsplit resonance appeared in the NMR spectrum showing that the molecular motions are not sufficiently anisotropic to cause any observable quadrupole splittings. With increasing temperature, resonances for both samples were narrowed, and the quadrupole splitting was reduced, reflecting more rapid reorientations of the surfactant molecules. DTIC

N93-26319# National Inst. of Standards and Technology, Boulder, CO. Thermophysics Div.

TABLES FOR THE THERMOPHYSICAL PROPERTIES OF ETHANE

D. G. Friend, J. F. Ely, and H. Ingham Jan. 1993 319 p See also NISTIR-3953

(PB93-160786; NIST/TN-1346) Avail: CASI HC A14/MF A03

The thermophysical properties of ethane are tabulated for a large range of the fluid state based on recently formulated correlations. For the thermodynamic properties, temperatures from 90 to 625 K at pressures less than 70 MPa are included; for the viscosity, the corresponding range is 90-500 K with pressures to 60 MPa; for the thermal conductivity the range is 90-600 K with pressures to 70 MPa. In addition to the tables of properties, algebraic expressions and associated tables of coefficients are given to allow additional property calculations. Graphical comparisons between experimental property determinations and the correlation are also given both for primary data used in the formulation of the correlations and for additional data. A listing of a FORTRAN program for the evaluation of ethane thermophysical properties is included. NTIS

N93-26323# National Inst. of Standards and Technology, Gaithersburg, MD. Applied and Computational Mathematics Div.

PHASE-FIELD MODELS FOR ANISOTROPIC INTERFACES

G. B. McFadden, A. A. Wheeler, R. J. Braun, S. R. Coriell, and R. F. Sekerka (Carnegie-Mellon Univ., Pittsburgh, PA.) Feb. 1993 28 p

(PB93-164564; NISTIR-5130) Avail: CASI HC A03/MF A01

The inclusion of anisotropic surface free energy and anisotropic linear interface kinetics in phase-field models is studied for the solidification of a pure material. The formulation is described for a two-dimensional system with a smooth crystal-melt interface and for a surface free energy that varies smoothly with orientation, in which case a quite general dependence of the surface free energy and kinetic coefficient on orientation can be treated; it is assumed that the anisotropy is mild enough that missing orientations do not occur. The method of matched asymptotic expansions is used to recover the appropriate anisotropic form of the Gibbs-Thomson equation in the sharp-interface limit in which the width of the diffuse interface is thin compared to its local radius of curvature. It is found that the surface free energy and the thickness of the diffuse interface have the same anisotropy, whereas the kinetic coefficient has an anisotropy characterized by the product of the interface thickness with the intrinsic mobility of the phase field. NTIS

N93-26402# Chicago Univ., IL.

DYNAMICS OF GAS-SURFACE INTERACTIONS Final Technical Report, 1 Jun. 1988 - 31 Oct. 1992

Steven J. Sibener 26 Jan. 1993 47 p

(Grant AF-AFOSR-0194-88)

(AD-A261402; AFOSR-93-0038TR) Avail: CASI HC A03/MF A01

This research initiative deals with the interaction of neutral particle, electron, and optical beams with well-characterized single crystal surfaces. These studies are motivated by a desire to understand and control surface reactions, such as surface oxidation, the technological need to characterize the physical properties of thin films and surfaces, and the desire to understand how energy and momentum are exchanged at the surface of a material when it is subjected to gas-surface collisions, electron-surface collisions, optical illumination, or chemical reaction. Experiments aimed at determining the surface phonon dispersion relations for a variety of clean and adsorbate covered systems play a central role in this program. Such measurements are crucial for elucidating how the force constants at e surface differ from those characteristic of the bulk for a given material, and how adsorption of atomic and molecular species modify the force constants, and hence electron density distributions, at and in the vicinity of the surface. The experimental program utilizes two, now fully operational, scattering laboratories that were constructed with significant DoD funding. One of these is a high resolution (energy and momentum) neutral particle scattering apparatus which routinely carries out single phonon inelastic as well as diffractive scattering measurements. The other laboratory houses an inelastic electron scattering instrument which also produces momentum-resolved inelastic scattering data. The capabilities of these two facilities complement each other in many important and useful ways. DTIC

N93-26439# Tennessee Univ., Knoxville. Dept. of Chemistry.

ELECTROCHEMICAL AND SPECTROSCOPIC STUDIES OF MOLTEN HALIDES Final Report, 15 Sep. 1988 - 14 Nov. 1992

Gleb Mamantov 8 Jan. 1993 76 p

(Grant AF-AFOSR-0307-88)

(AD-A261687; AFOSR-93-0101TR) Avail: CASI HC A05/MF A01

This program deals with chemistry and electrochemistry in molten halides, media which are used in the production of several important elements, such as aluminum, magnesium, and fluorine, in some high energy battery systems, as well as in other applications. The emphasis was placed on simple and complex chlorides and fluorides, for example the LiCl-KCl eutectic, the LiF-NaF-KF eutectic (FLINAK), alkali metal and organic tetrachloroaluminates, and cryolite. Pure fluorides usually have high melting points, for example cryolite, Na3AlF6, melts at 1000 C compared to NaAlCl4 which melts at 156 C. The use of molten mixtures of fluorides and chlorides can result in solute chemistry which is quite different from that observed in pure chloride. One complication which cannot be entirely avoided is caused by atmospheric contaminants. Even the parent alkali chloroaluminates contain millimolar quantities of complexed oxide which may result from the interaction of some melts with Pyrex glass. Therefore, studies of solute species at typical electrochemical or spectroscopic concentrations should take into account the presence of oxide species wherever possible. DTIC

N93-26502# Sandia National Labs., Albuquerque, NM.

VISIBLE LIGHT EMISSION FROM POROUS SILICON EXAMINED BY PHOTOLUMINESCENCE AND RAMAN SPECTROSCOPY

T. R. Guilinger, M. J. Kelly, D. R. Tallant, D. A. Redman, and D. M. Follstaedt 1992 9 p Presented at the 16th Material Research Society International Symposium on the Scientific Basis for Nuclear Waste Management Fall Meeting, Boston, MA, 30 Nov. - 5 Dec. 1992

(Contract DE-AC04-76DP-00789)

(DE93-006780; SAND-92-1560C; CONF-921101-100) Avail: CASI HC A02/MF A01

We describe the simultaneous acquisition of Raman and photoluminescence (PL) spectra on porous silicon (PS) samples that emit visible light. Spectra were acquired in both ex situ experiments (after exposure to air) as well as in situ experiments (with the PS covered either with the hydrofluoric acid electrolyte used in the formation process or water). In one set of ex situ experiments, we observed an inconsistency in the shift of the wavelength of maximum luminescence intensity for PS samples that exhibit oxygenated character in the Raman spectra. A higher current density produced a red shift in the PL spectra in one experiment, while chemical dissolution of the PS by hydrofluoric acid produced the well-known blue shift in another case. In two in situ experiments, we observed very weak and red-shifted PL for a PS sample immersed in HF (compared to the same sample measured later in air) while in another we immersed air-exposed PS in water and observed a 15-fold increase in PL intensity along with a blue shift in the luminescence maximum. DOE

N93-26505# Los Alamos National Lab., NM.

SPECTROSCOPIC EFFECTS OF DISORDER AND VIBRATIONAL LOCALIZATION IN MIXED-HALIDE METAL-HALIDE CHAIN SOLIDS

S. P. Love, B. Scott, L. A. Worl, S. C. Huckett, A. Saxena, X. Z. Huang, A. R. Bishop, and B. I. Swanson 1993 10 p Presented at the International Society for Optical Engineering (SPIE) Conference, Los Angeles, CA, 16-23 Jan. 1993

(Contract W-7405-eng-36)

(DE93-007361; LA-UR-93-0004; CONF-930159-11) Avail: CASI HC A02/MF A01

Resonance Raman techniques, together with lattice-dynamics and

Peierls-Hubbard modelling, are used to explore the electronic and vibrational dynamics of the quasi-one-dimensional metal-halogen chain solids (Pt(en)2)(Pt(en)2 X2)(ClO4)4, (en = C2H8N2 and X = Cl, Br), abbreviated 'PLX.' The mixed-halide materials PtCl(1-x)Br(x) and PtCl(1-x)I(x) consist of long mixed chains with heterojunctions between segments of the two constituent materials. Thus, in addition to providing mesoscale modulation of the chain electronic states, they serve as prototypes for elucidating the properties to be expected for macroscopic heterojunctions of these highly nonlinear materials. Once a detailed understanding of the various local vibrational modes occurring in these disordered solids is developed, the electronic structure of the chain segments and junctions can be probed by tuning the Raman excitation through their various electronic resonances. DOE

N93-26595# Ames Lab., IA.
THE SURFACE CHARACTERIZATION OF A SERIES OF HYDROXYBENZENES ON Ag(111): AN EELS AND TDS STUDY Ph.D. Thesis
B. S. Nielsen 27 Jan. 1993 262 p
(Contract W-7405-eng-82)
(DE93-007541; IS-T-1541) Avail: CASI HC A12/MF A03

Interaction of a series of hydroxybenzenes with Ag(111) is investigated by thermal desorption spectroscopy (TDS) and high resolution electron energy loss spectroscopy (EELS). The following were studied: mono-hydroxybenzene; phenol; the o-, m-, and p-dihydroxybenzenes; catechol; resorcinol; hydroquinone; and the 1,2.3-trihydroxybenzene, pyrogallol. Dehydrogenation of the hydroxyl groups upon adsorption is not directly observed in the TDS studies: however, the EELS results suggest possible dehydrogenation. The apparent O-H bond scission is attributed to hydrogen bonding between the surface molecules or to the orientation of the O-H bond aids with respect to the metal surface. Orientations of the mono- and dihydroxybenzene molecules are temperature dependent, whereas that of the trihydroxybenzene may be attributed to the number and position of the hydroxyl substitutents. Phenol and catechol both undergo an inclined-to-perpendicular orientational change. Resorcinol and hydroquinone undergo a perpendicular-to-inclined transformation. Finally, pyrogallol remains inclined at all temperatures until decomposition. DOE

N93-26599# California Univ., Berkeley. Lawrence Berkeley Lab.
BIMOLECULAR REACTION DYNAMICS FROM PHOTOELECTRON SPECTROSCOPY OF NEGATIVE IONS Ph.D. Thesis
S. E. Bradforth Nov. 1992 422 p
(Contract DE-AC03-76SF-00098)
(DE93-007669; LBL-33328) Avail: CASI HC A18/MF A04

The transition state region of a neutral bimolecular reaction may be experimentally investigated by photoelectron spectroscopy of an appropriate negative ion. The photoelectron spectrum provides information on the spectroscopy and dynamics of the short lived transition state and may be used to develop model potential energy surfaces that are semi-quantitative in this important region. The principles of bound (yields) bound negative ion photoelectron spectroscopy are illustrated by way of an example: a full analysis of the photoelectron bands of CN(-), NCO(-) and NCS(-). Transition state photoelectron spectra are presented for the following systems Br + HI, Cl + HI, F + HI, F + CH3OH, F + C2H5OH, F + OH, and F + H2. A time dependent framework for the simulation and interpretation of the bound (yields) free transition state photoelectron spectra is subsequently developed and applied to the hydrogen transfer reactions Br + HI, F + OH (yields) OP-3, D-1 + HF, and F + H2. The theoretical approach for the simulations is a fully quantum-mechanical wave packet propagation on a collinear model reaction potential surface. The connection between the wavepacket time evolution and the photoelectron spectrum is given by the time autocorrelation function. For the benchmark F + H2 system, comparisons with three-dimensional quantum calculations are made. DOE

N93-26602# Naval Postgraduate School, Monterey, CA.
ATOMIZATION AND COMBUSTION OF A GELLED, METALLIZED SLURRY FUEL M.S. Thesis
Bruce C. Urbon Dec. 1992 31 p
(AD-A261776) Avail: CASI HC A03/MF A01

Two commercially available atomizers were tested for their ability to atomize a gelled boron slurry fuel. Particle size distributions were measured in non-reacting flow using a Malvern 2600 HSD Laser Diffraction Particle Sizer. A sub-scale ramjet combustor was designed and fabricated which utilized a sudden expansion inlet dump together with inlet air swirl for flame stabilization. An airblast atomizer produced sufficiently small particles for good combustion, but at the cost of a high pressure drop across the atomizer, making it impractical for use in a slurry fueled ramjet. Sustained steady combustion of the slurry fuel was not achieved using the airblast atomizer. A whistle type ultrasonic atomizer also produced sufficiently small particles and at a much lower pressure drop across the atomizer. Sustained stable combustion was achieved using the ultrasonic atomizer which yielded a combustion efficiency of 76 percent at 96 psia and an equivalence ratio of 0.78. DTIC

N93-25037# Ecole Nationale Superieure de Mecanique et des Microtechniques, Besancon (France). Lab. de Chronometrie Electronique et Piezoelectricite.
ANISOTROPIC ETCHING OF SILICON IN KOH SOLUTIONS
A. Brahim-Bounab and C. R. Tellier *In* ESA, Frequency and Time Forum Jun. 1992 p 349-354 (For primary document see N93-24978 09-70)
Copyright Avail: CASI HC A02/MF A04

N93-26010 Naval Postgraduate School, Monterey, CA.
SOLID FUEL SUPERSONIC COMBUSTION
W. J. Angus, M. A. Witt, D. Laredo, and D. W. Netzer *In* JHU, 29th JANNAF Combustion Subcommittee Meeting, Volume 2 Oct. 1992 p 47-57 (For primary document see N93-26005 09-20)
Avail: CPIA, 10630 Little Patuxent Pkwy., Suite 202, Columbia, MD 21044-3200 HC

N93-26011 Wright Lab., Wright-Patterson AFB, OH. Special Projects Office.
GASP 1.3 RESULTS FOR THE TRANSVERSE HYDROGEN REACTING JET
Balu Sekar *In* JHU, 29th JANNAF Combustion Subcommittee Meeting, Volume 2 Oct. 1992 p 59-76 (For primary document see N93-26005 09-20)
Avail: CPIA, 10630 Little Patuxent Pkwy., Suite 202, Columbia, MD 21044-3200 HC

N93-26016 Rockwell International Corp., Canoga Park, CA. Rocketdyne Div.
DEVELOPMENT OF A SECOND GENERATION SPRAY COMBUSTION CODE
Pak-Yan Liang *In* JHU, 29th JANNAF Combustion Subcommittee Meeting, Volume 2 Oct. 1992 p 119-129 (For primary document see N93-26005 09-20)
Avail: CPIA, 10630 Little Patuxent Pkwy., Suite 202, Columbia, MD 21044-3200 HC

N93-26019 Jet Propulsion Lab., California Inst. of Tech., Pasadena.
HYBRID ROCKET FUEL COMBUSTION STUDY
L. D. Strand and N. S. Cohen (Cohen, Norman S. Professional Services, Inc., Redlands, CA.) *In* JHU, 29th JANNAF Combustion Subcommittee Meeting, Volume 2 Oct. 1992 p 149-154 (For primary document see N93-26005 09-20)
Avail: CPIA, 10630 Little Patuxent Pkwy., Suite 202, Columbia, MD 21044-3200 HC

N93-26021* Aerojet-General Corp., Iuka, MS.
IMPROVED BURN RATE DETERMINATION TECHNIQUES
T. J. Watson, F. W. Jordan, L. W. Stockham, and N. Leontsinis *In* JHU, 29th JANNAF Combustion Subcommittee Meeting, Volume 2 Oct. 1992 p 165-174 Sponsored by NASA. Marshall Space Flight Center (For primary document see N93-26005 09-20)
(Contract WE10E3640N)
Avail: CPIA, 10630 Little Patuxent Pkwy., Suite 202, Columbia, MD 21044-3200 HC

N93-26023* Aerojet-General Corp., Iuka, MS.
DETERMINATION OF BURN RATE REQUIREMENTS FROM ASRM PERFORMANCE SPECIFICATIONS
S. S. Schlueter, F. W. Jordan, and L. W. Stockham *In* JHU, 29th JANNAF Combustion Subcommittee Meeting, Volume 2 Oct. 1992

p 185-191 Sponsored by NASA. Marshall Space Flight Center (For primary document see N93-26005 09-20)
(Contract WE10E3640N)
Avail: CPIA, 10630 Little Patuxent Pkwy., Suite 202, Columbia, MD 21044-3200 HC

N93-26025 Army Research Lab., Aberdeen Proving Ground, MD.
FLAME STRUCTURE STUDIES OF A LEAN, 20 TORR H2/N2O/AR FLAME EMPLOYING MOLECULAR BEAM MASS SPECTROMETRY
D. C. Dayton, R. C. Sausa, and A. W. Miziolek *In* JHU, 29th JANNAF Combustion Subcommittee Meeting, Volume 2 Oct. 1992 p 197-203 (For primary document see N93-26005 09-20)
Avail: CPIA, 10630 Little Patuxent Pkwy., Suite 202, Columbia, MD 21044-3200 HC

N93-26026 Army Research Lab., Aberdeen Proving Ground, MD.
MODELING OF H2/N2O FLAMES
W. R. Anderson and C. M. Faust *In* JHU, 29th JANNAF Combustion Subcommittee Meeting, Volume 2 Oct. 1992 p 205-213 (For primary document see N93-26005 09-20)
Avail: CPIA, 10630 Little Patuxent Pkwy., Suite 202, Columbia, MD 21044-3200 HC

N93-26027 Princeton Univ., NJ. Dept. of Mechanical and Aerospace Engineering.
KINETIC STUDIES IN GAS-PHASE REACTION MECHANISMS IMPORTANT TO THE COMBUSTION PROCESS OF HIGH ENERGY DENSITY MATERIALS: THE H2/NO2 REACTION
R. A. Yetter, N. Ilincic, F. L. Dryer, M. Allen, and J. Gatto *In* JHU, 29th JANNAF Combustion Subcommittee Meeting, Volume 2 Oct. 1992 p 215-223 (For primary document see N93-26005 09-20)
Avail: CPIA, 10630 Little Patuxent Pkwy., Suite 202, Columbia, MD 21044-3200 HC

N93-26028 Army Research Lab., Aberdeen Proving Ground, MD.
DARK ZONE MODELING OF SOLID PROPELLANT FLAMES
J. A. Vanderhoff, W. R. Anderson, and A. J. Kotlar *In* JHU, 29th JANNAF Combustion Subcommittee Meeting, Volume 2 Oct. 1992 p 225-237 (For primary document see N93-26005 09-20)
Avail: CPIA, 10630 Little Patuxent Pkwy., Suite 202, Columbia, MD 21044-3200 HC

N93-26029 Army Research Lab., Aberdeen Proving Ground, MD.
DETECTION OF ATOMIC OXYGEN AND HYDROGEN IN SOLID PROPELLANT FLAMES AND PYROLYSIS GASES USING MULTIPHOTON LASER-INDUCED FLUORESCENCE
B. E. Forch *In* JHU, 29th JANNAF Combustion Subcommittee Meeting, Volume 2 Oct. 1992 p 239-248 (For primary document see N93-26005 09-20)
Avail: CPIA, 10630 Little Patuxent Pkwy., Suite 202, Columbia, MD 21044-3200 HC

N93-26030 Army Research Lab., Aberdeen Proving Ground, MD.
TOMOGRAPHIC ANALYSIS OF SIGHT INFRARED SPECTRA OF LOW PRESSURE FLAMES
Kevin L. McNesby and Robert A. Fifer *In* JHU, 29th JANNAF Combustion Subcommittee Meeting, Volume 2 Oct. 1992 p 249-262 (For primary document see N93-26005 09-20)
Avail: CPIA, 10630 Little Patuxent Pkwy., Suite 202, Columbia, MD 21044-3200 HC

N93-26031 Aerodyne Research, Inc., Billerica, MA.
INFRARED FIBER OPTIC DIAGNOSTIC FOR SOLID PROPELLANT COMBUSTION
J. Wormhoudt and P. L. Kebabian *In* JHU, 29th JANNAF Combustion Subcommittee Meeting, Volume 2 Oct. 1992 p 263-268 (For primary document see N93-26005 09-20)
Avail: CPIA, 10630 Little Patuxent Pkwy., Suite 202, Columbia, MD 21044-3200 HC

N93-26032 Army Research Lab., Aberdeen Proving Ground, MD.
CONDENSED-PHASE PROCESSES DURING SOLID PROPELLANT COMBUSTION. PART 4: CHEMICAL AND MICROSCOPIC EXAMINATION OF LASER-IRRADIATED PROPELLANT SAMPLES
M. A. Schroeder, R. A. Beyer, A. Cohen, R. A. Fifer, and R. A. Pesce-Rodriquez *In* JHU, 29th JANNAF Combustion Subcommittee Meeting, Volume 2 Oct. 1992 p 269-281 (For primary document see N93-26005 09-20)
Avail: CPIA, 10630 Little Patuxent Pkwy., Suite 202, Columbia, MD 21044-3200 HC

N93-26036 Naval Air Warfare Center, China Lake, CA. Weapons Div.
ADN PROPELLANT DIFFUSION FLAME STRUCTURE
Tim Parr and Donna Hanson-Parr *In* JHU, 29th JANNAF Combustion Subcommittee Meeting, Volume 2 Oct. 1992 p 313-327 (For primary document see N93-26005 09-20)
Avail: CPIA, 10630 Little Patuxent Pkwy., Suite 202, Columbia, MD 21044-3200 HC

N93-26041 Naval Air Warfare Center, China Lake, CA. Weapons Div.
FLAME RESPONSE IN OSCILLATORY SOLID PROPELLANT COMBUSTION
Tim Parr, Donna Hanson-Parr, and Jerry Finlinson *In* JHU, 29th JANNAF Combustion Subcommittee Meeting, Volume 2 Oct. 1992 p 369-374 (For primary document see N93-26005 09-20)
(Contract N00149-0-WX-24043)
Avail: CPIA, 10630 Little Patuxent Pkwy., Suite 202, Columbia, MD 21044-3200 HC

N93-26042 Illinois Univ., Urbana-Champaign. Department of Mechanical and Industrial Engineering.
AN EXPERIMENTAL AND ANALYTICAL STUDY OF THE UNSTEADY COMBUSTION OF HOMOGENEOUS ENERGETIC SOLIDS USING THE LASER-RECOIL METHOD
S. F. Son, M. H. Hites, and M. Q. Brewster *In* JHU, 29th JANNAF Combustion Subcommittee Meeting, Volume 2 Oct. 1992 p 375-385 (For primary document see N93-26005 09-20)
(Contract N00014-91-J-1977)
Avail: CPIA, 10630 Little Patuxent Pkwy., Suite 202, Columbia, MD 21044-3200 HC

N93-26043 Illinois Univ., Urbana-Champaign. Department of Mechanical and Industrial Engineering.
DYNAMIC BURNING RATE MEASUREMENTS OF METALIZED COMPOSITE PROPELLANTS USING THE LASER-RECOIL TECHNIQUE
M. Q. Brewster, M. H. Hites, and S. F. Son *In* JHU, 29th JANNAF Combustion Subcommittee Meeting, Volume 2 Oct. 1992 p 387-397 Sponsored by Thiokol Corporation (For primary document see N93-26005 09-20)
Avail: CPIA, 10630 Little Patuxent Pkwy., Suite 202, Columbia, MD 21044-3200 HC

N93-26079*# New Mexico State Univ., Las Cruces. Dept. of Chemical Engineering.
MODELING OF THE WSTF FRICTIONAL HEATING APPARATUS IN HIGH PRESSURE SYSTEMS Final Report
Christopher T. Skowlund *In* NASA. Johnson Space Center, National Aeronautics and Space Administration (NASA)/American Society for Engineering Education (ASEE) Summer Faculty Fellowship Program, 1992, Volume 2 Dec. 1992 p 13 (For primary document see N93-26070 09-99)
(Grant NGT-44-005-803)
Avail: CASI HC A03/MF A02

26 METALLIC MATERIALS

Includes physical, chemical, and mechanical properties of metals, e.g., corrosion; and metallurgy.

N93-25095# Engineering Science Software, Inc., Smithfield, RI.
A MICROMECHANICAL VISCOPLASTIC STRESS-STRAIN MODEL WITH GRAIN BOUNDARY SLIDING
K. P. Walker 28 Feb. 1993 5 p
(Contract DE-AC02-88ER-13895)
(DE93-009109; DOE/ER-13895/3) Avail: CASI HC A01/MF A01

This project was initiated to develop and experimentally verify a self-consistent micromechanics model of polycrystalline Hastelloy-X. A viscoplastic constitutive model was developed for the estimation of the overall mechanical behavior of Hastelloy-X polycrystalline metal from a knowledge of the single crystal behavior. The deformation behavior of the polycrystal was derived from that of single crystals by using a self-consistent method. The single crystal behavior was developed by summing postulated slip on crystallographic slip systems. Plasticity and creep were modeled using a unified viscoplastic model which includes the interaction between these phenomena at elevated temperatures. The validity of the model was directly tested by critical experiments on Hastelloy-X in both the single crystal and polycrystalline versions. DOE

N93-25128*# Case Western Reserve Univ., Cleveland, OH.
HOT CORROSION OF THE B2 NICKEL ALUMINIDES Final Report
David L. Ellis Mar. 1993 288 p
(Contract NCC3-94; RTOP 505-63-40)
(NASA-CR-191082; E-7621; NAS 1.26:191082) Avail: CASI HC A13/MF A03

The hot corrosion behavior of the B2 nickel aluminides was studied to determine the inherent hot corrosion resistance of the beta nickel aluminides and to develop a mechanism for the hot corrosion of the beta nickel aluminides. The effects of the prior processing of the material, small additions of zirconium, stoichiometry of the materials, and preoxidation of the samples were also examined. Additions of 2, 5, and 15 w/o chromium were used to determine the effect of chromium on the hot corrosion of the beta nickel aluminides and the minimum amount of chromium necessary for good hot corrosion resistance. The results indicate that the beta nickel aluminides have inferior inherent hot corrosion resistance despite their excellent oxidation resistance. Prior processing and zirconium additions had no discernible effect on the hot corrosion resistance of the alloys. Preoxidation extended the incubation period of the alloys only a few hours and was not considered to be an effective means of stopping hot corrosion. Stoichiometry was a major factor in determining the hot corrosion resistance of the alloys with the higher aluminum alloys having a definitely superior hot corrosion resistance. The addition of chromium to the alloys stopped the hot corrosion attack in the alloys tested. From a variety of experimental results, a complex hot corrosion mechanism was proposed. During the early stages of the hot corrosion of these alloys the corrosion is dominated by a local sulphidation/oxidation form of attack. During the intermediate stages of the hot corrosion, the aluminum depletion at the surface leads to a change in the oxidation mechanism from a protective external alumina layer to a mixed nickel-aluminum spinel and nickel oxide that can occur both externally and internally. The material undergoes extensive cracking during the later portions of the hot corrosion. Author

N93-25149# Ames Lab., IA.
PROCESSING AND PROPERTIES OF Ti5Si3
A. J. Thom, Y. Kim, and M. Akinc 1992 7 p Presented at the 16th Material Research Society International Symposium on the Scientific Basis for Nuclear Waste Management Fall Meeting, Boston, MA, 30 Nov. - 5 Dec. 1992
(Contract W-7405-eng-82)
(DE93-007284; IS-M-743; CONF-921101-82) Avail: CASI HC A02/MF A01

The mechanical properties and oxidation resistance of HIPed Ti5Si3 is measured. HIPing submicron size powder compacts produces a crack-free, fine grain microstructure with significantly higher hardness and toughness than a coarse grain microstructure which contains microcracks within larger grains. Oxidation resistance is also influenced by the grain size. Coarse-grained material has much lower mass gain in an oxidizing atmosphere and exhibits parabolic oxidation kinetics. Fine-grained material shows higher mass gain. The oxidation resistance of fine grained material was measured from 700-1000 C in air. At 700 C, the mass gain at 120 hours is 0.07 mg/sq. cm. At 900 C, cracking of the scale leads to linear oxidation kinetics and significantly higher mass gain. DOE

N93-25255# Westinghouse Hanford Co., Richland, WA.
MECHANICAL PROPERTIES OF MARTENSITIC ALLOY AISI 422
F. H. Huang, W. L. Hu, and M. L. Hamilton (Pacific Northwest Lab., Richland, WA.) Sep. 1992 16 p Presented at the 16th ASTM International Conference on Radiation Effect on Materials, Denver, CO, 22-25 Jun. 1992
(Contract DE-AC06-87RL-10930)
(DE93-006563; WHC-SA-1676; CONF-920673-16) Avail: CASI HC A03/MF A01

HT9 is a martensitic stainless steel that has been considered for structural applications in liquid metal reactors (LMR's) as well as in fusion reactors. AISI 422 is a commercially available martensitic stainless steel that closely resembles HT9, and was studied briefly under the auspices of the US LMR program. Previously unpublished tensile, fracture toughness, and charpy impact data on AISI 422 were reexamined for potential insights into the consequences of the compositional differences between the two alloys, particularly with respect to current questions concerning the origin of the radiation-induced embrittlement observed in HT9. DOE

N93-25336# Lawrence Livermore National Lab., CA.
RADIATION-INDUCED DISORDERING AND DEFECT PRODUCTION IN CuAu AND NiAl STUDIED BY MOLECULAR DYNAMICS SIMULATION
T. DiazdelaRubia, G. A. Janaway, M. W. Guinan, A. Caro (Paul Scherrer Inst., Villigen, Switzerland.), M. Spaczer (Paul Scherrer Inst., Villigen, Switzerland.), and M. Victoria (Paul Scherrer Inst., Villigen, Switzerland.) 17 Sep. 1992 19 p Presented at the 8th International Conference on Ion Beam Modification of Materials, Heidelberg, Germany, 7-11 Sep. 1992
(Contract W-7405-eng-48)
(DE93-007506; UCRL-JC-111660; CONF-9209200-7) Avail: CASI HC A03/MF A01

Molecular dynamics computer simulations are used to investigate the kinetics of disordering induced by energetic displacement cascades in two ordered intermetallics, Cu3Au and Ni3Al. The mechanisms of defect production in these systems are studied and the results are compared to recent findings in pure metals. Embedded atom potentials are employed which reproduce the main features of the phase diagram, including a disordering transition below the melting point T(sub m) in Cu3Au and an ordered compound up to T(sub m) in Ni3Al. Events with 5 keV recoil energy in crystals containing up to 157,216 atoms at 10 K are simulated. Results of the influence of the displacement cascade on the order parameters are presented and their temporal and spatial evolution are described. Atomic miding in the cascade regions in terms of the atomic mobilities in each sublattice are discussed. The influence of the ordering energy and the melting temperature in the behavior of the compounds is emphasized. DOE

N93-25428# Ames Lab., IA.
THEORETICAL PREDICTIONS OF PLATINUM-RHODIUM BIMETALLIC CATALYSTS Ph.D. Thesis
A. M. Schoeb 27 Jan. 1993 81 p
(Contract W-7405-eng-82)
(DE93-007540; IS-T-1635) Avail: CASI HC A05/MF A01

After a general introduction to supported bimetallic catalysts and automobile catalytic converters (supports, base metal promoters, noble metals, deterioration of 3-way catalysts, current/future technology), a paper is presented on the topic of surface segregation in bimetallic catalysts. The catalytic properties are influenced by the structure of the cluster surface. Two methods are described to treat this problem: the demanding corrected effective medium (CEM) theory (a non-self-consistent density functional based method); and the simple method of surface modified pair potentials. Predictions are compared with experiment for the heat of formation in Rh(x)Pt(1-x) alloys and for surface segregation in Rh(0.9)Pt(0.1)(111). Results on shape, site composition, and surface micromixing are shown for 201 atom clusters (dispersion of 0.6) and Rh(x)Pt(1-x)(111). The CEM calculated cohesive energy of Rh is slightly smaller than for Pt, but the surface energy of Rh is larger. The driving force for surface segregation is the

relative surface energies, not the relative cohesive energies. One can predict surface energy differences by accounting for the variation of the bond energy with coordination. Recommendations for the development of improved automobile exhaust catalysts are given. The Monte Carlo bimetallic simulation program is described. DOE

N93-25436 Surrey Univ., Guildford (England).
INTERNAL STRESSES AND THE CYCLIC DEFORMATION OF AN ALUMINUM MATRIX COMPOSITE Ph.D. Thesis
Birgir Johannesson 1992 221 p
Avail: Univ. Microfilms Order No. BRDX98103

The development of internal stresses in planar random Saffil fiber reinforced with a range of fiber volume fractions was studied theoretically and in monotonic and cyclic deformation (Bauschinger) experiments at room temperature and 77 K. The Eshelby S tensor for a planar random array of fibers is calculated. Because the aluminum/Saffil composites are not isotropic in the transverse directions, the plastic strain used in the calculations has to be determined experimentally. A method for quantifying the anisotropic plastic flow of the aluminum/Saffil composites is proposed and the results are used in calculations of the mean stress hardening rate. The measurements of the thermal stresses obtained in the Bauschinger experiments are in quantitative agreement with results obtained in monotonic tests. The magnitude of the thermal stress at room temperature or 77 K is independent of fiber volume fraction and a comparison with predictions shows that relaxation of the thermal stress increases with fiber volume fraction. Cycling in the Bauschinger experiments reduces the thermal stress and hence the separation of the mean and thermal stresses is essential for a reliable measurement of the mean stress hardening rate. Matrix hardening contributes considerably to the overall hardening of the composite, both at room temperature and 77 K. The modified Orowan-Wilson model, which enables the plastic friction coefficient to be measured in copper-tungsten composites, was applied to the aluminum/Saffil composites. The model requires both the mean stress and the peak stress curves obtained in Bauschinger experiments to be linear in plastic strain. The temperature dependence of the mean stress hardening rate suggests that relaxation is thermally activated. A model for relaxation of the mean stress is proposed. An equation is derived for the number of Orowan loops per fiber and it is assumed that the rate controlling mechanism of relaxation is cross slip of screw dislocations. The estimated activation energy is independent of fiber volume fraction, but the activation volume decreases with increasing fiber volume fraction. Dissert. Abstr.

N93-25464 Illinois Univ. at Urbana-Champaign, Savoy.
LASER INITIATED CORROSION PITS ON ALUMINUM Ph.D. Thesis
David Wayne Buzza 1992 191 p
Avail: Univ. Microfilms Order No. DA9305476

A laser initiation technique was developed that could control both the time and the location of pit initiation on a pure aluminum electrode that was immersed in 1.0 M NaCl, pH 11 solution and held under an applied potential. A new technique which was based on the laser initiation technique was invented to initiate an ordered array of pits of up to 61 pits that were spaced 100 micron apart. A study of the shape of single pits by a 3-D post electrolysis SEM method revealed detailed characteristics of pitting corrosion, such as: pit repassivation and secondary pit nucleation within a primary pit. The study also showed that single corrosion pits tended to be round and polished during the early stages of growth (less than 90 s) for applied potential of -0,7 to -0.52 V, SCE, which suggested that a precipitated electropolishing film was present on the pit surface. It was also found that the measured dependency of the current density and the radius of a single pit with time, agreed, for over 3 orders of magnitude of time, with a theoretical model which was based on the pit growth rate being limited by the diffusion controlled dissolution rate of a precipitated aluminum oxychloride film. Other experimental results were found to be inconsistent for a pit growth rate that was limited by the potential drop in solution. Therefore, for these conditions, it was concluded that the pit growth rate was limited by the diffusion controlled dissolution rate of a precipitated aluminum oxychloride film, despite the presence of a vigorous gas evolution reaction. Additional experimental results suggested that a condition for pit repassivation was the disapperance of the precipitated salt film. Once the salt film had disappeared, the pit stability was found to depend on both the (Cl(-)) in the solution adjacent to the pit surface and the applied potential. The pit stability criteria was found to be independent of the pit size. However, large pits were found to be more stable than smaller pits owing to the increased transport resistance for a larger pit. In conclusion, for this system, transport processes were found to be important in determining the pit growth rate and the pit stability. Dissert. Abstr.

N93-25492# Oak Ridge National Lab., TN.
HIGH TEMPERATURE FRACTURE TOUGHNESS OF Ni3Al ALLOY IC-396M
D. J. Alexander 1992 7 p The 16th Material Research Society International Symposium on the Scientific Basis for Nuclear Waste Management Fall Meeting held in Boston, MA, 30 Nov. - 5 Dec. 1992
(Contract DE-AC05-84OR-21400)
(DE93-008564; CONF-921101-97) Avail: CASI HC A02/MF A01

The fracture toughness of the nickel aluminide alloy IC-396M has been measured from room temperature to 800C. Material was tested in the as-cast condition. Specimens were oriented for crack growth either parallel or perpendicular to the dendritic structure (C-R and R-C orientations, respectively). Both orientations had acceptable levels of toughness from room temperature to 600C. At 650C the toughness decreased markedly with some recovery at 800C. Examination of the fracture surfaces revealed that the fracture mode changed from a ductile tearing mechanism at temperatures up to 600C to interdendritic fracture at 650C and higher temperatures. At 650C the crack grew along the dendrite axis for the C-R specimens, but for the R-C specimens the crack grew out-of-plane in attempting to follow the dendritic structure. It is believed that the presence of the sharp crack in the fracture toughness specimens allowed oxygen to penetrate to the crack tip, where straining exposed metal surfaces that were not protected by an oxide layer. The result was embrittlement of the interdendritic regions and low energy fracture, analogous to intergranular fracture in wrought materials. DOE

N93-25502# North Carolina State Univ., Raleigh. Dept. of Chemistry.
THEORETICAL STUDIES OF SURFACE REACTIONS ON METALS AND ELECTRONIC MATERIALS
J. L. Whitten 31 Jan. 1993 15 p
(Contract DE-FG05-90ER-45436)
(DE93-009761; DOE/ER-45436/4) Avail: CASI HC A03/MF A01

Studies of a variety of adsorbates on Ni have been completed; adsorption energies were determined for CH, CH2, CH3, H, NH3, H2O, and C6H6 on Ni(111). A refined calculation of the reaction of methane with Ni was completed. Other studies included H2 and SiH4 adsorption/decomposition on Si surfaces, Si-Si dimer bond length, activity energy barriers for reaction of CH4 and CH3F with Si(111). Studies were begun on deposition of C on Ni(111). New directions were explored for reaction of methane with transition metal surfaces; work was completed for a Ni(111) surface containing a substitutional iron atom. Twenty abstracts of papers are presented. DOE

N93-25519# Oak Ridge National Lab., TN.
ROOM TEMPERATURE FRACTURE OF FeCo
L. Zhao, I. Baker (Dartmouth Coll., Hanover, NH.), and E. P. George 1992 7 p Meeting of the Materials Research Society held in Pittsburgh, PA, 3 Nov. - 4 Dec. 1992
(Contracts DE-AC05-84OR-21400; DE-FG02-87ER-45311; DE-AC05-76OR-00033)
(DE93-008266; CONF-9211127-3) Avail: CASI HC A02/MF A01

FeCo is a B2 intermetallic compound which undergoes an order-disorder transformation. In this paper, the effects of changes in both constitutional and thermal disorder on the room temperature fracture of FeCo are presented. Tensile tests were performed on three compositions of FeCo, Fe30Co70, Fe50Co50, and Fe70Co30. The resulting fracture surfaces were examined by SEM and the grain boundary chemistry was investigated by Auger electron spectroscopy (AES). Ordered Fe50Co50 and Fe70Co30 were very brittle, fracture occurring before yielding, with intergranular fracture occurring in most grains. In contrast, ordered Fe30Co70 showed about 18 percent elongation and exhibited a dimple-type fracture. It was also found that disordering improved the ductility of each composition but had little influence on the fracture mode. AES showed that a low level of sulfur segregation was present at the grain boundaries, suggesting that sulfur segregation alone was not responsible for the brittle behavior of the ordered alloys. DOE

N93-25632# Naval Postgraduate School, Monterey, CA.
STUDY OF GRAIN REFINEMENT IN Al ALLOY 2519 USING BACKSCATTERING ORIENTATION-CONTRAST MODE IN THE SCANNING ELECTRON MICROSCOPE M.S. Thesis
Jeffrey R. Dunlap Dec. 1992 57 p
(AD-A260886) Avail: CASI HC A04/MF A01

The effects of variations in thermomechanical processing (TMP) parameters on grain refinement in 2519 Al-Cu alloy were studied. Refined grains enhance tensile ductility and are a prerequisite for superplastic response. The TMP variables were adjusted based on particle stimulated nucleation (PSN) theory. Process modifications included increased initial overaging time and decreased subsequent warm rolling temperatures. Backscatter orientation-contrast (BSOC) techniques for the scanning electron microscope (SEM) were developed to achieve grain-orientation contrast. An accelerating voltage of 5 kV resulted in increased intensities for atomic number and orientation contrast. Both grains and theta-phase (Al2Cu) precipitates were revealed on the same micrograph at higher resolutions than attainable in the optical microscope. Quantitative data from micrographs were obtained using image analysis methods. A method based on statistical considerations was developed to determine an approximate critical theta-phase particle diameter (d(sub crit)) for PSN. The theta-phase particle distribution was shown to be an important factor for grain refinement via PSN. DTIC

N93-25788# Southwest Research Inst., San Antonio, TX.
HIGH STRAIN RATE DAMAGE DEVELOPMENT AND FAILURE MECHANISMS IN TUNGSTEN HEAVY ALLOYS Final Report, 15 Sep. 1988 - 10 Sep. 1992
James Lankford, Jr. 30 Nov. 1992 16 p
(Contract DAAL03-88-K-0204)
(AD-A260856; SWRI-PN-06-2492; ARO-26167.5-MS-A) Avail: CASI HC A03/MF A01

A wide range of tungsten heavy alloy microstructures was subjected to high strain rate tensile and compressive loading. It is found that there exists a critical strain for the onset of unstable shear under compressive loading, which is related to the achievement of a viable mean free path for shear band propagation between tungsten particles. The critical strain thus relates to the W-grains, and not the matrix. Similarly, high strain rate tensile strength and toughness is degraded by the inherently weak W-W interfaces in all current alloys. The key to improvement in this case, will be the achievement of matrix wetting of these surfaces, and thereby ductilizing them. DTIC

N93-25843# Pratt and Whitney Aircraft, West Palm Beach, FL. Government Engines and Space Propulsion.
FATIGUE IN SINGLE CRYSTAL NICKEL SUPERALLOYS Technical Progress Report, 16 Dec. 1992 - 15 Jan. 1993
Charles Annis and Daniel P. DeLuca 15 Jan. 1993 6 p
(Contract N00014-91-C-0124)
(AD-A260709; PW/GESP-FR-21988-15) Avail: CASI HC A02/MF A01

This program investigates the seemingly unusual behavior of single crystal airfoil materials. The fatigue initiation processes in single crystal (SC) materials are significantly more complicated and involved than fatigue initiation and subsequent behavior of a (single) macrocrack in conventional, isotropic materials. To understand these differences is the major goal of this project. DTIC

N93-25895# Army Materials Technology Lab., Watertown, MA.
HYDROGEN-INDUCED STRESS CORROSION CRACKING SUSCEPTIBILITY ANALYSIS OF PITCH LINKS FROM THE AH-64 APACHE HELICOPTER Final Report
Paul Buckley, Milton Levy, John Beatty, and Richard Brown (Rhode Island Univ., Kingston.) Sep. 1992 19 p
(AD-A260692; MTL/TR-92-69) Avail: CASI HC A03/MF A01

AH-64 Apache helicopter pitch links were evaluated for degradation of mechanical properties due to service and susceptibility to hydrogen embrittlement. The pitch links were manufactured from 4340 electroslag remelted steel and heat treated to an HRC 52 hardness level and/or retempered to a HRC 38 hardness level and vacuum cadmium coated. Samples from fielded pitch links and virgin material were evaluated for comparison of mechanical behavior. Static torque-load tests on pitch links immersed in 3.5 percent NaCl at a potential of -1.2 V(SCE) were conducted for 1000 hours. Stress corrosion cracking resistance under hydrogen embrittlement conditions were determined. Mechanical and stress corrosion testing demonstrated no discernable change in properties due to service. Retempering the HRC 52 pitch links to HRC 38 resulted in properties similar to those expected from the 4340 ESR steel directly heat treated to the same hardness level. The immersion tests indicated no failure of the pitch links even at six times the service torque. The retempered material exhibited greater resistance to hydrogen-induced cracking. DTIC

N93-25903# Pennsylvania State Univ., University Park. Dept. of Materials Science and Engineering.
PREDICTION OF HYDROGEN ENTRY AND PERMEATION IN METALS AND ALLOYS Annual Report, 1 Oct. 1991 - 30 Sep. 1992
Howard W. Pickering Jan. 1993 49 p
(Contract N00014-91-J-1189)
(AD-A260580) Avail: CASI HC A03/MF A01

This report summarizes the past year's results of our continuing experiments into the problem of hydrogen entry and degradation of materials both of planar surfaces and for the more complicated recessed surface. For the planar surface, the hydrogen permeation and scanning tunneling microscopy (STM) techniques are being used, and for the recessed surface, the study uses the hydrogen permeation technique and a microscopy/electrochemical probe technique. In-situ STM of hydrogen adsorption from the gas phase on Si 111(7x7) demonstrates the feasibility of STM for atomic scale study of adsorbed hydrogen. In aqueous solutions, both acidification and chloride ion accumulation within recesses in iron surfaces cause enhanced proton reduction and hydrogen absorption. Flat, smooth surfaces can form or develop recesses as a result of corrosion or other reasons, e.g., grain boundary grooves that form during corrosion of Cr-depleted alloy in sensitized stainless steel. These recesses are found to be just as prone to proton discharge and hydrogen absorption as pre-existing recesses. DTIC

N93-25907# Brown Univ., Providence, RI. Div. of Engineering.
SHEAR BAND FORMATION IN A W-Ni-Fe ALLOY UNDER PLATE IMPACT Technical Report, 1 Nov. 1991 - 31 Oct. 1992
M. Zhou, R. J. Clifton, and A. Needleman Nov. 1992 16 p
(Contract DAAL03-91-G-0025)
(AD-A260702; ARO-28575.1-MS) Avail: CASI HC A03/MF A01

A thin foil of a W-Ni-Fe alloy, 50-200 micrometers in thickness, is sheared for 2 microseconds under plane wave conditions by plate impact. Shear bands observed show more intensely localized deformations than obtained in other experiments. The responses of the constituent phases, the tungsten grains and the matrix, as well as that of the composite alloy over a strain rate range of 10(exp -4)s(exp -1) to 7 x 10(exp 5)s(exp -1) are experimentally obtained and characterized by a viscoplastic model. The effects of strain hardening, thermal softening, material inertia, rate sensitivity, heat conduction and material microscopic inhomogeneity, on dynamic shear localization, are investigated through finite element simulations. DTIC

N93-26048*# National Aeronautics and Space Administration. Langley Research Center, Hampton, VA.
THERMAL COATINGS FOR TITANIUM-ALUMINUM ALLOYS
George R. Cunnington (Lockheed Missiles and Space Co., Palo Alto, CA.), Ronald K. Clark, and John C. Robinson (Lockheed Missiles and Space Co., Palo Alto, CA.) Apr. 1993 127 p
(RTOP 506-73-43-01)
(NASA-TM-107760; NAS 1.15:107760) Avail: CASI HC A07/MF A02

Titanium aluminides and titanium alloys are candidate materials for use in hot structure and heat-shield components of hypersonic vehicles because of their good strength-to-weight characteristics at elevated temperature. However, in order to utilize their maximum temperature capability, they must be coated to resist oxidation and to have a high total remittance. Also, surface catalysis for recombination of dissociated species in the aerodynamic boundary layer must be minimized. Very thin chemical vapor deposition (CVD) coatings are attractive candidates for this application because of durability and very light weight. To demonstrate this concept, coatings of boron-silicon and aluminum-boron-silicon compositions were applied to the titanium-aluminides alpha2 (Ti-14Al-21Nb), super-alpha2 (Ti-14Al-23-Nb-2V), and gamma (Ti-33Al-6Nb-1Ta) and to the titanium alloy beta-21S (Ti-15Mo-3Al-3Nb-0.2Si). Coated specimens of each alloy were

subjected to a set of simulated hypersonic vehicle environmental tests to determine their properties of oxidation resistance, surface catalysis, radiative emittance, and thermal shock resistance. Surface catalysis results should be viewed as relative performance only of the several coating-alloy combinations tested under the specific environmental conditions of the LaRC Hypersonic Materials Environmental Test System (HYMETS) arc-plasma-heated hypersonic wind tunnel. Tests were also conducted to evaluate the hydrogen transport properties of the coatings and any effects of the coating processing itself on fatigue life of the base alloys. Results are presented for three types of coatings, which are as follows: (1) a single layer boron silicon coating, (2) a single layer aluminum-boron-silicon coating, and (3) a multilayer coating consisting of an aluminum-boron-silicon sublayer with a boron-silicon outer layer. Author (revised)

N93-26197# Georgetown Univ., Washington, DC. Dept. of Chemistry.
Ir-Zr ALLOYS AS DIFFUSION BARRIERS BETWEEN Cu AND Si(100)
H. Yang, C. M. Gilmore, and D. E. Ramaker Dec. 1993 11 p
(Contract N00014-91-J-1896)
(AD-A261919; TR-65) Avail: CASI HC A03/MF A01

Ir-Zr alloys were studied as diffusion barriers between Cu and Si with XRD, AES, RBS, and resistivity measurements. An amorphous Ir(0.84)Zr alloy was found to be a better diffusion barrier than a polycrystalline Ir(2.85)Zr alloy, with the amorphous alloy serving as a satisfactory diffusion barrier up to 800 C. The diffusion constants were determined at various temperatures, and the activation energy for Si out-diffusion in Cu/Ir 0.84 Zr/Si was obtained. DTIC

N93-26201*# National Aeronautics and Space Administration. Lewis Research Center, Cleveland, OH.
EXTERNAL STRESS-CORROSION CRACKING OF A 1.22-m-DIAMETER TYPE 316 STAINLESS STEEL AIR VALVE
Thomas J. Moore, Jack Telesman, Allan S. Moore, Dereck F. Johnson, and David E. Kuivinen Washington Mar. 1993 21 p Original contains color illustrations
(RTOP 505-62-84)
(NASA-TP-3190; E-6810; NAS 1.60:3190) Avail: CASI HC A03/MF A01; 7 functional color pages

An investigation was conducted to determine the cause of the failure of a massive AISI Type 316 stainless steel valve which controlled combustion air to a jet engine test facility. Several through-the-wall cracks were present near welded joints in the valve skirt. The valve had been in outdoor service for 18 years. Samples were taken in the cracked regions for metallographic and chemical analyses. Insulating material and sources of water mist in the vicinity of the failed valve were analyzed for chlorides. A scanning electron microscope was used to determine whether foreign elements were present in a crack. On the basis of the information generated, the failure was characterized as external stress-corrosion cracking. The cracking resulted from a combination of residual tensile stress from welding and the presence of aqueous chlorides. Recommended countermeasures are included. Author

N93-26208# Allied-Signal Aerospace Co., Kansas City, MO.
AQUEOUS CLEANING OF FLUX RESIDUE FROM SOLDER JOINTS Final Report
Carol M. Krska, Don Bowlen, John Houtz, Roger Koelling, Wayne McLarren, and Bill Rowe Aug. 1992 26 p
(Contract DE-AC04-76DP-00613)
(KCP-613-4803) Avail: CASI HC A03/MF A01

Solder joints have traditionally been cleaned using chlorinated or fluorinated solvents. Alternate processing is addressed. One process involved using a saponifier/water solution to remove rosin flux residues; the other process involved using a water-soluble flux and water to remove the residues. Although both processes were satisfactory, the water-soluble flux with water cleaning proved to be the best. Author (revised)

N93-26234 Department of the Navy, Washington, DC.
METAL ALLOY AND METHOD OF PREPARATION THEREOF Patent
Raymond A. Satula, inventor (to Navy) and Frederick E. Wang, inventor (to Navy) 20 Oct. 1992 6 p Filed 5 May 1975
(AD-D015670; US-Patent-5,156,806; US-Patent-Appl-SN-575543) Avail: US Patent and Trademark Office

Ternary metallic alloys of the formula Li(x)B(y)M(z), wherein 0.05 less than or equal to x less than or equal to 0.90, 0.05 less than or equal to y less than or equal to 0.90, 0.05 less than or equal to z less than or equal to 0.90, and $x + y + z = 1$, and a method of preparing them are described. These alloys find use in areas where superlight weight, high specific strength (strength/weight ratio), and oxidation resistance are required. DTIC

N93-26235*# Georgia Inst. of Tech., Atlanta.
DEFORMATION MECHANISMS OF NiAl CYCLICLY DEFORMED NEAR THE BRITTLE-TO-DUCTILE TRANSITION TEMPERATURE Final Report
Cheryl L. Cullers (Georgia Inst. of Tech., Atlanta.) and Stephen D. Antolovich (Georgia Inst. of Tech., Atlanta.) Apr. 1993 105 p
(Contract NCC3-295; RTOP 505-63-5A)
(NASA-CR-191121; E-7745; NAS 1.26:191121) Avail: CASI HC A06/MF A02

The intermetallic compound NiAl is one of many advanced materials which is being scrutinized for possible use in high temperature, structural applications. Stoichiometric NiAl has a high melting temperature, excellent oxidation resistance, and good thermal conductivity. Past research has concentrated on improving monotonic properties. The encouraging results obtained on binary and micro-alloyed NiAl over the past ten years have led to the broadening of NiAl experimental programs. The purpose of this research project was to determine the low cycle fatigue properties and dislocation mechanisms of stoichiometric NiAl at temperatures near the monotonic brittle-to-ductile transition. The fatigue properties were found to change only slightly in the temperature range of 600 to 700 K; a temperature range over which monotonic ductility and fracture strength increase markedly. The shape of the cyclic hardening curves coincided with the changes observed in the dislocation structures. The evolution of dislocation structures did not appear to change with temperature. Author

N93-26264# Virginia Univ., Charlottesville. Dept. of Materials Science and Engineering.
MECHANICAL ALLOYING PROCESSING AND APPLICATION TO DEVELOPMENT OF STRUCTURAL MATERIALS Final Report, 1 Jun. 1991 - 15 Aug. 1992
Thomas H. Courtney 21 Sep. 1992 8 p
(Contract DAAL03-91-G-0092)
(AD-A261251; UVA/525272/MSE93/101; ARO-28639.2-MS) Avail: CASI HC A02/MF A01

This report summarizes results of several areas of research dealing with mechanical alloying of materials having potential structural use. The areas involve modeling of the process, synthesis of unique materials via mechanical alloying and consolidation of mechanically alloyed products. The latter area is one receiving most current attention as consolidation involves high temperatures and (usually) pressures. This can lead to a 'loss' of the unique structures produced by mechanical alloying. Thus, consolidation studies attempt to produce fully dense material maintaining many of the desirable properties manifested by mechanically alloyed powders. DTIC

N93-26282# United Technologies Corp., West Palm Beach, FL.
FATIGUE IN SINGLE CRYSTAL NICKEL SUPERALLOYS Technical Progress Report
Daniel P. DeLuca 16 Feb. 1993 6 p
(Contract N00014-91-C-0124)
(AD-A261742; FR21998-16) Avail: CASI HC A02/MF A01

This program investigates the seemingly unusual behavior of single crystal airfoil materials. The fatigue initiation processes in single crystal (SC) materials are significantly more complicated and involved than fatigue initiation and subsequent behavior of a (single) macrocrack in conventional, isotropic, materials. To understand these differences is the major goal of this project. DTIC

N93-26284# National Inst. of Standards and Technology, Gaithersburg, MD. Metallurgy Div.
SOLIDIFICATION PROCESSING AND PHASE TRANSFORMATIONS IN ORDERED HIGH TEMPERATURE ALLOYS Final Report, 30 Mar. 1990 - 30 Sep. 1992
William J. Boettinger, Leonid A. Bendersky, and Ursula R. Kattner 20 Jan. 1993 205 p

(DARPA Order 7469)
(AD-A261751) Avail: CASI HC A10/MF A03

Useful high temperature alloys generally have microstructures consisting of more than one phase. Multiphase microstructures are necessary to develop acceptable toughness and creep strength in high temperature intermetallic alloy matrices. The optimum microstructures must be developed by a careful selection of processing path that includes both solidification and solid state heat treatment. Research has been conducted on the rapid solidification of selected intermetallic alloys and on the phase transformation paths that occur during cooling, primarily in the Ti-Al-Nb system. This report describes research performed in the Metallurgy Division at NIST under DARPA order 7469 between 1/1/89 and 12/31/92. Various research tasks were completed and the results have been published or have been submitted for publication. DTIC

N93-26304# SRI International Corp., Menlo Park, CA.
FUNDAMENTAL ASPECTS OF METAL JOINING: THE STUDY OF STRONG INTERFACES Final Report
Anthony T. Paxton and Mark VanSchilfgaarde Dec. 1992 31 p
(Contract N00014-92-J-0006)
(AD-A261293) Avail: CASI HC A03/MF A01

Our aim for 1992 was to investigate whether modern quantum mechanical methods can be useful in the study of interfaces between dissimilar materials, and to complete at least a modest piece of work to demonstrate feasibility. This has been achieved. We developed an approximate quantum mechanical approach to the problem of dissimilar transition-metal interfaces. Because of its approximate nature, we have devoted a large effort to testing the scheme against experiment and first-principles theory. Our expertise in local density functional theory has allowed us to draw upon our first-principles capability both in determining parameters for our model Hamiltonian and in testing it. We have studied in some detail a lattice-mismatched interface between pure molybdenum and rhenium metals. Our conclusions concerning this system are that the shear strength of the interface is diminished from the theoretical strength by a factor of about twenty; the reduction is due to the presence of a misfit dislocation that glides in the interface during deformation. DTIC

N93-26500# Oak Ridge National Lab., TN.
POSITION SENSITIVE ATOM PROBE STUDY OF THE DECOMPOSITION OF A Cu-2.6 AT. PERCENT Co ALLOY
R. P. Setna (Oxford Univ., England.), J. M. Hyde (Oxford Univ., England.), A. Cerezo (Oxford Univ., England.), G. D. W. Smith (Oxford Univ., England.), and M. F. Chisholm Dec. 1992 23 p Presented at the 39th International Field Emission Symposium, Halifax, Nova Scotia, 9-14 Aug. 1992
(Contract DE-AC05-84OR-21400)
(DE93-006737; CONF-9208205-1) Avail: CASI HC A03/MF A01

This paper presents a Position Sensitive Atom Probe study of phase decomposition in a Cu-2.6 at. % Co alloy, aged at 723 K for various times up to 24 hours. The composition and ageing temperature of the alloy were chosen such that the free energy barrier to decomposition was small. Statistical techniques are used to characterize the fine-scale microstructures present in the early stages of phase separation and three-dimensional atomic reconstructions of the alloys are presented. The experimental results from the Position Sensitive Atom Probe are compared with Monte Carlo simulations and with the sub-regular solution-classical nucleation model to gain a greater insight into the nature of the processes taking place in the early stages of phase decomposition. Results demonstrate a complex range of behavior, from the development of enriched and partially diffuse regions of Co to the formation of Co-rich (alpha) precipitates. Monte Carlo simulations adequately mimic many of the features observed in the experimental data. DOE

27 NONMETALLIC MATERIALS

Includes physical, chemical, and mechanical properties of plastics, elastomers, lubricants, polymers, textiles, adhesives, and ceramic materials.

For composite materials see *24 Composite Materials.*

N93-24761*# Martin Marietta Labs., Baltimore, MD.
DEVELOPMENT OF DISPERSION-STRENGTHENED XD (TRADEMARK) Cu ALLOYS FOR HIGH HEAT-FLUX APPLICATIONS
K. Sharvan Kumar Apr. 1993 44 p Original contains color illustrations
(Contract NAS3-26474; RTOP 584-03-11)
(NASA-CR-191124; E-7701; NAS 1.26:191124) Avail: CASI HC A03/MF A01; 4 functional color pages

In a previous effort sponsored by NASA LeRC, the XD(trademark) process was used to produce ZrB2 particulate reinforcements in Cu and the resulting extruded material was microstructurally characterized and evaluated in tension over a range of temperatures. A problem that was encountered in that study was microstructural inhomogeneity resulting from the frequent presence of 'ZrB2 agglomerates' that were several microns in size. The presence of these agglomerates was attributed to improper mixing of powders in the green compact used in the XD process for elemental boron powder segregation. In this program, several milling parameters were examined in an effort to optimize this processing step; two levels of ZrB2 reinforcements were considered (7 vol. percent and 15 vol. percent). Microstructures of the reacted powder mass were examined to verify the absence of these agglomerates. Larger bathes of powder were then mixed, reacted, machined to size, canned, and extruded. The microstructure and tensile properties of these extrusions were examined, and the measured properties were correlated with the observed microstructure. Large unreacted or partially reacted Zr particles were present. These particles affected the mechanical properties deleteriously, and their presence is attributed to insufficient heat of reaction during XD synthesis. Alternate processing routes are recommended. Author (revised)

N93-24971# Sandia National Labs., Albuquerque, NM.
COLLOID FORMATION IN IMPLANTED GLASSES
G. W. Arnold, P. Mazzoldi (Padua Univ., Italy.), L. Tramontin (Padua Univ., Italy.), A. Boscolo-Boscoletto, and G. Battaglin (Venice Univ., Italy.) 1992 5 p Presented at the 16th Material Research Society International Symposium on the Scientific Basis for Nuclear Waste Management, Boston, MA, 30 Nov. - 5 Dec. 1992
(Contract DE-AC04-76DP-00789)
(DE93-006763; SAND-92-1596C; CONF-921101-91) Avail: CASI HC A01/MF A01

Metal colloids in glasses can yield an enhanced chi(sup 3) susceptibility which leads to an intensity dependent refractive index. Ion implantation is a convenient means of introducing the metal species. The host glass plays an important role in colloid formation. Ag-colloid formation was characterized in various silicate glasses and, in addition, the formation of colloids in Ag-doped phosphate glass as a function of N and H implantation were studied. Some preliminary results for Cu-implanted glasses are presented. DOE

N93-25078*# Jet Propulsion Lab., California Inst. of Tech., Pasadena.
AN INVESTIGATION OF THE DEGRADATION OF FLUORINATED ETHYLENE PROPYLENE (FEP) COPOLYMER THERMAL BLANKETING MATERIALS ABOARD LDEF IN THE LABORATORY
A. E. Stiegman, David E. Brinza, Mark S. Anderson, Timothy K. Minton, Eric G. Laue, and Ranty H. Liang 15 May 1991 25 p
(Contract NAS7-918)
(NASA-CR-192824; NAS 1.26:192824; JPL-Publ-91-10) Avail: CASI HC A03/MF A01

Samples of fluorinated ethylene propylene copolymer thermal blanketing material, recovered from the Long Duration Exposure Facility (LDEF), were investigated to determine the nature and the extent of degradation due to exposure to the low-Earth-orbit environment. Samples recovered from the ram-facing direction of LDEF, which received vacuum-ultraviolet (VUV) radiation and atomic-oxygen impingement, and samples from the trailing edge, which received almost exclusively VUV exposure, were investigated by scanning electron microscopy and atomic force microscopy. The most significant result of this investigation was found on samples that received

only VUV exposure. These samples possessed a hard, embrittled surface layer that was absent from the atomic-oxygen exposed sample and from unexposed control samples. This surface layer is believed to be responsible for the 'synergistic' effect between VUV and atomic oxygen. Overall, the investigation revealed dramatically different morphologies for the two samples. The sample receiving both atomic-oxygen and VUV exposure was deeply eroded and had a characteristic 'rolling' surface morphology, while the sample that received only VUV exposure showed mild erosion and a surface morphology characterized by sharp high-frequency peaks. The morphologies observed in the LDEF samples, including the embrittled surface layer, were successfully duplicated in the laboratory. Author

N93-25093*# National Aeronautics and Space Administration. Lewis Research Center, Cleveland, OH.

DETERMINATION OF THE THERMAL STABILITY OF PERFLUOROPOLYALKYL ETHERS BY TENSIMETRY

Larry A. Helmick (Cedarville Coll., OH.) and William R. Jones, Jr. May 1992 32 p Presented at the Society of Tribologists and Lubrication Engineers Annual Meeting, Philadelphia, PA, 4-7 May 1992; sponsored by the Society of Tribologists and Lubrication Engineers

(RTOP 505-53-1A)

(NASA-TM-106081; E-7699; NAS 1.15:106081) Avail: CASI HC A01/MF A01

The thermal decomposition temperatures of several perfluoropolyalkyl ether fluids were determined with a computerized tensimeter. In general, the decomposition temperatures of the commercial fluids were all similar and significantly higher than those for noncommercial fluids. Correlation of the decomposition temperatures with the molecular structures of the primary components of the commercial fluids revealed that the stability of the fluids was not affected by carbon chain length, branching, or adjacent difluoroformal groups. Instead, stability was limited by the presence of small quantities of thermally unstable material and/or chlorine-containing material arising from the use of chlorine containing solvents during synthesis. Finally, correlation of decomposition temperatures with molecular weights for two fluids supports a chain cleavage reaction mechanism for one and an unzipping reaction mechanism for the other. Author

N93-25359# Pacific Northwest Lab., Richland, WA.

TEMPERATURE-DEPENDENT ELECTRICAL CONDUCTIVITY OF SODA-LIME GLASS

L. Roy Bunnell and T. H. Vertrees (Kennewick High School, WA.) Nov. 1992 7 p Presented at the National Educator's Workshop, Oak Ridge, TN, 11-13 Nov. 1992

(Contract DE-AC06-76RL-01830)

(DE93-007872; PNL-SA-21577; CONF-9211178-2) Avail: CASI HC A02/MF A01

A laboratory procedure is given for demonstrating, for students at high school level or above, the difference between the electrical conductivity of metals and ceramics. DOE

N93-25361# Oak Ridge National Lab., TN.

DEVELOPMENT OF ASTM STANDARDS IN SUPPORT OF ADVANCED CERAMICS DEVELOPMENT

C. R. Brinkman, G. D. Quinn (National Inst. of Standards and Technology, Gaithersburg, MD.), and R. W. McClung 1993 28 p Presented at the 38th ASME International Gas Turbine and Aeroengine Congress and Exhibition, Cincinnati, OH, 24-27 May 1993

(Contract DE-AC05-84OR-21400)

(DE93-003024; CONF-930502-1) Avail: CASI HC A03/MF A01

The ASTM Committee C-28 on Advanced Ceramics was organized in 1986 when it became apparent that ceramics were being considered for extensive use in such applications as heat engines in the automotive and aerospace industries. It was determined that these standards should be written for the production, inspection, testing, data analysis, reliability, and probabilistic design for utilization of advanced ceramics. Advanced ceramics include both monolithic and composite materials. The ASTM Committee C-28 is organized into five subcommittees as follows: properties and performance, design and evaluation, characterization and processing, ceramic composites, and nomenclature. A summary overview is given of work performed to date and ongoing efforts in developing standards by these various subcommittees. DOE

N93-25372# Oak Ridge National Lab., TN.

STRUCTURE AND PROPERTIES OF a-C: N FILNS PREPARED BY PULSED EXCIMER LASER DEPOSITION

Fulin Xiong, R. P. H. Chang (Northwestern Univ., Evanston, IL.), and C. W. White 1992 6 p The 16th Material Research Society International Symposium on the Scientific Basis for Nuclear Waste Management Meeting held in Boston, MA, 30 Nov. - 5 Dec. 1992

(Contracts DE-AC05-84OR-21400; DE-FG02-87ER-45314)

(DE93-007908; CONF-921101-94) Avail: CASI HC A02/MF A01

We present results on the synthesis of a-C:N films deposited by pulsed excimer laser ablation of graphite in a nitrogen gas ambient. Analysis with RBS and forward recoil spectrometry show that the films are hydrogen-free and nitrogen can be incorporated up to 40 percent by varying the nitrogen gas pressure. Electron microscopy has identified these films to be amorphous. Raman spectroscopy, infrared spectroscopy, and electron energy loss spectroscopy have revealed carbon-nitrogen bonding structures. Compared to a-diamond films prepared by the same technique, the C:N films still possess the properties of high mechanical hardness, chemically inertness, and good wear resistance, but incorporation of nitrogen into the films generally degrades their diamond-like properties. Results suggest that nitrogen doping effect is presented in the films under the present process, instead of carbon-nitrogen compound formation. DOE

N93-25374# Oak Ridge National Lab., TN.

THE NATURE OF THE GLASS TRANSITION AND ITS DETERMINATION BY THERMAL ANALYSIS

B. Wunderlich (Tennessee Univ., Knoxville.) 1993 15 p Presented at the American Society of Testing and Materials (ASTM) Meeting on Glass Transition, Atlanta, GA, 4-5 Mar. 1993

(Contract DE-AC05-84OR-21400)

(DE93-006746; CONF-930398-1) Avail: CASI HC A03/MF A01

In this paper operational definitions of the glass transition and the pertinent condensed phases are given. This is followed by a description of the basic observations of glass transitions via thermal analysis using calorimetry, dilatometry, as well as thermomechanical, dielectric, and dynamic mechanical analysis. The time dependence of the glass transition causes hysteresis phenomena and physical ageing. Strain effects on the observation of the glass transition are identified. Complications resulting in symmetric and asymmetric broadening of the glass transition are linked to nanometer and micrometer scale phase separations. Finally, a rigid amorphous phase is identified in some semicrystalline polymers. DOE

N93-25382# Lawrence Livermore National Lab., CA.

SPUTTER DEPOSITION OF YTTRIUM-OXIDES

A. F. Jankowski, L. R. Schrawyer, and J. P. Hayes Nov. 1992 22 p Presented at the 39th National Symposium of the American Vacuum Society, Chicago, IL, 9-13 Nov. 1992

(Contract W-7405-eng-48)

(DE93-007499; UCRL-JC-110346; CONF-921129-7) Avail: CASI HC A03/MF A01

The yttrium-oxide phase diagram contains only one equilibrium compound, a Y2O3 cubic structure. The process of reactive sputter deposition is used to synthesize previously unreported, yttrium rich oxide compounds. A planar magnetron is operated in the dc mode using a working gas mixture of argon-20 percent oxygen. For low sputter gas pressure and flow conditions, the yttrium content of the coating is directly controlled as a function of the applied target power, i.e., the deposition rate. The composition and structure of the coatings are characterized using Auger depth profiling and x-ray diffraction. A continuous series of compounds are formed with an orthorhombic crystal structure for concentrations ranging from 40 to 75 at. percent yttrium. DOE

N93-25384# Lawrence Livermore National Lab., CA.

CORRELATION OF DAMAGE THRESHOLD AND SURFACE GEOMETRY OF NODULAR DEFECTS IN HR COATINGS AS DETERMINED BY IN-SITU ATOMIC FORCE MICROSCOPY

M. C. Staggs, M. R. Kozlowski, W. J. Siekhaus, and M. Balooch Oct. 1992 10 p Presented at the SPIE Symposium on Boulder Damage, Boulder, CO, 28-30 Oct. 1992

(Contract W-7405-eng-48)

(DE93-007509; UCRL-JC-111464; CONF-9210295-1) Avail: CASI HC A02/MF A01

Atomic force microscopy (AFM) was used to determine in-situ the correlation between the surface dimensions of defects in dielectric multilayer optical coatings and their susceptibility to damage by pulsed laser illumination. The primary surface defects studied were micron-scale domes associated with the classic nodule defect. The optical film studied was a highly reflective dielectric multilayer consisting of pairs of alternating HfO2 and SiO2 layers of quarter wave thickness at 1.06 microns. Nodule defect height and width dimensions were measured prior to laser illumination on two different samples. Correlation between these dimensions supported a simple model for the defect geometry. Defects with high nodule heights (greater than 0.6 micron) were found to be most susceptible to laser damage over a range of fluences between 0 - 35 J/sq cm (1.06 microns, 10 ns, and 1/e(exp 2) diameter of 1.3 mm). Crater defects, formed by nodules ejected from the coating prior to illumination, were also studied. None of the crater defects were damaged when they were illuminated in the same range of fluences as the nodule defects. DOE

N93-25444# Sandia National Labs., Albuquerque, NM.
TEMPERATURE DEPENDENT SENSOR RESPONSE CAUSED BY POLYMER-SOLVENT INTERACTIONS
M. A. Butler 1992 7 p Presented at the 183rd Electrochemical Society Meeting, Honolulu, HI, 16-21 May 1993
(Contract DE-AC04-76DP-00789)
(DE93-005368; SAND-92-2378C; CONF-930571-4) Avail: CASI HC A02/MF A01

Absorption of organic solvents by a range of polymers has been used as the chemical transduction mechanism for a variety of sensors. This paper examines the effect of the polymer-solvent interaction on the temperature dependence of the sensor response. Optical interferometric cavities are formed on the end of an optical fiber by plasma-deposition of a fluorocarbon polymer. Swelling of the polymer when exposed to various solvent vapors produces changes in the reflectivity of the fiber tip. The temperature dependence of the sensor response is related to the strength of the polymer-solvent interaction and the heat of vaporization of the solvent. DOE

N93-25446# Sandia National Labs., Albuquerque, NM.
CHROMATE-FREE CORROSION RESISTANT TALC COATINGS FOR ALUMINUM ALLOYS
R. G. Buchheit and G. E. Stoner (Virginia Univ., Charlottesville.) 1992 3 p Presented at the 183rd Electrochemical Society Meeting, Honolulu, HI, 16-21 May 1993
(Contract DE-AC04-76DP-00789)
(DE93-005370; SAND-92-2396C; CONF-930571-5) Avail: CASI HC A01/MF A01

Passivity developed by immersion in an alkaline Li salt solution is retained when the Al surface is exposed to an aggressive solution like aerated NaCl. A process for coating Al was developed using a method similar to the chromate conversion process. This process imparts appreciable corrosion resistance, but does not use or produce hazardous chemicals. Coatings are formed by immersion in 0.1 M Li carbonate solution whose pH is adjusted to 11.5-12.0 by LiOH additions. Immersion times of 1.5 to 90 min were used to produce talc coatings; up to this point, the best time has been 15 min. Increased corrosion resistance is obtained if the coating is sealed by elevated temperature treatment in air or distilled water. DOE

N93-25507# Los Alamos National Lab., NM.
A MODEL FOR THE FILLING OF COLD CAVITIES WITH SOLIDIFYING, SEMI-CRYSTALLINE POLYMERS
T. D. Papathanasiou (Imperial Coll. of Science and Technology, London, England.) and D. C. Guell 1992 17 p Presented at the ANTEC 1993 Society of Plastics Engineers Meeting, New Orleans, LA, 9-13 May 1993
(Contract W-7405-eng-36)
(DE93-003817; LA-UR-92-3668; CONF-930584-1) Avail: CASI HC A03/MF A01

A model for the filling stage of injection molding that includes wall solidification and crystallization was used to investigate the interaction between solidification and pressure drop during the filling of a rectangular plate with high-density polyethylene. We find that wall solidification affects the pressure drop in a complex way, reflecting the interplay between reduction in the area available for flow and thermal insulation of the still-molten polymer. Development of crystallinity on the surface of the part is also modelled under conditions of uniform and spatially varying cooling. Results indicate that nonuniform cooling can result in complex crystallinity distributions which are determined by thermal history of solidified polymer, duration of filling stage and by exact dependence of crystallization kinetics on temperature. DOE

N93-25524# Utah Univ., Salt Lake City. Dept. of Physics.
PHOTOMODULATION SPECTROSCOPY OF PHOTOCARRIER DYNAMICS, ELECTRONIC DEFECTS AND MORPHOLOGY OF CONDUCTING POLYMERS
Z. V. Vardeny 1993 14 p
(Contract DE-FG02-89ER-45409)
(DE93-010140; DOE/ER-45409/3) Avail: CASI HC A03/MF A01

A variety of techniques were used in this study: CW photomodulation, photomodulation in femtosecond and picosecond time ranges, CW resonant Raman scattering, transient photoinduced Raman scattering, electro-absorption, degenerate four-wave mixing, spin dependent photomodulation, and absorption detected magnetic resonance. The following conducting polymers were studied: polyacetylene, polythiophene, polydiacetylene 4-BCMU, polydiethynylsilanes, polysilane embedded in a-Si:H matrix, and fullerenes. DOE

N93-25642# Hunter Coll., New York, NY. Dept. of Physics and Astronomy.
NMR STUDIES OF ION MOBILITY AND ASSOCIATION IN POLYETHER-BASED POLYMER ELECTROLYTES Technical Report, Apr. 1992
Steven G. Greenbaum 25 Jan. 1993 69 p
(Contract N00014-92-J-1629)
(AD-A260662; TR-1) Avail: CASI HC A04/MF A01

The results of several investigations of polyether-based polymer electrolytes by nuclear magnetic resonance (NMR) spectroscopy conducted in the author's laboratory and by other groups are reviewed. For both Li-7 and Na-23 NMR, the onset of motional line-narrowing occurs at about the glass transition, illustrating the importance of polymer segmental motion to ion transport. Examples of the ability of NMR to probe cation-anion interactions are discussed. These include chemical shift variations corresponding to different Li(+) environments and nuclear quadrupole coupling and relaxation behavior as a probe of Na(+) environment. DTIC

N93-25816# Naval Air Warfare Center, Warminster, PA. Aircraft Div.
MACROMOLECULES FOR INHIBITION OF CORROSION AND WEAR Progress Report
Alfeo A. Conte, Jr. and Vinod S. Agarwala 14 Dec. 1992 30 p
(AD-A261041; NAWCADWAR-92112-60) Avail: CASI HC A03/MF A01

The phthalocyanines and Schiff base compounds are uniquely qualified inhibitors for corrosion. They are high electron density molecules for interaction with the metal surface, and possess large spatially arranged structures to serve as environmental barriers. Additionally, these compounds do stack-up as layered structures which provides shear planes, thus serving as lubricants. A number of these compounds have been synthesized and studied. Both electrochemical impedance spectroscopic and potentiostatic polarization techniques were used to determine their corrosion inhibition efficiencies. Wear studies were made using grease lubricated stainless steel miniature bearings. The results have shown that Schiff base compounds can be good additives for greases as they enhance wear life of bearings and inhibit corrosion by at least and order of magnitude. Although phthalocyanines, both monomers and polymers, provided a significant corrosion inhibition efficiencies (greater than 90 percent), they were not effective lubricants compared to the Schiff bases. DTIC

N93-25861# Missouri Univ., Columbia.
IN SITU SURFACE STUDIES OF CONVERSION COATINGS FOR STEEL AND ALUMINUM Final Report, 15 Apr. 1989 - 14 Sep. 1992
Henry W. White, Florian Mansfeld, and Paul Bryant 10 Nov. 1992 27 p
(Contract DAAL03-89-K-0084)
(AD-A261016; ARO-26400.7-MS) Avail: CASI HC A03/MF A01

The primary goals of the work were to develop mechanisms of corrosion protection for cerium based surface layers on aluminum alloys and on polyacrylic acid (PAA) complexed zinc phosphate conversion coatings on steel. Atomic force. microscopy (AFM) using tunnel current control was developed and applied to several problems. The cerium based coatings on

Al 6061-T6 are shown to consist of two principle components--a poorly ordered monohydrated aluminum oxide, and an insoluble cerium oxide which forms at areas concentrated with impurities and alloying elements. Electrochemical action during the surface modification process fosters the precipitation of cerium compounds which inhibit further attack. The addition of high molecular weight PAA to the phosphating bath can significantly improve both resistance to corrosion and top-coat adherence of zinc phosphate conversion coatings on steel. Raman spectra showed the compositions of both unmodified and PAA modified films to be zinc phosphate dihydrate. Single crystallite surfaces were imaged using AFM. The morphologies of the unmodified and modified films were in general quite similar, but subtle differences were apparent. Several other projects involving surface layers and adsorbates were carried out and are described. DTIC

N93-25940# Mission Research Corp., Costa Mesa, CA.
DUCT PROTECTION COATING CONCEPT DEVELOPMENT AND TEST. APPENDIX D, VOLUME 1: TEST SPECIMEN FABRICATION, CONDITIONING, AND TESTING DOCUMENTATION Final Report, period ending Feb. 1992
C. D. Newlander Jan. 1993 248 p
(Contract F40600-89-C-0002)
(AD-A261005) Avail: CASI HC A11/MF A03

The overall objective of the program was to develop and test a surface cleaning/preparation and corrosion resistant protective polymer coating for the interior of the AEDC Environment Test Facility ferrous metal air supply ducts. The types of cleaning techniques acceptable to the AEDC were basically limited to chemical approaches. Typically, sand or abrasive blasting is used to produce corrosion-free, clean surfaces for coating steel substrates. These particular techniques are strongly discouraged and basically outlawed at the AEDC facilities. Water blasting is an acceptable technique, but requires a high pressure water stream, expensive equipment, and considerable clean up. DTIC

N93-25995* National Aeronautics and Space Administration. Langley Research Center, Hampton, VA.
PROCESS FOR BONDING ELASTOMERS TO METALS Patent
George E. Dickerson, inventor (to NASA) and Henry L. Kelley, inventor (to NASA) 25 May 1993 5 p Filed 26 Jun. 1991 Supersedes N91-28424 (29 - 20, p 3327)
(NASA-Case-LAR-13645-1; US-Patent-5,213,739;
US-Patent-Appl-SN-721038; US-Patent-Class-264-135;
US-Patent-Class-156-245; US-Patent-Class-264-259;
US-Patent-Class-264-265; US-Patent-Class-264-DIG.65;
Int-Patent-Class-B29C-45/16) Avail: US Patent and Trademark Office

A process for bonding elastomeric material to a metal part includes coating a heat curable adhesive on the surfaces of the metal part to be bonded. The metal part is placed in a mold, a bottom plate and an upper transfer pot of a transfer molding machine is preheated to a predetermined cure temperature. A predetermined quantity of uncured elastomeric material is loaded into the transfer pot. The mold containing the adhesive coated metal part is clamped to the bottom plate, and almost contemporaneously, the uncured elastomeric material is pressed into the mold while maintaining heat and pressure in the mold for a time sufficient to vulcanize and thereby cure the elastomeric material simultaneously with the adhesive, whereby contacting surfaces of the metal part are strongly bonded to the vulcanized elastomeric material.
Official Gazette of the U.S. Patent and Trademark Office

N93-25997*# National Aeronautics and Space Administration. Langley Research Center, Hampton, VA.
POLYIMIDES WITH IMPROVED COMPRESSION MOLDABILITY Patent
Paul M. Hergenrother, inventor (to NASA), Stephen J. Havens, inventor (to NASA), and Mark W. Beltz, inventor (to NASA) 18 May 1993 9 p Filed 8 May 1990 Supersedes N92-11198 (30 - 2, p 218)
(NASA-Case-LAR-14457-1; US-Patent-5,212,276;
US-Patent-Appl-SN-520472; US-Patent-Class-528-125;
US-Patent-Class-528-128; US-Patent-Class-528-170;
US-Patent-Class-528-172; US-Patent-Class-528-173;
US-Patent-Class-528-176; US-Patent-Class-528-183) Avail: US Patent and Trademark Office

The semicrystalline polyimide prepared by reaction of 3,3',4,4' benzophenonetetracarboxylic (BTDA) and 1,3-bis(4-aminophenoxy 4' benzoyl) benzene (1,3-BABB) is modified so that it can be more readily processed to form adhesive bonds, moldings, and composites. The stoichiometric ratio of the two monomers, BTDA and 1,3-BABB is controlled so that the intermediate polyamide acid is of a calculated molecular weight. A polyimide acid with excess anhydride groups is then reacted with the stoichiometrically required amount of monofunctional aromatic or aliphatic amine required for complete endcapping. The stoichiometrically offset, encapped polyimide is processed at lower temperatures and pressures than the unmodified high molecular weight polyimide with the same repeat unit, and exhibits an improved melt stability.
Official Gazette of the U.S. Patent and Trademark Office

N93-25999* National Aeronautics and Space Administration. Langley Research Center, Hampton, VA.
POLYIMIDES CONTAINING THE CYCLOBUTENE-3,4-DIONE MOIETY Patent
Terry L. St.Clair, inventor (to NASA) 18 May 1993 5 p Filed 3 Mar. 1992 Supersedes N92-30313 (30 - 21, p 3601)
(NASA-Case-LAR-14753-1; US-Patent-5,212,283;
US-Patent-Appl-SN-845090; US-Patent-Class-528-353;
US-Patent-Class-528-125; US-Patent-Class-528-128;
US-Patent-Class-528-170; US-Patent-Class-528-172;
US-Patent-Class-528-173; US-Patent-Class-528-176) Avail: US Patent and Trademark Office

In the present invention, linear aromatic polyimides containing the cyclobutene-3,4-dione moiety were produced from the reaction of a substituted or unsubstituted 1,2-bis(4-aminoanilino) cyclobutene-3,4-dione (SQDA) with various aromatic dianhydrides. These polymers had high molecular weights and their glass transition temperatures (Tgs) were greater than 500 C. Despite the very high Tg, these polymers exhibited excellent adhesion to glass. In addition, the films of these polyimides increased in flexibility with increasing cure temperatures. The novelty of this invention lies in the linear aromatic polyimide containing the cyclobutene-3,4-dione moiety. The presence of this moiety causes such changes in properties as Tgs greater than 500 C, excellent adhesion to glass, and increased flexibility with increasing cure temperatures.
Official Gazette of the U.S. Patent and Trademark Office

N93-26155*# Missouri Univ., Rolla. Dept. of Chemistry.
NEW DIRECTIONS IN PHTHALOCYANINE PIGMENTS Final Report
Michael R. VanDeMark 9 Aug. 1992 44 p
(Contract NAS8-38259)
(NASA-CR-192443; NAS 1.26:192443) Avail: CASI HC A03/MF A01

The objectives were the following: (1) investigation of the synthesis of new phthalocyanines; (2) characterization of the new phthalocyanines synthesized; (3) investigate the properties of the newly synthesized phthalocyanines with emphasis on UV protection of plastics and coatings; and (4) utilize quantum mechanics to evaluate the structural relationships with possible properties and synthetic approaches. The proposed research targeted the synthesis of phthalocyanines containing an aromatic bridge between two phthalocyanine rings. The goal was to synthesize pigments which would protect plastics when exposed to the photodegradation effects of the sun in space. The stability and extended conjugation of the phthalocyanines offer a unique opportunity for energy absorption and numerous radiative and non-radiative energy loss mechanisms. Although the original targeted phthalocyanines were changed early in the project, several new and unique phthalocyanine compounds were prepared. The basic goals of this work were met and some unique and unexpected outcomes of the work were the result of the integral use of quantum mechanics and molecular modeling with the synthetic effort. Author

N93-26172# Colorado State Univ., Fort Collins. Dept. of Chemistry.
INORGANIC AND BIOLOGICAL ELECTRON TRANSFER ACROSS AN ELECTRONICALLY CONDUCTIVE COMPOSITE POLYMER MEMBRANE Interim Report
Del R. Lawson, Wenbin Liang, and Charles R. Martin 22 Feb. 1993 15 p
(Contract N00014-82-K-0612)
(AD-A261642; ONR-TR-81) Avail: CASI HC A03/MF A01

We describe in this paper an experiment involving an electronically conductive polymer that, to our knowledge, has not been described

previously. A free-standing conductive polymer (polypyrrole)-based membrane separates a solution of an electron donor from a solution of an electron acceptor. Because the conductive polymer is both electronically and anionically conductive, the membrane can transport electrons from the donor solution to the acceptor solution, and anions in the opposite direction, such that a sustainable electron-transfer reaction is driven across the conductive polymer membrane. We demonstrate such transmembrane electron/ion-transfer processes using both an inorganic and a biochemical electron donor/acceptor system. The biochemical case is of particular interest because we show that the reduced form of the enzyme glucose oxidase can give its electrons directly to the polypyrrolemembrane surface. Direct electron transfer is usually not possible at inorganic metals. DTIC

N93-26213# Allied-Signal Aerospace Co., Kansas City, MO. Kansas City Div.

CHARACTERIZATION OF THE SYNTHESIS OF M-61, A RANDOM EQUILIBRIUM SILICONE TERPOLYMER, USING DRY STARTING MATERIALS Final Report

J. W. Schneider, G. K. Baker, T. J. Reno, R. S. Sanders, and J. J. Wyckoff Dec. 1992 50 p

(Contract DE-AC04-76DP-00613)

(KCP-613-4985) Avail: CASI HC A03/MF A01

Process characterization of the synthesis of M-61, a random equilibrium silicon terpolymer, using 'dry' starting materials has been completed. Tests indicate considerable moisture is present in the starting materials: octamethyl cyclotetra siloxane, octaphenyl cyclotetra siloxane, tetramethyl cyclotetra siloxane, octaphenyl cyclotetra siloxane, tetramethyl tetravinyl cyclotetra siloxane, and a trimethyl endblocker. The presence of moisture provides -OH endblocking of the polymer chain and renders the trimethyl endblocker used to control the weight average molecular weight ineffective. The liquid starting materials were dried with molecular sieves while the octaphenyl cyclotetra siloxane powder was dried in an oven prior to use. Author

N93-26240# Pennsylvania Univ., Philadelphia. Dept. of Chemistry.

POLYMERS BY NON-REDOX PROCESSES: SYNTHESIS, PHYSICAL STUDIES, AND APPLICATION Final Report, 1 Nov. 1989 - 31 Dec. 1992

Alan G. MacDiarmid 31 Dec. 1992 24 p

(Contracts N00014-90-J-1559; N00014-86-K-0766)

(AD-A261064) Avail: CASI HC A03/MF A01

Included is a recapitulation of the research carried out during the time period of the grant, plus a complete list of 112 Technical Reports, 23 Patents Filed a/o Issued, and a complete listing of all personnel paid in whole or in part by the grant (and the previously connected Contract No. N00014-86-K-0766 covering period 9-16-86 to 10-31-89). DTIC

N93-26278# Mission Research Corp., Costa Mesa, CA.

DUCT PROTECTION COATING CONCEPT DEVELOPMENT AND TEST: TEST SPECIMEN FABRICATION, CONDITIONING, AND TESTING DOCUMENTATION. Final Report, period ending Feb. 1992

C. D. Newlander Jan. 1993 277 p

(Contract F40600-89-C-0002)

(AD-A261250; CDRL-A002; MRC-COM-R-92-0315;

AEDC-TR-92-23-App-D-Vol-2) Avail: CASI HC A13/MF A03

The overall objective of the program was to develop and test a surface cleaning/preparation and corrosion resistant protective polymer coating for the interior of the AEDC Environment Test Facility ferrous metal air supply ducts. The types of cleaning techniques acceptable to the AEDC were basically limited to chemical approaches. Typically, sand or abrasive blasting is used to produce corrosion-free, clean surfaces for coating steel substrates. These particular techniques are strongly discouraged and basically 'outlawed' at the AEDC facilities. Water blasting is an acceptable technique, but requires a high pressure water stream, expensive equipment, and considerable clean up. DTIC

N93-26303# Texas Univ., Austin. Dept. of Chemistry.

PHOSPHORUS-, NITROGEN-, SULFUR-, AND CHLORINE-CONTAINING MOLECULES ON SURFACES Final Report, 1 Sep. 1989 - 31 Aug. 1992

J. M. White 9 Oct. 1992 7 p LIMITED REPRODUCIBILITY: More than 20% of this document may be affected by microfiche quality

(Contract DAAL03-89-K-0107)

(AD-A261265; ARO-26822.12-CH) Avail: CASI HC A02/MF A01

The research is in the area of chemical reactions on surfaces and is concerned with molecules and solids that model systems of technological and environmental significance. In particular, we study heteroatom organic adsorbates containing halogens, sulfur, oxygen, phosphorus, and nitrogen. The fundamental surface chemical decomposition kinetics of selected molecules, especially simulants, are studied on metal and metal oxide substrates that model technological materials used to destroy and render them harmless. Our goal is to acquire fundamental and quantitative molecular level descriptions of heterogeneous chemical reactions at gas-solid interfaces. DTIC

N93-26341# Army Lab. Command, Fort Monmouth, NJ. Electronics Technology and Devices Lab.

EXTRUDED FILMS FROM MODIFIED POLYPROPYLENE RESIN: DIELECTRIC AND BREAKDOWN STUDIES Technical Report, Feb. - Aug. 1991

Robert J. Mammone, William L. Wade, Jr., and Michael Binder Apr. 1992 12 p

(AD-A261382; SLCET-TR-91-29) Avail: CASI HC A03/MF A01

Thin films (approximately 25 microns) formed by melt-extruding polypropylene resin after it had been briefly exposed to a low-pressure, low-temperature, CF4/O2 gas plasma had significantly increased dielectric breakdown strengths with very little accompanying changes in dielectric properties. DTIC

N93-26386# Minnesota Univ., Minneapolis. Dept. of Chemical Engineering and Materials Science.

ELECTROCHEMICAL PROCESSING OF ELECTRICALLY CONDUCTIVE POLYMER FIBERS Technical Report, 30 Jun. 1992 - 31 Mar. 1993

Shulong Li, Christopher W. Macosko, and Henry S. White 20 Mar. 1993 8 p

(Contract N00014-91-J-1927)

(AD-A261793; TR-25) Avail: CASI HC A02/MF A01

This article reviews recent developments in the synthesis of electrically conductive composite polymer fibers. DTIC

N93-26401# Ohio State Univ., Columbus.

ELECTRICAL CONDUCTIVITY OF ION IMPLANTED LADDER AND SEMI-LADDER POLYMERS Final Report, 1 Sep. 1990 - 31 Oct. 1991

Arthur J. Epstein Oct. 1992 35 p

(Contract F49620-90-C-0072)

(AD-A261401; AFOSR-93-0035TR) Avail: CASI HC A03/MF A01

Aromatic heterocyclic ordered rigid rod, ladder and semi-ladder polymers (including BBL, PBO, and BBB) combine exceptional high temperatures stability with excellent mechanical properties as well as environmental stability. We have carried out systemic coordinated investigation of the morphological, chemical, optical and electrical properties of ion implanted rigid rod, ladder and semi-ladder polymers, XPS data of films reveal significant reduction in the heteroatoms. An increase carbon content after implantation together with the scanning electron microscopy and Raman studies indicate that the implanted material is no longer polymeric but perhaps better described as a carbon network, The implanted polymers have a featureless broad optical absorption from the infrared to the UV. They have a very weakly temperature-dependent conductivity (typically -100 S/cm at room temperature). The initial conductivity, thermoelectric power and magnetotransport studies suggest that these implanted polymers behave as disordered metals. Further studies on are necessary to elucidate the role of implant ion beam energy and current as well as to determine the microscopic charge conduction mechanism. DTIC

N93-26432# Army Materials Technology Lab., Watertown, MA.

DENSIFICATION OF CERAMICS BY GAS OVERPRESSURE SINTERING

George E. Gazza and R. Nathan Katz Jul. 1992 14 p Presented at the Materials Research Society Meeting, Boston, MA, 4 Dec. 1991 Submitted for publication

(DA Proj. 1L1-62105-AH-84)

(MTL-TR-92-45) Avail: CASI HC A03/MF A01

The use of various gas pressure sintering (GPS) techniques for densifying ceramics are reviewed for both oxides and non-oxides. Variations of the process are discussed with respect to process parameters selected, process sequence, and microstructural development. Theoretical considerations

underlying the technique are presented. GPS and hot isostatic pressing are compared and the advantages and disadvantages of each are briefly discussed. Author

N93-26433# Army Materials Technology Lab., Watertown, MA.
ADHESION AND CORROSION BEHAVIOR OF Al-Zn AND TiN/Ti/TiN COATINGS ON A DU-0.75 WT. PERCENT Ti ALLOY
F. C. Chang, M. Levy, R. Huie, M. Kane, P. Buckley, T. Z. Kattamis (Connecticut Univ., Storrs.), and G. R. Lakshminarayan (Army Armament Research, Development and Engineering Center, Picatinny Arsenal, NJ.) Aug. 1992 13 p Presented at the 1991 International Conference on Metallurgical Coatings and Thin Films Submitted for publication
(MTL-TR-92-56) Avail: CASI HC A03/MF A01

Al-Zn alloy and multilayer TiN/Ti/TiN thin coatings were deposited on DU-0.75Ti alloy specimens by a cathodic arc plasma physical vapor deposition process. The quality, soundness, and adhesion of the coatings to the substrate were evaluated by automatic scratch testing, in combination with optical and scanning electron microscopy examination of the scratch morphology. The galvanic corrosion behavior of DU-0.75Ti alloy coupled to the coated alloys and aluminum alloy 7075-T6 was also investigated by electrochemical tests in a 0.5 N NaCl aqueous solution. Author

N93-26437# Colorado State Univ., Fort Collins. Dept. of Chemistry.
TEMPLATE SYNTHESIS OF ELECTRONICALLY CONDUCTIVE POLYMERS: A NEW ROUTE FOR ACHIEVING HIGHER ELECTRONIC CONDUCTIVITIES Interim Technical Report
Charles R. Martin, R. Parthasarathy, and V. Menon 22 Feb. 1993 8 p Submitted for publication Sponsored in part by AFOSR LIMITED REPRODUCIBILITY: More than 20% of this document may be affected by microfiche quality
(Contract N00014-82-K-0612)
(AD-A261616; ONR-TR-82) Avail: Issuing Activity (Defense Technical Information Center (DTIC))

We have recently developed a method for synthesizing microscopic fibers and tubules of electronically conductive polymers. This method entails synthesis of the polymer within the pores of a microporous host membrane. Conductivities in the narrowest of these 'template-synthesized' tubules and fibers can be significantly higher than in conventional forms (e.g. powders or thin films) of the analogous polymer. These previous conductivity data were based on a two-point measurement of the resistance of the host membrane after synthesis of the conductive polymer fibers within this membrane. In this paper we will show results of conductivity measurements on thin films composed of the template-synthesized tubules and fibers. A four-point conductivity measurement was used on these thin films. These four-point measurements corroborate the earlier two-point conductivity data and show that the template-synthesized materials are significantly more conductive. DTIC

N93-26506# Argonne National Lab., IL.
WORKSHOP ON DIAMOND AND DIAMOND-LIKE-CARBON FILMS FOR THE TRANSPORTATION INDUSTRY
F. A. Nichols, ed. and D. K. Moores, ed. Jan. 1993 385 p Workshop held in Argonne, IL, 4-5 Feb. 1992
(Contract W-31-109-eng-38)
(DE93-007491; CONF-920262) Avail: CASI HC A17/MF A04

Applications exist in advanced transportation systems as well as in manufacturing processes that would benefit from superior tribological properties of diamond, diamond-like-carbon and cubic boron nitride coatings. Their superior hardness make them ideal candidates as protective coatings to reduce adhesive, abrasive and erosive wear in advanced diesel engines, gas turbines and spark-ignited engines and in machining and manufacturing tools as well. The high thermal conductivity of diamond also makes it desirable for thermal management not only in tribological applications but also in high-power electronic devices and possibly large braking systems. A workshop has been recently held at Argonne National Laboratory entitled 'Diamond and Diamond-Like-Carbon Films for Transportation Applications' which was attended by 85 scientists and engineers including top people involved in the basic technology of these films and also representatives from many US industrial companies. A working group on applications endorsed 18 different applications for these films in the transportation area alone. Separate abstracts have been prepared. DOE

N93-26576# Cambridge Univ. (England).
EUROPEAN TRI-SERVICE ADVANCED MATERIALS WORKSHOP ON COMPRESSIVE STRENGTH IN RIGID-ROD POLYMERS
Anselm C. Griffin 5 Sep. 1992 18 p Workshop held in Cambridge, England, 3-5 Sep. 1992
(Contract DAJA45-92-M-0268)
(AD-A261517) Avail: CASI HC A03/MF A01

The First European Tri-Service Advanced Materials Workshops: Compressive Strength in Rigid-Rod Polymers was held at Pembroke College, University of Cambridge, 3-5 Sep. 1992. The Workshop brings together a small and select group of experts in the Physics, Engineering, Chemistry, and Materials aspects of compressive problems in these polymers. The abstracts which follow reflect the lectures by the distinguished scientists at the Workshop. It is the intent that as a result of intensive discussion concerning origins and manifestations of compressive failure in rigid-rod polymer systems, rational approaches for solving these problems may arise. DTIC

N93-26588# Argonne National Lab., IL.
PUBLISHED ASSESSMENTS BEARING ON THE FUTURE USE OF CERAMIC SUPERCONDUCTORS BY THE ELECTRIC POWER SECTOR
R. F. Giese and A. M. Wolsky 25 Aug. 1992 157 p
(Contract W-31-109-eng-38)
(DE93-007737; ANL-93007737) Avail: CASI HC A08/MF A02

Much has been written about ceramic superconductors since their discovery in 1986. Most of this writing reports and describes scientific research. However, some authors have sought to put this research in context: to assess where the field stands, what might be technically feasible, what might be economically feasible, and what potential impacts ceramic superconductors will bring to the electric power sector. This report's purpose is to make the results of already published assessments readily available. To that end, this report lists and provides abstracts for various technical and economic assessments related to applications of High-Temperature Superconductors (HTS) to the electric power sector. Those studies deemed most important are identified and summarized. These assessments were identified by two means. First, members of the Executive Committee identified some reports as worthy of consideration and forwarded them to Argonne National Laboratory. Twelve assessments were selected. Each of these is listed and summarized in the following section. Second, a bibliographic search was performed on five databases: INSPEC, NTIS, COMPENDEX, Energy Science & Technology, and Electric Power Database. The search consisted of first selecting all papers related to High Temperature Superconductors. Then papers related to SMES, cables, generators, motors, fault current limiters, or electric utilities were selected. When suitable variants of the above terms were included, this resulted in a selection of 493 citations. These citations were subjected to review by the authors. A number of citations were determined to be inappropriate (e.g., a number referred to digital transmission lines for electronics and communications applications). The reduced list consisted of 200 entries. Each of these citations, with an abstract, is presented in the following sections. DOE

N93-25562*# Idaho National Engineering Lab., Idaho Falls.
INEL SPRAY-FORMING RESEARCH
Kevin M. McHugh and James F. Key *In* NASA, Washington, Technology 2002: The Third National Technology Transfer Conference and Exposition, Volume 1 Feb. 1993 p 15-24 (For primary document see N93-25561 09-99)
(Contract DE-AC07-76ID-01570)
Avail: CASI HC A02/MF A04

N93-25563*# Midwest Research Inst., Golden, CO.
FILM FABRICATION TECHNOLOGIES AT NREL
Robert D. McConnell *In* NASA, Washington, Technology 2002: The Third National Technology Transfer Conference and Exposition, Volume 1 Feb. 1993 p 25-29 (For primary document see N93-25561 09-99)
Avail: CASI HC A01/MF A04

N93-25564*# National Aeronautics and Space Administration. Lewis Research Center, Cleveland, OH.
OPTICAL AND SCRATCH RESISTANT PROPERTIES OF DIAMONDLIKE CARBON FILMS DEPOSITED WITH SINGLE AND DUAL ION BEAMS
Michael T. Kussmaul (Sverdrup Technology, Inc., Brook Park, OH.), Michael

S. Bogdanski (Case Western Reserve Univ., Cleveland, OH.), Bruce A. Banks, and Michael J. Mirtich *In* NASA, Washington, Technology 2002: The Third National Technology Transfer Conference and Exposition, Volume 1 Feb. 1993 p 30-40 (For primary document see N93-25561 09-99)
Avail: CASI HC A03/MF A04

N93-25565*# National Aeronautics and Space Administration. Lewis Research Center, Cleveland, OH.
PROPERTIES OF EXTRUDED PS-212 TYPE SELF-LUBRICATING MATERIALS
W. J. Waters (Sverdrup Technology, Inc., Cleveland, OH.), H. E. Sliney, and R. F. Soltis (Cortez 3 Services Corp., Brook Park, OH.) *In* NASA, Washington, Technology 2002: The Third National Technology Transfer Conference and Exposition, Volume 1 Feb. 1993 p 41-55 (For primary document see N93-25561 09-99)
Avail: CASI HC A03/MF A04

N93-25585*# Bureau of Mines, Tuscaloosa, AL.
PRODUCTION OF ULTRAFINE, HIGH-PURITY CERAMIC POWDERS USING THE US BUREAU OF MINES DEVELOPED TURBOMILL
Jesse L. Hoyer *In* NASA, Washington, Technology 2002: The Third National Technology Transfer Conference and Exposition, Volume 1 Feb. 1993 p 231-240 (For primary document see N93-25561 09-99)
Avail: CASI HC A02/MF A04

N93-25607*# Army Research Lab., Fort Belvoir, VA. Engineering Materials and Coatings Div.
ELASTOMER COMPOUND DEVELOPED FOR HIGH WEAR APPLICATIONS
D. Crawford, H. Feuer, D. Flanagan, G. Rodriguez, A. Teets, and P. Touchet *In* NASA, Washington, Technology 2002: The Third National Technology Transfer Conference and Exposition, Volume 1 Feb. 1993 p 438-445 (For primary document see N93-25561 09-99)
Avail: CASI HC A02/MF A04

28 PROPELLANTS AND FUELS

Includes rocket propellants, igniters, and oxidizers; their storage and handling procedures; and aircraft fuels.

For related information see also *07 Aircraft Propulsion and Power, 20 Spacecraft Propulsion and Power,* and *44 Energy Production and Conversion.*

N93-24745*# Illinois Univ., Urbana-Champaign. Dept. of Aeronautical and Astronautical Engineering.
IGNITION AND COMBUSTION OF LUNAR PROPELLANTS Final Technical Report, 11 Jun. 1990 - 10 Jun. 1992
Rodney L. Burton, Ted A. Roberts, and Herman Krier Apr. 1993 317 p
(Grant NAG3-1184)
(NASA-CR-192814; NAS 1.26:192814; AAE-93-04; UIUL-93-0504) Avail: CASI HC A14/MF A03

The ignition and combustion of Al, Mg, and Al/Mg alloy particles in 99 percent O2/1 percent N2 mixtures is investigated at high temperatures and pressures for rocket engine applications. The 20 micron particles contain 0, 5, 10, 20, 40, 60, 80, and 100 weight percent Mg alloyed with Al, and are ignited in oxygen using the reflected shock in a shock tube near the endwall. Using this technique, the ignition delay and combustion times of the particles are measured at temperatures up to 3250 K as a function of Mg content for oxygen pressures of 8.5, 17, and 34 atm. An ignition model is developed which employs a simple lumped capacitance energy equation and temperature and pressure dependent particle and gas properties. Good agreement is achieved between the measured and predicted trends in the ignition delay times. For the particles investigated, the contribution of heterogeneous reaction to the heating of the particle is found to be significant at lower temperatures, but may be neglected as gas temperatures above 3000 K. As little as 10 percent Mg reduces the ignition delay time substantially at all pressures tested. The particle ignition delay times decrease with increasing Mg content, and this reduction becomes less pronounced as oxidizer temperature and pressure are increased.
Author (revised)

N93-25111# Delaware Univ., Newark. Center for Catalytic Science and Technology.
DESIGN OF A HIGH ACTIVITY AND SELECTIVITY ALCOHOL CATALYST Quarterly Report No. 7, 7 Feb. - 7 May 1992
H. C. Foley and G. A. Mills Jun. 1992 4 p
(Contract DE-FG22-90PC-90291)
(DE93-008101; DOE/PC-90291/T8) Avail: CASI HC A01/MF A01

In order to explore the secondary dehydration of methanol over gamma-Al2O3 support and over bimetallic Rh-Mo/gamma-Al2O3, a new series of K-doped Rh-Mo/gamma-Al2O3 catalysts was synthesized. Work on synthesis of bimetallic Rh-Mo clusters is reported. DOE

N93-25112# Delaware Univ., Newark. Center for Catalytic Science and Technology.
DESIGN OF A HIGH ACTIVITY AND SELECTIVITY ALCOHOL CATALYST Quarterly Report No. 9, 7 Aug. - 7 Nov. 1992
H. C. Foley and G. A. Mills 30 Nov. 1992 25 p
(Contract DE-FG22-90PC-90291)
(DE93-008103; DOE/PC-90291/T10) Avail: CASI HC A03/MF A01

Efforts to synthesize bimetallic cluster-derived Rh-Mo catalysts for CO and CO2 hydrogenation to preferentially produce oxygenates. The rhodium-molybdenum cluster, (PPh3)2RhMO(CO)(mu-CO)2Cp, was employed as a precursor to alumina- and silica-supported catalysts which were in CO hydrogenation. When compared to catalysts made from the distinct organometallic complexes, RhH(CO)(PPh3)3 and MO(CO)3Cp2, the catalysts derived from a binuclear precursor show higher activities for CO hydrogenation and superior selectivities towards oxygenates, namely, methanol, dimethyl ether, and ethanol. Their product distributions depend on the support. Fourier transform infrared spectroscopy studies indicate that CO chemisorbs on cluster-derived catalysts as gem-dicarbonyls while it is chemisorbed only in the linear-carbonyl configuration on catalysts made from separate rhodium and molybdenum complexes. The particular oxygenate selectivity of the cluster-derived catalysts may be correlated to the strong electronic interaction between Rh and Mo. Carbon dioxide hydrogenation was also carried out on the catalysts mentioned above. Again, the cluster-derived catalysts show higher oxygenate selectivities. Finally, the catalysts were studied with regard to both CO and CO2 hydrogenation kinetics, apparent activation energies inferred. DOE

N93-25118# Pittsburgh Univ., PA. Dept. of Chemical and Petroleum Engineering.
A NOVEL PROCESS FOR METHANOL SYNTHESIS
J. W. Tierney and I. Wender 1992 12 p
(Contract DE-FG22-89PC-89786)
(DE93-008037; DOE/PC-89786/T14) Avail: CASI HC A03/MF A01

A bench-scale reactor is being used to study the conversion of synthesis gas to methanol (MEOH) in the liquid phase by a novel method. In previous reports, evidence for a two step reaction consisting of a carbonylation reaction taking place mainly in the 'film' close to a copper chromite surface followed by a hydrogenolysis reaction taking place on the surface of the copper chromite was provided. The interaction between the two catalysts enhances the rate of methanol formation. In this quarter, the equilibrium concentration for methyl formate was reexamined and data at higher loadings of copper chromite was obtained. DOE

N93-25119# Pittsburgh Univ., PA. Dept. of Chemical and Petroleum Engineering.
PROBE MOLECULE STUDIES: ACTIVE SPECIES IN ALCOHOL SYNTHESIS Quarterly Report No. 8, Jul. - Sep. 1992
D. G. Blackmond, I. Wender, R. Oukaci, and J. Wang Oct. 1992 9 p
(Contract DE-FG22-90PC-90305)
(DE93-008097; DOE/PC-90305/T9) Avail: CASI HC A02/MF A01

The goal is to understand the mechanisms of formation of alcohols and other oxygenates from syngas over supported catalysts. Work during this period included: (1) BET (Brunauer, Emmett, and Teller) surface areas and x ray diffraction (XRD) patterns of Cu/ZnO/Al2O3 and Co(5 percent)/Cu/ZnO/Al2O3 suggest that Co did not change the structure; (2) CO was hydrogenated over 10 percent Co catalyst; (3) C2H4 additions increased the isopropanol and decreased the methanol production. Blank runs with H 2/He/CH3OH/C2H4 showed that C2H4 does not react with CH3OH. DOE

N93-25192# Argonne National Lab., IL.
EMISSIONS FROM ETHANOL AND LPG FUELED VEHICLES
Mark E. Pitstick 1992 20 p Presented at the 72nd Transportation Research Board Meeting, Washington, DC, 10-14 Jan. 1993
(Contract W-31-109-eng-38)
(DE93-006410; ANL/ES/CP-78570; CONF-930120-4) Avail: CASI HC A03/MF A01

This paper addresses the environmental concerns of using neat ethanol and liquified petroleum gas (LPG) as transportation fuels in the US. Low-levelblends of ethanol (10 percent) with gasoline have been used as fuels in the US for more than a decade, but neat ethanol (85 percent or more) has only been used extensively in Brazil. LPG, which consists mostly of propane, is already used extensively as a vehicle fuel in the US, but its use has been limited primarily to converted fleet vehicles. Increasing US interest in alternative fuels has raised the possibility of introducing neat ethanol vehicles into the market and expanding the number of LPG vehicles. Use of such vehicles and increased production and consumption of fuel ethanol and LPG will undoubtedly have environmental impacts. If the impacts are determined to be severe, they could act as barriers to the introduction of neat ethanol and LPG vehicles. Environmental concerns include exhaust and evaporative emissions and their impact on ozone formation and global warming, toxic emissions from fuel combustion and evaporation, and agricultural emissions from production of ethanol. The paper is not intended to be judgemental regarding the overall attractiveness of ethanol or LPG compared to other transportation fuels. The environmental concerns are reviewed and summarized, but the only conclusion reached is that there is no single concern that is likely to prevent the introduction of neat ethanol fueled vehicles or the increase in LPG fueled vehicles. DOE

N93-25298# Argonne National Lab., IL. Center for Transportation Research.
MAGNITUDE AND VALUE OF ELECTRIC VEHICLE EMISSIONS REDUCTIONS FOR SIX DRIVING CYCLES IN FOUR US CITIES WITH VARYING AIR QUALITY PROBLEMS
Quanlu Wang (California Univ., Davis.) and Danilo L. Santini 1992 28 p Presented at the 72nd Transportation research Board Meeting, Washington, DC, 10-14 Jan. 1993
(Contract W-31-109-eng-38)
(DE93-006417; ANL/ES/CP-77429; CONF-930120-3) Avail: CASI HC A03/MF A01

The emissions of logically competing mid-1990 gasoline vehicles (GV's) and electric vehicles (EV's) are estimated as if the vehicles were driven in the same pattern of driving. Six different driving cycles are evaluated, ranging in speed from 7 to 49 miles per hour (mph). These steps are repeated using specifics of fuel composition, electric power mix, and environmental conditions applicable to Chicago, Denver, Los Angeles, and New York in the month of July. The year 2000 emissions differences for each of four regulated pollutants - HC, CO, NOx, SOx - are estimated. CO2 emissions are also estimated. With use of EV's, HC and CO emissions are consistently lowered by 98 percent or more. CO2 emissions reductions are uniformly large at low speed, but variable at high speed. It is found that initially introduced EV's could achieve 100 percent emission reductions in Chicago by using off-peak power from nuclear power plants for EV electricity generation. Emissions reductions occur for all combinations in Los Angeles, and for most combinations in New York, excepting SOx. NOx emissions are reduced in all four cities. An 'avoided cost' value for each regulated pollutant is estimated for each of the cities. The values for each city depend on severity of air quality violations. It is estimated that the emissions reduction value of EV's driven an average of one and one half hours per day in Los Angeles ranges from $1050 to $3,900; $590 to $2100 in New York; $270 to $1200 in Chicago; and $330 to $1250 in Denver (1989$). Assuming a range of about 100 miles in congested conditions with speeds of 10 mph or less, the estimates range from $3600 to $13300 for Los Angeles; $2004 to $7200 for New York; $930 to $2930 for Chicago; and $1120 to $4290 for Denver. Low estimates are obtained using EPA's draft Mobile5 model for GV emissions, high values by using California's EMFAC7EP-SCF1 model. The dollar value benefit estimates include no economic value. DOE

N93-25496# Arkansas Univ., Fayetteville. Dept. of Chemical Engineering.
BIOLOGICAL PRODUCTION OF ETHANOL FROM COAL
Oct. 1992 146 p
(Contract DE-AC22-89PC-89876)
(DE93-008947; DOE/PC-89876/T17) Avail: CASI HC A07/MF A02

The production of ethanol from synthesis gas by the anaerobic bacterium C. ljungdahlii has been demonstrated in continuous stirred tank reactors (CSTRs), CSTRs with cell recycle and trickle bed reactors. Various liquid media were utilized in these studies including basal medium, basal media with 1/2 B-vitamins and no yeast extract and a medium specifically designed for the growth of C. ljungdahlii in the CSTR. Ethanol production was successful in each of the three reactor types, although trickle bed operation with C. ljungdahlii was not as good as with the stirred tank reactors. Operation in the CSTR with cell recycle was particularly promising, producing 47 g/L ethanol with only minor concentrations of the by-product acetate. DOE

N93-25497# Colorado Univ., Boulder. Dept. of Chemical Engineering.
DIRECT METHANE CONVERSION TO METHANOL
J. L. Falconer and R. D. Noble 3 Dec. 1992 9 p
(Contract DE-FG21-90MC-27115)
(DE93-009183; DOE/MC-27115/3280) Avail: CASI HC A02/MF A01

The objective is to demonstrate the effectiveness of a catalytic membrane reactor (ceramic membrane combined with catalyst) to selectively produce methanol by partial oxidation of methane. None of the membranes tested in a high pressure system could selectively remove methanol, until a cooling tube was inserted inside the membrane reactor to quench the product stream; this effectively increased methanol selectivity 2 times during methane oxidation. For both conditions, combined selectivity for methanol and CO is constant, 85 percent. The remaining product is CO2. The membranes were broken when removed from the system; this was remedied when a cooling tube with a smaller diameter was used. DOE

N93-25523# Arkansas Univ., Fayetteville.
BIOLOGICAL CONVERSION OF SYNTHESIS GAS
M. D. Ackerson, E. C. Clausen, and J. L. Gaddy Jan. 1993 36 p
(Contract DE-FG21-90MC-27225)
(DE93-009092; DOE/MC-27225/3281) Avail: CASI HC A03/MF A01

Syngas is known to contain approximately 1 percent H2S, along with CO, CO2, H2, and CH4. Similarly, the syngas may become contaminated with oxygen, particularly during reactor start-up and during maintenance. Previous studies with the water-gas shift bacterium Rhodospirillum rubrum have shown that the bacterium is tolerant of small quantities of oxygen, but the effects of oxygen on CO-consumption are unknown. Similarly, R. rubrum is known to be tolerant of H2S, with high concentrations of H2S negatively affecting CO-uptake. Batch experiments were thus carried out to determine the effects of H2S and O2 on CO-uptake by R. rubrum. The results of these experiments were quantified by using Monod equations modified by adding terms for CO, H2S, and O2 inhibition. The techniques used in determining kinetic expressions previously shown for other gas-phase substrate bacterial systems including R. rubrum were utilized. DOE

N93-25769# Department of Defense Explosives Safety Board, Alexandria, VA.
MINUTES OF THE TWENTY-FIFTH EXPLOSIVES SAFETY SEMINAR, VOLUME 4
Aug. 1992 632 p Seminar held in Anaheim, CA, 18-20 Aug. 1992
(AD-A261116) Avail: CASI HC A99/MF A06

For a long time now experts on energetic materials and munitions have been using experimental tests to evaluate the vulnerability of such materials or munitions, or at least their sensitivity to various stimuli. Yet those tests are far from being representative of the scenarios of accidental or combat stimuli, and the interpretation of them itself sometimes needs to be treated cautiously, given the important decisions that may be made as the results of these trials, for the design of insensitive munitions. A study of many examples, such as bullet impact and cook-off, enables a critical evaluation of those tests and suggests that they be conducted in a more scientific purpose by coupling them with mathematical modeling. It concludes by advocating international cooperation, as the recent NIMIC workshop shows the way, on modeling the tests and their experimental adaptation to the requirements of the models. DTIC

N93-25818# Economic Research Service, Washington, DC. Resources and Technology Div.
EMERGING TECHNOLOGIES IN ETHANOL PRODUCTION
Neil Hohmann and C. Matthew Rendleman Jan. 1993 19 p
(PB93-157014; USDA/AIB-663) Avail: CASI HC A03/MF A01

The fuel ethanol industry is poised to adopt a wide range of technologies that would reduce costs at every stage of the production process. Improved enzymes and fermenter designs can reduce the time needed to convert corn to ethanol, and they can lower capital costs. Membrane filtration can allow the recovery of high-value coproducts such as lactic acid. Adoption of these and other innovations in the next 5 years is expected in new ethanol plants constructed to cope with new demand resulting from Clean Air Act stipulations for cleaner burning fuel. Biomass (agricultural residues, municipal and yard waste, and energy crops like switch grass) can also be converted to ethanol, although commercial-scale ventures are limited by current technology. While biomass requires more handling and sorting before conversion, those costs may be offset by the abundance of biomass relative to corn. Author (DTIC)

N93-25857# Army Research Lab., Aberdeen Proving Ground, MD.
THE BURNING RATE BEHAVIOR OF PURE NITROCELLULOSE PROPELLANT SAMPLES Final Report, Jan. 1979 - Dec. 1981
Frederick W. Robbins and Theresa Keys Mar. 1993 37 p
(DA Proj. 1L1-62618-AH-80)
(AD-A261009) Avail: CASI HC A03/MF A01

Closed bomb firings have been conducted to determine the burning rate behavior of pure nitrocellulose (NC) gun propellants. Samples produced and tested included nitration levels of 12.02, 12.65, 13.11 percent, in both zero and seven-perforated cylindrical geometries. A sample containing basic lead carbonate was also included. Burning rates derived from the closed bomb tests were compared to strand burner data measured on samples extruded from the same NC batches. The burning rate plots for the pure NC samples show the characteristic slope changes of propellants with additives. DTIC

N93-25902# Southwest Research Inst., San Antonio, TX. Belvoir Fuels and Lubricants Research Facility.
DEVELOPMENT OF A METHOD TO DETERMINE THE AUTOXIDATION OF TURBINE FUELS Final Report, Sep. 1987 - Apr. 1992
George E. Fodor and David W. Naegeli May 1992 255 p
(Contract N00014-87-K-2057)
(AD-A260578; BFLRF-280) Avail: CASI HC A12/MF A03

The report describes the development of a research grade test method that allows the precise evaluation of antioxidants and prediction of the rate of peroxide formation at ambient conditions from data obtained from accelerated oxidation experiments at elevated temperatures. The rates of peroxide formation in 10 model jet fuels were measured at several temperatures ranging from 43 to 120 C, with oxygen partial pressures ranging from approximately 10 to 1140 kPa. Results of rigorously controlled experiments agreed with a kinetic model of the autoxidation process, which showed that the peroxide concentration increased as the square of stress duration. Within the experimental limits, the rate of peroxide formation did not depend on the oxygen partial pressure. Arrhenius correlations of global rate constants determined from peroxide concentration time histories in accordance with the kinetic model showed that a single autoxidation was accountable for the results obtained in the 430 to 120 C temperature range. This method has also been used to evaluate the effectiveness of several hindered phenolic antioxidants to inhibit the formation of peroxides in two jet fuels at temperatures of 100 and 120 C and an oxygen partial pressure of 240 kPa (ca. 20 psig). Antioxidants were evaluated in terms of induction period duration and their rates of peroxide formation during the induction period and the initial linear segment of the post-induction time. The global rate constant for the formation of peroxides during the induction period was reduced by the antioxidant, whereas the post-induction rate remained unchanged. DTIC

N93-25914# Southwest Research Inst., San Antonio, TX. Belvoir Fuels and Lubricants Research Facility.
EFFECT OF A METAL DEACTIVATOR FUEL ADDITIVE ON FUEL DEPOSITION IN FUEL ATOMIZERS AT HIGH TEMPERATURE Interim Report, Nov. 1990 - Aug. 1992
Clifford A. Moses Aug. 1992 38 p
(Contracts DAAK70-92-C-0059; DAAK70-87-C-0043)
(AD-A260915; BFLRF-281) Avail: CASI HC A03/MF A01

Fuel additives that are metal deactivators have been shown to improve the thermal stability breakpoint temperature of aviation fuels as determined in the Jet Fuel Thermal Oxidation Tester (JFTOT). These additives therefore, offer the opportunity to upgrade fuels of marginal thermal stability. However, concern has been expressed over whether this upgrade would be realized in actual aircraft hardware. To address this concern, an experimental project has been conducted with fuel atomizers from the T700 engine to determine the effect of the additive DMD-2, a metal deactivator, on high-temperature fuel deposition. The tests were conducted with JP-5 fuel supplied by the Naval Air Warfare Center Aircraft Division, Trenton (NAWCADTRN). For some of the tests, the base fuel was contaminated with copper to a concentration between 400 and 500 ppb. In the uncontaminated fuel, the metal deactivator (MDA) additive was tested at a concentration of 1 ppm; in the contaminated fuel, MDA concentrations of 1 ppm and 5.7 ppm were tested. With uncontaminated fuel, the results showed that initially the additive significantly reduced the deposition rate, but then, after an induction period, the deposition rate sharply increased. With the copper-contaminated fuel, at 1 ppm, the additive showed a small effect, but did not completely passivate the copper. At 5.7 ppm, there was no significant deposition during the test, indicating the copper was passivated. It is concluded that the metal deactivators inhibit deposition for a period of time until the surface becomes coated with carbon deposition, and then, they no longer serve any function. These results are consistent with some single-tube heat exchanger experiments reported in the literature. DTIC

N93-25948# California Univ., Irvine. Dept. of Mechanical and Aerospace Engineering.
FUNDAMENTAL STUDIES OF DROPLET INTERACTIONS IN DENSE SPRAYS Final Report, 1 Nov. 1989 - 31 Oct. 1992
W. A. Sirignano, S. E. Elghobashi, I. Kim, and C. H. Chiang 31 Dec. 1992 136 p
(Grant AF-AFOSR-0064-90)
(AD-A261165; AFOSR-TR-93-0073) Avail: CASI HC A07/MF A02

The research addressed interactions amongst droplets in a dense spray. The effects of neighboring droplets, that were a few droplet diameters away, on a vaporizing droplet were examined by theoretical and computational analyses for two basic configurations: (1) the axisymmetric convective situation where two or three droplets moved in tandem and (2) the fully three-dimensional convective situation where droplets moved side-by-side. Droplets in the wake of other droplets experienced a reduction in drag force, transport rates, and vaporization rate, sometimes causing collisions. Sufficiently close droplets moving side-by-side, approximately in parallel, experienced a repulsive lift force and an increased drag force. Vaporizing liquid oxygen droplets in a hydrogen gas environment were studied at both subcritical and supercritical pressures considering the variable liquid density with the associated droplet swelling during heating and the dependence of the local critical state upon local composition. Droplet surface conditions could be subcritical even if pressures were supercritical for pure oxygen due to diffusing hydrogen. The critical surface regressed towards the droplet surface as the droplet heated. Engineering correlations for the drag coefficients, Nusselt numbers, and Sherwood numbers for hydrocarbon fuel droplets in dense sprays were obtained. DTIC

N93-26268# CFD Research Corp., Huntsville, AL.
INFLUENCE OF SUPERCRITICAL CONDITIONS ON PRE-COMBUSTION CHEMISTRY AND TRANSPORT BEHAVIOR OF JET FUELS Final Report, 9 Jul. 1992 - 9 Jan. 1993
Anantha Krishnan Feb. 1993 60 p
(Contract F49620-92-C-0030)
(AD-A261813; CFDRC-4240/2; AFOSR-93-0137TR) Avail: CASI HC A04/MF A01

The objective of the Phase 1 study was to investigate heat transfer characteristics in supercritical flows. Detailed models were formulated to compute transport properties (such as density, conductivity, viscosity, and specific heat) in the supercritical regime. The models were incorporated into a general purpose Computational Fluid Dynamics (CFD) code capable of modeling flow, heat transfer, and reactions in complex geometries. Two and three-dimensional simulations were performed for supercritical flow and heat transfer in a test cell. Parallel experimental work was done by

Professor L. D. Chen at the University of Iowa. The results of the Phase 1 work show that there is considerable augmentation of heat transfer near the critical point. Also, the large variation in density across the critical point has a significant effect on the near wall profiles of velocity and temperature. Ideal gas approximations of supercritical flows can result in gross errors in predicting heat transfer rates. The development of this supercritical transport model provides a basis for incorporating complex models for pre-combustion chemistry in jet fuels. DTIC

N93-26308# Chicago Univ., IL. Dept. of Chemistry.
ENERGETIC MATERIALS FROM CUBANE Final Technical Report, 1 Aug. 1985 - 31 Jul. 1992
Philip E. Eaton 16 Feb. 1993 5 p
(Contract N00014-84-K-0645)
(AD-A261317) Avail: CASI HC A01/MF A01

New generations of highly energetic materials are required for the modern Navy. Cubane is a very dense, exceptionally energetic hydrocarbon; its heat of formation, density, and strain energy are all extraordinarily high--in combination unexceeded by any other stable hydrocarbon. This dense, energetic system has 8 identical methine C-H groups at which hydrogen may be replaced by energy-rich substituents. The goal of this project is to understand the fundamental properties of the basic set of reactive intermediates that might be used for the functionalization of the cubane nucleus. Only cubane-1,4-dicarboxylic acid is available readily. Ways to introduce other substituents elsewhere on the cubane nucleus are needed. As cubanes are far from the ordinary in their chemical behavior, this necessitates the development of radically new methodology. DTIC

N93-26387# Sandia National Labs., Livermore, CA. Combustion Research Facility.
THERMAL DECOMPOSITION OF ENERGETIC MATERIALS. 4: DEUTERIUM ISOTOPE EFFECTS AND ISOTOPIC SCRAMBLING CONDENSED-PHASED DECOMPOSITION OF 1,3,5-TRINITROHEXAHYDRO-S-TRIAZINE Special Publication
Richard Behrens, Jr. and Suryanarayana Bulusu Feb. 1993 15 p
Sponsored by ARO and Army Armament Research, Development and Engineering Center
(AD-A261804; ARAED-SP-92004) Avail: CASI HC A03/MF A01

The inter- versus intramolecular origin of the products formed in the thermal decomposition of 1,3,5-trinitrohexahydro-s-triazine (RDX) has been traced by isotopic crossover experiments using mixtures of differently labeled analogues of RDX. The isotopic analogues of RDX used in the experiments include H-2, C-13, N-15, and O-18. The fraction of isotopic scrambling and the extent of the deuterium kinetic isotope effect (DKIE) are reported for the different thermal decomposition products. Isotopic scrambling is not observed for the N-N bond in N2O and only in small amounts (7%) in the C-H bonds in CH2O, consistent with a mechanism of their formation through methylene nitramine precursors. A product, oxy-s-triazine (OST, C3H3N3O), does not undergo isotopic scrambling in H/D, N-14/N-15, or C-14/O-18 experiments, and its rate of formation exhibits a DKIE of 1.5. These results are consistent with the formation of OST via unimolecular decomposition of RDX. Another product, 1-nitroso-3,5-dinitrohexahydro-s-triazine (ONDNTA, C3H6N6O5), is found to be formed with complete scrambling of the N-NO bond, suggesting an N-N bond cleavage and a radical recombination process in its formation. One of the hydrogen containing products, H2O, exhibits a DKIE of 1.5 +/- 0.1. In contrast, CH2O and ONDNTA have DKIEs of 1.05 +/- 0.1 and 1.05 +/- 0.2, respectively, indicating that hydrogen transfer is not involved in the rate-limiting step of the reaction pathway leading to the formation of these products. DTIC

N93-26493# Los Alamos National Lab., NM.
MOLECULAR COMPOSITION, STRUCTURE, AND SENSITIVITY OF EXPLOSIVES
C. B. Storm and J. R. Travis 1992 14 p Presented at the 16th Material Research Society International Symposium on the Scientific Basis for Nuclear Waste Management Fall Meeting, Boston, MA, 30 Nov. - 5 Dec. 1992
(Contract W-7405-eng-36)
(DE93-003850; LA-UR-92-3823; CONF-921101-14) Avail: CASI HC A03/MF A01

High explosives, blasting agents, propellants, and pyrotechnics are all metastable relative to reaction products and are termed energetic materials. They are thermodynamically unstable but the kinetics of decomposition at ambient conditions are sufficiently slow that they can be handled safely under controlled conditions. The ease with which an energetic material can be caused to undergo a violent reaction or detonation is called its sensitivity. Sensitivity tests for energetic materials are aimed at defining the response of the material to a specific situation, usually prompt shock initiation or a delayed reaction in an accident. The observed response is always due to a combination of the physical state and the molecular structure of the material. Modeling of any initiation process must consider both factors. The physical state of the material determines how and where the energy is deposited in the material. The molecular structure determines the mechanism of decomposition of the material and the rate of energy release. Slower inherent reaction chemistry leads to longer reaction zones in detonation and inherently safer materials. Slower chemistry also requires hot spots involved in initiation to be hotter and to survive for longer periods of time. High thermal conductivity also leads to quenching of small hot spots and makes a material more difficult to initiate. Early endothermic decomposition chemistry also delays initiation by delaying heat release to support hot spot growth. The growth to violent reaction or detonation also depends on the nature of the early reaction products. If chemical intermediates are produced that drive further accelerating autocatalytic decomposition the initiation will grow rapidly to a violent reaction. DOE

N93-26600# Naval Air Systems Command, Washington, DC.
MILITARY STANDARDIZATION HANDBOOK: AIRCRAFT REFUELING HANDBOOK
20 Oct. 1992 105 p
(AD-A261755; MIL-HDBK-844(AS)) Avail: CASI HC A06/MF A02

This handbook provides basic information on the properties and characteristics of aviation fuels along with general information on the standards, equipment, and operating principals related to the handling of these fuels at Navy and Marine Corps activities. It is designed to supplement the NATOPS AIRCRAFT REFUELING MANUAL, NATOPS 00-80T-109, by providing background information and guidance on the requirements and procedures contained in the NATOPS Manual. The contents are limited to technical and operational information of a general nature. Specific operating procedures and equipment requirements are contained in the NATOPS AIRCRAFT REFUELING MANUAL, NATOPS 00-80T-109. Accounting and stock control procedures are not included. There are basically two different types of aircraft fuels in use at Navy and Marine Corps air activities - turbine engine fuels and aviation gasolines (AVGAS). A knowledge of some of the basic properties and characteristics of these fuels is necessary in understanding the importance of delivering the proper fuel to the aircraft. Such knowledge is also valuable in understanding the need for safety and caution in handling aviation fuels. DTIC

N93-26013 University of Southern California, Los Angeles. Dept. of Mechanical Engineering.
PARTICLE SIZE AS A FACTOR IN AGGLOMERATION IN SLURRY FUELS
P. Roy Choudhury *In* JHU, 29th JANNAF Combustion Subcommittee Meeting, Volume 2 Oct. 1992 p 91-99 (For primary document see N93-26005 09-20)
Avail: CPIA, 10630 Little Patuxent Pkwy., Suite 202, Columbia, MD 21044-3200 HC

N93-26033 Sandia National Labs., Livermore, CA. Combustion Research Facility.
THERMAL DECOMPOSITION OF HMX, MONONITROSO-RDX, TNCHP AND K6 IN THE LIQUID PHASE: RESULTS FROM SIMULTANEOUS THERMOGRAVIMETRY MODULATED BEAM MASS SPECTROMETRY MEASUREMENTS
Richard Behrens, Jr. and Suryanarayana Bulusu (Army Armament Research and Development Command, Dover, NJ.) *In* JHU, 29th JANNAF Combustion Subcommittee Meeting, Volume 2 Oct. 1992 p 283-293
Supported by U.S. Army Research Office (For primary document see N93-26005 09-20)
Avail: CPIA, 10630 Little Patuxent Pkwy., Suite 202, Columbia, MD 21044-3200 HC

N93-26034 Sandia National Labs., Albuquerque, NM.
DEVELOPMENT OF RATE EXPRESSIONS FOR THE THERMAL DECOMPOSITION OF RDX
K. L. Erickson, R. Behrens, Jr. (Sandia National Labs., Livermore, CA.), and S. Bulusu (Army Armament Research and Development Command, Dover, NJ.) *In* JHU, e 2 Oct. 1992 p 295-305 e 2 p 295-311
Previously announced as N93-22502 (For primary document see N93-26005 09-20)
(Contract DE-AC04-76DP-00789)
Avail: CPIA, 10630 Little Patuxent Pkwy., Suite 202, Columbia, MD 21044-3200 HC

N93-26035 Los Alamos National Lab., NM.
CHEMISTRY DURING THE INDUCTION TIME IN HEATED NITRAMINES
M. M. Stinecipher *In* JHU, 29th JANNAF Combustion Subcommittee Meeting, Volume 2 Oct. 1992 p 307-311 (For primary document see N93-26005 09-20)
(Contract W-7405-eng-36)
Avail: CPIA, 10630 Little Patuxent Pkwy., Suite 202, Columbia, MD 21044-3200 HC

N93-26037 Pennsylvania State Univ., University Park.
PHYSICAL AND CHEMICAL PROCESSES GOVERNING THE CO2 LASER-INDUCED DEFLAGRATION OF AMMONIUM DINITRAMIDE (ADN)
B. L. Fetherolf and T. A. Litzinger *In* JHU, 29th JANNAF Combustion Subcommittee Meeting, Volume 2 Oct. 1992 p 329-338 (For primary document see N93-26005 09-20)
(Contract N00014-89-J-1238)
Avail: CPIA, 10630 Little Patuxent Pkwy., Suite 202, Columbia, MD 21044-3200 HC

N93-26038 Naval Surface Warfare Center, Silver Spring, MD.
THERMAL DECOMPOSITION AND STABILIZATION OF AMMONIUM DINITRAMIDE
T. P. Russell, A. G. Stern, W. M. Koppes, and C. D. Bedford *In* JHU, 29th JANNAF Combustion Subcommittee Meeting, Volume 2 Oct. 1992 p 339-345 (For primary document see N93-26005 09-20)
Avail: CPIA, 10630 Little Patuxent Pkwy., Suite 202, Columbia, MD 21044-3200 HC

N93-26039 Pennsylvania State Univ., University Park. Dept. of Mechanical Engineering.
INTERACTIONS OF ACOUSTIC WAVES AND COMBUSTION OF HOMOGENEOUS SOLID PROPELLANTS IN ROCKET MOTORS
V. Yang and I. S. Tseng *In* JHU, 29th JANNAF Combustion Subcommittee Meeting, Volume 2 Oct. 1992 p 347-358 (For primary document see N93-26005 09-20)
Avail: CPIA, 10630 Little Patuxent Pkwy., Suite 202, Columbia, MD 21044-3200 HC

29 MATERIALS PROCESSING

Includes space-based development of products and processes for commercial applications.

For biological materials see *55 Space Biology*.

N93-24774 Alabama Univ., Huntsville.
ELECTRODEPOSITION IN LOW GRAVITY Ph.D. Thesis
Hind Malaeb Abi-Akar 1992 214 p
Avail: Univ. Microfilms Order No. DA9306835

Materials development and enhancement is paramount to the advancement of science and the growing demand for new materials. The possibility of enhancing metal coatings by production in a low G environment was investigated in this work. Ni and Co metal films were produced by electrodeposition, with emphasis on the former. High deposition rates, encompassing or exceeding 80 mA/cm(sup 2) produced an anomalous form of Ni which was microcrystalline or amorphous by an x-ray criterion. Employed deposition conditions under reduced gravity seemed to mimic the results quenching techniques utilized in producing amorphous metals and metallic alloys. Electrocodeposition of particles and metals was also part of this research. Ni-diamond and Co-chromium carbide systems were studied. Reduced gravity proved to eliminate sedimentation and edge affects and promote easier particle dispersion in the electrolyte, yielding uniformly distributed particles in the metal matrix. This environment codeposited higher volume percentage of large nonconducting particles (45 micron diamond) than produced on earth under similar conditions. The opposite was found for submicron diamond. Custom designed and constructed experimental packages and state-of-the-art electronics were utilized to perform this experimentation. These experiments accumulated and compared data from flights on a KC-135 airplane, four Consort sounding rockets, and one shuttle mission. Dissert. Abstr.

N93-24946*# Case Western Reserve Univ., Cleveland, OH.
A MODEL OF CONCURRENT FLOW FLAME SPREAD OVER A THIN SOLID FUEL
Paul V. Ferkul Apr. 1993 156 p
(Grant NAG3-1046; RTOP 674-22-05)
(NASA-CR-191111; E-7726; NAS 1.26:191111) Avail: CASI HC A08/MF A02

A numerical model is developed to examine laminar flame spread and extinction over a thin solid fuel in lowspeed concurrent flows. The model provides a more precise fluid-mechanical description of the flame by incorporating an elliptic treatment of the upstream flame stabilization zone near the fuel burnout point. Parabolic equations are used to treat the downstream flame, which has a higher flow Reynolds number. The parabolic and elliptic regions are coupled smoothly by an appropriate matching of boundary conditions. The solid phase consists of an energy equation with surface radiative loss and a surface pyrolysis relation. Steady spread with constant flame and pyrolysis lengths is found possible for thin fuels and this facilitates the adoption of a moving coordinate system attached to the flame with the flame spread rate being an eigen value. Calculations are performed in purely forced flow in a range of velocities which are lower than those induced in a normal gravity buoyant environment. Both quenching and blowoff extinction are observed. The results show that as flow velocity or oxygen percentage is reduced, the flame spread rate, the pyrolysis length, and the flame length all decrease, as expected. The flame standoff distance from the solid and the reaction zone thickness, however, first increase with decreasing flow velocity, but eventually decrease very near the quenching extinction limit. The short, diffuse flames observed at low flow velocities and oxygen levels are consistent with available experimental data. The maximum flame temperature decreases slowly at first as flow velocity is reduced, then falls more steeply close to the quenching extinction limit. Low velocity quenching occurs as a result of heat loss. At low velocities, surface radiative loss becomes a significant fraction of the total combustion heat release. In addition, the shorter flame length causes an increase in the fraction of conduction downstream compared to conduction to the fuel. These heat losses lead to lower flame temperatures, and ultimately, extinction. This extinction mechanism differs from that of blowoff, where the flame is unable to be stabilized due to the high flow velocity. Author

N93-25194*# National Aeronautics and Space Administration, Washington, DC.
NASA MICROGRAVITY SCIENCE AND APPLICATIONS PROGRAM Annual Report, 1992
1992 48 p
(NASA-TM-108775; NAS 1.15:108775) Avail: CASI HC A03/MF A01

Key elements of the microgravity research program as conducted by the Microgravity Science and Applications Division (MSAD) within the Office of Space Science and Applications (OSSA) during fiscal year (FY) 1992 are described. This NASA funded program supported investigators from the university, industry, and government research communities. The program's goals, the approach taken to achieve those goals, and the resources that were available are summarized. It provides a 'snapshot' of the Program's status at the end of FY 1992 and reviews highlights and progress in the ground and flight-based research during the year. It also describes four major space missions that flew during FY 1992, the advanced technology development (ATD) activities, and the plans to use the research potential of Space Station Freedom and other advanced carriers. The MSAD program structure encompassed five research areas: (1) Biotechnology, (2) Combustion Science, (3) Fluid Physics, (4) Materials Science, and (5) Benchmark Physics. Author (revised)

N93-25218*# George Washington Univ., Washington, DC.
WHISKER GROWTH STUDIES UNDER CONDITIONS WHICH RESEMBLE THOSE AVAILABLE ON AN ORBITING SPACE STATION
Final Technical Report, 1 Jun. 1990 - 31 Dec. 1992
Herman H. Hobbs 31 Dec. 1992 16 p
(Grant NAG3-1142)
(NASA-CR-192701; NAS 1.26:192701) Avail: CASI HC A03/MF A01

Minimal funding was provided by NASA with one designated 'mission' being the clear demonstration of the relevance of previously supported whisker growth studies to microgravity research. While in one sense this work has shown the converse, namely, that ambient gravitational fields as high as 1 Earth normal have no relevance to growth of whiskers by hydrogen reduction of metal halides, a case is made that this does not demonstrate lack of relevance to microgravity research. On the contrary, the driving forces for this growth are precisely those which must be understood in order to understand growth in microgravity. The results described suggest that knowledge gained from this work may be highly fundamental to our understanding of the genesis of metal crystals. Time and money ran out before this work could be considered complete. At least another year's study and analysis will be required before publications could be justified. Author

N93-25337*# National Aeronautics and Space Administration. Lewis Research Center, Cleveland, OH.
LASER IGNITION APPLICATION IN A SPACE EXPERIMENT
Larry C. Liou and Dennis E. Culley Apr. 1993 15 p Presented at the OE/LASE'93 Conference, Los Angeles, CA, 19-20 Jan. 1993; sponsored by the Society of Photo-Optical Instrumentation Engineers
(RTOP 694-03-08)
(NASA-TM-106133; E-7805; NAS 1.15:106133) Avail: CASI HC A03/MF A01

A laser ignition system is proposed for the Combustion Experiment Module on an orbiting spacecraft. The results of a design study are given using the scheduled 'Flame Ball Experiment' as the design guidelines. Three laser ignition mechanisms and wavelengths are evaluated. A prototype laser is chosen and its specifications are given, followed by consideration of the beam optical arrangement, the ignition power requirement, the laser ignition system weight, size, reliability, and laser cooling and power consumption. Electromagnetic interference to the onboard electronics caused by the laser ignition process is discussed. Finally, ground tests are suggested. Author (revised)

N93-25390 Case Western Reserve Univ., Cleveland, OH.
MODELING OF BUBBLE AND DROP FORMATION IN FLOWING LIQUIDS IN TERRESTRIAL AND MICROGRAVITY ENVIRONMENTS Ph.D. Thesis
Iee-Hwan Kim 1992 201 p
Avail: Univ. Microfilms Order No. DA9236330

A theoretical model for the process of bubble and drop formation, which is applicable for both terrestrial and microgravity environments, has been developed by using a force balance. Two different flow systems are considered in which a nozzle is located either horizontally (co-flow system) or vertically (cross-flow system) in a flowing liquid through a pipe. The contact angle variation at the nozzle due to the inertia of the flowing liquid has been theoretically analyzed. The added mass coefficient of the bubble moving through a pipe is obtained analytically based on potential flow theory. The bubble formation process is assumed to take place in two stages, the expansion stage and the detachment stage. The important forces in a bubble formation process are nondimensionalized and the bubble motions during its expansion and detachment stages for the two different flow systems are analyzed by using nondimensional variables. The predictions of the present model are compared with available experimental results in the case of normal gravity and the agreement is satisfactory. The present model is applied for a gas-liquid system to estimate the bubble size for various conditions in microgravity. The effect of the nondimensional variables as well as the flow systems on the bubble size have been evaluated. The present model is also applied for the prediction of the flow pattern transition from bubble to slug flow in microgravity. The predictions are compared with the results of microgravity experiment and of groundbased experiment. It is indicated that flow patterns in microgravity are closely related to the bubble formation process as well as the entrance configuration. The predictions of the present model for the transition from bubble to slug flow show good qualitative agreement with experimental results. Dissert. Abstr.

N93-25465 Illinois Univ. at Urbana-Champaign, Savoy.
MODELLING OF MICROGRAVITY IGNITION PHENOMENA Ph.D. Thesis
Changjin Lee 1992 154 p
Avail: Univ. Microfilms Order No. DA9236514

The structure and stability of flame balls and the characteristics of the outwardly propagating spherical flames of sub-limit mixtures are studied both analytically and numerically in the context of an asymptotic analysis in which theta approaches infinity, and (1 - Le) = O(1/theta), where theta is the activation energy and Le is Lewis number. For flame balls, the heat loss mechanism necessary for stable solutions is the radiation from burnt gas. If heat loss is less than quenching value, there are two stationary solutions, but the small branch solution is always unstable to the one dimensional disturbances regardless of Lewis number when Le is less than or equal to 1. And the large branch solution is stable within a certain range of heat loss, if Lewis number is less than the critical Lewis number Le(sub c) (Le less than Le(sub c) less than 1). The flame balls with sufficiently large radius are always unstable to three dimensional disturbances, independent of Le. These results, therefore, reveal that flame balls can only be possible if Le is less than Le(sub c) where Le(sub c) is identified very close to unity. The three dimensional stability is not Lewis number but near field heat losses driven. For spherically propagating flames, the evolution of flame after the flame initiation subject to radiative heat loss and confinement effect (pressure rise of unburned mixture due to finite chamber volume) was studied using numerical calculation of asymptotically derived model. The Lewis number effect (Le less than 1) enhances flame intensity but radiative cooling attenuates the intensity through the inflow velocity behind flame front. The pressure rise enhances the burning as flame radius is comparable to the chamber radius. The exchange of these two competitive mechanism leads to self-extinguishing flames (SEF's), and the confinement effect causes flames to be extremely sensitive to the intial data. Dissert. Abstr.

N93-25740 Case Western Reserve Univ., Cleveland, OH.
GRAVITY-DEPENDENT TRANSPORT PHENOMENA IN ZEOLITE CRYSTAL GROWTH Ph.D. Thesis
Hao Zhang 1992 123 p
Avail: Univ. Microfilms Order No. DA9236352

It has been thought that large zeolite crystals with perfect quality can be grown in microgravity environments due to avoidance of particle settling and elimination of natural convection. However, there has been no detailed quantitative study in the literature to determine the nature and extent of these effects. We investigated the related transport phenomena to see if they play important roles in zeolite crystal growth. Natural convection due to temperature and concentration gradients is analyzed by estimating thermal and solutal Grashof numbers. The results suggest that the effect of natural convection on zeolite syntheses is negligible even on the earth. Moreover, several different effects caused by sedimentation are studied herein. The shear stress at the growing surface due to settling and buoyancy driven natural convection is shown to be many orders of magnitude smaller than that due to vessel shaking. Therefore, there is no reason to believe that the shear stress caused by particle settling and natural convection has a significant effect on the sizes of resultant zeolite crystals. Furthermore, it is commonly thought that because of crystal settling a nutrient-poor crystal sediment is formed at the bottom of the reactor where growth terminates. However, the settiing itself may help transfer more nutrient to the growing surface than diffusion alone can, thereby accelerating the growth rate. Zeolite crystal growth is a unique process which usually takes place within an amorphous solid gel plus an aqueous solution. It is found herein that, under normal gravity, a white opaque gel portion containing amorphous solid gel, crystals and aqueous solution shrinks to the bottom of the hydrothermal reactor due to depletion of the flocculated gel particles. A correlation for the shrinkage is derived which agrees very well with experimental observations. Also, a non-dimensional parameter is suggested as a criterion for the occurrence of gravity-caused secondary nucleation which has been believed to result in smaller crystal size. In addition, zeolite crystal growth under microgravity is discussed in terms of under what conditions reduced gravity might be beneficial based on our analyses.

The gel structure and behavior in the absence of a gravitational force is preliminary explored, which suggests the mass transfer rate will be reduced at microgravity. Dissert. Abstr.

31 ENGINEERING (GENERAL)

Includes vacuum technology; control engineering; display engineering; cryogenics; and fire prevention.

N93-24678*# National Aeronautics and Space Administration, Washington, DC.
READINGS IN SYSTEMS ENGINEERING
Francis T. Hoban, ed. and William M. Lawbaugh, ed. 1993 215 p (NASA-SP-6102; NAS 1.21:6102) Avail: CASI HC A10/MF A03

This present collection was inspired by seven papers prepared by the NASA Alumni League, illustrating the members' systems engineering experience. These papers make up the heart of this collection. We have supplemented them with papers describing industry processes and other governmental practices to illustrate the diversity of systems engineering as it is formulated and practiced. This is one discipline that clearly benefits from cross-fertilization and infusion of new ideas. There is also a wide variety of tools and techniques described herein, some standard and some unique. For individual titles, see N93-24679 through N93-24693.

N93-24679*# Defense Systems Management School, Fort Belvoir, VA.
THE SYSTEMS ENGINEERING OVERVIEW AND PROCESS (FROM THE SYSTEMS ENGINEERING MANAGEMENT GUIDE, 1990)
In NASA, Washington, Readings in Systems Engineering 1993 p 9-15 (For primary document see N93-24678 09-31)
Avail: CASI HC A02/MF A03

The past several decades have seen the rise of large, highly interactive systems that are on the forward edge of technology. As a result of this growth and the increased usage of digital systems (computers and software), the concept of systems engineering has gained increasing attention. Some of this attention is no doubt due to large program failures which possibly could have been avoided, or at least mitigated, through the use of systems engineering principles. The complexity of modern day weapon systems requires conscious application of systems engineering concepts to ensure producible, operable and supportable systems that satisfy mission requirements. Although many authors have traced the roots of systems engineering to earlier dates, the initial formalization of the systems engineering process for military development began to surface in the mid-1950s on the ballistic missile programs. These early ballistic missile development programs marked the emergence of engineering discipline 'specialists' which has since continued to grow. Each of these specialties not only has a need to take data from the overall development process, but also to supply data, in the form of requirements and analysis results, to the process. A number of technical instructions, military standards and specifications, and manuals were developed as a result of these development programs. In particular, MILSTD-499 was issued in 1969 to assist both government and contractor personnel in defining the systems engineering effort in support of defense acquisition programs. This standard was updated to MIL-STD499A in 1974, and formed the foundation for current application of systems engineering principles to military development programs.
Author

N93-24680*# Hughes Aircraft Co., Los Angeles, CA.
SYSTEMS ENGINEERING FOR VERY LARGE SYSTEMS
Paul E. Lewkowicz *In* NASA, Washington, Readings in Systems Engineering 1993 p 17-22 (For primary document see N93-24678 09-31)
Avail: CASI HC A02/MF A03

Very large integrated systems have always posed special problems for engineers. Whether they are power generation systems, computer networks or space vehicles, whenever there are multiple interfaces, complex technologies or just demanding customers, the challenges are unique. 'Systems engineering' has evolved as a discipline in order to meet these challenges by providing a structured, top-down design and development methodology for the engineer. This paper attempts to define the general class of problems requiring the complete systems engineering treatment and to show how systems engineering can be utilized to improve customer satisfaction and profit ability. Specifically, this work will focus on a design methodology for the largest of systems, not necessarily in terms of physical size, but in terms of complexity and interconnectivity.
Author

N93-24681*# National Aeronautics and Space Administration. Marshall Space Flight Center, Huntsville, AL.
WHAT IS A SYSTEM? NASA'S PHASED PROJECT DESCRIPTION
In NASA, Washington, Readings in Systems Engineering 1993 p 23-34 (For primary document see N93-24678 09-31)
Avail: CASI HC A03/MF A03

NASA phase A and B projects are addressed. The Phase A study is the preliminary analysis of a space concept. These concepts could have come from a pre-Phase A study or from other sources within or external to NASA. The majority of concepts that are studied at MSFC are assigned by NASA Headquarters and funded accordingly. The overall program schedule depicts important milestones that establish the start and finish dates of each study phase, including design, development, launch, and operations. The Phase B of the project consists of the refinement of preliminary requirements, cost estimates, schedules and risk assessments prior to starting final design and development. The goal of a concept definition activity is to determine the best and most feasible concept(s) that will satisfy the mission and science requirements.
CASI

N93-24682*# California Inst. of Tech., Pasadena.
MANAGEMENT ISSUES IN SYSTEMS ENGINEERING
Robert Shishko, Robert G. Chamberlain, Robert Aster, Vincent Bilardo, Kevin Forsberg, Hal Mooz, Lou Polaski, and Ron Wade *In* NASA, Washington, Readings in Systems Engineering 1993 p 35-77 (For primary document see N93-24678 09-31)
Avail: CASI HC A03/MF A03

When applied to a system, the doctrine of successive refinement is a divide-and-conquer strategy. Complex systems are sucessively divided into pieces that are less complex, until they are simple enough to be conquered. This decomposition results in several structures for describing the product system and the producing system. These structures play important roles in systems engineering and project management. Many of the remaining sections in this chapter are devoted to describing some of these key structures. Structures that describe the product system include, but are not limited to, the requirements tree, system architecture and certain symbolic information such as system drawings, schematics, and data bases. The structures that describe the producing system include the project's work breakdown, schedules, cost accounts and organization.
CASI

N93-24683*# National Aeronautics and Space Administration. Goddard Space Flight Center, Greenbelt, MD.
SPACECRAFT SYSTEMS ENGINEERING: AN INTRODUCTION TO THE PROCESS AT GSFC
Tony Fragomeni and Michael G. Ryschkewitsch *In* NASA, Washington, Readings in Systems Engineering 1993 p 79-86 (For primary document see N93-24678 09-31)
Avail: CASI HC A02/MF A03

The main objective in systems engineering is to devise a coherent total system design capable of achieving the stated requirements. Requirements should be rigid. However, they should be continuously challenged, rechallenged and/or validated. The systems engineer must specify every requirement in order to design, document, implement and conduct the mission. Each and every requirement must be logically considered, traceable and evaluated through various analysis and trade studies in a total systems design. Margins must be determined to be realistic as well as adequate. The systems engineer must also continuously close the loop and verify system performance against the requirements. The fundamental role of the systems engineer, however, is to engineer, not manage. Yet, in large, complex missions, where more than one systems engineer is required, someone needs to manage the systems engineers, and we call them 'systems managers.' Systems engineering management is an overview function which plans, guides, monitors and controls the technical execution of a project as implemented by the systems engineers. As the project moves on through Phases A and B into Phase C/D, the systems engineering tasks become a small portion of the total effort. The systems management role increases since discipline subsystem engineers are conducting analyses and reviewing test data for final review and acceptance by the systems managers.
Derived from text

N93-24684*# National Aeronautics and Space Administration. Langley Research Center, Hampton, VA.
SYSTEMS ENGINEERING AND INTEGRATION AND MANAGEMENT FOR MANNED SPACE FLIGHT PROGRAMS
Owen Morris *In* NASA, Washington, Readings in Systems Engineering 1993 p 87-104 (For primary document see N93-24678 09-31)
Avail: CASI HC A03/MF A03

This paper discusses the history of SE&I management of the overall program architecture, organizational structure and the relationship of SE&I to other program organizational elements. A brief discussion of the method of executing the SE&I process, a summary of some of the major lessons learned, and identification of things that have proven successful are included. Derived from text

N93-24685*# National Aeronautics and Space Administration, Washington, DC.
THE SE ROLE IN ESTABLISHING, VERIFYING AND CONTROLLING TOP-LEVEL PROGRAM REQUIREMENTS
Charles W. Mathews *In its* Readings in Systems Engineering 1993 p 105-114 (For primary document see N93-24678 09-31)
Avail: CASI HC A02/MF A03

The program objectives and requirements described in the preceding paragraphs emphasize mission demonstrations. Obtaining desired science or applications information is another type of program objective. The program requirements then state the need for specific data, usually specifying a particular instrument or instrument set; the operating conditions under which the data is to be obtained (e.g., orbit altitude, field of view, and pointing accuracy); and the data handling and use. Conversely, a new instrument may be conceived or created with the program objective to establish its use potential. The Multispectral Scanner employed in the Landsat program is an example. Derived from text

N93-24686*# National Aeronautics and Space Administration, Washington, DC.
THE IMPORTANCE OF COST CONSIDERATIONS IN THE SYSTEMS ENGINEERING PROCESS
John D. Hodge *In its* Readings in Systems Engineering 1993 p 115-125 (For primary document see N93-24678 09-31)
Avail: CASI HC A03/MF A03

This paper examines the question of cost, from the birth of a program to its conclusion, particularly from the point of view of large multi-center programs, and suggests how to avoid some of the traps and pitfalls. Emphasis is given to cost in the systems engineering process, but there is an inevitable overlap with program management. (These terms, systems engineering and program management, have never been clearly defined.) In these days of vast Federal budget deficits and increasing overseas competition, it is imperative that we get more for each research and development dollar. This is the only way we will retain our leadership in high technology and, in the long run, our way of life. Derived from text

N93-24687*# National Aeronautics and Space Administration, Washington, DC.
SYSTEMS ENGINEERING AND THE USER: INCORPORATION OF USER REQUIREMENTS INTO THE SE PROCESS
John E. Naugle *In its* Readings in Systems Engineering 1993 p 127-144 (For primary document see N93-24678 09-31)
Avail: CASI HC A03/MF A03

This paper is organized into four parts. In the Gestation Phase, I describe the process of starting a new mission and establishing its rough boundaries. Next I show how the scientific experiments are selected. Then we enter the Preliminary Design Phase, where we incorporate the scientist's instruments into the systems engineering process. Finally, I show how the Preliminary Design Review (PDR) assures NASA management and the scientists that the scientific requirements have been incorporated into the systems engineering process to everyone's satisfaction. Derived from text

N93-24688*# National Aeronautics and Space Administration. Lyndon B. Johnson Space Center, Houston, TX.
SYSTEMS ENGINEERING AND INTEGRATION PROCESSES INVOLVED WITH MANNED MISSION OPERATIONS
Eugene F. Kranz and Christopher C. Kraft *In* NASA, Washington, Readings in Systems Engineering 1993 p 145-156 (For primary document see N93-24678 09-31)
Avail: CASI HC A03/MF A03

This paper will discuss three mission operations functions that are illustrative of the key principles of operations SE&I and of the processes and products involved. The flight systems process was selected to illustrate the role of the systems product line in developing the depth and cross disciplinary skills needed for SE&I and providing the foundation for dialogue between participating elements. FDDD was selected to illustrate the need for a structured process to assure that SE&I provides complete and accurate results that consistently support program needs. The flight director's role in mission operations was selected to illustrate the complexity of the risk/gain tradeoffs involved in the development of the flight techniques and flight rules process as well as the absolute importance of the leadership role in developing the technical, operational, and political trades.
Derived from text

N93-24689*# National Aeronautics and Space Administration, Washington, DC.
SYSTEMS ENGINEERING CONSIDERATIONS FOR OPERATIONAL SUPPORT SYSTEMS
Robert O. Aller *In its* Readings in Systems Engineering 1993 p 157-162 (For primary document see N93-24678 09-31)
Avail: CASI HC A02/MF A03

Operations support as considered here is the infrastructure of people, procedures, facilities and systems that provide NASA with the capability to conduct space missions. This infrastructure involves most of the Centers but is concentrated principally at the Johnson Space Center, the Kennedy Space Center, the Goddard Space Flight Center, and the Jet Propulsion Laboratory. It includes mission training and planning, launch and recovery, mission control, tracking, communications, data retrieval and data processing. Derived from text

N93-24690*# National Aeronautics and Space Administration, Washington, DC.
POLITICAL AND INSTITUTIONAL FACTORS AFFECTING SYSTEMS ENGINEERING
John F. Yardley *In its* Readings in Systems Engineering 1993 p 163-171 (For primary document see N93-24678 09-31)
Avail: CASI HC A02/MF A03

External groups have a significant impact on NASA's programs. Ten groups affecting NASA are identified, and examples are given for some of the them. Methods of dealing with these external inputs are discussed, the most important being good and open two way communications and an objective attitude on the part of the NASA participants. The importance of planning ahead, of developing rapport with these groups, and of effective use of NASA contractors is covered. The need for an overall strategic plan for the U.S. space program is stressed. Derived from text

N93-24691*# Lockheed-Georgia Co., Marietta.
OPTIMIZATION IN THE SYSTEMS ENGINEERING PROCESS
Loren A. Lemmerman *In* NASA, Washington, Readings in Systems Engineering 1993 p 173-179 (For primary document see N93-24678 09-31)
Avail: CASI HC A02/MF A03

The essential elements of the design process consist of the mission definition phase that provides the system requirements, the conceptual design, the preliminary design and finally the detailed design. Mission definition is performed largely by operations analysts in conjunction with the customer. The result of their study is handed off to the systems engineers for documentation as the systems requirements. The document that provides these requirements is the basis for the further design work of the design engineers at the Lockheed-Georgia Company. The design phase actually begins with conceptual design, which is generally conducted by a small group of engineers using multidisciplinary design programs. Because of the complexity of the design problem, the analyses are relatively simple and generally dependent on parametric analyses of the configuration. The result of this phase is a baseline configuration from which preliminary design may be initiated. Derived from text

N93-24692*# National Aeronautics and Space Administration, Washington, DC.

THE INITIAL FLIGHT ANOMALIES OF SKYLAB 1 **c18**

In its Readings in Systems Engineering 1993 p 181-199 (For primary document see N93-24678 09-31)

Avail: CASI HC A03/MF A03

At approximately 63 seconds into the flight of Skylab 1 on May 14, 1973, an anomaly occurred which resulted in the complete loss of the meteoroid shield around the orbital workshop. This was followed by the loss of one of the two solar array systems on the workshop and a failure of the inter stage adapter to separate from the S-II stage of the Saturn V launch vehicle. The investigation reported herein identified the most probable cause of this flight anomaly to be the breakup and loss of the meteoroid shield due to aerodynamic loads that were not accounted for in its design. The breakup of the meteoroid shield, in turn, broke the tie downs that secured one of the solar array systems to the workshop. Complete loss of this solar array system occurred at 593 seconds when the exhaust plume of the S-II stage retro-rockets impacted the partially deployed solar array system. Falling debris from the meteoroid shield also damaged the S-II inter stage adapter ordnance system in such a manner as to preclude separation. Of several possible failure modes of the meteoroid shield that were identified, the most probable in this particular flight was internal pressurization of its auxiliary tunnel which acted to force the forward end of the meteoroid shield away from the shell of the workshop and into the supersonic air stream. The pressurization of the auxiliary tunnel was due to the existence of several openings in the aft region of the tunnel. Another possible failure mode was the separation of the leading edge of the meteoroid shield from the shell of the workshop (particularly in the region of the folded ordnance panel) of sufficient extent to admit ram air pressures under the shield. Derived from text

N93-24693*# National Aeronautics and Space Administration, Washington, DC.

REPORT OF THE SEASAT FAILURE REVIEW BOARD **c18**

In its Readings in Systems Engineering 1993 p 201-215 (For primary document see N93-24678 09-31)

Avail: CASI HC A03/MF A03

The Seasat spacecraft failed on October 9, 1978, after satisfactory operation in orbit for 105 days, as a result of a loss of electrical power in the Agena bus that was used as a part of the spacecraft. The loss of power was caused by a massive and progressive short in one of the slip ring assemblies that was used to connect the rotating solar arrays into the power subsystem. The most likely cause of this short was the initiation of an arc between adjacent slip ring brush assemblies. The triggering mechanism of this arc could have been either a wire-to-brush assembly contact, a brush-to-brush contact, or a momentary short caused by a contaminant that bridged internal components of opposite electrical polarity. Derived from text

N93-24970# Oak Ridge National Lab., TN.

COMPRESSOR CALORIMETER PERFORMANCE OF REFRIGERANT BLENDS: COMPARATIVE METHODS AND RESULTS FOR A REFRIGERATOR/FREEZER APPLICATION

C. K. Rice and J. R. Sand Jan. 1993 32 p Presented at the Winter Meeting of the American Society of Heating, Refrigeration and Air Conditioning Engineers, Chicago, IL, 23-27 Jan. 1993

(Contract DE-AC05-84OR-21400)

(DE93-006734; CONF-930118-4) Avail: CASI HC A03/MF A01

A protocol was developed to define calorimeter operating pressures for nonazeotropic refrigerant mixtures (NARM's) which corresponded with the saturated evaporator and condenser temperatures commonly used for pure refrigerants. Compressor calorimeter results were obtained using this equivalent-mean-temperature (EMT) approach and a generally applied Association of Home Appliance Manufacturers (AHAM) procedure at conditions characteristic of a domestic refrigerator-freezer application. Tests with R-12 and two NARM's indicate that compressor volumetric and isentropic efficiencies are nearly the same for refrigerants with similar capacities and pressure ratios. The liquid-line temperature conditions specified in the AHAM calorimeter rating procedure for refrigerator-freezer compressors were found to preferentially derate NARM performance relative to R-12. Conversion of calorimeter data taken with a fixed liquid-line temperature to a uniform minimal level of condenser subcooling is recommended as a fairer procedure when NARM's are involved. Compressor energy-efficiency-ratio (EER) and capacity data measured as a result of the EMT approach were compared to system performance calculated using an equivalent heat exchanger loading (EHXL) protocol based on a Lorenz-Meutzner (L-M) refrigerator-freezer modeling program. The EHXL protocol was used to transform the calorimeter results into a more relevant representation of potential L-M cycle performance. The EMT method used to set up the calorimeter tests and the AHAM liquid-line conditions combined to significantly understate the cycle potential of NARM's relative to that predicted at the more appropriate EHXL conditions. Compressor conditions representative of larger heat exchanger sizes were also found to give a smaller L-M cycle advantage relative to R-12. DOE

N93-25085*# National Aeronautics and Space Administration. Ames Research Center, Moffett Field, CA.

A SURVEY OF LIFE SUPPORT SYSTEM AUTOMATION AND CONTROL

Cory K. Finn Jan. 1993 11 p

(RTOP 199-61-12)

(NASA-TM-103977; A-92191; NAS 1.15:103977) Avail: CASI HC A03/MF A01

The level of automation and control necessary to support advanced life support systems for use in the manned space program is steadily increasing. As the length and complexity of manned missions increase, life support systems must be able to meet new space challenges. Longer, more complex missions create new demands for increased automation, improved sensors, and improved control systems. It is imperative that research in these key areas keep pace with current and future developments in regenerative life support technology. This paper provides an overview of past and present research in the areas of sensor development, automation, and control of life support systems for the manned space program, and it discusses the impact continued research in several key areas will have on the feasibility, operation, and design of future life support systems. Author

N93-25177*# National Aeronautics and Space Administration. Lewis Research Center, Cleveland, OH.

HEAT TRANSFER IN ROTATING SERPENTINE PASSAGES WITH SELECTED MODEL ORIENTATION FOR SMOOTH OR SKEWED TRIP WALLS

B. V. Johnson (United Technologies Research Center, East Hartford, CT.), J. H. Wagner (United Technologies Research Center, East Hartford, CT.), G. D. Steuber (Pratt and Whitney Aircraft, East Hartford, CT.), and F. C. Yeh Apr. 1993 10 p Prepared for presentation at the 38th International Gas Turbine and Aeroengine Congress and Exposition, Cincinnati, OH, 24-27 May 1993; sponsored by ASME

(RTOP 505-62-52)

(NASA-TM-106126; E-7793; NAS 1.15:106126) Avail: CASI HC A02/MF A01

Experiments were conducted to determine the effects of model orientation as well as buoyancy and Coriolis forces on heat transfer in turbine blade internal coolant passages. Turbine blades have internal coolant passage surfaces at the leading and trailing edges of the airfoil with surfaces at angles which are as large as +/- 50 to 60 degrees to the axis of rotation. Most of the previously-presented, multiple-passage, rotating heat transfer experiments have focused on radial passages aligned with the axis of rotation. Results from serpentine passages with orientations 0 and 45 degrees to the axis of rotation which simulate the coolant passages for the mid chord and trailing edge regions of the rotating airfoil are compared. The experiments were conducted with rotation in both directions to simulate serpentine coolant passages with the rearward flow of coolant or with the forward flow of coolant. The experiments were conducted for passages with smooth surfaces and with 45 degree trips adjacent to airfoil surfaces for the radial portion of the serpentine passages. At a typical flow condition, the heat transfer on the leading surfaces for flow outward in the first passage with smooth walls was twice as much for the model at 45 degrees compared to the model at 0 degrees. However, the differences for the other passages and with trips were less. In addition, the effects of buoyancy and Coriolis forces on heat transfer in the rotating passage were decreased with the model at 45 degrees, compared to the results at 0 degrees. The heat transfer in the turn regions and immediately downstream of the turns in the second passage with flow inward and in the third passage with flow outward was also a function of model orientation with

differences as large as 40 to 50 percent occurring between the model orientations with forward flow and rearward flow of coolant. Author

N93-25238# Cambridge Univ. (England). Dept. of Engineering.
THE EVALUATION OF TECHNICAL MODELS USED FOR MAJOR-ACCIDENT HAZARD INSTALLATIONS. REPORT TO COMMISSION OF THE EUROPEAN COMMUNITIES DIRECTORATE GENERAL 12
R. E. Britter Aug. 1991 46 p
(CUED/A-AERO/TR-19) Avail: CASI HC A03/MF A01

Models are used in many ways by individuals and organizations within the European Community. Within the context of major technological hazards decisions of considerable importance are based wholly, or partly, on these models. The quality, that is the fitness-for-purpose, of these models will differ and there is obviously an interest in both the relative quality of one model against another and the absolute quality of any particular model. This leads to the evaluation of model quality and to methods by which model quality might be improved. It is noted that models are a principal method for the transfer of technology but also that the nature, role, and limitations of models is frequently misunderstood. There is a widespread demand for guidance on model quality and consequently on the development of evaluation techniques. The CEC is an appropriate body to have a role in the study of the quality and the management of quality of technical models. The evaluation of the quality of technical models entails: (1) an assurance of correct coding of algorithms is required and this is probably straightforward; (2) a statistical model validation is required and this entails comparison with experimental data sets (considerable care is required in performing such a validation, in particular in determination of an appropriate protocol to ensure unambiguous conclusions to be drawn from the validation); and (3) a model assessment including a scientific review and other less objective aspects is also required and should be given equal weight to a statistical model validation. Actions which may lead to an improvement in model quality are presented. Author

N93-25427# Joint Publications Research Service, Arlington, VA.
JPRS REPORT: SCIENCE AND TECHNOLOGY. CENTRAL EURASIA: ENGINEERING AND EQUIPMENT
12 Mar. 1992 32 p Transl. into ENGLISH from various Russian articles
(JPRS-UEQ-92-003) Avail: CASI HC A03/MF A01

Translated articles cover the following topics: oscillation stability of simple pendulum on moving frame at upper and lower trajectory points; and calculating gas turbine engine parts' coefficient of strengthening by balls in ultrasonic field. CASI

N93-25447# Los Alamos National Lab., NM.
MALONE REFRIGERATION
G. W. Swift 1992 6 p Presented at the 6th International Stirling Engine Conference and Exhibition, Rotterdam, Netherlands, 26-28 May 1993
(Contract W-7405-eng-36)
(DE93-005439; LA-UR-92-4136; CONF-930525-1) Avail: CASI HC A02/MF A01

Malone refrigeration is the use of a liquid near its critical point, without evaporation, as the working fluid in a refrigeration cycle such as the Stirling cycle. We discuss relevant properties of appropriate liquids, and we describe two Malone refrigerators. The first, which was completed several years ago, established the basic principles of use for liquids in such cycles. The second, now under construction, is a linear, free-piston machine. DOE

N93-25498# Bureau of Mines, Pittsburgh, PA. Research Center.
HAZARDS OF EXPLOSIVES DUSTS: PARTICLE SIZE EFFECTS
K. L. Cashdollar, M. Hertzberg, and G. M. Green Feb. 1992 39 p
(Contract DE-AI01-90EH-89084)
(DE93-009380; DOE/EH-89084/T8) Avail: CASI HC A03/MF A01

At the request of the Department of Energy, the Bureau of Mines has investigated the hazards of military explosives dispersed as dust clouds in a 20-L test chamber. In this report, the effect of particle size for HMX, HNS, RDX, TATB, and TNT explosives dusts is studied in detail. The explosibility data for these dusts are also compared to those for pure fuel dusts. The data show that all of the sizes of the explosives dusts that were studied were capable of sustaining explosions as dust clouds dispersed in air. The finest sizes (less than 10 micron) of explosives dusts were less reactive than the intermediate sizes (20 to 60 micron); this is opposite to the particle size effect observed previously for the pure fuel dusts. At the largest sizes studied, the explosives dusts become somewhat less reactive as dispersed dust clouds. The six sizes of the HMX dust were also studied as dust clouds dispersed in nitrogen. DOE

N93-25937# Oak Ridge National Lab., TN.
RECOMMENDATIONS FOR A KALMAN FILTER TO ESTIMATE AND CONTROL FREEZE AND SUBLIME RATES OF GASEOUS DIFFUSION PLANT FREEZER/SUBLIMER SYSTEMS
F. R. Ruppel Sep. 1992 43 p
(Contract DE-AC05-84OR-21400)
(ORNL/TM-12183) Avail: CASI HC A03/MF A01

The purpose of gaseous diffusion plant freezer/sublimer systems is to control the inventory of UF6 in the process cascade. When it is desired to decrease process inventory, UF6 vapor is transferred from the process cascade into the freezer/sublimer and frozen out. When it is desired to increase process inventory, UF6 is sublimed out of the freezer/sublimer and transferred back to the process cascade. This process technology has proven to be economically attractive for gaseous diffusion plants because it enables the plant to increase power usage during periods of low electrical utility demands, such as at night when inexpensive, nonfirm power is available, and decrease power usage during periods of high electrical utility demands. Power usage is proportional to process inventory. Control of freeze rate and sublime rate is important to this operation, especially when several freezer/sublimer systems must operate in harmony during a major inventory swing. The purpose of this report is to recommend an improved method to estimate and control the freeze and sublime rates of freezer/sublimer systems. Author (revised)

N93-26101* National Aeronautics and Space Administration. Langley Research Center, Hampton, VA.
VACUUM POWDER INJECTOR AND METHOD OF IMPREGNATING FIBER WITH POWDER Patent
Dennis C. Working, inventor (to NASA) 25 May 1993 6 p Filed 5 Aug. 1991
(NASA-Case-LAR-14179-1; US-Patent-5,213,843;
US-Patent-Appl-SN-740526; US-Patent-Class-427-180;
US-Patent-Class-427-195; US-Patent-Class-427-294;
US-Patent-Class-427-295; US-Patent-Class-427-296;
US-Patent-Class-118-308; US-Patent-Class-118-325) Avail: US Patent and Trademark Office

A method and apparatus uniformly impregnate stranded material with dry powder such as low solubility, high melt flow polymer powder to produce, for example, composite prepregs. The stranded material is expanded in an impregnation chamber by an influx of air so that the powder, which may enter through the same inlet as the air, penetrates to the center of the stranded material. The stranded material then is contracted for holding the powder therein. The stranded material and powder may be pulled through the impregnation chamber in the same direction by vacuum. Larger particles of powder which do not fully penetrate the stranded material may be combed into the stranded material and powder which does not impregnate the stranded material may be collected and reused.
Official Gazette of the U.S. Patent and Trademark Office

N93-26206# Allied-Signal Aerospace Co., Kansas City, MO. Kansas City Div.
FINITE ELEMENT MODELING OF THE HYDROFORMING PRESS Final Report
M. G. Schrank and W. H. Smith Dec. 1992 29 p
(Contract DE-AC04-76DP-00613)
(KCP-613-4999) Avail: CASI HC A03/MF A01

Three-dimensional finite element analyses were conducted to simulate a sheet metal forming process. An explicit transient dynamics finite element code was used to analyze the essentially quasi-static process. In order to obtain numerical results in a reasonable time frame, the process was modeled in a substantially compressed time period. Analytical results were compared with data obtained from experimental forming trials. Predicted wrinkling patterns, as well as distribution of plastic strain, compared favorably with available experimental data. Author

N93-26207# Allied-Signal Aerospace Co., Kansas City, MO. Kansas City Div.
DEVELOPMENT OF A REPLACEMENT FOR TRICHLOROETHYLENE IN THE TWO-STAGE CLEANING PROCESS Topical Report
W. B. Harding Dec. 1992 17 p
(Contract DE-AC04-76DP-00613)
(KCP-613-4941) Avail: CASI HC A03/MF A01

Isopropyl alcohol, d-limonene, and a synthetic mineral spirits were compared for effectiveness as replacements for trichloroethylene in an ultrasonic cleaning process. All were found to be suitable. Isopropyl alcohol is recommended as the replacement. Author

N93-26212# Allied-Signal Aerospace Co., Kansas City, MO. Kansas City Div.
ADVANCED ENGINEERING ANALYSIS
W. R. Freeman, M. D. Lee, J. F. Mahoney, and M. G. Schrank Nov. 1992 41 p Original contains color illustrations
(Contract DE-AC04-76DP-00613)
(KCP-613-4967) Avail: CASI HC A03/MF A01

The Advanced Engineering Analysis project is being used to improve the breadth of engineering analysis types, the particular phenomena which may be simulated, and also increase the accuracy and usability of the results of both new and current types of simulations and analyses. This is an interim report covering several topics under this project. Information on two new implementations of failure criteria for metal forming, the implementation of coupled fluid flow/heat transfer analysis, a correction to a contact solution problem with a 3-D parabolic brick finite element, and the development and implementation of a file translator to link I-DEAS to DYNA3D is provided. Author

N93-26285# Naval Postgraduate School, Monterey, CA. Dept. of Mechanical Engineering.
AMPHIB: A USERS MANUAL Technical Report, Jan. 1992 - Dec. 1992
Devadatta Mukutmoni, Yogendra K. Joshi, and Matthew D. Kelleher 25 Jan. 1993 113 p
(AD-A261769; NPS-ME-93-001) Avail: CASI HC A06/MF A02

A general purpose three-dimensional code (AMPHIB) that solves electronic cooling problems is documented. In its present structure, the code is set up for computations in liquid immersion cooling of an m by n array of chips embedded in a substrate in a three-dimensional rectangular enclosure. Nevertheless, it can be modified to solve problems in forced, mixed and natural convection for a wide range of boundary conditions. The subroutines and the input are described in detail. A listing of the code and sample example problems are also included. DTIC

N93-26405*# Colorado Univ., Boulder. Center for Space Construction.
CENTER FOR SPACE CONSTRUCTION THIRD ANNUAL SYMPOSIUM
1991 298 p Symposium held in Boulder, CO, 21-22 Nov. 1991
(Grant NAGw-1334)
(NASA-CR-192688; NAS 1.26:192688) Avail: CASI HC A13/MF A03

Viewgraphs from presentations given at the symposium are presented. The topics covered include the following: orbital assembly, large space structures, space stations, expert systems, lunar regolith and structure mechanics, lunar shelter construction from lunar resources, telerobotic rovers, lunar construction equipment, lunar based equipment, and lunar construction. For individual titles, see N93-26406 through N93-26417.

N93-26406*# Colorado Univ., Boulder. Center for Space Construction.
DYNAMICS OF ON-ORBIT CONSTRUCTION PROCESS
J. C. Chiou, S. Alexander, M. C. Natori, M. Mikulas, and K. C. Park *In its* Center for Space Construction Third Annual Symposium 1991 26 p (For primary document see N93-26405 09-31)
Avail: CASI HC A03/MF A03

The topics covered are presented in viewgraph form and include the following: problem definition and motivation; survey of current technology; focus problems; approach; progress/discussion; and future direction and anticipated results. Derived from text

N93-26407*# Colorado Univ., Boulder. Center for Space Construction.
INTERACTION DYNAMICS AND CONTROL FOR ORBITAL ASSEMBLY
Renjeng Su and Jim Chapel *In its* Center for Space Construction Third Annual Symposium 1991 14 p (For primary document see N93-26405 09-31)
Avail: CASI HC A03/MF A03

The topics are presented in viewgraph form and include the following: dynamics and control problems of joining structures in orbit; spring-and-mass models; and a simple example. Derived from text

N93-26408*# Colorado Univ., Boulder. Center for Space Construction.
CONTROLS FOR ORBITAL ASSEMBLY OF LARGE SPACE STRUCTURES **c18**
Mark J. Balas, Roger Davidson, Ali A. Gooyabadi, Ralph Quan, Brian Reisenauer, L. Robertson, James Mohl (Ball Aerospace Systems Div., Boulder, CO.), Philip Good (Martin Marietta Corp., Denver, CO.), Loren Vredevoogd, and Jose Galvez et al *In its* Center for Space Construction Third Annual Symposium 1991 36 p (For primary document see N93-26405 09-31)
Avail: CASI HC A03/MF A03

The topics covered are presented in viewgraph form and include the following: flexible structure control; decentralized control for flexible multi-body systems; control of structures during assembly; decentralized control using structural partitioning; reduced-orded model-based controller design; ROM/residual mode filters (RMF) control of large flexible structures;RMF in a distributed parameter system (DPS); LSS active control simulation; 3-D truss beam; mobile transporter with RMS; and flexible robot manipulator. Derived from text

N93-26409*# Colorado Univ., Boulder. Center for Space Construction.
STRUCTURAL LOAD CONTROL DURING CONSTRUCTION
Martin Mikulas *In its* Center for Space Construction Third Annual Symposium 1991 14 p (For primary document see N93-26405 09-31)
Avail: CASI HC A03/MF A03

The topics are presented in viewgraph form and include the following: examples of high transient loadings on large space structures; energy absorbing/load limiting strut research objectives; scope of research on energy absorbing struts to date; energy characteristics of cantilevered trusses with a tip load; ten bay long resilient truss example; stored energy characteristics of one meter deep truss; energy absorbing potential for 10-bay 5-meter deep truss; schematic of energy absorbing strut; linear load and motion control actuator; rigid body response of a solar array to the shuttle thruster pressure impingement; solar array piecewise linear response; solar array characteristics; solar array tip deflection and required actuator stroke; solar array response from finite element analysis; 12 bay energy absorbing test bed dynamics; and new AERO-Lab with 12-bay test beam. Derived from text

N93-26410*# Colorado Univ., Boulder. Center for Space Construction.
SYSTEMS ENGINEERING STUDIES OF ON-ORBIT ASSEMBLY OPERATIONS
George W. Morgenthaler *In its* Center for Space Construction Third Annual Symposium 1991 26 p (For primary document see N93-26405 09-31)
Avail: CASI HC A03/MF A03

The topics are presented in viewgraph form and include the following: definition and scope of space construction; orbital assembly and construction; lunar base construction; and Mars base construction. Derived from text

N93-26411*# Colorado Univ., Boulder. Center for Space Construction.
EXPERT SYSTEMS FOR ASSEMBLY SEQUENCE EVALUATION
Steve Jolly *In its* Center for Space Construction Third Annual Symposium 1991 15 p (For primary document see N93-26405 09-31)
Avail: CASI HC A03/MF A03

The objective is to identify delivered orbital subassemblies derived from a phase A conceptual space vehicle design while minimizing on-orbit assembly complexity. The topics covered are presented in viewgraph form and include the following: an orbital assembly scenario; subassemblies; subassembly identification and simulation model; estimating subassembly interfaces by engineering functional allocation using MBR; representative data base of interface connections; vehicle decomposition model; connection interface estimation model results; knowledge-source 1 and 2 results; knowledge-source 3 -- connection-index results (Boeing NTR-2016 CI-profile); KS3 algorithm, and KS3 flight manifest results. Derived from text

N93-26412*# Colorado Univ., Boulder. Center for Space Construction.
LUNAR REGOLITH AND STRUCTURE MECHANICS
Frank Barnes, Hon-Yim Ko, Stein Sture, Tyrone R. Carter, Kraig A. Evenson, Mark P. Nathan, and Steve W. Perkins *In its* Center for Space Construction Third Annual Symposium 1991 31 p (For primary document see N93-26405 09-31)
Avail: CASI HC A03/MF A03

The topics are presented in viewgraph form and include the following: modeling of regolith-structure interaction in extraterrestrial constructed facilities; densification of lunar soil simulant; and vibration assisted penetration of lunar soil simulant. Derived from text

N93-26413*# Colorado Univ., Boulder. Center for Space Construction.
INDIGENOUS LUNAR CONSTRUCTION MATERIALS
Wayne Rogers and Stein Sture *In its* Center for Space Construction Third Annual Symposium 1991 16 p (For primary document see N93-26405 09-31)
Avail: CASI HC A03/MF A03

The objectives are the following: to investigate the feasibility of the use of local lunar resources for construction of a lunar base structure; to develop a material processing method and integrate the method with design and construction of a pressurized habitation structure; to estimate specifications of the support equipment necessary for material processing and construction; and to provide parameters for systems models of lunar base constructions, supply, and operations. The topics are presented in viewgraph form and include the following: comparison of various lunar structures; guidelines for material processing methods; cast lunar regolith; examples of cast basalt components; cast regolith process; processing equipment; mechanical properties of cast basalt; material properties and structural design; and future work. Derived from text

N93-26414*# Colorado Univ., Boulder. Center for Space Construction.
DESIGN CONCEPTS FOR PRESSURIZED LUNAR SHELTERS UTILIZING INDIGENOUS MATERIALS
John Amin Happel, Kaspar Willam, and Benson Shing *In its* Center for Space Construction Third Annual Symposium 1991 22 p (For primary document see N93-26405 09-31)
Avail: CASI HC A03/MF A03

The objective is to design a pressurized shelter build of indigenous lunar material. The topics are presented in viewgraph form and include the following: lunar conditions which impact design; secondary factors; review of previously proposed concepts; cross section of assembly facility; rationale for indigenous materials; indigenous material choices; cast basalt properties; design variables; design 1, cylindrical segments; construction sequence; design 2, arch-slabs with post-tensioned ring girders; and future research. Derived from text

N93-26415*# Colorado Univ., Boulder. Center for Space Construction.
CONFIGURATION OPTIMIZATION OF SPACE STRUCTURES
Carlos Felippa, Luis A. Crivelli, and David Vandenbelt *In its* Center for Space Construction Third Annual Symposium 1991 22 p (For primary document see N93-26405 09-31)
Avail: CASI HC A03/MF A03

The objective is to develop a computer aid for the conceptual/initial design of aerospace structures, allowing configurations and shape to be apriori design variables. The topics are presented in viewgraph form and include the following: Kikuchi's homogenization method; a classical shape design problem; homogenization method steps; a 3D mechanical component design example; forming a homogenized finite element; a 2D optimization problem; treatment of volume inequality constraint; algorithms for the volume inequality constraint; object function derivatives--taking advantage of design locality; stiffness variations; variations of potential; and schematics of the optimization problem. Derived from text

N93-26416*# Colorado Univ., Boulder. Center for Space Construction.
TELEROBOTIC ROVERS FOR EXTRATERRESTRIAL CONSTRUCTION
c37
Chris Grasso, Jane Pavlich, Wayne Jermstad, Mike Matthews, Gary Snyder, Chris Steffen, Jim Avery, Renjeng Su, and Walter Lund *In its* Center for Space Construction Third Annual Symposium 1991 20 p (For primary document see N93-26405 09-31)
Avail: CASI HC A03/MF A03

The topics are presented in viewgraph form and include the following: fundamental concepts; advantages of modularity; modular robot; robot design; motor control system; simple manipulator; 4 degree of freedom manipulator; intermodule communication; network layout; positioning system--IR-TROP; IR TROP system design; testbed layout; modularized control; and centralized control. The objectives are the following: to design small modular robots; to test robotic cooperation and teleoperation; to develop modular control software; to develop intermodule communication network; to develop high accuracy positioning system; and to explore distributed algorithms for coordination. Derived from text

N93-26417*# Colorado Univ., Boulder. Center for Space Construction.
LUNAR SURFACE STRUCTURAL CONCEPTS AND CONSTRUCTION STUDIES
Martin Mikulas *In its* Center for Space Construction Third Annual Symposium 1991 30 p (For primary document see N93-26405 09-31)
Avail: CASI HC A03/MF A03

The topics are presented in viewgraph form and include the following: lunar surface structures construction research areas; lunar crane related disciplines; shortcomings of typical mobile crane in lunar base applications; candidate crane cable suspension systems; NIST six-cable suspension crane; numerical example of natural frequency; the incorporation of two new features for improved performance of the counter-balanced actively-controlled lunar crane; lunar crane pendulum mechanics; simulation results; 1/6 scale lunar crane testbed using GE robot for global manipulation; basic deployable truss approaches; bi-pantograph elevator platform; comparison of elevator platforms; perspective of bi-pantograph beam; bi-pantograph synchronously deployable tower/beam; lunar module off-loading concept; module off-loader concept packaged; starburst deployable precision reflector; 3-ring reflector deployment scheme; cross-section of packaged starburst reflector; and focal point and thickness packaging considerations. Derived from text

N93-24987# European Space Agency. European Space Research and Technology Center, ESTEC, Noordwijk (Netherlands).
THE COLUMBUS METROLOGY SCIENCE TEAM: REPORT ON ACTIVITIES
A. D. A. M. Spallicci *In its* Frequency and Time Forum Jun. 1992 p 67 (For primary document see N93-24978 09-70)
Copyright Avail: CASI HC A01/MF A04

N93-25579*# Extrude Hone Corp., Irwin, PA.
ON MACHINE CAPACITANCE DIMENSIONAL AND SURFACE PROFILE MEASUREMENT SYSTEM
Ralph Resnick *In* NASA, Washington, Technology 2002: The Third National Technology Transfer Conference and Exposition, Volume 1 Feb. 1993 p 178-181 (For primary document see N93-25561 09-99)
Avail: CASI HC A01/MF A04

N93-25580*# Extrude Hone Corp., Irwin, PA.
ULTRASONIC POLISHING
Randy Gilmore *In* NASA, Washington, Technology 2002: The Third National Technology Transfer Conference and Exposition, Volume 1 Feb. 1993 p 182-192 (For primary document see N93-25561 09-99)
Avail: CASI HC A03/MF A04

N93-25604*# Automatix, Inc., Billerica, MA.
VISION-AIDED MONITORING AND CONTROL OF THERMAL SPRAY, SPRAY FORMING, AND WELDING PROCESSES
John E. Agapakis and Jon Bolstad (Control Vision, Inc., Idaho Falls, ID.) *In* NASA, Washington, Technology 2002: The Third National Technology Transfer Conference and Exposition, Volume 1 Feb. 1993 p 407-414 Sponsored in part by DOE (For primary document see N93-25561 09-99)
Avail: CASI HC A02/MF A04

N93-26063*# Florida International Univ., Miami. Industrial and Systems Engineering.
USE OF TAGUCHI DESIGN OF EXPERIMENTS TO OPTIMIZE AND INCREASE ROBUSTNESS OF PRELIMINARY DESIGNS Final Report
Hector R. Carrasco *In* NASA. Johnson Space Center, National Aeronautics

and Space Administration (NASA)/American Society for Engineering Education (ASEE) Summer Faculty Fellowship Program, 1992, Volume 1 Dec. 1992 14 p (For primary document see N93-26058 09-99)
(Grant NGT-44-005-803)
Avail: CASI HC A03/MF A02

N93-26083*# Florida International Univ., Miami. Industrial and Systems Engineering.
THE REUSE OF LOGISTICS CARRIERS FOR THE FIRST LUNAR OUTPOST ALTERNATIVE HABITAT STUDY Final Report
Carolina Vargas *In* NASA. Johnson Space Center, National Aeronautics and Space Administration (NASA)/American Society for Engineering Education (ASEE) Summer Faculty Fellowship Program, 1992, Volume 2 Dec. 1992 15 p (For primary document see N93-26070 09-99)
(Grant NGT-44-005-803)
Avail: CASI HC A03/MF A02

32 COMMUNICATIONS AND RADAR

Includes radar; land and global communications; communications theory; and optical communications.

For related information see also *04 Aircraft Communications and Navigation* and *17 Space Communications, Spacecraft Communications, Command and Tracking.* For search and rescue see *03 Air Transportation and Safety,* and *16 Space Transportation.*

N93-24659*# Jet Propulsion Lab., California Inst. of Tech., Pasadena.
THE TELECOMMUNICATIONS AND DATA ACQUISITION REPORT Progress Report, Oct. - Dec. 1992
E. C. Posner, ed. 15 Feb. 1993 153 p
(Contract NAS7-1000)
(NASA-CR-192887; NAS 1.26:192887; JPL-TDA-PR-42-112) Avail: CASI HC A08/MF A02

This quarterly publication provides archival reports on developments in programs managed by JPL's Office of Telecommunications and Data Acquisition (TDA). In space communications, radio navigation, radio science, and ground-based radio and radar astronomy, it reports on activities of the Deep Space Network (DSN) in planning, supporting research and technology, implementation, and operations. Also included are standards activity at JPL for space data and information systems and reimbursable DSN work performed for other space agencies through NASA. For individual titles, see N93-24660 through N93-24671.

N93-24660*# Jet Propulsion Lab., California Inst. of Tech., Pasadena.
FEASIBILITY STUDY OF A Ka-/Ka-BAND DICHROIC PLATE WITH STEPPED RECTANGULAR APERTURES
J. C. Chen *In its* The Telecommunications and Data Acquisition Report 15 Feb. 1993 p 1-7 (For primary document see N93-24659 09-32)
(RTOP 310-20-64-86-02)
Avail: CASI HC A02/MF A02

For the Cassini spacecraft mission, a dichroic plate is needed to pass Ka-band uplink (34.2 to 34.7 GHz) and to reflect Ka-band downlink (31.8 to 32.3 GHz) for dual-frequency operation in the Deep Space Network. The special characteristic of the Ka-/Ka-band dichroic plate is that the pass band and the reflective band are only 1.9 GHz (5.7 percent) apart. A thick dichroic plate with stepped rectangular apertures that function as resonator filters was chosen for the Ka-/Ka-band dichroic plate design. The results of the feasibility study are presented in this article. Author

N93-24661*# Jet Propulsion Lab., California Inst. of Tech., Pasadena.
A TECHNIQUE FOR COMPUTATION OF NOISE TEMPERATURE DUE TO A BEAM WAVEGUIDE SHROUD
W. Veruttipong and M. M. Franco *In its* The Telecommunications and Data Acquisition Report 15 Feb. 1993 p 8-16 (For primary document see N93-24659 09-32)
(RTOP 310-20-65-86-02)
Avail: CASI HC A02/MF A02

Direct analytical computation of the noise temperature of real beam waveguide (BWG) systems, including all mirrors and the surrounding shroud, is an extremely complex problem and virtually impossible to achieve. Yet the DSN antennas are required to be ultra low-noise in order to be effective, and a reasonably accurate prediction is essential. This article presents a relatively simple technique to compute a real BWG system noise temperature by combining analytical techniques with data from experimental tests. Specific expressions and parameters for X-band (8.45-GHz) BWG noise computation are obtained for DSS 13 and DSS 24, now under construction. These expressions are also valid for various conditions of the BWG feed systems, including horn sizes and positions, and mirror sizes, curvatures, and positions. Parameters for S- and Ka-bands (2.3 and 32.0 GHz) have not been determined; however, those can be obtained following the same procedure as for X-band. Author

N93-24662*# Jet Propulsion Lab., California Inst. of Tech., Pasadena.
SOFT DECODING A SELF-DUAL (48, 24; 12) CODE **c61**
G. Solomon *In its* The Telecommunications and Data Acquisition Report 15 Feb. 1993 p 17-18 (For primary document see N93-24659 09-32)
(RTOP 310-30-71-83-02)
Avail: CASI HC A01/MF A02

A self-dual (48,24;12) code comes from restricting a binary cyclic (63,18;36) code to a 6 x 7 matrix, adding an eighth all-zero column, and then adjoining six dimensions to this extended 6 x 8 matrix. These six dimensions are generated by linear combinations of row permutations of a 6 x 8 matrix of weight 12, whose sums of rows and columns add to one. A soft decoding using these properties and approximating maximum likelihood is presented here. This is preliminary to a possible soft decoding of the box (72,36;15) code that promises a 7.7-dB theoretical coding under maximum likelihood. Author (revised)

N93-24663*# Jet Propulsion Lab., California Inst. of Tech., Pasadena.
A (72, 36; 15) BOX CODE **c61**
G. Solomon *In its* The Telecommunications and Data Acquisition Report 19-21 (SEE N93-24659 09-32) 15 Feb. 1993 (For primary document see N93-24659 09-32)
(RTOP 310-30-71-83-02)
Avail: CASI HC A01/MF A02

A (72,36;15) box code is constructed as a 9 x 8 matrix whose columns add to form an extended BCH-Hamming (8,4;4) code and whose rows sum to odd or even parity. The newly constructed code, due to its matrix form, is easily decodable for all seven-error and many eight-error patterns. The code comes from a slight modification in the parity (eighth) dimension of the Reed-Solomon (8,4;5) code over GF(512). Error correction uses the row sum parity information to detect errors, which then become erasures in a Reed-Solomon correction algorithm. Author

N93-24664*# Jet Propulsion Lab., California Inst. of Tech., Pasadena.
THE ANALYSIS OF CONVOLUTIONAL CODES VIA THE EXTENDED SMITH ALGORITHM **c61**
R. J. McEliece and I. Onyszchuk *In its* The Telecommunications and Data Acquisition Report 15 Feb. 1993 p 22-30 (For primary document see N93-24659 09-32)
(RTOP 310-30-71-83-02)
Avail: CASI HC A02/MF A02

Convolutional codes have been the central part of most error-control systems in deep-space communication for many years. Almost all such applications, however, have used the restricted class of (n,1), also known as 'rate 1/n,' convolutional codes. The more general class of (n,k) convolutional codes contains many potentially useful codes, but their algebraic theory is difficult and has proved to be a stumbling block in the evolution of convolutional coding systems. In this article, the situation is improved by describing a set of practical algorithms for computing certain basic things about a convolutional code (among them the degree, the Forney indices, a minimal generator matrix, and a parity-check matrix), which are usually needed before a system using the code can be built. The approach is based on the classic Forney theory for convolutional codes, together with the extended Smith algorithm for polynomial matrices, which is introduced in this article. Author

N93-24665*# Jet Propulsion Lab., California Inst. of Tech., Pasadena.
IMAGE CODING BY WAY OF WAVELETS **c61**
M. Shahshahani *In its* The Telecommunications and Data Acquisition Report 15 Feb. 1993 p 31-36 (For primary document see N93-24659

09-32)
(RTOP 310-30-71-83-02)
Avail: CASI HC A02/MF A02

The application of two wavelet transforms to image compression is discussed. It is noted that the Haar transform, with proper bit allocation, has performance that is visually superior to an algorithm based on a Daubechies filter and to the discrete cosine transform based Joint Photographic Experts Group (JPEG) algorithm at compression ratios exceeding 20:1. In terms of the root-mean-square error, the performance of the Haar transform method is basically comparable to that of the JPEG algorithm. The implementation of the Haar transform can be achieved in integer arithmetic, making it very suitable for applications requiring real-time performance. Author (revised)

N93-24666*# Jet Propulsion Lab., California Inst. of Tech., Pasadena.
FAILURE MONITORING IN DYNAMIC SYSTEMS: MODEL CONSTRUCTION WITHOUT FAULT TRAINING DATA **c38**
P. Smyth and J. Mellstrom *In its* The Telecommunications and Data Acquisition Report 15 Feb. 1993 p 37-49 (For primary document see N93-24659 09-32)
(RTOP 310-20-65-91-00)
Avail: CASI HC A03/MF A02

Advances in the use of autoregressive models, pattern recognition methods, and hidden Markov models for on-line health monitoring of dynamic systems (such as DSN antennas) have recently been reported. However, the algorithms described in previous work have the significant drawback that data acquired under fault conditions are assumed to be available in order to train the model used for monitoring the system under observation. This article reports that this assumption can be relaxed and that hidden Markov monitoring models can be constructed using only data acquired under normal conditions and prior knowledge of the system characteristics being measured. The method is described and evaluated on data from the DSS 13 34-m beam wave guide antenna. The primary conclusion from the experimental results is that the method is indeed practical and holds considerable promise for application at the 70-m antenna sites where acquisition of fault data under controlled conditions is not realistic. Author

N93-24667*# Jet Propulsion Lab., California Inst. of Tech., Pasadena.
A FUNCTIONAL DESCRIPTION OF THE BUFFERED TELEMETRY DEMODULATOR (BTD) **c17**
H. Tsou, B. Shah, R. Lee, and S. Hinedi *In its* The Telecommunications and Data Acquisition Report 15 Feb. 1993 p 50-73 (For primary document see N93-24659 09-32)
(RTOP 314-30-61-02-02)
Avail: CASI HC A03/MF A02

This article gives a functional description of the buffered telemetry demodulator (BTD), which operates on recorded digital samples to extract the symbols from the received signal. The key advantages of the BTD are as follows: (1) its ability to reprocess the signal to reduce acquisition time; (2) its ability to use future information about the signal and to perform smoothing on past samples; and (3) its minimum transmission bandwidth requirement as each sub carrier harmonic is processed individually. The first application of the BTD would be the Galileo S-band contingency mission, where the signal is so weak that reprocessing to reduce the acquisition time is crucial. Moreover, in the event of employing antenna arraying with full spectrum combining, only the sub carrier harmonics need to be transmitted between sites, resulting in significant reduction in data rate transmission requirements. Software implementation of the BTD is described for various general-purpose computers. Author (revised)

N93-24668*# Jet Propulsion Lab., California Inst. of Tech., Pasadena.
SYMBOL SIGNAL-TO-NOISE RATIO LOSS IN SQUARE-WAVE SUBCARRIER DOWNCONVERSION
Y. Feria and J. Statman *In its* The Telecommunications and Data Acquisition Report 74-82 (SEE N93-24659 09-32) 15 Feb. 1993 (For primary document see N93-24659 09-32)
(RTOP 314-30-42-10-89)
Avail: CASI HC A02/MF A02

This article presents the simulated results of the signal-to-noise ratio (SNR) loss in the process of a square-wave subcarrier down conversion. In a previous article, the SNR degradation was evaluated at the output of the down converter based on the signal and noise power change. Unlike in the previous article, the SNR loss is defined here as the difference between the actual and theoretical symbol SNR's for the same symbol-error rate at the output of the symbol matched filter. The results show that an average SNR loss of 0.3 dB can be achieved with tenth-order infinite impulse response (IIR) filters. This loss is a 0.2-dB increase over the SNR degradation in the previous analysis where neither the signal distortion nor the symbol detector was considered. Author (revised)

N93-24669*# Jet Propulsion Lab., California Inst. of Tech., Pasadena.
DESIGN OF THE REDUCED LQG COMPENSATOR FOR THE DSS-13 ANTENNA
W. Gawronski *In its* The Telecommunications and Data Acquisition Report 15 Feb. 1993 p 83-106 (For primary document see N93-24659 09-32)
(RTOP 314-40-41-10-15)
Avail: CASI HC A03/MF A02

A linear-quadratic-Gaussian (LQG) compensator design procedure is proposed for the DSS-13 antenna. The procedure is based on two properties. It is shown that tracking and flexible motion of the antenna are almost independent (the separation property). As a consequence, compensators for the flexible and tracking parts can be designed separately. It is shown also that the balanced LQG compensator's effort is evenly divided between the controller and the estimator. This allows a minimization of the compensator order, which is important for implementation purposes. An efficient compensator reduction procedure that gives a stable low-order compensator of satisfactory performance is introduced. This approach is illustrated with a detailed compensator design for the DSS-13 antenna. The implementation of this compensator design requires an update of the antenna model. Author

N93-24670*# Jet Propulsion Lab., California Inst. of Tech., Pasadena.
PERFORMANCE RESULTS OF A 300-DEGREE LINEAR PHASE MODULATOR FOR SPACEBORNE COMMUNICATIONS APPLICATIONS
N. R. Mysoor and R. O. Mueller *In its* The Telecommunications and Data Acquisition Report 15 Feb. 1993 p 107-116 (For primary document see N93-24659 09-32)
(RTOP 314-30-55-30-01)
Avail: CASI HC A02/MF A02

A phase modulator capable of large linear phase deviation, low loss, and wide band operation with good thermal stability was developed for deep space spacecraft transponder (DST) applications at X-band (8.415 GHz) and Ka-band (32 GHz) downlinks. The design uses a two-stage circulator-coupled reflection phase shifter with constant gamma hyperabrupt varactors and an efficient modulator driver circuit to obtain a phase deviation of +/-2.5 rad with better than 8 percent linearity. The measured insertion loss is 6.6 dB +/- 0.35 dB at 8415 MHz. Measured carrier and relative sideband amplitudes resulting from phase modulation by sine wave and square modulating functions agree well with the predicted results.
Author (revised)

N93-24671*# Jet Propulsion Lab., California Inst. of Tech., Pasadena.
MANAGEMENT OF SPACE NETWORKS
R. W. Markley and B. F. Williams *In its* The Telecommunications and Data Acquisition Report 15 Feb. 1993 p 117-133 (For primary document see N93-24659 09-32)
(RTOP 316-30-19-41-04)
Avail: CASI HC A03/MF A02

NASA has proposed missions to the Moon and Mars that reflect three areas of emphasis: human presence, exploration, and space resource development for the benefit of Earth. A major requirement for such missions is a robust and reliable communications architecture. Network management--the ability to maintain some degree of human and automatic control over the span of the network from the space elements to the end users on Earth--is required to realize such robust and reliable communications. This article addresses several of the architectural issues associated with space network management. Round-trip delays, such as the 5- to 40-min delays in the Mars case, introduce a host of problems that must be solved by delegating significant control authority to remote nodes. Therefore, management hierarchy is one of the important architectural issues. The following article addresses these concerns, and proposes a network management approach based on emerging standards that covers the needs for fault, configuration, and performance management, delegated

control authority, and hierarchical reporting of events. A relatively simple approach based on standards was demonstrated in the DSN 2000 Information Systems Laboratory, and the results are described. Author

N93-25168 British Broadcasting Corp., Kingswood (England). Engineering Div.

LOW-FREQUENCY ROOM RESPONSES. PART 1: BACKGROUND AND QUALITATIVE CONSIDERATIONS

R. Walker 1992 18 p

(BBC-RD-1992/8-Pt-1) Copyright Avail: BBC, Kingswood Warren, Tadworth, Surrey, England

The problems inherent in the reproduction of high-quality sound in relatively small rooms are discussed. Methods of predicting the inevitably uneven low-frequency response from source to listener or microphone are also discussed. It is concluded that, even with perfect prediction methods, there would still be some compromises which could only be resolved by making subjective judgements. The use of additional low-frequency loudspeakers in control rooms permits an extra degree of freedom in the positioning of the loudspeakers to obtain the maximum degree of uniformity in response without compromising the stereophonic image localization. Author

N93-25169 British Broadcasting Corp., Kingswood (England). Engineering Div.

LOW-FREQUENCY ROOM RESPONSES. PART 2: CALCULATION METHODS AND EXPERIMENTAL RESULTS

R. Walker 1992 23 p Original contains color illustrations

(BBC-RD-1992/9-Pt-2) Copyright Avail: BBC, Kingswood Warren, Tadworth, Surrey, England

The development of a relatively simple method for predicting low-frequency responses for near-rectangular rooms based on the summation of modal responses and their coupling coefficients for the source and receiver positions is outlined. Comparisons between calculated and measured responses show that many of the response features can be reproduced. The question of optimum room shape is also addressed, and a method of illustrating the effects of room shape on the low-frequency modal distribution is developed. This uses a single criterion to plot contours of 'room quality' as a function of proportions. Author

N93-25170 British Broadcasting Corp., Kingswood (England). Engineering Div.

THE DESIGN OF A MODULAR SOUND ABSORBER FOR VERY LOW FREQUENCIES

J. A. Fletcher 1992 15 p

(BBC-RD-1992/10) Copyright Avail: BBC, Kingswood Warren, Tadworth, Surrey, England

Studios and sound control rooms usually have their walls acoustically treated to control the reverberation time. In the BBC, this treatment often takes the form of modular absorbers of which there are a number of BBC designed types for sound absorption in different frequency bands. This report describes an investigation of the feasibility of a modular absorber for the 50 - 100 Hz frequency range. A method of measuring absorption coefficient over a continuous frequency range using a standing wave duct is described. This allows a single modular absorber to be tested instead of requiring a batch of prototypes to be constructed for a reverberation room test. This technique was used to test a variety of absorbers, including porous, Helmholtz, and membrane types. These tests led to a design of membrane absorber, and a small batch of prototypes was constructed and tested in a reverberation room. This test verified that the prototype module had useful absorption in the frequency range of interest. Author

N93-25171 British Broadcasting Corp., Kingswood (England). Engineering Div.

A MODULAR WIDEBAND SOUND ABSORBER

G. D. Plumb 1992 15 p

(BBC-RD-1992/11) Copyright Avail: BBC, Kingswood Warren, Tadworth, Surrey, England

The absorption coefficients were measured of various depths of RW2 grade Rockwool laid directly on the floor of the ISO-Standard reverberation room at BBC Research Department. The Rockwool was very effective as a wideband sound absorber. A new absorber was designed and tested, having the dimensions of the existing BBC type A modular absorbers and containing RW2 Rockwool. The new absorber has a smoother absorption coefficient curve, a less complicated construction, and weighs less than the existing BBC wideband absorber (type A8/A9). It has been named type A11 and has an equivalent performance to that of BBC type A2 and A3 absorbers combined. It complements, very well, the performance of the A10 very low frequency absorber, described in a companion Report (BBC RD No. 1992/10). Author

N93-25181*# National Aeronautics and Space Administration. Hugh L. Dryden Flight Research Facility, Edwards, CA.

THE CONSTANT CURRENT LOOP: A NEW PARADIGM FOR RESISTANCE SIGNAL CONDITIONING

Karl F. Anderson 1993 16 p Proposed for presentation at the Instrument Society of America 39th International Instrumentation Symposium, Albuquerque, NM, 3-6 May 1993

(NASA-TM-108744; NAS 1.15:108744) Avail: CASI HC A03/MF A01

A practical, single, constant-current loop circuit for the signal conditioning of variable-resistance transducers was synthesized, analyzed, and demonstrated. The strain gage and the resistance temperature device are examples of variable-resistance sensors. Lead wires connect variable-resistance sensors to remotely located signal-conditioning hardware. The presence of lead wires in the conventional Wheatstone bridge signal-conditioning circuit introduces undesired effects that reduce the quality of the data from the remote sensors. A practical approach is presented for suppressing essentially all lead wire resistance effects while indicating only the change in resistance value. Theoretical predictions supported by laboratory testing confirm the following features of the approach: (1) the dc response; (2) the electrical output is unaffected by extremely large variations in the resistance of any or all lead wires; (3) the electrical output remains zero for no change in gage resistance; (4) the electrical output is inherently linear with respect to gage resistance change; (5) the sensitivity is double that of a Wheatstone bridge circuit; and (6) the same excitation and sense wires can serve multiple independent gages. An adaptation of the current loop circuit is presented that simultaneously provides an output signal voltage directly proportional to transducer resistance change and provides temperature information that is unaffected by transducer and lead wire resistance variations. These innovations are the subject of NASA patent applications. Author (revised)

N93-25198*# Hawaii Univ., Manoa. Dept. of Electrical Engineering.

A LOW-COMPLEXITY AND HIGH PERFORMANCE CONCATENATED CODING SCHEME FOR HIGH-SPEED SATELLITE COMMUNICATIONS

Shu Lin, DoJun Rhee, and Sandeep Rajpal 1 Feb. 1993 12 p

(Grant NAG5-931)

(NASA-CR-192715; Rept-93-001; NAS 1.26:192715) Avail: CASI HC A03/MF A01

This report presents a low-complexity and high performance concatenated coding scheme for high-speed satellite communications. In this proposed scheme, the NASA Standard Reed-Solomon (RS) code over GF(2(exp 8) is used as the outer code and the second-order Reed-Muller (RM) code of Hamming distance 8 is used as the inner code. The RM inner code has a very simple trellis structure and is decoded with the soft-decision Viterbi decoding algorithm. It is shown that the proposed concatenated coding scheme achieves an error performance which is comparable to that of the NASA TDRS concatenated coding scheme in which the NASA Standard rate-1/2 convolutional code of constraint length 7 and d sub free = 10 is used as the inner code. However, the proposed RM inner code has much smaller decoding complexity, less decoding delay, and much higher decoding speed. Consequently, the proposed concatenated coding scheme is suitable for reliable high-speed satellite communications, and it may be considered as an alternate coding scheme for the NASA TDRS system. Derived from text

N93-25210# Federal Aviation Administration, Atlantic City, NJ. Technical Center.

THE ATC EVALUATION OF THE PROTOTYPE AIRPORT SURVEILLANCE RADAR WIND SHEAR PROCESSOR (ASR-WSP) AT ORLANDO INTERNATIONAL AIRPORT Final Report

Radame Martinez Mar. 1993 21 p

(DOT/FAA/CT-TN92/48) Avail: CASI HC A03/MF A01

The Airport Surveillance Radar Wind Shear Processor (ASR-WSP), also known as Airport Surveillance Radar-9 (ASR-9) modification for low

altitude wind shear detection, is a production ASR-9 with an expanded weather channel for added processing capabilities. The primary mission of the ASR-WSP is to enhance the safety of air travel through the timely detection and reporting of hazardous wind shear in and near the terminal approach and departure zones of the airport. It will also improve the management of air traffic (AT) in the terminal area through the forecast of precipitation, and ultimately the detection of other hazardous weather phenomena. The ASR-WSP may be used as a stand-alone system at airports without a Terminal Doppler Weather Radar (TDWR) or Enhanced-Low Level Wind Shear Alert System (E-LLWAS), or in an integrated mode with either or both the TDWR and E-LLWAS. An operational evaluation of a prototype ASR-WSP, developed by Massachusetts Institute of Technology Lincoln Laboratories (MIT/LL), was conducted at the Orlando International Airport (MCO) in Orlando, Florida, during the period 29 Jun. to 31 Aug. 1992. The objective of the evaluation was to obtain Federal Aviation Administration (FAA) air traffic controller reaction to the prototype ASR-WSP weather data and display equipment. The following are highlights of the evaluation: (1) the ASW-WSP is very useful when making runway configuration changes; (2) the ASR-WSP is not perceived to be as accurate as the prototype TDWR; (3) the gust front prediction feature is not reliable; and (4) the information provided on both the RDT and the GSD is very useful. Author (revised)

N93-25239 British Broadcasting Corp., Kingswood (England). Engineering Div.

AN EXAMPLE OF A PHASE-SEGREGATED ENHANCED PAL BROADCASTING SYSTEM

M. G. Croll, J. O. Drewery, J. E. Easterbrook, R. Storey, and G. A. Thomas 1992 59 p Original contains color illustrations

(BBC-RD-1992/6) Copyright Avail: BBC, Kingswood Warren, Tadworth, Surrey, England

An enhanced phase alteration line (PAL) system is described which is fully compatible with the terrestrial broadcast system B/G, having a 5 MHz bandwidth. Elimination of luminance/chrominance cross-effects is achieved using the principle of phase-segregation which also allows enhanced luminance resolution. The source picture has a 16:9 aspect ratio and appears on the compatible display as a full letterbox, occupying three-quarters of the display height. Subjective assessment of critical picture material shows a significant improvement over conventional PAL, aside from the wider aspect ratio, whilst phase distortion in the transmission path does not re-introduce cross-effects. Author (revised)

N93-25299# Lawrence Livermore National Lab., CA.

ENERGY AND TECHNOLOGY REVIEW, OCTOBER - DECEMBER 1992

J. A. Sefcik, ed. 1992 58 p

(Contract W-7405-eng-48)

(DE93-007784; UCRL-52000-92-10-11-12) Avail: CASI HC A04/MF A01

Discussions on the following topics are included: armature concepts for a hypervelocity railgun; chromosome painting; digital mammography; three-dimensional computational electromagnetics; and neural networks on chips. DOE

N93-25300# Oak Ridge National Lab., TN.

AN OUTGOING ENERGY FLUX BOUNDARY CONDITION FOR FINITE DIFFERENCE ICRP ANTENNA MODELS

D. B. Batchelor and M. D. Carter Nov. 1992 20 p

(DE93-007788; ORNL/TM-12248) Avail: CASI HC A03/MF A01

For antennas at the ion cyclotron range of frequencies (ICRF), modeling in vacuum can now be carried out to a high level of detail such that shaping of the current straps, isolating septa, and discrete Faraday shield structures can be included. An efficient approach would be to solve for the fields in the vacuum region near the antenna in three dimensions by finite methods and to match this solution at the plasma-vacuum interface to a solution obtained in the plasma region in one dimension by Fourier methods. This approach has been difficult to carry out because boundary conditions must be imposed at the edge of the finite difference grid on a point-by-point basis, whereas the condition for outgoing energy flux into the plasma is known only in terms of the Fourier transform of the plasma fields. A technique is presented by which a boundary condition can be imposed on the computational grid of a three-dimensional finite difference, or finite element, code by constraining the discrete Fourier transform of the fields at the boundary points to satisfy an outgoing energy flux condition appropriate for the plasma. The boundary condition at a specific grid point appears as a coupling to other grid points on the boundary, with weighting determined by a kernel calculated from the plasma surface impedance matrix for the various plasma Fourier modes. This boundary condition was implemented in a finite difference solution of a simple problem in two dimensions, which can also be solved directly by Fourier transformation. Results are presented, and it is shown that the proposed boundary condition does enforce outgoing energy flux and yields the same solution as is obtained by Fourier methods. DOE

N93-25308# Volunteers in Technical Assistance, Inc., Arlington, VA.

THE PACSAT COMMUNICATIONS EXPERIMENT (PCE) Final Report, 13 Aug. 1990 - 12 Feb. 1992

12 Feb. 1993 6 p

(Contract DE-FG01-90CE-33017)

(DE93-008185; DOE/CE-33017/T1) Avail: CASI HC A02/MF A01

While VITA (Volunteers in Technical Assistance) is the recognized world leader in low earth orbiting (LEO) satellite technology (below 1 GHz), its involvement in communications technologies is to facilitate renewable energy technology transfer to developing countries. A communications payload was incorporated into the UoSat 2 satellite (Surrey Univ., UK), launched in 1984; a prototype satellite (PCE) was also launched Jan 1990. US DOE awarded a second grant to VITA to design and test the prototype ground stations (command and field), install field ground stations in several developing country sites, pursue the operational licensing process, and transfer the evaluation results to the design of an operating system. The principal tasks of the grant are discussed. DOE

N93-25332 Department of the Navy, Washington, DC.

FREQUENCY DIVERSITY SIDELOBE CANCELLER Patent

Ben H. Cantrell, inventor (to Navy) 10 Nov. 1992 7 p Filed 19 Feb. 1975

(AD-D015647; US-Patent-5,162,805; US-Patent-Appl-SN-550097) Avail: US Patent and Trademark Office

A new system and technique for cancelling interference in frequency agile receiving systems are described. Main and auxiliary signals are supplied to a pair of multiple loop side-lobe cancellers which are capable of being tuned to different frequencies. At the same time, under the control of a timing clock, plural frequencies are selected and multiplexed between two channels at the time of a radar pulse transmission. The side-lobe cancellers and radar are coupled to the channels such that each canceller operates at a given frequency for two consecutive pulse periods, with the radar transmitting at said given frequency during the second pulse period. By continuously cycling between the two channels, each canceller is operating at the proper frequency to cancel interference even though the radar is changing frequency on a pulse to pulse basis. DTIC

N93-25340 Essex Univ., Colchester (England).

PROPAGATION AT MICROWAVE FREQUENCIES IN THE PRESENCE OF TROPOSPHERIC STRATIFIED LAYERS Ph.D. Thesis

Gail D. Lochtie 1991 268 p

Avail: Univ. Microfilms Order No. BRD-97210

The problem of determining the attenuation between a transmitter and receiver, in the presence of a horizontally stratified troposphere, is examined for microwave frequencies. Existing tropospheric propagation models are discussed and their limitations are considered. From consideration of measured meteorological parameters, a tri-linear piecewise profile is deemed a reasonable representation of the refractive index profile. Models are developed which simulate the tropospheric refractive index by bi-linear and tri-linear functions. These models provide a closed form solution to the boundary value problem when an arbitrary radiating source is included. The attenuation predictions obtained from the bi-linear and tri-linear models are compared with concurrently measured refractive index and radio signal data. This was carried out for a number of periods where the observed attenuation was considerably less than the normal diffraction level. This comparison has shown that, in cases where horizontal homogeneity is assumed to hold, the tri-linear model provides a considerable improvement over the bi-linear simulation. Dissert. Abstr.

N93-25391 British Broadcasting Corp., Kingswood (England). Engineering Div.

EXPERIMENTS WITH THE HIVITS HDTV CONTRIBUTION CODED

A. D. R. Cotton and N. D. Wells 1992 11 p
(BBC-RD-1992/12) Copyright Avail: BBC, Kingswood Warren, Tadworth, Surrey, England

As more and more programs are made in high definition television (HDTV) formats, so the need to provide complete production facilities will increase. An important part of television production is the ability to transmit very high quality television signals over long distances for program contribution purposes. For example, this may be from an outside broadcast unit to a television studio center or a transatlantic satellite link for a live television interview. The BBC Research Department, in collaboration with Thomson-CSF/LER and TRT, a French subsidiary of Philips, as part of the RACE HIVITS project, has participated in the construction of 140 Mbit/s contribution-quality bit-rate reduction codec for the transmission of digital HDTV. This report describes the codec architecture, some of the problems that have arisen out of the necessity to perform parallel processing, results from buffer regulation optimization experiments, and results from the field trials conducted over satellite links. The architecture of this equipment was specially developed to allow the generation of an implementation-independent bit stream. The current equipment based on six conventional definition bit-rate reduction codecs working in parallel, will perform equally well with future generations of equipment based on fewer processing units operating in parallel. Indeed, the output bit stream is equivalent to a suitably scaled version of the current ETSI and CMTT standards for the coding of conventional definition television.

Author (revised)

N93-25635# Army Armament Research, Development and Engineering Center, Picatinny Arsenal, NJ.
MICROWAVE ABSORPTION MEASUREMENTS AND INTERFERENCE: EFFECTS FOR A LIQUID FUEL BETWEEN 2.5 AND 18 GHz
Donald A. Wiegand and Frank Murray Feb. 1993 20 p
(AD-A260607; ARAED-TR-92023) Avail: CASI HC A03/MF A01

The incident, reflected and transmitted powers were measured and the reflection and transmission coefficients calculated for a liquid fuel. Two sizes of double-ridge waveguide were used to cover the frequency ranges 2.5 to 7.5 and 7.5 to 18 GHz and corrections were made for waveguide losses. Strong interference effects were observed and the real part of the dielectric constant was obtained primarily from the separation of interference maxima and minima. The loss tangent was obtained by curve fitting to the normalized power loss, and the absorption coefficient was calculated as a function of frequency from the dielectric data. DTIC

N93-25639# Haskins Labs., Inc., New Haven, CT.
SPEECH RESEARCH Progress Status Report, Jan. - Jun. 1992
Jun. 1992 298 p
(Grant NSF BNS-88-20099)
(AD-A260643; SR-109/110) Avail: CASI HC A13/MF A03

Phonology is traditionally seen as the discipline that concerns itself with the building blocks of linguistic messages. It is the study of the structure of sound inventories of languages and of the participation of sounds in rules or processes. Phonetics, in contrast, concerns speech sounds as produced and perceived. Two extreme positions on the relationship between phonological messages and phonetic realizations are represented in the literature. One holds that the primary home for linguistic symbols, including phonological ones, is the human mind, itself housed in the human brain. The second holds that their primary home is the human vocal tract. DTIC

N93-25640# University of Southern California, Marina del Rey.
GIGABIT NETWORK COMMUNICATIONS RESEARCH Quarterly Status Report No. 8, 1 Jul. - 30 Sep. 1992
30 Sep. 1992 11 p
(Contract DABT63-91-C-0001)
(AD-A260644) Avail: CASI HC A03/MF A01

The ATOMIC project utilizes inexpensive fine-grain multicomputer components to create a multi-gigabit per second local area network. This is a unique approach that leverages recent DARPA-supported research at Caltech by Professor Charles Seitz and his students. That research has already produced dense and extremely fast Mosaic single-chip multicomputer nodes. ATOMIC is a unique example of network development that grows upwards from multicomputer machine networking into the domain of a LAN. The principal concerns for this quarter were the continued integration of the new SPARCstation ATOMIC SBus card, modification of the Address Consultant to recognize SBus hosts, and testing of the 3x3 ATOMIC mesh. DTIC

N93-25689# Surveillance Research Lab., Salisbury (Australia).
DISTORTION MEASUREMENTS ON BANDPASS FILTERS WITH POWDERED IRON TOROIDAL INDUCTORS
A. Sarti Jun. 1992 23 p
(AD-A260790; SRL-0076-TM; DODA-AR-006-752) Avail: CASI HC A03/MF A01

This paper reports the results of measurements of both in-band and out-of-band non-linear distortion for an 11-18 MHz bandpass filter which used powdered iron toroidal cores for the inductors. The results are compared with those from a bandpass filter of the same specification using air cored inductors. It is shown that a performance comparable in linearity to the air cored inductor case can be obtained with appropriately sized powdered iron toroidal cores, while still realizing to some extent the advantages of magnetic self shielding and smaller volume that are usually associated with the use of toroidal cores. DTIC

N93-25700# Naval Command, Control and Ocean Surveillance Center, San Diego, CA. RDT and E Div.
HIGH-PERFORMANCE VISUALIZATION APPLIED TO COMPUTATIONAL ELECTROMAGNETICS: METHOD-OF-MOMENTS ON A SILICON GRAPHICS WORKSTATION Final Report, Oct. 1991 - Sep. 1992
L. C. Russell and J. W. Rockway Oct. 1992 56 p
(AD-A260820; NRAD-TR-1564) Avail: CASI HC A04/MF A01

This investigation applied advanced visualization techniques to an existing computational electromagnetic code. The goal was to demonstrate that high-performance visualization can improve the utility of computational techniques used in ship electromagnetic designs. The code used was the Numerical Electromagnetics Code Method of Moments (NEC-MoM). The visualization platform was a Silicon Graphics 4D workstation. Two codes were developed to do pre- and post-processing visualization on NEC-MoM. This report lists several benefits that have resulted, or will result, from work done on this Independent Exploratory Development (IED) project. DTIC

N93-25767# Rome Lab., Griffiss AFB, NY.
AN SPW SOFTWARE SIMULATION MODEL OF A DISPERSIVE FADING MULTIPATH NARROWBAND HF CHANNEL Report, Sep. 1991 - Aug. 1992
Michael J. Medley Nov. 1992 66 p
(AF Proj. 4519)
(AD-A261101; RL-TR-92-281) Avail: CASI HC A04/MF A01

This report describes a simulation which was developed to emulate a narrowband high frequency communications channel. The simulation was developed to allow test and evaluation of signal processing concepts used to combat interference generated by Rayleigh fading channels. Such techniques will be used by the Air Force in developing and analyzing next-generation data communications network architectures and protocols and communications systems. DTIC

N93-25772# Rensselaer Polytechnic Inst., Troy, NY. Dept. of Mechanical Engineering, Aeronautical Engineering and Mechanics.
ELECTROELASTIC EQUATIONS FOR ELECTRODED THIN PLATES SUBJECT TO LARGE DRIVING VOLTAGES
H. F. Tiersten 18 Jan. 1993 17 p
(Contract DAAL03-92-G-0123)
(AD-A261123; ARO-30378.3-EG-URI) Avail: CASI HC A03/MF A01

Existing rotationally invariant electroelastic equations are reduced to the case of large electric fields and small strain. These latter equations are specialized to the case of thin plates with completely electroded major surfaces, and it is shown that in this case the charge equation of electrostatics is satisfied trivially to lowest order. It is further shown that for the thin stress-free polarized ferroelectric ceramic plate subject to large electric fields, the resulting equations readily account for experimental data in existence in the literature. DTIC

N93-25847# Georgia Inst. of Tech., Atlanta. School of Electrical Engineering.
SIGNAL PROCESSING IN IMPULSIVE ELECTROMAGNETIC INTERFERENCE
Serena M. Zabin 31 Dec. 1992 6 p
(Contract N00014-91-J-1334)
(AD-A260755) Avail: CASI HC A02/MF A01

Statistical signal processing functions such as signal detection, estimation, and identification play a key role in the development of effective communications, radar, and sonar systems. For example, advanced statistical methods are emerging as being particularly important in digital communications systems operating in channels corrupted by interference from such phenomena as multiple-access noise, intentional jamming, and impulsive noise sources. Conventional demodulation methods, such as coherent matched filtering, often suffer serious performance degradation when subjected to interference of these types; however, this degradation can frequently be eliminated through the use of more sophisticated signal processing techniques. A central issue in the design of effective signal processing procedures for systems operating in channels such as those noted above is that of channel identification. DTIC

N93-25855# Surface Optics Corp., San Diego, CA.
ENHANCED BACKSCATTERING FROM ROUGH SURFACES Final Report, Oct. 1989 - Sep. 1992
Zu-Han Gu Dec. 1992 21 p
(Contract DAAL03-89-C-0036)
(AD-A261000; SOC-R613-002-1292; ARO-27031.22-GS-S) Avail: CASI HC A03/MF A01

We have been conducting a combined theoretical and experimental research program in the field of enhanced backscattering from randomly rough metal and dielectric surfaces. The principal goal of this study is to improve our understanding of the mechanism responsible for the enhanced backscattering phenomenon. At the same time, the results we obtained will apply to remote sensing and radar clutter research. DTIC

N93-25866# Naval Postgraduate School, Monterey, CA.
AN INTRODUCTION TO DOPPLER EFFECT AND FADING IN MOBILE COMMUNICATIONS M.S. Thesis
Abdon B. DePaula Dec. 1992 88 p
(AD-A260976) Avail: CASI HC A05/MF A01

In this research we present an introductory analysis of a complex aspect of mobile communications: Doppler effect is evaluated in both Ricean and Rayleigh channels. A noncoherent 2-FSK scheme is selected to evaluate the behavior of the system under very strong fading channel conditions. The analysis is conducted for the binary case due to the possibility of developing closed form solutions. Therefore, the approach is simplified avoiding long lasting simulations that may obscure the concepts. The probability of bit error for the 2-FSK case can also be used as an initial bound for a M-FSK scheme. Diversity is evaluated as a means of combating fading and Doppler effects. Error correcting codes, in the form of a convolutional codes, are also used and applied to both effects. DTIC

N93-25912# Naval Postgraduate School, Monterey, CA.
EXPERIMENTAL STUDY OF THE EFFECT OF HELICAL GROOVES ON AN INFINITE CYLINDER M.S. Thesis
Thomas D. Suart Dec. 1992 124 p
(AD-A260890) Avail: CASI HC A06/MF A02

A series of low-speed wind-tunnel investigations were conducted to determine the aerodynamic behavior of a grooved inclined cylinder representing a long trailing wire antenna towed from an orbiting airplane. The large angle-of-attack range of the trailing wire required two different model configurations. The first configuration, using full-scale wire lengths suspended between steel stanchions, was mounted on a flush four-degree-of-freedom wall balance. The second configuration used a 15-scale grooved cylinder model with an ogive nose mounted on a six-degree-of-freedom sting balance. Wall balance wire data, valid for higher angles of attack, were integrated with low angle-of-attack sting balance data. Empirical relationships for the normal and axial force coefficients were verified with historical references for tested clean circular cylinders and extended for the grooved configurations. Existence of a side force coefficient due to circulation caused by the helical grooves was discovered, expressed analytically, and verified with flow-visualization techniques. Finally, the experimental coefficients were used to improve an existing simulation model describing the static equilibrium conditions of a cable towed by an airplane in a circular orbit. Inclusion of the side force influence in the static model proved consistent with the lateral skew angle and direction observed during flight test. DTIC

N93-26105*# Jet Propulsion Lab., California Inst. of Tech., Pasadena.
THE TELECOMMUNICATIONS AND DATA ACQUISITION REPORT Progress Report, Jan. - Mar. 1992
Edward C. Posner, ed. 15 May 1992 405 p
(Contract NAS7-918)
(NASA-CR-192804; JPL-TDA-PR-42-109; NAS 1.26:192804) Avail: CASI HC A18/MF A04

This quarterly publication provides archival reports on developments in programs managed by JPL's Telecommunications and Data Acquisition (TDA) Office. In the Search for Extraterrestrial Intelligence (SETI), the TDA Progress Report reports on implementation and operations for searching the microwave spectrum. In solar system radar, it reports on the uses of the Goldstone Solar System Radar for scientific exploration of the planets, their rings and satellites, asteroids, and comets. In radio astronomy, the areas of support include spectroscopy, very long baseline interferometry, and astrometry. These three programs are performed for NASA's Office of Space Science and Applications (OSSA) with the Office of Space Operations for funding DSN operational support. For individual titles, see N93-26106 through N93-26130.

N93-26106*# Jet Propulsion Lab., California Inst. of Tech., Pasadena.
A DETERMINATION OF THE RADIO-PLANETARY FRAME TIE FROM COMPARISON OF EARTH ORIENTATION PARAMETERS
Mark Harold Finger (Computer Sciences Corp., Beltsville, MD.) and William M. Folkner *In its* The Telecommunications and Data Acquisition Report 15 May 1992 p 1-21 (For primary document see N93-26105 09-32)
(RTOP 310-10-60-50-00)
Avail: CASI HC A03/MF A04

The orientation of the reference frame of radio source catalogs relative to that of planetary ephemerides, or 'frame tie,' can be a major systematic error source for interplanetary spacecraft orbit determination. This work presents a method of determining the radio-planetary frame tie from a comparison of very long baseline interferometry (VLBI) and lunar laser ranging (LLR) station coordinate and Earth orientation parameter estimates. A frame tie result is presented with an accuracy of 25 nrad.
Author (revised)

N93-26107*# Jet Propulsion Lab., California Inst. of Tech., Pasadena.
OCCULTATION OF A COMPACT RADIO SOURCE BY VENUS
R. Linfield *In its* The Telecommunications and Data Acquisition Report 15 May 1992 p 22-39 (For primary document see N93-26105 09-32)
(RTOP 310-10-60-60-00)
Avail: CASI HC A03/MF A04

An occultation of the compact radio source P 0507+17 by Venus on 19 July 1988, was observed in Tidbinbilla, Australia at a frequency of 2.3 GHz. The purpose of this observation was to measure the position of Venus in the radio reference frame. When data from both ingress (Venus day side) and egress (Venus nightside) were used to solve for the position of Venus in ecliptic longitude and latitude, the results were consistent with zero offsets from the nominal values, with an uncertainty of approximately 0.2 arcsec in both coordinates. By using the nightside data alone, a value of -0.026+/-0.04 arcsec was obtained for the linear combination delta(lamda) + 0.51delta(beta) where delta(lambda) and delta(beta) were the offsets from their nominal values of the ecliptic longitude and latitude of Venus. Distortion of a vacuum Fresnel fringe pattern by the Venus troposphere, and especially by the Venus ionosphere, was observed. The day side ionosphere of Venus caused very large distortions; the amplitude of the first Fresnel fringe in the ingress data was eight times larger than had been expected for an airless planet. The observed fringe patterns were modeled by using plausible ionospheres (i.e., consistent with spacecraft measurements of the Venus ionosphere and with solar extreme ultraviolet flux and solar wind pressure measurements at the occultation epoch). However, the range of Venus ionospheric profiles (electron density as a function of altitude) allowed by a priori constraints and by the occultation data was large (e.g., the ionopause height on the day side was uncertain by a factor of two). This ionospheric uncertainty (particularly on the day

side) translated into a large position uncertainty (0.2 arcsec for the day side and 0.04 arcsec for the nightside). If it had been possible to calibrate the Venus ionosphere by some external means, the accuracy in delta(lambda) and delta(beta) would have been 0.01 arcsec or better. Author (revised)

N93-26108*# Jet Propulsion Lab., California Inst. of Tech., Pasadena.
A NANORADIAN DIFFERENTIAL VLBI TRACKING DEMONSTRATION
R. N. Treuhaft and S. T. Lowe *In its* The Telecommunications and Data Acquisition Report 15 May 1992 p 40-55 (For primary document see N93-26105 09-32)
(RTOP 310-10-60-86-02)
Avail: CASI HC A03/MF A04

The shift due to Jovian gravitational deflection in the apparent angular position of the radio source P 0201+113 was measured with very long baseline interferometry (VLBI) to demonstrate a differential angular tracking technique with nanoradian accuracy. The ray path of the radio source P 0201+113 passed within 1 mrad of Jupiter (approximately 10 Jovian radii) on 21 Mar. 1988. Its angular position was measured 10 times over 4 hours on that date, with a similar measurement set on 2 Apr. 1988, to track the differential angular gravitational deflection of the ray path. According to general relativity, the expected gravitational bend of the ray path averaged over the duration of the March experiment was approximately 1.45 nrad projected onto the two California-Australia baselines over which it was measured. Measurement accuracies on the order of 0.78 nrad were obtained for each of the ten differential measurements. The Chi-squared per degree of freedom of the data for the hypothesis of general relativity was 0.6, which suggests that the modeled dominant errors due to system noise and tropospheric fluctuations fully accounted for the scatter in the measured angular deflections. The Chi-squared per degree of freedom for the hypothesis of no gravitational deflection by Jupiter was 4.1, which rejects the no-deflection hypothesis with greater than 99.999-percent confidence. The system noise contributed about 0.34 nrad per combined-baseline differential measurement and tropospheric fluctuations contributed about 0.70 nrad. Unmodeled errors were assessed, which could potentially increase the 0.78-nrad error by about 8 percent. The above Chi-squared values, which result from the full accounting of errors, suggest that the nanoradian gravitational deflection signature was successfully tracked.
Author (revised)

N93-26109*# Jet Propulsion Lab., California Inst. of Tech., Pasadena.
DEEP-SPACE NAVIGATION WITH DIFFERENCED DATA TYPES. PART 3: AN EXPANDED INFORMATION CONTENT AND SENSITIVITY ANALYSIS **c17**
J. A. Estefan and S. W. Thurman *In its* The Telecommunications and Data Acquisition Report 15 May 1992 p 56-73 (For primary document see N93-26105 09-32)
(RTOP 310-10-63-50-00)
Avail: CASI HC A03/MF A04

An approximate six-parameter analytic model for Earth-based differenced range measurements is presented and is used to derive a representative analytic approximation for differenced Doppler measurements. The analytical models are tasked to investigate the ability of these data types to estimate spacecraft geocentric angular motion, Deep Space Network station oscillator (clock/frequency) offsets, and signal-path calibration errors over a period of a few days, in the presence of systematic station location and transmission media calibration errors. Quantitative results indicate that a few differenced Doppler plus ranging passes yield angular position estimates with a precision on the order of 0.1 to 0.4 microrad, and angular rate precision on the order of 10 to 25(10)(exp -12) rad/sec, assuming no a priori information on the coordinate parameters. Sensitivity analyses suggest that troposphere zenith delay calibration error is the dominant systematic error source in most of the tracking scenarios investigated; as expected, the differenced Doppler data were found to be much more sensitive to troposphere calibration errors than differenced range. By comparison, results computed using wide band and narrow band (delta)VLBI under similar circumstances yielded angular precisions of 0.07 to 0.4 /microrad, and angular rate precisions of 0.5 to 1.0(10)(exp -12) rad/sec. Author (revised)

N93-26110*# Jet Propulsion Lab., California Inst. of Tech., Pasadena.
ORBITER-ORBITER AND ORBITER-LANDER TRACKING USING SAME-BEAM INTERFEROMETRY
William M. Folkner and J. S. Border *In its* The Telecommunications and Data Acquisition Report 15 May 1992 p 74-86 (For primary document see N93-26105 09-32)
(RTOP 310-10-63-88-01)
Avail: CASI HC A03/MF A04

Two spacecraft orbiting Mars will subtend a small angle as viewed from Earth. This angle will usually be smaller than the beam width of a single radio antenna. Thus the two spacecraft may be tracked simultaneously by a single Earth-based antenna. The same-beam interferometry (SBI) technique involves using two widely separated antennas, each observing the two spacecraft, to produce a measurement of the angular separation of the two spacecraft in the plane of the sky. The information content of SBI data is thus complementary to the line-of-sight information provided by conventional Doppler data. The inclusion of SBI data with the Doppler data in a joint orbit estimation procedure can desensitize the solution to gravity mismodeling and result in improved orbit determination accuracy. This article presents an overview of the SBI technique, a measurement error analysis, and an error covariance analysis of some examples of the application of SBI to orbit determination. For hypothetical scenarios involving the Mars Observer and the Russian Mars '94 spacecraft, orbit determination accuracy improvements of up to an order of magnitude are predicted, relative to the accuracy that can be obtained by using only Doppler data acquired separately from each spacecraft. Relative tracking between a Mars orbiter and a lander fixed on the surface of Mars is also studied. Results indicate that the lander location may be determined to a few meters, while the orbiter ephemeris may be determined with accuracy similar to the orbiter-orbiter case. Author

N93-26111*# Jet Propulsion Lab., California Inst. of Tech., Pasadena.
GEOMETRIC DISTORTION ANALYSIS OF A WIDE-FIELD ASTROGRAPH **c19**
W. M. Owen, Jr. and S. B. Shaklan *In its* The Telecommunications and Data Acquisition Report 15 May 1992 p 87-93 (For primary document see N93-26105 09-32)
(RTOP 310-10-63-92-01)
Avail: CASI HC A02/MF A04

Ground-based optical navigation seeks to determine the angular position of a star, Solar System body, or laser-emitting spacecraft relative to objects with precisely known coordinates. Measurement accuracies of 25 nrad would make optical techniques competitive with current radio metric technology. This article examines a proposed design for a wide-field astrograph and concludes that the deviation of an image centroid from the ideal projection can be modeled to the desired accuracy provided that the field of view does not exceed 5 deg on a side. Author (revised)

N93-26112*# Jet Propulsion Lab., California Inst. of Tech., Pasadena.
APPLICATIONS OF INERTIAL-SENSOR HIGH-INHERITANCE INSTRUMENTS TO DSN PRECISION ANTENNA POINTING **c19**
R. E. Goddard *In its* The Telecommunications and Data Acquisition Report 15 May 1992 p 94-104 (For primary document see N93-26105 09-32)
(RTOP 310-20-65-67-00)
Avail: CASI HC A03/MF A04

Laboratory test results of the initialization and tracking performance of an existing inertial-sensor-based instrument are given. The instrument, although not primarily designed for precision antenna pointing applications, demonstrated an on-average 10-hour tracking error of several millidegrees. The system-level instrument performance is shown by analysis to be sensor limited. Simulated instrument improvements show a tracking error of less than 1 mdeg, which would provide acceptable performance, i.e., low pointing loss, for the DSN 70-m antenna sub network, operating at Ka-band (1-cm wavelength). Author

N93-26113*# Jet Propulsion Lab., California Inst. of Tech., Pasadena.
PERFORMANCE OF A 12-GHz FIBER-OPTIC SYSTEM FOR BEAM-WAVEGUIDE ANTENNA STABILITY TESTING **c74**
T. Y. Otoshi, M. M. Franco, and G. F. Lutes *In its* The Telecommunications and Data Acquisition Report 15 May 1992 p 105-113 (For primary document see N93-26105 09-32)
(RTOP 310-20-65-92-01)
Avail: CASI HC A02/MF A04

A 12-GHz fiber-optic system is a critical part of a test configuration that was proposed for measuring the fractional frequency stability of the

DSS-13 beamwaveguide (BWG) antenna. This fiber-optic system is used to carry Ku-band (12 GHz) signals from a reference antenna to the DSS-13 BWG pedestal room. Tests performed only on the fiber-optic system portion of the overall test configuration showed that the 12-GHz fiber-optic system (installed at DSS-13) has a frequency stability of about 1.1(10)(exp -16) for sampling time tau = 1000 sec for a nighttime run. This preliminary result establishes the lowest noise floor that can probably be achieved for the test configuration that will be used to measure the frequency stability of the DSS-13 BWG antenna. Author (revised)

N93-26114*# Jet Propulsion Lab., California Inst. of Tech., Pasadena.
IMPROVEMENTS IN X-BAND TRANSMITTER PHASE STABILITY THROUGH KLYSTRON BODY TEMPERATURE REGULATION
R. M. Perez *In its* The Telecommunications and Data Acquisition Report 15 May 1992 p 114-120 (For primary document see N93-26105 09-32)
(RTOP 310-20-64-22-00)
Avail: CASI HC A02/MF A04

This article describes the techniques used and experimental results obtained in improving transmitter stability by control of the klystron body temperature. Related work in the measurement of klystron phase control parameters (pushing factors) is also discussed. The contribution of wave guide temperature excursions to uplink phase stability is presented. Suggestions are made as to the direction of future work in this area. Author

N93-26115*# Jet Propulsion Lab., California Inst. of Tech., Pasadena.
NOISE-OPTIMAL CONTROL OF HEMT LNA'S FOR COMPENSATION OF TEMPERATURE DEVIATIONS **c33**
C. MacCarley, J. J. Bautista, and P. A. Willis *In its* The Telecommunications and Data Acquisition Report 15 May 1992 p 121-129 (For primary document see N93-26105 09-32)
(RTOP 310-20-66-09-01)
Avail: CASI HC A02/MF A04

Noise-optimal control of high-electron mobility transistor low noise amplifier (HEMT LNA) bias voltage and current values was achieved at room temperature. The performance metric maximized was the amplifier gain divided by the amplifier input noise temperature, G/T(sub e). Additionally, the feasibility of automating the initial determination of bias settings was demonstrated in the laboratory. Simulation models of an HEMT were developed from available measurement data, installed on a Sun SPARC 1 workstation and used in investigating several optimization algorithms. Simple tracking-type algorithms, which follow changes in optimum settings if started at or near the global optimum point, produced the best performance. Implementation of the optimization algorithms was performed using a three-stage Field Effect Transistor (FET) LNA and an existing test apparatus. Software was written to control the bias settings of the first stage of the LNA and to perform noise and gain measurements by using the test apparatus. The optimization control was then integrated with existing test software to create a master test and optimization program for test apparatus use. Author (revised)

N93-26116*# Solomon (G.), Pasadena, CA.
GOLAY AND OTHER BOX CODES **c61**
G. Solomon *In* JPL, The Telecommunications and Data Acquisition Report 15 May 1992 p 130-135 (For primary document see N93-26105 09-32)
(RTOP 310-30-71-83-02)
Avail: CASI HC A02/MF A04

The (24,12;8) extended Golay Code can be generated as a 6x4 binary matrix from the (15,11;3) BCH-Hamming Code, represented as a 5 x 3 matrix, by adding a row and a column, both of odd or even parity. The odd-parity case provides the additional 12th dimension. Furthermore, any three columns and five rows of the 6 x 4 Golay form a BCH-Hamming (15,11;3) Code. Similarly a (80,58;8) code can be generated as a 10 x 8 binary matrix from the (63,57;3) BCH-Hamming Code represented as a 9 x 7 matrix by adding a row and a column both of odd and even parity. Furthermore, any seven columns along with the top nine rows is a BCH-Hamming (63,57;3) Code. A (80,40;16) 10 x 8 matrix binary code with weight structure identical to the extended (80,40;16) Quadratic Residue Code is generated from a (63,39;7) binary cyclic code represented as a 9 x 7 matrix, by adding a row and a column, both of odd or even parity. Author (revised)

N93-26117*# Jet Propulsion Lab., California Inst. of Tech., Pasadena.
FIGURE OF MERIT FOR DIRECT-DETECTION OPTICAL CHANNELS **c74**
C.-C. Chen *In its* The Telecommunications and Data Acquisition Report 15 May 1992 p 136-151 (For primary document see N93-26105 09-32)
(RTOP 310-20-67-59-00)
Avail: CASI HC A03/MF A04

The capacity and sensitivity of a direct-detection optical channel are calculated and compared to those of a white Gaussian noise channel. Unlike Gaussian channels in which the receiver performance can be characterized using the noise temperature, the performance of the direct-detection channel depends on both signal and background noise, as well as the ratio of peak to average signal power. Because of the signal-power dependence of the optical channel, actual performance of the channel can be evaluated only by considering both transmit and receive ends of the systems. Given the background noise power and the modulation bandwidth, however, the theoretically optimum receiver sensitivity can be calculated. This optimum receiver sensitivity can be used to define the equivalent receiver noise temperature and calculate the corresponding G/T product. It should be pointed out, however, that the receiver sensitivity is a function of signal power, and care must be taken to avoid deriving erroneous projections of the direct-detection channel performance. Author

N93-26118*# Jet Propulsion Lab., California Inst. of Tech., Pasadena.
OPTIMIZING THE G/T RATIO OF THE DSS-13 34-METER BEAM-WAVEGUIDE ANTENNA
M. S. Esquivel *In its* The Telecommunications and Data Acquisition Report 15 May 1992 p 152-161 (For primary document see N93-26105 09-32)
(RTOP 310-30-69-91-02)
Avail: CASI HC A02/MF A04

Calculations using Physical Optics computer software were done to optimize the gain-to-noise temperature (G/T) ratio of DSS-13, the DSN's 34-m beam-waveguide antenna, at X-band for operation with the ultra-low-noise amplifier maser system. A better G/T value was obtained by using a 24.2-dB far-field-gain smooth-wall dual-mode horn than by using the standard X-band 22.5-dB-gain corrugated horn. Author (revised)

N93-26119*# Jet Propulsion Lab., California Inst. of Tech., Pasadena.
DYNAMIC MODELING OF FLUID TRANSMISSION LINES OF THE DSN 70-METER ANTENNAS BY USING A LUMPED PARAMETER MODEL **c37**
R. D. Bartos *In its* The Telecommunications and Data Acquisition Report 15 May 1992 p 162-169 (For primary document see N93-26105 09-32)
(RTOP 310-30-42-10-87)
Avail: CASI HC A02/MF A04

Fluid transmission lines and fittings have been found to significantly affect the dynamic and steady state operation of the engineering system in which they are incorporated. Therefore, a better understanding of the operation of a system can be obtained by including the performance of the transmission lines and fittings within the system model. The most accurate model of a transmission line or fitting is obtained by using a distributed parameter model. However, a distributed parameter model tends to be very complex. This complexity can be avoided without significant loss of model accuracy by using a lumped parameter model when the length of the fluid path through the transmission line or fitting is short. This article develops a lumped parameter model for short fluid transmission lines and fittings, describes the conditions under which the model is valid, and presents the model parameters associated with the servo hydraulic system of the Deep Space Network (DSN) 70-meter antennas. Author (revised)

N93-26120*# Jet Propulsion Lab., California Inst. of Tech., Pasadena.
BANDWIDTH COMPRESSION OF NOISY SIGNALS WITH SQUARE-WAVE SUBCARRIER
Y. Feria and J. Statman *In its* The Telecommunications and Data Acquisition Report 15 May 1992 p 170-178 (For primary document

see N93-26105 09-32)
(RTOP 310-30-71-92-02)
Avail: CASI HC A02/MF A04

This article discusses a method for downconverting the square-wave subcarrier of spacecraft signals, such as the one from Galileo, which results in a compression bandwidth that lowers the sample rate significantly. The study is focused on three issues. The first is the selection of an adequate down-mixing signal for the resulting signal to have a format similar to that of the original signal, except at a lowersub carrier frequency. The second is the control of the noise level so that the signal to noise ratio is not degraded due to the downconversion. The third is to determine the bandwidth of the downconverted signal considering the uncertainty of the residual carrier frequency. Author

N93-26121*# Jet Propulsion Lab., California Inst. of Tech., Pasadena.
AN OSI ARCHITECTURE FOR THE DEEP SPACE NETWORK
W. R. Heuser *In its* The Telecommunications and Data Acquisition Report 15 May 1992 p 179-208 (For primary document see N93-26105 09-32)
(RTOP 310-40-73-89-01)
Avail: CASI HC A03/MF A04

This article presents an Open Systems Interconnection (OSI) architecture developed for the Deep Space Network. An historical review is provided to establish the context for current United States Government policy on interprocessor communication standards. An introduction to the OSI architecture, its seven-layer approach, and an overview of application service entities are furnished as a tutorial. Finally, the results of a prototype system developed for monitor and control of a Deep Space Station are also presented. Author

N93-26122*# Jet Propulsion Lab., California Inst. of Tech., Pasadena.
DSS-13 26-METER ANTENNA UPGRADED RADIOMETER SYSTEM
C. T. Stelzried, L. Skjerve, and G. Bury *In its* The Telecommunications and Data Acquisition Report 15 May 1992 p 209-220 (For primary document see N93-26105 09-32)
(RTOP 314-40-31-30-06)
Avail: CASI HC A03/MF A04

The DSS-13 26-m antenna radiometer system was upgraded with an IBM compatible computer-controlled configuration with improved supporting hardware and software. Software was generated to analyze results and correct for antenna mispointing, tropospheric loss, and other observing errors. This total power radiometer configuration provides a prototype for the new DSS-13 34-m antenna. The radiometer system is described in terms of the theory, instrumentation hardware, computer configuration, and operational features and performance. The system is used to obtain antenna efficiency and pointing model data and is useful for radio source calibrations required for radio astronomy. Some recent results are given.
Author (revised)

N93-26123*# Jet Propulsion Lab., California Inst. of Tech., Pasadena.
SEQUENTIAL DESIGN OF A LINEAR QUADRATIC CONTROLLER FOR THE DEEP SPACE NETWORK ANTENNAS
W. Gawronski *In its* The Telecommunications and Data Acquisition Report 15 May 1992 p 221-252 (For primary document see N93-26105 09-32)
(RTOP 314-40-41-10-15)
Avail: CASI HC A03/MF A04

A new linear quadratic controller design procedure is proposed for the NASA/JPL Deep Space Network antennas. The antenna model is divided into a tracking subsystem and a flexible subsystem. Controllers for the flexible and tracking parts are designed separately by adjusting the performance index weights. Ad hoc weights are chosen for the tracking part of the controller and the weights of the flexible part are adjusted. Next, the gains of the tracking part are determined, followed by the flexible controller final tune-up. In addition, the controller for the flexible part is designed separately for each mode; thus the design procedure consists of weight adjustment for small-size subsystems. Since the controller gains are obtained by adjusting the performance index weights, determination of the weight effect on system performance is a crucial task. A method of determining this effect that allows an on-line improvement of the tracking performance is presented in this article. The procedure is illustrated with the control system design for the DSS-13 antenna. Author

N93-26124*# Jet Propulsion Lab., California Inst. of Tech., Pasadena.
DSN ACQUISITION OF MAGELLAN HIGH-RATE TELEMETRY DATA **c17**
A. L. Berman and P. A. Au *In its* The Telecommunications and Data Acquisition Report 15 May 1992 p 253-264 (For primary document see N93-26105 09-32)
(RTOP 314-40-22-35-01)
Avail: CASI HC A03/MF A04

The Magellan Project levied the stringent requirement of a 98-percent high-rate telemetry data capture rate on the Deep Space Network (DSN) during the Magellan Prime Mapping Mission. To meet this requirement, the DSN undertook extensive development of the DSN Telemetry System, as well as extensive DSN operations planning and test and training. In actuality, the DSN substantially exceeded the requirement by achieving a Prime Mapping Mission high-rate telemetry data capture rate of 99.14 percent. This article details the DSN telemetry system development and DSN operations planning and test and training. In addition, the actual high-rate telemetry data outages are comprehensively presented and analyzed.
Author (revised)

N93-26125*# Jet Propulsion Lab., California Inst. of Tech., Pasadena.
GALILEO EARLY CRUISE, INCLUDING VENUS, FIRST EARTH, AND GASPRA ENCOUNTERS **c12**
P. E. Beyer, R. C. OConnor, and D. J. Mudgway (Mudgway, D. J., Pasadena, CA.) *In its* The Telecommunications and Data Acquisition Report 15 May 1992 p 265-281 (For primary document see N93-26105 09-32)
(RTOP 314-40-22-37-01)
Avail: CASI HC A03/MF A04

This article documents DSN support for the Galileo cruise to Jupiter. The mission's unique trajectory affords multiple encounters during this cruise phase. Each encounter had or will have unique requirements for data acquisition and DSN support configurations. An overview of the cruise and its encounters, up through the asteroid Gaspra encounter, is provided.
Author (revised)

N93-26126*# Jet Propulsion Lab., California Inst. of Tech., Pasadena.
DEEP SPACE NETWORK INFORMATION SYSTEM ARCHITECTURE STUDY **c82**
C. A. Beswick, R. W. Markley, ed., D. J. Atkinson, L. P. Cooper, R. C. Tausworthe, R. C. Masline, J. S. Jenkins, R. A. Crowe, J. L. Thomas, and M. J. Stoloff *In its* The Telecommunications and Data Acquisition Report 15 May 1992 p 282-355 (For primary document see N93-26105 09-32)
(RTOP 314-30-58-50-05)
Avail: CASI HC A04/MF A04

The purpose of this article is to describe an architecture for the DSN information system in the years 2000-2010 and to provide guidelines for its evolution during the 1990's. The study scope is defined to be from the front-end areas at the antennas to the end users (spacecraft teams, principal investigators, archival storage systems, and non-NASA partners). The architectural vision provides guidance for major DSN implementation efforts during the next decade. A strong motivation for the study is an expected dramatic improvement in information-systems technologies--i.e., computer processing, automation technology (including knowledge-based systems), networking and data transport, software and hardware engineering, and human-interface technology. The proposed Ground Information System has the following major features: unified architecture from the front-end area to the end user; open-systems standards to achieve interoperability; DSN production of level 0 data; delivery of level 0 data from the Deep Space Communications Complex, if desired; dedicated telemetry processors for each receiver; security against unauthorized access and errors; and highly automated monitor and control. Author (revised)

N93-26127*# Jet Propulsion Lab., California Inst. of Tech., Pasadena.
GENERALIZED PROBABILITY MODEL FOR CALCULATION OF INTERFERENCE TO THE DEEP SPACE NETWORK DUE TO CIRCULARLY EARTH-ORBITING SATELLITES
C. J. Ruggier *In its* The Telecommunications and Data Acquisition Report 15 May 1992 p 356-366 (For primary document see N93-26105 09-32)
(RTOP 315-20-50-00-06)
Avail: CASI HC A03/MF A04

The probability of exceeding interference power levels and the duration of interference at the Deep Space Network (DSN) antenna is calculated parametrically when the state vector of an Earth-orbiting satellite over the DSN station view area is not known. A conditional probability distribution function is derived, transformed, and then convolved with the interference signal uncertainties to yield the probability distribution of interference at any given instant during the orbiter's mission period. The analysis is applicable to orbiting satellites having circular orbits with known altitude and inclination angle. Author (revised)

N93-26128*# Jet Propulsion Lab., California Inst. of Tech., Pasadena.
Ka-BAND FEED ARRAYS FOR SPACECRAFT REFLECTOR ANTENNAS WITH LIMITED SCAN CAPABILITY: AN OVERVIEW
V. Jamnejad *In its* The Telecommunications and Data Acquisition Report 15 May 1992 p 367-376 (For primary document see N93-26105 09-32)
(RTOP 315-91-50-20-04)
Avail: CASI HC A02/MF A04

The Jet Propulsion Laboratory (JPL) and NASA are in the process of developing ground and spacecraft antenna systems at Ka-band frequencies for future deep space applications. The use of Ka-band (32-GHz down) communication will result in smaller ground and spacecraft antennas and associated equipment and will provide the larger bandwidths necessary for very high data rate communication and radio navigation. In this article, the use of a small phased array as a feed for a reflector antenna system with limited scan capability is addressed. Different feed and antenna configurations, as well as array architectures, are examined. Some theoretical and experimental parameters of a particular breadboard feed array developed by JPL and the University of Massachusetts are presented. Guidelines for the future direction of this effort are provided. Author (revised)

N93-26129*# Jet Propulsion Lab., California Inst. of Tech., Pasadena.
DSN OBSERVATIONS OF TITAN **c91**
R. M. Goldstein and R. F. Jurgens *In its* The Telecommunications and Data Acquisition Report 15 May 1992 p 377-379 (For primary document see N93-26105 09-32)
(RTOP 196-41-73-02-00)
Avail: CASI HC A01/MF A04

When using DSS 14 in a monostatic configuration, radar observations of Titan show that Titan is a diffuse reflector with a relative radar cross section of 0.14+/-0.03. No hot spots were observed. Author (revised)

N93-26130*# Jet Propulsion Lab., California Inst. of Tech., Pasadena.
GOLDSTONE SOLAR SYSTEM RADAR SIGNAL PROCESSING
R. F. Jurgens, E. Satorius, and O. Sanchez *In its* The Telecommunications and Data Acquisition Report 15 May 1992 p 380-397 (For primary document see N93-26105 09-32)
(RTOP 196-41-73-02-00)
Avail: CASI HC A03/MF A04

A performance analysis of the planetary radar data acquisition system is presented. These results extend previous computer simulation analysis and are facilitated by the development of a simple analytical model that predicts radar system performance over a wide range of operational parameters. The results of this study are useful to both the radar systems designer and the science investigator in establishing operational radar data acquisition parameters which result in the best systems performance for a given set of input conditions. Author

N93-26160# Federal Aviation Administration, Atlantic City, NJ.
THE DATA MULTIPLEXING NETWORK (DMN) PHASE 3 EXTENDED DISTANCE DATA CABLE (EDDC) TEST AND EVALUATION
Wayne E. Bell, Phillip P. Hoang, and Edward N. Lind May 1993 118 p
(DOT/FAA/CT-TN93/11) Avail: CASI HC A06/MF A02

This test report contains the results of the Extended Distance Data Cable (EDDC) Test and Evaluation of the Data Multiplexing Network (DMN) Phase 3B Commercial Off-The-Shelf (COTS) equipment. The test was accomplished at the Federal Aviation Administration (FAA) Technical Center. The test results determined the maximum cable length of low loss cable and octopus cable which can be installed with the DMN Phase 3B COTS equipment. Report ASM-300 will prepare the Network Engineering Drawing and Cable Management for the first Operational Readiness Demonstration (ORD) site, Minneapolis Air Route Traffic Control Center (ARTCC), based on the results of this test. Author (revised)

N93-26166# Naval Postgraduate School, Monterey, CA. Dept. of Computer Science.
PROOF OF FAULT COVERAGE FOR A FORMAL PROTOCOL TEST PROCEDURE M.S. Thesis
Michael A. Randall Dec. 1992 57 p
(AD-A261612) Avail: CASI HC A04/MF A01

Due to the speed and complexity of communication networks being designed today, it is imperative to ensure that they operate correctly. Todays fiber optic networks, which can transmit billions of bits per second over thousands of miles, are heavily dependent on sophisticated software and protocols which are becoming increasingly difficult to test. Conformance testing is a method that is used for this purpose: to test the design of a protocol against an implementation of the design. This thesis provides some insight into the conformance testing problem by first providing background on some current protocol test methods and then focusing on a newer method, which is based on a formal protocol specification. A proof is given that demonstrates the method's error detection capabilities. Two well known local area network protocols, Token Bus and Fiber Distributed Data Interface (FDDI), are used as examples to illustrate how the test method is applied to a specification. DTIC

N93-26226# Techno-Sciences, Inc., Lanham, MD.
REALTIME CONTROL OF MULTIPLE SENSOR SYSTEMS Final Report
Gilmer Blankenship, Charles Fletcher, and Anthony LaVigna 29 Jan. 1993 48 p
(Contract DAAL03-92-C-0025)
(AD-A261037; TSI-ARO-93-1) Avail: CASI HC A03/MF A01

The technical objectives of this project are the design and demonstration of methods for the optimal management of sensor systems. As a specific application, we consider the nonlinear filtering of a vector diffusion process, with several noisy vector observations. Any number of sensors can be utilized in the signal processing performed by the nonlinear filter. The problem considered is the optimal selection of a schedule of these sensors from the available set, so as to optimally estimate a function of the state at some given time. Solution of the optimal schedule is derived from solving a system of quasi-linear inequalities (QVI's). The schedule derived from these methods is optimal with respect to predetermined, but possibly varying, running and switching costs for the sensors, as well as some cost functional of the estimate of the dynamics. Methods include precise strategies for adapting the sensor configuration to the engagement at hand, including optimal timing of decisions to communicate or activate active sensors which reveal position. These strategies have been developed by TSI in the form of feedback control laws which are computationally efficient and simple to implement. DTIC

N93-26227# Naval Research Lab., Washington, DC.
ADMISSION CONTROL IN INTEGRATED VOICE/DATA MULTIHOP RADIO NETWORKS Interim Report, Dec. 1991 - Dec. 1992
Craig M. Barnhart, Jeffrey E. Wieselthier, and Anthony Ephremides 18 Jan. 1993 54 p
(Proj. RR0-1509)
(AD-A261055; NRL/MR/5521-93-7196) Avail: CASI HC A04/MF A01

In this report, we investigate the admission control problem for voice traffic in integrated multihop radio networks. We consider only those admission control policies that yield a 'coordinate convex' state space. This restriction, in conjunction with the use of a 'blocked-calls-cleared' mode of operation and the assumption that the voice process is Markovian, results in a product-form stationary distribution for the voice state of the system. The product-form distribution allows the straightforward evaluation of network performance when subject to different admission control policies. A large number of coordinate convex admission-control policies must be searched to determine the optimal policy. We develop a recursive procedure to speed the evaluation of a large number of different policies, as well as descent-search method to reduce significantly the number of policies that must be evaluated in searching for the optimal one. The numerical examples we present indicate that improved performance can be obtained by administering admission control, but this improvement is typically small unless different revenues or costs are associated with the various call types. DTIC

N93-26241# Mitre Corp., Bedford, MA.
EMERGING LARGE-SCREEN DISPLAY TECHNOLOGY Final Report
Richard J. Blaha Nov. 1992 54 p
(Contract F19628-89-C-0001)
(AD-A261066; M-92B0000010; ESD-TR-92-266) Avail: CASI HC A04/MF A01

Large-screen display technology is undergoing significant changes because of huge investments being expended to meet the potential high-definition television (HDTV) market. The expected result of this investment is display devices having improved quality and larger areas, which can be immediately used in military command and control operations. This report tracks recent display developments and their potential capabilities for command and control applications. DTIC

N93-26247# Massachusetts Univ., Lowell. Center for Atmospheric Research.
OTH-B RADAR SYSTEM: SYSTEM SUMMARY
Gary S. Sales May 1992 56 p
(Contract F19628-90-K-0029)
(AD-A261727; PL-TR-92-2134; AD-E201408; SR-7) Avail: CASI HC A04/MF A01

This report introduces the basics of radar technology with a strong emphasis on their application to high frequency (HF) over-the-horizon radar systems. It is intended for people who have to work with OTH radars, but have little experience with either radar systems or with the interaction of the radar signals with the ionosphere. The report covers the radar equation, receive and transmit antenna design, waveform analysis and signal processing. DTIC

N93-26261# Naval Postgraduate School, Monterey, CA. Dept. of Electrical and Computer Engineering.
NEW ALGORITHMS FOR THE DETECTION AND ELIMINATION OF SINE WAVES AND OTHER NARROW-BAND SIGNALS IN THE PRESENCE OF BROADBAND SIGNALS AND NOISE
Michael A. Soderstrand, K. V. Rangarao, and H. H. Loomis 1 Oct. 1992 80 p Sponsored in part by AF
(AD-A261811; NPS-EC-93-005) Avail: CASI HC A05/MF A01

Four different classes of adaptive signal cancelers can be used to eliminate narrow-band interference from a broadband signal: (1) cascaded second-order notch filters; (2) high-order in-line notch filters; (3) second-order bandpass noise cancelers; and (4) high-order bandpass noise cancelers. Of the four, a structure based on second-order bandpass filters used as signal cancelers is found to perform better than the other structures. An adaptive algorithm for these filters has been proposed. The structure can be reduced in hardware complexity without degrading performance using a new adaptive algorithm that out-performs any of the other known structures or algorithms. This new structure is particularly suited to the elimination of narrow-band interference in broadband Bi-Phase Shift-Key (BPSK) signals with and without background noise. DTIC

N93-26276# Palisades Inst. for Research Services, Inc., Arlington, VA.
SPECIAL TECHNOLOGY AREA REVIEW ON MICROWAVE PACKAGING TECHNOLOGY
Becky Terry Feb. 1993 41 p Sponsored by DOD
(AD-A261852) Avail: CASI HC A03/MF A01

Microwave (MW) and millimeter wave (MMW) multichip module (MCM) packaging is an emerging technology that is of great importance for both defense and commercial applications. Military applications such as radar, electronic warfare, communications, and smart munitions and commercial applications such as communications, direct broadcast satellite, cellular telephone, and automotive electronics all require MW and/or MMW electronics. The spectrum of needs ranges from low volume, high performance electronics to high volume, low cost applications. A significant aspect of realizing these components and systems will be the development of a broad range of packaging and interconnect technologies that have the required reliability and environmental protection and are affordable and applicable to both the military and commercial sectors. DTIC

N93-26280# Massachusetts Univ., Lowell. Center for Atmospheric Research.
HIGH FREQUENCY (HF) RADIOWAVE PROPAGATION
Gary S. Sales Apr. 1992 38 p
(Contract F19628-90-K-0029)
(AD-A261726; PL-TR-92-2123; AD-E201407; SR-6) Avail: CASI HC A03/MF A01

This report serves to introduce the basics of high frequency radiowave propagation in the earth's ionosphere. It is intended for people who are not fully acquainted with the physics of the problem but have had some experience working with or will have to work with over-the-horizon radar systems. This material, after an introduction to propagation theory and terminology, concentrates on the features of the OTH radar. First, backscatter ionogram is introduced as the primary diagnostic tool for the management of the radar in terms of the ionospheric environment. The synthesis of these ionograms is presented in detail as a way of leading to a better understanding of HF radiowave propagation. Special emphasis is placed on a description of the effects of ionospheric clutter and sporadic-E on the performance of the radar. DTIC

N93-26289# Mission Research Corp., Santa Barbara, CA.
STATISTICS OF SAMPLED RICIAN FADING Technical Report, 1 Jan. - 31 Jun. 1992
Roger A. Dana 1 Feb. 1993 61 p
(Contract DNA001-91-C-0010)
(AD-A261397; MRC-R-1410; DNA-TR-92-98) Avail: CASI HC A04/MF A01

Realizations of the channel impulse response function generated with Rician amplitude statistics have been used for many years to evaluate system performance in the regime between full Rayleigh fading and ambient non-fading conditions. While it is well known that Rician distributed realizations fail to match observed phase fluctuations, Rician statistics provide a worst case description of the occurrence of deep fades. Thus the use of Rician statistics is attractive in slow fading situations where system performance has been rendered insensitive to phase variations. The purposes of this report are to provide new information on the temporal statistics of Rician fading (mean fade duration and separation) and to determine sampling requirements on realizations of the channel impulse response function with Rician amplitude statistics. It is found that 400 decorrelation time (tau(sub 0)) realizations generated with 10 samples per tau(sub 0) and sampled at tau(sub 0)/40 accurately reproduce the temporal statistics of Rician fading. DTIC

N93-26372# Naval Postgraduate School, Monterey, CA.
IMPLEMENTATION OF CYCLIC SPECTRAL ANALYSIS METHODS M.S. Thesis
Nancy J. Carter Dec. 1992 112 p
(AD-A261715) Avail: CASI HC A06/MF A02

Phase-shift keyed (PSK) signal modulation methods are coming into increasing use in modem communications. This thesis describes the implementation of three methods of computing the cyclic spectrum to determine the presence of PSK signals. The Strip Spectral Correlation Algorithm (SSCA) and the Fast Fourier Transform (FFT) Accumulation Method (FAM) both estimate the cyclic spectral plane. The Sub-FFT Accumulation Method (SUBFAM) program computes the Spectral Correlation Function (SCF) for a set of possible spectral frequencies for a single cycle frequency. The results of algorithm performance are presented along with a discussion of promising areas for performance enhancement and automation of signal detection and classification. DTIC

N93-26383# Phraxos Research and Development, Inc., Santa Monica, CA.
MICROSTRIP ANTENNAS ON/IN ANISOTROPIC MATERIAL LAYERS Final Report, Aug. 1988 - Feb. 1991
Hung-Yu Yang, Jesse A. Castaneda, and Akifumi Nakatani Nov. 1992 97 p
(Contract F19628-88-C-0059)
(AD-A261700; RPT-91025; RL-TR-92-257) Avail: CASI HC A05/MF A02

Accurate fullwave analyses of microstrip dipoles on multi-layer substrates with generalized anisotropic permittivity and permeability have been developed. The solution to the problem of microstrip dipoles on/in gyrotropic substrates has been obtained. The potential of electronically shaped, scanned, and gain enhanced element factors with ferrite substrates has been theoretically demonstrated. The scattering and radiation problems were solved. The use of biased ferrite substrates to simultaneously reduce

RCS and preserve antenna in-band gain has also been described. Infinite phased arrays of microstrip dipoles and probe-fed patches on general anisotropic multi-layer substrates have been analyzed. All the solutions involve the dyadic Green's function for the anisotropic layered structure and the application of the method of moments to an electric field integral equation. DTIC

N93-26388# Naval Postgraduate School, Monterey, CA.
THE DESIGN AND EVALUATION OF TRANSMIT AND RECEIVE ANTENNAS FOR AN IONOSPHERIC COMMUNICATIONS PROBE SYSTEM. B: SLOPING-VEE BEAMS M.S. Thesis
Georgios T. Bougioukos Dec. 1992 112 p
(AD-A261866) Avail: CASI HC A06/MF A02

The purpose of this study was to design and evaluate the performance of a transmitting antenna for an HF communications probe system. Monterey, CA, was selected as the transmit site, and San Diego, CA, was selected as the receive site to establish an ionospheric communication link to test the equipment involved in the probe system. A sloping-vee antenna was chosen for initial shakedown tests to support the transmitting requirements of the probe system at 5.6, 11, and 16.8 MHz. The Eyring Ground Measurement Probe was used to measure the ground constants at the NPS beach site. The Numerical Electromagnetics Code (NEC) was utilized to analyze the performance of the antenna at the NPS beach, and for average, poor, fair and arctic ground conditions. The antenna provides a maximum gain of 1.46 dBi at 5.6 MHz, 5.56 dBi at 11 MHz, 8 dBi at 16.8 MHz, and positive gain at take-off angles between 3 deg and 33 deg at frequencies from 5.6 to 16.8 MHz. The VSWRs with a standard 600 Ohm to 50 Ohm impedance matching transformer (12:1) are 1.73 at 5.6 MHz, 1.77 at 11 MHz, and 1.53 at 16.8 MHz. DTIC

N93-26441# Naval Postgraduate School, Monterey, CA.
TRELLIS CODED CPFSK M.S. Thesis
Zafer Inceoglu 10 Dec. 1992 55 p
(AD-A261788) Avail: CASI HC A04/MF A01

Continuous Phase Frequency Shift Keying (CPFSK) is a potentially attractive modulation scheme with constant envelope and good spectral characteristics for energy constrained and band-limited satellite channels. This research deals with Orthogonal Frequency Shift Keying (FSK), Minimum Shift Keying (MSK) which is a special case of CPFSK, uncoded quaternary CPFSK, and finally coded quaternary CPFSK. Orthogonal FSK is simulated by making the modulation index (h) equal to one, and all of the other simulations are performed with h=1/2. A rate 1/2 convolutional encoder with constraint lengths (k), k=2, 3, and 4 are used in coded quaternary CPFSK simulations. Good coding gains are obtained with only a slight increase in receiver complexity. Soft decision with the Viterbi Algorithm was applied to all CPFSK and one MSK application. Hard decision was applied to Orthogonal FSK and another MSK application. DTIC

N93-26451# Naval Research Lab., Washington, DC.
NEW RESULTS IN SIGNAL DESIGN FOR THE AWGN CHANNEL
Michael J. Steiner 31 Jan. 1993 27 p
(AD-A261424; NRL/FR/5341-93-9524) Avail: CASI HC A03/MF A01

The design of M average power constrained signals in white Gaussian noise (AWGN) is addressed. The long-standing strong simplex conjecture which postulates that the optimal signals, under an average power constraint, are the vertices of a regular simplex, is disproven. A signal set is shown that performs better than the regular simplex at low signal-to-noise ratios for an M greater than or equal to 7. This leads to a theorem stating that for any fixed M greater than or equal to 7 no signal set exists that is optimal at all signal-to-noise ratios. Furthermore it is found that the optimal solution at low signal-to-noise ratios is not an equal energy solution for any M greater than or equal to 7. The regular simplex is shown to be the unique polytope that maximizes the minimum distance between signals. This result leads to the corollary that a signal set which maximizes the minimum distance is not necessarily optimum. However, the regular simplex is shown to be globally optimum in the sense of uniquely maximizing the union bound at all signal-to-noise ratios. DTIC

N93-26455# Naval Research Lab., Washington, DC. Radar Div.
RADAR SENSING OF PETROLEUM SEEPAGE GASES Final Report
Donald F. Hemenway, James P. Hansen, and Eugene G. George 17 Jan. 1993 62 p
(AD-A261431; NRL/MR/5300-93-7177) Avail: CASI HC A04/MF A01

Simple X-band radars have been used by a number of commercial exploration companies since 1972 in the search for gas and oil deposits. Uncertainty and controversy over the physical mechanism involved in the radar sensing of gas and oil led to the April/May 1992 radar investigation conducted by NRL. A low power X-band radar was used by NRL to acquire experimental data in Texas. The attributes of return signals observed over producing and prospective oil fields were found to have a unique set of characteristics which included the following: return signals were from weak, distributed targets: simultaneous amplitude and range variations were observed (10 dB or more in amplitude and +/- 60 ft in range) within time intervals of 1/3rd second and at ranges of from 500 to 2,000 ft, and at elevation angles of less than + 1 deg. The range and amplitude varying radar returns were suppressed by rain and/or a wet earth. Also during a single period of 24 hour observation, the varying signals disappeared during a period of high humidity (local night-time) and then re-appeared the next day when the relative humidity dropped below 50%. Radar returns from seepage gases heights greater than 25 feet as well as gas associated radar returns over cattle feed lots (methane and ammonia) were not confirmed. DTIC

N93-26460# Range Commanders Council, White Sands Missile Range, NM. Range Safety Group.
FLIGHT TERMINATION RECEIVER CATALOG
Feb. 1993 226 p Supersedes RSG-306-84
(AD-A261558; RSG-306-93) Avail: CASI HC A11/MF A03

This catalog provides reference information on ultra-high frequency flight termination receivers used at various U.S. missile ranges and test facilities. It is not intended to be a comprehensive review of all available flight termination receivers. Inclusion in this catalog does not constitute approval or endorsement for use at any government installation. Information in this catalog was extracted from manufacturers' specifications. DTIC

N93-26463*# Jet Propulsion Lab., California Inst. of Tech., Pasadena.
PROCEEDINGS OF THE 16TH NASA PROPAGATION EXPERIMENTERS MEETING (NAPEX 16) AND THE ADVANCED COMMUNICATIONS TECHNOLOGY SATELLITE (ACTS) PROPAGATION STUDIES MINIWORKSHOP
Faramaz Davarian, ed. 1 Aug. 1992 254 p Meeting and workshop held in Houston, TX, 29-30 May 1992
(Contract NAS7-918)
(NASA-CR-192800; NAS 1.26:192800; JPL-Publ-92-16) Avail: CASI HC A12/MF A03

The NASA Propagation Experimenters Meeting (NAPEX), supported by the NASA Propagation Program, is convened annually to discuss studies made on radio wave propagation by investigators from domestic and international organizations. NAPEX 16 was held on May 29, 1992 in Houston, Texas. The meeting was organized into two technical sessions. The first session was dedicated to slant path propagation studies and measurements. The second session focused on Olympus propagation measurements and results. Following NAPEX 16, the Advanced Communications Technology Satellite (ACTS) Miniworkshop was held to review ACTS propagation activities with emphasis on ACTS hardware development and experiment planning. Eight technical papers were presented by contributors from government agencies, private industry, and university research establishments. For individual titles, see N93-26464 through N93-26486.

N93-26464*# Jet Propulsion Lab., California Inst. of Tech., Pasadena.
OPENING REMARKS
Faramaz Davarian *In its* Proceedings of the 16th NASA Propagation Experimenters Meeting (NAPEX 16) and the Advanced Communications Technology Satellite (ACTS) Propagation Studies Miniworkshop 1 Aug. 1992 p 4-7 (For primary document see N93-26463 09-32)
Avail: CASI HC A01/MF A03

The year's accomplishments at the onset of the yearly NAPEX meetings are reviewed. Therefore, I will present the last year's accomplishments and the plans for the next year. The studies supported by the Propagation Program during the last year are listed: OLYMPUS data collection and analysis; the ACTS Propagation Program; low elevation angle 11-GHz measurements; satellite broadcast and mobile studies; radiometric

techniques; propagation models database; NASA Reference Publication 1274; CCIR activities; fade detection and compensation; rain rate measurements; and information dissemination. Author (revised)

N93-26465*# Jet Propulsion Lab., California Inst. of Tech., Pasadena.
THE ACTS PROPAGATION PROGRAM
D. Chakraborty and Faramaz Davarian *In its* Proceedings of the 16th NASA Propagation Experimenters Meeting (NAPEX 16) and the Advanced Communications Technology Satellite (ACTS) Propagation Studies Miniworkshop 1 Aug. 1992 p 13-16 (For primary document see N93-26463 09-32)
Avail: CASI HC A01/MF A03

The success or failure of the ACTS experiment will depend on how accurately the rain-fade statistics and fade dynamics can be predicted in order to derive an appropriate algorithm that will combat weather vagaries, specifically for links with small terminals, such as very small aperture terminals (VSAT's) where the power margin is a premium. The planning process and hardware development program that will comply with the recommendations of the ACTS propagation study groups are described. Author (revised)

N93-26466*# Texas Univ., Austin.
LARGE SCALE RAINFALL DIVERSITY AND SATELLITE PROPAGATION
H. P. Lin and W. J. Vogel *In* JPL, Proceedings of the 16th NASA Propagation Experimenters Meeting (NAPEX 16) and the Advanced Communications Technology Satellite (ACTS) Propagation Studies Miniworkshop 1 Aug. 1992 p 17-26 (For primary document see N93-26463 09-32)
Avail: CASI HC A02/MF A03

From the NOAA 15 minute precipitation file for the U.S., data was selected for 128 stations covering a 17 year period and the probability of simultaneous rainfall at several stations was calculated. We assumed that the chosen stations were located in separate beams of a multi-beam communications satellite with shared fade mitigation resources. In order to estimate the demands made on these resources, we determined the number of stations at which rainfall rates exceeded 10 to 40 mm/hr. We found a 1 percent probability that at least 5 of the 128 stations have rain at or over 10 mm/hr in any 15 minute interval. Rain at 2 stations was found to correlate over distances less than about 600 miles. Author (revised)

N93-26467*# Texas Univ., Austin.
L- AND K-BAND LMSS PROPAGATION MEASUREMENTS USING MARECS-B, OLYMPUS, AND ACTS
W. J. Vogel, G. W. Torrence, J. Goldhirsh (Johns Hopkins Univ., Laurel, MD.), and J. R. Rowland (Johns Hopkins Univ., Laurel, MD.) *In* JPL, Proceedings of the 16th NASA Propagation Experimenters Meeting (NAPEX 16) and the Advanced Communications Technology Satellite (ACTS) Propagation Studies Miniworkshop 1 Aug. 1992 p 27-33 (For primary document see N93-26463 09-32)
Avail: CASI HC A02/MF A03

L-band measurements of land mobile satellite systems (LMSS) propagation effects were last made at the end of 1988, but some voids were left in the database, making modeling of low elevation roadside tree shadowing and multipath reflections difficult for some path geometries. Transmission of a pilot tone from MARECS-B at 55 deg West during Sep. and Dec. 1991 gave an opportunity to fill the gaps in the experimental results. Two campaigns during which fade data were obtained at elevation angles from 7 deg to 40 deg are described. Below 15 deg, specular terrain reflections in a non-shadowing, hilly environment were observed to introduce significant fading. Although the reflecting surface was at a distance of up to several km, it is shown that the reflected signals are delayed by less than 1 microsec. Mobile measurements were also attempted receiving the 20 GHz Olympus beacon, but antenna pointing problems restricted first results to straight-line driving. Author (revised)

N93-26468*# Johns Hopkins Univ., Laurel, MD.
RAIN RATE AND MODELED FADE DISTRIBUTIONS AT 20 GHz AND 30 GHz DERIVED FROM FIVE YEARS OF NETWORK RAIN GAUGE MEASUREMENTS
Julius Goldhirsh, Vladimir Krichevsky (Micromat Research, Gaithersburg, MD.), and Norman Gebo *In* JPL, Proceedings of the 16th NASA Propagation Experimenters Meeting (NAPEX 16) and the Advanced Communications Technology Satellite (ACTS) Propagation Studies Miniworkshop 1 Aug. 1992 p 34-44 (For primary document see N93-26463 09-32)
(Contract N00039-91-C-0001)
Avail: CASI HC A03/MF A03

Five years of rain rate and modeled slant path attenuation distributions at 20 GHz and 30 GHz derived from a network of 10 tipping bucket rain gages was examined. The rain gage network is located within a grid 70 km north-south and 47 km east-west in the Mid-Atlantic coast of the United States in the vicinity of Wallops Island, Virginia. Distributions were derived from the variable integration time data and from one minute averages. It was demonstrated that for realistic fade margins, the variable integration time results are adequate to estimate slant path attenuations at frequencies above 20 GHz using models which require one minute averages. An accurate empirical formula was developed to convert the variable integration time rain rates to one minute averages. Fade distributions at 20 GHz and 30 GHz were derived employing Crane's Global model because it was demonstrated to exhibit excellent accuracy with measured COMSTAR fades at 28.56 GHz. Author

N93-26469*# Oklahoma Univ., Norman.
ON THE ESTIMATION OF RISK ASSOCIATED WITH AN ATTENUATION PREDICTION
R. K. Crane *In* JPL, Proceedings of the 16th NASA Propagation Experimenters Meeting (NAPEX 16) and the Advanced Communications Technology Satellite (ACTS) Propagation Studies Miniworkshop 1 Aug. 1992 p 45-63 (For primary document see N93-26463 09-32)
Avail: CASI HC A03/MF A03

Viewgraphs from a presentation on the estimation of risk associated with an attenuation prediction is presented. Topics covered include: link failure - attenuation exceeding a specified threshold for a specified time interval or intervals; risk - the probability of one or more failures during the lifetime of the link or during a specified accounting interval; the problem - modeling the probability of attenuation by rainfall to provide a prediction of the attenuation threshold for a specified risk; and an accounting for the inadequacy of a model or models. CASI

N93-26470*# Ministry of Posts and Telecommunications, Tokyo (Japan). Communications Research Lab.
ETS-5, ETS-6, AND COMETS PROJECTS IN JAPAN
Takashi Iida, Hiromitsu Wakana, and Noriaki Obara *In* JPL, Proceedings of the 16th NASA Propagation Experimenters Meeting (NAPEX 16) and the Advanced Communications Technology Satellite (ACTS) Propagation Studies Miniworkshop 1 Aug. 1992 p 64-69 (For primary document see N93-26463 09-32)
Avail: CASI HC A02/MF A03

Three satellite communication projects now in progress in Japan are described. The first is a project to establish a telecommunication network for tele-education, TV conference, and tele-medicine in the Asia-Pacific region by using the Japan's Engineering Test Satellite-5 (ETS-5). The second is a project of the ETS-6 satellite, to be launched in 1993, for inter-satellite communication, mobile and fixed communication, and millimeter wave personal communication experiments. The third is a project of the Communications and Broadcasting Engineering Test Satellite (COMETS), to be launched in 1997, for advanced mobile satellite communication, inter-satellite link, and advanced broadcasting experiments at higher frequencies. Author (revised)

N93-26471*# Colorado Univ., Boulder.
SATELLITE COMMUNICATIONS APPLICATION TO PACIFIC COUNTRIES ABOVE Ku BAND
Takashi Iida *In* JPL, Proceedings of the 16th NASA Propagation Experimenters Meeting (NAPEX 16) and the Advanced Communications Technology Satellite (ACTS) Propagation Studies Miniworkshop 1 Aug. 1992 p 70-75 (For primary document see N93-26463 09-32)
(Grant NAGw-1105)
Avail: CASI HC A02/MF A03

An application of satellite communications above the Ku band to the Pacific region is described, focusing on: (1) Lightsat system and (2) a high capacity satellite system. A small geostationary satellite system using Ku band for the Federated States of Micronesia is shown as an example. A concept of multi-gigabits/second high capacity communications system using

two satellites in the Ka band is described. The onboard bit-by-bit processing is very useful in the low link margin environment due to rain attenuation. These topics were obtained by the Asia Pacific Telecommunications Study granted by NASA conducted by the University of Colorado at Boulder.
Author (revised)

N93-26472*# Jet Propulsion Lab., California Inst. of Tech., Pasadena.
A DATABASE FOR PROPAGATION MODELS
Anil V. Kantak and Krisjani S. Suwitra *In its* Proceedings of the 16th NASA Propagation Experimenters Meeting (NAPEX 16) and the Advanced Communications Technology Satellite (ACTS) Propagation Studies Miniworkshop 1 Aug. 1992 p 76-80 (For primary document see N93-26463 09-32)
Avail: CASI HC A01/MF A03

In June 1991, a paper at the fifteenth NASA Propagation Experimenters Meeting (NAPEX 15) was presented outlining the development of a database for propagation models. The database is designed to allow the scientists and experimenters in the propagation field to process their data through any known and accepted propagation model. The architecture of the database also incorporates the possibility of changing the standard models in the database to fit the scientist's or the experimenter's needs. The database not only provides powerful software to process the data generated by the experiments, but is also a time- and energy-saving tool for plotting results, generating tables, and producing impressive and crisp hard copy for presentation and filing. Author (revised)

N93-26473*# Colorado Univ., Boulder. Wave Propagation Lab.
BRIGHTNESS TEMPERATURE AND ATTENUATION DIVERSITY STATISTICS AT 20.6 AND 31.65 GHz FOR THE COLORADO RESEARCH NETWORK
Ed R. Westwater, M. J. Falls, and E. Fionda (Fondazione Ugo Bordoni, Rome, Italy.) *In* JPL, Proceedings of the 16th NASA Propagation Experimenters Meeting (NAPEX 16) and the Advanced Communications Technology Satellite (ACTS) Propagation Studies Miniworkshop 1 Aug. 1992 p 81-96 (For primary document see N93-26463 09-32)
Avail: CASI HC A03/MF A03

A limited network of four dual-channel microwave radiometers, with frequencies of 20.6 and 31.65 GHz, was operated in the front range of eastern Colorado from 1985 to 1988. Data, from November 1987 through October 1988 are analyzed to determine both single-station and joint-station brightness temperature and attenuation statistics. Only zenith observations were made. The spatial separations of the stations varied from 50 km to 190 km. Before the statistics were developed, the data were screened by rigorous quality control methods. One such method, that of 20.6 vs. 31.65 GHz scatter plots, is analyzed in detail, and comparisons are made of measured vs calculated data. At 20.6 and 31.65 GHz, vertical attenuations of 5 and 8 dB are exceeded 0.01 percent of the time. For these four stations and at the same 0.01 percent level, diversity gains from 6 to 8 dB are possible with the 50 to 190 km separations. Author (revised)

N93-26474*# Colorado Univ., Boulder. Dept. of Electrical and Computer Engineering.
A PROPOSED STUDY OF MULTIPLE SCATTERING THROUGH CLOUDS UP TO 1 THz
G. C. Gerace and E. K. Smith *In* JPL, Proceedings of the 16th NASA Propagation Experimenters Meeting (NAPEX 16) and the Advanced Communications Technology Satellite (ACTS) Propagation Studies Miniworkshop 1 Aug. 1992 p 97-115 (For primary document see N93-26463 09-32)
Avail: CASI HC A03/MF A03

A rigorous computation of the electromagnetic field scattered from an atmospheric liquid water cloud is proposed. The recent development of a fast recursive algorithm (Chew algorithm) for computing the fields scattered from numerous scatterers now makes a rigorous computation feasible. A method is presented for adapting this algorithm to a general case where there are an extremely large number of scatterers. It is also proposed to extend a new binary PAM channel coding technique (El-Khamy coding) to multiple levels with non-square pulse shapes. The Chew algorithm can be used to compute the transfer function of a cloud channel. Then the transfer function can be used to design an optimum El-Khamy code. In principle, these concepts can be applied directly to the realistic case of a time-varying cloud (adaptive channel coding and adaptive equalization). A brief review is included of some preliminary work on cloud dispersive effects on digital communication signals and on cloud liquid water spectra and correlations.
Author

N93-26475*# Colorado Univ., Boulder.
WARC 92 AND SOME THOUGHTS AS TO ITS IMPACT ON THE NASA PROPAGATION PROGRAM
Warren L. Flock and Ernest K. Smith *In* JPL, Proceedings of the 16th NASA Propagation Experimenters Meeting (NAPEX 16) and the Advanced Communications Technology Satellite (ACTS) Propagation Studies Miniworkshop 1 Aug. 1992 p 116-122 (For primary document see N93-26463 09-32)
Avail: CASI HC A02/MF A03

The World Administrative Radio Conference of 1992 (WARC 92) was held in Torremolinos, Spain, 3 Feb. - 3 Mar. 1992. Major topics considered included shortwave broadcasting, mobile and mobile-satellite service, broadcasting satellite service (sound and HDTV), space services above 20 GHz, and space research. Considerable attention was given to the congested 1-3 GHz band in general and to Low Earth Orbit (LEO) Mobile-Satellite Service, including 'little' LEO's operating below 1 GHz and to 'big' LEO's operating above 1 GHz. Significant new allocations were made for generic Mobile-Satellite Services (MSS). Proposals for allocations for uplink power control beacons and for space research received favorable treatment.
Author (revised)

N93-26476*# National Aeronautics and Space Administration. Lewis Research Center, Cleveland, OH.
ALLOCATIONS BY THE 1992 WORLD ADMINISTRATIVE RADIO CONFERENCE
Ann O. Heyward *In* JPL, Proceedings of the 16th NASA Propagation Experimenters Meeting (NAPEX 16) and the Advanced Communications Technology Satellite (ACTS) Propagation Studies Miniworkshop 1 Aug. 1992 p 123-128 (For primary document see N93-26463 09-32)
Avail: CASI HC A02/MF A03

An overview of the 1992 World Administrative Radio Conference is presented with viewgraphs. Allocations of radio frequency spectrum are addressed. Mobile satellite service, broadcast satellite service, and uplink power control beacons are also addressed. CASI

N93-26477*# European Space Agency. European Space Research and Technology Center, ESTEC, Noordwijk (Netherlands).
ESA'S PLANNING AND COORDINATION OF THE OLYMPUS PROPAGATION EXPERIMENT
B. Arbesser-Rastburg *In* JPL, Proceedings of the 16th NASA Propagation Experimenters Meeting (NAPEX 16) and the Advanced Communications Technology Satellite (ACTS) Propagation Studies Miniworkshop 1 Aug. 1992 p 131-142 (For primary document see N93-26463 09-32)
Avail: CASI HC A03/MF A03

An overview of the organization of the OLYMPUS propagation experimenters group (OPEX) is given. Preparations, participation, and experiments are described. Some examples for first statistical results are also reported. OLYMPUS, a 3-axis stabilized communications satellite was launched in 1989 for providing experimental telecommunications payloads and a propagation beacon payload at 12, 20, and 30 GHz to the European Space Agency. From previous experience (OTS), the Agency undertook to carry out extensive preparations with an eye on obtaining the statistical results needed within the limited available lifetime of the spacecraft. The OLYMPUS propagation experiment was conceived as part of ESA's space telecommunications applications program (ESA/IPC/(79)83) with the emphasis on exploring the possibilities and limitations of Ka-band satellite communications. The objectives of the OLYMPUS propagation campaign were: (1) characterization of the slant-path propagation conditions at 20/30 GHz in the various climatic regions of Europe; (2) improvement of the understanding of the link between atmospheric observable (rain rate, cloud thickness, etc.) to propagation impairments such as attenuation, depolarization, scintillation, etc.; and (3) arrive at improved propagation prediction methods. Author (revised)

N93-26478*# Forschungsinstitut der Deutschen Bundespost, Darmstadt (Germany).
EFFECT-SPECIFIC ANALYSIS OF PROPAGATION PARAMETERS
G. Ortgies, F. Ruecker, F. Dintelmann, and R. Jakoby *In* JPL, Proceedings

of the 16th NASA Propagation Experimenters Meeting (NAPEX 16) and the Advanced Communications Technology Satellite (ACTS) Propagation Studies Miniworkshop 1 Aug. 1992 p 143-154 (For primary document see N93-26463 09-32)
Avail: CASI HC A03/MF A03

Results of propagation measurements with the satellite OLYMPUS carried out at 12.5, 20, and 30 GHz at the Research Center of the Deutsche Bundespost Telekom are discussed. In particular, attenuation, scintillation, and depolarization measurements are analyzed with special emphasis on frequency scaling of the various effects. Author (revised)

N93-26479*# Virginia Polytechnic Inst. and State Univ., Blacksburg. Dept. of Electrical Engineering.
THE VIRGINIA TECH OLYMPUS PROPAGATION EXPERIMENT
Tim Pratt and Warren Stutzman *In* JPL, Proceedings of the 16th NASA Propagation Experimenters Meeting (NAPEX 16) and the Advanced Communications Technology Satellite (ACTS) Propagation Studies Miniworkshop 1 Aug. 1992 p 155-165 (For primary document see N93-26463 09-32)
Avail: CASI HC A03/MF A03

Virginia Polytechnic Institute has been carrying out a comprehensive set of propagation measurements using the OLYMPUS satellite beacons at 12.5, 20, and 30 GHz since August 1990. Total power radiometers are also included in each terminal, and radiometer data are used both to set the absolute level of the beacon data and to predict path attenuation. Some results from the experiment set are presented. Author (revised)

N93-26480*# Communications Research Centre, Ottawa (Ontario). Dept. of Communications.
STATUS OF THE OLYMPUS EXPERIMENT AT CRC
David V. Rogers *In* JPL, Proceedings of the 16th NASA Propagation Experimenters Meeting (NAPEX 16) and the Advanced Communications Technology Satellite (ACTS) Propagation Studies Miniworkshop 1 Aug. 1992 p 166-170 (For primary document see N93-26463 09-32)
Avail: CASI HC A01/MF A03

The status of the Olympus Propagation Experiment of the Communications Research Centre in Ottawa, Canada, is briefly summarized. Path attenuation measurements at multiple frequencies correlated with concurrent dual polarized radar data provide a unique method to investigate propagation effects. An experiment of this type is being implemented by the Communications Research Centre (CRC) on the grounds of the National Research Council of Canada in Ottawa. Beacon receivers monitor signals from the Olympus satellite at 12.5, 19.77, and 29.66 GHz at a path elevation angle of 14.2 deg. Sky noise radiometers operating near the same frequencies and pointed along the same path provide additional propagation information. A colocated dual-polarized 9.6-GHz radar probes the precipitation state on the path, permitting identification of precipitation regimes that cause the observed impairments. The Olympus experiment configuration is displayed pictorially. Information on path propagation phenomena can be deduced by correlating the radar, beacon, and sky noise data. Melting layer effects and propagation losses for higher time percentages are prime interests. Data collected by Diversitel Communications during equipment verification tests are presented. Author (revised)

N93-26481*# National Aeronautics and Space Administration. Lewis Research Center, Cleveland, OH.
OLYMPUS/ACTS SCINTILLATION EXPERIMENT AT THE LEWIS RESEARCH CENTER
Noulie Theofylaktos *In* JPL, Proceedings of the 16th NASA Propagation Experimenters Meeting (NAPEX 16) and the Advanced Communications Technology Satellite (ACTS) Propagation Studies Miniworkshop 1 Aug. 1992 p 171-181 (For primary document see N93-26463 09-32)
Avail: CASI HC A03/MF A03

Details of the OLYMPUS/ACTS scintillation experiment at the Lewis Research Center are presented in viewgraph form. Temporal frequency spectra of log-amplitude fluctuations are given. CASI

N93-26482*# Communications Research Centre, Ottawa (Ontario).
OBSERVATIONS ON THE NASA PROPAGATION PROGRAM
David V. Rogers *In* JPL, Proceedings of the 16th NASA Propagation Experimenters Meeting (NAPEX 16) and the Advanced Communications Technology Satellite (ACTS) Propagation Studies Miniworkshop 1 Aug. 1992 p 182-183 (For primary document see N93-26463 09-32)
Avail: CASI HC A01/MF A03

Several personal observations are offered on the NASA Propagation Program. The Science Review of the NASA Propagation Program held in September 1986 resulted in 14 principal recommendations. Current activities of the program reveal that the recommendations have in the main been successfully implemented and the program has evolved beyond conditions prevailing at the time of the review. A personal assessment of the current program is offered here. Author (revised)

N93-26483*# Johns Hopkins Univ., Laurel, MD. Applied Physics Lab.
A COMPARATIVE ASSESSMENT OF R. M. YOUNG AND TIPPING BUCKET RAIN GAUGES **c47**
Julius Goldhirsh and Norman E. Gebo *In* JPL, Proceedings of the 16th NASA Propagation Experimenters Meeting (NAPEX 16) and the Advanced Communications Technology Satellite (ACTS) Propagation Studies Miniworkshop 1 Aug. 1992 p 204-216 (For primary document see N93-26463 09-32)
(Contract N00039-91-C-0001)
Avail: CASI HC A03/MF A03

Rain rates as derived from standard tipping bucket rain gauges have variable integration times corresponding to the interval between bucket tips. For example, the integration time for the Weathertronics rain gauge is given by delta(T) = 15.24/R (min), where R is the rain rate expressed in mm/h and delta(T) is the time between tips expressed in minutes. It is apparent that a rain rate of 1 mm/h has an integration time in excess of 15 minutes. Rain rates larger than 15.24 mm/h will have integration times smaller than 1 minute. The integration time is dictated by the time it takes to fill a small tipping bucket where each tip gives rise to 0.254 mm of rainfall. Hence, a uniform rain rate of 1 mm/h over a 15 minute period will give rise to the same rain rate as 0 mm/h rainfall over the first 14 minutes and 15 mm/h between 14 to 15 minutes from the reference tip. Hence, the rain intensity fluctuations may not be captured with the tipping bucket rain gauge for highly variable rates encompassing lower and higher values over a given integration time. The objective of this effort is to provide an assessment of the features of the R. M. Young capacitive gauge and to compare these features with those of the standard tipping bucket rain gauge. A number of rain rate-time series derived from measurements with approximately co-located gauges are examined.
Derived from text

N93-26484*# Virginia Polytechnic Inst. and State Univ., Blacksburg. Dept. of Electrical Engineering.
ACTS PROPAGATION TERMINAL UPDATE
Warren L. Stutzman and Tim Pratt *In* JPL, Proceedings of the 16th NASA Propagation Experimenters Meeting (NAPEX 16) and the Advanced Communications Technology Satellite (ACTS) Propagation Studies Miniworkshop 1 Aug. 1992 p 222-229 (For primary document see N93-26463 09-32)
Avail: CASI HC A02/MF A03

The activities at Virginia Polytechnic Institute and State University in preparation for the February 1993 launch of ACTS are summarized. ACTS propagation terminals (APT) are being constructed to receive the 20 and 27.5 GHz ACTS beacon signals. Total power radiometers operating at the same frequencies are integrated into the terminal for use in level setting. Recent progress and plans for APT's are reported. Author (revised)

N93-26485*# Jet Propulsion Lab., California Inst. of Tech., Pasadena.
RAIN COMPENSATION ALGORITHM USING ADAPTIVE LINEAR PREDICTION
Edgar Satorius *In its* Proceedings of the 16th NASA Propagation Experimenters Meeting (NAPEX 16) and the Advanced Communications Technology Satellite (ACTS) Propagation Studies Miniworkshop 1 Aug. 1992 p 230-234 (For primary document see N93-26463 09-32)
Avail: CASI HC A01/MF A03

Rain compensation algorithm using adaptive linear prediction is presented in viewgraph form. Topics covered include AMT scenario, summary of AMT-RCA, empirical basis for reducing attenuation extrapolation errors, and candidate adaptive 1-pole prediction filter for application to AMT-RCA (at the mobile terminal (MT)). CASI

N93-26486*# California Univ., San Diego, La Jolla. Dept. of Electrical and Computer Engineering.
MORE RAIN COMPENSATION RESULTS
D. D. Sworder and R. Vojak *In* JPL, Proceedings of the 16th NASA Propagation Experimenters Meeting (NAPEX 16) and the Advanced Communications Technology Satellite (ACTS) Propagation Studies Miniworkshop 1 Aug. 1992 p 235-244 (For primary document see N93-26463 09-32)
Avail: CASI HC A02/MF A03

To reduce the impact of rain-induced attenuation in the 20/30 GHz band, the attenuation at a specified signal frequency must be estimated and extrapolated forward in time on the basis of a noisy beacon measurement. Several studies have used model based procedures for solving this problem in statistical inference. Perhaps the most widely used model-based paradigm leads to the Kalman filter and its lineal variants. In this formulation, the dynamic features of the attenuation are represented by a state process (x(sub t)). The observation process (y(sub t)) is derived from beacon measurements. Some ideas relating to the signal processing problems related to uplink power control are presented. It is shown that some easily implemented algorithms hold promise for use in estimating rain induced fades. The algorithms were applied to actual data generated at the Virginia Polytechnic Institute and State University (VPI) test facility. Because only one such event was studied, it is not clear that the algorithms will have the same effectiveness when a wide range of events are studied. Derived from text

N93-26490# Harvard Univ., Cambridge, MA. Dept. of Psychology.
PERCEPTION AND THE TEMPORAL PROPERTIES OF SPEECH Final Report, Jul. 1989 - Jul. 1992
Peter C. Gordon 11 Jan. 1993 42 p
(Grant AF-AFOSR-0461-89)
(AD-A261439; AFOSR-93-0042TR) Avail: CASI HC A03/MF A01

This research examines the interaction of acoustic and lexical information in the identification of words in lexically ambiguous phoneme sequences. In Experiment 1, subjects show priming for the meaning of a large word like tulips when presented with a sequence of combinable short words like two lips. In Experiment 2 priming is found for the meaning of the second short word in similar sequences (e.g., lips in two lips). Finally, Experiment 3 demonstrates that listeners do not show priming for a short word like lips when it is pronounced as part of a larger word like tulips. The results of these experiments show that listeners sometimes access words other than those intended by speakers, and that they may simultaneously access words associated with several alternative parses of ambiguous sequences. Furthermore, they suggest that acoustic marking of word onsets places constraints on the success of lexical access. To account for these results, we present a new model of lexical access and segmentation, the Good Start model, which gives a principled account of these properties. DTIC

N93-26541# Army Engineer Waterways Experiment Station, Vicksburg, MS. Geotechnical Lab.
PROCEEDINGS OF THE GOVERNMENT USERS WORKSHOP ON GROUND PENETRATING RADAR APPLICATIONS AND EQUIPMENT Final Report
Dwain K. Butler Dec. 1992 97 p Workshop held in Vicksburg, MS, 26-27 Mar. 1992
(AD-A261873; WES/MP/GL-92-40) Avail: CASI HC A05/MF A02

The first Government Users Workshop on Ground Penetration Radar (GPR) Applications and Equipment attracted 60 attendees from 17 government agencies/offices and private industry. Presentations emphasized the wide variety of applications of GPR and current and emerging technology in GPR equipment. The workshop included field demonstrations at the Waterways Experiment Station Environmental Geophysics Training Facility. A concluding panel discussion summarized the highlights of the workshop and discussed research and development needs and requirements. DTIC

N93-26573# Air Force Inst. of Tech., Wright-Patterson AFB, OH.
PROPERTIES OF READINGS OF PERIODICALLY CORRELATED RANDOM PROCESSES
Ya P. Dragan 27 Jan. 1993 9 p Transl. into ENGLISH from Orbor i Peredacha Informatsii (USSR), no. 33, 1972 p 7-12
(AD-A261225; FASTC-ID(RS)T-0561-92) Avail: CASI HC A02/MF A01

Periodically correlated random processes, which serve as models for natural rhythmic phenomena, are a generalization of amplitude modulation. It is noted in work that the operation of modulation is not invariant, since the phase of the carrier introduces a specific time structure, but it is invariant in the case of carriers which are multiples of the period of the carriers. Therefore there is interest in the investigation of the properties of readings of a periodically correlated random process (PKSP) in points which are multiples of the period of the correlated state. DTIC

N93-26603# Naval Postgraduate School, Monterey, CA.
GEOLOCATION OF AN ELECTROMAGNETIC EMITTER USING A CYCLOSTATIONARY TIME DIFFERENCE OF ARRIVAL TECHNIQUE M.S. Thesis
Timothy A. Benson 17 Dec. 1992 88 p
(AD-A261781) Avail: CASI HC A05/MF A01

Many applications of signal processing require that the location of an electromagnetic emitter be determined. An algorithm is used to geolocate such an emitter. Special features of the algorithm not only allow the detection of cyclostationary signals in strong negative signal to noise ratio environments, but also discriminate against unwanted signals not of interest that may either occupy the same frequency band or have similar signal characteristics as the signal of interest. This is accomplished by determining spectral correlation densities for cycle frequencies equal to various exploitable features of the binary phase shift keying (bpsk) direct sequence spread spectrum signal. DTIC

N93-26604# Naval Postgraduate School, Monterey, CA.
A COMPARISON OF IONOSPHERIC PROPAGATION MODE DELAY PREDICTIONS FROM ADVANCED PROPHET 4.3 WITH MEASURED DATA M.S. Thesis
Jose L. Nadal 15 Dec. 1992 63 p
(AD-A261782) Avail: CASI HC A04/MF A01

The outputs of the ionospheric propagation prediction model ADVANCED PROPHET 4.3 are compared to measurements of propagation mode delay for a high frequency communications link between Monterey and San Diego, California. Mode delay variations throughout the day are presented for experimental data and PROPHET predictions. A margin of error of less than 0.5 msec was considered acceptable and the number of acceptable predictions per day was generated. Acceptable predicted data collected over the test period was analyzed to establish which hours of the day PROPHET accurately predicts propagation mode delay, independent of frequency, date, and power levels. During the first six hours of the day PROPHET data tracks experimental data for mode delay change patterns. On a daily basis, predictions are best between 1400 and 1700 GMT (0600 and 0900 local time), although patterns could not be established for other hours of the day. Predicted mode delay percentage distributions show greater correlation during the first three hours of the morning and at sunset. DTIC

N93-24893# Politecnico di Torino (Italy). Dipt. di Elettronica.
FRACTAL DETERMINATION OF PARAMETERS IN LIGHTNING AND ESD MODEL
Giuseppe Vecchi, D. Labate, and F. Canavero *In* FAA, The 1992 International Aerospace and Ground Conference on Lightning and Static Electricity: Addendum Nov. 1992 9 p (For primary document see N93-24875 09-47)
(Grant EEC-SC1-CT91-0690)
Avail: CASI HC A02/MF A03

N93-24999# TimeTech G.m.b.H., Stuttgart (Germany).
A NEW MODEM FOR MICROWAVE TIME SYNCHRONISATION VIA GEOSYNCHRONOUS TELECOMMUNICATION SATELLITES
Michael Dienert *In* ESA, Frequency and Time Forum Jun. 1992 p 143-147 (For primary document see N93-24978 09-70)
Copyright Avail: CASI HC A01/MF A04

N93-25061# Nippon Telegraph and Telephone Public Corp., Yokosuka (Japan). Transmission Systems Labs.
TIMING AND TIME SIGNAL DISTRIBUTION IN DIGITAL COMMUNICATIONS NETWORKS
Masami Kihara and Atushi Imaoka *In* ESA, Frequency and Time Forum Jun. 1992 p 489-492 (For primary document see N93-24978 09-70)
Copyright Avail: CASI HC A01/MF A04

N93-25062# American Telephone and Telegraph Co., Bedminster, NJ.
TIMING A NATIONAL TELECOMMUNICATIONS NETWORK USING GPS
E. W. Butterline, J. E. Abate (Bell Telephone Labs., Inc., Holmdel, NJ.), and G. P. Zampetti *In* ESA, Frequency and Time Forum Jun. 1992 p 493-496 (For primary document see N93-24978 09-70)
Copyright Avail: CASI HC A01/MF A04

N93-25063# Telecom Solutions Europe Ltd., Leatherhead (England).
STRATEGIES FOR SYNCHRONISATION IN AN EVOLVING TELECOMMUNICATIONS NETWORK
Rob Avery (Telecom Solutions Ltd., San Jose, CA.) *In* ESA, Frequency and Time Forum Jun. 1992 p 497-501 (For primary document see N93-24978 09-70)
Copyright Avail: CASI HC A01/MF A04

N93-25064# Telecom Solutions Ltd., San Jose, CA.
SYNOPSIS OF TIMING MEASUREMENT TECHNIQUES USED IN TELECOMMUNICATIONS
G. P. Zampetti *In* ESA, Frequency and Time Forum Jun. 1992 p 503-507 (For primary document see N93-24978 09-70)
Copyright Avail: CASI HC A01/MF A04

N93-25069# National Physical Lab., Teddington (England).
PROGRESS TOWARDS LABORATORY FREQUENCY STANDARDS FOR THE OPTICAL COMMUNICATION BANDS
D. J. E. Knight, K. I. Pharaoh, S. L. T. Drysdale, J. Meldau (Strathclyde Univ., Glasgow, Scotland.), G. Duxbury (Strathclyde Univ., Glasgow, Scotland.), and C. J. Hodges (Cambridge Univ., England.) *In* ESA, Frequency and Time Forum Jun. 1992 p 531-536 (For primary document see N93-24978 09-70)
Copyright Avail: CASI HC A02/MF A04

33 ELECTRONICS AND ELECTRICAL ENGINEERING

Includes test equipment and maintainability; components, e.g., tunnel diodes and transistors; microminiaturization; and integrated circuitry.

For related information see also *60 Computer Operations and Hardware* and *76 Solid-State Physics.*

N93-24746*# National Aeronautics and Space Administration. Lewis Research Center, Cleveland, OH.
RADIATION AND TEMPERATURE EFFECTS ON ELECTRONIC COMPONENTS INVESTIGATED UNDER THE CSTI HIGH CAPACITY POWER PROJECT
Gene E. Schwarze, Janis M. Niedra (Sverdrup Technology, Inc., Brook Park, OH.), Albert J. Frasca (Wittenberg Univ., Springfield, OH.), and William R. Wieserman (Pittsburgh Univ., Johnstown, PA.) Jan. 1993 15 p Presented at the 10th Symposium on Space Nuclear Power and Propulsion, Albuquerque, NM, 10-14 Jan. 1993; sponsored by New Mexico Univ.
(RTOP 467-01-21)
(NASA-TM-106096; E-7737; NAS 1.15:106096) Avail: CASI HC A03/MF A01

The effects of nuclear radiation and high temperature environments must be fully known and understood for the electronic components and materials used in both the Power Conditioning and Control subsystem and the reactor Instrumentation and Control subsystem of future high capacity nuclear space power systems. This knowledge is required by the designer of these subsystems in order to develop highly reliable, long-life power systems for future NASA missions. A review and summary of the experimental results obtained for the electronic components and materials investigated under the power management element of the Civilian Space Technology Initiative (CSTI) high capacity power project are presented: (1) neutron, gamma ray, and temperature effects on power semiconductor switches, (2) temperature and frequency effects on soft magnetic materials; and (3) temperature effects on rare earth permanent magnets. Author (revised)

N93-24951# National Inst. for Fusion Science, Nagoya (Japan).
R AND D OF TRANSMISSION LINES FOR ECH SYSTEM
K. Ohkubo, M. Hosokawa, S. Kubo, M. Sato, Y. Takita, and T. Kuroda Feb. 1993 21 p Submitted for publication
(NIFS-210) Avail: CASI HC A03/MF A01

The performance of oversized transmission elements for millimeter waves is measured and compared with the calculation which is based on the superposition of plane wave (SPW) and on Fresnel approximation in the Huygens-Kirchhoff integral. Mode conversion in the split waveguide is discussed from the viewpoint of on- and off-axes, and 90-degree elbow bend on phase correction is examined by using the SPW method. The design and experiment on the whispering gallery mode generator are described. A preliminary analysis of the rectangular wave guide with two corrugated plates and two plane walls is also carried out to obtain the Gaussian beam with a waist size of x-axis different from that of y-axis.
Derived from text

N93-24964# Brookhaven National Lab., Upton, NY. Dept. of Applied Science.
CHARACTERIZATION OF ELECTROCHEMICAL SYSTEMS AND BATTERIES: MATERIALS AND SYSTEMS
James McBreen 1992 12 p Presented at the DOE Battery Workshop, Argonne, IL, 16-17 Jun. 1992
(Contracts DE-AC02-76CH-00016; DE-FG05-89ER-45384)
(DE93-003472; BNL-48039; CONF-9206311-1) Avail: CASI HC A03/MF A01

Materials are a pacing problem in battery development. The battery environment, particularly in rechargeable batteries, places great demands on materials. Characterization of battery materials is difficult because of their complex nature. In many cases meaningful characterization requires in situ methods. Fortunately, several new electrochemical and spectroscopic techniques for in situ characterization studies have recently become available, and reports of new techniques have become more frequent. The opportunity now exists to utilize advanced instrumentation to define detailed features, participating chemical species, and interfacial structure of battery materials with a precision heretofore not possible. This overview gives key references to these techniques and discusses the application of x-ray absorption spectroscopy to the study of battery materials. DOE

N93-25113# Colorado State Univ., Fort Collins. Dept. of Physics.
PRESSURE DEPENDENCE OF CONDUCTIVITY
B. L. Bracewell and H. D. Hochheimer 1993 36 p Prepared for Los Alamos National Lab., NM
(Contract W-7405-eng-36)
(DE93-008466; LA-Sub-93-47) Avail: CASI HC A03/MF A01

The overall objectives of this work were to attempt the following: (1) Measure the pressure dependence of the electrical conductivity of several quasi-one-dimensional, charge-density-wave solids, including measurements along various crystal directions. (2) Measure photocurrents in selected MX solids at ambient and elevated pressures. (3) Measure the resonance Raman spectra for selected MX solids as a function of pressure. DOE

N93-25212 Department of the Navy, Washington, DC.
LIQUID FILLED VARIABLE CAPACITOR Patent
Ronald J. Gripshover, inventor (to Navy) and David B. Fenneman, inventor (to Navy) 10 Nov. 1992 5 p Filed 30 Mar. 1982
(AD-D015639; US-Patent-5,162,972; US-Patent-Appl-SN-363691) Avail: US Patent and Trademark Office

A liquid filled variable capacitor or PFL which provides variable frequency, impedance, and pulse length without changing the capacitor or PFL hardware is described. The capacitor is constructed from two or more conducting surfaces. A dielectric fluid mixture separates the conductors. A fluid supply system furnishes the dielectric fluid mixture to the conductors and provides for varying of the dielectric constant of the fluid and thus the capacitor operating characteristics, by varying the mixture composition. The fluid supply system has a mixing tank connected to both a supply of high dielectric constant fluid and a supply of low dielectric constant fluid. The high dielectric constant fluid and low dielectric constant fluid are mixed proportionally to obtain a dielectric fluid having the desired dielectric constant. A pump conveys the dielectric fluid between the mixing tank and the conductors while a heat exchanger controls the temperature of the dielectric fluid. DTIC

N93-25282 Purdue Univ., West Lafayette, IN.
NEW GROUND STATES IN UNCONVENTIONAL SUPERCONDUCTORS Ph.D. Thesis
Mario Palumbo 1992 129 p
Avail: Univ. Microfilms Order No. DA9301358

The properties of unconventional superconductors have recently been the subject of much theoretical inquiry, since both the high-T(sub c) and heavy fermion superconductors may have unconventional order parameters. The term unconventional refers to order parameters having a lower degree of symmetry than the normal state lattice. Such systems may therefore break rotational, time reversal, and translational symmetry, leading to a variety of novel effects. This thesis is devoted to the detailed analysis of one such effect. In particular, we show how an unconventional superconductor, in zero applied field, can be subject to a 'magnetic' instability, yielding a new ground state which breaks both translational and time reversal symmetry. From our analytic calculations we will make predictions about the form of the new ground state and the qualitative features of the H - T phase diagram. We continue our consideration of this system by performing global minimizations of the Ginzburg-Landau functional via the method of simulated annealing. This technique allows us to study the detailed form of the order parameter and magnetic field both with and without an applied field. We will present the results of these minimizations, and discuss to what degree they support out analytic work. Finally, we will present the results of microscopic calculations of the Ginzburg-Landau parameters using the weak coupling quasi-classical theory, including the effects of impurity scattering. The results of these calculations will be discussed in conjunction with the physical feasibility of our instability conditions. Dissert. Abstr.

N93-25313# Los Alamos National Lab., NM.
POLY-COIL DESIGN FOR A 60 TESLA QUASI-STATIONARY MAGNET
H. J. Boenig, L. J. Campbell, M. L. Hodgdon, E. A. Lopez, D. G. Rickel, J. D. Rogers, J. B. Schillig, J. R. Sims, P. Pernambuco-Wise, and H. J. Schneider-Muntau et al 1993 9 p Presented at the 6th International Conference on Megagauss Magnetic Field Generation and Related Topics, Albuquerque, NM, 9-12 Nov. 1992
(Contract W-7405-eng-36)
(DE93-007353; LA-UR-93-0047; CONF-921133-15) Avail: CASI HC A02/MF A01

Among the new facilities to be offered by the National Science Foundation through the National High Magnetic Field Laboratory (NHMFL) are pulsed fields that can only be achieved at a national user facility by virtue of their strength, duration, and volume. In particular, a 44 mm bore pulsed magnet giving a 60 tesla field for 100 ms is in the final design stage. This magnet will be powered by a 1.4 GW motor-generator at Los Alamos and is an important step toward proving design principles that will be needed for the higher field quasi-stationary pulsed magnets that this power source is capable of driving. DOE

N93-25365# California Univ., Berkeley. Lawrence Berkeley Lab.
THE SUB 60 ps TIMING RESOLUTION USING LARGE AREA SILICON AVALANCHE DIODES
A. Hauger, A. Hirsch, N. Porile, R. Scharenberg, B. C. Stringfellow, M. Tincknell (Purdue Univ., West Lafayette, IN.), and G. Rai Oct. 1992 4 p Presented at the IEEE Nuclear Science Symposium, Orlando, Fl, 26-31 Oct. 1992
(Contract DE-AC03-76SF-00098)
(DE93-007723; LBL-32289; CONF-921005-25) Avail: CASI HC A01/MF A01

The new generation of planned experiments in high energy and nuclear physics requires high pixel density time-of-flight detection systems which mark the occurrence of an event with sub-100 ps accuracy. Conventional fast phototubes and scintillators do not easily lend themselves to large scale mechanical and electrical integration and generally prove to be very expensive. As an alternative technology, we report on the development and optimization of Silicon Avalanche Diodes (AVD's). The project is in part strongly motivated by the STAR experiment planned for the Relativistic Heavy Ion Collider (RHIC) facility at BNL. The time-of-flight component of STAR is expected to operate in a 0.5T magnetic field and is highly segmented. DOE

N93-25377# Oak Ridge National Lab., TN.
RADIATION-HARDENED CONTROL SYSTEM
R. I. Vandermolen, S. F. Smith, and M. S. Emery 1993 6 p Presented at the 5th Topical Meeting on Robotics and Remote Systems, Knoxville, TN, 26-29 Apr. 1993
(Contract DE-AC05-84OR-21400)
(DE93-007248; CONF-930403-16) Avail: CASI HC A02/MF A01

A radiation-hardened bit-slice control system with associated input/output circuits was developed to prove that programmable circuits could be constructed to successfully implement intelligent functions in a highly radioactive environment. The goal for this effort was to design and test a programmable control system that could withstand a minimum total dose of 10(exp 7) rads gamma. The Radiation Hardened Control System (RHCS) was tested in operation at a dose rate that ranged up to 135 krad/h, with an average total dose of 10.75 Mrads. Further testing beyond the required 10(exp 7) rads was also conducted. RHCS performed properly through the target dose of 10(exp 7) rads, and sporadic intermittent failures in some programmable logic devices were noted after approximately 13 Mrads. DOE

N93-25392 Stanford Univ., CA.
ULTRAFAST MEASUREMENTS OF 200 GIGAHERTZ SCHOTTKY PHOTODIODES Ph.D. Thesis
Kathryn LiDessau 1992 139 p
Avail: Univ. Microfilms Order No. DA9302241

Photodetectors play a fundamental role in optical communication and measurement systems. In communications systems, faster detectors could enhance system bandwidths, increasing information transmission capacity. In measurement systems, high-speed photodetectors could measure picosecond optical waveforms from mode-locked lasers, and optical and optoelectronic devices. To date, the fastest reported Schottky photodiodes achieve bandwidths around 100 GHz. Because presently available oscilloscopes have bandwidths up to only 50 GHz, electro-optic sampling had to be used to measure the response of these photodetectors. The speed of the actual devices was indirectly determined by a deconvolution of the system response from the measured data. To overcome this measurement limitation, we have devised two new circuits which allow high-speed photodiodes to be used to measure laser pulses without using expensive sampling oscilloscopes or complex laser systems. The first is a high-speed Schottky photodiode monolithically integrated with an electronic sampler. With this circuit we were able to measure an impulse response with a 1.8 ps full-width at half-maximum, corresponding to a 3-dB bandwidth of 200 GHz. No deconvolution was required. The second circuit is a high-speed photodiode monolithically integrated with a microwave detector. By using this circuit to replace the nonlinear crystal in autocorrelation and cross-correlation setups, we were able to measure laser pulse durations with a temporal resolution of 1.4 ps. The main advantages that this second photodiode optoelectronic circuit has over the nonlinear crystal are that it is not wavelength specific and that it is sensitive to very low input optical powers. In addition in this thesis, electro-optic sampling measurements of a greater than 220 GHz GaAs Schottky photodiode are presented. Dissert. Abstr.

N93-25397# Lawrence Livermore National Lab., CA.
BBU CODE DEVELOPMENT FOR HIGH-POWER MICROWAVE GENERATORS
T. L. Houck, G. A. Westenskow, and S. S. Yu (California Univ., Berkeley. Lawrence Berkeley Lab.) Aug. 1992 5 p Presented at the 16th International LINAC Conference, Ottawa, Ontario, 23-28 Aug. 1992
(Contract W-7405-eng-48)
(DE93-007111; UCRL-JC-110197; CONF-9208109-75) Avail: CASI HC A01/MF A01

We are developing a two-dimensional, time-dependent computer code for the simulation of transverse instabilities in support of relativistic klystron-two beam accelerator research at LLNL. The code addresses transient effects as well as both cumulative and regenerative beam breakup modes. Although designed specifically for the transport of high current (kA) beams through traveling-wave structures, it is applicable to devices consisting of multiple combinations of standing-wave, traveling-wave, and induction accelerator structures. In this paper we compare code simulations to analytical solutions for the case where there is no RF coupling between

cavities, to theoretical scaling parameters for coupled cavity structures, and to experimental data involving beam breakup in the two traveling-wave output structure of our microwave generator. DOE

N93-25416# Sandia National Labs., Albuquerque, NM.
A COMPARISON OF MOISTURE RESISTANCE WITH DIFFERENT TYPES OF END-TERMINATIONS IN CERAMIC CAPACITORS
R. A. Brooks (Allied-Signal Aerospace Co., Kansas City, MO.), C. A. Hall, and G. M. Enke 1992 5 p Presented at the 13th Capacitor and Resistor Technology Symposium: CARTS 1993, Costa Mesa, CA, 8-11 Mar. 1993
(Contract DE-AC04-76DP-00789)
(DE93-007600; SAND-92-2103C; CONF-930394-2) Avail: CASI HC A01/MF A01

Failures (shorts) were observed in MIL-C-20 like, molded-case, radial-leaded, ceramic capacitors after a low-voltage, 85 percent -relative-humidity, 85 C test was performed. Case removal revealed silver whisker growth on the chips between the non-coated solder area of the end-terminations where the radial leads extend from the chip. Insulation-resistance failures were observed in MIL-C-123 like, molded-case, radial-leaded, ceramic capacitors after moisture resistance, normal voltage testing (MIL STD 202 Method 106) was performed. In the case of the MIL-C-123 capacitors, no silver migration was observed. Three lots of molded-case, radial-leaded, MIL-C-123 capacitors with experimental end-terminations, were fabricated by KEMET Electronics Corporation, Greenville, South Carolina from a single chip lot. Three control lots with standard silver end-terminations were also fabricated. Each of the control lots was processed with each of the experimental lots through the subsequent processing and testing steps. This paper describes the different end-terminations and testing and evaluation of these three experimental lots and their counterpart control lots. These included a 4,000-hour, 85 percent-relative humidity, 85 C test and multiple cycles of moisture, normal voltage (MIL STD 202 Method 106) tests. DOE

N93-25417# Sandia National Labs., Albuquerque, NM.
CHARACTERIZATION OF CERAMIC CAPACITORS FOR HIGH-VOLTAGE PULSE-DISCHARGE APPLICATIONS
C. A. Hall and E. L. Jacobs 1992 8 p Presented at the 13th Capacitor and Resistor Technology Symposium: CARTS 1993, Costa Mesa, CA, 8-11 Mar. 1993
(Contract DE-AC04-76DP-00789)
(DE93-007601; SAND-92-2120C; CONF-930394-3) Avail: CASI HC A02/MF A01

Energy-storage, high-current, pulse discharge capacitors have been of interest for some time in applications such as weapon firing sets, trigger circuits, and laser power sources. For high reliability and temperature stability reasons, these capacitors have typically utilized Mylar or mica-paper dielectrics for high-voltage applications in the 2 to 6-kV range with peak currents greater than 5 kA and rise times less than 100 ns. Because of their volumetric efficiency some multilayer ceramic (MLC) capacitors have been used for trigger applications to approximately 750 volts with 2 kA peak current and pulse widths of approximately 1.5 microns. More recently, MLC capacitors have been developed for output filters of switchmode, high-voltage power supplies. Dielectric materials and capacitor designs from several manufacturers have been characterized to explore higher voltage applications of MLC capacitors. This characterization includes high-current, pulse discharge mode testing at voltages up to 3.5 kV. This allows their applicability and reliability for the above applications to be assessed. Results of pulse discharge testing, employing a low inductance circuit, with typically 4 kA peak current and 200 ns pulse width, are reported. The usefulness and reliability of larger MLC capacitor values were explored for pulse widths up to 50 microns at typical peak currents of 700 A. Standard capacitor parameters for the various dielectrics also reported. Discharge life testing at varying temperatures and D.C. breakdown testing is used to provide initial estimates of reliability. Finally, MLC capacitor results are compared with a new relatively efficient dual dielectric (film/paper) design. DOE

N93-25429# Sandia National Labs., Albuquerque, NM.
DETECTING DAMAGED CABLES USING A PREIONIZED GAS TECHNIQUE
R. A. Vigil (Science and Engineering Associates, Inc., Albuquerque, NM.), M. J. Jacobus, and C. F. Nelson 1992 8 p The EPRI Workshop on Power Plant Cable Condition Monitoring held in San Francisco, CA, 9-11 Feb. 1993
(Contract DE-AC04-76DP-00789)
(DE93-007588; SAND-92-2917C; CONF-930254-2) Avail: CASI HC A02/MF A01

Because of the difficulty in conducting electrical tests on unshielded cables installed in conduits, experiments were conducted to develop a preionized gas condition monitoring technique to detect localized degradation of installed, unshielded cables in conduits. Breakdown testing of various types of damaged and undamaged cables was performed. Other test parameters examined were gas type, position of tie cable with respect to the conduit wall, length of cables, conduit configuration, conduit size, gas propagation in conduits, and other parameters necessary for practical implementation of the technique. The principal conclusion of the test program is that high potential testing of cables in the presence of preionized helium gas provides essentially the same information as high potential testing in water. Using helium requires no greater effort and eliminates the practical disadvantage of using water. A test criterion of 30 kVDC or 10 kVAC would detect when 5 mils of insulation remain on one particular tested cable. No undamaged cable was noted to break down at these voltages. A high concentration of helium is required to achieve these results, but this is easily attained. AC testing appears preferable to DC testing because of the variability testing. However, DC testing may warrant further investigation because of its inherent advantages. The level of damage that a cable can incur without compromising its functionality in an accident environment has not yet been determined and is a subject of ongoing research. DOE

N93-25491# Superconducting Super Collider Lab., Dallas, TX.
STUDIES OF AVALANCHE PHOTODIODES FOR SCINTILLATING FIBRE TRACKING READOUT
H. Fenker and J. Thomas Jan. 1993 12 p
(Contract DE-AC35-89ER-40486)
(DE93-008370; SSCL-611) Avail: CASI HC A03/MF A01

Avalanche Photodiodes (APDs) operating in 'Geiger Mode' have been studied in a fibre tracking readout environment. A fast recharge circuit has been developed for high rate data taking, and results obtained from a model fibre tracker in the test beam at Brookhaven National Laboratory are presented. A high rate calibrated light source has been developed using a commercially available laser diode and has been used to measure the efficiency of the devices. The transmission of the light from a 1mm fibre onto a 0.5mm diameter APD surface has been identified as the main problem in the use of these particular devices for scintillating fibre tracking in the Superconducting Supercollider environment. Solutions to this problem are proposed. DOE

N93-25618*# National Aeronautics and Space Administration. Goddard Space Flight Center, Greenbelt, MD.
WALSH FUNCTION GENERATOR FOR THE ELECTRONICALLY SCANNED THINNED ARRAY RADIOMETER (ESTAR) INSTRUMENT
William A. Chren, Jr. Washington Apr. 1993 17 p
(RTOP 740-00-00)
(NASA-TM-4449; NAS 1.15:4449; Rept-93B00030) Avail: CASI HC A03/MF A01

A prototype Walsh Function Generator (WFG) for the ESTAR (Electronically Scanned Thinned Array Radiometer) instrument has been designed and tested. Implemented in a single Xilinx XC3020PC68-50 Field Programmable Gate Array (FPGA), it generates a user-programmable set of 32 consecutive Walsh Functions for noise cancellation in the analog circuitry of the Front-End Modules (FEM's). It is implemented in a 68-pin plastic leaded chip carrier (PLCC) package, is fully testable, and can be used for noise cancellation periods as small as 2 msec. Author

N93-25619 Princeton Univ., NJ.
TUNED CIRCUIT ELECTRIC LEVITATION BEARINGS FOR MICROACTUATORS Ph.D. Thesis
Suresh Kumar 1992 197 p
Avail: Univ. Microfilms Order No. DA9235260

Micromachined sensors, actuators, and systems have recently come into their own as an exciting field with the promise of revolutionary applications in many diverse areas. At present, the ability of the micromotors

to reach their full potential is hindered by the presence of large friction forces that play a dominant role in the dynamic behavior. A novel design for substantially reducing or eliminating this friction by using tuned circuit electric levitation (TCEL) is examined in this thesis. This design utilizes a resonant circuit driven by a radio frequency AC voltage source for achieving stable levitation. The main advantages of TCEL are stable levitation without requiring a feedback sensor and the ability to produce torque and motion using identical components of an existing micromotor design. This thesis analyzes the dynamics of electrically levitated systems, and derives stability conditions for such systems. TCEL is shown to be statically stable if the frequency of the source is greater than the natural frequency of the resonant circuit at equilibrium. The analysis shows that some electrically levitated systems can exhibit dynamic instability, but most of the practical designs are stable. The analysis also reveals that four independent tuned circuits can be used to stabilize a freely levitated object in all six degrees of freedom. An experimental demonstration of the stability of a TCEL system is also presented in this thesis. A small flat plate is levitated using four tuned circuits, and its stability is confirmed by photographing the gap between the suspended plate and the stator seen through a microscope. In addition, measurements of the plate position and orientation are presented, which are in good agreement with the theory. An experimental actuator utilizing the electric levitation is also presented. The tuned circuits are used to provide vertical stability as well as part of the motive force in the experiment, demonstrating the use of TCEL as a microbearing.
Dissert. Abstr.

N93-25660# Palisades Inst. for Research Services, Inc., Arlington, VA.
MICROWAVE AND MILLIMETER WAVE MONOLITHIC INTEGRATED CIRCUITS (MIMIC) PROGRAM. MIMIC BRIEFS: SUMMARIES OF PHASE 3 TECHNOLOGY SUPPORT PROGRAMS Report, Jul. 1990 - Dec. 1992
Warner Kramer Jan. 1993 62 p
(Contract MDA972-89-C-0087)
(AD-A260914; SPC-PIRS-90-C-15) Avail: CASI HC A04/MF A01

This publication contains technical and contractual summaries of the MIMIC program's Phase 3 technology support programs. Each project description includes a discussion of the objectives of the effort, the approach pursued, and recent progress. Also identified are the performing organization(s), principal investigator and/or other key personnel, contract number, program funding and duration, and program monitor/COTR. Concluding the document is a directory of the personnel associated with these projects, from whom more information may be requested. DTIC

N93-25678# California Univ., Los Angeles.
VLSI FOR HIGH-SPEED DIGITAL SIGNAL PROCESSING Quarterly Progress Report, 1 Oct. - 31 Dec. 1992
Alan N. Willson, Jr. 31 Dec. 1992 9 p
(Contract N00014-91-J-1852)
(AD-A260754) Avail: CASI HC A02/MF A01

During the past quarter we have fabricated and tested a 12-bit by 16-bit multiplier based on our previous multiplier architecture but using third order recoding. That is, we use an 8-to-1 multiplexer selected by 3 input bits to form each partial product instead of the 4-to-1 multiplexer selected by 2 input bits as used previously. The partial products (1X, 3X, 5X, and 7X the coefficient value) are stored in an on-chip RAM. DTIC

N93-25782# Texas Univ., Austin. Dept. of Chemical Engineering.
THE 0.3 mm DIAMETER FLEXIBLE AMPEROMETRIC LACTATE PROBE Technical Report, Oct. 1992 - Nov. 1993
Dan L. Wang and Adam Heller 26 Jan. 1993 31 p
(AD-A260826; TR-003) Avail: CASI HC A03/MF A01

A flexible lactate electrode was made of 400 +/- 100 7 micrometers diameter carbon fibers, epoxy embedded in a 0.3 mm diameter polyimide tubing. The electrode was modified by precipitating on it the relatively insoluble complex formed between 1100 kd partially N-ethylamine quaternized poly((vinylpyridine)Os(bipyridine)2Cl)Cl (POs-EA) and lactate oxidase. The steady-state lactate electrooxidation current, at 2mM lactate concentration and at 22 C, was 4OO nA. The 5O +/- 10 microA/sq cm current density and the 2OmA/sq cm/M sensitivity decreased only by 5 percent upon increasing the partial pressure of oxygen from 0.0 to 0.2 atm. The electrode retains its sensitivity after dry storage at 4 C for 4 months in air but loses at 37 C half of its sensitivity in 7 hours through polymer desorption when operated at 0.4V (SCE). DTIC

N93-25820# Spire Corp., Bedford, MA.
MOCVD PROCESS TECHNOLOGY FOR AFFORDABLE, HIGH-YIELD, HIGH-PERFORMANCE MESFET STRUCTURES. PHASE 3: MIMIC Final Report
26 Jan. 1993 51 p
(Contract N00019-89-C-0152)
(AD-A261178; FR-10119) Avail: CASI HC A04/MF A01

Under the MIMIC Program, Spire has pursued improvements in the manufacturing of low cost, high quality gallium arsenide MOCVD wafers for advanced MIMIC FET applications. As a demonstration of such improvements, Spire was tasked to supply MOCVD wafers for comparison to MBE wafers in the fabrication of millimeter and microwave integrated circuits. In this, the final technical report for Spire's two-year MIMIC contract, we report the results of our work. The main objectives of Spire's MIMIC Phase 3 Program, as outlined in the Statement of Work, were as follows: Optimize the MOCVD growth conditions for the best possible electrical and morphological gallium arsenide. Optimization should include substrate and source qualification as well as determination of the optimum reactor growth conditions; Perform all work on 75 millimeter diameter wafers, using a reactor capable of at least three wafers per run; and Evaluate epitaxial layers using electrical, optical, and morphological tests to obtain thickness, carrier concentration, and mobility data across wafers. DTIC

N93-25856# University of Southern California, Marina del Rey. Information Sciences Inst.
A DESIGN OF A FAST AND AREA EFFICIENT MULTI-INPUT MULLER C-ELEMENT Research Report
Tzyh-Yung Wuu and Sarma B. Vrudhula Jan. 1993 15 p
(Contract MDA903-92-D-0020)
(AD-A261002; ISI/RR-93-302) Avail: CASI HC A03/MF A01

A multi-input Muller C-element has frequently been used for joining signal transitions or completion time detection in self-timed circuits. This paper presents an n-input Muller C-element design which uses the multi-level login design technique and has a symmetric format for any integer n greater than 2. In comparison with series-parallel MOS structure implementations and C-element tree implementations, our design has fewer restrictions in terms of n, less path delay, less delay variance from inputs to output, and less area consumption. Experimental validation in this paper is based on an industrial standard cell library. DTIC

N93-25906# Honeywell, Inc., Bloomington, MN. Sensor and Systems Development Center.
MONOLITHIC INTEGRATION OF SEMICONDUCTOR AND SUPERCONDUCTOR COMPONENTS Final Report, 4 Sep. 1990 - 30 Sep. 1992
Paul W. Kruse and Burgess R. Johnson 31 Oct. 1992 126 p
(Contract N00014-90-C-0226; ARPA Order 7534)
(AD-A260589) Avail: CASI HC A07/MF A02

The objective of the contract was to conduct research to integrate semiconductor electronics with infrared sensors, based upon high transition temperature superconducting microbolometers, to make a 16 pixel (4x4) two-dimensional infrared staring array. This technology should enable us to eventually fabricate large area, high performance IR arrays using conventional silicon IC processing technology for cost-effective systems. Deliverables included quarterly reports, this final report, and a 16 pixel (4x4) two-dimensional superconducting microbolometer array including transistor switches at the pixels and drive electronics mounted in a Dewar. All items were delivered. DTIC

N93-25935# Defence Research Establishment, Ottawa (Ontario).
UTILIZATION OF AN ELECTRONIC CIRCUIT SIMULATOR IN CMOS LATCH-UP STUDIES
L. Varga Jun. 1992 42 p
(AD-A260877; DREO-1144) Avail: CASI HC A03/MF A01

The 2-D device simulator presented in this work allows the investigation of the effect of ionizing radiation dose rate on the performance of CMOS circuits. The simulator is composed of two parts, a diffusion current module and a lumped-element module. The first module solves the current transport equations with the aid of the HSPICE code. The lumped-element module then simulates the electrical characteristics of the parasitic pnpn structure (present in CMOS circuits) using the results from the first module as input

parameters. The model was applied to study the latch-up vulnerability of a CMOS inverter as a function of circuit layout and distribution of substrate contacts. Results of radiation hardening efforts are presented. DTIC

N93-26104* National Aeronautics and Space Administration. Goddard Space Flight Center, Greenbelt, MD.
PHASE DISCRIMINATING CAPACITIVE ARRAY SENSOR SYSTEM Patent
John M. Vranish, inventor (to NASA) and Wadi Rahim, inventor (to NASA) 25 May 1993 7 p Filed 28 May 1992
(NASA-Case-GSC-13460-1; US-Patent-5,214,388;
US-Patent-Appl-SN-889577; US-Patent-Class-324-683;
US-Patent-Class-324-662; US-Patent-Class-324-681;
US-Patent-Class-324-690; US-Patent-Class-340-870.37;
Int-Patent-Class-G01R-27/26) Avail: US Patent and Trademark Office

A phase discriminating capacitive sensor array system which provides multiple sensor elements which are maintained at a phase and amplitude based on a frequency reference provided by a single frequency stabilized oscillator. Sensor signals provided by the multiple sensor elements are controlled by multiple phase control units, which correspond to the multiple sensor elements, to adjust the sensor signals from the multiple sensor elements based on the frequency reference. The adjustment made to the sensor signals is indicated by output signals which indicate the proximity of the object. The output signals may also indicate the closing speed of the object based on the rate of change of the adjustment made, and the edges of the object based on a sudden decrease in the adjustment made. Official Gazette of the U.S. Patent and Trademark Office

N93-26142 Department of the Navy, Washington, DC.
CROSS-SWITCHED MICRAD SEEKER Patent
Frederick C. Alpers, inventor (to Navy) and Mervyn C. Hoover, inventor (to Navy) 3 Nov. 1992 13 p Filed 27 Aug. 1984
(AD-D015676; US-Patent-5,160,934; US-Patent-Appl-SN-649501;
US-Patent-Class-342-351) Avail: US Patent and Trademark Office

A MICrowave RADiometric (MICRAD) guidance system is disclosed which utilizes an antenna having four beams. The beams are designated right, left, up, and down. Information from the four beams is monitored essentially 100 percent of the time by passing through appropriate ferrite cross-switching means to four separate receivers. Information from two of the receivers passes through a first multiplexer and feedback gain balancer to provide a target azimuth output, and information from the remaining two receivers passes through a second multiplexer and feedback gain balancer to provide a target elevation output. A local oscillator heterodynes each of the four receivers in common, and a switch driver couples each of the multiplexers to the ferrite cross-switching means and gain balancers for appropriate selection. DTIC

N93-26171# Polytechnic Univ., Farmingdale, NY. Research Inst.
INVESTIGATIONS OF THE TRANSIENT BEHAVIOR OF THE CATHODE FALL REGION IN PLANAR AND HOLLOW CATHODES Final Report, 1 Jul. 1989 - 1 Jul. 1992
B. Cheo and D. Bruno 21 Dec. 1992 61 p
(Grant AF-AFOSR-0433-89)
(AD-A261636; AFOSR-93-0107TR) Avail: CASI HC A04/MF A01

Recently there has been a strong interest in producing negatively charged ion beams such as H-, for space based accelerators. The negative ions are generated in the plasma of an arc or glow discharge. The electrons are separated from the negative ions by a magnetic field. In such an environment, various plasma and discharge instabilities can occur resulting in an undesirable Megahertz noise of broad spectrum in the beam. It has been experimentally shown that the noise could be reduced by using a large ballast resistor in the discharge circuit. However to effectively suppress the noise, the value of the resistance would be prohibitively high. This report describes the design of a possible noise suppression circuit utilizing power transistors in a pulsed discharge. Using power transistors it is possible to obtain high dynamic impedance, but with sufficiently low D.C. resistance to stabilize the instabilities. The noise is present within a Negative Ion Source obtained from Los Alamos National Laboratory (AT division). This report describes the design of a Gate Turnoff Thyristor (GTO) pulsing circuit for the Negative Ion Source which includes the modification of an existing gate drive unit for a low power GTO. The Negative Ion Source had been pulsed by a capacitive bank discharge circuit. This GTO pulsing circuit has been successfully tested on a Hollow Cathode discharge. DTIC

N93-26233 Department of the Navy, Washington, DC.
VARIABLE PULSE RATE CIRCUIT Patent
Edwin E. Westerfield, inventor (to Navy), Larry L. Warnke, inventor (to Navy), and William S. Devereux, inventor (to Navy) 20 Oct. 1992 7 p Filed 28 Jan. 1988
(AD-D015675; US-Patent-5,157,695; US-Patent-Appl-SN-149298;
US-Patent-Class-375-96) Avail: US Patent and Trademark Office

A variable pulse rate circuit for correlating a locally generated code with a code that is being transmitted by a space vehicle is described. A computer means is used for providing a binary word to a latch. The binary word in the latch is used in turn by a delay line, to control the amount of delay that is presented to pulses. The pulses are emitted by a pulse generator having a fixed rate reference. The pulse rate, of pulses being emitted by of the delay line, is varied from the reference pulse rate. This variation is the result of computer means that rapidly changes the amount of delay of the delay line. The pulse rate and the pulse phase are varied in order to cause a locally generated code to become phase aligned with the code received from the space vehicle. The space vehicle is tracked using the variable pulse rate circuit. DTIC

N93-26272# Naval Postgraduate School, Monterey, CA.
INVESTIGATION OF A BACKGROUND SUPPRESSION TRANSIMPEDANCE AMPLIFIER FOR PHOTOVOLTAIC DETECTORS M.S. Thesis
Ferdinand J. Metzger, Jr. Dec. 1992 69 p
(AD-A261828) Avail: CASI HC A04/MF A01

The current generation of transimpedance amplifier based detector systems are limited by opamp saturation when operating at a high gain or in the presence of a large background signal. To eliminate saturation, an amplifier that is frequency dependent is developed. Additionally, the noise sources in the conventional transimpedance amplifier and photovoltaic detector are quantified for comparison to any modified circuit. Initial results indicate that the frequency dependent detector system is a viable system, however, further development is required. Further research of this technology is expected to support future infrared and long range detection applications. DTIC

N93-26299# Army Research Lab., Fort Monmouth, NJ.
MAGNETIC FIELD SOURCE FOR BI-CHAMBERED ELECTRON BEAM DEVICES Technical Report
Anup S. Tilak, Douglas J. Basarab, Herbert A. Leupold, and Ernest Potenziani, II Nov. 1992 20 p
(DA Proj. 1L1-61102-AH-47)
(AD-A261316; SLCET-TR-91-11) Avail: CASI HC A03/MF A01

Certain gyro-type electron beam devices require two tandem coaxial chambers with different uniform axial magnetic fields in their interiors. Therefore, there is a step in the field profile in the vicinity of the junction of the two chambers, which are sometimes of different diameter as well. An electric solenoid is usually employed to furnish such a field but the sources are bulky, cumbersome, and consumptive of energy, and provide only rough approximations to the ideal field profile. This report describes a permanent magnet field source that was designed to provide a constant axial field of 2 kOe in the larger of the two chambers and 0.5 kOe in the smaller. The basic field is provided by two tandem permanent magnet solenoids. The rather broad transition between the field values in the two chambers is considerably narrowed (approximately 50 percent) by the placement of a radially magnetized ring internal to the junction of the two solenoids. The field profile can be made to conform to that specified to within a few percent by addition of two axially magnetized rings. DTIC

N93-26311# Hughes Aircraft Co., Torrance, CA. Electron Dynamics Div.
RF VACUUM MICROELECTRONICS Quarterly Technical Report No. 3, 1 Oct. - 31 Dec. 1992
31 Dec. 1992 14 p
(Contract MDA972-92-C-0034; ARPA Order 8162)
(AD-A261343) Avail: CASI HC A03/MF A01

Findings from the first mask set that influenced the design of the second mask set were as follows: (1) The original size of a chip was

based on experience with semiconductor devices and was too small to dice adequately on the silver substrates; (2) The one micron emitter tips were too small and had fully open gate apertures on only a few samples. As a result, the relative number of one micron pyramids should be much less than 1.5, 2.0 and 2.5 micrometer pyramids. The three larger sizes were, in general, properly formed on all samples; (3) As a result of the large number of arrays on each chip, only a small fraction could be bonded to the header. Furthermore, the bonding pad arrangement made it difficult to run bond wires in certain directions without the wires crossing over an emitter array; (4) Scribe streets were located too near the bond pads and may have resulted in some emitter to gate short circuits; and (5) Dimensional stability of the silver substrates caused some misalignment of the gate metal to the emitter tips resulting in emitters on the edge of an array not being properly formed. DTIC

N93-26334# Rome Lab., Griffiss AFB, NY.
DYNAMIC BEHAVIOR OF HELIX INTERACTION CIRCUITS In-House Report, Oct. 1990 - May 1992
Peter J. Rocci Dec. 1992 39 p
(AD-A261362; RL-TR-92-298) Avail: CASI HC A03/MF A01

The dynamic behavior of a high power traveling wave tube's (TWT) helix interaction circuit was determined while operating in its system environment. The purpose of this effort was to develop a fundamental knowledge base of material interactions under thermal loading, develop an understanding of long-term thermal effects on materials and to develop a relationship to TWT performance and reliability. The interaction circuit for the TWT analyzed consists of a variable pitch tungsten helix, three beryllia support rods spaced at equal 120 degree intervals around the helix, and a stainless steel barrel which encloses the vacuum envelope. A three-dimensional finite element model was constructed that represented the entire interaction circuit (89 helix turns in length). There was a great deal of complexity associated with the development of this model due to the irregular 'T-shaped' cross-section of the support rods and variation in pitch of the helix. Upon completion, the model contained approximately 18,000 elements and 45,000 nodes. DTIC

N93-26366# Stanford Univ., CA. Dept. of Electrical Engineering.
MULTIVARIABLE CONTROL FOR FLEXIBLE IC PROCESSING Final Annual Report, 1 Oct. 1991 - 30 Sep. 1992
Thomas Kailath 30 Nov. 1992 21 p
(Contract F49620-90-C-0014; DARPA Order 7149)
(AD-A261685; AFOSR-93-0108TR) Avail: CASI HC A03/MF A01

The objective of this DARPA research project was to develop real-time control systems using in-situ sensors for semiconductor manufacturing. Our initial application was the development of a temperature control system for Rapid Thermal Processing (RTP) equipment. We developed mathematical models of RTP, analyzed them. identified and validated these models, deduced several control algorithms, and finally applied them to real systems at Stanford University and at Texas Instruments. Also, based on our analysis, we modified the design of the system hardware (lamp array) and also proposed an optimal lamp array design technique. DTIC

N93-26501# Sandia National Labs., Albuquerque, NM.
INTERNAL CURRENT PROBING OF INTEGRATED CIRCUITS USING MAGNETIC FORCE MICROSCOPY
A. N. Campbell, E. I. Cole, Jr., B. A. Dodd, and R. E. Anderson 1992 31 p Presented at the International Reliability Physics Conference, Atlanta, GA, 22-25 Mar. 1993
(Contract DE-AC04-76DP-00789)
(DE93-006752; SAND-92-2067C; CONF-930354-2) Avail: CASI HC A03/MF A01

Magnetic force microscopy (MFM) has been applied to image currents in internal IC conductors. We present a model for the MFM imaging of IC currents, describe MFM signal generation, and demonstrate the ability to analyze current direction and magnitude with a sensitivity of approximately 1 micro-A dc and approximately 1 micro-A ac. Our experimental results are a significant improvement on the 100 mA ac resolution previously reported using an electron beam to detect IC currents. DOE

N93-26539# California Univ., Berkeley. Electronics Research Lab.
JOINT SERVICES ELECTRONICS PROGRAM Annual Progress Report, 1 Mar. 1992 - 28 Feb. 1993
Chenming Hu and Michael A. Lieberman 5 Mar. 1993 58 p
(Contract F49620-90-C-0029)
(AD-A261801; UCB/ERL-90/3) Avail: CASI HC A04/MF A01

The 1992 annual report of research conducted in the Electronics Research Laboratory at University of California at Berkeley under the sponsorship of the Joint Services Electronics Program is presented. The research covers the following project areas: (1) quantum electronic devices: nonlinear optics in compound semiconductors, ultrafast optical techniques, and optical probing of semiconductor devices and interfaces by electro-optic and photo-elastic effects; (2) electronic devices: 0.1 micron BiCMOS devices in sulk and SOI substrates, conductive oxides and ferroelectrics for programmable devices, and insulated-gate GaAs field effect transistors; and (3) neural networks and parallel computation: stochastic neural networks and application to signal processing, learning and generalization by neural networks, reconfigurable analog elements for neural nets, and architectural issues in parallel computation. There is also a section concerning significant accomplishments. Two supplemental reports are included. An appendix of all publications, papers, and presentations forms a second part. It is bound under separate cover. DTIC

N93-26565# Honeywell, Inc., Bloomington, MN. Sensor and System Development Center.
RF VACUUM MICROELECTRONICS Quarterly Technical Report, 1 Oct. - 31 Dec. 1992
A. I. Akinwande, P. Bauhahn, and D. Arch 5 Mar. 1993 15 p
(Contract MDA972-91-C-0030; DARPA Order 8162)
(AD-A261784) Avail: CASI HC A03/MF A01

We summarize our fifth quarter results and discuss plans for the remainder of the baseline program which is to demonstrate a thin film edge emitter triode with 10 micro-A/micrometer emission current density at less than 250V and which can be modulated at 1 GHz for 1 hour. We completed fabrication of the first thin film edge emitter vacuum transistors this quarter. Extensive DC characterization has been carried out. Triode characteristics have been observed on many devices. Low frequency (1 KHz) modulation of the devices has been shown. Parametric testing shows these devices to have the high currents (50 micro-A), high current densities (10 micro-A/mM) and transconductances (1.5 micro-S necessary to achieve 1 GHz operation. High frequency testing is currently underway. DTIC

N93-26598# California Univ., Berkeley. Lawrence Berkeley Lab.
LARGE AREA, LOW CAPACITANCE Si(Li) DETECTORS FOR HIGH RATE X RAY APPLICATIONS
C. S. Rossington, P. M. Fine, and N. W. Madden Oct. 1992 7 p Presented at the Institute of Electrical and Electronic Engineers (IEEE) Nuclear Science Symposium, Orlando, FL, 26-31 Oct. 1992
(Contract DE-AC03-76SF-00098)
(DE93-007661; LBL-32243; CONF-921005-26) Avail: CASI HC A02/MF A01

Large area, single-element Si(Li) detectors have been fabricated using a novel geometry which yields detectors with reduced capacitance and hence reduced noise at short amplifier pulse-processing times. A typical device employing the new geometry with a thickness of 6 mm and an active area of 175 mm 2 has a capacitance of only 0.5 pf, compared to 2.9 pf for a conventional planar device with equivalent dimensions. These new low capacitance detectors, used in conjunction with low capacitance field effect transistors, will result in x-ray spectrometers capable of operating at very high count rates while still maintaining excellent energy resolution. The spectral response of the low capacitance detectors to a wide range of x-ray energies at 80 K is comparable to typical state-of-the-art conventional Si(Li) devices. In addition to their low capacitance, the new devices offer other advantages over conventional detectors. Detector fabrication procedures, I-V and C-V characteristics, noise performance, and spectral response to 2-60 keV x-rays are described. DOE

N93-24881# United Kingdom Atomic Energy Authority, Abingdon (England). Lightning Test and Technology.
EQUIPMENT TESTING WITH DAMPED SINEWAVES BETWEEN 1 AND 50 MHz
C. John Hardwick and R. E. Baldwin *In* FAA, The 1992 International Aerospace and Ground Conference on Lightning and Static Electricity: Addendum Nov. 1992 10 p Sponsored by British Aerospace Aircraft Group; Civil Aviation Authority; Construcciones Aeronauticas S.A.; Dept. of

Trade and Industry; Rolls-Royce Ltd.; Saab-Scania; Short Bros. and Harland Ltd.; and Westland Helicopters Ltd. (For primary document see N93-24875 09-47)
Avail: CASI HC A02/MF A03

N93-24882# Ktech Corp., Lexington Park, MD.
AN INTEGRATED APPROACH TO 300 kV ELECTROSTATIC DISCHARGE APPLICATION DURING COMPONENT TESTING THAT WILL SATISFY MIL-STD-331B APPENDIX F
Monty R. Lehmann, Jack Nial (Naval Surface Warfare Center, Indian Head, MD.), and Mike Whitaker (Naval Air Warfare Center, Patuxent River, MD.) *In* FAA, The 1992 International Aerospace and Ground Conference on Lightning and Static Electricity: Addendum Nov. 1992 7 p (For primary document see N93-24875 09-47)
Avail: CASI HC A02/MF A03

N93-24889*# National Aeronautics and Space Administration. Lewis Research Center, Cleveland, OH.
A SYSTEM TO MEASURE LIGHTNING-INDUCED TRANSIENTS ON SPACECRAFT UMBILICAL LINES
Jeffrey C. Brown, Noel B. Sargent, and Carl J. Wenzler *In* FAA, The 1992 International Aerospace and Ground Conference on Lightning and Static Electricity: Addendum Nov. 1992 8 p (For primary document see N93-24875 09-47)
Avail: CASI HC A02/MF A03

N93-24903# United Kingdom Atomic Energy Authority, Abingdon (England). Lightning Test and Technology.
ALTERNATIVE EQUIPMENT TEST PROCEDURES FOR SIMULTANEOUS CURRENT INJECTION ON MULTIPLE CABLE BUNDLES
C. John Hardwick, Stephen J. Haigh, and R. E. Baldwin *In* FAA, The 1992 International Aerospace and Ground Conference on Lightning and Static Electricity: Addendum Nov. 1992 9 p Sponsored by British Aerospace Aircraft Group; Civil Aviation Authority; Construcciones Aeronauticas S. A.; Dept. of Trade and Industry; Rolls-Royce Ltd.; Saab-Scania; and Short Bros. and Harland Ltd. (For primary document see N93-24875 09-47)
Avail: CASI HC A02/MF A03

N93-24982*# Jet Propulsion Lab., California Inst. of Tech., Pasadena.
MICROWAVE FREQUENCY DISCRIMINATOR WITH A CRYOGENIC SAPPHIRE RESONATOR FOR ULTRA-LOW PHASE NOISE
G. John Dick and David G. Santiago *In* ESA, Frequency and Time Forum Jun. 1992 p 35-39 Sponsored by NASA (For primary document see N93-24978 09-70)
Copyright Avail: CASI HC A01/MF A04

N93-25002# Franche-Comte Univ., Besancon (France). Lab. de Physique et Metrologie des Oscillateurs.
OSCCAR: OSCILLATOR-COMPENSATED WITH A CAPACITANCE ARRAY
W. Daniau and G. Marianneau *In* ESA, Frequency and Time Forum Jun. 1992 p 165-167 (For primary document see N93-24978 09-70)
Copyright Avail: CASI HC A01/MF A04

N93-25003# Franche-Comte Univ., Besancon (France). Lab. de Physique et Metrologie des Oscillateurs.
DESIGN OF A LOW PHASE NOISE UHF OSCILLATOR USING A PARTLY METALLIZED DIELECTRIC RESONATOR
R. E. Elcheikh and M. Olivier *In* ESA, Frequency and Time Forum Jun. 1992 p 169-171 (For primary document see N93-24978 09-70)
Copyright Avail: CASI HC A01/MF A04

N93-25004# Compagnie d'Electronique et de Piezo-Electricite, Argenteuil (France).
MINIATURIZATION AND STABILITY: A NEW GENERATION OF OVENISED OSCILLATORS
J. P. Aubry, G. Wagner, and V. Candelier *In* ESA, Frequency and Time Forum Jun. 1992 p 173-177 (For primary document see N93-24978 09-70)
Copyright Avail: CASI HC A01/MF A04

N93-25010# Tele Quartz Group G.m.b.H., Neckarbischofsheim (Germany).
A STATE-OF-THE-ART CRYSTAL FILTER DESIGN PACKAGE USING WINDOWS 3.0 TECHNIQUES
Markus Frey and Bernd W. Neubig *In* ESA, Frequency and Time Forum Jun. 1992 p 209-216 (For primary document see N93-24978 09-70)
Copyright Avail: CASI HC A02/MF A04

N93-25029# Oulu Univ. (Finland).
USE OF THE TV-SIGNAL IN STABILIZING A LOCAL RUBIDIUM OSCILLATOR
Reijo Kivelae *In* ESA, Frequency and Time Forum Jun. 1992 p 309-313 (For primary document see N93-24978 09-70)
Copyright Avail: CASI HC A01/MF A04

N93-25033# Kayser Threde G.m.b.H., Munich (Germany).
FIRST EXPERIENCE WITH THE ASN-16 GLONASS RECEIVER
B. Eissfeller, N. Balteas, A. Jansche, and V. Liebig *In* ESA, Frequency and Time Forum Jun. 1992 p 329-332 (For primary document see N93-24978 09-70)
Copyright Avail: CASI HC A01/MF A04

N93-25034# Franche-Comte Univ., Besancon (France). Lab. de Physique et Metrologie des Oscillateurs.
STABILITY OF NONLINEAR PHASE MOTION FROM THE STUDY OF OSCILLATOR MAPPINGS
M. Planat *In* ESA, Frequency and Time Forum Jun. 1992 p 333-336 (For primary document see N93-24978 09-70)
Copyright Avail: CASI HC A01/MF A04

N93-25038# Frequency Electronics, Inc., Mitchel AFB, NY.
MICROWAVE SYNTHESIZERS IN SPACE
A. Vulcan and M. Bloch *In* ESA, Frequency and Time Forum Jun. 1992 p 355-359 (For primary document see N93-24978 09-70)
Copyright Avail: CASI HC A01/MF A04

N93-25039# Wall (Peter K.) ElectroAcoustics, Penrith (England).
VERY WIDE BANDWIDTH HF CRYSTAL FILTERS
Peter K. Wall *In* ESA, Frequency and Time Forum Jun. 1992 p 361-364 (For primary document see N93-24978 09-70)
Copyright Avail: CASI HC A01/MF A04

N93-25041# Haut Commissariat a la Recherche, Algiers (Algeria). Lab. de Physique Nucleaire.
A FREQUENCY GENERATING SOURCE: FREQUENCY SYNTHESIZERS
N. Yahyabey and S. Hassani (CDTA, Algiers, Algeria.) *In* ESA, Frequency and Time Forum Jun. 1992 p 369-370 (For primary document see N93-24978 09-70)
Copyright Avail: CASI HC A01/MF A04

N93-25052# Johns Hopkins Univ., Laurel, MD. Applied Physics Lab.
QUARTZ OSCILLATORS, FREQUENCY SYNTHESIZERS, AND TIMING SYSTEMS FOR GEODESY AND RADIO SCIENCE APPLICATIONS
J. J. Suter, J. M. Cloeren, J. R. Norton, and M. J. Reinhart *In* ESA, Frequency and Time Forum Jun. 1992 p 427-429 (For primary document see N93-24978 09-70)
Copyright Avail: CASI HC A01/MF A04

N93-25053# Centre National d'Etudes Spatiales, Toulouse (France).
SPACE RADIATION SUSCEPTIBILITY OF ULTRA STABLE CRYSTAL OSCILLATORS
M. Brunet, J. F. Dutrey, J. B. Laporte, J. Bourriau (Centre d'Etudes et de Recherches, Toulouse, France.), and P. Calvel (Alcatel Espace, Toulouse, France.) *In* ESA, Frequency and Time Forum Jun. 1992 p 431-440 (For primary document see N93-24978 09-70)
Copyright Avail: CASI HC A02/MF A04

N93-25054# Alcatel Bell Telephone, Antwerp (Belgium).
FREQUENCY GENERATION AND SYNTHESIS IN THE DRSS
P. VanLoock and J. DeVlieghere *In* ESA, Frequency and Time Forum Jun. 1992 p 441-444 (For primary document see N93-24978 09-70)
Copyright Avail: CASI HC A01/MF A04

N93-25055# Compagnie d'Electronique et de Piezo-Electricite, Argenteuil (France).
OSCILLATORS FOR MOBILE GPS RECEIVERS
J. P. Aubry, P. Canzian, and V. Candelier *In* ESA, Frequency and Time Forum Jun. 1992 p 445-450 (For primary document see N93-24978 09-70)
Copyright Avail: CASI HC A02/MF A04

N93-25057# SEPA S.p.A., Turin (Italy). Fiat Ciei S.p.A.
HIGH RESOLUTION DIGITAL SYNTHESIZER FOR A Rb FREQUENCY STANDARD
E. Detoma, G. Pedrotto, A. Stern (Time and Frequency Ltd., Holon, Israel.), B. Levi (Time and Frequency Ltd., Holon, Israel.), and M. Bootnik (Time and Frequency Ltd., Holon, Israel.) *In* ESA, Frequency and Time Forum Jun. 1992 p 457-469 (For primary document see N93-24978 09-70)
Copyright Avail: CASI HC A03/MF A04

N93-25066# Observatoire Cantonal, Neuchatel (Switzerland).
LINE INHOMOGENEITY EFFECTS AND POWER SHIFT IN MINIATURIZED RUBIDIUM FREQUENCY STANDARDS
G. Mileti, I. Rueedi, and H. Schweda *In* ESA, Frequency and Time Forum Jun. 1992 p 515-519 Sponsored in part by Swiss Commission for the Encouragement of Research (For primary document see N93-24978 09-70)
(Contract ESTEC-9099/90/NL/US(SC))
Copyright Avail: CASI HC A01/MF A04

N93-25581*# Phillips Lab., Kirtland AFB, NM.
TWO- AND THREE-DIMENSIONAL HIGH PERFORMANCE, PATTERNED OVERLAY MULTI-CHIP MODULE TECHNOLOGY
James Lyke *In* NASA, Washington, Technology 2002: The Third National Technology Transfer Conference and Exposition, Volume 1 Feb. 1993 p 195-204 (For primary document see N93-25561 09-99)
Avail: CASI HC A02/MF A04

N93-25582*# Army Research Lab., Fort Monmouth, NJ. Electronics and Power Sources Directorate.
IMPROVED PERFORMANCE AND SAFETY FOR HIGH ENERGY BATTERIES THROUGH USE OF HAZARD ANTICIPATION AND CAPACITY PREDICTION
Terrill Atwater *In* NASA, Washington, Technology 2002: The Third National Technology Transfer Conference and Exposition, Volume 1 Feb. 1993 p 205-212 (For primary document see N93-25561 09-99)
Avail: CASI HC A02/MF A04

N93-25583*# EIC, Inc., Norwood, MA.
THIN RECHARGEABLE BATTERIES FOR CMOS SRAM MEMORY PROTECTION
Dennis N. Crouse *In* NASA, Washington, Technology 2002: The Third National Technology Transfer Conference and Exposition, Volume 1 Feb. 1993 p 213-218 (For primary document see N93-25561 09-99)
Avail: CASI HC A02/MF A04

N93-25596*# IsoGen Radioisotopic Research Lab., Oregon City, OR.
SOLID-STATE ISOTOPIC POWER SOURCE FOR COMPUTER MEMORY CHIPS
Paul M. Brown *In* NASA, Washington, Technology 2002: The Third National Technology Transfer Conference and Exposition, Volume 1 Feb. 1993 p 335-340 (For primary document see N93-25561 09-99)
Avail: CASI HC A02/MF A04

N93-25598*# Army Research Lab., Fort Monmouth, NJ. Pulse Power Components Branch.
HIGH SPEED SOLID STATE CIRCUIT BREAKER
Thomas F. Podlesak *In* NASA, Washington, Technology 2002: The Third National Technology Transfer Conference and Exposition, Volume 1 Feb. 1993 p 345-352 (For primary document see N93-25561 09-99)
Avail: CASI HC A02/MF A04

N93-25599*# Colorado Univ., Boulder. Dept. of Electrical and Computer Engineering.
VARIABLE-SPEED GENERATORS WITH FLUX WEAKENING
A. A. Fardoun, E. F. Fuchs, and P. W. Carlin (Midwest Research Inst., Golden, CO.) *In* NASA, Washington, Technology 2002: The Third National Technology Transfer Conference and Exposition, Volume 1 Feb. 1993 p 353-362 (For primary document see N93-25561 09-99)
Avail: CASI HC A02/MF A04

N93-26115*# Jet Propulsion Lab., California Inst. of Tech., Pasadena.
NOISE-OPTIMAL CONTROL OF HEMT LNA'S FOR COMPENSATION OF TEMPERATURE DEVIATIONS
C. MacCarley, J. J. Bautista, and P. A. Willis *In its* The Telecommunications and Data Acquisition Report 15 May 1992 p 121-129 (For primary document see N93-26105 09-32)
(RTOP 310-20-66-09-01)
Avail: CASI HC A02/MF A04

34 FLUID MECHANICS AND HEAT TRANSFER

Includes boundary layers; hydrodynamics; fluidics; mass transfer; and ablation cooling.

For related information see also *02 Aerodynamics* and *77 Thermodynamics and Statistical Physics.*

N93-24759*# National Aeronautics and Space Administration. Lewis Research Center, Cleveland, OH.
A THREE-DIMENSIONAL ALGEBRAIC GRID GENERATION SCHEME FOR GAS TURBINE COMBUSTORS WITH INCLINED SLOTS Final Report
S. L. Yang, M. C. Cline (Los Alamos National Lab., NM.), R. Chen, and Y. L. Chang Mar. 1993 25 p
(Grant NAG3-1109; RTOP 537-02-20)
(NASA-CR-191095; E-7674; NAS 1.26:191095) Avail: CASI HC A03/MF A01

A 3D algebraic grid generation scheme is presented for generating the grid points inside gas turbine combustors with inclined slots. The scheme is based on the 2D transfinite interpolation method. Since the scheme is a 2D approach, it is very efficient and can easily be extended to gas turbine combustors with either dilution hole or slot configurations. To demonstrate the feasibility and the usefulness of the technique, a numerical study of the quick-quench/lean-combustion (QQ/LC) zones of a staged turbine combustor is given. Preliminary results illustrate some of the major features of the flow and temperature fields in the QQ/LC zones. Formation of co- and counter-rotating bulk flow and shape temperature fields can be observed clearly, and the resulting patterns are consistent with experimental observations typical of the confined slanted jet-in-cross flow. Numerical solutions show the method to be an efficient and reliable tool for generating computational grids for analyzing gas turbine combustors with slanted slots. Author

N93-24766 Washington Univ., Saint Louis, MO.
COMPUTATION OF HYPERSONIC VISCOUS FLOWFIELDS USING THE PARABOLIZED NAVIER-STOKES EQUATIONS Ph.D. Thesis
Reinhold Alfred Gerbsch 1992 205 p
Avail: Univ. Microfilms Order No. DA9235897

A new, explicit, non-iterative, finite-volume algorithm based on Osher's upwind method is applied to the three-dimensional parabolized Navier-Stokes equations to model hypersonic flowfields. The algorithm includes real-gas effects and turbulence modeling and is second-order accurate. Flux limiters are added to make the scheme total variation diminishing. The streamwise pressure gradient is limited to the subsonic regions to maintain a hyperbolic inviscid equation set. Second-order central-differencing is applied to the viscous terms and upwind differencing is applied to the inviscid terms in both the subsonic and supersonic portions of the flowfield. The new algorithm is validated by computing laminar and turbulent-flow cases in both two and three dimensions. Results are compared with experimental data, analytical solutions and results from other numerical algorithms. Solutions obtained with the new algorithm agree well with other computational techniques and experimental data. The upwind technology results in robust algorithm which exhibits excellent shock capturing and the capability to resolve discontinuities. For the class of flows studied, the different upwind methods yield very similar results. Dissert. Abstr.

N93-24906 Indiana Univ., Bloomington.
A CONVERGENT FINITE DIFFERENCE SCHEME FOR THE NAVIER-STOKES EQUATIONS OF NONISENTROPIC COMPRESSIBLE FLUID FLOW Ph.D. Thesis
Jing Zhao 1992 184 p
Avail: Univ. Microfilms Order No. DA9301485

The main result of this work is an analysis of a finite difference scheme for the Navier-Stokes equations which model nonisentropic, compressible fluid flow in one space dimension. Convergence is proved and error bounds are derived for the scheme. The error is measured in the L(exp 2) norm for u and e; and in the piecewise H(exp 1) norm for v. It is noteworthy that the error bounds dominate sup-norm error bounds for discontinuous variable v. It is shown that the scheme converges at a rate of O(delta x(sup r)) (r less than 1/12) if the initial data is discontinuous, and a O(delta x(sup 1/2)) if the initial data is continuous. Numerical results are also presented in the last part of the dissertation. Dissert. Abstr.

N93-24954# Stanford Univ., CA. Petroleum Research Inst.
ULTRASONIC RATE MEASUREMENT OF MULTIPHASE FLOW
David A. Dannert and Roland N. Horne Jan. 1993 33 p
(Contract DE-FG22-90BC-14600)
(DE93-000112; DOE/BC-14600/38; SUPRI-TR-89) Avail: CASI HC A03/MF A01

One of the most important tools in production logging and well testing is the downhole flowmeter. Unfortunately, existing tools are inaccurate outside of an idealized single phase flow regime. Spinner tools are inaccurate at extremely high or low flow rates and when the flow rate is variable. Radioactive tracer tools have similar inaccuracies and are extremely sensitive to the flow regime. Both tools completely fail in the presence of multiphase flow, whether for gas/oil, gas/water, or fluid/solid. Downhole flowmetering is important for locating producing zones and thief zones and monitoring production and injection rates. The effects of stimulation can also be determined. The goal of this project is the investigation of accurate downhole flowmetering techniques for all single phase flow regimes and multiphase flows. The measurement method investigated in this report is the use of ultrasound. There are two ways to use ultrasound for fluid velocity measurement. The first method, examined in Chapter 2, is the contrapropagation, or transit-time, method which compares travel times with and against fluid flow. Chapter 3 details the second method which measures the Doppler frequency shift of a reflected sound wave in the moving fluid. Both of these technologies need to be incorporated in order to build a true multiphase flowmeter. Chapter 4 describes the proposed downhole multiphase flowmeter. DOE

N93-24963# Clarkson Univ., Potsdam, NY. Dept. of Chemical Engineering.
AN ANALYSIS OF LIFT FORCES ON AEROSOLS IN A WALL BOUNDED TURBULENT SHEAR FLOW
P. Cherukat and J. B. McLaughlin 1992 10 p Presented at the 13th Symposium on Turbulence, Rolla, MO, 22 Sep. 1992
(Contract DE-FG02-88ER-13919)
(DE93-003362; CONF-9209273-1) Avail: CASI HC A02/MF A01

This paper describes work that is expected to lead to a better understanding of the role of lift forces in the deposition of aerosols on the walls bounding a turbulent shear flow. After providing some background information about aerosol trajectories that was obtained from computer simulations, new results for the lift force in the relevant parameter ranges are presented. DOE

N93-24966# Argonne National Lab., Idaho Falls, ID. Fuel Cycle Division.
MINIMIZATION OF HEAT SLAB NODES WITH HIGHER ORDER BOUNDARY CONDITIONS
Charles W. Solbrig 1992 12 p Presented at the Joint American Nuclear Society (ANS)/European Nuclear Society (ENS) International Meeting on Fifty Years of Controlled Nuclear Chain Reaction: Past, Present, and Future, Chicago, IL, 15-20 Nov. 1992
(Contract W-31-109-eng-38)
(DE93-004238; ANL/CP-76463; CONF-921102-48) Avail: CASI HC A03/MF A01

The accuracy of a numerical solution can be limited by the numerical approximation to the boundary conditions rather than the accuracy of the equations which describe the interior. The study presented in this paper compares the results from two different numerical formulations of the convective boundary condition on the face of a heat transfer slab. The standard representation of the boundary condition in a test problem yielded an unacceptable error even when the heat transfer slab was partitioned into over 300 nodes. A higher order boundary condition representation was obtained by using a second order approximation for the first derivative at the boundary and combining it with the general equation used for inner nodes. This latter formulation produced reasonable results when as few as ten nodes were used. DOE

N93-24976# Cornell Univ., Ithaca, NY. School of Chemical Engineering.
EXPERIMENTAL AND THEORETICAL STUDIES OF DENSE FLUID MIXTURES
Dec. 1992 5 p
(Contract DE-FG02-86ER-13623)
(DE93-006070; DOE/ER-13623/3) Avail: CASI HC A01/MF A01

During the thirty-one months of this grant, extensive measurements of the speed of sound in three alternative refrigerants and in SF6 were conducted. Modifications and improvements were made to the equipment for measuring interfacial tension in pure fluids and mixtures, and a new set of measurements of interfacial tension over a wide range of temperature and pressure conditions for three mixtures of simple fluids was conducted. The results of these interfacial tension measurements were used to show that the new corresponding states theory of the variation of surface tension with temperature and composition is superior to the previous corresponding states theory. Computer simulations were performed on a system of molecules interacting via a Lennard-Jones potential that contained two liquid-vapor interfaces. Careful attention to the parameters of the simulation and to achievement of equilibrium illuminated problems that had plagued earlier simulations. DOE

N93-25082*# National Aeronautics and Space Administration. Ames Research Center, Moffett Field, CA.
PROPAGATION VELOCITY AND SPACE-TIME CORRELATION OF PERTURBATIONS IN TURBULENT CHANNEL FLOW
John Kim and Fazle Hussain (Houston Univ., TX.) May 1992 49 p
(RTOP 505-60-00)
(NASA-TM-103932; A-92088; NAS 1.15:103932) Avail: CASI HC A03/MF A01

A database obtained from direct numerical simulation of a turbulent channel flow is analyzed to extract the propagation velocity V of velocity, vorticity, and pressure fluctuations from their space-time correlations. A surprising result is that V is approximately the same as the local mean velocity for most of the channel, except for the near-wall region. For y(+) is less than or equal to 15, V is virtually constant, implying that perturbations of all flow variables propagate like waves near the wall. In this region V is 55 percent of the centerline velocity U(sub c) for velocity and vorticity perturbations and 75 percent of U(sub c) for pressure perturbations. Scale-dependence of V is also examined by analyzing the bandpass filtered flow fields. Comprehensive documentation of the propagation velocities and space-time correlation data, which should prove useful in the evaluation of Taylor's hypothesis is presented. An attempt was made to explain some of the data in terms of our current understanding of organized structures, although not all of the data can be explained this way. Author (revised)

N93-25087*# Vigyan Research Associates, Inc., Hampton, VA.
A FEASIBILITY STUDY OF USING LANGLEY 0.3-m TRANSONIC CRYOGENIC TUNNEL SIDEWALL BOUNDARY-LAYER REMOVAL SYSTEM FOR HEAVY GAS TESTING Final Report
A. V. Murthy, S. Balakrishna, and W. Allen Kilgore Mar. 1993 25 p
(Contract NAS1-18585; RTOP 505-59-86-02)
(NASA-CR-191438; NAS 1.26:191438) Avail: CASI HC A03/MF A01

This report presents the results of a preliminary study for using the 0.3-m Transonic Cryogenic Tunnel sidewall boundary-layer removal system with heavy gas sulfur hexafluoride as the test medium. It is shown that the drive motor speed/power of the existing system and the additional heat load on the tunnel heat exchanger are the major problems limiting the boundary-layer removal system performance. Overcoming these problems can provide the capability to remove about 1.5 percent of the test section mass flow at Mach number M = 0.8 and about 5 percent at M = 0.25.

Previous studies have shown that these boundary-layer mass flow removal rates can reduce the boundary-layer thickness by a factor of two at the model station. Also the effect of upstream boundary-layer removal on the airfoil test data is not likely to be significant under high lifting conditions. Near design conditions, corrections to the test Mach number may be necessary to account for sidewall boundary-layer effects. Author (revised)

N93-25109*# Duke Univ., Durham, NC. Dept. of Mechanical Engineering and Materials Science.

PREDICTION OF UNSTEADY FLOWS IN TURBOMACHINERY USING THE LINEARIZED EULER EQUATIONS ON DEFORMING GRIDS Final Technical Report

William S. Clark and Kenneth C. Hall Apr. 1993 110 p

(Grant NAG3-1192)

(NASA-CR-192919; NAS 1.26:192919) Avail: CASI HC A06/MF A02

A linearized Euler solver for calculating unsteady flows in turbomachinery blade rows due to both incident gusts and blade motion is presented. The model accounts for blade loading, blade geometry, shock motion, and wake motion. Assuming that the unsteadiness in the flow is small relative to the nonlinear mean solution, the unsteady Euler equations can be linearized about the mean flow. This yields a set of linear variable coefficient equations that describe the small amplitude harmonic motion of the fluid. These linear equations are then discretized on a computational grid and solved using standard numerical techniques. For transonic flows, however, one must use a linear discretization which is a conservative linearization of the nonlinear discretized Euler equations to ensure that shock impulse loads are accurately captured. Other important features of this analysis include a continuously deforming grid which eliminates extrapolation errors and hence, increases accuracy, and a new numerically exact, nonreflecting far-field boundary condition treatment based on an eigenanalysis of the discretized equations. Computational results are presented which demonstrate the computational accuracy and efficiency of the method and demonstrate the effectiveness of the deforming grid, far-field nonreflecting boundary conditions, and shock capturing techniques. A comparison of the present unsteady flow predictions to other numerical, semi-analytical, and experimental methods shows excellent agreement. In addition, the linearized Euler method presented requires one to two orders-of-magnitude less computational time than traditional time-marching techniques making the present method a viable design tool for aeroelastic analyses.

Author (revised)

N93-25124# Los Alamos National Lab., NM.

IMPLEMENTATION OF THE TURN FUNCTION METHOD IN A THREE-DIMENSIONAL, PARALLELIZED HYDRODYNAMICS CODE

P. J. ORourke and M. S. Fairfield 1992 22 p Presented at the 1993 International Simulators Conference on High Performance Computing, Arlington, VA, 29 Mar. - 1 Apr. 1993

(Contract W-7405-eng-36)

(DE93-003744; LA-UR-92-3468; CONF-930372-1) Avail: CASI HC A03/MF A01

The implementation of the Turn Function Method in KIVA-F90, a version of the KIVA computer program written in the FORTRAN 90 programming language that is used on some massively parallel computers is described. The Turn Function Method solves both linear momentum and vorticity equations in numerical calculations of compressible fluid flow. Solving a vorticity equation allows vorticity to be both conserved and transported more accurately than in traditional methods for computing compressible flow. This first implementation of the Turn Function Method in a three-dimensional hydrodynamics code involved some modification of the original method and some numerical difference approximations. In particular, a penalty method is used to keep the divergence of the computed vorticity field close to zero. Difference operators are also defined in such a way that the finite difference analog of del(del x u) = 0 is exactly satisfied. Three example problems show the increased computational cost and the accuracy to be gained by using the Turn Function Method in calculations of flows with rotational motion. Use of the Method can increase by 60 percent the computational times of the Euler equation solver in KIVA-F90, but it is concluded that this increased cost is justified by the increased accuracy. DOE

N93-25175*# National Aeronautics and Space Administration. Lewis Research Center, Cleveland, OH.

NONLINEAR EVOLUTION OF THE FIRST MODE SUPERSONIC OBLIQUE WAVES IN COMPRESSIBLE BOUNDARY LAYERS. PART 1: HEATED/COOLED WALLS

J. S. B. Gajjar (Manchester Univ., England.) Mar. 1993 32 p

(Contract NCC3-233; RTOP 505-62-21)

(NASA-TM-106087; ICOMP-93-08; E-7718; NAS 1.15:106087) Avail: CASI HC A03/MF A01

The nonlinear stability of an oblique mode propagating in a two-dimensional compressible boundary layer is considered under the long wave-length approximation. The growth rate of the wave is assumed to be small so that the concept of unsteady nonlinear critical layers can be used. It is shown that the spatial/temporal evolution of the mode is governed by a pair of coupled unsteady nonlinear equations for the disturbance vorticity and density. Expressions for the linear growth rate show clearly the effects of wall heating and cooling and in particular how heating destabilizes the boundary layer for these long wavelength inviscid modes at O(1) Mach numbers. A generalized expression for the linear growth rate is obtained and is shown to compare very well for a range of frequencies and wave-angles at moderate Mach numbers with full numerical solutions of the linear stability problem. The numerical solution of the nonlinear unsteady critical layer problem using a novel method based on Fourier decomposition and Chebychev collocation is discussed and some results are presented. Author (revised)

N93-25176*# National Aeronautics and Space Administration. Langley Research Center, Hampton, VA.

COMBINED LAURA-UPS HYPERSONIC SOLUTION PROCEDURE

William A. Wood and Richard A. Thompson Mar. 1993 24 p

(RTOP 506-40-91-01)

(NASA-TM-107682; NAS 1.15:107682) Avail: CASI HC A03/MF A01

A combined solution procedure for hypersonic flowfields around blunted slender bodies was implemented using a thin-layer Navier-Stokes code (LAURA) in the nose region and a parabolized Navier-Stokes code (UPS) on the after body region. Perfect gas, equilibrium air, and non-equilibrium air solutions to sharp cones and a sharp wedge were obtained using UPS alone as a preliminary step. Surface heating rates are presented for two slender bodies with blunted noses, having used LAURA to provide a starting solution to UPS downstream of the sonic line. These are an 8 deg sphere-cone in Mach 5, perfect gas, laminar flow at 0 and 4 deg angles of attack and the Reentry F body at Mach 20, 80,000 ft equilibrium gas conditions for 0 and 0.14 deg angles of attack. The results indicate that this procedure is a timely and accurate method for obtaining aerothermodynamic predictions on slender hypersonic vehicles.

Author (revised)

N93-25193# State Univ. of New York, Albany. Research Foundation.

THE MODELING OF COMPLEX CONTINUA: FUNDAMENTAL OBSTACLES AND GRAND CHALLENGES

Jan. 1993 19 p

(Contract DE-FG02-90ER-25084)

(DE93-006507; DOE/ER/25084-3) Avail: CASI HC A03/MF A01

The research is divided into the following areas: discontinuities and adaptive computation, chaotic flows, dispersion of flow in porous media, and nonlinear waves and nonlinear materials. The research program has emphasized innovative computation and theory. The approach depends on abstracting mathematical concepts and computational methods from individual applications to a wide range of problems involving complex continua. The generic difficulties in the modeling of continua that guide this abstraction are multiple length and time scales, microstructures (bubbles, droplets, vortices, crystal defects), and chaotic or random phenomena described by a statistical formulation. DOE

N93-25208*# Virginia Polytechnic Inst. and State Univ., Blacksburg. Dept. of Aerospace and Ocean Engineering.

FLOW VISUALIZATIONS OF PERPENDICULAR BLADE VORTEX INTERACTIONS Semiannual Progress Report

Michael C. Rife and William J. Davenport 15 Oct. 1992 94 p

(Grant NAG1-1119)

(NASA-CR-192725; NAS 1.26:192725) Avail: CASI HC A05/MF A01

Helium bubble flow visualizations have been performed to study

perpendicular interaction of a turbulent trailing vortex and a rectangular wing in the Virginia Tech Stability Tunnel. Many combinations of vortex strength, vortex-blade separation (Z(sub s)) and blade angle of attack were studied. Photographs of representative cases are presented. A range of phenomena were observed. For Z(sub s) greater than a few percent chord the vortex is deflected as it passes the blade under the influence of the local streamline curvature and its image in the blade. Initially the interaction appears to have no influence on the core. Downstream, however, the vortex core begins to diffuse and grow, presumably as a consequence of its interaction with the blade wake. The magnitude of these effects increases with reduction in Z(sub s). For Z(sub s) near zero the form of the interaction changes and becomes dependent on the vortex strength. For lower strengths the vortex appears to split into two filaments on the leading edge of the blade, one passing on the pressure and one passing on the suction side. At higher strengths the vortex bursts in the vicinity of the leading edge. In either case the core of its remnants then rapidly diffuse with distance downstream. Increase in Reynolds number did not qualitatively affect the flow apart from decreasing the amplitude of the small low-frequency wandering motions of the vortex. Changes in wing tip geometry and boundary layer trip had very little effect. Author

N93-25221*# North Carolina Univ., Charlotte. Dept. of Mechanical Engineering and Engineering Science.

TWO-PHASE/TWO-PHASE HEAT EXCHANGER ANALYSIS Final Report

Rhyn H. Kim Nov. 1992 19 p

(Grant NAG5-1503)

(NASA-CR-192783; NAS 1.26:192783) Avail: CASI HC A03/MF A01

A capillary pumped loop (CPL) system with a condenser linked to a double two-phase heat exchanger is analyzed numerically to simulate the performance of the system from different starting conditions to a steady state condition based on a simplified model. Results of the investigation are compared with those of similar apparatus available in the Space Station applications of the CPL system with a double two-phase heat exchanger. Author

N93-25237 Dayton Univ., OH.

AN INVESTIGATION OF LASER VELOCIMETRY MEASUREMENTS WITHIN HIGH SPEED, COMPLEX FLOWS Ph.D. Thesis

Mark S. Maurice 1992 212 p

Avail: Univ. Microfilms Order No. DA9239537

Laser velocimetry (LV) is a nonintrusive, optical method that measures particle velocities within a flow. Therefore, if LV measurements are to represent the structure of a flowfield, the particles must follow the dynamic motion of the fluid. However, in high speed, complex flows, the lag in particle response to fluid gradients can be substantial. In order to quantify velocity lag bias in high speed, mean velocity measurements, several flowfields are investigated experimentally and computationally. From measurements within the vortical flowfield of a supersonic delta wing at Mach 1.9, and for expansion flows at Mach 5.76, it is found that by coupling a particle equation of motion with the computational flowfield solutions, particle trajectories and velocity lag within complex flows can be predicted. For two primary flow structures, potential vortices and two-dimensional ideal shocks, it is found that relaxation distances can be quantified in terms of three dimensionless parameters. Results for these cases are presented graphically as an aid for test design and data analysis over a wide range of conditions. However, any analysis of velocity lag bias requires knowledge of the particle size distribution, which is often unknown in high speed flows. For a ten degree half-angle wedge at Mach Three, a methodology is presented which determines the mean particle diameter from measurements downstream of the shock, and then examines the remaining LV data throughout the flow. To extend this approach to flows with highly polydispersed particle sizes, an algorithm is developed which extracts the size distribution from the shape of LV velocity histograms. This method is applied to the investigation of a hypersonic inlet at Mach 5.76. Results show that despite the problem of velocity lag, measurements can still be used for computational code validation. In this final case, the developing boundary layer along the inlet ramp is accurately predicted, but the algebraic eddy viscosity model overestimates the turbulence production at the shock wave - boundary layer interactions. Dissert. Abstr.

N93-25247*# National Aeronautics and Space Administration. Ames Research Center, Moffett Field, CA.

ASSESSMENT OF CLOSURE COEFFICIENTS FOR COMPRESSIBLE-FLOW TURBULENCE MODELS

P. G. Huang (Eloret Corp., Palo Alto, CA.), P. Bradshaw (Stanford Univ., CA.), and T. J. Coakley Oct. 1992 15 p

(RTOP 505-59-53)

(NASA-TM-103882; A-91212; NAS 1.15:103882) Avail: CASI HC A03/MF A01

A critical assessment is made of the closure coefficients used for turbulence length scale in existing models of the transport equation, with reference to the extension of these models to compressible flow. It is shown that to satisfy the compressible 'law of the wall', the model coefficients must actually be functions of density gradients. The magnitude of the errors that result from neglecting this dependence on density varies with the variable used to specify the length scale. Among the models investigated, the k-omega model yields the best performance, although it is not completely free from errors associated with density terms. Models designed to reduce the density-gradient effect to an insignificant level are proposed. Author

N93-25252 Stanford Univ., CA.

SHOCK TUBE APPLICATION TO THE STUDY OF COMPRESSIBLE TURBULENT BOUNDARY LAYER WITH MASS INJECTION Ph.D. Thesis

Jiunn-Yih Liaw 1992 109 p

Avail: Univ. Microfilms Order No. DA9302240

The dissertation explores the feasibility of using the shock tube in studying the heat transfer in the compressible turbulent boundary layer with mass injection. The flow under consideration is the asymptotically steady region induced behind the shock wave. The test model is a flat plate with a 2-D 30 deg slot. The shock-induced flow was computed numerically for both the quasi-steady and the asymptotically steady region. The results were presented in a x-t diagram to estimate the available testing time in a steady state sense. The injection flow was measured by using the slot as a flow measuring device. Heat transfer data were measured by using the thin-film heat gauges. Some preliminary heat transfer data were obtained at the flow Mach number 0.9, gas-to-wall temperature ratio 1.6, and Reynolds number 4.62 x 10(exp 7) (per meter). The data upstream of the slot, through slightly lower, agree with existing theory within measurement uncertainty. The data downstream of the slot were compared with other sets of data obtained at flow Mach numbers 0.03 and 0.55. This comparison reveals a possible Mach number effect on film-cooling. An attempt was made by using the Prandtl-Glauert formula to model this effect. More experimental data and further analysis are needed to confirm this finding. Final remarks will discuss the feasibility and propose further improvements based on the experience learned from this study. Dissert. Abstr.

N93-25259 Stanford Univ., CA.

DIRECT SOLUTIONS OF THE NAVIER-STOKES EQUATIONS WITH APPLICATION TO STATIC AEROELASTICITY Ph.D. Thesis

Fort Fraser Felker 1992 146 p

Avail: Univ. Microfilms Order No. DA9234093

A method was developed to directly calculate solutions to the steady, compressible, Navier-Stokes equations. Direct solutions do not involve an advance in time of an unsteady analysis, and neither time nor any 'time-like' variable appears in the system. The steady Navier-Stokes equations were discretized in space, and the resulting nonlinear system of algebraic equations was solved using Newton's method. The method exhibits rapid convergence, with the residual reduced to machine zero in approximately ten iterations. One of the benefits of this solution method is that it is straightforward to include the effects of other physical phenomena on the fluid dynamics, and the effects of the fluid dynamics on the other phenomena. As an illustration of this, the direct solution method was extended to calculate the steady flow about a flexible body. The shape of the body depends on the fluid flow, and the fluid flow depends upon the shape of the body. There is no iteration between separate fluid dynamics and structures analyses. Rather, the solution for the complete aeroelastic system is found using the direct solution technique. The techniques used in the direct solution method, and the fluid/structure coupling are described. Important issues which arose during the implementation of the method, and their resolution, are reviewed. Sample calculations are presented for several two-dimensional, transonic, convergent-divergent nozzles, both with

rigid and flexible walls. These calculations serve to illustrate the accuracy and efficiency of the direct solution method. Recommendations are provided for the directions of future research in this area. Dissert. Abstr.

N93-25264 British Columbia Univ., Vancouver.
THE STEADY NAVIER-STOKES PROBLEM FOR LOW REYNOLDS NUMBER VISCOUS JETS Ph.D. Thesis
Huakang Chang 1991 81 p
Avail: Univ. Microfilms Order No. DANN69767

The classical existence theorem for the steady Navier-Stokes equations, based on a bound for the solution's Dirichlet integral, provides little qualitative information about the solution. In particular, if a domain is unbounded, it is not evident that the solutions will be unique even when the data are small. Inspired by the works of Odqvist for the interior problem and of Finn for the problem of flow past an obstacle, we give a potential theoretic construction of a solution of the steady Navier-Stokes equations in several domains with noncompact boundaries. We begin by studying a scalar quasilinear elliptic problem in a half space, which serves as a model problem for the development of some of the methods which are later applied to the Navier-Stokes equations. Then, we consider Navier-Stokes flow in a half space, modeling such phenomena as a juet emanating from a wall, with prescribed boundary values. The solution which is obtained decays like /x/(exp -2) at infinity and has a finite Dirichlet integral. Finally, we solve the problem of flow through an aperture in a wall between two half spaces, with a prescribed net flux through the aperture, or with a prescribed pressure drop between the two half space. A steady solution is constructed which decays like /x/(exp -2) at infinity. For small data, uniqueness is proven with the class of functions which decay like /x/(exp -1) at infinity and have finite Dirichlet integrals. Dissert. Abstr.

N93-25266*# Pennsylvania State Univ., University Park. Gas Dynamics Lab.
AN EXPERIMENTAL STUDY OF THE SOURCES OF FLUCTUATING PRESSURE LOADS BENEATH SWEPT SHOCK/BOUNDARY-LAYER INTERACTIONS Final Technical Report, 1 Jan. 1990 - 31 Dec. 1992
G. S. Settles and S. Garg Apr. 1993 34 p
(Grant NAG1-1070)
(NASA-CR-192918; NAS 1.26:192918; PSGDL-R-92/93-0002) Avail: CASI HC A03/MF A01

An experimental research program providing basic knowledge and establishing a database on the fluctuating pressure loads produced on aerodynamic surfaces beneath three dimensional shock wave/boundary layer interactions is described. Such loads constitute a fundamental problem of critical concern to future supersonic and hypersonic flight vehicles. A turbulent boundary layer on a flat plate is subjected to interactions with swept planar shock waves generated by sharp fins at angle of attack. Fin angles from 10 to 20 deg at freestream Mach numbers of 3 and 4 produce a variety of interaction strengths from weak to very strong. Miniature Kulite pressure transducers flush-mounted in the flat plate are used to measure interaction-induced wall pressure fluctuations. The distributions of properties of the pressure fluctuations, such as their ring levels, amplitude distributions, and power spectra, are also determined. Measurements were made for the first time in the aft regions of these interactions, revealing fluctuating pressure levels as high as 160 dB. These fluctuations are dominated by low frequency (0-5 kHz) signals. The maximum ring levels in the interactions show an increasing trend with increasing interaction strength. On the other hand, the maximum ring levels in the forward portion of the interactions decrease linearly with increasing interaction sweep back. These ring pressure distributions and spectra are correlated with the features of the interaction flowfield. The unsteadiness of the off-surface flowfield is studied using a new, non-intrusive technique based on the shadow graph method. The results indicate that the entire lambda-shock structure generated by the interaction undergoes relatively low-frequency oscillations. Some regions where particularly strong fluctuations are generated were identified. Fluctuating pressure measurements are also made along the line of symmetry of an axisymmetric jet impinging upon a flat plate at an angle. This flow was chosen as a simple analog to the impinging jet region found in the rear portion of the shock wave/boundary layer interactions under study. It is found that a sharp peak in ring pressure level exists at or near the mean stagnation point. It is suggested that the phenomena responsible for this peak may be active in the swept interactions as well, and may cause the extremely high fluctuating pressures observed in the impinging jet region in the present experimental program. Author (revised)

N93-25277# National Inst. for Fusion Science, Nagoya (Japan).
TRACKING SHARP INTERFACE OF TWO FLUIDS BY THE CIP (CUBIC-INTERPOLATED PROPAGATION) SCHEME
T. Yabe (Gunma Univ., Japan.) and F. Xiao (Gunma Univ., Japan.) 6 Jan. 1993 19 p Submitted for publication
(NIFS-206) Avail: CASI HC A03/MF A01

A method to treat a sharp discontinuity by the density function is proposed. The surface of the density function is described by one grid throughout the calculation even when the surface is largely distorted. This description is made possible by the CIP method combined with variable transformation. This scheme is applied to the linear wave propagation in one- and two-dimensions. In the nonlinear case, the injection of heavier fluid into lighter fluid is calculated and the winding of mushroom structure is successfully treated by the density function. Author (revised)

N93-25295 Illinois Univ. at Urbana-Champaign, Savoy.
CONSEQUENCES OF SPONTANEOUS AND ANOMALOUS SYMMETRY BREAKING FOR THE ORBITAL AND MASS FLOW HYDRODYNAMICS OF He-3 - A Ph.D. Thesis
Frank Paul Gaitan 1992 119 p
Avail: Univ. Microfilms Order No. DA9305531

In this thesis we address three problems associated with the mass flow and orbital hydrodynamics of He-3 - A. The first concerns the form of the T = 0 mass current in local equilibrium; the second is a paradox associated with the non-conservation of superfluid linear momentum at T = 0; and the third involves a longstanding disagreement between past calculations of the intrinsic angular momentum in He-3 - A. These problems are more fully described in chapter 1 along with a brief review of the generalized Hartree-Fock approach to the Bardeen-Cooper-Schrieffer theory of superconductivity. In chapter 2 we describe our formulation of the quasiparticle dynamics. In chapter 3 we demonstrate the occurrence of anomalous symmetry breaking in He-3 - A, and in chapter 4 we see how the first two problems can be understood as consequences of this anomalous symmetry breaking. In chapter 5 we calculate the intrinsic orbital angular momentum via a Berry phase argument and also through a calculation that is careful to account for backflow currents which are necessary for the maintenance of particle number conservation in the superfluid phase. On the basis of the latter calculation we propose an explanation for the disagreement in past calculations of the intrinsic orbital angular momentum in He-3 - A. Dissert. Abstr.

N93-25306# General Electric Co., Schenectady, NY.
MEASUREMENT OF VELOCITIES IN GAS-LIQUID TWO-PHASE FLOW USING LASER DOPPLER VELOCIMETRY
P. F. Vassallo, T. A. Trabold, W. E. Moore, and G. J. Kirouac Sep. 1992 29 p
(Contract DE-AC12-76SN-00052)
(DE93-008083; KAPL-4738) Avail: CASI HC A03/MF A01

Measurements of bubble and liquid velocities in two-phase flow were made using a new forward/backward scattering Laser Doppler Velocimetry (LDV) technique. This work was performed in a 6.4 by 11.1 mm vertical duct using known air/water mixtures. A standard LDV fiber optic probe was used to measure the bubble velocity, using direct backscattered light. A retro-reflector and lens assembly permitted the same probe to measure the liquid velocity with direct forward-scattered light. The bubble velocity was confirmed by independent measurements with a high-speed video system. The liquid velocity was confirmed by demonstrating the dominance of the liquid seed data rate in the forward-scatter measurement. Experimental data are presented to demonstrate the accuracy of the technique for a wide range of flow conditions, from bubbles as small as 0.75-mm-diam to slugs as large as 10-mm wide by 30-mm long. In the slug regime, the LDV technique performed velocity measurements for both phases, for void fractions up to 50 percent, which was the upper limit of our experimental investigation. DOE

N93-25309# Carnegie-Mellon Univ., Pittsburgh, PA. Dept. of Chemical Engineering.
PREDICTIVE MODELING OF PARTICLE-LADEN, TURBULENT FLOWS Quarterly Progress Report No. 1, 1 Sep. - 1 Dec. 1992

J. L. Sinclair 1992 18 p
(Contract DE-FG22-92PC-92540)
(DE93-008208; DOE/PC-92540/T1) Avail: CASI HC A03/MF A01

The successful prediction of particle-laden, turbulent flows relies heavily on the representation of turbulence in the gas phase. Several types of turbulence models for single-phase gas flow have been developed which compare reasonably well with experimental data. A low-Reynolds k-epsilon, closure model is chosen to describe the Reynolds stresses associated with gas-phase turbulence. This closure scheme, which involves transport equations for the turbulent kinetic energy and its dissipation rate, is valid in the turbulent core as well as the viscous sublayer. Several versions of the low-Reynolds k-epsilon closure are documented in the literature. However, even those models which are similar in theory often differ considerably in their quantitative and qualitative predictions, making the selection of such a model a difficult task. The purpose of this progress report is to document findings on the performance of ten different versions of the low-Reynolds k-epsilon model on predicting fully developed pipe flow. The predictions are compared with the experimental data. With the exception of the model put forth by Hoffman (1975), the predictions of all the closures show reasonable agreement for the mean velocity profile. However, important quantitative differences exist for the turbulent kinetic energy profile. In addition, the predicted eddy viscosity profile and the wall-region profile of the turbulent kinetic energy dissipation rate exhibit both quantitative and qualitative differences. An effort to extend the present comparisons to include experimental measurements of other researchers is recommended in order to further evaluate the performance of the models.
DOE

N93-25334 Stanford Univ., CA.
DATA PARALLEL FINITE ELEMENT TECHNIQUES FOR LARGE-SCALE COMPUTATIONAL FLUID DYNAMICS Ph.D. Thesis
Zdenek Johan 1992 108 p
Avail: Univ. Microfilms Order No. DA9302226

The objective of this work is to address two major issues arising in the computation of large-scale flow problems: storage and computing cost. A Galerkin/least-squares finite element formulation is used to solve the compressible Navier-Stokes equations. Structural heating is also considered by performing a classical Galerkin finite element discretization and by having a fully implicit coupling with the fluid. A matrix free implicit iterative solver based on the Generalized Minimal Residual Algorithm (GMRES) is developed to solve the nonlinear system of equations arising from the finite element discretizations. It is shown that the performance of this solver compares favorably with traditional implicit iterative techniques while reducing substantially the memory requirements. The computing cost issue is addressed through a data parallel implementation of the finite element solver on the Connection Machine massively parallel computers. A blocking strategy is presented to facilitate the handling of several element types in the same mesh. Two communication algorithms performing the gather and scatter operations required by the finite element implementation are proposed. The first algorithm makes use of communication primitives available in the Connection Machine Scientific Software Library. The second algorithm preserves data locality by partitioning the mesh using a parallel implementation of the spectral partitioning algorithm. The mesh decomposition leads to a reduction in the amount of data to be communicated between processing nodes. Fluid-structural heating interaction problems and compressible flow problems using meshes with close to one million elements, such as flow over a complete airplane, demonstrate the efficiency of the data parallel computing and communication strategies.
Dissert. Abstr.

N93-25341 Washington Univ., Saint Louis, MO.
A COMPACT HIGH-ORDER EULER SOLVER FOR UNSTRUCTURED GRIDS Ph.D. Thesis
David W. Halt 1992 151 p
Avail: Univ. Microfilms Order No. DA9235899

A compact high-order scheme is developed for solving the Euler equations in two or three dimensions. The flow domain is discretized by triangles in 2D or tetrahedra in 3D. A novel scheme is introduced which implements a set of characteristic-based split-flux formulas along the element boundaries in a conservation framework. Polynomials of order 0 through 3 are used in each cell to represent the conservation flow variables. Solutions are demonstrated to achieve up to fourth order accuracy. Comparisons are shown for a variety of flow applications with other numerical results, wind tunnel data, and an analytical solution. Numerical results demonstrate a substantial gain in efficiency using compact higher-order elements over the lower-order elements.
Dissert. Abstr.

N93-25342 Case Western Reserve Univ., Cleveland, OH.
NUMERICAL SIMULATION OF A SHOCK WAVE/TURBULENT BOUNDARY LAYER INTERACTION IN A DUCT Ph.D. Thesis
Wei-Li Yang 1992 219 p
Avail: Univ. Microfilms Order No. DA9236308

A numerical investigation of the interaction of an incident oblique shock wave with a turbulent duct flow is presented. The investigation consisted of solving the three dimensional, unsteady, compressible, and mass averaged Navier-Stokes equations. An implicit finite volume lower-upper time marching code (RPLUS) has been employed and modified. A three dimensional Baldwin-Lomax turbulence model has been programmed in conjunction with the code. Computed results are obtained at Mach number 2.9 for a turning angle of 12.99 degrees and Reynolds number based on duct width of 1.36 x 10(exp 7). Under various inlet conditions, the results clearly depict the flow characteristics including the shock structure, the separated flow region, the wall pressure distribution, and the skin friction distribution. The findings provide a physical understanding of the three dimensional vortex structure of the flow in a duct in which a shock wave interacts with a turbulent boundary layer. The results show that the ratio of the boundary layer thickness to the duct width is the critical parameter in determining the separation structure. The computational results also show that the corner vortices and center separation structures are closely related. However, the non-uniformities and secondary flows in the approach boundary layer do not change the separation structure qualitatively.
Dissert. Abstr.

N93-25348 Rice Univ., Houston, TX.
COMBINING PARTICLES AND WAVES FOR FLUID ANIMATION Ph.D. Thesis
Mark Hall 1992 80 p
Avail: Univ. Microfilms Order No. DA9234390

Modeling fluid motion is a problem largely unsolved by traditional modeling techniques. Animation of fluid motion has been possible only in special cases, falling into one of two general categories. Upper surface representations model wave phenomena for fluid in placid situations, such as calm ocean waves. Particle systems define the chaotic motion of fluid in highly volatile states, like waterfalls. Each technique can mimic physical motion of liquid only in limited situations. We propose a system unifying previous techniques. We describe a system containing fluid of both categories. Two representations for fluid, corresponding to previous methods, allow modeling a wide range of situations. Automatic transitions between representations allow using the most appropriate technique for a given physical situation. Fluid is represented by two types of primitives: drops and pools. The drops constitute a particle system describing small, independent components. Pools model large bodies of fluid in more placid situations. The notion of support differentiates the situations that each representation models best. In general terms, fluid is supported when there is a solid underneath the fluid. Previous techniques generally either assume that support is omnipresent or that support is nonexistent. In our system, support determines which representation should be used and when transitions between the two should occur. Supported drops flatten and become pools. Unsupported pools spawn drops. Combining the two techniques into a single system allows mimicking fluid in a broader range of physical situations than previous methods. The resulting system models fluid motion based on physical properties of the environment. Gravity causes fluid to fall or flow downward. Solids restrict fluid motion, changing the course of flowing fluid and defining the shape of contained fluid.
Dissert. Abstr.

N93-25349 Illinois Univ., Urbana-Champaign.
SOME NEW RESULTS FOR SOLVING LINEAR SYSTEMS ARISING FROM COMPUTATIONAL FLUID DYNAMICS PROBLEMS Ph.D. Thesis
Gang Lou 1992 149 p
Avail: Univ. Microfilms Order No. DA9236525

In this thesis, we consider the numerical solution of four kinds of linear systems: saddle-point problems, Stokes problems, symmetric systems (positive definite or indefinite), and unsymmetric systems. These systems

are related, and all of them arise from the numerical solution of partial differential equations. For saddle-point problems, we introduce a class of expansion methods based on new solution representation of the general problem. Many difficult computations involved in Uzawa and projection type methods for saddle-point problems are avoided in our approach. For the Stokes problems, by introducing a new variable, we split the linear system into several smaller systems according to its sparse structure. This new variable is then updated so that the split systems eventually produce the solution of the original problem. For symmetric systems that are indefinite and do not have a special sparse structure like saddle-point problems, we propose a class of nested iterative methods to handle them. We study how the convergence rate of the outer iteration is related to the convergence rate of the inner iterations. For symmetric positive definite systems, we propose a class of nested preconditioners and analyze properties of these preconditioners. Some necessary and sufficient conditions for the optimality of these nested preconditioners are established. Finally, for unsymmetric systems, we generalize the concept of spectral equivalence for symmetric positive definite systems to these general systems, We also study some properties of spectrally equivalent matrices and consider their applications for constructing efficient iterative methods. Dissert. Abstr.

N93-25438 Surrey Univ., Guildford (England).
VORTEX SHEDDING IN OSCILLATORY FLOW Ph.D. Thesis
Khalfan Al-Asmi 1992 316 p
Avail: Univ. Microfilms Order No.BRDX98100

Measurements of the response to inline flow oscillations of vortex shedding from certain bluff bodies were made. Four cylinders with fixed separation points were exposed to a mean stream with controlled sinusoidal oscillations at defined frequency ratios and amplitudes. Attention was concentrated on the highly sensitive reduced velocity regime around the inverse of twice the Strouhal number, 1/2S. Synchronization of vortex formation was first established; then, for conditions at which synchronization occurred, threshold amplitude was measured. In order to determine the common and distinguishing features of bluff body shape the response from cylinders having 'zero' and finite after body were investigated. Finally, for a selected cylinder, the influence, in the presence of oscillations, of turbulence intensity (of defined scale), solid blockage, and aspect ratio to the synchronous range were examined. It was found that amplitudes of oscillations of the order of 0.025 were sufficient to induce frequency lock-in when the reduce velocity was close to 1/2S and, provided the amplitude was sufficiently large, limited synchronization could also be induced near the upper and lower reduce velocities of 1/S and 1/4S. Synchronization is accompanied by enhanced vortex shedding which, in turn, can lead to increased base suction (and therefore increase in drag force). Flow visualization revealed that the near wake vortex arrangement can vary a great deal depending on the ratio of Strouhal numbers at the forced and self-excited frequencies (N/n(sub o)). It was concluded that the behavior of the base pressure reflected this situation and that the range of synchronization depended strongly on the stability of the prevailing mode of vortex shedding. The precise details of the flow were found to be highly dependent on body geometry and the frequency ratio N/n(sub o). In the smaller tunnel, having a working section size of 0.3 x 0.3 m, it was possible to produce sinusoidal variations of the working section flow, having peak to peak amplitude of up to 60 percent of the mean flow speed and frequencies up to, typically, that corresponding to the acoustic quarter-wavelength frequency determined by the tunnel length. Over the viable working range, the device is shown to produce high quality periodic flow with negligible harmonic distortion or acoustic noise difficulties.
Dissert. Abstr.

N93-25472 Colorado Univ., Boulder.
NUMERICAL SIMULATION OF TIME-DEPENDENT THERMOCAPILLARY CONVECTION IN LAYERED FLUID SYSTEMS Ph.D. Thesis
Leonard Joel Peltier 1992 271 p
Avail: Univ. Microfilms Order No. DA9304596

Time-dependent thermocapillary convection in single and encapsulated fluid layers is considered. Through a parametric study of thermocapillary convection in a single layer of a Prandtl number 6.78 fluid, a thermal-convective mechanism for oscillatory thermocapillary convection is explored. The instability is shown to depend upon temporal coupling between large scale thermal structures within the flow field and the temperature sensitive free surface. This interaction is initiated by cooling of the free surface from below by a cool finger of fluid convected from the cold wall beneath the large central eddy. A primary result is the development of a stability diagram for the Cartesian thermocapillary system presenting the critical Marangoni number separating steady from the time-dependent flow states as a function of aspect ratio for the range of values between 2.3 and 3.8. A minimum critical aspect ratio near 2.3 and a minimum Marangoni number near 2000 are predicted. Below these critical parameters, steady convection is found within the parameter ranges investigated. Extension of this work to encapsulated systems of moderate Prandtl number fluids targets both (1) water encapsulation of Fluorinert FC-75 and (2) ethylene glycol encapsulated by FC-75 from below and hexadecane from above. Particular attention is focused on modes of time-dependence and on the implications of using Antonow's Rule to predict the thermal coefficient of interface tension from surface tension data. The primary findings are that similar mechanisms for time-dependent thermocapillary convection exist for single layer and encapsulated layer fluid systems, gravity has a stabilizing influence on buoyant/thermocapillary convection with respect to time-dependence up to the transition from steady to time-dependent buoyancy driven convection, shear effects at a thermocapillary interface may reduce convection in the encapsulated fluid layer, and the absence of reliable data on the thermal coefficients of interface tension is a primary impediment to simulations of targeted fluid systems. The computer program developed for this work integrates the two-dimensional, time-dependent Navier-Stokes equations and the energy equation by a time-accurate method on a stretched, staggered mesh. Flat free surfaces and fluid/fluid interfaces are assumed.
Dissert. Abstr.

N93-25473 Michigan Univ., Ann Arbor.
LIQUID SURFACE BREAKUP OF NONTURBULENT AND TURBULENT LIQUIDS Ph.D. Thesis
Pei-Kuan Wu 1992 157 p
Avail: Univ. Microfilms Order No. DA9303841

An experimental study of the primary breakup in the near-injector region of large diameter (3.6-9.5 mm) liquid jets in still gases is described. The experiments involve the injection of different test liquids at a variety of velocities into various gas environments, with slug flow and fully-developed turbulent pipe flow at the jet exit. Measurements included flash photography, pulsed shadowgraphy, and single- and double-pulse holography. Drop sizes after primary breakup were found to satisfy Simmons' universal root-normal distribution with the ratio of the mass median diameter (MMD) and Sauter mean diameter (SMD), MMD/SMD = 1.2; therefore, the drop size distribution can be characterized solely by the SMD. For nonturbulent primary breakup, the SMD increased with distance from the jet exit and then remained nearly constant within a fully-developed primary breakup regime. SMD measurements in the fully-developed regime did not agree with existing unstable wave growth theories, however, the SMD could be correlated with an expression involving the thickness of an injector passage wall boundary layer at the jet exit. Drops formed by this primary breakup mechanism are intrinsically unstable to aerodynamic secondary breakup. When the liquid/gas density ratio is larger than 500, turbulent primary breakup is controlled by liquid properties alone and mass weighted streamwise and cross-stream drop velocities were comparable to mean streamwise and cross-stream rms fluctuating velocities in the liquid, respectively. The drop sizes at the onset of breakup could be correlated by comparing the surface tension work required to form a drop with the kinetic energy of radial velocity fluctuations. The SMD variation of turbulent primary breakup with distance from the jet exit could be correlated with a Rayleigh breakup mechanism which provides the time required to complete the drop detachment process from a liquid surface. When the liquid/gas density ratio was less than 500, aerodynamic effects affected turbulent primary breakup and final drop sizes were reduced by merging of turbulent primary breakup and aerodynamic secondary breakup; a good correlation of the final drop sizes due to this behavior was obtained by combining correlations for turbulent primary breakup and aerodynamic secondary breakup. Dissert. Abstr.

N93-25478 Cranfield Inst. of Tech., Bedford (England).
ANNULAR FLOW ENHANCED TWO-PHASE EVAPORATIVE HEAT EXCHANGER FOR SPACE-BASED SYSTEMS Ph.D. Thesis
D. Nikanpour 1991 191 p
Avail: Univ. Microfilms Order No. BRDX98015

The development of multi-kilowatt space-based systems requires the

transport of waste heat loads over long distances in micro-gravity conditions. In this context two-phase heat transport systems are attractive enabling a high rate of heat transport with low pump powers compared to single phase systems. In this context the design of a two-phase heat exchanger to transfer heat from a single-phase fluid (water) to a two-phase fluid (Freon 114) is discussed. Until reliable micro-gravity (less than 10-3g) test data on the heat transfer and pressure drop in a two-phase flows are available, it is deemed necessary that the design of heat exchanger's passages should promote gravity-independent flow regimes. This would make the design and test data, obtained at ground conditions, applicable in micro-gravity environments. The design concept investigated hinges on utilizing a set of helical flow passages (with small cross sectional area) to ensure a predictable flow regime, annular flow, up to high vapor qualities (greater than 0.8), in both micro-gravity and one 'g' environments. The concept was applied to the design of a 5 kW helically coiled evaporative heat exchanger for space-based systems, which was subsequently manufactured and tested. Ground tests gave results close to analytical predictions based on computer simulations of the heat transfer and pressure drops in helical flow passages. Finally design guideline for a two-phase evaporative heat exchanger for space-based systems is provided, along with conclusions and areas to be further researched. Dissert. Abstr.

N93-25483 Colorado Univ., Boulder.
SPATIAL SIMULATION OF TRANSITION IN WALL-BOUNDED SHEAR FLOWS: ACTIVE CONTROL AND EFFECTS OF SURFACE ROUGHNESS Ph.D. Thesis
Gokhan Danabasoglu 1992 295 p
Avail: Univ. Microfilms Order No. DA9304550

Spatial numerical simulations of instabilities in wall-bounded shear flows are discussed. In the first part, secondary instability in a three-dimensional plane channel flow is investigated. Also studied is the applicability of active control by periodic suction blowing to suppress the instability waves. In the second part, the effects of a two-dimensional, isolated roughness element on the spatial evolution of disturbances in boundary layer flows are considered. The mathematical model incorporates the incompressible, time-dependent, three-dimensional, full Navier-Stokes equations. These equations are integrated on a nonstaggered mesh using a mixed finite difference/spectral method with a time-splitting technique which decouples the momentum and pressure equations. For the problems involving the roughness element, a multidomain solution procedure was developed. The computer programs are optimized for operation on the CRAY-2S and CRAY Y-MP. The comparisons of the numerical results with the parallel linear stability theory reveal excellent agreement showing that the scheme accurately captures the evolution of disturbances both in time and space. Computations are performed to detail the secondary instability of the plane channel flow revealing good agreement with the experimental investigations. A local energy transfer rate analysis for the relevant wave triads is also performed considering only the nonlinear terms, and it is shown that the Tollmien-Schlichting wave acts only as a catalyst in agreement with the previous theoretical studies and temporal numerical simulations. It is also found that active control by period suction blowing successfully attenuates instability waves even at high (non-linear) amplitudes, reducing disturbance amplitudes very significantly and delaying transition to turbulence. The upstream effects of the control wave is shown to be confined to a small region in the vicinity of the control slot and does not propagate upstream. Finally, boundary layer simulations with surface roughness conclusively show that frequencies which are in the shear (mixing) layer instability range (but, stable according to the parallel linear stability theory) have higher growth rates than the Tollmien-Schlichting frequencies when the roughness element is large. Hence, the stability of the separation zone behind the roughness element is governed by the stability of the shear layer at its edge.
Dissert. Abstr.

N93-25485 California Univ., San Diego.
THE INTERACTION OF MODULATED VORTEX PAIRS WITH A FREE SURFACE Ph.D. Thesis
Christian Ernst Willert 1992 190 p
Avail: Univ. Microfilms Order No. DA9303277

Spatially modulated vortex pairs were generated below a free surface by two counter-rotating flaps whose edges approximate a sinusoid. The surface interactions of the vertically approaching vortex pairs were visualized by the shadowgraph technique. For certain initial conditions each modulated vortex core was seen to form a line of circular surface depressions. Subsequent digital particle image velocimetry (DPIV) measurements of several vortex pair cross-sections and the subsurface plane confirmed the existence of vortex core terminations at the surface - the modulated vortex tube was broken into a line of U-vortices. A prerequisite for reconnection of the vortex with the surface is that the flow's kinematics force the vortex core, that is regions of high vorticity, toward the surface. The ensuing locally concentrated viscous flux of surface-parallel vorticity through the surface is balanced by a local surface deceleration. Surface-normal vorticity appears on either side of the decelerated region whose gradually increasing circulation is directly balanced by the loss of circulation of the surface-parallel vortex. The circulation transfer for the Re = Gamma/(pi nu) approx. equals 2000 vortex tube lasts approximately 1 second. However, shear forces caused by small amounts of surface contamination (surface active agents) and its associated subsurface boundary layer inhibit the reconnection process by preventing the essential viscous flux of parallel vorticity through the surface. This work makes extensive use of digital particle image velocimetry (DPIV) in obtaining instantaneous flow field information from two-dimensional spatial cuts through the flow domain. A large number of laser-sheet illuminated particles are imaged by a solid state sensor yielding image sequences of single-exposed particles. A local interrogation of a pair of consecutive images by means of a local two-dimensional cross-correlation extracts the average displacement of the sample particle images whose velocity is then inferred from the magnification factor and time difference between the particle illumination. The acquisition of image sequences gives insight to the temporal evolution of the images flow field. Although the image acquisition rate is limited to the 30 Hz video standard, asynchronous particle illumination in conjunction with a specially configured camera yield particle image pairs whose time difference is on the order of 2 milliseconds. Dissert. Abstr.

N93-25534 Case Western Reserve Univ., Cleveland, OH.
AN EXPERIMENTAL STUDY OF PARTICLE-LADEN JET INTERACTIONS WITH COCURRENT FLOWS Ph.D. Thesis
Periasamy Chinnapalaniandi 1992 159 p
Avail. Univ. Microfilms Order No. DA9306096

The interactions of a particle laden jet with cocurrent flow was studied experimentally. To improve sorbent utilization an understanding of particle and fluid interaction within the turbulent mixing zone is necessary. To improve the understanding of this phenomenon, one needs to obtain measurements of the particle size, velocity, concentration, and gas phase velocity within the shear layer region of particle-laden jet. A particle injection test facility was designed specifically to study the interaction of particle laden jets using non-intrusive, laser-based optical techniques. Spherical glass particles in the size range of 2-100 micron were used. The mass loading was varied between 0 to 10. The Particle Dynamics Analyzer, which utilizes phase Doppler interferometry and laser Doppler anemometry was used for measuring the particle velocities, sizes, and concentration as well as gas phase velocities in the flow field. Phase discrimination between the particle phase and gas phase was accomplished by utilizing particle velocity and size statistics. Single phase, particle and gas phases mean velocities and fluctuating turbulent intensities, and concentration profiles were obtained. Single phase velocity measurements were used as baseline data for comparison with particle laden flows. The decay rate of mean gas phase centerline velocity for particle laden flows less than that for single phase flows. This resulted from the momentum transfer from particles to the gas phase. The axial and radial rms velocities of the particle and gas phases decrease with increase in mass loading. The spreading rate of particle laden jet is also reduced. This decrease resulted from the reduction in the radial fluctuating velocity. Entrainment increases with higher jet velocity and reduced mass loading. Higher mass loading reduces the turbulence level; therefore there is a reduction in mixing and entrainment. For the range of particle sizes used, larger particles tend to concentrate around the centerline of the jet. For a higher mass loading, the particles are concentrated in a smaller radial distance, and there is a resulting reduction in dispersion and mixing of particles. Dissert. Abstr.

N93-25540 Rice Univ., Houston, TX.
NUMERICAL STUDY OF CAVITY NATURAL CONVECTION FLOW WITH AUGMENTING AND COUNTERACTING EFFECTS BY PROJECTION FINITE ELEMENT METHOD Ph.D. Thesis

Tswen-Chyuan Jue 1992 182 p
Avail: Univ. Microfilms Order No. DA9234421

A numerical study of natural convection in cavities under the effects of thermocapillarity and gravity modulation is conducted in this research. Three different algorithms which are first-order explicit, second-order Taylor-Galerkin and semi-implicit schemes based on the projection finite element method (FEM) are developed. Each algorithm presents its own characteristics and advantages. By considering the problem characteristics and computational efficiency, the semi-implicit method is a better choice for this research. In this thesis, the physical investgation of cavity natural convection with augmenting or counteracting effects is divided into four parts. At first, the cavity flow with buoyancy force and thermocapillary effect is studied for different Marangoni numbers and aspects ratios. Next, the Benard convection with gravity modulation effects in normal gravity and zero-g gravity is investigated. The natural convection flow exhibits dramatically different flow structure under the influence of different modulation directions and frequencies. In addition, the natural convection with combined thermocapillarity and gravity modulation is explored for different modulation directions, frequencies and Marangoni numbers. Finally, the cavity natural convection flow with a deformable free surface is analyzed for different Grashof numbers and Marangoni numbers. Results of this research show that the surface tension provides a strong influence in the natural convection flow in both normal gravity and microgravity states. Particularly, the low aspect ratio and microgravity environments favor the development of thermocapillary-driven flow. On the other hand, the existence of gravity modulation makes the flow field different from the constant gravity state by applying different modulation directions and frequencies. The simultaneous presence of thermocapillarity and g-jitter creates a dramatically different flow pattern when compared to the results without thermocapillary effect. When a deformable free surface is considered, the flow field and heat transfer rate at the corners of free surface are changed due to the deformation of free surface shape. Dissert. Abstr.

N93-25546# Cornell Univ., Ithaca, NY.
IMPLICIT MULTIGRID SOLUTION OF THE COMPRESSIBLE NAVIER-STOKES EQUATIONS WITH APPLICATION TO DISTRIBUTED PARALLEL PROCESSING Ph.D. Thesis
Thomas Lee Tysinger 1992 185 p
Avail: Univ. Microfilms Order No. DA9236051

Efficient numerical procedures are developed for the solution of the Navier-Stokes equations. The Navier-Stokes equations are a system of conservation laws which govern the motion of compressible, viscous, heat-conducting fluids. A conservative finite volume formulation is used for spatial discretization of the governing equations, resulting in a system of ordinary differential equations. To advance the system in time, an Alternating Direction Implicit (ADI) procedure suitable for the Navier-Stokes equations is developed. The resulting implicit system is diagonalized to improve the computational efficiency of the scheme. Viscous contributions are added to the scheme implicitly in a way that enhances the stability, yet does not disturb the efficiency of the algorithm. Rapid convergence to a steady state solution is achieved with a recursive multigrid algorithm. The stability and efficiency of the scheme are demonstrated with simulations of flow over wing sections. Furthermore, the algorithm has been implemented within the framework of multiple-block structured grids in which the spatial domain is decomposed into multiple blocks and the solution is advanced in parallel on the different blocks. Generic utilities have been developed to implement such a scheme in distributed computing environments. The multiple-block algorithm is designed so that the explicit residual calculation is identical to that of the single-block scheme, and therefore converged solutions for both schemes must be the same. To accelerate convergence, horizontal, vertical, and asynchronous multigrid algorithms are tested. Significant speedups have been achieved in a multiprocessor environment, while convergence rates similar to those of the single-clock schemes are observed. Dissert. Abstr.

N93-25548 Houston Univ., TX.
DYNAMICS OF TURBULENT SLUGGING IN TRANSITIONAL PIPE FLOW Ph.D. Thesis
Joel Patrick Jenkinson 1992 318 p
Avail: Univ. Microfilms Order No. DA9235925

This dissertation examines the phenomenon of turbulent slugging (with particular focus on periodic slugging), a persistent type of transitional pipe flow. Turbulent slugging occurs either periodically or not. Which occurs is found to depend on the manner in which the flow is controlled; slugging is periodic when the pressure difference between the pipe inlet and exit is held constant, nonperiodic when Re(sub D) is held constant. In periodic slugging, deviations from exact periodicity--up to 5 percent of the mean period--are noted. These deviations are analyzed (in an effort to find chaos in an 'open' flow, using methods derived from information theory) and found to be nondeterministic. Turbulent slugs are the manifestation of a convective instability; systems having convective instabilities are often found to be noise driven, which is the case for nonperiodic slugging. For periodic slugging, the flow is 'closed' by strong feedback; the dynamics are intrinsic. Periodic slugging is analyzed as a dynamical system. Dimensionless pressure difference bar-(delta)P* is identified as the appropriate bifurcation parameter, Re(sub D)(t) and turbulent flow fraction Gamma(t) as dynamical variables, and pipe L/D as an auxiliary parameter. A bifurcation picture is constructed from experiments in a pipe with L/D = 1.181 x 10(exp 3). Experiments in which L/D is varied (from 1.17 x 10(exp 3) to 4.10 x 10(exp 3)) demonstrate that the slugging frequency is properly nondimensionalized as f(sub s)L/bar-U, not f(sub s)D/bar-U. A heuristic computer model which is quite successful in reproducing experimental results for periodic slugging is developed. The model is used to identify important or potentially important effects; in particular, comparisons of model and experimental results suggest the importance of bulk flow unsteadiness (acceleration/deceleration) on flow stability, transition, and turbulence production. The model is also used to examine effects of varying L/D, up to L/D is approximately 10(exp 6); an asymptotic range in bar-(delta)P* for periodic slugging is approached for L/D greater than 10(exp 4). Some preliminary results on effects of low-amplitude random and periodic forcing of bar-(delta)P* are also presented. In the latter case, only periodic and quasi-periodic (no chaotic) flows are found. Dissert. Abstr.

N93-25551 Old Dominion Univ., Norfolk, VA.
LAMINAR AND TURBULENT NATURAL CONVECTION HEAT TRANSFER IN TROMBE WALL CHANNELS Ph.D. Thesis
Tony D. T. Chen 1992 246 p
Avail: Univ. Microfilms Order No. DA9301142

The natural convective heat transfer and air movement in a Trombe wall solar passive system has been studied analytically and numerically. Three Trombe wall channel geometries including the parallel channel with axial inlet and exit, parallel channel with side vents and Trombe wall channel coupled to the room have been considered. For the parallel channel with axial inlet and exit geometry, a momentum-integral method has been used to solve parabolic governing equations for two dimensional laminar flow. This formulation leads to a second order ordinary differential equation for pressure defect in the Trombe wall channel. The solution of this equation leads to prediction of velocity, temperature and pressure fields, and Nusselt number correlations that are in good agreement with previously reported finite difference solution of natural convection boundary layer equations. For the side-vented channel case, results are obtained for both two dimensional laminar and turbulent natural convective flow regimes. Due to presence of recirculating flow patterns in this geometry, full Navier-Stokes equations in two-dimensions are employed. The turbulent flow characteristics are modeled by a two-equation (k-epsilon) model. The governing equations for steady laminar as well as turbulent flows are solved by a finite volume technique that uses the quadratic upwind differencing scheme to discretize non-linear governing equations to form algebraic equations which govern physical variables at the various numerical grid points. The coupled algebraic equations are solved by a semi-implicit algorithm known as SIMPLER. Flow patterns, isotherms and heat transfer characteristics are obtained for aspect ratios of 10 and 20, and Grashof number ranging from 1.4 x 10(exp 3) to 1.4 x 10(exp 8). The effect of the free pressure boundary location of flow characteristics is also analyzed. Results show that the mass flow rates induced and net energy delivered by the system is governed by the channel Grashof number and the channel vent size. The total vent loss coefficient for the side-vented cavity shows a minimum at Gr = 1.4 x 10(exp 4) for which the dimensionless mass flow rate also shows a maximum value. Dissert. Abstr.

N93-25553 Colorado Univ., Boulder.
THE EFFECTS OF LARGE-AMPLITUDE, LOW-FREQUENCY EXCITATION ON A THREE-DIMENSIONAL JET Ph.D. Thesis

Robert Bois Farrington 1992 874 p
Avail: Univ. Microfilms Order No. DA9304555

Large-amplitude, low-frequency excitation can increase the mixing and spreading in the two-dimensional region of a large aspect ratio slot jet and accelerate its transition from a two-dimensional form to an axisymmetric form. The average jet Reynolds number was 7240 and temperature differences were less than 10 C. A rotating damper was used to excite the flow at frequencies up to 56 Hz resulting in Strouhal numbers up to 0.32. Hot-wire anemometry was used to determine profiles of velocity and velocity fluctuations. Digital analysis of infrared images provided quantitative results on average spatial temperature distributions, temperature profiles, jet edge profiles, axial temperature decay rates, and mixing efficiencies. Large-amplitude, low-frequency excitation considerably distorts the velocity and velocity fluctuation profiles. Lower frequencies affect near-nozzle behavior and relatively higher frequencies affect the flow further from the nozzle. Decomposition of the temporal velocity profile into its phase-averaged mean, periodic, and random components show that most of the fluctuation is due to the periodic component with the random component contributing only 2 percent to 5 percent of the total velocity fluctuation. Depending on the excitation frequency, the half-harmonic and occasionally the quarter-harmonic can dominate the fundamental frequency. Higher excitation frequencies interact quickly with the flow structures generating multiple subharmonics and then dissipate while lower frequencies interact with structures near the nozzle exit without generating many subharmonics and then propagate with less interaction with flow structures. Excitation leads to increased velocity and temperature jet widths and accelerated decay of the centerline velocity and temperature. Infrared imaging shows that excitation does not distort the temperature profile as much as it does the velocity profile. Excitation enhanced the longitudinal 'saddle-back' profiles of the velocity and temperature. Both hot-wire anemometry and infrared imaging show that excitation accelerates the transformation of a rectangular jet to an axisymmetric form. Entrainment is not only increased in the two-dimensional regime but higher entrainment occurs sooner due to accelerated transformation to the axisymmetric regime, where entrainment increased linearly with distance rather than as the square root of the distance as in the two-dimensional regime. Dissert. Abstr.

N93-25560 California Univ., Los Angeles.
THE INSTABILITY OF A LIQUID JET IN A COMPRESSIBLE AIRSTREAM Ph.D. Thesis
Hsi-Shang Li 1992 180 p
Avail: Univ. Microfilms Order No. DA9302442

The instability of a liquid jet in a coflowing compressible airstream has been studied, motivated by the experimentally observed surface wave phenomenon and breakup of a liquid jet injected transversely into a compressible gas flow. The linear stability analysis of a two-dimensional plane liquid jet in a compressible airstream is formulated first to correlate the instability characteristics with the compressibility of the airstream. The small-amplitude disturbances superimposed on the mean flow inside and outside the jet are governed by Laplace's equation and the convective wave equation, respectively, along with suitable boundary conditions at the interfaces. The conditions for a valid linearization of the convective wave equation are obtained. It is established that the transient motion of the gas can dominate so that the nonlinear term due to accumulation of disturbances in the basic flow can be negligible even as the Mach number approaches unity. The dispersion relation has been developed and studied for both temporally and spatially growing modes. A physical understanding of how compressibility affects the growth rate has been made clear by applying a 1D compressible continuity equation at the interface region and studying the convection and accumulation of vorticity. Furthermore, the kinetic energy of the disturbed liquid jet is examined to see how surface tension and airstream pressure transfer energy between the liquid jet and the compressible airstream. A similar linear study using a circular liquid jet model is then formulated in order to further investigate the behavior of the axisymmetric and non-axisymmetric unstable modes. The empirically obtained sonic point criterion for predicting jet breakup has been partially explained by studying both the maximum growth rates and the transition from convective instability to absolute instability near M approx. 1 as obtained through these linear instability analyses. Furthermore, numerical simulations of the interfacial instability of a 2D plane liquid jet and of an axisymmetrical circular liquid jet in a compressible airstream are performed to investigate the nonlinear aspects of these problems. A high resolution scheme which has second order accuracy in space and time is coupled with a Lagrangian marker particle algorithm to visualize the large scale motion of the interfaces in compressible flow. A numerical algorithm based on an approximate equation of state of a compressible liquid is developed to allow this two-fluid system to be governed by the nonlinear Euler equations in conservative form. The initial growth of small disturbances given by the simulations agrees well with the instability characteristics of the jet flow established by the linear theory. The process of the jet disruption in compressible flow involves the formation of spikes and the stretching and detachment of the liquid main center core. Dissert. Abstr.

N93-25662 California Univ., San Diego.
ENERGY DISSIPATION IN INELASTIC FLOW OF COHESIONLESS GRANULAR MEDIA Ph.D. Thesis
Naoyuki Okada 1992 176 p
Avail: Univ. Microfilms Order No. DA9303271

In a granular mass which supports the externally applied loads through contact friction, the external work is partly stored and partly dissipated by friction or other mechanisms. In many applications involving relatively small pressures and hard granules, the dissipation by frictional sliding constitutes the major energy absorbing mechanism. Based on micromechanics, it is shown that the external work supplied to a water-saturated sand mass is mainly dissipated through friction between contacting granules. The frictional energy is formulated as a linear function of effective pressure. The model results are compared with the cyclic shearing experiments. A large hollow cylindrical torsional apparatus is used for the experiments, with sand as the test material. This thesis consists of three related parts. First, the results of a study of the cyclic shear deformation behavior under undrained conditions are presented. Experiments are conducted under strain-controlled conditions with various strain amplitudes. The relation between the excess pore water pressure and the corresponding external work in cyclic shearing is studied experimentally. Then, the results of a micromechanical model are compared with the experimental measurements. It is shown that the internal energy dissipation can be expressed as the history of the effective pressure and a single parameter. Second, the cyclic shear deformation behavior under drained conditions is studied. It is shown experimentally that the total volume decreases after each cycle, while the corresponding shear modulus increases. It is found that the energy dissipation coefficient is not constant in drained tests, but that these coefficients for undrained and drained tests approach each other as the number of cycles is increased. Third, the effect of the residual strain on the undrained cyclic shear deformation characteristics is experimentally studied. Experiments are conducted under both stress- and strain-controlled conditions, and the corresponding effects are investigated. It is shown that the shear deformation characteristics are significantly influenced by the residual strain under both strain- and stress-controlled conditions. In the stress-controlled tests, the shear resistance depends on the magnitude of residual strain. In the strain-controlled tests, however, the shear resistance does not seem to be strongly influenced by the magnitude of the residual strain. Dissert. Abstr.

N93-25663 Minnesota Univ., Minneapolis.
STABILIZED FINITE ELEMENT METHODS FOR INCOMPRESSIBLE FLOWS WITH EMPHASIS ON MOVING BOUNDARIES AND INTERFACES Ph.D. Thesis
Marek Antoni Behr 1992 233 p
Avail: Univ. Microfilms Order No. DA9303369

Two finite element formulations for incompressible fluid dynamics are presented. The space-time velocity-pressure formulation is used for flow problems involving moving boundaries and interfaces. The formulation is based on a time-discontinuous Galerkin method, supplemented with least-squares-type stabilization terms. The discussion centers on the application of the method to various problems with deforming domains. In particular, the formulation is employed to simulate three-dimensional sloshing in a storage tank subjected to external vibrations. The stress-velocity-pressure formulation is developed, essentially for viscoelastic flows. Treatment of stress as a separate unknown allows for inclusion of complex constitutive relations. Least-squares-type stabilization terms provide, once more, robustness to otherwise potentially unstable formulation. The method is first tested on Newtonian fluid flows past a circular cylinder in two dimensions. Then, by using simple viscoelastic constitutive model, the formulation is applied to a standard test problem. The strategies for the

solution of large systems of equations arising from the finite element discretization of the above formulations are also discussed. Particular emphasis is placed on iterative methods and the implementations on massively parallel supercomputers, paving the way for solving very large-scale practical problems, including those in three dimensions.
Dissert. Abstr.

N93-25683 Illinois Univ. at Urbana-Champaign, Savoy.
ASYMPTOTIC STUDIES OF GRAVITY-DRIVEN REACTING COATING FLOWS AND PULTRUSION PROCESSES Ph.D. Thesis
Quan Qi 1992 242 p
Avail: Univ. Microfilms Order No. DA9305658

Coating flows have many very important applications in engineering. The first part of this thesis deals with gravity-driven reacting coating flows down an inclined plane. When the reaction activation energy is large and heat release is significant, long wave theory and large activation energy asymptotics are applied jointly to derive a consistent set of governing equations, which describe wave formation on the free surface and evolution of the reaction front. The key feature shown by the solution is the coupling of the free surface with the reaction front. When the reaction activation energy is small and heat release is insignificant, long wave theory leads to a single governing equation for wave formation on the free surface. Unlike its traditional counterpart, this equation has variable coefficients attributed to the effect of variable viscosity. The solution of this equation shows that linear, as well as, nonlinear wave formations differ appreciably from the constant viscosity coating flows. Pultrusion is a composite manufacturing process. Issues such as variable viscosity resin flows etc., are examined in the second part of this thesis. Dissert. Abstr.

N93-25698 Manchester Univ. (England).
COMPUTATIONAL MODELLING OF 3D FLOW IN COMPLEX DUCTS AND PASSAGES Ph.D. Thesis
Fue-Sang Lien 1992 557 p
Avail: Univ. Microfilms Order No. BRD-97662

A computational procedure has been developed for predicting separated turbulent flows in complex two-dimensional and three-dimensional geometries. The procedure is based on the fully conservative, structured finite volume framework, within which the volume are non-orthogonal and collocated such that all discrete fields of flow variables are stored at one and the same set of nodes. To ease the task of discretization and to enhance the conservative property of the scheme, a Cartesian decomposition of the velocity field has been used, rather than a contravariant, coordinated directed decomposition. As an alternative, an adaptive decomposition has also been included, in which one velocity component is allowed to adapt itself to a pre-defined, essentially arbitrary datum line, with the other two components normal to that adapted. This latter decomposition has been provided with the view to the procedure being preferentially applied to curved three-dimensional duct of variable cross-sectional area. The solution algorithm is iterative in nature, approaching the steady-state solution by a sequential solution for velocity components and pressure with the aid of a pressure-correction algorithm. Convection is approximated with a range of schemes, among them first-order, second-order and third-order upstream-weighted schemes, and with a Total Variation Diminishing MUSCL scheme, the last applied specifically to transport equations governing turbulence properties. A broad range of flows, totalling some 20 configurations, have been computed within an extensive validation exercise, encompassing inviscid, laminar and turbulent flows, both compressible and incompressible, some two-dimensional and others three-dimensional. A number of geometries have been computed principally in order to verify or examine the adequacy of numerical practices or the performance of the multigrid convergence acceleration scheme. Many, however, involve the investigation of turbulence-model performance by reference to detailed experimental results. Among the most challenging flows computed are: shock-induced separation over bumps, computed with second-moment closure; separated flow through a sinusoidal constriction, also computed with second-moment closure; and three-dimensional flow through a S-shaped diffuser calculated with low-Reynolds-number models. Dissert. Abstr.

N93-25705 Pennsylvania State Univ., University Park.
HEAT TRANSFER MEASUREMENTS IN SWEPT SHOCK WAVE/TURBULENT BOUNDARY-LAYER INTERACTIONS Ph.D. Thesis
Yeol Lee 1992 187 p
Avail: Univ. Microfilms Order No. DA9236860

An experimental research program providing basic knowledge and establishing a database on the heat transfer in three-dimensional shock wave/boundary-layer interaction is described. High thermal loading in such interactions constitutes a fundamental problem of critical concern to future supersonic and hypersonic flight vehicles. A turbulent boundary-layer on a flat plate is subjected to interactions with swept planar shock waves generated by a sharp fin. Fin angles from 10 deg to 20 deg at freestream Mach numbers 3.0 and 4.0 produce a variety of interaction strengths from weak to very strong. A foil heater generates a uniform heat flux over the surface of interest and thin-film resistance thermometers mounted on it are used to measure the local surface temperature. The heat convection equation is then used to calculate the local heat transfer coefficients. The present heat transfer technique is applied to measure heat transfer distributions for 5 different interaction cases. The experimental data are compared with numerical Navier-Stokes solutions. The estimation of total uncertainty of the present measurements is about plus or minus 10 percent, which makes them suitable for CFD code validation purposes. The measured peak heat transfer data are correlated with the normal Mach number based on the concept of the quasi-conical nature of such interactions, and the results show good agreement with other experimental data.
Dissert. Abstr.

N93-25708 Colorado State Univ., Fort Collins.
THE RATE FORM OF EQUILIBRIUM EQUATION FOR PROBLEMS OF STEADY-STATE, ELASTIC, VISCOUS FLOWS Ph.D. Thesis
Lung John Tsai 1992 82 p
Avail: Univ. Microfilms Order No. DA9303900

The development of a numerical simulation for steady-state, elastic, viscous flows in two dimensions is presented. A mixed finite element method is used to couple the rate-equilibrium and the rate-constitutive equations by using successive substitution to solve for the velocity field and the stress field simultaneously. The method is applied to the flow analysis of co-rotational Maxwell (CRM), upper convective Maxwell (UCM), and four-element UCM fluid models. A flow through contraction problem is analyzed for the CRM, UCM and four-element UCM models. For both the CRM and UCM modles, the purely elastic case is compared to a solution found by using a linear formulation and it is found to compare favorably. For the purely viscous case, comparison is made with results obtained using the mixed formulation for velocity and pressure. Again, the results compare quite favorably. For the four-element UCM model, it is compared with the conventional UCM model. For the purely elastic and the purely viscous cases both models compare very well, and two examples are given for simulating both the Oldroyd-B and the Kelvin-Voigt models. From this illustration, the four-element UCM model is shown to work well for a wide range of constitutive behaviors. A second example presents an analysis of a metal forming rolling problem in the presence of free surfaces. For the purely elastic case, a decent solution of the velocity and stress distributions in the control volume for both CRM and UCM fluids is found. However, when the viscous effect is increased in the material, the free surface exhibits a continual swelling on the downstream side and the accuracy of the stress distribution deteriorates. In spite of the progress made on the free surface problem, the solutions for free surface problem presented in this dissertation are not yet of sufficient accuracy to be directly applicable to practical forming process design or analysis. The final example is an application of the rate-equilibrium formulation for elastic, nonlinear-viscous flows. It is shown that the method converges to reasonable solutions and hence the procedure has possible applications to metal forming processes. Dissert. Abstr.

N93-25725 Minnesota Univ., Minneapolis.
FLOW AND HEAT TRANSFER EXPERIMENTS IN THE TURBINE AIRFOIL/ENDWALL REGION Ph.D. Thesis
Jin Taek Chung 1992 277 p
Avail: Univ. Microfilms Order No. DA9236936

An experimental investigation of the three-dimensional flow and heat transfer near the junction between the endwall and suction wall of a gas turbine was performed. A large-scale, two-half-blade facility which simulates a turbine cascade was introduced. The simulator consists of two large half-blade sections, one wall simulating the pressure surface and the other wall simulating the suction surface. The advantage of this configuration is

that the features of the secondary flow are large, because of the relatively large test section, and the flow is easily accessible with probes. Qualification of this simulator was by comparison to a multi-blade cascade flow. Various flow visualization techniques--oil and lampblack, ink and oil of wintergeeen, a single tuft probe, and a tuft grid--were employed to confirm that the important features of the cascade flow were replicated in this simulator. The triangular region on the suction surface, which was affected by the passage vortex, and the endwall secondary crossflow were observed by shear stress visualization and the liquid crystal measurement techniques. In order to investigate the effects of the turbulence level on the secondary flow in a turbine passage, a turbulence generator, designed to reproduce the characteristics of a combustor exit flow, was built. The generator was designed not only to generate a high turbulence level but to produce three main features of a combustor exit flow. The generator produced a turbulence intensity level of about 10 percent and an integral length scale of 5 centimeters. It was observed that the endwall secondary flow, including the passage vortex, is not significantly influenced by freestream turbulence levels up to 10 percent. A flow management technique using a boundary layer fence designed to reduce some harmful effects of secondary flow in the endwall region of a turbine passage was introduced. The boundary layer fence is effective in changing the passage of the vortex and reducing the influence of the vortex near the suction wall. The fence was even more effective in reducing secondary flows for high levels of freestream turbulence (approximately 10 percent). Dissert. Abstr.

N93-25737 Missouri Univ., Rolla.
TWO-DIMENSIONAL FIN ANALYSIS Ph.D. Thesis
Hyung Suk Kang 1992 110 p
Avail: Univ. Microfilms Order No. DA9224672

This dissertation deals with the variation of heat loss from the fin and the temperature distribution within the fin using a two-dimensional analysis for rectangular and triangular fins. For the rectangular fins, the root temperature is assumed to vary as cosine function across the fin root and the surface convection coefficients of the fin are assumed to be constant but unequal. The analysis is restricted to Biot numbers (= hl/k) such that 0 is less than or equal to B2 is less than or equal to B1 is less than or equal to 1, and B1 = 1, 0.1, 0.01, where B1 is the Biot number of the top surface and B2 is the Biot number of the bottom surface. For the triangular fins, the root temperature and surface convection coefficient are assumed to be constant. A comparison of the two dimensional temperature distribution within the fin and heat transfer rate from the fine, computed using a non-traditional (forced) analytic method and finite difference method, is made. Finally a one-dimensional analyses of the triangular fin is made using a statistical method. The results of these analyses will be helpful when the actual experimental set up is built and used in the laboratory. For the rectangular fins, the results show that the value of the tip Biot number is not important in the heat loss predictions when B1 and B2 are large. Under certain circumstances, the heat loss from the fin is essentially independent of the ratio of the fin length to the fin half width. For the triangular fins, the results show that when the Biot number is less than 0.1 (i.e., under usual circumstances), the forced analytic method is applicable. The statistical method yields a reasonably accurate value of the convection coefficient, h, using actual experimental data. Dissert. Abstr.

N93-25738 New Jersey Inst. of Tech., Newark.
PARTICLE DYNAMICS MODELING OF BOUNDARY EFFECTS IN GRANULAR COUETTE FLOW Ph.D. Thesis
Hyeong-Jin Kim 1992 299 p
Avail: Univ. Microfilms Order No. DA9235729

This study provides insights in understanding boundary effects on the flow of dry granular materials composed of identical, smooth, inelastic spheres between parallel, bumpy walls in the absence of gravity. The results of this study are useful in providing a basis upon which developing theories can be modified as well as substantiating previous and current experiments. This in turn has a major importance in many industries which are concerned with handling of particulates, such as coal, mineral processing, powder metallurgy, and agriculture. The particle dynamics or discrete element method is used to model this flow, thereby providing a means of obtaining macroscopic information from the detailed particle-level multi-body dynamics. A shearing flow is induced by allowing the upper and lower walls to move with the same constant velocity in opposite directions. The wall geometry is characterized by several parameters - the spacing between the wall half-spheres and their geometric arrangement, diameter ratio of the wall to flow spheres, shear gap height and particle inelasticity measured by a constant normal restitution coefficient. Boundary roughness is either increased or decreased by appropriately adjusting the spacing between wall half-spheres or by changing the diameter ratio. For 'small' systems, a large stress drop occurs for dense flows when the wall particles are tightly packed. In this case, a layered shearing flow is present. However, as the shear gap height is increased while maintaining the same wall conditions, the stress drop does not occur. Computed wall stress components and slip velocities are very sensitive to boundary parameters. The ratio of shear to normal wall stresses is found to be independent of shear gap heights for fixed wall conditions. As wall roughness increases or flow particles become more elastic, slip velocity decreases thereby reducing the effectiveness of the walls in supplying momentum to the flow. A pronounced reduction in slip velocity is observed with increasing wall roughness for relatively elastic particles. Dissert. Abstr.

N93-25746 Maryland Univ., College Park.
AN EXPERIMENTAL STUDY OF PASSIVE DRAG REDUCTION IN A TURBULENT BOUNDARY LAYER BY A RIBLET SURFACE Ph.D. Thesis
Seong-Ryong Park 1992 232 p
Avail: Univ. Microfilms Order No. DA9304378

An experimental study was performed with a single-sensor hot-wire probe in the wall region of a nominally zero pressure gradient turbulent boundary layer over smooth and V-groove riblet plates of h(+) approximately 14, s(+) approximately 28 at Re(sub theta) is approximately equal to 1200. The shear stress variation in the span wise direction and the alteration of the turbulent characteristics were directly measured. The span wise average shear stress on riblet groove was obtained and contour lines were fitted to the measurement for all the statistics. Net drag reduction of about 4 percent was found for this case, in substantial agreement with previous direct measurement. The synthetic analysis, at y(+) approximately 30, of a modified Kovasznay-type probe was performed and an improvement algorithm was developed. The performance of a cross-shaped four-sensor probe in the turbulent boundary layer in the highly sheared region (y+ approximately 4) is also presented. To further understand the flow structure inside the riblet, four-sensor hot wire probes of a modified version of the original Kovaszny-type and of a cross-shaped were used over the two test surfaces at Re is approximately equal to 2500 and 2100, respectively. Statistical properties of the fluctuating velocity components and the Reynolds stress, including joint probability density functions and frequency spectra of data obtained over the smooth and the peak and over the valley of the riblet plate are presented. Dissert. Abstr.

N93-25747 Pittsburgh Univ., PA.
FLOW BETWEEN FINITE ROTATING DISKS AND ITS LINEAR STABILITY Ph.D. Thesis
Dong Fu 1992 184 p
Avail: Univ. Microfilms Order No. DA9236113

The flow between finite rotating disks with a large aspect ratio (beta = R/d, where d is the gap between the disks and R is the radius of the disk) and its linear stability are studied. Through an analysis of the singular points of the governing equations, some quasi-similar properties of basic flow with respect to certain parameters are obtained. Extensive numerical experiments on the basic flows are conducted by projecting governing equations onto a polynomial subspace with a B-spline basis. The numerical results have very good agreement with the experimental data of Szeri and strongly support the theoretical predictions. The linear stability of the basic flow, with beta(sup 2) = 406.5 and beta(sup 2) = 1975.3, is studied in detail. The perturbation equations which characterize the stability of the finite disk flow are derived and solved numerically. Three types of unstable modes are found. These are: (1) S(sub W), introduced by and located near the side wall; (2) S(sub L), consisting of spiral-like vortices, which occurs at mid radius; and (3) S(sub R), appearing when the Reynolds number of the basic flow is large. The numerical predictions for critical Reynolds number are in good agreement with the experimental data of Sirivat. Dissert. Abstr.

N93-25753 Maryland Univ., College Park.
LARGE-EDDY SIMULATION OF TEMPORALLY DEVELOPING BOUNDARY LAYERS WITH EMBEDDED STREAMWISE VORTICES

Ph.D. Thesis
Hossein Esmaili 1992 147 p
Avail: Univ. Microfilms Order No. DA9234560

The interaction of streamwise vortices with turbulent boundary layer has been investigated using large-eddy simulation. The embedded vortices are a pair of counter-rotating Oseen vortices with flow between them directed towards the wall (common-flow-down), superimposed on various instantaneous realizations of flat plate and sink flow turbulent boundary layers. The time development of the vortices and their interaction with the boundary layer are studied by integrating the filtered Navier-Stokes equations in time. The most important effects of the vortices on the boundary layer are the thinning of the boundary layer in the downwash region between the vortices and its thickening in the upwash region. The Reynolds stress profiles highlight the highly three-dimensional structure of the turbulent boundary layer modified by the vortices. The presence of significant turbulent activity near the vortex center and in the upwash region where inflectional velocity profiles are observed, suggests that localized instability mechanisms in addition to the convection of turbulent energy by the secondary flow are responsible for this effect. High levels of secondary stresses in the vicinity of the vortex center are also observed. These simulations also indicate that eddy viscosity models should be expected to perform poorly in the vortex core region. The numerical results for the flat plate turbulent boundary layer show good agreement with the experimental results of Pauley and Eaton (1988a,b). The mean features of flow show the same patterns for both the flat plate and sink flow turbulent boundary layers.
Dissert. Abstr.

N93-25779# Naval Postgraduate School, Monterey, CA.
THERMOCAPILLARY FLOW NEAR A COLD WALL Technical Report, Jan. - Dec. 1992
David Canright 20 Jan. 1993 43 p
(AD-A261050; NPS-MA-93-011) Avail: CASI HC A03/MF A01

The following model problem examines the thermocapillary feedback mechanism important at the edge of weld pools and other materials processes. A pool of liquid with a flat horizontal free surface is bounded on one side by a vertical solid wall, which is maintained at a cold temperature to unit depth, and at a warmer temperature below; far away the fluid is at the warmer temperature. Surface tension is a decreasing function of temperature, so that the surface thermal gradient drives flow toward the corner. When convection is vigorous, the flow compresses the thermal gradient which is driving the flow; this positive feedback results in small local length scales and high velocities near the corner. This problem is examined through a detailed scaling analysis and through numerical simulation for a range of parameters.
DTIC

N93-25885# Coast Guard Academy, New London, CT. Center for Advanced Studies.
CORRELATIONS BETWEEN ORGANIZED TURBULENT STRUCTURES AND WALL PRESSURE FLUCTUATIONS
Vincent Wilczynski and Mario J. Casarella (Catholic Univ. of America, Washington, DC.) Sep. 1992 19 p
(PB93-156479; USCGA-TR-11-92) Avail: CASI HC A03/MF A01

The investigation examines the relationship between flow structures observed across the boundary layer and their wall pressure signatures. Experimental data of simultaneous wall pressure and velocity fluctuations have been obtained in a low noise flow facility and analyzed using statistical and spectral methods. First, the individual properties were examined to observe their unique features in the inner and outer regions. Next, the joint probability and cross-spectra between stream wise and wall-normal velocity fluctuations were investigated to study distinctive features of both the Reynolds stress within the boundary layer, and the observed irrotational motion at the edge of the boundary layer. Finally, to evaluate a proposed correlation between the spatial locations of turbulent sources and the frequency bands of the wall pressure spectrum, cross-spectral data between the wall pressure spectrum and velocity fluctuations are examined. The distinct contributions to the wall pressure spectrum from the band-limited irrotational motion, and regions of high turbulent production are identified.
NTIS

N93-25951# North Carolina Agricultural and Technical State Univ., Greensboro. Dept. of Mechanical Engineering.
UNIFORM ROUGHNESS STUDIES Final Report, Sep. 1987 - Mar. 1992
D. E. Klett and M. Kithcart May 1992 82 p
(Contract F33615-C-87-3022)
(WL-TR-92-3041) Avail: CASI HC A05/MF A01

Heat transfer, skin friction, turbulence intensity, and velocity profile data were obtained for 22 different rough surfaces in turbulent subsonic boundary layer air flow. The rough surfaces consisted of hemispherical dimples, hemispherical protrusions, and rectangular protrusions. The rectangular roughness plates were tested with the tops of the elements flush with the upstream smooth surface and with the tops protruding above the smooth surface. The surfaces with protrusions were designed to have values of the Simpson roughness shape/spacing parameter that bracket the peak in the equivalent sand-grain correlation. The data was used for comparison with predictions from a discrete element rough surface boundary layer code in an attempt to improve the code's performance for cases of closely spaced roughness elements when wakes behind individual elements overlap. An anomaly was discovered in the code that causes wide variations in predicted drag and heat transfer for small variations in element drag coefficient C(sub d). The problem lies in the effect of C(sub d) on the velocity calculation giving rise to inflections in the calculated velocity profile near the crests of the roughness elements. A remedy to the problem has not, as yet, been found.
Author (revised)

N93-25953# Army Materials Technology Lab., Watertown, MA. Polymer Research Branch.
NUMERICAL SIMULATION OF PERMEATION FROM DEPOSITED DROPLETS: MODEL EXPANSION Final Report
Geralda Severe and Jerry H. Meldon Apr. 1992 69 p
(DA Proj. 1L1-62105-AH-84)
(MTL-TR-92-23) Avail: CASI HC A04/MF A01

A previously published model of permeation from a droplet has been expanded. The effects of downstream mass transfer resistance and concentration dependence of the diffusion coefficient are included. An attempt was made to fit experimental results for the permeation of di-iso-propyl- methyl-phosphonate (DIMP) through Neoprene and natural rubber. Simulated data do not reproduce the initial pronounced delay of experimental permeation. Furthermore, no rationale was identified for the anomalous dependence of 'breakthrough time' upon barrier thickness observed with several experimental systems.
Author (revised)

N93-25987# Los Alamos National Lab., NM.
DSD TECHNOLOGY: A DETONATION REACTIVE HUYGENS CODE
John Bdzil and Wildon Fickett Jul. 1992 52 p
(LA-12235-MS; UC-741; UC-705) Avail: CASI HC A04/MF A01

The length of the reaction zone strongly influences the speed of propagation of detonation in multi-dimensional explosive pieces. Detonation Shock Dynamics (DSD) properly accounts for these effects in detonation wave-spreading problems when the radius of curvature of the multi-dimensional detonation shock is large compared to the explosive's reaction-zone length. This report is a user manual for our two-dimensional implementation of this method, a FORTRAN subroutine called DSD Technology.
Author (revised)

N93-26000* National Aeronautics and Space Administration. Langley Research Center, Hampton, VA.
METHOD OF MEASURING CROSS-FLOW VORTICES BY USE OF AN ARRAY OF HOT-FILM SENSORS Patent
Aval K. Agarwal, inventor (to NASA), Dal V. Maddalon, inventor (to NASA), and Siva M. Mangalam, inventor (to NASA) 11 May 1993 9 p Filed 7 Jan. 1992 Supersedes N92-30390 (30 - 21, p 3628)
(NASA-Case-LAR-14824-1-SB; US-Patent-5,209,111;
US-Patent-Appl-SN-823805; US-Patent-Class-73-147;
US-Patent-Class-73-178R; US-Patent-Class-73-204.11;
Int-Patent-Class-G01M-9/00) Avail: US Patent and Trademark Office

The invention is a method for measuring the wavelength of cross-flow vortices of air flow having streamlines of flow traveling across a swept airfoil. The method comprises providing a plurality of hot-film sensors. Each hot-film sensor provides a signal which can be processed, and each hot-film sensor is spaced in a straight-line array such that the distance between successive hot-film sensors is less than the wavelength of the cross-flow vortices being measured. The method further comprises determining the direction of travel of the streamlines across the airfoil and positioning the straight-line array of hot film sensors perpendicular to the

direction of travel of the streamlines, such that each sensor has a spanwise location. The method further comprises processing the signals provided by the sensors to provide root-mean-square values for each signal, plotting each root-mean-square value as a function of its spanwise location, and determining the wavelength of the cross-flow vortices by noting the distance between two maxima or two minima of root-mean-square values.
Official Gazette of the U.S. Patent and Trademark Office

N93-26163# California Inst. of Tech., Pasadena. Graduate Aeronautical Labs.
IMAGE CORRELATION VELOCIMETRY Technical Report, 1 Jun. - 1 Nov. 1992
P. T. Tokumaru and P. E. Dimotakis 1 Feb. 1993 32 p
(Contract F49620-92-J-0290)
(AD-A261599; GALCIT-FM92-1; AFOSR-93-0133TR) Avail: CASI HC A03/MF A01

This paper focuses on the correlation of two successive scalar images for the purpose of measuring imaged fluid motions. A method is presented for deforming, or transforming, one image to another. Taylor series expansions of the Lagrangian displacement field are used, in conjunction with an integral form of the equations of motion, to approximate this transformation. The proposed method locally correlates images for displacements, rotations, deformations, and higher order displacement gradient fields and applies a global minimization procedure to insure a global consistency in the results. An integral form of the equations of motion is employed and, as a consequence, no spatial or temporal differentiation of the image data is required in estimating the displacement field. Successive two-dimensional digital CCD images of fluid motion marked with dye are used to verify the capabilities of the method. The utility of the method is also illustrated using a pair of Voyager 2 images of Jupiter.
DTIC

N93-26167# Naval Postgraduate School, Monterey, CA.
MODEL FAN PASSAGE FLOW SIMULATION M.S. Thesis
David D. Myre Dec. 1992 172 p
(AD-A261613) Avail: CASI HC A08/MF A02

Two-dimensional experimental and numerical simulations of a transonic fan blade passage were conducted at a Mach number of 1.4 to provide baseline data for the study of the effects of vortex generating devices on the suction surface shock-boundary layer interaction. In the experimental program, a probe and traverse system were designed and constructed. A new data acquisition system was adapted to record data from probe measurements and multiple scans of static pressure ports. Impact pressure behind two model fan passages and static pressures across the shock-boundary layer interaction were measured for a design and one off-design flow incidence in a blow-down wind tunnel. The passage shocks were positioned in similar locations by rotating the model to a decreased flow incidence. Fan passage losses were obtained by integrating probe measurements. The losses compared favorably with a numerical Navier-Stokes solution and one engineering loss model, Static pressure distributions were also found to compare favorably with numerical results.
DTIC

N93-26203*# National Aeronautics and Space Administration. Lewis Research Center, Cleveland, OH.
AN EXTENDED LAGRANGIAN METHOD
Meng-Sing Liou May 1992 28 p
(RTOP 505-62-52)
(NASA-TM-106129; E-7798; NAS 1.15:106129) Avail: CASI HC A03/MF A01

A unique formulation of describing fluid motion is presented. The method, referred to as 'extended Lagrangian method', is interesting from both theoretical and numerical points of view. The formulation offers accuracy in numerical solution by avoiding numerical diffusion resulting from mixing of fluxes in the Eulerian description. Meanwhile, it also avoids the inaccuracy incurred due to geometry and variable interpolations used by the previous Lagrangian methods. Unlike the Lagrangian method previously imposed which is valid only for supersonic flows, the present method is general and capable of treating subsonic flows as well as supersonic flows. The method proposed in this paper is robust and stable. It automatically adapts to flow features without resorting to clustering, thereby maintaining rather uniform grid spacing throughout and large time step. Moreover, the method is shown to resolve multi-dimensional discontinuities with a high level of accuracy, similar to that found in one-dimensional problems.
Author

N93-26269# Michigan Univ., Ann Arbor. Dept. of Electrical Engineering and Computer Science.
MASSIVELY-PARALLEL COMPUTATIONAL FLUID DYNAMICS Final Report, 15 Oct. 1989 - 14 Oct. 1992
Donald Calahan 14 Oct. 1992 5 p
(Grant AF-AFOSR-0020-90)
(AD-A261815; AFOSR-93-0139TR) Avail: CASI HC A01/MF A01

The effort has had several components since it was initiated in Oct of 1989; all of these had as their objective the assistance of Dr. Joseph Shang at WRDC in the redirection of his effort toward use of massively-parallel architectures. The major objective was to gain algorithm experience in conversion of two Air Force production CFD codes to a general format applicable to a variety of commercial message-passing architectures. Earlier, an explicit N-S 3D code from WRDC had been converted to the NCUBE. This was used as a model for parallelized production code developed at WRDC under DARPA sponsorship. This effort was completed with the conversion of a serial full 3D Navier-Stokes Beam-Warming CFD code to a 1024-node scalar NCUBE hypercube at SANDIA (Albuquerque).
DTIC

N93-26328# Naval Undersea Warfare Center, Newport, RI. Weapons Technology and Underseas Systems Dept.
PROCEEDINGS OF THE NUWC DIVISION NEWPORT SEMINAR SERIES ON TURBULENCE AND ITS CONTROL
P. R. Bandyopadhyay, comp. and J. C. S. Meng, comp. 1 Oct. 1992 204 p Seminars held in Newport, RI, summer 1992
(NUWC-NPT-TM-922089) Avail: CASI HC A10/MF A03

The proceedings of a four-part seminar series on turbulence and its control sponsored by the Naval Undersea Warfare Center Division, Newport, RI, during the summer of 1992 are presented. Topics covered include: new aspects of vortex dynamics and hydrodynamic turbulence; renormalization group theory for turbulence transport modeling; direct control of wall shear-stress in a turbulent boundary layer; and bluff-body and other shear flows.
Author (revised)

N93-26360# California Univ., San Diego, La Jolla. Dept. of Applied Mechanics and Engineering Sciences.
INTERACTION OF VORTICITY WITH A FREE SURFACE Report, 15 Mar. - 30 Sep. 1992
Morteza Gharib 30 Sep. 1992 8 p
(Contract N00014-92-J-1610)
(AD-A261524) Avail: CASI HC A02/MF A01

We intend to combine numerical, theoretical and experimental efforts to systematically extend our capabilities to understand and model vortical and turbulent flows near a free surface.
DTIC

N93-26379# California Inst. of Tech., Pasadena. Graduate Aeronautical Labs.
MEASUREMENTS OF SCALAR POWER SPECTRA IN HIGH SCHMIDT NUMBER TURBULENT JETS Technical Report, 1 Jun. - 1 Nov. 1992
Paul L. Miller and Paul E. Dimotakis 9 Nov. 1992 25 p
(Contract F49620-92-J-0290)
(AD-A261542; AFOSR-93-0132TR) Avail: CASI HC A03/MF A01

Single-point, jet-fluid concentration measurements obtained from high Schmidt number (Sc approximately equal to 1.9 x 10(exp 3)) turbulent jets permit an investigation of temporal scalar power spectra, for jet Reynolds numbers in the range of 1.25 less than or equal to Re x 10(exp -4) less than or equal to 7.2. At intermediate scales, we find a spectrum with a logarithmic derivative (slope) that is increasing with Reynolds number, in absolute value, but less than 5/3 at the highest Reynolds number in our experiments. At the smallest scales, our spectra exhibit no 1-k power-law behavior, possessing a log-normal region over a range of scales exceeding a factor of 40, in some cases.
DTIC

N93-26400# Virginia Polytechnic Inst. and State Univ., Blacksburg.
COMPUTATIONAL METHODS FOR FLOW PROBLEMS: PARALLEL ALGORITHMS, FLOW CONTROL, AND NOVEL APPROACHES Final Technical Report, 1 Mar. 1990 - 30 Nov. 1992

Max D. Gunzburger 30 Nov. 1992 19 p
(Grant AF-AFOSR-0179-90)
(AD-A261400; AFOSR-93-0041TR) Avail: CASI HC A03/MF A01

A review of the research that has been carried out under the sponsorship of Air Force Office of Scientific Research grant number AFOSR-90-0179 is given. Details are given about two research programs, namely flow control and superconductivity. In both instances we have modeled realistic physical problems, we have performed rigorous analysis on the mathematical models, we have developed approximation schemes which we have also analyzed, and we have written computer codes implementing our computational method. In both instances, were the first to carry out such a comprehensive research program, and in so doing, have developed robust and useful algorithms that also embarked on a joint research program with personnel at AEDC facility in Tullahoma, Tennessee. We also briefly discuss other accomplishments related to this grant, including other research project invited talks, journal articles, etc. DTIC

N93-26535# National Inst. of Standards and Technology, Boulder, CO. Chemical Engineering Div.
FLOW CONDITIONER LOCATION EFFECTS IN ORIFICE FLOWMETERS
J. L. Scott, C. F. Sindt, and M. A. Lewis Jan. 1993 72 p See also PB92-189521 and PB92-183730
(PB93-159457; NIST/TN-1356) Avail: CASI HC A04/MF A01; SOD HC

Tests sponsored by Gas Research Institute were conducted with orifice flowmeters of two nominal sizes: 104 mm and 52 mm. For the 104 mm orifice meter, the authors compared discharge coefficients measured in two common piping configurations used by laboratories to establish baseline flow conditions. The discharge coefficients are similar for beta ratios of 0.43, 0.55, and 0.67, but not for the 0.73 beta ratio plate. For other tests with the orifice meter, a 90 degree elbow or a reducer was located upstream of the orifice plate and flow conditioner. Two beta ratios (0.54, 0.67) were tested in the 52 mm orifice meter in baseline configuration and with an elbow at 17D and a flow conditioner at 12D. For many of the tests, differential pressures were measured at more than one flange tap location. Placing the flow conditioner too close to the orifice plate in either meter yields discharge coefficients below baseline values. The location of the flow conditioner with respect to the orifice plate appears to influence meter performance more significantly than the type or location of flow disturbance upstream of it. NTIS

N93-26543# Air Force Academy, CO.
ANOTHER LOOK AT THE DRIVEN CAVITY PROBLEM Final Report
Max A. Stafford 2 Nov. 1992 41 p
(AD-A261903; USAFA-TR-92-4) Avail: CASI HC A03/MF A01

Numerical analysis of a lid driven cavity is a standard computational fluid dynamics problem. A semi-discrete method known as the method of lines is used to reduce the problem to one of solving a coupled system of first-order linear differential equations and linear algebraic equations. The spectrum of the coefficient matrix in the first-order system of differential equations is analyzed as the flow field evolves from rest to steady state. By examining the pattern of this eigenvalue migration, it is possible to estimate the time to steady state by using very coarse grids. A simple relationship between the Reynolds number and time to steady state is also apparent from analyzing the coefficient matrix. DTIC

N93-26554*# National Aeronautics and Space Administration. Lewis Research Center, Cleveland, OH.
INCOMPRESSIBLE SPECTRAL-ELEMENT METHOD: DERIVATION OF EQUATIONS
Russell G. DeAnna Apr. 1993 88 p
(DA Proj. 1L1-61102-AH-45; RTOP 505-62-OK)
(NASA-TM-106109; E-7758; NAS 1.15:106109; AVSCOM-TR-92-C-022)
Avail: CASI HC A05/MF A01

A fractional-step splitting scheme breaks the full Navier-Stokes equations into explicit and implicit portions amenable to the calculus of variations. Beginning with the functional forms of the Poisson and Helmholtz equations, we substitute finite expansion series for the dependent variables and derive the matrix equations for the unknown expansion coefficients. This method employs a new splitting scheme which differs from conventional three-step (nonlinear, pressure, viscous) schemes. The nonlinear step appears in the conventional, explicit manner, the difference occurs in the pressure step. Instead of solving for the pressure gradient using the nonlinear velocity, we add the viscous portion of the Navier-Stokes equation from the previous time step to the velocity before solving for the pressure gradient. By combining this 'predicted' pressure gradient with the nonlinear velocity in an explicit term, and the Crank-Nicholson method for the viscous terms, we develop a Helmholtz equation for the final velocity. Author (revised)

N93-26008* National Aeronautics and Space Administration. Langley Research Center, Hampton, VA.
WORKSHOP REPORT: A VALIDATION STUDY OF NAVIER-STOKES CODES FOR TRANSVERSE INJECTION INTO A MACH 2 FLOW
Dean R. Eklund (Analytical Services and Materials, Inc., Hampton, VA.), G. Burton Northam, J. C. McDaniel (Virginia Univ., Charlottesville.), and Cliff Smith (CFD Research Corp., Huntsville, AL.) *In* JHU, 29th JANNAF Combustion Subcommittee Meeting, Volume 2 Oct. 1992 p 19-34 Previously announced as A93-21330 (For primary document see N93-26005 09-20)
Avail: CPIA, 10630 Little Patuxent Pkwy., Suite 202, Columbia, MD 21044-3200 HC

35 INSTRUMENTATION AND PHOTOGRAPHY

Includes remote sensors; measuring instruments and gages; detectors; cameras and photographic supplies; and holography.

For aerial photography see *43 Earth Resources and Remote Sensing*. For related information see also *06 Aircraft Instrumentation*, and *19 Spacecraft Instrumentation*.

N93-24737*# National Aeronautics and Space Administration. Lewis Research Center, Cleveland, OH.
ICE THICKNESS MEASUREMENT SYSTEM FOR THE ICING RESEARCH TUNNEL CALIBRATION
Theresa L. Gibson and John M. DeArmon (Sverdrup Technology, Inc., Brook Park, OH.) Jun. 1993 8 p Proposed for presentation at the 1993 SWE National Convention and Student Conference, Chicago, IL, 21-27 Jun. 1993; sponsored by the Society of Women Engineers
(RTOP 505-62-84)
(NASA-TM-106095; E-7735; NAS 1.15:106095) Avail: CASI HC A02/MF A01

To measure icing patterns across a test section of the Icing Research Tunnel, an automated rotating bar measurement system was developed at NASA LeRC. In comparison with the previously used manual measurement system, this system provides a number of improvements: increased accuracy and repeatability, increased number of data points, reduced tunnel operating time, and improved documentation. The automated system uses a linear variable differential transformer (LVDT) to measure ice accretion. This instrument is driven along the bar by means of an intelligent stepper motor which also controls data recording. This paper describes the rotating bar calibration measurement system. Author (revised)

N93-25076*# National Aeronautics and Space Administration. Ames Research Center, Moffett Field, CA.
MEASUREMENTS OF DENSITY, TEMPERATURE, AND THEIR FLUCTUATIONS IN TURBULENT SUPERSONIC FLOW USING UV LASER SPECTROSCOPY
Douglas G. Fletcher and R. L. McKenzie Oct. 1992 9 p Presented at the 6th International Symposium on Applications of Laser Techniques to Fluid Mechanics, Lisbon, Portugal, 20-23 Jul. 1992
(RTOP 505-59-00)
(NASA-TM-103943; A-92120; NAS 1.15:103943) Avail: CASI HC A02/MF A01

Nonintrusive measurements of density, temperature, and their turbulent fluctuation levels were obtained in the boundary layer of an unseeded, Mach 2 wind tunnel flow. The spectroscopic technique that was used to make the measurements is based on the combination of laser-induced oxygen fluorescence and Raman scattering by oxygen and nitrogen from the same laser pulse. Results from this demonstration experiment are compared with previous measurements obtained in the same facility using conventional probes and an earlier spectroscopic technique. Densities and temperatures measured with the current technique agree with the previous surveys to within 3 percent and 2 percent, respectively. The fluctuation

amplitudes for both variables agree with the measurements obtained using the earlier spectroscopic technique and show evidence of an unsteady, weak shock wave that perturbs the boundary layer. Author (revised)

N93-25173*# National Aeronautics and Space Administration. Lewis Research Center, Cleveland, OH.

DEVELOPMENT OF THIN FILM THERMOCOUPLES ON CERAMIC MATERIALS FOR ADVANCED PROPULSION SYSTEM APPLICATIONS

Raymond Holanda Feb. 1993 16 p Presented at the Conference for Preparation for Temperature: Its Measurement and Control in Science and Industry, Toronto, Ontario, 28 Apr. - 2 May 1992; sponsored by AIP, ISA, NIST, and NRC

(RTOP 510-01-50)

(NASA-TM-106017; E-7574; NAS 1.15:106017) Avail: CASI HC A03/MF A01

Thin film thermocouples were developed for use on metal parts in jet engines to 1000 C. However, advanced propulsion systems are being developed that will use ceramic materials and reach higher temperatures. The purpose is to develop thin film thermocouples for use on ceramic materials. The new thin film thermocouples are Pt13Rh/Pt fabricated by the sputtering process. Lead wires are attached using the parallel-gap welding process. The ceramic materials tested are silicon nitride, silicon carbide, aluminum oxide, and mullite. Both steady state and thermal cycling furnace tests were performed in the temperature range to 1500 C. High-heating-rate tests were performed in an arc lamp heat-flux-calibration facility. The fabrication of the thin film thermocouples is described. The thin film thermocouple output was compared to a reference wire thermocouple. Drift of the thin film thermocouples was determined, and causes of drift are discussed. The results of high heating rate tests up to 2500 C/sec are presented. The stability of the ceramic materials is examined. It is concluded that Pt13Rh/Pt thin film thermocouples are capable of meeting lifetime goals of 50 hr or more up to temperatures of 1500 C depending on the stability of the particular ceramic substrate.

Author (revised)

N93-25191*# National Aeronautics and Space Administration. Lewis Research Center, Cleveland, OH.

ATOMIZING-GAS TEMPERATURE EFFECT ON CRYOGENIC SPRAY DROPSIZE

Robert D. Ingebo Jun. 1993 12 p Prepared for presentation at the 29th Joint Propulsion Conference and Exhibit, Monterey, CA, 28-30 Jun. 1993; sponsored by AIAA, SAE, ASME, and ASEE

(RTOP 505-62-52)

(NASA-TM-106106; E-7754; NAS 1.15:106106) Avail: CASI HC A03/MF A01

Correlating expressions for two-phase flow breakup of liquid nitrogen, LN2, jets in sonic velocity nitrogen gasflows were obtained for an atomizing-gas temperature range of 111 to 442 K. The correlations were based on characteristic dropsize measurements obtained with a scattered-light scanner. The effect of droplet vaporization on the measurements of the volume-median dropsize was calculated by using previously determined heat and momentum transfer expressions for droplets evaporating in high-velocity gasflow. Finally, the dropsize of the originally unvaporized spray was calculated, normalized with respect to jet diameter and correlated with atomizing-gas flowrate and temperature. Author

N93-25291 Colorado Univ., Boulder.

AN ACTIVE SOLID STATE RING LASER GYROSCOPE Ph.D. Thesis

Timothy Joseph Valle 1992 174 p

Avail: Univ. Microfilms Order No. DA9304610

The properties of an active, solid state ring laser gyroscope were investigated. Two laser diode pumped monolithic nonplanar ring oscillators (NPRO), forced to lase in opposite directions, formed the NPRO-Gyro. It was unique in being an active ring laser gyroscope with a homogeneously broadened gain medium. This work examined sources of technical and fundamental noise. Associated calculations accounted for aspects of the NPRO-Gyro performance, suggested design improvements, and outlined limitations. The work brought out the need to stabilize the NPRO environment in order to achieve performance goals. Two Nd:YAG NPRO's were mounted within an environment short term stabilized to microdegrees Celsius. The Allan variance of the NPRO-Gyro beat note was 500 Hz for a one second time delay. Unequal treatment of the NPRO's appeared as noise on the beat frequency, therefore reducing its rotation sensitivity. The sensitivity to rotation was limited by technical noise sources. Dissert. Abstr.

N93-25345*# Iowa State Univ. of Science and Technology, Ames.

NOVEL APPROACHES TO THE CONSTRUCTION OF MINIATURIZED ANALYTICAL INSTRUMENTATION

Marc D. Porter, Ronald P. OToole, Shelley J. Coldiron, William D. Deninger, Randall S. Deinhammer, Stanley G. Burns, Glenn J. Bastiaans, Steve D. Braymen, and Howard R. Shanks [1992] 20 p

(Grant NAG2-722)

(NASA-CR-191988; NAS 1.26:191988) Avail: CASI HC A03/MF A01

This paper focuses on the design, construction, preliminary testing, and potential applications of three forms of miniaturized analytical instrumentation. The first is an optical fiber instrument for monitoring pH and other cations in aqueous solutions. The instrument couples chemically selective indicators that were immobilized at porous polymeric films with a hardware package that provides the excitation light source, required optical components, and detection and data processing hardware. The second is a new form of a piezoelectric mass sensor. The sensor was fabricated by the deposition of a thin (5.5 micron) film of piezoelectric aluminum nitride (AlN). The completed deposition process yields a thin film resonator (TFR) that is shaped as a 400 micron square and supports a standing bulk acoustic wave in a longitudinal mode at frequencies of approx. 1 GHz. Various deposition and vapor sorption studies indicate that the mass sensitivity of the TFR's rival those of the most sensitive mass sensors currently available, though offering such performance in a markedly smaller device. The third couples a novel form of liquid chromatography with microlithographic miniaturization techniques. The status of the miniaturization effort, the goal of which is to achieve chip-scale separations, is briefly discussed. Author (revised)

N93-25515# Lawrence Livermore National Lab., CA.

HIGH SPEED X RAY GATING CAMERAS FOR ICF IMAGING APPLICATIONS

P. M. Bell, J. D. Kilkenny, O. Landen, D. B. Ress, J. D. Wiedwald, D. K. Bradley (Rochester Univ., NY.), J. Oertel, and R. Watt (Los Alamos National Lab., NM.) Dec. 1992 22 p Presented at the 20th International Congress on High Speed Photography and Photonics, Victoria, Ontario, 25-26 Sep. 1992

(Contract W-7405-eng-48)

(DE93-007500; UCRL-JC-112256; CONF-9209188-8) Avail: CASI HC A03/MF A01

High speed, high x-ray energy imaging of implosions is a key diagnostic technique in the glass laser implosion program in the USA. With the correct x-ray energy, time gated images can measure the symmetry and mix of the imploding shell into the stagnated fuel if the spatial resolution of 10 or 5 microns is matched by a temporal resolution of 100 or 50 psec. Several 100 psec microchannelplate (MCP) x-ray pin hole cameras were installed and run on large laser systems with improving reliability. To increase the sensitivity of the imaging system, a ring aperture microscope was coupled to a gated MCP detector allowing imaging at up to 8 keV. To achieve 40 psec resolution, thinner MCP's are required. On line tests with a thin low gain, but high speed MCP, followed by a d.c. MCP for higher gain have demonstrated 40 psec gating, but the second plate may lead to an unacceptable sensitivity of the camera to hard x-rays. Off line tests have extensively investigated the properties of thinner MCP's and good agreement is seen with modeling. DOE

N93-25634# Sensors Unltd., Inc., Princeton, NJ.

A HIGH PERFORMANCE ROOM-TEMPERATURE NEAR-INFRARED CAMERA Final Report, 1 Jul. - 31 Dec. 1992

Marshall J. Cohen, Gregory H. Olsen, and Robert Trew 20 Jan. 1993 22 p

(Contract DAAL03-92-C-0040)

(AD-A260602; ARO-30479.1-EL-SBI) Avail: CASI HC A03/MF A01

The objective of this program is to advance InGaAs materials technology to allow high performance imaging at room temperature in the 1.0-2.6 micron near infrared band. During Phase I, 128x128 pixel lattice-matched In(.53)Ga(.47)As focal plane arrays from 1-1.7 micron were fabricated. The detectivity, D*, was 10(exp 13) cm-Hz(exp .5)/W at room temperature and greater than 3x10(exp 14) at 230K - a value very nearly background

limited. The standard deviation in D* was 14 percent of the mean value and 98 percent of the pixels has a D* greater than 50 percent of the mean value. These results significantly advance the state-of-the-art and all of the objectives of Phase I were met or exceeded. The goals of Phase II will be to advance the materials growth and processing technologies of lattice mismatched InGaAs so as to lower the dark current sufficiently that room temperature imaging in the 1.0-2.6 micron band can be performed. This goal has proven elusive despite investments of tens of millions of dollars over more than a decade. Potential applications of this research include remote atmospheric sensing, LIDAR, satellite imaging, and near infrared spectroscopy. DTIC

N93-25677# Kopin Corp., Taunton, MA.
SMART MICROSENSORS FOR HIGH TEMPERATURE APPLICATIONS
D. P. Vu, M. W. Batty, and J. C. Fan 4 Jan. 1993 42 p
(Contract DAAL03-90-C-0029)
(AD-A260747; ARO-28148.2-EL-SB2) Avail: CASI HC A03/MF A01

The following document details the results of efforts to develop a high temperature sensor technology based in Kopin's proprietary ISE SOI material. Results are presented from a detailed analysis of the piezoresistive properties, and of the internal stress in the layer. These results show the material to be electrically similar to bulk, with very low internal stress. This makes ISE(tm) an ideal material choice for this application. A full sensor process sequence, with mask set, and enabling process equipment and techniques, was developed for this program. In parallel with the process development, extensive circuit analysis and modeling was performed to identify the best high temperature sensing circuit for this task. After modeling, test circuits were fabricated in bulk wafers to evaluate the design. The final design, a switching capacitive MOS circuit with proportional output, is expected to produce a sensor with 0.1 percent accuracy over the temperature range of -60 C to 300 C. Kopin is currently pursuing industrial financing for Phase 3 of this work to complete the integration of this work for commercial application. DTIC

N93-25686# Eagle-Picher Industries, Inc., Colorado Springs, CO. Couples Dept.
INTRODUCTION TO LEAD SALT INFRARED DETECTORS Technical Report, Sep. 1990 - Sep. 1992
David A. Kondas Feb. 1993 26 p
(AD-A260781; ARFSD-TR-92024) Avail: CASI HC A03/MF A01

This technical report establishes the background necessary to understand how lead sulfide (PbS) and lead selenide (PbSe) infrared detectors operate. Both detectors, which are members of the lead salt family of infrared detectors, use the photoconductive effect to detect energy residing within the infrared region of the electromagnetic spectrum. PbS detectors are useful for detecting energies in the 1 to 3 micrometer region, while PbSe detectors can detect energies in the 1 to 7 micrometer region. They are essentially polycrystalline thin films which are fabricated by chemical deposition techniques in either single element or multi-element array configurations. The significance of the electronic structure of these crystalline films and the effects of temperature on their operation and performance are discussed. The history of the development of lead salt detectors from the early years before World War I to the more recent developments is detailed. In addition, an overview of a typical infrared system is also presented. DTIC

N93-25696# Rome Lab., Griffiss AFB, NY.
HIGH LEVEL DESIGN FOR DISTRIBUTED APPLICATION INSTRUMENTATION
Vaughn T. Combs and Cheryl L. Blake Sep. 1992 55 p
(AF Proj. 5581)
(AD-A260812; RL-TR-92-181) Avail: CASI HC A04/MF A01

This paper describes the high level design for a distributed application instrumentation package. The instrumentation package provides monitoring tools to aid application designers in developing and understanding the behavior of their applications within an object-oriented distributed environment. The package consists of a general query-based system for the collection of events that occur within an application and a display system for processing and presenting the events. These events are collected through the use of probes which register events with a distributed database. Calls to these probes are embedded within the code to be instrumented in order to mark the occurrence of a specific event. The instrumentation package will provide a library of predefined probes based on events that adhere to the object/thread model (e.g. thread entrances into objects, thread exits from objects, etc.) and will also allow for user-defined probes. The display to be provided will represent object/thread interactions. The design is built flexibly so as to permit a wide range of events and displays to be used with the package. DTIC

N93-26044# Sea Tech, Inc., Corvallis, OR.
DEVELOPMENT OF AN EXPENDABLE PARTICLE SENSOR Progress Report, Dec. 1992 - Jan. 1993
Robert Bartz 30 Nov. 1992 14 p
(Contract N00014-90-C-0123)
(AD-A261127) Avail: CASI HC A03/MF A01

This report addresses progress on the Phase 2 development of the Expendable Particle Sensor (EPS) for the period from Dec. 1992 through Jan. 1993. Work during this time period focused on both technical and administrative problems. DTIC

N93-26092 Department of the Navy, Washington, DC.
APPARATUS FOR DETERMINING THE ATTITUDE OF A VEHICLE Patent
Raymond G. Schmidt, inventor (to Navy) 15 Dec. 1992 19 p Filed 6 Dec. 1991
(AD-D015667; US-Patent-5,172,323; US-Patent-Appl-SN-804627;
US-Patent-Class-364-453) Avail: US Patent and Trademark Office

A method of automatically determining attitude of a moving vehicle is described. Acceleration of the moving vehicle is measured with gyro stabilized accelerometers. The measurement is converted to a motion related vector in a first frame of reference. The coordinates are read into a computer. The cosine value and the sine value for an Euler rotation of the first frame of reference are read into the computer. The computer produces coordinates of the vector in a rotated frame of reference. The above two steps are repeated a number of times to arrive at a final frame of reference. The attitude of the vehicle is provided with respect to a final frame of reference with the aid of final produced coordinates. DTIC

N93-26103* National Aeronautics and Space Administration. Goddard Space Flight Center, Greenbelt, MD.
METHOD AND APPARATUS FOR DEFLECTION MEASUREMENTS USING EDDY CURRENT EFFECTS Patent
Engmin J. Chern, inventor (to NASA) 25 May 1993 8 p Filed 25 Jun. 1992
(NASA-Case-GSC-13506-1; US-Patent-5,214,379;
US-Patent-Appl-SN-904308; US-Patent-Class-324-220;
US-Patent-Class-33-542; US-Patent-Class-324-207.16;
US-Patent-Class-324-262; Int-Patent-Class-G01B-7/28;
Int-Patent-Class-G01B-5/20; Int-Patent-Class-G01N-27/72) Avail: US Patent and Trademark Office

A method and apparatus for inserting and moving a sensing assembly with a mechanical positioning assembly to a desired remote location of a surface of a specimen under test and measuring angle and/or deflection by sensing the change in the impedance of at least one sensor coil located in a base plate which has a rotatable conductive plate pivotally mounted thereon so as to uncover the sensor coil(s) whose impedance changes as a function of deflection away from the center line of the base plate in response to the movement of the rotator plate when contacting the surface of the specimen under test is presented. The apparatus includes the combination of a system controller, a sensing assembly, an eddy current impedance measuring apparatus, and a mechanical positioning assembly driven by the impedance measuring apparatus to position the sensing assembly at a desired location of the specimen.
Official Gazette of the U.S. Patent and Trademark Office

N93-26141 Department of the Navy, Washington, DC.
MAGNETIC MULTILAYER STRAIN GAGE Patent
Marilyn Wun-Fogle, inventor (to Navy), Arthur E. Clark, inventor (to Navy), and Kristl B. Hathaway, inventor (to Navy) 8 Dec. 1992 4 p Filed 1 Nov. 1991
(AD-D015672; US-Patent-5,168,760; US-Patent-Appl-SN-786641;
US-Patent-Class-73-779) Avail: US Patent and Trademark Office

A strain gauge is discussed. The gauge is comprised of a magnetic multilayer assembly exhibiting spin-valve effect with individual ferromagnetic

layers possessing magnetostrictive properties. A magnetic field source is used to bias the magnetic moments of the ferromagnetic layers in a given direction whereby stress applied causes previously antiferromagnetically coupled moments to be angularly realigned toward a ferromagnetic arrangement. Such realignment causes a corresponding resistance change of unexpectedly high magnitude thereby providing a highly sensitive strain gauge. DTIC

N93-26154*# Alabama Univ., Huntsville. Center for Applied Optics.
ADVANCED TECHNOLOGY DEVELOPMENT MULTI-COLOR HOLOGRAPHY Final Report, 24 Mar. 1992 - 24 Jan. 1993
Chandra S. Vikram 15 Jan. 1993 39 p
(Contract NAS8-38609)
(NASA-CR-192451; NAS 1.26:192451; UAH-5-32892) Avail: CASI HC A03/MF A01

This is the final report of the Multi-color Holography project. The comprehensive study considers some strategic aspects of multi-color holography. First, various methods of available techniques for accurate fringe counting are reviewed. These are heterodyne interferometry, quasi-heterodyne interferometry, and phase-shifting interferometry. Phase-shifting interferometry was found to be the most suitable for multi-color holography. Details of experimentation with a sugar solution are also reported where better than 1/200 of a fringe order measurement capability was established. Rotating plate glass phase shifter was used for the experimentation. The report then describes the possible role of using more than two wavelengths with special reference-to-object beam intensity ratio needs in multicolor holography. Some specific two- and three-color cases are also described in detail. Then some new analysis methods of the reconstructed wavefront are considered. These are deflectometry, speckle metrology, confocal optical signal processing, and phase shifting technique related applications. Finally, design aspects of an experimental breadboard are presented. Author

N93-26324# International Trade Administration, Washington, DC. Office of Computers and Business Equipment.
PHOTOGRAPHIC INDUSTRY AND ELECTRONIC IMAGING: THE EMERGENCE OF ELECTRONIC STILL PHOTOGRAPHY
J. V. Watson 1993 60 p
(PB93-169399) Avail: CASI HC A04/MF A01

The study examines the current structure of the photographic industry and the effects of electronic photography. It also suggests that the industry will continue to find avenues for future growth in the emerging electronic imaging industry and the broader information management industry. NTIS

N93-24900# Lightning Location and Protection, Inc., Tucson, AZ.
A SINGLE-POINT WARNING SYSTEM FOR THUNDERSTORMS AND ELECTRIC FIELDS
W. T. Neumann, K. L. Cummins, and E. Philip Krider (Arizona Univ., Tucson.) *In* FAA, The 1992 International Aerospace and Ground Conference on Lightning and Static Electricity: Addendum Nov. 1992 8 p (For primary document see N93-24875 09-47)
Avail: CASI HC A02/MF A03

N93-24901# Veda, Inc., Lexington Park, MD.
COMMERCIAL PRECIPITATION STATIC (P-STATIC) TEST EQUIPMENT
R. Wayne Devereux *In* FAA, The 1992 International Aerospace and Ground Conference on Lightning and Static Electricity: Addendum Nov. 1992 10 p (For primary document see N93-24875 09-47)
Avail: CASI HC A02/MF A03

N93-25009# Franche-Comte Univ., Besancon (France). Lab. de Physique et Metrologie des Oscillateurs.
ELASTIC PLATE MODE SENSITIVITIES TO MASS LOADING APPLICATIONS TO GAS SENSORS
M. Hoummady and D. Hauden *In* ESA, Frequency and Time Forum Jun. 1992 p 203-207 (For primary document see N93-24978 09-70)
Copyright Avail: CASI HC A01/MF A04

N93-25011# Office National d'Etudes et de Recherches Aerospatiales, Paris (France).
MONOLITHIC QUARTZ VIBRATING BEAM ACCELEROMETER
F. Deyzac, D. Janiaud, and S. Muller *In* ESA, Frequency and Time Forum Jun. 1992 p 217-218 (For primary document see N93-24978 09-70)
Copyright Avail: CASI HC A01/MF A04

N93-25578*# Industrial Technology Inst., Ann Arbor, MI.
APPLICATION OF AN ON-MACHINE GAGE FOR DIAMETER MEASUREMENTS
Kevin G. Harding *In* NASA, Washington, Technology 2002: The Third National Technology Transfer Conference and Exposition, Volume 1 Feb. 1993 p 170-177 (For primary document see N93-25561 09-99)
(Contract F33615-91-C-5704)
Avail: CASI HC A02/MF A04

N93-25608*# Naval Surface Warfare Center, Silver Spring, MD.
DYNAMIC HARDNESS TESTER AND CURE METER
Walter M. Madigosky and Ralph B. Fiorito *In* NASA, Washington, Technology 2002: The Third National Technology Transfer Conference and Exposition, Volume 1 Feb. 1993 p 446-450 (For primary document see N93-25561 09-99)
Avail: CASI HC A01/MF A04

N93-25614*# National Aeronautics and Space Administration. Goddard Space Flight Center, Greenbelt, MD.
PRELIMINARY STUDIES LEADING TOWARD THE DEVELOPMENT OF A LIDAR BATHYMETRY MAPPING INSTRUMENT
John M. Hill (Houston Advanced Research Center, The Woodlands, TX.), Brendan D. Krenek (Houston Advanced Research Center, The Woodlands, TX.), Terry D. Kunz (Houston Advanced Research Center, The Woodlands, TX.), William Krabill, and Fran Stetina *In* NASA, Washington, Technology 2002: The Third National Technology Transfer Conference and Exposition, Volume 1 Feb. 1993 p 503-514 (For primary document see N93-25561 09-99)
Avail: CASI HC A03/MF A04

N93-26024 Sandia National Labs., Albuquerque, NM.
HERO RESISTANT SEMICONDUCTOR BRIDGE IGNITER
R. W. Bickes, Jr., D. Greenway, M. C. Grubelich, W. J. Meyer, J. K. Hartman (SCB Technologies, Inc., Albuquerque, NM.), and C. B. McCampbell (SCB Technologies, Inc., Albuquerque, NM.) *In* JHU, 29th JANNAF Combustion Subcommittee Meeting, Volume 2 Oct. 1992 p 193-196 (For primary document see N93-26005 09-20)
(Contract DE-AC04-76DP-00789)
Avail: CPIA, 10630 Little Patuxent Pkwy., Suite 202, Columbia, MD 21044-3200 HC

36 LASERS AND MASERS

Includes parametric amplifiers.
For related information see also *76 Solid-State Physics.*

N93-24961# Lawrence Livermore National Lab., CA.
A COMPACT AND VERSATILE PULSE GENERATION AND SHAPING SUBSYSTEM FOR HIGH ENERGY LASER SYSTEMS
B. M. VanWontergfhem, D. R. Speck, M. Norman, R. B. Wilcox, V. P. Karpenko, and J. B. Richards Jan. 1993 14 p Presented at the International Society for Optical Engineering Conference, Los Angeles, CA, 16-23 Jan. 1993
(Contract W-7405-eng-48)
(DE93-007114; UCRL-JC-111452; CONF-930159-14) Avail: CASI HC A03/MF A01

The amplifier and beam shaping section of a new pulse generation system that will drive the Beamlet laser at Lawrence Livermore National Laboratory (LLNL) is described. The master oscillator and pulse shaping system are described in an accompanying contribution. A modified regenerative amplifier produces a gain of 10(exp 9) to bring the oscillator pulses to the mJ-level. A serrated aperture and birefringent beam shaper produce a flat-topped square beam with high fill factor. A single four-passed Nd:glass rod amplifier provides sufficient gain to generate the desired 12 J output energy in a 3 nsec pulse with very small beam profile, wavefront, and pulse shape distortion. A description of the system components is

presented followed by a discussion of its performance, based upon over 150 full front end shots being completed since its assembly. DOE

N93-24967# Los Alamos National Lab., NM.
SURFACE DISCHARGE PHOTOINITIATION OF PULSED CHEMICAL LASERS
20 Oct. 1992 92 p Prepared in cooperation with Schafer (W.J.) Associates, Inc., Chelmsford, MA
(Contract W-7405-eng-36)
(DE93-006337; LA-SUB-93-13; WJSA-R-92-B-012) Avail: CASI HC A05/MF A01

This report summarizes the work carried out under the contract entitled Surface Discharge (SD) Photoinitiation Pulsed Chemical Lasers. This work consisted of technical analyzes, memos, and on-site test support. We considered SD design issues for both pulsed chemical lasers and photodissociation iodine lasers. Due to the similarity in the absorption band, the requirements on the SD light source are very similar. The SD systems can be utilized for either type of laser. Both rectangular and cylindrical SD configurations were analyzed. The cylindrical configuration is simpler, provides direct ultraviolet coupling into the laser medium, is smaller and lighter, and is better for voltage stand-off in multiple module configurations. But the impedance matching between the electrical circuit and the SD plasma is more difficult with the cylindrical geometry, unless small diameter cavities can be employed. A cylindrical configuration is preferred if the laser energy density is high enough for the diameter to be less than about 10 cm. A single rectangular SD module was tested for the first time at high voltage and worked very well. The four module system was integrated into the laser and SD tests conducted. Laser operation both in the DF-CO2 mode at 10.6 microns and the DF mode at about 3.8 microns were investigated. This is the first time an SD has been used in this configuration to produce laser energy outputs at the levels achieved. A weight scaling analysis of the pulsed power system was undertaken to support the application of this laser system. The pulsed power system will weigh 50 to 100 lbs, and provide 10 to 100 shots at repetition rates of less then 1 Hz. We concluded that the most practical approach to producing efficient ultraviolet emission from the SD at the short pulses needed for photoinitiation, and on the SD areas needed for the laser operation, employs a single capacitor bank rather than a pulser-sustainer approach. DOE

N93-25150# Los Alamos National Lab., NM.
LASER DESORPTION IN AN ION TRAP MASS SPECTROMETER
G. C. Eiden, M. E. Cisper, M. L. Alexander, P. H. Hemberger, and N. S. Nogar 1993 12 p Presented at the International Society for Optical Engineering Conference, Los Angeles, CA, 16-23 Jan. 1993
(Contract W-7405-eng-36)
(DE93-007330; LA-UR-93-370; CONF-930159-9) Avail: CASI HC A03/MF A01

Laser desorption in a ion-trap mass spectrometer shows significant promise for both qualitative and trace analysis. Several aspects of this methodology are discussed in this work. We previously demonstrated the generation of both negative and positive ions by laser desorption directly within a quadrupole ion trap. In the present work, we explore various combinations of d.c., r.f., and time-varying fields in order to optimize laser generated signals. In addition, we report on the application of this method to analyze samples containing compounds such as amines, metal complexes, carbon clusters, and polynuclear aromatic hydrocarbons. In some cases, the ability to rapidly switch between positive and negative ion modes provides sufficient specificity to distinguish different compounds of a mixture with a single stage of mass spectrometry. In other experiments, we combined intensity variation studies with tandem mass spectrometry experiments and positive and negative ion detection to further enhance specificity. DOE

N93-25280 Tennessee Univ., Knoxville.
PARTICLE SIMULATION FOR 10.6 MICRON PICOSECOND LASER-INDUCED BREAKDOWN IN GASES Ph.D. Thesis
Quan Zhang 1992 109 p
Avail: Univ. Microfilms Order No. DA9233601

A theoretical model was developed to explain experimental observations in free electron laser experiments. Argon plasmas were initiated and sustained by a free electron laser operating at a wavelength of 10.6 microns with a sequence of 10 ps pulses, and attempts to obtain optical breakdown with the same laser in nitrogen and hydrogen proved unsuccessful. The particle simulation method was used in this model to calculate the electron density increase and the electron energy distribution during the gas breakdown process. A Monte Carlo collision method was incorporated into the particle simulation method to calculate collisions between particles. The theoretical model also included three-body recombination and gasdynamic expansion effects. The calculated results showed that the argon plasma breakdown in the free electron laser experiments was the result of a cumulative growth of the electron density during 27 pulses. Hydrogen and nitrogen did not reach breakdown at the free electron laser experiment conditions because the electron energy decayed more rapidly in these gases during the interval between pulses. The reduction of electron energy permits a much faster electron recombination rate which depletes the electron density during the interval between pulses. The particle simulation predicts that hydrogen and nitrogen can reach breakdown at a power threshold which is higher than that which was used in the free electron laser experiments. Author (revised)

N93-25344 Illinois Univ. at Urbana-Champaign, Savoy.
ELECTRON-BEAM-PUMPED RECOMBINATION LASERS Ph.D. Thesis
Robert Lewis Rhoades 1992 81 p
Avail: Univ. Microfilms Order No. DA9236577

The first known instance of electron-beam pumping of the 546.1 nm mercury laser is reported. This has been achieved using high-energy electrons to create intense ionization in a coaxial diode chamber containing a mixture of noble gases with a small amount of mercury vapor. Also, the results of a study of the 585.3 nm neon laser in He:Ne:Ar mixtures under similar experimental conditions are reported. Both of these lasers are believed to be predominantly pumped by recombination. For the mercury laser, kinetic processes in the partially ionized plasma following the excitation pulse of high-energy electrons should favor the production of atomic mercury ions and molecular ions containing mercury. Subsequent recombination with electrons heavily favors the production of the 7(sup 3)S and 6(sup 3)D states of Hg, of which 7(sup 3)S is the upper level of the reported laser. For the neon laser, the dominant recombining ion has been previously shown to be Ne2(+). One of the dominant roles of helium in recombination lasers is inferred from the data for the neon laser at low helium concentrations. Helium appears to be necessary for the rapid relaxation of the electron energy which then increases the reaction rates for all known recombination processes thus increasing the pump rate into the upper state. Dissert. Abstr.

N93-25363# Lawrence Livermore National Lab., CA.
PROGRESS IN IMAGING MICROSCOPY WITH X RAY LASERS AT LLNL
L. B. DaSilva, J. E. Trebes, S. Mrowka, B. J. MacGowan, J. A. Koch, D. L. Matthews, T. W. Barbee, Jr., R. Balhorn, J. Gray, and E. Anderson et al 28 Jul. 1992 8 p Presented at the 3rd International Colloquium on X Ray Lasers, Schliersee, Germany, 18-22 May 1992
(Contract W-7405-eng-48)
(DE93-007508; UCRL-JC-111296; CONF-920523-7) Avail: CASI HC A02/MF A01

Imaging microscopy with short pulse (200 ps) x-ray lasers offers the opportunity of high resolution three-dimensional imaging of specimens in an aqueous environment without the blurring effects associated with natural motion and radiation induced chemical decomposition. As a first step towards this goal, we have performed imaging experiments with the Ni-like Ta x-ray laser (lambda=44.8 A) which have clearly resolved 500 A features on a gold test pattern. In addition, we have taken images of gold labeled dried rat sperm as a basis for comparison in future wet specimen imaging. The results of these experiments are described. DOE

N93-25378# Brookhaven National Lab., Upton, NY.
LASER FIELD ASSISTED PHOTOEMISSION USING FEMTOSECOND LASER PULSES
T. Srinivasan-Rao, J. Fischer, and T. Tsang Nov. 1992 7 p Presented at the Quantum Electronics and Laser Science Conference, Baltimore, MD, 2-7 May 1993
(Contract DE-AC02-76CH-00016)
(DE93-007277; BNL-48308; CONF-930586-3) Avail: CASI HC A02/MF A01

Photoemission from Cu mirror at a laser fluence of 10(exp 11) W/cm(exp 2), 300 fs, pulse is investigated for various angles of incidence, intensities

and polarizations. Electron emission is enhanced by approximately 20 from s to p polarization and by 4 on changing the angle of incidence from 0 to 73 degree. DOE

N93-25379# Los Alamos National Lab., NM.
MERCURY: THE LOS ALAMOS ICF KrF LASER SYSTEM
S. J. Czuchlewski, G. W. York, I. J. Bigio, J. Brucker, D. Hanson, E. M. Honig, N. Kurnit, W. Leland, A. W. McCown, and J. McLeod et al 19 Jan. 1993 12 p Presented at the 1992 International Conference on Lasers, Houston, TX, 7 Dec. 1992
(Contract W-7405-eng-36)
(DE93-007363; LA-UR-93-330; CONF-921256-2) Avail: CASI HC A03/MF A01

The Mercury KrF laser facility at Los Alamos is being built with the benefit of lessons learned from the Aurora system. An increased understanding of KrF laser engineering, and the designed implementation of system flexibility, will permit Mercury to serve as a testbed for a variety of advanced KrF technology concepts. DOE

N93-25381# Los Alamos National Lab., NM.
SIMULTANEOUS DETERMINATION OF GAIN PARAMETERS IN STEADY STATE LASERS
C. C. Jensen, D. A. Branning, and R. D. Marchbanks 1993 9 p Presented at the 1992 International Conference on Lasers, Houston, TX, 7 Dec. 1992
(Contract W-7405-eng-36)
(DE93-007389; LA-UR-93-289; CONF-921256-1) Avail: CASI HC A02/MF A01

The optical gain parameters of pulsed steady-state lasers, such as dye and excimer lasers, are determined from a single set of experiments from either a laser oscillator or an amplifier. The gain parameters determined by this technique are the small-signal gain coefficient, the saturation intensity for stimulated emission, the saturation fluence for stimulated emission, and the non-saturable absorption coefficient. The measured saturation properties of laser amplifiers and oscillators are used in a data fitting routine that finds all of the gain parameters simultaneously. The values of the gain parameters are determined with greater accuracy than by the conventional methods of measuring each of the parameters individually. The knowledge of the values of all the gain parameters allows for the determination of fluorescence lifetime of a gain medium. DOE

N93-25389 American Univ., Washington, DC.
INJECTION SEEDED, DIODE-PUMPED, SHORT PULSE Nd:YAG RING LASER FOR SPACE-BASED LASER RANGING Ph.D. Thesis
Donald Barry Coyle 1992 136 p
Avail: Univ. Microfilms Order No. DA9237217

In the near future, NASA plans to deploy LIDAR (Light Detection And Ranging) systems in space for the purpose of measuring geophysical quantities such as tectonic plate movement, crustal deformation near faults, and volcanic activity. Information on other quantities such as ice floes, cloud movemen t heights, and sea levels are also of interest. These measurements will require a spaceborne laser system which can operate unattended for extended periods of time and be able to make reliable sub-centimeter distance determinations from space. One system concept is the Geodynamic Laser Ranging System (GLRS) (Cohen et al. 1987). Optical pulses of 100 ps, or less, will be required from a Nd:YAG laser. The fundamental wavelength will provide altimetry information while the second and third harmonic frequencies will be generated to measure distances with high accuracy through two-color ranging techniques. Sub-100 ps pulses can be produced using either pulse pumped or continuous wave (CW) pumped mode-locked lasers. Shorter pulses are frequently achieved through CW pumping but the pulse energy is low, typically less than 10(exp -8) J. A method of achieving the pulse width of a CW mode-locked laser and pulse energy of a pulse pumped laser involves using regenerative amplification. The presented work covers one possible method of short pulse amplification. A pulsed Nd:YAG ring regenerative amplifier, pumped by laser diode-arrays and injection seeded by a 100 ps source, has been constructed. It was shown that high total optical gains can be achieved while holding the stringent alignment and timing specifications of regenerative amplification to a minimum. The construction of this laser/amplifier provided data on the behavior of 100 ps pulses when used as a temporal seed in a typical oscillator cavity with multiple optical surfaces. Dissert. Abstr.

N93-25393 Oxford Univ. (England).
COLLISIONAL RECOMBINATION LASERS Ph.D. Thesis
Damien Gerard Loveland 1992 195 p
Avail: Univ. Microfilms Order No. BRD-98051

An introduction to and extensive review of the field of strontium vapor recombination lasers is given. This includes coverage of both the theoretical aspects of the physics responsible for laser action and details of the technical features of a wide range of different laser designs. A description is given of an air-cooled strontium vapor laser of upgraded design which provides greater stability and improved ease of control over the output, together with increased running periods between the essential reloading of the strontium reservoir. A new type of design of strontium laser is investigated which employs water-cooling of the plasma tube, and it is shown that this is beneficial to obtaining increased output powers compared to natural-convection air-cooling the same laser, running at the same buffer gas pressure. Detailed experimental measurements are performed, of the electron temperature and strontium ion (Sr^+) excitation temperature in the immediate afterglow corresponding to the time of laser action, and of the spatially and temporally resolved electron density for the whole of the interpulse period. These experiments, which have not previously been attempted in such depth, provide an abundance of new data describing the properties of the discharge plasma of the strontium vapor laser. The use of strontium halides as an alternative to metallic strontium is also investigated. Dissert. Abstr.

N93-25420 Illinois Univ. at Urbana-Champaign, Savoy.
EXPERIMENTAL AND THEORETICAL STUDY OF cw HF CHEMICAL LASER OVERTONE PERFORMANCE Ph.D. Thesis
David Leon Carroll 1992 337 p
Avail: Univ. Microfilms Order No. DA9236413

The overtone performance of the UIUC supersonic cw HF chemical laser was characterized as a function of flow rates, cavity pressure, mode volume, mirror reflectivity and method of He injection. The overtone performance was optimized by the same set of flow rates that optimized the fundamental performance. When the absorption/scattering losses of the mirrors were taken into account, an overtone efficiency of 70-90 percent was achieved, which is the highest reported to date. The overtone efficiency was a strong function of media saturation. There was no significant change in overtone power and efficiency as the mode volume increased. However, there were an increase in the number of lasing lines and a shift to higher J lines. Overtone performance was as sensitive to cavity pressure as fundamental performance. There was no significant change in overtone efficiency when the method of the injection was changed. Base region absorption by ground state HF has a significant effect on fundamental and overtone performance. Even with very high degrees of saturation, approximately 10 percent of the total power was lost when the He purge was turned off. For a laser having an extensive data base with well characterized mirrors to firmly establish the Rigrod parameters g(0) and I(sat), the accuracy to which the mirror reflectivities can be deduced using measured mirror transmissivities, measured outcoupled power and Rigrod theory is approximately plus or minus 0.07 percent for high reflectivity overtone mirrors. Rigrod theory shows that a higher media saturation yields a higher overall overtone efficiency, but does not necessarily yield a higher measurable power (power in the bucket). For low absorption/scattering loss overtone mirrors and a 5 percent penalty in outcoupled power, the intracavity flux and hence the mirror loading can be reduced by more than a factor of two when the gain length is long enough to well saturate the media. The inclusion of HF-H2 multi-quantum VV transfer reactions in the ORNECL model significantly improved the prediction of the zero power gains for the H2 rich UI supersonic laser. The inclusion of absorption by SFx molecules in the model significantly improved the prediction of the Fabry-Perot spectra. Dissert. Abstr.

N93-25508# Oak Ridge National Lab., TN.
FAST DIAGNOSTICS OF LASER ABLATION USED FOR PULSED LASER DEPOSITION
D. B. Geohegan 1993 7 p Presented at the Quantum Electronics and Laser Science Conference, Baltimore, MD, 2-7 May 1993
(Contract DE-AC05-84OR-21400)
(DE93-005155; CONF-930586-2) Avail: CASI HC A02/MF A01

The mechanisms of the laser ablation process for pulsed laser deposition thin film growth will be discussed by describing results from several

implementable in situ diagnostic techniques, including gated ICCD photography, optical emission and absorption spectroscopy, ion probes and gate photon counting. DOE

N93-25721 Illinois Univ. at Urbana-Champaign, Savoy.
EXPERIMENTAL AND THEORETICAL STUDY OF CW HF CHEMICAL LASER RESIDUAL FUNDAMENTAL GAIN Ph.D. Thesis
Panagiotis Theodoros Theodoropoulos 1992 354 p
Avail: Univ. Microfilms Order No. DA9236606

A new technique that uses a multi-line probe beam to measure the gain on several lines simultaneously was developed. This new technique was used to measure the gains of the peak fundamental lines P1(4-9) and P2(4-9) while lasing on the overtone, for three levels of media saturation. The suppression of the fundamental gains obtained at relatively high media saturation with 99.7/99.7 percent reflective mirrors was essentially the same as that obtained with 55 percent higher intracavity flux with 99.8/99.8 percent reflective mirrors. The gains of the low J lines P1(4-6) and P2(4-6) were suppressed 41 percent to 84 percent; the gains of the high J lines P1(7-9) and P2(7-9) were suppressed 3 percent to 43 percent. The 1 to 0 lines were suppressed more than the 2 to 1 lines. The maximum suppression occurred between 2 and 6 mm downstream from the nozzle exit plane, near the center of the 9 mm overtone beam. Simulation of the experiments with a rotational nonequilibrium computer model showed that the fundamental gains are determined by three independent mechanisms when lasing occurs on the overtone. First, overtone lasing decreases the gains of the P1(J) and P2(J) lines whose upper or lower levels are directly involved in P20(J) overtone lasing. Second, overtone lasing reduces the rate at which the low J v = 2 states are populated by rotational relaxation and increases the rate at which the low J v = 0 states are populated by rotational relaxation, resulting in suppression of the low J fundamental gains whose upper or lower levels are not directly involved in overtone lasing. Third, overtone lasing reduces the rate at which the HF(0,J) and HF(1,J) states are populated by the various collisional deactivation processes. With 10 percent of the original rotational relaxation rate, the computer model was in reasonable agreement with the measured zero power gain profiles. The model overpredicted the fundamental gain suppression (Delta alpha) for the P1(8,9) and P2(8,9) lines whose upper or lower levels were directly involved in overtone lasing, and underpredicted the suppression for lines P1(4) and P2(4,5). The model predicted the suppression for lines P1(5-7) and P2(6,7) reasonably well. With the original rotational relaxation rate, the model was in reasonable agreement with the measured suppression of all P1(4-9) and P2(4-9) lines. However, with the original RR rate, the model's agreement with the experimental zero power gain profiles was not adequate. Dissert. Abstr.

N93-25761 University of Technology, Loughborough (England).
GENERATION OF ACOUSTIC WAVES BY FOCUSED INFRARED NEODYMIUM-LASER RADIATION Ph.D. Thesis
Barry Ward 1991 295 p
Avail: Univ. Microfilms Order No. BRDX98211

When the radiation from a sufficiently powerful pulsed laser is focused into the transparent gaseous, liquid or solid media, dielectric breakdown may occur around the beam waist giving rise to a short-lived high-temperature plasma which quickly heats the surrounding material. As a consequence of various energy-coupling mechanisms, this phenomenon causes the emission of one or more high-frequency ultrasonic acoustic waves whose speeds of propagation are dependent upon the physical properties of the host medium. In the high-speed photographic studies described, the 1.06 micron near-infrared radiation from an 8-ns, 10-mJ Q-switched Nd:YAG laser is focused in or onto a variety of fluid and solid materials. The rapid variations in density around the resulting plasma events are visualized using a Mach-Zehnder interferometer with a sub-nanosecond dye-laser light source and a video-imaging system. Calculations of the corresponding transient pressure distributions are then enacted from the digitally-recorded interferograms using a semi-automatic procedure under the control of a personal computer. Measurements of position, displacement, and velocity are also carried out using the same optical apparatus in schlieren and focused shadowgraph high-speed photographic measurements. The experimental work outlined in the following chapters is divided into three broad fields of interest. In the first of these, a study of the laser-generation of spherical shock waves in atmospheric air is carried out. In the second, the neodymium-laser beam is focused onto different solid-fluid interfaces resulting in the formation of bulk longitudinal and shear waves and surface acoustic waves. The interactions of these waves with various obstacles and defects are investigated with reference to their application to non-destructive testing. In the third and most important field, a detailed study of the dynamics of laser-induced cavitation bubbles in water is carried out. With regard to the associated phenomenon of cavitation erosion, particular attention is paid to the formation of spherical acoustic waves by radially-oscillating vapor cavities at various distances from transparent rigid boundaries. Dissert. Abstr.

N93-25774# University of Central Florida, Orlando. Center for Research in Electro-Optics and Lasers.
TIME RESOLVED STUDIES OF IN-WELL AND CROSS-WELL CARRIER TRANSPORT IN MQW SEMICONDUCTOR STRUCTURES Final Report, 15 May 1991 - 30 Sep. 1992
Alan Miller 8 Dec. 1992 33 p
(Contract DAAL03-91-G-0133)
(AD-A261170; ARO-28594.5-EL) Avail: CASI HC A03/MF A01

The objective of this research project was to establish a better understanding of in-well and cross-well carrier transport in multiple quantum well (MQW) semiconductors. Carrier emission from both multiple and single quantum well devices have been studied in detail in p-i-n doped MQW SEED-type modulator structures and in waveguides. Simultaneous measurements of electron and hole emission rates has been accomplished for the first time leading to important conclusions concerning thermionic emission models for quantum wells. Extensive modeling of the dynamical optical response relating to cross-well carrier transport has been carried out. Spin relaxation has also been used successfully to monitor carrier dynamics in MQW devices. A new family of mode-locked lasers have been developed for time resolved measurements which are looking extremely attractive as ultrashort pulse sources for GaAs-based optoelectronic devices. DTIC

N93-25869# Rochester Univ., NY. Inst. of Optics.
LIQUID CRYSTALS FOR LASER APPLICATIONS
S. D. Jacobs, K. L. Marshall, and A. Schmid 14 Oct. 1992 108 p
(Contract DAAL03-92-G-0147)
(AD-A261209; ARO-30367.2-PH-UIR) Avail: CASI HC A06/MF A02

This article highlights some of the advances made in the use of liquid crystals for laser applications from 1982 through 1992. New materials and new effects were discovered, many new devices were developed, and novel applications for well-understood phenomena were conceived. This was quite an eventful time period. Several new books were published on the broad subject of LC's, and the international scientific community organized a society devoted to encouraging further scientific and educational advancement in the field. Attention was focused on LC's in October of 1991 when the Nobel Prize in Physics was awarded to Pierre-Gilles de Gennes for his pioneering work toward understanding order phenomena in LC's and polymers. This article is divided into four sections. The first section discusses new materials, specifically ferroelectric LC's and LC polymers. The former have opened up the realm of submicrosecond response for LC devices, and the latter have significantly reduced the sensitivity of LC optics to temperature. Some new insights into the optical properties of materials are also mentioned. The second section reviews new developments in passive applications for cholesterics and nematics. Included here are the fabrication of cholesteric laser mirrors and apodizers, the use of LC polymers for notch filters and as optical storage media, and some novel nematic retarder concepts such as the distributed polarization rotator. DTIC

N93-26217# Florence Univ. (Italy). Dept. of Physics.
LASER PROPAGATION THROUGH TURBULENCE Final Technical Report, Sep. 1990 - Sep. 1992
Anna Consortini Nov. 1992 75 p
(Contract DAJA45-90-C-0029)
(AD-A260712; R/D-6458-EE-01) Avail: CASI HC A04/MF A01

A large data base of intensity fluctuations of laser radiation through the turbulent atmosphere has been analyzed. The base had been previously obtained in a joint measurement campaign of the Department of Physics, University of Florence, Italy, and the Wave Propagation Laboratory of NOAA/ERL, Boulder, Colorado, U.S.A. It included good quality data collected through continuously evolving atmospheric turbulence, comprising low,

moderate and high turbulence levels, as well as structure parameter (the so called structure constant) and inner scale, values, simultaneously measured. Results have been obtained on the four topics of the present contract. (1) The effect of the inner scale of the turbulence on the normalized variance of the intensity (scintillation index) was experimentally demonstrated, for the first time. Plots of intensity variance versus structure parameter, for fixed ranges of the inner scale, allowed an experimental determination of the role played by inner scale and structure parameter. They constitute a reference for comparison with results from theory or numerical simulations. (2) The evolution of the probability distributions with changing propagation conditions was examined. Some comparisons with existing theoretical distributions were made. Necessity for further investigation resulted. (3) A numerical deconvolution procedure was developed, to remove a broad noise from intensity fluctuation histograms, and applied to low intensity data measured with very small apertures. The results were positive (4) Spectral analyses of experimental data as well as time correlations of intensity fluctuations were made. The contribution to scintillation of the high frequency components, related to the wave coherence length, was shown. DTIC

N93-26296# Naval Surface Warfare Center, Panama City, FL. Coastal Systems Station.

LOSS OF TEMPORAL COHERENCE OF LASER LIGHT PROPAGATED THROUGH SIMULATED COASTAL WATERS Interim Report, FY92

N. L. Swanson Jan. 1993 26 p

(AD-A261303; CSS-TM-627-92) Avail: CASI HC A03/MF A01

Research is currently underway to investigate the physical mechanisms that cause loss of temporal coherence in scattered light. The results of experiments that measure coherence length versus temperature, optical path length, and water quality are reported. It is shown that the loss of temporal coherence is caused by spectral broadening. Based on these results and research into the causes of spectral broadening, experiments are proposed to measure each type of broadening mechanism, with a much higher degree of accuracy. DTIC

N93-26297# Stanford Univ., CA. Physics Lab.

EFFICIENT NONLINEAR OPTICAL CONVERSION OF 1.319-MICRON LASER RADIATION

Robert L. Byer and Robert C. Eckardt 14 Jan. 1993 14 p

(Contract DAAL03-89-K-0155)

(AD-A261309; ARO-27418.4-PH) Avail: CASI HC A03/MF A01

The accomplishments of this program are in the development and application of periodically poled nonlinear optical materials for nonlinear frequency-conversion. We have demonstrated the use of periodically poled lithium niobate (PPLN) as a bulk material for external resonant cavity second-harmonic generation with continuous-wave (cw) output power of 1.7 W. Work that is following this investigation is showing that planar waveguides of PPLN may well be the most satisfactory method of generation of 10's of mW of the 659-nm harmonic of the 1.32-micrometer Nd:YAG laser. We encountered major obstacles obtaining multilayer dielectric coatings necessary to pursue our proposed design of monolithic bulk optical harmonic generators. Additional alternative approaches such as discrete component resonant second harmonic generation employing single domain and periodically poled bulk crystals and monolithic single domain resonators formed by total internal reflection remain under investigation. DTIC

N93-26363# Potomac Photonics, Inc., Lanham, MD.

ULTRAVIOLET WAVEGUIDE LASERS FOR PHASED ARRAY LIDAR Final Report, 10 Jul. 1989 - 30 Jun. 1992

C. P. Christensen 1 Feb. 1993 33 p

(Contract DNA001-89-C-0064)

(AD-A261657; DNA-TR-92-78) Avail: CASI HC A03/MF A01

This is the final report for a SBIR Phase 2 investigation of xenon Chloride waveguide laser arrays. Using electrodeless microwave discharge techniques, we have constructed an optimized XeCl waveguide laser that could serve as the basic building block for a XeCl laser array with average power in the watt range. The beam produced by the laser is highly multimode. This has been shown to limit the efficiency of the laser, and will hinder its application to coherent arrays. DTIC

N93-26445# Naval Research Lab., Washington, DC.

START-UP IMPRINTING AND SHOCK DYNAMICS IN LASER-TARGET INTERACTION Interim Report

Mark H. Emergy 10 Dec. 1992 27 p

(NR Proj. 8068)

(AD-A261384; NRL/MR/6440-92-7174) Avail: CASI HC A03/MF A01

Improved uniformity of the laser for-al spot profile is a necessary criterion for the success of high intensity laser fusion and to improve the quality of data from moderate intensity laser driven shock experiments in solids. Recently developed laser smoothing techniques rely on both temporal smoothing and thermal smoothing to produce uniform ablation pressures on the target surface. Thermal smoothing is not effective during the low intensity portion of a laser pulse and the resultant shock structure mirrors the residual laser nonuniformities. The impact of the first (nonuniform) shock can be diminished by using foam layers, a precursor flash, shallow angles of incidence, and by adiabatically compressing the target with a temporally long, slowly rising laser pulse. DTIC

N93-26503# Lawrence Livermore National Lab., CA.

FEASIBILITY EXPERIMENT FOR SODIUM-LAYER LASER GUIDE STARS AT THE LAWRENCE LIVERMORE NATIONAL LABORATORY

C. Max, K. Avicola, H. Bissinger, J. Brase, D. Gavel, H. Friedman, J. Morris, S. Oliver, J. T. Salmon, and K. Waltjen Mar. 1992 9 p Presented at the Laser Guide Star Adaptive Optics Workshop, Albuquerque, NM, 10-12 Mar. 1992

(Contract W-7405-eng-48)

(DE93-007115; UCRL-JC-109526; CONF-9203139-3) Avail: CASI HC A02/MF A01

We are developing a feasibility experiment to demonstrate closed-loop adaptive optics using a sodium-layer laser guide star. We will use the copper-vapor-pumped dye lasers developed for LLNL's Atomic Vapor Laser Isotope Separation Program to create the laser guide star. Closed-loop adaptive corrections will be accomplished using a 69-subaperture adaptive optics system on a one-meter telescope at LLNL. The laser beam will be projected upwards from a beam director approximately 5 meters away from the main telescope, and is expected to form a spot about a meter in diameter at the atmospheric sodium layer (at an altitude of 95 km). Details of the adaptive optics components and an analysis of the expected performance will be presented in companion papers for this Workshop. Here we summarize the overall architecture and system objectives. The long-term goal of our effort is to develop laser guide stars and adaptive optics for large astronomical telescopes. DOE

N93-26524# Stanford Univ., CA. Physics Lab.

LASER PHYSICS AND LASER TECHNIQUES Final Report, 15 Mar. 1989 - 14 Mar. 1992

A. E. Siegman Jan. 1993 19 p

(Contract F49620-89-K-0004)

(AD-A261595; AFOSR-93-0059TR) Avail: CASI HC A03/MF A01

The Final Report summarizes accomplishments over the 3-year period in several different areas of Laser Physics and Laser Techniques, including ultrafast optical measurements using tunable laser-induced gratings; development of a new subpicosecond photodetector technique; generation of tunable picosecond pulses in the IR using parametric mode locking; new developments in laser resonators and laser mode computations; experimental progress toward measuring an important and fundamental excess spontaneous emission or excess quantum noise mechanism in laser oscillators; and the development of new techniques for laser beam characterization and laser beam measurement. DTIC

N93-26597# Sandia National Labs., Albuquerque, NM.

FALCON NUCLEAR-REACTOR-PUMPED LASER PROGRAM AND WIRELESS POWER TRANSMISSION

R. J. Lipinski and P. S. Pickard 1992 11 p Presented at the 1st Annual Wireless Power Transmission Conference, San Antonio, TX, 23-25 Feb. 1993

(Contract DE-AC04-76DP-00789)

(DE93-007607; SAND-92-1973C; CONF-930258-1) Avail: CASI HC A03/MF A01

FALCON is a high-power, reactor-pumped laser concept. The major strengths of a reactor-pumped laser are as follows: (1) simple, modular construction; (2) long-duration, closed-cycle capability; (3) self-contained

power; (4) compact size; and (5) a variety of wavelengths (from visible to infrared). Reactor-pumped lasing has been demonstrated experimentally in various mixtures of xenon, argon, neon, and helium at wavelengths of 585, 703, 725, 1271, 1733, 1792, 2032, 2630, 2650, and 3370 nm with intrinsic efficiency as high as 2.5 percent. Powers up to 300 W for 2 ms have been demonstrated. Projected beam quality for FALCON is good enough that frequency doubling at reasonable efficiencies could be expected to yield wavelengths at 353, 363, 636, 867, 896, 1016, 1315, 1325, and 1685 nm. Appropriate missions for FALCON are described and include the following: power beaming to satellites, the moon, and unmanned surveillance planes; lunar mapping; space debris removal; and laser propulsion. DOE

N93-26601# Naval Postgraduate School, Monterey, CA.
VERY LOW FREQUENCY SIGNALS AND WHISTLER-MODE AMPLIFICATION IN THE MAGNETOSPHERE AND LIMIT-CYCLE BEHAVIOR IN THE CECAF INFRARED FREE ELECTRONIC LASER M.S. Thesis
Daryl L. Caudle Dec. 1992 113 p
(AD-A261776) Avail: CASI HC A06/MF A02

Very low frequency (VLF) electromagnetic wave injection experiments were conducted on 23-24 Jan. 1988 from a 42-km horizontal dipole antenna located at Siple Station, Antarctica. The experiment consisted of a diagnostic format transmitted for one minute every five minutes, for a 10 hour period between 1700 UT and 0300 UT. These signals were received and recorded at the conjugate magnetic field point location at Lake Mistissini, Canada. A detailed analysis of this data clearly demonstrates hot plasma effects such as saturated power levels, exponential growth rates, sideband formation, and triggered emissions due to wave-particle interactions. These hot plasma effects remain constant over a time scale of 30 seconds but show large variations over a time scale of 5 minutes. These VLF signals were used to simulate whistler waves which occur naturally and are amplified by energetic electrons spiraling around magnetic field lines near the geomagnetic equator. Navy VLF communications are strongly affected by the presence of whistler waves. The electron and whistler wave interaction can be described by a theoretical model which is very similar to that used for free electron lasers (FEL). DTIC

N93-24980*# National Aeronautics and Space Administration. Marshall Space Flight Center, Huntsville, AL.
HYDROGEN MASERS FOR SPACE
R. F. C. Vessot (Smithsonian Astrophysical Observatory, Cambridge, MA.), E. M. Mattison (Smithsonian Astrophysical Observatory, Cambridge, MA.), G. U. Nystrom (Smithsonian Astrophysical Observatory, Cambridge, MA.), L. M. Coyle (Smithsonian Astrophysical Observatory, Cambridge, MA.), R. Decher, S. J. Feltham (European Space Agency. European Space Research and Technology Center, ESTEC, Noordwijk, Netherlands.), G. Busca (Observatoire Cantonal, Neuchatel, Switzerland.), S. Starker (Deutsche Forschungsanstalt fuer Luft- und Raumfahrt, Oberpfaffenhofen, Germany.), and S. Leschiutta (Politecnico di Torino, Italy.) *In* ESA, Frequency and Time Forum Jun. 1992 p 19-25 Sponsored by Smithsonian Institution Research Opportunities Funds (For primary document see N93-24978 09-70)
(Contract NAS8-39194)
Copyright Avail: CASI HC A02/MF A04

N93-25005# Ministry of Posts and Telecommunications, Tokyo (Japan). Communications Research Lab.
A SYSTEM DESIGN FOR LASER TIME SYNCHRONIZATION VIA GEODETIC SATELLITE AJISAI
Hiroo Kunimori, Fujinobu Takahashi, and Atsushi Yamamoto (Maritime Safety Agency, Tokyo, Japan.) *In* ESA, Frequency and Time Forum Jun. 1992 p 181-185 (For primary document see N93-24978 09-70)
Copyright Avail: CASI HC A01/MF A04

N93-25024# Observatoire Cantonal, Neuchatel (Switzerland).
BASIC DESIGN OF A SPACEBORNE HYDROGEN MASER
L. G. Bernier *In* ESA, Frequency and Time Forum Jun. 1992 p 283-286 (For primary document see N93-24978 09-70)
Copyright Avail: CASI HC A01/MF A04

N93-25030# Academia Sinica, Wuhan (China). Lab. of Magnetic Resonance and Atomic and Molecular Physics.
EXPERIMENTS ON A DIODE-LASER-PUMPED Rb-87 MASER
Deng Jinquan, Tan Yongfang, Xiang Yuanhai, and Zhu Xiwen *In* ESA, Frequency and Time Forum Jun. 1992 p 315-317 (For primary document see N93-24978 09-70)
Copyright Avail: CASI HC A01/MF A04

N93-25048# Shanghai Observatory (China).
THE DEVELOPMENT PROGRESSES OF HYDROGEN MASERS AT SHANGHAI OBSERVATORY
Z. C. Zhai, H. X. Huang, J. W. He, C. F. Lin, G. X. Jiang, W. H. Luo, and J. F. Lu *In* ESA, Frequency and Time Forum Jun. 1992 p 405-408 (For primary document see N93-24978 09-70)
Copyright Avail: CASI HC A01/MF A04

N93-25049# KVARZ, Nishnij Novgorod (Russia). Inst. of Electronic Measurements.
INVESTIGATIONS OF THE FREQUENCY INSTABILITY OF CH1-75 HYDROGEN MASERS
N. A. Demidov, E. M. Ezhov, B. A. Sakharov, B. A. Uljanov, A. Bauch (Physikalisch-Technische Bundesanstalt, Brunswick, Germany.), and B. Fischer (Physikalisch-Technische Bundesanstalt, Brunswick, Germany.) *In* ESA, Frequency and Time Forum Jun. 1992 p 409-414 (For primary document see N93-24978 09-70)
Copyright Avail: CASI HC A02/MF A04

N93-25065# Observatoire Cantonal, Neuchatel (Switzerland).
A COMPACT AND HIGH-PERFORMANCE REFERENCE CELL FOR LASER FREQUENCY STABILIZATION
G. Dudle and T. Thomann *In* ESA, Frequency and Time Forum Jun. 1992 p 511-514 Sponsored in part by Swiss National Fund for Scientific Research (For primary document see N93-24978 09-70)
(Contract ESTEC-9099/90/NL/US(SC))
Copyright Avail: CASI HC A01/MF A04

N93-25067# Observatoire Cantonal, Neuchatel (Switzerland).
NOISE MEASUREMENTS IN SINGLE-MODE GaAlAs DIODE LASERS
N. Sagna, C. Mandache (Bucharest Univ., Romania.), and P. Thomann *In* ESA, Frequency and Time Forum Jun. 1992 p 521-525 Sponsored by Swiss National Fund for Scientific Research (For primary document see N93-24978 09-70)
Copyright Avail: CASI HC A01/MF A04

N93-25068# Tokyo Inst. of Tech., Yokahama (Japan).
FUNDAMENTAL CHARACTERISTICS OF A LASER-DIODE-PUMPED RUBIDIUM MASER WITH AN EXTERNAL FEEDBACK LOOP
Nobunori Oura, Naimu Kuramochi, Wataru Domon, Tamotsu Komiyama, and Ryota Shirato *In* ESA, Frequency and Time Forum Jun. 1992 p 527-530 (For primary document see N93-24978 09-70)
Copyright Avail: CASI HC A01/MF A04

37 MECHANICAL ENGINEERING

Includes auxiliary systems (nonpower); machine elements and processes; and mechanical equipment.

N93-24751*# National Aeronautics and Space Administration. Lewis Research Center, Cleveland, OH.
GLOBAL DYNAMIC MODELING OF A TRANSMISSION SYSTEM Final Report
F. K. Choy (Akron Univ., OH.) and W. Qian (Akron Univ., OH.) Apr. 1993 163 p
(Grant NAG3-900; RTOP 505-62-10)
(NASA-CR-191117; E-7731; NAS 1.26:191117; ARL-CR-11) Avail: CASI HC A08/MF A02

The work performed on global dynamic simulation and noise correlation of gear transmission systems at the University of Akron is outlined. The objective is to develop a comprehensive procedure to simulate the dynamics of the gear transmission system coupled with the effects of gear box vibrations. The developed numerical model is benchmarked with results

from experimental tests at NASA Lewis Research Center. The modal synthesis approach is used to develop the global transient vibration analysis procedure used in the model. Modal dynamic characteristics of the rotor-gear-bearing system are calculated by the matrix transfer method while those of the gear box are evaluated by the finite element method (NASTRAN). A three-dimensional, axial-lateral coupled bearing model is used to couple the rotor vibrations with the gear box motion. The vibrations between the individual rotor systems are coupled through the nonlinear gear mesh interactions. The global equations of motion are solved in modal coordinates and the transient vibration of the system is evaluated by a variable time-stepping integration scheme. The relationship between housing vibration and resulting noise of the gear transmission system is generated by linear transfer functions using experimental data. A nonlinear relationship of the noise components to the fundamental mesh frequency is developed using the hypercoherence function. The numerically simulated vibrations and predicted noise of the gear transmission system are compared with the experimental results from the gear noise test rig at NASA Lewis Research Center. Results of the comparison indicate that the global dynamic model developed can accurately simulate the dynamics of a gear transmission system. Author (revised)

N93-25100# Oak Ridge National Lab., TN.
POSITION AND FORCE CONTROL OF A VEHICLE WITH TWO OR MORE STEERABLE DRIVE WHEELS
D. B. Reister and M. A. Unseren 1992 20 p Presented at the Institute of Electrical and Electronics Engineers International Conference on Robotics and Automation, Atlanta, GA, 2-7 May 1993
(Contract DE-AC05-84OR-21400)
(DE92-041301; CONF-930519-2) Avail: CASI HC A03/MF A01

When a vehicle with two or more steerable drive wheels is traveling in a circle, the motion of the wheels is constrained. The wheel translational velocity divided by the radius to the center of rotation must be the same for all wheels. When the drive wheels are controlled independently using position control, the motion of the wheels may violate the constraints and the wheels may slip. Consequently, substantial errors can occur in the orientation of the vehicle. A vehicle with N drive wheels has (N - 1) constraints and one degree of freedom. We have developed a new approach to the control of a vehicle with N steerable drive wheels. The novel aspect of our approach is the use of force control. To control the vehicle, we have one degree of freedom for the position on the circle and (N - 1) forces that can be used to reduce errors. Recently, Kankaanranta and Koivo developed a control architecture that allows the force and position degrees of freedom to be decoupled. In the work of Kankaanranta and Koivo the force is an exogenous input. We have made the force endogenous by defining the force in terms of the errors in satisfying the rigid body kinematic constraints. We have applied the control architecture to the HERMIES-M robot and have measured a dramatic reduction in error (more than a factor of 20) compared to rations without force control. DOE

N93-25228 Department of the Navy, Washington, DC.
APPARATUS AND METHODS FOR DETERMINING BALANCE OF A CYLINDRICAL VEHICLE Patent
David M. Nugent, inventor (to Navy) 8 Dec. 1992 11 p Filed 28 Aug. 1991
(AD-D015637; US-Patent-5,168,749; US-Patent-Appl-SN-750998) Avail: US Patent and Trademark Office

Apparatus and methods for determining balance of a cylindrical vehicle are presented. The apparatus comprises a frame adapted for horizontal disposition, first and second support assemblies mounted on the frame for receiving the vehicle, first and second load cells mounted, respectively, on the first and second support assemblies. Upon placement of the vehicle on the support assemblies, the load cells are adapted to provide readings indicative of the weight of the vehicle. From these readings, the center of gravity of the vehicle may be determined . A torsion cell assembly is mounted on the frame and adapted for connection to the vehicle and for providing indications of righting moment and static heel of the vehicle.
Official Gazette of the U.S. Patent and Trademark Office

N93-25268 Oxford Univ. (England).
TURBINE TURBOBRAKE SYSTEMS Ph.D. Thesis
Michael I. Goodisman 1991 253 p
Avail: Univ. Microfilms Order No. BRD-98278

Short duration rotating turbine facilities are a recent development in the field of turbine research. Turbine braking devices can be used to maintain the turbine at the desired test speed, resulting in a longer usable test time. The Isentropic Light Piston Cascade at the Defence Research Agency in Pyestock will perform heat transfer and aerodynamic tests on the first stage of a Rolls-Royce turbine (MT1) linked to a new type of brake, the 'axial turbo brake'. The axial turbo brake is driven by the turbine's exhaust gas and is isolated from the turbine by a choked throat. The turbo brake's power absorption must be controlled to match the power developed by the turbine stage for a constant speed run. Both the turbo brake blade shape and novel power control system were developed from tests on a 0.17 scale test rig. The turbo brake's braking is controlled through by-pass of flow over the blade tips and partial blockage of the turbo brake's exit annulus. Also described is the mechanical design, development and manufacture of the full size turbo brake, turbine disc and turbine blades, which have been successfully spun tested to their overspeed condition. Finally, a theory for self-pumping turbo brakes is developed. These devices would have additional applications because they do not require a supply of high pressure gas to drive them. Dissert. Abstr.

N93-25412 Stanford Univ., CA.
FORMULATION AND TREATMENT OF FRICTIONAL CONTACT PROBLEMS USING FINITE ELEMENTS Ph.D. Thesis
Tod Alan Laursen 1992 209 p
Avail: Univ. Microfilms Order No. DA9302237

In recent years, problems involving the mechanical contact between deformable bodies have received increasing attention from the computational solid mechanics community. Such problems, usually called contact problems, are particularly challenging in the presence of large deformations and inelastic response, as are found, for example, in dynamic impacts between bodies, metal forming applications, mechanical (hardness) testing, and post buckling response. The introduction of friction is an additional complication which has important consequences, both in the underlying mathematical structure of the problem and in the design of efficient solution algorithms. In this work, a new comprehensive approach is presented which enables the solution of frictional contact problems within a Lagrangian framework. The approach is suitable for the solution of static or low frequency dynamic problems using implicit time integration. Novel features of the work include: (1) a continuum basis for the formulation, making it suitable for arbitrary discretizations and two or three spatial dimensions; (2) the presence of an exact linearization for the discrete global equations, such that optimal convergence properties are attained when using a Newton-Raphson strategy for solving the nonlinear equation system; and (3) penalty and augmented Lagrangian enforcement of constraints, leading to efficient solution of the global equations while circumventing ill-conditioning. The augmented Lagrangian treatment presented includes a reliable algorithmic symmetrization of the frictional response, lending the formulation a high level of compatibility with existing structural and solid mechanics finite element codes. In presenting the proposed formulation, many details of the discretization process are given, including explicit expressions for the contact contributions to the global equation system. A full set of numerical simulations, demonstrating the utility of the proposed methodology, is also presented. Dissert. Abstr.

N93-25413# Texas Univ., Austin. Dept. of Mechanical Engineering.
A CONTROL STRUCTURE FOR FAULT-TOLERANT OPERATION OF ROBOTIC MANIPULATORS
Yung Ting, S. Tosunoglu, and D. Tesar 1993 8 p Presented at the Institute of Electrical and Electronics Engineers International Conference on Robotics and Automation, Atlanta, GA, 2-7 May 1993
(Contract DE-FG02-86NE-37966)
(DE93-005783; DOE/NE-37966/2; CONF-930519-7) Avail: CASI HC A02/MF A01

Failure of any component of a robotic system during operation is a matter of concern. This work investigates internal shock phenomena due to the failure of joint actuation, and a recovery algorithm for both serial and parallel mechanisms under such circumstances. A control algorithm is studied that consists of a model reference algorithm and computed torque method in the feedforward process, and a simple PID controller in the feedback process. Simulation results illustrate the effectiveness of this recovery algorithm which attempts to reduce the internal shock when failure occurs, and accomplish the tracking of the given end-effector trajectory.

The outlined recovery algorithms, which include two stages of robot control, path planning and path tracking, are expected to be applied not only to a case where some joint is fully failed, but also to cases where some joints experience partial failure. DOE

N93-25435 Loughborough Univ. of Technology (England).
LASER WELDING OF SELECTED AEROSPACE ALLOYS Ph.D. Thesis
Gracie E. Ebadan 1989 331 p
Avail: Univ. Microfilms Order No. BRDX98033

The study was aimed at developing an understanding of the microstructural effects of the laser welding process on the alloys, and assessing the structural integrity of the resultant welds. The effect of laser processing parameters such as laser power, laser beam traverse speed, lens focal length, and the manipulation of these parameters on the welding efficiency and weld area integrity was also investigated. Other tasks within the project included a study on the possibility of using an anodic film to enhance the laser weld ability of Al 6061. Finally, attempts were made to identify phases observed in the weld area of the composite materials. Nimonics C263 and PE11 exhibited laser welds free of cracks and porosity. The difference in composition between the two alloys did not result in any significant dissimilarities in their response to the laser welding process. The welds in both alloys exhibited a fine columnar dendritic microstructure, and while carbides were observed in the interdendritic regions of the welds, electron optical analysis did not reveal any gamma' precipitates in this region. It was concluded that for the welding of thin gage materials above a threshold laser power the resultant welding efficiency shows a greater dependence on laser beam mode, and laser spot size, than on laser power, and beam traverse speed. Aluminum 6061 was not easily welded with a laser in its as received form, and the welds showed some degree of porosity. Anodizing was found to improve the welding efficiency in this material. While the presence of an anodic film on the metal surface increased the welding efficiency of the alloy, no relationship was found between the thickness of the anodic film and welding efficiency in the range of film thicknesses investigated. Weld regions were observed to be cellular dendritic in structure, with narrow heat affected zones. No precipitates or low melting point phases could be identified in the weld region. Melt zones were successfully produced in the composite materials, with the main problem encountered being that of porosity adjacent to the weld bead. It was shown that manipulation of the laser welding parameters resulted in a decrease in this porosity. Dissert. Abstr.

N93-25449# Oak Ridge National Lab., TN.
NUMERICAL KINEMATIC TRANSFORMATION CALCULATIONS FOR A PARALLEL LINK MANIPULATOR
S. M. Killough 1993 8 p Presented at the Institute of Electrical and Electronics Engineers International Conference on Robotics and Automation, Atlanta, GA, 2-7 May 1993
(Contract DE-AC05-84OR-21400)
(DE93-005778; CONF-930519-8) Avail: CASI HC A02/MF A01

Parallel link manipulators are often considered for particular robotic applications because of the unique advantages they provide. Unfortunately, they have significant disadvantages with respect to calculating the kinematic transformations because of the high-order equations that must be solved. A manipulator design that exploits the mechanical advantages of parallel links yet also has a corresponding numerical kinematic solution that can be solved in real time on common microcomputers is presented. DOE

N93-25672*# National Aeronautics and Space Administration. Lewis Research Center, Cleveland, OH.
EVALUATION OF A VIBRATION DIAGNOSTIC SYSTEM FOR THE DETECTION OF SPUR GEAR PITTING FAILURES
Dennis P. Townsend and James J. Zakrajsek Jun. 1993 11 p Proposed for presentation at the 29th Joint Propulsion Conference and Exhibit, Monterey, CA, 28-30 Jun. 1993; sponsored by the AIAA, SAE, ASME, and ASEE
(DA Proj. 1L1-62211-A-47-A; RTOP 505-62-10)
(NASA-TM-106103; E-7752; NAS 1.15:106103; AIAA Paper 93-2298; ARL-TR-11) Avail: CASI HC A03/MF A01

A vibration diagnostic system was used to detect spur gear surface pitting fatigue in a closed-loop spur gear fatigue test rig. The diagnostic system, comprising a personal computer with an analog-to-digital conversion board, a diagnostic system unit, and software, uses time-synchronous averaging of the vibration signal to produce a vibration image of each tooth on any gear in a transmission. Several parameters were analyzed including gear pair stress wave and raw baseband vibration, kurtosis, peak ratios, and others. The system provides limits for the various parameters and gives a warning when the limits are exceeded. Several spur gear tests were conducted with this system and vibration data analyzed at 5-min. intervals. The results presented herein show that the system is fairly effective at detecting spur gear tooth surface fatigue pitting failures. Author

N93-25682# Army Belvoir Research and Development Center, Fort Belvoir, VA.
EVALUATION OF THE MIGRATING COMBUSTION CHAMBER (MCC) ENGINE Final Report
K. M. Miller and Dorin Morar Jan. 1993 43 p
(AD-A260780; BRDEC-2538) Avail: CASI HC A03/MF A01

The Belvoir Research, Development and Engineering Center (BRDEC) tested three Migrating Combustion Chamber (MCC) engines built by Engine Research Associates (ERA) for Natick RD and E Center. The MCC concept attempts to provide a lightweight, quiet engine having a cool exhaust gas stream. The cool exhaust is attained by capturing additional energy from expansion beyond that achievable in conventional engines by the use of gas porting to multiple expansion chambers; this provides a more efficient engine operation than is otherwise attainable for the configuration. The testing included determining the engine torque-speed-power characteristics and the Brake Specific Fuel Consumption (BSFC) under a variety of load conditions. Startability and operability were concerns; starting under normal ambient conditions was difficult. All testing was performed using a 10:1 fuel/oil mixture of low lead gasoline with AMZOIL synthetic lubricating oil for two-stroke engines. The maximum power achieved was 0.25 horsepower at 4,400 rpm. The peak torque observed was 69 oz.-in. at 3,200 rpm. It was not possible to make noise and vibration measurements during the testing cycle, but they appeared to be low. The MCC engines tested had relatively short lives, operating for less than 25 hours. Performance and durability improvements are necessary before this MCC design can be considered as a viable alternative to commercially available two-cycle engines. DTIC

N93-25697# Cincinnati Univ., OH.
BIPED CONTROL VIA NONLINEAR DYNAMICS Ph.D. Thesis
Hatem M. Hmam 1992 188 p
Avail: Univ. Microfilms Order No. DA9302395

This thesis applies nonlinear techniques to actuate a biped system and provides a rigorous analysis of the resulting motion. From observation of human locomotion, it is believed that the 'complex' dynamics developed by the aggregation of multiple muscle systems can be generated by a reduced order system which captures the rough details of the locomotion process. The investigation is begun with a simple model of a biped system. Since the locomotion process is cyclic in nature, we focus on applying the topologically similar concept of limit cycles to the simple model in order to generate the desired gaits. A rigorous analysis of the biped dynamics shows that the controlled motion is robust against dynamical disturbances. In addition, different biped gaits are generated by merely adjusting some of the limit cycle parameters. More dynamical and actuation complexities are then added for realism. First, two small foot components are added and the overall biped motion under the same control actuation is analyzed. Due to the physical constraints on the feet, it is shown using singular perturbation theory how the gross behavior of the biped dynamics are dictated by those of the reduced model. Next, an analysis of the biped dynamics under added nonlinear elasticities in the legs is carried out. Moreover, using a slightly modified model, forward motion is generated in the sagittal plane. At each step, a small amount of energy is consistently derived from the vertical plane and converted into a forward motion. Stability of the forward dynamics is guaranteed by appropriate foot placement. Finally, the robustness of the controlled biped dynamics is rigorously analyzed and illustrated through extensive computer simulations. Dissert. Abstr.

N93-25727 Salford Univ. (England).
THE INDUCTION OF ELASTIC FINE MOTION IN ROBOTIC GRASPS Ph.D. Thesis
Abdul Ghafoor 1992 283 p
Avail: Univ. Microfilms Order No. BRD-98219

The purpose of this thesis is to explore the possibilities of inducing elastic fine motions to the object held by a robotic gripper through a number of contacts. The problems of grasping are discussed explicitly to establish basis of imparting fine motions to the grasped objects. The recent studies in grasping and manipulation have suggested different kinds of models of the contacts between the grasped object and the gripping devices. Amongst those, the point contacts have commonly been used in grasping. Depending upon the nature of the objects and the contacts, further surface properties such as friction need to be analyzed. The analysis of these types of grasps are statically indeterminate. There is a need for a simple and general technique by which we are able to establish and analyze a statically indeterminate grasp. The use of the theory of elasticity in the form of elastic finger-tips solves the indeterminacy of the grasping problems. The compression of elastic systems in the finger-tips by the application of appropriate preloads provides a means of inducing fine movements to the grasped rigid objects. The contact elasticity is exploited in achieving this, while at the same time ensuring that the grasp is maintained. In the most general case, it may not always be possible to achieve a particular defined fine motion of the grasped object. In such cases approximate solutions are demonstrated. Many examples related to the basis of the theoretical analysis are also discussed. These cover the grasp of the objects and the induction of fine motion of the grasped objects, by considering elastic point contacts with and without friction. The analysis presented in this thesis is mainly based upon the assumption of point contacts, but a comparison between point contacts and cluster (a combination of point contacts) is also included. A brief description is also given of the preliminary experiments which were designed to demonstrate practically the induction of fine motions by the application of preloads through the normals of the elastic contacts. The experiments confirm the theoretical results.

Dissert. Abstr.

N93-25745 Salford Univ. (England).

ANALYSIS AND DESIGN OF A NOVEL ROBOTIC FINGER-TIP SENSOR FOR ADAPTIVE GRASPING Ph.D. Thesis

M. K. Mortazavi 1991 303 p

Avail: Univ. Microfilms Order No. BRD-98234

The need arises in a robotic grasping environment to determine in a non-contact manner the distance of the surface to be grasped and its relative orientation from a robot finger-tip. The research described deals with the design and development of a system to solve this problem. The investigation was developed in four major stages. Initially, a practical study of robotic grasping instrumentation problems and methods of grasping and the limitation of instrumentation of conventional robot grippers was carried out. The purpose was to explore a suitable technique to identify the direction of the contact normal to the surface to be contacted in relation to the known orientation of grasping device. Next, a theory supporting an optical robotic sensor was developed in both principle and practices. The method involves projection of three collimated beams diverging from central finger-based reference direction towards the object which is assumed to have locally flat surface. A geometric model relates the position of three light points on the object surface to surface orientation and to the distance between the object and the finger-tip and vice-versa. In order to measure the position of light beams intersecting a given test surface, a number of light-beam producing techniques using incandescent and laser sources, and then detecting the resulting projection points by sensing elements were investigated. Feasible operational ranges of distance and orientation parameters for the laser and photo-detectors were established. These parameters were used to demonstrate and evaluate the feasibility and applicability of the proposed theory with reference to the accuracy of the direction of the contact normal. Dissert. Abstr.

N93-25771# Rensselaer Polytechnic Inst., Troy, NY. Dept. of Electrical Computer and Systems Engineering.

PASSIVITY MOTIVATED CONTROLLER DESIGN FOR FLEXIBLE STRUCTURES

Declan Hughes and John T. Wen 18 Jan. 1993 25 p

(Contract DAAL03-92-G-0123)

(AD-A261122; ARO-30378.1-EG-URI) Avail: CASI HC A03/MF A01

When actuators and sensors on a controlled mechanical structure form naturally passive pairs, which usually requires physical collocation, very robust stabilizing controllers can be constructed. If the number of such naturally passive pairs is small, the closed loop performance may not be satisfactory. To address this problem, additional sensors, which are usually cheaper, lighter, and easier to instrument than actuators are frequently added to the control system. However, the passivity properly no longer holds for these sensors with respect to the existing actuators. This paper presents some results on extending the passivity based design to incorporate these noncollocated sensors by using some nominal model information to synthesize a fictitious strictly passive output. The design approach was applied to a single rotating flexible beam with encouraging results. DTIC

N93-25884*# Cincinnati Univ., OH.

COMPUTATIONAL GEARING MECHANICS Final Report

Ronald L. Huston Apr. 1993 11 p

(Grant NsG-3188; DA Proj. 1L1-62211-A-47-A; RTOP 505-62-10)

(NASA-CR-191127; E-7808; NAS 1.26:191127; ARL-CR-43) Avail: CASI HC A03/MF A01

This is an expository report summarizing the research efforts and results under NASA Grant NSG-3188 to the University of Cincinnati. Since the grant has now ended this report also serves as a final report for the grant. The focus of the research has been computational gearing mechanics. Research on gear geometry, gear stress, and gear dynamics is discussed. Current research and planned future efforts are also discussed. A comprehensive bibliography is presented. Author

N93-26001* National Aeronautics and Space Administration. Marshall Space Flight Center, Huntsville, AL.

RADIAL SPLINE ASSEMBLY FOR ANTIFRICTION BEARINGS Patent

Jerry H. Moore, inventor (to NASA) 18 May 1993 7 p Filed 7 Oct. 1992 Supersedes N93-17084 (31 - 5, p 1179)

(NASA-Case-MFS-28629-1; US-Patent-5,211,489;

US-Patent-Appl-SN-957128; US-Patent-Class-384-585;

US-Patent-Class-384-493; US-Patent-Class-384-537;

Int-Patent-Class-F16C-43/04; Int-Patent-Class-F16C-19/52) Avail: US Patent and Trademark Office

An outer race carrier is constructed for receiving an outer race of an antifriction bearing assembly. The carrier in turn is slidably fitted in an opening of a support wall to accommodate slight axial movements of a shaft. A plurality of longitudinal splines on the carrier are disposed to be fitted into matching slots in the opening. A deadband gap is provided between sides of the splines and slots, with a radial gap at ends of the splines and slots and a gap between the splines and slots sized larger than the deadband gap. With this construction, operational distortions (slope) of the support wall are accommodated by the larger radial gaps while the deadband gaps maintain a relatively high springrate of the housing. Additionally, side loads applied to the shaft are distributed between sides of the splines and slots, distributing such loads over a larger surface area than a race carrier of the prior art.

Official Gazette of the U.S. Patent and Trademark Office

N93-26144# Department of the Navy, Washington, DC.

POSITIVE DISPLACEMENT ROTARY PUMP Patent Application

Paul E. Moody, inventor (to Navy) 1 Dec. 1992 12 p

(AD-D015678; US-Patent-Appl-SN-983957) Avail: CASI HC A03/MF A01

An eccentric drive rotates inside a ring that is hinged to a plate, and an elastomeric curtain is wrapped around the ring and across an articulated plate. The curtain moves along a cylindrical wall inside the pump cavity to move fluid from an inlet to an outlet end of the chamber. Two or more chambers can be coupled in series or in parallel with one another. DTIC

N93-26244 Department of the Navy, Washington, DC.

PNEUMATIC ACTUATOR WITH HYDRAULIC CONTROL Patent

Hobart R. Everett, Jr., inventor (to Navy) 10 Nov. 1992 9 p Filed 24 Jun. 91

(AD-D015652; US-Patent-5,161,449; US-Patent-Appl-SN-719436;

US-Patent-Class-91-42) Avail: US Patent and Trademark Office

The present invention provides a pneumatically powered actuator having hydraulic control for both locking and controlling the velocity of an output rod without any sponginess. The invention includes a double-acting pneumatic actuator having a bore, a piston slidably engaged within the bore, and a control rod connected to the piston. The double-acting pneumatic actuator is mounted to a frame. A first double-acting hydraulic actuator having a bore, a piston slidably engaged within the bore, and a follower

rod mounted to the piston is mounted to the frame such that the follower rod is fixedly connected to the control rod. The maximum translation of the piston within the bore of the first double-acting hydraulic actuator provides a volumetric displacement V1. The present invention also includes a second double-acting hydraulic actuator having a bore, a piston slidably engaged within the bore, and an output rod mounted to the piston. The maximum translation of the piston within the bore of the second double-acting hydraulic actuator provides a volumetric displacement V2, where V2=V1. A pair of fluid ports in each of the first and second double-acting hydraulic cylinders are operably connected by fluid conduits, one of which includes a valve circuit which may be used to control the velocity of the output rod or to lock the output rod in a static position by regulating the flow of hydraulic fluid between the double-acting cylinders. DTIC

N93-26249# Naval Postgraduate School, Monterey, CA.
A SURFACE INTEGRAL ALGORITHM FOR THE MOTION PLANNING OF NONHOLONOMIC MECHANICAL SYSTEMS M.S. Thesis
David P. Anderson Dec. 1992 66 p
(AD-A261746) Avail: CASI HC A04/MF A01

The number of coordinates needed to completely describe the configuration of a holonomic mechanical system is equal to the number of degrees of freedom possessed by that system. In contrast, nonholonomic systems always require more coordinates for their description than their degrees of freedom due to the nonintegrable nature of the governing velocity constraints. The task of nonholonomic motion planning applied to a given system is to develop trajectories of the independent coordinate variables such that the entire system is driven to some desired point in its configuration space. An algorithm for constructing these trajectories is presented. In this algorithm, the independent variables are first converged to their desired values. The dependent variables are subsequently converged using closed trajectories of the independent variables. The requisite closed trajectories are planned using Stoke's Theorem which converts the problem of finding a closed path in the space of the independent variables to that of finding a surface area in that same space such that the dependent variables converge to their desired values as the independent variables traverse along the boundary of the surface area. The use of Stoke's Theorem simplifies the motion planning process and also answers important questions pertaining to the system. The salient features of the algorithm are apparent in the two examples discussed: a planar space robot and a disk rolling without slipping on a flat surface. DTIC

N93-26534# Texas Univ., Austin. Center for Transportation Research.
COST-EFFECTIVENESS ANALYSIS OF TxDOT CNG FLEET CONVERSION, VOLUME 2 Interim Research Report
M. A. Euritt, D. B. Taylor, and H. Mahmassani Aug. 1992 326 p See also PB92-218049 and PB93-134542 Sponsored by Federal Highway Administration and Texas Dept. of Transportation
(PB93-159432; CTR-3-4-90/2-93-2/2-Vol-2; FHWA/TX-92+983-2-Vol-2)
Avail: CASI HC A15/MF A03

Increased emphasis on energy efficiency and air quality has resulted in a number of state and federal initiatives examining the use of alternative fuels for motor vehicles. Texas' program for alternate fuels includes compressed natural gas (CNG). Based on an analysis of 30-year life-cycle costs, development of a natural gas vehicle (NGV) program for the Texas Department of Transportation (TxDOT) would cost about $47 million (in 1991 dollars). These costs include savings from lower priced natural gas, infrastructure costs for a fast-fueling station, vehicle costs, and operating costs. The 30-year life-cycle costs translate into an average annual vehicle cost increase of $596, or about 4.9 cents more per vehicle mile of travel. Based on the cost-effectiveness analysis and assumptions, there are currently no TxDOT stations suitable for conversion to compressed natural gas NTIS

N93-26564# Engineered Designs, Inc., Cincinnati, OH.
ADVANCED BRISTLE SEALS FOR GAS TURBINE ENGINES Final Report, May - Nov. 1992
Jerry L. Cabe 28 Jan. 1993 45 p
(Contract DAAJ02-92-C-0008)
(AD-A261296; FR9201-01) Avail: CASI HC A03/MF A01

A seven month proof-of-concept program was conducted for an advanced bristle seal, called a bush seal, for use in gas turbine engines. This program was performed as a Small Business Innovation Research (SBIR) Phase 1 project. Bush seal specimen and a full ring bush seal were designed, evaluated, and manufactured for testing. An analytical study of the potential of the bush seal relative to a labyrinth seal was conducted. Static and dynamic testing of the bush seal was performed to determine the behavior of the bristles under pressurization and during contact with a rotating labyrinth tooth. Stable behavior of the bristle elements was observed during static pressurization of a full ring bush seal. The dynamic testing of various configurations of bush seal against a rotating labyrinth tooth showed minimal wear of the bristles relative to a conventional labyrinth seal. The development and application of the bush seal concept to gas turbine engines has the potential of improving the engine's performance while decreasing the degradation of the seal performance over time. DTIC

N93-26585# Texas Univ., Austin. Center for Transportation Research.
COST-EFFECTIVENESS ANALYSIS OF TxDOT CNG FLEET CONVERSION, VOLUME 1 Interim Research Report
M. A. Euritt, D. B. Taylor, and H. Mahmassani Aug. 1992 187 p See also PB93-165611 and PB93-159432 Sponsored by Federal Highway Administration and Texas Dept. of Transportation
(PB93-165603; CTR-3-4-90/2-983-2/1-Vol-1; FHWA/TX-92+983-2-Vol-1)
Avail: CASI HC A09/MF A02

Increased emphasis on energy efficiency and air quality has resulted in a number of state and federal initiatives examining the use of alternative fuels for motor vehicles. A Texas program for alternate fuels includes compressed natural gas (CNG). Based on analysis of 30-year life-cycle costs, development of a natural gas vehicle (NGV) program for the Texas Department of Transportation (TxDOT) would cost about $47 million (in 1991 dollars). These costs include savings from lower-priced natural gas, infrastructure costs for a fast-fueling station, vehicle costs, and operating costs. The 30-year life-cycle costs translate into an average annual vehicle cost increase of $596, or about 4.9 cents more per vehicle mile of travel. NTIS

N93-26590# Texas Univ., Austin. Center for Transportation Research.
DOCUMENTATION FOR PROPANE FLEET CONVERSION COST-EFFECTIVENESS MODEL Interim Research Report
D. Taylor, M. Euritt, and H. Mahmassani Oct. 1992 50 p See also PB93-165603 Sponsored by Federal Highway Administration and Texas Dept. of Transportation
(PB93-165611; CTR-3-4-90/2-983-3; FHWA/TX-92+983-3) Avail: CASI HC A03/MF A01

Increased emphasis on energy efficiency and air quality has resulted in a number of state and federal initiatives examining the use of alternative fuels for motor vehicles. Texas instituted an alternative fuels program for public fleet operations beginning in the 1991-92 fiscal year. Life-cycle cost/benefit models for evaluating the economic implications of the action have been developed at the University of Texas at Austin Center for Transportation Research for both compressed natural gas (CNG) and propane. The report documents the various input data, calculations, and assumptions of the Propane Net Present Value (NPV) model. A similar report (number 983-1) documents the same for the CNG model. Input data with constant values across different fleets and locations are discussed first and include basic parameters for on-board storage capacity, vehicle conversion costs, equipment salvage values, etc. Variable input data, reflecting a given fleet size, composition, and location, include the number and types of vehicles, fuel consumption, etc. The next section presents the formulas for the internal model calculations. The final section discusses the basic assumptions underlying the model. NTIS

N93-25605*# Boeing Defense and Space Group, Huntsville, AL.
ROBOTIC VARIABLE POLARITY PLASMA ARC (VPPA) WELDING
Waris S. Jaffery *In* NASA, Washington, Technology 2002: The Third National Technology Transfer Conference and Exposition, Volume 1 Feb. 1993 p 415-424 (For primary document see N93-25561 09-99)
(Contract NAS8-50000)
Avail: CASI HC A02/MF A04

N93-25609*# National Aeronautics and Space Administration. Langley Research Center, Hampton, VA.
INSTRUMENTATION FOR MEASUREMENT OF GAS PERMEABILITY OF POLYMERIC MEMBRANES
Billy T. Upchurch, George M. Wood, Kenneth G. Brown (Old Dominion

Univ., Norfolk, VA.), and Karen S. Burns (Old Dominion Univ., Norfolk, VA.) *In* NASA, Washington, Technology 2002: The Third National Technology Transfer Conference and Exposition, Volume 1 Feb. 1993 p 451-460 (For primary document see N93-25561 09-99)
Avail: CASI HC A02/MF A04

N93-26119*# Jet Propulsion Lab., California Inst. of Tech., Pasadena.
DYNAMIC MODELING OF FLUID TRANSMISSION LINES OF THE DSN 70-METER ANTENNAS BY USING A LUMPED PARAMETER MODEL
R. D. Bartos *In its* The Telecommunications and Data Acquisition Report 15 May 1992 p 162-169 (For primary document see N93-26105 09-32)
(RTOP 310-30-42-10-87)
Avail: CASI HC A02/MF A04

N93-26416*# Colorado Univ., Boulder. Center for Space Construction.
TELEROBOTIC ROVERS FOR EXTRATERRESTRIAL CONSTRUCTION
Chris Grasso, Jane Pavlich, Wayne Jermstad, Mike Matthews, Gary Snyder, Chris Steffen, Jim Avery, Renjeng Su, and Walter Lund *In its* Center for Space Construction Third Annual Symposium 1991 20 p (For primary document see N93-26405 09-31)
Avail: CASI HC A03/MF A03

38 QUALITY ASSURANCE AND RELIABILITY

Includes product sampling procedures and techniques; and quality control.

N93-25451*# Dayton Univ., OH.
INTERNAL STRAIN ANALYSIS OF CERAMICS USING SCANNING LASER ACOUSTIC MICROSCOPY Final Report
Renee M. Kent Mar. 1993 144 p
(Contract NCC3-81; RTOP 510-01-50)
(NASA-CR-191118; E-7308; NAS 1.26:191118) Avail: CASI HC A07/MF A02

Quantitative studies of material behavior characteristics are essential for predicting the functionality of a material under its operating conditions. A nonintrusive methodology for measuring the in situ strain of small dimeter (to 11 microns) ceramic fibers under uniaxial tensile loading and the local internal strains of ceramics and ceramic composites under flexural loading is introduced. The strain measurements and experimentally observed mechanical behavior are analyzed in terms of the microstructural development and fracture behavior of each test specimen evaluated. Measurement and analysis of Nicalon silicon carbide (SiC) fiber (15 microns diameter) indicate that the mean elastic modulus of the individual fiber is 185.3 GPa. Deviations observed in the experimentally determined elastic modulus values between specimens were attributed to microstructural variations which occur during processing. Corresponding variations in the fracture surface morphology were also observed. The observed local mechanical behavior of a lithium alumino-silicate (LAS) glass ceramic, a LAS/SiC monofilament composite, and a calcium alumino-silicate (CAS)/SiC fully reinforced composite exhibits nonlinearities and apparent hysteresis due to the subcritical mechanical loading. Local hysteresis in the LAS matrices coincided with the occurrence of multiple fracture initiation sites, localized microcracking, and secondary cracking. The observed microcracking phenomenon was attributed to stress relaxation of residual stresses developed during processing, and local interaction of the crack front with the microstructure. The relaxation strain and stress predicted on apparent mechanical hysteresis effects were defined and correlated with the magnitude of the measured fracture stress for each specimen studied. This quantitative correlation indicated a repeatable measure of the stress at which matrix microcracking occurred for stress relief of each material system. Stress relaxation occurred prior to the onset of steady state cracking conditions. The relaxation stress occurred at 18.5 percent of the fracture stress in LAS and 11.0 percent of the yield stress in CAS/SiC. The relaxation stress ratio was dependent upon the dominant fracture mode of the LAS/SiC specimens. Relaxation stress ratios greater than 0.30 were observed for specimens which fractured due to shear at the fiber matrix interface; specimens which fracture due to tensile cracking had relaxation stress ratios less than 0.30. The stress relaxation ratio appeared to be a specific characteristic of the glass ceramic material. The measured stress relaxation for LAS indicated a measure of the inherent residual stresses in the material due to processing and suggested localized toughening mechanisms for brittle material structures. Author (revised)

N93-25518# Iowa State Univ. of Science and Technology, Ames. Center for Aviation Systems Reliability.
INVESTIGATION OF CORROSION IN ALUMINUM/ADHESIVE LAP-SPLICES USING PULSE-ECHO ULTRASONIC TECHNIQUES
T. C. Patton and D. K. Hsu 1992 8 p Presented at the Review of Progress in Quantitative Non Destructive Evaluation, La Jolla, CA, 19-24 Jul. 1992
(Contract W-7405-eng-82)
(DE93-008074; IS-M-740; CONF-920799-5) Avail: CASI HC A02/MF A01

In this paper we have shown that aluminum skin samples corroded in the laboratory by an electrochemical process are similar to corrosion that occurs naturally. Incorporating the corroded skins into several sets of characterized aluminum/adhesive lap-splices with first and second layer corrosion defects, we have shown qualitative agreement in PP signal amplitude between a low frequency ultrasonic model and experiment. The model suggests, and the experimental evidence agrees, that the trailing signal PP amplitude of a low frequency tri-polar pulse can be used to discriminate metal thinning in the second layer due to corrosion. Further work is in progress to address the issues of frequency selection and errors caused by layer parameter approximation. DOE

N93-25939# Allied-Signal Corp., Kansas City, MO. Technical Communications.
NONDESTRUCTIVE EVALUATION OF FERRITE c-CORES Final Report
J. W. Ekis Nov. 1992 18 p
(Contract DE-AC04-76DP-00613)
(KCP-613-4677) Avail: CASI HC A03/MF A01

A set of ultrasonic references for the ferrite c-cores for a strong link safety component were designed and manufactured. Ten sets of references were made for both the primary and the secondary c-cores. One set of each will be used to inspect loose piece parts. Second sets of each were mounted into transformer subassemblies. Third sets of each were mounted into transformers and welded into housing assemblies. These sets will be used to inspect their corresponding assemblies. All of these reference units were characterized using an ultrasonic test inspection system and calibrated by metrology. These reference units are now ready for use in product inspection. Author

N93-26135*# Cornell Univ., Ithaca, NY. Dept. of Computer Science.
VIRTUALLY-SYNCHRONOUS COMMUNICATION BASED ON A WEAK FAILURE SUSPECTOR
Andre Schiper (Ecole Polytechnique Federale de Lausanne, Switzerland.) and Aleta Ricciardi 28 Apr. 1993 24 p Sponsored in part by IBM and Siemens Corp.
(Grant NAG2-593)
(NASA-CR-193003; NAS 1.16:193003; CU-TR-93-1339) Avail: CASI HC A03/MF A01

Failure detectors (or, more accurately Failure Suspectors (FS)) appear to be a fundamental service upon which to build fault-tolerant, distributed applications. This paper shows that a FS with very weak semantics (i.e., that delivers failure and recovery information in no specific order) suffices to implement virtually-synchronous communication (VSC) in an asynchronous system subject to process crash failures and network partitions. The VSC paradigm is particularly useful in asynchronous systems and greatly simplifies building fault-tolerant applications that mask failures by replicating processes. We suggest a three-component architecture to implement virtually-synchronous communication: (1) at the lowest level, the FS component; (2) on top of it, a component (2a) that defines new views; and (3) a component (2b) that reliably multicasts messages within a view. The issues covered in this paper also lead to a better understanding of the various membership service semantics proposed in recent literature. Author (revised)

N93-26137*# National Aeronautics and Space Administration. Goddard Space Flight Center, Greenbelt, MD.
AUTOMATED INSPECTION OF SOLDER JOINTS FOR SURFACE MOUNT TECHNOLOGY

Robert M. Savage, Hyun Soo Park (Paramax Systems Corp., Lanham, MD.), and Mark S. Fan (Paramax Systems Corp., Lanham, MD.) Washington Mar. 1993 32 p Sponsored by NASA. Washington (RTOP 310-39-09-01-25)
(NASA-TM-104580; NAS 1.15:104580; Rept-93B00035) Avail: CASI HC A03/MF A01

Researchers at NASA/GSFC evaluated various automated inspection systems (AIS) technologies using test boards with known defects in surface mount solder joints. These boards were complex and included almost every type of surface mount device typical of critical assemblies used for space flight applications: X-ray radiography; X-ray laminography; Ultrasonic Imaging; Optical Imaging; Laser Imaging; and Infrared Inspection. Vendors, representative of the different technologies, inspected the test boards with their particular machine. The results of the evaluation showed limitations of AIS. Furthermore, none of the AIS technologies evaluated proved to meet all of the inspection criteria for use in high-reliability applications. It was found that certain inspection systems could supplement but not replace manual inspection for low-volume, high-reliability, surface mount solder joints. Author (revised)

N93-26246# Naval Postgraduate School, Monterey, CA.
EXPLORING THE LINK BETWEEN INTRINSIC MOTIVATION AND QUALITY M.S. Thesis
Steven M. Christy Dec. 1992 80 p
(AD-A261722) Avail: CASI HC A05/MF A01

This thesis proposes that it is workers' intrinsic motivation that leads them to produce quality work. It reviews two different types of evidence-expert opinion and empirical studies--to attempt to evaluate a link between intrinsic motivation and work quality. The thesis reviews the works of Total Quality writers and behavioral scientists for any connection they might have made between intrinsic motivation and quality. The thesis then looks at the works of Deming and his followers in an attempt to establish a match between Deming's motivational assumptions and the four task rewards in the Thomas/Tymon model of intrinsic motivation: choice, competence, meaningfulness, and progress. Based upon this analysis, it is proposed that the four Thomas/Tymon task rewards are a promising theoretical foundation for explaining the motivational basis of quality for workers in Total Quality organizations. DTIC

N93-26337# Delaware Univ., Newark. Dept. of Mathematical Sciences.
INVERSE PROBLEMS IN NONDESTRUCTIVE EVALUATIONS Final Report, 1 Sep. 1991 - 31 Aug. 1992
Fadil Santosa 31 Aug. 1992 7 p
(Grant AF-AFOSR-0360-91)
(AD-A261370) Avail: CASI HC A02/MF A01

The PI collaborated with Prof. Michael Vogelius on several problems. The research resulted in several reports, some of which have already been accepted for publication. The main research proposed was to investigate various aspects of the problem of electrical impedance tomography. In electrical impedance tomography, the problem is to image the interior of an object from static electrical measurements conducted on the boundary. The techniques of electrical impedance tomography may be applied to nondestructive evaluation of structures. The grant was directly responsible for two major accomplishments - (1) Inversion from real data and (2) Sensitivity of electrical impedance tomography. DTIC

N93-26434# Army Materials Technology Lab., Watertown, MA.
NDT STANDARDS FROM THE PERSPECTIVE OF THE DEPARTMENT OF DEFENSE
Bernard Strauss Sep. 1992 15 p Submitted for publication
(MTL-TR-92-68) Avail: CASI HC A03/MF A01

The interaction of the DoD non-Government Society (NGS) bodies in the area of nondestructive testing (NDT) are illustrated. The adoption process for NGS is outlined including the criteria for adoption, what adoption means, and the advantages of DoD/NGS interaction. The tasks of the DoD's Standardization Program Plan for NDT are described along with DoD's efforts on a Joint Army, Navy, Air Force (JANNAF) NDE Subcommittee and on an international standardization group (America, Britain, Canada, and Australia) called the Quadripartite Working Group on Proofing, Inspection, and Quality Assurance. Author (revised)

N93-26526# Boeing Defense and Space Group, Seattle, WA.
X-RAY COMPUTED TOMOGRAPHY FOR CASTING DEVELOPMENT Interim Report, May 1991 - Feb. 1992
Gary E. Georgeson, Alan R. Crews, and Richard H. Bossi 30 Sep. 1992 52 p
(Contract F33615-88-C-5404; AF Proj. 3153)
(AD-A261786; WL-TR-92-4032) Avail: CASI HC A04/MF A01

Computed tomography (CT) has been used to evaluate specific sand casting product examples for technical and economic benefits. The representative results are applicable to other casting technologies as well. CT has been shown to be cost effective in the development of new castings. The areas which would benefit include internal dimensional measurements (eliminating destructive sectioning), specific region inspections, flaw characterization in critical regions (to allow passing or informed repair of castings), and geometric acquisition for CAD/CAM. The quantitative capability of CT allows an engineering evaluation of castings based upon a correlation with performance. This quantitative measurement capability has also been used to measure the benefit of hot isostatic pressing in casting production. CT is also cost effective for engineering design and analysis by providing rapid geometry acquisition for input to computer aided design systems. This is particularly beneficial for components that do not have existing drawings or cannot be adequately defined until they are made for any reason. Presently CT can serve as an engineering aid to casting manufacturing. In order for CT evaluation to become routine in foundry applications, however, casting designers need to call it out as a measurement technique in the original casting design drawings, specifications on the application of CT must be written, contracts must include CT evaluation as a means for accepting casting quality, and lower cost CT systems must be available. DTIC

N93-26527# Boeing Defense and Space Group, Seattle, WA.
X RAY COMPUTED TOMOGRAPHY FOR FAILURE ANALYSIS Interim Report, May 1991 - Jan. 1992
Richard H. Bossi, Alan R. Crews, and Gary E. Georgeson 31 Aug. 1992 56 p
(Contract F33615-88-C-5404)
(AD-A261884; WL-TR-91-4102) Avail: CASI HC A04/MF A01

Under a preliminary testing task assignment of the Advanced Development of X-Ray Computed Tomography Application program, computed tomography (CT) has been studied for its potential as a tool to assist in failure analysis investigations. CT provides three-dimensional spatial distribution of material that can be used to assess internal configurations and material conditions nondestructively. This capability has been used in failure analysis studies to determine the position of internal components and their operation. CT is particularly advantageous on complex systems, composite failure studies, and testing under operational or environmental conditions. CT plays an important role in reducing the time and effort of a failure analysis investigation. Aircraft manufacturing or logistical facilities perform failure analysis operations routinely and could be expected to reduce schedules, reduce costs and/or improve evaluation on about 10 to 30 percent of the problems they investigate by using CT. DTIC

N93-26546# National Goals Research Staff, Washington, DC. Center for Policy Research and Analysis.
DESIGNING AND IMPLEMENTING A STATE QUALITY AWARD
E. N. Dobson Feb. 1993 55 p Sponsored by National Inst. of Standards and Technology
(PB93-154458; NIST/GCR-92/620) Avail: CASI HC A04/MF A01

To remain competitive in today's global economy, businesses need to ensure customer satisfaction by offering high-quality products and services. Governors and state governments can play a critical role in ensuring the economic health of the business in their state by encouraging the adoption of quality practices and recognizing successful efforts by firms to improve quality and productivity. The manual is intended to help state government officials and other individuals implement a state quality award program. NTIS

N93-24666*# Jet Propulsion Lab., California Inst. of Tech., Pasadena.
FAILURE MONITORING IN DYNAMIC SYSTEMS: MODEL CONSTRUCTION WITHOUT FAULT TRAINING DATA
P. Smyth and J. Mellstrom *In its* The Telecommunications and Data Acquisition Report 15 Feb. 1993 p 37-49 (For primary document see

N93-24659 09-32)
(RTOP 310-20-65-91-00)
Avail: CASI HC A03/MF A02

N93-25588*# Aeronautical Radio, Inc., Annapolis, MD.
EXPERT SYSTEM FOR UNIX SYSTEM RELIABILITY AND AVAILABILITY ENHANCEMENT
Catherine Q. Xu *In* NASA, Washington, Technology 2002: The Third National Technology Transfer Conference and Exposition, Volume 1 Feb. 1993 p 259-267 (For primary document see N93-25561 09-99)
Avail: CASI HC A02/MF A04

N93-26074*# Pennsylvania State Univ., University Park. Dept. of Industrial and Systems Engineering.
IMPLEMENTATION OF QUALITY IMPROVEMENT TECHNIQUES FOR MANAGEMENT AND TECHNICAL PROCESSES IN THE ACRV PROJECT Final Report
Laura B. Raiman *In* NASA. Johnson Space Center, National Aeronautics and Space Administration (NASA)/American Society for Engineering Education (ASEE) Summer Faculty Fellowship Program, 1992, Volume 2 Dec. 1992 9 p (For primary document see N93-26070 09-99)
(Grant NGT-44-005-803)
Avail: CASI HC A02/MF A02

39 STRUCTURAL MECHANICS

Includes structural element design and weight analysis; fatigue; and thermal stress.

For applications see *05 Aircraft Design, Testing and Performance* and *18 Spacecraft Design, Testing and Performance.*

N93-24765 Virginia Polytechnic Inst. and State Univ., Blacksburg.
VIBRATION, BUCKLING, AND POSTBUCKLING OF LAMINATED COMPOSITES WITH DELAMINATIONS Ph.D. Thesis
Jaehong Lee 1992 234 p
Avail: Univ. Microfilms Order No. DA9229606

Free vibration, buckling, and postbuckling analyses of laminated composite plates with multiple delaminations are presented. A finite element method based on a layer-wise laminated composite plate theory is developed to formulate the problem. Geometric nonlinearity in the sense of von Karman and the imperfection in the plate in the form of initial global deflection and initial delamination openings are included. A simple contact algorithm which precludes the physically inadmissible overlapping between delaminated surfaces is proposed and incorporated in the analysis. A sublaminate concept is adopted in the analysis to reduce the computational efforts. The concept was found to be efficient. Numerical results are obtained for through-the-width, circular and rectangular delaminations addressing the effects of the number of delaminations, their lengths and through-the-thickness and axial locations on the critical buckling load, and buckling mode shapes as well as free vibration frequency and modes. Postbuckling responses are investigated with respect to different magnitudes and directions of initial imperfections. The effects of material anisotropy and contact condition between delaminated surfaces are also considered. It is found that the proposed approach is very efficient and powerful for solving the above mentioned problems. Dissert. Abstr.

N93-24909*# National Aeronautics and Space Administration. Lewis Research Center, Cleveland, OH.
EVALUATION OF MARC FOR THE ANALYSIS OF ROTATING COMPOSITE BLADES
Karen F. Bartos and Michael A. Ernst Washington Mar. 1993 27 p
(RTOP 535-03-10)
(NASA-TM-4423; E-7163; NAS 1.15:4423) Avail: CASI HC A03/MF A01

The suitability of the MARC code for the analysis of rotating composite blades was evaluated using a four-task process. A nonlinear displacement analysis and subsequent eigenvalue analysis were performed on a rotating spring mass system to ensure that displacement-dependent centrifugal forces were accounted for in the eigenvalue analysis. Normal modes analyses were conducted on isotropic plates with various degrees of twist to evaluate MARC's ability to handle blade twist. Normal modes analyses were conducted on flat composite plates to validate the newly developed coupled COBSTRAN-MARC methodology. Finally, normal modes analyses were conducted on four composite propfan blades that were designed, analyzed, and fabricated at NASA Lewis Research Center. Results were compared with experimental data. The research documented herein presents MARC as a viable tool for the analysis of rotating composite blades. Author

N93-24912*# Naval Surface Warfare Center, Bethesda, MD. Carderock Div.
AXISYMMETRIC DEFORMATIONS AND STRESSES OF UNSYMMETRICALLY LAMINATED COMPOSITE CYLINDERS IN AXIAL COMPRESSION WITH THERMALLY-INDUCED PRELOADING EFFECTS
Peter J. Paraska Mar. 1993 183 p
(Grant NAG1-901)
(NASA-CR-192788; NAS 1.26:192788; CARDEROCKDIV-U-SSM-65-93/03)
Avail: CASI HC A09/MF A02

This report documents an analytical study of the response of unsymmetrically laminated cylinders subjected to thermally-induced preloading effects and compressive axial load. Closed-form solutions are obtained for the displacements and intralaminar stresses and recursive relations for the interlaminar shear stress were obtained using the closed-form intralaminar stress solutions. For the cylinder geometries and stacking sequence examples analyzed, several important and as yet undocumented effects of including thermally-induced preloading in the analysis are observed. It should be noted that this work is easily extended to include uniform internal and/or external pressure loadings and the application of strain and stress failure theories. Derived from text

N93-24913*# National Aeronautics and Space Administration. Lewis Research Center, Cleveland, OH.
HIGH TEMPERATURE COMPOSITE ANALYZER (HITCAN) THEORETICAL MANUAL, VERSION 1.0
J. J. Lackney (Sverdrup Technology, Inc., Brook Park, OH.), P. L. N. Murthy, and P. K. Gotsis Apr. 1993 58 p
(Contract NAS3-25266; RTOP 505-63-5B)
(NASA-TM-106001; E-7544; NAS 1.15:106001) Avail: CASI HC A04/MF A01

This manual outlines some of the theoretical aspects embedded in the computer code, HITCAN (High Temperature Composite ANalyzer). HITCAN is a general purpose computer program for predicting nonlinear global structural and local stress-strain response of arbitrarily oriented, multilayered high temperature metal matrix composite structures. This code combines composite mechanics and laminate theory with an internal data base of the constituents (matrix, fiber and interface) material properties. The thermal and mechanical properties of the constituents are considered to be nonlinearly dependent on several parameters including temperature, stress and stress rate. The computational procedure for the analysis of the composite structure uses the finite element method. HITCAN consists of three modules: COBSTRAN, METCAN and MHOST. COBSTRAN generates the geometry (pre-processor) and defines the layup of the different plies. METCAN computes the material behavior of the composite and of the constituents. Finally, MHOST is a finite element program based on the mixed iterative solution technique. MHOST has a library for 2D and 3D isoparametric elements. HITCAN is written in FORTRAN 77 computer language and has been configured and executed on the NASA Lewis Research Center CRAY XMP and YMP computers. Author

N93-24957# Los Alamos National Lab., NM.
SEISMIC BUCKLING CAPACITY OF UNSTIFFENED, FREE-STANDING STEEL CONTAINMENTS
Charles R. Farrar, Thomas A. Duffey, Peggy A. Goldman, and Joel G. Bennett Jul. 1992 150 p
(Contract W-7405-eng-36)
(DE93-005325; LA-12359-MS) Avail: CASI (US Sales Only)

An investigation of the seismic buckling capacity of two unstiffened, freestanding steel containments is reported. The first structure studied is a proposed next-generation containment whose geometry is driven by the need for a passive cooling mechanism. For the second structure, a survey of commercial nuclear reactor containments was used to develop a generic design indicative of existing unstiffened, free-standing containments. This generic structure is also assumed to be indicative of a smaller scale version of the next-generation, passively cooled containments. A simple

three-degree-of-freedom (3-DOF), axisymmetric model of the containments is analyzed using response spectrum methods to determine the zero-period acceleration that would produce a case of incipient buckling. Then, more refined numerical time-history analyses were performed using the ABAQUS finite element code. The numerical models were subjected to measured earthquake acceleration-time histories and to artificial earthquake acceleration-time histories whose response spectra matched the Reg. Guide 1.60 design spectra, an eastern U.S. site-specific design spectra, and a spectrum that includes soil-structure interaction effects. The effects of containment construction methods and the effects of the internal negative air pressure on containment buckling are examined. Additionally, applications of the work presented in this study to the development of a simplified margins assessment method are discussed. Finally, a summary of buckling concerns, which the authors feel have been inadequately addressed in Code Case N-284, is presented. In the conclusion, the level of safety of a proposed next-generation containment design for seismically induced buckling is compared with the level of safety of existing commercial nuclear power plant containments for this failure mode. DOE

N93-25070*# National Aeronautics and Space Administration. Lewis Research Center, Cleveland, OH.

HIGH TEMPERATURE COMPOSITE ANALYZER (HITCAN) USER'S MANUAL, VERSION 1.0

J. J. Lackney (Sverdrup Technology, Inc., Brook Park, OH.), S. N. Singhal (Sverdrup Technology, Inc., Brook Park, OH.), P. L. N. Murthy, and P. Gotsis Apr. 1993 180 p

(RTOP 505-63-5B)

(NASA-TM-106002; E-7545; NAS 1.15:106002) Avail: CASI HC A09/MF A02

This manual describes 'how-to-use' the computer code, HITCAN (HIgh Temperature Composite ANalyzer). HITCAN is a general purpose computer program for predicting nonlinear global structural and local stress-strain response of arbitrarily oriented, multilayered high temperature metal matrix composite structures. This code combines composite mechanics and laminate theory with an internal data base for material properties of the constituents (matrix, fiber and interphase). The thermo-mechanical properties of the constituents are considered to be nonlinearly dependent on several parameters including temperature, stress and stress rate. The computation procedure for the analysis of the composite structures uses the finite element method. HITCAN is written in FORTRAN 77 computer language and at present has been configured and executed on the NASA Lewis Research Center CRAY XMP and YMP computers. This manual describes HITCAN's capabilities and limitations followed by input/execution/output descriptions and example problems. The input is described in detail including (1) geometry modeling, (2) types of finite elements, (3) types of analysis, (4) material data, (5) types of loading, (6) boundary conditions, (7) output control, (8) program options, and (9) data bank. Author

N93-25260*# Auburn Univ., AL. Space Power Inst. and Materials Engineering.

HYPERVELOCITY IMPACT STUDY: THE EFFECT OF IMPACT ANGLE ON CRATER MORPHOLOGY Interim Report

Gary Crawford, David Hill, Frank E. Rose, Ralph Zee, Steve Best, and Mike Crumpler 15 Mar. 1993 11 p

(Grant NAG1-1329)

(NASA-CR-192711; NAS 1.26:192711) Avail: CASI HC A03/MF A01

The Space Power Institute (SPI) of Auburn University has conducted preliminary tests on the effects of impact angle on crater morphology for hypervelocity impacts. Copper target plates were set at angles of 30 deg and 60 deg from the particle flight path. For the 30 deg impact, the craters looked almost identical to earlier normal incidence impacts. The only difference found was in the apparent distribution of particle residue within the crater, and further research is needed to verify this. The 60 deg impacts showed marked differences in crater symmetry, crater lip shape, and particle residue distribution. Further research on angle effects is planned, because the particle velocities for these shots were relatively slow (7 km/s or less). Author (revised)

N93-25270 Maryland Univ., College Park.

NONHOLONOMIC GEOMETRY, MECHANICS AND CONTROL Ph.D. Thesis

Rui Yang 1992 174 p

Avail: Univ. Microfilms Order No. DA9304413

This dissertation is concerned with dynamic modeling and kinematic control of constrained mechanical systems with symmetry from a geometric point of view. Constraints are defined via the characteristics of distributions or codistributions on the tangent bundle (velocity phase space) of configuration space. Lie symmetry groups acting on the systems are assumed to leave both Lagrangian and constraints invariant. As a special case of mechanical systems with holonomic constraints, we rigorously analyze the kinematics and dynamics of floating, planar four-bar linkages. The analyses include a topological description of the configuration space, symplectic and Poisson reductions of the dynamics, and bifurcation of relative equilibria. For kinematic control of nonholonomic systems, we mainly study the related optimal control problem for a system consisting of a rigid body with two oscillators. In particular, the intrinsic formulation and explicit solvability of necessary conditions for the optimal control are investigated from a Hamiltonian point of view. In the study of the dynamics of Lagrangian systems with constraints, the nonholonomic distributions are defined via arbitrary choices of principal connections. We show that, under our hypotheses on constraints and exterior force, the dynamics of a nonholonomic Lagrangian system with non-Abelian symmetry can be reduced to a lower dimensional space determined by the principal fiber bundle. The reduced dynamic equations are formulated explicitly. This formulation generalizes the one for classical Chaplygin systems which possess Abelian symmetry and the one having non-Abelian symmetry but with linear constraints. In addition, if a special principal connection, that is, the mechanical connection by Kummer and Smale, is considered, our formulation for nonholonomic systems also leads to the one in Lagrangian reduction discovered recently by Marsden and Scheurle. The results of this dissertation have direct application in space robotics and nonholonomic motion planning in robotics. Dissert. Abstr.

N93-25273 Colorado Univ., Boulder.

EQUILIBRIUM CONSTRAINED ASSUMED NATURAL COORDINATE STRAIN FINITE ELEMENTS FOR SHELL ANALYSIS Ph.D. Thesis

Daniel Duane Jensen 1992 229 p

Avail: Univ. Microfilms Order No. DA9304569

Substantial enhancements have been made in the Assumed Natural-coordinate Strain (ANS) finite elements leading to a new class of plate and shell finite elements entitled Equilibrium Constrained Assumed Natural-coordinate Strain (ANS-EC). Hierarchical degrees of freedom (dof) augment the standard dof in these new elements. These hierarchical dof are then eliminated using 'kinematic' and 'strong form equilibrium' constraints at selected discrete points. Kinematic constraints are used to reduce the polynomial order of the transverse shear strains. Equilibrium based constraints enforce the strong form of both the 'moment-transverse shear' equilibrium and the 'membrane resultant-transverse shear' equilibrium at discrete locations in each element. This combination of constraints causes the elements to avoid shear locking in the thin limit. The elements are fully integrated, which eliminates spurious mechanisms. As with all of the ANS elements, a full tensor transformation replaces the Jacobian transformation used in isoparametric formulations resulting in reduced distortion sensitivity. These element modifications are completely contained in the strain-displacement matrix. This formulation produces a modified shape function matrix for use in creating consistent nodal loads. The result is a set of elements which has substantial improvements in stress accuracy as well as improved displacement convergence. Dissert. Abstr.

N93-25328# Polish Academy of Sciences, Warsaw. Inst. Podstawowych Problemow Techniki.

ON THE EFFECTIVE REFLECTION PROPERTIES OF THE RANDOMLY SEGMENTED ELASTIC BAR

Zbigniew Kotulski 1992 44 p Sponsored by Komitet Badan Naukowych

Avail: CASI HC A03/MF A01

In the paper transition of the wave pulses through bars with random properties is investigated. It is assumed that the bar is built of several homogeneous segments. It is permitted that the lengths of the segments as well as their material parameters are random variables. The overall properties of such bars are studied. The discussion of obtained results is illustrated with numerical calculations. Author

N93-25335 Purdue Univ., West Lafayette, IN.
THREE-DIMENSIONAL BOUNDARY ELEMENT ANALYSIS OF CONTACT AND FRACTURE PROBLEMS Ph.D. Thesis
Minzhu Liu 1992 138 p
Avail: Univ. Microfilms Order No. DA9301341

A general purpose three dimensional boundary element method is developed for elastic solids. Emphasis is placed on the unique requirements of contact and fracture problems. In order to allow efficient and detailed calculations near the region of contact, special infinite elements that include the exact effects of infinite boundaries are developed. It is shown that these infinite elements can be used to accurately calculate contact stresses with very few elements. The effect of naturally occurring three dimensional defects on stresses and fatigue life is calculated. A void reduces the maximum allowable fatigue limit design pressure by 75 percent while a hard inclusion reduces it by 25 percent. The modified crack closure integral is used to accurately calculate the three-dimensional stress intensity factors. A multidomain approach is utilized for mixed mode cracks. In general the error of prediction of the stress intensity factors is within +/- 1.5 percent. Finally, the sliding blister field model of sliding micro indentation fracture is shown to give qualitative agreement with experimentally observed crack growth. Dissert. Abstr.

N93-25357# Oak Ridge National Lab., TN.
DETAILED SOLUTION TO A COMPLEX KINEMATICS CHAIN MANIPULATOR
S. March-Leuba, J. F. Jansen, R. L. Kress, and S. M. Babcock 1992 10 p Presented at the Institute of Electrical and Electronics Engineers International Conference on Robotics and Automation, Atlanta, GA, 2-7 May 1993
(Contract DE-AC05-84OR-21400)
(DE93-004619; CONF-930519-6) Avail: CASI HC A02/MF A01

A relatively simple method based on planar geometry to analyze the inverse kinematics for closed kinematics chain (CKC) mechanisms is presented. Although the general problem and method of approach are well defined, the study of the inverse kinematics of a closed-chain mechanism is a very complicated one. The current methodology allows closed-form solutions to be found, if a solution exists, for the displacements and velocities of all manipulator joints. Critical design parameters can be identified and optimized by using symbolic models. Focus is on planar closed-chain structures extended with a rotational base. However, with open and CKC mechanisms combined in different planes, the extension to the case is straightforward. Further, real-time algorithms are developed that can be handled by existing microprocessor technology. To clarify the methodology, the Soldier Robot Interface Project (SRIP) manipulator is analyzed, and a graphic simulation is presented as a verification of the results. This manipulator has 17 links, 24 one-degree-of-freedom (DOF) joints, and 7 CKC loops working in a plane and a rotational base, which determine its 3 DOF's. The SRIP manipulator allows a decoupled linear motion along the vertical or horizontal directions using only one of its linear actuators. The symbolic solution for the inverse kinematics allows optimization to be performed to further decouple the Cartesian motions by changing link lengths of the manipulator. The conclusion achieved by the optimization is that only two link lengths need to be changed to tune the manipulator for a perfect decoupling at each area of the workspace. DOE

N93-25373# Oak Ridge National Lab., TN.
ANALYSIS OF PULL-TESTS FOR DETERMINING THE EFFECTS OF ION IMPLANTATION ON THE ADHESION OF IRON FILMS TO SAPPHIRE SUBSTRATES
J. E. Pawel and C. J. McHargue (Tennessee Univ., Knoxville.) 1992 19 p Presented at the International Symposium on Adhesion Measurement of Films and Coatings, Cambridge, MA, 5-7 Dec. 1992
(Contracts DE-AC05-84OR-21400; DE-AC05-76OR-00033)
(DE93-006732; CONF-921257-1) Avail: CASI HC A03/MF A01

Various chemical species were implanted at the interface between evaporated iron films and their sapphire substrates. From interfacial free energy considerations, it was postulated that implantation of Cr ions should increase the strength of the bond between iron. and sapphire, whereas implantation of Ni ions should weaken the bonds. Implantation of Fe ions should cause changes due to irradiation-produced defects but exhibit no chemical effect. The pull test was used to evaluate the bond strength of unimplanted and implanted specimens. Since there was large scatter in the data, it was necessary to conduct a statistical analysis. It was assumed that the separation of the film from the substrate was nucleated by interfacial defects in the bond. Because the Weibull analysis was developed to describe the failure probability due to a population of flaw-induced cracks, this technique was used to interpret the data. DOE

N93-25394 Michigan Univ., Ann Arbor.
NUMERICALLY DISSIPATIVE TIME INTEGRATION ALGORITHMS FOR STRUCTURAL DYNAMICS Ph.D. Thesis
Jintai Chung 1992 129 p
Avail: Univ. Microfilms Order No. DA9303717

New dissipative time integration algorithms are presented for solving systems of second-order ordinary differential equations that typically arise from the spatial discretization of elastodynamics problems. The new algorithms are: (1) a family of implicit generalized-alpha methods, (2) a family of explicit generalized-alpha methods, and (3) a family of single step Houbolt methods (implicit and implicit/explicit). Analyses of the algorithms are carried out systematically with particular emphasis on numerical dissipation, accuracy and stability. The implicit generalized-alpha method possesses numerical dissipation that can be controlled by the user. In particular, it is shown that the generalized-alpha method achieves high-frequency dissipation while minimizing unwanted low-frequency dissipation. Comparisons are given of the generalized-alpha method with other numerically dissipative methods; these results highlight the improved performance of the new algorithm. The new algorithm can be easily implemented into programs that include standard time integration methods. The explicit generalized-alpha method possesses controllable high-frequency algorithmic damping; moreover, in the presence of physical damping, the algorithm simultaneously maintains a truly explicit form and second-order accuracy. A numerical example is given to compare the proposed method with the central difference method; the result demonstrates the effectiveness of the new method. The implicit single-step Houbolt method is unconditionally stable, second-order accurate and asymptotically annihilating. It is spectrally equivalent to Houbolt's method but is cast in the more convenient single-step form rather than multi-step form. An explicit predictor-corrector algorithm based upon the new implicit scheme is spectrally equivalent to the central difference method. The two algorithms are merged into an implicit-explicit method, resulting in an improved algorithm for solving structural dynamics problems composed of 'soft' and 'stiff' domains. Dissert. Abstr.

N93-25411 Purdue Univ., West Lafayette, IN.
NUMERICAL INVESTIGATIONS ON FRACTURE BEHAVIOR OF DUCTILE MATERIALS Ph.D. Thesis
Tung-Li Weng 1992 227 p
Avail: Univ. Microfilms Order No. DA9301407

The objective of the present work was to establish a criterion to characterize the fracture behavior of crack extension in ductile materials. The first part of this dissertation explored some useful techniques dealing with the fracture behavior of nonlinear elastic solid as the ideal model for ductile material. Five different methods of calculation of non-linear strain energy release rates were investigated. Their efficiencies and accuracies were compared and discussed. The present work identified the cause of deviations between the numerical result and the HRR solution. The present result showed that all field components near the crack tip converged to the HRR solutions in all directions if FEM meshes were sufficiently refined, and that the HRR fields exist not only for small scale yielding, but also for general yielding. Moreover, the near tip field solutions for incremental plasticity are almost identical to those for deformation plasticity. For incremental plasticity, however, the crack tip fields progressively deviate from the HRR solutions as elastic unloading occurs. The present work also investigated the plastic crack tip fields in the presence of residual stresses. To establish a ductile fracture criterion, several potential fracture parameters were investigated in simulations of crack extensions by combining numerical techniques with existing experimental results. Based on the present observations, a fracture criterion, the Global-Local Fracture Criterion (GLFC) was proposed. The feasibility of the proposed fracture criterion in predicting the ductile fracture behavior was extensively verified. It was shown that the GLFC is highly accurate and is satisfactory for ductile fracture analyses. Dissert. Abstr.

N93-25419# Liege Univ. (Belgium). Dept. of Bridges and Framework.
FATIGUE RESISTANCE OF ORTHOTROPIC PLATES WITH TRAPEZOIDAL STIFFENERS
J. Thonnard and J. Janss Aug. 1985 39 p
(TRL-Trans-T3908; MT-161) Avail: CASI HC A03/MF A01

The use of trapezoidal-shaped, continuous, closed stiffeners, in the construction of metal bridges with orthotropic plates has increased considerably. The welded joints between stiffeners and the floor plate must be designed and made in such a way as to prevent any risk of fatigue failure when in service. This is why the Ministry of Public Works, the main user of orthotropic plates in Belgium, imposes a certain number of requirements for the construction of such plates. However, these requirements are costly, and one wonders whether they are really indispensable, given the usual dimensions of trapezoidal stiffeners and the real stresses imposed on bridges. The behavior of welded joints between closed stiffeners (6 mm thick) and floor plate (12 mm thick) under dynamic loadings is studied. The welds were made according to less strict requirements than is usual in Belgium. The tests showed that the range of fluctuations of transverse stresses sigma in the stiffener, at the root of the weld beads, which equals 80 N/mm(sup 2), may be considered the endurance limit, if the lack of union between plate and stiffener is 0.5 mm or less, the lack of penetration of the weld is in the region of 4 mm and the edges of the stiffeners have not been specially prepared.
Author (revised)

N93-25437# Polish Academy of Sciences, Warsaw. Inst. Podstawowych Problemow Techniki.
ON EXISTENCE OF SOLUTIONS AND DUALITY FOR A MODEL OF NON-LINEAR ELASTIC PLATES WITH TRANSVERSE SHEAR DEFORMATIONS
Wlodzimierz Robert Bielski and Jozef Joachim Telega 1992 27 p
Sponsored by the State Committee for Scientific Research
Avail: CASI HC A03/MF A01

Two problems are solved for Reddy's model of non-linear elastic plates with transverse shear deformations. An existence theorem is formulated and proved for a class of boundary conditions. The dual problem is derived and the minimax or Lagrangian approach is discussed. The material of the plate may be anisotropic.
Author

N93-25484 Virginia Polytechnic Inst. and State Univ., Blacksburg.
STOCHASTIC AND SEISMIC DESIGN RESPONSE OF LINEAR AND NONLINEAR STRUCTURES Ph.D. Thesis
Gustavo Omar Maldonado 1992 288 p
Avail: Univ. Microfilms Order No. DA9302671

New methods for calculating the stochastic and seismic design response of linear and nonlinear structures are presented. For linear structures, two approaches are developed: (1) the modified mode displacement approach for classically as well as non-classically damped structures; and (2) the generalized force derivative approach for classically damped structures. Both techniques improve the calculation of the pseudostatic contribution of the truncated modes without including them in the analysis. In particular, the modified mode displacement approach is a useful tool for the calculation of seismic design responses affected by the contributions of higher modes. It properly considers the modal correlations as well as the correlation between retained and truncated modes. It is as fast as the mode acceleration method of structural dynamics and it only requires the commonly used ground response spectra employed by the classical mode displacement approach. On the other hand, the generalized force derivative approach requires the input to be defined in terms of its power spectral density function, but it improves even further the estimation of the missing mass effect due to the truncation of modes. For nonlinear structures, the stochastic equivalent linearization technique is employed to develop response spectrum approaches for hysteretic shear buildings and for two dimensional frames with plastic hinges. For this purpose, a generalized modal analysis technique is successfully employed. The proposed response spectrum approaches require the input be defined in terms of the response spectrum of first order oscillators as well as in terms of the commonly used ground response spectra. For shear buildings, the work is extended to include the calculation of floor response spectra. A simulation study is performed to compare the results obtained by the proposed approach.
Dissert. Abstr.

N93-25489# Sandia National Labs., Albuquerque, NM.
PYROSHOCK: BIBLIOGRAPHY
R. M. Zimmerman 1993 8 p The 39th Annual Technical Meeting of the Institute of Environmental Sciences, held in Las Vegas, NV, 2-7 May 1993
(Contract DE-AC04-76DP-00789)
(DE93-007605; SAND-93-0331C; CONF-930529-1) Avail: CASI HC A02/MF A01

This paper represents a review copy for text that is to be included in the Shock and Vibration Recommended Practice Document. This section on pyroshock is written as a general introduction to and description of the topic leading to presentation of an extensive bibliography on the subject. Pyroshock is an evolving science that needs continued focus on both achieving improvements in testing and measurement techniques and advancing instrumentation capabilities. Pyroshock phenomena are associated with separation systems of missiles, spacecraft, and in some cases airplanes. During launch, a rocket driven vehicle may be exposed to 19 to 30 g's of acceleration with predominant frequencies less than 200 Hz. After launch or takeoff, sections or parts of vehicles may be separated rapidly using explosive driven release mechanisms. Separations can involve stage disconnections for spacecraft sections or payload ejections from missiles and airplanes. At separation, localized pyrotechnic induced accelerations may range from 1000 to over 100,000 g's at frequencies much higher than 1000 Hz. These pyroshocks are characterized by high intensity, high frequency transients that decay rapidly. Pyroshock impulses have insignificant velocity changes.
DOE

N93-25533 Virginia Polytechnic Inst. and State Univ., Blacksburg.
STRESS AND RELIABILITY ANALYSES OF MULTILAYERED COMPOSITE CYLINDER UNDER THERMAL AND MECHANICAL LOADS Ph.D. Thesis
Xiaohua Wang 1992 217 p
Avail: Univ. Microfilms Order No. DA9306161

The coupling resulting from the mutual influence of material thermal and mechanical parameters is examined in the thermal stress analysis of a multilayered isotropic composite cylinder subjected to sudden axisymmetric external and internal temperature. The method of complex frequency response functions together with the Fourier transform technique is utilized. Because the coupling parameters for some composite materials, such as carbon-carbon, are very small, the effect of coupling is neglected in the orthotropic thermal stress analysis. The stress distributions in multilayered orthotropic cylinders subjected to sudden axisymmetric temperature loading combined with dynamic pressure as well as asymmetric temperature loading are also obtained. The method of Fourier series together with the Laplace transform is utilized in solving the heat conduction equation and thermal stress analysis. For brittle materials, like carbon-carbon composites, the strength variability is represented by two or three parameter Weibull distributions. The 'weakest link' principle which takes into account both the carbon-carbon composite cylinders. The complex frequency response analysis is performed on a multilayered orthotropic cylinder under asymmetrical thermal load. Both deterministic and random thermal stress and reliability analyses can be based on the results of this frequency response analysis. The stress and displacement distributions and reliability of rocket motors under static or dynamic line loads are analyzed by an elasticity approach. Rocket motors are modeled as long hollow multilayered cylinders with an air core, a thick isotropic propellant inner layer and a thin orthotropic kevlar-epoxy case. The case is treated as a single orthotropic layer or a ten layered orthotropic structure. Five material properties and the load are treated as random variable with normal distributions when the reliability of the rocket motor is analyzed by the first-order, second-moment method (FOSM).
Dissert. Abstr.

N93-25638# Aeronautical Research Inst. of Sweden, Stockholm.
RELIABLE STRESS AND FRACTURE MECHANICS ANALYSIS OF COMPLEX AIRCRAFT COMPONENTS USING A h-p VERSION OF FEM
Borje Andersson, Ivo Babuska, Tobias VonPetersdorff, and Urban Falk Aug. 1992 51 p
(Contract N00014-90-J-1030)
(AD-A260628; FFA-TN-1992-17) Avail: CASI HC A04/MF A01

Effective approaches are developed with which complex three-dimensional components may be analyzed with a high and virtually guaranteed accuracy. The main computational tool is a h-p version of

FEM practically realized with the p-version program STRIPE having a mesh generator for automatic mesh refinement at edges and vertices. Use of advanced extraction methods and new theoretical approaches give exponential convergence rates for accuracies in all engineering data of interest. New methods for reliable calculation of local stresses and stress intensity data at edges and vertices to be used for fatigue dimensioning at fillets, damage tolerance assessment of three-dimensional flaws etc. are given. A complex real-life problem is reliably analyzed in order to demonstrate the practical usefulness of the procedures advocated. The technical details are given in forthcoming papers. DTIC

N93-25647# Illinois Univ., Urbana. Dept. of Computer Science.
CONTINUUM AND MICROMECHANICS TREATMENT OF CONSTRAINT IN FRACTURE Final Report
R. H. Dodds, Jr., C. F. Shih, and Ted L. Anderson Jan. 1993 46 p
(Contracts N00167-92-K-0038; N61533-92-R-0030)
(AD-A260927; UILU-ENG-92-2014; CDNSWC/SME-19-92) Avail: CASI HC A03/MF A01

This report explores the fundamental concepts of the J-Q description of crack-tip fields, the fracture toughness locus, and micromechanics approaches to predict the variability of macroscopic fracture toughness with constraint under elastic-plastic conditions. While these concepts are derived from plane-strain considerations, initial applications in fully 3D geometries are very promising. Computational results are presented for a surface cracked plate containing a 6:1 semi-elliptical, alpha = t/4 flaw subjected to remote uniaxial and biaxial tension. Crack-tip stress fields consistent with the J-Q theory are demonstrated to exist at each location along the crack front. The micromechanics model employs the J-Q description of crack-front stress to interpret fracture toughness values measured on laboratory specimens for fracture assessment of the surface cracked plate. The computational results suggest only a minor effect of the biaxial loading on the crack tip stress fields and, consequently, on the propensity for fracture relative to the uniaxial loading. DTIC

N93-25658# Naval Postgraduate School, Monterey, CA. Dept. of Mechanical Engineering.
THERMOELASTIC STRESSES IN MULTI-LAYERED MEDIA IN NON-UNIFORM TEMPERATURE FIELDS Final Report, Jan. - Dec. 1992
David Salinas, Young W. Kwon, and Michael J. Neibert 31 Dec. 1992 43 p
(AD-A260901; NPS-ME-92-005) Avail: CASI HC A03/MF A01

The objective of this investigation is to determine the shear and peeling stresses in a multilayered media in a nonuniform temperature field. The temperature field is obtained by a finite element solution of the energy equation with a flux generation term in one of the media layers. The resulting thermoelastic stresses are then obtained from a finite element mode which uses a recently developed beam element with only displacement degrees of freedom. Compared to the standard beam element with rotational degrees of freedom, this element without rotational degrees of freedom more readily provides displacement continuity along interfaces between medial layers. As a result of the differences in properties such as Young's moduli, Poisson's ratio, and coefficients of thermal expansion, thermoelastic stresses develop when the multilayered media is subjected to a thermal environment. DTIC

N93-25681 Virginia Polytechnic Inst. and State Univ., Blacksburg.
AN EFFICIENT TECHNIQUE FOR STRUCTURAL RELIABILITY WITH APPLICATIONS Ph.D. Thesis
Ibrahim Mustafa Janajreh 1992 200 p
Avail: Univ. Microfilms Order No. DA9306158

An efficient reliability technique has been developed based on Response Surface Methodology (RSM) in conjunction with the First Order Second Moment (FOSM) reliability method. The technique is applied when the limit state function cannot be obtained explicitly in terms of the design variables, i.e., when the analysis is performed using numerical techniques such as finite elements. The technique has proven to be efficient because it can handle problems with large numbers of design variables and correlated as well as nonnormal random variables. When compared with analytical results, the method has shown excellent agreement. The technique contains a sensitivity analysis scheme which can be used to reduce the computation time resulting in nearly the same accuracy. This technique allows the extension of most finite element codes to account for probabilistic analysis, where statistical variations can be added to the design variables. An explicit solution for rocket motors consisting of propellant and steel case under environmental temperature variations is compared to the RSM technique. The method is then used for the analysis of rocket motors subjected to mechanical loads for which the stress analysis is performed using the finite element method. The technique is also applied to study the reliability of a laminated composite plate with geometric nonlinearity subjected to static and time dependent loadings. Different failure modes were considered as well as different meshes. Results have shown that when the relative size of the element is introduced into the probabilistic model, the same reliability value is obtained regardless of the number of elements in the mesh. This is good because it allows the technique to be used for problems where the failure region is unknown. Dissert. Abstr.

N93-25690# Pennsylvania State Univ., University Park. Materials Research Lab.
PASSIVE VIBRATION DAMPING MATERIALS: PIEZOELECTRIC CERAMICS COMPOSITES FOR VIBRATION DAMPING APPLICATIONS Annual Technical Report, 1 Jan. 1992 - 31 Jan. 1993
Shoko Yoshikawa and S. K. Kurtz 11 Feb. 1993 24 p
(Contract N00014-92-J-1391)
(AD-A260792) Avail: CASI HC A03/MF A01

For application of the shunted passive piezoelectric damping of structural composites, piezoelectric ceramic fibers (PZT and its family) of several tens of micron diameter were made using sol-gel spinning process. Both acetate and acetylacetonate processes were examined as lead sources. Using the properly chosen spinneret and fiber drawing apparatus, PZT and modified PZT fibers of 10 to 100 micrometers diameter have been successfully produced. Different heat treatments gave different microstructure. Modeling analysis was also performed to estimate achievable damping levels for the composites. The results indicate high damping potential for shunted piezoelectric passive damping composites. DTIC

N93-25718 Tennessee Univ., Knoxville.
DEVELOPMENT AND APPLICATION OF AN ADVANCED DUCTILE FRACTURE MECHANICS METHODOLOGY Ph.D. Thesis
Zhen Zhou 1992 317 p
Avail: Univ. Microfilms Order No. DA9233603

An advanced ductile fracture mechanics methodology is presented here. This methodology takes a load versus displacement result from a laboratory specimen test to predict the load versus displacement for a structural component containing crack-like defect. To use this methodology, three steps need to be followed. First a test record from laboratory experiment needs to be reduced into two pieces of information, the calibration function and the fracture toughness. The calibration function relates load, displacement and crack size. The fracture toughness relates crack driving force and crack extension in terms of a J-R curve. The second step is to transfer this information to a structural component to be analyzed. After the calibration function and the fracture toughness for the structural component are determined, the last step is to use a ductile fracture methodology proposed by Ernst and Landes to predict the load versus displacement behavior of the structural component. Traditionally the J-R curve has been developed according to the ASTM standard. Crack growth is usually estimated by instrumentation. This does not always work well for non-side grooved specimens and polymeric materials. To ensure accurate data reduction, the normalization method for J-R curve calculation is further developed by introducing the LMN function as the calibration function. The new version of the normalization method works well for both metallic and polymeric materials. It is more reliable and versatile than the compliance method. Two procedures for the determination of the LMN function are introduced. Two procedures are developed for generating the calibration function for a structural component of interest. One is the transformation procedure that can be applied to the case where the limit load solution for the structural component is known. The other procedure is based on numerical simulation incorporating with the load separation method. This procedure can be used to any structural component whose behavior can be represented by load versus displacement. The methodology has been used to predict the behavior of different structural components with various cracks. The predictions are compared with the experimental results for most cases. In general, the predictions are accurate and successful.
Dissert. Abstr.

N93-25750 Cornell Univ., Ithaca, NY.
MODELS OF CRACK GROWTH ALONG POLYMER INTERFACES Ph.D. Thesis
Daben Xu 1992 176 p
Avail: Univ. Microfilms Order No. DA9236086

Several models of crack growth along polymer/polymer interfaces are investigated in this work. The core spirit of these models is the use of a cohesive zone to study the effect of rate dependent inelastic deformation and damage directly ahead of the tip of a growing crack at the polymer interfaces. For each interface model studied, the fracture toughness of the interface is predicted as a function of the crack growth rate, the interface constitutive behavior and the properties of bulk materials surrounding the interface. In chapter 1, we present a general formulation of cohesive zone models in an elastic medium. Asymptotic behavior at the two ends of the cohesive zone is derived. Detailed analyses are carried out for the special case of a crack growing along a power-law creeping interface under steady state condition. Asymptotic and numerical solutions in the cohesive zone for this model are obtained. In chapter 2, we study the problem of steady state crack growth along the interface of two immiscible homopolymers. The interface is strengthened by the addition of a small amount of diblock copolymer. A interface constitutive model based on the concept of polymer chain pull-out is proposed and the results of the analysis are compared with experimental results. In chapter 3 and chapter 4, we study the fracture behavior of weakly joined adhesives between two viscoelastic polymers. In this case, the energy dissipation due to viscoelastic deformation in the bulk materials outside the interface contributes significantly to the measured interface fracture toughness. The presence of viscoelastic deformation implies that the loading parameters governing the crack tip fields are in general dependent on the specimen dimensions as well as the crack growth rate. Therefore, analyses are carried out for both infinite and finite specimens. Our results are compared to some experimental observations. The dependence of the fracture toughness of the interface on the properties of adhesive and the viscoelastic bulk material are derived and discussed.
Dissert. Abstr.

N93-25784# California Univ., Davis. Dept. of Electrical and Computer Engineering.
EXPLOITATION OF CYCLOSTATIONARITY FOR SIGNAL-PARAMETER ESTIMATION AND SYSTEM IDENTIFICATION Semiannual Report, 1 Jul. - 31 Dec. 1992
William A. Gardner and Stephan V. Schell 31 Dec. 1992 5 p
(Contract N00014-92-J-1218)
(AD-A260833) Avail: CASI HC A01/MF A01

The cyclostationarity property of communications and telemetry signals enables the generation of spectral lines with appropriate nonlinear transformations and renders fluctuations in distinct spectral bands statistically dependent. The frequencies at which spectral lines can be generated are directly related to the separations between dependent spectral bands, which in turn are directly related to carrier frequencies, keying rates, pulse rates, and so on, in the signal. These inherent properties of cyclostationary signals can be exploited to great advantage for numerous tasks in signal processing. The objectives of the research being conducted are to investigate new cyclostationarity-exploiting methods for (1) signal-selective high-resolution direction finding using sensor arrays, (2) selectively locating emitters by time difference and frequency difference measurement with one or more pairs of sensors, (3) identifying the kernels in the Volterra series representation of nonlinear time-invariant and multiply-periodic systems.
DTIC

N93-25785# Metz Univ. (France). Lab. of Physics and Mechanics of Materials.
APPROXIMATE ANALYSIS ON STRAIN RATE EFFECTS AND BEHAVIOR OF STRESS AND STRAIN FIELDS AT THE CRACK TIP IN MODE 2 IN METALLIC MATERIALS, APPENDIX NO. 1
I. V. Varfolomeyev and J. R. Klepaczko Oct. 1992 97 p
(Contract DAJA45-90-C-0052)
(AD-A260836) Avail: CASI HC A05/MF A02

Analysis of conditions for crack initiation and fracture toughness in the case of metallic materials under various loading rates are problems of great interest in fracture mechanics. Several investigations have been carried out to reveal the loading rate effect on fracture toughness. At the same time, systematic analyses have been performed for a majority of structural materials to study strain rate effect on the yield stress, ultimate stress, material strain hardening, etc. Some correlations between fracture toughness and parameters of stress-strain diagram at different strain rates have been derived. The theoretical background of such correlations consists of solutions for elastic and elastic-plastic stress-strain fields near a crack tip. Analyses of stress distribution at the tip of a stationary crack under dynamic loading have been performed by Freund (1990) and Lee and Freund (1990). Another important application of fracture mechanics arises from a relationship between loading rate and specimen thickness for fracture toughness measurements.
DTIC

N93-25825 Utah Univ., Salt Lake City.
A THREE-DIMENSIONAL MODEL FOR THE RESIDUAL STRESSES IN A UNIDIRECTIONAL COMPOSITE PLATE Ph.D. Thesis
Jianhui Liu 1992 132 p
Avail: Univ. Microfilms Order No. DA9236254

A three-dimensional (3-D) micromechanical model has been developed to represent a unidirectional composite plate that is subjected to a residual stress induced by temperature mismatch. The model assumes the fibers to be cylindrical inclusions that are periodically embedded into an epoxy matrix. At the interface of fiber and matrix, perfect bonding conditions are assumed to prevail. The method used in the thesis is based on a 3-D analytic investigation. The analytical solution shows the maximum stresses are located at theta = 0 for the graphite/epoxy composite plate. The location of the maximum stresses, however, may change for other material systems, particularly, for small shear moduli ratios mu(2)/mu(1). The solution also shows that the shear moduli ratio mu(2)/mu(1) (fiber to matrix), the geometric ratios a/h (fiber radius to thickness of the plate) and a/b (fiber radius to separation distance between adjacent fibers) have a great effect on the displacement and stress distributions. On the other hand, the ratio of thermal expansion coefficients alpha(2)/alpha(1) (fiber to matrix) presents a linear action to the displacement and stress fields. The stress profiles along a fiber length are shown to be constant except in neighborhood of the fiber edge where a boundary layer is shown to prevail. In the region, a stress singularity is confirmed that is a departure from the results given by macromechanical theories. In the limit, as a/b approaches 0, the result of one fiber model is recovered; as a/h approaches infinity the plane stress solution is recovered. Similarly, as mu(2)/mu(1) approaches 0 the result of a plate with a periodic array of holes is recovered.
Dissert. Abstr.

N93-25838# Virginia Polytechnic Inst. and State Univ., Blacksburg.
NONLINEAR VIBRATIONS, STABILITY, AND DYNAMICS OF STRUCTURES AND MECHANISMS Final Report
A. H. Nayfeh and D. T. Mook Nov. 1992 167 p Fourth Conference held in Blacksburg, VA, 7-11 Jun. 1992
(Contract DAAL03-92-G-0211)
(AD-A260871; ARO-28756.1-EG-CF) Avail: CASI HC A08/MF A02

The conference was held as scheduled. Abstracts of the presentations appear in a report distributed by the Virginia Polytechnic Institute and State University Sessions included identification and control, analytical methods, impact dynamics, dynamics and control, applications to cables, optimization and computational methods, coupled oscillators, applications to mechanical systems, random vibrations, analytical and symbolic methods, applications to structural elements, multibody dynamics, and flow-induced vibrations and computational methods.
DTIC

N93-25842# Illinois Univ., Chicago. Dept. of Mechanical Engineering.
DYNAMICS OF DEFORMABLE MULTIBODY SYSTEMS USING RECURSIVE PROJECTION METHODS Final Report, 30 Nov. 1989 - 29 Nov. 1992
A. A. Shabana Dec. 1992 13 p
(Contract DAAL03-90-G-0007)
(AD-A260698; ARO-26934.8-EG) Avail: CASI HC A03/MF A01

In this investigation, generalized Newton-Euler equations are developed for deformable bodies that undergo large translational and rotational displacements. The configuration of the deformable body is identified using coupled sets of reference and elastic variables. The nonlinear generalized Newton-Euler equations are formulated in terms of a set of time invariant scalars and matrices that depend on the spatial coordinates as well as the assumed displacement field. These time-invariant quantities appear in the nonlinear terms that represent the dynamic coupling between the rigid body modes and the elastic deformation. A set of recursive kinematic

equations, in which the absolute accelerations are expressed in terms of the joint and elastic accelerations are developed for several joint types. The recursive kinematic equations and the joint reaction relationships are combined with the generalized Newton-Euler equations in order to obtain a system of loosely coupled equations which have sparse matrix structure. Using matrix partitioning and recursive projection techniques based on optimal block factorization an order n solution for the system equations is obtained. DTIC

N93-25846# Rensselaer Polytechnic Inst., Troy, NY. Dept. of Civil Engineering.
DESIGN OF FLEXIBLE RODS WITH EMBEDDED SMA ACTUATORS
H. J. Pfaeffle, Dimitris C. Lagoudas, Iradj Tadjbakhsh, and Kevin C. Craig 18 Jan. 1993 13 p
(Contract DAAL03-92-G-0123)
(AD-A260742; ARO-30378.5-EG-URI) Avail: CASI HC A03/MF A01

The shape change of a stress free cylindrical flexible rod with embedded SMA actuators is modeled in this paper for rods with single or multiple SMA actuators placed parallel to the long axis of the rod for the first heating the SMA actuators. The distributed axial compressive force, transverse normal force, and bending moments that act on the rod due to the shape recovery of the SMA actuators have been given by Lagoudas and Tadjbakhsh. The deformed shape of the rod is found by solving the nonlinear equations of equilibrium of the rod. For multiple actuators the resultant forces and moments are considered. A design analysis is performed for the active rod with a single SMA actuator. Key design variables are Erod, the thermal bond strength of the rod to the SMA actuator, and the rod dimensions. Key design parameters are: maximum rod/actuator interfacial shear stress, rod strain, rod slenderness ratio, and rod deflection. An analysis is then performed which investigates the influence of the design variables on each of the design parameters. DTIC

N93-25901# Paris VI Univ. (France). Lab. de Mecanique et Technologie.
MICROMECHANICS OF FATIGUE Final Report, 15 Mar. 1989 - 14 Mar. 1992
Jean Lemaitre and Rene Billardon Jun. 1992 81 p
(Grant AF-AFOSR-0329-89)
(AD-A260577; Rept-134; AFOSR-93-0016TR) Avail: CASI HC A05/MF A01

In this final report, the results given in the first two annual reports are recalled. Application of the derived tools to Alpha-Two-Titanium Aluminide Alloy is made with a first series of strain controlled fatigue tests. The locally coupled model is first identified and then checked on a second series of stress controlled fatigue tests. The good agreement allows us to use this locally coupled method to predict fatigue crack initiation on brittle or quasibrittle materials. DTIC

N93-25911# Naval Postgraduate School, Monterey, CA.
OPTIMIZATION TECHNIQUES FOR CONTACT STRESS ANALYSIS M.S. Thesis
Eric S. McDonald Dec. 1992 90 p
(AD-A260846) Avail: CASI HC A05/MF A01

The analysis of stresses induced by contact between two bodies is inherently difficult because the size of the contact zone is unknown and constantly changing throughout loading. To overcome these difficulties, two approximation methods have been developed to determine the magnitude of contact stresses using the Rayleigh-Ritz method and the finite element method. Numerical optimization methods are employed to solve the contact problem. The solution techniques are compared to known analytical solutions and shown to yield accurate results. An application of this approach to solving the contact problem is illustrated by examining the response of a clamped sandwich composite beam to low velocity impact. It was found that the maximum shear stress is insensitive to lamina thickness, however an increase in the contact layer thickness resulted in a reduction in interfacial shear stress. In addition, it was noted that a nonlinear bending stress distribution in the contact layer intensified as the thickness of this layer increased. This phenomenon was found to be localized to the region of contact. Finally, it was found that the compressive transverse normal stresses increased as the thickness of the contact lamina increased. DTIC

N93-25938# Puerto Rico Univ., Mayaguez. Dept. of Civil Engineering.
JOINT FLEXIBILITY EFFECTS ON THE DYNAMIC RESPONSE OF STRUCTURES. PART 2: STOCHASTIC ANALYSIS Final Report
Luis E. Suarez and Enrique E. Matheu Dec. 1992 66 p
(Contract DAAL03-90-G-0214)
(AD-A261003; ARO-28374.6-EG-H-Pt-2) Avail: CASI HC A04/MF A01

The objective of this study is to quantify the effect of flexible connections with random stiffness on the modal properties and dynamic response of structures. Since the mass and stiffness matrices contain random parameters, the modal decomposition solution of the equations of motion lead to a random eigenvalue problem. A second order perturbation technique is used for the solution of the random eigenproblem. Closed form expressions for the mean and variance of the natural frequencies and vibration modes are provided. The response of systems with random parameters subjected to deterministic loads is examined next beginning with single degree of freedom systems. When standard perturbation methods are applied to calculate the statistics of the response, the expressions obtained become nonuniform as time grows. A detailed discussion about the cause of the problem is presented. A new formulation based on the method of multiple scales used for nonlinear systems is proposed to overcome the problem. The response analysis is extended to multi-degree-of-freedom systems. Conclusions and recommendations for further research are presented. DTIC

N93-25941# Rensselaer Polytechnic Inst., Troy, NY.
VARIATIONAL THEORY OF MOTION OF CURVED, TWISTED AND EXTENSIBLE ELASTIC RODS Technical Report
Iradj Tadjbakhsh and Dimitris C. Lagoudas 18 Jan. 1993 15 p
(Contract DAAL03-92-G-0123)
(AD-A261028; ARO-30378.6-EG-URI) Avail: CASI HC A03/MF A01

The variational theory of three dimensional motion of curved twisted and extensible elastic rods is obtained based entirely on the kinematical variables of position and rotations. The constitutive relations that define the resistive couples and the axial force as gradients of the strain energy function are established. A candidate for the strain energy function, derived on the basis of classical assumptions, is presented. DTIC

N93-25950# Rensselaer Polytechnic Inst., Troy, NY. Dept. of Civil Engineering.
DEFORMATIONS OF ACTIVE FLEXIBLE RODS WITH EMBEDDED LINE ACTUATORS
D. C. Lagoudas and I. G. Tadjbakhsh 18 Jan. 1993 30 p
(Contract DAAL03-92-G-0123)
(AD-A261207; ARO-30378.8-EG-URI) Avail: CASI HC A03/MF A01

The 3-D formulation of flexible rods with embedded line actuators is presented in this paper. Both the rods and the line actuator are assumed to be initially curved and relatively positioned in an arbitrary way. The deformed configurations of the rod and actuator are connected by assuming that the principal planes of the rod remain in plane and inextensible in the deformed configuration. The resultant forces and moments in the rod and actuator are found by solving the equilibrium equations for both the rod and actuator and applying continuity of tractions on the rod-actuator interface. The formulation is reduced to 2-D and applied to the case of a Shape Memory Alloy (SMA) fiber embedded in a cylindrical rod. The deformed shapes of the rod under repeated thermal actuation and the resulting shape memory loss due to the development of residual stresses are evaluated. Finally, the inverse problem of finding the required actuation force and initial curvature, to acquire a predetermined deformed shape, is solved in closed form for the 2-D cases. DTIC

N93-26102* National Aeronautics and Space Administration. Langley Research Center, Hampton, VA.
METHODS OF DETERMINING LOADS AND FIBER ORIENTATIONS IN ANISOTROPIC NON-CRYSTALLINE MATERIALS USING ENERGY FLUX DEVIATION Patent
William H. Prosser, inventor (to NASA), Ronald D. Kriz, inventor (to NASA), and Dale W. Fitting, inventor (to NASA) 11 May 1993 8 p Filed 22 Nov. 1991
(NASA-Case-LAR-14399-1; US-Patent-5,209,123;
US-Patent-Appl-SN-797507; US-Patent-Class-73-788;
US-Patent-Class-73-641; Int-Patent-Class-G01N-3/00) Avail: US Patent and Trademark Office

An ultrasonic wave is applied to an anisotropic sample material in an initial direction and an angle of flux deviation of the ultrasonic wave front is measured from this initial direction. This flux deviation angle is induced by the unknown applied load. The flux shift is determined between this flux deviation angle and a previously determined angle of flux deviation of an ultrasonic wave applied to a similar anisotropic reference material under an initial known load condition. This determined flux shift is then compared to a plurality of flux shifts of a similarly tested, similar anisotropic reference material under a plurality of respective, known load conditions, whereby the load applied to the particular anisotropic sample material is determined. A related method is disclosed for determining the fiber orientation from known loads and a determined flux shift.

Official Gazette of the U.S. Patent and Trademark Office

N93-26177# Lawrence Livermore National Lab., CA.

ANALYSIS OF SHAPED CHARGE JET PENETRATION EXPERIMENTS WITH PEN

S. Christian Simonson, III May 1992 33 p

(Contract W-7405-eng-48)

(UCRL-LR-110773) Avail: CASI HC A03/MF A01

The 'Pen' computer program has been applied to the analysis of two shaped charge jet penetration experiments. This analysis has served as a test of the Pen algorithms and as an illustration of the methods of applying the code. As part of the analysis, an experimental value of 14.4 +/- 1.9 kbar has been obtained for the effective strength of hardened A4340 steel under jet impact. From radiographs and hydrocode calculations, the critical radius at breakup of the copper jets in these experiments was found to follow a linear relationship, r(sub cr) = 3.5 x 10(exp -4) 1.9 x 10(exp -6) (t - t(sub 0)), where r(sub cr) is expressed in charge diameters and (t - t(sub 0)) is the time in microsec referred to the virtual origin of the jet. (These coefficients may vary by a factor of 2 depending on design and manufacture.) Timing data from embedded foil switches yielded a set of penetration efficiency factors, which varied between 1.34 near the tip to 0.78 near the tail. Interference was found to set in at a constriction point a few centimeters inside the target entrance. By matching the jet arrival times and the hole profiles for the primary penetration, the effective strength of the steel was obtained. The increase of about 25 percent above the nominal yield strength of 11.5 kbar is attributed to work hardening and pressure effects. Author

N93-26178# Lawrence Livermore National Lab., CA.

ALGORITHMS FOR THE ANALYSIS OF PENETRATION BY SHAPED CHARGE JETS

S. Christian Simonson, III Apr. 1992 35 p

(Contract W-7405-eng-48)

(UCRL-LR-109887) Avail: CASI HC A03/MF A01

A set of algorithms has been developed for the analysis of penetration by shaped charge jets into homogeneous armor targets. Standard expressions are included for calculating the depth of penetration by a stretching jet (Bernoulli's equation) and for calculating the radius of the hole (by means of an energy balance). Special methods are developed for calculating the onset of particulation and for calculating the depth of penetration by the particulated portion of a jet. These methods are provided in order to evaluate the performance of new types of jets, some of which have unconventional mass and velocity distributions that are unsuited to analysis by previous methods. In particular, the onset of breakup for each portion of the jet is calculated by treating the critical radius as a linear function of the inverse local stretching rate. A method for calculating interference with the hole is included, and the jet profile for maximum penetration is derived. Author

N93-26202*# National Aeronautics and Space Administration. Lewis Research Center, Cleveland, OH.

FABRICATION OF COMPOSITE PROPFAN BLADES FOR A CRUISE MISSILE WIND TUNNEL MODEL

E. Brian Fite Apr. 1993 30 p

(RTOP 535-03-10)

(NASA-TM-105270; E-7327; NAS 1.15:105270) Avail: CASI HC A03/MF A01

This report outlines the procedures that were employed in fabricating prototype graphite-epoxy composite prop fan blades. These blades were used in wind tunnel tests that investigated prop fan propulsion system interactions with a missile airframe in order to study the feasibility of an advanced-technology-propfan-propelled missile. Major phases of the blade fabrication presented include machining of the master blade, mold fabrication, ply cutting and assembly, blade curing, and quality assurance. Specifically, four separate designs were fabricated, 18 blades of each geometry, using the same fabrication technique for each design. Author

N93-26279# Hughes Aircraft Co., Fullerton, CA. Ground Systems Group.

STEP STRESS TESTING OF RECEIVER/TRANSMITTER UNITS Final Report, Jun. 1991 - 1992

Steve Burnett, David Huch, Larry James, Stephen Mueller, and Peggy Tran Feb. 1993 517 p

(Contract F30602-89-D-0100)

(AD-A261286; RL-TR-93-21-Pt-2) Avail: CASI HC A22/MF A04

This report has been prepared to summarize a test validation effort for an accelerated life testing model which uses a wide parametric Bayesian Analysis Methodology. Step stress testing was performed on seven Joint Tactical Information Distribution System (JTIDS) Class 1 synthesizer detector, radio frequency assemblies. Failure data and analyses are provided. The report addresses issues concerning how to demonstrate high reliability (Mean-Time-Between-Failure values of 10,000 hours or more) on procured Air Force systems without incurring excessive testing costs. DTIC

N93-26320# Scripps Institution of Oceanography, La Jolla, CA.

IMPROVED FATIGUE LIFE FOR MOORINGS

R. J. Seymour and S. A. Massey Dec. 1992 25 p

(Grant NA89AA-D-SG138; Proj. NOAA-R/OE-14)

(PB93-161198; SIO-REF-92-33) Avail: CASI HC A03/MF A01

Moorings are ubiquitous in man's useful occupation of the ocean. They are used to secure instruments and other unattended apparatus for scientific, civil and military uses and to fix the location for various lengths of time of manned platforms for mineral and hydrocarbon extraction and for marine transportation and ocean construction applications. Subject to wave and current loads, vibration from eddy shedding, and a hostile chemical environment, moorings fatigue and eventually fail if not replaced in time. The research is directed toward significantly improving the reliability and the service life of ocean mooring systems by developing the use of nonconventional materials (particularly advanced composites) and constructions. The work will extend previous and present research by the investigators in highly related areas. Subscale mooring elements (lines, terminations, and flexures) will be tested for fatigue resistance in a seawater environment in the laboratory. The overall project objective is to make substantial improvements in the service life and reliability of ocean moorings by using materials and constructions that are significantly less sensitive to fatigue and stress corrosion than conventional components. NTIS

N93-26361# Michigan Technological Univ., Houghton.

ON THE STABILITY OF FINITE PLASTIC DEFORMATIONS

H. M. Zbib and E. C. Aifantis 1992 12 p

(Contract NSF MSS-89-07748; DAAL03-90-G-0151; NSF CES-88-00459; NSF MSS-89-20700)

(AD-A261526; ARO-27409.1-EG) Avail: CASI HC A03/MF A01

The stability of inelastic deformation and the formation of shear bands are examined by considering a recently developed gradient-dependent theory of elasto-viscoplasticity. The main issues addressed in the present work are the role of viscosity, inertia and higher order strain gradients in providing internal length scales, as well as the effect of back stress (deformation induced anisotropy) and plastic spin (texture development) on the structure of the shear bands in the post localization regime. DTIC

N93-26362# California Univ., Santa Barbara. Dept. of Materials.

EXPERIMENTAL STUDIES OF STRESS MANAGEMENT BY OPTICAL FLUORESCENCE Annual Report

David R. Clarke Dec. 1992 90 p

(Contract N00014-91-J-1875)

(AD-A261539) Avail: CASI HC A05/MF A01

In this program the measurement of stresses in ceramics using their optical fluorescence is being developed. The technique is based on the phenomena of piezospectroscopy, namely the shift in optical fluorescence of a material produced by a stress. In the course of the program to data we have derived for the first time a general relationship between an observed shift in fluorescence frequency and the state of stress, applied it to the

determination of both applied and residual stresses in single crystal and polycrystalline materials, and begun to exploit the technique to the measurement of stresses in a variety of composite materials. These are described in detail in the accompanying technical reports appended here. As part of this investigation we have also found that in ruby (Chromium(3+) doped sapphire) the observed optical fluorescence shift as a function of chromium concentration is a direct measure of the 'image stress'.
Author (DTIC)

N93-26390# Illinois Univ., Urbana. Dept. of Civil Engineering.
J AND CTOD ESTIMATION EQUATIONS FOR SHALLOW CRACKS IN SINGLE EDGE NOTCH BEND SPECIMENS
Mark T. Kirk and Robert H. Dodds, Jr. Jan. 1993 28 p
(Contract N61533-92-R-0030)
(AD-A261679; UILU-ENG-91-2013; CDNSWC/SME-CR-17-92; NUREG-CR-5669) Avail: CASI HC A03/MF A01

Results from two dimensional plane strain finite-element analyses are used to develop J and CTOD estimation strategies appropriate for application to both shallow and deep crack SE(B) specimens. Crack depth to specimen width (a/W) ratios between 0.05 and 0.70 are modelled using Ramberg-Osgood strain hardening exponents (n) between 4 and 50. The estimation formulas divide J and CTOD into small scale yielding (SSY) and large scale yielding (LSY) components. For each case, the SSY components is determined by the linear elastic stress intensity factor, K(sub I). The formulas differ in evaluation of the LSY component. The techniques considered include: estimating J or CTOD from plastic work based on load line displacement (A(sub pl)/ILLD), from plastic work based on crack mouth opening displacement (A(sub pl)/CMOD(sub pl)), and from the plastic component of crack mouth opening displacement (CMOD(sub pl)). A(sub pl)CMOD provides the most accurate J estimation possible. CTOD estimates based on scalar proportionality of CTOD(sub Isy) and CMOD(sub pl) are highly inaccurate, especially for materials with considerable strain hardening, where errors up to 38% occur. DTIC

N93-26459# Metz Univ. (France).
ANALYSIS OF LONGITUDINAL IMPACT ON SEMI-INFINITE CIRCULAR BARS AND TUBES. APPENDIX NO. 2 Final Technical Report
J. R. Klepaczko and S. J. Matysiak (Warsaw Univ., Poland.) Oct. 1992 28 p LIMITED REPRODUCIBILITY: More than 20% of this document may be affected by microfiche quality
(Contract DAJA45-90-C-0052)
(AD-A261556) Avail: CASI HC A03

The problems of pressure shock and longitudinal impact on a semi-infinite circular tube are studied. The considerations are performed within the framework of the linear theory of elasticity. The problems were reduced to the system of Bessel differential equations by using double integral transforms. The solutions are obtained in the terms of Fourier and Laplace integrals which could be evaluated by numerical methods. DTIC

N93-26507# Lawrence Livermore National Lab., CA.
BEHAVIOR OF A STEEL-LINER-AND-BOLTS SYSTEM UNDER VERY HIGH THERMAL AND MECHANICAL LOADING: THE CONVEX LINER ADD-ON TO DIAMOND FORTUNE
F. E. Heuze, R. P. Swift, L. R. Hill (Sandia National Labs., Albuquerque, NM.), and W. H. Barrett (Sandia National Labs., Albuquerque, NM.) Jan. 1993 13 p Presented at the Symposium on Numerical Modeling Applications in Mining and Geomechanics, Montreal, Quebec, 27-30 Mar. 1993
(Contracts W-7405-eng-48; DE-AC04-76DP-00789)
(DE93-007512; UCRL-JC-112455; CONF-9303102-1) Avail: CASI HC A03/MF A01

This work involved the response of a liner-bolt system installed on the wall of the DIAMOND FORTUNE cavity, a 22-m diameter nearly semi-spherical chamber in tuff, at the Nevada Test Site. DIAMOND FORTUNE is a low-yield nuclear test of the Defense Nuclear Agency which was performed in April, 1992. A 1.4-m square, 2.5-cm thick steel plate was anchored by 9-m long bolts: four 2.5-cm diameter bolts at the corners and a 5-cm diameter bolt at the center. The bolt ends daylighted in a tunnel surrounding the cavity, and were tensioned from there. The system was aped with 20 data channels for strain, acceleration, contact pressure, and temperature. We relate the thermal analyses and the 3-dimensional dynamic analyses performed for this project, and we present the test results which indicated the excellent response of this system to the high dynamic loads and temperatures. DOE

N93-26516# Illinois Univ., Urbana. Dept. of Computer Science.
APPROXIMATE TECHNIQUES FOR PREDICTING SIZE EFFECTS ON CLEAVAGE FRACTURE TOUGHNESS (J(SUB c)) Final Report
Mark T. Kirk and Robert H. Dodds, Jr. Jan. 1993 40 p
(Contract N61533-92-R-0030)
(AD-A261591; UILU-ENG-92-2016; CDNSWC/SME-CR-18-92; NUREG/CR-5970) Avail: CASI HC A03/MF A01

This investigation examines the ability of an elastic T-stress coupled with a modified boundary layer (MBL) solution to predict stresses ahead of a crack tip in a variety of planar geometries. The approximate stresses are used as input to estimate the effective driving force for cleavage fracture (J(sub o)) using the micromechanically based approach. Finite element analyses for a wide variety of planar cracked geometries are conducted which have elastic biaxiality parameters (beta) ranging from -0.99 (very low constraint) to +2.96 (very high constraint). The magnitude and sign of beta indicate the rate at which crack-tip constraint changes with increasing applied load. All results pertain to a moderately strain hardening material (strain hardening exponent (n) of 10). These analyses suggest that beta is an effective indicator of both the accuracy of T-MBL estimates of J(sub o) and of applicability limits on evolving fracture analysis methodologies (i.e. T-MBL, J-Q, and J/J(sub o)). DTIC

N93-26522# Brunel Univ., Uxbridge (England). Inst. of Computational Mathematics.
USE AND ANALYSIS OF FINITE ELEMENT METHODS FOR PROBLEMS OF SOLID MECHANICS AND FRACTURE Final Report, Sep. 1989 - Nov. 1992
J. R. Whiteman 19 Jan. 1993 8 p LIMITED REPRODUCIBILITY: More than 20% of this document may be affected by microfiche quality
(Contract DAJA45-89-C-0023)
(AD-A261574; Rept-6078-MA-01) Avail: CASI HC A02

In this project, the principal investigator and his co-workers wish to exploit their expertise in the theoretical analysis, particularly regarding superconvergence, and practical application of finite element methods to produce and analyze new finite element schemes for treating difficult linear and nonlinear problems of solid mechanics and fracture mechanics. The difficulties arise from the presence of effects such as material nonlinearities, nonhomogeneity, time dependence, and stationary and moving cracks. In particular, they wish to apply new retrieval techniques of finite elements to define new adaptive procedures for producing numerical solutions with enhanced properties for some problems of linear elasticity and linear elastic fracture, elasto-plasticity and nonlinear fracture, viscoelasticity, and viscoelastic fracture. Contexts in which these new techniques will be applied include the deformation and fracture of timbers, and elasto-plastic deformation and fracture of metals with work hardening and the viscoelastic deformation and fracture of various polymers. Attention will also be given to some composite structures in these contexts. Whenever possible the numerical results will be compared with experimental results. DTIC

N93-26550*# National Aeronautics and Space Administration. Lewis Research Center, Cleveland, OH.
THE INFLUENCE OF PRIMARY AND SECONDARY ORIENTATIONS ON THE ELASTIC RESPONSE OF A NICKEL-BASE SINGLE-CRYSTAL SUPERALLOY
Ali Abdul-Aziz (Sverdrup Technology, Inc., Brook Park, OH.), Sreeramesh Kalluri (Sverdrup Technology, Inc., Brook Park, OH.), and Michael A. McGaw Apr. 1993 13 p Presented at the 38th ASME International Gas Turbine and Aeroengine Congress and Exposition, Cincinnati, OH, 24-27 May 1993; sponsored by ASME
(RTOP 553-13-00)
(NASA-TM-106125; E-7801; NAS 1.15:106125) Avail: CASI HC A03/MF A01

The influence of primary orientation on the elastic response of a (001)-oriented nickel-base single-crystal superalloy, PWA 1480, was investigated under mechanical, thermal, and combined thermal and mechanical loading conditions using finite element techniques. Elastic stress analyses were performed using the MARC finite element code on a square plate of PWA 1480 material. Primary orientation of the single crystal

superalloy was varied in increments of 2 deg, from 0 to 10 deg, from the (001) direction. Two secondary orientations (0 and 45 deg) were considered, with respect to the global coordinate system, as the primary orientation angle was varied. The stresses developed within the single crystal plate were determined for each loading condition. In this paper, the influence of the angular offset between the primary crystal orientation and the loading direction on the elastic stress response of the PWA 1480 plate is presented for different loading conditions. The influence of primary orientation angle, when constrained between the bounds considered, was not found to be as significant as the influence of the secondary orientation angle, which is not typically controlled. Author (revised)

N93-25834*# Massachusetts Inst. of Tech., Cambridge. Dept. of Mechanical Engineering.

USING INPUT COMMAND PRE-SHAPING TO SUPPRESS MULTIPLE MODE VIBRATION

James M. Hyde and Warren P. Seering *In its* MIT Space Engineering Research Center Dec. 1990 19 p (For primary document see N93-25833 09-63)

(Contract NAGw-1335; N00014-86-K-0685)

Avail: CASI HC A03/MF A02

42 GEOSCIENCES (GENERAL)

N93-24915*# National Aeronautics and Space Administration. Goddard Space Flight Center, Greenbelt, MD.

PROCEEDINGS OF THE OCEAN CLIMATE DATA WORKSHOP

James Churgin, comp. 1992 375 p Workshop held in Greenbelt, MD, 18-21 Feb. 1992 Sponsored in cooperation with Commission of the European Communities; International Council of Scientific Unions; Intergovernmental Oceanographic Commission; and WMO Prepared in cooperation with National Oceanic and Atmospheric Administration, Washington, DC

(NASA-TM-108711; NAS 1.15:108711) Avail: CASI HC A16/MF A03

The First Consultative Meeting on Responsible National Oceanographic Data Centres (RNODC's) and Climate DataServices met in February 1988 and made a number of recommendations related to improving services to meet the needs of climate programmes. Included in these discussions was a recommendation for a Workshop on Ocean Climate Data Management. This workshop will be talking about ways to establish a Global Ocean Observing System (GOOS). For individual titles, see N93-24916 through N93-24942.

N93-24916*# / Naval Observatory, Washington, DC.

THE ROLE OF OCEAN CLIMATE DATA IN OPERATIONAL NAVAL OCEANOGRAPHY **c48**

Radm G. Chesbrough *In* NASA. Goddard Space Flight Center, Proceedings of the Ocean Climate Data Workshop 1992 p 27-43 (For primary document see N93-24915 09-42)

Avail: CASI HC A03/MF A03

Local application of global-scale models describes the U.S. Navy's basic philosophy for operational oceanography in support of fleet operations. Real-time data, climatologies, coupled air/ocean models, and large scale computers are the essential components of the Navy's system for providing the war fighters with the performance predictions and tactical decision aids they need to operate safely and efficiently. In peacetime, these oceanographic predictions are important for safety of navigation and flight. The paucity and uneven distribution of real-time data mean we have to fall back on climatology to provide the basic data to operate our models. The Navy is both a producer and user of climatologies; it provides observations to the national archives and in turn employs data from these archives to establish data bases. Suggestions for future improvements to ocean climate data are offered. Author

N93-24917*# Commonwealth Scientific and Industrial Research Organization, Hobart (Australia).

INTERNATIONAL ORGANISATION OF OCEAN PROGRAMS: MAKING A VIRTUE OF NECESSITY **c48**

Angus McEwan *In* NASA. Goddard Space Flight Center, Proceedings of the Ocean Climate Data Workshop 1992 p 45-49 (For primary document see N93-24915 09-42)

Avail: CASI HC A01/MF A03

When faced with the needs of climate prediction, a sharp contrast is revealed between existing networks for the observation of the atmosphere and for the ocean. Even the largest and longest-serving ocean data networks were created for their value to a specific user (usually with a defence, fishing or other maritime purpose) and the major compilations of historical data have needed extensive scientific input to reconcile the differences and deficiencies of the various sources. Vast amounts of such data remain inaccessible or unusable. Observations for research purposes have been generally short lived and funded on the basis of single initiatives. Even major programs such as FGGE, TOGA and WOCE have been driven by the dedicated interest of a surprisingly small number of individuals, and have been funded from a wide variety of temporary allocations. Recognising the global scale of ocean observations needed for climate research, international cooperation and coordination is an unavoidable necessity, resulting in the creation of such bodies as the Committee for Climatic Changes and the Ocean (CCCO), with the tasks of: (1) defining the scientific elements of research and ocean observation which meet the needs of climate prediction and amelioration; (2) translating these elements into terms of programs, projects or requirements that can be understood and participated in by individual nations and marine agencies; and (3) the sponsorship of specialist groups to facilitate the definition of research programs, the implementation of cooperative international activity and the dissemination of results. Derived from text

N93-24918*# State Oceanographic Inst., Moscow (USSR). Hydrometeorology Committee.

ROLE OF THE OCEAN IN CLIMATE CHANGES **c48**

Sergey K. Gulev *In* NASA. Goddard Space Flight Center, Proceedings of the Ocean Climate Data Workshop 1992 p 51-64 (For primary document see N93-24915 09-42)

Avail: CASI HC A03/MF A03

The present program aimed at the study of ocean climate change is prepared by a group of scientists from State Oceanographic Institute, Academy of Science of Russia, Academy of Science of Ukraine and Moscow State University. It appears to be a natural evolution of ideas and achievements that have been developed under national and international ocean research projects such as SECTIONS, WOCE, TOGA, JGOFS and others. The two primary goals are set in the program ROCC. (1) Quantitative description of the global interoceanic 'conveyor' and it's role in formation of the large scale anomalies in the North Atlantic. The objectives on the way to this goal are: to get the reliable estimates of year-to-year variations of heat and water exchange between the Atlantic Ocean and the atmosphere; to establish and understand the physics of long period variations in meridianal heat and fresh water transport (MHT and MFWT) in the Atlantic Ocean; to analyze the general mechanisms, that form the MHT and MFWT in low latitudes (Ekman flux), middle latitudes (western boundary currents) and high latitudes (deep convection) of the North Atlantic; to establish and to give quantitative description of the realization of global changes in SST, surface salinity, sea level and sea ice data. (2) Development of the observational system pointed at tracing the climate changes in the North Atlantic. This goal merges the following objectives: to find the proper sites that form the inter annual variations of MHT; to study the deep circulation in the 'key' points; to develop the circulation models reflecting the principle features of interoceanic circulation; and to define global and local response of the atmosphere circulation to large scale processes in the Atlantic Ocean. Derived from text

N93-24919*# Delaware Univ., Lewes. Coll. of Marine Studies.

THE ROLE OF THE WORLD DATA CENTERS IN HANDLING OCEAN CLIMATE DATA **c48**

Ferris Webster *In* NASA. Goddard Space Flight Center, Proceedings of the Ocean Climate Data Workshop 1992 p 65-73 (For primary document see N93-24915 09-42)

Avail: CASI HC A02/MF A03

The World Data Center System, set up for the International Geophysical Year in 1957, is an international network of data centers that links data contributors to data users in the geosciences. It includes means for the synthesis, analysis, and preparation of data products. It was set up in response to the needs of the international scientific community, and is still

overseen by non-governmental scientific organizations. Because it is freely available to researchers in all countries, the World Data Center System has a special role to play in support of ocean climate research and monitoring programs. The World Data Centers face a number of challenges today. Apathy is probably the greatest, since many scientists take the system for granted. There is need to improve access and exploit new technology. The system must establish new links to assure continuity in a world with political changes. The multidisciplinary needs of global change research will demand capabilities for data and information management that go beyond the traditional emphasis on geophysics. Author

N93-24920*# Ministry of the Environment, Ottawa (Ontario). Dept. of Fisheries and Oceans.

THE GLOBAL OCEAN OBSERVING SYSTEM: ONE PERSPECTIVE c48

J. Ron Wilson *In* NASA. Goddard Space Flight Center, Proceedings of the Ocean Climate Data Workshop 1992 p 79-84 (For primary document see N93-24915 09-42)

Avail: CASI HC A02/MF A03

This document presents a possible organization for a Global Ocean Observing System (GOOS) within the Intergovernmental Oceanographic Commission and the joint ocean programs with the World Meteorological Organization. The document and the organization presented here is not intended to be definitive, complete or the best possible organization for such an observation program. It is presented at this time to demonstrate three points. The first point to be made is that an international program office for GOOS along the lines of the WOCE and TOGA IPOs is essential. The second point is that national programs will have to continue to collect data at the scale of WOCE plus TOGA and more. The third point is that there are many existing groups and committees within the IOC and joint IOC/WMO ocean programs that can contribute essential experience to and form part of the basis of a Global Ocean Observing System. It is particularly important to learn from what has worked and what has not worked in the past if a successful ocean observing system is to result. Author (revised)

N93-24921*# Climate Analysis Center, Washington, DC.

OPERATIONAL SEASONAL AND INTERANNUAL PREDICTIONS OF OCEAN CONDITIONS c48

Ants Leetmaa *In* NASA. Goddard Space Flight Center, Proceedings of the Ocean Climate Data Workshop 1992 p 85-86 (For primary document see N93-24915 09-42)

Avail: CASI HC A01/MF A03

Dr. Leetmaa described current work at the U.S. National Meteorological Center (NMC) on coupled systems leading to a seasonal prediction system. He described the way in which ocean thermal data is quality controlled and used in a four dimensional data assimilation system. This consists of a statistical interpolation scheme, a primitive equation ocean general circulation model, and the atmospheric fluxes that are required to force this. This whole process generated dynamically consist thermohaline and velocity fields for the ocean. Currently routine weekly analyses are performed for the Atlantic and Pacific oceans. These analyses are used for ocean climate diagnostics and as initial conditions for coupled forecast models. Specific examples of output products were shown both in the Pacific and the Atlantic Ocean. Derived from text

N93-24922*# Bedford Inst. of Oceanography, Dartmouth (Nova Scotia). Atlantic Oceanographic Lab.

WORLD OCEAN CIRCULATION EXPERIMENT c48

R. Allyn Clarke *In* NASA. Goddard Space Flight Center, Proceedings of the Ocean Climate Data Workshop 1992 p 87-94 (For primary document see N93-24915 09-42)

Avail: CASI HC A02/MF A03

The oceans are an equal partner with the atmosphere in the global climate system. The World Ocean Circulation Experiment is presently being implemented to improve ocean models that are useful for climate prediction both by encouraging more model development but more importantly by providing quality data sets that can be used to force or to validate such models. WOCE is the first oceanographic experiment that plans to generate and to use multiparameter global ocean data sets. In order for WOCE to succeed, oceanographers must establish and learn to use more effective methods of assembling, quality controlling, manipulating and distributing oceanographic data. Author

N93-24923*# Naval Sea Systems Command, Washington, DC. Office of the Chief Scientist.

THE GLOBAL OCEAN OBSERVING SYSTEM Abstract Only c48

Dana Kester *In* NASA. Goddard Space Flight Center, Proceedings of the Ocean Climate Data Workshop 1992 p 95 (For primary document see N93-24915 09-42)

Avail: CASI HC A01/MF A03

A Global Ocean Observing System (GOOS) should be established now with international coordination (1) to address issues of global change, (2) to implement operational ENSO forecasts, (3) to provide the data required to apply global ocean circulation models, and (4) to extract the greatest value from the one billion dollar investment over the next ten years in ocean remote sensing by the world's space agencies. The objectives of GOOS will focus on climatic and oceanic predictions, on assessing coastal pollution, and in determining the sustainability of living marine resources and ecosystems. GOOS will be a complete system including satellite observations, in situ observations, numerical modeling of ocean processes, and data exchange and management. A series of practical and economic benefits will be derived from the information generated by GOOS. In addition to the marine science community, these benefits will be realized by the energy industries of the world, and by the world's fisheries. The basic oceanic variables that are required to meet the oceanic and predictability objectives of GOOS include wind velocity over the ocean, sea surface temperature and salinity, oceanic profiles of temperature and salinity, surface current, sea level, the extent and thickness of sea ice, the partial pressure of CO2 in surface waters, and the chlorophyll concentration of surface waters. Ocean circulation models and coupled ocean-atmosphere models can be used to evaluate observing system design, to assimilate diverse data sets from in situ and remotely sensed observations, and ultimately to predict future states of the system. The volume of ocean data will increase enormously over the next decade as new satellite systems are launched and as complementary in situ measuring systems are deployed. These data must be transmitted, quality controlled, exchanged, analyzed, and archived with the best state-of-the-art computational methods. Author

N93-24924*# Australian Oceanographic Data Centre, North Sydney.

GLOBAL TEMPERATURE AND SALINITY PILOT PROJECT c48

Ben Searle *In* NASA. Goddard Space Flight Center, Proceedings of the Ocean Climate Data Workshop 1992 p 97-108 (For primary document see N93-24915 09-42)

Avail: CASI HC A03/MF A03

Data exchange and data management programs have been evolving over many years. Within the international community there are two main programs to support the exchange, management and processing of real time and delayed mode data. The Intergovernmental Oceanographic Commission (IOC) operate the International Oceanographic Data and Information Exchange (IODE) program which coordinates the exchange of delayed mode data between national oceanographic data centers, World Data Centers and the user community. The Integrated Global Ocean Services System is a joint IOC/World Meteorological Organization (WMO) program for the exchange and management of real-time data. These two programs are complemented by mechanisms that have been established within scientific programs to exchange and manage project data sets. In particular TOGA and WOCE have identified a data management requirement and established the appropriate infrastructure to achieve this. Where GTSPP fits into this existing framework is discussed. Derived from text

N93-24925*# Commonwealth Scientific and Industrial Research Organization, Hobart (Australia). Marine Labs.

INDIAN OCEAN ANALYSES c48

Gary Meyers *In* NASA. Goddard Space Flight Center, Proceedings of the Ocean Climate Data Workshop 1992 p 109-129 (For primary document see N93-24915 09-42)

Avail: CASI HC A03/MF A03

The background and goals of Indian Ocean thermal sampling are discussed from the perspective of a national project which has research goals relevant to variation of climate in Australia. The critical areas of SST variation are identified. The first goal of thermal sampling at this stage is to develop a climatology of thermal structure in the areas and a description of the annual variation of major currents. The sampling strategy is reviewed. Dense XBT sampling is required to achieve accurate, monthly maps of isotherm-depth because of the high level of noise in the measurements

caused by aliasing of small scale variation. In the Indian Ocean ship routes dictate where adequate sampling can be achieved. An efficient sampling rate on available routes is determined based on objective analysis. The statistical structure required for objective analysis is described and compared at 95 locations in the tropical Pacific and 107 in the tropical Indian Oceans. XBT data management and quality control methods at CSIRO are reviewed. Results on the mean and annual variation of temperature and baroclinic structure in the South Equatorial Current and Pacific/Indian Ocean Throughflow are presented for the region between northwest Australia and Java-Timor. The mean relative geostrophic transport (0/400 db) of Throughflow is approximately 5 x 106 m3/sec. A nearly equal volume transport is associated with the reference velocity at 400 db. The Throughflow feeds the South Equatorial Current, which has maximum westward flow in August/September, at the end of the southeasterly Monsoon season. A strong semiannual oscillation in the South Java Current is documented. The results are in good agreement with the Semtner and Chervin (1988) ocean general circulation model. The talk concludes with comments on data inadequacies (insufficient coverage, timeliness) particular to the Indian Ocean and suggestions on the future role that can be played by Data Centers, particularly with regard to quality control of data as research bodies are replaced by operational bodies in the Global Ocean Observing System. Author

N93-24926*# Jet Propulsion Lab., California Inst. of Tech., Pasadena.
SATELLITE MONITORING OF THE GLOBAL OCEAN SURFACE DURING 1987-1989 **c48**
David Halpern *In* NASA. Goddard Space Flight Center, Proceedings of the Ocean Climate Data Workshop 1992 p 131-143 (For primary document see N93-24915 09-42)
Avail: CASI HC A03/MF A03

Long-term simultaneous global coverage of AVHRR sea surface temperature, SSMI surface wind speed, GEOSAT sea surface height, and ARGOS buoy drift began in 1987. Methodology to create annual atlases of monthly mean distributions is described. Author

N93-24927*# Lisbon Univ. (Portugal). Dept. de Fisica.
THE USE OF REMOTELY SENSED DATA FOR OPERATIONAL FISHERIES OCEANOGRAPHY **c48**
Armando F. G. Fiuza *In* NASA. Goddard Space Flight Center, Proceedings of the Ocean Climate Data Workshop 1992 p 145-152 Sponsored in part by Commission of the European Communities (For primary document see N93-24915 09-42)
Avail: CASI HC A02/MF A03

Satellite remote sensing data are used under two contexts in fisheries: as a tool for fisheries research and as a means to provide operational support to fishing activities. Fishing operations need synoptic data provided timely; fisheries research needs that type of data and, also, good short-term climatologies. A description is given of several experiences conducted around the world which have employed or are using satellite data for operational fisheries problems. An overview is included of the Portuguese program for fisheries support using remotely sensed data provided by satellites and in situ observations conducted by fishermen. Environmental products useful for fisheries necessarily combine satellite and in situ data. The role of fishermen as a source of good, near-real-time in situ environmental data is stressed; so far, this role seems to have been largely overlooked. Author

N93-24928*# National Ocean Service, Monterey, CA.
OCEAN-PC AND A DISTRIBUTED NETWORK FOR OCEAN DATA **c48**
Douglas R. McLain *In* NASA. Goddard Space Flight Center, Proceedings of the Ocean Climate Data Workshop 1992 p 153-160 (For primary document see N93-24915 09-42)
Avail: CASI HC A02/MF A03

The Intergovernmental Oceanographic Commission (IOC) wishes to develop an integrated software package for oceanographic data entry and access in developing countries. The software, called 'OCEAN-PC', would run on low cost PC microcomputers and would encourage and standardize: (1) entry of local ocean observations; (2) quality control of the local data; (3) merging local data with historical data; (4) improved display and analysis of the merged data; and (5) international data exchange. OCEAN-PC will link existing MS-DOS oceanographic programs and data sets with table-driven format conversions. Since many ocean data sets are now being distributed on optical discs (Compact Discs - Read Only Memory, CD-ROM, Mass et al. 1987), OCEAN-PC will emphasize access to CD-ROMs.
Derived from text

N93-24929*# National Ocean Service, Rockville, MD.
SEA LEVEL VARIATION Abstract Only **c48**
Bruce C. Douglas *In* NASA. Goddard Space Flight Center, Proceedings of the Ocean Climate Data Workshop 1992 p 161 (For primary document see N93-24915 09-42)
Avail: CASI HC A01/MF A03

Published values for the long-term, global mean sea level rise determined from tide gauge records range from about one to three mm per year. The scatter of the estimates appears to arise largely from the use of data from gauges located at convergent tectonic plate boundaries where changes of land elevation give fictitious sea level trends, and the effects of large interdecadal and longer sea level variations on short (less than 50+ years) or sappy records. In addition, virtually all gauges undergo subsidence or uplift due to isostatic rebound from the last deglaciation at a rate comparable to or greater than the secular rise of sea level. Modeling rebound by the ICE-3G model of Tushingham and Peltier (1990) and avoiding tide gauge records in areas of converging tectonic plates produces a highly consistent set of long sea level records. A global set of 21 such stations in nine oceanic regions with an average record length of 76 years during the period 1880-1980 yields the global sea level rise value 1.8 mm/year +/- 0.1. Greenhouse warming scenarios commonly forecast an additional acceleration of global sea level in the next 5 or 6+ decades in the range 0.1-0.2 mm/yr2. Because of the large power at low frequencies in the sea level spectrum, very long tide gauge records (75 years minimum) have been examined for past apparent sea level acceleration. For the 80-year period 1905-1985, 23 essentially complete tide gauge records in 10 geographic groups are available for analysis. These yielded the apparent global acceleration -0.011 (+/- 0.012) mm/yr2. A larger, less uniform set of 37 records in the same 10 groups with 92 years average length covering the 141 years from 1850-1991 gave 0.001 (+/- 0.008) mm/yr2. Thus there is no evidence for an apparent acceleration in the past 100+ years that is significant either statistically, or in comparison to values associated with global warming. Unfortunately, the large interdecadal fluctuations of sea level severely affect estimates of global sea level acceleration for time spans of less than about 50 years. This means that tide gauges alone cannot serve as a reliable leading indicator of climate change in less than many decades. This time required can be significantly reduced if the interdecadal fluctuations of sea level can be understood in terms of their forcing mechanisms, and then removed from the tide gauge records.
Author

N93-24930*# National Geodetic Survey, Rockville, MD.
SATELLITE ALTIMETRY **c43**
Robert E. Cheney *In* NASA. Goddard Space Flight Center, Proceedings of the Ocean Climate Data Workshop 1992 p 169-170 (For primary document see N93-24915 09-42)
Avail: CASI HC A01/MF A03

Since altimetry data are not really old enough to use the term data archaeology, Mr. Cheney referred to the stewardship of these data. He noted that it is very important to document the basis for an altimetry data set as the algorithms and corrections used to arrive at the Geophysical Data Record (GDR) have been improving and are continuing to improve the precision of sea level data derived from altimetry. He noted that the GEOSAT Exact Repeat Mission (ERM) data set has recently been reprocessed by his organization in the National Ocean Service of NOAA and made available to the scientific community on CD/ROM disks by the National Oceanographic Data Center of the U.S. (NODC). The new data set contains a satellite orbit more precise by an order of magnitude together with an improved water vapor correction. A new, comprehensive GDR Handbook has also been prepared. Author (revised)

N93-24931*# International Council for the Exploration of the Sea, Copenhagen (Denmark).
DATA ARCHAEOLOGY AT ICES **c82**
Harry D. Dooley *In* NASA. Goddard Space Flight Center, Proceedings of the Ocean Climate Data Workshop 1992 p 173-185 (For primary document see N93-24915 09-42)
Avail: CASI HC A03/MF A03

This paper provides a brief overview of the function of the International Council for the Exploration of the Sea (ICES), both past and present, in particular in the context of its interest in compiling oceanographic data sets. Details are provided of the procedures it adopted to ensure adequate internationally collaborative marine investigations during the first part of the century, such as how it provided a forum for action by its member states, how it coordinated and published the results of scientific programs, and how it provided a foundation, through scientists employed in the ICES Office, for the establishment of the original oceanographic marine databases and associated products, and the scientific interpretation of the results. The growth and expansion of this area of ICES activity is then traced, taking into account the changing conditions for oceanographic data management resulting from the establishment of the National Data Centres, as well as the World Data Centres for Oceanography, which were created to meet the needs of the International Geophysical Year (IGY). Finally, there is a discussion of the way in which the very existence of ICES has proved to be a valuable source of old data, some of which have not yet been digitized, but which can be readily retrieved because they have been very carefully documented throughout the years. Lessons from this activity are noted, and suggestions are made on how the past experiences of ICES can be utilized to ensure the availability of marine data to present and future generations of scientists. Author

N93-24932*# Academy of Sciences (USSR), Moscow. Oceanographic Data Centre.

DATA AVAILABILITY AND DATA ARCHEOLOGY FROM THE FORMER SOVIET UNION **c82**

Yuri Sychev and Nickolai N. Mikhailov *In* NASA. Goddard Space Flight Center, Proceedings of the Ocean Climate Data Workshop 1992 p 187-192 (For primary document see N93-24915 09-42)

Avail: CASI HC A02/MF A03

Acquisition of data on the ocean is believed to start in 1872, when the Royal Navy ship 'Challenger' performed oceanographic stations in its round-world voyage (1872-1876). The first oceanographic studies of the World Ocean refer to the 80s second half of the 19th century. During its round-world expedition 'Vityaz' (1886-1889) headed by S.O. Markov, performed hydrological measurements in the Baltic Sea, Atlantic and Pacific Oceans. According to information available the regular expedition observations (prototype of future complex international program on the ocean research) started in the second half of 80s last century under the auspice of Kiev commission for exploration of German Seas. Systematic hydrological observations were organized by Hydrographic Department of Russia in 1876-1879 according to the program similar to the Kiev one and observations were regularly made by ships of custom service over the Russian area of the Baltic Sea. The increasing demands in oceanographic data contributed to considerable progress in exploration of the World Ocean during current century whole tendency to increase and become more significant has been observed for the last 30-40 years. Most probably various expeditions which were carried out during International Geophysical Year in different regions of the World Ocean are to be reference point in performing intensive oceanographic observations of Marine environment. In the former USSR oceanographic observations are made by research and hydrographic vessels, commercial and fishery ships as well as oil production platforms, coastal hydrometeorological station and other observing platforms. Oceanographic observations data, available from main sources of information on the ocean-research vessels, are also considered in the report.

Derived from text

N93-24933*# Lagos Univ. (Nigeria). Dept. of Geography.

OCEAN CLIMATE DATA FOR USER COMMUNITY IN WEST AND CENTRAL AFRICA: NEEDS, OPPORTUNITIES, AND CHALLENGES **c82**

S. O. Ojo *In* NASA. Goddard Space Flight Center, Proceedings of the Ocean Climate Data Workshop 1992 p 193-199 (For primary document see N93-24915 09-42)

Avail: CASI HC A02/MF A03

The urgent need to improve data delivery systems needed by scientists studying ocean role in climate and climate characteristics has been manifested in recent years because of the unprecedented climatic events experienced in many parts of the world. Indeed, there has been a striking and growing realization by governments and the general public indicating that national economies and human welfare depend on climate and its variability. In West and Central Africa, for instance climatic events, which have resulted in floods and droughts, have caused a lot of concern to both governments and people of the region. In particular, the droughts have been so widespread that greater awareness and concern have become generated for the need to find solutions to the problems created by the consequences of the climatic events. Particularly in the southern border regions of the Sahara Desert as well as in the Sahel region, the drought episodes considerably reduced food production and led to series of socioeconomic problems, not only in the areas affected by the droughts, but also in the other parts of West Africa. The various climatic variabilities which have caused the climatic events are no doubt related to the ocean-atmosphere interactions. Unfortunately, not much has been done on the understanding of these interactions, particularly as they affect developing countries. Indeed, not much has been done to develop programs which will reflect the general concerns and needs for researching into the ocean-atmosphere systems and their implications on man-environmental systems in many developing countries. This is for example, true of West and Central Africa, where compared with the middle latitude countries, much less is known about the characteristics of the ocean-atmosphere systems and their significance on man-environmental systems of the area.

Author

N93-24934*# Maryland Univ., Cambridge. Marine Labs.

THE JGOFS NORTH ATLANTIC BLOOM EXPERIMENT: AN OVERVIEW **c48**

Hugh W. Ducklow *In* NASA. Goddard Space Flight Center, Proceedings of the Ocean Climate Data Workshop 1992 p 205-227 (For primary document see N93-24915 09-42)

Avail: CASI HC A03/MF A03

The North Atlantic Bloom Experiment (NABE) of JGOFS presents a unique opportunity and challenge to the data management community because of the diversity and large size of biogeochemical data sets collected. NABE was a pilot study for JGOFS and has also served as a pilot study within the U.S. NODC for management and archiving of the data sets. Here I present an overview to some of the scientific results of NABE, which will be published as an Introduction to a special volume of NABE results in Deep-Sea Research later this year. An overview of NABE data management is given elsewhere in the present report. This is the first collection of papers from the Joint Global Ocean Flux Study (JGOFS). Formed as an international program in 1987, JGOFS has four principal elements: modelling and data management, multidisciplinary regional process studies, a global survey of biogeochemical properties and long-term time series observatories. In 1989-1990 JGOFS conducted a pilot process study of the spring phytoplankton bloom, the North Atlantic Bloom Experiment (NABE). JGOFS decided to conduct a large scale, internationally-coordinated pilot study in the North Atlantic because of its proximity to the founding nations of the project, the size and predictability of the bloom and its fundamental impact on ocean bio-geochemistry (Billett et al., 1983; Watson and Whitfield, 1985; Pfannkuche, 1992). In 1989, six research vessels from Canada, Germany, The Netherlands, the United Kingdom and the USA and over 200 scientists and students from more than a dozen nations participated in NABE. Some of their initial results are reported in this volume.

Author

N93-24935*# Massachusetts Inst. of Tech., Cambridge. Center for Meteorology and Physical Oceanography.

DATA MANAGEMENT FOR JGOFS: THEORY AND DESIGN **c82**

Glenn R. Flierl, James K. B. Bishop, David M. Glover, and Satish Paranjpe *In* NASA. Goddard Space Flight Center, Proceedings of the Ocean Climate Data Workshop 1992 p 229-249 (For primary document see N93-24915 09-42)

Avail: CASI HC A03/MF A03

The Joint Global Ocean Flux Study (JGOFS), currently being organized under the auspices of the Scientific Committee for Ocean Research (SCOR), is intended to be a decade long internationally coordinated program. The main goal of JGOFS is to determine and understand on a global scale the processes controlling the time-varying fluxes of carbon and associated biogenic elements in the ocean and to evaluate the related exchanges with the atmosphere, sea floor and continental boundaries. 'A long-term goal of JGOFS will be to establish strategies for observing, on long time scales, changes in ocean biogeochemical cycles in relation to climate change'. Participation from a large number of U.S. and foreign institutions is expected. JGOFS investigators have begun a set of time-series

measurements and global surveys of a wide variety of biological, chemical and physical quantities, detailed process-oriented studies, satellite observations of ocean color and wind stress and modeling of the bio-geochemical processes. These experiments will generate data in amounts unprecedented in the biological and chemical communities; rapid and effortless exchange of these data will be important to the success of JGOFS. Derived from text

N93-24936*# Proudman Oceanographic Lab., Birkenhead (England).
DATA MANAGEMENT FOR COMMUNITY RESEARCH PROJECTS: A JGOFS CASE STUDY **c82**
Roy K. Lowry *In* NASA. Goddard Space Flight Center, Proceedings of the Ocean Climate Data Workshop 1992 p 251-273 (For primary document see N93-24915 09-42)
Avail: CASI HC A03/MF A03

Since the mid 1980s, much of the marine science research effort in the United Kingdom has been focused into large scale collaborative projects involving public sector laboratories and university departments, termed Community Research Projects. Two of these, the Biogeochemical Ocean Flux Study (BOFS) and the North Sea Project incorporated large scale data collection to underpin multidisciplinary modeling efforts. The challenge of providing project data sets to support the science was met by a small team within the British Oceanographic Data Centre (BODC) operating as a topical data center. The role of the data center was to both work up the data from the ship's sensors and to combine these data with sample measurements into online databases. The working up of the data was achieved by a unique symbiosis between data center staff and project scientists. The project management, programming and data processing skills of the data center were combined with the oceanographic experience of the project communities to develop a system which has produced quality controlled, calibrated data sets from 49 research cruises in 3.5 years of operation. The data center resources required to achieve this were modest and far outweighed by the time liberated in the scientific community by the removal of the data processing burden. Two online project databases have been assembled containing a very high proportion of the data collected. As these are under the control of BODC their long term availability as part of the UK national data archive is assured. The success of the topical data center model for UK Community Research Project data management has been founded upon the strong working relationships forged between the data center and project scientists. These can only be established by frequent personal contact and hence the relatively small size of the UK has been a critical factor. However, projects covering a larger, even international scale could be successfully supported by a network of topical data centers managing online databases which are interconnected by object oriented distributed data management systems over wide area networks. Author

N93-24937*# Plymouth Marine Lab. (England).
THE CONTINUOUS PLANKTON RECORDER SURVEY: A LONG-TERM, BASIN-SCALE OCEANIC TIME SERIES **c48**
John C. Gamble and Harold G. Hunt *In* NASA. Goddard Space Flight Center, Proceedings of the Ocean Climate Data Workshop 1992 p 277-293 (For primary document see N93-24915 09-42)
Avail: CASI HC A03/MF A03

In the 1920s, before the advent of echo sounders, fishery biologists were greatly concerned with assisting the fisherman to locate schools of pelagic fish. One of the approaches they developed was to relate the distribution of the planktonic food organisms to the presence of the schools of predators such as herring (Clupea harengus). The British planktologist, Alister Hardy, who had already carried out extensive studies on the feeding preferences of herring (Hardy, 1926a), initiated a program to examine the fishermen's contention that herring schools avoided 'green', i.e., phytoplankton-rich, water but could be correlated with high concentrations of zooplankton. This practical program was centered on the use of a specially developed instrument, the 'Plankton Indicator', designed to be used by the fisherman to assist in the search for suitable waters. It had limited success in its main aim but, as a collecting device, it embodied several profoundly important features. It was a simple instrument which was robust enough to be deployed and recovered by the crew of commercial vessels (in this case fishing vessels) while they were underway. The Indicator however, was no more than a high speed net which integrated the plankton over the area of sampling, but Hardy had also become interested in describing the patchiness of planktonic populations. He thus developed the Continuous Plankton Recorder (CPR) where he substituted the fixed filter screen of the Indicator by a continually moving length of silk mesh. The screen traversed at constant speed across the path of the incoming water and the trapped organisms were retained in place by sandwiching beneath an additional second mesh screen. Thus, knowing the speed of the towing vessel and the shooting and hauling positions, the spatial patterns of the plankton could be determined. Hardy took the first CPR to the Antarctic where he used it in the Southern Atlantic (Hardy, 1926b) and later deployed it in the North Sea to make some of the earliest contiguous records of plankton patchiness. Author

N93-24938*# Bermuda Biological Station for Research, Inc., Ferry Reach.
OCEAN TIME-SERIES NEAR BERMUDA: HYDROSTATION S AND THE US JGOFS BERMUDA ATLANTIC TIME-SERIES STUDY **c48**
Anthony F. Michaels and Anthony H. Knap *In* NASA. Goddard Space Flight Center, Proceedings of the Ocean Climate Data Workshop 1992 p 295-315 (For primary document see N93-24915 09-42)
(Grants NSF OCE-86-13904; NSF OCE-88-01089; NSF OCE-90-17173; NSF OCE-90-16990; NSF BSR-90-18298)
Avail: CASI HC A03/MF A03

Bermuda is the site of two ocean time-series programs. At Hydrostation S, the ongoing biweekly profiles of temperature, salinity and oxygen now span 37 years. This is one of the longest open-ocean time-series data sets and provides a view of decadal scale variability in ocean processes. In 1988, the U.S. JGOFS Bermuda Atlantic Time-series Study began a wide range of measurements at a frequency of 14-18 cruises each year to understand temporal variability in ocean biogeochemistry. On each cruise, the data range from chemical analyses of discrete water samples to data from electronic packages of hydrographic and optics sensors. In addition, a range of biological and geochemical rate measurements are conducted that integrate over time-periods of minutes to days. This sampling strategy yields a reasonable resolution of the major seasonal patterns and of decadal scale variability. The Sargasso Sea also has a variety of episodic production events on scales of days to weeks and these are only poorly resolved. In addition, there is a substantial amount of mesoscale variability in this region and some of the perceived temporal patterns are caused by the intersection of the biweekly sampling with the natural spatial variability. In the Bermuda time-series programs, we have added a series of additional cruises to begin to assess these other sources of variation and their impacts on the interpretation of the main time-series record. However, the adequate resolution of higher frequency temporal patterns will probably require the introduction of new sampling strategies and some emerging technologies such as biogeochemical moorings and autonomous underwater vehicles. Author

N93-24939*# University of Southern California, Los Angeles. Ocean Physics Group.
AUTOMATED IN SITU OBSERVATIONS OF UPPER OCEAN BIOGEOCHEMISTRY, BIO-OPTICS, AND PHYSICS AND THEIR POTENTIAL USE FOR GLOBAL STUDIES **c48**
Tommy D. Dickey, Timothy C. Granata, and Isabelle Taupier-Letage *In* NASA. Goddard Space Flight Center, Proceedings of the Ocean Climate Data Workshop 1992 p 317-353 Sponsored in part by NOAA and CNRS (For primary document see N93-24915 09-42)
(Contract N00014-89-J-1498; NSF OCE-90-13896)
Avail: CASI HC A03/MF A03

The processes controlling the flux of carbon in the upper ocean have dynamic ranges in space and time of at least nine orders of magnitude. These processes depend on a broad suite of inter-related biogeochemical, bio-optical, and physical variables. These variables should be sampled on scales matching the relevant phenomena. Traditional ship-based sampling, while critical for detailed and more comprehensive observations, can span only limited portions of these ranges because of logistical and financial constraints. Further, remote observations from satellite platforms enable broad horizontal coverage which is restricted to the upper few meters of the ocean. For these main reasons, automated subsurface measurement systems are important for the fulfillment of research goals related to the regional and global estimation and modeling of time varying biogeochemical fluxes. Within the past few years, new sensors and systems capable of autonomously measuring several of the critical variables have been

developed. The platforms for deploying these systems now include moorings and drifters and it is likely that autonomous underwater vehicles (AUV's) will become available for use in the future. Each of these platforms satisfies particular sampling needs and can be used to complement both shipboard and satellite observations. In the present review, (1) sampling considerations will be summarized, (2) examples of data obtained from some of the existing automated in situ sampling systems will be highlighted, (3) future sensors and systems will be discussed, (4) data management issues for present and future automated systems will be considered, and (5) the status of near real-time data telemetry will be outlined. Finally, we wish to make it clear at the outset that the perspectives presented here are those of the authors and are not intended to represent those of the United States JGOFS program, the International JGOFS program, NOAA's C&GC program, or other global ocean programs. Author

N93-24940*# Department of Fisheries and Oceans, Winnipeg (Manitoba). Physical and Chemical Science Directorate.
WRAP-UP SESSION **c48**
Geoffrey Holland *In* NASA. Goddard Space Flight Center, Proceedings of the Ocean Climate Data Workshop 1992 p 357-364 (For primary document see N93-24915 09-42)
Avail: CASI HC A02/MF A03

Listening to the case studies that were presented it became quite evident that the best data management systems were the ones where data managers and research scientists worked as a team developed in the early stages of project planning. Examples that were given included WOCE Data Assembly Centres e.g., Drifters, the Global Temperature Salinity Pilot Project (GTSPP) collaboration with Joint Analyses Centres in the U.S. and Australia, and JGOFS/BOFS development of Topical Centres. While each of these has some elements unique to the project, each had brought together 'teams' of Principal Investigators (PI's) and data management experts at an early stage of project development. Conversely, projects which had considered data management as a totally separate activity with lower priority often failed to provide the service required to meet scientific objectives. Therefore, the following actions should be brought to the attention of relevant groups within the IOC and other international organizations: (1) Publicize, at the national and international level, underway data/scientist collaborations that may be used as models in planning for the future. (2) Reduce adversarial situations where data managers and scientists appear to be in competition. (3) Colocation and other forms of collaboration often results in very high quality data sets and more timely data submission. Improved timeliness of data submissions was a common theme throughout the workshop and must be considered an important element in all future plans. Improvements in timely submission of data were noted. In order to continue this trend the advantages of timely submission of data must be stressed to those planning new ocean science projects. Author

N93-24941*# Department of Fisheries and Oceans, Winnipeg (Manitoba). Physical and Chemical Science Directorate.
INTERNATIONAL OCEAN SERVICES: IS IT TIME - WILL IT EVER BE TIME? **c48**
Geoffrey Holland *In* NASA. Goddard Space Flight Center, Proceedings of the Ocean Climate Data Workshop 1992 p 381-387 (For primary document see N93-24915 09-42)
Avail: CASI HC A02/MF A03

Considering the objectives of the Ocean Data Climate Workshop this week and trying to select a related, but not too technical subject, I decided to look at the services needed for ocean clients. I thought that it would make an interesting theme to consider how the acceptance of international ocean services is progressing over the years. Or is it? Are we closer to having a global observing system than we were twenty years ago? If so, what has changed between then and now? What is different between the efforts of twenty years or so ago to get the Integrated Global Ocean Stations System (IGOSS) off the ground and the present attempts to establish the Global Ocean Observing System (GOOS)? Is there a window of opportunity now that didn't exist then? If it doesn't happen now, a legitimate question could well be asked.... Will it ever happen? At least on historical topics I am on firm ground, having been attending IOC meetings for many years, in fact, it was in 1970 that I attended my first IGOSS meeting and a couple of years later I started what was to become regular attendances at the IOC Governing Body sessions. Despite the numbing effect of sitting through IOC related meetings for a total of what must add up to two or three years, I can still defend the IOC as an essential intergovernmental body for the oceans. One can accept the value of medicine, but one doesn't have to enjoy the taste. Author

N93-24942*# National Aeronautics and Space Administration. Goddard Space Flight Center, Greenbelt, MD.
COMPUTER SYSTEMS **c60**
Lola Olsen *In its* Proceedings of the Ocean Climate Data Workshop 1992 p 391-408 (For primary document see N93-24915 09-42)
Avail: CASI HC A03/MF A03

In addition to the discussions, Ocean Climate Data Workshop hosts gave participants an opportunity to hear about, see, and test for themselves some of the latest computer tools now available for those studying climate change and the oceans. Six speakers described computer systems and their functions. The introductory talks were followed by demonstrations to small groups of participants and some opportunities for participants to get hands-on experience. After this familiarization period, attendees were invited to return during the course of the Workshop and have one-on-one discussions and further hands-on experience with these systems. Brief summaries or abstracts of introductory presentations are addressed. Author

N93-25398# Joint Publications Research Service, Arlington, VA.
JPRS REPORT: SCIENCE AND TECHNOLOGY. CENTRAL EURASIA: EARTH SCIENCES
22 Apr. 1992 25 p Transl. into ENGLISH from various Russian articles (JPRS-UES-92-003) Avail: CASI HC A03/MF A01

Translated articles cover the following topics: oceanography; physics of atmosphere; and ecology. CASI

N93-25399# Joint Publications Research Service, Arlington, VA.
JPRS REPORT: SCIENCE AND TECHNOLOGY. CENTRAL EURASIA: LIFE SCIENCES
12 Feb. 1993 45 p Transl. into ENGLISH from various Russian articles (JPRS-ULS-93-002) Avail: CASI HC A03/MF A01

Translated articles cover the following topics: semiconductor biosensors: immobilization and properties of urease films; and technical bioenergetics and ecosystem biotechnology. CASI

N93-25401# Joint Publications Research Service, Arlington, VA.
JPRS REPORT: SCIENCE AND TECHNOLOGY. CENTRAL EURASIA: EARTH SCIENCES
3 Oct. 1992 32 p Transl. into ENGLISH from various Russian articles (JPRS-UES-92-005) Avail: CASI HC A03/MF A01

Translated articles cover the following topics: arctic, antarctic research; geology; oceanography; physics of atmosphere; and ecology. CASI

N93-25426# Joint Publications Research Service, Arlington, VA.
JPRS REPORT: SCIENCE AND TECHNOLOGY. CENTRAL EURASIA: EARTH SCIENCES
21 Apr. 1992 43 p Transl. into ENGLISH from various Russian articles (JPRS-UES-92-002) Avail: CASI HC A03/MF A01

Translated articles cover the following topics: oceanic acoustic research; overview of remote sensing methods; and laser monitoring of atmosphere. CASI

43 EARTH RESOURCES AND REMOTE SENSING

Includes remote sensing of earth resources by aircraft and spacecraft; photogrammetry; and aerial photography.

For instrumentation see *35 Instrumentation and Photography.*

N93-24775# European Space Agency, Paris (France).
ENVIRONMENT OBSERVATION AND CLIMATE MODELLING THROUGH INTERNATIONAL SPACE PROJECTS. VOLUME 2: REMOTE SENSING FOR ENVIRONMENTAL MONITORING AND RESOURCE MANAGEMENT
T. Duc Guyenne, ed. and James J. Hunt, ed. 1992 500 p Conference held in Munich, Germany, 30 Mar. - 4 Apr. 1992; sponsored by EEC, ESA, Deutsche Agentur fuer Raumfahrtangelegenheiten, and the European Association for the International Space Year

(ESA-ISY-1-Vol-2; ETN-93-93503) Copyright Avail: CASI HC A21/MF A04; ESA, EPD, ESTEC, Noordwijk, Netherlands, HC

The European International Space Year conference was held with the specific theme of the practical use of space derived information for environmental research and monitoring and resource management. This main theme, 'Mission to Planet Earth,' was maintained, but it was recognized that other fields needed to be equally addressed to provide a balanced view on space activities. Space sciences, space navigation and communications, and manned space activities were also represented. The present volume consists of papers addressing the following topics: general topics, methodology, and meteorology; geology, environment, and land cover; disaster monitoring; operational status of remote sensing; coastal zones and inland water; forestry; agriculture; and instrumentation and systems. For individual titles, see N93-24776 through N93-24874.

N93-24776# Ludwig-Maximilians-Univ., Munich (Germany). Arbeitsgruppe Fernerkundung.

USE OF AIRBORNE IMAGING SPECTROMETRY TO THE DEFINITION OF OPTIMISED SPECIFICATIONS FOR LAND APPLICATIONS WITH FUTURE SPACEBORNE IMAGING SPECTROMETERS

J. Bodechtel, S. Sommer, H. Bach, and W. Mauser *In* ESA, Environment Observation and Climate Modelling Through International Space Projects. Volume 2: Remote Sensing for Environmental Monitoring and Resource Management 1992 p 405-409 (For primary document see N93-24775 09-43)

Copyright Avail: CASI HC A01/MF A04; ESA, EPD, ESTEC, Noordwijk, Netherlands, HC

Airborne and ground data obtained from different test sites in Europe are used for a comparative analysis of the spectral signatures of various land surfaces (vegetation, bare soils and rocks, and mixed soil/rock vegetation) as seen from different imaging spectrometers. Recent experience with airborne imaging spectrometers has demonstrated the advantages of narrowband sensors over broadband scanners such as LANDSAT TM for characterizing the nature and physical status of typical land surfaces. Information on key spectral features associated with various land surfaces can be obtained from the data of airborne imaging spectrometers, which can be used to simulate spaceborne high spectral resolution data and to assess their information content if comprehensive underpinning is provided by ground data. ESA

N93-24777# Deutsche Forschungsanstalt fuer Luft- und Raumfahrt, Oberpfaffenhofen (Germany). Inst. fuer Hochfrequenztechnik.

THE USE OF POLARIMETRIC MULTIFREQUENCY SAR FOR CHARACTERIZING TERRAIN CLASSES

R. Glitz *In* ESA, Environment Observation and Climate Modelling Through International Space Projects. Volume 2: Remote Sensing for Environmental Monitoring and Resource Management 1992 p 411-417 (For primary document see N93-24775 09-43)

Copyright Avail: CASI HC A02/MF A04; ESA, EPD, ESTEC, Noordwijk, Netherlands, HC

The calibration of data acquired with NASA DC-8 SAR (Synthetic Aperture Radar) is reported. Signatures and polarimetric features of terrain classes are extracted and explained with respect to frequency and incidence angle dependence. Applications of polarimetric contrast enhancement, separation, and classification of object classes are demonstrated, and an approach to assess and optimize feature information is proposed. Summarizing the various topics of remote sensing applications and the analysis results discussed, the superiority of polarimetric SAR sensors with multifrequency capability against conventional SAR systems is demonstrated. ESA

N93-24778# Deutsche Forschungsanstalt fuer Luft- und Raumfahrt, Oberpfaffenhofen (Germany). Inst. fuer Hochfrequenztechnik.

THE SCOPE OF DLR'S SAR CALIBRATION PROGRAM

H. Kietzmann *In* ESA, Environment Observation and Climate Modelling Through International Space Projects. Volume 2: Remote Sensing for Environmental Monitoring and Resource Management 1992 p 419-421 (For primary document see N93-24775 09-43)

Copyright Avail: CASI HC A01/MF A04; ESA, EPD, ESTEC, Noordwijk, Netherlands, HC

The preparation of SAR (Synthetic Aperture Radar) calibration experiments concerning the SAR spaceborne remote sensing missions X-SAR/SIR-C, ERS-1, JERS-1, and PRIRODA, is reported. These SAR missions will deliver a large number of different SAR image products which are of special interest for various kinds of scientific disciplines. For an optimum use of these products, the best possible calibration is necessary. Therefore, a series of calibration experiments approved by the mission relevant review boards is being performed. To perform such a calibration, the main error sources and the error contributions of essential system parts like sensor, antenna, and external calibration references were investigated separately. For obtaining the experiment objectives, a large number of high precision trihedral and dihedral corner reflectors and especially designed calibration receivers and active radar calibrators are available. ESA

N93-24779# Consiglio Nazionale delle Ricerche, Venice (Italy).

REMOTE SENSED SPECTRAL SIGNATURES CLASSIFICATION AND RECOGNITION BY NEURAL NETWORKS: AN APPROACH TO UNSUPERVISED TECHNIQUES

L. Alberotanza and M. Pavanati (Venice Univ., Italy.) *In* ESA, Environment Observation and Climate Modelling Through International Space Projects. Volume 2: Remote Sensing for Environmental Monitoring and Resource Management 1992 p 423-428 (For primary document see N93-24775 09-43)

Copyright Avail: CASI HC A02/MF A04; ESA, EPD, ESTEC, Noordwijk, Netherlands, HC

The use of an adaptive resonance neural networks scheme to analyze multispectral remotely sensed images on a lagoon environment and coastal waters is reported. An attempt was made to develop a substantially unsupervised classifier, obtaining an algorithm capable of independently organizing the learning stage on the basis of the same data under analysis. Information is requested from the external operator to limit the number of classes to be recognized. It is not necessary to use models for samples of spectral signature. The experience acquired can be transferred to successive recognitions. The method makes use of the separation of color information from that of the intensity of the analyzed radiation, and derives from radiometric corrections and calibrations. ESA

N93-24780# Valencia Univ., Burjassot (Spain). Remote Sensing Unit.

CORRELATION BETWEEN NDVI VALUES DERIVED FROM NOAA AVHRR HRPT DATA AND GROUND MEASUREMENTS OF PRECIPITATION IN THE EFEDA STUDY AREA (SPAIN)

Jose F. Moreno, E. Lopez-Baeza, Joaquin Melia, D. Segarra, and J. Tamayo (National Inst. of Meteorology, Valencia, Spain.) *In* ESA, Environment Observation and Climate Modelling Through International Space Projects. Volume 2: Remote Sensing for Environmental Monitoring and Resource Management 1992 p 429-434 (For primary document see N93-24775 09-43)

Copyright Avail: CASI HC A02/MF A04; ESA, EPD, ESTEC, Noordwijk, Netherlands, HC

Research within the context of the EFEDA (ECHIVAL Field Experiment on a Desertification threatened Area) experiment, a European contribution to the International Geosphere-Biosphere Program (IGBP), is presented. The study area is located in the Spanish region of Castilla-La Mancha, and the main field campaign took place in Jun. 1991. The study is intended to characterize the conditions under which the field experiment was carried out, within the framework of a retrospective climatological study. The analysis of the correlation between NDVI and precipitation was addressed in two different ways: a point to point approach between the precipitation value of each station and the averaged value of NDVI (derived from AVHRR (Advanced Very High Resolution Radiometer) data) over an area of 25 sq km around the location of the station; and an image to image correlation approach between the NDVI map derived from AVHRR data and a precipitation map derived from the network of meteorological stations. The NDVI precipitation correlation shows a significant dependence on the spatial scale. Only at coarse scales is it possible to understand such correlation because of the complexity of the hydrological structure of the EFEDA study area. ESA

N93-24781# VERTIC, London (England).

VERIFICATION OF A CLIMATE CONVENTION: ROLE AND LIMITATIONS OF A SPACE BASED REMOTE SENSING SYSTEM

J. F. Lanchbery, W. Fischer (Kernforschungszentrum G.m.b.H., Karlsruhe, Germany.), R. Katscher (Kernforschungszentrum G.m.b.H., Karlsruhe, Germany.), and G. Stein (Kernforschungszentrum G.m.b.H., Karlsruhe,

Germany.) *In* ESA, Environment Observation and Climate Modelling Through International Space Projects. Volume 2: Remote Sensing for Environmental Monitoring and Resource Management 1992 p 435-447 (For primary document see N93-24775 09-43)

Copyright Avail: CASI HC A03/MF A04; ESA, EPD, ESTEC, Noordwijk, Netherlands, HC

Techniques currently under discussion for verifying compliance with an international climate convention are discussed. The protocols of such a system are likely to include space based remote sensing systems. Present and potential verification sectors for such systems and the likely technical demands of the verification system user are indicated. Space based remote sensors currently offer the prospect of being used to monitor changes in vegetation on the Earth's surface and could thus be used as tools to verify compliance with a forest protocol and possible land use or agriculture agreements. The capabilities and limitations of currently available remote sensing techniques in this type of application are discussed and some of the technical requirements of remote sensors in other areas likely to need verifying under a climate convention are explored. ESA

N93-24782# Bulgarian Academy of Sciences, Sofia. Solar Terrestrial Influences Lab.

ANOVA METHOD TO ESTIMATE VEGETATION INDICES SENSITIVITY ASSESSING NITROGEN FERTILIZING INFLUENCE ON SPECTRAL REFLECTANCE COEFFICIENTS

Tony K. Yanev, Rumiana H. Kancheva, and Valentina S. Boycheva *In* ESA, Environment Observation and Climate Modelling Through International Space Projects. Volume 2: Remote Sensing for Environmental Monitoring and Resource Management 1992 p 449-451 (For primary document see N93-24775 09-43)

Copyright Avail: CASI HC A01/MF A04; ESA, EPD, ESTEC, Noordwijk, Netherlands, HC

The sensitivity of Vegetation Indices (VI) to changes in the spectral reflectance data, by which the VI values were calculated, was estimated by the ANOVA (variance analysis) method. Greenhouse evidence for Spring barley, which was fertilized by nitrogen and grown from emergence to ripeness, was processed. The ANOVA method is a model free method and provides the possibility of a comparative analysis of the VI sensitivity to be performed without the requirement of the knowledge of model correlationships between VI and bioparameters. ESA

N93-24783# Colorado School of Mines, Golden.

SPECTRAL REMOTE SENSING OF ANOMALOUS MINERALOGY INDUCED BY HYDROCARBON MIGRATION AND URANIUM MINERALIZATION, SAN RAFAEL SWELL, UTAH, USA

Hayati Koyuncu (Hacettepe Univ., Ankara, Turkey.) *In* ESA, Environment Observation and Climate Modelling Through International Space Projects. Volume 2: Remote Sensing for Environmental Monitoring and Resource Management 1992 p 455-460 Sponsored in part by Ministry of Education, Turkey, and Geological Survey, Denver, CO (For primary document see N93-24775 09-43)

Copyright Avail: CASI HC A02/MF A04; ESA, EPD, ESTEC, Noordwijk, Netherlands, HC

Landsat Thematic Mapper (TM) data were digitally processed, analyzed, and interpreted for iron oxide, carbonate, and hydroxyl bearing mineral anomalies associated with hydrocarbon induced alteration and/or uranium mineralization in the San Rafael Swell, Utah. Discrimination of these minerals or mineral assemblages was possible based on their absorption features (spectral properties) that fall within TM spectral passbands. For this purpose, band ratios were calculated and combined to produce a Color Ratio Composite (CRC) image on which altered rocks were characterized by color differences. The colors of the CRC were further analyzed and classified numerically by digitally transforming the CRC digital numbers into Munsell color coordinates (intensity, hue, and saturation). Subsequent field checks and laboratory spectral, X-ray diffraction, and microscopic analyses of rock samples were performed to determine alteration minerals and/or mineral assemblages, and to establish a mineralogic basis for the spectral anomalies (altered versus unaltered rock) observed on the images. The TM data discriminated limonitic rocks from nonlimonitic rocks, as well as clays and carbonates, although an unambiguous identification of which of these minerals was present could not be made and required field checking. ESA

N93-24784# Bundesanstalt fuer Geowissenschaften und Rohstoffe, Hannover (Germany).

SATELLITE REMOTE SENSING FOR ENVIRONMENTAL GEOLOGY: THE BANDUNG (WEST JAVA) EXPERIENCE

Dietrich Bannert, P. H. Silitonga (Directorate of Environmental Geology, Bandung, Indonesia.), and Michael Siebenhuener (German Environmental Geological Advisory Team, Bandung, Indonesia.) *In* ESA, Environment Observation and Climate Modelling Through International Space Projects. Volume 2: Remote Sensing for Environmental Monitoring and Resource Management 1992 p 461-464 (For primary document see N93-24775 09-43)

Copyright Avail: CASI HC A01/MF A04; ESA, EPD, ESTEC, Noordwijk, Netherlands, HC

Experience in satellite remote sensing for environmental geology of greater Bandung in Java (Indonesia) is discussed. The details of the following are described: data collection, remote sensing, groundwater data, industrial minerals and rocks, soil data, and landslide inventory. Greater Bandung is rapidly expanding and poses great problems for the environment. The land is intensively used and future changes in land use will have to be carefully planned in order to minimize the risk of future environmental damage. The compilation of various data leads to a complete assessment of the natural and environmental potential of the area. SPOT image interpretation was among the most important data sources for actualization of the urban and land use map and for the evaluation and identification of environmental and engineering geological problems. ESA

N93-24785# Fernerkundungszentrum, Potsdam (Germany).

APPLICATION OF REMOTE SENSING DATA FOR THE INVESTIGATION OF ENVIRONMENTAL DEGRADATION SITES IN EAST GERMANY

Karl-Heinz Marek *In* ESA, Environment Observation and Climate Modelling Through International Space Projects. Volume 2: Remote Sensing for Environmental Monitoring and Resource Management 1992 p 465-469 (For primary document see N93-24775 09-43)

Copyright Avail: CASI HC A01/MF A04; ESA, EPD, ESTEC, Noordwijk, Netherlands, HC

Environmental problems, specifically those brought about by anthropogenic change and degradation of landscapes--which is marked by the decreasing use of land for agricultural and forestry purposes and the increasing use of land for open coal mining, military bases, and waste sites--are addressed. The availability and practical use of remote sensing data from space for environmental monitoring and recycling of such suspected areas was demonstrated at damaged sites in the eastern part of Germany. The methodological approach of the assessment is based on deriving environmental indicators like land use pattern, thermal pattern, vegetation, and other indices from space-based remote sensing data. The multitemporal analysis and combination of these complex indicators allow recognition of the environmental processes. ESA

N93-24786# Institute of Geodesy and Cartography, Warsaw (Poland). Remote Sensing and Spatial Information Centre.

APPLICATION OF REMOTE SENSING TO ENVIRONMENTAL MONITORING IN POLAND

Bogdan I. Ney *In* ESA, Environment Observation and Climate Modelling Through International Space Projects. Volume 2: Remote Sensing for Environmental Monitoring and Resource Management 1992 p 471-472 (For primary document see N93-24775 09-43)

Copyright Avail: CASI HC A01/MF A04; ESA, EPD, ESTEC, Noordwijk, Netherlands, HC

Aerial panchromatic and false color infrared photographs and thermal scanner images were the first sources of information to study environmental change in Poland since the beginning of the seventies. A full range of available satellite data (Landsat Multispectral Scanner and Thematic Mapper, SPOT, NOAA, and Soviet space photographs acquired by automatic satellites of the Cosmos series and manned space missions) are now in use. More than 200 research and application projects were completed during the sixteen years of activity of the Polish remote sensing center. These projects were connected with forest appraisal studies, agricultural studies (soil moisture, evapotranspiration, statistics), surveys on land use changes (including detailed studies of man induced transformation of the environment), and water and air pollution studies. The geographical information system SINUS, which is oriented to monitoring of the environment at regional level, was developed at the center. The Polish National Point of the GRID

program was established in 1991. Many projects are conducted within the Intercosmos program, and current participation is in establishing the PRIRODA project. Collaboration has also started with ESA and national space agencies in western Europe, and it is hoped that ERS-1 and other programs will be effective for environmental monitoring and studies in Poland. ESA

N93-24787# Commission of the European Communities, Brussels (Belgium).

LAND COVER, AN ESSENTIAL COMPONENT OF THE CORINE INFORMATION SYSTEM ON THE ENVIRONMENT: GIS IMPLICATIONS

M.-H. Cornaert and J. Maes *In* ESA, Environment Observation and Climate Modelling Through International Space Projects. Volume 2: Remote Sensing for Environmental Monitoring and Resource Management 1992 p 473-481 (For primary document see N93-24775 09-43)

Copyright Avail: CASI HC A02/MF A04; ESA, EPD, ESTEC, Noordwijk, Netherlands, HC

Aspects of the Commission of the European Communities' CORINE (Coordination of Information on the Environment) program are presented. The results of this program will constitute an essential input to the setting up of the European Environment Agency. The results are of three types: European expert networks to work together at common targets; common methods and nomenclatures; and a series of thematic data bases integrated in the CORINE Geographical Information System (GIS). The main GIS data sets concern biotopes (sites important for nature conservation), soil quality and erosion risk, coastal erosion risk, emissions into the air, land cover as well as geographic and socio-economic background information. The use of these data in a GIS environment, linked to data base management and statistical packages, provides a powerful tool for the generation of information for environment and physical planning policies, at Community, national and regional levels. ESA

N93-24788# Ceskoslovenska Akademie Ved, Prague. Information Theory and Automation Inst.

THE REGIONAL PLANNING AND CONTROL USING THE SATELLITE DATA

Dana Klimesova, Jan Havel, and Stanislav Saic *In* ESA, Environment Observation and Climate Modelling Through International Space Projects. Volume 2: Remote Sensing for Environmental Monitoring and Resource Management 1992 p 483-487 (For primary document see N93-24775 09-43)

Copyright Avail: CASI HC A01/MF A04; ESA, EPD, ESTEC, Noordwijk, Netherlands, HC

The results of a project concerning the use of remote sensing information in environmental protection are presented. This project is closely connected with the CORINE (Coordination of Information in the Environment) land cover project, whose capabilities it extends into the regional sphere by using 1:50,000 scale and greater resolution of input data. Much of the obtained information is directly applicable in regional planning and control. Image analysis and classification were applied on Landsat Thematic Mapper data and SPOT images covering the area of two districts. The land units containing risk factors were covered by the aerial photographs, time series of photos, or videotape data. ESA

N93-24789# Winand Staring Centre, Wageningen (Netherlands).

LAND COVER MONITORING IN THE NETHERLANDS APPLYING SATELLITE REMOTE SENSING

G. J. A. Nieuwenhuis, J. D. vanAmsterdam, C. G. J. Schotten, and H. A. M. Thunnissen *In* ESA, Environment Observation and Climate Modelling Through International Space Projects. Volume 2: Remote Sensing for Environmental Monitoring and Resource Management 1992 p 489-495 (For primary document see N93-24775 09-43)

Copyright Avail: CASI HC A02/MF A04; ESA, EPD, ESTEC, Noordwijk, Netherlands, HC

The production of a complete digital land cover database of the Netherlands with Landsat TM (Thematic Mapper) images, mainly acquired in the Summer of 1986, is reported. For several reasons only one image was applied during the growing season, hence, less accurate results were obtained for specific land cover classes. On a relatively global scale (1:100,000 and smaller), the available database can be applied on a national level, while derived statistics are applicable at a regional level, especially for agricultural areas. Methods were developed to improve the classification results based on a multitemporal analysis of satellite data and on integration with ancillary data such as digitized topographical maps and soil maps. The developed method was tested for a province in the southern part of the Netherlands. Since, in humid regions such as the Netherlands, data acquisition in the short wave range of the electromagnetic spectrum may cause problems, the application of ERS-1 radar images, in addition to images taken in the short wave range, was investigated. The first results were promising. ESA

N93-24790# Osnabrueck Univ. (Germany).

MONITORING AND ANALYSIS OF URBAN TRENDS USING MULTITEMPORAL SATELLITE-IMAGERY (CASE-STUDY: GREATER CAIRO)

Marion Czeranka *In* ESA, Environment Observation and Climate Modelling Through International Space Projects. Volume 2: Remote Sensing for Environmental Monitoring and Resource Management 1992 p 497-501 (For primary document see N93-24775 09-43)

Copyright Avail: CASI HC A01/MF A04; ESA, EPD, ESTEC, Noordwijk, Netherlands, HC

The use of a LANDSAT Thematic Mapper and SPOT data to examine the metropolitan area of Greater Cairo (Egypt), in the context of serious problems caused by the rapid increase in population and the resulting dynamic development, is reported. The monitored period of 10 years required different sensor data for the time points in 1979, 1982, and 1988. Consequently, a method was developed using a combination of unsupervised classification, image interpretation, and overlay techniques to perform a post classification comparison. The resulting land use/land cover changes provide current information about regional development patterns. Thus, it is possible to point out some differences in development concerning trends on arable land and on desert land, as well as for different political units within the conurbation. This feasibility study shows that, especially for large urban areas with uncontrolled development, monitoring within multitemporal satellite data is, indeed, appropriate to meet planners needs if there is a lack of fundamental and up to date data. ESA

N93-24791# National Center for Scientific Research of Vietnam, Hanoi. Remote Sensing Application Div.

DETECTION OF LAND USE/LAND COVER CHANGES USING REMOTE SENSING AND GIS IN VIETNAM

Pham Trung Luong *In* ESA, Environment Observation and Climate Modelling Through International Space Projects. Volume 2: Remote Sensing for Environmental Monitoring and Resource Management 1992 p 503-507 (For primary document see N93-24775 09-43)

Copyright Avail: CASI HC A01/MF A04; ESA, EPD, ESTEC, Noordwijk, Netherlands, HC

A study to develop a procedure for application of remote sensing and GIS (Geographic Information System) to analysis of land use/land cover changes is described. The study was carried out for coastal areas of the Red and Mekong river plains, where the land use/land cover is most changed according to human activities. The multitemporal land use/land cover maps produced from visual interpretation of different sensing data were digitized and integrated into GIS. The land use/land over were analyzed by a GIS overlay technique. ESA

N93-24792# Technische Univ., Munich (Germany). Standing Work Group Remote Sensing.

GEOLOGIC AND HYDROGEOLOGIC MAPPING OF ICELAND WITH MULTISENSOR DATA (JERS-1, ERS-1, SPOT, LANDSAT AND SEASAT)

U. Muenzer and C. Boehm *In* ESA, Environment Observation and Climate Modelling Through International Space Projects. Volume 2: Remote Sensing for Environmental Monitoring and Resource Management 1992 p 509-511 (For primary document see N93-24775 09-43)

Copyright Avail: CASI HC A01/MF A04; ESA, EPD, ESTEC, Noordwijk, Netherlands, HC

Tasks for a program of geological, hydrogeological petrographic, tectonic, and environmental research on Iceland, to be carried out from 1992-1994, are outlined. A major objective is the compilation and interpretation of maps based on multisensor and multitemporal remote sensing data obtained from JERS-1 (optical sensors and SAR (Synthetic Aperture Radar)), ERS-1 (SAR), Landsat (multispectral scanner and Thematic Mapper), SPOT High Resolution Visible (HRV), and SEASAT (SAR). Spectrometric in situ measurements and laboratory analyses are to be made as well. Results

are expected to greatly facilitate the identification and interpretation of terrain features to lead to greater detail and accuracy in cartographic work. ESA

N93-24793# Byelorussian Scientific and Technical Centre of Environment Remote Diagnostics (Byelarus).

AEROSPACE TECHNIQUES IN RADIATION AND ECOLOGICAL MONITORING OF THE REPUBLIC BELARUS

I. I. Lishtvan, L. I. Kiselevskii, A. A. Kovalyov, S. B. Kostyukevich, and V. S. Dragun *In* ESA, Environment Observation and Climate Modelling Through International Space Projects. Volume 2: Remote Sensing for Environmental Monitoring and Resource Management 1992 p 513-517 (For primary document see N93-24775 09-43)

Copyright Avail: CASI HC A01/MF A04; ESA, EPD, ESTEC, Noordwijk, Netherlands, HC

Remote sensing techniques used for monitoring radiation and ecological contamination in Belarus (U.S.S.R.) caused by the Chernobyl catastrophe and technogenic activity are reported. An international project of complex radiation and ecological monitoring, using aerospace, mobile, and ground technical facilities was created. Maps of exposure rates and cesium-137 and potassium-40 distribution were made and published on the basis of helicopter measurement data received by the aero-gammaspectrometer 'Macfar 2' and ground measurement results. A number of ecological maps were created. ESA

N93-24794# Telespazio, S.p.A., Rome (Italy).

DETERMINATION OF ENVIRONMENTAL DYNAMICS USING NOAA SATELLITE DATA AND A WATER BALANCE MODEL FOR THE MEDITERRANEAN LANDSCAPE

P. Peroni, A. DEpifanio, and C. Martellacci *In* ESA, Environment Observation and Climate Modelling Through International Space Projects. Volume 2: Remote Sensing for Environmental Monitoring and Resource Management 1992 p 519-523 (For primary document see N93-24775 09-43)

Copyright Avail: CASI HC A01/MF A04; ESA, EPD, ESTEC, Noordwijk, Netherlands, HC

The analysis of vegetation condition during the critical season in the Mediterranean area (Summer period) was performed. The analysis was carried out with a synthetic approach to the study of the vegetation dynamics in terms of the physiological state, which is a function of the main components: vegetation cover, water availability, and photosynthetic activity. A synthetic stress index was defined from the integration of static (land use map) and dynamic information coming from NOAA AVHRR (Advanced Very High Reolution Radiometer) satellite data and from the output of the Thornthwaite water balance model. Applications to the island of Sardinia and preliminary results for the year 1989 are presented. Results suggest that an integrated approach to a dynamic phenomenon can represent a useful instrument in regional control planning for forest fire prevention. ESA

N93-24795# Telespazio, S.p.A., Rome (Italy). Remote Sensing Dept.

AGROCLIMATOLOGICAL ZONATION BY AVHRR DATA FOR VEGETATION MONITORING

R. Benedetti, P. Rossini, and M. Sernicola *In* ESA, Environment Observation and Climate Modelling Through International Space Projects. Volume 2: Remote Sensing for Environmental Monitoring and Resource Management 1992 p 525-530 (For primary document see N93-24775 09-43)

Copyright Avail: CASI HC A02/MF A04; ESA, EPD, ESTEC, Noordwijk, Netherlands, HC

A study which aims firstly, to define areas with homogeneous time NDVI (Normalized Difference Vegetation Index) profile characterized by a similar vegetation composition and timing, and then to select and identify, within these zones, areas with different photosynthetic potential and productivity is presented. Advanced Very High Resolution Radiometer (AVHRR) images from NOAA 9 and 11 were used. The method chosen is an unsupervised classification of each single pixel NDVI profile, with a posteriori interpretation of each class obtained. The timeframe chosen is the four year span between 1986 and 1989, and the study area considered is the Mediterranean region centered on Italy. Thirty-nine (39) homogeneous areas with different photosynthetic potential and timing are produced and grouped in 17 main typologies of land cover. ESA

N93-24796# Centro Studi ed Applicazioni in Tecnologie Avanzate, Bari (Italy).

A KNOWLEDGE-BASED APPROACH TO WASTE DISPOSAL SITES DETECTION THROUGH INTEGRATION OF LANDSAT-TM IMAGERY AND GEOGRAPHICAL CONTEXT INFORMATION

R. Loguercio-Polosa, C. Piccinni, N. Sciacovelli, and A. M. Tonelli *In* ESA, Environment Observation and Climate Modelling Through International Space Projects. Volume 2: Remote Sensing for Environmental Monitoring and Resource Management 1992 p 531-534 (For primary document see N93-24775 09-43)

Copyright Avail: CASI HC A01/MF A04; ESA, EPD, ESTEC, Noordwijk, Netherlands, HC

A satellite image interpretation methodology using a knowledge based approach is presented. The methodology integrates traditional image processing techniques and knowledge of spectral, spatial, and contextual properties. The method is intended for use on Landsat TM (Thematic Mapper) imagery in processes of waste disposal site detection. The integration model used is based on the Dempster Shafer theory of evidence which offers a suitable data fusion and uncertainty handling framework. The knowledge necessary to drive the detection process is derived from the results of spectral and spatial analyses performed on the training Landsat TM scene and from other information relating to specific properties and features of dump sites. ESA

N93-24797# Consiglio Nazionale delle Ricerche, Naples (Italy). Land Planning Inst.

USE OF REMOTE SENSING AND GIS FOR THE ENVIRONMENTAL PLANNING PROPOSAL OF THE SARNO RIVER VALLEY (CAMPANIA, SOUTHERN ITALY) Final Report

F. Jemma *In* ESA, Environment Observation and Climate Modelling Through International Space Projects. Volume 2: Remote Sensing for Environmental Monitoring and Resource Management 1992 p 535-539 (For primary document see N93-24775 09-43)

Copyright Avail: CASI HC A01/MF A04; ESA, EPD, ESTEC, Noordwijk, Netherlands, HC

The final report of a multidisciplinary research project into the definition and experimentation, in a pilot area, of an environmental planning methodology is presented. The methodology is thought of as a continuous process of territorial management coherent with the hydrogeological reclamation of the study area and the reduction to the miniumum level of the water pollution hazard. The environmental water planning methodology together with the contribution that Geographic Information System (GIS) and satellite remote sensing give for the land use data collection, analysis, processing, and management, are reported and discussed. ESA

N93-24798# Bulgarian Academy of Sciences, Sofia. Space Research Inst.

COMPLEX INVESTIGATION OF A SYSTEM INDUSTRIAL SITE-ENVIRONMENT USING REMOTE SENSING AND LANDSCAPE-GEOCHEMICAL METHODS

H. Spiridonov, E. Roumenina, and L. Milenova *In* ESA, Environment Observation and Climate Modelling Through International Space Projects. Volume 2: Remote Sensing for Environmental Monitoring and Resource Management 1992 p 541-545 (For primary document see N93-24775 09-43)

Copyright Avail: CASI HC A01/MF A04; ESA, EPD, ESTEC, Noordwijk, Netherlands, HC

A prerequisite for the successful development of a complex of measures for protection of the environment and the rational exploration of natural resources in industrially loaded landscapes is the investigation of qualitative and quantitative characteristics of pollutants, emitted into environment. The basic results are presented from the complex application of remote sensing and landscape-geochemical methods in one region within the territory of Bulgaria. Thematic and landscape geochemical and water pollution data maps are drawn using aero and space images. The character of industrial emission is investigated. The accumulation of industrial emissions in soils and vegetation is followed for each separate elementary landscape. The results obtained from the complex investigation work on the territory of the industrial site environment system are used in determining the points for operative pollution control of elementary landscapes in areas of industrial impact for the purpose of environmental status, assessment, and prognostication. ESA

N93-24799# Consiglio Nazionale delle Ricerche, Florence (Italy). Ist. di Ricerca sulle Onde Elettromagnetiche.

ARCHAEOLOGICAL, HISTORICAL AND GEOELECTRICAL DATA AS GROUND TRUTH FOR LANDSAT TM IMAGERY APPLICATION TO COASTAL PLAIN EVOLUTION STUDIES

V. Alessandro, F. Maselli, M. Pieri (REDAT, Rome, Italy.), E. Pranzini (Florence Univ., Italy.), and V. Zichella (Florence Univ., Italy.) *In* ESA, Environment Observation and Climate Modelling Through International Space Projects. Volume 2: Remote Sensing for Environmental Monitoring and Resource Management 1992 p 547-551 (For primary document see N93-24775 09-43)

Copyright Avail: CASI HC A01/MF A04; ESA, EPD, ESTEC, Noordwijk, Netherlands, HC

Some examples of the integration of archaeological, historical, and geoelectrical data with Thematic Mapper (TM) remotely sensed data are presented. The different case studies were drawn from research carried out on the Tuscan coastal plains (Italy) where this procedure allowed reliable results to be obtained. Archaeological and historical data have both aided the interpretation of remotely sensed images and directed image processing towards the highlighting of specific features whose existence they suggest. Geoelectrical soundings have solved some problems arising from the disagreement between remotely sensed data and archaeological and/or historical ones. The various types of data are concluded to serve as ground truth in remote sensing when this is applied to the study of the geomorphological evolution of coastal plains. Archaeological findings as well as literary sources and old maps give detailed information that can be used to date forms and processes. Vertical geoelectrical soundings can sometimes explain anomalous spectral behaviors of the soil surface and help in relating image interpretation with 'remote' data. ESA

N93-24800# Palermo Univ. (Italy). Ist. di Agronomia Generale e Coltivazione Erbacee.

THE PHOTOINTERPRETATION OF THE AREA TAKEN OVER FROM AGRICULTURE BY INTENSE URBANIZATION AT VILLABATE (PALERMO, ITALY)

Salvatore Raimondi *In* ESA, Environment Observation and Climate Modelling Through International Space Projects. Volume 2: Remote Sensing for Environmental Monitoring and Resource Management 1992 p 553-556 (For primary document see N93-24775 09-43)

Copyright Avail: CASI HC A01/MF A04; ESA, EPD, ESTEC, Noordwijk, Netherlands, HC

A study on area taken away from agricultural activity in the territory of the commune of Villabate (Palermo, Sicily) between 1968 and 1987 by photointerpretation is reported. The results showed up the effects of next few years urban expansion on the studied areas and damages on the soils with high agronomic potentiality. The wise choice of an area, based on pedological studies and interpretations of the latter, could save soils with high productive capacities for agriculture, while those with lower potentiality could be used for nonagricultural purposes. ESA

N93-24801# Technical Research Centre of Finland, Espoo. Instrument Lab.

DEMONSTRATION OF SEASONAL CHANGES IN THE TERRITORY OF FINLAND USING MULTITEMPORAL NOAA-AVHRR DATA

Kaj Andersson *In* ESA, Environment Observation and Climate Modelling Through International Space Projects. Volume 2: Remote Sensing for Environmental Monitoring and Resource Management 1992 p 557-558 (For primary document see N93-24775 09-43)

Copyright Avail: CASI HC A01/MF A04; ESA, EPD, ESTEC, Noordwijk, Netherlands, HC

Work to demonstrate the possibilities of remote sensing in monitoring the Earth environment is reported. An image display system was developed for displaying sets of consecutive remote sensing images on a powerful UNIX workstation. The first image set gave the impression that the viewer was approaching the Earth from outer space. In the uppermost level the whole Earth globe could be seen and the following images showed the views from Meteosat, NOAA, Landsat MSS (Multispectral Scanner), Landsat TM (Thematic Mapper), SPOT and scanned aircraft images. The lowest level image was constructed from different sets of geophysical data and it showed the 'scene' from below the surface of the Earth. The second image set consisted of partly cloud free NOAA AVHRR satellite images acquired over Finland in 1991 and were displayed in a sequence to demonstrate the seasonal changes in the nature. ESA

N93-24802# Ghent Univ. (Belgium). Regional Geography and Landscape Science Lab.

THE USE OF REMOTE SENSING AND GIS FOR THE ASSESSMENT OF ENVIRONMENTAL DEGRADATION CAUSED BY FIRES, APPLIED UPON SOUTH-EUBOIA (CENTRAL GREECE)

Beata Maria DeVliegher *In* ESA, Environment Observation and Climate Modelling Through International Space Projects. Volume 2: Remote Sensing for Environmental Monitoring and Resource Management 1992 p 559-564 (For primary document see N93-24775 09-43)

Copyright Avail: CASI HC A02/MF A04; ESA, EPD, ESTEC, Noordwijk, Netherlands, HC

A study to map the risk of environmental degradation by fires using a multisource and multitemporal data set and a combined and integrated research using the ILWIS (Integrated Land and Watershed Information System) is presented. Five thematic maps together with the localization map of the fires during 1981-1989 are stored in the GIS (Geographic Information System). Additional data about the area, date, owner and type of vegetation were also imported. The factors form part of a hierarchical system indicating the influence: vegetation, altitude/aspects, slope/accessibility. In correspondence with the rank, a weight is given; a score is assigned for each category according to the risk. The combination of the single risk for each factor gives the fire risk which is ranked into four classes (none to severe). ESA

N93-24803# Musee Royal de l'Afrique Centrale, Tervuren (Belgium). Lab. de Teledetection Aerospatiale.

LITHOLOGIC MAPPING WITH LANDSAT THEMATIC MAPPER GUIDED BY LABORATORY SPECTRAL MEASUREMENTS, AIR, NIGER (AFRICA)

P. Trefois and C. Volon *In* ESA, Environment Observation and Climate Modelling Through International Space Projects. Volume 2: Remote Sensing for Environmental Monitoring and Resource Management 1992 p 565-570 (For primary document see N93-24775 09-43)

Copyright Avail: CASI HC A02/MF A04; ESA, EPD, ESTEC, Noordwijk, Netherlands, HC

The identification of different lithologies in the Air Massif (Niger, Africa) from satellite data is based on the knowledge of the spectral signatures from minerals and rocks collected during several field surveys. This spectral study is thus performed by a deterministic type of image processing. High resolution spectral reflectance signatures of these samples were measured in the laboratory and interpreted. The link with the remotely sensed data is established through a calibration procedure, using the 5S atmospheric correction model. After calibrating TM (Thematic Mapper) data to reflectance factors, a ratio technique was adopted in order to minimize the effects of topography. Color composite of a combination of TM bands ratios (5/7, 5/1, (3+5)/4; Crippen, 1988), is displayed and interpreted to emphasize the spectral features related to hydroxil or carbonate band absorptions, and to the presence of ferrous and ferric ions. ESA

N93-24804# United Nations, New York, NY. Outer Space Affairs Div.

NATURAL DISASTERS AND THEIR MITIGATION USING SPACE TECHNOLOGY

Adigun Ade Abiodun *In* ESA, Environment Observation and Climate Modelling Through International Space Projects. Volume 2: Remote Sensing for Environmental Monitoring and Resource Management 1992 p 573-580 (For primary document see N93-24775 09-43)

Copyright Avail: CASI HC A02/MF A04; ESA, EPD, ESTEC, Noordwijk, Netherlands, HC

The attribution of a significant number of events that are classified as natural disasters to environmental mismanagement is addressed. These contributing factors and the roles of space science and technology in their understanding and mitigation are reviewed. Potential future ground and space based programs specifically dedicated to disaster mitigation are highlighted. The need to address other associated elements that could enhance the effectiveness of a disaster mitigation program is emphasized. ESA

N93-24805# Bristol Univ. (England). Remote Sensing Unit.
ALTERNATIVE STRATEGIES FOR THE USE OF SATELLITE DATA ANALYSIS SYSTEMS FOR HAZARD MONITORING AND DISASTER MITIGATION
Eric C. Barrett and Michael J. Beaumont *In* ESA, Environment Observation and Climate Modelling Through International Space Projects. Volume 2: Remote Sensing for Environmental Monitoring and Resource Management 1992 p 581-586 (For primary document see N93-24775 09-43)
Copyright Avail: CASI HC A02/MF A04; ESA, EPD, ESTEC, Noordwijk, Netherlands, HC

A feasibility study to identify and evaluate comparatively the range of options for a satellite based snow monitoring operation in the United Kingdom, to improve near real time intelligence on snow area, type, depth and water equivalence, dependent advisories on flood potential and peaks of river water acidity, and the organization of disaster mitigation responses, is presented. The arguments and conclusions arrived at through this study are reviewed and compared with those encountered in Pakistan, a developing country, for which a more broadly based satellite environmental monitoring system was designed. The parameters already involved in this case include rainfall and vegetation productivity in addition to snow, and others considered for future incorporation in the system include temperatures at or near the ground, fires, and intense storms (both mesoscale, for example severe convective storms, and synoptic scale, for example tropical cyclones). Key factors identified as affecting the choice of satellite system for such operational uses in different types of countries are reviewed and discussed. It is concluded that quite different satellite environmental monitoring infrastructural strategies might be necessary in countries in different stages of development. ESA

N93-24806# Dornier System G.m.b.H., Friedrichshafen (Germany). Earth Observation Data Service.
SATELLITE BORNE REMOTE SENSING DATA: A TOOL FOR NATURAL DISASTER REDUCTION
F. Jaskolla and U. Lohr *In* ESA, Environment Observation and Climate Modelling Through International Space Projects. Volume 2: Remote Sensing for Environmental Monitoring and Resource Management 1992 p 587-590 (For primary document see N93-24775 09-43)
Copyright Avail: CASI HC A01/MF A04; ESA, EPD, ESTEC, Noordwijk, Netherlands, HC

The recently available ERS-1 data offers for the first time the opening up of new fields of application due to their unique capability to provide information independent of weather or illumination conditions. Although the fact that ERS-1 is not an operational system providing environmental data, it can be demonstrated, that the phenomena to be measurable by ERS-1 can be designated as of utmost significance for the task in mind. In particular, the relatively simple detectability of flooded areas or the differentiability of areas affected by volcanic eruptions underline the generally high potential of this type of data. ESA

N93-24807# Ludwig-Maximilians-Univ., Munich (Germany). Remote Sensing Working Group.
APPLICATION OF MULTITEMPORAL LANDSAT-MSS AND -TM DATA FOR THE DEVELOPMENT OF AN INUNDATION-RISK-MAP
H. Mehl and K. Hiller (Deutsche Forschungsanstalt fuer Luft- und Raumfahrt, Oberpfaffenhofen, Germany.) *In* ESA, Environment Observation and Climate Modelling Through International Space Projects. Volume 2: Remote Sensing for Environmental Monitoring and Resource Management 1992 p 591-594 Sponsored by BMFT (For primary document see N93-24775 09-43)
Copyright Avail: CASI HC A01/MF A04; ESA, EPD, ESTEC, Noordwijk, Netherlands, HC

Investigation carried out in the northwest of the province Buenos Aires (Argentina) to assess temporal and spatial surface changes of inundated areas with Landsat data (MSS (Multispectral Scanner), TM (Thematic Mapper)) are reported. For preparation of an inundation risk map, different approaches involving both simple image processing techniques and more sophisticated IHS (Intensity, Hue, Saturation) processing procedures were analyzed. The use of ratios gave suitable results for the extraction of water masks and their transformation into a map meeting cartographical standards. However, the procedure leading to the final map is very cost intensive. Therefore, a different multitemporal IHS approach was realized. Based on the multitemporal response of the principle components and the suitable use of an IHS transformation a new concept for the derivation of a computer based multitemporal product similar to a conventional risk map is demonstrated. ESA

N93-24808# Natural Resources Inst., Chatham (England).
SUSTAINABLE REMOTE SENSING: A MAJOR IMPROVEMENT FOR REALTIME RESOURCE MANAGEMENT AND DISASTER EARLY WARNING IN DEVELOPING COUNTRIES
J. B. Williams, J. Stephenson (Bradford Univ., England.), G. DSouza (Cranfield Inst. of Tech., Bedford, England.), and J. R. Milford (Reading Univ., England.) *In* ESA, Environment Observation and Climate Modelling Through International Space Projects. Volume 2: Remote Sensing for Environmental Monitoring and Resource Management 1992 p 595-598 (For primary document see N93-24775 09-43)
Copyright Avail: CASI HC A01/MF A04; ESA, EPD, ESTEC, Noordwijk, Netherlands, HC

To become sustainable and realize their potential for environmental monitoring in most developing countries, remote sensing techniques must be practical and be integrated into existing operational activities with minimal running costs. A program of technology transfer starting with direct Meteosat reception, continuing with NOAA, and leading on to higher resolution satellite applications appears to constitute a pragmatic and sustainable approach for even the poorest countries. Experience gained from working with a dozen operational low cost satellite receivers in developing countries is summarized. ESA

N93-24809# Compagnia Italiana Servizi Tecnici, Rome. Space Div.
USE OF REMOTE SENSING SPACECRAFTS IN REAL TIME SUPPORT TO DISASTER MANAGEMENT: INTERFACES WITH GROUND SEGMENT FACILITIES AND SERVICES
A. TortoriciMontaperto and F. Rossi *In* ESA, Environment Observation and Climate Modelling Through International Space Projects. Volume 2: Remote Sensing for Environmental Monitoring and Resource Management 1992 p 599-604 (For primary document see N93-24775 09-43)
Copyright Avail: CASI HC A02/MF A04; ESA, EPD, ESTEC, Noordwijk, Netherlands, HC

The demands by the current and planned utilization of remote sensing spacecraft in disaster management for facilities and services able to provide products characterized by fast delivery from acquisition, optimum source selection and integration of several data into a metadata, is addressed. This demand imposes on the existing space related infrastructure functional and performance requirements to build up an integrated system. Research to identify, detail, and assign to relevant entities the upgrading requirements, taking into account what already exists in terms of spacecrafts (and related payloads) and of ground infrastructure, is reported. This is performed by analyzing the interfaces of the regional operations center with the space related facilities (payload coordination center, user centers, processing and archiving facilities, acquisition stations). A key aspect addressed in this context is the concept of metadata, with respect to its applicability within real time environment monitoring. ESA

N93-24810# International Inst. for Aerospace Survey and Earth Sciences, Enschede (Netherlands). Applied Geomorphology Div.
A METHOD FOR SEQUENTIAL IMAGE ANALYSIS OF HAZARD AREAS
Jan J. Nossin *In* ESA, Environment Observation and Climate Modelling Through International Space Projects. Volume 2: Remote Sensing for Environmental Monitoring and Resource Management 1992 p 605-610 (For primary document see N93-24775 09-43)
Copyright Avail: CASI HC A02/MF A04; ESA, EPD, ESTEC, Noordwijk, Netherlands, HC

A method is presented for digitizing air photos in time sequence, and digitally referencing them to SPOT imagery, or to a topographic map. The sequential analysis allows the monitoring of the development of geomorphic hazards over time, and forecasting their possible further development. The eastern Colombian Andes front serves as a study area, where mass movements and fluvial dynamics are analyzed. Equipment used is an Agfa-Focus 2 flatbed scanner with MacView 2 2.0 software, and an EarthProbeOne image processing system. ESA

N93-24811# SPOT Image Corp., Toulouse (France).
THE USE OF SPOT DATA IN NATURAL DISASTER PREVENTION AND DAMAGE ASSESSMENT

J. C. Rivereau *In* ESA, Environment Observation and Climate Modelling Through International Space Projects. Volume 2: Remote Sensing for Environmental Monitoring and Resource Management 1992 p 611-613 (For primary document see N93-24775 09-43)
Copyright Avail: CASI HC A01/MF A04; ESA, EPD, ESTEC, Noordwijk, Netherlands, HC

SPOT can efficiently contribute to gather valuable information in disaster prevention and preparedness, damage assessment and disaster relief. In disaster prevention, risk analysis requires the compilation of information extracted from SPOT data: land use, infrastructures, topography and morphology (DEM (Digital Elevation Model)), hydrography, geology, soil types. The information is introduced into geographic information systems to establish hazard maps and risk potentialities. Vulnerability maps and contingency plans are thus derived by adding socio-economic factors. In case of disaster, the assessment of damage is vital to undertake relief measures and in the long term recovery and rehabilitation planning. In remote areas, SPOT images are often the only means of investigation if timely data can be obtained. For immediate disaster relief purposes, the use of SPOT is hampered by the difficulty to acquire good data in a very short period of time. But preparedness and disaster mitigation is strongly improved, in hazard prone areas, by establishing well in advance contingency studies to plan prevention means and measures. These documents are particularly useful to authorities to anticipate and plan energy actions according to actual situation and prevailing conditions. In the long term, SPOT data efficiently contribute to reconstruction and rehabilitation planning. ESA

N93-24812# Academy of Sciences (USSR), Moscow. MAB WG Aerospace Methods.
AEROSPACE MONITORING FOR ECOLOGICAL HAZARD AND DISASTER MITIGATION
B. V. Vinogradov and D. E. Frolov *In* ESA, Environment Observation and Climate Modelling Through International Space Projects. Volume 2: Remote Sensing for Environmental Monitoring and Resource Management 1992 p 615-618 (For primary document see N93-24775 09-43)
Copyright Avail: CASI HC A01/MF A04; ESA, EPD, ESTEC, Noordwijk, Netherlands, HC

The analysis of long term (no less than 10 to 30 years) aerial and space surveys for regional disaster monitoring in Russia is reported. Trend analysis of the aerospace monitoring of expansion of drift sands over the Kalmykia during 1954-1984 was used to predict full disaster degradation to 1992. More advanced technology based on a system approach using Markovian chains permitted forecasting of land desertification over the Amudarya delta to 2010. The verification of such a forecast revealed the error to be near 10 percent for 5 predicted years. Operations on models based on space supported dynamic models revealed the nonstability date of turning points which fell at the beginning of the 1970s. The format of the Dynamic EcoGeoInformation System was developed. ESA

N93-24813# GKSS-Forschungszentrum Geesthacht (Germany).
THE NEED FOR SPACEBORNE OBSERVATIONS FOR METEOROLOGY AND CLIMATOLOGY **c46**
E. Raschke *In* ESA, Environment Observation and Climate Modelling Through International Space Projects. Volume 2: Remote Sensing for Environmental Monitoring and Resource Management 1992 p 621-623 (For primary document see N93-24775 09-43)
Copyright Avail: CASI HC A01/MF A04; ESA, EPD, ESTEC, Noordwijk, Netherlands, HC

A discussion on the global availability of observations for Earth weather and climate analyses is presented. Some examples of presently available spaceborne information for weather analyses are given. Concentration is only on the climate system from the troposphere down to the ground. Thermodynamic properties of the atmosphere and surface, atmospheric wind fields, and various relevant properties of the surface, are discussed. Other information for climate research, including radiation budget parameters and precipitation, are described. The lack of efficient and accurate methodologies to derive quantities describing the weather and Earth climate from satellite measurement is discussed. A recommendation for major investment in data analysis techniques and verification studies is made. ESA

N93-24814# Technische Univ., Munich (Germany). Remote Sensing Working Group.
REMOTE SENSING OF NON-RENEWABLE RESOURCES
J. Bodechtel *In* ESA, Environment Observation and Climate Modelling Through International Space Projects. Volume 2: Remote Sensing for Environmental Monitoring and Resource Management 1992 p 625-628 (For primary document see N93-24775 09-43)
Copyright Avail: CASI HC A01/MF A04; ESA, EPD, ESTEC, Noordwijk, Netherlands, HC

The application objectives of remote sensing in geological and mineralogical sciences and the use of optical remote sensing are described. A comparison of the measurement capabilites of several scanner systems and the reflectivity properties of common surface minerals is given. Physical properties to be measured for nonrenewable resources are given. Advantages of microwave remote sensing are discussed. Existing remote sensing data sources are reviewed. User requirements for future satellite systems to extend the possibilities for the application of remote sensing data from space and to enable thematic evaluation on a scale of 1:50,000 to 1:100,000 are listed. The missions which these requirements call for are described. For nonrenewable resources, where phenomena can be analyzed directly only under certain optimum conditions using either multispectral or backscattered microwave information, a multisensor and multidata approach for identifying geology or pedology dependent indicators is essential. A payload combining an optical and a SAR (Synthetic Aperture Radar) sensor could provide the optimum operational capability, with the optical instrument yielding information about spectral behavior of the phenomena/indicators, and the radar giving the indispensable information on soil moisture, surface roughness, penetration and relief. ESA

N93-24815# Bundesanstalt fuer Geowissenschaften und Rohstoffe, Hannover (Germany).
REMOTE SENSING GEOLOGY
Dietrich Bannert *In* ESA, Environment Observation and Climate Modelling Through International Space Projects. Volume 2: Remote Sensing for Environmental Monitoring and Resource Management 1992 p 629-632 (For primary document see N93-24775 09-43)
Copyright Avail: CASI HC A01/MF A04; ESA, EPD, ESTEC, Noordwijk, Netherlands, HC

Earth resources satellite data for geological research is discussed. Imagery, as well as spectral data are widely used in lithological and structural mapping, groundwater, mineral and hydrocarbon prospecting, and in environmental geological investigations. Spectroradiometry supports field and remote sensing work. The discussion focuses on the indipensable need of the human interpretation of satellite derived data. From the side of the interpreter it requires a sound education in his geological or geoscientific profession. From the side of the image processing, it requires an optimized image for the task at hand. Sensor development and higher spatial resolution of future satellites cannot replace the human interpretation of the acquired data. Better data, however, will improve the results of the human interpreter. ESA

N93-24816# Zurich Univ. (Switzerland). Remote Sensing Labs.
REMOTE SENSING IN HYDROLOGY AND WATER MANAGEMENT
H. Haefner and A. H. Schumann (Ruhr Univ., Bochum, Germany.) *In* ESA, Environment Observation and Climate Modelling Through International Space Projects. Volume 2: Remote Sensing for Environmental Monitoring and Resource Management 1992 p 633-637 (For primary document see N93-24775 09-43)
Copyright Avail: CASI HC A01/MF A04; ESA, EPD, ESTEC, Noordwijk, Netherlands, HC

For water management activities runoff is the most important component of the hydrological cycle, and remote sensing applications serve to increase knowledge of the temporal and spatial distribution of runoff from rain and snow. A review on the methods and models used to assess, monitor, and forecast hydrological relevant input, process, and output variables related to runoff, using various remote sensing systems, and on future possibilities with advanced sensor system is presented. These sensors penetrate clouds and overcome the weather and daylight dependence of optical remote sensing data. In particular ERS-1 and similar satellites will augment water management applications. ESA

N93-24817# Freiburg Univ. (Germany).
POTENTIAL OPERATIONAL USE OF REMOTE SENSING FROM SPACE IN FORESTRY
G. Hildebrandt *In* ESA, Environment Observation and Climate Modelling Through International Space Projects. Volume 2: Remote Sensing for Environmental Monitoring and Resource Management 1992 p 639-646 (For primary document see N93-24775 09-43)
Copyright Avail: CASI HC A02/MF A04; ESA, EPD, ESTEC, Noordwijk, Netherlands, HC

The different information requirements for remote sensing for forestry purposes are described and the question as to how far remote sensing from space can accomplish these requirements is answered. The main problems and methodic ways to overcome these (at least to a satisfying extent) are discussed. This includes visual analysis of object related enhanced color composites, optimized digital classification and hybrid approaches for the evaluation, the prestratification of the survey area, the role of ancillary and multitemporal data, atmospheric corrections, and so on. Guided by latest examples it is demonstrated that much more information can be reliably extracted from high resolution optical satellite imagery as it is often described. An assessment of the various remote sensing systems is given. ESA

N93-24818# Joint Research Centre of the European Communities, Ispra (Italy). Inst. for Remote Sensing Applications.
REMOTE SENSING APPLIED TO AGRICULTURE STATE OF THE ART AND NEW TRENDS
Jean Meyer-Roux *In* ESA, Environment Observation and Climate Modelling Through International Space Projects. Volume 2: Remote Sensing for Environmental Monitoring and Resource Management 1992 p 647-649 (For primary document see N93-24775 09-43)
Copyright Avail: CASI HC A01/MF A04; ESA, EPD, ESTEC, Noordwijk, Netherlands, HC

The monitoring of agriculture using specific remote sensing methodology, such as that developed in the pilot project MARS (Monitoring Agriculture by Remote Sensing) is discussed. Crop inventories and control, requirements, and trends, are discussed. Successful remote sensing techniques have used mainly cartographic visual products. For continuous monitoring, some stable techniques are being implemented. Real time applications are also being implemented at the level of the Commission of the European Community. There are still strong limitations such as cloud cover preventing image acquisition, but at the same time, data such as ERS-1 are appearing on the market which could overcome some of these problems. Methodologies are rapidly improving for large scale applications specially with the implementation of geographic information systems, whose techniques are quite complementary with remote sensing techniques. ESA

N93-24819# Rijkswaterstaat, Delft (Netherlands). Survey Dept.
APPLICATIONS OF REMOTE SENSING FOR TIDAL WATERS, COASTAL AREAS AND INLAND WATERS
Roeland Allewijn *In* ESA, Environment Observation and Climate Modelling Through International Space Projects. Volume 2: Remote Sensing for Environmental Monitoring and Resource Management 1992 p 651-654 (For primary document see N93-24775 09-43)
Copyright Avail: CASI HC A01/MF A04; ESA, EPD, ESTEC, Noordwijk, Netherlands, HC

A review of the main aquatic applications of spaceborne and airborne remote sensing techniques is given. Examples of the use of remote sensing for operational management of Dutch tidal waters, coastal areas and inland waters are presented. Some priorities for further research on applications of remote sensing for water management are given. In conclusion, for future remote sensing research two priorities can be defined: a strong emphasis on the applications of remote sensing for which the information needs of users should form the starting point; and the need for integration of data acquisition and analysis methods to solve the many environmental problems of the Earth. ESA

N93-24820# Institute of Terrestrial Ecology, Bangor (Wales).
EUROPEAN APPLICATIONS OF SPACE-BORNE EARTH OBSERVATION FOR LAND COVER MAPPING
B. K. Wyatt and R. M. Fuller *In* ESA, Environment Observation and Climate Modelling Through International Space Projects. Volume 2: Remote Sensing for Environmental Monitoring and Resource Management 1992 p 655-659 Sponsored by British National Space Center; Dept. of the Environment, and Natural Environment Research Council (For primary document see N93-24775 09-43)
Copyright Avail: CASI HC A01/MF A04; ESA, EPD, ESTEC, Noordwijk, Netherlands, HC

Information on land surface cover and the manner with which this changes over time is needed for a variety of operational purposes. Data from spaceborne Earth observation offers a means of generating over extensive areas consistent and cost effective information in digital form, suitable for overlay with other geographically referenced data sets or for incoporation directly into numerical models. A number of recent initiatives in Europe are building on earlier experimental work in the use of digital remotely sensed imagery for land surface mapping and have resulted in large scale operational schemes for national and international applications. Such a program, currently in progress in the United Kingdom, with the objective of compiling a national digital map of land cover, is described. This land cover mapping project, based on the use of multitemporal Landsat Thematic Mapper imagery, is placed in its broader European context, with emphasis on the need to achieve intercompatibility between individual national initiatives and systems developed to service the requirements of the wider international community. ESA

N93-24821# Lisbon Univ. (Portugal). Grupo de Oceanografia.
SUPPORTING THE PORTUGUESE FISHERIES WITH SATELLITES
A. Miguel P. Santos and Armando F. G. Fiuza *In* ESA, Environment Observation and Climate Modelling Through International Space Projects. Volume 2: Remote Sensing for Environmental Monitoring and Resource Management 1992 p 663-668 (For primary document see N93-24775 09-43)
(Grant BD/123/90-IG)
Copyright Avail: CASI HC A02/MF A04; ESA, EPD, ESTEC, Noordwijk, Netherlands, HC

The operational support of the Portuguese tuna and swordfish fisheries by provision with near real time products based on satellite measurements of sea surface temperature is reported. These products include charts with the location of thermal fronts and isotherms. Besides these operational activities, three research programs are being carried out to investigate the relations between tuna, swordfish and sardine aggregations and the distributions of oceanographic parameters as observed by the fishermen and using satellite data. A preliminary finding of this research is that sardines concentrate in moderately cool, relatively old upwelling waters, on the inner shelf off western Portugal. On the other hand, swordfish and tunas are preferentially found seaward of the semipermanent thermal front separating coastal waters from the warmer open ocean. ESA

N93-24822# Japan Fisheries Information Service Center, Tokyo.
APPLICATION OF SATELLITE IMAGERIES DATA TO FISHERIES IN JAPAN
Hideo Tameishi, Osamu Honda, Toshiyuki Kohguti, Shin Fujita, and Katsuya Saitoh *In* ESA, Environment Observation and Climate Modelling Through International Space Projects. Volume 2: Remote Sensing for Environmental Monitoring and Resource Management 1992 p 669-674 (For primary document see N93-24775 09-43)
Copyright Avail: CASI HC A02/MF A04; ESA, EPD, ESTEC, Noordwijk, Netherlands, HC

The Japan Fisheries Information Service Center (JAFIC) makes satellite aided oceanographic condition charts with NOAA AVHRR (Advanced Very High Resolution Radiometer) data and sends these charts to fishing vessels at sea experimentally, because, it was shown that the NOAA AVHRR data were applicable to fishing ground forecasting. The indexes of fishing ground forecasting are as follows: the first index for monitoring fishing grounds is the most favorable temperature range of a target fish; the second index is an oceanographic environment such as warm/cold current, warm/cold eddy, front and intrusion of warm/cold water which is produced as a fisheries oceanographic chart by JAFIC; the third index will be ocean color which corresponds to distribution of phytoplanckton, that is pray condition, but which is not described here. JAFIC developed a discriminant prediction system of skipjack fishing ground formation using the NOAA AVHRR data (1982-1985). ESA

N93-24823# Catania Univ. (Italy). Inst. of Machinery.
OIL POLLUTION AND WATER QUALITY MAPPING OF AUGUSTA BAY, ITALY USING REMOTE SENSING TECHNIQUES
Alberto L. Geraci and Agatino LaRosa (Italia Telerilevamento s.r.l., Catania.) *In* ESA, Environment Observation and Climate Modelling Through International Space Projects. Volume 2: Remote Sensing for Environmental Monitoring and Resource Management 1992 p 675-680 (For primary document see N93-24775 09-43)
Copyright Avail: CASI HC A02/MF A04; ESA, EPD, ESTEC, Noordwijk, Netherlands, HC

Remotely sensed data for oil pollution and water quality mapping over Augusta Bay in Sicily, Italy, since 1977, to investigate the usefulness of remote sensing techniques to the analysis of resource related problems, is reported. LANDSAT MSS (Multispectral Scanner) and TM (Thematic Mapper) data, along with MSS data, thermal infrared imagery, ultraviolet and infrared photography from lightplanes and helicopters are among the data acquired. Color coded imagery, showing oil pollution, distinguishing different types of it and calculating their extension were obtained. Color coded images, each depicting the distribution of a selected water quality parameter, were produced. ESA

N93-24824# Nansen Remote Sensing Center, Bergen (Norway).
NORSMAP 1989: NORWEGIAN REMOTE SENSING SPECTROMETRY FOR MAPPING AND MONITORING OF ALGAL BLOOMS AND POLLUTION
Lasse H. Pettersson, Ola M. Johannessen, and Oeyvind Frette *In* ESA, Environment Observation and Climate Modelling Through International Space Projects. Volume 2: Remote Sensing for Environmental Monitoring and Resource Management 1992 p 681-686 (For primary document see N93-24775 09-43)
Copyright Avail: CASI HC A02/MF A04; ESA, EPD, ESTEC, Noordwijk, Netherlands, HC

The increased frequencies of toxic algal blooms in for example the North Sea and Adriatic Sea, which have caused severe problems to the human activities ranging from aquaculture to tourism are discussed. A multi-institutional research program, Norwegian Remote Sensing Spectrometry and Pollution (NORSMAP) between Norway and Canada was established to evaluate the potential of airborne imaging spectrometry for monitoring of such events in Norwegian waters. The Canadian Compact Airborne Spectrographic Imager (CASI) was used for a three week period in May 1989. Water masses covering a wide range of optical properties were analyzed and chlorophyll concentrations in the range from 0.8 to 5 micro-g/l were observed. A good large scale match between the in situ and airborne data are found, although the point to point comparisons are not convincing. ESA

N93-24825# Officine Galileo S.p.A., Florence (Italy).
SEOMAR: AN ITALIAN APPROACH TO THE OBSERVATION OF THE MEDITERRANEAN AREA
A. Buccheri, R. Bonsignori, and P. Pili *In* ESA, Environment Observation and Climate Modelling Through International Space Projects. Volume 2: Remote Sensing for Environmental Monitoring and Resource Management 1992 p 687-691 (For primary document see N93-24775 09-43)
Copyright Avail: CASI HC A01/MF A04; ESA, EPD, ESTEC, Noordwijk, Netherlands, HC

The design of a set of electrooptical instruments in the spectral bands from the visible to the infrared (SEOMAR) to satisfy the most important needs for environmental observation of the Mediterranean area, in terms of spatial and spectral resolution, radiometric sensitivity, swath width, and frequency of observations, is reported. The SEOMAR instrument package was designed for frequent monitoring of the sea and land at Mediterranean latitudes, with very high spectral resolution and moderate spatial resolution. Starting with a description of an airborne spectrometer already developed, the SEOMAR overall system aspects and the technological concepts of the main instrument (VNIR), a programmable imaging spectrometer in the visible, are presented, along with an overview of possible applications. ESA

N93-24826# Department of Resources, Surveys and Remote Sensing, Nairobi (Kenya).
THE EXTENT AND STATUS OF MANGROVES IN MOMBASA DISTRICT, KENYA: A CASE STUDY BASED ON REMOTE SENSING
P. O. Gang *In* ESA, Environment Observation and Climate Modelling Through International Space Projects. Volume 2: Remote Sensing for Environmental Monitoring and Resource Management 1992 p 693-698 (For primary document see N93-24775 09-43)
Copyright Avail: CASI HC A02/MF A04; ESA, EPD, ESTEC, Noordwijk, Netherlands, HC

The distribution and present utilization of the mangroves are outlined. Mangrove vegetation communities are an important component of the Mombasa district environment. They form the only gazetted forest cover within the 275 sq km district. These forests are undergoing constant changes in response to human activities within the peri-urban environment. The study area has a variety of mangrove types including regeneration stages, dense old stands, and saltish dry banks almost devoid of halophytes. The study was carried out in the Mombasa mangroves based on a double sampling approach starting with SPOT multispectral satellite imagery followed by ground checks to provide information on species composition, density, and distribution of mangroves. Other forms of land uses around and within the mangroves were determined. This report outlines the distribution and present utilization of the mangroves. It is recommended that map products from SPOT data should be digitized using a geographic information system. This will keep record and allow for further overlay analysis with other resource maps and also for monitoring purposes. ESA

N93-24827# Petroleum Research Centre, Tripoli (Libya).
REMOTE SENSING OF COASTAL ZONE SABKHA DEPOSITS, GULF OF SIRT, LIBYA
Y. AlFasatwi, M. ElAlami, A. Sghir, and I. ElAradi (Bironi Remote Sensing Centre, Tripoli, Libya.) *In* ESA, Environment Observation and Climate Modelling Through International Space Projects. Volume 2: Remote Sensing for Environmental Monitoring and Resource Management 1992 p 699-702 (For primary document see N93-24775 09-43)
Copyright Avail: CASI HC A01/MF A04; ESA, EPD, ESTEC, Noordwijk, Netherlands, HC

The mapping of the complex coastal sabkhas of the western Gulf of Sirt, Libya, from Landsat Thematic Mapper and SPOT data is reported. The main objectives are to examine the use of remote sensing data for coastal zone mapping, and to study the effect of sabkha sediments and depth of the ground water table in spectral reflectance of these sediments. Differences in spectral reflectances of different zones of sabkha in remote sensing images represents the differences in type of sediments and the effect of the soil wettness which is related to the thickness of capillary zone. The geomorphology and drainage system suggest that these sabkhas are more close to land sabkhas than marine sabkhas and the continental recharge is more likely. ESA

N93-24828# Max-Planck-Inst. fuer Meteorologie, Hamburg (Germany).
INHERENT OPTICAL PROPERTIES OF LAKES AS MEASURED BY LANDSAT 5 THEMATIC MAPPER
Waltraud Jahnen and Hartmut Grassl *In* ESA, Environment Observation and Climate Modelling Through International Space Projects. Volume 2: Remote Sensing for Environmental Monitoring and Resource Management 1992 p 703-708 (For primary document see N93-24775 09-43)
Copyright Avail: CASI HC A02/MF A04; ESA, EPD, ESTEC, Noordwijk, Netherlands, HC

Lakes at different altitudes in different seasons are investigated by using the spectral measurements of all seven channels of Landsat 5 Thematic Mapper (TM). The calibration of these channels had to be improved. Then an atmospheric correction with help of a radiative transfer model was carried out to make the lake's signals comparable for different altitudes and seasons. Due to the different penetration of light into the water, the information content of each channel of the TM belongs to a different water depth. The channels in the middle infrared are used to investigate the existence and structure of surface films. ESA

N93-24829# University of Western Australia, Nedlands. Centre for Water Research.
MULTI-DATE ALGORITHMS FOR PREDICTING SURFACE WATER QUALITY PARAMETERS IN ESTUARINE AND COASTAL WATERS USING LANDSAT TM DATA
Charitha Pattiaratchi, P. Lavery, A. Wyllie (Remote Sensing Applications Centre, Perth, Australia.), and Peter T. Hick (Commonwealth Scientific and Industrial Research Organization, Floreat Park, Australia.) *In* ESA,

Environment Observation and Climate Modelling Through International Space Projects. Volume 2: Remote Sensing for Environmental Monitoring and Resource Management 1992 p 709-713 Sponsored by Waterways Commission of Western Australia and Environmental Protection Agency of Western Australia (For primary document see N93-24775 09-43)
(ED-659-CP) Copyright Avail: CASI HC A01/MF A04; ESA, EPD, ESTEC, Noordwijk, Netherlands, HC

An assessment of Landsat TM (Thematic Mapper) data as a tool for monitoring south western Australian coast waters and estuaries for surface chlorophyll concentration and Secchi disk depth (a measure of the water clarity), undertaken using Cockburn Sound and Peel Harvey Estuary as study sites, is reported. Algorithms were developed for atmospheric effects and water quality data obtained at the time of the satellite overpass. It is shown that in both of these systems a high confidence may be placed on the predictions using these algorithms and therefore offers a cost effective tool for complementary regular monitoring programs. ESA

N93-24830# Telespazio, S.p.A., Rome (Italy).
REMOTE SENSING MONITORING AND HINDCASTING OF THE ACCIDENT OCCURRED TO THE TANKER HAVEN IN THE GULF OF GENOA (ITALY)
P. Cecamore, A. Ciappa, and V. Perusini *In* ESA, Environment Observation and Climate Modelling Through International Space Projects. Volume 2: Remote Sensing for Environmental Monitoring and Resource Management 1992 p 715-718 (For primary document see N93-24775 09-43)
Copyright Avail: CASI HC A01/MF A04; ESA, EPD, ESTEC, Noordwijk, Netherlands, HC

Remote sensing data from high resolution sensors (Landsat Thematic Mapper and SPOT High Resolution Visible) and high frequency of acquisition sensors (NOAA AVHRR (Advanced Very High Resolution Radiometer)) were used to monitor and hindcast the movements of the oil spill generated by the accident which occurred to the tanker 'Haven' in the Gulf of Genoa in Apr. 1991. High resolution data was used to accurately locate the oil slick and estimate its extension. NOAA AVHRR data provided information about sea surface circulation during the wreck days. These data, together with wind field data, were used as input for a pollution dispersion model. ESA

N93-24831# Telespazio, S.p.A., Rome (Italy).
ALGAL BLOOMS AND GEL PRODUCTION IN ADRIATIC SEA OBSERVED BY REMOTE SENSING TECHNIQUES
R. Ligi, B. Azzara, G. Borzelli, P. Cecamore, and A. Ciappa *In* ESA, Environment Observation and Climate Modelling Through International Space Projects. Volume 2: Remote Sensing for Environmental Monitoring and Resource Management 1992 p 719-722 (For primary document see N93-24775 09-43)
Copyright Avail: CASI HC A01/MF A04; ESA, EPD, ESTEC, Noordwijk, Netherlands, HC

The ability of aerospace remote sensing technology for the observation of the phenomenon of gel production in Adriatic Sea is presented. The observation activity carried out in Summer 1991, by the use of satellite (NOAA AVHRR (Advanced Very High Resolution Radiometer), SPOT High Resolution Visible (multispectral mode), and Landsat Thematic Mapper)) and airborne CZCS (Coastal Zone Color Scanner) data, made possible the detection of intense filaments and aggregations of gel hyperproduction over the northern and central parts of the Adriatic Sea. Some results of the observations and analysis performed in Summer 1991 are presented, proving the good capability of monitoring this phenomenon. ESA

N93-24832# Szczecin Univ., Lodz (Poland). Inst. of Marine Sciences.
HEL'S PENINSULA COASTAL ZONE CHANGES IN THE LAST 40 YEARS ON A BASE OF REMOTE SENSING METHODS
K. Furmanczyk and S. Musielak *In* ESA, Environment Observation and Climate Modelling Through International Space Projects. Volume 2: Remote Sensing for Environmental Monitoring and Resource Management 1992 p 723-728 (For primary document see N93-24775 09-43)
Copyright Avail: CASI HC A02/MF A04; ESA, EPD, ESTEC, Noordwijk, Netherlands, HC

A project to find a long term change trend of the coast at Hel, a narrow sandy peninsula about 34 km long in the north west part of Gdansk Bay (Poland), and to indicate parts of the coast with erosion hazard, is reported. On the basis of aerial photographs taken in 1957 and 1991 the maps were made as listed below: photointerpretation map of coastal zone on the scale 1:5000; classification of Hel peninsula coast changes in the period of time 1957-1991 on the scale 1:100,000; complex photointerpretation map of Hel peninsula coast condition at 2 Sep. 1991 on the scale 1:50,000; and map of the Hel peninsula coastal erosion hazard in the scale 1:100,000. An attempt to find the reason for so big an erosion of the peninsula's coast was made. The dune base line location changes were taken for classification. ESA

N93-24833# Florence Univ. (Italy). Dipt. Scienze della Terra.
EVALUATION OF NEARSHORE SUSPENDED SEDIMENT CONCENTRATION THROUGH LANDSAT TM DATA: FIRST RESULTS
Giuliana Profeti, Fabio Maselli (Consiglio Nazionale delle Ricerche, Florence, Italy.), and Enzo Pranzini *In* ESA, Environment Observation and Climate Modelling Through International Space Projects. Volume 2: Remote Sensing for Environmental Monitoring and Resource Management 1992 p 729-733 (For primary document see N93-24775 09-43)
Copyright Avail: CASI HC A01/MF A04; ESA, EPD, ESTEC, Noordwijk, Netherlands, HC

An approach to evaluate the concentration of suspended sediment in coastal waters through Landsat Thematic Mapper data is reported. A modification of a standard methodology taking into account the influence of a homogeneous sea bottom in order to retrieve suspended sediment concentration is proposed. The contribution of the bottom is quantified and removed from the global reflected signal through an iterative procedure. This methodology was tested on two images of the Ombrone river mouth (southern Tuscany, Italy). The first results show its effectiveness in removing radiance coming from the sea bottom. Some problems concerning the applicability of this method to coastal water quality assessment are discussed. ESA

N93-24834# Institute of Meteorology and Hydrology, Bucharest (Romania). Remote Sensing Lab.
MONITORING AND EVALUATION OF MORPHOHYDROGRAPHICAL CHANGES IN THE DANUBE DELTA BY REMOTE-SENSING
G. Stancalie, H. Grumazescu, and S. Tuplea *In* ESA, Environment Observation and Climate Modelling Through International Space Projects. Volume 2: Remote Sensing for Environmental Monitoring and Resource Management 1992 p 735-738 (For primary document see N93-24775 09-43)
Copyright Avail: CASI HC A01/MF A04; ESA, EPD, ESTEC, Noordwijk, Netherlands, HC

The results obtained after several years of sustained research for assessing the modifications recorded over the last two decades in the area of the Danube Delta are presented. The studies were made by means of data obtained by processing large scale air photos resulting from successive air photos (since 1969) and by processing multi spectral scanner LANDSAT recordings (beginning with those made in 1975), correlated with ground observation and measurement data in test areas. For identifying and mapping the morphohydrographical characteristics, several methods, such as optical and optoelectronical methods and methods of supervised digital processing of images were used. ESA

N93-24835# University of Western Australia, Nedlands. Centre for Water Research.
COASTAL ENVIRONMENTAL MAPPING USING LANDSAT DATA
Charitha Pattiaratchi *In* ESA, Environment Observation and Climate Modelling Through International Space Projects. Volume 2: Remote Sensing for Environmental Monitoring and Resource Management 1992 p 739-743 (For primary document see N93-24775 09-43)
(ED-658-CP) Copyright Avail: CASI HC A01/MF A04; ESA, EPD, ESTEC, Noordwijk, Netherlands, HC

With the availability of high spatial resolution data from Landsat 5 and SPOT satellites, remote sensing, with its capability to provide synoptic information, is an excellent cost effective tool for coastal investigations. Applications of this data are presented and discussed in relation to: the extraction of bathymetric data; quantitative estimates of suspended sediment or chlorophyll concentrations; dipersion of effluent discharges; dispersal of river discharges; estimation of sea surface temperature; and monitoring of coastal circulation using suspended material in the surface as a passive tracer. ESA

N93-24836# Instituto de Pesquisas Espaciais, Sao Jose dos Campos (Brazil).

WORLD FOREST WATCH: A GLOBAL FOREST MONITORING TEST

Roberto PereiradaCunha and Jean Paul Malingreau (Joint Research Centre of the European Communities, Ispra, Italy.) *In* ESA, Environment Observation and Climate Modelling Through International Space Projects. Volume 2: Remote Sensing for Environmental Monitoring and Resource Management 1992 p 747-749 (For primary document see N93-24775 09-43)

Copyright Avail: CASI HC A01/MF A04; ESA, EPD, ESTEC, Noordwijk, Netherlands, HC

The World Forest Watch is a joint project between the National Institute of Space Research of Brazil (INPE) and the Joint Research Center of the CEC (Commission of the European Communities) (Europe, JRC). The main objective of the project is to obtain both global and regional remote sensing satellite data in order to cover most parts of the tropical forest belt and some isolate temperate forest areas. The global forest coverage is currently being done by JRC (Italy) using NOAA AVHRR (Advanced Very High Resolution Radiometer) data at 1 km resolution. Embedded in the 1 km global coverage, regional high resolution data sets (for example LANDSAT) will be acquired for deforestation quantification. The regional projects are to be developed at 1:250,000 scale and will consist of wall to wall data sets. One example of this is the pan-Amazonia project which will cover the entire Amazonian forest for all countries. Examples and preliminary results of the pan-Amazonia deforestation project are presented. ESA

N93-24837# Deutsche Forschungsanstalt fuer Luft- und Raumfahrt, Oberpfaffenhofen (Germany).

THE NATIONAL PARKS OF BAVARIAN FOREST AND SUMAVA: A LANDSAT TM PERSPECTIVE ON THE STRUCTURE AND DYNAMICS OF THE LARGEST WOODLAND OF CENTRAL EUROPE

M. Keil, B. Coenradie (Technische Univ., Munich, Germany.), H. Rall (National Park Administration of Bavarian Forest, Grafenau, Germany.), and M. Sima (Ceskoslovenska Akademie Ved, Ceske Budejovice.) *In* ESA, Environment Observation and Climate Modelling Through International Space Projects. Volume 2: Remote Sensing for Environmental Monitoring and Resource Management 1992 p 751-755 (For primary document see N93-24775 09-43)

Copyright Avail: CASI HC A01/MF A04; ESA, EPD, ESTEC, Noordwijk, Netherlands, HC

After the opening of the German/Czechoslovakian border, the government of the Czech Republic used the chance to declare the National Park of Sumava (Bohemian Forest) bordered to the National Park of Bavarian Forest. Tasks of landscape assessment in the region can be remarkably facilitated by methods of satellite remote sensing. The ability of Landsat TM (Thematic Mapper) evaluation could be demonstrated for the assessment of forest structure. In a subarea of 30 km by 30 km, covering the National Park of Bavarian Forest, a forest type classification and dead wood mapping was performed combining TM data and ancillary data. In another subarea, Landsat TM data of 1985, 1987, and 1989 were used on landscape change detection (appearance of coniferous forest parts) and also in studies for change explanation. ESA

N93-24838# Technische Univ., Dresden (German D.R.). Inst. fuer Photogrammetrie und Fernerkundung.

APPLICATION OF PHOTOGRAPHIC REMOTE SENSING DATA FROM SPACE FOR INFORMATION ABOUT FORESTS

E. Pelz, K. Fritsche, and D. Hertel *In* ESA, Environment Observation and Climate Modelling Through International Space Projects. Volume 2: Remote Sensing for Environmental Monitoring and Resource Management 1992 p 757-760 (For primary document see N93-24775 09-43)

Copyright Avail: CASI HC A01/MF A04; ESA, EPD, ESTEC, Noordwijk, Netherlands, HC

The investigation of the possibilities of the application of photographic satellite images for forestry purposes is reported. Radiometric evaluation of different image points or of the same object points in different images proved to be problematic without knowledge of the optical and sensitometric transmission parameters. With a KFA-1000 (Soviet camera) image, tests were carried out in the eastern Erzgebirge mountains and in the Tharandt forest (Germany). The analog classification of the Erzgebirge was much poorer because of the extreme damages of forests. Therefore a special classification is necessary. ESA

N93-24839# Sveriges Lantbruksuniv., Umea. Dept. of Biometry and Forest Management.

INTERPRETATION AND SEGMENTATION OF CHANGED FOREST STANDS FROM DIFFERENCE IMAGERY BASED ON REGRESSION FUNCTIONS

Haakan Olsson and Jan Ericsson *In* ESA, Environment Observation and Climate Modelling Through International Space Projects. Volume 2: Remote Sensing for Environmental Monitoring and Resource Management 1992 p 761-765 Sponsored in part by Swedish Board for Space Activities (For primary document see N93-24775 09-43)

Copyright Avail: CASI HC A01/MF A04; ESA, EPD, ESTEC, Noordwijk, Netherlands, HC

Difference imagery derived from both SPOT panchromatic and Landsat TM (Thematic Mapper) satellite data from 1989 and 1991 were generated by regression techniques. In a test with visual interpretation, all clearfelled areas and all soil scarifications were readily detected. About 1/3 of the cleaning cuttings and thinning cuttings could be easily detected. However, with prior knowledge about the approximate position some 2/3 of the cleaning and thinning cuttings could be delineated. All these changes turned out light in the difference imagery. A problem with difference imagery computed from regression functions was that also bright unchanged regions became too light in the difference imagery. Discriminant analysis of spectral mean values for automatically computed segments was also evaluated. Only Landsat TM data were used. The results suggest that automatic methods can aid the visual interpretation. ESA

N93-24840# European Space Agency. European Space Research and Technology Center, ESTEC, Noordwijk (Netherlands).

THE ESA ISY INITIATIVES FOR FOREST INVENTORY IN EUROPE

K. Pseiner, F. Gampe, and B. Pfeiffer *In its* Environment Observation and Climate Modelling Through International Space Projects. Volume 2: Remote Sensing for Environmental Monitoring and Resource Management 1992 p 767-768 (For primary document see N93-24775 09-43)

Copyright Avail: CASI HC A01/MF A04; ESA, EPD, ESTEC, Noordwijk, Netherlands, HC

Forest inventory on a site, regional and global scale, based on remote sensing data, has become a key item of applied forestry and applications research. Scientific studies with high resolution data address the possibilities to establish forest inventories, the ways to distinguish between different forest categories (age, species, canopy density, etc.) and to monitor forest change and damage. Within the frame of the International Space Year (ISY) various field studies were performed or are underway to either show forest phenomena on a regional or even detailed site level (ISY Remote Sensing Forest Atlas) and to map forests on a Continental European Scale (Remote Sensing Forest Map for ISY). ESA

N93-24841# Swedish Space Corp., Solna.

TROPICAL FOREST MONITORING WITH HIGH RESOLUTION SATELLITE DATA

H. Oesterlund and L. Bjoerk (Sveriges Lantbruksuniv., Umea.) *In* ESA, Environment Observation and Climate Modelling Through International Space Projects. Volume 2: Remote Sensing for Environmental Monitoring and Resource Management 1992 p 769-772 (For primary document see N93-24775 09-43)

Copyright Avail: CASI HC A01/MF A04; ESA, EPD, ESTEC, Noordwijk, Netherlands, HC

In order to develop operational methods for tropical forest monitoring a feasible low cost approach was used and evaluated with promising results. Digital satellite imagery is digitally coregistered and enhanced to produce color hardcopies. These are visually interpreted and area cover classes are manually delineated. An adopted point sampling design is used to estimate area cover. Using time coincident reference data the interpretation accuracy is evaluated and the area estimates calibrated. The methodology was tested and evaluated for the Chiang Rai province in northern Thailand. Landsat imagery from the same season of 1977, 1984, and 1990 was used. ESA

N93-24842# Ghent Univ. (Belgium). Satellite Remote Sensing Research Program.

ASSESSMENT OF STORM DAMAGE IN FORESTS USING SPOT IMAGERY

Marc M. Leysen, Boudewijn P. DeRoover, Roland E. Goossens, and Robert

R. DeWulf *In* ESA, Environment Observation and Climate Modelling Through International Space Projects. Volume 2: Remote Sensing for Environmental Monitoring and Resource Management 1992 p 773-777 (For primary document see N93-24775 09-43)
Copyright Avail: CASI HC A01/MF A04; ESA, EPD, ESTEC, Noordwijk, Netherlands, HC

The possibilities of assessing the impact of storms on forests by satellite remote sensing are evaluated. Two main objectives are put forward: the location of the damaged zones and the establishment of a quantitative relation between timber volume losses and spectral changes. Different modes, acquisition dates, and change detection techniques are compared. The change detection method elaborated is based on the combination of two coregistered panchromatic images, together with their difference image, on a color composite. Supervised minimum distance classification of this composite image results in accurate delineation of seriously damaged areas. Quantitative parameters of the spectral change of the forest stands, extracted from the difference image by averaging and level slicing, are regressed against the field data. Results indicate that the extraction of reliable information on storm damage from satellite imagery is restricted to stands where severe damage occurs, that is, where groups of trees were thrown. ESA

N93-24843# Akademie der Wissenschaften und der Literatur, Mainz (Germany). Arbeitsstelle Geooekologie.
MAPPING OF WINDFALL DAMAGE IN THE HUNSRUECK PLATEAU WITH LANDSAT TM-DATA
Johannes Wieczorek *In* ESA, Environment Observation and Climate Modelling Through International Space Projects. Volume 2: Remote Sensing for Environmental Monitoring and Resource Management 1992 p 779-782 (For primary document see N93-24775 09-43)
Copyright Avail: CASI HC A01/MF A04; ESA, EPD, ESTEC, Noordwijk, Netherlands, HC

Using data from the Landsat 5 TM (Thematic Mapper), a mapping of windfall areas in the region of the eastern, Hunsrueck plateau (Germany) is carried out. The first step is to make a general exposition of the usefulness of geographical information systems. Subsequently, it is found by classifying the data that the species most affected is spruce (Picea abies) grown in monocultures. By correlating these results with digitized soil data, it is possible to identify the static wet soils which, in combination with flat rooting spruce, show the highest potential for windfall damage. A prediction of potentially endangered areas can be made. ESA

N93-24844# Italian Space Agency, Rome.
A PROTOTYPE SYSTEM FOR FOREST FIRE PREVENTION AND CONTROL
L. DeFusco, C. Martellacci (Telespazio, S.p.A., Rome, Italy.), P. Peroni (Telespazio, S.p.A., Rome, Italy.), and M. Bagni (Telespazio, S.p.A., Rome, Italy.) *In* ESA, Environment Observation and Climate Modelling Through International Space Projects. Volume 2: Remote Sensing for Environmental Monitoring and Resource Management 1992 p 783-788 (For primary document see N93-24775 09-43)
Copyright Avail: CASI HC A02/MF A04; ESA, EPD, ESTEC, Noordwijk, Netherlands, HC

A prototype system for forest fire prevention and related control activities, consisting of two SPARC stations that simulate an operative center and an intervention mobile unit is presented. Methodologies and algorithms using remote sensing data and a geographic information system are implemented to support agencies operating in the areas of environmental and human life protection and natural disaster prevention. The system identifies three main phases: risk evaluation, fire event control and management, and damage evaluation. Applications at regional and local scale in a Mediterranean region are performed and preliminary results are presented. ESA

N93-24845# Ludwig-Maximilians-Univ., Munich (Germany). Lehrstuhl fuer Landnutzungsplanung und Naturschutz.
THE USE OF POLARIMETRIC RADAR REMOTE SENSING DATA FOR APPLICATION IN FORESTRY
B. Koch, B. Foerster, and U. Ammer *In* ESA, Environment Observation and Climate Modelling Through International Space Projects. Volume 2: Remote Sensing for Environmental Monitoring and Resource Management 1992 p 789-793 (For primary document see N93-24775 09-43)
Copyright Avail: CASI HC A01/MF A04; ESA, EPD, ESTEC, Noordwijk, Netherlands, HC

Investigations on airborne polarimetric radar remote sensing data were carried out to evaluate its use for the discrimination of forest classes. Signature analysis was carried out in reference to different orientation angles. The results showed that P band is most effective to differentiate between forests and agriculture land. Within the forest classes deciduous, pine, and spruce stands were separated in certain bands and for certain orientation angles. ESA

N93-24846# Swedish Environmental Protection Board, Skane.
FOREST DECLINE MONITORING USING LANDSAT TM, DIGITAL STAND DATA AND DEMs
Sam Ekstrand *In* ESA, Environment Observation and Climate Modelling Through International Space Projects. Volume 2: Remote Sensing for Environmental Monitoring and Resource Management 1992 p 795-800 (For primary document see N93-24775 09-43)
Copyright Avail: CASI HC A02/MF A04; ESA, EPD, ESTEC, Noordwijk, Netherlands, HC

The complication of the utilization of satellite data for forest decline assessment by topographic effects and variations in stand characteristics such as species composition and density is addressed. The possibility of using DEM's (Digital Elevation Models) and digitized stand data to reduce this problem was investigated for a forest region of Sweden. Variations in the hardwood component with 5 percent affected the accuracy of the Landsat TM (Thematic Mapper) based defoliation estimation, as did variations in the pine component with 12 to 15 percent and slope gradients as low as 4 to 5 deg. Based on the results a spruce defoliation model that uses slope/aspect data from elevation models and stand data from digitized forest maps to account for the mentioned error sources was developed. The resulting defoliation estimation was of adequate accuracy. The amount of work needed to digitize forest maps is considerable, but the method seems feasible on a provincial scale. ESA

N93-24847# Swedish Space Corp., Solna.
SWEDISH FOREST INFORMATION ATLAS
M. Rosengren, L.-E. Gustafsson, and H. Oesterlund *In* ESA, Environment Observation and Climate Modelling Through International Space Projects. Volume 2: Remote Sensing for Environmental Monitoring and Resource Management 1992 p 801-804 (For primary document see N93-24775 09-43)
Copyright Avail: CASI HC A01/MF A04; ESA, EPD, ESTEC, Noordwijk, Netherlands, HC

The production of a Swedish Forest Information Atlas (SFIA) derived from a digital terrain type classification database covering all of Sweden is reported. The database includes 900 map files each covering an area of 25 by 25 km with 50 m pixel size. Landsat TM (Thematic Mapper) and 12 SPOT scenes acquired 1988-90 were geocoded and classified into 13 terrain type classes. The statistical overall classification accuracy measured was 78 percent, while merging into 8 more generalized classes gave an overall accuracy of 84 percent. The SFIA was derived by extracting the classes of the Atlas as percentage images, describing the percentage of 50 m pixels within a 500 by 500 m area. The Forest Atlas comprises three forest classes extracted from these 'percentage images', open and closed coniferous forests, deciduous forest, as well as water, urban, and open areas. Additional cartographic elements will be superimposed on this classification. The atlas will be produced as printed maps and in digital format with a pixel size of 500 m. ESA

N93-24848# Technische Univ., Berlin (Germany). Dept. of Landscape Planning, Landscape Management and Nature Conservation.
OBSERVATION OF FOREST DAMAGES IN THE HARZ MOUNTAINS BY MEANS OF SATELLITE REMOTE SENSING
H. Kenneweg, M. Schardt, and H. Sagischewski *In* ESA, Environment Observation and Climate Modelling Through International Space Projects. Volume 2: Remote Sensing for Environmental Monitoring and Resource Management 1992 p 805-810 (For primary document see N93-24775 09-43)
Copyright Avail: CASI HC A02/MF A04; ESA, EPD, ESTEC, Noordwijk, Netherlands, HC

The use of satellite data for forest damage inventory in the Harz

mountains (Germany) is reported. From the results of signature analyses and of previous classifications the necessity to integrate auxiliary information by means of a geographic information system could be deduced. Digital terrain model forest planning data and soil maps are particularly useful for this purpose. In addition to the LANDSAT TM (Thematic Mapper) data, intensive field work and the interpretation of color infrared photos are needed as ground truth for: control areas representing damage classes, stand parameters and topographic influences on illumination; and control of accuracy of classification results. Data, methods, and resulting maps and tables are discussed. Change detection ('monitoring') is a matter of increasing importance, and this requires absolutely precise methods for geometrical and radiometrical correction of satellite data. ESA

N93-24849# FOMI Remote Sensing Center, Budapest (Hungary).
TOWARD A SATELLITE BASED CROP INFORMATION SYSTEM IN HUNGARY
Gabor Csornai *In* ESA, Environment Observation and Climate Modelling Through International Space Projects. Volume 2: Remote Sensing for Environmental Monitoring and Resource Management 1992 p 813-815 Sponsored by Ministry of Agriculture, Hungary; State Board of Technical Development, Hungary; and Hungarian Academy of Sciences (For primary document see N93-24775 09-43)
Copyright Avail: CASI HC A01/MF A04; ESA, EPD, ESTEC, Noordwijk, Netherlands, HC

The validation of Landsat TM (Thematic Mapper) based crop area estimation methods on a complex 1.7 million hectares, three counties sample (19 percent) in Hungary is reported. In the stratification and sampling design procedures, historical production data were utilized. The area estimates for the major crops were very good, using satellite data. The study clearly indicated the potential of monotemporal Landsat TM data for crop area assessment, however, there are some problems left to be resolved. After the better understanding of the discrimination of the minor crop classes, the main problem will probably be stratification and sampling design. The extension of the methods to other areas and growing seasons is supposed to be relatively easy as well as the adaption of methods to multitemporal images. ESA

N93-24850# Bonn Univ. (Germany). Lehrstuhl fuer Allgemeinen Pflanzenbau.
REMOTE SENSING OF LAND RESOURCE MANAGEMENT IN AGRICULTURE WITH REGARD TO ITS INFLUENCE ON THE ENVIRONMENT
K. Dockter and W. Kuehbauch *In* ESA, Environment Observation and Climate Modelling Through International Space Projects. Volume 2: Remote Sensing for Environmental Monitoring and Resource Management 1992 p 817-821 (For primary document see N93-24775 09-43)
Copyright Avail: CASI HC A01/MF A04; ESA, EPD, ESTEC, Noordwijk, Netherlands, HC

The capability of remote sensing techniques (Landsat Thematic Mapper) for monitoring agricutural land management is described. Crop species identification and estimation of crop status, performed by remote sensing, enable analysts to assess the intensity level of land use. This information can be used to evaluate the influence of agricultural practices on the Earth's ecosystem. Remote sensing may help to control the extensification of today's high input farming. Satellite images reliably show crop rotation systems to comprise a high percentage of cereals. Nitrogen fertilization level can be monitored by remote sensing looking at the wavelength shift of the red edge inflection point. This is demonstrated for sugar beet and natural grassland. Both monoculture and intensive nitrogen fertilization lead to serious environmental problems and need to be monitored, as the protection of the natural resources becomes more and more important. ESA

N93-24851# Consiglio Nazionale delle Ricerche, Florence (Italy). Ist. di Analisi Ambientalee Telerilevamento Applicati all'Agricoltura.
ASSESSMENT AND FORECASTING OF CROP YIELD IN NIGER THROUGH NOAA NDVI DATA
F. Maselli, C. Conese, M. A. Gilabert (Valencia Univ., Burjassot, Spain.), and L. Petkov *In* ESA, Environment Observation and Climate Modelling Through International Space Projects. Volume 2: Remote Sensing for Environmental Monitoring and Resource Management 1992 p 823-827 (For primary document see N93-24775 09-43)
Copyright Avail: CASI HC A01/MF A04; ESA, EPD, ESTEC, Noordwijk, Netherlands, HC

NOAA NDVI (Normalized Different Vegetation Index) data were previously demonstrated to be correlated with annual rainfall and primary productivity in Sahelian areas, but these correlations are strongly affected by several environmental factors and were tested only with satellite data accumulated during whole rainy seasons. A methodology of NOAA AVHRR (Advanced Very High Resolution Radiometer) data processing is presented which utilizes NDVI computed only in the first part of some rainy reasons and statistically takes into account the geographical variability on land resources. Good results were obtained from an application of the methodology to Niger, especially for yield forecasting. ESA

N93-24852# National Oceanic and Atmospheric Administration, Washington, DC. Satellite Research Lab.
GLOBAL DROUGHT MONITORING FROM NOAA POLAR ORBITING SATELLITES
Felix N. Kogan *In* ESA, Environment Observation and Climate Modelling Through International Space Projects. Volume 2: Remote Sensing for Environmental Monitoring and Resource Management 1992 p 829-833 (For primary document see N93-24775 09-43)
Copyright Avail: CASI HC A01/MF A04; ESA, EPD, ESTEC, Noordwijk, Netherlands, HC

The study of satellite data in the form of vegetation indices for monitoring weather disasters is reported. Particularly, the AVHRR (Advanced Very High Resolution Radiometer) based Vegetation Condition Index (VCI) showed excellent utility for drought monitoring on continental and regional scales. Several independent large areas tests comparing VCI with ground observations in the U.S. and sub-Sahara Africa showed very promising results. The principles of this index, its development, and some validation results are described. ESA

N93-24853# Toulouse Univ. (France). Purpan Graduate School of Agriculture.
INTEREST OF COMPLEMENTARY DATA OF COARSE AND HIGH SPATIAL RESOLUTION FOR AGRO-CLIMATIC CROP MONITORING
Ph. Puyou-Lascassies, M. Gay, and D. Peccoud *In* ESA, Environment Observation and Climate Modelling Through International Space Projects. Volume 2: Remote Sensing for Environmental Monitoring and Resource Management 1992 p 835-840 Sponsored by CNES (For primary document see N93-24775 09-43)
Copyright Avail: CASI HC A02/MF A04; ESA, EPD, ESTEC, Noordwijk, Netherlands, HC

The development of a deconvolution method for NOAA AVHRR (Advanced Very High Resolution Radiometer) data through knowledge of land use (SPOT data) is reported. The use of AVHRR temporal series to characterize the changes in land cover is still difficult in the complex agriculture landscapes of temperate countries. Complementary use of coarse and high spatial resolution data may make it possible to extract the part due to each of the agricultural themes present from the AVHRR signal. The method presented allows deconvolution of the AVHRR signal date to date on a local scale. The method was developed using SPOT data only, the coarse resolution signal being simulated by degrading the SPOT images. Because of the possibility that this simulation provided control of all the parameters, it enabled the reliability and sensitivity of the model to be studied. ESA

N93-24854# Cranfield Inst. of Tech., Bedford (England). Remote Sensing Unit.
NORTH-CENTRAL MEXICO BLUE GRAMA RANGELAND BIOMASS ASSESSMENT AT THE END OF THE RAINY SEASON USING NOAA-AVHRR-LAC
R. Rene Garcia-Daguer *In* ESA, Environment Observation and Climate Modelling Through International Space Projects. Volume 2: Remote Sensing for Environmental Monitoring and Resource Management 1992 p 841-844 Sponsored by British Council, and CONACYT (For primary document see N93-24775 09-43)
Copyright Avail: CASI HC A01/MF A04; ESA, EPD, ESTEC, Noordwijk, Netherlands, HC

Normalized Difference Vegetation Index (NDVI) Local Area Coverage (LAC) data derived from the AVHRR (Advanced Very High Resolution

Radiometer) NOAA satellite for the 1990 end season growing period for the Mexican blue grama (Bouteloua gracilis) are compared with biomass estimates. A ground survey program was conducted in Aguascalientes, north central Mexico, involving both visual estimates and clipped plots (double sampling technique). Field measurements of biomass of herbaceous species were made for 22 sites in Nov. 1990. The sites were 1 sq km and were representative of the blue grama rangeland vegetation type. Relationship between NDVI and biomass was obtained through regression analysis. The correlation obtained was r squared = 0.79 when sites covered with trees were eliminated from the data set. ESA

N93-24855# Environmental Agency of Andalucia, Seville (Spain).
CARTOGRAPHY AND STATISTICS OF CROPS UNDER IRRIGATION IN THE DONANA AREA OF ANDALUCIA THROUGH THE USE OF LANDSAT-TM IMAGERY AND ITS INCORPORATION INTO A GIS
A. FernandezPalacios and A. GonsalezF. *In* ESA, Environment Observation and Climate Modelling Through International Space Projects. Volume 2: Remote Sensing for Environmental Monitoring and Resource Management 1992 p 845-850 (For primary document see N93-24775 09-43)
Copyright Avail: CASI HC A02/MF A04; ESA, EPD, ESTEC, Noordwijk, Netherlands, HC

The effect of an irrigation land use expansion in the surrounding area of the Donana National Park (Andalucia, Spain) since early 1970s is discussed. This is seriously disturbing the local aquifer reserves and, thereby, the conservation of the natural spaces. In order to better understand and anticipate management policies, a procedure involving sample methods, digital processing of Landsat data, and Geographic Information System (GIS) databases was developed to account for irrigated crops area estimation and spatial distribution. Because of the low cost and readily adaptable attitude, remote sensing approaches proved to be powerful tools versus traditional procedures when dealing with dynamic spatial phenomenon such as the one analyzed. ESA

N93-24856# Norwegian Defence Research Establishment, Kjeller.
REGISTRATION OF THE USE OF AGRICULTURAL FIELDS AND SOIL EROSION USING SATELLITE REMOTE SENSING
Dan Johan Weydahl and Rune Solberg (Norwegian Computing Center, Oslo.) *In* ESA, Environment Observation and Climate Modelling Through International Space Projects. Volume 2: Remote Sensing for Environmental Monitoring and Resource Management 1992 p 851-856 Sponsored by State-Pollution Control Authority, Norway (For primary document see N93-24775 09-43)
Copyright Avail: CASI HC A02/MF A04; ESA, EPD, ESTEC, Noordwijk, Netherlands, HC

The use of optical satellite for detecting tillage practices is discussed and the classification of fields using ERS-1 SAR (Synthetic Aperture Radar) images is described. Under the North Sea Agreement, Norway is obliged to reduce the discharge of nutrient salts from agricultural fields by 50 percent by 1995. Remote sensing from satellites can be used to monitor soil tillage in the areas concerned. An experiment was carried out which shows that it is possible to classify the different agricultural classes with a high degree of accuracy using either SPOT or LANDSAT Thematic Mapper images. However, cloud conditions in late Autumn make it interesting to investigate the use of satellite SAR images to detect tillage. The results of classifying SAR speckle reduced images, show that ploughed and stubble fields can be discriminated with a high degree of confidence when the soil moisture level is high. The best result is obtained using a field by field classification method. In an operational system, corrected SAR images should be used as a supplement to the optical images. ESA

N93-24857# Joint Research Centre of the European Communities, Ispra (Italy). Remote Sensing Applications Group.
APPLICTION OF REMOTE SENSING TO FORESTRY MAPPING: EXPERIENCE FROM THE EUROPEAN COLLABORATIVE PROGRAMME FOR THE LESS FAVOURED AREAS
Sten Folving *In* ESA, Environment Observation and Climate Modelling Through International Space Projects. Volume 2: Remote Sensing for Environmental Monitoring and Resource Management 1992 p 857-861 (For primary document see N93-24775 09-43)
Copyright Avail: CASI HC A01/MF A04; ESA, EPD, ESTEC, Noordwijk, Netherlands, HC

The European Collaborative Programme is primarily meant as an external activity to promote the use of remotely sensed data in the less favored areas of the European Economic Community and to adapt the methods and applications to the social need in the management of these regions. One of the themes of the program concentrated on forestry. Several institutes and laboratories cooperated on studies on application of satellite imagery in forest management and mapping. The studies contribute to define the basis for a European digital forest cover map and contribute to the definition of a specific methodology for application of remote sensing in local forest management, especially in national parks and other nature reserves. ESA

N93-24858# Deutsche Forschungsanstalt fuer Luft- und Raumfahrt, Cologne (Germany).
BIODIVERSITY INDICATION BY EARTH OBSERVATION DATA
Thomas Allner, Robert Backhaus, Steve Gaito (Forschungszentrum Juelich G.m.b.H., Germany.), and Jacqueline McGlade (Forschungszentrum Juelich G.m.b.H., Germany.) *In* ESA, Environment Observation and Climate Modelling Through International Space Projects. Volume 2: Remote Sensing for Environmental Monitoring and Resource Management 1992 p 863-867 (For primary document see N93-24775 09-43)
Copyright Avail: CASI HC A01/MF A04; ESA, EPD, ESTEC, Noordwijk, Netherlands, HC

An approach to biodiversity monitoring is presented. With the thematic approach, the range of Earth observation data suitable for application is limited by the number of objects (geophysical formations, vegetation classes, landscape elements, types of habitats, etc.) which can be positively identified with a reasonable degree of certainty. The thematic approach, however, does not take into account another type of information which may be derived from existing and future Earth observation data sets merely by virtue of their topological structure. From recent results and theoretical considerations, it is assumed that suitable indicators of habitat diversity can be derived from the structural/topological information content of multispectral satellite data covering specific ecosystems. To further evaluate and demonstrate this information potential of satellite data, a diversity index is proposed, which was tentatively applied to a LANDSAT Thematic Mapper scene of the Bavarian Forest National Park. First results are presented, and implications of these results with relation to the feasibility of biodiversity indication based on the information content of satellite image data are discussed. ESA

N93-24859# Wageningen Agricultural Univ. (Netherlands). Dept. of Landsurveying and Remote Sensing.
MEASURING THE INTENSITY OF NITROGEN FERTILIZATION OF GRASSLAND BY MEANS OF REMOTE SENSING
C. Bueker, J. G. P. W. Clevers, and W. Kuehbauch (Bonn Univ., Germany.) *In* ESA, Environment Observation and Climate Modelling Through International Space Projects. Volume 2: Remote Sensing for Environmental Monitoring and Resource Management 1992 p 869-872 (For primary document see N93-24775 09-43)
Copyright Avail: CASI HC A01/MF A04; ESA, EPD, ESTEC, Noordwijk, Netherlands, HC

An investigation of the red edge shift in imaging spectrometer data of a grassland site in Somerset (England) showed that nitrogen treatment effects could be ascertained with larger power by means of the red edge shift than by means of a vegetation index. Moreover, the position of the red edge index was best correlated with canopy parameters like biomass and chlorophyll concentration. The research showed that the position of the red edge reveals the level of nitrogen fertilization with good precision and therefore offers valuable additional information for agricultural research. Four narrow spectral bands at 670, 700, 740, and 780 nm can be used for determining the position of the red infrared slope. ESA

N93-24860# Bulgarian Academy of Sciences, Sofia. Solar Terrestrial Influences Lab.
CROP AGROECOLOGICAL DIAGNOSTICS BY REMOTE SENSING TECHNIQUE
Rumiana H. Kancheva, Alexandar H. Krumov, and Valentina S. Boycheva *In* ESA, Environment Observation and Climate Modelling Through International Space Projects. Volume 2: Remote Sensing for Environmental Monitoring and Resource Management 1992 p 873-879 (For primary document see N93-24775 09-43)
Copyright Avail: CASI HC A02/MF A04; ESA, EPD, ESTEC, Noordwijk, Netherlands, HC

The possibility of indicating canopy heavy metal pollution stress and quantitatively estimating heavy metal concentration in the soil using spectral reflectance data is investigated. Greenhouse experiments were conducted with spring barley on acid and neutral soil types with nickel introduction. Reflectance and crop parameters data were collected and statistically modeled. The regression models are suggested as indicators of toxic stress on crop morphology and physiology and predictors of heavy metal concentration in the soil, although their uniqueness requires further examination. ESA

N93-24861# Cranfield Inst. of Tech., Bedford (England).
COMBINING SPECTRAL INFORMATION WITH CROP ROTATION KNOWLEDGE FOR CROP CLASSIFICATIONS
Changyuan Ji *In* ESA, Environment Observation and Climate Modelling Through International Space Projects. Volume 2: Remote Sensing for Environmental Monitoring and Resource Management 1992 p 881-884 Sponsored by EEC (For primary document see N93-24775 09-43)
Copyright Avail: CASI HC A01/MF A04; ESA, EPD, ESTEC, Noordwijk, Netherlands, HC

First and second order state transition matrices were derived from crop rotation system knowledge, which represent the temporal relationship of crop transitions in a two and three year lap respectively. Classifications were implemented using SPOT High Resolution Visible data together with the transition matrices. Knowledge of crop temporal relationships represented by state transition matrices is concluded to improve crop classification when combined with spectral data of satellite images. The increase depends on the spectral separability of the image data. Depending on the data set used, the overall accuracy of eight agricultural classes is increased by 5 to 15 percent over the standard maximum likelihood classifications using the first order matrices. The 2nd order transition matrices, together with the 1st order matrices, even further improve crop classifications. It is recommended that the method be applied when ground data of cropping information are available. ESA

N93-24862# Freiburg Univ. (Germany). Abt. Luftbildmessung und Fernerkundung.
ATMOSPHERIC CORRECTION OF LANDSAT/TM DATA OVER MOUNTAINOUS TERRAIN FOR FORESTRY APPLICATIONS
G. Kattenborn *In* ESA, Environment Observation and Climate Modelling Through International Space Projects. Volume 2: Remote Sensing for Environmental Monitoring and Resource Management 1992 p 885-890 (For primary document see N93-24775 09-43)
Copyright Avail: CASI HC A02/MF A04; ESA, EPD, ESTEC, Noordwijk, Netherlands, HC

A method to correct atmospheric effects on Landsat TM (Thematic Mapper) data over mountainous terrain in the solar spectrum, developed primarily for forestry applications, and which can also be adapted to other sensors and applications is described. The algorithm automatically identifies patches of dark, dense vegetation as controllable dark surfaces for the estimation of the aerosol optical thickness. Thereby, a network of radiometric control points is laid over the scene which supply horizontal as well as relief induced vertical changes in atmospheric conditions. Atmospheric parameters calculated with the LOWTRAN program over these pixels are smoothed and interpolated by cubic spline regression. With these values, atmospherically corrected ground reflectances are calculated pixelwise by iteration of a correction model. Improvements in visual interpretation, in the standardization of photoproducts, and in the use of calibrated data with multitemporal applications are discussed. ESA

N93-24863# Sveriges Lantbruksuniv., Umea. Remote Sensing Lab.
STANDWISE FOREST INVENTORY AND MAPPING FOR OPERATIONAL MANAGEMENT PLANNING
Olle Hagner *In* ESA, Environment Observation and Climate Modelling Through International Space Projects. Volume 2: Remote Sensing for Environmental Monitoring and Resource Management 1992 p 891-892 Sponsored by Swedish Board for Space Activities; Swedish Board of Forestry; and Sveriges Lantbruksuniv. (For primary document see N93-24775 09-43)
Copyright Avail: CASI HC A01/MF A04; ESA, EPD, ESTEC, Noordwijk, Netherlands, HC

A concept for updating and revision of forest maps and associated tabular data using satellite remote sensing and GIS (Geographic Information System) techniques is presented. The method is based on integrated use of visual interpretation, image segmentation, ocular field inventory, and statistical estimation techniques. The methodology was implemented on a PC based GIS/remote sensing workstation for forestry. The system was used by a forest company for update and revision of a 5083 hectare management unit. The experiences gained indicated a potential for substantial cost savings and several other advantages compared to the conventional methods used in practice. The experiment also showed that the technique can be customized to be used at the local level in the forestry organization. ESA

N93-24864# Finnish Meteorological Inst., Helsinki. Air Quality Dept.
FOREST DAMAGE DETECTION AND REFLECTION OF CONIFERS: FROM MICRO TO FIELD LEVEL
Outi Heikkilae *In* ESA, Environment Observation and Climate Modelling Through International Space Projects. Volume 2: Remote Sensing for Environmental Monitoring and Resource Management 1992 p 893-896 (For primary document see N93-24775 09-43)
Copyright Avail: CASI HC A01/MF A04; ESA, EPD, ESTEC, Noordwijk, Netherlands, HC

The reflection of Scots pine (Pinus sylvestris L.) needles was examined in Autumn in traffic environment in order to study the usability of reflection information for forest damage detection. The atmospheric concentrations of nitrogen oxides, ozone, and sulphur dioxide were measured and a mapping of epiphytic lichens, indicating the biological effects of the measured atmospheric impurities, was performed. The trees, forming a line perpendicular to a highway and thus suffering from different amounts of environmental stress factors at different distances, were photographed in the field on black and white infrared film. Needle samples were also collected for macro and microscopical IR photography, scanning electron and light microscopy, and chemical analysis. The reflection of single needles was then studied more accurately by spectrometer measurements both beside the highway and in background area. ESA

N93-24865# Southampton Univ. (England). Dept. of Geography.
SCALE DEPENDENCE IN THE REFLECTANCE OF DECIDUOUS WOODLAND: EVIDENCE FROM A HELICOPTER-MOUNTED SPECTRORADIOMETER
G. A. Blackburn and E. J. Milton *In* ESA, Environment Observation and Climate Modelling Through International Space Projects. Volume 2: Remote Sensing for Environmental Monitoring and Resource Management 1992 p 897-900 Sponsored by Natural Environment Research Council, United Kingdom (For primary document see N93-24775 09-43)
Copyright Avail: CASI HC A01/MF A04; ESA, EPD, ESTEC, Noordwijk, Netherlands, HC

Spectral measurements were made from a helicopter at four different altitudes for a range of types of deciduous woodland. For seminatural woodlands, while visible reflectance remained constant, near infrared reflectance decreased as the size of area being sensed by the spectroradiometer increased. This raises important implications for the remote sensing of complex vegetation canopies. In remotely sensed imagery from different sensors, and from the same sensor at different altitudes, the area covered by a pixel varies. Therefore, as a result of the scale dependence identified in this experiment, the remotely sensed signal recorded from the same area of deciduous woodland will be different in the images from these different sources. This may impose limitations on the use of such data both in terms of the information from broadband analysis (for example estimating leaf area index) and from specific spectral features such as the red edge (for example monitoring stress). ESA

N93-24866# Surveying and Mapping Agency of Northrhine-Westfalia, Bonn-Bad Godesberg (Germany).
OPERATIONAL USE OF MOMS-02 (P2) DATA
K. Barwinski and W. Kickbusch *In* ESA, Environment Observation and Climate Modelling Through International Space Projects. Volume 2: Remote Sensing for Environmental Monitoring and Resource Management 1992 p 903-905 (For primary document see N93-24775 09-43)
Copyright Avail: CASI HC A01/MF A04; ESA, EPD, ESTEC, Noordwijk, Netherlands, HC

The field of planned activities with regard to the expected MOMS-02 (Modular Optoelectronic Multispectral Scanner) (P2) data is presented. The MOM-02 is to be installed on Priroda, a multisensor multidisciplinary research

platform coupled to the Space Station Mir. Activities relate to surveying and mapping, topography, statistical land use information, land uses and pollution monitoring, hydrogeology, natural resources and environment monitoring, agriculture, ecology, and forestry. ESA

N93-24867# Nippon Electric Co. Ltd., Yokohama (Japan). Space Development Div.

HIGH RESOLUTION STEREO IMAGING AND DATA COMPRESSION

Riichi Nagura *In* ESA, Environment Observation and Climate Modelling Through International Space Projects. Volume 2: Remote Sensing for Environmental Monitoring and Resource Management 1992 p 907-912 (For primary document see N93-24775 09-43)

Copyright Avail: CASI HC A02/MF A04; ESA, EPD, ESTEC, Noordwijk, Netherlands, HC

Studies undertaken for the forthcoming high resolution and stereo imaging system for the Japanese JERS-1 are reported. Typical stereo imaging systems are investigated and an effective stereo imaging method using wide angle optics and precise charge coupled device is shown. Concerning the rapid increase of data rates, some data reduction methods with high quality images are shown. Some forthcoming compact stereo imaging systems with the highest resolution of 2 to approximately 4 m are presented. ESA

N93-24868# Saga Univ. (Japan).

INFLUENCE DUE TO ANTENNA PATTERN CHANGE IN BRIGHTNESS TEMPERATURE ESTIMATION FOR A SPACE-BASED MICROWAVE RADIOMETER

Kohei Arai, Kenbu Teramoto, and Toshio Imatani (Mitsubishi Electric Corp., Kanagawa, Japan.) *In* ESA, Environment Observation and Climate Modelling Through International Space Projects. Volume 2: Remote Sensing for Environmental Monitoring and Resource Management 1992 p 913-916 (For primary document see N93-24775 09-43)

Copyright Avail: CASI HC A01/MF A04; ESA, EPD, ESTEC, Noordwijk, Netherlands, HC

An assessment of the influence due to antenna pattern changes in brightness temperature estimation taking into account antenna pattern correction for a space based microwave radiometer is reported. Boresight direction and asymmetry of the antenna pattern, in general, are changed in space due to thermal stress, mechanical stress or vibrations, and so forth. In order to estimate brightness temperature of targets, antenna pattern correction is necessary. In such a case, although an accurate real antenna pattern is needed, it is not possible in space. Therefore, some assessments of the influence due to antenna pattern changes in brightness temperature is required. Simulated antenna pattern was generated using actual antenna pattern taking into account a realistic distortion due to the aforementioned defects. The results show the influence for the case with antenna pattern correction is greater than that for the case without antenna pattern correction. The results suggest a required accuracy in antenna pattern measurement and allowable noise. ESA

N93-24869# Academy of Sciences (USSR), Alma-Ata. Cryophysics Lab.

CONDENSATION ON COOLED SURFACES OF OPTICAL DEVICES AT THE COSMIC CONDITIONS

A. Drobyshev, R. Atchoh, N. Atapina, D. Garipogly, S. Maximov, and V. Parfenov *In* ESA, Environment Observation and Climate Modelling Through International Space Projects. Volume 2: Remote Sensing for Environmental Monitoring and Resource Management 1992 p 917-921 (For primary document see N93-24775 09-43)

Copyright Avail: CASI HC A01/MF A04; ESA, EPD, ESTEC, Noordwijk, Netherlands, HC

The change in optical characteristics of surfaces cooled to low temperatures caused by gas condensation during heat and mass transfer at cosmos conditions, is investigated. The results of the experimental study of solidified gas layers growth rate and of change of some surfaces' optical parameters at various temperatures and pressures are presented. The main components of the cosmic apparatus atmosphere, such as CO2, H2O, etc., were investigated. The thickness of the films was grown up to 10 to 12 mm. The wavelength region, for which the results are presented, extends from 400 to 8300 nm. ESA

N93-24870# Bulgarian Academy of Sciences, Sofia. Solar Terrestrial Influences Lab.

DATA PROCESSING AND CONTROL IN A TRANSPUTER SYSTEM FOR REMOTE SENSING OF THE EARTH **c45**

Doino Petkov, Tomas Zdravev, Dora Krezhova, Georgi Georgiev, Valentina Boytcheva, Christo Nikolov, Anton Velitchkov, and Miroslav Ivanov *In* ESA, Environment Observation and Climate Modelling Through International Space Projects. Volume 2: Remote Sensing for Environmental Monitoring and Resource Management 1992 p 923-927 Sponsored by National Fund of Scientific Investigations, Hungary (For primary document see N93-24775 09-43)

Copyright Avail: CASI HC A01/MF A04; ESA, EPD, ESTEC, Noordwijk, Netherlands, HC

The creation of a program for adaptive control of data acquisition and processing of video data and multichannel images is discussed. Systems for remote sensing of the Earth and environment monitoring generate large volumes of information. Large space projects need special expensive technical means for data and image acquisition. A way to reconcile the controversy between the ever increasing volume of data and the time for its processing is believed to be the use of a specific transputer computing architecture in airborne and space measurement systems. The transputer concept makes use most efficiently of the natural parallelisms in the data streams, their mutual correlation, and information redundancy. ESA

N93-24871# Technische Univ., Munich (Germany).

EUROSTARS: A SYSTEM FOR THEMATIC ANALYSIS OF REMOTE SENSED DATA

S. Pfleger, A. Siebert, and M. Cantone (Bonifica S.p.A., Rome, Italy.) *In* ESA, Environment Observation and Climate Modelling Through International Space Projects. Volume 2: Remote Sensing for Environmental Monitoring and Resource Management 1992 p 929-932 (For primary document see N93-24775 09-43)

Copyright Avail: CASI HC A01/MF A04; ESA, EPD, ESTEC, Noordwijk, Netherlands, HC

The central point of the EUROSTARS (European System for Thematic Analysis of Remote Sensed Data) project, started in 1991, is the development of a new methodology of geographical analysis based on remote sensed images (satellite data) using neural networks and knowledge based terrain modeling. The processes of segmenting and classifying the information content of an image are guided by a neural network, which is able to correctly interpret the results related to the attributes of the extracted features like context, form, geometry, texture, and radiance. Classification will assign a semantic meaning to the extracted features, based on a specified human classification criterion. Self learning experiments based on examples will support an optimal calibration of the neural network; the accuracy of the obtained results will be evaluated by comparing them with the results obtained by traditional image processing and interpretation procedures. ESA

N93-24872# Buero fuer Angewandte Geowissenschaftliche Fernerkundung, Stockach (Germany).

EARTHQUAKE VULNERABILITY MAP OF THE LAKE CONSTANCE AREA

B. Theilen-Willige *In* ESA, Environment Observation and Climate Modelling Through International Space Projects. Volume 2: Remote Sensing for Environmental Monitoring and Resource Management 1992 p 933-935 (For primary document see N93-24775 09-43)

Copyright Avail: CASI HC A01/MF A04; ESA, EPD, ESTEC, Noordwijk, Netherlands, HC

The combined interpretation of geophysical, structural geological, geomorphological, and remote sensing data serves as a data base for an earthquake vulnerability map of the Lake Constance area (Europe). Linear features visible on satellite images and topographic lineaments such as linear valleys or ridges were mapped and correlated with known tectonic features and seismotectonic lines. ESA

N93-24873# Naples Univ. (Italy). Dept. of Zoology.

ANOMALOUS BIOELECTRIC POTENTIALS OF SILK TREES IN NAPLES ZOO (ITALY) PRIOR TO AN EARTHQUAKE IN MAY, 1991

G. Matteucig and H. Toriyama (Tokyo Woman's Christian Univ., Japan.) *In* ESA, Environment Observation and Climate Modelling Through International Space Projects. Volume 2: Remote Sensing for Environmental

Monitoring and Resource Management 1992 p 937-938 (For primary document see N93-24775 09-43)
Copyright Avail: CASI HC A01/MF A04; ESA, EPD, ESTEC, Noordwijk, Netherlands, HC

The attempted measurement of the bioelectric potential of silk trees in Naples zoo is reported. Many small earthquakes occur in the south of Italy, and on 26 May 1991 a moderate earthquake (M = 4.6) occurred in the Lucania area. The anomalous bioelectric potential changes in the silk trees on 25 May (about 24 hours before the earthquake) are presented. The development of interdisciplinary studies regarding physics, geoelectromagnetics, geochemistry, electroengineering, plant physiology, and animal physiology is suggested as an eventual way to predict earthquakes. ESA

N93-24874# Eurimage, Rome (Italy).
CURRENT TRENDS IN SATELLITE DATA SUPPLY FOR ENVIRONMENTAL MONITORING
Mikael Stern *In* ESA, Environment Observation and Climate Modelling Through International Space Projects. Volume 2: Remote Sensing for Environmental Monitoring and Resource Management 1992 p 939-942 (For primary document see N93-24775 09-43)
Copyright Avail: CASI HC A01/MF A04; ESA, EPD, ESTEC, Noordwijk, Netherlands, HC

Some of the current trends regarding the supply of remote sensing data are presented. Specifically, those trends which are relevant, and how they are relevant, for environmental monitoring are mentioned. Patterns noticed during the last few years and those known to continue for the next three years might be valid for ongoing monitoring projects. The discussed trends range from satellite technology to data delivery concepts. ESA

N93-25154*# JJM Systems, Inc., Ivyland, PA.
AN EXPERT SYSTEM SHELL FOR INFERRING VEGETATION CHARACTERISTICS: INRERFACE FOR THE ADDITION OF TECHNIQUES (TASK H) Report, Mar. - Apr. 1993
P. Ann Harrison 22 Apr. 1993 34 p
(Contract NAS5-30127; RTOP 462-61-14)
(NASA-CR-192897; NAS 1.26:192897; C931021-U-2R07) Avail: CASI HC A03/MF A01

All the NASA VEGetation Workbench (VEG) goals except the Learning System provide the scientist with several different techniques. When VEG is run, rules assist the scientist in selecting the best of the available techniques to apply to the sample of cover type data being studied. The techniques are stored in the VEG knowledge base. The design and implementation of an interface that allows the scientist to add new techniques to VEG without assistance from the developer were completed. A new interface that enables the scientist to add techniques to VEG without assistance from the developer was designed and implemented. This interface does not require the scientist to have a thorough knowledge of Knowledge Engineering Environment (KEE) by Intellicorp or a detailed knowledge of the structure of VEG. The interface prompts the scientist to enter the required information about the new technique. It prompts the scientist to enter the required Common Lisp functions for executing the technique and the left hand side of the rule that causes the technique to be selected. A template for each function and rule and detailed instructions about the arguments of the functions, the values they should return, and the format of the rule are displayed. Checks are made to ensure that the required data were entered, the functions compiled correctly, and the rule parsed correctly before the new technique is stored. The additional techniques are stored separately from the VEG knowledge base. When the VEG knowledge base is loaded, the additional techniques are not normally loaded. The interface allows the scientist the option of adding all the previously defined new techniques before running VEG. When the techniques are added, the required units to store the additional techniques are created automatically in the correct places in the VEG knowledge base. The methods file containing the functions required by the additional techniques is loaded. New rule units are created to store the new rules. The interface that allow the scientist to select which techniques to use is updated automatically to include the new techniques. Task H was completed. The interface that allows the scientist to add techniques to VEG was implemented and comprehensively tested. The Common Lisp code for the Add Techniques system is listed in Appendix A. Author (revised)

N93-25422 York Univ. (Ontario).
PASSIVE MICROWAVE REMOTE SENSING OF SNOW-COVERED FLOATING ICE DURING SPRING CONDITIONS IN THE ARCTIC AND ANTARCTIC Ph.D. Thesis
Caren Garrity 1991 350 p
(ISBN-0-315-70444-6) Avail: Univ. Microfilms Order No. DANN70444

It is possible to classify first year from multi-year ice during the onset of melt period using a dual-polarized 37 GHz radiometer. The classification is based on the emission from the snow cover instead of from the sea ice when the snow is not dry. There can be large diurnal fluctuations in the brightness temperature, as large as 80K, but there is a particular time of day when there will be a separation in the brightness temperature of first year compared to multi-year ice. This separation is due to the stage of metamorphism of the snow, which is a function of the temperature gradient in the snow and will be different for each ice type. A snow cover on first year ice is typically thinner than for multi-year ice. This thinner snow cover is influenced by environmental conditions at a faster rate than for a thicker snow cover due to the insulating property of snow. Generally, the afternoon period is a good time for ice classification using a passive microwave sensor. However, during the initial stages of the onset of melt, the morning hours would be a better time for a satellite overpass. This indicates that for ice classification, an overpass of a radiometer bearing satellite, such as the Special Sensor Microwave Imager (SSM/I), would be best in the morning during the mid-spring, and afternoon during the later spring for the high Arctic. A curve showing the stages of snow metamorphism from snow covered sea ice has been established using 37 GHz brightness temperatures. Therefore, the stage of metamorphism in a snow cover can be obtained from the curve. The onset of melt is well defined from the brightness temperature. If the brightness temperature is greater than that for sea ice, the snow cover contains from 1 percent to 6 percent free-water by volume. If the brightness temperature is lower than that measured for sea ice, and the signal is depolarized (vertical and horizontal brightness temperatures are similar), then the snow is dry. The amount of volume scattering in a dry snow cover will decrease the brightness temperature with increasing snow depth. Once snow depth and density are obtained, the amount of water a snow cover contains, known as water equivalent, can be determined. If the brightness temperature is low and polarized, there could be slush at the snow-ice interface. Mapping of slush on sea ice would be a useful parameter to shipping since slush will reduce the speed of a ship. Dissert. Abstr.

N93-25430 Purdue Univ., West Lafayette, IN.
INTEGRATING SATELLITE IMAGERY AND DIGITAL ELEVATION DATA FOR GEOBOTANICAL MAPPING IN QUETICO PROVINCIAL PARK, ONTARIO, CANADA Ph.D. Thesis
Timothy Andrew Warner 1992 93 p
Avail: Univ. Microfilms Order No. DA9301405

This geobotanical remote sensing study of a granite-greenstone terrain in eastern Quetico Provincial Park, north-western Ontario, Canada, is based on a topographic analysis of digital elevation data. The greenstone units consist of metamorphosed mafic and occasional ultramafic lithologies, surrounded by granites and granodiorites. Glacial till is thin and capped by loess in places. The soils are mainly Inceptisols, Histosols and Boralfs. The vegetation is dominantly boreal in nature. The digital elevation data analysis identified four microclimate and drainage classes. Landsat Thematic Mapper (TM) data were transformed into the nPDF Deciduous Forest Index and then density sliced in six informational classes of various deciduous and coniferous cover. The distribution of forest classes on each of the two lithologies shows that stands growing on mafic lithologies are enriched in deciduous species, compared to those growing on granites. Of the cover classes found on mafics, the highest coniferous component was on north facing slopes, and the highest deciduous component on south facing slopes. By contrast, granites showed no appreciable variation between site classes. These associations were then applied in an integrated, rule-based classification that utilizes average community vegetation, topographic landscape units and aeromagnetic anomalies to separate greenstone belts from surrounding granitic areas. The procedure, called Topoveg, is not overtly hampered by scattered clouds in the area, since areas that are obscured or have no forests on adjacent south facing slopes are assumed to be similar to their surrounding areas. Topoveg achieved an 85.0 percent accuracy in a classification of the 10 by 13 kilometer primary test site. A

standard maximum likelihood classification had an accuracy of only 71.3 percent, and produces output that has a distinctive noisy texture, compared to the large, homogenous classes of Topoveg. In a neighboring test site to the north, Topoveg accuracy was similarly high (86.3 percent). The southern test site, however, had an increased percentage of deciduous species on south facing granitic sites, and consequently a lower accuracy (78.6 percent). Thus these particular classification rules may be used with confidence in areas to the north, east and west. New rules should be developed for classification of areas to the south. Dissert. Abstr.

N93-25434 California Univ., Santa Barbara.
MULTI-TEMPORAL SATELLITE IMAGE ANALYSIS FOR CROP INVENTORIES IN THE PO RIVER VALLEY (ITALY) Ph.D. Thesis
Daniele Ehrlich 1992 180 p
Avail: Univ. Microfilms Order No. DA9303185

This dissertation describes satellite data image processing for crop area estimation in Veneto region (Italy). Several quantitative image analysis exercises were carried out to investigate the information content of Landsat Thematic Mapper imagery with reference to the landscape of the Veneto region. These exercises include multi-temporal image normalization, multi-temporal image classification of selected study sites, 'greenness' temporal profile modeling and development of an advanced agricultural information system for the integration of different data types describing the landscape for an optimal crop area estimation. Multi-temporal image normalization was performed using the procedure which relies only on spectral information contained in satellite imagery. The procedure is extendible to different images and to images acquired in different growing season. The procedure worked well especially for correcting systematic radiometric variation such as offsets in radiometric calibration coefficients, sun angle differences and uniform variation in atmosphere turbidity. Multi-temporal image classification at selected study sites was conducted to identify pattern of crop growth as detected from spectral imagery. Three study sites, each containing four annual crops under study were classified using several pattern recognition techniques. The image analysis revealed phenology related spectral crop pattern which were used to separate the crop under study. Crop classification accuracies as computed in the study sites yielded accuracies which range between 71 percent to 82 percent according to the crop and the area under investigation. Greenness temporal profile modeling, an image processing technique which exploits graphical shape rather than statistical characteristic of the image was also attempted for an improved crop type classification. Temporal profile analysis provided additional information on spectral properties of crops through time. Classification accuracy results obtained with temporal profile analysis resulted being comparable to pattern recognition techniques. Finally, knowledge on the information content of Landsat Thematic Mapper images combined with knowledge on the processes occurring on the landscape were combined in an image processing procedure which uses both image processing algorithms and geographic information system operations. Image analysis has been conducted within the framework of an advanced agricultural information system (AAIS). The AAIS is a raster based geographic information system which integrates several data types including satellite imagery, analog map data and ancillary information in the form of knowledge about the processes occurring in the landscape. The system is open to new input and can continuously be updated upon the arrival of new information. As such AAIS is a model which quantitatively describes some important components of the agricultural system and can be used to predict physical as well as social processes in the landscape. Dissert. Abstr.

N93-25441 North Carolina State Univ., Raleigh.
AERIAL PHOTOGRAPHIC SAMPLING FOR STATEWIDE RESOURCE INVENTORY Ph.D. Thesis
Glenn Paul Catts 1992 295 p
Avail: Univ. Microfilms Order No. DA9305422

The land use and forest resource conditions of the state of North Carolina were photointerpreted from 1:12,000 scale, color infrared aerial photography. Nearly 400 circular plots, of 1000 acres in area, were type mapped by two photointerpreters according to classification definitions adopted from those of the Southeastern Forest Inventory and Analysis (SE FIA) unit of the U.S. Forest Service. Photo plots were arranged in a statewide systematic layout. Four classification levels were used. The initial 1000 acre plot size was further subdivided into six smaller concentric plot sizes. Acreage photointerpreted was converted into a percentage estimate for each plot by forming a ratio of the number of acres type mapped in the class over the total number of acres in the plot. Regional and statewide percentage estimates for all classes in all classification schemes and for all plot sizes were produced separately. Fieldwork was conducted at nearly 300 locations imaged by the aerial photography. Results of coincident fieldwork and photointerpretation were cross-tabulated into a series of error matrices used to adjust the initial percentage estimates for classification bias. The precision of the percentage estimates was calculated using a Monte Carlo simulation technique known as bootstrapping. Accuracy of the percentage estimates was assessed by comparison with temporally coincident SE FIA 5th Survey results (1982-1984). The influence on precision of the numbers and size of the sample plots photointerpreted, and the number of coincident plots used to build the error matrix was investigated. An optimization model was formulated with the objective of finding a minimum total cost for a multiresource survey design meeting predetermined, class specific precision requirements. Photointerpretation was found to be accurate and consistent among the most experienced individuals. Adjusted class percentage estimates were closer to SE FIA estimates than were unadjusted for many classes. Bootstrapped confidence intervals contained SE FIA field survey estimates. Solutions to the minimization model indicated that photointerpretation of plots in sizes above 800 acres were most cost effective in an example examined. Optimization modeling could assist resource managers in choosing most efficient multiresource survey designs. Dissert. Abstr.

N93-25460*# National Aeronautics and Space Administration. Goddard Space Flight Center, Greenbelt, MD.
EARTH OBSERVING SYSTEM. OUTPUT DATA PRODUCTS AND INPUT REQUIREMENTS, VERSION 2.0. VOLUME 1: INSTRUMENT DATA PRODUCT CHARACTERISTICS
Yun-Chi Lu, Hyo Duck Chang, Brian Krupp, Ravindra Kumar, and Anand Swaroop Aug. 1992 189 p
(NASA-TM-108770; NAS 1.15:108770) Avail: CASI HC A09/MF A02

Information on Earth Observing System (EOS) output data products and input data requirements that has been compiled by the Science Processing Support Office (SPSO) at GSFC is presented. Since Version 1.0 of the SPSO Report was released in August 1991, there have been significant changes in the EOS program. In anticipation of a likely budget cut for the EOS Project, NASA HQ restructured the EOS program. An initial program consisting of two large platforms was replaced by plans for multiple, smaller platforms, and some EOS instruments were either deselected or descoped. Updated payload information reflecting the restructured EOS program superseding the August 1991 version of the SPSO report is included. This report has been expanded to cover information on non-EOS data products, and consists of three volumes (Volumes 1, 2, and 3). Volume 1 provides information on instrument outputs and input requirements. Volume 2 is devoted to Interdisciplinary Science (IDS) outputs and input requirements, including the 'best' and 'alternative' match analysis. Volume 3 provides information about retrieval algorithms, non-EOS input requirements of instrument teams and IDS investigators, and availability of non-EOS data products at seven primary Distributed Active Archive Centers (DAAC's). Author (revised)

N93-25461*# National Aeronautics and Space Administration. Goddard Space Flight Center, Greenbelt, MD.
EARTH OBSERVING SYSTEM. OUTPUT DATA PRODUCTS AND INPUT REQUIREMENTS, VERSION 2.0. VOLUME 2: ANALYSIS OF IDS INPUT REQUIREMENTS
Yun-Chi Lu, Hyo Duck Chang, Brian Krupp, Ravindra Kumar, and Anand Swaroop Aug. 1992 197 p
(NASA-TM-108771; NAS 1.15:108771) Avail: CASI HC A09/MF A03

On 18 Jan. 1991, NASA confirmed 29 Inter-Disciplinary Science (IDS) teams, each involving a group of investigators, to conduct interdisciplinary research using data products from Earth Observing System (EOS) instruments. These studies are multi-disciplinary and require output data products from multiple EOS instruments, including both FI and PI instruments. The purpose of this volume is to provide information on output products expected from IDS investigators, required input data, and retrieval algorithms. Also included in this volume is the revised analysis of the 'best' and 'alternative' match data products for IDS input requirements. The original analysis presented in the August 1991 release of the SPSO Report was revised to incorporate the restructuring of the EOS platform. As a result of

the reduced EOS payload, some of EOS instruments were deselected and their data products would not be available for IDS research. Information on these data products is also presented. Author (revised)

N93-25462*# National Aeronautics and Space Administration. Goddard Space Flight Center, Greenbelt, MD.
EARTH OBSERVING SYSTEM. OUTPUT DATA PRODUCTS AND INPUT REQUIREMENTS, VERSION 2.0. VOLUME 3: ALGORITHM SUMMARY TABLES AND NON-EOS DATA PRODUCTS
Yun-Chi Lu, Hyo Duck Chang, Brian Krupp, Ravindar Kumar, and Anand Swaroop Aug. 1992 227 p
(NASA-TM-108769; NAS 1.15:108769) Avail: CASI HC A11/MF A03

Volume 3 assists Earth Observing System (EOS) investigators in locating required non-EOS data products by identifying their non-EOS input requirements and providing the information on data sets available at various Distributed Active Archive Centers (DAAC's), including those from Pathfinder Activities and Earth Probes. Volume 3 is intended to complement, not to duplicate, the the EOSDIS Science Data Plan (SDP) by providing detailed data set information which was not presented in the SDP. Section 9 of this volume discusses the algorithm summary tables containing information on retrieval algorithms, expected outputs and required input data. Section 10 describes the non-EOS input requirements of instrument teams and IDS investigators. Also described are the current and future data holdings of the original seven DAACS and data products planned from the future missions and projects including Earth Probes and Pathfinder Activities. Section 11 describes source of information used in compiling data set information presented in this volume. A list of data set attributes used to describe various data sets is presented in section 12 along with their descriptions. Finally, Section 13 presents the SPSO's future plan to improve this report . Author

N93-25505# Oak Ridge National Lab., TN.
REAL-TIME CONSTRUCTION OF THREE-DIMENSIONAL OCCUPANCY MAPS
J. P. Jones 1992 7 p Presented at the Institute of Electrical and Electronics Engineers International Conference on Robotics and Automation, Atlanta, GA, 2-7 May 1993
(Contract DE-AC05-84OR-21400)
(DE93-001645; CONF-930519-4) Avail: CASI HC A02/MF A01

This paper describes a preliminary sensory system for real-time sensor-based navigation in a three-dimensional, dynamic environment. Data from a laser range camera are processed on an iWarp parallel computer to create a 3D occupancy map. This map is rendered using raytracing. The construction and rendering consume less than 800 milliseconds. DOE

N93-25516# Oak Ridge National Lab., TN.
REAL-TIME CONSTRUCTION AND RENDERING OF THREE-DIMENSIONAL OCCUPANCY MAPS
J. P. Jones 1993 9 p Presented at the 11th Society of Photo-Optical Instrumentation Engineering Applications of Artificial Intelligence, Orlando, FL, 12-16 Apr. 1993
(Contract DE-AC05-84OR-21400)
(DE93-007818; CONF-930493-1) Avail: CASI HC A02/MF A01

This paper describes a preliminary sensory system for real-time sensor-based navigation in a three-dimensional, dynamic environment. Data from a laser range camera are processed on an iWarp parallel computer to create a 3D occupancy map. This map is rendered using raytracing. The construction and rendering consume less than 800 milliseconds. DOE

N93-25653# Purdue Univ., West Lafayette, IN. Robot Vision Lab.
EFFICIENT GENERATION OF SYNTHETIC TERRAIN IMAGERY FOR AUTOMATIC TARGET RECOGNITION Final Report, 1 May 1989 - 30 Jun. 1992
A. C. Kak, R. L. Cromwell, S. G. Blask, L. L. Grewe, and H. Kang 23 Oct. 1992 11 p
(Contract DAAL03-89-K-0090)
(AD-A260705; ARO-26697.1-EL) Avail: CASI HC A03/MF A01

We have developed an integrated framework for the efficient synthesis of realistic images of three dimensional terrain with man-made objects and natural clutter. We have shown how many phenomenological aspects of the placement of road networks, tree clusters, populated areas, buildings, etc., can be captured in a computationally-efficient pseudorandom image-generation framework. We generate the underlying terrain with a fast Fourier based procedure. This procedure is seeded with a pseudorandom sequence, so a small number of parameters can characterize a distinctive class of terrain. Within each class, arbitrarily many scenes can be synthesized. We have used procedural definitions for objects; targets or clutter are represented by different models depending on range. For example, at a great distance trees may look like simple cones. But, as the viewpoint nears a tree, finer details will become visible. Procedural definitions also eliminate the need to explicitly store boundary representations for every object placed in the scene. A single procedural definition for an object, such as a tree, can be used at render time by a Z-buffer algorithm to create as many instances as are necessary, with each instance being unique since it uses a unique pseudorandom seed. DTIC

N93-25679# New Mexico Inst. of Mining and Technology, Socorro.
REMOTE SENSING OF PRECIPITATION AND ELECTRIFICATION WITH A DUAL-POLARIZATION, COHERENT, WIDEBAND RADAR SYSTEM Interim Report No. 2, 15 Jul. 1990 - 14 Jul. 1991
Paul R. Krehbiel and Grant Gray 15 Sep. 1992 9 p
(Grant AF-AFOSR-0450-89)
(AD-A260779; AFOSR-92-1002TR) Avail: CASI HC A02/MF A01

The radar has been upgraded through improvements to the receiver and addition of an inexpensive PC-based Digital Signal Processing system to allow real-time processing and display of radar parameters. A Sun Microsystems SPARCstation was added to the system for processed data archive as well as post analysis. The radar system was shipped to Kennedy Space Center for electrification studies during the summer of 1991. DTIC

N93-25694# Naval Research Lab., Bay Saint Louis, MS. Mapping, Charting and Geodesy Branch.
DIGITAL NAUTICAL CHART Final Report
James H. Hammack and S. D. Coughlan Jan. 1993 14 p
(AD-A260810; NRL/MR/7441-93-7011) Avail: CASI HC A03/MF A01

The Defense Mapping Agency (DMA) has tasked the Naval Research Laboratory (NRL) to develop a product specification for a Digital Nautical Chart (DNC) database. The DNC will be used by the Department of Defense in nautical Electronic Chart Display and Information Systems. This paper will describe the structure and content of the DNC database. DTIC

N93-25707 Louisiana State Univ., Baton Rouge.
DETECTING THE SCALE AND RESOLUTION EFFECTS IN REMOTE SENSING AND GIS Ph.D. Thesis
Changyong Cao 1992 222 p
Avail: Univ. Microfilms Order No. DA9302893

The relationship between resolution and fractal dimensions of remotely sensed images is examined. Based on the results of testing for the reliability of the algorithms on hypothetical surfaces, the isarithm algorithm is selected for determining the fractal dimensions of remotely sensed images. This algorithm is then applied to simulated fractal Brownian motion images and four calibrated airborne multispectral remotely sensed image data sets with different true and artificial resolutions for Puerto Rico. The results from applying the fractal method to images at different levels of resolution suggest that the higher the resolution of an image, the higher the fractal dimension of the image and the more complex the image surface. This relationship between resolution and fractal dimension is further verified by results from analysis employing the local variance method for the same data sets; where it is found that the higher the resolution, the higher the local variance or the more complex the image surface. The images with artificial resolutions were found to be unrealistic in simulating images with different resolutions because the aggregate method used in generating these images does not exactly simulate the sensor's response to resolution changes. The aggregate method was widely used in image resampling and cautious use of this algorithm is suggested in future studies. The findings show that the fractal method is a useful tool in detecting the scale and resolution effects of remotely sensed images and in evaluating the trade-offs between data volume and data accuracy. More studies employing fractals and other spatial statistics to images with different artificial resolutions generated using better aggregation algorithms are needed in the future in order to further detect the scale and resolution effects in remote sensing and Geographic Information Systems (GIS). Dissert. Abstr.

N93-25868# Naval Research Lab., Bay Saint Louis, MS.
RELATIONS BETWEEN BLUE WHITING BIOMASS AND SATELLITE DERIVED PHYTOPLANKTON AND TEMPERATURE IN THE NORWEGIAN SEA Final Report
R. A. Arnone, R. A. Oriol, and R. Nero Sep. 1992 28 p
(AD-A261205; NRL/MR/7240-92-7009; NOARL-TN-153) Avail: CASI HC A03/MF A01

The abundance of blue whiting in the Norwegian Sea is correlated with surface phytoplankton concentration and sea surface temperature (SST) measured from satellite. The distribution and abundance of fish has significant impact on active acoustic volume reverberation. Acoustic fish abundance ship surveys conducted in the Norwegian Sea in August from 1984 to 1986 were analyzed for relationships with the monthly coincident average surface phytoplankton and SST. Little correlation was observed between blue whiting and phytoplankton or SST separately suggesting that fish distributions are better coupled with a multiparameter approach. The spatial and temporal averaging of high resolution satellite imagery may inhibit correlations. Features such as ocean fronts are prime contributors to fish abundance distribution. Average ocean properties (such as phytoplankton concentration or SST) can mask the local ocean events that are partially responsible for fish distribution. DTIC

N93-26354# Texas Univ., Austin. Center for Space Research.
LAGEOS LASER RANGING EARTH ROTATION Final Report, 1 Apr. 1991 - 30 Sep. 1992
B. D. Tapley, B. E. Schutz, and R. L. Duncombe 30 Sep. 1992 3 p
LIMITED REPRODUCIBILITY: More than 20% of this document may be affected by microfiche quality
(Contract N00600-91-C-0920)
(AD-A261471) Avail: Issuing Activity (Defense Technical Information Center (DTIC))

This report summarizes the progress made under USNO funding on the topic of rapid service operational production of Earth orientation and rotation parameters. The purpose of this grant was to support the production of weekly rapid service Earth orientation using satellite laser ranging (SLR) observations to Lageos. DTIC

N93-26369# Army Topographic Engineering Center, Fort Belvoir, VA.
US ARMY EVALUATION OF THE ELECTRONIC MAP DATA (EMD) PROTOTYPE Technical Report, Nov. 1990 - Dec. 1991
John P. Bradley Dec. 1992 135 p
(AD-A261693; TEC-0026) Avail: CASI HC A07/MF A02

This report provides a consolidated U.S. Army evaluation of the Electronic Map Data (EMD) prototype. This prototype was developed by the Digital Concepts and Analysis Center (DCAC) of the U.S. Army Topographic Engineering Center (USATEC). The intent of this prototype was to refine Army map background requirements by providing a real example of an alternative product. Participants in the evaluation included program managers and support contractors representing the Army components, government agencies, and private industry. Overall, evaluator comments indicated that EMD, as defined by the prototype, cannot be definitively recommended as the Army's standard map background product. Although the color separate approach does provide desirable capabilities not afforded by a composite image map, these advantages are outweighed by inherent limitations associated with decluttering by color. From user feedback indications, the original documented map background requirement submitted to DMA, which was for a product that contains declutterable feature data, requires minimal storage, and provides normalized color across map sheets, remains unchanged. DTIC

N93-26429*# National Aeronautics and Space Administration, Washington, DC.
ATMOS: LONG TERM ATMOSPHERIC MEASUREMENTS FOR MISSION TO PLANET EARTH
1992 15 p Original contains color illustrations
(NASA-TM-108720; NAS 1.15:108720) Avail: CASI HC A03/MF A01; 10 functional color pages

A long-term, space-based measurement program, together with continued balloon and aircraft-borne investigations, is essential to monitor the predicted effects in the atmosphere, to determine to what extent the concentration measurements agree with current models of stratospheric chemistry, and to determine the condition of the ozone layer. The Atmospheric Trace Molecule Spectroscopy (ATMOS) Experiment is currently making comprehensive, global measurements of Earth's atmosphere as part of the Atmospheric Laboratory for Applications and Science (ATLAS) program on the Space Shuttle. Part of NASA's Mission to Planet Earth, ATLAS is a continuing series of missions to study Earth and the Sun and provide a more fundamental understanding of the solar influences on Earth's atmosphere. The ATMOS program, instruments, and science results are presented. Derived from text

N93-26440# Army Engineer Waterways Experiment Station, Vicksburg, MS. Environmental Lab.
BIBLIOGRAPHY OF REMOTE SENSING TECHNIQUES USED IN WETLAND RESEARCH Final Report
Janet L. Lampman Jan. 1993 196 p
(AD-A261704; WES/TR/EL-WRP-SM-2) Avail: CASI HC A09/MF A03

Within the Wetlands Research Program, a work unit under the Stewardship and Management Task Area, 'Techniques for Characterizing Changes to Wetlands,' is investigating the application of remote sensing technology for detecting changes in wetland environments. This report documents a bibliographic search conducted as part of that work unit on applications of remote sensing techniques in wetland research. Results were used to guide research efforts on the use of remote sensing technology for wetland change detection and assessment. The citations are presented in three appendixes, organized by wetland type, sensor type, and author. DTIC

N93-26448# Carnegie-Mellon Univ., Pittsburgh, PA. School of Computer Science.
EXPERIMENTS IN MULTIPLE-BASELINE STEREO Research Report
Tomoharu Nakahara and Takeo Kanade Aug. 1992 37 p
(Contract F33615-90-C-1465)
(AD-A261415; CMU-CS-92-103) Avail: CASI HC A03/MF A01

This paper presents the results of our experiments with a unique multiple-baseline stereo technique. This algorithm for producing precise, unambiguous depth maps from a set of multiple stereo pairs was developed by Okutomi and Kanade. Early versions of the algorithm were shown to perform well under controlled conditions in the Calibrated Imaging Laboratory (CIL). In this paper, the algorithm is further applied to complex outdoor scenes with variable lighting conditions and large depth ranges. While Okutomi and Kanade used stereo pairs acquired by moving a camera horizontally, we also investigated the use of stereo pairs taken by moving a camera in both horizontal and vertical directions. The use of stereo images with two orthogonal baseline orientations removes ambiguity and increases precision without the problems associated with the orientation of the features in a scene. We also show that the shapes of the sum of squared-difference (SSD) curve indicates the reliability of the match, and suggest a method to classify matches into various types and to improve estimates when a false match occurs. Finally, results are presented to show the effectiveness of this algorithm and the classification method. DTIC

N93-26574# Naval Research Lab., Bay Saint Louis, MS.
IMPLEMENTATION OF CUSTOM COLORS IN THE DECWINDOWS ENVIRONMENT
Stephanie A. Myrick and Perry B. Wischow Dec. 1992 12 p Presented at the DECUS Fall Symposium held in Las Vegas, NV, 5-11 Dec. 1992
(AD-A261456; NRLD-PR-92-085-351) Avail: CASI HC A03/MF A01

This paper describes the implementation of user-defined, or custom, colors in the DECwindows environment. Custom colors can be used to augment the standard color set that is associated with the hardware colormap. The custom color set that is included in this paper consists of 240 distinct colors, each of which is comprised of red, green, and blue intensities. Intensity levels range from zero (no intensity) to 255 (maximum intensity). The DECwindow and Xwindow statements, which are required to implement the custom color set, are identified and described. Some of the tasks performed by these statements include creating and installing a colormap and accessing individual colors. Using a VAX C programming language platform, examples of proper invocation and syntax of these statements are provided. Some familiarization with C, DECwindows and Xwindows is assumed. DTIC

N93-24930*# National Geodetic Survey, Rockville, MD.
SATELLITE ALTIMETRY
Robert E. Cheney *In* NASA. Goddard Space Flight Center, Proceedings of the Ocean Climate Data Workshop 1992 p 169-170 (For primary document see N93-24915 09-42)
Avail: CASI HC A01/MF A03

N93-25615*# National Aeronautics and Space Administration. John C. Stennis Space Center, Bay Saint Louis, MS.
COMMERCIAL APPLICATIONS MULTISPECTRAL SENSOR SYSTEM
Ronald J. Birk (Sverdrup Technology, Inc., Bay Saint Louis, MS.) and Bruce Spiering *In* NASA, Washington, Technology 2002: The Third National Technology Transfer Conference and Exposition, Volume 1 Feb. 1993 p 515-526 Previously announced in IAA as A93-28081 (For primary document see N93-25561 09-99)
Avail: CASI HC A03/MF A04

44 ENERGY PRODUCTION AND CONVERSION

Includes specific energy conversion systems, e.g., fuel cells; global sources of energy; geophysical conversion; and windpower.

For related information see also *07 Aircraft Propulsion and Power, 20 Spacecraft Propulsion and Power,* and *28 Propellants and Fuels.*

N93-24975# Pacific Northwest Lab., Richland, WA.
AN EVALUATION OF THERMAL ENERGY STORAGE OPTIONS FOR PRECOOLING GAS TURBINE INLET AIR
Z. I. Antoniak, D. R. Brown, and M. K. Drost Dec. 1992 32 p
(Contract DE-AC06-76RL-01830)
(DE93-005980; PNL-8427) Avail: CASI HC A03/MF A01

Several approaches have been used to reduce the temperature of gas turbine inlet air. One of the most successful uses off-peak electric power to drive vapor-compression-cycle ice makers. The ice is stored until the next time high ambient temperature is encountered, when the ice is used in a heat exchanger to cool the gas turbine inlet air. An alternative concept would use seasonal thermal energy storage to store winter chill for inlet air cooling. The objective of this study was to compare the performance and economics of seasonal thermal energy storage in aquifers with diurnal ice thermal energy storage for gas turbine inlet air cooling. The investigation consisted of developing computer codes to model the performance of a gas turbine, energy storage system, heat exchangers, and ancillary equipment. The performance models were combined with cost models to calculate unit capital costs and levelized energy costs for each concept. The levelized energy cost was calculated for three technologies in two locations (Minneapolis, Minnesota and Birmingham, Alabama). Precooling gas turbine inlet air with cold water supplied by an aquifer thermal energy storage system provided lower cost electricity than simply increasing the size of the turbine for meteorological and geological conditions existing in the Minneapolis vicinity. A 15 to 20 percent cost reduction resulted for both 0.05 and 0.2 annual operating factors. In contrast, ice storage precooling was found to be between 5 and 20 percent more expensive than larger gas turbines for the Minneapolis location. In Birmingham, aquifer thermal energy storage precooling was preferred at the higher capacity factor and ice storage precooling was the best option at the lower capacity factor. In both cases, the levelized cost was reduced by approximately 5 percent when compared to larger gas turbines. DOE

N93-25096# Helsinki Univ. of Technology, Otaniemi (Finland).
COMPUTATIONAL AND EXPERIMENTAL STUDIES ON LARGE SCALE SOLAR HEATING Ph.D. Thesis
S. Peltola 1992 60 p
(DE93-769942; TKK-NEMO-19) Avail: CASI HC A04/MF A01

The experimental part of the work deals mainly with the experiences gained from the Kerava Solar Village (KSV) but some additional remarks are presented from international studies. The measured thermal performance of the KSV heating system indicates considerably poorer performance than original design values. Reasons for this are studied by means of computational analyses. Fundamental problems with KSV systems was too small storage size with respect both to installed collector area and connected load. From an operational point of view, the frequent heat pump failures were the most severe problem. Computational tools for large solar heating system design and analyses are presented. Numerical models developed in this work, the KERCONT and SUPERSOL, are validated with measured performance from the KSV indicating reasonably good accuracy. The tools have been applied for detecting KSV heating system problems and for finding solutions for them as well as for re-design of the system. More general analyses are presented on the applicability of the KSV system principle in other load sizes and locations. A new approach for preliminary studies on Central Solar Heating Plants with Seasonal Storage (CSHPSS) is described. The analytical model, SOLCHIPS, is shown to be a very effective tool for pre-design studies. The validity of SOLCHIPS approach is studied by comparing the results against results from validated numerical model, MINSUN. In the last part of the work, preliminary results from numerical simulations of summer time district solar heating with short term storage are presented. According to the analyses, these systems should provide heat at or below the cost achievable with seasonal storage systems. DOE

N93-25097# Helsinki Univ. of Technology, Otaniemi (Finland).
ADVANCED ENERGY SYSTEMS AND TECHNOLOGIES - NATIONAL R AND D PROGRAMME
P. D. Lund Aug. 1992 64 p
(DE93-769943; TKK-NEMO-21) Avail: CASI HC A04/MF A01

The energy R and D in Finland is accomplished through the energy research programs of the Ministry of Trade and Industry. Today there are some 12 R and D programs in operation covering the various aspects of the energy sector. The NEMO-program deals with advanced new energy technologies and systems. The NEMO-program was launched in 1988 and it ends at the end of 1992. Helsinki University of Technology has been responsible for the coordination and most of the universities, research centers, and companies on new advanced energy technologies have been involved in the realization of NEMO. The objectives of the program have been to assess the potential of new technologies in the Finnish energy supply system, encourage and support businesses, and to create necessary research tradition in Finland. At the beginning in year 1988, several new technologies were included, but as the knowledge has increased, focusing on the most promising fields has taken place. Wind and solar energy show the best promises in respect to business activities and possibilities for utilization in Finland. Energy storage some other advanced technologies such as fuel cells and hydrogen technologies represented in the NEMO-program have an important role, but the commercial applications lie more distant in the future. The NEMO-program has reached its objectives. The international evaluation in fall 1990 gave very positive feedback and the scientific quality of the work was found good. At the same time, the contents was still focused more on commercial applications to support national industries in the field. The descriptions of the ongoing NEMO research projects are included in this report. DOE

N93-25098# Georgia Tech Research Inst., Atlanta.
NEW CONCEPTS FOR HIGH EFFICIENCY ENERGY CONVERSION: THE AVALANCHE HETEROSTRUCTURE AND SUPERLATTICE SOLAR CELLS
C. J. Summers, A. Rohatgi, A. Torabi, and H. M. Harris Jan. 1993 118 p Prepared for Midwest Research Inst., Golden, CO
(Contract DE-AC02-83CH-10093)
(DE92-010592; NREL/TP-410-4960) Avail: CASI HC A06/MF A02

This report describes an investigation into the theory and technology of a novel heterojunction or superlattice, single-junction solar cell, which injects electrons across the heterointerface to produce highly efficient impact ionization of carriers in the lowband-gap side of the junction, thereby conserving their total energy. Also, the superlattice structure has the advantage of relaxing the need for perfect lattice matching at the p-n interface and will inhibit the cross diffusion of dopant atoms that typically occurs in heavy doping. This structure avoids the use of tunnel junctions that make it very difficult to achieve the predicted efficiencies in cascade cells, thus making it possible to obtain energy efficiencies that are competitive with those predicted for cascade solar cells with reduced complexity and cost. This cell structure could also be incorporated into other solar cell structures designed for wider spectral coverage. DOE

N93-25102# Research Triangle Inst., Research Triangle Park, NC.
AN INVERTED AlGaAs/GaAs PATTERNED-Ge TUNNEL JUNCTION CASCADE CONCENTRATOR SOLAR CELL
R. Venkatasubramanian Jan. 1993 74 p Prepared for Midwest Research Inst., Golden, CO
(Contract DE-AC02-83CH-10093)
(DE93-000073; NREL/TP-411-5289) Avail: CASI HC A04/MF A01

This report describes work to develop inverted-grown Al(0.34)Ga(0.66)As/GaAs cascades. Several significant developments are reported on as follows: (1) The AM1.5 1-sun total-area efficiency of the top Al(0.34)Ga(0.66)As cell for the cascade was improved from 11.3 to 13.2 percent (NREL measurement total-area). (2) The 'cycled' organometallic vapor phase epitaxy growth (OMVPE) was studied in detail utilizing a combination of characterization techniques including Hall-data, photoluminescence, and secondary ion mass spectroscopy. (3) A technique called eutectic-metal-bonding (EMB) was developed by strain-free mounting of thin GaAs-AlGaAs films (based on lattice-matched growth on Ge substrates and selective plasma etching of Ge substrates) onto Si carrier substrates. Minority-carrier lifetime in an EMB GaAs double-heterostructure was measured as high as 103 nsec, the highest lifetime report for a freestanding GaAs thin film. (4) A thin-film, inverted-grown GaAs cell with a 1-sun AM1.5 active-area efficiency of 20.3 percent was obtained. This cell was eutectic-metal-bonded onto Si. (5) A thin-film inverted-grown, Al(0.34)Ga(0.66)As/GaAs cascade with AM1.5 efficiency of 19.9 and 21 percent at 1-sun and 7-suns, respectively, was obtained. This represents an important milestone in the development of an AlGaAs/GaAs cascade by OMVPE utilizing a tunnel interconnect and demonstrates a proof-of-concept for the inverted-growth approach. DOE

N93-25136*# National Aeronautics and Space Administration. Lewis Research Center, Cleveland, OH.
TEST RESULTS OF A STIRLING ENGINE UTILIZING HEAT EXCHANGER MODULES WITH AN INTEGRAL HEAT PIPE
Robert C. Skupinski (Sverdrup Technology, Inc., Brook Park, OH.), Leonard K. Tower (Sverdrup Technology, Inc., Brook Park, OH.), Frank J. Madi (Sverdrup Technology, Inc., Brook Park, OH.), and Kevin D. Brusk Apr. 1993 13 p
(RTOP 590-13-11)
(NASA-TM-105883; E-7681; NAS 1.15:105883) Avail: CASI HC A03/MF A01

The Heat Pipe Stirling Engine (HP-1000), a free-piston Stirling engine incorporating three heat exchanger modules, each having a sodium filled heat pipe, has been tested at the NASA-Lewis Research Center as part of the Civil Space Technology Initiative (CSTI). The heat exchanger modules were designed to reduce the number of potential flow leak paths in the heat exchanger assembly and incorporate a heat pipe as the link between the heat source and the engine. An existing RE-1000 free-piston Stirling engine was modified to operate using the heat exchanger modules. This paper describes heat exchanger module and engine performance during baseline testing. Condenser temperature profiles, brake power, and efficiency are presented and discussed. Author

N93-25183# Pacific Northwest Lab., Richland, WA.
AQUIFER THERMAL ENERGY (HEAT AND CHILL) STORAGE
E. A. Jenne, ed. Nov. 1992 134 p Presented at the 27th Intersociety Energy Conversion Engineering Conference, San Diego, CA, 3-7 Aug. 1992
(Contract DE-AC06-76RL-01830)
(DE93-006446; PNL-8381; CONF-920801) Avail: CASI HC A07/MF A02

As part of the 1992 Intersociety Conversion Engineering Conference (IECEC), held in San Diego, California, 3 - 7 Aug. 1992, the Seasonal Thermal Energy Storage Program coordinated five sessions dealing specifically with aquifer thermal energy storage technologies (ATES). Researchers from Sweden, The Netherlands, Germany, Switzerland, Denmark, Canada, and the United States presented papers on a variety of ATES related topics. With special permission from the Society of Automotive Engineers, host society for the 1992 IECEC, these papers are being republished here as a standalone summary of ATES technology status. Individual papers are indexed separately. DOE

N93-25253# Midwest Research Inst., Golden, CO. National Renewable Energy Lab.
NON-H2Se, ULTRA-THIN CIS DEVICES
A. E. Delahoy, J. Britt, and Z. Kiss Feb. 1993 61 p Prepared in cooperation with Energy Photovoltaics, Inc., Princeton, NJ
(Contract DE-AC02-83CH-10093)
(DE93-000078; NREL/TP-413-5334) Avail: CASI HC A04/MF A01

This report describes work done during Phase 1 of a 3-phase, cost-shared contract. Objective of the subcontract is to demonstrate 12 percent total-area efficiency copper indium diselenide (CIS) solar cells and 50-W CIS modules average at least 8 W/ft(exp 2) in the third year. At the end of Phase 1, EPV delivered to NREL a 1.1 cm(exp 2) CIS cell with an active area efficiency of 10.5 percent. The corresponding total-area efficiency is 7.9 percent. DOE

N93-25504# Colorado State Univ., Fort Collins.
ROLE OF POLYCRYSTALLINITY IN CdTe AND CuInSe2 PHOTOVOLTAIC CELLS
J. R. Sites Nov. 1992 34 p Prepared for Midwest Research Inst., Golden, CO
(Contract DE-AC02-83CH-10093)
(DE93-000045; NREL/TP-451-5190) Avail: CASI HC A03/MF A01

The limiting role of polycrystallinity in thin-film solar cells has been reduced somewhat during the past year, and efficiencies of both CdTe and CuInSe2 cells are approaching 15 percent. Quantitative separation of loss mechanisms shows that individual losses, with the exception of forward recombination current, can be made comparable to their single crystal counterparts. One general manifestation of the extraneous trapping states in that the voltage of all polycrystalline thin-film cells drifts upward by 10-50 mV following the onset of illumination. DOE

N93-26310# Naval Postgraduate School, Monterey, CA. Dept. of Physics.
BASIC RESEARCH THERMOACOUSTIC HEAT TRANSPORT Annual Summary Report, 1 Oct. 1991 - 30 Sep. 1992
Anthony A. Atchley Nov. 1992 35 p
(AD-A261334; NPS-PH-93-006) Avail: CASI HC A03/MF A01

This annual report details progress in basic research in thermoacoustic heat transport made during the period October 1, 1991 through September 30, 1992. Our major research efforts were concentrated in two areas during FY92: (1) a standing wave analysis of the low amplitude performance of thermoacoustic prime movers both below and above the onset of self-oscillation and (2) a study of finite amplitude standing waves in both harmonic and anharmonic tubes. In addition to these areas, FY92 research efforts also included the investigation of heat driven refrigerators and preliminary work on investigations of thermoacoustic engines with laser Doppler anemometry. This technical report summarizes the important results of these projects. A publications, patents, presentations, and honors report is also included. DTIC

N93-25572*# Recotech Corp., Aurora, OH.
CONVERTING ENVIRONMENTAL WASTES INTO VALUABLE RESOURCES
Leonard A. Duval *In* NASA, Washington, Technology 2002: The Third National Technology Transfer Conference and Exposition, Volume 1 Feb. 1993 p 118-120 (For primary document see N93-25561 09-99)
Avail: CASI HC A01/MF A04

N93-25597*# Naval Surface Warfare Center, Panama City, FL.
PHOTOVOLTAIC POWER WITHOUT BATTERIES FOR CONTINUOUS CATHODIC PROTECTION
W. W. Muehl, Sr. *In* NASA, Washington, Technology 2002: The Third National Technology Transfer Conference and Exposition, Volume 1 Feb. 1993 p 341-344 (For primary document see N93-25561 09-99)
Avail: CASI HC A01/MF A04

45 ENVIRONMENT POLLUTION

Includes atmospheric, noise, thermal, and water pollution.

N93-24673# Westinghouse Savannah River Co., Aiken, SC. Savannah River Center.
A COMPARISON OF THE WIND SYSTEM ATMOSPHERIC MODELS AND MATS DATA
Jerome D. Fast, Stephen Berman, and Robert P. Addis 14 Jul. 1992 15 p Presented at the 10th Symposium on Turbulence and Diffusion, Portland, OR, 29 Sep. - 2 Oct. 1992
(Contract DE-AC-9-89SR-18035)
(DE93-002687; WSRC-MS-92-178; CONF-9209158-9) Avail: CASI HC A03/MF A01

Atmospheric transport and diffusion models have been developed by the Environmental Technology Section (ETS) of the Savannah River Technology Center to calculate the location and concentration of toxic or radioactive materials during an accidental release at the Savannah River Site (SRS). The output from these models has been used to support initial on-site and off-site emergency response activities such as protective action decision making and field monitoring coordination. These atmospheric transport and diffusion models have been incorporated into an automated computer-based system called the Weather INformation and Display (WIND) System and linked to real-time meteorological and radiological monitoring instruments to provide timely information for these emergency response activities. This study will compare two of the WIND System atmospheric models, PUFF/PLUME and 2DPUF, with a select group of MATS experiments and examine the results in detail to determine the performance of the models. Additional results from this study can be found in Fast et al. DOE

N93-24674# Los Alamos National Lab., NM.
HEALTH AND ENVIRONMENTAL CHEMISTRY: ANALYTICAL TECHNIQUES, DATA MANAGEMENT, AND QUALITY ASSURANCE
Margaret A. Gautier, ed. Oct. 1992 368 p
(Contract W-7405-eng-36)
(DE93-002853; LA-10300-M-Vol-1) Avail: CASI HC A16/MF A03

Analytical procedures are described for the determination of organic compounds, metals, and radioisotopes in environmental materials, human tissue, urine, feces, and waste water. DOE

N93-24675# Pacific Northwest Lab., Richland, WA.
AN ASSESSMENT OF ALTERNATIVES AND TECHNOLOGIES FOR REPLACING OZONE-DEPLETING SUBSTANCES AT DOE FACILITIES
C. W. Purcell, K. B. Miller, J. R. Friedman, R. D. Rapoport, D. R. Conover, P. L. Hendrickson, and T. C. Koss (Department of Energy, Richland, WA.) Oct. 1992 77 p
(Contract DE-AC-6-76RL-01830)
(DE93-002862; PNL-8222) Avail: CASI HC A05/MF A01

Title 6 of the Clean Air Act, as amended, mandates a production phase-out for ozone-depleting substances (ODSs). These requirements will have a significant impact on US Department of Energy (DOE) facilities. Currently, DOE uses ODS's in three major activities: fire suppression (halon), refrigeration and cooling (chlorofluorocarbons (CFC's)), and cleaning that requires solvents (CFC's, methyl chloroform, and carbon tetrachloride). This report provides basic information on methods and strategies to phase out use of ODS's at DOE facilities. DOE

N93-24676# Oak Ridge National Lab., TN.
AN INTRODUCTORY GUIDE TO UNCERTAINTY ANALYSIS IN ENVIRONMENTAL AND HEALTH RISK ASSESSMENT
F. O. Hoffman and J. S. Hammonds Oct. 1992 34 p
(Contracts DE-AC05-84OR-21400; DE-AC05-76OR-00001)
(DE93-002873; ES/ER/TM-35) Avail: CASI HC A03/MF A01

To compensate for the potential for overly conservative estimates of risk, using standard US Environmental Protection Agency methods, an uncertainty analysis should be performed as an integral part of each risk assessment. Uncertainty analyses allow one to obtain quantitative results in the form of confidence intervals that will aid in decision making and will provide guidance for the acquisition of additional data. To perform an uncertainty analysis, one must frequently rely on subjective judgment in the absence of data to estimate the range and a probability distribution describing the extent of uncertainty about a true but unknown value for each parameter of interest. This information is formulated from professional judgment based on an extensive review of literature, analysis of the data, and interviews with experts. Various analytical and numerical techniques are available to allow statistical propagation of the uncertainty in the model parameters to a statement of uncertainty in the risk to a potentially exposed individual. Although analytical methods may be straightforward for relatively simple models, they rapidly become complicated for more involved risk assessments. Because of the tedious efforts required to mathematically derive analytical approaches to propagate uncertainty in complicated risk assessments, numerical methods such as Monte Carlo simulation should be employed. The primary objective of this report is to provide an introductory guide for performing uncertainty analysis in risk assessments being performed for Superfund sites. DOE

N93-24908 Georgia Inst. of Tech., Atlanta.
ATMOSPHERIC REACTIVE NITROGEN OXIDES AND THEIR RELATIONSHIP WITH URBAN AND RURAL OZONE FORMATION Ph.D. Thesis
Tao Wang 1992 230 p
Avail: Univ. Microfilms Order No. DA9303153

NO(x)(NO + NO2), HNO3, particulate NO3(-) and PAN are the primary forms of the reactive nitrogen oxides in the lower troposphere. NO(x) serves as catalyst and plays a key role in generating elevated ozone in the polluted boundary layer. PAN, HNO3, and NO3(-) are, like O3, the products of complex photochemistry involving hydrocarbons and nitrogen oxides. This work focuses on investigation of these nitrogen species in the ambient atmosphere of the southeastern U.S. including urban, suburban, and rural environments. These results indicate that for all environments encountered outside of the urban core, NO(x) is the limiting species in the formation of photochemical ozone. Dissert. Abstr.

N93-24952# Oak Ridge National Lab., TN. Carbon Dioxide Information Analysis Center.
SELECTED TRANSLATED ABSTRACTS OF RUSSIAN-LANGUAGE CLIMATE-CHANGE PUBLICATIONS: 1. SURFACE ENERGY BUDGET
Marvel D. Burtis, comp. Sep. 1992 62 p
(Contract DE-AC05-84OR-21400)
(DE93-003189; ORNL/CDIAC-57) Avail: CASI HC A04/MF A01

This report presents abstracts (translated into English) of important Russian-language literature concerning the surface energy budget as it relates to climate change. In addition to the bibliographic citations and abstracts translated into English, this report presents the original citations and abstracts in Russian. Author and title indexes are included, to assist the reader in locating abstracts of particular interest. DOE

N93-24955# Westinghouse Environmental Management Co. of Ohio, Cincinnati. Fernald Environmental Management Project.
USE OF THE ENVIRONMENTAL RESOURCE MANAGEMENT AND ANALYSIS SYSTEM AT THE FERNALD ENVIRONMENTAL MANAGEMENT PROJECT
J. L. Erjavec Jun. 1992 6 p Presented at the 104th Annual Meeting of the Geological Society of America, Inc., Cincinnati, OH, 26-29 Oct. 1992 Prepared in cooperation with Parsons Environmental Services, Inc., Fairfield, OH
(Contract DE-AC05-86OR-21600)
(DE93-002943; FEMP/SUB-052; CONF-921058-1) Avail: CASI HC A02/MF A01

In the past, hazardous waste site characterization and remediation using computer-based technologies has been a difficult and time-consuming process because of the need to analyze data using non-interfaced computer and software environments. The Environmental Resource Management and Analysis System (ERMA) was developed as an innovative approach to the management, analyses, and depiction of data collected during a hazardous site remediation. A modular, multi-disciplined software package, ERMA integrates an environmental database management system with a variety of Geographic Information System technologies. ERMA capabilities include spatial analysis, three-dimensional subsurface geologic interpretation and modeling, terrain modeling, and groundwater flow and contaminant transport modeling. ERMA's data management is provided through a set of user-modifiable, graphic interface tools that permit complex data queries,

data modification and reporting. An ERMA prototype has been implemented at the Fernald Environmental Management Project using groundwater monitoring and elevation data collected over the last few years. DOE

N93-24956# Argonne National Lab., IL.
A NEW METHOD FOR INFRARED IMAGING OF AIR CURRENTS IN AND AROUND CRITICAL HAZARD FUME HOODS
William A. Mulac, James R. McCreary, and Henry Schmalz 1992 17 p Presented at the IAQ '92 Conference: Environments for People, San Francisco, CA, 18-21 Oct. 1992; sponsored by the American Society of Heating, Refrigerating and Air Conditioning Engineers, Inc.
(Contract W-31-109-eng-38)
(DE93-003009; ANL/CHM/CP-75284; CONF-921095-2) Avail: CASI HC A03/MF A01

A real-time method of measuring and recording the efficacy of vapor containment in and around critical hazard fume hoods is being developed. An infrared camera whose response is restricted to a spectral range that overlaps a strong absorption band in a non-toxic gas is used to render real-time video images of the presence and flow of the gas. The gas, nitrous oxide, is ejected in a continuous stream in and around fume hoods that are to be certified capable of containing hazardous fumes. The principle advantage is that various scenarios of air flow displacement in and outside the hood can be easily investigated; the principle limitation is the necessity of high tracer gas concentration to obtain strong visualizations. We hope that this technique can be found to be an effective and safe method to test hoods in locations that were built before present regulations were promulgated. DOE

N93-24977# Los Alamos National Lab., NM.
ANALYSIS OF LARI SENSOR SYSTEM Final Report
Richard N. Pfisterer (Breault Research Organization, Tucson, AZ.), Gary L. Peterson (Breault Research Organization, Tucson, AZ.), and Robert P. Breault (Breault Research Organization, Tucson, AZ.) 25 Nov. 1992 18 p Prepared in cooperation with Breault Research Organization, Inc., Tucson, AZ
(Contract W-7405-eng-36)
(DE93-006334; LA-SUB-93-4) Avail: CASI HC A03/MF A01

Los Alamos National Labs (LANL) is developing a new space sensor for examination of global warming effects. This sensor is called LARI (Los Alamos Radiometric Instrument) and is a next generation follow-on to the ERBE instrument launched several years ago. Breault Research Organization, Inc. (BRO) is pleased to offer engineering consulting services for the development of this sensor. The goal of the consultation is to assist LANL engineers with the conceptual design of the LARI instrument. While the contract specifically stated that computer analyses would not be performed, we felt that some minimum level of computation effort would add more substance to the conclusions. DOE

N93-25122# Lawrence Livermore National Lab., CA.
THE AFTAC MODEL INTEGRATION PROJECT Annual Progress Report
D. J. Rodriguez and R. M. Moore Oct. 1992 33 p
(Contract W-7405-eng-48)
(DE93-003334; UCRL-ID-112129) Avail: CASI HC A03/MF A01

The Lawrence Livermore National Laboratory (LLNL) has completed its third year of research and development on the Basic Interactive Prototype (BIP), a term that describes both the modeling capability and the supporting environment for simulating the dispersion of pollutant plumes over great distances and for displaying the results. For purposes of organization, several major components of the system are identified and then their state of completion is described. However, the reader should be aware of, and always strive to understand, the interrelationships between the individual components. The reader's attention is drawn to these interconnections throughout the report. DOE

N93-25126# Los Alamos National Lab., NM.
EFFICIENT INSPECTION OF NETWORK POLLUTION DATA
L. H. Auer and J. P. Mutschlecner 1992 12 p Presented at the International Symposium on Air Pollution, Monterrey, Mexico, 16-25 Feb. 1993
(Contract W-7405-eng-36)
(DE93-003810; LA-UR-92-3655; CONF-930208-1) Avail: CASI HC A03/MF A01

A package of tools for the rapid survey of data from a pollution monitoring network was developed. It was designed to help in the recognition of regularities as well as peculiarities in a data set. Critical features are interactive user control, real-time graphic presentation in alternative formats, and simple modification of code to permit new options. The graphics used include movies of the spatial development, time-series, and scatter diagrams modulo the diurnal or weekly cycles. DOE

N93-25143# Argonne National Lab., IL. Environmental Assesment and Informational Sciences Div.
AQUIS: A PC-BASED AIR INVENTORY AND PERMIT MANAGER
Albert E. Smith, Craig C. Huber, John Tschanz, and S. James Ryckman, Jr. (Air Force Materials Lab., Wright-Patterson AFB, OH.) 1992 8 p Presented at the International Symposium on Emission Inventory Issues and Progress, Research Triangle Park, NC, 19-22 Oct. 1992
(Contract W-31-109-eng-38)
(DE93-003006; ANL/EAIS/CP-77721; CONF-921060-1) Avail: CASI HC A02/MF A01

The Air Quality Utility Information System (AQUIS) was developed to calculate and track sources, emissions, stacks, permits, and related information. The system runs on IBM-compatible personal computers with dBASE 4 and tracks more than 1,200 data items distributed among various source categories. AQUIS is currently operating at nine US Air Force facilities that have up to 1,000 sources. The system provides a flexible reporting capability that permits users who are unfamiliar with database structure to design and prepare reports containing user-specified information. In addition to six criteria pollutants, AQUIS calculates compound-specific emissions and allows users to enter their own emission estimates. DOE

N93-25144# Oak Ridge National Lab., TN. Carbon Dioxide Information Analysis Center.
TRENDS '91: A COMPENDIUM OF DATA ON GLOBAL CHANGE. HIGHLIGHTS
Thomas A. Boden, ed., Robert J. Sepanski, ed., and Frederick W. Stoss, ed. Mar. 1992 71 p
(Contract DE-AC05-84OR-21400)
(DE93-003112; ORNL/CDIAC-49) Avail: CASI HC A04/MF A01

The Carbon Dioxide Information Analysis Center (CDIAC) at Oak Ridge National Laboratory (ORNL) was prompted to produce the series Trends, a concise inventory of data in response to heightened concern about global environmental issues, in particular climate changes induced by the greenhouse effect. Extracts from Trends '91 are presented to illustrate the content, style, and presentation of data contained in the full 700-page report. A listing of the investigators contributing data for Trends '91 is included. In addition, it contains the abstract, foreward, and acknowledgements, as well as the introduction and a sample data record from each of the reports's five chapters. The topics covered are atmospheric CO2, atmospheric CH4, other trace gases, CO2 emissions, and temperature. Appendix A provides information about CDIAC and its activities related to global environmental issues. Appendix B lists the contents of the full report. An order form for obtaining a free copy of Trends '91 is found in Appendix C. DOE

N93-25145# Lawrence Livermore National Lab., CA. Program for Climate Model Diagnosis and Intercomparison.
THE EFFECTS OF SAMPLING FREQUENCY ON THE CLIMATE STATISTICS OF THE ECMWF GENERAL CIRCULATION MODEL
Thomas J. Phillips, W. Lawrence Gates, and Klaus Arpe (Max-Planck-Inst. fuer Meteorologie, Hamburg, Germany.) Sep. 1992 26 p
(Contract W-7405-eng-48)
(DE93-003338; UCRL-ID-108226; PCMDI-5) Avail: CASI HC A03/MF A01

The effects of sampling frequency on the first- and second-moment statistics of selected European Center (EC) model variables are investigated in a simulation of 'perpetual July' with a diurnal cycle included and with surface and atmospheric fields saved at hourly intervals. The shortest characteristic time scales (as determined by the enfolding time of lagged autocorrelation functions) are those of ground heat fluxes and temperatures, precipitation and run-off, convective processes, cloud properties, and atmospheric vertical motion, while the longest time scales are exhibited by soil temperature and moisture, surface pressure, and atmospheric specific

humidity, temperature, and wind. The time scales of surface heat and momentum fluxes and of convective processes are substantially shorter over land than over the oceans. DOE

N93-25146# Lawrence Livermore National Lab., CA.
GLOBAL WARMING POTENTIAL FOR CF4
Donald J. Wuebbles and Allen S. Grossman 16 Nov. 1992 3 p
(Contract W-7405-eng-48)
(DE93-005740; UCRL-ID-112295) Avail: CASI HC A01/MF A01

With sufficient emissions, fluorinated gases such as CF4 could contribute significantly to the concerns about global warming because they are greenhouse gases, are chemically very inert, and have long accumulation lifetimes in the atmosphere. At this time, the only significant known source of CF4 is primary aluminum smelting. While current emissions are small, additional sources could make CF4 an important contribution to climate forcing in the future. DOE

N93-25147# Lawrence Livermore National Lab., CA.
A CORRELATED K-DISTRIBUTION MODEL OF THE HEATING RATES FOR H2O AND A MOLECULAR MIXTURE IN THE 0-2500 cm(EXP -1) WAVELENGTH REGION IN THE ATMOSPHERE BETWEEN 0 AND 60 km
Allen S. Grossman and Keith Grant 16 Nov. 1992 9 p
(Contract W-7405-eng-48)
(DE93-005741; UCRL-ID-112296) Avail: CASI HC A02/MF A01

A prototype infrared radiative transfer model using a correlated k-distribution technique to calculate the transmission between atmospheric levels was used to calculate the radiative fluxes and heating rates for H2O and a mixture of the major molecular absorbers in the atmosphere between 0 and 60 km. The mixture consists of H2O, CO2, O3, CH4, and N2O. The wave number range considered is 0-2500 cm(exp -1). The use of the k-distribution method allows 25 cm(exp -1) wave number bins to produce fluxes and heating rates which are within ten percent of the results of detailed line by line calculations. DOE

N93-25157*# National Aeronautics and Space Administration, Washington, DC.
THE ATMOSPHERIC EFFECTS OF STRATOSPHERIC AIRCRAFT. REPORT OF THE 1992 MODELS AND MEASUREMENTS WORKSHOP. VOLUME 1: WORKSHOP OBJECTIVES AND SUMMARY
Michael J. Prather, ed. and Ellis E. Remsburg, ed. (National Aeronautics and Space Administration. Langley Research Center, Hampton, VA.) Mar. 1993 132 p Workshop held in Satellite Beach, FL, 3-7 Feb. 1992
(NASA-RP-1292-Vol-1; NAS 1.61:1292-Vol-1) Avail: CASI HC A07/MF A02

This Workshop on Stratospheric Models and Measurements (M&M) marks a significant expansion in the history of model intercomparisons. It provides a foundation for establishing the credibility of stratospheric models used in environmental assessments of chlorofluorocarbons, aircraft emissions, and climate-chemistry interactions. The core of the M&M comparisons involves the selection of observations of the current stratosphere (i.e., within the last 15 years): these data are believed to be accurate and representative of certain aspects of stratospheric chemistry and dynamics that the models should be able to simulate. Author

N93-25158*# National Aeronautics and Space Administration, Washington, DC.
THE ATMOSPHERIC EFFECTS OF STRATOSPHERIC AIRCRAFT. REPORT OF THE 1992 MODELS AND MEASUREMENTS WORKSHOP. VOLUME 2: COMPARISONS WITH GLOBAL ATMOSPHERIC MEASUREMENTS
Michael J. Prather, ed. and Ellis E. Remsberg, ed. (National Aeronautics and Space Administration. Langley Research Center, Hampton, VA.) Mar. 1993 254 p Workshop held in Satellite Beach, FL, 3-7 Feb. 1992
(NASA-RP-1292-Vol-2; NAS 1.61:1292-Vol-2) Avail: CASI HC A12/MF A03

This Workshop on Stratospheric Models and Measurements (M&M) marks a significant expansion in the history of model intercomparisons. It provides a foundation for establishing the credibility of stratospheric models used in environmental assessments of chlorofluorocarbons, aircraft emissions, and climate-chemistry interactions. The core of the M&M comparisons involves the selection of observations of the current stratosphere (i.e., within the last 15 years): these data are believed to be accurate and representative of certain aspects of stratospheric chemistry and dynamics that the models should be able to simulate. Author (revised)

N93-25159*# National Aeronautics and Space Administration, Washington, DC.
THE ATMOSPHERIC EFFECTS OF STRATOSPHERIC AIRCRAFT. REPORT OF THE 1992 MODELS AND MEASUREMENTS WORKSHOP. VOLUME 3: SPECIAL DIAGNOSTIC STUDIES
Michael J. Prather, ed. and Ellis E. Remsberg, ed. (National Aeronautics and Space Administration. Langley Research Center, Hampton, VA.) Mar. 1993 335 p Workshop held in Satellite, FL, 3-7 Feb. 1992
(NASA-RP-1292-Vol-3; NAS 1.61:1292-Vol-3) Avail: CASI HC A15/MF A03

This Workshop on Stratospheric Models and Measurements (M&M) marks a significant expansion in the history of model intercomparisons. It provides a foundation for establishing the credibility of stratospheric models used in environmental assessments of chlorofluorocarbons, aircraft emissions, and climate-chemistry interactions. The core of the M&M comparisons involves the selection of observations of the current stratosphere (i.e., within the last 15 years): these data are believed to be accurate and representative of certain aspects of stratospheric chemistry and dynamics that the models should be able to simulate. Author

N93-25166# Los Alamos National Lab., NM.
APPLICATIONS OF WAVELET-BASED COMPRESSION TO MULTIDIMENSIONAL EARTH SCIENCE DATA
J. N. Bradley and C. M. Brislawn 1993 13 p Presented at the 1993 Space and Earth Science Data Compression Workshop, Snowbird, UT, 2 Apr. 1993
(Contract W-7405-eng-36)
(DE93-007348; LA-UR-93-299; CONF-930490-1) Avail: CASI HC A03/MF A01

A data compression algorithm involving vector quantization (VQ) and the discrete wavelet transform (DWT) is applied to two different types of multidimensional digital earth-science data. The algorithm (WVQ) is optimized for each particular application through an optimization procedure that assigns VQ parameters to the wavelet transform subbands subject to constraints on compression ratio and encoding complexity. Preliminary results of compressing global ocean model data generated on a Thinking Machines CM-200 supercomputer are presented. The WVQ scheme is used in both a predictive and nonpredictive mode. Parameters generated by the optimization algorithm are reported, as are signal-to-noise ratio (SNR) measurements of actual quantized data. The problem of extrapolating hydrodynamic variables across the continental landmasses in order to compute the DWT on a rectangular grid is discussed. Results are also presented for compressing Landsat TM 7-band data using the WVQ scheme.The formulation of the optimization problem is presented along with SNR measurements of actual quantized data. Postprocessing applications are considered in which the seven spectral bands are clustered into 256 clusters using a k-means algorithm and analyzed using the Los Alamos multispectral data analysis program, SPECTRUM, both before and after being compressed using the WVQ program. DOE

N93-25184# Mitre Corp., McLean, VA.
CHAMMP
H. Abarbanel, R. Chervin, P. Colella, F. Dyson, S. Flatte, M. Freeman, M. Gregg, S. Koonin, C. Leith, and G. MacDonald et al Dec. 1992 57 p
(Contract DE-AI05-90ER-30174)
(DE93-007290; JSR-91-310) Avail: CASI HC A04/MF A01

The US global change research program embraces three important classes of activities. One is the long-term monitoring of climatic variables to detect and measure global change. A second class comprises detailed short-term studies of the processes that govern the climate system. The third activity involves the construction of climate models (e.g., ocean and atmospheric general circulation models - GCM's) incorporating the results of process studies to improve the ability to predict and eventually to respond to global change. The CHAMMP program clearly falls within the third class of activities (modeling) and complements DOE's Atmospheric Radiation Measurement Program (ARM) of process studies in the atmosphere, and NASA's Earth Observing System (EOS) program, aimed primarily at monitoring. CHAMMP's stated goal is to develop, verify, and

apply a new generation of climate model within a coordinated framework, that: (1) incorporates the best available scientific and numerical approaches to represent physical, biogeochemical, and ecological processes; (2) fully utilizes the hardware and software capabilities of new computer architectures; (3) probes the limits of climate predictability; and (4) can be used to address the challenging problem of understanding the greenhouse climate issue through the ability of models to simulate time-dependent climatic changes over extended times with regional resolution. DOE

N93-25244*# Maryland Univ., College Park. Dept. of Meteorology.
WINTER WARMING FROM LARGE VOLCANIC ERUPTIONS
Alan Robock and Jianping Mao 1992 11 p
(Grant NAG5-1835)
(NASA-CR-192848; NAS 1.26:192848) Avail: CASI HC A03/MF A01

An examination of the Northern Hemisphere winter surface temperature patterns after the 12 largest volcanic eruptions from 1883-1992 shows warming over Eurasia and North America and cooling over the Middle East which are significant at the 95 percent level. This pattern is found in the first winter after tropical eruptions, in the first or second winter after midlatitude eruptions, and in the second winter after high latitude eruptions. The effects are independent of the hemisphere of the volcanoes. An enhanced zonal wind driven by heating of the tropical stratosphere by the volcanic aerosols is responsible for the regions of warming, while the cooling is caused by blocking of incoming sunlight. Author

N93-25263 Illinois Inst. of Tech., Chicago.
A STUDY OF MASS SIZE DISTRIBUTIONS AND PARTICLE DEPOSITION VELOCITIES IN AMBIENT AIR Ph.D. Thesis
Guor Cheng Fang 1992 233 p
Avail: Univ. Microfilms Order No. DA9301983

Atmospheric coarse, fine particle, and elemental (Al, Ca, Fe, Mg, Na, Si, Ti, Cd, Cr, Cu, Mn, Pb, V, Zn) mass-size distributions were measured with the Noll Rotary Impactor (NRI) and cascade impactor in Chicago, Illinois. Simultaneously dry deposition fluxes were measured with a smooth surrogate surface. The elements of crustal origin (Al, Ca, Fe, Mg, Na, Si, Ti) tend to associate with the coarse particle mode while the metals of anthropogenic origin (Cd, Cr, Cu, Mn, Pb, V, Zn) were associated with the fine particle mode. The data analyzed have shown that the concentration of heavy metals and particles exist in both fine and coarse ranges and that their distribution changed with wind direction. Samples taken with wind over Lake Michigan and lower concentrations than those with wind originating over the land. The mass deposition velocities for coarse and fine particles were calculated with a multiple regression method to be 6.0 and 0.50 cm/sec for the coarse and fine particles, respectively. Multiple regression method combined with Slinn and Slinn 1-step method yield 0.451 and 0.107 cn/sec deposition velocities for the coarse and fine particles. Using these methods of multiple regression it found that coarse particles are responsible for the majority (greater than 85 percent) of the dry deposition flux for the mass and all the elements. Dissert. Abstr.

N93-25287*# New Hampshire Univ., Durham. Inst. for the Study of Earth, Oceans and Space.
MEASUREMENTS OF NITRIC ACID, CARBOXYLIC ACIDS, AND SELECTED AEROSOL SPECIES FOR THE NASA/GTE PACIFIC MISSION - WEST (PEM-WEST) Final Report, 9 Apr. 1991 - 8 Apr. 1993
Robert W. Talbot and Jack E. Dibb Apr. 1993 27 p
(Grant NAG1-1233)
(NASA-CR-192976; NAS 1.26:192976) Avail: CASI HC A03/MF A01

The research investigation funded through this grant to the University of New Hampshire was performed during a major field expedition conducted by the NASA Tropospheric Chemistry Program. The NASA Global Tropospheric Experiment (GTE) executed an airborne science mission (PEM-WEST A) aboard the NASA Ames DC-8 over the Pacific Ocean during Sep./Oct. 1981. The atmosphere over the central Pacific Ocean is the only major region in the Northern Hemisphere that is relatively free from direct anthropogenic influence. Thus, this environment is ideally suited to study the natural biogeochemical cycles of carbon, nitrogen, ozone, sulfur, and aerosols without serious confounding problems related to anthropogenic emissions. Asian sources account for about 17 percent of the global budgets of nitrogen oxides (NO(x)) and sulfur dioxide (SO2). The Pacific Rim region therefore provides the opportunity to study the anthropogenic impact on natural atmospheric chemical cycles. The PEM-WEST A flights were focused on contrasting the chemistry of 'clean' air over the central Pacific with anthropogenically impacted air advected off the Asian continent. The principal objectives of PEM-WEST A were to investigate the atmospheric chemistry of ozone (O3) and its precursors, and to study important aspects of the atmospheric sulfur cycle over the western Pacific Ocean. Measurements conducted by the University of New Hampshire contributed directly to both of these objectives. Subsequent PEM-WEST field missions are planned by GTE in the mid-1990's to contrast atmospheric chemistry documented during PEM-WEST A with other time periods. This report presents preliminary findings from the PEM-WEST A field mission. Data interpretation is currently ongoing with the goal of manuscript submission of scientific results to a special issue of the Journal of Geophysical Research-Atmospheres in Feb. 1994. The reader is strongly encouraged to review this suite of profession articles to appreciate the overall scientific findings and benefits of the PEM-WEST A field mission. Derived from text

N93-25329# Polish Academy of Sciences, Warsaw. Instytud Podstawowych Problemow Techniki.
NON-LOCAL DESCRIPTION OF POLLUTION TRANSPORT IN RANDOM MEDIUM
Zbigniew Kotulski and Kazimierz Sobczyk 1992 23 p
Avail: CASI HC A03/MF A01

In the paper the convection-diffusion equation with the velocity of the flow being a random field is considered. For such a problem the effective equation for the mean concentration is obtained. In the general case it is non-local in space and time. Some attempts of the localization of such an equation are undertaken. The results are illustrated with numerical calculations. Author

N93-25360# Ekono Ympaeristoetekniikka, Helsinki (Finland). Devecon-Rhymae Oy.
SIHTI: THE RESEARCH AND DEVELOPMENT PROGRAM OF ENERGY AND ENVIRONMENTAL TECHNOLOGY
Seppo Pietila 1991 117 p Sponsored by Ministry of Trade and Industry
(DE93-769925; NEI-FI-179) Avail: CASI HC A06/MF A02

The SIHTI program consists of the environmental part of the energy research programs in Finland funded by the Ministry of Trade and Industry. Also, industry participates in the funding of the projects, especially the development projects. The main subject areas of the SIHTI program are: monitoring of international energy and environmental technology and national solution models, emissions from energy production, traffic emissions and emissions and discharges from fuel chains. DOE

N93-25370# Argonne National Lab., IL. Mathematics and Computer Science Div.
FORTRAN M AS A LANGUAGE FOR BUILDING EARTH SYSTEM MODELS
I. Foster 1992 8 p The 5th ECMWF Workshop on Parallel Processing in Meteorology held in Reading, England, 23 Nov. 1992 - 27 Nov. 1993
(Contract W-31-109-eng-38)
(DE93-007897; ANL/MCS/CP-78729; CONF-9211198-1) Avail: CASI HC A02/MF A01

FORTRAN M is a small set of extensions to FORTRAN 77 that supports a modular or object-oriented approach to the development of parallel programs. In this paper, I discuss the use of FORTRAN M as a tool for building earth system models on massively parallel computers. I hypothesize that the use of FORTRAN M has software engineering advantages and outline experiments that we are conducting to investigate this hypothesis. DOE

N93-25385# Lawrence Livermore National Lab., CA.
APPLICATION OF NON-THERMAL PLASMAS TO POLLUTION CONTROL
B. M. Penetrante, G. E. Vogtlin, J. N. Bardsley, P. A. Vitello, and P. H. Wallman Jan. 1993 12 p Presented at the 2nd International Plasma Symposium on World Progress in Plasma Applications, Palo Alto, CA, 9-11 Feb. 1993
(Contract W-7405-eng-48)
(DE93-007515; UCRL-JC-112689; CONF-930256-1) Avail: CASI HC A03/MF A01

Non-thermal plasma techniques can be used to destroy many types of hazardous molecules. They are particularly efficient when the toxic materials are present in very small concentrations. This paper discusses three particular applications of non-thermal plasmas: (1) decomposition of hydrogen sulfide (H2S); (2) removal of trichloroethylene (TCE); and (3) removal of nitric oxides (NO(x)). Emphasis is placed on the energy cost for implementing the decomposition or removal of these pollutants. Some of the factors affecting the energy cost are discussed. We discuss in detail our work at LLNL on pulsed plasma processing for the treatment of NO(x) in diesel engine exhaust. Our results suggest that our plasma reactor can remove up to 70 percent of NO(x) with relatively high initial concentrations (up to 500 ppM) at a power consumption cost of 2.5 percent for an engine with an output of 14 kW and an exhaust gas flow rate of 1200 liters per minute. DOE

N93-25431*# Iowa State Univ. of Science and Technology, Ames. Dept. of Physics and Astronomy.

KELVIN WAVES IN TOTAL COLUMN OZONE

J. R. Ziemke and J. L. Stanford Apr. 1993 10 p

(Grant NAG5-1519)

(NASA-CR-192984; NAS 1.26:192984) Avail: CASI HC A02/MF A01

Tropical Kelvin waves have been observed previously in ozone mixing ratio data from the SBUV (Solar Backscatter Ultraviolet) and LIMS (Limb Infrared Monitor of the Stratosphere) instruments on board the Nimbus-7 satellite. Kelvin wave features in total column ozone, using version 6 data from the Total Ozone Mapping Spectrometer (TOMS) instrument (also on board Nimbus-7) are investigated. Results show eastward-propagating zonal waves 1-2 with periods approximately 5-15 days, amplitudes approximately 3-5 DU, and latitudinal symmetry typical of Kelvin waves. A simplified model calculation suggests that the primary source for the perturbations is slow Kelvin waves in the lower-to-middle stratosphere. Maximum Kelvin wave signatures occur in conjunction with westward lower-to-middle stratospheric equatorial zonal winds (a quasi-biennial oscillation (QBO) wind modulation effect). Author (revised)

N93-25432*# Iowa State Univ. of Science and Technology, Ames. Dept. of Physics and Astronomy.

ROSSBY-GRAVITY WAVES IN TROPICAL TOTAL OZONE DATA

J. L. Stanford and J. R. Ziemke Mar. 1993 10 p

(Grant NAG5-1519)

(NASA-CR-192983; NAS 1.26:192983) Avail: CASI HC A02/MF A01

Evidence for Rossby-gravity waves in tropical data fields produced by the European Center for Medium Range Weather Forecasts (ECMWF) was recently reported. Similar features are observable in fields of total column ozone from the Total Ozone Mapping Spectrometer (TOMS) satellite instrument. The observed features are episodic, have zonal (east-west) wavelengths of 6,000-10,000 km, and oscillate with periods of 5-10 days. In accord with simple linear theory, the modes exhibit westward phase progression and eastward group velocity. The significance of finding Rossby-gravity waves in total ozone fields is that (1) the report of similar features in ECMWF tropical fields is corroborated with an independent data set and (2) the TOMS data set is demonstrated to possess surprising versatility and sensitivity to relatively smaller scale tropical phenomena. Author (revised)

N93-25443# California Univ., Berkeley. Lawrence Berkeley Lab.

ENVIRONMENTAL RISKS AND FUTURE GENERATIONS: CRITERIA FOR PUBLIC POLICY

R. B. Howarth Oct. 1992 16 p Presented at the Conference on Clean Water and the American Economy, Arlington, VA, 19-21 Oct. 1992

(Contract DE-AC03-76SF-00098)

(DE93-004691; LBL-32993; CONF-9210256-1) Avail: CASI HC A03/MF A01

This paper examines alternative normative approaches to the policy challenges posed by long-term environmental problems such as toxic and radioactive waste disposal, stratospheric ozone depletion, and climate change. The paper argues that cost-benefit analysis is limited in its ability to handle the issues of intergenerational equity and uncertainty that are intrinsic to such problems. Also considered is the precautionary principle, which holds that policies should seek to reduce threats to the welfare of future generations if the costs of doing so would not significantly reduce the subjective well-being of existing persons. Although the precautionary principle depends on an explicit value judgement, it yields a policy criterion that is operationally decisive under a wide array of circumstances. DOE

N93-25476 Delaware Univ., Newark.

EVALUATING CLIMATE-VEGETATION INTERACTIONS AT CLIMATE MODEL SUB-GRID SCALES Ph.D. Thesis

Katherine Margaret Klink 1992 165 p

Avail: Univ. Microfilms Order No. DA9301764

Land surfaces are an integral part of the global climate system, since most of the energy that drives the atmospheric circulation is absorbed and re-released from the surface of the earth. Terrestrial vegetation forms an important component of this surface because different vegetation types can significantly alter the character of the surface energy balance. In addition, vegetation characteristics are highly variable, both geographically and temporally. General circulation or global climate models (GCMs) that include a vegetation parameterization consider these properties to be homogeneous across large areas--typically 4 deg of latitude by 5 deg of longitude. These coarse-resolution characterizations seriously misrepresent the true heterogeneous nature of the earth's surface, and this introduces an additional (and largely unknown) degree of uncertainty into model results. To assess the role of surface heterogeneity at sub-GCM grid scales, a land-surface energy balance model is developed and is coupled to a mesoscale at atmospheric model. The land-surface model includes the effects on the surface energy balance of vegetation physical and physiological characteristics, as well as the influence of soil physical properties. This coupled system allows the surface and the atmosphere to be examined at the scale of a single GCM grid square. Two types of geographic surfaces were examined with the model. Each contained two different surface covers, either grass and bare soil, grass and deciduous trees, or grass and coniferous trees. In addition, both dry and moist soil environments were simulated. Model results showed that changes in vegetation geographic distribution resulted in differences in surface temperatures and evaporation amounts for each vegetation type as well as for the entire model domain. Maximum temperature differences ranged from 0.3 C to as much as 4 C over the course of the simulations, and latent heat flux differences were as large as 100 W m(exp -2). Differences in the nature and magnitude of the vertical velocities over each geographic surface were identified as the primary mechanism that produced these changes. Dissert. Abstr.

N93-25517# Oak Ridge National Lab., TN.

CLIMATE DATA BASES OF THE PEOPLE'S REPUBLIC OF CHINA, 1841-1988

Dale Kaiser, Shiyan Tao (Academia Sinica, Beijing, China.), Congbin Fu (Academia Sinica, Beijing, China.), Zhaomei Zeng (Academia Sinica, Beijing, China.), Qingyun Zhang (Academia Sinica, Beijing, China.), Wie-Chyung Wang (State Univ. of New York, Albany.), and Thomas Karl (National Climatic Data Center, Asheville, NC.) Jan. 1993 203 p Prepared in cooperation with Academia Sinica, Beijing, BJ (China); Inst. of Atmospheric Physics, State Univ. of New York, Albany, NY; Atmospheric Sciences Research Center, National Climatic Data Center, Asheville, NC

(Contract DE-AC05-84OR-21400)

(DE93-007907; DOE/NBB-0091T) Avail: CASI HC A10/MF A03

A data base containing meteorological observations from the People's Republic of China (PRC) is described. These data were compiled in accordance with a joint research agreement signed by the United States Department of Energy and the PRC Chinese Academy of Sciences (CAS) on 19 Aug. 1987. CAS's Institute of Atmospheric Physics (Beijing, PRC) has provided records from 296 stations, organized into five data sets: (1) a 60-station data set containing monthly measurements of barometric pressure, surface air temperature, precipitation amount, relative humidity, sunshine duration, cloud amount, wind direction and speed, and number of days with snow cover; (2) a 205-station data set containing monthly mean temperatures and monthly precipitation totals; (3) a 40-station subset of the 205-station data set containing monthly mean maximum and minimum temperatures and monthly extreme maximum and minimum temperatures; (4) a 180-station data set containing daily precipitation totals; and (5) a 147-station data set containing 10-day precipitation totals. Sixteen stations from these data sets (13 from the 60-station set and 3 from the 205-station set) have temperature and/or precipitation records that begin prior to 1900, whereas the remaining stations began observing in the early to mid-1900's.

Records from most stations extend through 1988. These data can be used in defining regional climate changes, establishing relationships between regional and large-scale climates, studying the climatic impacts of urbanization and increased concentrations of greenhouse gases, and in assembling large-scale climate data bases. Additional uses could include examining impacts of periodic events such as volcanic eruptions or the El Nino/Southern Oscillation. These data sets represent the most comprehensive, long-term instrumental Chinese climate data currently available. DOE

N93-25666*# Colorado Univ., Boulder. Cooperative Inst. for Research in Environmental Science.

INVERSE SEQUENTIAL PROCEDURES FOR THE MONITORING OF TIME SERIES Progress Report No. 3

Uwe Radok and Timothy Brown 30 Apr. 1993 56 p

(Grant NAGw-2706)

(NASA-CR-192959; NAS 1.26:192959) Avail: CASI HC A04/MF A01

Climate changes traditionally have been detected from long series of observations and long after they happened. The 'inverse sequential' monitoring procedure is designed to detect changes as soon as they occur. Frequency distribution parameters are estimated both from the most recent existing set of observations and from the same set augmented by 1,2,...j new observations. Individual-value probability products ('likelihoods') are then calculated which yield probabilities for erroneously accepting the existing parameter(s) as valid for the augmented data set and vice versa. A parameter change is signaled when these probabilities (or a more convenient and robust compound 'no change' probability) show a progressive decrease. New parameters are then estimated from the new observations alone to restart the procedure. The detailed algebra is developed and tested for Gaussian means and variances, Poisson and chi-square means, and linear or exponential trends; a comprehensive and interactive Fortran program is provided in the appendix. Author (revised)

N93-25765# Air Force Inst. of Tech., Wright-Patterson AFB, OH. School of Engineering.

AN ENVIRONMENTAL AUDIT MANAGEMENT PLAN FOR THE ROYAL AUSTRALIAN AIR FORCE M.S. Thesis

Warren L. Lear Sep. 1992 223 p

(AD-A261092; AFIT/GEE/CEV/92S-13) Avail: CASI HC A10/MF A03

The purpose of this research was to develop an Environmental Audit Management Plan (EAMP) tailored to meet the specific requirements of the Royal Australian Air Force (RAAF). The research also examined the resources which would be required to introduce the proposed EAMP into the RAAF. The literature on environmental compliance auditing identifies a number of essential characteristics required for an effective environmental auditing program. These characteristics, in conjunction with the USEPA design guidelines for the development of audit programs for government agencies, were used to guide the development of the RAAF EAMP. Information on Australian environmental legislation, DOD/RAAF policies and regulations, and details of the RAAF Base Tindal Environmental Management Plan were placed within this framework to produce the EAMP. The USAF Environmental Compliance Assessment and Management Program (ECAMP) was also used as a practical example of an existing audit management plan to provide further guidance in the preparation of the RAAF EAMP. To determine what would be required to implement the proposed EAMP, data on the implementation and operation of ECAMP was collected and analysed. From this, estimates of the resources required for the EAMP were prepared. DTIC

N93-25837# Mitre Corp., McLean, VA. Program Office.

SMALL SATELLITES AND RPA'S IN GLOBAL-CHANGE RESEARCH

P. Banks, J. Cornwall, F. Dyson, N. Fortson, and R. Garwin 1 Dec. 1992 207 p

(AD-A260762; JSR-91-330) Avail: CASI HC A10/MF A03

This report contains an investigation of those global change science problems that can be addressed by remotely piloted aircraft or by small satellites, including the relationship to the NASA EOS program. New types of measurements that could be made possible by such satellite or aircraft platforms are pointed out. Issues of technical feasibility and cost are examined, as well as the role of new technology developed through DOD and other programs. Possible joint DOD/Global Science satellite missions are also discussed. DTIC

N93-25850# Environmental Protection Agency, Research Triangle Park, NC.

NATIONAL AIR POLLUTANT EMISSION ESTIMATES Annual Report, 1990 - 1991

Oct. 1992 182 p

(PB93-157808; EPA/454/R-92/013) Avail: CASI HC A09/MF A02

The document presents the most recent estimates of national and regional emissions of the criteria pollutants. The report is published annually. Emission estimates are presented for NO(x), SO(x), and VOC from 1900-1991, for CO and total particulate from 1940-1991, for lead from 1970-1991 and for PM-10 from 1985-1991 . NTIS

N93-25851# Environmental Protection Agency, Washington, DC. Office of Communications and Public Affairs.

GLOSSARY OF ENVIRONMENTAL TERMS AND ACRONYM LIST

Dec. 1989 33 p

(PB93-158004; EPA-19K-1002) Avail: CASI HC A03/MF A01

The glossary is designed to explain the more commonly used environmental terms and acronyms appearing in U.S. Environmental Protection Agency (EPA) publications, news releases, and other Agency documents available to the public. Although it is obviously necessary to use some scientific terminology, the terms and definitions were selected to give a general sense of what a term or phrase means in relatively nontechnical language. The glossary replaces 'Common Environmental Terms', published by EPA in 1974 and revised in 1978. NTIS

N93-25864# Air Force Inst. of Tech., Wright-Patterson AFB, OH. School of Engineering.

DEVELOPMENT OF A HEURISTIC KNOWLEDGE BASE FOR THE SELECTION OF APPLICABLE OR RELEVANT AND APPROPRIATE ENVIRONMENTAL REQUIREMENTS M.S. Thesis

Scott J. Borg and Gerald B. Puetz Sep. 1992 108 p

(AD-A261038; AFIT/GEE/CEC/92S-5) Avail: CASI HC A06/MF A02

Applicable or Relevant and Appropriate Requirements (ARAR's) are the basis used in establishing threshold limits for hazardous waste cleanups performed under the Comprehensive Environmental Response, Compensation and Liability Act (CERCIA). ARAR's selections must be applied consistently at numerous cleanup locations concurrently. The purpose of this research was to analyze activities required for the development of a heuristic knowledge base used for selection of ARAR's. The problem domain for the research was limited CERCLA cleanups of contaminated groundwater, through the use of a pump and treat strategy, using air stripping as the as the cleanup technology. The research examined literature concerning the importance of ARAR's in the CERCLA restoration process and the knowledge acquisition and representation methods. The research then analyzed the activities required to acquire and represent the knowledge required for the selection of ARAR's. A byproduct of the research was a proof-of-concept prototype expert system which was used to validate knowledge acquired and represented in the problem domain. Prototype validation included comparing the results of consultations with the expert system with ARAR's identified in the-Record of Decisions (ROD's) for actual CERCLA cleanups. In three of four cases, the expert system successfully identified all ARAR's germane to the cleanups. DTIC

N93-25873# North Dakota Univ., Grand Forks.

REDISTRIBUTION OF TRACE CHEMICAL SPECIES BY A SMALL CONVECTIVE CLOUD

J. L. Stith, A. J. Alkezweeny, J. E. Pleim (Environmental Protection Agency, Research Triangle Park, NC.), and J. K. S. Ching (Environmental Protection Agency, Research Triangle Park, NC.) 1993 9 p Sponsored in part by EPA

(Contracts NOAA NA-17RA021801; NDARB-UND-NOAA91)

(PB93-156164; EPA/600/A-93/025) Avail: CASI HC A02/MF A01

The paper describes a new experiment with an SF6 tracer to determine the mixing history of a small region of cloud-base air. In situ measurements of the SF6 are made to follow the region, and simultaneous measurements of natural trace gases are used to determine the dilution of the tagged region as it is affected by the cloud. After describing the experimental method, the results from an experiment with a small cumulus, which was ideally suited for the experiment, are explained. The goal of the paper is to better understand how convective clouds redistribute trace constituents (e.g., moisture, trace gases) in the vertical. Author (DTIC)

N93-25875# Environmental Quality Systems, Inc., Washington, DC. Office of Pollution Prevention.

POLLUTION PREVENTION 1991: PROGRESS ON REDUCING INDUSTRIAL POLLUTANTS

Sheila A. Ferguson, ed., Jo-Ann McNally, ed., Barbara F. Bass, Sarah E. Evans, Donna Churyk Huijing, Kathleen Matusik, Catherine G. Miller, Douglas C. Muir, Warren R. Muir, and Stephanie Murphy et al Oct. 1991 150 p

(PB93-157725; EPA-21P-3003) Avail: CASI HC A07/MF A02

Pollution Prevention 1991 is the first study to provide an overview of the range of activities in pollution prevention nationally. Its focus is on industrial pollution prevention where the greatest amount of activity has been occurring. The authors have tried to capture as many of the numerous activities that are underway within manufacturing facilities and in the policy discussions of government and citizens. The report briefly discusses the impact of pollution, prevention policies and programs for the consumer, agricultural, energy, and municipal sectors was well as for the conservation of significant resources, in future years the authors may see that these areas are a major focus of pollution prevention activities. NTIS

N93-25876# Environmental Protection Agency, Cincinnati, OH.

QUALITY CONTROL: VARIABILITY IN PROTOCOLS

G. Y. Simes Sep. 1991 33 p

(PB93-157790; EPA/600/9-91/034) Avail: CASI HC A03/MF A01

The document Variability in Protocols (VIP) was initially designed as a quick reference for personnel performing QA audits, but it also has found its place in serving as a reference source for laboratory managers as well as personnel reviewing or developing QA Project Plans. Variability in Protocols contains tabular summaries of the quality control differences and similarities for some of the most frequently used analytical methods for water, soils, and other environmental samples. The document has been prepared in an attempt to bring together the separate methods that became a product of the major environmental statutes. Noticeable differences between methods are evidenced in method detection limits, calibration methods, blanks, spikes, and several other parameters included in the summary. The tabular format provides quick and easy access to important, needed information. VIP can provide guidance when preparing Quality Assurance Project Plans. Managers, field sampling team members, auditors, and laboratory personnel alike will find the document helpful in determining the most suitable method of chemical analysis for their various purposes. NTIS

N93-25878# Council on Environmental Quality, Washington, DC.

INCORPORATING BIODIVERSITY CONSIDERATIONS INTO ENVIRONMENTAL IMPACT ANALYSIS UNDER THE NATIONAL ENVIRONMENTAL POLICY ACT

Jan. 1993 40 p

(PB93-139806) Avail: CASI HC A03/MF A01

The report presents the results of consultations by the Council on Environmental Quality (CEQ) concerning the consideration of biological diversity in analyses prepared under the National Environmental Policy Act (NEPA). The report is intended to provide background on the emerging, complex subject of biodiversity, outline some general concepts that underlie biological diversity analysis and management, describe how the issue is currently addressed in NEPA analyses, and provide options for agencies undertaking NEPA analyses that consider biodiversity. The report does not establish new requirements for such analyses. It is not, and should not be viewed as, formal CEQ guidance on the matter, nor are the recommendations in the report intended to be legally binding. The report does not mean to suggest the biodiversity analyses should be included in every NEPA document, without regard to the degree of potential impact on biodiversity of the action under review. NTIS

N93-26243# Sorbent Technologies Corp., Twinsburg, OH.

DEVELOPMENT AND DEMONSTRATION OF A NEW FILTER SYSTEM TO CONTROL EMISSIONS DURING JET ENGINE TESTING Final Report, Feb. 1990 - Sep. 1992

B. W. Nelson, D. A. VanStone, and S. G. Nelson 15 Oct. 1992 79 p

(Contract F08635-90-C-0053)

(AD-A261203; CEL-TR-92-49) Avail: CASI HC A05/MF A01

Measurable quantities of NO(x), CO and small particulates are produced and are emitted into the atmosphere during the testing of aircraft engines in jet engine test cells (JETC's). These emissions have been and are a concern to the Air Force and to others who test aircraft engines. The large quantities of exhaust gases that are generated, the wide range of testing conditions that are normally employed, and the sensitivity of engines to back pressures make control difficult and the use of conventional control technologies impractical. A need exists for a simple, low-cost method to control the emissions. In a Phase 1 SBIR project, Sorbent Technologies Corporation (Sorbtech) explored the ability of vermiculite to reduce or capture contaminants in exhaust gas streams. During the Phase 2 SBIR project described in this report, Sorbtech investigated how vermiculite might be employed in a commercial system to control emissions from JETC's and how chemical additions to vermiculite might enhance its NO(x)-removal abilities. The objectives of the Phase 11 project were to develop and to demonstrate a suitable filter design involving vermiculite that will control NO(x), CO, and small-particulate emissions during jet-engine testing. DTIC

N93-26292# Washington Univ., Seattle.

SUMMARY BY THE CLOUD AND AEROSOL RESEARCH GROUP FOR ASTEX Final Report, 15 Apr. - 31 Dec. 1992

31 Dec. 1992 7 p

(Contract N00014-92-J-1587)

(AD-A261292) Avail: CASI HC A02/MF A01

Activity during the 1992 calendar year centered around the ASTEX project in the Azores and what has been, essentially, a small follow-up experiment conducted off of the Washington-Oregon coast, at least partially in conjunction with a series of test flights by the newly outfitted NRL blimp. The main experiment, conducted during ASTEX, had several objectives: (1) evaluate data for the occurrence of significant relationships between DMS, SO(2) SO equal 4 and CCN concentrations, (2) evaluate the strength of the relationship between boundary layer CCN concentration and cloud drop concentration in capping stratocumulus decks, (3) investigate the evolution of the particle size distribution in the boundary layer and (4) assess the effect of ship-induced aerosol flux on cloud dynamics and chemistry. The west coast experiment concentrated on only the fourth objective of the ASTEX study. A review of data reliability has been undertaken, and some preliminary data analysis as well. DTIC

N93-26315# Federal Emergency Management Agency, Washington, DC.

HANDBOOK OF CHEMICAL HAZARD ANALYSIS PROCEDURES

1993 512 p See also PB86-155256 and PB86-155264 Sponsored by EPA, Washington Prepared in cooperation with DOT, Washington LIMITED REPRODUCIBILITY: More than 20% of this document may be affected by microfiche quality

(PB93-158756) Avail: CASI HC A22/MF A04

The fact that hazardous materials pose a threat to public safety and the environment is of vital concern to industry and all levels of government, particularly in the aftermath of the tragedy in Bhophal, India, that took over 2000 lives and injured tens of thousands of others in the course of a few hours. The primary purpose of the handbook and its associated computer program is to provide emergency planning personnel with the resources necessary to undertake comprehensive evaluations of potentially hazardous facilities and activities within their respective jurisdictions and thereby formulate a basis for their planning efforts. NTIS

N93-26316# Corvallis Environmental Research Lab., OR.

USING TERRESTRIAL PLANTS IN BIOMONITORING

T. G. Pfleeger, H. C. Ratsch, and R. A. Shimabuku 1993 18 p Presented at the American Society Testing and Materials Second Symposium on Environmental Toxicology and Risk Assessment: Aquatic, Plant, and Terrestrial, Pittsburgh, PA, 26-30 Apr. 1993

(PB93-158780; EPA/600/A-93/029) Avail: CASI HC A03/MF A01

Visible foliar injury on Bell W-3 Tobacco was developed as an indicator of ozone pollution. The Tradescantia stamen hair system has been successfully used for a number of years as a monitor for chemical mutagenesis for air and water systems. However, plants have rarely been used as an indicator for chronic exposure to organic chemical pollutants. A test using Arabidopsis was developed for chronic root exposure to both metal and organic toxicants. A chronic shoot exposure test using a short life cycle Brassica was developed for monitoring aerial deposition of spray, fog, and gases. Preliminary work has begun on using terrestrial plants as biomonitors in detecting nontarget foliar injury from sulfonylurea herbicides. NTIS

N93-26327# RAND Corp., Santa Monica, CA.
AEROSPACE-PLANE FLIGHTS AND STRATOSPHERIC OZONE: REVIEW AND PRELIMINARY ASSESSMENT OF THE NATIONAL AEROSPACE PLANE (NASP) OPERATIONS
S. K. Liu 1992 63 p
(Contract F49620-91-C-0003)
(RAND/N-3464-AF) Avail: CASI HC A04/MF A01

The United States is now engaged in a major National Aerospace Plane (NASP) effort keyed to the goal of achieving low earth orbit using an air-breathing single-stage-to-orbit (SSTO) vehicle, the X-30. This goal requires meeting many sensitive technology and integration challenges. The NASP program management office fully recognizes these challenges and has mounted numerous concerted projects to achieve the required technology advances, in many instances accelerating progress substantially in fields several decades old. RAND undertook a study under sponsorship of Air Force's Directorate of Program Planning and Integration (SAF/AQX) to provide an integrated overview of the benefits, cost, and technical risks of potential NASP-derived vehicles (NDV). One task of this larger study was to examine some of the critical environmental aspects of the NASP program, specifically the effect of operational NDV's on stratospheric ozone and on noise intensity from sonic booms. The stratospheric ozone research and first-order estimates of the possible perturbation of water vapor and NOx content induced by the operation of the National Aerospace Plane (NASP) is reviewed. The primary purpose of this analysis is to assess the effect on stratospheric ozone from an operational fleet of NDV's.
Author (revised)

N93-26427*# North Carolina State Univ., Raleigh. Dept. of Chemical Engineering.
HETEROGENEOUS PHOTOCATALYTIC OXIDATION OF ATMOSPHERIC TRACE CONTAMINANTS Semiannual Progress Report No. 4, 1 May - 31 Oct. 1992
David F. Ollis 2 Apr. 1993 34 p
(Grant NAG2-684)
(NASA-CR-192937; NAS 1.26:192937) Avail: CASI HC A03/MF A01

The progress report on heterogeneous photocatalytic oxidation of atmospheric trace contaminants covering the period from 1 May - 31 Oct. 1992 is presented. The two topics discussed are photoreactor monolith fundamental studies and monolith reactor operation: batch recirculation system. Concentration profiles are shown.
CASI

N93-26495# Pacific Northwest Lab., Richland, WA.
HUMAN FACTORS IN ENVIRONMENTAL MANAGEMENT: NEW DIRECTIONS FROM THE HANFORD SITE
J. A. Wise and S. F. Savage Oct. 1992 7 p Presented at the Human Factors Society (HFS) Annual Meeting, Atlanta, GA, 12-16 Oct. 1992
(Contract DE-AC06-76RL-01830)
(DE93-004337; PNL-SA-21232; CONF-921048-7) Avail: CASI HC A02/MF A01

Environmental management is the general term given to modern attempts to seek technological solutions to certain constrained environmental problems. It involves developing and applying new technologies that respond to changes in environmental policy. It does not eliminate the need for 'environmental ethics' in society. Nor does it substitute for the fundamental changes in political and social structures that are needed for dealing with large-scale environmental issues. The scope of these issues can be illustrated by looking at the Hanford Site. Since 1943, the 560-square-mile Hanford Site in southeastern Washington state has been the production source of much of the nuclear weapons-grade radioactive materials for the United States. The legacy of 50 years of producing fissile materials has been an environmental cleanup problem of impressive proportions. In 1989, with the Cold War winding down, Secretary of Energy James Watkins established a new vision for Hanford as 'the flagship for waste management research.' As plans and preparations for cleanup work proceed at the Hanford Site and around the world, the need for well-orchestrated environmental management methodologies has become increasingly apparent. In 1990, a Human Factors Engineering Group was established in the Technology Planning and Analysis Center at PNL to provide appropriate support for the Laboratory's research efforts. At an ever-increasing rate, these research efforts require integrating human performance into complex environmental technology systems. The endeavor of responding to the Laboratory's research needs has provided innovative opportunities for the application of the concept of Human Factors. Discussed are some of the major applications of Human Factors to environmental management. DOE

N93-26496# Argonne National Lab., IL. Mathematics and Computer Science Div.
THE EARTH'S CLIMATE AS A DYNAMICAL SYSTEM
I. Foster, H. Kaper, and M. K. Kwong Oct. 1992 178 p Presented at The Earth's Climate as a Dynamical System, Argonne, IL, 25-26 Sep. 1992
(Contract W-31-109-eng-38)
(DE93-004666; ANL/MCS-TM-170; CONF-9209281) Avail: CASI HC A09/MF A02

This report constitutes the proceedings of a two-day workshop on climate models which was held at Argonne National Laboratory, September 25 and 26, 1992. It contains the abstracts of the presentations and copies of the overhead transparencies used by the speakers.
DOE

N93-26497# Pacific Northwest Lab., Richland, WA.
LONG TERM MODELING OF THE LINKS BETWEEN ECONOMICS, TECHNICAL PROGRESS, AND ENVIRONMENT: EVOLUTION OF APPROACHES AND NEW TRENDS
J. Edmonds Oct. 1992 17 p Presented at the Prospective Modeling, Decision Criteria and International Negotiation on Sustainable Development: The Case of Climate Change, Paris, France, 25-30 Oct. 1992
(Contract DE-AC06-76RL-01830)
(DE93-005035; PNL-SA-21613; CONF-9210252-1) Avail: CASI HC A03/MF A01

This paper examines the evolution of modeling on greenhouse as emissions. The paper briefly highlights the origins and early efforts to model greenhouse gas emissions, efforts subsequent to 1988, and the shape of the next generation of greenhouse gas emissions models. Particular emphasis is placed on the author's own contributions, including the Edmonds-Reilly Model and the second generation model.
DOE

N93-26510# Corvallis Environmental Research Lab., OR.
RESPONSE AND FEEDBACKS OF FOREST ECOSYSTEMS TO GLOBAL CLIMATE CHANGE
R. K. Dixon 1993 16 p Presented at the 3rd Workshop on Closed Ecological Systems, Salt Lake City, UT See also PB91-104240 LIMITED REPRODUCIBILITY: More than 20% of this document may be affected by microfiche quality
(PB93-167252; EPA/600/A-93/049) Avail: CASI HC A03

The accumulation of greenhouse gases in the atmosphere over the past century is projected to cause a warming of the Earth. Climate change predictions vary by region and terrestrial biosphere response, and feedbacks will be ecosystem specific. Forests play a major role in the Earth's carbon cycle through assimilation of CO2, storage of carbon, and emission of greenhouse gases. Simulation models have been employed to examine the possible responses of global forest ecosystems to climate change. Major shifts in forest species distribution and composition are predicted in response to projected climate change within the next 50-80 years. The ultimate responses and feedbacks of forests will be influenced by the direction and magnitude of climate change, site quality and other stress agents.
NTIS

N93-26511# Maryland Univ., Solomons. Chesapeake Biological Lab.
INORGANIC NITROGEN AND PHOSPHORUS DYNAMICS IN THE WATER COLUMN OF THE PATUXENT RIVER Final Technical Report, 1 Jul. 1989 - 31 Dec. 1991
D. G. Capone, V. Miller, J. Love, and L. Duguay 1992 59 p LIMITED REPRODUCIBILITY: More than 20% of this document may be affected by microfiche quality
(Grant DI-14-08-0001-G1734)
(PB93-172955) Avail: CASI HC A04

An analysis was made of nitrogen (N) and phosphorus (P) dynamics in the water column of the Patuxent River, Maryland, over a 2 year cycle. Specifically, inorganic N and P assimilation were determined by isotopic tracer methods at 3 stations along the salinity gradient of the river on a monthly basis. The authors determined the concentrations of particulate N and P and the major dissolved species. Among inorganic species, nitrate showed the greatest seasonal variation, particularly at the upstream stations.

Nitrate, which increased going upstream, tended to dominate the inorganic N pools. Ammonium, nitrate and phosphate uptake varied over a wide range among and within sites. Values tended to increase moving upstream. Nitrate uptake dominated inorganic N assimilation upstream while ammonium uptake was of greater importance at the most saline station. With respect to indices of nutrient limitation, except for the summer, dissolved inorganic N was in excess relative to inorganic P, suggestive of P limitation. NTIS

N93-26529# Little (Arthur D.), Inc., Cambridge, MA.
IMPROVED SELECTIVE CATALYTIC NOx CONTROL TECHNOLOGY FOR COMPRESSOR STATION RECIPROCATING ENGINES Final Report, Sep. 1991 - Sep. 1992
C. E. Benson, K. R. Benedek, and P. J. Loftus Sep. 1992 89 p See also PB86-110186
(Contract GRI-5091-254-2235)
(PB93-158566; GRI-92/0364) Avail: CASI HC A05/MF A01

The objective of the program was to identify and assess improvements to Selective Catalytic Reduction (SCR) exhaust gas NO(x) control processes for stationary reciprocating engines at pipeline compressor stations. Based on commercial application experience in Europe and the U.S., it is evident that SCR systems have been successfully applied to control NO(x) emissions from natural gas fueled stationary engines. Nevertheless, cost, maintenance, and automation related aspects of most commercial SCR systems currently render the technology an unattractive NO(x) control option for pipeline compressor station engines. Desirable and feasible improvements to SCR technology were defined through interaction with technology consumers (pipeline companies) and technology suppliers (SCR manufacturers), followed by independent analyses. The key technologies recommended for advancement include: a non-extractive, continuous emissions monitoring system, integration and automation of optimized engine/SCR systems, engine NOx emission mapping and feed-forward control of the SCR process, and qualification and use of commercially available low phosphorus lubricating oils. NTIS

N93-26533# Pennsylvania State Univ., University Park. Propulsion Engineering Research Center.
OXIDES OF NITROGEN EMISSIONS FROM TURBULENT HYDROCARBON/AIR JET DIFFUSION FLAMES, PHASE 2 Final Report, Jan. 1990 - Aug. 1992
S. R. Turns and R. V. Bandaru Sep. 1992 111 p See also PB91-184952
(Contract GRI-5086-260-1308)
(PB93-152478; PSU-ME-R-90/91-0005-Phase-2; GRI-92/0470-Phase-2)
Avail: CASI HC A06/MF A02

Measurements of oxides of nitrogen and carbon monoxide emission indices, flame radiant fractions, and visual flame dimensions were made for turbulent jet diffusion flames covering a wide range of test conditions. Parameters investigated included: initial jet velocity, jet diameter, fuel type, fuel dilution with inerts, partial premixing with air, and location and quantity of radial air injection. Detailed temperature measurements were also obtained for selected test conditions. The objectives of the study were (1) to develop a well-characterized data base to guide modeling efforts, and (2) to understand the relationships among NO(x) and CO emissions and flow conditions, fuel variables, and flame radiation. A major finding of the study was that the effects on NO(x) of residence time, flame temperature, and departure of the radical pool from equilibrium, whether caused by variations in initial jet velocity, jet diameter, fuel type, fuel dilution, or partial premixing, were well-characterized using two parameters: a characteristic nonadiabatic flame temperature, and a global residence time. Additional fuel-type dependencies, relating to the relative importance of prompt NO, were also found. NTIS

N93-26536# Nevada Univ., Las Vegas. Environmental Research Center.
TANK ISSUES: DESIGN AND PLACEMENT OF VAPOR MONITORING WELLS Final Report
M. S. Bedinger Feb. 1993 6 p See also PB89-195184, PB93-161149 and PB93-161156
(Grant EPA-R-814701)
(PB93-161131; EPA/600/9-90/044) Avail: CASI HC A02/MF A01

Vapor monitors are relatively easy to install at many sites and may be suitable devices for monitoring underground storage tanks and piping systems for leaks. The paper discusses the use of vapor monitors at new and old tank installations for detecting leaks from underground hydrocarbon storage tanks. The paper discusses the site conditions under which vapor monitors can be effectively used and conditions which can mitigate or prevent the effective use of vapor monitors. NTIS

N93-26559# Geological Survey, Reston, VA.
MODEL FOR TRANSPORT OF FLOATING DEBRIS IN THE OCEAN
Y. C. Su and E. R. Holley Feb. 1993 192 p Sponsored by Geological Survey, Reston, VA LIMITED REPRODUCIBILITY: More than 20% of this document may be affected by microfiche quality
(Grant DI-14-08-0001-G1728)
(PB93-172997; CRWR-236) Avail: Issuing Activity (Defense Technical Information Center (DTIC))

A model was developed to simulate the effects of wind, waves, ocean currents, and diffusion on the transport of floating debris in the ocean. Floating spheres with various sizes and specific gravities were considered in the applications. For advection, simulated wind profiles were established from previous experiments and were used with current velocities, water particle velocities computed from Stokes second-order wave theory, and gravitational settling on the inclined wave faces to determine the drag and added-mass for the spheres. The resulting unsteady force balance equations were solved numerically. When the advection became periodic, the time-averaged advective velocity of spheres was obtained. The cloud grows due to the combined effects of atmospheric and oceanic diffusion. A methodology based on statistics and diffusion theories was developed to yield approximate longitudinal and transverse diffusion coefficients which were used to obtain the size of the debris cloud. Several test cases showed that, except for very light floating objects, the transport is governed primarily by water drag. NTIS

N93-26567# Eastern Research Group, Inc., Lexington, MA.
REGULATORY IMPACT ANALYSIS OF THE PART 503 SEWAGE SLUDGE REGULATION Final Report
S. Burris 25 Nov. 1992 482 p
(Contract EPA-68-CO-0080)
(PB93-110625; EPA/821/R-93/006) Avail: CASI HC A21/MF A04

The report evaluates the costs, benefits, and economic impacts of the final 40 CFR Part 503 regulation governing the use of disposal of sewage sludge generated during the treatment of domestic sewage in a treatment works and domestic septage. The report begins by describing some relevant characteristics of treatment works and domestic septage haulers. The report focuses on the costs, risks, and benefits of the Part 503 regulation. NTIS

N93-26592# Los Alamos National Lab., NM.
TREATMENT OF HAZARDOUS ORGANIC WASTES USING SILENT DISCHARGE PLASMAS
L. A. Rosocha, G. K. Anderson, L. A. Bechtold, J. J. Coogan, H. G. Heck, M. Kang, W. H. McCulla, R. A. Tennant, and P. J. Wantuck 1992 34 p Presented at the Advanced Research Workshop on Non-Thermal Plasma Techniques for Pollution Control, Cambridge, England, 21-25 Sep. 1992
(Contract W-7405-eng-36)
(DE93-003789; LA-UR-92-3554; CONF-920967-1) Avail: CASI HC A03/MF A01

During the past two decades, interest in applying non-equilibrium plasmas to the removal of hazardous chemicals from gaseous media has been growing, in particular from heightened concerns over the pollution of our environment and a growing body of environmental regulations. At the Los Alamos National Laboratory, we are currently engaged in a project to develop non-equilibrium plasma technology for hazardous waste treatment. Our present focus is on dielectric-barrier discharges, which are historically called silent electrical discharges. This type of plasma is also named a silent discharge plasma (SDP). We have chosen this method due to its potential for high energy efficiency, its scientific and technological maturity, and its scalability. The SDP process has been demonstrated to be reliable and economical for the industrial-scale synthesis of ozone, where municipal water treatment plants frequently require the on-site generation of thousands of kilograins per day. The related methods of corona processing are presently the focus of work at other institutions, particularly for flue gas processing. Both SDP and corona processes are characterized by the production of large quantities of highly reactive free radicals, especially atomic oxygen O(3P) and the hydroxyl OH, in the gaseous medium and their subsequent reaction with contaminants. Our primary objective is to convert hazardous

or toxic chemicals into non-hazardous compounds or into materials which are more amenable to treatment. In the ideal case, the hazardous wastes are destructively oxidized to simpler, non-hazardous compounds plus CO2 and H2O. Sometimes the reaction products are still potentially hazardous, but are easily treated by conventional methods to yield non-hazardous products. DOE

N93-24870# Bulgarian Academy of Sciences, Sofia. Solar Terrestrial Influences Lab.
DATA PROCESSING AND CONTROL IN A TRANSPUTER SYSTEM FOR REMOTE SENSING OF THE EARTH
Doino Petkov, Tomas Zdravev, Dora Krezhova, Georgi Georgiev, Valentina Boytcheva, Christo Nikolov, Anton Velitchkov, and Miroslav Ivanov *In* ESA, Environment Observation and Climate Modelling Through International Space Projects. Volume 2: Remote Sensing for Environmental Monitoring and Resource Management 1992 p 923-927 Sponsored by National Fund of Scientific Investigations, Hungary (For primary document see N93-24775 09-43)
Copyright Avail: CASI HC A01/MF A04; ESA, EPD, ESTEC, Noordwijk, Netherlands, HC

N93-25571*# Brookhaven National Lab., Upton, NY. Dept. of Applied Science.
RECLAMATION WITH RECOVERY OF RADIONUCLIDES AND TOXIC METALS FROM CONTAMINATED MATERIALS, SOILS, AND WASTES
A. J. Francis and C. J. Dodge *In* NASA, Washington, Technology 2002: The Third National Technology Transfer Conference and Exposition, Volume 1 Feb. 1993 p 109-117 (For primary document see N93-25561 09-99)
(Contract DE-AC02-76CH-00016)
Avail: CASI HC A02/MF A04

N93-25573*# Bureau of Mines, Tuscaloosa, AL.
LOW COST DEWATERING OF WASTE SLURRIES
J. B. Peterson, S. K. Sharma, R. H. Church, and B. J. Scheiner *In* NASA, Washington, Technology 2002: The Third National Technology Transfer Conference and Exposition, Volume 1 Feb. 1993 p 121-126 (For primary document see N93-25561 09-99)
Avail: CASI HC A02/MF A04

46 GEOPHYSICS

Includes aeronomy; upper and lower atmosphere studies; ionospheric and magnetospheric physics; and geomagnetism.

For space radiation see *93 Space Radiation.*

N93-24672# Westinghouse Savannah River Co., Aiken, SC. Savannah River Technology Center.
USE OF THE 1991 ASCOT FIELD STUDY DATA IN A MESOSCALE MODEL EMPLOYING A FOUR-DIMENSIONAL DATA ASSIMILATION TECHNIQUE
Jerome D. Fast and B. Lance Osteen 1992 15 p Presented at the 6th Conference on Mountain Meteorlogy, Portland, OR, 29 Sep. - 2 Oct. 1992
(Contract DE-AC-9-89SR-18035)
(DE93-002683; WSRC-MS-92-161; CONF-9209163-5) Avail: CASI HC A03/MF A01

In this study, a four-dimensional data assimilation technique based on Newtonian relaxation is incorporated into the Colorado State University (CSU) Regional Atmospheric Modeling System (RAMS) and evaluated using data taken from one experiment of the US Department of Energy's (DOE) 1991 Atmospheric Studies in COmplex Terrain (ASCOT) field study along the front range of the Rockies in Colorado. The main objective of this study is to determine the ability of the model to predict small-scale circulations influenced by terrain, such as drainage flows, and assess the impact of data assimilation on the numerical results. In contrast to previous studies in which the smallest horizontal grid spacing was 10 km and 8 km, data assimilation is applied in this study to domains with a horizontal grid spacing as small as 1 km. The prognostic forecasts made by RAMS are evaluated by comparing simulations that employ static initial conditions, with simulations that incorporate continuous data assimilation, and data assimilation for a fixed period of time (dynamic initialization). This paper will also elaborate on the application and limitation of the Newtonian relaxation technique in limited-area mesoscale models with a relatively small grid spacing. DOE

N93-24910*# New Orleans Univ., LA. Dept. of Physics.
DETERMINATION OF DESIGN AND OPERATION PARAMETERS FOR UPPER ATMOSPHERIC RESEARCH INSTRUMENTATION TO YIELD OPTIMUM RESOLUTION WITH DECONVOLUTION, APPENDIX 4 Final Report
George E. Ioup and Juliette W. Ioup Dec. 1989 144 p
(Grant NAG1-804)
(NASA-CR-192834; NAS 1.26:192834) Avail: CASI HC A07/MF A02

The power spectrum for a stationary random process can be defined with the Wiener-Khintchine Theorem, which says that the power spectrum and the auto correlation function are a Fourier transform pair. To implement this theorem for signals that are discrete and of finite length we can use the Blackman-Tukey method. Blackman and Tukey (1958) show that a function w(tau), called a lag window, can be applied to the auto correlation estimates to obtain power spectrum estimates that are statistically stable. The Fourier transform of w(r) is called a spectral window. Typical choices for spectral windows show a distinct trade-off between the main lobe width and side lobe strength. A new idea for designing windows by taking linear combinations of the standard windows to produce hybrid windows was introduced by Smith (1985). We implement Smith's idea to obtain spectral windows with narrow main lobes and smaller (compared with typical windows) near side lobes. One of the main contributions of this thesis is that we show that Smith's problem is equivalent to a Quadratic Programming (QP) problem with linear equality and inequality constraints. A computer program was written to produce hybrid windows by setting up and solving the QP problem. We also developed and solved two variations of the original problem. The two variations involved changing the inequality constraints in both cases from non negativity on the combination coefficients to non negativity on the hybrid lag window itself. For the second variation, the window functions used to construct the hybrid window were changed to a frequency-variable set of truncated cosinusoids. A series of tests was run with the three computer programs to investigate the behavior of the hybrid spectral and lag windows. Emphasis was put on obtaining spectral windows with both relatively narrow main lobes and the lowest possible (for these algorithms) near side lobes. Some success was achieved for this goal. A 10 dB peak side lobe reduction over the rectangular spectral window without significant main lobe broadening was achieved. Also, average side lobe levels of -117 dB were reached at a cost of doubling the main lobe width (at the -3 dB point). Author

N93-24945*# Georgia Univ., Griffin. Dept. of Crop and Soil Sciences.
SURFACE ENERGY FLUXES AT CENTRAL FLORIDA DURING THE CONVECTION AND PRECIPITATION ELECTRIFICATION EXPERIMENT Final Report
D. Nie, T. D. Demetriades-Shah, and E. T. Kanemasu Apr. 1993 37 p
(Grant NAG8-910)
(NASA-CR-192826; NAS 1.26:192826) Avail: CASI HC A03/MF A01

One of the objectives of CaPE is to better understand the convective process in central and south Florida during the warm season. The energy and moisture exchanges between the surface and the atmosphere are closely related to this process. Some recent studies have shown that the surface energy balance plays an important role in the climatic fields (Shukla and Mintz, 1982; Sud and Smith, 1985; Sato et. al, 1989). Surface energy fluxes and related surface processes such as evapotranspiration and sensible heat transfer directly effect the temperature, humidity, cloud formation and precipitation. For example, mesoscale circulation around a discontinuity in vegetation type were shown to be stronger with wet soil than with dry soil using an evapotranspiration model (Pinty et. al, 1989). In order to better describe the processes in the atmosphere at various scales and improve our ability of modeling and predicting weather related events, it is crucial to understand the mechanism of surface energy transfer in relation to atmospheric events. Surface energy flux measurements are required to fully understand the interactions between the atmosphere and the surface. Derived from text

N93-25081*# California Univ., Los Angeles. Inst. of Geophysics and Planetary Physics.

ANOMALOUS ASPECTS OF MAGNETOSHEATH FLOW AND OF THE SHAPE AND OSCILLATIONS OF THE MAGNETOPAUSE DURING AN INTERVAL OF STRONGLY NORTHWARD INTERPLANETARY MAGNETIC FIELD

Sheng-Hsien Chen, Margaret G. Kivelson, Jack T. Gosling (Los Alamos National Lab., NM.), Raymond T. Walker, and Allan J. Lazarus (Massachusetts Inst. of Tech., Cambridge.) 15 Sep. 1992 39 p

(Grant NAG5-1529)

(NASA-CR-192851; NAS 1.26:192851) Avail: CASI HC A03/MF A01

On 15 Feb. 1978, the orientation of the interplanetary magnetic field (IMF) remained steadily northward for more than 12 hours. The ISEE 1 and 2 spacecraft were located near apogee on the dawn side flank of the magnetotail. IMP 8 was almost symmetrically located in the magnetosheath on the dusk flank and IMP 7 was upstream in the solar wind. Using plasma and magnetic field data, we show the following: (1) the magnetosheath flow speed on the flanks of the magnetotail steadily exceeded the solar wind speed by 20 percent; (2) surface waves with approximately a 5-min period and very non-sinusoidal waveform were persistently present on the dawn magnetopause and waves of similar period were present in the dusk magnetosheath; and (3) the magnetotail ceased to flare at an antisunward distance of 15 R(sub E). We propose that the acceleration of the magnetosheath flow is achieved by magnetic tension in the draped field configuration for northward IMF and that the reduction of tail flaring is consistent with a decreased amount of open magnetic flux and a larger standoff distance of the subsolar magnetopause. Results of a three-dimensional magnetohydrodynamic simulation support this phenomenological model. Author (revised)

N93-25086*# Alabama Univ., Huntsville.

PARAMETRIC ANALYSIS OF ATMOSPHERIC PROCESSES Final Report

M. Elshamy 23 Apr. 1993 39 p

(Contract NAS8-36955)

(NASA-CR-192523; NAS 1.26:192523) Avail: CASI HC A03/MF A01

The different phases of the space shuttle mission operations and systems analyses are influenced by several random perturbations due to the dynamics of atmospheric processes. From the mission planning point of view, there are few atmospheric conditions of interest, such as thunderstorm, precipitation, cloud ceiling, peak surface wind speed, etc. These atmospheric conditions, called parametsrs, are actually constraints on the mission operations. An atmospheric parameter is a random variable which attains either a permissible or not permissible value. As such, each of these atmospheric parameters is assigned the values of either 0 or 1, for GO or NOGO outcomes, respectively. These atmospheric parameters are inherently dependent random variables. An important part of mission planning is being able to provide, ahead of time, a good assessment of GO/NOGO status for different atmospheric parameters as well as conditional probabilities involving GO and/or NOGO outcomes. Specifically, it is of interest to effectively address certain questions pertaining to the assigned constraints the different mission phases of the space vehicle. The questions of interest involve: (1) the probability that the assigned atmospheric constraints will (or will not) occur during a particular time; (2) the probability that the assigned atmospheric constraints will (or will not) occur for N consecutive days, at a particular time of the day; (3) given that the assigned constraints have occurred (or have not occurred) for n consecutive days, at a particular time of the day, what is the probability that the constraints will continue for N additional days?; (4) the probabilities of runs of GO and NOGO outcomes; and (5) estimating certain conditional probabilities involving GO and/or NOGO outcomes. Effectively addressing and giving specific answers to these types of questions are useful in many ways: (1) to determine design criteria for the space vehicle; (2) to establish flight operational rules; and (3) to set up effective cost assessments. The purpose of this technical report is to present an analytical study of the topics involved, such as the theories of runs and Markov chains, as well as an attempt to give answers to the questions raised above. We construct probabilistic models based on the nature of the problem, as well as certain assumptions relevant to atmospheric conditions. These models lay the ground work to establish a theory that would support a GO-NOGO decision. Author

N93-25088*# New Orleans Univ., LA. Dept. of Physics.

DETERMINATION OF DESIGN AND OPERATION PARAMETERS FOR UPPER ATMOSPHERIC RESEARCH INSTRUMENTATION TO YIELD OPTIMUM RESOLUTION WITH DECONVOLUTION, APPENDIX 2 Final Report

George E. Ioup and Juliette W. Ioup Aug. 1988 122 p

(Grant NAG1-804)

(NASA-CR-192833; NAS 1.26:192833) Avail: CASI HC A06/MF A02

This thesis reviews the technique established to clear channels in the Power Spectral Estimate by applying linear combinations of well known window functions to the autocorrelation function. The need for windowing the auto correlation function is due to the fact that the true auto correlation is not generally used to obtain the Power Spectral Estimate. When applied, the windows serve to reduce the effect that modifies the auto correlation by truncating the data and possibly the autocorrelation has on the Power Spectral Estimate. It has been shown in previous work that a single channel has been cleared, allowing for the detection of a small peak in the presence of a large peak in the Power Spectral Estimate. The utility of this method is dependent on the robustness of it on different input situations. We extend the analysis in this paper, to include clearing up to three channels. We examine the relative positions of the spikes to each other and also the effect of taking different percentages of lags of the auto correlation in the Power Spectral Estimate. This method could have application wherever the Power Spectrum is used. An example of this is beam forming for source location, where a small target can be located next to a large target. Other possibilities extend into seismic data processing. As the method becomes more automated other applications may present themselves. Author

N93-25160*# National Aeronautics and Space Administration. Goddard Space Flight Center, Greenbelt, MD.

EMPIRICAL WIND MODEL FOR THE MIDDLE AND LOWER ATMOSPHERE. PART 1: LOCAL TIME AVERAGE

A. E. Hedin, E. L. Fleming (Applied Research Corp., Landover, MD.), A. H. Manson (Saskatchewan Univ., Saskatoon.), F. J. Schmidlin, S. K. Avery (Colorado Univ., Boulder.), and S. J. Franke (Illinois Univ., Urbana.) Apr. 1993 89 p

(RTOP 910-00-00)

(NASA-TM-104581; Rept-93B00069; NAS 1.15:104581) Avail: CASI HC A05/MF A01

The HWM90 thermospheric wind model was revised in the lower thermosphere and extended into the mesosphere and lower atmosphere to provide a single analytic model for calculating zonal and meridional wind profiles representative of the climatological average for various geophysical conditions. Gradient winds from CIRA-86 plus rocket soundings, incoherent scatter radar, MF radar, and meteor radar provide the data base and are supplemented by previous data driven model summaries. Low-order spherical harmonics and Fourier series are used to describe the major variations throughout the atmosphere including latitude, annual, semiannual, and longitude (stationary wave 1). The model represents a smoothed compromise between the data sources. Although agreement between various data sources is generally good, some systematic differences are noted, particularly near the mesopause. Root mean square differences between data and model are on the order of 15 m/s in the mesosphere and 10 m/s in the stratosphere for zonal wind, and 10 m/s and 4 m/s, respectively, for meridional wind. Author

N93-25179 Pittsburgh Univ., PA.

A STUDY OF ViBRATIONALLY EXCITED N2(+) IONS IN THE DAYTIME THERMOSPHERE Ph.D. Thesis

Lan-Sheng Hsu 1992 138 p

Avail: Univ. Microfilms Order No. DA9304232

The role of vibrationally excited N2(+) ions in the daytime thermosphere is studied. Ionization rates of the neutrals N2(+), O2(+), and O by solar extreme ultraviolet radiations with wavelengths below lambda 1050A and by impact of photoelectrons with energies between 10 to 500 eV are calculated. A photochemical model with ambipolar diffusion of ions included is used to obtain the altitude profiles of N2(+), O2(+), O(+), O(+)(P-2), O(+)(D-2), O2(+)(a(sup 4)pi(sub u)), NO(+), and N(+) ion densities. Vibrational level densities and vibrational distribution of the X(sup 2)((sigma(sub g)))(sup +), A(sup 2)pi(sub u), and B(sup 2)((sigma(sub u)))(sup +) electronic states of N2(+) ions are then calculated by taking into

consideration the direct ionization-excitation of N2(+) ions by solar extreme ultraviolet radiations and photoelectron impacts, fluorescent scattering of sunlight, chemical reactions, collision with neutrals, and radiative emissions. Column emission rates for the (0,0) band at lambda 3914A, (0,1) band at lambda 4277A, (1,2) band at lambda 4236A, an (2,3) band at lambda 4199A of the N2(+) first negative band system are then computed and compared with rocket flight data. Dissert. Abstr.

N93-25201*# University of Southern Illinois, Carbondale. Dept. of Geology.

IMPROVED DETERMINATION OF VECTOR LITHOSPHERIC MAGNETIC ANOMALIES FROM MAGSAT DATA Final Report, 15 May 1992 - 31 Jan. 1993

Dhananjay Ravat Jan. 1993 59 p

(Grant NAG5-1972)

(NASA-CR-192784; NAS 1.26:192784) Avail: CASI HC A04/MF A01

Scientific contributions made in developing new methods to isolate and map vector magnetic anomalies from measurements made by Magsat are described. In addition to the objective of the proposal, the isolation and mapping of equatorial vector lithospheric Magsat anomalies, isolation of polar ionospheric fields during the period were also studied. Significant progress was also made in isolation of polar delta(Z) component and scalar anomalies as well as integration and synthesis of various techniques of removing equatorial and polar ionospheric effects. The significant contributions of this research are: (1) development of empirical/analytical techniques in modeling ionospheric fields in Magsat data and their removal from uncorrected anomalies to obtain better estimates of lithospheric anomalies (this task was accomplished for equatorial delta(X), delta(Z), and delta(B) component and polar delta(Z) and delta(B) component measurements; (2) integration of important processing techniques developed during the last decade with the newly developed technologies of ionospheric field modeling into an optimum processing scheme; and (3) implementation of the above processing scheme to map the most robust magnetic anomalies of the lithosphere (components as well as scalar). Author (revised)

N93-25202*# Massachusetts Inst. of Tech., Cambridge. Dept. of Earth, Atmospheric and Planetary Sciences.

LOW-FREQUENCY SOURCE PARAMETERS OF TWELVE LARGE EARTHQUAKES M.S. Thesis

Paolo Harabaglia (Trieste Univ., Italy.) Jun. 1993 114 p

(Grants NAG5-549; NAGw-1905)

(NASA-CR-192806; NAS 1.26:192806) Copyright Avail: CASI HC A06/MF A02

A global survey of the low-frequency (1-21 mHz) source characteristics of large events are studied. We are particularly interested in events unusually enriched in low-frequency and in events with a short-term precursor. We model the source time function of 12 large earthquakes using teleseismic data at low frequency. For each event we retrieve the source amplitude spectrum in the frequency range between 1 and 21 mHz with the Silver and Jordan method and the phase-shift spectrum in the frequency range between 1 and 11 mHz with the Riedesel and Jordan method. We then model the source time function by fitting the two spectra. Two of these events, the 1980 Irpinia, Italy, and the 1983 Akita-Oki, Japan, are shallow-depth complex events that took place on multiple faults. In both cases the source time function has a length of about 100 seconds. By comparison Westaway and Jackson find 45 seconds for the Irpinia event and Houston and Kanamori about 50 seconds for the Akita-Oki earthquake. The three deep events and four of the seven intermediate-depth events are fast rupturing earthquakes. A single pulse is sufficient to model the source spectra in the frequency range of our interest. Two other intermediate-depth events have slower rupturing processes, characterized by a continuous energy release lasting for about 40 seconds. The last event is the intermediate-depth 1983 Peru-Ecuador earthquake. It was first recognized as a precursive event by Jordan. We model it with a smooth rupturing process starting about 2 minutes before the high frequency origin time superimposed to an impulsive source. Author (revised)

N93-25424 California Univ., Santa Cruz.

GEOLOGIC STRUCTURE AND PROCESSES OF THE EASTERN PACIFIC MARGIN: CALIFORNIA AND COSTA RICA Ph.D. Thesis

Kirk Duncan McIntosh 1992 181 p

Avail: Univ. Microfilms Order No. DA9235716

The margin of the eastern Pacific has been sculpted during Tertiary geologic times by convergent and transcurrent plate motion along both continental and oceanic plate boundaries. Interpretations of central California geology predict margin development by Early Tertiary plate convergence, the transition to a transform plate boundary, and subsequent modification of that boundary. Deep penetration seismic reflection transects (EDGE profiles) provide new data to refine these interpretations. These data support the interpretation that a plate fragment related to the Farallon plate may be continued to subduct off California after the Pacific/North America transform boundary was established to the north and south. These seismic data also reveal structures related to probable Miocene transtensional development of the offshore Santa Maria Basin after subduction eventually ceased in this area. The final stage of margin development is one of compressional deformation. This stage is documented by folding and thrust faulting, that appear to be concentrated near the zones of earlier extension and include examples of basin inversion. The Tertiary history of Costa Rica is one of plate convergence in an oceanic island arc setting. In particular, the plate boundary off the Nicoya Peninsula, Costa Rica, is an accretionary convergent margin in a low sediment supply environment. Seismic reflection data, including regional 2D profiles and a 3D survey over a portion of the lower trench slope, show mechanisms of sediment accretion, subsequent compressional deformation, and upper slope extension. The mechanisms of sediment accretion include offscraping at the trench, but the dominant process is underplating. With low sediment supply (no trench turbidites) the sedimentary cover on the subducting Cocos plate is thin and is accreted in small blocks. Variation in the basement structure of the Cocos plate perturbs the accretion processes and affects the arrangement of sedimentary blocks as they are accreted to the prism. The resulting prism structure varies rapidly along strike. The upper slope of the Costa Rica margin features an approximately 20 km wide zone of predominantly landward dipping normal faults. Seismic data show that the faults cut the entire 2 km thick slope apron section and penetrate the underlying accretionary prism. Dissert. Abstr.

N93-25433 Stanford Univ., CA.

ELASTIC MODELING AND MIGRATION IN EARTH MODELS Ph.D. Thesis

Carlos Alves FilhoCunha 1992 135 p

Avail: Univ. Microfilms Order No. DA9302197

Migration and inversion of marine seismic data using the elastic wave equation requires the transformation of the recorded pressure data into a vector particle-displacement field. This can be done easily when the recording geometry samples the wavefield both horizontally and vertically. However, only experimental surveys have cables located at different depths. Using a few assumptions, I derive a method for performing this transformation, which is applicable to standard surveys. The assumptions are: smooth water surface, cable nearly parallel to water surface, and perfect seismic-reflection at the water surface. Results in a realistic example, where these assumptions are only partially fulfilled, demonstrate that the method is robust. Elastic, reverse-time migration/inversion schemes in the space-time domain are usually implemented by finite-difference or finite-element methods. When imaging beyond structures, a dynamically accurate scheme must be used. For models characterized by layers with sharp boundaries, traditional finite-difference methods fail to correctly describe the dynamics of the propagation process. Failure comes from the lack of distinction between model and field variables; the same difference operator is applied to discontinuous (model) and continuous (wavefield) components. The problem is solved with a modified finite-difference scheme (dual-operator), which uses long operators for wave-fields, short operators for elastic parameters, Shoenberg-Muir (1989) equivalence relations, and a modified Virieux (1984) staggered grid scheme. Tests show that the dual-operator is dynamically more accurate than traditional finite-difference schemes and comparable to Haskell-Thomson schemes. In structurally complex media, accurate recovery of angle-dependent reflectivities requires elastic prestack migration. Mode separation can be done before or after depth extrapolation. Though more complex, the latter is more complete because it images mode-converted waves. Standard depth-extrapolation and imaging approaches are unsuitable for true-reflectivity recovery. I introduce an extrapolation method which properly compensates for transmission/conversion losses. This method is combined with an imaging condition that performs the plane-wave decomposition of the downward

extrapolated data to define the plane-wave-response (PWD) migration. The four image-cubes generated by the PWD migration correspond to the plane-wave angle-dependent reflectivities for PP, PS, SP, and SS modes, and directly relate to the Zoeppritz equations because they represent the in-depth plane-wave response of the medium. Dissert. Abstr.

N93-25529*# California Inst. of Tech., Pasadena. Div. of Geological and Planetary Sciences.
INTRAPLATE DEFORMATION, STRESS IN THE LITHOSPHERE AND THE DRIVING MECHANISM FOR PLATE MOTIONS Final Technical Report, period ending 31 Dec. 1991
Arden L. Albee 10 Mar. 1993 5 p
(Grant NAG5-842)
(NASA-CR-192782; NAS 1.26:192782) Avail: CASI HC A01/MF A01

The initial research proposed was to use the predictions of geodynamical models of mantle flow, combined with geodetic observations of intraplate strain and stress, to better constrain mantle convection and the driving mechanism for plate motions and deformation. It is only now that geodetic observations of intraplate strain are becoming sufficiently well resolved to make them useful for substantial geodynamical inference to be made. A model of flow in the mantle that explains almost 90 percent of the variance in the observed longwavelength nonhydrostatic geoid was developed.
Derived from text

N93-25535 Colorado Univ., Boulder.
THE ROLE OF MULTIPLE SCATTERING IN TWILIGHT ZENITH SKY OBSERVATIONS OF ATMOSPHERIC ABSORBERS: DIURNAL PHOTOCHEMISTRY AND AIRMASS FACTORS Ph.D. Thesis
Lori Mac Perliski 1992 186 p
Avail: Univ. Microfilms Order No. DA9304597

The ability to properly interpret UV-visible twilight absorption measurements of atmospheric chemical constituents is dependent on how well the optical path, or airmass factor, of light collected by the spectrometer is understood. In the case of direct light measurement, the airmass factor may be calculated from simple geometrical considerations for a spherical atmosphere. In the case of scattered light, a spherical radiative transfer model must be used. A simple single scattering model and a Monte Carlo radiative transfer scheme were developed to study the effects of multiple scattering, aerosol scattering, albedo and refraction on scattered light airmass factors. Stratospheric airmass factors are found to be relatively insensitive to multiple scattering, albedo, refraction and aerosol scattering by background aerosols at fairly short visible wavelengths (about 450 nm). Tropospheric airmass factors, on the other hand, are very sensitive to these processes. Ground albedo, refraction, multiple scattering and aerosol scattering are also important in determining photolysis rates of atmospheric species. It is found that one-dimensional photochemical model calculations of vertical column abundances of several stratospheric chemical constituents are relatively insensitive to changes in photolysis rates due to albedo, refraction and background aerosol scattering, although they are sensitive to multiple scattering. Following the June 1991 eruption of Mt. Pinatubo, OClO and BrO were observed at Fritz Peak Observatory for the first time every. The radiative and photochemical effects of the presence of Pinatubo volcanic aerosols are examined using a one-dimensional photochemical model coupled to a spherical matrix inversion radiative transfer model. Although the heterogeneous removal of NO(x) is not explicitly considered in the photochemical model, the photochemical effects of NO(x) removal may be studied by prescribing the amount of NO(x) removed by heterogeneous chemistry. Measured OClO and BrO column abundances are found to be consistent with model calculations of OClO and BrO column abundances for which 75-98 percent of NO(x) has been removed. Dissert. Abstr.

N93-25547 York Univ. (Ontario).
GRAVITY WAVES FROM O2 AIRGLOW Ph.D. Thesis
Shengpan Zhang 1991 281 p
Avail: Univ. Microfilms Order No. DANN70397

This thesis mainly consists of two parts: the method of data analysis for a new ground-based optical instrument MORTI which observes the O2 (0-1) airglow, and the theoretical interpretation of the results from the data collected by MORTI during the AIDA '89 campaign. Two algorithms of the data analysis have been developed. The first algorithm is a curve fitting method for calculating the rotational temperature with precision plus or minus K, the emission rate with precision plus or minus 5 percent, and the background continuum. Using this method, 22 nights of observation over Puerto Rico during April and May of 1989 were analyzed. The results show that the nightly average rotational temperatures were between 172K and 220K, and the nightly emission rates were between 271R and 917R. The second algorithm is for calculating the gravity wave parameters using the Lomb-Scargle method for unevenly spaced data. The horizontal wave direction and wave speed can be derived from the twelve-point measurements by MORTI. A total of fourteen gravity waves were found, two evanescent waves and twelve internal waves. The apparent wave periods of these waves were between 45 minutes and 360 minutes, their horizontal wavelengths were between 200 km and 2900 km, and the horizontal wave speeds were between 48 m/s and 282 m/s. The observed eta, the ratio of emission rate fluctuations to temperature fluctuations, were between 3.5 and 5.5, and temperature and emission rate fluctuations were generally in phase. The dependencies of eta on the wave parameters and chemical parameters are developed using a new model for the O2 airglow's response to a gravity wave. The model is in the Eulerian frame of reference using the traditional linearization and perturbation method. Two photochemical mechanisms, the three-body recombination and mechanism and the two-step transfer mechanism, and two kinds of waves, evanescent and internal, were separately discussed in detail. The predictions by this model agree with MORTI's observations fairly well, better than other available theoretical predictions. Both the measurements and the theory show the emission rate exhibits larger fluctuations than the temperature, and it is more reliable for detecting wave parameters and measuring airglow variation. The wave characteristics measured by MORTI are important for further study of the energy and moment transmission by waves in the mesopause region. Dissert. Abstr.

N93-25556 Guelph Univ. (Ontario).
LOCAL AND REGIONAL ESTIMATES OF SENSIBLE AND LATENT HEAT FLUX DENSITIES FROM A PATCH-WORK SURFACE Ph.D. Thesis
Alan George Barr 1991 241 p
(ISBN-0-315-70882-4) Avail: Univ. Microfilms Order No. DANN70882

Regional, surface sensible and latent heat flux densities (H and LE) are important in climatology and hydrology. This study assesses the feasibility of estimating day-time H and LE from surface and upper-air weather data. The regional, upper-air estimates are compared with local, surface measurements above a surface patch-work of agricultural land and forest. Local surface H, LE and CO2 flux density were measured above nearby deciduous forest and alfalfa by the Bowen ratio method and eddy correlation (forest only). The day-time Bowen ratios (on average 0.15 forest and 0.17 alfalfa) and transpiration ratios (123 kg H2O kg(exp -1) CO2 forest and 135 kg H2O kg(exp -1) O2 alfalfa) were similar above forest and alfalfa. On some days, H averaged to near zero. Two approaches were used to estimate regional H and LE. The first used rawindsonde soundings of upper-air temperature and humidity. The second used an integral, convective boundary-layer (CBL) model, driven by surface temperature and humidity. Both approaches assumed that horizontal advection and subsidence were negligible, and that H and LE equalled the upper-air, integral storage changes of sensible and latent heat, integrated to well above the CBL.
Dissert. Abstr.

N93-25688 Michigan Univ., Ann Arbor.
THERMAL INFRARED RADIATION TRANSFER IN THE PLANETARY BOUNDARY LAYER Ph.D. Thesis
Wenzhong Zhao 1992 220 p
Avail: Univ. Microfilms Order No. DA9303846

A high spectral resolution thermal infrared radiation transfer program has been developed. It uses the emissivity growth method to calculate transmittances along in homogeneous paths from a line-by-line calculated database for homogeneous paths. This program offers high accuracy and reduces the computing time by about two orders of magnitude in comparison with the line-by-line method. Critical to the program are the choice of appropriate grid points for transmittance calculation, the double quadratic interpolation, and an appropriate stratification of the atmosphere. A criterion for evaluating grid points has been developed that can reduce interpolation errors significantly. This research reviewed and evaluated current measurements and theories on water vapor continuum absorption. By including the most current data, this radiation transfer program showed the significant effects of water vapor continuum absorption and produced

simulation results which agree with available measurements. The sensitivities of thermal radiation fluxes to a doubling of CO2 were significantly affected by the temperature and the water vapor profiles. Sensitivity studies also showed the extreme importance of the lower part of the boundary layer to the diurnal variation of the down-welling flux and the surface radiative energy budget. In the standard atmosphere, about 30 percent of the down-welling flux comes from the lowest 0.6 millibars and about 50 percent from the lowest 3 millibars. This research clearly showed that a widely used extrapolated profile cannot represent a daily average profile. The extrapolated profile overestimated the surface net radiation by 50 percent. A layer of fog was parameterized as a grey body for certain absorptions in radiation transfer simulations. The primary results of the one parameter model were consistent with observations. Dissert. Abstr.

N93-25709 California Univ., Los Angeles.
A STATISTICAL STUDY OF FIELD-ALIGNED CURRENTS IN THE EARTH'S INNER MAGNETOSPHERE Ph.D. Thesis
Francis Keoki Chun 1992 406 p
Avail: Univ. Microfilms Order No. DA9301538

Field-aligned currents (FAC's) play a major role in the solar wind-magnetospheric interaction by electrodynamically coupling magnetospheric and ionospheric plasmas, so that stresses applied to the outer magnetospheric plasma are transmitted to the ionosphere and ultimately to the upper atmosphere. FAC's have been studied extensively since 1967 and all of our knowledge and understanding of this coupling mechanism is based on data from low altitude polar orbiting satellites. The purpose of this dissertation is to address some of the questions related to the persistence of magnetospheric FAC's during low levels of geomagnetic activity, their motion throughout the magnetosphere and their possible source mechanisms. We detrend and rotate ISEE-1 and 2 magnetometer data into a field-aligned coordinate system using the Tsyganenko (1987) magnetic field model in order to identify current sheet crossings. We calculate the properties of the FAC's to include their current intensity, density, velocity and thickness and discuss the technique used to extrapolate those properties to the ionosphere. We also determine the location and orientation of the FAC's as well as a measure of how closely they resemble sheets of current. We identify two types of FAC's in the magnetosphere; one that is quasi-stationary and another that is moving quickly so that it is observed simultaneously by the spacecraft. The quasi-stationary FAC's are magnetospheric extensions of the low altitude region 1 and 2 currents while the fast moving FAC's are possibly current carrying waves and/or transient phenomena. Both currents are highly responsive to geomagnetic activity with the fast moving currents responding strongly to high activity. During periods of quiet activity, magnetospheric FAC's are infrequently observed except for a region on the dusk night side from mid to high L-values suggesting that global convection does drive the dusk FAC's but that the three dimensional current system is non existent on the dawn side. We also examine the night side quasi-stationary FAC's with respect to substorm phase and find that when classified as a region 1 or 2 sense current, the night side region 2 currents are responsive to internal magnetospheric stresses due to night side reconnection whereas the night side region 1 currents are responsive to variations in the stress assiciated with both day side and night side reconnection. Dissert. Abstr.

N93-25732 California Univ., Berkeley.
SOUNDING ROCKET OBSERVATIONS OF PRECIPITATING IONS IN THE MORNING AURORAL REGION Ph.D. Thesis
James Hart Clemmons 1992 142 p
Avail: Univ. Microfilms Order No. DA9304882

The origin of highly-structured ion fluxes measured by a sounding rocket launched into the morning auroral region on January 23, 1985 is investigated. The energy spectra of the precipitating ions exhibit an energy-time dependence in which particles of higher energies arrived at the rocket before those of lower energies. The spectra are interpreted as being due to the impulsive injection of particles onto high-altitude magnetic field lines, followed by their subsequent drift down the field lines to rocket altitudes. The dispersal to low energies with increasing time is explained as a time-of-flight effect in which the slower particles take longer times to traverse the distance. The ion signatures are used to constrain several possible physical models which characterize the source region. Source locations in the nightside magnetopause boundary layer are deduced through the examination of electron energy spectra and the use of a magnetospheric magnetic field model. The modeling efforts indicate that the data are consistent with sources located in the mid-latitude region of the flank boundary layer on the morning side of the magnetosphere, being in the range of 20-30 earth radii down the geomagnetic tail from the earth. Multiple injections of ions are observed, with a deduced quasi-periodicity of 100-200 s. Several candidate injection mechanisms are examined, with a mechanism related to the propagation of waves on the surface of the boundary layer found to be the most plausible explanation for the observations. Comparison is made to similar analyses by others and suggestions for future work are made. Dissert. Abstr.

N93-25739 Oxford Univ. (England).
THE PRESSURE MODULATION SYSTEM IN THE IMPROVED STRATOSPHERIC AND MESOSPHERIC SOUNDER Ph.D. Thesis
Peter Venters 1991 273 p
Avail: Univ. Microfilms Order No. BRD-97308

The technique of pressure modulation radiometry has been successfully used for the measurement of atmospheric pressures, temperatures and minor constituent amounts from orbiting spacecraft. This thesis describes the system used to effect the pressure modulation in the latest such instrument, the Improved Stratospheric and Mesospheric Sounder (ISAMS), which incorporates a number of further refinements to the technique. In particular, two matched pistons running in opposition are used to effect the modulation while considerably reducing the vibrational output of the mechanism. Considerable care has also been taken to design a chemically clean modulator, with no organic materials on the inside of the system. The dynamics of the double piston modulator are described, and simple approximations used to explain the main features of its behavior. In order to calculate the behavior of the gas in the modulator with sufficient accuracy to enable useful atmospheric measurements to be made, a detailed numerical model of the modulator was written. The predictions of the model were first validated against a comprehensive set of pressure cycle measurements made using a test modulator. Good agreement was obtained except for a modulator containing water vapor. It is shown that this discrepancy can be accounted for by the absorption of water vapor on the internal surfaces of the modulator. The performance of the modulators installed in the ISAMS is reviewed, and the numerical model used in the construction of an error analysis for the knowledge of the gas modulation. A preliminary discussion of the effects of these errors on the retrieval of atmospheric measurements is presented, and it is concluded that the prospects for the ISAMS to make a significant contribution to the understanding of the upper atmosphere are good. Dissert. Abstr.

N93-25756 Georgia Inst. of Tech., Atlanta.
AN INVESTIGATION OF THE ROLE OF FLUX DIVERGENCE IN THE TURBULENT KINETIC ENERGY BALANCE OF THE ATMOSPHERIC SURFACE LAYER Ph.D. Thesis
Christoph Alexander Vogel 1992 190 p
Avail. Univ. Microfilms Order No. DA9303151

The results of an investigation of the role of flux divergence contributions in the turbulent kinetic energy balance of the atmospheric surface layer are presented. Mechanisms of interest include the vertical divergence of the vertical turbulent flux of turbulent kinetic energy and the vertical divergence of the pressure-velocity covariance. Measurements for this analysis were made in a field experiment conducted in the fall of 1991 near Hay, New South Wales, Australia. Because the contributions of the pressure-velocity mechanism could not be measured directly, the effects of this term were determined as a residual in the TKE balance. All other terms in the governing equation were measured in the field. These included: the mechanical production of turbulence due to wind shear, the production (or damping) of turbulence due to buoyancy, the removal of turbulence due to viscous dissipation, and the redistribution of turbulence through the vertical divergence of the turbulent kinetic energy flux. The behavior of each of these mechanisms was determined over a range of stability and summarized in the form of an empirical function. As one result of this investigation, a significantly different behavior for the production of turbulence due to wind shear was found, thus defining an empirical relation more consistent with dimensional predictions. in addition, the behavior of the normalized viscous dissipation rate was found to be significantly different from the widely-accepted results of the Kansas experiments of the late 1960s. Further, the turbulence transport divergence was shown to remove turbulence at a significant rate in unstable conditions but to be negligibly

small in weakly stable conditions. The flux divergence of the pressure-velocity correlation was found to be an important source of turbulence in unstable conditions. Finally, one of the more significant results of this study was that the net contribution of the two flux divergence mechanisms was almost never negligible as had been previously assumed; that is, turbulence almost never dissipates locally in the atmospheric surface layer. Dissert. Abstr.

N93-25757 Colorado Univ., Boulder.
COMPUTATION OF MOISTURE FLUX FROM OCEAN TO ATMOSPHERE USING A SYNERGY OF SSM/I-DERIVED PRECIPITABLE WATER AND ECMWF ANALYSES Ph.D. Thesis
Charles Leslie Norris 1992 140 p
Avail: Univ. Microfilms Order No. DA9304590

Precipitable water (PW) measurements from the Special Sensor Microwave/Imager (SSM/I) are a source of atmospheric information that is not currently included in atmospheric analysis from the European Center for Medium Range Weather Forecasts (ECMWF). The SSM/I has better temporal and spatial coverage than other data sources which are currently used in ECMWF analyses. Estimates of ocean surface moisture flux (evaporation minus precipitation, or E-P) derived from a combination of SSM/I data and ECMWF analyses should be an improvement over estimates derived from ECMWF analyses alone. Surface moisture flux can be computed using the mass continuity equation for water vapor, which can be formulated in such a way as to take maximum advantage of precipitable water information. Three SSM/I-based PW algorithms from the current literature were tested against a statistically large set of radiosonde soundings to determine their suitability for global PW determination. Two of these algorithms were found to be acceptable for global PW computation, so final selection was based on convenience considerations. Daily maps of surface moisture flux were computed by solving the water vapor mass continuity equation for E-P for all areas receiving coverage by the SSM/I on two consecutive days. Daily flux maps for a one year period were then averaged together into monthly and annual means. Comparisons between the computed annual mean moisture flux and climatological estimates of E-P show good correlation. Differences between the computed annual mean and the climatology were of magnitude and distribution that would be expected due to interannual variability. Comparisons between monthly mean surface moisture flux and precipitation estimates show reasonable correlation, with areas receiving large amounts of precipitation generally showing strong negative moisture flux. Dissert. Abstr.

N93-25790# California Univ., Berkeley.
FURTHER ANALYSIS OF ECOM-721 DATA Final Report, 1 Feb. 1989 - 31 Jan. 1992
Supriya Chakrabarti 3 Feb. 1993 7 p
(Contract DAAL03-89-K-0057)
(AD-A260863; ARO-26404.1-GS) Avail: CASI HC A02/MF A01

During the period between February 1, 1989 and September 30, 1992, the U.S. Army grant, number DAAL03-89-K-0057, has funded auroral and airglow analysis of the ECOM-721 Extreme Ultraviolet Spectrometer Data. Some of the important work that we accomplished with the support of this grant includes transferring the data to a more accessible storage format, creating a quick look archive, further development of a solar EUV flux model which is crucial to the ECOM airglow analyses, development of a spherical radiative transfer model, and the analysis of atomic nitrogen dayglow as well as proton aurora STP78-1 data. DTIC

N93-25830 Princeton Univ., NJ.
PARTICLE SIMULATION OF AURORAL DOUBLE LAYERS Ph.D. Thesis
Bruce Lee Smith 1992 166 p
Avail: Univ. Microfilms Order No. DA9230259

Externally driven magnetic reconnection has been proposed as a possible mechanism for production of auroral electrons during magnetic substorms. Fluid simulations of magnetic reconnection lead to strong plasma flows towards the increasing magnetic field of the earth. These plasma flows must generate large scale potential drops to preserve global charge neutrality. We have examined currentless injection of plasma along a dipole magnetic field into a bounded region using both analytic techniques and particle simulation. Our analysis shows that the maximum potential for cold ions and electrons, mass ratio m/M, is: q delta-V = K (1-m/M)/2 varies as mu delta-B, where mu is their common magnetic moment, K is the kinetic energy of the injected ions, and delta-B is the difference between the maximum magnetic field strength, B(MAX), and that at injection, B(sub 0). With thermal spread in particle magnetic moments the potential depends on their temperature ratios, T(i)/T(e), and with thermal injection velocities the magnetic field mirror ratio, B MAX/B(sub 0). An expression for the leading order potential for drifting isotropic Maxwellians is given. This potential is a boundary condition for the local field solution. While global charge neutrality must be maintained in steady-state, the local potential is determined by the Vlasov-Poisson equations. Several authors obtained quasineutral solutions (n(sub i) = n(sub e)) to this boundary value problem. However, single-valued quasineutral solutions are only accessible to special combinations of fields and particle distributions. In our case multivalued solutions to the quasineutral equation arise for particular values of electric and magnetic fields. A double layer is that solution which preserves gross quasineutrality within its volume while permitting momentum balance between incident accelerated particles. The potential of the double layer is limited by the ion kinetic energy but need not match the global potential required for overall charge neutrality. One and two dimensional electrostatic particle simulations verify both double layer solutions and dependence of potentials on the injected energy. The difference between global and local potentials is absorbed in a sheath opposite the injection boundary. Potential formations are strictly dependent on the self-consistent charge distributions they support. Microinstabilities cause changes in particle distributions. Double layer motion is associated with exchange of momentum between particles and these fields. Dissert. Abstr.

N93-25852# Massachusetts Inst. of Tech., Cambridge.
THEORETICAL STUDY OF TOPSIDE IONOSPHERIC CLUTTER Final Report, 28 Mar. 1990 - 27 Mar. 1992
Min-Chang Lee and Keith M. Groves 15 Jul. 1992 115 p
(Contract F19628-90-K-0024)
(AD-A260982; PL-TR-92-2162) Avail: CASI HC A06/MF A02

The sponsored research is aimed at understanding the small scale topside ionospheric plasma structures first observed at Millstone Hill, Massachusetts with the 440 MHz incoherent scatter radar. These small scale obliquely propagating plasma modes occurring in the vicinity of the mid-latitude ionospheric trough, have large radar cross-sections and narrow spectral widths. They have, until recently, been dismissed solely as hard target contamination of the incoherent scatter radar. The geophysical conditions associated with the ionospheric trough, such as the field aligned current activity and steep plasma density gradients, suggest that these recently discovered small scale topside ionospheric plasma structures may also appear in the auroral and polar regions. This speculation has been corroborated by our preliminary experiments and data analyses at Tromso, Norway and Sondrestromfjord, Greenland. Presented in this final report are our research results and Arecibo experiments simulating the geophysical conditions of generating these topside ionospheric plasma structures. Recommendation for the future research is also given. DTIC

N93-25886*# Alabama Univ., Huntsville. Dept. of Chemistry.
CRRES: COMBINED RELEASE AND RADIATION EFFECTS SATELLITE PROGRAM SUMMARY
Laura D. Layman and George P. Miller 4 Mar. 1993 85 p
(Contract NAS8-38609)
(NASA-CR-192469; NAS 1.15:192469) Avail: CASI HC A05/MF A01

The experiments that comprise the Combined Release and Radiation Effects Satellite Program (CRRES) (Apr. 1990 - Jul. 1992) are presented. The experiments are as follows: PEGSAT; El Coqui; the Kwajalein Campaign; and experiments G1 - G14. CASI

N93-25889# National Inst. of Polar Research, Tokyo (Japan).
JARE DATA REPORTS. NO. 171 (UPPER ATMOSPHERE PHYSICS 9). DATA, SYOWA AND ASUKA STATIONS, 1989
Akira Kadokura, Kunio Uchida, Noriyuki Kurihara, Kenichi Kimura, Hiroshi Okamura, Hidetoshi Ariyoshi (Nippon Electric Co. Ltd., Yokohama, Japan.), Akira Yukimatsu (Kyoto Univ., Japan.), Masaki Ejiri, ed., Takao Hoshiai, ed., and Takeo Hirasawa, ed. Feb. 1992 338 p
Avail: CASI HC A15/MF A03

This data book summarizes upper atmosphere physics data acquired by the Upper Atmosphere Physics Monitoring Systems at Syowa Station and Asuka Station in 1989. Observations were made at Syowa Station in the following areas: (1) geomagnetism; (2) ELF-VLF waves; (3) the ionosphere; and (4) auroras. The following are observation items from the

Asuka Station: (1) geomagnetism; (2) the ionosphere; and (3) the aurora. The Upper Atmosphere Physics Monitoring Systems were installed at Syowa Station in Jan. 1981 and at Asuka Station in Jan. 1987. An outline of the systems is given. Specifications of the observation instruments and the data acquisition systems are presented. The recording periods are also listed. The format of the compiled digital data is shown. Magnetograms and frequency-time spectra of magnetic pulsations in the period of 1 Jan. - 31 Dec. 1989 for Syowa Station and Asuka Station are given.
Author (revised)

N93-25891# Naval Research Lab., Bay Saint Louis, MS.
A PREDICTED GEOMAGNETIC FIELD MODEL FOR EPOCH 1990.0 Final Report
Malcolm G. McLeod Jan. 1993 18 p
(AD-A260669; NRL/FR/7442-92-9414) Avail: CASI HC A03/MF A01

An epoch 1990.0 geomagnetic field model will be produced by the Naval Oceanographic Office (NAVOCEANO) using magnetic field measurements from the recently launched (April 1990) Polar Orbiting Geomagnetic Survey satellite for part of the input data. To aid in the production and evaluation of this model, NAVOCEANO requested that the Naval Oceanographic and Atmospheric Research Laboratory (NOARL) develop a predicted field model for 1990.0. A predicted model of the geomagnetic field for epoch 1990.0 has been developed. The model is based on the Definitive Geomagnetic Reference Field (DGRF) model for 1980.0 updated to 1990.0 by use of a secular variation model for 1980.0 developed at NOARL. The NOARL secular variation model is based upon annual means of vector geomagnetic field components from 73 magnetic observatories for years 1976.5 through 1983.5. The predicted model is of spherical harmonic degree and order 10. The rms error of the predicted model is estimated to be 200 nT relative to an accurate degree 10 field model for epoch 1990.0. Peak errors relative to an accurate model are estimated to be 500 nT for vector field error magnitude and +/-350, +250, and +/-500 nT for north, east, and vertical field components errors, respectively. If the DGRF model for 1980.0 were used without updating to represent the degree 10 field for 1990.0, estimated errors would be about four times as large.
DTIC

N93-25946# Pennsylvania State Univ., University Park. Dept. of Meteorology.
SAR-RELATED STRESS VARIABILITY IN THE MARINE ATMOSPHERIC BOUNDARY LAYER Final Report, 1 Jun. 1990 - 30 Sep. 1992
Hampton N. Shier and George S. Young 30 Sep. 1992 113 p
(Contract N00014-90-J-4012)
(AD-A261129) Avail: CASI HC A06/MF A02

Satellite- or aircraft-bourne synthetic aperture radars (SAR) have the potential to serve as a powerful and essential part of the global meteorological/oceanographic observation system. While the potential of SAR systems is enormous, quantitative interpretation of SAR signals has clearly been frustrated by our incomplete understanding of the relationships between the radar backscatter cross section and a complicated heterogeneous and constantly changing state of the sea surface. In the first phase of our High-Res ARI work summarized here, we began developing two new marine atmosphere boundary layer models of the surface stress caused by submesoscale boundary layer coherent structures and we finished obtaining plainview patterns of surface stress variability caused by MABL updrafts and downdrafts. We began turning our attention to such mesoscale atmospheric circulations as the solenoidal circulation over the sea surface temperature front, the coastal sea breeze circulation, and the flow between the Bermuda High and the diurnally varying pressure through on the coastal plain. In this report, we briefly review our progress on the work that will be continued and extended during the second phase of the project from October 1, 1992 to September 30, 1995. In Appendix A and Appendix B we give two manuscripts of journal articles summarizing our results. The first one by Sikora and Young (1993) discusses the plainview patterns of surface stress variability. The second one by Wells et al. (1993) discusses a new method for estimating the correlation dimension of boundary layer turbulent time series.
DTIC

N93-26084*# New Orleans Univ., LA. Dept. of Physics.
DETERMINATION OF DESIGN AND OPERATION PARAMETERS FOR UPPER ATMOSPHERIC RESEARCH INSTRUMENTATION TO YIELD OPTIMUM RESOLUTION WITH DECONVOLUTION Final Report, 1 Aug. 1987 - 31 Dec. 1991
George E. Ioup and Juliette W. Ioup 31 Dec. 1991 163 p
(Grant NAG1-804)
(NASA-CR-192832; NAS 1.26:192832) Avail: CASI HC A08/MF A02

The final report for work on the determination of design and operation parameters for upper atmospheric research instrumentation to yield optimum resolution with deconvolution is presented. Papers and theses prepared during the research report period are included. Among all the research results reported, note should be made of the specific investigation of the determination of design and operation parameters for upper atmospheric research instrumentation to yield optimum resolution with deconvolution. A methodology was developed to determine design and operation parameters for error minimization when deconvolution is included in data analysis. An error surface is plotted versus the signal-to-noise ratio (SNR) and all parameters of interest. Instrumental characteristics will determine a curve in this space. The SNR and parameter values which give the projection from the curve to the surface, corresponding to the smallest value for the error, are the optimum values. These values are constrained by the curve and so will not necessarily correspond to an absolute minimum in the error surface.
Derived from text

N93-26151*# Lockheed Missiles and Space Co., Palo Alto, CA. Space Sciences Lab.
IMAGING THE MAGNETOSPHERE IN THE EXTREME ULTRAVIOLET
Y. T. Chiu 6 Feb. 1993 38 p
(Contract NASw-4529)
(NASA-CR-192218; NAS 1.26:192218) Avail: CASI HC A03/MF A01

A final report on research on magnetosphere imaging in the extreme ultraviolet is presented. The objectives of the research contract can be summarized in three related items: (1) investigate the feasibility of the EUV imaging concept by using Lockheed in-situ ion measurement data; (2) investigate the technical resources required to make scientific interpretations of such EUV images by end-to-end simulations of the imaging concept; and (3) construct and test the key element for EUV magnetosphere imaging, the multilayer mirror with normal-incidence reflectance designed for the selected solar resonance line.
Derived from text

N93-26159*# SRI International Corp., Menlo Park, CA. Geoscience and Engineering Center.
STUDY OF AURORAL DYNAMICS WITH COMBINED SPACECRAFT AND INCOHERENT-SCATTER RADAR DATA Quarterly Progress Report No. 5, 1 Sep. - 31 Dec. 1992
Juergen Watermann 1 Feb. 1993 27 p Original contains color illustrations
(Contract NASw-4063; SRI Proj. 2781)
(NASA-CR-192224; NAS 1.26:192224) Avail: CASI HC A03/MF A01; 1 functional color page

We have examined Sondrestrom incoherent-scatter radar observations of ionospheric plasma density and temperature distributions, as well as measurements of F-region ion drifts that were made during a prenoon pass by the DMSP-F7 satellite through the radar field of view. The spacecraft traversed a region of intense electron precipitation with a characteristic energy below approximately 200 eV. Particles with such low characteristic energies are believed to originate, either directly or indirectly, in the magnetosheath. The precipitation region had a width of about 2 deg invariant latitude. The corotating radar observed a patch of enhanced electron density and elevated electron temperature in the F2 region between about 10.5 and 12 magnetic local time in the same invariant latitude range where DMSP-F7 detected the soft-electron flux. The ion drift pattern, also obtained by radar, shows that it is unlikely that the plasma patch was produced by solar radiation and advected into the radar field of view. We suggest that the radar observed modifications of the ionospheric plasma distribution, which resulted from direct entry of magnetosheath electrons into the magnetosphere and down to ionospheric altitudes. Model calculations of the ionospheric response to the observed electron flux support our interpretation.
Author (revised)

N93-26283# Massachusetts Univ., Lowell. Center for Atmospheric Research.
DIGITAL OBLIQUE REMOTE IONOSPHERIC SENSING (DORIS) PROGRAM DEVELOPMENT
Walter Kuklinski, Jon Hazelwood, and Bodo W. Reinisch Apr. 1992 46 p
(Contract F19628-90-K-0029)
(AD-A261750; PL-TR-92-2113; AD-E201414; SR-5) Avail: CASI HC A03/MF A01

The development and performance of a complete oblique ionogram autoscaling and inversion algorithm is presented. The inversion algorithm uses a three layer quasiparabolic model of the midpoint electron density profile. The inversion process is formulated as an optimization problem that uses a two-stage simulated annealing optimization algorithm. The inversion algorithm was tested using both synthetic data and oblique ionogram data obtained for a link between Goose Bay and Wallops Island. The results of the inversion were compared with midpoint electron density profiles recorded at the Maine OTH radar. DTIC

N93-26348# Clarkson Univ., Potsdam, NY. Dept. of Mathematics and Computer Science.
NONLINEAR WAVE PHENOMENA RELATED TO INTERACTIONS IN THE IONOSPHERE Final Report, 1 Sep. 1989 - 31 Aug. 1992
D. J. Kaup and A. S. Fokas 21 Jan. 1993 8 p
(Grant AF-AFOSR-0510-89)
(AD-A261450; AFOSR-93-0064TR) Avail: CASI HC A02/MF A01

A very important mechanism for the decay of upper hybrid waves into electron Bernstein waves was investigated. This mechanism operates only in a very narrow resonance region around the harmonics of the electron cyclotron frequency. The researchers calculated the width of these resonances and compared the analytical results with experimental observations. They found very good agreement with all available data. They found a simple mechanism for the generation of upper hybrid waves from the pump made by direct conversion. Simple estimates indicate how extremely large amplitude waves can be generated. DTIC

N93-26421*# National Aeronautics and Space Administration. Goddard Space Flight Center, Greenbelt, MD.
STEADY INDUCTION EFFECTS IN GEOMAGNETISM. PART 1B: GEOMAGNETIC ESTIMATION OF STEADY SURFICIAL CORE MOTIONS: A NON-LINEAR INVERSE PROBLEM
Coerte V. Voorhies Washington Apr. 1993 25 p
(RTOP 676-40-02; RTOP 579-31-07)
(NASA-TP-3272-Pt-1B; Rept-92B00100-Pt-1B; NAS 1.60:3272-Pt-1B)
Avail: CASI HC A03/MF A01

The problem of estimating a steady fluid velocity field near the top of Earth's core which induces the secular variation (SV) indicated by models of the observed geomagnetic field is examined in the source-free mantle/frozen-flux core (SFI/VFFC) approximation. This inverse problem is non-linear because solutions of the forward problem are deterministically chaotic. The SFM/FFC approximation is inexact, and neither the models nor the observations they represent are either complete or perfect. A method is developed for solving the non-linear inverse motional induction problem posed by the hypothesis of (piecewise, statistically) steady core surface flow and the supposition of a complete initial geomagnetic condition. The method features iterative solution of the weighted, linearized least-squares problem and admits optional biases favoring surficially geostrophic flow and/or spatially simple flow. Two types of weights are advanced radial field weights for fitting the evolution of the broad-scale portion of the radial field component near Earth's surface implied by the models, and generalized weights for fitting the evolution of the broad-scale portion of the scalar potential specified by the models. Author

N93-26430# Naval Research Lab., Washington, DC.
A CHANNEL SIMULATION PROCESSOR FOR THE MULTI-NODE TACTICAL NETWORK SIMULATOR
Joseph P. Macker 17 Jan. 1993 27 p
(AD-A261810; NRL/MR/5523-93-7184) Avail: CASI HC A03/MF A01

The design and development of a digital signal processor (DSP) based groundwave and ionospheric communication channel simulator is described. The primary objective is to simulate communication channel perturbations for a network of communication via an array of DSP modules operating in real-time. This array of channel simulator processors is a subsystem of the multimode tactical network simulator (TACNETSIM) being developed by the Information Technology Division at the Naval Research Laboratory (NRL). The propagation model developed is based upon intra-battlegroup high frequency (HF) communications. The communication channel model consists of two modes of propagation: HF groundwave and HF skywave. The HF skywave component is simulated via a Watterson ionospheric model. The real-time DSP implementation of the Watterson ionospheric model is described in terms of subprocesses. The performance of each subprocess is shown to be within established statistical parameters. Detailed specifications are given of both the hardware and software design. The simulator is designed for dynamic channel modeling and includes a data interface for real-time program control. DTIC

N93-26454# Naval Postgraduate School, Monterey, CA. Dept. of Physics.
CHAOS METRICS FOR TESTING LAGRANGIAN PARTICLE MODELS Technical Report, Mar. - Dec. 1992
R. F. Kamada 31 Jan. 1993 113 p
(AD-A261429; NPS-PH-93-007) Avail: CASI HC A06/MF A02

The Lorenz and Henon attractors and two atmospheric Lagrangian particle models were tested using self-affine fractal dimension, D(A), Shannon information entropy, S, and the Lyapunov exponent, lambda, along with turbulent kinetic energy, vertical variance, and Brunt-Vaisala Frequency. Results show that (1) chaos metrics are a new set of tools to assess the micro behavior of Lagrangian particle models. (2) that periodicity in bifurcatory systems differs from wave behavior in fluids, since wave states are not limited to amplitude extrema. (3) Non-spectral particle models lead to unrealistic variations in 'the chaos metrics with changes in buoyant stability. (4) S and D(A) behave oppositely at times, implying that diffusion and dispersion are not equivalent, even in the absence of mean windflow. DTIC

N93-26548# National Center for Atmospheric Research, Boulder, CO.
EFFECTS OF SURFACE THERMAL FORCING ON STRATIFIED FLOW PAST AN ISOLATED OBSTACLE Ph.D. Thesis - Iowa State Univ.
J. Reisner 1992 107 p Sponsored by NSF
(PB93-156776; NCAR/CT-140) Avail: CASI HC A06/MF A02

Scorer (1968) has pointed out that most experimental studies tend to overemphasize the effects of upstream stratification instead of the equally or perhaps more important effects of the localized heating and cooling of the surface of a three-dimensional (3-D) obstacle. Indeed, as shown, surface heating can lead to dramatic changes in the flow such as allowing for the disappearance of the upwind stagnation (defined as surface flow that is either zero or in opposite direction to the incoming flow). To understand how surface heating of mesoscale obstacles, such as the Hawaiian Archipelago, affects the flow, it is important to realize that heating will not only influence the surface flow but, perhaps more importantly, can also modify elevated flow structures such as internal gravity waves, columnar disturbances, and lee vortices. Basic aspects of the flow of a density-stratified fluid past three-dimensional obstacles for Froude number approximately O(1) and isolated surface thermal forcing representative of diurnally varying mesoscale flows past mountainous islands such as Hawaii are investigated. NTIS

N93-24813# GKSS-Forschungszentrum Geesthacht (Germany).
THE NEED FOR SPACEBORNE OBSERVATIONS FOR METEOROLOGY AND CLIMATOLOGY
E. Raschke *In* ESA, Environment Observation and Climate Modelling Through International Space Projects. Volume 2: Remote Sensing for Environmental Monitoring and Resource Management 1992 p 621-623
(For primary document see N93-24775 09-43)
Copyright Avail: CASI HC A01/MF A04; ESA, EPD, ESTEC, Noordwijk, Netherlands, HC

N93-25570*# Corps of Engineers, Vicksburg, MS.
DEVELOPMENT OF A CONE PENETROMETER FOR MEASURING SPECTRAL CHARACTERISTICS OF SOILS IN SITU
Landris T. Lee, Jr. and Philip G. Malone *In* NASA, Washington, Technology 2002: The Third National Technology Transfer Conference and Exposition, Volume 1 Feb. 1993 p 99-108 Sponsored in part by Army Toxic and

Hazardous Materials Agency (For primary document see N93-25561 09-99)
Avail: CASI HC A02/MF A04

47 METEOROLOGY AND CLIMATOLOGY

Includes weather forecasting and modification.

N93-24742*# National Aeronautics and Space Administration. Langley Research Center, Hampton, VA.
WCRP SURFACE RADIATION BUDGET SHORTWAVE DATA PRODUCT DESCRIPTION, VERSION 1.1
C. H. Whitlock, T. P. Charlock, W. F. Staylor, R. T. Pinker (Maryland Univ., College Park.), I. Laszlo (Maryland Univ., College Park.), R. C. DiPasquale (Lockheed Engineering and Sciences Co., Hampton, VA.), and N. A. Ritchey (Lockheed Engineering and Sciences Co., Hampton, VA.) Mar. 1993 28 p
(RTOP 578-12-23-70)
(NASA-TM-107747; NAS 1.15:107747) Avail: CASI HC A03/MF A01

Shortwave radiative fluxes which reach the Earth's surface are key elements that influence both atmospheric and oceanic circulation. The World Climate Research Program has established the Surface Radiation Budget climatology project with the ultimate goal of determining the various components of the surface radiation budget from satellite data on a global scale. This report describes the first global product that is being produced and archived as part of that effort. The interested user can obtain the monthly global data sets free of charge using e-mail procedures.
Author (revised)

N93-24747*# Little (Arthur D.), Inc., Cambridge, MA.
WEATHER FORECASTING EXPERT SYSTEM STUDY Final Report
Dec. 1985 165 p
(Contract NAS10-11333)
(NASA-CR-192929; NAS 1.26:192929) Avail: CASI HC A08/MF A02

Weather forecasting is critical to both the Space Transportation System (STS) ground operations and the launch/landing activities at NASA Kennedy Space Center (KSC). The current launch frequency places significant demands on the USAF weather forecasters at the Cape Canaveral Forecasting Facility (CCFF), who currently provide the weather forecasting for all STS operations. As launch frequency increases, KSC's weather forecasting problems will be great magnified. The single most important problem is the shortage of highly skilled forecasting personnel. The development of forecasting expertise is difficult and requires several years of experience. Frequent personnel changes within the forecasting staff jeopardize the accumulation and retention of experience-based weather forecasting expertise. The primary purpose of this project was to assess the feasibility of using Artificial Intelligence (AI) techniques to ameliorate this shortage of experts by capturing aria incorporating the forecasting knowledge of current expert forecasters into a Weather Forecasting Expert System (WFES) which would then be made available to less experienced duty forecasters. Author

N93-24875# Federal Aviation Administration, Atlantic City, NJ.
THE 1992 INTERNATIONAL AEROSPACE AND GROUND CONFERENCE ON LIGHTNING AND STATIC ELECTRICITY: ADDENDUM
Nov. 1992 309 p Conference held in Atlantic City, NJ, 6-8 Oct. 1992 Sponsored in part by National Interagency Coordinating Group and Florida Inst. of Tech.
(DOT/FAA/CT-92/20-Add-1) Avail: CASI HC A14/MF A03

This report supplements the compilation of papers presented at the 1992 International Aerospace and Ground Conference on Lightning and Static Electricity. It includes papers concerning lightning phenomenology, lightning characterization, modeling and simulation, test criteria and techniques, and protection of both airborne and ground systems. For individual titles, see N93-24876 through N93-24903.

N93-24876*# National Aeronautics and Space Administration. John F. Kennedy Space Center, Cocoa Beach, FL.
LAUNCH PAD LIGHTNING PROTECTION ENHANCEMENT BY INDUCED STREAMERS **c14**
James R. Stahmann (Boeing Aerospace Co., Cocoa Beach, FL.) and E. Ron Bentti *In* FAA, The 1992 International Aerospace and Ground Conference on Lightning and Static Electricity: Addendum Nov. 1992 17 p (For primary document see N93-24875 09-47)
Avail: CASI HC A03/MF A03

Estimations of the effectiveness of launch pad lightning protection systems on protected points within the cone of protection usually ignore the effects of streamers that propagate out to meet down coming lightning leaders. Multiple streamers develop when the lightning leader is close enough to cause high electric fields and air breakdown on the structures. The tips of the streamers propagate toward the leader tip; and the longest and fastest streamers capture the stroke. Improved operational television at the launch pads has produced TV pictures of this process. The lightning protection enhancement caused by this streamer extension of the protective systems can be estimated. Author

N93-24877# New Mexico Inst. of Mining and Technology, Socorro. Langmuir Lab. for Atmospheric Research.
LIGHTNING PRECURSOR SIGNATURES FROM DUAL-POLARIZATION RADAR MEASUREMENTS OF STORMS
Paul Krehbiel, Tiehan Chen, Stephen McCrary, William Rison, Grant Gray, and Marx Brook *In* FAA, The 1992 International Aerospace and Ground Conference on Lightning and Static Electricity: Addendum Nov. 1992 6 p (For primary document see N93-24875 09-47)
(Grant AF-AFOSR-0450-89)
Avail: CASI HC A02/MF A03

Real-time correlation and display of the co-polar and cross-polar radar returns from electrically active storms has provided dramatic indications of the buildup of electric stress in the storms, and of the collapse of the stress at the time of lightning. Following up on the pioneering work of Hendry and McCormick, strong correlations are observed above the 0 degree C level in the middle and upper parts of storms that are indicative of the presence of electrically aligned particles. Regions of strong correlation are readily identified in scanning a storm and provide an excellent indicator of the potential for lightning in the storm. The correlation values have been used to predict the occurrence of individual lightning discharges in storms. In addition, they have been used to detect the onset of electrification in storms and to tell when a storm is finished producing lightning. Author

N93-24878*# National Aeronautics and Space Administration. John F. Kennedy Space Center, Cocoa Beach, FL.
APPLICATIONS OF TRIGGERED LIGHTNING TO SPACE VEHICLE OPERATIONS Abstract Only **c18**
William Jafferis, Rocco Sanicandro (Boeing Aerospace Co., Cocoa Beach, FL.), John Rompalla (Wisconsin-Stout Univ., Menomonie.), and Richard Wohlman (University of Western Carolina, Cullowhee, NC.) *In* FAA, The 1992 International Aerospace and Ground Conference on Lightning and Static Electricity: Addendum Nov. 1992 1 p (For primary document see N93-24875 09-47)
Copyright Avail: CASI HC A01/MF A03

Kennedy Space Center (KSC) and the USAF Eastern Space Missile Center (ESMC) covering an area of 25 x 40 km are frequently called America's Spaceport. This title is earned through the integration, by labor and management, of many skills in a wide variety of engineering fields to solve many technical problems that occur during the launch processing of space vehicles. Weather is one of these problems, and although less frequent in time and duration when compared to engineering type problems, has caused costly and life threatening situations. This sensitivity to weather, especially lightning, was recognized in the very early pioneer days of space operations. The need to protect the many vfacilities, space flight hardware, and personnel from electrified clouds capable of producing lightning was a critical element in improving launch operations. A KSC lightning committee was formed and directed to improve lightning protection, detection, and measuring systems and required that all theoretical studies be confirmed by KSC field data. Over the years, there have been several lightning incidents involving flight vehicles during ground processing as well as launch. Subsequent investigations revealed the need to improve these systems as well as the knowledge of the electrical atmosphere and its effects on operations in regard to cost and safety. Presented here is how, KSC Atmospheric Science Field Laboratory (AFSL), in particular Rocket Triggered Lightning, is being used to solve these problems. Author

N93-24879# Aerospatiale, Suresnes (France). Centre Commun de Recherches.

NUMERICAL MODELLING OF INDUCED EFFECTS OF LIGHTNING STRIKE ON AN ALL COMPOSITE HELICOPTER **c03**

Pascal Gondot, G. Donnet (Nucletudes, Montreuil, France.), and Patrick Trochet (Nucletudes, Montreuil, France.) *In* FAA, The 1992 International Aerospace and Ground Conference on Lightning and Static Electricity: Addendum Nov. 1992 11 p (For primary document see N93-24875 09-47)

Avail: CASI HC A03/MF A03

The use of Carbon Fiber Composite in airframe construction arouses an increase of interest to protect sensitive avionic systems against indirect effects of lightning. In the SAE-AE4L recommendation, a long duration waveform is specified for equipment tests, especially in the case of an all composite structure. An all composite helicopter has been modeled with a FDTD method including internal structures and cables network. Then, the induced currents on shielded cables have been calculated for three lightning strike configurations. The purpose of this study is to discuss a specification for equipment tests based on calculations which permit us to distinguish typical waveforms and levels of transient for every equipment. Author

N93-24880# Rockwell International Corp., Downey, CA. Space Systems Div.

ZONING OF AIRCRAFT: A REVIEW OF THE DEFINITIONS **c03**

Nathaniel G. Bankston *In* FAA, The 1992 International Aerospace and Ground Conference on Lightning and Static Electricity: Addendum Nov. 1992 16 p (For primary document see N93-24875 09-47)

Avail: CASI HC A03/MF A03

The assignment of lightning strike zones to the surface areas of aircraft is a necessary first step in the protection design and certification process. Lightning strike zones are defined with respect to an external environment that has been synthesized from the important characteristics of natural lightning. Based on recent discussions in the Society of Automotive Engineers (SAE) AE4-L committee on lightning standards, it is apparent that the zone definitions are not intuitively clear. This paper presents a review of the zone definitions and discusses some of the problems associated with these definitions, including the problem of making probability statements in the definitions. Author

N93-24881# United Kingdom Atomic Energy Authority, Abingdon (England). Lightning Test and Technology.

EQUIPMENT TESTING WITH DAMPED SINEWAVES BETWEEN 1 AND 50 MHz **c33**

C. John Hardwick and R. E. Baldwin *In* FAA, The 1992 International Aerospace and Ground Conference on Lightning and Static Electricity: Addendum Nov. 1992 10 p Sponsored by British Aerospace Aircraft Group; Civil Aviation Authority; Construcciones Aeronauticas S.A.; Dept. of Trade and Industry; Rolls-Royce Ltd.; Saab-Scania; Short Bros. and Harland Ltd.; and Westland Helicopters Ltd. (For primary document see N93-24875 09-47)

Avail: CASI HC A02/MF A03

Present lightning equipment test standards such as RTCA DO160C call for damped sinusoidal tests at 1 and 10 MHz. There has been some discussion in the lightning community about extending these tests to 50 frequencies in the region 1-50 MHz. This paper presents characteristics of such tests on cable bundles and notes the relationship between bundle current and injected voltage; important parameters are the cable loss and Q of the driving waveform. Author

N93-24882# Ktech Corp., Lexington Park, MD.

AN INTEGRATED APPROACH TO 300 kV ELECTROSTATIC DISCHARGE APPLICATION DURING COMPONENT TESTING THAT WILL SATISFY MIL-STD-331B APPENDIX F **c33**

Monty R. Lehmann, Jack Nial (Naval Surface Warfare Center, Indian Head, MD.), and Mike Whitaker (Naval Air Warfare Center, Patuxent River, MD.) *In* FAA, The 1992 International Aerospace and Ground Conference on Lightning and Static Electricity: Addendum Nov. 1992 7 p (For primary document see N93-24875 09-47)

Avail: CASI HC A02/MF A03

The widely differing methods of producing and applying a 300 kV electrostatic stimulus to components during testing to satisfy MIL-STD-331B Appendix F has resulted in uncertainty about the validity of some test results data. Problems encountered in test methodology are examined and possible solutions are proposed. The resulting integrated systematic approach is presented; specific equipment is described, and sample waveforms are shown. Test procedures are presented in a standardized format. Author

N93-24883# Galaxy Scientific Corp., Pleasantville, NJ.

LIGHTNING DATA ACQUISITION

Rosemarie L. McDowall, J. Anderson Plumer (Lightning Technologies, Inc., Pittsfield, MA.), and Michael S. Glynn (Federal Aviation Administration, Atlanta, GA.) *In* FAA, The 1992 International Aerospace and Ground Conference on Lightning and Static Electricity: Addendum Nov. 1992 7 p (For primary document see N93-24875 09-47)

Avail: CASI HC A02/MF A03

Three data collection programs are being pursued to acquire data which may be useful in the Federal Aviation Administration (FAA) lightning databases. The Commercial Lightning Database (CLD) program solicits lightning strike data from commercial and general aviation pilots via a form filled out by the pilot when his aircraft is struck. Current airline participants are American and Delta. Another source of data is the Bureau of Land Management (BLM) which runs a network of lightning sensors covering the 11 western states of the United States. Data on approximately 13 million strikes between 1985 and 1990 have been reviewed. In addition to these two sources, the Organization of Flying Adjusters (OFA) and the Aircraft Owners and Pilots Association (AOPA) are starting to supply data from their files. Author

N93-24884# Electro Magnetic Applications, Inc., Denver, CO.

DIGITIZATION OF ANALOG DATA FROM IN-FLIGHT LIGHTNING STRIKES

James R. Elliott and Henry S. Weigel *In* FAA, The 1992 International Aerospace and Ground Conference on Lightning and Static Electricity: Addendum Nov. 1992 10 p (For primary document see N93-24875 09-47)

(Contracts DTFA03-86-C-60027; DTFA03-86-C-00042)

Avail: CASI HC A02/MF A03

Analog recorded data from in flight lightning strikes has been converted for installation in the FAA Research and Development Electromagnetic Database (FRED). One second of data associated with a lightning event is digitized for each of an ensemble of electromagnetic sensors. The digitization and conversion process, which yields as many as 4 million samples for a sensor, is described. Author

N93-24885# Northrop Corp., Pico Rivera, CA.

A PROCEDURE FOR DEFINING LIGHTNING RISK TO AIR VEHICLES **c03**

David Beeman and Naomi Morita *In* FAA, The 1992 International Aerospace and Ground Conference on Lightning and Static Electricity: Addendum Nov. 1992 18 p (For primary document see N93-24875 09-47)

Avail: CASI HC A03/MF A03

The risk of a lightning-induced failure is a function of the atmospheric conditions which produce lightning and the protective characteristics of the vehicle. Contemporary air vehicle designs - which incorporate 'wet' wings and extensive composite skin and structures - require thorough consideration of this risk to balance performance of lightning protection measures against other performance parameters (i.e., cost, weight, manufacturability, maintainability). An analytic procedure to investigate the risk of lightning-induced fuel vapor ignition is described in this paper. Sensitivity of the risk to various atmospheric and air vehicle design parameters was examined and is discussed. Author

N93-24886# United Kingdom Atomic Energy Authority, Abingdon (England). Lightning Test and Technology.

PARAMETERS INFLUENCING THE HOT-SPOT IGNITION OF AVIATION FUEL/AIR AND ETHYLENE/AIR MIXTURES **c03**

Stephen J. Haigh and C. John Hardwick *In* FAA, The 1992 International Aerospace and Ground Conference on Lightning and Static Electricity: Addendum Nov. 1992 9 p Sponsored by British Aerospace Aircraft Group; Civil Aviation Authority; Construcciones Aeronauticas S.A.; Dept. of Trade and Industry; Rolls-Royce Ltd.; Saab-Scania; and Short Bros. and

Harland Ltd. (For primary document see N93-24875 09-47)
Avail: CASI HC A02/MF A03

Lightning attachments to aircraft skins can lead to the creation of local areas of heating or 'hotspots', which may be able to ignite fuel/air vapor mixtures contained within the skin. The characteristic temperature/time histories of such hot-spots are very different depending on whether the skins are metallic or carbon fiber. This report describes experimental work carried out under the Lightning Club program to determine the ability of transient hot-spots in metal foil to ignite JP4/air mixtures. The influence of parameters such as hot-spot size and duration is considered, as well as fuel concentration and oxygen enrichment. To establish the validity of simulation testing techniques in which ethylene is used to detect hotspots, some experiments are also carried out using mixtures of this gas with air. We make comparison of these with results with other reported work in this field. Author

N93-24887# SRI International Corp., Menlo Park, CA.
COMPARISON OF THE ELECTRICAL CHARGING AND DISCHARGING ENVIRONMENTS OF MULTIPLE AIRCRAFT-BORNE ELECTRIC-FIELD MEASUREMENT SYSTEMS **c03**
Kathy L. Giori and J. E. Nanevicz *In* FAA, The 1992 International Aerospace and Ground Conference on Lightning and Static Electricity: Addendum Nov. 1992 10 p (For primary document see N93-24875 09-47)
Avail: CASI HC A02/MF A03

Various aircraft and particle charging and discharging mechanisms can adversely affect the performance of aircraft-borne electric-field measurement systems. Samples of data collected both during coordinated flight maneuvers (T-28 and SPTVAR aircraft) and from similar flight environments (Learjets 24B and 36A) have been analyzed and compared. These comparisons help in the identification and interpretation of the possible effects of (1) charged particles, and (2) aircraft charging and discharging phenomena on the respective electric-field measuring systems. It was found that the SPTVAR generally became more highly charged than the T-28, and the Learjet 36A more than the 24B. Such comparisons offer a better understanding of the electrical characteristics and of the measurement accuracies of these systems. Author

N93-24888# Tokyo Univ. (Japan). Inst. of Industrial Science.
OBSERVATION OF RADIATION FROM LIGHTNING DISCHARGES BY LPATS
Masaru Ishii, Junichi Hojo, T. Yamamoto (Tokyo Electric Power Co., Inc., Japan.), E. Zaima (Tokyo Electric Power Co., Inc., Japan.), J. Sawada (Tokyo Electric Power Co., Inc., Japan.), and N. Fukiyama (Tokyo Electric Power Co., Inc., Japan.) *In* FAA, The 1992 International Aerospace and Ground Conference on Lightning and Static Electricity: Addendum Nov. 1992 16 p (For primary document see N93-24875 09-47)
Avail: CASI HC A03/MF A03

A lightning location system known by the name of LPATS was installed on the central region of the Honshu Island as its third system in Japan. Calibration of the sensitivity of this system was completed in 1991, and a function to distinguish electromagnetic field waveforms having small peak-to-zero times was added at that time. By these modifications, the system has almost become able to distinguish negative cloud-to-ground strokes in summer, but still misinterprets many cloud-discharge pulses in summer as positive return strokes. Majority of such misinterpreted field waveforms had rather small range-normalized signal strengths, and were identified as bipolar pulses originating from cloud-discharge processes. In winter, such a difference depending on the polarity of return strokes becomes remarkably less, suggesting seasonal variation in the occurrence of cloud-discharge pulses. Author

N93-24889*# National Aeronautics and Space Administration. Lewis Research Center, Cleveland, OH.
A SYSTEM TO MEASURE LIGHTNING-INDUCED TRANSIENTS ON SPACECRAFT UMBILICAL LINES **c33**
Jeffrey C. Brown, Noel B. Sargent, and Carl J. Wenzler *In* FAA, The 1992 International Aerospace and Ground Conference on Lightning and Static Electricity: Addendum Nov. 1992 8 p (For primary document see N93-24875 09-47)
Avail: CASI HC A02/MF A03

Spacecraft electrical systems are potentially vulnerable during ground operations to damage from lightning-induced transients coupled onto umbilical cables. Limited data are available to compare spacecraft design protection levels with actual transient magnitudes. A system has been designed to accurately measure these transients and verify that spacecraft protection levels have not been exceeded. This paper describes the design and operation of the system and its installation at Launch Complex 36 on the Cape Canaveral Air Force Station (CCAFS). Author

N93-24890# British Aerospace Public Ltd. Co., Bristol (England). Research Centre.
A COMPUTATIONAL APPROACH TO PREDICTING THE EXTENT OF ARC ROOT DAMAGE IN CFC PANELS **c24**
Nicholas Jennings and C. John Hardwick (United Kingdom Atomic Energy Authority, Abingdon, England.) *In* FAA, The 1992 International Aerospace and Ground Conference on Lightning and Static Electricity: Addendum Nov. 1992 8 p Sponsored in part by Rolls-Royce Ltd.; Construcciones Aeronauticas S.A.; Saab-Scania; Civil Aviation Authority; Dept. of Trade and Industry; and Short Bros. and Harland Ltd. (For primary document see N93-24875 09-47)
Avail: CASI HC A02/MF A03

It is important to understand the mechanism of lightning arc root damage to carbon fiber composite panels in view of their increasing use in airframe construction. A computer model has been developed which contains coupled models of current and heat flow and predicts the extent of panel damage. Both initial stroke and continuing current components can be modelled, and the CFC parameters may be temperature dependent. Results and some comparisons with observations are presented. Author

N93-24891# Dornier Luftfahrt G.m.b.H., Friedrichshafen (Germany).
COMPARISON OF THE DAMAGE FOR VARIOUS TYPES OF FIBRE REINFORCED COMPOSITES DUE TO DIFFERENT LIGHTNING TEST STANDARDS (MIL-STD-1757A, GERMAN MILITARY VG-STANDARD 96903) **c24**
Juergen Wiedmann, Jan-Uwe Roth, and Alexander W. Kern (Universitaet der Bundeswehr Muenchen, Neubiberg, Germany.) *In* FAA, The 1992 International Aerospace and Ground Conference on Lightning and Static Electricity: Addendum Nov. 1992 16 p Sponsored by Ministry of Defence (For primary document see N93-24875 09-47)
Avail: CASI HC A03/MF A03

This paper provides experimental results on the extent and nature of damage on various types of aircraft FRC (fiber reinforced composites) caused by lightning arc attachment. Two different lightning test parameter sets were applied corresponding to MIL-STD-1757A and the German military VG-standard 96903 part 71. Concerning direct effects, the VG-standard differs from MIL-STD especially in the higher action integral (10 MJ/omega), the most important damage parameter with respect to FRC. Lightning tests with VG-standard are not known yet. The various types of tested aircraft FRC comprise unprotected and protected CFC and SFC/CFC-hybrid structures as well as novel, multilayered electromagnetic structures. The visible damage areas caused by impulse currents are strongly correlated to the action integrals. Metal protection meshes seem to suffer more from higher action integrals than the underlaying structures. The protection effectiveness of a new homogeneous protection system is proved. Author

N93-24892# Tohoku Electric Power Co., Inc., Sendai (Japan). Electricity Technology Research and Development Center.
LIGHTNING CHARACTERISTICS IN THE NORTH-EAST PART OF JAPAN OBSERVED BY A MAGNETIC DIRECTION-FINDER NETWORK
Noriyasu Honma, H. Komuro, Masaru Ishii (Tokyo Univ., Japan.), and Junichi Hojo (Tokyo Univ., Japan.) *In* FAA, The 1992 International Aerospace and Ground Conference on Lightning and Static Electricity: Addendum Nov. 1992 10 p (For primary document see N93-24875 09-47)
Avail: CASI HC A02/MF A03

Observations of lightning ground flashes have been made by a magnetic direction-finder network in the Tohoku region, located in the north-east part of the island of Honshu in Japan. The performance of this system has been evaluated and improved through close observations and ongoing analysis. Based on the data obtained to date, the density and the polarity of ground flashes were analyzed, focusing on various geographical and seasonal variations. It was concluded that the surrounding sea was the primary factor affecting ground flash characteristics. Author

N93-24893# Politecnico di Torino (Italy). Dipt. di Elettronica.
FRACTAL DETERMINATION OF PARAMETERS IN LIGHTNING AND ESD MODEL **c32**
Giuseppe Vecchi, D. Labate, and F. Canavero *In* FAA, The 1992 International Aerospace and Ground Conference on Lightning and Static Electricity: Addendum Nov. 1992 9 p (For primary document see N93-24875 09-47)
(Grant EEC-SC1-CT91-0690)
Avail: CASI HC A02/MF A03

In this paper, the radiation from a geometrically fractal (i.e., arbitrarily irregular) discharge channel is investigated from the point of view of fractal geometry. Numerical results are presented for lightning return stroke radiation, which demonstrate that the time waveform of radiated field (in the Fraunhofer region) is a fractal with the same fractal dimension as the channel path. Some implications of this finding are discussed. Author

N93-24894# United Kingdom Atomic Energy Authority, Abingdon (England). Lightning Test and Technology.
ZONING OF AIRCRAFT BY ELECTRIC FIELD MODELLING **c03**
C. John Hardwick and V. K. Thompson *In* FAA, The 1992 International Aerospace and Ground Conference on Lightning and Static Electricity: Addendum Nov. 1992 10 p Sponsored by British Aerospace Aircraft Group; Construcciones Aeronauticas S.A.; Rolls-Royce Ltd.; Saab-Scania; Short Bros. and Harland Ltd.; Westland Helicopters Ltd.; Civil Aviation Authority; and Dept. of Trade and Industry (For primary document see N93-24875 09-47)
Avail: CASI HC A02/MF A03

The accurate determination of the zoning of aircraft has become more important with the increasing use of CFC materials in airframe construction. In-flight evidence suggests previous rules such as those given in the FAA AC20-53A are unsatisfactory. The proposed AC20-53B recommends substantially increased areas for Zone 1A. This paper presents an approach for calculating the initial attachment zones which, unlike the rolling sphere model, explicitly takes field concentration factors into account. Author

N93-24895# Lightning Technologies, Inc., Pittsfield, MA.
LIGHTNING PHENOMENOLOGY BASES FOR FULL THREAT RETURN STROKE OCCURRENCE FOLLOWING EXTENDED LEADER SWEEP AT FLIGHT ALTITUDES
J. Anderson Plumer *In* FAA, The 1992 International Aerospace and Ground Conference on Lightning and Static Electricity: Addendum Nov. 1992 18 p (For primary document see N93-24875 09-47)
Avail: CASI HC A03/MF A03

It has been recognized that lightning leaders sweep aft from initial attachment points on aircraft forward extremities prior to arrival of the first return stroke, which, in a cloud-to-earth flash, is not initiated until a branch of the leader reaches the earth. This process has lead to more realistic procedures for locating lightning strike Zone 1A on aircraft surfaces, with the result that Zone 1A covers considerably more of the aircraft surfaces than previous zone location methods (i.e., 'the 18-inch criteria') would indicate. Some observers have suggested that, whereas the leader may indeed sweep a considerable distance alongside fast moving aircraft at flight altitudes, the intensity of the ensuing first return stroke will be less than it would be at the ground terminus of the lightning channel, because a portion of leader charge is below, not above, the airplane. Analytical models of lightning channels are often cited to support this, since such models often show reduction of the stroke intensity (i.e., peak current and action integral) with distance from the earth terminus. Physical damage on aircraft struck in flight belies this contention, however, as damage indicative of severe return strokes is often seen well beyond 18 inches aft of initial leader attachments. This paper discusses the natural lightning characteristics that explain why severe first return strokes may arrive well aft of forward extremity tips of aircraft, and why zone location methods must account for this. It is the third paper in a series begun in 1980 by the author on the topic of swept leader and zone location methodology, and presented at these conferences. Author

N93-24896# National Severe Storms Lab., Norman, OK.
POSITIVE CLOUD-TO-GROUND FLASHES IN SEVERE STORMS
Donald R. MacGorman, Donald W. Burgess (National Weather Service, Norman, OK.), and Carolyn D. Morgenstern (Oklahoma Univ., Norman.) *In* FAA, The 1992 International Aerospace and Ground Conference on Lightning and Static Electricity: Addendum Nov. 1992 8 p (For primary document see N93-24875 09-47)
Avail: CASI HC A02/MF A03

We examine positive cloud-to-ground lightning in 25 mesoscale convective systems (MCS's) and in 15 severe storms. The signal amplitude distributions of positive ground flashes in MCS's that produced severe weather almost always either peaked at relatively large amplitudes or peaked at small amplitudes and decreased slowly with increasing amplitude. In the 15 severe storms we examined, cloud-to-ground flashes were dominated by positive flashes for periods ranging from 30 min to several hours. The geographic region in which positive or negative flashes dominated sequential storms on a given day appeared similar from storm to storm. In most cases observed by Doppler radar, storms dominated by positive flashes were low-precipitation or classic supercell storms. If negative ground flashes subsequently became dominant, the storm often became a classic or heavy-precipitation supercell storm. Large hail usually was reported during the period when positive ground flashes dominated, and the reported frequency and diameter of hail usually decreased after the dominant polarity of ground flashes switched to negative. In tornadic storms, the strongest tornado usually began after the positive ground flash rate decreased from its maximum value. Although many hailstorms and tornadic storms are dominated by negative flashes, tornadic storms and hailstorms comprise a small fraction of storms dominated by frequent negative flashes, but appear to comprise an overwhelming majority of storms dominated by frequent positive flashes. Author

N93-24897# Universidad Nacional Autonoma de Mexico, Mexico City. Center for Atmospheric Sciences.
STUDY OF ATMOSPHERIC ELECTRICAL EVENTS ABOVE COMPLEX TERRAIN
Oscar Troncoso-Lozada *In* FAA, The 1992 International Aerospace and Ground Conference on Lightning and Static Electricity: Addendum Nov. 1992 7 p (For primary document see N93-24875 09-47)
Avail: CASI HC A02/MF A03

From the middle of 1982, there has been, in our institution, an interest in thunderstorm studies, aided greatly by advances in instrumentation and data processing. As a result, several cloud systems were analyzed and studied, and results are presented in this paper. The emphasis of the study was to investigate when and where the electrical discharge typically occur in relation to the lightning detection network. The sensor system consisted of two punctual discharge detectors, three radio noise detectors at frequencies of 10, 27, and 100 kHz, and a tipping-bucket rain-gauge adjacent to the sensors. The instrumentation used in this study has been described by Troncoso (1987). Author

N93-24898# Naval Air Warfare Center, Patuxent River, MD. Aircraft Div.
APPLICATIONS OF STRESS ENVELOPE CONCEPTS TO AIRCRAFT EMP AND LIGHTNING SURVIVABILITY **c03**
Sam Frazier *In* FAA, The 1992 International Aerospace and Ground Conference on Lightning and Static Electricity: Addendum Nov. 1992 6 p (For primary document see N93-24875 09-47)
Avail: CASI HC A02/MF A03

The Naval Air Warfare Center Aircraft Division is conducting research into the modeling of aircraft electromagnetic transient response data. One result has been the development of a test point stress waveform which combines multiple responses. This single stress waveform bounds the test point stress responses collected during different test phases; each contributing waveform contains coupling response data from various polarizations, orientations, and configurations relative to the external threat environment. This new waveform, termed the 'Stress Envelope', has significant applications in the area of inductively coupled direct-drive, reducing test uncertainties, and permitting better estimates of system margins.
Author

N93-24899# Electro Magnetic Applications, Inc., Lakewood, CO.
DEVELOPMENT OF MODELS FOR PREDICTING THE TRIGGERING OF LIGHTNING BY LAUNCH VEHICLES **c15**
Rodney A. Perala, Terence H. Rudolph, and Calvin C. Easterbrook *In* FAA, The 1992 International Aerospace and Ground Conference on Lightning and Static Electricity: Addendum Nov. 1992 11 p (For primary document see N93-24875 09-47)
Avail: CASI HC A03/MF A03

As evidenced by incidents on Apollo 12 and AC-67 launches, the threat to launch vehicles from triggered lightning is real. Even in the absence of naturally occurring lightning, it is possible for a launch vehicle with attached plume to amplify atmospheric electric fields to an extent such that an electrical discharge can happen. Therefore, launch rules which are based on the presence of natural lightning in the vicinity may be inadequate to ensure that a triggered strike cannot occur. In order to develop adequate launch guidelines with respect to triggered lightning, it is necessary to first thoroughly understand the physical mechanisms leading to the triggered strike. To this end, we have begun to develop a triggered lightning model which will allow one to predict in advance the conditions under which a lightning strike will occur to a launch vehicle during ascent. The purpose of this paper is to describe the project and the technical issues, and to present some preliminary results. Author

N93-24900# Lightning Location and Protection, Inc., Tucson, AZ.
A SINGLE-POINT WARNING SYSTEM FOR THUNDERSTORMS AND ELECTRIC FIELDS **c35**
W. T. Neumann, K. L. Cummins, and E. Philip Krider (Arizona Univ., Tucson.) *In* FAA, The 1992 International Aerospace and Ground Conference on Lightning and Static Electricity: Addendum Nov. 1992 8 p (For primary document see N93-24875 09-47)
Avail: CASI HC A02/MF A03

In this paper, we describe a single-point warning system that combines a single-station thunderstorm warning sensor with a static electric field sensor. This integrated system monitors nearby cloud-to-ground lightning and overhead electrification, allowing a wide variety of potentially hazardous meteorological conditions to be monitored. The paper discusses relevant sensing technologies, public safety and aviation applications for the system, recent field experience, and future development options. Author

N93-24901# Veda, Inc., Lexington Park, MD.
COMMERCIAL PRECIPITATION STATIC (P-STATIC) TEST EQUIPMENT **c35**
R. Wayne Devereux *In* FAA, The 1992 International Aerospace and Ground Conference on Lightning and Static Electricity: Addendum Nov. 1992 10 p (For primary document see N93-24875 09-47)
Avail: CASI HC A02/MF A03

The aircraft industry requires commercially available, safe and reliable, test equipment to support Precipitation Static (P-static) Research, Development, Test and Evaluation (RDT&E). The test equipment must be able to simulate the in-flight P-static charging environment and acquire the P-static interference data for analysis of specification compliance. Using P-static test equipment, the aircraft industry can locate P-static problem areas, compare these results to specification limits, identify potential fixes, and evaluate fixes effectiveness. This paper describes the commercially available portable P-static test equipment designed, from a user's perspective, to meet the Royal Australian Navy's (RAN) aircraft ground support equipment's (GSE) needs. Author

N93-24902# International Protection Consultants Proprietary Ltd., Hobart (Australia).
COMPARATIVE PERFORMANCE OF LIGHTNING AIR TERMINALS UNDER NATURAL STORM CONDITIONS
J. R. Gumley and Philip J. Jones (Lightning Protection International Proprietary Ltd., Hobart, Australia.) *In* FAA, The 1992 International Aerospace and Ground Conference on Lightning and Static Electricity: Addendum Nov. 1992 7 p (For primary document see N93-24875 09-47)
Avail: CASI HC A02/MF A03

During August 1992, a test site was established in Florida to assess the upward leader initiation capability of air terminals under natural storm conditions. Five types of air terminals were mounted independently on 10 m masts and grounded through one ohm resistors to sense emission currents. Two terminals were corona forming types, and three were spherical in design. Coaxial feeders conveyed the derived voltages to digitizer cards located in a personal computer with hard disc and tape drive storage. The two types of events described were recorded from very close lightning. The first showed marked differences in the emission currents of the spherical and corona forming terminals at the commencement of the return stroke. The latter exhibited strong negative polarity while the 3 spheres simultaneously produced a strong positive deflection. Several events displayed this type of characteristic. The second type of event recorded pulse currents of 10-15 amperes with polarity consistent to that expected for upward streamer initiation. These emissions were generated from the floating spheres 30-150 microseconds ahead of the return stroke. No significant or similar emissions were recorded in the same period from the conventional sphere or from the Franklin Rod. The reference Franklin Rod showed the lowest predischarge activity in 75 percent of recorded events. Author

N93-24903# United Kingdom Atomic Energy Authority, Abingdon (England). Lightning Test and Technology.
ALTERNATIVE EQUIPMENT TEST PROCEDURES FOR SIMULTANEOUS CURRENT INJECTION ON MULTIPLE CABLE BUNDLES **c33**
C. John Hardwick, Stephen J. Haigh, and R. E. Baldwin *In* FAA, The 1992 International Aerospace and Ground Conference on Lightning and Static Electricity: Addendum Nov. 1992 9 p Sponsored by British Aerospace Aircraft Group; Civil Aviation Authority; Construcciones Aeronauticas S. A.; Dept. of Trade and Industry; Rolls-Royce Ltd.; Saab-Scania; and Short Bros. and Harland Ltd. (For primary document see N93-24875 09-47)
Avail: CASI HC A02/MF A03

Simple equipment tests can be accomplished by injecting currents into interconnect cables and adjusting the voltage injected into the loop under test or current in the cable until the ETDL is reached. However, for more complicated systems with several cables, this simple procedure is inadequate. This paper compares measurements made on cable bundles in a fuselage with both injection into the fuselage and injection on bundles to illustrate the problem and proposes alternative test methods. Author

N93-25125# Los Alamos National Lab., NM.
APPLICATION OF OPTICAL REMOTE SENSING TO THE STUDY OF SURFACE FLUXES RELATED TO CLOUD FORMATION
W. M. Porch and W. I. Shaw (Pacific Northwest Lab., Richland, WA.) 1992 6 p Presented at the Optical Society of America Meeting on Optical Remote Sensing of the Atmosphere, Salt Lake City, UT, 8-12 Mar. 1993
(Contract W-7405-eng-36)
(DE93-003783; LA-UR-92-3500; CONF-930346-1) Avail: CASI HC A02/MF A01

Optical scintillation instrumentation was applied to studies of cloud effects on surface fluxes. Spatial averaging of optical-turbulence-based estimates of fluxes can be made much faster than conventional tower techniques. DOE

N93-25220# National Oceanic and Atmospheric Administration, Washington, DC.
A SYSTEMATIC SATELLITE APPROACH FOR ESTIMATING CENTRAL PRESSURES OF MID-LATTITUDE OCEANIC STORMS
Frank J. Smigielski and H. Michael Mogil Dec. 1992 71 p
(NOAA-TR-NESDIS-63) Avail: CASI HC A04/MF A01

The development and applications of the Smigielski-Mogil-Burtt technique, used to assess central pressures of mid-latitude Atlantic Ocean cyclones are described. The technique combines attributes of the Junker-Haller technique (1980) and Dvorak tropical cyclone analysis technique (1984) in a flow chart format. It is based on the analysis of 50 full-latitude cyclone developments during the colder months, as well as operational feedback provided by National Weather Service and the U.S. Navy forecasters. The paper was also written to supplement training courses conducted by the authors. Forecasters should read the background material in the first four sections before completing the case to make independent assessments on a storm's central pressure before finding out 'solutions.' Author (revised)

N93-25275 Oklahoma Univ., Norman.
THE CHARGE AND SIZE OF PRECIPITATION PARTICLES INSIDE THUNDERSTORMS AND MESOSCALE CONVECTIVE SYSTEMS ON THE GREAT PLAINS Ph.D. Thesis
Monte Gene Bateman 1992 154 p
Avail: Univ. Microfilms Order No. DA9305953

We created a new balloon-borne instrument that measures the charge (q) and size (d) of precipitation particles; we call it the q-d instrument. It is capable of measuring particle sizes ranging from 0.8 to 8.0 mm diameter

and charges ranging from plus or minus 4 to plus or minus 400 pC. The q-d instruments were flown into thunderstorms and mesoscale convective systems. We did not find any dependence of precipitation charge on ambient thermodynamic or electrical conditions. Both polarities of charge were found to coexist at nearly all altitudes within and below most storms. The exception was that only particles with positive and no detectable charge were measured within and below a decaying thunderstorm. The fraction of all particles that carried no detectable charge ranged from 17-77 percent and did not depend on the magnitude of the vertical electric field. We found evidence of positive charging by melting. When we compared the charge density due to precipitation with the total charge density calculated from the vertical electric field profile using Gauss's law, we found the former to be a factor of 2-100 smaller. This implies that much charge was carried on particles smaller than 0.8 mm diameter. Dissert. Abstr.

N93-25293 Georgia Inst. of Tech., Atlanta.
CLOUD PROPERTIES AS INFERRED FROM HIRS/2 MULTI-SPECTRAL DATA Ph.D. Thesis
Eric Otto Schmidt 1991 156 p
Avail: Univ. Microfilms Order No. DA9238476

Cloud properties and types are inferred from analysis of the 3.74 micron, 6.7 micron, and 11.1 micron data from the HIRS/2 instrument. The data analyzed was recorded on September 14 and 15, 1988 in the Ohio valley area. The approach uniquely uses the 6.7 micron water vapor channel data to improve detection of clouds by exploring discrimination between high and low clouds. Information on cloud height, cloud fraction, and emissivity is determined from the Baum multi-spectral multi-resolution (MSMR) method and used in determination of cloud optical depth and type. Improved identification of cloudy pixels by the MSMR method is a feature of the technique, as is the application of a brightness temperature difference comparison for the 6.7 micron and 11.1 micron channels. Multi-spectral image classification supports the presence of clouds, including subvisual cirrus, for these two days. The spectral classification and analyses incorporate the AVHRR GAC data at 3.74 microns, 10.8 microns, and 12.0 microns, while the MSMR method also utilizes HIRS/2 CO2 and infrared window channels. All cloud types in the image are identified and their optical properties (optical depth, cloud-top pressure height, emissivity, cloud fraction, and cloud-top equivalent brightness temperature) determined. Comparison of the spectral data with radiative transfer model results establishes limits on determinable cloud parameters and suggests further study of the effects of multiple layers in complex cloud systems.
Dissert. Abstr.

N93-25294 Florida State Univ., Tallahassee.
INITIALIZATION OF A MODELED CONVECTIVE STORM USING DOPPLER RADAR-DERIVED FIELDS Ph.D. Thesis
Ying Lin 1992 125 p
Avail: Univ. Microfilms Order No. DA9306039

A method is developed to initialize convective storm simulations with Doppler radar-derived fields. Input fields for initialization include velocity, rain water derived from radar reflectivity, and pressure and temperature fields obtained through thermodynamic retrieval. A procedure has been developed to fill in missing wind data, followed by a variational adjustment to the filled wind field to minimize 'shocks' that would otherwise cause the simulated fields to deteriorate rapidly. A series of experiments using data from a simulated storm establishes the feasibility of the initialization method. Multiple Doppler radar observations from the 20 May 1977 Del City tornadic storm are used for the initialization experiments. Simulation results initialized from observations taken at two different stages of storm development are shown and compared to observations taken at later times. A simulation initialized from one of the observation times showed good agreement with subsequent observations, though the simulated storm appeared to be evolving much faster than observed. Possible mechanisms for error growth are discussed. Dissert. Abstr.

N93-25352 Colorado State Univ., Fort Collins.
A DYNAMICAL THEORY FOR HURRICANE SPIRAL BANDS Ph.D. Thesis
Thomas Alan Guinn 1992 190 p
Avail: Univ. Microfilms Order No. DA9303868

A dynamical theory is presented for two classes of hurricane spiral bands--inner and outer. Inner bands, which typically form within 500 km of the vortex center, can result from both potential vorticity (PV) wave breaking and vortex merger. PV wave breaking is found to occur when the PV field is asymmetric. This process ejects a relatively high PV air down gradient into regions of relatively low PV air in the form of spiral bands. Vortex merger occurs when a vortex moves sufficiently close to a PV source. This process also produces inner spiral bands. The inner bands modeled in this study were found to project almost entirely onto the rotational modes, thus suggesting they are a slow-manifold phenomenon rather than a gravity wave phenomenon as previously proposed. Outer bands, which typically form at a radius greater than 500 km from the vortex center, are found to occur as a result of the intertropical convergence zone (TICZ) breakdown. Both types of bands are found to be stabilized by the adverse shear created by the main vortex. All theories are tested through the integration of a limited area, normal mode, spectral model. Dissert. Abstr.

N93-25549 Maryland Univ., College Park.
OBSERVED ANNUAL AND INTERANNUAL VARIATIONS IN TROPOSPHERIC WATER VAPOR Ph.D. Thesis
Dian Judith Gaffen 1992 245 p
Avail: Univ. Microfilms Order No. DA9238477

Radiosonde observations from a global network of 56 radiosonde stations for 1973-1990 are used to describe and quantify annual and interannual variations of tropospheric water vapor. Taking care to identify data inhomogeneities related to changes in instruments or observing practices, monthly mean and anomaly data sets are constructed for dew point, specific humidity, relative humidity, temperature and precipitable water from the surface to 500 mb. Local annual cycles of tropospheric humidity can be classified according to the amplitude and phase of humidity variations which define five humidity regimes. For two regimes, both in middle and high latitudes, relative humidity is fairly constant while the annual cycle of precipitable water is in phase with that of temperature. At some midlatitude stations with a monsoon-like climate, seasonal relative humidity variations are large. In the tropics, seasonal relative humidity variations, especially above the boundary layer, dominate the annual cycle of precipitable water, and precipitable water variations are not related to temperature variations. Correlations of temperature and specific humidity anomalies are generally positive outside the tropics, suggesting that atmospheric warming is associated with increases in water vapor content. However, correlations of temperature and relative humidity anomalies are sometimes not significant and are often negative (e.g., in mid- and high latitude continental regions). Thus relative humidity is not always insensitive to temperature changes. In the tropics, tropospheric water vapor and temperature variations are not well correlated. An empirical orthogonal function analysis of tropical specific humidity variations identified two important modes of variability. The first is a step-like increase in specific humidity that occurred in about 1976-1977, and the second is associated with the El Nino phenomenon. The increase is consistent with the results of an extensive trend analysis of the data, which showed evidence for increases in precipitable water at about half of the 39 studied, decreases at three and no statistically significant trend at the others. Precipitable water trends were closely related to trends in dew point and specific humidity, as one would expect, but they were not always related to temperature trends. In addition, statistically significant relative humidity trends, both positive and negative, were found. Dissert. Abstr.

N93-25557 Utah Univ., Salt Lake City.
ON THE VERTICAL STRUCTURE OF SEASONAL, INTERANNUAL AND INTRASEASONAL FLOWS Ph.D. Thesis
Steven Reino Gilbert 1992 216 p
Avail: Univ. Microfilms Order No. DA9305145

The vertical structure of the height and wind fields associated with the seasonal, interannual, and intraseasonal cycles is documented by making use of global ECMWF operational analyses for seven pressure levels (1000-100 mb) and spanning a 10 year period (1980-89). The role of tropical convection is examined for each of these time scales. The seasonal cycle is described through the structure of the geopotential height field standing waves, the vertical structure of the first seven wavenumbers of the rotational and divergent winds, and latitude/time cross-sections for the vertical structure of the planetary waves. The change in the vertical structure from the internal mode combinations found in the tropics to a dominant external mode of the extratropics occurs rapidly and within 10 degrees of the convective source regions. Extensive use is made of a primitive equation (PE) model, as a diagnostic tool, to explore the extent to which tropical

heating might influence the extratropical vertical structure. The PE response indicates the possibility that 25-40 percent of the Northern Hemisphere and 30-55 percent of the Southern Hemisphere kinematic vertical structure could be the result of tropical heating. Two significant El Nino/Southern Oscillation (ENSO) events occur during this 10 year period and their vertical structures are examined. The cold phase is found to be dominated by higher internal modes than the warm phase. This may be linked to different air-sea interactive processes during cold and warm ENSO phases. The tie to tropical convection is also seen in the PE model response which shows wave trains and zonal wind maxima moving westward from the war to cold phase of the ENSO events, consistent with observations. The intraseasonal oscillation, as found in the near-equatorial 200 mb velocity potential, is composited for three seasons. A link between this oscillation and tropical convection is only clearly established during the convective phase, when convective activity is present across the Western Pacific and Indian Oceans. Composite cases for each season are selected to be in phase with one another and during times when the convective phase of the intraseasonal oscillation is strong. It is found that, when convective regions in the composites are collocated with those present in the seasonal average, the kinematic vertical structure is dominated by the two deepest vertical modes. This is different for other locations, where the convection in the composites does not coincide with regions of convection in the seasonal average. In this case the kinematic vertical structure favors higher internal modes.

Dissert. Abstr.

N93-25633# Naval Postgraduate School, Monterey, CA.

AN ANALYSIS OF MESOSCALE CONVECTIVE SYSTEMS OBSERVED DURING THE 1992 TROPICAL CYCLONE MOTION FIELD EXPERIMENT M.S. Thesis

Eric J. McKinley Dec. 1992 113 p

(AD-A260889) Avail: CASI HC A06/MF A02

An analysis of two tropical Mesoscale Convective Systems (MCS) observed during the Tropical Cyclone Motion-92 (TCM-92) mini-field experiment is accomplished. A discussion of TCM-92, its primary and secondary missions, and the resulting data sets is provided. Primary data sets for the two cases include high-density (one minute) WC-130 aircraft data, 44 omega dropwindsondes, and visual and infrared (IR) geostationary satellite imagery. The observed characteristics exhibited by the tropical MCS's of the two cases are related to the hypothesized characteristics of midlatitude MCS's. Thus, the goal of the analyses is to document, for the first time, the horizontal and vertical scales in terms of the expected structure and evolution of the tropical MCS. The MCS's of the two cases were in the mature and decaying stages of the convective life cycle. Mid-level (500 mb) vortices that are apparently created in the stratiform rain regions of the MCS's are clearly discernable in the wind fields. In both cases, these vortices are seen to build upward to 300 mb or originate higher than the 500 mb surface. Downward translation of the vortex to 700 mb is evident in both aircraft and satellite data in one case. Convective signatures in the temperature and dewpoint fields are not as significant as the wind fields. Because signatures are observed in the synoptic scale, such as anticyclonic outflow in the MCS regions, these systems apparently were significant mesoscale features of sufficient intensity and duration to alter the large-scale regime for over 24 h. DTIC

N93-25645# Massachusetts Inst. of Tech., Lexington.

SETTING VALUES FOR TDWR/LLWAS 3 INTEGRATION PARAMETERS

Rodney E. Cole and Russell F. Todd 5 Feb. 1993 21 p

(Contracts DTFA01-89-Z-02033; F19628-90-C-0002)

(AD-A260740; DOT/FAA/NR-92/12) Avail: CASI HC A03/MF A01

In 1993 the FAA will begin deploying the Terminal Doppler Weather Radar (TDWR) at selected airports in the United States. Forty-five TDWRs will be collocated with LLWAS 3 systems, and the FAA has decided that all TDWRs collocated with LLWAS 3 systems must be integrated with LLWAS 3 prior to commissioning. The algorithm chosen to perform this integration must be supplied with a set of site-specific parameters. This report gives guidance on how to set the values of theme integration parameters. DTIC

N93-25685 Florida State Univ., Tallahassee.

LAND SURFACE PROCESSES AND CLIMATE MODELING Ph.D. Thesis

Lahouari Bounoua 1992 210 p

Avail: Univ. Microfilms Order No. DA9306028

A simple but realistic parameterization of ground wetness is developed and implemented in the FSUGSM to model in climate. Specifically, a soil moisture parameter based on a moisture budget, is introduced to estimate the Bowen ratio. It is expressed as an evolutive function of the model predicted rainfall, surface temperature and takes into account ground characteristics through its dependence on albedo and surface elevation. This scheme is used in conjunction with a prognostic equation for surface temperature to determine the surface fluxes. A global spectral model is used to perform two parallel forecasts, one of which includes the new scheme. Monthly situations for selected variables are presented. Comparison of the components of the surface energy balance are carried out for different types of climatic regime over Africa during summer. The new scheme captures the essence of the known physics in simple formulation of the processes and introduced interesting modulation of the fluxes. Reduction of the surface temperature and its diurnal cycle is observed. This is particularly evident over arid zones. An important and coherent interaction between the physical processes has resulted from the introduction of the scheme and led to better representation of the distribution of the heat sources at the surface. Realistic rainfall rates and distribution are obtained over the Sahelian region. Significant improvement has been introduced in the prediction of primary variables near the surface. The effect of the new land surface processes parameterization was, however, not clearly discernible in the upper level model atmosphere structure.

Dissert. Abstr.

N93-25714 Colorado State Univ., Fort Collins.

TROPICAL CYCLOGENESIS IN THE WESTERN NORTH PACIFIC Ph.D. Thesis

Raymond Milton Zehr 1992 231 p

Avail: Univ. Microfilms Order No. DA9303909

Tropical cyclogenesis in the western North Pacific is characterized by an early convective maximum which precedes the initial appearance of a tropical depression. The convection is quantified from cloud areas specified by cold infrared temperature thresholds with 3-hourly GMS satellite data. It is hypothesized that this convective maximum represents an important process associated with tropical cyclogenesis and is a response to large-scale (synoptic-scale) forcing. A conceptual model is described in which the early convective maximum is viewed as a necessary but not sufficient condition for tropical cyclone formation. An important change in the wind field takes place in response to the convective maximum. A weak mesoscale vortex is initiated and is located within the larger broad-scale cyclonic circulation of the pre-existing tropical disturbance. However, the first substantial decrease in central sea-level pressure and resultant increase in surface wind speed occur at a later stage of tropical cyclogenesis. Typically, the early convective maximum and associated mesoscale vortex formation precede first designation as a tropical storm by 2-3 days. The 850 mb and 200 mb objective analyses of conventional data are used to classify different synoptic-scale patterns associated with the formation of fifty individual tropical storms and typhoons during 1983-1984. Animated satellite imagery and aircraft reconnaissance data provide observations of deep convection and low-level winds for more detailed analysis. Twenty-four non-developing tropical disturbances which persisted for at least two days in the climatologically favorable genesis region are also investigated. Quantitative IR satellite analysis and 850 mb and 200 mb objective analyses of relative vorticity, divergence, and vertical wind shear allow comparisons among individual non-developing and developing disturbances. Small vertical wind shear, sufficient low-level convergence, and sufficient low-level relative vorticity are shown to be necessary conditions for tropical cyclogenesis. One or more of the three conditions can usually be identified as being deficient with individual cases of non-developing disturbances.

Dissert. Abstr.

N93-25724 Wisconsin Univ., Madison.

PRESSURE TORQUES AND CIRCULATION CHANGES IN ROCKY MOUNTAIN LEE CYCLONES Ph.D. Thesis

Alan C. Czarnetzki 1992 232 p

Avail: Univ. Microfilms Order No. DA9231196

The transfer of absolute dynamic circulation across the earth-atmosphere interface by pressure stresses in Rocky Mountain lee cyclones is examined through the use of Bjerknes' (1937) relation between stress and the tendency of absolute dynamic circulation. The pressure stress that leads to the horizontal acceleration of atmospheric circulation at the earth-atmosphere

interface results from the horizontal component of the hydrostatic weight of the atmosphere resting against the sloped terrain. The azimuthally-integrated pressure torque is the azimuthal integral of the tangential component of the pressure gradient force. It is equal to the azimuthal integral of the vertical derivative of the horizontal surfaces of the coordinate system being utilized and the contribution from the azimuthal pressure stress where the coordinate surfaces intersect the mountain. A positive (negative) vertically-integrated torque indicates a transfer of absolute dynamic circulation from (to) the earth. The tendencies of absolute dynamic circulation and the pressure torque are found to be the same order of magnitude. Negative pressure torque dominates the lower-tropospheric layers of all four simulations, indicating the transfer of absolute dynamic circulation from the atmosphere to the earth. The presence of higher pressure to the north of the lee cyclone and a pressure trough extending to the south of the cyclone are found to be crucial to explaining the sign and intensity of the pressure torque. The vertically-integrated west-to-east component of pressure drag per unit length across the Rocky Mountains is also computed. The results aid in the development of a conceptual model of the relation between the earth-atmosphere transfer of storm angular momentum on the cyclone scale and the angular momentum component along the earth's axis of rotation on the planetary scale. The pressure distributions which produces the negative mountain-induced pressure torque, and thus removes angular momentum from the cyclone, also returns eastward angular momentum to the earth by enhancing the pressure drag across the mountains to the south of the lee cyclone. This indicates that the transfer of the two components of absolute angular momentum between the atmosphere and earth are coupled. Dissert. Abstr.

N93-25731 York Univ. (Ontario).
POLARIZING MICHELSON INTERFEROMETER FOR MEASURING THERMOSPHERIC WINDS Ph.D. Thesis
John C. Bird 1991 219 p
(ISBN-0-315-70442-X) Avail: Univ. Microfilms Order No. DANN70442

The Polarizing Atmospheric Michelson Interferometer, PAMI, a new version of the Wide Angle Michelson Interferometer, is used to measure winds in the thermosphere. In the polarizing instrument, the optical path difference is changed simply by rotating a polarizing filter external to the interferometer. This allows a very simple scanning mechanism. PAMI's general behavior has been modeled in terms of Meuller matrices providing a framework for the analysis of partial polarization states within the Michelson Interferometer (MI). A field instrument based on the above concept was designed and built. PAMI is similar to other instruments such as WAMDII (Shepherd et al., 1985) that measure thermospheric winds and temperatures, retaining the benefits of high light throughput, while offering advantages including lower cost, simplicity, and portability. PAMI was constructed from readily available components wherever possible to facilitate replacement. The instrument is highly sensitive and thus is designed to be used for field measurements at locations far from city lights. Results are shown from the AIDA observation campaign in Puerto Rico (17 deg 57 min 0 sec N, 66 deg 52 min 42 sec W) where coordinated observations were made by PAMI along with other optical and radio measurements during April and May 1989. Intensities of the green line layer at 95 km were compared to those observed by several other instruments. For example, MORTI (Mesopause Oxygen Rotational Temperature Imager), a colocated instrument which was looking at the 94 km 867.6 nm molecular oxygen emission. MORTI and PAMI emission rates were found to show the same trends. PAMI intensities were also compared to two green-line photometers. In these comparisons the trends in observed emission rates were the same for all three instruments. On the brightest night recorded during April, the zenith emission rate reached over 400 Rayleighs; emission enhancements were sometimes related to auroral events. During the observing period of April 4 to April 11, 1989, most of the observations of the 95 km airglow were after midnight where the winds were found to be generally towards the north east at about 50 to 100 m/s. During auroral activity this wind vector always turned counterclockwise, towards the west. During the nights of May 2 and May 6 these wind vectors follow a wave-like variation in magnitude and direction. It is concluded that auroral activity changes the global circulation in a way that sometimes transports increased amounts of oxygen atoms over Arecibo. Wind comparisons were made with a Fabry-Perot interferometer operating at the same time at the Arecibo observatory, 60 km away. The agreement was generally good, with some differences in detail, in some cases, for the eastward wind component. Dissert. Abstr.

N93-25741 Colorado State Univ., Fort Collins.
TROPICAL CYCLONE/UPPER-ATMOSPHERIC INTERACTION AS INFERRED FROM SATELLITE TOTAL OZONE OBSERVATIONS Ph.D. Thesis
Edward Burton Rodgers 1992 291 p
Avail: Univ. Microfilms Order No. DA9303893

The Nimbus-7 Total Ozone Mapping Spectrometer (TOMS) was used to map the distribution of total ozone within and surrounding western North Atlantic and North Pacific tropical cyclones that occurred from 1979-1982. It was found from numerical model simulations and diagnostics and satellite observations that the distribution of total ozone within the subtropical upper-tropospheric waves during the tropical cyclone season correspond well with the variation of thermodynamic parameters (i.e., temperature, thickness, geopotential heights) near the tropopause and the regions of strong stratospheric and tropospheric exchange processes. These results are similar to previous middle latitudinal observations. It was also found that the three-dimensional transport processes associated with both the western North Atlantic and Pacific tropical cyclone's outflow jet induced secondary circulation and the strong vertical motions associated with active deep convective and eye regions helped to modify the total ozone distribution that is usually observed within these subtropical upper-tropospheric waves. The tropical cyclone induced modifications of the total ozone in the upper-tropospheric waves became greater as the tropical cyclone became more intense and the three-dimensional transpost processes associated with the outflow jet, convection and eye strengthened. The strong relationship between total ozone distribution and the variation of the tropopause topography, made it possible to use TOMS to monitor the propagation of the subtropical upper-tropospheric waves and the mutual adjustment between tropical cyclones and their upper-tropospheric and lower-stratospheric environment when these tropical cyclones and the upper-tropospheric waves interacted. These total ozone patterns during tropical cyclone and upper-tropospheric wave interaction reflected the three-dimensional upper-tropospheric transport processes that were conducive for storm intensification, weakening, or recurvature. The total ozone distribution indicated that high latitude western North Atlantic and North Pacific tropical cyclones that intensify (do not intensify) are (1) within 10 degrees (15 degrees) latitude of weak (strong) upper-tropospheric troughs that are moderately rich (very rich) in total ozone; (2) have outflow channels that extend (do not extend) large distances from their centers; and (3) have (do not have) subsiding ozone rich stratospheric air southwest of their centers. The total ozone distribution indicated that low latitude North Pacific tropical cyclones that intensify (do not intensify) com (do not come) into close proximity with weak upper-troposphere troughs that are moderately rich in ozone and have outflow channels that do (do not) extend large distances from the centers. Finally, the total ozone distribution indicated that western North Pacific tropical cyclones that turn left (right) are within approximately 15 degrees latitude downstream of an ozone-poor (ozone-rich) upper-tropospheric ridge (trough). Dissert. Abstr.

N93-25743 Colorado State Univ., Fort Collins.
VECTOR RADIATIVE TRANSFER MODEL: APPLICATION TO RAINFALL RETRIEVAL WITH MICROWAVE RADIOMETRIC DATA Ph.D. Thesis
Fuzhong Weng 1992 202 p
Avail: Univ. Microfilms Order No. DA9303904

A new vector radiative transfer model is developed. The physical processes included are thermal emission, scattering, absorption, and bidirectional reflection and emission at the lower boundary. The medium may be forced at the top boundary by polarized parallel or diffuse radiation and by polarized internal and boundary thermal sources as well. The model is unconditionally stable for an arbitrarily large number of streams and arbitrarily large optical depths. Brightness temperature structures of mesoscale precipitation systems (MPS's) from radiative transfer modeling are presented and analyzed. The analysis reveals several results. Polarization brightness temperatures at 85.50 GHz well reflect structures of convective and stratiform precipitation in the MPS's. Distinct contrasts between PCT's at 85.50 GHz in the convective and stratiform regions in the MPS's exist. Horizontally polarized brightness temperatures at 19.35 and 37.00 GHz are more sensitive to the light rain over ocean than those at other frequencies and polarization states. The PCT's at 37.00 and 85.50 GHz well correlate

the precipitation ice water path in the MPS's and the PCT at 19.35 GHz correlates the precipitation liquid water path. Inversion relations between PCT's and rain rates are derived from radiative transfer calculations in terms of a new precipitation model. This model includes precipitation-sized ice hydrometeors, raindrops, and cloud-sized hydrometeors. Error sensitivity study shows that variations of cloud water content are major causes responsible for errors of retrieved rain rates and that light rain rates retrieved from low frequency inversion relations include larger uncertainty than those from high frequency inversion relations. A microwave multi-channel algorithm is developed for retrieving monthly precipitation over global land and ocean. The probability density function of rain rates is employed in the algorithm. Retrieved monthly precipitation exhibits consistency with presently existing precipitation data in terms of large scale features and discrepancy in terms of detailed structures. Dissert. Abstr.

N93-25775# National Weather Service, Portland, OR.
NATIONAL WEATHER SERVICE WINTER WEATHER WORKSHOP
Dec. 1992 289 p Workshop held in Portland, OR, 15-18 Sep. 1992
(PB93-146785; NOAA-TM-NWS-WR-218) Avail: CASI HC A13/MF A03

The workshop's papers covered a variety of topics related to forecasting and observations of various winter weather phenomena in the United States. Papers were given on storm models and theories, applications of computer and satellite data for weather forecasting, quantitative descriptions of specific storms, and overviews of winter climate in several areas of the United States. Author (DTIC)

N93-25776# North Dakota Atmospheric Resource Board, Bismarck.
THE NORTH DAKOTA THUNDERSTORM PROJECT Final Report, Apr. 1989 - Mar. 1991
20 Nov. 1991 61 p
(Grant NA89RA-H-09088)
(PB93-153039) Avail: CASI HC A04/MF A01

The North Dakota Thunderstorm Project (NDTP) was a national scale research program conducted in central North Dakota during June and July, 1989. The program was hosted and coordinated by the North Dakota Atmospheric Resource Board and funded jointly by the National Oceanic and Atmospheric Administration (NOAA), the State of North Dakota, and the National Science Foundation. Data collection with four Doppler radars, six aircraft, and a variety of supporting instrumentation began 12 June 1989, and continued through 22 July 1989. In all, 106 of the nineteen various predefined experiments were conducted, though severe storms were fewer in number than expected. Several different atmospheric tracer techniques were employed including gaseous (sulfur hexafluoride), radar chaff, natural (ozone, carbon monoxide), and fluorescent beads. Author (DTIC)

N93-25777# Florida State Univ., Gainesville. Dept. of Meteorology.
PREDICTION OF GLOBAL CLOUD COVER WITH A VERY HIGH RESOLUTION GLOBAL SPECTRAL MODEL Interim Report, 15 Nov. 1990 - 14 Nov. 1992
T. N. Krishnamurti 29 Dec. 1992 4 p
(Grant AF-AFOSR-0023-91)
(AD-A261047; AFOSR-93-0135TR) Avail: CASI HC A01/MF A01

Currently in numerical weather prediction, two avenues for cloud forecasting are being pursued by the research community. The conventional one defines cloud coverage as a function of prevailing relative humidity. The new method explicitly predicts clouds as a variable of the model. Our research effort covers both avenues. The major results of our research are: (1) The threshold relative humidity approach exhibits a decay of cloud fractions during the medium range weather forecasts. The major errors in the prediction appear to occur in the first 24 hours, an initialization problem. Observed clouds appear to exhibit more of a resilience than is demonstrated by the models. Long lasting cloud debris (i.e., nonprecipitating elements) are not reasonably handled by the model. This deficiency is related to the strong selection rules imposed by the model for the existence of clouds; (2) The explicit treatment of clouds where the cloud water mixing ratio is used as a dependent variable of the model, appears to handle long lasting clouds in a more realistic manner. It does not show the rapid spin-down feature present in the threshold relative humidity approach; and (3) A large effort on physical initialization is currently underway in our global modeling effort. This provides a consistent analysis of the humidity variable with respect to the rain rates (as seen from satellite based measurements). DTIC

N93-25849# Desert Research Inst., Reno, NV. Atmospheric Sciences Center.
INVESTIGATION OF WINTER MOUNTAIN STORMS IN UTAH DURING THE 1989 UTAH/NOAA FIELD PROGRAM Final Report, Feb. 1989 - Mar. 1990
Arlen W. Huggins Sep. 1990 112 p
(Grant NA89RA-H-09090)
(PB93-153021) Avail: CASI HC A06/MF A02

A field research effort was conducted in the vicinity of the Tushar Mountains of southern Utah as part of the Federal-State Program in Atmospheric Modification Research involving the National Oceanic and Atmospheric Administration and the State of Utah. The field study took place in February and March 1989 and emphasized the studies of supercooled liquid water evolution in winter storms and attempts to measure the effects of ground-based silver iodide cloud seeding. Results of the field effort are presented. NTIS

N93-25870# National Center for Atmospheric Research, Boulder, CO. Advanced Study Program.
SYNOPTIC AND MESOSCALE METEOROLOGY INSTRUCTION WORKSHOP
1991 230 p Workshop held in Boulder, CO, 18-22 Jun. 1991 Sponsored by NSF Prepared in cooperation with University Corp. for Atmospheric Research, Boulder, CO
(PB93-156347) Avail: CASI HC A11/MF A03

The workshop was sponsored by the National Science Foundation and conducted jointly by the Advanced Study Program of the National Center for Atmospheric Research (NCAR), together with the Unidata Users Committee and COMET program of the University Corporation for Atmospheric Research, and the STORM Projects Office of NCAR at Boulder, Colorado, 18-22 Jun. 1991. Session headings include the following: current support for interactive computing for meteorological instruction; McIDAS instructional/classroom techniques; SDM instruction techniques; computer driven displays in a large classroom; campus distribution systems; GEMPAK instructional techniques; COMET mesoscale instruction; experiences with integrated educational labs; future applications of interactive computing. Author (DTIC)

N93-25871# National Oceanic and Atmospheric Administration, Boulder, CO. Environmental Research Labs.
CLIMATE MONITORING AND DIAGNOSTICS LABORATORY Summary Report No. 20, 1991
Eldon E. Ferguson, ed. and Rita M. Rosson, ed. Dec. 1992 140 p
(PB93-156388) Avail: CASI HC A07/MF A02

The report of activities of the Climate Monitoring Diagnostics Laboratory of the National Oceanic and Atmospheric Administration for 1991 is presented. The report summarizes the following: the activities and programs of the various observatories--the carbon cycle, aerosols, radiation, ozone, and water vapor; acquisitions and data management; nitrous oxide and halocarbons divisions; activities of the director's office; and activities of the cooperative programs. Special projects reported include studies of atmospheric aerosols generated by Mt. Pinatubo and the effects of the Mt. Pinatubo eruption on stratospheric ozone. Author (DTIC)

N93-25872# Illinois State Water Survey, Champaign. Midwest Climate Center.
RAINFALL FREQUENCY ATLAS OF THE MIDWEST
Floyd A. Huff and James R. Angel 1992 151 p Sponsored by Climate Analysis Center and National Environmental Satellite Service
(PB93-164606; ISWS/BUL-71; MCC-RR-92-03) Avail: CASI HC A08/MF A02

The report presents the results and methodology of an intense study of rainfall frequency relationships throughout the Midwest (Illinois, Indiana, Iowa, Kentucky, Michigan, Minnesota, Missouri, Ohio, and Wisconsin). Using the 275 long-term daily reporting stations from the National Weather Service (NWS) cooperative network, supplemented by 134 daily reporting stations with shorter records, rainfall amounts have been determined for recurrence intervals from 2 months to 100 years and for durations of 5 minutes to 10 days. The results are presented as maps and as climate division averages

in tabular form. Several special rainage networks were used to develop relationships between amounts for 24 hours and less. The report also examines the time distributions of heavy rainfall over time and other storm characteristics such as storm orientation and movement. The assumption of spatially independent observations between stations is also discussed.
Author (DTIC)

N93-25874# Nevada Univ. System, Reno. Atmospheric Sciences Center.
NATURAL AND AUGMENTED SNOWFALL GROWTH PROCESSES AND THEIR INTERACTIONS WITH THE NATURAL AND MODIFIED AEROSOL Final Report, 1 Mar. 1989 - 30 Apr. 1990
J. Warburton Jul. 1991 57 p
(Grant NA89RA-H-09087)
(PB93-153096) Avail: CASI HC A04/MF A01

The second annual report describes the activities performed under seven separate tasks. These tasks dealt with the development of a trace chemical method of assessing the effects of seeding in a snow producing environment and the use of the stable isotopes of water for assessing the regions of ice-phase water capture in the cloud systems from which precipitation fell in the study regions. They also dealt with the theoretical aspects of these trace chemical programs of study and with the roles which trace impurities can play in affecting the growth characteristics of ice particles in supercooled clouds and of the shapes and number fluxes of ice crystals which occur under both natural and artificially seeded conditions. These tasks also included studies of the supercooled liquid water and ice contents of winter storms over the central Sierra Nevada, both spatially and temporally through the use of ground-based remote sensing radar and microwave radiometers. Some work was also conducted on the further development of new aircraft instrumentation for measuring atmospheric motions and the microphysical composition of winter orographic clouds.
Author (DTIC)

N93-25892# Florida State Univ., Tallahassee.
TYPHOON PREDICTION (RECURVATURE - 1990 EXPERIMENT) Final Report, 1 Nov. 1988 - 30 Apr. 1992
30 Apr. 1992 35 p
(Contract N00014-89-J-1476)
(AD-A260673) Avail: CASI HC A03/MF A01

A recent review paper, to appear in the journal Advances in Atmospheric Sciences, summarizes the work completed under this grant. A copy of this review is enclosed as an appendix to the report. The approach we have followed is to first make a very high resolution model forecast of a recurving typhoon. Given a good forecast on the medium range with a comprehensive physical-dynamical model we next proceeded to evaluate residue-free budgets of vorticity and divergence following the model's output history. The residue-free budgets follow the model equations and thus carry a lot of useful information on the recurvature dynamics. Specifically, we have evaluated the residue-free budgets of vorticity and divergence for a 6 day period.
DTIC

N93-26156*# FWG Associates, Inc., Tullahoma, TN.
RAIN RATE INSTRUMENT FOR DEPLOYMENT AT SEA, PHASE 2 Final Report, 10 Apr. 1990 - 10 Mar. 1992
Jimmy W. Steele 30 Mar. 1992 126 p Original contains color illustrations
(Contract NAS8-38481; SBIR-08.02-1982)
(NASA-CR-192442; NAS 1.26:192442) Avail: CASI HC A07/MF A02; 7 functional color pages

This report describes, in detail, the SBIR Phase 2 contracting effort provided for by NASA Contract Number NAS8-38481 in which a prototype Rain Rate Sensor was developed. FWG Model RP101A is a fully functional rain rate and droplet size analyzing instrument. The RP101A is a fully functional rain rate and droplet size analyzing instrument. The RP101A consists of a fiber optic probe containing a 32-fiber array connected to an electronic signal processor. When interfaced to an IBM compatible personal computer and configured with appropriate software, the RP101A is capable of measuring rain rates and particles ranging in size from around 300 microns up to 6 to 7 millimeters. FWG Associates, Inc. intends to develop a production model from the prototype and continue the effort under NASA's SBIR Phase 3 program.
Author

N93-26245# Naval Postgraduate School, Monterey, CA.
A CLIMATOLOGY OF POLAR LOW OCCURRENCES IN THE NORDIC SEAS AND AN EXAMINATION OF KATABATIC WINDS AS A TRIGGERING MECHANISM M.S. Thesis
Kenneth A. Wos Dec. 1992 154 p
(AD-A261719) Avail: CASI HC A08/MF A02

This study examines polar low formation frequency, origin region and storm tracks in the entire Nordic Sea region for a complete polar low season and identifies the prevailing synoptic situation common to polar low formation. The number of polar lows detected through TIROS-N satellite imagery between September 1988 and May 1989 was significantly greater than one would expect from previous studies. Many polar lows were detected over the land areas of Greenland, Iceland and Svalbard away from a direct surface heat source. The storms detected over Greenland generally formed at the outflows of glacial valleys. To determine probable formation areas, polar lows were linearly backtracked along the reciprocal of their storm tracks. A significant number were backtracked to glacier outflows. These formation locations suggest a katabatic influence on storm formation, possibly due to vortex stretching, or the enhancement and distortion of an over-ice or over-land boundary layer baroclinic zone. Katabatic flows were examined by analyzing one month of regional surface synoptic observations and NOGAP 1000 mb height gradients. To develop aids to enhance polar low forecasting, monthly mean 1000 and 500 mb fields for chart times closest to polar low detection, or time backtracked to Northern, Central and Southern Greenland, were calculated from archived NOGAPS 12 hourly analyses and compared to the monthly averaged climatology fields of height and temperature.
DTIC

N93-26270# Naval Postgraduate School, Monterey, CA.
EFFECTS OF TAIWAN OROGRAPHY ON THE MOTION AND STRUCTURE OF TYPHOONS M.S. Thesis
Tien C. Yeh Dec. 1992 308 p
(AD-A261819) Avail: CASI HC A14/MF A03

Effects of steep island terrain on typhoon motion and structure changes are studied by both observational analyses and numerical simulations. The analyses involve calculation of center position deviations from a second-order polynomial curve fitted to the best tracks, and an empirical orthogonal function analysis to determine the terrain-induced surface structures. The simulations use a limited-area model, with a elliptical-shaped barrier and a 'spun-up vortex' to represent the typhoon, to demonstrate the sensitivity on track and structure relative to vortex intensity, approach direction and translation speed. Both observational and simulation studies show that the orography induces significant track deflections and structure distortions, especially for a weaker and slowly moving typhoon approaching central or southern Taiwan. As the typhoon approaches, the outer edge of the circulation accentuates the blocking effect of the barrier. Asymmetric gyres are induced by a vortex-terrain interaction as the vortex moves closer to the barrier, which accounts for the significant track deflections from a simple barrier effect. The simulations suggest that a center-following algorithm based on the wind field would be more representative than on the pressure field. A track discontinuity occurs when the secondary vortex created from flow deflections around the barrier becomes the primary center downstream.
DTIC

N93-26273# Naval Academy, Annapolis, MD.
AN INVESTIGATION INTO THE CAUSATIVE MECHANISMS FOR EXPLOSIVE CYCLONE DEVELOPMENT OVER THE ATLANTIC Final Report, 1991 - 1992
Susan S. Minton 8 May 1992 72 p
(AD-A261831; USNA-TSPR-191) Avail: CASI HC A04/MF A01

Explosive cyclogenesis is defined as the rapid intensification of a marine cyclone at the rate of 24 mb in a 24 hour period (Sanders, 1980). Such cyclones produce very intense storms which result in gale-force winds, heavy precipitation, and severe sea states along the East Coast of the United States. Green (1988) suggested that an atmospheric inversion (or lid) may play an important role in the explosive development of marine cyclones. The atmospheric lid condition is present prior to and upwind of cyclone development. This study examines three ERICA, the Experiment on Rapidly Intensifying Cyclones over the Atlantic, cases for the presence of the atmospheric lid condition. Results show that the lid condition was present 12-48 hours prior to explosive cyclone development in ERICA cases IOP 4 and 5, while the lid condition was not present in the control

case, LOP 6P. Moreover, the prediction of explosive marine cyclones would be improved with the use of operational numerical weather prediction models, such as the Nested Grid Model, provided these models have adequate vertical resolution. DTIC

N93-26286# Naval Postgraduate School, Monterey, CA.
AN OBSERVATIONAL STUDY OF THE LOCAL AND REMOTE RESPONSE OF THE EQUATORIAL PACIFIC TO WESTERLY WIND EVENTS DURING THE 1991-92 EL NINO M.S. Thesis
Grant A. Cooper, IV Dec. 1992 109 p
(AD-A261777) Avail: CASI HC A06/MF A02

The upper equatorial Pacific ocean response to anomalous westerly wind forcing during the 1991-92 El Nino was examined using observed oceanographic and atmospheric data from equatorial moorings and the Navy's operational atmospheric analyses. A strong 30-60 day signal was observed in the zonal winds and is mainly a result of westerly wind events. The local response to anomalous westerly winds differed between the western and eastern equatorial Pacific. In the western Pacific, westerly wind events tended to produce rapid decreases in sea surface temperature (SST) (up to 1 deg C). These decreases were followed several days later by SST increases due to horizontal warm water advection and downwelling. In the central and eastern equatorial Pacific, westerly wind events were expressed mainly as weakenings of the easterlies. These weakenings caused decreases in equatorial upwelling and SST increases. Westerly wind events in the western Pacific were also associated with large thermocline temperature fluctuations (on the order of 10 deg C) in the central and eastern equatorial Pacific. These fluctuations propagated eastward at phase speeds consistent with first baroclinic equatorial Kelvin wave dynamics (i.e., 2.0 - 3.5 m/s). The ocean temperature fluctuations indicate basin wide wavelengths (about 15 x 103 km), with periods of 30-60 days. DTIC

N93-26351# Pennsylvania State Univ., University Park. Dept. of Meteorology.
DEVELOPMENT AND TESTING OF IMPROVED TECHNIQUES FOR MODELING THE HYDROLOGIC CYCLE IN A MESOSCALE WEATHER PREDICTION SYSTEM Annual Technical Report, 15 Dec. 1991 - 14 Dec. 1992
Thomas Warner, Toby N. Carlson, and J. M. Fritsch Jan. 1993 11 p
(Contract F49620-92-J-0118)
(AD-A261454; AFOSR-93-0045TR) Avail: CASI HC A03/MF A01

Soil-water content is the single most important land-surface variable in atmospheric prediction models. Sophisticated surface physics-soil hydrology parameterization schemes are beginning to be used in mesoscale weather prediction models; however, soil-water content is not measured over large enough areas on a regular basis where it could provide suitable initial conditions for those models. Therefore, the initialization of the soil-water content profile has to depend on a knowledge of the hydrological balance of the soil in the area represented by each mesoscale-model grid point. In turn, this information must be obtained from a knowledge of the precipitation, evaporation, and substrate recharge from the water table. We have undertaken the task to develop a systematic means for providing initial values of the soil-water-content profile for the Penn State/NCAR Mesoscale Model. This task is composed of three phases. The first phase is to develop an off-line, one-dimensional hydrological model that is driven by conventional meteorological, soil, and vegetation data. The second phase is to develop the database to drive the hydrological model in a form that is compatible with the surface physics-soil hydrology parameterization scheme utilized in the mesoscale model (i.e., the Biosphere-Atmosphere Transfer Scheme (BATS)). The last phase consists of generating an automated update of the soil-water content profile at each of the mesoscale-model grid points. DTIC

N93-26352# Manchester Univ. (England). Inst. of Science and Technology.
THE INITIATION OF LIGHTNING AND THE GROWTH OF ELECTRIC FIELDS IN THUNDERSTORMS Annual Report, 10 Jul. 1991 - 9 Jul. 1992
John Latham Dec. 1992 90 p
(Contract F49620-92-J-0020)
(AD-A261455; AFOSR-93-0046TR) Avail: CASI HC A05/MF A01

As specified in the original proposal, there exits mounting evidence that the growth of strong electric fields--culminating in lightning--in the great majority of thunderstorms is intimately linked with--and probably contingent upon--the concomitant development of the ice-phase. Thus, significant progress in the elucidation of electrification mechanisms requires an improved understanding of the complex set of processes involved in cloud glaciation. Accordingly, primary emphasis has been devoted in this first year of a proposed 3-year study, to the analysis and interpretation of data emanating from major airborne experiments in which a primary objective was to seek a superior understanding of the initiation and development in cumulus clouds of the type which often become strongly electrified. DTIC

N93-26492*# South Dakota School of Mines and Technology, Rapid City. Inst. of Atmospheric Sciences.
THE EFFECTS OF CLOUD INHOMOGENEITIES UPON RADIATIVE FLUXES, AND THE SUPPLY OF A CLOUD TRUTH VALIDATION DATASET Semiannual Progress Report, 1 Jul. - 31 Dec. 1992
Ronald M. Welch 1993 103 p
(Contract NAS5-31718)
(NASA-CR-191711; NAS 1.26:191711; SA-2) Avail: CASI HC A06/MF A02

A series of cloud and sea ice retrieval algorithms are being developed in support of the Advanced Spaceborne Thermal Emission and Reflection Radiometer (ASTER) Science Team objectives. These retrievals include the following: cloud fractional area, cloud optical thickness, cloud phase (water or ice), cloud particle effective radius, cloud top heights, cloud base height, cloud top temperature, cloud emissivity, cloud 3-D structure, cloud field scales of organization, sea ice fractional area, sea ice temperature, sea ice albedo, and sea surface temperature. Due to the problems of accurately retrieving cloud properties over bright surfaces, an advanced cloud classification method was developed which is based upon spectral and textural features and artificial intelligence classifiers. Author

N93-26513# Scripps Institution of Oceanography, La Jolla, CA.
BOUNDARY LAYER COUPLING BETWEEN AN EXPLOSIVE CYCLONE AND THE GULF STREAM DURING ERICA Final Report, 1 Oct. 1990 - 30 Sep. 1991
Warren B. White and Dave Rogers 1 Mar. 1993 17 p
(Contract N00014-90-J-1716)
(AD-A261577) Avail: CASI HC A03/MF A01

Oceanographic and atmospheric observations collected during the Experiment on Rapidly Intensifying Cyclones over the Atlantic (ERICA) were analyzed for an explosive cyclone event occurring in 13-14 Dec. 1989, labeled IOP-2. This explosive cyclone formed over the Gulf Stream Front adjacent to Cape Hatteras; it developed independently of upper air baroclinicity and subsequently tracked the Gulf Stream to the east from 74 deg W to 60 deg W over the following two-day period. A kind of boundary layer coupling that existed between the Gulf Stream and the explosive cyclone, with the Gulf Stream Front shown able to alter the boundary layer characteristics of the explosive cyclone and the explosive cyclone, in turn, shown able to alter the frontal character of the Gulf Stream was shown to exist. The effect of this boundary layer coupling, which amounted to a positive feedback between ocean and atmosphere, was to increase the gradient structure of the Gulf Stream by 10-20 percent from 73 deg - 60 deg W over just a few days. The effect of the boundary layer coupling upon the explosive cyclone is unknown. The atmospheric model employed was that of the planetary boundary layer. DTIC

N93-26545# Naval Postgraduate School, Monterey, CA.
A THREE-DIMENSIONAL STUDY OF THE INFLUENCE OF MOUNTAINS ON A FRONT M.S. Thesis
Shang-Wu Li Dec. 1992 142 p
(AD-A261927) Avail: CASI HC A07/MF A02

Mountain effects on a frontal system in three dimensions is investigated. A numerical hydrostatic primitive-equation model is employed. The frontal system is developed in the model from the most unstable Eady wave in a baroclinic state and is then introduced into a new model domain that contains mountain ridges of different sizes, shapes, and orientations. DTIC

N93-26570# National Weather Service, Fort Worth, TX. Southern Region.
GUIDE FOR CONDUCTING CONVECTIVE WINDSTORM SURVEYS

W. F. Bunting and B. E. Smith Feb. 1993 49 p See also PB93-148435
(PB93-148427; NOAA-TM-NWS-SR-146) Avail: CASI HC A03/MF A01

Guidelines for performing convective windstorm damage surveys are presented. The resource guide was written as an introduction to the challenge of conducting damage surveys. The material covers a range of topics including logistics of damage surveys, basic structural engineering principles, and methods of recording and interpreting damage information. NTIS

N93-26584# National Weather Service, Fort Worth, TX. Southern Region.
TORNADO: AN ENGINEERING-ORIENTED PERSPECTIVE
J. E. Minor, J. R. McDonald, and K. C. Mehta Feb. 1993 209 p See also PB93-148427 and PB-281860
(PB93-148435; NOAA-TM-NWS-SR-147) Avail: CASI HC A10/MF A03

The report is concerned with the tornado from an engineering point of view. The engineering perspective of tornado-induced damage should aid the meteorologist in his assessments of the tornadic windfield while, at the same time, draw the attention of the engineer who is concerned with developing wind resistant designs. A basic discussion of building failure mechanisms in windstorms is presented, since an understanding of failure phenomena is important to the treatment of subsequent topics. Following the development of background information on failure modes are treatments of tornadic windspeeds and near-ground windfields. These perspectives may be of value to both the meteorologist and the engineer. A major section on housing points out the usefulness, and limitations, of housing damage as an indicator of windspeed and windfield geometry. Further, the evaluation identifies deficiencies in design which should draw the attention of builders, architects, and engineers. Final topics include the role of atmospheric pressure change in inducing damage, tornado generated missiles, and discussions of unusual events. NTIS

N93-25616*# National Weather Service, Silver Spring, MD. Office of Hydrology.
INTERACTIVE FORECASTING WITH THE NATIONAL WEATHER SERVICE RIVER FORECAST SYSTEM
George F. Smith and Donna Page *In* NASA, Washington, Technology 2002: The Third National Technology Transfer Conference and Exposition, Volume 1 Feb. 1993 p 527-536 (For primary document see N93-25561 09-99)
Avail: CASI HC A02/MF A04

N93-26483*# Johns Hopkins Univ., Laurel, MD. Applied Physics Lab.
A COMPARATIVE ASSESSMENT OF R. M. YOUNG AND TIPPING BUCKET RAIN GAUGES
Julius Goldhirsh and Norman E. Gebo *In* JPL, Proceedings of the 16th NASA Propagation Experimenters Meeting (NAPEX 16) and the Advanced Communications Technology Satellite (ACTS) Propagation Studies Miniworkshop 1 Aug. 1992 p 204-216 (For primary document see N93-26463 09-32)
(Contract N00039-91-C-0001)
Avail: CASI HC A03/MF A03

48 OCEANOGRAPHY

Includes biological, dynamic, and physical oceanography; and marine resources.

For related information see also *43 Earth Resources and Remote Sensing.*

N93-24769 North Carolina Univ., Chapel Hill.
OBSERVATIONS OF AN INTRATHERMOCLINE VORTEX Ph.D. Thesis
Lucy Marguerite OKeefe 1992 156 p
Avail: Univ. Microfilms Order No. DA9302556

This study describes the temperature and velocity structure of an intrathermocline vortex. We first estimate and discuss the vortex's propagation velocity. On this basis, we employ the 'frozen field' hypothesis to map time series into spatial sampling of the vortex. This yields an estimate of vortex structure. The chief priority of this study is to present this overview of the structure of an intrathermocline vortex. We add to the current state of knowledge by employing data which (unlike the hydrographic data which is generally employed in studies of these objects) is finely sampled in the horizontal dimension, at five depths from 300 meters below sea surface down to 5 meters above sea surface. The focus of further analysis of these observations is on delineation of interactions between the vortex and its background. The study will present observations which appear to characterize interactions between the vortex and its Gulf Stream background, and also between the vortex and the deep ocean flow.
Dissert. Abstr.

N93-24960# Lawrence Livermore National Lab., CA.
SELECTED RESULTS FROM LLNL-HUGHES RAR FOR WEST COAST SCOTLAND EXPERIMENT 1991
Sean K. Lehman, Brooks Johnston, Richard Twogood, Melvin Wieting, Thomas Yorkey, Harry Robey, David Whelan (Hughes Aircraft Co., Los Angeles, CA.), and Ray Nagele (Hughes Aircraft Co., Los Angeles, CA.) 5 Jan. 1993 71 p
(Contract W-7405-eng-48)
(DE93-006972; UCRL-ID-112755) Avail: CASI HC A04/MF A01

The joint US-UK 1991 West Coast Scotland Experiment (WCSEX) was held from 5-12 Jul. 1991, in Upper Loch Linnhe, and from 18-26 Jul. 1991, in the Sound of Sleat. The LLNL-Hughes team fielded a fully polarimetric x-band hill-side real aperture radar to collect internal wave wake data. A sample data set of the best radar runs is presented. DOE

N93-25276 Florida State Univ., Tallahassee.
ON THE GENERATION AND DISPERSION OF YANAI WAVES WITH A SPECTRAL CHEBYSHEV-COLLOCATION REDUCED-GRAVITY OCEAN MODEL Ph.D. Thesis
Brian Gerard Joseph Kelly 1992 129 p
Avail. Univ. Microfilms Order No. DA9306235

A spectral Chebyshev-collocation method is devised for the 1-1/2 layer non-linear reduced-gravity equations. Following a general description of spectral methods with their application to meteorological and oceanographic problems the implementation of the numerical technique is described. A bicharacteristic scheme is applied to solve the equations at the boundaries incorporating the boundary conditions. This treatment enables stable time integrations (spectral methods in general are very sensitive to boundary errors). A simple transfinite grid generation method is used to construct grids over irregular (non-rectangular) simply-connected domains. The model is used in a study of the dynamics of Yanai (or mixed Rossby-gravity) wave packets. These are of interest because of the observations of equatorial instability waves (which have the characteristics of Yanai waves) and their role in the momentum and heat budgets in the tropics. A series of experiments is performed to investigate the generation of the waves by simple cross-equatorial wind stress forcings in various configurations and the influence of a western boundary on them. They may be generated in the interior ocean as well as from a western boundary. The observations from all the oceans indicate that the waves have a preferential period and wavelength of around 26 days and 1000 km respectively. This is seen in the model results too and a plausible explanation is provided as being due to the dispersive properties of Yanai waves.
Dissert. Abstr.

N93-25354 Miami Univ., Coral Gables, FL.
DYNAMICS OF GULF STREAM MEANDERS AND FRONTAL EDDIES IN THE SOUTH ATLANTIC BIGHT Ph.D. Thesis
Jerry L. Miller 1992 139 p
Avail: Univ. Microfilms Order No. DA9301242

As the Gulf Stream flows along the outer edge of the southeastern United States' continental shelf, it meanders on and offshore creating frontal eddies which influence the exchange of water between the shelf and the adjacent Atlantic Ocean on weekly time scales. The dynamics controlling the development of such features in this region, the 'South Atlantic Bight' (SAB) were investigated. Analyses of the low-frequency low-wavenumber behavior of the Gulf Stream front revealed two modes of meandering which have maximum amplitudes in the vicinity of the Charleston Bump and periods of a few months to a year. In the southern one-third of the SAB, these modes have small amplitudes and the frontal fluctuations are predominantly due to the meander/frontal eddy processes. The Princeton Ocean Model was tuned for conditions which prevail in the southern SAB and idealized numerical simulations of Gulf Stream meanders and associated frontal eddies were performed. The system was found to be sensitive to

both the amplitude and period of a small perturbation applied at the southern boundary and a case which produced events most similar to those observed in nature was studied in detail. The energetics indicate that the development of these features is controlled by a mixture of both baroclinic and barotropic instabilities of the mean Gulf Stream flow. The corresponding momentum balances are equally complex. While the along-isobath flow is predominantly in geostrophic balance, several of the nonlinear advection terms in both horizontal momentum equations play important roles in the space-time development of the flow. In particular, the vertical advection of horizontal momentum as well as frictional dissipation are now recognized as important contributions to the dynamical balances in the vicinity of the steep continental slope. Dissert. Abstr.

N93-25445 Maryland Univ., College Park.
NUMERICAL SIMULATION OF THE SEASONAL AND INTERANNUAL VARIABILITY OF THE TROPICAL ATLANTIC OCEAN CIRCULATION DURING THE 1980'S Ph.D. Thesis
Bohua Huang 1992 229 p
Avail: Univ. Microfilms Order No. DA9304336

A nine-year (1980-88) surface wind stress data set over the tropical Atlantic ocean is constructed based on the European Center for Medium Range Weather Forecasts (ECMWF) twice-daily wind analysis. Its quality is checked against an independent data set based on ship observations. A comprehensive analysis of these two data sets shows a strong seasonal cycle of the wind stress over the equatorial Atlantic ocean. Interannually, the stress field is dominated by a seesaw between the northeast and southeast trade winds, with anomalously strong (weak) southeast (northeast) trade winds during 1980-83 and a reversed pattern during 1984-88. Two nine-year simulations of the tropical Atlantic ocean circulation are performed with a general circulation model, one forced by the twice-daily, and second by monthly averaged ECMWF surface wind stresses. Comparisons with available observations show that the seasonal ocean circulation and interannual signals of the sea surface temperature (SST), i.e., the dipole oscillation and abnormal warmings, are reproduced qualitatively by both simulations. Further analysis shows that the seasonal cycle of the subtropical and tropical Atlantic wind stress and the interannual SST dipole oscillation is generally in balance with the seesaw pattern of the trade wind systems although wave processes are important during the transition of phase. In 1984, the transition of the SST dipole from north-warm/south-cold to its opposite occurred during an equatorial warming event. This warming event was initiated by the relaxation of equatorial easterly wind, which stimulated heat transfer first eastward along the equator, then to the southern ocean and caused a deepening of the thermocline in the Gulf of Guinea and the southern ocean. Another warming event occurred in 1987-88 which restored the disappearing north-cold/south-warm dipole. A comparison of the two simulations shows the effects of high frequency wind forcing on the oceanic circulation. In midlatitudes, high frequency wind fluctuations cool the upper ocean through increasing the transport of the sensible and evaporative heat to the atmosphere. Near the equator, high frequency wind fluctuations enhance vertical mixing in the upper ocean, increasing temperature near the thermocline. The high frequency wind also generates oceanic waves near the equator. However, these waves only have a small effect on the seasonal and interannual variability of the ocean circulation.
Dissert. Abstr.

N93-25469 Oxford Univ. (England).
SIMULATION AND PREDICTION OF TROPICAL SST WITH A COUPLED OCEAN-ATMOSPHERE MODEL Ph.D. Thesis
Timothy N. Stockdale 1992 256 p
Avail: Univ. Microfilms Order No. BRD-98048

An ocean general circulation model (OGCM) is adapted to represent the tropical Pacific ocean. The model is tuned and tested by attempting to simulate the climatological seasonal cycle of the equatorial Pacific Ocean, with particular regard to the quantitative reproduction of the observed sea surface temperatures (SST's) and heat fluxes. Several errors in the model simulation are noted, the most serious being a cold bias in the central equatorial ocean. Possible causes of this cold bias (known to afflict many OGCM's) are investigated, and it is concluded that errors in the model representation of the Equatorial Undercurrent are partly responsible, while errors in the vertical mixing of heat may also be important. Two versions of a single baroclinic mode, equilibrium atmosphere model are developed. One of these is a usual Gill type model, and the other uses the same formalism to represent a boundary layer model of the atmosphere. The boundary layer atmosphere model enables explicit calculation of all the parameters for the Gill equations, and successfully reproduces observed stress anomalies. A coupled model is constructed from the OGCM, an atmosphere model, and a parameterization of heat flux. The atmosphere and heat flux models run in anomaly mode (i.e., they are driven by SST anomalies only), while the OGCM simulates the full state of the ocean. Coupled interactions in the model produce a slow eastward motion of the west Pacific warm pool, and this motion is sensitive to various model parameters. Although the model is able to give rise to some interesting types of long term behavior, realistic interannual variability similar to the observed El Nino and the Southern Oscillation is not produced. The coupled model is configured for forecasting future changes in SST, and a number of preliminary experiments made. Although the OGCM alone gives some indication of future large scale SST changes, the coupled model is not successful. The potential for short range prediction of detailed SST patterns is considered.
Dissert. Abstr.

N93-25558 Colorado Univ., Boulder.
CRUSTAL DEFORMATION STUDIES IN SUBAERIAL PARTS OF THE WORLD OCEANIC RIFT SYSTEM: ICELAND AND AFAR Ph.D. Thesis
Freysteinn Sigmundson 1992 119 p
Avail: Univ. Microfilms Order No. DA9304603

Crustal deformation in Iceland and Afar, both subaerial parts of the oceanic rift system, is studied for a better understanding of tectonic processes and rheology in these areas. This thesis evaluates the mechanics of the 1991 Hekla eruption in Iceland, rheology and glacio-isostatic crustal movements around the Vatnajoekull ice cap in Iceland, and strain accommodation between overlapping spreading centers in Afar. Between January 17 and March 11, 1991, 0.15 cu km of lava erupted initially from several radial fissures and subsequently from a single fissure on the SE flank of the Hekla volcano in Iceland. Hekla is within an array of geodetic control points that were measured in 1989 using the Global Positioning System and re-measured during and after the eruption. Measurements of the lake level of Lake Langisjor at the SW edge of the Vatnajoekull ice cap in Iceland indicate a tilt of 0.26 plus or minus 0.06 microrad/year away from the ice cap between 1959-1991. The tilt is too large to be explained as an elastic response to the earth to ice retreat during this century or caused by change in the gravitational pull of the ice cap. Rather, it can be explained by sub-lithospheric viscous adjustment when the sub-lithospheric viscosity is 1 x 10(exp 18) - 5 x 10(exp 19) Pa s. Regional subsidence in historical times in SE Iceland can similarly be attributed to viscous adjustment resulting from the increased load of Vatnajoekull during the Little Ice Age. A GPS geodetic network was installed in the area to monitor further elevation changes. In August 1989 a sequence of m(sub b) 5-6 normal faulting earthquakes occurred in the area between the Ghoubbet Asal-Manda Inakir and Manda Haroro-Abhe Bad rifts in central Afar. Relocation of the events suggest they occurred on major faults in the Dobi graben located midway between the principal rift zones. The earthquakes are evidence that extensional strain is still occurring in the area. A previously proposed 'bookshelf' tectonic model for central and southern Afar has been modified to account for ongoing extension in the area between the principal rifts as well as distributed shear.
Dissert. Abstr.

N93-25657# Naval Postgraduate School, Monterey, CA.
ERRORS CAUSED BY INCOMPATIBLE WIND AND BUOYANCY FORCING IN THE OCEAN GENERAL CIRCULATION MODELS M.S. Thesis
Yu-Heng Kuo Dec. 1992 73 p
(AD-A260894) Avail: CASI HC A04/MF A01

The Geophysical Fluid Dynamics Laboratory Modular Ocean Model (GFDL-MOM) is used to investigate the model difference between compatible and incompatible surface wind and buoyancy forcing. The atmosphere is a physical system in which surface wind and temperature fields are related, however in most ocean numerical models, the wind stress and buoyancy forcing are usually specified separately, i.e., no constraint between the surface wind stress and surface air temperature is considered. In reality, only one of these two fields can be prescribed in the atmosphere-driven ocean models. When the surface wind field is prescribed, the surface air temperature should be derived, and vice versa. If the two related fields are treated as totally independent in forcing the ocean models the results

will be distorted. Since the model solutions depend upon the atmospheric forcing, it is important that we study the compatibility between the wind and buoyancy forcings and the effect which incompatibility might have on the ocean numerical models. This study shows that the surface wind and buoyancy forcing widely used in ocean numerical models are incompatible. Such an incompatibility results in 21 percent error in the total northward transport of heat, 16 percent error in the total northward transport of salt, 25 percent error in v velocity, and 16 percent error in w velocity. DTIC

N93-26050*# Kansas Univ., Lawrence. Radar Systems and Remote Sensing Lab.

RADAR BACKSCATTER MEASUREMENTS FROM ARCTIC SEA ICE DURING THE FALL FREEZE-UP

S. Beaven, S. P. Gogineni, M. Shanableh, A. Gow (Army Cold Regions Research and Engineering Lab., Hanover, NH.), W. Tucker (Army Cold Regions Research and Engineering Lab., Hanover, NH.), and K. Jezek (Ohio State Univ., Columbus.) Feb. 1993 69 p

(Contract NAGw-1984; N00014-89-J-1456)

(NASA-CR-193100; NAS 1.26:193100; RSL-TR-8241-1; RSL-TR-8243-1; AD-A261843) Avail: CASI HC A04/MF A01

Radar backscatter measurements from sea ice during the fall freeze-up were performed by the United States Coast Guard Icebreaker Polar Star as a part of the International Arctic Ocean Expedition (IAOE'91) from Aug. to Sep. 1991. The U.S. portion of the experiment took place on board the Polar Star and was referred to as TRAPOLEX '91 (Transpolar expedition) by some investigators. Before prematurely aborting its mission because of mechanical failure of her port shaft, the Polar Star reached 84 deg 57 min N latitude at 35 deg E longitude. The ship was in the ice (greater than 50 percent coverage) from 14 Aug. until 3 Sep. and was operational for all but 6 days due to two instances of mechanical problems with the port shaft. The second was fatal to the ship's participation in the expedition. During the expedition, radar backscatter was measured at C-band under a variety of conditions. These included measurements from young ice types as well as from multiyear and first-/second-year sea ice during the fall freeze-up. The sea ice types were determined by measurement of the ice properties at several of the stations and by visual inspection on others. Radar backscatter measurements were performed over a large portion of the ship's transit into the Arctic ice pack. These were accompanied by in situ sea ice property characterization by the U.S. Army Cold Regions Research and Engineering Laboratory (CRREL) at several stations and, when snow was present, its properties were documented by The Microwave Group, Ottawa River (MWG). Author (revised)

N93-26164# Coastal Engineering Research Center, Vicksburg, MS.

ADCIRC: AN ADVANCED THREE-DIMENSIONAL CIRCULATION MODEL FOR SHELVES, COASTS, AND ESTUARIES. REPORT 1: THEORY AND METHODOLOGY OF ADCIRC-2DDI AND ADCIRC-3DL

R. A. Luettich, Jr., J. J. Westerink, and Norman W. Scheffner Nov. 1992 143 p

(AD-A261608; CERC-TR-DRP-92-6) Avail: CASI HC A07/MF A02

This report describes the theory, methodology, and verification of the ADCIRC (ADvanced CIRCulation) finite element numerical models. The ADCIRC-2DDI model is a two-dimensional, depth-integrated hydrodynamic model. The ADCIRC-3DL model is a three-dimensional model that couples the external mode solution generated by ADCIRC-2DDI to a locally one-dimensional internal mode solution. The numerical internal mode solution can be obtained using either velocity or stress as the dependent variable. The ADCIRC model was developed to simulate hydrodynamic circulation along shelves, coasts, and within estuaries. To allow long numerical simulations (on the order of a year) over very large computational domains (for example, the entire east coast of the United States), ADCIRC was designed to have high computational efficiency and has been tested extensively for both hydrodynamic accuracy and numerical stability. The results of these tests are included in this report. DTIC

N93-26170# Office of Naval Research, Arlington, VA.

ISOLATION AND ANALYSIS OF KEY COMPONENTS OF SEAFLOOR RELIEF Final Technical Report, 1 Oct. 1991 - 30 Sep. 1992

Dennis E. Hayes 1992 10 p

(Contract N00014-92-J-1049)

(AD-A261635) Avail: CASI HC A02/MF A01

We are continuing to investigate several hypotheses regarding the processes that are responsible for forming the various components of seafloor relief and the composite seafloor roughness. We have put forward the hypothesis that the composite seafloor relief can be meaningfully divided into three or more distinctive spatial wavebands each of which can be related to different physical processes. Our goal is to understand the operative geological processes well enough to be able to better predict the complete seafloor/basement roughness characteristics where it has not been measured and for regions where it is difficult or impossible to measure accurately (e.g., buried basement relief). DTIC

N93-26298# California Univ., San Diego, La Jolla.

EXPERIMENTS ON THE PHYSICS OF TURBULENT MIXING IN STABLY STRATIFIED OCEAN LAYERS Final Report, 1 Oct. 1991 - 30 Sep. 1992

Charles W. VanAtta 30 Sep. 1992 4 p

(Contract N00014-92-J-1121)

(AD-A261312) Avail: CASI HC A01/MF A01

Our research goals are to understand, quantify, and parameterize mixing processes in stably stratified fluids. The research is intended to provide a sound scientific basis for making accurate quantitative estimates of ocean mixing from limited observations at sea. DTIC

N93-26331# Scripps Institution of Oceanography, La Jolla, CA.

WIND-DRIVEN COASTAL GENERATION OF ANNUAL MESOSCALE EDDY ACTIVITY IN THE CALIFORNIA CURRENT Final Report, 1 Oct. 1990 - 30 Nov. 1991

Alejandro Pares-Sierra, Warren B. White, and C. K. Tai Feb. 1993 14 p

(Contract N00014-91-J-1278)

(AD-A261355) Avail: CASI HC A03/MF A01

Two candidate sources for the generation of mesoscale eddy activity in the California Current are local baroclinic instability and/or the wind stress adjacent to the coast. The latter constitutes remote forcing with eddy activity propagating westward from the coast into California Current via Rossby wave dynamics. In this study, two wind-driven models are utilized to test the relative significance of these two sources. One is an eddy resolving quasigeostrophic (QG) model, with the ability to represent baroclinic instability but not the coastal response to winds. The other is a 1 1/2-layer primitive equation (PE) model with the ability to represent the coastal response to winds but not baroclinic instability. Both models have the same spatial grid (i.e.. approximately 20 km) and are driven by the same coarse-grid wind stress forcing fields over the same one year time period (i.e. January 1987 to December 1987). The PE model is able to simulate qualitatively this distribution of the eddy variance as it appears in altimetric sea level, yielding significant coherence and phrase between model and observed sea-level residuals along longitude/time matrices at 30 deg N and 40 deg N. The QG model on the other hand, is found incapable of simulating the main features of this distribution of eddy variance. DTIC

N93-26384# Woods Hole Oceanographic Inst., MA.

COASTAL OCEAN PROCESSES: A SCIENCE PROSPECTUS

K. H. Brink, J. M. Bane, T. M. Church, C. W. Fairall, and G. L. Geernaert Apr. 1992 101 p

(Grant NSF OCE-91-08993)

(AD-A261702; WHOI-92-18) Avail: CASI HC A06/MF A02

CoOP (Coastal Ocean Processes) is an organization meant to study major interdisciplinary scientific problems in the coastal ocean. Its goal is to obtain a new level of quantitative understanding of the processes that dominate the transformations, transports and fates of biologically, chemically and geologically important matter on the continental margin. Central to obtaining this understanding will be advances in observing and modeling the cross-shelf component of transport. More specific objectives are to understand (1) cross-margin exchanges, (2) air-sea exchanges, (3) benthic-pelagic exchanges, (4) terrestrial inputs, and (5) biological and chemical transformations within the water column. CoOP research will be carried out primarily through a series of process-oriented field studies, each involving about two years of measurements. Each of these field studies is to be initiated and defined through a community workshop. In addition to the process studies, CoOP will also involve modeling, long time series, exploratory studies, remote sensing, technological innovation, data archiving and communications. A CoOP pilot study has been approved for

funding by the National Science Foundation, and funding will begin in 1992. The CoOP science effort is thus already underway. DTIC

N93-26578# Woods Hole Oceanographic Inst., MA.
INTERACTION OF AN EDDY WITH A CONTINENTAL SLOPE Ph.D. Thesis
Xiaoming Wang Sep. 1992 220 p
(AD-A261550; WHOI-92-40) Avail: CASI HC A10/MF A03

The barotropic interactions between a mesoscale eddy and a straight monotonic bottom topography are studied. Through simple to relatively complicated modeling effort, some of the fundamental properties of the interaction are investigated. The fundamental aspects of the interaction are examined using a simple contour dynamics model. With the simplest model configuration of an ideal vortex and a step topography, the basic dynamical features of the observed oceanic eddy-topography interaction are qualitatively reproduced. The results consist of eddy-induced cross-topography exchange, formation of topographic eddies, eddy propagation, and generation of topographic waves. A more complicated primitive equation model is used to investigate a mesoscale eddy interacting with an exponential continental shelf/slope topography on both f and beta-planes. The roles of the eddy size and strength and the geometry of topography are studied. It is seen that the multiple anticyclonic eddy-slope interactions strongly affect the total cross-slope volume transport and the evolution of both the original anticyclone and the topographic eddy. Since a cyclone is trapped at the slope and eventually moves on to the slope, it is most effective in causing perturbation on the shelf and slope. The responses on the shelf and slope are mainly wavelike with dispersion relation obeying that of the free shelf-trapped wave modes. It is found that the straight eddy incident is more effective in achieving large onslope eddy penetration distance than the oblique eddy incident. DTIC

N93-26586*# National Aeronautics and Space Administration. Goddard Inst. for Space Studies, New York, NY.
A COASTAL HAZARDS DATA BASE FOR THE US EAST COAST
V. M. Gornitz, T. W. White (Oak Ridge National Lab., TN.), and R. C. Daniels (Tennessee Univ., Knoxville.) Aug. 1992 172 p
(Contract DE-AC05-84OR-21400)
(NASA-TM-108265; NAS 1.15:108265; DE93-003678; ORNL/CDIAC-45; NDP-043A; ESDP-3913) Avail: CASI HC A08/MF A02

This document describes the contents of a digital data base that may be used by raster or vector geographic information systems (GIS) and non-GIS data bases to assess the risk of coastlines to erosion or sea level rise. The data base integrates point, line, and polygon data for the US East Coast into 0.250 latitude (times) 0.250 longitude grid cells. Each coastal grid cell contains data on geology, geomorphology, elevation, wave heights, tidal ranges, shoreline displacement (erosion), and sea-level trends. These data are available as a Numeric Data Package (NDP), from the Carbon Dioxide Information Analysis Center, consisting of this document and a set of computerized data files. The documentation contains information on the methods used in calculating each variable, detailed descriptions of file contents and formats, and a discussion of the sources, restrictions, and limitations of the data. The data files are available on magnetic tape, on floppy diskettes, or through INTERNET. DOE

N93-24916*# Naval Observatory, Washington, DC.
THE ROLE OF OCEAN CLIMATE DATA IN OPERATIONAL NAVAL OCEANOGRAPHY
Radm G. Chesbrough *In* NASA. Goddard Space Flight Center, Proceedings of the Ocean Climate Data Workshop 1992 p 27-43 (For primary document see N93-24915 09-42)
Avail: CASI HC A03/MF A03

N93-24917*# Commonwealth Scientific and Industrial Research Organization, Hobart (Australia).
INTERNATIONAL ORGANISATION OF OCEAN PROGRAMS: MAKING A VIRTUE OF NECESSITY
Angus McEwan *In* NASA. Goddard Space Flight Center, Proceedings of the Ocean Climate Data Workshop 1992 p 45-49 (For primary document see N93-24915 09-42)
Avail: CASI HC A01/MF A03

N93-24918*# State Oceanographic Inst., Moscow (USSR). Hydrometeorology Committee.
ROLE OF THE OCEAN IN CLIMATE CHANGES
Sergey K. Gulev *In* NASA. Goddard Space Flight Center, Proceedings of the Ocean Climate Data Workshop 1992 p 51-64 (For primary document see N93-24915 09-42)
Avail: CASI HC A03/MF A03

N93-24919*# Delaware Univ., Lewes. Coll. of Marine Studies.
THE ROLE OF THE WORLD DATA CENTERS IN HANDLING OCEAN CLIMATE DATA
Ferris Webster *In* NASA. Goddard Space Flight Center, Proceedings of the Ocean Climate Data Workshop 1992 p 65-73 (For primary document see N93-24915 09-42)
Avail: CASI HC A02/MF A03

N93-24920*# Ministry of the Environment, Ottawa (Ontario). Dept. of Fisheries and Oceans.
THE GLOBAL OCEAN OBSERVING SYSTEM: ONE PERSPECTIVE
J. Ron Wilson *In* NASA. Goddard Space Flight Center, Proceedings of the Ocean Climate Data Workshop 1992 p 79-84 (For primary document see N93-24915 09-42)
Avail: CASI HC A02/MF A03

N93-24921*# Climate Analysis Center, Washington, DC.
OPERATIONAL SEASONAL AND INTERANNUAL PREDICTIONS OF OCEAN CONDITIONS
Ants Leetmaa *In* NASA. Goddard Space Flight Center, Proceedings of the Ocean Climate Data Workshop 1992 p 85-86 (For primary document see N93-24915 09-42)
Avail: CASI HC A01/MF A03

N93-24922*# Bedford Inst. of Oceanography, Dartmouth (Nova Scotia). Atlantic Oceanographic Lab.
WORLD OCEAN CIRCULATION EXPERIMENT
R. Allyn Clarke *In* NASA. Goddard Space Flight Center, Proceedings of the Ocean Climate Data Workshop 1992 p 87-94 (For primary document see N93-24915 09-42)
Avail: CASI HC A02/MF A03

N93-24923*# Naval Sea Systems Command, Washington, DC. Office of the Chief Scientist.
THE GLOBAL OCEAN OBSERVING SYSTEM Abstract Only
Dana Kester *In* NASA. Goddard Space Flight Center, Proceedings of the Ocean Climate Data Workshop 1992 p 95 (For primary document see N93-24915 09-42)
Avail: CASI HC A01/MF A03

N93-24924*# Australian Oceanographic Data Centre, North Sydney.
GLOBAL TEMPERATURE AND SALINITY PILOT PROJECT
Ben Searle *In* NASA. Goddard Space Flight Center, Proceedings of the Ocean Climate Data Workshop 1992 p 97-108 (For primary document see N93-24915 09-42)
Avail: CASI HC A03/MF A03

N93-24925*# Commonwealth Scientific and Industrial Research Organization, Hobart (Australia). Marine Labs.
INDIAN OCEAN ANALYSES
Gary Meyers *In* NASA. Goddard Space Flight Center, Proceedings of the Ocean Climate Data Workshop 1992 p 109-129 (For primary document see N93-24915 09-42)
Avail: CASI HC A03/MF A03

N93-24926*# Jet Propulsion Lab., California Inst. of Tech., Pasadena.
SATELLITE MONITORING OF THE GLOBAL OCEAN SURFACE DURING 1987-1989
David Halpern *In* NASA. Goddard Space Flight Center, Proceedings of the Ocean Climate Data Workshop 1992 p 131-143 (For primary document see N93-24915 09-42)
Avail: CASI HC A03/MF A03

N93-24927*# Lisbon Univ. (Portugal). Dept. de Fisica.
THE USE OF REMOTELY SENSED DATA FOR OPERATIONAL FISHERIES OCEANOGRAPHY
Armando F. G. Fiuza *In* NASA. Goddard Space Flight Center, Proceedings of the Ocean Climate Data Workshop 1992 p 145-152 Sponsored in part by Commission of the European Communities (For primary document see N93-24915 09-42)
Avail: CASI HC A02/MF A03

N93-24928*# National Ocean Service, Monterey, CA.
OCEAN-PC AND A DISTRIBUTED NETWORK FOR OCEAN DATA
Douglas R. McLain *In* NASA. Goddard Space Flight Center, Proceedings of the Ocean Climate Data Workshop 1992 p 153-160 (For primary document see N93-24915 09-42)
Avail: CASI HC A02/MF A03

N93-24929*# National Ocean Service, Rockville, MD.
SEA LEVEL VARIATION Abstract Only
Bruce C. Douglas *In* NASA. Goddard Space Flight Center, Proceedings of the Ocean Climate Data Workshop 1992 p 161 (For primary document see N93-24915 09-42)
Avail: CASI HC A01/MF A03

N93-24934*# Maryland Univ., Cambridge. Marine Labs.
THE JGOFS NORTH ATLANTIC BLOOM EXPERIMENT: AN OVERVIEW
Hugh W. Ducklow *In* NASA. Goddard Space Flight Center, Proceedings of the Ocean Climate Data Workshop 1992 p 205-227 (For primary document see N93-24915 09-42)
Avail: CASI HC A03/MF A03

N93-24937*# Plymouth Marine Lab. (England).
THE CONTINUOUS PLANKTON RECORDER SURVEY: A LONG-TERM, BASIN-SCALE OCEANIC TIME SERIES
John C. Gamble and Harold G. Hunt *In* NASA. Goddard Space Flight Center, Proceedings of the Ocean Climate Data Workshop 1992 p 277-293 (For primary document see N93-24915 09-42)
Avail: CASI HC A03/MF A03

N93-24938*# Bermuda Biological Station for Research, Inc., Ferry Reach.
OCEAN TIME-SERIES NEAR BERMUDA: HYDROSTATION S AND THE US JGOFS BERMUDA ATLANTIC TIME-SERIES STUDY
Anthony F. Michaels and Anthony H. Knap *In* NASA. Goddard Space Flight Center, Proceedings of the Ocean Climate Data Workshop 1992 p 295-315 (For primary document see N93-24915 09-42)
(Grants NSF OCE-86-13904; NSF OCE-88-01089; NSF OCE-90-17173; NSF OCE-90-16990; NSF BSR-90-18298)
Avail: CASI HC A03/MF A03

N93-24939*# University of Southern California, Los Angeles. Ocean Physics Group.
AUTOMATED IN SITU OBSERVATIONS OF UPPER OCEAN BIOGEOCHEMISTRY, BIO-OPTICS, AND PHYSICS AND THEIR POTENTIAL USE FOR GLOBAL STUDIES
Tommy D. Dickey, Timothy C. Granata, and Isabelle Taupier-Letage *In* NASA. Goddard Space Flight Center, Proceedings of the Ocean Climate Data Workshop 1992 p 317-353 Sponsored in part by NOAA and CNRS (For primary document see N93-24915 09-42)
(Contract N00014-89-J-1498; NSF OCE-90-13896)
Avail: CASI HC A03/MF A03

N93-24940*# Department of Fisheries and Oceans, Winnipeg (Manitoba). Physical and Chemical Science Directorate.
WRAP-UP SESSION
Geoffrey Holland *In* NASA. Goddard Space Flight Center, Proceedings of the Ocean Climate Data Workshop 1992 p 357-364 (For primary document see N93-24915 09-42)
Avail: CASI HC A02/MF A03

N93-24941*# Department of Fisheries and Oceans, Winnipeg (Manitoba). Physical and Chemical Science Directorate.
INTERNATIONAL OCEAN SERVICES: IS IT TIME - WILL IT EVER BE TIME?
Geoffrey Holland *In* NASA. Goddard Space Flight Center, Proceedings of the Ocean Climate Data Workshop 1992 p 381-387 (For primary document see N93-24915 09-42)
Avail: CASI HC A02/MF A03

51 LIFE SCIENCES (GENERAL)

N93-25104# Oak Ridge National Lab., TN.
KINETIC STUDIES OF INTERFACIAL PHOTOCURRENTS IN PLATINIZED CHLOROPLASTS
E. Greenbaum 1992 2 p Presented at the 183rd Electrochemical Society Meeting, Honolulu, HI, 16-21 May 1993
(Contract DE-AC05-84OR-21400)
(DE93-002344; CONF-930571-1) Avail: CASI HC A01/MF A01

The present experiments focus on kinetic studies of photocurrents generated in a photobioelectrochemical cell constructed from platinized chloroplast membranes. These chloroplast membranes although separated from the CO2-reducing enzymes of the Calvin-Benson cycle, contain the full complement of photosystem 1 and 2 reaction centers along with the electron transport chain linking these two centers. The vectorial model of photosynthesis indicates that the orientation of the reaction centers in the photosynthetic membranes is such that electrons emerge from the membranes into the stroma region of the chloroplasts. Since the flattened saclike vesicles of the thylakoid membranes are topologically equivalent to spheres, it follows that, irrespective of the rotational orientation of the membranes, the photogenerated electrons emerge from the reaction centers in a radial direction away from the intra-thylakoid region. DOE

N93-25195* Lockheed Engineering and Sciences Co., Washington, DC.
DIGEST OF RUSSIAN SPACE LIFE SCIENCES, ISSUE 33
Lydia Razran Stone, ed., Ronald Teeter, ed., and Joseph Rowe, ed. (Library of Congress, Washington, DC.) Washington NASA Mar. 1993 108 p
(Contract NASw-4292)
(NASA-CR-3922(39); NAS 1.26:3922(39)) Avail: CASI HC A06

This is the thirty-third issue of NASA's USSR Space Life Sciences Digest. It contains abstracts of 55 papers published in Russian journals. The abstracts in this issue have been identified as relevant to the following areas of space biology and medicine: biological rhythms, body fluids, botany, cardiovascular and respiratory systems, developmental biology, endocrinology, equipment and instrumentation, gastrointestinal system, genetics, hematology, human performance, metabolism, microbiology, musculoskeletal system, neurophysiology, nutrition, operational medicine, psychology, radiobiology, and reproductive system. Author

N93-25242*# National Aeronautics and Space Administration. Ames Research Center, Moffett Field, CA.
SPACE BIOLOGY RESEARCH DEVELOPMENT Final Report, 1 Apr. 1989 - 31 Mar. 1993
Sjoerd L. Bonting 31 Mar. 1993 15 p
(Contract NCC2-614)
(NASA-CR-192830; NAS 1.26:192830) Avail: CASI HC A03/MF A01

The purpose of the Search for Extraterrestrial Intelligence (SETI) Institute is to conduct and promote research related activities regarding the search for extraterrestrial life, particularly intelligent life. Such research encompasses the broad discipline of 'Life in the Universe', including all scientific and technological aspects of astronomy and the planetary sciences, chemical evolution, the origin of life, biological evolution, and cultural evolution. The primary purpose was to provide funding for the Principal Investigator to collaborate with the personnel of the SETI Institute and the NASA-Ames Research center in order to plan and develop space biology research on and in connection with Space Station Freedom; to promote cooperation with the international partners in the space station; to conduct a study on the use of biosensors in space biology research and life support system operation; and to promote space biology research through the initiation of

an annual publication 'Advances in Space Biology and Medicine'.
Author (revised)

N93-25405# Joint Publications Research Service, Arlington, VA.
JPRS REPORT: SCIENCE AND TECHNOLOGY. CENTRAL EURASIA: LIFE SCIENCES
25 Nov. 1992 49 p Transl. into ENGLISH from various Russian articles
(JPRS-ULS-92-025) Avail: CASI HC A03/MF A01

The translated article covers the following topic: changes in the psychophysiological characteristics in the visual system with different retina and visual nerve pathology in humans with low vision as a result of transcutaneous stimulation of visual path periphery. CASI

N93-25406# Joint Publications Research Service, Arlington, VA.
JPRS REPORT: SCIENCE AND TECHNOLOGY. CENTRAL EURASIA: LIFE SCIENCES
4 Aug. 1992 34 p Transl. into ENGLISH from various Russian articles
(JPRS-ULS-92-020) Avail: CASI HC A03/MF A01

The translated article covers the following topic: satellite monitoring and normative prognosis for ecosystem dynamics in the Amudar Delta.
Author

N93-25457# President's Council of Advisors on Science and Technology, Washington, DC.
ACHIEVING THE PROMISE OF THE BIOSCIENCE REVOLUTION: THE ROLE OF THE FEDERAL GOVERNMENT
Dec. 1992 19 p Original contains color illustrations
(PB93-139970) Avail: CASI HC A03/MF A01

This report deals with the role of the federal government in achieving two goals: (1) promoting the health of the American people and all mankind through research in the biosciences; and (2) fostering a vigorous American biotechnology industry. These goals are inter-related. Discoveries in the biosciences are the basis for industrial development of more effective ways to prevent or treat illness, produce more nutritious foods, make use of renewable energy sources, and protect the environment. A critical factor in the continued success of America's biotechnology industry is the strength of the nation's bioscience research enterprise. Author

N93-25764# State Univ. of New York, Buffalo. Dept. of Biophysical Sciences.
EFFECT OF CYTOSKELETAL REAGENTS ON STRETCH ACTIVATED ION CHANNELS Final Report, 15 Mar. 1989 - 14 Jun. 1992
Frederick Sachs 12 Nov. 1992 5 p
(Contract DAAL03-89-K-0064)
(AD-A261089; ARO-26099.9-LS) Avail: CASI HC A01/MF A01

Mechanically sensitive ion channels have been proposed to respond to membrane tension. We have developed methods to measure the membrane tension in a patch and have examine the stress strain relationship. The results show that, in general, tension is the critical variable. However, we have also found one channel in glial cells whose gating is additionally dependent upon the curvature of the membrane. Stresses in a patch caused by suction lead to lipid flow along the wall of the pipette, but the flow is constrained by the highly extensible cytoskeleton whose area elastic constant is ca. 50 dyn/cm. We developed tools to use high voltage electron microscopy to study the structure of patches and have characterized the placement of cytoskeleton, lipids, and receptors in a variety of preparations. We also developed a new algorithm to align projections for tomography in order to examine the three dimensional structure of patches. We have demonstrated mechanically induced release of calcium via stretch activated ion channels in heart cells extending work on the molecular level to the whole cell level. DTIC

N93-25877# Corvallis Environmental Research Lab., OR.
ANATOMY AND PHYSIOLOGY OF PLANT CONDUCTIVE SYSTEMS
Craig McFarlane, ed. and S. Trapp, ed. 1993 42 p Repr. from Modeling Anthropogenic Organic Chemicals in Plants (New York), Marcel Decker Publishing Corp., 1993
(PB93-156032; EPA/600/A-93/017) Avail: CASI HC A03/MF A01

Mathematical models considered in the book are representations of the physical features and chemical reactions that define interactions between plants and their environment. By centering attention on equations, it is easy to lose sight of the intricate and complex nature of the problem. The particular chapter describes the anatomy of important plant features and briefly discuss some physiological principles that will help to visualize and perceive the conditions which are represented in the models. Because of the many competing interactions, the fate of chemicals in the soil/plant/air environment is not obvious. Models were thus developed to intelligently integrate available knowledge, to increase understanding of the complex interactions, to aid in presentation of plant functions, and to help make predictions about chemical fate. NTIS

N93-25994* National Aeronautics and Space Administration. Pasadena Office, CA.
PSEUDOMONAS SCREENING ASSAY Patent
Ruth Margalit, inventor (to NASA) (Jet Propulsion Lab., California Inst. of Tech., Pasadena.) 11 May 1993 4 p Filed 30 Mar. 1990 Supersedes N90-27239 (29 - 21, p 3032)
(NASA-Case-NPO-17653-1-CU; US-Patent-5,210,019;
US-Patent-Appl-SN-501908; US-Patent-Class-435-7.32;
US-Patent-Class-435-7.92; US-Patent-Class-435-874;
US-Patent-Class-436-518; Int-Patent-Class-G01N-33/569) Avail: US Patent and Trademark Office

A method for the detection of Pseudomonas bacteria is described where an Azurin-specific antibody is employed for detecting the presence of Azurin in a test sample. The detection of the presence of Azurin in the sample is a conclusive indicator of the presence of the Pseudomonas bacteria since the Azurin protein is a specific marker for this bacterial strain.
Official Gazette of the U.S. Patent and Trademark Office

N93-26259# Trinity Univ., San Antonio, TX.
EFFECTS OF SPACE RADIATION ON HUMORAL AND CELLULAR IMMUNITY IN RHESUS MONKEYS Final Report, May 1990 - Mar. 1991
William H. Stone and Michael L. Miller (Childrens Memorial Hospital, Chicago, IL.) Dec. 1992 21 p
(Contract F33615-87-D-0626)
(AD-A261808; AL-TR-1992-0101) Avail: CASI HC A03/MF A01

The objective of this study was to complete profiles of immune competence in rhesus monkeys more than 25 years after single exposures to protons of different energies. Access to irradiated animals provided a unique opportunity to study late effects on the immune systems of nonhuman primates; late immunological defects could be relevant to astronauts and high-flying pilots. Working with the primate model allowed us to assess the possible late effects of ionizing radiations on parameters associated with B-cell and T-cell functions. Antibody-mediated immune (AMI) function was investigated by measuring immunoglobulin (Ig) levels, hemolytic complement activity, and autoantibodies. Cell-mediated immune (CMI) function was evaluated by measuring selected T- and B-cell activities as well as responses to mitogens and interleukin production. There were no significant differences between control and irradiated animals for most parameters measured in this survey, but some reduction in spontaneous proliferation was noted in irradiated primates. With regard to late risks for humans following exposure(s) to ionizing radiations, it is encouraging that few late immunobiological effects were exhibited by primate survivors of low and intermediate doses of protons. DTIC

N93-26587# Oak Ridge National Lab., TN.
DEVELOPMENT OF RESONANCE IONIZATION SPECTROSCOPY FOR GENOME MAPPING AND DNA SEQUENCING USING STABLE ISOTOPES AS DNA LABELS
K. B. Jacobson, M. J. Doktycz, R. A. Sachleben, G. M. Brown, F. W. Larimer, and H. F. Arlinghaus (Atom Sciences, Inc., Oak Ridge, TN.) 1993 10 p Presented at the International Society for Optical Engineering (SPIE) Conference, Los Angeles, CA, 16-23 Jan. 1993
(Contracts DE-AC05-84OR-21400; DE-FG05-91ER-81235)
(DE93-007815; CONF-930159-16) Avail: CASI HC A02/MF A01

Stable isotopes can be used as alternatives to radioisotopes or fluorescent DNA labels. After the labeled DNA has been banded on electrophoresis gels, the stable isotopes may be located by scanning the gel with resonance ionization spectroscopy. Methods for synthesizing appropriate labels and for detecting isotopes of iron and tin directly on polyacrylamide gels are described. DOE

N93-25566*# National Aeronautics and Space Administration. Lyndon B. Johnson Space Center, Houston, TX.
MEASURING THE METASTATIC POTENTIAL OF CANCER CELLS
Dennis R. Morrison, Howard Gratzner (DNA Sciences, Houston, TX.), and M. Z. Atassi (Baylor Coll. of Medicine, Houston, TX.) *In* NASA, Washington, Technology 2002: The Third National Technology Transfer Conference and Exposition, Volume 1 Feb. 1993 p 59-70 (For primary document see N93-25561 09-99)
Avail: CASI HC A03/MF A04

N93-26066*# Houston Univ., TX. Dept. of Biological and Environmental Sciences.
METABOLIC RESPONSE OF ENVIRONMENTALLY ISOLATED MICROORGANISMS TO INDUSTRIAL EFFLUENTS: USE OF A NEWLY DESCRIBED CELL CULTURE ASSAY Final Report
Robert N. Ferebee *In* NASA. Johnson Space Center, National Aeronautics and Space Administration (NASA)/American Society for Engineering Education (ASEE) Summer Faculty Fellowship Program, 1992, Volume 1 15 Sep. 1992 10 p (For primary document see N93-26058 09-99)
Avail: CASI HC A02/MF A02

N93-26069*# University of Western Illinois, Macomb. Dept. of Mathematics.
ANALYSIS OF THE LETTUCE DATA FROM THE VARIABLE PRESSURE GROWTH CHAMBER AT NASA JOHNSON SPACE CENTER: A THREE-STAGE NESTED DESIGN MODEL Final Report
Tze-San Lee *In* NASA. Johnson Space Center, National Aeronautics and Space Administration (NASA)/American Society for Engineering Education (ASEE) Summer Faculty Fellowship Program, 1992, Volume 1 Dec. 1992 14 p (For primary document see N93-26058 09-99)
(Grant NGT-44-005-803)
Avail: CASI HC A03/MF A02

N93-26073*# Mercer Univ., Macon, GA. Dept. of Electrical and Computer Engineering.
INVESTIGATION INTO THE COMMON MODE REJECTION RATIO OF THE PHYSIOLOGICAL SIGNAL CONDITIONER CIRCUIT Final Report
Edward M. OBrien *In* NASA. Johnson Space Center, National Aeronautics and Space Administration (NASA)/American Society for Engineering Education (ASEE) Summer Faculty Fellowship Program, 1992, Volume 2 Dec. 1992 10 p (For primary document see N93-26070 09-99)
(Grant NGT-44-005-803)
Avail: CASI HC A02/MF A02

N93-26077*# Louisiana Tech Univ., Ruston. Dept. of Health and Physical Education.
UTILIZATION OF THE GRADED UNIVERSAL TESTING SYSTEM TO INCREASE THE EFFICIENCY FOR ASSESSING AEROBIC AND ANAEROBIC CAPACITY Final Report
Sandra L. Rodgers *In* NASA. Johnson Space Center, National Aeronautics and Space Administration (NASA)/American Society for Engineering Education (ASEE) Summer Faculty Fellowship Program, 1992, Volume 2 Dec. 1992 9 p (For primary document see N93-26070 09-99)
(Grant NGT-44-005-803)
Avail: CASI HC A02/MF A02

52 AEROSPACE MEDICINE

Includes physiological factors; biological effects of radiation; and effects of weightlessness on man and animals.

N93-24738*# Monterey Technologies, Inc., Carmel, CA.
AUTONOMIC PHYSIOLOGICAL DATA ASSOCIATED WITH SIMULATOR DISCOMFORT
James C. Miller, Thomas J. Sharkey, Glenna A. Graham, and Michael E. McCauley Feb. 1993 28 p Sponsored by U.S. Army Aerroflight Dynamics Directorate
(Contract NAS2-12927)
(NASA-CR-177609; A-93026; NAS 1.26:177609; USAATCOM-TR-92-A-001)
Avail: CASI HC A03/MF A01

The development of a physiological monitoring capability for the Army's advanced helicopter simulator facility is reported. Additionally, preliminary physiological data is presented. Our objective was to demonstrate the sensitivity of physiological measures in this simulator to self-reported simulator sickness. The data suggested that heart period, hypergastria, and skin conductance level were more sensitive to simulator sickness than were vagal tone and normal electrogastric activity. Author (revised)

N93-24763*# Brown Univ., Providence, RI. Dept. of Pathology.
MECHANICAL STIMULATION OF SKELETAL MUSCLE MITIGATES GLUCOCORTICOID INDUCED DECREASES IN PROSTAGLANDIN SYNTHESIS
Joseph A. Chromiak and Herman H. Vandenburgh 1993 35 p
(Grant NAG2-414)
(NASA-CR-193040; NAS 1.26:193040) Avail: CASI HC A03/MF A01

The glucocorticoid dexamethasone (Dex) induces a decline in protein synthesis and protein content of tissue cultured, avian skeletal muscle cells, and this atrophy is attenuated by repetitive mechanical stretch. Since the prostaglandin synthesis inhibitor indomethacin mitigated this stretch attenuation of muscle atrophy, the role of prostaglandins as growth modulators in these processes was examined. Dex at 10(exp -8) M reduced PGF(sub 2(alpha)) production 55 percent - 65 percent and PGE(sub 2) production 84 - 90 percent after 24 - 72 h of incubation in static cultures. Repetitive 10 percent stretch-relaxations of the non-Dex treated cultures increased PGF(sub 2(alpha)) efflux 41 percent at 24 h and 276 percent at 72 h and increased PGE(sub 2) production 51 percent at 24 h and 236 percent at 72 h. Mechanical stimulation of Dex treated cultures increased PGF(sub 2(alpha)) production 162 percent after 24 h, thus returning PGF(sub 2(alpha)) efflux to the level of non-Dex treated cultures. At 72 h, stretch increased PGF(sub 2(alpha)) efflux 65 percent in Dex treated cultures, but PGF(sub 2(alpha)) production was 45-84 percent less than non-Dex treated cultures. Mechanical stimulation of Dex treated cultures increased PGE(sub 2) production at 24 h, but not at 72 h. Dex reduced prostaglandin H synthase (PGHS) activity in the muscle cultures by 70 percent after 8 - 24 h of incubation, and mechanical stimulation increased PGHS activity of the Dex treated cultures by 98 percent. It is concluded that repetitive mechanical stimulation attenuates the catabolic effects of Dex on cultured skeletal muscle cells in part by reversing the Dex-induced declines in PGHS activity and prostaglandin production. Author (revised)

N93-25186# Los Alamos National Lab., NM.
BIOMAGNETIC LOCALIZATION FROM TRANSIENT QUASI-STATIC EVENTS
J. C. Mosher, R. M. Leahy, and P. S. Lewis 1993 5 p Presented at the IEEE International Conference on Acoustics, Speech, and Signal Processing, Minneapolis, MN, 27-30 Apr. 1993
(Contract W-7405-eng-36)
(DE93-007328; LA-UR-93-402; CONF-930489-1) Avail: CASI HC A01/MF A01

Sensory stimuli, such as auditory, visual, or somatosensory, evoke neural responses in very localized regions of the brain. A SQUID biomagnetometer can measure the very weak fields that are generated outside of the head by this response. A simple source and head model of current dipoles inside a conducting sphere is typically used to interpret these magnetic field measurements or magnetoencephalogram (MEG). Locating dipole sources using data recorded from an array of biomagnetic sensors is distinguished from conventional array source localization techniques by the quasi-static transient nature of the data. Here, the basic MEG model is reviewed, then a localization example is given to motivate the need for partitioning the data to improve estimator performance. Tune-eigenspectrum analysis is introduced as a means of partitioning and interpreting spatio-temporal biomagnetic data. Examples using both simulated and somatosensory data are presented. DOE

N93-25214# Federal Aviation Administration, Oklahoma City, OK. Civil Aeromedical Inst.
THE PREVALENCE OF ARTIFICIAL LENS IMPLANTS IN THE CIVIL AIRMAN POPULATION Final Report
Van B. Nakagawara, Faredoon K. Loochan, and Kathryn J. Wood Mar. 1992 18 p
(FAA Proj. AM-A-91-PHY-144)
(DOT/FAA/AM-92/14) Avail: CASI HC A03/MF A01

The use of artificial lens implants to correct for aphakia has become

increasingly prevalent in the United States. This study analyzes the distribution of intraocular lens (IOL) implants in the civil airman population by type (unilateral, bilateral), class of medical certificate, and gender for a 4-year period (1982-85). Medical records were evaluated for all certified airmen who were carrying pathology codes for aphakia artificial lenses was higher for bilateral, second-class medical certificate holders, and female aphakics. However, the incidence of total and unilateral artificial lens implants declined in 1985. The implications of the study's findings for aeromedical certification are discussed. A change in the methods used to evaluate trends in the use of IOL in the airman population is recommended.

Author

N93-25407# Joint Publications Research Service, Arlington, VA.
JPRS REPORT: SCIENCE AND TECHNOLOGY. CENTRAL EURASIA: LIFE SCIENCES
30 Sep. 1992 92 p Transl. into ENGLISH from various Russian articles
(JPRS-ULS-92-022) Avail: CASI HC A05/MF A01

The translated article covers the following topic: results of blood tests among EO-2, -3, and -4 Space Crews. CASI

N93-25629# Los Alamos National Lab., NM. Life Sciences Div.
THE ACUTE INHALATION TOXICITY OF PYROLYSIS PRODUCTS OF HALON 1301 Final Report, 1 Apr. 1987 - 30 Sep. 1992
Bruce E. Lehnert 31 Dec. 1992 96 p
(DA Proj. 3M1-62787-A-875)
(AD-A260874) Avail: CASI HC A05/MF A01

This final report summarizes investigations conducted during this project. During the course of the project, investigations were undertaken to address the following objectives: (1) to develop exposure systems and methodology to deliver pure, stable atmospheres of HF, HBr, or HCl to laboratory rats; (2) to determine the toxicological equivalency of inhaled HF, HBr, and HCl in the upper and lower respiratory tract; (3) characterize the anatomical sites of injury caused by HF, HCl, and HBr when inhaled at high mass concentrations through the nasal (NB) and oral (MB) pathways; (4) to assess the relative toxicities of the above halides when inhaled at high mass concentrations during mouth and nose breathing; (5) to characterize the upper and lower respiratory tract lesion(s) produced by HCl inhalation in the nose breathing (NB) and mouth breathing (MB) rats during CO2-induced increased minute ventilation; (6) to examine the toxicity of HF when administered directly into the rat's lung; (7) to determine if work performance incapacitation occurs after acute high concentration inhalation of HCl via the nose (NB) or the mouth (MB); (8) to assess post-exposure exercise as a potentiator of the severity of expression of halide-induced respiratory tract injury; and (9) to initiate studies to determine whether or not lung injury becomes more pronounced after halides are breathed in combination with a particulate phase. DTIC

N93-25900# CryoLife, Inc., Marietta, GA.
CELLULAR AND TISSUE INJURY DURING NONFREEZING COLD INJURY AND FROSTBITE Triannual Report No. 6, Sep. - Nov. 1992
8 Dec. 1992 6 p
(Contract N00014-91-C-0044)
(AD-A260574) Avail: CASI HC A02/MF A01

Metabolic perturbation and enzyme structure-function studies are presented. We have now almost completed our investigation of the structure-function relationships that are thought to be involved with regulating the activity of phosphofructokinase (PFK) in vivo. Specifically, we set out to study how alterations in quaternary structure account for enzyme inhibition in red blood cells under cold, acidotic conditions. Prior in vitro studies have shown that phosphofructokinase from erythrocytes (and several other mammalian cells and tissues) dissociates from active tetrameres into inactive dimers and monomers at low Ph. In addition, we have previously demonstrated that this reversible phenomenon accounts for the inhibition of PFK activity in vivo in ischemic myocardium. DTIC

N93-25944# Duke Univ., Durham, NC. Medical Center.
PRIMARY EVENTS IN OLFACTORY RECEPTION Final Report
Robert R. Anholt 8 Jan. 1993 13 p
(Contract DAAL03-89-K-0178)
(AD-A260562; ARO-26767.6-LS) Avail: CASI HC A03/MF A01

This project was designed to characterize olfactory tissue-specific proteins previously identified with a library of monoclonal antibodies raised against frog olfactory cilia. First, we showed that our olfactory tissue-specific monoclonal antibodies all recognize different molecular forms of the same protein. We named this protein 'olfactomedin'. We then proceeded to purify olfactomedin and characterize it biochemically and immunohistochemically. We showed that olfactomedin is produced only in olfactory tissue by sustentacular cells and Bowman's glands and that it is deposited in the lower mucus layer of olfactory neuroepithelium. Next, we extracted mRNA from olfactory tissue and constructed a cDNA library. We obtained partial sequence information of the N-terminus of purified olfactomedin and used these data to design a degenerate oligonucleotide probe for the identification of a full-length cDNA clone which encodes olfactomedin. This clone was sequenced and found to encode a 448 amino acid protein preceded by a leader peptide of 16 amino acids. Analysis of the sequence showed no homologies with any known protein. Examination of its amino acid sequence by Chou-Fasman analysis in combination with biochemical and immunochemical evidence obtained previously enabled us to construct a model for olfactomedin which identifies this protein as a novel olfactory tissue-specific extracellular matrix protein, which forms the main structural component of the extracellular mucous matrix of olfactory neuroepithelium and which may trigger the growth and differentiation of the dendritic knob and its olfactory cilia that house the olfactory transduction machinery.

DTIC

N93-26133*# National Aeronautics and Space Administration. Ames Research Center, Moffett Field, CA.
VASCULAR UPTAKE OF REHYDRATION FLUIDS IN HYPOHYDRATED MEN AT REST AND EXERCISE
J. E. Greenleaf (Shaklee US, Inc., San Francisco, CA.), G. Geelen (Shaklee US, Inc., San Francisco, CA.), G. R. Jackson (Shaklee US, Inc., San Francisco, CA.), J.-L. Saumet (Shaklee US, Inc., San Francisco, CA.), L. T. Juhos (Shaklee US, Inc., San Francisco, CA.), L. C. Keil (Shaklee US, Inc., San Francisco, CA.), D. Fegan-Meyer (Shaklee US, Inc., San Francisco, CA.), A. Dearborn (Shaklee US, Inc., San Francisco, CA.), H. Hinghofer-Szalkay (Shaklee US, Inc., San Francisco, CA.), and J. H. Whittam (Shaklee US, Inc., San Francisco, CA.) Aug. 1992 49 p
(RTOP 199-18-12-07)
(NASA-TM-103942; A-92113; NAS 1.15:103942) Avail: CASI HC A03/MF A01

The purpose of this study was to formulate and to evaluate rehydration drinks, which would restore total body water and plasma volume (PV), for astronauts to consume before and during extravehicular activity, a few hours before reentry, and immediately after landing. In the first experiment (rest, sitting), five healthy men (23-41 yr), previously dehydrated for 24 hr., drank six (1a, 2, 4, 5, 6, 7) fluid formulations (one each at weekly intervals) and then sat for 70 min. Pre-test PV were measured with Evans blue dye and changes in PV were calculated with the hematocrit-hemoglobin transformation equation. This rest experiment simulated hypohydrated astronauts preparing for reentry. The second experiment (exercise, supine) followed the same protocol except four healthy men (30-46 yr) worked for 70 min. in the supine position on a cycle ergometer at a mean load of 71 +/-1 percent of their peak aerobic work capacity. This exercise experiment simulated conditions for astronauts with reduced total body water engaging in extravehicular activity. Author (revised)

N93-26218# Army Aeromedical Research Lab., Fort Rucker, AL.
THE USE OF EXTENDED WEAR CONTACT LENSES IN THE AVIATION ENVIRONMENT: AN ARMY-WIDE STUDY Final Report
Morris R. Lattimore and Rhonda L. Cornum Sep. 1992 185 p
(DA Proj. 3M1-62787-A-8879)
(AD-A260938; USAARL-92-35) Avail: CASI HC A09/MF A02

Standard refractive error correction options for the M-43 protective mask have proven to be incompatible with the Helmet Display Unit (HDU) component of the AH-64 Apache Integrated Helmet and Display Sighting System (IHADSS). Glue-on and outsert packages push the HDU, a Maxwellian-view virtual imaging system, far enough from the spectacle-wearing aviator's eye to significantly reduce the available field-of-view. Consequently, portions of critical peripheral instrumentation and weapon system overlays cannot be visualized. In November 1988, the U.S. Army Aeromedical Research Laboratory (USAARL) initiated the AH-64 contact lens research protocol to provide both an interim readiness fix and to develop a comprehensive database on contact lens wear in a variety of environments. The protocol was organized from three perspectives with

concerns directed toward operational and flight safety, ocular health, and corneal physiology issues, and concluded at the end of September 1991. Fundamental operational and safety data were chronicled, along with written questionnaires, to assess subjective effectiveness of routine contact lens use. Ocular health complications were collated from the aviation medicine, optometric, and ophthalmological communities. Clinical and physiological data were gathered by one USAARL optometrist, and two contract civilian optometrists and their supporting technicians. DTIC

N93-25567*# National Inst. of Health, Bethesda, MD. Office of Technology Transfer.
IMMUNOCONJUGATES: MAGIC BULLETS FOR CANCER THERAPY?
Daniel R. Passeri and Jack Spiegel *In* NASA, Washington, Technology 2002: The Third National Technology Transfer Conference and Exposition, Volume 1 Feb. 1993 p 71-76 (For primary document see N93-25561 09-99)
Avail: CASI HC A02/MF A04

N93-25568*# Johns Hopkins Univ., Laurel, MD. Applied Physics Lab.
AUTOMATED SYSTEM FOR EARLY BREAST CANCER DETECTION IN MAMMOGRAMS
Isaac N. Bankman, Dong W. Kim, William A. Christens-Barry, Irving N. Weinberg, Olga B. Gatewood, and William R. Brody *In* NASA, Washington Technology 2002: The Third National Technology Transfer Conference and Exposition, Volume 1 Feb. 1993 p 77-85 (For primary document see N93-25561 09-99)
Avail: CASI HC A02/MF A04

N93-25569*# Johns Hopkins Univ., Laurel, MD. Applied Physics Lab.
THE DESIGN OF MECHANICALLY COMPATIBLE FASTENERS FOR HUMAN MANDIBLE RECONSTRUCTION
Jack C. Roberts, John A. Ecker, and Paul J. Biermann *In* NASA, Washington, Technology 2002: The Third National Technology Transfer Conference and Exposition, Volume 1 Feb. 1993 p 86-95 (For primary document see N93-25561 09-99)
Avail: CASI HC A02/MF A04

N93-25592*# Johns Hopkins Univ., Laurel, MD. Applied Physics Lab.
AUTOMATIC DETECTION OF SEIZURES WITH APPLICATIONS
Dale E. Olsen, John C. Harris, Protagoras N. Cutchis, John A. Cristion, Ronald P. Lesser (Johns Hopkins Univ., Baltimore, MD.), and W. Robert S. Webber (Johns Hopkins Univ., Baltimore, MD.) *In* NASA, Washington, Technology 2002: The Third National Technology Transfer Conference and Exposition, Volume 1 Feb. 1993 p 301-307 (For primary document see N93-25561 09-99)
Avail: CASI HC A02/MF A04

N93-25593*# National Aeronautics and Space Administration. Lewis Research Center, Cleveland, OH.
A FIBER OPTIC PROBE FOR THE DETECTION OF CATARACTS
Rafat R. Ansari and Harbans S. Dhadwal (State Univ. of New York, Stony Brook.) *In* NASA, Washington, Technology 2002: The Third National Technology Transfer Conference and Exposition, Volume 1 Feb. 1993 p 308-316 (For primary document see N93-25561 09-99)
Avail: CASI HC A02/MF A04

N93-25594*# General Electric Co., Houston, TX. Government Services.
MAC TO VAX CONNECTIVITY: HEARTRATE SPECTRAL ANALYSIS SYSTEM
Hasan H. Rahman and Monazer Faruque *In* NASA, Washington, Technology 2002: The Third National Technology Transfer Conference and Exposition, Volume 1 Feb. 1993 p 317-321 Prepared for NASA. Johnson Space Center, Houston, TX (For primary document see N93-25561 09-99)
Avail: CASI HC A01/MF A04

N93-26068*# Pennsylvania State Univ., University Park. Dept. of Nutrition.
THE ROLE OF PYRIDOXINE AS A COUNTERMEASURE FOR IN-FLIGHT LOSS OF LEAN BODY MASS Final Report
Joyce A. Gilbert *In* NASA. Johnson Space Center, National Aeronautics and Space Administration (NASA)/American Society for Engineering Education (ASEE) Summer Faculty Fellowship Program, 1992, Volume 1 Dec. 1992 4 p (For primary document see N93-26058 09-99)
(Grant NGT-44-005-803)
Avail: CASI HC A01/MF A02

53 BEHAVIORAL SCIENCES

Includes psychological factors; individual and group behavior; crew training and evaluation; and psychiatric research.

N93-25203# Federal Aviation Administration, Oklahoma City, OK. Civil Aeromedical Inst.
ORGANIZATIONAL POLITICS, PARTICIPATION IN DECISION-MAKING, AND JOB SATISFACTION Final Report
L. A. Witt Apr. 1992 15 p
(FAA Proj. AM-C-92-HRR-122)
(DOT/FAA/AM-92/17) Avail: CASI HC A03/MF A01

The study tested two hypotheses: (1) that organizational politics as measured by the Kacmar and Ferris (1991) Perceptions of Organizational Politics Scale would be negatively related to feelings of job satisfaction; and (2) that participation in decision-making (PDM) would moderate that relationship. In line with concerns for dispositional affect as a contributor to method variance and the possibility that biodata may explain some of the effects of organizational politics and PDM on job satisfaction, dispositional affect and biodata variables were included in the analyses. Hierarchical moderated multiple regression analyses conducted on data collected from 1,083 Federal employees confirmed the hypotheses. Author

N93-25213# Federal Aviation Administration, Oklahoma City, OK. Civil Aeromedical Inst.
A LONGITUDINAL EXAMINATION OF APPLICANTS TO THE AIR TRAFFIC CONTROL SUPERVISORY IDENTIFICATION AND DEVELOPMENT PROGRAM Final Report
Jennifer G. Myers, ed. Apr. 1992 57 p
(FAA Proj. AM-C-92-HRR-125)
(DOT/FAA/AM-92/16) Avail: CASI HC A04/MF A01

The Federal Aviation Administration began development of an extensive longitudinal database on its air traffic controller workforce following the strike of 1981. Since that time, data have been collected on thousands of air traffic controllers, spanning a period which covers their application to the federal government for employment to their achievement of a first-line supervisor position. This collection of papers examines a subset of air traffic control specialists who have completed the agency's supervisor selection program, beginning with their performance on the Office of Personnel Management test battery and other cognitive tests administered prior to completion of the air traffic controller Screen Program. Measures of academic, laboratory, and overall Screen performance were examined in relationship to aspects of performance in the supervisor selection program. Field training profiles were analyzed to determine differences between successful and unsuccessful supervisor selection program candidates and relationship with selection program performance. Finally, performance in the supervisor selection program was compared for those who were selected as first-line supervisors and those who were not. Author

N93-25654# Texas Univ., San Antonio. Health Science Center.
PROCEEDINGS OF WORKSHOP 1: THE HUMAN BRAINMAP DATABASE Final Report, 15 Apr. 1991 - 31 Aug. 1992
Peter T. Fox and Jack L. Lancaster 17 Feb. 1993 89 p Workshop held in San Antonio, TX, 29 Nov. - 1 Dec. 1991
(Contract N00014-91-J-1903)
(AD-A260720) Avail: CASI HC A05/MF A01

The Human BrainMap Database is a software environment for meta-analysis of functional brain mapping experiments. In brief, BrainMap relates brain locations with behavioral functions. For any brain region, the behavioral conditions associated with that region can be returned. Conversely, for any behavioral function, the brain regions supporting that behavior can be retrieved. BrainMap is composed of three main parts: a relational database, graphical user interface (GUI), and a data-entry interface. BrainMap's database is constructed in a natural hierarchy. The highest level is the paper. Each paper is divided into one or more experiments. An experiment is a grouping (typically a pairing) of behavioral conditions

for which differentially activated locations are reported. Behavioral conditions are specified for each experiment. Methodological details are specified for each experiment, including imaging modality, tracer, patient population, etc. Each experiment reports one or more activated locations, the lowest level of the hierarchy. Each location (i.e., each x-y-z coordinate) carries its links up the hierarchy, allowing formation at the experiment and paper levels to be rapidly retrieved. DTIC

N93-25736*# National Aeronautics and Space Administration. Lyndon B. Johnson Space Center, Houston, TX.

EVALUATION OF LENS DISTORTION ERRORS IN VIDEO-BASED MOTION ANALYSIS

Jeffrey Poliner (Lockheed Engineering and Sciences Co., Houston, TX.), Robert Wilmington (Lockheed Engineering and Sciences Co., Houston, TX.), Glenn K. Klute, and Angelo Micocci (Lockheed Engineering and Sciences Co., Houston, TX.) May 1993 41 p

(Contract NAS9-17900)

(NASA-TP-3266; S-721; NAS 1.60:3266) Avail: CASI HC A03/MF A01

In an effort to study lens distortion errors, a grid of points of known dimensions was constructed and videotaped using a standard and a wide-angle lens. Recorded images were played back on a VCR and stored on a personal computer. Using these stored images, two experiments were conducted. Errors were calculated as the difference in distance from the known coordinates of the points to the calculated coordinates. The purposes of this project were as follows: (1) to develop the methodology to evaluate errors introduced by lens distortion; (2) to quantify and compare errors introduced by use of both a 'standard' and a wide-angle lens; (3) to investigate techniques to minimize lens-induced errors; and (4) to determine the most effective use of calibration points when using a wide-angle lens with a significant amount of distortion. It was seen that when using a wide-angle lens, errors from lens distortion could be as high as 10 percent of the size of the entire field of view. Even with a standard lens, there was a small amount of lens distortion. It was also found that the choice of calibration points influenced the lens distortion error. By properly selecting the calibration points and avoidance of the outermost regions of a wide-angle lens, the error from lens distortion can be kept below approximately 0.5 percent with a standard lens and 1.5 percent with a wide-angle lens. Author (revised)

N93-25815# Air Force Human Resources Lab., Wright-Patterson AFB, OH. Logistics Research Div.

A COGNITIVE ARCHITECTURE FOR HUMAN PERFORMANCE PROCESS MODEL RESEARCH Interim Report, Dec. 1991 - Jul. 1992

Michael J. Young Nov. 1992 38 p

(AD-A261040; AL-TP-1992-0054) Avail: CASI HC A03/MF A01

This Technical Paper proposes a new cognitive architecture for human performance process (HPP) model research. HPP models are engineering models of human performance. They represent the human information-processing system as a series of subsystems consisting of input and output, memory, and processing subsystems. HPP models are used in engineering studies of new systems where the goal of the study is to predict human performance. This report proposes a new cognitive architecture for HPP model research. This new architecture is based upon the holon theory of mind previously proposed by Arthur Koestler. The holon theory of mind proposes that mind is both highly modular and hierarchically organized. The report provides an overview of HPP model research, describes the holon theory of mind, and discusses how this theory can form the basis of a new cognitive architecture for HPP model research. DTIC

N93-26138# Civil Aeromedical Inst., Oklahoma City, OK.

CONTRIBUTION OF PERSONALITY TO THE PREDICTION OF SUCCESS IN INITIAL AIR TRAFFIC CONTROL SPECIALIST TRAINING Final Report

David J. Schroeder, Dana Broach, and Willie C. Young Apr. 1993 32 p

Presented at the 34th Annual Meeting of the Aerospace Medical Association, Miami, FL Sponsored by Office of Aviation Medicine

(DOT/FAA/AM-93/4) Avail: CASI HC A03/MF A01

Reviews have consistently concluded that the validity of personality as a predictor of job performance is low. However, a 1991 meta-analysis of studies of personality and job performance demonstrated the utility of the 'Big Five' model of personality in personnel selection and training. This study was designed to evaluate the utility of personality in predicting student success in the FAA's Air Traffic Control Specialist (ATCS) Nonradar Screen Program ('the Screen'). The Screen follows the miniature training, testing, and evaluation paradigm, in which individuals with no prior knowledge of the occupation are taught critical aspects of the job and then assessed on a pass/fail basis for their potential to succeed as controllers. The NEO personality Inventory was administered to 723 men and 307 women at entry into the 9-week Screen. NEO-PI scale scores and cognitive aptitude measures were used to predict final composite scores (COMP) of students. Men and women air traffic students exhibited lower average scores in Neuroticism, higher average scores in Extroversion, Openness to Experience, and Conscientiousnous, and no difference on Agreeableness when compared to normative samples. Correlations between the personality scales and COMP were low for both sexes, ranging from .000 with Impulsiveness, a facet of Neuroticism, to -0.148 with Excitement-seeking, a facet of the Extraversion dimension. Despite the low zero-order correlations, several of the personality facets proved useful in a regression equation, explaining an additional 3 percent of variance in performance over that explained by cognitive aptitude measures. These included the following: Excitement-seeking, Fantasy, Activity, and Ideas. While these results were not entirely consistent with Barrick and Mount (1991), they do offer some support for the role of personality variables in the prediction of success in the ATCS Screen. Continued research is needed to assess the relationship of theoretically-based measures of personality to success on the job over time. Author (revised)

N93-26307# Columbia Univ., New York, NY. Dept. of Psychology.

VISUAL PERCEPTION OF ELEVATION Annual Report, 1 Jan. - 31 Dec. 1992

Leonard Matin 25 Jan. 1993 12 p

(Grant AF-AFOSR-0146-91)

(AD-A261394; Rept-002; AFOSR-93-0084TR) Avail: CASI HC A03/MF A01

The work at the Columbia laboratory concentrated on two matters: (1) expansion of the work on uncovering the laws of spatial summation between and within members of parallel line sets with regard to the influence on the setting of visually perceived eye level (VPEL); and (2) initial work on the separation of components of the body-referenced mechanism and to determine their separate influence on VPEL. The work on summation was reported at 4 presentations at professional meetings in 1992 and a fifth set of experiments has been submitted for presentation in 1993. The completed experimental work on the body-referenced mechanism has been submitted for presentation in 1993. In addition to the above, at Columbia we have begun work in which eye movements are being measured (scleral search coil technique) in conjunction with variation of visual field pitch with the first interest in determining whether a subject's setting of eye level to VPEL is differently influenced by the visual field than is the discrimination of VPEL. DTIC

N93-26347# Harvard Univ., Cambridge, MA.

NEUROPSYCHOLOGICAL COMPONENTS OF OBJECT IDENTIFICATION Final Technical Report, Dec. 1990 - Nov. 1992

Stephen M. Kosslyn 29 Jan. 1993 19 p

(Grant AF-AFOSR-0100-91)

(AD-A261449; AFOSR-93-0070TR) Avail: CASI HC A03/MF A01

The research supported by this grant focused on the structure of high-level visual processing. Five types of research were conducted: (1) We performed case studies of individual brain-damaged patients. We found evidence that curved edges are processed separately from straight edges and that location information sometimes can be used to encode some characteristics of shape. (2) We tested groups of brain-damaged patients with specific types of lesions. We found evidence that metric information may be used to encode spatial categories (such as above/below), and that imagery may involve some structures that are intact even when the visual field is disrupted. (3) We developed a computerized visual/spatial test battery, and administered it to a group of 19 brain-damaged patients. The results indicate that most of the visual/spatial abilities we examined can be impaired independently, suggesting that at least some distinct subsystems carry out each ability. (4) We implemented computer models and found support for the distinction between subsystems that compute two distinct kinds of spatial relations (metric and category). (5) Some of the tasks we developed to study deficits in brain-damaged patients were

used to study the visual-spatial abilities of Air Force pilots; we found that pilots are particularly good at mental rotation and encoding metric distance information. DTIC

N93-26349# California Univ., San Diego, La Jolla.
NEURAL BASIS OF MOTION PERCEPTION Annual Report, 1 Apr. 1991 - 31 May 1992
V. S. Ramachandran 31 May 1992 5 p
(Grant AF-AFOSR-0414-89)
(AD-A261452; AFOSR-93-0050TR) Avail: CASI HC A01/MF A01

Our research is concerned with 'high level' vision with a strong biological slant. The last two or three decades have seen breathtaking progress in the three disciplines--cognitive psychology, AI, and visual neurophysiology--but they have been pursued more or less independently. We believe that the time is now ripe for forging links between these disciplines for an integrated approach to vision. We have had two goals in mind: (1) to develop conceptual links between neurophysiology and perception; and (2) to develop specific tests for computational models of human vision. Our research has called into question several widely accepted dogmas concerning the mechanisms of early vision. Also, we have been able to discover several novel visual phenomena (e.g., motion capture, stereo-capture, etc.) and have identified a wide range of new 'natural constraints' that govern the perception of shape from shading structure from motion and motion correspondence. Also, we have discovered striking perceptual correlates of several well-known physiological observations (e.g., 'phantom contours'-stimuli which selectively activate the magnocellular pathway). DTIC

N93-26353# Army Intelligence Center and School, Fort Huachuca, AZ.
UNITED STATES ARMY SPACE EXPERIMENT 601
Terra Scout 29 Jul. 1992 195 p
(AD-A261460) Avail: CASI HC A09/MF A03

The original purpose of the Terra Scout experiment was to collect data which could be used to determine the ability of a specialist, in this case an Imagery Analyst (IA), on-board an orbiting platform, to collect valuable information in real time. During seven years of development, the experiment evolved and expanded in scope to include a variety of research and developmental issues described later in this report. DTIC

N93-26356# New York Univ., New York.
FACILITATION AND INTERFERENCE IN IDENTIFICATION OF PICTURES AND WORDS Annual Report, 1 Dec. 1991 - 30 Nov. 1992
Joan G. Snodgrass 10 Jan. 1993 16 p
(Contract F49620-92-J-0119)
(AD-A261484; AFOSR-93-0085TR) Avail: CASI HC A03/MF A01

This research is concerned with facilitation and interference in the identification of pictures and words. We study facilitation by presenting subjects with fragmented stimuli to identify during study and then test the ability of various types of study stimuli to prime or improve performance on the same stimuli presented again. An important finding from our previous research is that subjects show more priming when they study a picture which is moderately fragmented during study than one which is either very fragmented or almost intact. We accounted for this phenomenon by the perceptual closure hypothesis, which says that experiencing perceptual closure, or completion of an incomplete figure during a study episode, has the most facilitative effect on subsequent identification. We study interference by presenting more degraded versions of a picture or word just prior to the identification test. Perceptual interference is generally observed if a picture or word is preceded by more fragmented versions of itself just prior to identification. Much of our work on this aspect of the research concerns discovering the reason for the perceptual interference. DTIC

N93-26364# Stanford Univ., CA. Dept. of Psychology.
SPONTANEOUS DISCOVERY AND USE OF CATEGORICAL STRUCTURE Annual Technical Report, 15 Jan. 1992 - 14 Jan. 1993
John P. Clapper and Gordon H. Bower 15 Feb. 1993 31 p
(Grant AF-AFOSR-0144-91)
(AD-A261658; AFOSR-93-0093TR) Avail: CASI HC A03/MF A01

These experiments investigated unsupervised category learning using tasks in which subjects attempted to memorize the features of training instances from two contrasting categories. On each trial, subjects studied a verbal feature list (training instance) for 24 seconds, after which they were given multiple choice recognition tests to evaluate their memory for each list item. The amount of time spent looking at each feature during the study phase, and the accuracy of recognition during the test phase, provided two separate indices of unsupervised learning on each trial. The main independent variable in these experiments was the specific sequence in which instances from the two categories were presented. The effects of these sequence manipulations on learning provided strong evidence for the use of an explicit, non-incremental, category invention process to capture the consistent structure of the stimulus domain. The present experiments also showed the selective encoding process and enhanced memory for instances predicted by standard, schema-based, theories of learning. DTIC

N93-26391# SAM Technology, Inc., San Francisco, CA.
PHYSIOLOGICAL INDICES OF MENTAL WORKLOAD Interim Technical Report, 15 Dec. 1991 - 14 Dec. 1992
Alan Gevins and H. M. Leong 14 Dec. 1992 7 p
(Contract F49620-92-C-0013)
(AD-A261692; AFOSR-93-0086TR) Avail: CASI HC A02/MF A01

We are working on an enabling technology to facilitate the development of physiological indices of mental workload that could be used in high performance aircraft. To date, we have designed and implemented the core components of a neural-network based algorithm for deriving continuous mental workload indices from continuous recordings of brain, scalp muscle, eye and heart electrical activity. We have also designed an experiment to test the adequacy of this algorithm, and have developed technologies to perform the experiment including: (1) designing a task battery to initially test the ability of the network algorithm to generalize across cognitive functions relevant to piloting aircraft; and (2) implementing a software library that could be used to efficiently present the task stimuli using the same personal computer which also collects 32 channels of electrophysiological data. We have tested the integrated system and have found it capable of providing accurate timing of task stimuli, subject responses, and electrophysiological data. DTIC

N93-26435# New York Univ., New York.
DURATION OF ALPHA SUPPRESSION INCREASES WITH ANGLE IN A MENTAL ROTATION TASK Report, 1 Feb. 1992 - 14 Feb. 1993
C. M. Michel, L. Kaufman, and S. J. Williamson 1 Feb. 1993 27 p
(Grant AF-AFOSR-0221-90)
(AD-A261592; Rept-92-6; AFOSR-93-0055TR) Avail: CASI HC A03/MF A01

Magnetic and electric recordings of average power within the restricted alpha band (10-12 Hz) were made over the parietal and occipital areas of the human scalp while subjects were engaged in the mental imagery task of comparing an object with one previously seen but rotated and perhaps also mirror reflected. Alpha power was found to be suppressed while the subjects were engaged in the comparison, and the duration of suppression increased with the minimum rotation angle to achieve a match. This is additional evidence that the visual cortex is engaged in the process of mental imagery. Moreover, for large rotation angles, where the task is markedly more difficult, a shift in the spatial pattern of suppression indicates that the left parietal area of the cortex becomes involved. DTIC

N93-26436# New York Univ., New York.
IMAGING REGIONAL CHANGES IN THE SPONTANEOUS ACTIVITY OF THE BRAIN: AN EXTENSION OF THE MINIMUM-NORM LEAST-SQUARES ESTIMATE Manuscript Report, 1 Feb. 1992 - 14 Feb. 1993
Jia Z. Wang, Lloyd Kaufman, and Samuel J. Williamson 20 Jan. 1993 16 p
(Grants AF-AFOSR-0401-91; AF-AFOSR-0221-90)
(AD-A261593; Rept-92-5; AFOSR-93-0054TR) Avail: CASI HC A03/MF A01

A method was developed to determine the distribution of average spontaneous neuronal activity across the cerebral cortex from measurements of the field pattern across the human scalp. Computations of the mean short-term power, as well as the covariance between pairs of sensors, provide sufficient information to obtain a best estimate for the distribution of mean short-term image current power, as well as the covariance of image current between different locations on cerebral cortex. This method

has applications for determining the spatial locations of alpha power suppression as regions of cortex participate in sensory or cognitive functions. DTIC

N93-26446# California Univ., San Diego, La Jolla. Dept. of Neurosciences.
COMPARATIVE ANALYTICAL STUDY OF EVOKED AND EVENT RELATED POTENTIALS AS CORRELATES OF COGNITIVE PROCESSES Final Technical Report, 1 Feb. 1991 - 31 Oct. 1992
Theodore H. Bullock 21 Dec. 1992 5 p
(Grant AF-AFOSR-0191-91)
(AD-A261388; AFOSR-93-0043TR) Avail: CASI HC A01/MF A01

This project permitted collaboration between Prof. Erol Basar in Lubeck and Dr. Bullock on new views and analyses of cognitive Event Related Potentials (ERP's), evoked oscillations (induced Rhythms, IR's) and their relations to the EEG. ERP's have been found for the first time in nonmammalian models (fish, turtles), especially Omitted Stimulus Potentials (OSP's) and oddball ERP' and Mismatch Potentials. To compare the dynamics of these models with human ERP's, a new series of human subjects has been run, extending the range of interstimulus intervals; this showed two types of OSP with distinct dynamics - including a short ISI type not heretofore recognized. Basar and Bullock co-edited a book on a new theme: Induced Rhythms in the Brain (Birkhauser Boston, 1992), with 22 chapters by invited experts. The phenomenon of triggered or modulated oscillations has been known for more than 50 years but not been recognized or studied as a category of brain responses; it is now under active investigation in ours and several other laboratories as a possible correlate of certain kinds of cognition. DTIC

N93-26449# Maryland Univ., College Park. Office of Research Administration and Advancement.
COORDINATED ACTION IN 3-D SPACE Annual Report, 15 Jan. 1992 - 14 Jan. 1993
Robert M. Steinman 24 Feb. 1993 7 p
(Grant AF-AFOSR-0124-91)
(AD-A261418; AFOSR-93-0136TR) Avail: CASI HC A02/MF A01

This grant: (1) tests alternative hypotheses about the mechanism that controls gaze-shifts when nearby objects are manipulated: Two quite different mechanisms have been proposed, namely, on-line feedback, and learned, preplanned patterns of coordinated movements, and (2) studies the speed and accuracy of visually-guided hand movements and the correlation of these performance measures with binocular gaze-errors. The latter studies seek to determine how accurate binocular fixation must be to assure rapid and accurate manual performance in nearby 3-D space. The answer to this (and derivative questions) is not known because, until recently, binocular gaze-errors could not be measured accurately when nearby objects were handled by a subject free to move naturally. During this past year, a unique movement monitoring instrument (the Maryland RFM) was used to make the first measurements that can be used to answer these questions. More than 200 Mb of eye and head movement data were recorded, and detailed analyses are underway. Arrangements have been made to disseminate the answers obtained widely at a number of international conferences during the remaining months of 1993. Manuscripts testing models of shape and size perception and reading of unspaced texts have been in preparation for submission publication soon. DTIC

N93-26489# New Hampshire Univ., Durham. Vision Lab.
RECEPTORAL AND NEURAL ALIASING Final Report, 1 Nov. 1989 - 30 Apr. 1992
Robert A. Smith 30 Jan. 1993 46 p
(Grant AF-AFOSR-0126-89)
(AD-A261438; AFOSR-93-0060TR) Avail: CASI HC A03/MF A01

This project saw some unexpected successes, and some even more unexpected failures. Chief among the latter was our total failure to replicate Williams' observations of receptoral aliasing, either in the fovea or the parafovea. Despite much communication between us and Williams, no explanation of this discrepancy has been found. We present substantial evidence below to eliminate the possibility of technical failure in our experiments. Unable to study aliasing directly, we pursued a very different approach to the problems of retinal geometry and aliasing: we studied methods to directly map the parafoveal visual field into its constituent summation areas (presumably receptive fields). Although we have not fully solved the very difficult problem of eye-movements, several successful studies were performed, notably: (1) the development of a precise new method for measuring fixation accuracy using afterimages, and (2) studies of spatial summation for isoluminant spots in the parafovea. In addition, a computer model was designed that produces sample ganglion cell lattices and models the process of chromatic identification. Finally, we diverged considerably from the original focus of the project to design what we believe to be the most powerful stimulus display for visual research currently available. This is now a commercial product, showing both scientific and financial success. DTIC

N93-26521# New York Univ., New York.
NEUROMAGNETIC INVESTIGATION OF CORTICAL REGIONS UNDERLYING SHORT-TERM MEMORY Technical Report, 1 Jul. 1991 - 30 Jun. 1992
Z. L. Lu, S. J. Williamson, and L. Kaufman 20 Dec. 1992 8 p
(Grant AF-AFOSR-0401-91)
(AD-A261445; Rept-92-4; AFOSR-93-0056TR) Avail: CASI HC A02/MF A01

Magnetic source imaging (MSI) makes it possible to identify the cortical area in the human brain whose activity reflects the decay of sensory storage of information about sounds (echoic memory). The lifetime for decay of the neuronal activation trace in primary auditory cortex is found to range from 0.8 sec to 3.4 sec for the subjects studied. Extensive behavioral studies that determine the duration of memory for the loudness of a tone show that these physiological measures predict the lifetime of echoic memory to within the uncertainty of 0.2 sec for each of the subjects. DTIC

N93-25595*# National Aeronautics and Space Administration. Lyndon B. Johnson Space Center, Houston, TX.
THE APPLICATION OF INTEGRATED KNOWLEDGE-BASED SYSTEMS FOR THE BIOMEDICAL RISK ASSESSMENT INTELLIGENT NETWORK (BRAIN)
Karin C. Loftin (Krug Life Sciences, Inc., Houston, TX.), Bebe Ly, Laurie Webster, James Verlander (Krug Life Sciences, Inc., Houston, TX.), Gerald R. Taylor, Gary Riley, Chris Culbert, Tina Holden (Lockheed Engineering and Sciences Co., Houston, TX.), and Marianne Rudisill *In* NASA, Washington, Technology 2002: The Third National Technology Transfer Conference and Exposition, Volume 1 Feb. 1993 p 322-331 (For primary document see N93-25561 09-99)
Avail: CASI HC A02/MF A04

N93-26082*# Houston Univ., TX. Dept. of Curriculum and Instruction.
THE ADULT LITERACY EVALUATOR: AN INTELLIGENT COMPUTER-AIDED TRAINING SYSTEM FOR DIAGNOSING ADULT ILLITERATES Final Report
David B. Yaden, Jr. *In* NASA. Johnson Space Center, National Aeronautics and Space Administration (NASA)/American Society for Engineering Education (ASEE) Summer Faculty Fellowship Program, 1992, Volume 2 Dec. 1992 p 16 (For primary document see N93-26070 09-99)
(Grant NAG9-562)
Avail: CASI HC A03/MF A02

54 MAN/SYSTEM TECHNOLOGY AND LIFE SUPPORT

Includes human engineering; biotechnology; and space suits and protective clothing.

For related information see also *16 Space Transportation.*

N93-25099# Oak Ridge National Lab., TN.
INITIAL EXPERIMENTS WITH A MYOELECTRIC-BASED MUSCLE SENSOR
J. F. Jansen 1992 21 p Presented at the Institute of Electrical and Electronics Engineers International Conference on Robotics and Automation, Atlanta, GA, 2-7 May 1993
(Contract DE-AC05-84OR-21400)
(DE92-016034; CONF-930519-1) Avail: CASI HC A03/MF A01

This paper describes initial experiments in which a myoelectric-based

sensor is used to measure local muscle activity in the human body -- specifically the hand muscles. Applications of this sensor are twofold: (1) to quantify the voluntary muscular activity of specific muscles for human factors studies and (2) to allow a human operator to control a mechanical hand in teleoperation mode. Discussions are focused mainly on the measurement of muscle activity and how it relates to controlling a mechanical hand. Supportive experimental results are given. DOE

N93-25318# Sandia National Labs., Albuquerque, NM.
A HEAT TRANSFER ANALYSIS OF A MOBILE VEHICLE RADIATION-SHIELDED OPERATOR COMPARTMENT
K. W. Snyder Dec. 1992 19 p
(Contract DE-AC04-76DP-00789)
(DE93-007428; SAND-92-2392) Avail: CASI HC A03/MF A01

Solar heat gain inside a radiation-shielded forklift operator compartment can be a significant problem due to the 'greenhouse effect'. Battery power prohibits the use of a refrigerant type of air-conditioning system, which limits the interior temperature to be approximately equal to the outside ambient temperature through alternative cooling methods. A heat transfer analysis is performed to determine the amount of solar heat gain in this type of mobile vehicle shelter. Various results are presented that depend on exterior surface finish and temperature difference between inside and outside ambient. An amount of forced air flow along with several design recommendations are then specified to rid the compartment of this excess heat. DOE

N93-25415# Oak Ridge National Lab., TN.
HUMAN FACTORS ENGINEERING: A KEY ELEMENT OF INSTRUMENTATION AND CONTROL SYSTEM DESIGN
H. E. Knee 1992 10 p Presented at the 39th International Instrumentation Symposium, Albuquerque, NM, 2-6 May 1993
(Contract DE-AC05-84OR-21400)
(DE93-006731; CONF-930561-1) Avail: CASI HC A02/MF A01

Human factors engineering (HFE) has been in existence for a number of decades. Up until recently, however, its application to the design and operation of complex process control environments has been relatively conservative. In the nuclear industry, it took a major accident such as that at Three Mile Island - Unit 2 (TMI-2) to focus attention on the need for systematically accounting for the roles of humans in the control and maintenance of nuclear power plants (NPPs). Since TMI, the nuclear industry has made significant strides in fostering the use of HFE principals. This progress has been slowed to some degree due to the relatively anemic state of the US commercial nuclear power industry; however, new evolutionary and revolutionary nuclear design concepts are utilizing HFE principals and supporting research for advanced HFE concepts. Furthermore, a new Department of Energy (DOE) standard on HFE design criteria is being developed. Since instrumentation and controls (I&C) provide the interface between humans and the systems to be monitored, diagnosed and controlled, much of the HFE work is key to successful I&C. This paper will discuss HFE in the nuclear industry, its recent role in nuclear I&C, and will discuss recent applications and future directions. DOE

N93-25531 Michigan Univ., Ann Arbor.
HELMETED HEAD AND NECK DYNAMICS UNDER WHOLE-BODY VIBRATION Ph.D. Thesis
Barclay Phelps Butler 1992 165 p
Avail: Univ. Microfilms Order No. DA9303701

The military aviator's helmet functions as both protective gear and as an equipment mounting platform for devices that enhance aviator performance. These devices include night vision goggles, head-up displays, sighting systems, and other gear such as multiple visors and chemical protective masks. This additional equipment alters the helmet mass and center of mass, which in turn, increases the load on the muscles of the neck. Sagitally symmetric changes in head supported mass (M) and center of mass (CM) for effects on head and neck posture, acceleration, and neck myoelectric responses under whole-body vibration are investigated. Twelve volunteer male aviators were exposed to short duration axially swept sinusoidal vibration while wearing twelve different helmet configurations. These configurations consisted of three masses of 2, 3, and 4 Kg, and four center of masses of -2, 0, 2 and 4 cm measured relative to the head center of mass in the Anterior/Posterior (AP) direction. Acceleration measurements were made obtaining pitch, AP, and axial motion at T1 and the AO complex. Postural measurements were made using high speed video recordings of the subject's profile. Myoelectric responses were measured using bipolar surface electrodes placed over the right and left infrahyoid, sternocleidomastoid, splenius capitus, and trapezius muscles. Results showed that postural static moments remained constant with no significant changes in head, neck, or trunk angle as a function of vibration frequency, M, or CM parameters. Acceleration measurements showed significant increases in head pitch acceleration at resonance, but no changes in resonant frequency, for changes in M and CM. Consistent resonant frequencies suggest the head and neck system is not a passive system but is actively controlled by the muscles of the neck. Myoelectric responses in the neck showed significant increases in peak RMS activity for posterior muscles and were highly correlated with head pitch acceleration (r greater than 0.80). Force calculations about the combined head and helmet center of mass were correlated (r greater than 0.85) with calibrated posterior neck muscle responses. Acceleration, myoelectric, and force calculation results suggest that significant differences are seen in the responses when added helmet mass exceeds 82 plus or minus 23 N cm relative to the AO complex. Dissert. Abstr.

N93-25628# Army Natick Research and Development Command, MA.
ASSESSING PATTERNS OF CHANGE IN ANTHROPOMETRIC DIMENSIONS: SECULAR TRENDS OF US ARMY FEMALES, 1946-1988 Final Report, 1 Oct. 1991 - 31 Aug. 1992
Thomas M. Greiner and Claire C. Gordon Jan. 1993 75 p
(AD-A260869; NATICK/TR-93/013) Avail: CASI HC A04/MF A01

This report presents an analysis of data gathered in 1946, 1977, and 1988 anthropometric surveys of U.S. Army women to assess long-term changes in body dimensions. Fifteen dimensions are analyzed for two racial/cultural groups: Whites and Blacks. The results of these analyses describe trends that are slow, erratic, and yet statistically significant as linear models. Several hypotheses, drawn from conventional explanations of secular trends, are tested against the anthropometric trends observed in Army women. The application of these hypotheses, however, was deemed to be either inappropriate for these data or unsatisfactory in the ability to explain the observed phenomenon. It is concluded that shifting cultural forces that influence which women join the Army are the most likely cause of the observed patterns. Because these cultural actions have undergone so much change in the last half of the 20th century, it is impossible to establish a basis for predicting the anthropometric dimensions of future populations. Therefore, it is recommended that race-specific data from the most recent anthropometric survey of Army women (1988) be utilized with appropriate race-specific weights to predict Army women's body dimension values in the near future. DTIC

N93-25778# Smith-Kettlewell Inst. of Visual Sciences, San Francisco, CA.
VISUAL PROCESSING OF OBJECT VELOCITY AND ACCELERATION Annual Technical Report, 16 Jan. 1992 - 15 Jan. 1993
Suzanne McKee 14 Feb. 1993 3 p
(Contract F49620-92-J-0156)
(AD-A261048; AFOSR-93-0134TR) Avail: CASI HC A01/MF A01

The visual system can use local speed information to determine whether one surface or two transparent surfaces are visible. The local speed signals are very noisy, so a large difference in speed is necessary to produce surface segregation. Once the segregation has occurred, the visual system then integrates the local speed signals associated with each surface to improve the precision of the speed information. To study this phenomenon, speed discrimination was measured for a display composed of random dots all moving in one direction, but at two different speeds. When the speeds were sufficiently different to create the perception of two transparent planes, speed discrimination was as precise for either of the two speeds as when each was viewed alone. The local motion vectors specifying the two speeds had to be present simultaneously to produce segregation (and good speed discrimination). If all dots alternated rapidly between the two speeds in synchrony, no segregation was observed. On the other hand, asynchronous alternation, in which different subsets of dots changed speed in every frame, produced excellent segregation. DTIC

N93-25787# Air Force Human Resources Lab., Brooks AFB, TX.
MEASURING HEARING PROTECTION DEVICE PERFORMANCE USING THE METROSONICS db-3100 SOUND LEVEL ANALYZER (DOSIMETER) Final Report, 15 Apr. - 31 Jul. 1992
Andrew T. Wells and Phillip L. Hopper Nov. 1992 23 p
(AD-A260852; AL-TR-1992-0132) Avail: CASI HC A03/MF A01

This report provides detailed operating instructions to be used by base-level bioenvironmental engineers and technicians to determine appropriate personal hearing protection devices (HPD) and to calculate allowable exposure times for individuals wearing different HPD's in hazardous noise. In addition, this report presents a computer program that uses dosimeter time histories from Metrosonics noise dosimeters to streamline and increase the accuracy of HPD assessments. DTIC

N93-25840# Mitre Corp., Bedford, MA.
MEASURES OF USER-SYSTEM INTERFACE EFFECTIVENESS: AN ENCODING SCHEME AND INDICATORS FOR ASSESSING THE USABILITY OF GRAPHICAL, DIRECT-MANIPULATION STYLE USER INTERFACES
Donna L. Cuomo and Charles D. Bowen Jan. 1993 106 p
(AD-A260606; MTR-92B0000047V3) Avail: CASI HC A06/MF A02

The purpose of this MITRE Sponsored Research project was to develop methods and measures for evaluating user-system interface effectiveness for command and control systems with graphical, direct manipulation style interfaces. Due to the increased use of user interface prototyping during concept definition and demonstration/validation phases, the opportunity exists for human factors engineers to apply evaluation methodologies early enough in the life cycle to make an impact on system design. Understanding and improving user-system interface (USI) evaluation techniques is critical to this process. In 1986, Norman proposed a descriptive 'stages of user activity' model of human-computer interaction (HCI). Hutchins, Hollan, and Norman (1986) proposed concepts of measures based on the model which would assess the directness of the engagements between the user and the interface at each stage of the model. We created operational definitions of the concepts of directness, and derived observable indicators that certain types of indirectness may exist in the interface design. This phase of our research program involved using these concepts as a basis for a methodology of analyzing data collected during usability studies. A usability study was performed on the Military Airspace Management System (MAMS) prototype; four participants' and one user interface expert's data were used for further analysis. DTIC

N93-25859# Naval Aerospace Medical Research Lab., Pensacola, FL.
SIMULATED SUSTAINED FLIGHT OPERATIONS AND PERFORMANCE. PART 1: EFFECTS OF FATIGUE
D. F. Neri, S. A. Shappell, and C. A. DeJohn Jul. 1992 22 p
(AD-A261012) Avail: CASI HC A03/MF A01

Sustained flight operations are likely to produce fatigue and performance decrement in aviators. We assessed changes in cognitive performance using a work/rest schedule modeled on successive long-range attack missions. Twelve subjects performed several subtests of the Unified Tri-Service Cognitive Performance Assessment Battery an the Walter Reed Performance Assessment Battery 18 times during a simulated sustained operation. The scenario consisted of a 9-hr planning session followed by a 4-hr rest period and a 14-hr daytime mission. After 6 hr of rest, subjects repeated this schedule with a nighttime mission. For two spatial tests, subjects showed linear increases in response rate and one of its components, error rate. Subjects appeared to change strategy as the study progressed, possibly exchanging a higher failure rate for a savings in time. Any tendency to take chances when fatigued may serious implications for aircrew in sustained operations. DTIC

N93-25867# Naval Postgraduate School, Monterey, CA.
MODELING OF A FULL VISION SYSTEM USING COMBINED VISUAL/HAPTIC SEARCH FOR REMOTE OBJECT IDENTIFICATION M.S. Thesis
David L. Klein Dec. 1992 65 p
(AD-A260977) Avail: CASI HC A04/MF A01

It is proposed that a hybrid sensory feedback system comprising a visual peripheral component together with a haptic component corresponding to that of visual foveal information, is equivalent to that of full visual sensory feedback. Such a system is constructed and the ability of subjects to perceive objects using it is investigated by observing and classifying their search strategy. Although the provision of a peripheral component provides advantages over a purely haptic system, it is concluded that subjects rely heavily on the haptic data, and the resulting hybrid system is not equivalent to full vision. DTIC

N93-25888*# Spectra Research Systems, Inc., Huntsville, AL.
ADVANCED LIFE SUPPORT STUDY. MODIFICATION 10: ECLSS LOGISTICAL SUPPORT ANALYSIS FOR SPACE STATION FREEDOM Final Report
30 Jan. 1993 9 p
(Contract NAS8-38781)
(NASA-CR-192481; NAS 1.26:192481; SRS/STG-PR93-5738/17) Avail: CASI HC A02/MF A01

This addendum to the final report provides a description of the work performed under the subject contract. This report describes the work that was performed by SRS Technologies from Jan. 1992 - Jan. 1993. The work that was performed included the following: (1) a study of the Space Station Freedom (SSF) Preliminary Design Review (PDR) data package and an identification of the maintenance concept, structure, implementation plans, training plan, and the LSAR approach; development of a working ability with the ALSTAR and DATA Express software; (3) a review of the SSF maintenance concept; and (4) an update of the ALSTAR data base. CASI

N93-25904# Materials Research Labs., Ascot Vale (Australia).
MEMBRANE TECHNOLOGY: A SEARCH FOR MEMBRANES FOR SUBMARINE ATMOSPHERE CONTROL
S. P. Roe 1992 12 p
(AD-A260581; MRL-GD-0040; DODA-AR-006-899) Avail: CASI HC A03/MF A01

This overview of membrane technology covers the development of devices which can separate carbon dioxide from air and many other feed gases and the factors influencing selection and performance of such systems. Of the polymeric materials investigated for the separation of carbon dioxide from air, dimethyl silicone (25 percent) rubber membranes exhibit the highest permeability for carbon dioxide, while cellulose acetate exhibits the highest separation factor (10.9) of carbon dioxide to oxygen. However, an immobilized film membrane (IFM) device constructed of a cellulose acetate membrane impregnated with a cesium bicarbonate and sodium arsenite solution exhibits the highest recorded separation factor of 4100. Since a membrane must exhibit a separation factor of at least 100 in order to be effective in any life support system, the IFM method is at present the only approach worthy of further research and development in support of submarine atmosphere control. DTIC

N93-26047*# Maryland Univ., College Park. Dept. of Computer Science.
ARCHITECTURE OF AUTONOMOUS SYSTEMS Final Report
Piyush Dikshit, Katia Guimaraes, Maya Ramamurthy, Ashok Agrawala, and Ronald L. Larsen Nov. 1986 56 p
(Contract NCC2-414)
(NASA-CR-192974; NAS 1.26:192974; SDAG-TN-86-01) Avail: CASI HC A04/MF A01

Automation of Space Station functions and activities, particularly those involving robotic capabilities with interactive or supervisory human control, is a complex, multi-disciplinary systems design problem. A wide variety of applications using autonomous control can be found in the literature, but none of them seem to address the problem in general. All of them are designed with a specific application in mind. In this report, an abstract model is described which unifies the key concepts underlying the design of automated systems such as those studied by the aerospace contractors. The model has been kept as general as possible. The attempt is to capture all the key components of autonomous systems. With a little effort, it should be possible to map the functions of any specific autonomous system application to the model presented here. Author (revised)

N93-26088*# Life Systems, Inc., Cleveland, OH.
INTEGRATED OXYGEN RECOVERY SYSTEM Technical Progress Report No. 2, 9 Mar. - 7 May 1993
M. Gene Lee and Ronald J. Davenport 7 May 1993 22 p
(Contract NAS8-39843)

(NASA-CR-192982; NAS 1.26:192982; TR-1619-1-2) Avail: CASI HC A03/MF A01

Life Systems has conceptualized an innovative Integrated Oxygen Recovery System (IORS) applicable to advanced mission air revitalization. The IORS provides the capability to electrochemically generate metabolic oxygen (O2) and recover O2 from the space habitat atmosphere via a carbon dioxide (CO2) reduction process within a single assembly. To achieve this capability, the IORS utilizes a Solid Metal Cathode (SMC) water electrolysis unit that simultaneously serves as the Sabatier CO2 reduction reactor. The IORS enables two major life support systems currently baselined in closed loop air revitalization systems to be combined into one smaller, less complex system. This concept reduces fluidic and electrical interface requirements and eliminates a hydrogen (H2) interface. Life Systems is performing an evaluation of the IORS process directed at demonstrating performance and quantifying key physical characteristics including power, weight, and volume. The results of the checkout, shakedown, and initial parametric tests are summarized. Author (revised)

N93-26089# Galaxy Scientific Corp., Pleasantville, NJ.
HUMAN FACTORS IN AVIATION MAINTENANCE, PHASE 2 Final Report
Apr. 1993 200 p
(DOT/FAA/AM-93/5) Avail: CASI HC A09/MF A03

In the second phase of research on Human Factors in Aviation Maintenance, the emphasis evolved from problem definition to development of demonstrations and prototypes. These demonstrations include a computer-based training simulation for troubleshooting an airliner environmental control system and a software system to store and display documents. Laboratory and workplace evaluations of work cards, lighting, experimental systems for inspection training, and the initial effects of communication training for maintenance workers are described. A chapter of the Human Factors Guide for Aircraft Maintenance is described. Author (revised)

N93-26153*# National Aeronautics and Space Administration. Ames Research Center, Moffett Field, CA.
AUTOMATION AND ROBOTICS HUMAN PERFORMANCE Annual Report, FY 1989
Robert W. Mah 17 Jan. 1990 135 p
(NASA-CR-193049; NAS 1.26:193049) Avail: CASI HC A07/MF A02

The scope of this report is limited to the following: (1) assessing the feasibility of the assumptions for crew productivity during the intra-vehicular activities and extra-vehicular activities; (2) estimating the appropriate level of automation and robotics to accomplish balanced man-machine, cost-effective operations in space; (3) identifying areas where conceptually different approaches to the use of people and machines can leverage the benefits of the scenarios; and (4) recommending modifications to scenarios or developing new scenarios that will improve the expected benefits. The FY89 special assessments are grouped into the five categories shown in the report. The high level system analyses for Automation & Robotics (A&R) and Human Performance (HP) were performed under the Case Studies Technology Assessment category, whereas the detailed analyses for the critical systems and high leverage development areas were performed under the appropriate operations categories (In-Space Vehicle Operations or Planetary Surface Operations). The analysis activities planned for the Science Operations technology areas were deferred to FY90 studies. The remaining activities such as analytic tool development, graphics/video demonstrations and intelligent communicating systems software architecture were performed under the Simulation & Validations category. Author (revised)

N93-26229# Naval Health Research Center, San Diego, CA.
COMBINED STRENGTH AND ENDURANCE TRAINING: FUNCTIONAL AND MORPHOLOGICAL ADAPTATIONS TO TEN WEEKS OF TRAINING Final Report, May - Sep. 1991
J. McCarthy, P. Griffith, W. K. Prusaczyk, H. W. Goforth, Jr., and A. Vailas 29 Sep. 1992 20 p
(AD-A261059; NHRC-92-26) Avail: CASI HC A03/MF A01

The literature suggests that muscular strength development can be inhibited when endurance and strength training programs are combined. The purpose of this study was to examine the effects of strength and endurance training programs, individually and in combination, on performance changes and associated muscle adaptations. Sedentary males (n=30) were randomly assigned to one of three training groups: strength-only (STR), endurance-only (END), or combined strength and endurance (COM). Subjects trained three days per week for ten weeks. Strength training consisted of select upper and lower body resistance exercises (three maximal effort sets, five to seven repetitions per set). Endurance training consisted of continuous cycling for 50 min at 70% heart rate reserve (HRR). Subjects in COM engaged in both the strength and endurance training programs on the same day. Anthropometric characteristics, strength, and peak oxygen uptake (cycling) were measured; biopsies were taken from the vastus lateralis muscle; and computed tomography (CT) scans were performed on mid-thigh before and after ten weeks of training. Groups STR and COM showed significant (p less than 0.05) increases in: one-repetition maximum squat (23%, 22%) and bench press (18%, 18%); vertical jump (6%, 9%); lean body weight (3%, 5%); mid-thigh girth (3%, 4%); fast twitch (FT) muscle fiber area (24%, 28%); mean muscle fiber area (21%, 23%); thigh extensor (12%, 14%) and flexor (7%, 6%) areas. All groups exhibited significant increases in peak oxygen uptake following training END (18%), COM (16%), and STR (9%). These results suggest that combining strength and endurance training programs can produce significant concurrent gains in muscular strength and power, muscle hypertrophy, and peak oxygen uptake. DTIC

N93-26265# Army Aeromedical Research Lab., Fort Rucker, AL. Sensory Research Div.
INTERPUPILLARY AND VERTEX DISTANCE EFFECTS ON FIELD-OF-VIEW AND ACUITY WITH ANVIS Final Report
James M. King and Stephen E. Morse Jan. 1993 44 p
(DA Proj. 3M1-62787-A-879)
(AD-A261259; USAARL-93-9) Avail: CASI HC A03/MF A01

Third generation Aviation Night Vision Imaging Systems (ANVIS) employ vertical, tilt, interpupillary distance, vertex distance, and focus adjustments. ANVIS field-of-view is nominally 40 degrees but can be limited by adjustments. Interpupillary distance effects on ANVIS field-of-view have been computed, but seldom measured. There have been reports of acuity loss at the periphery of ANVIS fields-of-view. Fields-of-view were measured in 10 subjects, acuities in 8. ANVIS were used with a 10-foot working distance. Acuities were Assessed using Bailey-Lovie charts. At the 18 mm vertex distance, binocular and monocular fields-of-view decreased with decentration. At the 32 mm vertex distance, binocular and monocular fields-of-view were reduced at optimal interpupillary distance, and decreased with increasing decentration. The total horizontal field-of-view at 32 mm vertex distance was increased by increasing decentration, offsetting the reduction caused by increased vertex distance. Acuity was relatively insensitive to changes in vertex distance and interpupillary distance, but was substantially reduced in the periphery of the field-of-view, and under low contrast. DTIC

N93-26404# Army Natick Research and Development Command, MA.
ANTHROPOMETRY OF THE FOOT AND LOWER LEG OF U.S. ARMY SOLDIERS: FORT JACKSON, SC Final Report, Jun. 1985 - Dec. 1988
Kenneth R. Parham, Claire C. Gordon, and Carolyn K. Bensel Sep. 1992 358 p
(AD-A261405; NATICK/TR-92/028) Avail: CASI HC A16/MF A03

In 1985, a fit test for a leather combat boot, which was recently adopted by the US Army, was conducted at Fort Jackson, South Carolina by the US Army Natick Research, Development and Engineering Center. In conjunction with the fit test, a series of 33 anthropometric measurements of the foot and lower leg (including stature and weight) was obtained on 867 male and female soldiers. This report presents statistical information for those data on the full male sample (n=293) and on a female subsample (n=491), which has been reconfigured to represent more closely the demographic composition of the current US Army female population. In addition to measurement descriptions and summary statistics for each variable by gender, bivariate and multivariate relationships in the data are also presented. This includes bivariate tables, correlation coefficients, and both simple and multiple regression equations. These data represent the most comprehensive anthropometric information on the foot collected to date. As such, the statistical information presented in this report should be of value to scientists and to developers of both military and civilian footwear. DTIC

N93-25617*# Lockheed Missiles and Space Co., Sunnyvale, CA.
SPACE LIFE SUPPORT TECHNOLOGY APPLICATIONS TO TERRESTRIAL ENVIRONMENTAL PROBLEMS
Steven H. Schwartzkopf and Howard L. Sleeper *In* NASA, Washington, Technology 2002: The Third National Technology Transfer Conference and Exposition, Volume 1 Feb. 1993 p 537-543 (For primary document see N93-25561 09-99)
Avail: CASI HC A02/MF A04

N93-26061*# Nebraska Univ., Lincoln. Dept. of Industrial and Management Systems Engineering.
INVESTIGATION OF THE EFFECTS OF EXTRA VEHICULAR ACTIVITY (EVA) AND LAUNCH AND ENTRY (LES) GLOVES ON PERFORMANCE Final Report
Ram R. Bishu *In* NASA. Johnson Space Center, National Aeronautics and Space Administration (NASA)/American Society for Engineering Education (ASEE) Summer Faculty Fellowship Program, 1992, Volume 1 Dec. 1992 15 p (For primary document see N93-26058 09-99)
(Grant NGT-44-005-803)
Avail: CASI HC A03/MF A02

N93-26076*# Bevill State Community Coll., Fayette, AL. Div. of Natural Sciences.
DEVELOPMENT OF A PYROLYSIS WASTE RECOVERY MODEL WITH DESIGNS, TEST PLANS, AND APPLICATIONS FOR SPACE-BASED HABITATS Final Report
Bobby J. Roberson *In* NASA. Johnson Space Center, National Aeronautics and Space Administration (NASA)/American Society for Engineering Education (ASEE) Summer Faculty Fellowship Program, 1992, Volume 2 Dec. 1992 13 p (For primary document see N93-26070 09-99)
(Grant NGT-44-005-803)
Avail: CASI HC A03/MF A02

55 SPACE BIOLOGY

Includes exobiology; planetary biology; and extraterrestrial life.

N93-26157*# Wisconsin Univ., Milwaukee. Center for Great Lakes Studies.
PLANETARY BIOLOGY AND MICROBIAL ECOLOGY: MOLECULAR ECOLOGY AND THE GLOBAL NITROGEN CYCLE
Molly Stone Nealson, ed. and Kenneth H. Nealson, ed. Washington Mar. 1993 194 p
(Grant NAGw-2436)
(NASA-CR-4497; NAS 1.26:4497) Avail: CASI HC A09/MF A03

This report summarizes the results of the Planetary Biology and Molecular Ecology's summer 1991 program, which was held at the Marine Biological Laboratory in Woods Hole, Massachusetts. The purpose of the interdisciplinary PBME program is to integrate, via lectures and laboratory work, the contributions of university and NASA scientists and student interns. The goals of the 1991 program were to examine several aspects of the biogeochemistry of the nitrogen cycle and to teach the application of modern methods of molecular genetics to field studies of organisms. Descriptions of the laboratory projects and protocols and abstracts and references of the lectures are presented. Author (revised)

59 MATHEMATICAL AND COMPUTER SCIENCES (GENERAL)

N93-25084*# Institute for Computer Applications in Science and Engineering, Hampton, VA.
[CURRENT RESEARCH ACTIVITIES: APPLIED AND NUMERICAL MATHEMATICS, FLUID MECHANICS, EXPERIMENTS IN TRANSITION AND TURBULENCE AND AERODYNAMICS, AND COMPUTER SCIENCE] Semiannual Final Report, 1 Apr. - 30 Sep. 1992
Washington Dec. 1992 93 p Sponsored by NASA. Langley Research Center
(Contracts NAS1-18605; NAS1-19480; RTOP 505-90-52-01)
(NASA-CR-191408; NAS 1.26:191408) Avail: CASI HC A05/MF A01

Research conducted at the Institute for Computer Applications in Science and Engineering in applied mathematics, numerical analysis, fluid mechanics including fluid dynamics, acoustics, and combustion, aerodynamics, and computer science during the period 1 Apr. 1992 - 30 Sep. 1992 is summarized. Author (revised)

N93-25235*# National Aeronautics and Space Administration. Ames Research Center, Moffett Field, CA.
SCENE SEGMENTATION OF NATURAL IMAGES USING TEXTURE MEASURES AND BACK-PROPAGATION
Banavar Sridhar, Anil Phatak, and Gano Chatterji Mar. 1993 27 p
(RTOP 505-64-36)
(NASA-TM-104003; A-93043; NAS 1.15:104003) Avail: CASI HC A03/MF A01

Knowledge of the three-dimensional world is essential for many guidance and navigation applications. A sequence of images from an electro-optical sensor can be processed using optical flow algorithms to provide a sparse set of ranges as a function of azimuth and elevation. A natural way to enhance the range map is by interpolation. However, this should be undertaken with care since interpolation assumes continuity of range. The range is continuous in certain parts of the image and can jump at object boundaries. In such situations, the ability to detect homogeneous object regions by scene segmentation can be used to determine regions in the range map that can be enhanced by interpolation. The use of scalar features derived from the spatial gray-level dependence matrix for texture segmentation is explored. Thresholding of histograms of scalar texture features is done for several images to select scalar features which result in a meaningful segmentation of the images. Next, the selected scalar features are used with a neural net to automate the segmentation procedure. Back-propagation is used to train the feed forward neural network. The generalization of the network approach to subsequent images in the sequence is examined. It is shown that the use of multiple scalar features as input to the neural network result in a superior segmentation when compared with a single scalar feature. It is also shown that the scalar features, which are not useful individually, result in a good segmentation when used together. The methodology is applied to both indoor and outdoor images. Author

N93-25921*# National Aeronautics and Space Administration. Goddard Space Flight Center, Greenbelt, MD.
THE SPACE AND EARTH SCIENCE DATA COMPRESSION WORKSHOP
James C. Tilton, ed. 1993 145 p Workshop held at the Snowbird Conference Center, Snowbird, UT, 27 Mar. 1992
(RTOP 590-32-14-01)
(NASA-CP-3183; NAS 1.55:3183) Avail: CASI HC A07/MF A02

This document is the proceedings from a Space and Earth Science Data Compression Workshop, which was held on March 27, 1992, at the Snowbird Conference Center in Snowbird, Utah. This workshop was held in conjunction with the 1992 Data Compression Conference (DCC '92), which was held at the same location, March 24-26, 1992. The workshop explored opportunities for data compression to enhance the collection and analysis of space and Earth science data. The workshop consisted of eleven papers presented in four sessions. These papers describe research that is integrated into, or has the potential of being integrated into, a particular space and/or Earth science data information system. Presenters were encouraged to take into account the scientists's data requirements, and the constraints imposed by the data collection, transmission, distribution, and archival system. For individual titles, see N93-25922 through N93-25932.

N93-25922*# National Aeronautics and Space Administration. Lewis Research Center, Cleveland, OH.
SUBBAND CODING FOR IMAGE DATA ARCHIVING **c82**
Daniel Glover and S. C. Kwatra (Toledo Univ., OH.) *In* NASA. Goddard Space Flight Center, The Space and Earth Science Data Compression Workshop 1993 p 3-16 (For primary document see N93-25921 09-59)
Avail: CASI HC A03/MF A02

The use of subband coding on image data is discussed. An overview

of subband coding is given. Advantages of subbanding for browsing and progressive resolution are presented. Implementations for lossless and lossy coding are discussed. Algorithm considerations and simple implementations of subband systems are given. Author

N93-25923*# Universities Space Research Association, Greenbelt, MD.
ADJUSTABLE LOSSLESS IMAGE COMPRESSION BASED ON A NATURAL SPLITTING OF AN IMAGE INTO DRAWING, SHADING, AND FINE-GRAINED COMPONENTS **c82**
Dmitry A. Novik and James C. Tilton (National Aeronautics and Space Administration. Goddard Space Flight Center, Greenbelt, MD.) *In its* The Space and Earth Science Data Compression Workshop 1993 p 17-25 (For primary document see N93-25921 09-59)
Avail: CASI HC A02/MF A02

The compression, or efficient coding, of single band or multispectral still images is becoming an increasingly important topic. While lossy compression approaches can produce reconstructions that are visually close to the original, many scientific and engineering applications require exact (lossless) reconstructions. However, the most popular and efficient lossless compression techniques do not fully exploit the two-dimensional structural links existing in the image data. We describe here a general approach to lossless data compression that effectively exploits two-dimensional structural links of any length. After describing in detail two main variants on this scheme, we discuss experimental results. Author

N93-25924*# Cambridge Univ. (England). Computer Lab.
ENTROPY REDUCTION VIA SIMPLIFIED IMAGE CONTOURIZATION **c82**
Martin J. Turner *In* NASA. Goddard Space Flight Center, The Space and Earth Science Data Compression Workshop 1993 p 27-42 (For primary document see N93-25921 09-59)
Avail: CASI HC A03/MF A02

The process of contourization is presented which converts a raster image into a set of plateaux or contours. These contours can be grouped into a hierarchical structure, defining total spatial inclusion, called a contour tree. A contour coder has been developed which fully describes these contours in a compact and efficient manner and is the basis for an image compression method. Simplification of the contour tree has been undertaken by merging contour tree nodes thus lowering the contour tree's entropy. This can be exploited by the contour coder to increase the image compression ratio. By applying general and simple rules derived from physiological experiments on the human vision system, lossy image compression can be achieved which minimizes noticeable artifacts in the simplified image. Author

N93-25925*# General Electric Co., Philadelphia, PA. Astro-Space Div.
COMPRESSION OF SPECTRAL METEOROLOGICAL IMAGERY **c82**
Kristo Miettinen *In* NASA. Goddard Space Flight Center, The Space and Earth Science Data Compression Workshop 1993 p 43-57 (For primary document see N93-25921 09-59)
Avail: CASI HC A03/MF A02

Data compression is essential to current low-earth-orbit spectral sensors with global coverage, e.g., meteorological sensors. Such sensors routinely produce in excess of 30 Gb of data per orbit (over 4 Mb/s for about 110 min) while typically limited to less than 10 Gb of downlink capacity per orbit (15 minutes at 10 Mb/s). Astro-Space Division develops spaceborne compression systems for compression ratios from as little as three to as much as twenty-to-one for high-fidelity reconstructions. Current hardware production and development at Astro-Space Division focuses on discrete cosine transform (DCT) systems implemented with the GE PFFT chip, a 32x32 2D-DCT engine. Spectral relations in the data are exploited through block mean extraction followed by orthonormal transformation. The transformation produces blocks with spatial correlation that are suitable for further compression with any block-oriented spatial compression system, e.g., Astro-Space Division's Laplacian modeler and analytic encoder of DCT coefficients. Author

N93-25926*# MacDonald, Dettwiler and Associates Ltd., Richmond (British Columbia).
METHODS OF EVALUATING THE EFFECTS OF CODING ON SAR DATA **c82**
Melanie Dutkiewicz and Ian Cumming *In* NASA. Goddard Space Flight Center, The Space and Earth Science Date Compression Workshop 1993 p 59-72 (For primary document see N93-25921 09-59)
Avail: CASI HC A03/MF A02

It is recognized that mean square error (MSE) is not a sufficient criterion for determining the acceptability of an image reconstructed from data that has been compressed and decompressed using an encoding algorithm. In the case of Synthetic Aperture Radar (SAR) data, it is also deemed to be insufficient to display the reconstructed image (and perhaps error image) alongside the original and make a (subjective) judgment as to the quality of the reconstructed data. In this paper we suggest a number of additional evaluation criteria which we feel should be included as evaluation metrics in SAR data encoding experiments. These criteria have been specifically chosen to provide a means of ensuring that the important information in the SAR data is preserved. The paper also presents the results of an investigation into the effects of coding on SAR data fidelity when the coding is applied in (1) the signal data domain, and (2) the image domain. An analysis of the results highlights the shortcomings of the MSE criterion, and shows which of the suggested additional criterion have been found to be most important. Author

N93-25927*# Iterated Systems, Inc., Norcross, GA.
FRACTAL IMAGE COMPRESSION: A RESOLUTION INDEPENDENT REPRESENTATION FOR IMAGERY **c82**
Alan D. Sloan *In* NASA. Goddard Space Flight Center, The Space and Earth Science Data Compression Workshop 1993 p 73-79 (For primary document see N93-25921 09-59)
Avail: CASI HC A02/MF A02

A deterministic fractal is an image which has low information content and no inherent scale. Because of their low information content, deterministic fractals can be described with small data sets. They can be displayed at high resolution since they are not bound by an inherent scale. A remarkable consequence follows. Fractal images can be encoded at very high compression ratios. This fern, for example is encoded in less than 50 bytes and yet can be displayed at resolutions with increasing levels of detail appearing. The Fractal Transform was discovered in 1988 by Michael F. Barnsley. It is the basis for a new image compression scheme which was initially developed by myself and Michael Barnsley at Iterated Systems. The Fractal Transform effectively solves the problem of finding a fractal which approximates a digital 'real world image'. Author

N93-25928*# National Aeronautics and Space Administration. Goddard Space Flight Center, Greenbelt, MD.
THE IMPLEMENTATION OF A LOSSLESS DATA COMPRESSION MODULE IN AN ADVANCED ORBITING SYSTEM: ANALYSIS AND DEVELOPMENT **c82**
Pen-Shu Yeh, Warner H. Miller, Jack Venbrux (Idaho Univ., Moscow.), Norley Liu (Idaho Univ., Moscow.), and Robert F. Rice (Jet Propulsion Lab., California Inst. of Tech., Pasadena.) *In its* The Space and Earth Science Data Compression Workshop 1993 p 81-94 (For primary document see N93-25921 09-59)
(Grant NAGw-1406)
Avail: CASI HC A03/MF A02

Data compression has been proposed for several flight missions as a means of either reducing on board mass data storage, increasing science data return through a bandwidth constrained channel, reducing TDRSS access time, or easing ground archival mass storage requirement. Several issues arise with the implementation of this technology. These include the requirement of a clean channel, onboard smoothing buffer, onboard processing hardware and on the algorithm itself, the adaptability to scene changes and maybe even versatility to the various mission types. This paper gives an overview of an ongoing effort being performed at Goddard Space Flight Center for implementing a lossless data compression scheme for space flight. We will provide analysis results on several data systems issues, the performance of the selected lossless compression scheme, the status of the hardware processor and current development plan. Author

N93-25929*# Hughes STX, Inc., Lanham, MD.
LOSSLESS COMPRESSION OF IMAGE DATA PRODUCTS ON TH E FIFE CD-ROM SERIES **c82**
Jeffrey A. Newcomer and Donald E. Strebel (Versar, Inc., Columbia, MD.) *In* NASA. Goddard Space Flight Center, The Space and Earth Science Data Compression Workshop 1993 p 95-10 Sponsored in part by the

FIFT Project and VERSAR, Inc. (For primary document see N93-25921 09-59)
Avail: CASI HC A03/MF A02

How do you store enough of the key data sets, from a total of 120 gigabytes of data collected for a scientific experiment, on a collection of CD-ROM's, small enough to distribute to a broad scientific community? In such an application where information loss in unacceptable, lossless compression algorithms are the only choice. Although lossy compression algorithms can provide an order of magnitude improvement in compression ratios over lossless algorithms the information that is lost is often part of the key scientific precision of the data. Therefore, lossless compression algorithms are and will continue to be extremely important in minimizing archiving storage requirements and distribution of large earth and space (ESS) data sets while preserving the essential scientific precision of the data. Author

N93-25930*# National Aeronautics and Space Administration. Ames Research Center, Moffett Field, CA.
THE EFFECTS OF VIDEO COMPRESSION ON ACCEPTABILITY OF IMAGES FOR MONITORING LIFE SCIENCES' EXPERIMENTS **c82**
Richard F. Haines and Sherry L. Chuang *In* NASA. Goddard Space Flight Center, The Space and Earth Science Data Compression Workshop 1993 p 109-116 (For primary document see N93-25921 09-59)
Avail: CASI HC A02/MF A02

Current plans indicate that there will be a large number of life science experiments carried out during the thirty year-long mission of the Biological Flight Research Laboratory (BFRL) on board Space Station Freedom (SSF). Non-human life science experiments will be performed in the BFRL. Two distinct types of activities have already been identified for this facility: (1) collect, store, distribute, analyze and manage engineering and science data from the Habitats, Glovebox and Centrifuge, (2) perform a broad range of remote science activities in the Glovebox and Habitat chambers in conjunction with the remotely located principal investigator (PI). These activities require extensive video coverage, viewing and/or recording and distribution to video displays on board SSF and to the ground. This paper concentrates mainly on the second type of activity. Each of the two BFRL habitat racks are designed to be configurable for either six rodent habitats per rack, four plant habitats per rack, or a combination of the above. Two video cameras will be installed in each habitat with a spare attachment for a third camera when needed. Therefore, a video system that can accommodate up to 12-18 camera inputs per habitat rack must be considered. Author

N93-25931*# Colorado Univ., Boulder. Joint Inst. for Lab. Astrophysics.
HIGH-PERFORMANCE COMPRESSION OF ASTRONOMICAL IMAGES **c82**
Richard L. White (Space Telescope Science Inst., Baltimore, MD.) *In* NASA. Goddard Space Flight Center, The Space and Earth Science Data Compression Workshop 1993 p 117-123 (For primary document see N93-25921 09-59)
(Grant NAGw-2166)
Avail: CASI HC A02/MF A02

Astronomical images have some rather unusual characteristics that make many existing image compression techniques either ineffective or inapplicable. A typical image consists of a nearly flat background sprinkled with point sources and occasional extended sources. The images are often noisy, so that lossless compression does not work very well; furthermore, the images are usually subjected to stringent quantitative analysis, so any lossy compression method must be proven not to discard useful information, but must instead discard only the noise. Finally, the images can be extremely large. For example, the Space Telescope Science Institute has digitized photographic plates covering the entire sky, generating 1500 images each having 14000 x 14000 16-bit pixels. Several astronomical groups are now constructing cameras with mosaics of large CCD's (each 2048 x 2048 or larger); these instruments will be used in projects that generate data at a rate exceeding 100 MBytes every 5 minutes for many years. An effective technique for image compression may be based on the H-transform (Fritze et al. 1977). The method that we have developed can be used for either lossless or lossy compression. The digitized sky survey images can be compressed by at least a factor of 10 with no noticeable losses in the astrometric and photometric properties of the compressed images. The method has been designed to be computationally efficient: compression or decompression of a 512 x 512 image requires only 4 seconds on a Sun SPARCstation 1. The algorithm uses only integer arithmetic, so it is completely reversible in its lossless mode, and it could easily be implemented in hardware for space applications. Author

N93-25932*# Utah State Univ., Logan. Dept. of Electrical Engineering.
MULTI-RATE, REAL TIME IMAGE COMPRESSION FOR IMAGES DOMINATED BY POINT SOURCES **c82**
A. Kris Huber, Scott E. Budge, and Richard W. Harris *In* NASA. Goddard Space Flight Center, The Space and Earth Science Data Compression Workshop 1993 p 125-135 Sponsored by Space Dynamics Lab. (For primary document see N93-25921 09-59)
Avail: CASI HC A03/MF A02

An image compression system recently developed for compression of digital images dominated by point sources is presented. Encoding consists of minimum-mean removal, vector quantization, adaptive threshold truncation, and modified Huffman encoding. Simulations are presented showing that the peaks corresponding to point sources can be transmitted losslessly for low signal-to-noise ratios (SNR) and high point source densities while maintaining a reduced output bit rate. Encoding and decoding hardware has been built and tested which processes 552,960 12-bit pixels per second at compression rates of 10:1 and 4:1. Simulation results are presented for the 10:1 case only. Author

60 COMPUTER OPERATIONS AND HARDWARE

Includes hardware for computer graphics, firmware, and data processing.

For components see *33 Electronics and Electrical Engineering.*

N93-25130*# California Univ., Berkeley. Computer Science Div.
ROBO-LINE STORAGE: LOW LATENCY, HIGH CAPACITY STORAGE SYSTEMS OVER GEOGRAPHICALLY DISTRIBUTED NETWORKS
Randy H. Katz, Thomas E. Anderson, John K. Ousterhout, and David A. Patterson Sep. 1991 27 p
(Grant NAG2-591)
(NASA-CR-192910; NAS 1.26:192910; UCB/CSD-91/651) Avail: CASI HC A03/MF A01

Rapid advances in high performance computing are making possible more complete and accurate computer-based modeling of complex physical phenomena, such as weather front interactions, dynamics of chemical reactions, numerical aerodynamic analysis of airframes, and ocean-land-atmosphere interactions. Many of these 'grand challenge' applications are as demanding of the underlying storage system, in terms of their capacity and bandwidth requirements, as they are on the computational power of the processor. A global view of the Earth's ocean chlorophyll and land vegetation requires over 2 terabytes of raw satellite image data. In this paper, we describe our planned research program in high capacity, high bandwidth storage systems. The project has four overall goals. First, we will examine new methods for high capacity storage systems, made possible by low cost, small form factor magnetic and optical tape systems. Second, access to the storage system will be low latency and high bandwidth. To achieve this, we must interleave data transfer at all levels of the storage system, including devices, controllers, servers, and communications links. Latency will be reduced by extensive caching throughout the storage hierarchy. Third, we will provide effective management of a storage hierarchy, extending the techniques already developed for the Log Structured File System. Finally, we will construct a prototype high capacity file server, suitable for use on the National Research and Education Network (NREN). Such research must be a Cornerstone of any coherent program in high performance computing and communications.
Author (revised)

N93-25165# Los Alamos National Lab., NM.
SUPERCOMPUTER DEBUGGING WORKSHOP 1992
J. S. Brown 1993 355 p Workshop held in Dallas, TX, 7-9 Oct. 1992
(Contract W-7405-eng-36)
(DE93-007322; LA-UR-93-341; CONF-9210293) Avail: CASI HC A16/MF A03

This report contains papers or viewgraphs on the following topics: The ABC's of Debugging in the 1990s; Cray Computer Corporation; Thinking

Machines Corporation; Cray Research, Incorporated; Sun Microsystems, Inc; Kendall Square Research; The Effects of Register Allocation and Instruction Scheduling on Symbolic Debugging; Debugging Optimized Code: Currency Determination with Data Flow; A Debugging Tool for Parallel and Distributed Programs; Analyzing Traces of Parallel Programs Containing Semaphore Synchronization; Compile-time Support for Efficient Data Race Detection in Shared-Memory Parallel Programs; Direct Manipulation Techniques for Parallel Debuggers; Transparent Observation of XENOOPS Objects; A Parallel Software Monitor for Debugging and Performance Tools on Distributed Memory Multicomputers; Profiling Performance of Inter-Processor Communications in an iWarp Torus; The Application of Code Instrumentation Technology in the Los Alamos Debugger; and CXdb: The Road to Remote Debugging. DOE

N93-25233*# California Univ., Berkeley. Computer Science Div.
RAID-2: DESIGN AND IMPLEMENTATION OF A LARGE SCALE DISK ARRAY CONTROLLER
R. H. Katz, P. M. Chen, A. L. Drapeau, E. K. Lee, K. Lutz, E. L. Miller, S. Seshan, and D. A. Patterson 6 Oct. 1992 18 p
(Grant NAG2-591)
(NASA-CR-192911; NAS 1.26:192911; UCB/CSD-92/705) Avail: CASI HC A03/MF A01

We describe the implementation of a large scale disk array controller and subsystem incorporating over 100 high performance 3.5 inch disk drives. It is designed to provide 40 MB/s sustained performance and 40 GB capacity in three 19 inch racks. The array controller forms an integral part of a file server that attaches to a Gb/s local area network. The controller implements a high bandwidth interconnect between an interleaved memory, an XOR calculation engine, the network interface (HIPPI), and the disk interfaces (SCSI). The system is now functionally operational, and we are tuning its performance. We review the design decisions, history, and lessons learned from this three year university implementation effort to construct a truly large scale system assembly. Author (revised)

N93-25267*# California Univ., Berkeley. Computer Science Div.
STRIPED TAPE ARRAYS
Ann L. Drapeau and Randy H. Katz 1992 10 p
(Grant NAG2-591)
(NASA-CR-192914; NAS 1.26:192914) Avail: CASI HC A02/MF A01

A growing number of applications require high capacity, high throughput tertiary storage systems. How data striping ideas apply to arrays of magnetic tape drives is investigated. Data striping increases throughput and reduces response time for large accesses to a storage system. Striped magnetic tape systems are particularly appealing because many inexpensive magnetic tape drives have low bandwidth; striping may offer dramatic performance improvements for these systems. There are several important issues in designing striped tape systems: the choice of tape drives and robots, whether to stripe within or between robots, and the choice of the best scheme for distributing data on cartridges. One of the most troublesome problems in striped tape arrays is the synchronization of transfers across tape drives. Another issue is how improved devices will affect the desirability of striping in the future. The results of simulations comparing the performance of striped tape systems to non-striped systems are presented.
Author (revised)

N93-25650# Florida Univ., Gainesville.
VERY HIGH-SPEED ARITHMETIC PROCESSORS (THE GAUSS MACHINE) Final Report
Fred J. Taylor 29 Oct. 1992 173 p
(Contract DAAL03-89-K-0147)
(AD-A260693; ARO-26735.1-EL) Avail: CASI HC A08/MF A02

Our VHSAP ARO study has lead to a number of accomplishments including an original VLSI processor and a system with a high residue number system (RNS) content called the Gauss Machine. The Gauss machine is a SIMD systolic array architecture which takes advantage of the Galois-enhanced quadratic residue number system (GEQRNS) to form reduced complexity arithmetic elements. The Gauss machine is targeted at front-end signal and image processing applications. With a 2x2 array of GEQRNS multiplier accumulators operating at 10 MHz, the Gauss machine can achieve a peak equivalent throughput of 320 million operations per second when performing complex arithmetic. The Gauss machine is designed for a broader, more general class of problems other than RNS based systems which have been constructed: the Gauss machine may be used to accelerate computations which involve or may be expressed as matrix-matrix (level 3), matrix-vector (level 2), or vector-vector (level 1) operations. This paper describes the implementation of the Gauss machine and how it may be used to accelerate signal processing operations. DTIC

N93-25841# Carnegie-Mellon Univ., Pittsburgh, PA. School of Computer Science.
SET BASED PROGRAM ANALYSIS Ph.D. Thesis
Nevin Heintze Oct. 1992 373 p
(Contract F19628-91-C-0168; DARPA Order 8313)
(AD-A260979; CMU-CS-92-201) Avail: CASI HC A16/MF A03

The central component of standard approaches to compile-time program analysis is an abstract domain for approximating program values. Importantly, the domain must be chosen so that an iterative fixed point computation over the domain terminates. This requirement represents a substantial restriction on the accuracy of the analysis. Furthermore, it leads to complex and often chaotic behavior. We present an alternative approach to program analysis, called set based analysis. A key feature of set based analysis is that reasoning about a program's run-time behavior is reduced to reasoning about constraints on sets of program values. Set based analysis incorporates just a single notion of approximation: all dependencies arising from the treatment of program variables are ignored. The main advantage of set based analysis is improved accuracy, due to the absence of an abstract domain. Additionally, the use of a very simple and uniform notion of approximation leads to program analysis that is easier to understand and less sensitive to minor program modifications. DTIC

N93-25848# Rutgers - The State Univ., New Brunswick, NJ. Dept. of Computer Science.
COMPUTER-AIDED DESIGN PACKAGE FOR DESIGNERS OF DIGITAL OPTICAL COMPUTERS
Miles Murdocca Feb. 1993 4 p
(Contract N00014-90-J-4018)
(AD-A260757) Avail: CASI HC A01/MF A01

This report covers progress for the period 10/1/92 - 12/31/93 on a jointly sponsored ONR/AFOSR grant to Rutgers University which supports research into the architecture and design of digital optical computers. During this reporting period Murdocca developed the notion of a reconfigurable logic/interconnection component (RELIC) as part of an investigation into the architectural implications of reconfiguration optical interconnects. Prof. Thomas Stone made progress on the study of hybrid micro-macro optics for optical interconnection, achromatic optical interconnects, and the use of birefringent materials for optical interconnection. In addition, our experimental facilities have improved and related work has progressed at the Photonics Center at Rome Laboratory where we have found a good opportunity for technology transfer. DTIC

N93-25858# Naval Postgraduate School, Monterey, CA.
AN INVESTIGATION OF MEMORY LATENCY REDUCTION USING AN ADDRESS PREDICTION BUFFER M.S. Thesis
Arthur B. Billingsley Dec. 1992 39 p
(AD-A261010) Avail: CASI HC A03/MF A01

Developing memory systems to support high-speed processors is a major challenge to computer architects. Cache memories can improve system performance but the latency of main memory remains a major penalty for a cache-miss. A novel approach to improve system performance is the use of a memory prediction buffer. The memory prediction buffer (MPB) is inserted between the cache and main memory. The MPB predicts the next cache-miss address and pre-fetches the data. The use of an MPB in a computer system is shown to decrease main-memory latency and increase system performance . DTIC

N93-25934# Naval Postgraduate School, Monterey, CA.
THE DESIGN AND IMPLEMENTATION OF A READ PREDICTION BUFFER M.S. Thesis
Gary J. Nowicki Dec. 1992 204 p
(AD-A260902) Avail: CASI HC A10/MF A03

Cache memories, which are the level of memory between the central processing unit (CPU) and the main memory, hold small amounts of data and instructions and allow the CPU to access the contents in them very quickly. This significantly reduces the read access time for the CPU if the

required information is available in the cache. However, caches are small and can only hold the most commonly used data and instructions required by the CPU. When information requested does not appear in the cache, a 'cache miss' occurs and the CPU must fetch the required data from the main memory. The Read Prediction Buffer reduces this time-costly read access by attempting to predict the possible miss address, and pre-fetch the read data. DTIC

N93-26131# President's Council of Advisors on Science and Technology, Washington, DC.
HIGH PERFORMANCE COMPUTING AND COMMUNICATIONS PANEL REPORT
Dec. 1992 12 p
Avail: CASI HC A03/MF A01

In FY-92, a presidential initiative was launched, aimed at securing U.S. preeminence in high performance computing and related communication technologies. The initiative, entitled High Performance Computing and Communications (HPCC), is one of five initiatives coordinated by the Federal Coordinating Council for Science, Engineering, and Technology (FCCSET) process. Nine federal agencies are currently involved, with the Defense Advanced Research Project Agency, the Department of Energy, the National Aeronautics and Space Administration, and the National Science Foundation providing the principal program funding and direction. Lesser but important roles are being played by the National Oceanic and Atmospheric Administration, the National Institute of Standards and Technology, the Environmental Protection Agency, the Department of Education, and the National Institutes of Health. The stated goal of the initiative is threefold: extend U.S. technological leadership in high performance computing and computer communications; provide wide dissemination and application of the technologies; and spur gains in U.S. productivity and industrial competitiveness, all within the context of the mission needs of federal agencies. The strategy for accomplishing the goals and the program components are highlighted in the report 'Grand Challenges: High Performance Computing and Communications,' published as a supplement to the fiscal year 1992 and 1993 budgets. Author (revised)

N93-26291# Defense Information Systems Agency, Arlington, VA. Center for Information Management.
HUMAN COMPUTER INTERFACE STYLE GUIDE, VERSION 2.0 Final Report
30 Sep. 1992 565 p Supersedes DoD HCI Style Guide V1.0, AD-A253475
(AD-A261280) Avail: CASI HC A24/MF A04

The purpose of this Style Guide is to provide a common framework for HCI design and implementation. Through this framework, the long-term functional goals, objectives, and requirements of the HCI will be defined and documented. Interface implementation options will be standardized, enabling all DoD applications to appear and operate in a reasonably consistent manner. DTIC

N93-26293# North Carolina Univ., Chapel Hill. Dept. of Computer Science.
ADVANCED TECHNOLOGY FOR PORTABLE PERSONAL VISUALIZATION Progress Report, Jul. 1992 - Jan. 1993
Frederick P. Brooks, Jr. and Henry Fuchs Jan. 1993 61 p
(Contract DAEA18-90-C-0044)
(AD-A261294) Avail: CASI HC A04/MF A01

Despite the recent avalanche of publicity on virtual reality, the state of the art in head-mounted displays (HMD) is still at the almost-works stage. Although extravagant claims are made almost daily on television and in the popular press, there is very little that can be usefully accomplished today with virtual reality technologies. We at UNC have been working since the early 1970s on aspects of these technologies and have been advancing the state of the art by a driving problem approach; we let the needs of selected applications stimulate the direction of the technological developments and then test new results by observing their impact on solving the original application. We are working on three application areas: molecular modeling, 3D medical imaging, and modeling of architectural interiors. We have developed complete systems that include the head-mounted display device, the display generation hardware, and a head and hand tracker. We have access to a force-feedback ARM that is owned by the GRIP project. DTIC

N93-26294# Naval Postgraduate School, Monterey, CA.
CONSIDERATIONS FOR SPACE AND NAVAL AVIATION APPLICATIONS OF FERROELECTRIC MEMORY M.S. Thesis
Theodore A. Vetter Dec. 1992 77 p
(AD-A261300) Avail: CASI HC A05/MF A01

The purpose of this thesis is to introduce the reader to Ferroelectric memory and discuss considerations for possible space and Naval aviation applications. Ferroelectric memory's characteristics and basic mechanism are discussed. A broad spectrum of existing computer memory types are presented for comparison. The memory requirements of Space Shuttle, Landsat, Intelsat VI and Hubble Space Telescope as well as the Navy E-2 Hawkeye and EA-6B Prowler aircraft are given as possible examples of space and Naval aviation applications of ferroelectric memory. DTIC

N93-26403# Naval Surface Warfare Center, Dahlgren, VA.
PROCEEDINGS OF THE COMPLEX SYSTEMS ENGINEERING SYNTHESIS AND ASSESSMENT TECHNOLOGY WORKSHOP
Cuong M. Nguyen 24 Jul. 1992 618 p Workshop held in Silver Spring, MD, 20-24 Jul. 1992
(AD-A261404; NSWCDD/MP-92/304) Avail: CASI HC A99/MF A06

The emphasis of CSESAW'92 is on exploring system-level design synthesis and assessment capabilities for mission critical computer systems. These capabilities will facilitate the development of such systems from informal system requirements, through the design phase prototyping, and into implementation and post deployment. Component products produced by these capabilities are specifications that subenvironments will receive. The focus of this workshop is the development and integration of these multiple technologies and the exploration of the creation of a system-level engineering discipline with support technologies to provide potential high payoff solutions to the difficult problems encountered by designers, developers, and maintainers of large, complex, real-time systems. The emphasis is on resolving system-level technology issues that cut across component boundaries, such as those associated with system behavior requirements of real time, fault tolerance, and security. DTIC

N93-26569# National Technical Information Service, Springfield, VA. Federal Computer Products Center.
DIRECTORY OF US GOVERNMENT SOFTWARE FOR MAINFRAMES AND MICROCOMPUTERS, 1993 Annual Report
Jan. 1993 174 p Supersedes PB92-100106
(PB93-111565; ISBN-0-934213-37-2) Avail: CASI HC A08/MF A02

The directory contains descriptions of some 550 mainframe and microcomputer programs made available from more than 100 Federal agencies, or their contractors, since 1984. The major government agencies whose computer programs are included in the directory are the Departments of Defense, Energy, and Health and Human Services; the Environmental Protection Agency; the Food and Drug Administration; the National Library of Medicine; and the National Bureau of Standards. The directory is an essential reference tool for users who wish to tap the wealth of U.S. Government software. The annual listing is the only complete record of government-produced computer programs. NTIS

N93-24942*# National Aeronautics and Space Administration. Goddard Space Flight Center, Greenbelt, MD.
COMPUTER SYSTEMS
Lola Olsen *In its* Proceedings of the Ocean Climate Data Workshop 1992 p 391-408 (For primary document see N93-24915 09-42)
Avail: CASI HC A03/MF A03

N93-25577*# Rome Lab., Griffiss AFB, NY.
THE DATABASE QUERY SUPPORT PROCESSOR (QSP)
In NASA, Washington, Technology 2002: The Third National Technology Transfer Conference and Exposition, Volume 1 Feb. 1993 p 156-165 (For primary document see N93-25561 09-99)
Avail: CASI HC A02/MF A04

N93-25606*# National Aeronautics and Space Administration. Goddard Space Flight Center, Greenbelt, MD.
FIRMWARE DEVELOPMENT IMPROVES SYSTEM EFFICIENCY
E. James Chern and David W. Butler *In* NASA, Washington, Technology 2002: The Third National Technology Transfer Conference and Exposition,

Volume 1 Feb. 1993 p 425-434 (For primary document see N93-25561 09-99)
Avail: CASI HC A02/MF A04

61 COMPUTER PROGRAMMING AND SOFTWARE

Includes computer programs, routines, alogorithms, and specific applications, e.g., CAD/CAM.

N93-24750*# Old Dominion Univ., Norfolk, VA. Dept. of Computer Science.
GEOMETRIC MODELING FOR COMPUTER AIDED DESIGN Progress Report, period ending 1 Jan. 1993
James L. Schwing Apr. 1993 152 p
(Contract NCC1-99)
(NASA-CR-192891; NAS 1.26:192891) Avail: CASI HC A08/MF A02

Over the past several years, it has been the primary goal of this grant to design and implement software to be used in the conceptual design of aerospace vehicles. The work carried out under this grant was performed jointly with members of the Vehicle Analysis Branch (VAB) of NASA LaRC, Computer Sciences Corp., and Vigyan Corp. This has resulted in the development of several packages and design studies. Primary among these are the interactive geometric modeling tool, the Solid Modeling Aerospace Research Tool (smart), and the integration and execution tools provided by the Environment for Application Software Integration and Execution (EASIE). In addition, it is the purpose of the personnel of this grant to provide consultation in the areas of structural design, algorithm development, and software development and implementation, particularly in the areas of computer aided design, geometric surface representation, and parallel algorithms. Author (revised)

N93-24944*# California Univ., Santa Cruz. Computer and Information Sciences.
RAPID EXPLORATION OF CURVILINEAR GRIDS USING DIRECT VOLUME RENDERING
Allen VanGelder and Jane Wilhelms 16 Mar. 1993 14 p
(Contract NCC2-717)
(NASA-CR-192765; NAS 1.26:192765; UCSC-CRL-93-02) Avail: CASI HC A03/MF A01

Fast techniques for direct volume rendering over curvilinear grids of hexahedral cells are developed. This type of 3D grid is common in computational fluid dynamics and finite element analysis. Four new projection methods are presented and compared with each other and with previous methods for tetrahedral grids and rectilinear grids. All four methods use polygon-rendering hardware for speed. A simplified algorithm for visibility ordering, which is based on a combination of breadth-first and depth-first searches, is described. A new multi-pass blending method is described that reduces visual artifacts that are introduced by linear interpolation in hardware where exponential interpolation is needed. Multi-pass blending is of equal interest to hardware-oriented projection methods used on rectilinear grids. Visualization tools that permit rapid data banding and cycling through transfer functions, as well as region restrictions, are described. Author

N93-24947*# Analex Corp., Brook Park, OH.
FEDERAL COMMUNICATIONS COMMISSION (FCC) TRANSPONDER LOADING DATA CONVERSION SOFTWARE. USER'S GUIDE AND SOFTWARE MAINTENANCE MANUAL, VERSION 1.2
Paul G. Mallasch Jan. 1993 82 p
(Contract NAS3-25776; RTOP 144-10-10)
(NASA-CR-191067; E-7570; NAS 1.26:191067) Avail: CASI HC A05/MF A01

This volume contains the complete software system documentation for the Federal Communications Commission (FCC) Transponder Loading Data Conversion Software (FIX-FCC). This software was written to facilitate the formatting and conversion of FCC Transponder Occupancy (Loading) Data before it is loaded into the NASA Geosynchronous Satellite Orbital Statistics Database System (GSOSTATS). The information that FCC supplies NASA is in report form and must be converted into a form readable by the database management software used in the GSOSTATS application. Both the User's Guide and Software Maintenance Manual are contained in this document. This volume of documentation passed an independent quality assurance review and certification by the Product Assurance and Security Office of the Planning Research Corporation (PRC). The manuals were reviewed for format, content, and readability. The Software Management and Assurance Program (SMAP) life cycle and documentation standards were used in the development of this document. Accordingly, these standards were used in the review. Refer to the System/Software Test/Product Assurance Report for the Geosynchronous Satellite Orbital Statistics Database System (GSOSTATS) for additional information. Author

N93-24962# EG and G Energy Measurements, Inc., Idaho Falls. INEL Supercomputing Center.
EXCHANGE
J. C. Boltz, ed. Jan. 1993 14 p
(Contract DE-AC07-76ID-01570)
(DE93-007227; EGG-CODP-10620(1-93)) Avail: CASI HC A03/MF A01

The following topics are discussed: automated data processing equipment/resources (ADPE) acquisition process made easy with short range plan (SRP); scientific reference material available; occurrence reporting and processing system (ORPS) WordPerfect macro setup procedure; system managed storage is here; LIBSPOOL for MVS mainframe end-users; training center course schedule for February 1993; enjoy NJOY; scientific user services staff decreased; new release of Forwarn, a static source code analysis tool for FORTRAN programs; out of the cold with HEAT; coping cells from one table to another in word perfect; used PC equipment pool; and video training. DOE

N93-25073*# Computer Sciences Corp., Hampton, VA.
A COMPARISON USING APPL AND PVM FOR A PARALLEL IMPLEMENTATION OF AN UNSTRUCTURED GRID GENERATION PROGRAM
Trey Arthur and Michael J. Bockelie Jan. 1993 16 p
(Contract NAS1-19038; RTOP 505-90-53-02)
(NASA-CR-191425; NAS 1.26:191425; TAO-60322) Avail: CASI HC A03/MF A01

Efforts to parallelize the VGRIDSG unstructured surface grid generation program are described. The inherent parallel nature of the grid generation algorithm used in VGRIDSG was exploited on a cluster of Silicon Graphics IRIS 4D workstations using the message passing libraries Application Portable Parallel Library (APPL) and Parallel Virtual Machine (PVM). Comparisons of speed up are presented for generating the surface grid of a unit cube and a Mach 3.0 High Speed Civil Transport. It was concluded that for this application, both APPL and PVM give approximately the same performance, however, APPL is easier to use. Author (revised)

N93-25107*# Cornell Univ., Ithaca, NY. Dept. of Computer Science.
ON THE ROBUSTNESS OF HERLIHY'S HIERARCHY
Prasad Jayanti Mar. 1993 35 p Sponsored in part by the IBM Endicott Programming Lab. and Siemens Corp.
(Grants NAG2-593; NSF CCR-89-01780; NSF CCR-91-02231)
(NASA-CR-193002; NAS 1.26:193002; CU-TR-93-1332) Avail: CASI HC A03/MF A01

A wait-free hierarchy maps object types to levels in Z(+) U (infinity) and has the following property: if a type T is at level N, and T' is an arbitrary type, then there is a wait-free implementation of an object of type T', for N processes, using only registers and objects of type T. The infinite hierarchy defined by Herlihy is an example of a wait-free hierarchy. A wait-free hierarchy is robust if it has the following property: if T is at level N, and S is a finite set of types belonging to levels N - 1 or lower, then there is no wait-free implementation of an object of type T, for N processes, using any number and any combination of objects belonging to the types in S. Robustness implies that there are no clever ways of combining weak shared objects to obtain stronger ones. Contrary to what many researchers believe, we prove that Herlihy's hierarchy is not robust. We then define some natural variants of Herlihy's hierarchy, which are also infinite wait-free hierarchies. With the exception of one, which is still open, these are not robust either. We conclude with the open question of whether non-trivial robust wait-free hierarchies exist. Author (revised)

N93-25131*# California Univ., Berkeley. Computer Science Div.
AN ANALYSIS OF FILE MIGRATION IN A UNIX SUPERCOMPUTING ENVIRONMENT
Ethan L. Miller and Randy H. Katz Nov. 1992 13 p
(Grant NAG2-591)
(NASA-CR-192908; NAS 1.26:192908; UCB/CSD-92/712) Avail: CASI HC A03/MF A01

The super computer center at the National Center for Atmospheric Research (NCAR) migrates large numbers of files to and from its mass storage system (MSS) because there is insufficient space to store them on the Cray supercomputer's local disks. This paper presents an analysis of file migration data collected over two years. The analysis shows that requests to the MSS are periodic, with one day and one week periods. Read requests to the MSS account for the majority of the periodicity; as write requests are relatively constant over the course of a week. Additionally, reads show a far greater fluctuation than writes over a day and week since reads are driven by human users while writes are machine-driven.
Author

N93-25152*# Cornell Univ., Ithaca, NY. Dept. of Computer Science.
PUTTING TIME INTO PROOF OUTLINES
Fred B. Schneider, Bard Bloom, and Keith Marzullo 10 Mar. 1993 33 p
Sponsored in part by IBM Endicott Programming Lab. and Siemens Corp.
(Contract NAG2-593; N00014-91-J-1219; NSF CCR-87-01103; NSF CCR-90-14363)
(NASA-CR-192978; NAS 1.26:192978; CU-TR-93-1333) Avail: CASI HC A03/MF A01

A logic for reasoning about timing properties of concurrent programs is presented. The logic is based on Hoare-style proof outlines and can handle maximal parallelism as well as certain resource-constrained execution environments. The correctness proof for a mutual exclusion protocol that uses execution timings in a subtle way illustrates the logic in action. A soundness proof using structural operational semantics is outlined in the appendix.
Author

N93-25246*# National Aeronautics and Space Administration. Ames Research Center, Moffett Field, CA.
USING A CRAY Y-MP AS AN ARRAY PROCESSOR FOR A RISC WORKSTATION
Hugh LaMaster and Sarah J. Rogallo Nov. 1992 17 p
(RTOP 505-59-00)
(NASA-TM-103961; A-92158; NAS 1.15:103961) Avail: CASI HC A03/MF A01

As microprocessors increase in power, the economics of centralized computing has changed dramatically. At the beginning of the 1980's, mainframes and super computers were often considered to be cost-effective machines for scalar computing. Today, microprocessor-based RISC (reduced-instruction-set computer) systems have displaced many uses of mainframes and supercomputers. Supercomputers are still cost competitive when processing jobs that require both large memory size and high memory bandwidth. One such application is array processing. Certain numerical operations are appropriate to use in a Remote Procedure Call (RPC)-based environment. Matrix multiplication is an example of an operation that can have a sufficient number of arithmetic operations to amortize the cost of an RPC call. An experiment which demonstrates that matrix multiplication can be executed remotely on a large system to speed the execution over that experienced on a workstation is described.
Author

N93-25250*# California Univ., Berkeley. Computer Science Div.
ZEBRA: A STRIPED NETWORK FILE SYSTEM
John H. Hartman and John K. Ousterhout 28 Apr. 1992 11 p Presented at the USENIX Workshop on File Systems, May 1992
(Grants NAG2-591; NSF CCR-89-00029)
(NASA-CR-192912; NAS 1.26:192912; UCB/CSD-92/683) Avail: CASI HC A03/MF A01

The design of Zebra, a striped network file system, is presented. Zebra applies ideas from log-structured file system (LFS) and RAID research to network file systems, resulting in a network file system that has scalable performance, uses its servers efficiently even when its applications are using small files, and provides high availability. Zebra stripes file data across multiple servers, so that the file transfer rate is not limited by the performance of a single server. High availability is achieved by maintaining parity information for the file system. If a server fails its contents can be reconstructed using the contents of the remaining servers and the parity information. Zebra differs from existing striped file systems in the way it stripes file data: Zebra does not stripe on a per-file basis; instead it stripes the stream of bytes written by each client. Clients write to the servers in units called stripe fragments, which are analogous to segments in an LFS. Stripe fragments contain file blocks that were written recently, without regard to which file they belong. This method of striping has numerous advantages over per-file striping, including increased server efficiency, efficient parity computation, and elimination of parity update.
Author (revised)

N93-25257*# George Mason Univ., Fairfax, VA. Dept. of Operations Research and Applied Statistics.
STATISTICAL MODELLING OF SOFTWARE RELIABILITY Semiannual Status Report No. 1, 1 Apr. - 30 Sep. 1991
Douglas R. Miller 30 Sep. 1991 45 p
(Grant NAG1-1241)
(NASA-CR-192985; NAS 1.26:192985) Avail: CASI HC A03/MF A01

During the six-month period from 1 April 1991 to 30 September 1991 the following research papers in statistical modeling of software reliability appeared: (1) A Nonparametric Software Reliability Growth Model; (2) On the Use and the Performance of Software Reliability Growth Models; (3) Research and Development Issues in Software Reliability Engineering; (4) Special Issues on Software; and (5) Software Reliability and Safety.
Author (revised)

N93-25303# Los Alamos National Lab., NM.
PROTOTYPE PC USER INTERFACE
1993 12 p
(Contract W-7405-eng-36)
(DE93-008008; LA-Sub-93-29) Avail: CASI HC A03/MF A01

The conceptual model of analytical director is implemented to simulate a robotic analytical laboratory. In this model, the robotic table is represented by an abstract workbench; and the laboratory activities are represented by a set of primitive operations. A PC version user interface is developed based on the conceptual model using Microsoft Windows 3.0 programming and object-oriented design technique. With the interface, a user can design a robotic procedure on conceptual level.
DOE

N93-25307# Allied-Signal Aerospace Co., Kansas City, MO.
CAD DATA EXCHANGE DEVELOPMENT Final Report
J. W. Havenhill Feb. 1993 56 p
(Contract DE-AC04-76DP-00613)
(DE93-008085; KCP-613-4864) Avail: CASI HC A04/MF A01

The capability to automatically transfer electronic product definition files was developed. This data exchange capability provides for automatic transmission of electronic files between an external sending site and Allied-Signal Inc., Kansas City Division (KCD), the receiving site. Data exchange was completely integrated with internal KCD systems and requires no human intervention as incoming and outgoing files are processed by several computers for preparation and routing over networks to the end user.
DOE

N93-25315# Los Alamos National Lab., NM.
PCG: A SOFTWARE PACKAGE FOR THE ITERATIVE SOLUTION OF LINEAR SYSTEMS ON SCALAR, VECTOR AND PARALLEL COMPUTERS
W. Joubert and G. F. Carey 1993 5 p Presented at the 6th Society for Industrial and Applied Mathematics Conference on Parallel Processing for Scientific Computing, Norfolk, VA, 21-24 Mar. 1993
(Contract W-7405-eng-36)
(DE93-007366; LA-UR-93-303; CONF-930331-2) Avail: CASI HC A01/MF A01

The expanded use of parallel computers heightens the need for numerical software which meets the joint requirements of ease of use, transportability across different architectures, state-of-the-art methods, and high megaflop rates. The PCG package which is currently being developed to solve sparse systems of linear equations by preconditioned gradient iterative methods is discussed. The basic design and some of the features of the package are described. Issues involved in designing the software to be

transportable across different architectures are discussed. Finally, some preliminary timings for a model test problem are given to verify feasibility. DOE

N93-25386# Sandia National Labs., Albuquerque, NM.
AN IMPROVED SPECTRAL LOAD BALANCING METHOD
B. Hendrickson and R. Leland 1993 8 p Presented at the 6th Society for Industrial and Applied Mathematics Conference on Parallel Processing for Scientific Computing, Norfolk, VA, 21-24 Mar. 1993
(Contract DE-AC04-76DP-00789)
(DE93-007582; SAND-93-0164C; CONF-930331-4) Avail: CASI HC A02/MF A01

We describe an algorithm for the static load balancing of scientific computations that generalizes and improves upon spectral bisection. Through a novel use of multiple eigenvectors, our new spectral algorithm can divide a computation into 4 or 8 pieces at once. This leads to balanced partitions that have lower communication overhead and are less expensive to compute than those of spectral bisection. In addition, our approach automatically works to minimize message contention on a hypercube or mesh architecture. DOE

N93-25453# Defence Research Agency, Malvern (England).
LANGUAGES FOR REQUIREMENTS SPECIFICATIONS
G. P. Randell Mar. 1992 21 p
(RSRE-Memo-4585; BR310395) Copyright Avail: CASI HC A03/MF A01

This memorandum discusses 11 desirable features that make a requirements specification language a 'good' language. Current languages are assessed to determine which of these features they possess, and where they are lacking. Conclusions are drawn as to the current state of requirements specification languages, and topics for further research are proposed. Author

N93-25627# CSA Engineering, Inc., Palo Alto, CA.
ASTROS-ID: SOFTWARE FOR SYSTEM IDENTIFICATION USING MATHEMATICAL PROGRAMMING Final Report, Jun. 1991 - Dec. 1991
Warren C. Gibson Sep. 1992 45 p
(Contract F33615-90-C-3211)
(AD-A260867; ASIAC-TR-92-2; WL-TR-92-3100) Avail: CASI HC A03/MF A01

The multidisciplinary optimization computer program, ASTROS, which was developed for Wright Laboratory, is discussed. It seeks minimum weight structural designs subject to constraints on displacements, stresses, vibration frequencies, flutter speeds, etc. The program is based on a versatile set of software tools including a relational database, a matrix programming language, and an input description facility, all of which make the program readily extensible by knowledgeable users. This report documents an extension to ASTROS (called ASTROS-ID) which makes it possible to tune finite element models to enhance their correspondence with measured frequencies and mode shapes. The existing ASTROS optimization package is used to construct a constrained minimization problem where the user may choose to include particular frequencies and mode shape entries either in the objective function, in a least squares sense, or in constraints which require conformance within a given tolerance. Other terms include an excursion penalty and a weight deviation penalty. At the time of writing, ASTROS-ID was still in the research stage and had not been subject to beta testing. DTIC

N93-25669*# Mississippi State Univ., Mississippi State. NSF Engineering Research Center for Computational Field Simulation.
TRANSFORMATION OF TWO AND THREE-DIMENSIONAL REGIONS BY ELLIPTIC SYSTEMS Semiannual Status Report, 1 Oct. 1992 - 30 Mar. 1993
C. Wayne Mastin 29 Apr. 1993 10 p
(Grant NsG-1577)
(NASA-CR-192955; NAS 1.26:192955) Avail: CASI HC A02/MF A01

During this contract period, our work has focused on improvements to elliptic grid generation methods. There are two principle objectives in this project. One objective is to make the elliptic methods more reliable and efficient, and the other is to construct a modular code that can be incorporated into the National Grid Project (NGP), or any other grid generation code. Progress has been made in meeting both of these objectives. The two objectives are actually complementary. As the code development for the NGP progresses, we see many areas where improvements in algorithms can be made. Derived from text

N93-25699# Iowa State Univ. of Science and Technology, Ames. Center for Emerging Manufacturing Technology.
A VIRTUAL ENVIRONMENT FOR MANUFACTURING SYSTEMS Quarterly Progress Report, Oct. - Dec. 1992
J. H. Oliver, L. L. Chen, and M. J. Vanderploeg Dec. 1992 2 p
(Contract N00014-92-J-4092)
(AD-A260813) Avail: CASI HC A01/MF A01

From October to December 1992, the research on Assembly Planning Through Visualization has been focused on the development and implementation of algorithms for proposing disassembly trajectories. One of the graduate students has been working on the development of a new set of algorithms for generating potential assembly/disassembly directions for components with free-form surfaces. To generate potentially feasible disassembly directions, an O(n vector 2 alpha(n)) time algorithm has been developed for computing the spherical convex hull of a possibly self intersecting spherical curve consisting of n algebraic curved segments, where alpha(n) is the functional inverse of Ackermann's function and is an extremely slow growing function of n. DTIC

N93-25711# Institute for Defense Analyses, Alexandria, VA.
FIDELITY AND VALIDITY IN DISTRIBUTED INTERACTIVE SIMULATION: QUESTIONS AND ANSWERS Final Report, Nov. 1991 - Nov. 1992
Norman E. Lane and Earl A. Alluisi Nov. 1992 37 p
(Contract MDA903-89-C-0003)
(AD-A260971; IDA-D-1066; IDA/HQ-91-40476) Avail: CASI HC A03/MF A01

Distributed Interactive Simulation (DIS) involves the on-line networking of large numbers of participants operating through simulators, actual equipment, or computer models of friendly and opposing forces in free-play exercises on a simulated battlefield. The DIS employs new simulation-related technologies that can be used to support innovative applications generally not feasible with the older technologies of conventional simulation. It has the potential of revolutionizing future work in the following areas: (1) collective training; (2) the development and evaluation of tactical concepts and doctrine; (3) system test and evaluation; and (4) weapon system concept analysis. Its potential importance is sufficiently great to suggest that special attention be given to issues regarding the desirability or necessity of relevant simulator characteristics. Two such issues are addressed in this document. Specifically, in this document, simulator fidelity and validity issues and applications-based fidelity requirements are addressed in a question-and-answer dialogue format. Secondly, four key drivers of fidelity requirements are identified: (1) the mission to be simulated; (2) the objective(s) of the simulation; (3) the fidelity dimensions; and (4) the simulation components. Thirdly, some conclusions about DIS and the associated fidelity issues are discussed. It is suggested that two parallel trends--the emergence of affordable technology and the continuing drawdowns in military resources--will interact to increase the importance of DIS as a problem-solving tool across a wide variety of potential application areas. It is suggested that the advantages and disadvantages of such DIS applications should be examined carefully and logically for they are capable of providing a powerful supplement or alternative to large-scale field exercises. DTIC

N93-25786# Naval Postgraduate School, Monterey, CA.
A DIGITAL HARDWARE TEST SYSTEM ANALYSIS WITH TEST VECTOR TRANSLATION M.S. Thesis
James T. Loeblein Dec. 1992 106 p
(AD-A260849) Avail: CASI HC A06/MF A02

Digital logic testing occurs in two different test environments, digital simulation and actual hardware testing. A computer aided design (CAD) tool applies a set of stimulus/response test vector patterns to check the functionality of a digital circuit design. Once manufactured, the chip with this design is tested by a hardware tester system (i.e., automatic test equipment (ATE)). The ATE performs many tests in addition to the functionality test. However, the stimulus/response test vector formats used in these two environments are different and, therefore, incompatible in present form. This thesis is aimed at two major objectives. First, a system study will be performed on the GenRad-125 VLSI Hardware Tester System,

including its usage, test capabilities and limitations. Secondly, this thesis addresses the problem of test vector format incompatibility between the two testing environments. Special UNIX tools, Lex and Yacc, are used to create a software translator which changes the CAD simulation file into the GenRad-125 Hardware Test System format. DTIC

N93-25791# Honeywell, Inc., Minneapolis, MN. Systems and Research Center.

SOFTWARE LIFECYCLE SUPPORT ENVIRONMENT (SLCSE) KNOWLEDGE-BASED ENHANCEMENTS Final Report, Sep. 1989 - Jun. 1992

Bhavesh Damania Oct. 1992 41 p

(Contract F30602-89-C-0199)

(AD-A261042; RL-TR-92-249) Avail: CASI HC A03/MF A01

This report summarizes the assessment of the Rome Laboratory Software Life Cycle Support Environment (SLCSE) for potential application of knowledge-based technology. The work performed under this contract included three major tasks: Task 1: Analyze SLCSE; Task 2: Specify Approaches for inserting knowledge-based techniques; Task 3: Develop a Software Requirements Specification and Software Development Plan for incorporating near-term knowledge-based enhancements into the SLCSE. This report provides an overview of these three tasks, and concludes with areas for further evaluation. DTIC

N93-25845# Illinois Univ., Urbana. Dept. of Civil Engineering.

APPLICATIONS OF PARALLEL AND VECTOR ALGORITHMS IN NONLINEAR STRUCTURAL DYNAMICS USING THE FINITE ELEMENT METHOD

Brian E. Healy, David A. Pecknold, and Robert H. Dodds, Jr. Sep. 1992 116 p

(Contract DE-FG02-85ER-25001)

(AD-A260716; UILU-ENG-92-2011; SRS-571) Avail: CASI HC A06/MF A02

This research is directed toward the numerical analysis of large, three dimensional, nonlinear dynamic problems in structural and solid mechanics. Such problems include those exhibiting large deformations, displacements, or rotations, those requiring finite strain plasticity material models that couple geometric and material nonlinearities, and those demanding detailed geometric modeling. A finite element code was developed, designed around the 3D isoparametric family of elements, and using a Total Lagrangian formulation and implicit integration of the global equations of motion. The research was conducted using the Alliant FX/8 and Convex C240 supercomputers. The research focuses on four main areas: Development of element computation algorithms that exploit the inherent opportunities for concurrency and vectorization present in the finite element method; Comparison of the preconditioned conjugate gradient method to a representative direct solver; Investigation of various nonlinear solution algorithms, such as modified Newton-Raphson, secant-Newton, and nonlinear preconditioned conjugate gradient; and, Discovery of an accurate, robust finite strain plasticity material model. DTIC

N93-25942# Defence Research Agency, Malvern (England).

THE SWORD MULTILEVEL SECURE DBMS

Andrew W. Wood, Sharon R. Lewis, and Simon R. Wiseman Feb. 1992 23 p

(RSRE-92005) Copyright Avail: CASI HC A03/MF A01

SWORD is a multilevel secure relational database management system. It adopts the 'Insert Low' approach to the provision of confidentiality controls, rather than the more commonly adopted technique of 'Polyinstantiation'. This allows SWORD to enforce confidentiality and elementary integrity constraints, such as uniqueness. Special techniques allow a multilevel SWORD database to be created and maintained by untrusted database clients working at a single level. In particular, 'Place Holders' allow fields to be created so that the classification of the field's contents dominates the classification of its existence. The report presents an informal description of SWORD and provides a general discussion of the issues. Author (revised)

N93-25943# Los Alamos National Lab., NM.

THE STATE OF COMPUTING AT LOS ALAMOS NATIONAL LABORATORY, FY 1991

Vanessa A. DeLaCruz, ed., Ira A. Agins, Comp., C. Slocomb, M. Trainor, and D. Land Aug. 1992 42 p

(LA-12326-MS; UC-905) Avail: CASI HC A03/MF A01

This study is an effort to provide quantitative data concerning the state of computing at the Los Alamos National Laboratory as of the end of FY-91. It includes information pertaining to the Laboratory's computing equipment inventory, costs associated with the acquisition and support of the Laboratory's computing efforts during that fiscal year, and information related to the Laboratory's central and distributed computing and networking capabilities. The bulk of the data was obtained from the Laboratory's central property and financial databases. Additional information was obtained from the Computing and Communications Division's personal computer and network support organizations. Author (revised)

N93-26150*# George Mason Univ., Fairfax, VA. Dept. of Computer Science.

PERCEPTUAL FACTORS THAT INFLUENCE USE OF COMPUTER ENHANCED VISUAL DISPLAYS Final Report

David Littman and Debbie Boehm-Davis 31 Mar. 1993 37 p

(Grant NAG1-1425)

(NASA-CR-192961; NAS 1.26:192961) Avail: CASI HC A03/MF A01

This document is the final report for the NASA/Langley contract entitled 'Perceptual Factors that Influence Use of Computer Enhanced Visual Displays.' The document consists of two parts. The first part contains a discussion of the problem to which the grant was addressed, a brief discussion of work performed under the grant, and several issues suggested for follow-on work. The second part, presented as Appendix I, contains the annual report produced by Dr. Ann Fulop, the Postdoctoral Research Associate who worked on-site in this project. The main focus of this project was to investigate perceptual factors that might affect a pilot's ability to use computer generated information that is projected into the same visual space that contains information about real world objects. For example, computer generated visual information can identify the type of an attacking aircraft, or its likely trajectory. Such computer generated information must not be so bright that it adversely affects a pilot's ability to perceive other potential threats in the same volume of space. Or, perceptual attributes of computer generated and real display components should not contradict each other in ways that lead to problems of accommodation and, thus, distance judgments. The purpose of the research carried out under this contract was to begin to explore the perceptual factors that contribute to effective use of these displays. Derived from text

N93-26221# Oregon State Univ., Corvallis. Computer Center.

REAL-TIME VALUE-DRIVEN MONITORING AND REPAIR Final Report, 1 Sep. 1990 - 31 Aug. 1992

Bruce Dambrosio 30 Dec. 1992 39 p

(Grant AF-AFOSR-0348-90)

(AD-A260959; OSU-CS-92-30-08; AFOSR-93-0141TR) Avail: CASI HC A03/MF A01

Monitoring and repair (diagnosis, for short) are often thought of as isolated tasks in theoretical reasoning (reasoning with the goal of updating our beliefs about the world). We present a decision-theoretic interpretation of diagnosis as a task in practical reasoning (reasoning with the goal of acting in the world), and sketch components of our approach to this task. These components include an abstract problem description, a decision-theoretic model of the basic task, a set of inference methods suitable for evaluating the decision representation in real-time, and a control architecture to provide the needed continuing coordination between the agent and its environment. A principal contribution of this work is the representation and inference methods we have developed, which extend previously available probabilistic inference methods and narrow, somewhat, the gap between probabilistic and logical models of diagnosis. DTIC

N93-26253# Pittsburgh Univ., PA. Learning Research and Development Center.

ANALYSIS OF SYMBOLIC PARAMETER MODELS Quarterly Progress Report, 1 Oct. - 30 Dec. 1992

Kurt VanLehn 4 Mar. 1993 3 p

(Contract N00014-91-J-1529)

(AD-A261930) Avail: CASI HC A01/MF A01

This letter is the quarterly progress report for the grant entitled 'Analysis of Symbolic Parameter Models.' This report covers only the work done at

the University of Pittsburgh. The report period is 1 Oct. to 30 Dec. 1992. Early in this report period we finally got enough bugs into Deb so that we could see the expected combinatorial explosion. We began exploring some standard techniques for reducing its search. Because Deb is implemented in Prolog and uses its chronological backtracking technique, our first attempt was to try dependency-directed backtracking, which is usually called intelligent backtracking in the Prolog community. Although there are several versions of intelligent backtracking, we discovered that none of them would reduce Deb's research. The results of our research are discussed. DTIC

N93-26257# Arizona Univ., Tucson. Optical Sciences Center.
BAYESIAN CROSS-ENTROPY RECONSTRUCTION OF COMPLEX IMAGES Final Report, 1 Jul. 1991 - 30 Jun. 1992
B. R. Frieden and Anisa T. Bajkova 16 Nov. 1992 21 p
(Contract N00014-91-J-4056)
(AD-A261812) Avail: CASI HC A03/MF A01

Bajkova's generalized maximum entropy method (GMEM) for reconstruction of complex signals has been further generalized through the use of Kullback-Leibler cross entropy. This permits a priori information in the form of bias functions to be inserted into the algorithm, with resulting benefits to reconstruction quality. Also, the cross-entropy term is imbedded within an overall m.a.p. (maximum a posteriori probability) approach that includes a noise-rejection term. A further modification is transformation of the large, two-dimensional problem due to modest-sized 2-D images into a sequence of one-dimensional problems. Finally, the added operation of three-point median window filtration of each intermediary, one-dimensional output is shown to suppress edge-top overshoots while augmenting edge gradients. Applications to simulated complex images are shown. DTIC

N93-26271# Naval Postgraduate School, Monterey, CA.
THE DESIGN AND IMPLEMENTATION OF A REUSABLE COMPONENT LIBRARY AND A RETRIEVAL/INTEGRATION SYSTEM M.S. Thesis
Dogan Ozdemir Dec. 1992 344 p
(AD-A261827) Avail: CASI HC A15/MF A03

Rapid prototyping with automated retrieval of reusable software components is a software development method to construct software systems expeditiously. This thesis describes a tool to enhance the practice of software reuse within the Computer Aided Prototyping System (CAPS). A software base interface provides prototype designers with the means to retrieve components and integrate them into new applications. Reusable components are retrieved from the software base using a formal specification as the search key or through a browser. The specification language used is the Prototype System Description Language (PSDL). The software base stores the reusable components in an object oriented database management system (ONTOS) with an appropriate PSDL specification. Following a query conducted by the PSDL specification, chosen retrieved components are transformed and integrated to the system under development. All software base procedures, including the storage, retrieval, and integration of the components, are conducted through a graphical user interface which is designed to demonstrate and manipulate available software base operations. DTIC

N93-26275# Synectics Corp., Rome, NY.
ARC DIGITAL RASTER IMAGERY (ADRI) DEVELOPMENT Final Report, Feb. - Oct. 1991
Bradley A. Rogers Dec. 1992 39 p
(Contract F30602-91-D-0003)
(AD-A261850; RL-TR-92-265) Avail: CASI HC A03/MF A01

This document gives a general overview of the software developed and is intended to provide the knowledge necessary to understand the capabilities and general operation. A full set of design and testing documents were produced. This document is not intended to be a stand-alone user's manual or maintenance manual. The ADRI development system provides a baseline capability to exploit the ADRI product. It provides the ability to perform point positioning against ADRI, as well as the ability to create a compressed ADRI product. The point positioning capability can be performed utilizing either compressed or noncompressed ADRI. The ADRI data compression subsystem provides the capability to take a raw, noncompressed, ADRI product and compress it by a factor of approximately 18:1. DTIC

N93-26290# Rice Univ., Houston, TX. Dept. of Mathematical Sciences.
LINEAR-PROGRAMMING TOOLS IN INTEGER PROGRAMMING: THE TRAVELING SALESMAN Final Report, 1 Nov. 1991 - 31 Oct. 1992
Robert Bixby 31 Oct. 1992 5 p
(Contract F49620-92-J-0053)
(AD-A261398; AFOSR-93-0092TR) Avail: CASI HC A01/MF A01

New branching rules and new methods to control the size of LP's resulted in a world's record for the solution of large traveling salesman problems. DTIC

N93-26321# National Inst. of Standards and Technology, Gaithersburg, MD. Advanced Systems Div.
SYNTHETIC-PERTURBATION TUNING OF MIMD PROGRAMS
G. Lyon, R. Snelick, and R. Kacker Feb. 1993 30 p See also PB91-222588 Sponsored by DARPA
(PB93-161339; NISTIR-5131) Avail: CASI HC A03/MF A01

Synthetic-perturbation tuning (SPT) is a novel technique for assaying and improving the performance of programs on Multiple-instruction Multiple-data (MIMD) systems. Conceptually, SPT brings the powerful, mathematical perspective of statistically designed experiments (DEX) to the interdependent, sometimes refractory aspects of MIMD program tuning. Practically, SPT provides a needed reconfiguration mechanism via synthetic delays for what otherwise would be ad hoc, hand-tailored program setups for DEX. Overall, the technique identifies bottlenecks in programs directly as quantitative effects upon response time. SPT works on programs for both shared and distributed-memory and it scales well with increasing system size. NTIS

N93-26336# Naval Postgraduate School, Monterey, CA. Dept. of Computer Science.
RESEARCH DIRECTIONS IN SOFTWARE ANALYSIS, SYNTHESIS AND CERTIFICATION
31 Dec. 1992 13 p
(AD-A261367; NPSCS-92-018) Avail: CASI HC A03/MF A01

This paper presents a view of research directions relevant to producing reliable and useful software systems. Appropriate research goals are identified for achieving improvements in software quality via formalization and computer aid for software analysis, synthesis, and certification tasks at all stages of software development and evolution. DTIC

N93-26368# Texas Univ., El Paso.
TOWARDS A FORMALISM FOR PROGRAM GENERATION Final Report, 15 Jun. 1989 - 29 Dec. 1992
Daniel E. Cooke Dec. 1992 31 p
(Contract F49620-89-C-0074)
(AD-A261689; AFOSR-93-0083TR) Avail: CASI HC A03/MF A01

The following was accomplished over the period of the contract: (1) Studied the interaction between iterative and data structures; (2) Completed denotational semantics of BagL; (3) Initiated work on a logic semantic for BagL; (4) Initiated work on a visual interface for BagL; (5) Initiated work on semantic extensions to support software maintenance in BagL; (6) Initiated a revision of BagL semantics; and (7) Initiated work on a BagL interpreter. In the coming years, the researchers hope to complete the BagL interpreter, the logical semantic, and establish the expressiveness of BagL. In the long term, it is hoped to apply results of nonmonotonic logic research to BagL for the purpose of software evolution automation. They also hope to develop a visual interface based upon the formal language. DTIC

N93-26375# Naval Surface Warfare Center, Dahlgren, VA.
AEGIS MEASURES DEFINITION Final Report
Edward J. Dudash and David E. McConnell Mar. 1992 45 p
(AD-A261494; NSWCDD/TR-92/119) Avail: CASI HC A03/MF A01

As part of an effort to improve the development and maintenance processes for AEGIS computer programs at the Naval Surface Warfare Center Dahlgren Division, a software measurement program has been initiated. The measurement program is based on a structure representing the process employed, the products involved, the resources required, and the management controls specified. A standard set of attributes is defined across the software engineering entities as a means of obtaining complete measurement coverage. A life-cycle process model is specified to standardize the collection of required data. Then a set of measures that spans the

entities and attributes and a method for validation of the defined measures is described. The defined measures are intended to be employed as part of a mechanism to provide the objective management necessary to support continuous improvement of AEGIS lifetime processes. DTIC

N93-26378# Carnegie-Mellon Univ., Pittsburgh, PA. School of Computer Science.
SOURCE-LEVEL DEBUGGING OF AUTOMATICALLY PARALLELIZED PROGRAMS Ph.D. Thesis
Robert Cohn 23 Oct. 1992 138 p
(Contract MDA972-90-C-0035; ARPA Order 7330)
(AD-A261520; CMU-CS-92-204) Avail: CASI HC A07/MF A02

Parallelizing compilers automatically translate a sequential program into a parallel program. They simplify parallel programming by freeing the user from the need to consider the details of the parallel architecture and the parallel decomposition. A source-level debugger for automatically parallelized programs hides the parallelism from the user by providing the illusion that the original sequential program is executing. To provide a source-level view, a debugger has two tasks. The first task is to make it appear that programs execute operations in source order. The second task is to hide the decomposition of data and computation. This thesis describes a method for implementing dynamic order restoration and structural mapping in a debugger for automatically parallelized programs. Examples are taken from the domain of loop-based parallelism. DTIC

N93-26431# Naval Postgraduate School, Monterey, CA. Dept. of Mechanical Engineering.
PSEUDO WIGNER-VILLE DISTRIBUTION, COMPUTER PROGRAM, AND ITS APPLICATIONS TO TIME-FREQUENCY DOMAIN PROBLEMS Report, 1 Oct. 1992 - 28 Feb. 1993
Jae-Jin Jeon and Young S. Shin 1 Mar. 1993 87 p
(AD-A261839; NPS-ME-93-002) Avail: CASI HC A05/MF A01

Machinery operating in non-stationary mode generates a signature which at each instant of time has a distinct frequency. A time-frequency domain representation is needed to characterize such a signature.The pseudo-Wigner-Ville distribution is ideally suited for portraying non-stationary signals in the time-frequency domain and is carried out by adapting the fast Fourier transform algorithm. The important parameters affecting the pseudo-Wigner-Ville distribution are discussed and sensitivity analyses are also performed. Practical examples of an actual transient signal are used to illustrate its dynamic features jointly in time and frequency. DTIC

N93-26450# Wisconsin Univ., Madison.
COMPUTATION AND THEORY IN LARGE-SCALE OPTIMIZATION Final Report, 15 Nov. 1990 - 14 Nov. 1992
Stephen M. Robinson 13 Jan. 1993 5 p
(Grant AF-AFOSR-0089-91)
(AD-A261419; AFOSR-93-0144TR) Avail: CASI HC A01/MF A01

The principal objectives of this research project were (1) improvement of algorithms for solving large-scale, block-structured convex programming problems, (2) approximation of optimization problems for purposes of computational solution, and (3) improvement of algorithms for nonsmooth optimization, as well as (4) use of the research results to improve problem-solving ability in application areas. Progress was achieved in all of these areas, and was documented in eight papers prepared for journal publication as well as one Ph.D. dissertation and two technical reports. DTIC

N93-26453# Naval Postgraduate School, Monterey, CA. Dept. of Computer Science.
MANAGING REAL-TIME SOFTWARE PROJECTS: PROBLEMS AND ISSUES
M. S. Luqi, V. Berzins, and L. Chmura 31 Dec. 1992 12 p
(AD-A261428; NPS-CS-92-016) Avail: CASI HC A03/MF A01

Hard real-time systems are defined as those software system in which the correctness of the system depends not only on the logical result of computation, but also on the time at which the results are produced. Hard real-time systems of interest to DoD are tailored specifically to their applications, employ various degrees of fault-tolerance, and are typically embedded in larger systems. The process of design and development of these systems is often plagued with uncertainty, ambiguity and inconsistency. This report examines problems and issues in managing real-time software projects. DTIC

N93-26461# Institute for Defense Analyses, Alexandria, VA.
CALS-HSC DATA ELEMENT DICTIONARY Final Report, Mar. 1991 - Oct. 1992
Earl A. Alluisi Oct. 1992 113 p
(Contract MDA903-89-C-0003)
(AD-A261560; IDA-D-1183; IDA/HQ-92-42001; AD-E501629) Avail: CASI HC A06/MF A02

The data element dictionary (DED) presented was developed under a human system integration (HSI) effort to integrate all human system components (HSC) into the weapon system acquisition process as part of a joint Department of Defense (DoD)-industry initiative in computer-assisted acquisition and logistic support/concurrent engineering (CALS/CE). The present version of the CALS-HSC data element dictionary evolved from an earlier CALS-Training DED developed at the Defense Training and Performance Data Center, Orlando, Florida, and augmented later with HSC data elements that extend beyond training. The final set of over 430 data elements was coordinated through the CALS-HSC Work Group with representatives of the DoD and industry, first in May 1990 and more recently in April, May, and June 1992. Although the materials presented constitute a current baseline for the CALS-HSC DED, they are viewed as comprising a living document to be amended and updated continuously. DTIC

N93-26563# Mystech Associates, Inc., Middletown, RI.
SYSTEM CONCEPT OF OPERATIONS EVALUATOR (SCOPE) Final Report, Mar. 1991 - Sep. 1992
Terry R. Raymond and David A. Hathaway Nov. 1992 37 p
(Contract N66604-90-D-0104)
(AD-A261257; D-N01-92; AL-TR-1992-0161) Avail: CASI HC A03/MF A01

Command and control centers and operations centers are environments in which information must be collected, processed, integrated and analyzed in order to accomplish specific missions. To be operationally and economically effective, the system design of these centers and the design of their concept of operations must be coordinated. This is a complex task due to the myriad of information available, the variety and limits of technologies that can be incorporated into the center, and the very large number of activities and information that the technology must support. The System Concept of Operations Evaluator (SCOPE) provides the designer with a tool to address this problem. It enables the designers to capture the complex relationships between various system objects using an object-oriented representation. Furthermore, it facilitates the comparison of alternatives by providing a layered construction process where all the alternatives in a layer utilize the same knowledge defined in the underlying layer. The designer can then analyze either the static relationships of a model or simulate a scenario using discrete event simulation. This report describes the model building concepts and tools concepts of SCOPE. DTIC

N93-26583# Software Productivity Consortium, Herndon, VA.
THREE VIEW LANGUAGE: A GRAPHICS-BASED LANGUAGE FOR REQUIREMENTS DEFINITION, VERSION 01.00.00
Paul Ward Mar. 1993 23 p
(Contract MDA972-92-J-1018)
(AD-A261732; SPC-92114-CMC) Avail: CASI HC A03/MF A01

Viewgraphs on Three View Language (3VL): a graphics-based language for requirements definition are presented. 3VL is an extension of the Harel statechart-activity chart notation which provides a comprehensive operational semantics encompassing the data, functional, and behavioral views and provides dynamic creation adn deletion of objects. 3VL is designed explicitly for use on an interactive electronic display medium, extensive use is made of colors and textures to aid comprehension. CASI

N93-24662*# Jet Propulsion Lab., California Inst. of Tech., Pasadena.
SOFT DECODING A SELF-DUAL (48, 24; 12) CODE
G. Solomon *In its* The Telecommunications and Data Acquisition Report 15 Feb. 1993 p 17-18 (For primary document see N93-24659 09-32)
(RTOP 310-30-71-83-02)
Avail: CASI HC A01/MF A02

N93-24663*# Jet Propulsion Lab., California Inst. of Tech., Pasadena.
A (72, 36; 15) BOX CODE
G. Solomon *In its* The Telecommunications and Data Acquisition Report 19-21 (SEE N93-24659 09-32) 15 Feb. 1993 (For primary document see N93-24659 09-32)
(RTOP 310-30-71-83-02)
Avail: CASI HC A01/MF A02

N93-24664*# Jet Propulsion Lab., California Inst. of Tech., Pasadena.
THE ANALYSIS OF CONVOLUTIONAL CODES VIA THE EXTENDED SMITH ALGORITHM
R. J. McEliece and I. Onyszchuk *In its* The Telecommunications and Data Acquisition Report 15 Feb. 1993 p 22-30 (For primary document see N93-24659 09-32)
(RTOP 310-30-71-83-02)
Avail: CASI HC A02/MF A02

N93-24665*# Jet Propulsion Lab., California Inst. of Tech., Pasadena.
IMAGE CODING BY WAY OF WAVELETS
M. Shahshahani *In its* The Telecommunications and Data Acquisition Report 15 Feb. 1993 p 31-36 (For primary document see N93-24659 09-32)
(RTOP 310-30-71-83-02)
Avail: CASI HC A02/MF A02

N93-24709*# McDonnell-Douglas Space Systems Co., Huntington Beach, CA.
COMPUTATIONALLY EFFICIENT ALGORITHMS FOR REAL-TIME ATTITUDE ESTIMATION
Steven R. Pringle *In* NASA. Goddard Space Flight Center, Flight Mechanics/Estimation Theory Symposium, 1992 Feb. 1993 p 217-225 (For primary document see N93-24694 09-13)
Copyright Avail: CASI HC A02/MF A04

N93-24711*# National Aeronautics and Space Administration. Goddard Space Flight Center, Greenbelt, MD.
POLAR DECOMPOSITION FOR ATTITUDE DETERMINATION FROM VECTOR OBSERVATIONS
Itzhack Y. Bar-Itzhack (Technion - Israel Inst. of Tech., Haifa.) *In its* Flight Mechanics/Estimation Theory Symposium, 1992 Feb. 1993 p 243-257 (For primary document see N93-24694 09-13)
Copyright Avail: CASI HC A03/MF A04

N93-24722*# Lockheed Technical Operations Co., Crofton, MD.
ANALYSIS OF THE COMMAND AND CONTROL SEGMENT (CCS) ATTITUDE ESTIMATION ALGORITHM
Catherine Stockwell *In* NASA. Goddard Space Flight Center, Flight Mechanics/Estimation Theory Symposium, 1992 Feb. 1993 p 413-421 Prepared for Consolidated Space Test Center, Onizuka AFB, CA (For primary document see N93-24694 09-13)
Copyright Avail: CASI HC A02/MF A04

N93-24731*# National Aeronautics and Space Administration. Goddard Space Flight Center, Greenbelt, MD.
ATTITUDE DETERMINATION USING VECTOR OBSERVATIONS: A FAST OPTIMAL MATRIX ALGORITHM
F. Landis Markley *In its* Flight Mechanics/Estimation Theory Symposium, 1992 Feb. 1993 p 537-551 (For primary document see N93-24694 09-13)
Copyright Avail: CASI HC A03/MF A04

N93-25575*# Supercomputer Research Center, Bowie, MD.
SPLASH 2
Jeffrey M. Arnold, Duncan A. Buell, and Walter J. Kleinfelder *In* NASA, Washington, Technology 2002: The Third National Technology Transfer Conference and Exposition, Volume 1 Feb. 1993 p 139-145 (For primary document see N93-25561 09-99)
Avail: CASI HC A02/MF A04

N93-25589*# National Aeronautics and Space Administration. Goddard Space Flight Center, Greenbelt, MD.
THE GENERIC SPACECRAFT ANALYST ASSISTANT (GenSAA): A TOOL FOR DEVELOPING GRAPHICAL EXPERT SYSTEMS
Peter M. Hughes *In* NASA, Washington, Technology 2002: The Third National Technology Transfer Conference and Exposition, Volume 1 Feb. 1993 p 268-278 (For primary document see N93-25561 09-99)
Avail: CASI HC A03/MF A04

N93-25590*# National Aeronautics and Space Administration. Lyndon B. Johnson Space Center, Houston, TX.
TARGET: RAPID CAPTURE OF PROCESS KNOWLEDGE
C. J. Ortiz, H. V. Ly, T. Saito (Computer Sciences Corp., Houston, TX.), and R. B. Loftin (Houston Univ., TX.) *In* NASA, Washington, Technology 2002: The Third National Technology Transfer Conference and Exposition, Volume 1 Feb. 1993 p 279-288 (For primary document see N93-25561 09-99)
Avail: CASI HC A02/MF A04

N93-25591*# Research Inst. for Advanced Computer Science, Moffett Field, CA.
TREE CLASSIFICATION SOFTWARE
Wray Buntine *In* NASA, Washington, Technology 2002: The Third National Technology Transfer Conference and Exposition, Volume 1 Feb. 1993 p 289-298 (For primary document see N93-25561 09-99)
Avail: CASI HC A02/MF A04

N93-25600*# Sterling Software, Moffett Field, CA.
SCIENTIFIC VISUALIZATION USING THE FLOW ANALYSIS SOFTWARE TOOLKIT (FAST)
Gordon V. Bancroft, Paul G. Kelaita, R. Kevin McCabe, Fergus J. Merritt, Todd C. Plessel, Timothy A. Sandstrom, and John T. West *In* NASA, Washington, Technology 2002: The Third National Technology Transfer Conference and Exposition, Volume 1 Feb. 1993 p 366-375 (For primary document see N93-25561 09-99)
Avail: CASI HC A02/MF A04

N93-25601*# National Aeronautics and Space Administration. Langley Research Center, Hampton, VA.
INTEGRATION OF DESIGN, THERMAL, STRUCTURAL, AND OPTICAL ANALYSIS, INCLUDING THERMAL ANIMATION
Ruth M. Amundsen *In* NASA, Washington, Technology 2002: The Third National Technology Transfer Conference and Exposition, Volume 1 Feb. 1993 p 376-384 (For primary document see N93-25561 09-99)
Avail: CASI HC A02/MF A04

N93-25602*# National Aeronautics and Space Administration. Goddard Space Flight Center, Greenbelt, MD.
DATA SYSTEMS DYNAMIC SIMULATOR
Christopher Rouff, Melana Clark, Bill Davenport, and Philip Message (Stanford Telecommunications, Inc., Seabrook, MD.) *In* NASA, Washington, Technology 2002: The Third National Technology Transfer Conference and Exposition, Volume 1 Feb. 1993 p 385-393 (For primary document see N93-25561 09-99)
Avail: CASI HC A02/MF A04

N93-25603*# Johns Hopkins Univ., Laurel, MD. Electro-Optical Systems Group.
A NOVEL OPTICAL/DIGITAL PROCESSING SYSTEM FOR PATTERN RECOGNITION
Bradley G. Boone and Oodaye B. Shukla *In* NASA, Washington, Technology 2002: The Third National Technology Transfer Conference and Exposition, Volume 1 Feb. 1993 p 397-406 (For primary document see N93-25561 09-99)
Avail: CASI HC A02/MF A04

N93-25613*# National Aeronautics and Space Administration. Lyndon B. Johnson Space Center, Houston, TX.
A GENETIC ALGORITHM TOOL (SPLICER) FOR COMPLEX SCHEDULING PROBLEMS AND THE SPACE STATION FREEDOM RESUPPLY PROBLEM
Lui Wang and Manuel Valenzuela-Rendon (Instituto Technologico y de

Estudios Superiores de Monterrey, Mexico.) *In* NASA, Washington, Technology 2002: The Third National Technology Transfer Conference and Exposition, Volume 1 Feb. 1993 p 491-500 Sponsored in part by Inst. Technologico y de Estudios Superiores de Monterrey (For primary document see N93-25561 09-99)
(Contract NCC9-16)
Avail: CASI HC A02/MF A04

N93-25799*# National Aeronautics and Space Administration. Ames Research Center, Moffett Field, CA.
CONSTRUCTION OF AN ADVANCED SOFTWARE TOOL FOR PLANETARY ATMOSPHERIC MODELING
Peter Friedland, Richard M. Keller, Christopher P. McKay, Michael H. Sims, and David E. Thompson *In* Colorado Univ., Applied Information Systems Research Program (AISRP). Workshop 2: Meeting Proceedings 1992 2 p (For primary document see N93-25792 09-82)
Avail: CASI HC A01/MF A03

N93-26075*# Ambassador Coll., Big Sandy, TX. Dept. of Computer Information Systems.
DISTRIBUTED PROJECT SCHEDULING AT NASA: REQUIREMENTS FOR MANUAL PROTOCOLS AND COMPUTER-BASED SUPPORT Final Report
Stephen F. Richards *In* NASA. Johnson Space Center, National Aeronautics and Space Administration (NASA)/American Society for Engineering Education (ASEE) Summer Faculty Fellowship Program, 1992, Volume 2 Dec. 1992 13 p (For primary document see N93-26070 09-99)
(Grant NGT-44-005-803)
Avail: CASI HC A03/MF A02

N93-26116*# Solomon (G.), Pasadena, CA.
GOLAY AND OTHER BOX CODES
G. Solomon *In* JPL, The Telecommunications and Data Acquisition Report 15 May 1992 p 130-135 (For primary document see N93-26105 09-32)
(RTOP 310-30-71-83-02)
Avail: CASI HC A02/MF A04

62 COMPUTER SYSTEMS

Includes computer networks and special application computer systems.

N93-24748*# Illinois Univ., Urbana-Champaign. Coordinated Science Lab.
ANALYSIS OF LARGE SYSTEM BLACK BOX VERIFICATION TEST DATA
Kenneth C. Clapp (Bell Telephone Labs., Inc., Naperville, IL.) and Ravishankar Krishnan Iyer Apr. 1993 51 p
(Contract NAG1-613; N00014-91-J-1116)
(NASA-CR-192885; NAS 1.26:192885; UILU-ENG-93-2212; CRHC-93-05)
Avail: CASI HC A04/MF A01

Issues regarding black box, large systems verification are explored. It begins by collecting data from several testing teams. An integrated database containing test, fault, repair, and source file information is generated. Intuitive effectiveness measures are generated using conventional black box testing results analysis methods. Conventional analysts methods indicate that the testing was effective in the sense that as more tests were run, more faults were found. Average behavior and individual data points are analyzed. The data is categorized and average behavior shows a very wide variation in number of tests run and in pass rates (pass rates ranged from 71 percent to 98 percent). The 'white box' data contained in the integrated database is studied in detail. Conservative measures of effectiveness are discussed. Testing efficiency (ratio of repairs to number of tests) is measured at 3 percent, fault record effectiveness (ratio of repairs to fault records) is measured at 55 percent, and test script redundancy (ratio of number of failed tests to minimum number of tests needed to find the faults) ranges from 4.2 to 15.8. Error prone source files and subsystems are identified. A correlational mapping of test functional area to product subsystem is completed. A new adaptive testing process based on real-time generation of the integrated database is proposed. Author (revised)

N93-24749*# Illinois Univ., Urbana-Champaign. Coordinated Science Lab.
OPTIMAL MESSAGE LOG RECLAMATION FOR INDEPENDENT CHECKPOINTING
Yi-Min Wang and W. Kent Fuchs 14 Apr. 1993 22 p Sponsored in part by ICLASS
(Contract NAG1-613; N00014-91-J-1283)
(NASA-CR-192886; NAS 1.26:192886; UILU-ENG-93-2213; CRHC-93-07)
Avail: CASI HC A03/MF A01

Independent (uncoordinated) check pointing for parallel and distributed systems allows maximum process autonomy but suffers from possible domino effects and the associated storage space overhead for maintaining multiple checkpoints and message logs. In most research on check pointing and recovery, it was assumed that only the checkpoints and message logs older than the global recovery line can be discarded. It is shown how recovery line transformation and decomposition can be applied to the problem of efficiently identifying all discardable message logs, thereby achieving optimal garbage collection. Communication trace-driven simulation for several parallel programs is used to show the benefits of the proposed algorithm for message log reclamation. Author (revised)

N93-25251*# California Univ., Berkeley. Computer Science Div.
A TRACE-DRIVEN ANALYSIS OF NAME AND ATTRIBUTE CACHING IN A DISTRIBUTED SYSTEM
Ken W. Shirriff and John K. Ousterhout May 1992 18 p
(Grants NAG2-591; NSF CCR-89-00029)
(NASA-CR-192899; NAS 1.26:192899) Avail: CASI HC A03/MF A01

This paper presents the results of simulating file name and attribute caching on client machines in a distributed file system. The simulation used trace data gathered on a network of about 40 workstations. Caching was found to be advantageous: a cache on each client containing just 10 directories had a 91 percent hit rate on name look ups. Entry-based name caches (holding individual directory entries) had poorer performance for several reasons, resulting in a maximum hit rate of about 83 percent. File attribute caching obtained a 90 percent hit rate with a cache on each machine of the attributes for 30 files. The simulations show that maintaining cache consistency between machines is not a significant problem; only 1 in 400 name component look ups required invalidation of a remotely cached entry. Process migration to remote machines had little effect on caching. Caching was less successful in heavily shared and modified directories such as /tmp, but there weren't enough references to /tmp overall to affect the results significantly. We estimate that adding name and attribute caching to the Sprite operating system could reduce server load by 36 percent and the number of network packets by 30 percent.
Author (revised)

N93-25297*# California Univ., Berkeley.
RAMA: A FILE SYSTEM FOR MASSIVELY PARALLEL COMPUTERS
Ethan L. Miller and Randy H. Katz 1993 7 p
(Grant NAG2-591)
(NASA-CR-192906; NAS 1.26:192906) Avail: CASI HC A02/MF A01

This paper describes a file system design for massively parallel computers which makes very efficient use of a few disks per processor. This overcomes the traditional I/O bottleneck of massively parallel machines by storing the data on disks within the high-speed interconnection network. In addition, the file system, called RAMA, requires little inter-node synchronization, removing another common bottleneck in parallel processor file systems. Support for a large tertiary storage system can easily be integrated in lo the file system; in fact, RAMA runs most efficiently when tertiary storage is used. Author

N93-25304# Lawrence Livermore National Lab., CA.
PROCEEDINGS OF THE SECOND SISAL USERS' CONFERENCE
J. T. Feo, ed., C. Frerking, ed., and P. J. Miller, ed. Dec. 1992 273 p Conference held in San Diego, CA, 4-5 Oct. 1992
(Contract W-7405-eng-48)
(DE93-008019; CONF-9210270) Avail: CASI HC A12/MF A03

Papers on the following topics are included: a Sisal code for computing the fourier transform on S(sub N); five ways to fill your knapsack; simulating material dislocation motion in Sisal; candis as an interface for Sisal; parallelization and performance of the burg algorithm on a shared-memory multiprocessor; use of genetic algorithm in Sisal to solve the file design

problem; implementing FFT's in Sisal; programming and evaluating the performance of signal processing applications in the Sisal programming environment; Sisal and Von Neumann-based languages: translation and intercommunication; an IF2 code generator for ADAM architecture; program partitioning for NUMA multiprocessor computer systems; mapping functional parallelism on distributed memory machines; implicit array copying: prevention is better than cure; mathematical syntax for Sisal; an approach for optimizing recursive functions; implementing arrays in Sisal 2.0; Fol: an object oriented extension to the Sisal language; twine: a portable, extensible sisal execution kernel; and investigating the memory performance of the optimizing sisal compiler. DOE

N93-25316# Los Alamos National Lab., NM.
STRUCTURED ADAPTIVE MESH REFINEMENT ON THE CONNECTION MACHINE
M. J. Berger and J. S. Saltzman 1993 5 p Presented at the 6th Society for Industrial and Applied Mathematics Conference on Parallel Processing for Scientific Computing, Norfolk, VA, 21-24 Mar. 1993
(Contract W-7405-eng-36)
(DE93-007368; LA-UR-93-302; CONF-930331-1) Avail: CASI HC A01/MF A01

Adaptive mesh refinement has proven itself to be a useful tool in a large collection of applications. By refining only a small portion of the computational domain, computational savings of up to a factor of 80 in 3 dimensional calculations have been obtained on serial machines. A natural question is, can this algorithm be used on massively parallel machines and still achieve the same efficiencies? A data layout scheme for mapping grid points to processors that preserves locality and minimizes global communication was designed for the CM-200. The effect of the data layout scheme is that at the finest level nearby grid points from adjacent grids in physical space are in adjacent memory locations. Furthermore, coarse grid points are arranged in memory to be near their associated fine grid points. Applications of the algorithm to inviscid compressible fluid flow in two space dimensions is shown. DOE

N93-25414# Oak Ridge National Lab., TN.
TOWARD A PARALLEL RECURSIVE SPECTRAL BISECTION MAPPING TOOL
C. A. Leete, B. W. Peyton, and R. F. Sincovec 1993 6 p Presented at the 6th Society for Industrial and Applied Mathematics (SIAM) Conference on Parallel Processing for Scientific Computing, Norfolk, VA, 21-24 Mar. 1993
(Contract DE-AC05-84OR-21400)
(DE93-006632; CONF-930331-3) Avail: CASI HC A02/MF A01

Recent work has shown that the recursive spectral bisection (RSB) partitioning algorithm results in good load balance and low communication costs for PDE calculations on a distributed- multiprocessor. We have enhanced a recent implementation of the method in the following three ways: we have (1) developed parallel implementation, (2) used simple 'proportional mapping' ideas to handle an arbitrary number of processes, and (3) implemented a more flexible load balancing technique. Our tests indicate that the latter two enhancements are quite effective. We also report timings obtained on an Intel iPSC/860. DOE

N93-25458*# California Univ., Berkeley.
INTERFACING A HIGH PERFORMANCE DISK ARRAY FILE SERVER TO A GIGABIT LAN
Srinivasan Seshan and Randy H. Katz 21 Apr. 1993 19 p
(Grant NAG2-591)
(NASA-CR-192898; NAS 1.26:192898) Avail: CASI HC A03/MF A01

Our previous prototype, RAID-1, identified several bottlenecks in typical file server architectures. The most important bottleneck was the lack of a high-bandwidth path between disk, memory, and the network. Workstation servers, such as the Sun-4/280, have very slow access to peripherals on busses far from the CPU. For the RAID-2 system, we addressed this problem by designing a crossbar interconnect, Xbus board, that provides a 40MB/s path between disk, memory, and the network interfaces. However, this interconnect does not provide the system CPU with low latency access to control the various interfaces. To provide a high data rate to clients on the network, we were forced to carefully and efficiently design the network software. A block diagram of the system hardware architecture is given. In the following subsections, we describe pieces of the RAID-2 file server hardware that had a significant impact on the design of the network interface. Derived from text

N93-25481 Florida Univ., Gainesville.
A SOFTWARE DEVELOPMENT APPROACH FOR PARALLEL PROCESSING SYSTEMS INTEGRATING OBJECT-ORIENTED AND FUNCTIONAL PARADIGMS Ph.D. Thesis
Doo-Hwan Bae 1992 167 p
Avail: Univ. Microfilms Order No. DA9303966

Although there are many parallel computers available, the effective use of their computing power is difficult to achieve due to the lack of proper software development methods and techniques for parallel processing systems. In this dissertation, we present a computation model, called PROOF (PaRallel Object-Oriented Functional) as a basis for expressing parallelism, and an intermediate form, called IPR (Intermediate Program Representation) as a basis for exploiting parallelism in software development for parallel processing systems. We also present grain size determination techniques on different types of parallelism. We develop the computation model PROOF in which the object-oriented paradigm is integrated with the functional paradigm without sacrificing the advantages of either. The major features of our computation model include expressing the various granularity levels of parallelism, integrating the referential transparency and history sensitivity, and supporting inheritance and synchronization without interference. The computation model PROOF serves as a basis for developing our approach to the software development for parallel processing systems. We develop the IPR, which is used for representing all the parallelism in the software and performing partitioning analysis. We develop transformation rules from a PROOF code to the IPR and from the IPR to a target code and show that the transformation rules preserve the correctness of the original PROOF programs. For efficient exploitation of parallelism, we present the grain size determination algorithms on various patterns of parallelism and compare them with the existing approaches. Software development based on PROOF has the following distinct advantages: First, parallel aspects of the software can be treated as a prime issue, using object-oriented concepts. Second, our approach can reduce the communication and synchronization errors by automatically embedding proper codes during the transformation stage. Third, the use of the IPR improves portability of the software by separating architecture-dependent issues from the semantics of the software.
Dissert. Abstr.

N93-25521# Argonne National Lab., IL.
PARALLELIZING THE SPECTRAL TRANSFORM METHOD: A COMPARISON OF ALTERNATIVE PARALLEL ALGORITHMS
I. Foster and P. H. Worley (Oak Ridge National Lab., TN.) 1993 9 p Presented at the 6th Society for Industrial and Applied Mathematics Conference on Parallel Processing for Scientific Computing, Norfolk, VA, 21-24 Mar. 1993
(Contract W-31-109-eng-38)
(DE93-008664; ANL/MCS/CP-78727; CONF-930331-6) Avail: CASI HC A02/MF A01

The spectral transform method is a standard numerical technique for solving partial differential equations on the sphere and is widely used in global climate modeling. In this paper, we outline different approaches for parallelizing the method and describe experiments that we are conducting to evaluate the efficiency of these approaches on parallel computers. The experiments are conducted using a testbed code that solves the nonlinear shallow water equations on a sphere, but are designed to permit evaluation in the context of a global model. They allow us to evaluate the relative merits of the approaches as a function of problem size and number of processors. The results of this study are guiding ongoing work on PCCM2, a parallel implementation of the Community Climate Model developed at the National Center for Atmospheric Research. DOE

N93-25522# Argonne National Lab., IL.
DETERMINISTIC PARALLEL FORTRAN
K. M. Chandy (California Inst. of Tech., Pasadena.) and I. Foster 1993 9 p Presented at the 6th Society for Industrial and Applied Mathematics Conference on Parallel Processing for Scientific Computing, Norfolk, VA, 21-24 Mar. 1993
(Contract W-31-109-eng-38; NSF CCR-88-09615)

(DE93-008665; ANL/MCS/CP-78728; CONF-930331-7) Avail: CASI HC A02/MF A01

We describe FORTRAN M. FORTRAN M is comprised of message-passing extensions to FORTRAN 77 that provide deterministic execution and information hiding while preserving the desirable properties of message passing. DOE

N93-26169# Johns Hopkins Univ., Baltimore, MD.
COMPLEXITY OF CONNECTIONIST AND CONSTRAINT-SATISFACTION NETWORKS Final Report, 1 Dec. 1988 - 30 Apr. 1992
Simon Kasif 30 Apr. 1992 10 p
(Grant AF-AFOSR-0151-89)
(AD-A261617; AFOSR-93-0074TR) Avail: CASI HC A02/MF A01

Since the beginning of the funding of the grant, we established a substantial effort in the area of connectionist optimization algorithms, relaxation networks, and geometrical learning algorithms. All of the above are highly interconnected research projects. We have achieved several significant results that have increased our understanding of the computational capabilities and limitations, of connectionist and constraint network. Our most significant contributions thus far are in the area of parallel complexity of constraint networks, comparative experimentation with learning algorithms, and geometric concept learning. Our results in the area of parallel constraint networks are the subject of several publications in journals and conferences. Our experimental research achieves the best results on several well established benchmarks. Most notably our group achieved the best results (in terms of predictions accuracy) in the area of protein folding. The technical results of the research investigations are summarized in the following sections. DTIC

N93-26277# Minnesota Supercomputer Center, Inc., Minneapolis.
VERY HIGH-SPEED REPORT FILE SYSTEM Final Report, 20 Sep. 1991 - 19 Sep. 1992
Timothy J. Salo, John D. Cavanaugh, and Michael K. Spengler 15 Dec. 1992 71 p
(Contract DAAL03-91-C-0049)
(AD-A261068; ARO-29396.1-MA) Avail: CASI HC A04/MF A01

The Minnesota Supercomputer Center, Inc. (MSCI), under its Very High-Speed Remote File System (VHSRFS) contract with the Army Research Office, conducted research in: Technologies for integrating TCP/EP protocols with ATM networks; Technologies which will enable gigabit-per-second local area networks (LAN's) and high-performance hosts to use gigabit-speed ATM wide-area networks; Methods by which high-performance, massively parallel processors (MPP's) can connect to high-speed wide-area networks; and Protocols and other technologies required to develop a shared, remote file system capable of transferring data to multiple remote supercomputers over gigabit wide-area networks. The research results of the VHSRFS contract were intended to provide some of the foundation for research in the MAGIC Gigabit Testbed, which has been funded by DARPA. DTIC

N93-26338# Carnegie-Mellon Univ., Pittsburgh, PA. School of Computer Science.
SIGNED VECTOR TIMESTAMPS: A SECURE PROTOCOL FOR PARTIAL ORDER TIME
Sean W. Smith and J. D. Tygar Feb. 1993 17 p Sponsored in part by ONR
(Contract F33615-90-C-1465; NSF CCR-88-58087)
(AD-A261371; CMU-CS-93-116-REV) Avail: CASI HC A03/MF A01

The language of partial order time expresses the issues central to many problems in asynchronous distributed systems. A secure partial order time service would provide a general method to develop secure protocols for these problems. In this paper, we sketch out these issues and develop one such protocol: signed vector timestamps. The majority of this paper is drawn verbatim from the first author's October 1991 thesis proposal, the first research into security issues for non-scalar time services and the original presentation of the SVT protocol. DTIC

N93-25576*# Symbiotics, Inc., Cambridge, MA.
OBJECT-ORIENTED TOOLS FOR DISTRIBUTED COMPUTING
Richard M. Adler *In* NASA, Washington, Technology 2002: The Third National Technology Transfer Conference and Exposition, Volume 1 Feb. 1993 p 146-155 (For primary document see N93-25561 09-99)
(Contracts NAS10-11606; NAS10-11882; NAS5-31920; NAS8-39343; DAAB10-87-C-0053)
Avail: CASI HC A02/MF A04

63 CYBERNETICS

Includes feedback and control theory, artificial intelligence, robotics and expert systems.

For related information see also *54 Man/System Technology and Life Support.*

N93-24743*# Rensselaer Polytechnic Inst., Troy, NY. Dept. of Electrical, Computer, and Systems Engineering.
USING NEURAL NETWORKS AND DYNA ALGORITHM FOR INTEGRATED PLANNING, REACTING AND LEARNING IN SYSTEMS
Pedro Lima and Randal Beard Aug. 1992 27 p
(Grant NAGw-1333)
(NASA-CR-193018; NAS 1.26:193018; CIRSSE-122) Avail: CASI HC A03/MF A01

The traditional AI answer to the decision making problem for a robot is planning. However, planning is usually CPU-time consuming, depending on the availability and accuracy of a world model. The Dyna system generally described in earlier work, uses trial and error to learn a world model which is simultaneously used to plan reactions resulting in optimal action sequences. It is an attempt to integrate planning, reactive, and learning systems. The architecture of Dyna is presented. The different blocks are described. There are three main components of the system. The first is the world model used by the robot for internal world representation. The input of the world model is the current state and the action taken in the current state. The output is the corresponding reward and resulting state. The second module in the system is the policy. The policy observes the current state and outputs the action to be executed by the robot. At the beginning of program execution, the policy is stochastic and through learning progressively becomes deterministic. The policy decides upon an action according to the output of an evaluation function, which is the third module of the system. The evaluation function takes the following as input: the current state of the system, the action taken in that state, the resulting state, and a reward generated by the world which is proportional to the current distance from the goal state. Originally, the work proposed was as follows: (1) to implement a simple 2-D world where a 'robot' is navigating around obstacles, to learn the path to a goal, by using lookup tables; (2) to substitute the world model and Q estimate function Q by neural networks; and (3) to apply the algorithm to a more complex world where the use of a neural network would be fully justified. In this paper, the system design and achieved results will be described. First we implement the world model with a neural network and leave Q implemented as a look up table. Next, we use a lookup table for the world model and implement the Q function with a neural net. Time limitations prevented the combination of these two approaches. The final section discusses the results and gives clues for future work. Derived from text

N93-24757*# Tennessee State Univ., Nashville. Center for Excellence in Information Systems.
ROBUST CONTROLS WITH STRUCTURED PERTURBATIONS Final Report
Leehyun Keel May 1993 47 p
(Grant NAG1-863)
(NASA-CR-192956; NAS 1.26:192956) Avail: CASI HC A03/MF A01

This final report summarizes the recent results obtained by the principal investigator and his coworkers on the robust stability and control of systems containing parametric uncertainty. The starting point is a generalization of Kharitonov's theorem obtained in 1989, and its generalization to the multilinear case, the singling out of extremal stability subsets, and other ramifications now constitutes an extensive and coherent theory of robust parametric stability that is summarized in the results contained here. Author (revised)

N93-25137*# Stanford Univ., CA. Dept. of Electrical Engineering.
TWO NEURAL NETWORK ALGORITHMS FOR DESIGNING OPTIMAL TERMINAL CONTROLLERS WITH OPEN FINAL TIME
Edward S. Plumer Oct. 1992 24 p

(Grant NGT-50642)
(NASA-CR-177599; A-92194; NAS 1.26:177599) Avail: CASI HC A03/MF A01

Multilayer neural networks, trained by the backpropagation through time algorithm (BPTT), have been used successfully as state-feedback controllers for nonlinear terminal control problems. Current BPTT techniques, however, are not able to deal systematically with open final-time situations such as minimum-time problems. Two approaches which extend BPTT to open final-time problems are presented. In the first, a neural network learns a mapping from initial-state to time-to-go. In the second, the optimal number of steps for each trial run is found using a line-search. Both methods are derived using Lagrange multiplier techniques. This theoretical framework is used to demonstrate that the derived algorithms are direct extensions of forward/backward sweep methods used in N-stage optimal control. The two algorithms are tested on a Zermelo problem and the resulting trajectories compare favorably to optimal control results. Author

N93-25138*# National Aeronautics and Space Administration. Lyndon B. Johnson Space Center, Houston, TX.

HOW TO COMBINE PROBABILISTIC AND FUZZY UNCERTAINTIES IN FUZZY CONTROL

Hung T. Nguyen (Tokyo Inst. of Tech., Yokahama, Japan.), Vladik Ya. Kreinovich (Texas Univ., El Paso.), and Robert Lea 1991 4 p
(Grants NAG9-482; NSF CDA-90-15006)
(NASA-TM-108746; NAS 1.15:108746) Avail: CASI HC A01/MF A01

Fuzzy control is a methodology that translates natural-language rules, formulated by expert controllers, into the actual control strategy that can be implemented in an automated controller. In many cases, in addition to the experts' rules, additional statistical information about the system is known. It is explained how to use this additional information in fuzzy control methodology. Author (revised)

N93-25141*# National Aeronautics and Space Administration. Lyndon B. Johnson Space Center, Houston, TX.

MAXIMUM ENTROPY APPROACH TO FUZZY CONTROL

Arthur Ramer (New South Wales Univ., Kensington, Australia.) and Vladik Ya. Kreinovich (Texas Univ., El Paso.) 1992 5 p
(Grants NAG9-482; NSF CDA-90-15006)
(NASA-CR-192949; NAS 1.26:192949) Avail: CASI HC A01/MF A01

For the same expert knowledge, if one uses different &- and V-operations in a fuzzy control methodology, one ends up with different control strategies. Each choice of these operations restricts the set of possible control strategies. Since a wrong choice can lead to a low quality control, it is reasonable to try to loose as few possibilities as possible. This idea is formalized and it is shown that it leads to the choice of min(a + b,1) for V and min(a,b) for &. This choice was tried on NASA Shuttle simulator; it leads to a maximally stable control. Author (revised)

N93-25142*# National Aeronautics and Space Administration. Lyndon B. Johnson Space Center, Houston, TX.

HOW TO CONTROL IF EVEN EXPERTS ARE NOT SURE: ROBUST FUZZY CONTROL

Hung T. Nguyen (Tokyo Inst. of Tech., Yokahama, Japan.), Vladik Ya. Kreinovich (Texas Univ., El Paso.), Robert Lea, and Dana Tolbert 1992 10 p
(Grants NAG9-482; NSF CDA-90-15006)
(NASA-TM-108745; NAS 1.15:108745) Avail: CASI HC A02/MF A01

In real life, the degrees of certainty that correspond to one of the same expert can differ drastically, and fuzzy control algorithms translate these different degrees of uncertainty into different control strategies. In such situations, it is reasonable to choose a fuzzy control methodology that is the least vulnerable to this kind of uncertainty. It is shown that this 'robustness' demand leads to min and max for &- and V-operations, to 1-x for negation, and to centroid as a defuzzification procedure. Author (revised)

N93-25155*# Tennessee State Univ., Nashville. Center of Excellence in Information Systems.

THE 32ND CDC: SYSTEM IDENTIFICATION USING INTERVAL DYNAMIC MODELS

L. H. Keel, J. S. Lew, and S. P. Bhattacharyya (Texas A&M Univ., College Station.) 1992 18 p
(Grant NAG5-2109)
(NASA-CR-192895; NAS 1.26:192895) Avail: CASI HC A03/MF A01

Motivated by the recent explosive development of results in the area of parametric robust control, a new technique to identify a family of uncertain systems is identified. The new technique takes the frequency domain input and output data obtained from experimental test signals and produces an 'interval transfer function' that contains the complete frequency domain behavior with respect to the test signals. This interval transfer function is one of the key concepts in the parametric robust control approach and identification with such an interval model allows one to predict the worst case performance and stability margins using recent results on interval systems. The algorithm is illustrated by applying it to an 18 bay Mini-Mast truss structure. Author (revised)

N93-25156*# Texas A&M Univ., College Station. Dept. of Electrical Engineering.

THE 32ND CDC: ROBUST STABILIZER SYNTHESIS FOR INTERVAL PLANTS USING NEVANLINA-PICK THEORY

Saikat Bhattacharya, L. H. Keel (Tennessee State Univ., Nashville.), and S. P. Bhattacharyya 1989 24 p
(Grant NAG5-2109)
(NASA-CR-192894; NAS 1.26:192894) Avail: CASI HC A03/MF A01

The synthesis of robustly stabilizing compensators for interval plants, i.e., plants whose parameters vary within prescribed ranges is discussed. Well-known H(sup infinity) methods are used to establish robust stabilizability conditions for a family of plants and also to synthesize controllers that would stabilize the whole family. Though conservative, these methods give a very simple way to come up with a family of robust stabilizers for an interval plant. Author (revised)

N93-25190*# National Aeronautics and Space Administration. Lyndon B. Johnson Space Center, Houston, TX.

FAST PARALLEL ALGORITHMS THAT COMPUTE TRANSITIVE CLOSURE OF A FUZZY RELATION

Vladik Ya. Kreinovich (Texas Univ., El Paso.) Jan. 1993 9 p
(Grants NAG9-482; NSF CDA-90-15006)
(NASA-CR-192950; NAS 1.26:192950; CFL-93-002) Avail: CASI HC A02/MF A01

The notion of a transitive closure of a fuzzy relation is very useful for clustering in pattern recognition, for fuzzy databases, etc. The original algorithm proposed by L. Zadeh (1971) requires the computation time O(n(sup 4)), where n is the number of elements in the relation. In 1974, J. C. Dunn proposed a O(n(sup 2)) algorithm. Since we must compute n(n-1)/2 different values s(a, b) (a not equal to b) that represent the fuzzy relation, and we need at least one computational step to compute each of these values, we cannot compute all of them in less than O(n(sup 2)) steps. So, Dunn's algorithm is in this sense optimal. For small n, it is ok. However, for big n (e.g., for big databases), it is still a lot, so it would be desirable to decrease the computation time (this problem was formulated by J. Bezdek). Since this decrease cannot be done on a sequential computer, the only way to do it is to use a computer with several processors working in parallel. We show that on a parallel computer, transitive closure can be computed in time O((log(sub 2)(n))2). Author (revised)

N93-25196*# National Aeronautics and Space Administration. Lyndon B. Johnson Space Center, Houston, TX.

HOW TO HELP INTELLIGENT SYSTEMS WITH DIFFERENT UNCERTAINTY REPRESENTATIONS COOPERATE WITH EACH OTHER

Vladik Ya. Kreinovich (Texas Univ., El Paso.) and Sundeep Kumar (Texas Univ., El Paso.) 1991 6 p Repr. from Cybernetics and Systems: An International Journal, Hemisphere Publishing Corp., no. 22, 1991 p 217-222
(Grants NAG9-482; NSF CDA-90-15006)
(NASA-CR-192947; NAS 1.26:192947) Copyright Avail: CASI HC A02/MF A01

In order to solve a complicated problem one must use the knowledge from different domains. Therefore, if one wants to automatize the solution of these problems, one has to help the knowledge-based systems that correspond to these domains cooperate, that is, communicate facts and conclusions to each other in the process of decision making. One of the main obstacles to such cooperation is the fact that different intelligent

systems use different methods of knowledge acquisition and different methods and formalisms for uncertainty representation. So an interface f is needed, 'translating' the values x, y, which represent uncertainty of the experts' knowledge in one system, into the values f(x), f(y) appropriate for another one. The problem of designing such an interface as a mathematical problem is formulated and solved. It is shown that the interface must be fractionally linear: f(x) = (ax + b)/(cx + d). Author (revised)

N93-25197*# National Aeronautics and Space Administration. Lyndon B. Johnson Space Center, Houston, TX.

NEURAL NETWORKS: WHAT NON-LINEARITY TO CHOOSE

Vladik Ya. Kreinovich (Texas Univ., El Paso.) and Chris Quintana (Texas Univ., El Paso.) 1991 11 p

(Grants NAG9-482; NSF CDA-90-15006)

(NASA-CR-192948; NAS 1.26:192948) Avail: CASI HC A03/MF A01

Neural networks are now one of the most successful learning formalisms. Neurons transform inputs (x(sub 1),...,x(sub n)) into an output f(w(sub 1)x(sub 1) + ... + w(sub n)x(sub n)), where f is a non-linear function and w, are adjustable weights. What f to choose? Usually the logistic function is chosen, but sometimes the use of different functions improves the practical efficiency of the network. The problem of choosing f as a mathematical optimization problem is formulated and solved under different optimality criteria. As a result, a list of functions f that are optimal under these criteria are determined. This list includes both the functions that were empirically proved to be the best for some problems, and some new functions that may be worth trying. Author (revised)

N93-25226*# Tennessee State Univ., Nashville. Center of Excellence in Information Systems.

STABILITY MARGINS FOR MULTILINEAR INTERVAL SYSTEMS BY WAY OF PHASE CONDITIONS: A UNIFIED APPROACH

L. H. Keel and S. P. Bhattacharyya (Texas A&M Univ., College Station.) 1992 5 p

(Grant NAG5-2109)

(NASA-CR-192893; NAS 1.26:192893) Avail: CASI HC A01/MF A01

A simple way of checking the stability with respect to an arbitrary stability region of a family of polynomials containing a vector of parameters varying within prescribed intervals is discussed. It is assumed that the parameters appear affine multilinearly in the characteristic polynomial coefficients. The condition proposed is simply to check the phase difference of the vertex polynomials. This test based on the mapping theorem significantly reduces computational complexity. Mathematical proofs are omitted. The results can be used to determine various stability margins of control systems containing interconnected interval subsystems. These include the gain, phase, time-delay, H(sup infinity), and nonlinear sector bounded stability margins of multilinear interval systems. Author (revised)

N93-25278 Michigan Univ., Ann Arbor.

DYNAMIC ERROR ANALYSIS OF NUMERICAL METHODS FOR SIMULATION OF STATE-VARIABLE DERIVATIVES WITH DISCONTINUITIES Ph.D. Thesis

Amadi Nwankpa 1992 172 p

Avail: Univ. Microfilms Order No. DA9226976

One of the most difficult computer simulation problems is the simulation of dynamic systems which include discontinuous nonlinear elements. When real-time simulation is required, the selection of integration algorithms used to simulate the system is limited to fixed-step methods with inputs compatible with real time. In order to assess the comparative accuracy of the different integration methods and to develop improved algorithms, it is important to have a general method to evaluate the dynamic errors in simulating discontinuous nonlinearities. Procedures to predict dynamic errors in open-loop and closed-loop systems which include discontinuous nonlinearities are introduced in this thesis. The procedures use the concept of a uniform distribution of 'step-begin' times over the integration step containing the discontinuity as well as the concept of ergodicity in order to predict mean-square errors in the frequency domain. These procedures are applied to specific systems, but are shown to be more general, i.e., applicable to a wide range of nonlinear systems which, except for the discontinuous derivative function, can otherwise be linearized for analysis purposes. With the procedures developed in the thesis, the accuracy of different integration algorithms is compared. Simulation experiments are performed on both the bang-bang and effort-limited control systems to confirm the accuracy of the analysis procedures. Finally, a time-domain simulation experiment is performed to show that frequency domain analysis can be used to predict errors in the time-domain. Dissert. Abstr.

N93-25296*# Tennessee State Univ., Nashville. Center of Excellence in Information Systems.

PARAMETRIC STABILITY MARGIN FOR MULTILINEAR INTERVAL CONTROL SYSTEMS

L. H. Keel and S. P. Bhattacharyya (Texas A&M Univ., College Station.) 1992 5 p

(Grant NAG5-2109)

(NASA-CR-192892; NAS 1.26:192892) Avail: CASI HC A01/MF A01

Recently, a necessary and sufficient condition to determine the robust stability of a multilinear interval control system has been reported as an extension of the well-known Box theorem which deals with the linear affine case. A simple but computationally efficient algorithm, based on the above result, to check the robust stability of such systems is introduced. The method is also extended to find the parametric stability margin of such a system. Author (revised)

N93-25343 Maryland Univ., College Park.

OPTIMAL CONTROL OF LARGE SPACE STRUCTURES Ph.D. Thesis

Mohamed ElBaraka 1992 212 p

Avail: Univ. Microfilms Order No. DA9234558

A computational spectral factorization method is presented to solve the optimal state feedback control problem for flexible structures with the following features: (1) mathematically rigorous; (2) wide range of applicability; (3) flexibility of design; (4) fast and efficient; and (5) mini-computer (versus super-computer) implementation. This method is applied to the following systems: (1) a membrane; (2) a string; (3) an Euler-Bernoulli/Timoshenko beam models; and (4) a beam with structural damping and boundary control. Dissert. Abstr.

N93-25410 Michigan Univ., Ann Arbor.

OPTIMAL THRUST MAGNITUDE ON A SINGULAR ARC IN ATMOSPHERIC FLIGHT Ph.D. Thesis

Sudhakar Medepalli 1992 180 p

Avail: Univ. Microfilms Order No. DA9303785

In optimal control theory, the cases where the second order necessary conditions are trivially satisfied are named the singular cases and the corresponding controls, the singular controls. These are shown to occur quite frequently in a wide variety of practical applications and play an important role. Lie and Poisson brackets can be used to express these singular controls in a very elegant and systematic manner. However, in the literature, Lie bracket solutions are derived only for the simplest cases of a single or multiple inputs appearing linearly in the equations of motion. These come under a category called the totally singular arcs, where all the controls are singular simultaneously. The cases where both singular and non-singular cases occur together, however, are quite common in the literature, especially in trajectory optimization problems. These are called partially singular arcs. This dissertation extends the Lie and Poisson bracket solutions to partially singular arcs of order one. The significance of singular controls in trajectory optimization is illustrated through an example orbital plane change problem. A general trajectory optimization problem in the atmosphere is shown to be partially singular with the thrust magnitude being the singular control and the aerodynamic controls being non-singular. The extended Lie bracket solution is then applied to obtain the thrust magnitude expression on the singular arc. This is shown to be identical to the expression derived by conventional means. It is also shown to be computationally more efficient and to preserve any symmetry properties in the problem. Some interesting sub-cases are studied with the help of the general expression. Further extensions of the Lie bracket solution are suggested for constrained arcs and higher order singular arcs. Vector formulation is used throughout the thesis to make the results concise and independent of the choice of the coordinate system. An example canonical transformation to flight path variables is derived to illustrate how all the results in vector form can be translated in terms of any desired set of variables. Dissert. Abstr.

N93-25425*# National Aeronautics and Space Administration. Lyndon B. Johnson Space Center, Houston, TX.
STRONGLY TRANSITIVE FUZZY RELATIONS: A MORE ADEQUATE WAY TO DESCRIBE SIMILARITY
Vladik Ya. Kreinovich (Texas Univ., El Paso.) 1992 10 p
(Grants NAG9-482; NSF CDA-90-15006)
(NASA-CR-192951; NAS 1.26:192951) Avail: CASI HC A02/MF A01

The notion of a transitive closure of a fuzzy relation is very useful for clustering in pattern recognition, for fuzzy databases, etc. It is based on translating the standard definition of transitivity and transitive closure into fuzzy terms. This definition works fine, but to some extent it does not fully capture our understanding of transitivity. The reason is that this definition is based on fuzzifying only the positive side of transitivity: if R(a,b) and R(b,c), then R(a,c); but transitivity also includes a negative side: if R(a,b) and not R(a,c), then not R(b,c). In classical logic, this negative statement follows from the standard 'positive' definition of transitivity. In fuzzy logic, this negative part of the transitivity has to be formulated as an additional demand. A strongly transitive fuzzy relation as the one that satisfies both the positive and the negative transitivity demands is defined, the existence of strongly transitive closure is proven, and the relationship between strongly transitive similarity and clustering are found. Author (revised)

N93-25452*# Texas Univ., El Paso. Dept. of Computer Science.
MIN AND MAX ARE THE ONLY CONTINUOUS AMPERSAND-, V-OPERATIONS FOR FINITE LOGICS
Vladik Kreinovich 1992 11 p
(Grants NAG9-482; NSF CDA-90-15006)
(NASA-CR-192952; NAS 1.26:192952) Avail: CASI HC A03/MF A01

Experts usually express their degrees of belief in their statements by the words of a natural language (like 'maybe', 'perhaps', etc.). If an expert system contains the degrees of beliefs t(A) and t(B) that correspond to the statements A and B, and a user asks this expert system whether 'A&B' is true, then it is necessary to come up with a reasonable estimate for the degree of belief of A&B. The operation that processes t(A) and t(B) into such an estimate t(A&B) is called an &-operation. Many different &-operations have been proposed. Which of them to choose? This can be (in principle) done by interviewing experts and eliciting a &-operation from them, but such a process is very time-consuming and therefore, not always possible. So, usually, to choose a &-operation, the finite set of actually possible degrees of belief is extended to an infinite set (e.g., to an interval (0,1)), define an operation there, and then restrict this operation to the finite set. Only this original finite set is considered. It is shown that a reasonable assumption that an &-operation is continuous (i.e., that gradual change in t(A) and t(B) must lead to a gradual change in t(A&B)), uniquely determines min as an &-operation. Likewise, max is the only continuous V-operation. These results are in good accordance with the experimental analysis of 'and' and 'or' in human beliefs. Author (revised)

N93-25459*# National Aeronautics and Space Administration. Lyndon B. Johnson Space Center, Houston, TX.
WHAT PROCEDURE TO CHOOSE WHILE DESIGNING A FUZZY CONTROL? TOWARDS MATHEMATICAL FOUNDATIONS OF FUZZY CONTROL
Vladik Ya. Kreinovich (Texas Univ., El Paso.), Chris Quintana (Texas Univ., El Paso.), and Robert Lea 1991 8 p
(Grants NAG9-482; NSF CDA-90-15006)
(NASA-TM-108719; NAS 1.15:108719) Avail: CASI HC A02/MF A01

Fuzzy control has been successfully applied in industrial systems. However, there is some caution in using it. The reason is that it is based on quite reasonable ideas, but each of these ideas can be implemented in several different ways, and depending on which of the implementations chosen different results are achieved. Some implementations lead to a high quality control, some of them not. And since there are no theoretical methods for choosing the implementation, the basic way to choose it now is experimental. But if one chooses a method that is good for several examples, there is no guarantee that it will work fine in all of them. Hence the caution. A theoretical basis for choosing the fuzzy control procedures is provided. In order to choose a procedure that transforms a fuzzy knowledge into a control, one needs, first, to choose a membership function for each of the fuzzy terms that the experts use, second, to choose operations of uncertainty values that corresponds to 'and' and 'or', and third, when a membership function for control is obtained, one must defuzzy it, that is, somehow generate a value of the control u that will be actually used. A general approach that will help to make all these choices is described: namely, it is proved that under reasonable assumptions membership functions should be linear or fractionally linear, defuzzification must be described by a centroid rule and describe all possible 'and' and 'or' operations. Thus, a theoretical explanation of the existing semi-heuristic choices is given and the basis for the further research on optimal fuzzy control is formulated. Author (revised)

N93-25468 Virginia Polytechnic Inst. and State Univ., Blacksburg.
ANALYTICAL AND EXPERIMENTAL STUDY OF CONTROL EFFORT ASSOCIATED WITH MODEL REFERENCE ADAPTIVE CONTROL Ph.D. Thesis
Richard Scott Messer 1992 164 p
Avail: Univ. Microfilms Order No. DA9234277

During the past decade, researchers have shown much interest in control and identification of Large Space Structures (LSS). Our inability to model these LSS accurately has generated extensive research into robust controllers capable of maintaining stability in the presence of large structural uncertainties as well as changing structural characteristics. In this work the performance of Model Reference Adaptive Control (MRAC) is studied in numerical simulations and verified experimentally, to understand how differences between the plant and the reference model affect the control effort. MRAC is applied analytically and experimentally to a single-degree-of-freedom system and analytically to a multi-degree-of-freedom system and analytically to a multi-degree-of-freedom system with multi-inputs and multi-outputs. Good experiments and it is shown that MRAC does an excellent job of controlling the structures and achieving the desired performance even when large differences between the plant and ideal reference model exist. However, it is shown that reasonable differences between the reference model and the plant significantly increase the required control effect. The effects of increased damping in the reference model are considered, and it is shown that requiring the controller to provide increased damping actually decreases the required control effort when differences between the plant and reference model exist. This result is very useful because one of the first attempts to counteract the increased control effort due to differences between the plant and reference model might be to require less damping, however, this would actually increase the control effort. The use of optimization to successfully improve performance and reduce control effort is shown to be limited, because the actual control-structure system cannot realize all the performance improvements of the analytical optimal system. Finally, it is shown that very large sampling rates may be required to accurately implement MRAC. Dissert. Abstr.

N93-25648# California Univ., Berkeley.
CONSTRUCTION OF A CONNECTIONIST NETWORK SUPERCOMPUTER Technical Progress Report, 1 Nov. 1992 - 1 Feb. 1993
1 Feb. 1993 4 p
(Contract N00014-92-J-1617)
(AD-A260929) Avail: CASI HC A01/MF A01

The first finding is that, in the assessment of our reviewers, the project is technically sound. In particular, there was general agreement that the motivations are reasonable, the physical packaging scheme is plausible, the processor interconnection network is satisfactory, and the VLSI task is attainable. The software strategy was only briefly presented; a more complete software review is planned at a later time. There were several minor points made by the reviewers which are being incorporated in the CNS-1 Architecture Specification. However, we also received suggestion for making better use of industry and academic 'standards', thereby allowing more widespread use of the CNS-1 by others in the field. The subsequent consideration of these suggestions led to the second major result of the review. We are adopting an industry standard instruction set architecture (ISA) for the scalar processor within the Torrent VLSI chip. Although this decision directly only affects about 15 percent of the silicon die area (making it slightly more complex to design), the repercussions are extensive in the software area. By using a standard ISA (we have selected the MIPS R3000), we will be able to take advantage of suitable commercially available and public domain system software, tools, and application libraries. In addition, machines executing the R3000 instruction set are widely available and will be used as development platforms throughout the life of CNS-1. The basic architecture of the Torrent chip

remains the same; it is a scalar processor with a SIMD array of moderate precision datapaths for neural computation. The SIMD array now interfaces to the scalar processor as a vector coprocessor. DTIC

N93-25821# Pennsylvania Univ., Philadelphia. Dept. of Electrical Engineering.
COMPUTATION AND LEARNING IN NEURAL NETWORKS WITH BINARY WEIGHTS Final Report, 1 Sep. 1989 - 31 Aug. 1992
Santosh S. Venkatesh 28 Nov. 1992 325 p
(Grant AF-AFOSR-0523-89)
(AD-A261182; AFOSR-93-0066TR) Avail: CASI HC A14/MF A03

Under the aegis of the AFOSR grant they have been investigating computational learning attributes of networks of formal neurons. The formal neurons considered are linear threshold elements which produce binary outputs based on the sign of a linear form of a set of inputs. The researchers have been interested in (1) exploring the theoretical limitations on what can be computed or learnt in neural network architectures, and (2) developing and analysing learning algorithms which specify weights as a function of a set of examples of a computation. DTIC

N93-25833*# Massachusetts Inst. of Tech., Cambridge.
MIT SPACE ENGINEERING RESEARCH CENTER
Edward F. Crawley and David W. Miller Dec. 1990 187 p
(Grant NAGw-1335)
(NASA-CR-192879; NAS 1.26:192879; MIT-SERC-17-90-R) Avail: CASI HC A09/MF A02

The Space Engineering Research Center (SERC) at MIT, started in Jul. 1988, has completed two years of research. The Center is approaching the operational phase of its first testbed, is midway through the construction of a second testbed, and is in the design phase of a third. We presently have seven participating faculty, four participating staff members, ten graduate students, and numerous undergraduates. This report reviews the testbed programs, individual graduate research, other SERC activities not funded by the Center, interaction with non-MIT organizations, and SERC milestones. Published papers made possible by SERC funding are included at the end of the report. For individual titles, see N93-25834 through N93-25836.

N93-25834*# Massachusetts Inst. of Tech., Cambridge. Dept. of Mechanical Engineering.
USING INPUT COMMAND PRE-SHAPING TO SUPPRESS MULTIPLE MODE VIBRATION **c39**
James M. Hyde and Warren P. Seering *In its* MIT Space Engineering Research Center Dec. 1990 19 p (For primary document see N93-25833 09-63)
(Contract NAGw-1335; N00014-86-K-0685)
Avail: CASI HC A03/MF A02

Spacecraft, space-borne robotic systems, and manufacturing equipment often utilize lightweight materials and configurations that give rise to vibration problems. Prior research has led to the development of input command pre-shapers that can significantly reduce residual vibration. These shapers exhibit marked insensitivity to errors in natural frequency estimates and can be combined to minimize vibration at more than one frequency. This paper presents a method for the development of multiple mode input shapers which are simpler to implement than previous designs and produce smaller system response delays. The new technique involves the solution of a group of simultaneous non-linear impulse constraint equations. The resulting shapers were tested on a model of MACE, an MIT/NASA experimental flexible structure. Author

N93-25835*# Massachusetts Inst. of Tech., Cambridge.
THE MODE FAMILY OF ON-ORBIT EXPERIMENTS: THE MIDDECK ACTIVE CONTROL EXPERIMENT (MACE) **c12**
Edward F. Crawley, David W. Miller, Javier deLuis (Payload Systems, Inc., Cambridge, MA.), Mel Waldman (Lockheed Missiles and Space Co., Greenbelt, MD.), and Andy Bicos (McDonnell-Douglas Space Systems Co., Washington, DC.) *In its* MIT Space Engineering Research Center Dec. 1990 45 p (For primary document see N93-25833 09-63)
Avail: CASI HC A03/MF A02

A flight experiment entitled the Middeck Active Control Experiment (MACE), proposed by the Space Engineering Research Center (SERC) at the Massachusetts Institute of Technology, is described. This is the second in a family of flight experiments being developed at MIT. The first is the Middeck 0-Gravity Dynamics Experiment (MODE) which investigates the nonlinear behavior of contained fluids and truss structures in zero gravity. The objective of the MACE program is to investigate and validate the modeling of the dynamics of an actively controlled flexible, articulating, multibody platform free floating in zero gravity. A rationale and experimental approach for the program are presented. The rationale shows that on-orbit testing, coupled with ground testing and a strong analytical program, is necessary in order to fully understand both how flexibility of the platform affects the pointing problem, as well as how gravity perturbs this structural flexibility causing deviations between 1- and 0-gravity behavior. The experimental approach captures the essential physics of multibody platforms, by identifying the appropriate attributes, tests, and performance metrics of the test article and defines the tests required to successfully validate the analytical framework. Author (revised)

N93-25836*# Massachusetts Inst. of Tech., Cambridge.
MIT'S INTERFEROMETER CST TESTBED **c14**
Tupper Hyde, Ed Kim, Eric Anderson, Gary Blackwood, and Leonard Lublin *In its* MIT Space Engineering Research Center Dec. 1990 20 p (For primary document see N93-25833 09-63)
(Grant NAGw-1335)
Avail: CASI HC A03/MF A02

The MIT Space Engineering Research Center (SERC) has developed a controlled structures technology (CST) testbed based on one design for a space-based optical interferometer. The role of the testbed is to provide a versatile platform for experimental investigation and discovery of CST approaches. In particular, it will serve as the focus for experimental verification of CSI methodologies and control strategies at SERC. The testbed program has an emphasis on experimental CST--incorporating a broad suite of actuators and sensors, active struts, system identification, passive damping, active mirror mounts, and precision component characterization. The SERC testbed represents a one-tenth scaled version of an optical interferometer concept based on an inherently rigid tetrahedral configuration with collecting apertures on one face. The testbed consists of six 3.5 meter long truss legs joined at four vertices and is suspended with attachment points at three vertices. Each aluminum leg has a 0.2 m by 0.2 m by 0.25 m triangular cross-section. The structure has a first flexible mode at 31 Hz and has over 50 global modes below 200 Hz. The stiff tetrahedral design differs from similar testbeds (such as the JPL Phase B) in that the structural topology is closed. The tetrahedral design minimizes structural deflections at the vertices (site of optical components for maximum baseline) resulting in reduced stroke requirements for isolation and pointing of optics. Typical total light path length stability goals are on the order of lambda/20, with a wavelength of light, lambda, of roughly 500 nanometers. It is expected that active structural control will be necessary to achieve this goal in the presence of disturbances. Author (revised)

N93-25853# Massachusetts Inst. of Tech., Cambridge.
CENTER FOR INTELLIGENT CONTROL SYSTEMS Final Report, 1 Oct. 1986 - 30 Jun. 1992
Sanjoy K. Mitter Dec. 1992 57 p
(Contract DAAL03-86-K-0171)
(AD-A260995; ARO-24635.430-MA-UIR) Avail: CASI HC A04/MF A01

This report contains results of research on perceptual systems, multiscale signal and image analysis, intelligent control, learning control of linear and nonlinear systems, computation, communication and distributed computation. It also contains a list of 359 reports. DTIC

N93-25880 Oklahoma State Univ., Stillwater.
AN OPTIMAL SCHEDULING OF PICK-PLACE OPERATIONS OF A ROBOT-VISION-TRACKING SYSTEM BY USING NEURAL NETWORKS AND RULE-BASED SYSTEMS Ph.D. Thesis
Keqi Feng 1992 166 p
Avail: Univ. Microfilms Order No. DA9236738

In this research program, a scheduling of pick-place operations of a robot-vison tracking system which handles multi-type and multi-size objects presented randomly on a moving conveyer has been identified and formulated as a real-time repetitive optimization problem. A mathematical model for calculating robot processing times in a constrained environment is constructed, and the strategy to deal with constraint violation situations is also proposed. The real-time repetitive optimization problem can be

viewed as an associative mapping problem. A scheme which uses both the back-propagation and Hamming networks is proposed to implement the mapping in an attempt to overcome difficulties raised by using traditional methods. To improve the training time, an alternative neural network, a Modified ARTMAP (Adaptive Resonance Theory Networks), which is based on the ARTMAP introduced by Carpenter, et al. has been investigated to solve the optimal scheduling problem. The main modification is that a matching check mechanism is added to the system such that the Modified ARTMAP can cope with situations appearing in the optimal scheduling problem, whereas the original ARTMAP cannot, without using the complement coding technique. The repetitive optimization problem may also be viewed as an on-line decision making problem. A rule-based system can be constructed to conduct the on-line decision making directly is some rules are available. The discrimination net approach is designed for cases where all needed rules can be obtained; the partial search approach is designed for cases where only some of the rules are available. The heuristic approach is proposed for the cases of variable object patterns. Both neural network and ruled-based system approaches are implemented, and the experimental results have shown that time savings of up to 21 percent with only 4 different objects are possible, over first-come, first-served schemes currently used in industry. Dissert. Abstr.

N93-25961*# National Aeronautics and Space Administration. Goddard Space Flight Center, Greenbelt, MD.

THE 1993 GODDARD CONFERENCE ON SPACE APPLICATIONS OF ARTIFICIAL INTELLIGENCE

Carl F. Hostetter, ed. Washington 1993 280 p Conference held in Greenbelt, MD, 10-13 May 1993

(NASA-CP-3200; NAS 1.55:3200) Avail: CASI HC A13/MF A03

This publication comprises the papers presented at the 1993 Goddard Conference on Space Applications of Artificial Intelligence held at the NASA/Goddard Space Flight Center, Greenbelt, MD on May 10-13, 1993. The purpose of this annual conference is to provide a forum in which current research and development directed at space applications of artificial intelligence can be presented and discussed. For individual titles, see N93-25962 through N93-25984.

N93-25962*# National Aeronautics and Space Administration. Goddard Space Flight Center, Greenbelt, MD.

USING AI/EXPERT SYSTEM TECHNOLOGY TO AUTOMATE PLANNING AND REPLANNING FOR THE HST SERVICING MISSIONS

L. Bogovich (Bendix Field Engineering Corp., Seabrook, MD.), J Johnson (Bendix Field Engineering Corp., Seabrook, MD.), A. Tuchman (Bendix Field Engineering Corp., Seabrook, MD.), D. McLean (Bendix Field Engineering Corp., Seabrook, MD.), B. Page (Bendix Field Engineering Corp., Seabrook, MD.), A. Kispert (Bendix Field Engineering Corp., Seabrook, MD.), C. Burkhardt (Bendix Field Engineering Corp., Seabrook, MD.), R. Littlefield (Bendix Field Engineering Corp., Seabrook, MD.), and W. Potter *In its* The 1993 Goddard Conference on Space Applications of Artificial Intelligence 1993 p 3-10 (For primary document see N93-25961 09-63)

(Contract NAS5-27772)

Avail: CASI HC A02/MF A03

This paper describes a knowledge-based system that has been developed to automate planning and scheduling for the Hubble Space Telescope (HST) Servicing Missions. This new system is the Servicing Mission Planning and Replanning Tool (SM/PART). SM/PART has been delivered to the HST Flight Operations Team (FOT) at Goddard Space Flight Center (GSFC) where it is being used to build integrated time lines and command plans to control the activities of the HST, Shuttle, Crew and ground systems for the next HST Servicing Mission. SM/PART reuses and extends AI/expert system technology from Interactive Experimenter Planning System (IEPS) systems to build or rebuild time lines and command plans more rapidly than was possible for previous missions where they were built manually. This capability provides an important safety factor for the HST, Shuttle and Crew in case unexpected events occur during the mission. Author

N93-25963*# Honeywell, Inc., Minneapolis, MN.

KNOWLEDGE-BASED CONTROL FOR ROBOT SELF-LOCALIZATION

Bonnie Kathleen Holt Bennett *In* NASA. Goddard Space Flight Center, The 1993 Goddard Conference on Space Applicati ons of Artificial Intelligence 1993 p 13-27 Sponsored in part by DARPA Prepared in cooperation with Saint Thomas Coll., Saint Paul, MN (For primary document see N93-25961 09-63)

(Grant NSF IRI-91-96146)

Avail: CASI HC A03/MF A03

Autonomous robot systems are being proposed for a variety of missions including the Mars rover/sample return mission. Prior to any other mission objectives being met, an autonomous robot must be able to determine its own location. This will be especially challenging because location sensors like GPS, which are available on Earth, will not be useful, nor will INS sensors because their drift is too large. Another approach to self-localization is required. In this paper, we describe a novel approach to localization by applying a problem solving methodology. The term 'problem solving' implies a computational technique based on logical representational and control steps. In this research, these steps are derived from observing experts solving localization problems. The objective is not specifically to simulate human expertise but rather to apply its techniques where appropriate for computational systems. In doing this, we describe a model for solving the problem and a system built on that model, called localization control and logic expert (LOCALE), which is a demonstration of concept for the approach and the model. The results of this work represent the first successful solution to high-level control aspects of the localization problem. Author

N93-25964*# Institute for Space and Terrestrial Science, York (Ontario).

PARAMETRIC MOTION CONTROL OF ROBOTIC ARMS: A BIOLOGICALLY BASED APPROACH USING NEURAL NETWORKS

O. Bock, G. M. T. D'Eleuterio (Toronto Univ., Ontario.), J. Lipitkas (Toronto Univ., Ontario.), and J. J. Grodski (Defence and Civil Inst. of Environmental Medicine, Toronto, Ontario.) *In* NASA. Goddard Space Flight Center, The 1993 Goddard Conference on Space Applicati ons of Artificial Intelligence 1993 p 29-37 (For primary document see N93-25961 09-63)

(Contract W7711-0-7118)

Avail: CASI HC A02/MF A03

A neural network based system is presented which is able to generate point-to-point movements of robotic manipulators. The foundation of this approach is the use of prototypical control torque signals which are defined by a set of parameters. The parameter set is used for scaling and shaping of these prototypical torque signals to effect a desired outcome of the system. This approach is based on neurophysiological findings that the central nervous system stores generalized cognitive representations of movements called synergies, schemas, or motor programs. It has been proposed that these motor programs may be stored as torque-time functions in central pattern generators which can be scaled with appropriate time and magnitude parameters. The central pattern generators use these parameters to generate stereotypical torque-time profiles, which are then sent to the joint actuators. Hence, only a small number of parameters need to be determined for each point-to-point movement instead of the entire torque-time trajectory. This same principle is implemented for controlling the joint torques of robotic manipulators where a neural network is used to identify the relationship between the task requirements and the torque parameters. Movements are specified by the initial robot position in joint coordinates and the desired final end-effector position in Cartesian coordinates. This information is provided to the neural network which calculates six torque parameters for a two-link system. The prototypical torque profiles (one per joint) are then scaled by those parameters. After appropriate training of the network, our parametric control design allowed the reproduction of a trained set of movements with relatively high accuracy, and the production of previously untrained movements with comparable accuracy. We conclude that our approach was successful in discriminating between trained movements and in generalizing to untrained movements. Author

N93-25965*# Allied-Signal Aerospace Co., Columbia, MD.

DETECTION OF BEARING FAILURE IN MECHANICAL DEVICES USING NEURAL NETWORKS

Richard A. Burne, Paul F. Payer, R. Paul Gorman, and Dan T. Horak *In* NASA. Goddard Space Flight Center, The 1993 Goddard Conference on Space Applicati ons of Artificial Intelligence 1993 p 39-45 (For primary document see N93-25961 09-63)

Avail: CASI HC A02/MF A03

We present a novel time-domain method for the detection of faulty

bearings that has direct applicability to monitoring the health of the turbo pumps on the Space Shuttle Main Engine. A feed-forward neural network was trained to detect modelled roller bearing faults on the basis of the periodicity of impact pulse trains. The network's performance was dependent upon the number of pulses in the network's input window and the signal-to-noise ratio of the input signal. To test the model's validity, we fit the model's parameters to an actual vibration signal generated by a faulty roller element bearing and applied the network trained on this model to detect faults in actual vibration data. When this network was tested on the actual vibration data, it correctly identified the vibration signal as a fault condition 76 percent of the time. Author

N93-25966*# Boeing Defense and Space Group, Huntsville, AL. Advanced Computing Lab.

MACHINE LEARNING TECHNIQUES FOR FAULT ISOLATION AND SENSOR PLACEMENT

James R. Carnes and Douglas H. Fisher (Vanderbilt Univ., Nashville, TN.) *In* NASA. Goddard Space Flight Center, The 1993 Goddard Conference on Space Applicati ons of Artificial Intelligence 1993 p 47-58 (For primary document see N93-25961 09-63)

Avail: CASI HC A03/MF A03

Fault isolation and sensor placement are vital for monitoring and diagnosis. A sensor conveys information about a system's state that guides troubleshooting if problems arise. We are using machine learning methods to uncover behavioral patterns over snapshots of system simulations that will aid fault isolation and sensor placement, with an eye towards minimality, fault coverage, and noise tolerance. Author

N93-25967*# Harris Corp., Melbourne, FL.

ADAPTIVE LASER LINK RECONFIGURATION USING CONSTRAINT PROPAGATION **c66**

M. S. Crone, P. M. Julich, and L. M. Cook *In* NASA. Goddard Space Flight Center, The 1993 Goddard Conference on Space Applicati ons of Artificial Intelligence 1993 p 59-73 (For primary document see N93-25961 09-63)

(Contract F30602-89-D-0096)

Avail: CASI HC A03/MF A03

This paper describes Harris AI research performed on the Adaptive Link Reconfiguration (ALR) study for Rome Lab, and focuses on the application of constraint propagation to the problem of link reconfiguration for the proposed space based Strategic Defense System (SDS) Brilliant Pebbles (BP) communications system. According to the concept of operations at the time of the study, laser communications will exist between BP's and to ground entry points. Long-term links typical of RF transmission will not exist. This study addressed an initial implementation of BP's based on the Global Protection Against Limited Strikes (GPALS) SDI mission. The number of satellites and rings studied was representative of this problem. An orbital dynamics program was used to generate line-of-site data for the modeled architecture. This was input into a discrete event simulation implemented in the Harris developed COnstraint Propagation Expert System (COPES) Shell, developed initially on the Rome Lab BM/C3 study. Using a model of the network and several heuristics, the COPES shell was used to develop the Heuristic Adaptive Link Ordering (HALO) Algorithm to rank and order potential laser links according to probability of communication. A reduced set of links based on this ranking would then be used by a routing algorithm to select the next hop. This paper includes an overview of Constraint Propagation as an Artificial Intelligence technique and its embodiment in the COPES shell. It describes the design and implementation of both the simulation of the GPALS BP network and the HALO algorithm in COPES. This is described using a 59 Data Flow Diagram, State Transition Diagrams, and Structured English PDL. It describes a laser communications model and the heuristics involved in rank-ordering the potential communication links. The generation of simulation data is described along with its interface via COPES to the Harris developed View Net graphical tool for visual analysis of communications networks. Conclusions are presented, including a graphical analysis of results depicting the ordered set of links versus the set of all possible links based on the computed Bit Error Rate (BER). Finally, future research is discussed which includes enhancements to the HALO algorithm, network simulation, and the addition of an intelligent routing algorithm for BP. Author

N93-25968*# Houston Univ., TX.

AN ARCHITECTURE FOR OBJECT-ORIENTED INTELLIGENT CONTROL OF POWER SYSTEMS IN SPACE

Sven G. Holmquist, Prakash Jayaram, and Ben H. Jansen *In* NASA. Goddard Space Flight Center, The 1993 Goddard Conference on Space Applicati ons of Artificial Intelligence 1993 p 75-82 (For primary document see N93-25961 09-63)

Avail: CASI HC A02/MF A03

A control system for autonomous distribution and control of electrical power during space missions is being developed. This system should free the astronauts from localizing faults and reconfiguring loads if problems with the power distribution and generation components occur. The control system uses an object-oriented simulation model of the power system and first principle knowledge to detect, identify, and isolate faults. Each power system component is represented as a separate object with knowledge of its normal behavior. The reasoning process takes place at three different levels of abstraction: the Physical Component Model (PCM) level, the Electrical Equivalent Model (EEM) level, and the Functional System Model (FSM) level, with the PCM the lowest level of abstraction and the FSM the highest. At the EEM level the power system components are reasoned about as their electrical equivalents, e.g, a resistive load is thought of as a resistor. However, at the PCM level detailed knowledge about the component's specific characteristics is taken into account. The FSM level models the system at the subsystem level, a level appropriate for reconfiguration and scheduling. The control system operates in two modes, a reactive and a proactive mode, simultaneously. In the reactive mode the control system receives measurement data from the power system and compares these values with values determined through simulation to detect the existence of a fault. The nature of the fault is then identified through a model-based reasoning process using mainly the EEM. Compound component models are constructed at the EEM level and used in the fault identification process. In the proactive mode the reasoning takes place at the PCM level. Individual components determine their future health status using a physical model and measured historical data. In case changes in the health status seem imminent the component warns the control system about its impending failure. The fault isolation process uses the FSM level for its reasoning base. Author

N93-25969*# College of William and Mary, Williamsburg, VA. Dept. of Computer Science.

THE USE OF MULTIPLE MODELS IN CASE-BASED DIAGNOSIS

Stamos T. Karamouzis and Stefan Feyock *In* NASA. Goddard Space Flight Center, The 1993 Goddard Conference on Space Applicati ons of Artificial Intelligence 1993 p 83-90 (For primary document see N93-25961 09-63)

(Contract NCC1-159)

Avail: CASI HC A02/MF A03

The work described in this paper has as its goal the integration of a number of reasoning techniques into a unified intelligent information system that will aid flight crews with malfunction diagnosis and prognostication. One of these approaches involves using the extensive archive of information contained in aircraft accident reports along with various models of the aircraft as the basis for case-based reasoning about malfunctions. Case-based reasoning draws conclusions on the basis of similarities between the present situation and prior experience. We maintain that the ability of a CBR program to reason about physical systems is significantly enhanced by the addition to the CBR program of various models. This paper describes the diagnostic concepts implemented in a prototypical case based reasoner that operates in the domain of in-flight fault diagnosis, the various models used in conjunction with the reasoner's CBR component, and results from a preliminary evaluation. Author

N93-25970*# New South Wales Univ., Kensington (Australia). Dept. of Computer Science and Engineering.

AN AUTONOMOUS SATELLITE ARCHITECTURE INTEGRATING DELIBERATIVE REASONING AND BEHAVIOURAL INTELLIGENCE

Craig A. Lindley *In* NASA. Goddard Space Flight Center, The 1993 Goddard Conference on Space Applicati ons of Artificial Intelligence 1993 p 91-106 (For primary document see N93-25961 09-63)

Avail: CASI HC A03/MF A03

This paper describes a method for the design of autonomous spacecraft, based upon behavioral approaches to intelligent robotics. First, a number

of previous spacecraft automation projects are reviewed. A methodology for the design of autonomous spacecraft is then presented, drawing upon both the European Space Agency technological center (ESTEC) automation and robotics methodology and the subsumption architecture for autonomous robots. A layered competency model for autonomous orbital spacecraft is proposed. A simple example of low level competencies and their interaction is presented in order to illustrate the methodology. Finally, the general principles adopted for the control hardware design of the AUSTRALIS-1 spacecraft are described. This system will provide an orbital experimental platform for spacecraft autonomy studies, supporting the exploration of different logical control models, different computational metaphors within the behavioral control framework, and different mappings from the logical control model to its physical implementation. Author

N93-25971*# National Oceanic and Atmospheric Administration, Camp Springs, MD.

ANOMALOUS EVENT DIAGNOSIS FOR ENVIRONMENTAL SATELLITE SYSTEMS **c18**

Bruce H. Ramsay *In* NASA. Goddard Space Flight Center, The 1993 Goddard Conference on Space Applicati ons of Artificial Intelligence 1993 p 107-116 (For primary document see N93-25961 09-63)

Avail: CASI HC A02/MF A03

The National Oceanic and Atmospheric Administration's (NOAA) National Environmental Satellite, Data, and Information Service (NESDIS) is responsible for the operation of the NOAA geostationary and polar orbiting satellites. NESDIS provides a wide array of operational meteorological and oceanographic products and services and operates various computer and communication systems on a 24-hour, seven days per week schedule. The Anomaly Reporting System contains a database of anomalous events regarding the operations of the Geostationary Operational Environmental Satellite (GOES), communication, or computer systems that have degraded or caused the loss of GOES imagery. Data is currently entered manually via an automated query user interface. There are 21 possible symptoms (e.g., No Data), and 73 possible causes (e.g., Sectorizer - World Weather Building) of an anomalous event. The determination of an event's cause(s) is made by the on-duty computer operator, who enters the event in a paper based daily log, and by the analyst entering the data into the reporting system. The determination of the event's cause(s) impacts both the operational status of these systems, and the performance evaluation of the on-site computer and communication operations contractor. Author

N93-25972*# National Aeronautics and Space Administration. Goddard Space Flight Center, Greenbelt, MD.

THE PROBABILISTIC NEURAL NETWORK ARCHITECTURE FOR HIGH SPEED CLASSIFICATION OF REMOTELY SENSED IMAGERY

Samir R. Chettri and Robert F. Cromp *In its* The 1993 Goddard Conference on Space Applications of Artificial Intelligence 1993 p 119-132 (For primary document see N93-25961 09-63)

Avail: CASI HC A03/MF A03

In this paper we discuss a neural network architecture (the Probabilistic Neural Net or the PNN) that, to the best of our knowledge, has not previously been applied to remotely sensed data. The PNN is a supervised non-parametric classification algorithm as opposed to the Gaussian maximum likelihood classifier (GMLC). The PNN works by fitting a Gaussian kernel to each training point. The width of the Gaussian is controlled by a tuning parameter called the window width. If very small widths are used, the method is equivalent to the nearest neighbor method. For large windows, the PNN behaves like the GMLC. The basic implementation of the PNN requires no training time at all. In this respect it is far better than the commonly used backpropagation neural network which can be shown to take O(N6) time for training where N is the dimensionality of the input vector. In addition the PNN can be implemented in a feed forward mode in hardware. The disadvantage of the PNN is that it requires all the training data to be stored. Some solutions to this problem are discussed in the paper. Finally, we discuss the accuracy of the PNN with respect to the GMLC and the backpropagation neural network (BPNN). The PNN is shown to be better than GMLC and not as good as the BPNN with regards to classification accuracy. Author

N93-25973*# National Aeronautics and Space Administration. Goddard Space Flight Center, Greenbelt, MD.

IMAGE ANALYSIS BY INTEGRATION OF DISPARATE INFORMATION

Jacqueline LeMoigne *In its* The 1993 Goddard Conference on Space Applications of Artificial Intelligence 1993 p 133-144 (For primary document see N93-25961 09-63)

Avail: CASI HC A03/MF A03

Image analysis often starts with some preliminary segmentation which provides a representation of the scene needed for further interpretation. Segmentation can be performed in several ways, which are categorized as pixel based, edge-based, and region-based. Each of these approaches are affected differently by various factors, and the final result may be improved by integrating several or all of these methods, thus taking advantage of their complementary nature. In this paper, we propose an approach that integrates pixel-based and edge-based results by utilizing an iterative relaxation technique. This approach has been implemented on a massively parallel computer and tested on some remotely sensed imagery from the Landsat-Thematic Mapper (TM) sensor. Author

N93-25974*# Caelum Research Corp., Silver Spring, MD.

DATA FUSION WITH ARTIFICIAL NEURAL NETWORKS (ANN) FOR CLASSIFICATION OF EARTH SURFACE FROM MICROWAVE SATELLITE MEASUREMENTS

Y. M. Fleming Lure, Norman C. Grody (National Oceanic and Atmospheric Administration, Washington, DC.), Y. S. Peter Chiou, and H. Y. Michael Yeh *In* NASA. Goddard Space Flight Center, The 1993 Goddard Conference on Space Applicati ons of Artificial Intelligence 1993 p 145-154 (For primary document see N93-25961 09-63)

(Contract F30602-89-C-0130)

Avail: CASI HC A02/MF A03

A data fusion system with artificial neural networks (ANN) is used for fast and accurate classification of five earth surface conditions and surface changes, based on seven SSMI multichannel microwave satellite measurements. The measurements include brightness temperatures at 19, 22, 37, and 85 GHz at both H and V polarizations (only V at 22 GHz). The seven channel measurements are processed through a convolution computation such that all measurements are located at same grid. Five surface classes including non-scattering surface, precipitation over land, over ocean, snow, and desert are identified from ground-truth observations. The system processes sensory data in three consecutive phases: (1) pre-processing to extract feature vectors and enhance separability among detected classes; (2) preliminary classification of Earth surface patterns using two separate and parallely acting classifiers: back-propagation neural network and binary decision tree classifiers; and (3) data fusion of results from preliminary classifiers to obtain the optimal performance in overall classification. Both the binary decision tree classifier and the fusion processing centers are implemented by neural network architectures. The fusion system configuration is a hierarchical neural network architecture, in which each functional neural net will handle different processing phases in a pipelined fashion. There is a total of around 13,500 samples for this analysis, of which 4 percent are used as the training set and 96 percent as the testing set. After training, this classification system is able to bring up the detection accuracy to 94 percent compared with 88 percent for back-propagation artificial neural networks and 80 percent for binary decision tree classifiers. The neural network data fusion classification is currently under progress to be integrated in an image processing system at NOAA and to be implemented in a prototype of a massively parallel and dynamically reconfigurable Modular Neural Ring (MNR). Author

N93-25975*# National Aeronautics and Space Administration. Goddard Space Flight Center, Greenbelt, MD.

NEURAL NETWORKS FOR ATMOSPHERIC RETRIEVALS

Howard E. Motteler, J. A. Gualtieri, L. Larrabee Strow (Maryland Univ. Baltimore County, Catonsville.), and Larry McMillin (National Oceanic and Atmospheric Administration, Camp Springs, MD.) *In its* The 1993 Goddard Conference on Space Applications of Artificial Intelligence 1993 p 155-167 (For primary document see N93-25961 09-63)

Avail: CASI HC A03/MF A03

We use neural networks to perform retrievals of temperature and water fractions from simulated clear air radiances for the Atmospheric Infrared Sounder (AIRS). Neural networks allow us to make effective use of the large AIRS channel set, and give good performance with noisy input. We retrieve surface temperature, air temperature at 64 distinct pressure levels, and water fractions at 50 distinct pressure levels. Using 728 temperature and surface sensitive channels, the RMS error for temperature retrievals

with 0.2K input noise is 1.2K. Using 586 water and temperature sensitive channels, the mean error with 0.2K input noise is 16 percent. Our implementation of backpropagation training for neural networks on the 16,000-processor MasPar MP-1 runs at a rate of 90 million weight updates per second, and allows us to train large networks in a reasonable amount of time. Once trained, the network can be used to perform retrievals quickly on a workstation of moderate power. Author

N93-25976*# National Aeronautics and Space Administration. Goddard Space Flight Center, Greenbelt, MD.

CLASSIFYING MULTISPECTRAL DATA BY NEURAL NETWORKS

Brian A. Telfer (Naval Surface Warfare Center, Silver Spring, MD.), Harold H. Szu (Naval Surface Warfare Center, Silver Spring, MD.), and Richard K. Kiang *In its* The 1993 Goddard Conference on Space Applications of Artificial Intelligence 1993 p 169-177 (For primary document see N93-25961 09-63)

Avail: CASI HC A02/MF A03

Several energy functions for synthesizing neural networks are tested on 2-D synthetic data and on Landsat-4 Thematic Mapper data. These new energy functions, designed specifically for minimizing misclassification error, in some cases yield significant improvements in classification accuracy over the standard least mean squares energy function. In addition to operating on networks with one output unit per class, a new energy function is tested for binary encoded outputs, which result in smaller network sizes. The Thematic Mapper data (four bands were used) is classified on a single pixel basis, to provide a starting benchmark against which further improvements will be measured. Improvements are underway to make use of both subpixel and superpixel (i.e. contextual or neighborhood) information in tile processing. For single pixel classification, the best neural network result is 78.7 percent, compared with 71.7 percent for a classical nearest neighbor classifier. The 78.7 percent result also improves on several earlier neural network results on this data. Author

N93-25977*# National Aeronautics and Space Administration. Goddard Space Flight Center, Greenbelt, MD.

THE WorkPlace DISTRIBUTED PROCESSING ENVIRONMENT

Troy Ames and Scott Henderson (Computer Technology Associates, Inc., Rockville, MD.) *In its* The 1993 Goddard Conference on Space Applications of Artificial Intelligence 1993 p 181-188 (For primary document see N93-25961 09-63)

Avail: CASI HC A02/MF A03

Real time control problems require robust, high performance solutions. Distributed computing can offer high performance through parallelism and robustness through redundancy. Unfortunately, implementing distributed systems with these characteristics places a significant burden on the applications programmers. Goddard Code 522 has developed WorkPlace to alleviate this burden. WorkPlace is a small, portable, embeddable network interface which automates message routing, failure detection, and re-configuration in response to failures in distributed systems. This paper describes the design and use of WorkPlace, and its application in the construction of a distributed blackboard system. Author

N93-25978*# National Aeronautics and Space Administration. Goddard Space Flight Center, Greenbelt, MD.

MODEL-BASED REASONING FOR SYSTEM AND SOFTWARE ENGINEERING: THE KNOWLEDGE FROM PICTURES (KFP) ENVIRONMENT

Sydney Bailin (Computer Technology Associates, Inc., Rockville, MD.), Frank Paterra (Computer Technology Associates, Inc., Rockville, MD.), Scott Henderson (Computer Technology Associates, Inc., Rockville, MD.), and Walt Truszkowski *In its* The 1993 Goddard Conference on Space Applications of Artificial Intelligence 1993 p 189-200 (For primary document see N93-25961 09-63)

Avail: CASI HC A03/MF A03

This paper presents a discussion of current work in the area of graphical modeling and model-based reasoning being undertaken by the Automation Technology Section, Code 522.3, at Goddard. The work was initially motivated by the growing realization that the knowledge acquisition process was a major bottleneck in the generation of fault detection, isolation, and repair (FDIR) systems for application in automated Mission Operations. As with most research activities this work started out with a simple objective: to develop a proof-of-concept system demonstrating that a draft rule-base for a FDIR system could be automatically realized by reasoning from a graphical representation of the system to be monitored. This work was called Knowledge From Pictures (KFP) (Truszkowski et. al. 1992). As the work has successfully progressed the KFP tool has become an environment populated by a set of tools that support a more comprehensive approach to model-based reasoning. This paper continues by giving an overview of the graphical modeling objectives of the work, describing the three tools that now populate the KFP environment, briefly presenting a discussion of related work in the field, and by indicating future directions for the KFP environment. Author

N93-25979*# University of Central Florida, Orlando. Dept. of Computer Science.

INFERRING HEURISTIC CLASSIFICATION HIERARCHIES FROM NATURAL LANGUAGE INPUT

Richard Hull and Fernando Gomez *In* NASA. Goddard Space Flight Center, The 1993 Goddard Conference on Space Applicati ons of Artificial Intelligence 1993 p 201-215 (For primary document see N93-25961 09-63)

(Grant NAG10-0058)

Avail: CASI HC A03/MF A03

A methodology for inferring hierarchies representing heuristic knowledge about the check out, control, and monitoring sub-system (CCMS) of the space shuttle launch processing system from natural language input is explained. Our method identifies failures explicitly and implicitly described in natural language by domain experts and uses those descriptions to recommend classifications for inclusion in the experts' heuristic hierarchies. Author

N93-25980*# Vigyan Research Associates, Inc., Hampton, VA.

MULTI-VIEWPOINT CLUSTERING ANALYSIS

Mala Mehrotra and Chris Wild (Old Dominion Univ., Norfolk, VA.) *In* NASA. Goddard Space Flight Center, The 1993 Goddard Conference on Space Applicati ons of Artificial Intelligence 1993 p 217-231 (For primary document see N93-25961 09-63)

(Contract NAS9-18706)

Avail: CASI HC A03/MF A03

In this paper, we address the feasibility of partitioning rule-based systems into a number of meaningful units to enhance the comprehensibility, maintainability and reliability of expert systems software. Preliminary results have shown that no single structuring principle or abstraction hierarchy is sufficient to understand complex knowledge bases. We therefore propose the Multi View Point - Clustering Analysis (MVP-CA) methodology to provide multiple views of the same expert system. We present the results of using this approach to partition a deployed knowledge-based system that navigates the Space Shuttle's entry. We also discuss the impact of this approach on verification and validation of knowledge-based systems. Author

N93-25981*# National Aeronautics and Space Administration. Goddard Space Flight Center, Greenbelt, MD.

AN APPLICATION OF MACHINE LEARNING TO THE ORGANIZATION OF INSTITUTIONAL SOFTWARE REPOSITORIES **c82**

Sidney Bailin (Computer Technology Associates, Inc., Rockville, MD.), Scott Henderson (Computer Technology Associates, Inc., Rockville, MD.), and Walt Truszkowski *In its* The 1993 Goddard Conference on Space Applications of Artificial Intelligence 1993 p 235-248 (For primary document see N93-25961 09-63)

Avail: CASI HC A03/MF A03

Software reuse has become a major goal in the development of space systems, as a recent NASA-wide workshop on the subject made clear. The Data Systems Technology Division of Goddard Space Flight Center has been working on tools and techniques for promoting reuse, in particular in the development of satellite ground support software. One of these tools is the Experiment in Libraries via Incremental Schemata and Cobweb (ElvisC). ElvisC applies machine learning to the problem of organizing a reusable software component library for efficient and reliable retrieval. In this paper we describe the background factors that have motivated this work, present the design of the system, and evaluate the results of its application. Author

N93-25982*# Analytic Sciences Corp., Reading, MA.
VISUALIZING THE SEMANTIC CONTENT OF LARGE TEXT DATABASES USING TEXT MAPS **c82**
Nathan Combs *In* NASA. Goddard Space Flight Center, The 1993 Goddard Conference on Space Applicati ons of Artificial Intelligence 1993 p 249-261 (For primary document see N93-25961 09-63)
Avail: CASI HC A03/MF A03

A methodology for generating text map representations of the semantic content of text databases is presented. Text maps provide a graphical metaphor for conceptualizing and visualizing the contents and data interrelationships of large text databases. Described are a set of experiments conducted against the TIPSTER corpora of Wall Street Journal articles. These experiments provide an introduction to current work in the representation and visualization of documents by way of their semantic content. Author

N93-25983*# Loyola Univ., New Orleans, LA.
IN SEARCH OF META-KNOWLEDGE **c82**
Antonio M. Lopez, Jr. *In* NASA. Goddard Space Flight Center, The 1993 Goddard Conference on Space Applicati ons of Artificial Intelligence 1993 p 263-269 (For primary document see N93-25961 09-63)
Avail: CASI HC A02/MF A03

Development of an Intelligent Information System (IIS) involves application of numerous artificial intelligence (AI) paradigms and advanced technologies. The National Aeronautics and Space Administration (NASA) is interested in an IIS that can automatically collect, classify, store and retrieve data, as well as develop, manipulate and restructure knowledge regarding the data and its application (Campbell et al., 1987, p.3). This interest stems in part from a NASA initiative in support of the interagency Global Change Research program. NASA's space data problems are so large and varied that scientific researchers will find it almost impossible to access the most suitable information from a software system if meta-information (metadata and meta-knowledge) is not embedded in that system. Even if more, faster, larger hardware is used, new innovative software systems will be required to organize, link, maintain, and properly archive the Earth Observing System (EOS) data that is to be stored and distributed by the EOS Data and Information System (EOSDIS) (Dozier, 1990). Although efforts are being made to specify the metadata that will be used in EOSDIS, meta-knowledge specification issues are not clear. With the expectation that EOSDIS might evolve into an IIS, this paper presents certain ideas on the concept of meta-knowledge and demonstrates how meta-knowledge might be represented in a pixel classification problem. Author

N93-25984*# Johns Hopkins Univ., Laurel, MD. Applied Physics Lab.
THE StarView INTELLIGENT QUERY MECHANISM
R. D. Semmel and D. P. Silberberg (Space Telescope Science Inst., Baltimore, MD.) *In* NASA. Goddard Space Flight Center, The 1993 Goddard Conference on Space Applicati ons of Artificial Intelligence 1993 p 271-285 (For primary document see N93-25961 09-63)
Avail: CASI HC A03/MF A03

The StarView interface is being developed to facilitate the retrieval of scientific and engineering data produced by the Hubble Space Telescope. While predefined screens in the interface can be used to specify many common requests, ad hoc requests require a dynamic query formulation capability. Unfortunately, logical level knowledge is too sparse to support this capability. In particular, essential formulation knowledge is lost when the domain of interest is mapped to a set of database relation schemas. Thus, a system known as QUICK has been developed that uses conceptual design knowledge to facilitate query formulation. By heuristically determining strongly associated objects at the conceptual level, QUICK is able to formulate semantically reasonable queries in response to high-level requests that specify only attributes of interest. Moreover, by exploiting constraint knowledge in the conceptual design, QUICK assures that queries are formulated quickly and will execute efficiently. Author

N93-25986*# Rensselaer Polytechnic Inst., Troy, NY. Center for Intelligent Robotic Systems for Space Exploration.
NASA CENTER FOR INTELLIGENT ROBOTIC SYSTEMS FOR SPACE EXPLORATION
Sep. 1990 37 p Revised
(Grant NAGw-1333)
(NASA-CR-193208; NAS 1.26:193208) Avail: CASI HC A03/MF A01

NASA's program for the civilian exploration of space is a challenge to scientists and engineers to help maintain and further develop the United States' position of leadership in a focused sphere of space activity. Such an ambitious plan requires the contribution and further development of many scientific and technological fields. One research area essential for the success of these space exploration programs is Intelligent Robotic Systems. These systems represent a class of autonomous and semi-autonomous machines that can perform human-like functions with or without human interaction. They are fundamental for activities too hazardous for humans or too distant or complex for remote telemanipulation. To meet this challenge, Rensselaer Polytechnic Institute (RPI) has established an Engineering Research Center for Intelligent Robotic Systems for Space Exploration (CIRSSE). The Center was created with a five year $5.5 million grant from NASA submitted by a team of the Robotics and Automation Laboratories. The Robotics and Automation Laboratories of RPI are the result of the merger of the Robotics and Automation Laboratory of the Department of Electrical, Computer, and Systems Engineering (ECSE) and the Research Laboratory for Kinematics and Robotic Mechanisms of the Department of Mechanical Engineering, Aeronautical Engineering, and Mechanics (ME,AE,&M), in 1987. This report is an examination of the activities that are centered at CIRSSE. Author (revised)

N93-26162# Massachusetts Inst. of Tech., Cambridge. Dept. of Brain and Cognitive Sciences.
USING MODULAR NEURAL NETWORKS WITH LOCAL REPRESENTATIONS TO CONTROL DYNAMIC SYSTEMS Final Report, 1 Sep. 1989 - 31 Aug. 1992
Christopher G. Atkeson 18 Dec. 1992 11 p
(Grant AF-AFOSR-0500-89)
(AD-A261597; AFOSR-93-0062TR) Avail: CASI HC A03/MF A01

The objective of the research was to develop an artificial neural network with very fast learning. Many areas of activity and approaches have convinced us that we can perform training and access sufficiently quickly to allow real-time learning. DTIC

N93-26333# California Univ., Santa Barbara. Dept. of Electrical and Computer Engineering.
NONLINEAR SYSTEM DESIGN: ADAPTIVE FEEDBACK LINEARIZATION WITH UNMODELED DYNAMICS Final Technical Report, 1 Oct. 1989 - 30 Sep. 1992
Petar V. Kokotovic 22 Dec. 1992 16 p
(Contract F49620-92-J-0004)
(AD-A261360; AFOSR-93-0098TR) Avail: CASI HC A03/MF A01

The main goal of this research has been to develop a unified geometric-asymptotic-adaptive methodology for feedback design of nonlinear control systems. Such a methodology is needed because the existing differential geometric results are restrictive and often violated by small modeling errors. Effects of these errors can be analyzed asymptotically by singular perturbation methods, which, however, are still lacking a clear geometric interpretation. Neither geometric, nor perturbational problem formulations can cope with large parametric uncertainty, for which an adaptive approach seems suitable. Conversely, both geometric and asymptotic techniques can become constructive steps in the design of an adaptive scheme and in the analysis of its robustness. In our research these three heretofore separate techniques have been to be merged into a methodology which eliminates their individual shortcomings. In a separate research direction we have initiated a study of systems with practically important nondifferentiable nonlinearities such as dead-zone, backlash and hysteresis. These systems can not be analyzed by existing methods. DTIC

N93-26365# Integrated Systems, Inc., Santa Clara, CA.
ADAPTIVE CONTROL OF NONLINEAR FLEXIBLE SYSTEMS Final Report, 1 Aug. 1990 - 31 Jul. 1992
Robert L. Kosut and M. G. Kabuli 18 Jan. 1993 55 p
(Contract F49620-90-C-0064)
(AD-A261676; ISI-5878-2; AFOSR-93-0081TR) Avail: CASI HC A04/MF A01

The objective is the development of adaptive control methods which can significantly improve closed-loop performance for a broad class of

nonlinear flexible systems. Towards this end, a nonlinear controller, applicable to a broad class of nonlinear systems, was devised. The controller consists of a feedforward signal generator which incorporates a model estimate together with a global feedback linearizer. There is an inner feedback controller which modifies control action in accordance with output errors between the feedforward ideal output and the actual sensed output. The adaptive scheme studied uses measured data to update the model in the feedforward signal generator. It was discovered in many simulations that this two-level approach to adaptive feedback linearization can perform significantly better than feedback linearizers using an observer network. DTIC

N93-26487# Carnegie-Mellon Univ., Pittsburgh, PA. School of Computer Science.
REINFORCEMENT LEARNING FOR ROBOTS USING NEURAL NETWORKS Ph.D. Thesis
Long-Ji Lin 6 Jan. 1993 165 p
(Contract F33615-90-C-1465; ARPA Order 7597)
(AD-A261434; CMU-CS-93-103) Avail: CASI HC A08/MF A02

Reinforcement learning agents are adaptive, reactive, and self-supervised. The aim of this dissertation is to extend the state of the art of reinforcement learning and enable its applications to complex robot-learning problems. In particular, it focuses on two issues. First, learning from sparse and delayed reinforcement signals is hard and in general a slow process. Techniques for reducing learning time must be devised. Second, most existing reinforcement learning methods assume that the world is a Markov decision process. This assumption is too strong for many robot tasks of interest, This dissertation demonstrates how we can possibly overcome the slow learning problem and tackle non-Markovian environments, making reinforcement learning more practical for realistic robot tasks. DTIC

N93-26596# Sandia National Labs., Albuquerque, NM.
DIGITAL FILTER CONTROL OF REMOTELY OPERATED FLEXIBLE ROBOTIC STRUCTURES
J. T. Feddema 1992 6 p Presented at the 5th Topical Meeting on Robotics and Remote Systems, Knoxville, TN, 26-29 Apr. 1993
(Contract DE-AC04-76DP-00789)
(DE93-007587; SAND-92-1630C; CONF-930403-19) Avail: CASI HC A02/MF A01

This paper presents an infinite impulse response (IIR) filtering technique for reducing structural vibration in remotely operated robotic systems. The technique uses a discrete filter between the operator's joy stick and the robot controller to alter the inputs of the system so that residual vibration and swing are reduced. A linearized plant model of the system is analyzed in the discrete time domain, and the filter is designed using pole-zero placement in the z-plane. This technique has been successfully applied to a two link flexible arm and a gantry crane with a suspended payload. DOE

N93-25610*# Naval Surface Warfare Center, Silver Spring, MD.
A SOFTWARE PACKAGE FOR NEURAL NETWORK APPLICATIONS DEVELOPMENT
Robert H. Baran *In* NASA, Washington, Technology 2002: The Third National Technology Transfer Conference and Exposition, Volume 1 Feb. 1993 p 463-472 Sponsored in part by Office of Naval Technology (For primary document see N93-25561 09-99)
Avail: CASI HC A02/MF A04

N93-25611*# Johns Hopkins Univ., Laurel, MD. Applied Physics Lab.
CONTROL OF COMPLEX DYNAMIC SYSTEMS BY NEURAL NETWORKS
James C. Spall and John A. Cristion *In* NASA, Washington, Technology 2002: The Third National Technology Transfer Conference and Exposition, Volume 1 Feb. 1993 p 473-482 (For primary document see N93-25561 09-99)
(Contract N00039-91-C-0001)
Avail: CASI HC A02/MF A04

N93-25612*# Bureau of Mines, Tuscaloosa, AL.
ADAPTIVE PROCESS CONTROL WITH FUZZY LOGIC AND GENETIC ALGORITHMS
C. L. Karr *In* NASA, Washington, Technology 2002: The Third National Technology Transfer Conference and Exposition, Volume 1 Feb. 1993 p 483-490 (For primary document see N93-25561 09-99)
Avail: CASI HC A02/MF A04

N93-26071*# Wyoming Univ., Laramie. Dept. of Computer Science.
A VISION ARCHITECTURE FOR THE EXTRAVEHICULAR ACTIVITY RETRIEVER Final Report
Michael Magee *In* NASA. Johnson Space Center, National Aeronautics and Space Administration (NASA)/American Society for Engineering Education (ASEE) Summer Faculty Fellowship Program, 1992, Volume 2 Dec. 1992 10 p (For primary document see N93-26070 09-99)
(Grant NGT-44-005-803)
Avail: CASI HC A02/MF A02

N93-26072*# Oklahoma State Univ., Stillwater. Dept. of Computer Science.
A STUDY OF MAPPING EXOGENOUS KNOWLEDGE REPRESENTATIONS INTO CONFIG Final Report
Blayne E. Mayfield *In* NASA. Johnson Space Center, National Aeronautics and Space Administration (NASA)/American Society for Engineering Education (ASEE) Summer Faculty Fellowship Program, 1992, Volume 2 Dec. 1992 15 p (For primary document see N93-26070 09-99)
(Grant NGT-44-005-803)
Avail: CASI HC A03/MF A02

64 NUMERICAL ANALYSIS

Includes iteration, difference equations, and numerical approximation.

N93-24973# Brookhaven National Lab., Upton, NY. Dept. of Nuclear Energy.
ALGORITHMS FOR OPTIMAL REDUNDANCY ALLOCATION
J. Vandenkieboom and R. Youngblood 1993 7 p Presented at the Probabilistic Safety Assessment International Topical Meeting, Clearwater Beach, FL, 27-29 Jan. 1993
(Contract DE-AC02-76CH-00016)
(DE93-005709; BNL-48250; CONF-930116-30) Avail: CASI HC A02/MF A01

Heuristic and exact methods for solving the redundancy allocation problem are compared to an approach based on genetic algorithms. The various methods are applied to the bridge problem, which has been used as a benchmark in earlier work on optimization methods. Comparisons are presented in terms of the best configuration found by each method and the computation effort which was necessary in order to find it. DOE

N93-25103# Sandia National Labs., Albuquerque, NM.
PROBABILISTIC ANALYSIS OF MANIPULATION TASKS: A RESEARCH AGENDA
R. C. Brost and A. D. Christiansen (Grenoble-1 Univ., France.) 1992 10 p Presented at the Institute of Electrical and Electronics Engineers International Conference on Robotics and Automation, Atlanta, GA, 2-7 May 1993
(Contract DE-AC04-76DP-00789)
(DE93-000713; SAND-92-2032C; CONF-930519-3) Avail: CASI HC A02/MF A01

This paper addresses the problem of manipulation planning in the presence of uncertainty. We begin by reviewing the worst-case planning techniques introduced in and show that these methods are hampered by an information gap inherent to worst-case analysis techniques. As the task uncertainty increases, these methods fail to produce useful information even though a high-quality plan may exist. To fill this gap, we present the probabilistic backprojection, which describes the likelihood that a given action will achieve the task goal from a given initial state. We provide a constructive definition of the probabilistic backprojection and related probabilistic models of manipulation task mechanics, and show how these models unify and enhance several past results in manipulation planning. These models capture the fundamental nature of the task behavior, but appear to be very complex. Methods for computing these models are sketched, but efficient computational methods remain unknown. DOE

N93-25140*# National Aeronautics and Space Administration. Lyndon B. Johnson Space Center, Houston, TX.

MONTE-CARLO METHODS MAKE DEMPSTER-SHAFER FORMALISM FEASIBLE

Vladik Ya. Kreinovich (Texas Univ., El Paso.), Andrew Bernat (Texas Univ., El Paso.), Walter Borrett (Texas Univ., El Paso.), Yvonne Mariscal (Texas Univ., El Paso.), and Elsa Villa (Texas Univ., El Paso.) 1991 17 p

(Grants NAG9-482; NSF CDA-90-15006)

(NASA-CR-192945; NAS 1.26:192945) Avail: CASI HC A03/MF A01

One of the main obstacles to the applications of Dempster-Shafer formalism is its computational complexity. If we combine m different pieces of knowledge, then in general case we have to perform up to 2(sup m) computational steps, which for large m is infeasible. For several important cases algorithms with smaller running time were proposed. We prove, however, that if we want to compute the belief bel(Q) in any given query Q, then exponential time is inevitable. It is still inevitable, if we want to compute bel(Q) with given precision epsilon. This restriction corresponds to the natural idea that since initial masses are known only approximately, there is no sense in trying to compute bel(Q) precisely. A further idea is that there is always some doubt in the whole knowledge, so there is always a probability p(sub o) that the expert's knowledge is wrong. In view of that it is sufficient to have an algorithm that gives a correct answer a probability greater than 1-p(sub o). If we use the original Dempster's combination rule, this possibility diminishes the running time, but still leaves the problem infeasible in the general case. We show that for the alternative combination rules proposed by Smets and Yager feasible methods exist. We also show how these methods can be parallelized, and what parallelization model fits this problem best. Author (revised)

N93-25151# Los Alamos National Lab., NM.

ASYMPTOTIC DERIVATION OF THE SIMPLIFIED P(SUB N) EQUATIONS

E. W. Larsen (Michigan Univ., Ann Arbor.), J. E. Morel, and J. M. McGhee 1993 13 p Presented at the International Topical Meeting on Mathematical Methods and Supercomputing in Nuclear Applications (M and C Plus SNA 1993), Karlsruhe, Germany, 19-23 Apr. 1993

(Contracts W-7405-eng-36; DE-FG02-92ER-75709)

(DE93-007342; LA-UR-93-180; CONF-930404-5) Avail: CASI HC A03/MF A01

The diffusion and simplified P(sub N) equations are derived from the transport equation by means of an asymptotic expansion in which the diffusion equation is the leading order approximation and the simplified P(sub N) equations are higher-order approximations. In addition, the simplified P(sub N) equations are reformulated in a 'canonical' form that greatly facilitates the formulation of boundary conditions and the implementation of the resulting problem in a conventional multigroup diffusion code. Numerical comparisons of S(sub N), diffusion, and simplified P(sub N) solutions show that the simplified P(sub N) solutions often contain most of the transport corrections for the diffusion approximation. DOE

N93-25223*# California Inst. of Tech., Pasadena. Div. of Geological and Planetary Sciences.

USING A MULTIFRONTAL SPARSE SOLVER IN A HIGH PERFORMANCE, FINITE ELEMENT CODE

Scott D. King, Robert Lucas (Supercomputer Research Center, Bowie, MD.), and Arthur Raefsky (Stanford Univ., CA.) 1990 47 p

(Grants NAG5-1132; NSF EAR-86-18744)

(NASA-CR-192718; NAS 1.26:192718) Avail: CASI HC A03/MF A01

We consider the performance of the finite element method on a vector supercomputer. The computationally intensive parts of the finite element method are typically the individual element forms and the solution of the global stiffness matrix both of which are vectorized in high performance codes. To further increase throughput, new algorithms are needed. We compare a multifrontal sparse solver to a traditional skyline solver in a finite element code on a vector supercomputer. The multifrontal solver uses the Multiple-Minimum Degree reordering heuristic to reduce the number of operations required to factor a sparse matrix and full matrix computational kernels (e.g., BLAS3) to enhance vector performance. The net result in an order-of-magnitude reduction in run time for a finite element application on one processor of a Cray X-MP. Author

N93-25262*# Vanderbilt Univ., Nashville, TN. Dept. of Computer Science.

IMPROVING PERFORMANCE THROUGH CONCEPT FORMATION AND CONCEPTUAL CLUSTERING Final Technical Report, 1 Jun. 1989 - 31 Oct. 1992

Douglas H. Fisher 31 Oct. 1992 51 p

(Contract NCC2-645)

(NASA-CR-192726; NAS 1.26:192726) Avail: CASI HC A04/MF A01

Research from June 1989 through October 1992 focussed on concept formation, clustering, and supervised learning for purposes of improving the efficiency of problem-solving, planning, and diagnosis. These projects resulted in two dissertations on clustering, explanation-based learning, and means-ends planning, and publications in conferences and workshops, several book chapters, and journals; a complete Bibliography of NASA Ames supported publications is included. The following topics are studied: clustering of explanations and problem-solving experiences; clustering and means-end planning; and diagnosis of space shuttle and space station operating modes. Derived from text

N93-25687# Maryland Univ., College Park. Dept. of Computer Science.

PARALLEL MATRIX COMPUTATIONS Final Report, 15 Apr. 1987 - 14 Oct. 1992

G. W. Stewart and Dianne P. OLeary 14 Oct. 1992 21 p

(Grant AF-AFOSR-0188-87)

(AD-A260783; AFORS-TR-93-0014) Avail: CASI HC A03/MF A01

This project concerns the design and analysis of algorithms for matrix computations to be run in a processor-rich environment. The researchers focused on algorithms that require no global control and that can be run on systems with only local connections among processors. They investigated these algorithms both theoretically and practically. The final year's work has focused on subspace updating, granularity of communication, projection methods for eigenvalue problems, polynomial preconditioners for conjugate gradients, and other topics. DTIC

N93-25762# Colorado Univ., Denver.

MULTILEVEL TECHNIQUES IN LARGE SCALE COMPUTATION Final Report, 1 Feb. 1991 - 30 Sep. 1992

Stephen F. McCormick Oct. 1992 9 p

(Grant AF-AFOSR-0156-91)

(AD-A261082; AFOSR-93-0065TR) Avail: CASI HC A02/MF A01

Techniques have been demonstrated for time dependent problems that allow rare activation of finest grids; new multiscale approaches in statistical mechanics and many particle problems; fast integral transforms and solvers for integro-differential equations; fast Dirac solvers; and multigrid algorithms on decomposed domains. DTIC

N93-25773# Aeronautical Research Labs., Melbourne (Australia).

ESTIMATION OF COEFFICIENTS IN A RATIONAL FUNCTION FROM OBSERVED VALUES

Betty Emslie Dec. 1992 22 p

(AD-A261126; ARL-TR-8; DODA-AR-007-116) Avail: CASI HC A03/MF A01

A method for estimating the coefficients in a rational function representation of the frequency response function of a dynamic system is presented. A nonlinear least squares approach is used and this requires initial estimates for the coefficients. The first attempt to find initial estimates was not satisfactory, but a second approach, which can be thought of as a linear approximation to the nonlinear problem, was much more successful. Tests have been carried out with both generated and experimental data and reasonable estimates have been achieved. DTIC

N93-25905# Yale Univ., New Haven, CT. Dept. of Computer Science.

THE RAPID SOLUTION OF THE LAPLACE EQUATION ON REGIONS WITH FRACTAL BOUNDARIES

J. H. Ma 21 Oct. 1992 85 p

(Contract N00014-89-J-1527; NSF DMS-90-12751)

(AD-A260585; YaleU/DCS/RR-927) Avail: CASI HC A05/MF A01

Interest in the numerical solution of the Laplace equation on regions with fractal boundaries arises both in mathematics and physics. In mathematics, examples include harmonic measure of fractals, complex iteration theory, and potential theory. In physics, examples include Brownian motion, crystallization, electrodeposition, viscous fingering, and

diffusion-limited aggregation. In a typical application, the numerical simulation has to be on a very large scale involving at least tens of thousands of equations with as many unknowns in order to obtain any meaningful results. Attempts to use conventional techniques have encountered insurmountable difficulties, due to excessive CPU time requirements of the computations involved. Indeed, conventional direct algorithms for the solution of linear systems require order O(N(exp 3)) operations for the solution of an N x N-problem, while classical iterative methods require order O(N(exp 2)) operations, with the constant strongly dependent on the problem in question. In either case, the computational expense is prohibitive for large-scale problems. We present a direct algorithm for the solution of the Laplace equation on regions with fractal boundaries. The algorithm requires O(N) operations with a constant dependent only on the geometry of the fractal boundaries. The performance of the algorithm is demonstrated by numerical examples, and applications and generalizations of the scheme are discussed. DTIC

N93-26199# North Carolina Univ., Charlotte. Dept. of Mathematics.
ACTIVITY REPORT Report, 1 Oct. 1991 - 1 Oct. 1992
Michael V. Klibanov and Semion Gutman 1 Oct. 1992 11 p
(Contract N00014-92-J-1008)
(AD-A261933) Avail: CASI HC A03/MF A01

We have been working on the following issues: (1) Numerical methods and computational experiments for the multidimensional Inverse Scattering Problem (ISP) for the Helmholtz equation; (2) Numerical methods for the 3-dimensional ISP in random media; (3) Global convergence of numerical methods for 3-D ISP with time dependent data; (4) Phaseless 1-dimensional ISP; and (5) Quasi-Reversibility method for nonclassical Cauchy problems. DTIC

N93-26222# Illinois Univ., Chicago. Dept. of Mathematics, Statistics and Computer Science.
PDE: DIFFERENTIAL, GEOMETRIC AND ALGEBRAIC METHODS IN NONLINEAR FILTERING Final Report, 21 Aug. 1989 - 20 Aug. 1992
Stephen S. Yau 7 Jan. 1993 11 p
(Contract DAAL03-89-K-0123)
(AD-A260967; ARO-26674.6-MA) Avail: CASI HC A03/MF A01

We have constructed explicitly the most general class of finite dimensional filters which include both Kalman-Bucy filters and Benes filters as special cases. We also proved that if the state space dimension is less than three, then generically all finite dimensional filters must be those constructed by us from the Lie algebraic point of view. Without making any assumption on the drift term of the filtering system, we can write down the asymptotic solution to the famous Kolmogorov equation which is a fundamental equation in Applied Science. Moreover we have an explicit algorithm to construct the convergent solution from this formal asymptotic solution. DTIC

N93-26228# Naval Postgraduate School, Monterey, CA.
ELASTIC CURVES ON THE SPHERE Technical Report, Sep. - Nov. 1992
Guido Brunnett and Peter E. Crouch 16 Dec. 1992 22 p
(AD-A261057; NPS-MA-93-010) Avail: CASI HC A03/MF A01

This paper deals with the derivation of equations suitable for the computation of elastic curves on the sphere. To this end equations for the main invariants of spherical elastic curves are given. A new method for solving geometrically constraint differential equations is used to compute the curves for given initial values. A classification of the fundamental forms of the curves is presented. DTIC

N93-26344# Rice Univ., Houston, TX. Dept. of Mathematical Sciences.
INTEGRATED APPROACHES TO PARALLELISM IN OPTIMIZATION AND THE SOLUTION OF INVERSE PROBLEMS Final Report, 1 Apr. - 30 Sep. 1992
John E. Dennis and Richard A. Tapia 30 Sep. 1992 6 p
(Contract F49620-92-J-0203)
(AD-A261490; AFOSR-93-0091TR) Avail: CASI HC A02/MF A01

New primal-dual interior point methods for linear programming were developed. Convergence properties were determined. DTIC

N93-26345# Massachusetts Univ., Amherst. Dept. of Computer and Information Science.
INTELLIGENT, REAL-TIME PROBLEM SOLVING, PHASE 3 Final Report, 1 Nov. 1990 - 30 Apr. 1992
Paul R. Cohen, Victor R. Lesser, and David M. Hart 30 Apr. 1992 37 p
(Grant AF-AFOSR-0067-91)
(AD-A261441; AFOSR-93-0063TR) Avail: CASI HC A03/MF A01

Progress was made in the IRTPS initiative in five areas: resolving the relationship between deliberative and reactive planning with a framework for their effective combination; modeling the real-time performance of the Phoenix planner through the application of a powerful statistical technique--path analysis--that can be used to build causal models from observed behavior; developing and applying design-to-time scheduling to design a solution that uses all available resources to maximize solution quality within available time; extending previous work on the real-time monitoring and control structure we call envelopes; and finally, in a new body of research started in Phase 3, delineating a taxonomy of monitoring problems found in real-time domains, and developing optimal monitoring strategies to address these problems. DTIC

N93-26370# Naval Postgraduate School, Monterey, CA.
POWER ITERATIONS AND THE DOMINANT EIGENVALUE PROBLEM Technical Report, Mar. - Jun. 1992
Jeffery J. Leader 15 Dec. 1992 23 p LIMITED REPRODUCIBILITY: Availability: Document partially illegible
(AD-A261695; NPS-MA-93-007) Avail: CASI HC A03/MF A01

The orbits of an iterative numerical method for the dominant eigenvalue problem are analyzed from a discrete dynamical systems perspective. It is shown that the method can extract more information than the standard power method but at greater computational cost. DTIC

N93-26452# Naval Postgraduate School, Monterey, CA. Dept. of Mathematics.
BOUNDEDNESS AND ASYMPTOTICS OF THE GENERALIZED THEODORUS ITERATION Technical Report, Mar. - Jun. 1992
Jeffrey J. Leader 15 Dec. 1992 26 p
(AD-A261427; NPS-MA-93-006) Avail: CASI HC A03/MF A01

A weakly chaotic iteration, called the Generalized Theodorus Iteration, is analyzed with respect to its boundedness and asymptotics. The limit sets, which often are strange attractors, are also considered. Applications are discussed. DTIC

N93-26519# Yale Univ., New Haven, CT.
SOLUTION OF NONLINEAR BOUNDARY VALUE PROBLEM ON SUCCESSIVELY REFINED GRIDS Final Report, 1 Aug. 1988 - 30 Apr. 1992
Mitchell Smooke 30 Apr. 1992 8 p
(Contract F49620-88-C-0096)
(AD-A261395; AFOSR-93-0090TR) Avail: CASI HC A02/MF A01

Our AFOSR supported research (F49620-88-C-0096DEF) has focused on four main areas: (1) the development and analysis of adaptive continuation methods for the solution of nonlinear two-point boundary value problems; (2) the investigation of flame stretch and flame curvature in tubular premixed laminar flames; (3) the study of fresh reactant-hot product counterflow flames; and (4) the formulation of a parallel multidimensional elliptic boundary value solver for use in complex chemistry combustion problems. DTIC

N93-26560*# National Aeronautics and Space Administration. Lewis Research Center, Cleveland, OH.
A BRIEF DESCRIPTION OF A NEW NUMERICAL FRAMEWORK FOR SOLVING CONSERVATION LAWS: THE METHOD OF SPACE-TIME CONSERVATION ELEMENT AND SOLUTION ELEMENT
Sin-Chung Chang and Wai-Ming To (Sverdrup Technology, Inc., Brook Park, OH.) Jul. 1992 17 p Presented at the 13th International Conference on Numerical Methods in Fluid Dynamics, Rome, Italy, 6-10 Jul. 1992
(RTOP 505-62-52)
(NASA-TM-105757; E-7169; NAS 1.26:105757) Avail: CASI HC A03/MF A01

A new numerical method for solving conservation laws is being developed. It differs substantially from the well established methods, i.e., finite difference, finite volume, finite element, and spectral methods, in both concept and

methodology. It is much simpler than a typical high resolution method. No flux limiter or any technique related to characteristics is involved. No artificial viscosity or smoothing is introduced, and no moving mesh is used. Yet this method is capable of generating highly accurate shock tube solutions. The slight numerical overshoot and/or oscillations generated can be removed if a simple averaging formula initially used is replaced by a weighted formula. This modification has little effect on other parts of the solution. Because of its simplicity, generalization of this new method for multi-dimensional problems is straightforward. Derived from text

N93-24729*# State Univ. of New York, Buffalo. Dept. of Mechanical and Aerospace Engineering.
SCALAR GAIN INTERPRETATION OF LARGE ORDER FILTERS
Paul A. C. Mason and D. Joseph Mook *In* NASA. Goddard Space Flight Center, Flight Mechanics/Estimation Theory Symposium, 1992 Feb. 1993 p 507-521 Sponsored by NASA. Langley Research Center (For primary document see N93-24694 09-13)
Copyright Avail: CASI HC A03/MF A04

65 STATISTICS AND PROBABILITY

Includes data sampling and smoothing; Monte Carlo method; and stochastic processes.

N93-25860# Stanford Univ., CA.
TIME SERIES ANALYSIS AND MULTIVARIATE ANALYSIS Final Report, 12 Oct. 1992
Theodore W. Anderson 12 Oct. 1992 7 p
(Contract DAAL03-89-K-0033)
(AD-A261014; ARO-26394.8-MA) Avail: CASI HC A02/MF A01
The final report includes the following: summary of results, list of scientific personnel; list of technical reports, and list of publications. DTIC

N93-25863# Princeton Univ., NJ.
PROBABILITY AND STATISTICS APPLIED TO THE THEORY OF ALGORITHMS Final Report, 1 Jul. 1989 - 31 Oct. 1990
J. M. Steele 15 Oct. 1992 11 p
(Contract DAAL03-89-G-0092)
(AD-A261019; ARO-26158.24-MA) Avail: CASI HC A03/MF A01
This final report summarizes the contribution of the fourteen articles and two doctoral dissertations that were supported by this grant. The central aim of the work has been to understand the asymptotic behavior of the objective function of problems of classical combinatorial optimization, both in the stochastically modeled cases and in the deterministic worst-case. One of the engaging developments of this investigation has been that there are close parallels in these two problems, despite substantial differences in technique. In addition to reviewing the main contributions, there is a brief discussion of two articles that responded to targets of opportunity. One of these articles received the Wilcoxon Prize for Best Application Paper in 'Technometrics.' DTIC

N93-26255# Rome Lab., Griffiss AFB, NY.
CONSIDERATIONS OF THE ERROR VARIANCES OF TIME-AVERAGED ESTIMATORS FOR CORRELATED PROCESSES Report, Jun. 1991 - Oct. 1992
James H. Michels Dec. 1992 113 p
(AF Proj. 4506)
(AD-A261796; RL-TR-92-339) Avail: CASI HC A06/MF A02
This report considers the sample and error variances of both time-averaged correlation function and parameter estimators for stationary discrete complex processes. Analytic expressions for the variance of the biased, time-averaged auto, and cross-channel correlation function estimators of stationary discrete complex processes are developed. These expressions relate the variance of these estimators not only to the size of the observation windows used to obtain the estimates, but also to the correlation of the processes as well. They provide a performance measure which can be used to specify the window size of the observation interval required to achieve a specific value of this variance. A unique aspect of this development is the determination of the functional dependence of these expressions in terms of the process temporal and cross-channel correlation. Validation of the analytic expressions is obtained using Monte-Carlo simulation. Furthermore, computed results are presented for the error variances of several parameter estimators for which analytical expressions are lacking. Their performance is compared to that of the exact Cramer-Rao bound as a function of process correlation and data window size. Both Gaussian and non-Gaussian processes are considered as well as both single and multichannel processes. DTIC

N93-26262# Aerospace Technical Intelligence Center, Wright-Patterson AFB, OH.
SUBSTANTIATION OF A STOCHASTIC MODEL OF RHYTHMIC PHENOMENA
Ya P. Dragan 4 Feb. 1993 15 p Transl. into ENGLISH from Otbor i Peredacha Informatsii (USSR), no. 31, 1972 p 21-27
(AD-A261232; FASTC-ID(RS)T-0562-92) Avail: CASI HC A03/MF A01
In a number of areas of science and technology it is necessary to deal with rhythmic processes, such as the parasitic modulation of shot fluctuations in radio-electronic equipment, changes in the levels of stability of oscillatory parameters of biological systems, modulation of an acoustic field in a layer of water due to heaving of its surface change in meteorological parameters under the action of tidal forces, etc. Many investigators note the advisability of using methods of the theory of stationary random processes for analyzing such essentially nonstationary phenomena as biological, etc. rhythms, and stress the necessity of developing statistical methods, based directly on the properties of this type of nonstationary processes and having an explicit interpretation. DTIC

N93-26317# National Inst. of Standards and Technology, Gaithersburg, MD. Applied and Computational Mathematics Div.
MONTE CARLO APPROACH TO THE APPROXIMATION OF INVARIANT MEASURES
F. Y. Hunt Jan. 1993 27 p
(PB93-159069; NISTIR-4980) Avail: CASI HC A03/MF A01
Approximation of absolutely continuous measures of maps of the interval and the closely related tasks of computing Lyapunov exponents and metric entropy are accomplished in principle by iterating the map to produce a sufficiently long trajectory. There is an alternative approach based on approximating the fixed point of the Frobenius-Perron operator. The authors present a Monte-Carlo implementation of the original piecewise constant method proposed by Ulam. The method has the advantage of not requiring explicit evaluation of the elements of the approximate Frobenius-Perron operator. Convergence rates of Ulam's method and some recently proposed higher order variants are discussed. Using the classical Bohman-Korovkin theorems of approximation theory the optimality of the rates are shown to be a consequence of the saturation phenomenon. Finally Ulam's scheme is used to estimate the leading Lyapunov exponent of a one dimensional map with an absolutely continuous measure. The authors propose an analytical criterion for comparing the results of using this method with an estimate obtained by iterating a long trajectory and illustrate its use in a numerical example. NTIS

N93-26318# National Inst. of Standards and Technology, Gaithersburg, MD. Physics Lab.
GUIDELINES FOR EVALUATING AND EXPRESSING THE UNCERTAINTY OF NIST MEASUREMENTS RESULTS Final Technical Report
B. N. Taylor and C. E. Kuyatt Jan. 1993 20 p
(PB93-159465; NIST/TN-1297) Avail: CASI HC A03/MF A01; SOD HC
The Technical Note presents, in the context of the new NIST policy on uncertainty statements, those aspects of the Guide to the Expression of Uncertainty in Measurement being developed internationally that will be of most use to the NIST staff in implementing that policy. (The Guide is expected to be published by the International Organization for Standardization (ISO) during the first half of 1993 in the name of the ISO and the six other international organizations that sponsored its development). Also included are suggestions not contained in the Guide or policy. However, none of the guidance given in the Technical Note is to be interpreted as NIST policy unless it is directly quoted from the policy itself. NTIS

66 SYSTEMS ANALYSIS

Includes mathematical modeling; network analysis; and operations research.

N93-26330# Institute for Defense Analyses, Alexandria, VA.
SOFTWARE TESTING INITIATIVE FOR STRATEGIC DEFENSE SYSTEMS Final Report
Bill Brykczynski, Reginald N. Meeson, Christine Youngblut, and David A. Wheeler Mar. 1992 78 p
(Contract MDA903-89-C-0003)
(AD-A261350; IDA-P-2701; IDA/HQ-92-41141) Avail: CASI HC A05/MF A01

SDIO is planning to develop and deploy a ballistic missile defense system called Global Protection Against Limited Strikes (GPALS). Testing of GPALS software will play a critical role in ensuring the cost-effective development and reliable execution of the GPALS system. An earlier IDA study examined the states of the art and practice in the field of software testing. The study identified deficiencies in SDI software testing capabilities and recommended that SDIO launch a technical initiative to address these deficiencies. The current study lays the groundwork for this initiative. Emphasis is placed on three areas: (1) improving current and near-term SDI software testing practices by promoting consistent use of effective technology, (2) identifying promising new testing techniques that can add significantly to the reliability, cost-effectiveness, and quality of SDI software, and (3) fostering research into several fundamental problems of testing large-scale, concurrent, distributed, real-time, and fault-tolerant software systems. DTIC

N93-25967*# Harris Corp., Melbourne, FL.
ADAPTIVE LASER LINK RECONFIGURATION USING CONSTRAINT PROPAGATION
M. S. Crone, P. M. Julich, and L. M. Cook *In* NASA. Goddard Space Flight Center, The 1993 Goddard Conference on Space Applicati ons of Artificial Intelligence 1993 p 59-73 (For primary document see N93-25961 09-63)
(Contract F30602-89-D-0096)
Avail: CASI HC A03/MF A03

67 THEORETICAL MATHEMATICS

Includes topology and number theory.

No abstracts in this category.

70 PHYSICS (GENERAL)

For precision time and time interval (PTTI) see *35 Instrumentation and Photography;* for geophysics, astrophysics or solar physics see *46 Geophysics, 90 Astrophysics,* or *92 Solar Physics.*

N93-24978# European Space Agency, Paris (France).
FREQUENCY AND TIME FORUM
James J. Hunt, ed. Jun. 1992 502 p In ENGLISH and FRENCH The 6th forum was held in Noordwijk, Netherlands, 17-19 Mar. 1992
(ESA-SP-340; ISBN-92-9092-202-8; ETN-93-93497) Copyright Avail: CASI HC A22/MF A04

Conference papers for the following sessions are presented: space applications; fundamentals of time and frequency; optically pumped cesium atomic frequency space applications; quartz oscillators; dissemination of time and frequency; quartz filters and sensors; time and frequency activities relating to GPS (Global Positioning System) and GLONASS (Russian Global space Navigation System); a plenary poster session; quartz materials; atomic frequency standards, masers and trapped ion frequency sources; quartz space oscillators; electronics of atomic frequency standards; network synchronization; and miscellaneous studies relating to atomic frequency standards. For individual titles, see N93-24979 through N93-25069.

N93-24979# Stuttgart Univ. (Germany). Inst. of Navigation.
THE ADVANCES IN F AND T TECHNOLOGY: THEIR BENEFITS OF AND FOR SPACE SCIENCE AND TECHNOLOGY
Ph. Hartl *In* ESA, Frequency and Time Forum Jun. 1992 p 9-15 (For primary document see N93-24978 09-70)
Copyright Avail: CASI HC A02/MF A04

The keynote address to the Frequency and Time (F and T) forum is presented. Time is an indispensable parameter for numerous types of physical measurements. It is also the most accurately measurable physical quantity. Space science and technology apply F and T measurements for time tagging of scientific and technical data, for time complexing in the fields of telecommunication, for radiometric tracking, and orbit determination. F and T measurements constitute means for detection and quantification of various phenomena of interest for fundamental science, geoscience, and navigation. Space technology offers special opportunities for time distribution and for new markets of F and T applications, one of which is satellite navigation techniques. ESA

N93-24980*# National Aeronautics and Space Administration. Marshall Space Flight Center, Huntsville, AL.
HYDROGEN MASERS FOR SPACE **c36**
R. F. C. Vessot (Smithsonian Astrophysical Observatory, Cambridge, MA.), E. M. Mattison (Smithsonian Astrophysical Observatory, Cambridge, MA.), G. U. Nystrom (Smithsonian Astrophysical Observatory, Cambridge, MA.), L. M. Coyle (Smithsonian Astrophysical Observatory, Cambridge, MA.), R. Decher, S. J. Feltham (European Space Agency. European Space Research and Technology Center, ESTEC, Noordwijk, Netherlands.), G. Busca (Observatoire Cantonal, Neuchatel, Switzerland.), S. Starker (Deutsche Forschungsanstalt fuer Luft- und Raumfahrt, Oberpfaffenhofen, Germany.), and S. Leschiutta (Politecnico di Torino, Italy.) *In* ESA, Frequency and Time Forum Jun. 1992 p 19-25 Sponsored by Smithsonian Institution Research Opportunities Funds (For primary document see N93-24978 09-70)
(Contract NAS8-39194)
Copyright Avail: CASI HC A02/MF A04

A program for the design and testing of atomic hydrogen (H) masers for general use in space and methods for high precision space to Earth time and frequency comparisons are described. Because of the similarity of the space masers' basic components to those of existing terrestrial masers, their frequency stability is expected to reach well below 1 part in 10(exp 15) for intervals between 1000 and 100,000 sec. A NASA funded development program at the Smithsonian Astrophysical Observatory (SAO), currently in a conceptual design phase, is specifically directed toward producing an H laser for space and testing it for 6 months in the ESA Eureca spacecraft. The maser design will have the capability to cope with stringent dynamic load test levels and will have sufficient lifetime for long term continuous operation in future deep space missions such as a close approach solar probe. The time comparison system for the Eureca test mission will use high precision (less than 50 ps) pulsed laser time transfer between the spacecraft and H maser equipped laser ranging Earth stations. European studies of the proposed inclusion of a second H maser for direct onboard frequency comparisons and of a modified PRARE (Precise Range and Range rate Equipment) microwave system (in addition to the laser system) for worldwide time synchronization are also discussed. ESA

N93-24981# Laboratoire Primaire du Temps et des Frequences, Paris (France).
A SIMPLE AND COMPACT SOURCE OF COLD ATOMS FOR CESIUM FOUNTAINS AND MICROGRAVITY CLOCKS **c72**
A. Clairon, P. Laurent, A. Nadir, M. Drewsen (Ecole Normale Superieure, Paris, France.), D. Grison (Ecole Normale Superieure, Paris, France.), B. Lounis (Ecole Normale Superieure, Paris, France.), and C. Salomon (Ecole Normale Superieure, Paris, France.) *In* ESA, Frequency and Time Forum Jun. 1992 p 27-33 (For primary document see N93-24978 09-70)
Copyright Avail: CASI HC A02/MF A04

The use of very cold atoms for a pulsed fountain clock is addressed. Laser cooling and trapping of atoms has opened up new possibilites in the field of ultrastable atomic frequency standards. A narrow (2 Hz) Ramsey resonance in a Cesium fountain was recently observed, and the expected performances of an optimized fountain clock was discussed. A crucial element in such a fountain as well as in future microgravity clocks is the

source of cold atoms. A simple and compact source using a magnetooptical trap, or simply, optical molasses in a low vapor pressure cell, is presented and performances are discussed. ESA

N93-24982*# Jet Propulsion Lab., California Inst. of Tech., Pasadena.
MICROWAVE FREQUENCY DISCRIMINATOR WITH A CRYOGENIC SAPPHIRE RESONATOR FOR ULTRA-LOW PHASE NOISE **c33**
G. John Dick and David G. Santiago *In* ESA, Frequency and Time Forum Jun. 1992 p 35-39 Sponsored by NASA (For primary document see N93-24978 09-70)
Copyright Avail: CASI HC A01/MF A04

Results of an X-band frequency discriminator using a cooled sapphire microwave resonator are presented. These results show a lower close-in (1 Hz to 1 kHz offset) phase noise measurement floor than any oscillator presently available. This performance is made possible by a sapphire 'Whispering gallery' mode resonator which shows the highest quality factor (with Q's up to 30 million) for any RF, microwave, or acoustic resonator at temperatures down to 77K. Performance is further increased by the use of novel phase detection circuitry. The sapphire discriminator was used to characterize the phase noise of a single crystal quartz oscillator of the highest quality, without the use of a second similar oscillator as reference. ESA

N93-24983# Stuttgart Univ. (Germany). Inst. of Navigation.
THE APPLICATION OF THE PRARE PRINCIPLE FOR PRECISE TWO-WAY TIME TRANSFER TO SPACE-BASED ATOMIC CLOCKS
Wolfgang Schaefer *In* ESA, Frequency and Time Forum Jun. 1992 p 41-47 (For primary document see N93-24978 09-70)
(Grant BMFT-01-QS-154)
Copyright Avail: CASI HC A02/MF A04

System requirements, system layout, performance, and planned improvements, are outlined. The PRARE (Precise Range and Range rate Equipment) principle was originally intended as a universal tool for precise orbit determination of Earth orbiting spacecraft. Its primary purpose was to provide exact measurements of physical quantities required for this task and to avoid, as far as possible, the use of orbit and signal propagation models. Systematic errors were reduced by choosing a near optimum topology. The paper demonstrated that the very demanding requirements of time transfer between an orbiting H maser clock and the ground could be met by the instrument in its basic configuration, provided that the carried phase measurement resolution is increased and the onboard calibration provisions are specifically tailored for this task. An estimation of the expected residual instrumentation error is given in conclusion. ESA

N93-24984# Bureau International des Poids et Mesures, Sevres (France).
ATOMIC TIME SCALES FOR DYNAMICAL ASTRONOMY **c89**
B. Guinot *In* ESA, Frequency and Time Forum Jun. 1992 p 51-56 (For primary document see N93-24978 09-70)
Copyright Avail: CASI HC A02/MF A04

A series of recommendations on space-time references issued in the framework of the general theory of relativity in 1991 by the International Astronomical Unions (IAU) is presented. The recommendations, their background, the difficulties that were met, and the connection with previous recommendations--with an emphasis on time--are given. For simplicity of theoretical developments in celestial mechanics, several coordinate systems must be defined. The implied definitions of new coordinate times are presented together with their relation between themselves and to other times. International Atomic Time (TAI) is not affected by these recommendations, but appears now as a realization of the ideal terrestrial time having a clear scientific definition. ESA

N93-24985# Bureau International des Poids et Mesures, Sevres (France).
HOW CAN MILLISECOND PULSARS IMPROVE THE LONG TERM STABILITY OF ATOMIC TIME SCALES?
G. Petit, P. Tavella (Istituto Elettrotecnico Nazionale, Turin, Italy.), and C. Thomas *In* ESA, Frequency and Time Forum Jun. 1992 p 57-60 (For primary document see N93-24978 09-70)
Copyright Avail: CASI HC A01/MF A04

The use of millisecond pulsars to improve the long term stability of atomic time scales is addressed. Millisecond pulsars are galactic objects that exhibit a very stable period of rotation. Since the first discovery in 1982, radioastronomers have carried out timing observations, which measure the time of arrival of the radio pulses relative to an atomic time scale. Several tens of millisecond pulsars have now been discovered, located in different parts of the sky. If they are observed regularly for many years, they can be considered as an ensemble of clocks, which although they are affected by frequency drifts, allow an average time scale to be deduced through a stability algorithm. The basis for such an algorithm is presented and applied to simulated pulsar data. The properties of the resulting time scale and how it could monitor the stability of the atomic time scale are discussed. ESA

N93-24986# European Space Agency. European Space Research and Technology Center, ESTEC, Noordwijk (Netherlands).
RELATIVISTIC EFFECTS FOR LOW EARTH ORBIT SATELLITES USING GPS **c13**
A. Spallicci, C. Jimenez (Zaragoza Univ., Spain.), G. Prisco, and N. Ashby (Colorado Univ., Boulder.) *In its* Frequency and Time Forum Jun. 1992 p 61-65 (For primary document see N93-24978 09-70)
Copyright Avail: CASI HC A01/MF A04

The relativistic corrections for a low Earth orbit satellite are evaluated. The GPS (Global Positioning System) satellite clock rate is slowed before launch by 4.465 x 10(exp -10), called the 'factory offset', for time dilation and gravitational frequency shift. This offset cancels the main constant relativistic effects for terrestrial users, which in order to operate in coordinate time have only to process the GPS orbital eccentricities, a sinusoidal function whose peaks are in the order of tens of ns, and the Sagnac effect. For a space user the situation greatly differs, because a large part of the relativistic effects are still present due to the high velocity of the satellite and its location in the Earth gravitational field. Past tests and proposals for future measurements with GPS--perigee advance, Shapiro time delay, preferred frame independence, Lense Thirring effect, light bending and gravitational waves--are reviewed. ESA

N93-24987# European Space Agency. European Space Research and Technology Center, ESTEC, Noordwijk (Netherlands).
THE COLUMBUS METROLOGY SCIENCE TEAM: REPORT ON ACTIVITIES **c31**
A. D. A. M. Spallicci *In its* Frequency and Time Forum Jun. 1992 p 67 (For primary document see N93-24978 09-70)
Copyright Avail: CASI HC A01/MF A04

The activities of the Columbus metrology science team are summarized. The Columbus Attached Pressurized Laboratory of the Freedom Space Station, the Columbus Free Flyer Laboratory, Eureca, and Spacelab might offer the potential for experiments in fundamental metrology. In order to identify the specific opportunities offered by these microgravity carriers, a Columbus metrology science team was sponsored by ESA. A Pico Gravity Box (PGB) for gravitation science experiments and a proposal regarding maser clocks to fly aboard Eureca are mentioned. ESA

N93-24988# National Service of Metrology, Delft (Netherlands).
PROSPECTS OF TWO-WAY INTERNATIONAL TIME SCALE COMPARISONS
Gerrit deJong *In* ESA, Frequency and Time Forum Jun. 1992 p 69-73 (For primary document see N93-24978 09-70)
Copyright Avail: CASI HC A01/MF A04

The two way time comparison technique is introduced, and the effects of non-reciprocity are discussed. The results obtained to this point are reported. The support and activities of international bodies are described, and the prospects of using a satellite for both regional use and transatlantic use in North America and western Europe are given. ESA

N93-24989# Laboratoire Primaire du Temps et des Frequences, Paris (France).
PRELIMINARY RESULTS ON AN OPTICALLY-PUMPED Cs BEAM FREQUENCY STANDARD
P. Aynie, J. P. Berthet, S. Bouzid, A. Clairon, E. deClercq, B. Dahmani, A. H. Gerard, P. Leclerc, M. Lours, and G. D. Rovera et al *In* ESA, Frequency and Time Forum Jun. 1992 p 77-81 (For primary document see N93-24978 09-70)
Copyright Avail: CASI HC A01/MF A04

A laboratory, optically pumped Cs-beam frequency standard is described.

The measured short term stability is sigma y(tau) - 2.2 x 10(exp -12)/tau(exp -1/2) for tau greater than 100 s. The velocity distribution in the atomic beam is verified to be Maxwellian weighted by 1/nu as expected. The main frequency shifts were estimated. There is an unexpected power dependent frequency shift which needs further experiments to be explained. ESA

N93-24990# Laboratoire de l'Horloge Atomique, Orsay (France).
MINIATURE OPTICALLY-PUMPED CESIUM BEAM RESONATOR
P. Petit, V. Giordano, N. Dimarcq, P. Cerez, C. Audoin, and G. Theobald *In* ESA, Frequency and Time Forum Jun. 1992 p 83-86 Sponsored by STEI, France (For primary document see N93-24978 09-70)
Copyright Avail: CASI HC A01/MF A04

The design of a miniature optically pumped cesium beam resonator is described. It is of the flop in type but with a phase difference of 180 deg between the two oscillating fields. In the present circumstances, this small machine operating at low oven temperature (85 C) exhibits a rather outstanding short term frequency stability. This phi = 180 deg cavity configuration makes a lowering of a number of frequency shifts possible. ESA

N93-24991# Laboratoire de l'Horloge Atomique, Orsay (France).
ACTUAL LIMITS OF FLUORESCENCE S/N RATIO IN AN OPTICALLY-PUMPED CESIUM BEAM RESONATOR
N. Dimarcq, V. Giordano, P. Cerez, and G. Theobald *In* ESA, Frequency and Time Forum Jun. 1992 p 87-90 Sponsored by Bureau National de Metrologie (For primary document see N93-24978 09-70)
Copyright Avail: CASI HC A01/MF A04

The effect of laser noise on the Signal/Noise (S/N) ratio is reported and limits of this ratio are derived. The frequency stability of an optically pumped cesium beam resonator crucially depends on the fluorescence S/N ratio in the detection region. The total noise results from various noise sources: atomic shot noise, photon noise, laser frequency noise, and signal detection noise. A model which gives the fluorescence S/N ratio as a function of the main parameters characterizing the interaction between the atoms and the laser beam is developed. Variations of the S/N ratio with the atomic beam intensity and laser linewidth are presented for various excitation schemes. A good agreement is found between experiments and theory. ESA

N93-24992# Ecole Nationale Superieure de Mecanique et des Microtechniques, Besancon (France). Lab. de Chronometrie Electronique et Piezoelectricite.
LONG TERM DRIFT AND GAMMA-IRRADIATION EFFECT **c72**
J. J. Boy, A. Berthaut, D. Thiebaud, and K. Yamni (Besancon Univ., France.) *In* ESA, Frequency and Time Forum Jun. 1992 p 93-98 (For primary document see N93-24978 09-70)
Copyright Avail: CASI HC A02/MF A04

The frequency and motional resistance characteristics versus temperature of SC (Stress Compensation) cut resonators were measured before, during, and after irradiation, in order to correlate the influence of the selected chemical impurities on their electrical behavior. The long term drifts were discussed and compared to the Al(3+) ion content. These measurements were performed on BVA (electrodeless quartz resonator) SC cut, which were manufactured using either synthetic (swept or unswept) or natural quartz crystals. The results obtained show that a link could be established between the gamma irradiation sensitivity and the aluminum content and hence, the large difference, on one hand, between natural and synthetic raw material and, on the other hand, between unswept and swept quartz crystals. ESA

N93-24993# Franche-Comte Univ., Besancon (France). Lab. de Physique et Metrologie des Oscillateurs.
WEAK MAGNETIC FIELD SENSITIVITY OF QUARTZ CRYSTAL OSCILLATORS **c76**
R. Brendel and E. Robert (Centre National d'Etudes Spatiales, Toulouse, France.) *In* ESA, Frequency and Time Forum Jun. 1992 p 99-104 (For primary document see N93-24978 09-70)
(Contract CNES/CNRS-932-88-53-474-00)
Copyright Avail: CASI HC A02/MF A04

The magnetic sensitivity curves for selected quartz crystal resonators in the range of +/- 40 gauss are presented. It is shown that in most cases the sensitivity to a small magnetic field can hardly be extrapolated from the high field measurements. Also, the frequency versus magnetic field curves often exhibit a strong hysteresis which makes questionable the definition of the resonator's magnetic sensitivity. Although the main cause of this sensitivity remains the ferromagnetic nature of the material used in the plate support, it is shown that the mounting technique can be of great importance. ESA

N93-24994# Paris VI Univ. (France).
SYNCHROTRON RADIATION X RAY TOPOGRAPHY STUDY OF LATERAL FIELD RESONATORS
B. Capelle, J. Detaint (Centre National d'Etudes des Telecommunications, Bagneux, France.), J. Schwartzel (Centre National d'Etudes des Telecommunications, Bagneux, France.), Y. Zheng, and A. Zarka *In* ESA, Frequency and Time Forum Jun. 1992 p 105-109 (For primary document see N93-24978 09-70)
Copyright Avail: CASI HC A01/MF A04

Using synchrotron radiation, plano-convex AT resonators excited by a lateral field were studied by the X-ray topography technique. Different overtones and anharmonics of the three types of the thickness modes were observed. The study showed that it is possible to excite more modes with the lateral field excitation than with the thickness field excitation. These modes can present intrinsic interest due to the values of the temperature coefficient and/or of the coupling coefficient. The new degree of freedom, given by the possibility of choosing the direction of the excitation field, permits interesting applications such as the suppression or excitation of one type of mode. This study can help to understand the coupled modes which appear in the thickness excitation resonators. ESA

N93-24995# Tele Quartz Group G.m.b.H., Neckarbischofsheim (Germany).
IMPROVED PI-NETWORK MEASUREMENT OF ALL QUARTZ CRYSTAL PARAMETERS BY APPROPRIATE MODELLING OF THE TEST FIXTURE
B. Neubig and L. Schulzke (KVG G.m.b.H., Neckarbischofsheim, Germany.) *In* ESA, Frequency and Time Forum Jun. 1992 p 111-117 (For primary document see N93-24978 09-70)
Copyright Avail: CASI HC A02/MF A04

The measurement of quartz crystal units is standardized in IEC 444. This means that different test fixtures and additional elements must be used, for example in the determination of the load resonance parameters (IEC 444-4) or for the physical static capacitance compensation (IEC 444-3). A method introducing a general approach, which allows the precise determination of all quartz crystal parameters with one test fixture only by appropriate modeling, is presented: inductances in series to the inserted crystal modeling the electrical connection; a capacitance between the PI network ports modeling the crosstalk; and complex impedance of the PI network. All these elements are computed by a calibration routine with an open, a short, and a calibration resistor in the complete frequency range. The quartz crystal parameters are determined by complex mathematical algorithms for the measurement data. Measurement results with different hardware are presented in comparison to the standardized hardware based methods of IEC 444. ESA

N93-24996# Roditi International Corp. Ltd., London (England).
THE MEASUREMENT OF THE RESONANT FREQUENCY OF QUARTZ CRYSTAL UNITS: AN ONGOING SAGA
Eric Kentley *In* ESA, Frequency and Time Forum Jun. 1992 p 119-122 (For primary document see N93-24978 09-70)
Copyright Avail: CASI HC A01/MF A04

The history of practical methods of industrial measurement leading to the present situation is traced. Resonant frequency measurement of a quartz crystal unit has always presented problems due to the fact that a quartz crystal unit is not an absolute frequency determining device. The frequency of oscillation of a quartz crystal unit in an oscillator circuit is a function of the crystal unit and the maintaining oscillator circuit. Since the introduction of zero phase type measurements in a passive network by the I.E.C. in the early 1970's many of these measurement problems have been eliminated or much reduced, but there are still some problem areas. Using the computer aided test methods now available, automatic crystal measurements can be made. These can cause what might be termed computer aided correlation errors due to slightly different measuring procedures and methods of computation. ESA

N93-24997# Centre National d'Etudes Spatiales, Toulouse (France).
DORIS PRECISE ORBIT DETERMINATION AND LOCATION SYSTEM PERFORMANCES OF ULTRA STABLE OSCILLATORS **c13**
M. Brunet *In* ESA, Frequency and Time Forum Jun. 1992 p 125-136 (For primary document see N93-24978 09-70)
Copyright Avail: CASI HC A03/MF A04

Elements of the DORIS (Doppler precise positioning System) performances and performances of the DORIS USO (Ultra Stable Oscillators) are described. The DORIS system was designed and developed to meet new needs in precision orbit determination and high accuracy beacon location. DORIS payload was integrated on three French SPOT satellites and on the Topex-Poseidon NASA satellite. The first model DORIS SPOT 2 began operating on 22 Jan. 1990. The fundamental measurement precision depends strongly on the stability of USO, which are used in the onboard receiver, and in ground location beacons. ESA

N93-24998# Consiglio Nazionale delle Ricerche, Bologna (Italy). Ist. di Radioastronomia.
PRECISE DOPPLER TRACKING FROM THE MEDICINA VLBI STATION **c13**
R. Ambrosini, G. Comoretto (Osservatorio Astrofisico di Arcetri, Florence, Italy.), L. Iess (Consiglio Nazionale delle Ricerche, Frascati, Italy.), and A. Messeri (Consiglio Nazionale delle Ricerche, Frascati, Italy.) *In* ESA, Frequency and Time Forum Jun. 1992 p 137-142 (For primary document see N93-24978 09-70)
Copyright Avail: CASI HC A02/MF A04

The first opposition test of Doppler tracking the Ulysses spacecraft from the Medicina VLBI (Very Long Base Interferometry) station (Italy) proved its capability to perform a systematic search for gravitational waves. In house and JPL (Jet Propulsion Laboratory) data analysis showed that the target Allan variance of 3 x 10(exp -14) at 1000 s, planned for the DSN antennas was also achieved from the station. The main observation campaign during the second opposition phase will last for thirty continuous nights--from mid Feb. to mid Mar. 1992. The main hardware and software features developed for this application, together with some results of the first opposition test, are described. ESA

N93-24999# TimeTech G.m.b.H., Stuttgart (Germany).
A NEW MODEM FOR MICROWAVE TIME SYNCHRONISATION VIA GEOSYNCHRONOUS TELECOMMUNICATION SATELLITES **c32**
Michael Dienert *In* ESA, Frequency and Time Forum Jun. 1992 p 143-147 (For primary document see N93-24978 09-70)
Copyright Avail: CASI HC A01/MF A04

A study illustrating the two way time transfer technique and describing the use of this technique with the MITREX (Microwave Time and Range Experiment) SATRE (Satellite Time and Range Experiment) modems is presented. The two way time transfer technique via geosynchronous telecom satellites is one of the most accurate methods for synchronization and comparison of remote clocks. Most of the unknown propagation delays can be eliminated by the two way principle. The use of a coherent spread spectrum technique with a truncated pseudonoise code offers a resolution better than 30 ps of the measured time interval. The receiver is built around a Delay Locked Loop (DLL), which correlates the received signal with the known PN sequence to derive the control signal of the loop. In the locked state both PN sequences are synchronous and tracking errors of less than 30 ps are possible. Results showing the accuracy of the modem depending on signal to noise ratio and variation of total input power levels are presented and show that the expected improvement of the jitter of the internal delay by an increase of the chip rate is possible. ESA

N93-25000# Alcatel Bell Telephone, Antwerp (Belgium). Space Ground Systems.
SYNCHRONISATION, ACQUISITION AND TRACKING FOR TELEMETRY AND DATA RECEPTION **c17**
A. VanDoninck *In* ESA, Frequency and Time Forum Jun. 1992 p 149-155 (For primary document see N93-24978 09-70)
Copyright Avail: CASI HC A02/MF A04

The important parameters of synchronization, acquisition, and tracking are addressed, and each function is highlighted separately. The following sequence is such as the functions occur in the system in time and for the type of data to be received, with distinction between telemetry and data reception, between direct carrier modulation or the use of a subcarrier, and between deep space and normal reception. For the telemetry reception the acquisition is described taking into account the difference in performances as geostationary or polar orbits, and the dependencies on the different Doppler offsets and rates are distinguished. The related functions and parameters are covered and the specifications of an average receiver are summarized. The synchronization of the valid data is described with a distinction for data directly modulated or via a subcarrier, the type of modulation and bitrate. The relevant functions and parameters of the average receiver/demodulator are summarized. The tracking of the signal in the course of the operational phase is described and relevant parameters of an actual system are presented. The reception of real data is handled and a sequence of acquisition, synchronization, and tracking is applied. Here higher bitrates and direct modulation schemes play an important role. The market equipment with the relevant parameters are discussed. The three functions in cases where deep reception is needed are covered. The high performance receiver/demodulator functions and how the acquisition, synchronization, and tracking is handled in such application, are explained. ESA

N93-25001# Composants Quartz et Electronique, Pont Sainte Marie (France).
A MICROCOMPUTER COMPENSATED CRYSTAL OSCILLATOR MCXO **c76**
P. Collet, G. Putois, and F. Vignaud *In* ESA, Frequency and Time Forum Jun. 1992 p 159-163 Sponsored by STTE, France (For primary document see N93-24978 09-70)
Copyright Avail: CASI HC A01/MF A04

A Microcomputer Compensated Crystal Oscillator (MCXO) using a resonator operating in a dual mode is described. Modern communications systems demand a more stable frequency than currenty available with a TCXO (Temperature Compensated Crystal Oscillator) and consume considerably less power than an OCXO (Oven Controlled Crystal Oscillator). The MCXO ideally fills this requirement, frequency stability of +/- 20 ppb over the military temperature range consuming less than 50 mWatt being achievable. The current status and future time scales of the project are given. ESA

N93-25002# Franche-Comte Univ., Besancon (France). Lab. de Physique et Metrologie des Oscillateurs.
OSCCAR: OSCILLATOR-COMPENSATED WITH A CAPACITANCE ARRAY **c33**
W. Daniau and G. Marianneau *In* ESA, Frequency and Time Forum Jun. 1992 p 165-167 (For primary document see N93-24978 09-70)
Copyright Avail: CASI HC A01/MF A04

A study based on the realization of a Capacitance Switch Array (CSA), usable on a Digitally Temperature Compensated Crystal Osillator (DTCXO) is presented. An original design method of the CSA was proposed, and a prototype and an experimental DTCXO using the CSA was realized. The design of the CSA and the results obtained with the DTXCO are presented. The firt prototype has a frequency stability of +/- 2.2 times 10 to the minus 7th power within the range of temperature 0 to 80 C, with a power consumption of 25 mW and a supply voltage of 5V. ESA

N93-25003# Franche-Comte Univ., Besancon (France). Lab. de Physique et Metrologie des Oscillateurs.
DESIGN OF A LOW PHASE NOISE UHF OSCILLATOR USING A PARTLY METALLIZED DIELECTRIC RESONATOR **c33**
R. E. Elcheikh and M. Olivier *In* ESA, Frequency and Time Forum Jun. 1992 p 169-171 (For primary document see N93-24978 09-70)
Copyright Avail: CASI HC A01/MF A04

A type of oscillator composed of a Dielectric Resonator (DR), which is part of a Microwave Integrated Circuit (MIC), is presented. For this oscillator, the oscillating characteristics can be controlled by several parameters, such as the dimensions, the position of the DR in its environment, and the bias voltage of the oscillator. With this technique, a frequency stability sigma(sub y)(tau) of less than 5 times 10 to the minus 9th power for tau = 1s, an output power of 17 dBm and phase noise as low as -106 dBc at 1kHz from the carrier in the 800-1000 MHz frequency band are obtained. ESA

N93-25004# Compagnie d'Electronique et de Piezo-Electricite, Argenteuil (France).

MINIATURIZATION AND STABILITY: A NEW GENERATION OF OVENISED OSCILLATORS **c33**

J. P. Aubry, G. Wagner, and V. Candelier *In* ESA, Frequency and Time Forum Jun. 1992 p 173-177 (For primary document see N93-24978 09-70)

Copyright Avail: CASI HC A01/MF A04

The design procedure and the electrical performances obtained with very small ovenized oscillators are presented. The sizes were reduced to 40 by 30 by 19, 40 by 30 by 16, and 36 by 26 by 19 cu mm. The oscillator designs offer 'intrinsic' high performances regarding either aging, frequency stability, or phase noise in the way that these performances can be compared to the one achieved from actual standard oscillators designed in a larger package. One of the keys in getting ovenized oscillators in small package is the resonator definition. The use of SC cut allow good performances in ageing, thermal stability and phase noise, in smaller size than an equivalent AT cut. Miniaturized and stable oscillator specifications can be met by using state of the art of oscillators design and manufacture concepts. The experimental results show that tight requirements are obtained with very good oscillator yields. ESA

N93-25005# Ministry of Posts and Telecommunications, Tokyo (Japan). Communications Research Lab.

A SYSTEM DESIGN FOR LASER TIME SYNCHRONIZATION VIA GEODETIC SATELLITE AJISAI **c36**

Hiroo Kunimori, Fujinobu Takahashi, and Atsushi Yamamoto (Maritime Safety Agency, Tokyo, Japan.) *In* ESA, Frequency and Time Forum Jun. 1992 p 181-185 (For primary document see N93-24978 09-70)

Copyright Avail: CASI HC A01/MF A04

A laser time synchronization system based on a satellite laser ranging system developed in 1990 is described. The target satellite is the Japanese geodetic satellite Ajisai, which is equipped with corner cubes and mirrors. Feasibility of the experiment is studied including the time transfer equation, the observation system, the link budget, and distribution of reflected beam. Simulation study indicates that two stations thousands of km from each other can be linked by a laser beam with a signal strength of more than 10 photons. The images of the laser beam from the Ajisai mirrors are uniformly distributed on the ground and two stations have many chances to link in a single Ajisai pass. ESA

N93-25006# Technical Research Centre of Finland, Espoo. Metrology Research Inst.

THE ACCURACY OF SYLT- AND RNS-BASED TIME SCALES AT MTI AND SNT DURING 1990-1991

Tapio Mansten, Kalevi Kalliomaeki (Oulu Univ., Finland.), and Bengt Selin (Swedish National Time and Frequency Lab.) *In* ESA, Frequency and Time Forum Jun. 1992 p 187-190 (For primary document see N93-24978 09-70)

Copyright Avail: CASI HC A01/MF A04

The phases of transmissions from Norwegian Sea Loran Sylt and Soviet Radionavigation System (RNS) Bryansk stations were measured at MTI (Metrology National Time and Frequency Laboratory) (Finland) and SNT (Swedish National Time and Frequency Laboratory) (Sweden) daily for two years to find out the uncertainty of time scales based on them. The phases were traced back to UTC by using BIPM time circulars and appropriate time information letters for other laboratories. The reference time scale at MTI is a GPS receiver. The reference time scale at SNT is based on one of three Cs clocks which contribute to UTC. The results show that by common view Sylt measurements, a Loran C based time scale can be maintained at 100 ns level/10 days. By using RNS common view measurements, a time scale at about 500 ns/10 day level is achievable. ESA

N93-25007# Oulu Univ. (Finland). Dept. of Electrical Engineering.

CONTROL OF ENVIRONMENTAL AND CLOCK PARAMETERS IN TIME AND FREQUENCY STANDARDS LABORATORY

Kalevi Kalliomaeki and Tapio Mansten (Technical Research Centre of Finland, Espoo.) *In* ESA, Frequency and Time Forum Jun. 1992 p 191-194 (For primary document see N93-24978 09-70)

Copyright Avail: CASI HC A01/MF A04

The measurement of environmental parameters and frequencies of rubidium and precision crystal oscillators in two time and frequency laboratories are reported. The effects of ambient fluctuations to oscillator frequencies were studied using multiple linear regression. Laboratory temperature seems to be the most significant factor even in air conditioned rooms. Additional thermally controlled cabinets were built to reduce temperature effects. ESA

N93-25008# National Physical Lab., Teddington (England).

ANALYTICAL TECHNIQUES FOR IMPROVED TIME TRANSFER USING COMMON VIEW OF DIRECT BROADCASTING SATELLITES

John A. Davis and Peter R. Pearce *In* ESA, Frequency and Time Forum Jun. 1992 p 195-199 Sponsored by the United Kingdom Measurement System Program for Time and Frequency (For primary document see N93-24978 09-70)

Copyright Avail: CASI HC A01/MF A04

Time transfer using television signals from direct broadcasting satellites is an accurate and inexpensive method of comparing atomic clocks at distant locations. The major source of error arises from the residual motion of the geostationary satellite. Previous work showed that it is possible to determine the components of the satellite motion by observing two widely spaced geostationary satellites simultaneously from three locations. A method where the common view measurements are corrected for the variation of the positions of the satellites is developed. In contrast to previous work, there is no requirement to calculate explicitly the coordinate of the satellites. Time transfers with uncertainties of a few parts in 10 exp 14 were obtained. The longitudinal drift and periodic variations of the satellite positions were determined. ESA

N93-25009# Franche-Comte Univ., Besancon (France). Lab. de Physique et Metrologie des Oscillateurs.

ELASTIC PLATE MODE SENSITIVITIES TO MASS LOADING APPLICATIONS TO GAS SENSORS **c35**

M. Hoummady and D. Hauden *In* ESA, Frequency and Time Forum Jun. 1992 p 203-207 (For primary document see N93-24978 09-70)

Copyright Avail: CASI HC A01/MF A04

The theoretical analysis of the possibility of measuring mass loading variations by means of bulk wave modes generated with Interdigital Transducers (IDT) is addressed. Elastic waves are generated and detected by means of IDT transducers plated on piezoelectric fields or substrates. It was shown that both surface and bulk elastic waves can be launched by IDT's. The type of elastic wave excited is related to the piezoelectric material properties and its crystallographic orientation. In a thin piezoelectric plate, surface and bulk vibrations propagate in the volume of the plate. Thus, propagating plate modes are stationary in the plate thickness. Two kinds of modes can be distinguished: Shear Horizontal (SH) and Lamb modes. To adapt a plate mode device to a gas sensor, it is necessary to deposit a selectivity sensitive film which can absorb the gas to be detected. The velocity of the wave is then modified because the induced variation of the mass loading of the film changes the boundary conditions. The theoretical study of the mass loading sensitity of both SH and Lamb modes is presented. For instance, expected sensitivity for the SH mode of a gas sensor is in the order of 1 ng of the gas for 1 sq cm of sensitive film. ESA

N93-25010# Tele Quartz Group G.m.b.H., Neckarbischofsheim (Germany).

A STATE-OF-THE-ART CRYSTAL FILTER DESIGN PACKAGE USING WINDOWS 3.0 TECHNIQUES **c33**

Markus Frey and Bernd W. Neubig *In* ESA, Frequency and Time Forum Jun. 1992 p 209-216 (For primary document see N93-24978 09-70)

Copyright Avail: CASI HC A02/MF A04

A company owned software package TeleQuartz (TQ) WINFIL for systematic design of crystal filters is reported. TQ WINFIL offers access to several levels of the filter synthesis: the pole-zero plane, the normalized low pass domain, and the synthesis of the final crystal filter circuit. At each synthesis level, an analysis module as well as an optimization module are included. This allows the user to analyze the theoretical models as well as the real crystal filter circuit including losses, component tolerances, and nonideal characteristics such as spurious responses of the crystals. The optimization modules make it possible to search iteratively for a network solution from a starting set of values in order to meet special requirements. Frequency unsymmetric responses can be computed by a frequency transformation module, which effects the bilinear transformation of all circuit

components of the filter. Any parameter changes in the synthesis and any action of the optimization module not only cause changes of the desired response, they also influence the other characteristics of the filter. The Windows graphical user interface allows the simultaneous display of all interesting parameters and results during the whole cycle of synthesis, analysis, optimization, and transformation. ESA

N93-25011# Office National d'Etudes et de Recherches Aerospatiales, Paris (France).

MONOLITHIC QUARTZ VIBRATING BEAM ACCELEROMETER c35

F. Deyzac, D. Janiaud, and S. Muller *In* ESA, Frequency and Time Forum Jun. 1992 p 217-218 (For primary document see N93-24978 09-70)

Copyright Avail: CASI HC A01/MF A04

A monolithic quartz vibrating beam accelerometer is described. The objective is machining, by chemical etching process, miniature accelerometers suitable for various applications, like guidance systems, and vehicle dynamic control. The monolithic quartz active part includes two vibrating beams, the proof mass, and its articulation in a base. It is obtained by a process similar to the one used in watch crystal manufacturing, so the potential cost is very low. The simplicity of piezoelectric excitation and the numerical output (frequency signal) are key features to reduce dimensions and cost. The expected accuracy of this sensor is 0.003 in a harsh environment. First experimental results are presented. ESA

N93-25012# Franche-Comte Univ., Besancon (France). Lab. de Physique et Metrologie des Oscillateurs.

SURFACE TRANSVERSE WAVE (STW) QUARTZ RESONATORS IN THE GHz RANGE

E. Bigler, E. Gavignet, B. A. Auld (Stanford Univ., CA.), E. Ritz (Tektronix, Inc., Beaverton, OR.), and E. Sang (Tektronix, Inc., Beaverton, OR.) *In* ESA, Frequency and Time Forum Jun. 1992 p 219-222 (For primary document see N93-24978 09-70)

Copyright Avail: CASI HC A01/MF A04

A model predicting the influence of various design parameters on fundamental properties such as resonant frequency, Q factor, and insertion losses is presented. STW resonators offer several advantages over conventional Rayleigh wave SAW (Surface Acoustic Wave) resonators, one of the most interesting advantages being higher operating frequencies (+60 percent) for given geometrices of the transducers and reflectors. A model to compute the resonant frequency of a three grating STW resonator is presented and and the influence of important design parameters, cavity length, metal thickness, grating periodicities, and finger to gap ratio is discussed. Starting from first experimental results, obtained in metal strip (37 deg Y rotated) quartz STW resonators at 500 MHz, new devices at 1 GHz were fabricated and tested. Experimental results are presented and discussed. ESA

N93-25013# Centre National d'Etudes des Telecommunications, Bagneux (France).

COMPARISON OF ENERGY TRAPPING RESONATORS AND FILTERS USING THE AT CUT OF QUARTZ, BERLINITE AND GALLIUM PHOSPHATE c76

J. Detaint, J. Schwartzel, C. Joly, B. Capelle (Paris VI Univ., France.), A. Zarka (Paris VI Univ., France.), Y. Zheng (Paris VI Univ., France.), Y. Toudic (Centre National d'Etudes des Telecommunications, Lannion, France.), and E. Philippot (Montpellier Univ., France.) *In* ESA, Frequency and Time Forum Jun. 1992 p 223-227 (For primary document see N93-24978 09-70)

Copyright Avail: CASI HC A01/MF A04

The properties of the AT cuts of quartz, berlinite, and gallium phosphate are compared (velocity of the shear waves, coupling coefficient, and thermal behavior). A more precise evaluation of the properties of AT cut resonators using the quartz analogs is made in considering the computed properties of energy trapped resonators. The computed properties of resonators are obtained using a three dimensional model based upon the theory of the essentially thickness modes. Using computed equivalent schemes, the bandwidths achievable at 20 MHz are calculated for 4 poles Jaumann filters having a Chebishev response with 14 dB ripple and a maximal termination impedance of 2 kohm. The obtained results indicate that berlinite and gallium phosphate produce a filter with much larger bandwidth than quartz. They suggest that the use of new designs (resonators with elliptical electrodes and/or grooved electrodes, integrated filters etc.) will further lower the equivalent inductance and/or the influence of the stray capacitances. Such designs would lead with the high coupling quartz analogs to much better characteristics than the usual designs using round electrodes. Experimental results (equivalent scheme of resonators, observed mode shape etc.) are successfully compared with computed ones to validate the model use for the computations. ESA

N93-25014# Edgerton, Germeshausen and Grier, Inc., Salem, MA. Frequency and Time Dept.

RUBIDIUM ATOMIC FREQUENCY STANDARDS FOR GPS BLOCK 2R

William K. Riley, Jr. *In* ESA, Frequency and Time Forum Jun. 1992 p 231-238 (For primary document see N93-24978 09-70)

Copyright Avail: CASI HC A02/MF A04

The design, improvements, test results, and progress of the Rubinium Atomic Frequency Standards (RAFS) for the GPS (Global Positioning System) Block 2R Navstar satellites are described. These satellites will replenish and upgrade the space segment of the GPS in the mid 1990's. The RAFS offer an aging rate in the low pp 10 to the 14th power/day range and a drift corrected 1 day stability in the low pp 10 to the 14th power range. The Block 2R version of these devices will have improved performance, higher reliability, smaller size, and greater radiation hardness. The GPS Block 2R atomic clocks have a 'natural frequency' configuration whereby they output a frequency of about 13.4 MHz that is a submultiple of the atomic resonance. The RAFS operate at a low fixed C field for increased stability. The unit was repackaged into a smaller 4.6 by 8.5 by 5.8 inch outline, but is somewhat heavier (12 lbs.) because of additional radiation shielding. Elimination of the ground tuning logic and the secondary loop synthesizer (with its ovenized crystal oscillator) reduced the RAFS complexity and improved its reliability to 0.80 for the 7.5 year mission. The RAFS power consumption is only 13 W at +20 C in vacuum. ESA

N93-25015# Aerospace Corp., El Segundo, CA.

MIXED CONSTELLATION SYNCHRONIZATION OF GPS TIME

A. L. Satin, C. H. Yinger, and W. A. Feess *In* ESA, Frequency and Time Forum Jun. 1992 p 239-242 (For primary document see N93-24978 09-70)

Copyright Avail: CASI HC A01/MF A04

The Global Positioning System (GPS) will consist of a mixed constellation of Block 2/2A ground navigated and Block 2R autonomously navigated (Autonav) satellites for many years starting in 1996. The GPS time references for these two types of subconstellations must be synchronized to within a few nanoseconds if user navigation accuracy is to be preserved. A technique for achieving Root Mean Square (RMS) phase and rate synchronization of 2.9 ns and 0.13 ns/hr, by steering the ground system to Autonav, is described and validated by simulation. Coincidental with synchronization steering, it is shown that Autonav ensemble time (for a subconstellation of as few as four satellites) can be maintained to within 20.7 ns of Universal Time Coordinated (UTC) using a drift rate steering control law. ESA

N93-25016# Bureau International des Poids et Mesures, Sevres (France).

GPS STANDARDIZATION FOR THE NEEDS OF TIME TRANSFER

W. Lewandowski, G. Petit, and C. Thomas *In* ESA, Frequency and Time Forum Jun. 1992 p 243-248 (For primary document see N93-24978 09-70)

Copyright Avail: CASI HC A02/MF A04

The need to develop standards in GPS (Global Positioning Systems) receiver software and hardware, in particular with the implementation of Selective Availability (SA) is reported. The most recent activities of the CGGTTS (CCDS Group on GPS Time Transfer Standards) are reported. It has been clear for some time that a desirable and necessary step for improvement of the accuracy of GPS time comparisons is to establish GPS standards which may be adopted by receiver designers and users. For this reason, a formal body, the CGGTTS was created in 1991. The implementation of SA is described and examples of deficiencies caused by a lack of standardization are discussed. ESA

N93-25017# Leeds Univ. (England).

COMPARISON OF GLONASS AND GPS TIME TRANSFERS

P. Daly, N. B. Koshelyaevsky (All-Union Research Inst. for Physical and Radiotechnical Measurements, Mendeleevo, USSR.), W. Lewandowski

(Bureau International des Poids et Mesures, Sevres, France.), G. Petit (Bureau International des Poids et Mesures, Sevres, France.), and C. Thomas (Bureau International des Poids et Mesures, Sevres, France.) *In* ESA, Frequency and Time Forum Jun. 1992 p 249-252 (For primary document see N93-24978 09-70)

Copyright Avail: CASI HC A01/MF A04

The Russian Global Space Navigation System GLONASS could provide a technique similar to GPS (Global Positioning System) for international time comparison. The main limitation to its use for time transfer lies in the lack of commercially available time receivers. The building of a GPS/GLONASS receiver and continuous information collected about GLONASS time and its comparison with GPS time are reported. Russian built GLONASS navigation receivers built for time comparisons are addressed. Since June 1991, a GPS time receiver has been operating. This offered for the first time an opportunity for direct comparison of time transfers using GPS and GLONASS. This 7 month experiment shows that even with relatively imprecise data recordings and processing, in terms of time metrology, GLONASS can provide continental time transfer at a level of several tens of nanoseconds. ESA

N93-25018# Kayser Threde G.m.b.H., Munich (Germany).

AN EXPERIMENTAL HEALTH MONITORING UNIT FOR GPS AND GLONASS **c04**

B. Eissfeller, M. Haunschild (Maschinenfabrik Augsburg-Nuernberg A.G., Munich, Germany.), A. Jansche, and N. Niklasch (Maschinenfabrik Augsburg-Nuernberg A.G., Munich, Germany.) *In* ESA, Frequency and Time Forum Jun. 1992 p 253-257 (For primary document see N93-24978 09-70)

(Contract ESA-9281/91/F/RD(SC))

Copyright Avail: CASI HC A01/MF A04

The development of an experimental Health Monitoring Unit (HMU) for GPS (Global Positioning System) and GLONASS (Russian Global Space Navigation System) is reported. The purpose of the HMU is to provide timely warnings to the navigation users if the satellite navigation systems should not be used for navigation. The monitoring unit is a key element in the integrity channel concept of a civil overlay Navsat to GPS and GLONASS. The most stringent requirements are those of civil aviation: in the nonprecision approach phase horizontal position errors exceeding the 600 m SPE threshold have to be reported within 10 seconds. The concept of the HMU is to use a GPS receiver as well as a GLONASS reveiver in a known location in order to detect large pseudorange errors and to identify the malfunctioning satellites. This means that the station is able to work autonomously. But it will also provide pseudorange errors compatible with the American RTCA SC-159 approach and for a future wide area DGPS (Differential GPS) system. ESA

N93-25019# Leeds Univ. (England). Dept. of Electronic and Electrical Engineering.

COLLABORATION IN THE UK ON TIME TRANSFER USING THE GLONASS SYSTEM

P. Daly, D. J. E. Knight (National Physical Lab., Teddington, England.), R. Jefferies (National Physical Lab., Teddington, England.), and B. R. Swabey (National Physical Lab., Teddington, England.) *In* ESA, Frequency and Time Forum Jun. 1992 p 259-261 Sponsored by United Kingdom National Measurement System Program for Time and Frequency (For primary document see N93-24978 09-70)

Copyright Avail: CASI HC A01/MF A04

Collaboration in the UK (United Kingdom) on the use of the GLONASS (Russian Global Space Navigation System) satellite navigation system for time transfer, and the main results obtained, are reported. The GLONASS clock stability and GLONASS system time has been monitored since 1988 within an accuracy of about +/- 50 ns. Current news of the GLONASS system is given, and measures towards improving accuracy are discussed. ESA

N93-25020# Ecole Nationale Superieure de Mecanique et des Microtechniques, Besancon (France). Equipe de Physique et Electronique des Capteurs.

DEDICATED OSCILLATOR FOR IMMERSED CRYSTAL SENSOR **c76**

G. Bardeche, C. Filiatre, and J.-P. Valentin *In* ESA, Frequency and Time Forum Jun. 1992 p 265-268 (For primary document see N93-24978 09-70)

Copyright Avail: CASI HC A01/MF A04

A study performed with the circuit simulation software PSPICE on the design of an oscillator is presented. For chemical applications a quartz oscillator may be successfully implemented. For these applications, the quartz crystal is generally immersed in liquid medium. Therefore, the quality factor and the motional resistance are very different compared to usual cases. The oscillator circuit must therefore be strongly modified in order to obtain oscillation of the immersed crystal. The characteristics of an immersed quartz crystal are determined, and, from the measured values, an electronic design is proposed. The quartz crystal works in series resonance with a grounded electrode. This circuit can be considered like an approximation of the optimal curcuit where the resonant element is loaded by the zero impedance of a current controlled voltage source. ESA

N93-25021# National Physical Lab., New Delhi (India).

RADIATION EFFECTS IN GERMANIUM DOPED QUARTZ **c76**

Harish Bahadur *In* ESA, Frequency and Time Forum Jun. 1992 p 269-272 Sponsored by Sandia National Labs. and RADC (For primary document see N93-24978 09-70)

Copyright Avail: CASI HC A01/MF A04

Cultured quartz crystals doped heavily with Ge (Ge concentration approximately 3000 ppm) were studied for their infrared spectral characteristics as a function of irradiation temperature. The irradiation was done in sequence at 77 K, 300 K, and finally again at 77 K. Infrared spectra show that in addition to the growth defect bands the previously unreported peak at 3656/cm is caused due to the presence of Ge in quartz. Intense irradiation at 77 K in prior 300 K irradiated samples exhibit the presence of a band at 3400/cm which is a different defect center than the growth defect band at this frequency. Production curve for this band shows a linear dose dependence. ESA

N93-25022# Ecole Nationale Superieure de Mecanique et des Microtechniques, Besancon (France). Lab. de Chronometrie Electronique et Piezoelectricite.

TRAPPED ENERGY QUARTZ CRYSTAL RESONATOR ON WEDGE-SHAPED PLATE **c76**

R. Bourquin *In* ESA, Frequency and Time Forum Jun. 1992 p 273-277 (For primary document see N93-24978 09-70)

Copyright Avail: CASI HC A01/MF A04

Based upon the general relation of dispersion for a quartz plate of doubly rotated cut, an analytical model is presented. It describes the modes shapes of a resonator exhibiting a linear thickness variation along in-plane directions and is only submitted to the following assumptions: small wave numbers along the plate plane and slowly varying thickness. The proposed model allows a direct computation of overtones and anharmonic mode frequencies, as well as the motional elements of the resonator, as functions of the tilt angle. ESA

N93-25023# Tekelec-Systemes, Les Ulis (France).

TIME AND FREQUENCY REFERENCE FOR A TRAJECTORY MEASUREMENT SYSTEM

G. Boime *In* ESA, Frequency and Time Forum Jun. 1992 p 279-282 (For primary document see N93-24978 09-70)

Copyright Avail: CASI HC A01/MF A04

A time and frequency reference installed on a ship for dating and synchronization of all the different measurement instruments is described. There is a requirement of precise time and frequency referencing in trajectory measurement which allows tracking of long range missiles. Time and frequency are provided to different systems such as radar, optical sighting, and telemetry. The time and frequency system is made up from a main clock reference and secondary clocks synchronized via a local area network. This redundant architecture improves the reliability and allows time and frequency distribution even when the main clock is unavailable. ESA

N93-25024# Observatoire Cantonal, Neuchatel (Switzerland).

BASIC DESIGN OF A SPACEBORNE HYDROGEN MASER **c36**

L. G. Bernier *In* ESA, Frequency and Time Forum Jun. 1992 p 283-286 (For primary document see N93-24978 09-70)

Copyright Avail: CASI HC A01/MF A04

The construction of a space qualified atomic hydrogen maser to be flown on Eureca 3 in a technology demonstration experiment is addressed.

The basic issues in the design of the physics package at the feasibility level are discussed. The main topics are the choice of the microwave resonator, the choice of the basic operational parameters, the hydrogen storage, distribution and pumping, the magnetic shielding, and the storage bulb coating. Foreseeable critical issues are the mechanical thermal and magnetic designs. ESA

N93-25025# Societe Industrielle de Combustible Nucleaire, Annecy (France).

CRYSTAL GROWTH OF BERLINITE: METHODS FOR GROWING LONGER CRYSTALS AND IMPROVING THE QUALITY **c76**

X. Buisson, A. Zarka (Paris VI Univ., France.), R. Arnaud, B. Capelle (Paris VI Univ., France.), Y. Zheng (Paris VI Univ., France.), J. Schwartzel (Centre National d'Etudes des Telecommunications, Bagneux, France.), J. Detaint (Centre National d'Etudes des Telecommunications, Bagneux, France.), and T. Toudic (Centre National d'Etudes des Telecommunications, Lannion, France.) *In* ESA, Frequency and Time Forum Jun. 1992 p 287-291 (For primary document see N93-24978 09-70)

Copyright Avail: CASI HC A01/MF A04

A study to find a hydrothermal method for growing berlinite crystals of sufficently large sizes to use as piezoelectric materials is presented. Natural berlinite of large size are not known. Studies of the optimal conditions of growth were performed using extension of different techniques previously applied particularly to quartz crystals. Two growth techniques obtained large crystals of good quality. The first starts by joining several crystals of the same orientation to make a single seed. If this is not sufficient, a second 'crossed growth' technique can be used. To control the quality of the obtained crystals, x ray topographic studies were done and typical features of the samples are presented. ESA

N93-25026# Time and Frequency Ltd., Holon (Israel).

TF-4020A: TFL'S NEW COMPACT MILITARY RUBIDIUM STANDARD

E. Eltsufin and A. Stern *In* ESA, Frequency and Time Forum Jun. 1992 p 293-296 (For primary document see N93-24978 09-70)

Copyright Avail: CASI HC A01/MF A04

A military rubidium frequency standard model TF-4020A is described and analyzed. It is a compact (volume less than 500 cc) military rubidium standard and meets MIL-E-5400 (airborne electronic equipment) class 2 (-55 C to +71 C, 70,000 ft). The physics package shown is extremely small (87 cc) and comprises lamp and cavity subassembly and a twofold magnetic field. The oscillator is a miniature oven controlled crystal oscillator with a SC (Stress Compensated) cut crystal for a low vibration susceptibility. The main effort during the design process was concentrated on the design of reliable circuits: general reliability, stability and low susceptibility to external and internal influences like temperature, vibration and electromagnetic interference (EMI). Key features of the unit are: compact design; extremely small physics package (87 cc) with a special rugged design to withstand strong vibration; high stability over the wide operating temperature range of -55 C to +71 C; low susceptibility to EMI; low sensitivity to external DC and AC magnetic field; excellent short term stability of 7 x 10(exp -12)/square root of tau for tau greater than 0.1 s and less than 300 s; excellent long term stability of 1 x 10(exp -11) per month; and versatility to adopt versions without size increase. ESA

N93-25027# Frequency Electronics, Inc., Mitchel AFB, NY.

ULTRA STABLE OSCILLATORS FOR SATELLITE APPLICATIONS **c19**

John C. Ho *In* ESA, Frequency and Time Forum Jun. 1992 p 297-300 (For primary document see N93-24978 09-70)

Copyright Avail: CASI HC A01/MF A04

An ultrastable 5 mHz reference oscillator performance specification and a list of satellites that use source ultrastable crystal oscillators are presented. The circuit design and physical package provides an output frequency noise of -145 dBc/Hz 10 Hz from carrier; short term frequency stability is better than 5 pp 10 to the 13th power/second; temperature coefficient is less than 2 pp 10 to the 12th power/C over the operating temperature -20 C to +50 C; vibration 'g' sensitivity less than 6 pp 10 to the 10th power/g; and long term frequency stability less than 5 pp 10 to the 12th power/day in the actual space environment. These precision oscillators have frequency update capability allowing them to be tuned from the ground by command. A built-up 12 bit D/A converter with either parallel or series command codes controls the oscillator frequency. This tuning ability enables the oscillator to remain at an accurate frequency for missions of 10 to 15 years. Radiation hardening protection is also incorporated as required. ESA

N93-25028# Compagnie d'Electronique et de Piezo-Electricite, Argenteuil (France).

PRELIMINARY RESULTS OF A NEWLY DESIGNED MINI-OCXO OSCILLATOR ESPECIALLY DEDICATED TO SPACE APPLICATIONS **c19**

Evelyne Gerard and Gerard Wagner *In* ESA, Frequency and Time Forum Jun. 1992 p 301-307 (For primary document see N93-24978 09-70)

Copyright Avail: CASI HC A02/MF A04

The different steps of the development phase, a short description of the design, and the first results obtained on the breadboard model of the 'Mini OCXO (Oven Controlled Crystal Oscillator)', are presented. The product will be available in frequency range 5 to 20 MHz in a low weight (160 g maximum) small holder (83 by 50 by 34.6 mm), with stabilities for the higher version in the range 10(exp -9) and 10(exp -8). ESA

N93-25029# Oulu Univ. (Finland).

USE OF THE TV-SIGNAL IN STABILIZING A LOCAL RUBIDIUM OSCILLATOR **c33**

Reijo Kivelae *In* ESA, Frequency and Time Forum Jun. 1992 p 309-313 (For primary document see N93-24978 09-70)

Copyright Avail: CASI HC A01/MF A04

The methods and results of using the 15625 Hz frame synchronizing frequency of a normal television (TV) broadcast as a reference to automatically stabilize a local rubidium oscillator are described. The characteristics of the Finnish TV network were studied. Consequently, TVCRO (TV Controlled Rubidium Oscillator) microcomputer control algorithms and TVCRO prototype hardware were designed. Prototype measurements showed that the daily frequency can be maintained within 5 x 10(exp -12) (peak to peak). The standard deviation around the mean value is 0.9 x 10(exp -12). During a 40 day test run, the TVCRO output phase was within 0.8 microseconds of the TV phase. The long term drift of the TVCRO is in the order of a few parts on 10(exp -13) per year when referenced to transmission center frequency. ESA

N93-25030# Academia Sinica, Wuhan (China). Lab. of Magnetic Resonance and Atomic and Molecular Physics.

EXPERIMENTS ON A DIODE-LASER-PUMPED Rb-87 MASER **c36**

Deng Jinquan, Tan Yongfang, Xiang Yuanhai, and Zhu Xiwen *In* ESA, Frequency and Time Forum Jun. 1992 p 315-317 (For primary document see N93-24978 09-70)

Copyright Avail: CASI HC A01/MF A04

The demonstration of self sustained oscillations of a diode laser pumped Rb-87 maser is reported. The output powers of the laser in various pumping light intensities and cell temperatures were measured. The largest output power obtained with the diode laser power of 3.6 mW was 1 x 10(exp -10) W at the optimal cell temperature of 58 C. ESA

N93-25031# Ministry of Posts and Telecommunications, Kobe (Japan). Kansai Advanced Research Center.

OPTICAL DETECTION OF LASER-COOLED IONS IN A PENNING TRAP **c72**

Hidetsuka Imajo, Shinji Urabe, Kazuhiro Hayasaka, and Masayoshi Watanabe *In* ESA, Frequency and Time Forum Jun. 1992 p 319-322 (For primary document see N93-24978 09-70)

Copyright Avail: CASI HC A01/MF A04

The use of a Penning trap to trap Be(+) ions, which are then cooled by a laser to approximately 300 mK is described. The eigenmotions of the cooled ions were measured optically by using the laser fluorescence technique. In addition, several kinds of ions were trapped with Be(+) ions and their motional frequencies were measured. A small number of the cooled Be(+) ions were trapped and their fluorescence was also observed. ESA

N93-25032# Ecole Nationale Superieure de Mecanique et des Microtechniques, Besancon (France). Lab. de Chronometrie Electronique et Piezoelectricite.

QUARTZ CRYSTAL TWINNING UNDER MECHANICAL STRESS: FINITE ELEMENT ANALYSIS **c76**

J. J. Boy, B. Dulmet, and P. Conraux (Framasoft + CSI, Lyon, France.) *In* ESA, Frequency and Time Forum Jun. 1992 p 323-327 (For primary document see N93-24978 09-70)

Copyright Avail: CASI HC A01/MF A04

Some tools to describe the switching process of electrical twinning in various cuts of quartz are proposed. In all cases, the principle of minimal energy, together with a threshold condition is applied to the proper thermodynamic potential to determine which twin will survive the exerted stresses on a quartz sample. An analytical expression useful for samples submitted to a known homogeneous compressive stress is given. For more general stress states, a finite element approach is chosen to study the propagation of the switching process. It is founded upon a bielastic stress-strain relationship introduced into the plasticity model for nonlinear transient analysis in the SYSTUS (trademark) program. ESA

N93-25033# Kayser Threde G.m.b.H., Munich (Germany).

FIRST EXPERIENCE WITH THE ASN-16 GLONASS RECEIVER **c33**

B. Eissfeller, N. Balteas, A. Jansche, and V. Liebig *In* ESA, Frequency and Time Forum Jun. 1992 p 329-332 (For primary document see N93-24978 09-70)

Copyright Avail: CASI HC A01/MF A04

Experience with the ASN-16 GLONASS (Russian Global Space Navigation System), a slow sequencing C/A code receiver working on one channel, is described. It is basically designed for airborne applications but can also be used in terrestrial and maritime applications. It consists of a navigation computer; an RF unit, a control and display unit as well as antenna and preamplifier. An ARINC 429 compatible interface enables data transfer between receiver and external units (input of inertial aiding data, output of position, velocity, and time). A software upgrade also provides access to ephemeris, almanac, pseudorange, and pseudodoppler measurements. The ASN-16 equipment is described on hardware and software level. The first results of test measurements and material on the actual GLONASS constellation is presented. During the test period horizontal position errors of up to 30 m were measured within 24 hours in stationary mode. ESA

N93-25034# Franche-Comte Univ., Besancon (France). Lab. de Physique et Metrologie des Oscillateurs.

STABILITY OF NONLINEAR PHASE MOTION FROM THE STUDY OF OSCILLATOR MAPPINGS **c33**

M. Planat *In* ESA, Frequency and Time Forum Jun. 1992 p 333-336 (For primary document see N93-24978 09-70)

Copyright Avail: CASI HC A01/MF A04

A fundamental approach to study the intrinsic stability of phase motion at resonances of oscillator differential equations is reported. An averaging technique was developed to replace the continuous problem by a discrete phase mapping. A criterium of structural stability of resonances was found to numerically plot the diagram of frequency locked states. Typical diagrams have several layers corresponding to seperate power laws in the frequency fluctuation. By studying Hoedler continuity of frequency in parameter space (Omega, c) the phenomenon of Hoedler exponent resonance associated to fractal sets was discovered. In the case epsilon = 0, previous power laws associated to mode lock-in or irrational windings are recovered. Scaling laws associated to the decay in time of frequency fluctuations are studied. In the case of a small epsilon not equal to 0, a wide region of 1/f frequency noise is observed at the bottom of Arnold tongues. ESA

N93-25035# Oulu Univ. (Finland). Dept. of Electrical Engineering.

EXPERIMENTAL RESULTS OF THE PERFORMANCE OF THE NEW PHASE AND FREQUENCY CONTROLLER

Jari Mannermaa and Kalevi Kalliomaeki *In* ESA, Frequency and Time Forum Jun. 1992 p 337-341 (For primary document see N93-24978 09-70)

Copyright Avail: CASI HC A01/MF A04

The application of the Maximum Entropy Method (MEM) to control phase locked crystals of Loran C receivers is reported. Performance optimization of the MEM controller achieved the result of 9 ns and 7 x 10(exp -12) for phase and frequency residuals, respectively. These values are comparable with 100 ns and 9 x 10(exp -12) of the older conventional PI controller, respectively. The performance of the MEM controlled Loran C receiver is at least 50 percent better when compared with the identical receiver equipped with the PI controller. The results verify the presumed superiority of the MEM controller over the conventional PI. ESA

N93-25036# Observatoire de Besancon (France).

TIME STABILITY: AN IMPROVEMENT OF THE MULTI-VARIANCE METHOD FOR THE OSCILLATOR NOISE ANALYSIS

F. Vernotte and E. Lantz (Besancon Univ., France.) *In* ESA, Frequency and Time Forum Jun. 1992 p 343-347 (For primary document see N93-24978 09-70)

Copyright Avail: CASI HC A01/MF A04

A study attempting to improve the measurement accuracy in oscillator instabilities in order to better distinguish the different types of noises is presented. The different notions, tools, and mathematical models used in the frequency and time field are presented and the classical measurement method using one single variance is recalled. The multivariance method, based on the use of several variances, is described. An improvement of this multivariance method is proposed and the measurements accuracy of these methods compared. ESA

N93-25037# Ecole Nationale Superieure de Mecanique et des Microtechniques, Besancon (France). Lab. de Chronometrie Electronique et Piezoelectricite.

ANISOTROPIC ETCHING OF SILICON IN KOH SOLUTIONS **c25**

A. Brahim-Bounab and C. R. Tellier *In* ESA, Frequency and Time Forum Jun. 1992 p 349-354 (For primary document see N93-24978 09-70)

Copyright Avail: CASI HC A02/MF A04

Procedures which can be used to predict etched shapes encountered in anisotropic micromachining processes which start with the dissolution slowness surface are reported. Changes in the etch rate and in dissolution shapes of differently oriented silicon plates are analyzed to obtain the slowness surface describing the anisotropic etching of silicon in KOH solutions. Theoretical etched shapes are derived and compared with experimental results. The proposed three dimensional representation of the slowness surface is discussed. ESA

N93-25038# Frequency Electronics, Inc., Mitchel AFB, NY.

MICROWAVE SYNTHESIZERS IN SPACE **c33**

A. Vulcan and M. Bloch *In* ESA, Frequency and Time Forum Jun. 1992 p 355-359 (For primary document see N93-24978 09-70)

Copyright Avail: CASI HC A01/MF A04

An overview of synthesizers used in the space environment including direct and indirect synthesizers is presented. Synthesizers are used in satellites as local oscillators, reference signal generators for phase locked loops, sources for calibration systems, and any other purposes. The design drivers are small size, low weight, high reliability, and low power consumption. The frequency sources are used in redundant configurations to ensure that there are no single point failures. Space synthesizers have many self test telemetry outputs which provide indications of the unit health and operating mode. They operate either directly from the spacecraft primary power bus or from a centralized DC to DC converter whose outputs are semiregulated voltages. The long term frequency stability depends upon the reference source which may or may not be internal to the synthesizer. Atomic frequency standards or quartz crystal oscillators are used depending on mission stability requirements. ESA

N93-25039# Wall (Peter K.) ElectroAcoustics, Penrith (England).

VERY WIDE BANDWIDTH HF CRYSTAL FILTERS **c33**

Peter K. Wall *In* ESA, Frequency and Time Forum Jun. 1992 p 361-364 (For primary document see N93-24978 09-70)

Copyright Avail: CASI HC A01/MF A04

Measurements on 1 MHz wide crystal filters at 20 MHz with less than 6 dB insertion loss, 1 dB unwanted response heights, and with high selectivity and stopband attenuation are presented. Calculations show that unwanted responses in the 100,000 ohm region are required. Measurements of crystals made for these filters are presented. They show that these levels of unwanted response are achievable. Comparisons with a high accuracy reference method show acceptable correlation. ESA

N93-25040# Polish Academy of Sciences, Warsaw. Tele- and Radio Research Inst.

MEASUREMENT RESULTS OF THE CRYSTALLOGRAPHIC ORIENTATION OF THE SC CUT ROUND PLATES **c76**

K. Weiss *In* ESA, Frequency and Time Forum Jun. 1992 p 365-367 (For primary document see N93-24978 09-70)

Copyright Avail: CASI HC A01/MF A04

Investigations and analysis of the main measurement errors of crystallographic orientation of doubly rotated cuts are reported. On the basis of the results, a procedure to measure the crystal orientation of rectangular and round plates using the standard double reflection goniometer with simple additional equipment was developed. Using this procedure the crystallographic orientation measurements of SC (Stress Compensation) cut plates with reference to selected atomic planes were carried out. A review of factors involving the measurement inaccuracy measurement procedure, as well as measurement and calculation results for the SC round plates is given. The achieved measurement accuracy of crystallographic orientation of these plates was better than 5 seconds (for selected atomic planes). The time consumption of one plate orientation measurement was not longer than 5 minutes. ESA

N93-25041# Haut Commissariat a la Recherche, Algiers (Algeria). Lab. de Physique Nucleaire.

A FREQUENCY GENERATING SOURCE: FREQUENCY SYNTHESIZERS **c33**

N. Yahyabey and S. Hassani (CDTA, Algiers, Algeria.) *In* ESA, Frequency and Time Forum Jun. 1992 p 369-370 (For primary document see N93-24978 09-70)

Copyright Avail: CASI HC A01/MF A04

A mode of fractional frequency harmonic generation obtained by the modulation of a square wave reference signal is considered. The produced spectrum exhibits a particular structure. The longer the fractional part of the frequency of the modulating wave is, the more figures the value of the frequency of the harmonic has. A comparison in terms of design purposes of component frequency generator blocks of frequency synthesizers is carried out. ESA

N93-25042# Politecnico di Milano (Italy). Dipt. di Elettronica.

PHASE DIFFERENCES OF THE FIELDS IN A RAMSEY RESONATOR FOR SUBMILLIMETRIC FREQUENCY STANDARDS

E. Bava and P. Tavella (Istituto Elettrotecnico Nazionale, Galileo Ferraris, Turin, Itlay.) *In* ESA, Frequency and Time Forum Jun. 1992 p 371-374 Sponsored in part by CNR (For primary document see N93-24978 09-70)

Copyright Avail: CASI HC A01/MF A04

The study of an open resonator suitable for standards operating in the submillimeter region, such as Mg and Ca beams and hopefully in the infrared region, is addressed. The structure is obtained by weakly coupling two resonators by means of a very thin splitter. One of the resonators is doubly folded, to allow the Ramsey technique, and it is fed in a nearly symmetric way by the other one. The resonances of the overall structure are studied, as they appear at the input, to distinguish the high excitation from the low excitation ones of the folded resonator. This analysis is firstly performed supposing a lossless structure, then the phase relationships between the two separated fields are evaluated in a few special cases for a real structure. ESA

N93-25043# Compagnie d'Electronique et de Piezo-Electricite, Argenteuil (France).

CONTROLLED DISSOLUTION OF A PIEZOELECTRIC MATERIAL BERLINITE (AlPO4) [DISSOLUTION CONTROLEE D'UN MATERIAU PIEZOELECTRIQUE, LA BERLINITE (ALPO4)] **c76**

O. Cambon, A. Goiffon (Montpellier Univ., France.), A. Ibanez (Montpellier Univ., France.), and E. Philippot (Montpellier Univ., France.) *In* ESA, Frequency and Time Forum Jun. 1992 p 377-381 In FRENCH (For primary document see N93-24978 09-70)

Copyright Avail: CASI HC A01/MF A04

The results on the controlled dissolution of berlinite aimed at realizing AT high frequency (75 Hz) resonators are presented. The dissolution takes place in acid solutions (H3PO4 or H2SO4) of aluminum phosphate. The dissolution kinetics and evolution of the surface state are controlled during the chemical machining process by frequency variation of resonance and roughometry. After systematic study, the controlled dissolution bath giving the best results is used to prepare AT berlinite resonators. Theses are characterized by their piezoelectric performances and compared to resonators obtained by ion bombardment or to similarly oriented quartz resonators. ESA

N93-25044# Montpellier Univ. (France).

CRYSTAL GROWTH AND PHYSICAL CHARACTERIZATIONS OF GaPO4 **c76**

E. Philippot, A. Ibanez, A. Goiffon, B. Capelle (Paris VI Univ., France.), A. Zarka (Paris VI Univ., France.), J. Schwartzel (Centre National d'Etudes des Telecommunications, Bagneux, France.), and J. Detaint (Centre National d'Etudes des Telecommunications, Bagneux, France.) *In* ESA, Frequency and Time Forum Jun. 1992 p 383-388 (For primary document see N93-24978 09-70)

Copyright Avail: CASI HC A02/MF A04

An investigation concerning GaPO4 crystal growth in sulphuric and phosphoric acid media through the slow heating and vertical reverse temperature gradient methods is reported. Systematic study of growth parameters shows a Vx growth rate always much greater than the two other ones: Vz and Vy. The most interesting result is the ability to do GaPO4 epitaxy in large berlinite seems in sulphuric acid and, after that, to use them for GaPO4 crystal growth in phosphoric acid. The good epitaxy process and the crystalline quality were checked by x ray topography. The (OH) content, followed by infrared spectrometry, seems to prove a lower OH concentration than in the berlinite case for approximately the same crystal growth conditions. First piezoelectric characterizations of resonators near the AT cut show GaPO4 to be a very promising piezoelectric material with a large coupling coefficient near 16 percent, a quartz like thermal stability, and a Q factor already nearly sufficient for the applications. ESA

N93-25045# Nancy Univ. (France). Lab. Infrarouge.

THERMIONIC CURRENT MEASUREMENT IN QUARTZ [MESURE DE COURANTS THERMOIONIQUES DANS LE QUARTZ] **c76**

G. Jeandel, A. Warin, C. Poignon, J. P. Aubry (Compagnie d'Electronique et de Piezo-Electricite, Argenteuil, France.), and G. Morlot *In* ESA, Frequency and Time Forum Jun. 1992 p 389-392 In FRENCH Sponsored by Direction des Recherches, Etudes et Techniques (For primary document see N93-24978 09-70)

Copyright Avail: CASI HC A01/MF A04

The characterization of quartz samples by a thermionic current measurement called Ionic Thermal Current (ITC) is reported. A better understanding of impurity migration, under applied electric field, would enable a more efficient control of the electromigration process used for quartz purification: 'sweeping'. Several blocks originating from the same zone were cut off in the same crystal. The laminas were cut in each of the blocks of perpendicular to the Z or Y axes. Two crystals were studied: one of the I quality (number 272) and the other of standard quality (number 511). The ITC measurements of these two types of crystal are presented. Thermionic currents of laminas cut off more or less further from the nucleus are compared. The effects of 'sweeping' on the ITC current is shown. ESA

N93-25046# York Univ. (Ontario). Piezoelectricity Research Lab.

THE THIRD-ORDER PERMITTIVITY OF QUARTZ OBTAINED BY DIFFERENT METHODS **c76**

Carl K. Hruska *In* ESA, Frequency and Time Forum Jun. 1992 p 393-395 Sponsored in part by Natural Sciences and Engineering Research Council of Canada and York Univ. (For primary document see N93-24978 09-70)

Copyright Avail: CASI HC A01/MF A04

A comparison of three values of the third order permittivity constant of quartz obtained independently by three different methods is presented. Each method produces a value of a different order of magnitude and there is no uniformity in sign among them. The difference between the value obtained by the resonator method and the older, original value obtained by the capacitor method, is not statistically significant. On the other hand, the values obtained by the transit time method differs significantly from the previous two results. ESA

N93-25047# Army Electronics Technology and Devices Lab., Fort Monmouth, NJ.
THERMOELASTICITY IN QUARTZ **c76**
J. A. Kosinski, J. G. Gualtieri, and A. Ballato *In* ESA, Frequency and Time Forum Jun. 1992 p 397-402 (For primary document see N93-24978 09-70)
Copyright Avail: CASI HC A02/MF A04

A critical analysis of experimental measurements of alpha quartz thermal expansion reported in the literature is presented. A recommended set of best measured values over the temperature range -50 to +150C was determined, as were values for the coefficient of thermal linear expansion and the thermoelastic coefficients alpha(sub ij)(sup (n)). The new alpha(sub ij)(sup (n)) values are: alpha(sub 11)(sup (1)) = 13.65 times 10 to the minus 6th power/K, alpha(sub 33)(sup (1)) = 7.50 x 10(exp -6)/K, alpha(sub 11)(sup (2)) = 11.02 x 10 (exp 1 9)/K squared, alpha(sub 33)(sup (2)) = 8.00 x 10(exp - 9)/K squared, alpha(sub 11)(sup (3)) = -19.32 x 10(exp 1 12)/K cubed, alpha(sub 33)(sup (3)) = -10.44 x 10(exp -12)/K cubed. The impact of using the new alpha(sub ij)(sup (n)) on determinations of quartz material temperature coefficients and on the calculation of temperature coefficients of frequency for the case of the AT cut are discussed. ESA

N93-25048# Shanghai Observatory (China).
THE DEVELOPMENT PROGRESSES OF HYDROGEN MASERS AT SHANGHAI OBSERVATORY **c36**
Z. C. Zhai, H. X. Huang, J. W. He, C. F. Lin, G. X. Jiang, W. H. Luo, and J. F. Lu *In* ESA, Frequency and Time Forum Jun. 1992 p 405-408 (For primary document see N93-24978 09-70)
Copyright Avail: CASI HC A01/MF A04

The developments, performances, and applications of hydrogen masers are summarized. After the success of the first Chinese hydrogen maser, five more hydrogen masers with several improvements to the maser design, but still traditional structures, were made for VLBI (Very Long Base Interferometry) observations and timekeeping. To equip the Chinese VLBI network, a new generation of hydrogen maser, an integrated, rugged and easily transportable maser, was developed successfully. For timekeeping with hydrogen masers, a kind of one maser autotuning system was developed. Meanwhile, the third generation of hydrogen maser, an oscillating compact hydrogen maser which employs a compact cavity design, resulting in significant size and weight reductions compared to a conventional maser, is being developed. This kind of maser is suitable for timekeeping because of its excellent long term stability. ESA

N93-25049# KVARZ, Nishnij Novgorod (Russia). Inst. of Electronic Measurements.
INVESTIGATIONS OF THE FREQUENCY INSTABILITY OF CH1-75 HYDROGEN MASERS **c36**
N. A. Demidov, E. M. Ezhov, B. A. Sakharov, B. A. Uljanov, A. Bauch (Physikalisch-Technische Bundesanstalt, Brunswick, Germany.), and B. Fischer (Physikalisch-Technische Bundesanstalt, Brunswick, Germany.) *In* ESA, Frequency and Time Forum Jun. 1992 p 409-414 (For primary document see N93-24978 09-70)
Copyright Avail: CASI HC A02/MF A04

The construction and characteristics of the Russian CH1-75 active hydrogen maser are described. Technical features providing low frequency instability are detailed. Methods and problems of microwave cavity autotuning are analyzed. Frequency instability caused by the autotuning microwave cavity system and the crystal oscillator synchronization system are discussed. The comparison between two CH1-75 H masers mutually and with primary clocks CS1 and CS2 during a 1 year period are presented. ESA

N93-25050# Physikalisch-Technische Bundesanstalt, Brunswick (Germany).
ION TRAP FREQUENCY STANDARD RESEARCH AT PTB
D. Schnier, A. Bauch, R. Schroeder, and C. Tamm *In* ESA, Frequency and Time Forum Jun. 1992 p 415-420 (For primary document see N93-24978 09-70)
Copyright Avail: CASI HC A02/MF A04

The transition between the hyperfine levels F = 1, m(sub F) = 0 and F = 0, m(sub F) = 0 in the ground state of 171-Yb(+) is investigated as a reference transition for a trapped ion frequency standard. A description of the experimental setup and the measurement procedure is given. The line was recorded with a linewidth of 16 MHz. Results of the frequency instability and the first steps of an evaluation of the uncertainty contributions are given. ESA

N93-25051# Hamburg Univ. (Germany). Inst. fuer Laser-Physik.
CONTROLLING AN OPTICAL FREQUENCY BY A SINGLE ION
I. Siemers, V. Enders, R. Blatt, W. Neuhauser, and P. E. Toschek *In* ESA, Frequency and Time Forum Jun. 1992 p 421-424 (For primary document see N93-24978 09-70)
Copyright Avail: CASI HC A01/MF A04

The control of the oscillation frequency of a single mode signal laser by a narrow resonance of a single trapped ion may result in frequency generation of both satisfactory precision and unprecendented accuracy. The signature of resonant excitation cannot be derived from the very weak fluorescence on the control transition. Instead, the rate of dark intervals of simultaneously excited resonance light may be used as a discriminant for the signal resonance. Alternatively, two lasers may excite an E2 transition whose resonance is indicated by a 'dark line' in the resonance fluorescence. Perturbative effects in the dark lines of a single trapped Ba(+) ion, the narrowest of which is 63 kHz, are quantitatively studied and a dark line of a single Yb(+) ion is demonstrated. Systematic shifts of the signal frequency may be eliminated with residual inaccuracy smaller than 10 to the minus 15th power. ESA

N93-25052# Johns Hopkins Univ., Laurel, MD. Applied Physics Lab.
QUARTZ OSCILLATORS, FREQUENCY SYNTHESIZERS, AND TIMING SYSTEMS FOR GEODESY AND RADIO SCIENCE APPLICATIONS **c33**
J. J. Suter, J. M. Cloeren, J. R. Norton, and M. J. Reinhart *In* ESA, Frequency and Time Forum Jun. 1992 p 427-429 (For primary document see N93-24978 09-70)
Copyright Avail: CASI HC A01/MF A04

Recent advances in improvements to a series of high quality frequency standards, including quartz crystal oscillators, frequency synthesizers, and hydrogen masers, are discussed. The performance of spaceflight BVA (electrodeless quartz resonator) oscillators and frequency synthesizers developed for the Topex Poseidon mission is reported. Data on the performance of atomic clocks is presented. The ongoing developments of quartz crystal oscillators and synthesizers address the needs of several U.S. and European geodesy and radio science space programs. ESA

N93-25053# Centre National d'Etudes Spatiales, Toulouse (France).
SPACE RADIATION SUSCEPTIBILITY OF ULTRA STABLE CRYSTAL OSCILLATORS **c33**
M. Brunet, J. F. Dutrey, J. B. Laporte, J. Bourriau (Centre d'Etudes et de Recherches, Toulouse, France.), and P. Calvel (Alcatel Espace, Toulouse, France.) *In* ESA, Frequency and Time Forum Jun. 1992 p 431-440 (For primary document see N93-24978 09-70)
Copyright Avail: CASI HC A02/MF A04

The radiation susceptibility of several quartz oscillators for space use (USO) with classical and BVA (electrodeless quartz resonator) type resonators, AT and SC (Stress Compensation) cut, is reported. Susceptibility of each USO was measured at low dose rate, 1 and 0.1 rad per hour, using a cobalt 60 source. In parallel, a space radiation exposure analysis was made taking into account the radation environment during the in flight data recording. A deposited dose calculation analysis was conducted using an up to data three dimensional Monte Carlo transport code. Results of aging rate per day are then compared to several in flight data. ESA

N93-25054# Alcatel Bell Telephone, Antwerp (Belgium).
FREQUENCY GENERATION AND SYNTHESIS IN THE DRSS **c33**
P. VanLoock and J. DeVlieghere *In* ESA, Frequency and Time Forum Jun. 1992 p 441-444 (For primary document see N93-24978 09-70)
Copyright Avail: CASI HC A01/MF A04

The feasibility of a Tunable Frequency Converter (TFC) concept envisaged on board of the Data Relay System Satellites (DRSS), which requires a synthesizer with state of the art phase noise performance that is locked to a common, ultrastable oscillator, is addressed. The DRSS Ka band communication links are discussed with reference to the DRS system and the TCF. The aim is to provide an autonomous TCF unit demonstrating that the advanced channel selection scheme, with all frequency translations locked to one common reference, is feasible. Concept tradeoff and key elements of the frequency synthesizer are outlined. White noise filtering

and reference frequency selection of the reference generator are discussed. The TFC unit allows payload reconfigurability via the frequency setting. The concept is extendable to all TFC types on board of the DRSS. ESA

N93-25055# Compagnie d'Electronique et de Piezo-Electricite, Argenteuil (France).

OSCILLATORS FOR MOBILE GPS RECEIVERS **c33**

J. P. Aubry, P. Canzian, and V. Candelier *In* ESA, Frequency and Time Forum Jun. 1992 p 445-450 (For primary document see N93-24978 09-70)

Copyright Avail: CASI HC A02/MF A04

The design procedure and optimization of oscillators for mobile GPS (Global Positioning System) receivers and typical results regarding the resonator's performance are presented. The GPS oscillators were designed to meet the GPS system requirements, either for time transfer or localization, in different environment. These oscillators focus either on the absolute accuracy, through low G sensitivity and high stability for the naval ones, or in the warm up, through the use of the airborne TXCO (Temperature Compensated Crystal Oscillator), which provides an accuracy good enough with low power and low size. One of the key points is that most of the applications require low oscillator size. That means that the low G sensitivity must now be achieved with a low size resonator. Significant improvements were carried on HC37 can resonators which can exhibit now G sensitivity better than 5 times 10 to the minus 10th power per G. ESA

N93-25056# Laboratoire de l'Horloge Atomique, Orsay (France).

MICROWAVE INTERROGATION FREQUENCY NOISE AND CLOCK FREQUENCY STABILITY: EXPERIMENTAL RESULTS

R. Barillet, V. Giordano, J. Viennet, and C. Audoin *In* ESA, Frequency and Time Forum Jun. 1992 p 453-456 Sponsored by Direction des Recherches, Etudes et Techniques (For primary document see N93-24978 09-70)

Copyright Avail: CASI HC A01/MF A04

Theoretical study shows that the frequency noise of the microwave interrogation may limit the short term frequency stability of passive atomic frequency standards. In order to investigate experimentally this effect, two identical microwave interrogation systems were realized. The phase shift difference of their frequency noise can be increased and measured. The validity of the theoretical model is confirmed by the experimental results. Measurements shows that the frequency stability of an experimental cesium beam tube is close to the limit associated with the use of a high quality 10 MHz VCXO. It will be necessary to take care of this effect in future passive frequency standards using optical pumping and/or cooled atoms. ESA

N93-25057# SEPA S.p.A., Turin (Italy). Fiat Ciei S.p.A.

HIGH RESOLUTION DIGITAL SYNTHESIZER FOR A Rb FREQUENCY STANDARD **c33**

E. Detoma, G. Pedrotto, A. Stern (Time and Frequency Ltd., Holon, Israel.), B. Levi (Time and Frequency Ltd., Holon, Israel.), and M. Bootnik (Time and Frequency Ltd., Holon, Israel.) *In* ESA, Frequency and Time Forum Jun. 1992 p 457-469 (For primary document see N93-24978 09-70)

Copyright Avail: CASI HC A03/MF A04

Work in implementing a Rb frequency standard with an internal high resolution synthesizer and incorporating a novel technique of AC C field modulation is presented. The aim was to develop a device in which the output frequency can be accurately set without changing the C field, in order to achieve a good settability in time and frequency without perturbing the conditions of the atomic interrogation. The modulation technique being used (square wave FM) allowed a straightforward implementation of the proposed AC C field modulation, the latter technique being specifically intended to reduce the magnetic sensitivity of the Rb frequency standard. Some communication network and space applications are discussed. ESA

N93-25058# Istituto Elettrotecnico Nazionale (Galileo Ferraris), Turin (Itlay).

SOLID STATE FREQUENCY SYNTHESIS UP TO 600 GHz: AN APPLICATION TO THE Mg FREQUENCY STANDARD **c76**

A. Godone and C. Novero *In* ESA, Frequency and Time Forum Jun. 1992 p 471-475 (For primary document see N93-24978 09-70)

Copyright Avail: CASI HC A01/MF A04

An all solid state frequency multiplication chain from 5 MHz to 601.3 GHz with spectral purity and output power suitable to excite the (sup 3)P(sub 1) - (sup 3)P(sub 0) Delta(m(sub j)) = 0 transition in the metastable triplet of Mg is presented. The chain is described and the frequency modulation spectrum of the free running Gunn oscillator and the Gunn oscillator phase locked loop are described. By use of this chain the Mg frequency is remeasured with an uncertainty of +/- 4 x 10(exp -12) with respect to the Cs standard, corresponding to an improvement of an order of magnitude with respect to the previous data. ESA

N93-25059# National Inst. of Standards and Technology, Boulder, CO. Time and Frequency Div.

DESIGNING FOR FREQUENCY AND TIME METROLOGY AT THE 10 TO THE MINUS 18 POWER LEVEL

F. L. Walls, L. M. Nelson, and G. R. Valdez *In* ESA, Frequency and Time Forum Jun. 1992 p 477-481 Sponsored in part by CECOM Center for Space Systems (For primary document see N93-24978 09-70)

Copyright Avail: CASI HC A01/MF A04

Some of the key parameters that significantly affect the overall architecture of a system that is being designed to measure frequency or time accuracy to 3 by 10(exp -18) are examined. Specifically, the following are investigated: the timing errors in signal transmission for distances up to 100 m; the effect of changes in temperature and RF amplitude on timing (low frequency) errors in several available phase detectors; and the influence of measurement algorithms on the allowable level of white phase noise in the system as a function of the carrier frequency. ESA

N93-25060# Tekelec-Systemes, Les Ulis (France).

TIME GENERATION AND DISTRIBUTION SYSTEM FOR A MILITARY NATIONAL SYNCHRONIZATION

V. Mourier *In* ESA, Frequency and Time Forum Jun. 1992 p 485-488 (For primary document see N93-24978 09-70)

Copyright Avail: CASI HC A01/MF A04

The requirements, concept, and principle of a French air force time generation and distribution system are presented. The system provides homogeneous dating of events throughout the country. It generates and distributes time codes and precise frequency used for high precision measurements, telecommunications, etc. Accordingly the need is to provide on each operational site an accurate and stable time reference based on UTC time scale. The system consists of a common reference (GPS (Global Positioning System)) independent clocks and time distribution that provides time to all the user equipment on each operational site. ESA

N93-25061# Nippon Telegraph and Telephone Public Corp., Yokosuka (Japan). Transmission Systems Labs.

TIMING AND TIME SIGNAL DISTRIBUTION IN DIGITAL COMMUNICATIONS NETWORKS **c32**

Masami Kihara and Atushi Imaoka *In* ESA, Frequency and Time Forum Jun. 1992 p 489-492 (For primary document see N93-24978 09-70)

Copyright Avail: CASI HC A01/MF A04

The timing signal distribution characteristics of a digital communications network are evaluated to determine the Maximum Time Interval Error (MTIE) of the network; reference is made to the performance of network components such as transmission systems, slave clocks and timing distribution systems in intraoffices. The MTIE of each component is measured and used to determine the allowable MTIE of that component. The maximum number of slave node chains is shown to be 20. Time signal distribution performance is detailed. It is shown that time synchronization accuracy is of the order of submicroseconds between nodes separated by 2400 km over a two year period. For intra-office time signal distribution, the relative time accuracy is less than 3 nanoseconds using an 8 Mb/s round trip digital interface to connect a time signal supply in an office to dispersed equipment. ESA

N93-25062# American Telephone and Telegraph Co., Bedminster, NJ.

TIMING A NATIONAL TELECOMMUNICATIONS NETWORK USING GPS **c32**

E. W. Butterline, J. E. Abate (Bell Telephone Labs., Inc., Holmdel, NJ.), and G. P. Zampetti *In* ESA, Frequency and Time Forum Jun. 1992 p 493-496 (For primary document see N93-24978 09-70)

Copyright Avail: CASI HC A01/MF A04

The use of signals from the Global Positioning System (GPS) to synchronize national telecommunications networks is addressed. The GPS

based system, termed a Primary Reference Clock (PRC), employs a GPS receiver providing long term timing accuracy along with duplicated disciplined rubidium oscillators providing short term (one day) stability. The PRC system produces a digital signal used to synchronize a master clock in the node which in turn produces a signal that is used to synchronize all other clocks in the node, and distributed on a dedicated digital basis to all neighboring nodes. By use of monitoring equipment at each PRC, the performance of the master clock at every network node will be verified against the PRC signal. For the first time, a national telecommunications network is monitored and verified to be performing to a precision better than existing international standards. ESA

N93-25063# Telecom Solutions Europe Ltd., Leatherhead (England).
STRATEGIES FOR SYNCHRONISATION IN AN EVOLVING TELECOMMUNICATIONS NETWORK **c32**
Rob Avery (Telecom Solutions Ltd., San Jose, CA.) *In* ESA, Frequency and Time Forum Jun. 1992 p 497-501 (For primary document see N93-24978 09-70)
Copyright Avail: CASI HC A01/MF A04

The achievement of precise synchronization in the telecommunications environment is addressed. Transmitting the timing from node to node has been the inherent problem for all digital networks. Traditional network equipment used to transfer synchronization, such as digital switching ststems, adds impairments to the once traceable signal. As the synchronization signals are passed from node to node, they lose stability by passing through intervening clocks. Timing would be an integrated part of all new network and service deployments. New transmission methods, such as the Synchronous Digital Hierarchy (SDH), survivable network topologies and the issues that arise from them, necessitate a review of current network synchronization strategies. Challenges that face the network are itemized. A demonstration of why localized Primary Reference Clocks (PRC) in key nodes and the Synchronization Supply Unit (SSU) clock architecture of transit and local node clocks is a technically and economically viable solution to the issues facing network planners today is given. ESA

N93-25064# Telecom Solutions Ltd., San Jose, CA.
SYNOPSIS OF TIMING MEASUREMENT TECHNIQUES USED IN TELECOMMUNICATIONS **c32**
G. P. Zampetti *In* ESA, Frequency and Time Forum Jun. 1992 p 503-507 (For primary document see N93-24978 09-70)
Copyright Avail: CASI HC A01/MF A04

Historically, Maximum Time Interval Error (MTIE) and Maximum Relative Time Interval Error (MRTIE) have been the main measurement techniques used to characterize timing performance in telecommunications networks. Recently, a new measurement technique, Time Variance (TVAR) has gained acceptance in the North American (ANSI) standards body. TVAR was developed in concurrence to address certain inadequacies in the MTIE approach. The advantages and disadvantages of each of these approaches are outlined. Real measurement examples are presented to illustrate the critical issues in actual telecommunication applications. An MTIE measurement is proposed (ZTIE) that complements TVAR. The basic concept behind ZTIE is that a peak power measure is needed to complement TVAR. Together, TVAR and ZTIE provide a very good characterization of network timing. ESA

N93-25065# Observatoire Cantonal, Neuchatel (Switzerland).
A COMPACT AND HIGH-PERFORMANCE REFERENCE CELL FOR LASER FREQUENCY STABILIZATION **c36**
G. Dudle and T. Thomann *In* ESA, Frequency and Time Forum Jun. 1992 p 511-514 Sponsored in part by Swiss National Fund for Scientific Research (For primary document see N93-24978 09-70)
(Contract ESTEC-9099/90/NL/US(SC))
Copyright Avail: CASI HC A01/MF A04

Frequency stabilized lasers are required for many applications such as length metrology, telecommunications and optically pumped atomic frequency standards. Linear and saturated absorption atomic vapor cells are traditionally used as frequency discriminators to lock the laser frequency to an atomic transmition (for example, the D1 and D2 lines in Cs or Rb). The problems associated with these discriminators may be overcome by using a short and intense atomic beam as a reference. Theoretical considerations show that with a proper design of the atomic beam collimator, an atomic beam discriminator can combine a small residual Doppler width with a high signal to noise ratio and signal to background ratio. The experimental results obtained in a Cs beam show that this high performance discriminator can be realized in practice in a very compact sealed cell, comparable in size with a simple absorption cell. ESA

N93-25066# Observatoire Cantonal, Neuchatel (Switzerland).
LINE INHOMOGENEITY EFFECTS AND POWER SHIFT IN MINIATURIZED RUBIDIUM FREQUENCY STANDARDS **c33**
G. Mileti, I. Rueedi, and H. Schweda *In* ESA, Frequency and Time Forum Jun. 1992 p 515-519 Sponsored in part by Swiss Commission for the Encouragement of Research (For primary document see N93-24978 09-70)
(Contract ESTEC-9099/90/NL/US(SC))
Copyright Avail: CASI HC A01/MF A04

The role of the line inhomogeneity in determining the overall performances of a compact rubidium frequency standard is analyzed. The possibility of zero power shift operation is discussed and the effects of the main physical parameters of the standards on this particular operation mode is investigated experimentally. The power shift varies as function of the cell temperature, but only very little with the light intensity. Light attenuation and filtering appears as the main cause. Different C field gradients show variations in the power shift which was predominantly positive in all cases. It was possible to find a C field configuration, and a working point, in which, in addition to zero temperature coefficient, and zero light shift, the power shift is reduced to less than 3 times 10 to the minus 12th power/micro W. This performance was possible at very low operating RF power, less than 0.5 microW, due to an improved microwave structure. ESA

N93-25067# Observatoire Cantonal, Neuchatel (Switzerland).
NOISE MEASUREMENTS IN SINGLE-MODE GaAlAs DIODE LASERS **c36**
N. Sagna, C. Mandache (Bucharest Univ., Romania.), and P. Thomann *In* ESA, Frequency and Time Forum Jun. 1992 p 521-525 Sponsored by Swiss National Fund for Scientific Research (For primary document see N93-24978 09-70)
Copyright Avail: CASI HC A01/MF A04

Laser diodes may bring significant improvements to the performance of Cs and Rb frequency standards, as well as new possibilities for their miniaturization. However, the requirements on the laser are stringent, particularly as far as frequency noise are concerned. The requirements are viewed and compared with measurements of several types of single mode lasers including Fabry-Perot CSP, quantum well and distributed Bragg reflector structures. ESA

N93-25068# Tokyo Inst. of Tech., Yokahama (Japan).
FUNDAMENTAL CHARACTERISTICS OF A LASER-DIODE-PUMPED RUBIDIUM MASER WITH AN EXTERNAL FEEDBACK LOOP **c36**
Nobunori Oura, Naimu Kuramochi, Wataru Domon, Tamotsu Komiyama, and Ryota Shirato *In* ESA, Frequency and Time Forum Jun. 1992 p 527-530 (For primary document see N93-24978 09-70)
Copyright Avail: CASI HC A01/MF A04

A small Rb-87 maser with a TE(sub 011) mode cavity is studied. The feedback loop technique similar to that of a compact H maser is utilized. The continuous oscillation is confirmed from the fact that the oscillation began only when the laser diode light irradiated an Rb-87 maser cell in the cavity. In addition to the Rb-87 maser, the continuous oscillation of maser using a natural Rb cell is also obtained. ESA

N93-25069# National Physical Lab., Teddington (England).
PROGRESS TOWARDS LABORATORY FREQUENCY STANDARDS FOR THE OPTICAL COMMUNICATION BANDS **c32**
D. J. E. Knight, K. I. Pharaoh, S. L. T. Drysdale, J. Meldau (Strathclyde Univ., Glasgow, Scotland.), G. Duxbury (Strathclyde Univ., Glasgow, Scotland.), and C. J. Hodges (Cambridge Univ., England.) *In* ESA, Frequency and Time Forum Jun. 1992 p 531-536 (For primary document see N93-24978 09-70)
Copyright Avail: CASI HC A02/MF A04

Some frequency reference points in the 1.5 micrometer optical communication band are reviewed, and experimental results on frequency references for the 1.52 micrometers He-Ne laser are presented. A 15-NH3 absorption within the tuning range of the laser is found to be weak and not saturable. A diode laser was used to investigate to 1.52 micrometers

Ne transition observed via the optogalvanic effect in a hollow cathode discharge. Using a similar discharge tube intracavity in a He-Ne laser, optogalvanic saturated absorption dips of about 6 were found in 20-Ne discharges at about 1 torr (133 Pa) pressure. The full width at half maximum was about 100 MHz. ESA

N93-25402# Joint Publications Research Service, Arlington, VA.
JPRS REPORT: SCIENCE AND TECHNOLOGY. CENTRAL EURASIA: PHYSICS AND MATHEMATICS
25 Jun. 1992 34 p Transl. into ENGLISH from various Russian articles (JPRS-UPM-92-004) Avail: CASI HC A03/MF A01

Translated articles cover the following topics: acoustics; crystals, laser glasses, semiconductors; gas dynamics; lasers; optics, spectroscopy; plasma physics; superconductivity; technical physics; and theoretical physics. CASI

N93-25403# Joint Publications Research Service, Arlington, VA.
JPRS REPORT: SCIENCE AND TECHNOLOGY. CENTRAL EURASIA: PHYSICS AND MATHEMATICS
18 May 1992 32 p Transl. into ENGLISH from various Russian articles (JPRS-UPM-92-003) Avail: CASI HC A03/MF A01

Translated articles cover the following topics: acoustics, crystals, laser glasses, semiconductors; lasers; optics, spectroscopy; plasma physics; superconductivity; and theoretical physics. CASI

N93-25404# Joint Publications Research Service, Arlington, VA.
JPRS REPORT: SCIENCE AND TECHNOLOGY. CENTRAL EURASIA: PHYSICS AND MATHEMATICS
28 Jan. 1993 34 p Transl. into ENGLISH from various Russian articles (JPRS-UPM-93-001) Avail: CASI HC A03/MF A01

Translated articles cover the following topics: acoustics; crystals, laser glasses, and semiconductors; high-temperature physics; lasers; optics, spectroscopy; plasma physics; superconductivity; theoretical physics; and operations research. CASI

N93-25520# Sandia National Labs., Albuquerque, NM.
STABILITY ANALYSIS AND MODELING OF ROTATING FLEXIBLE STRUCTURES
C. R. Dohrmann Jan. 1993 99 p
(Contract DE-AC04-76DP-00789)
(DE93-008493; SAND-92-2537) Avail: CASI HC A05/MF A02

A method is presented for determining the nonlinear stability of undamped flexible structures spinning about a principal axis of inertia. Equations of motion are developed for structures that are free of applied forces and moments. The development makes use of a floating reference frame which follows the overall rigid body motion. Within this frame, elastic deformations are assumed to be given functions of n generalized coordinates. A transformation of variables is devised which shows the equivalence of the equations of motion to a Hamiltonian system with n + 1 degrees of freedom. Using this equivalence, stability criteria are developed based upon the normal form of the Hamiltonian. It is shown that a motion which is spin stable in the linear approximation may be unstable when nonlinear terms are included. A stability analysis of a simple flexible structure is provided to demonstrate the application of the stability criteria. Results from numerical integration of the equations of motion are shown to be consistent with the predictions of the stability analysis. A new method for modeling the dynamics of rotating flexible structures is developed and investigated. The method is similar to conventional assumed displacement (modal) approaches with the addition that quadratic terms are retained in the kinematics of deformation. Retention of these terms is shown to account for the geometric stiffening effects which occur in rotating structures. Computational techniques are developed for the practical implementation of the method. The techniques make use of finite element analysis results and thus, are applicable to a wide variety of structures. Motion studies of specific problems are provided to demonstrate the validity of the method. Excellent agreement is found both with simulations presented in the literature for different approaches and with results from a commercial finite element analysis code. The computational advantages of the method are demonstrated. DOE

71 ACOUSTICS

Includes sound generation, transmission and attenuation.
For noise pollution see *45 Environmental Pollution.*

N93-25094*# United Technologies Corp., Windsor Locks, CT. Standard Div.
THEORY FOR NOISE OF PROPELLERS IN ANGULAR INFLOW WITH PARAMETRIC STUDIES AND EXPERIMENTAL VERIFICATION Final Report
Donald B. Hanson and David J. Parzych Washington NASA. Lewis Research Center Mar. 1993 111 p
(Contract NAS3-24222; RTOP 535-03-10)
(NASA-CR-4499; E-7601; NAS 1.26:4499) Avail: CASI HC A06/MF A02

This report presents the derivation of a frequency domain theory and working equations for radiation of propeller harmonic noise in the presence of angular inflow. In applying the acoustic analogy, integration over the tangential coordinate of the source region is performed numerically, permitting the equations to be solved without approximation for any degree of angular inflow. Inflow angle is specified in terms of yaw, pitch, and roll angles of the aircraft. Since these can be arbitrarily large, the analysis applies with equal accuracy to propellers and helicopter rotors. For thickness and loading, the derivation is given in complete detail with working equations for near and far field. However, the quadrupole derivation has been carried only far enough to show feasibility of the numerical approach. Explicit formulas are presented for computation of source elements, evaluation of Green's functions, and location of observer points in various visual and retarded coordinate systems. The resulting computer program, called WOBBLE has been written in FORTRAN and follows the notation of this report very closely. The new theory is explored to establish the effects of varying inflow angle on axial and circumferential directivity. Also, parametric studies were performed to evaluate various phenomena outside the capabilities of earlier theories, such as an unsteady thickness effect. Validity of the theory was established by comparison with test data from conventional propellers and Prop Fans in flight and in wind tunnels under a variety of operating conditions and inflow angles. Author

N93-25189*# National Aeronautics and Space Administration. Langley Research Center, Hampton, VA.
ON THE EFFECT OF ACOUSTIC COUPLING ON RANDOM AND HARMONIC PLATE VIBRATIONS
A. Frendi (Analytical Services and Materials, Inc., Hampton, VA.) and J. H. Robinson Mar. 1993 20 p
(RTOP 505-63-50-10)
(NASA-TM-107740; NAS 1.15:107740) Avail: CASI HC A03/MF A01

The effect of acoustic coupling on random and harmonic plate vibrations is studied using two numerical models. In the coupled model, the plate response is obtained by integration of the nonlinear plate equation coupled with the nonlinear Euler equations for the surrounding acoustic fluid. In the uncoupled model, the nonlinear plate equation with an equivalent linear viscous damping term is integrated to obtain the response of the plate subject to the same excitation field. For a low-level, narrow-band excitation, the two models predict the same plate response spectra. As the excitation level is increased, the response power spectrum predicted by the uncoupled model becomes broader and more shifted towards the high frequencies than that obtained by the coupled model. In addition, the difference in response between the coupled and uncoupled models at high frequencies becomes larger. When a high intensity harmonic excitation is used, causing a nonlinear plate response, both models predict the same frequency content of the response. However, the level of the harmonics and subharmonics are higher for the uncoupled model. Comparisons to earlier experimental and numerical results show that acoustic coupling has a significant effect on the plate response at high excitation levels. Its absence in previous models may explain the discrepancy between predicted and measured responses. Author

N93-25637# Naval Postgraduate School, Monterey, CA.
SPECTRA OF STABLE SONOLUMINESCENCE M.S. Thesis
Stephen D. Lewis Dec. 1992 94 p
(AD-A260621) Avail: CASI HC A05/MF A01

The continuous emission of picosecond pulses of light has been observed

to originate from a bubble trapped at the pressure antinode of a resonant sound field in water and in water/glycerin mixtures. The spectra of this light in several solutions has been measured with a scanning monochrometer/photomultiplier detector system. The spectra are broadband and show strong emission in the UV region. A comparison of this measurement to two other independently produced spectra is made. The spectra are also modeled by a blackbody radiation distribution to determine an effective blackbody temperature and a size is deduced as if Sonoluminescence were characterized by blackbody radiation. DTIC

N93-25643# Open Univ., Milton (England). Faculty of Technology.
PROCEEDINGS OF THE 5TH INTERNATIONAL SYMPOSIUM ON LONG RANGE SOUND PROPAGATION
1992 457 p Symposium held in Milton, England, 24-26 May 1992
(Contract DAJA45-91-M-0345)
(AD-A260666; R/D-6792-EN-02) Avail: CASI HC A20/MF A04

The symposium consisted of five main technical sessions devoted respectively to ground effects, refraction, turbulence and scattering, topography and screens and instrumentation and measurement methods. The sixth and final session gave an opportunity for other acoustics-related work at the Open University to be presented and for a plenary discussion on the way forward, briefly reported above. The papers in this session although not strictly related to the topic of the conference are included for the sake of completeness. DTIC

N93-25649# Aeronautical Research Labs., Melbourne (Australia).
IN-FLIGHT EVALUATION OF NOISE LEVELS AND ASSESSMENT OF ACTIVE NOISE REDUCTION SYSTEMS IN THE SEAHAWK S-70B-2 HELICOPTER
R. B. King and D. A. Foran 1992 46 p
(AD-A260689; ARL-TR-9; DODA-AR-007-077) Avail: CASI HC A03/MF A01

Cabin and at-ear sound spectra in the S-70B-2 at various crew positions and flight conditions were measured in order to determine the noise attenuation properties of the ALPHA helmet and the effectiveness of active noise reduction (ANR) systems developed by the Defence Research Agency-Aerospace Division (formerly the Royal Aerospace Establishment) and the BOSE Corporation. Results show that if newly proposed hearing conservation guidelines are adopted, aircrew wearing the ALPHA helmet would require additional attenuation devices. It is recommended that an ANR system be incorporated into the S-70B-2 as such a system would allow realistic flight duration to be maintained, improve voice communication, and reduce aircrew fatigue. DTIC

N93-25651# Arizona State Univ., Tempe. Dept. of Mechanical and Aerospace Engineering.
FAR FIELD ROTOR NOISE Final Report
Valana L. Wells 22 Jan. 1993 27 p
(Contract DAAL03-90-G-0221)
(AD-A260703; ARO-28002.1-EG) Avail: CASI HC A03/MF A01

The work covered two main areas of research--the aerodynamics of rotor blades including viscous and high angle of attack effects and, secondly, the propagation of noise from the rotor blade, particularly the nonlinear propagation. The aerodynamics work included the development and testing of a Navier-Stokes computational solver for rotor blades which incorporates rotating, translating, flapping and feathering motions. Results, which focus on the British Experimental Rotor Programme (BERP) blade, clearly show the importance of including all motions in the calculation of aerodynamic-forces. The acoustics research concentrates on the development of a method for computing the nonlinear propagation of acoustic signals in the atmosphere. The method is based on a boundary-element discretization of the time-dependent, nonlinear wave equation. Results, computed for a spherically symmetric domain, show an equivalence with Whitham's method up to the formation of a shock. DTIC

N93-25717 Tennessee Univ., Knoxville.
A COMPUTATIONAL METHOD FOR THE ANALYSIS OF ACOUSTIC RADIATION FROM TURBOFAN INLETS Ph.D. Thesis
G. K. Raviprakash 1992 159 p
Avail: Univ. Microfilms Order No. DA9233579

A computational method is presented for the analysis of the noise radiation from turbofan inlets. The method developed considers the effect of mean flow and can be used at high frequencies. The techniques for generating the grid, solving the acoustic equations, applying radiating conditions on the far-field boundary, imposing inlet-fan interface conditions as well as solving the steady compressible flow equations are embodied in the Inlet Acoustic Analysis Method. The theoretical basis, formulated for 3-D acoustics within an axisymmetric domain, considers the effect of non-uniform mean flow. The discretization of the field equations is done using a finite volume type differencing. This leads to a block tri-diagonal system of equations which is then efficiently solved. A new and powerful method is developed for the application of radiating conditions. A layer potential representation is used in obtaining numerically local radiating conditions. The locally radiating conditions, developed using the single layer source representation, can be used even at the interior eigenvalues. Using this technique, the radiating conditions can be applied very close to the inlet, and hence the computational efficiency can be significantly increased. The irrotationality conditions for the axisymmetric compressible flow are discretized for solving the mean flow field. An iterative scheme is developed to solve for the stream function, the density, and the speed of sound. The inlet-fan interface conditions are incorporated to properly specify the source of noise. The noise source is either directly specified or the interface potential distribution is split into a combination of an imposed right traveling disturbance and an unknown combination of left traveling disturbances, that come out as part of the solution process. The grid generation procedure utilizes algebraic transformations as well as the grid blending techniques. This process is automated to accommodate variations in the grid geometry. Several aspects of the numerical techniques are verified by demonstration problems and comparison with analytical solutions. The noise radiation from a typical inlet with a center-body at different frequencies and circumferential modes is presented including cases with mean flow. The results for a Bellmouth inlet are compared with experimental data and are in good agreement. The noise radiation at a typical blade passing frequency for an inlet with a center-body is also presented.
Dissert. Abstr.

N93-25915# Southeastern Center for Electrical Engineering Education, Inc., Saint Cloud, FL.
DESIGN, FABRICATION, AND TESTING OF A THREE-DIMENSIONAL ACOUSTIC ORIENTATION INSTRUMENT (3-D AOI): DRAWINGS, ENGINEERING AND ASSOCIATED LISTS (CONCEPTUAL AND DEVELOPMENT DESIGN) Final Report, 1 May 1989 - 15 Apr. 1991
Dan D. Fulgham and Jeffrey Gabelmann Dec. 1992 133 p
(Contract F33615-87-D-0609)
(AD-A260934; SWRI-PN-12-3384; AL-TR-1992-0154) Avail: CASI HC A07/MF A02

Subcontractor (Southwest Research Institute) provides a description of the hardware assembled and software created to develop the 3-D AOI. A Macintosh 2x computer is the heart of the system acting as a general controller and processor of data flowing from the Flight Information Package to the Audio Localization Cue Synthesizer, audio mixer, headphones, and data recording equipment. A National Instruments NB-DSP2300 digital signal processing board and NB-A2100 audio 1/0 board generate the audio signals, and National instruments LabView software is used to control the auditory display. The majority of this report is a description of the 18 LabView software modules created to control the 3-D AOI display. DTIC

N93-26086*# National Aeronautics and Space Administration. Langley Research Center, Hampton, VA.
ON THE CROSS-STREAM SPECTRAL METHOD FOR THE ORR-SOMMERFELD EQUATION
William E. Zorumski and Steven L. Hodge Mar. 1993 47 p
(RTOP 505-59-52)
(NASA-TM-107737; NAS 1.15:107737) Avail: CASI HC A03/MF A01

Cross-stream models are defined as solutions to the Orr-Sommerfeld equation which are propagating normal to the flow direction. These models are utilized as a basis for a Hilbert space to approximate the spectrum of the Orr-Sommerfeld equation with plane Poiseuille flow. The cross-stream basis leads to a standard eigenvalue problem for the frequencies of Poiseuille flow instability waves. The coefficient matrix in the eigenvalue problem is shown to be the sum of a real matrix and a negative-imaginary diagonal matrix which represents the frequencies of the cross-stream modes. The real coefficient matrix is shown to approach a Toeplitz matrix when the row and column indices are large. The Toeplitz matrix is diagonally dominant,

and the diagonal elements vary inversely in magnitude with diagonal position. The Poiseuille flow eigenvalues are shown to lie within Gersgorin disks with radii bounded by the product of the average flow speed and the axial wavenumber. It is shown that the eigenvalues approach the Gersgorin disk centers when the mode index is large, so that the method may be used to compute spectra with an essentially unlimited number of elements. When the mode index is large, the real part of the eigenvalue is the product of the axial wavenumber and the average flow speed, and the imaginary part of the eigen value is identical to the corresponding cross-stream mode frequency. The cross-stream method is numerically well-conditioned in comparison to Chebyshev based methods, providing equivalent accuracy for small mode indices and superior accuracy for large indices. Author

N93-26165# Florida State Univ., Tallahassee. Dept. of Mathematics.
COMPUTATION OF BROADBAND MIXING NOISE FROM TURBOMACHINERY Final Report, 1 Mar. 1989 - 28 Feb. 1993
Christopher Tam 28 Feb. 1993 6 p
(Contract N00014-89-J-1836)
(AD-A261611) Avail: CASI HC A02/MF A01

The original objectives of the investigation were as follows: (1) development of a computational aeroacoustics methodology for direct numerical solution of acoustic propagation and scattering problems associated with turbomachinery mixing noise; and (2) development of a (computation oriented) theory for the prediction of turbulent mixing noise. DTIC

N93-26179# Texas Univ., Austin. Applied Research Labs.
PROPAGATION OF FINITE AMPLITUDE SOUND IN A WAVEGUIDE WITH A PARABOLIC SOUND VELOCITY PROFILE
Douglas E. Reckamp 17 Jun. 1992 61 p
(ARL-TR-92-11) Avail: CASI HC A04/MF A01

The propagation of finite amplitude sound in a waveguide with a parabolic sound velocity profile is investigated theoretically. It is assumed that the primary wave propagates in a single mode at a frequency that is large compared with the cutoff frequency. The energy is therefore concentrated near the axis of the sound channel. Both the primary wave and the nonlinearly generated second harmonic component have mode shapes that are described by Gauss-Hermite eigen functions. For a primary wave in mode m, the second harmonic component is generated in all even modes up to 2m, with most of the energy contained in mode 2m. A nonlinear Schrodinger equation is derived for the envelope of a narrow band pulse that propagates in a single mode. Analytical expressions are derived for the coefficients in the Schrodinger equation, and it is found that only dark envelope solitons can propagate without distortion in the waveguide. Otherwise, the pulses are expected to disperse with distance. Author

N93-26358# Connecticut Univ., Farmington. Health Center.
MONAURAL AND BINAURAL PROCESSING OF COMPLEX WAVEFORMS Annual Technical Report, 1 Nov. 1991 - 31 Oct. 1992
Constantine Trahiotis and Leslie R. Bernstein 5 Jan. 1993 12 p
(Contract F49620-92-J-0062)
(AD-A261659; AFOSR-93-0094TR) Avail: CASI HC A03/MF A01

Data were collected concerning the amount of comodulation masking release (CMR) obtained when coherent envelope information is presented successively rather than simultaneously. It was determined that off-frequency information, which produces a CMR, can provide only a small release from masking when presented prior and subsequent to the temporal interval containing the signal. Three papers were published and a fourth is undergoing revision. One assessed sensitivity to interaural correlation of the envelope of high-frequency waveforms and whether such sensitivity might account for detectability in an MLD paradigm. Another showed sensitivity to antiphasic sinusoids added only to the envelopes of high-frequency bands of noise as a function of the frequency of the sinusoid and the bandwidth of the masker. A third, with Dr. R. M. Stem, depicts how straightness weighting can be accomplished by a second, physiologically demonstrated, stage of neural processing. The complex, cross-correlation-based model was extended to account for how interaural insensitive disparities in combination with interaural temporal disparities affects lateralization. Software was written for experiments concerning effects of forward masking fringes on the high-frequency MLD and to perform the theoretical analyses of stimuli used in the successive CMR paradigm. DTIC

N93-26374# Florida Univ., Gainesville. Dept. of Psychology.
COMPLEX AUDITORY SIGNALS Annual Report, 1 Jan. - 31 Dec. 1992
David M. Green 31 Dec. 1992 8 p
(Contract F49620-92-J-0139)
(AD-A261491; AFOSR-93-0079TR) Avail: CASI HC A02/MF A01

The main area of research continues to be spectral shape discrimination, what I have called profile analysis. Three areas continue to receive considerable attention. They are: (1) the cues available for detecting spectral changes as a function of the bandwidth of the stimulus, (2) how the number of components or density of the spectrum affects the ability to hear spectral changes, and (3) temporal effects--how duration of the stimulus appears to interact with other variables to influence the listener's ability to hear spectral changes. In the first two areas, we have used Berg's COSS analysis to great advantage, and we anticipate that we shall continue to utilize that procedure in our research. DTIC

N93-26376# Mitre Corp., McLean, VA. Jason Program Office.
STRUCTURAL ACOUSTICS: A GENERAL FORM OF RECIPROCITY PRINCIPLES IN ACOUSTICS
K. Case 14 Jan. 1993 17 p
(DA Proj. 8503Z)
(AD-A261515; JSR-91-193) Avail: CASI HC A03/MF A01

A generalized Reciprocity Principle for Acoustics is obtained. By specialization, various principles which appear in the literature are obtained. DTIC

N93-26551*# National Aeronautics and Space Administration. Lewis Research Center, Cleveland, OH.
A LARGE HEMI-ANECHOIC ENCLOSURE FOR COMMUNITY-COMPATIBLE AEROACOUSTIC TESTING OF AIRCRAFT PROPULSION SYSTEMS
Beth A. Cooper Apr. 1993 15 p Presented at Noise-Con'93, Williamsburg, VA, 2-5 May 1993; sponsored by Noise-Con
(RTOP 537-02-22)
(NASA-TM-106015; E-7572-1; NAS 1.15:106015) Avail: CASI HC A03/MF A01

A large hemianechoic (absorptive walls and acoustically hard floor) noise control enclosure was erected around a complex of test stands at the NASA Lewis Research Center in Cleveland, Ohio. This new state-of-the art Aeroacoustic Propulsion Laboratory (APL) provides an all-weather, semi secure test environment while limiting noise to acceptable levels in surrounding residential neighborhoods. The 39.6-m- (130-ft-) diameter geodesic dome houses the new nozzle aeroacoustic test rig (NATR), an ejector-powered Mach 0.3 free jet facility for acoustic testing of supersonic aircraft exhaust nozzles and turbomachinery. A multiaxis, force-measuring, powered lift facility (PLF) stand for testing short takeoff vertical-landing (STOVL) vehicles is also located in the dome. The design of the Aeroacoustic Propulsion Laboratory efficiently accommodates the research functions of two separate test rigs, one of which (NATR) requires a specialized environment for taking acoustic measurements. An absorptive fiberglass wedge treatment on the interior surface of the dome provides a hemianechoic environment for obtaining the accurate acoustic measurements required to meet research program goals. The APL is the first known geodesic dome structure to incorporate transmission-loss properties as well as interior absorption in a free-standing, community-compatible, hemianechoic test facility. Author

72 ATOMIC AND MOLECULAR PHYSICS

Includes atomic structure, electron properties, and molecular spectra.

N93-24959# Lawrence Livermore National Lab., CA.
NOTES ON RADIAL DRIFT FOR DALITZ DETECTION
James H. Thomas 21 Aug. 1992 6 p
(Contract W-7405-eng-48)
(DE93-006971; UCRL-ID-111522) Avail: CASI HC A02/MF A01

One solution to the problem of identifying electron pairs due to dalitz decay is to exploit the large difference in energy lose by electrons and pions at momenta below 150 MeV/C. The 'restricted' energy loss is measured by averaging the bottom 60 percent of the energy loss samples

in order to avoid the wide fluctuations caused by the Landau tails. Note that the electrons are fully relativistic and well up on the relativistic rise of the dE/dx curve at a momentum of 30 MeV/C whereas the pions are still moving down off the peak of the Bragg curve and are more heavily ionizing than the electrons. The separation between pions and electrons is very good up to about the pion rest mass and so we can in principle separate the species all through the kinematically allowed range for Dalitz decay but, in practice, the dE/dx resolution will eventually limit the technique to the range well below where the curves crossover. We then might need an additional technique for e/pi separation above 110 MeV/C or so. Time of Flight would be a suitable technique. We propose to use a radial drift Time Expansion Chamber (TEC, or sometimes known as at Time Projection Chamber, TPC) to simultaneously measure the energy loss and momentum of electrons and pions. The detector would be placed at Y = 0 and extend to plus or minus 0.5 units of rapidity and the secondary electrons generated by a track would drift radially away from the vertex towards a sensepad plane. The detector would be inside the magnetic field of the RE2 detector and the drift direction would be perpendicular to the field direction. DOE

N93-25114# Ohio State Univ., Columbus.
MOLECULAR/POLYMERIC MAGNETISM
1993 11 p
(Contract DE-FG02-86ER-45271)
(DE93-008635; DOE/ER-45271/T6) Avail: CASI HC A03/MF A01

New materials were synthesized to test the generality of magnetism in molecular/polymeric systems. The first room temperature molecular based magnet V(TCNE)(sub x) y(solvent) (1) is disclosed. The ferromagnetic and related transitions were studied in decamethylferrocenium tetracyanoethanide (TCNE), (1), and related materials. Our and others' models were tested for ferromagnetic and antiferromagnetic exchange between local sites; models for control of (Tc) were also tested. DOE

N93-25148# Oak Ridge National Lab., TN. Joint Inst. for Heavy Ion Research.
DIABATICITY OF NUCLEAR MOTION: PROBLEMS AND PERSPECTIVES
W. Nazarewicz 1992 27 p Presented at the 1992 International Symposium on Rapidly Rotating Nuclei, Tokyo, Japan, 26-30 Oct. 1992
(Contracts DE-AC05-84OR-21400; DE-FG05-87ER-40361)
(DE93-007252; CONF-9210249-5) Avail: CASI HC A03/MF A01

The assumption of adiabatic motion lies in foundations of many models of nuclear collective motion. To what extend can nuclear modes be treated adiabatically? Due to the richness and complexity of the nuclear many-body problem there is no unique answer to this question. The challenges of nuclear collective dynamics invite exciting interactions between several areas of physics such as nuclear structure, field theory, nonlinear dynamics, transport theory, and quantum chaos. DOE

N93-25256# Oak Ridge Y-12 Plant, TN.
A METHOD FOR TRANSIENT, THREE-DIMENSIONAL NEUTRON TRANSPORT CALCULATIONS
M. W. Waddell, Jr. (Martin Marietta Energy Systems, Inc., Oak Ridge, TN.) and H. L. Dodds (Tennessee Univ., Oak Ridge.) 28 Dec. 1992 15 p
(Contract DE-AC05-84OR-21400)
(DE93-007243; Y/DD-586) Avail: CASI HC A03/MF A01

The development and evaluation of a method for solving the time-dependent, three-dimensional Boltzmann transport model with explicit representation of delayed neutrons is described. A hybrid stochastic/deterministic technique is utilized with a Monte Carlo code embedded inside of a quasi-static kinetics framework. The time-dependent flux amplitude, which is usually fast varying, is computed deterministically by a conventional point kinetics algorithm. The point kinetics parameters, reactivity, and generation time as well as the flux shape, which is usually slowly varying in time, are computed stochastically during the random walk of the Monte Carlo calculation. To verify the accuracy of this new method, several computational benchmark problems from the Argonne National Laboratory benchmark book, ANL-7416, were calculated. The results are shown to be in reasonably good agreement with other independently obtained solutions. The results obtained indicate that the method/code is working properly and that it is economically feasible for many practical applications provided a dedicated high performance workstation is available. DOE

N93-25310# State Univ. of New York, Stony Brook.
IONIZATION PROBES OF MOLECULAR STRUCTURE AND CHEMISTRY
Progress Report, 15 Jan. 1992 - 14 Jan. 1993
P. M. Johnson Jan. 1993 7 p
(Contract DE-FG02-86ER-13590)
(DE93-008211; DOE/ER-13590/12) Avail: CASI HC A02/MF A01

Development of laser ionization tools toward study of spectroscopy and dynamics of molecules relevant to combustion processes is discussed. Ionization versus dissociation was studied in CO2; the intensity dependence of vibrational structure in photoelectron spectra had no changes over almost a 2(times) factor, indicating that the CO2 multiphoton ionization through its Rydberg states proceeds by autoionization of bound, neutral dissociative states at the four photon level. Variants of threshold ionization spectroscopy were used for studying ions, aromatics, diazines, azines, etc. In collaboration with BNL people, rotational structure of the combustion radicals trans-HOCO and DOCO, and vacuum UV photodissociation of three chlorofluoromethanes were studied. DOE

N93-25323# Stanford Linear Accelerator Center, CA.
TOPICS IN CP VIOLATION
H. R. Quinn Feb. 1993 8 p Presented at the 3rd Symposium on Particles, Strings and Cosmology and the 16th Texas Symposium on Relativistic Astrophysics Conference, Berkeley, CA, 13-18 Dec. 1992
(Contract DE-AC03-76SF-00515)
(DE93-007615; SU-SLAC-PUB-6053; CONF-921261-1) Avail: CASI HC A02/MF A01

Given the varied backgrounds of the members of this audience this talk will be a grab bag of topics related to the general theme of CP Violation. I do not have time to dwell in detail on any of them. First, for the astronomers and astrophysicists among you, I want to begin by reviewing the experimental status of evidence for CP violation in particle processes. There is only one system where this has been observed, and that is in the decays of neutral K mesons. DOE

N93-25326# California Univ., Berkeley. Lawrence Berkeley Lab.
STRANGENESS PRODUCTION IN S + Pb AND p + Pb COLLISIONS AT 200 GeV/c PER NUCLEON NUCLEON
I. Sakrejda Sep. 1992 12 p Presented at the Conference on Hadron Structures, Stara Lesna,Czechoslovakia, 6-11 Sep. 1992
(Contract DE-AC03-76SF-00098)
(DE93-007654; LBL-33145; CONF-9209127-1) Avail: CASI HC A03/MF A01

Results from CERN experiment NA36 are reported. Cross sections for the production of singly strange particles in the S + Pb and p + Pb reactions were measured in the rapidity range 1.25 is less than y is less than 3.5 and for p(sub t) is greater than 0.2 GeV. A significant difference in the rapidity distributions of the lambda particles originating from these reactions suggests a fundamental difference in the strangeness production mechanism. DOE

N93-25355 Colorado Univ., Boulder.
LINE FORMATION AND THE POYNTING-ROBERTSON EFFECT IN ACCRETION DISCS Ph.D. Thesis
Douglas Lee Carroll 1992 222 p
Avail: Univ. Microfilms Order No. DA9304546

A combination of the Sobolev method and a linearization method is used to calculate line profiles from accretion discs which have outer parts optically thin in the continuum, but optically thick in the lines. The Sobolev method is used to find the mean intensity in the lines. The level populations are assumed to be in statistical equilibrium, and it is only the equation governing this equilibrium that is linearized. The temperature in the outer parts is specified as a function of radius. The computed line profiles are compared with those observed from the dwarf nova U Geminorum. The special relativistic equations of motion for a particle and the general relativistic equations of motion for a fluid in an arbitrary radiation field are formulated. The Poynting-Robertson forces are manifested in some of the velocity dependent terms so obtained. Newtonian approximations to the equations of motion are solved for a particle in orbit about a spherically symmetric source of radiation, where the angular size of the source as seen from the orbit is arbitrary. Situations are considered in which the absorption cross section of the particle is independent of frequency as well as when the particle is an atom absorbing in a spectral line. In both

instances it is found that the finite size of the source of radiation leads to Poynting-Robertson drags greater than those caused by a point source of the same luminosity. The Newtonian equations are solved for a particle moving radially outward from the source. Limits for the velocities of high speed particles due to Poynting-Robertson drags are obtained. The fluid equations are discussed briefly in their relation to theoretical treatments of relativistic jets and accretion discs. Dissert. Abstr.

N93-25364# California Univ., Berkeley. Lawrence Berkeley Lab.
RESULTS FROM THE NA36 ON STRANGENESS PRODUCTION IN 200 GeV/c PER NUCLEON S + Pb AND p - Pb REACTIONS
D. E. Greiner Jul. 1992 12 p Presented at the 22nd International Symposium on Multiparticle Dynamics, Santiago de Compostela, Spain, 13-17 Jul. 1992
(Contracts DE-AC03-76SF-00098; DE-FG02-91ER-40652)
(DE93-007711; LBL-33345; CONF-9207169-3) Avail: CASI HC A03/MF A01

Recent results from CERN experiment NA36 are discussed and compared with models. These results refer to reactions of sulfur and protons of momentum 200 GeV/c per nucleon on a lead target. The lambda spectrum for the sulfur beam was found to peak at mid-rapidity rather than target rapidity as observed in the proton induced reactions. This result indicates different reaction mechanisms are active. We discuss in some detail the analysis methods used. The data are consistent with the assumption of a fireball of high strangeness content being created at mid-rapidity in S plus Pb reactions. DOE

N93-25366# California Univ., Berkeley. Lawrence Berkeley Lab.
DETECTION OF FRAGMENTS ARISING FROM GREATER THAN 10 GeV ELECTRON-NUCLEUS COLLISIONS
D. M. Moltz, K. A. Griffioen (Pennsylvania Univ., Philadelphia.), and K. VanBibber (Lawrence Livermore National Lab., CA.) Nov. 1992 12 p Presented at the International Seminar on High Energy Physics Problems, Dubna, Russia, 7-12 Sep. 1992
(Contracts DE-AC03-76SF-00098; W-7405-eng-48)
(DE93-007725; LBL-33171; CONF-9209279-3) Avail: CASI HC A03/MF A01

Much is understood about the interaction of both high energy electrons with nucleons and lower energy electrons with nucleons and nuclei. Although a number of experiments involving high energy inelastic scattering of electrons from quarks bound in nuclei have been performed, many interpretations of the data are still discussed. A project called PEGASYS was conceived at PEP to further investigate this physics. Unfortunately, the termination of PEP operations curtailed this experiment and much of the physics remains unexplored. In this paper, we present some details of one proposed part of this project (tagged nuclear structure functions) and some considerations made in designing a detector suitable for observing very low momentum nuclear fragments around a cold-cluster gas target. DOE

N93-25368# Argonne National Lab., IL.
PRELIMINARY DESIGN OF THE BPM ELECTRONICS MEMORY SCANNER/DUAL BOXCAR AVERAGER FOR THE ADVANCED PHOTON SOURCE
A. J. Votaw 1992 8 p Workshop of the 1992 Accelerator Instrumentation Workshop held in Berkeley, CA, 27-30 Oct. 1992
(Contract W-31-109-eng-38)
(DE93-007893; ANL/ASD/CP-77461; CONF-9210246-17) Avail: CASI HC A02/MF A01

The memory scanner/dual boxcar averager are VXI modules that are part of the Advanced Photon Source (APS) beam position monitor (BPM) data acquisition system. Each pair of modules is designed to gather and process digital data from up to nine digital channels transmitting the BPM data from the storage ring (360 locations) and the synchrotron (80 locations). They store beam history in a buffer, store the latest scan of all channels, and provide boxcar averaged X and Y position data for the global orbit feedback system, provide boxcar average X and Y position data for beam diagnostics, and a buffered output of SCDU data as it is scanned for the beam abort interlock system. The system's capability to support single pass, closed orbit, and tune measurement functions is also be briefly described. DOE

N93-25371# Argonne National Lab., IL.
FEEDING AND DECAY OF SUPERDEFORMED STATES
T. L. Khoo, T. Lauritsen, I. Ahmad, M. P. Carpenter, P. B. Fernandez, R. V. F. Janssens, E. F. Moore, F. L. H. Wolfs, Ph. Benet, and P. J. Daly (Purdue Univ., West Lafayette, IN.) et al 1992 15 p Presented at the 1992 International Symposium on Rapidly Rotating Nuclei, Tokyo, Japan, 26-30 Oct. 1992
(Contract W-31-109-eng-38)
(DE93-007899; ANL/PHY/CP-78720; CONF-9210249-6) Avail: CASI HC A03/MF A01

The mechanisms for feeding and decay of superdeformed (SD) bands are examined. Data connected with both processes in Hg-192 are compared with model calculations. The calculations successfully reproduce the data, suggesting that the mechanisms for both processes are understood. Constraints on the energy of the SD band energies and on the well-depths at low and high spins have been obtained. At the point of decay around spin 10, we suggest that the SD band is 3.3-4.3 MeV above the normal yrast line and that the well depths at spin 10 and 40 are 0.5-1.3 and 3.5-4.5 MeV, respectively. DOE

N93-25376# Oak Ridge National Lab., TN.
THE INTERACTION OF SWIFT ELECTRONS WITH SURFACE EXCITATIONS
R. H. Ritchie (Tennessee Univ., Knoxville.) 1992 10 p Presented at the 7th Latin-American Symposium on Surface Science, Bariloche, Argentina, 14-21 Nov. 1992
(Contract DE-AC05-84OR-21400)
(DE93-007245; CONF-9211193-1) Avail: CASI HC A02/MF A01

For many decades swift electrons have comprised a powerful tool for the study of the dynamical properties of condensed matter. The development of this technique has involved much important physics. Here we sketch the historical background of the field and some important developments in theory and experiment. Possible directions for future research are indicated. DOE

N93-25450*# Eloret Corp., Palo Alto, CA.
THE STRUCTURE AND ENERGETICS OF Cr(CO)6 AND Cr(CO)5
Leslie A. Barnes, Bowen Liu (International Business Machines Corp., San Jose, CA.), and Roland Lindh (Lund Univ., Sweden.) 1992 34 p Revised
(Contract NCC2-741)
(NASA-CR-192889; NAS 1.26:192889) Avail: CASI HC A03/MF A01

The geometric structure of Cr(CO)6 is optimized at the modified coupled pair functional (MCPF), single and double excitation coupled-cluster (CCSD) and CCSD(T) levels of theory (including a perturbational estimate for connected triple excitations), and the force constants for the totally symmetric representation are determined. The geometry of Cr(CO)5 is partially optimized at the MCPF, CCSD, and CCSD(T) levels of theory. Comparison with experimental data shows that the CCSD(T) method gives the best results for the structures and force constants, and that remaining errors are probably due to deficiencies in the one-particle basis sets used for CO. The total binding energies of Cr(CO)6 and Cr(CO)5 are also determined at the MCPF, CCSD, and CCSD(T) levels of theory. The CCSD(T) method gives a much larger total binding energy than either the MCPF or CCSD methods. An analysis of the basis set superposition error (BSSE) at the MCPF level of treatment points out limitations in the one-particle basis used. Calculations using larger basis sets reduce the BSSE, but the total binding energy of Cr(CO)6 is still significantly smaller than the experimental value, although the first CO bond dissociation energy of Cr(CO)6 is well described. An investigation of 3s3p correlation reveals only a small effect. In the largest basis set, the total CO binding energy of Cr(CO)6 is estimated to be 140 kcal/mol at the CCSD(T) level of theory, or about 86 percent of the experimental value. The remaining discrepancy between the experimental and theoretical value is probably due to limitations in the one-particle basis, rather than limitations in the correlation treatment. In particular an additional d function and an f function on each C and O are needed to obtain quantitative results. This is underscored by the fact that even using a very large primitive set (1042 primitive functions contracted to 300 basis functions), the superposition error for the total binding energy of Cr(CO)6 is 22 kcal/mol at the MCPF level of treatment. Author (revised)

N93-25488# Michigan Univ., Ann Arbor. Dept. of Atmospheric, Oceanic and Space Sciences.
ENERGY TRANSFER PROPERTIES AND MECHANISMS
J. R. Barker 20 Oct. 1992 4 p
(Contract DE-FG02-85ER-13442)
(DE93-008540; DOE/ER-13442/7) Avail: CASI HC A01/MF A01

The overall objective of the research carried out under this program is to determine the principles of collisional energy transfer and use them in predictive models and theories. In order to accomplish this goal, energy transfer properties must be determined and then analyzed to discern the underlying principles involved. In this laboratory, the experimental determination of energy transfer parameters is based on techniques that use physical properties to monitor the amount of energy in excited molecules. These techniques differ from chemical methods, based on unimolecular reaction studies, which are susceptible to interferences from complex chemical mechanisms and other complications. The physical methods have their own weaknesses and limitations, however, and much of our effort has been directed toward gaining a better understanding of these deficiencies. Two physical techniques have been proved to be particularly useful: time-resolved infrared fluorescence (IRF) and time-dependent thermal lensing (TDTL). As described later, we will shortly begin work using resonance enhanced multiphoton ionization (REMPI) techniques to investigate energy transfer in bulbs and 'half collisions' in free jets. We also have completed some experiments and model calculations which explore the approximations we previously have used in calculating infrared emission from highly excited molecules. DOE

N93-25509# Nebraska Univ., Lincoln. Dept. of Physics and Astronomy.
DYNAMICS OF COLLISION PROCESSES
A. F. Starace Jan. 1993 4 p
(Contract DE-FG02-88ER-13955)
(DE93-007143; DOE/ER-13955/15) Avail: CASI HC A01/MF A01

Investigations have been carried out of two- and three-photon detachment of the negative hydrogen ion (H(-)) including effects of electron correlations, of two-color detachment of H(-) with excitation of H(n=2), and of the (sup 3)P(sup e) state of H(-). Striking effects of long-range dipole field interactions have been demonstrated. Electron correlation effects on detachment cross sections have been quantified. Variational R-matrix calculations of photodetachment of Li(-) have provided state-of-the-art agreement with recent experimental results. Electric field effects on photodetachment of H(-) above the H(n=2) threshold have also been elucidated. DOE

N93-25644# SRI International Corp., Menlo Park, CA.
PHOTOEXCITATION OF CARBON FULLERENES Final Report, 30 Sep. 1991 - 29 Sep. 1992
H. Helm, D. C. Lorents, and Y. K. Bae Dec. 1992 19 p
(Contract DAAL03-91-K-0001)
(AD-A260739; ARO-28955.1-PH) Avail: CASI HC A03/MF A01

Photoexcitation processes in cold and thermal C60 and C70 molecules in the gas phase were studied. We set up a supersonic beam source of cold fullerenes and use measure the beam energies for helium and krypton as driving gas. We studied thermionic emission from fullerenes following multiphoton pumping using laser pulses of 20 ns, 1 ps, and 150 fs duration. The wavelength dependence for REMPI was investigated from 315 to 335 nm. Multiphoton fragmentation processes and ultrafast dynamics of fullerenes were investigated. DTIC

N93-25659# Utah Univ., Salt Lake City. Dept. of Chemistry.
COLLISIONAL ENERGY TRANSFER IN BIOMOLECULAR ION-MOLECULE DYNAMICS Technical Report
Maciej Gutowski, Mark Roberson, Jon Ru, and Jack Simons, II 25 Jan. 1993 50 p
(Contract N00014-89-J-1497)
(AD-A260911; TR-30) Avail: CASI HC A03/MF A01

Guided ion beam kinetic energy thresholds in the ion-molecule reactions M(+) + H2 yields MH(+) + H where M(+) = B(+), Al(+), and Ga(+) exceed by 0.4 to ca. 5 eV the thermodynamic energy requirements or theoretically computed barrier heights of these reactions. In addition, the formation of MD(+) occurs at a significantly lower threshold than MH(+) when M(+) reacts with HD. Moreover, the measured reaction cross sections for production of MH(+) productions are very small (10(exp -17) to 10(exp -20) sq cm.). These facts suggest that a 'dynamical bottleneck' may be operative in these reactions. In this work, the eigenvalues of the mass-weighted Hessian matrix, which provide local normal mode frequencies, are used to identify locations on the ground-state MH2(+) potential energy surfaces where collisional to internal energy transfer can readily take place. In particular, the potential energies at geometries where eigenvalues corresponding to inter-fragment and to internal motions undergo avoided crossings are related to the kinetic energies of apparent reaction thresholds. This near resonance energy transfer model, applied to M(+) + HD reactions, displays the experimentally observed preference to form MD(+) at lower collision energies than MH(+) as well as the fact that reaction thresholds may greatly exceed thermodynamic energy requirements. DTIC

N93-25734# California Univ., Irvine.
[DEVELOPING AND IMPROVING NUMERICAL ALGORITHMS TO STUDY INTRINSICALLY CORRELATED ELECTRON SYSTEMS]
Steven R. White 1992 6 p
(Contract N00014-91-J-1143)
(AD-A261214) Avail: CASI HC A02/MF A01

Over the last two years, we have used several different numerical techniques to study a variety of intrinsically correlated electron systems. The three main types of numerical techniques we have used are as follows: (1) finite-temperature quantum Monte Carlo (QMC); (2) exact diagonalization; and (3) numerical renormalization groups. We have made substantial progress both on developing and improving the numerical algorithms and in using these methods to study interesting systems. We have developed techniques for analytically continuing imaginary-time QMC data to obtain dynamical properties, and we have used these techniques to study pseudogap and gap formation in the repulsive and attractive Hubbard models. We have developed a program to calculate two particle interaction vertices with full frequency and momentum dependence using QMC, and we have studied possible magnetic and superconducting instabilities in the Hubbard model. DTIC

N93-25823# Honeywell, Inc., Bloomington, MN. Sensor and System Development Center.
RESEARCH ON LEAD TITANATE FILMS FOR RADIATION DETECTION Final Report, 5 Sep. 1989 - 30 Sep. 1992
Barrett E. Cole, Robert D. Horning, and Paul W. Kruse 4 Nov. 1992 33 p
(AD-A261187; ARO-26791.2-EL) Avail: CASI HC A03/MF A01

The objectives of the contract were to prepare thin films of PbTiO3, measure their properties, and determine their performance for pyroelectric detection of infrared and millimeter-wave (94 GHz) radiation. Thin films of PbTiO3 were deposited on silicon microstructures consisting of Si3N4 membranes over etch pits in silicon substrates. Upper and lower Pt electrodes formed electrical contacts to the PbTiO3 pyroelectric films. Aluminum metallizations in the form of full-wave and half-wave dipoles contacting the PbTiO3 pixels were developed for detection of 94 GHz radiation. Infrared detection was by direct absorption in the PbTiO3 pixel. Two process runs incorporating single pixels and linear arrays were carried out and the results described. DTIC

N93-26173# Yap Analytics, Inc., Lexington, MA.
MODELING OF ATOM-DIATOM SCATTERING
J. M. Sindoni 30 May 1992 46 p
(Contract F19628-89-C-0033)
(AD-A261645; YAI-TR-106; PL-TR-92-2132; AD-E201405; SR-3) Avail: CASI HC A03/MF A01

This report entails the work performed on modeling atom-diatom scattering processes utilizing the Impulse Approach (IA). Results of the model, obtained with a computer code, have proven to be in remarkable agreement with laboratory measurements for several atom-diatom scattering systems. Two scattering systems, in particular, that were successfully modeled and compared to measurements were Ar-KBr and Ar-CsF. The IA model provided an explanation for the rapid deactivation evident in the Ar-KBr system. Experimental results in the Ar-CsF experiment that could not be explained by conventional models were also successfully modeled using the IA. Results fit the experimental observations. DTIC

N93-26267# Pennsylvania State Univ., University Park. Dept. of Chemistry.
STATE-SELECTED STUDIES OF ATOMS AND MOLECULES EJECTED FROM ION BOMBARDED SURFACES Technical Report
Nicholas Winograd Jan. 1993 11 p
(Contract N00014-91-J-1410)
(AD-A261275; TR-61) Avail: CASI HC A03/MF A01

A fundamental understanding of the essential physics which contributes to the formation of secondary ions requires a global view of the energy transfer processes which occur subsequent to the ion bombardment event. Many different pathways are known which must contribute to this global view including the desorption of ground state and excited state neutral atoms, desorption of molecules and clusters in various rotation and vibrational excited states, and desorption of species induced by electronic transitions. In many experimental configurations the SIMS component is a minor fraction of the total possible energy-loss pathways. DTIC

N93-26281# Yap Analytics, Inc., Lexington, MA.
PROGRESS IN IMPULSE APPROACH RESEARCH
H. Dothe and J. M. Sindoni 30 Oct. 1992 108 p
(Contract F19628-91-C-0142)
(AD-A261728; YAI-TR-107; PL-TR-92-2296; AD-E201422; SR-1) Avail: CASI HC A06/MF A02

This report entails the progress made during the first contract year in the research of Impulse Approach (IA) modeling. The IA technique was successfully applied to the Ar-CsF scattering system with results that compared favorably with observations. Limitations and discrepancies were also found in the treatment of other scattering systems which were attributed to the confinement of the IA method to the single collision T matrix. Work is at the present progressing on extending the approach to the double collision T Matrix. The Distorted Wave Impulse Approach (DWIA) is also being developed to model observed distributions of rotational transitional probabilities of the Li(+)-N2 scattering system. DTIC

N93-26287# George Washington Univ., Washington, DC. Dept. of Chemistry.
RESONANCE ELECTRON SCATTERING BY O2 MONOLAYERS ON GRAPHITES: REINTERPRETED
Hideo Sambe and David E. Ramaker Jan. 1993 4 p
(Contract N00014-91-J-1896)
(AD-A261851; TR-63) Avail: CASI HC A01/MF A01

Electron angular distributions of inelastic electron scattering from O2 physisorbed on graphite have been studied extensively by Palmer and coworkers. Their results have been published in more than sight papers over the past four years and summarized in two recent review articles. We have reinterpreted their data and in some aspects come to different conclusions. DTIC

N93-26288# Princeton Univ., NJ. Dept. of Physics.
THE PHYSICS OF SPIN POLARIZED GASES Final Report, 1 Mar. 1988 - 29 Feb. 1992
G. D. Cates 2 Jan. 1993 20 p
(Grant AF-AFOSR-0165-88)
(AD-A261396; AFOSR-93-0103TR) Avail: CASI HC A03/MF A01

Over the four year period covered by this grant, we have carried out extensive research involving polarized atoms and nuclei. Using laser optical pumping, high polarizations can be produced in alkali-metal vapors. From this starting point, angular momentum can be transferred to other atoms and nuclei through several different types of spin-exchange collisions. This powerful technique enables us to study a wide variety of spin interactions and spin related phenomena. Among the systems we work with are polarized noble gases, which display extremely long spin-relaxation times that vary from several minutes to many weeks. The use of optical pumping and spin exchange has grown enormously over the past four years. DTIC

N93-26314# National Inst. of Standards and Technology, Gaithersburg, MD. Ionizing Radiation Div.
PROTON MONTE CARLO TRANSPORT PROGRAM PTRAN
M. J. Berger Jan. 1993 47 p See also PB93-146033 Sponsored by National Cancer Inst.
(PB93-158673; NISTIR-5113) Avail: CASI HC A03/MF A01

The report describes the structure and use of Monte Carlo programs that calculate the transport of proton beams through extended media. Although more generally applicable, the programs have been designed to deal with the penetration of 50- to 250-MeV beams through water phantoms. The Monte Carlo model takes into account multiple-scattering deflections and energy-loss straggling due to Coulomb interactions of protons with atoms and orbital electrons. Nonelastic nuclear interactions are treated as an absorptive effect. The PTRAN system at present consists of several cross-section preparation programs and two main codes, PTRAN3D and PTRAN1D. PTRAN3D applies to an incident narrow pencil beam, and calculates (1) the deposition of energy as function of depth and radial distance from the beam axis, and (2) the energy spectra of the primary protons as function of depth. Program PTRAN1D is a simplified version which runs faster and omits the calculation of the radial distribution of energy deposition. NTIS

N93-26346# Chicago Univ., IL. Dept. of Chemistry.
PENNING DETACHMENT: A NEW FRONTIER Final Report, 1 Feb. 1989 - 31 Jul. 1992
R. S. Berry 19 Jan. 1993 8 p
(Grant AF-AFOSR-0256-89)
(AD-A261447; AFOSR-93-0039TR) Avail: CASI HC A02/MF A01

The main objective of this project is a first exploration of a process not heretofore studied systematically, the detachment of electrons from negative ions when the ions collide with electronically excited neutral atoms or molecules. A steppingstone experiment, the two-color, two-photon photodetachment of the electrons from negative ions, is a part of the project as it is now being done. This report describes the completion of the apparatus for the steppingstone experiment and the first photodetachment results and outlines precisely what the goals for the next few months will be, based on the success of the ion source and the laser. The steppingstone experiment is being conducted with Cl-ions to determine the dependence of the detachment probability on the total energy and the difference in energies of the two photons; when this is complete, the ion optics and target cell for the collisional detachment experiment will be completed while the photodetachment work is extended to the study of the CN-ion. DTIC

N93-26367# Florida Univ., Gainesville. Quantum Theory Project.
MOLECULAR INTERACTIONS AND PROPERTIES WITH MANY-BODY METHODS Final Report, 1 Dec. 1991 - 30 Nov. 1992
Rodney J. Bartlett 30 Nov. 1992 7 p
(Grant AF-AFOSR-0079-90)
(AD-A261688; AFOSR-93-0104TR) Avail: CASI HC A02/MF A01

A variety of Air Force applications require highly detailed information about atoms, molecules, and their interactions. This information is necessary in problems ranging from chemical laser development, to the detection and identification of rocket plumes, to nonlinear optics electron beam technology, and high density and energy fuels. The crucial component needed to understand molecular reactions is the potential energy surfaces (PES) that serve to describe the attractions among the atoms and molecules. However, such information is not easy to obtain. In many cases, the most direct approach to obtaining accurate potential surfaces for molecules, and detailed information about their excited states, vibrational spectra, and a wealth of other quantities is high level ab initio solutions of the Schrodinger equation. DTIC

N93-26443# Minnesota Univ., Minneapolis. Dept. of Chemical Engineering and Materials Science.
HALOGEN ADLAYERS ON Ag(111) Technical Report, 30 Jun. 1992 - 31 Mar. 1993
Joachim H. Schott and Henry S. White 20 Mar. 1993 24 p
(Contract N00014-91-J-1927)
(AD-A261792; TR-17) Avail: CASI HC A03/MF A01

Atomically smooth halogen adlayers on Ag(111) (AgX, where X = I, Br, Cl, and F) have been prepared by quenching of heated Ag samples in concentrated acid halide (HX) solutions. The AgX adlayers are chemically stable in air for several hours, allowing detailed characterization of the adlayer atomic structures by scanning tunneling microscopy (STM). STM images of I adlayers are consistent with a nearly perfect square root of 3 times the square root of 3/R30 structure; F, Cl and Br adlayers, however, are characterized by a parallel double row structure of adsorbed halogen atoms, oriented along the (110) direction on the Ag(111) substrate. The

row structure observed by STM for Cl and Br adlayers is shown to be consistent with low-energy-electron-diffraction (LEED) patterns, but inconsistent with the corresponding structures derived from LEED. The degree of symmetry in the various adlayers decreases with increasing adatom electronegativity, indicating that the local charge distribution around the adlayer atom, and its size, are the controlling factors in determining the adlayer structure. DTIC

N93-26514# Hunter Coll., New York, NY. Dept. of Physics and Astronomy.
DEUTERON AND OXYGEN-17 NMR STUDIES OF MOLECULAR MOTION IN METHANOL-SATURATED NAFION MEMBRANES Interim Technical Report
R. S. Chen, J. R. Jayakody, and S. G. Greenbaum 25 Jan. 1993 9 p
(Contract N00014-92-J-1629)
(AD-A261579; TR-2) Avail: CASI HC A02/MF A01

Deuteron and oxygen-17 nuclear magnetic resonance (NMR) linewidth and spin-lattice relaxation measurements in Nafion-117 films containing methanol at approximately 75 percent and approximately 100 percent saturation are reported. Molecular motion probed by room temperature measurements in stretched films and low T measurements in unstretched films is found to be quite rapid compared to previous results obtained for Nafion-117 containing water. DTIC

N93-26518# Pittsburgh Univ., PA. Dept. of Chemistry.
INTRAMOLECULAR BRIDGE/TERMINAL OXO EXCHANGE WITHIN (MoV2O3) (4+) COMPLEXES CONTAINING LINEAR OXO BRIDGES Interim Technical Report, Jun. 1990 - Feb. 1993
Robert L. Thompson, Samkeun Lee, Steven J. Geib, and N. J. Cooper 15 Feb. 1993 47 p
(Contract N00014-90-J-1762)
(AD-A261230; TR-4) Avail: CASI HC A03/MF A01

Oxo complexes play a central role in the biological and inorganic chemistry of molybdenum. In the 5(+) oxidation state, molybdenum oxo chemistry is dominated by the (Mo(5+)2O3)(4+) unit, which contains a linear oxo bridge which spin pairs two d(1) centers while two terminal oxo ligands adopt syn- or anti-orientations perpendicular to the oxo bridge. DTIC

N93-26525# Johns Hopkins Univ., Baltimore, MD. Dept. of Chemistry.
THEORETICAL TREATMENT OF SPIN-FORBIDDEN AND ELECTRONICALLY NONADIABATIC PROCESSES. METHODS AND APPLICATIONS Final Report, 1 Nov. 1989 - 31 Oct. 1992
David R. Yarkony 10 Jan. 1993 23 p
(Grant AF-AFOSR-0051-90)
(AD-A261596; AFOSR-93-0061TR) Avail: CASI HC A03/MF A01

This research program focusses on the electronic structure aspects of radiationless decay processes related to the stability and formation of high energy density materials. We have also begun theoretical studies on electronic nonadiabaticity in ion-molecule reactions. These studies are enabled by a unique system of electronic structure algorithms, the BROOKLYN programs, which we have developed over the last decade. These programs provide advanced capabilities for the study of the electronic structure aspects of spin-forbidden and spin-allowed electronically nonadiabatic processes. The methodology we have developed is based exclusively on large scale configuration state function expansions. These methods, which we believe define the state of the art in these areas, have permitted us to make significant contributions to the understanding of electronically nonadiabatic processes. Problems of particular relevance to the high energy density materials program include studies of the stability of the potential energetic species a-N2O2, tetrahedral N4 and the dication HS2(+). We have also initiated a research program in ion-molecule chemistry reporting for the first time a seam of crossings of two states of the same symmetry for the prototypical charge transfer reaction H(+) + NO yields H + NO(+). Finally, a new phase of program development has been initiated with the goal of extending our capabilities for the direct determination of actual/allowed/avoided crossing hyperlines and hyperplanes. The algorithms under development will permit systematic determination of (1) actual/allowed crossing seams passing through a minimum energy crossing point, and (2) avoided crossing seams as a function of an arbitrary set of internal coordinates. DTIC

N93-24981# Laboratoire Primaire du Temps et des Frequences, Paris (France).
A SIMPLE AND COMPACT SOURCE OF COLD ATOMS FOR CESIUM FOUNTAINS AND MICROGRAVITY CLOCKS
A. Clairon, P. Laurent, A. Nadir, M. Drewsen (Ecole Normale Superieure, Paris, France.), D. Grison (Ecole Normale Superieure, Paris, France.), B. Lounis (Ecole Normale Superieure, Paris, France.), and C. Salomon (Ecole Normale Superieure, Paris, France.) *In* ESA, Frequency and Time Forum Jun. 1992 p 27-33 (For primary document see N93-24978 09-70)
Copyright Avail: CASI HC A02/MF A04

N93-24992# Ecole Nationale Superieure de Mecanique et des Microtechniques, Besancon (France). Lab. de Chronometrie Electronique et Piezoelectricite.
LONG TERM DRIFT AND GAMMA-IRRADIATION EFFECT
J. J. Boy, A. Berthaut, D. Thiebaud, and K. Yamni (Besancon Univ., France.) *In* ESA, Frequency and Time Forum Jun. 1992 p 93-98 (For primary document see N93-24978 09-70)
Copyright Avail: CASI HC A02/MF A04

N93-25031# Ministry of Posts and Telecommunications, Kobe (Japan). Kansai Advanced Research Center.
OPTICAL DETECTION OF LASER-COOLED IONS IN A PENNING TRAP
Hidetsuka Imajo, Shinji Urabe, Kazuhiro Hayasaka, and Masayoshi Watanabe *In* ESA, Frequency and Time Forum Jun. 1992 p 319-322 (For primary document see N93-24978 09-70)
Copyright Avail: CASI HC A01/MF A04

73 NUCLEAR AND HIGH-ENERGY PHYSICS

Includes elementary and nuclear particles; and reactor theory. For space radiation see *93 Space Radiation.*

N93-25301# Argonne National Lab., IL. High Energy Physics Div.
RECENT EXPERIMENTS ON SPIN PHYSICS IN HIGH ENERGY HADRON INTERACTIONS
Akihiko Yokosawa 1993 10 p Presented at the 10th International Symposium on High-Energy Spin Physics, Nagoya, Japan, 9-14 Nov. 1992
(Contract W-31-109-eng-38)
(DE93-007900; ANL-HEP-CP-93-06; CONF-921131-6) Avail: CASI HC A02/MF A01

Recent spin-physics experiments in high-energy hadron interactions, significant physics accomplished, and future prospects are reviewed. DOE

N93-25314# Los Alamos National Lab., NM.
LOG-RATIO SIGNAL-PROCESSING TECHNIQUE FOR BEAM POSITION MONITORS
R. E. Shafer 1993 10 p Presented at the 1992 Accelerator Instrumentation Workshop, Berkeley, CA, 27-30 Oct. 1992
(Contract W-7405-eng-36)
(DE93-007356; LA-UR-93-43; CONF-9210246-13) Avail: CASI HC A02/MF A01

Two basic signal-processing techniques are presently in wide use for the processing of signals from beam position monitors (BPM's); difference-over-sum, and amplitude-modulation-to-phase-modulation (AM-PM) conversion. Difference-over-sum offers simplicity and low cost, but poor real-time normalized response and amplitude dynamic range. AM-PM offers fast real-time response and large dynamic range, but is costly and difficult to implement. Logarithmic-ratio processing, a technique using newly available inexpensive hybrid circuits, appears to offer the advantages of both, and the disadvantages of neither. The features of all three processing techniques are reviewed, and the features of the log-ratio technique are highlighted. Among the advantages of log-ratio is a beam-displacement response linearity that is superior to either difference-over-sum or AM-PM for circular-aperture BPM's. DOE

N93-25325# California Univ., Berkeley. Lawrence Berkeley Lab.
BEAM POSITION AND TOTAL CURRENT MONITOR FOR HEAVY ION FUSION BEAMS
D. Berners and L. L. Reginato Oct. 1992 7 p Presented at the 1992

Accelerator Instrumentation Workshop, Berkeley, CA, 27-30 Oct. 1992
(Contract DE-AC03-76SF-00098)
(DE93-007653; LBL-32918; CONF-9210246-12) Avail: CASI HC A02/MF A01

Heavy ion fusion requires moderate currents, 1-10 A, for a duration of about 1 microsec. For accurate beam transport, the center of charge must be located to within plus or minus 100 microns. Beam position and intensity may be excited at frequencies approaching 10 MHz, and the monitoring system must have adequate bandwidth to respond at these frequencies. The Rogowski technique was modified by using distributed reactance multiturn magnetic loops so that it is suitable for measuring current position as well as amplitude. Four identical stripline coils are wound one per quadrant around a nonmagnetic core. The sensitivity is similar to that of a lumped coil system, with the added advantage of increased bandwidth. The voltages induced on the four separate coils are compared and suitable signal conditioning is performed to recover beam position and intensity information. DOE

N93-25375# Lawrence Livermore National Lab., CA.
TRANSVERSE INSTABILITIES IN A RELATIVISTIC KLYSTRON TWO-BEAM ACCELERATOR
G. A. Westenskow, T. L. Houck, and S. S. Yu (California Univ., Berkeley. Lawrence Berkeley Lab.) Aug. 1992 7 p Presented at the 16th International LINAC Conference, Ottawa, Ontario, 23-28 Aug. 1992
(Contract W-7405-eng-48)
(DE93-007110; UCRL-JC-110195; CONF-9208109-76) Avail: CASI HC A02/MF A01

Transverse beam instabilities have been observed in the traveling-wave output structures of high-power microwave generators driven by induction accelerators. The relativistic klystron two-beam accelerator concept involves the transport of kiloamperes of current through many microwave output sections. Energy in both the cumulative and regenerative beam breakup modes could grow in these two-beam accelerator systems to levels that beam loss would occur. For induction accelerators the current term can be several orders of magnitude larger than values common for RF accelerators, presenting a difficult challenge for beam stability. In this paper we present experimental evidence of beam breakup in the output section of a high-power microwave generator, methods used to suppress the higher order modes in the power extraction sections, and computer modeling for transverse instabilities in larger relativistic klystron two-beam accelerator systems. DOE

N93-25380# Los Alamos National Lab., NM.
HIGH-ENERGY PION-NUCLEUS SCATTERING AT LAMPF
C. L. Morris 1993 12 p Workshop on New Vistas in Physics with High-Energy Pion Beams held in Santa Fe, NM, 14 Oct. 1992
(Contract W-7405-eng-36)
(DE93-007364; LA-UR-93-322; CONF-9210292-1) Avail: CASI HC A03/MF A01

Recent data obtained for pion-nucleus interactions above the (triangle)(1232) is presented. The expected long mean-free path at pion energies above the (3,3) resonance is demonstrated in elastic scattering. Evidence for unexpected nuclear transparency for outgoing pions at resonance energies is presented. A new technique measuring virtual (triangle) components of the nuclear wave function is suggested. DOE

N93-25676# Oklahoma State Univ., Stillwater. Dept. of Chemistry.
CHEMICAL DYNAMICS STUDIES OF HIGH ENERGY SPECIES Final Report, 1 Nov. 1989 - 31 Oct. 1992
Donald L. Thompson 16 Nov. 1992 29 p
(Grant AF-AFOSR-0048-90)
(AD-A260743; AFOSR-93-0018TR) Avail: CASI HC A03/MF A01

We report the results of a theoretical/computational research program to develop methods and to investigate the fundamental chemical dynamics of elementary processes important in systems that can potentially yield large amounts of energy when they react. We describe a research program designed to further develop methods and to perform dynamics calculations for fundamental reactions in polyatomic molecules in which tunneling, electronic nonadiabatic processes, and vibrationally mode-selected reactions occur using theoretical methods based on classical trajectories and transition-state theory. Semiclassical corrections were employed to treat nonclassical processes such as tunneling and electronic transitions. DTIC

N93-26322# National Inst. of Standards and Technology, Gaithersburg, MD. Reactor Radiation Div.
NIST REACTOR: SUMMARY OF ACTIVITIES, JULY 1991 THROUGH SEPTEMBER 1992
Feb. 1993 132 p See also PB92-149731
(PB93-162873; NISTIR-5120) Avail: CASI HC A07/MF A02

The report summarizes all the programs which use the NIST reactor. It covers the period for July 1991 through September 1992. The programs range from the use of neutron beams to study the structure and dynamics of materials through nuclear physics and neutron standards to sample irradiations for activation analysis, isotope production, neutron radiography, and nondestructive evaluation. NTIS

74 OPTICS

Includes light phenomena; and optical devices.
For lasers see *36 Lasers and Masers.*

N93-25127# Los Alamos National Lab., NM.
INTERFEROMETRIC FIBER-OPTIC RADIATION SENSOR
P. R. Forman 1992 6 p Presented at the 9th Optical Fiber Sensors Conference, Florence, Italy, 4-6 May 1993
(Contract W-7405-eng-36)
(DE93-003841; LA-UR-92-3790; CONF-930588-1) Avail: CASI HC A02/MF A01

Interferometric fiber-optic radiation sensors based on the Kramers-Kronig relation are investigated. Both high frequency time integral and low frequency instantaneous sensors are proposed. DOE

N93-25182# Allied-Signal Aerospace Co., Kansas City, MO. Technical Communications.
SURFACE PREPARATION AND CHARACTERIZATION OF A 400 MICROMETER DIAMETER FUSED SILICA OPTICAL FIBER FOR DIRECT OPTICAL INITIATION (DOI) APPLICATIONS
P. E. Klingsporn, Theresa Morris, and Donnie Moore Nov. 1992 37 p
(Contract DE-AC04-76DP-00613)
(DE93-005485; KCP-613-4969) Avail: CASI HC A03/MF A01

Studies were conducted to determine the effect of lapping and polishing variables on fiber optic surface finish, flatness, perpendicularity to axis, and subsurface characteristics. The studies were done with a fiber having a 400 micron diameter fused silica core and a 440 micron outer diameter fused silica cladding used for DOI (direct optical initiation) system developmental work. On fibers polished to the best level of surface finish, laser-induced damage studies conducted at Sandia National Laboratory (SNL) showed that seventy percent of the fibers passed optical power densities in excess of 5 GW/sq cm, without surface damage. The geometry of two fiber optic-connector pairs mated along a common axis in an adapter was investigated to determine the tolerances necessary to achieve a desired degree of angular and positional alignment of the mating fiber surfaces. DOE

N93-25281*# Stanford Univ., CA. Dept. of Applied Physics.
ADVANCES IN NONLINEAR OPTICAL MATERIALS AND DEVICES
Robert L. Byer [1991] 14 p Partially supported by NASA, Army Research Office,Office of Naval Research, DARPA, NSF, and Sony Corp.
(NASA-CR-192681; NAS 1.26:192681) Avail: CASI HC A03/MF A01

The recent progress in the application of nonlinear techniques to extend the frequency of laser sources has come from the joint progress in laser sources and in nonlinear materials. A brief summary of the progress in diode pumped solid state lasers is followed by an overview of progress in nonlinear frequency extension by harmonic generation and parametric processes. Improved nonlinear materials including bulk crystals, quasiphasematched interactions, guided wave devices, and quantum well intersubband studies are discussed with the idea of identifying areas of future progress in nonlinear materials and devices. Author (revised)

N93-25358# Department of the Navy, Washington, DC.
APPARATUS FOR IMAGING AN OBJECT IN OR THROUGH A SCATTERING MEDIUM USING COHERENT ANTI-STOKES RAMAN SCATTERING Patent Application
Mark Bashkansky, inventor (to Navy) and John F. Reintjes, inventor (to

Navy) 13 Nov. 1992 24 p
(AD-D015642; US-Patent-Appl-SN-970886; Navy-Case-74286) Avail: CASI HC A03/MF A01

A method and apparatus for imaging an object that is part of, embedded in, or viewed through a scattering medium is provided. A first broadband beam generator, such as a broadband pulse laser, provides a first broadband beam. A second broadband beam generator, such as a Raman Stokes generator disposed to receive the first broadband beam, generates a second broadband beam capable of correlation with the first broadband beam. A coherent anti-Stokes Raman scattering material is disposed to receive the second broadband beam after dispersion in the scattering medium. A variable delay path also illuminates the coherent anti-Stokes Raman scattering material with the first broadband beam. The coherent anti-Stokes Raman scattering material produces an anti-Stokes beam which contains an extracted image of an object in the scattering medium, whose image is recorded on a photodetector. DTIC

N93-25550# California Univ., Berkeley. Lawrence Berkeley Lab.
SURFACE DIFFUSION STUDIES BY OPTICAL DIFFRACTION TECHNIQUES Ph.D. Thesis
X. D. Xiao Nov. 1992 165 p
(Contract DE-AC03-76SF-00098)
(DE93-007707; LBL-33248) Avail: CASI HC A08/MF A02

The newly developed optical techniques have been combined with either second harmonic (SH) diffraction or linear diffraction off of a monolayer adsorbate grating for surface diffusion measurement. Anisotropy of surface diffusion of CO on Ni(110) was used as a demonstration for the second harmonic (SH) diffraction method. The linear diffraction method, which possesses a much higher sensitivity than the SH diffraction method, was employed to study the effect of adsorbate-adsorbate interaction on CO diffusion on Ni(110) surface. Results showed that only the short range direct CO-CO orbital overlapping interaction influences CO diffusion, but not the long range dipole-dipole and CO-NI-CO interactions. Effects of impurities and defects on surface diffusion were further explored by using linear diffraction method on CO/Ni(110) system. It was found that a few percent S impurity can alter the CO diffusion barrier height to a much higher value through changing the Ni(110) surface. The point defects of Ni(l10) surface seem to speed up CO diffusion significantly. A mechanism with long jumps over multiple lattice distance initiated by CO filled vacancy is proposed to explain the observed defect effect. DOE

N93-25646# Wisconsin Univ., Madison. Dept. of Physics.
THEORETICAL AND EXPERIMENTAL RESEARCH IN INFRARED TECHNOLOGY Final Report, 26 Mar. 1986 - 30 Sep. 1992
Chun C. Lin 31 Dec. 1992 58 p
(Contract F19628-86-C-0076)
(AD-A260926; PL-TR-92-2252) Avail: CASI HC A04/MF A01

This report includes research on the following topics: (1) electron-impact ionization of oxygen atoms; (2) rate constants for three-body recombination of electrons with atomic oxygen ions; (3) electronic structure of Rydberg oxygen molecules; (4) electron-impact excitation of Rydberg oxygen molecules; (5) electron impact emission cross sections of the oxygen Second Negative Bands; and (6) formation of highly excited states by electron recombination with atomic and molecular oxygen ions. DTIC

N93-25748 Heriot-Watt Univ., Edinburgh (Scotland).
FIBRE OPTIC SENSORS FOR HEAT TRANSFER STUDIES Ph.D. Thesis
Pranay G. Sinha 1991 349 p
Avail: Univ. Microfilms Order No. BRDX97916

This thesis describes the design and development of a prototype sensor, based on a miniature optical fiber Fabry-Perot interferometer, for heat transfer studies on model turbomachinery components in transient flow wind tunnels. These sensors overcome a number of difficulties which are often encountered in using conventional electrical thin-film resistance gauges such as in the measurement of rapidly varying heat transfer rates, spatial resolution, electromagnetic interference, calibration and signal processing. The special features of the optical sensor are: (1) short length (less than 5 mm), and therefore embeddable in thin structures of model components; (2) direct measurement of heat flux rates; (3) calorimetric operation with temperature resolution of less than 25 mK over a measurement bandwidth of 100 kHz; (4) capability of measuring heat flux less than 5 kWm(exp -2) with measurement range in excess of 10 MWm(exp -2); (5) temporal response time of less than 10 microseconds; (6) minimal thermal disturbances because models are often made of ceramic materials with thermal properties similar to those of the optical fiber from which sensors are made;(7) possibility of using in models with dissimilar thermal properties to the optical fiber, for example, metals; (8) spatial resolution of less than 5 microns; (9) remote operation; (10) an ability to be multiplexed; and (11) immunity to electromagnetic interference. A detailed discussion of the design considerations for the sensor, system development, evaluation of the sensor performance both in the laboratory and wind tunnel environments is presented in this thesis. The performance of the sensor compared favorably with electrical gauges namely, platinum thin-film resistance thermometers. A 4-sensor multiplexed system has been successfully operated, and is reported in the thesis. A brief discussion is also included to indicate that the same sensor design may be considered for applications in other engineering areas. Dissert. Abstr.

N93-25766# SRI International Corp., Menlo Park, CA.
IR MATERIALS PRODUCIBILITY Quarterly Report No. 1, 1 Nov. 1992 - 31 Jan. 1993
A. Sher, M. A. Berding, and A. T. Paxton Feb. 1993 20 p
(Contract MDA972-92-C-0053; ARPA Order 8557)
(AD-A261099) Avail: CASI HC A03/MF A01

We have begun the calculation of relaxation of the near neighbors about the native defects in HgCdTe. We have found that approximate self-consistent schemes are inadequate for the large displacements of the highly strained defects, and therefore these calculations are being done self-consistently. The fields produced by long-range strain fields of dislocations via the piezoelectric effect and charged dislocation cores have been calculated for HgCdTe. The impact of dislocation core charges depends on the location of the dislocation and is greater in the depletion region where the screening is reduced and smaller in the neutral regions of the device. We also find that their impact decreases as the temperature is increased. We have completed the calculations of the unrelaxed native point defect energies in ZnSe within the local density approximation and have begun the calculation of the gradient correction to these energies. Based on these preliminary numbers, we predict the zinc vacancy and the zinc antisite, and the zinc interstitial to be the dominant defects in ZnSe. We are currently calculating the relaxation about the most important defects in ZnSe. DTIC

N93-25822# Oregon Univ., Eugene.
EXPERIMENTAL STUDIES OF FUNDAMENTAL PROBLEMS IN QUANTUM OPTICS Final Report, 11 Jan. 1988 - 31 Jul. 1992
Thomas W. Mossberg and Michael G. Raymer 30 Nov. 1992 8 p
(Contract DAAL02-89-K-0004)
(AD-A261183; ARO-25546.16-PH) Avail: CASI HC A02/MF A01

Extensive experimental and theoretical results obtained in the two research areas supported by this grant are summarized. These diverse areas include the statistical properties of light produced via stimulated Raman scattering and the operational and technical properties of the time-domain frequency-selective approach to optical data storage. DTIC

N93-25839# University of Southern California, Los Angeles. Dept. of Electrical Engineering.
SECOND-HARMONIC GENERATION IN OPTICAL FIBERS AND GLASS Final Report, Aug. 1989 - Aug. 1992
Vincent G. Dominic 30 Sep. 1992 34 p
(Contract DAAL03-89-G-0077)
(AD-A260592; ARO-27005.2-EL-F) Avail: CASI HC A03/MF A01

We report on our investigation into the unusual and unexpected effect of second-harmonic generation in optical fibers and optical fiber preforms. We make three important conclusions: Experimental investigations into this effect are simpler and more controllable if carried out in bulk glass samples (optical fiber preforms) rather than in the optical fibers themselves. The induced second-order nonlinearity arises from a DC electric field which is induced inside the glass by light beams containing a fundamental frequency (omega) and its second harmonic (2 omega). The light beams induce the DC electric field through a multiple-photon process. Specifically, we believe that the interference between several multi-photon ionization channels gives rise to anisotropic emission of photoelectrons. The ejected electrons create a photogalvanic current that builds the DC electric field. DTIC

N93-25898# Purdue Univ., West Lafayette, IN. School of Aeronautics and Astronautics.

A HIERARCHICAL TARGET EXTRACTION, RECOGNITION, AND TRACKING (HiTert) SYSTEM Final Report, 1 Apr. 1989 - 31 Mar. 1992

Jun Lu, Dominick Andrisani, II, and M. F. Tenorio 31 Mar. 1992 132 p (Contract DAAL03-89-K-0086)

(AD-A260567; ARO-26813.5-EL) Avail: CASI HC A07/MF A02

This research contributed to the development of a hierarchical target extraction, identification, and tracking system based on imaging sensors. The work suggests that passive tracking of ground targets is a desirable possibility. Our work involved computer rendering of a color image database containing 1000 images of a maneuvering tank; the use of image derived data to help track a violently maneuvering tank; the use of the Cantata Visual Programming Language to design the multiple interconnected algorithms in an intuitive and extensible manner; the delivery of this software to the U.S. Army Armament Research and Development Center (ARDEC) at Picatinny Arsenal, New Jersey; and presentation of a one day short course to engineers at ARDEC concerning the design and use of the software. This final report describes that software. Our research has suggested the need for the following future work: improved realism in the computer generated image database; development of additional higher level image processing and tracking modules using Cantata; and implementation of a way to communicate between competing algorithms. DTIC

N93-26091 Department of the Navy, Washington, DC.

VIDEO SCAN RATE CONVERSION METHOD AND APPARATUS FOR ACHIEVING SAME Patent

George T. Mills, inventor (to Navy) 1 Dec. 1992 9 p Filed 1 Aug. 1991

(AD-D015661; US-Patent-5,168,359; US-Patent-Appl-SN-742235; US-Patent-Class-358-140) Avail: US Patent and Trademark Office

In a video system, a video signal operates at a vertical scan rate to generate a first video frame characterized by a first number of lines per frame. A method and apparatus are provided to convert the first video frame into a second video frame characterized by a second number of lines per frame. The first video frame is stored at the vertical scan rate as digital samples. A portion of the stored digital samples from each line of the first video frame are retrieved at the vertical scan rate. The number of digital samples in the retrieved portion from each line of the first video frame is governed by a ratio equal to the second number divided by the first number, such that the retrieved portion from the first video frame is the second video frame. DTIC

N93-26183*# Smithsonian Astrophysical Observatory, Cambridge, MA.

VETA-I X RAY TEST ANALYSIS Interim Report

R. J. V. Brissenden, G. Chartas, M. D. Freeman, J. P. Hughes, E. M. Kellogg, W. A. Podgorski, D. A. Schwartz, and P. Zhao 23 Oct. 1992 138 p

(Contract NAS8-36123)

(NASA-CR-192321; NAS 1.26:192321; SAO-AXAF-DR-92-012) Avail: CASI HC A07/MF A02

This interim report presents some definitive results from our analysis of the VETA-I x-ray testing data. It also provides a description of the hardware and software used in the conduct of the VETA-I x-ray test program performed at the MSFC x-ray Calibration Facility (XRCF). These test results also serve to supply data and information to include in the TRW final report required by DPD 692, DR XC04. To provide an authoritative compendium of results, we have taken nine papers as published in the SPIE Symposium, 'Grazing Incidence X-ray/EUV Optics for Astronomy and Projection Lithography' and have reproduced them as the content of this report. For individual titles, see N93-26184 through N93-26192.

N93-26184*# Smithsonian Astrophysical Observatory, Cambridge, MA.

INTENSITY DISTRIBUTION OF THE X RAY SOURCE FOR THE AXAF VETA-I MIRROR TEST

Ping Zhao, Edwin M. Kellogg, Daniel A. Schwartz, Yibo Shao, and M. Ann Fulton *In its* VETA-I X Ray Test Analysis 23 Oct. 1992 14 p (For primary document see N93-26183 09-74)

Avail: CASI HC A03/MF A02

The X-ray generator for the AXAF VETA-I mirror test is an electron impact X-ray source with various anode materials. The source sizes of different anodes and their intensity distributions were measured with a pinhole camera before the VETA-I test. The pinhole camera consists of a 30 micrometers diameter pinhole for imaging the source and a Microchannel Plate Imaging Detector with 25 micrometers FWHM spatial resolution for detecting and recording the image. The camera has a magnification factor of 8.79, which enables measuring the detailed spatial structure of the source. The spot size, the intensity distribution, and the flux level of each source were measured with different operating parameters. During the VETA-I test, microscope pictures were taken for each used anode immediately after it was brought out of the source chamber. The source sizes and the intensity distribution structures are clearly shown in the pictures. They are compared and agree with the results from the pinhole camera measurements. This paper presents the results of the above measurements. The results show that under operating conditions characteristic of the VETA-I test, all the source sizes have a FWHM of less than 0.45 mm. For a source of this size at 528 meters away, the angular size to VETA is less than 0.17 arcsec which is small compared to the on ground VETA angular resolution (0.5 arcsec, required and 0.22 arcsec, measured). Even so, the results show the intensity distributions of the sources have complicated structures. These results were crucial for the VETA data analysis and for obtaining the on ground and predicted in orbit VETA Point Response Function. Author

N93-26185*# Smithsonian Astrophysical Observatory, Cambridge, MA. Center for Astrophysics.

VETA-1 X RAY DETECTION SYSTEM

W. A. Podgorski, Kathy A. Flanagan, Mark D. Freeman, R. G. Goddard, Edwin M. Kellogg, T. J. Norton, J. P. Ouellette, A. G. Roy, and Daniel A. Schwartz *In its* VETA-I X Ray Test Analysis 23 Oct. 1992 15 p (For primary document see N93-26183 09-74)

Avail: CASI HC A03/MF A02

The alignment and X-ray imaging performance of the Advanced X-ray Astrophysics Facility (AXAF) Verification Engineering Test Article-I (VETA-I) was measured by the VETA-I X-Ray Detection System (VXDS). The VXDS was based on the X-ray detection system utilized in the AXAF Technology Mirror Assembly (TMA) program, upgraded to meet the more stringent requirements of the VETA-I test program. The VXDS includes two types of X-ray detectors: (1) a High Resolution Imager (HRI) which provides X-ray imaging capabilities, and (2) sealed and flow proportional counters which, in conjunction with apertures of various types and precision translation stages, provide the most accurate measurement of VETA-I performance. Herein we give an overview of the VXDS hardware including X-ray detectors, translation stages, apertures, proportional counters and flow counter gas supply system and associated electronics. We also describe the installation of the VXDS into the Marshall Space Flight Center (MSFC) X-Ray Calibration Facility (XRCF). We discuss in detail the design and performance of those elements of the VXDS which have not been discussed elsewhere; translation systems, flow counter gas supply system, apertures and thermal monitoring system. Author

N93-26186*# Smithsonian Astrophysical Observatory, Cambridge, MA.

VETA X RAY DATA ACQUISITION AND CONTROL SYSTEM

Roger J. V. Brissenden, Mark T. Jones, Malin Ljungberg, Dan T. Nguyen, and John B. Roll, Jr. *In its* VETA-I X Ray Test Analysis 23 Oct. 1992 10 p (For primary document see N93-26183 09-74)

Avail: CASI HC A02/MF A02

We describe the X-ray Data Acquisition and Control System (XDACS) used together with the X-ray Detection System (XDS) to characterize the X-ray image during testing of the AXAF P1/H1 mirror pair at the MSFC X-ray Calibration Facility. A variety of X-ray data were acquired, analyzed and archived during the testing including: mirror alignment, encircled energy, effective area, point spread function, system housekeeping and proportional counter window uniformity data. The system architecture is presented with emphasis placed on key features that include a layered UNIX tool approach, dedicated subsystem controllers, real-time X-window displays, flexibility in combining tools, network connectivity and system extensibility. The VETA test data archive is also described. Author

N93-26187*# Smithsonian Astrophysical Observatory, Cambridge, MA. Center for Astrophysics.

CORRECTING X RAY SPECTRA OBTAINED FROM THE AXAF VETA-I MIRROR CALIBRATION FOR PILEUP, CONTINUUM, BACKGROUND AND DEADTIME

G. Chartas, Kathy Flanagan, John P. Hughes, Edwin M. Kellogg, D. Nguyen, M. Zombeck, M. Joy, and J. Kolodziejezak *In its* VETA-I X Ray Test Analysis 23 Oct. 1992 10 p (For primary document see N93-26183 09-74)
Avail: CASI HC A02/MF A02

The VETA-I mirror was calibrated with the use of a collimated soft X-ray source produced by electron bombardment of various anode materials. The FWHM, effective area and encircled energy were measured with the use of proportional counters that were scanned with a set of circular apertures. The pulsers from the proportional counters were sent through a multichannel analyzer that produced a pulse height spectrum. In order to characterize the properties of the mirror at different discrete photon energies one desires to extract from the pulse height distribution only those photons that originated from the characteristic line emission of the X-ray target source. We have developed a code that fits a modeled spectrum to the observed X-ray data, extracts the counts that originated from the line emission, and estimates the error in these counts. The function that is fitted to the X-ray spectra includes a Prescott function for the resolution of the detector a second Prescott function for a pileup peak and a X-ray continuum function. The continuum component is determined by calculating the absorption of the target Bremsstrahlung through various filters correcting for the reflectivity of the mirror and convolving with the detector response. Author

N93-26188*# Smithsonian Astrophysical Observatory, Cambridge, MA. Center for Astrophysics.
AXAF VETA-I MIRROR ENCIRCLED ENERGY MEASUREMENTS AND DATA REDUCTION
Ping Zhao, Mark D. Freeman, John P. Hughes, Edwin M. Kellogg, Dan T. Nguyen, Marshall Joy, and Jeffery J. Kolodziejczak *In its* VETA-I X Ray Test Analysis 23 Oct. 1992 16 p (For primary document see N93-26183 09-74)
Avail: CASI HC A03/MF A02

The AXAF VETA-I mirror encircled energy was measured with a series of apertures and two flow gas proportional counters at five X-ray energies ranging from 0.28 to 2.3 keV. The proportional counter has a thin plastic window with an opaque wire mesh supporting grid. Depending on the counter position, this mesh can cause the X-ray transmission to vary as much as +/-9 percent, which directly translates into an error in the encircled energy. In order to correct this wire mesh effect, window scan measurements were made, in which the counter was scanned in both horizontal (Y) and vertical (Z) directions with the aperture fixed. Post VETA measurement of the VXDS setup were made to determine the exact geometry and position of the mesh grid. Computer models of the window mesh were developed to simulate the X-ray transmission based on this measurement. The window scan data were fitted to such mesh models and corrections were made. After this study, the mesh effect was well understood and the final results of the encircled energy were obtained with an uncertainty of less than 0.8 percent. Author

N93-26189*# Smithsonian Astrophysical Observatory, Cambridge, MA. Center for Astrophysics.
PRECISION OF THE CALIBRATION OF THE AXAF ENGINEERING TEST ARTICLE (VETA) MIRRORS
D. A. Schwartz, G. Chartas, John P. Hughes, Edwin M. Kellogg, and Ping Zhao *In its* VETA-I X Ray Test Analysis 23 Oct. 1992 20 p (For primary document see N93-26183 09-74)
Avail: CASI HC A03/MF A02

Measurements of the VETA encircled energies have been performed at 5 energies within 16 radii ranging from 0.05 to 200 arcseconds. We report here on the analysis of the accuracy of those measurements. A common 'error tree' structure applies, and we present representative numbers for the larger terms. At 0.277, 1.5, and 2.07 keV, and for radii of 3 arcsec and larger, our measurements have estimated 1 sigma errors of 0.6 to 1.5 percent. Effects of measurement statistics and of the VETA test mount limit the accuracy at smaller angles, and modulation by the counter window support structure together with the imperfect position repeatability limit the accuracy for the 0.93 and 2.3 keV energies. We expect to mitigate these limitations when calibrating the complete AXAF flight mirror assembly. Author

N93-26190*# Smithsonian Astrophysical Observatory, Cambridge, MA. Center for Astrophysics.
IMAGE ANALYSIS OF THE AXAF VETA-I X RAY MIRROR
Mark D. Freeman, John P Hughes, L. VanSpeybroeck, M. Weisskopf, and J. Bilbro *In its* VETA-I X Ray Test Analysis 23 Oct. 1992 16 p (For primary document see N93-26183 09-74)
Avail: CASI HC A03/MF A02

Initial core scan data of the VETA-I x-ray mirror proved disappointing, showing considerable unpredicted image structure and poor measured FWHM. 2-D core scans were performed, providing important insight into the nature of the distortion. Image deconvolutions using a ray traced model PSF was performed successfully to reinforce our conclusion regarding the origin of the astigmatism. A mechanical correction was made to the optical structure, and the mirror was tested successfully (FWHM 0.22 arcsec) as a result. Author

N93-26191*# Smithsonian Astrophysical Observatory, Cambridge, MA. Center for Astrophysics.
SURFACE FINISH QUALITY OF THE OUTER AXAF MIRROR PAIR BASED ON X RAY MEASUREMENTS OF THE VETA-I
John P. Hughes, Daniel A. Schwartz, Andrew Szentgyorgyi, Leon VanSpeybroeck, and Ping Zhao *In its* VETA-I X Ray Test Analysis 23 Oct. 1992 10 p (For primary document see N93-26183 09-74)
Avail: CASI HC A02/MF A02

We employ the X-ray measurements of the VETA-I taken at the X-Ray Calibration Facility (XRCF) of the Marshall Space Flight Center (MSFC) to extract information about the surface finish quality of the outermost pair of AXAF mirrors. The particular measurements we consider are one dimensional scans of the core of the point response function (PRF) (full width half maximum (FWHM) scans), the encircled energy as a function of radius, and one dimensional scans of the wings of the PRF. We discuss briefly our ray trace model which incorporates the numerous effects present in the VETA-I test, such as the finite source distance, the size and shape of the X-ray source, the residual gravitational distortions of the optic, the despace of the VETA-I, and particulate contamination. We show how the data constrain the amplitude of mirror surface deviations for spatial frequencies greater than about 0.1 mm(exp -1). Constraints on the average amplitude of circumferential slope errors are derived as well. Author

N93-26192*# Smithsonian Astrophysical Observatory, Cambridge, MA. Center for Astrophysics.
THE X RAY REFLECTIVITY OF THE AXAF VETA-I OPTICS
Edwin M. Kellogg, G. Chartas, D. Graessle, John P. Hughes, Leon VanSpeybroeck, Ping Zhao, M. C. Weisskopf, R. F. Elsner, and S. L. ODell *In its* VETA-I X Ray Test Analysis 23 Oct. 1992 8 p (For primary document see N93-26183 09-74)
Avail: CASI HC A02/MF A02

The x-ray reflectivity of the VETA-I optic, the outermost shell of the AXAF x-ray telescope, with a bare Zerodur surface, is measured and compared with theoretical predictions. Measurements made at energies of 0.28, 0.9, 1.5, 2.1, and 2.3 keV are compared with predictions based on ray trace calculations. The data were obtained at the x-ray calibrations facility at Marshall Space Flight Center with an electron impact x-ray source located 528 m from the grazing incidence mirror. The source used photoelectric absorption filters to eliminate bremsstrahlung continuum. The mirror has a diameter of 1.2 m and a focal length of 10 m. The incident and reflected x-ray flux are detected using two proportional counters, one located in the incident beam of x-rays at the entrance aperture of the VETA-I, and the other in the focal plane behind an aperture of variable size. Results on the variation of the reflectivity with energy as well as the absolute value of the reflectivity are presented. We also present a synchrotron reflectivity measurement with high energy resolution over the range 0.26 to 1.8 keV on a flat Zerodur sample, done at NSLS. We present evidence for contamination of the flat by a thin layer of carbon on the surface, and the possibility of alteration of the surface composition of the VETA-I mirror perhaps by the polishing technique. The overall agreement between the measured and calculated effective area of VETA-I is between 2.6 percent and 10 percent, depending on which model for the surface composition is adopted. Measurements at individual energies deviate from the best-fitting calculation to 0.3 to 0.8 percent, averaging 0.6 percent at energies below the high energy cutoff of the mirror reflectivity, and are as

high as 20.7 percent at the cutoff. We also discuss the approach to the final preflight calibration of the full AXAF flight mirror. Author

N93-26224# Pennsylvania State Univ., University Park. Materials Research Lab.
NEW PYRO-OPTIC TECHNIQUES FOR IMAGING OF LONG WAVELENGTH IR-RADIATION (PYRO-OPTIC INITIATION PROGRAM) Final Report, 31 Mar. - 30 Sep. 1992
L. E. Cross and A. S. Bhalla 21 Dec. 1992 20 p
(Contract DAAL03-92-G-0036)
(AD-A260969; ARO-28784.1-PH) Avail: CASI HC A03/MF A01

From a simple consideration of the thermal conversation efficiency which can be realized in the non contact pyro-optic system it is shown that for f/1 optics a scene temperature change of 0.1 deg C will realize a change at the detector of 0.001 deg C for a detector thickness of 0.1 micrometer, chopping frequency of 25 Hz. For a simple pixel element 50 micron x 50 micron x 0.1 micron the RMS thermal noise limit in SBSI is calculated to be 3.5 x 10 to the -5 deg C well below the expected signal level. Using a very simple ellipsometric setup working into a photomultiplier detector it is shown that for SbSI single crystals and thin films, temperature oscillations of 0.001 deg C can be detected above noise level. DTIC

N93-26256# Stanford Univ., CA. Dept. of Electrical Engineering.
ADVANCED OPTICAL FIBER COMMUNICATION SYSTEMS Status Report, 1 Aug. 1992 - 28 Feb. 1993
Leonid G. Kazovsky 28 Feb. 1993 19 p
(Contract N00014-91-J-1857)
(AD-A261802) Avail: CASI HC A03/MF A01

Our research is focused on theoretical investigations of advanced optical fiber communication systems and can be grouped into three broad areas: WDM networks, coherent analog links, and optical fiber nonlinearities. In the area of WDM networks, we proposed and investigated a novel WDM network architecture (STARNET), a novel combined phase/amplitude modulation format, and a high-speed optics-to-computer interface for STARNET. In the area of coherent analog links, we investigated angle and amplitude modulated systems for linewidth-insensitive analog applications and direct-frequency-modulated subcarrier-multiplexed systems. In the area of fiber nonlinearities, we investigated four-wave mixing, thermally induced parasitic phase modulation, and a new type of soliton. DTIC

N93-26266# Optical Society of America, Washington, DC.
OPTICAL COMPUTING. VOLUME 6: ORGANIZATION OF THE OPTICAL SOCIETY OF AMERICA PHOTONIC SCIENCE TOPICAL MEETING SERIES Final Report, 1 Jan. - 31 Dec. 1991
J. W. Quinn 22 May 1992 327 p Meeting held in Salt Lake City, UT, 4-6 Mar. 1991
(Grant AF-AFOSR-0176-91)
(AD-A261267; AFOSR-92-0517TR) Avail: CASI HC A15/MF A03

Summaries of papers are included that address the following subjects: Photorefractive Materials, Effects, and Devices; Integrated Photonics Research; Nonlinear Guided Wave Phenomena; Optical Amplifiers and Their Applications; Optical computing; Picosecond Electronics and Optoelectronics; Quantum Optoelectronics; Photonic Switching; Microphysics of Surfaces; Beam Induced Processes; Soft X-ray Projection Lithography; Short Wavelength Coherent Radiation, Generation and Applications; and Persistent Spectral Hole-Buring; Science and Applications. DTIC

N93-26306# Columbia Univ., New York, NY. Dept. of Electrical Engineering.
MULTICHIP MODULE HIGH SPEED TESTING Quarterly Progress Report, 1 Oct. - 31 Dec. 1992
Robert J. Davis and David H. Auston 31 Dec. 1992 3 p
(Contract N00014-91-J-4045)
(AD-A261391) Avail: CASI HC A01/MF A01

Work is proceeding on the testing of high-speed circuits using poled electrooptic polymers. Coplanar electrodes with thin layer (3 microns) coatings of a copolymer system have been obtained from Allied Signal. The samples were poled at their glass transition temperature of 132 C at a poling field of 0.50 MV/cm. The response was measured in transmission mode through the electrode gap using a Ti:sapphire laser and a lock-in amplifier. DTIC

N93-26309# HCC Science and Technology Co., Summit, NJ.
DEVELOPMENT OF ORGANIC NONLINEAR OPTICAL MATERIALS Final Report, 1 Aug. 1989 - 30 Oct. 1992
J. Sounik, R. Norwood, I. McCulloch, K. Song, and R. DeMartino 22 Oct. 1992 167 p LIMITED REPRODUCIBILITY: More than 20% of this document may be affected by microfiche quality
(Contract F49620-89-C-0097)
(AD-A261332; AFOSR-93-0036TR) Avail: CASI HC A08/MF A02

The design of organic polymers as active mediums for nonlinear optics has attracted much attention because their nature of versatility in synthetic chemistry and in fabrication. A series of new side chain polymers were synthesized and characterized for the second and third order NLO applications. Linear copolymers containing maleic anhydride as an active functional group on the main chain were prepared in this work. The maleic anhydride group reacts, by ring opening esterification with an appropriate alcohol containing an NLO functionality. These copolymers were also found to be suitable for branching or crosslinking reactions with alpha, omega-diols. A series of substituted silicon and aluminum phthalocyanines has been synthesized to study their third order nonlinear responses. A nitro/amino substituted aluminum phthalocyanine has been made along with mixtures of benzo-substituted silicon phthalocyanines. A synthetic route has been investigated to directly give donor acceptor phthalocyanines. To increase mechanical property of phthalocyanine compounds, copolymers with MMA have been synthesized and characterized. All of the copolymers show excellent film forming characteristics. DTIC

N93-26343# Brown Univ., Providence, RI. Div. of Engineering.
RESEARCH SUPPORT FOR THE LABORATORY FOR LIGHTWAVE TECHNOLOGY Final Report, 1 Jan. 1990 - 31 Dec. 1992
T. F. Morse 31 Dec. 1992 101 p
(Grant AF-AFOSR-0062-90)
(AD-A261488; AFOSR-93-0102TR) Avail: CASI HC A06/MF A02

The Laboratory for Lightwave Technology at Brown University is one of the few university laboratories at which it is possible to design, fabricate, and characterize optical fibers of not only traditional, but of unusual design. These fibers have an increasingly important role in a host of applications of significance to the defense requirements of the United States. Among these are the following: fiber lasers for the measurement of clear air turbulence (in an important eye-safe region of the spectrum); and fiber sensors for the measurement of temperature and strain, not only in high temperature composite materials, but in structural concrete, which is important for roads, runways, and buildings. We are also engaged in research, an outgrowth of our work in optical fibers, on novel techniques for the formation of nanophase oxide particles, both ceramic and amorphous. The work on amorphous oxides is associated with our MCVD and OVD laboratories. In these labs, we have proposed and studied a new technique for the formation of multi-component oxides to be used in the doping of optical fiber preforms. In this synthesis, an aerosol of organometallic precursors is convectively transported into a reaction zone where it is pyrolized. The liquid aerosol is homogeneous at the molecular level, so that subsequent reactions produce glasses that are not phase separated. This has also been used to study the synthesis of high temperature ceramic nanophase single crystal oxides that may be produced at a high rate. The synthesis of both glasses and ceramics using novel techniques has meshed with our research in novel optical fibers and fiber sensors. In this report, we discuss the general activities of our laboratory. DTIC

N93-26457# Massachusetts Inst. of Tech., Cambridge. Research Lab. of Electronics.
INTERFEROMETRIC MEASUREMENT WITH SQUEEZED LIGHT Annual Technical Report, 1 Feb. 1992 - 31 Jan. 1993
Hermann A. Haus 29 Jan. 1993 5 p
(Contract N00014-92-J-1302)
(AD-A260910) Avail: CASI HC A01/MF A01

The progress report on interferometric measurement with squeezed light covering the period from 1 Feb. 1992 - 31 Jan. 1993 is presented. Topics discussed include phase measurement below the shot noise level; pulsed excitation of a resonant ring gyro; squeezing with short pulses; and quantum theory of nonlinear optics. CASI

N93-26488# Carnegie-Mellon Univ., Pittsburgh, PA. School of Computer Science.
UNCERTAINTY IN OBJECT POSE DETERMINATION WITH THREE LIGHT-STRIPE RANGE MEASUREMENTS
Keiichi Kemmotsu and Takeo Kanade Jan. 1993 7 p
(Contract F33615-90-C-1465; ARPA Order 7597)
(AD-A261435; CMU-CS-93-100) Avail: CASI HC A02/MF A01

The pose (position and orientation) of a polyhedral object can be determined with sparse range data obtained from simple light-stripe range finders. However, the sensing data inherently contains some error which introduces uncertainty in the determination of the object's pose. This paper presents a method for estimating the uncertainty in determining the pose of an object when using several light-stripe range finders. Three dimensional line segments obtained by the range finders are matched to model faces based on an interpretation tree search. The object pose is obtained by a least squares fit of the segment-face pairings. We show that the uncertainty in the position of the object can be estimated using the covariance matrix of the endpoint positions of the sensed line segments. Experiments with three light-stripe range finders show that our method makes it possible to estimate how accurately the pose of an object can be determined. DTIC

N93-26515# Minnesota Mining and Mfg. Co., Saint Paul. Fiber Optics Lab.
OPTICAL FIBER FOR ACOUSTIC SENSOR APPLICATIONS Final Technical Report, 30 Sep. 1989 - 31 Oct. 1992
James R. Onstott Feb. 1993 120 p
(Contract N00014-89-C-2455)
(AD-A261580) Avail: CASI HC A06/MF A02

Development, fabrication, and delivery to Naval Research Laboratory (NRL) of 48 km of optical fiber are summarized. The fiber was designed to have a cladding diameter of 80 micrometers and to be single mode at 1300 micrometers. Development of thin single layer coatings for the fiber is reported. Fabrication of fiber with unusually small cladding and coating diameters is reported. DTIC

N93-26542# Space Computer Corp., Santa Monica, CA.
ALGORITHMS FOR SPACE-BASED INFRARED SURVEILLANCE Final Technical Report, Aug. 1990 - Aug. 1992
Alan D. Stocker Feb. 1993 10 p
(Contract N00014-90-C-2183)
(AD-A261891; SCC-R-181F) Avail: CASI HC A02/MF A01

The objective of the study summarized was to develop and evaluate algorithms for detecting low-observable air vehicle targets from a space-based imaging infrared sensor. The effort consisted of theoretical and simulation studies in three areas: frame registration, velocity filtering, and multispectral processing. In the first area, a generalization of the well-known phase-correlation approach for frame registration and clutter suppression was developed. This new approach is significantly more accurate and robust than the standard correlation technique. Also, an improved approach to image interpolation for multi-frame clutter suppression applications was formulated. A major feature of this new approach is the application of the same in-band filtering to every registered frame in order to minimize structured clutter leakage when the frames are differenced. In the second area (velocity filtering), the standard velocity filter approach was extended from fixed-contrast to variable-contrast targets. In the third area (multispectral processing), techniques were developed for clutter suppression and target enhancement for both stationary and moving targets. DTIC

N93-26544# Optical Society of America, Washington, DC.
1992 TECHNICAL DIGEST SERIES VOLUME 16. CONFERENCE EDITION: SUMMARIES OF PAPERS PRESENTED AT THE NONLINEAR DYNAMICS IN OPTICAL SYSTEMS TOPICAL MEETING
26 Jun. 1992 361 p Topical meeting held in Alpbach, Austria, 22-26 Jun. 1992 Sponsored by AFOSR
(AD-A261915) Avail: CASI HC A16/MF A03

Summaries of papers presented at the Nonlinear Dynamics in Optical Systems meeting held on 22-26 Jun. 1992 are included. Topics covered include: dynamics of pulse formation; laser instabilities; control of chaos; multiwave mixing and phase conjugation; spatial pattern formation and dynamics; semiconductor device dynamics; laser array dynamics; and optical chaos and noise. CASI

N93-26566# Wright Lab., Wright-Patterson AFB, OH.
OPTICALLY SMART SURFACES SURVIVABILITY TESTING AT MACH 3 Final Report
Linda G. Smith and Glenn W. Williams Jan. 1993 13 p
(AD-A261785; WL-TM-93-300) Avail: CASI HC A02/MF A01

Optically smart surfaces are being developed as wind tunnel diagnostic techniques for the Wright Laboratory. The optically smart surfaces are holographic optical elements constructed by flow coating an aluminum plate with photoresist as the emulsion material. Survivability of these optically smart surfaces was tested in the Mach 3 High Reynolds Number Facility. The surfaces did not survive at angle of attack to the freestream flow for higher Reynolds numbers and did survive when the surface was parallel to the freestream flow. DTIC

N93-26593# Lawrence Livermore National Lab., CA.
MODELING OF ELECTRIC-FIELD ENHANCEMENT AT NODULAR DEFECTS IN DIELECTRIC MIRROR COATINGS
J. F. DeFord and M. R. Kozlowski Oct. 1992 17 p Presented at the SPIE Symposium on Boulder Damage, Boulder, CO, 28-30 Oct. 1992
(Contract W-7405-eng-48)
(DE93-007513; UCRL-JC-111462; CONF-9210295-2) Avail: CASI HC A03/MF A01

In dielectric multilayer optical coatings, laser induced damage is often associated withmicron-sca le surface defects such as the well known nodule defect. The interaction mechanism of the laser light with the coating defects is not understood, however. Historically, laser damage has been associated with peaks in the standing-wave electric-field distribution within the multilayer films. In the present work we use a finite-difference time-domain electromagnetic modeling code to study the influence of 3-D nodule defects on the E-field distribution. The coating studied is a dielectric multilayer HR consisting of alternating quarter-wave layers of HfO2 and SiO2 at 1.06 microns. The nodule is modeled as a parabolic defect initiated at a spherical seed. The modeling results show that E-field enhancements as large as a factor of 4 can be present at the defects. The enhancement shows a complex dependence on the size, depth, and dielectric constant of the seed material. In general, defects initiated by large, shallow seeds produce the largest E-fields. Voids at the nodule boundary influence the E-field distribution, but have a small effect on the peak field. DOE

N93-26113*# Jet Propulsion Lab., California Inst. of Tech., Pasadena.
PERFORMANCE OF A 12-GHz FIBER-OPTIC SYSTEM FOR BEAM-WAVEGUIDE ANTENNA STABILITY TESTING
T. Y. Otoshi, M. M. Franco, and G. F. Lutes *In its* The Telecommunications and Data Acquisition Report 15 May 1992 p 105-113 (For primary document see N93-26105 09-32)
(RTOP 310-20-65-92-01)
Avail: CASI HC A02/MF A04

N93-26117*# Jet Propulsion Lab., California Inst. of Tech., Pasadena.
FIGURE OF MERIT FOR DIRECT-DETECTION OPTICAL CHANNELS
C.-C. Chen *In its* The Telecommunications and Data Acquisition Report 15 May 1992 p 136-151 (For primary document see N93-26105 09-32)
(RTOP 310-20-67-59-00)
Avail: CASI HC A03/MF A04

75 PLASMA PHYSICS

Includes magnetohydrodynamics and plasma fusion.

For ionospheric plasmas see *46 Geophysics*. For space plasmas see *90 Astrophysics*.

N93-24950# National Inst. for Fusion Science, Nagoya (Japan).
DENSITY DEPENDENCE OF LINE INTENSITIES AND APPLICATION TO PLASMA DIAGNOSTICS
Kuniaki Masai Feb. 1993 26 p Submitted for publication
(NIFS-209) Avail: CASI HC A03/MF A01

Electron density dependence of spectral lines are discussed in view of application to density diagnostics of plasmas. The dependence arises from competitive level population processes and radiative and collisional transitions from the excited states. Results of the measurement on tokamak

plasmas are presented to demonstrate the usefulness of line intensity ratios for density diagnostics. Also, general characteristics related to density dependence are discussed with atomic-number scaling for H-like and He-like systems to be helpful for application to higher density plasmas.
Derived from text

N93-24968# Tennessee Univ. Space Inst., Tullahoma.
EVALUATION OF A CANDIDATE MATERIAL FOR A COAL-FIRED MAGNETOHYDRODYNAMIC (MHD) HIGH TEMPERATURE RECUPERATIVE AIR HEATER
J. Winkler, N. B. Dahotre, and W. Boss 1993 8 p Presented at the 17th Annual Conference on Composites and Advanced Ceramics, Cocoa Beach, FL, 11-15 Jan. 1993
(Contract DE-AC02-79ET-10815)
(DE93-006630; DOE/ET-10815/203; CONF-930164-8) Avail: CASI HC A02/MF A01

In order to achieve the desired efficiency in the magnetohydrodynamic (MHD) cycle, one of two procedures must be employed. The first is to inject pure oxygen during combustion in order to achieve higher combustion temperatures which will yield better conversion efficiencies. The other is to preheat the combustor air through the use of high temperature air heaters (HTAH). A recuperative air heater heats the combustor air directly by passing it through tubes which are in the exhaust gas flow before sending it into the combustor. The procedure of passing air through the furnace requires a material for the tubes which will withstand the high temperatures and corrosive environment of the furnace and should have a high heat transfer coefficient. All of the necessary properties seem to exist in ceramic materials, so ceramics have begun to be studied for high temperature air heaters as well as other high temperature applications. One such effort to evaluate the performance of a ceramic composite tube in a coal fired MHD facility in order to determine any changes in the tube material after exposure to high temperature and a highly corrosive environment is outlined. A recuperative high temperature air heater (HTAH) would be positioned in the radiant furnace, because the radiant furnace provides conditions comparable to an actual MHD facility and is adequate for testing HTAH materials. The temperature conditions in the furnace range from approximately 1600 C to 1890 C, and velocities of approximately 12 m/s to 100 m/s were measured depending on the location in the furnace. The evaluated tube was placed in the furnace in a reducing environment with approximately 14 m/s velocity, 1650 C gas temperature, and 1230 C tube temperature. DOE

N93-24969# Tennessee Univ. Space Inst., Tullahoma.
ASSESSMENT OF TORSATRONS AS REACTORS
J. F. Lyon and S. L. Painter (Australian National Univ., Canberra.) Dec. 1992 32 p
(Contract DE-AC05-84OR-21400)
(DE93-006721; ORNL/TM-12189) Avail: CASI HC A03/MF A01

Stellarators have significant operational advantages over tokamaks as ignited steady-state reactors because stellarators have no dangerous disruptions and no need for continuous current drive or power recirculated to the plasma, both easing the first wall, blanket, and shield design; less severe constraints on the plasma parameters and profiles; and better access for maintenance. A reactor based on the torsatron configuration (a stellarator variant) could also have up to double the mass utilization efficiency (MUE) and a significantly lower cost of electricity (COE) than a conventional tokamak reactor (ARIES-I) for a range of assumptions. Torsatron reactors can have much smaller coil systems than tokamak reactors because the coils are closer to the plasma and they have a smaller cross section (higher average current density because of the lower magnetic field). The reactor optimization approach and the costing and component models are those used in the current stage of the ARIES-I tokamak reactor study. Typical reactor parameters for a 1-GW(e) Compact Torsatron reactor example are major radius R(sub 0) = 6.6-8.8 m, on-axis magnetic field B(sup 0) = 4.8-7.5 T, B(sub max)(on coils) = 16 T, MUE 140-210 kW(e)/ton, and COE (in constant 1990 dollars) = 67-79 mill/kW(e)h. The results are relatively sensitive to assumptions on the level of confinement improvement and the blanket thickness under the inboard half of the helical windings but relatively insensitive to other assumptions. DOE

N93-25092# National Inst. for Fusion Science, Nagoya (Japan).
PLASMA HEATING IN TOROIDAL SYSTEMS
Masao Okamoto and Sadayoshi Murakami Feb. 1993 17 p Presented at the 4th International Toki Conference on Plasma Physics and Controlled Fusion: ITC-4 Fusion and Astrophysical Plasmas, Toki, Japan, 17-20 Nov. 1992 Submitted for publication
(NIFS-208) Avail: CASI HC A03/MF A01

The present status of plasma heating in toroidal systems is reviewed (mainly tokamaks and helical systems) for astrophysical plasma scientists. The main method of plasma heating in toroidal systems or tori is to utilize fast ions (NBI heating and alpha heating). The maximum ion temperature of 3D keV has been achieved at the plasma center by neutral beam injections (NBI's) in the JT-60U tokamak. Ripple trapped losses of fast ions produced by NBI's have been measured also in the JT-60U. The first tokamak discharges in deuterium-tritium fuel led mixtures have been carried out successfully in the JET tokamak. These experimental results are compared with the theoretical predictions based on the Coulomb collisions. Another powerful method is the ICRF heating (Ion Cyclotron Range of Frequency). However, this article is focused mainly on the NBI and alpha heatings. Related to plasma heating, the current drive will be mentioned briefly placing an emphasis on the bootstrap current. Author

N93-25167# Los Alamos National Lab., NM.
MODELING OF PLASMA FLOW SWITCHES AT LOW, INTERMEDIATE AND HIGH ENERGIES
R. L. Bowers, J. H. Brownell, A. E. Greene, D. L. Peterson, N. Roderick, and P. Turchi 1992 9 p Presented at the 6th International Conference on Megagauss Magnetic Field Generation and Related Topics, Albuquerque, NM, 9-12 Nov. 1992
(Contract W-7405-eng-36)
(DE93-007359; LA-UR-93-0014; CONF-921133-16) Avail: CASI HC A02/MF A01

Inductively stored pulsed power technology has been used over the past thirty years to produce multi-megaamp currents to implode low inductance loads and produce x-radiation. Because of the large difference in timescales for the delivery of magnetic energy to the load and the desire for high power x-radiation output (short timescale for the implosion), most inductively stored systems require at least one opening switch. The design and understanding of fast, efficient opening switches for multi-megaamp systems represents a long standing problem in pulsed power research. The Los Alamos Foil Implosion Project uses inductively stored magnetic energy to implode thin metallic liners. A plasma flow switch (PFS) has been investigated as the final pulse shaping step for this system. The PFS consists of a wire array and a barrier foil located upstream from the load region. Several stages can be identified in the performance of the plasma flow switch. These are: (1) the vaporization of the wire array; (2) the assembly of the initiated plasma on tie barrier foil to form the switch plasma; (3) the motion of the switch plasma down the coaxial barrel; and (4) current switching to the load (the actual switching stage). The fourth stage affects the switch's efficiency, as well as the quality of the load implosion. Instabilities may develop during any of these four stages, and their presence may seriously degrade the structure of the switch plasma. Two primary criteria may be used to characterize good switching. The first is switching efficiency. A second criterion is transferred to the load during or after switching. This paper summarizes the computational design of the PFS experiments carried out on Pegasus 1. We conclude by considering the implications of these results for the design of a PFS for the higher energy regime (Procyon) regime. DOE

N93-25187# Los Alamos National Lab., NM.
SUMMARY OF PROGRESS IN INERTIAL CONFINEMENT FUSION
S. M. Younger 1992 9 p Presented at the 14th International Conference on Plasma Physics and Controlled Nuclear Fusion Research, Wurzburg, Germany, Oct. 1992
(Contract W-7405-eng-36)
(DE93-007350; LA-UR-93-297; CONF-9210315-1) Avail: CASI HC A02/MF A01

Progress in inertial confinement fusion (ICF) has been very rapid over the past two years. Significant advances have been made in the production of smooth laser beams, the focusing of light ions beams, and the development of heavy ion accelerators. The availability of advanced target diagnostics on several major drivers has resulted in an extensive database of target performance over a wide range of conditions. Theoretical models of ICF targets are approaching the predictive level with two and even

three dimensional calculations becoming routine. Within the next several years information should be available to allow confident extrapolation to ignition on the next generation driver. DOE

N93-25206*# Jet Propulsion Lab., California Inst. of Tech., Pasadena.
STATIONARY PLASMA THRUSTER EVALUATION IN RUSSIA
John R. Brophy 15 Mar. 1992 35 p
(Contract NAS7-918)
(NASA-CR-192823; NAS 1.26:192823; JPL-Publ-92-4) Avail: CASI HC A03/MF A01

A team of electric propulsion specialists from U.S. government laboratories experimentally evaluated the performance of a 1.35-kW Stationary Plasma Thruster (SPT) at the Scientific Research Institute of Thermal Processes in Moscow and at 'Fakel' Enterprise in Kaliningrad, Russia. The evaluation was performed using a combination of U.S. and Russian instrumentation and indicated that the actual performance of the thruster appears to be close to the claimed performance. The claimed performance was a specific impulse of 16,000 m/s, an overall efficiency of 50 percent, and an input power of 1.35 kW, and is superior to the performance of western electric thrusters at this specific impulse. The unique performance capabilities of the stationary plasma thruster, along with claims that more than fifty of the 660-W thrusters have been flown in space on Russian spacecraft, attracted the interest of western spacecraft propulsion specialists. A two-phase program was initiated to evaluate the stationary plasma thruster performance and technology. The first phase of this program, to experimentally evaluate the performance of the thruster with U.S. instrumentation in Russia, is described in this report. The second phase objective is to determine the suitability of the stationary plasma thruster technology for use on western spacecraft. This will be accomplished by bringing stationary plasma thrusters to the U.S. for quantification of thruster erosion rates, measurements of the performance variation as a function of long-duration operation, quantification of the exhaust beam divergence angle, and determination of the non-propellant efflux from the thruster. These issues require quantification in order to maximize the probability for user application of the SPT technology and significantly increase the propulsion capabilities of U.S. spacecraft. Author (revised)

N93-25215# National Inst. for Fusion Science, Nagoya (Japan).
EFFECT OF CONTINUOUS EIGENVALUE SPECTRUM ON PLASMA TRANSPORT IN TOROIDAL SYSTEMS
Tomejiro Yamagishi (Fukui Inst. of Tech., Japan.) Mar. 1993 25 p Submitted for publication
(NIFS-214) Avail: CASI HC A03/MF A01

The effect of the continuous eigenvalue of the Vlasov equation on the cross field ion thermal flux is investigated. The continuum contribution due to the toroidal drift resonance is found to play an important role in ion transport particularly near the edge, which may apply to the interpretation of the sharp increase of ion heat conductivity near the periphery observed in large tokamaks. Author

N93-25216# National Inst. for Fusion Science, Nagoya (Japan).
SOME FEATURES OF PARTICLE ORBIT BEHAVIOR IN LHD CONFIGURATIONS
A. A. Shishkin, K. Y. Watanabe, K. Yamazaki, O. Motojima, D. L. Grekov (Kharkov Polytechnical Inst., USSR.), M. S. Smirnova (Kharkov Polytechnical Inst., USSR.), and A. V. Zolotukhin (Kharkov Polytechnical Inst., USSR.) Mar. 1993 49 p Submitted for publication
(NIFS-211) Avail: CASI HC A03/MF A01

Localizations of helically trapped particle losses on the last closed magnetic surface in different large helical devices (LHD) configurations are studied. The effects of electric field, finite beta, and bootstrap current are taken into account. It is shown that the angular location of the helically trapped particle losses may be controlled by the change of vertical field coil currents. Author (revised)

N93-25227# National Inst. for Fusion Science, Nagoya (Japan).
DEMONSTRATION FOR NOVEL SELF-ORGANIZATION THEORY BY THREE-DIMENSIONAL MAGNETOHYDRODYNAMIC SIMULATION
Yoshiomi Kondoh (Gunma Univ., Japan.), Yasuo Hosaka (Gunma Univ., Japan.), and Jia-Ling Liang (Gunma Univ., Japan.) Mar. 1993 21 p Submitted for publication
(NIFS-212) Avail: CASI HC A03/MF A01

It is demonstrated by three-dimensional simulations for resistive magnetohydrodynamic (MHD) plasmas with both 'spatially nonuniform resistivity eta' and 'uniform eta' that the attractor of the dissipative structure in the resistive MHD plasmas is given by del x (eta)j) = (alpha/2)B which is derived from a self-organization theory based on the minimum dissipation rate profile. It is shown by the simulations that the attractor is reduced to del x B = (lambda)B in the special case with the 'uniform eta' and no pressure gradient. Author (revised)

N93-25248# National Inst. for Fusion Science, Nagoya (Japan).
TWO-STREAM INSTABILITY FOR A LIGHT ION BEAM-PLASMA SYSTEM WITH EXTERNAL MAGNETIC FIELD
T. Okada (Tokyo Univ. of Agriculture and Technology, Japan.) and H. Tazawa (Tokyo Univ. of Agriculture and Technology, Japan.) 3 Dec. 1992 14 p Submitted for publication
(NIFS-204) Avail: CASI HC A03/MF A01

For inertial confinement fusion, a focused light ion beam (LIB) is required to propagate stably through a chamber to a target. The applied external magnetic field is important for LIB propagation. To investigate the influence of the external magnetic field on the LIB propagation, the electrostatic dispersion relation of magnetized light ion beam-plasma system was analyzed. The particle in-cell (PIC) simulation results are presented for a light ion beam-plasma system with external magnetic field. Author (revised)

N93-25290 Maryland Univ., College Park.
ION TEMPERATURE MEASUREMENTS IN THE MARYLAND SPHEROMAK Ph.D. Thesis
Jean-Luc Gauvreau 1992 137 p
Avail: Univ. Microfilms Order No. DA9304323

Initial spectroscopic data from MS showed evidence of ion heating as deduced from the line widths of different ion species. Detailed measurements of O IV spectral emission line profiles in space and time revealed that heating takes place at early time, before spheromak formation and is occurring within the current discharge. The measured ion temperature is several times the electron temperature and cannot be explained by classical (Spitzer) resistivity. Classically, ions are expected to have lower temperatures than the electrons and therefore, lower temperatures than observed. High ion temperatures have been observed in different RFP's and Spheromaks but are usually associated with relaxation to the Taylor state and occur in the sustainment phase. During formation, the current delivered to start the discharge is not axisymmetric and as a consequence, X-points appear in the magnetic flux. A two dimensional analysis predicts that magnetic reconnection occurring at an X-point can give rise to high ion heating rates. A simple 0-dimensional calculation showed that within the first 20 microsec, a conversion of mass flow kinetic energy into ion temperature could take place due to viscosity. Dissert. Abstr.

N93-25302# New York Univ., New York. Inst. of Mathematical Sciences.
BOUNDARY PLASMA MODELLING FOR ITER
B. J. Braams Jan. 1993 9 p
(Contract DE-FG02-92ER-54165)
(DE93-007963; DOE/ER-54165/1) Avail: CASI HC A02/MF A01

Computer programs were developed to model the effect of nonaxisymmetric magnetic perturbations upon divertor heat load, and have explored what kind of externally applied perturbations are the most effective for heat load reduction without destroying core plasma confinement. We find that a carefully tuned set of coils located about 0.3 m outside the separatrix can be used to spread the heat load over about 0.1 m perpendicular to flux surfaces at the ITER divertor plate, even at a very low level of anomalous cross-field heat transport. As such a spreading would significantly extend the permissible regime of operation for ITER, it is recommended that this study be pursued at the level of detail required for engineering design. In other work under this grant, the B2 code is being modified to handle correctly a non-orthogonal geometry. DOE

N93-25324# California Univ., Berkeley. Lawrence Berkeley Lab.
METAL ION IMPLANTATION FOR LARGE SCALE SURFACE MODIFICATION
I. G. Brown Oct. 1992 21 p Presented at the 39th National Symposium of the American Vacuum Society, Chicago, IL, 9-13 Nov. 1992

(Contract DE-AC03-76SF-00098)
(DE93-007649; LBL-32203; CONF-921129-6) Avail: CASI HC A03/MF A01

Intense energetic beams of metal ions can be produced by using a metal vapor vacuum arc as the plasma discharge from which the ion beam is formed. A number of ion sources of this kind were developed and a metal ion implantation facility was built which can produce repetitively pulsed ion beams with mean ion energy up to several hundred keV, pulsed beam current of more than an ampere, and time averaged current of several tens of milliamperes delivered onto a downstream target. Also some preliminary work was done on scaling up this technology to very large size. For example, a 50-cm diameter (2000 cm(sup 2)) set of beam formation electrodes was used to produce a pulsed titanium beam with ion current over 7 amperes at a mean ion energy of 100 keV. Separately, a dc embodiment was used to produce a dc titanium ion beam with current over 600 mA, power supply limited, and up to 6 amperes of dc plasma ion current was maintained for over an hour. In a related program, a plasma immersion method was developed for applying thin metallic and compound films in which the added species is atomically mixed to the substrate. By adding a gas flow to the process, well-bonded compound films can also be formed; metallic films and multilayers as well as oxides and nitrides with mixed transition zones some hundreds of angstroms thick were synthesized. These parallel metal-plasma-based research programs are outlined and the hardware that was developed and some of the surface modification research that was done with it are described. DOE

N93-25346# National Inst. for Fusion Science, Nagoya (Japan).
THERMAL AND ELECTRIC OSCILLATION DRIVEN BY ORBIT LOSS IN HELICAL SYSTEMS
K. Itoh, H. Sanuki, and S.-I. Itoh (Kyushu Univ., Fukuoka, Japan.) Mar. 1993 22 p Submitted for publication
(NIFS-213) Avail: CASI HC A03/MF A01

Coupled oscillation of the radial electric field, the heating power, and the plasma temperature in helical systems is analyzed. This oscillation is caused by the influence of the radial electric field on the direct loss of injected fast ions. The damped oscillations of the radial electric field, temperature, and fast-ion loss are predicted. Conditions for the mode and the dependence of the frequency are discussed. Author (revised)

N93-25347# National Inst. for Fusion Science, Nagoya (Japan).
A COMPACT NEUTRON COUNTER TELESCOPE WITH THICK RADIATOR (Cotetra) FOR FUSION EXPERIMENT
M. Osakabe, S. Itoh (Nagoya Univ., Japan.), Y. Gotoh, M. Sasao, and J. Fujita Jan. 1993 33 p Submitted for publication
(NIFS-205) Avail: CASI HC A03/MF A01

A new type of neutron spectrometer, based on recoil proton measurement, was developed for diagnosing a DT fusion plasma. This spectrometer has such advantages as: (1) direct measurement of the neutron energy without the unfolding procedure, (2) relatively high detection efficiency for 14 MeV neutrons, (3) a wide dynamic range of counting rate, and (4) perfect n-gamma discrimination. To examine the performance of this spectrometer, a Monte Carlo simulation code was developed. It predicts that we may achieve energy resolution up to 3 percent with a detection efficiency of 10(exp -5) (count cm(sup 2)/n) if we could successfully adjust the condition of the spectrometer. A prototype spectrometer was constructed and was compared with the Monte Carlo prediction. The energy resolution of 5.3 plus or minus 0.7 percent for 14 MeV neutron was obtained for the prototype spectrometer and the calculation agrees with the experimental results within its margin of error if we take into account the intrinsic energy resolution of the detector that is used in the prototype.
Author (revised)

N93-25356# National Inst. for Fusion Science, Nagoya (Japan).
SIMULATION STUDY OF MHD DYNAMO: CONVECTION IN A ROTATING SPHERICAL SHELL
A. Kageyama (Hiroshima Univ., Japan.), K. Watanabe, and T. Sato Feb. 1993 46 p Submitted for publication Original contains color illustrations
(NIFS-207) Avail: CASI HC A03/MF A01

Numerical simulations on the thermal convection of a neutral fluid (without the magnetic field) in a rotating spherical shell have been performed. The results indicate that if the rotation is sufficiently rapid, the fluid results in a strong differential rotation where an equatorial acceleration is remarkable. The formation dynamics of convection columns aligned to the rotation axis is studied extensively. A new model of generation mechanism of the differential rotation is then proposed which concludes that the fluid motion generates an equatorial acceleration by selectively exciting the cyclonic columns in the spherical shell. Author

N93-25493# Oak Ridge National Lab., TN.
TSC PLASMA HALO SIMULATION OF A D3-D VERTICAL DISPLACEMENT EPISODE
R. O. Sayer, Y. K. M. Peng, S. C. Jardin (Princeton Univ., NJ.), A. G. Kellman, and J. C. Wesley (General Atomic Co., San Diego, CA.) Jan. 1993 35 p
(Contract DE-AC05-84OR-21400)
(DE93-008688; ORNL/TM-12281) Avail: CASI HC A03/MF A01

A benchmark of the Tokamak Simulation Code (TSC) plasma halo model has been achieved by calibration against a DIII-D vertical displacement episode (VDE) consisting of vertical drift, thermal quench, and current quench. Inclusion of a 1-to 4-eV halo surrounding the main plasma was found to be necessary to match simulation and experimental results for plasma current decay, trajectory, toroidal and poloidal vessel currents, and magnetic probe and flux loop values for the entire VDE. DOE

N93-25626# SRI International Corp., Menlo Park, CA.
DIAGNOSTICS OF DIAMOND FILM DEPOSITION PLASMAS Final Report, 19 Sep. 1989 - 18 Sep. 1992
Kenneth R. Stalder and Jay B. Jeffries Nov. 1992 20 p
(Contract DAAL03-89-K-0157)
(AD-A260866; SRI-MP-257; ARO-26959.5-PH) Avail: CASI HC A03/MF A01

Diagnostic methods were developed and applied toward understanding the gas phase processes occurring in diamond film deposition plasmas. Diagnostics were applied in plasma arcjet environments, hot filament systems, and in radio frequency plasma systems. The diagnostic methods included optical emission spectroscopy, surface Raman spectroscopy, scanning electron microscopy, laser-induced fluorescence, and surface analysis by laser ionization. The parameters that were measured included radical concentrations and temperatures, ground-state and excited-state temperatures of C2 and CH molecules, electron temperatures and energy distribution functions, ion densities, and the observation of acetylene and other hydrocarbon species. Some modeling and comparison of experimental results to model predictions were also performed. DTIC

N93-25641# Pennsylvania State Univ., University Park. Applied Research Lab.
STUDIES OF SEVERAL SMALL SEAWATER MHD THRUSTERS USING THE HIGH-FIELD SOLENOID OF MIT'S BITTER MAGNET LABORATORY Annual Report, 1 Feb. 1992 - 31 Jan. 1993
T. F. Lin, D. L. Aumiller, J. B. Gilbert, and M. J. Coslo Feb. 1993 100 p
(Contract N00014-89-J-1693)
(AD-A260645) Avail: CASI HC A05/MF A02

The performance of several small, seawater magnetohydrodynamic (MHD) thrusters was studied in a closed loop environment. Three different thrusters were designed, constructed, and evaluated. For the first time, videographic and photographic recordings of flow through MHD thrusters were obtained. The MHD induced flowrate, thrust, and mechanical efficiency was measured/calculated for each thruster at different combinations of electric current and magnetic field strength. Direct determination of thrust, and subsequently of efficiency were not possible. Therefore, the hydraulic resistance of each different thruster was correlated with flowrate. This information was used in conjunction with the measured MHD induced flowrate to calculate the thrust and efficiency of each thruster. Experimental results were repeatable. A theoretical model was developed to predict the performance of each thruster. The results of this model are presented for one thruster at several magnetic field strengths at various electric currents. These predictions corresponded well with the measured/calculated values of MHD induced flowrate and mechanical efficiency. Finally, several MHD thrusters with radically different configurations are proposed. DTIC

N93-25730 Glasgow Univ. (Scotland).
THE GENERATION OF LANGMUIR WAVES BY THICK TARGET ELECTRON BEAMS IN SOLAR FLARES Ph.D. Thesis
Kenneth George McClements 1987 183 p
Avail: Univ. Microfilms Order No. BRDX98127

This thesis is concerned with the generation of Langmuir waves by collimated beams of electrons. In Chapter 1 we review observations of solar flares across the electromagnetic spectrum. Particular emphasis is given to the impulsive phase, and to those observations which provide strong evidence for the existence of electron beams. Solar flare theory, insofar as it is pertinent to the original work of this thesis, is reviewed in Chapter 2. After briefly discussing models of primary energy release and particle acceleration, we consider in detail the theoretical interpretation of hard X-ray and microwave observations. In Chapter 3 we use the quasi-linear theory to determine the conditions required for the stability of a steady state electron beam propagating in the solar corona. The growth rate for electron plasma waves in a magnetized plasma is evaluated, with the electron distribution being given by an analytic solution of the linearized Fokker-Planck equation. A stability boundary in parameter space is determined, indicating that electron beams must be highly collimated at injection to be Langmuir unstable at any point in space. In Chapters 4 and 5 we investigate the quasi-linear dynamics of thick target electron beams, using a combination of analytical and numerical techniques. In Chapter 4, one dimensional quasi-linear equations are derived from the general three dimensional equations for an axisymmetric beam in a magnetized collisional plasma. Numerical computations of the thick target electron distribution and the associated Langmuir wave level are presented in Chapter 5. It is shown that the energy deposition rate and bremsstrahlung X-ray signature of a thick target beam are essentially unaffected by the presence of Langmuir turbulence. In Chapter 6 we consider Langmuir wave generation by a time dependent beam. It is shown that the steady state model remains valid if the electrons are injected on a time scale greater than about 1s. If the injection time scale is as short as 100ms, however, the energy density of Langmuir waves produced by a given instantaneous flux of electrons may be amplified by as much as an order of magnitude. In Chapter 7 we consider thick target beam relaxation in an inhomogeneous plasma, and the induced scattering of Langmuir waves on thermal ions.
Dissert. Abstr.

N93-25829 Alaska Univ., Fairbanks.
THE FORMATION AND CHARACTERISTICS OF E-REGION THIN IONIZATION LAYERS AT HIGH LATITUDES Ph.D. Thesis
William Albert Bristow 1992 186 p
Avail: Univ. Microfilms Order No. DA9303405

Thin layers of ionization are often observed in the E region ionosphere. The layers are 1 to 3 km in thickness and are of high density, often as high as 5 x 10(exp 5) cm(exp -3). The density of the layers is a large enhancement over the background density. The layers are primarily composed of metallic ions, which have long lifetimes and can accumulate to high densities. Thin ionization layers at mid-latitudes are formed by the action of neutral wind shears redistributing the background ionization. At high latitudes wind-shears are not as effective at the redistribution of ionization, and it is found that the high-latitude electric fields may cause layer formation. Here the mechanism for high-latitude layer formation is studied through numerical simulation and incoherent-scatter radar observations. A one-dimensional simulation examined high-latitude layer formation in detail, in particular it examined the effects of the direction of the electric field. It was found that thin ionization layers formed for electric fields directed in the north-west and south-west quadrants. The layers formed by electric fields in the south-west quadrant form at altitudes which are consistent with observations, while fields in the north-west quadrant resulted in layer altitudes which were higher than usually observed. It was also found that the neutral wind acting in concert with the electric field may affect the altitude and thinness of layers. The one-dimensional simulation was extended to a three-dimensional model of the polar cap ionosphere. The three dimensional simulation showed that large areas of thin ionization layers may form for widely varying geophysical conditions. Incoherent-scatter radar observations showed the presence of thin ionization layers on 12 out of 16 nights of observation. High-resolution spectral data showed that the average ion mass within the layers was higher than that in the background ionization, demonstrating the presence of heavy metallic ions. Concurrent observation of thin layers and electric fields showed layers present for field directions between 40 degrees and 140 degrees west of the magnetic north, which agrees with the simulation however the range of angles is more limited than was predicted. Antenna scanning observations examined the latitudinal extent of the layers, and found the layers were of a limited extent; the largest extent observed was about 200 km. Dissert. Abstr.

N93-25831 California Univ., Irvine.
DIRECT MEASUREMENT OF VELOCITY SPACE TRANSPORT IN A PLASMA Ph.D. Thesis
Jeffrey Henry Bowles 1992 156 p
Avail: Univ. Microfilms Order No. DA9306174

This work reports the direct measurement of velocity space transport in a plasma. Transport is interpreted in terms of diffusion and convection coefficients. These coefficients are compared to the Fokker-Planck coefficients for a fully ionized plasma. Measurements were made in a quiet (low fluctuation level) plasma and in a plasma with drift waves or broadband electrostatic ion cyclotron waves present. The measured coefficients agree with classical collision theory in the quiet plasma. Coefficients measured in the presence of fluctuations are generally larger and have different velocity dependences than those measured in a quiet plasma. Test particle distributions are created and interrogated using the method of optical tagging in a Q-machine plasma (T sub i = T sub e = 0.17 eV, 5 x 10(exp 8) less than or = n less than or = 8 x 10(exp 9) cm(exp -3)). The short time (much less than 90 deg collision time) relaxation of the test particle distribution function was measured as a function of density and temperature of the background plasma and as a function of the velocity of the test particle distribution. The values of the convection and diffusion coefficients were extracted from these measurements. Additionally, in the quiet plasma case, the relaxation of the test particle distribution was measured for a time that was a significant fraction of the 90 deg collision time. The short time coefficients were used to predict the long time shape of the distribution and this was compared to the measured distributions. The diffusion of the distribution was seen to be accurately predicted while the measurement of the convection suffered from experimental difficulties. The short-time relaxation of test-particle distributions was also measured in the presence of drift waves and EIC waves. Drift waves were destabilized by a density gradient across the plasma column. The EIC waves were created by the parametric decay of lower hybrid waves. Coefficients measured under these conditions were generally larger and had different velocity dependencies than those predicted classically.
Dissert. Abstr.

N93-26504# Los Alamos National Lab., NM.
COMPUTATIONAL MODELING OF MAGO AND OTHER MAGNETIZED TARGET FUSION CONCEPTS
I. R. Lindemuth, R. C. Kirkpatrick, R. E. Reinovsky, P. T. Sheehey, R. S. Thurston, and F. J. Wysocki 1993 9 p Presented at the 6th International Conference on Megagauss Magnetic Field Generation and Related Topics, Albuquerque, NM, 9-12 Nov. 1992
(Contract W-7405-eng-36)
(DE93-007354; LA-UR-93-0045; CONF-921133-18) Avail: CASI HC A02/MF A01

One possible way to obtain a preheated and magnetized plasma suitable for subsequent implosion is the 'MAGO' concept. The unique MAGO discharge consists of two chambers, with electrical current flowing in one chamber accelerating plasma flow into an implosion chamber. Up to 4 x 10(sup 13) D-T neutrons have been produced in the MAGO discharge. In this paper, we discuss our computational modeling of MAGO. Our objectives are to characterize the plasma, compare with the limited diagnostics available, and to understand the neutron production. We also discuss, briefly, some other possible means for creating a magnetized plasma.
DOE

N93-26512# Los Alamos National Lab., NM.
SENSITIVITY OF MAGNETIC FLUX COMPRESSION IN CYLINDRICAL IMPLOSIONS TO MODEL PARAMETERS
C. Lund, M. Sheppard, J. Brownell, C. M. Fowler, and B. Freeman 1992 10 p Presented at the 6th International Conference on Megagauss Magnetic Field Generation and Related Topics, Albuquerque, NM, 9-12 Nov. 1992
(Contract W-7405-eng-36)

(DE93-003819; LA-UR-92-3712; CONF-921133-8) Avail: CASI HC A02/MF A01

The ultra-high magnetic fields produced by cylindrical implosions are expected to be of increasing interest for solid state physics applications, plasma compression for fusion, and isentropic compression of condensed matter. Calculated one-dimensional time-dependent radius and magnetic field behavior during the compression process will depend on the descriptions of material equations of state, conductivities, strength of materials, high-explosive type and model, temperature, geometric dimensions of the implosion system, and the numerical models. The influence of some these parameters on calculations of the magnetic field and liner properties is described in this paper. DOE

N93-26520# Ohio State Univ., Columbus. Research Foundation.
IR AND FIR LASER DIAGNOSTICS FOR PLASMA THRUSTERS USING A CW CO2 RADIATION SOURCE Final Report
Thomas M. York Nov. 1992 52 p
(Grant AF-AFOSR-0201-91)
(AD-A261399) Avail: CASI HC A04/MF A01

This research involves diagnostic studies of plasma thrusters. This effort will use the new, high resolution diagnostic techniques that will determine electron densities, local magnetic fields, and density fluctuations indicating anomalous transport. DTIC

N93-26528# National Inst. of Standards and Technology, Boulder, CO. Time and Frequency Div.
LIQUID AND SOLID ION PLASMAS Annual Report, 1 Oct. 1991 - 31 Sep. 1992
D. J. Wineland and J. J. Bollinger 22 Oct. 1992 9 p
(Contract N00014-92-F-0038)
(AD-A261888) Avail: CASI HC A02/MF A01

Atomic ions which are stored in electromagnetic fields are an example of nonneutral plasmas. Laser techniques allow control of plasma angular momentum and provide plasma cooling to temperatures much less than 1 K. Using imaging techniques, plasma spatial information is achieved. Laser spectroscopic techniques allow measurement of plasma velocity distribution functions. Liquid and solid behavior of ion plasmas is studied. DTIC

76 SOLID-STATE PHYSICS

Includes superconductivity.

For related information, see also *33 Electronics and Electrical Engineering* and *36 Lasers and Masers.*

N93-24953# Midwest Research Inst., Golden, CO. National Renewable Energy Lab.
FUNDAMENTAL STUDIES OF DEFECT GENERATION IN AMORPHOUS SILICON ALLOYS GROWN BY REMOTE PLASMA-ENHANCED CHEMICAL-VAPOR DEPOSITION (REMOTE PECVD) Annual Report, 1 Sep. 1990 - 31 Aug. 1991
G. Lucovsky (North Carolina State Univ., Raleigh.), R. J. Nemanich (North Carolina State Univ., Raleigh.), J. Bernholc (North Carolina State Univ., Raleigh.), J. Whitten (North Carolina State Univ., Raleigh.), C. Wang (North Carolina State Univ., Raleigh.), B. Davidson (North Carolina State Univ., Raleigh.), M. Williams (North Carolina State Univ., Raleigh.), D. Lee (North Carolina State Univ., Raleigh.), C. Bjorkman (North Carolina State Univ., Raleigh.), and Z. Jing (North Carolina State Univ., Raleigh.) Jan. 1993 58 p Prepared in cooperation with North Carolina State Univ., Raleigh, NC
(Contract DE-AC02-83CH-10093)
(DE92-010560; NREL/TP-451-4852) Avail: CASI HC A04/MF A01

We demonstrated that the remote PECVD process can be used to deposit heavily doped n-type and p-type a-Si:H thin films. We optimized conditions for depositing undoped, near-intrinsic and heavily doped thin films of micro-c(microcrystalline)-Si by remote PECVD. We extended the remote PECVD process to the deposition of undoped and doped a-Si,C:H and micro-c-Si,C alloy films. We analyzed transport data for the dark conductivity in undoped and doped a-Si:H, a-Si,C:H, micro-c-Si and micro-c-Si,C films. We studied the properties of doped a-Si:H and micro-c-Si in MOS capacitors using approximately 10 Omega-cm p-type crystalline substrates and thermally grown SiO2 dielectric layers. We collaborated with a group at RWTH in Aachen, Germany, and studied the contributions of process induced defect states to the recombination of photogenerated electron pairs. We applied a tight-binding model to Si-Bethe lattice structures to investigate the effects of bond angle, and dihedral angle disorder. We used ab initio and empirical calculations to study non-random bonding arrangements in a-Si,O:H and doped a-Si:H films. DOE

N93-24958# Sandia National Labs., Albuquerque, NM.
PHOTOLUMINESCENCE OF SILICON NANOSTRUCTURES FORMED BY ION BEAM IMPLANTATION
D. A. Redman, D. M. Follstaedt, T. Guilinger, and M. Kelly 1992 7 p Presented at the 16th Material Research Society International Symposium on the Scientific Basis for Nuclear Waste Management, Boston, MA, 30 Nov. - 5 Dec. 1992
(Contract DE-AC04-76DP-00789)
(DE93-006777; SAND-92-1487C; CONF-921101-86) Avail: CASI HC A02/MF A01

A new method was used to fabricate nanometer-scale structures in Si for photoluminescence (PL) studies. He ions were implanted to form a dense subsurface layer of small cavities (1-8 nm diameters). The implanted specimens were either annealed in H or anodized with HF to evaluate the quantum confinement model for PL from porous Si. Incomplete passivation apparently prevented PL in the H-annealed specimens. Implantation combined with anodization produced a substantial blue shift relative to anodization alone, which is consistent with quantum confinement. DOE

N93-25108*# Maryland Univ., College Park.
STUDYING THE KINETICS OF MAGNETIZATION IN HIGH Tc SUPERCONDUCTORS Final Report
Marina Turchinskaya 8 Feb. 1993 11 p
(Grant NAG5-1890)
(NASA-CR-192916; NAS 1.26:192916) Avail: CASI HC A03/MF A01

The first microscopic maps of magnetic induction in YBa2Cu3O(7-x) crystals which directly show the dependence of flux flow on twin density and polytwin block and twin boundary orientation are reported. These maps were obtained by means of a recently-improved magneto-optical imaging technique. Pinning was lowest in untwinned regions and increased with increasing twin density. An isotropy in twin boundary pinning, defined as the ratio of the magnetic induction gradient across twin boundaries to that along twin boundaries, was 10 at 17 K; this ratio increased with increasing temperature. In polycrystals, twin boundaries also had a strongly anisotropic effect on flux flow into a grain from a grain boundary. Author (revised)

N93-25163# Midwest Research Inst., Golden, CO. National Renewable Energy Lab.
RESEARCH ON STABLE, HIGH-EFFICIENCY AMORPHOUS SILICON MULTIJUNCTION MODULES
M. Ghosh, J. DelCueto, J. Xi, and F. Kampus Feb. 1993 13 p Prepared in cooperation with Advanced Photovoltaic Systems, Princeton, NJ
(Contract DE-AC02-82CH-10093)
(DE93-000072; NREL/TP-411-5327) Avail: CASI HC A03/MF A01

Results from the first phase of a three-phase contract for the development of stable, high-efficiency, same-band-gap, amorphous silicon (a-Si) multijunction photovoltaic (PV) modules are described. The program involved improving the properties of individual layers of semiconductor and non-semiconductor materials and small-area single-junction and multijunction devices, as well as the multijunction modules. The semiconductor materials research was performed on a-Si p, i, and n layers, and on microcrystalline silicon n layers. These were deposited using plasma-enhanced chemical vapor deposition. The non-semiconductor materials studied were tin oxide, for use as a transparent-conducting-oxide (TCO), and zinc oxide, for use as a back reflector and as a buffer layer between the TCO and the semiconductor layers. Tin oxide was deposited using atmospheric-pressure chemical vapor deposition. Zinc oxide was deposited using magnetron sputtering. The research indicated that the major challenge in the fabrication of a-Si multijunction PV modules is the contact between the two p-i-n cells. A structure that has low optical absorption but that also facilitates the recombination of electrons from the first p-i-n structure with holes from the second p-i-n structure is required. Non-semiconductor layers and a-Si semiconductor layers were tested without achieving the desired result. DOE

N93-25219*# Clemson Univ., SC. Dept. of Ceramic Engineering.
DEVELOPMENT OF HIGH Tc (GREATER THAN 100 K) Bi, Tl AND Y-BASED MATERIALS AS SUPERCONDUCTING CIRCUIT ELEMENTS Annual Report, Feb. 1992-1993
Gene Haertling, Gregory Grabert, and Phillip Gilmour 31 Mar. 1993 107 p
(Grant NAG1-1108)
(NASA-CR-192344; NAS 1.26:192344) Avail: CASI HC A06/MF A02

Results on this project over the past three years have shown that the Bi and Tl-based superconducting materials in bulk form are noticeably different from the Y-based 123 material in that superconductivity is considerably harder to achieve, maintain and reproduce. This is due primarily to the difficulty in obtaining the higher Tc phase in pure form since it commonly co-exists with other undesirable, lower Tc phases. In particular, it has been found that long processing times for calcining and firing (20 - 200 hrs.) and close control of temperatures which are very near the melting point are required in order to obtain higher proportions of the desirable, high Tc (2223) phase. Author

N93-25225*# Alabama Univ., Huntsville. Dept. of Physics.
FNAS COMPUTATIONAL MODELING Final Report No. 4, 18 Aug. 1992 - 17 Feb. 1993
J. R. Franz 17 Feb. 1993 11 p
(Contract NAS8-38609)
(NASA-CR-192512; NAS 1.26:192512) Avail: CASI HC A03/MF A01

Numerical calculations of the electronic properties of liquid II-VI semiconductors, particularly CdTe and ZnTe were performed. The measured conductivity of these liquid alloys were modeled by assuming that the dominant temperature effect is the increase in the number of dangling bonds with increasing temperature. For low to moderate values of electron correlation, the calculated conductivity as a function of dangling bond concentration closely follows the measured conductivity as a function of temperature. Both the temperature dependence of the chemical potential and the thermal smearing in region of the Fermi surface have a large effect on calculated values of conductivity. Author (revised)

N93-25265 Lehigh Univ., Bethlehem, PA.
QUANTUM CONDUCTANCE FLUCTUATIONS IN SELF-ALIGNED, PINCH-NARROWED MOSFETs Ph.D. Thesis
David Allen Slimmer 1992 96 p
Avail: Univ. Microfilms Order No. DA9302834

We have investigated transport phenomena in pinch-narrowed p-channel accumulation mode metal-oxide-semiconductor field-effect-transistors (MOSFETs). The devices were fabricated using a conventional twin well complementary MOS process with gate widths of order 1.3 microns. Biasing the pinch electrodes was found to be an effective means for changing the dimensions of the conducting channel. Measurements with these devices have been made at temperatures down to 0.75 K and in magnetic fields up to 8 Tesla. At temperatures below 8 K, we observe fluctuations from ordinary linear MOSFET behavior in the channel conductance as a function of gate voltage. These fluctuations, the well known signature of quantum phenomena in mesoscopic systems, are aperiodic and reproducible between thermal cycling. Similar observations have been reported in n-channel systems of comparable design, but with the pinch regions formed with diffusion over 1 micron. The n(+) pinch electrodes in these devices are anticipated to produce uniform channel widths because they were ion implanted with the gate structure serving as the mask. These are also the first observations of mesoscopic conductance fluctuations in p-channel systems. We calculate the expected magnitude of the variations according to the theory of universal conductance fluctuations from measured device parameters. A technique has been constructed in order to extract fluctuations due to the constriction based upon the effective channel dimensions and the total device conductance. The values we obtain for the fluctuation amplitudes and correlation ranges in Fermi energy are in good agreement with the theoretical predictions. Dissert. Abstr.

N93-25362# Ames Lab., IA.
RHEOLOGY OF YBa2Cu3O(7-x) PRECURSORS
Timothy M. Green and Mufit Akinc 1992 5 p Presented at the Symposium on Rheology of Dense Suspensions, Boston, MA, 30 Nov. - 4 Dec. 1992
(Contract W-7405-eng-82)
(DE93-007285; IS-M-745; CONF-9211189-1) Avail: CASI HC A01/MF A01

Nitrate and acetate precursors to YBa2Cu3O(7-x) (123) are prepared using a molten salt technique. The viscosity and shear stress of the paste are controlled by evaporation of water from the paste. The pastes contain approximately 20-80 vol. percent solids. Rheometry over strain rates of 0-200 sec(exp -1) shows both systems are shear-thinning. Both systems are thixotropic. The nitrate system may be described by a two-stage Bingham Plastic model, the acetate by a Hershel-Bulkley model. The existence of more than one region of flow behavior suggests that there are at least two mechanisms which contribute to flow. In the low strain rate region, flow resistance is due to the existence of flocs in the colloidal assembly. At higher strain rates, flow is probably controlled by interlaminar drag interactions. Precursors produced by both methods have been used to form fibers of YBa2Cu3O(7-x), by ram extrusion. DOE

N93-25367# California Univ., Berkeley. Lawrence Berkeley Lab.
CORRELATED WAVEFUNCTION QUANTUM MONTE CARLO APPROACH TO SOLIDS
S. G. Louie Oct. 1992 13 p Presented at the 15th Taniguchi International Symposium on Condensed Matter Theory, Kashikojima, Japan, 19-23 Oct. 1992
(Contract DE-AC03-76SF-00098)
(DE93-007730; LBL-33057; CONF-9210314-1) Avail: CASI HC A03/MF A01

A method for calculating the electronic and structural properties of solids using correlated wavefunctions together with quantum Monte Carlo techniques is described. The approach retains the exact Coulomb interaction between the electrons and employs a many-electron wavefunction of the Jastrow-Slater form. Several examples are given to illustrate the utility of the method. Topics discussed include the cohesive properties of bulk semiconductors, the magnetic field induced Wigner crystal in two dimensions, and the magnetic structure of bcc hydrogen. Landau level mixing is shown to be important in determining the transition between the fractional quantum Hall liquid and the Wigner crystal. Information on electron correlations such as the pair correlation functions which are not accessible to one-electron theories is also obtained. DOE

N93-25369# Argonne National Lab., IL.
MAGNETIC EXCITATIONS IN ANTIFERROMAGNETICALLY COUPLED SUPERLATTICES: Fe/Mo AND Fe/Cr
M. Grimsdtich, S. Kumar, and E. E. Fullerton Jan. 1993 10 p Presented at the 7th Latin-American Symposium on Surface Science, Bariloche, Argentina, 14-21 Nov. 1992
(Contract W-31-109-eng-38)
(DE93-007894; ANL/MSD/CP-78798; CONF-9211193-2) Avail: CASI HC A02/MF A01

We report the results of a Brillouin light scattering (BLS) study of magnetic excitations in antiferromagnetically (AF) coupled Fe/Mo and Fe/Cr superlattices. This technique, already having been applied to AF coupled tri-layer films, shows that these systems reflect coupling (ferromagnetic and antiferromagnetic) between ferromagnetic layers. However, since in ordinary magnetic superlattices, new collective modes exist resulting from dipolar coupling of the ferromagnetic layers, it could be expected that these new antiferromagnetic systems will also show novel behavior. Only the magnetization and BLS results are presented and discussed. DOE

N93-25387# Sandia National Labs., Albuquerque, NM.
METASTABLE SiC AND SiGeC ALLOYS BY CARBON IMPLANTATION AND SOLID PHASE EPITAXY
J. W. Strane, W. J. Edwards (Cornell Univ., Ithaca, NY.), J. W. Mayer (Arizona State Univ., Tempe.), H. S. Stein, S. R. Lee, B. L. Doyle, and S. T. Picraux 1992 4 p Fall Meeting of the 16th Material Research Society Internation Symposium on the Scientific Basis for Nuclear Waste Management held in Boston, MA, 30 Nov. - 5 Dec. 1992
(Contract DE-AC04-76DP-00789)
(DE93-007594; SAND-92-1617C; CONF-921101-89) Avail: CASI HC A01/MF A01

We demonstrate the formation of metastable Si(1-y)C(y) and Si(1-y-x)Ge(x)C(y) alloys by C ion implantation and solid phase epitaxial regrowth. Carbon was introduced into Si and SiGe layers by 5, 12, and 25

keV implants to achieve nearly uniform profiles of 0.7 and 1.4 at. percent C. The 0.7 at. percent C specimens exhibit the highest quality epitaxial layers after SPE regrowth, whereas in higher C concentration specimens solid phase regrowth was impeded. The localized vibrational mode of C occupying substitutional lattice sites in the diamond lattice provides a signature of the metastable phase and is used to monitor the loss of stability due to precipitation of silicon carbide. The SiC and SiGeC alloys retained substitutional carbon during 30 minute isochronal anneals up to 850 C. DOE

N93-25454# Royal Signals and Radar Establishment, Malvern (England).
LASER INDUCED PHONONS (LIPs) IN MBE GROWN ZnSe
K. Welford Oct. 1991 15 p
(RSRE-Memo-4544; BR307779) Copyright Avail: CASI HC A03/MF A01

Thin film ZnSe, grown by the MBE method, has been examined using the technique of degenerate four wave mixing, DFWM, using laser illumination at 532 nm. Laser induced phonons are observed in this thin film material but are not seen in a sample of bulk polycrystalline ZnSe. This observation of laser induced phonons is the first reported in ZnSe. Author

N93-25490# California Univ., Berkeley. Lawrence Berkeley Lab.
THE DX CENTERS IN THREE TO FIVE SEMICONDUCTORS UNDER HYDROSTATIC PRESSURE Ph.D. Thesis
J. A. Wolk Nov. 1992 176 p
(Contract DE-AC03-76SF-00098)
(DE93-007701; LBL-33379) Avail: CASI HC A09/MF A02

The DX centers are deep level defects found in some 3-5 semiconductors. They have persistent photoconductivity and large difference between thermal and optical ionization energies. Hydrostatic pressure was used to study microstructure of these defects. A new local vibrational mode (LVM) was observed in hydrostatically stressed, Si-doped GaAs. Corresponding infrared absorption peak is distinct from the Si(sub Ga) shallow donor LVM peak, which is the only other LVM peak observed in our samples, and is assigned to the Si DX center. Analysis of the relative intensities of the Si DX LVM and the Si shallow donor LVM peaks, combined with Hall effect and resistivity indicate that the Si DX center is negatively charged. Frequency of this new mode provides clues to the structure of this defect. A pressure induced deep donor level in S-doped InP was also discovered which has the properties of a DX center. Pressure at which the new defect becomes more stable than the shallow donor is 82 kbar. Optical ionization energy and energy dependence of the optical absorption cross section was measured for this new effect. The capture barriers from the conduction band into the DX state were also determined. That DX centers can be formed in InP by pressure suggests that DX states should be common in n-type 3-5 semiconductors. A method is suggested for predicting under what conditions these defects will be the most stable form of the donor impurity. DOE

N93-25503# Missouri Univ., Columbia. Research Reactor Facility.
INELASTIC SCATTERING IN CONDENSED MATTER WITH HIGH INTENSITY MOESSBAUER RADIATION
W. B. Yelon and G. Schupp Feb. 1993 34 p
(Contract DE-FG02-85ER-45200)
(DE93-008763; DOE/ER-45200/T2) Avail: CASI HC A03/MF A01

The QUEGS facility at MURR has produced a number of new results and demonstrated the range of potential applications of high resolution, high intensity Moessbauer scattering. This work has been carried out by both MU and Purdue researchers and includes published results on Na, W, pentadecane, polydimethylsiloxane and other systems, manuscripts submitted on alkali halides (Phys. Rev. B) and accurate Moessbauer lineshape measurements (Phys. Rev. C), and manuscripts in preparation on glycerol, NiAl and Moessbauer spectra obtained by modulating a scattering crystal. Recently, new collaborations have been initiated which will substantially enhance our efforts. These are with W. Steiner (Vienna), G. Coddens (Saclay), and R. D. Taylor (Los Alamos). Steiner is experienced with Fe-57 Moessbauer scattering, while Coddens specializes in quasielastic neutron scattering; both of these areas naturally complement our work. R. D. Taylor has pioneered Moessbauer spectroscopy from the time of its discovery and has already made important contributions to our study of lattice dynamics and superconductivity for lead alloyed with small quantities of tin. At the same time, a significant instrument upgrade is underway, funded in part by the DOE-URIP program. DOE

N93-25506# Westinghouse Savannah River Co., Aiken, SC.
ENVIRONMENTAL TEST PROGRAM FOR SUPERCONDUCTING MATERIALS AND DEVICES
H. Randolph and D. Verebelyi 1992 24 p
(Contract DE-AC09-89SR-18035)
(DE93-003646; WSRC-TR-91-673) Avail: CASI HC A03/MF A01

The properties of YBa2Cu3O(7-x) superconducting tapes designed and fabricated into SAFIRE-type, encapsulated, grounding links by the Ceramic Engineering Department at Clemson University were investigated. Testing at the Savannah River Site included gamma irradiation, vibration, magnetic field, and long-term evaluation. Irradiation and vibration did not change the physical or electrical properties of the tested samples. An applied magnetic field of 1000 Gauss increased the superconduction resistance and invoked semiconductor electrical properties of some samples. The long-term testing began in January 1991 and resistance data showed no increases. No gaseous decomposition has been found. DOE

N93-25528 Florida State Univ., Gainesville.
THERMODYNAMIC, KINETIC, AND STRUCTURAL PROPERTIES OF LINEAR POLYETHYLENE CRYSTALLIZED FROM POLYMER-DILUENT MIXTURE Ph.D. Thesis
Lida Lu 1992 228 p
Avail: Univ. Microfilms Order No. DA9303354

The crystallization behavior in the extremes of crystallization of pure polymer and from dilute solution have been extensively studied. However, studies over the intervening concentration range are very sparse. Therefore, studies have been carried out toward the structural properties, morphology and crystallization kinetics of polyethylene crystallized from solution, over a wide concentration range (from dilute to pure polymer), and a wide range of molecular weights (from low to very high molecular weight) using many analytical techniques. By the use of Raman spectroscopy, the phase structure of the three major regions of crystalline polymer, i.e., the ordered crystalline region, the disordered liquid-like interlamellar region, and the interfacial region, has been examined. The major parameters obtained are the thicknesses and mass fraction of the three regions. The mass fraction of ordered crystalline region showed a sharp increase in the range of 10-20 percent polymer concentration, and the mass fraction of interfacial region showed a sharp drop at a similar concentration. It is shown that chain entanglements play a very important role in determining the final structure crystallized from solution. The entanglement effect on the interfacial structure is very significant. When entanglements are trapped in the interphase, the amount of tight adjacent chain folds is reduced, and the interfacial thickness and the interfacial free energy increase. Studies of crystallization kinetics, over the large composition and molecular weight range also reveal the influence of entanglements and a correlation with resulting properties. The crystallization behavior in concentrated solution differs from that in dilute solution because of the entanglement effect. The supermolecular structure developed are very sensitive to the polymer concentration and molecular weight. Significant changes take place in the morphological map with dilution. Very high molecular weights, which from randomly oriented lamellar structure in the melt, can develop spherulitic structure in solution. Under particular conditions of composition, molecular weight and temperature very large polyethylene spherulites develop. Dissert. Abstr.

N93-25655# Pennsylvania State Univ., University Park. Dept. of Electrical and Computer Engineering.
ADAPTIVE LIQUID CRYSTAL TV BASED JOINT TRANSFORM CORRELATOR AS APPLIED TO REAL-TIME PATTERN RECOGNITION Final Report, 15 Apr. 1991 - 14 Dec. 1992
Francis T. Yu 5 Jan. 1993 172 p
(Contract DAAL03-91-G-0112)
(AD-A260724; ARO-28502.1-PH) Avail: CASI HC A08/MF A02

The primary goal of this research is to study a programmable joint-transform correlator (JTC) using liquid crystal television (LCTV) panels for adaptive realtime pattern recognition applications. The technique can improve the pattern recognition and identification technology that is of interest to the U.S. Army. The technique we studied is a real-time programmable electro-optical architecture. There are several reasons for selecting the optical technique over their digital and electronic counterparts,

as follows: Optical technique is capable of handling a large space-bandwidth image; optical technique is capable of performing parallel operations; optics can perform massive interconnections; optical transformation can be operated at high speed, etc. By using the LCTV, the pattern under observation can be correlated with a large number of recallable image memories. In addition, the LCTV technique is rather simple and economical to operate. The LCTV-optical correlator, in principle, can be designed into a compact portable form for in situ application. Brief outlines of the major research findings and publications are provided in this report. DTIC

N93-25667*# Houston Univ., TX. Inst. for Beam Particle Dynamics.
AEROSPACE DEVICES FOR MAGNETIC REPLICAS Final Report
Roy Weinstein 1 May 1993 67 p
(Grant NAG9-592)
(NASA-CR-192958; NAS 1.26:192958) Avail: CASI HC A04/MF A01

Retained persistent magnetic field has been studied and improved in the superconductor YBa2Cu3O7 (Y123). During the study, trapped magnetic field, B(t), has been increased by over a factor of 10(exp 5). Methods used to improve magnetic field trapping were principally: (1) the adoption of the Melt Texturing process to increase grain size; (2) the addition of excess Y to disperse deposits of Y2BaCuO5 (Y211) and again increase grain size; (3) irradiation with high energy particles including 1H+, 3He++, 4He++, and fission fragments; and (4) utilizing temperatures below 77 K has also been quantified as a way to increase trapped field. In addition, in our study of B(t), we have found laws governing creep, activation, temperature dependence, creep vs. current flow, etc. In the range 20 K less than or equal to T less than or equal to 65 K, and for B less than 10 Tesla, a simple empirical relationship was found: B(trap) (T2) = B(trap) (T1) ((Tc - T2)/(Tc - T1))squared where Tc is the critical temperature. The highest experimental trapped field was B(trap) = 3.96 Tesla, at 65 K. We believe this to be the highest persistent field ever produced, by any method. A two component model of the persistent currents has been developed. This accurately reproduces the data, using as parameters only the magnitude of a constant surface current, J(s), and a constant volume current J(v). The model successfully predicts B(t) (xyz) for the case of maximum trapped field, for all samples observed. It has also been extended to describe the unsaturated case either zero field cooled, or field cooled. Loss of strap with time has been studied for the critical state (Bt,max), and non critical state (Bt less than Bt,max), for times from a few minutes to a few months, for unirradiated material, for irradiation by 1H+, 3He++, 4He++, high z projectiles, and neutrons, and for all materials used in the overall study. We conclude that: (1) multi Tesla trapped fields are attained; (2) fields over 10 T are achievable; (3) creep is not a large problem; (4) application is feasible to motors, generators, magnets for particle beam optics, separators, levitating bearings, energy storage, shielding, and transportation. Author (revised)

N93-25703 State Univ. of New York, Buffalo.
ELECTRIC FIELD EFFECTS ON QUANTUM-CONFINED SEMICONDUCTOR STRUCTURES Ph.D. Thesis
Byungsu Yoo 1992 275 p
Avail: Univ. Microfilms Order No. DA9301926

Effects of electric field on quantum well systems have been studied by FIR magneto-spectroscopy. Two systems have been investigated; One is an external electric field applied to the QW's system doped with shallow donors in the wells. In this case the effect of the electric field with the shallow impurities confined in quantum wells was determined. A p-'i'-n diode structure was used to produce the controllable electric field, and the states of donors doped in the well center were monitored by far-infrared magnetospectroscopy. A broadened, impurity-related peak is observed, which changes significantly both in shape and in position with electric field. In order to provide a basis for interpretation of the experimental data, a variational calculation was carried out for the low lying energy states of an effective-mass electron in the presence of an electric field at zero magnetic field. Also the absorption line profile that incorporates the impurity distribution within the well was calculated for comparison with experiment. Observed shifts of the position of the minimum are in good agreement with the variational calculation. The observed line-shape evolution with increasing electric field is explained by considering the impurity distribution in the well. With a rectangular distribution displaced by about 30A along the growth direction, qualitative agreement with experiment is obtained. The second case considered is that of built-in electric fields in strained-layer superlattices (SLS's). Significant strain-induced electric fields are known to occur in (111)-oriented strained-layer superlattices. Hole cyclotron resonance was observed in both nominally undoped InGaAs/AlGaAs SLS samples. Magnetoreflectivity spectra show features whose magnetic field dependence demonstrates their excitonic origin. A doublet structure observed in the reflectivity spectra is correlated with Landau-level-confinement-subband coupling experiments in cyclotron resonance (CR) in a tilted magnetic field which gives a subband separation of 11 meV. Hall measurements were performed to verify that CR was due to holes. To provide a basis for interpretation, subband energy separations and interband energy separations are calculated as a function of electric field. The parameter combinations are varied to fit to the observed experimental data. A perturbation method was used to calculate the energy splitting in the Landau-level-confinement-subband coupling experiments. Finally, from these calculations and comparison with experiments the strength of the built-in electric field was estimated on one of the SLS sample. The obtained value (3 x 10(exp 4)V/cm) is substantially smaller than predicted (approx. 1 x 10(exp 5)V/cm) from the piezoelectric coefficients and strain expected from pseudomorphic growth. Dissert. Abstr.

N93-25715 Illinois Univ. at Urbana-Champaign, Savoy.
TRANSMISSION ELECTRON MICROSCOPY INVESTIGATION OF ION IMPLANTATION DAMAGE IN GaAs AND OTHER SEMICONDUCTORS Ph.D. Thesis
Michael Wayne Bench 1992 189 p
Avail: Univ. Microfilms Order No. DA9305465

The crystalline-to-amorphous transition induced by ion implantation was investigated in GaAs and GaP using transmission electron microscopy. The experiments included those performed in situ using the HVEM-Tandem Accelerator Facility at Argonne National Laboratory and also those performed using high-resolution TEM. The implantations were made with Ar+, Kr+, Xe+, and Au+ ions (energy 50 or 80 keV) at 30 and 300 K. The high-resolution experiments confirmed the amorphous nature of the damage produced in individual displacement cascades. The in situ experiments at 30 K showed that amorphous zones are produced within isolated cascades with high probability. It was found that the efficiency of production of amorphous damage increases with increasing ion mass. The probability that an individual cascade will generate an amorphous region decreases when the implantation is performed at room temperature in GaAs but remains the same for GaP. Annealing experiments in the 30-300 K range demonstrated that there is significant damage recovery below 300 K in GaAs but none in GaP. Calculations of the energy density deposited in the cascades, determined through Monte-Carlo simulations, suggest that the formation and subsequent quenching of a molten zone may be responsible for the production of the amorphous damage. In addition to the experiments on damage production, electron beam induced recrystallization of isolated amorphous zones was investigated in GaAs, GaP, Si, and Ge. Regrowth was induced in all materials at electron energies below the threshold displacement energy. However, a minimum energy threshold was found only in Si. Results in the other three materials, particularly Ge, suggest that beam-induced ionization may be playing a role in the solid-phase epitaxial regrowth process in each of those materials. Dissert. Abstr.

N93-25744 Stanford Univ., CA.
ANALYSIS OF THE GAP IN HIGH-TEMPERATURE SUPERCONDUCTORS USING PHOTOEMISSION SPECTROSCOPY Ph.D. Thesis
Barrett Otis Wells 1992 144 p
Avail: Univ. Microfilms Order No. DA9302335

The discovery of the cuprate superconductors had led to intensive research activity aimed at discovering the mechanism of high temperature superconductivity. A key feature in the electronic structure of a superconductor is the energy gap in the excitation spectrum. While gaps have been detected in the cuprate superconductors, traditional techniques for measuring the gap often give confusing or inconsistent results. The high transition temperatures and correspondingly large gaps of the cuprate superconductors have allowed photoemission spectroscopy to be used for the first time as a technique for studying the superconducting gap. Advantages of photoemission include that is is a direct measure of the gap, the surface studied is by necessity a clean, well defined region with variable depth, and the gap can be measured as a function of position in

k-space. The largest disadvantage of photoemission as tool for studying the gap is that the best resolution available so far is only on the order of the gap size. This makes a determination of gap size difficult. We have used photoemission to study the behavior of the gap near the surface of Bi2Sr2CaCu2O(8 + delta) and its variation as a function of k position. We have found that the gap does not diminish near the surface, an indication of the highly two dimensional nature of these materials. Our photoemission experiment has shown no evidence of a proximity effect in a metal overlayer. We have also found that the gap is anisotropic in k space within the planes themselves. In particular, by measuring how the gap varies with k, we can gain information on the symmetry of the gap function. Our data is consistent with a mixed s+id symmetry gap and possibly with a pure d wave gap. Determining the symmetry of the gap provides one of the most stringent experimental constraints on the theory of high T(sub c) superconductivity yet found. We compare our result with other experiments which measure the gap in order to attempt to provide a complete and consistent picture of what is presently known of the behavior of the superconducting gap in cuprate superconductors. Dissert. Abstr.

N93-25749 Harvard Univ., Cambridge, MA.
CRACK TIP FIELDS IN DUCTILE CRYSTALS AND BICRYSTALS Ph.D. Thesis
Maryam Saeedvafa 1992 167 p
Avail: Univ. Microfilms Order No. DA9228274

Crack tip fields are analyzed in order to explain fracture processes in ductile crystals. The focus is to understand the stress and deformation fields, and cracking mechanisms. Both asymptotic and finite element models based on continuum plasticity for single crystals are used. The ductility of interfacial in sigma-9 copper bicrystals has been observed experimentally to depend on the cracking direction, with the (114) being the brittle cracking direction and the (114) the ductile one. Although the continuum plasticity solutions given here show that the tensile stresses ahead of the crack is essentially identical for the two cracking directions, the overall plastic zone size is much larger in the ductile case. Also, the orientations of the zones of concentrated shearing ahead of the crack, observed in the ideally plastic model, suggest two different dislocation shearing mechanisms. Analysis of the crack tip field for an ideally plastic NiAl single crystal which has only 3 independent slip systems at room temperature (the (100) /100/ systems), shows that the stress field has a lnr type singularity, with a shearing discontinuity at 90 degrees. The largest zone over which the stresses on either (110) /111/ or (112) /111/ systems exceeds the critical resolved shear stress on the (110) /100/ system is of the same order as the plastic zone site, although very close to the crack tip the stresses on some of these systems become significant due to the stress singularity, and thus they may become activated. A finite element model based on a single crystal plasticity was adopted to examine the domain of validity of HRR fields. The results show that domain of validity of HRR stress fields increases from 0.4 to 0.5 percent of the overall plastic zone sizes as the hardening exponent n increases from 3 to 20. Both the finite element and the HRR asymptotic results coverage to the discontinuous stress field of Rice's (1987) solution for ideally plastic material as n gets larger. Even though clear the displacements remain continuous in the ideally plastic limit, zones of very high slopes located across the sector boundaries can be observed in the finite element results. Dissert. Abstr.

N93-25781# Puerto Rico Univ., Rio Piedras. Dept. of Physics.
A NUMERICAL SIMULATION OF ADSORPTION ONTO A CRYSTALLINE SURFACE
J. A. Hernando (Comision Nacional de Energia Atomica, Buenos Aires, Argentina.) and L. Blum 15 Jan. 1993 5 p
(AD-A261079; TR-25) Avail: CASI HC A01/MF A01

A particular model for the adsorption of a dense fluid onto a crystalline surface has been studied. The fluid is arbitrary and the crystalline surface is modelled by a hard wall decorated with a triangular lattice of sticky sites. This model can be mapped on a lattice gas model with interaction potentials related to the particle distribution functions of the smooth (undecorated) wall problem. Approximate adsorption isotherms in the theta-p plane (fraction of occupied sites vs. bulk density) have also been drawn. However, the effect that the three particle distribution function has on the critical point has also been estimated, and it is quite important. We have performed Monte Carlo simulations of a model system inspired on this work. It is a 2D system interacting via a hard sphere plus a triangular well potential and immersed in an external field described by a triangular lattice of sticky sites. We have studied its phase diagram paying some attention also to its behavior in the limit of infinitesimally small sticky adhesion. DTIC

N93-25789# Worcester Polytechnic Inst., MA.
MEASUREMENT OF OPTICAL PROPERTIES OF INFRARED BANDGAP SUPERLATTICES Final Report, 18 Jan. 1989 - 17 Jul. 1992
Donald F. Nelson Oct. 1992 17 p
(Contract DAAL03-89-K-0030)
(AD-A260859; ARO-26188.4-EL) Avail: CASI HC A03/MF A01

The lattice-matched bandgap-tunable heterostructure system Ga(x)In(1-x)As(y)P(1-y)/InP is technologically important because the bandgap can be tuned with composition between 1.55 and 0.90 micron wavelengths. Because the range of bandgaps in this heterostructure system is further into the infrared when compared to the much studied GaAs/Ga(x)Al(1-x)As system, many spectroscopic techniques are more difficult. For example, prior to this study no inelastic light scattering had been done in this heterostructure system for laser wavelengths longer than the InP bandgap wavelength, that is, in a region where resonant interaction with the confined states of the wells is possible and where four polarization combinations of incident and scattered light are possible (rather than only two when backscattering is done at an opaque wavelength). Utilizing this technique was one of the primary goals of this project. A second goal was to attempt to clarify a confusing situation in this heterostructure system in which previous photoluminescence measurement gave huge discrepancies with predicted emission photon energies of between 50 and 200 meV. This contrasted sharply with the GaAs/GaAlAs system in which agreement was in 1 to 2 meV range. DTIC

N93-25854# Nebraska Univ., Lincoln.
MOLECULAR DEVICES BASED ON NEW MONOLAYER-FORMING SYSTEMS Final Report, 1 Sep 1989 - 31 Oct. 1992
Craig J. Eckhardt 21 Dec. 1992 6 p
(Contract DAAL03-89-G-0094)
(AD-A260996; ARO-27195.1-CH-SM) Avail: CASI HC A02/MF A01

The formation of novel planar lattices formed by monolayers of new amphiphilic molecules is reported. The rigid amphiphiles have cross-sections designed to provide two-dimensional crystals of the hexagonal, rectangular and oblique crystal classes. The packings are studied by atomic force microscopy. One amphiphile of triangular cross-section forms a hexagonal lattice. Two other amphiphiles, a tetracyclic and binapthyl, are chiral and synthesized as racemates. The single binapthyl amphiphile forms two commensurate lattices, rectangular and oblique, in the same monolayer. The tetracyclic amphiphile shows three phases on water and upon transfer at their respective formation pressures onto mica, three phases are observed: glass-like, rectangular and oblique. The oblique phase results as a phase separation of the enantiomers as a result of spontaneous resolution in two dimensions. Atom-atom potential calculation are shown to be essential to the design and understanding of these planar lattices. The results have important implications beyond monolayer chemistry and physics for fields such as liquid crystals and biophysics. DTIC

N93-25897# Pennsylvania State Univ., University Park. Dept. of Electrical and Computer Engineering.
SHORT-PERIOD SUPERLATTICE MATERIALS FOR HETEROJUNCTION BIPOLAR TRANSISTORS Final Report, 1 May 1989 - 31 Dec. 1992
David L. Miller 30 Jan. 1993 9 p
(Contract DAAL03-89-K-0093)
(AD-A260701; ARO-26444.4-EL) Avail: CASI HC A02/MF A01

This is the final report of the project Short-period Superlattice Materials for Heterojunction Bipolar Transistors, for the period 5/01/89-12/31/92. The goal of this project was to investigate the usefulness of short-period superlattices (SPSL) of InAs/GaAs and InAs/AlAs for heterojunction bipolar transistors (HBT's). Because of difficulties encountered early in the project in growing high structural quality SPSL's, the emphasis of the project was shifted to attempting to understand the growth of HBT material at low temperatures using migration-enhanced epitaxy and the incorporation of that material into HBT's. To summarize our technical results, we have grown InAs/GaAs SPSL on InP and GaAs and determined their surface roughening behavior with thickness and InAs content; correlated x-ray line widths with RHEED observations of roughening; developed methods to

use migration-enhanced epitaxy to grow doped GaAs on (111) and (100) substrates, with material on both orientations having good mobilities; studied the properties of low-temperature conducting GaAs, determining Schottky barrier heights; and applied the migration-enhanced epitaxy technique to the low temperature growth of Be-doped base materials for HBT's with usable gain and no Be diffusion during growth. DTIC

N93-25899# University of South Florida, Tampa.
FUNDAMENTAL AND APPLIED ASPECTS OF DEFECT ENGINEERING IN GaAs Final Report, 12 Jan. 1990 - 30 Sep. 1992
Jacek Lagowski 8 Dec. 1992 20 p
(Contract DAAL03-90-G-0020)
(AD-A260573; ARO-27764.1-MS) Avail: CASI HC A03/MF A01

The program was aimed at advancing the fundamental and applied knowledge required for defect engineering in bulk GaAs. It was focussed on deep level defects, especially antisite defects such as arsenic-antisite related EL2 defect and gallium antisite acceptor defects. Using non-stoichiometric crystal methods, with controlled cooling rates, we established, for the first time, quantitative temperature characteristics of the EL2 formation rate. We determined melt stoichiometry and Fermi energy dependence of the native acceptor concentration. The latter results has stimulated theoretical interest and ab initio calculations by the Xerox group of the negative 'U' property of the Ga(sub As) antisite. Recently we also completed a study on the hetero-antisite defect, Sb(sub Ga). Using our knowledge of EL2 formation/annihilation, we were able to engineer defect structures in arsenic-rich crystal leading to very low EL2 and EL3 concentrations. This enabled the first positive identification of both, single and double levels of Sb(sub Ga) defects otherwise marked by the EL2 and EL3 defects. The program has also lead to the discovery of a non-contract, no preparation, wafer scale, deep level defect characterization method based on the surface photovoltage transient. DTIC

N93-25947# Aerospace Corp., El Segundo, CA. Technology Operations.
ANALYSIS OF TRANSIENT PHOTOLUMINESCENCE MEASUREMENTS ON GaAs AND AlGaAs DOUBLE HETEROSTRUCTURES
Dean C. Marvin, Steven C. Moss, and Linda F. Halle 13 Jan. 1993 58 p
(Contract F04701-88-C-0089)
(AD-A261154; TR-0091(6925-11)-2; SMC-TR-93-03) Avail: CASI HC A04/MF A01

We discuss the analysis of transient photoluminescence measurements and the extraction of carrier recombination lifetimes in GaAs and AlGaAs double heterostructures. In contrast to recently reported claims, we demonstrate that even in regions where the measured decay curves show single exponential behavior, the slopes do not, in general, correspond to any single physical carrier lifetime, such as the minority carrier lifetime. A series of measurements over a range of incident optical intensities is required to extract such lifetimes. DTIC

N93-26090 Department of the Navy, Washington, DC.
CONTROL OF CRYSTALLITE SIZE IN DIAMOND FILM CHEMICAL VAPOR DEPOSITION Patent
Mark B. Moran, inventor (to Navy), Linda F. Johnson, inventor (to Navy), and Karl A. Klemm, inventor (to Navy) 8 Dec. 1992 8 p Filed 16 May 1991
(AD-D015660; US-Patent-5,169,676; US-Patent-Appl-SN-702663) Avail: US Patent and Trademark Office

In depositing an adhering, continuous, polycrystalline diamond film of optical or semiconductor quality on a substrate, as by forming on the substrate a layer of a refractory nitride interlayer and depositing diamond on the interlayer without mechanical treatment or seeding of the substrate or the interlayer, the substrate is heated in a vacuum chamber containing a microwave activated mixture of hydrogen and a gas including carbon, and the size of deposited diamond crystallites and their rate of deposition selectively varied by a bias voltage applied to the substrate. DTIC

N93-26140 Department of the Navy, Washington, DC.
METHOD OF JOINING DIAMOND STRUCTURES Patent
Lawrence T. Kabacoff, inventor (to Navy) and John Barkyoumb, inventor (to Navy) 5 Jan. 1993 5 p Filed 8 Jul. 1991
(AD-D015671; US-Patent-5,176,788; US-Patent-Appl-SN-726483) Avail: US Patent and Trademark Office

A process for bonding two diamond surfaces together is described. The method is as follows: (1) form a layer of opaque non-diamond carbon material between the two diamond surfaces; (2) press the diamond surfaces together with the opaque non-diamond material sandwiched between the diamond surfaces; (3) use pulse lased light to quickly melt all the opaque non-diamond carbon material before a significant amount of heat is lost through the diamond surface; and then (4) allow the resulting carbon melt to cool and solidify as polycrystalline diamond which grows homoepitaxially from the diamond surfaces bonding those surfaces together. DTIC

N93-26193# Colorado State Univ., Fort Collins. Dept. of Electrical Engineering.
OPTOELECTRONIC III-V HETEROSTRUCTURES ON Si SUBSTRATES Final Report, 15 Sep. 1989 - 14 Sep. 1992
Gary Y. Robinson 14 Sep. 1992 26 p
(Grant AF-AFOSR-0153-89)
(AD-A261651; AFOSR-93-0106TR) Avail: CASI HC A03/MF A01

The results of a three-year program to investigate the epitaxial growth of the 3-5 semiconductors, particularly the InGaAsP/InP materials system, on Si substrates is presented. The heterostructures were grown by gas-source molecular beam epitaxy (GSMBE) and were designed for applications in optoelectronics. With regard to growth of InP and InGaAsP alloys on Si, the research program was successful in reducing misfit dislocations and stacking faults resulting from the 8 percent lattice mismatch between InP and Si. A strained layer superlattice of In(x)Ga(1-x)P/In(y)Ga(1-y)P (X not equal Y) was used as a buffer layer. The use of InGaP as buffer layers led to extensive development, in parallel with the InP-on-Si work, of InGaP layers by GSMBE. The Schottky barrier energies for both n-type and p-type materials were measured for the first time for the wide bandgap alloys InGaP and InGaAlP when lattice matched to GaAs. DTIC

N93-26194# Polytechnic Univ., Brooklyn, NY. Dept. of Physics.
EXPERIMENTAL AND THEORETICAL STUDIES OF PROXIMITY EFFECT AND COULOMB BLOCKADE PHENOMENA IN JOSEPHSON JUNCTIONS Final Report, 15 May 1989 - 29 Mar. 1992
E. L. Wolf and B. Laikhtman 27 Jan. 1993 35 p
(Grant AF-AFOSR-0338-89)
(AD-A261652; AFOSR-93-0105TR) Avail: CASI HC A03/MF A01

The topics of theoretical and experimental interest in this research are as follows: behavior of ultrasmall low capacitance (Coulbomb-blockaded) Josephson and normal metal tunnel junction microstructures; and experimental evaluation of the associated microstructures (STM). A particular interest is in the fundamentally new mechanisms of interaction with radiation believed to operate in these systems. The Proximity Induced Josephson Effect (PIJE), an effect occurring at a Normal Metal/Superconductor (N/S) interface which displays many of the features of the Josephson effect, and whose device potential has not been at all explored, is also researched. Related topics in our research in this project have been methods to form Josephson junctions using cuprate superconductors and methods to prepare and modify the surface of cuprate superconductors to make Josephson junctions and other electronic devices. DTIC

N93-26223# Illinois Univ., Chicago. Dept. of Physics.
STUDY OF SURFACE BEHAVIOR IN FUNCTION OF TEMPERATURE OF THE QUATERNARY SYSTEM (Hg, Cd, Zn)Te Final Report, 1 Aug. 1986 - 31 Aug. 1989
James W. Garland and Paul M. Raccah 17 Jul. 1992 8 p
(Contract DAAL03-86-K-0131)
(AD-A260968; ARO-23662.7-EL) Avail: CASI HC A02/MF A01

The work performed under this contract represents an extension of our past work on mercury cadmium telluride (MCT). Under this contract we have focussed on the use of spectroscopic ellipsometry (SE) and the development of new theoretical and analytical tools for the analysis of SE data. Our major achievement was the demonstration of an excellent, physically understandable correlation between the low-temperature dark storage time of MIS devices built on bulk MCT samples and a parameter measured by room-temperature electrolyte electroreflectance (EER) on those samples. The analysis which led to this result required the input of SE data obtained under this contract as well as the EER data. The other experimental results obtained under this grant were the determination of the nature of the broadening of critical-point transition energies in

semiconductor alloys and compounds and SE measurements of critical-point energies and of the thickness of the ZnSe epilayers for ZnSe/GaAs heterojunctions. Theoretical and analytical work performed under this contract included the determination of the origin of the quasiperiodic oscillations in numerically differentiated SE data, a procedure to minimize those oscillations, the development of a method to obtain more accurate values of critical-point energies and linewidths from SE data, and the initial work on the development of a greatly improved model for the optical dielectric function. DTIC

N93-26252# Puerto Rico Univ., Rio Piedras. Dept. of Physics.
PROCEEDINGS OF THE 16TH INTERNATIONAL WORKSHOP ON CONDENSED MATTER THEORIES
L. Blum and F. B. Malik 15 Jan. 1993 15 p Workshop held in San Juan, Puerto Rico, 1-5 Jun. 1992 Prepared in cooperation with University of Southern Illinois, Carbondale
(Contract N00014-90-J-1263)
(AD-A261078; TR-21) Avail: CASI HC A03/MF A01

This report outlines the proceedings of the XVI International Workshop on Condensed Matter Physics containing contributions to solid, liquid, interfacial, quantum and classical physics. The 16th International Workshop on Condensed Matter Theories (CMT) was held in San Juan, Puerto Rico between June 1 and 5, 1992. A number of outstanding lectures were given on solid state physics, density functional theory, diffusion limited aggregation, cellular automata, superconductivity, quantum fluids (Bose and Fermi liquids), theory of inhomogeneous classical fluids, nonequilibrium and equilibrium fluids, phase transitions, nuclear structure, lattices, as well as a number of excellent posters. DTIC

N93-26254# Minnesota Univ., Minneapolis. Dept. of Chemical Engineering and Materials Science.
RESONANT TUNNELING THROUGH CHEMISORBED HALOGEN ATOMS ON Ag(111) Technical Report, 30 Jun. 1992 - 31 Mar. 1993
Joachim H. Schott and Henry S. White 20 Mar. 1993 17 p
(Contract N00014-91-J-1927)
(AD-A261794; TR-18) Avail: CASI HC A03/MF A01

Tunneling spectroscopy measurements performed with a scanning tunneling microscope (STM) on Ag(111) surfaces coated with a monolayer of halogen atoms (F, Cl, Br, and I) are reported. Maxima in the tunneling spectra are assigned to resonance tunneling through both the occupied p- and virtual bound states of the halogen atoms. The observed minimum tunneling resistance at resonance is pi(h)/e(exp 2) (is approximately 12.6 k-ohms), in agreement with theoretical predictions. DTIC

N93-26258# George Washington Univ., Washington, DC. Dept. of Chemistry.
ACCURATE DETERMINATION OF AUGER LINE SHAPE BINDING ENERGIES
N. H. Turner, D. E. Ramaker, and F. L. Hutson Jan. 1993 16 p
(Contract N00014-91-J-1896)
(AD-A261803; TR-64) Avail: CASI HC A03/MF A01

A quantitative comparison between an experimental and a theoretical description of any Auger spectrum requires a common energy reference point such as the Fermi level. With non-conductors this is problematic, since the Fermi level is not well defined and charging may shift the Fermi level. A common approach to overcome this problem employs spectra containing the Auger peak, core, and valence band (VB) photoemission peaks. One then has only to locate a common reference point in the Auger and VB spectra relative to the core level peak. We have developed a procedure where a comparison is made between model theoretical and experimental spectra so that a large energy range (about 20 eV) of each spectrum can be utilized to locate the common reference points. We have found that this method enables accurate reference points to be determined even with severe sample charging. The method is precise enough to observe what may be a differential charging effect in the polyethylene (PE) spectra. This suggests that the photoelectron and Auger peaks may not shift an equal amount with charging in all instances. Although much smaller than that previously reported, a breakdown in the Cini-Sawatzky expression as modified for covalent systems still is suggested for PE. DTIC

N93-26302# Harvard Univ., Cambridge, MA. Div. of Applied Sciences.
SINGLE ELECTRON CHARGING EFFECTS IN MESOSCOPIC SYSTEMS Interim Technical Report
Ashraf E. Hanna Oct. 1992 156 p
(Contracts N00014-89-J-1023; N00014-89-J-1565)
(AD-A261228; TR-34) Avail: CASI HC A08/MF A02

We report the investigation of two ultra-small tunnel junctions in series. These junctions have capacitances on the order of 10-18 to 10-19 F each. In this regime the charging energy associated with a single electron tunneling event (e2/2C) can be made significantly larger than thermal fluctuations (kBT) at liquid helium temperatures. As such, measurements of the tunneling current as a function of voltage show unique features associated with individual electron tunneling events. DTIC

N93-26312# Kulite Semi-Conductor Products, Inc., Leonia, NJ.
SiC MICROSENSOR WITH PIEZORESISTIVE DIAMOND SENSING ELEMENTS Final Report, Jul. - Dec. 1992
J. S. Shor, J. L. Davidson, and A. D. Kurtz 31 Dec. 1992 25 p
LIMITED REPRODUCIBILITY: More than 20% of this document may be affected by microfiche quality
(Contract DAAL03-92-C-0043)
(AD-A261346; ARO-30676.1-EL-SBI) Avail: CASI HC A03/MF A01

Advanced microfabrication processes have been developed for novel high temperature pressure sensors utilizing diamond and SiC materials. Such sensors represent a new generation of high temperature piezoresistive sensors. The accomplishments of Phase 1 include the following: (1) Growth of polycrystalline diamond on Beta-SiC substrates; (2) The first isolated p-type diamond resistive elements grown on intrinsic diamond; (3) Establishment of microfabrication processes for sensor manufacture; (4) Demonstration of a large piezoresistive effect in poly-diamond; and (5) Demonstration of a new field-assisted-bonding process which allows dielectrically isolated SiC elements to be formed. DTIC

N93-26332# Virginia Polytechnic Inst. and State Univ., Blacksburg.
INVESTIGATION OF COUPLED ANALYSIS TECHNIQUES FOR ADAPTIVE MATERIAL STRUCTURAL SYSTEMS Final Technical Report, 15 Sep. 1991 - 14 Sep. 1992
Craig A. Rogers 15 Nov. 1992 112 p
(Grant AF-AFOSR-0416-91)
(AD-A261359; AFOSR-93-0146TR) Avail: CASI HC A06/MF A02

The objective of this research program is to investigate coupled analysis techniques for adaptive material structural systems. There are two aspects of this research: one is to develop a nonlinear full-field constitutive model for ferroelectric materials, including piezoelectric and electrostrictive materials; the other is to develop an impedance-based analysis technique for adaptive material systems. A coupled electro-thermal-mechanical nonlinear constitutive relation for piezoelectric materials has been developed and verified based on experimental data from the literature. This model uses the polarization fraction as a newly established internal variable. This internal variable is related to other parameters such as electric field, stress, frequency, etc., using a hyperbolic tangent function, which accurately describes the nonlinearity, including the hysteresis of ferroelectric materials. The same approach has also been utilized in the modeling of relaxor ferroelectric PMN-PT materials. An impedance methodology for the dynamic analysis of adaptive material systems has been developed. This approach can provide accurate theoretical prediction of the dynamic response of a structure driven by any type of actuator and yet reflect the physical essence of the actuator/structure interaction. This model has been experimentally verified. DTIC

N93-26357# Gordon Research Conferences, Inc., Kingston, RI.
GORDON CONFERENCE ON POINT DEFECTS, LINE DEFECTS AND INTERFACES IN SEMICONDUCTORS Final Report, 15 Jul. - 3 Dec. 1992
Alexander Cruickshank 3 Dec. 1992 10 p Conference held in Plymouth, NH, 20-24 Jul. 1992
(Contract F49620-92-J-0409)
(AD-A261485; AFOSR-93-0099TR) Avail: CASI HC A02/MF A01

By any number of measures the 1992 Gordon Research Conference on Point Defects, Line Defects, and Interfaces in Semiconductors was very successful. The Gordon conference organization evaluates all of its conferences by means of a questionnaire to all participants. Our conference was ranked 20 out of 134 conferences held during the summer of 1992. This is especially good for a field that is so mature. Good choices of discussion leaders and speakers were key to this success. Speakers from

related fields where new and important defect problems are emerging generated a lot of excitement. The 23 invited talks were presented in sessions run by 11 different discussion leaders. In addition 59 posters were presented. The total number of participants was about 125. In this year of reduced travel budgets, many key people would not have been able to participate without financial support. Having so many younger scientists among the participants was also important. The conference finances are summarized on the attached sheet. Since no conference proceedings or abstract book was printed, I have submitted the final program along with a complete list of the poster presentations as the final report. DTIC

N93-26381# Conductus, Inc., Sunnyvale, CA.
ADVANCED HTS S-N-S DEVICES Final Report, 1 Jul. - 24 Dec. 1992
Randy W. Simon and Kookrin Char 30 Dec. 1992 20 p
(Contract F49620-92-C-0044)
(AD-A261552; SB92-A-02; AFOSR-93-0058TR) Avail: CASI HC A03/MF A01

Superconductor-normal-superconductor Josephson junctions are a prime candidate for the active devices in electronic circuits based on high-temperature superconductors. In this program, CaRuO3 was used as a normal metal layer and yttrium barium copper oxide as the superconducting layers to produce Josephson junctions in edge-junction geometry. These superconductor-normal-superconductor junctions have been studied to determine their suitability for use in integrated circuits. The devices worked as Josephson junctions at temperatures up to at least 77 K with characteristic voltages in the range of 100-750 microvolts over most of their operating temperature range. The resistance of the junctions was dominated by the interface region rather than by the barrier layer itself. The properties of dc SQUIDs made from the junctions were excellent at 77 K. The variation in junction parameters over multiple devices was on the order of plus-or-minus thirty percent, which is encouraging but not yet sufficient for integrated circuit applications. Further process refinements may lead to more desirable device uniformity. DTIC

N93-26385# Washington State Univ., Pullman. Dept. of Physics.
DEFECT INITIATION/GROWTH AND ENERGY DISSIPATION INDUCED BY DEFORMATION AND FRACTURE Annual Technical Report, 15 Jun. 1991 - 14 Dec. 1992
J. T. Dickinson Jan. 1993 313 p
(Contract F49620-91-C-0093)
(AD-A261703; FRACTO-1992; AFOSR-93-0078TR) Avail: CASI HC A14/MF A03

Based on our capabilities to (1) detect and characterize particle release from surfaces on fast time scales, (2) to measure rapid electrical transients, and (3) to obtain high resolution topographical information utilizing scanning tunneling and atomic force microscopy, we present new results on the time sequence of events leading up to defect initiation and growth which ultimately leads to fracture. We employ dynamic methods as well as post-fracture examination in polymers, ceramics, metals, and interfaces. We emphasize mechanisms, with interpretation and connections between these results and the creation and evolution of defects in materials under mechanical stress. In many cases, the information we are acquiring has important implications concerning dissipation of energy (e.g., plastic deformation, microcracking, crack branching, and crack deflection) which play critical roles in controlling the strength and toughness of materials. DTIC

N93-26494# Los Alamos National Lab., NM.
TEMPERATURE DEPENDENCE OF RADIATION DAMAGE AND ITS ANNEALING IN SILICON DETECTORS
H. J. Ziock, J. G. Boissevain, K. Holzscheiter, J. S. Kapustinsky, A. P. T. Palounek, W. E. Sondheim, E. Barberis (California Univ., Santa Cruz.), N. Cartiglia (California Univ., Santa Cruz.), J. Leslie (California Univ., Santa Cruz.), and D. Pitzl (California Univ., Santa Cruz.) et al 1992 6 p
Presented at the Institute of Electrical and Electronic Engineers (IEEE) Nuclear Science Symposium, Orlando, FL, 26-31 Oct. 1992
(Contract W-7405-eng-36)
(DE93-003854; LA-UR-92-3827; CONF-921005-8) Avail: CASI HC A02/MF A01

The radiation damage resulting from the large particle fluences predicted at the Superconducting Super Collider will induce significant leakage currents in silicon detectors. In order to limit those currents, we plan to operate the detectors at reduced temperatures (approximately 0 deg C). In this paper, we present the results of a study of temperature effects on both the initial radiation damage and the long-term annealing of that damage in silicon PIN detectors. Depletion voltage results are reported. The detectors were exposed to approximately 10(sup 14)/cm(sup 2) 650 MeV protons. Very pronounced temperature dependencies were observed. DOE

N93-26540# Cincinnati Univ., OH. Dept. of Physics.
LOW TEMPERATURE HALL AND SHUBNIKOV-DE HAAS EFFECTS Final Report, 1 Sep. 1990 - 30 Apr. 1992
R. S. Newrock Dec. 1992 18 p
(Contract F33615-90-C-5958)
(AD-A261871; WL-TR-93-4008) Avail: CASI HC A03/MF A01

The goals of this program were to develop the facilities necessary to measure the quantum Hall effect and Shubnikov - de Haas effects at magnetic fields up to 9 Tesla and at temperatures down to 0.5 Kelvin or below. Theses goals were accomplished and AlGaAs/GaAs high electron mobility samples were measured, owing the effectiveness of the high fields and low temperatures. A He-3 refrigerator was designed and constructed and coupled with a superconducting magnet. A PC based computer control program was written in QuickBasic to control the experiment. DTIC

N93-26547# National Inst. of Standards and Technology, Gaithersburg, MD.
COMPUTATION OF COMPLEX SOLIDIFICATION MORPHOLOGIES USING A PHASE-FIELD MODEL
B. T. Murray, A. A. Wheeler (Bristol Univ., England.), W. J. Boettinger, and G. B. McFadden Feb. 1993 23 p
(PB93-156743; NISTIR-5124) Avail: CASI HC A03/MF A01

An anisotropic phase-field model is used to calculate numerically the solidification patterns of a pure material into an undercooled liquid in a two-dimensional rectangular region. In the phase-field approach, the solid-liquid interface is treated as diffuse, and a dynamic equation for the phase variable is introduced in addition to the equation for heat flow. The phase-field model equations are solved using finite-difference techniques on a uniform mesh. Calculations for dendritic growth are presented for both four-fold and six-fold anisotropy, and the effect of the level of anisotropy on the growth of a dendrite is investigated. A previous study has shown that performing computations with an interface that is sufficiently thin for the numerical solution to accurately represent a sharp interface model is computationally demanding. However, even with a relatively thick interface, the computations using the phase-field model show many of the qualitative features of dendritic growth, and the method is well suited for handling the evolution of very complex, realistic interface shapes. NTIS

N93-26577# Colorado State Univ., Fort Collins. Dept. of Chemistry.
TRANSITION METAL CHELATE-FULLERIDE COMPOUNDS: ELECTROCRYSTALLIZATION OF SEMICONDUCTING (Ru(bpy)S)(C60)2 Interim Report
Colby A. Foss, Jr., Daniel L. Feldheim, Del R. Lawson, Peter K. Dorhout, C. M. Elliott, C. R. Martin, and B. A. Parkinson Feb. 1992 13 p
(Contract N00014-82-K-0612)
(AD-A261549; ONR-TR-83) Avail: CASI HC A03/MF A01

Two recent breakthroughs in the chemistry of fullerenes have provided the impetus for using fullerenes to prepare solid state materials: a method to produce large amounts of C60 and related materials, and the discovery of superconductivity in fullerides of K, Rb, and Cs. The superconducting alkali metal compounds, which appear to contain C60(3-) show a trend toward higher transition temperatures upon increasing the size of the unit cell up to the composition Rb2CsC60. It was thought that the synthesis of new compounds of reduced fullerenes with large cations might produce materials with interesting properties. Transition metal complexes with neutral chelating ligands (e.g., Ru(bpy)3(2+), where bpy = 2,2' bipyridine) seemed like good candidates as cations for C60 salts. Such complex cation have a rich electrochemistry and photochemistry. Furthermore, the electronic and optical properties can be varied via ligand and metal substitution, providing a route for tuning the properties of the new materials. DTIC

N93-26581# North Carolina Agricultural and Technical State Univ., Greensboro. Dept. of Electrical Engineering.
OPTICAL CHARACTERIZATION OF Ga(1-x)In(x)As(y)Sb(1 y)/GaSb ALLOY AND DEVICE APPLICATION Final Report, 1 Nov. 1988 - 30 Oct. 1992
S. Iyer and A. Abul-Fadl 15 Dec. 1992 80 p
(Contract F46920-89-C-0004)
(AD-A261713; TR-3; AFOSR-93-0096TR) Avail: CASI HC A05/MF A01

GaSb and GaInAsSb layers of excellent optical quality with compositions corresponding to the room temperature photoluminescence peak wavelength of 1.7 microns to 2.32 microns were grown by liquid phase electroepitaxial (LPEE) technique. These layers were characterized using x-ray diffraction, energy dispersive X-ray analysis, and low temperature Fourier transform photoluminescence (PL) with emphasis on the latter. The variation in the low temperature photoluminescence spectra of these alloys as a function of the alloy compositions was the subject of detailed investigation. The nature of the recombination processes was identified from the temperature and intensity dependence of the PL spectra. N-type doping of the layers was achieved using tellurium. The PL spectra become increasingly complicated and considerable change in the PL spectra with the excitation intensity is also observed. A systematic and quantitative evaluation of the effects of compensation in GaSb was examined as a function of Te concentration in the layers under both low and high excitation conditions. Photoreflectance spectroscopy was assembled for the characterization of semiconductor band structure and surface, PIN photodiode device was fabricated using the doped layers and characterized using I-V and C-V measurements. DTIC

N93-26594# Lawrence Livermore National Lab., CA.
LASER DAMAGE TO PRODUCTION- AND RESEARCH-GRADE KDP CRYSTALS
F. Rainer, L. J. Atherton, and J. J. DeYoreo Oct. 1992 13 p Presented at the SPIE Symposium on Boulder Damage, Boulder, CO, 28-30 Oct. 1992
(Contract W-7405-eng-48)
(DE93-007517; UCRL-JC-111463; CONF-9210295-3) Avail: CASI HC A03/MF A01

We present the results of laser damage measurements conducted on potassium dihydrogen phosphate (KDP) and deuterated potassium dihydrogen phosphate (KD0P) crystals that were grown recently for both production and research applications by several sources. We have measured extrinsic damage thresholds that cover wavelengths from 1064 nm to 266 nm at pulse durations in the 3- to 10-ns regime. Many of the samples were extracted from boules grown specifically to yield large-area crystals, up to 32-sq cm, for laser fusion applications. These crystals were the result of efforts, both by the Lawrence Livermore National Laboratory (LLNL) and commercial crystal-growth companies, to yield high-threshold KDP. In particular we have established that such crystals can reliably survive fluences exceeding 15 j/sq cm at 355 nm and 20 j/sq cm at 1064 nm when irradiated with 3-ns pulses. We present details of how bulk and surface damage to these crystals scale with pulse duration and wavelength as well as of morphological effects due to laser conditioning. DOE

N93-24993# Franche-Comte Univ., Besancon (France). Lab. de Physique et Metrologie des Oscillateurs.
WEAK MAGNETIC FIELD SENSITIVITY OF QUARTZ CRYSTAL OSCILLATORS
R. Brendel and E. Robert (Centre National d'Etudes Spatiales, Toulouse, France.) *In* ESA, Frequency and Time Forum Jun. 1992 p 99-104 (For primary document see N93-24978 09-70)
(Contract CNES/CNRS-932-88-53-474-00)
Copyright Avail: CASI HC A02/MF A04

N93-25001# Composants Quartz et Electronique, Pont Sainte Marie (France).
A MICROCOMPUTER COMPENSATED CRYSTAL OSCILLATOR MCXO
P. Collet, G. Putois, and F. Vignaud *In* ESA, Frequency and Time Forum Jun. 1992 p 159-163 Sponsored by STTE, France (For primary document see N93-24978 09-70)
Copyright Avail: CASI HC A01/MF A04

N93-25013# Centre National d'Etudes des Telecommunications, Bagneux (France).
COMPARISON OF ENERGY TRAPPING RESONATORS AND FILTERS USING THE AT CUT OF QUARTZ, BERLINITE AND GALLIUM PHOSPHATE
J. Detaint, J. Schwartzel, C. Joly, B. Capelle (Paris VI Univ., France.), A. Zarka (Paris VI Univ., France.), Y. Zheng (Paris VI Univ., France.), Y. Toudic (Centre National d'Etudes des Telecommunications, Lannion, France.), and E. Philippot (Montpellier Univ., France.) *In* ESA, Frequency and Time Forum Jun. 1992 p 223-227 (For primary document see N93-24978 09-70)
Copyright Avail: CASI HC A01/MF A04

N93-25020# Ecole Nationale Superieure de Mecanique et des Microtechniques, Besancon (France). Equipe de Physique et Electronique des Capteurs.
DEDICATED OSCILLATOR FOR IMMERSED CRYSTAL SENSOR
G. Bardeche, C. Filiatre, and J.-P. Valentin *In* ESA, Frequency and Time Forum Jun. 1992 p 265-268 (For primary document see N93-24978 09-70)
Copyright Avail: CASI HC A01/MF A04

N93-25021# National Physical Lab., New Delhi (India).
RADIATION EFFECTS IN GERMANIUM DOPED QUARTZ
Harish Bahadur *In* ESA, Frequency and Time Forum Jun. 1992 p 269-272 Sponsored by Sandia National Labs. and RADC (For primary document see N93-24978 09-70)
Copyright Avail: CASI HC A01/MF A04

N93-25022# Ecole Nationale Superieure de Mecanique et des Microtechniques, Besancon (France). Lab. de Chronometrie Electronique et Piezoelectricite.
TRAPPED ENERGY QUARTZ CRYSTAL RESONATOR ON WEDGE-SHAPED PLATE
R. Bourquin *In* ESA, Frequency and Time Forum Jun. 1992 p 273-277 (For primary document see N93-24978 09-70)
Copyright Avail: CASI HC A01/MF A04

N93-25025# Societe Industrielle de Combustible Nucleaire, Annecy (France).
CRYSTAL GROWTH OF BERLINITE: METHODS FOR GROWING LONGER CRYSTALS AND IMPROVING THE QUALITY
X. Buisson, A. Zarka (Paris VI Univ., France.), R. Arnaud, B. Capelle (Paris VI Univ., France.), Y. Zheng (Paris VI Univ., France.), J. Schwartzel (Centre National d'Etudes des Telecommunications, Bagneux, France.), J. Detaint (Centre National d'Etudes des Telecommunications, Bagneux, France.), and T. Toudic (Centre National d'Etudes des Telecommunications, Lannion, France.) *In* ESA, Frequency and Time Forum Jun. 1992 p 287-291 (For primary document see N93-24978 09-70)
Copyright Avail: CASI HC A01/MF A04

N93-25032# Ecole Nationale Superieure de Mecanique et des Microtechniques, Besancon (France). Lab. de Chronometrie Electronique et Piezoelectricite.
QUARTZ CRYSTAL TWINNING UNDER MECHANICAL STRESS: FINITE ELEMENT ANALYSIS
J. J. Boy, B. Dulmet, and P. Conraux (Framasoft + CSI, Lyon, France.) *In* ESA, Frequency and Time Forum Jun. 1992 p 323-327 (For primary document see N93-24978 09-70)
Copyright Avail: CASI HC A01/MF A04

N93-25040# Polish Academy of Sciences, Warsaw. Tele- and Radio Research Inst.
MEASUREMENT RESULTS OF THE CRYSTALLOGRAPHIC ORIENTATION OF THE SC CUT ROUND PLATES
K. Weiss *In* ESA, Frequency and Time Forum Jun. 1992 p 365-367 (For primary document see N93-24978 09-70)
Copyright Avail: CASI HC A01/MF A04

N93-25043# Compagnie d'Electronique et de Piezo-Electricite, Argenteuil (France).
CONTROLLED DISSOLUTION OF A PIEZOELECTRIC MATERIAL BERLINITE (AlPO4) [DISSOLUTION CONTROLEE D'UN MATERIAU PIEZOELECTRIQUE, LA BERLINITE (ALPO4)]
O. Cambon, A. Goiffon (Montpellier Univ., France.), A. Ibanez (Montpellier Univ., France.), and E. Philippot (Montpellier Univ., France.) *In* ESA, Frequency and Time Forum Jun. 1992 p 377-381 In FRENCH (For primary document see N93-24978 09-70)
Copyright Avail: CASI HC A01/MF A04

N93-25044# Montpellier Univ. (France).
CRYSTAL GROWTH AND PHYSICAL CHARACTERIZATIONS OF GaPO4
E. Philippot, A. Ibanez, A. Goiffon, B. Capelle (Paris VI Univ., France.), A. Zarka (Paris VI Univ., France.), J. Schwartzel (Centre National d'Etudes des Telecommunications, Bagneux, France.), and J. Detaint (Centre National d'Etudes des Telecommunications, Bagneux, France.) *In* ESA, Frequency and Time Forum Jun. 1992 p 383-388 (For primary document see N93-24978 09-70)
Copyright Avail: CASI HC A02/MF A04

N93-25045# Nancy Univ. (France). Lab. Infrarouge.
THERMIONIC CURRENT MEASUREMENT IN QUARTZ [MESURE DE COURANTS THERMOIONIQUES DANS LE QUARTZ]
G. Jeandel, A. Warin, C. Poignon, J. P. Aubry (Compagnie d'Electronique et de Piezo-Electricite, Argenteuil, France.), and G. Morlot *In* ESA, Frequency and Time Forum Jun. 1992 p 389-392 In FRENCH Sponsored by Direction des Recherches, Etudes et Techniques (For primary document see N93-24978 09-70)
Copyright Avail: CASI HC A01/MF A04

N93-25046# York Univ. (Ontario). Piezoelectricity Research Lab.
THE THIRD-ORDER PERMITTIVITY OF QUARTZ OBTAINED BY DIFFERENT METHODS
Carl K. Hruska *In* ESA, Frequency and Time Forum Jun. 1992 p 393-395 Sponsored in part by Natural Sciences and Engineering Research Council of Canada and York Univ. (For primary document see N93-24978 09-70)
Copyright Avail: CASI HC A01/MF A04

N93-25047# Army Electronics Technology and Devices Lab., Fort Monmouth, NJ.
THERMOELASTICITY IN QUARTZ
J. A. Kosinski, J. G. Gualtieri, and A. Ballato *In* ESA, Frequency and Time Forum Jun. 1992 p 397-402 (For primary document see N93-24978 09-70)
Copyright Avail: CASI HC A02/MF A04

N93-25058# Istituto Elettrotecnico Nazionale (Galileo Ferraris), Turin (Itlay).
SOLID STATE FREQUENCY SYNTHESIS UP TO 600 GHz: AN APPLICATION TO THE Mg FREQUENCY STANDARD
A. Godone and C. Novero *In* ESA, Frequency and Time Forum Jun. 1992 p 471-475 (For primary document see N93-24978 09-70)
Copyright Avail: CASI HC A01/MF A04

N93-25584*# Johns Hopkins Univ., Laurel, MD. Applied Physics Lab.
A NOVEL METHOD FOR CHARACTERIZATION OF SUPERCONDUCTORS: PHYSICAL MEASUREMENTS AND MODELING OF THIN FILMS
B. F. Kim, K. Moorjani, T. E. Phillips, F. J. Adrian, J. Bohandy, and Q. E. Dolecek *In* NASA, Washington, Technology 2002: The Third National Technology Transfer Conference and Exposition, Volume 1 Feb. 1993 p 223-230 (For primary document see N93-25561 09-99)
Avail: CASI HC A02/MF A04

77 THERMODYNAMICS AND STATISTICAL PHYSICS

Includes quantum mechanics; theoretical physics; and Bose and Fermi statistics.

For related information see also *25 Inorganic and Physical Chemistry* and *34 Fluid Mechanics and Heat Transfer.*

N93-25423 Oxford Univ. (England).
TWISTOR DIAGRAMS AND A QUANTUM FIELD THEORY Ph.D. Thesis
Lewis ODonald 1992 145 p
Avail: Univ. Microfilms Order No. BRD-98304

This thesis uses twistor diagram theory, as developed by Penrose (1975) and Hodges (1990c), to try to approach some of the difficulties inherent in the standard quantum field theoretic description of particle interactions. The resolution of these issues is the eventual goal of the twistor diagram program. First twistor diagram theory is introduced from a physical view-point, with the aim of studying larger diagrams than have been typically explored. Methods are evolved to tackle the double box and triple box diagrams. These lead to three methods of constructing an amplitude for the double box, and two ways for the triple box. Next this theory is applied to translate the channels of a Yukawa Feynman diagram, which has more than four external states, into various twistor diagrams. This provides a test of the skeleton hypothesis (of Hodges, l990c) in these cases, and also shows that conformal breaking must enter into twistor diagrams before the translation of loop level Feynman diagrams. The issue of divergent Feynman diagrams is then considered. By using a twistor equivalent of the sum-over-states idea of quantum field theory, twistor translations of loop diagrams are conjectured. The various mass less propagator corrections and vacuum diagrams calculated give results consistent with Feynman theory. Two diagrams are also found that give agreement with the finite parts of the Feynman 'fish' diagrams of phi(sup 4)-theory. However it is found that a more rigorous translation for the time-like fish requires new boundaries to be added to the twistor sum-over-states. The twistor diagram obtained is found to give the finite part of the relevant Feynman diagram. Dissert. Abstr.

N93-25742 Princeton Univ., NJ.
FROM FRACTALS TO WORMHOLES VIA STRING THEORY Ph.D. Thesis
Andrew George Felce 1992 110 p
Avail: Univ. Microfilms Order No. DA9302070

The thesis is in two parts. The first part is devoted to a study of the definition of mass for soliton solutions in string theory. In the context of the low-energy effective field theory, there are three distinct quantities from which one can extract the mass of a soliton: the ADM mass, the static action and the kinetic energy. The three corresponding masses are carefully defined and shown to be equal for a representative class of string solitons, the so-called 'black fivebranes'. Along the way a potential confusion in the definition of the action is cleared up, and it is shown that the kinetic energy of a moving soliton is given in terms of a surface integral at spacelike infinity. This result for the kinetic energy is used to motivate a conjecture about the exact value of soliton masses in string theory: That in conformal field theory the kinetic mass is realized as the norm of the (1,1) deformation induced by the collective coordinate. Such deformations are usually treated as unphysical because they appear to be pure gauge and have zero norm. In a soliton conformal field theory, a finite number of these gauge transformations become physical because of a subtlety involving the boundary at spatial infinity. Some proposals for concrete exploration of this phenomenon are discussed. The second part of the thesis concerns the connection between string theory and an important problem in condensed matter physics. It has recently been shown that the dissipative Hofstadter model (dissipative quantum mechanics of an electron subject to uniform magnetic field and periodic potential in two dimensions) exhibits critical behavior on a network of lines in the dissipation/magnetic field plane. Apart from their obvious condensed matter interest, the corresponding critical theories represent non-trivial solutions of open string field theory containing a tachyon and gauge field background. A detailed account of their properties would be interesting from several points of view. The thesis reports the results of an initial investigation of the free energy, N-point functions and boundary state for this type of critical theory.

Although the primary goal is to study the magnetic field dependence of these quantities, some new results are presented which bear on the zero magnetic field case as well. Dissert. Abstr.

N93-26250# Naval Postgraduate School, Monterey, CA.
INTRODUCTION OF CHAOTIC DYNAMICAL SYSTEMS M.S. Thesis
Michael A. Bernhard Dec. 1992 78 p
(AD-A261747) Avail: CASI HC A05/MF A01

The emerging discipline known as chaos theory is a relatively new field of study with a diverse range of applications (economics, biology, meteorology, etc.). Despite this, there is not as yet a universally accepted definition for 'chaos' as it applies to general dynamical systems. Various approaches range from topological methods of a qualitative description, to physical notions of randomness, information, and entropy in ergodic theory, to the development of computational definitions and algorithms designed to obtain quantitative information. This thesis develops some of the current definitions and discusses several quantitative measures of chaos. It is intended to stimulate the interest of undergraduate and graduate students and is accessible to those with a knowledge of advanced calculus and ordinary differential equations. In covering chaos for continuous systems it serves as a complement to the work done by Philip Beaver which details chaotic dynamics for discrete systems. DTIC

N93-26509# Texas A&M Univ., College Station. Dept. of Chemical Engineering.
THERMODYNAMIC PROPERTIES OF NATURAL GAS MIXTURES Annual Report, 1 Jan. - 31 Dec. 1990
James C. Holste and Kenneth R. Hall Nov. 1992 21 p See also PB93-156818 and PB93-162816 LIMITED REPRODUCIBILITY: More than 20% of this document may be affected by microfiche quality
(Contract GRI-5087-260-1449; GRI Proj. 5696)
(PB93-167112; GRI-93/0004) Avail: CASI HC A03

The objective of the project is to provide PVT and calorimetric data for fluids and fluid mixtures which are components of natural gas or synthetic gas. In the report the authors present data collected on two apparatus: a pycnometer and a Burnett. These data range from 225 - 350 K and from 0 - 70 MPa and include densities and virial coefficients. The fluids covered are five gravimetrically prepared standard reference gases representative of key natural gas in the USA and Europe. NTIS

N93-26558# Gas Research Inst., Chicago, IL.
THERMODYNAMIC PROPERTIES OF NATURAL GAS MIXTURES Annual Report, 1 Jan. - 31 Dec. 1991
J. C. Holste and K. R. Hall Nov. 1992 15 p See also PB93-162816 Sponsored by Gas Research Inst. LIMITED REPRODUCIBILITY: More than 20% of this document may be affected by microfiche quality
(Contract GRI-5087-260-1449)
(PB93-156818; GRI-93/0005) Avail: Issuing Activity (Defense Technical Information Center (DTIC))

The objective of the project is to provide PVT and calorimetric data for fluids and fluid mixtures which are components of natural gas or synthetic gas. In the report the authors present data collected on two apparatus: a pycnometer and a Burnett. These data range from 225 - 350 K and from 0 - 70 MPa and include densities and virial coefficients. The fluids covered are five gravimetrically prepared standard reference gases representative of key natural gas in the USA and Europe. Experimental measurements have been completed and evaluation is underway at van der Waals Laboratory. NTIS

80 SOCIAL SCIENCES (GENERAL)

Includes educational matters.

N93-26051*# National Aeronautics and Space Administration, Washington, DC.
THE 1993/1994 NASA GRADUATE STUDENT RESEARCHERS PROGRAM
Sep. 1992 98 p Original contains color illustrations
(NASA-EP-283; NAS 1.19:283) Avail: CASI HC A05/MF A02; 17 functional color pages

The NASA Graduate Student Researchers Program (GSRP) attempts to reach a culturally diverse group of promising U.S. graduate students whose research interests are compatible with NASA's programs in space science and aerospace technology. Each year we select approximately 100 new awardees based on competitive evaluation of their academic qualifications, their proposed research plan and/or plan of study, and their planned utilization of NASA research facilities. Fellowships of up to $22,000 are awarded for one year and are renewable, based on satisfactory progress, for a total of three years. Approximately 300 graduate students are, thus, supported by this program at any one time. Students may apply any time during their graduate career or prior to receiving their baccalaureate degree. An applicant must be sponsored by his/her graduate department chair or faculty advisor; this book discusses the GSRP in great detail.
Author (revised)

81 ADMINISTRATION AND MANAGEMENT

Includes management planning and research.

N93-25204# Federal Aviation Administration, Oklahoma City, OK. Civil Aeromedical Inst.
PROCEDURAL JUSTICE, OCCUPATIONAL IDENTIFICATION, AND ORGANIZATIONAL COMMITMENT Final Report
L. A. Witt Jun. 1992 13 p
(FAA Proj. AM-C-92-HRR-122)
(DOT/FAA/AM-92/21) Avail: CASI HC A03/MF A01

Extending Tyler's (1989) group-value model, the present study tested the hypothesis that procedural justice may be of differential salience in the development of organizational commitment among individuals who identify primarily with their employing organization versus their occupation. Data collected from 1,235 FAA employees indicated that procedural justice scores were moderately related to commitment scores. Contrary to the hypothesis, occupational identification had no moderating effect on the procedural justice-organizational commitment relationship. Consistent with the multiple commitment literature, employees identifying primarily with their occupation perceived more procedural justice, but expressed less commitment to the organization, than those identifying with their organization. These results provide little support for this extension of the group-value model of procedural justice but some support for the multiple commitment approach to the study of work commitment. Author

N93-25735# Applied Economics Group, Inc., Knoxville, TN.
SMALL BUSINESS ACCESS TO EQUITY CAPITAL Final Report
Robert J. Gaston 7 Aug. 1992 112 p
(Contract SBA-5654-OA-90)
(PB93-144582) Avail: CASI HC A06/MF A02

An entrepreneur's own contribution to the equity capital of their business is constrained by their wealth. If those constraints are binding, entrepreneurs often seek to attract equity capital from external sources. Because formal investors in small businesses incur relatively high transaction costs, some small business owners seek to attract informal investors. The report uses special survey data to explore how and where entrepreneurs find equity capital. Author (DTIC)

N93-26205*# National Aeronautics and Space Administration. Lewis Research Center, Cleveland, OH.
DESIGN AND IMPLEMENTATION OF A PILOT ORIENTATION PROGRAM FOR NEW NASA ENGINEERING EMPLOYEES
Ronald E. Graham, Randall B. Furnas, and Maria Babula May 1993 14 p
(NASA-TM-105907; E-7687; NAS 1.15:105907) Avail: CASI HC A03/MF A01

This paper describes the design and field testing of an orientation program for new employees of NASA Lewis Research Center's Engineering Directorate. A group of new employees designed the program using a series of TQM analysis techniques. The program objectives were: provide consistent treatment for new employees; assist management and clerical staff with their responsibility for orientation; introduce the employee to as many facets of the organization as possible; allow the employee to feel like a member of the organization as early as possible; maximize the use of existing services; and use up-to-date information. The major aspects of the program included: training of management and clerical staff; lab tours

and briefings describing the organization; shepherding, using senior employees as shepherds; a handbook of information about the center and the directorate; a package of information about northeast Ohio; and social activities involving the new employees and shepherds. The program was tested on a pilot group of six new employees over a four month period and was considered to be highly successful by both the employees and management. Aspects of the program have subsequently been adopted for center-wide use. Author

N93-26342# Washington Univ., Seattle. Dept. of Mathematics.
METHODS OF OPTIMIZATION UNDER UNCERTAINTY Final Report
R. T. Rockafellar 29 Dec. 1992 14 p
(Grant AF-AFOSR-0081-89)
(AD-A261487; AFOSR-93-0089TR) Avail: CASI HC A03/MF A01

Research under this grant has focused on a large-scale optimization methodology connected with the solution of problems in which decisions must be made in the face of uncertainty: stochastic programming problems. The principal techniques developed for modeling such problems have made use of various kinds of decomposition--into small-scale optimization problems in extended linear-quadratic programming. Extended linear-quadratic programming goes beyond ordinary linear and quadratic programming in allowing for objective functions to incorporate penalty terms and other features which create piecewise linear or quadratic formulas. The new decomposition techniques include the following: primal-dual Lagrangian decomposition; and forward-backward splitting. DTIC

N93-26418*# National Aeronautics and Space Administration. John F. Kennedy Space Center, Cocoa Beach, FL.
TCMS OPERATIONS AND MAINTENANCE PHILOSOPHY
David P. Buehler and Rock E. Griffin 25 Feb. 1992 32 p
(NASA-TM-108756; NAS 1.15:108756; TS-TCMS-92001) Avail: CASI HC A03/MF A01

The purpose is to describe the basic philosophies of operating and maintaining the Test, Control, and Monitor System (TCMS) equipment. TCMS is a complex and sophisticated checkout system. Operations and maintenance processes developed to support it will be based upon current experience, but will be focused on the specific needs of TCMS in support of Space Station Freedom Program (SSFP) and related activities. An overview of the operations and maintenance goals and philosophies are presented. The assumptions, roles and responsibilities, concepts and interfaces for operation, on-line maintenance, off-line support, and Operations and Maintenance (O&M) personnel training on all TCMS equipment located at KSC are described. Author (revised)

N93-26419*# McDonnell-Douglas Space Systems Co., Cocoa Beach, FL.
TEST, CONTROL AND MONITOR SYSTEM (TCMS) OPERATIONS PLAN
C. K. Macfarlane and M. P. Conroy 29 Jan. 1993 132 p
(Contract NAS10-11400)
(NASA-CR-193098; NAS 1.26:193098; TS-TCMS-92002) Avail: CASI HC A07/MF A02

The purpose is to provide a clear understanding of the Test, Control and Monitor System (TCMS) operating environment and to describe the method of operations for TCMS. TCMS is a complex and sophisticated checkout system focused on support of the Space Station Freedom Program (SSFP) and related activities. An understanding of the TCMS operating environment is provided and operational responsibilities are defined. NASA and the Payload Ground Operations Contractor (PGOC) will use it as a guide to manage the operation of the TCMS computer systems and associated networks and workstations. All TCMS operational functions are examined. Other plans and detailed operating procedures relating to an individual operational function are referenced within this plan. This plan augments existing Technical Support Management Directives (TSMD's), Standard Practices, and other management documentation which will be followed where applicable. Author (revised)

N93-26420*# McDonnell-Douglas Space Systems Co., Cocoa Beach, FL.
TEST, CONTROL AND MONITOR SYSTEM MAINTENANCE PLAN
David P. Buehler and M. J. Lougheed 19 Jan. 1993 163 p
(Contract NAS10-11400)
(NASA-CR-193099; NAS 1.26:193099; TS-TCMS-92003) Avail: CASI HC A08/MF A02

The maintenance requirements for Test, Control, and Monitor System (TCMS) and the method for satisfying these requirements prior to First Need Date (FND) of the last TCMS set are described. The method for satisfying maintenance requirements following FND of the last TCMS set will be addressed by a revision to this plan. This maintenance plan serves as the basic planning document for maintenance of this equipment by the NASA Payloads Directorate (CM) and the Payload Ground Operations Contractor (PGOC) at KSC. The terms TCMS Operations and Maintenance (O&M), Payloads Logistics, TCMS Sustaining Engineering, Payload Communications, and Integrated Network Services refer to the appropriate NASA and PGOC organization. For the duration of their contract, the Core Electronic Contractor (CEC) will provide a Set Support Team (SST). One of the primary purposes of this team is to help NASA and PGOC operate and maintain TCMS. It is assumed that SST is an integral part of TCMS O&M. The purpose of this plan is to describe the maintenance concept for TCMS hardware and system software in order to facilitate activation, transition planning, and continuing operation. When software maintenance is mentioned in this plan, it refers to maintenance of TCMS system software. Author (revised)

N93-26428# Advisory Group for Aerospace Research and Development, Neuilly-Sur-Seine (France).
AGARD MEMBERSHIP, 1993 [LES MEMBRES DE L'AGARD, 1993]
Mar. 1993 83 p
(AGARD-MEMB-93) Copyright Avail: CASI HC A05/MF A01

The mission of the Advisory Group for Aerospace Research and Development (AGARD) is to bring together the leading personalities of the NATO nations in the fields of science and technology relating to aerospace. Lists of members of the National Delegates Board of AGARD, Steering Committee, AGARD National Coordinators, Technical Panels, and Aerospace Applications Studies Committee as of 1 Jan. 1993 are given. CASI

82 DOCUMENTATION AND INFORMATION SCIENCE

Includes information management; information storage and retrieval technology; technical writing; graphic arts; and micrography.

For computer documentation see *61 Computer Programming and Software.*

N93-24677# Lawrence Livermore National Lab., CA.
CROSSING THE FRONTIER BETWEEN PUBLISHING AND INFORMATION SERVICE
Howard L. Lentzner 1 Jul. 1992 7 p Presented at the IEEE International Pofessional Communications Conference, Sante Fe, NM, 30 Sep. 1992
(Contract W-7405-eng-48)
(DE93-002894; UCRL-JC-111017; CONF-9209142-9) Avail: CASI HC A02/MF A01

The changing role of libraries and librarians is discussed with respect to the use of interlinked, high-speed, digital networks and information dissemination methods. DOE

N93-24905 New Mexico State Univ., Las Cruces.
IMPROVING INFORMATION SEARCH AT THE USER INTERFACE: THE IMPACT OF GRAPHICAL INNOVATION ON QUERY FORMULATION AND EXPRESSION Ph.D. Thesis
Troy Cannon Beecroft 1992 129 p
Avail: Univ. Microfilms Order No. DA9302035

The performance of current textual information retrieval systems is limited by informationally impoverished topic descriptions. User-interface innovation may be a suitable method for diminishing human difficulties in query specification. The utility of graphical user-interface artifacts was assessed in several problem areas. First, graphical network displays of index term relations are compared with list displays for their effectiveness in conveying the topical content of a database. Next, queries formed while referring to either a list or network term display are compared, with respect to composition and effectiveness, to a no-display condition. Finally, a traditional syntax for articulating Boolean queries was compared with a novel graphical specification. In each of the above cases, the graphical user-interface components demonstrated a potential to positively impact the query specification process. Dissert. Abstr.

N93-25139*# National Aeronautics and Space Administration. Lyndon B. Johnson Space Center, Houston, TX.
HOW FAR WE ARE FROM THE COMPLETE KNOWLEDGE: COMPLEXITY OF KNOWLEDGE ACQUISITION IN DEMPSTER-SHAFER APPROACH
Bassam A. Chokr (Texas Univ., El Paso.) and Vladik Ya. Kreinovich (Texas Univ., El Paso.) 1991 21 p
(Grants NAG9-482; NSF CDA-90-15006)
(NASA-CR-192944; NAS 1.26:192944) Avail: CASI HC A03/MF A01

When a knowledge base represents the experts' uncertainty, then it is reasonable to ask how far we are from the complete knowledge, that is, how many more questions do we have to ask (to these experts, to nature by means of experimenting, etc) in order to attain the complete knowledge. Of course, since we do not know what the real world is, we cannot get the precise number of questions from the very beginning: it is quite possible, for example, that we ask the right question first and thus guess the real state of the world after the first question. So we have to estimate this number and use this estimate as a natural measure of completeness for a given knowledge base. We give such estimates for Dempster-Shafer formalism. Namely, we show that this average number of questions can be obtained by solving a simple mathematical optimization problem. In principle this characteristic is not always sufficient to express the fact that sometimes we have more knowledge. For example, it has the same value if we have an event with two possible outcomes and nothing else is known, and if there is an additional knowledge that the probability of every outcome is 0.5. We'll show that from the practical viewpoint this is not a problem, because the difference between the necessary number of questions in both cases is practically negligible. Author

N93-25209 University of Technology, Loughborough (England).
THE GENERAL INFORMATION PROGRAMME (PGI) AND DEVELOPING COUNTRIES: A CASE STUDY OF IRAQ Ph.D. Thesis
Victoria Yousip Zado 1990 231 p
Avail: Univ. Microfilms Order No. BRDX97669

The existing information services in Iraq are inefficient and inadequate. They are contributing very little to the development process in the country. Therefore, they need to be improved and developed. The majority of the developing countries, of which Iraq is one and with which we are especially concerned, are undergoing a development process which, in itself, forms a force that develops demand for information services (libraries, documentation, and archives centers). The present situation of information services in Iraq are described, their deficiencies examined, and the possibility of establishing effective guidelines for their development within the conceptual framework of the General Information Programme (GPI) of Unesco, so that they can contribute to the national development plans of the country is considered. The vital role of information services in development and the functions of collecting, organizing, retrieving and disseminating information at the national, regional and international level is explained. The factors that are hindering the development of information services are identified. The measures and steps that must be taken to bring about a fundamental change in the development of these services in Iraq and that might be useful for other developing countries, especially Arab countries are identified.
Dissert. Abstr.

N93-25254# Midwest Research Inst., Golden, CO. National Renewable Energy Lab.
AN ADVANCED DATA-ACQUISITION SYSTEM FOR WIND ENERGY PROJECTS
D. A. Simms and K. L. Cousineau Oct. 1992 10 p Presented at the Windpower '92, Seattle, WA, 19-23 Oct. 1992 Prepared in cooperation with Zond Systems, Inc., Tehachapi, CA
(Contract DE-AC02-83CH-10093)
(DE93-000079; NREL/TP-442-5102; CONF-921049-9) Avail: CASI HC A02/MF A01

NREL has subcontracted with Zond Systems, Inc. to develop an advanced data-acquisition system (ADAS) for wind energy projects. The ADAS can be used to simplify the process of making accurate measurements and analyzing. The system utilizes state-of-the-art electronics and telemetry to provide distributed multi-source, multi-channel data acquisition. Local stand-alone microprocessor-based data acquisition modules (DAMs) can be located near sources of measurement. These allow analog data values to be digitized close to the measurement source, thus eliminating the need for long data runs and slip rings. Signals from digital sensors and transducers can also be directly input to the local DAMS. A PC-based ground station is used to coordinate data transmission to and from all remote DAMS, display real-time values, archive data sets, and process and analyze results. The system is capable of acquiring synchronized time-series data from sensors and transducers under a variety of test configurations in an operational wind-park environment. Data acquisition needs of the wind industry differ significantly from those of most other technologies. Most conventional system designs do not handle data coming from multiple distributed sources, nor do they provide telemetry or the ability to mesh multiple incoming digital data streams. This paper describes the capabilities of the ADAS, and how its design and cost objectives are geared to meet anticipated US wind industry needs. DOE

N93-25258 Florida State Univ., Tallahassee.
USE OF FUZZY RELATIONAL INFORMATION RETRIEVAL TECHNIQUE FOR GENERATING CONTROL STRATEGIES IN RESOLUTION-BASED AUTOMATED REASONING Ph.D. Thesis
Yong-Gi Kim 1992 270 p
Avail: Univ. Microfilms Order No. DA9233293

Current resolution based automated theorem provers, such as ITP and OTTER, adopt strategies to avoid many fruitless paths by their judicious and 'informed' application. Without a suitable strategy guiding the inference, too many often irrelevant clauses may derive, and those clauses may lead the program easily into a blind alley. Therefore, the strategies are the must in any serious use of automated reasoning. Weighting strategy is one of the necessary strategies to produce an answer in allowably short time and space along with the set of support strategy in the area of the resolution based automated reasoning. But, the weighting strategy is still based on the user's knowledge or intuition of the problem to be solved. A method for control of inferential strategies of resolution based architectures is suggested, and then the method is applied to some of domains in automated reasoning fields to inspect the effect of the new scheme. Also, the results of using the various fuzzy implication operators were compared by means of the new weighting mechanism to give a choice of a fuzzy implication operator in a specific domain of automated reasoning. The method for speeding up the logical inference is tested in conjunction with both of the theorem provers called ITP and OTTER. The new weighting mechanism will help the user of the resolution based mechanical theorem prover decide the weighting pattern and the weights to reduce the deduction time and space automatically from the given input problem. The new mechanism employs the triangle fuzzy relational products and fast fuzzy relational algorithm. Dissert. Abstr.

N93-25271 Illinois Univ. at Urbana-Champaign, Savoy.
CONCURRENCY CONTROL IN REAL-TIME DATABASE SYSTEMS Ph.D. Thesis
Oezguer Ulusoy 1992 214 p
Avail: Univ. Microfilms Order No. DA9305720

A 'real-time database system (RTDBS)' is a database system designed to provide real-time information to data-intensive applications. Each RTDB transaction is associated with a timing constraint, typically in the form of a deadline. It is difficult, in a RTDBS, to meet all timing constraints due to the consistency requirements of the underlying database. Efficient resource scheduling algorithms and concurrency control protocols are required to maximize the number of transactions satisfying their timing constraints. In our work, we concentrated on the concurrency control problem in RTDBS's. We evaluated the real-time performance of existing concurrency control approaches in RTDBS's, and we proposed new concurrency control protocols to improve the performance. The protocols take the real-time requirements of the transactions into account in ordering data accesses, while maintaining data consistency via enforcing serializability. The relative performance of the protocols was evaluated in both single-site and distributed RTDBS environments in terms of fraction of satisfied deadlines and average lateness of the tardy transactions. We also investigated the performance impact of different aspects of data distribution and data replication in distributed RTDBS's. Dissert. Abstr.

N93-25288*# Foothill-De Anza Community Coll., Los Altos Hills, CA.
OPTIMIZATION OF KNOWLEDGE-BASED SYSTEMS AND EXPERT SYSTEM BUILDING TOOLS Final Technical Report, 1 Jan. 1986 - 31 Mar. 1993

Phyllis Yasuda and Donald McKellar 31 Mar. 1993 4 p
(Contract NCC2-342)
(NASA-CR-192763; NAS 1.26:192763) Avail: CASI HC A01/MF A01

The objectives of the NASA-AMES Cooperative Agreement were to investigate, develop, and evaluate, via test cases, the system parameters and processing algorithms that constrain the overall performance of the Information Sciences Division's Artificial Intelligence Research Facility. Written reports covering various aspects of the grant were submitted to the co-investigators for the grant. Research studies concentrated on the field of artificial intelligence knowledge-based systems technology. Activities included the following areas: (1) AI training classes; (2) merging optical and digital processing; (3) science experiment remote coaching; (4) SSF data management system tests; (5) computer integrated documentation project; (6) conservation of design knowledge project; (7) project management calendar and reporting system; (8) automation and robotics technology assessment; (9) advanced computer architectures and operating systems; and (10) honors program. Derived from text

N93-25319# Lawrence Livermore National Lab., CA.
A DISTRIBUTED HETEROGENEOUS CLIENT-SERVER ENVIRONMENT
W. M. Buckley and J. B. Carlson Apr. 1992 10 p Presented at the North American Ingres Users Association Meeting, Tarpan Springs, FL, May 1992
(Contract W-7405-eng-48)
(DE93-007496; UCRL-JC-109178; CONF-9205138-3) Avail: CASI HC A02/MF A01

What we have done and will be doing to facilitate operations in a networked multi-vendor environment used by chemists who will not need to know details of how their data migrates between various environments is addressed. The Nuclear Chemistry Division at Lawrence Livermore National Laboratory (LLNL) is using Ingres Release 6.3 in VMS and Sun-OS environments on VAXes, Suns, and Solbournes to manage and analyze data that support the division's missions. The database and applications reside in both the VMS and UNIX environments. Additionally, they have to exchange data and otherwise cooperate with MS-DOS PC's, Macintoshes, remote Ingres databases, and other commercial database products. This environment is relatively seamless and transparent to the users and we strive to use commercial off-the-shelf solutions wherever practical. A very general client-server computing environment is described, but neither a leading-edge client-server environment nor federated or other multidatabase concepts are described. What is described is a cooperative environment that is heterogeneous with respect to hardware and software vendors, network protocols, and user community. Our approach to constructing this cooperative environment and some aspects of our management of that environment are discussed. DOE

N93-25350 Stanford Univ., CA.
HIERARCHICAL DYNAMICS IN DISTRIBUTED INFORMATION PROCESSING Ph.D. Thesis
Erik Daniel Lumer 1992 127 p
Avail: Univ. Microfilms Order No. DA9234132

The large size of distributed processing systems, the nontrivial dynamics of their local processes, and the emergence of collective states having a computational interpretation, call for new theories which predict the behavior of these systems and point at the relevant macroscopic measures with which to characterize them. This dissertation focuses on the collective computation that arises in the context of two phenomena: decentralized resource allocation in distributed system, and visual processing with large assemblies of oscillators. In the study of decentralized resource allocation, a renormalization group analysis elucidates the relationship between individual interactions and global migration of resources among clusters when the interactions follow a hierarchy of time scales. From this study, a formal hierarchy that manages computational resources is derived and its dynamics in the face of delays and so-called informal links is investigated theoretically. Experiments on a hypercube parallel computer confirm the predicted regimes. For the model of visual processing, the basic conditions under which collective rhythmic activity can exist in a population of phase coupled oscillators with a hierarchy of coupling strengths and a distribution of intrinsic frequencies are established. Novel regimes, such as a cascade of discrete phase transitions into global synchrony, are also exhibited. These regimes are interpreted in terms of grouping and segmentation operations in the visual system. A solution to the problem of internal access to the perceptual groups constructed in this way is given in the form of a dynamic network called the phase-tracker of attention. Simulations show that the network's behavior matches a number of psychophysical observations on human visual attention. Dissert. Abstr.

N93-25395 Pittsburgh Univ., PA.
AN EXPERIMENTAL EXAMINATION OF THE EFFECTS OF EXPERTISE AND PROBLEM-SOLVING CUES ON THE IDENTIFICATION OF IDEAS FOR STRATEGIC INFORMATION SYSTEMS Ph.D. Thesis
Jeffrey Lynn Sampler 1992 280 p
Avail: Univ. Microfilms Order No. DA9304198

The topic of developing strategic information systems, and potentially using them to gain competitive advantage, has been a focus of much research activity over the past decade. The result of this literature has been the development of several frameworks to aid in the identification of strategic information applications. Unfortunately, only one comparative study evaluating these techniques has been performed, and this study did not examine the role of expertise of subjects solving the task (Bergeron, Buteau, and Raymond, 1991). The purpose of this dissertation was to look at the role of individual expertise and problem solving cues as they affect the definition of the strategic information system. These questions were investigated in a 2 x 2 x 4 factorial designed experiment with factors of: (1) type of expertise (banking and IS); (2) level of expertise (expert and novice); and (3) problem solving cue (control, 'Be Creative', Competitive Forces, and CRLC). Using multivariate and univariate analysis of variance, it appears that expertise in both banking and IS is necessary to develop solutions of high quality, usefulness, and feasibility. Also, banking expertise is necessary to develop solutions that are specific, detailed, and well justified. The problem solving cue used by subjects had no significant effect on the quality of the solutions developed. In one treatment of the dependent variables, there was a significant interaction effect between IS expertise and problem solving cues. Dissert. Abstr.

N93-25421 Temple Univ., Philadelphia, PA.
FACTORS ASSOCIATED WITH PERCEPTIONS OF PRODUCTIVITY AND USAGE OF INFORMATION TECHNOLOGY IN A SERVICE ORGANIZATION Ph.D. Thesis
Shashi Rao Karpur 1992 174 p
Avail: Univ. Microfilms Order No. DA9302118

One of the most important issues facing organizations is to evaluate the value gained from information and communication technologies, particularly in terms of productivity. While there have been numerous economic justifications for implementing information systems, this study argues for the importance of defining productivity from an end-user point of view. The objective of this study was to understand user perceptions of productivity from utilizing information technology in their work environment, to examine the relationship between these perceptions and usage of the technology, and to explore the association of individual, organizational and technical factors with these dependent variables. Data for the study was collected using survey methodology from 289 users of banking automation systems at a large Northeast regional bank. Self-report survey data was enhanced with actual data on system usage. Four hypotheses were proposed that tested a research model outlining the relationship between perceived productivity, system usage, and individual, organizational, and technical variables. Results showed that users perceived their productivity to have increased from using the banking automation system. These perceptions were attributed to feelings of being more efficient and competent because of the system, having the ability to be creative and flexible, and from just having the access to using the technology. Perceptions of productivity were most strongly associated with users' satisfaction with technical characteristics of the system, with their attitude towards computers, their rating of their skill level, and with their satisfaction with system-relevant communication and training. Satisfaction with enhancements to the system also proved important. Although a significant relationship between user perceptions of productivity and usage of the system was established, the strength of the relationship was only moderate. Again, satisfaction with technical characteristics and organizational support variables were most significantly associated with usage. The study also found that self-reports on usage when compared with actual data was reasonably reliable. The study provided directions to increase the value of information technology by highlighting factors most important to enhancing user perceptions of productivity and their usage of the technology. Dissert. Abstr.

N93-25448# Los Alamos National Lab., NM.
WAVELET TRANSFORM-VECTOR QUANTIZATION COMPRESSION OF SUPERCOMPUTER OCEAN MODEL SIMULATION OUTPUT
J. N. Bradley and C. M. Brislawn 12 Nov. 1992 13 p Presented at the 1993 Data Compression Conference, Snowbird, UT, 30 Mar. - 1 Apr. 1993
(Contract W-7405-eng-36)
(DE93-005453; LA-UR-92-4002; CONF-930390-1) Avail: CASI HC A03/MF A01

We describe a new procedure for the efficient compression of digital information for storage and transmission purposes. The algorithm involves a discrete wavelet transform subband decomposition of the data set. This is followed by vector quantization of the wavelet transform coefficients using application-specific vector quantizers. The new vector quantizer design procedure optimizes the assignment of both memory resources and vector dimensions to the transform subbands by minimizing an exponential rate-distortion functional subject to constraints on both overall bit-rate and encoder complexity. The wavelet-vector quantization method, which originates in digital image compression, is applicable to the compression of other multidimensional data sets possessing some degree of smoothness. In this paper, we discuss the use of this technique for compressing the output of supercomputer simulations of global climate models. The data presented here comes from Semtner-Chervin global ocean models run at the National Center for Atmospheric Research and at the Los Alamos Advanced Computing Laboratory. DOE

N93-25466 Florida Univ., Gainesville.
A LOGIC-BASED APPROACH TO FEDERATED DATABASES Ph.D. Thesis
Whan-Kyu Whang 1992 149 p
Avail: Univ. Microfilms Order No. DA9304071

Current systems for federated database management have concentrated on either schema integration using semantic models or query processing by the relational model, but not both issues in a single framework. In this dissertation we explored an alternative approach to database integration based on using Horn-clause logic as a canonical, intermediate form. First-order logic is used as a language for specifying an integration of component schemas as well as expressing integrity constraints associated with global and component schemas. A first-order logic-based language is rich enough to be used for canonical representation at the intermediate level. Global to local query mapping is done using unification in logic programming. Query optimization is performed using integrity constraints such as functional, inclusion, and data integration dependencies. Moreover, the logic programming language PROLOG can provide a tool for implementation. Therefore, the logic-based approach increases processing capability by providing a single formal framework for design and implementation of integrating heterogeneous databases. In this dissertation we deal with schemas of relational databases as component schemas. To generate a single integrated schema from component schemas at the initial phase of schema integration, five types of equivalences (EQUAL, CONTAIN, CONTAINED IN, OVERLAP, DISJOINT) are to be identified between a pair of relations. An algorithm is developed to aid the designer in deriving new equivalences from partially known equivalences as well as to check the consistency of equivalences that are previously specified. To provide set operations on the component relations related to one another by the five types of equivalences, we have developed an extended SQL (ESQL). The set operations in ESQL are expressed non-procedurally in a single statement, unlike conventional SQL which requires blocks of code with set operations among the blocks. The overall approach to processing of queries in ESQL, their optimization, and decomposition against component databases is discussed. Several parts of the proposed architecture are implemented using PROLOG. Dissert. Abstr.

N93-25475 Kentucky Univ., Lexington.
ADAPTIVE DECISION SUPPORT SYSTEMS: CONCEPTS, CHARACTERIZATION, AND AN APPLICATION Ph.D. Thesis
Jigish Shirish Zaveri 1992 306 p
Avail: Univ. Microfilms Order No. DA9303651

An examination of machine learning strategies employed in existing decision support system (DSS) paradigms suggests that problem processing knowledge (PPK) is acquired through one or more supervised learning strategies. Therefore, specific instances of these paradigms are dependent, to varying degrees, upon external agents for acquiring needed PPK. Such dependence imposes two limitations on a system: (1) the extent of its intelligence is largely governed by the agent's intelligence, and (2) in typical, dynamic contexts, the system soon becomes obsolete unless its PPK is continually updated with the aid of an agent. A possible alternative is to construct a system with the ability to independently acquire, utilize, and dispose of some or all of the needed PPK during the course of one or more problem processing episodes, and to generalize what has been learned to other, similar problem instances. Such an approach is especially desirable in complex domains where predefinition of PPK may be impossible and/or undesirable. A new DSS paradigm called the Adaptive DSS (AdDSS) is proposed, it is characterized in terms of key problem processing features, it is contrasted with existing paradigms, and a prototype system within one application context is constructed and tested. By our definition, an AdDSS possesses a problem processor which makes heavy use of some form of unsupervised induction, in addition to rote and, perhaps, other forms of learning. Thus, unlike earlier paradigns, AdDSS has the ability to acquire some or much of its PPK without the assistance of an external entity. In order to examine the viability of developing useful AdDSS's in practice, the paradigm is applied in developing a DSS to support static scheduling decisions in flexible manufacturing contexts and study its performance through a series of experiments. This system uses generic algorithms in conjunction with predefined algorithmic search knowledge to effectively combine unsupervised induction with rote learning. Our experiments seek to contrast the performance of the AdDSS with systems relying wholly on memorization, analyze its learning behavior, and assess its ability to automatically specify some of the needed input parameters.
Dissert. Abstr.

N93-25482# Ohio State Univ., Columbus.
DESIGN AND ANALYSIS OF ALGORITHMS FOR PROCESSING QUERIES IN DATABASE SYSTEMS Ph.D. Thesis
Shu-Shang Sam Wei 1992 174 p
Avail: Univ. Microfilms Order No. DA9238296

This dissertation studies various strategies for reducing I/O costs in database systems in the following perspectives. (1) Join operations in relational database system. While an indexed file structure is available for each operand relation, join operations are usually modeled by page connectivity graphs. In such graphs, each node represents a page of a relation and two nodes are linked with an edge if their corresponding pages contain tuples that may need to be joined. Two problems regarding reducing I/O costs are widely studied. They are the minimum page retrieval problem and the minimum buffer size problem. The minimum page retrieval problem asks for a page retrieval sequence to perform a join operation such that the number of disk pages retrieved into a given fixed size memory buffer is minimum. The minimum buffer size problem asks for a page retrieval sequence to perform a join operation such that each page is retrieved at most once and the size of the memory buffer required is minimum. These two problems are both known to be NP-hard in general cases. We first show that the minimum page retrieval problem remains NP-hard when the page connectivity graph is bipartite. Then we discover that the page connectivity graphs of many frequently encountered join operations belong to a special class of graphs called 'forward-convex bipartite graphs'. For such graphs, we propose an efficient algorithm for each of the above problems. (2) Composition operation is relational database systems. The page connectivity graphs do not model composition operations as successfully as they do join operations. For composition operation, we propose a heuristic algorithm which uses a new hot-spot technique. (3) Linear recursive rules in deductive database systems. The page connectivity graphs are also useless for describing the processing of recursive rules in deductive databases. In such cases, we develop a methodology that utilizes a multiple query optimization technique to generate a query processing plan where the number of relations accessed is minimum. Dissert. Abstr.

N93-25554 California Univ., Berkeley.
PERFORMANCE STUDIES OF CACHE CONSISTENCY AND CONCURRENCY CONTROL ALGORITHMS IN A DISTRIBUTED CLIENT/SERVER DBMS ARCHITECTURE Ph.D. Thesis
Yongdong Wang 1992 206 p
Avail: Univ. Microfilms Order No. DA9305108

This dissertation presents a performance study of database concurrency control and application program cache consistency algorithms in a distributed

client/server database system (DBMS) architecture. The database resides on the server and application programs. To reduce object access latency and network and server load, objects are cached in the application program. Mechanisms must be provided to guarantee that concurrent transactions accessing the cached objects and the database do not interfere with each other. We distinguished between caching within a transaction (intra-transaction) and between transactions (inter-transaction). Two intra-transaction cache consistency algorithms and five inter-transaction cache consistency algorithms are described. A simulator was developed to compare the average transaction response time and server throughput rate for these algorithms under different workloads and system configurations. The simulator supported an innovative object reference model. Four workloads were included in our experiments: small batch transactions, large batch transactions, interactive transactions, and mixed transactions. System configurations included a system where the server CPU was the bottleneck, a system where the server disk was the bottleneck, a system where the network was the bottleneck, and systems with different client cache sizes. Our simulation experiments show that two-phase locking and call-back locking dominate no-wait locking and no-wait locking with notification where the server or the network is a bottleneck. Callback locking is better than two-phase locking when the intertransaction locality is high and the probability of object update is low because it avoids handshake with the server when accessing cached objects. Two-phase locking is better when write probability is high because it causes the least number of transaction restarts. When the server disk is a bottleneck, no-wait locking with notification performs the best because it propagates updates to clients directly and hence saves server disk I/O's. It is critical for client caches to be larger than the working set of the applications on a client. Dissert. Abstr.

N93-25722 Stanford Univ., CA.
DISTRIBUTED INFORMATION STORAGE Ph.D. Thesis
James Richard Roche 1992 130 p
Avail: Univ. Microfilms Order No. DA9234155

Information is distributed in many different applications. In conventional parallel processing, for example, data is distributed in order to speed up computation. We consider the less-studied problem of distributing data among different sites for fault-tolerance. The primary example that we consider involves storing information on a network of disks so that the information can be recovered reliably even when some of the disks fail. The techniques developed in this thesis apply equally well, however, to problems in which communication links can fail and information packets can be lost. Using techniques from Galois field theory and network flow theory, we show how to store information at different sites with an absolute minimum of redundancy so as to prevent any loss of data if several sites become inaccessible. We allow the different sites to have different storage capacities and to be arranged in a variety of network topologies. The theoretical results on reliable information storage derived for general networks can be specialized to a particular configuration of disks that is widely used in practice. Although the information storage scheme for this configuration is simple in principle, there are practical difficulties because of the need to update parity-check blocks continually as data blocks are modified. For the setup above, the delay between reading a parity block and writing its updated value back onto the disk can seriously degrade the performance of a disk array. We analyze a technique called floating parity track that dramatically reduces the average delay between reading and writing a parity block. We find that the delay can typically be reduced by a factor of thirty in return for a slight decrease in storage efficiency.
Dissert. Abstr.

N93-25754 University of Technology, Loughborough (England).
A FRAMEWORK FOR THE DESIGN OF USABLE ELECTRONIC TEXT Ph.D. Thesis
Andrew Patrick Dillon 1991 258 p
Avail: Univ. Microfilms Order No. BRDX97673

This thesis examines the human issues underlying the design and usability of electronic text systems. In so doing it develops a framework for the conceptualization of these issues that aims to guide designers of electronic texts in their attempts to produce usable systems. The thesis commences with a review of the traditional human factors literature on electronic text according to three basic themes: its concern with perceptual, manipulatory and structural issues. From this examination it is concluded that shortcomings in translating this work into design result from the adoption of overly narrow uni-disciplinary views of reading taken from cognitive psychology and information science which are inappropriate to serve the needs of electronic text designers. In an attempt to provide a more relevant description of the reading process a series of studies examining readers and their views as well as uses of texts if reported. In the first, a repertory grid based investigation revealed that all texts can be described in reader-relevant terms according to three criteria: why a text is read, what a text contains and how it is read. These criteria then form the basis of two investigations of reader-text interaction using academic journals and user manuals. The results of these studies highlighted the need to consider readers' models of a document's structure in discussing text usability. Subsequent experimental work on readers' models of academic articles demonstrated not only that such models are important aspects of reader-text interaction but that data of this form could usefully be employed in the design of an electronic text system. The proposed framework provides a broad, qualitative model of the important issues for designers to consider when developing a product. It consists of four interactive elements that focus attention on aspects of reading that have been identified as central to usability. Simple tests of the utility and validity of the framework are reported and it is shown that the framework both supports reasoned analysis and subsequent prediction of reader behavior as well as providing a parsimonious account of their verbal utterances while reading. The thesis concludes with an analysis of the likely uses of such a framework and the potential for electronic text systems in an increasingly information-hungry world. Dissert. Abstr.

N93-25763# Texas A&M Univ., College Station. Knowledge Based Systems Lab.
INTEGRATED DEVELOPMENT SUPPORT ENVIRONMENT (IDSE) Interim Report, Jan. 1990 - Mar. 1991
Richard J. Mayer, Martha S. Wells, and Michael K. Painter Nov. 1992 68 p
(Contract MIPR-FQ7624-90-00010; AF Proj. 2940)
(AD-A261088; AL-TP-1992-0052) Avail: CASI HC A04/MF A01

Businesses today are rapidly recognizing that information assets are a resource that belongs to, and can be more effectively used by, the enterprise as a whole to realize major advancements in competitiveness. Attempts to leverage and reuse these assets, however, have long been plagued by the inability of our information systems to adapt and evolve gracefully to a changing environment. The ability to leverage corporate information assets therefore necessitates an altogether new way of thinking about, and developing, enterprise information systems. If information is to be controlled and managed as a global enterprise resource, then enterprise information systems will require the consistent, long-term involvement of large numbers of individuals, many of whom are not computer specialists. An Integrated Development Support Environment (IDSE) provides a system which supports user-driven development and evolution of information systems through graceful change to both (1) the information needs to be supported, and (2) the degree and types of automation. This report describes the design concepts for an IDSE centering around a scalable architectural design strategy enabling enterprise-level evaluation towards the desired levels of integration, automation, and sophistication. DTIC

N93-25792*# Colorado Univ., Boulder. Lab. for Atmospheric and Space Physics.
APPLIED INFORMATION SYSTEMS RESEARCH PROGRAM (AISRP). WORKSHOP 2: MEETING PROCEEDINGS
1992 262 p Workshop held in Boulder, CO, 11-13 Aug. 1992 Sponsored by NASA. Washington
(NASA-CR-193096; NAS 1.26:193096) Avail: CASI HC A12/MF A03

The Earth and space science participants were able to see where the current research can be applied in their disciplines and computer science participants could see potential areas for future application of computer and information systems research. The Earth and Space Science research proposals for the High Performance Computing and Communications (HPCC) program were under evaluation. Therefore, this effort was not discussed at the AISRP Workshop. OSSA's other high priority area in computer science is scientific visualization, with the entire second day of the workshop devoted to it. For individual titles, see N93-25793 through N93-25814.

N93-25793*# Illinois Univ., Urbana.
AN INTERACTIVE ENVIRONMENT FOR THE ANALYSIS OF LARGE EARTH OBSERVATION AND MODEL DATA SETS Abstract Only
Kenneth P. Bowman, John E. Walsh, and Robert B. Wilhelmson *In* Colorado Univ., Applied Information Systems Research Program (AISRP). Workshop 2: Meeting Proceedings 1992 1 p (For primary document see N93-25792 09-82)
Avail: CASI HC A01/MF A03

We propose to develop an interactive environment for the analysis of large Earth science observation and model data sets. We will use a standard scientific data storage format and a large capacity (greater than 20 GB) optical disk system for data management; develop libraries for coordinate transformation and regridding of data sets; modify the NCSA X Image and X Data Slice software for typical Earth observation data sets by including map transformations and missing data handling; develop analysis tools for common mathematical and statistical operations; integrate the components described above into a system for the analysis and comparison of observations and model results; and distribute software and documentation to the scientific community. Author

N93-25794*# National Center for Atmospheric Research, Boulder, CO.
INTERACTIVE INTERFACE FOR NATIONAL CENTER FOR ATMOSPHERIC RESEARCH (NCAR) GRAPHICS Abstract Only
William Buzbee and Robert L. Lackman *In* Colorado Univ., Applied Information Systems Research Program (AISRP). Workshop 2: Meeting Proceedings 1992 1 p (For primary document see N93-25792 09-82)
Avail: CASI HC A01/MF A03

NCAR Graphics is a FORTRAN 77 library of over 30 high-level graphics modules which are heavily used by science and engineering researchers at over 1500 sites world-wide including many universities and government agencies. These Earth science oriented modules now have a FORTRAN callable subroutine interface which excludes their use by non-programming researchers. This proposal outlines the development of a fully interactive 'point and click' menu-based interface using the prevailing toolkit standard for the X-window systems. Options for direct output to the display window and/or output to a Computer Graphics Metafile (CGM) will be provided. X, PEX, and PHIGS will be implemented as the underlying windowing and graphics standards. Associated meteorological and geometric data sets would exploit the network extended NASA Common Data Format, netCDF. Author

N93-25795*# California Univ., Berkeley.
DEVELOPMENT OF A TOOL-SET FOR SIMULTANEOUS, MULTI-SITE OBSERVATIONS OF ASTRONOMICAL OBJECTS Abstract Only c89
Supriya Chakrabarti, J. Garrett Jernigan, and Herman L. Marshall *In* Colorado Univ., Applied Information Systems Research Program (AISRP). Workshop 2: Meeting Proceedings 1992 1 p (For primary document see N93-25792 09-82)
Avail: CASI HC A01/MF A03

A network of ground and space based telescopes can provide continuous observation of astronomical objects. In a 'Target of Opportunity' scenario triggered by the system, any telescope on the network may request supporting observations. We propose to develop a set of data collection and display tools to support these observations. We plan to demonstrate the usefulness of this tool set for simultaneous multi-site observations of astronomical targets. Possible candidates for the proposed demonstration include the Extreme Ultraviolet Explorer, International Ultraviolet Explorer, ALEXIS, and sounding rocket experiments. Ground based observations operated by the University of California, Berkeley; the Jet Propulsion Laboratory; and Fairborn Observatory, Mesa, Arizona will be used to demonstrate the proposed concept. Although the demonstration will involve astronomical investigations, these tools will be applicable to a large number of scientific disciplines. The software tools and systems developed as a result of our work will be made available to the scientific community. Author

N93-25796*# California Inst. of Tech., Pasadena. Dept. of Astronomy.
MULTIVARIATE STATISTICAL ANALYSIS SOFTWARE TECHNOLOGIES FOR ASTROPHYSICAL RESEARCH INVOLVING LARGE DATA BASES
Stanislav Djorgovski *In* Colorado Univ., Applied Information Systems Research Program (AISRP). Workshop 2: Meeting Proceedings 1992 2 p (For primary document see N93-25792 09-82)
Avail: CASI HC A01/MF A03

The existing and forthcoming data bases from NASA missions contain an abundance of information whose complexity cannot be efficiently tapped with simple statistical techniques. Powerful multivariate statistical methods already exist which can be used to harness much of the richness of these data. Automatic classification techniques have been developed to solve the problem of identifying known types of objects in multi parameter data sets, in addition to leading to the discovery of new physical phenomena and classes of objects. We propose an exploratory study and integration of promising techniques in the development of a general and modular classification/analysis system for very large data bases, which would enhance and optimize data management and the use of human research resources. Author

N93-25797*# Colorado Univ., Boulder. Center for Astrodynamics Research.
A LAND-SURFACE TESTBED FOR EOSDIS Abstract Only
William Emery, Jeff Dozier (California Univ., Santa Barbara.), and Paul Rotar (National Center for Atmospheric Research, Boulder, CO.) *In its* Applied Information Systems Research Program (AISRP). Workshop 2: Meeting Proceedings 1992 1 p (For primary document see N93-25792 09-82)
Avail: CASI HC A01/MF A03

We propose to develop an on-line data distribution and interactive display system for the collection, archival, distribution and analysis of operational weather satellite data for applications in land surface studies. A 1,000 sq km scene of the western U.S. (centered on the Colorado Rockies) will be extracted from Advanced Very High Resolution Radiometer (AVHRR) imagery collected from morning and afternoon passes of the NOAA polar-orbiters at the direct readout stations operated by CU/CCAR. All five channels of these AVHRR data will be navigated and map registered at CU/CCAR and then be transferred to NCAR for storage in an on-line data system. Software will also be available at NCAR to process and navigate the raw AVHRR data as needed. A display workstation software, based on a Macintosh II computer, will be developed that will display and further process the AVHRR data for studies of vegetation monitoring and snowpack assessment. Various options of presently used techniques for both vegetation and snowpack monitoring will be implemented in the workstation software to provide the individual investigator with the freedom to interact with the satellite image data. The display software will be freely distributed online to interested investigators and the AVHRR data will be made available on-line to anyone interested. In addition, potential users will be sought out and connected to the on-line data archive. This experiment with an active on-line archive and interactive analysis systems will provide experience with a small scale EOSDIS. Author

N93-25798*# Jet Propulsion Lab., California Inst. of Tech., Pasadena.
GEOGRAPHIC INFORMATION SYSTEM FOR FUSION AND ANALYSIS OF HIGH-RESOLUTION REMOTE SENSING AND GROUND TRUTH DATA Abstract Only
Anthony Freeman, Jo Bea Way, Pascale DuBois, and Franz Leberl (Vexcel Corp., Boulder, CO.) *In* Colorado Univ., Applied Information Systems Research Program (AISRP). Workshop 2: Meeting Proceedings 1992 2 p (For primary document see N93-25792 09-82)
Avail: CASI HC A01/MF A03

We seek to combine high-resolution remotely sensed data with models and ground truth measurements, in the context of a Geographical Information System, integrated with specialized image processing software. We will use this integrated system to analyze the data from two Case Studies, one at a bore AI forest site, the other a tropical forest site. We will assess the information content of the different components of the data, determine the optimum data combinations to study biogeophysical changes in the forest, assess the best way to visualize the results, and validate the models for the forest response to different radar wavelengths/polarizations. During the 1990's, unprecedented amounts of high-resolution images from space of the Earth's surface will become available to the applications scientist from the LANDSAT/TM series, European and Japanese ERS-1 satellites, RADARSAT and SIR-C missions. When the Earth Observation Systems (EOS) program is operational, the amount of data available for a particular site can only increase. The interdisciplinary scientist, seeking to

use data from various sensors to study his site of interest, may be faced with massive difficulties in manipulating such large data sets, assessing their information content, determining the optimum combinations of data to study a particular parameter, visualizing his results and validating his model of the surface. The techniques to deal with these problems are also needed to support the analysis of data from NASA's current program of Multi-sensor Airborne Campaigns, which will also generate large volumes of data. In the Case Studies outlined in this proposal, we will have somewhat unique data sets. For the Bonanza Creek Experimental Forest (Case I) calibrated DC-8 SAR data and extensive ground truth measurement are already at our disposal. The data set shows documented evidence to temporal change. The Belize Forest Experiment (Case II) will produce calibrated DC-8 SAR and AVIRIS data, together with extensive measurements on the tropical rain forest itself. The extreme range of these sites, one an Arctic forest, the other a tropical rain forest, has been deliberately chosen to find common problems which can lead to generalized observations and unique problems with data which raise issues for the EOS System. Author

N93-25799*# National Aeronautics and Space Administration. Ames Research Center, Moffett Field, CA.

CONSTRUCTION OF AN ADVANCED SOFTWARE TOOL FOR PLANETARY ATMOSPHERIC MODELING c61

Peter Friedland, Richard M. Keller, Christopher P. McKay, Michael H. Sims, and David E. Thompson *In* Colorado Univ., Applied Information Systems Research Program (AISRP). Workshop 2: Meeting Proceedings 1992 2 p (For primary document see N93-25792 09-82)

Avail: CASI HC A01/MF A03

Scientific model-building can be a time intensive and painstaking process, often involving the development of large complex computer programs. Despite the effort involved, scientific models cannot be distributed easily and shared with other scientists. In general, implemented scientific models are complicated, idiosyncratic, and difficult for anyone but the original scientist/programmer to understand. We propose to construct a scientific modeling software tool that serves as an aid to the scientist in developing, using and sharing models. The proposed tool will include an interactive intelligent graphical interface and a high-level domain-specific modeling language. As a test bed for this research, we propose to develop a software prototype in the domain of planetary atmospheric modeling. Author

N93-25800*# Canada Centre for Remote Sensing, Ottawa (Ontario).

SYSTEM OF EXPERTS FOR INTELLIGENT DATA MANAGEMENT (SEIDAM) Abstract Only

David G. Goodenough, Joji Iisaka, and Ko Fung (Ottawa Univ., Ontario.) *In* Colorado Univ., Applied Information Systems Research Program (AISRP). Workshop 2: Meeting Proceedings 1992 1 p (For primary document see N93-25792 09-82)

Avail: CASI HC A01/MF A03

It is proposed to conduct research and development on a system of expert systems for intelligent data management (SEIDAM). CCRS has much expertise in developing systems for integrating geographic information with space and aircraft remote sensing data and in managing large archives of remotely sensed data. SEIDAM will be composed of expert systems grouped in three levels. At the lowest level, the expert systems will manage and integrate data from diverse sources, taking account of symbolic representation differences and varying accuracies. Existing software can be controlled by these expert systems, without rewriting existing software into an Artificial Intelligence (AI) language. At the second level, SEIDAM will take the interpreted data (symbolic and numerical) and combine these with data models. At the top level, SEIDAM will respond to user goals for predictive outcomes given existing data. The SEIDAM Project will address the research areas of expert systems, data management, storage and retrieval, and user access and interfaces. Author

N93-25801*# Jet Propulsion Lab., California Inst. of Tech., Pasadena.

KNOWLEDGE-BASED ASSISTANCE FOR SCIENCE VISUALIZATION AND ANALYSIS USING LARGE DISTRIBUTED DATABASES Abstract Only

Thomas H. Handley, Jr., Allan S. Jacobson, Richard J. Doyle, and Donald J. Collins *In* Colorado Univ., Applied Information Systems Research Program (AISRP). Workshop 2: Meeting Proceedings 1992 1 p (For primary document see N93-25792 09-82)

Avail: CASI HC A01/MF A03

Within this decade, the growth in complexity of exploratory data analysis and the sheer volume of space data require new and innovative approaches to support science investigators in achieving their research objectives. To date, there have been numerous efforts addressing the individual issues involved in inter-disciplinary, multi-instrument investigations. However, while successful in small scale, these efforts have not proven to be open and scaleable. This proposal addresses four areas of significant need: scientific visualization and analysis; science data management; interactions in a distributed, heterogeneous environment; and knowledge-based assistance for these functions. The fundamental innovation embedded within this proposal is the integration of three automation technologies, namely, knowledge-based expert systems, science visualization and science data management. This integration is based on the concept called the Data Hub. With the Data Hub concept, NASA will be able to apply a more complete solution to all nodes of a distributed system. Both computation nodes and interactive nodes will be able to effectively and efficiently use the data services (access, retrieval, update, etc.) with a distributed, interdisciplinary information system in a uniform and standard way. This will allow the science investigators to concentrate on their scientific endeavors, rather than to involve themselves in the intricate technical details of the systems and tools required to accomplish their work. Thus, science investigators need not be programmers. The emphasis will be on the definition and prototyping of system elements with sufficient detail to enable data analysis and interpretation leading to publishable scientific results. In addition, the proposed work includes all the required end-to-end components and interfaces to demonstrate the completed concept. Author

N93-25802*# Colorado Univ., Boulder.

EXPERIMENTER'S LABORATORY FOR VISUALIZED INTERACTIVE SCIENCE Abstract Only

Elaine R. Hansen, Marjorie K. Klemp, Sally W. Lasater, Marti R. Szczur (National Aeronautics and Space Administration. Goddard Space Flight Center, Greenbelt, MD.), and Joseph B. Klemp (National Center for Atmospheric Research, Boulder, CO.) *In its* Applied Information Systems Research Program (AISRP). Workshop 2: Meeting Proceedings 1992 1 p (For primary document see N93-25792 09-82)

Avail: CASI HC A01/MF A03

The science activities of the 1990's will require the analysis of complex phenomena and large diverse sets of data. In order to meet these needs, we must take advantage of advanced user interaction techniques: modern user interface tools; visualization capabilities; affordable, high performance graphics workstations; and interoperable data standards and translator. To meet these needs, we propose to adopt and upgrade several existing tools and systems to create an experimenter's laboratory for visualized interactive science. Intuitive human-computer interaction techniques have already been developed and demonstrated at the University of Colorado. A Transportable Applications Executive (TAE+), developed at GSFC, is a powerful user interface tool for general purpose applications. A 3D visualization package developed by NCAR provides both color shaded surface displays and volumetric rendering in either index or true color. The Network Common Data Form (NetCDF) data access library developed by Unidata supports creation, access and sharing of scientific data in a form that is self-describing and network transparent. The combination and enhancement of these packages constitutes a powerful experimenter's laboratory capable of meeting key science needs of the 1990's. This proposal encompasses the work required to build and demonstrate this capability. Author

N93-25803*# Massachusetts Inst. of Tech., Cambridge.

TOPOGRAPHY FROM SHADING AND STEREO Abstract Only

Berthold P. Horn and Michael Caplinger (Arizona State Univ., Tempe.) *In* Colorado Univ., Applied Information Systems Research Program (AISRP). Workshop 2: Meeting Proceedings 1992 1 p (For primary document see N93-25792 09-82)

Avail: CASI HC A01/MF A03

Methods exploiting photometric information in images that have been developed in machine vision can be applied to planetary imagery. Present techniques, however, focus on one visual cue, such as shading or binocular

stereo, and produce results that are either not very accurate in an absolute sense or provide information only at few points on the surface. We plan to integrate shape from shading, binocular stereo and photometric stereo to yield a robust system for recovering detailed surface shape and surface reflectance information. Such a system will be useful in producing quantitative information from the vast volume of imagery being received, as well as in helping visualize the underlying surface. The work will be carried out on a popular computing platform so that it will be easily accessible to other workers. Author

N93-25804*# Jet Propulsion Lab., California Inst. of Tech., Pasadena.
A DISTRIBUTED SYSTEM FOR VISUALIZING AND ANALYZING MULTIVARIATE AND MULTIDISCIPLINARY DATA Abstract Only
Allan S. Jacobson, Mark Allen, Michael Bailey, Ronald Blom, Leo Blume, and Lee Elson *In* Colorado Univ., Applied Information Systems Research Program (AISRP). Workshop 2: Meeting Proceedings 1992 1 p (For primary document see N93-25792 09-82)
Avail: CASI HC A01/MF A03

The Linked Windows Interactive Data System (Link Winds) is being developed with NASA support. The objective of this proposal is to adapt and apply that system in a complex network environment containing elements to be found by scientists working multidisciplinary teams on very large scale and distributed data sets. The proposed three year program will develop specific visualization and analysis tools, to be exercised locally and remotely in the Link Winds environment, to demonstrate visual data analysis, interdisciplinary data analysis and cooperative and interactive televisualization and analysis of data by geographically separated science teams. These demonstrations will involve at least two science disciplines with the aim of producing publishable results. Author

N93-25805*# Maryland Univ., College Park. Dept. of Meteorology.
THE GRID ANALYSIS AND DISPLAY SYSTEM (GRADS): A PRACTICAL TOOL FOR EARTH SCIENCE VISUALIZATION Abstract Only
James L. Kinter, III (Maryland Univ., College Park.) *In* Colorado Univ., Applied Information Systems Research Program (AISRP). Workshop 2: Meeting Proceedings 1992 1 p (For primary document see N93-25792 09-82)
Avail: CASI HC A01/MF A03

We propose to develop and enhance a workstation based grid analysis and display software system for Earth science data set browsing, sampling and manipulation. The system will be coupled to a super computer in a distributed computing environment for near real-time interaction between scientists and computational results. Author

N93-25806*# Wisconsin Univ., Madison. Space Science and Engineering Center.
PLANETARY DATA ANALYSIS AND DISPLAY SYSTEM: A VERSION OF PC-McIDAS Abstract Only
Sanjay S. Limaye, L. A. Sromovsky, R. S. Saunders (Jet Propulsion Lab., California Inst. of Tech., Pasadena.), and Michael Martin (Jet Propulsion Lab., California Inst. of Tech., Pasadena.) *In* Colorado Univ., Applied Information Systems Research Program (AISRP). Workshop 2: Meeting Proceedings 1992 1 p (For primary document see N93-25792 09-82)
Avail: CASI HC A01/MF A03

We propose to develop a system for access and analysis of planetary data from past and future space missions based on an existing system, the PC-McIDAS workstation. This system is now in use in the atmospheric science community for access to meteorological satellite and conventional weather data. The proposed system would be usable by not only planetary atmospheric researchers but also by the planetary geologic community. By providing the critical tools of an efficient system architecture, newer applications and customized user interfaces can be added by the end user within such a system. Author

N93-25807*# Jet Propulsion Lab., California Inst. of Tech., Pasadena.
MULTI-LAYER HOLOGRAPHIC BIFURCATIVE NEURAL NETWORK SYSTEM FOR REAL-TIME ADAPTIVE EOS DATA ANALYSIS
Hua-Kuang Liu, K. Huang (University of Southern California, Los Angeles.), and J. Diep *In* Colorado Univ., Applied Information Systems Research Program (AISRP). Workshop 2: Meeting Proceedings 1992 2 p (For primary document see N93-25792 09-82)
Avail: CASI HC A01/MF A03

Optical data processing techniques have the inherent advantage of high data throughout, low weight and low power requirements. These features are particularly desirable for onboard spacecraft in-situ real-time data analysis and data compression applications. The proposed multi-layer optical holographic neural net pattern recognition technique will utilize the nonlinear photorefractive devices for real-time adaptive learning to classify input data content and recognize unexpected features. Information can be stored either in analog or digital form in a nonlinear photorefractive device. The recording can be accomplished in time scales ranging from milliseconds to microseconds. When a system consisting of these devices is organized in a multi-layer structure, a feed forward neural net with bifurcating data classification capability is formed. The interdisciplinary research will involve the collaboration with top digital computer architecture experts at the University of Southern California. Author

N93-25808*# Space Telescope Science Inst., Baltimore, MD.
DEVELOPMENT OF AN EXPERT DATA REDUCTION ASSISTANT
Glenn E. Miller, Mark D. Johnston, and Robert J. Hanisch *In* Colorado Univ., Applied Information Systems Research Program (AISRP). Workshop 2: Meeting Proceedings 1992 1 p (For primary document see N93-25792 09-82)
Avail: CASI HC A01/MF A03

We propose the development of an expert system tool for the management and reduction of complex data sets. The proposed work is an extension of a successful prototype system for the calibration of CCD images developed by Dr. Johnston in 1987. The reduction of complex multi-parameter data sets presents severe challenges to a scientist. Not only must a particular data analysis system be mastered, (e.g. IRAF/SDAS/MIDAS), large amounts of data can require many days of tedious work and supervision by the scientist for even the most straightforward reductions. The proposed Expert Data Reduction Assistant will help the scientist overcome these obstacles by developing a reduction plan based on the data at hand and producing a script for the reduction of the data in a target common language. Author

N93-25809*# Maryland Univ., College Park.
VIEWCACHE: AN INCREMENTAL POINTER-BASED ACCESS METHOD FOR AUTONOMOUS INTEROPERABLE DATABASES Abstract Only
N. Roussopoulos and Timos Sellis *In* Colorado Univ., Applied Information Systems Research Program (AISRP). Workshop 2: Meeting Proceedings 1992 1 p (For primary document see N93-25792 09-82)
Avail: CASI HC A01/MF A03

One of biggest problems facing NASA today is to provide scientists efficient access to a large number of distributed databases. Our pointer-based incremental database access method, VIEWCACHE, provides such an interface for accessing distributed data sets and directories. VIEWCACHE allows database browsing and search performing inter-database cross-referencing with no actual data movement between database sites. This organization and processing is especially suitable for managing Astrophysics databases which are physically distributed all over the world. Once the search is complete, the set of collected pointers pointing to the desired data are cached. VIEWCACHE includes spatial access methods for accessing image data sets, which provide much easier query formulation by referring directly to the image and very efficient search for objects contained within a two-dimensional window. We will develop and optimize a VIEWCACHE External Gateway Access to database management systems to facilitate distributed database search. Author

N93-25810*# Hughes Aircraft Co., Culver City, CA.
ADVANCED DATA VISUALIZATION AND SENSOR FUSION: CONVERSION OF TECHNIQUES FROM MEDICAL IMAGING TO EARTH SCIENCE Abstract Only
Richard C. Savage, Chin-Tu Chen (Chicago Univ., IL.), Charles Pelizzari (Chicago Univ., IL.), and Veerabhadran Ramanathan (Chicago Univ., IL.) *In* Colorado Univ., Applied Information Systems Research Program (AISRP). Workshop 2: Meeting Proceedings 1992 1 p (For primary document see N93-25792 09-82)
Avail: CASI HC A01/MF A03

Hughes Aircraft Company and the University of Chicago propose to transfer existing medical imaging registration algorithms to the area of

multi-sensor data fusion. The University of Chicago's algorithms have been successfully demonstrated to provide pixel by pixel comparison capability for medical sensors with different characteristics. The research will attempt to fuse GOES, AVHRR, and SSM/I sensor data which will benefit a wide range of researchers. The algorithms will utilize data visualization and algorithm development tools created by Hughes in its EOSDIS prototyping. This will maximize the work on the fusion algorithms since support software (e.g. input/output routines) will already exist. The research will produce a portable software library with documentation for use by other researchers. Author

N93-25811*# Brandeis Univ., Waltham, MA.
HIGH PERFORMANCE COMPRESSION OF SCIENCE DATA Abstract Only
James A. Storer and Martin Cohn *In* Colorado Univ., Applied Information Systems Research Program (AISRP). Workshop 2: Meeting Proceedings 1992 1 p (For primary document see N93-25792 09-82)
Avail: CASI HC A01/MF A03

In the future, NASA expects to gather over a tera-byte per day of data requiring space for levels of archival storage. Data compression will be a key component in systems that store this data (e.g., optical disk and tape) as well as in communications systems (both between space and Earth and between scientific locations on Earth). We propose to develop algorithms that can be a basis for software and hardware systems that compress a wide variety of scientific data with different criteria for fidelity/bandwidth tradeoffs. The algorithmic approaches we consider are specially targeted for parallel computation where data rates of over 1 billion bits per second are achievable with current technology. Author

N93-25812*# Science Applications, Inc., McLean, VA. Lab. for Atmospheric and Space Sciences.
SAVS: A SPACE ANALYSIS AND VISUALIZATION SYSTEM Abstract Only
Edward P. Szuszczewicz, Alan Mankofsky, and Charles C. Goodrich (Maryland Univ., College Park.) *In* Colorado Univ., Applied Information Systems Research Program (AISRP). Workshop 2: Meeting Proceedings 1992 1 p (For primary document see N93-25792 09-82)
Avail: CASI HC A01/MF A03

We propose to develop, test, demonstrate, and deliver to NASA a powerful and versatile data acquisition, manipulation, analysis and visualization system which will enhance scientific capabilities in the display and interpretation of diverse and distributed data within an integrated user-friendly environment. Our approach exploits existing technologies and combines three major elements into an easy-to-use interactive package: (1) innovative visualization software; (2) advanced database techniques; and (3) a rich set of mathematical and image processing tools. Visualization capabilities will include one-, two-, and three-dimensional displays, along with animation, compression, warping and slicing functions. Analysis tools will include generic mathematical and statistical techniques along with the ability to use large scale models for interactive interpretation of large volume data sets. Our system will be implemented on Sun and DEC UNIX workstations and on the Stardent Graphics Super computer. Our final deliverable will include complete documentation and a NASA/NSF-CDAW/SUNDIAL campaign demonstration. Author

N93-25813*# National Aeronautics and Space Administration. Goddard Space Flight Center, Greenbelt, MD.
A SPATIAL ANALYSIS AND MODELING SYSTEM (SAMS) FOR ENVIRONMENT MANAGEMENT
Charles H. Vermillion, Fran Stetina, John Hill (Louisiana State Univ., Baton Rouge.), Paul Chan (Science Systems and Applications, Inc., Greenbelt, MD.), Robert Jaske (Federal Emergency Management Agency, Denver, CO.), and Gilbert Rochon (Dillard Univ., New Orleans, LA.) *In* Colorado Univ., Applied Information Systems Research Program (AISRP). Workshop 2: Meeting Proceedings 1992 1 p (For primary document see N93-25792 09-82)
Avail: CASI HC A01/MF A03

This is a proposal to develop a uniform global environmental data gathering and distribution system to support the calibration and validation of remotely sensed data. SAMS is based on an enhanced version of FE MA's Integrated Emergency Management Information Systems and the Department of Defense's Air Land Battlefield Environment Software Systems. This system consists of state-of-the-art graphics and visualization techniques, simulation models, database management and expert systems for conducting environmental and disaster preparedness studies. This software package will be integrated into various Landsat and UNEP-GRID stations which are planned to become direct readout stations during the EOS timeframe. This system would be implemented as a pilot program to support the Tropical Rainfall Measuring Mission (TRMM). This will be a joint NASA-FEMA-University-Industry project. Author

N93-25814*# Illinois Univ., Urbana.
A DISTRIBUTED ANALYSIS AND VISUALIZATION SYSTEM FOR MODEL AND OBSERVATIONAL DATA Abstract Only
Robert Wilhelmson and Steven Koch (National Aeronautics and Space Administration. Goddard Space Flight Center, Greenbelt, MD.) *In* Colorado Univ., Applied Information Systems Research Program (AISRP). Workshop 2: Meeting Proceedings 1992 1 p (For primary document see N93-25792 09-82)
Avail: CASI HC A01/MF A03

The objective of this proposal is to develop an integrated and distributed analysis and display software system which can be applied to all areas of the Earth System Science to study numerical model and earth observational data from storm to global scale. This system will be designed to be easy to use, portable, flexible and easily extensible and to adhere to current and emerging standards whenever possible. It will provide an environment for visualization of the massive amounts of data generated from satellites and other observational field measurements and from model simulations during or after their execution. Two- and three-dimensional animation will also be provided. This system will be based on a widely used software package from NASA called GEMPAK and prototype software for three dimensional interactive displays built at NCSA. The underlying foundation of the system will be a set of software libraries which can be distributed across a UNIX based supercomputer and workstations. Author

N93-25824# Army Engineer Waterways Experiment Station, Vicksburg, MS. Information Technology Lab.
INTELLIGENT ACCESS TO MULTIPLE RELATIONAL DATABASE SYSTEMS Final Report
Peggy Wright Nov. 1992 183 p
(AD-A261198; WES/TR/ITL-92-9) Avail: CASI HC A09/MF A02

The combination of artificial intelligence (AI) and database technology allows the capability of extending the usefulness of existing database applications. More specifically, the use of AI provides the means to develop an intelligent front end to allow nonintrusive assess to multiple relational databases. A knowledge source is built for each participating database application. A meta-knowledge source, constructed from all knowledge sources in the system, is consulted to determine the appropriate application to which a database request is channeled. This report introduces a proposed architecture and presents a prototype developed to accomplish this task. DTIC

N93-25826 Rutgers - The State Univ., New Brunswick, NJ.
AGREEMENT IN NAMING OBJECTS AND CONCEPTS FOR INFORMATION RETRIEVAL Ph.D. Thesis
Lourdes Y. Collantes 1992 395 p
Avail: Univ. Microfilms Order No. DA9232906

The naming of objects and concepts in information retrieval contexts by users themselves was explored because of the vocabulary problem in communication between users and information system. How do people name things? Can they find information about these things by using these names? The study investigated the representation of users' knowledge (names of objects and concepts), database representation for similar objects/concepts, and degree of agreement among users and between users and information system. Three groups of users (undergraduates, graduate students, librarians) were asked to give names to 20 illustrations and 20 texts. Names generated were compared with each other and with LC subject headings on exact and keyword basis. Degree of agreement was calculated using similarity measures. Analysis was on name and user levels. Cross product ratio analysis was used to explore the relationship between agreement on names and retrieval of information. The study identified patterns of naming and patterns of agreement in naming objects and concepts. Findings suggest wide variability in naming. The number of names differed greatly from one stimulus to another. Agreement on particular

names was low but at least one name for each item was relatively popular among users. Agreement between pairs of users averaged 25 to 26 percent. While some users tend to agree more than others, there is no difference among user groups in number of names generated or in agreement on names. Levels of agreement, in descending order, were highest for names given to illustrations, followed by abstracts and lowest for names given to search statements. Average match with LCSH was 6 names per item and 7.68 names based on keywords. Name-LCSH agreement was low but names with higher agreement among users were more likely to match LCSH. Naming of objects and concepts indicated a pattern of agreement and variability. Retrieval system design and document representation should accommodate the characteristics of naming and the natural pattern of users' naming behavior. Naming seems to be user specific and object/concept specific, suggesting that any naming paradigm should be broadened to include aspects both internal and external with respect to the user. Dissert. Abstr.

N93-25844# Carnegie-Mellon Univ., Pittsburgh, PA. School of Computer Science.

A METHODOLOGY AND SOFTWARE ENVIRONMENT FOR TESTING PROCESS MODEL'S SEQUENTIAL PREDICTIONS WITH PROTOCOLS M.S. Thesis

Frank E. Ritter 21 Dec. 1992 210 p

(Contract F33615-90-C-1465; ARPA Order 7597)

(AD-A260980; CMU-CS-93-101) Avail: CASI HC A10/MF A03

Getting the most out of information processing models requires that testing and refining them be straightforward. This requires that (1) large amounts of data be easily compared with the model's performance, (2) descriptions of how and where the model mismatches are readily available and easy to interpret, and (3) the models themselves can be refined in a straightforward way. Current methods for testing the sequential predictions of process models provides none of these. It is a difficult, time consuming, boring task, requiring the full attention of a skilled analyst despite the importance and and difficulty of testing process models against protocol data, and in contrast to the rich methodology for analyzing samples of numerical data, there is no explicit methodology or set of tools for automatically or semi-automatically doing this task. This thesis specifies a methodology for testing process models sequential predictions through comparison with verbal and non-verbal protocols. Each of its steps are delineated, and the requirements to perform these steps developed. DTIC

N93-26096# General Accounting Office, Washington, DC. Information Management and Technology Div.

DEPARTMENT OF ENERGY: BETTER INFORMATION RESOURCES MANAGEMENT NEEDED TO ACCOMPLISH MISSIONS. REPORT TO THE SECRETARY OF ENERGY

Sep. 1992 64 p

(GAO/IMTEC-92-53; B-248529) Avail: CASI HC A04/MF A01; GAO, PO Box 6015, Gaithersburg, MD 20877 HC

The Department of Energy (DOE) is responsible for multiple energy and defense missions that are important to economic growth, public health and safety, and the nation's security. DOE also faces complex challenges, such as massive environmental damage and unsafe nuclear weapons production facilities, and management problems, such as weak controls over contractor activities. To successfully accomplish DOE'S missions and correct existing problems, the Secretary and departmental and contractor managers need timely, reliable, and relevant information. GAO examined key aspects of the Department's information resources management (IRM) program, focusing primarily on the environmental restoration, safety and health management, nuclear weapons production, and security mission areas. GAO'S objectives were to determine whether (1) information shortfalls impair managers' ability to fulfill their responsibilities, (2) DOE's strategic IRM planning is linked to strategic mission planning, and (3) management control over the acquisition and operation of information systems is adequate to ensure compliance with federal and DOE IRM policies and requirements. Author

N93-26097# General Accounting Office, Washington, DC.

STRATEGIC INFORMATION PLANNING: FRAMEWORK FOR DESIGNING AND DEVELOPING SYSTEM ARCHITECTURES

Jun. 1992 34 p

(GAO/IMTEC-92-51) Avail: CASI HC A03/MF A01; GAO, PO Box 6015, Gaithersburg, MD 20877 HC

Managing and modernizing the federal government's information resources is an enormously complex task. The purposes of government information systems vary widely from business applications, such as payroll or personnel, to worldwide military command, control, and communications systems. Identifying the best solution to a problem in terms of operational effectiveness, flexibility, maintenance, and cost requires detailed, structured analyses of user needs and identification of technical alternatives and supporting technologies for the system's software, hardware, communications, data management, and security infrastructures. This framework is intended to (1) provide a basis for systematically determining information needs, (2) identify and analyze information and data needs and relationships, (3) identify and analyze alternative ways to satisfy information needs, and (4) provide factors to be considered in arriving at the best way to satisfy information needs. The framework is not meant to be a 'cookbook,' but a guide for systematically identifying and evaluating an organization's information needs and laying out a disciplined process to satisfy those needs. Methodologies for identifying information needs and planning acquisitions to fill those needs were devised. The assessment and evaluation of the various methodologies resulted in this generic framework for analyzing, designing, and developing open and flexible information system architectures that can be used to meet any information processing need. Author (revised)

N93-26230# Defense Information Systems Agency, Arlington, VA. Center for Information Management.

DEPARTMENT OF DEFENSE TECHNICAL ARCHITECTURE FRAMEWORK FOR INFORMATION MANAGEMENT. VOLUME 3: REFERENCE MODEL AND STANDARDS PROFILE, VERSION 1.3

John Keane 31 Dec. 1992 113 p

(AD-A261913) Avail: CASI HC A06/MF A02

This document provides the conceptual model for information system services and the standards profile for implementing the services. The Reference Model for Information Management (IM) with additions covering support applications services and standards, communications services and standards, and legacy interface standards is also provided. DTIC

N93-26231*# National Aeronautics and Space Administration, Washington, DC.

OSSA INFORMATION SYSTEMS PROGRAM Annual Report, 1992

David H. Brown 1993 30 p

(Grant NAGw-4561)

(NASA-TM-108774; NAS 1.15:108774) Avail: CASI HC A03/MF A01

The Office of Space Science and Applications' (OSSA) Information Systems Program was established to coordinate and enhance activities that support the processing analysis, transport, archival, and access of space science data. Within OSSA, the science discipline divisions have the ultimate responsibility for the proper management of the data generated by their missions. The OSSA Information Systems Branch works in concert with the divisions to provide an infrastructure of information system services and expertise in operations, policy, planning, and technology. Discipline specific and infrastructure activities are coordinated through participation in the OSSA Information Systems Management Board. The Information Systems Program is organized into four program areas: Scientific Computing, Networking, Data Management and Archiving, and Applied Information Systems Technology. Together, these program areas form a solid technical and policy development base that supports the overall OSSA information systems strategy. The underlying theme of each element is to facilitate science research and ensure the efficient implementation and utilization of OSSA information systems resources. The annual report for 1992 is presented. Derived from text

N93-26242# School of Aerospace Medicine, Brooks AFB, TX.

PROCEEDINGS OF THE 33RD ANNUAL MILITARY LIBRARIANSWORKSHOP Final Report

Thomas H. Kerns Dec. 1992 181 p Workshop held in San Antonio, TX, 18-20 Oct. 1989

(AD-A261071; USAFSAM-PROC-89-29) Avail: CASI HC A09/MF A02

The theme of the Thirty-Third Annual Military Librarians Workshop was Technology in Transition. The workshop, sponsored by the USAF School of Aerospace Medicine, was held at the Sheraton Gunter Hotel in downtown

San Antonio. Discussion topics included Hypermedia, Local Area Networks, CD-ROM Catalogs, Emerging Technologies, and Total Quality Management. DTIC

N93-26313# Institute for Defense Analyses, Alexandria, VA.
FY92 CONTRIBUTIONS TO THE DATABASE MANAGEMENT SYSTEM INTERFACE STANDARDS WORKING GROUP OF THE NAVY NEXT GENERATION COMPUTER RESOURCES PROGRAM Final Report
Karen D. Gordon Oct. 1992 34 p
(Contract MDA903-89-C-0003)
(AD-A261348; IDA-D-1244; IDA/HQ-92-42853) Avail: CASI HC A03/MF A01

The Next Generation Computer Resources (NGCR) Program is a Navy standardization effort designed to fulfill the Navy's needs for standard computer resources while at the same time allowing it to take advantage of commercial products and investments and to field new technology more quickly and effectively. The program is centered around the selection and adoption of open system standards in several areas, including backplanes, local area networks, operating systems, project support environments, graphics, and database management systems. IDA is providing support through participation in a recently formed group known as the NGCR Database Management System (DBMS) Interface Standards Working Group (DISWG). The objective of the NGCR DISWG is to identify and help define nonproprietary industry-based database management system interface standards for use in the development and maintenance of future Navy mission-critical computing systems. The document is a compilation of IDA written contributions to the NGCR DISWG from April 1992 through September 1992. DTIC

N93-26350# Knowledge Based Systems, Inc. College Station, TX.
DESIGN KNOWLEDGE MANAGEMENT SYSTEM (DKMS) BETA TEST REPORT Interim Report, Nov. 1990 - Jun. 1992
Richard J. Mayer, Thomas M. Blinn, David C. Browne, Matthew A. Grisius, Arthur A. Keen, Jeffrey C. Lockledge, and Les Sanders Nov. 1992 73 p
(Contract F33615-90-C-0011)
(AD-A261453; AL-TP-1992-0043) Avail: CASI HC A04/MF A01

The Beta Test Report documents potential use of the Design Knowledge Management System (DKMS) in research and industry. Industry concerns, gathered from surveys, are addressed in each subsection. The appendix gives an in-depth overview of the entire DKMS. The DKMS consists of the following components: Container Object System--a flexible means of storing computer objects and constraints, so that a design can easily evolve as information changes; Model Design Support Environment--a method for automatic solution and code generation based on the problem, the 'givens', and the real-world equations that rule the environment; High-Productivity CAD--a toolbox for CAD designers; Shape-based Design Knowledge Representation and Reasoning--a component which allows shape information as a key factor in the design; and Integration Platform--a component which helps user select and translate services. DTIC

N93-26377# Army Research Lab., Adelphi, MD.
INFORMATION TRANSMISSION USING CHAOS Final Report, May - Aug. 1992
Scott Hayes, Celso Grebogi, and Edward Ott Feb. 1993 13 p
(AD-A261519; ARL-TR-94) Avail: CASI HC A03/MF A01

The use of chaos to transmit information is described. Chaotic dynamical systems, such as electrical oscillators with very simple structures, naturally produce complex waveforms. We show that the symbolic dynamics of a chaotic oscillator can be made to follow a desired symbol sequence by using small perturbations, thus allowing us to encode a message in the waveform. We illustrate this using a simple numerical electrical oscillator model. DTIC

N93-26389# Carnegie-Mellon Univ., Pittsburgh, PA. School of Computer Science.
FAST MUTUAL EXCLUSION FOR UNIPROCESSORS
Brian N. Bershad, David D. Redell (Digital Equipment Corp., Palo Alto, CA.), and John R. Ellis (Digital Equipment Corp., Palo Alto, CA.) Oct. 1992 13 p
(Contract MDA972-90-C-0035; ARPA Order 7330)
(AD-A261663; CMU-CS-92-183) Avail: CASI HC A03/MF A01

In this paper we describe restartable atomic sequences, an optimistic mechanism for implementing simple atomic operations (such as Test-and-Set) on a uniprocessor. A thread that is suspended within a restartable atomic sequence is resumed by the operating system at the beginning of the sequence, rather than at the point of suspension. This guarantees that the thread eventually executes the sequence atomically. A restartable atomic sequence has significantly less overhead than other software-based synchronization mechanisms, such as kernel emulation or software, reservation. Consequently, it is an attractive alternative for use on uniprocessors that do not support atomic operations. Even on processors that do support atomic operations in hardware, restartable atomic sequences can have lower overhead. We describe different implementations of restartable atomic sequences for the Mach 3.0 and Taos operating systems. These systems' thread management packages rely on atomic operations to implement higher-level mutual exclusion facilities. We show that improving the performance of low-level atomic operations, and therefore mutual exclusion mechanisms, improves application performance. DTIC

N93-26423*# Space Telescope Science Inst., Baltimore, MD.
HUBBLE SPACE TELESCOPE: THE ARCHIVED EXPOSURES CATALOG, VERSION 2.0
Kirk Borne and Pete Reppert Apr. 1993 401 p Sponsored by NASA. Washington
(NASA-CR-192896; NAS 1.26:192896) Avail: CASI HC A18/MF A04

The archived exposures catalog for the Hubble Space Telescope is presented. Information is in table format. CASI

N93-26442# Cornell Univ., Ithaca, NY. Inst. for the Study of the Continents.
A GEOLOGICAL AND GEOPHYSICAL INFORMATION SYSTEM FOR EURASIA Technical Report, 30 Apr. - 30 Oct. 1992
Eric J. Fielding, Bryan L. Isacks, and Muawia Barazangi 15 Dec. 1992 21 p
(Contract F29601-91-K-DB08)
(AD-A261789) Avail: CASI HC A03/MF A01

Topography and crustal structure variations have significant effects on the propagation of regional seismic phases. Geological and geophysical data are also useful for other aspects of the problems of nonproliferation, verification, and yield estimation. We are collecting datasets for Eurasia, China, the Middle East, and North Africa. Available now are digital databases of topography, crustal thicknesses, and sedimentary basin depths. Work continues on collecting and organizing available topographical, geological, and geophysical datasets. We store the data in an information system with a network-accessible server to which we can connect client modules of future versions of the Intelligent Monitoring System (IMS) running at the Center for Seismic Studies and other DARPA researchers. We have created regularly spaced grids of the crustal and sediment thickness values from preliminary maps that can be used to create profiles of crustal structure. These profiles can be compared by an analyst or an automatic program with the crustal seismic phases received along the propagation path to better understand and predict the path effects on phase amplitudes, a key to estimating magnitudes and yields. The gridded data can also be used to model propagation of crustal phases in three dimensions. The data server at Cornell allows clients to directly connect to databases that we are generating and improving. This allows IMS users and other DARPA researchers to utilize data as soon as it is available. We encourage researchers to contact us about access to these databases and with suggestions for improvements. DTIC

N93-26491*# National Aeronautics and Space Administration, Washington, DC.
OSSA INFORMATION SYSTEMS PROGRAM Annual Report, 1992
Center for Space and Advanced Technology 1993 30 p
(Contract NASw-4561)
(NASA-TM-108758; NAS 1.15:108758) Avail: CASI HC A03/MF A01

The Office of Space Science Applications (OSSA) Information Systems Program was established to coordinate and enhance activities that support the processing, analysis, transport, archival, and access of space science data. Within OSSA, the science discipline divisions have the ultimate responsibility for the proper management of the data generated by their missions. A program overview is presented followed by sections covering

the following topics: scientific computing; networking, data management and archiving, applied information system technology, and an acronyms reference guide. Derived from text

N93-26523# Texas A&M Univ., College Station. Knowledge Based Systems Lab.

IDEF6: A DESIGN RATIONALE CAPTURE METHOD CONCEPT PAPER Interim Report, Jan. 1990 - Mar. 1991

Richard J. Mayer, Patricia A. Griffith, and Christopher P. Menzel Nov. 1992 28 p

(Contract FQ7624-90-00010)

(AD-A261594; AL-TP-1992-0050) Avail: CASI HC A03/MF A01

When explicitly captured, design rationale typically exists in the form of unstructured textual comments. In addition to making it difficult, if not impossible to find relevant information on demand, lack of a structured method for organizing and providing completeness criteria for design rationale capture makes it unlikely that important information will be documented. Unlike design methods which serve to document WHAT a design is (Design Specification), the IDEF6 Design Rationale Capture Method is targeted at capturing WHY a design is the way it is -- or WHY it is not manifested in some other form -- together with HOW the final design configuration was reached. IDEF6 was intended to be a method with the representational capability to capture information system design rationale and associate that rationale with the design models and documentation for the end system. Thus, IDEF6 attempts to capture the logic underlying the decisions contributing to, or resulting in, the final design. The explicit capture of design rationale serves to help avoid repeating past mistakes, provides a direct means for determining the impact of proposed design changes, forces the explicit statement of goals and assumptions, and aids in the communication of final system specifications. DTIC

N93-26530# National Inst. of Standards and Technology, Gaithersburg, MD. Semiconductor Electronics Div.

ELECTRONICS AND ELECTRICAL ENGINEERING LABORATORY TECHNICAL PUBLICATION ANNOUNCEMENTS COVERING LABORATORY PROGRAMS, JULY TO SEPTEMBER 1992 WITH 1992/1993 EEEL EVENTS CALENDAR

J. M. Rohrbaugh Jan. 1993 118 p See also PB93-147163

(PB93-158632; NISTIR-5114) Avail: CASI HC A06/MF A02

The report is the thirty-third issue of a quarterly publication providing information on the technical work of the National Institute of Standards and Technology, Electronics and Electrical Engineering Laboratory. The issue of the EEEL Technical Publication Announcements covers the second quarter of calendar year 1992. Abstracts are provided by technical area for papers published this quarter. Major subject headings include the following: Fundamental electrical measurements; Semiconductor microelectronics; Signal acquisition, processing, and transmission; and Electrical systems. NTIS

N93-26531# Defense Information Systems Agency, Arlington, VA. Center for Information Management.

DEPARTMENT OF DEFENSE TECHNICAL ARCHITECTURE FRAMEWORK FOR INFORMATION MANAGEMENT. VOLUME 1: IMPLEMENTATION CONCEPT, VERSION 1.1

John Keane 21 Oct. 1992 37 p

(AD-A261911) Avail: CASI HC A03/MF A01

This document provides a broad overview of the technical architecture framework program in the context of the DoD Information Management (IM) initiatives, such as Information Technology Reuse (ITRUS). It describes the relationships to the ITRUS and Software Reuse Program and how the Technical Architecture Framework is used by developers and integrators to build information systems. The DoD technical infrastructure includes support applications, computing platforms, and communications networks. The current DoD technical infrastructure consists largely of stove-piped, single-purpose, and inflexible systems which are costly to develop and maintain. The evolving DoD enterprise vision for Information Management (IM) emphasizes integration, interoperability, flexibility and efficiency through the development of a common, multi-purpose, standards-based technical infrastructure. DTIC

N93-26532# Defense Information Systems Agency, Arlington, VA. Center for Information Management.

DEPARTMENT OF DEFENSE TECHNICAL ARCHITECTURE FRAMEWORK FOR INFORMATION MANAGEMENT. VOLUME 2: ARCHITECTURE GUIDANCE AND DESIGN CONCEPTS, VERSION 1.1

John Keane 21 Oct. 1992 151 p

(AD-A261912) Avail: CASI HC A08/MF A02

This document provides the overall guidance and concepts needed to develop technical architectures in the DoD. An information system (IS) consists of three elements: data; mission-specific applications; and a technical infrastructure consisting of support applications, computing platforms, and communications networks. Each of these IS elements has a unique life-cycle which requires distinct development and maintenance approaches. For example, data definitions and formats may have a useful life that is many times longer than the applications that manipulate and use the data definitions, and the hardware and software that comprise the technical infrastructure may have a half-life that is less than the applications. Based on the necessity to manage the IS elements according to different life-cycles, an information system architecture includes a data architecture, an application software architecture (mission-specific), and a technical (i.e., support applications, computing platforms and communications networks) architecture. DTIC

N93-26562*# National Aeronautics and Space Administration. Marshall Space Flight Center, Huntsville, AL.

SPACE SCIENCE LABORATORY PUBLICATIONS AND PRESENTATIONS Technical Memorandum, 1 Jan. - 31 Dec. 1992

T. W. Moorehead, comp. Apr. 1993 63 p

(NASA-TM-108402; NAS 1.15:108402) Avail: CASI HC A04/MF A01

This document lists the significant publications and presentations of the Space Science Laboratory during the period January 1 - December 31, 1992. Entries in the main part of the document are categorized according to NASA Reports (arranged by report number), Open Literature, and Presentations (arranged alphabetically by title). Also included for completeness is an Appendix (arranged by report number) listing preprints issued by the Laboratory during this reporting period. Some of the preprints have not been published; those already published are so indicated. Most of the articles listed under Open Literature have appeared in refereed professional journals, books, monographs, or conference proceedings. Although many published abstracts are eventually expanded into full papers for publications in scientific and technical journals, they are often sufficiently comprehensive to include the significant results of the research reported. Therefore, published abstracts are listed separately in a subsection under Open Literature. The organizational code of the cognizant SSL branch or office is given at the end of each entry. Author (revised)

N93-26568# Meridian Research, Inc., Silver Spring, MD.

DEVELOPMENT OF A CONCEPT FOR A NATIONAL CONSTRUCTION INDUSTRY HEALTH AND SAFETY DATA BASE Final Report

M. Kent, W. Perry, and R. Burt 27 Aug. 1992 158 p

(Contract NIOSH-CDC-299-90-2847)

(PB93-159325) Avail: CASI HC A08/MF A02

An operations oriented data base concept was developed for health and safety data for the construction industry. Construction industry hazards were investigated, and potential users were surveyed. Possible data base designs were identified. Resources for development and maintenance of a data base were determined, and methods for distributing the data base were identified. Sources of information were examined. The data base concept as developed was operations oriented as opposed to bibliographic or technology oriented in order to best serve the industry. The data base would be continually updated with information concerned with safety, health and ergonomic hazards associated with the industry. Information on the control methods used to combat the hazards would also be included in the data base. Methods for distributing the data base were briefly considered; multiple distribution methods eventually may be used. NTIS

N93-26575# Naval Surface Warfare Center, Dahlgren, VA.

NSWC LIBRARY OF MATHEMATICS SUBROUTINES

Alfred H. Morris, Jr. Jan. 1993 464 p LIMITED REPRODUCIBILITY: More than 20% of this document may be affected by microfiche quality

(AD-A261511; NSWCDD/TR-92-425) Avail: Issuing Activity (Defense Technical Information Center (DTIC))

The Naval Surface Warfare Center (NSWC) library is a library of general purpose Fortran subroutines that provide a basic computational capability for a variety of mathematical activities. Emphasis was placed on the transportability of the codes. Subroutines are available in the following areas: elementary operations, geometry, special functions, polynomials, vectors, matrices, large dense systems of linear equations, banded matrices, sparse matrices, eigenvalues and eigenvectors, solution of linear equations, least-squares solution of linear equations, optimization, transforms, approximation of functions, curve fitting, surface fitting, manifold fitting, numerical integration, integral equations, ordinary differential equations, partial differential equations, and random number generation. DTIC

N93-26582# West Virginia Univ., Morgantown. Dept. of Management.
A HYPERTEXT FRAMEWORK FOR GROUP SUPPORT SYSTEMS
Interim Report, Jul. - Dec. 1991
Michael D. Wolfe and Kenneth J. Moen Nov. 1992 47 p
(AD-A261731; AL-TR-1992-0165) Avail: CASI HC A03/MF A01

The formula, generic description, and framework for the study of Decision Support Systems (DSS's) developed by Bonczek, Change, Holsapple, and Whinston is extended to Group Support Systems (GSS's). The original description was based on three components: a language system, a knowledge system, and a problem processing system. This was later extended to a hyperknowledge framework, which was a comprehensive foundational framework. The hyperknowledge framework for DSS is extended to a GSS framework which includes multiple copies of individual DSS (IDSS), the communications between the IDSS, and a special system for a facilitator. A representative selection of the most common commercially available GSS's are presented together; these are all shown to fit the framework. In addition, the framework suggests directions for the design of an architecture to support multicultural GSS, which may cross international and/or interfunctional boundaries. DTIC

N93-24931*# International Council for the Exploration of the Sea, Copenhagen (Denmark).
DATA ARCHAEOLOGY AT ICES
Harry D. Dooley *In* NASA. Goddard Space Flight Center, Proceedings of the Ocean Climate Data Workshop 1992 p 173-185 (For primary document see N93-24915 09-42)
Avail: CASI HC A03/MF A03

N93-24932*# Academy of Sciences (USSR), Moscow. Oceanographic Data Centre.
DATA AVAILABILITY AND DATA ARCHEOLOGY FROM THE FORMER SOVIET UNION
Yuri Sychev and Nickolai N. Mikhailov *In* NASA. Goddard Space Flight Center, Proceedings of the Ocean Climate Data Workshop 1992 p 187-192 (For primary document see N93-24915 09-42)
Avail: CASI HC A02/MF A03

N93-24933*# Lagos Univ. (Nigeria). Dept. of Geography.
OCEAN CLIMATE DATA FOR USER COMMUNITY IN WEST AND CENTRAL AFRICA: NEEDS, OPPORTUNITIES, AND CHALLENGES
S. O. Ojo *In* NASA. Goddard Space Flight Center, Proceedings of the Ocean Climate Data Workshop 1992 p 193-199 (For primary document see N93-24915 09-42)
Avail: CASI HC A02/MF A03

N93-24935*# Massachusetts Inst. of Tech., Cambridge. Center for Meteorology and Physical Oceanography.
DATA MANAGEMENT FOR JGOFS: THEORY AND DESIGN
Glenn R. Flierl, James K. B. Bishop, David M. Glover, and Satish Paranjpe *In* NASA. Goddard Space Flight Center, Proceedings of the Ocean Climate Data Workshop 1992 p 229-249 (For primary document see N93-24915 09-42)
Avail: CASI HC A03/MF A03

N93-24936*# Proudman Oceanographic Lab., Birkenhead (England).
DATA MANAGEMENT FOR COMMUNITY RESEARCH PROJECTS: A JGOFS CASE STUDY
Roy K. Lowry *In* NASA. Goddard Space Flight Center, Proceedings of the Ocean Climate Data Workshop 1992 p 251-273 (For primary document see N93-24915 09-42)
Avail: CASI HC A03/MF A03

N93-25922*# National Aeronautics and Space Administration. Lewis Research Center, Cleveland, OH.
SUBBAND CODING FOR IMAGE DATA ARCHIVING
Daniel Glover and S. C. Kwatra (Toledo Univ., OH.) *In* NASA. Goddard Space Flight Center, The Space and Earth Science Data Compression Workshop 1993 p 3-16 (For primary document see N93-25921 09-59)
Avail: CASI HC A03/MF A02

N93-25923*# Universities Space Research Association, Greenbelt, MD.
ADJUSTABLE LOSSLESS IMAGE COMPRESSION BASED ON A NATURAL SPLITTING OF AN IMAGE INTO DRAWING, SHADING, AND FINE-GRAINED COMPONENTS
Dmitry A. Novik and James C. Tilton (National Aeronautics and Space Administration. Goddard Space Flight Center, Greenbelt, MD.) *In its* The Space and Earth Science Data Compression Workshop 1993 p 17-25 (For primary document see N93-25921 09-59)
Avail: CASI HC A02/MF A02

N93-25924*# Cambridge Univ. (England). Computer Lab.
ENTROPY REDUCTION VIA SIMPLIFIED IMAGE CONTOURIZATION
Martin J. Turner *In* NASA. Goddard Space Flight Center, The Space and Earth Science Data Compression Workshop 1993 p 27-42 (For primary document see N93-25921 09-59)
Avail: CASI HC A03/MF A02

N93-25925*# General Electric Co., Philadelphia, PA. Astro-Space Div.
COMPRESSION OF SPECTRAL METEOROLOGICAL IMAGERY
Kristo Miettinen *In* NASA. Goddard Space Flight Center, The Space and Earth Science Data Compression Workshop 1993 p 43-57 (For primary document see N93-25921 09-59)
Avail: CASI HC A03/MF A02

N93-25926*# MacDonald, Dettwiler and Associates Ltd., Richmond (British Columbia).
METHODS OF EVALUATING THE EFFECTS OF CODING ON SAR DATA
Melanie Dutkiewicz and Ian Cumming *In* NASA. Goddard Space Flight Center, The Space and Earth Science Date Compression Workshop 1993 p 59-72 (For primary document see N93-25921 09-59)
Avail: CASI HC A03/MF A02

N93-25927*# Iterated Systems, Inc., Norcross, GA.
FRACTAL IMAGE COMPRESSION: A RESOLUTION INDEPENDENT REPRESENTATION FOR IMAGERY
Alan D. Sloan *In* NASA. Goddard Space Flight Center, The Space and Earth Science Data Compression Workshop 1993 p 73-79 (For primary document see N93-25921 09-59)
Avail: CASI HC A02/MF A02

N93-25928*# National Aeronautics and Space Administration. Goddard Space Flight Center, Greenbelt, MD.
THE IMPLEMENTATION OF A LOSSLESS DATA COMPRESSION MODULE IN AN ADVANCED ORBITING SYSTEM: ANALYSIS AND DEVELOPMENT
Pen-Shu Yeh, Warner H. Miller, Jack Venbrux (Idaho Univ., Moscow.), Norley Liu (Idaho Univ., Moscow.), and Robert F. Rice (Jet Propulsion Lab., California Inst. of Tech., Pasadena.) *In its* The Space and Earth Science Data Compression Workshop 1993 p 81-94 (For primary document see N93-25921 09-59)
(Grant NAGw-1406)
Avail: CASI HC A03/MF A02

N93-25929*# Hughes STX, Inc., Lanham, MD.
LOSSLESS COMPRESSION OF IMAGE DATA PRODUCTS ON TH E FIFE CD-ROM SERIES
Jeffrey A. Newcomer and Donald E. Strebel (Versar, Inc., Columbia, MD.) *In* NASA. Goddard Space Flight Center, The Space and Earth Science Data Compression Workshop 1993 p 95-10 Sponsored in part by the

FIFT Project and VERSAR, Inc. (For primary document see N93-25921 09-59)
Avail: CASI HC A03/MF A02

N93-25930*# National Aeronautics and Space Administration. Ames Research Center, Moffett Field, CA.
THE EFFECTS OF VIDEO COMPRESSION ON ACCEPTABILITY OF IMAGES FOR MONITORING LIFE SCIENCES' EXPERIMENTS
Richard F. Haines and Sherry L. Chuang *In* NASA. Goddard Space Flight Center, The Space and Earth Science Data Compression Workshop 1993 p 109-116 (For primary document see N93-25921 09-59)
Avail: CASI HC A02/MF A02

N93-25931*# Colorado Univ., Boulder. Joint Inst. for Lab. Astrophysics.
HIGH-PERFORMANCE COMPRESSION OF ASTRONOMICAL IMAGES
Richard L. White (Space Telescope Science Inst., Baltimore, MD.) *In* NASA. Goddard Space Flight Center, The Space and Earth Science Data Compression Workshop 1993 p 117-123 (For primary document see N93-25921 09-59)
(Grant NAGw-2166)
Avail: CASI HC A02/MF A02

N93-25932*# Utah State Univ., Logan. Dept. of Electrical Engineering.
MULTI-RATE, REAL TIME IMAGE COMPRESSION FOR IMAGES DOMINATED BY POINT SOURCES
A. Kris Huber, Scott E. Budge, and Richard W. Harris *In* NASA. Goddard Space Flight Center, The Space and Earth Science Data Compression Workshop 1993 p 125-135 Sponsored by Space Dynamics Lab. (For primary document see N93-25921 09-59)
Avail: CASI HC A03/MF A02

N93-25981*# National Aeronautics and Space Administration. Goddard Space Flight Center, Greenbelt, MD.
AN APPLICATION OF MACHINE LEARNING TO THE ORGANIZATION OF INSTITUTIONAL SOFTWARE REPOSITORIES
Sidney Bailin (Computer Technology Associates, Inc., Rockville, MD.), Scott Henderson (Computer Technology Associates, Inc., Rockville, MD.), and Walt Truszkowski *In its* The 1993 Goddard Conference on Space Applications of Artificial Intelligence 1993 p 235-248 (For primary document see N93-25961 09-63)
Avail: CASI HC A03/MF A03

N93-25982*# Analytic Sciences Corp., Reading, MA.
VISUALIZING THE SEMANTIC CONTENT OF LARGE TEXT DATABASES USING TEXT MAPS
Nathan Combs *In* NASA. Goddard Space Flight Center, The 1993 Goddard Conference on Space Applicati ons of Artificial Intelligence 1993 p 249-261 (For primary document see N93-25961 09-63)
Avail: CASI HC A03/MF A03

N93-25983*# Loyola Univ., New Orleans, LA.
IN SEARCH OF META-KNOWLEDGE
Antonio M. Lopez, Jr. *In* NASA. Goddard Space Flight Center, The 1993 Goddard Conference on Space Applicati ons of Artificial Intelligence 1993 p 263-269 (For primary document see N93-25961 09-63)
Avail: CASI HC A02/MF A03

N93-26126*# Jet Propulsion Lab., California Inst. of Tech., Pasadena.
DEEP SPACE NETWORK INFORMATION SYSTEM ARCHITECTURE STUDY
C. A. Beswick, R. W. Markley, ed., D. J. Atkinson, L. P. Cooper, R. C. Tausworthe, R. C. Masline, J. S. Jenkins, R. A. Crowe, J. L. Thomas, and M. J. Stoloff *In its* The Telecommunications and Data Acquisition Report 15 May 1992 p 282-355 (For primary document see N93-26105 09-32)
(RTOP 314-30-58-50-05)
Avail: CASI HC A04/MF A04

N93-26398*# National Aeronautics and Space Administration. Goddard Space Flight Center, Greenbelt, MD.
EnviroNET
Tim VanSant *In* NASA. Lewis Research Center, Electrical and Chemical Interactions at Mars Workshop. Part 2: Appendix 1992 p 93-105 (For primary document see N93-26392 09-91)
Avail: CASI HC A03/MF A02

83 ECONOMICS AND COST ANALYSIS

Includes cost effectiveness studies.

N93-26158# Commerce Dept., Washington, DC. Office of Business Analysis.
SPACE BUSINESS INDICATORS
Jun. 1992 61 p
Avail: CASI HC A04/MF A01

This report is intended as a one-stop collection of economic data and information on space business industries. Initiated by the Office of Space Commerce, the Economics and Statistics Administration was selected to compile business-related statistics on the markets for space-related goods and services using the best available sources, public and private. In-depth analysis of the industries monitored by the International Trade Administration--satellites and launch services--is also included. Although the focus is on the commercial sector, data and information on Government space programs are also included because many space commerce companies have government, as well as private, customers. With its emphasis on the business side of space activity, the report will be useful for investors, market and financial planners, entrepreneurs, market analysts, and policymakers. The report is divided into two sections: an introductory text with industry analysis and forecasts; and a large section of statistical tables and charts. We welcome suggestions for improvement in industry coverage and accuracy. Author (revised)

N93-26305# Assistant Secretary of Defense (Intelligence), Washington, DC.
FUNCTIONAL ECONOMIC ANALYSIS GUIDEBOOK, VERSION 1.1 Final Report
15 Jan. 1993 156 p
(AD-A261390) Avail: CASI HC A08/MF A02

Functional Economic Analysis is an evolving methodology. It will change as new techniques and tools are developed and as experience is gained in applying the methodology. This Guidebook shows how to prepare an FEA through practical examples and illustrations that are consistent with OSD policy. Also, this Guidebook shows that FEA is most effectively done in conjunction with functional process improvement analysis. DTIC

84 LAW, POLITICAL SCIENCE AND SPACE POLICY

Includes NASA appropriation hearings; aviation law; space law and policy; international law; international cooperation; and patent policy.

N93-25232# President's Council of Advisors on Science and Technology, Washington, DC.
SCIENCE, TECHNOLOGY, AND NATIONAL SECURITY
Dec. 1992 24 p
Avail: CASI HC A03/MF A01

During nearly half a century of cold war, America used technological superiority to offset the numerical advantage of Soviet military power. More recently, the spectacular performance of U.S. defense and intelligence technology in Operation Desert Storm graphically demonstrated to the world an American technological prowess that is matched by no other nation. Leadership in science and technology helped make American leadership in world affairs effective. Yet science and technology are forever moving forward: today's cutting edge can easily become tomorrow's trailing edge. Thus, continuation of America's advantage cannot be taken for granted, but must be constantly renewed through vigorous and far-sighted policies and programs. The panel has been given the task of proposing policies that will provide to future Presidents as wide a lead in national security technology as America enjoys today. In its deliberations, the panel has identified six critical objectives for presidential attention: (1) preserving and

extending our capability to gather and interpret essential intelligence by exploiting advanced science and technology for intelligence; (2) staving off proliferation of weapons of mass destruction and advanced conventional weapons, which opponents will try to use to undercut our unmatched capability for intense, precision, conventional warfare; (3) restructuring government's approach to applying technology and acquiring new high-tech defense and intelligence systems, so we can continue to have modern forces despite budget cutbacks; (4) attracting and retaining technically qualified people to serve in key national security posts; (5) giving a new emphasis to exploring defensive technology, so that have options to defend our nation, our allies, and our forces in proliferation does occur; and (6) enunciating a presidential strategy for continued superiority in science and technology, so that government and industry leaders clearly recognize that the advantage we displayed in Desert Storm must be preserved in the future. Author

N93-26499# State Dept., Washington, DC.
SCIENCE, TECHNOLOGY, AND INDUSTRIAL POLICY IN THE FORMER SOVIET UNION
1992 27 p Conference held in Washington, DC, 27-28 Apr. 1992 Prepared in cooperation with Commerce Dept., Washington, DC and Carnegie Commission on Science, Technology, and Goverment, New York, NY
(Contract DE-AI01-92IN-00554)
(DE93-006528; CONF-9204225-Summ) Avail: CASI HC A03/MF A01

The conference was intended to give members of the American government and business communities a better understanding of the changes taking place in science, technology and industry in the Former Soviet Union. Science and technology issues were accorded a prominent place in the program of perestroika. In the six turbulent years of perestroika great strides were made in identifying problems, shortcomings and difficult relationships. But implementation of solutions to the problems has been far more modest. The science and technology community has been affected by the turmoil in the country, and continues to search for a viable and productive future. The objective of the conference was to examine the current state of science, technology and industry in Russia and the other states of the Commonwealth, and consider its possible future development. The specific topics and questions conference speakers were asked to address included: Analyze current science, technology and industrial policy. What is the new legal framework for science, technology and industry? How are property rights and intellectual property rights being handled? What has been done to insure individual rights and freedoms? What are the organizational and management structures at the national level and at lower levels? What impact is decentralization having on priorities and funding? What industries are being de-nationalized? What will be the relationship between private and government sponsored research? To what extent will reductions in the budget for military R&D affect non-defense S&T funding? How will reductions in military R&D affect the long-term outlook for research? How serious has the brain-drain become in the military R&D sector. What has been the effect of glasnost on the R&D community. How might improved international contacts affect S&T? What economic forecasting, if any, is feasible?. DOE

85 URBAN TECHNOLOGY AND TRANSPORTATION

Includes applications of space technology to urban problems; technology transfer; technology assessment; and surface and mass transportation.

For related information see also *03 Air Transportation and Safety, 16 Space Transportation,* and *44 Energy Production and Conversion.*

N93-24965# Department of Energy, Washington, DC.
TECHNOLOGY TRANSFER 92/93
Jan. 1993 193 p Presented at the National Technology Initiative Conference, St. Louis, MO, 25 Jun. 1992
(DE93-003623; DOE/ST-0005P) Avail: CASI HC A09/MF A03

Technology transfer is one of the primary missions of the US Department of Energy (DOE). The purpose of Technology Transfer 92/93 is as follows: to reflect the depth and breadth of DOE's scientific and technical capabilities; describe its technology transfer activities; and indicate opportunities for industry, academia, state and local governments, and others to join DOE in these activities for the overall enhancement of US technical competitiveness. This document also introduces those unfamiliar with DOE to its major programs, laboratories, and facilities, and it provides information about the various mechanisms available for working with DOE in research and development, technology transfer, and commercialization of technological innovations. It is designed to serve as a guide for pinpointing the most appropriate DOE program office or laboratory to meet specific needs or interests. In short, this document tells how to contact the right person in the right office so work can get started quickly. DOE

N93-26458# Executive Office of the President, Washington, DC.
TECHNOLOGY FOR AMERICA'S ECONOMIC GROWTH: A NEW DIRECTION TO BUILD ECONOMIC STRENGTH
William J. Clinton and Albert Gore, Jr. 22 Feb. 1993 47 p
(AD-A261553) Avail: CASI HC A03/MF A01

Investing in technology is investing in America's future: a growth economy with more high-skill, high-wage jobs for American workers; a cleaner environment where energy efficiency increases profits and reduces pollution; a stronger, more competitive private sector able to maintain U.S. leadership in critical world markets; an educational system where every student is challenged; and an inspired scientific and technological research community focused on ensuring not just our national security but our very quality of life. American technology must move in a new direction to build economic strength and spur economic growth. The traditional federal role in technology development has been limited to support of basic science and mission-oriented research in the Defense Department, NASA, and other agencies. This strategy was appropriate for a previous generation but not for today's profound challenges. We cannot rely on the serendipitous application of defense technology to the private sector. We must aim directly at these new challenges and focus our efforts on the new opportunities before us, recognizing that government can play a role helping private firms develop and profit from innovations. DTIC

88 SPACE SCIENCES (GENERAL)

N93-25442*# TRW Space Technology Labs., Redondo Beach, CA. Applied Technology Div.
GAS-GRAIN SIMULATION FACILITY (GGSF). VOLUME 1: STAGE 1 FACILITY DEFINITION STUDIES
Nahum Gat (TRW Space Technology Labs., Redondo Beach, CA.) Mar. 1993 231 p
(Contract NAS2-13408; RTOP 107-20-06)
(NASA-CR-177606; A-93055; NAS 1.26:177606) Avail: CASI HC A11/MF A03

The Gas-Grain Simulation Facility (GGSF) is a facility-type payload to be included in the Space Station Freedom (SSF). The GGSF is a multidisciplinary facility that will accommodate several classes of experiments, including exobiology, planetary science, atmospheric science, and astrophysics. The physical mechanisms envisioned to be investigated include crystal growth, aggregation, nucleation, coagulation, condensation, collisions, fractal growth, cycles of freezing and evaporation, scavenging, longevity of bacteria, and more. TRW performed a Phase A study that included analyses of the science and technical (S&T) requirements, the development of facility functional requirements, and a conceptual design of the facility. The work that was performed under Stage 1 of the Phase A study and the results to date are summarized. In this stage, facility definition studies were conducted in sufficient detail to establish the technical feasibility of the candidate strawman experiments. The studies identified technical difficulties, identified required facility subsystems, surveyed existing technology studies and established preliminary facility weight, volume, power consumption, data systems, interface definition, and crew time requirements. The results of this study served as the basis for Stage 2 of the Phase A study in which a conceptual design and a reference design were performed. The results also served as a basis for a related study for a Gas-Grain Simulation Experiment Module (GGSEM), which is an apparatus intended to perform a subset of the GGSF experiments on board a low-Earth-orbiting platform.
Author (revised)

N93-25887# Swedish Board for Space Activities, Stockholm.
SPACE RESEARCH IN SWEDEN, 1990-1991
K. Fredga, ed. Swedish National Space Board 1992 133 p Presented at the COSPAR Meeting, Washington, DC, 28 Aug. - 5 Sep. 1992
Avail: CASI HC A07/MF A02

A review of the space sciences as practiced in Sweden during the years 1990-1991 is presented. Summaries of the following organizational bodies and areas are presented: National Organization of Space Activities; international cooperation; national scientific space programs; Space Research Groups; Space Application Programs; Esrange; space-related facilities and installations; and publications during 1990 and 1991. CASI

89 ASTRONOMY

Includes radio, gamma-ray, and infrared astronomy, and astrometry.

N93-25135*# Jamieson Science and Engineering, Inc., Scotts Valley, CA.
AN ATLAS OF SELECTED CALIBRATED STELLAR SPECTRA
Russell G. Walker and Martin Cohen Sep. 1992 256 p
(Contract NAS2-13327; RTOP 188-41-53)
(NASA-CR-177604; A-93022; NAS 1.26:177604) Avail: CASI HC A12/MF A03

Five hundred and fifty six stars in the IRAS PSC-2 that are suitable for stellar radiometric standards and are brighter than 1 Jy at 25 microns were identified. In addition, 123 stars that meet all of our criteria for calibration standards, but which lack a luminosity class were identified. An approach to absolute stellar calibration of broadband infrared filters based upon new models of Vega and Sirius due to Kurucz (1992) is presented. A general technique used to assemble continuous wide-band calibrated infrared spectra is described and an absolutely calibrated 1-35 micron spectrum of alpha(Tau) is constructed and the method using new and carefully designed observations is independently validated. The absolute calibration of the IRAS Low Resolution Spectrometer (LRS) database is investigated by comparing the observed spectrum of alpha(Tau) with that assumed in the original LRS calibration scheme. Neglect of the SiO fundamental band in alpha(Tau) has led to the presence of a specious 'emission' feature in all LRS spectra near 8.5 microns, and to an incorrect spectral slope between 8 and 12 microns. Finally, some of the properties of asteroids that effect their utility as calibration objects for the middle and far infrared region are examined. A technique to determine, from IRAS multiwaveband observations, the basic physical parameters needed by various asteroid thermal models that minimize the number of assumptions required is developed. Author (revised)

N93-25172*# Michigan Univ., Ann Arbor.
CORRELATIVE STUDIES OF ASTROPHYSICAL SOURCES OF VERY HIGH AND ULTRA HIGH ENERGY GAMMA-RAYS Final Report
Carl W. Akerlof 20 Jan. 1993 5 p
(Grant NAG5-1591)
(NASA-CR-192781; NAS 1.26:192781) Avail: CASI HC A01/MF A01

During the period of this contract, June 1, 1991 to November 14, 1992, the major results of our research effort have come from the Whipple air shower experiment in Tucson, AZ. The most notable development has been the discovery of TeV photons from the BL Lac object, Markarian 421. This result depended critically on the identification of Mrk 421 by the EGRET team as a source of GeV gamma rays. Derived from text

N93-25286 Sussex Univ., Brighton (England).
RADIAL VELOCITY STUDIES OF THE SECONDARY IN CATACLYSMIC VARIABLES M.S. Thesis
J. S. Martin 1988 177 p
Avail: Univ. Microfilms Order No. BRDX98316

The derivation and use of radial velocity curves of the secondary star to determine the component masses in cataclysmic variables is investigated. A brief review of these objects, especially their observational properties and possible evolutionary history is presented. This highlights the uncertain state of understanding in this area and shows the need for accurate component masses. A critical review of the various methods which have been employed for mass determinations is presented. The observational procedure and data reduction methods are covered. CCD spectroscopy in the near infra-red is used to detect the spectrum of the secondary star in four systems (IP Peg, CN Ori, AM Her, and U Gem), the first two of which are new detections. Radial velocity curves are produced by cross-correlation against the spectra of field stars. The observed spectra and radial velocity curves are reported together with the results of orbital fits to the curves. In three systems, a significant apparent eccentricity is detected. This may be due to irradiation of the inner face of the secondary or contamination by disc emission. To correct the orbital parameters for the effect of irradiation as well as tidal distortion and variation in surface gravity, a computer simulation of the secondary radial velocity curve was developed. The assumptions and methods used to produce simulated spectra and derive radial velocity curves from them are described. The observational consequences of the above effects ruling out all but the reduction of line strength by irradiation as significant sources of eccentricity (contamination from the disc was not included) are investigated. The corrections derived from the simulation are applied to the observations to produce masses for the four systems. The main findings are summarized and further work needed in this field is suggested. Dissert. Abstr.

N93-25289*# Arizona Univ., Tucson.
A STUDY OF THE LARGE-SCALE INFRARED EMISSION FROM A SELECTED DARK CLOUD Final Technical Report, 15 Aug. 1989 - 14 Sep. 1990
Erick T. Young 14 Sep. 1990 6 p
(Grant NAG5-1221)
(NASA-CR-192775; NAS 1.26:192775) Avail: CASI HC A02/MF A01

An investigation of the infrared emission energetics and embedded population in the rho Ophiuchi dark cloud is summarized. With a distance of approximately 140 pc, the rho Ophiuchi cloud is one of the closest regions of recent star formation. It is also one of the best studied such regions with numerous observations at all wavelengths. The IRAS data of the cloud provided a new glimpse of the overall structure of the cloud. In particular, the interaction of radiation from the Sco-Oph OB Association on the external heating of the cloud was very evident on Skyflux and Survey Co-Add images produced by IRAS. The infrared survey also revealed a number of new embedded sources in the cloud which have subsequently been observed from the ground. An earlier study explored the overall energetics of the cloud using the IRAS data. The main conclusions of that work were: (1) the overall luminosity of the cloud is well explained by the emission of the known B-stars, HD 147889, SR-3, and S1, along with a 15 percent contribution from the external radiation field; (2) the dust physical temperatures were significantly lower than the observed CO gas temperatures; and (3) dust grains are heated to only 10 percent to 20 percent of the total depth into the cloud. This analysis is extended by drawing on data from large-scale CO maps and from near-infrared surveys of the embedded population. Author (revised)

N93-25320# Lawrence Livermore National Lab., CA.
DEVELOPMENT OF LASER GUIDE STARS AND ADAPTIVE OPTICS FOR LARGE ASTRONOMICAL TELESCOPES
C. E. Max, K. Avicola, H. Bissinger, J. M. Brase, D. T. Gavel, H. Friedman, J. R. Morris, S. S. Olivier, D. Rapp, and J. T. Salmon et al 29 Jun. 1992 10 p Presented at the Progress in Telescope and Instrumentation Technologies, Garching, Germany, 27-30 Apr. 1992
(Contract W-7405-eng-48)
(DE93-007511; UCRL-JC-107218; CONF-920401-1) Avail: CASI HC A02/MF A01

A feasibility experiment to demonstrate high-order adaptive optics using a sodium-layer laser guide star is described. The copper-vapor-pumped dye lasers developed for LLNL's atomic Vapor Laser Isotope Separation program is used to create the laser guide star. Closed-loop adaptive corrections will be accomplished using a 69-subaperture adaptive optics system on a one-meter telescope at LLNL. The laser beam is projected upwards from a beam director approximately 5 meters away from the main telescope, and is expected to form a spot 1-2 meters in diameter at the atmospheric sodium layer (95 km altitude). The overall system architecture and adaptive optics components are described, and the expected performance is analyzed. Our long-term goal is to develop sodium-layer laser guide stars and adaptive optics for large astronomical telescopes. Preliminary design trade-offs for the Keck Telescope at Mauna Kea are discussed. DOE

N93-25331*# State Univ. of New York, Stony Brook. Astronomy Program.

THE STRUCTURE OF THE NEARBY UNIVERSE TRACED BY THEIRAS GALAXIES Final Report

Amos Yahil 8 Apr. 1993 4 p

(Grant NAG5-1228)

(NASA-CR-192809; NAS 1.26:192809) Avail: CASI HC A01/MF A01

One of the most important discoveries of the Infrared Astronomical Satellite (IRAS) has been the detection of about 20,000 galaxies with 60 microns fluxes above 0.5 Jy. From the observational point of view, the IRAS galaxies are ideal tracers of density, since they are homogeneously detected over most of the sky, and their fluxes are unaffected by galactic extinction. The nearby universe was mapped by the IRAS galaxies to a distance of approximately 200 h(exp -1) Mpc for the absolute value of b less than 5 deg. The ability to map down to such low galactic latitudes has proven to be particularly imporant, since some of the most important nearby large-scale structures, such as the Great Attractor, the Perseus-Pisces region, and the Shapley concentration, all lie there. Two major results of the U.S. IRAS redshift survey are discussed. Derived from text

N93-25440 California Univ., Berkeley.

A SUPERCONDUCTING TUNNEL JUNCTION RECEIVER FOR SUBMILLIMETER ASTRONOMY, AND ANALYSIS OF OBSERVATIONS OF POST-AGB STAR MOLECULAR ENVELOPES Ph.D. Thesis

Paul Aloysius Jaminet 1992 150 p

Avail: Univ. Microfilms Order No. DA9304952

A heterodyne receiver designed for astronomical use between 450 and 520 GHz has been constructed. Very low capacitance (C approximately = 5-10 fF) Superconductor-Insulator-Superconductor (SIS) junctions have been fabricated as the detectors; these junctions lie on the edges of niobium thin films and form Nb-Al-Al2O3-Al-Nb sandwiches. The double sideband (DSB) receiver noise temperature is between 400 K and 800 K throughout the 70 GHz band. In addition, detailed modelling and analysis of astronomical observations of two post-AGB (Asymptotic Giant Branch) stars was performed. The observations were made with an SIS receiver designed for 345 GHz. CO observations and modelling of the young planetary nebula NGC 7027 provided the best determination yet of its AGB mass loss rate, the first direct evidence for bipolarity in its AGB mass loss, evidence for close hydrodynamic coupling between the planetary nebula and the relic AGB wind, and evidence for evolution in the metallicity of the stellar wind. Observations of the proto-planetary nebula CRL 2688 found evidence for spatially extended fast wind emission with a non-bipolar morphology, and evidence for evolution in elemental abundances in the stellar wind. Dissert. Abstr.

N93-25536 Oxford Univ. (England).

THE TAURID METEOROID COMPLEX Ph.D. Thesis

D. J. Asher 1991 211 p

Avail: Univ. Microfilms Order No. BRD-98276

The aim of this work is to produce quite a detailed model, consistent with observations, of the evolution of the Taurid complex of interplanetary objects. The Taurids do not produce a spectacular meteor shower but the great breadth of the Taurid stream means that it is a major stream with regard to amount of material. The real size of the stream is evidenced by the fact that the activity lasts at least three months at both relevant times of year. As observations have been done over the years, new names have been given to showers coming from different longitudes in the sky, the Taurids not having as localized a radiant as many of the well-known and more compact streams. But despite the fact that the orbits of meteors in the various showers are comparatively spread out, they are still well enough aligned, and of similar size and shape, that they must be related (i.e., have a common origin). Around three quarters of meteors are sporadic rather than belonging to well-defined streams, although the dividing line is not clear-cut, perhaps 20 percent of meteors sometimes classified as sporadic actually occur as part of minor showers. The sporadic meteoroids move on similar orbits to meteoroids that are part of what is generally recognized as the Taurid stream, but there is a somewhat greater dispersion of elements in the sporadic stream. We point out the existence of a apex (AP) source which dominates for fainter (10th magnitude, say) meteors. There is a tendency for larger orbits in the Taurid stream to be at greater longitudes (cf. trends with longitude calculated by Stohl and Porubcan 1990). This is because of the differential effect of Jupiter on the rate of longitude precession on orbits of different sizes. We shall see that this dispersal in longitude is associated with a timescale of (is) approximately (or equivalent, similar) 10 kyr (1 kyr = 1000 years). One of the main questions will be the mechanism for generating the range in size of orbits (which then undergo differential precession due to Jupiter). We shall see that the distribution of Taurid meteor orbits as detected by photography and radar is best explained by a model in which large cometary fragments split from the parent object (the Encke progenitor) at perihelion and these fragments then undergo catastrophic collisions with objects in the astroid belt. Dissert. Abstr.

N93-25621 California Univ., Santa Cruz.

TULLY-FISHER DISTANCES AND MOTIONS IN THE NORTHERN SKY Ph.D. Thesis

Stephane Courteau 1992 275 p

Avail: Univ. Microfilms Order No. DA9235704

The results of a study to test for large-scale velocity deviations in a uniformly expanding universe are presented. At the onset of this work, galaxy motions in the northern hemisphere, contrary to the impressive sky coverage in the south, were still very poorly mapped. To improve on this situation, we identified a well-defined sample of 380 northern Sb-Sc UGC spirals in the range of 2000-10000 km sec(exp -1). Distances are estimated using the Tully-Fisher relation but with rotation velocities measured from long slit spectra in lieu of 21 cm delta V's. Surface brightness profiles and total magnitudes are extracted for 820 r-band images, and (H alpha + (NII)) rotation curves, fluxes, and rotation profiles are measured from 450 red spectra. The galaxy magnitudes are accurate internally to plus or minus 0(exp m)022 and the delta V's agree internally to plus or minus 12 km s(exp -1). A tight linear correlation of optical versus radio velocity widths with a scatter of 25 km s(exp -1) is also derived. We find evidence for large-scale motions near the concentration of Perseus-Pisces (PP), but identify a vast region of unperturbed, quiet Hubble flow (QHF) perpendicular to PP. The peculiar velocity (PV) data are corrected for uniform density Malmquist bias when they are analyzed in estimated distance space; an empirical correction for selection effects mainly due to magnitude cutoff is derived from the QHF region and applied to the PVs in redshift space. Both analyses are consistent in showing the PP Supercluster as streaming in bulk towards the Local Group at 392 plus or minus 79 km s(exp -1) (with respect to the microwave background restframe). The cause for such motion remains undetermined. Gravitational collapse within PP is detected, but the statistical error is large. An emerging picture of large-scale velocity fields shows the main infall regions to be correlated with the observed clumpiness of luminous matter. Our data, combined with published PV surveys, provide strong support for the existence of low-amplitude perturbations in the universe on scales not yet probed by current samples (approxmately greater than 120h(exp -1)Mpc). The implications of cosmic bulk motions with such large coherence lengths pose a serious challenge for models of generation of structure in the universe. Dissert. Abstr.

N93-25624 Delaware Univ., Newark.

STEADY-STATE NUMERICAL MODELS OF ACCRETING NEUTRON STARS: THE EFFECT OF ATMOSPHERIC CNO DEPLETION AND DIFFUSION Ph.D. Thesis

Jason Clark Tillett 1992 114 p

Avail: Univ. Microfilms Order No. DA9301779

We use the observed variation of burst properties of x-ray burst sources, with the persistent flux to determine if nuclear reactions are proceeding in a carbon poor or carbon rich environment. We find that by reducing the CNO cycle burning rate, which corresponds to a carbon poor environment, we cannot reproduce observed variations in the burst properties with persistent flux. Recent work on the surface boundary conditions of accreting neutron stars indicates that appreciable amounts of CNO elements can be destroyed by spallation. Previous authors assume an accretion of near solar abundance material which is not altered by boundary effects. Here we construct steady-state models of accreting neutron stars assuming all but traces of metals are destroyed due to spallation in the surface layers. We also construct models with solar accretion for comparison. The models are compared with EXOSAT observations of 4U/MXB 1636-53. We find that the simplification introduced by assuming CNO destruction does not bring theory closer to describing what is observed. Elemental diffusion has never been incorporated into the equations of stellar structure when solving for the steady-state structure of an accreting neutron star. A simple order

of magnitude estimate of the timescale for diffusion indicates that this process may be important, particularly for bursts with long recurrence intervals. We solve the equations of stellar structure with diffusion and show that the results indicate that the star may not be in a steady-state.
Dissert. Abstr.

N93-25712 Durham Univ. (England).
OPTICAL AND INFRARED STUDIES OF DISTANT GALAXIES Ph.D. Thesis
Alfonso Aragon-Salamanca 1991 278 p
Avail: Univ. Microfilms Order No. BRD-97956

This thesis investigates the evolution of galaxies as a function of look-back time, concentrating on early-type cluster galaxies. We demonstrate that selecting galaxies in the near-infrared produces samples that are representative of the galaxy population at intermediate and high redshift, and that such samples are likely to contain approximately the same proportion of all galaxy classes independently of z, avoiding the biases introduced by optical selection criteria. We have developed observing and data processing techniques using infrared arrays that yield high precision near-infrared photometry to very faint limits. Combining such data with optical photometry for the galaxy samples, we have been able to quantify the amount of color evolution in early-type cluster galaxies up to redshifts z approx. 0.9. At z = 0.37 the mean color-luminosity (c-L) relation for early-type cluster galaxies is compatible in slope and zero point with that of present-day ellipticals, indicating that the bulk of the stellar population at that epoch does not show any significant color evolution. However, the scatter around the main c-L line is significantly larger than the observational errors, and distinctively non-Gaussian. We interpret this as evidence that a large fraction (approx. 60 percent) of the early-type members have suffered a burst of star formation (involving approx. 10 percent of the galaxy mass) approx. 1 Gyr prior to the epoch of observation. In the redshift range 0.5 less than z less than 0.9, we detect systematic color evolution with redshift in the red cluster galaxies. In particular, at z approx. 0.9 there are no galaxies as red as present day ellipticals at all wavelengths. The detected evolution is compatible with the passive aging of stellar populations formed before z approx. equals 2. Superimposed on that, there is evidence for subsequent bursts of star formation happening on a substantial fraction of the cluster galaxies, but affecting only a small fraction of the total galaxy mass. We suggest this may be related to the Butcher-Oemler effect observed at lower redshifts. We did not detect significant amounts of galaxy luminosity evolution at 2 microns, in contrast with the results for radio galaxies. We finally propose and test three new approaches to the study of normal field and cluster galaxies beyond z = 1: a study of gravitationally lensed galaxies, a search for galaxies producing clustered metallic absorption lines in QSO's and an infrared follow-up of ROSAT X-ray detected high redshift clusters.
Dissert. Abstr.

N93-25755*# Yale Univ., New Haven, CT.
FAR-INFRARED EMISSION, GAS, AND ULTRALUMINOUS HII REGIONS IN M101 Final Report
J. D. P. Kenney and N. Z. Scoville 1992 1 p
(Grant NAG5-1803)
(NASA-CR-192791; NAS 1.26:192791) Avail: CASI HC A01/MF A01

We have made deconvolved maps of M101 in each of the 4 IRAS bands using a new maximum-entropy based model for reconstructing distributions with correlated structure on multiple scales. This new deconvolution procedure, developed by Weir (1992, J.Opt.Soc.Am., submitted), is superior to other maximum entropy-based techniques for several reasons. For our purposes, an important advantage is that it has less artifacts and greatly reduced systematic biases compared with the 'HiRes' maps of M101 produced by Aumann, Fowler, and Melnyk (1990, AJ, 99, 1674), thus it is accurate enough to perform aperture photometry. The deconvolved maps have a maximum resolution of approximately 30 sec, sufficient to resolve the brightest HII complexes and much of the spiral structure. The new maps and our comparison of the far-infrared, gas, and optical distributions are being written up in Kenney, Weir & Scoville (1992, in preparation). The quality of the reconstructed far-infrared maps is good enough for us to carry out most of the analyses outlined in the original proposal. From a ratio of the 60 micron and 100 micron maps, we have found that the ultraluminous HII complexes in the outer galaxy have the hottest dust temperatures with T approximately 50-60 K, which is twice as hot as most of the disk. Their extraordinary luminosity in the far-infrared is due to a relatively small amount of dust being heated to high temperatures, rather than a large concentration of dust and gas. A map of the dust opacity at 60 microns shows good overall agreement with a map of cold gas (HI+H2), indicating that throughout most of the galaxy only approximately 20 percent of the dust is warm enough to be detected by IRAS. The ultraluminous HII complexes have a high luminosity-to-gas mass ratio, independent of whether the far-infrared or the H-alpha emission line is used to measure the luminosity, which implies that gas is being converted into high mass stars more rapidly in these complexes compared to other locations in the disk.
Author (revised)

N93-26002*# National Aeronautics and Space Administration. Goddard Space Flight Center, Greenbelt, MD.
CAPE PHOTOGRAPHIC DURCHMUSTERUNG, VOLUME 1
Washington May 1993 429 p
(Contract NAS5-30960; RTOP 633-00-00)
(NASA-RP-1300-Vol-1; Rept-93B00049-Vol-1; NAS 1.61:1300-Vol-1) Avail: CASI HC A19/MF A04

The Cape Photographic Durchmusterung (CPD Gill and Kapteyn 1895-1900) is a photographic survey of southern stars in the declination range -18 to -90 degrees. This volume covers the declination range -18 through -37 degrees. Positions are given for the 1875 equinox. The summary of the positional uncertainties quoted in the third volume of the published catalog gives +/- 0.28 sec (R.A.) +/- 0.044 arcmin (Dec.) for zones -18 to -57 degrees. The probable error of a photographic magnitude as determined by combining results for different magnitudes and weighting proportionately according to the numbers of stars in each class of magnitude is given as +/- 0.055 mag. From an analysis of the taint magnitude limits on the plates discussed in the third volume introduction, the catalog as a whole can be considered complete to photographic magnitude 9.2 but it is stated that it will be found practically complete in or near the Milky Way, to magnitude 9.5.
Author

N93-26003*# National Aeronautics and Space Administration. Goddard Space Flight Center, Greenbelt, MD.
CAPE PHOTOGRAPHIC DURCHMUSTERUNG, VOLUME 2
Washington May 1993 445 p
(Contract NAS5-30960; RTOP 633-00-00)
(NASA-RP-1300-Vol-2; Rept-93B00049-Vol-2; NAS 1.61:1300-Vol-2) Avail: CASI HC A19/MF A04

The Cape Photographic Durchmusterung (CPD, Gill and Kapteyn 1895-1900) is a Photographic survey of southern stars in the declination range -18 to -90 degrees. This volume covers the declination range -53 through -89 degrees. Positions are given for 1875 equinox. The summary of the positional uncertainties quoted in the third volume of the published catalog gives +/- 0.28 sec (R.A.), +/- 0.044 arcmin (Dec.) for zones - 18 to -57 degrees, + 0.157 sec + 0.0764/cos(delta) sec (R.A.), +/- 0.056 arcmin (Dec.) for zones -58 to -85 degrees, +0.157 sec + 0.0353/cos (delta) sec (R.A.), + 0.0127 arcmin (Dec.) for the polar plate where, as explained in the introduction to the third volume, many positions were derived from rectangular coordinates (these are positions reported to 0.1 SCC (R.A.) and 0.001 arcmin (Dec.) in the -86 to -89 degree zones in the catalog). The probable error of a photographic magnitude, as determined by combining results for different magnitudes and weighting proportionately according to the numbers of stars in each class of magnitude, is given as +0.055 mag. From an analysis of the faint magnitude limits on the plates discussed in the third volume introduction, the catalog as a whole can be considered complete to photographic magnitude 9.2, but it is stated that it will be found practically complete, in or near the Milky Way, to magnitude 9.5.
Author

N93-26004*# National Aeronautics and Space Administration. Goddard Space Flight Center, Greenbelt, MD.
CAPE PHOTOGRAPHIC DURCHMUSTERUNG, VOLUME 3
Washington May 1993 406 p
(Contract NAS5-30960; RTOP 633-00-00)
(NASA-RP-1300-Vol-3; Rept-93B00049-Vol-3; NAS 1.61:1300-Vol-3) Avail: CASI HC A18/MF A04

The Cape Photographic Durchmusterung (CPD, Gill and Kapleyn 1895-1900) is a photographic survey of southern stars in the declination range -18 to -90 degrees. This volume covers the declination range -53 through -89 degrees. Positions are given for the 1875 equinox. The summary

of the positional uncertainties quoted in the third volume of the published catalog gives +/- 0.28 sec (R.A.), + 0.044 arcmin (Dec.) for zones -18 to -57 degrees, + 0.157 sec + 0.0764/cos(delta) sec (R.A.), +/- 0.056 arcmin (Dec.) for zones -58 to -85 degrees, +0.157 sec + 0.0353/cos(delta) sec (R.A.), +/- 0.0127 arcmin (Dec.) for the polar plate where, as explained in the introduction to the third volume, many positions were derived from rectangular coordinates (these are positions reported to 0.1 sec (R.A.) and 0.001 arcmin (Dec.) in the -86 to -89 degree zones in the catalog). The probable error of a photographic magnitude, as determined by combining results for different magnitudes and weighting proportionately according to the numbers of stars in each class of magnitude, is given as +0.055 mag. From an analysis of the faint magnitude limits on the plates discussed in the third volume introduction, the catalog as a whole can be considered complete to photographic magnitude 9.2, but it is stated that it will be found practically complete, in or near the Milky Way, to magnitude 9.5.
Author

N93-26139*# Lockheed Missiles and Space Co., Palo Alto, CA. Research Lab.
ROSAT INVESTIGATION OF FLARING AND ACTIVITY ON PROX CEN Final Report, 5 May 1992 - 4 May 1993
Bernhard Haisch 4 May 1993 30 p
(Contract NAS5-31844)
(NASA-CR-192972; NAS 1.26:192972) Avail: CASI HC A03/MF A01

The objective of this program was to investigate with high sensitivity the low-level flare activity which may underlie coronal heating. This was done. The ROSAT observations of Prox Cen were scheduled for 50 ks spread out from 26 Feb. - 10 Mar. 1992. Unfortunately because of spacecraft problems many of these pointings turned out to contain no useful data or extremely truncated valid data sets. Considerable time was spent trying to determine which of the data would be scientifically useful and which would not. Fortunately, several developments took place to augment the original data in such a way that the scientific goal of advancing the study of flaring and variability was able to be achieved after all. These are as follows: (1) a second round of ROSAT observations was carried out in Feb. 1993 which only came to the attention of the PI in Apr. 1993 when a new data tape arrived; (2) simultaneous IUE observations were requested and obtained; (3) data from the UK WFC are available via the collaboration with Dr. G. Bromage; and (4) the 'cleaned-up' original data set was found to include one major flare and 2 moderate flares. Because of the problems with the original data set, the unexpected acquisition of new data only two months ago, and the availability of IUE and WFC data, an article on Prox Cen for publication is not ready at this time. Such an article is being developed and can be completed as part of ongoing ROSAT research efforts on stellar coronae and flaring. Author (revised)

N93-26426*# Pennsylvania State Univ., University Park. Dept. of Astronomy and Astrophysics.
ROSAT X RAY SURVEY OBSERVATIONS OF ACTIVE CHROMOSPHERIC BINARY SYSTEMS AND OTHER SELECTED SOURCES Final Technical Report
Lawrence W. Ramsey 24 Apr. 1993 7 p
(Grant NAG5-1435)
(NASA-CR-192933; NAS 1.26:192933) Avail: CASI HC A02/MF A01

The connection between processes that produce optical chromospheric activity indicators and those that produce x-rays in RS CVn binary systems by taking advantage of the ROSAT All-Sky Survey (RASS) results and our unique ground-based data set was investigated. In RS CVn systems, excess emission in the Ca 2 resonance (K & H) and infrared triplet (IRT) lines and in the Balmer lines of hydrogen is generally cited as evidence for chromospheric activity, which is usually modeled as scaled up solar-type activity. X-ray emission in RS CVn systems is believed to arise from coronal loop structures. Results from spectra data obtained from RASS observations are discussed and presented. Derived from text

N93-24723*# Hughes Danbury Optical Systems, Inc., CT.
OPTIMIZING THE FINE LOCK PERFORMANCE OF THE HUBBLE SPACE TELESCOPE FINE GUIDANCE SENSORS
David J. Eaton, Richard Whittlesey, Linda Abramowicz-Reed, and Robert Zarba *In* NASA. Goddard Space Flight Center, Flight Mechanics/Estimation Theory Symposium, 1992 Feb. 1993 p 423-437 (For primary document see N93-24694 09-13)
(Contracts NAS8-32700; NAS8-38494)
Copyright Avail: CASI HC A03/MF A04

N93-24724*# Hughes Danbury Optical Systems, Inc., CT.
THE HUBBLE SPACE TELESCOPE FINE GUIDANCE SYSTEM OPERATING IN THE COARSE TRACK POINTING CONTROL MODE
Richard Whittlesey *In* NASA. Goddard Space Flight Center, Flight Mechanics/Estimation Theory Symposium, 1992 Feb. 1993 p 439-452 (For primary document see N93-24694 09-13)
(Contract NAS5-38494)
Copyright Avail: CASI HC A03/MF A04

N93-24984# Bureau International des Poids et Mesures, Sevres (France).
ATOMIC TIME SCALES FOR DYNAMICAL ASTRONOMY
B. Guinot *In* ESA, Frequency and Time Forum Jun. 1992 p 51-56 (For primary document see N93-24978 09-70)
Copyright Avail: CASI HC A02/MF A04

N93-25795*# California Univ., Berkeley.
DEVELOPMENT OF A TOOL-SET FOR SIMULTANEOUS, MULTI-SITE OBSERVATIONS OF ASTRONOMICAL OBJECTS Abstract Only
Supriya Chakrabarti, J. Garrett Jernigan, and Herman L. Marshall *In* Colorado Univ., Applied Information Systems Research Program (AISRP). Workshop 2: Meeting Proceedings 1992 1 p (For primary document see N93-25792 09-82)
Avail: CASI HC A01/MF A03

90 ASTROPHYSICS

Includes cosmology; celestial mechanics; space plasmas; and interstellar and interplanetary gases and dust.

For related information see also *75 Plasma Physics*.

N93-24770 North Carolina Univ., Chapel Hill.
OBSERVATIONS AND MODELS OF SHOCK STRUCTURES IN HERBIG-HARO OBJECTS Ph.D. Thesis
Jon Arthur Morse 1992 215 p
Avail: Univ. Microfilms Order No. DA9302552

Herbig-Haro objects are emission-line nebulae that result from radiative shock waves formed by the interaction of a collimated supersonic stellar wind, driven by an embedded young stellar object, with the ambient molecular material out of which the star formed. This dissertation is a study of these energetic outflows using detailed spectrophotometry of the emitting gas and dynamical models of the wind/cloud interactions. Three stellar jets with prominent bow-shaped Herbig-Haro objects have been studied, with the following principal results: (1) the stellar jets all show signs of being velocity-variable (i.e., non-steady); (2) the densities in the jets are approximately 10 times the densities in the ambient environments; and (3) magnetic fields do not appear to play a major role in the dynamics of the outflows, at least in the regions of the outer bow shocks. Dissert. Abstr.

N93-24907 Wisconsin Univ., Milwaukee.
COSMIC STRING COSMOLOGY Ph.D. Thesis
Robert Reynolds Caldwell 1992 151 p
Avail: Univ. Microfilms Order No. DA9300075

Cosmological aspects of cosmic strings are studied. The formation, growth, and evolution of small scale structure on cosmic strings are studied. It is found that the accumulation of small scale structure alters the appearance and behavior of the cosmic string network and changes the means by which cosmic strings may contribute to the formation of large scale structure from loops to long strings. Next, the density of gravitational radiation produced by a realistic cosmic string network, evolving in a realistic universe, is calculated. Cosmological observations of nucleosynthesis and noise in pulsar timing measurements are used to constrain the density of cosmic string gravitational radiation. It is found that cosmic string scenarios which may realistically contribute to the formation of large scale structure are heavily restricted. Dissert. Abstr.

N93-24949 Illinois Univ. at Urbana-Champaign, Savoy.
PROPAGATION OF RADIATION IN ASTROPHYSICAL MEDIA: GRAVITATIONAL LENSES AND ASTROPHYSICAL MASERS Ph.D. Thesis
Gerardo Angelo Scappaticci 1992 146 p
Avail: Univ. Microfilms Order No. DA9305679

In Part 1 the time variability of the radiation emitted by astrophysical masers is studied by numerically solving the system of time dependent non-linear partial differential equations of radiative transfer through a masing gas. The calculations demonstrate for the first time how oscillations, with periods which are comparable to the light travel time through the maser, might develop as a result of radiative instabilities. In addition, we perform a linear stability analysis of the radiative transfer equations and the rate equations for the molecular populations of the masing transition. We use this stability analysis to determine the conditions and parameters for which an astrophysical maser would become unstable. Our results are in agreement with recent observations of astrophysical masers in which fluctuations are found on time scales as short as one thousand seconds. In Part 2 statistical methods are applied to analytically calculate the properties of the fluctuations, in intensity and luminosity, of gravitationally lensed images of quasars, due to compact masses lying within the deflecting galaxy. We compute the fluctuations in intensity, and apparent luminosity, of the gravitationally lensed source as measured by quantities such as the standard deviation, autocorrelation function, and power spectrum. We also compare our results with numerical data we received from P. Schneider and A. Weiss, which for the first time directly compares a Monte Carlo type method with a totally analytical calculation. Dissert. Abstr.

N93-25164# Idaho National Engineering Lab., Idaho Falls.
NEAR EARTH OBJECT FUELS (NEO-FUELS): DISCOVERY, PROSPECTING AND USE
Anthony C. Zuppero and Michael G. Jacox 25 Aug. 1992 9 p Presented at the 43rd Congress of the International Astronautical Federation, Washington, DC, 28 Aug. - 5 Sep. 1992
(Contract DE-AC07-76ID-01570)
(DE93-005185; EGG-M-92057; CONF-9208154-2) Avail: CASI HC A02/MF A01

The 1992 discovery of a water-ice, near-Earth object (NEO) in the space near Earth is evaluated as a source of rocket fuel and life support materials for Earth orbit use. Nuclear thermal rockets using steam propellant are evaluated and suggested. The space geological formation containing such water-rich NEO's is described. An architecture couples near-Earth object fuels (neo-fuel) extraction with use in Earth orbits. Preliminary mass payback analyses show that space tanker systems fueled from space can return in excess of 100 times their launched mass from the NEO, per trip. Preliminary cost estimates indicate neo-fuel costs at Earth orbit can be 3 orders of magnitude below today's cost. A suggested resource verification plan is presented. DOE

N93-25200*# Molecular Research Inst., Palo Alto, CA.
[THEORETICAL CALCULATIONS ON THE ELECTRON ABSORPTION SPECTRA OF SELECTED POLYCYCLIC AROMATIC HYDROCARBONS (PAH) AND DERIVATIVES] Final Technical Report
Ping Du 5 Apr. 1993 55 p Submitted for publication
(Contract NCC2-733)
(NASA-CR-192762; NAS 1.26:192762) Avail: CASI HC A04/MF A01

As a theoretical component of the joint effort with the laboratory of Dr. Lou Allamandola to search for potential candidates for interstellar organic carbon compound that are responsible for the visible diffuse interstellar absorption bands (DIB's), quantum mechanical calculations were performed on the electron absorption spectra of selected polycyclic aromatic hydrocarbons (PAH) and derivatives. In the completed project, 15 different species of naphthalene, its hydrogen abstraction and addition derivatives, and corresponding cations and anions were studied. Using semiempirical quantum mechanical method INDO/S, the ground electronic state of each species was evaluated with restricted Hartree-Fock scheme and limited configuration interaction. The lowest energy spin state for each species was used for electron absorption calculations. Results indicate that these calculations are accurate enough to reproduce the spectra of naphthalene cation and anion observed in neon matrix. The spectral pattern of the hydrogen abstraction and addition derivatives predicted based on these results indicate that the electron configuration of the pi orbitals of these species is the dominant determinant. A combined list of 19 absorptions calculated from 4500 A to 10,400 A were compiled and suggested as potential candidates that are relevant for the DIB's absorptions. Continued studies on pyrene and derivatives revealed the ground state symmetries and multiplicities of its neutral, anionic, and cationic species. Spectral calculations show that the cation (B(sub 3g)-2) and the anion (A(sub u)-2) are more likely to have low energy absorptions in the regions between 10 kK and 20 kK, similar to naphthalene. These absorptions, together with those to be determined from the hydrogen abstraction and addition derivatives of pyrene, can be used to provide additional candidates and suggest experimental work in the search for interstellar compounds that are responsible for DIB's. Author (revised)

N93-25211*# California Univ., San Diego, La Jolla. Center for Astrophysics and Space Sciences.
STARBURST GALAXIES: HARD X-RAY SPECTRA AND CONTRIBUTION TO THE DIFFUSE BACKGROUND Final Report
Duane E. Gruber 3 Mar. 1993 5 p
(Grant NAG5-1385)
(NASA-CR-192790; NAS 1.26:192790) Avail: CASI HC A01/MF A01

During the period of this grant two main tasks were performed: a determination of a selection criterion for starburst galaxies most likely to emit X-rays, and performance of a pilot study of the X-ray emission from nine such systems. Starburst galaxies may be expected to emit flat-spectrum X-ray at energies above 10 keV resulting from the various remnants of the short-lived massive stars which characterize the starburst. The investigation to determine the optimum sample resulted in a change from an X-ray selected (HEAO-2) sample to infrared selection based on the IRAS catalogue. A much broader sample thereby available for study, and selection could be limited to only the nearest objects and still obtain a reasonably large sample. A sample of 99 of the brightest infrared starburst galaxies was settled on for the X-ray survey. For a set of practical size, this was then reduced to a subset of 53, based on luminosity and nearness. X-ray emission from these objects was individually measured from the UCSD HEAO-1 all-sky survey in four energy bands between 13 keV to 160 keV. This data base consists of about 20 optical disk volumes. Net significance for the result was roughly two sigma, and a very hard spectral shape is indicated for the net spectrum of the surveyed galaxies. With the possibility of detection of the class, it was then felt worthwhile to examine fluxes from these sources in other archival data. This was performed with the HEAO-1 A2 data and the HEAO-2 (EINSTEIN) main archive and slew survey. Positive results were also obtained for the sample, but again at weak significance. With three independent measures of weak X-ray fluxes from nearby starburst galaxies, we wrote a letter to the Astrophysical Journal (enclosed) discussing these results and their likely significance, in particular, for the contribution to the cosmic diffuse x-ray background, perhaps as much as 25 percent. Author

N93-25230*# National Aeronautics and Space Administration. Goddard Space Flight Center, Greenbelt, MD.
FAR INFRARED SPECTRA OF AMORPHOUS AND CRYSTALLINE WATER ICE AND CHANGES IN THESE PHASES AS THE RESULT OF PROTON IRRADIATION
Reggie L. Hudson (Eckerd Coll., Saint Petersburg, FL.) and Marla H. Moore Chicago, IL University of Chicago Press 20 Nov. 1992 25 p Submitted for publication
(Grants NAG5-1843; NsG-5172)
(NASA-CR-192849; NAS 1.26:192849) Avail: CASI HC A03/MF A01

Far infrared spectra from 20 microns (500 cm(sup -1)) to 100 microns (100 cm(sup -1)) of water ice were measured. Amorphous ice deposited at 13 K has one absorption band at 45 microns (220 cm(sup -1)). Amorphous ice evolves into a crystalline form with absorptions at 44 microns (229 cm(sup -1)) and 62 microns (162 cm(sup -1)) as the temperature is increased to 155 K. Spectra documenting this phase change are presented as well as spectra of crystalline ice at temperatures between 13 K and 155 K. Far infrared spectra of amorphous and crystalline water ice before and after proton irradiation are also presented. Changes in these two forms are discussed in relation to ices in comets, grains, and planetary satellites in various radiation environments. Observations of non-terrestrial clathrate hydrates are still lacking despite the fact that clathrates first were suggested to exist in cometary and interstellar ices over forty years ago. Spectroscopy, the most direct method of astronomical detection, has been hampered by

the similarity of clathrate hydrate spectra to those of unenclathrated guest molecules and solid H2O. A methanol (CH3OH) clathrate hydrate, using a recently published procedure, was prepared and its far-IR spectrum investigated. The spectrum is quite differenct from that of either unenclathrated CH3OH or solid H2O and so should be of value in astronomical searches for this clathrate. Author (revised)

N93-25245 Sussex Univ., Brighton (England).
ORIGIN AND EVOLUTION OF CATACLYSMIC VARIABLES M.S. Thesis
D. Thomas 1988 268 p
Avail: Univ. Microfilms Order No. BRDX98319

The basic model of a cataclysmic variable, incorporating a low mass dwarf transferring material via an accretion disc to a white dwarf, is well founded. However, the details of how such systems form and evolve is still uncertain. Some of the problems are discussed in the background presented in Part 1. One obstacle to a solution of these evolutionary problems is the lack of accurate information on component masses. Part 2 presents the results of an observing program aimed at providing further information for use in mass determinations. Chapter 3 reports on survey of 65 cataclysmic variables in which 16 secondary stars were detected through the lambda 8190 A NaI doublet. Several other interesting spectroscopic features are also discussed. In Chapters 4 and 5, radial velocity studies of five secondaries are presented. Improved periods are determined for three objects and preliminary mass determinations are carried out for all, using mass ratios found from the rotational broadening and white dwarf radial velocity semi-amplitudes. Chapter 6 presents a preliminary kinematic study of cataclysmic variables using gamma velocities from secondary star observations. Unfortunately, radial velocity measurements using the lambda 8190 A doublet are often severely distorted by line flux variations caused by irradiation and contamination. Such effects were observed as apparently eccentric orbits in CH UMa and SS Aur. Corrections may be calculated by measuring the line flux variations. This was attempted for RU Peg and SS Cyg in Chapter 7. No significant eccentricities or line flux variations were detected, but the results indicate that direct NaI line flux measurements are difficult. The secondary star in RU Peg, CH UMa, MU Cen, SS Cyg, and DO Dra appears cooler than expected if it obeys the often assumed main sequence mass-radius relation. Part 3 reports evolutionary calculations, using the latest theories for disc and stellar magnetic braking, aimed at explaining this over-cool tendency. The most likely explanation is that the single star mass-radius relations are not valid for cataclysmic variable secondaries. For the longer period systems, mass determinations imply the secondaries have evolved significantly across the main sequence. Different rates of angular momentum loss may also explain the different appearances of secondary stars in systems with similar periods. Part 4 provides a detailed summary of the preceding work and suggests possible approaches for the future. Dissert. Abstr.

N93-25477# Massachusetts Univ., Boston.
STRUCTURE AND STAR FORMING ACTIVITIES OF THE COLD MASSIVE MOLECULAR CLOUD G216-2.5 Ph.D. Thesis
Youngung Lee 1992 181 p
Avail: Univ. Microfilms Order No. DA9305858

The gas and dust properties and the star forming activity in G216-2.5 (also called Maddalena's cloud), a cold, massive giant molecular cloud (GMC) that has no evidence for star formation are studied. We have mapped 11 square degrees in the J = 1-0 transitions of CO-12 and CO-13 using the QUARRY fifteen-beam array receiver on the 14 m telescope at FCRAO. We have confirmed the results of Maddalena and Thaddeus (1985) that the cloud is unusually cold and has very broad linewidths (delta(V) is approximately 8 km/s). The visual extinction to CO-13 column density ratio is found to be similar to that in local molecular clouds, suggesting that if the gas to dust ratio is normal, the CO-13 abundance relative to molecular hydrogen in this cloud is similar to that found for clouds near the sun. The low gas and dust temperatures found for this cloud are largely due to the absence of heating by massive stars. The exceptionally low gas temperature can be explained if the cosmic-ray heating rate is reduced by a factor of two in the outer Galaxy. Low luminosity, and presumably low mass, young stars were identified in this cloud. These young stars are found preferentially on the edge of the cloud. Clusters of T Tauri stars are found in two locations within G216-2.5. The mass of the cloud was established by several techniques and masses between 1 x 10(exp 5) and 6 x 10(exp 5) M solar magnitudes were obtained. It is suggested that G216-2.5 is a remnant cloud from a past episode of massive star formation for the following reasons. First, the cloud has a relatively large velocity dispersion for a non-star-forming GMC. Second, there is clear evidence for shells and rings within the cloud, which may be the fossil remains of its earlier star formation activity. Third, the kinematics of the cloud is dominated by a global velocity gradient suggesting that the cloud is part of a very large expanding shell. Lastly, the discrepancy between the local thermodynamic equilibrium (LTE) and virial masses may be explained if the cloud has been severely perturbed and is currently expanding. G216-2.5 may be part of a larger star forming complex that includes the adjacent H 2 region S287 and its molecular cloud.
Dissert. Abstr.

N93-25537 Florida Univ., Gainesville.
NUMERICAL MODELING OF BARRED SPIRAL GALAXIES Ph.D. Thesis
Elizabeth Mary Moore 1992 250 p
Avail: Univ. Microfilms Order No. DA9304032

A two-component, self-consistent computer code to model spiral galaxies was written and tested and a method of inducing and controlling bar formation is developed. This work presents a departure from former modeling work done at the University of Florida, which depended on the beam scheme, a hydrodynamical code with a number of limitations. In particular, only the gas component could be modeled, no self-gravitational forces were included, and the viscosity inherent to the code could not be controlled easily. These shortcomings are overcome in the new algorithm. Most importantly, an attempt has been made to keep the models self-consistent. No perturbing potentials are imposed or required to excite bar and spiral structure. The code can model both the stellar and the gaseous component of a spiral galaxy. The stellar component feels only gravitational forces, while the gas component feels both gravitational and viscous forces. In addition, a halo force can be imposed for the purpose of stabilizing the disk. The code is a hybrid grid/smooth particle code. The gravitational forces are calculated on a Cartesian grid using a Fast Fourier Transform, while the gas viscous forces are calculated in a smooth particle manner. A mechanism for creating warm, featureless, stable disks is developed by taking moments of the collision less Boltzmann equation. In order to induce and control bar and spiral arm formation, the stabilizing stellar velocity dispersions are reduced in the center of the disk, but maintained in the outer regions. A bar forms naturally in the interior and the rotation of this bar helps maintain spiral structure in the outer gas disk. Realistic-looking spiral features are maintained in the gas component for as long as the models are calculated. A wide variety of bar and spiral structure can be formed by varying the size of the unstable central region, the rate of 'turn on', of the heating and the halo mass. We would like to test the model results by comparing them with observations and so a second part of the thesis consists of observing and reducing 21 cm line data of NGC 1398 and NGC 1784 at the Very Large Array. Low (C/D array) and high (B/C) resolution data were obtained, calibrated and combined to make maps of the integrated column density and mean radial velocity of the neutral hydrogen. In the future, the code will be used to try to model these galaxies. Dissert. Abstr.

N93-25555 Massachusetts Univ., Boston.
SHELLS, OUTFLOWS AND STAR FORMATION IN THE GIANT MOLECULAR CLOUD MONOCEROS R2 Ph.D. Thesis
Taoling Xie 1992 241 p
Avail: Univ. Microfilms Order No. DA9305918

To improve our understanding about giant molecular clouds (GMC) associated with R-associations, a CO-12 J = 1-0 map of 167,000 spectra with 45 inch resolution and 25 inch spacing, a CO-13 J = 1-0 map of approximately 40,000 spectra with 1.5 foot resolution and 1 foot spacing, IRAS BIGMAP images, and maps of high density molecular tracers for the dense cores are obtained for the GMC Monoceros R2 (D = 830 plus or minus 50 pc). These data reveal that the large-scale structure of Mon R2 is dominated by an expanding bubble shell (approximately 30 pc) with front side moving towards us at a radial velocity of approximately 4-5 km/s. Distortions of this shell are obvious, suggesting of the inhomogeneity of the cloud before the formation of the bubble. There is no evidence for red-shifted shell at the far side of the bubble. There are at least two generations of star formation in Mon R2. The older generation of stars with an age of 6-10 x 10(exp 6) years are represented mostly by reflection nebulae. The younger generation of stars with an age of approximately

10(exp 5) years are represented mostly by IRAS point sources. It is proposed that the large-scale expanding bubble shell is the result of combined effects of ionizing flux and stellar winds originating from the older generation of young stellar objects, but perhaps dominated by O type stars which either are obscured or left main sequence. It is suggested that the formation of the younger generation of stars has been triggered by the older generation of stars. The main and the GGD12-15 cores are located on the large-scale expanding shell, and their harboring both generations of stars can be explained were the cores preexisting clumps. Our CO data reveal an eggplant-shaped bipolar outflow shell, whose shape can be satisfactorily modeled with radially directed stellar winds sweeping up ambient material with momentum conservation. An inversion method is implemented for analyzing dust emission spectra at FIR wavelengths in terms of a continuous dust temperature distribution, and was applied to IRAS BIGMAP images of Mon R2. Computer programs are developed for identifying clumps and determining their properties in molecular emission maps. The results support the reality of size-linewidth and mass-linewidth relations for clumps in individual GMC's. Dissert. Abstr.

N93-25559 Colorado Univ., Boulder.
30 DORADUS IN THE LARGE MAGELLANIC CLOUD: THE STELLAR CONTENT AND INITIAL MASS FUNCTION Ph.D. Thesis
Joel William Parker 1992 240 p
Avail: Univ. Microfilms Order No. DA9304594

UBV photometry for 2400 stars in the OB associations of 30 Doradus in the LMC and new spectroscopic classifications for 54 stars including 23 O stars are presented. The entire catalog (exclusive of the dense core cluster R 136) is photometrically complete to V = B = 18(sup m) and U = 17(sup m), although the completeness magnitudes are fainter for regions with less nebular contamination. From these data, I have determined the effective temperatures and bolometric magnitudes of the stars and placed them on the theoretical H-R diagram. Using stellar evolution models, I then bin the stars by mass to obtain the initial mass function (IMF), which is the number distribution as a function of mass. The IMF shows marked curvature, flattening out to lower masses, even for masses above which the photometry is complete. Best estimates of the IMF slope yield values of gamma = -1.3 to -1.5 for M approximately greater than 12 solar mass, where the Salpeter slope is gamma = -1.35. However, there are indications that different regions of 30 Doradus have different IMF slopes, perhaps as the result of sequential star formation effects. Calculations of the Lyman continuum photon luminosity, N(sub Ly), lead to the result that approximately 3.2 x 10(exp 51) photons s(sup -1) are being produced by the observed stars in 30 Doradus. Less than 60 percent of this luminosity comes from the 150 stars with spectroscopic classifications, implying that there still remain a large number of OB stars yet to be observed spectroscopically. This, along with stellar evolution effects, could explain the IMF curvature and the apparent deficiency of stars in the most massive bins of the IMF. For an ionization-bounded H 2 region, the H alpha luminosity due to the Lyman continuum photons produced by the stars would be L(sub H alpha) is approximately equal to 4.5 x 10(exp 39) erg s(exp -1). This value agrees with the luminosity determined from the observed H alpha flux, but is a lower limit since the effects of W-R stars and the unresolved cluster of R 136 were not included. Dissert. Abstr.

N93-25620 Wisconsin Univ., Madison.
THE EFFECTS OF ROTATION ON THE WINDS FROM HOT STARS Ph.D. Thesis
Jon Eric Bjorkman 1992 186 p
Avail: Univ. Microfilms Order No. DA9221466

We present three studies in which we attempt to develop an understanding of both the geometry and origin of circumstellar disks in the winds from Be stars. In the first study, we develop analytic expressions for the infrared excess and optical intrinsic polarization produced by an ad hoc density distribution that permits us to study the effect of the disk thickness and inclination angle on the observed IR flux and intrinsic polarization. Fits to the data predict a disk that is either very thin (HWHM approx. equals 0.5 degrees), or relatively thick (HWHM approx. equals 43 degrees). In the second study, we address the origin of the disk. We present a simple approximation that permits us to obtain the axisymmetric 2-D supersonic solution of a rotating radiation driven stellar wind from a 1-D model of the equatorial flow. Our solution predicts the formation of a dense equatorial disk of the rotation rate of the star is above a threshold value. We find that the disk forms because the supersonic wind that leaves the stellar surface at high latitudes travels along trajectories that carry it down to the equatorial plane, where it passes through a standing oblique shock on top of the disk. The disk is predicted to be quite thin (approx. equals 0.5 degrees opening angle) and has a density enhancement rho(sub eq)/rho(sub pole) approx. equals 10(exp 3). Adjacent to the disk, the standing shock heats the flow that enters the equatorial region to temperatures of 10(exp 5) to 10(exp 6) K before the material finally mixes with the disk. This temperature is sufficient to produce the observed degree of superionization in the winds of Be stars. In the final study, we develop the fluid equations for a 1-D model of an equatorial circumstellar disk with finite thickness while accounting for the addition of mass and momentum from the stellar wind of a rapidly rotating star. We find that the disk rotation speed initially falls faster than 1/r. We also find that the location of the disk in our model is determined by a critical point condition in the disk outflow. Dissert. Abstr.

N93-25622 Stanford Univ., CA.
DISKOSEISMOLOGY: PROBING RELATIVISTIC ACCRETION DISKS Ph.D. Thesis
Michael Allen Nowak 1992 126 p
Avail: Univ. Microfilms Order No. DA9302280

Helioseismology has provided a wealth of information about the structure of the solar atmosphere. Little is known, however, about the structure of accretion disks that are thought to exist around black holes and neutron stars. In this thesis we present calculations of modes that are trapped in thin Keplerian accretion disks. We hope to use observations of thes modes to elucidate the structure of the inner relativistic regions of accretion disks. Our calculations assume that the thin disk is terminated by an innermost stable orbit, as would occur around a slowly rotating black hole or weakly magnetized compact neutron star. The dominant relativistic effects, which allow modes to be trapped within the inner region of the disk, are approximated via a modified Newtonian potential. Using the Lagrangian formulation of Friedman and Schutz, we develop a general formalism for investigating the adiabatic oscillations of arbitrary unperturbed disk models. First we consider the special case of acoustic waves in disks with isothermal atmospheres. Next we describe the Lagrangian perturbation vectors in terms of the derivatives of a scalar potential, as has been done by Ipser and Lindblom. Using this potential, we derive a single partial differential equation governing the oscillations of a disk. The eigenfunctions and eigenfrequencies of a variety of disk models are found to fall into two main classes which are analogous to the p-modes and g-modes in the sun. Specifically we use the potential formalism to compute the g-modes for disks with isothermal atmospheres. Physical arguments show that both the p-modes and g-modes belong to the same family of modes as the p-modes and g-modes in the sun, just viewed in a different parameter regime. With the aid of the Lagrangian formalism we consider possible growth or damping mechanisms and compute the (assumed) relatively small rates of growth or damping of the modes. Specifically, we consider gravitational radiation reaction and parameterized models of viscosity. Both isotropic and anisotropic viscosity models are considered. We find that isotropic viscosity models tend to lead toward mode growth, while anisotropic viscosity models tend to lead toward damping. We consider possible physical explanations for this effect. Finally, by considering the stochastic driving of the modes by free turbulence (i.e. shear driven turbulence) we present estimates of the mode amplitudes. These estimates, coupled with simple estimates of the luminosity variations caused by the modes, are used to gauge the observational appearance of the modes. We calculate the expected fractional variation of the R-band magnitude for parameters suitable to the study of Active Galactic Nuclei. We explore various criteria for selecting suitable objects in which to search for these modes, and present a preliminary list of candidate objects. Dissert. Abstr.

N93-25623 California Inst. of Tech., Pasadena.
PHOTOSPHERIC ABUNDANCE ANALYSIS OF LOW-MASS PRE-MAIN SEQUENCE STARS Ph.D. Thesis
Deborah Lynne Padgett 1992 222 p
Avail: Univ. Microfilms Order No. DA9232213

This thesis investigation uses photospheric abundance analysis techniques to determine metal abundances both for individual weakly active T Tauri stars and the molecular clouds with which these stars are associated. Using the high resolution echelle spectrographs of the Palomar 1.5m and

the Las Campanas Observatory 2.5m telescopes, high signal-to-noise ratio spectra have been obtained for 53 low pre-main sequence stars in six major northern and southern hemisphere star formation regions. Spectra were also taken of 14 main sequence stars with known effective temperatures and metallicity to serve as spectral standards. Equivalent widths of a large number of Fe I absorption lines have been measured, as well as lines of Ca I, Al I, V I, Ni I, Ti I, K I, and Li I. Temperature-sensitive line ratios of neutral iron and vanadium calibrated against the spectral standards are used to derive effective temperatures for 30 weak-line T Tauri stars, which are much improved over the low resolution spectral classifications found for these objects in the literature. Microturbulent velocities have also been found for 16 of the pre-main sequence stars in the sample. Several stars with abnormally high microturbulences for their spectral type have been found. Using these improved stellar parameters, metallicities of a large number of T Tauri stars have been determined for the first time. Abundance analyses of iron, aluminum, calcium, nickel, and titanium are performed on 30 low masses, pre-main sequence stars. In the star-formation regions of Taurus-Auriga, Orion, Chamaeleon, and Ophiuchus, which each contributed five or more association members to the young star survey, bulk metallicities have been determined. The results indicate that the current metal abundances in these clouds are near or slightly above solar values. Cloud material metallicities are then used to calibrate ultraviolet line-of-sight metal depletion studies for the Orion and rho Ophiuchi clouds. The final chapter of this work is a lithium abundance analysis for the entire sample of 53 pre-main sequence stars. Dissert. Abstr.

N93-25713 California Univ., Los Angeles.
RADIAL VELOCITY MEASUREMENTS OF CARBON STARS Ph.D. Thesis
Cecilia Syfert Barnbaum 1992 236 p
Avail: Univ. Microfilms Order No. DA9303482

This is a study of the atmospheric structure of AGB carbon stars. I have measured the radial velocities of individual transitions in the optical region, both in absorption and emission. The data are high resolution echelle spectra ranging from 5085 A to 7800 A on 87 optically bright carbon stars in the solar neighborhood, using the 3 m Shane Telescope at Lick Observatory. It has been known for some time that the atmospheric velocities of another group of evolved star, oxygen-rich in composition, are consistently redshifted from center-of-mass motion. I have found the same trend for carbon-rich Mira variables and have shown that carbon-rich SR variables do not show a redshift bias, suggesting that either the atmospheric dynamics or the composition of the dusty circumstellar envelopes differ between the two kinds of carbon stars. Also, I have found a number of differences in the velocity behavior with time between Mira and SR carbon stars: Miras have (1) stronger emission lines, (2) greater amplitude of atmospheric velocity variation with phase, and (3) greater velocity dispersion among atomic lines. In Miras for which I have obtained adequate phase coverage, the velocities of atomic and molecular lines converge near minimum light and have their greatest differences from each other near maximum light, whereas the fluctuations in SR velocities are much smaller and are not as obviously correlated with phase. Also presented for the first time are the emission lines in inverse (Mg I) and classical (K I) P Cygni profiles for 15 carbon stars, all Miras. Using the velocities of these lines and other absorption features, I present a qualitative model of the atmosphere. Another important result from this study is the identification of a broadened spectrum in one carbon star, V Hya. The broadened optical spectrum indicates that this star is rotating rapidly. Models which explain bipolar outflows invoke either binary systems, rotation, or common envelope evolution in which a close companion is engulfed by the giant primary star. If the optical broadening of V Hya is correctly ascribed to rotation, models for asymmetric mass loss, which call on binarity, rotation or common evolution, merge into a coherent picture. Dissert. Abstr.

N93-25728 Arizona Univ., Tucson.
INVERSE PROBLEM WITH CONTINUOUS PARAMETERS FOR SOLAR OSCILLATIONS Ph.D. Thesis
Yeming Gu 1992 180 p
Avail: Univ. Microfilms Order No. DA9303296

Solar seismology is a relatively new field in solar astrophysics. It provides us a way of 'looking' into the deep interior of the Sun. The goal of solar seismology is to derive information about the internal structure of the Sun from the observed properties of solar oscillations. This is called the inverse problem of solar seismology. This project is to explore a new set of methods and algorithms to solve the inverse problem. The continuous orthonormalization (CON) method and the adjoint method adapted by Rosenwald can be used to compute the eigenfrequency sensitivities to the solar structure parameters in a very efficient way. In this work, the computational algorithm for using these methods has been modified and improved. Continuous parameterization for the internal structure of the Sun is introduced. The solar interior is subdivided into sections, and polynomial fits are applied to the solar structure parameters in each section. The eigenfrequency sensitivities to these polynomial coefficients - the continuous parameters - are computed. These sensitivities can be used to predict the change in solar eigenfrequencies when the structure parameters are perturbed (with the necessary physical constraints satisfied). The inverse problem for the solar internal structure is formulated by using these sensitivities. The generalized inverse technique is used to solve the nonlinear inverse problem in an iterative process. Observed data of low-degree g-modes have been used for a preliminary inversion. The nonlinearity of the solar seismic inverse problem is demonstrated. A nonlinear inversion process has been successfully performed and the results analyzed. The inversion results indicate that the standard solar model is a good approximation of the real Sun. Only relatively small peturbations to the model are needed to explain the frequency deviations between observation and theory. Dissert. Abstr.

N93-25832 Michigan Univ., Ann Arbor.
THE PHYSICAL PROPERTIES OF LOW SURFACE BRIGHTNESS GALAXIES Ph.D. Thesis
Stacy Sutton McGaugh 1992 179 p
Avail: Univ. Microfilms Order No. DA9303781

Low Surface Brightness (LSB) galaxies are those with central disk surface brightnesses many standard deviations fainter than the canonical value. Severe selection effects stemming from the contrast relative to the arbitrary level of the sky background act to limit knowledge of the LSB component of the galaxy population. This component could be numerically dominant, yet very little is known about the physical properties of such galaxies. This situation is addressed by making a detailed examination of a large sample of LSB galaxies. Structurally, LSB galaxies are similar to high surface brightness (HSB) spiral galaxies. They are comparable in size, and span an enormous range in both surface brightness and luminosity. There is no correlation between size and surface brightness, and galaxies occupy the entire plane defined by these parameters. Physically, LSB galaxies are observed to typically be metal poor, very blue, and possess large gas mass fractions and small mass to light ratios. These indicate a relatively unevolved state, with less of the original gas converted into stars than in HSB galaxies. The blue colors are extreme and are difficult to understand, but probably indicate stellar populations with young mean ages and underpopulated giant branches. There are some cases of galaxies which may be undergoing their first episode of star formation. The elemental abundance ratios indicate either very peculiar star formation histories and IMFs, or some external source of enrichment. The latter provides a better empirical fit, but is not readily explicable without altering standard primordial nucleosynthesis. The low degree of evolution of LSB galaxies is caused by the low surface densities of their atomic gas disks. These remain predominantly below the threshold for star formation, so that this occurs only sporadically, and evolution proceeds gradually. The low densities of LSB galaxies are a natural consequence of their formation from modest initial density fluctuations. From this, it follows that LSB galaxies should be common at all masses, though they may be subject to destruction in high density environments. Thus, observational selection effects may indeed have severely limited knowledge of the majority of the galaxy population. Dissert. Abstr.

N93-26147# Aerospace Corp., El Segundo, CA. Engineering and Technology Group.
MAGNETOTAIL PROCESSES ASSOCIATED WITH AURORAL SURGE FORMATION
L. R. Lyons 15 Apr. 1993 16 p Sponsored by NSF
(Grant NSF ATM-88-00602)
(ATR-90(7186)-1) Avail: CASI HC A03/MF A01

The current wedge that forms during substorms is associated with significant magnetic field (B) changes and particle injections observed at synchronous orbit. It is argued that the B changes associated with the

current wedge lead to a distortion of the separatrix between open and closed field lines that extends from the ionosphere to at least x = -22 R(sub e) in the tail. It is suggested that the distortion forms the auroral bulge observed in the ionosphere during the expansion phase of substorms and that it causes the plasma sheet to expand at longitudes within the current wedge and to thin at longitudes near, but outside, the current wedge. A number of important substorm phenomena observed in the tail beyond synchronous orbit can be interpreted to be a result of the distortion of the separatrix. These include plasma sheet thinning and concurrent enhanced stretching of B after expansion phase onset, plasma sheet expansion that follows thinning and should be concurrent with a field dipolarization, and tailward plasma flows and associated negative B(sub z)'s during some expansion phases. The above phenomena are expected to occur at longitudes outside the current wedge that forms at onset. At longitudes within the initial current wedge, dispersionless particle injection and concurrent dipolarization of B is expected at onset as has recently been observed out to x = -22 R(sub e). Author (revised)

N93-26340# Air Force Environmental Technical Applications Center, Scott AFB, IL.
BIT HIT/SOLAR ACTIVITY CORRELATION STUDY
Mary L. Hart Dec. 1992 35 p
(AD-A261381; USAFETAC/PR-92/007) Avail: CASI HC A03/MF A01

This report documents a study of statistical correlations between Global Positioning System (GPS) satellite anomalies (bit hits) and the state of the actual space environment from 1 October 1984 through 31 March 1991. The study compared distributions of space environmental data with GPS anomalies to determine the correlations (if any) of GPS anomaly occurrences with space environment variables such as global geomagnetic index and proton/electron counts. Using stepwise linear regression and discriminant analysis, correlations were found to be very low. Regression equations were found to predict the probability of satellite anomalies only slightly better than random chance. DTIC

N93-26508# Virginia Univ., Charlottesville. Dept. of Astronomy.
CHROMOSPHERIC ACTIVITY IN ALGOL BINARIES Annual Report, 1 Oct. 1991 - 30 Sep. 1992
Mercedes T. Richards 10 Aug. 1992 4 p
(Contract F49620-92-J-0024)
(AD-A261440; AFOSR-93-0044TR) Avail: CASI HC A01/MF A01

A literature search was performed for the probable magnetic properties of 15 Algol-type binaries. The properties examined included detection of Calcium, Hydrogen and Potassium emission, the x-ray luminosity determined from x-ray flares, detection of radio emission and type of polarization, evidence of variations in the brightness of the cool secondary and changes in the orbital periods of the binary which can be linked to changes in the polarity of the magnetic field of the cool star. The technique of Doppler Tomography was used in an attempt to isolate the source of the emission seen in the Hydrogen alpha difference profiles of Algol. The Doppler images indicate that most of the emission is not associated with the cool star but with the mass transfer process and, in particular, with gas found between the two stars. DTIC

N93-26062*# Arkansas Coll., Batesville. Natural Science and Mathematics Div.
VOLATILES IN INTERPLANETARY DUST PARTICLES: A COMPARISON WITH CI AND CM CHONDRITES Final Report
Roberta Bustin *In* NASA. Johnson Space Center, National Aeronautics and Space Administration (NASA)/American Society for Engineering Education (ASEE) Summer Faculty Fellowship Program, 1992, Volume 1 Dec. 1992 14 p (For primary document see N93-26058 09-99)
(Grant NGT-44-005-803)
Avail: CASI HC A03/MF A02

N93-26067*# Stockton State Coll., Pomona, NJ. Dept. of Geology.
GEOCHEMISTRY AND PETROLOGY OF PRIMITIVE ACHONDRITE METEORITES LEW 88280, MAC 88177, ALHA 81187, EET 84302, AND LEW 88663 Final Report
Stephen W. Field *In* NASA. Johnson Space Center, National Aeronautics and Space Administration (NASA)/American Society for Engineering Education (ASEE) Summer Faculty Fellowship Program, 1992, Volume 1 14 Aug. 1992 17 p (For primary document see N93-26058 09-99)
(Grant NGT-44-005-803)
Avail: CASI HC A03/MF A02

91 LUNAR AND PLANETARY EXPLORATION

Includes planetology; and manned and unmanned flights.
For spacecraft design or space stations see *18 Spacecraft Design, Testing and Performance.*

N93-25285 Colorado Univ., Boulder.
THE VENUS 130-nm DAYGLOW AS A DIAGNOSTIC OF THERMOSPHERIC STRUCTURE AND DYNAMICS Ph.D. Thesis
M. Joan Alexander 1992 159 p
Avail: Univ. Microfilms Order No. DA9304538

The bright emission at 130-nm from atomic oxygen in the Venus thermosphere, as measured by the Pioneer Venus Orbiter Ultraviolet Spectrometer (PVOUVS), can serve as a diagnostic of Venus thermospheric structure. Images from the PVOUVS at this wavelength reveal unusual large-scale patterns in the emission which can be interpreted as variations in the O/CO2 ratio in the middle thermosphere. Through analysis of these images, a high-contrast asymmetry in local-time has been revealed which has not previously been observed or predicted by any existing models. The asymmetry can be interpreted as up to a factor of two increase in PM oxygen densities over corresponding AM times, and this basic pattern has been present in every image examined, spanning the period 1980-1990. This local-time asymmetry in O can be understood in the context of the subsolar-to-antisolar flow pattern which dominates the thermospheric circulation: gravity waves, originating in the middle atmosphere of Venus where a westward zonal flow pattern dominates, will preferentially enhance eddy mixing in the morning hours if these waves propagate into the thermosphere. Enhanced eddy mixing tends to lower thermospheric O. This sam mechanism can also explain zonal asymmetries known to be present in the thermospheric subsolar-to-antisolar wind pattern, since these waves provide a net transport of westward momentum to the thermosphere. Dissert. Abstr.

N93-25321# Sandia National Labs., Albuquerque, NM.
A MISSION CONCEPT FOR NEAR TERM LUNAR EXPLORATION
J. W. Purvis 1993 4 p Presented at the 5th Topical Meeting on Robotics and Remote Systems, Knoxville, TN, 26-29 Apr. 1993
(Contract DE-AC04-76DP-00789)
(DE93-007598; SAND-93-0099C; CONF-930403-18) Avail: CASI HC A01/MF A01

A robotic precursor mission to the Lunar surface is proposed. The objective of the mission is to place six to ten 15-kg micro-rovers on the planet to investigate equipment left behind during the Apollo missions and to perform other science and exploration duties. The micro-rovers are teleoperated from Earth. All equipment on the rovers is existing technology from NASA, DOE, SDIO, DoD, and industry. The mission is designed to involve several NASA centers, the National Laboratories, multiple universities, and the private sector. A major long-term goal which is addressed is the educational outreach aspect of space exploration. DOE

N93-25439# Colorado Univ., Boulder.
MARS: THE DYNAMICS OF ORBITING SATELLITES AND GRAVITY MODEL DEVELOPMENT Ph.D. Thesis
Frank George Rodrigu Lemoine 1992 448 p
Avail: Univ. Microfilms Order No. DA9304574

Three major questions are addressed: (1) what is the sensitivity of satellites to the Mars gravity field?; (2) can the range measurements to the Viking Orbiters be used to improve the solutions for the Mars gravity field?; and (3) what improvements can be made to the force models for spacecraft in orbit about Mars? Mars orbiting satellites, including the Mariner 9 spacecraft, the two Viking Orbiters, the Mars Observer spacecraft (scheduled for launch in September 1992), and the natural Martian satellites of Phobos and Deimos have orbits with different periods and geometries. Kaula's (1966) linear theory of orbit element perturbations was used to analyze the sensitivity of these satellites to the Mars gravity field. Numerical procedures were developed to evaluate the Kaula eccentricity functions, and to determine the RMS position and velocity sensitivity of the highly

eccentric Viking and Mariner 9 orbits. The amplitude and frequency of the orbit perturbations were characterized. This information was used to optimize the processing of the Viking and Mariner 9 tracking data for the task of Mars gravity field determination. Over the course of the Viking mission 26,000 range measurements to the two Viking Orbiters were obtained. This observable has not previously been incorporated into Mars gravity solutions. A portion of the range data was processed simultaneously with the Doppler data to develop spherical harmonic models of the Mars gravity field. Tests with orbit overlaps, orbit predictions, and with the gravity field covariances show that the range data contribute positively to the gravity field solutions. This research indicates that the range measurements to the Mars Observer spacecraft can be used to supplement the Doppler data by improving the determination of both orbit and the gravity field. Previous analyses have not incorporated the perturbing force due to the Martian moons, and due to the Mars radiation pressure on the trajectories of Mars orbiting satellites. The magnitude of these perturbations was calculated for Mariner 9 and the Viking Orbiters, as well as for Mars Observer. It is shown that Phobos produces measurable third-body perturbations on the orbits of both Mariner 9 and the Vikings. The Infrared Thermal Mapper (IRTM) measurements of the Mars albedo and thermal emission (obtained by Viking Orbiters 1 and 2) were used to develop zonal spherical harmonic models of the Mars albedo, and third degree and order spherical harmonic models of the Mars thermal emission. These models were applied to the Mars Observer (MO) mapping orbit. This research shows that the Mars radiation pressure will produce perturbations on the orbit of MO that exceed the planned precision of the X-band Doppler data (0.1 mm/s). The effects of the Mars radiation pressure must be included in the trajectory force model for this spacecraft. Dissert. Abstr.

N93-26094*# National Aeronautics and Space Administration. Lyndon B. Johnson Space Center, Houston, TX.

EVALUATING SCIENCE RETURN IN SPACE EXPLORATION INITIATIVE ARCHITECTURES

Nancy Ann Budden and Paul D. Spudis (Lunar and Planetary Inst., Houston, TX.) Washington Mar. 1993 13 p

(NASA-TP-3339; S-704; NAS 1.60:3339) Avail: CASI HC A03/MF A01

Science is an important aspect of the Space Exploration Initiative, a program to explore the Moon and Mars with people and machines. Different SEI mission architectures are evaluated on the basis of three variables: access (to the planet's surface), capability (including number of crew, equipment, and supporting infrastructure), and time (being the total number of man-hours available for scientific activities). This technique allows us to estimate the scientific return to be expected from different architectures and from different implementations of the same architecture. Our methodology allows us to maximize the scientific return from the initiative by illuminating the different emphases and returns that result from the alternative architectural decisions. Author

N93-26392*# National Aeronautics and Space Administration. Lewis Research Center, Cleveland, OH.

ELECTRICAL AND CHEMICAL INTERACTIONS AT MARS WORKSHOP. PART 2: APPENDIX

1992 120 p Workshop held in Cleveland, OH, 19-20 Nov. 1991

(RTOP 506-41-41)

(NASA-CP-10093-Pt-2; E-7016-2-Pt-2; NAS 1.55:10093-Pt-2) Avail: CASI HC A06/MF A02

The objectives of the workshop were the following: (1) to identify issues related to electrical and chemical interactions between systems and their local environments at Mars; and (2) to recommend means of addressing those issues, including the dispatch of robotic spacecraft to Mars to acquire necessary information. Presentations about Mars' surface and orbital environments, Space Exploration Initiative (SEI) systems, environmental interactions, modeling and analysis, and plans for exploration are presented in viewgraph form. For individual titles, see N93-26393 through N93-26399.

N93-26393*# Michigan Univ., Ann Arbor. Space Physics Research Lab.

THE UPPER ATMOSPHERE AND IONOSPHERE OF MARS

Larry H. Brace *In* NASA. Lewis Research Center, Electrical and Chemical Interactions at Mars Workshop. Part 2: Appendix 1992 p 25-38 (For primary document see N93-26392 09-91)

Avail: CASI HC A03/MF A02

The topics discussed include the following: the dynamic atmosphere of Mars; possible similarities with Earth and Venus; the atmosphere and ionosphere of Mars; solar wind interactions; future approved missions; and possible future mission. Derived from text

N93-26394*# National Aeronautics and Space Administration. Ames Research Center, Moffett Field, CA.

THE MARTIAN LOWER ATMOSPHERE

Robert M. Haberle *In* NASA. Lewis Research Center, Electrical and Chemical Interactions at Mars Workshop. Part 2: Appendix 1992 p 39-52 (For primary document see N93-26392 09-91)

Avail: CASI HC A02/MF A02

The topics are presented in viewgraph form and include the following: mass and composition; photochemical processes; temperatures and winds; general circulation; and dust storms. Derived from text

N93-26395*# National Aeronautics and Space Administration. Lewis Research Center, Cleveland, OH.

REPRESENTATIVE SYSTEMS FOR SPACE EXPLORATION

Scott R. Graham *In its* Electrical and Chemical Interactions at Mars Workshop. Part 2: Appendix 1992 p 55-68 (For primary document see N93-26392 09-91)

Avail: CASI HC A03/MF A02

The topics are presented in viewgraph form and include the following: an overview of the synthesis report; specific architecture 4 implementations; and specific power systems/environment issues. Derived from text

N93-26396*# National Aeronautics and Space Administration. Lewis Research Center, Cleveland, OH.

SPACE ENVIRONMENTAL INTERACTIONS FOR THE SPACE EXPLORATION INITIATIVE

Dale C. Ferguson *In its* Electrical and Chemical Interactions at Mars Workshop. Part 2: Appendix 1992 p 69-85 (For primary document see N93-26392 09-91)

Avail: CASI HC A03/MF A02

The topics are presented in viewgraph form and include the following: atomic oxygen attack; arcing and discharges; micrometeoroids and debris; state-of-the-art computer tools; current collection and snapover; effluents--neutral and ionized; and winds, dust, and contamination. Derived from text

N93-26397*# Systems Science and Software, San Diego, CA.

MODELING AND ANALYSIS TOOLS

Gary Jongeward *In* NASA. Lewis Research Center, Electrical and Chemical Interactions at Mars Workshop. Part 2: Appendix 1992 p 87-92 (For primary document see N93-26392 09-91)

Avail: CASI HC A02/MF A02

The topics covered are presented in viewgraph form and include the following: the effect of the Mars environment on systems; the design of models and modeling tools; space environment interaction information dissemination; tools used in the development and validation of models; Space Exploration Initiative planning; and systems integration. Derived from text

N93-26398*# National Aeronautics and Space Administration. Goddard Space Flight Center, Greenbelt, MD.

EnviroNET **c82**

Tim VanSant *In* NASA. Lewis Research Center, Electrical and Chemical Interactions at Mars Workshop. Part 2: Appendix 1992 p 93-105 (For primary document see N93-26392 09-91)

Avail: CASI HC A03/MF A02

EnviroNET is a service/facility that provides users with on-line, dial-up technical information concerning environmental conditions likely to be encountered by instruments and experimental arrangements carried aboard spacecraft. EnviroNET incorporates at present a combination of expository text and numerical tables amounting to about two million characters (bytes), plus FORTRAN programs that model the space environment. The topics covered are presented in viewgraph form and include the following: advantages of EnviroNET; thermal and humidity; vibration and acoustics; electromagnetic interference; loads and low frequency dynamics; microbial and toxic contaminants; molecular contamination; natural environment; orbiter motion; particulate environment; surface interactions; spacecraft anomalies; and interactive graphics facility. Derived from text

N93-26399*# National Aeronautics and Space Administration, Washington, DC.
MARS EXPLORATION PLANNING
Tamara L. Dickinson *In* NASA. Lewis Research Center, Electrical and Chemical Interactions at Mars Workshop. Part 2: Appendix 1992 p 107-126 (For primary document see N93-26392 09-91)
Avail: CASI HC A03/MF A02

The topics are presented in viewgraph form and include the following: Mars Observer; Mars Environmental Survey (MESUR); and the Small Rovers and Sample Return missions. Derived from text

N93-26424*# Jet Propulsion Lab., California Inst. of Tech., Pasadena.
V-GRAM: MAGELLAN BULLETIN ABOUT VENUS AND THE RADAR MAPPING MISSION
Mona Jasnow, ed. Apr. 1993 22 p
(NASA-CR-192923; JPL-410-11-20; NAS 1.26:192923) Avail: CASI HC A03/MF A01

Papers on the following topics are presented: Magellan project update; summary of Magellan science findings; excerpt from 'Acquisition and Analysis of Magellan Gravity Data'; Magellan gravity; and Magellan stereo image data. CASI

N93-26517*# Jet Propulsion Lab., California Inst. of Tech., Pasadena.
REVEALING THE FACE OF VENUS: MAGELLAN
Mar. 1993 28 p Original contains color illustrations
(NASA-CR-192922; JPL-400-494; NAS 1.26:192922; ISBN-0-16-042197-7)
Avail: CASI HC A03/MF A01; SOD HC 14 functional color pages

An overview of the Magellan spacecraft and mission is presented. Topics covered include: a description of the Magellan spacecraft; Venus geology; Venus gravity; synthetic aperture radar; and radar sensing. CASI

N93-26571# Coast Guard Academy, New London, CT. Center for Advanced Studies.
RESIDUAL MEAN MERIDIONAL CIRCULATION IN TITAN'S MIDDLE ATMOSPHERE Final Report
J. R. Dire Oct. 1992 17 p
(PB93-162931; USCGA-17-92) Copyright Avail: CASI HC A03/MF A01

The Transformed Eulerian-Mean Equations are solved to yield an elliptical partial differential equation in the stream function. The PDE is solved numerically and the meridional and vertical mean residual speeds are calculated from the stream function. Newtonian cooling provides the thermal forcing. The mechanical forcing in the present model is due to Rayleigh friction and molecular diffusion. The nominal model atmosphere assumes an isothermal tropopause and at 0.4 mbar the temperature at 85 degrees N is approximately 8 degrees lower than at 85 degrees S. The vertical temperature profile is after Lindal et al (1983, Icarus, 53, 348) and eddy coefficients are taken from Yung et al (1984, Astrophys. J. Suppl., 55, 465). The zonal speeds are estimated using the gradient wind balance. The nominal model results in meridional Hadley cells with little transport across the equator. The effects on the meridional circulation and hemispheric transport by varying the forcing parameters will be shown. NTIS

N93-26059*# LeTourneau Coll., Longview, TX. Div. of Natural Sciences.
DATA ANALYSIS AND INTERPRETATION OF LUNAR DUST EXOSPHERE Final Report
George A. Andrews, Jr. *In* NASA. Johnson Space Center, National Aeronautics and Space Administration (NASA)/American Society for Engineering Education (ASEE) Summer Faculty Fellowship Program, 1992, Volume 1 Dec. 1992 11 p (For primary document see N93-26058 09-99)
(Grant NGT-44-005-803)
Avail: CASI HC A03/MF A02

N93-26129*# Jet Propulsion Lab., California Inst. of Tech., Pasadena.
DSN OBSERVATIONS OF TITAN
R. M. Goldstein and R. F. Jurgens *In its* The Telecommunications and Data Acquisition Report 15 May 1992 p 377-379 (For primary document see N93-26105 09-32)
(RTOP 196-41-73-02-00)
Avail: CASI HC A01/MF A04

92 SOLAR PHYSICS

Includes solar activity, solar flares, solar radiation and sunspots. For related information see *93 Space Radiation.*

N93-25101# Midwest Research Inst., Golden, CO.
SUMMARY INFORMATION AND DATA SETS FOR NREL'S SOLAR RADIATION RESEARCH LABORATORY, 1981 - 1991
W. Marion Jan. 1993 76 p
(Contract DE-AC02-83CH-10093)
(DE93-000052; NREL/TP-463-5217) Avail: CASI HC A05/MF A01

This report summarizes the solar radiation and meteorological data collected at the Solar Radiation Research Laboratory in Golden, Colorado, from 1981 through 1991. The data collection was part of the National Renewable Energy Laboratory's Solar Radiation Resource Assessment Project. The report includes long-term averages and monthly and annual variability for key solar radiation elements and describes the hourly data sets for 1981 through 1991. Described in the report are how the elements were measured and how the data were collected and processed into hourly values. Procedures used for quality assessment of the hourly data values are presented, and the position of the solar radiation and meteorological elements in the data sets are defined; samples of read statements are provided. DOE

N93-25180 Maryland Univ., College Park.
AN INVESTIGATION OF NEUTRINO PROPERTIES THROUGH STUDY OF THE SUN, SUPERNOVAE, THE EARLY UNIVERSE AND LAB DATA Ph.D. Thesis
Ira Ziv Rothstein 1992 119 p
Avail: Univ. Microfilms Order No. DA9304386

In this thesis I propose theories to explain two experiments whose results are incompatible with the standard model of particle physics. More specifically, these experiments indicate a need for considerable augmentation in the neutrino sector of the Weinberg-Salam model. The first part of this thesis deals with explaining the results of the search for solar neutrinos. Three solar neutrino experiments have been performed and all see only a fraction of the expected number of neutrinos. Moreover, one of the experiments (seems to) see an anti-correlation of the neutrino flux with the magnetic field intensity in the convective zone of the sun, while the second does not (the third has not been running long enough to see any time variation). Here it is shown that by assuming that the neutrinos have masses, as well as considerable magnetic moments, it is possible to explain not only the dearth in the flux but also its time variation. The second part of this work is dedicated to explaining the results of the recent experiments which claim the existence of a 17 keV neutrino which mixes with the electron neutrino with a mixing angle of 10 percent. Such a neutrino is especially meddlesome to theorists because of the encyclopedic constraints from lab data, supernovae, and big-bang nucleosynthesis. In this thesis I show that such a neutrino is compatible with all the constraints if one is willing to go well beyond the standard model. Dissert. Abstr.

N93-25222*# Ohio State Univ., Columbus. Dept. of Astronomy.
COMPARISON OF HIGH-RESOLUTION SOLAR IRRADIANCE SPECTRA AND THE SOLAR LUMINOSITY IN THE PERIOD 1980-1989 Final Report
Walter E. Mitchell, Jr. Apr. 1992 17 p
(Grant NAG5-1326; RF Proj. 768121/723186)
(NASA-CR-192776; NAS 1.26:192776) Avail: CASI HC A03/MF A01

In this research, we aim to determine to what extent the solar irradiance changes measured through the 1980's from orbiting vehicles are accompanied by spectroscopic irradiance changes observable from the ground. We describe fractional changes in line absorption as 'blanketing'. In section 2, we briefly review results obtained in an earlier project and which have been published. Section 3 describes the data of this investigation; section 4 describes the data reduction; section 5 describes the observational results in terms of blanketing; and section 6 describes the interpretation of the measured changes. Section 7 contains an outline of possible uses for Doppler-shift data that emerges with the measurements of the blanketing variations. Section 8 is an outline for future research suggested by our results in this project. Author

N93-25327# California Univ., Berkeley. Lawrence Berkeley Lab.
THE SUDBURY NEUTRINO OBSERVATORY
E. B. Norman, Y. D. Chan, A. Garcia, K. T. Lesko, A. R. Smith, R. G. Stokstad, I. Zlimen, H. C. Evans (Queens Univ., Kingston, Ontario.), G. T. Ewan (Queens Univ., Kingston, Ontario.), and A. Hallin (Queens Univ., Kingston, Ontario.) et al Nov. 1992 3 p Presented at the Meeting of the Division of Particles and Fields of the American Physics Society, Batavia, IL, 10-14 Nov. 1992
(Contract DE-AC03-76SF-00098)
(DE93-007697; LBL-33304; CONF-921122-42) Avail: CASI HC A01/MF A01

Two experiments now in progress have reported measurements of the flux of high energy neutrinos from the Sun. Since about 1970, Davis and his co-workers have been using a (Cl-37)-based detector to measure the Be-7 and B-8 solar neutrino flux and have found it to be at least a factor of three lower than that predicted by the Standard Solar Model (SSM). The Kamiokande collaborations has been taking data since 1986 using a large light-water Cerenkov detector and have confirmed that the flux is about two times lower than predicted. Recent results from the SAGE and GALLEX gallium-based detectors show that there is also a deficit of the low energy pp solar neutrinos. These discrepancies between experiment and theory could arise because of inadequacies in the theoretical models of solar energy generation or because of previously unobserved properties of neutrinos. The Sudbury Neutrino Observatory (SNO) will provide the information necessary to decide which of these solutions to the 'solar neutrino problem' is correct. DOE

N93-26537# National Geophysical Data Center, Boulder, CO.
SOLAR-GEOPHYSICAL DATA NUMBER 581, JANUARY 1993. PART 1: (PROMPT REPORTS). DATA FOR DECEMBER, NOVEMBER 1992, AND LATE DATA
Helen E. Coffey, ed. Jan. 1993 121 p See also PB93-150332 and Part 2, PB93-161750
(PB93-161743; SGD-581-Pt-1) Avail: CASI HC A06/MF A02

The contents are as follows: Detailed Index for 1992; Data for December 1992 - Solar-Terrestrial Environment; IUWDS Alert Periods (Advance and Worldwide); Solar Activity Indices; Solar Flares; Solar Radio Emission; and Standard Mean Solar Magnetic Field. NTIS

N93-26538# National Geophysical Data Center, Boulder, CO.
SOLAR-GEOPHYSICAL DATA NUMBER 581, JANUARY 1993. PART 2: (COMPREHENSIVE REPORTS). DATA FOR JULY 1992 AND MISCELLANEOUS
Helen E. Coffey, ed. Jan. 1993 88 p See also PB93-150340 and Part 1, PB93-161743
(PB93-161750; SGD-581-Pt-2) Avail: CASI HC A05/MF A01

The contents are as follows: Detailed Index for 1992; Data for July 1992 - Solar Flares; Solar Radio Bursts at Fixed Frequencies; Solar X-ray Radiation from GOES Satellite; Mass Ejections from the Sun; Active Prominences and Filaments; Solar Irradiance; and IMP-8 Polar Wind Plot. NTIS

N93-26556*# National Center for Atmospheric Research, Boulder, CO. High Altitude Observatory.
A REVISED AND EXPANDED CATALOGUE OF MASS EJECTIONS OBSERVED BY THE SOLAR MAXIMUM MISSION CORONAGRAPH
J. T. Burkepile and O. C. St.Cyr Jan. 1993 223 p
(NASA Order S-04167-D)
(NASA-CR-193146; NAS 1.26:193146; PB93-156826; NCAR/TN-369+STR) Avail: CASI HC A10/MF A03

A revised and expanded catalog of coronal mass ejections identified in data from the High Altitude Observatory's coronograph aboard NASA's Solar Maximum Mission spacecraft is presented. The list includes events observed during 1980 and the period 1984 - 1989. Th first edition was published in July 1990. Descriptions and measurements of mass ejections included in the first catalog were expanded and revised. A few additional mass ejections were identified in the data and were added to the listing. The catalog was expanded to include morphological descriptions of each event and apparent speed measurements, whenever possible. Author (revised)

N93-24716*# National Aeronautics and Space Administration. Goddard Space Flight Center, Greenbelt, MD.
NONLINEAR TECHNIQUES FOR FORECASTING SOLAR ACTIVITY DIRECTLY FROM ITS TIME SERIES
S. Ashrafi (Computer Sciences Corp., Lanham, MD.), L. Roszman (Computer Sciences Corp., Lanham, MD.), and J. Cooley *In its* Flight Mechanics/Estimation Theory Symposium, 1992 Feb. 1993 p 319-335 Previously announced as N92-28870 (For primary document see N93-24694 09-13)
(Contract NAS5-31500)
Copyright Avail: CASI HC A03/MF A04

93 SPACE RADIATION

Includes cosmic radiation; and inner and outer earth's radiation belts.

For biological effects of radiation see *52 Aerospace Medicine.* For theory see *73 Nuclear and High-Energy Physics.*

N93-24752*# Minnesota Univ., Minneapolis. Dept. of Astronomy.
TIME DEPENDENT SIMULATION OF COSMIC-RAY SHOCKS INCLUDING ALFVEN TRANSPORT
T. W. Jones 1993 10 p
(Grants NAGw-2548; NSF AST-91-00486)
(NASA-CR-192931; NAS 1.26:192931) Avail: CASI HC A02/MF A01

Time evolution of plane, cosmic-ray modified shocks was simulated numerically for the case with parallel magnetic fields. Computations were done in a 'three-fluid' dynamical model incorporating cosmic-ray and Alfven wave energy transport equations. Nonlinear feedback from the cosmic-rays and Alfven waves is included in the equation of motion for the underlying plasma, as is the finite propagation speed and energy dissipation of the Alfven waves. Exploratory results confirm earlier, steady state analyses that found these Alfven transport effects to be potentially important when the upstream Alfven speed and gas sound speeds are comparable. As noted earlier Alfven transport effects tend to reduce the transfer of energy through a shock from gas to energetic particles. These studies show as well that the time scale for modification of the shock is altered in nonlinear ways. It is clear, however, that the consequences of Alfven transport are strongly model dependent and that both advection of cosmic-rays by the waves and dissipation of wave energy in the plasma will be important to model correctly when quantitative results are needed. Comparison is made between simulations based on a constant diffusion coefficient and more realistic diffusion models allowing the diffusion coefficient to vary in response to changes in Alfven wave intensity. No really substantive differences were found between them. Author (revised)

N93-25161*# Minnesota Univ., Minneapolis. Dept. of Astronomy.
ALFVEN WAVE TRANSPORT EFFECTS IN THE TIME EVOLUTION OF PARALLEL COSMIC-RAY MODIFIED SHOCKS
T. W. Jones 1993 33 p
(Grants NAGw-2548; NSF AST-91-00486)
(NASA-CR-192932; NAS 1.26:192932) Avail: CASI HC A03/MF A01

Some of the issues associated with a more complete treatment of Alfven transport in cosmic ray shocks are explored qualitatively. The treatment is simplified in some important respects, but some new issues are examined and for the first time a nonlinear, time dependent study of plane cosmic ray mediated shocks with both the entropy producing effects of wave dissipation and effects due to the Alfven wave advection of the cosmic ray relative to the gas is included. Examination of the direct consequences of including the pressure and energy of the Alfven waves in the formalism began. Author (revised)

N93-25185# Los Alamos National Lab., NM.
THE ALEXIS DATA PROCESSING PACKAGE: AN UPDATE
J. J. Bloch, B. W. Smith, and B. C. Edwards 1993 4 p Presented at the Astronomical Data Analysis Software and Systems, Boston, MA, 2-4 Nov. 1992
(Contract W-7405-eng-36)
(DE93-007374; LA-UR-93-263; CONF-9211188-1) Avail: CASI HC A01/MF A01

The ALEXIS experiment (Array of Low Energy X Ray Imaging Sensors),

is a mini-satellite containing six wide angle EUV/ultrasoft x ray telescopes. Its purpose is to map out the sky in three narrow (5 percent) bandpasses around 66, 71, and 93 eV. The 66 and 71 eV bandpasses are centered on intense Fe emission lines which are characteristic of million-degree plasmas such as the one thought to produce the soft x ray background. The 93 eV bandpass is not near any strong emission lines and is more sensitive to continuum sources. The mission will be launched on the Pegasus Air-Launched Vehicle in early 1993 into a 400-nautical-mile, high-inclination orbit and will be controlled entirely from a small ground station located at Los Alamos. The project is a collaborative effort between Los Alamos National Laboratory, Sandia National Laboratory, and the University of California-Berkeley Space Sciences Laboratory. DOE

N93-25241*# Chicago Univ., IL.
COSMIC RAY COMPOSITION INVESTIGATIONS USING ICE/ISEE-3
Mark E. Wiedenbeck 1992 9 p
(Grant NAG5-308)
(NASA-CR-192808; NAS 1.26:192808) Avail: CASI HC A02/MF A01

The analysis of data from the high energy cosmic experiment on ISEE-3 and associated modeling and interpretation activities are discussed. The ISEE-3 payload included two instruments capable of measuring the composition of heavy cosmic rays. The designs of these two instruments incorporated innovations which made it possible, for the first time, to measure isotopic as well as the chemical composition for a wide range of elements. As the result of the demonstrations by these two instruments of the capability to resolve individual cosmic ray isotopes, a new generation of detectors was developed using very similar designs, but having improved reliability and increased sensitive area. The composition measurements which were obtained from the ISEE-3 experiment are summarized. Derived from text

N93-25625 Washington Univ., Seattle.
GRAVITATIONAL RADIATION FROM COALESCING BINARY STAR SYSTEMS Ph.D. Thesis
Alan Gray Wiseman 1992 119 p
Avail: Univ. Microfilms Order No. DA9305287

Nonlinear contributions to the gravitational radiation emitted during the late stages of a binary-star coalescence involving neutron stars or black holes are investigated using a post-Newtonian approximation to general relativity. A waveform which is accurate to (post)(exp 3/2)-Newtonian order is obtained. It includes corrections of O((Gm/rc(exp 2))(exp 3/2)) approx. equals O((v/c)(exp 3)) beyond the lowest order quadrupole radiation, where m is the total mass of the system, r is the separation of the bodies, v is the relative velocity of the bodies, G is the gravitational constant, and c is the speed of light. This waveform is used to examine the post-Newtonian correction to the linear momentum carried off in the radiation, thus allowing an estimate of the upper bound of the center of mass recoil velocity for coalescing neutron star systems, V(sub C.M.) less than or equal to km s(exp -1). At (post)(exp 3/2)-Newtonian order the effects of the gravitational wave 'tail' also enter the waveform. The tail of the radiation, which is caused by scatter of the radiation from the background spacetime curvature, does not depend solely on the instantaneous state of the system at the retarded time, but rather depends on the integrated past history of the system. However, we show the dependence on the remote past of the system is quite weak. The nonlinear contribution to the gravitational radiation which has as its source the quadrupole radiation itself is studied. This effect is shown to enter the waveform at the (post)(exp 5/2)-Newtonian order. The detectability of these contributions to the waveform by laser interferometric gravitational wave observatories (LIGO) is discussed.
Dissert. Abstr.

N93-25828 Princeton Univ., NJ.
GRAVITATIONAL LENSING AND GAMMA RAY BURSTS Ph.D. Thesis
Shude Mao 1992 116 p
Avail: Univ. Microfilms Order No. DA9302076

This thesis is divided into two parts, the first part (chapters 2-4) is on gravitational lensing, and the second part (chapters 5-8) on gamma ray bursts (GRBs). In chapter 2, the assumptions in the analysis of gravitational lensing statistics are examined. It is shown that a redshift cutoff model, which may result from galaxy evolution, can reduce the lensing probability and explain the large mean separation of gravitational lenses. We show that the reduction of the lensing probability due to the finite core radii of galaxies is likely to be no more than a factor of 2 and the most recent galaxy luminosity function gives a lensing probability that is smaller than previously estimated by a factor of approximately 3. In chapter 3, gravitational microlensing by a single star plus external shear is discussed. It is shown analytically that for a general cusp the magnification probability distribution follows p(sub c)(A)dA is approximately A(exp -7/2)dA asymptotically, in excellent agreement with the numerical results obtained from an adaptive grid technique. In chapter 4, gravitational microlensing by double lenses is applied to the galactic bulge stars. We estimate that approximately 10 percent of all lensing episodes of the galactic bulge stars will display complicated light curves due to the binary nature of the lens. The effect is strong even if the companion is a planet. A search for microlensing of the galactic bulge stars may lead to a discovery of extrasolar planetary systems. In chapter 5, statistical properties of GRBs are calculated for a large number of luminosity functions and density profiles assuming that the sources are galactic. We find that no galactic disk model can be reconciled with the statistical properties observed by the Burst and Transient Source Experiment (BATSE), and a galactic halo distribution must have a core radius R(sub c) greater than 18 kpc (3 sigma) to have no measured dipole anisotropy. In chapter 6, statistical properties of GRBs are analyzed assuming that the sources are cosmological. The range of observations is estimated to be z approximately equals 1.5 for BATSE, and z approximately equals 0.2 for the Pioneer Venus Orbiter. Assuming isotropic radiation, the rate of events is approximately 2 x 10(exp -6) yr(exp -1) per L* galaxy, approximately 3,000 yr(exp -1) in the whole observable universe, and their peak luminosity is approximately 2 x 10(exp 51) h(sub 100)(exp -2) erg s(exp -1). In chapters 7 and 8, gravitational lensing of GRBs is studied. The lensing frequency of GRBs by galaxies is approximately 0.1 percent, while that by black holes (M greater than 10(exp 6) solar M) for the Gnedin & Ostriker model is approximately 5 percent. BATSE may observe several lensing events and thus provide an unambiguous determination of the origin of GRBs.
Dissert. Abstr.

N93-25890*# National Aeronautics and Space Administration. Goddard Space Flight Center, Greenbelt, MD.
NEUTRON ENERGY DETERMINATION WITH A HIGH-PURITY GERMANIUM DETECTOR Final Report, 1989 - 1992
Gene A. Beck 20 Feb. 1992 37 p
(Grant NAG5-1273)
(NASA-CR-192773; NAS 1.26:192773) Avail: CASI HC A03/MF A01

Two areas that are related to planetary gamma-ray spectrometry are investigated. The first task was the investigation of gamma rays produced by high-energy charged particles and their secondaries in planetary surfaces by means of thick target bombardments. The second task was the investigation of the effects of high-energy neutrons on gamma-ray spectral features obtained with high-purity Ge-detectors. For both tasks, as a function of the funding level, the experimental work was predominantly tied to that of other researchers, whenever there was an opportunity to participate in bombardment experiments at large or small accelerators for charged particles.
Author (revised)

N93-26132*# Minnesota Univ., Minneapolis. Dept. of Astronomy.
OBLIQUE MHD COSMIC-RAY MODIFIED SHOCKS: TWO-FLUID NUMERICAL SIMULATIONS
Adam Frank, T. W. Jones, and Dongsu Ryu (Princeton Univ. Observatory, NJ.) 1991 14 p
(Grants NAGw-2548; NSF AST-91-00486)
(NASA-CR-192930; NAS 1.26:192930) Avail: CASI HC A03/MF A01

We present the first results of time dependent, two-fluid, cosmic-ray (CR) modified, MHD shock simulations. The calculations were carried out with a new numerical code for 1-D ideal MHD. By coupling this code with the CR energy transport equation we can simulate the time-dependent evolution of MHD shocks including the acceleration of the CR and their feedback on the shock structures. We report tests of the combined numerical method including comparisons with analytical steady state results published earlier by Webb, as well as internal consistency checks for more general MHD CR shock structures after they appear to have converged to dynamical steady states. We also present results from an initial time dependent simulation which extend the parameter space domain of previous analytical models. These new results support Webb's suggestion that equilibrium oblique shocks are less effective than parallel shocks in the acceleration of CR. However, for realistic models of anisotropic CR diffusion, oblique

shocks may achieve dynamical equilibrium on shorter timescale than parallel shocks. Author (revised)

99 GENERAL

N93-24974# Lawrence Livermore National Lab., CA.
ENERGY AND TECHNOLOGY REVIEW, AUGUST-SEPTEMBER 1992
Joseph A. Sefcik, ed. 1992 20 p
(Contract W-7405-eng-48)
(DE93-005882; UCRL-52000-92-8/9) Avail: CASI HC A03/MF A01

This issue of Energy and Technology Review focuses on cooperative research and development agreements (CRADA's)--one of the Laboratory's most effective means of technology transfer. The first article chronicles the legislative evolution of these agreements. The second article examines the potential beneficial effects of CRADA's on the national economy and discusses their role in the development and marketing of Laboratory technologies. The third article provides information on how to initiate and develop CRADA's at LLNL, and the fourth and fifth articles describe the Laboratory's two most prominent technology transfer projects. One is a 30-month CRADA with General Motors to develop advanced lasers for cutting, welding, and heat-treating operations. The cover photograph shows this laser cutting through a piece of steel 1/16 of an inch thick. The other project is a three-year CRADA with Amoco, Chevron-Conoco, and Unocal to refine our oil shale retorting process. DOE

N93-25188*# National Aeronautics and Space Administration. Lyndon B. Johnson Space Center, Houston, TX.
JSC RESEARCH AND TECHNOLOGY Annual Report, 1992
1993 167 p
(NASA-TM-104763; S-713; NAS 1.15:104763) Avail: CASI HC A08/MF A02

The primary roles and missions of JSC incorporate all aspects of human presence in space. Therefore, the Center is involved in the development of technology that will allow humans to stay longer in Earth orbit, allow safe flight in space, and provide capabilities to explore the Moon and Mars. The Center's technology emphasis areas include human spacecraft development, human support systems and infrastructure, and human spacecraft operations. Safety and reliability are critical requirements for the technologies that JSC pursues for long-duration use in space. One of the objectives of technology development at the Center is to give employees the opportunity to enhance their technological expertise and project management skills by defining, designing, and developing projects that are vital to the Center's strategy for the future. This report is intended to communicate within and outside the Agency our research and technology (R&T) accomplishments, as well as inform Headquarters program managers and their constituents of the significant accomplishments that have promise for future Agency programs. While not inclusive of all R&T efforts, the report presents a comprehensive summary of JSC projects in which substantial progress was made in the 1992 fiscal year. At the beginning of each project description, names of the Principal Investigator (PI) and the Technical Monitor (TM) are given, followed by their JSC mail codes or their company or university affiliations. The funding sources and technology focal points are identified in the index. Derived from text

N93-25418# Joint Publications Research Service, Arlington, VA.
JPRS REPORT: SCIENCE AND TECHNOLOGY. JAPAN. 30TH NATIONAL AEROSPACE LABORATORY CONFERENCE
9 Mar. 1993 54 p Transl. into ENGLISH of NAL (Tokyo, Japan), 20 Oct. 1992 p 1-42 Conference held in Tokyo, Japan, 20 Oct. 1992
(JPRS-JST-93-009) Avail: CASI HC A04/MF A01

Selected articles from the 30th National Aerospace Laboratory Conference held on 20 Oct. 1992 in Tokyo are included. Topics covered include: (1) ultrahigh bypass ratio engine; (2) research into supersonic intakes; (3) research into robust flight control system; (4) summary of research into liquid oxygen turbopumps; (5) microgravity fluid experiments; (6) research into antifriction bearings for use in space; (7) statistical distribution of compressive strength for smoothed testpiece of carbon/polyimide laminated material; and (8) experimental research into thermal/aerodynamic topics for hypersonic transport plane. CASI

N93-25561*# National Aeronautics and Space Administration, Washington, DC.
TECHNOLOGY 2002: THE THIRD NATIONAL TECHNOLOGY TRANSFER CONFERENCE AND EXPOSITION, VOLUME 1
Michael Hackett, comp. Feb. 1993 524 p Conference and Exposition held in Baltimore, MD, 1-3 Dec. 1992
(NASA-CP-3189-Vol-1; NAS 1.55:3189-Vol-1) Avail: CASI HC A22/MF A04

The proceedings from the conference are presented. The topics covered include the following: computer technology, advanced manufacturing, materials science, biotechnology, and electronics. For individual titles, see N93-25562 through N93-25617.

N93-25562*# Idaho National Engineering Lab., Idaho Falls.
INEL SPRAY-FORMING RESEARCH **c27**
Kevin M. McHugh and James F. Key *In* NASA, Washington, Technology 2002: The Third National Technology Transfer Conference and Exposition, Volume 1 Feb. 1993 p 15-24 (For primary document see N93-25561 09-99)
(Contract DE-AC07-76ID-01570)
Avail: CASI HC A02/MF A04

Spray forming is a near-net-shape fabrication technology in which a spray of finely atomized liquid droplets is deposited onto a suitably shaped substrate or mold to produce a coherent solid. The technology offers unique opportunities for simplifying materials processing without sacrificing, and oftentimes substantially improving, product quality. Spray forming can be performed with a wide range of metals and nonmetals, and offers property improvements resulting from rapid solidification (e.g., refined microstructures, extended solid solubilities and reduced segregation). Economic benefits result from process simplification and the elimination of unit operations. Researchers at the Idaho National Engineering Laboratory (INEL) are developing spray-forming technology for producing near-net-shape solids and coatings of a variety of metals, polymers, and composite materials. Results from several spray forming programs are presented to illustrate the range of capabilities of the technique as well as the accompanying technical and economic benefits. Low-carbon steel strip greater than 0.75 mm thick and polymer membranes for gas/gas and liquid/liquid separations that were spray formed are discussed; recent advances in spray forming molds, dies, and other tooling using low-melting-point metals are described. Author

N93-25563*# Midwest Research Inst., Golden, CO.
FILM FABRICATION TECHNOLOGIES AT NREL **c27**
Robert D. McConnell *In* NASA, Washington, Technology 2002: The Third National Technology Transfer Conference and Exposition, Volume 1 Feb. 1993 p 25-29 (For primary document see N93-25561 09-99)
Avail: CASI HC A01/MF A04

The National Renewable Energy Laboratory (NREL) has extensive capabilities for fabricating a variety of high-technology films. Much of the in-house work in NREL's large photovoltaics (PV) program involves the fabrication of multiple thin-film semiconducting layers constituting a thin-film PV device. NREL's smaller program in superconductivity focuses on the fabrication of superconducting films on long, flexible tape substrates. This paper focuses on four of NREL's in-house research groups and their film fabrication techniques, developed for a variety of elements, alloys, and compounds to be deposited on a variety of substrates. As is the case for many national laboratories, NREL's technology transfer efforts are focusing on Cooperative Research and Development Agreements (CRADA's) between NREL researchers and private industry researchers. Author

N93-25564*# National Aeronautics and Space Administration. Lewis Research Center, Cleveland, OH.
OPTICAL AND SCRATCH RESISTANT PROPERTIES OF DIAMONDLIKE CARBON FILMS DEPOSITED WITH SINGLE AND DUAL ION BEAMS **c27**
Michael T. Kussmaul (Sverdrup Technology, Inc., Brook Park, OH.), Michael S. Bogdanski (Case Western Reserve Univ., Cleveland, OH.), Bruce A. Banks, and Michael J. Mirtich *In* NASA, Washington, Technology 2002: The Third National Technology Transfer Conference and Exposition, Volume 1 Feb. 1993 p 30-40 (For primary document see N93-25561 09-99)
Avail: CASI HC A03/MF A04

Amorphous diamond-like carbon (DLC) films were deposited using both

single and dual ion beam techniques utilizing filament and hollow cathode ion sources. Continuous DLC films up to 3000 A thick were deposited on fused quartz plates. Ion beam process parameters were varied in an effort to create hard, clear films. Total DLC film absorption over visible wavelengths was obtained using a Perkin-Elmer spectrophotometer. An ellipsometer, with an Ar-He laser (wavelength 6328 A) was used to determine index of refraction for the DLC films. Scratch resistance, frictional, and adherence properties were determined for select films. Applications for these films range from military to the ophthalmic industries. Author

N93-25565*# National Aeronautics and Space Administration. Lewis Research Center, Cleveland, OH.

PROPERTIES OF EXTRUDED PS-212 TYPE SELF-LUBRICATING MATERIALS **c27**

W. J. Waters (Sverdrup Technology, Inc., Cleveland, OH.), H. E. Sliney, and R. F. Soltis (Cortez 3 Services Corp., Brook Park, OH.) *In* NASA, Washington, Technology 2002: The Third National Technology Transfer Conference and Exposition, Volume 1 Feb. 1993 p 41-55 (For primary document see N93-25561 09-99)

Avail: CASI HC A03/MF A04

Research has been underway at the NASA Lewis Research Center since the 1960's to develop high temperature, self-lubricating materials. The bulk of the research has been done in-house by a team of researchers from the Materials Division. A series of self-lubricating solid material systems has been developed over the years. One of the most promising is the composite material system referred to as PS-212 or PM-212. This material is a powder metallurgy product composed of metal bonded chromium carbide and two solid lubricating materials known to be self-lubricating over a wide temperature range. NASA feels this material has a wide potential in industrial applications. Simplified processing of this material would enhance its commercial potential. Processing changes have the potential to reduce processing costs, but tribological and physical properties must not be adversely affected. Extrusion processing has been employed in this investigation as a consolidation process for PM-212/PS-212. It has been successful in that high density bars of EX-212 (extruded PM-212) can readily be fabricated. Friction and strength data indicate these properties have been maintained or improved over the P.M. version. A range of extrusion temperatures have been investigated and tensile, friction, wear, and microstructural data have been obtained. Results indicate extrusion temperatures are not critical from a densification standpoint, but other properties are temperature dependent. Author

N93-25566*# National Aeronautics and Space Administration. Lyndon B. Johnson Space Center, Houston, TX.

MEASURING THE METASTATIC POTENTIAL OF CANCER CELLS **c51**

Dennis R. Morrison, Howard Gratzner (DNA Sciences, Houston, TX.), and M. Z. Atassi (Baylor Coll. of Medicine, Houston, TX.) *In* NASA, Washington, Technology 2002: The Third National Technology Transfer Conference and Exposition, Volume 1 Feb. 1993 p 59-70 (For primary document see N93-25561 09-99)

Avail: CASI HC A03/MF A04

Cancer cells must secrete proteolytic enzymes to invade adjacent tissues and migrate to a new metastatic site. Urokinase (uPA) is a key enzyme related to metastasis in cancers of the lung, colon, gastric, uterine, breast, brain, and malignant melanoma. A NASA technology utilization project has combined fluorescence microscopy, image analysis, and flow cytometry, using fluorescent dyes, and urokinase-specific antibodies to measure uPA and abnormal DNA levels (related to cancer cell proliferation) inside the cancer cells. The project is focused on developing quantitative measurements to determine if a patient's tumor cells are actively metastasizing. If a significant number of tumor cells contain large amounts of uPA (esp. membrane-bound) then the post-surgical chemotherapy or radiotherapy can be targeted for metastatic cells that have already left the primary tumor. These analytical methods have been applied to a retrospective study of biopsy tissues from 150 node negative, stage 1 breast cancer patients. Cytopathology and image analysis has shown that uPA is present in high levels in many breast cancer cells, but not found in normal breast. Significant amounts of uPA also have been measured in glioma cell lines cultured from brain tumors. Commercial applications include new diagnostic tests for metastatic cells, in different cancers, which are being developed with a company that provides a medical testing service using flow cytometry for DNA analysis and hormone receptors on tumor cells from patient biopsies. This research also may provide the basis for developing a new 'magic bullet' treatment against metastasis using chemotherapeutic drugs or radioisotopes attached to urokinase-specific monoclonal antibodies that will only bind to metastatic cells. Author

N93-25567*# National Inst. of Health, Bethesda, MD. Office of Technology Transfer.

IMMUNOCONJUGATES: MAGIC BULLETS FOR CANCER THERAPY? **c52**

Daniel R. Passeri and Jack Spiegel *In* NASA, Washington, Technology 2002: The Third National Technology Transfer Conference and Exposition, Volume 1 Feb. 1993 p 71-76 (For primary document see N93-25561 09-99)

Avail: CASI HC A02/MF A04

Conjugating cytotoxic agents to antibodies allows for site-specific delivery of the agent to tumor cells and should provide increased efficacy and reduced non-specific toxicity. These site-specific cytotoxic agents are known as immunoconjugates or 'magic bullets' and have demonstrated great promise as therapeutic agents for cancer and other diseases. The historical developments and future potential of this new approach to cancer therapy are reviewed. Author

N93-25568*# Johns Hopkins Univ., Laurel, MD. Applied Physics Lab.

AUTOMATED SYSTEM FOR EARLY BREAST CANCER DETECTION IN MAMMOGRAMS **c52**

Isaac N. Bankman, Dong W. Kim, William A. Christens-Barry, Irving N. Weinberg, Olga B. Gatewood, and William R. Brody *In* NASA, Washington Technology 2002: The Third National Technology Transfer Conference and Exposition, Volume 1 Feb. 1993 p 77-85 (For primary document see N93-25561 09-99)

Avail: CASI HC A02/MF A04

The increasing demand on mammographic screening for early breast cancer detection, and the subtlety of early breast cancer signs on mammograms, suggest an automated image processing system that can serve as a diagnostic aid in radiology clinics. We present a fully automated algorithm for detecting clusters of microcalcifications that are the most common signs of early, potentially curable breast cancer. By using the contour map of the mammogram, the algorithm circumvents some of the difficulties encountered with standard image processing methods. The clinical implementation of an automated instrument based on this algorithm is also discussed. Author

N93-25569*# Johns Hopkins Univ., Laurel, MD. Applied Physics Lab.

THE DESIGN OF MECHANICALLY COMPATIBLE FASTENERS FOR HUMAN MANDIBLE RECONSTRUCTION **c52**

Jack C. Roberts, John A. Ecker, and Paul J. Biermann *In* NASA, Washington, Technology 2002: The Third National Technology Transfer Conference and Exposition, Volume 1 Feb. 1993 p 86-95 (For primary document see N93-25561 09-99)

Avail: CASI HC A02/MF A04

Mechanically compatible fasteners for use with thin or weakened bone sections in the human mandible are being developed to help reduce large strain discontinuities across the bone/implant interface. Materials being considered for these fasteners are a polyetherertherketone (PEEK) resin with continuous quartz or carbon fiber for the screw. The screws were designed to have a shear strength equivalent to that of compact/trabecular bone and to be used with a conventional nut, nut plate, or an expandable shank/blind nut made of a ceramic filled polymer. Physical and finite element models of the mandible were developed in order to help select the best material fastener design. The models replicate the softer inner core of trabecular bone and the hard outer shell of compact bone. The inner core of the physical model consisted of an expanding foam and the hard outer shell consisted of ceramic particles in an epoxy matrix. This model has some of the cutting and drilling attributes of bone and may be appropriate as an educational tool for surgeons and medical students. The finite element model was exercised to establish boundary conditions consistent with the stress profiles associated with mandible bite forces and muscle loads. Work is continuing to compare stress/strain profiles of a reconstructed mandible with the results from the finite element model. When optimized, these design and fastening techniques may be applicable, not only to other skeletal structures, but to any composite structure. Author

N93-25570*# Corps of Engineers, Vicksburg, MS.
DEVELOPMENT OF A CONE PENETROMETER FOR MEASURING SPECTRAL CHARACTERISTICS OF SOILS IN SITU **c46**
Landris T. Lee, Jr. and Philip G. Malone *In* NASA, Washington, Technology 2002: The Third National Technology Transfer Conference and Exposition, Volume 1 Feb. 1993 p 99-108 Sponsored in part by Army Toxic and Hazardous Materials Agency (For primary document see N93-25561 09-99)
Avail: CASI HC A02/MF A04

A patent was recently granted to the U.S. Army for an adaptation of a soil cone penetrometer that can be used to measure the spectral characteristics (fluorescence or reflectance) of soils adjacent to the penetrometer rod. The system can use a variety of light sources and spectral analytical equipment. A laser induced fluorescence measuring system has proven to be of immediate use in mapping the distribution of oil contaminated soil at waste disposal and oil storage areas. The fiber optic adaptation coupled with a cone penetrometer permits optical characteristics of the in-situ soil to be measured rapidly, safely, and inexpensively. The fiber optic cone penetrometer can be used to gather spectral data to a depth of approximately 25 to 30 m even in dense sands or stiff clays and can investigate 300 m of soil per day. Typical detection limits for oil contamination in sand is on the order of several hundred parts per million. Author

N93-25571*# Brookhaven National Lab., Upton, NY. Dept. of Applied Science.
RECLAMATION WITH RECOVERY OF RADIONUCLIDES AND TOXIC METALS FROM CONTAMINATED MATERIALS, SOILS, AND WASTES **c45**
A. J. Francis and C. J. Dodge *In* NASA, Washington, Technology 2002: The Third National Technology Transfer Conference and Exposition, Volume 1 Feb. 1993 p 109-117 (For primary document see N93-25561 09-99)
(Contract DE-AC02-76CH-00016)
Avail: CASI HC A02/MF A04

A process has been developed at Brookhaven National Laboratory (BNL) for the removal of metals and radionuclides from contaminated materials, soils, and waste sites. In this process, citric acid, a naturally occurring organic complexing agent, is used to extract metals such as Ba, Cd, Cr, Ni, Zn, and radionuclides Co, Sr, Th, and U from solid wastes by formation of water soluble, metal-citrate complexes. Citric acid forms different types of complexes with the transition metals and actinides, and may involve formation of a bidentate, tridentate, binuclear, or polynuclear complex species. The extract containing radionuclide/metal complex is then subjected to microbiological degradation followed by photochemical degradation under aerobic conditions. Several metal citrate complexes are biodegraded, and the metals are recovered in a concentrated form with the bacterial biomass. Uranium forms binuclear complex with citric acid and is not biodegraded. The supernatant containing uranium citrate complex is separated and upon exposure to light, undergoes rapid degradation resulting in the formation of an insoluble, stable polymeric form of uranium. Uranium is recovered as a precipitate (polyuranate) in a concentrated form for recycling or for appropriate disposal. This treatment process, unlike others which use caustic reagents, does not create additional hazardous wastes for disposal and causes little damage to soil which can then be returned to normal use. Author

N93-25572*# Recotech Corp., Aurora, OH.
CONVERTING ENVIRONMENTAL WASTES INTO VALUABLE RESOURCES **c44**
Leonard A. Duval *In* NASA, Washington, Technology 2002: The Third National Technology Transfer Conference and Exposition, Volume 1 Feb. 1993 p 118-120 (For primary document see N93-25561 09-99)
Avail: CASI HC A01/MF A04

This concept employs a viable energy saving method that uses a solvent to separate oil from particle matter; it can be used in metal forming industries to deoil sludges, oxides, and particle matter that is presently committed to landfill. If oily particles are used in their oily state, severe consequences to environmental control systems such as explosions or filter blinding, occur in the air handling equipment. This is due to the presence of hydrocarbons in the stack gasses resulting from the oily particles. After deoiling, the particles can be recycled and the separated oil can be used as a fuel. The process does not produce a waste of it's own and does not harm air or water. It demonstrates the dual benefits of it being commercially viable and in the national interest of conserving resources. Author

N93-25573*# Bureau of Mines, Tuscaloosa, AL.
LOW COST DEWATERING OF WASTE SLURRIES **c45**
J. B. Peterson, S. K. Sharma, R. H. Church, and B. J. Scheiner *In* NASA, Washington, Technology 2002: The Third National Technology Transfer Conference and Exposition, Volume 1 Feb. 1993 p 121-126 (For primary document see N93-25561 09-99)
Avail: CASI HC A02/MF A04

The U.S. Bureau of Mines has developed a technique for dewatering mineral waste slurries which utilizes polymer and a static screen. A variety of waste slurries from placer gold mines and crushed stone operations have been successfully treated using the system. Depending on the waste, a number of polymers have been used successfully with polymer costs ranging from $0.05 to $0.15 per 1,000 gal treated. The dewatering is accomplished using screens made from either ordinary window screen or wedge wire. The screens used are 8 ft wide and 8 ft long. The capacity of the screens varies from 3 to 7 gpm/sq. ft. The water produced is acceptable for recycling to the plant or for discharge to the environment. For example, a fine grain dolomite waste slurry produced from a crushed stone operation was dewatered from a nominal 2.5 pct solids to greater than 50 pct solids using $0.10 to $0.15 worth of polymer per 1,000 gal of slurry. The resulting waste water had a turbidity of less than 50 NTU and could be discharged or recycled. The paper describes field tests conducted using the polymer-screen dewatering system. Author

N93-25574*# National Aeronautics and Space Administration. Langley Research Center, Hampton, VA.
USE OF HIGH PERFORMANCE NETWORKS AND SUPERCOMPUTERS FOR REAL-TIME FLIGHT SIMULATION **c09**
Jeff I. Cleveland, II *In* NASA, Washington, Technology 2002: The Third National Technology Transfer Conference and Exposition, Volume 1 Feb. 1993 p 129-138 (For primary document see N93-25561 09-99)
Avail: CASI HC A02/MF A04

In order to meet the stringent time-critical requirements for real-time man-in-the-loop flight simulation, computer processing operations must be consistent in processing time and be completed in as short a time as possible. These operations include simulation mathematical model computation and data input/output to the simulators. In 1986, in response to increased demands for flight simulation performance, NASA's Langley Research Center (LaRC), working with the contractor, developed extensions to the Computer Automated Measurement and Control (CAMAC) technology which resulted in a factor of ten increase in the effective bandwidth and reduced latency of modules necessary for simulator communication. This technology extension is being used by more than 80 leading technological developers in the United States, Canada, and Europe. Included among the commercial applications are nuclear process control, power grid analysis, process monitoring, real-time simulation, and radar data acquisition. Personnel at LaRC are completing the development of the use of supercomputers for mathematical model computation to support real-time flight simulation. This includes the development of a real-time operating system and development of specialized software and hardware for the simulator network. This paper describes the data acquisition technology and the development of supercomputing for flight simulation. Author

N93-25575*# Supercomputer Research Center, Bowie, MD.
SPLASH 2 **c61**
Jeffrey M. Arnold, Duncan A. Buell, and Walter J. Kleinfelder *In* NASA, Washington, Technology 2002: The Third National Technology Transfer Conference and Exposition, Volume 1 Feb. 1993 p 139-145 (For primary document see N93-25561 09-99)
Avail: CASI HC A02/MF A04

Splash 2 is an attached processor system for Sun SPARC 2 workstations that uses Xilinx 4010 Field Programmable Gate Arrays (FPGA's) as its processing elements. The purpose of this paper is to describe Splash 2. The predecessor system, Splash 1, was designed to be used as a systolic processing system. Although it was very successful in that mode, there were many other applications that were not systolic, but which were successful, nonetheless, on Splash 1, or that were not implemented

successfully due to one or more architectural limitations, most notably I/O bandwidth and interprocessor communication. Although other uses to increase computational performance have been found for the Xilinx FPGA's that are Splash's processing elements. Splash is unique in its goal to be programmable in a general sense. Author

N93-25576*# Symbiotics, Inc., Cambridge, MA.
OBJECT-ORIENTED TOOLS FOR DISTRIBUTED COMPUTING **c62**
Richard M. Adler *In* NASA, Washington, Technology 2002: The Third National Technology Transfer Conference and Exposition, Volume 1 Feb. 1993 p 146-155 (For primary document see N93-25561 09-99)
(Contracts NAS10-11606; NAS10-11882; NAS5-31920; NAS8-39343; DAAB10-87-C-0053)
Avail: CASI HC A02/MF A04

Distributed computing systems are proliferating, owing to the availability of powerful, affordable microcomputers and inexpensive communication networks. A critical problem in developing such systems is getting application programs to interact with one another across a computer network. Remote interprogram connectivity is particularly challenging across heterogeneous environments, where applications run on different kinds of computers and operating systems. NetWorks! (trademark) is an innovative software product that provides an object-oriented messaging solution to these problems. This paper describes the design and functionality of NetWorks! and illustrates how it is being used to build complex distributed applications for NASA and in the commercial sector. Author

N93-25577*# Rome Lab., Griffiss AFB, NY.
THE DATABASE QUERY SUPPORT PROCESSOR (QSP) **c60**
In NASA, Washington, Technology 2002: The Third National Technology Transfer Conference and Exposition, Volume 1 Feb. 1993 p 156-165 (For primary document see N93-25561 09-99)
Avail: CASI HC A02/MF A04

The number and diversity of databases available to users continues to increase dramatically. Currently, the trend is towards decentralized, client server architectures that (on the surface) are less expensive to acquire, operate, and maintain than information architectures based on centralized, monolithic mainframes. The database query support processor (QSP) effort evaluates the performance of a network level, heterogeneous database access capability. Air Force Material Command's Rome Laboratory has developed an approach, based on ANSI standard X3.138 - 1988, 'The Information Resource Dictionary System (IRDS)' to seamless access to heterogeneous databases based on extensions to data dictionary technology. To successfully query a decentralized information system, users must know what data are available from which source, or have the knowledge and system privileges necessary to find out this information. Privacy and security considerations prohibit free and open access to every information system in every network. Even in completely open systems, time required to locate relevant data (in systems of any appreciable size) would be better spent analyzing the data, assuming the original question was not forgotten. Extensions to data dictionary technology have the potential to more fully automate the search and retrieval for relevant data in a decentralized environment. Substantial amounts of time and money could be saved by not having to teach users what data resides in which systems and how to access each of those systems. Information describing data and how to get it could be removed from the application and placed in a dedicated repository where it belongs. The result simplified applications that are less brittle and less expensive to build and maintain. Software technology providing the required functionality is off the shelf. The key difficulty is in defining the metadata required to support the process. The database query support processor effort will provide quantitative data on the amount of effort required to implement an extended data dictionary at the network level, add new systems, adapt to changing user needs, and provide sound estimates on operations and maintenance costs and savings. Author

N93-25578*# Industrial Technology Inst., Ann Arbor, MI.
APPLICATION OF AN ON-MACHINE GAGE FOR DIAMETER MEASUREMENTS **c35**
Kevin G. Harding *In* NASA, Washington, Technology 2002: The Third National Technology Transfer Conference and Exposition, Volume 1 Feb. 1993 p 170-177 (For primary document see N93-25561 09-99)
(Contract F33615-91-C-5704)
Avail: CASI HC A02/MF A04

This paper describes the design analysis and application of a laser based gage made specifically for measuring parts on the machine tool to a high accuracy. The tri-beam gage uses three beams of light to measure the local curvature of the part in a manner similar to a V-block gage. The properties of this design include: calibration that is independent of the machine tool scales, non-contact damage free operation, low cost of the gage, and the ability to measure parts in motion. Author

N93-25579*# Extrude Hone Corp., Irwin, PA.
ON MACHINE CAPACITANCE DIMENSIONAL AND SURFACE PROFILE MEASUREMENT SYSTEM **c31**
Ralph Resnick *In* NASA, Washington, Technology 2002: The Third National Technology Transfer Conference and Exposition, Volume 1 Feb. 1993 p 178-181 (For primary document see N93-25561 09-99)
Avail: CASI HC A01/MF A04

A program was awarded under the Air Force Machine Tool Sensor Improvements Program Research and Development Announcement to develop and demonstrate the use of a Capacitance Sensor System including Capacitive Non-Contact Analog Probe and a Capacitive Array Dimensional Measurement System to check the dimensions of complex shapes and contours on a machine tool or in an automated inspection cell. The manufacturing of complex shapes and contours and the subsequent verification of those manufactured shapes is fundamental and widespread throughout industry. The critical profile of a gear tooth; the overall shape of a graphite EDM electrode; the contour of a turbine blade in a jet engine; and countless other components in varied applications possess complex shapes that require detailed and complex inspection procedures. Current inspection methods for complex shapes and contours are expensive, time-consuming, and labor intensive. Author

N93-25580*# Extrude Hone Corp., Irwin, PA.
ULTRASONIC POLISHING **c31**
Randy Gilmore *In* NASA, Washington, Technology 2002: The Third National Technology Transfer Conference and Exposition, Volume 1 Feb. 1993 p 182-192 (For primary document see N93-25561 09-99)
Avail: CASI HC A03/MF A04

The ultrasonic polishing process makes use of the high-frequency (ultrasonic) vibrations of an abradable tool which automatically conforms to the work piece and an abrasive slurry to finish surfaces and edges on complex, highly detailed, close tolerance cavities in materials from beryllium copper to carbide. Applications range from critical deburring of guidance system components to removing EDM recast layers from aircraft engine components to polishing molds for forming carbide cutting tool inserts or injection molding plastics. A variety of materials including tool steels, carbides, and even ceramics can be successfully processed. Since the abradable tool automatically conforms to the work piece geometry, the ultrasonic finishing method described offers a number of important benefits in finishing components with complex geometries. Author (revised)

N93-25581*# Phillips Lab., Kirtland AFB, NM.
TWO- AND THREE-DIMENSIONAL HIGH PERFORMANCE, PATTERNED OVERLAY MULTI-CHIP MODULE TECHNOLOGY **c33**
James Lyke *In* NASA, Washington, Technology 2002: The Third National Technology Transfer Conference and Exposition, Volume 1 Feb. 1993 p 195-204 (For primary document see N93-25561 09-99)
Avail: CASI HC A02/MF A04

A two- and three-dimensional multi-chip module technology was developed in response to the continuum in demand for increased performance in electronic systems, as well as the desire to reduce the size, weight, and power of space systems. Though developed to satisfy the needs of military programs, such as the Strategic Defense Initiative Organization, the technology, referred to as High Density Interconnect, can also be advantageously exploited for a wide variety of commercial applications, ranging from computer workstations to instrumentation and microwave telecommunications. The robustness of the technology, as well as its high performance, make this generality in application possible. More encouraging is the possibility of this technology for achieving low cost through high volume usage. Author (revised)

N93-25582*# Army Research Lab., Fort Monmouth, NJ. Electronics and Power Sources Directorate.

IMPROVED PERFORMANCE AND SAFETY FOR HIGH ENERGY BATTERIES THROUGH USE OF HAZARD ANTICIPATION AND CAPACITY PREDICTION **c33**

Terrill Atwater *In* NASA, Washington, Technology 2002: The Third National Technology Transfer Conference and Exposition, Volume 1 Feb. 1993 p 205-212 (For primary document see N93-25561 09-99)
Avail: CASI HC A02/MF A04

Prediction of the capacity remaining in used high rate, high energy batteries is important information to the user. Knowledge of the capacity remaining in used batteries results in better utilization. This translates into improved readiness and cost savings due to complete, efficient use. High rate batteries, due to their chemical nature, are highly sensitive to misuse (i.e., over discharge or very high rate discharge). Battery failure due to misuse or manufacturing defects could be disastrous. Since high rate, high energy batteries are expensive and energetic, a reliable method of predicting both failures and remaining energy has been actively sought. Due to concerns over safety, the behavior of lithium/sulphur dioxide cells at different temperatures and current drains was examined. The main thrust of this effort was to determine failure conditions for incorporation in hazard anticipation circuitry. In addition, capacity prediction formulas have been developed from test data. A process that performs continuous, real-time hazard anticipation and capacity prediction was developed. The introduction of this process into microchip technology will enable the production of reliable, safe, and efficient high energy batteries. Author (revised)

N93-25583*# EIC, Inc., Norwood, MA.

THIN RECHARGEABLE BATTERIES FOR CMOS SRAM MEMORY PROTECTION **c33**

Dennis N. Crouse *In* NASA, Washington, Technology 2002: The Third National Technology Transfer Conference and Exposition, Volume 1 Feb. 1993 p 213-218 (For primary document see N93-25561 09-99)
Avail: CASI HC A02/MF A04

New rechargeable battery technology is described and compared with classical primary battery back-up of SRAM PC cards. Thin solid polymer electrolyte cells with the thickness of TSOP memory components (1 mm nominal, 1.1 mm max) and capacities of 14 mAh/sq cm can replace coin cells. The SRAM PC cards with permanently installed rechargeable cells and optional electrochromic low battery voltage indicators will free the periodic PC card user from having to 'feed' their PC cards with coin cells and will allow a quick visual check of stored cards for their battery voltage status. Author (revised)

N93-25584*# Johns Hopkins Univ., Laurel, MD. Applied Physics Lab.

A NOVEL METHOD FOR CHARACTERIZATION OF SUPERCONDUCTORS: PHYSICAL MEASUREMENTS AND MODELING OF THIN FILMS **c76**

B. F. Kim, K. Moorjani, T. E. Phillips, F. J. Adrian, J. Bohandy, and Q. E. Dolecek *In* NASA, Washington, Technology 2002: The Third National Technology Transfer Conference and Exposition, Volume 1 Feb. 1993 p 223-230 (For primary document see N93-25561 09-99)
Avail: CASI HC A02/MF A04

A method for characterization of granular superconducting thin films has been developed which encompasses both the morphological state of the sample and its fabrication process parameters. The broad scope of this technique is due to the synergism between experimental measurements and their interpretation using numerical simulation. Two novel technologies form the substance of this system: the magnetically modulated resistance method for characterizing superconductors; and a powerful new computer peripheral, the Parallel Information Processor card, which provides enhanced computing capability for PC computers. This enhancement allows PC computers to operate at speeds approaching that of supercomputers. This makes atomic scale simulations possible on low cost machines. The present development of this system involves the integration of these two technologies using mesoscale simulations of thin film growth. A future stage of development will incorporate atomic scale modeling. Author (revised)

N93-25585*# Bureau of Mines, Tuscaloosa, AL.

PRODUCTION OF ULTRAFINE, HIGH-PURITY CERAMIC POWDERS USING THE US BUREAU OF MINES DEVELOPED TURBOMILL **c27**

Jesse L. Hoyer *In* NASA, Washington, Technology 2002: The Third National Technology Transfer Conference and Exposition, Volume 1 Feb. 1993 p 231-240 (For primary document see N93-25561 09-99)
Avail: CASI HC A02/MF A04

Turbomilling, an innovative grinding technology developed by the U.S. Bureau of Mines in the early 1960's for delaminating filler-grade kaolinitic clays, has been expanded into the areas of particle size reduction, material mixing, and process reaction kinetics. The turbomill, originally called an attrition grinder, has been used for particle size reduction of many minerals, including natural and synthetic mica, pyrophyllite, talc, and marble. In recent years, an all-polymer version of the turbomill has been used to produce ultrafine, high-purity, advanced ceramic powders such as SiC, Si3N4, TiB2, and ZrO2. In addition to particle size reduction, the turbomill has been used to produce intimate mixtures of high surface area powders and whiskers. Raw materials, TiN, AlN, and Al2O3, used to produce a titanium nitride/aluminum oxynitride (TiN/AlON) composite, were mixed in the turbomill, resulting in strength increases over samples prepared by dry ball milling. Using the turbomill as a leach vessel, it was found that 90.4 pct of the copper was extracted from the chalcopyrite during a 4-hour leach test in ferric sulfate versus conventional processing which involves either roasting of the ore for Cu recovery or leaching of the ore for several days.
Author (revised)

N93-25586*# Naval Surface Warfare Center, Silver Spring, MD.

MULLITE WHISKERS AND MULLITE-WHISKER FELT **c24**

Inna G. Talmy and Deborah A. Haught *In* NASA, Washington, Technology 2002: The Third National Technology Transfer Conference and Exposition, Volume 1 Feb. 1993 p 241-249 Sponsored in part by Office of Naval Technology (For primary document see N93-25561 09-99)
Avail: CASI HC A02/MF A04

The Naval Surface Warfare Center has developed processes for the preparation of mullite (3(Al2O3)(dot)2(SiO2)) whiskers and mullite-whisker felt. Three patents on the technology were issued in 1990. The processes are based on chemical reactions between AlF3, Al2O3, and SiO2. The felt is formed in-situ during the processing of shaped powdered precursors. It consists of randomly oriented whiskers which are mutually intergrown forming a rigid structure. The microstructure and properties of the felt and size of the whiskers can be modified by varying the amount of Al2O3 in the starting mixture. Loose mullite whiskers can be used as a reinforcement for polymer-, metal-, and ceramic-matrix composites. The felt can be used as preforms for fabricating composite materials as well as for thermal insulation and high temperature, chemically stable filters for liquids (melts) and gases. Author (revised)

N93-25587*# National Aeronautics and Space Administration. Lewis Research Center, Cleveland, OH.

GRAPHITE/EPOXY COMPOSITE LAMINATES WITH CO-CURED INTERLAMINAR DAMPING LAYERS **c24**

J. Michael Pereira *In* NASA, Washington, Technology 2002: The Third National Technology Transfer Conference and Exposition, Volume 1 Feb. 1993 p 250-255 (For primary document see N93-25561 09-99)
Avail: CASI HC A02/MF A04

Damped composite laminates were fabricated by co-curing viscoelastic damping film with graphite/epoxy prepreg plies. The dynamic response of the damped plates was measured using an impulse response technique and compared with the response of similar undamped laminates. Modal damping was computed from the frequency response data. Micrographs of the damped laminates showed that the damping layers retained their integrity during the fabrication process. The layers significantly increased the damping in the composite laminates. The use of the constrained viscoelastic film as an integral part of composite structures appears to be a feasible approach to passive vibration control. Composite plates manufactured with co-cured damping layers may have commercial applications in cases where light weight, strength, and vibration and noise reduction are important considerations. Author (revised)

N93-25588*# Aeronautical Radio, Inc., Annapolis, MD.

EXPERT SYSTEM FOR UNIX SYSTEM RELIABILITY AND AVAILABILITY ENHANCEMENT **c38**

Catherine Q. Xu *In* NASA, Washington, Technology 2002: The Third National Technology Transfer Conference and Exposition, Volume 1 Feb. 1993 p 259-267 (For primary document see N93-25561 09-99)
Avail: CASI HC A02/MF A04

Highly reliable and available systems are critical to the airline industry. However, most off-the-shelf computer operating systems and hardware do not have built-in fault tolerant mechanisms, the UNIX workstation is one example. In this research effort, we have developed a rule-based Expert System (ES) to monitor, command, and control a UNIX workstation system with hot-standby redundancy. The ES on each workstation acts as an on-line system administrator to diagnose, report, correct, and prevent certain types of hardware and software failures. If a primary station is approaching failure, the ES coordinates the switch-over to a hot-standby secondary workstation. The goal is to discover and solve certain fatal problems early enough to prevent complete system failure from occurring and therefore to enhance system reliability and availability. Test results show that the ES can diagnose all targeted faulty scenarios and take desired actions in a consistent manner regardless of the sequence of the faults. The ES can perform designated system administration tasks about ten times faster than an experienced human operator. Compared with a single workstation system, our hot-standby redundancy system downtime is predicted to be reduced by more than 50 percent by using the ES to command and control the system. Author (revised)

N93-25589*# National Aeronautics and Space Administration. Goddard Space Flight Center, Greenbelt, MD.

THE GENERIC SPACECRAFT ANALYST ASSISTANT (GenSAA): A TOOL FOR DEVELOPING GRAPHICAL EXPERT SYSTEMS **c61**

Peter M. Hughes *In* NASA, Washington, Technology 2002: The Third National Technology Transfer Conference and Exposition, Volume 1 Feb. 1993 p 268-278 (For primary document see N93-25561 09-99)

Avail: CASI HC A03/MF A04

During numerous contacts with a satellite each day, spacecraft analysts must closely monitor real-time data. The analysts must watch for combinations of telemetry parameter values, trends, and other indications that may signify a problem or failure. As the satellites become more complex and the number of data items increases, this task is becoming increasingly difficult for humans to perform at acceptable performance levels. At NASA GSFC, fault-isolation expert systems are in operation supporting this data monitoring task. Based on the lessons learned during these initial efforts in expert system automation, a new domain-specific expert system development tool named the Generic Spacecraft Analyst Assistant (GenSAA) is being developed to facilitate the rapid development and reuse of real-time expert systems to serve as fault-isolation assistants for spacecraft analysts. Although initially domain-specific in nature, this powerful tool will readily support the development of highly graphical expert systems for data monitoring purposes throughout the space and commercial industry. Author (revised)

N93-25590*# National Aeronautics and Space Administration. Lyndon B. Johnson Space Center, Houston, TX.

TARGET: RAPID CAPTURE OF PROCESS KNOWLEDGE **c61**

C. J. Ortiz, H. V. Ly, T. Saito (Computer Sciences Corp., Houston, TX.), and R. B. Loftin (Houston Univ., TX.) *In* NASA, Washington, Technology 2002: The Third National Technology Transfer Conference and Exposition, Volume 1 Feb. 1993 p 279-288 (For primary document see N93-25561 09-99)

Avail: CASI HC A02/MF A04

TARGET (Task Analysis/Rule Generation Tool) represents a new breed of tool that blends graphical process flow modeling capabilities with the function of a top-down reporting facility. Since NASA personnel frequently perform tasks that are primarily procedural in nature, TARGET models mission or task procedures and generates hierarchical reports as part of the process capture and analysis effort. Historically, capturing knowledge has proven to be one of the greatest barriers to the development of intelligent systems. Current practice generally requires lengthy interactions between the expert whose knowledge is to be captured and the knowledge engineer whose responsibility is to acquire and represent the expert's knowledge in a useful form. Although much research has been devoted to the development of methodologies and computer software to aid in the capture and representation of some types of knowledge, procedural knowledge has received relatively little attention. In essence, TARGET is one of the first tools of its kind, commercial or institutional, that is designed to support this type of knowledge capture undertaking. This paper will describe the design and development of TARGET for the acquisition and representation of procedural knowledge. The strategies employed by TARGET to support use by knowledge engineers, subject matter experts, programmers and managers will be discussed. This discussion includes the method by which the tool employs its graphical user interface to generate a task hierarchy report. Next, the approach to generate production rules for incorporation in and development of a CLIPS based expert system will be elaborated. TARGET also permits experts to visually describe procedural tasks as a common medium for knowledge refinement by the expert community and knowledge engineer making knowledge consensus possible. The paper briefly touches on the verification and validation issues facing the CLIPS rule generation aspects of TARGET. A description of efforts to support TARGET's interoperability issues on PCs, Macintoshes and UNIX workstations concludes the paper. Author (revised)

N93-25591*# Research Inst. for Advanced Computer Science, Moffett Field, CA.

TREE CLASSIFICATION SOFTWARE **c61**

Wray Buntine *In* NASA, Washington, Technology 2002: The Third National Technology Transfer Conference and Exposition, Volume 1 Feb. 1993 p 289-298 (For primary document see N93-25561 09-99)

Avail: CASI HC A02/MF A04

This paper introduces the IND Tree Package to prospective users. IND does supervised learning using classification trees. This learning task is a basic tool used in the development of diagnosis, monitoring and expert systems. The IND Tree Package was developed as part of a NASA project to semi-automate the development of data analysis and modelling algorithms using artificial intelligence techniques. The IND Tree Package integrates features from CART and C4 with newer Bayesian and minimum encoding methods for growing classification trees and graphs. The IND Tree Package also provides an experimental control suite on top. The newer features give improved probability estimates often required in diagnostic and screening tasks. The package comes with a manual, Unix 'man' entries, and a guide to tree methods and research. The IND Tree Package is implemented in C under Unix and was beta-tested at university and commercial research laboratories in the United States. Author (revised)

N93-25592*# Johns Hopkins Univ., Laurel, MD. Applied Physics Lab.

AUTOMATIC DETECTION OF SEIZURES WITH APPLICATIONS **c52**

Dale E. Olsen, John C. Harris, Protagoras N. Cutchis, John A. Cristion, Ronald P. Lesser (Johns Hopkins Univ., Baltimore, MD.), and W. Robert S. Webber (Johns Hopkins Univ., Baltimore, MD.) *In* NASA, Washington, Technology 2002: The Third National Technology Transfer Conference and Exposition, Volume 1 Feb. 1993 p 301-307 (For primary document see N93-25561 09-99)

Avail: CASI HC A02/MF A04

There are an estimated two million people with epilepsy in the United States. Many of these people do not respond to anti-epileptic drug therapy. Two devices can be developed to assist in the treatment of epilepsy. The first is a microcomputer-based system designed to process massive amounts of electroencephalogram (EEG) data collected during long-term monitoring of patients for the purpose of diagnosing seizures, assessing the effectiveness of medical therapy, or selecting patients for epilepsy surgery. Such a device would select and display important EEG events. Currently many such events are missed. A second device could be implanted and would detect seizures and initiate therapy. Both of these devices require a reliable seizure detection algorithm. A new algorithm is described. It is believed to represent an improvement over existing seizure detection algorithms because better signal features were selected and better standardization methods were used. Author (revised)

N93-25593*# National Aeronautics and Space Administration. Lewis Research Center, Cleveland, OH.

A FIBER OPTIC PROBE FOR THE DETECTION OF CATARACTS **c52**

Rafat R. Ansari and Harbans S. Dhadwal (State Univ. of New York, Stony Brook.) *In* NASA, Washington, Technology 2002: The Third National Technology Transfer Conference and Exposition, Volume 1 Feb. 1993 p 308-316 (For primary document see N93-25561 09-99)

Avail: CASI HC A02/MF A04

A compact fiber optic probe developed for on-orbit science experiments was used to detect the onset of cataracts, a capability that could eliminate physicians' guesswork and result in new drugs to 'dissolve' or slow down the cataract formation before surgery is necessary. The probe is based upon dynamic light scattering (DLS) principles. It has no moving parts, no

apertures, and requires no optical alignment. It is flexible and easy to use. Results are presented for excised but intact human eye lenses. In a clinical setting, the device can be easily incorporated into a slit-lamp apparatus (ophthalmoscope) for complete eye diagnostics. In this set-up, the integrated fiber optic probe, the size of a pencil, delivers a low power cone of laser light into the eye of a patient and guides the light which is backscattered by the protein molecules of the lens through a receiving optical fiber to a photo detector. The non-invasive DLS measurements provide rapid determination of protein crystalline size and its size distribution in the eye lens. Author (revised)

N93-25594*# General Electric Co., Houston, TX. Government Services.
MAC TO VAX CONNECTIVITY: HEARTRATE SPECTRAL ANALYSIS SYSTEM **c52**
Hasan H. Rahman and Monazer Faruque *In* NASA, Washington, Technology 2002: The Third National Technology Transfer Conference and Exposition, Volume 1 Feb. 1993 p 317-321 Prepared for NASA. Johnson Space Center, Houston, TX (For primary document see N93-25561 09-99)
Avail: CASI HC A01/MF A04

The heart rate Spectral Analysis System (SAS) acquires and analyzes, in real-time, the Space Shuttle onboard electrocardiograph (EKG) experiment signals, calculates the heartrate, and applies a Fast Fourier Transformation (FFT) to the heart rate. The system also calculates other statistical parameters such as the 'mean heart rate' over specific time period and heart rate histogram. This SAS is used by NASA Principal Investigators as a research tool to determine the effects of weightlessness on the human cardiovascular system. This is also used to determine if Lower Body Negative Pressure (LBNP) is an effective countermeasure to the orthostatic intolerance experienced by astronauts upon return to normal gravity. In microgravity, astronauts perform the LBNP experiment in the mid deck of the Space Shuttle. The experiment data are downlinked by the orbiter telemetry system, then processed and analyzed in real-time by the integrated Life Sciences Data Acquisition (LSDS) - Spectral Analysis System. The data system is integrated within the framework of two different computer systems, VAX and Macintosh (Mac), using the networking infrastructure to assist the investigators in further understanding the most complex machine on Earth--the human body. Author (revised)

N93-25595*# National Aeronautics and Space Administration. Lyndon B. Johnson Space Center, Houston, TX.
THE APPLICATION OF INTEGRATED KNOWLEDGE-BASED SYSTEMS FOR THE BIOMEDICAL RISK ASSESSMENT INTELLIGENT NETWORK (BRAIN) **c53**
Karin C. Loftin (Krug Life Sciences, Inc., Houston, TX.), Bebe Ly, Laurie Webster, James Verlander (Krug Life Sciences, Inc., Houston, TX.), Gerald R. Taylor, Gary Riley, Chris Culbert, Tina Holden (Lockheed Engineering and Sciences Co., Houston, TX.), and Marianne Rudisill *In* NASA, Washington, Technology 2002: The Third National Technology Transfer Conference and Exposition, Volume 1 Feb. 1993 p 322-331 (For primary document see N93-25561 09-99)
Avail: CASI HC A02/MF A04

One of NASA's goals for long duration space flight is to maintain acceptable levels of crew health, safety, and performance. One way of meeting this goal is through the Biomedical Risk Assessment Intelligent Network (BRAIN), an integrated network of both human and computer elements. The BRAIN will function as an advisor to flight surgeons by assessing the risk of in-flight biomedical problems and recommending appropriate countermeasures. This paper describes the joint effort among various NASA elements to develop BRAIN and an Infectious Disease Risk Assessment (IDRA) prototype. The implementation of this effort addresses the technological aspects of the following: (1) knowledge acquisition; (2) integration of IDRA components; (3) use of expert systems to automate the biomedical prediction process; (4) development of a user-friendly interface; and (5) integration of the IDRA prototype and Exercise Countermeasures Intelligent System (ExerCISys). Because the C Language, CLIPS (the C Language Integrated Production System), and the X-Window System were portable and easily integrated, they were chosen as the tools for the initial IDRA prototype. The feasibility was tested by developing an IDRA prototype that predicts the individual risk of influenza. The application of knowledge-based systems to risk assessment is of great market value to the medical technology industry. Author (revised)

N93-25596*# IsoGen Radioisotopic Research Lab., Oregon City, OR.
SOLID-STATE ISOTOPIC POWER SOURCE FOR COMPUTER MEMORY CHIPS **c33**
Paul M. Brown *In* NASA, Washington, Technology 2002: The Third National Technology Transfer Conference and Exposition, Volume 1 Feb. 1993 p 335-340 (For primary document see N93-25561 09-99)
Avail: CASI HC A02/MF A04

Recent developments in materials technology now make it possible to fabricate nonthermal thin-film radioisotopic energy converters (REC) with a specific power of 24 W/kg and a 10 year working life at 5 to 10 watts. This creates applications never before possible, such as placing the power supply directly on integrated circuit chips. The efficiency of the REC is about 25 percent which is two to three times greater than the 6 to 8 percent capabilities of current thermoelectric systems. Radio isotopic energy converters have the potential to meet many future space power requirements for a wide variety of applications with less mass, better efficiency, and less total area than other power conversion options. These benefits result in significant dollar savings over the projected mission lifetime.
Author (revised)

N93-25597*# Naval Surface Warfare Center, Panama City, FL.
PHOTOVOLTAIC POWER WITHOUT BATTERIES FOR CONTINUOUS CATHODIC PROTECTION **c44**
W. W. Muehl, Sr. *In* NASA, Washington, Technology 2002: The Third National Technology Transfer Conference and Exposition, Volume 1 Feb. 1993 p 341-344 (For primary document see N93-25561 09-99)
Avail: CASI HC A01/MF A04

The objective of this project was to successfully demonstrate that renewable energy can efficiently and economically replace dedicated non-renewable power sources. The COASTSYSTA designed, installed, and started up on 20 Jan. 1990, a state-of-the-art photovoltaic powered impressed current cathodic protection system (PVCPSYS) for steel and iron submerged structures. This system does not require any auxiliary/battery backup power. The PVCPSYS installed on 775 ft. of steel sheet piling of a Navy bulkhead is continuing to provide complete, continuous corrosion protection. This installation is well documented by COASTSYSTA and was verified on-site by the U.S. Army Corps of Engineers. The PVCPSYS uses only renewable energy and is environmentally clean. A patent is pending on the new technology. Other possible PVCPSYS applications are mothballed ships, docks, dams, locks, bridges, marinas, and pipelines. The Department of Defense Photovoltaic Review Committee and Sandia National Laboratories consider this successful and cost effective system a major advance in the application of photovoltaics. Author (revised)

N93-25598*# Army Research Lab., Fort Monmouth, NJ. Pulse Power Components Branch.
HIGH SPEED SOLID STATE CIRCUIT BREAKER **c33**
Thomas F. Podlesak *In* NASA, Washington, Technology 2002: The Third National Technology Transfer Conference and Exposition, Volume 1 Feb. 1993 p 345-352 (For primary document see N93-25561 09-99)
Avail: CASI HC A02/MF A04

The U.S. Army Research Laboratory, Fort Monmouth, NJ, has developed and is installing two 3.3 MW high speed solid state circuit breakers at the Army's Pulse Power Center. These circuit breakers will interrupt 4160V three phase power mains in no more than 300 microseconds, two orders of magnitude faster than conventional mechanical contact type circuit breakers. These circuit breakers utilize Gate Turnoff Thyristors (GTO's) and are currently utility type devices using air cooling in an air conditioned enclosure. Future refinements include liquid cooling, either water or two phase organic coolant, and more advanced semiconductors. Each of these refinements promises a more compact, more reliable unit. Author

N93-25599*# Colorado Univ., Boulder. Dept. of Electrical and Computer Engineering.
VARIABLE-SPEED GENERATORS WITH FLUX WEAKENING **c33**
A. A. Fardoun, E. F. Fuchs, and P. W. Carlin (Midwest Research Inst., Golden, CO.) *In* NASA, Washington, Technology 2002: The Third National Technology Transfer Conference and Exposition, Volume 1 Feb. 1993 p 353-362 (For primary document see N93-25561 09-99)
Avail: CASI HC A02/MF A04

A cost-competitive, permanent-magnet 20 kW generator is designed such that the following criteria are satisfied: an (over) load capability of at

least 30 kW over the entire speed range of 60-120 rpm, generator weight of about 550 lbs with a maximum radial stator flux density of 0.82 T at low speed, unity power factor operation, acceptably small synchronous reactances and operation without a gear box. To justify this final design four different generator designs are investigated: the first two designs are studied to obtain a speed range from 20 to 200 rpm employing rotor field weakening, and the latter two are investigated to obtain a maximum speed range of 40 to 160 rpm based on field weakening via the stator excitation. The generator reactances and induced voltages are computed using finite element/difference solutions. Generator losses and efficiencies are presented for all four designs at rated temperature of Tr=120C. Author

N93-25600*# Sterling Software, Moffett Field, CA.
SCIENTIFIC VISUALIZATION USING THE FLOW ANALYSIS SOFTWARE TOOLKIT (FAST) **c61**
Gordon V. Bancroft, Paul G. Kelaita, R. Kevin McCabe, Fergus J. Merritt, Todd C. Plessel, Timothy A. Sandstrom, and John T. West *In* NASA, Washington, Technology 2002: The Third National Technology Transfer Conference and Exposition, Volume 1 Feb. 1993 p 366-375 (For primary document see N93-25561 09-99)
Avail: CASI HC A02/MF A04

Over the past few years the Flow Analysis Software Toolkit (FAST) has matured into a useful tool for visualizing and analyzing scientific data on high-performance graphics workstations. Originally designed for visualizing the results of fluid dynamics research, FAST has demonstrated its flexibility by being used in several other areas of scientific research. These research areas include earth and space sciences, acid rain and ozone modelling, and automotive design, just to name a few. This paper describes the current status of FAST, including the basic concepts, architecture, existing functionality and features, and some of the known applications for which FAST is being used. A few of the applications, by both NASA and non-NASA agencies, are outlined in more detail. Described in the Outlines are the goals of each visualization project, the techniques or 'tricks' used lo produce the desired results, and custom modifications to FAST, if any, done to further enhance the analysis. Some of the future directions for FAST are also described. Author

N93-25601*# National Aeronautics and Space Administration. Langley Research Center, Hampton, VA.
INTEGRATION OF DESIGN, THERMAL, STRUCTURAL, AND OPTICAL ANALYSIS, INCLUDING THERMAL ANIMATION **c61**
Ruth M. Amundsen *In* NASA, Washington, Technology 2002: The Third National Technology Transfer Conference and Exposition, Volume 1 Feb. 1993 p 376-384 (For primary document see N93-25561 09-99)
Avail: CASI HC A02/MF A04

In many industries there has recently been a concerted movement toward 'quality management' and the issue of how to accomplish work more efficiently. Part of this effort is focused on concurrent engineering; the idea of integrating the design and analysis processes so that they are not separate, sequential processes (often involving design rework due to analytical findings) but instead form an integrated system with smooth transfers of information. Presented herein are several specific examples of concurrent engineering methods being carried out at Langley Research Center (LaRC): integration of thermal, structural and optical analyses to predict changes in optical performance based on thermal and structural effects; integration of the CAD design process with thermal and structural analyses; and integration of analysis and presentation by animating the thermal response of a system as an active color map -- a highly effective visual indication of heat flow. Author

N93-25602*# National Aeronautics and Space Administration. Goddard Space Flight Center, Greenbelt, MD.
DATA SYSTEMS DYNAMIC SIMULATOR **c61**
Christopher Rouff, Melana Clark, Bill Davenport, and Philip Message (Stanford Telecommunications, Inc., Seabrook, MD.) *In* NASA, Washington, Technology 2002: The Third National Technology Transfer Conference and Exposition, Volume 1 Feb. 1993 p 385-393 (For primary document see N93-25561 09-99)
Avail: CASI HC A02/MF A04

The Data System Dynamic Simulator (DSDS) is a discrete event simulation tool. It was developed for NASA for the specific purpose of evaluating candidate architectures for data systems of the Space Station era. DSDS provides three methods for meeting this requirement. First, the user has access to a library of standard pre-programmed elements. These elements represent tailorable components of NASA data systems and can be connected in any logical manner. Secondly, DSDS supports the development of additional elements. This allows the more sophisticated DSDS user the option of extending the standard element set. Thirdly, DSDS supports the use of data streams simulation. Data streams is the name given to a technique that ignores packet boundaries, but is sensitive to rate changes. Because rate changes are rare compared to packet arrivals in a typical NASA data system, data stream simulations require a fraction of the CPU run time. Additionally, the data stream technique is considerably more accurate than another commonly-used optimization technique. Author

N93-25603*# Johns Hopkins Univ., Laurel, MD. Electro-Optical Systems Group.
A NOVEL OPTICAL/DIGITAL PROCESSING SYSTEM FOR PATTERN RECOGNITION **c61**
Bradley G. Boone and Oodaye B. Shukla *In* NASA, Washington, Technology 2002: The Third National Technology Transfer Conference and Exposition, Volume 1 Feb. 1993 p 397-406 (For primary document see N93-25561 09-99)
Avail: CASI HC A02/MF A04

This paper describes two processing algorithms that can be implemented optically: the Radon transform and angular correlation. These two algorithms can be combined in one optical processor to extract all the basic geometric and amplitude features from objects embedded in video imagery. We show that the internal amplitude structure of objects is recovered by the Radon transform, which is a well-known result, but, in addition, we show simulation results that calculate angular correlation, a simple but unique algorithm that extracts object boundaries from suitably threshold images from which length, width, area, aspect ratio, and orientation can be derived. In addition to circumventing scale and rotation distortions, these simulations indicate that the features derived from the angular correlation algorithm are relatively insensitive to tracking shifts and image noise. Some optical architecture concepts, including one based on micro-optical lenslet arrays, have been developed to implement these algorithms. Simulation test and evaluation using simple synthetic object data will be described, including results of a study that uses object boundaries (derivable from angular correlation) to classify simple objects using a neural network. Author

N93-25604*# Automatix, Inc., Billerica, MA.
VISION-AIDED MONITORING AND CONTROL OF THERMAL SPRAY, SPRAY FORMING, AND WELDING PROCESSES **c31**
John E. Agapakis and Jon Bolstad (Control Vision, Inc., Idaho Falls, ID.) *In* NASA, Washington, Technology 2002: The Third National Technology Transfer Conference and Exposition, Volume 1 Feb. 1993 p 407-414 Sponsored in part by DOE (For primary document see N93-25561 09-99)
Avail: CASI HC A02/MF A04

Vision is one of the most powerful forms of non-contact sensing for monitoring and control of manufacturing processes. However, processes involving an arc plasma or flame such as welding or thermal spraying pose particularly challenging problems to conventional vision sensing and processing techniques. The arc or plasma is not typically limited to a single spectral region and thus cannot be easily filtered out optically. This paper presents an innovative vision sensing system that uses intense stroboscopic illumination to overpower the arc light and produce a video image that is free of arc light or glare and dedicated image processing and analysis schemes that can enhance the video images or extract features of interest and produce quantitative process measures which can be used for process monitoring and control. Results of two SBIR programs sponsored by NASA and DOE and focusing on the application of this innovative vision sensing and processing technology to thermal spraying and welding process monitoring and control are discussed. Author

N93-25605*# Boeing Defense and Space Group, Huntsville, AL.
ROBOTIC VARIABLE POLARITY PLASMA ARC (VPPA) WELDING **c37**
Waris S. Jaffery *In* NASA, Washington, Technology 2002: The Third National Technology Transfer Conference and Exposition, Volume 1 Feb. 1993 p 415-424 (For primary document see N93-25561 09-99)
(Contract NAS8-50000)
Avail: CASI HC A02/MF A04

The need for automated plasma welding was identified in the early stages of the Space Station Freedom Program (SSFP) because it requires approximately 1.3 miles of welding for assembly. As a result of the Variable Polarity Plasma Arc Welding (VPPAW) process's ability to make virtually defect-free welds in aluminum, it was chosen to fulfill the welding needs. Space Station Freedom will be constructed of 2219 aluminum utilizing the computer controlled VPPAW process. The 'Node Radial Docking Port', with it's saddle shaped weld path, has a constantly changing surface angle over 360 deg of the 282 inch weld. The automated robotic VPPAW process requires eight-axes of motion (six-axes of robot and two-axes of positioner movement). The robot control system is programmed to maintain Torch Center Point (TCP) orientation perpendicular to the part while the part positioner is tilted and rotated to maintain the vertical up orientation as required by the VPPAW process. The combined speed of the robot and the positioner are integrated to maintain a constant speed between the part and the torch. A laser-based vision sensor system has also been integrated to track the seam and map the surface of the profile during welding. Author

N93-25606*# National Aeronautics and Space Administration. Goddard Space Flight Center, Greenbelt, MD.

FIRMWARE DEVELOPMENT IMPROVES SYSTEM EFFICIENCY c60

E. James Chern and David W. Butler *In* NASA, Washington, Technology 2002: The Third National Technology Transfer Conference and Exposition, Volume 1 Feb. 1993 p 425-434 (For primary document see N93-25561 09-99)

Avail: CASI HC A02/MF A04

Most manufacturing processes require physical pointwise positioning of the components or tools from one location to another. Typical mechanical systems utilize either stop-and-go or fixed feed-rate procession to accomplish the task. The first approach achieves positional accuracy but prolongs overall time and increases wear on the mechanical system. The second approach sustains the throughput but compromises positional accuracy. A computer firmware approach has been developed to optimize this point wise mechanism by utilizing programmable interrupt controls to synchronize engineering processes 'on the fly'. This principle has been implemented in an eddy current imaging system to demonstrate the improvement. Software programs were developed that enable a mechanical controller card to transmit interrupts to a system controller as a trigger signal to initiate an eddy current data acquisition routine. The advantages are: (1) optimized manufacturing processes, (2) increased throughput of the system, (3) improved positional accuracy, and (4) reduced wear and tear on the mechanical system. Author

N93-25607*# Army Research Lab., Fort Belvoir, VA. Engineering Materials and Coatings Div.

ELASTOMER COMPOUND DEVELOPED FOR HIGH WEAR APPLICATIONS c27

D. Crawford, H. Feuer, D. Flanagan, G. Rodriguez, A. Teets, and P. Touchet *In* NASA, Washington, Technology 2002: The Third National Technology Transfer Conference and Exposition, Volume 1 Feb. 1993 p 438-445 (For primary document see N93-25561 09-99)

Avail: CASI HC A02/MF A04

The U.S. Army is currently spending 300 million dollars per year replacing rubber track pads. An experimental rubber compound has been developed which exhibits 2 to 3 times greater service life than standard production pad compounds. To improve the service life of the tank track pads various aspects of rubber chemistry were explored including polymer, curing and reinforcing systems. Compounds that exhibited superior physical properties based on laboratory data were then fabricated into tank pads and field tested. This paper will discuss the compounding studies, laboratory data and field testing that led to the high wear elastomer compound. Author

N93-25608*# Naval Surface Warfare Center, Silver Spring, MD.

DYNAMIC HARDNESS TESTER AND CURE METER c35

Walter M. Madigosky and Ralph B. Fiorito *In* NASA, Washington, Technology 2002: The Third National Technology Transfer Conference and Exposition, Volume 1 Feb. 1993 p 446-450 (For primary document see N93-25561 09-99)

Avail: CASI HC A01/MF A04

The Shore hardness tester is used extensively throughout industry to determine the static modulus of materials. The new apparatus described here extends the capability of an indentor-type tester into the dynamic regime, and provides a measurement of the dynamic shear or Young's modulus and loss factor as a function of frequency. The instrument, model and data of typical rubber samples are given and compared to other dynamic measurements. Author

N93-25609*# National Aeronautics and Space Administration. Langley Research Center, Hampton, VA.

INSTRUMENTATION FOR MEASUREMENT OF GAS PERMEABILITY OF POLYMERIC MEMBRANES c37

Billy T. Upchurch, George M. Wood, Kenneth G. Brown (Old Dominion Univ., Norfolk, VA.), and Karen S. Burns (Old Dominion Univ., Norfolk, VA.) *In* NASA, Washington, Technology 2002: The Third National Technology Transfer Conference and Exposition, Volume 1 Feb. 1993 p 451-460 (For primary document see N93-25561 09-99)

Avail: CASI HC A02/MF A04

A mass spectrometric 'Dynamic Delta' method for the measurement of gas permeability of polymeric membranes has been developed. The method is universally applicable for measurement of the permeability of any gas through polymeric membrane materials. The usual large sample size of more than 100 square centimeters required for other methods is not necessary for this new method which requires a size less than one square centimeter. The new method should fulfill requirements and find applicability for industrial materials such as food packaging, contact lenses and other commercial materials where gas permeability or permselectivity properties are important. Author

N93-25610*# Naval Surface Warfare Center, Silver Spring, MD.

A SOFTWARE PACKAGE FOR NEURAL NETWORK APPLICATIONS DEVELOPMENT c63

Robert H. Baran *In* NASA, Washington, Technology 2002: The Third National Technology Transfer Conference and Exposition, Volume 1 Feb. 1993 p 463-472 Sponsored in part by Office of Naval Technology (For primary document see N93-25561 09-99)

Avail: CASI HC A02/MF A04

Original Backprop (Version 1.2) is an MS-DOS package of four stand-alone C-language programs that enable users to develop neural network solutions to a variety of practical problems. Original Backprop generates three-layer, feed-forward (series-coupled) networks which map fixed-length input vectors into fixed length output vectors through an intermediate (hidden) layer of binary threshold units. Version 1.2 can handle up to 200 input vectors at a time, each having up to 128 real-valued components. The first subprogram, TSET, appends a number (up to 16) of classification bits to each input, thus creating a training set of input output pairs. The second subprogram, BACKPROP, creates a trilayer network to do the prescribed mapping and modifies the weights of its connections incrementally until the training set is leaned. The learning algorithm is the 'back-propagating error correction procedures first described by F. Rosenblatt in 1961. The third subprogram, VIEWNET, lets the trained network be examined, tested, and 'pruned' (by the deletion of unnecessary hidden units). The fourth subprogram, DONET, makes a TSR routine by which the finished product of the neural net design-and-training exercise can be consulted under other MS-DOS applications. Author

N93-25611*# Johns Hopkins Univ., Laurel, MD. Applied Physics Lab.

CONTROL OF COMPLEX DYNAMIC SYSTEMS BY NEURAL NETWORKS c63

James C. Spall and John A. Cristion *In* NASA, Washington, Technology 2002: The Third National Technology Transfer Conference and Exposition, Volume 1 Feb. 1993 p 473-482 (For primary document see N93-25561 09-99)

(Contract N00039-91-C-0001)

Avail: CASI HC A02/MF A04

This paper considers the use of neural networks (NN's) in controlling a nonlinear, stochastic system with unknown process equations. The NN is used to model the resulting unknown control law. The approach here is based on using the output error of the system to train the NN controller without the need to construct a separate model (NN or other type) for the unknown process dynamics. To implement such a direct adaptive control approach, it is required that connection weights in the NN be estimated while the system is being controlled. As a result of the feedback of the unknown process dynamics, however, it is not possible to determine the

gradient of the loss function for use in standard (back-propagation-type) weight estimation algorithms. Therefore, this paper considers the use of a new stochastic approximation algorithm for this weight estimation, which is based on a 'simultaneous perturbation' gradient approximation that only requires the system output error. It is shown that this algorithm can greatly enhance the efficiency over more standard stochastic approximation algorithms based on finite-difference gradient approximations. Author

N93-25612*# Bureau of Mines, Tuscaloosa, AL.
ADAPTIVE PROCESS CONTROL WITH FUZZY LOGIC AND GENETIC ALGORITHMS **c63**
C. L. Karr *In* NASA, Washington, Technology 2002: The Third National Technology Transfer Conference and Exposition, Volume 1 Feb. 1993 p 483-490 (For primary document see N93-25561 09-99)
Avail: CASI HC A02/MF A04

Researchers at the U.S. Bureau of Mines have developed adaptive process control systems in which genetic algorithms (GA's) are used to augment fuzzy logic controllers (FLC's). GA's are search algorithms that rapidly locate near-optimum solutions to a wide spectrum of problems by modeling the search procedures of natural genetics. FLC's are rule based systems that efficiently manipulate a problem environment by modeling the 'rule-of-thumb' strategy used in human decision-making. Together, GA's and FLC's possess the capabilities necessary to produce powerful, efficient, and robust adaptive control systems. To perform efficiently, such control systems require a control element to manipulate the problem environment, an analysis element to recognize changes in the problem environment, and a learning element to adjust to the changes in the problem environment. Details of an overall adaptive control system are discussed. A specific laboratory acid-base pH system is used to demonstrate the ideas presented. Author

N93-25613*# National Aeronautics and Space Administration. Lyndon B. Johnson Space Center, Houston, TX.
A GENETIC ALGORITHM TOOL (SPLICER) FOR COMPLEX SCHEDULING PROBLEMS AND THE SPACE STATION FREEDOM RESUPPLY PROBLEM **c61**
Lui Wang and Manuel Valenzuela-Rendon (Instituto Technologico y de Estudios Superiores de Monterrey, Mexico.) *In* NASA, Washington, Technology 2002: The Third National Technology Transfer Conference and Exposition, Volume 1 Feb. 1993 p 491-500 Sponsored in part by Inst. Technologico y de Estudios Superiores de Monterrey (For primary document see N93-25561 09-99)
(Contract NCC9-16)
Avail: CASI HC A02/MF A04

The Space Station Freedom will require the supply of items in a regular fashion. A schedule for the delivery of these items is not easy to design due to the large span of time involved and the possibility of cancellations and changes in shuttle flights. This paper presents the basic concepts of a genetic algorithm model, and also presents the results of an effort to apply genetic algorithms to the design of propellant resupply schedules. As part of this effort, a simple simulator and an encoding by which a genetic algorithm can find near optimal schedules have been developed. Additionally, this paper proposes ways in which robust schedules, i.e., schedules that can tolerate small changes, can be found using genetic algorithms. Author

N93-25614*# National Aeronautics and Space Administration. Goddard Space Flight Center, Greenbelt, MD.
PRELIMINARY STUDIES LEADING TOWARD THE DEVELOPMENT OF A LIDAR BATHYMETRY MAPPING INSTRUMENT **c35**
John M. Hill (Houston Advanced Research Center, The Woodlands, TX.), Brendan D. Krenek (Houston Advanced Research Center, The Woodlands, TX.), Terry D. Kunz (Houston Advanced Research Center, The Woodlands, TX.), William Krabill, and Fran Stetina *In* NASA, Washington, Technology 2002: The Third National Technology Transfer Conference and Exposition, Volume 1 Feb. 1993 p 503-514 (For primary document see N93-25561 09-99)
Avail: CASI HC A03/MF A04

The National Aeronautics and Space Administration (NASA) at Goddard Space Flight Center (GSFC) has developed a laser ranging device (LIDAR) which provides accurate and timely data of earth features. NASA/GSFC recently modified the sensor to include a scanning capability to produce LIDAR swaths. They have also integrated a Global Positioning System (GPS) and an Inertial Navigation System (INS) to accurately determine the absolute aircraft location and aircraft attitude (pitch, yaw, and roll), respectively. The sensor has been flown in research mode by NASA for many years. The LIDAR has been used in different configurations or modes to acquire such data as altimetry (topography), bathymetry (water depth), laser-induced fluorosensing (tracer dye movements, oil spills and oil thickness, chlorophyll and plant stress identification), forestry, and wetland discrimination studies. NASA and HARC are developing a commercial version of the instrument for topographic mapping applications. The next phase of the commercialization project will be to investigate other applications such as wetlands mapping and coastal bathymetry. In this paper we report on preliminary laboratory measurements to determine the feasibility of making accurate depth measurements in relatively shallow water (approximately 2 to 6 feet deep) using a LIDAR system. The LIDAR bathymetry measurements are relatively simple in theory. The water depth is determined by measuring the time interval between the water surface reflection and the bottom surface reflection signals. Depth is then calculated by dividing by the index of refraction of water. However, the measurements are somewhat complicated due to the convolution of the water surface return signal with the bottom surface return signal. Therefore in addition to the laboratory experiments, computer simulations of the data were made to show these convolution effects in the return pulse waveform due to: (1) water depth, and (2) changes in bottom surface reflectivity. Author

N93-25615*# National Aeronautics and Space Administration. John C. Stennis Space Center, Bay Saint Louis, MS.
COMMERCIAL APPLICATIONS MULTISPECTRAL SENSOR SYSTEM **c43**
Ronald J. Birk (Sverdrup Technology, Inc., Bay Saint Louis, MS.) and Bruce Spiering *In* NASA, Washington, Technology 2002: The Third National Technology Transfer Conference and Exposition, Volume 1 Feb. 1993 p 515-526 Previously announced in IAA as A93-28081 (For primary document see N93-25561 09-99)
Avail: CASI HC A03/MF A04

NASA's Office of Commercial Programs is funding a multispectral sensor system to be used in the development of remote sensing applications. The Airborne Terrestrial Applications Sensor (ATLAS) is designed to provide versatility in acquiring spectral and spatial information. The ATLAS system will be a test bed for the development of specifications for airborne and spaceborne remote sensing instrumentation for dedicated applications. This objective requires spectral coverage from the visible through thermal infrared wavelengths, variable spatial resolution from 2-25 meters; high geometric and geo-location accuracy; on-board radiometric calibration; digital recording; and optimized performance for minimized cost, size, and weight. ATLAS is scheduled to be available in 3rd quarter 1992 for acquisition of data for applications such as environmental monitoring, facilities management, geographic information systems data base development, and mineral exploration. Author

N93-25616*# National Weather Service, Silver Spring, MD. Office of Hydrology.
INTERACTIVE FORECASTING WITH THE NATIONAL WEATHER SERVICE RIVER FORECAST SYSTEM **c47**
George F. Smith and Donna Page *In* NASA, Washington, Technology 2002: The Third National Technology Transfer Conference and Exposition, Volume 1 Feb. 1993 p 527-536 (For primary document see N93-25561 09-99)
Avail: CASI HC A02/MF A04

The National Weather Service River Forecast System (NWSRFS) consists of several major hydrometeorologic subcomponents to model the physics of the flow of water through the hydrologic cycle. The entire NWSRFS currently runs in both mainframe and minicomputer environments, using command oriented text input to control the system computations. As computationally powerful and graphically sophisticated scientific workstations became available, the National Weather Service (NWS) recognized that a graphically based, interactive environment would enhance the accuracy and timeliness of NWS river and flood forecasts. Consequently, the operational forecasting portion of the NWSRFS has been ported to run under a UNIX operating system, with X windows as the display environment on a system of networked scientific workstations. In addition, the NWSRFS Interactive Forecast Program was developed to provide a graphical user

interface to allow the forecaster to control NWSRFS program flow and to make adjustments to forecasts as necessary. The potential market for water resources forecasting is immense and largely untapped. Any private company able to market the river forecasting technologies currently developed by the NWS Office of Hydrology could provide benefits to many information users and profit from providing these services. Author

N93-25617*# Lockheed Missiles and Space Co., Sunnyvale, CA.
SPACE LIFE SUPPORT TECHNOLOGY APPLICATIONS TO TERRESTRIAL ENVIRONMENTAL PROBLEMS **c54**
Steven H. Schwartzkopf and Howard L. Sleeper *In* NASA, Washington, Technology 2002: The Third National Technology Transfer Conference and Exposition, Volume 1 Feb. 1993 p 537-543 (For primary document see N93-25561 09-99)
Avail: CASI HC A02/MF A04

Many of the problems now facing the human race on Earth are, in fact, life support issues. Decline of air Quality as a result of industrial and automotive emissions, pollution of ground water by organic pesticides or solvents, and the disposal of solid wastes are all examples of environmental problems that we must solve to sustain human life. The technologies currently under development to solve the problems of supporting human life for advanced space missions are extraordinarily synergistic with these environmental problems. The development of these technologies (including both physicochemical and bioregenerative types) is increasingly focused on closing the life support loop by removing and recycling contaminants and wastes to produce the materials necessary to sustain human life. By so doing, this technology development effort also focuses automatically on reducing resupply logistics requirements and increasing crew safety through increased self-sufficiency. This paper describes several technologies that have been developed to support human life in space and illustrates the applicability of the technologies to environmental problems including environmental remediation and pollution prevention. Author

N93-25710# Armed Forces Radiobiology Research Inst., Bethesda, MD.
AFRRI RESEARCH, FISCAL YEAR 1991 Annual Research Report, 1 Oct. 1990 - 30 Sep. 1991
1992 161 p
(AD-A260933; ARR-20) Avail: CASI HC A08/MF A02

This report reviews the scientific program and describes the status of in-house research at AFRRI for the period 1 Oct. 1990 through 30 Sep. 1991. DTIC

N93-25893# Air Force Office of Scientific Research, Bolling AFB, Washington, DC.
AIR FORCE OFFICE OF SCIENTIFIC RESEARCH Annual Quarterly Status Report, Jul. - Sep. 1992
Sep. 1992 72 p LIMITED REPRODUCIBILITY: Availability: Document partially illegible
(AD-A260675; AFOSR-TR-92-1010) Avail: CASI HC A04/MF A01

The Research Proposal Quarterly Status Report is published in March, June, September, and December by the Air Force Office of Scientific Research (AFOSR). It lists all the research proposals received by AFOSR in the previous six months along with the action taken (Initiated, Declined or Withdrawn) on each report. The report is divided into two parts. The Institution index lists proposals alphabetically by institution. This is followed by a more detailed listing by Directorate, and by Program Manager within the Directorate. This Report is designed to inform other Government sponsoring agencies of the proposals received by the AFOSR and the action taken on these proposals. Readers must keep in mind that declined proposals should not necessarily be considered as scientifically unacceptable; many declinations result from a lack of funds or as a result of special programmatic emphasis. DTIC

N93-25910# Rome Lab., Griffiss AFB, NY.
ROME LABORATORY JOURNAL, 1992
1992 232 p
(AD-A260821) Avail: CASI HC A11/MF A03

The Rome Laboratory is the Air Force's center of expertise for advancing the state-of-the-art in command, control, communications, and intelligence. This mission is accomplished by: (1) Conducting vigorous research, development, and test programs in all applicable technologies; (2) Transitioning technology to current and future Air Force systems to improve operational capability, readiness, and supportability; (3) Providing a full range of technical support to AFSC product divisions and other Air Force organizations; and (4) Conducting selected acquisition programs for low volume, limited quantity intelligence and software systems. The Laboratory maintains leading edge technological expertise in the following areas: surveillance, communications, command and control, intelligence, reliability science, electromagnetic technology, photonics, signal processing, and computational science. The Laboratory is organized into four major staff directorates and four mission directorates: Surveillance and Photonics, Command Control and Communications, Intelligence and Reconnaissance and Electromagnetics and Reliability. We recognize that a system approach, integrating efforts across the Laboratory's organizational structure, is required to develop effective C3I systems. Journal papers are presented. DTIC

N93-26058*# National Aeronautics and Space Administration. Lyndon B. Johnson Space Center, Houston, TX.
NATIONAL AERONAUTICS AND SPACE ADMINISTRATION (NASA)/AMERICAN SOCIETY FOR ENGINEERING EDUCATION (ASEE) SUMMER FACULTY FELLOWSHIP PROGRAM, 1992, VOLUME 1
Richard B. Bannerot, ed. and Stanley H. Goldstein, ed. Dec. 1992 142 p Prepared in cooperation with Houston Univ, TX
(Grant NGT-44-005-803)
(NASA-CR-188242-Vol-1; NAS 1.26:188242-Vol-1) Avail: CASI HC A07/MF A02

The 1992 Johnson Space Center (JSC) National Aeronautics and Space Administration (NASA)/American Society for Engineering Education (ASEE) Summer Faculty Fellowship Program was conducted by the University of Houston and JSC. The program at JSC, as well as the programs at other NASA Centers, was funded by the Office of University Affairs, Washington, DC. The objectives of the program, which began nationally in 1964 and at JSC in 1965, are (1) to further the professional knowledge of qualified engineering and science faculty members; (2) to stimulate an exchange of ideas between participants and NASA; (3) to enrich and refresh the research and teaching activities of participants' institutions; and (4) to contribute to the research objective of the NASA Centers. This document is a compilation of the final reports 1 through 12. For individual titles, see N93-26059 through N93-26069.

N93-26059*# LeTourneau Coll., Longview, TX. Div. of Natural Sciences.
DATA ANALYSIS AND INTERPRETATION OF LUNAR DUST EXOSPHERE Final Report **c91**
George A. Andrews, Jr. *In* NASA. Johnson Space Center, National Aeronautics and Space Administration (NASA)/American Society for Engineering Education (ASEE) Summer Faculty Fellowship Program, 1992, Volume 1 Dec. 1992 11 p (For primary document see N93-26058 09-99)
(Grant NGT-44-005-803)
Avail: CASI HC A03/MF A02

The lunar horizon glow observed by Apollo astronauts and captured on film during the Surveyor mission is believed to result from the scattering of sunlight off lunar fines suspended in a dust layer over the lunar surface. For scale heights on the order of tens of kilometers, it is anticipated that the size of the dust particles will be small enough to admit Rayleigh scattering. Such events would result in scattered light which is polarized to a degree which is a function of observation angle and produce spectra containing large high frequency components ('bluing'). Believing these signatures to be observable from ground based telescopes, observational data has been collected from McDonald Observatory and the task of reduction and analysis of this data is the focus of the present report. Author

N93-26060*# Rice Univ., Houston, TX. Dept. of Mechanical Engineering and Materials Science.
COMPOSITE MATERIALS FOR THE EXTRAVEHICULAR MOBILITY UNIT Final Report **c24**
Enrique V. Barrera and Hector M. Tello *In* NASA. Johnson Space Center, National Aeronautics and Space Administration (NASA)/American Society for Engineering Education (ASEE) Summer Faculty Fellowship Program, 1992, Volume 1 Dec. 1992 15 p (For primary document see N93-26058 09-99)
(Grant NGT-44-005-803)
Avail: CASI HC A03/MF A02

The extravehicular mobility unit (EMU), commonly known as the astronaut space suit assembly (SSA) and primary life support system (PLSS), has evolved through the years to incorporate new and innovative materials in order to meet the demands of the space environment. The space shuttle program which is seeing an increasing level of extravehicular activity (EVA), also called space walks, along with interest in an EMU for Lunar-Mars missions means even more demanding conditions are being placed on the suit and PLSS. The project for this NASA-ASEE Summer Program was to investigate new materials for these applications. The focus was to emphasize the use of composite materials for every component of the EMU to enhance the properties while reducing the total weight of the EMU. To accomplish this, development of new materials called fullerene reinforced materials (FRM's) was initiated. Fullerenes are carbon molecules which when added to a material significantly reduce the weight of that material. The Faculty Fellow worked directly on the development of the fullerene reinforced materials. A chamber for fullerene production was designed and assembled and first generation samples were processed. He also supervised with the JSC Colleague, a study of composite materials for the EMU conducted by the student participant in the NASA-ASEE Program, Hector Tello a Rice University graduate student, and by a NASA Aerospace Technologist (Materials Engineer) Evelyne Orndoff, in the Systems Engineering Analysis Office (EC7), also a Rice University graduate student. Hector Tello conducted a study on beryllium and Be alloys and initiated a study of carbon and glass reinforced composites for space applications. Evelyne Orndoff compiled an inventory of the materials on the SSA. Ms. Orndoff also reviewed SSA material requirements and cited aspects of the SSA design where composite materials might be further considered. Hector Tello spent part of his time investigating the solar radiation sensitivity of anodic coatings. This project was directed toward the effects of ultra-violet radiation on high emissivity anodic coatings. The work of both Evelyne Orndoff and Hector Tello is of interest to the Engineering Directorate at NASA/JSC and is also directed toward their research as Rice University graduate students. Author

N93-26061*# Nebraska Univ., Lincoln. Dept. of Industrial and Management Systems Engineering.

INVESTIGATION OF THE EFFECTS OF EXTRA VEHICULAR ACTIVITY (EVA) AND LAUNCH AND ENTRY (LES) GLOVES ON PERFORMANCE Final Report **c54**

Ram R. Bishu *In* NASA. Johnson Space Center, National Aeronautics and Space Administration (NASA)/American Society for Engineering Education (ASEE) Summer Faculty Fellowship Program, 1992, Volume 1 Dec. 1992 15 p (For primary document see N93-26058 09-99)
(Grant NGT-44-005-803)
Avail: CASI HC A03/MF A02

Human capabilities such as dexterity, manipulability, and tactile perception are unique and render the hand as a very versatile, effective and a multipurpose tool. This is especially true for unknown environments such as the EVA environment. In the microgravity environment interfaces, procedures, and activities are too complex, diverse, and defy advance definition. Under these conditions the hand becomes the primary means of locomotion, restraint, and material handling. Facilitation of these activities, with simultaneous protection from the cruel EVA environment are the two, often conflicting, objectives of glove design. The objectives of this study was (1) to assess the effects of EVA gloves at different pressures on human hand capabilities, (2) to devise a protocol for evaluating EVA gloves, (3) to develop force time relations for a number of EVA glove pressure combinations, and (4) to evaluate two types of launch and entry suit gloves. The objectives were achieved through three experiments. The experiments for achieving objectives 1, 2, and 3 were performed in the glove box in building 34. In experiment 1 three types of EVA gloves were tested at five pressure differentials. A number of performance measures were recorded. In experiment 2 the same gloves as in experiment 1 were evaluated in a reduced number of pressure conditions. The performance measure was endurance time. Six subjects participated in both the experiments. In experiment 3 two types of launch and entry suit gloves were evaluated using a paradigm similar to experiment 1. Currently the data is being analyzed. However for this report some summary analyses have been performed. The results indicate that a) With EVA gloves strength is reduced by nearly 50 percent, b) performance decrements increase with increasing pressure differential, c) TMG effects are not consistent across the three gloves tested, d) some interesting gender glove interactions were observed, some of which may have been due to the extent (or lack of) fit of the glove to the hand, and e) differences in performance exist between partial pressure suit glove and full pressure suit glove, especially in the unpressurized condition. Author

N93-26062*# Arkansas Coll., Batesville. Natural Science and Mathematics Div.

VOLATILES IN INTERPLANETARY DUST PARTICLES: A COMPARISON WITH CI AND CM CHONDRITES Final Report **c90**

Roberta Bustin *In* NASA. Johnson Space Center, National Aeronautics and Space Administration (NASA)/American Society for Engineering Education (ASEE) Summer Faculty Fellowship Program, 1992, Volume 1 Dec. 1992 14 p (For primary document see N93-26058 09-99)
(Grant NGT-44-005-803)
Avail: CASI HC A03/MF A02

In an effort to classify and determine the origin of interplanetary dust particles (IDPs), 14 of these particles were studied using a laser microprobe/mass spectrometer. The mass spectra for these particles varied dramatically. Some particles released hydroxide or water which probably originated in hydroxide-bearing minerals or hydrates. Others produced spectra which included a number of hydrocarbons and resembled meteorite spectra. However, none of the individual IDPs gave spectra which could be matched identically with a particular meteorite type such as a CI or CM carbonaceous chondrite. We believe this was due to the fact that 10-20 micron size IDPs are too small to be representative of the parent body. To verify that the diversity was due primarily to the small particle sizes, small grains of approximately the same size range as the IDPs were obtained from two primitive meteorites, Murchison and Orgueil, and these small meteorite particles were treated exactly like the IDPs. Considerable diversity was observed among individual grains, but a composite spectrum of all the grains from one meteorite closely resembled the spectrum obtained from a much larger sample of that meteorite. A composite spectrum of the 14 IDPs also resembled the spectra of the CM and CI meteorites, pointing to a possible link between IDPs and carbonaceous chondrites. This also illustrates that despite the inherent diversity in particles as small as 10-20 micron, conclusions can be drawn about the possible origin and overall composition of such particles by looking not only at results from individual particles but also by including many particles in a study and basing conclusions on some kind of composite data. Author

N93-26063*# Florida International Univ., Miami. Industrial and Systems Engineering.

USE OF TAGUCHI DESIGN OF EXPERIMENTS TO OPTIMIZE AND INCREASE ROBUSTNESS OF PRELIMINARY DESIGNS Final Report **c31**

Hector R. Carrasco *In* NASA. Johnson Space Center, National Aeronautics and Space Administration (NASA)/American Society for Engineering Education (ASEE) Summer Faculty Fellowship Program, 1992, Volume 1 Dec. 1992 14 p (For primary document see N93-26058 09-99)
(Grant NGT-44-005-803)
Avail: CASI HC A03/MF A02

The research performed this summer includes the completion of work begun last summer in support of the Air Launched Personnel Launch System parametric study, providing support on the development of the test matrices for the plume experiments in the Plume Model Investigation Team Project, and aiding in the conceptual design of a lunar habitat. After the conclusion of last years Summer Program, the Systems Definition Branch continued with the Air Launched Personnel Launch System (ALPLS) study by running three experiments defined by L27 Orthogonal Arrays. Although the data was evaluated during the academic year, the analysis of variance and the final project review were completed this summer. The Plume Model Investigation Team (PLUMMIT) was formed by the Engineering Directorate to develop a consensus position on plume impingement loads and to validate plume flowfield models. In order to obtain a large number of individual correlated data sets for model validation, a series of plume experiments was planned. A preliminary 'full factorial' test matrix indicated that 73,024 jet firings would be necessary to obtain all of the information requested. As this was approximately 100 times more firings than the scheduled use of Vacuum Chamber A would permit, considerable effort was needed to reduce the test matrix and optimize it with respect to the specific objectives of the program. Part of the First Lunar Outpost Project deals with Lunar Habitat. Requirements for the habitat include radiation

protection, a safe haven for occasional solar flare storms, an airlock module as well as consumables to support 34 extra vehicular activities during a 45 day mission. The objective for the proposed work was to collaborate with the Habitat Team on the development and reusability of the Logistics Modules. Author

N93-26064*# Texas Technological Univ., Lubbock. Dept. of Mechanical Engineering.

STUDY OF PLATE-FIN HEAT EXCHANGER AND COLD PLATE FOR THE ACTIVE THERMAL CONTROL SYSTEM OF SPACE STATION Final Report **c18**

Ming-C. Chyu *In* NASA. Johnson Space Center, National Aeronautics and Space Administration (NASA)/American Society for Engineering Education (ASEE) Summer Faculty Fellowship Program, 1992, Volume 1 Dec. 1992 15 p (For primary document see N93-26058 09-99)
(Grant NGT-44-005-803)
Avail: CASI HC A03/MF A02

Plate-fin heat exchangers will be employed in the Active Thermal Control System of Space Station Freedom. During ground testing of prototypic heat exchangers, certain anomalous behaviors have been observed. Diagnosis has been conducted to determine the cause of the observed behaviors, including a scrutiny of temperature, pressure, and flow rate test data, and verification calculations based on such data and more data collected during the ambient and thermal/vacuum tests participated by the author. The test data of a plate-fin cold plate have been also analyzed. Recommendation was made with regard to further tests providing more useful information of the cold plate performance. Author

N93-26065*# City Univ. of New York, Bronx. Dept. of Physics.

A PROTOTYPE FOR SIMULATION OF THE SPACE-TO-GROUND ASSEMBLY/CONTINGENCY SYSTEM OF SPACE STATION FREEDOM Final Report **c18**

Louis A. DeAcetis *In* NASA. Johnson Space Center, National Aeronautics and Space Administration (NASA)/American Society for Engineering Education (ASEE) Summer Faculty Fellowship Program, 1992, Volume 1 Dec. 1992 7 p (For primary document see N93-26058 09-99)
(Grant NGT-44-005-803)
Avail: CASI HC A02/MF A02

This project was a continuation of work started during the Summer of 1991 when techniques and methods were investigated for simulating equipment components of the Communications and Tracking System on Space Station Freedom (SSF). The current work involved developing a design for simulation of the entire Assembly/Contingency Subsystem (ACS), which includes the Baseband Signal Processor, standard TDRSS Transponder and the RF Group antenna assembly. A design prototype of the ACS was developed. Methods to achieving 'high fidelity' real-time simulations of the ACS components on IBM-PC compatible computers were considered. The intention is to have separate component simulations running on separate personal computers (PC's), with the capability of substituting actual equipment units for those being simulated when such equipment becomes available for testing. To this end, a scheme for communication between the various simulated ACS components was developed using the serial ports of the PC's hosting the simulations. In addition, control and monitoring of ACS equipment on SSF will be via a MIL-STD 1553B bus. The proposed simulation includes actual 1553B hardware as part of the test bed. Author

N93-26066*# Houston Univ., TX. Dept. of Biological and Environmental Sciences.

METABOLIC RESPONSE OF ENVIRONMENTALLY ISOLATED MICROORGANISMS TO INDUSTRIAL EFFLUENTS: USE OF A NEWLY DESCRIBED CELL CULTURE ASSAY Final Report **c51**

Robert N. Ferebee *In* NASA. Johnson Space Center, National Aeronautics and Space Administration (NASA)/American Society for Engineering Education (ASEE) Summer Faculty Fellowship Program, 1992, Volume 1 15 Sep. 1992 10 p (For primary document see N93-26058 09-99)
Avail: CASI HC A02/MF A02

An environmental application using a microtiter culture assay to measure the metabolic sensitivity of microorganisms to petrochemical effluents will be tested. The Biomedical Operations and Research Branch at NASA JSC has recently developed a rapid and nondestructive method to measure cell growth and metabolism. Using a colorimetric procedure the uniquely modified assay allows the metabolic kinetics of prokaryotic and eukaryotic cells to be measured. Use of such an assay if adapted for the routine monitoring of waste products, process effluents, and environmentally hazardous substances may prove to be invaluable to the industrial community. The microtiter method as described will be tested using microorganisms isolated from the Galveston Bay aquatic habitat. The microbial isolates will be identified prior to testing using the automated systems available at JSC. Sodium dodecyl sulfate (SDS), cadmium, and lead will provide control toxic chemicals. The toxicity of industrial effluent from two industrial sites will be tested. An effort will be made to test the efficacy of this assay for measuring toxicity in a mixed culture community. Author

N93-26067*# Stockton State Coll., Pomona, NJ. Dept. of Geology.

GEOCHEMISTRY AND PETROLOGY OF PRIMITIVE ACHONDRITE METEORITES LEW 88280, MAC 88177, ALHA 81187, EET 84302, AND LEW 88663 Final Report **c90**

Stephen W. Field *In* NASA. Johnson Space Center, National Aeronautics and Space Administration (NASA)/American Society for Engineering Education (ASEE) Summer Faculty Fellowship Program, 1992, Volume 1 14 Aug. 1992 17 p (For primary document see N93-26058 09-99)
(Grant NGT-44-005-803)
Avail: CASI HC A03/MF A02

Primitive achondrites are meteorites that have mineral and bulk chemical compositions similar to the most primitive meteorites (chondrites) but have textures similar to more evolved meteorites (achondrites). The unique geochemistry and texture of the primitive achondrites suggest these meteorites may be genetic intermediates between chondrites and achondrites and may preserve evidence of processes occurring in the early solar system. Five primitive achondrites LEW 88280, MAC 88177, ALHA 81187, EET 84302, and LEW 88663 were examined in this study in order to classify the meteorites and to determine processes that have affected them. Bulk chemical analyses of Nap, K2O, CaO, FeO, Cr, Co, Ni, Sc, Ir, Au, As, Sb, Se, Br, Cs, Ba, La, Ce, Nd, Sm, Eu, Tb, Yb, and Lu were determined for each meteorite by Instrumental Neutron Activation Analysis (INAA). Concentrations of Hf, U, and Th were determined for some meteorites. Polished thin sections of the five meteorites were examined in transmitted and reflected light microscopy to identify minerals and examine petrographic relationships. Minerals found in the meteorites include olivine, orthopyroxene, clinopyroxene, plagioclase, Cr-spinel, phosphates, troilite, kamecite, and taenite along with other minor phases. Mineral compositions were determined with an electron microprobe. The initial study suggests that the meteorites have been altered by metamorphic processes although igneous processes may also have played a role in the evolution of these rocks. Further studies of isotope and bulk chemistry are planned for these meteorites. Author

N93-26068*# Pennsylvania State Univ., University Park. Dept. of Nutrition.

THE ROLE OF PYRIDOXINE AS A COUNTERMEASURE FOR IN-FLIGHT LOSS OF LEAN BODY MASS Final Report **c52**

Joyce A. Gilbert *In* NASA. Johnson Space Center, National Aeronautics and Space Administration (NASA)/American Society for Engineering Education (ASEE) Summer Faculty Fellowship Program, 1992, Volume 1 Dec. 1992 4 p (For primary document see N93-26058 09-99)
(Grant NGT-44-005-803)
Avail: CASI HC A01/MF A02

Ground based and in flight research has shown that humans, under conditions of microgravity, sustain a loss of lean body tissue (protein) and changes in several biological processes including, reductions in red blood cell mass, and neurotransmitters. The maintenance of muscle mass, the major component of lean body mass, is required to meet the needs of space station EVAs. Central to the biosynthesis of amino acids, the building blocks of protein, is pyridoxine (vitamin B-6). Muscle mass integrity requires the availability of vitamin B-6 for protein metabolism and neurotransmitter synthesis. Furthermore, the formation of red blood cells require pyridoxine as a cofactor in the biosynthesis of hemoglobin, a protein that carries oxygen to tissues. In its active form, pyridoxal-5'-phosphate (PLP), vitamin B-6 serves as a link between amino acid and carbohydrate metabolism through intermediates of glycolysis and the tricarboxylic acid cycle. In addition to its role in energy metabolism, PLP is involved in the biosynthesis of hemoglobin and neurotransmitter which are necessary for neurological

functions. Alterations in pyridoxine metabolism may affect countermeasures designed to overcome some of these biochemical changes. The focus of this research is to determine the effects of microgravity on the metabolic utilization of vitamin B-6, integrating nutrition as an integral component of the countermeasure (exercise) to maintain lean body mass and muscle strength. The objectives are: 1) to determine whether microgravity effects the metabolic utilization of pyridoxine and 2) to quantitate changes in B-6 vitamer distribution in tissue and excreta relative to loss of lean body tissue. The rationale for this study encompasses the unique challenge to control biochemical mechanisms effected during space travel and the significance of pyridoxine to maintain and counter muscle integrity for EVA activities. This experiment will begin to elucidate the importance of biochemical interactions between micronutrients and the homeostasis condition of biological processes in the space environment. To address this research topic a simulated microgravity model has been developed. The experiment uses radioisotopically labelled pyridoxine administered as an oral dose to rats which are maintained by tail suspension to simulate a microgravity environment. At the termination of the study, liver, muscle, blood and urine are collected and analyzed by reverse phase high pressure liquid chromatography to determine the quantity and distribution of the B-6 vitamers in tissue and excreta relative to lean body tissue loss. Earlier studies, published by this investigator, have shown that differences in vitamer distribution among samples from experimental versus control subjects indicate changes in metabolic utilization and storage of vitamin B-6.

Author

N93-26069*# University of Western Illinois, Macomb. Dept. of Mathematics.

ANALYSIS OF THE LETTUCE DATA FROM THE VARIABLE PRESSURE GROWTH CHAMBER AT NASA JOHNSON SPACE CENTER: A THREE-STAGE NESTED DESIGN MODEL Final Report **c51**

Tze-San Lee *In* NASA. Johnson Space Center, National Aeronautics and Space Administration (NASA)/American Society for Engineering Education (ASEE) Summer Faculty Fellowship Program, 1992, Volume 1 Dec. 1992 14 p (For primary document see N93-26058 09-99)
(Grant NGT-44-005-803)
Avail: CASI HC A03/MF A02

A model of three-stage nested experimental design was applied to analyze the lettuce data obtained from the variable pressure growth chamber test bed at NASA-Johnson Space Center. From the results of an application of the analysis of variance and covariance on the data set, it was noted that all of the (uncontrollable) factors, Side, Zone, Height and (controllable) PAR (photosynthetically active radiation), had nonhomogeneous effects on the dry weight of the edible biomass of lettuce per pot. Incidentally, the variations accountable to the (uncontrollable) factorial heterogeneities are merely 9 percent and 17 percent of the total variation for both the first and second crop test, respectively. After adjusting for the PAR as a covariate in the no-intercept model, the accountable variations to all the four factors are 94 percent and 92 percent for the first and the second crop test, respectively. With the use of a no-intercept simple linear regression model, the accountable variations to the factor PAR are 92 percent and 90 percent for the first and the second crop test, respectively. Evidently, the (controllable) factor PAR is the dominating one. Author

N93-26070*# National Aeronautics and Space Administration. Lyndon B. Johnson Space Center, Houston, TX.

NATIONAL AERONAUTICS AND SPACE ADMINISTRATION (NASA)/AMERICAN SOCIETY FOR ENGINEERING EDUCATION (ASEE) SUMMER FACULTY FELLOWSHIP PROGRAM, 1992, VOLUME 2

Richard B. Bannerot, ed. and Stanley H. Goldstein, ed. Dec. 1992 165 p Prepared in cooperation with Houston Univ., TX
(Grant NGT-44-005-803)
(NASA-CR-188242-Vol-2; NAS 1.26:188242-Vol-2) Avail: CASI HC A08/MF A02

The 1992 Johnson Space Center (JSC) National Aeronautics and Space Administration (NASA)/American Society for Engineering Education (ASEE) Summer Faculty Fellowship Program was conducted by the University of Houston and JSC. The program at JSC, as well as the programs at other NASA Centers, was funded by the Office of University Affairs, NASA Headquarters Washington, DC. The objectives of the program, which began nationally in 1964 and at JSC in 1965, are (1) to further the professional knowledge of qualified engineering and science faculty members; (2) to stimulate an exchange of ideas between participants and NASA; (3) to enrich and refresh the research and teaching activities of participants' institutions; and (4) to contribute to the research objective of the NASA Centers. This document contains reports 13 through 24. For individual titles, see N93-26071 through N93-26083.

N93-26071*# Wyoming Univ., Laramie. Dept. of Computer Science.

A VISION ARCHITECTURE FOR THE EXTRAVEHICULAR ACTIVITY RETRIEVER Final Report **c63**

Michael Magee *In* NASA. Johnson Space Center, National Aeronautics and Space Administration (NASA)/American Society for Engineering Education (ASEE) Summer Faculty Fellowship Program, 1992, Volume 2 Dec. 1992 10 p (For primary document see N93-26070 09-99)
(Grant NGT-44-005-803)
Avail: CASI HC A02/MF A02

The Extravehicular Activity Retriever (EVAR) is a robotic device currently being developed by the Automation and Robotics Division at the NASA Johnson Space Center to support activities in the neighborhood of the Space Shuttle or Space Station Freedom. As the name implies, the Retriever's primary function will be to provide the capability to retrieve tools, equipment or other objects which have become detached from the spacecraft, but it will also be able to rescue a crew member who may have become inadvertently de-tethered. Later goals will include cooperative operations between a crew member and the Retriever such as fetching a tool that is required for servicing or maintenance operations. This report documents a preliminary design for a Vision System Planner (VSP) for the EVAR that is capable of achieving visual objectives provided to it by a high level task planner. Typical commands which the task planner might issue to the VSP relate to object recognition, object location determination, and obstacle detection. Upon receiving a command from the task planner, the VSP then plans a sequence of actions to achieve the specified objective using a model-based reasoning approach. This sequence may involve choosing an appropriate sensor, selecting an algorithm to process the data, reorienting the sensor, adjusting the effective resolution of the image using lens zooming capability, and/or requesting the task planner to reposition the EVAR to obtain a different view of the object. An initial version of the Vision System Planner which realizes the above capabilities using simulated images has been implemented and tested. The remaining sections describe the architecture and capabilities of the VSP and its relationship to the high level task planner. In addition, typical plans that are generated to achieve visual goals for various scenarios will be discussed. Specific topics to be addressed will include object search strategies, repositioning of the EVAR to improve the quality of information obtained from the sensors, complementary usage of the sensors and redundant capabilities. Author

N93-26072*# Oklahoma State Univ., Stillwater. Dept. of Computer Science.

A STUDY OF MAPPING EXOGENOUS KNOWLEDGE REPRESENTATIONS INTO CONFIG Final Report **c63**

Blayne E. Mayfield *In* NASA. Johnson Space Center, National Aeronautics and Space Administration (NASA)/American Society for Engineering Education (ASEE) Summer Faculty Fellowship Program, 1992, Volume 2 Dec. 1992 15 p (For primary document see N93-26070 09-99)
(Grant NGT-44-005-803)
Avail: CASI HC A03/MF A02

Qualitative reasoning is reasoning with a small set of qualitative values that is an abstraction of a larger and perhaps infinite set of quantitative values. The use of qualitative and quantitative reasoning together holds great promise for performance improvement in applications that suffer from large and/or imprecise knowledge domains. Included among these applications are the modeling, simulation, analysis, and fault diagnosis of physical systems. Several research groups continue to discover and experiment with new qualitative representations and reasoning techniques. However, due to the diversity of these techniques, it is difficult for the programs produced to exchange system models easily. The availability of mappings to transform knowledge from the form used by one of these programs to that used by another would open the doors for comparative analysis of these programs in areas such as completeness, correctness, and performance. A group at the Johnson Space Center (JSC) is working to develop CONFIG, a prototype qualitative modeling, simulation, and analysis tool for fault diagnosis applications in the U.S. space program. The availability

of knowledge mappings from the programs produced by other research groups to CONFIG may provide savings in CONFIG's development costs and time, and may improve CONFIG's performance. The study of such mappings is the purpose of the research described in this paper. Two other research groups that have worked with the JSC group in the past are the Northwest University Group and the University of Texas at Austin Group. The former has produced a qualitative reasoning tool named SIMGEN, and the latter has produced one named QSIM. Another program produced by the Austin group is CC, a preprocessor that permits users to develop input for eventual use by QSIM, but in a more natural format. CONFIG and CC are both based on a component-connection ontology, so a mapping from CC's knowledge representation to CONFIG's knowledge representation was chosen as the focus of this study. A mapping from CC to CONFIG was developed. Due to differences between the two programs, however, the mapping transforms some of the CC knowledge to CONFIG as documentation rather than as knowledge in a form useful to computation. The study suggests that it may be worthwhile to pursue the mappings further. By implementing the mapping as a program, actual comparisons of computational efficiency and quality of results can be made between the QSIM and CONFIG programs. A secondary study may reveal that the results of the two programs augment one another, contradict one another, or differ only slightly. If the latter, the qualitative reasoning techniques may be compared in other areas, such as computational efficiency. Author

N93-26073*# Mercer Univ., Macon, GA. Dept. of Electrical and Computer Engineering.

INVESTIGATION INTO THE COMMON MODE REJECTION RATIO OF THE PHYSIOLOGICAL SIGNAL CONDITIONER CIRCUIT Final Report **c51**

Edward M. OBrien *In* NASA. Johnson Space Center, National Aeronautics and Space Administration (NASA)/American Society for Engineering Education (ASEE) Summer Faculty Fellowship Program, 1992, Volume 2 Dec. 1992 10 p (For primary document see N93-26070 09-99)
(Grant NGT-44-005-803)
Avail: CASI HC A02/MF A02

The common mode rejection ratio (CMRR) of the single operational amplifier (op amp) differential amplifier and of the three operational amplifier differential amplifier was investigated. The three op amp differential amplifier circuit is used in the signal conditioner circuit which amplifies signals such as the electromyograph or electrocardiogram. The investigation confirmed via SPICE modeling what has been observed by others in the recent literature that the CMRR for the circuit can be maximized without precision resistor values or precisely matched op amps. This can be done if one resistor in the final stage can be adjusted either by a potentiometer or by laser trimming in the case of hybrid circuit fabrication. Author

N93-26074*# Pennsylvania State Univ., University Park. Dept. of Industrial and Systems Engineering.

IMPLEMENTATION OF QUALITY IMPROVEMENT TECHNIQUES FOR MANAGEMENT AND TECHNICAL PROCESSES IN THE ACRV PROJECT Final Report **c38**

Laura B. Raiman *In* NASA. Johnson Space Center, National Aeronautics and Space Administration (NASA)/American Society for Engineering Education (ASEE) Summer Faculty Fellowship Program, 1992, Volume 2 Dec. 1992 9 p (For primary document see N93-26070 09-99)
(Grant NGT-44-005-803)
Avail: CASI HC A02/MF A02

Total Quality Management (TQM) is a cooperative form of doing business that relies on the talents of everyone in an organization to continually improve quality and productivity, using teams and an assortment of statistical and measurement tools. The objective of the activities described in this paper was to implement effective improvement tools and techniques in order to build work processes which support good management and technical decisions and actions which are crucial to the success of the ACRV project. The objectives were met by applications in both the technical and management areas. The management applications involved initiating focused continuous improvement projects with widespread team membership. The technical applications involved applying proven statistical tools and techniques to the technical issues associated with the ACRV Project. Specific activities related to the objective included working with a support contractor team to improve support processes, examining processes involved in international activities, a series of tutorials presented to the New Initiatives Office and support contractors, a briefing to NiO managers, and work with the NIO Q+ Team. On the technical side, work included analyzing data from the large-scale W.A.T.E.R. test, landing mode trade analyses, and targeting probability calculations. The results of these efforts will help to develop a disciplined, ongoing process for producing fundamental decisions and actions that shape and guide the ACRV organization . Author

N93-26075*# Ambassador Coll., Big Sandy, TX. Dept. of Computer Information Systems.

DISTRIBUTED PROJECT SCHEDULING AT NASA: REQUIREMENTS FOR MANUAL PROTOCOLS AND COMPUTER-BASED SUPPORT Final Report **c61**

Stephen F. Richards *In* NASA. Johnson Space Center, National Aeronautics and Space Administration (NASA)/American Society for Engineering Education (ASEE) Summer Faculty Fellowship Program, 1992, Volume 2 Dec. 1992 13 p (For primary document see N93-26070 09-99)
(Grant NGT-44-005-803)
Avail: CASI HC A03/MF A02

The increasing complexity of space operations and the inclusion of interorganizational and international groups in the planning and control of space missions lead to requirements for greater communication, coordination, and cooperation among mission schedulers. These schedulers must jointly allocate scarce shared resources among the various operational and mission oriented activities while adhering to all constraints. This scheduling environment is complicated by such factors as the presence of varying perspectives and conflicting objectives among the schedulers, the need for different schedulers to work in parallel, and limited communication among schedulers. Smooth interaction among schedulers requires the use of protocols that govern such issues as resource sharing, authority to update the schedule, and communication of updates. This paper addresses the development and characteristics of such protocols and their use in a distributed scheduling environment that incorporates computer-aided scheduling tools. An example problem is drawn from the domain of Space Shuttle mission planning. Author

N93-26076*# Bevill State Community Coll., Fayette, AL. Div. of Natural Sciences.

DEVELOPMENT OF A PYROLYSIS WASTE RECOVERY MODEL WITH DESIGNS, TEST PLANS, AND APPLICATIONS FOR SPACE-BASED HABITATS Final Report **c54**

Bobby J. Roberson *In* NASA. Johnson Space Center, National Aeronautics and Space Administration (NASA)/American Society for Engineering Education (ASEE) Summer Faculty Fellowship Program, 1992, Volume 2 Dec. 1992 13 p (For primary document see N93-26070 09-99)
(Grant NGT-44-005-803)
Avail: CASI HC A03/MF A02

Extensive literature searches revealed the numerous advantages of using pyrolysis as a means of recovering usable resources from inedible plant biomass, paper, plastics, other polymers, and human waste. A possible design of a pyrolysis reactor with test plans and applications for use on a space-based habitat are proposed. The proposed system will accommodate the wastes generated by a four-person crew while requiring solar energy as the only power source. Waste materials will be collected and stored during the 15-day lunar darkness periods. Resource recovery will occur during the daylight periods. Usable gases such as methane and hydrogen and a solid char will be produced while reducing the mass and volume of the waste to almost infinitely small levels. The system will be operated economically, safely, and in a non-polluting manner. Author

N93-26077*# Louisiana Tech Univ., Ruston. Dept. of Health and Physical Education.

UTILIZATION OF THE GRADED UNIVERSAL TESTING SYSTEM TO INCREASE THE EFFICIENCY FOR ASSESSING AEROBIC AND ANAEROBIC CAPACITY Final Report **c51**

Sandra L. Rodgers *In* NASA. Johnson Space Center, National Aeronautics and Space Administration (NASA)/American Society for Engineering Education (ASEE) Summer Faculty Fellowship Program, 1992, Volume 2 Dec. 1992 9 p (For primary document see N93-26070 09-99)
(Grant NGT-44-005-803)
Avail: CASI HC A02/MF A02

The in-flight exercise test performed by cosmonauts as part of the Russian Exercise Countermeasure Program is limited to 5 minutes due to

communication restrictions. During a recent graded exercise test on a U.S. Shuttle flight, the test was terminated early due to an upcoming loss of signal (LOS) with the ground. This exercise test was a traditional test where the subject's exercise capacity dictates the length of the test. For example, one crew member may take 15 minutes to complete the test, while another may take 18 minutes. The traditional exercise test limits the flight schedulers to large blocks of space flight time in order to provide medical and research personnel information on the fitness capacity (maximal oxygen uptake: VO2max) of crew members during flight. A graded exercise test that would take a finite amount of time and a set preparation and recovery time would ease this problem by allowing flight schedulers to plan exercise tests in advance of LOS. The Graded Universal Testing System (GUTS) was designed to meet this goal. Fitness testing of astronauts before and after flight provides pertinent data on many variables. The Detailed Supplemental Objective (DSO608) protocol (6) is one of the graded exercise tests (GXT) currently used in astronaut testing before and after flight. Test times for this protocol have lasted from 11 to 18 minutes. Anaerobic capacity is an important variable that is currently not being evaluated before and after flight. Recent reports (1,2,5) from the literature have suggested that the oxygen deficit at supramaximal exercise is a measure of anaerobic capacity. We postulated that the oxygen deficit at maximal exercise would be an indication of anaerobic capacity. If this postulate can be accepted, then the efficiency of acquiring data from a graded exercise test would increase at least twofold. To examine this hypothesis anaerobic capacity was measured using a modified treadmill test (3,4) designed to exhaust the anaerobic systems in approximately 45 to 75 seconds. Lactate concentration in the blood was analyzed after all tests, since lactate is the end-product of anaerobic energy production. Therefore, the peak lactate response is an additional indication of anaerobic capacity. A preliminary comparison of the GUTS and the DSO608 suggests that the GUTS protocol would increase the efficiency of VO2max testing of astronauts before and after flight. Results for anaerobic capacity have not been tabulated. Author

N93-26078*# Houston Univ., TX. Dept. of Mathematics.
A HYBRID MULTIGRID TECHNIQUE FOR COMPUTING STEADY-STATE SOLUTIONS TO SUPERSONIC FLOWS Final Report **c02**
Richard Sanders *In* NASA. Johnson Space Center, National Aeronautics and Space Administration (NASA)/American Society for Engineering Education (ASEE) Summer Faculty Fellowship Program, 1992, Volume 2 Dec. 1992 p 16 (For primary document see N93-26070 09-99)
(Grant NGT-44-001-800)
Avail: CASI HC A03/MF A02

Recently, Li and Sanders have introduced a class of finite difference schemes to approximate generally discontinuous solutions to hyperbolic systems of conservation laws. These equations have the form together with relevant boundary conditions. When modelling hypersonic spacecraft reentry, the differential equations above are frequently given by the compressible Euler equations coupled with a nonequilibrium chemistry model. For these applications, steady state solutions are often sought. Many tens (to hundreds) of super computer hours can be devoted to a single three space dimensional simulation. The primary difficulty is the inability to rapidly and reliably capture the steady state. In these notes, we demonstrate that a particular variant from the schemes presented can be combined with a particular multigrid approach to capture steady state solutions to the compressible Euler equations in one space dimension. We show that the rate of convergence to steady state coming from this multigrid implementation is vastly superior to the traditional approach of artificial time relaxation. Moreover, we demonstrate virtual grid independence. That is, the rate of convergence does not depend on the degree of spatial grid refinement. Author

N93-26079*# New Mexico State Univ., Las Cruces. Dept. of Chemical Engineering.
MODELING OF THE WSTF FRICTIONAL HEATING APPARATUS IN HIGH PRESSURE SYSTEMS Final Report **c25**
Christopher T. Skowlund *In* NASA. Johnson Space Center, National Aeronautics and Space Administration (NASA)/American Society for Engineering Education (ASEE) Summer Faculty Fellowship Program, 1992, Volume 2 Dec. 1992 p 13 (For primary document see N93-26070 09-99)
(Grant NGT-44-005-803)
Avail: CASI HC A03/MF A02

In order to develop a computer program able to model the frictional heating of metals in high pressure oxygen or nitrogen a number of additions have been made to the frictional heating model originally developed for tests in low pressure helium. These additions include: (1) a physical property package for the gases to account for departures from the ideal gas state; (2) two methods for spatial discretization (finite differences with quadratic interpolation or orthogonal collocation on finite elements) which substantially reduce the computer time required to solve the transient heat balance; (3) more efficient programs for the integration of the ordinary differential equations resulting from the discretization of the partial differential equations; and (4) two methods for determining the best-fit parameters via minimization of the mean square error (either a direct search multivariable simplex method or a modified Levenburg-Marquardt algorithm). The resulting computer program has been shown to be accurate, efficient and robust for determining the heat flux or friction coefficient vs. time at the interface of the stationary and rotating samples. Author

N93-26080*# Memphis State Univ., TN. Dept. of Electrical Engineering.
SPACELAB, SPACEHAB, AND SPACE STATION FREEDOM PAYLOAD INTERFACE PROJECTS Final Report **c18**
Dean Lance Smith *In* NASA. Johnson Space Center, National Aeronautics and Space Administration (NASA)/American Society for Engineering Education (ASEE) Summer Faculty Fellowship Program, 1992, Volume 2 Dec. 1992 5 p (For primary document see N93-26070 09-99)
(Grant NGT-44-005-803)
Avail: CASI HC A01/MF A02

Contributions were made to several projects. Howard Nguyen was assisted in developing the Space Station RPS (Rack Power Supply). The RPS is a computer controlled power supply that helps test equipment used for experiments before the equipment is installed on Space Station Freedom. Ron Bennett of General Electric Government Services was assisted in the design and analysis of the Standard Interface Rack Controller hardware and software. An analysis was made of the GPIB (General Purpose Interface Bus), looking for any potential problems while transmitting data across the bus, such as the interaction of the bus controller with a data talker and its listeners. An analysis was made of GPIB bus communications in general, including any negative impact the bus may have on transmitting data back to Earth. A study was made of transmitting digital data back to Earth over a video channel. A report was written about the study and a revised version of the report will be submitted for publication. Work was started on the design of a PC/AT compatible circuit board that will combine digital data with a video signal. Another PC/AT compatible circuit board is being designed to recover the digital data from the video signal. A proposal was submitted to support the continued development of the interface boards after the author returns to Memphis State University in the fall. A study was also made of storing circuit board design software and data on the hard disk server of a LAN (Local Area Network) that connects several IBM style PCs. A report was written that makes several recommendations. A preliminary design review was started of the AIVS (Automatic Interface Verification System). The summer was over before any significant contribution could be made to this project. Author

N93-26081*# Cincinnati Univ., OH. Dept. of Aerospace Engineering.
MODEL REDUCTION FOR SPACE STATION FREEDOM Final Report **c18**
Trevor Williams *In* NASA. Johnson Space Center, National Aeronautics and Space Administration (NASA)/American Society for Engineering Education (ASEE) Summer Faculty Fellowship Program, 1992, Volume 2 Dec. 1992 p 15 (For primary document see N93-26070 09-99)
(Grant NGT-44-005-803)
Avail: CASI HC A03/MF A02

Model reduction is an important practical problem in the control of flexible spacecraft, and a considerable amount of work has been carried out on this topic. Two of the best known methods developed are modal truncation and internal balancing. Modal truncation is simple to implement but can give poor results when the structure possesses clustered natural frequencies, as often occurs in practice. Balancing avoids this problem but has the disadvantages of high computational cost, possible numerical sensitivity problems, and no physical interpretation for the resulting balanced 'modes'. The purpose of this work is to examine the performance of the

subsystem balancing technique developed by the investigator when tested on a realistic flexible space structure, in this case a model of the Permanently Manned Configuration (PMC) of Space Station Freedom. This method retains the desirable properties of standard balancing while overcoming the three difficulties listed above. It achieves this by first decomposing the structural model into subsystems of highly correlated modes. Each subsystem is approximately uncorrelated from all others, so balancing them separately and then combining yields comparable results to balancing the entire structure directly. The operation count reduction obtained by the new technique is considerable: a factor of roughly r(exp 2) if the system decomposes into r equal subsystems. Numerical accuracy is also improved significantly, as the matrices being operated on are of reduced dimension, and the modes of the reduced-order model now have a clear physical interpretation; they are, to first order, linear combinations of repeated-frequency modes. Author

N93-26082*# Houston Univ., TX. Dept. of Curriculum and Instruction.
THE ADULT LITERACY EVALUATOR: AN INTELLIGENT COMPUTER-AIDED TRAINING SYSTEM FOR DIAGNOSING ADULT ILLITERATES Final Report **c53**
David B. Yaden, Jr. *In* NASA. Johnson Space Center, National Aeronautics and Space Administration (NASA)/American Society for Engineering Education (ASEE) Summer Faculty Fellowship Program, 1992, Volume 2 Dec. 1992 p 16 (For primary document see N93-26070 09-99)
(Grant NAG9-562)
Avail: CASI HC A03/MF A02

An important part of NASA's mission involves the secondary application of its technologies in the public and private sectors. One current application being developed is The Adult Literacy Evaluator, a simulation-based diagnostic tool designed to assess the operant literacy abilities of adults having difficulties in learning to read and write. Using ICAT system technology in addition to speech recognition, closed-captioned television (CCTV), live video and other state-of-the art graphics and storage capabilities, this project attempts to overcome the negative effects of adult literacy assessment by allowing the client to interact with an intelligent computer system which simulates real-life literacy activities and materials and which measures literacy performance in the actual context of its use. The specific objectives of the project are as follows: (1) To develop a simulation-based diagnostic tool to assess adults' prior knowledge about reading and writing processes in actual contexts of application; (2) to provide a profile of readers' strengths and weaknesses; and (3) to suggest instructional strategies and materials which can be used as a beginning point for remediation. In the first and developmental phase of the project, descriptions of literacy events and environments are being written and functional literacy documents analyzed for their components. Examples of literacy events and situations being considered included interactions with environmental print (e.g., billboards, street signs, commercial marquees, storefront logos, etc.), functional literacy materials (e.g., newspapers, magazines, telephone books, bills, receipts, etc.) and employment related communication (i.e., job descriptions, application forms, technical manuals, memorandums, newsletters, etc.). Each of these situations and materials is being analyzed for its literacy requirements in terms of written display (i.e., knowledge of printed forms and conventions), meaning demands (i.e., comprehension and word knowledge) and social situation. From these descriptions, scripts are being generated which define the interaction between the student, an on-screen guide and the simulated literacy environment. The proposed outcome of the Evaluator is a diagnostic profile which will present broad classifications of literacy behaviors across the major areas of metacognitive abilities, word recognition, vocabulary knowledge, comprehension and writing. From these classifications, suggestions for materials and strategies for instruction with which to begin corrective action will be made. The focus of the Literacy Evaluator will be essentially to provide an expert diagnosis and an interpretation of that assessment which then can be used by a human tutor to further design and individualize a remedial program as needed through the use of an authoring system. Author

N93-26083*# Florida International Univ., Miami. Industrial and Systems Engineering.
THE REUSE OF LOGISTICS CARRIERS FOR THE FIRST LUNAR OUTPOST ALTERNATIVE HABITAT STUDY Final Report **c31**
Carolina Vargas *In* NASA. Johnson Space Center, National Aeronautics and Space Administration (NASA)/American Society for Engineering Education (ASEE) Summer Faculty Fellowship Program, 1992, Volume 2 Dec. 1992 15 p (For primary document see N93-26070 09-99)
(Grant NGT-44-005-803)
Avail: CASI HC A03/MF A02

The Systems Definition Branch deals with preliminary concepts/designs of various projects currently in progress at NASA. One of these projects is called the First Lunar Outpost. The First Lunar Outpost (FLO) is a proposed permanent lunar base to be located on the moon. In order to better understand the Lunar Habitat, a detailed analysis of the lunar environment as well as conceptual studies of the physical living arrangements for the support crew is necessary. The habitat will be inhabited for a period of 45 days followed by a six month dormant period. Requirements for the habitat include radiation protection, a safe haven for occasional solar flare storms, an airlock module and consumables to support a crew of 4 with a schedule of 34 extra vehicular activities. Consumables in order to sustain a crew of four for 45 days ranges from 430 kg of food to only 15 kg for personal hygiene items. These consumables must be brought to the moon with every mission. They are transported on logistics carriers. The logistics carrier must be pressurized in order to successfully transport the consumables. Refrigeration along with other types of thermal control and variation in pressure are defined by the list of necessary consumables. The objective of the proposed work was to collaborate the Habitat Team with their study on Logistic Carriers as possible alternatives for additional habitable volume. Options for possible reuses was also determined. From this analysis, a recommended design is proposed. Author

N93-26326# Lawrence Livermore National Lab., CA.
ENGINEERING: RESEARCH DEVELOPMENT AND TECHNOLOGY Thrust Area Report, FY 1991
Jul. 1992 274 p
(Contract W-7405-eng-48)
(UCRL-53868-91) Avail: CASI HC A12/MF A03

The mission of the Engineering Research, Development, and Technology Program at Lawrence Livermore National Laboratory (LLNL) is to develop technical staff and the technology needed to support current and future LLNL programs. To accomplish this mission, the Engineering Research, Development, and Technology Program has two important goals: (1) to identify key technologies and (2) conduct high quality work to enhance our capabilities in these key technologies. To help focus our efforts, technology thrust areas are identified. The thrust areas are integrated engineering activities and, rather than being based on individual disciplines, they are staffed by personnel from Electronics Engineering, Mechanical Engineering, and other LLNL organizations, as appropriate. This annual report, organized by thrust area, describes activities conducted within the Program for the fiscal year, 1991. Its intent is to provide timely summaries of objectives, theories, methods, and results. Readers desiring more information are encouraged to contact the individual thrust area leaders or authors. Thrust areas include: computational electronics and electromagnetics, computational mechanics, diagnostics and microelectronics, fabrication technology, materials science and engineering, microwave and pulsed power, nondestructive evaluation, remote sensing and imaging, signal engineering, and emerging technologies. Derived from text

N93-26359# Michigan Univ., Ann Arbor. Dept. of Chemical Engineering.
SUMMARY REPORT OF THE DEFENSE SCIENCES RESEARCH COUNCIL SUMMER CONFERENCE
M. J. Sinnott Jul. 1992 270 p Conference held in La Jolla, CA, 6-31 Jul. 1992
(Contract N00014-87-J-1217)
(AD-A261375) Avail: CASI HC A12/MF A03

This technical report contains information on Layered Materials; Advanced Intelligent Processing of Materials; Comments on Workshop on Advanced Intelligent Processing of Materials; Complex Oxide Thin Films; Workshop on Rapid Prototyping (Solid Freeform Fabrication); Computation and Materials; Process Control and Signal Processing in Microelectronics Manufacturing; Multi-Spectral IR Systems; The Future of CMOS; Optical Arrays and Packaging; Workshop on Terabit Memories; Three-Dimensional Patterning and Processing; Optical Interconnect Technology; Head-Mounted Display; Tutorial on Perception and Cognition; On Neutral Holes in Tailored, Layered Sheets; Crosstalk and Error Probability in Counter-Beam Lambda-Multiplexed Digital Holograms; DARPA Supercritical Water Oxidation Project (GA); and DARPA/DSRC Wargaming. DTIC

N93-26380# Air Force Office of Scientific Research, Bolling AFB, Washington, DC.

AFOSR TECHNICAL REPORT SUMMARIES Quarterly Report, Oct. - Dec. 1992

Debra L. Tyrrell Dec. 1992 170 p

(AD-A261551; AFOSR-TR-93-0051) Avail: CASI HC A08/MF A02

The AFOSR Technical Report Summaries are published quarterly of each calendar year. They consist of a brief summary of each AFOSR technical report received in the Technical Information Division and submitted to the Defense Technical Information Center for that quarter. DTIC

Typical Subject Index Listing

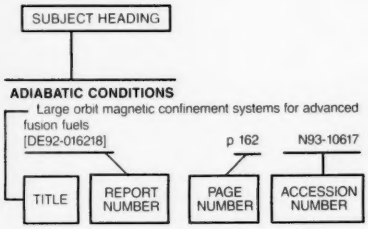

The subject heading is a key to the subject content of the document. Titles, report numbers, and accession numbers of pertinent documents are provided under each subject heading. When the title is insufficiently descriptive of the document content, a title extension has been added, separated from the title by three hyphens. The report number helps to indicate the type of document cited (e.g., NASA report, NASA translation, NASA contractor report). The accession number is the number by which the document abstracts are arranged in this journal and by which the document is sold or requested. The page number helps you locate the the citation in the abstract section. The titles, with title extensions if present, are arranged under each subject heading in ascending accession number order. The subject headings have been selected from the latest revision of the *NASA Thesaurus*.

A

ABERRATION
Optimizing the fine lock performance of the Hubble Space Telescope fine guidance sensors
p 2604 N93-24723
Miniature Optical Wide-Angle-Lens Startracker (Mini-OWLS) p 2606 N93-24728

ABORT TRAJECTORIES
External tank aerothermal design criteria verification
| NASA-CR-192514 | p 2618 N93-26055

ABRASION RESISTANCE
Optical and scratch resistant properties of diamondlike carbon films deposited with single and dual ion beams
p 2658 N93-25564

ABRASIVES
Ultrasonic polishing p 2670 N93-25580
Duct protection coating concept development and test. Appendix D, volume 1: Test specimen fabrication, conditioning, and testing documentation
| AD-A261005 | p 2656 N93-25940

ABSORBERS
The design of a modular sound absorber for very low frequencies
| BBC-RD-1992/10 | p 2673 N93-25170
A modular wideband sound absorber
| BBC-RD-1992/11 | p 2673 N93-25171

ABSORPTION
Optical and scratch resistant properties of diamondlike carbon films deposited with single and dual ion beams
p 2658 N93-25564

ABSORPTION SPECTRA
Theoretical calculations on the electron absorption spectra of selected Polycyclic Aromatic Hydrocarbons (PAH) and derivatives
| NASA-CR-192762 | p 2892 N93-25200
Tomographic analysis of sight infrared spectra of low pressure flames p 2628 N93-26030
Loss of temporal coherence of laser light propagated through simulated coastal waters
| AD-A261303 | p 2715 N93-26296

ABSORPTION SPECTROSCOPY
Fast diagnostics of laser ablation used for pulsed laser deposition
| DE93-005155 | p 2713 N93-25508
Microwave absorption measurements and interference: Effects for a liquid fuel between 2.5 and 18 GHz
| AD-A260607 | p 2675 N93-25635

ABSORPTIVITY
Simultaneous determination of gain parameters in steady state lasers
| DE93-007389 | p 2713 N93-25381

ABSTRACTS
Selected translated abstracts of Russian-language climate-change publications: 1. Surface energy budget
| DE93-003189 | p 2760 N93-24952
Digest of Russian Space Life Sciences, issue 33
| NASA-CR-3922(39) | p 2792 N93-25195
Bibliography on propulsion airframe integration technologies for high-speed civil transport applications, 1980-1991
| NASA-TM-105602 | p 2573 N93-26136
Planetary Biology and Microbial Ecology: Molecular Ecology and the Global Nitrogen cycle
| NASA-CR-4497 | p 2803 N93-26157
European tri-service advanced materials workshop on compressive strength in rigid-rod polymers
| AD-A261517 | p 2658 N93-26576

ACCELERATED LIFE TESTS
Step stress testing of receiver/transmitter units
| AD-A261286 | p 2730 N93-26279

ACCELERATION (PHYSICS)
Tsien's method for generating non-Keplerian trajectories. Part 2: The question of thrust to orbit a sphere and the restricted three-body problem
p 2603 N93-24718
Visual processing of object velocity and acceleration
| AD-A261048 | p 2800 N93-25778

ACCELERATION TOLERANCE
Step stress testing of receiver/transmitter units
| AD-A261286 | p 2730 N93-26279

ACCELEROMETERS
Monolithic quartz vibrating beam accelerometer
p 2711 N93-25011
Apparatus for determining the attitude of a vehicle
| AD-D015667 | p 2710 N93-26092

ACCEPTABILITY
The effects of video compression on acceptability of images for monitoring life sciences' experiments
p 2805 N93-25930

ACCESS CONTROL
Interfacing a high performance disk array file server to a Gigabit LAN
| NASA-CR-192898 | p 2816 N93-25458

ACCESS TIME
The design and implementation of a read prediction buffer
| AD-A260902 | p 2806 N93-25934

ACCIDENT PREVENTION
Handbook of chemical hazard analysis procedures
| PB93-158756 | p 2766 N93-26315

ACCIDENTS
A comparison of the WIND System atmospheric models and MATS data
| DE93-002687 | p 2760 N93-24673
The evaluation of technical models used for major-accident hazard installations. Report to Commission of the European Communities Directorate General 12
| CUED/A-AERO/TR-19 | p 2668 N93-25238
A review of civil aviation propeller-to-person accidents: 1980-1989
| AD-A260695 | p 2583 N93-25896
HERO resistant semiconductor bridge igniter
p 2627 N93-26024

ACCRETION DISKS
Line formation and the Poynting-Robertson effect in accretion discs p 2847 N93-25355
Diskoseismology: Probing relativistic accretion disks
p 2894 N93-25622

ACCUMULATORS
Nozzle diffuser for use with an open test section of a wind tunnel
| NASA-CASE-LAR-14424-1-SB | p 2598 N93-25996

ACCURACY
The accuracy of SYLT- and RNS-based time scales at MTI and SNT during 1990-1991 p 2835 N93-25006
Classifying multispectral data by neural networks
p 2825 N93-25976
Guidelines for evaluating and expressing the uncertainty of NIST measurements results
| PB93-159465 | p 2830 N93-26318

ACETATES
Rheology of YBa2Cu3O(7-x) precursors
| DE93-007285 | p 2863 N93-25362

ACHONDRITES
Geochemistry and petrology of primitive achondrite meteorites LEW 88280, MAC 88177, ALHA 81187, EET 84302, and LEW 88663 p 2896 N93-26067

ACOUSTIC ATTENUATION
The design of a modular sound absorber for very low frequencies
| BBC-RD-1992/10 | p 2673 N93-25170
A modular wideband sound absorber
| BBC-RD-1992/11 | p 2673 N93-25171
In-flight evaluation of noise levels and assessment of active noise reduction systems in the Seahawk S-70B-2 helicopter
| AD-A260689 | p 2845 N93-25649

ACOUSTIC COUPLING
Low-frequency room responses. Part 2: Calculation methods and experimental results
| BBC-RD-1992/9-PT-2 | p 2673 N93-25169
On the effect of acoustic coupling on random and harmonic plate vibrations
| NASA-TM-107740 | p 2844 N93-25189

ACOUSTIC DUCTS
The design of a modular sound absorber for very low frequencies
| BBC-RD-1992/10 | p 2673 N93-25170

ACOUSTIC EMISSION
Monitoring damage growth in titanium matrix composites using acoustic emission
| NASA-TM-107742 | p 2634 N93-25072

ACOUSTIC EXCITATION
Initial streamwise vorticity formation in a two-stream mixing layer p 2579 N93-25752

ACOUSTIC MEASUREMENT
Measuring hearing protection device performance using the metrosonics db-3100 sound level analyzer (dosimeter)
| AD-A260852 | p 2801 N93-25787
Rotating rake design for unique measurement of fan-generated spinning acoustic modes
| NASA-TM-105946 | p 2595 N93-26161

ACOUSTIC PROPAGATION
A modular wideband sound absorber
| BBC-RD-1992/11 | p 2673 N93-25171
Computation of broadband mixing noise from turbomachinery
| AD-A261611 | p 2846 N93-26165

ACOUSTIC PROPERTIES
Low-frequency room responses. Part 1: Background and qualitative considerations
| BBC-RD-1992/8-PT-1 | p 2673 N93-25168
Development of a flight instrument package
| AD-A260830 | p 2591 N93-25783
Rotating rake design for unique measurement of fan-generated spinning acoustic modes
| NASA-TM-105946 | p 2595 N93-26161

ACOUSTIC SCATTERING
Proceedings of the 5th International Symposium on Long Range Sound Propagation
| AD-A260666 | p 2845 N93-25643
Computation of broadband mixing noise from turbomachinery
| AD-A261611 | p 2846 N93-26165

ACOUSTIC VELOCITY
Experimental and theoretical studies of dense fluid mixtures
| DE93-006070 | p 2695 N93-24976

Atomizing-gas temperature effect on cryogenic spray dropsize
| NASA-TM-106106 | p 2709 N93-25191
A computational method for the analysis of acoustic radiation from turbofan inlets p 2845 N93-25717
Propagation of finite amplitude sound in a waveguide with a parabolic sound velocity profile
| ARL-TR-92-11 | p 2846 N93-26179
Basic research thermoacoustic heat transport
| AD-A261334 | p 2759 N93-26310

ACOUSTICS
Low-frequency room responses. Part 1: Background and qualitative considerations
| BBC-RD-1992/8-PT-1 | p 2673 N93-25168
JPRS report: Science and technology. Central Eurasia: Physics and mathematics
| JPRS-UPM-92-004 | p 2844 N93-25402
JPRS report: Science and technology. Central Eurasia: Physics and mathematics
| JPRS-UPM-92-003 | p 2844 N93-25403
JPRS report: Science and technology. Central Eurasia: Physics and mathematics
| JPRS-UPM-93-001 | p 2844 N93-25404
Development of a flight instrument package
| AD-A260830 | p 2591 N93-25783
Measurement of droplet vaporization rate enhancement caused by acoustic disturbances p 2626 N93-26015
Experimental investigation of flow turning losses in unstable rocket motors p 2630 N93-26040
Structural acoustics: A general form of reciprocity principles in acoustics
| AD-A261515 | p 2846 N93-26376
Optical fiber for acoustic sensor applications
| AD-A261580 | p 2857 N93-26515

ACQUISITION
Synchronisation, acquisition and tracking for telemetry and data reception p 2614 N93-25000

ACTINIDE SERIES
Reclamation with recovery of radionuclides and toxic metals from contaminated materials, soils, and wastes p 2769 N93-25571

ACTIVATION ANALYSIS
NIST reactor: Summary of activities, July 1991 through September 1992
| PB93-162873 | p 2852 N93-26322

ACTIVATION ENERGY
Modelling of microgravity ignition phenomena p 2664 N93-25465
Asymptotic studies of gravity-driven reacting coating flows and pultrusion processes p 2704 N93-25683
Ir-Zr alloys as diffusion barriers between Cu and Si(100)
| AD-A261919 | p 2652 N93-26197

ACTIVE CONTROL
Spatial simulation of transition in wall-bounded shear flows: Active control and effects of surface roughness p 2701 N93-25483
In-flight evaluation of noise levels and assessment of active noise reduction systems in the Seahawk S-70B-2 helicopter
| AD-A260689 | p 2845 N93-25649
Active control of NITINOL-reinforced structural composites
| AD-A261062 | p 2638 N93-25780
MIT Space Engineering Research Center
| NASA-CR-192879 | p 2821 N93-25833
Using input command pre-shaping to suppress multiple mode vibration p 2732 N93-25834
The MODE family of on-orbit experiments: The Middeck Active Control Experiment (MACE) p 2599 N93-25835
MIT's interferometer CST testbed p 2609 N93-25836
Study of plate-fin heat exchanger and cold plate for the active thermal control system of Space Station p 2619 N93-26064
Active stabilization of aeromechanical systems
| AD-A261366 | p 2595 N93-26335

ACTS
Proceedings of the 16th NASA Propagation Experimenters Meeting (NAPEX 16) and the Advanced Communications Technology Satellite (ACTS) Propagation Studies Miniworkshop
| NASA-CR-192800 | p 2682 N93-26463
Opening remarks p 2682 N93-26464
The ACTS propagation program p 2683 N93-26465
Large scale rainfall diversity and satellite propagation p 2683 N93-26466
OLYMPUS/ACTS scintillation experiment at the Lewis Research Center p 2685 N93-26481
ACTS propagation terminal update p 2685 N93-26484

ACTUATORS
Handbook of actuators and edge alignment sensors
| NASA-CR-193203 | p 2620 N93-25317
Firmware development improves system efficiency p 2807 N93-25606
Tuned circuit electric levitation bearings for microactuators p 2689 N93-25619
Passivity motivated controller design for flexible structures
| AD-A261122 | p 2719 N93-25771
MIT's interferometer CST testbed p 2609 N93-25836
Design of flexible rods with embedded SMA actuators
| AD-A260742 | p 2729 N93-25846
Primary events in olfactory reception
| AD-A260562 | p 2795 N93-25944
Damage detection and mitigation of composite structures using smart materials
| AD-A261121 | p 2639 N93-25945
Deformations of active flexible rods with embedded line actuators
| AD-A261207 | p 2729 N93-25950
Parametric motion control of robotic arms: A biologically based approach using neural networks p 2822 N93-25964
Pneumatic actuator with hydraulic control
| AD-D015652 | p 2719 N93-26244
Structural load control during construction p 2669 N93-26409

ACUITY
Interpupillary and vertex distance effects on field-of-view and acuity with ANVIS
| AD-A261259 | p 2802 N93-26265

ADAPTATION
Adaptive decision support systems: Concepts, characterization, and an application p 2876 N93-25475

ADAPTIVE CONTROL
Data processing and control in a transputer system for remote sensing of the Earth p 2753 N93-24870
Control of complex dynamic systems by neural networks p 2827 N93-25611
Adaptive process control with fuzzy logic and genetic algorithms p 2827 N93-25612
Nonlinear dynamics and attitude control of articulated flexible space structures p 2617 N93-25726
Nonlinear system design: Adaptive feedback linearization with unmodeled dynamics
| AD-A261360 | p 2826 N93-26333
Adaptive control of nonlinear flexible systems
| AD-A261676 | p 2826 N93-26365

ADAPTIVE OPTICS
Handbook of actuators and edge alignment sensors
| NASA-CR-193203 | p 2620 N93-25317
Development of laser guide stars and adaptive optics for large astronomical telescopes
| DE93-007511 | p 2888 N93-25320
Feasibility experiment for sodium-layer laser guide stars at the Lawrence Livermore National Laboratory
| DE93-007115 | p 2715 N93-26503

ADDITIVES
Effect of a metal deactivator fuel additive on fuel deposition in fuel atomizers at high temperature
| AD-A260915 | p 2661 N93-25914

ADHESION
Analysis of pull-tests for determining the effects of ion implantation on the adhesion of iron films to sapphire substrates
| DE93-006732 | p 2725 N93-25373
Effect of water immersion on fiber/matrix adhesion
| AD-A260704 | p 2636 N93-25652
Adhesion and corrosion behavior of Al-Zn and TiN/Ti/TiN coatings on a DU-0.75 wt. percent Ti alloy
| MTL-TR-92-56 | p 2658 N93-26433

ADHESIVES
Process for bonding elastomers to metals
| NASA-CASE-LAR-13645-1 | p 2656 N93-25995

ADIABATIC CONDITIONS
Diabaticity of nuclear motion: Problems and perspectives
| DE93-007252 | p 2847 N93-25148

ADIABATIC EQUATIONS
Diabaticity of nuclear motion: Problems and perspectives
| DE93-007252 | p 2847 N93-25148

ADIABATIC FLOW
Diabaticity of nuclear motion: Problems and perspectives
| DE93-007252 | p 2847 N93-25148

ADJUSTING
Adjustable lossless image compression based on a natural splitting of an image into drawing, shading, and fine-grained components p 2804 N93-25923

ADRIATIC SEA
Algal blooms and gel production in Adriatic Sea observed by remote sensing techniques p 2747 N93-24831

ADSORPTION
Theoretical studies of surface reactions on metals and electronic materials
| DE93-009761 | p 2650 N93-25502
Surface diffusion studies by optical diffraction techniques
| DE93-007707 | p 2853 N93-25550
A numerical simulation of adsorption onto a crystalline surface
| AD-A261079 | p 2866 N93-25781
Prediction of hydrogen entry and permeation in metals and alloys
| AD-A260580 | p 2651 N93-25903
The interaction of HCN/DCN with Si(100)-2x1
| AD-A260837 | p 2645 N93-25920
Structure of sodium 4-(1'-heptylnonyl) benzenesulfonate adsorbed on alumina using H-2 NMR
| AD-A261224 | p 2645 N93-26300
Phosphorus-, nitrogen-, sulfur-, and chlorine-containing molecules on surfaces
| AD-A261265 | p 2657 N93-26303
Halogen adlayers on Ag(111)
| AD-A261792 | p 2850 N93-26443
The surface characterization of a series of hydroxybenzenes on Ag(111): An EELS and TDS study
| DE93-007541 | p 2647 N93-26595

ADVANCED LAUNCH SYSTEM (STS)
Task 5: Architecture sensitivity to STME performance
| MCR-92-5010 | p 2609 N93-26176
Advanced Launch System (ALS) test requirements
| MCR-91-5004 | p 2610 N93-26181

ADVANCED SOLID ROCKET MOTOR (STS)
ASRM design philosophy and modelling challenges p 2627 N93-26022
Determination of burn rate requirements from ASRM performance specifications p 2627 N93-26023

ADVANCED VERY HIGH RESOLUTION RADIOMETER
Correlation between NDVI values derived from NOAA AVHRR HRPT data and ground measurements of precipitation in the EFEDA study area (Spain) p 2738 N93-24780
Determination of environmental dynamics using NOAA satellite data and a water balance model for the Mediterranean landscape p 2741 N93-24794
Demonstration of seasonal changes in the territory of Finland using multitemporal NOAA-AVHRR data p 2742 N93-24801
Application of satellite imageries data to fisheries in Japan p 2745 N93-24822
Assessment and forecasting of crop yield in Niger through NOAA NDVI data p 2750 N93-24851
Interest of complementary data of coarse and high spatial resolution for agro-climatic crop monitoring p 2750 N93-24853
North-central Mexico blue grama rangeland biomass assessment at the end of the rainy season using NOAA-AVHRR-LAC p 2750 N93-24854

AERIAL PHOTOGRAPHY
A method for sequential image analysis of hazard areas p 2743 N93-24810

AERIAL RECONNAISSANCE
Commercial applications multispectral sensor system p 2758 N93-25615

AEROACOUSTICS
Theory for noise of propellers in angular inflow with parametric studies and experimental verification
| NASA-CR-4499 | p 2844 N93-25094
Rotating rake design for unique measurement of fan-generated spinning acoustic modes
| NASA-TM-105946 | p 2595 N93-26161
Computation of broadband mixing noise from turbomachinery
| AD-A261611 | p 2846 N93-26165
A large hemi-anechoic enclosure for community-compatible aeroacoustic testing of aircraft propulsion systems
| NASA-TM-106015 | p 2846 N93-26551

AEROASSIST
Space transfer vehicle concepts and requirements study. Volume 2, book 4: Integrated advanced technology development
| NASA-CR-192528 | p 2611 N93-25512

AEROBES
Utilization of the graded universal testing system to increase the efficiency for assessing aerobic and anaerobic capacity p 2794 N93-26077

AERODYNAMIC BALANCE
An integrated finite-state model for rotor deformation, nonlinear airloads, inflow, and trim p 2588 N93-25538

AERODYNAMIC CHARACTERISTICS
Aerodynamic design and synthesis of the oblique flying wing supersonic transport p 2587 N93-24768
Computational study of the aerodynamics and control by blowing of asymmetric vortical flows over delta wings p 2574 N93-24772
Grid sensitivity for aerodynamic optimization and flow analysis
| NASA-CR-192980 | p 2575 N93-25117
Integrated aerodynamic-structural wing design optimization p 2587 N93-25279

Computation of transonic flow over a porous surface projectile p 2577 N93-25409
Structural and aerodynamic optimization of joined-wing aircraft p 2588 N93-25526
Tangential fuselage blowing on an ogive cylinder p 2578 N93-25545
Structural dynamic analysis of bearingless rotor blade p 2590 N93-25719
Experimental study of the effect of helical grooves on an infinite cylinder
| AD-A260890 | p 2676 N93-25912
Jet-induced ground effects on a parametric flat-plate model in hover
| NASA-TM-104001 | p 2581 N93-26099

AERODYNAMIC COEFFICIENTS
Aerodynamic foundations for use of unsteady aerodynamic effects in flight control p 2576 N93-25274

AERODYNAMIC CONFIGURATIONS
A computational aerodynamic design optimization method using sensitivity analysis p 2589 N93-25552

AERODYNAMIC DRAG
Aerodynamic design and synthesis of the oblique flying wing supersonic transport p 2587 N93-24768
Fundamental studies of droplet interactions in dense sprays
| AD-A261165 | p 2661 N93-25948
Uniform roughness studies
| WL-TR-92-3041 | p 2706 N93-25951
Modified point mass trajectory simulation for base-burn projectiles
| BRL-TR-3321 | p 2609 N93-25985

AERODYNAMIC FORCES
Prediction of forces and moments for hypersonic flight vehicle control effectors
| NASA-CR-193033 | p 2595 N93-24762
Optimal finite-thrust time-bounded direct-ascent interception p 2607 N93-25272
Aerodynamic foundations for use of unsteady aerodynamic effects in flight control p 2576 N93-25274
Helicopter forced response vibration analysis method RTVIB20
| AD-A261809 | p 2597 N93-26260

AERODYNAMIC HEATING
SRB environment evaluation and analysis. Volume 1: Redesigned SRB flight heating evaluation
| NASA-CR-192517 | p 2631 N93-26053

AERODYNAMIC LOADS
General aviation aircraft: Normal acceleration data analysis and collection project
| DOT/FAA/CT-91/20 | p 2586 N93-24739
A feasibility study of using Langley 0.3-m transonic cryogenic tunnel sidewall boundary-layer removal system for heavy gas testing
| NASA-CR-191438 | p 2695 N93-25087
An integrated finite-state model for rotor deformation, nonlinear airloads, inflow, and trim p 2588 N93-25538

AERODYNAMIC NOISE
Far field rotor noise
| AD-A260703 | p 2845 N93-25651

AERODYNAMIC STABILITY
AEW aircraft design
| AD-A261800 | p 2590 N93-26444

AERODYNAMICS
A multimission three-axis stabilized spacecraft flight dynamics ground support system p 2603 N93-24714
Goddard Space Flight Center (GSFC) Flight Dynamics Facility (FDF) calibration of the Upper Atmosphere Research Satellite (UARS) sensors p 2606 N93-24733
Applied aerodynamics: Challenges and expectations
| NASA-TM-103963 | p 2575 N93-25091
Digest of Russian Space Life Sciences, issue 33
| NASA-CR-3922(39) | p 2792 N93-25195
Optimal thrust magnitude on a singular arc in atmospheric flight p 2819 N93-25410
A computational aerodynamic design optimization method using sensitivity analysis p 2589 N93-25552
Numerical simulation of hypersonic aerodynamics and the computational needs for the design of an aerospace plane
| AD-A260681 | p 2580 N93-25894
Radial inflow turbine study
| AD-A260767 | p 2594 N93-25917

AEROELASTICITY
An aeroelastic model structure investigation for a manned real-time rotorcraft simulation p 2574 N93-24756
Application of finite-state inflow to flap-lag-torsion damping in hover p 2587 N93-25486
Aeroelastic response and aeromechanical stability of helicopters with elastically coupled composite rotor blades p 2588 N93-25530
An integrated finite-state model for rotor deformation, nonlinear airloads, inflow, and trim p 2588 N93-25538
Supersonic aeroelastic instability results for a NASP-like wing model
| NASA-TM-107739 | p 2591 N93-26553

AEROMANEUVERING
Space transfer vehicle concepts and requirements study. Volume 2, book 4: Integrated advanced technology development
| NASA-CR-192528 | p 2611 N93-25512

AERONAUTICAL ENGINEERING
JPRS report: Central Eurasia. Aviation and cosmonautics, no. 9, September 1992
| JPRS-UAC-93-003 | p 2574 N93-26325

AERONAUTICS
JPRS report: Central Eurasia. Aviation and cosmonautics, no. 9, September 1992
| JPRS-UAC-93-003 | p 2574 N93-26325

AEROSOLS
An analysis of lift forces on aerosols in a wall bounded turbulent shear flow
| DE93-003362 | p 2695 N93-24963
Measurements of nitric acid, carboxylic acids, and selected aerosol species for the NASA/GTE Pacific Mission - West (PEM-WEST)
| NASA-CR-192976 | p 2763 N93-25287
The role of multiple scattering in twilight zenith sky observations of atmospheric absorbers: Diurnal photochemistry and airmass factors p 2772 N93-25535
Natural and augmented snowfall growth processes and their interactions with the natural and modified aerosol
| PB93-153096 | p 2786 N93-25874
Summary by the cloud and aerosol research group for ASTEX
| AD-A261292 | p 2766 N93-26292

AEROSPACE ENGINEERING
Digest of Russian Space Life Sciences, issue 33
| NASA-CR-3922(39) | p 2792 N93-25195
Former Soviet Republic capabilities in space and science
| DE93-007613 | p 2598 N93-25322
Scientific visualization using the Flow Analysis Software Toolkit (FAST) p 2814 N93-25600
Space life support technology applications to terrestrial environmental problems p 2803 N93-25617
MIT Space Engineering Research Center
| NASA-CR-192879 | p 2821 N93-25833
Space research in Sweden, 1990-1991 p 2888 N93-25887
Aeronautics in NACA and NASA
| NASA-NP-156 | p 2574 N93-26422
AGARD membership, 1993
| AGARD-MEMB-93 | p 2873 N93-26428

AEROSPACE ENVIRONMENTS
Composite materials for the extravehicular mobility unit p 2642 N93-26060
The role of pyridoxine as a countermeasure for in-flight loss of lean body mass p 2796 N93-26068
Electrical and Chemical Interactions at Mars Workshop. Part 2: Appendix
| NASA-CP-10093-PT-2 | p 2897 N93-26392
Space environmental interactions for the space exploration initiative p 2897 N93-26396
EnviroNET p 2886 N93-26398

AEROSPACE INDUSTRY
Applied aerodynamics: Challenges and expectations
| NASA-TM-103963 | p 2575 N93-25091
Development of ASTM standards in support of advanced ceramics development
| DE93-003024 | p 2654 N93-25361
Space business indicators p 2886 N93-26158

AEROSPACE MEDICINE
Digest of Russian Space Life Sciences, issue 33
| NASA-CR-3922(39) | p 2792 N93-25195
The prevalence of artificial lens implants in the civil airman population
| DOT/FAA/AM-92/14 | p 2794 N93-25214
Space biology research development
| NASA-CR-192830 | p 2792 N93-25242
JPRS report: Science and technology. Central Eurasia: Life sciences
| JPRS-ULS-92-022 | p 2795 N93-25407
The application of integrated knowledge-based systems for the Biomedical Risk Assessment Intelligent Network (BRAIN) p 2799 N93-25595
Simulated sustained flight operations and performance. Part 1: Effects of fatigue
| AD-A261012 | p 2801 N93-25859
The use of extended wear contact lenses in the aviation environment: An Army-wide study
| AD-A260938 | p 2795 N93-26218

AEROSPACE PLANES
Trajectory optimization for the National aerospace plane
| NASA-CR-192954 | p 2589 N93-25670
Numerical simulation of hypersonic aerodynamics and the computational needs for the design of an aerospace plane
| AD-A260681 | p 2580 N93-25894
Supersonic aeroelastic instability results for a NASP-like wing model
| NASA-TM-107739 | p 2591 N93-26553

AEROSPACE SAFETY
Contributions of microgravity test results to the design of spacecraft fire safety systems
| NASA-TM-106093 | p 2614 N93-24755
A review of civil aviation propeller-to-person accidents: 1980-1989
| AD-A260695 | p 2583 N93-25896
Nuclear safety policy working group recommendations on nuclear propulsion safety for the space exploration initiative
| NASA-TM-105705 | p 2632 N93-26200
PROAV Cable Warning System (CWS) - U.S. Army aircraft Integration assessment and OCONUS field evaluation
| AD-A261233 | p 2583 N93-26263

AEROSPACE SCIENCES
JPRS report: Science and technology. Japan. 30th National Aerospace Laboratory Conference
| JPRS-JST-93-009 | p 2901 N93-25418
Applied Information Systems Research Program (AISRP). Workshop 2: Meeting Proceedings
| NASA-CR-193096 | p 2877 N93-25792
The Space and Earth Science Data Compression Workshop
| NASA-CP-3183 | p 2803 N93-25921
OSSA Information Systems Program
| NASA-TM-108774 | p 2882 N93-26231
Aeronautics in NACA and NASA
| NASA-NP-156 | p 2574 N93-26422
Space Science Laboratory Publications and Presentations
| NASA-TM-108402 | p 2884 N93-26562

AEROSPACE SYSTEMS
The Telecommunications and Data Acquisition Report
| NASA-CR-192887 | p 2671 N93-24659
An application of machine learning to the organization of institutional software repositories p 2825 N93-25981
Assured crew return vehicle man-systems integration standards
| NASA-CR-193065 | p 2614 N93-26329

AEROSPACE TECHNOLOGY TRANSFER
JPRS report: Science and technology. Japan. 30th National Aerospace Laboratory Conference
| JPRS-JST-93-009 | p 2901 N93-25418

AEROSPACE VEHICLES
Geometric modeling for computer aided design
| NASA-CR-192891 | p 2808 N93-24750
Contributions of microgravity test results to the design of spacecraft fire safety systems
| NASA-TM-106093 | p 2614 N93-24755
Maneuvering a reentry body via magneto-gasdynamic forces p 2615 N93-25207
Aerospace vehicle model simplification for feedback control p 2596 N93-25292
Characterization of aerospace grade resins and composites through pressurized volumetric dilatometry
| AD-A260794 | p 2639 N93-25918

AEROTHERMODYNAMICS
Development and application of computational aerothermodynamics flowfield computer codes
| NASA-CR-192940 | p 2574 N93-24736
Fuel Injector: Air swirl characterization aerothermal modeling, phase 2, volume 2
| NASA-CR-189193 | p 2592 N93-25106

AGENA ROCKET VEHICLES
Report of the Seasat Failure Review Board p 2619 N93-24693

AGGLOMERATION
Particle size as a factor in agglomeration in slurry fuels p 2625 N93-26013

AGING (MATERIALS)
Control of environmental and clock parameters in Time and Frequency Standards Laboratory p 2835 N93-25007
Study of grain refinement in Al alloy 2519 using backscattering orientation-contrast mode in the scanning electron microscope
| AD-A260886 | p 2651 N93-25632

AGREEMENTS
Energy and Technology Review, August-September 1992
| DE93-005882 | p 2901 N93-24974

AGRICULTURE
The photointerpretation of the area taken over from agriculture by intense urbanization at Villabate (Palermo, Italy) p 2742 N93-24800
Remote sensing applied to agriculture state of the art and new trends p 2745 N93-24818

Toward a satellite based crop information system in Hungary p 2750 N93-24849
Remote sensing of land resource management in agriculture with regard to its influence on the environment p 2750 N93-24850

AGROCLIMATOLOGY
Agroclimatological zonation by AVHRR data for vegetation monitoring p 2741 N93-24795

AH-64 HELICOPTER
Hydrogen-induced stress corrosion cracking susceptibility analysis of pitch links from the AH-64 Apache helicopter
| AD-A260692 | p 2651 N93-25895

AIR
Parameters influencing the hot-spot ignition of aviation fuel/air and ethylene/air mixtures p 2583 N93-24886
Development and use of hydrogen-air torches in an altitude facility
| NASA-TM-106047 | p 2598 N93-26214

AIR BREATHING ENGINES
Screening studies of advanced control concepts for airbreathing engines
| NASA-TM-106042 | p 2592 N93-25079
Turbulence interacting with chemical kinetics in airbreathing combustion of ducted rockets p 2625 N93-26012

AIR COOLING
An evaluation of thermal energy storage options for precooling gas turbine inlet air
| DE93-005980 | p 2758 N93-24975

AIR CURRENTS
A new method for infrared imaging of air currents in and around critical hazard fume hoods
| DE93-003009 | p 2761 N93-24956

AIR DEFENSE
An environmental audit management plan for the Royal Australian Air Force
| AD-A261092 | p 2765 N93-25765

AIR DUCTS
Duct protection coating concept development and test. Appendix D, volume 1: Test specimen fabrication, conditioning, and testing documentation
| AD-A261005 | p 2656 N93-25940

AIR FILTERS
Development and demonstration of a new filter system to control emissions during jet engine testing
| AD-A261203 | p 2766 N93-26243

AIR FLOW
Use of the 1991 ASCOT field study data in a mesoscale model employing a four-dimensional data assimilation technique
| DE93-002683 | p 2769 N93-24672
A new method for infrared imaging of air currents in and around critical hazard fume hoods
| DE93-003009 | p 2761 N93-24956
Uniform roughness studies
| WL-TR-92-3041 | p 2706 N93-25951
Method of measuring cross-flow vortices by use of an array of hot-film sensors
| NASA-CASE-LAR-14824-1-SB | p 2706 N93-26000
Visualization of a Mach 2 reacting flow using Planar Laser-Induced Fluorescence (PLIF) p 2598 N93-26006

AIR INTAKES
An evaluation of thermal energy storage options for precooling gas turbine inlet air
| DE93-005980 | p 2758 N93-24975

AIR JETS
Fuel injector: Air swirl characterization aerothermal modeling, phase 2, volume 1
| NASA-CR-189193 | p 2592 N93-24754
Fuel Injector: Air swirl characterization aerothermal modeling, phase 2, volume 2
| NASA-CR-189193 | p 2592 N93-25106

AIR LAND INTERACTIONS
Surface energy fluxes at Central Florida during the convection and precipitation electrification experiment
| NASA-CR-192826 | p 2769 N93-24945
Effects of Taiwan orography on the motion and structure of typhoons
| AD-A261819 | p 2786 N93-26270

AIR MASSES
The role of multiple scattering in twilight zenith sky observations of atmospheric absorbers: Diurnal photochemistry and airmass factors p 2772 N93-25535

AIR POLLUTION
Atmospheric reactive nitrogen oxides and their relationship with urban and rural ozone formation p 2760 N93-24908
The AFTAC model integration project
| DE93-003334 | p 2761 N93-25122
AQUIS: A PC-based air inventory and permit manager
| DE93-003006 | p 2761 N93-25143
Trends '91: A compendium of data on global change. Highlights
| DE93-003112 | p 2761 N93-25144
A study of mass size distributions and particle deposition velocities in ambient air p 2763 N93-25263
Measurements of nitric acid, carboxylic acids, and selected aerosol species for the NASA/GTE Pacific Mission - West (PEM-WEST)
| NASA-CR-192976 | p 2763 N93-25287
Magnitude and value of electric vehicle emissions reductions for six driving cycles in four US cities with varying air quality problems
| DE93-006417 | p 2660 N93-25298
SIHTI: The research and development program of energy and environmental technology
| DE93-769925 | p 2763 N93-25360
National air pollutant emission estimates
| PB93-157808 | p 2765 N93-25850
Using terrestrial plants in biomonitoring
| PB93-158780 | p 2766 N93-26316
Particulate emissions from gas turbine engines
| AD-A261374 | p 2595 N93-26339
Improved selective catalytic NOx control technology for compressor station reciprocating engines
| PB93-158566 | p 2768 N93-26529
Oxides of nitrogen emissions from turbulent hydrocarbon/air jet diffusion flames, phase 2
| PB93-152478 | p 2768 N93-26533

AIR PURIFICATION
Integrated oxygen recovery system
| NASA-CR-192982 | p 2801 N93-26088

AIR QUALITY
An assessment of alternatives and technologies for replacing ozone-depleting substances at DOE facilities
| DE93-002862 | p 2760 N93-24675
AQUIS: A PC-based air inventory and permit manager
| DE93-003006 | p 2761 N93-25143
Measurements of nitric acid, carboxylic acids, and selected aerosol species for the NASA/GTE Pacific Mission - West (PEM-WEST)
| NASA-CR-192976 | p 2763 N93-25287
Magnitude and value of electric vehicle emissions reductions for six driving cycles in four US cities with varying air quality problems
| DE93-006417 | p 2660 N93-25298
Space life support technology applications to terrestrial environmental problems p 2803 N93-25617
Emerging technologies in ethanol production
| PB93-157014 | p 2661 N93-25818
Membrane technology: A search for membranes for submarine atmosphere control
| AD-A260581 | p 2801 N93-25904
Cost-effectiveness analysis of TxDOT CNG fleet conversion, volume 2
| PB93-159432 | p 2720 N93-26534
Cost-effectiveness analysis of TxDOT CNG fleet conversion, volume 1
| PB93-165603 | p 2720 N93-26585

AIR TO AIR MISSILES
ASTROS-ID: Software for system identification using mathematical programming
| AD-A260867 | p 2810 N93-25627

AIR TRAFFIC
The ATC evaluation of the prototype Airport Surveillance Radar Wind Shear Processor (ASR-WSP) at Orlando International Airport
| DOT/FAA/CT-TN92/48 | p 2673 N93-25210
Design of an air traffic computer simulation system to support investigation of civil tiltrotor aircraft operations
| NASA-CR-192920 | p 2585 N93-26052

AIR TRAFFIC CONTROL
The ATC evaluation of the prototype Airport Surveillance Radar Wind Shear Processor (ASR-WSP) at Orlando International Airport
| DOT/FAA/CT-TN92/48 | p 2673 N93-25210
A longitudinal examination of applicants to the air traffic control supervisory identification and development program
| DOT/FAA/AM-92/16 | p 2796 N93-25213
Runway Visual Range (RVR) Operational Test and Evaluation (OT&E) integration and OT&E operational test report
| DOT/FAA/CT-TN93/37 | p 2584 N93-25243
Design of a cooperative problem-solving system for enroute flight planning: An empirical study of its use by airline dispatchers
| NASA-CR-192709 | p 2585 N93-25330
Design of an air traffic computer simulation system to support investigation of civil tiltrotor aircraft operations
| NASA-CR-192920 | p 2585 N93-26052
Piloted simulation of an air-ground profile negotiation process in a time-based Air Traffic Control environment
| NASA-TM-107748 | p 2585 N93-26087
Contribution of personality to the prediction of success in initial air traffic control specialist training
| DOT/FAA/AM-93/4 | p 2797 N93-26138
The Data Multiplexing Network (DMN) phase 3 Extended Distance Data Cable (EDDC) test and evaluation
| DOT/FAA/CT-TN93/11 | p 2680 N93-26160

AIR TRAFFIC CONTROLLERS (PERSONNEL)
A longitudinal examination of applicants to the air traffic control supervisory identification and development program
| DOT/FAA/AM-92/16 | p 2796 N93-25213
Conversion of the CTA, Inc., en route operations concepts database into a formal sentence outline job task taxonomy
| AD-A261410 | p 2586 N93-26447

AIR WATER INTERACTIONS
Simulation and prediction of tropical SST with a coupled ocean-atmosphere model p 2789 N93-25469
Errors caused by incompatible wind and buoyancy forcing in the ocean general circulation models
| AD-A260894 | p 2789 N93-25657
An investigation into the causative mechanisms for explosive cyclone development over the Atlantic
| AD-A261831 | p 2786 N93-26273
An observational study of the local and remote response of the equatorial Pacific to westerly wind events during the 1991-92 El Nino
| AD-A261777 | p 2787 N93-26286
Experiments on the physics of turbulent mixing in stably stratified ocean layers
| AD-A261312 | p 2790 N93-26298
Wind-driven coastal generation of annual mesoscale eddy activity in the California current
| AD-A261355 | p 2790 N93-26331
Coastal ocean processes: A science prospectus
| AD-A261702 | p 2790 N93-26384

AIRBORNE EQUIPMENT
Use of airborne imaging spectrometry to the definition of optimised specifications for land applications with future spaceborne imaging spectrometers p 2738 N93-24776
Comparison of the electrical charging and discharging environments of multiple aircraft-borne electric-field measurement systems p 2583 N93-24887
Commercial applications multispectral sensor system p 2758 N93-25615

AIRBORNE/SPACEBORNE COMPUTERS
Orbit determination and orbit control for the Earth Observing System (EOS) AM spacecraft p 2601 N93-24705
Computationally efficient algorithms for real-time attitude estimation p 2602 N93-24709
Upper Atmosphere Research Satellite (UARS) onboard attitude determination using a Kalman filter p 2606 N93-24732
Walsh function generator for the Electronically Scanned Thinned Array Radiometer (ESTAR) instrument
| NASA-TM-4449 | p 2689 N93-25618

AIRCRAFT ACCIDENT INVESTIGATION
Aircraft accident report: Tomy International, Inc., d/b/a Scenic Air Tours flight 22, Beech Model E18S, N342E in-flight collision with terrain, Mount Haleakala, Maui, Hawaii, 22 April 1992
| PB93-910401 | p 2583 N93-25827
The use of multiple models in case-based diagnosis p 2823 N93-25969

AIRCRAFT ACCIDENTS
Aircraft accident report: Tomy International, Inc., d/b/a Scenic Air Tours flight 22, Beech Model E18S, N342E in-flight collision with terrain, Mount Haleakala, Maui, Hawaii, 22 April 1992
| PB93-910401 | p 2583 N93-25827
A review of civil aviation propeller-to-person accidents: 1980-1989
| AD-A260695 | p 2583 N93-25896
The use of multiple models in case-based diagnosis p 2823 N93-25969

AIRCRAFT ANTENNAS
Experimental study of the effect of helical grooves on an infinite cylinder
| AD-A260890 | p 2676 N93-25912

AIRCRAFT APPROACH SPACING
Visual approach data collection at St. Louis Lambert Field (STL)
| DOT/FAA/CT-TN93/2 | p 2584 N93-24948
The dependent converging instrument approach procedure: An analysis of its safety and applicability
| DOE/FAA/RD-93/6 | p 2585 N93-25456

AIRCRAFT COMPARTMENTS
In-flight evaluation of noise levels and assessment of active noise reduction systems in the Seahawk S-70B-2 helicopter
| AD-A260689 | p 2845 N93-25649

AIRCRAFT CONFIGURATIONS
Structural and aerodynamic optimization of joined-wing aircraft p 2588 N93-25526
An approach to configuration design synthesis of subsonic transport aircraft using artificial intelligence techniques p 2589 N93-25692

AIRCRAFT CONSTRUCTION MATERIALS
Numerical modelling of induced effects of lightning strike on an all composite helicopter p 2583 N93-24879
Comparison of the damage for various types of fibre reinforced composites due to different lightning test standards (MIL-STD-1757A, German military VG-standard 96903) p 2642 N93-24891
Fatigue in single crystal nickel superalloys
| AD-A261742 | p 2652 N93-26282

AIRCRAFT CONTROL
Prediction of forces and moments for hypersonic flight vehicle control effectors
| NASA-CR-193033 | p 2595 N93-24762
Robust nonlinear control of vectored thrust aircraft
| NASA-CR-192727 | p 2596 N93-25199
Control and optimization of aircraft trajectories p 2596 N93-25543

AIRCRAFT DESIGN
Aerodynamic design and synthesis of the oblique flying wing supersonic transport p 2587 N93-24768
A procedure for defining lightning risk to air vehicles p 2583 N93-24885
Screening studies of advanced control concepts for airbreathing engines
| NASA-TM-106042 | p 2592 N93-25079
Grid sensitivity for aerodynamic optimization and flow analysis
| NASA-CR-192980 | p 2575 N93-25117
Integrated aerodynamic-structural wing design optimization p 2587 N93-25279
Structural and aerodynamic optimization of joined-wing aircraft p 2588 N93-25526
An approach to configuration design synthesis of subsonic transport aircraft using artificial intelligence techniques p 2589 N93-25692
ASTOVL combat aircraft design synthesis and optimization p 2589 N93-25704
Techniques for designing rotorcraft control systems
| NASA-CR-192960 | p 2597 N93-26046
AEW aircraft design
| AD-A261800 | p 2590 N93-26444

AIRCRAFT ENGINES
Aerodynamic design and synthesis of the oblique flying wing supersonic transport p 2587 N93-24768
Screening studies of advanced control concepts for airbreathing engines
| NASA-TM-106042 | p 2592 N93-25079
Simulation of aircraft gas turbine engine p 2594 N93-25751
Development and demonstration of a new filter system to control emissions during jet engine testing
| AD-A261203 | p 2766 N93-26243
Particulate emissions from gas turbine engines
| AD-A261374 | p 2595 N93-26339
A large hemi-anechoic enclosure for community-compatible aeroacoustic testing of aircraft propulsion systems
| NASA-TM-106015 | p 2846 N93-26551

AIRCRAFT EQUIPMENT
Alternative equipment test procedures for simultaneous current injection on multiple cable bundles p 2693 N93-24903
Special tooling disposition for aircraft entering post production support
| AD-A261614 | p 2573 N93-26168

AIRCRAFT FUEL SYSTEMS
Military standardization handbook: Aircraft refueling handbook
| AD-A261755 | p 2662 N93-26600

AIRCRAFT GUIDANCE
Discrete range clustering using Monte Carlo methods
| NASA-TM-104004 | p 2584 N93-24914
Control and optimization of aircraft trajectories p 2596 N93-25543
Image-based ranging and guidance for rotorcraft
| NASA-CR-177608 | p 2586 N93-26549

AIRCRAFT HAZARDS
The 1992 International Aerospace and Ground Conference on Lightning and Static Electricity: Addendum
| DOT/FAA/CT-92/20-ADD-1 | p 2777 N93-24875
Lightning phenomenology bases for full threat return stroke occurrence following extended leader sweep at flight altitudes p 2780 N93-24895
Applications of stress envelope concepts to aircraft EMP and lightning survivability p 2584 N93-24898
PROAV Cable Warning System (CWS) - U.S. Army aircraft Integration assessment and OCONUS field evaluation
| AD-A261233 | p 2583 N93-26263

AIRCRAFT INSTRUMENTS
Comparison of the electrical charging and discharging environments of multiple aircraft-borne electric-field measurement systems p 2583 N93-24887

AIRCRAFT LANDING
Visual approach data collection at St. Louis Lambert Field (STL)
| DOT/FAA/CT-TN93/2 | p 2584 N93-24948

AIRCRAFT MAINTENANCE
Reliability assessment at airline inspection facilities. Volume 1: A generic protocol for inspection reliability experiments
| DOT/FAA/CT-92/12-VOL-1 | p 2582 N93-25110
Investigation of corrosion in aluminum/adhesive lap-splices using pulse-echo ultrasonic techniques
| DE93-008074 | p 2721 N93-25518
Human Factors in Aviation Maintenance, phase 2
| DOT/FAA/AM-93/5 | p 2802 N93-26089
An analysis of the reliability and maintainability of the Jian 6 and Jian 7 aircraft and ways to improve them
| AD-A261060 | p 2574 N93-26238

AIRCRAFT MODELS
A computational approach to predicting the extent of arc root damage in CFC panels p 2642 N93-24890
Fabrication of composite propfan blades for a cruise missile wind tunnel model
| NASA-TM-105270 | p 2730 N93-26202

AIRCRAFT NOISE
Rotating rake design for unique measurement of fan-generated spinning acoustic modes
| NASA-TM-105946 | p 2595 N93-26161

AIRCRAFT PERFORMANCE
Applications of stress envelope concepts to aircraft EMP and lightning survivability p 2584 N93-24898
Experimental performance of a ventral nozzle with pitch and yaw vectoring capability for SSTOVL aircraft
| NASA-TM-106054 | p 2592 N93-25129
Generic hypersonic vehicle performance model
| NASA-CR-192953 | p 2587 N93-25162
Jet-induced ground effects on a parametric flat-plate model in hover
| NASA-TM-104001 | p 2581 N93-26099

AIRCRAFT PILOTS
Simulated sustained flight operations and performance. Part 1: Effects of fatigue
| AD-A261012 | p 2801 N93-25859
Performance-based testing and success in Naval advanced flight training
| AD-A260838 | p 2590 N93-25933
The use of extended wear contact lenses in the aviation environment: An Army-wide study
| AD-A260938 | p 2795 N93-26218

AIRCRAFT PRODUCTION
Special tooling disposition for aircraft entering post production support
| AD-A261614 | p 2573 N93-26168

AIRCRAFT RELIABILITY
An analysis of the reliability and maintainability of the Jian 6 and Jian 7 aircraft and ways to improve them
| AD-A261060 | p 2574 N93-26238

AIRCRAFT SAFETY
The 1992 International Aerospace and Ground Conference on Lightning and Static Electricity: Addendum
| DOT/FAA/CT-92/20-ADD-1 | p 2777 N93-24875
Zoning of aircraft: A review of the definitions p 2583 N93-24880
A procedure for defining lightning risk to air vehicles p 2583 N93-24885
Parameters influencing the hot-spot ignition of aviation fuel/air and ethylene/air mixtures p 2583 N93-24886
Lightning phenomenology bases for full threat return stroke occurrence following extended leader sweep at flight altitudes p 2780 N93-24895
Narrow-body aircraft water spray optimization study
| DOT/FAA/CT-TN93/3 | p 2582 N93-25224
A review of civil aviation propeller-to-person accidents: 1980-1989
| AD-A260695 | p 2583 N93-25896
Military standardization handbook: Aircraft refueling handbook
| AD-A261755 | p 2662 N93-26600

AIRCRAFT STRUCTURES
Crashworthiness of composite seats for civil aircraft p 2582 N93-24773
Numerical modelling of induced effects of lightning strike on an all composite helicopter p 2583 N93-24879
A procedure for defining lightning risk to air vehicles p 2583 N93-24885
Comparison of the damage for various types of fibre reinforced composites due to different lightning test standards (MIL-STD-1757A, German military VG-standard 96903) p 2642 N93-24891
Grid sensitivity for aerodynamic optimization and flow analysis
| NASA-CR-192980 | p 2575 N93-25117
Design and analysis of curved composite components for rotorcraft fuselage frames p 2589 N93-25701
Hydrogen-induced stress corrosion cracking susceptibility analysis of pitch links from the AH-64 Apache helicopter
| AD-A260692 | p 2651 N93-25895
Thermally induced stresses in a composite exposed to fire
| AD-A261714 | p 2641 N93-26371

AIRCRAFT SURVIVABILITY
Applications of stress envelope concepts to aircraft EMP and lightning survivability p 2584 N93-24898

AIRFOILS
Aerodynamic foundations for use of unsteady aerodynamic effects in flight control p 2576 N93-25274
Flow control of low heat load turbine airfoils
| AD-A260941 | p 2595 N93-26219
Fatigue in single crystal nickel superalloys
| AD-A261742 | p 2652 N93-26282

AIRFRAMES
A computational approach to predicting the extent of arc root damage in CFC panels p 2642 N93-24890
Zoning of aircraft by electric field modelling p 2583 N93-24894
Helicopter forced response vibration analysis method RTVIB20
| AD-A261809 | p 2597 N93-26260
AEW aircraft design
| AD-A261800 | p 2590 N93-26444

AIRGLOW
Gravity waves from O2 airglow p 2772 N93-25547
Further analysis of ECOM-721 data
| AD-A260863 | p 2774 N93-25790

AIRLINE OPERATIONS
Design concepts for the development of cooperative problem-solving systems
| NASA-CR-192708 | p 2585 N93-25261
Expert system for UNIX system reliability and availability enhancement p 2723 N93-25588

AIRPORTS
Visual approach data collection at St. Louis Lambert Field (STL)
| DOT/FAA/CT-TN93/2 | p 2584 N93-24948
The dependent converging instrument approach procedure: An analysis of its safety and applicability
| DOE/FAA/RD-93/6 | p 2585 N93-25456
Expedient repair of structural facilities
| AD-A260727 | p 2598 N93-25656

AIRSPEED
General aviation aircraft: Normal acceleration data analysis and collection project
| DOT/FAA/CT-91/20 | p 2586 N93-24739

ALBEDO
Small satellites and RPA's in global-change research
| AD-A260762 | p 2765 N93-25837

ALCOHOLS
Design of a high activity and selectivity alcohol catalyst
| DE93-008101 | p 2659 N93-25111
Design of a high activity and selectivity alcohol catalyst
| DE93-008103 | p 2659 N93-25112
Catalytic conversion of light alkanes
| DE93-009646 | p 2644 N93-25499

ALGAE
NORSMAP 1989: Norwegian remote sensing spectrometry for mapping and monitoring of algal blooms and pollution p 2746 N93-24824
Algal blooms and gel production in Adriatic Sea observed by remote sensing techniques p 2747 N93-24831

ALGEBRA
A three-dimensional algebraic grid generation scheme for gas turbine combustors with inclined slots
| NASA-CR-191095 | p 2694 N93-24759
Tables for the thermophysical properties of ethane
| PB93-160786 | p 2646 N93-26319

ALGORITHMS
A (72, 36; 15) box code p 2671 N93-24663
The analysis of convolutional codes via the extended Smith algorithm p 2671 N93-24664
Image coding by way of wavelets p 2671 N93-24665
Failure monitoring in dynamic systems: Model construction without fault training data p 2672 N93-24666
Star tracker operation in a high density proton field p 2600 N93-24699
A ground track control algorithm for the Topographic Mapping Laser Altimeter (TMLA) p 2602 N93-24707
Computationally efficient algorithms for real-time attitude estimation p 2602 N93-24709
Polar decomposition for attitude determination from vector observations p 2602 N93-24711
Rate determination from vector observations p 2603 N93-24713
Analysis of the Command and Control Segment (CCS) attitude estimation algorithm p 2604 N93-24722

Attitude determination using vector observations: A fast optimal matrix algorithm p 2606 N93-24731
Using neural networks and Dyna algorithm for integrated planning, reacting and learning in systems
|NASA-CR-193018| p 2817 N93-24743
Optimal message log reclamation for independent checkpointing
|NASA-CR-192886| p 2815 N93-24749
Geometric modeling for computer aided design
|NASA-CR-192891| p 2808 N93-24750
Satellite altimetry p 2734 N93-24930
Algorithms for optimal redundancy allocation
|DE93-005709| p 2827 N93-24973
How can millisecond pulsars improve the long term stability of atomic time scales? p 2832 N93-24985
Improved PI-network measurement of all quartz crystal parameters by appropriate modelling of the test fixture p 2833 N93-24995
An experimental health monitoring unit for GPS and GLONASS p 2586 N93-25018
A contribution to the great Riemann solver debate
|NASA-CR-191409| p 2575 N93-25083
Two neural network algorithms for designing optimal terminal controllers with open final time
|NASA-CR-177599| p 2817 N93-25137
A low-complexity and high performance concatenated coding scheme for high-speed satellite communications
|NASA-CR-192715| p 2673 N93-25198
Use of fuzzy relational information retrieval technique for generating control strategies in resolution-based automated reasoning p 2874 N93-25258
Concurrency control in real-time database systems p 2874 N93-25271
Toward a parallel recursive spectral bisection mapping tool
|DE93-006632| p 2816 N93-25414
Wavelet transform-vector quantization compression of supercomputer ocean model simulation output
|DE93-005453| p 2876 N93-25448
A software development approach for parallel processing systems integrating object-oriented and functional paradigms p 2816 N93-25481
Design and analysis of algorithms for processing queries in database systems p 2876 N93-25482
Parallelizing the spectral transform method: A comparison of alternative parallel algorithms
|DE93-008664| p 2816 N93-25521
Performance studies of cache consistency and concurrency control algorithms in a distributed client/server DBMS architecture p 2876 N93-25554
Tree classification software p 2814 N93-25591
Automatic detection of seizures with applications p 2796 N93-25592
A software package for neural network applications development p 2827 N93-25610
Control of complex dynamic systems by neural networks p 2827 N93-25611
Adaptive process control with fuzzy logic and genetic algorithms p 2827 N93-25612
Setting values for TDWR/LLWAS 3 integration parameters
|AD-A260740| p 2783 N93-25645
Efficient generation of synthetic terrain imagery for automatic target recognition
|AD-A260705| p 2756 N93-25653
Developing and improving numerical algorithms to study intrinsically correlated electron systems
|AD-A261214| p 2849 N93-25734
Multilevel techniques in large scale computation
|AD-A261082| p 2828 N93-25762
Effect of cytoskeletal reagents on stretch activated ion channels
|AD-A261089| p 2793 N93-25764
High performance compression of science data p 2881 N93-25811
Applications of parallel and vector algorithms in nonlinear structural dynamics using the finite element method
|AD-A260716| p 2811 N93-25845
Probability and statistics applied to the theory of algorithms
|AD-A261019| p 2830 N93-25863
A Hierarchical Target Extraction, Recognition, and Tracking (HiTert) system
|AD-A260567| p 2854 N93-25898
The rapid solution of the Laplace equation on regions with fractal boundaries
|AD-A260585| p 2828 N93-25905
Subband coding for image data archiving p 2803 N93-25922
Methods of evaluating the effects of coding on SAR data p 2804 N93-25926
Adaptive laser link reconfiguration using constraint propagation p 2823 N93-25967
A vision architecture for the extravehicular activity retriever p 2827 N93-26071
Complexity of connectionist and constraint-satisfaction networks
|AD-A261617| p 2817 N93-26169
Algorithms for the analysis of penetration by shaped charge jets
|UCRL-LR-109887| p 2730 N93-26178
New algorithms for the detection and elimination of sine waves and other narrow-band signals in the presence of broadband signals and noise
|AD-A261811| p 2681 N93-26261
The effects of cloud inhomogeneities upon radiative fluxes, and the supply of a cloud truth validation dataset
|NASA-CR-191711| p 2787 N93-26492

ALIPHATIC HYDROCARBONS
An assessment of alternatives and technologies for replacing ozone-depleting substances at DOE facilities
|DE93-002862| p 2760 N93-24675

ALKALI METAL COMPOUNDS
Transition metal chelate-fulleride compounds: Electrocrystallization of semiconducting (Ru(bpy)s)(C60)2
|AD-A261549| p 2869 N93-26577

ALKALI METALS
The physics of spin polarized gases
|AD-A261396| p 2850 N93-26288
Electrochemical and spectroscopic studies of molten halides
|AD-A261687| p 2646 N93-26439

ALKANES
Catalytic conversion of light alkanes
|DE93-009646| p 2644 N93-25499

ALKENES
Energetic materials from cubane
|AD-A261317| p 2662 N93-26308

ALKYL COMPOUNDS
Energetic materials from cubane
|AD-A261317| p 2662 N93-26308

ALLOYING
Mechanical alloying processing and application to development of structural materials
|AD-A261251| p 2652 N93-26264

ALLOYS
Ir-Zr alloys as diffusion barriers between Cu and Si(100)
|AD-A261919| p 2652 N93-26197

ALTERNATING CURRENT
Structure and properties of a-C: N films prepared by pulsed excimer laser deposition
|DE93-007908| p 2654 N93-25372

ALTERNATING DIRECTION IMPLICIT METHODS
Implicit multigrid solution of the compressible Navier-Stokes equations with application to distributed parallel processing p 2702 N93-25546

ALTERNATIVES
An assessment of alternatives and technologies for replacing ozone-depleting substances at DOE facilities
|DE93-002862| p 2760 N93-24675

ALTITUDE
What is the relationship between altitude and weight in a model rocket? p 2603 N93-24715

ALUMINIDES
Hot corrosion of the B2 nickel aluminides
|NASA-CR-191082| p 2649 N93-25128
High temperature fracture toughness of Ni3Al alloy IC-396M
|DE93-008564| p 2650 N93-25492
Micromechanics of fatigue
|AD-A260577| p 2729 N93-25901
Thermal coatings for titanium-aluminum alloys
|NASA-TM-107760| p 2651 N93-26048

ALUMINUM
Laser initiated corrosion pits on aluminum p 2650 N93-25464
Investigation of corrosion in aluminum/adhesive lap-splices using pulse-echo ultrasonic techniques
|DE93-008074| p 2721 N93-25518

ALUMINUM ALLOYS
Ignition and combustion of lunar propellants
|NASA-CR-192814| p 2659 N93-24745
Hot corrosion of the B2 nickel aluminides
|NASA-CR-191082| p 2649 N93-25128
Dynamic deformations and analysis of a metal matrix composite p 2634 N93-25234
Processing and mechanical properties of laminated metal composites of Al/Al-25 vol. percent SiC and ultrahigh carbon steel/brass
|DE93-007504| p 2635 N93-25383
Laser welding of selected aerospace alloys p 2718 N93-25435
Chromate-free corrosion resistant talc coatings for aluminum alloys
|DE93-005370| p 2655 N93-25446
High temperature fracture toughness of Ni3Al alloy IC-396M
|DE93-008564| p 2650 N93-25492
Study of grain refinement in Al alloy 2519 using backscattering orientation-contrast mode in the scanning electron microscope
|AD-A260886| p 2651 N93-25632
The corrosion of metal matrix composites p 2638 N93-25723
In situ surface studies of conversion coatings for steel and aluminum
|AD-A261016| p 2655 N93-25861

ALUMINUM ARSENIDES
Short-period superlattice materials for heterojunction bipolar transistors
|AD-A260701| p 2866 N93-25897

ALUMINUM BORON COMPOSITES
Finite element micromechanics modeling of inelastic deformation of unidirectionally fiber-reinforced composites p 2637 N93-25680

ALUMINUM COMPOUNDS
Comparison of energy trapping resonators and filters using the AT cut of quartz, berlinite and gallium phosphate p 2836 N93-25013
Crystal growth of berlinite: Methods for growing longer crystals and improving the quality p 2838 N93-25025
Controlled dissolution of a piezoelectric material berlinite (AlPO4) p 2840 N93-25043

ALUMINUM GALLIUM ARSENIDES
Noise measurements in single-mode GaAlAs diode lasers p 2716 N93-25067
An inverted AlGaAs/GaAs patterned-Ge tunnel junction cascade concentrator solar cell
|DE93-000073| p 2759 N93-25102
Analysis of transient photoluminescence measurements on GaAs and AlGaAs double heterostructures
|AD-A261154| p 2867 N93-25947

ALUMINUM OXIDES
Dynamic deformations and analysis of a metal matrix composite p 2634 N93-25234
Transformation plasticity and fracture behavior of ceria-TZP/alumina composites p 2638 N93-25760
Structure of sodium 4-(1'-heptylnonyl) benzenesulfonate adsorbed on alumina using H-2 NMR
|AD-A261224| p 2645 N93-26300

AMBIENT TEMPERATURE
An evaluation of thermal energy storage options for precooling gas turbine inlet air
|DE93-005980| p 2758 N93-24975
Control of environmental and clock parameters in Time and Frequency Standards Laboratory p 2835 N93-25007

AMBIPOLAR DIFFUSION
A study of vibrationally excited N2(+) ions in the daytime thermosphere p 2770 N93-25179

AMINES
Polyimides with improved compression moldability
|NASA-CASE-LAR-14457-1| p 2656 N93-25997

AMMONIUM CHLORIDES
Flow and morphological conditions associated with the directional solidification of aqueous ammonium chloride
|DE93-008886| p 2644 N93-25495

AMMONIUM COMPOUNDS
Physical and chemical processes governing the CO2 laser-induced deflagration of ammonium dinitramide (ADN) p 2629 N93-26037
Thermal decomposition and stabilization of ammonium dinitramide p 2630 N93-26038

AMMONIUM NITRATES
Thermal decomposition and stabilization of ammonium dinitramide p 2630 N93-26038

AMMUNITION
Minutes of the Twenty-Fifth Explosives Safety Seminar, volume 4
|AD-A261116| p 2660 N93-25769

AMORPHOUS MATERIALS
Structure and properties of a-C: N films prepared by pulsed excimer laser deposition
|DE93-007908| p 2654 N93-25372
The nature of the glass transition and its determination by thermal analysis
|DE93-006746| p 2654 N93-25374
Optical and scratch resistant properties of diamondlike carbon films deposited with single and dual ion beams p 2658 N93-25564
Ir-Zr alloys as diffusion barriers between Cu and Si(100)
|AD-A261919| p 2652 N93-26197
Research support for the Laboratory for Lightwave Technology
|AD-A261488| p 2856 N93-26343

AMORPHOUS SILICON
Fundamental studies of defect generation in amorphous silicon alloys grown by remote plasma-enhanced chemical-vapor deposition (Remote PECVD)
|DE92-010560| p 2862 N93-24953
Research on stable, high-efficiency amorphous silicon multijunction modules
|DE93-000072| p 2862 N93-25163

AMPLIFICATION
Scalar gain interpretation of large order filters p 2606 N93-24729
Stability margins for multilinear interval systems by way of phase conditions: A unified approach
|NASA-CR-192893| p 2819 N93-25226
AMPLIFIERS
Investigation of a background suppression transimpedance amplifier for photovoltaic detectors
|AD-A261828| p 2691 N93-26272
AMPLITUDE MODULATION
Advanced optical fiber communication systems
|AD-A261802| p 2856 N93-26256
Properties of readings of periodically correlated random processes
|AD-A261225| p 2686 N93-26573
ANALOG DATA
Digitization of analog data from in-flight lightning strikes p 2778 N93-24884
ANALOG TO DIGITAL CONVERTERS
Digitization of analog data from in-flight lightning strikes p 2778 N93-24884
Evaluation of a vibration diagnostic system for the detection of spur gear pitting failures
|NASA-TM-106103| p 2718 N93-25672
ANALOGIES
Strongly transitive fuzzy relations: A more adequate way to describe similarity
|NASA-CR-192951| p 2820 N93-25425
The use of multiple models in case-based diagnosis p 2823 N93-25969
ANALYSIS OF VARIANCE
ANOVA method to estimate vegetation indices sensitivity assessing nitrogen fertilizing influence on spectral reflectance coefficients p 2739 N93-24782
ANATOMY
Proceedings of Workshop 1: The Human Brainmap Database
|AD-A260720| p 2796 N93-25654
Anatomy and physiology of plant conductive systems
|PB93-156032| p 2793 N93-25877
ANECHOIC CHAMBERS
A large hemi-anechoic enclosure for community-compatible aeroacoustic testing of aircraft propulsion systems
|NASA-TM-106015| p 2846 N93-26551
ANGLE OF ATTACK
The transient development of vortices over delta wings p 2576 N93-25269
Computation of transonic flow over a porous surface projectile p 2577 N93-25409
Conical Euler analysis and active roll suppression for unsteady vortical flows about rolling delta wings
|NASA-TP-3259| p 2581 N93-26134
ANGULAR DISTRIBUTION
Resonance electron scattering by O2 monolayers on graphites: Reinterpreted
|AD-A261851| p 2850 N93-26287
ANGULAR MOMENTUM
Testing of the on-board attitude determination and control algorithms for SAMPEX p 2600 N93-24698
Liquid and solid ion plasmas
|AD-A261888| p 2862 N93-26528
ANGULAR VELOCITY
A nanoradian differential VLBI tracking demonstration p 2677 N93-26108
Deep-space navigation with differenced data types. Part 3: An expanded information content and sensitivity analysis p 2614 N93-26109
ANHYDRIDES
Polyimides with improved compression moldability
|NASA-CASE-LAR-14457-1| p 2656 N93-25997
Polyimides containing the cyclobutene-3,4-dione moiety
|NASA-CASE-LAR-14753-1| p 2656 N93-25999
ANIMATION
Combining particles and waves for fluid animation p 2699 N93-25348
ANIONS
Penning detachment: A new frontier
|AD-A261447| p 2850 N93-26346
ANISOTROPIC MEDIA
Methods of determining loads and fiber orientations in anisotropic non-crystalline materials using energy flux deviation
|NASA-CASE-LAR-14399-1| p 2729 N93-26102
ANISOTROPY
Anisotropic etching of silicon in KOH solutions p 2647 N93-25037
Surface diffusion studies by optical diffraction techniques
|DE93-007707| p 2853 N93-25550
Electrorheological fluids: A structural approach to mechanisms
|AD-A260563| p 2645 N93-25879
Oblique MHD cosmic-ray modified shocks: Two-fluid numerical simulations
|NASA-CR-192930| p 2900 N93-26132
Phase-field models for anisotropic interfaces
|PB93-164564| p 2646 N93-26323
Microstrip antennas on/in anisotropic material layers
|AD-A261700| p 2681 N93-26383
ANNEALING
The interaction of HCN/DCN with Si(100)-2x1
|AD-A260837| p 2645 N93-25920
Temperature dependence of radiation damage and its annealing in silicon detectors
|DE93-003854| p 2869 N93-26494
ANNUAL VARIATIONS
Demonstration of seasonal changes in the territory of Finland using multitemporal NOAA-AVHRR data p 2742 N93-24801
Role of the ocean in climate changes p 2732 N93-24918
Operational seasonal and interannual predictions of ocean conditions p 2733 N93-24921
Indian Ocean analyses p 2733 N93-24925
Satellite monitoring of the global ocean surface during 1987-1989 p 2734 N93-24926
Control of environmental and clock parameters in Time and Frequency Standards Laboratory p 2835 N93-25007
Summary information and data sets for NREL's Solar Radiation Research Laboratory, 1981 - 1991
|DE93-000052| p 2898 N93-25101
Numerical simulation of the seasonal and interannual variability of the tropical Atlantic Ocean circulation during the 1980's p 2789 N93-25445
Observed annual and interannual variations in tropospheric water vapor p 2782 N93-25549
On the vertical structure of seasonal, interannual and intraseasonal flows p 2782 N93-25557
ANNULAR FLOW
Annular flow enhanced two-phase evaporative heat exchanger for space-based systems p 2700 N93-25478
ANODES
Anode power deposition in coaxial MPD thrusters p 2623 N93-25665
ANODIC COATINGS
Adhesion and corrosion behavior of Al-Zn and TiN/Ti/TiN coatings on a DU-0.75 wt. percent Ti alloy
|MTL-TR-92-56| p 2658 N93-26433
ANODIZING
Laser welding of selected aerospace alloys p 2718 N93-25435
ANOMALIES
The initial flight anomalies of Skylab 1 p 2619 N93-24692
Anomalous event diagnosis for environmental satellite systems p 2619 N93-25971
ANTARCTIC REGIONS
Passive microwave remote sensing of snow-covered floating ice during spring conditions in the Arctic and Antarctic
|ISBN-0-315-70444-6| p 2754 N93-25422
JARE data reports. No. 171 (upper atmosphere physics 9). Data, Syowa and Asuka Stations, 1989 p 2774 N93-25889
ANTENNA ARRAYS
A functional description of the Buffered Telemetry Demodulator (BTD) p 2614 N93-24667
Ka-band feed arrays for spacecraft reflector antennas with limited scan capability: An overview p 2680 N93-26128
Microstrip antennas on/in anisotropic material layers
|AD-A261700| p 2681 N93-26383
ANTENNA DESIGN
DSS-13 26-meter antenna upgraded radiometer system p 2679 N93-26122
Sequential design of a linear quadratic controller for the Deep Space Network antennas p 2679 N93-26123
Ka-band feed arrays for spacecraft reflector antennas with limited scan capability: An overview p 2680 N93-26128
ANTENNA RADIATION PATTERNS
Influence due to antenna pattern change in brightness temperature estimation for a space-based microwave radiometer p 2753 N93-24868
ANTENNAS
Design of the reduced LQG compensator for the DSS-13 antenna p 2672 N93-24669
ANTHROPOMETRY
Assessing patterns of change in anthropometric dimensions: Secular trends of US Army females, 1946-1988
|AD-A260869| p 2800 N93-25628
Anthropometry of the foot and lower leg of U.S. Army soldiers: Fort Jackson, SC
|AD-A261405| p 2802 N93-26404
ANTIBODIES
Measuring the metastatic potential of cancer cells p 2794 N93-25566
Primary events in olfactory reception
|AD-A260562| p 2795 N93-25944
Pseudomonas screening assay
|NASA-CASE-NPO-17653-1-CU| p 2793 N93-25994
ANTIFERROMAGNETISM
Molecular/polymeric magnetism
|DE93-008635| p 2847 N93-25114
Magnetic excitations in antiferromagnetically coupled superlattices: Fe/Mo and Fe/Cr
|DE93-007894| p 2863 N93-25369
Magnetic multilayer strain gage
|AD-D015672| p 2710 N93-26141
ANTIFRICTION BEARINGS
Radial spline assembly for antifriction bearings
|NASA-CASE-MFS-28629-1| p 2719 N93-26001
ANTIOXIDANTS
Development of a method to determine the autoxidation of turbine fuels
|AD-A260578| p 2661 N93-25902
ANTIREFLECTION COATINGS
Correlation of damage threshold and surface geometry of nodular defects in HR coatings as determined by in-situ atomic force microscopy
|DE93-007509| p 2654 N93-25384
Modeling of electric-field enhancement at nodular defects in dielectric mirror coatings
|DE93-007513| p 2857 N93-26593
APERTURES
Feasibility study of a Ka-/Ka-band dichroic plate with stepped rectangular apertures p 2671 N93-24660
Optimizing the fine lock performance of the Hubble Space Telescope fine guidance sensors p 2604 N93-24723
A fiber optic probe for the detection of cataracts p 2796 N93-25593
Correcting x ray spectra obtained from the AXAF VETA-I mirror calibration for pileup, continuum, background and deadtime p 2854 N93-26187
APPLICATIONS OF MATHEMATICS
Current research activities: Applied and numerical mathematics, fluid mechanics, experiments in transition and turbulence and aerodynamics, and computer science
|NASA-CR-191408| p 2803 N93-25084
Strongly transitive fuzzy relations: A more adequate way to describe similarity
|NASA-CR-192951| p 2820 N93-25425
APPLICATIONS PROGRAMS (COMPUTERS)
Orbit determination and orbit control for the Earth Observing System (EOS) AM spacecraft p 2601 N93-24705
A ground track control algorithm for the Topographic Mapping Laser Altimeter (TMLA) p 2602 N93-24707
Geometric modeling for computer aided design
|NASA-CR-192891| p 2808 N93-24750
A computational approach to predicting the extent of arc root damage in CFC panels p 2642 N93-24890
OCEAN-PC and a distributed network for ocean data p 2734 N93-24928
Use of the Environmental Resource Management and Analysis System at the Fernald Environmental Management Project
|DE93-002943| p 2760 N93-24955
EXCHANGE
|DE93-007227| p 2808 N93-24962
PCG: A software package for the iterative solution of linear systems on scalar, vector and parallel computers
|DE93-007366| p 2809 N93-25315
A software package for neural network applications development p 2827 N93-25610
Experimenter's laboratory for visualized interactive science p 2879 N93-25802
A Spatial Analysis and Modeling System (SAMS) for environment management p 2881 N93-25813
A distributed analysis and visualization system for model and observational data p 2881 N93-25814
DSD Technology: A detonation reactive Huygens code
|LA-12235-MS| p 2706 N93-25987
Techniques for designing rotorcraft control systems
|NASA-CR-192960| p 2597 N93-26046
EnviroNET p 2886 N93-26398
Department of Defense technical architecture framework for information management. Volume 2: Architecture guidance and design concepts, version 1.1
|AD-A261912| p 2884 N93-26532
Directory of US Government software for mainframes and microcomputers, 1993
|PB93-111565| p 2807 N93-26569
APPROACH
Visual approach data collection at St. Louis Lambert Field (STL)
|DOT/FAA/CT-TN93/2| p 2584 N93-24948

APPROACH CONTROL
The dependent converging instrument approach procedure: An analysis of its safety and applicability
| DOE/FAA/RD-93/6 | p 2585 N93-25456
Control of complex dynamic systems by neural networks p 2827 N93-25611
APPROXIMATION
Estimation of coefficients in a rational function from observed values
| AD-A261126 | p 2828 N93-25773
Approximate analysis on strain rate effects and behavior of stress and strain fields at the crack tip in Mode 2 in metallic materials, appendix no. 1
| AD-A260836 | p 2728 N93-25785
Monte Carlo approach to the approximation of invariant measures
| PB93-159069 | p 2830 N93-26317
AQUEOUS SOLUTIONS
Novel approaches to the construction of miniaturized analytical instrumentation
| NASA-CR-191988 | p 2709 N93-25345
AQUIFERS
Aquifer thermal energy (heat and chill) storage
| DE93-006446 | p 2759 N93-25183
ARC DISCHARGES
Conversion of light hydrocarbon gases to metal carbides for production of liquid fuels and chemicals
| DE93-009707 | p 2644 N93-25500
Investigations of the transient behavior of the cathode fall region in planar and hollow cathodes
| AD-A261636 | p 2691 N93-26171
ARCHAEOLOGY
Archaeological, historical and geoelectrical data as ground truth for Landsat TM imagery application to coastal plain evolution studies p 2742 N93-24799
ARCHITECTURE (COMPUTERS)
Data processing and control in a transputer system for remote sensing of the Earth p 2753 N93-24870
A comparison using APPL and PVM for a parallel implementation of an unstructured grid generation program
| NASA-CR-191425 | p 2808 N93-25073
RAMA: A file system for massively parallel computers
| NASA-CR-192906 | p 2815 N93-25297
Interfacing a high performance disk array file server to a Gigabit LAN
| NASA-CR-192898 | p 2816 N93-25458
Real-time construction of three-dimensional occupancy maps
| DE93-001645 | p 2756 N93-25505
Performance studies of cache consistency and concurrency control algorithms in a distributed client/server DBMS architecture p 2876 N93-25554
Splash 2 p 2814 N93-25575
A novel method for characterization of superconductors: Physical measurements and modeling of thin films p 2871 N93-25584
Data systems dynamic simulator p 2814 N93-25602
Construction of a connectionist network supercomputer
| AD-A260929 | p 2820 N93-25648
Very high-speed arithmetic processors (The Gauss Machine)
| AD-A260693 | p 2806 N93-25650
Integrated Development Support Environment (IDSE)
| AD-A261088 | p 2877 N93-25763
An SPW software simulation model of a dispersive fading multipath narrowband HF channel
| AD-A261101 | p 2675 N93-25767
Planetary data analysis and display system: A version of PC-McIDAS p 2880 N93-25806
Multi-layer holographic bifurcative neural network system for real-time adaptive EOS data analysis p 2880 N93-25807
Computation and learning in neural networks with binary weights
| AD-A261182 | p 2821 N93-25821
Intelligent access to multiple relational database systems
| AD-A261198 | p 2881 N93-25824
Information requirements analyses for transatmospheric vehicles
| AD-A261189 | p 2590 N93-25949
Strategic information planning: Framework for designing and developing system architectures
| GAO/IMTEC-92-51 | p 2882 N93-26097
National Launch System. Task 4: System architecture options analysis
| MCR-92-5011 | p 2609 N93-26098
An OSI architecture for the Deep Space Network p 2679 N93-26121
Deep Space Network information system architecture study p 2679 N93-26126
Source-level debugging of automatically parallelized programs
| AD-A261520 | p 2813 N93-26378
Department of Defense technical architecture framework for information management. Volume 2: Architecture guidance and design concepts, version 1.1
| AD-A261912 | p 2884 N93-26532
ARCS
Optimal thrust magnitude on a singular arc in atmospheric flight p 2819 N93-25410
ARCTIC OCEAN
Radar backscatter measurements from Arctic sea ice during the fall freeze-up
| NASA-CR-193100 | p 2790 N93-26050
ARCTIC REGIONS
Passive microwave remote sensing of snow-covered floating ice during spring conditions in the Arctic and Antarctic
| ISBN-0-315-70444-6 | p 2754 N93-25422
Radar backscatter measurements from Arctic sea ice during the fall freeze-up
| NASA-CR-193100 | p 2790 N93-26050
A climatology of polar low occurrences in the Nordic Seas and an examination of katabatic winds as a triggering mechanism
| AD-A261719 | p 2786 N93-26245
ARGON PLASMA
Particle simulation for 10.6 micron picosecond laser-induced breakdown in gases p 2712 N93-25280
ARITHMETIC
Very high-speed arithmetic processors (The Gauss Machine)
| AD-A260693 | p 2806 N93-25650
ARITHMETIC AND LOGIC UNITS
Very high-speed arithmetic processors (The Gauss Machine)
| AD-A260693 | p 2806 N93-25650
ARMED FORCES (FOREIGN)
An environmental audit management plan for the Royal Australian Air Force
| AD-A261092 | p 2765 N93-25765
ARMED FORCES (UNITED STATES)
Assessing patterns of change in anthropometric dimensions: Secular trends of US Army females, 1946-1988
| AD-A260869 | p 2800 N93-25628
Aircraft electrical and environmental systems, AFSCs 452x5, 454x5, and 454x6
| AD-A261213 | p 2590 N93-25733
United States Army space experiment 601
| AD-A261460 | p 2798 N93-26353
ARMOR
Algorithms for the analysis of penetration by shaped charge jets
| UCRL-LR-109887 | p 2730 N93-26178
ARRAYS
Splash 2 p 2814 N93-25575
Walsh function generator for the Electronically Scanned Thinned Array Radiometer (ESTAR) instrument
| NASA-TM-4449 | p 2689 N93-25618
Method of measuring cross-flow vortices by use of an array of hot-film sensors
| NASA-CASE-LAR-14824-1-SB | p 2706 N93-26000
ARTIFICIAL INTELLIGENCE
Weather forecasting expert system study
| NASA-CR-192929 | p 2777 N93-24747
An expert system shell for inferring vegetation characteristics: Inrerface for the addition of techniques (Task H)
| NASA-CR-192897 | p 2754 N93-25154
Optimization of knowledge-based systems and expert system building tools
| NASA-CR-192763 | p 2874 N93-25288
Radiation-hardened control system
| DE93-007248 | p 2688 N93-25377
Real-time construction and rendering of three-dimensional occupancy maps
| DE93-007818 | p 2756 N93-25516
An approach to configuration design synthesis of subsonic transport aircraft using artificial intelligence techniques p 2589 N93-25692
System of Experts for Intelligent Data Management (SEIDAM) p 2879 N93-25800
Development of an expert data reduction assistant p 2880 N93-25808
Intelligent access to multiple relational database systems
| AD-A261198 | p 2881 N93-25824
Center for intelligent control systems
| AD-A260995 | p 2821 N93-25853
The 1993 Goddard Conference on Space Applications of Artificial Intelligence
| NASA-CP-3200 | p 2822 N93-25961
Using AI/expert system technology to automate planning and replanning for the HST servicing missions p 2822 N93-25962
Adaptive laser link reconfiguration using constraint propagation p 2823 N93-25967
An architecture for object-oriented intelligent control of power systems in space p 2823 N93-25968
An autonomous satellite architecture integrating deliberative reasoning and behavioural intelligence p 2823 N93-25970
Visualizing the semantic content of large text databases using text maps p 2826 N93-25982
The StarView intelligent query mechanism p 2826 N93-25984
NASA Center for Intelligent Robotic Systems for Space Exploration
| NASA-CR-193208 | p 2826 N93-25986
Using modular neural networks with local representations to control dynamic systems
| AD-A261597 | p 2826 N93-26162
Complexity of connectionist and constraint-satisfaction networks
| AD-A261617 | p 2817 N93-26169
Real-time value-driven monitoring and repair
| AD-A260959 | p 2811 N93-26221
Neural basis of motion perception
| AD-A261452 | p 2798 N93-26349
Design Knowledge Management System (DKMS) Beta Test Report
| AD-A261453 | p 2883 N93-26350
IDEF6: A design rationale capture method concept paper
| AD-A261594 | p 2884 N93-26523
ARTIFICIAL SATELLITES
Tsien's method for generating non-Keplerian trajectories. Part 2: The question of thrust to orbit a sphere and the restricted three-body problem p 2603 N93-24718
Mars: The dynamics of orbiting satellites and gravity model development p 2896 N93-25439
Orbital parameter estimation using an extended Kalman filter
| AD-A260618 | p 2608 N93-25636
Small satellites and RPA's in global-change research
| AD-A260762 | p 2765 N93-25837
Space research in Sweden, 1990-1991 p 2888 N93-25887
A Biphase Shift Keying (BPSK), direct sequence, spread spectrum modem for Petite Amateur Navy Satellite (PANSAT)
| AD-A261301 | p 2618 N93-26295
Trellis coded CPFSK
| AD-A261788 | p 2682 N93-26441
ASCENT TRAJECTORIES
Optimal finite-thrust time-bounded direct-ascent interception p 2607 N93-25272
ASIA
A geological and geophysical information system for Eurasia
| AD-A261789 | p 2883 N93-26442
ASSAYING
Pseudomonas screening assay
| NASA-CASE-NPO-17653-1-CU | p 2793 N93-25994
ASSEMBLING
A virtual environment for manufacturing systems
| AD-A260813 | p 2810 N93-25699
ASSESSMENTS
An introductory guide to uncertainty analysis in environmental and health risk assessment
| DE93-002873 | p 2760 N93-24676
The application of integrated knowledge-based systems for the Biomedical Risk Assessment Intelligent Network (BRAIN) p 2799 N93-25595
ASSIMILATION
Use of the 1991 ASCOT field study data in a mesoscale model employing a four-dimensional data assimilation technique
| DE93-002683 | p 2769 N93-24672
ASTROGRAPHY
Geometric distortion analysis of a wide-field astrograph p 2621 N93-26111
ASTROMETRY
The Telecommunications and Data Acquisition Report
| NASA-CR-192804 | p 2676 N93-26105
ASTRONAUTICS
JPRS report: Central Eurasia. Aviation and cosmonautics, no. 9, September 1992
| JPRS-UAC-93-003 | p 2574 N93-26325
ASTRONAUTS
Space Nuclear Thermal Propulsion Test Facilities Subpanel
| NASA-TM-105708 | p 2622 N93-25105
Vascular uptake of rehydration fluids in hypohydrated men at rest and exercise
| NASA-TM-103942 | p 2795 N93-26133
ASTRONOMICAL CATALOGS
30 Doradus in the Large Magellanic Cloud: The stellar content and initial mass function p 2894 N93-25559
Cape Photographic Durchmusterung, volume 1
| NASA-RP-1300-VOL-1 | p 2890 N93-26002

Cape Photographic Durchmusterung, volume 2
| NASA-RP-1300-VOL-2 | p 2890 N93-26003
Cape Photographic Durchmusterung, volume 3
| NASA-RP-1300-VOL-3 | p 2890 N93-26004
Hubble Space Telescope: The archived exposures catalog, version 2.0
| NASA-CR-192896 | p 2883 N93-26423

ASTRONOMICAL MODELS
Observations and models of shock structures in Herbig-Haro objects p 2891 N93-24770
Numerical modeling of barred spiral galaxies p 2893 N93-25537

ASTRONOMICAL PHOTOMETRY
Observations and models of shock structures in Herbig-Haro objects p 2891 N93-24770

ASTRONOMICAL SPECTROSCOPY
Observations and models of shock structures in Herbig-Haro objects p 2891 N93-24770

ASTRONOMY
Development of a tool-set for simultaneous, multi-site observations of astronomical objects p 2878 N93-25795
High-performance compression of astronomical images p 2805 N93-25931

ASTROPHYSICS
Propagation of radiation in astrophysical media: Gravitational lenses and astrophysical masers p 2892 N93-24949
Correlative studies of astrophysical sources of very high and ultra high energy gamma-rays
| NASA-CR-192781 | p 2888 N93-25172
Multivariate statistical analysis software technologies for astrophysical research involving large data bases p 2878 N93-25796
VIEWCACHE: An incremental pointer-based access method for autonomous interoperable databases p 2880 N93-25809

ASYMPTOTIC GIANT BRANCH STARS
A superconducting tunnel junction receiver for submillimeter astronomy, and analysis of observations of post-AGB star molecular envelopes p 2889 N93-25440
Radial velocity measurements of carbon stars p 2895 N93-25713

ASYMPTOTIC METHODS
Asymptotic studies of gravity-driven reacting coating flows and pultrusion processes p 2704 N93-25683
Nonlinear system design: Adaptive feedback linearization with unmodeled dynamics
| AD-A261360 | p 2826 N93-26333

ASYMPTOTIC PROPERTIES
Control of nonlinear systems under input constraints with applications to flight control p 2596 N93-25353
Boundedness and asymptotics of the generalized theodorus iteration
| AD-A261427 | p 2829 N93-26452

ASYMPTOTIC SERIES
Asymptotic derivation of the simplified P(sub N) equations
| DE93-007342 | p 2828 N93-25151
Modelling of microgravity ignition phenomena p 2664 N93-25465
Phase-field models for anisotropic interfaces
| PB93-164564 | p 2646 N93-26323

ATLANTIC OCEAN
The JGOFS North Atlantic Bloom Experiment: An overview p 2735 N93-24934
Numerical simulation of the seasonal and interannual variability of the tropical Atlantic Ocean circulation during the 1980's p 2789 N93-25445
Relations between blue whiting biomass and satellite derived phytoplankton and temperature in the Norwegian Sea
| AD-A261205 | p 2757 N93-25868

ATLANTIS (ORBITER)
STS-44 Space Shuttle mission report
| NASA-TM-108735 | p 2612 N93-25988

ATMOSPHERIC ATTENUATION
Effect-specific analysis of propagation parameters p 2684 N93-26478
The Virginia Tech OLYMPUS propagation experiment p 2685 N93-26479

ATMOSPHERIC BOUNDARY LAYER
An investigation of the role of flux divergence in the turbulent kinetic energy balance of the atmospheric surface layer p 2773 N93-25756
SAR-related stress variability in the marine atmospheric boundary layer
| AD-A261129 | p 2775 N93-25946

ATMOSPHERIC CHEMISTRY
Applications of triggered lightning to space vehicle operations p 2619 N93-24878
Atmospheric reactive nitrogen oxides and their relationship with urban and rural ozone formation p 2760 N93-24908
Selected translated abstracts of Russian-language climate-change publications: 1. Surface energy budget
| DE93-003189 | p 2760 N93-24952
Measurements of nitric acid, carboxylic acids, and selected aerosol species for the NASA/GTE Pacific Mission - West (PEM-WEST)
| NASA-CR-192976 | p 2763 N93-25287
Planetary data analysis and display system: A version of PC-McIDAS p 2880 N93-25806
Electrical and Chemical Interactions at Mars Workshop. Part 2: Appendix
| NASA-CP-10093-PT-2 | p 2897 N93-26392
The Martian lower atmosphere p 2897 N93-26394
Long term modeling of the links between economics, technical progress, and environment: Evolution of approaches and new trends
| DE93-005035 | p 2767 N93-26497

ATMOSPHERIC CIRCULATION
Use of the 1991 ASCOT field study data in a mesoscale model employing a four-dimensional data assimilation technique
| DE93-002683 | p 2769 N93-24672
A comparison of the WIND System atmospheric models and MATS data
| DE93-002687 | p 2760 N93-24673
Empirical wind model for the middle and lower atmosphere. Part 1: Local time average
| NASA-TM-104581 | p 2770 N93-25160
A dynamical theory for hurricane spiral bands p 2782 N93-25352
FORTRAN M as a language for building earth system models
| DE93-007897 | p 2763 N93-25370
Evaluating climate-vegetation interactions at climate model sub-grid scales p 2764 N93-25476
An analysis of mesoscale convective systems observed during the 1992 Tropical Cyclone Motion field experiment
| AD-A260889 | p 2783 N93-25633
Pressure torques and circulation changes in Rocky Mountain lee cyclones p 2783 N93-25724
Tropical cyclone/upper-atmospheric interaction as inferred from satellite total ozone observations p 2784 N93-25741
SAR-related stress variability in the marine atmospheric boundary layer
| AD-A261129 | p 2775 N93-25946
Effects of surface thermal forcing on stratified flow past an isolated obstacle
| PB93-156776 | p 2776 N93-26548
Residual mean meridional circulation in titan's middle atmosphere
| PB93-162931 | p 2898 N93-26571

ATMOSPHERIC COMPOSITION
Trends '91: A compendium of data on global change. Highlights
| DE93-003112 | p 2761 N93-25144
Aspects of the design of a satellite borne infra-red radiometer p 2620 N93-25474
Climate Monitoring and Diagnostics Laboratory
| PB93-156388 | p 2785 N93-25871
Redistribution of trace chemical species by a small convective cloud
| PB93-156164 | p 2765 N93-25873
Heterogeneous photocatalytic oxidation of atmospheric trace contaminants
| NASA-CR-192937 | p 2767 N93-26427
ATMOS: Long term atmospheric measurements for mission to planet Earth
| NASA-TM-108720 | p 2757 N93-26429
Long term modeling of the links between economics, technical progress, and environment: Evolution of approaches and new trends
| DE93-005035 | p 2767 N93-26497

ATMOSPHERIC CORRECTION
Inherent optical properties of lakes as measured by Landsat 5 Thematic Mapper p 2746 N93-24828
Atmospheric correction of Landsat/TM data over mountainous terrain for forestry applications p 2752 N93-24862

ATMOSPHERIC DIFFUSION
Chaos metrics for testing lagrangian particle models
| AD-A261429 | p 2776 N93-26454

ATMOSPHERIC EFFECTS
The atmospheric effects of stratospheric aircraft. Report of the 1992 Models and Measurements Workshop. Volume 1: Workshop objectives and summary
| NASA-RP-1292-VOL-1 | p 2762 N93-25157
The atmospheric effects of stratospheric aircraft. Report of the 1992 Models and Measurements Workshop. Volume 2: Comparisons with global atmospheric measurements
| NASA-RP-1292-VOL-2 | p 2762 N93-25158
The atmospheric effects of stratospheric aircraft. Report of the 1992 Models and Measurements Workshop. Volume 3: Special diagnostic studies
| NASA-RP-1292-VOL-3 | p 2762 N93-25159
Laser propagation through turbulence
| AD-A260712 | p 2714 N93-26217

ATMOSPHERIC ELECTRICITY
The 1992 International Aerospace and Ground Conference on Lightning and Static Electricity: Addendum
| DOT/FAA/CT-92/20-ADD-1 | p 2777 N93-24875
Launch pad lightning protection enhancement by induced streamers p 2609 N93-24876
Applications of triggered lightning to space vehicle operations p 2619 N93-24878
Zoning of aircraft: A review of the definitions p 2583 N93-24880
Observation of radiation from lightning discharges by LPATS p 2779 N93-24888
Lightning characteristics in the north-east part of Japan observed by a magnetic direction-finder network p 2779 N93-24892
Zoning of aircraft by electric field modelling p 2583 N93-24894
Lightning phenomenology bases for full threat return stroke occurrence following extended leader sweep at flight altitudes p 2780 N93-24895
Study of atmospheric electrical events above complex terrain p 2780 N93-24897
Development of models for predicting the triggering of lightning by launch vehicles p 2610 N93-24899
A single-point warning system for thunderstorms and electric fields p 2711 N93-24900
Commercial Precipitation Static (P-static) test equipment p 2711 N93-24901
Comparative performance of lightning air terminals under natural storm conditions p 2781 N93-24902

ATMOSPHERIC GENERAL CIRCULATION MODELS
The effects of sampling frequency on the climate statistics of the ECMWF general circulation model
| DE93-003338 | p 2761 N93-25145
Empirical wind model for the middle and lower atmosphere. Part 1: Local time average
| NASA-TM-104581 | p 2770 N93-25160
CHAMMP
| DE93-007290 | p 2762 N93-25184
Rossby-gravity waves in tropical total ozone data
| NASA-CR-192983 | p 2764 N93-25432
Numerical simulation of the seasonal and interannual variability of the tropical Atlantic Ocean circulation during the 1980's p 2789 N93-25445

ATMOSPHERIC HEATING
Numerical simulation of the seasonal and interannual variability of the tropical Atlantic Ocean circulation during the 1980's p 2789 N93-25445

ATMOSPHERIC IONIZATION
A study of vibrationally excited N2(+) ions in the daytime thermosphere p 2770 N93-25179

ATMOSPHERIC LASERS
Development of laser guide stars and adaptive optics for large astronomical telescopes
| DE93-007511 | p 2888 N93-25320

ATMOSPHERIC MODELS
Use of the 1991 ASCOT field study data in a mesoscale model employing a four-dimensional data assimilation technique
| DE93-002683 | p 2769 N93-24672
A comparison of the WIND System atmospheric models and MATS data
| DE93-002687 | p 2760 N93-24673
The AFTAC model integration project
| DE93-003334 | p 2761 N93-25122
The atmospheric effects of stratospheric aircraft. Report of the 1992 Models and Measurements Workshop. Volume 1: Workshop objectives and summary
| NASA-RP-1292-VOL-1 | p 2762 N93-25157
The atmospheric effects of stratospheric aircraft. Report of the 1992 Models and Measurements Workshop. Volume 2: Comparisons with global atmospheric measurements
| NASA-RP-1292-VOL-2 | p 2762 N93-25158
The atmospheric effects of stratospheric aircraft. Report of the 1992 Models and Measurements Workshop. Volume 3: Special diagnostic studies
| NASA-RP-1292-VOL-3 | p 2762 N93-25159
Applications of wavelet-based compression to multidimensional earth science data
| DE93-007348 | p 2762 N93-25166
Initialization of a modeled convective storm using Doppler radar-derived fields p 2782 N93-25294
Propagation at microwave frequencies in the presence of tropospheric stratified layers p 2674 N93-25340
A dynamical theory for hurricane spiral bands p 2782 N93-25352
FORTRAN M as a language for building earth system models
| DE93-007897 | p 2763 N93-25370
Wavelet transform-vector quantization compression of supercomputer ocean model simulation output
| DE93-005453 | p 2876 N93-25448

Simulation and prediction of tropical SST with a coupled ocean-atmosphere model p 2789 N93-25469
Evaluating climate-vegetation interactions at climate model sub-grid scales p 2764 N93-25476
Parallelizing the spectral transform method: A comparison of alternative parallel algorithms
| DE93-008664 | p 2816 N93-25521
Land surface processes and climate modeling p 2783 N93-25685
Prediction of global cloud cover with a very high resolution global spectral model
| AD-A261047 | p 2785 N93-25777
Construction of an advanced software tool for planetary atmospheric modeling p 2815 N93-25799
A channel simulation processor for the multi-node tactical network simulator
| AD-A261810 | p 2776 N93-26430
Chaos metrics for testing lagrangian particle models
| AD-A261429 | p 2776 N93-26454
The Earth's climate as a dynamical system
| DE93-004666 | p 2767 N93-26496
Long term modeling of the links between economics, technical progress, and environment: Evolution of approaches and new trends
| DE93-005035 | p 2767 N93-26497
Boundary layer coupling between an explosive cyclone and the Gulf Stream during ERICA
| AD-A261577 | p 2787 N93-26513
Residual mean meridional circulation in titan's middle atmosphere
| PB93-162931 | p 2898 N93-26571

ATMOSPHERIC MOISTURE
Surface energy fluxes at Central Florida during the convection and precipitation electrification experiment
| NASA-CR-192826 | p 2769 N93-24945
Observed annual and interannual variations in tropospheric water vapor p 2782 N93-25549
Computation of moisture flux from ocean to atmosphere using a synergy of SSM/I-derived precipitable water and ECMWF analyses p 2774 N93-25757
A proposed study of multiple scattering through clouds up to 1 THz p 2684 N93-26474

ATMOSPHERIC OPTICS
Laser propagation through turbulence
| AD-A260712 | p 2714 N93-26217

ATMOSPHERIC PHYSICS
Applications of triggered lightning to space vehicle operations p 2619 N93-24878
JPRS report: Science and technology. Central Eurasia: Earth sciences
| JPRS-UES-92-003 | p 2737 N93-25398
JPRS report: Science and technology. Central Eurasia: Earth sciences
| JPRS-UES-93-001 | p 2599 N93-25400
JPRS report: Science and technology. Central Eurasia: Earth sciences
| JPRS-UES-92-002 | p 2737 N93-25426
Climate data bases of the People's Republic of China, 1841-1988
| DE93-007907 | p 2764 N93-25517
Planetary data analysis and display system: A version of PC-McIDAS p 2880 N93-25806
JARE data reports. No. 171 (upper atmosphere physics 9). Data, Syowa and Asuka Stations, 1989 p 2774 N93-25889

ATMOSPHERIC PRESSURE
A systematic satellite approach for estimating central pressures of mid-latitude oceanic storms
| NOAA-TR-NESDIS-63 | p 2781 N93-25220
The pressure modulation system in the Improved Stratospheric and Mesospheric Sounder p 2773 N93-25739
Tornado: An engineering-oriented perspective
| PB93-148435 | p 2788 N93-26584

ATMOSPHERIC RADIATION
WCRP surface radiation budget shortwave data product description, version 1.1
| NASA-TM-107747 | p 2777 N93-24742
Gravity waves from O2 airglow p 2772 N93-25547

ATMOSPHERIC REFRACTION
Proceedings of the 5th International Symposium on Long Range Sound Propagation
| AD-A260666 | p 2845 N93-25643

ATMOSPHERIC SCATTERING
Proceedings of the 5th International Symposium on Long Range Sound Propagation
| AD-A260666 | p 2845 N93-25643
High Frequency (HF) radiowave propagation
| AD-A261726 | p 2681 N93-26280
Brightness temperature and attenuation diversity statistics at 20.6 and 31.65 GHz for the Colorado Research Network p 2684 N93-26473
A proposed study of multiple scattering through clouds up to 1 THz p 2684 N93-26474

ATMOSPHERIC SOUNDING
The pressure modulation system in the Improved Stratospheric and Mesospheric Sounder p 2773 N93-25739
Digital Oblique Remote Ionospheric Sensing (DORIS) program development
| AD-A261750 | p 2776 N93-26283

ATMOSPHERIC STRATIFICATION
SAR-related stress variability in the marine atmospheric boundary layer
| AD-A261129 | p 2775 N93-25946

ATMOSPHERIC TEMPERATURE
Winter warming from large volcanic eruptions
| NASA-CR-192848 | p 2763 N93-25244
Aspects of the design of a satellite borne infra-red radiometer p 2620 N93-25474
Observed annual and interannual variations in tropospheric water vapor p 2782 N93-25549
Errors caused by incompatible wind and buoyancy forcing in the ocean general circulation models
| AD-A260894 | p 2789 N93-25657
The Martian lower atmosphere p 2897 N93-26394

ATMOSPHERIC TURBULENCE
An investigation of the role of flux divergence in the turbulent kinetic energy balance of the atmospheric surface layer p 2773 N93-25756
Laser propagation through turbulence
| AD-A260712 | p 2714 N93-26217

ATOMIC BEAMS
Preliminary results on an optically-pumped Cs beam frequency standard p 2832 N93-24989
Miniature optically-pumped cesium beam resonator p 2833 N93-24990
Actual limits of fluorescence S/N ratio in an optically-pumped cesium beam resonator p 2833 N93-24991
Phase differences of the fields in a Ramsey resonator for submillimetric frequency standards p 2840 N93-25042
A compact and high-performance reference cell for laser frequency stabilization p 2716 N93-25065

ATOMIC CLOCKS
Frequency and Time Forum
| ESA-SP-340 | p 2831 N93-24978
The advances in F and T technology: Their benefits of and for space science and technology p 2831 N93-24979
Hydrogen masers for space p 2716 N93-24980
A simple and compact source of cold atoms for cesium fountains and microgravity clocks p 2831 N93-24981
The application of the PRARE principle for precise two-way time transfer to space-based atomic clocks p 2832 N93-24983
Relativistic effects for low Earth orbit satellites using GPS p 2608 N93-24986
A new modem for microwave time synchronisation via geosynchronous telecommunication satellites p 2686 N93-24999
Control of environmental and clock parameters in Time and Frequency Standards Laboratory p 2835 N93-25007
Rubidium atomic frequency standards for GPS block 2R p 2836 N93-25014
Collaboration in the UK on time transfer using the GLONASS system p 2837 N93-25019
Microwave interrogation frequency noise and clock frequency stability: Experimental results p 2842 N93-25056
Solid state frequency synthesis up to 600 GHz: An application to the Mg frequency standard p 2842 N93-25058
A compact and high-performance reference cell for laser frequency stabilization p 2716 N93-25065

ATOMIC COLLISIONS
Progress in impulse approach research
| AD-A261728 | p 2850 N93-26281

ATOMIC ENERGY LEVELS
Solid state frequency synthesis up to 600 GHz: An application to the Mg frequency standard p 2842 N93-25058

ATOMIC EXCITATIONS
State-selected studies of atoms and molecules ejected from ion bombarded surfaces
| AD-A261275 | p 2850 N93-26267

ATOMIC PHYSICS
The physics of spin polarized gases
| AD-A261396 | p 2850 N93-26288

ATOMIC STRUCTURE
Correlated wavefunction quantum Monte Carlo approach to solids
| DE93-007730 | p 2863 N93-25367
Theoretical predictions of platinum-rhodium bimetallic catalysts
| DE93-007540 | p 2649 N93-25428
A novel method for characterization of superconductors: Physical measurements and modeling of thin films p 2871 N93-25584
Study of grain refinement in Al alloy 2519 using backscattering orientation-contrast mode in the scanning electron microscope
| AD-A260886 | p 2651 N93-25632
Theoretical and experimental research in infrared technology
| AD-A260926 | p 2853 N93-25646
Fundamental aspects of metal joining: The study of strong interfaces
| AD-A261293 | p 2653 N93-26304
Halogen adlayers on Ag(111)
| AD-A261792 | p 2850 N93-26443
Theoretical treatment of spin-forbidden and electronically nonadiabatic processes. Methods and applications
| AD-A261596 | p 2851 N93-26525
Liquid and solid ion plasmas
| AD-A261888 | p 2862 N93-26528

ATOMIZERS
Effect of a metal deactivator fuel additive on fuel deposition in fuel atomizers at high temperature
| AD-A260915 | p 2661 N93-25914
Atomization and combustion of a gelled, metallized slurry fuel
| AD-A261778 | p 2647 N93-26602

ATOMIZING
Fuel injector: Air swirl characterization aerothermal modeling, phase 2, volume 1
| NASA-CR-189193 | p 2592 N93-24754
Fuel Injector: Air swirl characterization aerothermal modeling, phase 2, volume 2
| NASA-CR-189193 | p 2592 N93-25106
Atomizing-gas temperature effect on cryogenic spray dropsize
| NASA-TM-106106 | p 2709 N93-25191
A summary of the JANNAF workshop on liquid rocket atomization p 2625 N93-26014

ATOMS
Liquid and solid ion plasmas
| AD-A261888 | p 2862 N93-26528

ATROPHY
Mechanical stimulation of skeletal muscle mitigates glucocorticoid induced decreases in prostaglandin synthesis
| NASA-CR-193040 | p 2794 N93-24763

ATTITUDE (INCLINATION)
Flight Mechanics/Estimation Theory Symposium, 1992
| NASA-CP-3186 | p 2599 N93-24694
The results of the in-flight attitude sensor calibration for the Arthur Holly Compton Gamma Ray Observatory p 2600 N93-24697
Resolution of the COBE Earth sensor anomaly p 2600 N93-24700
Real-time attitude determination and gyro calibration p 2602 N93-24708
Computationally efficient algorithms for real-time attitude estimation p 2602 N93-24709
Improvements in ERBS attitude determination without gyros p 2602 N93-24710
Polar decomposition for attitude determination from vector observations p 2602 N93-24711
Attitude analysis in Flatland: The plane truth p 2603 N93-24712
Rate determination from vector observations p 2603 N93-24713
Analysis of the Command and Control Segment (CCS) attitude estimation algorithm p 2604 N93-24722
SCATHA mission termination report p 2605 N93-24725
Accurate attitude determination of the LACE satellite p 2605 N93-24726
Attitude control of the LACE satellite: A gravity gradient stabilized spacecraft p 2605 N93-24727
Quaternion normalization in spacecraft attitude determination p 2606 N93-24730
Attitude determination using vector observations: A fast optimal matrix algorithm p 2606 N93-24731
Upper Atmosphere Research Satellite (UARS) onboard attitude determination using a Kalman filter p 2606 N93-24732
Goddard Space Flight Center (GSFC) Flight Dynamics Facility (FDF) calibration of the Upper Atmosphere Research Satellite (UARS) sensors p 2606 N93-24733
Solar array thermal snap and the characteristics of its effect on UARS p 2607 N93-24734
Upper Atmosphere Research Satellite (UARS) attitude accuracy using coarse attitude sensors p 2607 N93-24735
Apparatus for determining the attitude of a vehicle
| AD-D015667 | p 2710 N93-26092

ATTITUDE CONTROL
Momentum accumulation due to solar radiation torque, and reaction wheel sizing, with configuration optimization p 2600 N93-24695
Analysis of the Command and Control Segment (CCS) attitude estimation algorithm p 2604 N93-24722
Nonlinear stability analysis of the attitude motion of spin-stabilized thrusting spacecraft p 2617 N93-25527
Nonlinear dynamics and attitude control of articulated flexible space structures p 2617 N93-25726
Apparatus for determining the attitude of a vehicle
| AD-D015667 | p 2710 N93-26092
Dynamics of on-orbit construction process p 2669 N93-26406

ATTITUDE GYROS
Real-time attitude determination and gyro calibration p 2602 N93-24708
Upper Atmosphere Research Satellite (UARS) onboard attitude determination using a Kalman filter p 2606 N93-24732
Solar array thermal snap and the characteristics of its effect on UARS p 2607 N93-24734

ATTITUDE INDICATORS
Flight Mechanics/Estimation Theory Symposium, 1992
| NASA-CP-3186 | p 2599 N93-24694
The results of the in-flight attitude sensor calibration for the Arthur Holly Compton Gamma Ray Observatory p 2600 N93-24697
Testing of the on-board attitude determination and control algorithms for SAMPEX p 2600 N93-24698
Resolution of the COBE Earth sensor anomaly p 2600 N93-24700
Real-time attitude determination and gyro calibration p 2602 N93-24708
Computationally efficient algorithms for real-time attitude estimation p 2602 N93-24709
Improvements in ERBS attitude determination without gyros p 2602 N93-24710
Polar decomposition for attitude determination from vector observations p 2602 N93-24711
Rate determination from vector observations p 2603 N93-24713
A multimission three-axis stabilized spacecraft flight dynamics ground support system p 2603 N93-24714
Accurate attitude determination of the LACE satellite p 2605 N93-24726
Quaternion normalization in spacecraft attitude determination p 2606 N93-24730
Attitude determination using vector observations: A fast optimal matrix algorithm p 2606 N93-24731
Upper Atmosphere Research Satellite (UARS) onboard attitude determination using a Kalman filter p 2606 N93-24732
Goddard Space Flight Center (GSFC) Flight Dynamics Facility (FDF) calibration of the Upper Atmosphere Research Satellite (UARS) sensors p 2606 N93-24733
Solar array thermal snap and the characteristics of its effect on UARS p 2607 N93-24734
Upper Atmosphere Research Satellite (UARS) attitude accuracy using coarse attitude sensors p 2607 N93-24735

ATTITUDE STABILITY
Spacecraft detumbling through energy dissipation p 2600 N93-24696

AUDIO DATA
Design, fabrication, and testing of a three-dimensional acoustic orientation instrument (3-D AOI): Drawings, engineering and associated lists (conceptual and development design)
| AD-A260934 | p 2845 N93-25915

AUDIO EQUIPMENT
Inflight evaluation of an acoustic orientation instrument
| AD-A260752 | p 2591 N93-25909

AUDIO FREQUENCIES
Neuromagnetic investigation of cortical regions underlying short-term memory
| AD-A261445 | p 2799 N93-26521

AUDIO SIGNALS
Design, fabrication, and testing of a three-dimensional acoustic orientation instrument (3-D AOI): Drawings, engineering and associated lists (conceptual and development design)
| AD-A260934 | p 2845 N93-25915

AUDITORY PERCEPTION
Speech research
| AD-A260643 | p 2675 N93-25639
Complex auditory signals
| AD-A261491 | p 2846 N93-26374

AUDITORY SIGNALS
Inflight evaluation of an acoustic orientation instrument
| AD-A260752 | p 2591 N93-25909
Design, fabrication, and testing of a three-dimensional acoustic orientation instrument (3-D AOI): Drawings, engineering and associated lists (conceptual and development design)
| AD-A260934 | p 2845 N93-25915
Complex auditory signals
| AD-A261491 | p 2846 N93-26374

AUGER SPECTROSCOPY
Accurate determination of Auger line shape binding energies
| AD-A261803 | p 2868 N93-26258

AURORAL ZONES
Sounding rocket observations of precipitating ions in the morning auroral region p 2773 N93-25732

AURORAS
Mercury: The Los Alamos ICF KrF laser system
| DE93-007363 | p 2713 N93-25379
Further analysis of ECOM-721 data
| AD-A260863 | p 2774 N93-25790
Particle simulation of auroral double layers p 2774 N93-25830
JARE data reports. No. 171 (upper atmosphere physics 9). Data, Syowa and Asuka Stations, 1989 p 2774 N93-25889
Study of auroral dynamics with combined spacecraft and incoherent-scatter radar data
| NASA-CR-192224 | p 2775 N93-26159

AUSTRALIA
An environmental audit management plan for the Royal Australian Air Force
| AD-A261092 | p 2765 N93-25765

AUTOCORRELATION
Determination of design and operation parameters for upper atmospheric research instrumentation to yield optimum resolution with deconvolution, appendix 4
| NASA-CR-192834 | p 2769 N93-24910
Determination of design and operation parameters for upper atmospheric research instrumentation to yield optimum resolution with deconvolution, appendix 2
| NASA-CR-192833 | p 2770 N93-25088
Spontaneous discovery and use of categorical structure
| AD-A261658 | p 2798 N93-26364

AUTOIONIZATION
Ionization probes of molecular structure and chemistry
| DE93-008211 | p 2847 N93-25310

AUTOMATIC CONTROL
A ground track control algorithm for the Topographic Mapping Laser Altimeter (TMLA) p 2602 N93-24707
Ice thickness measurement system for the icing research tunnel calibration
| NASA-TM-106095 | p 2708 N93-24737
A survey of life support system automation and control
| NASA-TM-103977 | p 2667 N93-25085
How to combine probabilistic and fuzzy uncertainties in fuzzy control
| NASA-TM-108746 | p 2818 N93-25138
Automated system for early breast cancer detection in mammograms p 2796 N93-25568
An architecture for object-oriented intelligent control of power systems in space p 2823 N93-25968
Architecture of autonomous systems
| NASA-CR-192974 | p 2801 N93-26047
DSS-13 26-meter antenna upgraded radiometer system p 2679 N93-26122
Automated inspection of solder joints for surface mount technology
| NASA-TM-104580 | p 2721 N93-26137

AUTOMATIC FLIGHT CONTROL
Discrete range clustering using Monte Carlo methods
| NASA-TM-104004 | p 2584 N93-24914

AUTOMATIC FREQUENCY CONTROL
Investigations of the frequency instability of CH1-75 hydrogen masers p 2716 N93-25049
Frequency generation and synthesis in the DRSS p 2693 N93-25054

AUTOMATIC TEST EQUIPMENT
A digital hardware test system analysis with test vector translation
| AD-A260849 | p 2810 N93-25786

AUTOMATION
Use of fuzzy relational information retrieval technique for generating control strategies in resolution-based automated reasoning p 2874 N93-25258

AUTOMOBILE FUELS
Emissions from ethanol and LPG fueled vehicles
| DE93-006410 | p 2660 N93-25192
Cost-effectiveness analysis of TxDOT CNG fleet conversion, volume 2
| PB93-159432 | p 2720 N93-26534
Cost-effectiveness analysis of TxDOT CNG fleet conversion, volume 1
| PB93-165603 | p 2720 N93-26585
Documentation for propane fleet conversion cost-effectiveness model
| PB93-165611 | p 2720 N93-26590

AUTOMOBILES
Magnitude and value of electric vehicle emissions reductions for six driving cycles in four US cities with varying air quality problems
| DE93-006417 | p 2660 N93-25298
Development of ASTM standards in support of advanced ceramics development
| DE93-003024 | p 2654 N93-25361
Theoretical predictions of platinum-rhodium bimetallic catalysts
| DE93-007540 | p 2649 N93-25428

AUTONOMIC NERVOUS SYSTEM
Autonomic physiological data associated with simulator discomfort
| NASA-CR-177609 | p 2794 N93-24738

AUTONOMOUS NAVIGATION
Using neural networks and Dyna algorithm for integrated planning, reacting and learning in systems
| NASA-CR-193018 | p 2817 N93-24743
Real-time construction and rendering of three-dimensional occupancy maps
| DE93-007818 | p 2756 N93-25516

AUTONOMY
Experimental modal survey of the probe mass mock-up
| DE93-008846 | p 2617 N93-25494
VIEWCACHE: An incremental pointer-based access method for autonomous interoperable databases p 2880 N93-25809
Knowledge-based control for robot self-localization p 2822 N93-25963
An architecture for object-oriented intelligent control of power systems in space p 2823 N93-25968
An autonomous satellite architecture integrating deliberative reasoning and behavioural intelligence p 2823 N93-25970
NASA Center for Intelligent Robotic Systems for Space Exploration
| NASA-CR-193208 | p 2826 N93-25986
Architecture of autonomous systems
| NASA-CR-192974 | p 2801 N93-26047

AUTOREGRESSIVE PROCESSES
Failure monitoring in dynamic systems: Model construction without fault training data p 2672 N93-24666
Considerations of the error variances of time-averaged estimators for correlated processes
| AD-A261796 | p 2830 N93-26255

AVAILABILITY
GPS standardization for the needs of time transfer p 2836 N93-25016

AVALANCHE DIODES
The sub 60 ps timing resolution using large area silicon avalanche diodes
| DE93-007723 | p 2688 N93-25365
Studies of avalanche photodiodes for scintillating fibre tracking readout
| DE93-008370 | p 2689 N93-25491

AVALANCHES
New concepts for high efficiency energy conversion: The avalanche heterostructure and superlattice solar cells
| DE92-010592 | p 2758 N93-25098
Advanced technology for portable personal visualization
| AD-A261294 | p 2807 N93-26293

AVIATION METEOROLOGY
The 1992 International Aerospace and Ground Conference on Lightning and Static Electricity: Addendum
| DOT/FAA/CT-92/20-ADD-1 | p 2777 N93-24875
Applications of triggered lightning to space vehicle operations p 2619 N93-24878
A procedure for defining lightning risk to air vehicles p 2583 N93-24885

AVIONICS
Alternative equipment test procedures for simultaneous current injection on multiple cable bundles p 2693 N93-24903
Aircraft electrical and environmental systems, AFSCs 452x5, 454x5, and 454x6
| AD-A261213 | p 2590 N93-25733
Technical operating report on the Data Integration and Collection Environment (DICE) instrumentation system design
| AD-A261105 | p 2591 N93-26572

AXIAL FLOW
The WINCOF-I code: Detailed description
| NASA-CR-190779 | p 2573 N93-24760

AXIAL LOADS
Axisymmetric deformations and stresses of unsymmetrically laminated composite cylinders in axial compression with thermally-induced preloading effects
| NASA-CR-192788 | p 2723 N93-24912

Continuum and micromechanics treatment of constraint in fracture
| AD-A260927 | p 2727 N93-25647
In-situ ultrasonic C-scanner
| AD-A261113 | p 2638 N93-25768

AXIAL STRAIN
Axisymmetric deformations and stresses of unsymmetrically laminated composite cylinders in axial compression with thermally-induced preloading effects
| NASA-CR-192788 | p 2723 N93-24912

AXISYMMETRIC FLOW
Simulation of vortex bursting p 2580 N93-25881

AZIMUTH
Tsien's method for generating non-Keplerian trajectories. Part 2: The question of thrust to orbit a sphere and the restricted three-body problem p 2603 N93-24718

AZORES
Summary by the cloud and aerosol research group for ASTEX
| AD-A261292 | p 2766 N93-26292

B

B STARS
The effects of rotation on the winds from hot stars p 2894 N93-25620

BACKGROUND NOISE
Figure of merit for direct-detection optical channels p 2678 N93-26117
New algorithms for the detection and elimination of sine waves and other narrow-band signals in the presence of broadband signals and noise
| AD-A261811 | p 2681 N93-26261

BACKGROUND RADIATION
Starburst Galaxies: Hard X-ray spectra and contribution to the diffuse background
| NASA-CR-192790 | p 2892 N93-25211
Investigation of a background suppression transimpedance amplifier for photovoltaic detectors
| AD-A261828 | p 2691 N93-26272
Analysis of the IBSS spectra of Space Shuttle control engine exhaust
| AD-A261749 | p 2632 N93-26373

BACKSCATTERING
A fiber optic probe for the detection of cataracts p 2796 N93-25593
Study of grain refinement in Al alloy 2519 using backscattering orientation-contrast mode in the scanning electron microscope
| AD-A260886 | p 2651 N93-25632
Enhanced backscattering from rough surfaces
| AD-A261000 | p 2676 N93-25855
Radar backscatter measurements from Arctic sea ice during the fall freeze-up
| NASA-CR-193100 | p 2790 N93-26050
High Frequency (HF) radiowave propagation
| AD-A261726 | p 2681 N93-26280

BACTERIA
Biological production of ethanol from coal
| DE93-008947 | p 2660 N93-25496
Biological conversion of synthesis gas
| DE93-009092 | p 2660 N93-25523

BALANCE
Development and testing of improved techniques for modeling the hydrologic cycle in a mesoscale weather prediction system
| AD-A261454 | p 2787 N93-26351

BALANCING
An improved spectral load balancing method
| DE93-007582 | p 2810 N93-25386
Toward a parallel recursive spectral bisection mapping tool
| DE93-006632 | p 2816 N93-25414

BALLOON-BORNE INSTRUMENTS
The charge and size of precipitation particles inside thunderstorms and mesoscale convective systems on the Great Plains p 2781 N93-25275

BALTIC SEA
Data availability and data archeology from the former Soviet Union p 2735 N93-24932

BANDPASS FILTERS
Distortion measurements on bandpass filters with powdered iron toroidal inductors
| AD-A260790 | p 2675 N93-25689
New algorithms for the detection and elimination of sine waves and other narrow-band signals in the presence of broadband signals and noise
| AD-A261811 | p 2681 N93-26261

BANDSTOP FILTERS
New algorithms for the detection and elimination of sine waves and other narrow-band signals in the presence of broadband signals and noise
| AD-A261811 | p 2681 N93-26261

BANDWIDTH
Robo-line storage: Low latency, high capacity storage systems over geographically distributed networks
| NASA-CR-192910 | p 2805 N93-25130
Striped tape arrays
| NASA-CR-192914 | p 2806 N93-25267
Bandwidth compression of noisy signals with square-wave subcarrier p 2678 N93-26120
Complex auditory signals
| AD-A261491 | p 2846 N93-26374

BAROCLINIC INSTABILITY
Dynamics of Gulf Stream meanders and frontal eddies in the South Atlantic Bight p 2788 N93-25354
Wind-driven coastal generation of annual mesoscale eddy activity in the California current
| AD-A261355 | p 2790 N93-26331

BAROTROPIC FLOW
Dynamics of Gulf Stream meanders and frontal eddies in the South Atlantic Bight p 2788 N93-25354

BARRED GALAXIES
Numerical modeling of barred spiral galaxies p 2893 N93-25537

BARYONS
High-energy pion-nucleus scattering at LAMPF
| DE93-007364 | p 2852 N93-25380

BASALT
Indigenous lunar construction materials p 2670 N93-26413

BASE FLOW
Modified point mass trajectory simulation for base-burn projectiles
| BRL-TR-3321 | p 2609 N93-25985

BASE PRESSURE
Modified point mass trajectory simulation for base-burn projectiles
| BRL-TR-3321 | p 2609 N93-25985

BATCH PROCESSING
TDRSS-user orbit determination using batch least-squares and sequential methods p 2601 N93-24703

BATHYMETERS
Preliminary studies leading toward the development of a LIDAR bathymetry mapping instrument p 2711 N93-25614

BATTERY CHARGERS
Characterization of electrochemical systems and batteries: Materials and systems
| DE93-003472 | p 2687 N93-24964

BAUSCHINGER EFFECT
Internal stresses and the cyclic deformation of an aluminum matrix composite p 2650 N93-25436

BAYES THEOREM
Bayesian cross-entropy reconstruction of complex images
| AD-A261812 | p 2812 N93-26257
Step stress testing of receiver/transmitter units
| AD-A261286 | p 2730 N93-26279

BCH CODES
Soft decoding a self-dual (48, 24; 12) code p 2671 N93-24662
A (72, 36; 15) box code p 2671 N93-24663
Golay and other box codes p 2678 N93-26116

BEACONS
DORIS precise orbit determination and location system performances of ultra stable oscillators p 2608 N93-24997

BEAM CURRENTS
Metal ion implantation for large scale surface modification
| DE93-007649 | p 2859 N93-25324
Beam position and total current monitor for heavy ion fusion beams
| DE93-007653 | p 2851 N93-25325

BEAM INJECTION
Plasma heating in toroidal systems
| NIFS-208 | p 2858 N93-25092

BEAM WAVEGUIDES
A technique for computation of noise temperature due to a beam waveguide shroud p 2671 N93-24661
Performance of a 12-GHz fiber-optic system for beam-waveguide antenna stability testing p 2677 N93-26113
Optimizing the G/T ratio of the DSS-13 34-meter beam-waveguide antenna p 2678 N93-26118

BEAMFORMING
A compact and versatile pulse generation and shaping subsystem for high energy laser systems
| DE93-007114 | p 2711 N93-24961
Analysis and design of a novel robotic finger-tip sensor for adaptive grasping p 2719 N93-25745

BEAMS (RADIATION)
Log-ratio signal-processing technique for beam position monitors
| DE93-007356 | p 2851 N93-25314
Preliminary design of the BPM electronics memory scanner/dual boxcar averager for the advanced photon source
| DE93-007893 | p 2848 N93-25368

BEARINGLESS ROTORS
Structural dynamic analysis of bearingless rotor blade p 2590 N93-25719

BEARINGS
Tuned circuit electric levitation bearings for microactuators p 2689 N93-25619
Evaluation of a vibration diagnostic system for the detection of spur gear pitting failures
| NASA-TM-106103 | p 2718 N93-25672
Macromolecules for inhibition of corrosion and wear
| AD-A261041 | p 2655 N93-25816

BEECHCRAFT AIRCRAFT
Development of a flight instrument package
| AD-A260830 | p 2591 N93-25783

BENDING
Transformation plasticity and fracture behavior of ceria-TZP/alumina composites p 2638 N93-25760

BENZENE
Intramolecular bridge/terminal oxo exchange within (MoV2O3) (4+) complexes containing linear oxo bridges
| AD-A261230 | p 2851 N93-26518

BERMUDA
Ocean time-series near Bermuda: Hydrostation S and the US JGOFS Bermuda Atlantic time-series study p 2736 N93-24938

BIAS
Magnetic multilayer strain gage
| AD-D015672 | p 2710 N93-26141
Bayesian cross-entropy reconstruction of complex images
| AD-A261812 | p 2812 N93-26257

BIBLIOGRAPHIES
Selected translated abstracts of Russian-language climate-change publications: 1. Surface energy budget
| DE93-003189 | p 2760 N93-24952
Pyroshock: Bibliography
| DE93-007605 | p 2726 N93-25489
Bibliography on propulsion airframe integration technologies for high-speed civil transport applications, 1980-1991
| NASA-TM-105602 | p 2573 N93-26136
Bibliography of remote sensing techniques used in wetland research
| AD-A261704 | p 2757 N93-26440
Space Science Laboratory Publications and Presentations
| NASA-TM-108402 | p 2884 N93-26562

BICRYSTALS
Crack tip fields in ductile crystals and bicrystals p 2866 N93-25749

BIMETALS
Design of a high activity and selectivity alcohol catalyst
| DE93-008101 | p 2659 N93-25111
Theoretical predictions of platinum-rhodium bimetallic catalysts
| DE93-007540 | p 2649 N93-25428

BINARY CODES
Soft decoding a self-dual (48, 24; 12) code p 2671 N93-24662
Golay and other box codes p 2678 N93-26116
A proposed study of multiple scattering through clouds up to 1 THz p 2684 N93-26474

BINARY DATA
Goldstone solar system radar signal processing p 2680 N93-26130

BINARY PHASE SHIFT KEYING
New algorithms for the detection and elimination of sine waves and other narrow-band signals in the presence of broadband signals and noise
| AD-A261811 | p 2681 N93-26261
A Biphase Shift Keying (BPSK), direct sequence, spread spectrum modem for Petite Amateur Navy Satellite (PANSAT)
| AD-A261301 | p 2618 N93-26295
Geolocation of an electromagnetic emitter using a cyclostationary time difference of arrival technique
| AD-A261781 | p 2686 N93-26603

BINARY STARS
Gravitational radiation from coalescing binary star systems p 2900 N93-25625
Chromospheric activity in algol binaries
| AD-A261440 | p 2896 N93-26508

BINAURAL HEARING
Monaural and binaural processing of complex waveforms
| AD-A261659 | p 2846 N93-26358

BINOCULAR VISION
Coordinated action in 3-D space
| AD-A261418 | p 2799 N93-26449

BIOACOUSTICS
Neuromagnetic investigation of cortical regions underlying short-term memory
| AD-A261445 | p 2799 N93-26521
BIOASSAY
Health and environmental chemistry: Analytical techniques, data management, and quality assurance
| DE93-002853 | p 2760 N93-24674
BIOCHEMISTRY
Primary events in olfactory reception
| AD-A260562 | p 2795 N93-25944
The role of pyridoxine as a countermeasure for in-flight loss of lean body mass p 2796 N93-26068
Inorganic and biological electron transfer across an electronically conductive composite polymer membrane
| AD-A261642 | p 2656 N93-26172
Intramolecular bridge/terminal oxo exchange within (MoV2O3) (4+) complexes containing linear oxo bridges
| AD-A261230 | p 2851 N93-26518
BIOCONVERSION
Biological conversion of synthesis gas
| DE93-009092 | p 2660 N93-25523
BIODEGRADATION
Reclamation with recovery of radionuclides and toxic metals from contaminated materials, soils, and wastes p 2769 N93-25571
BIODYNAMICS
Evaluation of lens distortion errors in video-based motion analysis
| NASA-TP-3266 | p 2797 N93-25736
BIOELECTRIC POTENTIAL
Anomalous bioelectric potentials of silk trees in Naples zoo (Italy) prior to an earthquake in May, 1991 p 2753 N93-24873
Comparative analytical study of evoked and event related potentials as correlates of cognitive processes
| AD-A261388 | p 2799 N93-26446
BIOELECTRICITY
Anomalous bioelectric potentials of silk trees in Naples zoo (Italy) prior to an earthquake in May, 1991 p 2753 N93-24873
Biomagnetic localization from transient quasi-static events
| DE93-007328 | p 2794 N93-25186
BIOGEOCHEMISTRY
The JGOFS North Atlantic Bloom Experiment: An overview p 2735 N93-24934
Data management for JGOFS: Theory and design p 2735 N93-24935
Data management for community research projects: A JGOFS case study p 2736 N93-24936
Ocean time-series near Bermuda: Hydrostation S and the US JGOFS Bermuda Atlantic time-series study p 2736 N93-24938
Automated in situ observations of upper ocean biogeochemistry, bio-optics, and physics and their potential use for global studies p 2736 N93-24939
Planetary Biology and Microbial Ecology: Molecular Ecology and the Global Nitrogen cycle
| NASA-CR-4497 | p 2803 N93-26157
BIOINSTRUMENTATION
JPRS report: Science and technology. Central Eurasia: Life sciences
| JPRS-ULS-93-002 | p 2737 N93-25399
BIOLOGICAL MODELS (MATHEMATICS)
Anatomy and physiology of plant conductive systems
| PB93-156032 | p 2793 N93-25877
BIOLOGY
Achieving the promise of the bioscience revolution: The role of the Federal Government
| PB93-139970 | p 2793 N93-25457
BIOMAGNETISM
Biomagnetic localization from transient quasi-static events
| DE93-007328 | p 2794 N93-25186
Neuromagnetic investigation of cortical regions underlying short-term memory
| AD-A261445 | p 2799 N93-26521
BIOMASS
North-central Mexico blue grama rangeland biomass assessment at the end of the rainy season using NOAA-AVHRR-LAC p 2750 N93-24854
Biodiversity indication by Earth observation data p 2751 N93-24858
Emerging technologies in ethanol production
| PB93-157014 | p 2661 N93-25818
Relations between blue whiting biomass and satellite derived phytoplankton and temperature in the Norwegian Sea
| AD-A261205 | p 2757 N93-25868
Analysis of the lettuce data from the variable pressure growth chamber at NASA Johnson Space Center: A three-stage nested design model p 2794 N93-26069
Development of a pyrolysis waste recovery model with designs, test plans, and applications for space-based habitats p 2803 N93-26076
BIOREACTORS
Biological production of ethanol from coal
| DE93-008947 | p 2660 N93-25496
Biological conversion of synthesis gas
| DE93-009092 | p 2660 N93-25523
BIOSYNTHESIS
Biological production of ethanol from coal
| DE93-008947 | p 2660 N93-25496
The role of pyridoxine as a countermeasure for in-flight loss of lean body mass p 2796 N93-26068
BIOTECHNOLOGY
JPRS report: Science and technology. Central Eurasia: Life sciences
| JPRS-ULS-93-002 | p 2737 N93-25399
Achieving the promise of the bioscience revolution: The role of the Federal Government
| PB93-139970 | p 2793 N93-25457
Technology 2002: The Third National Technology Transfer Conference and Exposition, volume 1
| NASA-CP-3189-VOL-1 | p 2901 N93-25561
The application of integrated knowledge-based systems for the Biomedical Risk Assessment Intelligent Network (BRAIN) p 2799 N93-25595
BIPOLAR TRANSISTORS
Short-period superlattice materials for heterojunction bipolar transistors
| AD-A260701 | p 2866 N93-25897
Monolithic integration of semiconductor and superconductor components
| AD-A260589 | p 2690 N93-25906
BIRDS
Mechanical stimulation of skeletal muscle mitigates glucocorticoid induced decreases in prostaglandin synthesis
| NASA-CR-193040 | p 2794 N93-24763
BISMUTH OXIDES
Development of high Tc (greater than 100 K) Bi, Tl and Y-based materials as superconducting circuit elements
| NASA-CR-192344 | p 2863 N93-25219
BIT SYNCHRONIZATION
Resolution of the COBE Earth sensor anomaly p 2600 N93-24700
BL LACERTAE OBJECTS
Correlative studies of astrophysical sources of very high and ultra high energy gamma-rays
| NASA-CR-192781 | p 2888 N93-25172
BLACK BODY RADIATION
Spectra of stable sonoluminescence
| AD-A260621 | p 2844 N93-25637
BLACK HOLES (ASTRONOMY)
Diskoseismology: Probing relativistic accretion disks p 2894 N93-25622
Gravitational radiation from coalescing binary star systems p 2900 N93-25625
BLADE-VORTEX INTERACTION
Flow visualizations of perpendicular blade vortex interactions
| NASA-CR-192725 | p 2696 N93-25208
BLADES
Flow visualizations of perpendicular blade vortex interactions
| NASA-CR-192725 | p 2696 N93-25208
BLASIUS FLOW
Instability of flow in a streamwise corner
| NASA-CR-191410 | p 2576 N93-25153
BLAST LOADS
Minutes of the Twenty-Fifth Explosives Safety Seminar, volume 4
| AD-A261116 | p 2660 N93-25769
BLOOD PLASMA
Vascular uptake of rehydration fluids in hypohydrated men at rest and exercise
| NASA-TM-103942 | p 2795 N93-26133
BLOOD VOLUME
Vascular uptake of rehydration fluids in hypohydrated men at rest and exercise
| NASA-TM-103942 | p 2795 N93-26133
BLOWING
Computational study of the aerodynamics and control by blowing of asymmetric vortical flows over delta wings p 2574 N93-24772
Tangential fuselage blowing on an ogive cylinder p 2578 N93-25545
BLUFF BODIES
Vortex shedding in oscillatory flow p 2700 N93-25438
BOATTAILS
Computation of transonic flow over a porous surface projectile p 2577 N93-25409
BODY CENTERED CUBIC LATTICES
Correlated wavefunction quantum Monte Carlo approach to solids
| DE93-007730 | p 2863 N93-25367
BODY FLUIDS
Vascular uptake of rehydration fluids in hypohydrated men at rest and exercise
| NASA-TM-103942 | p 2795 N93-26133
BODY-WING CONFIGURATIONS
Experimental effects of wing location on wing-body pressures at supersonic speeds
| NASA-TM-4434 | p 2581 N93-26085
BOLTS
Behavior of a steel-liner-and-bolts system under very high thermal and mechanical loading: The CONVEX Liner Add-On to DIAMOND FORTUNE
| DE93-007512 | p 2731 N93-26507
BOLTZMANN TRANSPORT EQUATION
A method for transient, three-dimensional neutron transport calculations
| DE93-007243 | p 2847 N93-25256
BONDED JOINTS
Models of crack growth along polymer interfaces p 2728 N93-25750
BONDING
Processing and mechanical properties of laminated metal composites of Al/Al-25 vol. percent SiC and ultrahigh carbon steel/brass
| DE93-007504 | p 2635 N93-25383
Method of joining diamond structures
| AD-D015671 | p 2867 N93-26140
BONES
The design of mechanically compatible fasteners for human mandible reconstruction p 2796 N93-25569
BOOSTER ROCKET ENGINES
SRB environment evaluation and analysis. Volume 3: ASRB plume induced environments
| NASA-CR-192519 | p 2631 N93-26054
SRB environment evaluation and analysis. Volume 2: RSRB joint filling test/analysis improvements
| NASA-CR-192518 | p 2631 N93-26057
Liquid Rocket Booster (LRB) for the Space Transportation System (STS) Systems Study. Amendment 13: Orientation meeting
| NASA-CR-192515 | p 2614 N93-26152
Space transportation booster engine thrust chamber technology, large scale injector
| NASA-CR-192531 | p 2633 N93-26557
BORANES
Mechanisms of decomposition and oxidation of borane compounds
| AD-A261137 | p 2645 N93-26045
BORESIGHTS
Testing of the on-board attitude determination and control algorithms for SAMPEX p 2600 N93-24698
BORON
Development of dispersion-strengthened XD (trademark) Cu alloys for high heat-flux applications
| NASA-CR-191124 | p 2653 N93-24761
BORON NITRIDES
Workshop on Diamond and Diamond-Like-Carbon Films for the Transportation Industry
| DE93-007491 | p 2658 N93-26506
BOROSILICATE GLASS
Ceramic fiber reinforced glass-ceramic matrix composite
| NASA-CASE-LEW-15262-1 | p 2640 N93-26100
BOTANY
Anatomy and physiology of plant conductive systems
| PB93-156032 | p 2793 N93-25877
BOULES
Laser damage to production- and research-grade KDP crystals
| DE93-007517 | p 2870 N93-26594
BOUNDARIES
High resolution interface nanochemistry and structure
| DE93-009750 | p 2635 N93-25501
BOUNDARY CONDITIONS
Minimization of heat slab nodes with higher order boundary conditions
| DE93-004238 | p 2695 N93-24966
High-order cyclo-difference techniques: An alternative to finite differences
| NASA-TM-107745 | p 2575 N93-25074
Asymptotic derivation of the simplified P(sub N) equations
| DE93-007342 | p 2828 N93-25151
An outgoing energy flux boundary condition for finite difference ICRP antenna models
| DE93-007788 | p 2674 N93-25300
BOUNDARY ELEMENT METHOD
Three-dimensional boundary element analysis of contact and fracture problems p 2725 N93-25335
BOUNDARY LAYER COMBUSTION
Hybrid rocket fuel combustion study p 2626 N93-26019
BOUNDARY LAYER CONTROL
Stationary crossflow instability on an infinite swept wing p 2580 N93-25865

BOUNDARY LAYER FLOW
Surface and flow field measurements in a symmetric crossing shock wave/turbulent boundary-layer interaction
| NASA-TM-106086 | p 2575 N93-24911
Measurements of density, temperature, and their fluctuations in turbulent supersonic flow using UV laser spectroscopy
| NASA-TM-103943 | p 2708 N93-25076
A feasibility study of using Langley 0.3-m transonic cryogenic tunnel sidewall boundary-layer removal system for heavy gas testing
| NASA-CR-191438 | p 2695 N93-25087
Spatial simulation of transition in wall-bounded shear flows: Active control and effects of surface roughness p 2701 N93-25483
Particle dynamics modeling of boundary effects in granular Couette flow p 2705 N93-25738
Large-eddy simulation of temporally developing boundary layers with embedded streamwise vortices p 2705 N93-25753
Model fan passage flow simulation
| AD-A261613 | p 2707 N93-26167

BOUNDARY LAYER PLASMAS
Boundary plasma modelling for ITER
| DE93-007963 | p 2859 N93-25302

BOUNDARY LAYER SEPARATION
Development of an expendable particle sensor
| AD-A261127 | p 2710 N93-26044
Model fan passage flow simulation
| AD-A261613 | p 2707 N93-26167

BOUNDARY LAYER STABILITY
Instability of flow in a streamwise corner
| NASA-CR-191410 | p 2576 N93-25153
Large-eddy simulation of temporally developing boundary layers with embedded streamwise vortices p 2705 N93-25753

BOUNDARY LAYERS
An analysis of lift forces on aerosols in a wall bounded turbulent shear flow
| DE93-003362 | p 2695 N93-24963
A feasibility study of using Langley 0.3-m transonic cryogenic tunnel sidewall boundary-layer removal system for heavy gas testing
| NASA-CR-191438 | p 2695 N93-25087
Numerical simulation of leading-edge receptivity to freestream vorticity p 2577 N93-25388

BOUNDARY VALUE PROBLEMS
Solution of nonlinear boundary value problem on successively refined grids
| AD-A261395 | p 2829 N93-26519

BRAIN
Biomagnetic localization from transient quasi-static events
| DE93-007328 | p 2794 N93-25186
Proceedings of Workshop 1: The Human Brainmap Database
| AD-A260720 | p 2796 N93-25654
Imaging regional changes in the spontaneous activity of the brain: An extension of the minimum-norm least-squares estimate
| AD-A261593 | p 2798 N93-26436
Neuromagnetic investigation of cortical regions underlying short-term memory
| AD-A261445 | p 2799 N93-26521

BRAIN DAMAGE
Neuropsychological components of object identification
| AD-A261449 | p 2797 N93-26347

BRAKES (FOR ARRESTING MOTION)
Turbine turbobrake systems p 2717 N93-25268

BRAKING
Turbine turbobrake systems p 2717 N93-25268

BREADBOARD MODELS
Preliminary results of a newly designed mini-OCXO oscillator especially dedicated to space applications p 2621 N93-25028

BREATHING APPARATUS
Inward contaminant leakage tests of the S-Tron Corporation emergency escape breathing device. Phase 1: Tests of the original design. Phase 2: Tests with the redesigned neck seal
| DOT/FAA/AM-92/18 | p 2582 N93-25205

BRICKS
Advanced engineering analysis
| KCP-613-4967 | p 2669 N93-26212

BRIDGES (STRUCTURES)
Fatigue resistance of orthotropic plates with trapezoidal stiffeners
| TRL-TRANS-T3908 | p 2726 N93-25419

BRIGHTNESS TEMPERATURE
Influence due to antenna pattern change in brightness temperature estimation for a space-based microwave radiometer p 2753 N93-24868
Cloud properties as inferred from HIRS/2 multi-spectral data p 2782 N93-25293
Spectra of stable sonoluminescence
| AD-A260621 | p 2844 N93-25637
Vector radiative transfer model: Application to rainfall retrieval with microwave radiometric data p 2784 N93-25743
Brightness temperature and attenuation diversity statistics at 20.6 and 31.65 GHz for the Colorado Research Network p 2684 N93-26473

BRILLOUIN EFFECT
Magnetic excitations in antiferromagnetically coupled superlattices: Fe/Mo and Fe/Cr
| DE93-007894 | p 2863 N93-25369

BRITTLENESS
Micromechanics of fatigue
| AD-A260577 | p 2729 N93-25901
Deformation mechanisms of NiAl cyclicly deformed near the brittle-to-ductile transition temperature
| NASA-CR-191121 | p 2652 N93-26235

BROADBAND
Very wide bandwidth HF crystal filters p 2693 N93-25039
A modular wideband sound absorber
| BBC-RD-1992/11 | p 2673 N93-25171
Apparatus for imaging an object in or through a scattering medium using coherent anti-Stokes Raman scattering
| AD-D015642 | p 2852 N93-25358
Computation of broadband mixing noise from turbomachinery
| AD-A261611 | p 2846 N93-26165
New algorithms for the detection and elimination of sine waves and other narrow-band signals in the presence of broadband signals and noise
| AD-A261811 | p 2681 N93-26261

BROADCASTING
An example of a phase-segregated enhanced PAL broadcasting system
| BBC-RD-1992/6 | p 2674 N93-25239
Experiments with the HIVITS HDTV contribution CODED
| BBC-RD-1992/12 | p 2674 N93-25391
WARC 92 and some thoughts as to its impact on the NASA propagation program p 2684 N93-26475

BROKEN SYMMETRY
Consequences of spontaneous and anomalous symmetry breaking for the orbital and mass flow hydrodynamics of He-3 - A p 2698 N93-25295

BROMIDES
The acute inhalation toxicity of pyrolysis products of halon 1301
| AD-A260874 | p 2795 N93-25629

BSCCO SUPERCONDUCTORS
Development of high Tc (greater than 100 K) Bi, Tl and Y-based materials as superconducting circuit elements
| NASA-CR-192344 | p 2863 N93-25219
Analysis of the gap in high-temperature superconductors using photoemission spectroscopy p 2865 N93-25744

BUBBLES
Modeling of bubble and drop formation in flowing liquids in terrestrial and microgravity environments p 2664 N93-25390
Simulation of vortex bursting p 2580 N93-25881

BUCKLING
Vibration, buckling, and postbuckling of laminated composites with delaminations p 2723 N93-24765
Seismic buckling capacity of unstiffened, free-standing steel containments
| DE93-005325 | p 2723 N93-24957
The damage, repair and design of fiber composite structural materials p 2635 N93-25532

BUFFER STORAGE
An investigation of memory latency reduction using an address prediction buffer
| AD-A261010 | p 2806 N93-25858
The design and implementation of a read prediction buffer
| AD-A260902 | p 2806 N93-25934

BUILDINGS
Stochastic and seismic design response of linear and nonlinear structures p 2726 N93-25484
Tornado: An engineering-oriented perspective
| PB93-148435 | p 2788 N93-26584

BULKHEADS
Photovoltaic power without batteries for continuous cathodic protection p 2759 N93-25597

BUOYANCY
Heat transfer in rotating serpentine passages with selected model orientation for smooth or skewed trip walls
| NASA-TM-106126 | p 2667 N93-25177
Errors caused by incompatible wind and buoyancy forcing in the ocean general circulation models
| AD-A260894 | p 2789 N93-25657

BURNING RATE
Calculations of combustion response profiles and oscillations
| NASA-TM-106135 | p 2623 N93-25236
The burning rate behavior of pure nitrocellulose propellant samples
| AD-A261009 | p 2661 N93-25857
Thermal radiation in non-metalized solid rocket motors: Effect on burning rate and temperature sensitivity p 2626 N93-26020
Improved burn rate determination techniques p 2627 N93-26021
Determination of burn rate requirements from ASRM performance specifications p 2627 N93-26023
Flame response in oscillatory solid propellant combustion p 2630 N93-26041
An experimental and analytical study of the unsteady combustion of homogeneous energetic solids using the laser-recoil method p 2630 N93-26042
Dynamic burning rate measurements of metalized composite propellants using the laser-recoil technique p 2631 N93-26043

BURNING TIME
Improved burn rate determination techniques p 2627 N93-26021

BURNOUT
A model of concurrent flow flame spread over a thin solid fuel
| NASA-CR-191111 | p 2663 N93-24946

BY-PRODUCTS
Biological production of ethanol from coal
| DE93-008947 | p 2660 N93-25496

BYPASS RATIO
Transient performance of fan engine with water ingestion
| NASA-CR-190778 | p 2573 N93-25134

C

C (PROGRAMMING LANGUAGE)
A software package for neural network applications development p 2827 N93-25610
Implementation of custom colors in the DECwindows environment
| AD-A261456 | p 2757 N93-26574

CABLES
Equipment testing with damped sinewaves between 1 and 50 MHz p 2692 N93-24881
A system to measure lightning-induced transients on spacecraft umbilical lines p 2693 N93-24889
Alternative equipment test procedures for simultaneous current injection on multiple cable bundles p 2693 N93-24903

CADMIUM TELLURIDES
Role of polycrystallinity in CdTe and CuInSe2 photovoltaic cells
| DE93-000045 | p 2759 N93-25504
IR materials producibility
| AD-A261099 | p 2853 N93-25766

CALCIUM OXIDES
Temperature-dependent electrical conductivity of soda-lime glass
| DE93-007872 | p 2654 N93-25359

CALCULUS OF VARIATIONS
Incompressible spectral-element method: Derivation of equations
| NASA-TM-106109 | p 2708 N93-26554

CALIBRATING
The results of the in-flight attitude sensor calibration for the Arthur Holly Compton Gamma Ray Observatory p 2600 N93-24697
Real-time attitude determination and gyro calibration p 2602 N93-24708
Goddard Space Flight Center (GSFC) Flight Dynamics Facility (FDF) calibration of the Upper Atmosphere Research Satellite (UARS) sensors p 2606 N93-24733
Ice thickness measurement system for the icing research tunnel calibration
| NASA-TM-106095 | p 2708 N93-24737
The use of polarimetric multifrequency SAR for characterizing terrain classes p 2738 N93-24777
The scope of DLR's SAR calibration program p 2738 N93-24778
Observation of radiation from lightning discharges by LPATS p 2779 N93-24888
An atlas of selected calibrated stellar spectra
| NASA-CR-177604 | p 2888 N93-25135
Thermal expansion measurements of polymer matrix composites and syntactics
| MTL-TR-92-27 | p 2640 N93-25954
System for calibrating a gyro navigator
| AD-D015668 | p 2586 N93-26093
Deep-space navigation with differenced data types. Part 3: An expanded information content and sensitivity analysis p 2614 N93-26109
VETA-I x ray test analysis
| NASA-CR-192321 | p 2854 N93-26183

Precision of the calibration of the AXAF engineering test article (VETA) mirrors p 2855 N93-26189
Surface finish quality of the outer AXAF mirror pair based on x ray measurements of the VETA-I p 2855 N93-26191
The x ray reflectivity of the AXAF VETA-I optics p 2855 N93-26192

CALIFORNIA
Geologic structure and processes of the eastern Pacific margin: California and Costa Rica p 2771 N93-25424

CALORIMETERS
Compressor calorimeter performance of refrigerant blends: Comparative methods and results for a refrigerator/freezer application
| DE93-006734 | p 2667 N93-24970

CAMBER
Aerodynamic foundations for use of unsteady aerodynamic effects in flight control p 2576 N93-25274

CAMERAS
High speed x ray gating cameras for ICF imaging applications
| DE93-007500 | p 2709 N93-25515
A high performance room-temperature near-infrared camera
| AD-A260602 | p 2709 N93-25634

CANADA
Integrating satellite imagery and digital elevation data for geobotanical mapping in Quetico Provincial Park, Ontario, Canada p 2754 N93-25430

CANCER
Measuring the metastatic potential of cancer cells p 2794 N93-25566
Immunoconjugates: Magic bullets for cancer therapy? p 2796 N93-25567
Automated system for early breast cancer detection in mammograms p 2796 N93-25568

CANONICAL FORMS
Asymptotic derivation of the simplified P(sub N) equations
| DE93-007342 | p 2828 N93-25151

CAP CLOUDS
Natural and augmented snowfall growth processes and their interactions with the natural and modified aerosol
| PB93-153096 | p 2786 N93-25874

CAPACITANCE
On machine capacitance dimensional and surface profile measurement system p 2670 N93-25579
Single electron charging effects in mesoscopic systems
| AD-A261228 | p 2868 N93-26302
Large area, low capacitance Si(Li) detectors for high rate x ray applications
| DE93-007661 | p 2692 N93-26598

CAPACITANCE SWITCHES
OSCCAR: Oscillator-compensated with a capacitance array p 2693 N93-25002

CAPACITANCE-VOLTAGE CHARACTERISTICS
Liquid filled variable capacitor
| AD-D015639 | p 2687 N93-25212

CAPACITORS
Fundamental studies of defect generation in amorphous silicon alloys grown by remote plasma-enhanced chemical-vapor deposition (Remote PECVD)
| DE92-010560 | p 2862 N93-24953
Liquid filled variable capacitor
| AD-D015639 | p 2687 N93-25212
A comparison of moisture resistance with different types of end-terminations in ceramic capacitors
| DE93-007600 | p 2689 N93-25416
Characterization of ceramic capacitors for high-voltage pulse-discharge applications
| DE93-007601 | p 2689 N93-25417

CAPE KENNEDY LAUNCH COMPLEX
Weather forecasting expert system study
| NASA-CR-192929 | p 2777 N93-24747
Launch pad lightning protection enhancement by induced streamers p 2609 N93-24876
Applications of triggered lightning to space vehicle operations p 2619 N93-24878
A system to measure lightning-induced transients on spacecraft umbilical lines p 2693 N93-24889

CAPILLARY FLOW
Two-phase/two-phase heat exchanger analysis
| NASA-CR-192783 | p 2697 N93-25221
Numerical simulation of time-dependent thermocapillary convection in layered fluid systems p 2700 N93-25472
Thermocapillary flow near a cold wall
| AD-A261050 | p 2706 N93-25779

CARBIDES
Metastable SiC and SiGeC alloys by carbon implantation and solid phase epitaxy
| DE93-007594 | p 2863 N93-25387
Conversion of light hydrocarbon gases to metal carbides for production of liquid fuels and chemicals
| DE93-009707 | p 2644 N93-25500

CARBON
Metastable SiC and SiGeC alloys by carbon implantation and solid phase epitaxy
| DE93-007594 | p 2863 N93-25387
Optical and scratch resistant properties of diamondlike carbon films deposited with single and dual ion beams p 2658 N93-25564
Method of joining diamond structures
| AD-D015671 | p 2867 N93-26140
Workshop on Diamond and Diamond-Like-Carbon Films for the Transportation Industry
| DE93-007491 | p 2658 N93-26506

CARBON COMPOUNDS
Structure and properties of a-C: N filns prepared by pulsed excimer laser deposition
| DE93-007908 | p 2654 N93-25372

CARBON DIOXIDE
The properties of and analytical methods for detection of LiOH and Li2CO3
| NASA-CR-192771 | p 2643 N93-25240
Membrane technology: A search for membranes for submarine atmosphere control
| AD-A260581 | p 2801 N93-25904
Physical and chemical processes governing the CO2 laser-induced deflagration of ammonium dinitramide (ADN) p 2629 N93-26037
Long term modeling of the links between economics, technical progress, and environment: Evolution of approaches and new trends
| DE93-005035 | p 2767 N93-26497
IR and FIR laser diagnostics for plasma thrusters using a CW CO2 radiation source
| AD-A261399 | p 2862 N93-26520

CARBON DIOXIDE LASERS
IR and FIR laser diagnostics for plasma thrusters using a CW CO2 radiation source
| AD-A261399 | p 2862 N93-26520

CARBON FIBER REINFORCED PLASTICS
Effect of water immersion on fiber/matrix adhesion
| AD-A260704 | p 2636 N93-25652

CARBON FIBERS
Numerical modelling of induced effects of lightning strike on an all composite helicopter p 2583 N93-24879
A computational approach to predicting the extent of arc root damage in CFC panels p 2642 N93-24890
Zoning of aircraft by electric field modelling p 2583 N93-24894
Effect of water immersion on fiber/matrix adhesion
| AD-A260704 | p 2636 N93-25652
The corrosion of metal matrix composites p 2638 N93-25723
The 0.3 mm diameter flexible amperometric lactate probe
| AD-A260826 | p 2690 N93-25782

CARBON MONOXIDE
Oxides of nitrogen emissions from turbulent hydrocarbon/air jet diffusion flames, phase 2
| PB93-152478 | p 2768 N93-26533

CARBON STARS
Radial velocity measurements of carbon stars p 2895 N93-25713

CARBON STEELS
Processing and mechanical properties of laminated metal composites of Al/Al-25 vol. percent SiC and ultrahigh carbon steel/brass
| DE93-007504 | p 2635 N93-25383

CARBON TETRAFLUORIDE
Global warming potential for CF4
| DE93-005740 | p 2762 N93-25146

CARBON-CARBON COMPOSITES
Stress and reliability analyses of multilayered composite cylinder under thermal and mechanical loads p 2726 N93-25533
Characterization of aerospace grade resins and composites through pressurized volumetric dilatometry
| AD-A260794 | p 2639 N93-25918

CARBONACEOUS CHONDRITES
Volatiles in interplanetary dust particles: A comparison with CI and CM chondrites p 2896 N93-26062

CARBONYL COMPOUNDS
A novel process for methanol synthesis
| DE93-008037 | p 2659 N93-25118
The structure and energetics of Cr(CO)6 and Cr(CO)5
| NASA-CR-192889 | p 2848 N93-25450

CARBOXYL GROUP
Intramolecular bridge/terminal oxo exchange within (MoV2O3) (4+) complexes containing linear oxo bridges
| AD-A261230 | p 2851 N93-26518

CARBOXYLIC ACIDS
Measurements of nitric acid, carboxylic acids, and selected aerosol species for the NASA/GTE Pacific Mission - West (PEM-WEST)
| NASA-CR-192976 | p 2763 N93-25287
Energetic materials from cubane
| AD-A261317 | p 2662 N93-26308

CARDIOVASCULAR SYSTEM
MAC to VAX connectivity: Heartrate spectral analysis system p 2796 N93-25594
Vascular uptake of rehydration fluids in hypohydrated men at rest and exercise
| NASA-TM-103942 | p 2795 N93-26133

CARDS
Thin rechargeable batteries for CMOS SRAM memory protection p 2694 N93-25583
A novel method for characterization of superconductors: Physical measurements and modeling of thin films p 2871 N93-25584

CARRIER INJECTION
Alternative equipment test procedures for simultaneous current injection on multiple cable bundles p 2693 N93-24903

CARRIER WAVES
Bandwidth compression of noisy signals with square-wave subcarrier p 2678 N93-26120

CASCADE FLOW
Flow and heat transfer experiments in the turbine airfoil/endwall region p 2704 N93-25725

CASING
Design and performance of nozzle-less volute casings for inward flow radial turbines p 2593 N93-25471

CASSINI MISSION
Feasibility study of a Ka-/Ka-band dichroic plate with stepped rectangular apertures p 2671 N93-24660

CASTINGS
High temperature fracture toughness of Ni3Al alloy IC-396M
| DE93-008564 | p 2650 N93-25492
Indigenous lunar construction materials p 2670 N93-26413
X-ray computed tomography for casting development
| AD-A261786 | p 2722 N93-26526

CASTS
Indigenous lunar construction materials p 2670 N93-26413

CATACLYSMIC VARIABLES
Origin and evolution of cataclysmic variables p 2893 N93-25245
Radial velocity studies of the secondary in cataclysmic variables p 2888 N93-25286

CATALOGS (PUBLICATIONS)
A revised and expanded catalogue of mass ejections observed by the Solar Maximum Mission coronagraph
| NASA-CR-193146 | p 2899 N93-26556

CATALYSIS
Improved selective catalytic NOx control technology for compressor station reciprocating engines
| PB93-158566 | p 2768 N93-26529

CATALYSTS
Design of a high activity and selectivity alcohol catalyst
| DE93-008101 | p 2659 N93-25111
Design of a high activity and selectivity alcohol catalyst
| DE93-008103 | p 2659 N93-25112
Probe molecule studies: Active species in alcohol synthesis
| DE93-008097 | p 2659 N93-25119
Theoretical predictions of platinum-rhodium bimetallic catalysts
| DE93-007540 | p 2649 N93-25428
Direct methane conversion to methanol
| DE93-009183 | p 2660 N93-25497
Catalytic conversion of light alkanes
| DE93-009646 | p 2644 N93-25499
Activation of methane by clean and chemically modified single crystal oxide surfaces
| PB93-157295 | p 2644 N93-25817

CATARACTS
A fiber optic probe for the detection of cataracts p 2796 N93-25593

CATHODE RAY TUBES
Emerging large-screen display technology
| AD-A261066 | p 2681 N93-26241

CATHODIC COATINGS
Photovoltaic power without batteries for continuous cathodic protection p 2759 N93-25597

CAUCHY PROBLEM
Activity report
| AD-A261933 | p 2829 N93-26199

CAVITIES
Surface discharge photoinitiation of pulsed chemical lasers
| DE93-006337 | p 2712 N93-24967
Poly-coil design for a 60 tesla quasi-stationary magnet
| DE93-007353 | p 2688 N93-25313
A model for the filling of cold cavities with solidifying, semi-crystalline polymers
| DE93-003817 | p 2655 N93-25507
Ultrasonic polishing p 2670 N93-25580

Another look at the driven cavity problem
| AD-A261903 | p 2708 N93-26543

CAVITY FLOW
Numerical study of cavity natural convection flow with augmenting and counteracting effects by projection finite element method p 2701 N93-25540
Navier-Stokes simulations of unsteady transonic flow phenomena p 2578 N93-25542

CAVITY RESONATORS
Basic design of a spaceborne hydrogen maser p 2716 N93-25024
Efficient nonlinear optical conversion of 1.319-micron laser radiation
| AD-A261309 | p 2715 N93-26297

CD-ROM
OCEAN-PC and a distributed network for ocean data p 2734 N93-24928
Satellite altimetry p 2734 N93-24930
US Army evaluation of the Electronic Map Data (EMD) prototype
| AD-A261693 | p 2757 N93-26369

CELESTIAL MECHANICS
Atomic time scales for dynamical astronomy p 2832 N93-24984

CELESTIAL REFERENCE SYSTEMS
Atomic time scales for dynamical astronomy p 2832 N93-24984

CELLS (BIOLOGY)
Mechanical stimulation of skeletal muscle mitigates glucocorticoid induced decreases in prostaglandin synthesis
| NASA-CR-193040 | p 2794 N93-24763
Measuring the metastatic potential of cancer cells p 2794 N93-25566
Effect of cytoskeletal reagents on stretch activated ion channels
| AD-A261089 | p 2793 N93-25764

CELLULOSE NITRATE
The burning rate behavior of pure nitrocellulose propellant samples
| AD-A261009 | p 2661 N93-25857

CEMENTATION
Particle size as a factor in agglomeration in slurry fuels p 2625 N93-26013

CENTAURUS CONSTELLATION
ROSAT investigation of flaring and activity on Prox Cen
| NASA-CR-192972 | p 2891 N93-26139

CENTER OF GRAVITY
Experimental performance of a ventral nozzle with pitch and yaw vectoring capability for SSTOVL aircraft
| NASA-TM-106054 | p 2592 N93-25129
Apparatus and methods for determining balance of a cylindrical vehicle
| AD-D015637 | p 2717 N93-25228

CENTER OF MASS
Helmeted head and neck dynamics under whole-body vibration p 2800 N93-25531

CENTRAL PROCESSING UNITS
Using a Cray Y-MP as an array processor for a RISC Workstation
| NASA-TM-103961 | p 2809 N93-25246
The database Query Support Processor (QSP) p 2807 N93-25577
The design and implementation of a read prediction buffer
| AD-A260902 | p 2806 N93-25934

CENTRIFUGAL COMPRESSORS
Numerical modelling of viscous turbomachinery flows with a pressure correction method p 2594 N93-25702

CENTRIFUGAL FORCE
A numerical and experimental studies of flow characteristics in centrifugal fans p 2577 N93-25339

CENTROIDS
Geometric distortion analysis of a wide-field astrograph p 2621 N93-26111

CERAMIC FIBERS
Internal strain analysis of ceramics using scanning laser acoustic microscopy
| NASA-CR-191118 | p 2721 N93-25451
Passive vibration damping materials: Piezoelectric ceramics composites for vibration damping applications
| AD-A260792 | p 2727 N93-25690
The corrosion of metal matrix composites p 2638 N93-25723
International Workshop on Advances in Inorganic Fibre Technology
| AD-A260719 | p 2639 N93-25908
Ceramic fiber reinforced glass-ceramic matrix composite
| NASA-CASE-LEW-15262-1 | p 2640 N93-26100

CERAMIC MATRIX COMPOSITES
Development of ASTM standards in support of advanced ceramics development
| DE93-003024 | p 2654 N93-25361
Internal strain analysis of ceramics using scanning laser acoustic microscopy
| NASA-CR-191118 | p 2721 N93-25451
High resolution interface nanochemistry and structure
| DE93-009750 | p 2635 N93-25501
Mullite whiskers and mullite-whisker felt p 2642 N93-25586
Transformation plasticity and fracture behavior of ceria-TZP/alumina composites p 2638 N93-25760
International Workshop on Advances in Inorganic Fibre Technology
| AD-A260719 | p 2639 N93-25908
Processing and properties of silicon carbide reinforced reaction bonded silicon nitride composites
| AD-A260570 | p 2640 N93-26236
Three-dimensional analysis and verification of fracture growth mechanisms in fiber-reinforced ceramic composites
| AD-A261483 | p 2641 N93-26355

CERAMICS
Evaluation of a candidate material for a coal-fired magnetohydrodynamic (MHD) high temperature recuperative air heater
| DE93-006630 | p 2858 N93-24968
Development of thin film thermocouples on ceramic materials for advanced propulsion system applications
| NASA-TM-106017 | p 2709 N93-25173
Temperature-dependent electrical conductivity of soda-lime glass
| DE93-007872 | p 2654 N93-25359
Development of ASTM standards in support of advanced ceramics development
| DE93-003024 | p 2654 N93-25361
A comparison of moisture resistance with different types of end-terminations in ceramic capacitors
| DE93-007600 | p 2689 N93-25416
Characterization of ceramic capacitors for high-voltage pulse-discharge applications
| DE93-007601 | p 2689 N93-25417
The design of mechanically compatible fasteners for human mandible reconstruction p 2796 N93-25569
Production of ultrafine, high-purity ceramic powders using the US Bureau of Mines developed turbomill p 2659 N93-25585
Electroelastic equations for electroded thin plates subject to large driving voltages
| AD-A261123 | p 2675 N93-25772
Vickers indentation hardness of stoichiometric and reduced single crystal TiO2 (rutile) from 25 to 800 C
| NASA-TM-105959 | p 2633 N93-26204
Processing and properties of silicon carbide reinforced reaction bonded silicon nitride composites
| AD-A260570 | p 2640 N93-26236
Research support for the Laboratory for Lightwave Technology
| AD-A261488 | p 2856 N93-26343
Densification of ceramics by gas overpressure sintering
| MTL-TR-92-45 | p 2657 N93-26432
Published assessments bearing on the future use of ceramic superconductors by the electric power sector
| DE93-007737 | p 2658 N93-26588

CEREBRAL CORTEX
Duration of alpha suppression increases with angle in a mental rotation task
| AD-A261592 | p 2798 N93-26435
Imaging regional changes in the spontaneous activity of the brain: An extension of the minimum-norm least-squares estimate
| AD-A261593 | p 2798 N93-26436
Neuromagnetic investigation of cortical regions underlying short-term memory
| AD-A261445 | p 2799 N93-26521

CERENKOV COUNTERS
The Sudbury Neutrino Observatory
| DE93-007697 | p 2899 N93-25327

CERIUM OXIDES
In situ surface studies of conversion coatings for steel and aluminum
| AD-A261016 | p 2655 N93-25861

CERTIFICATION
General aviation aircraft: Normal acceleration data analysis and collection project
| DOT/FAA/CT-91/20 | p 2586 N93-24739
Zoning of aircraft: A review of the definitions p 2583 N93-24880

CESIUM
A simple and compact source of cold atoms for cesium fountains and microgravity clocks p 2831 N93-24981
Preliminary results on an optically-pumped Cs beam frequency standard p 2832 N93-24989
Miniature optically-pumped cesium beam resonator p 2833 N93-24990
Actual limits of fluorescence S/N ratio in an optically-pumped cesium beam resonator p 2833 N93-24991
A compact and high-performance reference cell for laser frequency stabilization p 2716 N93-25065

CHANGE DETECTION
The regional planning and control using the satellite data p 2740 N93-24788
Monitoring and analysis of urban trends using multitemporal satellite-imagery (case-study: Greater Cairo) p 2740 N93-24790
Detection of land use/land cover changes using remote sensing and GIS in Vietnam p 2740 N93-24791
Hel's peninsula coastal zone changes in the last 40 years on a base of remote sensing methods p 2747 N93-24832
Monitoring and evaluation of morphohydrographical changes in the Danube Delta by remote-sensing p 2747 N93-24834
The national parks of Bavarian Forest and Sumava: A Landsat TM perspective on the structure and dynamics of the largest woodland of Central Europe p 2748 N93-24837
Interpretation and segmentation of changed forest stands from difference imagery based on regression functions p 2748 N93-24839
Assessment of storm damage in forests using SPOT imagery p 2748 N93-24842
Observation of forest damages in the Harz mountains by means of satellite remote sensing p 2749 N93-24848

CHANNEL FLOW
Propagation velocity and space-time correlation of perturbations in turbulent channel flow
| NASA-TM-103932 | p 2695 N93-25082
Spatial simulation of transition in wall-bounded shear flows: Active control and effects of surface roughness p 2701 N93-25483
Computational modelling of 3D flow in complex ducts and passages p 2704 N93-25698

CHANNELS (DATA TRANSMISSION)
Figure of merit for direct-detection optical channels p 2678 N93-26117
Statistics of sampled Rician fading
| AD-A261397 | p 2681 N93-26289

CHAOS
Introduction of chaotic dynamical systems
| AD-A261747 | p 2872 N93-26250
Information transmission using CHAOS
| AD-A261519 | p 2883 N93-26377
Chaos metrics for testing lagrangian particle models
| AD-A261429 | p 2776 N93-26454
1992 technical digest series volume 16. Conference edition: Summaries of papers presented at the Nonlinear Dynamics in Optical Systems Topical Meeting
| AD-A261915 | p 2857 N93-26544

CHAPLYGIN EQUATION
Nonholonomic geometry, mechanics and control p 2724 N93-25270

CHARACTERIZATION
Use of the Environmental Resource Management and Analysis System at the Fernald Environmental Management Project
| DE93-002943 | p 2760 N93-24955
Characterization of electrochemical systems and batteries: Materials and systems
| DE93-003472 | p 2687 N93-24964
Crystal growth and physical characterizations of GaPO4 p 2840 N93-25044
Interface engineering in oxide fiber/oxide matrix composites
| AD-A261705 | p 2641 N93-26579

CHARGE COUPLED DEVICES
Star tracker operation in a high density proton field p 2600 N93-24699
High resolution stereo imaging and data compression p 2753 N93-24867

CHARGE DISTRIBUTION
Halogen adlayers on Ag(111)
| AD-A261792 | p 2850 N93-26443

CHARGE TRANSFER
Halogen adlayers on Ag(111)
| AD-A261792 | p 2850 N93-26443
Theoretical treatment of spin-forbidden and electronically nonadiabatic processes. Methods and applications
| AD-A261596 | p 2851 N93-26525

CHARGED PARTICLES
Comparison of the electrical charging and discharging environments of multiple aircraft-borne electric-field measurement systems p 2583 N93-24887
Neutron energy determination with a high-purity germanium detector
| NASA-CR-192773 | p 2900 N93-25890

CHARPY IMPACT TEST
Mechanical properties of martensitic alloy AISI 422
| DE93-006563 | p 2649 N93-25255

CHEBYSHEV APPROXIMATION
An approach for finding long period elliptical orbits for precursor SEI missions p 2604 N93-24720
CHECKOUT
Source-level debugging of automatically parallelized programs
| AD-A261520 | p 2813 N93-26378
TCMS operations and maintenance philosophy
| NASA-TM-108756 | p 2873 N93-26418
Test, Control and Monitor System (TCMS) operations plan
| NASA-CR-193098 | p 2873 N93-26419
CHELATES
Transition metal chelate-fulleride compounds: Electrocrystallization of semiconducting (Ru(bpy)s)(C60)2
| AD-A261549 | p 2869 N93-26577
CHEMICAL ANALYSIS
Health and environmental chemistry: Analytical techniques, data management, and quality assurance
| DE93-002853 | p 2760 N93-24674
Ocean time-series near Bermuda: Hydrostation S and the US JGOFS Bermuda Atlantic time-series study p 2736 N93-24938
Studies of the analyte-carrier interface in flow injection analysis
| DE93-008374 | p 2644 N93-25311
High resolution interface nanochemistry and structure
| DE93-009750 | p 2635 N93-25501
Natural and augmented snowfall growth processes and their interactions with the natural and modified aerosol
| PB93-153096 | p 2786 N93-25874
Quality control: Variability in protocols
| PB93-157790 | p 2766 N93-25876
Handbook of chemical hazard analysis procedures
| PB93-158756 | p 2766 N93-26315
CHEMICAL BONDS
The interaction of HCN/DCN with Si(100)-2x1
| AD-A260837 | p 2645 N93-25920
Theoretical treatment of spin-forbidden and electronically nonadiabatic processes. Methods and applications
| AD-A261596 | p 2851 N93-26525
CHEMICAL CLEANING
Duct protection coating concept development and test. Appendix D, volume 1: Test specimen fabrication, conditioning, and testing documentation
| AD-A261005 | p 2656 N93-25940
Aqueous cleaning of flux residue from solder joints
| KCP-613-4803 | p 2652 N93-26208
CHEMICAL COMPOSITION
Characterization of electrochemical systems and batteries: Materials and systems
| DE93-003472 | p 2687 N93-24964
Cosmic ray composition investigations using ICE/ISEE-3
| NASA-CR-192808 | p 2900 N93-25241
Room temperature fracture of FeCo
| DE93-008266 | p 2650 N93-25519
Modeling of H2/N2O flames p 2627 N93-26026
CHEMICAL EQUILIBRIUM
A novel process for methanol synthesis
| DE93-008037 | p 2659 N93-25118
NMR studies of ion mobility and association in polyether-based polymer electrolytes
| AD-A260662 | p 2655 N93-25642
CHEMICAL EXPLOSIONS
Hazards of explosives dusts: Particle size effects
| DE93-009380 | p 2668 N93-25498
CHEMICAL LASERS
Surface discharge photoinitiation of pulsed chemical lasers
| DE93-006337 | p 2712 N93-24967
Experimental and theoretical study of cw HF chemical laser overtone performance p 2713 N93-25420
Experimental and theoretical study of CW HF chemical laser residual fundamental gain p 2714 N93-25721
Molecular interactions and properties with many-body methods
| AD-A261688 | p 2850 N93-26367
CHEMICAL MACHINING
Monolithic quartz vibrating beam accelerometer p 2711 N93-25011
Controlled dissolution of a piezoelectric material berlinite (AlPO4) p 2840 N93-25043
CHEMICAL PROPERTIES
Electrical and Chemical Interactions at Mars Workshop. Part 2: Appendix
| NASA-CP-10093-PT-2 | p 2897 N93-26392
Electrochemical and spectroscopic studies of molten halides
| AD-A261687 | p 2646 N93-26439
CHEMICAL REACTIONS
Design and synthesis of reactive separation systems
| DE93-008764 | p 2642 N93-25115
The properties of and analytical methods for detection of LiOH and Li2CO3
| NASA-CR-192771 | p 2643 N93-25240
Mechanistic studies of the CVD of silicon nitride from SiF4 and NH3
| DE93-004500 | p 2644 N93-25312
Energy transfer properties and mechanisms
| DE93-008540 | p 2849 N93-25488
Chemical dynamics studies of high energy species
| AD-A260743 | p 2852 N93-25676
Physical and chemical processes governing the CO2 laser-induced deflagration of ammonium dinitramide (ADN) p 2629 N93-26037
Phosphorus-, nitrogen-, sulfur-, and chlorine-containing molecules on surfaces
| AD-A261265 | p 2657 N93-26303
Energetic materials from cubane
| AD-A261317 | p 2662 N93-26308
Electrical and Chemical Interactions at Mars Workshop. Part 2: Appendix
| NASA-CP-10093-PT-2 | p 2897 N93-26392
CHEMICAL REACTORS
Direct methane conversion to methanol
| DE93-009183 | p 2660 N93-25497
CHEMISORPTION
Design of a high activity and selectivity alcohol catalyst
| DE93-008103 | p 2659 N93-25112
Resonant tunneling through chemisorbed halogen atoms on Ag(111)
| AD-A261794 | p 2868 N93-26254
CHEMOTHERAPY
Measuring the metastatic potential of cancer cells p 2794 N93-25566
Immunoconjugates: Magic bullets for cancer therapy? p 2796 N93-25567
CHINA
Climate data bases of the People's Republic of China, 1841-1988
| DE93-007907 | p 2764 N93-25517
CHINESE AIRCRAFT
An analysis of the reliability and maintainability of the Jian 6 and Jian 7 aircraft and ways to improve them
| AD-A261060 | p 2574 N93-26238
CHIPS (ELECTRONICS)
Two- and three-dimensional high performance, patterned overlay multi-chip module technology p 2694 N93-25581
Improved performance and safety for high energy batteries through use of hazard anticipation and capacity prediction p 2694 N93-25582
Solid-state isotopic power source for computer memory chips p 2694 N93-25596
Gigabit network communications research
| AD-A260644 | p 2675 N93-25640
Construction of a connectionist network supercomputer
| AD-A260929 | p 2820 N93-25648
Thermoelastic stresses in multi-layered media in non-uniform temperature fields
| AD-A260901 | p 2727 N93-25658
VLSI for high-speed digital signal processing
| AD-A260754 | p 2690 N93-25678
The design and implementation of a read prediction buffer
| AD-A260902 | p 2806 N93-25934
AMPHIB: A users manual
| AD-A261769 | p 2669 N93-26285
Considerations for space and naval aviation applications of ferroelectric memory
| AD-A261300 | p 2807 N93-26294
Multichip module high speed testing
| AD-A261391 | p 2856 N93-26306
RF vacuum microelectronics
| AD-A261343 | p 2691 N93-26311
CHIPS (MEMORY DEVICES)
Solid-state isotopic power source for computer memory chips p 2694 N93-25596
CHLOROCARBONS
An assessment of alternatives and technologies for replacing ozone-depleting substances at DOE facilities
| DE93-002862 | p 2760 N93-24675
CHLOROETHYLENE
Development of a replacement for trichloroethylene in the two-stage cleaning process
| KCP-613-4941 | p 2669 N93-26207
CHLOROFLUOROCARBONS
An assessment of alternatives and technologies for replacing ozone-depleting substances at DOE facilities
| DE93-002862 | p 2760 N93-24675
CHLOROPLASTS
Kinetic studies of interfacial photocurrents in platinized chloroplasts
| DE93-002344 | p 2792 N93-25104
CHROMATES
Chromate-free corrosion resistant talc coatings for aluminum alloys
| DE93-005370 | p 2655 N93-25446
CHROMIUM CARBIDES
Electrodeposition in low gravity p 2663 N93-24774
Properties of extruded PS-212 type self-lubricating materials p 2659 N93-25565
CHROMIUM STEELS
Interaction of O2 with the Fe(.84)Cr(.16) (001) surface studied by photoelectron spectroscopy
| AD-A261065 | p 2645 N93-26251
CHROMOSPHERE
ROSAT x ray survey observations of active chromospheric binary systems and other selected sources
| NASA-CR-192933 | p 2891 N93-26426
Chromospheric activity in algol binaries
| AD-A261440 | p 2896 N93-26508
CIRCUIT BOARDS
Aqueous cleaning of flux residue from solder joints
| KCP-613-4803 | p 2652 N93-26208
CIRCUIT BREAKERS
High speed solid state circuit breaker p 2694 N93-25598
CIRCUIT RELIABILITY
Dynamic behavior of helix interaction circuits
| AD-A261362 | p 2692 N93-26334
CIRCUITS
The constant current loop: A new paradigm for resistance signal conditioning
| NASA-TM-108744 | p 2673 N93-25181
Development of high Tc (greater than 100 K) Bi, Tl and Y-based materials as superconducting circuit elements
| NASA-CR-192344 | p 2863 N93-25219
Radiation-hardened control system
| DE93-007248 | p 2688 N93-25377
Tuned circuit electric levitation bearings for microactuators p 2689 N93-25619
A design of a fast and area efficient multi-input Muller C-element
| AD-A261002 | p 2690 N93-25856
Utilization of an electronic circuit simulator in CMOS latch-up studies
| AD-A260877 | p 2690 N93-25935
Investigation into the common mode rejection ratio of the physiological signal conditioner circuit p 2794 N93-26073
Dynamic behavior of helix interaction circuits
| AD-A261362 | p 2692 N93-26334
CIRCULAR CYLINDERS
Experimental study of the effect of helical grooves on an infinite cylinder
| AD-A260890 | p 2676 N93-25912
CIRCULAR ORBITS
Momentum accumulation due to solar radiation torque, and reaction wheel sizing, with configuration optimization p 2600 N93-24695
Optimal finite-thrust time-bounded direct-ascent interception p 2607 N93-25272
Generalized probability model for calculation of interference to the Deep Space Network due to circularly Earth-orbiting satellites p 2679 N93-26127
CIRCULAR TUBES
Analysis of longitudinal impact on semi-infinite circular bars and tubes. Appendix no. 2
| AD-A261556 | p 2731 N93-26459
CIRCULATION DISTRIBUTION
Supersonic shock wave/vortex interaction
| NASA-CR-192917 | p 2576 N93-25249
CITRIC ACID
Reclamation with recovery of radionuclides and toxic metals from contaminated materials, soils, and wastes p 2769 N93-25571
CIVIL AVIATION
Design concepts for the development of cooperative problem-solving systems
| NASA-CR-192708 | p 2585 N93-25261
A review of civil aviation propeller-to-person accidents: 1980-1989
| AD-A260695 | p 2583 N93-25896
Design of an air traffic computer simulation system to support investigation of civil tiltrotor aircraft operations
| NASA-CR-192920 | p 2585 N93-26052
Bibliography on propulsion airframe integration technologies for high-speed civil transport applications, 1980-1991
| NASA-TM-105602 | p 2573 N93-26136
CLADDING
Surface preparation and characterization of a 400 micrometer diameter fused silica optical fiber for direct optical initiation (DOI) applications
| DE93-005485 | p 2852 N93-25182
CLASSIFICATIONS
The use of polarimetric multifrequency SAR for characterizing terrain classes p 2738 N93-24777

Remote sensed spectral signatures classification and recognition by neural networks: An approach to unsupervised techniques p 2738 N93-24779
The regional planning and control using the satellite data p 2740 N93-24788
A knowledge-based approach to waste disposal sites detection through integration of Landsat-TM imagery and geographical context information p 2741 N93-24796
European applications of space-borne Earth observation for land cover mapping p 2745 N93-24820
The national parks of Bavarian Forest and Sumava: A Landsat TM perspective on the structure and dynamics of the largest woodland of Central Europe p 2748 N93-24837
Application of photographic remote sensing data from space for information about forests p 2748 N93-24838
The use of polarimetric radar remote sensing data for application in forestry p 2749 N93-24845
Swedish forest information atlas p 2749 N93-24847
Cartography and statistics of crops under irrigation in the Donana area of Andalucia through the use of Landsat-TM imagery and its incorporation into a GIS p 2751 N93-24855
Registration of the use of agricultural fields and soil erosion using satellite remote sensing p 2751 N93-24856
Appliction of remote sensing to forestry mapping: Experience from the European collaborative programme for the less favoured areas p 2751 N93-24857
Biodiversity indication by Earth observation data p 2751 N93-24858
Combining spectral information with crop rotation knowledge for crop classifications p 2752 N93-24861
Tree classification software p 2814 N93-25591
The SWORD multilevel secure DBMS
|RSRE-92005| p 2811 N93-25942
The probabilistic neural network architecture for high speed classification of remotely sensed imagery p 2824 N93-25972
Data fusion with artificial neural networks (ANN) for classification of earth surface from microwave satellite measurements p 2824 N93-25974
Classifying multispectral data by neural networks p 2825 N93-25976
Inferring heuristic classification hierarchies from natural language input p 2825 N93-25979

CLASSIFIERS
The effects of cloud inhomogeneities upon radiative fluxes, and the supply of a cloud truth validation dataset
|NASA-CR-191711| p 2787 N93-26492

CLATHRATES
Far infrared spectra of amorphous and crystalline water ice and changes in these phases as the result of proton irradiation
|NASA-CR-192849| p 2892 N93-25230

CLAYS
Production of ultrafine, high-purity ceramic powders using the US Bureau of Mines developed turbomill p 2659 N93-25585

CLEAN ENERGY
Documentation for propane fleet conversion cost-effectiveness model
|PB93-165611| p 2720 N93-26590

CLEAN FUELS
Catalytic conversion of light alkanes
|DE93-009646| p 2644 N93-25499

CLEAR AIR TURBULENCE
Research support for the Laboratory for Lightwave Technology
|AD-A261488| p 2856 N93-26343

CLIMATE
WCRP surface radiation budget shortwave data product description, version 1.1
|NASA-TM-107747| p 2777 N93-24742
Environment Observation and Climate Modelling Through International Space Projects. Volume 2: Remote Sensing for Environmental Monitoring and Resource Management
|ESA-ISY-1-VOL-2| p 2737 N93-24775
Verification of a climate convention: Role and limitations of a space based remote sensing system p 2738 N93-24781
Proceedings of the Ocean Climate Data Workshop
|NASA-TM-108711| p 2732 N93-24915
International organisation of ocean programs: Making a virtue of necessity p 2732 N93-24917
Role of the ocean in climate changes p 2732 N93-24918
The role of the World Data Centers in handling ocean climate data p 2732 N93-24919
Operational seasonal and interannual predictions of ocean conditions p 2733 N93-24921
Indian Ocean analyses p 2733 N93-24925
Ocean climate data for user community in West and Central Africa: Needs, opportunities, and challenges p 2735 N93-24933
International ocean services: Is it time - will it ever be time? p 2737 N93-24941
Computer systems p 2737 N93-24942
FORTRAN M as a language for building earth system models
|DE93-007897| p 2763 N93-25370
Evaluating climate-vegetation interactions at climate model sub-grid scales p 2764 N93-25476
Climate data bases of the People's Republic of China, 1841-1988
|DE93-007907| p 2764 N93-25517
Parallelizing the spectral transform method: A comparison of alternative parallel algorithms
|DE93-008664| p 2816 N93-25521
Land surface processes and climate modeling p 2783 N93-25685
National Weather Service Winter Weather Workshop
|PB93-146785| p 2785 N93-25775
Climate Monitoring and Diagnostics Laboratory
|PB93-156388| p 2785 N93-25871
Rainfall frequency atlas of the Midwest
|PB93-164606| p 2785 N93-25872
The Earth's climate as a dynamical system
|DE93-004666| p 2767 N93-26496

CLIMATE CHANGE
Environment Observation and Climate Modelling Through International Space Projects. Volume 2: Remote Sensing for Environmental Monitoring and Resource Management
|ESA-ISY-1-VOL-2| p 2737 N93-24775
Role of the ocean in climate changes p 2732 N93-24918
Sea level variation p 2734 N93-24929
Data management for JGOFS: Theory and design p 2735 N93-24935
Selected translated abstracts of Russian-language climate-change publications: 1. Surface energy budget
|DE93-003189| p 2760 N93-24952
Analysis of LARI sensor system
|DE93-006334| p 2761 N93-24977
Application of optical remote sensing to the study of surface fluxes related to cloud formation
|DE93-003783| p 2781 N93-25125
Trends '91: A compendium of data on global change. Highlights
|DE93-003112| p 2761 N93-25144
CHAMMP
|DE93-007290| p 2762 N93-25184
Climate data bases of the People's Republic of China, 1841-1988
|DE93-007907| p 2764 N93-25517
Inverse sequential procedures for the monitoring of time series
|NASA-CR-192959| p 2765 N93-25666
Response and feedbacks of forest ecosystems to global climate change
|PB93-167252| p 2767 N93-26510

CLIMATOLOGY
WCRP surface radiation budget shortwave data product description, version 1.1
|NASA-TM-107747| p 2777 N93-24742
Correlation between NDVI values derived from NOAA AVHRR HRPT data and ground measurements of precipitation in the EFEDA study area (Spain) p 2738 N93-24780
The need for spaceborne observations for meteorology and climatology p 2744 N93-24813
World Ocean Circulation Experiment p 2733 N93-24922
The Global Ocean Observing System p 2733 N93-24923
Indian Ocean analyses p 2733 N93-24925
The use of remotely sensed data for operational fisheries oceanography p 2734 N93-24927
Ocean climate data for user community in West and Central Africa: Needs, opportunities, and challenges p 2735 N93-24933
The effects of sampling frequency on the climate statistics of the ECMWF general circulation model
|DE93-003338| p 2761 N93-25145
Climate data bases of the People's Republic of China, 1841-1988
|DE93-007907| p 2764 N93-25517
Parallelizing the spectral transform method: A comparison of alternative parallel algorithms
|DE93-008664| p 2816 N93-25521
Local and regional estimates of sensible and latent heat flux densities from a patch-work surface
|ISBN-0-315-70882-4| p 2772 N93-25556
National Weather Service Winter Weather Workshop
|PB93-146785| p 2785 N93-25775
Climate Monitoring and Diagnostics Laboratory
|PB93-156388| p 2785 N93-25871
Rainfall frequency atlas of the Midwest
|PB93-164606| p 2785 N93-25872
A climatology of polar low occurrences in the Nordic Seas and an examination of katabatic winds as a triggering mechanism
|AD-A261719| p 2786 N93-26245

CLINICAL MEDICINE
Automated system for early breast cancer detection in mammograms p 2796 N93-25568

CLOCKS
Timing a national telecommunications network using GPS p 2687 N93-25062
Strategies for synchronisation in an evolving telecommunications network p 2687 N93-25063

CLOSED CIRCUIT TELEVISION
The adult literacy evaluator: An intelligent computer-aided training system for diagnosing adult illiterates p 2799 N93-26082

CLOSED CYCLES
FALCON nuclear-reactor-pumped laser program and wireless power transmission
|DE93-007607| p 2715 N93-26597

CLOSED ECOLOGICAL SYSTEMS
A survey of life support system automation and control
|NASA-TM-103977| p 2667 N93-25085

CLOSURE LAW
Fast parallel algorithms that compute transitive closure of a fuzzy relation
|NASA-CR-192950| p 2818 N93-25190

CLOUD COVER
Application of optical remote sensing to the study of surface fluxes related to cloud formation
|DE93-003783| p 2781 N93-25125
Prediction of global cloud cover with a very high resolution global spectral model
|AD-A261047| p 2785 N93-25777

CLOUD GLACIATION
The initiation of lightning and the growth of electric fields in thunderstorms
|AD-A261455| p 2787 N93-26352

CLOUD SEEDING
Investigation of winter mountain storms in Utah during the 1989 Utah/NOAA field program
|PB93-153021| p 2785 N93-25849
Natural and augmented snowfall growth processes and their interactions with the natural and modified aerosol
|PB93-153096| p 2786 N93-25874

CLOUDS (METEOROLOGY)
WCRP surface radiation budget shortwave data product description, version 1.1
|NASA-TM-107747| p 2777 N93-24742
Cloud properties as inferred from HIRS/2 multi-spectral data p 2782 N93-25293

CLUSTER ANALYSIS
Discrete range clustering using Monte Carlo methods
|NASA-TM-104004| p 2584 N93-24914
Improving performance through concept formation and conceptual clustering
|NASA-CR-192726| p 2828 N93-25262

CLUTTER
Theoretical study of topside ionospheric clutter
|AD-A260982| p 2774 N93-25852
High Frequency (HF) radiowave propagation
|AD-A261726| p 2681 N93-26280

CMOS
Thin rechargeable batteries for CMOS SRAM memory protection p 2694 N93-25583
Smart microsensors for high temperature applications
|AD-A260747| p 2710 N93-25677
A design of a fast and area efficient multi-input Muller C-element
|AD-A261002| p 2690 N93-25856
Utilization of an electronic circuit simulator in CMOS latch-up studies
|AD-A260877| p 2690 N93-25935

COAL
Biological production of ethanol from coal
|DE93-008947| p 2660 N93-25496

COAL DERIVED LIQUIDS
Production of low-cost hydrogen
|DE93-008070| p 2643 N93-25305

COAL GASIFICATION
Production of low-cost hydrogen
|DE93-008070| p 2643 N93-25305

COAL LIQUEFACTION
Production of low-cost hydrogen
|DE93-008070| p 2643 N93-25305

COASTAL CURRENTS
Wind-driven coastal generation of annual mesoscale eddy activity in the California current
|AD-A261355| p 2790 N93-26331

COASTAL ECOLOGY
Oil pollution and water quality mapping of Augusta Bay, Italy using remote sensing techniques p 2746 N93-24823

Hel's peninsula coastal zone changes in the last 40 years on a base of remote sensing methods
p 2747 N93-24832

COASTAL PLAINS
Archaeological, historical and geoelectrical data as ground truth for Landsat TM imagery application to coastal plain evolution studies p 2742 N93-24799
Remote sensing of coastal zone Sabkha deposits, Gulf of Sirt, Libya p 2746 N93-24827

COASTAL WATER
Multi-date algorithms for predicting surface water quality parameters in estuarine and coastal waters using Landsat TM data
| ED-659-CP | p 2746 N93-24829
Evaluation of nearshore suspended sediment concentration through Landsat TM data: First results
p 2747 N93-24833
Coastal environmental mapping using Landsat data
| ED-658-CP | p 2747 N93-24835
Loss of temporal coherence of laser light propagated through simulated coastal waters
| AD-A261303 | p 2715 N93-26296

COASTS
Applications of remote sensing for tidal waters, coastal areas and inland waters p 2745 N93-24819
Supporting the Portuguese fisheries with satellites
p 2745 N93-24821
ADCIRC: An advanced three-dimensional circulation model for shelves, coasts, and estuaries. Report 1: Theory and methodology of ADCIRC-2DDI and ADCIRC-3DL
| AD-A261608 | p 2790 N93-26164
Coastal ocean processes: A science prospectus
| AD-A261702 | p 2790 N93-26384
A coastal hazards data base for the US East Coast
| NASA-TM-108265 | p 2791 N93-26586

COATING
Asymptotic studies of gravity-driven reacting coating flows and pultrusion processes p 2704 N93-25683
Duct protection coating concept development and test: Test specimen fabrication, conditioning, and testing documentation.
| AD-A261250 | p 2657 N93-26278

COATINGS
Process for bonding elastomers to metals
| NASA-CASE-LAR-13645-1 | p 2656 N93-25995
New directions in phthalocyanine pigments
| NASA-CR-192443 | p 2656 N93-26155
Optically smart surfaces survivability testing at Mach 3
| AD-A261785 | p 2857 N93-26566

COAXIAL PLASMA ACCELERATORS
Preliminary investigation of power flow and electrode phenomena in a multi-megawatt coaxial plasma thruster
| NASA-CR-191084 | p 2633 N93-26555

COBALT ALLOYS
Room temperature fracture of FeCo
| DE93-008266 | p 2650 N93-25519
Position sensitive atom probe study of the decomposition of a Cu-2.6 at. percent Co alloy
| DE93-006737 | p 2653 N93-26500

CODERS
Entropy reduction via simplified image contourization
p 2804 N93-25924
Compression of spectral meteorological imagery
p 2804 N93-25925
Trellis coded CPFSK
| AD-A261788 | p 2682 N93-26441

CODING
The analysis of convolutional codes via the extended Smith algorithm p 2671 N93-24664
Image coding by way of wavelets
p 2671 N93-24665
Experiments with the HIVITS HDTV contribution CODED
| BBC-RD-1992/12 | p 2674 N93-25391
Subband coding for image data archiving
p 2803 N93-25922
Adjustable lossless image compression based on a natural splitting of an image into drawing, shading, and fine-grained components p 2804 N93-25923
Methods of evaluating the effects of coding on SAR data p 2804 N93-25926
Multi-rate, real time image compression for images dominated by point sources p 2805 N93-25932
Variable pulse rate circuit
| AD-D015675 | p 2691 N93-26233

COEFFICIENTS
Thermoelasticity in quartz p 2841 N93-25047
Estimation of coefficients in a rational function from observed values
| AD-A261126 | p 2828 N93-25773
Thermal expansion measurements of polymer matrix composites and syntactics
| MTL-TR-92-27 | p 2640 N93-25954

COGNITION
Facilitation and interference in identification of pictures and words
| AD-A261484 | p 2798 N93-26356
Duration of alpha suppression increases with angle in a mental rotation task
| AD-A261592 | p 2798 N93-26435
Comparative analytical study of evoked and event related potentials as correlates of cognitive processes
| AD-A261388 | p 2799 N93-26446

COGNITIVE PSYCHOLOGY
A cognitive architecture for human performance process model research
| AD-A261040 | p 2797 N93-25815
Neural basis of motion perception
| AD-A261452 | p 2798 N93-26349
Facilitation and interference in identification of pictures and words
| AD-A261484 | p 2798 N93-26356
Spontaneous discovery and use of categorical structure
| AD-A261658 | p 2798 N93-26364
Neuromagnetic investigation of cortical regions underlying short-term memory
| AD-A261445 | p 2799 N93-26521

COHERENT LIGHT
Loss of temporal coherence of laser light propagated through simulated coastal waters
| AD-A261303 | p 2715 N93-26296

COHERENT RADAR
Remote sensing of precipitation and electrification with a dual-polarization, coherent, wideband radar system
| AD-A260779 | p 2756 N93-25679

COHERENT SCATTERING
Apparatus for imaging an object in or through a scattering medium using coherent anti-Stokes Raman scattering
| AD-D015642 | p 2852 N93-25358

COHESION
Theoretical predictions of platinum-rhodium bimetallic catalysts
| DE93-007540 | p 2649 N93-25428

COLD FRONTS
A three-dimensional study of the influence of mountains on a front
| AD-A261927 | p 2787 N93-26545

COLD GAS
Far-infrared emission, gas, and ultraluminous HII regions in M101
| NASA-CR-192791 | p 2890 N93-25755

COLD SURFACES
Numerical simulation of time-dependent thermocapillary convection in layered fluid systems
p 2700 N93-25472
Thermocapillary flow near a cold wall
| AD-A261050 | p 2706 N93-25779

COLD TOLERANCE
Cellular and tissue injury during nonfreezing cold injury and frostbite
| AD-A260574 | p 2795 N93-25900

COLD TRAPS
Optical detection of laser-cooled ions in a Penning trap p 2838 N93-25031

COLLISIONS
Energy transfer properties and mechanisms
| DE93-008540 | p 2849 N93-25488
Aircraft accident report: Tomy International, Inc., d/b/a Scenic Air Tours flight 22, Beech Model E18S, N342E in-flight collision with terrain, Mount Haleakala, Maui, Hawaii, 22 April 1992
| PB93-910401 | p 2583 N93-25827

COLLOCATION
Optimal cooperative power-limited rendezvous
p 2607 N93-24904

COLLOIDS
Colloid formation in implanted glasses
| DE93-006763 | p 2653 N93-24971

COLOR
Relations between blue whiting biomass and satellite derived phytoplankton and temperature in the Norwegian Sea
| AD-A261205 | p 2757 N93-25868
Advanced technology development multi-color holography
| NASA-CR-192451 | p 2711 N93-26154
Implementation of custom colors in the DECwindows environment
| AD-A261456 | p 2757 N93-26574

COLOR TELEVISION
An example of a phase-segregated enhanced PAL broadcasting system
| BBC-RD-1992/6 | p 2674 N93-25239

COLUMBUS SPACE STATION
The Columbus Metrology Science Team: Report on activities p 2670 N93-24987

COMBINATIONS (MATHEMATICS)
Monte-Carlo methods make Dempster-Shafer formalism feasible
| NASA-CR-192945 | p 2828 N93-25140

COMBINATORIAL ANALYSIS
Probability and statistics applied to the theory of algorithms
| AD-A261019 | p 2830 N93-25863

COMBUSTIBLE FLOW
A basic research model of natural gas combustion in turbulent flow, phase 2
| PB93-158509 | p 2644 N93-25819
Influence of supercritical conditions on pre-combustion chemistry and transport behavior of jet fuels
| AD-A261813 | p 2661 N93-26268

COMBUSTION
Catalytic conversion of light alkanes
| DE93-009646 | p 2644 N93-25499
Fundamental studies of droplet interactions in dense sprays
| AD-A261165 | p 2661 N93-25948
The 29th JANNAF Combustion Subcommittee Meeting, volume 2
| CPIA-PUB-593-VOL-2 | p 2624 N93-26005
Particle size as a factor in agglomeration in slurry fuels p 2625 N93-26013
A summary of the JANNAF workshop on liquid rocket atomization p 2625 N93-26014
Development of a second generation spray combustion code p 2626 N93-26016
Kinetic studies in gas-phase reaction mechanisms important to the combustion process of high energy density materials: The H2/NO2 reaction p 2628 N93-26027
Chemistry during the induction time in heated nitramines p 2629 N93-26035
An experimental and analytical study of the unsteady combustion of homogeneous energetic solids using the laser-recoil method p 2630 N93-26042

COMBUSTION CHAMBERS
Fuel injector: Air swirl characterization aerothermal modeling, phase 2, volume 1
| NASA-CR-189193 | p 2592 N93-24754
A three-dimensional algebraic grid generation scheme for gas turbine combustors with inclined slots
| NASA-CR-191095 | p 2694 N93-24759
Evaluation of the Migrating Combustion Chamber (MCC) engine
| AD-A260780 | p 2718 N93-25682
Particle behavior in solid propellant rocket motors and plumes
| AD-A260900 | p 2624 N93-25913
The effect of entrance radius and film injection on wall heating in scramjet nozzles p 2625 N93-26009
Solid fuel supersonic combustion
p 2625 N93-26010
Gasp 1.3 results for the transverse hydrogen reacting jet p 2625 N93-26011
Turbulence interacting with chemical kinetics in airbreathing combustion of ducted rockets
p 2625 N93-26012
A summary of the JANNAF workshop on liquid rocket atomization p 2625 N93-26014
Measurement of droplet vaporization rate enhancement caused by acoustic disturbances p 2626 N93-26015
A new approach to cooled combustion chambers: The 40K formed platelet chamber p 2626 N93-26018

COMBUSTION CHEMISTRY
Turbulence interacting with chemical kinetics in airbreathing combustion of ducted rockets
p 2625 N93-26012
Condensed-phase processes during solid propellant combustion. Part 4: Chemical and microscopic examination of laser-irradiated propellant samples
p 2628 N93-26032

COMBUSTION EFFICIENCY
Solid fuel supersonic combustion
p 2625 N93-26010
Gasp 1.3 results for the transverse hydrogen reacting jet p 2625 N93-26011
Development and use of hydrogen-air torches in an altitude facility
| NASA-TM-106047 | p 2598 N93-26214

COMBUSTION PHYSICS
A premixed laminar flame interacting with a vortex resulting in flame stretch and quenching
p 2642 N93-24771
A model of concurrent flow flame spread over a thin solid fuel
| NASA-CR-191111 | p 2663 N93-24946
Calculations of combustion response profiles and oscillations
| NASA-TM-106135 | p 2623 N93-25236
Ionization probes of molecular structure and chemistry
| DE93-008211 | p 2847 N93-25310
Modelling of microgravity ignition phenomena
p 2664 N93-25465

The 29th JANNAF Combustion Subcommittee Meeting, volume 2
| CPIA-PUBL-593-VOL-2 | p 2624 N93-26005
Visualization of a Mach 2 reacting flow using Planar Laser-Induced Fluorescence (PLIF)
p 2598 N93-26006
Solution of nonlinear boundary value problem on successively refined grids
| AD-A261395 | p 2829 N93-26519

COMBUSTION PRODUCTS
SIHTI: The research and development program of energy and environmental technology
| DE93-769925 | p 2763 N93-25360
Experimental investigation of flow turning losses in unstable rocket motors p 2630 N93-26040
Development and demonstration of a new filter system to control emissions during jet engine testing
| AD-A261203 | p 2766 N93-26243
Particulate emissions from gas turbine engines
| AD-A261374 | p 2595 N93-26339
Analysis of the IBSS spectra of Space Shuttle control engine exhaust
| AD-A261749 | p 2632 N93-26373
Improved selective catalytic NOx control technology for compressor station reciprocating engines
| PB93-158566 | p 2768 N93-26529
Oxides of nitrogen emissions from turbulent hydrocarbon/air jet diffusion flames, phase 2
| PB93-152478 | p 2768 N93-26533

COMBUSTION STABILITY
Calculations of combustion response profiles and oscillations
| NASA-TM-106135 | p 2623 N93-25236
Modelling of microgravity ignition phenomena
p 2664 N93-25465
The 29th JANNAF Combustion Subcommittee Meeting, volume 2
| CPIA-PUBL-593-VOL-2 | p 2624 N93-26005
Space transportation booster engine thrust chamber technology, large scale injector
| NASA-CR-192531 | p 2633 N93-26557

COMBUSTION TEMPERATURE
Evaluation of a candidate material for a coal-fired magnetohydrodynamic (MHD) high temperature recuperative air heater
| DE93-006630 | p 2858 N93-24968

COMMAND AND CONTROL
Analysis of the Command and Control Segment (CCS) attitude estimation algorithm p 2604 N93-24722
Expert system for UNIX system reliability and availability enhancement p 2723 N93-25588
Fidelity and validity in distributed interactive simulation: Questions and answers
| AD-A260971 | p 2810 N93-25711
Rome Laboratory Journal, 1992
| AD-A260821 | p 2911 N93-25910
Flight termination receiver catalog
| AD-A261558 | p 2682 N93-26460
System Concept of Operations Evaluator (SCOPE)
| AD-A261257 | p 2813 N93-26563

COMMERCE
Advanced energy systems and technologies - National R and D programme
| DE93-769943 | p 2758 N93-25097
Small business access to equity capital
| PB93-144582 | p 2872 N93-25735

COMMERCIAL AIRCRAFT
Evaluation of advanced displays for engine monitoring and control
| NASA-CR-191418 | p 2591 N93-24764
Lightning data acquisition p 2778 N93-24883
Applied aerodynamics: Challenges and expectations
| NASA-TM-103963 | p 2575 N93-25091

COMMUNICATION EQUIPMENT
The design and evaluation of transmit and receive antennas for an ionospheric communications probe system. B: Sloping-vee beams
| AD-A261866 | p 2682 N93-26388

COMMUNICATION NETWORKS
Crossing the frontier between publishing and information service
| DE93-002894 | p 2873 N93-24677
Time generation and distribution system for a military national synchronization p 2842 N93-25060
Timing and time signal distribution in digital communications networks p 2686 N93-25061
Timing a national telecommunications network using GPS p 2687 N93-25062
Strategies for synchronisation in an evolving telecommunications network p 2687 N93-25063
Robo-line storage: Low latency, high capacity storage systems over geographically distributed networks
| NASA-CR-192910 | p 2805 N93-25130
The PACSAT Communications Experiment (PCE)
| DE93-008185 | p 2674 N93-25308
Object-oriented tools for distributed computing
p 2817 N93-25576
The database Query Support Processor (QSP)
p 2807 N93-25577
An SPW software simulation model of a dispersive fading multipath narrowband HF channel
| AD-A261101 | p 2675 N93-25767
Adaptive laser link reconfiguration using constraint propagation p 2823 N93-25967
An OSI architecture for the Deep Space Network
p 2679 N93-26121
Deep Space Network information system architecture study p 2679 N93-26126
High performance computing and communications panel report p 2807 N93-26131
The Data Multiplexing Network (DMN) phase 3 Extended Distance Data Cable (EDDC) test and evaluation
| DOT/FAA/CT-TN93/11 | p 2680 N93-26160
Admission control in integrated voice/data multihop radio networks
| AD-A261055 | p 2680 N93-26227
Advanced optical fiber communication systems
| AD-A261802 | p 2856 N93-26256
Very high-speed report file system
| AD-A261068 | p 2817 N93-26277
FY92 contributions to the Database Management System Interface Standards Working Group of the Navy Next Generation Computer Resources Program
| AD-A261348 | p 2883 N93-26313
The design and evaluation of transmit and receive antennas for an ionospheric communications probe system. B: Sloping-vee beams
| AD-A261866 | p 2682 N93-26388
EnviroNET p 2886 N93-26398
Telerobotic rovers for extraterrestrial construction
p 2670 N93-26416
A channel simulation processor for the multi-node tactical network simulator
| AD-A261810 | p 2776 N93-26430
ETS-5, ETS-6, and COMETS projects in Japan
p 2683 N93-26470
OSSA Information Systems Program
| NASA-TM-108758 | p 2883 N93-26491
Department of Defense technical architecture framework for information management. Volume 1: Implementation concept, version 1.1
| AD-A261911 | p 2884 N93-26531
Department of Defense technical architecture framework for information management. Volume 2: Architecture guidance and design concepts, version 1.1
| AD-A261912 | p 2884 N93-26532
A comparison of ionospheric propagation mode delay predictions from ADVANCED PROPHET 4.3 with measured data
| AD-A261782 | p 2686 N93-26604

COMMUNICATION SATELLITES
The PACSAT Communications Experiment (PCE)
| DE93-008185 | p 2674 N93-25308
Investigation of liquid sloshing in spin-stabilized satellites
| AD-A261671 | p 2619 N93-26438
ETS-5, ETS-6, and COMETS projects in Japan
p 2683 N93-26470

COMMUTER AIRCRAFT
General aviation aircraft: Normal acceleration data analysis and collection project
| DOT/FAA/CT-91/20 | p 2586 N93-24739

COMPARISON
Prospects of two-way international time scale comparisons p 2832 N93-24988
Comparison of GLONASS and GPS time transfers
p 2836 N93-25017

COMPENSATORS
Design of the reduced LQG compensator for the DSS-13 antenna p 2672 N93-24669
The 32nd CDC: Robust stabilizer synthesis for interval plants using Nevanlina-pick theory
| NASA-CR-192894 | p 2818 N93-25156

COMPETITION
Energy and Technology Review, August-September 1992
| DE93-005882 | p 2901 N93-24974

COMPLEX SYSTEMS
Control of complex dynamic systems by neural networks p 2827 N93-25611
The rapid solution of the Laplace equation on regions with fractal boundaries
| AD-A260585 | p 2828 N93-25905
Proceedings of the complex systems engineering synthesis and assessment technology workshop
| AD-A261404 | p 2807 N93-26403

COMPOSITE MATERIALS
Method for providing EMI/EMP hardening and breakdown protection in composite materials
| AD-D015638 | p 2634 N93-25283
Numerical and experimental analyses of large composite skeletal satellite systems p 2616 N93-25463
Design and validation of optimal experiments for estimating thermal properties of composite materials
p 2635 N93-25541
Determination of the elastic constants of composite materials from ultrasonic group velocity measurements
p 2635 N93-25544
INEL spray-forming research p 2658 N93-25562
Properties of extruded PS-212 type self-lubricating materials p 2659 N93-25565
Improved composite fabrication process
| AD-D015679 | p 2640 N93-26145

COMPOSITE PROPELLANTS
Dynamic burning rate measurements of metalized composite propellants using the laser-recoil technique
p 2631 N93-26043

COMPOSITE STRUCTURES
Numerical modelling of induced effects of lightning strike on an all composite helicopter p 2583 N93-24879
A procedure for defining lightning risk to air vehicles
p 2583 N93-24885
A computational approach to predicting the extent of arc root damage in CFC panels p 2642 N93-24890
Axisymmetric deformations and stresses of unsymmetrically laminated composite cylinders in axial compression with thermally-induced preloading effects
| NASA-CR-192788 | p 2723 N93-24912
High Temperature Composite Analyzer (HITCAN) theoretical manual, version 1.0
| NASA-TM-106001 | p 2723 N93-24913
High temperature composite analyzer (HITCAN) user's manual, version 1.0
| NASA-TM-106002 | p 2724 N93-25070
Determination of the elastic constants of composite materials from ultrasonic group velocity measurements
p 2635 N93-25544
The design of mechanically compatible fasteners for human mandible reconstruction p 2796 N93-25569
Graphite/epoxy composite laminates with co-cured interlaminar damping layers p 2642 N93-25587
Low-velocity impact of composite sandwich plate
p 2637 N93-25695
Design and analysis of curved composite components for rotorcraft fuselage frames p 2589 N93-25701
A three-dimensional model for the residual stresses in a unidirectional composite plate p 2728 N93-25825
Damage detection and mitigation of composite structures using smart materials
| AD-A261121 | p 2639 N93-25945
Improved fatigue life for moorings
| PB93-161198 | p 2730 N93-26320
Thermally induced stresses in a composite exposed to fire
| AD-A261714 | p 2641 N93-26371
Use and analysis of finite element methods for problems of solid mechanics and fracture
| AD-A261574 | p 2731 N93-26522
Japanese Technology Evaluation Center Workshop on Advanced Manufacturing Technology for Polymer Composite Structures in Japan
| PB93-165249 | p 2641 N93-26589

COMPOUND A
Sputter deposition of yttrium-oxides
| DE93-007499 | p 2654 N93-25382

COMPRESSED GAS
Cost-effectiveness analysis of TxDOT CNG fleet conversion, volume 2
| PB93-159432 | p 2720 N93-26534
Cost-effectiveness analysis of TxDOT CNG fleet conversion, volume 1
| PB93-165603 | p 2720 N93-26585

COMPRESSIBILITY
European tri-service advanced materials workshop on compressive strength in rigid-rod polymers
| AD-A261517 | p 2658 N93-26576

COMPRESSIBILITY EFFECTS
The effects of video compression on acceptability of images for monitoring life sciences' experiments
p 2805 N93-25930

COMPRESSIBLE BOUNDARY LAYER
Nonlinear evolution of the first mode supersonic oblique waves in compressible boundary layers. Part 1: Heated/cooled walls
| NASA-TM-106087 | p 2696 N93-25175
Shock tube application to the study of compressible turbulent boundary layer with mass injection
p 2697 N93-25252

COMPRESSIBLE FLOW
A convergent finite difference scheme for the Navier-Stokes equations of nonisentropic compressible fluid flow p 2695 N93-24906
Implementation of the Turn Function Method in a three-dimensional, parallelized hydrodynamics code
| DE93-003744 | p 2696 N93-25124

Assessment of closure coefficients for compressible-flow turbulence models
| NASA-TM-103882 | p 2697 N93-25247
Structured adaptive mesh refinement on the connection machine
| DE93-007368 | p 2816 N93-25316
Implicit multigrid solution of the compressible Navier-Stokes equations with application to distributed parallel processing p 2702 N93-25546
Unsteady airfoil flow solutions on moving zonal grids
| AD-A261925 | p 2582 N93-26198

COMPRESSING
Polyimides with improved compression moldability
| NASA-CASE-LAR-14457-1 | p 2656 N93-25997

COMPRESSION LOADS
Axisymmetric deformations and stresses of unsymmetrically laminated composite cylinders in axial compression with thermally-induced preloading effects
| NASA-CR-192788 | p 2723 N93-24912
Numerical simulation of damage and progressive failures in composite laminates using the layerwise plate theory p 2636 N93-25661

COMPRESSION RATIO
Compression of spectral meteorological imagery p 2804 N93-25925
Fractal image compression: A resolution independent representation for imagery p 2804 N93-25927

COMPRESSION TESTS
Transformation plasticity and fracture behavior of ceria-TZP/alumina composites p 2638 N93-25760

COMPRESSIVE STRENGTH
European tri-service advanced materials workshop on compressive strength in rigid-rod polymers
| AD-A261517 | p 2658 N93-26576

COMPRESSOR BLADES
The effects of reaction on axial compressor performance p 2594 N93-25882
Model fan passage flow simulation
| AD-A261613 | p 2707 N93-26167

COMPRESSORS
The WINCOF-I code: Detailed description
| NASA-CR-190779 | p 2573 N93-24760
Improved selective catalytic NOx control technology for compressor station reciprocating engines
| PB93-158566 | p 2768 N93-26529

COMPUTATION
Attitude determination using vector observations: A fast optimal matrix algorithm p 2606 N93-24731
An improved spectral load balancing method
| DE93-007582 | p 2810 N93-25386
Parallel matrix computations
| AD-A260783 | p 2828 N93-25687
Knowledge-based assistance for science visualization and analysis using large distributed databases p 2879 N93-25801
High performance compression of science data p 2881 N93-25811
Computation and learning in neural networks with binary weights
| AD-A261182 | p 2821 N93-25821
Power iterations and the dominant eigenvalue problem
| AD-A261695 | p 2829 N93-26370

COMPUTATIONAL FLUID DYNAMICS
Prediction of forces and moments for hypersonic flight vehicle control effectors
| NASA-CR-193033 | p 2595 N93-24762
Computation of hypersonic viscous flowfields using the parabolized Navier-Stokes equations p 2694 N93-24766
Computational study of the aerodynamics and control by blowing of asymmetric vortical flows over delta wings p 2574 N93-24772
A convergent finite difference scheme for the Navier-Stokes equations of nonisentropic compressible fluid flow p 2695 N93-24906
Rapid exploration of curvilinear grids using direct volume rendering
| NASA-CR-192765 | p 2808 N93-24944
Propagation velocity and space-time correlation of perturbations in turbulent channel flow
| NASA-TM-103932 | p 2695 N93-25082
A contribution to the great Riemann solver debate
| NASA-CR-191409 | p 2575 N93-25083
Prediction of unsteady flows in turbomachinery using the linearized Euler equations on deforming grids
| NASA-CR-192919 | p 2696 N93-25109
Implementation of the Turn Function Method in a three-dimensional, parallelized hydrodynamics code
| DE93-003744 | p 2696 N93-25124
Transient performance of fan engine with water ingestion
| NASA-CR-190778 | p 2573 N93-25134
Instability of flow in a streamwise corner
| NASA-CR-191410 | p 2576 N93-25153
The modeling of complex continua: Fundamental obstacles and grand challenges
| DE93-006507 | p 2696 N93-25193
Assessment of closure coefficients for compressible-flow turbulence models
| NASA-TM-103882 | p 2697 N93-25247
Direct solutions of the Navier-Stokes equations with application to static aeroelasticity p 2697 N93-25259
The steady Navier-Stokes problem for low Reynolds number viscous jets p 2698 N93-25264
Data parallel finite element techniques for large-scale computational fluid dynamics p 2699 N93-25334
A compact high-order Euler solver for unstructured grids p 2699 N93-25341
Some new results for solving linear systems arising from computational fluid dynamics problems p 2699 N93-25349
Numerical simulation of leading-edge receptivity to freestream vorticity p 2577 N93-25388
Spatial simulation of transition in wall-bounded shear flows: Active control and effects of surface roughness p 2701 N93-25483
Numerical study of cavity natural convection flow with augmenting and counteracting effects by projection finite element method p 2701 N93-25540
Navier-Stokes simulations of unsteady transonic flow phenomena p 2578 N93-25542
Implicit multigrid solution of the compressible Navier-Stokes equations with application to distributed parallel processing p 2702 N93-25546
Dynamics of turbulent slugging in transitional pipe flow p 2702 N93-25548
A computational aerodynamic design optimization method using sensitivity analysis p 2589 N93-25552
The instability of a liquid jet in a compressible airstream p 2703 N93-25560
Stabilized finite element methods for incompressible flows with emphasis on moving boundaries and interfaces p 2703 N93-25663
Computational modelling of 3D flow in complex ducts and passages p 2704 N93-25698
Analysis of wing wake roll-up using a vortex-in-cell method p 2579 N93-25706
Flow between finite rotating disks and its linear stability p 2705 N93-25747
Large-eddy simulation of temporally developing boundary layers with embedded streamwise vortices p 2705 N93-25753
A new LU-SGS flow solver for calculating reentry flows p 2579 N93-25759
Stationary crossflow instability on an infinite swept wing p 2580 N93-25865
Simulation of vortex bursting p 2580 N93-25881
Numerical simulation of hypersonic aerodynamics and the computational needs for the design of an aerospace plane
| AD-A260681 | p 2580 N93-25894
Workshop Report: A validation study of Navier-Stokes codes for transverse injection into a Mach 2 flow p 2624 N93-26008
Development of a second generation spray combustion code p 2626 N93-26016
Eulerian-Eulerian treatment of turbulent dense spray combustion in a bipropellant liquid rocket engine p 2626 N93-26017
External tank aerothermal design criteria verification
| NASA-CR-192514 | p 2618 N93-26055
An extended Lagrangian method
| NASA-TM-106129 | p 2707 N93-26203
Influence of supercritical conditions on pre-combustion chemistry and transport behavior of jet fuels
| AD-A261813 | p 2661 N93-26268
Massively-parallel computational fluid dynamics
| AD-A261815 | p 2707 N93-26269
Computational methods for flow problems: Parallel algorithms, flow control, and novel approaches
| AD-A261400 | p 2707 N93-26400
Another look at the driven cavity problem
| AD-A261903 | p 2708 N93-26543
Effects of surface thermal forcing on stratified flow past an isolated obstacle
| PB93-156776 | p 2776 N93-26548
Incompressible spectral-element method: Derivation of equations
| NASA-TM-106109 | p 2708 N93-26554
A brief description of a new numerical framework for solving conservation laws: The method of space-time conservation element and solution element
| NASA-TM-105757 | p 2829 N93-26560

COMPUTATIONAL GRIDS
Use of the 1991 ASCOT field study data in a mesoscale model employing a four-dimensional data assimilation technique
| DE93-002683 | p 2769 N93-24672
A three-dimensional algebraic grid generation scheme for gas turbine combustors with inclined slots
| NASA-CR-191095 | p 2694 N93-24759
Rapid exploration of curvilinear grids using direct volume rendering
| NASA-CR-192765 | p 2808 N93-24944
A contribution to the great Riemann solver debate
| NASA-CR-191409 | p 2575 N93-25083
Prediction of unsteady flows in turbomachinery using the linearized Euler equations on deforming grids
| NASA-CR-192919 | p 2696 N93-25109
Grid sensitivity for aerodynamic optimization and flow analysis
| NASA-CR-192980 | p 2575 N93-25117
A compact high-order Euler solver for unstructured grids p 2699 N93-25341
Transformation of two and three-dimensional regions by elliptic systems
| NASA-CR-192955 | p 2810 N93-25669
Analysis of wing wake roll-up using a vortex-in-cell method p 2579 N93-25706
Multilevel techniques in large scale computation
| AD-A261082 | p 2828 N93-25762
Unsteady airfoil flow solutions on moving zonal grids
| AD-A261925 | p 2582 N93-26198
An extended Lagrangian method
| NASA-TM-106129 | p 2707 N93-26203
Solution of nonlinear boundary value problem on successively refined grids
| AD-A261395 | p 2829 N93-26519

COMPUTER AIDED DESIGN
Geometric modeling for computer aided design
| NASA-CR-192891 | p 2808 N93-24750
A state-of-the-art crystal filter design package using Windows 3.0 techniques p 2693 N93-25010
Integration of design, thermal, structural, and optical analysis, including thermal animation p 2814 N93-25601
An approach to configuration design synthesis of subsonic transport aircraft using artificial intelligence techniques p 2589 N93-25692
High-performance visualization applied to computational electromagnetics: Method-of-moments on a silicon graphics workstation
| AD-A260820 | p 2675 N93-25700
ASTOVL combat aircraft design synthesis and optimization p 2589 N93-25704
A digital hardware test system analysis with test vector translation
| AD-A260849 | p 2810 N93-25786
Computer-aided design package for designers of digital optical computers
| AD-A260757 | p 2806 N93-25848
An autonomous satellite architecture integrating deliberative reasoning and behavioural intelligence p 2823 N93-25970
Model reduction for Space Station Freedom p 2620 N93-26081
Design Knowledge Management System (DKMS) Beta Test Report
| AD-A261453 | p 2883 N93-26350
IDEF6: A design rationale capture method concept paper
| AD-A261594 | p 2884 N93-26523
X-ray computed tomography for casting development
| AD-A261786 | p 2722 N93-26526
System Concept of Operations Evaluator (SCOPE)
| AD-A261257 | p 2813 N93-26563

COMPUTER AIDED MANUFACTURING
A virtual environment for manufacturing systems
| AD-A260813 | p 2810 N93-25699
X-ray computed tomography for casting development
| AD-A261786 | p 2722 N93-26526

COMPUTER AIDED TOMOGRAPHY
Intraplate deformation, stress in the lithosphere and the driving mechanism for plate motions
| NASA-CR-192782 | p 2772 N93-25529
X-ray computed tomography for casting development
| AD-A261786 | p 2722 N93-26526
X ray computed tomography for failure analysis
| AD-A261884 | p 2722 N93-26527

COMPUTER ASSISTED INSTRUCTION
Integrated Development Support Environment (IDSE)
| AD-A261088 | p 2877 N93-25763
Computation and learning in neural networks with binary weights
| AD-A261182 | p 2821 N93-25821
Human Factors in Aviation Maintenance, phase 2
| DOT/FAA/AM-93/5 | p 2802 N93-26089

COMPUTER DESIGN
Computer-aided design package for designers of digital optical computers
| AD-A260757 | p 2806 N93-25848

COMPUTER GRAPHICS
Demonstration of seasonal changes in the territory of Finland using multitemporal NOAA-AVHRR data p 2742 N93-24801
Improving information search at the user interface: The impact of graphical innovation on query formulation and expression p 2873 N93-24905
A state-of-the-art crystal filter design package using Windows 3.0 techniques p 2693 N93-25010
Efficient inspection of network pollution data
| DE93-003810 | p 2761 N93-25126
Scientific visualization using the Flow Analysis Software Toolkit (FAST) p 2814 N93-25600
Interactive interface for National Center for Atmospheric Research (NCAR) Graphics p 2878 N93-25794
Measures of user-system interface effectiveness: An encoding scheme and indicators for assessing the usability of graphical, direct-manipulation style user interfaces
| AD-A260606 | p 2801 N93-25840
Advanced technology for portable personal visualization
| AD-A261294 | p 2807 N93-26293
Three view language: A graphics-based language for requirements definition, version 01.00.00
| AD-A261732 | p 2813 N93-26583

COMPUTER INFORMATION SECURITY
The database Query Support Processor (QSP) p 2807 N93-25577
The SWORD multilevel secure DBMS
| RSRE-92005 | p 2811 N93-25942

COMPUTER NETWORKS
Crossing the frontier between publishing and information service
| DE93-002894 | p 2873 N93-24677
EXCHANGE
| DE93-007227 | p 2808 N93-24962
On the robustness of Herlihy's hierarchy
| NASA-CR-193002 | p 2808 N93-25107
Robo-line storage: Low latency, high capacity storage systems over geographically distributed networks
| NASA-CR-192910 | p 2805 N93-25130
Zebra: A striped network file system
| NASA-CR-192912 | p 2809 N93-25250
A trace-driven analysis of name and attribute caching in a distributed system
| NASA-CR-192899 | p 2815 N93-25251
CAD data exchange development
| DE93-008085 | p 2809 N93-25307
A distributed heterogeneous client-server environment
| DE93-007496 | p 2875 N93-25319
Object-oriented tools for distributed computing p 2817 N93-25576
The database Query Support Processor (QSP) p 2807 N93-25577
Fidelity and validity in distributed interactive simulation: Questions and answers
| AD-A260971 | p 2810 N93-25711
Distributed information storage p 2877 N93-25722
The state of computing at Los Alamos National Laboratory, FY 1991
| LA-12326-MS | p 2811 N93-25943
An OSI architecture for the Deep Space Network p 2679 N93-26121
Deep Space Network information system architecture study p 2679 N93-26126
High performance computing and communications panel report p 2807 N93-26131
The Data Multiplexing Network (DMN) phase 3 Extended Distance Data Cable (EDDC) test and evaluation
| DOT/FAA/CT-TN93/11 | p 2680 N93-26160
Complexity of connectionist and constraint-satisfaction networks
| AD-A261617 | p 2817 N93-26169
Very high-speed report file system
| AD-A261068 | p 2817 N93-26277
FY92 contributions to the Database Management System Interface Standards Working Group of the Navy Next Generation Computer Resources Program
| AD-A261348 | p 2883 N93-26313
Test, Control and Monitor System (TCMS) operations plan
| NASA-CR-193098 | p 2873 N93-26419
OSSA Information Systems Program
| NASA-TM-108758 | p 2883 N93-26491
Department of Defense technical architecture framework for information management. Volume 2: Architecture guidance and design concepts, version 1.1
| AD-A261912 | p 2884 N93-26532

COMPUTER PROGRAM INTEGRITY
The SWORD multilevel secure DBMS
| RSRE-92005 | p 2811 N93-25942

COMPUTER PROGRAMMING
Geometric modeling for computer aided design
| NASA-CR-192891 | p 2808 N93-24750
Putting time into proof outlines
| NASA-CR-192978 | p 2809 N93-25152
Using a Cray Y-MP as an array processor for a RISC Workstation
| NASA-TM-103961 | p 2809 N93-25246
Deterministic parallel FORTRAN
| DE93-008665 | p 2816 N93-25522
Technology 2002: The Third National Technology Transfer Conference and Exposition, volume 1
| NASA-CP-3189-VOL-1 | p 2901 N93-25561
Splash 2 p 2814 N93-25575
Proceedings of Workshop 1: The Human Brainmap Database
| AD-A260720 | p 2796 N93-25654
Software lifecycle support environment (SLCSE) knowledge-based enhancements
| AD-A261042 | p 2811 N93-25791
Set based program analysis
| AD-A260979 | p 2806 N93-25841
Model-based reasoning for system and software engineering: The Knowledge From Pictures (KFP) environment p 2825 N93-25978
The design and implementation of a reusable component library and a retrieval/integration system
| AD-A261827 | p 2812 N93-26271
FY92 contributions to the Database Management System Interface Standards Working Group of the Navy Next Generation Computer Resources Program
| AD-A261348 | p 2883 N93-26313
Research directions in software analysis, synthesis and certification
| AD-A261367 | p 2812 N93-26336
Towards a formalism for program generation
| AD-A261689 | p 2812 N93-26368
AEGIS measures definition
| AD-A261494 | p 2812 N93-26375
Managing real-time software projects: Problems and issues
| AD-A261428 | p 2813 N93-26453
Three view language: A graphics-based language for requirements definition, version 01.00.00
| AD-A261732 | p 2813 N93-26583

COMPUTER PROGRAMS
Development and application of computational aerothermodynamics flowfield computer codes
| NASA-CR-192940 | p 2574 N93-24736
Experimentation in the low-density plume of a simulated electrothermal thruster for computer code validation
| NASA-CR-191112 | p 2622 N93-24758
Evaluation of MARC for the analysis of rotating composite blades
| NASA-TM-4423 | p 2723 N93-24909
High Temperature Composite Analyzer (HITCAN) theoretical manual, version 1.0
| NASA-TM-106001 | p 2723 N93-24913
Federal Communications Commission (FCC) Transponder Loading Data Conversion Software. User's guide and software maintenance manual, version 1.2
| NASA-CR-191067 | p 2808 N93-24947
A state-of-the-art crystal filter design package using Windows 3.0 techniques p 2693 N93-25010
High temperature composite analyzer (HITCAN) user's manual, version 1.0
| NASA-TM-106002 | p 2724 N93-25070
Supercomputer Debugging Workshop 1992
| DE93-007322 | p 2805 N93-25165
Using a multifrontal sparse solver in a high performance, finite element code
| NASA-CR-192718 | p 2828 N93-25223
BBU code development for high-power microwave generators
| DE93-007111 | p 2688 N93-25397
Use of high performance networks and supercomputers for real-time flight simulation p 2598 N93-25574
TARGET: Rapid capture of process knowledge p 2814 N93-25590
Scientific visualization using the Flow Analysis Software Toolkit (FAST) p 2814 N93-25600
Simulation of aircraft gas turbine engine p 2594 N93-25751
Development of a flight instrument package
| AD-A260830 | p 2591 N93-25783
Interactive interface for National Center for Atmospheric Research (NCAR) Graphics p 2878 N93-25794
Construction of an advanced software tool for planetary atmospheric modeling p 2815 N93-25799
Advanced data visualization and sensor fusion: Conversion of techniques from medical imaging to Earth science p 2880 N93-25810
High performance compression of science data p 2881 N93-25811
An application of machine learning to the organization of institutional software repositories p 2825 N93-25981
Development of a second generation spray combustion code p 2626 N93-26016
Eulerian-Eulerian treatment of turbulent dense spray combustion in a bipropellant liquid rocket engine p 2626 N93-26017
Design of an air traffic computer simulation system to support investigation of civil tiltrotor aircraft operations
| NASA-CR-192920 | p 2585 N93-26052
A study of mapping exogenous knowledge representations into CONFIG p 2827 N93-26072
Modeling of the WSTF frictional heating apparatus in high pressure systems p 2648 N93-26079
Spacelab, Spacehab, and Space Station Freedom payload interface projects p 2620 N93-26080
DSS-13 26-meter antenna upgraded radiometer system p 2679 N93-26122
Analysis of shaped charge jet penetration experiments with Pen
| UCRL-LR-110773 | p 2730 N93-26177
VETA-I x ray test analysis
| NASA-CR-192321 | p 2854 N93-26183
Analysis of symbolic parameter models
| AD-A261930 | p 2811 N93-26253
Arc Digital Raster Imagery (ADRI) development
| AD-A261850 | p 2812 N93-26275
AMPHIB: A users manual
| AD-A261769 | p 2669 N93-26285
Handbook of chemical hazard analysis procedures
| PB93-158756 | p 2766 N93-26315
Software testing initiative for strategic defense systems
| AD-A261350 | p 2831 N93-26330
AEGIS measures definition
| AD-A261494 | p 2812 N93-26375
Pseudo Wigner-Ville distribution, computer program, and its applications to time-frequency domain problems
| AD-A261839 | p 2813 N93-26431
METal matrix composite ANalyzer (METCAN): Theoretical manual
| NASA-TM-106025 | p 2641 N93-26552
Directory of US Government software for mainframes and microcomputers, 1993
| PB93-111565 | p 2807 N93-26569

COMPUTER STORAGE DEVICES
Robo-line storage: Low latency, high capacity storage systems over geographically distributed networks
| NASA-CR-192910 | p 2805 N93-25130
An analysis of file migration in a UNIX supercomputing environment
| NASA-CR-192908 | p 2809 N93-25131
Thin rechargeable batteries for CMOS SRAM memory protection p 2694 N93-25583
Considerations for space and naval aviation applications of ferroelectric memory
| AD-A261300 | p 2807 N93-26294

COMPUTER SYSTEMS DESIGN
Technology 2002: The Third National Technology Transfer Conference and Exposition, volume 1
| NASA-CP-3189-VOL-1 | p 2901 N93-25561
Deep Space Network information system architecture study p 2679 N93-26126
Very high-speed report file system
| AD-A261068 | p 2817 N93-26277
Proceedings of the complex systems engineering synthesis and assessment technology workshop
| AD-A261404 | p 2807 N93-26403

COMPUTER SYSTEMS PERFORMANCE
Robo-line storage: Low latency, high capacity storage systems over geographically distributed networks
| NASA-CR-192910 | p 2805 N93-25130
RAID-2: Design and implementation of a large scale disk array controller
| NASA-CR-192911 | p 2806 N93-25233
Expert system for UNIX system reliability and availability enhancement p 2723 N93-25588
An investigation of memory latency reduction using an address prediction buffer
| AD-A261010 | p 2806 N93-25858
Proof of fault coverage for a formal protocol test procedure
| AD-A261612 | p 2680 N93-26166
Complexity of connectionist and constraint-satisfaction networks
| AD-A261617 | p 2817 N93-26169
NSWC library of mathematics subroutines
| AD-A261511 | p 2884 N93-26575

COMPUTER SYSTEMS PROGRAMS
Interfacing a high performance disk array file server to a Gigabit LAN
| NASA-CR-192898 | p 2816 N93-25458
Multi-viewpoint clustering analysis p 2825 N93-25980

COMPUTER TECHNIQUES
Computer systems p 2737 N93-24942
Analysis of LARI sensor system
| DE93-006334 | p 2761 N93-24977

Current research activities: Applied and numerical mathematics, fluid mechanics, experiments in transition and turbulence and aerodynamics, and computer science
| NASA-CR-191408 | p 2803 N93-25084
Robo-line storage: Low latency, high capacity storage systems over geographically distributed networks
| NASA-CR-192910 | p 2805 N93-25130
Design concepts for the development of cooperative problem-solving systems
| NASA-CR-192708 | p 2585 N93-25261
Automatic detection of seizures with applications p 2796 N93-25592
Proceedings of Workshop 1: The Human Brainmap Database
| AD-A260720 | p 2796 N93-25654
Computational gearing mechanics
| NASA-CR-191127 | p 2719 N93-25884
Distributed project scheduling at NASA: Requirements for manual protocols and computer-based support p 2815 N93-26075
The adult literacy evaluator: An intelligent computer-aided training system for diagnosing adult illiterates p 2799 N93-26082
FY92 contributions to the Database Management System Interface Standards Working Group of the Navy Next Generation Computer Resources Program
| AD-A261348 | p 2883 N93-26313

COMPUTER VISION
Real-time construction and rendering of three-dimensional occupancy maps
| DE93-007818 | p 2756 N93-25516
Topography from shading and stereo p 2879 N93-25803
Center for intelligent control systems
| AD-A260995 | p 2821 N93-25853
Modeling of a full vision system using combined Visual/Haptic search for remote object identification
| AD-A260977 | p 2801 N93-25867
Uncertainty in object pose determination with three light-stripe range measurements
| AD-A261435 | p 2857 N93-26488
Receptoral and neural aliasing
| AD-A261438 | p 2799 N93-26489

COMPUTERIZED SIMULATION
Upper Atmosphere Research Satellite (UARS) onboard attitude determination using a Kalman filter p 2606 N93-24732
Dynamics and control of maneuverable tethered flight vehicles p 2615 N93-24767
Crashworthiness of composite seats for civil aircraft p 2582 N93-24773
High-order cyclo-difference techniques: An alternative to finite differences
| NASA-TM-107745 | p 2575 N93-25074
Rotor design optimization using a free wake analysis
| NASA-CR-177612 | p 2575 N93-25075
A contribution to the great Riemann solver debate
| NASA-CR-191409 | p 2575 N93-25083
Plasma sheath effects on ion collection by a pinhole
| NASA-TM-106098 | p 2615 N93-25090
Computational and experimental studies on large scale solar heating
| DE93-769942 | p 2758 N93-25096
The effects of sampling frequency on the climate statistics of the ECMWF general circulation model
| DE93-003338 | p 2761 N93-25145
Two-stream instability for a light ion beam-plasma system with external magnetic field
| NIFS-204 | p 2859 N93-25248
Dynamic error analysis of numerical methods for simulation of state-variable derivatives with discontinuities p 2819 N93-25278
Particle simulation for 10.6 micron picosecond laser-induced breakdown in gases p 2712 N93-25280
Radial velocity studies of the secondary in cataclysmic variables p 2888 N93-25286
Initialization of a modeled convective storm using Doppler radar-derived fields p 2782 N93-25294
Boundary plasma modelling for ITER
| DE93-007963 | p 2859 N93-25302
Radiation-induced disordering and defect production in CuAu and NiAl studied by molecular dynamics simulation
| DE93-007506 | p 2649 N93-25336
Propagation at microwave frequencies in the presence of tropospheric stratified layers p 2674 N93-25340
A compact neutron counter telescope with thick radiator (Cotetra) for fusion experiment
| NIFS-205 | p 2860 N93-25347
Simulation study of MHD dynamo: Convection in a rotating spherical shell
| NIFS-207 | p 2860 N93-25356
Detailed solution to a complex kinematics chain manipulator
| DE93-004619 | p 2725 N93-25357
Transverse instabilities in a relativistic klystron two-beam accelerator
| DE93-007110 | p 2852 N93-25375
BBU code development for high-power microwave generators
| DE93-007111 | p 2688 N93-25397
Computation of transonic flow over a porous surface projectile p 2577 N93-25409
Wavelet transform-vector quantization compression of supercomputer ocean model simulation output
| DE93-005453 | p 2876 N93-25448
Annular flow enhanced two-phase evaporative heat exchanger for space-based systems p 2700 N93-25478
TSC plasma halo simulation of a D3-D vertical displacement episode
| DE93-008688 | p 2860 N93-25493
Use of high performance networks and supercomputers for real-time flight simulation p 2598 N93-25574
Data systems dynamic simulator p 2814 N93-25602
A novel optical/digital processing system for pattern recognition p 2814 N93-25603
Efficient generation of synthetic terrain imagery for automatic target recognition
| AD-A260705 | p 2756 N93-25653
Gas turbine system simulation: An object-oriented approach
| NASA-TM-106044 | p 2593 N93-25673
Thermal infrared radiation transfer in the planetary boundary layer p 2772 N93-25688
Fidelity and validity in distributed interactive simulation: Questions and answers
| AD-A260971 | p 2810 N93-25711
A computational method for the analysis of acoustic radiation from turbofan inlets p 2845 N93-25717
Simulation of aircraft gas turbine engine p 2594 N93-25751
An SPW software simulation model of a dispersive fading multipath narrowband HF channel
| AD-A261101 | p 2675 N93-25767
A numerical simulation of adsorption onto a crystalline surface
| AD-A261079 | p 2866 N93-25781
A basic research model of natural gas combustion in turbulent flow, phase 2
| PB93-158509 | p 2644 N93-25819
Computer modelling of cyclic deformation of high-temperature materials
| AD-A260978 | p 2639 N93-25936
Analysis of transient photoluminescence measurements on GaAs and AlGaAs double heterostructures
| AD-A261154 | p 2867 N93-25947
Dark zone modeling of solid propellant flames p 2628 N93-26028
Design of an air traffic computer simulation system to support investigation of civil tiltrotor aircraft operations
| NASA-CR-192920 | p 2585 N93-26052
A prototype for simulation of the space-to-ground assembly/contingency system of Space Station Freedom p 2619 N93-26065
A study of mapping exogenous knowledge representations into CONFIG p 2827 N93-26072
Goldstone solar system radar signal processing p 2680 N93-26130
AXAF VETA-I mirror encircled energy measurements and data reduction p 2855 N93-26188
Advanced engineering analysis
| KCP-613-4967 | p 2669 N93-26212
Effect of image update rate on moving-target identification range
| AD-A261562 | p 2591 N93-26462
A database for propagation models p 2684 N93-26472
Very low frequency signals and whistler-mode amplification in the magnetosphere and limit-cycle behavior in the CECAF infrared free electronic laser
| AD-A261776 | p 2716 N93-26601

COMPUTERS
Computer systems p 2737 N93-24942
EXCHANGE
| DE93-007227 | p 2808 N93-24962
High performance compression of science data p 2881 N93-25811

CONCATENATED CODES
A low-complexity and high performance concatenated coding scheme for high-speed satellite communications
| NASA-CR-192715 | p 2673 N93-25198

CONDENSED MATTER PHYSICS
The interaction of swift electrons with surface excitations
| DE93-007245 | p 2848 N93-25376
Inelastic scattering in condensed matter with high intensity Moessbauer radiation
| DE93-008763 | p 2864 N93-25503
From fractals to wormholes via string theory p 2871 N93-25742
Proceedings of the 16th International Workshop on Condensed Matter Theories
| AD-A261078 | p 2868 N93-26252
Sensitivity of magnetic flux compression in cylindrical implosions to model parameters
| DE93-003819 | p 2861 N93-26512

CONDENSERS (LIQUEFIERS)
Two-phase/two-phase heat exchanger analysis
| NASA-CR-192783 | p 2697 N93-25221

CONDENSING
Condensation on cooled surfaces of optical devices at the cosmic conditions p 2753 N93-24869
The nature of the glass transition and its determination by thermal analysis
| DE93-006746 | p 2654 N93-25374

CONDUCTING FLUIDS
Maneuvering a reentry body via magneto-gasdynamic forces p 2615 N93-25207

CONDUCTING POLYMERS
Photomodulation spectroscopy of photocarrier dynamics, electronic defects and morphology of conducting polymers
| DE93-010140 | p 2655 N93-25524
Polymers by non-redox processes: Synthesis, physical studies, and application
| AD-A261064 | p 2657 N93-26240
Electrical conductivity of ion implanted ladder and semi-ladder polymers
| AD-A261401 | p 2657 N93-26401

CONDUCTION BANDS
The DX centers in three to five semiconductors under hydrostatic pressure
| DE93-007701 | p 2864 N93-25490

CONDUCTIVE HEAT TRANSFER
Stress and reliability analyses of multilayered composite cylinder under thermal and mechanical loads p 2726 N93-25533

CONDUCTIVITY
Template synthesis of electronically conductive polymers: A new route for achieving higher electronic conductivities
| AD-A261616 | p 2658 N93-26437

CONES
Development of a cone penetrometer for measuring spectral characteristics of soils in situ p 2776 N93-25570

CONFERENCES
Flight Mechanics/Estimation Theory Symposium, 1992
| NASA-CP-3186 | p 2599 N93-24694
The 1992 International Aerospace and Ground Conference on Lightning and Static Electricity: Addendum
| DOT/FAA/CT-92/20-ADD-1 | p 2777 N93-24875
Frequency and Time Forum
| ESA-SP-340 | p 2831 N93-24978
Aquifer thermal energy (heat and chill) storage
| DE93-006446 | p 2759 N93-25183
JPRS report: Science and technology. Japan. 30th National Aerospace Laboratory Conference
| JPRS-JST-93-009 | p 2901 N93-25418
Technology 2002: The Third National Technology Transfer Conference and Exposition, volume 1
| NASA-CP-3189-VOL-1 | p 2901 N93-25561
National Weather Service Winter Weather Workshop
| PB93-146785 | p 2785 N93-25775
Nonlinear vibrations, stability, and dynamics of structures and mechanisms
| AD-A260871 | p 2728 N93-25838
International Workshop on Advances in Inorganic Fibre Technology
| AD-A260719 | p 2639 N93-25908
The 1993 Goddard Conference on Space Applications of Artificial Intelligence
| NASA-CP-3200 | p 2822 N93-25961
Proceedings of the 33rd Annual Military LibrariansWorkshop
| AD-A261071 | p 2882 N93-26242
Proceedings of the 16th International Workshop on Condensed Matter Theories
| AD-A261078 | p 2868 N93-26252
Optical computing. Volume 6: Organization of the Optical Society of America photonic science topical meeting series
| AD-A261267 | p 2856 N93-26266
Gordon Conference on Point Defects, Line Defects and Interfaces in Semiconductors
| AD-A261485 | p 2868 N93-26357
Summary report of the Defense Sciences Research Council Summer Conference
| AD-A261375 | p 2917 N93-26359
Proceedings of the complex systems engineering synthesis and assessment technology workshop
| AD-A261404 | p 2807 N93-26403
Center for Space Construction Third Annual Symposium
| NASA-CR-192688 | p 2669 N93-26405

The Earth's climate as a dynamical system
| DE93-004666 | p 2767 N93-26496
Workshop on Diamond and Diamond-Like-Carbon Films for the Transportation Industry
| DE93-007491 | p 2658 N93-26506
European tri-service advanced materials workshop on compressive strength in rigid-rod polymers
| AD-A261517 | p 2658 N93-26576
Japanese Technology Evaluation Center Workshop on Advanced Manufacturing Technology for Polymer Composite Structures in Japan
| PB93-165249 | p 2641 N93-26589

CONFIGURATION INTERACTION
Theoretical calculations on the electron absorption spectra of selected Polycyclic Aromatic Hydrocarbons (PAH) and derivatives
| NASA-CR-192762 | p 2892 N93-25200

CONFIGURATION MANAGEMENT
Management of space networks p 2672 N93-24671

CONFINEMENT
Assessment of torsatrons as reactors
| DE93-006721 | p 2858 N93-24969
Modelling of microgravity ignition phenomena p 2664 N93-25465

CONICAL BODIES
Investigation of liquid sloshing in spin-stabilized satellites
| AD-A261671 | p 2619 N93-26438

CONICAL NOZZLES
Experimentation in the low-density plume of a simulated electrothermal thruster for computer code validation
| NASA-CR-191112 | p 2622 N93-24758
An experimental study of under-expanded jets p 2577 N93-25467

CONICAL SCANNING
Accurate attitude determination of the LACE satellite p 2605 N93-24726

CONIFERS
Forest damage detection and reflection of conifers: From micro to field level p 2752 N93-24864

CONJUGATE GRADIENT METHOD
Configuration optimization of space structures p 2670 N93-26415

CONJUGATION
Immunoconjugates: Magic bullets for cancer therapy? p 2796 N93-25567

CONNECTION MACHINE
Structured adaptive mesh refinement on the connection machine
| DE93-007368 | p 2816 N93-25316

CONNECTORS
A comparison of moisture resistance with different types of end-terminations in ceramic capacitors
| DE93-007600 | p 2689 N93-25416

CONSERVATION LAWS
A brief description of a new numerical framework for solving conservation laws: The method of space-time conservation element and solution element
| NASA-TM-105757 | p 2829 N93-26560

CONSISTENCY
Concurrency control in real-time database systems p 2874 N93-25271
Performance studies of cache consistency and concurrency control algorithms in a distributed client/server DBMS architecture p 2876 N93-25554

CONSTITUTIVE EQUATIONS
Investigation of coupled analysis techniques for adaptive material structural systems
| AD-A261359 | p 2868 N93-26332

CONSTRAINTS
Adaptive laser link reconfiguration using constraint propagation p 2823 N93-25967

CONSTRUCTION
Seismic buckling capacity of unstiffened, free-standing steel containments
| DE93-005325 | p 2723 N93-24957
Novel approaches to the construction of miniaturized analytical instrumentation
| NASA-CR-191988 | p 2709 N93-25345
Real-time construction of three-dimensional occupancy maps
| DE93-001645 | p 2756 N93-25505
Construction of a connectionist network supercomputer
| AD-A260929 | p 2820 N93-25648
Construction of an advanced software tool for planetary atmospheric modeling p 2815 N93-25799
Center for Space Construction Third Annual Symposium
| NASA-CR-192688 | p 2669 N93-26405
Dynamics of on-orbit construction process p 2669 N93-26406
Systems engineering studies of on-orbit assembly operations p 2669 N93-26410
Indigenous lunar construction materials p 2670 N93-26413
Design concepts for pressurized lunar shelters utilizing indigenous materials p 2670 N93-26414
Lunar surface structural concepts and construction studies p 2670 N93-26417

CONSTRUCTION INDUSTRY
Development of a concept for a national construction industry health and safety data base
| PB93-159325 | p 2884 N93-26568

CONSTRUCTION MATERIALS
Indigenous lunar construction materials p 2670 N93-26413

CONTACT LENSES
The use of extended wear contact lenses in the aviation environment: An Army-wide study
| AD-A260938 | p 2795 N93-26218

CONTACT LOADS
Optimization techniques for contact stress analysis
| AD-A260846 | p 2729 N93-25911

CONTAINMENT
A new method for infrared imaging of air currents in and around critical hazard fume hoods
| DE93-003009 | p 2761 N93-24956
Seismic buckling capacity of unstiffened, free-standing steel containments
| DE93-005325 | p 2723 N93-24957

CONTAMINANTS
Non-local description of pollution transport in random medium p 2763 N93-25329
National air pollutant emission estimates
| PB93-157808 | p 2765 N93-25850
Pollution prevention 1991: Progress on reducing industrial pollutants
| PB93-157725 | p 2766 N93-25875
Effects of moisture and other contaminants in friction composites
| AD-A261226 | p 2640 N93-26301
Using terrestrial plants in biomonitoring
| PB93-158780 | p 2766 N93-26316
Particulate emissions from gas turbine engines
| AD-A261374 | p 2595 N93-26339
Inorganic nitrogen and phosphorus dynamics in the water column of the Patuxent River
| PB93-172955 | p 2767 N93-26511
Model for transport of floating debris in the ocean
| PB93-172997 | p 2768 N93-26559

CONTAMINATION
Development of a cone penetrometer for measuring spectral characteristics of soils in situ p 2776 N93-25570
Military standardization handbook: Aircraft refueling handbook
| AD-A261755 | p 2662 N93-26600

CONTINENTAL SHELVES
Interaction of an eddy with a continental slope
| AD-A261550 | p 2791 N93-26578

CONTINUITY (MATHEMATICS)
Min and max are the only continuous ampersand-, V-operations for finite logics
| NASA-CR-192952 | p 2820 N93-25452

CONTINUOUS SPECTRA
Effect of continuous eigenvalue spectrum on plasma transport in toroidal systems
| NIFS-214 | p 2859 N93-25215

CONTINUOUS WAVE LASERS
Experimental and theoretical study of cw HF chemical laser overtone performance p 2713 N93-25420
Experimental and theoretical study of CW HF chemical laser residual fundamental gain p 2714 N93-25721

CONTINUUM MECHANICS
Development and application of computational aerothermodynamics flowfield computer codes
| NASA-CR-192940 | p 2574 N93-24736

CONTINUUMS
Continuum and micromechanics treatment of constraint in fracture
| AD-A260927 | p 2727 N93-25647

CONTOURS
Entropy reduction via simplified image contourization p 2804 N93-25924

CONTROL SIMULATION
Use of high performance networks and supercomputers for real-time flight simulation p 2598 N93-25574

CONTROL STABILITY
Design of the reduced LQG compensator for the DSS-13 antenna p 2672 N93-24669
Robust controls with structured perturbations
| NASA-CR-192956 | p 2817 N93-24757
The 32nd CDC: Robust stabilizer synthesis for interval plants using Nevanlina-pick theory
| NASA-CR-192894 | p 2818 N93-25156
Robust nonlinear control of vectored thrust aircraft
| NASA-CR-192727 | p 2596 N93-25199
Stability margins for multilinear interval systems by way of phase conditions: A unified approach
| NASA-CR-192893 | p 2819 N93-25226
Parametric stability margin for multilinear interval control systems
| NASA-CR-192892 | p 2819 N93-25296
Control of nonlinear systems under input constraints with applications to flight control p 2596 N93-25353

CONTROL SURFACES
Development and testing of the digital control system for the Archytas unmanned air vehicle
| AD-A261656 | p 2597 N93-26196

CONTROL SYSTEMS DESIGN
Robust controls with structured perturbations
| NASA-CR-192956 | p 2817 N93-24757
Screening studies of advanced control concepts for airbreathing engines
| NASA-TM-106042 | p 2592 N93-25079
A survey of life support system automation and control
| NASA-TM-103977 | p 2667 N93-25085
Two neural network algorithms for designing optimal terminal controllers with open final time
| NASA-CR-177599 | p 2817 N93-25137
The 32nd CDC: System identification using interval dynamic models
| NASA-CR-192895 | p 2818 N93-25155
Robust nonlinear control of vectored thrust aircraft
| NASA-CR-192727 | p 2596 N93-25199
Dynamic error analysis of numerical methods for simulation of state-variable derivatives with discontinuities p 2819 N93-25278
Aerospace vehicle model simplification for feedback control p 2596 N93-25292
Parametric stability margin for multilinear interval control systems
| NASA-CR-192892 | p 2819 N93-25296
Identification and control of lightly damped, large space structures: An experimental evaluation p 2616 N93-25351
Application of non-thermal plasmas to pollution control
| DE93-007515 | p 2763 N93-25385
A control structure for fault-tolerant operation of robotic manipulators
| DE93-005783 | p 2717 N93-25413
Human factors engineering: A key element of instrumentation and control system design
| DE93-006731 | p 2800 N93-25415
What procedure to choose while designing a fuzzy control? Towards mathematical foundations of fuzzy control
| NASA-TM-108719 | p 2820 N93-25459
Dynamics and robust control of a sampled data system for large space structures. Volume 2: The LQG/LTR methodology for the discrete-time system and the design of reduced order robust digital controller for orbiting flexible shallow spherical shell system
| AD-A260793 | p 2599 N93-25693
Nonlinear dynamics and attitude control of articulated flexible space structures p 2617 N93-25726
Control and stabilization of nonholonomic dynamic systems p 2596 N93-25729
Passivity motivated controller design for flexible structures
| AD-A261122 | p 2719 N93-25771
Center for intelligent control systems
| AD-A260995 | p 2821 N93-25853
Recommendations for a Kalman filter to estimate and control freeze and sublime rates of gaseous diffusion plant freezer/sublimer systems
| ORNL/TM-12183 | p 2668 N93-25937
Techniques for designing rotorcraft control systems
| NASA-CR-192960 | p 2597 N93-26046
Sequential design of a linear quadratic controller for the Deep Space Network antennas p 2679 N93-26123
Nonlinear system design: Adaptive feedback linearization with unmodeled dynamics
| AD-A261360 | p 2826 N93-26333

CONTROL THEORY
Robust controls with structured perturbations
| NASA-CR-192956 | p 2817 N93-24757
Maximum entropy approach to fuzzy control
| NASA-CR-192949 | p 2818 N93-25141
How to control if even experts are not sure: Robust fuzzy control
| NASA-TM-108745 | p 2818 N93-25142
The 32nd CDC: Robust stabilizer synthesis for interval plants using Nevanlina-pick theory
| NASA-CR-192894 | p 2818 N93-25156
Optimal thrust magnitude on a singular arc in atmospheric flight p 2819 N93-25410
Control of complex dynamic systems by neural networks p 2827 N93-25611
Control and stabilization of nonholonomic dynamic systems p 2596 N93-25729
Digital filter control of remotely operated flexible robotic structures
| DE93-007587 | p 2827 N93-26596

CONTROLLABILITY
The Hubble Space Telescope fine guidance system operating in the coarse track pointing control mode p 2605 N93-24724
CONTROLLED ATMOSPHERES
Membrane technology: A search for membranes for submarine atmosphere control
| AD-A260581 | p 2801 N93-25904
CONTROLLED FUSION
R and D of transmission lines for ECH system
| NIFS-210 | p 2687 N93-24951
CONTROLLERS
Design of the reduced LQG compensator for the DSS-13 antenna p 2672 N93-24669
Experimental results of the performance of the new phase and frequency controller p 2839 N93-25035
Two neural network algorithms for designing optimal terminal controllers with open final time
| NASA-CR-177599 | p 2817 N93-25137
RAID-2: Design and implementation of a large scale disk array controller
| NASA-CR-192911 | p 2806 N93-25233
Identification and control of lightly damped, large space structures: An experimental evaluation p 2616 N93-25351
A control structure for fault-tolerant operation of robotic manipulators
| DE93-005783 | p 2717 N93-25413
The design of a propulsion system using vent gas from a liquid helium cryogenic system p 2623 N93-25539
Firmware development improves system efficiency p 2807 N93-25606
Adaptive process control with fuzzy logic and genetic algorithms p 2827 N93-25612
Dynamics and robust control of a sampled data system for large space structures. Volume 2: The LQG/LTR methodology for the discrete-time system and the design of reduced order robust digital controller for orbiting flexible shallow spherical shell system
| AD-A260793 | p 2599 N93-25693
Nonlinear dynamics and attitude control of articulated flexible space structures p 2617 N93-25726
Passivity motivated controller design for flexible structures
| AD-A261122 | p 2719 N93-25771
Techniques for designing rotorcraft control systems
| NASA-CR-192960 | p 2597 N93-26046
Spacelab, Spacehab, and Space Station Freedom payload interface projects p 2620 N93-26080
Sequential design of a linear quadratic controller for the Deep Space Network antennas p 2679 N93-26123
VETA x ray data acquisition and control system p 2854 N93-26186
Development and testing of the digital control system for the Archytas unmanned air vehicle
| AD-A261656 | p 2597 N93-26196
Adaptive control of nonlinear flexible systems
| AD-A261676 | p 2826 N93-26365
Controls for orbital assembly of large space structures p 2620 N93-26408
CONVECTION
Surface energy fluxes at Central Florida during the convection and precipitation electrification experiment
| NASA-CR-192826 | p 2769 N93-24945
Minimization of heat slab nodes with higher order boundary conditions
| DE93-004238 | p 2695 N93-24966
Initialization of a modeled convective storm using Doppler radar-derived fields p 2782 N93-25294
Simulation study of MHD dynamo: Convection in a rotating spherical shell
| NIFS-207 | p 2860 N93-25356
Flow and morphological conditions associated with the directional solidification of aqueous ammonium chloride
| DE93-008886 | p 2644 N93-25495
On the vertical structure of seasonal, interannual and intraseasonal flows p 2782 N93-25557
Tropical cyclogenesis in the western North Pacific p 2783 N93-25714
Two-dimensional fin analysis p 2705 N93-25737
Gravity-dependent transport phenomena in zeolite crystal growth p 2664 N93-25740
Direct measurement of velocity space transport in a plasma p 2861 N93-25831
CONVECTION CLOUDS
Redistribution of trace chemical species by a small convective cloud
| PB93-156164 | p 2765 N93-25873
CONVECTION CURRENTS
An analysis of mesoscale convective systems observed during the 1992 Tropical Cyclone Motion field experiment
| AD-A260889 | p 2783 N93-25633
CONVECTION-DIFFUSION EQUATION
Non-local description of pollution transport in random medium p 2763 N93-25329
CONVECTIVE FLOW
Numerical study of cavity natural convection flow with augmenting and counteracting effects by projection finite element method p 2701 N93-25540
Laminar and turbulent natural convection heat transfer in Trombe wall channels p 2702 N93-25551
Thermocapillary flow near a cold wall
| AD-A261050 | p 2706 N93-25779
CONVECTIVE HEAT TRANSFER
Laminar and turbulent natural convection heat transfer in Trombe wall channels p 2702 N93-25551
Two-dimensional fin analysis p 2705 N93-25737
Thermocapillary flow near a cold wall
| AD-A261050 | p 2706 N93-25779
CONVENTIONS
Verification of a climate convention: Role and limitations of a space based remote sensing system p 2738 N93-24781
CONVERGENCE
Activity report
| AD-A261933 | p 2829 N93-26199
Integrated approaches to parallelism in optimization and the solution of inverse problems
| AD-A261490 | p 2829 N93-26344
CONVERGENT-DIVERGENT NOZZLES
Direct solutions of the Navier-Stokes equations with application to static aeroelasticity p 2697 N93-25259
CONVERSION
Direct methane conversion to methanol
| DE93-009183 | p 2660 N93-25497
CONVOLUTION INTEGRALS
The analysis of convolutional codes via the extended Smith algorithm p 2671 N93-24664
Interest of complementary data of coarse and high spatial resolution for agro-climatic crop monitoring p 2750 N93-24853
COOLING
A simple and compact source of cold atoms for cesium fountains and microgravity clocks p 2831 N93-24981
Optical detection of laser-cooled ions in a Penning trap p 2838 N93-25031
Winter warming from large volcanic eruptions
| NASA-CR-192848 | p 2763 N93-25244
A heat transfer analysis of a mobile vehicle radiation-shielded operator compartment
| DE93-007428 | p 2800 N93-25318
Two-dimensional fin analysis p 2705 N93-25737
AMPHIB: A users manual
| AD-A261769 | p 2669 N93-26285
COOLING SYSTEMS
Two-phase/two-phase heat exchanger analysis
| NASA-CR-192783 | p 2697 N93-25221
High speed solid state circuit breaker p 2694 N93-25598
COORDINATE TRANSFORMATIONS
Orbital parameter estimation using an extended Kalman filter
| AD-A260618 | p 2608 N93-25636
COORDINATES
Atomic time scales for dynamical astronomy p 2832 N93-24984
Evaluation of lens distortion errors in video-based motion analysis
| NASA-TP-3266 | p 2797 N93-25736
Occultation of a compact radio source by Venus p 2676 N93-26107
COPOLYMERS
An investigation of the degradation of Fluorinated Ethylene Propylene (FEP) copolymer thermal blanketing materials aboard LDEF in the laboratory
| NASA-CR-192824 | p 2653 N93-25078
Multichip module high speed testing
| AD-A261391 | p 2856 N93-26306
Development of organic nonlinear optical materials
| AD-A261332 | p 2856 N93-26309
COPPER ALLOYS
Development of dispersion-strengthened XD (trademark) Cu alloys for high heat-flux applications
| NASA-CR-191124 | p 2653 N93-24761
Study of grain refinement in Al alloy 2519 using backscattering orientation-contrast mode in the scanning electron microscope
| AD-A260886 | p 2651 N93-25632
Position sensitive atom probe study of the decomposition of a Cu-2.6 at. percent Co alloy
| DE93-006737 | p 2653 N93-26500
COPPER SELENIDES
Non-H2Se, ultra-thin CIS devices
| DE93-000078 | p 2759 N93-25253
Role of polycrystallinity in CdTe and CuInSe2 photovoltaic cells
| DE93-000045 | p 2759 N93-25504
CORE FLOW
Steady induction effects in geomagnetism. Part 1B: Geomagnetic estimation of steady surficial core motions: A non-linear inverse problem
| NASA-TP-3272-PT-1B | p 2776 N93-26421
CORIOLIS EFFECT
Heat transfer in rotating serpentine passages with selected model orientation for smooth or skewed trip walls
| NASA-TM-106126 | p 2667 N93-25177
CORN
Emerging technologies in ethanol production
| PB93-157014 | p 2661 N93-25818
CORNER FLOW
Instability of flow in a streamwise corner
| NASA-CR-191410 | p 2576 N93-25153
CORONAGRAPHS
A revised and expanded catalogue of mass ejections observed by the Solar Maximum Mission coronagraph
| NASA-CR-193146 | p 2899 N93-26556
CORRECTION
Relativistic effects for low Earth orbit satellites using GPS p 2608 N93-24986
Analytical techniques for improved time transfer using common view of direct broadcasting satellites p 2835 N93-25008
AXAF VETA-I mirror encircled energy measurements and data reduction p 2855 N93-26188
CORRELATION
Correlation between NDVI values derived from NOAA AVHRR HRPT data and ground measurements of precipitation in the EFEDA study area (Spain) p 2738 N93-24780
Atomizing-gas temperature effect on cryogenic spray dropsize
| NASA-TM-106106 | p 2709 N93-25191
Correlated wavefunction quantum Monte Carlo approach to solids
| DE93-007730 | p 2863 N93-25367
Correlation of damage threshold and surface geometry of nodular defects in HR coatings as determined by in-situ atomic force microscopy
| DE93-007509 | p 2654 N93-25384
Tables for the thermophysical properties of ethane
| PB93-160786 | p 2646 N93-26319
Properties of readings of periodically correlated random processes
| AD-A261225 | p 2686 N93-26573
CORROSION
Laser initiated corrosion pits on aluminum p 2650 N93-25464
The corrosion of metal matrix composites p 2638 N93-25723
CORROSION PREVENTION
Chromate-free corrosion resistant talc coatings for aluminum alloys
| DE93-005370 | p 2655 N93-25446
Photovoltaic power without batteries for continuous cathodic protection p 2759 N93-25597
Macromolecules for inhibition of corrosion and wear
| AD-A261041 | p 2655 N93-25816
In situ surface studies of conversion coatings for steel and aluminum
| AD-A261016 | p 2655 N93-25861
CORROSION RESISTANCE
Hot corrosion of the B2 nickel aluminides
| NASA-CR-191082 | p 2649 N93-25128
Chromate-free corrosion resistant talc coatings for aluminum alloys
| DE93-005370 | p 2655 N93-25446
Photovoltaic power without batteries for continuous cathodic protection p 2759 N93-25597
Macromolecules for inhibition of corrosion and wear
| AD-A261041 | p 2655 N93-25816
Duct protection coating concept development and test. Appendix D, volume 1: Test specimen fabrication, conditioning, and testing documentation
| AD-A261005 | p 2656 N93-25940
Duct protection coating concept development and test: Test specimen fabrication, conditioning, and testing documentation.
| AD-A261250 | p 2657 N93-26278
CORROSION TESTS
Hydrogen-induced stress corrosion cracking susceptibility analysis of pitch links from the AH-64 Apache helicopter
| AD-A260692 | p 2651 N93-25895
COSMIC BACKGROUND EXPLORER SATELLITE
Resolution of the COBE Earth sensor anomaly p 2600 N93-24700
Real-time attitude determination and gyro calibration p 2602 N93-24708
COSMIC DUST
Space environmental interactions for the space exploration initiative p 2897 N93-26396

COSMIC RAYS
Time dependent simulation of cosmic-ray shocks including Alfven transport
| NASA-CR-192931 | p 2899 N93-24752
Alfven wave transport effects in the time evolution of parallel cosmic-ray modified shocks
| NASA-CR-192932 | p 2899 N93-25161
Cosmic ray composition investigations using ICE/ISEE-3
| NASA-CR-192808 | p 2900 N93-25241
Oblique MHD cosmic-ray modified shocks: Two-fluid numerical simulations
| NASA-CR-192930 | p 2900 N93-26132
COSMOLOGY
Cosmic string cosmology p 2891 N93-24907
COSMONAUTS
Utilization of the graded universal testing system to increase the efficiency for assessing aerobic and anaerobic capacity p 2794 N93-26077
COST ANALYSIS
Orbit determination error analysis and comparison of station-keeping costs for Lissajous and halo-type libration point orbits and sensitivity analysis using experimental design techniques p 2604 N93-24721
Space transfer vehicle concepts and requirements study. Volume 3, book 1: Program cost estimates
| NASA-CR-192529 | p 2611 N93-25514
Space transfer concepts and analyses for exploration missions. Technical directive 12: Beamed power systems study
| NASA-CR-192532 | p 2599 N93-26146
Functional Economic Analysis Guidebook, version 1.1
| AD-A261390 | p 2886 N93-26305
Cost-effectiveness analysis of TxDOT CNG fleet conversion, volume 2
| PB93-159432 | p 2720 N93-26534
Regulatory impact analysis of the Part 503 sewage sludge regulation
| PB93-110625 | p 2768 N93-26567
COST EFFECTIVENESS
Environmental risks and future generations: Criteria for public policy
| DE93-004691 | p 2764 N93-25443
Space transfer vehicle concepts and requirements study. Volume 1: Executive summary
| NASA-CR-192524 | p 2610 N93-25479
Photovoltaic power without batteries for continuous cathodic protection p 2759 N93-25597
Variable-speed generators with flux weakening p 2694 N93-25599
Automation and robotics human performance
| NASA-CR-193049 | p 2802 N93-26153
X-ray computed tomography for casting development
| AD-A261786 | p 2722 N93-26526
Cost-effectiveness analysis of TxDOT CNG fleet conversion, volume 2
| PB93-159432 | p 2720 N93-26534
Cost-effectiveness analysis of TxDOT CNG fleet conversion, volume 1
| PB93-165603 | p 2720 N93-26585
Documentation for propane fleet conversion cost-effectiveness model
| PB93-165611 | p 2720 N93-26590
COST ESTIMATES
What is a system? NASA's phased project description p 2665 N93-24681
Magnitude and value of electric vehicle emissions reductions for six driving cycles in four US cities with varying air quality problems
| DE93-006417 | p 2660 N93-25298
Aerial photographic sampling for statewide resource inventory p 2755 N93-25441
Space transfer vehicle concepts and requirements study. Volume 3, book 1: Program cost estimates
| NASA-CR-192529 | p 2611 N93-25514
COST REDUCTION
Design and analysis of algorithms for processing queries in database systems p 2876 N93-25482
Emerging technologies in ethanol production
| PB93-157014 | p 2661 N93-25818
COSTA RICA
Geologic structure and processes of the eastern Pacific margin: California and Costa Rica p 2771 N93-25424
COSTS
Management issues in systems engineering p 2665 N93-24682
The importance of cost considerations in the systems engineering process p 2666 N93-24686
Data parallel finite element techniques for large-scale computational fluid dynamics p 2699 N93-25334
The state of computing at Los Alamos National Laboratory, FY 1991
| LA-12326-MS | p 2811 N93-25943
COUETTE FLOW
Navier-Stokes simulations of unsteady transonic flow phenomena p 2578 N93-25542
Particle dynamics modeling of boundary effects in granular Couette flow p 2705 N93-25738
COULOMB COLLISIONS
Plasma heating in toroidal systems
| NIFS-208 | p 2858 N93-25092
COUNTER ROTATION
The interaction of modulated vortex pairs with a free surface p 2701 N93-25485
COUNTERFLOW
Solution of nonlinear boundary value problem on successively refined grids
| AD-A261395 | p 2829 N93-26519
COUNTERMEASURES
The role of pyridoxine as a countermeasure for in-flight loss of lean body mass p 2796 N93-26068
COUPLING
Magnetic excitations in antiferromagnetically coupled superlattices: Fe/Mo and Fe/Cr
| DE93-007894 | p 2863 N93-25369
COUPLINGS
Aeroelastic response and aeromechanical stability of helicopters with elastically coupled composite rotor blades p 2588 N93-25530
COVALENCE
Accurate determination of Auger line shape binding energies
| AD-A261803 | p 2868 N93-26258
COVARIANCE
TDRSS orbit determination using short baseline differenced carrier phase p 2601 N93-24701
Attitude determination using vector observations: A fast optimal matrix algorithm p 2606 N93-24731
CRACK INITIATION
Approximate analysis on strain rate effects and behavior of stress and strain fields at the crack tip in Mode 2 in metallic materials, appendix no. 1
| AD-A260836 | p 2728 N93-25785
Micromechanics of fatigue
| AD-A260577 | p 2729 N93-25901
CRACK OPENING DISPLACEMENT
J and CTOD estimation equations for shallow cracks in single edge notch bend specimens
| AD-A261679 | p 2731 N93-26390
CRACK PROPAGATION
Numerical investigations on fracture behavior of ductile materials p 2725 N93-25411
High temperature fracture toughness of Ni3Al alloy IC-396M
| DE93-008564 | p 2650 N93-25492
Development and application of an advanced ductile fracture mechanics methodology p 2727 N93-25718
Models of crack growth along polymer interfaces p 2728 N93-25750
In-situ ultrasonic C-scanner
| AD-A261113 | p 2638 N93-25768
Three-dimensional analysis and verification of fracture growth mechanisms in fiber-reinforced ceramic composites
| AD-A261483 | p 2641 N93-26355
Use and analysis of finite element methods for problems of solid mechanics and fracture
| AD-A261574 | p 2731 N93-26522
CRACK TIPS
Continuum and micromechanics treatment of constraint in fracture
| AD-A260927 | p 2727 N93-25647
Crack tip fields in ductile crystals and bicrystals p 2866 N93-25749
Approximate analysis on strain rate effects and behavior of stress and strain fields at the crack tip in Mode 2 in metallic materials, appendix no. 1
| AD-A260836 | p 2728 N93-25785
J and CTOD estimation equations for shallow cracks in single edge notch bend specimens
| AD-A261679 | p 2731 N93-26390
Approximate techniques for predicting size effects on cleavage fracture toughness (J(sub c))
| AD-A261591 | p 2731 N93-26516
CRACKING (FRACTURING)
Quantifying distributed damage in composites via the thermoelastic effect p 2637 N93-25691
Crack tip fields in ductile crystals and bicrystals p 2866 N93-25749
CRACKS
Fracture of an elliptical inclusion and its implications for the properties of short fiber composites p 2634 N93-25333
Three-dimensional boundary element analysis of contact and fracture problems p 2725 N93-25335
Continuum and micromechanics treatment of constraint in fracture
| AD-A260927 | p 2727 N93-25647
In-situ ultrasonic C-scanner
| AD-A261113 | p 2638 N93-25768
Nondestructive evaluation of ferrite c-cores
| KCP-613-4677 | p 2721 N93-25939
External stress-corrosion cracking of a 1.22-m-diameter type 316 stainless steel air valve
| NASA-TP-3190 | p 2652 N93-26201
J and CTOD estimation equations for shallow cracks in single edge notch bend specimens
| AD-A261679 | p 2731 N93-26390
CRANES
Lunar surface structural concepts and construction studies p 2670 N93-26417
CRASHES
Virtually-synchronous communication based on a weak failure suspector
| NASA-CR-193003 | p 2721 N93-26135
CRASHWORTHINESS
Crashworthiness of composite seats for civil aircraft p 2582 N93-24773
CRATERS
Hypervelocity impact study: The effect of impact angle on crater morphology
| NASA-CR-192711 | p 2724 N93-25260
CRAY COMPUTERS
An analysis of file migration in a UNIX supercomputing environment
| NASA-CR-192908 | p 2809 N93-25131
Using a multifrontal sparse solver in a high performance, finite element code
| NASA-CR-192718 | p 2828 N93-25223
Using a Cray Y-MP as an array processor for a RISC Workstation
| NASA-TM-103961 | p 2809 N93-25246
CREEP PROPERTIES
Inelastic behavior of thermoplastic composites p 2636 N93-25674
Models of crack growth along polymer interfaces p 2728 N93-25750
CRITERIA
Environmental risks and future generations: Criteria for public policy
| DE93-004691 | p 2764 N93-25443
CRITICAL LOADING
Estimating turbine limit load
| NASA-CR-191105 | p 2580 N93-25883
CRITICAL POINT
Malone refrigeration
| DE93-005439 | p 2668 N93-25447
CRITICAL TEMPERATURE
Molecular/polymeric magnetism
| DE93-008635 | p 2847 N93-25114
Development of high Tc (greater than 100 K) Bi, Tl and Y-based materials as superconducting circuit elements
| NASA-CR-192344 | p 2863 N93-25219
CROP IDENTIFICATION
Remote sensing of land resource management in agriculture with regard to its influence on the environment p 2750 N93-24850
CROP INVENTORIES
Remote sensing applied to agriculture state of the art and new trends p 2745 N93-24818
Toward a satellite based crop information system in Hungary p 2750 N93-24849
Assessment and forecasting of crop yield in Niger through NOAA NDVI data p 2750 N93-24851
Multi-temporal satellite image analysis for crop inventories in the Po River Valley (Italy) p 2755 N93-25434
CROSS CORRELATION
Radial velocity studies of the secondary in cataclysmic variables p 2888 N93-25286
An investigation on planar velocimetry by spatial cross-correlation p 2578 N93-25664
Considerations of the error variances of time-averaged estimators for correlated processes
| AD-A261796 | p 2830 N93-26255
Monaural and binaural processing of complex waveforms
| AD-A261659 | p 2846 N93-26358
CROSS FLOW
Stationary crossflow instability on an infinite swept wing p 2580 N93-25865
Method of measuring cross-flow vortices by use of an array of hot-film sensors
| NASA-CASE-LAR-14824-1-SB | p 2706 N93-26000
Reduction in size and unsteadiness of a VTOL ground vortex by ground fences
| NASA-CR-192997 | p 2580 N93-26049
On the cross-stream spectral method for the Orr-Sommerfeld equation
| NASA-TM-107737 | p 2845 N93-26086
CROSS POLARIZATION
Lightning precursor signatures from dual-polarization radar measurements of storms p 2777 N93-24877
CROSSLINKING
Development of organic nonlinear optical materials
| AD-A261332 | p 2856 N93-26309

CRUISE MISSILES
Fabrication of composite propfan blades for a cruise missile wind tunnel model
| NASA-TM-105270 | p 2730 N93-26202
CRUISING FLIGHT
Optimized scramjet engine integration on a waverider airframe p 2593 N93-25480
CRUSTAL FRACTURES
Crustal deformation studies in subaerial parts of the world oceanic rift system: Iceland and Afar
p 2789 N93-25558
Proceedings of the Government Users Workshop on Ground Penetrating Radar Applications and Equipment
| AD-A261873 | p 2686 N93-26541
CRUSTS
Crustal deformation studies in subaerial parts of the world oceanic rift system: Iceland and Afar
p 2789 N93-25558
CRYODEPOSITS
Condensation on cooled surfaces of optical devices at the cosmic conditions p 2753 N93-24869
CRYOGENIC WIND TUNNELS
A feasibility study of using Langley 0.3-m transonic cryogenic tunnel sidewall boundary-layer removal system for heavy gas testing
| NASA-CR-191438 | p 2695 N93-25087
CRYOGENICS
Microwave frequency discriminator with a cryogenic sapphire resonator for ultra-low phase noise
p 2693 N93-24982
CRYOLITE
Electrochemical and spectroscopic studies of molten halides
| AD-A261687 | p 2646 N93-26439
CRYSTAL DEFECTS
Fundamental studies of defect generation in amorphous silicon alloys grown by remote plasma-enhanced chemical-vapor deposition (Remote PECVD)
| DE92-010560 | p 2862 N93-24953
Radiation-induced disordering and defect production in CuAu and NiAl studied by molecular dynamics simulation
| DE93-007506 | p 2649 N93-25336
The DX centers in three to five semiconductors under hydrostatic pressure
| DE93-007701 | p 2864 N93-25490
Photomodulation spectroscopy of photocarrier dynamics, electronic defects and morphology of conducting polymers
| DE93-010140 | p 2655 N93-25524
Optoelectronic III-V heterostructures on Si substrates
| AD-A261651 | p 2867 N93-26193
Defect initiation/growth and energy dissipation induced by deformation and fracture
| AD-A261703 | p 2869 N93-26385
CRYSTAL FILTERS
A state-of-the-art crystal filter design package using Windows 3.0 techniques p 2693 N93-25010
Very wide bandwidth HF crystal filters
p 2693 N93-25039
CRYSTAL GROWTH
Crystal growth and physical characterizations of GaPO4 p 2840 N93-25044
Whisker growth studies under conditions which resemble those available on an orbiting space station
| NASA-CR-192701 | p 2664 N93-25218
Fast diagnostics of laser ablation used for pulsed laser deposition
| DE93-005155 | p 2713 N93-25508
Gravity-dependent transport phenomena in zeolite crystal growth p 2664 N93-25740
Computation of complex solidification morphologies using a phase-field model
| PB93-156743 | p 2869 N93-26547
Laser damage to production- and research-grade KDP crystals
| DE93-007517 | p 2870 N93-26594
CRYSTAL LATTICES
Metastable SiC and SiGeC alloys by carbon implantation and solid phase epitaxy
| DE93-007594 | p 2863 N93-25387
A numerical simulation of adsorption onto a crystalline surface
| AD-A261079 | p 2866 N93-25781
Molecular devices based on new monolayer-forming systems
| AD-A260996 | p 2866 N93-25854
Fundamental aspects of metal joining: The study of strong interfaces
| AD-A261293 | p 2653 N93-26304
CRYSTAL OSCILLATORS
Weak magnetic field sensitivity of quartz crystal oscillators p 2833 N93-24993
A microcomputer compensated crystal oscillator MCXO p 2834 N93-25001
OSCCAR: Oscillator-compensated with a capacitance array p 2693 N93-25002
Control of environmental and clock parameters in Time and Frequency Standards Laboratory
p 2835 N93-25007
Dedicated oscillator for immersed crystal sensor
p 2837 N93-25020
TF-4020A: TFL's new compact military rubidium standard p 2838 N93-25026
Ultra stable oscillators for satellite applications
p 2621 N93-25027
Preliminary results of a newly designed mini-OCXO oscillator especially dedicated to space applications
p 2621 N93-25028
Use of the TV-signal in stabilizing a local rubidium oscillator p 2693 N93-25029
Quartz oscillators, frequency synthesizers, and timing systems for geodesy and radio science applications
p 2693 N93-25052
Space radiation susceptibility of ultra stable crystal oscillators p 2693 N93-25053
Oscillators for mobile GPS receivers
p 2694 N93-25055
CRYSTAL STRUCTURE
Sputter deposition of yttrium-oxides
| DE93-007499 | p 2654 N93-25382
Thermodynamic, kinetic, and structural properties of linear polyethylene crystallized from polymer-diluent mixture p 2864 N93-25528
The influence of primary and secondary orientations on the elastic response of a nickel-base single-crystal superalloy
| NASA-TM-106125 | p 2731 N93-26550
CRYSTAL SURFACES
A numerical simulation of adsorption onto a crystalline surface
| AD-A261079 | p 2866 N93-25781
Activation of methane by clean and chemically modified single crystal oxide surfaces
| PB93-157295 | p 2644 N93-25817
Dynamics of gas-surface interactions
| AD-A261402 | p 2646 N93-26402
CRYSTALLINITY
A model for the filling of cold cavities with solidifying, semi-crystalline polymers
| DE93-003817 | p 2655 N93-25507
CRYSTALLITES
Control of crystallite size in diamond film chemical vapor deposition
| AD-D015660 | p 2867 N93-26090
CRYSTALLIZATION
The nature of the glass transition and its determination by thermal analysis
| DE93-006746 | p 2654 N93-25374
A model for the filling of cold cavities with solidifying, semi-crystalline polymers
| DE93-003817 | p 2655 N93-25507
Thermodynamic, kinetic, and structural properties of linear polyethylene crystallized from polymer-diluent mixture p 2864 N93-25528
Transition metal chelate-fulleride compounds: Electrocrystallization of semiconducting (Ru(bpy)s)(C60)2
| AD-A261549 | p 2869 N93-26577
CRYSTALLOGRAPHY
Measurement results of the crystallographic orientation of the SC cut round plates p 2840 N93-25040
A micromechanical viscoplastic stress-strain model with grain boundary sliding
| DE93-009109 | p 2649 N93-25095
Vickers indentation hardness of stoichiometric and reduced single crystal TiO2 (rutile) from 25 to 800 C
| NASA-TM-105959 | p 2633 N93-26204
CRYSTALS
Correlated wavefunction quantum Monte Carlo approach to solids
| DE93-007730 | p 2863 N93-25367
Molecular devices based on new monolayer-forming systems
| AD-A260996 | p 2866 N93-25854
CUBANE
Energetic materials from cubane
| AD-A261317 | p 2662 N93-26308
CULTURE TECHNIQUES
Biological production of ethanol from coal
| DE93-008947 | p 2660 N93-25496
Metabolic response of environmentally isolated microorganisms to industrial effluents: Use of a newly described cell culture assay p 2794 N93-26066
CUMULUS CLOUDS
Redistribution of trace chemical species by a small convective cloud
| PB93-156164 | p 2765 N93-25873
The initiation of lightning and the growth of electric fields in thunderstorms
| AD-A261455 | p 2787 N93-26352
CURING
Process for bonding elastomers to metals
| NASA-CASE-LAR-13645-1 | p 2656 N93-25995
In-process cure monitoring of composites via fiber-optic fluorescence
| AD-A261712 | p 2641 N93-26580
CURRENT DENSITY
Assessment of torsatrons as reactors
| DE93-006721 | p 2858 N93-24969
Laser initiated corrosion pits on aluminum
p 2650 N93-25464
Anode power deposition in coaxial MPD thrusters
p 2623 N93-25665
CURVED BEAMS
Design and analysis of curved composite components for rotorcraft fuselage frames p 2589 N93-25701
CURVES (GEOMETRY)
Elastic curves on the sphere
| AD-A261057 | p 2829 N93-26228
CUTTING
The design of mechanically compatible fasteners for human mandible reconstruction p 2796 N93-25569
CYCLES
A comparison of moisture resistance with different types of end-terminations in ceramic capacitors
| DE93-007600 | p 2689 N93-25416
CYCLIC HYDROCARBONS
Measurements of soot formation and hydroxyl concentration in near critical equivalence ratio premixed ethylene flame
| NASA-CR-191099 | p 2642 N93-25116
CYCLIC LOADS
Internal stresses and the cyclic deformation of an aluminum matrix composite p 2650 N93-25436
CYCLOGENESIS
Tropical cyclogenesis in the western North Pacific
p 2783 N93-25714
An investigation into the causative mechanisms for explosive cyclone development over the Atlantic
| AD-A261831 | p 2786 N93-26273
CYCLONES
A systematic satellite approach for estimating central pressures of mid-lattitude oceanic storms
| NOAA-TR-NESDIS-63 | p 2781 N93-25220
An analysis of mesoscale convective systems observed during the 1992 Tropical Cyclone Motion field experiment
| AD-A260889 | p 2783 N93-25633
Tropical cyclogenesis in the western North Pacific
p 2783 N93-25714
Pressure torques and circulation changes in Rocky Mountain lee cyclones p 2783 N93-25724
Tropical cyclone/upper-atmospheric interaction as inferred from satellite total ozone observations
p 2784 N93-25741
An investigation into the causative mechanisms for explosive cyclone development over the Atlantic
| AD-A261831 | p 2786 N93-26273
Boundary layer coupling between an explosive cyclone and the Gulf Stream during ERICA
| AD-A261577 | p 2787 N93-26513
CYCLOTRON FREQUENCY
Optical detection of laser-cooled ions in a Penning trap p 2838 N93-25031
Nonlinear wave phenomena related to interactions in the ionosphere
| AD-A261450 | p 2776 N93-26348
CYCLOTRON RADIATION
Nonlinear wave phenomena related to interactions in the ionosphere
| AD-A261450 | p 2776 N93-26348
CYCLOTRON RESONANCE DEVICES
Theoretical and experimental investigation of electron beam acceleration and sub-millimeter wave generation
| AD-A261117 | p 2609 N93-25770
Magnetic field source for bi-chambered electron beam devices
| AD-A261316 | p 2691 N93-26299
CYLINDRICAL BODIES
Axisymmetric deformations and stresses of unsymmetrically laminated composite cylinders in axial compression with thermally-induced preloading effects
| NASA-CR-192788 | p 2723 N93-24912
Surface discharge photoinitiation of pulsed chemical lasers
| DE93-006337 | p 2712 N93-24967
Apparatus and methods for determining balance of a cylindrical vehicle
| AD-D015637 | p 2717 N93-25228
Tangential fuselage blowing on an ogive cylinder
p 2578 N93-25545
Positive displacement rotary pump
| AD-D015678 | p 2719 N93-26144
CYTOMETRY
Measuring the metastatic potential of cancer cells
p 2794 N93-25566

D

DAMAGE
Mapping of windfall damage in the Hunsrueck plateau with Landsat TM-data p 2749 N93-24843
Forest damage detection and reflection of conifers: From micro to field level p 2752 N93-24864
A computational approach to predicting the extent of arc root damage in CFC panels p 2642 N93-24890
Comparison of the damage for various types of fibre reinforced composites due to different lightning test standards (MIL-STD-1757A, German military VG-standard 96903) p 2642 N93-24891
Lightning phenomenology bases for full threat return stroke occurrence following extended leader sweep at flight altitudes p 2780 N93-24895
Analysis of matrix damage in unidirectional composites p 2634 N93-25338
The damage, repair and design of fiber composite structural materials p 2635 N93-25532
Expedient repair of structural facilities
|AD-A260727| p 2598 N93-25656
Numerical simulation of damage and progressive failures in composite laminates using the layerwise plate theory p 2636 N93-25661
Quantifying distributed damage in composites via the thermoelastic effect p 2637 N93-25691
Transmission electron microscopy investigation of ion implantation damage in GaAs and other semiconductors p 2865 N93-25715
Damage and failure analysis on continuous fiber-reinforced polymer composites p 2637 N93-25716
Computer modelling of cyclic deformation of high-temperature materials
|AD-A260978| p 2639 N93-25936
Damage detection and mitigation of composite structures using smart materials
|AD-A261121| p 2639 N93-25945
Remtech SSME nozzle design TPS
|NASA-CR-192516| p 2631 N93-26056
Electrostatic fiber spreader
|AD-D015677| p 2640 N93-26143

DAMAGE ASSESSMENT
The use of SPOT data in natural disaster prevention and damage assessment p 2743 N93-24811
Forest damage detection and reflection of conifers: From micro to field level p 2752 N93-24864
Comparison of the damage for various types of fibre reinforced composites due to different lightning test standards (MIL-STD-1757A, German military VG-standard 96903) p 2642 N93-24891
Lightning phenomenology bases for full threat return stroke occurrence following extended leader sweep at flight altitudes p 2780 N93-24895
In-situ ultrasonic C-scanner
|AD-A261113| p 2638 N93-25768
Damage detection and mitigation of composite structures using smart materials
|AD-A261121| p 2639 N93-25945
Guide for conducting convective windstorm surveys
|PB93-148427| p 2787 N93-26570

DAMPING
Application of finite-state inflow to flap-lag-torsion damping in hover p 2587 N93-25486

DATA ACQUISITION
The Telecommunications and Data Acquisition Report
|NASA-CR-192887| p 2671 N93-24659
Failure monitoring in dynamic systems: Model construction without fault training data p 2672 N93-24666
A functional description of the Buffered Telemetry Demodulator (BTD) p 2614 N93-24667
Ice thickness measurement system for the icing research tunnel calibration
|NASA-TM-106095| p 2708 N93-24737
Analysis of large system black box verification test data
|NASA-CR-192885| p 2815 N93-24748
A prototype system for forest fire prevention and control p 2749 N93-24844
Data processing and control in a transputer system for remote sensing of the Earth p 2753 N93-24870
Lightning data acquisition p 2778 N93-24883
A system to measure lightning-induced transients on spacecraft umbilical lines p 2693 N93-24889
Data availability and data archeology from the former Soviet Union p 2735 N93-24932
Visual approach data collection at St. Louis Lambert Field (STL)
|DOT/FAA/CT-TN93/2| p 2584 N93-24948
An analysis of file migration in a UNIX supercomputing environment
|NASA-CR-192908| p 2809 N93-25131
How to help intelligent systems with different uncertainty representations cooperate with each other
|NASA-CR-192947| p 2818 N93-25196
An advanced data-acquisition system for wind energy projects
|DE93-000079| p 2874 N93-25254
Preliminary design of the BPM electronics memory scanner/dual boxcar averager for the advanced photon source
|DE93-007893| p 2848 N93-25368
The North Dakota thunderstorm project
|PB93-153039| p 2785 N93-25776
Development of a tool-set for simultaneous, multi-site observations of astronomical objects p 2878 N93-25795
The Telecommunications and Data Acquisition Report
|NASA-CR-192804| p 2676 N93-26105
DSN acquisition of Magellan high-rate telemetry data p 2614 N93-26124
Galileo early cruise, including Venus, First Earth, and Gaspra encounters p 2599 N93-26125
Goldstone solar system radar signal processing p 2680 N93-26130
ROSAT investigation of flaring and activity on Prox Cen
|NASA-CR-192972| p 2891 N93-26139
Rain rate instrument for deployment at sea, phase 2
|NASA-CR-192442| p 2786 N93-26156
VETA x ray data acquisition and control system p 2854 N93-26186
Correcting x ray spectra obtained from the AXAF VETA-I mirror calibration for pileup, continuum, background and deadtime p 2854 N93-26187
Monaural and binaural processing of complex waveforms
|AD-A261659| p 2846 N93-26358
CALS-HSC data element dictionary
|AD-A261560| p 2813 N93-26461
Technical operating report on the Data Integration and Collection Environment (DICE) instrumentation system design
|AD-A261105| p 2591 N93-26572

DATA BASE MANAGEMENT SYSTEMS
Use of the Environmental Resource Management and Analysis System at the Fernald Environmental Management Project
|DE93-002943| p 2760 N93-24955
AQUIS: A PC-based air inventory and permit manager
|DE93-003006| p 2761 N93-25143
Concurrency control in real-time database systems p 2874 N93-25271
Optimization of knowledge-based systems and expert system building tools
|NASA-CR-192763| p 2874 N93-25288
A distributed heterogeneous client-server environment
|DE93-007496| p 2875 N93-25319
A logic-based approach to federated databases p 2876 N93-25466
Performance studies of cache consistency and concurrency control algorithms in a distributed client/server DBMS architecture p 2876 N93-25554
VIEWCACHE: An incremental pointer-based access method for autonomous interoperable databases p 2880 N93-25809
A Spatial Analysis and Modeling System (SAMS) for environment management p 2881 N93-25813
Intelligent access to multiple relational database systems
|AD-A261198| p 2881 N93-25824
The SWORD multilevel secure DBMS
|RSRE-92005| p 2811 N93-25942
OSSA Information Systems Program
|NASA-TM-108774| p 2882 N93-26231
FY92 contributions to the Database Management System Interface Standards Working Group of the Navy Next Generation Computer Resources Program
|AD-A261348| p 2883 N93-26313
A coastal hazards data base for the US East Coast
|NASA-TM-108265| p 2791 N93-26586

DATA BASES
Lightning data acquisition p 2778 N93-24883
Digitization of analog data from in-flight lightning strikes p 2778 N93-24884
Improving information search at the user interface: The impact of graphical innovation on query formulation and expression p 2873 N93-24905
The role of ocean climate data in operational Naval oceanography p 2732 N93-24916
Data archaeology at ICES p 2734 N93-24931
Data management for community research projects: A JGOFS case study p 2736 N93-24936
Propagation velocity and space-time correlation of perturbations in turbulent channel flow
|NASA-TM-103932| p 2695 N93-25082
Efficient inspection of network pollution data
|DE93-003810| p 2761 N93-25126
A longitudinal examination of applicants to the air traffic control supervisory identification and development program
|DOT/FAA/AM-92/16| p 2796 N93-25213
Concurrency control in real-time database systems p 2874 N93-25271
Earth observing system. Output data products and input requirements, version 2.0. Volume 3: Algorithm summary tables and non-EOS data products
|NASA-TM-108769| p 2756 N93-25462
A logic-based approach to federated databases p 2876 N93-25466
Space transfer vehicle concepts and requirements study. Volume 1: Executive summary
|NASA-CR-192524| p 2610 N93-25479
Design and analysis of algorithms for processing queries in database systems p 2876 N93-25482
Climate data bases of the People's Republic of China, 1841-1988
|DE93-007907| p 2764 N93-25517
Performance studies of cache consistency and concurrency control algorithms in a distributed client/server DBMS architecture p 2876 N93-25554
The database Query Support Processor (QSP) p 2807 N93-25577
ASTROS-ID: Software for system identification using mathematical programming
|AD-A260867| p 2810 N93-25627
Proceedings of Workshop 1: The Human Brainmap Database
|AD-A260720| p 2796 N93-25654
Digital Nautical Chart
|AD-A260810| p 2756 N93-25694
Multivariate statistical analysis software technologies for astrophysical research involving large data bases p 2878 N93-25796
Knowledge-based assistance for science visualization and analysis using large distributed databases p 2879 N93-25801
VIEWCACHE: An incremental pointer-based access method for autonomous interoperabie databases p 2880 N93-25809
SAVS: A Space Analysis and Visualization System p 2881 N93-25812
Intelligent access to multiple relational database systems
|AD-A261198| p 2881 N93-25824
Advanced life support study. Modification 10: ECLSS logistical support analysis for Space Station Freedom
|NASA-CR-192481| p 2801 N93-25888
The SWORD multilevel secure DBMS
|RSRE-92005| p 2811 N93-25942
Visualizing the semantic content of large text databases using text maps p 2826 N93-25982
The StarView intelligent query mechanism p 2826 N93-25984
Bibliography on propulsion airframe integration technologies for high-speed civil transport applications, 1980-1991
|NASA-TM-105602| p 2573 N93-26136
Department of Defense technical architecture framework for information management. Volume 3: Reference model and standards profile, version 1.3
|AD-A261913| p 2882 N93-26230
A geological and geophysical information system for Eurasia
|AD-A261789| p 2883 N93-26442
A database for propagation models p 2684 N93-26472
Department of Defense technical architecture framework for information management. Volume 1: Implementation concept, version 1.1
|AD-A261911| p 2884 N93-26531
Department of Defense technical architecture framework for information management. Volume 2: Architecture guidance and design concepts, version 1.1
|AD-A261912| p 2884 N93-26532
Oxides of nitrogen emissions from turbulent hydrocarbon/air jet diffusion flames, phase 2
|PB93-152478| p 2768 N93-26533
Development of a concept for a national construction industry health and safety data base
|PB93-159325| p 2884 N93-26568
A coastal hazards data base for the US East Coast
|NASA-TM-108265| p 2791 N93-26586
Published assessments bearing on the future use of ceramic superconductors by the electric power sector
|DE93-007737| p 2658 N93-26588

DATA COMPRESSION
Image coding by way of wavelets p 2671 N93-24665
High resolution stereo imaging and data compression p 2753 N93-24867
Applications of wavelet-based compression to multidimensional earth science data
|DE93-007348| p 2762 N93-25166

Wavelet transform-vector quantization compression of supercomputer ocean model simulation output
| DE93-005453 | p 2876 N93-25448
High performance compression of science data
p 2881 N93-25811
The Space and Earth Science Data Compression Workshop
| NASA-CP-3183 | p 2803 N93-25921
Adjustable lossless image compression based on a natural splitting of an image into drawing, shading, and fine-grained components p 2804 N93-25923
Compression of spectral meteorological imagery
p 2804 N93-25925
Methods of evaluating the effects of coding on SAR data p 2804 N93-25926
Fractal image compression: A resolution independent representation for imagery p 2804 N93-25927
The implementation of a lossless data compression module in an advanced orbiting system: Analysis and development p 2804 N93-25928
Lossless compression of image data products on th e FIFE CD-ROM series p 2804 N93-25929
The effects of video compression on acceptability of images for monitoring life sciences' experiments
p 2805 N93-25930
High-performance compression of astronomical images p 2805 N93-25931
Bandwidth compression of noisy signals with square-wave subcarrier p 2678 N93-26120

DATA CONVERSION ROUTINES
Federal Communications Commission (FCC) Transponder Loading Data Conversion Software. User's guide and software maintenance manual, version 1.2
| NASA-CR-191067 | p 2808 N93-24947

DATA CORRELATION
Propagation velocity and space-time correlation of perturbations in turbulent channel flow
| NASA-TM-103932 | p 2695 N93-25082
Determination of design and operation parameters for upper atmospheric research instrumentation to yield optimum resolution with deconvolution, appendix 2
| NASA-CR-192833 | p 2770 N93-25088

DATA FLOW ANALYSIS
CAD data exchange development
| DE93-008085 | p 2809 N93-25307
Data systems dynamic simulator p 2814 N93-25602

DATA INTEGRATION
A logic-based approach to federated databases
p 2876 N93-25466
Advanced data visualization and sensor fusion: Conversion of techniques from medical imaging to Earth science p 2880 N93-25810
Data fusion with artificial neural networks (ANN) for classification of earth surface from microwave satellite measurements p 2824 N93-25974
Technical operating report on the Data Integration and Collection Environment (DICE) instrumentation system design
| AD-A261105 | p 2591 N93-26572

DATA LINKS
Orbit determination support of the Ocean Topography Experiment (TOPEX)/Poseidon operational orbit
p 2601 N93-24704
A system design for laser time synchronization via geodetic satellite Ajisai p 2716 N93-25005
Frequency generation and synthesis in the DRSS
p 2693 N93-25054
Piloted simulation of an air-ground profile negotiation process in a time-based Air Traffic Control environment
| NASA-TM-107748 | p 2585 N93-26087
ETS-5, ETS-6, and COMETS projects in Japan
p 2683 N93-26470

DATA MANAGEMENT
Health and environmental chemistry: Analytical techniques, data management, and quality assurance
| DE93-002853 | p 2760 N93-24674
Proceedings of the Ocean Climate Data Workshop
| NASA-TM-108711 | p 2732 N93-24915
Global Temperature and Salinity Pilot Project
p 2733 N93-24924
Indian Ocean analyses p 2733 N93-24925
Data archaeology at ICES p 2734 N93-24931
The JGOFS North Atlantic Bloom Experiment: An overview p 2735 N93-24934
Data management for JGOFS: Theory and design
p 2735 N93-24935
Data management for community research projects: A JGOFS case study p 2736 N93-24936
Automated in situ observations of upper ocean biogeochemistry, bio-optics, and physics and their potential use for global studies p 2736 N93-24939
Wrap-up session p 2737 N93-24940
International ocean services: Is it time - will it ever be time? p 2737 N93-24941
An analysis of file migration in a UNIX supercomputing environment
| NASA-CR-192908 | p 2809 N93-25131
RAID-2: Design and implementation of a large scale disk array controller
| NASA-CR-192911 | p 2806 N93-25233
The database Query Support Processor (QSP)
p 2807 N93-25577
An interactive environment for the analysis of large Earth observation and model data sets p 2878 N93-25793
Multivariate statistical analysis software technologies for astrophysical research involving large data bases
p 2878 N93-25796
System of Experts for Intelligent Data Management (SEIDAM) p 2879 N93-25800
Knowledge-based assistance for science visualization and analysis using large distributed databases
p 2879 N93-25801
Development of an expert data reduction assistant
p 2880 N93-25808
Climate Monitoring and Diagnostics Laboratory
| PB93-156388 | p 2785 N93-25871
In search of meta-knowledge p 2826 N93-25983
Department of Defense technical architecture framework for information management. Volume 3: Reference model and standards profile, version 1.3
| AD-A261913 | p 2882 N93-26230
OSSA Information Systems Program
| NASA-TM-108774 | p 2882 N93-26231
FY92 contributions to the Database Management System Interface Standards Working Group of the Navy Next Generation Computer Resources Program
| AD-A261348 | p 2883 N93-26313
OSSA Information Systems Program
| NASA-TM-108758 | p 2883 N93-26491
Department of Defense technical architecture framework for information management. Volume 1: Implementation concept, version 1.1
| AD-A261911 | p 2884 N93-26531
Department of Defense technical architecture framework for information management. Volume 2: Architecture guidance and design concepts, version 1.1
| AD-A261912 | p 2884 N93-26532

DATA PROCESSING
Orbit determination support of the Ocean Topography Experiment (TOPEX)/Poseidon operational orbit
p 2601 N93-24704
Land cover, an essential component of the CORINE information system on the environment: GIS implications
p 2740 N93-24787
Agroclimatological zonation by AVHRR data for vegetation monitoring p 2741 N93-24795
The need for spaceborne observations for meteorology and climatology p 2744 N93-24813
Data processing and control in a transputer system for remote sensing of the Earth p 2753 N93-24870
Data management for community research projects: A JGOFS case study p 2736 N93-24936
Ocean time-series near Bermuda: Hydrostation S and the US JGOFS Bermuda Atlantic time-series study
p 2736 N93-24938
Efficient inspection of network pollution data
| DE93-003810 | p 2761 N93-25126
Applications of wavelet-based compression to multidimensional earth science data
| DE93-007348 | p 2762 N93-25166
The ALEXIS data processing package: An update
| DE93-007374 | p 2899 N93-25185
An advanced data-acquisition system for wind energy projects
| DE93-000079 | p 2874 N93-25254
A distributed heterogeneous client-server environment
| DE93-007496 | p 2875 N93-25319
Hierarchical dynamics in distributed information processing p 2875 N93-25350
Preliminary design of the BPM electronics memory scanner/dual boxcar averager for the advanced photon source
| DE93-007893 | p 2848 N93-25368
Earth observing system. Output data products and input requirements, version 2.0. Volume 3: Algorithm summary tables and non-EOS data products
| NASA-TM-108769 | p 2756 N93-25462
The database Query Support Processor (QSP)
p 2807 N93-25577
A novel optical/digital processing system for pattern recognition p 2814 N93-25603
Very high-speed arithmetic processors (The Gauss Machine)
| AD-A260693 | p 2806 N93-25650
A land-surface testbed for EOSDIS
p 2878 N93-25797
System of Experts for Intelligent Data Management (SEIDAM) p 2879 N93-25800
A distributed system for visualizing and analyzing multivariate and multidisciplinary data
p 2880 N93-25804
The Grid Analysis and Display System (GRADS): A practical tool for Earth science visualization
p 2880 N93-25805
Planetary data analysis and display system: A version of PC-McIDAS p 2880 N93-25806
Development of an expert data reduction assistant
p 2880 N93-25808
SAVS: A Space Analysis and Visualization System
p 2881 N93-25812
A distributed analysis and visualization system for model and observational data p 2881 N93-25814
Subband coding for image data archiving
p 2803 N93-25922
Adjustable lossless image compression based on a natural splitting of an image into drawing, shading, and fine-grained components p 2804 N93-25923
Entropy reduction via simplified image contourization
p 2804 N93-25924
Compression of spectral meteorological imagery
p 2804 N93-25925
Fractal image compression: A resolution independent representation for imagery p 2804 N93-25927
Data analysis support for the Shuttle Potential and Return Electron Experiment (SPREE) on the Tethered Satellite System 1 (TSS-1) flight
| AD-A261646 | p 2618 N93-26232
Step stress testing of receiver/transmitter units
| AD-A261286 | p 2730 N93-26279
Monaural and binaural processing of complex waveforms
| AD-A261659 | p 2846 N93-26358
IDEF6: A design rationale capture method concept paper
| AD-A261594 | p 2884 N93-26523
A hypertext framework for group support systems
| AD-A261731 | p 2885 N93-26582

DATA PROCESSING EQUIPMENT
Fast mutual exclusion for uniprocessors
| AD-A261663 | p 2883 N93-26389

DATA RECORDERS
US Army evaluation of the Electronic Map Data (EMD) prototype
| AD-A261693 | p 2757 N93-26369

DATA RECORDING
Ice thickness measurement system for the icing research tunnel calibration
| NASA-TM-106095 | p 2708 N93-24737
Design, fabrication, and testing of a three-dimensional acoustic orientation instrument (3-D AOI): Drawings, engineering and associated lists (conceptual and development design)
| AD-A260934 | p 2845 N93-25915
US Army evaluation of the Electronic Map Data (EMD) prototype
| AD-A261693 | p 2757 N93-26369
Technical operating report on the Data Integration and Collection Environment (DICE) instrumentation system design
| AD-A261105 | p 2591 N93-26572

DATA REDUCTION
A distributed system for visualizing and analyzing multivariate and multidisciplinary data
p 2880 N93-25804
Multi-layer holographic bifurcative neural network system for real-time adaptive EOS data analysis
p 2880 N93-25807
Development of an expert data reduction assistant
p 2880 N93-25808
High performance compression of science data
p 2881 N93-25811
The implementation of a lossless data compression module in an advanced orbiting system: Analysis and development p 2804 N93-25928
AXAF VETA-I mirror encircled energy measurements and data reduction p 2855 N93-26188
Data analysis support for the Shuttle Potential and Return Electron Experiment (SPREE) on the Tethered Satellite System 1 (TSS-1) flight
| AD-A261646 | p 2618 N93-26232
Step stress testing of receiver/transmitter units
| AD-A261286 | p 2730 N93-26279

DATA RETRIEVAL
Earth observing system. Output data products and input requirements, version 2.0. Volume 2: Analysis of IDS input requirements
| NASA-TM-108771 | p 2755 N93-25461

DATA SAMPLING
The Grid Analysis and Display System (GRADS): A practical tool for Earth science visualization
p 2880 N93-25805

DATA STORAGE
RAID-2: Design and implementation of a large scale disk array controller
| NASA-CR-192911 | p 2806 N93-25233
Striped tape arrays
| NASA-CR-192914 | p 2806 N93-25267
Distributed information storage p 2877 N93-25722
High performance compression of science data p 2881 N93-25811
Lossless compression of image data products on th e FIFE CD-ROM series p 2804 N93-25929
DATA STRUCTURES
Towards a formalism for program generation
| AD-A261689 | p 2812 N93-26368
DATA SYSTEMS
OCEAN-PC and a distributed network for ocean data p 2734 N93-24928
Ocean climate data for user community in West and Central Africa: Needs, opportunities, and challenges p 2735 N93-24933
Computer systems p 2737 N93-24942
Summary information and data sets for NREL's Solar Radiation Research Laboratory, 1981 - 1991
| DE93-000052 | p 2898 N93-25101
The database Query Support Processor (QSP) p 2807 N93-25577
Data systems dynamic simulator p 2814 N93-25602
Walsh function generator for the Electronically Scanned Thinned Array Radiometer (ESTAR) instrument
| NASA-TM-4449 | p 2689 N93-25618
A land-surface testbed for EOSDIS p 2878 N93-25797
A distributed system for visualizing and analyzing multivariate and multidisciplinary data p 2880 N93-25804
A Spatial Analysis and Modeling System (SAMS) for environment management p 2881 N93-25813
Subband coding for image data archiving p 2803 N93-25922
Adjustable lossless image compression based on a natural splitting of an image into drawing, shading, and fine-grained components p 2804 N93-25923
The implementation of a lossless data compression module in an advanced orbiting system: Analysis and development p 2804 N93-25928
DATA TRANSFER (COMPUTERS)
RAID-2: Design and implementation of a large scale disk array controller
| NASA-CR-192911 | p 2806 N93-25233
Interfacing a high performance disk array file server to a Gigabit LAN
| NASA-CR-192898 | p 2816 N93-25458
DATA TRANSMISSION
A functional description of the Buffered Telemetry Demodulator (BTD) p 2614 N93-24667
Symbol signal-to-noise ratio loss in square-wave subcarrier downconversion p 2672 N93-24668
Crossing the frontier between publishing and information service
| DE93-002894 | p 2873 N93-24677
CAD data exchange development
| DE93-008085 | p 2809 N93-25307
An SPW software simulation model of a dispersive fading multipath narrowband HF channel
| AD-A261101 | p 2675 N93-25767
Spacelab, Spacehab, and Space Station Freedom payload interface projects p 2620 N93-26080
Bandwidth compression of noisy signals with square-wave subcarrier p 2678 N93-26120
DSN acquisition of Magellan high-rate telemetry data p 2614 N93-26124
Galileo early cruise, including Venus, First Earth, and Gaspra encounters p 2599 N93-26125
Admission control in integrated voice/data multihop radio networks
| AD-A261055 | p 2680 N93-26227
Information transmission using CHAOS
| AD-A261519 | p 2883 N93-26377
DAYGLOW
The Venus 130-nm dayglow as a diagnostic of thermospheric structure and dynamics p 2896 N93-25285
DEACTIVATION
Effect of a metal deactivator fuel additive on fuel deposition in fuel atomizers at high temperature
| AD-A260915 | p 2661 N93-25914
DEBONDING (MATERIALS)
Damage and failure analysis on continuous fiber-reinforced polymer composites p 2637 N93-25716
DEBRIS
The initial flight anomalies of Skylab 1 p 2619 N93-24692
Model for transport of floating debris in the ocean
| PB93-172997 | p 2768 N93-26559
DECELERATION
Tsien's method for generating non-Keplerian trajectories. Part 2: The question of thrust to orbit a sphere and the restricted three-body problem p 2603 N93-24718
DECIDUOUS TREES
Scale dependence in the reflectance of deciduous woodland: Evidence from a helicopter-mounted spectroradiometer p 2752 N93-24865
DECISION MAKING
An introductory guide to uncertainty analysis in environmental and health risk assessment
| DE93-002873 | p 2760 N93-24676
Using neural networks and Dyna algorithm for integrated planning, reacting and learning in systems
| NASA-CR-193018 | p 2817 N93-24743
How to help intelligent systems with different uncertainty representations cooperate with each other
| NASA-CR-192947 | p 2818 N93-25196
Organizational politics, participation in decision-making, and job satisfaction
| DOT/FAA/AM-92/17 | p 2796 N93-25203
The evaluation of technical models used for major-accident hazard installations. Report to Commission of the European Communities Directorate General 12
| CUED/A-AERO/TR-19 | p 2668 N93-25238
Design of a cooperative problem-solving system for enroute flight planning: An empirical study of its use by airline dispatchers
| NASA-CR-192709 | p 2585 N93-25330
Adaptive process control with fuzzy logic and genetic algorithms p 2827 N93-25612
Knowledge-based decision support for Space Station assembly sequence planning
| NASA-CR-193048 | p 2599 N93-26095
A hypertext framework for group support systems
| AD-A261731 | p 2885 N93-26582
DECISION THEORY
Adaptive decision support systems: Concepts, characterization, and an application p 2876 N93-25475
Real-time value-driven monitoring and repair
| AD-A260959 | p 2811 N93-26221
DECODING
Soft decoding a self-dual (48, 24; 12) code p 2671 N93-24662
A (72, 36; 15) box code p 2671 N93-24663
A low-complexity and high performance concatenated coding scheme for high-speed satellite communications
| NASA-CR-192715 | p 2673 N93-25198
DECOMPOSITION
Polar decomposition for attitude determination from vector observations p 2602 N93-24711
Progress in imaging microscopy with x ray lasers at LLNL
| DE93-007508 | p 2712 N93-25363
Application of non-thermal plasmas to pollution control
| DE93-007515 | p 2763 N93-25385
Wavelet transform-vector quantization compression of supercomputer ocean model simulation output
| DE93-005453 | p 2876 N93-25448
Environmental test program for superconducting materials and devices
| DE93-003646 | p 2864 N93-25506
Mechanisms of decomposition and oxidation of borane compounds
| AD-A261137 | p 2645 N93-26045
Model reduction for Space Station Freedom p 2620 N93-26081
Phosphorus-, nitrogen-, sulfur-, and chlorine-containing molecules on surfaces
| AD-A261265 | p 2657 N93-26303
Methods of optimization under uncertainty
| AD-A261487 | p 2873 N93-26342
Position sensitive atom probe study of the decomposition of a Cu-2.6 at. percent Co alloy
| DE93-006737 | p 2653 N93-26500
DEEP SPACE
The advances in F and T technology: Their benefits of and for space science and technology p 2831 N93-24979
Deep-space navigation with differenced data types. Part 3: An expanded information content and sensitivity analysis p 2614 N93-26109
DEEP SPACE NETWORK
The Telecommunications and Data Acquisition Report
| NASA-CR-192887 | p 2671 N93-24659
Feasibility study of a Ka-/Ka-band dichroic plate with stepped rectangular apertures p 2671 N93-24660
A technique for computation of noise temperature due to a beam waveguide shroud p 2671 N93-24661
Failure monitoring in dynamic systems: Model construction without fault training data p 2672 N93-24666
A functional description of the Buffered Telemetry Demodulator (BTD) p 2614 N93-24667
Design of the reduced LQG compensator for the DSS-13 antenna p 2672 N93-24669
Performance results of a 300-degree linear phase modulator for spaceborne communications applications p 2672 N93-24670
Management of space networks p 2672 N93-24671
The Telecommunications and Data Acquisition Report
| NASA-CR-192804 | p 2676 N93-26105
Deep-space navigation with differenced data types. Part 3: An expanded information content and sensitivity analysis p 2614 N93-26109
Applications of inertial-sensor high-inheritance instruments to DSN precision antenna pointing p 2621 N93-26112
Dynamic modeling of fluid transmission lines of the DSN 70-meter antennas by using a lumped parameter model p 2678 N93-26119
An OSI architecture for the Deep Space Network p 2679 N93-26121
Sequential design of a linear quadratic controller for the Deep Space Network antennas p 2679 N93-26123
DSN acquisition of Magellan high-rate telemetry data p 2614 N93-26124
Galileo early cruise, including Venus, First Earth, and Gaspra encounters p 2599 N93-26125
Deep Space Network information system architecture study p 2679 N93-26126
Generalized probability model for calculation of interference to the Deep Space Network due to circularly Earth-orbiting satellites p 2679 N93-26127
DSN observations of Titan p 2680 N93-26129
DEFECTS
Vibration, buckling, and postbuckling of laminated composites with delaminations p 2723 N93-24765
Investigation of corrosion in aluminum/adhesive lap-splices using pulse-echo ultrasonic techniques
| DE93-008074 | p 2721 N93-25518
Automated inspection of solder joints for surface mount technology
| NASA-TM-104580 | p 2721 N93-26137
Effects of space radiation on humoral and cellular immunity in rhesus monkeys
| AD-A261808 | p 2793 N93-26259
DEFENSE PROGRAM
Photovoltaic power without batteries for continuous cathodic protection p 2759 N93-25597
Special tooling disposition for aircraft entering post production support
| AD-A261614 | p 2573 N93-26168
Department of Defense technical architecture framework for information management. Volume 3: Reference model and standards profile, version 1.3
| AD-A261913 | p 2882 N93-26230
AFOSR technical report summaries
| AD-A261551 | p 2918 N93-26380
Department of Defense technical architecture framework for information management. Volume 1: Implementation concept, version 1.1
| AD-A261911 | p 2884 N93-26531
Department of Defense technical architecture framework for information management. Volume 2: Architecture guidance and design concepts, version 1.1
| AD-A261912 | p 2884 N93-26532
DEFLAGRATION
Physical and chemical processes governing the CO2 laser-induced deflagration of ammonium dinitramide (ADN) p 2629 N93-26037
Flame response in oscillatory solid propellant combustion p 2630 N93-26041
DEFLECTION
Method and apparatus for deflection measurements using eddy current effects
| NASA-CASE-GSC-13506-1 | p 2710 N93-26103
A nanoradian differential VLBI tracking demonstration p 2677 N93-26108
DEFOLIATION
Forest decline monitoring using Landsat TM, digital stand data and DEMs p 2749 N93-24846
DEFORESTATION
World Forest Watch: A global forest monitoring test p 2748 N93-24836
Interpretation and segmentation of changed forest stands from difference imagery based on regression functions p 2748 N93-24839
DEFORMATION
Axisymmetric deformations and stresses of unsymmetrically laminated composite cylinders in axial compression with thermally-induced preloading effects
| NASA-CR-192788 | p 2723 N93-24912
Dynamic deformations and analysis of a metal matrix composite p 2634 N93-25234
On existence of solutions and duality for a model of non-linear elastic plates with transverse shear deformations p 2726 N93-25437
An integrated finite-state model for rotor deformation, nonlinear airloads, inflow, and trim p 2588 N93-25538

Crustal deformation studies in subaerial parts of the world oceanic rift system: Iceland and Afar
p 2789 N93-25558
Damage and failure analysis on continuous fiber-reinforced polymer composites
p 2637 N93-25716
Models of crack growth along polymer interfaces
p 2728 N93-25750
Computer modelling of cyclic deformation of high-temperature materials
| AD-A260978 | p 2639 N93-25936
Deformations of active flexible rods with embedded line actuators
| AD-A261207 | p 2729 N93-25950
Repair, evaluation, maintenance, and rehabilitation research program. Continuous Deformation Monitoring System (CDMS)
| AD-A261833 | p 2586 N93-26274
On the stability of finite plastic deformations
| AD-A261526 | p 2730 N93-26361
Use and analysis of finite element methods for problems of solid mechanics and fracture
| AD-A261574 | p 2731 N93-26522

DEGRADATION
Application of remote sensing data for the investigation of environmental degradation sites in East Germany
p 2739 N93-24785
The use of remote sensing and GIS for the assessment of environmental degradation caused by fires, applied upon South-Euboia (central Greece) p 2742 N93-24802
An investigation of the degradation of Fluorinated Ethylene Propylene (FEP) copolymer thermal blanketing materials aboard LDEF in the laboratory
| NASA-CR-192824 | p 2653 N93-25078
Detecting damaged cables using a preionized gas technique
| DE93-007588 | p 2689 N93-25429
New algorithms for the detection and elimination of sine waves and other narrow-band signals in the presence of broadband signals and noise
| AD-A261811 | p 2681 N93-26261

DEGREES OF FREEDOM
A nanoradian differential VLBI tracking demonstration
p 2677 N93-26108

DEHYDRATION
Design of a high activity and selectivity alcohol catalyst
| DE93-008101 | p 2659 N93-25111
Vascular uptake of rehydration fluids in hypohydrated men at rest and exercise
| NASA-TM-103942 | p 2795 N93-26133

DEHYDROGENATION
The surface characterization of a series of hydroxybenzenes on Ag(111): An EELS and TDS study
| DE93-007541 | p 2647 N93-26595

DELAMINATING
Vibration, buckling, and postbuckling of laminated composites with delaminations p 2723 N93-24765
Processing and mechanical properties of laminated metal composites of Al/Al-25 vol. percent SiC and ultrahigh carbon steel/brass
| DE93-007504 | p 2635 N93-25383
The damage, repair and design of fiber composite structural materials p 2635 N93-25532
Production of ultrafine, high-purity ceramic powders using the US Bureau of Mines developed turbomill
p 2659 N93-25585
Damage-survivable and damage-tolerant laminated composites with optimally placed piezoelectric layers
| AD-A260879 | p 2636 N93-25631
Investigation and modeling of penetration process for composite laminates impacted by a blunt-ended projectile p 2637 N93-25675
Low-velocity impact of composite sandwich plate
p 2637 N93-25695
Damage and failure analysis on continuous fiber-reinforced polymer composites
p 2637 N93-25716

DELAY
A new modem for microwave time synchronisation via geosynchronous telecommunication satellites
p 2686 N93-24999

DELAY CIRCUITS
Variable pulse rate circuit
| AD-D015675 | p 2691 N93-26233

DELTA WINGS
Computational study of the aerodynamics and control by blowing of asymmetric vortical flows over delta wings
p 2574 N93-24772
The transient development of vortices over delta wings p 2576 N93-25269
Experimental effects of wing location on wing-body pressures at supersonic speeds
| NASA-TM-4434 | p 2581 N93-26085
Conical Euler analysis and active roll suppression for unsteady vortical flows about rolling delta wings
| NASA-TP-3259 | p 2581 N93-26134

DELTAS
Monitoring and evaluation of morphohydrographical changes in the Danube Delta by remote-sensing
p 2747 N93-24834

DEMODULATION
Synchronisation, acquisition and tracking for telemetry and data reception p 2614 N93-25000

DEMODULATORS
A functional description of the Buffered Telemetry Demodulator (BTD) p 2614 N93-24667

DEMOGRAPHY
Assessing patterns of change in anthropometric dimensions: Secular trends of US Army females, 1946-1988
| AD-A260869 | p 2800 N93-25628

DENDRITIC CRYSTALS
High temperature fracture toughness of Ni3Al alloy IC-396M
| DE93-008564 | p 2650 N93-25492
Flow and morphological conditions associated with the directional solidification of aqueous ammonium chloride
| DE93-008886 | p 2644 N93-25495
Computation of complex solidification morphologies using a phase-field model
| PB93-156743 | p 2869 N93-26547

DENSIFICATION
Properties of extruded PS-212 type self-lubricating materials p 2659 N93-25565
Densification of ceramics by gas overpressure sintering
| MTL-TR-92-45 | p 2657 N93-26432

DENSITY (NUMBER/VOLUME)
The structure of the nearby universe traced by theIRAS galaxies
| NASA-CR-192809 | p 2889 N93-25331

DENSITY DISTRIBUTION
A study of vibrationally excited N2(+) ions in the daytime thermosphere p 2770 N93-25179

DENSITY MEASUREMENT
Measurements of density, temperature, and their fluctuations in turbulent supersonic flow using UV laser spectroscopy
| NASA-TM-103943 | p 2708 N93-25076

DEOXYRIBONUCLEIC ACID
Measuring the metastatic potential of cancer cells
p 2794 N93-25566
Development of resonance ionization spectroscopy for genome mapping and DNA sequencing using stable isotopes as DNA labels
| DE93-007815 | p 2793 N93-26587

DEPOSITION
A study of mass size distributions and particle deposition velocities in ambient air p 2763 N93-25263
Sputter deposition of yttrium-oxides
| DE93-007499 | p 2654 N93-25382
Theoretical studies of surface reactions on metals and electronic materials
| DE93-009761 | p 2650 N93-25502
Optical and scratch resistant properties of diamondlike carbon films deposited with single and dual ion beams
p 2658 N93-25564

DEPTH
Algorithms for the analysis of penetration by shaped charge jets
| UCRL-LR-109887 | p 2730 N93-26178

DESERTIFICATION
Aerospace monitoring for ecological hazard and disaster mitigation p 2744 N93-24812

DESIGN ANALYSIS
Optimization in the systems engineering process
p 2666 N93-24691
A procedure for defining lightning risk to air vehicles
p 2583 N93-24885
Miniaturization and stability: A new generation of ovenised oscillators p 2693 N93-25004
A state-of-the-art crystal filter design package using Windows 3.0 techniques p 2693 N93-25010
Surface Transverse Wave (STW) quartz resonators in the GHz range p 2836 N93-25012
TF-4020A: TFL's new compact military rubidium standard p 2838 N93-25026
Rotor design optimization using a free wake analysis
| NASA-CR-177612 | p 2575 N93-25075
Design concepts for the development of cooperative problem-solving systems
| NASA-CR-192708 | p 2585 N93-25261
Poly-coil design for a 60 tesla quasi-stationary magnet
| DE93-007353 | p 2688 N93-25313
A numerical and experimental studies of flow characteristics in centrifugal fans p 2577 N93-25339
Human factors engineering: A key element of instrumentation and control system design
| DE93-006731 | p 2800 N93-25415
Space transfer vehicle concepts and requirements study. Volume 2, book 3: STV system interfaces
| NASA-CR-192527 | p 2611 N93-25513
A computational aerodynamic design optimization method using sensitivity analysis p 2589 N93-25552
Application of an on-machine gage for diameter measurements p 2711 N93-25578
Variable-speed generators with flux weakening
p 2694 N93-25599
Integration of design, thermal, structural, and optical analysis, including thermal animation
p 2814 N93-25601
The effects of reaction on axial compressor performance p 2594 N93-25882
Advanced life support study. Modification 10: ECLSS logistical support analysis for Space Station Freedom
| NASA-CR-192481 | p 2801 N93-25888
A new approach to cooled combustion chambers: The 40K formed platelet chamber p 2626 N93-26018
ASRM design philosophy and modelling challenges
p 2627 N93-26022
Techniques for designing rotorcraft control systems
| NASA-CR-192960 | p 2597 N93-26046
SRB environment evaluation and analysis. Volume 1: Redesigned SRB flight heating evaluation
| NASA-CR-192517 | p 2631 N93-26053
External tank aerothermal design criteria verification
| NASA-CR-192514 | p 2618 N93-26055
Use of Taguchi design of experiments to optimize and increase robustness of preliminary designs
p 2670 N93-26063
Model reduction for Space Station Freedom
p 2620 N93-26081
Task 5: Architecture sensitivity to STME performance
| MCR-92-5010 | p 2609 N93-26176
Develop margin philosophy to attain robustness
| MCR-92-5005 | p 2610 N93-26182
Design concepts for pressurized lunar shelters utilizing indigenous materials p 2670 N93-26414
Configuration optimization of space structures
p 2670 N93-26415

DESIGN TO COST
Space transfer vehicle concepts and requirements study. Volume 3, book 1: Program cost estimates
| NASA-CR-192529 | p 2611 N93-25514

DESORPTION
Laser desorption in an ion trap mass spectrometer
| DE93-007330 | p 2712 N93-25150
Theoretical studies of surface reactions on metals and electronic materials
| DE93-009761 | p 2650 N93-25502
Resonance electron scattering by O2 monolayers on graphites: Reinterpreted
| AD-A261851 | p 2850 N93-26287
The surface characterization of a series of hydroxybenzenes on Ag(111): An EELS and TDS study
| DE93-007541 | p 2647 N93-26595

DESULFURIZING
An experimental study of particle-laden jet interactions with cocurrent flows p 2701 N93-25534

DETACHMENT
Dynamics of collision processes
| DE93-007143 | p 2849 N93-25509
Penning detachment: A new frontier
| AD-A261447 | p 2850 N93-26346

DETECTION
Detecting damaged cables using a preionized gas technique
| DE93-007588 | p 2689 N93-25429
Automated system for early breast cancer detection in mammograms p 2796 N93-25568
Automatic detection of seizures with applications
p 2796 N93-25592
Vision-aided monitoring and control of thermal spray, spray forming, and welding processes
p 2670 N93-25604
Detection of bearing failure in mechanical devices using neural networks p 2822 N93-25965
Model-based reasoning for system and software engineering: The Knowledge From Pictures (KFP) environment p 2825 N93-25978
Pseudomonas screening assay
| NASA-CASE-NPO-17653-1-CU | p 2793 N93-25994
VETA x ray data acquisition and control system
p 2854 N93-26186

DETONABLE GAS MIXTURES
Parameters influencing the hot-spot ignition of aviation fuel/air and ethylene/air mixtures p 2583 N93-24886

DETONATION
DSD Technology: A detonation reactive Huygens code
| LA-12235-MS | p 2706 N93-25987
Molecular composition, structure, and sensitivity of explosives
| DE93-003850 | p 2662 N93-26493

DETONATION WAVES
DSD Technology: A detonation reactive Huygens code
| LA-12235-MS | p 2706 N93-25987
DEUTERIUM
Structure of sodium 4-(1'-heptylnonyl) benzenesulfonate adsorbed on alumina using H-2 NMR
| AD-A261224 | p 2645 N93-26300
Thermal decomposition of energetic materials. 4: Deuterium isotope effects and isotopic scrambling condensed-phased decomposition of 1,3,5-trinitrohexahydro-s-triazine
| AD-A261804 | p 2662 N93-26387
DEUTERIUM COMPOUNDS
Structure of sodium 4-(1'-heptylnonyl) benzenesulfonate adsorbed on alumina using H-2 NMR
| AD-A261224 | p 2645 N93-26300
Laser damage to production- and research-grade KDP crystals
| DE93-007517 | p 2870 N93-26594
DEVELOPING NATIONS
The General Information Programme (PGI) and developing countries: A case study of Iraq
p 2874 N93-25209
The PACSAT Communications Experiment (PCE)
| DE93-008185 | p 2674 N93-25308
DEWATERING
Low cost dewatering of waste slurries
p 2769 N93-25573
DIAGNOSIS
Summary of progress in inertial confinement fusion
| DE93-007350 | p 2858 N93-25187
Fast diagnostics of laser ablation used for pulsed laser deposition
| DE93-005155 | p 2713 N93-25508
A fiber optic probe for the detection of cataracts
p 2796 N93-25593
Machine learning techniques for fault isolation and sensor placement p 2823 N93-25966
The use of multiple models in case-based diagnosis
p 2823 N93-25969
Anomalous event diagnosis for environmental satellite systems p 2619 N93-25971
Measurement of droplet vaporization rate enhancement caused by acoustic disturbances p 2626 N93-26015
Flame structure studies of a lean, 20 torr H2/N2O/AR flame employing molecular beam mass spectrometry
p 2627 N93-26025
Infrared fiber optic diagnostic for solid propellant combustion p 2628 N93-26031
ADN propellant diffusion flame structure
p 2629 N93-26036
DIAMETERS
Application of an on-machine gage for diameter measurements p 2711 N93-25578
DIAMOND FILMS
Diagnostics of diamond film deposition plasmas
| AD-A260866 | p 2860 N93-25626
Control of crystallite size in diamond film chemical vapor deposition
| AD-D015660 | p 2867 N93-26090
Workshop on Diamond and Diamond-Like-Carbon Films for the Transportation Industry
| DE93-007491 | p 2658 N93-26506
DIAMONDS
Electrodeposition in low gravity p 2663 N93-24774
Metastable SiC and SiGeC alloys by carbon implantation and solid phase epitaxy
| DE93-007594 | p 2863 N93-25387
Optical and scratch resistant properties of diamondlike carbon films deposited with single and dual ion beams
p 2658 N93-25564
Method of joining diamond structures
| AD-D015671 | p 2867 N93-26140
DIATOMIC MOLECULES
Modeling of atom-diatom scattering
| AD-A261645 | p 2849 N93-26173
Application of the Saha equation to high temperature (greater than or equal to) rocket exhaust
| AD-A261648 | p 2632 N93-26174
DICARBOXYLIC ACIDS
Energetic materials from cubane
| AD-A261317 | p 2662 N93-26308
DICHROISM
Feasibility study of a Ka-/Ka-band dichroic plate with stepped rectangular apertures p 2671 N93-24660
DICTIONARIES
The database Query Support Processor (QSP)
p 2807 N93-25577
Glossary of environmental terms and acronym list
| PB93-158004 | p 2765 N93-25851
CALS-HSC data element dictionary
| AD-A261560 | p 2813 N93-26461
DIELECTRIC PROPERTIES
Characterization of ceramic capacitors for high-voltage pulse-discharge applications
| DE93-007601 | p 2689 N93-25417
Extruded films from modified polypropylene resin: Dielectric and breakdown studies
| AD-A261382 | p 2657 N93-26341
DIELECTRICS
Design of a low phase noise UHF oscillator using a partly metallized dielectric resonator p 2693 N93-25003
Liquid filled variable capacitor
| AD-D015639 | p 2687 N93-25212
Correlation of damage threshold and surface geometry of nodular defects in HR coatings as determined by in-situ atomic force microscopy
| DE93-007509 | p 2654 N93-25384
Characterization of ceramic capacitors for high-voltage pulse-discharge applications
| DE93-007601 | p 2689 N93-25417
Microwave absorption measurements and interference: Effects for a liquid fuel between 2.5 and 18 GHz
| AD-A260607 | p 2675 N93-25635
Enhanced backscattering from rough surfaces
| AD-A261000 | p 2676 N93-25855
Electrorheological fluids: A structural approach to mechanisms
| AD-A260563 | p 2645 N93-25879
Extruded films from modified polypropylene resin: Dielectric and breakdown studies
| AD-A261382 | p 2657 N93-26341
Modeling of electric-field enhancement at nodular defects in dielectric mirror coatings
| DE93-007513 | p 2857 N93-26593
DIESEL ENGINES
Center for Advanced Propulsion Systems (fellowship)
| AD-A260571 | p 2632 N93-26216
DIFFERENTIAL AMPLIFIERS
Investigation into the common mode rejection ratio of the physiological signal conditioner circuit
p 2794 N93-26073
DIFFERENTIAL CALCULUS
Dynamic error analysis of numerical methods for simulation of state-variable derivatives with discontinuities p 2819 N93-25278
DIFFERENTIAL EQUATIONS
Stability of nonlinear phase motion from the study of oscillator mappings p 2693 N93-25034
On the effect of acoustic coupling on random and harmonic plate vibrations
| NASA-TM-107740 | p 2844 N93-25189
Numerically dissipative time integration algorithms for structural dynamics p 2725 N93-25394
Multilevel techniques in large scale computation
| AD-A261082 | p 2828 N93-25762
A basic research model of natural gas combustion in turbulent flow, phase 2
| PB93-158509 | p 2644 N93-25819
A hybrid multigrid technique for computing steady-state solutions to supersonic flows p 2582 N93-26078
NSWC library of mathematics subroutines
| AD-A261511 | p 2884 N93-26575
DIFFERENTIAL GEOMETRY
Elastic curves on the sphere
| AD-A261057 | p 2829 N93-26228
DIFFRACTION
Surface diffusion studies by optical diffraction techniques
| DE93-007707 | p 2853 N93-25550
DIFFUSION
Asymptotic derivation of the simplified P(sub N) equations
| DE93-007342 | p 2828 N93-25151
Oblique MHD cosmic-ray modified shocks: Two-fluid numerical simulations
| NASA-CR-192930 | p 2900 N93-26132
Ir-Zr alloys as diffusion barriers between Cu and Si(100)
| AD-A261919 | p 2652 N93-26197
DIFFUSION COEFFICIENT
Direct measurement of velocity space transport in a plasma p 2861 N93-25831
Numerical simulation of permeation from deposited droplets: Model expansion
| MTL-TR-92-23 | p 2706 N93-25953
DIFFUSION FLAMES
ADN propellant diffusion flame structure
p 2629 N93-26036
Oxides of nitrogen emissions from turbulent hydrocarbon/air jet diffusion flames, phase 2
| PB93-152478 | p 2768 N93-26533
DIFFUSION THEORY
Asymptotic derivation of the simplified P(sub N) equations
| DE93-007342 | p 2828 N93-25151
DIGITAL DATA
Crossing the frontier between publishing and information service
| DE93-002894 | p 2873 N93-24677
Wavelet transform-vector quantization compression of supercomputer ocean model simulation output
| DE93-005453 | p 2876 N93-25448
Digital Nautical Chart
| AD-A260810 | p 2756 N93-25694
US Army evaluation of the Electronic Map Data (EMD) prototype
| AD-A261693 | p 2757 N93-26369
Implementation of custom colors in the DECwindows environment
| AD-A261456 | p 2757 N93-26574
DIGITAL ELECTRONICS
High resolution digital synthesizer for a Rb frequency standard p 2694 N93-25057
A digital hardware test system analysis with test vector translation
| AD-A260849 | p 2810 N93-25786
Published assessments bearing on the future use of ceramic superconductors by the electric power sector
| DE93-007737 | p 2658 N93-26588
DIGITAL FILTERS
Digital filter control of remotely operated flexible robotic structures
| DE93-007587 | p 2827 N93-26596
DIGITAL SIMULATION
Forest decline monitoring using Landsat TM, digital stand data and DEMs p 2749 N93-24846
A digital hardware test system analysis with test vector translation
| AD-A260849 | p 2810 N93-25786
DIGITAL SYSTEMS
A digital hardware test system analysis with test vector translation
| AD-A260849 | p 2810 N93-25786
Development and testing of the digital control system for the Archytas unmanned air vehicle
| AD-A261656 | p 2597 N93-26196
Digital Oblique Remote Ionospheric Sensing (DORIS) program development
| AD-A261750 | p 2776 N93-26283
A channel simulation processor for the multi-node tactical network simulator
| AD-A261810 | p 2776 N93-26430
DIGITAL TECHNIQUES
Swedish forest information atlas p 2749 N93-24847
Digitization of analog data from in-flight lightning strikes p 2778 N93-24884
A microcomputer compensated crystal oscillator MCXO p 2834 N93-25001
Synopsis of timing measurement techniques used in telecommunications p 2687 N93-25064
DIGITAL TRANSDUCERS
An advanced data-acquisition system for wind energy projects
| DE93-000079 | p 2874 N93-25254
DIMENSIONAL MEASUREMENT
Application of an on-machine gage for diameter measurements p 2711 N93-25578
On machine capacitance dimensional and surface profile measurement system p 2670 N93-25579
A novel method for characterization of superconductors: Physical measurements and modeling of thin films
p 2871 N93-25584
X-ray computed tomography for casting development
| AD-A261786 | p 2722 N93-26526
DIMENSIONAL STABILITY
RF vacuum microelectronics
| AD-A261343 | p 2691 N93-26311
DIODES
Electric field effects on quantum-confined semiconductor structures p 2865 N93-25703
DIRAC EQUATION
Multilevel techniques in large scale computation
| AD-A261082 | p 2828 N93-25762
DIRECT BROADCAST SATELLITES
Analytical techniques for improved time transfer using common view of direct broadcasting satellites
p 2835 N93-25008
DIRECTION FINDING
Lightning characteristics in the north-east part of Japan observed by a magnetic direction-finder network
p 2779 N93-24892
DIRECTIONAL SOLIDIFICATION (CRYSTALS)
Flow and morphological conditions associated with the directional solidification of aqueous ammonium chloride
| DE93-008886 | p 2644 N93-25495
DIRECTORIES
A trace-driven analysis of name and attribute caching in a distributed system
| NASA-CR-192899 | p 2815 N93-25251
Directory of US Government software for mainframes and microcomputers, 1993
| PB93-111565 | p 2807 N93-26569
DIRICHLET PROBLEM
The steady Navier-Stokes problem for low Reynolds number viscous jets p 2698 N93-25264

DISASTERS
Natural disasters and their mitigation using space technology p 2742 N93-24804
Alternative strategies for the use of satellite data analysis systems for hazard monitoring and disaster mitigation p 2743 N93-24805
Satellite borne remote sensing data: A tool for natural disaster reduction p 2743 N93-24806
Use of remote sensing spacecrafts in real time support to disaster management: Interfaces with ground segment facilities and services p 2743 N93-24809
The use of SPOT data in natural disaster prevention and damage assessment p 2743 N93-24811
Aerospace monitoring for ecological hazard and disaster mitigation p 2744 N93-24812
DISCHARGE COEFFICIENT
Flow conditioner location effects in orifice flowmeters | PB93-159457 | p 2708 N93-26535
DISCONTINUITY
The modeling of complex continua: Fundamental obstacles and grand challenges | DE93-006507 | p 2696 N93-25193
Tracking sharp interface of two fluids by the CIP (Cubic-Interpolated Propagation) scheme | NIFS-206 | p 2698 N93-25277
Dynamic error analysis of numerical methods for simulation of state-variable derivatives with discontinuities p 2819 N93-25278
DISCOVERY (ORBITER)
STS-39 Space Shuttle mission report | NASA-CR-193063 | p 2611 N93-25955
STS-42 Space Shuttle mission report | NASA-CR-193059 | p 2613 N93-25989
STS-48 Space Shuttle mission report | NASA-CR-193060 | p 2613 N93-25990
DISK GALAXIES
Starburst Galaxies: Hard X-ray spectra and contribution to the diffuse background | NASA-CR-192790 | p 2892 N93-25211
DISK OPERATING SYSTEM (DOS)
OCEAN-PC and a distributed network for ocean data p 2734 N93-24928
DISPERSING
The AFTAC model integration project | DE93-003334 | p 2761 N93-25122
On the generation and dispersion of Yanai waves with a spectral Chebyshev-collocation reduced-gravity ocean model p 2788 N93-25276
DISPERSION
Hazards of explosives dusts: Particle size effects | DE93-009380 | p 2668 N93-25498
DISPLACEMENT
Equilibrium constrained assumed natural coordinate strain finite elements for shell analysis p 2724 N93-25273
TSC plasma halo simulation of a D3-D vertical displacement episode | DE93-008688 | p 2860 N93-25493
Positive displacement rotary pump | AD-D015678 | p 2719 N93-26144
DISPLAY DEVICES
A comparison of the WIND System atmospheric models and MATS data | DE93-002687 | p 2760 N93-24673
Evaluation of advanced displays for engine monitoring and control | NASA-CR-191418 | p 2591 N93-24764
Improving information search at the user interface: The impact of graphical innovation on query formulation and expression p 2873 N93-24905
The Grid Analysis and Display System (GRADS): A practical tool for Earth science visualization p 2880 N93-25805
Planetary data analysis and display system: A version of PC-McIDAS p 2880 N93-25806
SAVS: A Space Analysis and Visualization System p 2881 N93-25812
A distributed analysis and visualization system for model and observational data p 2881 N93-25814
Inflight evaluation of an acoustic orientation instrument | AD-A260752 | p 2591 N93-25909
Perceptual factors that influence use of computer enhanced visual displays | NASA-CR-192961 | p 2811 N93-26150
Experimental and theoretical studies of proximity effect and Coulomb blockade phenomena in Josephson junctions | AD-A261652 | p 2867 N93-26194
Emerging large-screen display technology | AD-A261066 | p 2681 N93-26241
Advanced technology for portable personal visualization | AD-A261294 | p 2807 N93-26293
Effect of image update rate on moving-target identification range | AD-A261562 | p 2591 N93-26462
Implementation of custom colors in the DECwindows environment | AD-A261456 | p 2757 N93-26574
DISSOLVING
Anisotropic etching of silicon in KOH solutions p 2647 N93-25037
Controlled dissolution of a piezoelectric material berlinite (AlPO4) p 2840 N93-25043
DISTANCE
Analytical techniques for improved time transfer using common view of direct broadcasting satellites p 2835 N93-25008
DISTILLATION
Design and synthesis of reactive separation systems | DE93-008764 | p 2642 N93-25115
DISTILLATION EQUIPMENT
Design and synthesis of reactive separation systems | DE93-008764 | p 2642 N93-25115
DISTORTION
An example of a phase-segregated enhanced PAL broadcasting system | BBC-RD-1992/6 | p 2674 N93-25239
Equilibrium constrained assumed natural coordinate strain finite elements for shell analysis p 2724 N93-25273
Tracking sharp interface of two fluids by the CIP (Cubic-Interpolated Propagation) scheme | NIFS-206 | p 2698 N93-25277
Distortion measurements on bandpass filters with powdered iron toroidal inductors | AD-A260790 | p 2675 N93-25689
Evaluation of lens distortion errors in video-based motion analysis | NASA-TP-3266 | p 2797 N93-25736
Geometric distortion analysis of a wide-field astrograph p 2621 N93-26111
Surface finish quality of the outer AXAF mirror pair based on x ray measurements of the VETA-I p 2855 N93-26191
DISTRIBUTED PROCESSING
Optimal message log reclamation for independent checkpointing | NASA-CR-192886 | p 2815 N93-24749
Data processing and control in a transputer system for remote sensing of the Earth p 2753 N93-24870
A comparison using APPL and PVM for a parallel implementation of an unstructured grid generation program | NASA-CR-191425 | p 2808 N93-25073
On the robustness of Herlihy's hierarchy | NASA-CR-193002 | p 2808 N93-25107
Using a Cray Y-MP as an array processor for a RISC Workstation | NASA-TM-103961 | p 2809 N93-25246
A trace-driven analysis of name and attribute caching in a distributed system | NASA-CR-192899 | p 2815 N93-25251
Proceedings of the Second SISAL Users' Conference | DE93-008019 | p 2815 N93-25304
Hierarchical dynamics in distributed information processing p 2875 N93-25350
Implicit multigrid solution of the compressible Navier-Stokes equations with application to distributed parallel processing p 2702 N93-25546
Object-oriented tools for distributed computing p 2817 N93-25576
Distributed information storage p 2877 N93-25722
Knowledge-based assistance for science visualization and analysis using large distributed databases p 2879 N93-25801
A distributed analysis and visualization system for model and observational data p 2881 N93-25814
The WorkPlace distributed processing environment p 2825 N93-25977
Signed vector timestamps: A secure protocol for partial order time | AD-A261371 | p 2817 N93-26338
DISTRIBUTION FUNCTIONS
Pseudo Wigner-Ville distribution, computer program, and its applications to time-frequency domain problems | AD-A261839 | p 2813 N93-26431
Liquid and solid ion plasmas | AD-A261888 | p 2862 N93-26528
DIURNAL VARIATIONS
Analysis of the effects of mean local node-crossing time on the evolution of Sun-synchronous orbits p 2602 N93-24706
Summary information and data sets for NREL's Solar Radiation Research Laboratory, 1981 - 1991 | DE93-000052 | p 2898 N93-25101
The role of multiple scattering in twilight zenith sky observations of atmospheric absorbers: Diurnal photochemistry and airmass factors p 2772 N93-25535
DIVERTERS
Boundary plasma modelling for ITER | DE93-007963 | p 2859 N93-25302
DOCUMENT STORAGE
Zebra: A striped network file system | NASA-CR-192912 | p 2809 N93-25250
DOLOMITE (MINERAL)
Low cost dewatering of waste slurries p 2769 N93-25573
DOMAINS
Intelligent, real-time problem solving, phase 3 | AD-A261441 | p 2829 N93-26345
DOPED CRYSTALS
Fundamental studies of defect generation in amorphous silicon alloys grown by remote plasma-enhanced chemical-vapor deposition (Remote PECVD) | DE92-010560 | p 2862 N93-24953
Radiation effects in germanium doped quartz p 2837 N93-25021
Structure and properties of a-C: N films prepared by pulsed excimer laser deposition | DE93-007908 | p 2654 N93-25372
Time resolved studies of in-well and cross-well carrier transport in MQW semiconductor structures | AD-A261170 | p 2714 N93-25774
Experimental studies of stress management by optical fluorescence | AD-A261539 | p 2730 N93-26362
Optical characterization of Ga(1-x)In(x)As(y)Sb(1-y)/GaSb alloy and device application | AD-A261713 | p 2870 N93-26581
DOPPLER EFFECT
An introduction to Doppler effect and fading in mobile communications | AD-A260976 | p 2676 N93-25866
Imaging the magnetosphere in the extreme ultraviolet | NASA-CR-192218 | p 2775 N93-26151
Trailing vortex/free-surface interaction | AD-A261654 | p 2581 N93-26195
DOPPLER NAVIGATION
The advances in F and T technology: Their benefits of and for space science and technology p 2831 N93-24979
DOPPLER RADAR
Positive cloud-to-ground flashes in severe storms p 2780 N93-24896
Initialization of a modeled convective storm using Doppler radar-derived fields p 2782 N93-25294
Setting values for TDWR/LLWAS 3 integration parameters | AD-A260740 | p 2783 N93-25645
The North Dakota thunderstorm project | PB93-153039 | p 2785 N93-25776
DOSAGE
Radiation-hardened control system | DE93-007248 | p 2688 N93-25377
Utilization of an electronic circuit simulator in CMOS latch-up studies | AD-A260877 | p 2690 N93-25935
DOSIMETERS
Measuring hearing protection device performance using the metrosonics db-3100 sound level analyzer (dosimeter) | AD-A260852 | p 2801 N93-25787
Detailed component design for a Compact Environmental Anomaly Sensor (CEASE) | AD-A261729 | p 2620 N93-26248
DOUBLE BASE PROPELLANTS
Modeling of H2/N2O flames p 2627 N93-26026
Dark zone modeling of solid propellant flames p 2628 N93-26028
DOWN-CONVERTERS
Symbol signal-to-noise ratio loss in square-wave subcarrier downconversion p 2672 N93-24668
Bandwidth compression of noisy signals with square-wave subcarrier p 2678 N93-26120
DOWNLINKING
Feasibility study of a Ka-/Ka-band dichroic plate with stepped rectangular apertures p 2671 N93-24660
Performance results of a 300-degree linear phase modulator for spaceborne communications applications p 2672 N93-24670
DRAG REDUCTION
Computation of transonic flow over a porous surface projectile p 2577 N93-25409
Structural and aerodynamic optimization of joined-wing aircraft p 2588 N93-25526
An experimental study of passive drag reduction in a turbulent boundary layer by a riblet surface p 2705 N93-25746
Modified point mass trajectory simulation for base-burn projectiles | BRL-TR-3321 | p 2609 N93-25985

DRIFT RATE
Analysis of the effects of mean local node-crossing time on the evolution of Sun-synchronous orbits p 2602 N93-24706
Mixed constellation synchronization of GPS time p 2836 N93-25015
Use of the TV-signal in stabilizing a local rubidium oscillator p 2693 N93-25029
Space radiation susceptibility of ultra stable crystal oscillators p 2693 N93-25053
DRILLING
The design of mechanically compatible fasteners for human mandible reconstruction p 2796 N93-25569
DRINKING
Vascular uptake of rehydration fluids in hypohydrated men at rest and exercise
| NASA-TM-103942 | p 2795 N93-26133
DROP SIZE
Liquid surface breakup of nonturbulent and turbulent liquids p 2700 N93-25473
DROP TOWERS
Contributions of microgravity test results to the design of spacecraft fire safety systems
| NASA-TM-106093 | p 2614 N93-24755
DROPS (LIQUIDS)
The WINCOF-I code: Detailed description
| NASA-CR-190779 | p 2573 N93-24760
Atomizing-gas temperature effect on cryogenic spray dropsize
| NASA-TM-106106 | p 2709 N93-25191
The modeling of complex continua: Fundamental obstacles and grand challenges
| DE93-006507 | p 2696 N93-25193
The structure of particle cloud premixed flames
| NASA-CR-192827 | p 2643 N93-25229
Modeling of bubble and drop formation in flowing liquids in terrestrial and microgravity environments p 2664 N93-25390
Fundamental studies of droplet interactions in dense sprays
| AD-A261165 | p 2661 N93-25948
Numerical simulation of permeation from deposited droplets: Model expansion
| MTL-TR-92-23 | p 2706 N93-25953
Particle size as a factor in agglomeration in slurry fuels p 2625 N93-26013
A summary of the JANNAF workshop on liquid rocket atomization p 2625 N93-26014
Measurement of droplet vaporization rate enhancement caused by acoustic disturbances p 2626 N93-26015
DROUGHT
Global drought monitoring from NOAA polar orbiting satellites p 2750 N93-24852
DRUGS
Immunoconjugates: Magic bullets for cancer therapy? p 2796 N93-25567
DRYING
Production of ultrafine, high-purity ceramic powders using the US Bureau of Mines developed turbomill p 2659 N93-25585
DUCTED FLOW
Numerical simulation of a shock wave/turbulent boundary layer interaction in a duct p 2699 N93-25342
Computational modelling of 3D flow in complex ducts and passages p 2704 N93-25698
DUCTED ROCKET ENGINES
Turbulence interacting with chemical kinetics in airbreathing combustion of ducted rockets p 2625 N93-26012
DUCTILITY
Numerical investigations on fracture behavior of ductile materials p 2725 N93-25411
Study of grain refinement in Al alloy 2519 using backscattering orientation-contrast mode in the scanning electron microscope
| AD-A260886 | p 2651 N93-25632
Development and application of an advanced ductile fracture mechanics methodology p 2727 N93-25718
Deformation mechanisms of NiAl cyclicly deformed near the brittle-to-ductile transition temperature
| NASA-CR-191121 | p 2652 N93-26235
DUCTS
Experimental investigation of flow turning losses in unstable rocket motors p 2630 N93-26040
Duct protection coating concept development and test: Test specimen fabrication, conditioning, and testing documentation.
| AD-A261250 | p 2657 N93-26278
DURABILITY
Damage-survivable and damage-tolerant laminated composites with optimally placed piezoelectric layers
| AD-A260879 | p 2636 N93-25631
DUST
Structure and star forming activities of the cold massive molecular cloud G216-2.5 p 2893 N93-25477
Hazards of explosives dusts: Particle size effects
| DE93-009380 | p 2668 N93-25498
DUST STORMS
The Martian lower atmosphere p 2897 N93-26394
DYE LASERS
Simultaneous determination of gain parameters in steady state lasers
| DE93-007389 | p 2713 N93-25381
DYES
Flow and morphological conditions associated with the directional solidification of aqueous ammonium chloride
| DE93-008886 | p 2644 N93-25495
DYNAMIC CHARACTERISTICS
Global dynamic modeling of a transmission system
| NASA-CR-191117 | p 2716 N93-24751
Dynamics and control of maneuverable tethered flight vehicles p 2615 N93-24767
Trapped energy quartz crystal resonator on wedge-shaped plate p 2837 N93-25022
Dynamic test apparatus for electro-rheological fluids
| AD-D015632 | p 2643 N93-25284
Computational gearing mechanics
| NASA-CR-191127 | p 2719 N93-25884
Dynamic behavior of helix interaction circuits
| AD-A261362 | p 2692 N93-26334
1992 technical digest series volume 16. Conference edition: Summaries of papers presented at the Nonlinear Dynamics in Optical Systems Topical Meeting
| AD-A261915 | p 2857 N93-26544
DYNAMIC CONTROL
Dynamics and control of maneuverable tethered flight vehicles p 2615 N93-24767
Nonholonomic geometry, mechanics and control p 2724 N93-25270
Identification and control of lightly damped, large space structures: An experimental evaluation p 2616 N93-25351
Analytical and experimental study of control effort associated with model reference adaptive control p 2820 N93-25468
The dynamics and control of large flexible asymmetric spacecraft p 2617 N93-25525
Dynamics and robust control of a sampled data system for large space structures. Volume 2: The LQG/LTR methodology for the discrete-time system and the design of reduced order robust digital controller for orbiting flexible shallow spherical shell system
| AD-A260793 | p 2599 N93-25693
Nonlinear dynamics and attitude control of articulated flexible space structures p 2617 N93-25726
Dynamics of on-orbit construction process p 2669 N93-26406
Interaction dynamics and control for orbital assembly p 2669 N93-26407
DYNAMIC MODELS
An aeroelastic model structure investigation for a manned real-time rotorcraft simulation p 2574 N93-24756
A simple, approximate model of parachute inflation
| DE93-002465 | p 2576 N93-25121
The 32nd CDC: System identification using interval dynamic models
| NASA-CR-192895 | p 2818 N93-25155
Dynamic hardness tester and cure meter p 2711 N93-25608
DYNAMIC PRESSURE
Stress and reliability analyses of multilayered composite cylinder under thermal and mechanical loads p 2726 N93-25533
DYNAMIC RANGE
Log-ratio signal-processing technique for beam position monitors
| DE93-007356 | p 2851 N93-25314
A compact neutron counter telescope with thick radiator (Cotetra) for fusion experiment
| NIFS-205 | p 2860 N93-25347
DYNAMIC RESPONSE
Surface Transverse Wave (STW) quartz resonators in the GHz range p 2836 N93-25012
Very wide bandwidth HF crystal filters p 2693 N93-25039
Stochastic and seismic design response of linear and nonlinear structures p 2726 N93-25484
Experimental modal survey of the probe mass mock-up
| DE93-008846 | p 2617 N93-25494
Aeroelastic response and aeromechanical stability of helicopters with elastically coupled composite rotor blades p 2588 N93-25530
Applications of parallel and vector algorithms in nonlinear structural dynamics using the finite element method
| AD-A260716 | p 2811 N93-25845
Joint flexibility effects on the dynamic response of structures. Part 2: Stochastic analysis
| AD-A261003 | p 2729 N93-25938
DYNAMIC STABILITY
Dynamics and control of maneuverable tethered flight vehicles p 2615 N93-24767
Nonlinear stability analysis of the attitude motion of spin-stabilized thrusting spacecraft p 2617 N93-25527
Biped control via nonlinear dynamics p 2718 N93-25697
Structural dynamic analysis of bearingless rotor blade p 2590 N93-25719
Supersonic aeroelastic instability results for a NASP-like wing model
| NASA-TM-107739 | p 2591 N93-26553
DYNAMIC STRUCTURAL ANALYSIS
On the effective reflection properties of the randomly segmented elastic bar p 2724 N93-25328
Optimal control of large space structures p 2819 N93-25343
Numerically dissipative time integration algorithms for structural dynamics p 2725 N93-25394
Numerical and experimental analyses of large composite skeletal satellite systems p 2616 N93-25463
Stochastic and seismic design response of linear and nonlinear structures p 2726 N93-25484
Structural dynamic analysis of bearingless rotor blade p 2590 N93-25719
Nonlinear dynamics and attitude control of articulated flexible space structures p 2617 N93-25726
Nonlinear vibrations, stability, and dynamics of structures and mechanisms
| AD-A260871 | p 2728 N93-25838
Dynamics of deformable multibody systems using recursive projection methods
| AD-A260698 | p 2728 N93-25842
Applications of parallel and vector algorithms in nonlinear structural dynamics using the finite element method
| AD-A260716 | p 2811 N93-25845
Computational gearing mechanics
| NASA-CR-191127 | p 2719 N93-25884
Helicopter forced response vibration analysis method RTVIB20
| AD-A261809 | p 2597 N93-26260
Structural load control during construction p 2669 N93-26409
Mechanics and control of multibody structural systems
| AD-A261576 | p 2619 N93-26456
DYNAMIC TESTS
Dynamic test apparatus for electro-rheological fluids
| AD-D015632 | p 2643 N93-25284
SRB environment evaluation and analysis. Volume 2: RSRB joint filling test/analysis improvements
| NASA-CR-192518 | p 2631 N93-26057
DYNAMICAL SYSTEMS
Dynamic error analysis of numerical methods for simulation of state-variable derivatives with discontinuities p 2819 N93-25278
Control and stabilization of nonholonomic dynamic systems p 2596 N93-25729
Estimation of coefficients in a rational function from observed values
| AD-A261126 | p 2828 N93-25773
Using modular neural networks with local representations to control dynamic systems
| AD-A261597 | p 2826 N93-26162
Introduction of chaotic dynamical systems
| AD-A261747 | p 2872 N93-26250
Power iterations and the dominant eigenvalue problem
| AD-A261695 | p 2829 N93-26370
Information transmission using CHAOS
| AD-A261519 | p 2883 N93-26377
The Earth's climate as a dynamical system
| DE93-004666 | p 2767 N93-26496
DYNAMO THEORY
Simulation study of MHD dynamo: Convection in a rotating spherical shell
| NIFS-207 | p 2860 N93-25356

E

E REGION
The formation and characteristics of E-region thin ionization layers at high latitudes p 2861 N93-25829
E-2 AIRCRAFT
AEW aircraft design
| AD-A261800 | p 2590 N93-26444
EAR PROTECTORS
Measuring hearing protection device performance using the metrosonics db-3100 sound level analyzer (dosimeter)
| AD-A260852 | p 2801 N93-25787
EARPHONES
Inflight evaluation of an acoustic orientation instrument
| AD-A260752 | p 2591 N93-25909

EARTH (PLANET)
Environment Observation and Climate Modelling Through International Space Projects. Volume 2: Remote Sensing for Environmental Monitoring and Resource Management
| ESA-ISY-1-VOL-2 | p 2737 N93-24775

EARTH ATMOSPHERE
A correlated K-distribution model of the heating rates for H2O and a molecular mixture in the 0-2500 cm(exp -1) wavelength region in the atmosphere between 0 and 60 km
| DE93-005741 | p 2762 N93-25147
ATMOS: Long term atmospheric measurements for mission to planet Earth
| NASA-TM-108720 | p 2757 N93-26429
Long term modeling of the links between economics, technical progress, and environment: Evolution of approaches and new trends
| DE93-005035 | p 2767 N93-26497

EARTH CRUST
Intraplate deformation, stress in the lithosphere and the driving mechanism for plate motions
| NASA-CR-192782 | p 2772 N93-25529

EARTH ENVIRONMENT
Land cover, an essential component of the CORINE information system on the environment: GIS implications p 2740 N93-24787
Demonstration of seasonal changes in the territory of Finland using multitemporal NOAA-AVHRR data p 2742 N93-24801

EARTH IONOSPHERE
Magnetotail processes associated with auroral surge formation
| ATR-90(7186)-1 | p 2895 N93-26147
High Frequency (HF) radiowave propagation
| AD-A261726 | p 2681 N93-26280

EARTH MAGNETOSPHERE
A statistical study of field-aligned currents in the Earth's inner magnetosphere p 2773 N93-25709
Sounding rocket observations of precipitating ions in the morning auroral region p 2773 N93-25732

EARTH MANTLE
Intraplate deformation, stress in the lithosphere and the driving mechanism for plate motions
| NASA-CR-192782 | p 2772 N93-25529

EARTH OBSERVATIONS (FROM SPACE)
Environment Observation and Climate Modelling Through International Space Projects. Volume 2: Remote Sensing for Environmental Monitoring and Resource Management
| ESA-ISY-1-VOL-2 | p 2737 N93-24775
The scope of DLR's SAR calibration program p 2738 N93-24778
Verification of a climate convention: Role and limitations of a space based remote sensing system p 2738 N93-24781
Application of remote sensing data for the investigation of environmental degradation sites in East Germany p 2739 N93-24785
Natural disasters and their mitigation using space technology p 2742 N93-24804
The need for spaceborne observations for meteorology and climatology p 2744 N93-24813
Operational use of MOMS-02 (P2) data p 2752 N93-24866
An interactive environment for the analysis of large Earth observation and model data sets p 2878 N93-25793
Geographic information system for fusion and analysis of high-resolution remote sensing and ground truth data p 2878 N93-25798

EARTH OBSERVING SYSTEM (EOS)
TDRSS-user orbit determination using batch least-squares and sequential methods p 2601 N93-24703
Orbit determination and orbit control for the Earth Observing System (EOS) AM spacecraft p 2601 N93-24705
UARS in-flight jitter study for EOS
| NASA-CR-191419 | p 2615 N93-25133
Earth observing system. Output data products and input requirements, version 2.0. Volume 1: Instrument data product characteristics
| NASA-TM-108770 | p 2755 N93-25460
Earth observing system. Output data products and input requirements, version 2.0. Volume 2: Analysis of IDS input requirements
| NASA-TM-108771 | p 2755 N93-25461
Earth observing system. Output data products and input requirements, version 2.0. Volume 3: Algorithm summary tables and non-EOS data products
| NASA-TM-108769 | p 2756 N93-25462
In search of meta-knowledge p 2826 N93-25983

EARTH ORBITAL ENVIRONMENTS
An investigation of the degradation of Fluorinated Ethylene Propylene (FEP) copolymer thermal blanketing materials aboard LDEF in the laboratory
| NASA-CR-192824 | p 2653 N93-25078
Plasma current collection of Z-93 thermal control paint as measured in the Lewis Research Center's plasma interaction facility
| NASA-TM-106132 | p 2618 N93-26215
Bit hit/solar activity correlation study
| AD-A261381 | p 2896 N93-26340

EARTH ORBITS
Near Earth object fuels (neo-fuels): Discovery, prospecting and use
| DE93-005185 | p 2892 N93-25164
United States Army space experiment 601
| AD-A261460 | p 2798 N93-26353
Lageos laser ranging earth rotation
| AD-A261471 | p 2757 N93-26354

EARTH ORIENTATION
A determination of the radio-planetary frame tie from comparison of Earth orientation parameters p 2676 N93-26106
Lageos laser ranging earth rotation
| AD-A261471 | p 2757 N93-26354

EARTH RESOURCES
Remote sensing of non-renewable resources p 2744 N93-24814

EARTH ROTATION
Lageos laser ranging earth rotation
| AD-A261471 | p 2757 N93-26354

EARTH SCIENCES
Applications of wavelet-based compression to multidimensional earth science data
| DE93-007348 | p 2762 N93-25166
JPRS report: Science and technology. Central Eurasia: Earth sciences
| JPRS-UES-92-003 | p 2737 N93-25398
JPRS report: Science and technology. Central Eurasia: Earth sciences
| JPRS-UES-93-001 | p 2599 N93-25400
JPRS report: Science and technology. Central Eurasia: Earth sciences
| JPRS-UES-92-005 | p 2737 N93-25401
JPRS report: Science and technology. Central Eurasia: Earth sciences
| JPRS-UES-92-002 | p 2737 N93-25426
Scientific visualization using the Flow Analysis Software Toolkit (FAST) p 2814 N93-25600
Applied Information Systems Research Program (AISRP). Workshop 2: Meeting Proceedings
| NASA-CR-193096 | p 2877 N93-25792
An interactive environment for the analysis of large Earth observation and model data sets p 2878 N93-25793
The Grid Analysis and Display System (GRADS): A practical tool for Earth science visualization p 2880 N93-25805
Advanced data visualization and sensor fusion: Conversion of techniques from medical imaging to Earth science p 2880 N93-25810
A distributed analysis and visualization system for model and observational data p 2881 N93-25814
The Space and Earth Science Data Compression Workshop
| NASA-CP-3183 | p 2803 N93-25921

EARTH SURFACE
Use of airborne imaging spectrometry to the definition of optimised specifications for land applications with future spaceborne imaging spectrometers p 2738 N93-24776
A land-surface testbed for EOSDIS p 2878 N93-25797
Data fusion with artificial neural networks (ANN) for classification of earth surface from microwave satellite measurements p 2824 N93-25974

EARTH-VENUS TRAJECTORIES
Galileo early cruise, including Venus, First Earth, and Gaspra encounters p 2599 N93-26125

EARTHQUAKE DAMAGE
Expedient repair of structural facilities
| AD-A260727 | p 2598 N93-25656

EARTHQUAKES
Earthquake vulnerability map of the Lake Constance area p 2753 N93-24872
Anomalous bioelectric potentials of silk trees in Naples zoo (Italy) prior to an earthquake in May, 1991 p 2753 N93-24873
Seismic buckling capacity of unstiffened, free-standing steel containments
| DE93-005325 | p 2723 N93-24957
Low-frequency source parameters of twelve large earthquakes
| NASA-CR-192806 | p 2771 N93-25202

ECCENTRIC ORBITS
Origin and evolution of cataclysmic variables p 2893 N93-25245

ECLIPTIC
Occultation of a compact radio source by Venus p 2676 N93-26107

ECOLOGY
Aerospace techniques in radiation and ecological monitoring of the Republic Belarus p 2741 N93-24793
Aerospace monitoring for ecological hazard and disaster mitigation p 2744 N93-24812
JPRS report: Science and technology. Central Eurasia: Earth sciences
| JPRS-UES-92-003 | p 2737 N93-25398
JPRS report: Science and technology. Central Eurasia: Earth sciences
| JPRS-UES-93-001 | p 2599 N93-25400
JPRS report: Science and technology. Central Eurasia: Earth sciences
| JPRS-UES-92-005 | p 2737 N93-25401
Planetary Biology and Microbial Ecology: Molecular Ecology and the Global Nitrogen cycle
| NASA-CR-4497 | p 2803 N93-26157
Bibliography of remote sensing techniques used in wetland research
| AD-A261704 | p 2757 N93-26440

ECONOMIC ANALYSIS
Aerodynamic design and synthesis of the oblique flying wing supersonic transport p 2587 N93-24768
Environmental risks and future generations: Criteria for public policy
| DE93-004691 | p 2764 N93-25443
Space business indicators p 2886 N93-26158
Functional Economic Analysis Guidebook, version 1.1
| AD-A261390 | p 2886 N93-26305
AEW aircraft design
| AD-A261800 | p 2590 N93-26444
Cost-effectiveness analysis of TxDOT CNG fleet conversion, volume 2
| PB93-159432 | p 2720 N93-26534

ECONOMIC DEVELOPMENT
Designing and implementing a state quality award
| PB93-154458 | p 2722 N93-26546

ECONOMIC FACTORS
Applied aerodynamics: Challenges and expectations
| NASA-TM-103963 | p 2575 N93-25091

ECONOMIC IMPACT
Regulatory impact analysis of the Part 503 sewage sludge regulation
| PB93-110625 | p 2768 N93-26567

ECONOMICS
Environmental risks and future generations: Criteria for public policy
| DE93-004691 | p 2764 N93-25443
Technology for America's economic growth: A new direction to build economic strength
| AD-A261553 | p 2887 N93-26458

ECOSYSTEMS
Biodiversity indication by Earth observation data p 2751 N93-24858
The Global Ocean Observing System p 2733 N93-24923
JPRS report: Science and technology. Central Eurasia: Life sciences
| JPRS-ULS-93-002 | p 2737 N93-25399
JPRS report: Science and technology. Central Eurasia: Life sciences
| JPRS-ULS-92-020 | p 2793 N93-25406
Response and feedbacks of forest ecosystems to global climate change
| PB93-167252 | p 2767 N93-26510

EDDY CURRENTS
Method and apparatus for deflection measurements using eddy current effects
| NASA-CASE-GSC-13506-1 | p 2710 N93-26103
Wind-driven coastal generation of annual mesoscale eddy activity in the California current
| AD-A261355 | p 2790 N93-26331

EDDY VISCOSITY
Gasp 1.3 results for the transverse hydrogen reacting jet p 2625 N93-26011

EDGES
Measuring the intensity of nitrogen fertilization of grassland by means of remote sensing p 2751 N93-24859
Neuropsychological components of object identification
| AD-A261449 | p 2797 N93-26347

EDUCATION
A software package for neural network applications development p 2827 N93-25610
Fidelity and validity in distributed interactive simulation: Questions and answers
| AD-A260971 | p 2810 N93-25711
Aircraft electrical and environmental systems, AFSCs 452x5, 454x5, and 454x6
| AD-A261213 | p 2590 N93-25733

MIT Space Engineering Research Center
| NASA-CR-192879 | p 2821 N93-25833
Performance-based testing and success in Naval advanced flight training
| AD-A260838 | p 2590 N93-25933
The 1993/1994 NASA Graduate Student Researchers Program
| NASA-EP-283 | p 2872 N93-26051
National Aeronautics and Space Administration (NASA)/American Society for Engineering Education (ASEE) Summer Faculty Fellowship Program, 1992, volume 1
| NASA-CR-188242-VOL-1 | p 2911 N93-26058
National Aeronautics and Space Administration (NASA)/American Society for Engineering Education (ASEE) Summer Faculty Fellowship Program, 1992, volume 2
| NASA-CR-188242-VOL-2 | p 2914 N93-26070
The adult literacy evaluator: An intelligent computer-aided training system for diagnosing adult illiterates p 2799 N93-26082
Contribution of personality to the prediction of success in initial air traffic control specialist training
| DOT/FAA/AM-93/4 | p 2797 N93-26138
Design and implementation of a pilot orientation program for new NASA engineering employees
| NASA-TM-105907 | p 2872 N93-26205
Spontaneous discovery and use of categorical structure
| AD-A261658 | p 2798 N93-26364

EFFICIENCY
Non-H2Se, ultra-thin CIS devices
| DE93-000078 | p 2759 N93-25253
Role of polycrystallinity in CdTe and CuInSe2 photovoltaic cells
| DE93-000045 | p 2759 N93-25504
Variable-speed generators with flux weakening p 2694 N93-25599
FALCON nuclear-reactor-pumped laser program and wireless power transmission
| DE93-007607 | p 2715 N93-26597

EFFLUENTS
Metabolic response of environmentally isolated microorganisms to industrial effluents: Use of a newly described cell culture assay p 2794 N93-26066

EIGENVALUES
Parallel matrix computations
| AD-A260783 | p 2828 N93-25687
Power iterations and the dominant eigenvalue problem
| AD-A261695 | p 2829 N93-26370

EIGENVECTORS
Demonstration for novel self-organization theory by three-dimensional magnetohydrodynamic simulation
| NIFS-212 | p 2859 N93-25227

EL NINO
On the vertical structure of seasonal, interannual and intraseasonal flows p 2782 N93-25557
An observational study of the local and remote response of the equatorial Pacific to westerly wind events during the 1991-92 El Nino
| AD-A261777 | p 2787 N93-26286

ELASTIC BARS
On the effective reflection properties of the randomly segmented elastic bar p 2724 N93-25328

ELASTIC BODIES
Dynamics of deformable multibody systems using recursive projection methods
| AD-A260698 | p 2728 N93-25842

ELASTIC DEFORMATION
Stability analysis and modeling of rotating flexible structures
| DE93-008493 | p 2844 N93-25520
Dynamics of deformable multibody systems using recursive projection methods
| AD-A260698 | p 2728 N93-25842
Investigation of liquid sloshing in spin-stabilized satellites
| AD-A261671 | p 2619 N93-26438

ELASTIC MEDIA
Numerical investigations on fracture behavior of ductile materials p 2725 N93-25411
The rate form of equilibrium equation for problems of steady-state, elastic, viscous flows p 2704 N93-25708

ELASTIC PLATES
On existence of solutions and duality for a model of non-linear elastic plates with transverse shear deformations p 2726 N93-25437

ELASTIC PROPERTIES
Fracture of an elliptical inclusion and its implications for the properties of short fiber composites p 2634 N93-25333
Determination of the elastic constants of composite materials from ultrasonic group velocity measurements p 2635 N93-25544
Inelastic behavior of thermoplastic composites p 2636 N93-25674
The induction of elastic fine motion in robotic grasps p 2718 N93-25727
Effect of cytoskeletal reagents on stretch activated ion channels
| AD-A261089 | p 2793 N93-25764
Variational theory of motion of curved, twisted and extensible elastic rods
| AD-A261028 | p 2729 N93-25941
On the stability of finite plastic deformations
| AD-A261526 | p 2730 N93-26361
Analysis of longitudinal impact on semi-infinite circular bars and tubes. Appendix no. 2
| AD-A261556 | p 2731 N93-26459
Use and analysis of finite element methods for problems of solid mechanics and fracture
| AD-A261574 | p 2731 N93-26522
The influence of primary and secondary orientations on the elastic response of a nickel-base single-crystal superalloy
| NASA-TM-106125 | p 2731 N93-26550

ELASTIC SCATTERING
High-energy pion-nucleus scattering at LAMPF
| DE93-007364 | p 2852 N93-25380

ELASTIC WAVES
Elastic plate mode sensitivities to mass loading applications to gas sensors p 2711 N93-25009
Elastic modeling and migration in Earth models p 2771 N93-25433

ELASTODYNAMICS
Numerically dissipative time integration algorithms for structural dynamics p 2725 N93-25394
Analysis of longitudinal impact on semi-infinite circular bars and tubes. Appendix no. 2
| AD-A261556 | p 2731 N93-26459

ELASTOMERS
Elastomer compound developed for high wear applications p 2659 N93-25607
Process for bonding elastomers to metals
| NASA-CASE-LAR-13645-1 | p 2656 N93-25995
Positive displacement rotary pump
| AD-D015678 | p 2719 N93-26144

ELASTOPLASTICITY
Use and analysis of finite element methods for problems of solid mechanics and fracture
| AD-A261574 | p 2731 N93-26522

ELECTRIC ARCS
Conversion of light hydrocarbon gases to metal carbides for production of liquid fuels and chemicals
| DE93-009707 | p 2644 N93-25500
Space environmental interactions for the space exploration initiative p 2897 N93-26396

ELECTRIC BATTERIES
Characterization of electrochemical systems and batteries: Materials and systems
| DE93-003472 | p 2687 N93-24964
Improved performance and safety for high energy batteries through use of hazard anticipation and capacity prediction p 2694 N93-25582
Thin rechargeable batteries for CMOS SRAM memory protection p 2694 N93-25583
Photovoltaic power without batteries for continuous cathodic protection p 2759 N93-25597
Electrochemical and spectroscopic studies of molten halides
| AD-A261687 | p 2646 N93-26439

ELECTRIC CHARGE
Commercial Precipitation Static (P-static) test equipment p 2711 N93-24901
The charge and size of precipitation particles inside thunderstorms and mesoscale convective systems on the Great Plains p 2781 N93-25275
Single electron charging effects in mesoscopic systems
| AD-A261228 | p 2868 N93-26302

ELECTRIC CONDUCTORS
NMR studies of ion mobility and association in polyether-based polymer electrolytes
| AD-A260662 | p 2655 N93-25642

ELECTRIC CONNECTORS
Two- and three-dimensional high performance, patterned overlay multi-chip module technology p 2694 N93-25581

ELECTRIC CORONA
Comparative performance of lightning air terminals under natural storm conditions p 2781 N93-24902
Treatment of hazardous organic wastes using silent discharge plasmas
| DE93-003789 | p 2768 N93-26592

ELECTRIC CURRENT
Kinetic studies of interfacial photocurrents in platinized chloroplasts
| DE93-002344 | p 2792 N93-25104
Pressure dependence of conductivity
| DE93-008466 | p 2687 N93-25113
Studies of several small seawater MHD thrusters using the high-field solenoid of MIT's Bitter Magnet Laboratory
| AD-A260645 | p 2860 N93-25641
Internal current probing of integrated circuits using magnetic force microscopy
| DE93-006752 | p 2692 N93-26501

ELECTRIC DISCHARGES
An integrated approach to 300 kV electrostatic discharge application during component testing that will satisfy MIL-STD-331B Appendix F p 2693 N93-24882
Comparison of the electrical charging and discharging environments of multiple aircraft-borne electric-field measurement systems p 2583 N93-24887
Electrical and Chemical Interactions at Mars Workshop. Part 2: Appendix
| NASA-CP-10093-PT-2 | p 2897 N93-26392
Space environmental interactions for the space exploration initiative p 2897 N93-26396
Treatment of hazardous organic wastes using silent discharge plasmas
| DE93-003789 | p 2768 N93-26592

ELECTRIC FIELDS
Launch pad lightning protection enhancement by induced streamers p 2609 N93-24876
Comparison of the electrical charging and discharging environments of multiple aircraft-borne electric-field measurement systems p 2583 N93-24887
Fractal determination of parameters in lightning and ESD model p 2686 N93-24893
Zoning of aircraft by electric field modelling p 2583 N93-24894
Development of models for predicting the triggering of lightning by launch vehicles p 2610 N93-24899
A single-point warning system for thunderstorms and electric fields p 2711 N93-24900
Dynamic test apparatus for electro-rheological fluids
| AD-D015632 | p 2643 N93-25284
Thermal and electric oscillation driven by orbit loss in helical systems
| NIFS-213 | p 2860 N93-25346
Dynamics of collision processes
| DE93-007143 | p 2849 N93-25509
Electric field effects on quantum-confined semiconductor structures p 2865 N93-25703
The initiation of lightning and the growth of electric fields in thunderstorms
| AD-A261455 | p 2787 N93-26352
Modeling of electric-field enhancement at nodular defects in dielectric mirror coatings
| DE93-007513 | p 2857 N93-26593

ELECTRIC FILTERS
Comparison of energy trapping resonators and filters using the AT cut of quartz, berlinite and gallium phosphate p 2836 N93-25013

ELECTRIC IGNITION
A procedure for defining lightning risk to air vehicles p 2583 N93-24885
Parameters influencing the hot-spot ignition of aviation fuel/air and ethylene/air mixtures p 2583 N93-24886

ELECTRIC MOTOR VEHICLES
Magnitude and value of electric vehicle emissions reductions for six driving cycles in four US cities with varying air quality problems
| DE93-006417 | p 2660 N93-25298

ELECTRIC POTENTIAL
Equipment testing with damped sinewaves between 1 and 50 MHz p 2692 N93-24881
Alternative equipment test procedures for simultaneous current injection on multiple cable bundles p 2693 N93-24903
The constant current loop: A new paradigm for resistance signal conditioning
| NASA-TM-108744 | p 2673 N93-25181
A comparison of moisture resistance with different types of end-terminations in ceramic capacitors
| DE93-007600 | p 2689 N93-25416
Characterization of ceramic capacitors for high-voltage pulse-discharge applications
| DE93-007601 | p 2689 N93-25417
Detecting damaged cables using a preionized gas technique
| DE93-007588 | p 2689 N93-25429
Noise-optimal control of HEMT LNA's for compensation of temperature deviations p 2678 N93-26115
Data analysis support for the Shuttle Potential and Return Electron Experiment (SPREE) on the Tethered Satellite System 1 (TSS-1) flight
| AD-A261646 | p 2618 N93-26232
Single electron charging effects in mesoscopic systems
| AD-A261228 | p 2868 N93-26302

ELECTRIC POWER PLANTS
An evaluation of thermal energy storage options for precooling gas turbine inlet air
| DE93-005980 | p 2758 N93-24975

Published assessments bearing on the future use of ceramic superconductors by the electric power sector
| DE93-007737 | p 2658 N93-26588

ELECTRIC POWER SUPPLIES
Published assessments bearing on the future use of ceramic superconductors by the electric power sector
| DE93-007737 | p 2658 N93-26588

ELECTRIC PROPULSION
Stationary plasma thruster evaluation in Russia
| NASA-CR-192823 | p 2859 N93-25206
Anode power deposition in coaxial MPD thrusters
p 2623 N93-25665
Minimum-fuel power-limited transfers between coplanar elliptic orbits p 2608 N93-25684
Measurement and analysis of a small nozzle plume in vacuum
| NASA-TM-106066 | p 2633 N93-26561

ELECTRICAL ENGINEERING
Investigations of the frequency instability of CH1-75 hydrogen masers p 2716 N93-25049
Engineering: Research development and technology
| UCRL-53868-91 | p 2917 N93-26326
Electronics and Electrical Engineering Laboratory technical publication announcements covering laboratory programs, July to September 1992 with 1992/1993 EEEL events calendar
| PB93-158632 | p 2884 N93-26530

ELECTRICAL FAULTS
Electrical and Chemical Interactions at Mars Workshop. Part 2: Appendix
| NASA-CP-10093-PT-2 | p 2897 N93-26392

ELECTRICAL IMPEDANCE
Inverse problems in nondestructive evaluations
| AD-A261370 | p 2722 N93-26337

ELECTRICAL INSULATION
A comparison of moisture resistance with different types of end-terminations in ceramic capacitors
| DE93-007600 | p 2689 N93-25416
Detecting damaged cables using a preionized gas technique
| DE93-007588 | p 2689 N93-25429

ELECTRICAL MEASUREMENT
Comparison of the electrical charging and discharging environments of multiple aircraft-borne electric-field measurement systems p 2583 N93-24887
Observation of radiation from lightning discharges by LPATS p 2779 N93-24888
A system to measure lightning-induced transients on spacecraft umbilical lines p 2693 N93-24889
Study of atmospheric electrical events above complex terrain p 2780 N93-24897
A single-point warning system for thunderstorms and electric fields p 2711 N93-24900
Commercial Precipitation Static (P-static) test equipment p 2711 N93-24901
Improved PI-network measurement of all quartz crystal parameters by appropriate modelling of the test fixture
p 2833 N93-24995
Thermionic current measurement in quartz
p 2840 N93-25045
The 0.3 mm diameter flexible amperometric lactate probe
| AD-A260826 | p 2690 N93-25782
Internal current probing of integrated circuits using magnetic force microscopy
| DE93-006752 | p 2692 N93-26501
Electronics and Electrical Engineering Laboratory technical publication announcements covering laboratory programs, July to September 1992 with 1992/1993 EEEL events calendar
| PB93-158632 | p 2884 N93-26530

ELECTRICAL PROPERTIES
FNAS computational modeling
| NASA-CR-192512 | p 2863 N93-25225
Electrochemical processing of electrically conductive polymer fibers
| AD-A261793 | p 2657 N93-26386
Electrical and Chemical Interactions at Mars Workshop. Part 2: Appendix
| NASA-CP-10093-PT-2 | p 2897 N93-26392

ELECTRICAL RESISTIVITY
Pressure dependence of conductivity
| DE93-008466 | p 2687 N93-25113
FNAS computational modeling
| NASA-CR-192512 | p 2863 N93-25225
Temperature-dependent electrical conductivity of soda-lime glass
| DE93-007872 | p 2654 N93-25359
The DX centers in three to five semiconductors under hydrostatic pressure
| DE93-007701 | p 2864 N93-25490
Ir-Zr alloys as diffusion barriers between Cu and Si(100)
| AD-A261919 | p 2652 N93-26197
Electrochemical processing of electrically conductive polymer fibers
| AD-A261793 | p 2657 N93-26386
Electrical conductivity of ion implanted ladder and semi-ladder polymers
| AD-A261401 | p 2657 N93-26401

ELECTRIFICATION
Lightning precursor signatures from dual-polarization radar measurements of storms p 2777 N93-24877
Remote sensing of precipitation and electrification with a dual-polarization, coherent, wideband radar system
| AD-A260779 | p 2756 N93-25679

ELECTRO-OPTICAL PHOTOGRAPHY
Photographic industry and electronic imaging: The emergence of electronic still photography
| PB93-169399 | p 2711 N93-26324

ELECTRO-OPTICS
Ultrafast measurements of 200 gigahertz Schottky photodiodes p 2688 N93-25392
Adaptive liquid crystal TV based joint transform correlator as applied to real-time pattern recognition
| AD-A260724 | p 2864 N93-25655
Advanced technology for portable personal visualization
| AD-A261294 | p 2807 N93-26293
Multichip module high speed testing
| AD-A261391 | p 2856 N93-26306

ELECTROCARDIOGRAPHY
MAC to VAX connectivity: Heartrate spectral analysis system p 2796 N93-25594
Investigation into the common mode rejection ratio of the physiological signal conditioner circuit
p 2794 N93-26073

ELECTROCHEMICAL CELLS
Composite nanostructured material fabrication by electrochemical scanning probe microscopy
| AD-A261017 | p 2639 N93-25862

ELECTROCHEMICAL CORROSION
Investigation of corrosion in aluminum/adhesive lap-splices using pulse-echo ultrasonic techniques
| DE93-008074 | p 2721 N93-25518
Adhesion and corrosion behavior of Al-Zn and TiN/Ti/TiN coatings on a DU-0.75 wt. percent Ti alloy
| MTL-TR-92-56 | p 2658 N93-26433

ELECTROCHEMICAL MACHINING
Anisotropic etching of silicon in KOH solutions
p 2647 N93-25037

ELECTROCHEMISTRY
Characterization of electrochemical systems and batteries: Materials and systems
| DE93-003472 | p 2687 N93-24964
Electrochemical processing of electrically conductive polymer fibers
| AD-A261793 | p 2657 N93-26386
Electrochemical and spectroscopic studies of molten halides
| AD-A261687 | p 2646 N93-26439

ELECTRODEPOSITION
Electrodeposition in low gravity p 2663 N93-24774
Composite nanostructured material fabrication by electrochemical scanning probe microscopy
| AD-A261017 | p 2639 N93-25862

ELECTRODES
Characterization of electrochemical systems and batteries: Materials and systems
| DE93-003472 | p 2687 N93-24964
Electroelastic equations for electroded thin plates subject to large driving voltages
| AD-A261123 | p 2675 N93-25772
The 0.3 mm diameter flexible amperometric lactate probe
| AD-A260826 | p 2690 N93-25782
Preliminary investigation of power flow and electrode phenomena in a multi-megawatt coaxial plasma thruster
| NASA-CR-191084 | p 2633 N93-26555

ELECTROENCEPHALOGRAPHY
Biomagnetic localization from transient quasi-static events
| DE93-007328 | p 2794 N93-25186
Automatic detection of seizures with applications
p 2796 N93-25592
Physiological indices of mental workload
| AD-A261692 | p 2798 N93-26391
Duration of alpha suppression increases with angle in a mental rotation task
| AD-A261592 | p 2798 N93-26435

ELECTROLYSIS
Integrated oxygen recovery system
| NASA-CR-192982 | p 2801 N93-26088

ELECTROLYTE METABOLISM
Vascular uptake of rehydration fluids in hypohydrated men at rest and exercise
| NASA-TM-103942 | p 2795 N93-26133

ELECTROLYTES
NMR studies of ion mobility and association in polyether-based polymer electrolytes
| AD-A260662 | p 2655 N93-25642

ELECTROLYTIC CELLS
The 0.3 mm diameter flexible amperometric lactate probe
| AD-A260826 | p 2690 N93-25782

ELECTROMAGNETIC ABSORPTION
The DX centers in three to five semiconductors under hydrostatic pressure
| DE93-007701 | p 2864 N93-25490

ELECTROMAGNETIC COUPLING
BBU code development for high-power microwave generators
| DE93-007111 | p 2688 N93-25397

ELECTROMAGNETIC FIELDS
Observation of radiation from lightning discharges by LPATS p 2779 N93-24888
Fractal determination of parameters in lightning and ESD model p 2686 N93-24893
PROAV Cable Warning System (CWS) - U.S. Army aircraft Integration assessment and OCONUS field evaluation
| AD-A261233 | p 2583 N93-26263
The design and evaluation of transmit and receive antennas for an ionospheric communications probe system. B: Sloping-vee beams
| AD-A261866 | p 2682 N93-26388
Liquid and solid ion plasmas
| AD-A261888 | p 2862 N93-26528

ELECTROMAGNETIC INTERFERENCE
Fractal determination of parameters in lightning and ESD model p 2686 N93-24893
Signal processing in impulsive electromagnetic interference
| AD-A260755 | p 2676 N93-25847

ELECTROMAGNETIC NOISE
Study of atmospheric electrical events above complex terrain p 2780 N93-24897
Microwave interrogation frequency noise and clock frequency stability: Experimental results
p 2842 N93-25056
Noise measurements in single-mode GaAlAs diode lasers p 2716 N93-25067

ELECTROMAGNETIC PROPERTIES
High-performance visualization applied to computational electromagnetics: Method-of-moments on a silicon graphics workstation
| AD-A260820 | p 2675 N93-25700

ELECTROMAGNETIC PULSES
Observation of radiation from lightning discharges by LPATS p 2779 N93-24888
Applications of stress envelope concepts to aircraft EMP and lightning survivability p 2584 N93-24898
Signal processing in impulsive electromagnetic interference
| AD-A260755 | p 2676 N93-25847
Interferometric measurement with squeezed light
| AD-A260910 | p 2856 N93-26457

ELECTROMAGNETIC RADIATION
Very low frequency signals and whistler-mode amplification in the magnetosphere and limit-cycle behavior in the CECAF infrared free electronic laser
| AD-A261776 | p 2716 N93-26601

ELECTROMAGNETIC SCATTERING
A proposed study of multiple scattering through clouds up to 1 THz p 2684 N93-26474

ELECTROMAGNETIC SHIELDING
Method for providing EMI/EMP hardening and breakdown protection in composite materials
| AD-D015638 | p 2634 N93-25283

ELECTROMAGNETISM
Energy and Technology Review, October - December 1992
| DE93-007784 | p 2674 N93-25299
The design and evaluation of transmit and receive antennas for an ionospheric communications probe system. B: Sloping-vee beams
| AD-A261866 | p 2682 N93-26388

ELECTROMECHANICS
X ray computed tomography for failure analysis
| AD-A261884 | p 2722 N93-26527

ELECTROMIGRATION
Thermionic current measurement in quartz
p 2840 N93-25045

ELECTRON ACCELERATORS
Theoretical and experimental investigation of electron beam acceleration and sub-millimeter wave generation
| AD-A261117 | p 2609 N93-25770

ELECTRON BEAMS
Plasma heating in toroidal systems
| NIFS-208 | p 2858 N93-25092
The generation of Langmuir waves by thick target electron beams in solar flares p 2861 N93-25730

Theoretical and experimental investigation of electron beam acceleration and sub-millimeter wave generation
| AD-A261117 | p 2609 N93-25770
Magnetic field source for bi-chambered electron beam devices
| AD-A261316 | p 2691 N93-26299

ELECTRON CYCLOTRON HEATING
R and D of transmission lines for ECH system
| NIFS-210 | p 2687 N93-24951

ELECTRON DENSITY (CONCENTRATION)
Density dependence of line intensities and application to plasma diagnostics
| NIFS-209 | p 2857 N93-24950
Developing and improving numerical algorithms to study intrinsically correlated electron systems
| AD-A261214 | p 2849 N93-25734
Digital Oblique Remote Ionospheric Sensing (DORIS) program development
| AD-A261750 | p 2776 N93-26283
IR and FIR laser diagnostics for plasma thrusters using a CW CO2 radiation source
| AD-A261399 | p 2862 N93-26520

ELECTRON DENSITY PROFILES
Particle simulation for 10.6 micron picosecond laser-induced breakdown in gases p 2712 N93-25280
Digital Oblique Remote Ionospheric Sensing (DORIS) program development
| AD-A261750 | p 2776 N93-26283

ELECTRON DISTRIBUTION
Resonance electron scattering by O2 monolayers on graphites: Reinterpreted
| AD-A261851 | p 2850 N93-26287

ELECTRON EMISSION
Time resolved studies of in-well and cross-well carrier transport in MQW semiconductor structures
| AD-A261170 | p 2714 N93-25774

ELECTRON ENERGY
Theoretical calculations on the electron absorption spectra of selected Polycyclic Aromatic Hydrocarbons (PAH) and derivatives
| NASA-CR-192762 | p 2892 N93-25200
High resolution interface nanochemistry and structure
| DE93-009750 | p 2635 N93-25501
Diagnostics of diamond film deposition plasmas
| AD-A260866 | p 2860 N93-25626
The surface characterization of a series of hydroxybenzenes on Ag(111): An EELS and TDS study
| DE93-007541 | p 2647 N93-26595

ELECTRON GUNS
Theoretical and experimental investigation of electron beam acceleration and sub-millimeter wave generation
| AD-A261117 | p 2609 N93-25770

ELECTRON IMPACT
Theoretical and experimental research in infrared technology
| AD-A260926 | p 2853 N93-25646

ELECTRON IRRADIATION
Radiation-induced disordering and defect production in CuAu and NiAl studied by molecular dynamics simulation
| DE93-007506 | p 2649 N93-25336

ELECTRON MICROSCOPES
Resonant tunneling through chemisorbed halogen atoms on Ag(111)
| AD-A261794 | p 2868 N93-26254

ELECTRON MOBILITY
Low temperature Hall and Shubnikov-de Haas effects
| AD-A261871 | p 2869 N93-26540

ELECTRON PHONON INTERACTIONS
Developing and improving numerical algorithms to study intrinsically correlated electron systems
| AD-A261214 | p 2849 N93-25734

ELECTRON PLASMA
The generation of Langmuir waves by thick target electron beams in solar flares p 2861 N93-25730

ELECTRON PRECIPITATION
Study of auroral dynamics with combined spacecraft and incoherent-scatter radar data
| NASA-CR-192224 | p 2775 N93-26159

ELECTRON PUMPING
Electron-beam-pumped recombination lasers p 2712 N93-25344

ELECTRON RECOMBINATION
Theoretical and experimental research in infrared technology
| AD-A260926 | p 2853 N93-25646

ELECTRON SCATTERING
Developing and improving numerical algorithms to study intrinsically correlated electron systems
| AD-A261214 | p 2849 N93-25734
Resonance electron scattering by O2 monolayers on graphites: Reinterpreted
| AD-A261851 | p 2850 N93-26287
Dynamics of gas-surface interactions
| AD-A261402 | p 2646 N93-26402

ELECTRON SPECTROSCOPY
Accurate determination of Auger line shape binding energies
| AD-A261803 | p 2868 N93-26258

ELECTRON STATES
Theoretical treatment of spin-forbidden and electronically nonadiabatic processes. Methods and applications
| AD-A261596 | p 2851 N93-26525

ELECTRON TRANSFER
Measuring the metastatic potential of cancer cells p 2794 N93-25566
NMR studies of ion mobility and association in polyether-based polymer electrolytes
| AD-A260662 | p 2655 N93-25642
Inorganic and biological electron transfer across an electronically conductive composite polymer membrane
| AD-A261642 | p 2656 N93-26172
Single electron charging effects in mesoscopic systems
| AD-A261228 | p 2868 N93-26302

ELECTRON TRANSITIONS
Resonance electron scattering by O2 monolayers on graphites: Reinterpreted
| AD-A261851 | p 2850 N93-26287

ELECTRON TUNNELING
Resonant tunneling through chemisorbed halogen atoms on Ag(111)
| AD-A261794 | p 2868 N93-26254
Single electron charging effects in mesoscopic systems
| AD-A261228 | p 2868 N93-26302

ELECTRON-ION RECOMBINATION
Electron-beam-pumped recombination lasers p 2712 N93-25344

ELECTRONIC AIRCRAFT
AEW aircraft design
| AD-A261800 | p 2590 N93-26444

ELECTRONIC EQUIPMENT
Thermoelastic stresses in multi-layered media in non-uniform temperature fields
| AD-A260901 | p 2727 N93-25658
Optoelectronic III-V heterostructures on Si substrates
| AD-A261651 | p 2867 N93-26193
Experimental and theoretical studies of proximity effect and Coulomb blockade phenomena in Josephson junctions
| AD-A261652 | p 2867 N93-26194
Electrical and Chemical Interactions at Mars Workshop. Part 2: Appendix
| NASA-CP-10093-PT-2 | p 2897 N93-26392
Joint services electronics program
| AD-A261801 | p 2692 N93-26539

ELECTRONIC EQUIPMENT TESTS
Equipment testing with damped sinewaves between 1 and 50 MHz p 2692 N93-24881
An integrated approach to 300 kV electrostatic discharge application during component testing that will satisfy MIL-STD-331B Appendix F p 2693 N93-24882
Alternative equipment test procedures for simultaneous current injection on multiple cable bundles p 2693 N93-24903
Step stress testing of receiver/transmitter units
| AD-A261286 | p 2730 N93-26279

ELECTRONIC MODULES
Preliminary design of the BPM electronics memory scanner/dual boxcar averager for the advanced photon source
| DE93-007893 | p 2848 N93-25368
Two- and three-dimensional high performance, patterned overlay multi-chip module technology p 2694 N93-25581

ELECTRONIC PACKAGING
Two- and three-dimensional high performance, patterned overlay multi-chip module technology p 2694 N93-25581
Special technology area review on microwave packaging technology
| AD-A261852 | p 2681 N93-26276

ELECTRONICS
Technology 2002: The Third National Technology Transfer Conference and Exposition, volume 1
| NASA-CP-3189-VOL-1 | p 2901 N93-25561

ELECTRONS
Notes on radial drift for dalitz detection
| DE93-006971 | p 2846 N93-24959
The interaction of swift electrons with surface excitations
| DE93-007245 | p 2848 N93-25376
Theoretical and experimental research in infrared technology
| AD-A260926 | p 2853 N93-25646
Particle simulation of auroral double layers p 2774 N93-25830
Investigations of the transient behavior of the cathode fall region in planar and hollow cathodes
| AD-A261636 | p 2691 N93-26171
Single electron charging effects in mesoscopic systems
| AD-A261228 | p 2868 N93-26302
Penning detachment: A new frontier
| AD-A261447 | p 2850 N93-26346

ELECTROPHORESIS
Development of resonance ionization spectroscopy for genome mapping and DNA sequencing using stable isotopes as DNA labels
| DE93-007815 | p 2793 N93-26587

ELECTROPHYSIOLOGY
Physiological indices of mental workload
| AD-A261692 | p 2798 N93-26391

ELECTROPOLISHING
Laser initiated corrosion pits on aluminum p 2650 N93-25464

ELECTRORHEOLOGICAL FLUIDS
Coarsening of a quiescent electrorheological fluid I: Experiment
| DE93-006776 | p 2642 N93-24972
Dynamic test apparatus for electro-rheological fluids
| AD-D015632 | p 2643 N93-25284
Electrorheological fluids: A structural approach to mechanisms
| AD-A260563 | p 2645 N93-25879

ELECTROSTATIC CHARGE
Improved composite fabrication process
| AD-D015679 | p 2640 N93-26145

ELECTROSTATICS
An integrated approach to 300 kV electrostatic discharge application during component testing that will satisfy MIL-STD-331B Appendix F p 2693 N93-24882
Fractal determination of parameters in lightning and ESD model p 2686 N93-24893
Electroelastic equations for electroded thin plates subject to large driving voltages
| AD-A261123 | p 2675 N93-25772
Electrostatic fiber spreader
| AD-D015677 | p 2640 N93-26143

ELECTROSTRICTION
Investigation of coupled analysis techniques for adaptive material structural systems
| AD-A261359 | p 2868 N93-26332

ELEMENTARY EXCITATIONS
Consequences of spontaneous and anomalous symmetry breaking for the orbital and mass flow hydrodynamics of He-3 - A p 2698 N93-25295

ELEVATION
Visual perception of elevation
| AD-A261394 | p 2797 N93-26307

ELLIPSOMETRY
Study of surface behavior in function of temperature of the quaternary system (Hg, Cd, Zn)Te
| AD-A260968 | p 2867 N93-26223

ELLIPTIC DIFFERENTIAL EQUATIONS
Transformation of two and three-dimensional regions by elliptic systems
| NASA-CR-192955 | p 2810 N93-25669

ELLIPTICAL GALAXIES
Prograde anomalous orbits in triaxial gravitational potentials that rotate about the long axis: VLA neutral hydrogen observations and modeling of the inclined rings around the galaxies NGC 2685 and NGC 660 p 2607 N93-25396

ELLIPTICAL ORBITS
An approach for finding long period elliptical orbits for precursor SEI missions p 2604 N93-24720
Minimum-fuel power-limited transfers between coplanar elliptic orbits p 2608 N93-25684

EMBEDDING
Deformations of active flexible rods with embedded line actuators
| AD-A261207 | p 2729 N93-25950

EMBRITTLEMENT
Mechanical properties of martensitic alloy AISI 422
| DE93-006563 | p 2649 N93-25255

EMERGENCY BREATHING TECHNIQUES
Inward contaminant leakage tests of the S-Tron Corporation emergency escape breathing device. Phase 1: Tests of the original design. Phase 2: Tests with the redesigned neck seal
| DOT/FAA/AM-92/18 | p 2582 N93-25205

EMISSION SPECTRA
Compression of spectral meteorological imagery p 2804 N93-25925
The effects of cloud inhomogeneities upon radiative fluxes, and the supply of a cloud truth validation dataset
| NASA-CR-191711 | p 2787 N93-26492

EMISSIVITY
The effects of cloud inhomogeneities upon radiative fluxes, and the supply of a cloud truth validation dataset
| NASA-CR-191711 | p 2787 N93-26492

EMITTANCE
Propagation of radiation in astrophysical media: Gravitational lenses and astrophysical masers
p 2892 N93-24949

EMITTERS
RF vacuum microelectronics
| AD-A261784 | p 2692 N93-26565

EMPLOYEE RELATIONS
Organizational politics, participation in decision-making, and job satisfaction
| DOT/FAA/AM-92/17 | p 2796 N93-25203

ENCAPSULATING
Numerical simulation of time-dependent thermocapillary convection in layered fluid systems
p 2700 N93-25472

END EFFECTORS
The induction of elastic fine motion in robotic grasps
p 2718 N93-25727
Analysis and design of a novel robotic finger-tip sensor for adaptive grasping p 2719 N93-25745

ENDURANCE
Combined strength and endurance training: Functional and morphological adaptations to ten weeks of training
| AD-A261059 | p 2802 N93-26229

ENERGY ABSORPTION
Photomodulation spectroscopy of photocarrier dynamics, electronic defects and morphology of conducting polymers
| DE93-010140 | p 2655 N93-25524
New directions in phthalocyanine pigments
| NASA-CR-192443 | p 2656 N93-26155

ENERGY BUDGETS
WCRP surface radiation budget shortwave data product description, version 1.1
| NASA-TM-107747 | p 2777 N93-24742
Surface energy fluxes at Central Florida during the convection and precipitation electrification experiment
| NASA-CR-192826 | p 2769 N93-24945
Selected translated abstracts of Russian-language climate-change publications: 1. Surface energy budget
| DE93-003189 | p 2760 N93-24952
An investigation of the role of flux divergence in the turbulent kinetic energy balance of the atmospheric surface layer p 2773 N93-25756

ENERGY CONSERVATION
Technology for America's economic growth: A new direction to build economic strength
| AD-A261553 | p 2887 N93-26458
Cost-effectiveness analysis of TxDOT CNG fleet conversion, volume 2
| PB93-159432 | p 2720 N93-26534
Cost-effectiveness analysis of TxDOT CNG fleet conversion, volume 1
| PB93-165603 | p 2720 N93-26585

ENERGY CONSUMPTION
Computational and experimental studies on large scale solar heating
| DE93-769942 | p 2758 N93-25096

ENERGY CONVERSION EFFICIENCY
New concepts for high efficiency energy conversion: The avalanche heterostructure and superlattice solar cells
| DE92-010592 | p 2758 N93-25098
Test results of a Stirling engine utilizing heat exchanger modules with an integral heat pipe
| NASA-TM-105883 | p 2759 N93-25136

ENERGY DISSIPATION
Spacecraft detumbling through energy dissipation
p 2600 N93-24696
Notes on radial drift for dalitz detection
| DE93-006971 | p 2846 N93-24959
Demonstration for novel self-organization theory by three-dimensional magnetohydrodynamic simulation
| NIFS-212 | p 2859 N93-25227
High-energy pion-nucleus scattering at LAMPF
| DE93-007364 | p 2852 N93-25380
High resolution interface nanochemistry and structure
| DE93-009750 | p 2635 N93-25501
Energy dissipation in inelastic flow of cohesionless granular media p 2703 N93-25662
The interaction of HCN/DCN with Si(100)-2x1
| AD-A260837 | p 2645 N93-25920
Proton Monte Carlo transport program PTRAN
| PB93-158673 | p 2850 N93-26314
Defect initiation/growth and energy dissipation induced by deformation and fracture
| AD-A261703 | p 2869 N93-26385
The surface characterization of a series of hydroxybenzenes on Ag(111): An EELS and TDS study
| DE93-007541 | p 2647 N93-26595

ENERGY GAPS (SOLID STATE)
Analysis of the gap in high-temperature superconductors using photoemission spectroscopy p 2865 N93-25744
Measurement of optical properties of infrared bandgap superlattices
| AD-A260859 | p 2866 N93-25789
Optoelectronic III-V heterostructures on Si substrates
| AD-A261651 | p 2867 N93-26193

ENERGY METHODS
Converting environmental wastes into valuable resources p 2759 N93-25572

ENERGY OF FORMATION
Energetic materials from cubane
| AD-A261317 | p 2662 N93-26308

ENERGY POLICY
SIHTI: The research and development program of energy and environmental technology
| DE93-769925 | p 2763 N93-25360
Cost-effectiveness analysis of TxDOT CNG fleet conversion, volume 2
| PB93-159432 | p 2720 N93-26534

ENERGY REQUIREMENTS
Collisional energy transfer in biomolecular ion-molecule dynamics
| AD-A260911 | p 2849 N93-25659

ENERGY SPECTRA
Proton Monte Carlo transport program PTRAN
| PB93-158673 | p 2850 N93-26314

ENERGY STORAGE
Advanced energy systems and technologies - National R and D programme
| DE93-769943 | p 2758 N93-25097
Aquifer thermal energy (heat and chill) storage
| DE93-006446 | p 2759 N93-25183

ENERGY TECHNOLOGY
Energy and Technology Review, August-September 1992
| DE93-005882 | p 2901 N93-24974
Advanced energy systems and technologies - National R and D programme
| DE93-769943 | p 2758 N93-25097
Energy and Technology Review, October - December 1992
| DE93-007784 | p 2674 N93-25299
The PACSAT Communications Experiment (PCE)
| DE93-008185 | p 2674 N93-25308
SIHTI: The research and development program of energy and environmental technology
| DE93-769925 | p 2763 N93-25360
Published assessments bearing on the future use of ceramic superconductors by the electric power sector
| DE93-007737 | p 2658 N93-26588

ENERGY TRANSFER
Time dependent simulation of cosmic-ray shocks including Alfven transport
| NASA-CR-192931 | p 2899 N93-24752
Surface energy fluxes at Central Florida during the convection and precipitation electrification experiment
| NASA-CR-192826 | p 2769 N93-24945
Energy transfer properties and mechanisms
| DE93-008540 | p 2849 N93-25488
Collisional energy transfer in biomolecular ion-molecule dynamics
| AD-A260911 | p 2849 N93-25659
Thermal infrared radiation transfer in the planetary boundary layer p 2772 N93-25688
Oblique MHD cosmic-ray modified shocks: Two-fluid numerical simulations
| NASA-CR-192930 | p 2900 N93-26132
FALCON nuclear-reactor-pumped laser program and wireless power transmission
| DE93-007607 | p 2715 N93-26597

ENGINE ANALYZERS
A three-dimensional algebraic grid generation scheme for gas turbine combustors with inclined slots
| NASA-CR-191095 | p 2694 N93-24759

ENGINE CONTROL
Evaluation of advanced displays for engine monitoring and control
| NASA-CR-191418 | p 2591 N93-24764
Screening studies of advanced control concepts for airbreathing engines
| NASA-TM-106042 | p 2592 N93-25079

ENGINE DESIGN
A preliminary sizing method for unmanned aircraft using multi-variate optimisation p 2587 N93-25408
Design and performance of nozzle-less volute casings for inward flow radial turbines p 2593 N93-25471
Optimized scramjet engine integration on a waverider airframe p 2593 N93-25480
Evaluation of the Migrating Combustion Chamber (MCC) engine
| AD-A260780 | p 2718 N93-25682
Task 5: Architecture sensitivity to STME performance
| MCR-92-5010 | p 2609 N93-26176
Center for Advanced Propulsion Systems (fellowship)
| AD-A260571 | p 2632 N93-26216

ENGINE MONITORING INSTRUMENTS
Evaluation of advanced displays for engine monitoring and control
| NASA-CR-191418 | p 2591 N93-24764

ENGINE PARTS
JPRS report: Science and technology. Central Eurasia: Engineering and equipment
| JPRS-UEQ-92-003 | p 2668 N93-25427
Design and performance of nozzle-less volute casings for inward flow radial turbines p 2593 N93-25471
Advanced bristle seals for gas turbine engines
| AD-A261296 | p 2720 N93-26564

ENGINE TESTING LABORATORIES
A large hemi-anechoic enclosure for community-compatible aeroacoustic testing of aircraft propulsion systems
| NASA-TM-106015 | p 2846 N93-26551

ENGINE TESTS
Test results of a Stirling engine utilizing heat exchanger modules with an integral heat pipe
| NASA-TM-105883 | p 2759 N93-25136
Stationary plasma thruster evaluation in Russia
| NASA-CR-192823 | p 2859 N93-25206
SRB environment evaluation and analysis. Volume 3: ASRB plume induced environments
| NASA-CR-192519 | p 2631 N93-26054
External stress-corrosion cracking of a 1.22-m-diameter type 316 stainless steel air valve
| NASA-TP-3190 | p 2652 N93-26201
Development and use of hydrogen-air torches in an altitude facility
| NASA-TM-106047 | p 2598 N93-26214
Development and demonstration of a new filter system to control emissions during jet engine testing
| AD-A261203 | p 2766 N93-26243
Analysis of the IBSS spectra of Space Shuttle control engine exhaust
| AD-A261749 | p 2632 N93-26373
A large hemi-anechoic enclosure for community-compatible aeroacoustic testing of aircraft propulsion systems
| NASA-TM-106015 | p 2846 N93-26551

ENGINEERING MANAGEMENT
The systems engineering overview and process (from the Systems Engineering Management Guide, 1990)
p 2665 N93-24679
Spacecraft systems engineering: An introduction to the process at GSFC p 2665 N93-24683
The importance of cost considerations in the systems engineering process p 2666 N93-24686
Rendezvous, proximity operations and capture quality function deployment report
| NASA-TM-108752 | p 2614 N93-25952

ENRICHMENT
National Aeronautics and Space Administration (NASA)/American Society for Engineering Education (ASEE) Summer Faculty Fellowship Program, 1992, volume 2
| NASA-CR-188242-VOL-2 | p 2914 N93-26070

ENTRAINMENT
An experimental study of particle-laden jet interactions with cocurrent flows p 2701 N93-25534

ENTROPY
Bayesian cross-entropy reconstruction of complex images
| AD-A261812 | p 2812 N93-26257

ENVIRONMENT EFFECTS
Application of remote sensing data for the investigation of environmental degradation sites in East Germany
p 2739 N93-24785
The use of remote sensing and GIS for the assessment of environmental degradation caused by fires, applied upon South-Euboia (central Greece) p 2742 N93-24802
Oil pollution and water quality mapping of Augusta Bay, Italy using remote sensing techniques
p 2746 N93-24823
Remote sensing of land resource management in agriculture with regard to its influence on the environment p 2750 N93-24850
Forest damage detection and reflection of conifers: From micro to field level p 2752 N93-24864
Measurements of nitric acid, carboxylic acids, and selected aerosol species for the NASA/GTE Pacific Mission - West (PEM-WEST)
| NASA-CR-192976 | p 2763 N93-25287
SIHTI: The research and development program of energy and environmental technology
| DE93-769925 | p 2763 N93-25360
Incorporating biodiversity considerations into environmental impact analysis under the National Environmental Policy Act
| PB93-139806 | p 2766 N93-25878
Aerospace-plane flights and stratospheric ozone: Review and preliminary assessment of the National Aerospace Plane (NASP) operations
| RAND/N-3464-AF | p 2767 N93-26327
Response and feedbacks of forest ecosystems to global climate change
| PB93-167252 | p 2767 N93-26510

ENVIRONMENT MANAGEMENT
Use of remote sensing and GIS for the environmental planning proposal of the Sarno River Valley (Campania, southern Italy) p 2741 N93-24797
Use of the Environmental Resource Management and Analysis System at the Fernald Environmental Management Project
| DE93-002943 | p 2760 N93-24955
Environmental risks and future generations: Criteria for public policy
| DE93-004691 | p 2764 N93-25443
An environmental audit management plan for the Royal Australian Air Force
| AD-A261092 | p 2765 N93-25765
A Spatial Analysis and Modeling System (SAMS) for environment management p 2881 N93-25813
Human factors in environmental management: New directions from the Hanford site
| DE93-004337 | p 2767 N93-26495
ENVIRONMENT MODELS
EnviroNET p 2886 N93-26398
ENVIRONMENT POLLUTION
Complex investigation of a system industrial site-environment using remote sensing and landscape-geochemical methods p 2741 N93-24798
Crop agroecological diagnostics by remote sensing technique p 2751 N93-24860
The atmospheric effects of stratospheric aircraft. Report of the 1992 Models and Measurements Workshop. Volume 1: Workshop objectives and summary
| NASA-RP-1292-VOL-1 | p 2762 N93-25157
The atmospheric effects of stratospheric aircraft. Report of the 1992 Models and Measurements Workshop. Volume 2: Comparisons with global atmospheric measurements
| NASA-RP-1292-VOL-2 | p 2762 N93-25158
The atmospheric effects of stratospheric aircraft. Report of the 1992 Models and Measurements Workshop. Volume 3: Special diagnostic studies
| NASA-RP-1292-VOL-3 | p 2762 N93-25159
Converting environmental wastes into valuable resources p 2759 N93-25572
Space life support technology applications to terrestrial environmental problems p 2803 N93-25617
ENVIRONMENT PROTECTION
An introductory guide to uncertainty analysis in environmental and health risk assessment
| DE93-002873 | p 2760 N93-24676
Complex investigation of a system industrial site-environment using remote sensing and landscape-geochemical methods p 2741 N93-24798
Appliction of remote sensing to forestry mapping: Experience from the European collaborative programme for the less favoured areas p 2751 N93-24857
Environmental risks and future generations: Criteria for public policy
| DE93-004691 | p 2764 N93-25443
An environmental audit management plan for the Royal Australian Air Force
| AD-A261092 | p 2765 N93-25765
Glossary of environmental terms and acronym list
| PB93-158004 | p 2765 N93-25851
Development of a heuristic knowledge base for the selection of applicable or relevant and appropriate environmental requirements
| AD-A261038 | p 2765 N93-25864
Incorporating biodiversity considerations into environmental impact analysis under the National Environmental Policy Act
| PB93-139806 | p 2766 N93-25878
Handbook of chemical hazard analysis procedures
| PB93-158756 | p 2766 N93-26315
ENVIRONMENT SIMULATORS
SRB environment evaluation and analysis. Volume 2: RSRB joint filling test/analysis improvements
| NASA-CR-192518 | p 2631 N93-26057
ENVIRONMENTAL CHEMISTRY
Health and environmental chemistry: Analytical techniques, data management, and quality assurance
| DE93-002853 | p 2760 N93-24674
The atmospheric effects of stratospheric aircraft. Report of the 1992 Models and Measurements Workshop. Volume 1: Workshop objectives and summary
| NASA-RP-1292-VOL-1 | p 2762 N93-25157
The atmospheric effects of stratospheric aircraft. Report of the 1992 Models and Measurements Workshop. Volume 2: Comparisons with global atmospheric measurements
| NASA-RP-1292-VOL-2 | p 2762 N93-25158
The atmospheric effects of stratospheric aircraft. Report of the 1992 Models and Measurements Workshop. Volume 3: Special diagnostic studies
| NASA-RP-1292-VOL-3 | p 2762 N93-25159
ENVIRONMENTAL CONTROL
A survey of life support system automation and control
| NASA-TM-103977 | p 2667 N93-25085
Converting environmental wastes into valuable resources p 2759 N93-25572
Advanced life support study. Modification 10: ECLSS logistical support analysis for Space Station Freedom
| NASA-CR-192481 | p 2801 N93-25888
ENVIRONMENTAL ENGINEERING
Control of environmental and clock parameters in Time and Frequency Standards Laboratory p 2835 N93-25007
Quartz oscillators, frequency synthesizers, and timing systems for geodesy and radio science applications p 2693 N93-25052
Trends '91: A compendium of data on global change. Highlights
| DE93-003112 | p 2761 N93-25144
ENVIRONMENTAL MONITORING
Environment Observation and Climate Modelling Through International Space Projects. Volume 2: Remote Sensing for Environmental Monitoring and Resource Management
| ESA-ISY-1-VOL-2 | p 2737 N93-24775
Satellite remote sensing for environmental geology: The Bandung (West Java) experience p 2739 N93-24784
Application of remote sensing data for the investigation of environmental degradation sites in East Germany p 2739 N93-24785
Application of remote sensing to environmental monitoring in Poland p 2739 N93-24786
Land cover, an essential component of the CORINE information system on the environment: GIS implications p 2740 N93-24787
Aerospace techniques in radiation and ecological monitoring of the Republic Belarus p 2741 N93-24793
Determination of environmental dynamics using NOAA satellite data and a water balance model for the Mediterranean landscape p 2741 N93-24794
Complex investigation of a system industrial site-environment using remote sensing and landscape-geochemical methods p 2741 N93-24798
Demonstration of seasonal changes in the territory of Finland using multitemporal NOAA-AVHRR data p 2742 N93-24801
Alternative strategies for the use of satellite data analysis systems for hazard monitoring and disaster mitigation p 2743 N93-24805
Sustainable remote sensing: A major improvement for realtime resource management and disaster early warning in developing countries p 2743 N93-24808
Use of remote sensing spacecrafts in real time support to disaster management: Interfaces with ground segment facilities and services p 2743 N93-24809
Aerospace monitoring for ecological hazard and disaster mitigation p 2744 N93-24812
Remote sensing geology p 2744 N93-24815
NORSMAP 1989: Norwegian remote sensing spectrometry for mapping and monitoring of algal blooms and pollution p 2746 N93-24824
SEOMAR: An Italian approach to the observation of the Mediterranean area p 2746 N93-24825
The extent and status of mangroves in Mombasa district, Kenya: A case study based on remote sensing p 2746 N93-24826
Multi-date algorithms for predicting surface water quality parameters in estuarine and coastal waters using Landsat TM data
| ED-659-CP | p 2746 N93-24829
Algal blooms and gel production in Adriatic Sea observed by remote sensing techniques p 2747 N93-24831
Hel's peninsula coastal zone changes in the last 40 years on a base of remote sensing methods p 2747 N93-24832
Monitoring and evaluation of morphohydrographical changes in the Danube Delta by remote-sensing p 2747 N93-24834
Coastal environmental mapping using Landsat data
| ED-658-CP | p 2747 N93-24835
World Forest Watch: A global forest monitoring test p 2748 N93-24836
Tropical forest monitoring with high resolution satellite data p 2748 N93-24841
Assessment of storm damage in forests using SPOT imagery p 2748 N93-24842
Forest decline monitoring using Landsat TM, digital stand data and DEMs p 2749 N93-24846
Observation of forest damages in the Harz mountains by means of satellite remote sensing p 2749 N93-24848
Global drought monitoring from NOAA polar orbiting satellites p 2750 N93-24852
Cartography and statistics of crops under irrigation in the Donana area of Andalucia through the use of Landsat-TM imagery and its incorporation into a GIS p 2751 N93-24855
Appliction of remote sensing to forestry mapping: Experience from the European collaborative programme for the less favoured areas p 2751 N93-24857
Crop agroecological diagnostics by remote sensing technique p 2751 N93-24860
Forest damage detection and reflection of conifers: From micro to field level p 2752 N93-24864
Data processing and control in a transputer system for remote sensing of the Earth p 2753 N93-24870
Current trends in satellite data supply for environmental monitoring p 2754 N93-24874
Lightning characteristics in the north-east part of Japan observed by a magnetic direction-finder network p 2779 N93-24892
AQUIS: A PC-based air inventory and permit manager
| DE93-003006 | p 2761 N93-25143
Emissions from ethanol and LPG fueled vehicles
| DE93-006410 | p 2660 N93-25192
Commercial applications multispectral sensor system p 2758 N93-25615
Glossary of environmental terms and acronym list
| PB93-158004 | p 2765 N93-25851
Quality control: Variability in protocols
| PB93-157790 | p 2766 N93-25876
Using terrestrial plants in biomonitoring
| PB93-158780 | p 2766 N93-26316
ENVIRONMENTAL QUALITY
Environmental risks and future generations: Criteria for public policy
| DE93-004691 | p 2764 N93-25443
ENVIRONMENTAL SURVEYS
Aerodynamic design and synthesis of the oblique flying wing supersonic transport p 2587 N93-24768
Incorporating biodiversity considerations into environmental impact analysis under the National Environmental Policy Act
| PB93-139806 | p 2766 N93-25878
Mars exploration planning p 2898 N93-26399
ENVIRONMENTAL TESTS
Star tracker operation in a high density proton field p 2600 N93-24699
An investigation of the degradation of Fluorinated Ethylene Propylene (FEP) copolymer thermal blanketing materials aboard LDEF in the laboratory
| NASA-CR-192824 | p 2653 N93-25078
Environmental test program for superconducting materials and devices
| DE93-003646 | p 2864 N93-25506
Duct protection coating concept development and test. Appendix D, volume 1: Test specimen fabrication, conditioning, and testing documentation
| AD-A261005 | p 2656 N93-25940
Thermal coatings for titanium-aluminum alloys
| NASA-TM-107760 | p 2651 N93-26048
Plasma current collection of Z-93 thermal control paint as measured in the Lewis Research Center's plasma interaction facility
| NASA-TM-106132 | p 2618 N93-26215
Duct protection coating concept development and test: Test specimen fabrication, conditioning, and testing documentation.
| AD-A261250 | p 2657 N93-26278
Using terrestrial plants in biomonitoring
| PB93-158780 | p 2766 N93-26316
ENZYMES
Kinetic studies of interfacial photocurrents in platinized chloroplasts
| DE93-002344 | p 2792 N93-25104
Measuring the metastatic potential of cancer cells p 2794 N93-25566
Emerging technologies in ethanol production
| PB93-157014 | p 2661 N93-25818
Cellular and tissue injury during nonfreezing cold injury and frostbite
| AD-A260574 | p 2795 N93-25900
Inorganic and biological electron transfer across an electronically conductive composite polymer membrane
| AD-A261642 | p 2656 N93-26172
EPHEMERIDES
Application of GPS tracking techniques to orbit determination for TDRS p 2601 N93-24702
TDRSS-user orbit determination using batch least-squares and sequential methods p 2601 N93-24703
A determination of the radio-planetary frame tie from comparison of Earth orientation parameters p 2676 N93-26106
EPIDEMIOLOGY
The prevalence of artificial lens implants in the civil airman population
| DOT/FAA/AM-92/14 | p 2794 N93-25214
EPILEPSY
Automatic detection of seizures with applications p 2796 N93-25592

EPITAXY
Metastable SiC and SiGeC alloys by carbon implantation and solid phase epitaxy
| DE93-007594 | p 2863 N93-25387
Method of joining diamond structures
| AD-D015671 | p 2867 N93-26140
EPOXY MATRIX COMPOSITES
The design of mechanically compatible fasteners for human mandible reconstruction p 2796 N93-25569
Quantifying distributed damage in composites via the thermoelastic effect p 2637 N93-25691
In-process cure monitoring of composites via fiber-optic fluorescence
| AD-A261712 | p 2641 N93-26580
EPOXY RESINS
The 0.3 mm diameter flexible amperometric lactate probe
| AD-A260826 | p 2690 N93-25782
Characterization of aerospace grade resins and composites through pressurized volumetric dilatometry
| AD-A260794 | p 2639 N93-25918
Thermal expansion measurements of polymer matrix composites and syntactics
| MTL-TR-92-27 | p 2640 N93-25954
EQUATIONS OF MOTION
Position and force control of a vehicle with two or more steerable drive wheels
| DE92-041301 | p 2717 N93-25100
Diabaticity of nuclear motion: Problems and perspectives
| DE93-007252 | p 2847 N93-25148
Stability analysis and modeling of rotating flexible structures
| DE93-008493 | p 2844 N93-25520
The dynamics and control of large flexible asymmetric spacecraft p 2617 N93-25525
EQUILIBRIUM EQUATIONS
The rate form of equilibrium equation for problems of steady-state, elastic, viscous flows p 2704 N93-25708
EQUILIBRIUM FLOW
Development of a second generation spray combustion code p 2626 N93-26016
EQUIPMENT SPECIFICATIONS
Military standardization handbook: Aircraft refueling handbook
| AD-A261755 | p 2662 N93-26600
EQUIVALENCE
Measurements of soot formation and hydroxyl concentration in near critical equivalence ratio premixed ethylene flame
| NASA-CR-191099 | p 2642 N93-25116
Stability analysis and modeling of rotating flexible structures
| DE93-008493 | p 2844 N93-25520
EQUIVALENT CIRCUITS
Method for providing EMI/EMP hardening and breakdown protection in composite materials
| AD-D015638 | p 2634 N93-25283
ERGODIC PROCESS
Considerations of the error variances of time-averaged estimators for correlated processes
| AD-A261796 | p 2830 N93-26255
EROSION
Modeling and analysis tools p 2897 N93-26397
A coastal hazards data base for the US East Coast
| NASA-TM-108265 | p 2791 N93-26586
ERROR ANALYSIS
Star tracker operation in a high density proton field p 2600 N93-24699
Resolution of the COBE Earth sensor anomaly p 2600 N93-24700
Improvements in ERBS attitude determination without gyros p 2602 N93-24710
Practical aspects of transfer from GTO to lunar orbit p 2604 N93-24719
Orbit determination error analysis and comparison of station-keeping costs for Lissajous and halo-type libration point orbits and sensitivity analysis using experimental design techniques p 2604 N93-24721
Optimizing the fine lock performance of the Hubble Space Telescope fine guidance sensors p 2604 N93-24723
The Hubble Space Telescope fine guidance system operating in the coarse track pointing control mode p 2605 N93-24724
Attitude determination using vector observations: A fast optimal matrix algorithm p 2606 N93-24731
Solar array thermal snap and the characteristics of its effect on UARS p 2607 N93-24734
Dynamic error analysis of numerical methods for simulation of state-variable derivatives with discontinuities p 2819 N93-25278
Initialization of a modeled convective storm using Doppler radar-derived fields p 2782 N93-25294
The use of multiple models in case-based diagnosis p 2823 N93-25969
A study of mapping exogenous knowledge representations into CONFIG p 2827 N93-26072
Determination of design and operation parameters for upper atmospheric research instrumentation to yield optimum resolution with deconvolution
| NASA-CR-192832 | p 2775 N93-26084
Orbiter-orbiter and orbiter-lander tracking using same-beam interferometry p 2677 N93-26110
Considerations of the error variances of time-averaged estimators for correlated processes
| AD-A261796 | p 2830 N93-26255
Statistics of sampled Rician fading
| AD-A261397 | p 2681 N93-26289
Bit hit/solar activity correlation study
| AD-A261381 | p 2896 N93-26340
ERROR CORRECTING CODES
Soft decoding a self-dual (48, 24; 12) code p 2671 N93-24662
A (72, 36; 15) box code p 2671 N93-24663
The analysis of convolutional codes via the extended Smith algorithm p 2671 N93-24664
Golay and other box codes p 2678 N93-26116
ERROR SIGNALS
Optimizing the fine lock performance of the Hubble Space Telescope fine guidance sensors p 2604 N93-24723
ERRORS
An experimental health monitoring unit for GPS and GLONASS p 2586 N93-25018
Timing and time signal distribution in digital communications networks p 2686 N93-25061
Synopsis of timing measurement techniques used in telecommunications p 2687 N93-25064
Aerial photographic sampling for statewide resource inventory p 2755 N93-25441
Evaluation of lens distortion errors in video-based motion analysis
| NASA-TP-3266 | p 2797 N93-25736
Model-based reasoning for system and software engineering: The Knowledge From Pictures (KFP) environment p 2825 N93-25978
Deep-space navigation with differenced data types. Part 3: An expanded information content and sensitivity analysis p 2614 N93-26109
ERS-1 (ESA SATELLITE)
Land cover monitoring in the Netherlands applying satellite remote sensing p 2740 N93-24789
Satellite borne remote sensing data: A tool for natural disaster reduction p 2743 N93-24806
Registration of the use of agricultural fields and soil erosion using satellite remote sensing p 2751 N93-24856
ERYTHROCYTES
Cellular and tissue injury during nonfreezing cold injury and frostbite
| AD-A260574 | p 2795 N93-25900
ESCAPE VELOCITY
Propagation of finite amplitude sound in a waveguide with a parabolic sound velocity profile
| ARL-TR-92-11 | p 2846 N93-26179
ESTIMATES
Local and regional estimates of sensible and latent heat flux densities from a patch-work surface
| ISBN-0-315-70882-4 | p 2772 N93-25556
Estimation of coefficients in a rational function from observed values
| AD-A261126 | p 2828 N93-25773
Considerations of the error variances of time-averaged estimators for correlated processes
| AD-A261796 | p 2830 N93-26255
On the estimation of risk associated with an attenuation prediction p 2683 N93-26469
ESTIMATING
Flight Mechanics/Estimation Theory Symposium, 1992
| NASA-CP-3186 | p 2599 N93-24694
Computationally efficient algorithms for real-time attitude estimation p 2602 N93-24709
Analysis of the Command and Control Segment (CCS) attitude estimation algorithm p 2604 N93-24722
Estimating spares requirements for Space Station Freedom using the M-SPARE model
| AD-A260878 | p 2617 N93-25630
Orbital parameter estimation using an extended Kalman filter
| AD-A260618 | p 2608 N93-25636
Estimation of coefficients in a rational function from observed values
| AD-A261126 | p 2828 N93-25773
Estimating turbine limit load
| NASA-CR-191105 | p 2580 N93-25883
ESTUARIES
Multi-date algorithms for predicting surface water quality parameters in estuarine and coastal waters using Landsat TM data
| ED-659-CP | p 2746 N93-24829
ADCIRC: An advanced three-dimensional circulation model for shelves, coasts, and estuaries. Report 1: Theory and methodology of ADCIRC-2DDI and ADCIRC-3DL
| AD-A261608 | p 2790 N93-26164
ETCHING
Monolithic quartz vibrating beam accelerometer p 2711 N93-25011
Anisotropic etching of silicon in KOH solutions p 2647 N93-25037
Controlled dissolution of a piezoelectric material berlinite (AlPO4) p 2840 N93-25043
ETHANE
Activation of methane by clean and chemically modified single crystal oxide surfaces
| PB93-157295 | p 2644 N93-25817
Tables for the thermophysical properties of ethane
| PB93-160786 | p 2646 N93-26319
ETHERS
Determination of the thermal stability of perfluoropolyalkyl ethers by tensimetry
| NASA-TM-106081 | p 2654 N93-25093
ETHYL ALCOHOL
Emissions from ethanol and LPG fueled vehicles
| DE93-006410 | p 2660 N93-25192
Biological production of ethanol from coal
| DE93-008947 | p 2660 N93-25496
Emerging technologies in ethanol production
| PB93-157014 | p 2661 N93-25818
ETHYLENE
Parameters influencing the hot-spot ignition of aviation fuel/air and ethylene/air mixtures p 2583 N93-24886
Measurements of soot formation and hydroxyl concentration in near critical equivalence ratio premixed ethylene flame
| NASA-CR-191099 | p 2642 N93-25116
ETHYLENE COMPOUNDS
An investigation of the degradation of Fluorinated Ethylene Propylene (FEP) copolymer thermal blanketing materials aboard LDEF in the laboratory
| NASA-CR-192824 | p 2653 N93-25078
EUCLIDEAN GEOMETRY
Attitude analysis in Flatland: The plane truth p 2603 N93-24712
EULER EQUATIONS OF MOTION
A contribution to the great Riemann solver debate
| NASA-CR-191409 | p 2575 N93-25083
A compact high-order Euler solver for unstructured grids p 2699 N93-25341
Dynamics of deformable multibody systems using recursive projection methods
| AD-A260698 | p 2728 N93-25842
A brief description of a new numerical framework for solving conservation laws: The method of space-time conservation element and solution element
| NASA-TM-105757 | p 2829 N93-26560
EURECA (ESA)
The Columbus Metrology Science Team: Report on activities p 2670 N93-24987
STS-46 Space Shuttle mission report
| NASA-CR-193058 | p 2613 N93-25991
EUROPE
Land cover, an essential component of the CORINE information system on the environment: GIS implications p 2740 N93-24787
A geological and geophysical information system for Eurasia
| AD-A261789 | p 2883 N93-26442
EUROPEAN COMMUNICATIONS SATELLITE
ESA's planning and coordination of the OLYMPUS propagation experiment p 2684 N93-26477
EUROPEAN SPACE PROGRAMS
Appliction of remote sensing to forestry mapping: Experience from the European collaborative programme for the less favoured areas p 2751 N93-24857
The Columbus Metrology Science Team: Report on activities p 2670 N93-24987
EUTECTICS
Electrochemical and spectroscopic studies of molten halides
| AD-A261687 | p 2646 N93-26439
EVALUATION
Methods of evaluating the effects of coding on SAR data p 2804 N93-25926
EVAPORATION
Computation of moisture flux from ocean to atmosphere using a synergy of SSM/I-derived precipitable water and ECMWF analyses p 2774 N93-25757
Measurement of droplet vaporization rate enhancement caused by acoustic disturbances p 2626 N93-26015
Eulerian-Eulerian treatment of turbulent dense spray combustion in a bipropellant liquid rocket engine p 2626 N93-26017
EVAPORATION RATE
Measurement of droplet vaporization rate enhancement caused by acoustic disturbances p 2626 N93-26015

EVAPORATORS
Two-phase/two-phase heat exchanger analysis
|NASA-CR-192783| p 2697 N93-25221
EVOKED RESPONSE (PSYCHOPHYSIOLOGY)
Comparative analytical study of evoked and event related potentials as correlates of cognitive processes
|AD-A261388| p 2799 N93-26446
EVOLUTION (DEVELOPMENT)
Archaeological, historical and geoelectrical data as ground truth for Landsat TM imagery application to coastal plain evolution studies p 2742 N93-24799
EXCIMER LASERS
Structure and properties of a-C: N films prepared by pulsed excimer laser deposition
|DE93-007908| p 2654 N93-25372
Simultaneous determination of gain parameters in steady state lasers
|DE93-007389| p 2713 N93-25381
EXCITATION
Monolithic quartz vibrating beam accelerometer p 2711 N93-25011
Magnetic excitations in antiferromagnetically coupled superlattices: Fe/Mo and Fe/Cr
|DE93-007894| p 2863 N93-25369
The interaction of swift electrons with surface excitations
|DE93-007245| p 2848 N93-25376
The effects of large-amplitude, low-frequency excitation on a three-dimensional jet p 2702 N93-25553
EXCLUSION
Fast mutual exclusion for uniprocessors
|AD-A261663| p 2883 N93-26389
EXERCISE PHYSIOLOGY
Combined strength and endurance training: Functional and morphological adaptations to ten weeks of training
|AD-A261059| p 2802 N93-26229
EXHAUST EMISSION
Emissions from ethanol and LPG fueled vehicles
|DE93-006410| p 2660 N93-25192
Magnitude and value of electric vehicle emissions reductions for six driving cycles in four US cities with varying air quality problems
|DE93-006417| p 2660 N93-25298
Theoretical predictions of platinum-rhodium bimetallic catalysts
|DE93-007540| p 2649 N93-25428
National air pollutant emission estimates
|PB93-157808| p 2765 N93-25850
Development and demonstration of a new filter system to control emissions during jet engine testing
|AD-A261203| p 2766 N93-26243
Particulate emissions from gas turbine engines
|AD-A261374| p 2595 N93-26339
Heterogeneous photocatalytic oxidation of atmospheric trace contaminants
|NASA-CR-192937| p 2767 N93-26427
EXHAUST FLOW SIMULATION
Measurement and analysis of a small nozzle plume in vacuum
|NASA-TM-106066| p 2633 N93-26561
EXHAUST GASES
Emissions from ethanol and LPG fueled vehicles
|DE93-006410| p 2660 N93-25192
An experimental study of under-expanded jets p 2577 N93-25467
Development and demonstration of a new filter system to control emissions during jet engine testing
|AD-A261203| p 2766 N93-26243
Molecular interactions and properties with many-body methods
|AD-A261688| p 2850 N93-26367
Analysis of the IBSS spectra of Space Shuttle control engine exhaust
|AD-A261749| p 2632 N93-26373
Improved selective catalytic NOx control technology for compressor station reciprocating engines
|PB93-158566| p 2768 N93-26529
EXHAUST NOZZLES
Particle behavior in solid propellant rocket motors and plumes
|AD-A260900| p 2624 N93-25913
EXHAUST SYSTEMS
Development and use of hydrogen-air torches in an altitude facility
|NASA-TM-106047| p 2598 N93-26214
EXOBIOLOGY
Analysis of reentry into the White Sands Missile Range (WSMR) for the LifeSat mission p 2603 N93-24717
Digest of Russian Space Life Sciences, issue 33
|NASA-CR-3922(39)| p 2792 N93-25195
Space biology research development
|NASA-CR-192830| p 2792 N93-25242
EXOSPHERE
Data analysis and interpretation of lunar dust exosphere p 2898 N93-26059
EXPERIMENT DESIGN
Laser ignition application in a space experiment
|NASA-TM-106133| p 2664 N93-25337
Temperature-dependent electrical conductivity of soda-lime glass
|DE93-007872| p 2654 N93-25359
Design and validation of optimal experiments for estimating thermal properties of composite materials p 2635 N93-25541
Use of Taguchi design of experiments to optimize and increase robustness of preliminary designs p 2670 N93-26063
Task 5: Architecture sensitivity to STME performance
|MCR-92-5010| p 2609 N93-26176
EXPERIMENTATION
Microwave interrogation frequency noise and clock frequency stability: Experimental results p 2842 N93-25056
EXPERT SYSTEMS
Weather forecasting expert system study
|NASA-CR-192929| p 2777 N93-24747
A knowledge-based approach to waste disposal sites detection through integration of Landsat-TM imagery and geographical context information p 2741 N93-24796
How to combine probabilistic and fuzzy uncertainties in fuzzy control
|NASA-TM-108746| p 2818 N93-25138
How to control if even experts are not sure: Robust fuzzy control
|NASA-TM-108745| p 2818 N93-25142
An expert system shell for inferring vegetation characteristics: Inrerface for the addition of techniques (Task H)
|NASA-CR-192897| p 2754 N93-25154
How to help intelligent systems with different uncertainty representations cooperate with each other
|NASA-CR-192947| p 2818 N93-25196
Optimization of knowledge-based systems and expert system building tools
|NASA-CR-192763| p 2874 N93-25288
Min and max are the only continuous ampersand-, V-operations for finite logics
|NASA-CR-192952| p 2820 N93-25452
What procedure to choose while designing a fuzzy control? Towards mathematical foundations of fuzzy control
|NASA-TM-108719| p 2820 N93-25459
Expert system for UNIX system reliability and availability enhancement p 2723 N93-25588
The Generic Spacecraft Analyst Assistant (GenSAA): A tool for developing graphical expert systems p 2814 N93-25589
TARGET: Rapid capture of process knowledge p 2814 N93-25590
Tree classification software p 2814 N93-25591
The application of integrated knowledge-based systems for the Biomedical Risk Assessment Intelligent Network (BRAIN) p 2799 N93-25595
Software lifecycle support environment (SLCSE) knowledge-based enhancements
|AD-A261042| p 2811 N93-25791
System of Experts for Intelligent Data Management (SEIDAM) p 2879 N93-25800
Knowledge-based assistance for science visualization and analysis using large distributed databases p 2879 N93-25801
Development of an expert data reduction assistant p 2880 N93-25808
A Spatial Analysis and Modeling System (SAMS) for environment management p 2881 N93-25813
A methodology and software environment for testing process model's sequential predictions with protocols
|AD-A260980| p 2882 N93-25844
Development of a heuristic knowledge base for the selection of applicable or relevant and appropriate environmental requirements
|AD-A261038| p 2765 N93-25864
Using AI/expert system technology to automate planning and replanning for the HST servicing missions p 2822 N93-25962
Adaptive laser link reconfiguration using constraint propagation p 2823 N93-25967
The WorkPlace distributed processing environment p 2825 N93-25977
Inferring heuristic classification hierarchies from natural language input p 2825 N93-25979
Multi-viewpoint clustering analysis p 2825 N93-25980
Expert systems for assembly sequence evaluation p 2669 N93-26411
The effects of cloud inhomogeneities upon radiative fluxes, and the supply of a cloud truth validation dataset
|NASA-CR-191711| p 2787 N93-26492
EXPLOITATION
Exploitation of cyclostationarity for signal-parameter estimation and system identification
|AD-A260833| p 2728 N93-25784
EXPLOSIVES
Pyroshock: Bibliography
|DE93-007605| p 2726 N93-25489
Hazards of explosives dusts: Particle size effects
|DE93-009380| p 2668 N93-25498
Minutes of the Twenty-Fifth Explosives Safety Seminar, volume 4
|AD-A261116| p 2660 N93-25769
DSD Technology: A detonation reactive Huygens code
|LA-12235-MS| p 2706 N93-25987
Molecular composition, structure, and sensitivity of explosives
|DE93-003850| p 2662 N93-26493
EXPOSURE
Effects of space radiation on humoral and cellular immunity in rhesus monkeys
|AD-A261808| p 2793 N93-26259
EXTERNAL TANKS
An in-depth probabilistic study of external tank attach ring
|NASA-TM-108403| p 2624 N93-25671
External tank aerothermal design criteria verification
|NASA-CR-192514| p 2618 N93-26055
EXTRACTION
Biological production of ethanol from coal
|DE93-008947| p 2660 N93-25496
Reclamation with recovery of radionuclides and toxic metals from contaminated materials, soils, and wastes p 2769 N93-25571
Vision-aided monitoring and control of thermal spray, spray forming, and welding processes p 2670 N93-25604
EXTRATERRESTRIAL LIFE
Space biology research development
|NASA-CR-192830| p 2792 N93-25242
EXTRATERRESTRIAL RADIATION
Space radiation susceptibility of ultra stable crystal oscillators p 2693 N93-25053
Effects of space radiation on humoral and cellular immunity in rhesus monkeys
|AD-A261808| p 2793 N93-26259
EXTRATERRESTRIAL RESOURCES
Near Earth object fuels (neo-fuels): Discovery, prospecting and use
|DE93-005185| p 2892 N93-25164
Representative systems for space exploration p 2897 N93-26395
EXTRAVEHICULAR ACTIVITY
Composite materials for the extravehicular mobility unit p 2642 N93-26060
Investigation of the effects of Extra Vehicular Activity (EVA) and Launch and Entry (LES) gloves on performance p 2803 N93-26061
The role of pyridoxine as a countermeasure for in-flight loss of lean body mass p 2796 N93-26068
A vision architecture for the extravehicular activity retriever p 2827 N93-26071
EXTRAVEHICULAR MOBILITY UNITS
The properties of and analytical methods for detection of LiOH and Li2CO3
|NASA-CR-192771| p 2643 N93-25240
Composite materials for the extravehicular mobility unit p 2642 N93-26060
EXTREME ULTRAVIOLET EXPLORER SATELLITE
Real-time attitude determination and gyro calibration p 2602 N93-24708
A multimission three-axis stabilized spacecraft flight dynamics ground support system p 2603 N93-24714
EXTREME ULTRAVIOLET RADIATION
Further analysis of ECOM-721 data
|AD-A260863| p 2774 N93-25790
Imaging the magnetosphere in the extreme ultraviolet
|NASA-CR-192218| p 2775 N93-26151
EXTREMELY HIGH FREQUENCIES
A technique for computation of noise temperature due to a beam waveguide shroud p 2671 N93-24661
Ka-band feed arrays for spacecraft reflector antennas with limited scan capability: An overview p 2680 N93-26128
L- and K-band LMSS propagation measurements using MARECS-B, OLYMPUS, and ACTS p 2683 N93-26467
EXTRUDING
Properties of extruded PS-212 type self-lubricating materials p 2659 N93-25565
EYE (ANATOMY)
The prevalence of artificial lens implants in the civil airman population
|DOT/FAA/AM-92/14| p 2794 N93-25214
A fiber optic probe for the detection of cataracts p 2796 N93-25593

Visual perception of elevation
| AD-A261394 | p 2797 N93-26307

EYE MOVEMENTS
Visual perception of elevation
| AD-A261394 | p 2797 N93-26307
Coordinated action in 3-D space
| AD-A261418 | p 2799 N93-26449

F

F REGION
Study of auroral dynamics with combined spacecraft and incoherent-scatter radar data
| NASA-CR-192224 | p 2775 N93-26159

FABRICATION
An inverted AlGaAs/GaAs patterned-Ge tunnel junction cascade concentrator solar cell
| DE93-000073 | p 2759 N93-25102
Environmental test program for superconducting materials and devices
| DE93-003646 | p 2864 N93-25506
INEL spray-forming research p 2658 N93-25562
Film fabrication technologies at NREL p 2658 N93-25563
Mullite whiskers and mullite-whisker felt p 2642 N93-25586
A high performance room-temperature near-infrared camera
| AD-A260602 | p 2709 N93-25634
MOCVD process technology for affordable, high-yield, high-performance MESFET structures. Phase 3: MIMIC
| AD-A261178 | p 2690 N93-25820
Composite nanostructured material fabrication by electrochemical scanning probe microscopy
| AD-A261017 | p 2639 N93-25862
Duct protection coating concept development and test. Appendix D, volume 1: Test specimen fabrication, conditioning, and testing documentation
| AD-A261005 | p 2656 N93-25940
A new approach to cooled combustion chambers: The 40K formed platelet chamber p 2626 N93-26018
Investigation into the common mode rejection ratio of the physiological signal conditioner circuit p 2794 N93-26073
Improved composite fabrication process
| AD-D015679 | p 2640 N93-26145
Fabrication of composite propfan blades for a cruise missile wind tunnel model
| NASA-TM-105270 | p 2730 N93-26202
Development of organic nonlinear optical materials
| AD-A261332 | p 2856 N93-26309
Research support for the Laboratory for Lightwave Technology
| AD-A261488 | p 2856 N93-26343

FABRY-PEROT INTERFEROMETERS
Fibre optic sensors for heat transfer studies p 2853 N93-25748

FAILURE
Failure monitoring in dynamic systems: Model construction without fault training data p 2672 N93-24666
Report of the Seasat Failure Review Board p 2619 N93-24693
Ultrasonic rate measurement of multiphase flow
| DE93-000112 | p 2695 N93-24954
Seismic buckling capacity of unstiffened, free-standing steel containments
| DE93-005325 | p 2723 N93-24957
A comparison of moisture resistance with different types of end-terminations in ceramic capacitors
| DE93-007600 | p 2689 N93-25416
Improved performance and safety for high energy batteries through use of hazard anticipation and capacity prediction p 2694 N93-25582
Numerical simulation of damage and progressive failures in composite laminates using the layerwise plate theory p 2636 N93-25661
Detection of bearing failure in mechanical devices using neural networks p 2822 N93-25965
Virtually-synchronous communication based on a weak failure suspector
| NASA-CR-193003 | p 2721 N93-26135
European tri-service advanced materials workshop on compressive strength in rigid-rod polymers
| AD-A261517 | p 2658 N93-26576

FAILURE ANALYSIS
A procedure for defining lightning risk to air vehicles p 2583 N93-24885
Tethered Satellite System Contingency Investigation Board
| NASA-TM-108704 | p 2616 N93-25231
Evaluation of a vibration diagnostic system for the detection of spur gear pitting failures
| NASA-TM-106103 | p 2718 N93-25672
Damage and failure analysis on continuous fiber-reinforced polymer composites p 2637 N93-25716
High strain rate damage development and failure mechanisms in tungsten heavy alloys
| AD-A260856 | p 2651 N93-25788
External stress-corrosion cracking of a 1.22-m-diameter type 316 stainless steel air valve
| NASA-TP-3190 | p 2652 N93-26201
Advanced engineering analysis
| KCP-613-4967 | p 2669 N93-26212
Thermally induced stresses in a composite exposed to fire
| AD-A261714 | p 2641 N93-26371
X ray computed tomography for failure analysis
| AD-A261884 | p 2722 N93-26527

FAILURE MODES
Monitoring damage growth in titanium matrix composites using acoustic emission
| NASA-TM-107742 | p 2634 N93-25072
Analysis of matrix damage in unidirectional composites p 2634 N93-25338
The damage, repair and design of fiber composite structural materials p 2635 N93-25532
Damage and failure analysis on continuous fiber-reinforced polymer composites p 2637 N93-25716
NLS operations concepts: Failure modes scenario simulation model analysis
| MCR-92-5013 | p 2609 N93-26175
Deformation mechanisms of NiAl cyclicly deformed near the brittle-to-ductile transition temperature
| NASA-CR-191121 | p 2652 N93-26235

FAN BLADES
Model fan passage flow simulation
| AD-A261613 | p 2707 N93-26167

FAR FIELDS
Fractal determination of parameters in lightning and ESD model p 2686 N93-24893
Far field rotor noise
| AD-A260703 | p 2845 N93-25651
Unsteady airfoil flow solutions on moving zonal grids
| AD-A261925 | p 2582 N93-26198
Three-dimensional analysis and verification of fracture growth mechanisms in fiber-reinforced ceramic composites
| AD-A261483 | p 2641 N93-26355

FAR INFRARED RADIATION
Far-infrared emission, gas, and ultraluminous HII regions in M101
| NASA-CR-192791 | p 2890 N93-25755

FARM CROPS
Cartography and statistics of crops under irrigation in the Donana area of Andalucia through the use of Landsat-TM imagery and its incorporation into a GIS p 2751 N93-24855
Crop agroecological diagnostics by remote sensing technique p 2751 N93-24860
Combining spectral information with crop rotation knowledge for crop classifications p 2752 N93-24861
Multi-temporal satellite image analysis for crop inventories in the Po River Valley (Italy) p 2755 N93-25434
Analysis of the lettuce data from the variable pressure growth chamber at NASA Johnson Space Center: A three-stage nested design model p 2794 N93-26069

FARMLANDS
Registration of the use of agricultural fields and soil erosion using satellite remote sensing p 2751 N93-24856

FAST FOURIER TRANSFORMATIONS
Implementation of cyclic spectral analysis methods
| AD-A261715 | p 2681 N93-26372

FASTENERS
The design of mechanically compatible fasteners for human mandible reconstruction p 2796 N93-25569

FATIGUE (BIOLOGY)
Simulated sustained flight operations and performance. Part 1: Effects of fatigue
| AD-A261012 | p 2801 N93-25859

FATIGUE (MATERIALS)
Fatigue resistance of orthotropic plates with trapezoidal stiffeners
| TRL-TRANS-T3908 | p 2726 N93-25419
Reliable stress and fracture mechanics analysis of complex aircraft components using a h-p version of FEM
| AD-A260628 | p 2726 N93-25638
Micromechanics of fatigue
| AD-A260577 | p 2729 N93-25901
Improved fatigue life for moorings
| PB93-161198 | p 2730 N93-26320

FATIGUE LIFE
Improved fatigue life for moorings
| PB93-161198 | p 2730 N93-26320

FATIGUE TESTS
General aviation aircraft: Normal acceleration data analysis and collection project
| DOT/FAA/CT-91/20 | p 2586 N93-24739
Evaluation of a vibration diagnostic system for the detection of spur gear pitting failures
| NASA-TM-106103 | p 2718 N93-25672
In-situ ultrasonic C-scanner
| AD-A261113 | p 2638 N93-25768
Micromechanics of fatigue
| AD-A260577 | p 2729 N93-25901
Improved fatigue life for moorings
| PB93-161198 | p 2730 N93-26320

FAULT TOLERANCE
Failure monitoring in dynamic systems: Model construction without fault training data p 2672 N93-24666
Optimal message log reclamation for independent checkpointing
| NASA-CR-192886 | p 2815 N93-24749
On the robustness of Herlihy's hierarchy
| NASA-CR-193002 | p 2808 N93-25107
A control structure for fault-tolerant operation of robotic manipulators
| DE93-005783 | p 2717 N93-25413
Expert system for UNIX system reliability and availability enhancement p 2723 N93-25588
Machine learning techniques for fault isolation and sensor placement p 2823 N93-25966
Virtually-synchronous communication based on a weak failure suspector
| NASA-CR-193003 | p 2721 N93-26135

FAULTS
The Generic Spacecraft Analyst Assistant (GenSAA): A tool for developing graphical expert systems p 2814 N93-25589
Machine learning techniques for fault isolation and sensor placement p 2823 N93-25966

FEASIBILITY
Feasibility study of a Ka-/Ka-band dichroic plate with stepped rectangular apertures p 2671 N93-24660
A feasibility study of using Langley 0.3-m transonic cryogenic tunnel sidewall boundary-layer removal system for heavy gas testing
| NASA-CR-191438 | p 2695 N93-25087

FEASIBILITY ANALYSIS
TDRSS orbit determination using short baseline differenced carrier phase p 2601 N93-24701
Weather forecasting expert system study
| NASA-CR-192929 | p 2777 N93-24747
Feasibility study of a long duration balloon flight with NASA/GSFC and Soviet Space Agency Gamma Ray Spectrometers
| NASA-CR-192934 | p 2573 N93-25077
Development of laser guide stars and adaptive optics for large astronomical telescopes
| DE93-007511 | p 2888 N93-25320

FECES
Health and environmental chemistry: Analytical techniques, data management, and quality assurance
| DE93-002853 | p 2760 N93-24674

FEED SYSTEMS
A technique for computation of noise temperature due to a beam waveguide shroud p 2671 N93-24661

FEEDBACK
Coordinated action in 3-D space
| AD-A261418 | p 2799 N93-26449

FEEDBACK CONTROL
Fundamental characteristics of a laser-diode-pumped rubidium maser with an external feedback loop p 2716 N93-25068
A neural network-based estimator for the mixture ratio of the Space Shuttle Main Engine
| NASA-TM-106070 | p 2622 N93-25089
Two neural network algorithms for designing optimal terminal controllers with open final time
| NASA-CR-177599 | p 2817 N93-25137
Dynamic error analysis of numerical methods for simulation of state-variable derivatives with discontinuities p 2819 N93-25278
Aerospace vehicle model simplification for feedback control p 2596 N93-25292
Optimal control of large space structures p 2819 N93-25343
Control of nonlinear systems under input constraints with applications to flight control p 2596 N93-25353
Detailed solution to a complex kinematics chain manipulator
| DE93-004619 | p 2725 N93-25357
Dynamics and robust control of a sampled data system for large space structures. Volume 2: The LQG/LTR methodology for the discrete-time system and the design of reduced order robust digital controller for orbiting flexible shallow spherical shell system
| AD-A260793 | p 2599 N93-25693

Nonlinear dynamics and attitude control of articulated flexible space structures p 2617 N93-25726
Passivity motivated controller design for flexible structures
| AD-A261122 | p 2719 N93-25771
Recommendations for a Kalman filter to estimate and control freeze and sublime rates of gaseous diffusion plant freezer/sublimer systems
| ORNL/TM-12183 | p 2668 N93-25937
Nonlinear system design: Adaptive feedback linearization with unmodeled dynamics
| AD-A261360 | p 2826 N93-26333
Adaptive control of nonlinear flexible systems
| AD-A261676 | p 2826 N93-26365
Interaction dynamics and control for orbital assembly p 2669 N93-26407

FEEDFORWARD CONTROL
Adaptive control of nonlinear flexible systems
| AD-A261676 | p 2826 N93-26365

FEET (ANATOMY)
Anthropometry of the foot and lower leg of U.S. Army soldiers: Fort Jackson, SC
| AD-A261405 | p 2802 N93-26404

FEMALES
Assessing patterns of change in anthropometric dimensions: Secular trends of US Army females, 1946-1988
| AD-A260869 | p 2800 N93-25628

FERMENTATION
Biological production of ethanol from coal
| DE93-008947 | p 2660 N93-25496

FERMIONS
New ground states in unconventional superconductors p 2688 N93-25282

FERRITES
Nondestructive evaluation of ferrite c-cores
| KCP-613-4677 | p 2721 N93-25939
Cross-switched MICRAD seeker
| AD-D015676 | p 2691 N93-26142

FERROELECTRICITY
Electroelastic equations for electroded thin plates subject to large driving voltages
| AD-A261123 | p 2675 N93-25772
Considerations for space and naval aviation applications of ferroelectric memory
| AD-A261300 | p 2807 N93-26294
Investigation of coupled analysis techniques for adaptive material structural systems
| AD-A261359 | p 2868 N93-26332

FERROMAGNETIC MATERIALS
Molecular/polymeric magnetism
| DE93-008635 | p 2847 N93-25114
Magnetic excitations in antiferromagnetically coupled superlattices: Fe/Mo and Fe/Cr
| DE93-007894 | p 2863 N93-25369
Magnetic multilayer strain gage
| AD-D015672 | p 2710 N93-26141

FERROMAGNETISM
Molecular/polymeric magnetism
| DE93-008635 | p 2847 N93-25114
Magnetic excitations in antiferromagnetically coupled superlattices: Fe/Mo and Fe/Cr
| DE93-007894 | p 2863 N93-25369

FERROUS METALS
Duct protection coating concept development and test. Appendix D, volume 1: Test specimen fabrication, conditioning, and testing documentation
| AD-A261005 | p 2656 N93-25940
Duct protection coating concept development and test: Test specimen fabrication, conditioning, and testing documentation.
| AD-A261250 | p 2657 N93-26278

FERTILIZERS
ANOVA method to estimate vegetation indices sensitivity assessing nitrogen fertilizing influence on spectral reflectance coefficients p 2739 N93-24782
Remote sensing of land resource management in agriculture with regard to its influence on the environment p 2750 N93-24850
Measuring the intensity of nitrogen fertilization of grassland by means of remote sensing p 2751 N93-24859

FIBER COMPOSITES
Numerical modelling of induced effects of lightning strike on an all composite helicopter p 2583 N93-24879
A computational approach to predicting the extent of arc root damage in CFC panels p 2642 N93-24890
Comparison of the damage for various types of fibre reinforced composites due to different lightning test standards (MIL-STD-1757A, German military VG-standard 96903) p 2642 N93-24891
Zoning of aircraft by electric field modelling p 2583 N93-24894
High Temperature Composite Analyzer (HITCAN) theoretical manual, version 1.0
| NASA-TM-106001 | p 2723 N93-24913
High temperature composite analyzer (HITCAN) user's manual, version 1.0
| NASA-TM-106002 | p 2724 N93-25070
Fracture of an elliptical inclusion and its implications for the properties of short fiber composites p 2634 N93-25333
Analysis of matrix damage in unidirectional composites p 2634 N93-25338
Internal stresses and the cyclic deformation of an aluminum matrix composite p 2650 N93-25436
The damage, repair and design of fiber composite structural materials p 2635 N93-25532
Effect of water immersion on fiber/matrix adhesion
| AD-A260704 | p 2636 N93-25652
Inelastic behavior of thermoplastic composites p 2636 N93-25674
Finite element micromechanics modeling of inelastic deformation of unidirectionally fiber-reinforced composites p 2637 N93-25680
Damage and failure analysis on continuous fiber-reinforced polymer composites p 2637 N93-25716
The corrosion of metal matrix composites p 2638 N93-25723
International Workshop on Advances in Inorganic Fibre Technology
| AD-A260719 | p 2639 N93-25908
Thermomechanical response of shape memory composites
| AD-A260828 | p 2639 N93-25919
Composite materials for the extravehicular mobility unit p 2642 N93-26060
Electrostatic fiber spreader
| AD-D015677 | p 2640 N93-26143
Smart structural composites with piezoelectric micro-constituents
| AD-A260970 | p 2640 N93-26225
Effects of moisture and other contaminants in friction composites
| AD-A261226 | p 2640 N93-26301
Improved fatigue life for moorings
| PB93-161198 | p 2730 N93-26320
Three-dimensional analysis and verification of fracture growth mechanisms in fiber-reinforced ceramic composites
| AD-A261483 | p 2641 N93-26355
Failure considerations in composite systems based on 3D micromechanical stress fields, part A
| AD-A261698 | p 2641 N93-26382
METal matrix composite ANalyzer (METCAN): Theoretical manual
| NASA-TM-106025 | p 2641 N93-26552

FIBER OPTICS
Interferometric fiber-optic radiation sensor
| DE93-003841 | p 2852 N93-25127
Surface preparation and characterization of a 400 micrometer diameter fused silica optical fiber for direct optical initiation (DOI) applications
| DE93-005485 | p 2852 N93-25182
Development of a cone penetrometer for measuring spectral characteristics of soils in situ p 2776 N93-25570
A fiber optic probe for the detection of cataracts p 2796 N93-25593
Fibre optic sensors for heat transfer studies p 2853 N93-25748
Infrared fiber optic diagnostic for solid propellant combustion p 2628 N93-26031
Performance of a 12-GHz fiber-optic system for beam-waveguide antenna stability testing p 2677 N93-26113
Rain rate instrument for deployment at sea, phase 2
| NASA-CR-192442 | p 2786 N93-26156
Proof of fault coverage for a formal protocol test procedure
| AD-A261612 | p 2680 N93-26166
Advanced optical fiber communication systems
| AD-A261802 | p 2856 N93-26256
Research support for the Laboratory for Lightwave Technology
| AD-A261488 | p 2856 N93-26343
Optical fiber for acoustic sensor applications
| AD-A261580 | p 2857 N93-26515
In-process cure monitoring of composites via fiber-optic fluorescence
| AD-A261712 | p 2641 N93-26580

FIBER ORIENTATION
Methods of determining loads and fiber orientations in anisotropic non-crystalline materials using energy flux deviation
| NASA-CASE-LAR-14399-1 | p 2729 N93-26102

FIBER STRENGTH
Interface engineering in oxide fiber/oxide matrix composites
| AD-A261705 | p 2641 N93-26579

FIBER VOLUME FRACTION
Failure considerations in composite systems based on 3D micromechanical stress fields, part A
| AD-A261698 | p 2641 N93-26382

FIBRILLATION
Electrorheological fluids: A structural approach to mechanisms
| AD-A260563 | p 2645 N93-25879

FIELD ALIGNED CURRENTS
A statistical study of field-aligned currents in the Earth's inner magnetosphere p 2773 N93-25709

FIELD EFFECT TRANSISTORS
Quantum conductance fluctuations in self-aligned, pinch-narrowed MOSFETs p 2863 N93-25265
Microwave and millimeter wave monolithic integrated circuits (MIMIC) program. MIMIC briefs: Summaries of phase 3 technology support programs
| AD-A260914 | p 2690 N93-25660
MOCVD process technology for affordable, high-yield, high-performance MESFET structures. Phase 3: MIMIC
| AD-A261178 | p 2690 N93-25820
Noise-optimal control of HEMT LNA's for compensation of temperature deviations p 2678 N93-26115
Large area, low capacitance Si(Li) detectors for high rate x ray applications
| DE93-007661 | p 2692 N93-26598

FIELD OF VIEW
Miniature Optical Wide-Angle-Lens Startracker (Mini-OWLS) p 2606 N93-24728
Evaluation of lens distortion errors in video-based motion analysis
| NASA-TP-3266 | p 2797 N93-25736
Interpupillary and vertex distance effects on field-of-view and acuity with ANVIS
| AD-A261259 | p 2802 N93-26265

FIELD THEORY (PHYSICS)
Topics in CP violation
| DE93-007615 | p 2847 N93-25323
Twistor diagrams and a quantum field theory p 2871 N93-25423

FIGHTER AIRCRAFT
Screening studies of advanced control concepts for airbreathing engines
| NASA-TM-106042 | p 2592 N93-25079
ASTOVL combat aircraft design synthesis and optimization p 2589 N93-25704
An analysis of the reliability and maintainability of the Jian 6 and Jian 7 aircraft and ways to improve them
| AD-A261060 | p 2574 N93-26238
Physiological indices of mental workload
| AD-A261692 | p 2798 N93-26391

FIGURE OF MERIT
Figure of merit for direct-detection optical channels p 2678 N93-26117

FILAMENT WINDING
Improved composite fabrication process
| AD-D015679 | p 2640 N93-26145

FILE MAINTENANCE (COMPUTERS)
An analysis of file migration in a UNIX supercomputing environment
| NASA-CR-192908 | p 2809 N93-25131
A trace-driven analysis of name and attribute caching in a distributed system
| NASA-CR-192899 | p 2815 N93-25251
RAMA: A file system for massively parallel computers
| NASA-CR-192906 | p 2815 N93-25297
Test, Control and Monitor System maintenance plan
| NASA-CR-193099 | p 2873 N93-26420

FILM COOLING
Measurements and computations of external heat transfer and film cooking in turbines
| RAE-TM-P-1223 | p 2592 N93-25455

FILTRATION
Emerging technologies in ethanol production
| PB93-157014 | p 2661 N93-25818

FINANCE
Small business access to equity capital
| PB93-144582 | p 2872 N93-25735
Gordon Conference on Point Defects, Line Defects and Interfaces in Semiconductors
| AD-A261485 | p 2868 N93-26357

FINITE DIFFERENCE THEORY
Numerical modelling of induced effects of lightning strike on an all composite helicopter p 2583 N93-24879
A convergent finite difference scheme for the Navier-Stokes equations of nonisentropic compressible fluid flow p 2695 N93-24906
High-order cyclo-difference techniques: An alternative to finite differences
| NASA-TM-107745 | p 2575 N93-25074
A hybrid multigrid technique for computing steady-state solutions to supersonic flows p 2582 N93-26078

FINITE ELEMENT METHOD
Evaluation of MARC for the analysis of rotating composite blades
| NASA-TM-4423 | p 2723 N93-24909

High Temperature Composite Analyzer (HITCAN) theoretical manual, version 1.0
| NASA-TM-106001 | p 2723 N93-24913
Rapid exploration of curvilinear grids using direct volume rendering
| NASA-CR-192765 | p 2808 N93-24944
Seismic buckling capacity of unstiffened, free-standing steel containments
| DE93-005325 | p 2723 N93-24957
Quartz crystal twinning under mechanical stress: Finite element analysis p 2839 N93-25032
High temperature composite analyzer (HITCAN) user's manual, version 1.0
| NASA-TM-106002 | p 2724 N93-25070
Stress distribution in composite flatwise tension test specimens
| NASA-TM-106074 | p 2634 N93-25071
UARS in-flight jitter study for EOS
| NASA-CR-191419 | p 2615 N93-25133
Using a multifrontal sparse solver in a high performance, finite element code
| NASA-CR-192718 | p 2828 N93-25223
Equilibrium constrained assumed natural coordinate strain finite elements for shell analysis p 2724 N93-25273
Data parallel finite element techniques for large-scale computational fluid dynamics p 2699 N93-25334
Formulation and treatment of frictional contact problems using finite elements p 2717 N93-25412
Experimental modal survey of the probe mass mock-up
| DE93-008846 | p 2617 N93-25494
Numerical study of cavity natural convection flow with augmenting and counteracting effects by projection finite element method p 2701 N93-25540
The design of mechanically compatible fasteners for human mandible reconstruction p 2796 N93-25569
Stabilized finite element methods for incompressible flows with emphasis on moving boundaries and interfaces p 2703 N93-25663
An in-depth probabilistic study of external tank attach ring
| NASA-TM-108403 | p 2624 N93-25671
Finite element micromechanics modeling of inelastic deformation of unidirectionally fiber-reinforced composites p 2637 N93-25680
An efficient technique for structural reliability with applications p 2727 N93-25681
Low-velocity impact of composite sandwich plate p 2637 N93-25695
The rate form of equilibrium equation for problems of steady-state, elastic, viscous flows p 2704 N93-25708
Active control of NiTINOL-reinforced structural composites
| AD-A261062 | p 2638 N93-25780
Applications of parallel and vector algorithms in nonlinear structural dynamics using the finite element method
| AD-A260716 | p 2811 N93-25845
Optimization techniques for contact stress analysis
| AD-A260846 | p 2729 N93-25911
Modeling of the WSTF frictional heating apparatus in high pressure systems p 2648 N93-26079
ADCIRC: An advanced three-dimensional circulation model for shelves, coasts, and estuaries. Report 1: Theory and methodology of ADCIRC-2DDI and ADCIRC-3DL
| AD-A261608 | p 2790 N93-26164
Finite element modeling of the hydroforming press
| KCP-613-4999 | p 2668 N93-26206
Advanced engineering analysis
| KCP-613-4967 | p 2669 N93-26212
Thermally induced stresses in a composite exposed to fire
| AD-A261714 | p 2641 N93-26371
J and CTOD estimation equations for shallow cracks in single edge notch bend specimens
| AD-A261679 | p 2731 N93-26390
Configuration optimization of space structures p 2670 N93-26415
Approximate techniques for predicting size effects on cleavage fracture toughness (J(sub c))
| AD-A261591 | p 2731 N93-26516
Use and analysis of finite element methods for problems of solid mechanics and fracture
| AD-A261574 | p 2731 N93-26522
The influence of primary and secondary orientations on the elastic response of a nickel-base single-crystal superalloy
| NASA-TM-106125 | p 2731 N93-26550

FINITE VOLUME METHOD
Computation of hypersonic viscous flowfields using the parabolized Navier-Stokes equations p 2694 N93-24766
Computational modelling of 3D flow in complex ducts and passages p 2704 N93-25698

FINLAND
SIHTI: The research and development program of energy and environmental technology
| DE93-769925 | p 2763 N93-25360

FINS
Two-dimensional fin analysis p 2705 N93-25737

FIRE CONTROL
Narrow-body aircraft water spray optimization study
| DOT/FAA/CT-TN93/3 | p 2582 N93-25224

FIRE DAMAGE
A prototype system for forest fire prevention and control p 2749 N93-24844

FIRE EXTINGUISHERS
The acute inhalation toxicity of pyrolysis products of halon 1301
| AD-A260874 | p 2795 N93-25629

FIRE FIGHTING
Narrow-body aircraft water spray optimization study
| DOT/FAA/CT-TN93/3 | p 2582 N93-25224

FIRE PREVENTION
Contributions of microgravity test results to the design of spacecraft fire safety systems
| NASA-TM-106093 | p 2614 N93-24755
A prototype system for forest fire prevention and control p 2749 N93-24844

FIRES
The use of remote sensing and GIS for the assessment of environmental degradation caused by fires, applied upon South-Euboia (central Greece) p 2742 N93-24802
Thermally induced stresses in a composite exposed to fire
| AD-A261714 | p 2641 N93-26371

FIRMWARE
Firmware development improves system efficiency p 2807 N93-25606

FISHERIES
Supporting the Portuguese fisheries with satellites p 2745 N93-24821
Application of satellite imageries data to fisheries in Japan p 2745 N93-24822
The use of remotely sensed data for operational fisheries oceanography p 2734 N93-24927
The continuous plankton recorder survey: A long-term, basin-scale oceanic time series p 2736 N93-24937

FISHES
Relations between blue whiting biomass and satellite derived phytoplankton and temperature in the Norwegian Sea
| AD-A261205 | p 2757 N93-25868

FISHING
The continuous plankton recorder survey: A long-term, basin-scale oceanic time series p 2736 N93-24937

FISSIONABLE MATERIALS
Human factors in environmental management: New directions from the Hanford site
| DE93-004337 | p 2767 N93-26495

FITTINGS
Dynamic modeling of fluid transmission lines of the DSN 70-meter antennas by using a lumped parameter model p 2678 N93-26119

FIXED WINGS
Unsteady airfoil flow solutions on moving zonal grids
| AD-A261925 | p 2582 N93-26198

FLAME PROPAGATION
Contributions of microgravity test results to the design of spacecraft fire safety systems
| NASA-TM-106093 | p 2614 N93-24755
A model of concurrent flow flame spread over a thin solid fuel
| NASA-CR-191111 | p 2663 N93-24946
The structure of particle cloud premixed flames
| NASA-CR-192827 | p 2643 N93-25229
Modelling of microgravity ignition phenomena p 2664 N93-25465
Interactions of acoustic waves and combustion of homogeneous solid propellants in rocket motors p 2630 N93-26039
Oxides of nitrogen emissions from turbulent hydrocarbon/air jet diffusion flames, phase 2
| PB93-152478 | p 2768 N93-26533

FLAME STABILITY
Atomization and combustion of a gelled, metallized slurry fuel
| AD-A261778 | p 2647 N93-26602

FLAME TEMPERATURE
Physical and chemical processes governing the CO2 laser-induced deflagration of ammonium dinitramide (ADN) p 2629 N93-26037

FLAMEOUT
A model of concurrent flow flame spread over a thin solid fuel
| NASA-CR-191111 | p 2663 N93-24946

FLAMES
Contributions of microgravity test results to the design of spacecraft fire safety systems
| NASA-TM-106093 | p 2614 N93-24755
Modelling of microgravity ignition phenomena p 2664 N93-25465
Flame structure studies of a lean, 20 torr H2/N2O/AR flame employing molecular beam mass spectrometry p 2627 N93-26025
Modeling of H2/N2O flames p 2627 N93-26026
Dark zone modeling of solid propellant flames p 2628 N93-26028
Detection of atomic oxygen and hydrogen in solid propellant flames and pyrolysis gases using multiphoton laser-induced fluorescence p 2628 N93-26029
Tomographic analysis of sight infrared spectra of low pressure flames p 2628 N93-26030
ADN propellant diffusion flame structure p 2629 N93-26036
Physical and chemical processes governing the CO2 laser-induced deflagration of ammonium dinitramide (ADN) p 2629 N93-26037
Interactions of acoustic waves and combustion of homogeneous solid propellants in rocket motors p 2630 N93-26039
Flame response in oscillatory solid propellant combustion p 2630 N93-26041

FLAMMABILITY
Contributions of microgravity test results to the design of spacecraft fire safety systems
| NASA-TM-106093 | p 2614 N93-24755

FLANGES
Design and analysis of curved composite components for rotorcraft fuselage frames p 2589 N93-25701

FLARE STARS
ROSAT investigation of flaring and activity on Prox Cen
| NASA-CR-192972 | p 2891 N93-26139

FLAT PLATES
Shock tube application to the study of compressible turbulent boundary layer with mass injection p 2697 N93-25252

FLEXIBILITY
Scientific visualization using the Flow Analysis Software Toolkit (FAST) p 2814 N93-25600
The MODE family of on-orbit experiments: The Middeck Active Control Experiment (MACE) p 2599 N93-25835
Joint flexibility effects on the dynamic response of structures. Part 2: Stochastic analysis
| AD-A261003 | p 2729 N93-25938

FLEXIBLE BODIES
Direct solutions of the Navier-Stokes equations with application to static aeroelasticity p 2697 N93-25259
Stability analysis and modeling of rotating flexible structures
| DE93-008493 | p 2844 N93-25520
Passivity motivated controller design for flexible structures
| AD-A261122 | p 2719 N93-25771
Using input command pre-shaping to suppress multiple mode vibration p 2732 N93-25834
The MODE family of on-orbit experiments: The Middeck Active Control Experiment (MACE) p 2599 N93-25835
Sequential design of a linear quadratic controller for the Deep Space Network antennas p 2679 N93-26123
Controls for orbital assembly of large space structures p 2620 N93-26408

FLEXIBLE SPACECRAFT
Optimal control of large space structures p 2819 N93-25343
The dynamics and control of large flexible asymmetric spacecraft p 2617 N93-25525
Nonlinear dynamics and attitude control of articulated flexible space structures p 2617 N93-25726
Model reduction for Space Station Freedom p 2620 N93-26081

FLEXIBLE WINGS
An aeroelastic model structure investigation for a manned real-time rotorcraft simulation p 2574 N93-24756

FLEXING
Damage and failure analysis on continuous fiber-reinforced polymer composites p 2637 N93-25716

FLIGHT CHARACTERISTICS
Applications of stress envelope concepts to aircraft EMP and lightning survivability p 2584 N93-24898
Nonlinear stability analysis of the attitude motion of spin-stabilized thrusting spacecraft p 2617 N93-25527

FLIGHT CONDITIONS
Aeroelastic response and aeromechanical stability of helicopters with elastically coupled composite rotor blades p 2588 N93-25530

FLIGHT CONTROL
Orbit determination and orbit control for the Earth Observing System (EOS) AM spacecraft p 2601 N93-24705
Prediction of forces and moments for hypersonic flight vehicle control effectors
| NASA-CR-193033 | p 2595 N93-24762

Robust nonlinear control of vectored thrust aircraft
| NASA-CR-192727 | p 2596 N93-25199
Aerodynamic foundations for use of unsteady aerodynamic effects in flight control
p 2576 N93-25274
Control of nonlinear systems under input constraints with applications to flight control p 2596 N93-25353
Use of high performance networks and supercomputers for real-time flight simulation p 2598 N93-25574

FLIGHT CREWS
Simulated sustained flight operations and performance. Part 1: Effects of fatigue
| AD-A261012 | p 2801 N93-25859

FLIGHT HAZARDS
The 1992 International Aerospace and Ground Conference on Lightning and Static Electricity: Addendum
| DOT/FAA/CT-92/20-ADD-1 | p 2777 N93-24875
Digitization of analog data from in-flight lightning strikes p 2778 N93-24884
Lightning phenomenology bases for full threat return stroke occurrence following extended leader sweep at flight altitudes p 2780 N93-24895
Applications of stress envelope concepts to aircraft EMP and lightning survivability p 2584 N93-24898
Development of models for predicting the triggering of lightning by launch vehicles p 2610 N93-24899
PROAV Cable Warning System (CWS) - U.S. Army aircraft Integration assessment and OCONUS field evaluation
| AD-A261233 | p 2583 N93-26263

FLIGHT INSTRUMENTS
Development of a flight instrument package
| AD-A260830 | p 2591 N93-25783
Aircraft accident report: Tomy International, Inc., d/b/a Scenic Air Tours flight 22, Beech Model E18S, N342E in-flight collision with terrain, Mount Haleakala, Maui, Hawaii, 22 April 1992
| PB93-910401 | p 2583 N93-25827
Design, fabrication, and testing of a three-dimensional acoustic orientation instrument (3-D AOI): Drawings, engineering and associated lists (conceptual and development design)
| AD-A260934 | p 2845 N93-25915
SRB environment evaluation and analysis. Volume 1: Redesigned SRB flight heating evaluation
| NASA-CR-192517 | p 2631 N93-26053

FLIGHT MANAGEMENT SYSTEMS
Piloted simulation of an air-ground profile negotiation process in a time-based Air Traffic Control environment
| NASA-TM-107748 | p 2585 N93-26087

FLIGHT MECHANICS
Flight Mechanics/Estimation Theory Symposium, 1992
| NASA-CP-3186 | p 2599 N93-24694

FLIGHT OPERATIONS
The Generic Spacecraft Analyst Assistant (GenSAA): A tool for developing graphical expert systems
p 2814 N93-25589
Expedient repair of structural facilities
| AD-A260727 | p 2598 N93-25656
Simulated sustained flight operations and performance. Part 1: Effects of fatigue
| AD-A261012 | p 2801 N93-25859
Design of an air traffic computer simulation system to support investigation of civil tiltrotor aircraft operations
| NASA-CR-192920 | p 2585 N93-26052

FLIGHT OPTIMIZATION
Optimal thrust magnitude on a singular arc in atmospheric flight p 2819 N93-25410

FLIGHT PATHS
Design concepts for the development of cooperative problem-solving systems
| NASA-CR-192708 | p 2585 N93-25261
Control and optimization of aircraft trajectories
p 2596 N93-25543

FLIGHT PLANS
Design of a cooperative problem-solving system for enroute flight planning: An empirical study of its use by airline dispatchers
| NASA-CR-192709 | p 2585 N93-25330

FLIGHT RULES
Systems engineering and integration processes involved with manned mission operations p 2666 N93-24688

FLIGHT SAFETY
The 1992 International Aerospace and Ground Conference on Lightning and Static Electricity: Addendum
| DOT/FAA/CT-92/20-ADD-1 | p 2777 N93-24875
Lightning phenomenology bases for full threat return stroke occurrence following extended leader sweep at flight altitudes p 2780 N93-24895
The ATC evaluation of the prototype Airport Surveillance Radar Wind Shear Processor (ASR-WSP) at Orlando International Airport
| DOT/FAA/CT-TN92/48 | p 2673 N93-25210
Aircraft accident report: Tomy International, Inc., d/b/a Scenic Air Tours flight 22, Beech Model E18S, N342E in-flight collision with terrain, Mount Haleakala, Maui, Hawaii, 22 April 1992
| PB93-910401 | p 2583 N93-25827
PROAV Cable Warning System (CWS) - U.S. Army aircraft Integration assessment and OCONUS field evaluation
| AD-A261233 | p 2583 N93-26263

FLIGHT SIMULATION
An aeroelastic model structure investigation for a manned real-time rotorcraft simulation
p 2574 N93-24756
Use of high performance networks and supercomputers for real-time flight simulation p 2598 N93-25574
Piloted simulation of an air-ground profile negotiation process in a time-based Air Traffic Control environment
| NASA-TM-107748 | p 2585 N93-26087
Effect of image update rate on moving-target identification range
| AD-A261562 | p 2591 N93-26462

FLIGHT SIMULATORS
Autonomic physiological data associated with simulator discomfort
| NASA-CR-177609 | p 2794 N93-24738
An aeroelastic model structure investigation for a manned real-time rotorcraft simulation
p 2574 N93-24756
Evaluation of advanced displays for engine monitoring and control
| NASA-CR-191418 | p 2591 N93-24764
Use of high performance networks and supercomputers for real-time flight simulation p 2598 N93-25574

FLIGHT TESTS
Summary and recommendations on nuclear electric propulsion technology for the space exploration initiative
| NASA-TM-105707 | p 2622 N93-24744
An aeroelastic model structure investigation for a manned real-time rotorcraft simulation
p 2574 N93-24756
In-flight evaluation of noise levels and assessment of active noise reduction systems in the Seahawk S-70B-2 helicopter
| AD-A260689 | p 2845 N93-25649
Development of a flight instrument package
| AD-A260830 | p 2591 N93-25783
SRB environment evaluation and analysis. Volume 1: Redesigned SRB flight heating evaluation
| NASA-CR-192517 | p 2631 N93-26053

FLIGHT TIME
General aviation aircraft: Normal acceleration data analysis and collection project
| DOT/FAA/CT-91/20 | p 2586 N93-24739

FLIGHT TRAINING
Performance-based testing and success in Naval advanced flight training
| AD-A260838 | p 2590 N93-25933

FLOODS
Application of multitemporal Landsat-MSS and -TM data for the development of an inundation-risk-map
p 2743 N93-24807

FLOORS
A modular wideband sound absorber
| BBC-RD-1992/11 | p 2673 N93-25171

FLORIDA
Comparative performance of lightning air terminals under natural storm conditions p 2781 N93-24902

FLOW CHARACTERISTICS
A numerical and experimental studies of flow characteristics in centrifugal fans p 2577 N93-25339

FLOW CHARTS
A systematic satellite approach for estimating central pressures of mid-lattitude oceanic storms
| NOAA-TR-NESDIS-63 | p 2781 N93-25220

FLOW COEFFICIENTS
Experimental effects of wing location on wing-body pressures at supersonic speeds
| NASA-TM-4434 | p 2581 N93-26085
Another look at the driven cavity problem
| AD-A261903 | p 2708 N93-26543

FLOW DISTORTION
Flow conditioner location effects in orifice flowmeters
| PB93-159457 | p 2708 N93-26535

FLOW DISTRIBUTION
A three-dimensional algebraic grid generation scheme for gas turbine combustors with inclined slots
| NASA-CR-191095 | p 2694 N93-24759
Computation of hypersonic viscous flowfields using the parabolized Navier-Stokes equations
p 2694 N93-24766
Computational study of the aerodynamics and control by blowing of asymmetric vortical flows over delta wings
p 2574 N93-24772
Surface and flow field measurements in a symmetric crossing shock wave/turbulent boundary-layer interaction
| NASA-TM-106086 | p 2575 N93-24911
Combined LAURA-UPS hypersonic solution procedure
| NASA-TM-107682 | p 2696 N93-25176
An experimental study of the sources of fluctuating pressure loads beneath swept shock/boundary-layer interactions
| NASA-CR-192918 | p 2698 N93-25266
A numerical and experimental studies of flow characteristics in centrifugal fans p 2577 N93-25339
Optimized scramjet engine integration on a waverider airframe p 2593 N93-25480
The interaction of modulated vortex pairs with a free surface p 2701 N93-25485
Experimental and computational investigation of helium injection into air at supersonic and hypersonic speeds
p 2577 N93-25487
A computational method for the analysis of acoustic radiation from turbofan inlets p 2845 N93-25717
An experimental study of passive drag reduction in a turbulent boundary layer by a riblet surface
p 2705 N93-25746
A new LU-SGS flow solver for calculating reentry flows p 2579 N93-25759
Visualization of a Mach 2 reacting flow using Planar Laser-Induced Fluorescence (PLIF)
p 2598 N93-26006
External tank aerothermal design criteria verification
| NASA-CR-192514 | p 2618 N93-26055
The blade curving effects in a turbine stator cascade with low aspect ratio
| AD-A261063 | p 2595 N93-26239
Another look at the driven cavity problem
| AD-A261903 | p 2708 N93-26543
Measurement and analysis of a small nozzle plume in vacuum
| NASA-TM-106066 | p 2633 N93-26561

FLOW EQUATIONS
Parallelizing the spectral transform method: A comparison of alternative parallel algorithms
| DE93-008664 | p 2816 N93-25521
A computational method for the analysis of acoustic radiation from turbofan inlets p 2845 N93-25717

FLOW MEASUREMENT
Surface and flow field measurements in a symmetric crossing shock wave/turbulent boundary-layer interaction
| NASA-TM-106086 | p 2575 N93-24911
Ultrasonic rate measurement of multiphase flow
| DE93-000112 | p 2695 N93-24954
An investigation of laser velocimetry measurements within high speed, complex flows p 2697 N93-25237
An investigation on planar velocimetry by spatial cross-correlation p 2578 N93-25664
Method of measuring cross-flow vortices by use of an array of hot-film sensors
| NASA-CASE-LAR-14824-1-SB | p 2706 N93-26000
Pulsed laser Rayleigh scattering diagnostic for hydrogen/oxygen rocket exit plane flowfield velocimetry
| NASA-TM-106098 | p 2631 N93-26149
Trailing vortex/free-surface interaction
| AD-A261654 | p 2581 N93-26195
Flow conditioner location effects in orifice flowmeters
| PB93-159457 | p 2708 N93-26535
Optically smart surfaces survivability testing at Mach 3
| AD-A261785 | p 2857 N93-26566

FLOW STABILITY
Instability of flow in a streamwise corner
| NASA-CR-191410 | p 2576 N93-25153
Vortex shedding in oscillatory flow
p 2700 N93-25438
Spatial simulation of transition in wall-bounded shear flows: Active control and effects of surface roughness
p 2701 N93-25483
The instability of a liquid jet in a compressible airstream p 2703 N93-25560
Flow between finite rotating disks and its linear stability p 2705 N93-25747
Stationary crossflow instability on an infinite swept wing p 2580 N93-25865
Development of an expendable particle sensor
| AD-A261127 | p 2710 N93-26044
ADCIRC: An advanced three-dimensional circulation model for shelves, coasts, and estuaries. Report 1: Theory and methodology of ADCIRC-2DDI and ADCIRC-3DL
| AD-A261608 | p 2790 N93-26164
Active stabilization of aeromechanical systems
| AD-A261366 | p 2595 N93-26335

FLOW VELOCITY
Ultrasonic rate measurement of multiphase flow
| DE93-000112 | p 2695 N93-24954
The interaction of modulated vortex pairs with a free surface p 2701 N93-25485

Studies of several small seawater MHD thrusters using the high-field solenoid of MIT's Bitter Magnet Laboratory
| AD-A260645 | p 2860 N93-25641
Experiments on the physics of turbulent mixing in stably stratified ocean layers
| AD-A261312 | p 2790 N93-26298

FLOW VISUALIZATION
Flow visualizations of perpendicular blade vortex interactions
| NASA-CR-192725 | p 2696 N93-25208
Scientific visualization using the Flow Analysis Software Toolkit (FAST) p 2814 N93-25600
An investigation of photothermal velocimetry for application to transient, high-speed gas flows p 2579 N93-25720
Image correlation velocimetry
| AD-A261599 | p 2707 N93-26163

FLOWMETERS
Ultrasonic rate measurement of multiphase flow
| DE93-000112 | p 2695 N93-24954
Flow conditioner location effects in orifice flowmeters
| PB93-159457 | p 2708 N93-26535

FLUE GASES
An experimental study of particle-laden jet interactions with cocurrent flows p 2701 N93-25534
Treatment of hazardous organic wastes using silent discharge plasmas
| DE93-003789 | p 2768 N93-26592

FLUID DYNAMICS
Combining particles and waves for fluid animation p 2699 N93-25348
Scientific visualization using the Flow Analysis Software Toolkit (FAST) p 2814 N93-25600
Fundamental studies of droplet interactions in dense sprays
| AD-A261165 | p 2661 N93-25948
Conceptual design for the Space Station Freedom fluid physics/dynamics facility
| NASA-TM-103663 | p 2618 N93-26209

FLUID FLOW
Ultrasonic rate measurement of multiphase flow
| DE93-000112 | p 2695 N93-24954
Grid sensitivity for aerodynamic optimization and flow analysis
| NASA-CR-192980 | p 2575 N93-25117
Studies of the analyte-carrier interface in flow injection analysis
| DE93-008374 | p 2644 N93-25311
Combining particles and waves for fluid animation p 2699 N93-25348
Advanced engineering analysis
| KCP-613-4967 | p 2669 N93-26212

FLUID INJECTION
Shock tube application to the study of compressible turbulent boundary layer with mass injection p 2697 N93-25252
Studies of the analyte-carrier interface in flow injection analysis
| DE93-008374 | p 2644 N93-25311

FLUID JETS
The steady Navier-Stokes problem for low Reynolds number viscous jets p 2698 N93-25264
Liquid surface breakup of nonturbulent and turbulent liquids p 2700 N93-25473
The instability of a liquid jet in a compressible airstream p 2703 N93-25560

FLUID MECHANICS
Development and application of computational aerothermodynamics flowfield computer codes
| NASA-CR-192940 | p 2574 N93-24736
Current research activities: Applied and numerical mathematics, fluid mechanics, experiments in transition and turbulence and aerodynamics, and computer science
| NASA-CR-191408 | p 2803 N93-25084

FLUID TRANSMISSION LINES
Dynamic modeling of fluid transmission lines of the DSN 70-meter antennas by using a lumped parameter model p 2678 N93-26119

FLUORESCENCE
Actual limits of fluorescence S/N ratio in an optically-pumped cesium beam resonator p 2833 N93-24991
Development of a cone penetrometer for measuring spectral characteristics of soils in situ p 2776 N93-25570
Experimental studies of stress management by optical fluorescence
| AD-A261539 | p 2730 N93-26362
In-process cure monitoring of composites via fiber-optic fluorescence
| AD-A261712 | p 2641 N93-26580

FLUOROHYDROCARBONS
An investigation of the degradation of Fluorinated Ethylene Propylene (FEP) copolymer thermal blanketing materials aboard LDEF in the laboratory
| NASA-CR-192824 | p 2653 N93-25078
The acute inhalation toxicity of pyrolysis products of halon 1301
| AD-A260874 | p 2795 N93-25629

FLUOROPOLYMERS
Determination of the thermal stability of perfluoropolyalkyl ethers by tensimetry
| NASA-TM-106081 | p 2654 N93-25093

FLUTTER
ASTROS-ID: Software for system identification using mathematical programming
| AD-A260867 | p 2810 N93-25627

FLUX DENSITY
Surface discharge photoinitiation of pulsed chemical lasers
| DE93-006337 | p 2712 N93-24967
An outgoing energy flux boundary condition for finite difference ICRP antenna models
| DE93-007788 | p 2674 N93-25300
Local and regional estimates of sensible and latent heat flux densities from a patch-work surface
| ISBN-0-315-70882-4 | p 2772 N93-25556
Variable-speed generators with flux weakening p 2694 N93-25599

FLUX PINNING
Studying the kinetics of magnetization in high Tc superconductors
| NASA-CR-192916 | p 2862 N93-25108

FLUX VECTOR SPLITTING
An extended Lagrangian method
| NASA-TM-106129 | p 2707 N93-26203

FOCUSING
Feasibility experiment for sodium-layer laser guide stars at the Lawrence Livermore National Laboratory
| DE93-007115 | p 2715 N93-26503

FORBIDDEN TRANSITIONS
Theoretical treatment of spin-forbidden and electronically nonadiabatic processes. Methods and applications
| AD-A261596 | p 2851 N93-26525

FORCED VIBRATION
Helicopter forced response vibration analysis method RTVIB20
| AD-A261809 | p 2597 N93-26260

FORECASTING
Use of the 1991 ASCOT field study data in a mesoscale model employing a four-dimensional data assimilation technique
| DE93-002683 | p 2769 N93-24672
Nonlinear techniques for forecasting solar activity directly from its time series p 2603 N93-24716
Supporting the Portuguese fisheries with satellites p 2745 N93-24821
Assessment and forecasting of crop yield in Niger through NOAA NDVI data p 2750 N93-24851
Anomalous bioelectric potentials of silk trees in Naples zoo (Italy) prior to an earthquake in May, 1991 p 2753 N93-24873

FOREST FIRES
A prototype system for forest fire prevention and control p 2749 N93-24844

FOREST MANAGEMENT
Potential operational use of remote sensing from space in forestry p 2745 N93-24817
The national parks of Bavarian Forest and Sumava: A Landsat TM perspective on the structure and dynamics of the largest woodland of Central Europe p 2748 N93-24837
Application of photographic remote sensing data from space for information about forests p 2748 N93-24838
The ESA ISY initiatives for forest inventory in Europe p 2748 N93-24840
Assessment of storm damage in forests using SPOT imagery p 2748 N93-24842
The use of polarimetric radar remote sensing data for application in forestry p 2749 N93-24845
Forest decline monitoring using Landsat TM, digital stand data and DEMs p 2749 N93-24846
Swedish forest information atlas p 2749 N93-24847
Observation of forest damages in the Harz mountains by means of satellite remote sensing p 2749 N93-24848
Appliction of remote sensing to forestry mapping: Experience from the European collaborative programme for the less favoured areas p 2751 N93-24857
Atmospheric correction of Landsat/TM data over mountainous terrain for forestry applications p 2752 N93-24862
Standwise forest inventory and mapping for operational management planning p 2752 N93-24863

FORESTS
The extent and status of mangroves in Mombasa district, Kenya: A case study based on remote sensing p 2746 N93-24826
Forest damage detection and reflection of conifers: From micro to field level p 2752 N93-24864
Scale dependence in the reflectance of deciduous woodland: Evidence from a helicopter-mounted spectroradiometer p 2752 N93-24865
Response and feedbacks of forest ecosystems to global climate change
| PB93-167252 | p 2767 N93-26510

FORMALISM
How far we are from the complete knowledge: Complexity of knowledge acquisition in Dempster-Shafer approach
| NASA-CR-192944 | p 2874 N93-25139
Monte-Carlo methods make Dempster-Shafer formalism feasible
| NASA-CR-192945 | p 2828 N93-25140
Neural networks: What non-linearity to choose
| NASA-CR-192948 | p 2819 N93-25197

FORMING TECHNIQUES
INEL spray-forming research p 2658 N93-25562
Advanced engineering analysis
| KCP-613-4967 | p 2669 N93-26212

FORTRAN
FORTRAN M as a language for building earth system models
| DE93-007897 | p 2763 N93-25370
Deterministic parallel FORTRAN
| DE93-008665 | p 2816 N93-25522
EnviroNET p 2886 N93-26398
NSWC library of mathematics subroutines
| AD-A261511 | p 2884 N93-26575

FOURIER ANALYSIS
A frequency generating source: Frequency synthesizers p 2693 N93-25041

FOURIER TRANSFORMATION
Stress and reliability analyses of multilayered composite cylinder under thermal and mechanical loads p 2726 N93-25533
Implementation of cyclic spectral analysis methods
| AD-A261715 | p 2681 N93-26372

FRACTALS
Fractal determination of parameters in lightning and ESD model p 2686 N93-24893
Detecting the scale and resolution effects in remote sensing and GIS p 2756 N93-25707
From fractals to wormholes via string theory p 2871 N93-25742
The rapid solution of the Laplace equation on regions with fractal boundaries
| AD-A260585 | p 2828 N93-25905
Fractal image compression: A resolution independent representation for imagery p 2804 N93-25927

FRACTOGRAPHY
Defect initiation/growth and energy dissipation induced by deformation and fracture
| AD-A261703 | p 2869 N93-26385

FRACTURE MECHANICS
Analysis of matrix damage in unidirectional composites p 2634 N93-25338
Numerical investigations on fracture behavior of ductile materials p 2725 N93-25411
Internal strain analysis of ceramics using scanning laser acoustic microscopy
| NASA-CR-191118 | p 2721 N93-25451
Reliable stress and fracture mechanics analysis of complex aircraft components using a h-p version of FEM
| AD-A260628 | p 2726 N93-25638
Low-velocity impact of composite sandwich plate p 2637 N93-25695
Development and application of an advanced ductile fracture mechanics methodology p 2727 N93-25718
Approximate analysis on strain rate effects and behavior of stress and strain fields at the crack tip in Mode 2 in metallic materials, appendix no. 1
| AD-A260836 | p 2728 N93-25785
Micromechanics of fatigue
| AD-A260577 | p 2729 N93-25901
Fatigue in single crystal nickel superalloys
| AD-A261742 | p 2652 N93-26282
Failure considerations in composite systems based on 3D micromechanical stress fields, part A
| AD-A261698 | p 2641 N93-26382
Defect initiation/growth and energy dissipation induced by deformation and fracture
| AD-A261703 | p 2869 N93-26385
J and CTOD estimation equations for shallow cracks in single edge notch bend specimens
| AD-A261679 | p 2731 N93-26390
Use and analysis of finite element methods for problems of solid mechanics and fracture
| AD-A261574 | p 2731 N93-26522

FRACTURE STRENGTH
Processing and mechanical properties of laminated metal composites of Al/Al-25 vol. percent SiC and ultrahigh carbon steel/brass
| DE93-007504 | p 2635 N93-25383
High temperature fracture toughness of Ni3Al alloy IC-396M
| DE93-008564 | p 2650 N93-25492
Continuum and micromechanics treatment of constraint in fracture
| AD-A260927 | p 2727 N93-25647
Development and application of an advanced ductile fracture mechanics methodology p 2727 N93-25718
Models of crack growth along polymer interfaces p 2728 N93-25750
Approximate analysis on strain rate effects and behavior of stress and strain fields at the crack tip in Mode 2 in metallic materials, appendix no. 1
| AD-A260836 | p 2728 N93-25785
Deformation mechanisms of NiAl cyclicly deformed near the brittle-to-ductile transition temperature
| NASA-CR-191121 | p 2652 N93-26235
Effects of moisture and other contaminants in friction composites
| AD-A261226 | p 2640 N93-26301
Improved fatigue life for moorings
| PB93-161198 | p 2730 N93-26320
J and CTOD estimation equations for shallow cracks in single edge notch bend specimens
| AD-A261679 | p 2731 N93-26390
Approximate techniques for predicting size effects on cleavage fracture toughness (J(sub c))
| AD-A261591 | p 2731 N93-26516
FRACTURES (MATERIALS)
Three-dimensional analysis and verification of fracture growth mechanisms in fiber-reinforced ceramic composites
| AD-A261483 | p 2641 N93-26355
FRACTURING
Fracture of an elliptical inclusion and its implications for the properties of short fiber composites p 2634 N93-25333
Three-dimensional boundary element analysis of contact and fracture problems p 2725 N93-25335
Room temperature fracture of FeCo
| DE93-008266 | p 2650 N93-25519
Continuum and micromechanics treatment of constraint in fracture
| AD-A260927 | p 2727 N93-25647
Development and application of an advanced ductile fracture mechanics methodology p 2727 N93-25718
Crack tip fields in ductile crystals and bicrystals p 2866 N93-25749
Transformation plasticity and fracture behavior of ceria-TZP/alumina composites p 2638 N93-25760
Three-dimensional analysis and verification of fracture growth mechanisms in fiber-reinforced ceramic composites
| AD-A261483 | p 2641 N93-26355
Defect initiation/growth and energy dissipation induced by deformation and fracture
| AD-A261703 | p 2869 N93-26385
FRAGMENTATION
Detection of fragments arising from greater than 10 GeV electron-nucleus collisions
| DE93-007725 | p 2848 N93-25366
Photoexcitation of carbon fullerenes
| AD-A260739 | p 2849 N93-25644
FRAGMENTS
Detection of fragments arising from greater than 10 GeV electron-nucleus collisions
| DE93-007725 | p 2848 N93-25366
FREE ELECTRON LASERS
Particle simulation for 10.6 micron picosecond laser-induced breakdown in gases p 2712 N93-25280
Electron-beam-pumped recombination lasers p 2712 N93-25344
Laser field assisted photoemission using femtosecond laser pulses
| DE93-007277 | p 2712 N93-25378
FREE ENERGY
Phase-field models for anisotropic interfaces
| PB93-164564 | p 2646 N93-26323
FREE JETS
Energy transfer properties and mechanisms
| DE93-008540 | p 2849 N93-25488
FREE VIBRATION
Vibration, buckling, and postbuckling of laminated composites with delaminations p 2723 N93-24765
FREQUENCIES
Occultation of a compact radio source by Venus p 2676 N93-26107
Pseudo Wigner-Ville distribution, computer program, and its applications to time-frequency domain problems
| AD-A261839 | p 2813 N93-26431
FREQUENCY CONTROL
Experimental results of the performance of the new phase and frequency controller p 2839 N93-25035
Controlling an optical frequency by a single ion p 2841 N93-25051
FREQUENCY CONVERTERS
Frequency generation and synthesis in the DRSS p 2693 N93-25054
FREQUENCY DISCRIMINATORS
Microwave frequency discriminator with a cryogenic sapphire resonator for ultra-low phase noise p 2693 N93-24982
A compact and high-performance reference cell for laser frequency stabilization p 2716 N93-25065
FREQUENCY DISTRIBUTION
Time and frequency reference for a trajectory measurement system p 2837 N93-25023
Inverse sequential procedures for the monitoring of time series
| NASA-CR-192959 | p 2765 N93-25666
Rainfall frequency atlas of the Midwest
| PB93-164606 | p 2785 N93-25872
FREQUENCY MEASUREMENT
Hydrogen masers for space p 2716 N93-24980
The measurement of the resonant frequency of quartz crystal units: An ongoing saga p 2833 N93-24996
The accuracy of SYLT- and RNS-based time scales at MTI and SNT during 1990-1991 p 2835 N93-25006
Dedicated oscillator for immersed crystal sensor p 2837 N93-25020
Time stability: An improvement of the multi-variance method for the oscillator noise analysis p 2839 N93-25036
Very wide bandwidth HF crystal filters p 2693 N93-25039
Investigations of the frequency instability of CH1-75 hydrogen masers p 2716 N93-25049
Designing for frequency and time metrology at the 10 to the minus 18 power level p 2842 N93-25059
Time generation and distribution system for a military national synchronization p 2842 N93-25060
Progress towards laboratory frequency standards for the optical communication bands p 2687 N93-25069
FREQUENCY MODULATION
High resolution digital synthesizer for a Rb frequency standard p 2694 N93-25057
FREQUENCY MULTIPLIERS
Theoretical and experimental investigation of electron beam acceleration and sub-millimeter wave generation
| AD-A261117 | p 2609 N93-25770
FREQUENCY RANGES
An aeroelastic model structure investigation for a manned real-time rotorcraft simulation p 2574 N93-24756
The design of a modular sound absorber for very low frequencies
| BBC-RD-1992/10 | p 2673 N93-25170
Pyroshock: Bibliography
| DE93-007605 | p 2726 N93-25489
Microwave absorption measurements and interference: Effects for a liquid fuel between 2.5 and 18 GHz
| AD-A260607 | p 2675 N93-25635
FREQUENCY RESPONSE
Stability of nonlinear phase motion from the study of oscillator mappings p 2693 N93-25034
Low-frequency room responses. Part 1: Background and qualitative considerations
| BBC-RD-1992/8-PT-1 | p 2673 N93-25168
Low-frequency room responses. Part 2: Calculation methods and experimental results
| BBC-RD-1992/9-PT-2 | p 2673 N93-25169
Flame response in oscillatory solid propellant combustion p 2630 N93-26041
FREQUENCY SHIFT
Preliminary results on an optically-pumped Cs beam frequency standard p 2832 N93-24989
Space radiation susceptibility of ultra stable crystal oscillators p 2693 N93-25053
Line inhomogeneity effects and power shift in miniaturized rubidium frequency standards p 2694 N93-25066
Frequency diversity sidelobe canceller
| AD-D015647 | p 2674 N93-25332
Trellis coded CPFSK
| AD-A261788 | p 2682 N93-26441
FREQUENCY SHIFT KEYING
An introduction to Doppler effect and fading in mobile communications
| AD-A260976 | p 2676 N93-25866
Trellis coded CPFSK
| AD-A261788 | p 2682 N93-26441
FREQUENCY STABILITY
Frequency and Time Forum
| ESA-SP-340 | p 2831 N93-24978
Hydrogen masers for space p 2716 N93-24980
Preliminary results on an optically-pumped Cs beam frequency standard p 2832 N93-24989
Miniature optically-pumped cesium beam resonator p 2833 N93-24990
DORIS precise orbit determination and location system performances of ultra stable oscillators p 2608 N93-24997
A microcomputer compensated crystal oscillator MCXO p 2834 N93-25001
OSCCAR: Oscillator-compensated with a capacitance array p 2693 N93-25002
Design of a low phase noise UHF oscillator using a partly metallized dielectric resonator p 2693 N93-25003
Miniaturization and stability: A new generation of ovenised oscillators p 2693 N93-25004
Collaboration in the UK on time transfer using the GLONASS system p 2837 N93-25019
Dedicated oscillator for immersed crystal sensor p 2837 N93-25020
TF-4020A: TFL's new compact military rubidium standard p 2838 N93-25026
Ultra stable oscillators for satellite applications p 2621 N93-25027
Preliminary results of a newly designed mini-OCXO oscillator especially dedicated to space applications p 2621 N93-25028
Experiments on a diode-laser-pumped Rb-87 maser p 2716 N93-25030
Stability of nonlinear phase motion from the study of oscillator mappings p 2693 N93-25034
Time stability: An improvement of the multi-variance method for the oscillator noise analysis p 2839 N93-25036
Microwave synthesizers in space p 2693 N93-25038
Investigations of the frequency instability of CH1-75 hydrogen masers p 2716 N93-25049
Space radiation susceptibility of ultra stable crystal oscillators p 2693 N93-25053
Oscillators for mobile GPS receivers p 2694 N93-25055
Microwave interrogation frequency noise and clock frequency stability: Experimental results p 2842 N93-25056
High resolution digital synthesizer for a Rb frequency standard p 2694 N93-25057
Designing for frequency and time metrology at the 10 to the minus 18 power level p 2842 N93-25059
A compact and high-performance reference cell for laser frequency stabilization p 2716 N93-25065
Performance of a 12-GHz fiber-optic system for beam-waveguide antenna stability testing p 2677 N93-26113
Improvements in X-band transmitter phase stability through Klystron body temperature regulation p 2678 N93-26114
FREQUENCY STANDARDS
Frequency and Time Forum
| ESA-SP-340 | p 2831 N93-24978
The advances in F and T technology: Their benefits of and for space science and technology p 2831 N93-24979
Hydrogen masers for space p 2716 N93-24980
A simple and compact source of cold atoms for cesium fountains and microgravity clocks p 2831 N93-24981
Preliminary results on an optically-pumped Cs beam frequency standard p 2832 N93-24989
Control of environmental and clock parameters in Time and Frequency Standards Laboratory p 2835 N93-25007
Rubidium atomic frequency standards for GPS block 2R p 2836 N93-25014
TF-4020A: TFL's new compact military rubidium standard p 2838 N93-25026
Ultra stable oscillators for satellite applications p 2621 N93-25027
Preliminary results of a newly designed mini-OCXO oscillator especially dedicated to space applications p 2621 N93-25028
Use of the TV-signal in stabilizing a local rubidium oscillator p 2693 N93-25029
Microwave synthesizers in space p 2693 N93-25038
Phase differences of the fields in a Ramsey resonator for submillimetric frequency standards p 2840 N93-25042
Ion trap frequency standard research at PTB p 2841 N93-25050
Quartz oscillators, frequency synthesizers, and timing systems for geodesy and radio science applications p 2693 N93-25052
Microwave interrogation frequency noise and clock frequency stability: Experimental results p 2842 N93-25056
High resolution digital synthesizer for a Rb frequency standard p 2694 N93-25057

Solid state frequency synthesis up to 600 GHz: An application to the Mg frequency standard
p 2842 N93-25058
Designing for frequency and time metrology at the 10 to the minus 18 power level p 2842 N93-25059
Time generation and distribution system for a military national synchronization p 2842 N93-25060
Line inhomogeneity effects and power shift in miniaturized rubidium frequency standards
p 2694 N93-25066
Progress towards laboratory frequency standards for the optical communication bands p 2687 N93-25069

FREQUENCY SYNCHRONIZATION
Hydrogen masers for space p 2716 N93-24980

FREQUENCY SYNTHESIZERS
Selected results from LLNL-Hughes RAR for West Coast Scotland Experiment 1991
| DE93-006972 | p 2788 N93-24960
A microcomputer compensated crystal oscillator MCXO p 2834 N93-25001
Microwave synthesizers in space
p 2693 N93-25038
A frequency generating source: Frequency synthesizers p 2693 N93-25041
Quartz oscillators, frequency synthesizers, and timing systems for geodesy and radio science applications
p 2693 N93-25052
Frequency generation and synthesis in the DRSS
p 2693 N93-25054
High resolution digital synthesizer for a Rb frequency standard p 2694 N93-25057
Solid state frequency synthesis up to 600 GHz: An application to the Mg frequency standard
p 2842 N93-25058

FRICTION
Effects of moisture and other contaminants in friction composites
| AD-A261226 | p 2640 N93-26301

FRICTION FACTOR
Formulation and treatment of frictional contact problems using finite elements p 2717 N93-25412
Modeling of the WSTF frictional heating apparatus in high pressure systems p 2648 N93-26079
Three-dimensional analysis and verification of fracture growth mechanisms in fiber-reinforced ceramic composites
| AD-A261483 | p 2641 N93-26355

FRONTS (METEOROLOGY)
Boundary layer coupling between an explosive cyclone and the Gulf Stream during ERICA
| AD-A261577 | p 2787 N93-26513

FROSTBITE
Cellular and tissue injury during nonfreezing cold injury and frostbite
| AD-A260574 | p 2795 N93-25900

FUEL CELLS
DC-DC power converter research for Orbiter/Station power exchange
| NASA-CR-192939 | p 2633 N93-26425

FUEL COMBUSTION
A procedure for defining lightning risk to air vehicles
p 2583 N93-24885
Parameters influencing the hot-spot ignition of aviation fuel/air and ethylene/air mixtures p 2583 N93-24886
Fuel Injector: Air swirl characterization aerothermal modeling, phase 2, volume 2
| NASA-CR-189193 | p 2592 N93-25106
Emissions from ethanol and LPG fueled vehicles
| DE93-006410 | p 2660 N93-25192
The structure of particle cloud premixed flames
| NASA-CR-192827 | p 2643 N93-25229
Solid fuel supersonic combustion
p 2625 N93-26010
Hybrid rocket fuel combustion study
p 2626 N93-26019
Military standardization handbook: Aircraft refueling handbook
| AD-A261755 | p 2662 N93-26600
Atomization and combustion of a gelled, metallized slurry fuel
| AD-A261778 | p 2647 N93-26602

FUEL CONTAMINATION
Effect of a metal deactivator fuel additive on fuel deposition in fuel atomizers at high temperature
| AD-A260915 | p 2661 N93-25914

FUEL CONTROL
A neural network-based estimator for the mixture ratio of the Space Shuttle Main Engine
| NASA-TM-106070 | p 2622 N93-25089

FUEL INJECTION
Fuel injector: Air swirl characterization aerothermal modeling, phase 2, volume 1
| NASA-CR-189193 | p 2592 N93-24754
A summary of the JANNAF workshop on liquid rocket atomization p 2625 N93-26014
Space transportation booster engine thrust chamber technology, large scale injector
| NASA-CR-192531 | p 2633 N93-26557

FUEL PRODUCTION
Near Earth object fuels (neo-fuels): Discovery, prospecting and use
| DE93-005185 | p 2892 N93-25164

FUEL SPRAYS
Fuel Injector: Air swirl characterization aerothermal modeling, phase 2, volume 2
| NASA-CR-189193 | p 2592 N93-25106
Atomizing-gas temperature effect on cryogenic spray dropsize
| NASA-TM-106106 | p 2709 N93-25191
The structure of particle cloud premixed flames
| NASA-CR-192827 | p 2643 N93-25229
Fundamental studies of droplet interactions in dense sprays
| AD-A261165 | p 2661 N93-25948

FUEL SYSTEMS
Cost-effectiveness analysis of TxDOT CNG fleet conversion, volume 2
| PB93-159432 | p 2720 N93-26534

FUELS
Development of a method to determine the autoxidation of turbine fuels
| AD-A260578 | p 2661 N93-25902
Particle size as a factor in agglomeration in slurry fuels p 2625 N93-26013

FULL SCALE TESTS
Narrow-body aircraft water spray optimization study
| DOT/FAA/CT-TN93/3 | p 2582 N93-25224

FULLERENES
Photomodulation spectroscopy of photocarrier dynamics, electronic defects and morphology of conducting polymers
| DE93-010140 | p 2655 N93-25524
Photoexcitation of carbon fullerenes
| AD-A260739 | p 2849 N93-25644
Transition metal chelate-fulleride compounds: Electrocrystallization of semiconducting (Ru(bpy)s)(C60)2
| AD-A261549 | p 2869 N93-26577

FUMES
A new method for infrared imaging of air currents in and around critical hazard fume hoods
| DE93-003009 | p 2761 N93-24956

FUNCTION GENERATORS
Walsh function generator for the Electronically Scanned Thinned Array Radiometer (ESTAR) instrument
| NASA-TM-4449 | p 2689 N93-25618

FUNCTIONAL ANALYSIS
Functional Economic Analysis Guidebook, version 1.1
| AD-A261390 | p 2886 N93-26305

FUNCTIONAL DESIGN SPECIFICATIONS
Gas-Grain Simulation Facility (GGSF). Volume 1: Stage 1 facility definition studies
| NASA-CR-177606 | p 2887 N93-25442
Determination of burn rate requirements from ASRM performance specifications p 2627 N93-26023
Human computer interface style guide, version 2.0
| AD-A261280 | p 2807 N93-26291

FUNCTIONS (MATHEMATICS)
Attitude determination using vector observations: A fast optimal matrix algorithm p 2606 N93-24731
NSWC library of mathematics subroutines
| AD-A261511 | p 2884 N93-26575

FUSELAGES
Alternative equipment test procedures for simultaneous current injection on multiple cable bundles
p 2693 N93-24903
Tangential fuselage blowing on an ogive cylinder
p 2578 N93-25545
Design and analysis of curved composite components for rotorcraft fuselage frames p 2589 N93-25701

FUZZY SETS
How to control if even experts are not sure: Robust fuzzy control
| NASA-TM-108745 | p 2818 N93-25142

FUZZY SYSTEMS
Probabilistic analysis of manipulation tasks: A research agenda
| DE93-000713 | p 2827 N93-25103
Using fuzzy behaviors for the outdoor navigation of a car with low-resolution sensors
| DE93-002428 | p 2584 N93-25120
How to combine probabilistic and fuzzy uncertainties in fuzzy control
| NASA-TM-108746 | p 2818 N93-25138
Maximum entropy approach to fuzzy control
| NASA-CR-192949 | p 2818 N93-25141
Fast parallel algorithms that compute transitive closure of a fuzzy relation
| NASA-CR-192950 | p 2818 N93-25190
Use of fuzzy relational information retrieval technique for generating control strategies in resolution-based automated reasoning p 2874 N93-25258
Strongly transitive fuzzy relations: A more adequate way to describe similarity
| NASA-CR-192951 | p 2820 N93-25425
What procedure to choose while designing a fuzzy control? Towards mathematical foundations of fuzzy control
| NASA-TM-108719 | p 2820 N93-25459
Adaptive process control with fuzzy logic and genetic algorithms p 2827 N93-25612

G

GALACTIC COSMIC RAYS
Analysis of reentry into the White Sands Missile Range (WSMR) for the LifeSat mission p 2603 N93-24717

GALACTIC EVOLUTION
Optical and infrared studies of distant galaxies
p 2890 N93-25712
The physical properties of low surface brightness galaxies p 2895 N93-25832

GALACTIC ROTATION
Prograde anomalous orbits in triaxial gravitational potentials that rotate about the long axis: VLA neutral hydrogen observations and modeling of the inclined rings around the galaxies NGC 2685 and NGC 660
p 2607 N93-25396

GALACTIC STRUCTURE
Prograde anomalous orbits in triaxial gravitational potentials that rotate about the long axis: VLA neutral hydrogen observations and modeling of the inclined rings around the galaxies NGC 2685 and NGC 660
p 2607 N93-25396
Numerical modeling of barred spiral galaxies
p 2893 N93-25537
The physical properties of low surface brightness galaxies p 2895 N93-25832

GALAXIES
The structure of the nearby universe traced by theIRAS galaxies
| NASA-CR-192809 | p 2889 N93-25331
Tully-Fisher distances and motions in the northern sky
p 2889 N93-25621
Optical and infrared studies of distant galaxies
p 2890 N93-25712
The physical properties of low surface brightness galaxies p 2895 N93-25832

GALERKIN METHOD
Stabilized finite element methods for incompressible flows with emphasis on moving boundaries and interfaces p 2703 N93-25663

GALILEO SPACECRAFT
Galileo early cruise, including Venus, First Earth, and Gaspra encounters p 2599 N93-26125

GALLIUM ARSENIDES
A high performance room-temperature near-infrared camera
| AD-A260602 | p 2709 N93-25634
Transmission electron microscopy investigation of ion implantation damage in GaAs and other semiconductors
p 2865 N93-25715
Time resolved studies of in-well and cross-well carrier transport in MQW semiconductor structures
| AD-A261170 | p 2714 N93-25774
MOCVD process technology for affordable, high-yield, high-performance MESFET structures. Phase 3: MIMIC
| AD-A261178 | p 2690 N93-25820
Short-period superlattice materials for heterojunction bipolar transistors
| AD-A260701 | p 2866 N93-25897
Fundamental and applied aspects of defect engineering in GaAs
| AD-A260573 | p 2867 N93-25899
Analysis of transient photoluminescence measurements on GaAs and AlGaAs double heterostructures
| AD-A261154 | p 2867 N93-25947

GALLIUM COMPOUNDS
Comparison of energy trapping resonators and filters using the AT cut of quartz, berlinite and gallium phosphate p 2836 N93-25013

GALLIUM PHOSPHIDES
Transmission electron microscopy investigation of ion implantation damage in GaAs and other semiconductors
p 2865 N93-25715

GAMMA RAY ASTRONOMY
Interferometric fiber-optic radiation sensor
| DE93-003841 | p 2852 N93-25127
Correlative studies of astrophysical sources of very high and ultra high energy gamma-rays
| NASA-CR-192781 | p 2888 N93-25172

GAMMA RAY BURSTS
Gravitational lensing and gamma ray bursts
p 2900 N93-25828

GAMMA RAY OBSERVATORY
The results of the in-flight attitude sensor calibration for the Arthur Holly Compton Gamma Ray Observatory p 2600 N93-24697
Real-time attitude determination and gyro calibration p 2602 N93-24708
STS-37 Space Shuttle mission report
|NASA-CR-193062| p 2612 N93-25956
GAMMA RAY SPECTROMETERS
Feasibility study of a long duration balloon flight with NASA/GSFC and Soviet Space Agency Gamma Ray Spectrometers
|NASA-CR-192934| p 2573 N93-25077
Neutron energy determination with a high-purity germanium detector
|NASA-CR-192773| p 2900 N93-25890
GAMMA RAYS
Long term drift and gamma-irradiation effect p 2833 N93-24992
Correlative studies of astrophysical sources of very high and ultra high energy gamma-rays
|NASA-CR-192781| p 2888 N93-25172
Radiation-hardened control system
|DE93-007248| p 2688 N93-25377
Inelastic scattering in condensed matter with high intensity Moessbauer radiation
|DE93-008763| p 2864 N93-25503
Environmental test program for superconducting materials and devices
|DE93-003646| p 2864 N93-25506
GANTRY CRANES
Digital filter control of remotely operated flexible robotic structures
|DE93-007587| p 2827 N93-26596
GAS ANALYSIS
Redistribution of trace chemical species by a small convective cloud
|PB93-156164| p 2765 N93-25873
GAS ATOMIZATION
Atomizing-gas temperature effect on cryogenic spray dropsize
|NASA-TM-106106| p 2709 N93-25191
GAS DETECTORS
Elastic plate mode sensitivities to mass loading applications to gas sensors p 2711 N93-25009
Tank issues: Design and placement of vapor monitoring wells
|PB93-161131| p 2768 N93-26536
GAS DYNAMICS
Generic hypersonic vehicle performance model
|NASA-CR-192953| p 2587 N93-25162
Supersonic shock wave/vortex interaction
|NASA-CR-192917| p 2576 N93-25249
JPRS report: Science and technology. Central Eurasia: Physics and mathematics
|JPRS-UPM-92-004| p 2844 N93-25402
GAS FLOW
A new method for infrared imaging of air currents in and around critical hazard fume hoods
|DE93-003009| p 2761 N93-24956
Predictive modeling of particle-laden, turbulent flows
|DE93-008208| p 2698 N93-25309
Mechanistic studies of the CVD of silicon nitride from SiF4 and NH3
|DE93-004500| p 2644 N93-25312
An experimental study of particle-laden jet interactions with cocurrent flows p 2701 N93-25534
The instability of a liquid jet in a compressible airstream p 2703 N93-25560
Instrumentation for measurement of gas permeability of polymeric membranes p 2720 N93-25609
An investigation of photothermal velocimetry for application to transient, high-speed gas flows p 2579 N93-25720
A basic research model of natural gas combustion in turbulent flow, phase 2
|PB93-158509| p 2644 N93-25819
SRB environment evaluation and analysis. Volume 2: RSRB joint filling test/analysis improvements
|NASA-CR-192518| p 2631 N93-26057
Flow conditioner location effects in orifice flowmeters
|PB93-159457| p 2708 N93-26535
GAS INJECTION
Experimental and computational investigation of helium injection into air at supersonic and hypersonic speeds p 2577 N93-25487
Workshop Report: A validation study of Navier-Stokes codes for transverse injection into a Mach 2 flow p 2624 N93-26008
Oxides of nitrogen emissions from turbulent hydrocarbon/air jet diffusion flames, phase 2
|PB93-152478| p 2768 N93-26533
GAS IONIZATION
Optical detection of laser-cooled ions in a Penning trap p 2838 N93-25031
GAS JETS
Atomizing-gas temperature effect on cryogenic spray dropsize
|NASA-TM-106106| p 2709 N93-25191
Experimental and computational investigation of helium injection into air at supersonic and hypersonic speeds p 2577 N93-25487
Gasp 1.3 results for the transverse hydrogen reacting jet p 2625 N93-26011
GAS LASERS
FALCON nuclear-reactor-pumped laser program and wireless power transmission
|DE93-007607| p 2715 N93-26597
GAS MIXTURES
The structure of particle cloud premixed flames
|NASA-CR-192827| p 2643 N93-25229
Development and use of hydrogen-air torches in an altitude facility
|NASA-TM-106047| p 2598 N93-26214
Thermodynamic properties of natural gas mixtures
|PB93-167112| p 2872 N93-26509
Thermodynamic properties of natural gas mixtures
|PB93-156818| p 2872 N93-26558
GAS PRESSURE
Modified point mass trajectory simulation for base-burn projectiles
|BRL-TR-3321| p 2609 N93-25985
Densification of ceramics by gas overpressure sintering
|MTL-TR-92-45| p 2657 N93-26432
GAS TEMPERATURE
A premixed laminar flame interacting with a vortex resulting in flame stretch and quenching p 2642 N93-24771
An evaluation of thermal energy storage options for precooling gas turbine inlet air
|DE93-005980| p 2758 N93-24975
GAS TURBINE ENGINES
A three-dimensional algebraic grid generation scheme for gas turbine combustors with inclined slots
|NASA-CR-191095| p 2694 N93-24759
Screening studies of advanced control concepts for airbreathing engines
|NASA-TM-106042| p 2592 N93-25079
JPRS report: Science and technology. Central Eurasia: Engineering and equipment
|JPRS-UEQ-92-003| p 2668 N93-25427
Gas turbine system simulation: An object-oriented approach
|NASA-TM-106044| p 2593 N93-25673
Simulation of aircraft gas turbine engine p 2594 N93-25751
Active stabilization of aeromechanical systems
|AD-A261366| p 2595 N93-26335
Particulate emissions from gas turbine engines
|AD-A261374| p 2595 N93-26339
Advanced bristle seals for gas turbine engines
|AD-A261296| p 2720 N93-26564
GAS TURBINES
An evaluation of thermal energy storage options for precooling gas turbine inlet air
|DE93-005980| p 2758 N93-24975
Flow and heat transfer experiments in the turbine airfoil/endwall region p 2704 N93-25725
Radial inflow turbine study
|AD-A260767| p 2594 N93-25917
Fatigue in single crystal nickel superalloys
|AD-A261742| p 2652 N93-26282
GAS-SOLID INTERACTIONS
Condensation on cooled surfaces of optical devices at the cosmic conditions p 2753 N93-24869
Gas-Grain Simulation Facility (GGSF). Volume 1: Stage 1 facility definition studies
|NASA-CR-177606| p 2887 N93-25442
Dynamics of gas-surface interactions
|AD-A261402| p 2646 N93-26402
GASEOUS DIFFUSION
Recommendations for a Kalman filter to estimate and control freeze and sublime rates of gaseous diffusion plant freezer/sublimer systems
|ORNL/TM-12183| p 2668 N93-25937
GASEOUS FUELS
The structure of particle cloud premixed flames
|NASA-CR-192827| p 2643 N93-25229
GASES
Instrumentation for measurement of gas permeability of polymeric membranes p 2720 N93-25609
GASOLINE
Emissions from ethanol and LPG fueled vehicles
|DE93-006410| p 2660 N93-25192
GATES (CIRCUITS)
Splash 2 p 2814 N93-25575
Walsh function generator for the Electronically Scanned Thinned Array Radiometer (ESTAR) instrument
|NASA-TM-4449| p 2689 N93-25618
RF vacuum microelectronics
|AD-A261343| p 2691 N93-26311
GEAR TEETH
Evaluation of a vibration diagnostic system for the detection of spur gear pitting failures
|NASA-TM-106103| p 2718 N93-25672
Computational gearing mechanics
|NASA-CR-191127| p 2719 N93-25884
GEARS
Global dynamic modeling of a transmission system
|NASA-CR-191117| p 2716 N93-24751
Computational gearing mechanics
|NASA-CR-191127| p 2719 N93-25884
GELLED PROPELLANTS
Atomization and combustion of a gelled, metallized slurry fuel
|AD-A261778| p 2647 N93-26602
GELS
Algal blooms and gel production in Adriatic Sea observed by remote sensing techniques p 2747 N93-24831
Development of resonance ionization spectroscopy for genome mapping and DNA sequencing using stable isotopes as DNA labels
|DE93-007815| p 2793 N93-26587
GENERAL AVIATION AIRCRAFT
General aviation aircraft: Normal acceleration data analysis and collection project
|DOT/FAA/CT-91/20| p 2586 N93-24739
Lightning data acquisition p 2778 N93-24883
GENETIC ALGORITHMS
Algorithms for optimal redundancy allocation
|DE93-005709| p 2827 N93-24973
Adaptive process control with fuzzy logic and genetic algorithms p 2827 N93-25612
A genetic algorithm tool (splicer) for complex scheduling problems and the Space Station Freedom resupply problem p 2814 N93-25613
GENETIC CODE
Development of resonance ionization spectroscopy for genome mapping and DNA sequencing using stable isotopes as DNA labels
|DE93-007815| p 2793 N93-26587
GENETICS
A genetic algorithm tool (splicer) for complex scheduling problems and the Space Station Freedom resupply problem p 2814 N93-25613
Primary events in olfactory reception
|AD-A260562| p 2795 N93-25944
Planetary Biology and Microbial Ecology: Molecular Ecology and the Global Nitrogen cycle
|NASA-CR-4497| p 2803 N93-26157
Development of resonance ionization spectroscopy for genome mapping and DNA sequencing using stable isotopes as DNA labels
|DE93-007815| p 2793 N93-26587
GEOBOTANY
Integrating satellite imagery and digital elevation data for geobotanical mapping in Quetico Provincial Park, Ontario, Canada p 2754 N93-25430
GEOCHEMISTRY
Complex investigation of a system industrial site-environment using remote sensing and landscape-geochemical methods p 2741 N93-24798
The JGOFS North Atlantic Bloom Experiment: An overview p 2735 N93-24934
Ocean time-series near Bermuda: Hydrostation S and the US JGOFS Bermuda Atlantic time-series study p 2736 N93-24938
Aquifer thermal energy (heat and chill) storage
|DE93-006446| p 2759 N93-25183
Geochemistry and petrology of primitive achondrite meteorites LEW 88280, MAC 88177, ALHA 81187, EET 84302, and LEW 88663 p 2896 N93-26067
GEODESY
Repair, evaluation, maintenance, and rehabilitation research program. Continuous Deformation Monitoring System (CDMS)
|AD-A261833| p 2586 N93-26274
GEODETIC SATELLITES
A system design for laser time synchronization via geodetic satellite Ajisai p 2716 N93-25005
GEODETIC SURVEYS
Intraplate deformation, stress in the lithosphere and the driving mechanism for plate motions
|NASA-CR-192782| p 2772 N93-25529
GEOGRAPHIC INFORMATION SYSTEMS
Land cover, an essential component of the CORINE information system on the environment: GIS implications p 2740 N93-24787
Detection of land use/land cover changes using remote sensing and GIS in Vietnam p 2740 N93-24791
A knowledge-based approach to waste disposal sites detection through integration of Landsat-TM imagery and geographical context information p 2741 N93-24796

Use of remote sensing and GIS for the environmental planning proposal of the Sarno River Valley (Campania, southern Italy) p 2741 N93-24797
The use of remote sensing and GIS for the assessment of environmental degradation caused by fires, applied upon South-Euboia (central Greece) p 2742 N93-24802
The use of SPOT data in natural disaster prevention and damage assessment p 2743 N93-24811
European applications of space-borne Earth observation for land cover mapping p 2745 N93-24820
Mapping of windfall damage in the Hunsrueck plateau with Landsat TM-data p 2749 N93-24843
Cartography and statistics of crops under irrigation in the Donana area of Andalucia through the use of Landsat-TM imagery and its incorporation into a GIS p 2751 N93-24855
Standwise forest inventory and mapping for operational management planning p 2752 N93-24863
EUROSTARS: A system for thematic analysis of remote sensed data p 2753 N93-24871
Use of the Environmental Resource Management and Analysis System at the Fernald Environmental Management Project
| DE93-002943 | p 2760 N93-24955
Multi-temporal satellite image analysis for crop inventories in the Po River Valley (Italy) p 2755 N93-25434
Commercial applications multispectral sensor system p 2758 N93-25615
Detecting the scale and resolution effects in remote sensing and GIS p 2756 N93-25707
Geographic information system for fusion and analysis of high-resolution remote sensing and ground truth data p 2878 N93-25798
A coastal hazards data base for the US East Coast
| NASA-TM-108265 | p 2791 N93-26586

GEOLOGICAL FAULTS
Low-frequency source parameters of twelve large earthquakes
| NASA-CR-192806 | p 2771 N93-25202

GEOLOGICAL SURVEYS
A geological and geophysical information system for Eurasia
| AD-A261789 | p 2883 N93-26442

GEOLOGY
Satellite remote sensing for environmental geology: The Bandung (West Java) experience p 2739 N93-24784
Geologic and hydrogeologic mapping of Iceland with multisensor data (JERS-1, ERS-1, SPOT, Landsat and SEASAT) p 2740 N93-24792
Remote sensing of non-renewable resources p 2744 N93-24814
Remote sensing geology p 2744 N93-24815
JPRS report: Science and technology. Central Eurasia: Earth sciences
| JPRS-UES-93-001 | p 2599 N93-25400
JPRS report: Science and technology. Central Eurasia: Earth sciences
| JPRS-UES-92-005 | p 2737 N93-25401
Isolation and analysis of key components of seafloor relief
| AD-A261635 | p 2790 N93-26170
A geological and geophysical information system for Eurasia
| AD-A261789 | p 2883 N93-26442
A coastal hazards data base for the US East Coast
| NASA-TM-108265 | p 2791 N93-26586

GEOMAGNETIC TAIL
Magnetotail processes associated with auroral surge formation
| ATR-90(7186)-1 | p 2895 N93-26147

GEOMAGNETISM
SCATHA mission termination report p 2605 N93-24725
A statistical study of field-aligned currents in the Earth's inner magnetosphere p 2773 N93-25709
JARE data reports. No. 171 (upper atmosphere physics 9). Data, Syowa and Asuka Stations, 1989 p 2774 N93-25889
A predicted geomagnetic field model for epoch 1990.0
| AD-A260669 | p 2775 N93-25891
Steady induction effects in geomagnetism. Part 1B: Geomagnetic estimation of steady surficial core motions: A non-linear inverse problem
| NASA-TP-3272-PT-1B | p 2776 N93-26421

GEOMORPHOLOGY
A method for sequential image analysis of hazard areas p 2743 N93-24810
Hypervelocity impact study: The effect of impact angle on crater morphology
| NASA-CR-192711 | p 2724 N93-25260

GEOPHYSICS
Archaeological, historical and geoelectrical data as ground truth for Landsat TM imagery application to coastal plain evolution studies p 2742 N93-24799
The role of the World Data Centers in handling ocean climate data p 2732 N93-24919
Satellite altimetry p 2734 N93-24930
Low-frequency source parameters of twelve large earthquakes
| NASA-CR-192806 | p 2771 N93-25202
A geological and geophysical information system for Eurasia
| AD-A261789 | p 2883 N93-26442
Solar-geophysical data number 581, January 1993. Part 1: (Prompt reports). Data for December, November 1992, and late data
| PB93-161743 | p 2899 N93-26537
Solar-geophysical data number 581, January 1993. Part 2: (Comprehensive reports). Data for July 1992 and miscellaneous
| PB93-161750 | p 2899 N93-26538
Proceedings of the Government Users Workshop on Ground Penetrating Radar Applications and Equipment
| AD-A261873 | p 2686 N93-26541

GEOPOTENTIAL
Orbit determination support of the Ocean Topography Experiment (TOPEX)/Poseidon operational orbit p 2601 N93-24704
Analysis of the effects of mean local node-crossing time on the evolution of Sun-synchronous orbits p 2602 N93-24706

GEOSAT SATELLITES
Satellite monitoring of the global ocean surface during 1987-1989 p 2734 N93-24926
Satellite altimetry p 2734 N93-24930

GEOSYNCHRONOUS ORBITS
Practical aspects of transfer from GTO to lunar orbit p 2604 N93-24719

GEOTECHNICAL ENGINEERING
Lunar regolith and structure mechanics p 2670 N93-26412

GERMANIUM
Radiation effects in germanium doped quartz p 2837 N93-25021

GERMANIUM ALLOYS
Metastable SiC and SiGeC alloys by carbon implantation and solid phase epitaxy
| DE93-007594 | p 2863 N93-25387

GET AWAY SPECIALS (STS)
STS-45 Space Shuttle mission report
| NASA-CR-193054 | p 2612 N93-25959
STS-47 Space Shuttle mission report
| NASA-CR-193056 | p 2612 N93-25960
STS-42 Space Shuttle mission report
| NASA-CR-193059 | p 2613 N93-25989

GIMBALS
Goddard Space Flight Center (GSFC) Flight Dynamics Facility (FDF) calibration of the Upper Atmosphere Research Satellite (UARS) sensors p 2606 N93-24733

GIRDERS
Design concepts for pressurized lunar shelters utilizing indigenous materials p 2670 N93-26414

GLACIOLOGY
Sea level variation p 2734 N93-24929

GLASS
Temperature-dependent electrical conductivity of soda-lime glass
| DE93-007872 | p 2654 N93-25359
The nature of the glass transition and its determination by thermal analysis
| DE93-006746 | p 2654 N93-25374
Second-harmonic generation in optical fibers and glass
| AD-A260592 | p 2853 N93-25839
Three-dimensional analysis and verification of fracture growth mechanisms in fiber-reinforced ceramic composites
| AD-A261483 | p 2641 N93-26355

GLASS FIBER REINFORCED PLASTICS
Damage and failure analysis on continuous fiber-reinforced polymer composites p 2637 N93-25716

GLASS FIBERS
Second-harmonic generation in optical fibers and glass
| AD-A260592 | p 2853 N93-25839
International Workshop on Advances in Inorganic Fibre Technology
| AD-A260719 | p 2639 N93-25908
Ceramic fiber reinforced glass-ceramic matrix composite
| NASA-CASE-LEW-15262-1 | p 2640 N93-26100

GLASS LASERS
High speed x ray gating cameras for ICF imaging applications
| DE93-007500 | p 2709 N93-25515

GLASS TRANSITION TEMPERATURE
Polyimides containing the cyclobutene-3,4-dione moiety
| NASA-CASE-LAR-14753-1 | p 2656 N93-25999

GLIDE PATHS
ILS mathematical modeling study of an ILS glide slope proposed for runway 19L at the Meridian Naval Air Station, Mississippi
| DOT/FAA/CT-TN93/8 | p 2584 N93-24741

GLOBAL AIR SAMPLING PROGRAM
Gasp 1.3 results for the transverse hydrogen reacting jet p 2625 N93-26011

GLOBAL ATMOSPHERIC RESEARCH PROGRAM
Data management for JGOFS: Theory and design p 2735 N93-24935

GLOBAL POSITIONING SYSTEM
Application of GPS tracking techniques to orbit determination for TDRS p 2601 N93-24702
Relativistic effects for low Earth orbit satellites using GPS p 2608 N93-24986
Rubidium atomic frequency standards for GPS block 2R p 2836 N93-25014
Mixed constellation synchronization of GPS time p 2836 N93-25015
GPS standardization for the needs of time transfer p 2836 N93-25016
Comparison of GLONASS and GPS time transfers p 2836 N93-25017
An experimental health monitoring unit for GPS and GLONASS p 2586 N93-25018
Oscillators for mobile GPS receivers p 2694 N93-25055
Timing a national telecommunications network using GPS p 2687 N93-25062
Preliminary studies leading toward the development of a LIDAR bathymetry mapping instrument p 2711 N93-25614
Knowledge-based control for robot self-localization p 2822 N93-25963
Methodology investigation: Global Positioning System integration (GPS)
| AD-A261054 | p 2586 N93-26237
Repair, evaluation, maintenance, and rehabilitation research program. Continuous Deformation Monitoring System (CDMS)
| AD-A261833 | p 2586 N93-26274
Bit hit/solar activity correlation study
| AD-A261381 | p 2896 N93-26340

GLOBAL WARMING
Sea level variation p 2734 N93-24929
Analysis of LARI sensor system
| DE93-006334 | p 2761 N93-24977
Global warming potential for CF4
| DE93-005740 | p 2762 N93-25146

GLOVES
Investigation of the effects of Extra Vehicular Activity (EVA) and Launch and Entry (LES) gloves on performance p 2803 N93-26061

GLOW DISCHARGES
Investigations of the transient behavior of the cathode fall region in planar and hollow cathodes
| AD-A261636 | p 2691 N93-26171

GLUCOSE
Inorganic and biological electron transfer across an electronically conductive composite polymer membrane
| AD-A261642 | p 2656 N93-26172

GODDARD TRAJECTORY DETERMINATION SYSTEM
TDRSS-user orbit determination using batch least-squares and sequential methods p 2601 N93-24703

GOGGLES
Interpupillary and vertex distance effects on field-of-view and acuity with ANVIS
| AD-A261259 | p 2802 N93-26265

GOLD
Low cost dewatering of waste slurries p 2769 N93-25573

GONIOMETERS
Measurement results of the crystallographic orientation of the SC cut round plates p 2840 N93-25040

GOVERNMENT/INDUSTRY RELATIONS
Energy and Technology Review, August-September 1992
| DE93-005882 | p 2901 N93-24974
Achieving the promise of the bioscience revolution: The role of the Federal Government
| PB93-139970 | p 2793 N93-25457
Designing and implementing a state quality award
| PB93-154458 | p 2722 N93-26546

GOVERNMENTS
Technology Transfer 92/93
| DE93-003623 | p 2887 N93-24965
Achieving the promise of the bioscience revolution: The role of the Federal Government
| PB93-139970 | p 2793 N93-25457

GRAIN BOUNDARIES
A micromechanical viscoplastic stress-strain model with grain boundary sliding
| DE93-009109 | p 2649 N93-25095
Studying the kinetics of magnetization in high Tc superconductors
| NASA-CR-192916 | p 2862 N93-25108
Room temperature fracture of FeCo
| DE93-008266 | p 2650 N93-25519
Ir-Zr alloys as diffusion barriers between Cu and Si(100)
| AD-A261919 | p 2652 N93-26197
GRAIN SIZE
Processing and properties of Ti5Si3
| DE93-007284 | p 2649 N93-25149
GRANTS
The 1993/1994 NASA Graduate Student Researchers Program
| NASA-EP-283 | p 2872 N93-26051
GRANULAR MATERIALS
Energy dissipation in inelastic flow of cohesionless granular media p 2703 N93-25662
GRAPH THEORY
Design and analysis of algorithms for processing queries in database systems p 2876 N93-25482
GRAPHITE
Resonance electron scattering by O2 monolayers on graphites: Reinterpreted
| AD-A261851 | p 2850 N93-26287
GRAPHITE-EPOXY COMPOSITES
Stress distribution in composite flatwise tension test specimens
| NASA-TM-106074 | p 2634 N93-25071
Graphite/epoxy composite laminates with co-cured interlaminar damping layers p 2642 N93-25587
Quantifying distributed damage in composites via the thermoelastic effect p 2637 N93-25691
A three-dimensional model for the residual stresses in a unidirectional composite plate p 2728 N93-25825
Fabrication of composite propfan blades for a cruise missile wind tunnel model
| N/ SA-TM-105270 | p 2730 N93-26202
Thermally induced stresses in a composite exposed to fire
| AD-A261714 | p 2641 N93-26371
GRAPHS (CHARTS)
Model-based reasoning for system and software engineering: The Knowledge From Pictures (KFP) environment p 2825 N93-25978
GRASSLANDS
Measuring the intensity of nitrogen fertilization of grassland by means of remote sensing p 2751 N93-24859
GRAUPEL
The initiation of lightning and the growth of electric fields in thunderstorms
| AD-A261455 | p 2787 N93-26352
GRAVITATIONAL EFFECTS
Contributions of microgravity test results to the design of spacecraft fire safety systems
| NASA-TM-106093 | p 2614 N93-24755
A model of concurrent flow flame spread over a thin solid fuel
| NASA-CR-191111 | p 2663 N93-24946
Relativistic effects for low Earth orbit satellites using GPS p 2608 N93-24986
Modeling of bubble and drop formation in flowing liquids in terrestrial and microgravity environments p 2664 N93-25390
Numerical study of cavity natural convection flow with augmenting and counteracting effects by projection finite element method p 2701 N93-25540
Gravity-dependent transport phenomena in zeolite crystal growth p 2664 N93-25740
GRAVITATIONAL FIELDS
Optimal cooperative power-limited rendezvous p 2607 N93-24904
Prograde anomalous orbits in triaxial gravitational potentials that rotate about the long axis: VLA neutral hydrogen observations and modeling of the inclined rings around the galaxies NGC 2685 and NGC 660 p 2607 N93-25396
Mars: The dynamics of orbiting satellites and gravity model development p 2896 N93-25439
GRAVITATIONAL LENSES
Gravitational lensing and gamma ray bursts p 2900 N93-25828
GRAVITATIONAL PHYSIOLOGY
JPRS report: Science and technology. Central Eurasia: Life sciences
| JPRS-ULS-92-022 | p 2795 N93-25407
GRAVITATIONAL WAVES
Cosmic string cosmology p 2891 N93-24907
Gravitational radiation from coalescing binary star systems p 2900 N93-25625
GRAVITY PROBE B
The design of a propulsion system using vent gas from a liquid helium cryogenic system p 2623 N93-25539
GRAVITY WAVES
Rossby-gravity waves in tropical total ozone data
| NASA-CR-192983 | p 2764 N93-25432
Gravity waves from O2 airglow p 2772 N93-25547
GRAZING INCIDENCE
VETA-I x ray test analysis
| NASA-CR-192321 | p 2854 N93-26183
The x ray reflectivity of the AXAF VETA-I optics p 2855 N93-26192
GREASES
Macromolecules for inhibition of corrosion and wear
| AD-A261041 | p 2655 N93-25816
GREAT PLAINS CORRIDOR (NORTH AMERICA)
The charge and size of precipitation particles inside thunderstorms and mesoscale convective systems on the Great Plains p 2781 N93-25275
GREEN'S FUNCTIONS
Structural acoustics: A general form of reciprocity principles in acoustics
| AD-A261515 | p 2846 N93-26376
GREENHOUSE EFFECT
Sea level variation p 2734 N93-24929
Selected translated abstracts of Russian-language climate-change publications: 1. Surface energy budget
| DE93-003189 | p 2760 N93-24952
Analysis of LARI sensor system
| DE93-006334 | p 2761 N93-24977
Trends '91: A compendium of data on global change. Highlights
| DE93-003112 | p 2761 N93-25144
CHAMMP
| DE93-007290 | p 2762 N93-25184
Climate data bases of the People's Republic of China, 1841-1988
| DE93-007907 | p 2764 N93-25517
Long term modeling of the links between economics, technical progress, and environment: Evolution of approaches and new trends
| DE93-005035 | p 2767 N93-26497
GRID GENERATION (MATHEMATICS)
A three-dimensional algebraic grid generation scheme for gas turbine combustors with inclined slots
| NASA-CR-191095 | p 2694 N93-24759
Rapid exploration of curvilinear grids using direct volume rendering
| NASA-CR-192765 | p 2808 N93-24944
A comparison using APPL and PVM for a parallel implementation of an unstructured grid generation program
| NASA-CR-191425 | p 2808 N93-25073
A contribution to the great Riemann solver debate
| NASA-CR-191409 | p 2575 N93-25083
Grid sensitivity for aerodynamic optimization and flow analysis
| NASA-CR-192980 | p 2575 N93-25117
On the generation and dispersion of Yanai waves with a spectral Chebyshev-collocation reduced-gravity ocean model p 2788 N93-25276
Structured adaptive mesh refinement on the connection machine
| DE93-007368 | p 2816 N93-25316
Transformation of two and three-dimensional regions by elliptic systems
| NASA-CR-192955 | p 2810 N93-25669
An extended Lagrangian method
| NASA-TM-106129 | p 2707 N93-26203
GRINDING (COMMINUTION)
Production of ultrafine, high-purity ceramic powders using the US Bureau of Mines developed turbomill p 2659 N93-25585
GROOVES
Experimental study of the effect of helical grooves on an infinite cylinder
| AD-A260890 | p 2676 N93-25912
GROUND BASED CONTROL
Piloted simulation of an air-ground profile negotiation process in a time-based Air Traffic Control environment
| NASA-TM-107748 | p 2585 N93-26087
GROUND OPERATIONAL SUPPORT SYSTEM
Weather forecasting expert system study
| NASA-CR-192929 | p 2777 N93-24747
A system to measure lightning-induced transients on spacecraft umbilical lines p 2693 N93-24889
Develop margin philosophy to attain robustness
| MCR-92-5005 | p 2610 N93-26182
TCMS operations and maintenance philosophy
| NASA-TM-108756 | p 2873 N93-26418
Test, Control and Monitor System (TCMS) operations plan
| NASA-CR-193098 | p 2873 N93-26419
Test, Control and Monitor System maintenance plan
| NASA-CR-193099 | p 2873 N93-26420
GROUND STATE
Theoretical calculations on the electron absorption spectra of selected Polycyclic Aromatic Hydrocarbons (PAH) and derivatives
| NASA-CR-192762 | p 2892 N93-25200
New ground states in unconventional superconductors p 2688 N93-25282
GROUND STATIONS
Precise Doppler tracking from the Medicina VLBI station p 2608 N93-24998
A system design for laser time synchronization via geodetic satellite Ajisai p 2716 N93-25005
GROUND SUPPORT EQUIPMENT
Commercial Precipitation Static (P-static) test equipment p 2711 N93-24901
GROUND SUPPORT SYSTEMS
A multimission three-axis stabilized spacecraft flight dynamics ground support system p 2603 N93-24714
The scope of DLR's SAR calibration program p 2738 N93-24778
Use of remote sensing spacecrafts in real time support to disaster management: Interfaces with ground segment facilities and services p 2743 N93-24809
GROUND TESTS
HERO resistant semiconductor bridge igniter p 2627 N93-26024
Study of plate-fin heat exchanger and cold plate for the active thermal control system of Space Station p 2619 N93-26064
GROUND TRACKS
A ground track control algorithm for the Topographic Mapping Laser Altimeter (TMLA) p 2602 N93-24707
GROUND TRUTH
Use of airborne imaging spectrometry to the definition of optimised specifications for land applications with future spaceborne imaging spectrometers p 2738 N93-24776
Archaeological, historical and geoelectrical data as ground truth for Landsat TM imagery application to coastal plain evolution studies p 2742 N93-24799
Geographic information system for fusion and analysis of high-resolution remote sensing and ground truth data p 2878 N93-25798
GROUND WATER
Aquifer thermal energy (heat and chill) storage
| DE93-006446 | p 2759 N93-25183
GROUND WIND
Parametric analysis of atmospheric processes
| NASA-CR-192523 | p 2770 N93-25086
Errors caused by incompatible wind and buoyancy forcing in the ocean general circulation models
| AD-A260894 | p 2789 N93-25657
GROUP VELOCITY
Determination of the elastic constants of composite materials from ultrasonic group velocity measurements p 2635 N93-25544
GUIDANCE SENSORS
Optimizing the fine lock performance of the Hubble Space Telescope fine guidance sensors p 2604 N93-24723
GULF STREAM
Observations of an intrathermocline vortex p 2788 N93-24769
Dynamics of Gulf Stream meanders and frontal eddies in the South Atlantic Bight p 2788 N93-25354
Boundary layer coupling between an explosive cyclone and the Gulf Stream during ERICA
| AD-A261577 | p 2787 N93-26513
GUN PROPELLANTS
Minutes of the Twenty-Fifth Explosives Safety Seminar, volume 4
| AD-A261116 | p 2660 N93-25769
The burning rate behavior of pure nitrocellulose propellant samples
| AD-A261009 | p 2661 N93-25857
Infrared fiber optic diagnostic for solid propellant combustion p 2628 N93-26031
GUSTS
General aviation aircraft: Normal acceleration data analysis and collection project
| DOT/FAA/CT-91/20 | p 2586 N93-24739
GYROSCOPES
The results of the in-flight attitude sensor calibration for the Arthur Holly Compton Gamma Ray Observatory p 2600 N93-24697
Resolution of the COBE Earth sensor anomaly p 2600 N93-24700
UARS in-flight jitter study for EOS
| NASA-CR-191419 | p 2615 N93-25133
GYROTROPISM
Microstrip antennas on/in anisotropic material layers
| AD-A261700 | p 2681 N93-26383

H

H II REGIONS
Far-infrared emission, gas, and ultraluminous HII regions in M101
| NASA-CR-192791 | p 2890 N93-25755

HABITABILITY
The reuse of logistics carriers for the first lunar outpost alternative habitat study p 2671 N93-26083

HABITATS
Biodiversity indication by Earth observation data p 2751 N93-24858
The effects of video compression on acceptability of images for monitoring life sciences' experiments p 2805 N93-25930
Use of Taguchi design of experiments to optimize and increase robustness of preliminary designs p 2670 N93-26063
Metabolic response of environmentally isolated microorganisms to industrial effluents: Use of a newly described cell culture assay p 2794 N93-26066
Analysis of the lettuce data from the variable pressure growth chamber at NASA Johnson Space Center: A three-stage nested design model p 2794 N93-26069
Development of a pyrolysis waste recovery model with designs, test plans, and applications for space-based habitats p 2803 N93-26076
The reuse of logistics carriers for the first lunar outpost alternative habitat study p 2671 N93-26083

HAIL
Positive cloud-to-ground flashes in severe storms p 2780 N93-24896

HAILSTORMS
Positive cloud-to-ground flashes in severe storms p 2780 N93-24896

HALIDES
Halogen adlayers on Ag(111)
| AD-A261792 | p 2850 N93-26443

HALL EFFECT
The DX centers in three to five semiconductors under hydrostatic pressure
| DE93-007701 | p 2864 N93-25490
Low temperature Hall and Shubnikov-de Haas effects
| AD-A261871 | p 2869 N93-26540

HALLEY'S COMET
Near Earth object fuels (neo-fuels): Discovery, prospecting and use
| DE93-005185 | p 2892 N93-25164

HALOGENS
Resonant tunneling through chemisorbed halogen atoms on Ag(111)
| AD-A261794 | p 2868 N93-26254
Phosphorus-, nitrogen-, sulfur-, and chlorine-containing molecules on surfaces
| AD-A261265 | p 2657 N93-26303
Halogen adlayers on Ag(111)
| AD-A261792 | p 2850 N93-26443

HALOS
TSC plasma halo simulation of a D3-D vertical displacement episode
| DE93-008688 | p 2860 N93-25493

HANDBOOKS
Handbook of actuators and edge alignment sensors
| NASA-CR-193203 | p 2620 N93-25317
Human computer interface style guide, version 2.0
| AD-A261280 | p 2807 N93-26291
Handbook of chemical hazard analysis procedures
| PB93-158756 | p 2766 N93-26315
Particulate emissions from gas turbine engines
| AD-A261374 | p 2595 N93-26339

HANDLING EQUIPMENT
Transmission system for a transfer device gripping a double wheel
| CA-PATENT-APPL-SN-2024585 | p 2597 N93-25178

HARDNESS
Processing and properties of Ti5Si3
| DE93-007284 | p 2649 N93-25149
Dynamic hardness tester and cure meter p 2711 N93-25608

HARDWARE
The implementation of a lossless data compression module in an advanced orbiting system: Analysis and development p 2804 N93-25928
Test, Control and Monitor System (TCMS) operations plan
| NASA-CR-193098 | p 2873 N93-26419

HARMONIC EXCITATION
On the effect of acoustic coupling on random and harmonic plate vibrations
| NASA-TM-107740 | p 2844 N93-25189

HARMONIC GENERATIONS
A frequency generating source: Frequency synthesizers p 2693 N93-25041
Advances in nonlinear optical materials and devices
| NASA-CR-192681 | p 2852 N93-25281
Second-harmonic generation in optical fibers and glass
| AD-A260592 | p 2853 N93-25839

HARMONIC GENERATORS
Theoretical and experimental investigation of electron beam acceleration and sub-millimeter wave generation
| AD-A261117 | p 2609 N93-25770

HARMONICS
Synchrotron radiation X ray topography study of lateral field resonators p 2833 N93-24994
Comparison of energy trapping resonators and filters using the AT cut of quartz, berlinite and gallium phosphate p 2836 N93-25013
On the effect of acoustic coupling on random and harmonic plate vibrations
| NASA-TM-107740 | p 2844 N93-25189

HASTELLOY (TRADEMARK)
A micromechanical viscoplastic stress-strain model with grain boundary sliding
| DE93-009109 | p 2649 N93-25095

HAZARDS
An introductory guide to uncertainty analysis in environmental and health risk assessment
| DE93-002873 | p 2760 N93-24676
Alternative strategies for the use of satellite data analysis systems for hazard monitoring and disaster mitigation p 2743 N93-24805
A method for sequential image analysis of hazard areas p 2743 N93-24810
A new method for infrared imaging of air currents in and around critical hazard fume hoods
| DE93-003009 | p 2761 N93-24956
The evaluation of technical models used for major-accident hazard installations. Report to Commission of the European Communities Directorate General 12
| CUED/A-AERO/TR-19 | p 2668 N93-25238
Hazards of explosives dusts: Particle size effects
| DE93-009380 | p 2668 N93-25498
Improved performance and safety for high energy batteries through use of hazard anticipation and capacity prediction p 2694 N93-25582
A review of civil aviation propeller-to-person accidents: 1980-1989
| AD-A260695 | p 2583 N93-25896
A coastal hazards data base for the US East Coast
| NASA-TM-108265 | p 2791 N93-26586

HEALTH
An introductory guide to uncertainty analysis in environmental and health risk assessment
| DE93-002873 | p 2760 N93-24676
Achieving the promise of the bioscience revolution: The role of the Federal Government
| PB93-139970 | p 2793 N93-25457
The application of integrated knowledge-based systems for the Biomedical Risk Assessment Intelligent Network (BRAIN) p 2799 N93-25595
Development of a concept for a national construction industry health and safety data base
| PB93-159325 | p 2884 N93-26568

HEALTH PHYSICS
AFRRI research, fiscal year 1991
| AD-A260933 | p 2911 N93-25710

HEARING
In-flight evaluation of noise levels and assessment of active noise reduction systems in the Seahawk S-70B-2 helicopter
| AD-A260689 | p 2845 N93-25649
Measuring hearing protection device performance using the metrosonics db-3100 sound level analyzer (dosimeter)
| AD-A260852 | p 2801 N93-25787
Design, fabrication, and testing of a three-dimensional acoustic orientation instrument (3-D AOI): Drawings, engineering and associated lists (conceptual and development design)
| AD-A260934 | p 2845 N93-25915

HEART
Effect of cytoskeletal reagents on stretch activated ion channels
| AD-A261089 | p 2793 N93-25764

HEART RATE
MAC to VAX connectivity: Heartrate spectral analysis system p 2796 N93-25594

HEAT ENGINES
Development of ASTM standards in support of advanced ceramics development
| DE93-003024 | p 2654 N93-25361

HEAT EXCHANGERS
Compressor calorimeter performance of refrigerant blends: Comparative methods and results for a refrigerator/freezer application
| DE93-006734 | p 2667 N93-24970
An evaluation of thermal energy storage options for precooling gas turbine inlet air
| DE93-005980 | p 2758 N93-24975
Test results of a Stirling engine utilizing heat exchanger modules with an integral heat pipe
| NASA-TM-105883 | p 2759 N93-25136
Two-phase/two-phase heat exchanger analysis
| NASA-CR-192783 | p 2697 N93-25221
Malone refrigeration
| DE93-005439 | p 2668 N93-25447
Annular flow enhanced two-phase evaporative heat exchanger for space-based systems p 2700 N93-25478
Study of plate-fin heat exchanger and cold plate for the active thermal control system of Space Station p 2619 N93-26064

HEAT FLUX
Development of dispersion-strengthened XD (trademark) Cu alloys for high heat-flux applications
| NASA-CR-191124 | p 2653 N93-24761
Application of optical remote sensing to the study of surface fluxes related to cloud formation
| DE93-003783 | p 2781 N93-25125
A correlated K-distribution model of the heating rates for H2O and a molecular mixture in the 0-2500 cm(exp -1) wavelength region in the atmosphere between 0 and 60 km
| DE93-005741 | p 2762 N93-25147
Effect of continuous eigenvalue spectrum on plasma transport in toroidal systems
| NIFS-214 | p 2859 N93-25215
Simulation and prediction of tropical SST with a coupled ocean-atmosphere model p 2789 N93-25469
Local and regional estimates of sensible and latent heat flux densities from a patch-work surface
| ISBN-0-315-70882-4 | p 2772 N93-25556
The effect of entrance radius and film injection on wall heating in scramjet nozzles p 2625 N93-26009
Flame response in oscillatory solid propellant combustion p 2630 N93-26041
Modeling of the WSTF frictional heating apparatus in high pressure systems p 2648 N93-26079

HEAT MEASUREMENT
Compressor calorimeter performance of refrigerant blends: Comparative methods and results for a refrigerator/freezer application
| DE93-006734 | p 2667 N93-24970
The nature of the glass transition and its determination by thermal analysis
| DE93-006746 | p 2654 N93-25374
Fibre optic sensors for heat transfer studies p 2853 N93-25748

HEAT OF FORMATION
Energetic materials from cubane
| AD-A261317 | p 2662 N93-26308

HEAT PIPES
Test results of a Stirling engine utilizing heat exchanger modules with an integral heat pipe
| NASA-TM-105883 | p 2759 N93-25136

HEAT RESISTANT ALLOYS
Fatigue in single crystal nickel superalloys
| AD-A260709 | p 2651 N93-25843
Fatigue in single crystal nickel superalloys
| AD-A261742 | p 2652 N93-26282
Solidification processing and phase transformations in ordered high temperature alloys
| AD-A261751 | p 2652 N93-26284
The influence of primary and secondary orientations on the elastic response of a nickel-base single-crystal superalloy
| NASA-TM-106125 | p 2731 N93-26550

HEAT SHIELDING
An investigation of the degradation of Fluorinated Ethylene Propylene (FEP) copolymer thermal blanketing materials aboard LDEF in the laboratory
| NASA-CR-192824 | p 2653 N93-25078

HEAT STORAGE
An evaluation of thermal energy storage options for precooling gas turbine inlet air
| DE93-005980 | p 2758 N93-24975
Aquifer thermal energy (heat and chill) storage
| DE93-006446 | p 2759 N93-25183

HEAT TRANSFER
Minimization of heat slab nodes with higher order boundary conditions
| DE93-004238 | p 2695 N93-24966
Heat transfer in rotating serpentine passages with selected model orientation for smooth or skewed trip walls
| NASA-TM-106126 | p 2667 N93-25177
Shock tube application to the study of compressible turbulent boundary layer with mass injection p 2697 N93-25252
Turbine turbobrake systems p 2717 N93-25268
Boundary plasma modelling for ITER
| DE93-007963 | p 2859 N93-25302
Measurements and computations of external heat transfer and film cooking in turbines
| RAE-TM-P-1223 | p 2592 N93-25455

Annular flow enhanced two-phase evaporative heat exchanger for space-based systems p 2700 N93-25478
Laminar and turbulent natural convection heat transfer in Trombe wall channels p 2702 N93-25551
Heat transfer measurements in swept shock wave/turbulent boundary-layer interactions p 2704 N93-25705
Flow and heat transfer experiments in the turbine airfoil/endwall region p 2704 N93-25725
Two-dimensional fin analysis p 2705 N93-25737
Fibre optic sensors for heat transfer studies p 2853 N93-25748
Uniform roughness studies | WL-TR-92-3041 | p 2706 N93-25951
A new approach to cooled combustion chambers: The 40K formed platelet chamber p 2626 N93-26018
Advanced engineering analysis | KCP-613-4967 | p 2669 N93-26212
Flow control of low heat load turbine airfoils | AD-A260941 | p 2595 N93-26219
Influence of supercritical conditions on pre-combustion chemistry and transport behavior of jet fuels | AD-A261813 | p 2661 N93-26268
AMPHIB: A users manual | AD-A261769 | p 2669 N93-26285
Basic research thermoacoustic heat transport | AD-A261334 | p 2759 N93-26310
Theoretical treatment of spin-forbidden and electronically nonadiabatic processes. Methods and applications | AD-A261596 | p 2851 N93-26525

HEAT TRANSFER COEFFICIENTS
Evaluation of a candidate material for a coal-fired magnetohydrodynamic (MHD) high temperature recuperative air heater | DE93-006630 | p 2858 N93-24968

HEAT TRANSMISSION
A computational approach to predicting the extent of arc root damage in CFC panels p 2642 N93-24890
Integration of design, thermal, structural, and optical analysis, including thermal animation p 2814 N93-25601

HEAT TREATMENT
Processing and mechanical properties of laminated metal composites of Al/Al-25 vol. percent SiC and ultrahigh carbon steel/brass | DE93-007504 | p 2635 N93-25383
Control of crystallite size in diamond film chemical vapor deposition | AD-D015660 | p 2867 N93-26090
Solidification processing and phase transformations in ordered high temperature alloys | AD-A261751 | p 2652 N93-26284

HEATING
Winter warming from large volcanic eruptions | NASA-CR-192848 | p 2763 N93-25244
Modeling of the WSTF frictional heating apparatus in high pressure systems p 2648 N93-26079

HEATING EQUIPMENT
Evaluation of a candidate material for a coal-fired magnetohydrodynamic (MHD) high temperature recuperative air heater | DE93-006630 | p 2858 N93-24968

HEAVY IONS
Testing of the on-board attitude determination and control algorithms for SAMPEX p 2600 N93-24698
Summary of progress in inertial confinement fusion | DE93-007350 | p 2858 N93-25187
Beam position and total current monitor for heavy ion fusion beams | DE93-007653 | p 2851 N93-25325
Results from the NA36 on strangeness production in 200 GeV/c per nucleon S + Pb and p - Pb reactions | DE93-007711 | p 2848 N93-25364
The sub 60 ps timing resolution using large area silicon avalanche diodes | DE93-007723 | p 2688 N93-25365

HELICAL WINDINGS
Assessment of torsatrons as reactors | DE93-006721 | p 2858 N93-24969

HELICOPTER CONTROL
Discrete range clustering using Monte Carlo methods | NASA-TM-104004 | p 2584 N93-24914
Helicopter low-speed yaw control | NASA-CASE-LAR-14219-1 | p 2597 N93-25998
Image-based ranging and guidance for rotorcraft | NASA-CR-177608 | p 2586 N93-26549

HELICOPTER DESIGN
Rotor design optimization using a free wake analysis | NASA-CR-177612 | p 2575 N93-25075

HELICOPTERS
Numerical modelling of induced effects of lightning strike on an all composite helicopter p 2583 N93-24879
Aeroelastic response and aeromechanical stability of helicopters with elastically coupled composite rotor blades p 2588 N93-25530
Structural dynamic analysis of bearingless rotor blade p 2590 N93-25719
Computational gearing mechanics | NASA-CR-191127 | p 2719 N93-25884
Helicopter low-speed yaw control | NASA-CASE-LAR-14219-1 | p 2597 N93-25998
Helicopter forced response vibration analysis method RTVIB20 | AD-A261809 | p 2597 N93-26260
PROAV Cable Warning System (CWS) - U.S. Army aircraft Integration assessment and OCONUS field evaluation | AD-A261233 | p 2583 N93-26263

HELIOSEISMOLOGY
Inverse problem with continuous parameters for solar oscillations p 2895 N93-25728

HELIUM
Detecting damaged cables using a preionized gas technique | DE93-007588 | p 2689 N93-25429
Experimental and computational investigation of helium injection into air at supersonic and hypersonic speeds p 2577 N93-25487

HELIUM IONS
Photoluminescence of silicon nanostructures formed by ion beam implantation | DE93-006777 | p 2862 N93-24958

HELIUM-NEON LASERS
Progress towards laboratory frequency standards for the optical communication bands p 2687 N93-25069

HELMET MOUNTED DISPLAYS
Perceptual factors that influence use of computer enhanced visual displays | NASA-CR-192961 | p 2811 N93-26150

HELMETS
Helmeted head and neck dynamics under whole-body vibration p 2800 N93-25531
In-flight evaluation of noise levels and assessment of active noise reduction systems in the Seahawk S-70B-2 helicopter | AD-A260689 | p 2845 N93-25649

HEMATOLOGY
JPRS report: Science and technology. Central Eurasia: Life sciences | JPRS-ULS-92-022 | p 2795 N93-25407

HERBIG-HARO OBJECTS
Observations and models of shock structures in Herbig-Haro objects p 2891 N93-24770

HERMITIAN POLYNOMIAL
Polar decomposition for attitude determination from vector observations p 2602 N93-24711

HERTZSPRUNG-RUSSELL DIAGRAM
30 Doradus in the Large Magellanic Cloud: The stellar content and initial mass function p 2894 N93-25559

HETEROCYCLIC COMPOUNDS
Electrical conductivity of ion implanted ladder and semi-ladder polymers | AD-A261401 | p 2657 N93-26401

HETERODYNING
Advanced technology development multi-color holography | NASA-CR-192451 | p 2711 N93-26154

HETEROGENEITY
Luminescence probe studies of ionomers. 3: Distribution of decay rate constants for tris bipyridyl ruthenium(2) in Nafion membranes | AD-A260764 | p 2645 N93-25916
Phosphorus-, nitrogen-, sulfur-, and chlorine-containing molecules on surfaces | AD-A261265 | p 2657 N93-26303

HETEROJUNCTIONS
New concepts for high efficiency energy conversion: The avalanche heterostructure and superlattice solar cells | DE92-010592 | p 2758 N93-25098
Short-period superlattice materials for heterojunction bipolar transistors | AD-A260701 | p 2866 N93-25897

HEURISTIC METHODS
Algorithms for optimal redundancy allocation | DE93-005709 | p 2827 N93-24973
Using a multifrontal sparse solver in a high performance, finite element code | NASA-CR-192718 | p 2828 N93-25223
Design and analysis of algorithms for processing queries in database systems p 2876 N93-25482
Adaptive laser link reconfiguration using constraint propagation p 2823 N93-25967
Inferring heuristic classification hierarchies from natural language input p 2825 N93-25979
Complexity of connectionist and constraint-satisfaction networks | AD-A261617 | p 2817 N93-26169

HF LASERS
Experimental and theoretical study of cw HF chemical laser overtone performance p 2713 N93-25420
Experimental and theoretical study of CW HF chemical laser residual fundamental gain p 2714 N93-25721

HIERARCHIES
Management of space networks p 2672 N93-24671
On the robustness of Herlihy's hierarchy | NASA-CR-193002 | p 2808 N93-25107
Hierarchical dynamics in distributed information processing p 2875 N93-25350
TARGET: Rapid capture of process knowledge p 2814 N93-25590
Inferring heuristic classification hierarchies from natural language input p 2825 N93-25979
Multi-viewpoint clustering analysis p 2825 N93-25980

HIGH CURRENT
BBU code development for high-power microwave generators | DE93-007111 | p 2688 N93-25397
Characterization of ceramic capacitors for high-voltage pulse-discharge applications | DE93-007601 | p 2689 N93-25417

HIGH DEFINITION TELEVISION
Experiments with the HIVITS HDTV contribution CODED | BBC-RD-1992/12 | p 2674 N93-25391

HIGH ELECTRON MOBILITY TRANSISTORS
Noise-optimal control of HEMT LNA's for compensation of temperature deviations p 2678 N93-26115

HIGH ENERGY ELECTRONS
Detection of fragments arising from greater than 10 GeV electron-nucleus collisions | DE93-007725 | p 2848 N93-25366

HIGH ENERGY INTERACTIONS
Recent experiments on spin physics in high energy hadron interactions | DE93-007900 | p 2851 N93-25301
Topics in CP violation | DE93-007615 | p 2847 N93-25323
The sub 60 ps timing resolution using large area silicon avalanche diodes | DE93-007723 | p 2688 N93-25365

HIGH FREQUENCIES
An SPW software simulation model of a dispersive fading multipath narrowband HF channel | AD-A261101 | p 2675 N93-25767
High Frequency (HF) radiowave propagation | AD-A261726 | p 2681 N93-26280
A comparison of ionospheric propagation mode delay predictions from ADVANCED PROPHET 4.3 with measured data | AD-A261782 | p 2686 N93-26604

HIGH POLYMERS
Vacuum powder injector and method of impregnating fiber with powder | NASA-CASE-LAR-14179-1 | p 2668 N93-26101

HIGH POWER LASERS
A compact and versatile pulse generation and shaping subsystem for high energy laser systems | DE93-007114 | p 2711 N93-24961
Start-up imprinting and shock dynamics in laser-target interaction | AD-A261384 | p 2715 N93-26445
FALCON nuclear-reactor-pumped laser program and wireless power transmission | DE93-007607 | p 2715 N93-26597

HIGH PRESSURE
Modeling of the WSTF frictional heating apparatus in high pressure systems p 2648 N93-26079

HIGH RESOLUTION
High resolution stereo imaging and data compression p 2753 N93-24867
Comparison of high-resolution solar irradiance spectra and the solar luminosity in the period 1980-1989 | NASA-CR-192776 | p 2898 N93-25222
High resolution interface nanochemistry and structure | DE93-009750 | p 2635 N93-25501
Inelastic scattering in condensed matter with high intensity Moessbauer radiation | DE93-008763 | p 2864 N93-25503
Prediction of global cloud cover with a very high resolution global spectral model | AD-A261047 | p 2785 N93-25777
Geographic information system for fusion and analysis of high-resolution remote sensing and ground truth data p 2878 N93-25798
VETA-1 x ray detection system p 2854 N93-26185
The x ray reflectivity of the AXAF VETA-I optics p 2855 N93-26192

HIGH SPEED
High speed x ray gating cameras for ICF imaging applications | DE93-007500 | p 2709 N93-25515

High speed solid state circuit breaker
p 2694 N93-25598
Very high-speed arithmetic processors (The Gauss Machine)
| AD-A260693 | p 2806 N93-25650
An investigation of photothermal velocimetry for application to transient, high-speed gas flows
p 2579 N93-25720

HIGH STRENGTH
Metal alloy and method of preparation thereof
| AD-D015670 | p 2652 N93-26234

HIGH TEMPERATURE
High temperature fracture toughness of Ni3Al alloy IC-396M
| DE93-008564 | p 2650 N93-25492
Application of the Saha equation to high temperature (greater than or equal to) rocket exhaust
| AD-A261648 | p 2632 N93-26174
Deformation mechanisms of NiAl cyclicly deformed near the brittle-to-ductile transition temperature
| NASA-CR-191121 | p 2652 N93-26235
SiC microsensor with piezoresistive diamond sensing elements
| AD-A261346 | p 2868 N93-26312

HIGH TEMPERATURE AIR
Evaluation of a candidate material for a coal-fired magnetohydrodynamic (MHD) high temperature recuperative air heater
| DE93-006630 | p 2858 N93-24968

HIGH TEMPERATURE ENVIRONMENTS
Radiation and temperature effects on electronic components investigated under the CSTI high capacity power project
| NASA-TM-106096 | p 2687 N93-24746
Characterization of ceramic capacitors for high-voltage pulse-discharge applications
| DE93-007601 | p 2689 N93-25417
Smart microsensors for high temperature applications
| AD-A260747 | p 2710 N93-25677

HIGH TEMPERATURE GASES
SRB environment evaluation and analysis. Volume 2: RSRB joint filling test/analysis improvements
| NASA-CR-192518 | p 2631 N93-26057

HIGH TEMPERATURE PLASMAS
Conversion of light hydrocarbon gases to metal carbides for production of liquid fuels and chemicals
| DE93-009707 | p 2644 N93-25500
Very low frequency signals and whistler-mode amplification in the magnetosphere and limit-cycle behavior in the CECAF infrared free electronic laser
| AD-A261776 | p 2716 N93-26601

HIGH TEMPERATURE SUPERCONDUCTORS
Development of high Tc (greater than 100 K) Bi, Tl and Y-based materials as superconducting circuit elements
| NASA-CR-192344 | p 2863 N93-25219
New ground states in unconventional superconductors
p 2688 N93-25282
Inelastic scattering in condensed matter with high intensity Moessbauer radiation
| DE93-008763 | p 2864 N93-25503
Analysis of the gap in high-temperature superconductors using photoemission spectroscopy p 2865 N93-25744
Published assessments bearing on the future use of ceramic superconductors by the electric power sector
| DE93-007737 | p 2658 N93-26588

HIGH TEMPERATURE TESTS
Development of thin film thermocouples on ceramic materials for advanced propulsion system applications
| NASA-TM-106017 | p 2709 N93-25173

HIGH VOLTAGES
Characterization of ceramic capacitors for high-voltage pulse-discharge applications
| DE93-007601 | p 2689 N93-25417
The interaction of high voltage systems with the environments of the Moon and Mars
| NASA-TM-106107 | p 2618 N93-26148

HILSCH TUBES
The interaction of modulated vortex pairs with a free surface p 2701 N93-25485

HISTOGRAMS
Scene segmentation of natural images using texture measures and back-propagation
| NASA-TM-104003 | p 2803 N93-25235

HISTORIES
Archaeological, historical and geoelectrical data as ground truth for Landsat TM imagery application to coastal plain evolution studies p 2742 N93-24799
Aeronautics in NACA and NASA
| NASA-NP-156 | p 2574 N93-26422

HMX
ADN propellant diffusion flame structure
p 2629 N93-26036
Flame response in oscillatory solid propellant combustion p 2630 N93-26041

HOLES (MECHANICS)
High speed x ray gating cameras for ICF imaging applications
| DE93-007500 | p 2709 N93-25515

HOLLOW CATHODES
Investigations of the transient behavior of the cathode fall region in planar and hollow cathodes
| AD-A261636 | p 2691 N93-26171

HOLOGRAPHIC INTERFEROMETRY
Advanced technology development multi-color holography
| NASA-CR-192451 | p 2711 N93-26154

HOLOGRAPHY
Miniature Optical Wide-Angle-Lens Startracker (Mini-OWLS) p 2606 N93-24728
Multi-layer holographic bifurcative neural network system for real-time adaptive EOS data analysis
p 2880 N93-25807
Advanced technology development multi-color holography
| NASA-CR-192451 | p 2711 N93-26154
Optically smart surfaces survivability testing at Mach 3
| AD-A261785 | p 2857 N93-26566

HOMING DEVICES
Cross-switched MICRAD seeker
| AD-D015676 | p 2691 N93-26142

HORIZONTAL FLIGHT
Aeroelastic response and aeromechanical stability of helicopters with elastically coupled composite rotor blades p 2588 N93-25530
Development and testing of the digital control system for the Archytas unmanned air vehicle
| AD-A261656 | p 2597 N93-26196

HORMONE METABOLISMS
Vascular uptake of rehydration fluids in hypohydrated men at rest and exercise
| NASA-TM-103942 | p 2795 N93-26133

HOT CORROSION
Hot corrosion of the B2 nickel aluminides
| NASA-CR-191082 | p 2649 N93-25128

HOT ISOSTATIC PRESSING
Processing and properties of Ti5Si3
| DE93-007284 | p 2649 N93-25149
Mechanical alloying processing and application to development of structural materials
| AD-A261251 | p 2652 N93-26264

HOT STARS
The effects of rotation on the winds from hot stars
p 2894 N93-25620

HOT-WIRE FLOWMETERS
An experimental study of passive drag reduction in a turbulent boundary layer by a riblet surface
p 2705 N93-25746

HOVERING
Application of finite-state inflow to flap-lag-torsion damping in hover p 2587 N93-25486
Aeroelastic response and aeromechanical stability of helicopters with elastically coupled composite rotor blades p 2588 N93-25530
Jet-induced ground effects on a parametric flat-plate model in hover
| NASA-TM-104001 | p 2581 N93-26099

HTPB PROPELLANTS
ADN propellant diffusion flame structure
p 2629 N93-26036

HUBBLE SPACE TELESCOPE
Optimizing the fine lock performance of the Hubble Space Telescope fine guidance sensors
p 2604 N93-24723
The Hubble Space Telescope fine guidance system operating in the coarse track pointing control mode
p 2605 N93-24724
Hubble Space Telescope: The archived exposures catalog, version 2.0
| NASA-CR-192896 | p 2883 N93-26423

HUMAN BEINGS
The adult literacy evaluator: An intelligent computer-aided training system for diagnosing adult illiterates p 2799 N93-26082
Vascular uptake of rehydration fluids in hypohydrated men at rest and exercise
| NASA-TM-103942 | p 2795 N93-26133
Contribution of personality to the prediction of success in initial air traffic control specialist training
| DOT/FAA/AM-93/4 | p 2797 N93-26138

HUMAN BODY
Initial experiments with a myoelectric-based muscle sensor
| DE92-016034 | p 2799 N93-25099
Assessing patterns of change in anthropometric dimensions: Secular trends of US Army females, 1946-1988
| AD-A260869 | p 2800 N93-25628
Visual perception of elevation
| AD-A261394 | p 2797 N93-26307

HUMAN FACTORS ENGINEERING
Crashworthiness of composite seats for civil aircraft
p 2582 N93-24773
Initial experiments with a myoelectric-based muscle sensor
| DE92-016034 | p 2799 N93-25099
A heat transfer analysis of a mobile vehicle radiation-shielded operator compartment
| DE93-007428 | p 2800 N93-25318
Human factors engineering: A key element of instrumentation and control system design
| DE93-006731 | p 2800 N93-25415
Helmeted head and neck dynamics under whole-body vibration p 2800 N93-25531
A framework for the design of usable electronic text
p 2877 N93-25754
Measures of user-system interface effectiveness: An encoding scheme and indicators for assessing the usability of graphical, direct-manipulation style user interfaces
| AD-A260606 | p 2801 N93-25840
Human Factors in Aviation Maintenance, phase 2
| DOT/FAA/AM-93/5 | p 2802 N93-26089
CALS-HSC data element dictionary
| AD-A261560 | p 2813 N93-26461
Human factors in environmental management: New directions from the Hanford site
| DE93-004337 | p 2767 N93-26495

HUMAN PERFORMANCE
A longitudinal examination of applicants to the air traffic control supervisory identification and development program
| DOT/FAA/AM-92/16 | p 2796 N93-25213
A cognitive architecture for human performance process model research
| AD-A261040 | p 2797 N93-25815
Simulated sustained flight operations and performance. Part 1: Effects of fatigue
| AD-A261012 | p 2801 N93-25859
Performance-based testing and success in Naval advanced flight training
| AD-A260838 | p 2590 N93-25933
Investigation of the effects of Extra Vehicular Activity (EVA) and Launch and Entry (LES) gloves on performance p 2803 N93-26061
Contribution of personality to the prediction of success in initial air traffic control specialist training
| DOT/FAA/AM-93/4 | p 2797 N93-26138
Automation and robotics human performance
| NASA-CR-193049 | p 2802 N93-26153

HUMAN WASTES
Development of a pyrolysis waste recovery model with designs, test plans, and applications for space-based habitats p 2803 N93-26076

HUMIDITY
A comparison of moisture resistance with different types of end-terminations in ceramic capacitors
| DE93-007600 | p 2689 N93-25416
Observed annual and interannual variations in tropospheric water vapor p 2782 N93-25549

HURRICANES
A dynamical theory for hurricane spiral bands
p 2782 N93-25352
Typhoon prediction (recurvature - 1990 experiment)
| AD-A260673 | p 2786 N93-25892

HUYGENS PRINCIPLE
DSD Technology: A detonation reactive Huygens code
| LA-12235-MS | p 2706 N93-25987

HYBRID PROPELLANT ROCKET ENGINES
Hybrid rocket fuel combustion study
p 2626 N93-26019

HYDRATES
Far infrared spectra of amorphous and crystalline water ice and changes in these phases as the result of proton irradiation
| NASA-CR-192849 | p 2892 N93-25230

HYDRAULIC CONTROL
Pneumatic actuator with hydraulic control
| AD-D015652 | p 2719 N93-26244

HYDRAULIC EQUIPMENT
Dynamic modeling of fluid transmission lines of the DSN 70-meter antennas by using a lumped parameter model
p 2678 N93-26119

HYDROCARBON COMBUSTION
Measurements of soot formation and hydroxyl concentration in near critical equivalence ratio premixed ethylene flame
| NASA-CR-191099 | p 2642 N93-25116

HYDROCARBON FUELS
Catalytic conversion of light alkanes
| DE93-009646 | p 2644 N93-25499
Conversion of light hydrocarbon gases to metal carbides for production of liquid fuels and chemicals
| DE93-009707 | p 2644 N93-25500
Fundamental studies of droplet interactions in dense sprays
| AD-A261165 | p 2661 N93-25948

HYDROCARBONS
Atmospheric reactive nitrogen oxides and their relationship with urban and rural ozone formation p 2760 N93-24908
Tank issues: Design and placement of vapor monitoring wells
| PB93-161131 | p 2768 N93-26536
HYDROCYANIC ACID
The interaction of HCN/DCN with Si(100)-2x1
| AD-A260837 | p 2645 N93-25920
HYDRODYNAMIC EQUATIONS
Implementation of the Turn Function Method in a three-dimensional, parallelized hydrodynamics code
| DE93-003744 | p 2696 N93-25124
HYDRODYNAMICS
Applications of wavelet-based compression to multidimensional earth science data
| DE93-007348 | p 2762 N93-25166
Consequences of spontaneous and anomalous symmetry breaking for the orbital and mass flow hydrodynamics of He-3 - A p 2698 N93-25295
Development of an expendable particle sensor
| AD-A261127 | p 2710 N93-26044
ADCIRC: An advanced three-dimensional circulation model for shelves, coasts, and estuaries. Report 1: Theory and methodology of ADCIRC-2DDI and ADCIRC-3DL
| AD-A261608 | p 2790 N93-26164
Algorithms for the analysis of penetration by shaped charge jets
| UCRL-LR-109887 | p 2730 N93-26178
HYDROFORMING
Finite element modeling of the hydroforming press
| KCP-613-4999 | p 2668 N93-26206
HYDROGEN
Whisker growth studies under conditions which resemble those available on an orbiting space station
| NASA-CR-192701 | p 2664 N93-25218
Detection of atomic oxygen and hydrogen in solid propellant flames and pyrolysis gases using multiphoton laser-induced fluorescence p 2628 N93-26029
Development and use of hydrogen-air torches in an altitude facility
| NASA-TM-106047 | p 2598 N93-26214
HYDROGEN BONDS
Femtosecond dynamics in hydrogen-bonding solvents: Formamides
| DE93-003476 | p 2643 N93-25123
HYDROGEN EMBRITTLEMENT
Hydrogen-induced stress corrosion cracking susceptibility analysis of pitch links from the AH-64 Apache helicopter
| AD-A260692 | p 2651 N93-25895
HYDROGEN IONS
Dynamics of collision processes
| DE93-007143 | p 2849 N93-25509
Prediction of hydrogen entry and permeation in metals and alloys
| AD-A260580 | p 2651 N93-25903
HYDROGEN MASERS
Hydrogen masers for space p 2716 N93-24980
The application of the PRARE principle for precise two-way time transfer to space-based atomic clocks p 2832 N93-24983
Basic design of a spaceborne hydrogen maser p 2716 N93-25024
The development progresses of hydrogen masers at Shanghai Observatory p 2716 N93-25048
Investigations of the frequency instability of CH1-75 hydrogen masers p 2716 N93-25049
Quartz oscillators, frequency synthesizers, and timing systems for geodesy and radio science applications p 2693 N93-25052
HYDROGEN OXYGEN ENGINES
Pulsed laser Rayleigh scattering diagnostic for hydrogen/oxygen rocket exit plane flowfield velocimetry
| NASA-TM-106098 | p 2631 N93-26149
HYDROGEN PRODUCTION
Production of low-cost hydrogen
| DE93-008070 | p 2643 N93-25305
Biological conversion of synthesis gas
| DE93-009092 | p 2660 N93-25523
HYDROGEN SULFIDE
Biological conversion of synthesis gas
| DE93-009092 | p 2660 N93-25523
HYDROGENATION
Design of a high activity and selectivity alcohol catalyst
| DE93-008103 | p 2659 N93-25112
HYDROGENOLYSIS
A novel process for methanol synthesis
| DE93-008037 | p 2659 N93-25118
HYDROGEOLOGY
Geologic and hydrogeologic mapping of Iceland with multisensor data (JERS-1, ERS-1, SPOT, Landsat and SEASAT) p 2740 N93-24792
HYDROGRAPHY
Observations of an intrathermocline vortex p 2788 N93-24769
Data availability and data archeology from the former Soviet Union p 2735 N93-24932
Ocean time-series near Bermuda: Hydrostation S and the US JGOFS Bermuda Atlantic time-series study p 2736 N93-24938
HYDROLOGICAL CYCLE
Remote sensing in hydrology and water management p 2744 N93-24816
World Ocean Circulation Experiment p 2733 N93-24922
Development and testing of improved techniques for modeling the hydrologic cycle in a mesoscale weather prediction system
| AD-A261454 | p 2787 N93-26351
HYDROLOGY
Monitoring and evaluation of morphohydrographical changes in the Danube Delta by remote-sensing p 2747 N93-24834
Aquifer thermal energy (heat and chill) storage
| DE93-006446 | p 2759 N93-25183
Non-local description of pollution transport in random medium p 2763 N93-25329
Local and regional estimates of sensible and latent heat flux densities from a patch-work surface
| ISBN-0-315-70882-4 | p 2772 N93-25556
Interactive forecasting with the National Weather Service River Forecast System p 2788 N93-25616
Development and testing of improved techniques for modeling the hydrologic cycle in a mesoscale weather prediction system
| AD-A261454 | p 2787 N93-26351
HYDROLOGY MODELS
Remote sensing in hydrology and water management p 2744 N93-24816
Development and testing of improved techniques for modeling the hydrologic cycle in a mesoscale weather prediction system
| AD-A261454 | p 2787 N93-26351
HYDROSTATIC PRESSURE
The DX centers in three to five semiconductors under hydrostatic pressure
| DE93-007701 | p 2864 N93-25490
HYDROSTATICS
A three-dimensional study of the influence of mountains on a front
| AD-A261927 | p 2787 N93-26545
HYDROTHERMAL CRYSTAL GROWTH
Crystal growth of berlinite: Methods for growing longer crystals and improving the quality p 2838 N93-25025
HYDROXYL RADICALS
Measurements of soot formation and hydroxyl concentration in near critical equivalence ratio premixed ethylene flame
| NASA-CR-191099 | p 2642 N93-25116
HYPERBOLIC TRAJECTORIES
Tsien's method for generating non-Keplerian trajectories. Part 2: The question of thrust to orbit a sphere and the restricted three-body problem p 2603 N93-24718
HYPERCUBE MULTIPROCESSORS
Hierarchical dynamics in distributed information processing p 2875 N93-25350
An improved spectral load balancing method
| DE93-007582 | p 2810 N93-25386
Massively-parallel computational fluid dynamics
| AD-A261815 | p 2707 N93-26269
HYPERFINE STRUCTURE
Ion trap frequency standard research at PTB p 2841 N93-25050
HYPERSONIC FLIGHT
Trajectory optimization for the National aerospace plane
| NASA-CR-192954 | p 2589 N93-25670
Information requirements analyses for transatmospheric vehicles
| AD-A261189 | p 2590 N93-25949
HYPERSONIC FLOW
Development and application of computational aerothermodynamics flowfield computer codes
| NASA-CR-192940 | p 2574 N93-24736
Prediction of forces and moments for hypersonic flight vehicle control effectors
| NASA-CR-193033 | p 2595 N93-24762
Computation of hypersonic viscous flowfields using the parabolized Navier-Stokes equations p 2694 N93-24766
An investigation of laser velocimetry measurements within high speed, complex flows p 2697 N93-25237
Experimental and computational investigation of helium injection into air at supersonic and hypersonic speeds p 2577 N93-25487
HYPERSONIC REENTRY
A hybrid multigrid technique for computing steady-state solutions to supersonic flows p 2582 N93-26078
HYPERSONIC SPEED
Combined LAURA-UPS hypersonic solution procedure
| NASA-TM-107682 | p 2696 N93-25176
HYPERSONIC VEHICLES
Prediction of forces and moments for hypersonic flight vehicle control effectors
| NASA-CR-193033 | p 2595 N93-24762
Generic hypersonic vehicle performance model
| NASA-CR-192953 | p 2587 N93-25162
Combined LAURA-UPS hypersonic solution procedure
| NASA-TM-107682 | p 2696 N93-25176
Optimized scramjet engine integration on a waverider airframe p 2593 N93-25480
Thermal coatings for titanium-aluminum alloys
| NASA-TM-107760 | p 2651 N93-26048
Supersonic aeroelastic instability results for a NASP-like wing model
| NASA-TM-107739 | p 2591 N93-26553
HYPERSONICS
Numerical simulation of hypersonic aerodynamics and the computational needs for the design of an aerospace plane
| AD-A260681 | p 2580 N93-25894
HYPERVELOCITY GUNS
Energy and Technology Review, October - December 1992
| DE93-007784 | p 2674 N93-25299
HYPERVELOCITY IMPACT
Hypervelocity impact study: The effect of impact angle on crater morphology
| NASA-CR-192711 | p 2724 N93-25260
HYPERVELOCITY PROJECTILES
Hypervelocity impact study: The effect of impact angle on crater morphology
| NASA-CR-192711 | p 2724 N93-25260

I

IBM PERSONAL COMPUTERS
DSS-13 26-meter antenna upgraded radiometer system p 2679 N93-26122
ICE
Ice thickness measurement system for the icing research tunnel calibration
| NASA-TM-106095 | p 2708 N93-24737
An evaluation of thermal energy storage options for precooling gas turbine inlet air
| DE93-005980 | p 2758 N93-24975
ICE CLOUDS
Natural and augmented snowfall growth processes and their interactions with the natural and modified aerosol
| PB93-153096 | p 2786 N93-25874
ICE FORMATION
Ice thickness measurement system for the icing research tunnel calibration
| NASA-TM-106095 | p 2708 N93-24737
The initiation of lightning and the growth of electric fields in thunderstorms
| AD-A261455 | p 2787 N93-26352
ICELAND
Geologic and hydrogeologic mapping of Iceland with multisensor data (JERS-1, ERS-1, SPOT, Landsat and SEASAT) p 2740 N93-24792
Crustal deformation studies in subaerial parts of the world oceanic rift system: Iceland and Afar p 2789 N93-25558
IDEAL GAS
Combined LAURA-UPS hypersonic solution procedure
| NASA-TM-107682 | p 2696 N93-25176
IDENTIFYING
A longitudinal examination of applicants to the air traffic control supervisory identification and development program
| DOT/FAA/AM-92/16 | p 2796 N93-25213
IGNITERS
HERO resistant semiconductor bridge igniter p 2627 N93-26024
IGNITION
Ignition and combustion of lunar propellants
| NASA-CR-192814 | p 2659 N93-24745
Modelling of microgravity ignition phenomena p 2664 N93-25465
HERO resistant semiconductor bridge igniter p 2627 N93-26024
Condensed-phase processes during solid propellant combustion. Part 4: Chemical and microscopic examination of laser-irradiated propellant samples p 2628 N93-26032
ADN propellant diffusion flame structure p 2629 N93-26036

Dynamic burning rate measurements of metalized composite propellants using the laser-recoil technique
p 2631 N93-26043
Development and use of hydrogen-air torches in an altitude facility
| NASA-TM-106047 | p 2598 N93-26214

IGNITION SYSTEMS
Laser ignition application in a space experiment
| NASA-TM-106133 | p 2664 N93-25337

IMAGE ANALYSIS
Remote sensed spectral signatures classification and recognition by neural networks: An approach to unsupervised techniques p 2738 N93-24779
Spectral remote sensing of anomalous mineralogy induced by hydrocarbon migration and uranium mineralization, San Rafael Swell, Utah, USA
p 2739 N93-24783
The regional planning and control using the satellite data p 2740 N93-24788
Monitoring and analysis of urban trends using multitemporal satellite-imagery (case-study: Greater Cairo) p 2740 N93-24790
A method for sequential image analysis of hazard areas p 2743 N93-24810
Potential operational use of remote sensing from space in forestry p 2745 N93-24817
EUROSTARS: A system for thematic analysis of remote sensed data p 2753 N93-24871
Earthquake vulnerability map of the Lake Constance area p 2753 N93-24872
Multi-temporal satellite image analysis for crop inventories in the Po River Valley (Italy)
p 2755 N93-25434
Evaluation of a vibration diagnostic system for the detection of spur gear pitting failures
| NASA-TM-106103 | p 2718 N93-25672
Evaluation of lens distortion errors in video-based motion analysis
| NASA-TP-3266 | p 2797 N93-25736
Center for intelligent control systems
| AD-A260995 | p 2821 N93-25853
Image analysis by integration of disparate information
p 2824 N93-25973
Image analysis of the AXAF VETA-I x ray mirror
p 2855 N93-26190
Uncertainty in object pose determination with three light-stripe range measurements
| AD-A261435 | p 2857 N93-26488
Image-based ranging and guidance for rotorcraft
| NASA-CR-177608 | p 2586 N93-26549

IMAGE CORRELATORS
Image correlation velocimetry
| AD-A261599 | p 2707 N93-26163

IMAGE ENHANCEMENT
The use of polarimetric multifrequency SAR for characterizing terrain classes p 2738 N93-24777
Application of multitemporal Landsat-MSS and -TM data for the development of an inundation-risk-map
p 2743 N93-24807

IMAGE PROCESSING
Image coding by way of wavelets
p 2671 N93-24665
Spectral remote sensing of anomalous mineralogy induced by hydrocarbon migration and uranium mineralization, San Rafael Swell, Utah, USA
p 2739 N93-24783
Monitoring and analysis of urban trends using multitemporal satellite-imagery (case-study: Greater Cairo) p 2740 N93-24790
A knowledgc-based approach to waste disposal sites detection through integration of Landsat-TM imagery and geographical context information p 2741 N93-24796
Lithologic mapping with LANDSAT Thematic Mapper guided by laboratory spectral measurements, Air, Niger (Africa) p 2742 N93-24803
Application of multitemporal Landsat-MSS and -TM data for the development of an inundation-risk-map
p 2743 N93-24807
A method for sequential image analysis of hazard areas p 2743 N93-24810
Remote sensing geology p 2744 N93-24815
Tropical forest monitoring with high resolution satellite data p 2748 N93-24841
Mapping of windfall damage in the Hunsrueck plateau with Landsat TM-data p 2749 N93-24843
Data processing and control in a transputer system for remote sensing of the Earth p 2753 N93-24870
Scene segmentation of natural images using texture measures and back-propagation
| NASA-TM-104003 | p 2803 N93-25235
Progress in imaging microscopy with x ray lasers at LLNL
| DE93-007508 | p 2712 N93-25363
Multi-temporal satellite image analysis for crop inventories in the Po River Valley (Italy)
p 2755 N93-25434
Real-time construction and rendering of three-dimensional occupancy maps
| DE93-007818 | p 2756 N93-25516
Automated system for early breast cancer detection in mammograms p 2796 N93-25568
A novel optical/digital processing system for pattern recognition p 2814 N93-25603
Vision-aided monitoring and control of thermal spray, spray forming, and welding processes
p 2670 N93-25604
Very high-speed arithmetic processors (The Gauss Machine)
| AD-A260693 | p 2806 N93-25650
Efficient generation of synthetic terrain imagery for automatic target recognition
| AD-A260705 | p 2756 N93-25653
Geographic information system for fusion and analysis of high-resolution remote sensing and ground truth data
p 2878 N93-25798
A distributed system for visualizing and analyzing multivariate and multidisciplinary data
p 2880 N93-25804
SAVS: A Space Analysis and Visualization System
p 2881 N93-25812
A Hierarchical Target Extraction, Recognition, and Tracking (HiTert) system
| AD-A260567 | p 2854 N93-25898
Adjustable lossless image compression based on a natural splitting of an image into drawing, shading, and fine-grained components p 2804 N93-25923
Entropy reduction via simplified image contourization
p 2804 N93-25924
Methods of evaluating the effects of coding on SAR data p 2804 N93-25926
Fractal image compression: A resolution independent representation for imagery p 2804 N93-25927
Lossless compression of image data products on th e FIFE CD-ROM series p 2804 N93-25929
The effects of video compression on acceptability of images for monitoring life sciences' experiments
p 2805 N93-25930
High-performance compression of astronomical images p 2805 N93-25931
Multi-rate, real time image compression for images dominated by point sources p 2805 N93-25932
Data fusion with artificial neural networks (ANN) for classification of earth surface from microwave satellite measurements p 2824 N93-25974
A vision architecture for the extravehicular activity retriever p 2827 N93-26071
US Army evaluation of the Electronic Map Data (EMD) prototype
| AD-A261693 | p 2757 N93-26369
Experiments in multiple-baseline stereo
| AD-A261415 | p 2757 N93-26448

IMAGERY
A novel optical/digital processing system for pattern recognition p 2814 N93-25603
Efficient generation of synthetic terrain imagery for automatic target recognition
| AD-A260705 | p 2756 N93-25653
Topography from shading and stereo
p 2879 N93-25803
Compression of spectral meteorological imagery
p 2804 N93-25925
Fractal image compression: A resolution independent representation for imagery p 2804 N93-25927
The probabilistic neural network architecture for high speed classification of remotely sensed imagery
p 2824 N93-25972
Image analysis by integration of disparate information
p 2824 N93-25973
Arc Digital Raster Imagery (ADRI) development
| AD-A261850 | p 2812 N93-26275

IMAGES
An example of a phase-segregated enhanced PAL broadcasting system
| BBC-RD-1992/6 | p 2674 N93-25239
Facilitation and interference in identification of pictures and words
| AD-A261484 | p 2798 N93-26356

IMAGING SPECTROMETERS
Use of airborne imaging spectrometry to the definition of optimised specifications for land applications with future spaceborne imaging spectrometers
p 2738 N93-24776
Measuring the intensity of nitrogen fertilization of grassland by means of remote sensing
p 2751 N93-24859

IMAGING TECHNIQUES
Accurate attitude determination of the LACE satellite
p 2605 N93-24726
Scene segmentation of natural images using texture measures and back-propagation
| NASA-TM-104003 | p 2803 N93-25235
Apparatus for imaging an object in or through a scattering medium using coherent anti-Stokes Raman scattering
| AD-D015642 | p 2852 N93-25358
Progress in imaging microscopy with x ray lasers at LLNL
| DE93-007508 | p 2712 N93-25363
High speed x ray gating cameras for ICF imaging applications
| DE93-007500 | p 2709 N93-25515
Firmware development improves system efficiency
p 2807 N93-25606
A high performance room-temperature near-infrared camera
| AD-A260602 | p 2709 N93-25634
Proceedings of Workshop 1: The Human Brainmap Database
| AD-A260720 | p 2796 N93-25654
An investigation of photothermal velocimetry for application to transient, high-speed gas flows
p 2579 N93-25720
Small satellites and RPA's in global-change research
| AD-A260762 | p 2765 N93-25837
A Hierarchical Target Extraction, Recognition, and Tracking (HiTert) system
| AD-A260567 | p 2854 N93-25898
ADN propellant diffusion flame structure
p 2629 N93-26036
Imaging the magnetosphere in the extreme ultraviolet
| NASA-CR-192218 | p 2775 N93-26151
Image correlation velocimetry
| AD-A261599 | p 2707 N93-26163
Intensity distribution of the x ray source for the AXAF VETA-I mirror test p 2854 N93-26184
New pyro-optic techniques for imaging of long wavelength IR-Radiation (pyro-optic initiation program)
| AD-A260969 | p 2856 N93-26224
Advanced technology for portable personal visualization
| AD-A261294 | p 2807 N93-26293
Photographic industry and electronic imaging: The emergence of electronic still photography
| PB93-169399 | p 2711 N93-26324
Imaging regional changes in the spontaneous activity of the brain: An extension of the minimum-norm least-squares estimate
| AD-A261593 | p 2798 N93-26436
Experiments in multiple-baseline stereo
| AD-A261415 | p 2757 N93-26448
Neuromagnetic investigation of cortical regions underlying short-term memory
| AD-A261445 | p 2799 N93-26521

IMMUNE SYSTEMS
Effects of space radiation on humoral and cellular immunity in rhesus monkeys
| AD-A261808 | p 2793 N93-26259

IMMUNOLOGY
Immunoconjugates: Magic bullets for cancer therapy?
p 2796 N93-25567
Effects of space radiation on humoral and cellular immunity in rhesus monkeys
| AD-A261808 | p 2793 N93-26259

IMPACT DAMAGE
Expedient repair of structural facilities
| AD-A260727 | p 2598 N93-25656
Investigation and modeling of penetration process for composite laminates impacted by a blunt-ended projectile p 2637 N93-25675

IMPACT FUSION
Computational modeling of MAGO and other magnetized target fusion concepts
| DE93-007354 | p 2861 N93-26504

IMPACT LOADS
Analysis of longitudinal impact on semi-infinite circular bars and tubes. Appendix no. 2
| AD-A261556 | p 2731 N93-26459

IMPACT RESISTANCE
Low-velocity impact of composite sandwich plate
p 2637 N93-25695
Shear band formation in a W-Ni-Fe alloy under plate impact
| AD-A260702 | p 2651 N93-25907

IMPACT TESTS
Investigation and modeling of penetration process for composite laminates impacted by a blunt-ended projectile p 2637 N93-25675

IMPACT TOLERANCES
Low-velocity impact of composite sandwich plate
p 2637 N93-25695

IMPEDANCE MATCHING
Surface discharge photoinitiation of pulsed chemical lasers
| DE93-006337 | p 2712 N93-24967

IMPELLERS
Numerical modelling of viscous turbomachinery flows with a pressure correction method p 2594 N93-25702

IMPINGEMENT
Three-dimensional analysis and verification of fracture growth mechanisms in fiber-reinforced ceramic composites
| AD-A261483 | p 2641 N93-26355
IMPLANTATION
The prevalence of artificial lens implants in the civil airman population
| DOT/FAA/AM-92/14 | p 2794 N93-25214
Analysis of pull-tests for determining the effects of ion implantation on the adhesion of iron films to sapphire substrates
| DE93-006732 | p 2725 N93-25373
IMPLOSIONS
High speed x ray gating cameras for ICF imaging applications
| DE93-007500 | p 2709 N93-25515
Sensitivity of magnetic flux compression in cylindrical implosions to model parameters
| DE93-003819 | p 2861 N93-26512
IMPREGNATING
Vacuum powder injector and method of impregnating fiber with powder
| NASA-CASE-LAR-14179-1 | p 2668 N93-26101
IMPULSES
Using input command pre-shaping to suppress multiple mode vibration p 2732 N93-25834
Modeling of atom-diatom scattering
| AD-A261645 | p 2849 N93-26173
Progress in impulse approach research
| AD-A261728 | p 2850 N93-26281
IMPURITIES
Thermionic current measurement in quartz p 2840 N93-25045
Surface diffusion studies by optical diffraction techniques
| DE93-007707 | p 2853 N93-25550
IN SITU MEASUREMENT
Comparison of the electrical charging and discharging environments of multiple aircraft-borne electric-field measurement systems p 2583 N93-24887
Development of a cone penetrometer for measuring spectral characteristics of soils in situ p 2776 N93-25570
IN-FLIGHT MONITORING
Digitization of analog data from in-flight lightning strikes p 2778 N93-24884
Comparison of the electrical charging and discharging environments of multiple aircraft-borne electric-field measurement systems p 2583 N93-24887
INCLINATION
Space Station Freedom assembly and operation at a 51.6 degree inclination orbit
| NASA-TM-107731 | p 2615 N93-25174
INCLUSIONS
Fracture of an elliptical inclusion and its implications for the properties of short fiber composites p 2634 N93-25333
INCOHERENT SCATTER RADAR
Theoretical study of topside ionospheric clutter
| AD-A260982 | p 2774 N93-25852
Study of auroral dynamics with combined spacecraft and incoherent-scatter radar data
| NASA-CR-192224 | p 2775 N93-26159
INCOMPRESSIBLE FLOW
Instability of flow in a streamwise corner
| NASA-CR-191410 | p 2576 N93-25153
Incompressible spectral-element method: Derivation of equations
| NASA-TM-106109 | p 2708 N93-26554
INCOMPRESSIBLE FLUIDS
Stabilized finite element methods for incompressible flows with emphasis on moving boundaries and interfaces p 2703 N93-25663
INDENTATION
Vickers indentation hardness of stoichiometric and reduced single crystal TiO2 (rutile) from 25 to 800 C
| NASA-TM-105959 | p 2633 N93-26204
INDEPENDENT VARIABLES
Spontaneous discovery and use of categorical structure
| AD-A261658 | p 2798 N93-26364
INDIAN OCEAN
Indian Ocean analyses p 2733 N93-24925
INDIUM ARSENIDES
A high performance room-temperature near-infrared camera
| AD-A260602 | p 2709 N93-25634
Short-period superlattice materials for heterojunction bipolar transistors
| AD-A260701 | p 2866 N93-25897
INDIUM COMPOUNDS
Non-H2Se, ultra-thin CIS devices
| DE93-000078 | p 2759 N93-25253
Role of polycrystallinity in CdTe and CuInSe2 photovoltaic cells
| DE93-000045 | p 2759 N93-25504
INDUCTION HEATING
Chemistry during the induction time in heated nitramines p 2629 N93-26035
Steady induction effects in geomagnetism. Part 1B: Geomagnetic estimation of steady surficial core motions: A non-linear inverse problem
| NASA-TP-3272-PT-1B | p 2776 N93-26421
INDUCTORS
Distortion measurements on bandpass filters with powdered iron toroidal inductors
| AD-A260790 | p 2675 N93-25689
INDUSTRIAL MANAGEMENT
Technology for America's economic growth: A new direction to build economic strength
| AD-A261553 | p 2887 N93-26458
Designing and implementing a state quality award
| PB93-154458 | p 2722 N93-26546
INDUSTRIAL PLANTS
Complex investigation of a system industrial site-environment using remote sensing and landscape-geochemical methods p 2741 N93-24798
Pollution prevention 1991: Progress on reducing industrial pollutants
| PB93-157725 | p 2766 N93-25875
X ray computed tomography for failure analysis
| AD-A261884 | p 2722 N93-26527
INDUSTRIAL SAFETY
Handbook of chemical hazard analysis procedures
| PB93-158756 | p 2766 N93-26315
Development of a concept for a national construction industry health and safety data base
| PB93-159325 | p 2884 N93-26568
INDUSTRIAL WASTES
Converting environmental wastes into valuable resources p 2759 N93-25572
Pollution prevention 1991: Progress on reducing industrial pollutants
| PB93-157725 | p 2766 N93-25875
Treatment of hazardous organic wastes using silent discharge plasmas
| DE93-003789 | p 2768 N93-26592
INDUSTRIES
Technology Transfer 92/93
| DE93-003623 | p 2887 N93-24965
An advanced data-acquisition system for wind energy projects
| DE93-000079 | p 2874 N93-25254
Converting environmental wastes into valuable resources p 2759 N93-25572
Space business indicators p 2886 N93-26158
Handbook of chemical hazard analysis procedures
| PB93-158756 | p 2766 N93-26315
Science, Technology, and Industrial Policy in the Former Soviet Union
| DE93-006528 | p 2887 N93-26499
INELASTIC COLLISIONS
Dynamics of collision processes
| DE93-007143 | p 2849 N93-25509
INELASTIC SCATTERING
Detection of fragments arising from greater than 10 GeV electron-nucleus collisions
| DE93-007725 | p 2848 N93-25366
Inelastic scattering in condensed matter with high intensity Moessbauer radiation
| DE93-008763 | p 2864 N93-25503
Measurement of optical properties of infrared bandgap superlattices
| AD-A260859 | p 2866 N93-25789
Modeling of atom-diatom scattering
| AD-A261645 | p 2849 N93-26173
Resonance electron scattering by O2 monolayers on graphites: Reinterpreted
| AD-A261851 | p 2850 N93-26287
INERTIA
Stability analysis and modeling of rotating flexible structures
| DE93-008493 | p 2844 N93-25520
INERTIAL CONFINEMENT FUSION
Summary of progress in inertial confinement fusion
| DE93-007350 | p 2858 N93-25187
Two-stream instability for a light ion beam-plasma system with external magnetic field
| NIFS-204 | p 2859 N93-25248
INERTIAL NAVIGATION
Preliminary studies leading toward the development of a LIDAR bathymetry mapping instrument p 2711 N93-25614
INERTIAL REFERENCE SYSTEMS
Apparatus for determining the attitude of a vehicle
| AD-D015667 | p 2710 N93-26092
INFINITE SPAN WINGS
Stationary crossflow instability on an infinite swept wing p 2580 N93-25865
INFLATING
A simple, approximate model of parachute inflation
| DE93-002465 | p 2576 N93-25121
INFORMATION
Information requirements analyses for transatmospheric vehicles
| AD-A261189 | p 2590 N93-25949
INFORMATION DISSEMINATION
Technology Transfer 92/93
| DE93-003623 | p 2887 N93-24965
The General Information Programme (PGI) and developing countries: A case study of Iraq p 2874 N93-25209
INFORMATION MANAGEMENT
Management of space networks p 2672 N93-24671
The role of the World Data Centers in handling ocean climate data p 2732 N93-24919
Distributed information storage p 2877 N93-25722
Department of Energy: Better information resources management needed to accomplish missions. Report to the Secretary of Energy
| GAO/IMTEC-92-53 | p 2882 N93-26096
Strategic information planning: Framework for designing and developing system architectures
| GAO/IMTEC-92-51 | p 2882 N93-26097
Department of Defense technical architecture framework for information management. Volume 3: Reference model and standards profile, version 1.3
| AD-A261913 | p 2882 N93-26230
Proceedings of the 33rd Annual Military LibrariansWorkshop
| AD-A261071 | p 2882 N93-26242
Photographic industry and electronic imaging: The emergence of electronic still photography
| PB93-169399 | p 2711 N93-26324
OSSA Information Systems Program
| NASA-TM-108758 | p 2883 N93-26491
Department of Defense technical architecture framework for information management. Volume 1: Implementation concept, version 1.1
| AD-A261911 | p 2884 N93-26531
Department of Defense technical architecture framework for information management. Volume 2: Architecture guidance and design concepts, version 1.1
| AD-A261912 | p 2884 N93-26532
INFORMATION PROCESSING (BIOLOGY)
Hierarchical dynamics in distributed information processing p 2875 N93-25350
Visual processing of object velocity and acceleration
| AD-A261048 | p 2800 N93-25778
A cognitive architecture for human performance process model research
| AD-A261040 | p 2797 N93-25815
Duration of alpha suppression increases with angle in a mental rotation task
| AD-A261592 | p 2798 N93-26435
INFORMATION RETRIEVAL
Improving information search at the user interface: The impact of graphical innovation on query formulation and expression p 2873 N93-24905
Use of fuzzy relational information retrieval technique for generating control strategies in resolution-based automated reasoning p 2874 N93-25258
Agreement in naming objects and concepts for information retrieval p 2881 N93-25826
Power iterations and the dominant eigenvalue problem
| AD-A261695 | p 2829 N93-26370
A geological and geophysical information system for Eurasia
| AD-A261789 | p 2883 N93-26442
The effects of cloud inhomogeneities upon radiative fluxes, and the supply of a cloud truth validation dataset
| NASA-CR-191711 | p 2787 N93-26492
INFORMATION SYSTEMS
Management of space networks p 2672 N93-24671
Crossing the frontier between publishing and information service
| DE93-002894 | p 2873 N93-24677
Land cover, an essential component of the CORINE information system on the environment: GIS implications p 2740 N93-24787
The role of the World Data Centers in handling ocean climate data p 2732 N93-24919
AQUIS: A PC-based air inventory and permit manager
| DE93-003006 | p 2761 N93-25143
Trends '91: A compendium of data on global change. Highlights
| DE93-003112 | p 2761 N93-25144
The General Information Programme (PGI) and developing countries: A case study of Iraq p 2874 N93-25209
Striped tape arrays
| NASA-CR-192914 | p 2806 N93-25267
Optimization of knowledge-based systems and expert system building tools
| NASA-CR-192763 | p 2874 N93-25288

A distributed heterogeneous client-server environment
| DE93-007496 | p 2875 N93-25319
An experimental examination of the effects of expertise and problem-solving cues on the identification of ideas for strategic information systems p 2875 N93-25395
Factors associated with perceptions of productivity and usage of information technology in a service organization p 2875 N93-25421
Earth observing system. Output data products and input requirements, version 2.0. Volume 2: Analysis of IDS input requirements
| NASA-TM-108771 | p 2755 N93-25461
Earth observing system. Output data products and input requirements, version 2.0. Volume 3: Algorithm summary tables and non-EOS data products
| NASA-TM-108769 | p 2756 N93-25462
The database Query Support Processor (QSP) p 2807 N93-25577
Digital Nautical Chart
| AD-A260810 | p 2756 N93-25694
A framework for the design of usable electronic text p 2877 N93-25754
Integrated Development Support Environment (IDSE)
| AD-A261088 | p 2877 N93-25763
Applied Information Systems Research Program (AISRP). Workshop 2: Meeting Proceedings
| NASA-CR-193096 | p 2877 N93-25792
Geographic information system for fusion and analysis of high-resolution remote sensing and ground truth data p 2878 N93-25798
Knowledge-based assistance for science visualization and analysis using large distributed databases p 2879 N93-25801
Experimenter's laboratory for visualized interactive science p 2879 N93-25802
The Space and Earth Science Data Compression Workshop
| NASA-CP-3183 | p 2803 N93-25921
The use of multiple models in case-based diagnosis p 2823 N93-25969
In search of meta-knowledge p 2826 N93-25983
Strategic information planning: Framework for designing and developing system architectures
| GAO/IMTEC-92-51 | p 2882 N93-26097
Deep Space Network information system architecture study p 2679 N93-26126
Task 2A: UNIS requirements and concepts
| MCR-92-5006-PT-A | p 2610 N93-26180
Department of Defense technical architecture framework for information management. Volume 3: Reference model and standards profile, version 1.3
| AD-A261913 | p 2882 N93-26230
OSSA Information Systems Program
| NASA-TM-108774 | p 2882 N93-26231
Proceedings of the 33rd Annual Military LibrariansWorkshop
| AD-A261071 | p 2882 N93-26242
Step stress testing of receiver/transmitter units
| AD-A261286 | p 2730 N93-26279
EnviroNET p 2886 N93-26398
A channel simulation processor for the multi-node tactical network simulator
| AD-A261810 | p 2776 N93-26430
A geological and geophysical information system for Eurasia
| AD-A261789 | p 2883 N93-26442
OSSA Information Systems Program
| NASA-TM-108758 | p 2883 N93-26491
IDEF6: A design rationale capture method concept paper
| AD-A261594 | p 2884 N93-26523
Department of Defense technical architecture framework for information management. Volume 1: Implementation concept, version 1.1
| AD-A261911 | p 2884 N93-26531
Department of Defense technical architecture framework for information management. Volume 2: Architecture guidance and design concepts, version 1.1
| AD-A261912 | p 2884 N93-26532
Development of a concept for a national construction industry health and safety data base
| PB93-159325 | p 2884 N93-26568
Task Type E report for National Launch Demonstration Center (NLDC) (Task 32)
| MCR-91-5010 | p 2610 N93-26591

INFORMATION THEORY

Information transmission using CHAOS
| AD-A261519 | p 2883 N93-26377

INFRARED ASTRONOMY

An atlas of selected calibrated stellar spectra
| NASA-CR-177604 | p 2888 N93-25135
A study of the large-scale infrared emission from a selected dark cloud
| NASA-CR-192775 | p 2888 N93-25289
Optical and infrared studies of distant galaxies p 2890 N93-25712

INFRARED ASTRONOMY SATELLITE

A study of the large-scale infrared emission from a selected dark cloud
| NASA-CR-192775 | p 2888 N93-25289
The structure of the nearby universe traced by theIRAS galaxies
| NASA-CR-192809 | p 2889 N93-25331

INFRARED DETECTORS

Introduction to lead salt infrared detectors
| AD-A260781 | p 2710 N93-25686
Research on lead titanate films for radiation detection
| AD-A261187 | p 2849 N93-25823
Small satellites and RPA's in global-change research
| AD-A260762 | p 2765 N93-25837
Monolithic integration of semiconductor and superconductor components
| AD-A260589 | p 2690 N93-25906
New pyro-optic techniques for imaging of long wavelength IR-Radiation (pyro-optic initiation program)
| AD-A260969 | p 2856 N93-26224
Investigation of a background suppression transimpedance amplifier for photovoltaic detectors
| AD-A261828 | p 2691 N93-26272
Algorithms for space-based infrared surveillance
| AD-A261891 | p 2857 N93-26542

INFRARED IMAGERY

A new method for infrared imaging of air currents in and around critical hazard fume hoods
| DE93-003009 | p 2761 N93-24956
Small satellites and RPA's in global-change research
| AD-A260762 | p 2765 N93-25837
Algorithms for space-based infrared surveillance
| AD-A261891 | p 2857 N93-26542

INFRARED LASERS

IR and FIR laser diagnostics for plasma thrusters using a CW CO2 radiation source
| AD-A261399 | p 2862 N93-26520
Laser physics and laser techniques
| AD-A261595 | p 2715 N93-26524

INFRARED PHOTOMETRY

Optical and infrared studies of distant galaxies p 2890 N93-25712
Far-infrared emission, gas, and ultraluminous HII regions in M101
| NASA-CR-192791 | p 2890 N93-25755

INFRARED RADIATION

A correlated K-distribution model of the heating rates for H2O and a molecular mixture in the 0-2500 cm(exp -1) wavelength region in the atmosphere between 0 and 60 km
| DE93-005741 | p 2762 N93-25147
A study of the large-scale infrared emission from a selected dark cloud
| NASA-CR-192775 | p 2888 N93-25289
Theoretical and experimental research in infrared technology
| AD-A260926 | p 2853 N93-25646
Thermal infrared radiation transfer in the planetary boundary layer p 2772 N93-25688
Generation of acoustic waves by focused infrared neodymium-laser radiation p 2714 N93-25761
IR materials producibility
| AD-A261099 | p 2853 N93-25766
Measurement of optical properties of infrared bandgap superlattices
| AD-A260859 | p 2866 N93-25789
Monolithic integration of semiconductor and superconductor components
| AD-A260589 | p 2690 N93-25906
Infrared fiber optic diagnostic for solid propellant combustion p 2628 N93-26031
Analysis of the IBSS spectra of Space Shuttle control engine exhaust
| AD-A261749 | p 2632 N93-26373
Algorithms for space-based infrared surveillance
| AD-A261891 | p 2857 N93-26542

INFRARED RADIOMETERS

Aspects of the design of a satellite borne infra-red radiometer p 2620 N93-25474

INFRARED SIGNATURES

Analysis of the IBSS spectra of Space Shuttle control engine exhaust
| AD-A261749 | p 2632 N93-26373

INFRARED SPECTRA

An atlas of selected calibrated stellar spectra
| NASA-CR-177604 | p 2888 N93-25135
Far infrared spectra of amorphous and crystalline water ice and changes in these phases as the result of proton irradiation
| NASA-CR-192849 | p 2892 N93-25230
Commercial applications multispectral sensor system p 2758 N93-25615
Theoretical and experimental research in infrared technology
| AD-A260926 | p 2853 N93-25646
Tomographic analysis of sight infrared spectra of low pressure flames p 2628 N93-26030
Condensed-phase processes during solid propellant combustion. Part 4: Chemical and microscopic examination of laser-irradiated propellant samples p 2628 N93-26032

INFRARED SPECTROSCOPY

Crystal growth and physical characterizations of GaPO4 p 2840 N93-25044
Modeling of atom-diatom scattering
| AD-A261645 | p 2849 N93-26173

INGESTION (ENGINES)

Transient performance of fan engine with water ingestion
| NASA-CR-190778 | p 2573 N93-25134

INHOMOGENEITY

Line inhomogeneity effects and power shift in miniaturized rubidium frequency standards p 2694 N93-25066
Use and analysis of finite element methods for problems of solid mechanics and fracture
| AD-A261574 | p 2731 N93-26522

INITIATION

Chemistry during the induction time in heated nitramines p 2629 N93-26035

INJECTION

Tracking sharp interface of two fluids by the CIP (Cubic-Interpolated Propagation) scheme
| NIFS-206 | p 2698 N93-25277

INJECTION MOLDING

A model for the filling of cold cavities with solidifying, semi-crystalline polymers
| DE93-003817 | p 2655 N93-25507

INJECTORS

A summary of the JANNAF workshop on liquid rocket atomization p 2625 N93-26014
Experimental investigation of flow turning losses in unstable rocket motors p 2630 N93-26040

INJURIES

Cellular and tissue injury during nonfreezing cold injury and frostbite
| AD-A260574 | p 2795 N93-25900
Using terrestrial plants in biomonitoring
| PB93-158780 | p 2766 N93-26316

INLAND WATERS

Applications of remote sensing for tidal waters, coastal areas and inland waters p 2745 N93-24819

INLET FLOW

Nozzle diffuser for use with an open test section of a wind tunnel
| NASA-CASE-LAR-14424-1-SB | p 2598 N93-25996

INLET NOZZLES

Nozzle diffuser for use with an open test section of a wind tunnel
| NASA-CASE-LAR-14424-1-SB | p 2598 N93-25996

INLET TEMPERATURE

Measurements and computations of external heat transfer and film cooking in turbines
| RAE-TM-P-1223 | p 2592 N93-25455

INORGANIC CHEMISTRY

Intramolecular bridge/terminal oxo exchange within (MoV2O3) (4+) complexes containing linear oxo bridges
| AD-A261230 | p 2851 N93-26518

INORGANIC COMPOUNDS

Inorganic nitrogen and phosphorus dynamics in the water column of the Patuxent River
| PB93-172955 | p 2767 N93-26511

INORGANIC NITRATES

Inorganic nitrogen and phosphorus dynamics in the water column of the Patuxent River
| PB93-172955 | p 2767 N93-26511

INSPECTION

Reliability assessment at airline inspection facilities. Volume 1: A generic protocol for inspection reliability experiments
| DOT/FAA/CT-92/12-VOL-1 | p 2582 N93-25110
Nondestructive evaluation of ferrite c-cores
| KCP-613-4677 | p 2721 N93-25939
Automated inspection of solder joints for surface mount technology
| NASA-TM-104580 | p 2721 N93-26137
NDT standards from the perspective of the Department of Defense
| MTL-TR-92-68 | p 2722 N93-26434

INSTRUMENT APPROACH

The dependent converging instrument approach procedure: An analysis of its safety and applicability
| DOE/FAA/RD-93/6 | p 2585 N93-25456

INSTRUMENT ERRORS

Aircraft accident report: Tomy International, Inc., d/b/a Scenic Air Tours flight 22, Beech Model E18S, N342E in-flight collision with terrain, Mount Haleakala, Maui, Hawaii, 22 April 1992
| PB93-910401 | p 2583 N93-25827

Applications of inertial-sensor high-inheritance instruments to DSN precision antenna pointing p 2621 N93-26112

INSTRUMENT LANDING SYSTEMS
ILS mathematical modeling study of an ILS glide slope proposed for runway 19L at the Meridian Naval Air Station, Mississippi
| DOT/FAA/CT-TN93/8 | p 2584 N93-24741

INSTRUMENT PACKAGES
Development of a flight instrument package
| AD-A260830 | p 2591 N93-25783

INSULATION
Detecting damaged cables using a preionized gas technique
| DE93-007588 | p 2689 N93-25429

INTEGERS
Linear-programming tools in integer programming: The traveling salesman
| AD-A261398 | p 2812 N93-26290

INTEGRAL EQUATIONS
Multilevel techniques in large scale computation
| AD-A261082 | p 2828 N93-25762
A surface integral algorithm for the motion planning of nonholonomic mechanical systems
| AD-A261746 | p 2720 N93-26249

INTEGRAL TRANSFORMATIONS
Multilevel techniques in large scale computation
| AD-A261082 | p 2828 N93-25762

INTEGRATED CIRCUITS
Design of a low phase noise UHF oscillator using a partly metallized dielectric resonator p 2693 N93-25003
A state-of-the-art crystal filter design package using Windows 3.0 techniques p 2693 N93-25010
Monolithic quartz vibrating beam accelerometer p 2711 N93-25011
Two- and three-dimensional high performance, patterned overlay multi-chip module technology p 2694 N93-25581
Solid-state isotopic power source for computer memory chips p 2694 N93-25596
Microwave and millimeter wave monolithic integrated circuits (MIMIC) program. MIMIC briefs: Summaries of phase 3 technology support programs
| AD-A260914 | p 2690 N93-25660
VLSI for high-speed digital signal processing
| AD-A260754 | p 2690 N93-25678
MOCVD process technology for affordable, high-yield, high-performance MESFET structures. Phase 3: MIMIC
| AD-A261178 | p 2690 N93-25820
Multichip module high speed testing
| AD-A261391 | p 2856 N93-26306
Multivariable control for flexible IC processing
| AD-A261685 | p 2692 N93-26366
Advanced HTS S-N-S devices
| AD-A261552 | p 2869 N93-26381
Internal current probing of integrated circuits using magnetic force microscopy
| DE93-006752 | p 2692 N93-26501
Electronics and Electrical Engineering Laboratory technical publication announcements covering laboratory programs, July to September 1992 with 1992/1993 EEEL events calendar
| PB93-158632 | p 2884 N93-26530

INTEGRATED GLOBAL OCEAN STATION SYSTEMS
International ocean services: Is it time - will it ever be time? p 2737 N93-24941

INTEGRITY
An experimental health monitoring unit for GPS and GLONASS p 2586 N93-25018

INTELLIGENCE
Science, technology, and national security p 2886 N93-25232

INTELSAT SATELLITES
Prospects of two-way international time scale comparisons p 2832 N93-24988

INTERACTIVE CONTROL
Architecture of autonomous systems
| NASA-CR-192974 | p 2801 N93-26047
Interaction dynamics and control for orbital assembly p 2669 N93-26407

INTERCEPTION
Optimal finite-thrust time-bounded direct-ascent interception p 2607 N93-25272

INTERDIGITAL TRANSDUCERS
Elastic plate mode sensitivities to mass loading applications to gas sensors p 2711 N93-25009

INTERFACIAL ENERGY
Analysis of pull-tests for determining the effects of ion implantation on the adhesion of iron films to sapphire substrates
| DE93-006732 | p 2725 N93-25373

INTERFACIAL TENSION
Experimental and theoretical studies of dense fluid mixtures
| DE93-006070 | p 2695 N93-24976
Effect of cytoskeletal reagents on stretch activated ion channels
| AD-A261089 | p 2793 N93-25764
Interaction of vorticity with a free surface
| AD-A261524 | p 2707 N93-26360

INTERFERENCE
Generalized probability model for calculation of interference to the Deep Space Network due to circularly Earth-orbiting satellites p 2679 N93-26127

INTERFEROMETERS
The Hubble Space Telescope fine guidance system operating in the coarse track pointing control mode p 2605 N93-24724
MIT's interferometer CST testbed p 2609 N93-25836

INTERFEROMETRY
Optimizing the fine lock performance of the Hubble Space Telescope fine guidance sensors p 2604 N93-24723
Interferometric fiber-optic radiation sensor
| DE93-003841 | p 2852 N93-25127
Temperature dependent sensor response caused by polymer-solvent interactions
| DE93-005368 | p 2655 N93-25444
Polarizing Michelson interferometer for measuring thermospheric winds
| ISBN-0-315-70442-X | p 2784 N93-25731
Orbiter-orbiter and orbiter-lander tracking using same-beam interferometry p 2677 N93-26110
Interferometric measurement with squeezed light
| AD-A260910 | p 2856 N93-26457

INTERLAMINAR STRESS
Numerical simulation of damage and progressive failures in composite laminates using the layerwise plate theory p 2636 N93-25661

INTERMETALLICS
Pressure dependence of conductivity
| DE93-008466 | p 2687 N93-25113
Radiation-induced disordering and defect production in CuAu and NiAl studied by molecular dynamics simulation
| DE93-007506 | p 2649 N93-25336
Room temperature fracture of FeCo
| DE93-008266 | p 2650 N93-25519
Deformation mechanisms of NiAl cyclicly deformed near the brittle-to-ductile transition temperature
| NASA-CR-191121 | p 2652 N93-26235
Solidification processing and phase transformations in ordered high temperature alloys
| AD-A261751 | p 2652 N93-26284

INTERNAL COMBUSTION ENGINES
Evaluation of the Migrating Combustion Chamber (MCC) engine
| AD-A260780 | p 2718 N93-25682
Center for Advanced Propulsion Systems (fellowship)
| AD-A260571 | p 2632 N93-26216
Improved selective catalytic NOx control technology for compressor station reciprocating engines
| PB93-158566 | p 2768 N93-26529

INTERNAL WAVES
Selected results from LLNL-Hughes RAR for West Coast Scotland Experiment 1991
| DE93-006972 | p 2788 N93-24960

INTERNATIONAL COOPERATION
CEOS Committee on Earth Observations Satellites consolidated report, 1992
| NASA-TM-108776 | p 2615 N93-25217
Former Soviet Republic capabilities in space and science
| DE93-007613 | p 2598 N93-25322
Space research in Sweden, 1990-1991 p 2888 N93-25887
AGARD membership, 1993
| AGARD-MEMB-93 | p 2873 N93-26428

INTERNATIONAL GEOPHYSICAL YEAR
Data archaeology at ICES p 2734 N93-24931

INTERNATIONAL RELATIONS
Science, technology, and national security p 2886 N93-25232

INTERNATIONAL SUN EARTH EXPLORER 1
Anomalous aspects of magnetosheath flow and of the shape and oscillations of the magnetopause during an interval of strongly northward interplanetary magnetic field
| NASA-CR-192851 | p 2770 N93-25081

INTERNATIONAL SUN EARTH EXPLORER 2
Anomalous aspects of magnetosheath flow and of the shape and oscillations of the magnetopause during an interval of strongly northward interplanetary magnetic field
| NASA-CR-192851 | p 2770 N93-25081

INTERNATIONAL TRADE
Space business indicators p 2886 N93-26158
Technology for America's economic growth: A new direction to build economic strength
| AD-A261553 | p 2887 N93-26458

INTERPLANETARY DUST
Volatiles in interplanetary dust particles: A comparison with CI and CM chondrites p 2896 N93-26062

INTERPLANETARY MAGNETIC FIELDS
Anomalous aspects of magnetosheath flow and of the shape and oscillations of the magnetopause during an interval of strongly northward interplanetary magnetic field
| NASA-CR-192851 | p 2770 N93-25081

INTERPLANETARY SPACECRAFT
A determination of the radio-planetary frame tie from comparison of Earth orientation parameters p 2676 N93-26106

INTERPOLATION
Unsteady airfoil flow solutions on moving zonal grids
| AD-A261925 | p 2582 N93-26198

INTERPROCESSOR COMMUNICATION
Splash 2 p 2814 N93-25575
Anomalous event diagnosis for environmental satellite systems p 2619 N93-25971
An OSI architecture for the Deep Space Network p 2679 N93-26121

INTERSTELLAR GAS
Far-infrared emission, gas, and ultraluminous HII regions in M101
| NASA-CR-192791 | p 2890 N93-25755

INTERVALS
Timing and time signal distribution in digital communications networks p 2686 N93-25061
Synopsis of timing measurement techniques used in telecommunications p 2687 N93-25064

INTRAVEHICULAR ACTIVITY
Automation and robotics human performance
| NASA-CR-193049 | p 2802 N93-26153

INVENTIONS
Polyimides containing the cyclobutene-3,4-dione moiety
| NASA-CASE-LAR-14753-1 | p 2656 N93-25999

INVENTORIES
The ESA ISY initiatives for forest inventory in Europe p 2748 N93-24840
Estimating spares requirements for Space Station Freedom using the M-SPARE model
| AD-A260878 | p 2617 N93-25630
The state of computing at Los Alamos National Laboratory, FY 1991
| LA-12326-MS | p 2811 N93-25943

INVERSE KINEMATICS
Detailed solution to a complex kinematics chain manipulator
| DE93-004619 | p 2725 N93-25357
Numerical kinematic transformation calculations for a parallel link manipulator
| DE93-005778 | p 2718 N93-25449

INVERSE SCATTERING
Activity report
| AD-A261933 | p 2829 N93-26199

INVERSIONS
Elastic modeling and migration in Earth models p 2771 N93-25433

INVERTERS
Utilization of an electronic circuit simulator in CMOS latch-up studies
| AD-A260877 | p 2690 N93-25935

INVESTMENT CASTING
X-ray computed tomography for casting development
| AD-A261786 | p 2722 N93-26526

INVISCID FLOW
Nonlinear evolution of the first mode supersonic oblique waves in compressible boundary layers. Part 1: Heated/cooled walls
| NASA-TM-106087 | p 2696 N93-25175
Navier-Stokes simulations of unsteady transonic flow phenomena p 2578 N93-25542

IODINE
Surface discharge photoinitiation of pulsed chemical lasers
| DE93-006337 | p 2712 N93-24967

IODINE LASERS
Surface discharge photoinitiation of pulsed chemical lasers
| DE93-006337 | p 2712 N93-24967

ION ACCELERATORS
Summary of progress in inertial confinement fusion
| DE93-007350 | p 2858 N93-25187

ION BEAMS
Two-stream instability for a light ion beam-plasma system with external magnetic field
| NIFS-204 | p 2859 N93-25248
Metal ion implantation for large scale surface modification
| DE93-007649 | p 2859 N93-25324
Beam position and total current monitor for heavy ion fusion beams
| DE93-007653 | p 2851 N93-25325

Optical and scratch resistant properties of diamondlike carbon films deposited with single and dual ion beams
p 2658 N93-25564
Collisional energy transfer in biomolecular ion-molecule dynamics
| AD-A260911 | p 2849 N93-25659
Investigations of the transient behavior of the cathode fall region in planar and hollow cathodes
| AD-A261636 | p 2691 N93-26171

ION CURRENTS
Thermionic current measurement in quartz
p 2840 N93-25045
Plasma sheath effects on ion collection by a pinhole
| NASA-TM-106098 | p 2615 N93-25090

ION CYCLOTRON RADIATION
Plasma heating in toroidal systems
| NIFS-208 | p 2858 N93-25092
An outgoing energy flux boundary condition for finite difference ICRP antenna models
| DE93-007788 | p 2674 N93-25300

ION DENSITY (CONCENTRATION)
A study of vibrationally excited N2(+) ions in the daytime thermosphere p 2770 N93-25179
Diagnostics of diamond film deposition plasmas
| AD-A260866 | p 2860 N93-25626

ION IMPLANTATION
Photoluminescence of silicon nanostructures formed by ion beam implantation
| DE93-006777 | p 2862 N93-24958
Colloid formation in implanted glasses
| DE93-006763 | p 2653 N93-24971
Metal ion implantation for large scale surface modification
| DE93-007649 | p 2859 N93-25324
Analysis of pull-tests for determining the effects of ion implantation on the adhesion of iron films to sapphire substrates
| DE93-006732 | p 2725 N93-25373
Metastable SiC and SiGeC alloys by carbon implantation and solid phase epitaxy
| DE93-007594 | p 2863 N93-25387
Transmission electron microscopy investigation of ion implantation damage in GaAs and other semiconductors
p 2865 N93-25715
Electrical conductivity of ion implanted ladder and semi-ladder polymers
| AD-A261401 | p 2657 N93-26401

ION IRRADIATION
Aerospace devices for magnetic replicas
| NASA-CR-192958 | p 2865 N93-25667
State-selected studies of atoms and molecules ejected from ion bombarded surfaces
| AD-A261275 | p 2850 N93-26267

ION PROPULSION
Nuclear electric propulsion for planetary science missions: NASA technology program planning
| NASA-TM-106139 | p 2632 N93-26210

ION SOURCES
Penning detachment: A new frontier
| AD-A261447 | p 2850 N93-26346

ION STORAGE
Ion trap frequency standard research at PTB
p 2841 N93-25050
Controlling an optical frequency by a single ion
p 2841 N93-25051

ION TEMPERATURE
Plasma heating in toroidal systems
| NIFS-208 | p 2858 N93-25092
Ion temperature measurements in the Maryland Spheromak p 2859 N93-25290

ION TRAPS (INSTRUMENTATION)
Laser desorption in an ion trap mass spectrometer
| DE93-007330 | p 2712 N93-25150

IONIC COLLISIONS
Strangeness production in S + Pb and p + Pb collisions at 200 GeV/c per nucleon nucleon
| DE93-007654 | p 2847 N93-25326

IONIC REACTIONS
Collisional energy transfer in biomolecular ion-molecule dynamics
| AD-A260911 | p 2849 N93-25659
Theoretical treatment of spin-forbidden and electronically nonadiabatic processes. Methods and applications
| AD-A261596 | p 2851 N93-26525

IONIZATION
Theoretical and experimental research in infrared technology
| AD-A260926 | p 2853 N93-25646
The formation and characteristics of E-region thin ionization layers at high latitudes p 2861 N93-25829
Development of resonance ionization spectroscopy for genome mapping and DNA sequencing using stable isotopes as DNA labels
| DE93-007815 | p 2793 N93-26587

IONOGRAMS
High Frequency (HF) radiowave propagation
| AD-A261726 | p 2681 N93-26280
Digital Oblique Remote Ionospheric Sensing (DORIS) program development
| AD-A261750 | p 2776 N93-26283

IONOSPHERIC COMPOSITION
The formation and characteristics of E-region thin ionization layers at high latitudes p 2861 N93-25829

IONOSPHERIC ION DENSITY
The formation and characteristics of E-region thin ionization layers at high latitudes p 2861 N93-25829

IONOSPHERIC PROPAGATION
Theoretical study of topside ionospheric clutter
| AD-A260982 | p 2774 N93-25852
Statistics of sampled Rician fading
| AD-A261397 | p 2681 N93-26289
Nonlinear wave phenomena related to interactions in the ionosphere
| AD-A261450 | p 2776 N93-26348
The design and evaluation of transmit and receive antennas for an ionospheric communications probe system. B: Sloping-vee beams
| AD-A261866 | p 2682 N93-26388
A comparison of ionospheric propagation mode delay predictions from ADVANCED PROPHET 4.3 with measured data
| AD-A261782 | p 2686 N93-26604

IONOSPHERIC SOUNDING
Sounding rocket observations of precipitating ions in the morning auroral region p 2773 N93-25732

IONOSPHERIC TEMPERATURE
Study of auroral dynamics with combined spacecraft and incoherent-scatter radar data
| NASA-CR-192224 | p 2775 N93-26159

IONS
Collisional energy transfer in biomolecular ion-molecule dynamics
| AD-A260911 | p 2849 N93-25659
Sounding rocket observations of precipitating ions in the morning auroral region p 2773 N93-25732
Particle simulation of auroral double layers
p 2774 N93-25830
Intramolecular bridge/terminal oxo exchange within (MoV2O3) (4 +) complexes containing linear oxo bridges
| AD-A261230 | p 2851 N93-26518
Theoretical treatment of spin-forbidden and electronically nonadiabatic processes. Methods and applications
| AD-A261596 | p 2851 N93-26525
Liquid and solid ion plasmas
| AD-A261888 | p 2862 N93-26528

IRAQ
The General Information Programme (PGI) and developing countries: A case study of Iraq
p 2874 N93-25209

IRON
Analysis of pull-tests for determining the effects of ion implantation on the adhesion of iron films to sapphire substrates
| DE93-006732 | p 2725 N93-25373
Prediction of hydrogen entry and permeation in metals and alloys
| AD-A260580 | p 2651 N93-25903

IRON ALLOYS
Room temperature fracture of FeCo
| DE93-008266 | p 2650 N93-25519
Shear band formation in a W-Ni-Fe alloy under plate impact
| AD-A260702 | p 2651 N93-25907

IRRADIANCE
Comparison of high-resolution solar irradiance spectra and the solar luminosity in the period 1980-1989
| NASA-CR-192776 | p 2898 N93-25222

IRRADIATION
Long term drift and gamma-irradiation effect
p 2833 N93-24992
Radiation effects in germanium doped quartz
p 2837 N93-25021

IRRIGATION
Cartography and statistics of crops under irrigation in the Donana area of Andalucia through the use of Landsat-TM imagery and its incorporation into a GIS
p 2751 N93-24855

ISOLATION
Isolation and analysis of key components of seafloor relief
| AD-A261635 | p 2790 N93-26170

ISOPARAMETRIC FINITE ELEMENTS
Applications of parallel and vector algorithms in nonlinear structural dynamics using the finite element method
| AD-A260716 | p 2811 N93-25845

ISOPROPYL ALCOHOL
Development of a replacement for trichloroethylene in the two-stage cleaning process
| KCP-613-4941 | p 2669 N93-26207

ISOTOPE EFFECT
Thermal decomposition of energetic materials. 4: Deuterium isotope effects and isotopic scrambling condensed-phased decomposition of 1,3,5-trinitrohexahydro-s-triazine
| AD-A261804 | p 2662 N93-26387

ISOTOPE SEPARATION
Development of laser guide stars and adaptive optics for large astronomical telescopes
| DE93-007511 | p 2888 N93-25320

ISOTOPIC LABELING
Development of resonance ionization spectroscopy for genome mapping and DNA sequencing using stable isotopes as DNA labels
| DE93-007815 | p 2793 N93-26587

ITERATION
Monte Carlo approach to the approximation of invariant measures
| PB93-159069 | p 2830 N93-26317
Power iterations and the dominant eigenvalue problem
| AD-A261695 | p 2829 N93-26370
Boundedness and asymptotics of the generalized theodorus iteration
| AD-A261427 | p 2829 N93-26452

ITERATIVE SOLUTION
PCG: A software package for the iterative solution of linear systems on scalar, vector and parallel computers
| DE93-007366 | p 2809 N93-25315
The rapid solution of the Laplace equation on regions with fractal boundaries
| AD-A260585 | p 2828 N93-25905
Power iterations and the dominant eigenvalue problem
| AD-A261695 | p 2829 N93-26370

J

J INTEGRAL
J and CTOD estimation equations for shallow cracks in single edge notch bend specimens
| AD-A261679 | p 2731 N93-26390

JAPAN
Application of satellite imageries data to fisheries in Japan p 2745 N93-24822
Lightning characteristics in the north-east part of Japan observed by a magnetic direction-finder network
p 2779 N93-24892
Japanese Technology Evaluation Center Workshop on Advanced Manufacturing Technology for Polymer Composite Structures in Japan
| PB93-165249 | p 2641 N93-26589

JET BOUNDARIES
Liquid surface breakup of nonturbulent and turbulent liquids p 2700 N93-25473

JET ENGINE FUELS
Development of a method to determine the autoxidation of turbine fuels
| AD-A260578 | p 2661 N93-25902
Influence of supercritical conditions on pre-combustion chemistry and transport behavior of jet fuels
| AD-A261813 | p 2661 N93-26268
Oxides of nitrogen emissions from turbulent hydrocarbon/air jet diffusion flames, phase 2
| PB93-152478 | p 2768 N93-26533

JET ENGINES
External stress-corrosion cracking of a 1.22-m-diameter type 316 stainless steel air valve
| NASA-TP-3190 | p 2652 N93-26201
Development and demonstration of a new filter system to control emissions during jet engine testing
| AD-A261203 | p 2766 N93-26243

JET FLOW
The steady Navier-Stokes problem for low Reynolds number viscous jets p 2698 N93-25264
Experimental and computational investigation of helium injection into air at supersonic and hypersonic speeds
p 2577 N93-25487
The instability of a liquid jet in a compressible airstream p 2703 N93-25560
Algorithms for the analysis of penetration by shaped charge jets
| UCRL-LR-109887 | p 2730 N93-26178
Measurements of scalar power spectra in high Schmidt number turbulent jets
| AD-A261542 | p 2707 N93-26379
Oxides of nitrogen emissions from turbulent hydrocarbon/air jet diffusion flames, phase 2
| PB93-152478 | p 2768 N93-26533

JET IMPINGEMENT
Reduction in size and unsteadiness of a VTOL ground vortex by ground fences
| NASA-CR-192997 | p 2580 N93-26049

JET MIXING FLOW
Experimental and computational investigation of helium injection into air at supersonic and hypersonic speeds p 2577 N93-25487
Measurements of scalar power spectra in high Schmidt number turbulent jets
| AD-A261542 | p 2707 N93-26379
JOINED WINGS
Structural and aerodynamic optimization of joined-wing aircraft p 2588 N93-25526
JOINTS (JUNCTIONS)
SRB environment evaluation and analysis. Volume 2: RSRB joint filling test/analysis improvements
| NASA-CR-192518 | p 2631 N93-26057
JOSEPHSON JUNCTIONS
A superconducting tunnel junction receiver for submillimeter astronomy, and analysis of observations of post-AGB star molecular envelopes p 2889 N93-25440
Experimental and theoretical studies of proximity effect and Coulomb blockade phenomena in Josephson junctions
| AD-A261652 | p 2867 N93-26194
Advanced HTS S-N-S devices
| AD-A261552 | p 2869 N93-26381
JP-5 JET FUEL
Effect of a metal deactivator fuel additive on fuel deposition in fuel atomizers at high temperature
| AD-A260915 | p 2661 N93-25914

K

K-EPSILON TURBULENCE MODEL
Fuel injector: Air swirl characterization aerothermal modeling, phase 2, volume 1
| NASA-CR-189193 | p 2592 N93-24754
Fuel Injector: Air swirl characterization aerothermal modeling, phase 2, volume 2
| NASA-CR-189193 | p 2592 N93-25106
Predictive modeling of particle-laden, turbulent flows
| DE93-008208 | p 2698 N93-25309
Studies in air/air supersonic mixing layers p 2582 N93-26007
Interactions of acoustic waves and combustion of homogeneous solid propellants in rocket motors p 2630 N93-26039
KALMAN FILTERS
Testing of the on-board attitude determination and control algorithms for SAMPEX p 2600 N93-24698
Orbit determination and orbit control for the Earth Observing System (EOS) AM spacecraft p 2601 N93-24705
Computationally efficient algorithms for real-time attitude estimation p 2602 N93-24709
Improvements in ERBS attitude determination without gyros p 2602 N93-24710
Rate determination from vector observations p 2603 N93-24713
Scalar gain interpretation of large order filters p 2606 N93-24729
Quaternion normalization in spacecraft attitude determination p 2606 N93-24730
Upper Atmosphere Research Satellite (UARS) onboard attitude determination using a Kalman filter p 2606 N93-24732
Orbital parameter estimation using an extended Kalman filter
| AD-A260618 | p 2608 N93-25636
Recommendations for a Kalman filter to estimate and control freeze and sublime rates of gaseous diffusion plant freezer/sublimer systems
| ORNL/TM-12183 | p 2668 N93-25937
System for calibrating a gyro navigator
| AD-D015668 | p 2586 N93-26093
On-line implementation of nonlinear parameter estimation for the Space Shuttle main engine
| NASA-TM-106097 | p 2632 N93-26211
PDE: Differential, geometric and algebraic methods in nonlinear filtering
| AD-A260967 | p 2829 N93-26222
More rain compensation results p 2686 N93-26486
KAONS
Topics in CP violation
| DE93-007615 | p 2847 N93-25323
Results from the NA36 on strangeness production in 200 GeV/c per nucleon S + Pb and p - Pb reactions
| DE93-007711 | p 2848 N93-25364
KENYA
The extent and status of mangroves in Mombasa district, Kenya: A case study based on remote sensing p 2746 N93-24826
KERNEL FUNCTIONS
Fast mutual exclusion for uniprocessors
| AD-A261663 | p 2883 N93-26389
KERR MAGNETOOPTICAL EFFECT
Femtosecond dynamics in hydrogen-bonding solvents: Formamides
| DE93-003476 | p 2643 N93-25123
KINEMATIC EQUATIONS
Numerical kinematic transformation calculations for a parallel link manipulator
| DE93-005778 | p 2718 N93-25449
KINEMATICS
Rate determination from vector observations p 2603 N93-24713
Position and force control of a vehicle with two or more steerable drive wheels
| DE92-041301 | p 2717 N93-25100
Equilibrium constrained assumed natural coordinate strain finite elements for shell analysis p 2724 N93-25273
On the vertical structure of seasonal, interannual and intraseasonal flows p 2782 N93-25557
Studies in air/air supersonic mixing layers p 2582 N93-26007
KINETIC ENERGY
Collisional energy transfer in biomolecular ion-molecule dynamics
| AD-A260911 | p 2849 N93-25659
An investigation of the role of flux divergence in the turbulent kinetic energy balance of the atmospheric surface layer p 2773 N93-25756
KINETICS
Thermal decomposition of HMX, mononitroso-RDX, TNCHP and K6 in the liquid phase: Results from simultaneous thermogravimetry modulated beam mass spectrometry measurements p 2628 N93-26033
Phase-field models for anisotropic interfaces
| PB93-164564 | p 2646 N93-26323
KLYSTRONS
Transverse instabilities in a relativistic klystron two-beam accelerator
| DE93-007110 | p 2852 N93-25375
BBU code development for high-power microwave generators
| DE93-007111 | p 2688 N93-25397
Improvements in X-band transmitter phase stability through Klystron body temperature regulation p 2678 N93-26114
KNOWLEDGE BASED SYSTEMS
How far we are from the complete knowledge: Complexity of knowledge acquisition in Dempster-Shafer approach
| NASA-CR-192944 | p 2874 N93-25139
How to help intelligent systems with different uncertainty representations cooperate with each other
| NASA-CR-192947 | p 2818 N93-25196
Min and max are the only continuous ampersand-, V-operations for finite logics
| NASA-CR-192952 | p 2820 N93-25452
Multi-viewpoint clustering analysis p 2825 N93-25980
Knowledge-based decision support for Space Station assembly sequence planning
| NASA-CR-193048 | p 2599 N93-26095
Design Knowledge Management System (DKMS) Beta Test Report
| AD-A261453 | p 2883 N93-26350
KNOWLEDGE BASES (ARTIFICIAL INTELLIGENCE)
How far we are from the complete knowledge: Complexity of knowledge acquisition in Dempster-Shafer approach
| NASA-CR-192944 | p 2874 N93-25139
Optimization of knowledge-based systems and expert system building tools
| NASA-CR-192763 | p 2874 N93-25288
Development of a heuristic knowledge base for the selection of applicable or relevant and appropriate environmental requirements
| AD-A261038 | p 2765 N93-25864
KNOWLEDGE REPRESENTATION
A knowledge-based approach to waste disposal sites detection through integration of Landsat-TM imagery and geographical context information p 2741 N93-24796
Min and max are the only continuous ampersand-, V-operations for finite logics
| NASA-CR-192952 | p 2820 N93-25452
TARGET: Rapid capture of process knowledge p 2814 N93-25590
A study of mapping exogenous knowledge representations into CONFIG p 2827 N93-26072
Design Knowledge Management System (DKMS) Beta Test Report
| AD-A261453 | p 2883 N93-26350
KOLMOGOROFF THEORY
PDE: Differential, geometric and algebraic methods in nonlinear filtering
| AD-A260967 | p 2829 N93-26222
KRYPTON FLUORIDE LASERS
Mercury: The Los Alamos ICF KrF laser system
| DE93-007363 | p 2713 N93-25379
KURTOSIS
Evaluation of a vibration diagnostic system for the detection of spur gear pitting failures
| NASA-TM-106103 | p 2718 N93-25672

L

LACTATES
The 0.3 mm diameter flexible amperometric lactate probe
| AD-A260826 | p 2690 N93-25782
LAGEOS (SATELLITE)
STS-52 Space Shuttle mission report
| NASA-CR-193061 | p 2613 N93-25993
LAGRANGIAN FUNCTION
Formulation and treatment of frictional contact problems using finite elements p 2717 N93-25412
Image correlation velocimetry
| AD-A261599 | p 2707 N93-26163
An extended Lagrangian method
| NASA-TM-106129 | p 2707 N93-26203
Chaos metrics for testing lagrangian particle models
| AD-A261429 | p 2776 N93-26454
LAKES
Inherent optical properties of lakes as measured by Landsat 5 Thematic Mapper p 2746 N93-24828
Earthquake vulnerability map of the Lake Constance area p 2753 N93-24872
LAMB WAVES
Elastic plate mode sensitivities to mass loading applications to gas sensors p 2711 N93-25009
LAMINAR FLOW
A premixed laminar flame interacting with a vortex resulting in flame stretch and quenching p 2642 N93-24771
Combined LAURA-UPS hypersonic solution procedure
| NASA-TM-107682 | p 2696 N93-25176
Laminar and turbulent natural convection heat transfer in Trombe wall channels p 2702 N93-25551
Stationary crossflow instability on an infinite swept wing p 2580 N93-25865
On the cross-stream spectral method for the Orr-Sommerfeld equation
| NASA-TM-107737 | p 2845 N93-26086
Solution of nonlinear boundary value problem on successively refined grids
| AD-A261395 | p 2829 N93-26519
LAMINATES
Vibration, buckling, and postbuckling of laminated composites with delaminations p 2723 N93-24765
Axisymmetric deformations and stresses of unsymmetrically laminated composite cylinders in axial compression with thermally-induced preloading effects
| NASA-CR-192788 | p 2723 N93-24912
High Temperature Composite Analyzer (HITCAN) theoretical manual, version 1.0
| NASA-TM-106001 | p 2723 N93-24913
High temperature composite analyzer (HITCAN) user's manual, version 1.0
| NASA-TM-106002 | p 2724 N93-25070
Stress distribution in composite flatwise tension test specimens
| NASA-TM-106074 | p 2634 N93-25071
Processing and mechanical properties of laminated metal composites of Al/Al-25 vol. percent SiC and ultrahigh carbon steel/brass
| DE93-007504 | p 2635 N93-25383
Graphite/epoxy composite laminates with co-cured interlaminar damping layers p 2642 N93-25587
Damage-survivable and damage-tolerant laminated composites with optimally placed piezoelectric layers
| AD-A260879 | p 2636 N93-25631
Numerical simulation of damage and progressive failures in composite laminates using the layerwise plate theory p 2636 N93-25661
Inelastic behavior of thermoplastic composites p 2636 N93-25674
Investigation and modeling of penetration process for composite laminates impacted by a blunt-ended projectile p 2637 N93-25675
Quantifying distributed damage in composites via the thermoelastic effect p 2637 N93-25691
Low-velocity impact of composite sandwich plate p 2637 N93-25695
Design and analysis of curved composite components for rotorcraft fuselage frames p 2589 N93-25701
Thermal expansion measurements of polymer matrix composites and syntactics
| MTL-TR-92-27 | p 2640 N93-25954
LAND MANAGEMENT
European applications of space-borne Earth observation for land cover mapping p 2745 N93-24820

Remote sensing of land resource management in agriculture with regard to its influence on the environment p 2750 N93-24850

LAND MOBILE SATELLITE SERVICE

Numerical and experimental analyses of large composite skeletal satellite systems p 2616 N93-25463

L- and K-band LMSS propagation measurements using MARECS-B, OLYMPUS, and ACTS p 2683 N93-26467

LAND SURFACE TEMPERATURE

Surface energy fluxes at Central Florida during the convection and precipitation electrification experiment | NASA-CR-192826 | p 2769 N93-24945

Evaluating climate-vegetation interactions at climate model sub-grid scales p 2764 N93-25476

LAND USE

Application of remote sensing data for the investigation of environmental degradation sites in East Germany p 2739 N93-24785

Land cover monitoring in the Netherlands applying satellite remote sensing p 2740 N93-24789

Detection of land use/land cover changes using remote sensing and GIS in Vietnam p 2740 N93-24791

The photointerpretation of the area taken over from agriculture by intense urbanization at Villabate (Palermo, Italy) p 2742 N93-24800

European applications of space-borne Earth observation for land cover mapping p 2745 N93-24820

Aerial photographic sampling for statewide resource inventory p 2755 N93-25441

LANDSAT SATELLITES

Bibliography of remote sensing techniques used in wetland research | AD-A261704 | p 2757 N93-26440

LANDSAT 4

Classifying multispectral data by neural networks p 2825 N93-25976

LANGMUIR-BLODGETT FILMS

Molecular devices based on new monolayer-forming systems | AD-A260996 | p 2866 N93-25854

LANGUAGES

Languages for requirements specifications | RSRE-MEMO-4585 | p 2810 N93-25453

LAP JOINTS

Investigation of corrosion in aluminum/adhesive lap-splices using pulse-echo ultrasonic techniques | DE93-008074 | p 2721 N93-25518

LAPLACE EQUATION

The rapid solution of the Laplace equation on regions with fractal boundaries | AD-A260585 | p 2828 N93-25905

LAPLACE TRANSFORMATION

Stress and reliability analyses of multilayered composite cylinder under thermal and mechanical loads p 2726 N93-25533

LARGE DEPLOYABLE REFLECTOR

Numerical and experimental analyses of large composite skeletal satellite systems p 2616 N93-25463

LARGE SPACE STRUCTURES

Optimal control of large space structures p 2819 N93-25343

Identification and control of lightly damped, large space structures: An experimental evaluation p 2616 N93-25351

Analytical and experimental study of control effort associated with model reference adaptive control p 2820 N93-25468

The dynamics and control of large flexible asymmetric spacecraft p 2617 N93-25525

Dynamics and robust control of a sampled data system for large space structures. Volume 2: The LQG/LTR methodology for the discrete-time system and the design of reduced order robust digital controller for orbiting flexible shallow spherical shell system | AD-A260793 | p 2599 N93-25693

Nonlinear dynamics and attitude control of articulated flexible space structures p 2617 N93-25726

Center for Space Construction Third Annual Symposium | NASA-CR-192688 | p 2669 N93-26405

Dynamics of on-orbit construction process p 2669 N93-26406

Interaction dynamics and control for orbital assembly p 2669 N93-26407

Controls for orbital assembly of large space structures p 2620 N93-26408

Structural load control during construction p 2669 N93-26409

LASER ABLATION

Structure and properties of a-C: N films prepared by pulsed excimer laser deposition | DE93-007908 | p 2654 N93-25372

Fast diagnostics of laser ablation used for pulsed laser deposition | DE93-005155 | p 2713 N93-25508

LASER ALTIMETERS

A ground track control algorithm for the Topographic Mapping Laser Altimeter (TMLA) p 2602 N93-24707

LASER APPLICATIONS

A compact and high-performance reference cell for laser frequency stabilization p 2716 N93-25065

Laser desorption in an ion trap mass spectrometer | DE93-007330 | p 2712 N93-25150

Laser ignition application in a space experiment | NASA-TM-106133 | p 2664 N93-25337

JPRS report: Science and technology. Central Eurasia: Physics and mathematics | JPRS-UPM-92-004 | p 2844 N93-25402

JPRS report: Science and technology. Central Eurasia: Physics and mathematics | JPRS-UPM-92-003 | p 2844 N93-25403

JPRS report: Science and technology. Central Eurasia: Physics and mathematics | JPRS-UPM-93-001 | p 2844 N93-25404

Laser Induced Phonons (LIPs) in MBE grown ZnSe | RSRE-MEMO-4544 | p 2864 N93-25454

Laser initiated corrosion pits on aluminum p 2650 N93-25464

Application of an on-machine gage for diameter measurements p 2711 N93-25578

Liquid crystals for laser applications | AD-A261209 | p 2714 N93-25869

Method of joining diamond structures | AD-D015671 | p 2867 N93-26140

Research support for the Laboratory for Lightwave Technology | AD-A261488 | p 2856 N93-26343

Molecular interactions and properties with many-body methods | AD-A261688 | p 2850 N93-26367

LASER ARRAYS

Ultraviolet waveguide lasers for phased array lidar | AD-A261657 | p 2715 N93-26363

LASER BEAMS

Laser beamed power: Satellite demonstration applications | NASA-CR-190793 | p 2623 N93-25132

Summary of progress in inertial confinement fusion | DE93-007350 | p 2858 N93-25187

Laser field assisted photoemission using femtosecond laser pulses | DE93-007277 | p 2712 N93-25378

Laser propagation through turbulence | AD-A260712 | p 2714 N93-26217

Loss of temporal coherence of laser light propagated through simulated coastal waters | AD-A261303 | p 2715 N93-26296

Efficient nonlinear optical conversion of 1.319-micron laser radiation | AD-A261309 | p 2715 N93-26297

Laser physics and laser techniques | AD-A261595 | p 2715 N93-26524

Modeling of electric-field enhancement at nodular defects in dielectric mirror coatings | DE93-007513 | p 2857 N93-26593

LASER CAVITIES

Fundamental characteristics of a laser-diode-pumped rubidium maser with an external feedback loop p 2716 N93-25068

LASER DAMAGE

Surface preparation and characterization of a 400 micrometer diameter fused silica optical fiber for direct optical initiation (DOI) applications | DE93-005485 | p 2852 N93-25182

Correlation of damage threshold and surface geometry of nodular defects in HR coatings as determined by in-situ atomic force microscopy | DE93-007509 | p 2654 N93-25384

Modeling of electric-field enhancement at nodular defects in dielectric mirror coatings | DE93-007513 | p 2857 N93-26593

Laser damage to production- and research-grade KDP crystals | DE93-007517 | p 2870 N93-26594

LASER DOPPLER VELOCIMETERS

An investigation of laser velocimetry measurements within high speed, complex flows p 2697 N93-25237

Measurement of velocities in gas-liquid two-phase flow using laser Doppler velocimetry | DE93-008083 | p 2698 N93-25306

Pulsed laser Rayleigh scattering diagnostic for hydrogen/oxygen rocket exit plane flowfield velocimetry | NASA-TM-106098 | p 2631 N93-26149

Trailing vortex/free-surface interaction | AD-A261654 | p 2581 N93-26195

LASER FUSION

Start-up imprinting and shock dynamics in laser-target interaction | AD-A261384 | p 2715 N93-26445

Laser damage to production- and research-grade KDP crystals | DE93-007517 | p 2870 N93-26594

LASER GUIDANCE

Feasibility experiment for sodium-layer laser guide stars at the Lawrence Livermore National Laboratory | DE93-007115 | p 2715 N93-26503

LASER GYROSCOPES

An active solid state ring laser gyroscope p 2709 N93-25291

Applications of inertial-sensor high-inheritance instruments to DSN precision antenna pointing p 2621 N93-26112

LASER INDUCED FLUORESCENCE

Measurements of soot formation and hydroxyl concentration in near critical equivalence ratio premixed ethylene flame | NASA-CR-191099 | p 2642 N93-25116

Development of a cone penetrometer for measuring spectral characteristics of soils in situ p 2776 N93-25570

Visualization of a Mach 2 reacting flow using Planar Laser-Induced Fluorescence (PLIF) p 2598 N93-26006

LASER MATERIALS

Laser damage to production- and research-grade KDP crystals | DE93-007517 | p 2870 N93-26594

LASER MODE LOCKING

Time resolved studies of in-well and cross-well carrier transport in MQW semiconductor structures | AD-A261170 | p 2714 N93-25774

Laser physics and laser techniques | AD-A261595 | p 2715 N93-26524

LASER MODES

Fundamental characteristics of a laser-diode-pumped rubidium maser with an external feedback loop p 2716 N93-25068

Laser physics and laser techniques | AD-A261595 | p 2715 N93-26524

LASER OUTPUTS

An active solid state ring laser gyroscope p 2709 N93-25291

Laser field assisted photoemission using femtosecond laser pulses | DE93-007277 | p 2712 N93-25378

Injection seeded, diode-pumped, short pulse Nd:YAG ring laser for space-based laser ranging p 2713 N93-25389

Experimental and theoretical study of cw HF chemical laser overtone performance p 2713 N93-25420

Experimental and theoretical study of CW HF chemical laser residual fundamental gain p 2714 N93-25721

Start-up imprinting and shock dynamics in laser-target interaction | AD-A261384 | p 2715 N93-26445

Laser physics and laser techniques | AD-A261595 | p 2715 N93-26524

Modeling of electric-field enhancement at nodular defects in dielectric mirror coatings | DE93-007513 | p 2857 N93-26593

FALCON nuclear-reactor-pumped laser program and wireless power transmission | DE93-007607 | p 2715 N93-26597

LASER PLASMA INTERACTIONS

Surface discharge photoinitiation of pulsed chemical lasers | DE93-006337 | p 2712 N93-24967

LASER PLASMAS

IR and FIR laser diagnostics for plasma thrusters using a CW CO2 radiation source | AD-A261399 | p 2862 N93-26520

LASER POWER BEAMING

Laser beamed power: Satellite demonstration applications | NASA-CR-190793 | p 2623 N93-25132

Handbook of actuators and edge alignment sensors | NASA-CR-193203 | p 2620 N93-25317

Space transfer concepts and analyses for exploration missions. Technical directive 12: Beamed power systems study | NASA-CR-192532 | p 2599 N93-26146

FALCON nuclear-reactor-pumped laser program and wireless power transmission | DE93-007607 | p 2715 N93-26597

LASER PUMPING

Experiments on a diode-laser-pumped Rb-87 maser p 2716 N93-25030

Fundamental characteristics of a laser-diode-pumped rubidium maser with an external feedback loop p 2716 N93-25068

Injection seeded, diode-pumped, short pulse Nd:YAG ring laser for space-based laser ranging p 2713 N93-25389

1992 technical digest series volume 16. Conference edition: Summaries of papers presented at the Nonlinear Dynamics in Optical Systems Topical Meeting
| AD-A261915 | p 2857 N93-26544

LASER RANGE FINDERS
A system design for laser time synchronization via geodetic satellite Ajisai p 2716 N93-25005
Injection seeded, diode-pumped, short pulse Nd:YAG ring laser for space-based laser ranging p 2713 N93-25389
Real-time construction and rendering of three-dimensional occupancy maps
| DE93-007818 | p 2756 N93-25516
Preliminary studies leading toward the development of a LIDAR bathymetry mapping instrument p 2711 N93-25614
A determination of the radio-planetary frame tie from comparison of Earth orientation parameters p 2676 N93-26106
Lageos laser ranging earth rotation
| AD-A261471 | p 2757 N93-26354

LASER TARGET INTERACTIONS
Start-up imprinting and shock dynamics in laser-target interaction
| AD-A261384 | p 2715 N93-26445

LASER WELDING
Laser welding of selected aerospace alloys p 2718 N93-25435

LASERS
Mercury: The Los Alamos ICF KrF laser system
| DE93-007363 | p 2713 N93-25379
Robotic Variable Polarity Plasma Arc (VPPA) welding p 2720 N93-25605
Adaptive laser link reconfiguration using constraint propagation p 2823 N93-25967
Efficient nonlinear optical conversion of 1.319-micron laser radiation
| AD-A261309 | p 2715 N93-26297

LASING
FALCON nuclear-reactor-pumped laser program and wireless power transmission
| DE93-007607 | p 2715 N93-26597

LATENT HEAT
Local and regional estimates of sensible and latent heat flux densities from a patch-work surface
| ISBN-0-315-70882-4 | p 2772 N93-25556

LATERAL CONTROL
Monaural and binaural processing of complex waveforms
| AD-A261659 | p 2846 N93-26358

LATTICE VIBRATIONS
Spectroscopic effects of disorder and vibrational localization in mixed-halide metal-halide chain solids
| DE93-007361 | p 2646 N93-26505

LAUNCH VEHICLE CONFIGURATIONS
National Launch System. Task 4: System architecture options analysis
| MCR-92-5011 | p 2609 N93-26098

LAUNCH VEHICLES
What is the relationship between altitude and weight in a model rocket? p 2603 N93-24715
Development of models for predicting the triggering of lightning by launch vehicles p 2610 N93-24899
Space transfer vehicle concepts and requirements study. Volume 1: Executive summary
| NASA-CR-192524 | p 2610 N93-25479
Space transfer vehicle concepts and requirements study. Volume 2, book 2: System and program requirements trade studies
| NASA-CR-192526 | p 2611 N93-25511
Space transfer vehicle concepts and requirements study. Volume 2, book 3: STV system interfaces
| NASA-CR-192527 | p 2611 N93-25513

LAUNCH WINDOWS
Practical aspects of transfer from GTO to lunar orbit p 2604 N93-24719

LAUNCHING
Systems engineering considerations for operational support systems p 2666 N93-24689
Investigation of the effects of Extra Vehicular Activity (EVA) and Launch and Entry (LES) gloves on performance p 2803 N93-26061
Use of Taguchi design of experiments to optimize and increase robustness of preliminary designs p 2670 N93-26063
Task 2A: UNIS requirements and concepts
| MCR-92-5006-PT-A | p 2610 N93-26180
Develop margin philosophy to attain robustness
| MCR-92-5005 | p 2610 N93-26182
Task Type E report for National Launch Demonstration Center (NLDC) (Task 32)
| MCR-91-5010 | p 2610 N93-26591

LAUNCHING BASES
A system to measure lightning-induced transients on spacecraft umbilical lines p 2693 N93-24889

LAUNCHING SITES
Launch pad lightning protection enhancement by induced streamers p 2609 N93-24876

LEACHING
Production of ultrafine, high-purity ceramic powders using the US Bureau of Mines developed turbomill p 2659 N93-25585

LEAD (METAL)
Results from the NA36 on strangeness production in 200 GeV/c per nucleon S + Pb and p - Pb reactions
| DE93-007711 | p 2848 N93-25364

LEAD SELENIDES
Introduction to lead salt infrared detectors
| AD-A260781 | p 2710 N93-25686

LEAD SULFIDES
Introduction to lead salt infrared detectors
| AD-A260781 | p 2710 N93-25686

LEAD TITANATES
Research on lead titanate films for radiation detection
| AD-A261187 | p 2849 N93-25823

LEADING EDGE FLAPS
Conical Euler analysis and active roll suppression for unsteady vortical flows about rolling delta wings
| NASA-TP-3259 | p 2581 N93-26134

LEADING EDGES
The transient development of vortices over delta wings p 2576 N93-25269
Numerical simulation of leading-edge receptivity to freestream vorticity p 2577 N93-25388

LEAKAGE
Inward contaminant leakage tests of the S-Tron Corporation emergency escape breathing device. Phase 1: Tests of the original design. Phase 2: Tests with the redesigned neck seal
| DOT/FAA/AM-92/18 | p 2582 N93-25205
Tank issues: Design and placement of vapor monitoring wells
| PB93-161131 | p 2768 N93-26536

LEAST SQUARES METHOD
TDRSS-user orbit determination using batch least-squares and sequential methods p 2601 N93-24703
Stabilized finite element methods for incompressible flows with emphasis on moving boundaries and interfaces p 2703 N93-25663
Estimation of coefficients in a rational function from observed values
| AD-A261126 | p 2828 N93-25773

LEG (ANATOMY)
Anthropometry of the foot and lower leg of U.S. Army soldiers: Fort Jackson, SC
| AD-A261405 | p 2802 N93-26404

LENNARD-JONES POTENTIAL
Experimental and theoretical studies of dense fluid mixtures
| DE93-006070 | p 2695 N93-24976

LENSES
The prevalence of artificial lens implants in the civil airman population
| DOT/FAA/AM-92/14 | p 2794 N93-25214
A fiber optic probe for the detection of cataracts p 2796 N93-25593

LESIONS
Neuropsychological components of object identification
| AD-A261449 | p 2797 N93-26347

LEVITATION
Tuned circuit electric levitation bearings for microactuators p 2689 N93-25619

LEWIS NUMBERS
A premixed laminar flame interacting with a vortex resulting in flame stretch and quenching p 2642 N93-24771
Modelling of microgravity ignition phenomena p 2664 N93-25465

LIAPUNOV FUNCTIONS
Control of nonlinear systems under input constraints with applications to flight control p 2596 N93-25353

LIBRARIES
Crossing the frontier between publishing and information service
| DE93-002894 | p 2873 N93-24677
Interactive interface for National Center for Atmospheric Research (NCAR) Graphics p 2878 N93-25794
Proceedings of the 33rd Annual Military LibrariansWorkshop
| AD-A261071 | p 2882 N93-26242

LIBRATION
Optimal transfers between libration-point orbits in the elliptic restricted three-body problem p 2608 N93-25758

LIBRATIONAL MOTION
Femtosecond dynamics in hydrogen-bonding solvents: Formamides
| DE93-003476 | p 2643 N93-25123

LIBYA
Remote sensing of coastal zone Sabkha deposits, Gulf of Sirt, Libya p 2746 N93-24827

LIFE (DURABILITY)
A new approach to cooled combustion chambers: The 40K formed platelet chamber p 2626 N93-26018

LIFE CYCLE COSTS
Space transfer concepts and analyses for exploration missions. Technical directive 12: Beamed power systems study
| NASA-CR-192532 | p 2599 N93-26146
Cost-effectiveness analysis of TxDOT CNG fleet conversion, volume 1
| PB93-165603 | p 2720 N93-26585

LIFE SCIENCES
JPRS report: Science and technology. Central Eurasia: Life sciences
| JPRS-ULS-93-002 | p 2737 N93-25399
JPRS report: Science and technology. Central Eurasia: Life sciences
| JPRS-ULS-92-025 | p 2793 N93-25405
The effects of video compression on acceptability of images for monitoring life sciences' experiments p 2805 N93-25930

LIFE SUPPORT SYSTEMS
A survey of life support system automation and control
| NASA-TM-103977 | p 2667 N93-25085
Near Earth object fuels (neo-fuels): Discovery, prospecting and use
| DE93-005185 | p 2892 N93-25164
Space life support technology applications to terrestrial environmental problems p 2803 N93-25617
Advanced life support study. Modification 10: ECLSS logistical support analysis for Space Station Freedom
| NASA-CR-192481 | p 2801 N93-25888
Membrane technology: A search for membranes for submarine atmosphere control
| AD-A260581 | p 2801 N93-25904
Integrated oxygen recovery system
| NASA-CR-192982 | p 2801 N93-26088

LIFT
An analysis of lift forces on aerosols in a wall bounded turbulent shear flow
| DE93-003362 | p 2695 N93-24963
Aerodynamic foundations for use of unsteady aerodynamic effects in flight control p 2576 N93-25274

LIGANDS
Intramolecular bridge/terminal oxo exchange within (MoV2O3) (4+) complexes containing linear oxo bridges
| AD-A261230 | p 2851 N93-26518

LIGHT BEAMS
A fiber optic probe for the detection of cataracts p 2796 N93-25593
Analysis and design of a novel robotic finger-tip sensor for adaptive grasping p 2719 N93-25745

LIGHT EMISSION
Visible light emission from porous silicon examined by photoluminescence and Raman spectroscopy
| DE93-006780 | p 2646 N93-26502

LIGHT EMITTING DIODES
Emerging large-screen display technology
| AD-A261066 | p 2681 N93-26241

LIGHT IONS
Summary of progress in inertial confinement fusion
| DE93-007350 | p 2858 N93-25187

LIGHT SCATTERING
Coarsening of a quiescent electrorheological fluid I: Experiment
| DE93-006776 | p 2642 N93-24972
Analysis of LARI sensor system
| DE93-006334 | p 2761 N93-24977
Magnetic excitations in antiferromagnetically coupled superlattices: Fe/Mo and Fe/Cr
| DE93-007894 | p 2863 N93-25369
The role of multiple scattering in twilight zenith sky observations of atmospheric absorbers: Diurnal photochemistry and airmass factors p 2772 N93-25535
A fiber optic probe for the detection of cataracts p 2796 N93-25593
Measurement of optical properties of infrared bandgap superlattices
| AD-A260859 | p 2866 N93-25789
Experimental studies of fundamental problems in quantum optics
| AD-A261183 | p 2853 N93-25822
Development of an expendable particle sensor
| AD-A261127 | p 2710 N93-26044
Pulsed laser Rayleigh scattering diagnostic for hydrogen/oxygen rocket exit plane flowfield velocimetry
| NASA-TM-106098 | p 2631 N93-26149
Loss of temporal coherence of laser light propagated through simulated coastal waters
| AD-A261303 | p 2715 N93-26296

LIGHT TRANSMISSION
The DX centers in three to five semiconductors under hydrostatic pressure
| DE93-007701 | p 2864 N93-25490
LIGHTING EQUIPMENT
Launch pad lightning protection enhancement by induced streamers p 2609 N93-24876
LIGHTNING
The 1992 International Aerospace and Ground Conference on Lightning and Static Electricity: Addendum
| DOT/FAA/CT-92/20-ADD-1 | p 2777 N93-24875
Launch pad lightning protection enhancement by induced streamers p 2609 N93-24876
Lightning precursor signatures from dual-polarization radar measurements of storms p 2777 N93-24877
Applications of triggered lightning to space vehicle operations p 2619 N93-24878
Numerical modelling of induced effects of lightning strike on an all composite helicopter p 2583 N93-24879
Zoning of aircraft: A review of the definitions p 2583 N93-24880
Equipment testing with damped sinewaves between 1 and 50 MHz p 2692 N93-24881
Lightning data acquisition p 2778 N93-24883
Digitization of analog data from in-flight lightning strikes p 2778 N93-24884
A procedure for defining lightning risk to air vehicles p 2583 N93-24885
Parameters influencing the hot-spot ignition of aviation fuel/air and ethylene/air mixtures p 2583 N93-24886
Observation of radiation from lightning discharges by LPATS p 2779 N93-24888
A system to measure lightning-induced transients on spacecraft umbilical lines p 2693 N93-24889
A computational approach to predicting the extent of arc root damage in CFC panels p 2642 N93-24890
Comparison of the damage for various types of fibre reinforced composites due to different lightning test standards (MIL-STD-1757A, German military VG-standard 96903) p 2642 N93-24891
Lightning characteristics in the north-east part of Japan observed by a magnetic direction-finder network p 2779 N93-24892
Fractal determination of parameters in lightning and ESD model p 2686 N93-24893
Zoning of aircraft by electric field modelling p 2583 N93-24894
Lightning phenomenology bases for full threat return stroke occurrence following extended leader sweep at flight altitudes p 2780 N93-24895
Positive cloud-to-ground flashes in severe storms p 2780 N93-24896
Study of atmospheric electrical events above complex terrain p 2780 N93-24897
Applications of stress envelope concepts to aircraft EMP and lightning survivability p 2584 N93-24898
Development of models for predicting the triggering of lightning by launch vehicles p 2610 N93-24899
A single-point warning system for thunderstorms and electric fields p 2711 N93-24900
Comparative performance of lightning air terminals under natural storm conditions p 2781 N93-24902
Remote sensing of precipitation and electrification with a dual-polarization, coherent, wideband radar system
| AD-A260779 | p 2756 N93-25679
The initiation of lightning and the growth of electric fields in thunderstorms
| AD-A261455 | p 2787 N93-26352
LIGHTNING SUPPRESSION
Applications of triggered lightning to space vehicle operations p 2619 N93-24878
Equipment testing with damped sinewaves between 1 and 50 MHz p 2692 N93-24881
Comparative performance of lightning air terminals under natural storm conditions p 2781 N93-24902
LINE OF SIGHT
Tomographic analysis of sight infrared spectra of low pressure flames p 2628 N93-26030
LINE SHAPE
Accurate determination of Auger line shape binding energies
| AD-A261803 | p 2868 N93-26258
LINE SPECTRA
Density dependence of line intensities and application to plasma diagnostics
| NIFS-209 | p 2857 N93-24950
Line formation and the Poynting-Robertson effect in accretion discs p 2847 N93-25355
Exploitation of cyclostationarity for signal-parameter estimation and system identification
| AD-A260833 | p 2728 N93-25784
Accurate determination of Auger line shape binding energies
| AD-A261803 | p 2868 N93-26258
LINEAR ARRAYS
Research on lead titanate films for radiation detection
| AD-A261187 | p 2849 N93-25823
LINEAR EQUATIONS
Some new results for solving linear systems arising from computational fluid dynamics problems p 2699 N93-25349
LINEAR FILTERS
Scalar gain interpretation of large order filters p 2606 N93-24729
LINEAR PREDICTION
Rain compensation algorithm using adaptive linear prediction p 2685 N93-26485
LINEAR PROGRAMMING
Linear-programming tools in integer programming: The traveling salesman
| AD-A261398 | p 2812 N93-26290
Methods of optimization under uncertainty
| AD-A261487 | p 2873 N93-26342
Integrated approaches to parallelism in optimization and the solution of inverse problems
| AD-A261490 | p 2829 N93-26344
LINEAR QUADRATIC GAUSSIAN CONTROL
Design of the reduced LQG compensator for the DSS-13 antenna p 2672 N93-24669
Identification and control of lightly damped, large space structures: An experimental evaluation p 2616 N93-25351
Dynamics and robust control of a sampled data system for large space structures. Volume 2: The LQG/LTR methodology for the discrete-time system and the design of reduced order robust digital controller for orbiting flexible shallow spherical shell system
| AD-A260793 | p 2599 N93-25693
LINEAR SYSTEMS
Robust controls with structured perturbations
| NASA-CR-192956 | p 2817 N93-24757
Stability margins for multilinear interval systems by way of phase conditions: A unified approach
| NASA-CR-192893 | p 2819 N93-25226
Parametric stability margin for multilinear interval control systems
| NASA-CR-192892 | p 2819 N93-25296
PCG: A software package for the iterative solution of linear systems on scalar, vector and parallel computers
| DE93-007366 | p 2809 N93-25315
Some new results for solving linear systems arising from computational fluid dynamics problems p 2699 N93-25349
Stochastic and seismic design response of linear and nonlinear structures p 2726 N93-25484
The rapid solution of the Laplace equation on regions with fractal boundaries
| AD-A260585 | p 2828 N93-25905
LINEARITY
Log-ratio signal-processing technique for beam position monitors
| DE93-007356 | p 2851 N93-25314
LINEARIZATION
Prediction of unsteady flows in turbomachinery using the linearized Euler equations on deforming grids
| NASA-CR-192919 | p 2696 N93-25109
Line formation and the Poynting-Robertson effect in accretion discs p 2847 N93-25355
LINGUISTICS
Speech research
| AD-A260643 | p 2675 N93-25639
LININGS
A new approach to cooled combustion chambers: The 40K formed platelet chamber p 2626 N93-26018
Behavior of a steel-liner-and-bolts system under very high thermal and mechanical loading: The CONVEX Liner Add-On to DIAMOND FORTUNE
| DE93-007512 | p 2731 N93-26507
LINKAGES
Nonholonomic geometry, mechanics and control p 2724 N93-25270
LIPIDS
Effect of cytoskeletal reagents on stretch activated ion channels
| AD-A261089 | p 2793 N93-25764
LIQUEFIED GASES
Emissions from ethanol and LPG fueled vehicles
| DE93-006410 | p 2660 N93-25192
LIQUID ALLOYS
FNAS computational modeling
| NASA-CR-192512 | p 2863 N93-25225
LIQUID CRYSTALS
Adaptive liquid crystal TV based joint transform correlator as applied to real-time pattern recognition
| AD-A260724 | p 2864 N93-25655
Liquid crystals for laser applications
| AD-A261209 | p 2714 N93-25869
LIQUID FLOW
The instability of a liquid jet in a compressible airstream p 2703 N93-25560
LIQUID FUELS
Catalytic conversion of light alkanes
| DE93-009646 | p 2644 N93-25499
Conversion of light hydrocarbon gases to metal carbides for production of liquid fuels and chemicals
| DE93-009707 | p 2644 N93-25500
Microwave absorption measurements and interference: Effects for a liquid fuel between 2.5 and 18 GHz
| AD-A260607 | p 2675 N93-25635
LIQUID HELIUM
The design of a propulsion system using vent gas from a liquid helium cryogenic system p 2623 N93-25539
LIQUID INJECTION
Liquid surface breakup of nonturbulent and turbulent liquids p 2700 N93-25473
The instability of a liquid jet in a compressible airstream p 2703 N93-25560
LIQUID METALS
Thermocapillary flow near a cold wall
| AD-A261050 | p 2706 N93-25779
LIQUID NITROGEN
Atomizing-gas temperature effect on cryogenic spray dropsize
| NASA-TM-106106 | p 2709 N93-25191
LIQUID PHASE EPITAXY
Optical characterization of Ga(1-x)In(x)As(y)Sb(1-y)/GaSb alloy and device application
| AD-A261713 | p 2870 N93-26581
LIQUID PHASES
The WINCOF-I code: Detailed description
| NASA-CR-190779 | p 2573 N93-24760
The nature of the glass transition and its determination by thermal analysis
| DE93-006746 | p 2654 N93-25374
Thermal decomposition of HMX, mononitroso-RDX, TNCHP and K6 in the liquid phase: Results from simultaneous thermogravimetry modulated beam mass spectrometry measurements p 2628 N93-26033
LIQUID PROPELLANT ROCKET ENGINES
A neural network-based estimator for the mixture ratio of the Space Shuttle Main Engine
| NASA-TM-106070 | p 2622 N93-25089
The 29th JANNAF Combustion Subcommittee Meeting, volume 2
| CPIA-PUBL-593-VOL-2 | p 2624 N93-26005
Eulerian-Eulerian treatment of turbulent dense spray combustion in a bipropellant liquid rocket engine p 2626 N93-26017
Liquid Rocket Booster (LRB) for the Space Transportation System (STS) Systems Study. Amendment 13: Orientation meeting
| NASA-CR-192515 | p 2614 N93-26152
Analysis of the IBSS spectra of Space Shuttle control engine exhaust
| AD-A261749 | p 2632 N93-26373
LIQUID ROCKET PROPELLANTS
The 29th JANNAF Combustion Subcommittee Meeting, volume 2
| CPIA-PUBL-593-VOL-2 | p 2624 N93-26005
Eulerian-Eulerian treatment of turbulent dense spray combustion in a bipropellant liquid rocket engine p 2626 N93-26017
LIQUID SLOSHING
Stabilized finite element methods for incompressible flows with emphasis on moving boundaries and interfaces p 2703 N93-25663
Investigation of liquid sloshing in spin-stabilized satellites
| AD-A261671 | p 2619 N93-26438
LIQUID SURFACES
Liquid surface breakup of nonturbulent and turbulent liquids p 2700 N93-25473
LIQUID-GAS MIXTURES
Parameters influencing the hot-spot ignition of aviation fuel/air and ethylene/air mixtures p 2583 N93-24886
Flow visualizations of perpendicular blade vortex interactions
| NASA-CR-192725 | p 2696 N93-25208
Measurement of velocities in gas-liquid two-phase flow using laser Doppler velocimetry
| DE93-008083 | p 2698 N93-25306
LIQUID-LIQUID INTERFACES
Tracking sharp interface of two fluids by the CIP (Cubic-Interpolated Propagation) scheme
| NIFS-206 | p 2698 N93-25277
LIQUID-SOLID INTERFACES
Computation of complex solidification morphologies using a phase-field model
| PB93-156743 | p 2869 N93-26547
LIQUID-VAPOR INTERFACES
The WINCOF-I code: Detailed description
| NASA-CR-190779 | p 2573 N93-24760
Experimental and theoretical studies of dense fluid mixtures
| DE93-006070 | p 2695 N93-24976

LIQUIDS
Liquid and solid ion plasmas
| AD-A261888 | p 2862 N93-26528
LITHIUM
Dynamics of collision processes
| DE93-007143 | p 2849 N93-25509
LITHIUM HYDROXIDES
The properties of and analytical methods for detection of LiOH and Li2CO3
| NASA-CR-192771 | p 2643 N93-25240
LITHIUM NIOBATES
Efficient nonlinear optical conversion of 1.319-micron laser radiation
| AD-A261309 | p 2715 N93-26297
LITHOGRAPHY
VETA-I x ray test analysis
| NASA-CR-192321 | p 2854 N93-26183
LITHOLOGY
Lithologic mapping with LANDSAT Thematic Mapper guided by laboratory spectral measurements, Air, Niger (Africa) p 2742 N93-24803
LITHOSPHERE
Improved determination of vector lithospheric magnetic anomalies from MAGSAT data
| NASA-CR-192784 | p 2771 N93-25201
LOAD DISTRIBUTION (FORCES)
Energy dissipation in inelastic flow of cohesionless granular media p 2703 N93-25662
Radial spline assembly for antifriction bearings
| NASA-CASE-MFS-28629-1 | p 2719 N93-26001
LOAD TESTS
Stress distribution in composite flatwise tension test specimens
| NASA-TM-106074 | p 2634 N93-25071
LOADS (FORCES)
Elastic plate mode sensitivities to mass loading applications to gas sensors p 2711 N93-25009
Apparatus and methods for determining balance of a cylindrical vehicle
| AD-D015637 | p 2717 N93-25228
Helmeted head and neck dynamics under whole-body vibration p 2800 N93-25531
Estimating turbine limit load
| NASA-CR-191105 | p 2580 N93-25883
Methods of determining loads and fiber orientations in anisotropic non-crystalline materials using energy flux deviation
| NASA-CASE-LAR-14399-1 | p 2729 N93-26102
LOCAL AREA NETWORKS
Time and frequency reference for a trajectory measurement system p 2837 N93-25023
RAID-2: Design and implementation of a large scale disk array controller
| NASA-CR-192911 | p 2806 N93-25233
Interfacing a high performance disk array file server to a Gigabit LAN
| NASA-CR-192898 | p 2816 N93-25458
Gigabit network communications research
| AD-A260644 | p 2675 N93-25640
Proof of fault coverage for a formal protocol test procedure
| AD-A261612 | p 2680 N93-26166
FY92 contributions to the Database Management System Interface Standards Working Group of the Navy Next Generation Computer Resources Program
| AD-A261348 | p 2883 N93-26313
LOCOMOTION
Biped control via nonlinear dynamics p 2718 N93-25697
LOGIC CIRCUITS
Walsh function generator for the Electronically Scanned Thinned Array Radiometer (ESTAR) instrument
| NASA-TM-4449 | p 2689 N93-25618
A digital hardware test system analysis with test vector translation
| AD-A260849 | p 2810 N93-25786
LOGIC DESIGN
A design of a fast and area efficient multi-input Muller C-element
| AD-A261002 | p 2690 N93-25856
IDEF6: A design rationale capture method concept paper
| AD-A261594 | p 2884 N93-26523
LOGIC PROGRAMMING
A logic-based approach to federated databases p 2876 N93-25466
LOGISTICS
Estimating spares requirements for Space Station Freedom using the M-SPARE model
| AD-A260878 | p 2617 N93-25630
The reuse of logistics carriers for the first lunar outpost alternative habitat study p 2671 N93-26083
LOGISTICS MANAGEMENT
Estimating spares requirements for Space Station Freedom using the M-SPARE model
| AD-A260878 | p 2617 N93-25630
LONG DURATION EXPOSURE FACILITY
An investigation of the degradation of Fluorinated Ethylene Propylene (FEP) copolymer thermal blanketing materials aboard LDEF in the laboratory
| NASA-CR-192824 | p 2653 N93-25078
LONG DURATION SPACE FLIGHT
JPRS report: Science and technology. Central Eurasia: Life sciences
| JPRS-ULS-92-022 | p 2795 N93-25407
The application of integrated knowledge-based systems for the Biomedical Risk Assessment Intelligent Network (BRAIN) p 2799 N93-25595
Analysis of the lettuce data from the variable pressure growth chamber at NASA Johnson Space Center: A three-stage nested design model p 2794 N93-26069
LONGITUDINAL CONTROL
Control of nonlinear systems under input constraints with applications to flight control p 2596 N93-25353
LORAN C
The accuracy of SYLT- and RNS-based time scales at MTI and SNT during 1990-1991 p 2835 N93-25006
Experimental results of the performance of the new phase and frequency controller p 2839 N93-25035
LOSSES
Symbol signal-to-noise ratio loss in square-wave subcarrier downconversion p 2672 N93-24668
Report of the Seasat Failure Review Board p 2619 N93-24693
The implementation of a lossless data compression module in an advanced orbiting system: Analysis and development p 2804 N93-25928
Lossless compression of image data products on th e FIFE CD-ROM series p 2804 N93-25929
High-performance compression of astronomical images p 2805 N93-25931
Experimental investigation of flow turning losses in unstable rocket motors p 2630 N93-26040
Loss of temporal coherence of laser light propagated through simulated coastal waters
| AD-A261303 | p 2715 N93-26296
LOUDNESS
Neuromagnetic investigation of cortical regions underlying short-term memory
| AD-A261445 | p 2799 N93-26521
LOUDSPEAKERS
Low-frequency room responses. Part 1: Background and qualitative considerations
| BBC-RD-1992/8-PT-1 | p 2673 N93-25168
LOW ASPECT RATIO
The blade curving effects in a turbine stator cascade with low aspect ratio
| AD-A261063 | p 2595 N93-26239
LOW ASPECT RATIO WINGS
Supersonic aeroelastic instability results for a NASP-like wing model
| NASA-TM-107739 | p 2591 N93-26553
LOW CARBON STEELS
INEL spray-forming research p 2658 N93-25562
LOW CONCENTRATIONS
Fundamental and applied aspects of defect engineering in GaAs
| AD-A260573 | p 2867 N93-25899
LOW COST
Robo-line storage: Low latency, high capacity storage systems over geographically distributed networks
| NASA-CR-192910 | p 2805 N93-25130
Low cost dewatering of waste slurries p 2769 N93-25573
MOCVD process technology for affordable, high-yield, high-performance MESFET structures. Phase 3: MIMIC
| AD-A261178 | p 2690 N93-25820
LOW FREQUENCIES
Low-frequency room responses. Part 1: Background and qualitative considerations
| BBC-RD-1992/8-PT-1 | p 2673 N93-25168
Low-frequency room responses. Part 2: Calculation methods and experimental results
| BBC-RD-1992/9-PT-2 | p 2673 N93-25169
The effects of large-amplitude, low-frequency excitation on a three-dimensional jet p 2702 N93-25553
LOW NOISE
A technique for computation of noise temperature due to a beam waveguide shroud p 2671 N93-24661
LOW PRESSURE
Tomographic analysis of sight infrared spectra of low pressure flames p 2628 N93-26030
LOW REYNOLDS NUMBER
The steady Navier-Stokes problem for low Reynolds number viscous jets p 2698 N93-25264
LOW SPEED
Helicopter low-speed yaw control
| NASA-CASE-LAR-14219-1 | p 2597 N93-25998
LOW VOLTAGE
Thin rechargeable batteries for CMOS SRAM memory protection p 2694 N93-25583
LOW WEIGHT
Metal alloy and method of preparation thereof
| AD-D015670 | p 2652 N93-26234
LOWER BODY NEGATIVE PRESSURE
MAC to VAX connectivity: Heartrate spectral analysis system p 2796 N93-25594
LUBRICANTS
Macromolecules for inhibition of corrosion and wear
| AD-A261041 | p 2655 N93-25816
LUBRICATION
Vickers indentation hardness of stoichiometric and reduced single crystal TiO2 (rutile) from 25 to 800 C
| NASA-TM-105959 | p 2633 N93-26204
LUMINAIRES
TF-4020A: TFL's new compact military rubidium standard p 2838 N93-25026
LUMINESCENCE
Luminescence probe studies of ionomers. 3: Distribution of decay rate constants for tris bipyridyl ruthenium(2) in Nafion membranes
| AD-A260764 | p 2645 N93-25916
LUMINOSITY
Propagation of radiation in astrophysical media: Gravitational lenses and astrophysical masers p 2892 N93-24949
Structure and star forming activities of the cold massive molecular cloud G216-2.5 p 2893 N93-25477
LUMPED PARAMETER SYSTEMS
Dynamic modeling of fluid transmission lines of the DSN 70-meter antennas by using a lumped parameter model p 2678 N93-26119
LUNAR BASED EQUIPMENT
Center for Space Construction Third Annual Symposium
| NASA-CR-192688 | p 2669 N93-26405
Design concepts for pressurized lunar shelters utilizing indigenous materials p 2670 N93-26414
Configuration optimization of space structures p 2670 N93-26415
Lunar surface structural concepts and construction studies p 2670 N93-26417
LUNAR BASES
Space Nuclear Thermal Propulsion Test Facilities Subpanel
| NASA-TM-105708 | p 2622 N93-25105
The reuse of logistics carriers for the first lunar outpost alternative habitat study p 2671 N93-26083
Center for Space Construction Third Annual Symposium
| NASA-CR-192688 | p 2669 N93-26405
Systems engineering studies of on-orbit assembly operations p 2669 N93-26410
Lunar regolith and structure mechanics p 2670 N93-26412
Indigenous lunar construction materials p 2670 N93-26413
Design concepts for pressurized lunar shelters utilizing indigenous materials p 2670 N93-26414
Configuration optimization of space structures p 2670 N93-26415
Lunar surface structural concepts and construction studies p 2670 N93-26417
LUNAR CONSTRUCTION EQUIPMENT
Center for Space Construction Third Annual Symposium
| NASA-CR-192688 | p 2669 N93-26405
Systems engineering studies of on-orbit assembly operations p 2669 N93-26410
Indigenous lunar construction materials p 2670 N93-26413
Design concepts for pressurized lunar shelters utilizing indigenous materials p 2670 N93-26414
Configuration optimization of space structures p 2670 N93-26415
Telerobotic rovers for extraterrestrial construction p 2670 N93-26416
Lunar surface structural concepts and construction studies p 2670 N93-26417
LUNAR DUST
Data analysis and interpretation of lunar dust exosphere p 2898 N93-26059
LUNAR ENVIRONMENT
Use of Taguchi design of experiments to optimize and increase robustness of preliminary designs p 2670 N93-26063
The reuse of logistics carriers for the first lunar outpost alternative habitat study p 2671 N93-26083
The interaction of high voltage systems with the environments of the Moon and Mars
| NASA-TM-106107 | p 2618 N93-26148
LUNAR EXPLORATION
A mission concept for near term Lunar exploration
| DE93-007598 | p 2896 N93-25321

LUNAR LANDING
Space Nuclear Thermal Propulsion Test Facilities Subpanel
| NASA-TM-105708 | p 2622 N93-25105
LUNAR ORBITS
Practical aspects of transfer from GTO to lunar orbit p 2604 N93-24719
LUNAR RESOURCES
Center for Space Construction Third Annual Symposium
| NASA-CR-192688 | p 2669 N93-26405
Indigenous lunar construction materials p 2670 N93-26413
Design concepts for pressurized lunar shelters utilizing indigenous materials p 2670 N93-26414
LUNAR ROCKS
Lunar regolith and structure mechanics p 2670 N93-26412
Indigenous lunar construction materials p 2670 N93-26413
Design concepts for pressurized lunar shelters utilizing indigenous materials p 2670 N93-26414
LUNAR ROVING VEHICLES
A mission concept for near term Lunar exploration
| DE93-007598 | p 2896 N93-25321
Telerobotic rovers for extraterrestrial construction p 2670 N93-26416
LUNAR SHELTERS
Center for Space Construction Third Annual Symposium
| NASA-CR-192688 | p 2669 N93-26405
Design concepts for pressurized lunar shelters utilizing indigenous materials p 2670 N93-26414
LUNAR SOIL
Lunar regolith and structure mechanics p 2670 N93-26412
Design concepts for pressurized lunar shelters utilizing indigenous materials p 2670 N93-26414
LUNAR SPACECRAFT
Space transfer vehicle concepts and requirements study. Volume 2, book 4: Integrated advanced technology development
| NASA-CR-192528 | p 2611 N93-25512
Space transfer vehicle concepts and requirements study. Volume 2, book 3: STV system interfaces
| NASA-CR-192527 | p 2611 N93-25513
LUNAR SURFACE
Data analysis and interpretation of lunar dust exosphere p 2898 N93-26059
LUNGS
The acute inhalation toxicity of pyrolysis products of halon 1301
| AD-A260874 | p 2795 N93-25629

M

MACH NUMBER
Aerodynamic design and synthesis of the oblique flying wing supersonic transport p 2587 N93-24768
Conical Euler analysis and active roll suppression for unsteady vortical flows about rolling delta wings
| NASA-TP-3259 | p 2581 N93-26134
MACH-ZEHNDER INTERFEROMETERS
Generation of acoustic waves by focused infrared neodymium-laser radiation p 2714 N93-25761
MACHINE LEARNING
Using neural networks and Dyna algorithm for integrated planning, reacting and learning in systems
| NASA-CR-193018 | p 2817 N93-24743
Two neural network algorithms for designing optimal terminal controllers with open final time
| NASA-CR-177599 | p 2817 N93-25137
Adaptive decision support systems: Concepts, characterization, and an application p 2876 N93-25475
Tree classification software p 2814 N93-25591
Computation and learning in neural networks with binary weights
| AD-A261182 | p 2821 N93-25821
Center for intelligent control systems
| AD-A260995 | p 2821 N93-25853
Machine learning techniques for fault isolation and sensor placement p 2823 N93-25966
An application of machine learning to the organization of institutional software repositories p 2825 N93-25981
Using modular neural networks with local representations to control dynamic systems
| AD-A261597 | p 2826 N93-26162
Reinforcement learning for robots using neural networks
| AD-A261434 | p 2827 N93-26487
MACHINE TOOLS
Application of an on-machine gage for diameter measurements p 2711 N93-25578
On machine capacitance dimensional and surface profile measurement system p 2670 N93-25579
MAGELLAN PROJECT (NASA)
DSN acquisition of Magellan high-rate telemetry data p 2614 N93-26124
V-GRAM: Magellan bulletin about Venus and the radar mapping mission
| NASA-CR-192923 | p 2898 N93-26424
Revealing the face of Venus: Magellan
| NASA-CR-192922 | p 2898 N93-26517
MAGELLAN SPACECRAFT (NASA)
V-GRAM: Magellan bulletin about Venus and the radar mapping mission
| NASA-CR-192923 | p 2898 N93-26424
Revealing the face of Venus: Magellan
| NASA-CR-192922 | p 2898 N93-26517
MAGELLANIC CLOUDS
30 Doradus in the Large Magellanic Cloud: The stellar content and initial mass function p 2894 N93-25559
MAGNESIUM
Solid state frequency synthesis up to 600 GHz: An application to the Mg frequency standard p 2842 N93-25058
MAGNESIUM ALLOYS
Ignition and combustion of lunar propellants
| NASA-CR-192814 | p 2659 N93-24745
MAGNESIUM OXIDES
Activation of methane by clean and chemically modified single crystal oxide surfaces
| PB93-157295 | p 2644 N93-25817
MAGNETIC ANOMALIES
Improved determination of vector lithospheric magnetic anomalies from MAGSAT data
| NASA-CR-192784 | p 2771 N93-25201
MAGNETIC BEARINGS
Tuned circuit electric levitation bearings for microactuators p 2689 N93-25619
MAGNETIC COILS
Poly-coil design for a 60 tesla quasi-stationary magnet
| DE93-007353 | p 2688 N93-25313
MAGNETIC EFFECTS
Steady induction effects in geomagnetism. Part 1B: Geomagnetic estimation of steady surficial core motions: A non-linear inverse problem
| NASA-TP-3272-PT-1B | p 2776 N93-26421
MAGNETIC FIELD CONFIGURATIONS
Some features of particle orbit behavior in LHD configurations
| NIFS-211 | p 2859 N93-25216
Correlated wavefunction quantum Monte Carlo approach to solids
| DE93-007730 | p 2863 N93-25367
MAGNETIC FIELD RECONNECTION
Particle simulation of auroral double layers p 2774 N93-25830
MAGNETIC FIELDS
Lightning characteristics in the north-east part of Japan observed by a magnetic direction-finder network p 2779 N93-24892
Weak magnetic field sensitivity of quartz crystal oscillators p 2833 N93-24993
Improved determination of vector lithospheric magnetic anomalies from MAGSAT data
| NASA-CR-192784 | p 2771 N93-25201
Two-stream instability for a light ion beam-plasma system with external magnetic field
| NIFS-204 | p 2859 N93-25248
New ground states in unconventional superconductors p 2688 N93-25282
Boundary plasma modelling for ITER
| DE93-007963 | p 2859 N93-25302
Poly-coil design for a 60 tesla quasi-stationary magnet
| DE93-007353 | p 2688 N93-25313
Magnetic excitations in antiferromagnetically coupled superlattices: Fe/Mo and Fe/Cr
| DE93-007894 | p 2863 N93-25369
Environmental test program for superconducting materials and devices
| DE93-003646 | p 2864 N93-25506
Studies of several small seawater MHD thrusters using the high-field solenoid of MIT's Bitter Magnet Laboratory
| AD-A260645 | p 2860 N93-25641
Investigations of the transient behavior of the cathode fall region in planar and hollow cathodes
| AD-A261636 | p 2691 N93-26171
Magnetic field source for bi-chambered electron beam devices
| AD-A261316 | p 2691 N93-26299
Imaging regional changes in the spontaneous activity of the brain: An extension of the minimum-norm least-squares estimate
| AD-A261593 | p 2798 N93-26436
Sensitivity of magnetic flux compression in cylindrical implosions to model parameters
| DE93-003819 | p 2861 N93-26512
Low temperature Hall and Shubnikov-de Haas effects
| AD-A261871 | p 2869 N93-26540
MAGNETIC FLUX
Studies of several small seawater MHD thrusters using the high-field solenoid of MIT's Bitter Magnet Laboratory
| AD-A260645 | p 2860 N93-25641
Sensitivity of magnetic flux compression in cylindrical implosions to model parameters
| DE93-003819 | p 2861 N93-26512
MAGNETIC INDUCTION
Studying the kinetics of magnetization in high Tc superconductors
| NASA-CR-192916 | p 2862 N93-25108
MAGNETIC MATERIALS
Electronics and Electrical Engineering Laboratory technical publication announcements covering laboratory programs, July to September 1992 with 1992/1993 EEEL events calendar
| PB93-158632 | p 2884 N93-26530
MAGNETIC MEASUREMENT
Electronics and Electrical Engineering Laboratory technical publication announcements covering laboratory programs, July to September 1992 with 1992/1993 EEEL events calendar
| PB93-158632 | p 2884 N93-26530
MAGNETIC MOMENTS
Magnetic multilayer strain gage
| AD-D015672 | p 2710 N93-26141
MAGNETIC PROPERTIES
Molecular/polymeric magnetism
| DE93-008635 | p 2847 N93-25114
Correlated wavefunction quantum Monte Carlo approach to solids
| DE93-007730 | p 2863 N93-25367
Magnetic excitations in antiferromagnetically coupled superlattices: Fe/Mo and Fe/Cr
| DE93-007894 | p 2863 N93-25369
MAGNETIC RESONANCE
Neuromagnetic investigation of cortical regions underlying short-term memory
| AD-A261445 | p 2799 N93-26521
MAGNETIC SHIELDING
Basic design of a spaceborne hydrogen maser p 2716 N93-25024
MAGNETIC STORMS
Magnetotail processes associated with auroral surge formation
| ATR-90(7186)-1 | p 2895 N93-26147
MAGNETIC TAPES
Striped tape arrays
| NASA-CR-192914 | p 2806 N93-25267
MAGNETIC VARIATIONS
JARE data reports. No. 171 (upper atmosphere physics 9). Data, Syowa and Asuka Stations, 1989 p 2774 N93-25889
A predicted geomagnetic field model for epoch 1990.0
| AD-A260669 | p 2775 N93-25891
MAGNETICALLY TRAPPED PARTICLES
Some features of particle orbit behavior in LHD configurations
| NIFS-211 | p 2859 N93-25216
Thermal and electric oscillation driven by orbit loss in helical systems
| NIFS-213 | p 2860 N93-25346
MAGNETIZATION
Studying the kinetics of magnetization in high Tc superconductors
| NASA-CR-192916 | p 2862 N93-25108
Molecular/polymeric magnetism
| DE93-008635 | p 2847 N93-25114
Magnetic excitations in antiferromagnetically coupled superlattices: Fe/Mo and Fe/Cr
| DE93-007894 | p 2863 N93-25369
Computational modeling of MAGO and other magnetized target fusion concepts
| DE93-007354 | p 2861 N93-26504
MAGNETO-OPTICS
A simple and compact source of cold atoms for cesium fountains and microgravity clocks p 2831 N93-24981
MAGNETOHYDRODYNAMIC FLOW
Modeling of plasma flow switches at low, intermediate and high energies
| DE93-007359 | p 2858 N93-25167
Maneuvering a reentry body via magneto-gasdynamic forces p 2615 N93-25207
Simulation study of MHD dynamo: Convection in a rotating spherical shell
| NIFS-207 | p 2860 N93-25356
Particle simulation of auroral double layers p 2774 N93-25830
Magnetotail processes associated with auroral surge formation
| ATR-90(7186)-1 | p 2895 N93-26147

MAGNETOHYDRODYNAMIC STABILITY
Modeling of plasma flow switches at low, intermediate and high energies
| DE93-007359 | p 2858 N93-25167
MAGNETOHYDRODYNAMIC WAVES
Time dependent simulation of cosmic-ray shocks including Alfven transport
| NASA-CR-192931 | p 2899 N93-24752
R and D of transmission lines for ECH system
| NIFS-210 | p 2687 N93-24951
Alfven wave transport effects in the time evolution of parallel cosmic-ray modified shocks
| NASA-CR-192932 | p 2899 N93-25161
MAGNETOHYDRODYNAMICS
Evaluation of a candidate material for a coal-fired magnetohydrodynamic (MHD) high temperature recuperative air heater
| DE93-006630 | p 2858 N93-24968
Modeling of plasma flow switches at low, intermediate and high energies
| DE93-007359 | p 2858 N93-25167
Demonstration for novel self-organization theory by three-dimensional magnetohydrodynamic simulation
| NIFS-212 | p 2859 N93-25227
Studies of several small seawater MHD thrusters using the high-field solenoid of MIT's Bitter Magnet Laboratory
| AD-A260645 | p 2860 N93-25641
Oblique MHD cosmic-ray modified shocks: Two-fluid numerical simulations
| NASA-CR-192930 | p 2900 N93-26132
MAGNETOMETERS
Accurate attitude determination of the LACE satellite p 2605 N93-24726
Goddard Space Flight Center (GSFC) Flight Dynamics Facility (FDF) calibration of the Upper Atmosphere Research Satellite (UARS) sensors p 2606 N93-24733
Upper Atmosphere Research Satellite (UARS) attitude accuracy using coarse attitude sensors p 2607 N93-24735
MAGNETOPAUSE
Anomalous aspects of magnetosheath flow and of the shape and oscillations of the magnetopause during an interval of strongly northward interplanetary magnetic field
| NASA-CR-192851 | p 2770 N93-25081
MAGNETOSHEATH
Anomalous aspects of magnetosheath flow and of the shape and oscillations of the magnetopause during an interval of strongly northward interplanetary magnetic field
| NASA-CR-192851 | p 2770 N93-25081
Study of auroral dynamics with combined spacecraft and incoherent-scatter radar data
| NASA-CR-192224 | p 2775 N93-26159
MAGNETOSPHERE-IONOSPHERE COUPLING
A statistical study of field-aligned currents in the Earth's inner magnetosphere p 2773 N93-25709
MAGNETOSPHERIC ION DENSITY
Imaging the magnetosphere in the extreme ultraviolet
| NASA-CR-192218 | p 2775 N93-26151
MAGNETOSTRICTION
Magnetic multilayer strain gage
| AD-D015672 | p 2710 N93-26141
MAGNETRONS
Optical detection of laser-cooled ions in a Penning trap p 2838 N93-25031
MAGNETS
Molecular/polymeric magnetism
| DE93-008635 | p 2847 N93-25114
Poly-coil design for a 60 tesla quasi-stationary magnet
| DE93-007353 | p 2688 N93-25313
MAINTAINABILITY
An analysis of the reliability and maintainability of the Jian 6 and Jian 7 aircraft and ways to improve them
| AD-A261060 | p 2574 N93-26238
MAINTENANCE
The damage, repair and design of fiber composite structural materials p 2635 N93-25532
Expedient repair of structural facilities
| AD-A260727 | p 2598 N93-25656
Anomalous event diagnosis for environmental satellite systems p 2619 N93-25971
AEGIS measures definition
| AD-A261494 | p 2812 N93-26375
TCMS operations and maintenance philosophy
| NASA-TM-108756 | p 2873 N93-26418
MAINTENANCE TRAINING
Human Factors in Aviation Maintenance, phase 2
| DOT/FAA/AM-93/5 | p 2802 N93-26089
TCMS operations and maintenance philosophy
| NASA-TM-108756 | p 2873 N93-26418
MALES
Vascular uptake of rehydration fluids in hypohydrated men at rest and exercise
| NASA-TM-103942 | p 2795 N93-26133
MAMMARY GLANDS
Energy and Technology Review, October - December 1992
| DE93-007784 | p 2674 N93-25299
Automated system for early breast cancer detection in mammograms p 2796 N93-25568
MAN ENVIRONMENT INTERACTIONS
Application of remote sensing data for the investigation of environmental degradation sites in East Germany p 2739 N93-24785
Aerospace monitoring for ecological hazard and disaster mitigation p 2744 N93-24812
Forest damage detection and reflection of conifers: From micro to field level p 2752 N93-24864
Measurements of nitric acid, carboxylic acids, and selected aerosol species for the NASA/GTE Pacific Mission - West (PEM-WEST)
| NASA-CR-192976 | p 2763 N93-25287
MAN MACHINE SYSTEMS
Human factors engineering: A key element of instrumentation and control system design
| DE93-006731 | p 2800 N93-25415
Automation and robotics human performance
| NASA-CR-193049 | p 2802 N93-26153
Assured crew return vehicle man-systems integration standards
| NASA-CR-193065 | p 2614 N93-26329
MAN-COMPUTER INTERFACE
Improving information search at the user interface: The impact of graphical innovation on query formulation and expression p 2873 N93-24905
Prototype PC user interface
| DE93-008008 | p 2809 N93-25303
TARGET: Rapid capture of process knowledge p 2814 N93-25590
Experimenter's laboratory for visualized interactive science p 2879 N93-25802
Measures of user-system interface effectiveness: An encoding scheme and indicators for assessing the usability of graphical, direct-manipulation style user interfaces
| AD-A260606 | p 2801 N93-25840
Department of Defense technical architecture framework for information management. Volume 3: Reference model and standards profile, version 1.3
| AD-A261913 | p 2882 N93-26230
Human computer interface style guide, version 2.0
| AD-A261280 | p 2807 N93-26291
Implementation of custom colors in the DECwindows environment
| AD-A261456 | p 2757 N93-26574
MANAGEMENT ANALYSIS
Use of the Environmental Resource Management and Analysis System at the Fernald Environmental Management Project
| DE93-002943 | p 2760 N93-24955
MANAGEMENT INFORMATION SYSTEMS
A Spatial Analysis and Modeling System (SAMS) for environment management p 2881 N93-25813
Design Knowledge Management System (DKMS) Beta Test Report
| AD-A261453 | p 2883 N93-26350
OSSA Information Systems Program
| NASA-TM-108758 | p 2883 N93-26491
MANAGEMENT METHODS
Organizational politics, participation in decision-making, and job satisfaction
| DOT/FAA/AM-92/17 | p 2796 N93-25203
Procedural justice, occupational identification, and organizational commitment
| DOT/FAA/AM-92/21 | p 2872 N93-25204
Design of a cooperative problem-solving system for enroute flight planning: An empirical study of its use by airline dispatchers
| NASA-CR-192709 | p 2585 N93-25330
Department of Energy: Better information resources management needed to accomplish missions. Report to the Secretary of Energy
| GAO/IMTEC-92-53 | p 2882 N93-26096
Bibliography of remote sensing techniques used in wetland research
| AD-A261704 | p 2757 N93-26440
MANAGEMENT PLANNING
Viewgraph description of Penn State's Propulsion Engineering Research Center: Activity highlights and future plans
| NASA-CR-192317 | p 2622 N93-24943
JSC research and technology
| NASA-TM-104763 | p 2901 N93-25188
Improving performance through concept formation and conceptual clustering
| NASA-CR-192726 | p 2828 N93-25262
Aircraft electrical and environmental systems, AFSCs 452x5, 454x5, and 454x6
| AD-A261213 | p 2590 N93-25733
An environmental audit management plan for the Royal Australian Air Force
| AD-A261092 | p 2765 N93-25765
Climate Monitoring and Diagnostics Laboratory
| PB93-156388 | p 2785 N93-25871
Knowledge-based decision support for Space Station assembly sequence planning
| NASA-CR-193048 | p 2599 N93-26095
Department of Energy: Better information resources management needed to accomplish missions. Report to the Secretary of Energy
| GAO/IMTEC-92-53 | p 2882 N93-26096
Handbook of chemical hazard analysis procedures
| PB93-158756 | p 2766 N93-26315
Observations on the NASA Propagation Program p 2685 N93-26482
MANAGEMENT SYSTEMS
Systems engineering for very large systems p 2665 N93-24680
Intelligent access to multiple relational database systems
| AD-A261198 | p 2881 N93-25824
Task 2A: UNIS requirements and concepts
| MCR-92-5006-PT-A | p 2610 N93-26180
Design Knowledge Management System (DKMS) Beta Test Report
| AD-A261453 | p 2883 N93-26350
MANDRELS
Improved composite fabrication process
| AD-D015679 | p 2640 N93-26145
MANEUVERABILITY
Experimental modal survey of the probe mass mock-up
| DE93-008846 | p 2617 N93-25494
MANEUVERABLE REENTRY BODIES
Maneuvering a reentry body via magneto-gasdynamic forces p 2615 N93-25207
MANEUVERS
A Hierarchical Target Extraction, Recognition, and Tracking (HiTert) system
| AD-A260567 | p 2854 N93-25898
MANIPULATORS
Initial experiments with a myoelectric-based muscle sensor
| DE92-016034 | p 2799 N93-25099
Probabilistic analysis of manipulation tasks: A research agenda
| DE93-000713 | p 2827 N93-25103
Detailed solution to a complex kinematics chain manipulator
| DE93-004619 | p 2725 N93-25357
A control structure for fault-tolerant operation of robotic manipulators
| DE93-005783 | p 2717 N93-25413
Numerical kinematic transformation calculations for a parallel link manipulator
| DE93-005778 | p 2718 N93-25449
The induction of elastic fine motion in robotic grasps p 2718 N93-25727
Modeling of a full vision system using combined Visual/Haptic search for remote object identification
| AD-A260977 | p 2801 N93-25867
Parametric motion control of robotic arms: A biologically based approach using neural networks p 2822 N93-25964
Controls for orbital assembly of large space structures p 2620 N93-26408
Telerobotic rovers for extraterrestrial construction p 2670 N93-26416
MANNED MARS MISSIONS
Space Nuclear Thermal Propulsion Test Facilities Subpanel
| NASA-TM-105708 | p 2622 N93-25105
MANNED SPACE FLIGHT
Systems engineering and integration and management for manned space flight programs p 2666 N93-24684
Space transfer vehicle concepts and requirements study. Volume 2, book 3: STV system interfaces
| NASA-CR-192527 | p 2611 N93-25513
MANNED SPACECRAFT
A survey of life support system automation and control
| NASA-TM-103977 | p 2667 N93-25085
MANUAL CONTROL
Architecture of autonomous systems
| NASA-CR-192974 | p 2801 N93-26047
MANUALS
The systems engineering overview and process (from the Systems Engineering Management Guide, 1990) p 2665 N93-24679
NASA Lewis 8- by 6-foot supersonic wind tunnel user manual
| NASA-TM-105771 | p 2597 N93-25080
Distributed project scheduling at NASA: Requirements for manual protocols and computer-based support p 2815 N93-26075

Arc Digital Raster Imagery (ADRI) development
| AD-A261850 | p 2812 N93-26275
Guide for conducting convective windstorm surveys
| PB93-148427 | p 2787 N93-26570

MANUFACTURING
Technology 2002: The Third National Technology Transfer Conference and Exposition, volume 1
| NASA-CP-3189-VOL-1 | p 2901 N93-25561
On machine capacitance dimensional and surface profile measurement system p 2670 N93-25579
Vision-aided monitoring and control of thermal spray, spray forming, and welding processes
p 2670 N93-25604
Firmware development improves system efficiency
p 2807 N93-25606
MOCVD process technology for affordable, high-yield, high-performance MESFET structures. Phase 3: MIMIC
| AD-A261178 | p 2690 N93-25820
Using input command pre-shaping to suppress multiple mode vibration p 2732 N93-25834
Special tooling disposition for aircraft entering post production support
| AD-A261614 | p 2573 N93-26168
RF vacuum microelectronics
| AD-A261343 | p 2691 N93-26311
Multivariable control for flexible IC processing
| AD-A261685 | p 2692 N93-26366
Japanese Technology Evaluation Center Workshop on Advanced Manufacturing Technology for Polymer Composite Structures in Japan
| PB93-165249 | p 2641 N93-26589

MANY BODY PROBLEM
Diabaticity of nuclear motion: Problems and perspectives
| DE93-007252 | p 2847 N93-25148
Correlated wavefunction quantum Monte Carlo approach to solids
| DE93-007730 | p 2863 N93-25367
Molecular interactions and properties with many-body methods
| AD-A261688 | p 2850 N93-26367
Mechanics and control of multibody structural systems
| AD-A261576 | p 2619 N93-26456

MAPPING
A ground track control algorithm for the Topographic Mapping Laser Altimeter (TMLA) p 2602 N93-24707
Geologic and hydrogeologic mapping of Iceland with multisensor data (JERS-1, ERS-1, SPOT, Landsat and SEASAT) p 2740 N93-24792
Agroclimatological zonation by AVHRR data for vegetation monitoring p 2741 N93-24795
European applications of space-borne Earth observation for land cover mapping p 2745 N93-24820
Oil pollution and water quality mapping of Augusta Bay, Italy using remote sensing techniques
p 2746 N93-24823
NORSMAP 1989: Norwegian remote sensing spectrometry for mapping and monitoring of algal blooms and pollution p 2746 N93-24824
Cartography and statistics of crops under irrigation in the Donana area of Andalucia through the use of Landsat-TM imagery and its incorporation into a GIS
p 2751 N93-24855
Appliction of remote sensing to forestry mapping: Experience from the European collaborative programme for the less favoured areas p 2751 N93-24857
Standwise forest inventory and mapping for operational management planning p 2752 N93-24863
Preliminary studies leading toward the development of a LIDAR bathymetry mapping instrument
p 2711 N93-25614

MAPS
Application of multitemporal Landsat-MSS and -TM data for the development of an inundation-risk-map
p 2743 N93-24807
Supporting the Portuguese fisheries with satellites
p 2745 N93-24821
Application of satellite imageries data to fisheries in Japan p 2745 N93-24822
US Army evaluation of the Electronic Map Data (EMD) prototype
| AD-A261693 | p 2757 N93-26369
Implementation of custom colors in the DECwindows environment
| AD-A261456 | p 2757 N93-26574

MARANGONI CONVECTION
Numerical simulation of time-dependent thermocapillary convection in layered fluid systems
p 2700 N93-25472

MARINE CHEMISTRY
The JGOFS North Atlantic Bloom Experiment: An overview p 2735 N93-24934

MARINE ENVIRONMENTS
Data availability and data archeology from the former Soviet Union p 2735 N93-24932
Summary by the cloud and aerosol research group for ASTEX
| AD-A261292 | p 2766 N93-26292

MARINE METEOROLOGY
Proceedings of the Ocean Climate Data Workshop
| NASA-TM-108711 | p 2732 N93-24915
The role of ocean climate data in operational Naval oceanography p 2732 N93-24916
Role of the ocean in climate changes
p 2732 N93-24918
The role of the World Data Centers in handling ocean climate data p 2732 N93-24919
Operational seasonal and interannual predictions of ocean conditions p 2733 N93-24921
Ocean climate data for user community in West and Central Africa: Needs, opportunities, and challenges
p 2735 N93-24933
Computer systems p 2737 N93-24942
A systematic satellite approach for estimating central pressures of mid-lattitude oceanic storms
| NOAA-TR-NESDIS-63 | p 2781 N93-25220
Tropical cyclogenesis in the western North Pacific
p 2783 N93-25714
An investigation into the causative mechanisms for explosive cyclone development over the Atlantic
| AD-A261831 | p 2786 N93-26273

MARINE TECHNOLOGY
High-performance visualization applied to computational electromagnetics: Method-of-moments on a silicon graphics workstation
| AD-A260820 | p 2675 N93-25700

MARKET RESEARCH
Space business indicators p 2886 N93-26158

MARKETING
Energy and Technology Review, August-September 1992
| DE93-005882 | p 2901 N93-24974

MARKOV CHAINS
Aerospace monitoring for ecological hazard and disaster mitigation p 2744 N93-24812
Parametric analysis of atmospheric processes
| NASA-CR-192523 | p 2770 N93-25086
JPRS report: Science and technology. Central Eurasia: Life sciences
| JPRS-ULS-92-020 | p 2793 N93-25406

MARKOV PROCESSES
Failure monitoring in dynamic systems: Model construction without fault training data
p 2672 N93-24666

MARS (PLANET)
Electrical and Chemical Interactions at Mars Workshop. Part 2: Appendix
| NASA-CP-10093-PT-2 | p 2897 N93-26392
The upper atmosphere and ionosphere of Mars
p 2897 N93-26393
The Martian lower atmosphere p 2897 N93-26394
Representative systems for space exploration
p 2897 N93-26395
Mars exploration planning p 2898 N93-26399
Systems engineering studies of on-orbit assembly operations p 2669 N93-26410

MARS ATMOSPHERE
Electrical and Chemical Interactions at Mars Workshop. Part 2: Appendix
| NASA-CP-10093-PT-2 | p 2897 N93-26392
The upper atmosphere and ionosphere of Mars
p 2897 N93-26393
The Martian lower atmosphere p 2897 N93-26394

MARS ENVIRONMENT
The interaction of high voltage systems with the environments of the Moon and Mars
| NASA-TM-106107 | p 2618 N93-26148
Electrical and Chemical Interactions at Mars Workshop. Part 2: Appendix
| NASA-CP-10093-PT-2 | p 2897 N93-26392
Modeling and analysis tools p 2897 N93-26397
Mars exploration planning p 2898 N93-26399

MARS LANDING
Space Nuclear Thermal Propulsion Test Facilities Subpanel
| NASA-TM-105708 | p 2622 N93-25105

MARS OBSERVER
Orbiter-orbiter and orbiter-lander tracking using same-beam interferometry p 2677 N93-26110
Mars exploration planning p 2898 N93-26399

MARS SAMPLE RETURN MISSIONS
Knowledge-based control for robot self-localization
p 2822 N93-25963
Mars exploration planning p 2898 N93-26399

MARS SATELLITES
Mars: The dynamics of orbiting satellites and gravity model development p 2896 N93-25439

MARS SURFACE
Orbiter-orbiter and orbiter-lander tracking using same-beam interferometry p 2677 N93-26110
Electrical and Chemical Interactions at Mars Workshop. Part 2: Appendix
| NASA-CP-10093-PT-2 | p 2897 N93-26392

MARSHLANDS
Bibliography of remote sensing techniques used in wetland research
| AD-A261704 | p 2757 N93-26440

MARTENSITIC STAINLESS STEELS
Mechanical properties of martensitic alloy AISI 422
| DE93-006563 | p 2649 N93-25255

MASERS
Propagation of radiation in astrophysical media: Gravitational lenses and astrophysical masers
p 2892 N93-24949
Experiments on a diode-laser-pumped Rb-87 maser
p 2716 N93-25030
Fundamental characteristics of a laser-diode-pumped rubidium maser with an external feedback loop
p 2716 N93-25068
Optimizing the G/T ratio of the DSS-13 34-meter beam-waveguide antenna p 2678 N93-26118
Efficient nonlinear optical conversion of 1.319-micron laser radiation
| AD-A261309 | p 2715 N93-26297

MASKING
RF vacuum microelectronics
| AD-A261343 | p 2691 N93-26311
Monaural and binaural processing of complex waveforms
| AD-A261659 | p 2846 N93-26358

MASS
What is the relationship between altitude and weight in a model rocket? p 2603 N93-24715

MASS BALANCE
Apparatus and methods for determining balance of a cylindrical vehicle
| AD-D015637 | p 2717 N93-25228

MASS DISTRIBUTION
Elastic plate mode sensitivities to mass loading applications to gas sensors p 2711 N93-25009
A study of mass size distributions and particle deposition velocities in ambient air p 2763 N93-25263

MASS FLOW
A feasibility study of using Langley 0.3-m transonic cryogenic tunnel sidewall boundary-layer removal system for heavy gas testing
| NASA-CR-191438 | p 2695 N93-25087
Consequences of spontaneous and anomalous symmetry breaking for the orbital and mass flow hydrodynamics of He-3 - A p 2698 N93-25295

MASS FLOW RATE
A feasibility study of using Langley 0.3-m transonic cryogenic tunnel sidewall boundary-layer removal system for heavy gas testing
| NASA-CR-191438 | p 2695 N93-25087
Modified point mass trajectory simulation for base-burn projectiles
| BRL-TR-3321 | p 2609 N93-25985

MASS SPECTRA
Volatiles in interplanetary dust particles: A comparison with CI and CM chondrites p 2896 N93-26062

MASS SPECTROMETERS
Laser desorption in an ion trap mass spectrometer
| DE93-007330 | p 2712 N93-25150

MASS SPECTROSCOPY
Laser desorption in an ion trap mass spectrometer
| DE93-007330 | p 2712 N93-25150
The properties of and analytical methods for detection of LiOH and Li2CO3
| NASA-CR-192771 | p 2643 N93-25240
Flame structure studies of a lean, 20 torr H2/N2O/AR flame employing molecular beam mass spectrometry
p 2627 N93-26025
Thermal decomposition of HMX, mononitroso-RDX, TNCHP and K6 in the liquid phase: Results from simultaneous thermogravimetry modulated beam mass spectrometry measurements p 2628 N93-26033
Development of rate expressions for the thermal decomposition of RDX p 2629 N93-26034

MASS TRANSFER
The WINCOF-I code: Detailed description
| NASA-CR-190779 | p 2573 N93-24760
Numerical simulation of permeation from deposited droplets: Model expansion
| MTL-TR-92-23 | p 2706 N93-25953

MASSIVE STARS
Starburst Galaxies: Hard X-ray spectra and contribution to the diffuse background
| NASA-CR-192790 | p 2892 N93-25211
Structure and star forming activities of the cold massive molecular cloud G216-2.5 p 2893 N93-25477

MASSIVELY PARALLEL PROCESSORS
RAMA: A file system for massively parallel computers
| NASA-CR-192906 | p 2815 N93-25297

FORTRAN M as a language for building earth system models
| DE93-007897 | p 2763 N93-25370
Image analysis by integration of disparate information p 2824 N93-25973
Massively-parallel computational fluid dynamics
| AD-A261815 | p 2707 N93-26269

MATERIALS HANDLING
Handbook of chemical hazard analysis procedures
| PB93-158756 | p 2766 N93-26315

MATERIALS RECOVERY
Reclamation with recovery of radionuclides and toxic metals from contaminated materials, soils, and wastes p 2769 N93-25571

MATERIALS SCIENCE
Technology 2002: The Third National Technology Transfer Conference and Exposition, volume 1
| NASA-CP-3189-VOL-1 | p 2901 N93-25561

MATHEMATICAL LOGIC
Algorithms for optimal redundancy allocation
| DE93-005709 | p 2827 N93-24973

MATHEMATICAL MODELS
Rate determination from vector observations p 2603 N93-24713
ILS mathematical modeling study of an ILS glide slope proposed for runway 19L at the Meridian Naval Air Station, Mississippi
| DOT/FAA/CT-TN93/8 | p 2584 N93-24741
Ignition and combustion of lunar propellants
| NASA-CR-192814 | p 2659 N93-24745
Global dynamic modeling of a transmission system
| NASA-CR-191117 | p 2716 N93-24751
Crashworthiness of composite seats for civil aircraft p 2582 N93-24773
Remote sensing monitoring and hindcasting of the accident occurred to the tanker Haven in the Gulf of Genoa (Italy) p 2747 N93-24830
Atmospheric correction of Landsat/TM data over mountainous terrain for forestry applications p 2752 N93-24862
The 1992 International Aerospace and Ground Conference on Lightning and Static Electricity: Addendum
| DOT/FAA/CT-92/20-ADD-1 | p 2777 N93-24875
Numerical modelling of induced effects of lightning strike on an all composite helicopter p 2583 N93-24879
A computational approach to predicting the extent of arc root damage in CFC panels p 2642 N93-24890
Fractal determination of parameters in lightning and ESD model p 2686 N93-24893
Zoning of aircraft by electric field modelling p 2583 N93-24894
Lightning phenomenology bases for full threat return stroke occurrence following extended leader sweep at flight altitudes p 2780 N93-24895
Development of models for predicting the triggering of lightning by launch vehicles p 2610 N93-24899
A model of concurrent flow flame spread over a thin solid fuel
| NASA-CR-191111 | p 2663 N93-24946
Improved PI-network measurement of all quartz crystal parameters by appropriate modelling of the test fixture p 2833 N93-24995
Surface Transverse Wave (STW) quartz resonators in the GHz range p 2836 N93-25012
Time stability: An improvement of the multi-variance method for the oscillator noise analysis p 2839 N93-25036
Parametric analysis of atmospheric processes
| NASA-CR-192523 | p 2770 N93-25086
A micromechanical viscoplastic stress-strain model with grain boundary sliding
| DE93-009109 | p 2649 N93-25095
Computational and experimental studies on large scale solar heating
| DE93-769942 | p 2758 N93-25096
Probabilistic analysis of manipulation tasks: A research agenda
| DE93-000713 | p 2827 N93-25103
Fuel Injector: Air swirl characterization aerothermal modeling, phase 2, volume 2
| NASA-CR-189193 | p 2592 N93-25106
Grid sensitivity for aerodynamic optimization and flow analysis
| NASA-CR-192980 | p 2575 N93-25117
A simple, approximate model of parachute inflation
| DE93-002465 | p 2576 N93-25121
The AFTAC model integration project
| DE93-003334 | p 2761 N93-25122
The effects of sampling frequency on the climate statistics of the ECMWF general circulation model
| DE93-003338 | p 2761 N93-25145
Global warming potential for CF4
| DE93-005740 | p 2762 N93-25146
A correlated K-distribution model of the heating rates for H2O and a molecular mixture in the 0-2500 cm(exp -1) wavelength region in the atmosphere between 0 and 60 km
| DE93-005741 | p 2762 N93-25147
Empirical wind model for the middle and lower atmosphere. Part 1: Local time average
| NASA-TM-104581 | p 2770 N93-25160
Generic hypersonic vehicle performance model
| NASA-CR-192953 | p 2587 N93-25162
Modeling of plasma flow switches at low, intermediate and high energies
| DE93-007359 | p 2858 N93-25167
Summary of progress in inertial confinement fusion
| DE93-007350 | p 2858 N93-25187
Maneuvering a reentry body via magneto-gasdynamic forces p 2615 N93-25207
FNAS computational modeling
| NASA-CR-192512 | p 2863 N93-25225
The evaluation of technical models used for major-accident hazard installations. Report to Commission of the European Communities Directorate General 12
| CUED/A-AERO/TR-19 | p 2668 N93-25238
A method for transient, three-dimensional neutron transport calculations
| DE93-007243 | p 2847 N93-25256
Integrated aerodynamic-structural wing design optimization p 2587 N93-25279
Particle simulation for 10.6 micron picosecond laser-induced breakdown in gases p 2712 N93-25280
An outgoing energy flux boundary condition for finite difference ICRP antenna models
| DE93-007788 | p 2674 N93-25300
Mechanistic studies of the CVD of silicon nitride from SiF4 and NH3
| DE93-004500 | p 2644 N93-25312
The Sudbury Neutrino Observatory
| DE93-007697 | p 2899 N93-25327
A numerical and experimental studies of flow characteristics in centrifugal fans p 2577 N93-25339
Combining particles and waves for fluid animation p 2699 N93-25348
Detailed solution to a complex kinematics chain manipulator
| DE93-004619 | p 2725 N93-25357
A preliminary sizing method for unmanned aircraft using multi-variate optimisation p 2587 N93-25408
Elastic modeling and migration in Earth models p 2771 N93-25433
Aerial photographic sampling for statewide resource inventory p 2755 N93-25441
Numerical and experimental analyses of large composite skeletal satellite systems p 2616 N93-25463
Spatial simulation of transition in wall-bounded shear flows: Active control and effects of surface roughness p 2701 N93-25483
Experimental modal survey of the probe mass mock-up
| DE93-008846 | p 2617 N93-25494
Intraplate deformation, stress in the lithosphere and the driving mechanism for plate motions
| NASA-CR-192782 | p 2772 N93-25529
Numerical modeling of barred spiral galaxies p 2893 N93-25537
On the vertical structure of seasonal, interannual and intraseasonal flows p 2782 N93-25557
Use of high performance networks and supercomputers for real-time flight simulation p 2598 N93-25574
Studies of several small seawater MHD thrusters using the high-field solenoid of MIT's Bitter Magnet Laboratory
| AD-A260645 | p 2860 N93-25641
Numerical modelling of viscous turbomachinery flows with a pressure correction method p 2594 N93-25702
Vector radiative transfer model: Application to rainfall retrieval with microwave radiometric data p 2784 N93-25743
A distributed analysis and visualization system for model and observational data p 2881 N93-25814
Anatomy and physiology of plant conductive systems
| PB93-156032 | p 2793 N93-25877
The rapid solution of the Laplace equation on regions with fractal boundaries
| AD-A260585 | p 2828 N93-25905
On the cross-stream spectral method for the Orr-Sommerfeld equation
| NASA-TM-107737 | p 2845 N93-26086
Goldstone solar system radar signal processing p 2680 N93-26130
Finite element modeling of the hydroforming press
| KCP-613-4999 | p 2668 N93-26206
Substantiation of a stochastic model of rhythmic phenomena
| AD-A261232 | p 2830 N93-26262
Progress in impulse approach research
| AD-A261728 | p 2850 N93-26281
Phase-field models for anisotropic interfaces
| PB93-164564 | p 2646 N93-26323
Investigation of coupled analysis techniques for adaptive material structural systems
| AD-A261359 | p 2868 N93-26332
Multivariable control for flexible IC processing
| AD-A261685 | p 2692 N93-26366
Thermally induced stresses in a composite exposed to fire
| AD-A261714 | p 2641 N93-26371
Modeling and analysis tools p 2897 N93-26397
EnviroNET p 2886 N93-26398
Computational methods for flow problems: Parallel algorithms, flow control, and novel approaches
| AD-A261400 | p 2707 N93-26400
Heterogeneous photocatalytic oxidation of atmospheric trace contaminants
| NASA-CR-192937 | p 2767 N93-26427
Rain rate and modeled fade distributions at 20 GHz and 30 GHz derived from five years of network rain gauge measurements p 2683 N93-26468
Computational modeling of MAGO and other magnetized target fusion concepts
| DE93-007354 | p 2861 N93-26504
Approximate techniques for predicting size effects on cleavage fracture toughness (J(sub c))
| AD-A261591 | p 2731 N93-26516
A three-dimensional study of the influence of mountains on a front
| AD-A261927 | p 2787 N93-26545
Computation of complex solidification morphologies using a phase-field model
| PB93-156743 | p 2869 N93-26547
Effects of surface thermal forcing on stratified flow past an isolated obstacle
| PB93-156776 | p 2776 N93-26548
METal matrix composite ANalyzer (METCAN): Theoretical manual
| NASA-TM-106025 | p 2641 N93-26552
Interaction of an eddy with a continental slope
| AD-A261550 | p 2791 N93-26578
Very low frequency signals and whistler-mode amplification in the magnetosphere and limit-cycle behavior in the CECAF infrared free electronic laser
| AD-A261776 | p 2716 N93-26601
A comparison of ionospheric propagation mode delay predictions from ADVANCED PROPHET 4.3 with measured data
| AD-A261782 | p 2686 N93-26604

MATHEMATICAL PROGRAMMING
ASTROS-ID: Software for system identification using mathematical programming
| AD-A260867 | p 2810 N93-25627
Computation and theory in large-scale optimization
| AD-A261419 | p 2813 N93-26450

MATRICES (MATHEMATICS)
The analysis of convolutional codes via the extended Smith algorithm p 2671 N93-24664
Polar decomposition for attitude determination from vector observations p 2602 N93-24711
Attitude determination using vector observations: A fast optimal matrix algorithm p 2606 N93-24731
Combining spectral information with crop rotation knowledge for crop classifications p 2752 N93-24861
Equilibrium constrained assumed natural coordinate strain finite elements for shell analysis p 2724 N93-25273
Parallel matrix computations
| AD-A260783 | p 2828 N93-25687
Golay and other box codes p 2678 N93-26116
Progress in impulse approach research
| AD-A261728 | p 2850 N93-26281

MATRIX MATERIALS
Analysis of matrix damage in unidirectional composites p 2634 N93-25338
Thermomechanical response of shape memory composites
| AD-A260828 | p 2639 N93-25919
Thermal expansion measurements of polymer matrix composites and syntactics
| MTL-TR-92-27 | p 2640 N93-25954

MAXIMUM ENTROPY METHOD
Experimental results of the performance of the new phase and frequency controller p 2839 N93-25035
Maximum entropy approach to fuzzy control
| NASA-CR-192949 | p 2818 N93-25141
Bayesian cross-entropy reconstruction of complex images
| AD-A261812 | p 2812 N93-26257

MEAN
General aviation aircraft: Normal acceleration data analysis and collection project
| DOT/FAA/CT-91/20 | p 2586 N93-24739

MEAN SQUARE VALUES
Methods of evaluating the effects of coding on SAR data p 2804 N93-25926

MEANDERS
Dynamics of Gulf Stream meanders and frontal eddies in the South Atlantic Bight p 2788 N93-25354
MEASURE AND INTEGRATION
A comparative assessment of R. M. Young and tipping bucket rain gauges p 2685 N93-26483
MEASURING INSTRUMENTS
A system to measure lightning-induced transients on spacecraft umbilical lines p 2693 N93-24889
Study of atmospheric electrical events above complex terrain p 2780 N93-24897
Determination of design and operation parameters for upper atmospheric research instrumentation to yield optimum resolution with deconvolution, appendix 4
| NASA-CR-192834 | p 2769 N93-24910
Determination of design and operation parameters for upper atmospheric research instrumentation to yield optimum resolution with deconvolution, appendix 2
| NASA-CR-192833 | p 2770 N93-25088
Apparatus and methods for determining balance of a cylindrical vehicle
| AD-D015637 | p 2717 N93-25228
Application of an on-machine gage for diameter measurements p 2711 N93-25578
Method of measuring cross-flow vortices by use of an array of hot-film sensors
| NASA-CASE-LAR-14824-1-SB | p 2706 N93-26000
Determination of design and operation parameters for upper atmospheric research instrumentation to yield optimum resolution with deconvolution
| NASA-CR-192832 | p 2775 N93-26084
MECHANICAL DEVICES
Detection of bearing failure in mechanical devices using neural networks p 2822 N93-25965
MECHANICAL ENGINEERING
Turbine turbobrake systems p 2717 N93-25268
Nonlinear vibrations, stability, and dynamics of structures and mechanisms
| AD-A260871 | p 2728 N93-25838
Engineering: Research development and technology
| UCRL-53868-91 | p 2917 N93-26326
Configuration optimization of space structures p 2670 N93-26415
MECHANICAL PROPERTIES
High Temperature Composite Analyzer (HITCAN) theoretical manual, version 1.0
| NASA-TM-106001 | p 2723 N93-24913
Processing and properties of Ti5Si3
| DE93-007284 | p 2649 N93-25149
Dynamic test apparatus for electro-rheological fluids
| AD-D015632 | p 2643 N93-25284
Processing and mechanical properties of laminated metal composites of Al/Al-25 vol. percent SiC and ultrahigh carbon steel/brass
| DE93-007504 | p 2635 N93-25383
MEDICAL EQUIPMENT
Automated system for early breast cancer detection in mammograms p 2796 N93-25568
MEDICAL SCIENCE
Achieving the promise of the bioscience revolution: The role of the Federal Government
| PB93-139970 | p 2793 N93-25457
Advanced data visualization and sensor fusion: Conversion of techniques from medical imaging to Earth science p 2880 N93-25810
MEDICAL SERVICES
Automated system for early breast cancer detection in mammograms p 2796 N93-25568
MEDITERRANEAN SEA
Determination of environmental dynamics using NOAA satellite data and a water balance model for the Mediterranean landscape p 2741 N93-24794
The use of remote sensing and GIS for the assessment of environmental degradation caused by fires, applied upon South-Euboia (central Greece) p 2742 N93-24802
MELTING POINTS
Electrochemical and spectroscopic studies of molten halides
| AD-A261687 | p 2646 N93-26439
MELTS (CRYSTAL GROWTH)
Fundamental and applied aspects of defect engineering in GaAs
| AD-A260573 | p 2867 N93-25899
MEMBRANE STRUCTURES
INEL spray-forming research p 2658 N93-25562
MEMBRANES
Kinetic studies of interfacial photocurrents in platinized chloroplasts
| DE93-002344 | p 2792 N93-25104
Direct methane conversion to methanol
| DE93-009183 | p 2660 N93-25497
Effect of cytoskeletal reagents on stretch activated ion channels
| AD-A261089 | p 2793 N93-25764
Emerging technologies in ethanol production
| PB93-157014 | p 2661 N93-25818
Membrane technology: A search for membranes for submarine atmosphere control
| AD-A260581 | p 2801 N93-25904
Luminescence probe studies of ionomers. 3: Distribution of decay rate constants for tris bipyridyl ruthenium(2) in Nafion membranes
| AD-A260764 | p 2645 N93-25916
Inorganic and biological electron transfer across an electronically conductive composite polymer membrane
| AD-A261642 | p 2656 N93-26172
Template synthesis of electronically conductive polymers: A new route for achieving higher electronic conductivities
| AD-A261616 | p 2658 N93-26437
MEMORY
A cognitive architecture for human performance process model research
| AD-A261040 | p 2797 N93-25815
Neuromagnetic investigation of cortical regions underlying short-term memory
| AD-A261445 | p 2799 N93-26521
MEMORY (COMPUTERS)
Performance studies of cache consistency and concurrency control algorithms in a distributed client/server DBMS architecture p 2876 N93-25554
Thin rechargeable batteries for CMOS SRAM memory protection p 2694 N93-25583
Solid-state isotopic power source for computer memory chips p 2694 N93-25596
An investigation of memory latency reduction using an address prediction buffer
| AD-A261010 | p 2806 N93-25858
The design and implementation of a read prediction buffer
| AD-A260902 | p 2806 N93-25934
Considerations for space and naval aviation applications of ferroelectric memory
| AD-A261300 | p 2807 N93-26294
MENTAL PERFORMANCE
A cognitive architecture for human performance process model research
| AD-A261040 | p 2797 N93-25815
Simulated sustained flight operations and performance. Part 1: Effects of fatigue
| AD-A261012 | p 2801 N93-25859
Facilitation and interference in identification of pictures and words
| AD-A261484 | p 2798 N93-26356
Physiological indices of mental workload
| AD-A261692 | p 2798 N93-26391
Duration of alpha suppression increases with angle in a mental rotation task
| AD-A261592 | p 2798 N93-26435
MERCURY CADMIUM TELLURIDES
IR materials producibility
| AD-A261099 | p 2853 N93-25766
Study of surface behavior in function of temperature of the quaternary system (Hg, Cd, Zn)Te
| AD-A260968 | p 2867 N93-26223
MERCURY ISOTOPES
Feeding and decay of superdeformed states
| DE93-007899 | p 2848 N93-25371
MERCURY TELLURIDES
IR materials producibility
| AD-A261099 | p 2853 N93-25766
MESH
Reduction in size and unsteadiness of a VTOL ground vortex by ground fences
| NASA-CR-192997 | p 2580 N93-26049
MESOMETEOROLOGY
Use of the 1991 ASCOT field study data in a mesoscale model employing a four-dimensional data assimilation technique
| DE93-002683 | p 2769 N93-24672
Synoptic and Mesoscale Meteorology Instruction Workshop
| PB93-156347 | p 2785 N93-25870
SAR-related stress variability in the marine atmospheric boundary layer
| AD-A261129 | p 2775 N93-25946
Development and testing of improved techniques for modeling the hydrologic cycle in a mesoscale weather prediction system
| AD-A261454 | p 2787 N93-26351
MESON-NUCLEON INTERACTIONS
High-energy pion-nucleus scattering at LAMPF
| DE93-007364 | p 2852 N93-25380
MESOSCALE PHENOMENA
Use of the 1991 ASCOT field study data in a mesoscale model employing a four-dimensional data assimilation technique
| DE93-002683 | p 2769 N93-24672
Positive cloud-to-ground flashes in severe storms p 2780 N93-24896
Surface energy fluxes at Central Florida during the convection and precipitation electrification experiment
| NASA-CR-192826 | p 2769 N93-24945
The charge and size of precipitation particles inside thunderstorms and mesoscale convective systems on the Great Plains p 2781 N93-25275
An analysis of mesoscale convective systems observed during the 1992 Tropical Cyclone Motion field experiment
| AD-A260889 | p 2783 N93-25633
Synoptic and Mesoscale Meteorology Instruction Workshop
| PB93-156347 | p 2785 N93-25870
SAR-related stress variability in the marine atmospheric boundary layer
| AD-A261129 | p 2775 N93-25946
Wind-driven coastal generation of annual mesoscale eddy activity in the California current
| AD-A261355 | p 2790 N93-26331
Development and testing of improved techniques for modeling the hydrologic cycle in a mesoscale weather prediction system
| AD-A261454 | p 2787 N93-26351
MESOSPHERE
Empirical wind model for the middle and lower atmosphere. Part 1: Local time average
| NASA-TM-104581 | p 2770 N93-25160
The pressure modulation system in the Improved Stratospheric and Mesospheric Sounder p 2773 N93-25739
MESSAGE PROCESSING
Deterministic parallel FORTRAN
| DE93-008665 | p 2816 N93-25522
MESSAGES
An improved spectral load balancing method
| DE93-007582 | p 2810 N93-25386
Deterministic parallel FORTRAN
| DE93-008665 | p 2816 N93-25522
Virtually-synchronous communication based on a weak failure suspector
| NASA-CR-193003 | p 2721 N93-26135
METABOLIC DISEASES
Cellular and tissue injury during nonfreezing cold injury and frostbite
| AD-A260574 | p 2795 N93-25900
METABOLISM
Cellular and tissue injury during nonfreezing cold injury and frostbite
| AD-A260574 | p 2795 N93-25900
Metabolic response of environmentally isolated microorganisms to industrial effluents: Use of a newly described cell culture assay p 2794 N93-26066
METAL BONDING
Process for bonding elastomers to metals
| NASA-CASE-LAR-13645-1 | p 2656 N93-25995
Fundamental aspects of metal joining: The study of strong interfaces
| AD-A261293 | p 2653 N93-26304
METAL COATINGS
Electrodeposition in low gravity p 2663 N93-24774
Duct protection coating concept development and test: Test specimen fabrication, conditioning, and testing documentation.
| AD-A261250 | p 2657 N93-26278
METAL CRYSTALS
Whisker growth studies under conditions which resemble those available on an orbiting space station
| NASA-CR-192701 | p 2664 N93-25218
Crack tip fields in ductile crystals and bicrystals p 2866 N93-25749
METAL FATIGUE
Fatigue in single crystal nickel superalloys
| AD-A260709 | p 2651 N93-25843
Deformation mechanisms of NiAl cyclicly deformed near the brittle-to-ductile transition temperature
| NASA-CR-191121 | p 2652 N93-26235
METAL FIBERS
Interface engineering in oxide fiber/oxide matrix composites
| AD-A261705 | p 2641 N93-26579
METAL FILMS
Fundamental studies of defect generation in amorphous silicon alloys grown by remote plasma-enhanced chemical-vapor deposition (Remote PECVD)
| DE92-010560 | p 2862 N93-24953
Metal ion implantation for large scale surface modification
| DE93-007649 | p 2859 N93-25324
Analysis of pull-tests for determining the effects of ion implantation on the adhesion of iron films to sapphire substrates
| DE93-006732 | p 2725 N93-25373
Research on lead titanate films for radiation detection
| AD-A261187 | p 2849 N93-25823
METAL FINISHING
Ultrasonic polishing p 2670 N93-25580

METAL FOILS
Shear band formation in a W-Ni-Fe alloy under plate impact
| AD-A260702 | p 2651 N93-25907
METAL FUELS
Effect of a metal deactivator fuel additive on fuel deposition in fuel atomizers at high temperature
| AD-A260915 | p 2661 N93-25914
METAL HALIDES
Whisker growth studies under conditions which resemble those available on an orbiting space station
| NASA-CR-192701 | p 2664 N93-25218
Spectroscopic effects of disorder and vibrational localization in mixed-halide metal-halide chain solids
| DE93-007361 | p 2646 N93-26505
METAL IONS
Metal ion implantation for large scale surface modification
| DE93-007649 | p 2859 N93-25324
The formation and characteristics of E-region thin ionization layers at high latitudes p 2861 N93-25829
METAL MATRIX COMPOSITES
High Temperature Composite Analyzer (HITCAN) theoretical manual, version 1.0
| NASA-TM-106001 | p 2723 N93-24913
High temperature composite analyzer (HITCAN) user's manual, version 1.0
| NASA-TM-106002 | p 2724 N93-25070
Monitoring damage growth in titanium matrix composites using acoustic emission
| NASA-TM-107742 | p 2634 N93-25072
Dynamic deformations and analysis of a metal matrix composite p 2634 N93-25234
Internal stresses and the cyclic deformation of an aluminum matrix composite p 2650 N93-25436
The corrosion of metal matrix composites p 2638 N93-25723
Electrostatic fiber spreader
| AD-D015677 | p 2640 N93-26143
METal matrix composite ANalyzer (METCAN): Theoretical manual
| NASA-TM-106025 | p 2641 N93-26552
METAL OXIDE SEMICONDUCTORS
Quantum conductance fluctuations in self-aligned, pinch-narrowed MOSFETs p 2863 N93-25265
Smart microsensors for high temperature applications
| AD-A260747 | p 2710 N93-25677
METAL OXIDES
Development of high Tc (greater than 100 K) Bi, Tl and Y-based materials as superconducting circuit elements
| NASA-CR-192344 | p 2863 N93-25219
Phosphorus-, nitrogen-, sulfur-, and chlorine-containing molecules on surfaces
| AD-A261265 | p 2657 N93-26303
METAL PARTICLES
A study of mass size distributions and particle deposition velocities in ambient air p 2763 N93-25263
METAL PLATES
Behavior of a steel-liner-and-bolts system under very high thermal and mechanical loading: The CONVEX Liner Add-On to DIAMOND FORTUNE
| DE93-007512 | p 2731 N93-26507
METAL PROPELLANTS
Particle behavior in solid propellant rocket motors and plumes
| AD-A260900 | p 2624 N93-25913
Effect of a metal deactivator fuel additive on fuel deposition in fuel atomizers at high temperature
| AD-A260915 | p 2661 N93-25914
Dynamic burning rate measurements of metalized composite propellants using the laser-recoil technique p 2631 N93-26043
METAL SHEETS
Finite element modeling of the hydroforming press
| KCP-613-4999 | p 2668 N93-26206
METAL SPRAYING
INEL spray-forming research p 2658 N93-25562
METAL STRIPS
INEL spray-forming research p 2658 N93-25562
METAL SURFACES
Hot corrosion of the B2 nickel aluminides
| NASA-CR-191082 | p 2649 N93-25128
Laser welding of selected aerospace alloys p 2718 N93-25435
Theoretical studies of surface reactions on metals and electronic materials
| DE93-009761 | p 2650 N93-25502
Macromolecules for inhibition of corrosion and wear
| AD-A261041 | p 2655 N93-25816
Enhanced backscattering from rough surfaces
| AD-A261000 | p 2676 N93-25855
In situ surface studies of conversion coatings for steel and aluminum
| AD-A261016 | p 2655 N93-25861
Prediction of hydrogen entry and permeation in metals and alloys
| AD-A260580 | p 2651 N93-25903
Process for bonding elastomers to metals
| NASA-CASE-LAR-13645-1 | p 2656 N93-25995
Interaction of O2 with the Fe(.84)Cr(.16) (001) surface studied by photoelectron spectroscopy
| AD-A261065 | p 2645 N93-26251
Dynamics of gas-surface interactions
| AD-A261402 | p 2646 N93-26402
METAL VAPOR LASERS
Electron-beam-pumped recombination lasers p 2712 N93-25344
Collisional recombination lasers p 2713 N93-25393
Feasibility experiment for sodium-layer laser guide stars at the Lawrence Livermore National Laboratory
| DE93-007115 | p 2715 N93-26503
METAL VAPORS
The physics of spin polarized gases
| AD-A261396 | p 2850 N93-26288
METAL WORKING
Converting environmental wastes into valuable resources p 2759 N93-25572
Advanced engineering analysis
| KCP-613-4967 | p 2669 N93-26212
METALLIC GLASSES
Colloid formation in implanted glasses
| DE93-006763 | p 2653 N93-24971
METALLICITY
Photospheric abundance analysis of low-mass pre-main sequence stars p 2894 N93-25623
METALLOGRAPHY
External stress-corrosion cracking of a 1.22-m-diameter type 316 stainless steel air valve
| NASA-TP-3190 | p 2652 N93-26201
METALORGANIC CHEMICAL VAPOR DEPOSITION
MOCVD process technology for affordable, high-yield, high-performance MESFET structures. Phase 3: MIMIC
| AD-A261178 | p 2690 N93-25820
METALS
Health and environmental chemistry: Analytical techniques, data management, and quality assurance
| DE93-002853 | p 2760 N93-24674
Crop agroecological diagnostics by remote sensing technique p 2751 N93-24860
Reclamation with recovery of radionuclides and toxic metals from contaminated materials, soils, and wastes p 2769 N93-25571
Use and analysis of finite element methods for problems of solid mechanics and fracture
| AD-A261574 | p 2731 N93-26522
METAMORPHISM (GEOLOGY)
Geochemistry and petrology of primitive achondrite meteorites LEW 88280, MAC 88177, ALHA 81187, EET 84302, and LEW 88663 p 2896 N93-26067
METASTABLE STATE
Metastable SiC and SiGeC alloys by carbon implantation and solid phase epitaxy
| DE93-007594 | p 2863 N93-25387
METEORITES
Volatiles in interplanetary dust particles: A comparison with CI and CM chondrites p 2896 N93-26062
Geochemistry and petrology of primitive achondrite meteorites LEW 88280, MAC 88177, ALHA 81187, EET 84302, and LEW 88663 p 2896 N93-26067
METEORITIC COMPOSITION
Geochemistry and petrology of primitive achondrite meteorites LEW 88280, MAC 88177, ALHA 81187, EET 84302, and LEW 88663 p 2896 N93-26067
METEOROIDS
The initial flight anomalies of Skylab 1 p 2619 N93-24692
METEOROLOGICAL INSTRUMENTS
A comparison of the WIND System atmospheric models and MATS data
| DE93-002687 | p 2760 N93-24673
METEOROLOGICAL PARAMETERS
The Global Ocean Observing System: One perspective p 2733 N93-24920
Parametric analysis of atmospheric processes
| NASA-CR-192523 | p 2770 N93-25086
Summary information and data sets for NREL's Solar Radiation Research Laboratory, 1981 - 1991
| DE93-000052 | p 2898 N93-25101
Propagation at microwave frequencies in the presence of tropospheric stratified layers p 2674 N93-25340
Climate data bases of the People's Republic of China, 1841-1988
| DE93-007907 | p 2764 N93-25517
Development and testing of improved techniques for modeling the hydrologic cycle in a mesoscale weather prediction system
| AD-A261454 | p 2787 N93-26351
The ACTS propagation program p 2683 N93-26465
METEOROLOGICAL RADAR
Lightning precursor signatures from dual-polarization radar measurements of storms p 2777 N93-24877
Positive cloud-to-ground flashes in severe storms p 2780 N93-24896
The ATC evaluation of the prototype Airport Surveillance Radar Wind Shear Processor (ASR-WSP) at Orlando International Airport
| DOT/FAA/CT-TN92/48 | p 2673 N93-25210
Initialization of a modeled convective storm using Doppler radar-derived fields p 2782 N93-25294
Setting values for TDWR/LLWAS 3 integration parameters
| AD-A260740 | p 2783 N93-25645
Remote sensing of precipitation and electrification with a dual-polarization, coherent, wideband radar system
| AD-A260779 | p 2756 N93-25679
Status of the Olympus experiment at CRC p 2685 N93-26480
METEOROLOGICAL SATELLITES
A land-surface testbed for EOSDIS p 2878 N93-25797
METEOROLOGICAL SERVICES
Interactive forecasting with the National Weather Service River Forecast System p 2788 N93-25616
National Weather Service Winter Weather Workshop
| PB93-146785 | p 2785 N93-25775
Experimenter's laboratory for visualized interactive science p 2879 N93-25802
Synoptic and Mesoscale Meteorology Instruction Workshop
| PB93-156347 | p 2785 N93-25870
Rainfall frequency atlas of the Midwest
| PB93-164606 | p 2785 N93-25872
METEOROLOGY
The need for spaceborne observations for meteorology and climatology p 2744 N93-24813
Global Temperature and Salinity Pilot Project p 2733 N93-24924
Parametric analysis of atmospheric processes
| NASA-CR-192523 | p 2770 N93-25086
Summary information and data sets for NREL's Solar Radiation Research Laboratory, 1981 - 1991
| DE93-000052 | p 2898 N93-25101
Winter warming from large volcanic eruptions
| NASA-CR-192848 | p 2763 N93-25244
On the generation and dispersion of Yanai waves with a spectral Chebyshev-collocation reduced-gravity ocean model p 2788 N93-25276
Planetary data analysis and display system: A version of PC-McIDAS p 2880 N93-25806
Compression of spectral meteorological imagery p 2804 N93-25925
Coastal ocean processes: A science prospectus
| AD-A261702 | p 2790 N93-26384
METEOSAT SATELLITE
Sustainable remote sensing: A major improvement for realtime resource management and disaster early warning in developing countries p 2743 N93-24808
METHANE
Direct methane conversion to methanol
| DE93-009183 | p 2660 N93-25497
Activation of methane by clean and chemically modified single crystal oxide surfaces
| PB93-157295 | p 2644 N93-25817
METHOD OF MOMENTS
High-performance visualization applied to computational electromagnetics: Method-of-moments on a silicon graphics workstation
| AD-A260820 | p 2675 N93-25700
METHYL ALCOHOL
Fuel Injector: Air swirl characterization aerothermal modeling, phase 2, volume 2
| NASA-CR-189193 | p 2592 N93-25106
A novel process for methanol synthesis
| DE93-008037 | p 2659 N93-25118
Probe molecule studies: Active species in alcohol synthesis
| DE93-008097 | p 2659 N93-25119
Direct methane conversion to methanol
| DE93-009183 | p 2660 N93-25497
Deuteron and oxygen-17 NMR studies of molecular motion in methanol-saturated Nafion membranes
| AD-A261579 | p 2851 N93-26514
METROLOGY
Frequency and Time Forum
| ESA-SP-340 | p 2831 N93-24978
Relativistic effects for low Earth orbit satellites using GPS p 2608 N93-24986
The Columbus Metrology Science Team: Report on activities p 2670 N93-24987
Designing for frequency and time metrology at the 10 to the minus 18 power level p 2842 N93-25059

MEXICO
North-central Mexico blue grama rangeland biomass assessment at the end of the rainy season using NOAA-AVHRR-LAC p 2750 N93-24854
MICHELSON INTERFEROMETERS
Polarizing Michelson interferometer for measuring thermospheric winds
|ISBN-0-315-70442-X| p 2784 N93-25731
MICROANALYSIS
Physical and chemical processes governing the CO2 laser-induced deflagration of ammonium dinitramide (ADN) p 2629 N93-26037
MICROBIOLOGY
Planetary Biology and Microbial Ecology: Molecular Ecology and the Global Nitrogen cycle
|NASA-CR-4497| p 2803 N93-26157
MICROCHANNEL PLATES
Intensity distribution of the x ray source for the AXAF VETA-I mirror test p 2854 N93-26184
MICROCOMPUTERS
Object-oriented tools for distributed computing p 2817 N93-25576
MICROCRACKS
Processing and properties of Ti5Si3
|DE93-007284| p 2649 N93-25149
Quantifying distributed damage in composites via the thermoelastic effect p 2637 N93-25691
Defect initiation/growth and energy dissipation induced by deformation and fracture
|AD-A261703| p 2869 N93-26385
MICROELECTRONICS
Microwave and millimeter wave monolithic integrated circuits (MIMIC) program. MIMIC briefs: Summaries of phase 3 technology support programs
|AD-A260914| p 2690 N93-25660
RF vacuum microelectronics
|AD-A261343| p 2691 N93-26311
SiC microsensor with piezoresistive diamond sensing elements
|AD-A261346| p 2868 N93-26312
Electronics and Electrical Engineering Laboratory technical publication announcements covering laboratory programs, July to September 1992 with 1992/1993 EEEL events calendar
|PB93-158632| p 2884 N93-26530
RF vacuum microelectronics
|AD-A261784| p 2692 N93-26565
MICROGRAVITY APPLICATIONS
NASA Microgravity Science and Applications Program
|NASA-TM-108775| p 2663 N93-25194
Whisker growth studies under conditions which resemble those available on an orbiting space station
|NASA-CR-192701| p 2664 N93-25218
Laser ignition application in a space experiment
|NASA-TM-106133| p 2664 N93-25337
MICROHARDNESS
Vickers indentation hardness of stoichiometric and reduced single crystal TiO2 (rutile) from 25 to 800 C
|NASA-TM-105959| p 2633 N93-26204
MICROMECHANICS
High Temperature Composite Analyzer (HITCAN) theoretical manual, version 1.0
|NASA-TM-106001| p 2723 N93-24913
A micromechanical viscoplastic stress-strain model with grain boundary sliding
|DE93-009109| p 2649 N93-25095
Continuum and micromechanics treatment of constraint in fracture
|AD-A260927| p 2727 N93-25647
Energy dissipation in inelastic flow of cohesionless granular media p 2703 N93-25662
Finite element micromechanics modeling of inelastic deformation of unidirectionally fiber-reinforced composites p 2637 N93-25680
A three-dimensional model for the residual stresses in a unidirectional composite plate p 2728 N93-25825
Micromechanics of fatigue
|AD-A260577| p 2729 N93-25901
Thermomechanical response of shape memory composites
|AD-A260828| p 2639 N93-25919
Failure considerations in composite systems based on 3D micromechanical stress fields, part A
|AD-A261698| p 2641 N93-26382
METal matrix composite ANalyzer (METCAN): Theoretical manual
|NASA-TM-106025| p 2641 N93-26552
MICROMETEOROIDS
Hypervelocity impact study: The effect of impact angle on crater morphology
|NASA-CR-192711| p 2724 N93-25260
MICROMOTORS
Tuned circuit electric levitation bearings for microactuators p 2689 N93-25619
MICROORGANISMS
Metabolic response of environmentally isolated microorganisms to industrial effluents: Use of a newly described cell culture assay p 2794 N93-26066
MICROPOROSITY
Template synthesis of electronically conductive polymers: A new route for achieving higher electronic conductivities
|AD-A261616| p 2658 N93-26437
MICROPROCESSORS
A microcomputer compensated crystal oscillator MCXO p 2834 N93-25001
MICROSCOPY
Progress in imaging microscopy with x ray lasers at LLNL
|DE93-007508| p 2712 N93-25363
Correlation of damage threshold and surface geometry of nodular defects in HR coatings as determined by in-situ atomic force microscopy
|DE93-007509| p 2654 N93-25384
Internal current probing of integrated circuits using magnetic force microscopy
|DE93-006752| p 2692 N93-26501
MICROSTRIP ANTENNAS
Microstrip antennas on/in anisotropic material layers
|AD-A261700| p 2681 N93-26383
MICROSTRUCTURE
Development of dispersion-strengthened XD (trademark) Cu alloys for high heat-flux applications
|NASA-CR-191124| p 2653 N93-24761
Processing and properties of Ti5Si3
|DE93-007284| p 2649 N93-25149
Laser welding of selected aerospace alloys p 2718 N93-25435
Internal strain analysis of ceramics using scanning laser acoustic microscopy
|NASA-CR-191118| p 2721 N93-25451
Properties of extruded PS-212 type self-lubricating materials p 2659 N93-25565
Mullite whiskers and mullite-whisker felt p 2642 N93-25586
Transformation plasticity and fracture behavior of ceria-TZP/alumina composites p 2638 N93-25760
High strain rate damage development and failure mechanisms in tungsten heavy alloys
|AD-A260856| p 2651 N93-25788
Research on lead titanate films for radiation detection
|AD-A261187| p 2849 N93-25823
Experimental and theoretical studies of proximity effect and Coulomb blockade phenomena in Josephson junctions
|AD-A261652| p 2867 N93-26194
External stress-corrosion cracking of a 1.22-m-diameter type 316 stainless steel air valve
|NASA-TP-3190| p 2652 N93-26201
Solidification processing and phase transformations in ordered high temperature alloys
|AD-A261751| p 2652 N93-26284
NIST reactor: Summary of activities, July 1991 through September 1992
|PB93-162873| p 2852 N93-26322
Position sensitive atom probe study of the decomposition of a Cu-2.6 at. percent Co alloy
|DE93-006737| p 2653 N93-26500
Interface engineering in oxide fiber/oxide matrix composites
|AD-A261705| p 2641 N93-26579
MICROWAVE ABSORPTION
Microwave absorption measurements and interference: Effects for a liquid fuel between 2.5 and 18 GHz
|AD-A260607| p 2675 N93-25635
MICROWAVE ANTENNAS
Ka-band feed arrays for spacecraft reflector antennas with limited scan capability: An overview p 2680 N93-26128
MICROWAVE ATTENUATION
Rain rate and modeled fade distributions at 20 GHz and 30 GHz derived from five years of network rain gauge measurements p 2683 N93-26468
More rain compensation results p 2686 N93-26486
MICROWAVE CIRCUITS
Microwave and millimeter wave monolithic integrated circuits (MIMIC) program. MIMIC briefs: Summaries of phase 3 technology support programs
|AD-A260914| p 2690 N93-25660
MOCVD process technology for affordable, high-yield, high-performance MESFET structures. Phase 3: MIMIC
|AD-A261178| p 2690 N93-25820
Special technology area review on microwave packaging technology
|AD-A261852| p 2681 N93-26276
MICROWAVE EMISSION
Propagation at microwave frequencies in the presence of tropospheric stratified layers p 2674 N93-25340
MICROWAVE IMAGERY
Remote sensing of non-renewable resources p 2744 N93-24814
Passive microwave remote sensing of snow-covered floating ice during spring conditions in the Arctic and Antarctic
|ISBN-0-315-70444-6| p 2754 N93-25422
Computation of moisture flux from ocean to atmosphere using a synergy of SSM/I-derived precipitable water and ECMWF analyses p 2774 N93-25757
Advanced data visualization and sensor fusion: Conversion of techniques from medical imaging to Earth science p 2880 N93-25810
MICROWAVE OSCILLATORS
Microwave frequency discriminator with a cryogenic sapphire resonator for ultra-low phase noise p 2693 N93-24982
Design of a low phase noise UHF oscillator using a partly metallized dielectric resonator p 2693 N93-25003
MICROWAVE POWER BEAMING
Preliminary results on an optically-pumped Cs beam frequency standard p 2832 N93-24989
MICROWAVE RADIOMETERS
Influence due to antenna pattern change in brightness temperature estimation for a space-based microwave radiometer p 2753 N93-24868
Vector radiative transfer model: Application to rainfall retrieval with microwave radiometric data p 2784 N93-25743
Cross-switched MICRAD seeker
|AD-D015676| p 2691 N93-26142
Brightness temperature and attenuation diversity statistics at 20.6 and 31.65 GHz for the Colorado Research Network p 2684 N93-26473
MICROWAVE RESONANCE
Basic design of a spaceborne hydrogen maser p 2716 N93-25024
Microwave synthesizers in space p 2693 N93-25038
Line inhomogeneity effects and power shift in miniaturized rubidium frequency standards p 2694 N93-25066
MICROWAVE SPECTRA
The Telecommunications and Data Acquisition Report
|NASA-CR-192804| p 2676 N93-26105
MICROWAVES
BBU code development for high-power microwave generators
|DE93-007111| p 2688 N93-25397
Microwave and millimeter wave monolithic integrated circuits (MIMIC) program. MIMIC briefs: Summaries of phase 3 technology support programs
|AD-A260914| p 2690 N93-25660
MIDDLE ATMOSPHERE
The Venus 130-nm dayglow as a diagnostic of thermospheric structure and dynamics p 2896 N93-25285
MIGRATION
Elastic modeling and migration in Earth models p 2771 N93-25433
MILITARY AIRCRAFT
Thermally induced stresses in a composite exposed to fire
|AD-A261714| p 2641 N93-26371
MILITARY AVIATION
Considerations for space and naval aviation applications of ferroelectric memory
|AD-A261300| p 2807 N93-26294
MILITARY OPERATIONS
Science, technology, and national security p 2886 N93-25232
Fidelity and validity in distributed interactive simulation: Questions and answers
|AD-A260971| p 2810 N93-25711
MILITARY SPACECRAFT
A Biphase Shift Keying (BPSK), direct sequence, spread spectrum modem for Petite Amateur Navy Satellite (PANSAT)
|AD-A261301| p 2618 N93-26295
MILITARY TECHNOLOGY
TF-4020A: TFL's new compact military rubidium standard p 2838 N93-25026
Science, technology, and national security p 2886 N93-25232
Summary report of the Defense Sciences Research Council Summer Conference
|AD-A261375| p 2917 N93-26359
Department of Defense technical architecture framework for information management. Volume 1: Implementation concept, version 1.1
|AD-A261911| p 2884 N93-26531
Department of Defense technical architecture framework for information management. Volume 2: Architecture guidance and design concepts, version 1.1
|AD-A261912| p 2884 N93-26532

MILKY WAY GALAXY
Cape Photographic Durchmusterung, volume 1
| NASA-RP-1300-VOL-1 | p 2890 N93-26002
Cape Photographic Durchmusterung, volume 2
| NASA-RP-1300-VOL-2 | p 2890 N93-26003
Cape Photographic Durchmusterung, volume 3
| NASA-RP-1300-VOL-3 | p 2890 N93-26004
MILLIMETER WAVES
A superconducting tunnel junction receiver for submillimeter astronomy, and analysis of observations of post-AGB star molecular envelopes
p 2889 N93-25440
Microwave and millimeter wave monolithic integrated circuits (MIMIC) program. MIMIC briefs: Summaries of phase 3 technology support programs
| AD-A260914 | p 2690 N93-25660
MIMD (COMPUTERS)
Synthetic-perturbation tuning of MIMD programs
| PB93-161339 | p 2812 N93-26321
MIMO (CONTROL SYSTEMS)
Scalar gain interpretation of large order filters
p 2606 N93-24729
Identification and control of lightly damped, large space structures: An experimental evaluation
p 2616 N93-25351
Analytical and experimental study of control effort associated with model reference adaptive control
p 2820 N93-25468
MINERALOGY
Spectral remote sensing of anomalous mineralogy induced by hydrocarbon migration and uranium mineralization, San Rafael Swell, Utah, USA
p 2739 N93-24783
Remote sensing of non-renewable resources
p 2744 N93-24814
MINERALS
Remote sensing of non-renewable resources
p 2744 N93-24814
Low cost dewatering of waste slurries
p 2769 N93-25573
Production of ultrafine, high-purity ceramic powders using the US Bureau of Mines developed turbomill
p 2659 N93-25585
MINIATURIZATION
Miniature Optical Wide-Angle-Lens Startracker (Mini-OWLS) p 2606 N93-24728
Miniaturization and stability: A new generation of ovenised oscillators p 2693 N93-25004
Novel approaches to the construction of miniaturized analytical instrumentation
| NASA-CR-191988 | p 2709 N93-25345
MINICOMPUTERS
Interactive forecasting with the National Weather Service River Forecast System p 2788 N93-25616
MINING
Low cost dewatering of waste slurries
p 2769 N93-25573
MINORITIES
The 1993/1994 NASA Graduate Student Researchers Program
| NASA-EP-283 | p 2872 N93-26051
MIR SPACE STATION
Operational use of MOMS-02 (P2) data
p 2752 N93-24866
MIRRORS
A system design for laser time synchronization via geodetic satellite Ajisai p 2716 N93-25005
Precision of the calibration of the AXAF engineering test article (VETA) mirrors p 2855 N93-26189
Image analysis of the AXAF VETA-I x ray mirror
p 2855 N93-26190
Surface finish quality of the outer AXAF mirror pair based on x ray measurements of the VETA-I
p 2855 N93-26191
The x ray reflectivity of the AXAF VETA-I optics
p 2855 N93-26192
Modeling of electric-field enhancement at nodular defects in dielectric mirror coatings
| DE93-007513 | p 2857 N93-26593
MIS (SEMICONDUCTORS)
Study of surface behavior in function of temperature of the quaternary system (Hg, Cd, Zn)Te
| AD-A260968 | p 2867 N93-26223
MISSILE CONFIGURATIONS
Fabrication of composite propfan blades for a cruise missile wind tunnel model
| NASA-TM-105270 | p 2730 N93-26202
MISSILE DESIGN
The systems engineering overview and process (from the Systems Engineering Management Guide, 1990)
p 2665 N93-24679
ASTROS-ID: Software for system identification using mathematical programming
| AD-A260867 | p 2810 N93-25627
MISSILE RANGES
Analysis of reentry into the White Sands Missile Range (WSMR) for the LifeSat mission p 2603 N93-24717
Applications of triggered lightning to space vehicle operations p 2619 N93-24878
Flight termination receiver catalog
| AD-A261558 | p 2682 N93-26460
MISSILE TRACKING
Time and frequency reference for a trajectory measurement system p 2837 N93-25023
MISSILES
Tornado: An engineering-oriented perspective
| PB93-148435 | p 2788 N93-26584
MISSION PLANNING
The systems engineering overview and process (from the Systems Engineering Management Guide, 1990)
p 2665 N93-24679
What is a system? NASA's phased project description
p 2665 N93-24681
Systems engineering and integration processes involved with manned mission operations p 2666 N93-24688
Systems engineering considerations for operational support systems p 2666 N93-24689
Summary and recommendations on nuclear electric propulsion technology for the space exploration initiative
| NASA-TM-105707 | p 2622 N93-24744
Parametric analysis of atmospheric processes
| NASA-CR-192523 | p 2770 N93-25086
JSC research and technology
| NASA-TM-104763 | p 2901 N93-25188
A mission concept for near term Lunar exploration
| DE93-007598 | p 2896 N93-25321
Space transfer vehicle concepts and requirements study. Volume 1: Executive summary
| NASA-CR-192524 | p 2610 N93-25479
Space transfer vehicle concepts and requirements study. Volume 2, book 1: STV concept definition and evaluation
| NASA-CR-192525 | p 2611 N93-25510
Space transfer vehicle concepts and requirements study. Volume 2, book 2: System and program requirements trade studies
| NASA-CR-192526 | p 2611 N93-25511
Space transfer vehicle concepts and requirements study. Volume 2, book 3: STV system interfaces
| NASA-CR-192527 | p 2611 N93-25513
Space transfer vehicle concepts and requirements study. Volume 3, book 1: Program cost estimates
| NASA-CR-192529 | p 2611 N93-25514
Using AI/expert system technology to automate planning and replanning for the HST servicing missions
p 2822 N93-25962
Evaluating science return in space exploration initiative architectures
| NASA-TP-3339 | p 2897 N93-26094
Knowledge-based decision support for Space Station assembly sequence planning
| NASA-CR-193048 | p 2599 N93-26095
NLS operations concepts: Failure modes scenario simulation model analysis
| MCR-92-5013 | p 2609 N93-26175
Nuclear safety policy working group recommendations on nuclear propulsion safety for the space exploration initiative
| NASA-TM-105705 | p 2632 N93-26200
Representative systems for space exploration
p 2897 N93-26395
Mars exploration planning p 2898 N93-26399
Department of Defense technical architecture framework for information management. Volume 2: Architecture guidance and design concepts, version 1.1
| AD-A261912 | p 2884 N93-26532
MIXERS
Design, fabrication, and testing of a three-dimensional acoustic orientation instrument (3-D AOI): Drawings, engineering and associated lists (conceptual and development design)
| AD-A260934 | p 2845 N93-25915
MIXING
A basic research model of natural gas combustion in turbulent flow, phase 2
| PB93-158509 | p 2644 N93-25819
MIXING LAYERS (FLUIDS)
Initial streamwise vorticity formation in a two-stream mixing layer p 2579 N93-25752
MOBILE COMMUNICATION SYSTEMS
An introduction to Doppler effect and fading in mobile communications
| AD-A260976 | p 2676 N93-25866
ETS-5, ETS-6, and COMETS projects in Japan
p 2683 N93-26470
WARC 92 and some thoughts as to its impact on the NASA propagation program p 2684 N93-26475
Allocations by the 1992 World Administrative Radio Conference p 2684 N93-26476
MOBILITY
NMR studies of ion mobility and association in polyether-based polymer electrolytes
| AD-A260662 | p 2655 N93-25642
MODAL RESPONSE
Global dynamic modeling of a transmission system
| NASA-CR-191117 | p 2716 N93-24751
Trapped energy quartz crystal resonator on wedge-shaped plate p 2837 N93-25022
Joint flexibility effects on the dynamic response of structures. Part 2: Stochastic analysis
| AD-A261003 | p 2729 N93-25938
MODEL REFERENCE ADAPTIVE CONTROL
Analytical and experimental study of control effort associated with model reference adaptive control
p 2820 N93-25468
MODELS
The evaluation of technical models used for major-accident hazard installations. Report to Commission of the European Communities Directorate General 12
| CUED/A-AERO/TR-19 | p 2668 N93-25238
ASRM design philosophy and modelling challenges
p 2627 N93-26022
Model reduction for Space Station Freedom
p 2620 N93-26081
MODEMS
A new modem for microwave time synchronisation via geosynchronous telecommunication satellites
p 2686 N93-24999
MODULARITY
Use of the Environmental Resource Management and Analysis System at the Fernald Environmental Management Project
| DE93-002943 | p 2760 N93-24955
MODULATION
Synchronisation, acquisition and tracking for telemetry and data reception p 2614 N93-25000
A frequency generating source: Frequency synthesizers p 2693 N93-25041
Monaural and binaural processing of complex waveforms
| AD-A261659 | p 2846 N93-26358
MODULATORS
Performance results of a 300-degree linear phase modulator for spaceborne communications applications
p 2672 N93-24670
Time resolved studies of in-well and cross-well carrier transport in MQW semiconductor structures
| AD-A261170 | p 2714 N93-25774
MODULES
Test results of a Stirling engine utilizing heat exchanger modules with an integral heat pipe
| NASA-TM-105883 | p 2759 N93-25136
Multichip module high speed testing
| AD-A261391 | p 2856 N93-26306
MODULUS OF ELASTICITY
Dynamic hardness tester and cure meter
p 2711 N93-25608
MOIRE FRINGES
In-situ ultrasonic C-scanner
| AD-A261113 | p 2638 N93-25768
MOISTURE
Effects of moisture and other contaminants in friction composites
| AD-A261226 | p 2640 N93-26301
MOISTURE CONTENT
Natural and augmented snowfall growth processes and their interactions with the natural and modified aerosol
| PB93-153096 | p 2786 N93-25874
MOISTURE RESISTANCE
A comparison of moisture resistance with different types of end-terminations in ceramic capacitors
| DE93-007600 | p 2689 N93-25416
MOLECULAR BEAM EPITAXY
Laser Induced Phonons (LIPs) in MBE grown ZnSe
| RSRE-MEMO-4544 | p 2864 N93-25454
MOCVD process technology for affordable, high-yield, high-performance MESFET structures. Phase 3: MIMIC
| AD-A261178 | p 2690 N93-25820
Optoelectronic III-V heterostructures on Si substrates
| AD-A261651 | p 2867 N93-26193
MOLECULAR BEAMS
Mechanistic studies of the CVD of silicon nitride from SiF4 and NH3
| DE93-004500 | p 2644 N93-25312
Flame structure studies of a lean, 20 torr H2/N2O/AR flame employing molecular beam mass spectrometry
p 2627 N93-26025
Modeling of atom-diatom scattering
| AD-A261645 | p 2849 N93-26173
MOLECULAR CLOUDS
Structure and star forming activities of the cold massive molecular cloud G216-2.5 p 2893 N93-25477
Shells, outflows and star formation in the giant molecular cloud Monoceros R2 p 2893 N93-25555

Photospheric abundance analysis of low-mass pre-main sequence stars p 2894 N93-25623

MOLECULAR COLLISIONS
Progress in impulse approach research
| AD-A261728 | p 2850 N93-26281

MOLECULAR DIFFUSION
Deuteron and oxygen-17 NMR studies of molecular motion in methanol-saturated Nafion membranes
| AD-A261579 | p 2851 N93-26514

MOLECULAR EXCITATION
The structure and energetics of Cr(CO)6 and Cr(CO)5
| NASA-CR-192889 | p 2848 N93-25450
Theoretical and experimental research in infrared technology
| AD-A260926 | p 2853 N93-25646
State-selected studies of atoms and molecules ejected from ion bombarded surfaces
| AD-A261275 | p 2850 N93-26267

MOLECULAR INTERACTIONS
Radiation-induced disordering and defect production in CuAu and NiAl studied by molecular dynamics simulation
| DE93-007506 | p 2649 N93-25336
Collisional energy transfer in biomolecular ion-molecule dynamics
| AD-A260911 | p 2849 N93-25659
Molecular interactions and properties with many-body methods
| AD-A261688 | p 2850 N93-26367
Theoretical treatment of spin-forbidden and electronically nonadiabatic processes. Methods and applications
| AD-A261596 | p 2851 N93-26525

MOLECULAR STRUCTURE
Ionization probes of molecular structure and chemistry
| DE93-008211 | p 2847 N93-25310
The structure and energetics of Cr(CO)6 and Cr(CO)5
| NASA-CR-192889 | p 2848 N93-25450
Structure of sodium 4-(1'-heptylnonyl) benzenesulfonate adsorbed on alumina using H-2 NMR
| AD-A261224 | p 2645 N93-26300
Thermal decomposition of energetic materials. 4: Deuterium isotope effects and isotopic scrambling condensed-phased decomposition of 1,3,5-trinitrohexahydro-s-triazine
| AD-A261804 | p 2662 N93-26387
Molecular composition, structure, and sensitivity of explosives
| DE93-003850 | p 2662 N93-26493
Intramolecular bridge/terminal oxo exchange within (MoV2O3) (4+) complexes containing linear oxo bridges
| AD-A261230 | p 2851 N93-26518

MOLECULAR WEIGHT
Polyimides containing the cyclobutene-3,4-dione moiety
| NASA-CASE-LAR-14753-1 | p 2656 N93-25999

MOLECULES
Experimental and theoretical studies of dense fluid mixtures
| DE93-006070 | p 2695 N93-24976
Application of non-thermal plasmas to pollution control
| DE93-007515 | p 2763 N93-25385
Macromolecules for inhibition of corrosion and wear
| AD-A261041 | p 2655 N93-25816
Phosphorus-, nitrogen-, sulfur-, and chlorine-containing molecules on surfaces
| AD-A261265 | p 2657 N93-26303
Penning detachment: A new frontier
| AD-A261447 | p 2850 N93-26346
Theoretical treatment of spin-forbidden and electronically nonadiabatic processes. Methods and applications
| AD-A261596 | p 2851 N93-26525
Bimolecular reaction dynamics from photoelectron spectroscopy of negative ions
| DE93-007669 | p 2647 N93-26599

MOLTEN SALTS
Rheology of YBa2Cu3O(7-x) precursors
| DE93-007285 | p 2863 N93-25362

MOLYBDENUM
Fundamental aspects of metal joining: The study of strong interfaces
| AD-A261293 | p 2653 N93-26304
Intramolecular bridge/terminal oxo exchange within (MoV2O3) (4+) complexes containing linear oxo bridges
| AD-A261230 | p 2851 N93-26518

MOMENTUM
Momentum accumulation due to solar radiation torque, and reaction wheel sizing, with configuration optimization p 2600 N93-24695
Accurate attitude determination of the LACE satellite p 2605 N93-24726
Implementation of the Turn Function Method in a three-dimensional, parallelized hydrodynamics code
| DE93-003744 | p 2696 N93-25124

MOMENTUM TRANSFER
Momentum accumulation due to solar radiation torque, and reaction wheel sizing, with configuration optimization p 2600 N93-24695
High-energy pion-nucleus scattering at LAMPF
| DE93-007364 | p 2852 N93-25380

MONITORS
An experimental health monitoring unit for GPS and GLONASS p 2586 N93-25018
Measuring hearing protection device performance using the metrosonics db-3100 sound level analyzer (dosimeter)
| AD-A260852 | p 2801 N93-25787

MONKEYS
Effects of space radiation on humoral and cellular immunity in rhesus monkeys
| AD-A261808 | p 2793 N93-26259

MONOMERS
Polyimides with improved compression moldability
| NASA-CASE-LAR-14457-1 | p 2656 N93-25997

MONTE CARLO METHOD
An introductory guide to uncertainty analysis in environmental and health risk assessment
| DE93-002873 | p 2760 N93-24676
Development and application of computational aerothermodynamics flowfield computer codes
| NASA-CR-192940 | p 2574 N93-24736
Discrete range clustering using Monte Carlo methods
| NASA-TM-104004 | p 2584 N93-24914
Monte-Carlo methods make Dempster-Shafer formalism feasible
| NASA-CR-192945 | p 2828 N93-25140
Correlated wavefunction quantum Monte Carlo approach to solids
| DE93-007730 | p 2863 N93-25367
The role of multiple scattering in twilight zenith sky observations of atmospheric absorbers: Diurnal photochemistry and airmass factors p 2772 N93-25535
An in-depth probabilistic study of external tank attach ring
| NASA-TM-108403 | p 2624 N93-25671
Developing and improving numerical algorithms to study intrinsically correlated electron systems
| AD-A261214 | p 2849 N93-25734
A numerical simulation of adsorption onto a crystalline surface
| AD-A261079 | p 2866 N93-25781
Considerations of the error variances of time-averaged estimators for correlated processes
| AD-A261796 | p 2830 N93-26255
Proton Monte Carlo transport program PTRAN
| PB93-158673 | p 2850 N93-26314
Monte Carlo approach to the approximation of invariant measures
| PB93-159069 | p 2830 N93-26317

MOORING
Improved fatigue life for moorings
| PB93-161198 | p 2730 N93-26320

MORNING
Sounding rocket observations of precipitating ions in the morning auroral region p 2773 N93-25732

MORPHOLOGY
Monitoring and evaluation of morphohydrographical changes in the Danube Delta by remote-sensing p 2747 N93-24834
Crop agroecological diagnostics by remote sensing technique p 2751 N93-24860
Flow and morphological conditions associated with the directional solidification of aqueous ammonium chloride
| DE93-008886 | p 2644 N93-25495
Photomodulation spectroscopy of photocarrier dynamics, electronic defects and morphology of conducting polymers
| DE93-010140 | p 2655 N93-25524
Luminescence probe studies of ionomers. 3: Distribution of decay rate constants for tris bipyridyl ruthenium(2) in Nafion membranes
| AD-A260764 | p 2645 N93-25916

MOSSBAUER EFFECT
Inelastic scattering in condensed matter with high intensity Moessbauer radiation
| DE93-008763 | p 2864 N93-25503

MOTION PERCEPTION
Visual processing of object velocity and acceleration
| AD-A261048 | p 2800 N93-25778
Neural basis of motion perception
| AD-A261452 | p 2798 N93-26349
Effect of image update rate on moving-target identification range
| AD-A261562 | p 2591 N93-26462

MOTION SICKNESS
Autonomic physiological data associated with simulator discomfort
| NASA-CR-177609 | p 2794 N93-24738

MOTION STABILITY
Investigation of liquid sloshing in spin-stabilized satellites
| AD-A261671 | p 2619 N93-26438

MOTIVATION
Exploring the link between intrinsic motivation and quality
| AD-A261722 | p 2722 N93-26246

MOTOR VEHICLES
A heat transfer analysis of a mobile vehicle radiation-shielded operator compartment
| DE93-007428 | p 2800 N93-25318
Cost-effectiveness analysis of TxDOT CNG fleet conversion, volume 2
| PB93-159432 | p 2720 N93-26534
Cost-effectiveness analysis of TxDOT CNG fleet conversion, volume 1
| PB93-165603 | p 2720 N93-26585

MOUNTAINS
Atmospheric correction of Landsat/TM data over mountainous terrain for forestry applications p 2752 N93-24862
A three-dimensional study of the influence of mountains on a front
| AD-A261927 | p 2787 N93-26545

MOVING TARGET INDICATORS
Effect of image update rate on moving-target identification range
| AD-A261562 | p 2591 N93-26462

MTBF
Step stress testing of receiver/transmitter units
| AD-A261286 | p 2730 N93-26279

MULLITES
Mullite whiskers and mullite-whisker felt p 2642 N93-25586

MULTIGRID METHODS
Implicit multigrid solution of the compressible Navier-Stokes equations with application to distributed parallel processing p 2702 N93-25546
Multilevel techniques in large scale computation
| AD-A261082 | p 2828 N93-25762

MULTIMEDIA
US Army evaluation of the Electronic Map Data (EMD) prototype
| AD-A261693 | p 2757 N93-26369

MULTIPATH TRANSMISSION
An SPW software simulation model of a dispersive fading multipath narrowband HF channel
| AD-A261101 | p 2675 N93-25767

MULTIPHASE FLOW
Ultrasonic rate measurement of multiphase flow
| DE93-000112 | p 2695 N93-24954
Numerical simulation of time-dependent thermocapillary convection in layered fluid systems p 2700 N93-25472

MULTIPHOTON ABSORPTION
Energy transfer properties and mechanisms
| DE93-008540 | p 2849 N93-25488
Photoexcitation of carbon fullerenes
| AD-A260739 | p 2849 N93-25644

MULTIPLEXING
Miniature Optical Wide-Angle-Lens Startracker (Mini-OWLS) p 2606 N93-24728
Cross-switched MICRAD seeker
| AD-D015676 | p 2691 N93-26142
The Data Multiplexing Network (DMN) phase 3 Extended Distance Data Cable (EDDC) test and evaluation
| DOT/FAA/CT-TN93/11 | p 2680 N93-26160

MULTIPROCESSING (COMPUTERS)
Supercomputer Debugging Workshop 1992
| DE93-007322 | p 2805 N93-25165
Proceedings of the Second SISAL Users' Conference
| DE93-008019 | p 2815 N93-25304
Toward a parallel recursive spectral bisection mapping tool
| DE93-006632 | p 2816 N93-25414
Gigabit network communications research
| AD-A260644 | p 2675 N93-25640

MULTISENSOR APPLICATIONS
Remote sensed spectral signatures classification and recognition by neural networks: An approach to unsupervised techniques p 2738 N93-24779
Monitoring and analysis of urban trends using multitemporal satellite-imagery (case-study: Greater Cairo) p 2740 N93-24790
Geologic and hydrogeologic mapping of Iceland with multisensor data (JERS-1, ERS-1, SPOT, Landsat and SEASAT) p 2740 N93-24792
Operational use of MOMS-02 (P2) data p 2752 N93-24866
Advanced data visualization and sensor fusion: Conversion of techniques from medical imaging to Earth science p 2880 N93-25810
Method of measuring cross-flow vortices by use of an array of hot-film sensors
| NASA-CASE-LAR-14824-1-SB | p 2706 N93-26000

Phase discriminating capacitive array sensor system
| NASA-CASE-GSC-13460-1 | p 2691 N93-26104
MULTISPECTRAL BAND SCANNERS
SEOMAR: An Italian approach to the observation of the Mediterranean area p 2746 N93-24825
Operational use of MOMS-02 (P2) data p 2752 N93-24866
MULTISPECTRAL PHOTOGRAPHY
Cloud properties as inferred from HIRS/2 multi-spectral data p 2782 N93-25293
MULTIVARIABLE CONTROL
Multivariable control for flexible IC processing
| AD-A261685 | p 2692 N93-26366
MULTIVARIATE STATISTICAL ANALYSIS
Time stability: An improvement of the multi-variance method for the oscillator noise analysis p 2839 N93-25036
Multivariate statistical analysis software technologies for astrophysical research involving large data bases p 2878 N93-25796
Time series analysis and multivariate analysis
| AD-A261014 | p 2830 N93-25860
MUSCLES
Mechanical stimulation of skeletal muscle mitigates glucocorticoid induced decreases in prostaglandin synthesis
| NASA-CR-193040 | p 2794 N93-24763
Initial experiments with a myoelectric-based muscle sensor
| DE92-016034 | p 2799 N93-25099
Helmeted head and neck dynamics under whole-body vibration p 2800 N93-25531
MUSCULAR FUNCTION
Initial experiments with a myoelectric-based muscle sensor
| DE92-016034 | p 2799 N93-25099
MUSCULOSKELETAL SYSTEM
Mechanical stimulation of skeletal muscle mitigates glucocorticoid induced decreases in prostaglandin synthesis
| NASA-CR-193040 | p 2794 N93-24763

N

N-TYPE SEMICONDUCTORS
Research on stable, high-efficiency amorphous silicon multijunction modules
| DE93-000072 | p 2862 N93-25163
The DX centers in three to five semiconductors under hydrostatic pressure
| DE93-007701 | p 2864 N93-25490
Optoelectronic III-V heterostructures on Si substrates
| AD-A261651 | p 2867 N93-26193
NAMING
Agreement in naming objects and concepts for information retrieval p 2881 N93-25826
NAP-OF-THE-EARTH NAVIGATION
Methodology investigation: Global Positioning System integration (GPS)
| AD-A261054 | p 2586 N93-26237
Image-based ranging and guidance for rotorcraft
| NASA-CR-177608 | p 2586 N93-26549
NAPHTHALENE
Theoretical calculations on the electron absorption spectra of selected Polycyclic Aromatic Hydrocarbons (PAH) and derivatives
| NASA-CR-192762 | p 2892 N93-25200
NARROWBAND
New algorithms for the detection and elimination of sine waves and other narrow-band signals in the presence of broadband signals and noise
| AD-A261811 | p 2681 N93-26261
NASA PROGRAMS
Space transfer vehicle concepts and requirements study. Volume 1: Executive summary
| NASA-CR-192524 | p 2610 N93-25479
The 1993/1994 NASA Graduate Student Researchers Program
| NASA-EP-283 | p 2872 N93-26051
National Aeronautics and Space Administration (NASA)/American Society for Engineering Education (ASEE) Summer Faculty Fellowship Program, 1992, volume 1
| NASA-CR-188242-VOL-1 | p 2911 N93-26058
National Aeronautics and Space Administration (NASA)/American Society for Engineering Education (ASEE) Summer Faculty Fellowship Program, 1992, volume 2
| NASA-CR-188242-VOL-2 | p 2914 N93-26070
High performance computing and communications panel report p 2807 N93-26131
Design and implementation of a pilot orientation program for new NASA engineering employees
| NASA-TM-105907 | p 2872 N93-26205
OSSA Information Systems Program
| NASA-TM-108758 | p 2883 N93-26491
NASA SPACE PROGRAMS
Former Soviet Republic capabilities in space and science
| DE93-007613 | p 2598 N93-25322
Aeronautics in NACA and NASA
| NASA-NP-156 | p 2574 N93-26422
NATIONAL AEROSPACE PLANE PROGRAM
Trajectory optimization for the National aerospace plane
| NASA-CR-192954 | p 2589 N93-25670
Numerical simulation of hypersonic aerodynamics and the computational needs for the design of an aerospace plane
| AD-A260681 | p 2580 N93-25894
Aerospace-plane flights and stratospheric ozone: Review and preliminary assessment of the National Aerospace Plane (NASP) operations
| RAND/N-3464-AF | p 2767 N93-26327
NATIONAL AIRSPACE SYSTEM
Runway Visual Range (RVR) Operational Test and Evaluation (OT&E) integration and OT&E operational test report
| DOT/FAA/CT-TN93/37 | p 2584 N93-25243
NATIONAL LAUNCH VEHICLE PROGRAM
National Launch System. Task 4: System architecture options analysis
| MCR-92-5011 | p 2609 N93-26098
NATURAL GAS
Catalytic conversion of light alkanes
| DE93-009646 | p 2644 N93-25499
A basic research model of natural gas combustion in turbulent flow, phase 2
| PB93-158509 | p 2644 N93-25819
Thermodynamic properties of natural gas mixtures
| PB93-167112 | p 2872 N93-26509
Improved selective catalytic NOx control technology for compressor station reciprocating engines
| PB93-158566 | p 2768 N93-26529
Cost-effectiveness analysis of TxDOT CNG fleet conversion, volume 2
| PB93-159432 | p 2720 N93-26534
Thermodynamic properties of natural gas mixtures
| PB93-156818 | p 2872 N93-26558
Cost-effectiveness analysis of TxDOT CNG fleet conversion, volume 1
| PB93-165603 | p 2720 N93-26585
NATURAL LANGUAGE (COMPUTERS)
Inferring heuristic classification hierarchies from natural language input p 2825 N93-25979
NAUTICAL CHARTS
Digital Nautical Chart
| AD-A260810 | p 2756 N93-25694
NAVIER-STOKES EQUATION
Computation of hypersonic viscous flowfields using the parabolized Navier-Stokes equations p 2694 N93-24766
Computational study of the aerodynamics and control by blowing of asymmetric vortical flows over delta wings p 2574 N93-24772
A convergent finite difference scheme for the Navier-Stokes equations of nonisentropic compressible fluid flow p 2695 N93-24906
Direct solutions of the Navier-Stokes equations with application to static aeroelasticity p 2697 N93-25259
The steady Navier-Stokes problem for low Reynolds number viscous jets p 2698 N93-25264
Data parallel finite element techniques for large-scale computational fluid dynamics p 2699 N93-25334
Numerical simulation of a shock wave/turbulent boundary layer interaction in a duct p 2699 N93-25342
Numerical simulation of leading-edge receptivity to freestream vorticity p 2577 N93-25388
Numerical simulation of time-dependent thermocapillary convection in layered fluid systems p 2700 N93-25472
Spatial simulation of transition in wall-bounded shear flows: Active control and effects of surface roughness p 2701 N93-25483
Navier-Stokes simulations of unsteady transonic flow phenomena p 2578 N93-25542
Tangential fuselage blowing on an ogive cylinder p 2578 N93-25545
Implicit multigrid solution of the compressible Navier-Stokes equations with application to distributed parallel processing p 2702 N93-25546
Numerical modelling of viscous turbomachinery flows with a pressure correction method p 2594 N93-25702
Stationary crossflow instability on an infinite swept wing p 2580 N93-25865
Simulation of vortex bursting p 2580 N93-25881
Workshop Report: A validation study of Navier-Stokes codes for transverse injection into a Mach 2 flow p 2624 N93-26008
Unsteady airfoil flow solutions on moving zonal grids
| AD-A261925 | p 2582 N93-26198
Incompressible spectral-element method: Derivation of equations
| NASA-TM-106109 | p 2708 N93-26554
NAVIGATION
The role of ocean climate data in operational Naval oceanography p 2732 N93-24916
Mixed constellation synchronization of GPS time p 2836 N93-25015
Collaboration in the UK on time transfer using the GLONASS system p 2837 N93-25019
NAVIGATION AIDS
Orbit determination and orbit control for the Earth Observing System (EOS) AM spacecraft p 2601 N93-24705
Digital Nautical Chart
| AD-A260810 | p 2756 N93-25694
NAVIGATION INSTRUMENTS
System for calibrating a gyro navigator
| AD-D015668 | p 2586 N93-26093
NAVIGATION SATELLITES
Application of GPS tracking techniques to orbit determination for TDRS p 2601 N93-24702
An experimental health monitoring unit for GPS and GLONASS p 2586 N93-25018
NAVSTAR SATELLITES
Rubidium atomic frequency standards for GPS block 2R p 2836 N93-25014
NAVY
Photovoltaic power without batteries for continuous cathodic protection p 2759 N93-25597
NEAR INFRARED RADIATION
A high performance room-temperature near-infrared camera
| AD-A260602 | p 2709 N93-25634
NEBULAE
Observations and models of shock structures in Herbig-Haro objects p 2891 N93-24770
NEGATIVE IONS
Dynamics of collision processes
| DE93-007143 | p 2849 N93-25509
Investigations of the transient behavior of the cathode fall region in planar and hollow cathodes
| AD-A261636 | p 2691 N93-26171
Penning detachment: A new frontier
| AD-A261447 | p 2850 N93-26346
Bimolecular reaction dynamics from photoelectron spectroscopy of negative ions
| DE93-007669 | p 2647 N93-26599
NEODYMIUM LASERS
Injection seeded, diode-pumped, short pulse Nd:YAG ring laser for space-based laser ranging p 2713 N93-25389
NERVES
JPRS report: Science and technology. Central Eurasia: Life sciences
| JPRS-ULS-92-025 | p 2793 N93-25405
Primary events in olfactory reception
| AD-A260562 | p 2795 N93-25944
NERVOUS SYSTEM
Biomagnetic localization from transient quasi-static events
| DE93-007328 | p 2794 N93-25186
Computation and learning in neural networks with binary weights
| AD-A261182 | p 2821 N93-25821
NETWORK CONTROL
An OSI architecture for the Deep Space Network p 2679 N93-26121
Admission control in integrated voice/data multihop radio networks
| AD-A261055 | p 2680 N93-26227
NETWORKS
Lightning characteristics in the north-east part of Japan observed by a magnetic direction-finder network p 2779 N93-24892
NEURAL NETS
Using neural networks and Dyna algorithm for integrated planning, reacting and learning in systems
| NASA-CR-193018 | p 2817 N93-24743
Remote sensed spectral signatures classification and recognition by neural networks: An approach to unsupervised techniques p 2738 N93-24779
EUROSTARS: A system for thematic analysis of remote sensed data p 2753 N93-24871
A neural network-based estimator for the mixture ratio of the Space Shuttle Main Engine
| NASA-TM-106070 | p 2622 N93-25089
Two neural network algorithms for designing optimal terminal controllers with open final time
| NASA-CR-177599 | p 2817 N93-25137
Neural networks: What non-linearity to choose
| NASA-CR-192948 | p 2819 N93-25197

Scene segmentation of natural images using texture measures and back-propagation
| NASA-TM-104003 | p 2803 N93-25235
Energy and Technology Review, October - December 1992
| DE93-007784 | p 2674 N93-25299
A software package for neural network applications development p 2827 N93-25610
Control of complex dynamic systems by neural networks p 2827 N93-25611
Construction of a connectionist network supercomputer
| AD-A260929 | p 2820 N93-25648
Multi-layer holographic bifurcative neural network system for real-time adaptive EOS data analysis p 2880 N93-25807
Computation and learning in neural networks with binary weights
| AD-A261182 | p 2821 N93-25821
An optimal scheduling of pick-place operations of a robot-vision-tracking system by using neural networks and rule-based systems p 2821 N93-25880
Parametric motion control of robotic arms: A biologically based approach using neural networks p 2822 N93-25964
Detection of bearing failure in mechanical devices using neural networks p 2822 N93-25965
The probabilistic neural network architecture for high speed classification of remotely sensed imagery p 2824 N93-25972
Data fusion with artificial neural networks (ANN) for classification of earth surface from microwave satellite measurements p 2824 N93-25974
Neural networks for atmospheric retrievals p 2824 N93-25975
Classifying multispectral data by neural networks p 2825 N93-25976
Using modular neural networks with local representations to control dynamic systems
| AD-A261597 | p 2826 N93-26162
Complexity of connectionist and constraint-satisfaction networks
| AD-A261617 | p 2817 N93-26169
Physiological indices of mental workload
| AD-A261692 | p 2798 N93-26391
Reinforcement learning for robots using neural networks
| AD-A261434 | p 2827 N93-26487
Joint services electronics program
| AD-A261801 | p 2692 N93-26539

NEUROLOGY
Proceedings of Workshop 1: The Human Brainmap Database
| AD-A260720 | p 2796 N93-25654
The role of pyridoxine as a countermeasure for in-flight loss of lean body mass p 2796 N93-26068
Neuropsychological components of object identification
| AD-A261449 | p 2797 N93-26347

NEUROPHYSIOLOGY
Neuropsychological components of object identification
| AD-A261449 | p 2797 N93-26347
Neural basis of motion perception
| AD-A261452 | p 2798 N93-26349
Imaging regional changes in the spontaneous activity of the brain: An extension of the minimum-norm least-squares estimate
| AD-A261593 | p 2798 N93-26436
Neuromagnetic investigation of cortical regions underlying short-term memory
| AD-A261445 | p 2799 N93-26521

NEUTRAL BEAMS
Plasma heating in toroidal systems
| NIFS-208 | p 2858 N93-25092
Dynamics of gas-surface interactions
| AD-A261402 | p 2646 N93-26402

NEUTRINOS
An investigation of neutrino properties through study of the sun, supernovae, the early universe and lab data p 2898 N93-25180

NEUTRON BEAMS
NIST reactor: Summary of activities, July 1991 through September 1992
| PB93-162873 | p 2852 N93-26322

NEUTRON COUNTERS
Feasibility study of a long duration balloon flight with NASA/GSFC and Soviet Space Agency Gamma Ray Spectrometers
| NASA-CR-192934 | p 2573 N93-25077
A compact neutron counter telescope with thick radiator (Cotetra) for fusion experiment
| NIFS-205 | p 2860 N93-25347

NEUTRON DIFFRACTION
NIST reactor: Summary of activities, July 1991 through September 1992
| PB93-162873 | p 2852 N93-26322

NEUTRON IRRADIATION
NIST reactor: Summary of activities, July 1991 through September 1992
| PB93-162873 | p 2852 N93-26322

NEUTRON RADIOGRAPHY
NIST reactor: Summary of activities, July 1991 through September 1992
| PB93-162873 | p 2852 N93-26322

NEUTRON SPECTROMETERS
A compact neutron counter telescope with thick radiator (Cotetra) for fusion experiment
| NIFS-205 | p 2860 N93-25347

NEUTRON STARS
Diskoseismology: Probing relativistic accretion disks p 2894 N93-25622
Steady-state numerical models of accreting neutron stars: The effect of atmospheric CNO depletion and diffusion p 2889 N93-25624
Gravitational radiation from coalescing binary star systems p 2900 N93-25625

NEUTRONS
Asymptotic derivation of the simplified P(sub N) equations
| DE93-007342 | p 2828 N93-25151
A method for transient, three-dimensional neutron transport calculations
| DE93-007243 | p 2847 N93-25256
Neutron energy determination with a high-purity germanium detector
| NASA-CR-192773 | p 2900 N93-25890

NEWTON METHODS
Direct solutions of the Navier-Stokes equations with application to static aeroelasticity p 2697 N93-25259
Dynamics of deformable multibody systems using recursive projection methods
| AD-A260698 | p 2728 N93-25842

NEWTONIAN FLUIDS
Thermocapillary flow near a cold wall
| AD-A261050 | p 2706 N93-25779

NICKEL ALLOYS
Hot corrosion of the B2 nickel aluminides
| NASA-CR-191082 | p 2649 N93-25128
High temperature fracture toughness of Ni3Al alloy IC-396M
| DE93-008564 | p 2650 N93-25492
Fatigue in single crystal nickel superalloys
| AD-A260709 | p 2651 N93-25843
Shear band formation in a W-Ni-Fe alloy under plate impact
| AD-A260702 | p 2651 N93-25907
Fatigue in single crystal nickel superalloys
| AD-A261742 | p 2652 N93-26282
Solidification processing and phase transformations in ordered high temperature alloys
| AD-A261751 | p 2652 N93-26284
The influence of primary and secondary orientations on the elastic response of a nickel-base single-crystal superalloy
| NASA-TM-106125 | p 2731 N93-26550

NIGER
Lithologic mapping with LANDSAT Thematic Mapper guided by laboratory spectral measurements, Air, Niger (Africa) p 2742 N93-24803

NIGHT VISION
Interpupillary and vertex distance effects on field-of-view and acuity with ANVIS
| AD-A261259 | p 2802 N93-26265

NITINOL ALLOYS
Active control of NiTINOL-reinforced structural composites
| AD-A261062 | p 2638 N93-25780

NITRAMINE PROPELLANTS
Modeling of H2/N2O flames p 2627 N93-26026
Dark zone modeling of solid propellant flames p 2628 N93-26028
Chemistry during the induction time in heated nitramines p 2629 N93-26035
Thermal decomposition of energetic materials. 4: Deuterium isotope effects and isotopic scrambling condensed-phased decomposition of 1,3,5-trinitrohexahydro-s-triazine
| AD-A261804 | p 2662 N93-26387

NITRATES
Rheology of YBa2Cu3O(7-x) precursors
| DE93-007285 | p 2863 N93-25362

NITRIC ACID
Atmospheric reactive nitrogen oxides and their relationship with urban and rural ozone formation p 2760 N93-24908
Measurements of nitric acid, carboxylic acids, and selected aerosol species for the NASA/GTE Pacific Mission - West (PEM-WEST)
| NASA-CR-192976 | p 2763 N93-25287

NITRIDES
Structure and properties of a-C: N films prepared by pulsed excimer laser deposition
| DE93-007908 | p 2654 N93-25372

NITROGEN
ANOVA method to estimate vegetation indices sensitivity assessing nitrogen fertilizing influence on spectral reflectance coefficients p 2739 N93-24782
Remote sensing of land resource management in agriculture with regard to its influence on the environment p 2750 N93-24850
Measuring the intensity of nitrogen fertilization of grassland by means of remote sensing p 2751 N93-24859
Structure and properties of a-C: N films prepared by pulsed excimer laser deposition
| DE93-007908 | p 2654 N93-25372
Planetary Biology and Microbial Ecology: Molecular Ecology and the Global Nitrogen cycle
| NASA-CR-4497 | p 2803 N93-26157
Inorganic nitrogen and phosphorus dynamics in the water column of the Patuxent River
| PB93-172955 | p 2767 N93-26511

NITROGEN OXIDES
Atmospheric reactive nitrogen oxides and their relationship with urban and rural ozone formation p 2760 N93-24908
Improved selective catalytic NOx control technology for compressor station reciprocating engines
| PB93-158566 | p 2768 N93-26529
Oxides of nitrogen emissions from turbulent hydrocarbon/air jet diffusion flames, phase 2
| PB93-152478 | p 2768 N93-26533

NITROUS OXIDES
A new method for infrared imaging of air currents in and around critical hazard fume hoods
| DE93-003009 | p 2761 N93-24956

NOAA SATELLITES
Analysis of the effects of mean local node-crossing time on the evolution of Sun-synchronous orbits p 2602 N93-24706
Correlation between NDVI values derived from NOAA AVHRR HRPT data and ground measurements of precipitation in the EFEDA study area (Spain) p 2738 N93-24780
Demonstration of seasonal changes in the territory of Finland using multitemporal NOAA-AVHRR data p 2742 N93-24801
Sustainable remote sensing: A major improvement for realtime resource management and disaster early warning in developing countries p 2743 N93-24808
Assessment and forecasting of crop yield in Niger through NOAA NDVI data p 2750 N93-24851
Global drought monitoring from NOAA polar orbiting satellites p 2750 N93-24852
Interest of complementary data of coarse and high spatial resolution for agro-climatic crop monitoring p 2750 N93-24853
North-central Mexico blue grama rangeland biomass assessment at the end of the rainy season using NOAA-AVHRR-LAC p 2750 N93-24854

NOBLE METALS
Theoretical predictions of platinum-rhodium bimetallic catalysts
| DE93-007540 | p 2649 N93-25428

NODULES
Correlation of damage threshold and surface geometry of nodular defects in HR coatings as determined by in-situ atomic force microscopy
| DE93-007509 | p 2654 N93-25384

NOISE (SOUND)
A computational method for the analysis of acoustic radiation from turbofan inlets p 2845 N93-25717
Measuring hearing protection device performance using the metrosonics db-3100 sound level analyzer (dosimeter)
| AD-A260852 | p 2801 N93-25787

NOISE GENERATORS
A computational method for the analysis of acoustic radiation from turbofan inlets p 2845 N93-25717

NOISE INTENSITY
Noise measurements in single-mode GaAlAs diode lasers p 2716 N93-25067
In-flight evaluation of noise levels and assessment of active noise reduction systems in the Seahawk S-70B-2 helicopter
| AD-A260689 | p 2845 N93-25649
Aerospace-plane flights and stratospheric ozone: Review and preliminary assessment of the National Aerospace Plane (NASP) operations
| RAND/N-3464-AF | p 2767 N93-26327

NOISE MEASUREMENT
Noise measurements in single-mode GaAlAs diode lasers p 2716 N93-25067
Noise-optimal control of HEMT LNA's for compensation of temperature deviations p 2678 N93-26115
NOISE PREDICTION (AIRCRAFT)
Theory for noise of propellers in angular inflow with parametric studies and experimental verification
| NASA-CR-4499 | p 2844 N93-25094
NOISE PROPAGATION
Far field rotor noise
| AD-A260703 | p 2845 N93-25651
Rotating rake design for unique measurement of fan-generated spinning acoustic modes
| NASA-TM-105946 | p 2595 N93-26161
NOISE REDUCTION
A numerical and experimental studies of flow characteristics in centrifugal fans p 2577 N93-25339
Graphite/epoxy composite laminates with co-cured interlaminar damping layers p 2642 N93-25587
Walsh function generator for the Electronically Scanned Thinned Array Radiometer (ESTAR) instrument
| NASA-TM-4449 | p 2689 N93-25618
In-flight evaluation of noise levels and assessment of active noise reduction systems in the Seahawk S-70B-2 helicopter
| AD-A260689 | p 2845 N93-25649
Rotating rake design for unique measurement of fan-generated spinning acoustic modes
| NASA-TM-105946 | p 2595 N93-26161
A large hemi-anechoic enclosure for community-compatible aeroacoustic testing of aircraft propulsion systems
| NASA-TM-106015 | p 2846 N93-26551
NOISE SPECTRA
Time stability: An improvement of the multi-variance method for the oscillator noise analysis p 2839 N93-25036
NOISE TEMPERATURE
A technique for computation of noise temperature due to a beam waveguide shroud p 2671 N93-24661
Noise-optimal control of HEMT LNA's for compensation of temperature deviations p 2678 N93-26115
Figure of merit for direct-detection optical channels p 2678 N93-26117
NOISE TOLERANCE
Machine learning techniques for fault isolation and sensor placement p 2823 N93-25966
NONADIABATIC CONDITIONS
Chemical dynamics studies of high energy species
| AD-A260743 | p 2852 N93-25676
NONDESTRUCTIVE TESTS
Monitoring damage growth in titanium matrix composites using acoustic emission
| NASA-TM-107742 | p 2634 N93-25072
Reliability assessment at airline inspection facilities. Volume 1: A generic protocol for inspection reliability experiments
| DOT/FAA/CT-92/12-VOL-1 | p 2582 N93-25110
Investigation of corrosion in aluminum/adhesive lap-splices using pulse-echo ultrasonic techniques
| DE93-008074 | p 2721 N93-25518
Determination of the elastic constants of composite materials from ultrasonic group velocity measurements p 2635 N93-25544
Fundamental and applied aspects of defect engineering in GaAs
| AD-A260573 | p 2867 N93-25899
Nondestructive evaluation of ferrite c-cores
| KCP-613-4677 | p 2721 N93-25939
Automated inspection of solder joints for surface mount technology
| NASA-TM-104580 | p 2721 N93-26137
NIST reactor: Summary of activities, July 1991 through September 1992
| PB93-162873 | p 2852 N93-26322
Inverse problems in nondestructive evaluations
| AD-A261370 | p 2722 N93-26337
NDT standards from the perspective of the Department of Defense
| MTL-TR-92-68 | p 2722 N93-26434
X-ray computed tomography for casting development
| AD-A261786 | p 2722 N93-26526
X ray computed tomography for failure analysis
| AD-A261884 | p 2722 N93-26527
NONEQUILIBRIUM FLOW
A new LU-SGS flow solver for calculating reentry flows p 2579 N93-25759
NONISENTROPICITY
A convergent finite difference scheme for the Navier-Stokes equations of nonisentropic compressible fluid flow p 2695 N93-24906
NONLINEAR EQUATIONS
Nonlinear evolution of the first mode supersonic oblique waves in compressible boundary layers. Part 1: Heated/cooled walls
| NASA-TM-106087 | p 2696 N93-25175
On the effect of acoustic coupling on random and harmonic plate vibrations
| NASA-TM-107740 | p 2844 N93-25189
Parallelizing the spectral transform method: A comparison of alternative parallel algorithms
| DE93-008664 | p 2816 N93-25521
Dynamics of deformable multibody systems using recursive projection methods
| AD-A260698 | p 2728 N93-25842
Investigation of liquid sloshing in spin-stabilized satellites
| AD-A261671 | p 2619 N93-26438
NONLINEAR FEEDBACK
Nonlinear system design: Adaptive feedback linearization with unmodeled dynamics
| AD-A261360 | p 2826 N93-26333
NONLINEAR FILTERS
PDE: Differential, geometric and algebraic methods in nonlinear filtering
| AD-A260967 | p 2829 N93-26222
Realtime control of multiple sensor systems
| AD-A261037 | p 2680 N93-26226
NONLINEAR OPTICS
IR materials producibility
| AD-A261099 | p 2853 N93-25766
Second-harmonic generation in optical fibers and glass
| AD-A260592 | p 2853 N93-25839
Advanced optical fiber communication systems
| AD-A261802 | p 2856 N93-26256
Efficient nonlinear optical conversion of 1.319-micron laser radiation
| AD-A261309 | p 2715 N93-26297
Development of organic nonlinear optical materials
| AD-A261332 | p 2856 N93-26309
Molecular interactions and properties with many-body methods
| AD-A261688 | p 2850 N93-26367
Interferometric measurement with squeezed light
| AD-A260910 | p 2856 N93-26457
Laser physics and laser techniques
| AD-A261595 | p 2715 N93-26524
NONLINEAR PROGRAMMING
Optimal cooperative power-limited rendezvous p 2607 N93-24904
NONLINEAR SYSTEMS
Two neural network algorithms for designing optimal terminal controllers with open final time
| NASA-CR-177599 | p 2817 N93-25137
Robust nonlinear control of vectored thrust aircraft
| NASA-CR-192727 | p 2596 N93-25199
Dynamic error analysis of numerical methods for simulation of state-variable derivatives with discontinuities p 2819 N93-25278
Control of nonlinear systems under input constraints with applications to flight control p 2596 N93-25353
On existence of solutions and duality for a model of non-linear elastic plates with transverse shear deformations p 2726 N93-25437
Stochastic and seismic design response of linear and nonlinear structures p 2726 N93-25484
Nonlinear stability analysis of the attitude motion of spin-stabilized thrusting spacecraft p 2617 N93-25527
Biped control via nonlinear dynamics p 2718 N93-25697
Nonlinear dynamics and attitude control of articulated flexible space structures p 2617 N93-25726
Using input command pre-shaping to suppress multiple mode vibration p 2732 N93-25834
The MODE family of on-orbit experiments: The Middeck Active Control Experiment (MACE) p 2599 N93-25835
Nonlinear vibrations, stability, and dynamics of structures and mechanisms
| AD-A260871 | p 2728 N93-25838
Applications of parallel and vector algorithms in nonlinear structural dynamics using the finite element method
| AD-A260716 | p 2811 N93-25845
Joint flexibility effects on the dynamic response of structures. Part 2: Stochastic analysis
| AD-A261003 | p 2729 N93-25938
On-line implementation of nonlinear parameter estimation for the Space Shuttle main engine
| NASA-TM-106097 | p 2632 N93-26211
Nonlinear system design: Adaptive feedback linearization with unmodeled dynamics
| AD-A261360 | p 2826 N93-26333
Adaptive control of nonlinear flexible systems
| AD-A261676 | p 2826 N93-26365
Solution of nonlinear boundary value problem on successively refined grids
| AD-A261395 | p 2829 N93-26519
NONLINEARITY
Nonlinear techniques for forecasting solar activity directly from its time series p 2603 N93-24716
The third-order permittivity of quartz obtained by different methods p 2840 N93-25046
Nonlinear evolution of the first mode supersonic oblique waves in compressible boundary layers. Part 1: Heated/cooled walls
| NASA-TM-106087 | p 2696 N93-25175
On the effect of acoustic coupling on random and harmonic plate vibrations
| NASA-TM-107740 | p 2844 N93-25189
Stability analysis and modeling of rotating flexible structures
| DE93-008493 | p 2844 N93-25520
Damage-survivable and damage-tolerant laminated composites with optimally placed piezoelectric layers
| AD-A260879 | p 2636 N93-25631
Far field rotor noise
| AD-A260703 | p 2845 N93-25651
Thermal expansion measurements of polymer matrix composites and syntactics
| MTL-TR-92-27 | p 2640 N93-25954
Nonlinear wave phenomena related to interactions in the ionosphere
| AD-A261450 | p 2776 N93-26348
NONUNIFORM MAGNETIC FIELDS
Maneuvering a reentry body via magneto-gasdynamic forces p 2615 N93-25207
NONUNIFORMITY
Thermoelastic stresses in multi-layered media in non-uniform temperature fields
| AD-A260901 | p 2727 N93-25658
NORMAL SHOCK WAVES
Supersonic shock wave/vortex interaction
| NASA-CR-192917 | p 2576 N93-25249
An investigation of photothermal velocimetry for application to transient, high-speed gas flows p 2579 N93-25720
NORMALIZING (STATISTICS)
Quaternion normalization in spacecraft attitude determination p 2606 N93-24730
NORTH ATLANTIC TREATY ORGANIZATION (NATO)
AGARD membership, 1993
| AGARD-MEMB-93 | p 2873 N93-26428
NORTH DAKOTA
The North Dakota thunderstorm project
| PB93-153039 | p 2785 N93-25776
NORTHERN HEMISPHERE
Measurements of nitric acid, carboxylic acids, and selected aerosol species for the NASA/GTE Pacific Mission - West (PEM-WEST)
| NASA-CR-192976 | p 2763 N93-25287
NORTHERN SKY
Tully-Fisher distances and motions in the northern sky p 2889 N93-25621
NOTCH STRENGTH
J and CTOD estimation equations for shallow cracks in single edge notch bend specimens
| AD-A261679 | p 2731 N93-26390
NOTCHES
J and CTOD estimation equations for shallow cracks in single edge notch bend specimens
| AD-A261679 | p 2731 N93-26390
NOZZLE DESIGN
Remtech SSME nozzle design TPS
| NASA-CR-192516 | p 2631 N93-26056
NOZZLE EFFICIENCY
The effect of entrance radius and film injection on wall heating in scramjet nozzles p 2625 N93-26009
NOZZLE FLOW
Experimentation in the low-density plume of a simulated electrothermal thruster for computer code validation
| NASA-CR-191112 | p 2622 N93-24758
Solid fuel supersonic combustion p 2625 N93-26010
Measurement and analysis of a small nozzle plume in vacuum
| NASA-TM-106066 | p 2633 N93-26561
NOZZLE WALLS
Particle behavior in solid propellant rocket motors and plumes
| AD-A260900 | p 2624 N93-25913
NUCLEAR BINDING ENERGY
The structure and energetics of Cr(CO)6 and Cr(CO)5
| NASA-CR-192889 | p 2848 N93-25450
Accurate determination of Auger line shape binding energies
| AD-A261803 | p 2868 N93-26258
NUCLEAR DEFORMATION
Feeding and decay of superdeformed states
| DE93-007899 | p 2848 N93-25371

NUCLEAR ELECTRIC PROPULSION
Nuclear thermal propulsion technology: Results of an interagency panel in FY 1991
| NASA-TM-105711 | p 2621 N93-24740
Summary and recommendations on nuclear electric propulsion technology for the space exploration initiative
| NASA-TM-105707 | p 2622 N93-24744
Space Nuclear Thermal Propulsion Test Facilities Subpanel
| NASA-TM-105708 | p 2622 N93-25105
Nuclear safety policy working group recommendations on nuclear propulsion safety for the space exploration initiative
| NASA-TM-105705 | p 2632 N93-26200
Nuclear electric propulsion for planetary science missions: NASA technology program planning
| NASA-TM-106139 | p 2632 N93-26210

NUCLEAR EXPLOSIONS
Behavior of a steel-liner-and-bolts system under very high thermal and mechanical loading: The CONVEX Liner Add-On to DIAMOND FORTUNE
| DE93-007512 | p 2731 N93-26507

NUCLEAR FUSION
Cosmic string cosmology p 2891 N93-24907

NUCLEAR INTERACTIONS
Proton Monte Carlo transport program PTRAN
| PB93-158673 | p 2850 N93-26314

NUCLEAR MAGNETIC RESONANCE
NMR studies of ion mobility and association in polyether-based polymer electrolytes
| AD-A260662 | p 2655 N93-25642
Structure of sodium 4-(1'-heptylnonyl) benzenesulfonate adsorbed on alumina using H-2 NMR
| AD-A261224 | p 2645 N93-26300
Deuteron and oxygen-17 NMR studies of molecular motion in methanol-saturated Nafion membranes
| AD-A261579 | p 2851 N93-26514

NUCLEAR MODELS
Diabaticity of nuclear motion: Problems and perspectives
| DE93-007252 | p 2847 N93-25148

NUCLEAR PHYSICS
Diabaticity of nuclear motion: Problems and perspectives
| DE93-007252 | p 2847 N93-25148
The sub 60 ps timing resolution using large area silicon avalanche diodes
| DE93-007723 | p 2688 N93-25365

NUCLEAR POWER PLANTS
Seismic buckling capacity of unstiffened, free-standing steel containments
| DE93-005325 | p 2723 N93-24957
Human factors engineering: A key element of instrumentation and control system design
| DE93-006731 | p 2800 N93-25415

NUCLEAR PROPULSION
Radiation and temperature effects on electronic components investigated under the CSTI high capacity power project
| NASA-TM-106096 | p 2687 N93-24746
Space exploration initiative candidate nuclear propulsion test facilities
| NASA-TM-105710 | p 2622 N93-24753
Nuclear safety policy working group recommendations on nuclear propulsion safety for the space exploration initiative
| NASA-TM-105705 | p 2632 N93-26200

NUCLEAR RADIATION
Radiation and temperature effects on electronic components investigated under the CSTI high capacity power project
| NASA-TM-106096 | p 2687 N93-24746
Aerospace techniques in radiation and ecological monitoring of the Republic Belarus
p 2741 N93-24793
AFRRI research, fiscal year 1991
| AD-A260933 | p 2911 N93-25710

NUCLEAR REACTORS
Seismic buckling capacity of unstiffened, free-standing steel containments
| DE93-005325 | p 2723 N93-24957

NUCLEAR SPIN
The physics of spin polarized gases
| AD-A261396 | p 2850 N93-26288

NUCLEAR STRUCTURE
Detection of fragments arising from greater than 10 GeV electron-nucleus collisions
| DE93-007725 | p 2848 N93-25366

NUCLEATION
Study of grain refinement in Al alloy 2519 using backscattering orientation-contrast mode in the scanning electron microscope
| AD-A260886 | p 2651 N93-25632
Position sensitive atom probe study of the decomposition of a Cu-2.6 at. percent Co alloy
| DE93-006737 | p 2653 N93-26500

NUCLEI (NUCLEAR PHYSICS)
Feeding and decay of superdeformed states
| DE93-007899 | p 2848 N93-25371

NUCLEONS
Results from the NA36 on strangeness production in 200 GeV/c per nucleon S + Pb and p - Pb reactions
| DE93-007711 | p 2848 N93-25364
Detection of fragments arising from greater than 10 GeV electron-nucleus collisions
| DE93-007725 | p 2848 N93-25366

NUMERICAL ANALYSIS
Minimization of heat slab nodes with higher order boundary conditions
| DE93-004238 | p 2695 N93-24966
Analytical techniques for improved time transfer using common view of direct broadcasting satellites
p 2835 N93-25008
Current research activities: Applied and numerical mathematics, fluid mechanics, experiments in transition and turbulence and aerodynamics, and computer science
| NASA-CR-191408 | p 2803 N93-25084
Developing and improving numerical algorithms to study intrinsically correlated electron systems
| AD-A261214 | p 2849 N93-25734
Activity report
| AD-A261933 | p 2829 N93-26199

NUMERICAL CONTROL
Position and force control of a vehicle with two or more steerable drive wheels
| DE92-041301 | p 2717 N93-25100
Using fuzzy behaviors for the outdoor navigation of a car with low-resolution sensors
| DE93-002428 | p 2584 N93-25120
Spacelab, Spacehab, and Space Station Freedom payload interface projects p 2620 N93-26080

NUMERICAL FLOW VISUALIZATION
Combining particles and waves for fluid animation
p 2699 N93-25348

NUMERICAL INTEGRATION
Numerically dissipative time integration algorithms for structural dynamics p 2725 N93-25394

NUMERICAL STABILITY
ADCIRC: An advanced three-dimensional circulation model for shelves, coasts, and estuaries. Report 1: Theory and methodology of ADCIRC-2DDI and ADCIRC-3DL
| AD-A261608 | p 2790 N93-26164

NUMERICAL WEATHER FORECASTING
Prediction of global cloud cover with a very high resolution global spectral model
| AD-A261047 | p 2785 N93-25777

NUTATION
SCATHA mission termination report
p 2605 N93-24725
Investigation of liquid sloshing in spin-stabilized satellites
| AD-A261671 | p 2619 N93-26438

O

OBJECT-ORIENTED PROGRAMMING
Prototype PC user interface
| DE93-008008 | p 2809 N93-25303
Proceedings of the Second SISAL Users' Conference
| DE93-008019 | p 2815 N93-25304
A software development approach for parallel processing systems integrating object-oriented and functional paradigms p 2816 N93-25481
Object-oriented tools for distributed computing
p 2817 N93-25576
Gas turbine system simulation: An object-oriented approach
| NASA-TM-106044 | p 2593 N93-25673
High level design for distributed application instrumentation
| AD-A260812 | p 2710 N93-25696

OBLIQUE SHOCK WAVES
Nonlinear evolution of the first mode supersonic oblique waves in compressible boundary layers. Part 1: Heated/cooled walls
| NASA-TM-106087 | p 2696 N93-25175
Supersonic shock wave/vortex interaction
| NASA-CR-192917 | p 2576 N93-25249
Numerical simulation of a shock wave/turbulent boundary layer interaction in a duct
p 2699 N93-25342

OBLIQUE WINGS
Aerodynamic design and synthesis of the oblique flying wing supersonic transport p 2587 N93-24768

OBSERVATION
The Global Ocean Observing System: One perspective p 2733 N93-24920
The development progresses of hydrogen masers at Shanghai Observatory p 2716 N93-25048
Development of a tool-set for simultaneous, multi-site observations of astronomical objects
p 2878 N93-25795

OBSERVATORIES
The Sudbury Neutrino Observatory
| DE93-007697 | p 2899 N93-25327

OBSTACLE AVOIDANCE
Discrete range clustering using Monte Carlo methods
| NASA-TM-104004 | p 2584 N93-24914
PROAV Cable Warning System (CWS) - U.S. Army aircraft Integration assessment and OCONUS field evaluation
| AD-A261233 | p 2583 N93-26263

OCCULTATION
Occultation of a compact radio source by Venus
p 2676 N93-26107

OCCUPATION
Aircraft electrical and environmental systems, AFSCs 452x5, 454x5, and 454x6
| AD-A261213 | p 2590 N93-25733

OCEAN BOTTOM
Isolation and analysis of key components of seafloor relief
| AD-A261635 | p 2790 N93-26170

OCEAN CURRENTS
Observations of an intrathermocline vortex
p 2788 N93-24769
World Ocean Circulation Experiment
p 2733 N93-24922
The Global Ocean Observing System
p 2733 N93-24923
Indian Ocean analyses p 2733 N93-24925
Errors caused by incompatible wind and buoyancy forcing in the ocean general circulation models
| AD-A260894 | p 2789 N93-25657
Wind-driven coastal generation of annual mesoscale eddy activity in the California current
| AD-A261355 | p 2790 N93-26331

OCEAN DYNAMICS
The Global Ocean Observing System
p 2733 N93-24923

OCEAN MODELS
World Ocean Circulation Experiment
p 2733 N93-24922
Applications of wavelet-based compression to multidimensional earth science data
| DE93-007348 | p 2762 N93-25166
CHAMMP
| DE93-007290 | p 2762 N93-25184
Dynamics of Gulf Stream meanders and frontal eddies in the South Atlantic Bight p 2788 N93-25354
JPRS report: Science and technology. Central Eurasia: Earth sciences
| JPRS-UES-92-003 | p 2737 N93-25398
Wavelet transform-vector quantization compression of supercomputer ocean model simulation output
| DE93-005453 | p 2876 N93-25448
Simulation and prediction of tropical SST with a coupled ocean-atmosphere model p 2789 N93-25469
Errors caused by incompatible wind and buoyancy forcing in the ocean general circulation models
| AD-A260894 | p 2789 N93-25657
Boundary layer coupling between an explosive cyclone and the Gulf Stream during ERICA
| AD-A261577 | p 2787 N93-26513

OCEAN SURFACE
Orbit determination support of the Ocean Topography Experiment (TOPEX)/Poseidon operational orbit
p 2601 N93-24704
Satellite monitoring of the global ocean surface during 1987-1989 p 2734 N93-24926
Computation of moisture flux from ocean to atmosphere using a synergy of SSM/I-derived precipitable water and ECMWF analyses p 2774 N93-25757
Relations between blue whiting biomass and satellite derived phytoplankton and temperature in the Norwegian Sea
| AD-A261205 | p 2757 N93-25868
Experiments on the physics of turbulent mixing in stably stratified ocean layers
| AD-A261312 | p 2790 N93-26298
Model for transport of floating debris in the ocean
| PB93-172997 | p 2768 N93-26559

OCEAN TEMPERATURE
Observations of an intrathermocline vortex
p 2788 N93-24769
An observational study of the local and remote response of the equatorial Pacific to westerly wind events during the 1991-92 El Nino
| AD-A261777 | p 2787 N93-26286

OCEANOGRAPHIC PARAMETERS
International organisation of ocean programs: Making a virtue of necessity p 2732 N93-24917

OCEANOGRAPHY
Orbit determination support of the Ocean Topography Experiment (TOPEX)/Poseidon operational orbit p 2601 N93-24704
Supporting the Portuguese fisheries with satellites p 2745 N93-24821
Proceedings of the Ocean Climate Data Workshop | NASA-TM-108711 | p 2732 N93-24915
The role of ocean climate data in operational Naval oceanography p 2732 N93-24916
Role of the ocean in climate changes p 2732 N93-24918
The Global Ocean Observing System: One perspective p 2733 N93-24920
World Ocean Circulation Experiment p 2733 N93-24922
The Global Ocean Observing System p 2733 N93-24923
Global Temperature and Salinity Pilot Project p 2733 N93-24924
The use of remotely sensed data for operational fisheries oceanography p 2734 N93-24927
OCEAN-PC and a distributed network for ocean data p 2734 N93-24928
Satellite altimetry p 2734 N93-24930
Data archaeology at ICES p 2734 N93-24931
Data availability and data archeology from the former Soviet Union p 2735 N93-24932
Data management for community research projects: A JGOFS case study p 2736 N93-24936
On the generation and dispersion of Yanai waves with a spectral Chebyshev-collocation reduced-gravity ocean model p 2788 N93-25276
JPRS report: Science and technology. Central Eurasia: Earth sciences | JPRS-UES-92-003 | p 2737 N93-25398
JPRS report: Science and technology. Central Eurasia: Earth sciences | JPRS-UES-93-001 | p 2599 N93-25400
JPRS report: Science and technology. Central Eurasia: Earth sciences | JPRS-UES-92-005 | p 2737 N93-25401
Relations between blue whiting biomass and satellite derived phytoplankton and temperature in the Norwegian Sea | AD-A261205 | p 2757 N93-25868
Development of an expendable particle sensor | AD-A261127 | p 2710 N93-26044
Coastal ocean processes: A science prospectus | AD-A261702 | p 2790 N93-26384

OCEANS
International organisation of ocean programs: Making a virtue of necessity p 2732 N93-24917
The Global Ocean Observing System: One perspective p 2733 N93-24920
Operational seasonal and interannual predictions of ocean conditions p 2733 N93-24921
The Global Ocean Observing System p 2733 N93-24923
OCEAN-PC and a distributed network for ocean data p 2734 N93-24928
Data availability and data archeology from the former Soviet Union p 2735 N93-24932
Ocean time-series near Bermuda: Hydrostation S and the US JGOFS Bermuda Atlantic time-series study p 2736 N93-24938
Automated in situ observations of upper ocean biogeochemistry, bio-optics, and physics and their potential use for global studies p 2736 N93-24939
Wrap-up session p 2737 N93-24940
International ocean services: Is it time - will it ever be time? p 2737 N93-24941
Coastal ocean processes: A science prospectus | AD-A261702 | p 2790 N93-26384

OFF-ON CONTROL
Dynamic error analysis of numerical methods for simulation of state-variable derivatives with discontinuities p 2819 N93-25278

OGIVES
Tangential fuselage blowing on an ogive cylinder p 2578 N93-25545

OIL EXPLORATION
Radar sensing of petroleum seepage gases | AD-A261431 | p 2682 N93-26455

OIL FIELDS
Radar sensing of petroleum seepage gases | AD-A261431 | p 2682 N93-26455

OIL POLLUTION
Oil pollution and water quality mapping of Augusta Bay, Italy using remote sensing techniques p 2746 N93-24823
Remote sensing monitoring and hindcasting of the accident occurred to the tanker Haven in the Gulf of Genoa (Italy) p 2747 N93-24830

OILS
Development of a cone penetrometer for measuring spectral characteristics of soils in situ p 2776 N93-25570

OLFACTORY PERCEPTION
Primary events in olfactory reception | AD-A260562 | p 2795 N93-25944

ON-LINE SYSTEMS
Expert system for UNIX system reliability and availability enhancement p 2723 N93-25588
Fidelity and validity in distributed interactive simulation: Questions and answers | AD-A260971 | p 2810 N93-25711
A framework for the design of usable electronic text p 2877 N93-25754
A land-surface testbed for EOSDIS p 2878 N93-25797
On-line implementation of nonlinear parameter estimation for the Space Shuttle main engine | NASA-TM-106097 | p 2632 N93-26211
EnviroNET p 2886 N93-26398

ONBOARD DATA PROCESSING
The implementation of a lossless data compression module in an advanced orbiting system: Analysis and development p 2804 N93-25928

ONBOARD EQUIPMENT
Testing of the on-board attitude determination and control algorithms for SAMPEX p 2600 N93-24698
Orbit determination and orbit control for the Earth Observing System (EOS) AM spacecraft p 2601 N93-24705
Rate determination from vector observations p 2603 N93-24713

ONTARIO
Integrating satellite imagery and digital elevation data for geobotanical mapping in Quetico Provincial Park, Ontario, Canada p 2754 N93-25430

OPERATING COSTS
Application of non-thermal plasmas to pollution control | DE93-007515 | p 2763 N93-25385
Cost-effectiveness analysis of TxDOT CNG fleet conversion, volume 2 | PB93-159432 | p 2720 N93-26534
Cost-effectiveness analysis of TxDOT CNG fleet conversion, volume 1 | PB93-165603 | p 2720 N93-26585

OPERATING SYSTEMS (COMPUTERS)
Experimenter's laboratory for visualized interactive science p 2879 N93-25802
Fast mutual exclusion for uniprocessors | AD-A261663 | p 2883 N93-26389

OPERATIONAL AMPLIFIERS
Investigation into the common mode rejection ratio of the physiological signal conditioner circuit p 2794 N93-26073

OPERATIONS RESEARCH
JPRS report: Science and technology. Central Eurasia: Physics and mathematics | JPRS-UPM-93-001 | p 2844 N93-25404

OPHIUCHI CLOUDS
A study of the large-scale infrared emission from a selected dark cloud | NASA-CR-192775 | p 2888 N93-25289

OPTICAL ACTIVITY
ROSAT x ray survey observations of active chromospheric binary systems and other selected sources | NASA-CR-192933 | p 2891 N93-26426

OPTICAL COMMUNICATION
Progress towards laboratory frequency standards for the optical communication bands p 2687 N93-25069
Adaptive laser link reconfiguration using constraint propagation p 2823 N93-25967
Figure of merit for direct-detection optical channels p 2678 N93-26117
Advanced optical fiber communication systems | AD-A261802 | p 2856 N93-26256
Electronics and Electrical Engineering Laboratory technical publication announcements covering laboratory programs, July to September 1992 with 1992/1993 EEEL events calendar | PB93-158632 | p 2884 N93-26530

OPTICAL COMPUTERS
A novel optical/digital processing system for pattern recognition p 2814 N93-25603
Computer-aided design package for designers of digital optical computers | AD-A260757 | p 2806 N93-25848
Optical computing, Volume 6: Organization of the Optical Society of America photonic science topical meeting series | AD-A261267 | p 2856 N93-26266

OPTICAL DATA PROCESSING
Multi-layer holographic bifurcative neural network system for real-time adaptive EOS data analysis p 2880 N93-25807
Optical computing, Volume 6: Organization of the Optical Society of America photonic science topical meeting series | AD-A261267 | p 2856 N93-26266

OPTICAL DENSITY
Surface preparation and characterization of a 400 micrometer diameter fused silica optical fiber for direct optical initiation (DOI) applications | DE93-005485 | p 2852 N93-25182

OPTICAL DISKS
Lossless compression of image data products on th e FIFE CD-ROM series p 2804 N93-25929

OPTICAL EMISSION SPECTROSCOPY
Fast diagnostics of laser ablation used for pulsed laser deposition | DE93-005155 | p 2713 N93-25508

OPTICAL EQUIPMENT
Advances in nonlinear optical materials and devices | NASA-CR-192681 | p 2852 N93-25281
United States Army space experiment 601 | AD-A261460 | p 2798 N93-26353
1992 technical digest series volume 16. Conference edition: Summaries of papers presented at the Nonlinear Dynamics in Optical Systems Topical Meeting | AD-A261915 | p 2857 N93-26544

OPTICAL FIBERS
Surface preparation and characterization of a 400 micrometer diameter fused silica optical fiber for direct optical initiation (DOI) applications | DE93-005485 | p 2852 N93-25182
Novel approaches to the construction of miniaturized analytical instrumentation | NASA-CR-191988 | p 2709 N93-25345
Temperature dependent sensor response caused by polymer-solvent interactions | DE93-005368 | p 2655 N93-25444
A fiber optic probe for the detection of cataracts p 2796 N93-25593
Second-harmonic generation in optical fibers and glass | AD-A260592 | p 2853 N93-25839
Advanced optical fiber communication systems | AD-A261802 | p 2856 N93-26256
Research support for the Laboratory for Lightwave Technology | AD-A261488 | p 2856 N93-26343
Optical fiber for acoustic sensor applications | AD-A261580 | p 2857 N93-26515

OPTICAL MATERIALS
Advances in nonlinear optical materials and devices | NASA-CR-192681 | p 2852 N93-25281
Correlation of damage threshold and surface geometry of nodular defects in HR coatings as determined by in-situ atomic force microscopy | DE93-007509 | p 2654 N93-25384
Optical and scratch resistant properties of diamondlike carbon films deposited with single and dual ion beams p 2658 N93-25564
IR materials producibility | AD-A261099 | p 2853 N93-25766
Efficient nonlinear optical conversion of 1.319-micron laser radiation | AD-A261309 | p 2715 N93-26297
Development of organic nonlinear optical materials | AD-A261332 | p 2856 N93-26309
Experimental studies of stress management by optical fluorescence | AD-A261539 | p 2730 N93-26362
Optically smart surfaces survivability testing at Mach 3 | AD-A261785 | p 2857 N93-26566

OPTICAL MEASUREMENT
Monitoring damage growth in titanium matrix composites using acoustic emission | NASA-TM-107742 | p 2634 N93-25072
Polarizing Michelson interferometer for measuring thermospheric winds | ISBN-0-315-70442-X | p 2784 N93-25731
Measurement of optical properties of infrared bandgap superlattices | AD-A260859 | p 2866 N93-25789
Summary by the cloud and aerosol research group for ASTEX | AD-A261292 | p 2766 N93-26292
Laser physics and laser techniques | AD-A261595 | p 2715 N93-26524

OPTICAL MEASURING INSTRUMENTS
Registration of the use of agricultural fields and soil erosion using satellite remote sensing p 2751 N93-24856
Application of optical remote sensing to the study of surface fluxes related to cloud formation | DE93-003783 | p 2781 N93-25125
Analysis and design of a novel robotic finger-tip sensor for adaptive grasping p 2719 N93-25745
Fibre optic sensors for heat transfer studies p 2853 N93-25748

MIT's interferometer CST testbed
p 2609 N93-25836

OPTICAL MEMORY (DATA STORAGE)
Experimental studies of fundamental problems in quantum optics
| AD-A261183 | p 2853 N93-25822

OPTICAL PATHS
Miniature Optical Wide-Angle-Lens Startracker (Mini-OWLS) p 2606 N93-24728

OPTICAL PROPERTIES
Inherent optical properties of lakes as measured by Landsat 5 Thematic Mapper p 2746 N93-24828
Optical and scratch resistant properties of diamondlike carbon films deposited with single and dual ion beams
p 2658 N93-25564
Measurement of optical properties of infrared bandgap superlattices
| AD-A260859 | p 2866 N93-25789
Optoelectronic III-V heterostructures on Si substrates
| AD-A261651 | p 2867 N93-26193
Electrochemical processing of electrically conductive polymer fibers
| AD-A261793 | p 2657 N93-26386
Optical characterization of Ga(1-x)In(x)As(y)Sb(1-y)/GaSb alloy and device application
| AD-A261713 | p 2870 N93-26581

OPTICAL PUMPING
Preliminary results on an optically-pumped Cs beam frequency standard p 2832 N93-24989
Miniature optically-pumped cesium beam resonator
p 2833 N93-24990
Actual limits of fluorescence S/N ratio in an optically-pumped cesium beam resonator
p 2833 N93-24991
FALCON nuclear-reactor-pumped laser program and wireless power transmission
| DE93-007607 | p 2715 N93-26597

OPTICAL PYROMETERS
New pyro-optic techniques for imaging of long wavelength IR-Radiation (pyro-optic initiation program)
| AD-A260969 | p 2856 N93-26224

OPTICAL RADAR
Remote sensing of non-renewable resources
p 2744 N93-24814
Injection seeded, diode-pumped, short pulse Nd:YAG ring laser for space-based laser ranging
p 2713 N93-25389
Preliminary studies leading toward the development of a LIDAR bathymetry mapping instrument
p 2711 N93-25614
Ultraviolet waveguide lasers for phased array lidar
| AD-A261657 | p 2715 N93-26363

OPTICAL RESONATORS
Phase differences of the fields in a Ramsey resonator for submillimetric frequency standards
p 2840 N93-25042
Temperature dependent sensor response caused by polymer-solvent interactions
| DE93-005368 | p 2655 N93-25444
Laser physics and laser techniques
| AD-A261595 | p 2715 N93-26524

OPTICAL SCANNERS
Video scan rate conversion method and apparatus for achieving same
| AD-D015661 | p 2854 N93-26091
Photographic industry and electronic imaging: The emergence of electronic still photography
| PB93-169399 | p 2711 N93-26324
Large area, low capacitance Si(Li) detectors for high rate x ray applications
| DE93-007661 | p 2692 N93-26598

OPTICAL TRACKING
An optimal scheduling of pick-place operations of a robot-vision-tracking system by using neural networks and rule-based systems p 2821 N93-25880
A Hierarchical Target Extraction, Recognition, and Tracking (HiTert) system
| AD-A260567 | p 2854 N93-25898
Geometric distortion analysis of a wide-field astrograph p 2621 N93-26111

OPTIMAL CONTROL
Dynamics and control of maneuverable tethered flight vehicles p 2615 N93-24767
Optimal cooperative power-limited rendezvous
p 2607 N93-24904
Two neural network algorithms for designing optimal terminal controllers with open final time
| NASA-CR-177599 | p 2817 N93-25137
Nonholonomic geometry, mechanics and control
p 2724 N93-25270
Optimal finite-thrust time-bounded direct-ascent interception p 2607 N93-25272
Optimal control of large space structures
p 2819 N93-25343
Optimal thrust magnitude on a singular arc in atmospheric flight p 2819 N93-25410
What procedure to choose while designing a fuzzy control? Towards mathematical foundations of fuzzy control
| NASA-TM-108719 | p 2820 N93-25459
Control and optimization of aircraft trajectories
p 2596 N93-25543
Realtime control of multiple sensor systems
| AD-A261037 | p 2680 N93-26226

OPTIMIZATION
Minimization of heat slab nodes with higher order boundary conditions
| DE93-004238 | p 2695 N93-24966
A state-of-the-art crystal filter design package using Windows 3.0 techniques p 2693 N93-25010
Grid sensitivity for aerodynamic optimization and flow analysis
| NASA-CR-192980 | p 2575 N93-25117
Neural networks: What non-linearity to choose
| NASA-CR-192948 | p 2819 N93-25197
Integrated aerodynamic-structural wing design optimization p 2587 N93-25279
A preliminary sizing method for unmanned aircraft using multi-variate optimisation p 2587 N93-25408
A computational aerodynamic design optimization method using sensitivity analysis p 2589 N93-25552
An optimal scheduling of pick-place operations of a robot-vision-tracking system by using neural networks and rule-based systems p 2821 N93-25880
Techniques for designing rotorcraft control systems
| NASA-CR-192960 | p 2597 N93-26046
Monte Carlo approach to the approximation of invariant measures
| PB93-159069 | p 2830 N93-26317
Integrated approaches to parallelism in optimization and the solution of inverse problems
| AD-A261490 | p 2829 N93-26344
Configuration optimization of space structures
p 2670 N93-26415
Computation and theory in large-scale optimization
| AD-A261419 | p 2813 N93-26450

OPTOELECTRONIC DEVICES
Discrete range clustering using Monte Carlo methods
| NASA-TM-104004 | p 2584 N93-24914
Ultrafast measurements of 200 gigahertz Schottky photodiodes p 2688 N93-25392
Investigation of a background suppression transimpedance amplifier for photovoltaic detectors
| AD-A261828 | p 2691 N93-26272

ORBIT CALCULATION
TDRSS orbit determination using short baseline differenced carrier phase p 2601 N93-24701
Application of GPS tracking techniques to orbit determination for TDRS p 2601 N93-24702
TDRSS-user orbit determination using batch least-squares and sequential methods
p 2601 N93-24703
Orbit determination support of the Ocean Topography Experiment (TOPEX)/Poseidon operational orbit
p 2601 N93-24704
Orbit determination and orbit control for the Earth Observing System (EOS) AM spacecraft
p 2601 N93-24705
Attitude analysis in Flatland: The plane truth
p 2603 N93-24712
Tsien's method for generating non-Keplerian trajectories. Part 2: The question of thrust to orbit a sphere and the restricted three-body problem
p 2603 N93-24718
Orbit determination error analysis and comparison of station-keeping costs for Lissajous and halo-type libration point orbits and sensitivity analysis using experimental design techniques p 2604 N93-24721
The advances in F and T technology: Their benefits of and for space science and technology
p 2831 N93-24979
The application of the PRARE principle for precise two-way time transfer to space-based atomic clocks
p 2832 N93-24983
DORIS precise orbit determination and location system performances of ultra stable oscillators
p 2608 N93-24997
A determination of the radio-planetary frame tie from comparison of Earth orientation parameters
p 2676 N93-26106
Orbiter-orbiter and orbiter-lander tracking using same-beam interferometry p 2677 N93-26110

ORBIT DECAY
A ground track control algorithm for the Topographic Mapping Laser Altimeter (TMLA) p 2602 N93-24707

ORBIT SPECTRUM UTILIZATION
Federal Communications Commission (FCC) Transponder Loading Data Conversion Software. User's guide and software maintenance manual, version 1.2
| NASA-CR-191067 | p 2808 N93-24947

ORBIT TRANSFER VEHICLES
Space transfer vehicle concepts and requirements study. Volume 2, book 1: STV concept definition and evaluation
| NASA-CR-192525 | p 2611 N93-25510
Space transfer vehicle concepts and requirements study. Volume 2, book 2: System and program requirements trade studies
| NASA-CR-192526 | p 2611 N93-25511
Space transfer vehicle concepts and requirements study. Volume 2, book 3: STV system interfaces
| NASA-CR-192527 | p 2611 N93-25513
Space transfer vehicle concepts and requirements study. Volume 3, book 1: Program cost estimates
| NASA-CR-192529 | p 2611 N93-25514
Space transfer concepts and analyses for exploration missions. Technical directive 12: Beamed power systems study
| NASA-CR-192532 | p 2599 N93-26146
Representative systems for space exploration
p 2897 N93-26395

ORBITAL ASSEMBLY
Space Station Freedom assembly and operation at a 51.6 degree inclination orbit
| NASA-TM-107731 | p 2615 N93-25174
A prototype for simulation of the space-to-ground assembly/contingency system of Space Station Freedom p 2619 N93-26065
Center for Space Construction Third Annual Symposium
| NASA-CR-192688 | p 2669 N93-26405
Dynamics of on-orbit construction process
p 2669 N93-26406
Interaction dynamics and control for orbital assembly
p 2669 N93-26407
Controls for orbital assembly of large space structures
p 2620 N93-26408
Structural load control during construction
p 2669 N93-26409
Systems engineering studies of on-orbit assembly operations p 2669 N93-26410
Expert systems for assembly sequence evaluation
p 2669 N93-26411

ORBITAL MANEUVERS
Rendezvous, proximity operations and capture quality function deployment report
| NASA-TM-108752 | p 2614 N93-25952

ORBITAL MECHANICS
Flight Mechanics/Estimation Theory Symposium, 1992
| NASA-CP-3186 | p 2599 N93-24694
Minimum-fuel power-limited transfers between coplanar elliptic orbits p 2608 N93-25684
Optimal transfers between libration-point orbits in the elliptic restricted three-body problem
p 2608 N93-25758

ORBITAL WORKSHOPS
The initial flight anomalies of Skylab 1
p 2619 N93-24692

ORDER-DISORDER TRANSFORMATIONS
Radiation-induced disordering and defect production in CuAu and NiAl studied by molecular dynamics simulation
| DE93-007506 | p 2649 N93-25336
Room temperature fracture of FeCo
| DE93-008266 | p 2650 N93-25519

ORGANIC COMPOUNDS
Health and environmental chemistry: Analytical techniques, data management, and quality assurance
| DE93-002853 | p 2760 N93-24674
Femtosecond dynamics in hydrogen-bonding solvents: Formamides
| DE93-003476 | p 2643 N93-25123

ORGANISMS
Analysis of reentry into the White Sands Missile Range (WSMR) for the LifeSat mission p 2603 N93-24717
Planetary Biology and Microbial Ecology: Molecular Ecology and the Global Nitrogen cycle
| NASA-CR-4497 | p 2803 N93-26157

ORGANIZATIONS
Rendezvous, proximity operations and capture quality function deployment report
| NASA-TM-108752 | p 2614 N93-25952
Functional Economic Analysis Guidebook, version 1.1
| AD-A261390 | p 2886 N93-26305

ORGANOMETALLIC COMPOUNDS
Design of a high activity and selectivity alcohol catalyst
| DE93-008103 | p 2659 N93-25112

ORIENTATION
Uncertainty in object pose determination with three light-stripe range measurements
| AD-A261435 | p 2857 N93-26488

ORIFICE FLOW
Flow conditioner location effects in orifice flowmeters
| PB93-159457 | p 2708 N93-26535

ORIFICES
Flow conditioner location effects in orifice flowmeters
| PB93-159457 | p 2708 N93-26535
OROGRAPHY
Effects of Taiwan orography on the motion and structure of typhoons
| AD-A261819 | p 2786 N93-26270
ORR-SOMMERFELD EQUATIONS
On the cross-stream spectral method for the Orr-Sommerfeld equation
| NASA-TM-107737 | p 2845 N93-26086
ORTHOTROPIC CYLINDERS
Stress and reliability analyses of multilayered composite cylinder under thermal and mechanical loads
p 2726 N93-25533
ORTHOTROPIC PLATES
Fatigue resistance of orthotropic plates with trapezoidal stiffeners
| TRL-TRANS-T3908 | p 2726 N93-25419
OSCILLATIONS
Propagation of radiation in astrophysical media: Gravitational lenses and astrophysical masers
p 2892 N93-24949
Experiments on a diode-laser-pumped Rb-87 maser
p 2716 N93-25030
Controlling an optical frequency by a single ion
p 2841 N93-25051
Anomalous aspects of magnetosheath flow and of the shape and oscillations of the magnetopause during an interval of strongly northward interplanetary magnetic field
| NASA-CR-192851 | p 2770 N93-25081
JPRS report: Science and technology. Central Eurasia: Engineering and equipment
| JPRS-UEQ-92-003 | p 2668 N93-25427
Vortex shedding in oscillatory flow
p 2700 N93-25438
Flame response in oscillatory solid propellant combustion p 2630 N93-26041
Substantiation of a stochastic model of rhythmic phenomena
| AD-A261232 | p 2830 N93-26262
OSCILLATORS
DORIS precise orbit determination and location system performances of ultra stable oscillators
p 2608 N93-24997
Miniaturization and stability: A new generation of ovenised oscillators p 2693 N93-25004
Stability of nonlinear phase motion from the study of oscillator mappings p 2693 N93-25034
Solid state frequency synthesis up to 600 GHz: An application to the Mg frequency standard
p 2842 N93-25058
Information transmission using CHAOS
| AD-A261519 | p 2883 N93-26377
OVER-THE-HORIZON RADAR
OTH-B radar system: System summary
| AD-A261727 | p 2681 N93-26247
High Frequency (HF) radiowave propagation
| AD-A261726 | p 2681 N93-26280
Digital Oblique Remote Ionospheric Sensing (DORIS) program development
| AD-A261750 | p 2776 N93-26283
OXIDASE
Inorganic and biological electron transfer across an electronically conductive composite polymer membrane
| AD-A261642 | p 2656 N93-26172
OXIDATION
The structure of particle cloud premixed flames
| NASA-CR-192827 | p 2643 N93-25229
Direct methane conversion to methanol
| DE93-009183 | p 2660 N93-25497
Mechanisms of decomposition and oxidation of borane compounds
| AD-A261137 | p 2645 N93-26045
Thermal coatings for titanium-aluminum alloys
| NASA-TM-107760 | p 2651 N93-26048
Interaction of O2 with the Fe(.84)Cr(.16) (001) surface studied by photoelectron spectroscopy
| AD-A261065 | p 2645 N93-26251
Dynamics of gas-surface interactions
| AD-A261402 | p 2646 N93-26402
Intramolecular bridge/terminal oxo exchange within (MoV2O3) (4 +) complexes containing linear oxo bridges
| AD-A261230 | p 2851 N93-26518
OXIDATION RESISTANCE
Hot corrosion of the B2 nickel aluminides
| NASA-CR-191082 | p 2649 N93-25128
Processing and properties of Ti5Si3
| DE93-007284 | p 2649 N93-25149
Thermal coatings for titanium-aluminum alloys
| NASA-TM-107760 | p 2651 N93-26048
Metal alloy and method of preparation thereof
| AD-D015670 | p 2652 N93-26234
Deformation mechanisms of NiAl cyclicly deformed near the brittle-to-ductile transition temperature
| NASA-CR-191121 | p 2652 N93-26235
OXIDATION-REDUCTION REACTIONS
Integrated oxygen recovery system
| NASA-CR-192982 | p 2801 N93-26088
OXIDE FILMS
Interaction of O2 with the Fe(.84)Cr(.16) (001) surface studied by photoelectron spectroscopy
| AD-A261065 | p 2645 N93-26251
OXIDES
Converting environmental wastes into valuable resources p 2759 N93-25572
Activation of methane by clean and chemically modified single crystal oxide surfaces
| PB93-157295 | p 2644 N93-25817
Research support for the Laboratory for Lightwave Technology
| AD-A261488 | p 2856 N93-26343
OXYGEN
Membrane technology: A search for membranes for submarine atmosphere control
| AD-A260581 | p 2801 N93-25904
Resonance electron scattering by O2 monolayers on graphites: Reinterpreted
| AD-A261851 | p 2850 N93-26287
Intramolecular bridge/terminal oxo exchange within (MoV2O3) (4 +) complexes containing linear oxo bridges
| AD-A261230 | p 2851 N93-26518
OXYGEN ATOMS
Detection of atomic oxygen and hydrogen in solid propellant flames and pyrolysis gases using multiphoton laser-induced fluorescence p 2628 N93-26029
Mechanisms of decomposition and oxidation of borane compounds
| AD-A261137 | p 2645 N93-26045
Space environmental interactions for the space exploration initiative p 2897 N93-26396
OXYGEN SPECTRA
Gravity waves from O2 airglow p 2772 N93-25547
OXYGEN SUPPLY EQUIPMENT
Integrated oxygen recovery system
| NASA-CR-192982 | p 2801 N93-26088
OZONE
Atmospheric reactive nitrogen oxides and their relationship with urban and rural ozone formation
p 2760 N93-24908
Kelvin waves in total column ozone
| NASA-CR-192984 | p 2764 N93-25431
Tropical cyclone/upper-atmospheric interaction as inferred from satellite total ozone observations
p 2784 N93-25741
Treatment of hazardous organic wastes using silent discharge plasmas
| DE93-003789 | p 2768 N93-26592
OZONE DEPLETION
An assessment of alternatives and technologies for replacing ozone-depleting substances at DOE facilities
| DE93-002862 | p 2760 N93-24675
Measurements of nitric acid, carboxylic acids, and selected aerosol species for the NASA/GTE Pacific Mission - West (PEM-WEST)
| NASA-CR-192976 | p 2763 N93-25287
Aerospace-plane flights and stratospheric ozone: Review and preliminary assessment of the National Aerospace Plane (NASP) operations
| RAND/N-3464-AF | p 2767 N93-26327
OZONOSPHERE
An assessment of alternatives and technologies for replacing ozone-depleting substances at DOE facilities
| DE93-002862 | p 2760 N93-24675
Rossby-gravity waves in tropical total ozone data
| NASA-CR-192983 | p 2764 N93-25432

P

P-I-N JUNCTIONS
Research on stable, high-efficiency amorphous silicon multijunction modules
| DE93-000072 | p 2862 N93-25163
Time resolved studies of in-well and cross-well carrier transport in MQW semiconductor structures
| AD-A261170 | p 2714 N93-25774
P-TYPE SEMICONDUCTORS
Research on stable, high-efficiency amorphous silicon multijunction modules
| DE93-000072 | p 2862 N93-25163
PACIFIC OCEAN
Measurements of nitric acid, carboxylic acids, and selected aerosol species for the NASA/GTE Pacific Mission - West (PEM-WEST)
| NASA-CR-192976 | p 2763 N93-25287
Tropical cyclogenesis in the western North Pacific
p 2783 N93-25714
An observational study of the local and remote response of the equatorial Pacific to westerly wind events during the 1991-92 El Nino
| AD-A261777 | p 2787 N93-26286
PACKAGING
Instrumentation for measurement of gas permeability of polymeric membranes p 2720 N93-25609
PAINTS
Plasma current collection of Z-93 thermal control paint as measured in the Lewis Research Center's plasma interaction facility
| NASA-TM-106132 | p 2618 N93-26215
PANELS
A computational approach to predicting the extent of arc root damage in CFC panels p 2642 N93-24890
PARABOLIC DIFFERENTIAL EQUATIONS
Computation of hypersonic viscous flowfields using the parabolized Navier-Stokes equations
p 2694 N93-24766
PARACHUTE DESCENT
A simple, approximate model of parachute inflation
| DE93-002465 | p 2576 N93-25121
PARALLEL COMPUTERS
Fast parallel algorithms that compute transitive closure of a fuzzy relation
| NASA-CR-192950 | p 2818 N93-25190
A software development approach for parallel processing systems integrating object-oriented and functional paradigms p 2816 N93-25481
Real-time construction and rendering of three-dimensional occupancy maps
| DE93-007818 | p 2756 N93-25516
PARALLEL PROCESSING (COMPUTERS)
Optimal message log reclamation for independent checkpointing
| NASA-CR-192886 | p 2815 N93-24749
Data processing and control in a transputer system for remote sensing of the Earth p 2753 N93-24870
A comparison using APPL and PVM for a parallel implementation of an unstructured grid generation program
| NASA-CR-191425 | p 2808 N93-25073
Monte-Carlo methods make Dempster-Shafer formalism feasible
| NASA-CR-192945 | p 2828 N93-25140
Supercomputer Debugging Workshop 1992
| DE93-007322 | p 2805 N93-25165
Fast parallel algorithms that compute transitive closure of a fuzzy relation
| NASA-CR-192950 | p 2818 N93-25190
RAMA: A file system for massively parallel computers
| NASA-CR-192906 | p 2815 N93-25297
PCG: A software package for the iterative solution of linear systems on scalar, vector and parallel computers
| DE93-007366 | p 2809 N93-25315
Structured adaptive mesh refinement on the connection machine
| DE93-007368 | p 2816 N93-25316
Data parallel finite element techniques for large-scale computational fluid dynamics p 2699 N93-25334
Hierarchical dynamics in distributed information processing p 2875 N93-25350
FORTRAN M as a language for building earth system models
| DE93-007897 | p 2763 N93-25370
An improved spectral load balancing method
| DE93-007582 | p 2810 N93-25386
Experiments with the HIVITS HDTV contribution CODED
| BBC-RD-1992/12 | p 2674 N93-25391
Toward a parallel recursive spectral bisection mapping tool
| DE93-006632 | p 2816 N93-25414
A software development approach for parallel processing systems integrating object-oriented and functional paradigms p 2816 N93-25481
Real-time construction of three-dimensional occupancy maps
| DE93-001645 | p 2756 N93-25505
Deterministic parallel FORTRAN
| DE93-008665 | p 2816 N93-25522
Implicit multigrid solution of the compressible Navier-Stokes equations with application to distributed parallel processing p 2702 N93-25546
Splash 2 p 2814 N93-25575
A novel method for characterization of superconductors: Physical measurements and modeling of thin films
p 2871 N93-25584
Adaptive liquid crystal TV based joint transform correlator as applied to real-time pattern recognition
| AD-A260724 | p 2864 N93-25655
Parallel matrix computations
| AD-A260783 | p 2828 N93-25687
Massively-parallel computational fluid dynamics
| AD-A261815 | p 2707 N93-26269

Integrated approaches to parallelism in optimization and the solution of inverse problems
| AD-A261490 | p 2829 N93-26344
Source-level debugging of automatically parallelized programs
| AD-A261520 | p 2813 N93-26378
Joint services electronics program
| AD-A261801 | p 2692 N93-26539

PARALLEL PROGRAMMING
Synthetic-perturbation tuning of MIMD programs
| PB93-161339 | p 2812 N93-26321
Source-level debugging of automatically parallelized programs
| AD-A261520 | p 2813 N93-26378

PARAMETERIZATION
Improved PI-network measurement of all quartz crystal parameters by appropriate modelling of the test fixture p 2833 N93-24995

PARAMETRIC AMPLIFIERS
Advances in nonlinear optical materials and devices
| NASA-CR-192681 | p 2852 N93-25281

PARITY
A (72, 36; 15) box code p 2671 N93-24663
Golay and other box codes p 2678 N93-26116

PARTIAL DIFFERENTIAL EQUATIONS
Some new results for solving linear systems arising from computational fluid dynamics problems p 2699 N93-25349
PDE: Differential, geometric and algebraic methods in nonlinear filtering
| AD-A260967 | p 2829 N93-26222

PARTIAL PRESSURE
Biological conversion of synthesis gas
| DE93-009092 | p 2660 N93-25523
Development of a method to determine the autoxidation of turbine fuels
| AD-A260578 | p 2661 N93-25902

PARTICLE CHARGING
Comparison of the electrical charging and discharging environments of multiple aircraft-borne electric-field measurement systems p 2583 N93-24887

PARTICLE COLLISIONS
Particle simulation for 10.6 micron picosecond laser-induced breakdown in gases p 2712 N93-25280
Strangeness production in S + Pb and p + Pb collisions at 200 GeV/c per nucleon nucleon
| DE93-007654 | p 2847 N93-25326
Detection of fragments arising from greater than 10 GeV electron-nucleus collisions
| DE93-007725 | p 2848 N93-25366
Collisional energy transfer in biomolecular ion-molecule dynamics
| AD-A260911 | p 2849 N93-25659
The physics of spin polarized gases
| AD-A261396 | p 2850 N93-26288

PARTICLE DIFFUSION
Asymptotic derivation of the simplified P(sub N) equations
| DE93-007342 | p 2828 N93-25151
A method for transient, three-dimensional neutron transport calculations
| DE93-007243 | p 2847 N93-25256
Direct measurement of velocity space transport in a plasma p 2861 N93-25831

PARTICLE INTERACTIONS
Notes on radial drift for dalitz detection
| DE93-006971 | p 2846 N93-24959
Twistor diagrams and a quantum field theory p 2871 N93-25423
An experimental study of particle-laden jet interactions with cocurrent flows p 2701 N93-25534

PARTICLE LADEN JETS
An experimental study of particle-laden jet interactions with cocurrent flows p 2701 N93-25534

PARTICLE MOTION
Diabaticity of nuclear motion: Problems and perspectives
| DE93-007252 | p 2847 N93-25148
An investigation of laser velocimetry measurements within high speed, complex flows p 2697 N93-25237
Particle dynamics modeling of boundary effects in granular Couette flow p 2705 N93-25738

PARTICLE PRECIPITATION
Sounding rocket observations of precipitating ions in the morning auroral region p 2773 N93-25732

PARTICLE PRODUCTION
Recent experiments on spin physics in high energy hadron interactions
| DE93-007900 | p 2851 N93-25301
Strangeness production in S + Pb and p + Pb collisions at 200 GeV/c per nucleon nucleon
| DE93-007654 | p 2847 N93-25326
Results from the NA36 on strangeness production in 200 GeV/c per nucleon S + Pb and p - Pb reactions
| DE93-007711 | p 2848 N93-25364

PARTICLE SIZE DISTRIBUTION
A study of mass size distributions and particle deposition velocities in ambient air p 2763 N93-25263
The charge and size of precipitation particles inside thunderstorms and mesoscale convective systems on the Great Plains p 2781 N93-25275
Liquid surface breakup of nonturbulent and turbulent liquids p 2700 N93-25473
Hazards of explosives dusts: Particle size effects
| DE93-009380 | p 2668 N93-25498
Particle behavior in solid propellant rocket motors and plumes
| AD-A260900 | p 2624 N93-25913
Rain rate instrument for deployment at sea, phase 2
| NASA-CR-192442 | p 2786 N93-26156
Summary by the cloud and aerosol research group for ASTEX
| AD-A261292 | p 2766 N93-26292
Atomization and combustion of a gelled, metallized slurry fuel
| AD-A261778 | p 2647 N93-26602

PARTICLE SPIN
Recent experiments on spin physics in high energy hadron interactions
| DE93-007900 | p 2851 N93-25301

PARTICLE THEORY
An investigation of neutrino properties through study of the sun, supernovae, the early universe and lab data p 2898 N93-25180

PARTICLE TRAJECTORIES
Plasma sheath effects on ion collection by a pinhole
| NASA-TM-106098 | p 2615 N93-25090
Some features of particle orbit behavior in LHD configurations
| NIFS-211 | p 2859 N93-25216

PARTICULATE REINFORCED COMPOSITES
Dynamic deformations and analysis of a metal matrix composite p 2634 N93-25234

PARTICULATES
Development of dispersion-strengthened XD (trademark) Cu alloys for high heat-flux applications
| NASA-CR-191124 | p 2653 N93-24761
Particle dynamics modeling of boundary effects in granular Couette flow p 2705 N93-25738
Electrorheological fluids: A structural approach to mechanisms
| AD-A260563 | p 2645 N93-25879
Particulate emissions from gas turbine engines
| AD-A261374 | p 2595 N93-26339

PASSIVITY
Chromate-free corrosion resistant talc coatings for aluminum alloys
| DE93-005370 | p 2655 N93-25446
Passivity motivated controller design for flexible structures
| AD-A261122 | p 2719 N93-25771

PATHOLOGY
The prevalence of artificial lens implants in the civil airman population
| DOT/FAA/AM-92/14 | p 2794 N93-25214

PATIENTS
Automatic detection of seizures with applications p 2796 N93-25592
A fiber optic probe for the detection of cataracts p 2796 N93-25593
Neuropsychological components of object identification
| AD-A261449 | p 2797 N93-26347

PATTERN METHOD (FORECASTING)
A systematic satellite approach for estimating central pressures of mid-lattitude oceanic storms
| NOAA-TR-NESDIS-63 | p 2781 N93-25220

PATTERN RECOGNITION
Failure monitoring in dynamic systems: Model construction without fault training data p 2672 N93-24666
The use of polarimetric multifrequency SAR for characterizing terrain classes p 2738 N93-24777
Remote sensed spectral signatures classification and recognition by neural networks: An approach to unsupervised techniques p 2738 N93-24779
EUROSTARS: A system for thematic analysis of remote sensed data p 2753 N93-24871
A novel optical/digital processing system for pattern recognition p 2814 N93-25603
Adaptive liquid crystal TV based joint transform correlator as applied to real-time pattern recognition
| AD-A260724 | p 2864 N93-25655
A vision architecture for the extravehicular activity retriever p 2827 N93-26071
Facilitation and interference in identification of pictures and words
| AD-A261484 | p 2798 N93-26356
Spontaneous discovery and use of categorical structure
| AD-A261658 | p 2798 N93-26364

PAYLOAD INTEGRATION
Assured crew return vehicle man-systems integration standards
| NASA-CR-193065 | p 2614 N93-26329

PAYLOAD STATIONS
STS-43 Space Shuttle mission report
| NASA-CR-193064 | p 2612 N93-25957

PAYLOADS
What is the relationship between altitude and weight in a model rocket? p 2603 N93-24715
Analysis of reentry into the White Sands Missile Range (WSMR) for the LifeSat mission p 2603 N93-24717
STS-39 Space Shuttle mission report
| NASA-CR-193063 | p 2611 N93-25955
STS-37 Space Shuttle mission report
| NASA-CR-193062 | p 2612 N93-25956
STS-47 Space Shuttle mission report
| NASA-CR-193056 | p 2612 N93-25960
STS-42 Space Shuttle mission report
| NASA-CR-193059 | p 2613 N93-25989
STS-48 Space Shuttle mission report
| NASA-CR-193060 | p 2613 N93-25990
STS-46 Space Shuttle mission report
| NASA-CR-193058 | p 2613 N93-25991
STS-50 Space Shuttle mission report
| NASA-CR-193057 | p 2613 N93-25992
STS-52 Space Shuttle mission report
| NASA-CR-193061 | p 2613 N93-25993
Spacelab, Spacehab, and Space Station Freedom payload interface projects p 2620 N93-26080

PECULIAR GALAXIES
Prograde anomalous orbits in triaxial gravitational potentials that rotate about the long axis: VLA neutral hydrogen observations and modeling of the inclined rings around the galaxies NGC 2685 and NGC 660 p 2607 N93-25396

PEEK
The design of mechanically compatible fasteners for human mandible reconstruction p 2796 N93-25569

PEELING
Thermoelastic stresses in multi-layered media in non-uniform temperature fields
| AD-A260901 | p 2727 N93-25658

PENDULUMS
JPRS report: Science and technology. Central Eurasia: Engineering and equipment
| JPRS-UEQ-92-003 | p 2668 N93-25427
Investigation of liquid sloshing in spin-stabilized satellites
| AD-A261671 | p 2619 N93-26438

PENETRATION
Method for providing EMI/EMP hardening and breakdown protection in composite materials
| AD-D015638 | p 2634 N93-25283
Investigation and modeling of penetration process for composite laminates impacted by a blunt-ended projectile p 2637 N93-25675
Analysis of shaped charge jet penetration experiments with Pen
| UCRL-LR-110773 | p 2730 N93-26177
Algorithms for the analysis of penetration by shaped charge jets
| UCRL-LR-109887 | p 2730 N93-26178

PENETROMETERS
Development of a cone penetrometer for measuring spectral characteristics of soils in situ p 2776 N93-25570

PENNING EFFECT
Optical detection of laser-cooled ions in a Penning trap p 2838 N93-25031

PERFLUORO COMPOUNDS
Determination of the thermal stability of perfluoropolyalkyl ethers by tensimetry
| NASA-TM-106081 | p 2654 N93-25093

PERFORMANCE
Task 5: Architecture sensitivity to STME performance
| MCR-92-5010 | p 2609 N93-26176

PERFORMANCE PREDICTION
Rotor design optimization using a free wake analysis
| NASA-CR-177612 | p 2575 N93-25075
Transient performance of fan engine with water ingestion
| NASA-CR-190778 | p 2573 N93-25134
Statistical modelling of software reliability
| NASA-CR-192985 | p 2809 N93-25257
A cognitive architecture for human performance process model research
| AD-A261040 | p 2797 N93-25815
The effects of reaction on axial compressor performance p 2594 N93-25882
On-line implementation of nonlinear parameter estimation for the Space Shuttle main engine
| NASA-TM-106097 | p 2632 N93-26211
Intelligent, real-time problem solving, phase 3
| AD-A261441 | p 2829 N93-26345

PERFORMANCE TESTS
A procedure for defining lightning risk to air vehicles p 2583 N93-24885
Precise Doppler tracking from the Medicina VLBI station p 2608 N93-24998
Miniaturization and stability: A new generation of ovenised oscillators p 2693 N93-25004
Test results of a Stirling engine utilizing heat exchanger modules with an integral heat pipe
| NASA-TM-105883 | p 2759 N93-25136
Measuring hearing protection device performance using the metrosonics db-3100 sound level analyzer (dosimeter)
| AD-A260852 | p 2801 N93-25787
Performance-based testing and success in Naval advanced flight training
| AD-A260838 | p 2590 N93-25933
The Data Multiplexing Network (DMN) phase 3 Extended Distance Data Cable (EDDC) test and evaluation
| DOT/FAA/CT-TN93/11 | p 2680 N93-26160
Synthetic-perturbation tuning of MIMD programs
| PB93-161339 | p 2812 N93-26321
Tank issues: Design and placement of vapor monitoring wells
| PB93-161131 | p 2768 N93-26536
PERIODIC FUNCTIONS
Properties of readings of periodically correlated random processes
| AD-A261225 | p 2686 N93-26573
PERIODIC VARIATIONS
Climate data bases of the People's Republic of China, 1841-1988
| DE93-007907 | p 2764 N93-25517
Substantiation of a stochastic model of rhythmic phenomena
| AD-A261232 | p 2830 N93-26262
PERMANENT MAGNETS
Variable-speed generators with flux weakening p 2694 N93-25599
PERMEABILITY
Instrumentation for measurement of gas permeability of polymeric membranes p 2720 N93-25609
Membrane technology: A search for membranes for submarine atmosphere control
| AD-A260581 | p 2801 N93-25904
PERMEATING
Prediction of hydrogen entry and permeation in metals and alloys
| AD-A260580 | p 2651 N93-25903
Numerical simulation of permeation from deposited droplets: Model expansion
| MTL-TR-92-23 | p 2706 N93-25953
PERMITTIVITY
The third-order permittivity of quartz obtained by different methods p 2840 N93-25046
Liquid filled variable capacitor
| AD-D015639 | p 2687 N93-25212
Electrorheological fluids: A structural approach to mechanisms
| AD-A260563 | p 2645 N93-25879
Modeling of electric-field enhancement at nodular defects in dielectric mirror coatings
| DE93-007513 | p 2857 N93-26593
PERMUTATIONS
Soft decoding a self-dual (48, 24; 12) code p 2671 N93-24662
PEROXIDES
Development of a method to determine the autoxidation of turbine fuels
| AD-A260578 | p 2661 N93-25902
PERSONAL COMPUTERS
A distributed heterogeneous client-server environment
| DE93-007496 | p 2875 N93-25319
Evaluation of a vibration diagnostic system for the detection of spur gear pitting failures
| NASA-TM-106103 | p 2718 N93-25672
The state of computing at Los Alamos National Laboratory, FY 1991
| LA-12326-MS | p 2811 N93-25943
Development and testing of the digital control system for the Archytas unmanned air vehicle
| AD-A261656 | p 2597 N93-26196
PERSONALITY
Contribution of personality to the prediction of success in initial air traffic control specialist training
| DOT/FAA/AM-93/4 | p 2797 N93-26138
PERSONNEL
JSC research and technology
| NASA-TM-104763 | p 2901 N93-25188
Organizational politics, participation in decision-making, and job satisfaction
| DOT/FAA/AM-92/17 | p 2796 N93-25203
Procedural justice, occupational identification, and organizational commitment
| DOT/FAA/AM-92/21 | p 2872 N93-25204
Assessing patterns of change in anthropometric dimensions: Secular trends of US Army females, 1946-1988
| AD-A260869 | p 2800 N93-25628
Aircraft electrical and environmental systems, AFSCs 452x5, 454x5, and 454x6
| AD-A261213 | p 2590 N93-25733
PERSONNEL DEVELOPMENT
Design and implementation of a pilot orientation program for new NASA engineering employees
| NASA-TM-105907 | p 2872 N93-26205
PERSONNEL MANAGEMENT
A longitudinal examination of applicants to the air traffic control supervisory identification and development program
| DOT/FAA/AM-92/16 | p 2796 N93-25213
Exploring the link between intrinsic motivation and quality
| AD-A261722 | p 2722 N93-26246
PERSONNEL SELECTION
Contribution of personality to the prediction of success in initial air traffic control specialist training
| DOT/FAA/AM-93/4 | p 2797 N93-26138
PERTURBATION
Robust controls with structured perturbations
| NASA-CR-192956 | p 2817 N93-24757
Parametric analysis of atmospheric processes
| NASA-CR-192523 | p 2770 N93-25086
Boundary plasma modelling for ITER
| DE93-007963 | p 2859 N93-25302
Cellular and tissue injury during nonfreezing cold injury and frostbite
| AD-A260574 | p 2795 N93-25900
Synthetic-perturbation tuning of MIMD programs
| PB93-161339 | p 2812 N93-26321
PERTURBATION THEORY
Biped control via nonlinear dynamics p 2718 N93-25697
PETROGRAPHY
Geochemistry and petrology of primitive achondrite meteorites LEW 88280, MAC 88177, ALHA 81187, EET 84302, and LEW 88663 p 2896 N93-26067
PETROLOGY
Geochemistry and petrology of primitive achondrite meteorites LEW 88280, MAC 88177, ALHA 81187, EET 84302, and LEW 88663 p 2896 N93-26067
PHASE CHANGE MATERIALS
Far infrared spectra of amorphous and crystalline water ice and changes in these phases as the result of proton irradiation
| NASA-CR-192849 | p 2892 N93-25230
PHASE CONJUGATION
1992 technical digest series volume 16. Conference edition: Summaries of papers presented at the Nonlinear Dynamics in Optical Systems Topical Meeting
| AD-A261915 | p 2857 N93-26544
PHASE CONTROL
Experimental results of the performance of the new phase and frequency controller p 2839 N93-25035
Phase discriminating capacitive array sensor system
| NASA-CASE-GSC-13460-1 | p 2691 N93-26104
Improvements in X-band transmitter phase stability through Klystron body temperature regulation p 2678 N93-26114
PHASE DEVIATION
Performance results of a 300-degree linear phase modulator for spaceborne communications applications p 2672 N93-24670
PHASE DIAGRAMS
New ground states in unconventional superconductors p 2688 N93-25282
Sputter deposition of yttrium-oxides
| DE93-007499 | p 2654 N93-25382
PHASE LOCKED SYSTEMS
A microcomputer compensated crystal oscillator MCXO p 2834 N93-25001
Experimental results of the performance of the new phase and frequency controller p 2839 N93-25035
PHASE MODULATION
Performance results of a 300-degree linear phase modulator for spaceborne communications applications p 2672 N93-24670
Advanced optical fiber communication systems
| AD-A261802 | p 2856 N93-26256
PHASE SHIFT
Stability of nonlinear phase motion from the study of oscillator mappings p 2693 N93-25034
Microwave interrogation frequency noise and clock frequency stability: Experimental results p 2842 N93-25056
Advanced technology development multi-color holography
| NASA-CR-192451 | p 2711 N93-26154
PHASE SHIFT KEYING
Implementation of cyclic spectral analysis methods
| AD-A261715 | p 2681 N93-26372
Trellis coded CPFSK
| AD-A261788 | p 2682 N93-26441
PHASE TRANSFORMATIONS
Coarsening of a quiescent electrorheological fluid I: Experiment
| DE93-006776 | p 2642 N93-24972
Far infrared spectra of amorphous and crystalline water ice and changes in these phases as the result of proton irradiation
| NASA-CR-192849 | p 2892 N93-25230
The nature of the glass transition and its determination by thermal analysis
| DE93-006746 | p 2654 N93-25374
Solidification processing and phase transformations in ordered high temperature alloys
| AD-A261751 | p 2652 N93-26284
Position sensitive atom probe study of the decomposition of a Cu-2.6 at. percent Co alloy
| DE93-006737 | p 2653 N93-26500
Computation of complex solidification morphologies using a phase-field model
| PB93-156743 | p 2869 N93-26547
PHASE VELOCITY
An experimental study of particle-laden jet interactions with cocurrent flows p 2701 N93-25534
PHASED ARRAYS
Ka-band feed arrays for spacecraft reflector antennas with limited scan capability: An overview p 2680 N93-26128
Ultraviolet waveguide lasers for phased array lidar
| AD-A261657 | p 2715 N93-26363
Microstrip antennas on/in anisotropic material layers
| AD-A261700 | p 2681 N93-26383
PHENOLS
The surface characterization of a series of hydroxybenzenes on Ag(111): An EELS and TDS study
| DE93-007541 | p 2647 N93-26595
PHENOMENOLOGY
Efficient generation of synthetic terrain imagery for automatic target recognition
| AD-A260705 | p 2756 N93-25653
PHENYLS
Intramolecular bridge/terminal oxo exchange within (MoV2O3) (4+) complexes containing linear oxo bridges
| AD-A261230 | p 2851 N93-26518
PHONEMES
Perception and the temporal properties of speech
| AD-A261439 | p 2686 N93-26490
PHONEMICS
Perception and the temporal properties of speech
| AD-A261439 | p 2686 N93-26490
PHONETICS
Speech research
| AD-A260643 | p 2675 N93-25639
PHOSPHATES
Comparison of energy trapping resonators and filters using the AT cut of quartz, berlinite and gallium phosphate p 2836 N93-25013
Crystal growth of berlinite: Methods for growing longer crystals and improving the quality p 2838 N93-25025
Controlled dissolution of a piezoelectric material berlinite (AlPO4) p 2840 N93-25043
In situ surface studies of conversion coatings for steel and aluminum
| AD-A261016 | p 2655 N93-25861
PHOSPHORUS
Inorganic nitrogen and phosphorus dynamics in the water column of the Patuxent River
| PB93-172955 | p 2767 N93-26511
PHOTOCHEMICAL REACTIONS
Atmospheric reactive nitrogen oxides and their relationship with urban and rural ozone formation p 2760 N93-24908
A study of vibrationally excited N2(+) ions in the daytime thermosphere p 2770 N93-25179
The role of multiple scattering in twilight zenith sky observations of atmospheric absorbers: Diurnal photochemistry and airmass factors p 2772 N93-25535
Reclamation with recovery of radionuclides and toxic metals from contaminated materials, soils, and wastes p 2769 N93-25571
The Martian lower atmosphere p 2897 N93-26394
PHOTOCONDUCTIVITY
The DX centers in three to five semiconductors under hydrostatic pressure
| DE93-007701 | p 2864 N93-25490
Photomodulation spectroscopy of photocarrier dynamics, electronic defects and morphology of conducting polymers
| DE93-010140 | p 2655 N93-25524
PHOTODETACHMENT
Dynamics of collision processes
| DE93-007143 | p 2849 N93-25509
Penning detachment: A new frontier
| AD-A261447 | p 2850 N93-26346

PHOTODIODES
Ultrafast measurements of 200 gigahertz Schottky photodiodes p 2688 N93-25392
Studies of avalanche photodiodes for scintillating fibre tracking readout
| DE93-008370 | p 2689 N93-25491
Optical characterization of Ga(1-x)In(x)As(y)Sb(1-y)/GaSb alloy and device application
| AD-A261713 | p 2870 N93-26581
PHOTODISSOCIATION
Surface discharge photoinitiation of pulsed chemical lasers
| DE93-006337 | p 2712 N93-24967
Ionization probes of molecular structure and chemistry
| DE93-008211 | p 2847 N93-25310
PHOTOELECTRIC EMISSION
Kinetic studies of interfacial photocurrents in platinized chloroplasts
| DE93-002344 | p 2792 N93-25104
Laser field assisted photoemission using femtosecond laser pulses
| DE93-007277 | p 2712 N93-25378
Accurate determination of Auger line shape binding energies
| AD-A261803 | p 2868 N93-26258
PHOTOELECTRON SPECTROSCOPY
Ionization probes of molecular structure and chemistry
| DE93-008211 | p 2847 N93-25310
Analysis of the gap in high-temperature superconductors using photoemission spectroscopy p 2865 N93-25744
The interaction of HCN/DCN with Si(100)-2x1
| AD-A260837 | p 2645 N93-25920
Interaction of O2 with the Fe(.84)Cr(.16) (001) surface studied by photoelectron spectroscopy
| AD-A261065 | p 2645 N93-26251
Bimolecular reaction dynamics from photoelectron spectroscopy of negative ions
| DE93-007669 | p 2647 N93-26599
PHOTOELECTRONS
Bimolecular reaction dynamics from photoelectron spectroscopy of negative ions
| DE93-007669 | p 2647 N93-26599
PHOTOEXCITATION
Photoexcitation of carbon fullerenes
| AD-A260739 | p 2849 N93-25644
PHOTOGRAPHIC EQUIPMENT
Photographic industry and electronic imaging: The emergence of electronic still photography
| PB93-169399 | p 2711 N93-26324
PHOTOGRAPHS
Cape Photographic Durchmusterung, volume 1
| NASA-RP-1300-VOL-1 | p 2890 N93-26002
Cape Photographic Durchmusterung, volume 2
| NASA-RP-1300-VOL-2 | p 2890 N93-26003
Cape Photographic Durchmusterung, volume 3
| NASA-RP-1300-VOL-3 | p 2890 N93-26004
Photographic industry and electronic imaging: The emergence of electronic still photography
| PB93-169399 | p 2711 N93-26324
PHOTOGRAPHY
Fast diagnostics of laser ablation used for pulsed laser deposition
| DE93-005155 | p 2713 N93-25508
The Taurid meteoroid complex p 2889 N93-25536
Photographic industry and electronic imaging: The emergence of electronic still photography
| PB93-169399 | p 2711 N93-26324
PHOTOINTERPRETATION
The photointerpretation of the area taken over from agriculture by intense urbanization at Villabate (Palermo, Italy) p 2742 N93-24800
Hel's peninsula coastal zone changes in the last 40 years on a base of remote sensing methods p 2747 N93-24832
Interpretation and segmentation of changed forest stands from difference imagery based on regression functions p 2748 N93-24839
Tropical forest monitoring with high resolution satellite data p 2748 N93-24841
Aerial photographic sampling for statewide resource inventory p 2755 N93-25441
PHOTOIONIZATION
Energy transfer properties and mechanisms
| DE93-008540 | p 2849 N93-25488
Photoexcitation of carbon fullerenes
| AD-A260739 | p 2849 N93-25644
PHOTOLUMINESCENCE
Photoluminescence of silicon nanostructures formed by ion beam implantation
| DE93-006777 | p 2862 N93-24958
Analysis of transient photoluminescence measurements on GaAs and AlGaAs double heterostructures
| AD-A261154 | p 2867 N93-25947
Visible light emission from porous silicon examined by photoluminescence and Raman spectroscopy
| DE93-006780 | p 2646 N93-26502
PHOTOLUMINESCENT BANDS
Optical characterization of Ga(1-x)In(x)As(y)Sb(1-y)/GaSb alloy and device application
| AD-A261713 | p 2870 N93-26581
PHOTOMAPPING
US Army evaluation of the Electronic Map Data (EMD) prototype
| AD-A261693 | p 2757 N93-26369
PHOTOMETERS
Apparatus for imaging an object in or through a scattering medium using coherent anti-Stokes Raman scattering
| AD-D015642 | p 2852 N93-25358
Laser physics and laser techniques
| AD-A261595 | p 2715 N93-26524
PHOTOMETRY
Topography from shading and stereo p 2879 N93-25803
PHOTON BEAMS
Preliminary design of the BPM electronics memory scanner/dual boxcar averager for the advanced photon source
| DE93-007893 | p 2848 N93-25368
Poster session: Fifth Users Meeting for the Advanced Photon Source
| DE93-006019 | p 2598 N93-26498
PHOTONICS
Optical computing, Volume 6: Organization of the Optical Society of America photonic science topical meeting series
| AD-A261267 | p 2856 N93-26266
PHOTONS
Correlative studies of astrophysical sources of very high and ultra high energy gamma-rays
| NASA-CR-192781 | p 2888 N93-25172
Preliminary design of the BPM electronics memory scanner/dual boxcar averager for the advanced photon source
| DE93-007893 | p 2848 N93-25368
PHOTOSPHERE
Photospheric abundance analysis of low-mass pre-main sequence stars p 2894 N93-25623
PHOTOSYNTHESIS
Kinetic studies of interfacial photocurrents in platinized chloroplasts
| DE93-002344 | p 2792 N93-25104
PHOTOTUBES
The sub 60 ps timing resolution using large area silicon avalanche diodes
| DE93-007723 | p 2688 N93-25365
PHOTOVOLTAIC CELLS
Research on stable, high-efficiency amorphous silicon multijunction modules
| DE93-000072 | p 2862 N93-25163
Role of polycrystallinity in CdTe and CuInSe2 photovoltaic cells
| DE93-000045 | p 2759 N93-25504
PHOTOVOLTAIC CONVERSION
An inverted AlGaAs/GaAs patterned-Ge tunnel junction cascade concentrator solar cell
| DE93-000073 | p 2759 N93-25102
Laser beamed power: Satellite demonstration applications
| NASA-CR-190793 | p 2623 N93-25132
Film fabrication technologies at NREL p 2658 N93-25563
Photovoltaic power without batteries for continuous cathodic protection p 2759 N93-25597
PHTHALOCYANIN
Macromolecules for inhibition of corrosion and wear
| AD-A261041 | p 2655 N93-25816
New directions in phthalocyanine pigments
| NASA-CR-192443 | p 2656 N93-26155
PHYSICAL EXERCISE
Utilization of the graded universal testing system to increase the efficiency for assessing aerobic and anaerobic capacity p 2794 N93-26077
Combined strength and endurance training: Functional and morphological adaptations to ten weeks of training
| AD-A261059 | p 2802 N93-26229
PHYSICAL FITNESS
Combined strength and endurance training: Functional and morphological adaptations to ten weeks of training
| AD-A261059 | p 2802 N93-26229
PHYSICAL OPTICS
ILS mathematical modeling study of an ILS glide slope proposed for runway 19L at the Meridian Naval Air Station, Mississippi
| DOT/FAA/CT-TN93/8 | p 2584 N93-24741
Optimizing the G/T ratio of the DSS-13 34-meter beam-waveguide antenna p 2678 N93-26118
PHYSIOLOGICAL EFFECTS
The acute inhalation toxicity of pyrolysis products of halon 1301
| AD-A260874 | p 2795 N93-25629
AFRRI research, fiscal year 1991
| AD-A260933 | p 2911 N93-25710
PHYSIOLOGICAL RESPONSES
Autonomic physiological data associated with simulator discomfort
| NASA-CR-177609 | p 2794 N93-24738
JPRS report: Science and technology. Central Eurasia: Life sciences
| JPRS-ULS-92-022 | p 2795 N93-25407
AFRRI research, fiscal year 1991
| AD-A260933 | p 2911 N93-25710
Metabolic response of environmentally isolated microorganisms to industrial effluents: Use of a newly described cell culture assay p 2794 N93-26066
PHYSIOLOGY
Autonomic physiological data associated with simulator discomfort
| NASA-CR-177609 | p 2794 N93-24738
Anatomy and physiology of plant conductive systems
| PB93-156032 | p 2793 N93-25877
Entropy reduction via simplified image contourization p 2804 N93-25924
Investigation into the common mode rejection ratio of the physiological signal conditioner circuit p 2794 N93-26073
Physiological indices of mental workload
| AD-A261692 | p 2798 N93-26391
PHYTOPLANKTON
Relations between blue whiting biomass and satellite derived phytoplankton and temperature in the Norwegian Sea
| AD-A261205 | p 2757 N93-25868
PICOSECOND PULSES
Spectra of stable sonoluminescence
| AD-A260621 | p 2844 N93-25637
Laser physics and laser techniques
| AD-A261595 | p 2715 N93-26524
PIEZOELECTRIC CERAMICS
Passive vibration damping materials: Piezoelectric ceramics composites for vibration damping applications
| AD-A260792 | p 2727 N93-25690
Damage detection and mitigation of composite structures using smart materials
| AD-A261121 | p 2639 N93-25945
PIEZOELECTRIC CRYSTALS
The measurement of the resonant frequency of quartz crystal units: An ongoing saga p 2833 N93-24996
Crystal growth of berlinite: Methods for growing longer crystals and improving the quality p 2838 N93-25025
Controlled dissolution of a piezoelectric material berlinite (AlPO4) p 2840 N93-25043
Crystal growth and physical characterizations of GaPO4 p 2840 N93-25044
IR materials producibility
| AD-A261099 | p 2853 N93-25766
PIEZOELECTRICITY
Monolithic quartz vibrating beam accelerometer p 2711 N93-25011
The third-order permittivity of quartz obtained by different methods p 2840 N93-25046
Novel approaches to the construction of miniaturized analytical instrumentation
| NASA-CR-191988 | p 2709 N93-25345
Damage-survivable and damage-tolerant laminated composites with optimally placed piezoelectric layers
| AD-A260879 | p 2636 N93-25631
Damage detection and mitigation of composite structures using smart materials
| AD-A261121 | p 2639 N93-25945
Smart structural composites with piezoelectric micro-constituents
| AD-A260970 | p 2640 N93-26225
Investigation of coupled analysis techniques for adaptive material structural systems
| AD-A261359 | p 2868 N93-26332
PIGMENTS
New directions in phthalocyanine pigments
| NASA-CR-192443 | p 2656 N93-26155
PILOT ERROR
Aircraft accident report: Tomy International, Inc., d/b/a Scenic Air Tours flight 22, Beech Model E18S, N342E in-flight collision with terrain, Mount Haleakala, Maui, Hawaii, 22 April 1992
| PB93-910401 | p 2583 N93-25827
PILOT PERFORMANCE
Perceptual factors that influence use of computer enhanced visual displays
| NASA-CR-192961 | p 2811 N93-26150
PILOT SELECTION
Performance-based testing and success in Naval advanced flight training
| AD-A260838 | p 2590 N93-25933

PILOTLESS AIRCRAFT
A preliminary sizing method for unmanned aircraft using multi-variate optimisation p 2587 N93-25408
PILOTS
Aircraft accident report: Tomy International, Inc., d/b/a Scenic Air Tours flight 22, Beech Model E18S, N342E in-flight collision with terrain, Mount Haleakala, Maui, Hawaii, 22 April 1992
| PB93-910401 | p 2583 N93-25827
PINHOLE CAMERAS
Intensity distribution of the x ray source for the AXAF VETA-I mirror test p 2854 N93-26184
PINHOLES
Plasma sheath effects on ion collection by a pinhole
| NASA-TM-106098 | p 2615 N93-25090
PIONS
Notes on radial drift for dalitz detection
| DE93-006971 | p 2846 N93-24959
High-energy pion-nucleus scattering at LAMPF
| DE93-007364 | p 2852 N93-25380
PIPE FLOW
Predictive modeling of particle-laden, turbulent flows
| DE93-008208 | p 2698 N93-25309
Modeling of bubble and drop formation in flowing liquids in terrestrial and microgravity environments p 2664 N93-25390
Dynamics of turbulent slugging in transitional pipe flow p 2702 N93-25548
Flow conditioner location effects in orifice flowmeters
| PB93-159457 | p 2708 N93-26535
PIPELINES
Tank issues: Design and placement of vapor monitoring wells
| PB93-161131 | p 2768 N93-26536
PIPES (TUBES)
Detecting damaged cables using a preionized gas technique
| DE93-007588 | p 2689 N93-25429
PISTON ENGINES
A preliminary sizing method for unmanned aircraft using multi-variate optimisation p 2587 N93-25408
Evaluation of the Migrating Combustion Chamber (MCC) engine
| AD-A260780 | p 2718 N93-25682
Improved selective catalytic NOx control technology for compressor station reciprocating engines
| PB93-158566 | p 2768 N93-26529
PITTING
Laser initiated corrosion pits on aluminum p 2650 N93-25464
Evaluation of a vibration diagnostic system for the detection of spur gear pitting failures
| NASA-TM-106103 | p 2718 N93-25672
PIXELS
The sub 60 ps timing resolution using large area silicon avalanche diodes
| DE93-007723 | p 2688 N93-25365
Monolithic integration of semiconductor and superconductor components
| AD-A260589 | p 2690 N93-25906
High-performance compression of astronomical images p 2805 N93-25931
Multi-rate, real time image compression for images dominated by point sources p 2805 N93-25932
PLANAR STRUCTURES
Multichip module high speed testing
| AD-A261391 | p 2856 N93-26306
PLANE STRAIN
Continuum and micromechanics treatment of constraint in fracture
| AD-A260927 | p 2727 N93-25647
PLANETARY ATMOSPHERES
Construction of an advanced software tool for planetary atmospheric modeling p 2815 N93-25799
Planetary data analysis and display system: A version of PC-McIDAS p 2880 N93-25806
PLANETARY BOUNDARY LAYER
Atmospheric reactive nitrogen oxides and their relationship with urban and rural ozone formation p 2760 N93-24908
Thermal infrared radiation transfer in the planetary boundary layer p 2772 N93-25688
Boundary layer coupling between an explosive cyclone and the Gulf Stream during ERICA
| AD-A261577 | p 2787 N93-26513
PLANETARY COMPOSITION
The Martian lower atmosphere p 2897 N93-26394
PLANETARY GRAVITATION
V-GRAM: Magellan bulletin about Venus and the radar mapping mission
| NASA-CR-192923 | p 2898 N93-26424
PLANETARY IONOSPHERES
Occultation of a compact radio source by Venus p 2676 N93-26107
The upper atmosphere and ionosphere of Mars p 2897 N93-26393
PLANETARY MASS
The Martian lower atmosphere p 2897 N93-26394
PLANETARY RADIATION
The Venus 130-nm dayglow as a diagnostic of thermospheric structure and dynamics p 2896 N93-25285
PLANETARY SURFACES
Neutron energy determination with a high-purity germanium detector
| NASA-CR-192773 | p 2900 N93-25890
PLANETARY WAVES
Interaction of an eddy with a continental slope
| AD-A261550 | p 2791 N93-26578
PLANKTON
The continuous plankton recorder survey: A long-term, basin-scale oceanic time series p 2736 N93-24937
PLANNING
Using neural networks and Dyna algorithm for integrated planning, reacting and learning in systems
| NASA-CR-193018 | p 2817 N93-24743
PLASMA ARC WELDING
Robotic Variable Polarity Plasma Arc (VPPA) welding p 2720 N93-25605
PLASMA CONTROL
Density dependence of line intensities and application to plasma diagnostics
| NIFS-209 | p 2857 N93-24950
Assessment of torsatrons as reactors
| DE93-006721 | p 2858 N93-24969
Boundary plasma modelling for ITER
| DE93-007963 | p 2859 N93-25302
Simulation study of MHD dynamo: Convection in a rotating spherical shell
| NIFS-207 | p 2860 N93-25356
PLASMA COOLING
Liquid and solid ion plasmas
| AD-A261888 | p 2862 N93-26528
PLASMA CURRENTS
TSC plasma halo simulation of a D3-D vertical displacement episode
| DE93-008688 | p 2860 N93-25493
Plasma current collection of Z-93 thermal control paint as measured in the Lewis Research Center's plasma interaction facility
| NASA-TM-106132 | p 2618 N93-26215
PLASMA DENSITY
Density dependence of line intensities and application to plasma diagnostics
| NIFS-209 | p 2857 N93-24950
Study of auroral dynamics with combined spacecraft and incoherent-scatter radar data
| NASA-CR-192224 | p 2775 N93-26159
Liquid and solid ion plasmas
| AD-A261888 | p 2862 N93-26528
PLASMA DIAGNOSTICS
Density dependence of line intensities and application to plasma diagnostics
| NIFS-209 | p 2857 N93-24950
Diagnostics of diamond film deposition plasmas
| AD-A260866 | p 2860 N93-25626
Direct measurement of velocity space transport in a plasma p 2861 N93-25831
IR and FIR laser diagnostics for plasma thrusters using a CW CO2 radiation source
| AD-A261399 | p 2862 N93-26520
PLASMA DISPLAY DEVICES
Emerging large-screen display technology
| AD-A261066 | p 2681 N93-26241
PLASMA DRIFT
Direct measurement of velocity space transport in a plasma p 2861 N93-25831
PLASMA DYNAMICS
IR and FIR laser diagnostics for plasma thrusters using a CW CO2 radiation source
| AD-A261399 | p 2862 N93-26520
PLASMA ENGINES
Stationary plasma thruster evaluation in Russia
| NASA-CR-192823 | p 2859 N93-25206
Anode power deposition in coaxial MPD thrusters p 2623 N93-25665
IR and FIR laser diagnostics for plasma thrusters using a CW CO2 radiation source
| AD-A261399 | p 2862 N93-26520
Preliminary investigation of power flow and electrode phenomena in a multi-megawatt coaxial plasma thruster
| NASA-CR-191084 | p 2633 N93-26555
PLASMA HEATING
Plasma heating in toroidal systems
| NIFS-208 | p 2858 N93-25092
An outgoing energy flux boundary condition for finite difference ICRP antenna models
| DE93-007788 | p 2674 N93-25300
Thermal and electric oscillation driven by orbit loss in helical systems
| NIFS-213 | p 2860 N93-25346
PLASMA INTERACTIONS
The interaction of high voltage systems with the environments of the Moon and Mars
| NASA-TM-106107 | p 2618 N93-26148
Plasma current collection of Z-93 thermal control paint as measured in the Lewis Research Center's plasma interaction facility
| NASA-TM-106132 | p 2618 N93-26215
The upper atmosphere and ionosphere of Mars p 2897 N93-26393
PLASMA JETS
Metal ion implantation for large scale surface modification
| DE93-007649 | p 2859 N93-25324
Investigations of the transient behavior of the cathode fall region in planar and hollow cathodes
| AD-A261636 | p 2691 N93-26171
PLASMA LAYERS
Modeling of plasma flow switches at low, intermediate and high energies
| DE93-007359 | p 2858 N93-25167
PLASMA OSCILLATIONS
Thermal and electric oscillation driven by orbit loss in helical systems
| NIFS-213 | p 2860 N93-25346
PLASMA PHYSICS
Simulation study of MHD dynamo: Convection in a rotating spherical shell
| NIFS-207 | p 2860 N93-25356
JPRS report: Science and technology. Central Eurasia: Physics and mathematics
| JPRS-UPM-92-004 | p 2844 N93-25402
JPRS report: Science and technology. Central Eurasia: Physics and mathematics
| JPRS-UPM-92-003 | p 2844 N93-25403
JPRS report: Science and technology. Central Eurasia: Physics and mathematics
| JPRS-UPM-93-001 | p 2844 N93-25404
PLASMA PROPULSION
Preliminary investigation of power flow and electrode phenomena in a multi-megawatt coaxial plasma thruster
| NASA-CR-191084 | p 2633 N93-26555
PLASMA SHEATHS
Plasma sheath effects on ion collection by a pinhole
| NASA-TM-106098 | p 2615 N93-25090
PLASMA TEMPERATURE
Ion temperature measurements in the Maryland Spheromak p 2859 N93-25290
Study of auroral dynamics with combined spacecraft and incoherent-scatter radar data
| NASA-CR-192224 | p 2775 N93-26159
PLASMA WAVES
The generation of Langmuir waves by thick target electron beams in solar flares p 2861 N93-25730
PLASMA-PARTICLE INTERACTIONS
Alfven wave transport effects in the time evolution of parallel cosmic-ray modified shocks
| NASA-CR-192932 | p 2899 N93-25161
Two-stream instability for a light ion beam-plasma system with external magnetic field
| NIFS-204 | p 2859 N93-25248
PLASMAS (PHYSICS)
Time dependent simulation of cosmic-ray shocks including Alfven transport
| NASA-CR-192931 | p 2899 N93-24752
Modeling of plasma flow switches at low, intermediate and high energies
| DE93-007359 | p 2858 N93-25167
A compact neutron counter telescope with thick radiator (Cotetra) for fusion experiment
| NIFS-205 | p 2860 N93-25347
Application of non-thermal plasmas to pollution control
| DE93-007515 | p 2763 N93-25385
TSC plasma halo simulation of a D3-D vertical displacement episode
| DE93-008688 | p 2860 N93-25493
Liquid and solid ion plasmas
| AD-A261888 | p 2862 N93-26528
Treatment of hazardous organic wastes using silent discharge plasmas
| DE93-003789 | p 2768 N93-26592
PLASMONS
The interaction of swift electrons with surface excitations
| DE93-007245 | p 2848 N93-25376
PLASTIC DEFORMATION
Internal stresses and the cyclic deformation of an aluminum matrix composite p 2650 N93-25436
Finite element micromechanics modeling of inelastic deformation of unidirectionally fiber-reinforced composites p 2637 N93-25680
On the stability of finite plastic deformations
| AD-A261526 | p 2730 N93-26361
Defect initiation/growth and energy dissipation induced by deformation and fracture
| AD-A261703 | p 2869 N93-26385

PLASTIC PROPERTIES
A micromechanical viscoplastic stress-strain model with grain boundary sliding
| DE93-009109 | p 2649 N93-25095
Inelastic behavior of thermoplastic composites
p 2636 N93-25674
Transformation plasticity and fracture behavior of ceria-TZP/alumina composites p 2638 N93-25760
Polyimides with improved compression moldability
| NASA-CASE-LAR-14457-1 | p 2656 N93-25997

PLASTICS
New directions in phthalocyanine pigments
| NASA-CR-192443 | p 2656 N93-26155
Extruded films from modified polypropylene resin: Dielectric and breakdown studies
| AD-A261382 | p 2657 N93-26341

PLATE THEORY
Vibration, buckling, and postbuckling of laminated composites with delaminations p 2723 N93-24765
On existence of solutions and duality for a model of non-linear elastic plates with transverse shear deformations p 2726 N93-25437
Numerical simulation of damage and progressive failures in composite laminates using the layerwise plate theory
p 2636 N93-25661

PLATELETS
A new approach to cooled combustion chambers: The 40K formed platelet chamber p 2626 N93-26018

PLATES (STRUCTURAL MEMBERS)
Vibration, buckling, and postbuckling of laminated composites with delaminations p 2723 N93-24765
Damage-survivable and damage-tolerant laminated composites with optimally placed piezoelectric layers
| AD-A260879 | p 2636 N93-25631
A three-dimensional model for the residual stresses in a unidirectional composite plate p 2728 N93-25825

PLOWING
Registration of the use of agricultural fields and soil erosion using satellite remote sensing
p 2751 N93-24856

PLUMES
Experimentation in the low-density plume of a simulated electrothermal thruster for computer code validation
| NASA-CR-191112 | p 2622 N93-24758
The AFTAC model integration project
| DE93-003334 | p 2761 N93-25122
Particle behavior in solid propellant rocket motors and plumes
| AD-A260900 | p 2624 N93-25913
SRB environment evaluation and analysis. Volume 3: ASRB plume induced environments
| NASA-CR-192519 | p 2631 N93-26054
Molecular interactions and properties with many-body methods
| AD-A261688 | p 2850 N93-26367
Measurement and analysis of a small nozzle plume in vacuum
| NASA-TM-106066 | p 2633 N93-26561

PNEUMATIC EQUIPMENT
Pneumatic actuator with hydraulic control
| AD-D015652 | p 2719 N93-26244

POINT DEFECTS
Surface diffusion studies by optical diffraction techniques
| DE93-007707 | p 2853 N93-25550
IR materials producibility
| AD-A261099 | p 2853 N93-25766
Gordon Conference on Point Defects, Line Defects and Interfaces in Semiconductors
| AD-A261485 | p 2868 N93-26357

POINT SOURCES
Shells, outflows and star formation in the giant molecular cloud Monoceros R2 p 2893 N93-25555
Multi-rate, real time image compression for images dominated by point sources p 2805 N93-25932

POINTING CONTROL SYSTEMS
The Hubble Space Telescope fine guidance system operating in the coarse track pointing control mode
p 2605 N93-24724
Applications of inertial-sensor high-inheritance instruments to DSN precision antenna pointing
p 2621 N93-26112

POINTS (MATHEMATICS)
Integrated approaches to parallelism in optimization and the solution of inverse problems
| AD-A261490 | p 2829 N93-26344

POLAND
Application of remote sensing to environmental monitoring in Poland p 2739 N93-24786

POLAR COORDINATES
Polar decomposition for attitude determination from vector observations p 2602 N93-24711

POLAR REGIONS
A climatology of polar low occurrences in the Nordic Seas and an examination of katabatic winds as a triggering mechanism
| AD-A261719 | p 2786 N93-26245

POLARIMETRY
The use of polarimetric multifrequency SAR for characterizing terrain classes p 2738 N93-24777
The scope of DLR's SAR calibration program
p 2738 N93-24778
The use of polarimetric radar remote sensing data for application in forestry p 2749 N93-24845
Selected results from LLNL-Hughes RAR for West Coast Scotland Experiment 1991
| DE93-006972 | p 2788 N93-24960

POLARIZATION (WAVES)
The use of polarimetric multifrequency SAR for characterizing terrain classes p 2738 N93-24777

POLARIZATION CHARACTERISTICS
Polarizing Michelson interferometer for measuring thermospheric winds
| ISBN-0-315-70442-X | p 2784 N93-25731

POLARIZED ELECTROMAGNETIC RADIATION
Lightning precursor signatures from dual-polarization radar measurements of storms p 2777 N93-24877
Recent experiments on spin physics in high energy hadron interactions
| DE93-007900 | p 2851 N93-25301

POLICIES
Political and institutional factors affecting systems engineering p 2666 N93-24690
Science, technology, and national security
p 2886 N93-25232
Environmental risks and future generations: Criteria for public policy
| DE93-004691 | p 2764 N93-25443
Functional Economic Analysis Guidebook, version 1.1
| AD-A261390 | p 2886 N93-26305
Guidelines for evaluating and expressing the uncertainty of NIST measurements results
| PB93-159465 | p 2830 N93-26318

POLISHING
Surface preparation and characterization of a 400 micrometer diameter fused silica optical fiber for direct optical initiation (DOI) applications
| DE93-005485 | p 2852 N93-25182
Ultrasonic polishing p 2670 N93-25580

POLITICS
Political and institutional factors affecting systems engineering p 2666 N93-24690
Organizational politics, participation in decision-making, and job satisfaction
| DOT/FAA/AM-92/17 | p 2796 N93-25203

POLLUTION CONTROL
SIHTI: The research and development program of energy and environmental technology
| DE93-769925 | p 2763 N93-25360
Application of non-thermal plasmas to pollution control
| DE93-007515 | p 2763 N93-25385
An experimental study of particle-laden jet interactions with cocurrent flows p 2701 N93-25534
Converting environmental wastes into valuable resources p 2759 N93-25572
Space life support technology applications to terrestrial environmental problems p 2803 N93-25617
Pollution prevention 1991: Progress on reducing industrial pollutants
| PB93-157725 | p 2766 N93-25875
Development and demonstration of a new filter system to control emissions during jet engine testing
| AD-A261203 | p 2766 N93-26243
Improved selective catalytic NOx control technology for compressor station reciprocating engines
| PB93-158566 | p 2768 N93-26529

POLLUTION MONITORING
Remote sensing monitoring and hindcasting of the accident occurred to the tanker Haven in the Gulf of Genoa (Italy) p 2747 N93-24830
Crop agroecological diagnostics by remote sensing technique p 2751 N93-24860
Efficient inspection of network pollution data
| DE93-003810 | p 2761 N93-25126
Using terrestrial plants in biomonitoring
| PB93-158780 | p 2766 N93-26316

POLLUTION TRANSPORT
Remote sensing monitoring and hindcasting of the accident occurred to the tanker Haven in the Gulf of Genoa (Italy) p 2747 N93-24830
Non-local description of pollution transport in random medium p 2763 N93-25329
Model for transport of floating debris in the ocean
| PB93-172997 | p 2768 N93-26559

POLYACETYLENE
Photomodulation spectroscopy of photocarrier dynamics, electronic defects and morphology of conducting polymers
| DE93-010140 | p 2655 N93-25524

POLYAMIDE RESINS
Polyimides with improved compression moldability
| NASA-CASE-LAR-14457-1 | p 2656 N93-25997

POLYATOMIC MOLECULES
Chemical dynamics studies of high energy species
| AD-A260743 | p 2852 N93-25676

POLYCRYSTALS
Laser Induced Phonons (LIPs) in MBE grown ZnSe
| RSRE-MEMO-4544 | p 2864 N93-25454
Method of joining diamond structures
| AD-D015671 | p 2867 N93-26140
Ir-Zr alloys as diffusion barriers between Cu and Si(100)
| AD-A261919 | p 2652 N93-26197

POLYESTERS
NMR studies of ion mobility and association in polyether-based polymer electrolytes
| AD-A260662 | p 2655 N93-25642

POLYETHYLENES
A model for the filling of cold cavities with solidifying, semi-crystalline polymers
| DE93-003817 | p 2655 N93-25507
Thermodynamic, kinetic, and structural properties of linear polyethylene crystallized from polymer-diluent mixture p 2864 N93-25528

POLYIMIDES
Polyimides with improved compression moldability
| NASA-CASE-LAR-14457-1 | p 2656 N93-25997
Polyimides containing the cyclobutene-3,4-dione moiety
| NASA-CASE-LAR-14753-1 | p 2656 N93-25999

POLYMER CHEMISTRY
Polyimides with improved compression moldability
| NASA-CASE-LAR-14457-1 | p 2656 N93-25997
Characterization of the synthesis of M-61, a random equilibrium silicone terpolymer, using dry starting materials
| KCP-613-4985 | p 2657 N93-26213

POLYMER MATRIX COMPOSITES
Damage and failure analysis on continuous fiber-reinforced polymer composites
p 2637 N93-25716
Thermal expansion measurements of polymer matrix composites and syntactics
| MTL-TR-92-27 | p 2640 N93-25954
Japanese Technology Evaluation Center Workshop on Advanced Manufacturing Technology for Polymer Composite Structures in Japan
| PB93-165249 | p 2641 N93-26589

POLYMERIC FILMS
Novel approaches to the construction of miniaturized analytical instrumentation
| NASA-CR-191988 | p 2709 N93-25345
INEL spray-forming research p 2658 N93-25562
Duct protection coating concept development and test: Test specimen fabrication, conditioning, and testing documentation.
| AD-A261250 | p 2657 N93-26278
Extruded films from modified polypropylene resin: Dielectric and breakdown studies
| AD-A261382 | p 2657 N93-26341

POLYMERIZATION
Polymers by non-redox processes: Synthesis, physical studies, and application
| AD-A261064 | p 2657 N93-26240

POLYMERS
Temperature dependent sensor response caused by polymer-solvent interactions
| DE93-005368 | p 2655 N93-25444
Thermodynamic, kinetic, and structural properties of linear polyethylene crystallized from polymer-diluent mixture p 2864 N93-25528
Models of crack growth along polymer interfaces
p 2728 N93-25750
Characterization of the synthesis of M-61, a random equilibrium silicone terpolymer, using dry starting materials
| KCP-613-4985 | p 2657 N93-26213
European tri-service advanced materials workshop on compressive strength in rigid-rod polymers
| AD-A261517 | p 2658 N93-26576

POLYNOMIALS
The analysis of convolutional codes via the extended Smith algorithm p 2671 N93-24664
Stability margins for multilinear interval systems by way of phase conditions: A unified approach
| NASA-CR-192893 | p 2819 N93-25226

POLYPROPYLENE
Extruded films from modified polypropylene resin: Dielectric and breakdown studies
| AD-A261382 | p 2657 N93-26341

POLYSILANES
Photomodulation spectroscopy of photocarrier dynamics, electronic defects and morphology of conducting polymers
| DE93-010140 | p 2655 N93-25524
POLYSTATION DOPPLER TRACKING SYSTEM
Precise Doppler tracking from the Medicina VLBI station p 2608 N93-24998
POPULATIONS
Biodiversity indication by Earth observation data p 2751 N93-24858
POROSITY
The modeling of complex continua: Fundamental obstacles and grand challenges
| DE93-006507 | p 2696 N93-25193
Novel approaches to the construction of miniaturized analytical instrumentation
| NASA-CR-191988 | p 2709 N93-25345
Computation of transonic flow over a porous surface projectile p 2577 N93-25409
POROUS MATERIALS
The modeling of complex continua: Fundamental obstacles and grand challenges
| DE93-006507 | p 2696 N93-25193
Visible light emission from porous silicon examined by photoluminescence and Raman spectroscopy
| DE93-006780 | p 2646 N93-26502
PORTABLE EQUIPMENT
Commercial Precipitation Static (P-static) test equipment p 2711 N93-24901
PORTABLE LIFE SUPPORT SYSTEMS
The properties of and analytical methods for detection of LiOH and Li2CO3
| NASA-CR-192771 | p 2643 N93-25240
Composite materials for the extravehicular mobility unit p 2642 N93-26060
POSEIDON SATELLITE
Orbit determination support of the Ocean Topography Experiment (TOPEX)/Poseidon operational orbit p 2601 N93-24704
POSITION (LOCATION)
DORIS precise orbit determination and location system performances of ultra stable oscillators p 2608 N93-24997
Analytical techniques for improved time transfer using common view of direct broadcasting satellites p 2835 N93-25008
An experimental health monitoring unit for GPS and GLONASS p 2586 N93-25018
Collaboration in the UK on time transfer using the GLONASS system p 2837 N93-25019
Optimal finite-thrust time-bounded direct-ascent interception p 2607 N93-25272
Firmware development improves system efficiency p 2807 N93-25606
Visualization of a Mach 2 reacting flow using Planar Laser-Induced Fluorescence (PLIF) p 2598 N93-26006
Flow conditioner location effects in orifice flowmeters
| PB93-159457 | p 2708 N93-26535
POSITION ERRORS
Star tracker operation in a high density proton field p 2600 N93-24699
TDRSS orbit determination using short baseline differenced carrier phase p 2601 N93-24701
First experience with the ASN-16 GLONASS receiver p 2693 N93-25033
POSITION INDICATORS
Observation of radiation from lightning discharges by LPATS p 2779 N93-24888
Log-ratio signal-processing technique for beam position monitors
| DE93-007356 | p 2851 N93-25314
System for calibrating a gyro navigator
| AD-D015668 | p 2586 N93-26093
POSITION SENSING
Method and apparatus for deflection measurements using eddy current effects
| NASA-CASE-GSC-13506-1 | p 2710 N93-26103
POSITIONING
Firmware development improves system efficiency p 2807 N93-25606
POSITIONING DEVICES (MACHINERY)
Preliminary design of the BPM electronics memory scanner/dual boxcar averager for the advanced photon source
| DE93-007893 | p 2848 N93-25368
Telerobotic rovers for extraterrestrial construction p 2670 N93-26416
POTASSIUM HYDRIDES
Laser damage to production- and research-grade KDP crystals
| DE93-007517 | p 2870 N93-26594
POTASSIUM HYDROXIDES
Temperature-dependent electrical conductivity of soda-lime glass
| DE93-007872 | p 2654 N93-25359
POTASSIUM PHOSPHATES
Laser damage to production- and research-grade KDP crystals
| DE93-007517 | p 2870 N93-26594
POTENTIAL ENERGY
Bimolecular reaction dynamics from photoelectron spectroscopy of negative ions
| DE93-007669 | p 2647 N93-26599
POWDER (PARTICLES)
Processing and properties of Ti5Si3
| DE93-007284 | p 2649 N93-25149
Production of ultrafine, high-purity ceramic powders using the US Bureau of Mines developed turbomill p 2659 N93-25585
Ceramic fiber reinforced glass-ceramic matrix composite
| NASA-CASE-LEW-15262-1 | p 2640 N93-26100
Vacuum powder injector and method of impregnating fiber with powder
| NASA-CASE-LAR-14179-1 | p 2668 N93-26101
Template synthesis of electronically conductive polymers: A new route for achieving higher electronic conductivities
| AD-A261616 | p 2658 N93-26437
POWDER METALLURGY
Properties of extruded PS-212 type self-lubricating materials p 2659 N93-25565
Mechanical alloying processing and application to development of structural materials
| AD-A261251 | p 2652 N93-26264
POWER AMPLIFIERS
A compact and versatile pulse generation and shaping subsystem for high energy laser systems
| DE93-007114 | p 2711 N93-24961
POWER CONVERTERS
DC-DC power converter research for Orbiter/Station power exchange
| NASA-CR-192939 | p 2633 N93-26425
POWER EFFICIENCY
Preliminary investigation of power flow and electrode phenomena in a multi-megawatt coaxial plasma thruster
| NASA-CR-191084 | p 2633 N93-26555
POWER GAIN
Experimental and theoretical study of CW HF chemical laser residual fundamental gain p 2714 N93-25721
POWER LIMITED SPACECRAFT
Optimal cooperative power-limited rendezvous p 2607 N93-24904
POWER LINES
Detecting damaged cables using a preionized gas technique
| DE93-007588 | p 2689 N93-25429
PROAV Cable Warning System (CWS) - U.S. Army aircraft Integration assessment and OCONUS field evaluation
| AD-A261233 | p 2583 N93-26263
POWER SPECTRA
Determination of design and operation parameters for upper atmospheric research instrumentation to yield optimum resolution with deconvolution, appendix 2
| NASA-CR-192833 | p 2770 N93-25088
DSN observations of Titan p 2680 N93-26129
Measurements of scalar power spectra in high Schmidt number turbulent jets
| AD-A261542 | p 2707 N93-26379
POWERED LIFT AIRCRAFT
Experimental performance of a ventral nozzle with pitch and yaw vectoring capability for SSTOVL aircraft
| NASA-TM-106054 | p 2592 N93-25129
POYNTING-ROBERTSON EFFECT
Line formation and the Poynting-Robertson effect in accretion discs p 2847 N93-25355
PRE-MAIN SEQUENCE STARS
Photospheric abundance analysis of low-mass pre-main sequence stars p 2894 N93-25623
PRECESSION
Analysis of the effects of mean local node-crossing time on the evolution of Sun-synchronous orbits p 2602 N93-24706
SCATHA mission termination report p 2605 N93-24725
PRECIPITATION (METEOROLOGY)
Correlation between NDVI values derived from NOAA AVHRR HRPT data and ground measurements of precipitation in the EFEDA study area (Spain) p 2738 N93-24780
Commercial Precipitation Static (P-static) test equipment p 2711 N93-24901
Remote sensing of precipitation and electrification with a dual-polarization, coherent, wideband radar system
| AD-A260779 | p 2756 N93-25679
Vector radiative transfer model: Application to rainfall retrieval with microwave radiometric data p 2784 N93-25743
Computation of moisture flux from ocean to atmosphere using a synergy of SSM/I-derived precipitable water and ECMWF analyses p 2774 N93-25757
Rainfall frequency atlas of the Midwest
| PB93-164606 | p 2785 N93-25872
Large scale rainfall diversity and satellite propagation p 2683 N93-26466
PRECIPITATION HARDENING
Development of dispersion-strengthened XD (trademark) Cu alloys for high heat-flux applications
| NASA-CR-191124 | p 2653 N93-24761
Computer modelling of cyclic deformation of high-temperature materials
| AD-A260978 | p 2639 N93-25936
PRECISION
Precision of the calibration of the AXAF engineering test article (VETA) mirrors p 2855 N93-26189
PRECOOLING
An evaluation of thermal energy storage options for precooling gas turbine inlet air
| DE93-005980 | p 2758 N93-24975
PREDATORS
The continuous plankton recorder survey: A long-term, basin-scale oceanic time series p 2736 N93-24937
PREDICTION ANALYSIS TECHNIQUES
Flight Mechanics/Estimation Theory Symposium, 1992
| NASA-CP-3186 | p 2599 N93-24694
What is the relationship between altitude and weight in a model rocket? p 2603 N93-24715
Nonlinear techniques for forecasting solar activity directly from its time series p 2603 N93-24716
Anomalous bioelectric potentials of silk trees in Naples zoo (Italy) prior to an earthquake in May, 1991 p 2753 N93-24873
The 1992 International Aerospace and Ground Conference on Lightning and Static Electricity: Addendum
| DOT/FAA/CT-92/20-ADD-1 | p 2777 N93-24875
A computational approach to predicting the extent of arc root damage in CFC panels p 2642 N93-24890
Development of models for predicting the triggering of lightning by launch vehicles p 2610 N93-24899
Operational seasonal and interannual predictions of ocean conditions p 2733 N93-24921
UARS in-flight jitter study for EOS
| NASA-CR-191419 | p 2615 N93-25133
Low-frequency room responses. Part 1: Background and qualitative considerations
| BBC-RD-1992/8-PT-1 | p 2673 N93-25168
Low-frequency room responses. Part 2: Calculation methods and experimental results
| BBC-RD-1992/9-PT-2 | p 2673 N93-25169
An in-depth probabilistic study of external tank attach ring
| NASA-TM-108403 | p 2624 N93-25671
Computer modelling of cyclic deformation of high-temperature materials
| AD-A260978 | p 2639 N93-25936
PREDICTIONS
Natural disasters and their mitigation using space technology p 2742 N93-24804
Aerospace monitoring for ecological hazard and disaster mitigation p 2744 N93-24812
International organisation of ocean programs: Making a virtue of necessity p 2732 N93-24917
World Ocean Circulation Experiment p 2733 N93-24922
Energy transfer properties and mechanisms
| DE93-008540 | p 2849 N93-25488
Contribution of personality to the prediction of success in initial air traffic control specialist training
| DOT/FAA/AM-93/4 | p 2797 N93-26138
PREFORMS
Mullite whiskers and mullite-whisker felt p 2642 N93-25586
PREMIXED FLAMES
A premixed laminar flame interacting with a vortex resulting in flame stretch and quenching p 2642 N93-24771
Measurements of soot formation and hydroxyl concentration in near critical equivalence ratio premixed ethylene flame
| NASA-CR-191099 | p 2642 N93-25116
The structure of particle cloud premixed flames
| NASA-CR-192827 | p 2643 N93-25229
Flame-turbulence interactions
| AD-A260957 | p 2645 N93-26220
Solution of nonlinear boundary value problem on successively refined grids
| AD-A261395 | p 2829 N93-26519
Oxides of nitrogen emissions from turbulent hydrocarbon/air jet diffusion flames, phase 2
| PB93-152478 | p 2768 N93-26533

PREPREGS
Graphite/epoxy composite laminates with co-cured interlaminar damping layers p 2642 N93-25587
Characterization of aerospace grade resins and composites through pressurized volumetric dilatometry
| AD-A260794 | p 2639 N93-25918
Vacuum powder injector and method of impregnating fiber with powder
| NASA-CASE-LAR-14179-1 | p 2668 N93-26101

PRESIDENTIAL REPORTS
Science, technology, and national security p 2886 N93-25232
High performance computing and communications panel report p 2807 N93-26131

PRESSING (FORMING)
Method of joining diamond structures
| AD-D015671 | p 2867 N93-26140

PRESSURE CHAMBERS
Analysis of the lettuce data from the variable pressure growth chamber at NASA Johnson Space Center: A three-stage nested design model p 2794 N93-26069

PRESSURE DEPENDENCE
Pressure dependence of conductivity
| DE93-008466 | p 2687 N93-25113

PRESSURE DISTRIBUTION
Surface and flow field measurements in a symmetric crossing shock wave/turbulent boundary-layer interaction
| NASA-TM-106086 | p 2575 N93-24911
Generic hypersonic vehicle performance model
| NASA-CR-192953 | p 2587 N93-25162
An experimental study of the sources of fluctuating pressure loads beneath swept shock/boundary-layer interactions
| NASA-CR-192918 | p 2698 N93-25266
The transient development of vortices over delta wings p 2576 N93-25269
Generation of acoustic waves by focused infrared neodymium-laser radiation p 2714 N93-25761
Experimental effects of wing location on wing-body pressures at supersonic speeds
| NASA-TM-4434 | p 2581 N93-26085
Model fan passage flow simulation
| AD-A261613 | p 2707 N93-26167

PRESSURE DRAG
Pressure torques and circulation changes in Rocky Mountain lee cyclones p 2783 N93-25724

PRESSURE EFFECTS
The DX centers in three to five semiconductors under hydrostatic pressure
| DE93-007701 | p 2864 N93-25490
Tornado: An engineering-oriented perspective
| PB93-148435 | p 2788 N93-26584

PRESSURE GRADIENTS
The effect of entrance radius and film injection on wall heating in scramjet nozzles p 2625 N93-26009

PRESSURE MEASUREMENT
Surface and flow field measurements in a symmetric crossing shock wave/turbulent boundary-layer interaction
| NASA-TM-106086 | p 2575 N93-24911
A systematic satellite approach for estimating central pressures of mid-lattitude oceanic storms
| NOAA-TR-NESDIS-63 | p 2781 N93-25220
An experimental study of the sources of fluctuating pressure loads beneath swept shock/boundary-layer interactions
| NASA-CR-192918 | p 2698 N93-25266
The transient development of vortices over delta wings p 2576 N93-25269
The pressure modulation system in the Improved Stratospheric and Mesospheric Sounder p 2773 N93-25739
Experimental effects of wing location on wing-body pressures at supersonic speeds
| NASA-TM-4434 | p 2581 N93-26085
Jet-induced ground effects on a parametric flat-plate model in hover
| NASA-TM-104001 | p 2581 N93-26099
Measurement and analysis of a small nozzle plume in vacuum
| NASA-TM-106066 | p 2633 N93-26561

PRESSURE OSCILLATIONS
Calculations of combustion response profiles and oscillations
| NASA-TM-106135 | p 2623 N93-25236
An experimental study of the sources of fluctuating pressure loads beneath swept shock/boundary-layer interactions
| NASA-CR-192918 | p 2698 N93-25266
Correlations between organized turbulent structures and wall pressure fluctuations
| PB93-156479 | p 2706 N93-25885

PRESSURE RATIO
Experimental performance of a ventral nozzle with pitch and yaw vectoring capability for SSTOVL aircraft
| NASA-TM-106054 | p 2592 N93-25129
Estimating turbine limit load
| NASA-CR-191105 | p 2580 N93-25883

PRESSURE REDUCTION
Crustal deformation studies in subaerial parts of the world oceanic rift system: Iceland and Afar p 2789 N93-25558

PRESSURE SENSORS
Smart microsensors for high temperature applications
| AD-A260747 | p 2710 N93-25677
SiC microsensor with piezoresistive diamond sensing elements
| AD-A261346 | p 2868 N93-26312

PRESTRESSING
Axisymmetric deformations and stresses of unsymmetrically laminated composite cylinders in axial compression with thermally-induced preloading effects
| NASA-CR-192788 | p 2723 N93-24912

PREVENTION
The use of SPOT data in natural disaster prevention and damage assessment p 2743 N93-24811

PROBABILITY DENSITY FUNCTIONS
Joint flexibility effects on the dynamic response of structures. Part 2: Stochastic analysis
| AD-A261003 | p 2729 N93-25938

PROBABILITY DISTRIBUTION FUNCTIONS
Equilibrium constrained assumed natural coordinate strain finite elements for shell analysis p 2724 N93-25273
Generalized probability model for calculation of interference to the Deep Space Network due to circularly Earth-orbiting satellites p 2679 N93-26127

PROBABILITY THEORY
Parametric analysis of atmospheric processes
| NASA-CR-192523 | p 2770 N93-25086
How to combine probabilistic and fuzzy uncertainties in fuzzy control
| NASA-TM-108746 | p 2818 N93-25138
How far we are from the complete knowledge: Complexity of knowledge acquisition in Dempster-Shafer approach
| NASA-CR-192944 | p 2874 N93-25139
An in-depth probabilistic study of external tank attach ring
| NASA-TM-108403 | p 2624 N93-25671
Probability and statistics applied to the theory of algorithms
| AD-A261019 | p 2830 N93-25863
Generalized probability model for calculation of interference to the Deep Space Network due to circularly Earth-orbiting satellites p 2679 N93-26127
Progress in impulse approach research
| AD-A261728 | p 2850 N93-26281
Penning detachment: A new frontier
| AD-A261447 | p 2850 N93-26346

PROBLEM SOLVING
Design concepts for the development of cooperative problem-solving systems
| NASA-CR-192708 | p 2585 N93-25261
Improving performance through concept formation and conceptual clustering
| NASA-CR-192726 | p 2828 N93-25262
Design of a cooperative problem-solving system for enroute flight planning: An empirical study of its use by airline dispatchers
| NASA-CR-192709 | p 2585 N93-25330
An experimental examination of the effects of expertise and problem-solving cues on the identification of ideas for strategic information systems p 2875 N93-25395
Linear-programming tools in integer programming: The traveling salesman
| AD-A261398 | p 2812 N93-26290
Intelligent, real-time problem solving, phase 3
| AD-A261441 | p 2829 N93-26345
Power iterations and the dominant eigenvalue problem
| AD-A261695 | p 2829 N93-26370
Computation and theory in large-scale optimization
| AD-A261419 | p 2813 N93-26450

PROCESS CONTROL (INDUSTRY)
Vision-aided monitoring and control of thermal spray, spray forming, and welding processes p 2670 N93-25604
Adaptive process control with fuzzy logic and genetic algorithms p 2827 N93-25612
Recommendations for a Kalman filter to estimate and control freeze and sublime rates of gaseous diffusion plant freezer/sublimer systems
| ORNL/TM-12183 | p 2668 N93-25937
Polyimides with improved compression moldability
| NASA-CASE-LAR-14457-1 | p 2656 N93-25997

PRODUCT DEVELOPMENT
Rendezvous, proximity operations and capture quality function deployment report
| NASA-TM-108752 | p 2614 N93-25952
Engineering: Research development and technology
| UCRL-53868-91 | p 2917 N93-26326

PRODUCTION COSTS
Emerging technologies in ethanol production
| PB93-157014 | p 2661 N93-25818

PRODUCTION ENGINEERING
Multivariable control for flexible IC processing
| AD-A261685 | p 2692 N93-26366

PRODUCTION MANAGEMENT
Managing real-time software projects: Problems and issues
| AD-A261428 | p 2813 N93-26453

PRODUCTION PLANNING
Special tooling disposition for aircraft entering post production support
| AD-A261614 | p 2573 N93-26168

PRODUCTIVITY
Factors associated with perceptions of productivity and usage of information technology in a service organization p 2875 N93-25421
Implementation of quality improvement techniques for management and technical processes in the ACRV project p 2723 N93-26074

PROFILES
On machine capacitance dimensional and surface profile measurement system p 2670 N93-25579

PROGRAM VERIFICATION (COMPUTERS)
Putting time into proof outlines
| NASA-CR-192978 | p 2809 N93-25152
Supercomputer Debugging Workshop 1992
| DE93-007322 | p 2805 N93-25165
High level design for distributed application instrumentation
| AD-A260812 | p 2710 N93-25696
Set based program analysis
| AD-A260979 | p 2806 N93-25841
Analysis of symbolic parameter models
| AD-A261930 | p 2811 N93-26253
Software testing initiative for strategic defense systems
| AD-A261350 | p 2831 N93-26330
Research directions in software analysis, synthesis and certification
| AD-A261367 | p 2812 N93-26336
AEGIS measures definition
| AD-A261494 | p 2812 N93-26375
Source-level debugging of automatically parallelized programs
| AD-A261520 | p 2813 N93-26378

PROGRAMMABLE LOGIC DEVICES
Radiation-hardened control system
| DE93-007248 | p 2688 N93-25377
Walsh function generator for the Electronically Scanned Thinned Array Radiometer (ESTAR) instrument
| NASA-TM-4449 | p 2689 N93-25618

PROGRAMMING ENVIRONMENTS
Proceedings of the Second SISAL Users' Conference
| DE93-008019 | p 2815 N93-25304
A methodology and software environment for testing process model's sequential predictions with protocols
| AD-A260980 | p 2882 N93-25844

PROGRAMMING LANGUAGES
Prototype PC user interface
| DE93-008008 | p 2809 N93-25303
Proceedings of the Second SISAL Users' Conference
| DE93-008019 | p 2815 N93-25304
Towards a formalism for program generation
| AD-A261689 | p 2812 N93-26368

PROJECT MANAGEMENT
Management issues in systems engineering p 2665 N93-24682
The importance of cost considerations in the systems engineering process p 2666 N93-24686
Systems engineering and integration processes involved with manned mission operations p 2666 N93-24688
Nuclear thermal propulsion technology: Results of an interagency panel in FY 1991
| NASA-TM-105711 | p 2621 N93-24740
Wrap-up session p 2737 N93-24940
Energy and Technology Review, August-September 1992
| DE93-005882 | p 2901 N93-24974
JSC research and technology
| NASA-TM-104763 | p 2901 N93-25188
Tree classification software p 2814 N93-25591
Climate Monitoring and Diagnostics Laboratory
| PB93-156388 | p 2785 N93-25871
Liquid Rocket Booster (LRB) for the Space Transportation System (STS) Systems Study. Amendment 13: Orientation meeting
| NASA-CR-192515 | p 2614 N93-26152

PROJECT PLANNING
Nuclear thermal propulsion technology: Results of an interagency panel in FY 1991
| NASA-TM-105711 | p 2621 N93-24740
Viewgraph description of Penn State's Propulsion Engineering Research Center: Activity highlights and future plans
| NASA-CR-192317 | p 2622 N93-24943
Space transfer vehicle concepts and requirements study. Volume 3, book 1: Program cost estimates
| NASA-CR-192529 | p 2611 N93-25514
Nuclear electric propulsion for planetary science missions: NASA technology program planning
| NASA-TM-106139 | p 2632 N93-26210
PROJECT SETI
Space biology research development
| NASA-CR-192830 | p 2792 N93-25242
The Telecommunications and Data Acquisition Report
| NASA-CR-192804 | p 2676 N93-26105
PROJECTILES
Computation of transonic flow over a porous surface projectile p 2577 N93-25409
Modified point mass trajectory simulation for base-burn projectiles
| BRL-TR-3321 | p 2609 N93-25985
PROLOG (PROGRAMMING LANGUAGE)
Analysis of symbolic parameter models
| AD-A261930 | p 2811 N93-26253
PROP-FAN TECHNOLOGY
Evaluation of MARC for the analysis of rotating composite blades
| NASA-TM-4423 | p 2723 N93-24909
Fabrication of composite propfan blades for a cruise missile wind tunnel model
| NASA-TM-105270 | p 2730 N93-26202
PROPAGATION MODES
A comparison of ionospheric propagation mode delay predictions from ADVANCED PROPHET 4.3 with measured data
| AD-A261782 | p 2686 N93-26604
PROPAGATION VELOCITY
Observations of an intrathermocline vortex p 2788 N93-24769
Propagation velocity and space-time correlation of perturbations in turbulent channel flow
| NASA-TM-103932 | p 2695 N93-25082
PROPANE
Emissions from ethanol and LPG fueled vehicles
| DE93-006410 | p 2660 N93-25192
Documentation for propane fleet conversion cost-effectiveness model
| PB93-165611 | p 2720 N93-26590
PROPELLANT ADDITIVES
Dynamic burning rate measurements of metalized composite propellants using the laser-recoil technique p 2631 N93-26043
PROPELLANT COMBUSTION
Ignition and combustion of lunar propellants
| NASA-CR-192814 | p 2659 N93-24745
Dynamic burning rate measurements of metalized composite propellants using the laser-recoil technique p 2631 N93-26043
PROPELLANT GRAINS
Particle behavior in solid propellant rocket motors and plumes
| AD-A260900 | p 2624 N93-25913
PROPELLANT SENSITIVITY
Minutes of the Twenty-Fifth Explosives Safety Seminar, volume 4
| AD-A261116 | p 2660 N93-25769
Molecular composition, structure, and sensitivity of explosives
| DE93-003850 | p 2662 N93-26493
PROPELLANT TESTS
Minutes of the Twenty-Fifth Explosives Safety Seminar, volume 4
| AD-A261116 | p 2660 N93-25769
The burning rate behavior of pure nitrocellulose propellant samples
| AD-A261009 | p 2661 N93-25857
PROPELLANTS
An experimental and analytical study of the unsteady combustion of homogeneous energetic solids using the laser-recoil method p 2630 N93-26042
PROPELLER BLADES
Evaluation of MARC for the analysis of rotating composite blades
| NASA-TM-4423 | p 2723 N93-24909
A review of civil aviation propeller-to-person accidents: 1980-1989
| AD-A260695 | p 2583 N93-25896
PROPELLER FANS
Evaluation of MARC for the analysis of rotating composite blades
| NASA-TM-4423 | p 2723 N93-24909
Theory for noise of propellers in angular inflow with parametric studies and experimental verification
| NASA-CR-4499 | p 2844 N93-25094
A numerical and experimental studies of flow characteristics in centrifugal fans p 2577 N93-25339
Fabrication of composite propfan blades for a cruise missile wind tunnel model
| NASA-TM-105270 | p 2730 N93-26202
PROPELLER NOISE
Theory for noise of propellers in angular inflow with parametric studies and experimental verification
| NASA-CR-4499 | p 2844 N93-25094
PROPORTIONAL COUNTERS
VETA-1 x ray detection system p 2854 N93-26185
Correcting x ray spectra obtained from the AXAF VETA-I mirror calibration for pileup, continuum, background and deadtime p 2854 N93-26187
AXAF VETA-I mirror encircled energy measurements and data reduction p 2855 N93-26188
PROPOSALS
Air Force Office of Scientific Research
| AD-A260675 | p 2911 N93-25893
PROPULSION SYSTEM CONFIGURATIONS
Nuclear thermal propulsion technology: Results of an interagency panel in FY 1991
| NASA-TM-105711 | p 2621 N93-24740
Aerodynamic design and synthesis of the oblique flying wing supersonic transport p 2587 N93-24768
PROPULSION SYSTEM PERFORMANCE
Nuclear thermal propulsion technology: Results of an interagency panel in FY 1991
| NASA-TM-105711 | p 2621 N93-24740
Screening studies of advanced control concepts for airbreathing engines
| NASA-TM-106042 | p 2592 N93-25079
Test results of a Stirling engine utilizing heat exchanger modules with an integral heat pipe
| NASA-TM-105883 | p 2759 N93-25136
Liquid Rocket Booster (LRB) for the Space Transportation System (STS) Systems Study. Amendment 13: Orientation meeting
| NASA-CR-192515 | p 2614 N93-26152
On-line implementation of nonlinear parameter estimation for the Space Shuttle main engine
| NASA-TM-106097 | p 2632 N93-26211
Development and use of hydrogen-air torches in an altitude facility
| NASA-TM-106047 | p 2598 N93-26214
PROPYLENE
An investigation of the degradation of Fluorinated Ethylene Propylene (FEP) copolymer thermal blanketing materials aboard LDEF in the laboratory
| NASA-CR-192824 | p 2653 N93-25078
PROSTAGLANDINS
Mechanical stimulation of skeletal muscle mitigates glucocorticoid induced decreases in prostaglandin synthesis
| NASA-CR-193040 | p 2794 N93-24763
PROSTHETIC DEVICES
The design of mechanically compatible fasteners for human mandible reconstruction p 2796 N93-25569
PROTECTION
Method for providing EMI/EMP hardening and breakdown protection in composite materials
| AD-D015638 | p 2634 N93-25283
Duct protection coating concept development and test. Appendix D, volume 1: Test specimen fabrication, conditioning, and testing documentation
| AD-A261005 | p 2656 N93-25940
PROTECTIVE COATINGS
Mechanistic studies of the CVD of silicon nitride from SiF4 and NH3
| DE93-004500 | p 2644 N93-25312
Chromate-free corrosion resistant talc coatings for aluminum alloys
| DE93-005370 | p 2655 N93-25446
In situ surface studies of conversion coatings for steel and aluminum
| AD-A261016 | p 2655 N93-25861
Duct protection coating concept development and test. Appendix D, volume 1: Test specimen fabrication, conditioning, and testing documentation
| AD-A261005 | p 2656 N93-25940
Thermal coatings for titanium-aluminum alloys
| NASA-TM-107760 | p 2651 N93-26048
Duct protection coating concept development and test: Test specimen fabrication, conditioning, and testing documentation.
| AD-A261250 | p 2657 N93-26278
Workshop on Diamond and Diamond-Like-Carbon Films for the Transportation Industry
| DE93-007491 | p 2658 N93-26506
PROTEIN SYNTHESIS
Mechanical stimulation of skeletal muscle mitigates glucocorticoid induced decreases in prostaglandin synthesis
| NASA-CR-193040 | p 2794 N93-24763
PROTEINS
Primary events in olfactory reception
| AD-A260562 | p 2795 N93-25944
Pseudomonas screening assay
| NASA-CASE-NPO-17653-1-CU | p 2793 N93-25994
PROTOCOL (COMPUTERS)
An SPW software simulation model of a dispersive fading multipath narrowband HF channel
| AD-A261101 | p 2675 N93-25767
A methodology and software environment for testing process model's sequential predictions with protocols
| AD-A260980 | p 2882 N93-25844
Distributed project scheduling at NASA: Requirements for manual protocols and computer-based support p 2815 N93-26075
An OSI architecture for the Deep Space Network p 2679 N93-26121
Proof of fault coverage for a formal protocol test procedure
| AD-A261612 | p 2680 N93-26166
Signed vector timestamps: A secure protocol for partial order time
| AD-A261371 | p 2817 N93-26338
PROTON BEAMS
Proton Monte Carlo transport program PTRAN
| PB93-158673 | p 2850 N93-26314
PROTON IRRADIATION
Far infrared spectra of amorphous and crystalline water ice and changes in these phases as the result of proton irradiation
| NASA-CR-192849 | p 2892 N93-25230
Effects of space radiation on humoral and cellular immunity in rhesus monkeys
| AD-A261808 | p 2793 N93-26259
PROTONS
Star tracker operation in a high density proton field p 2600 N93-24699
Results from the NA36 on strangeness production in 200 GeV/c per nucleon S + Pb and p - Pb reactions
| DE93-007711 | p 2848 N93-25364
Prediction of hydrogen entry and permeation in metals and alloys
| AD-A260580 | p 2651 N93-25903
Proton Monte Carlo transport program PTRAN
| PB93-158673 | p 2850 N93-26314
PROTOTYPES
Prototype PC user interface
| DE93-008008 | p 2809 N93-25303
Data systems dynamic simulator p 2814 N93-25602
Knowledge-based assistance for science visualization and analysis using large distributed databases p 2879 N93-25801
Development of an expert data reduction assistant p 2880 N93-25808
Advanced data visualization and sensor fusion: Conversion of techniques from medical imaging to Earth science p 2880 N93-25810
A distributed analysis and visualization system for model and observational data p 2881 N93-25814
A prototype for simulation of the space-to-ground assembly/contingency system of Space Station Freedom p 2619 N93-26065
A study of mapping exogenous knowledge representations into CONFIG p 2827 N93-26072
A Biphase Shift Keying (BPSK), direct sequence, spread spectrum modem for Petite Amateur Navy Satellite (PANSAT)
| AD-A261301 | p 2618 N93-26295
PROVING
Analysis of large system black box verification test data
| NASA-CR-192885 | p 2815 N93-24748
Verification of a climate convention: Role and limitations of a space based remote sensing system p 2738 N93-24781
The evaluation of technical models used for major-accident hazard installations. Report to Commission of the European Communities Directorate General 12
| CUED/A-AERO/TR-19 | p 2668 N93-25238
Proof of fault coverage for a formal protocol test procedure
| AD-A261612 | p 2680 N93-26166
PROXIMITY
Rendezvous, proximity operations and capture quality function deployment report
| NASA-TM-108752 | p 2614 N93-25952
PSEUDOMONAS
Pseudomonas screening assay
| NASA-CASE-NPO-17653-1-CU | p 2793 N93-25994

PSEUDORANDOM SEQUENCES
Efficient generation of synthetic terrain imagery for automatic target recognition
| AD-A260705 | p 2756 N93-25653
PSYCHOLOGICAL TESTS
Performance-based testing and success in Naval advanced flight training
| AD-A260838 | p 2590 N93-25933
Spontaneous discovery and use of categorical structure
| AD-A261658 | p 2798 N93-26364
Neuromagnetic investigation of cortical regions underlying short-term memory
| AD-A261445 | p 2799 N93-26521
PSYCHOLOGY
Neuropsychological components of object identification
| AD-A261449 | p 2797 N93-26347
PSYCHOMOTOR PERFORMANCE
Proceedings of Workshop 1: The Human Brainmap Database
| AD-A260720 | p 2796 N93-25654
PSYCHOPHYSIOLOGY
JPRS report: Science and technology. Central Eurasia: Life sciences
| JPRS-ULS-92-025 | p 2793 N93-25405
Comparative analytical study of evoked and event related potentials as correlates of cognitive processes
| AD-A261388 | p 2799 N93-26446
PULSARS
Cosmic string cosmology p 2891 N93-24907
How can millisecond pulsars improve the long term stability of atomic time scales? p 2832 N93-24985
PULSE AMPLITUDE
Correcting x ray spectra obtained from the AXAF VETA-I mirror calibration for pileup, continuum, background and deadtime p 2854 N93-26187
PULSE COMMUNICATION
Timing and time signal distribution in digital communications networks p 2686 N93-25061
Timing a national telecommunications network using GPS p 2687 N93-25062
Strategies for synchronisation in an evolving telecommunications network p 2687 N93-25063
A channel simulation processor for the multi-node tactical network simulator
| AD-A261810 | p 2776 N93-26430
A proposed study of multiple scattering through clouds up to 1 THz p 2684 N93-26474
PULSE DURATION MODULATION
Testing of the on-board attitude determination and control algorithms for SAMPEX p 2600 N93-24698
Development and testing of the digital control system for the Archytas unmanned air vehicle
| AD-A261656 | p 2597 N93-26196
PULSE GENERATORS
A compact and versatile pulse generation and shaping subsystem for high energy laser systems
| DE93-007114 | p 2711 N93-24961
Variable pulse rate circuit
| AD-D015675 | p 2691 N93-26233
PULSE RADAR
Frequency diversity sidelobe canceller
| AD-D015647 | p 2674 N93-25332
PULSE RATE
Variable pulse rate circuit
| AD-D015675 | p 2691 N93-26233
PULSED LASER DEPOSITION
Structure and properties of a-C: N films prepared by pulsed excimer laser deposition
| DE93-007908 | p 2654 N93-25372
Fast diagnostics of laser ablation used for pulsed laser deposition
| DE93-005155 | p 2713 N93-25508
PULSED LASERS
Surface discharge photoinitiation of pulsed chemical lasers
| DE93-006337 | p 2712 N93-24967
Apparatus for imaging an object in or through a scattering medium using coherent anti-Stokes Raman scattering
| AD-D015642 | p 2852 N93-25358
Progress in imaging microscopy with x ray lasers at LLNL
| DE93-007508 | p 2712 N93-25363
Structure and properties of a-C: N films prepared by pulsed excimer laser deposition
| DE93-007908 | p 2654 N93-25372
Laser field assisted photoemission using femtosecond laser pulses
| DE93-007277 | p 2712 N93-25378
Simultaneous determination of gain parameters in steady state lasers
| DE93-007389 | p 2713 N93-25381
Correlation of damage threshold and surface geometry of nodular defects in HR coatings as determined by in-situ atomic force microscopy
| DE93-007509 | p 2654 N93-25384
Injection seeded, diode-pumped, short pulse Nd:YAG ring laser for space-based laser ranging p 2713 N93-25389
Laser physics and laser techniques
| AD-A261595 | p 2715 N93-26524
PULTRUSION
Asymptotic studies of gravity-driven reacting coating flows and pultrusion processes p 2704 N93-25683
PUMPS
Positive displacement rotary pump
| AD-D015678 | p 2719 N93-26144
PYRIDOXINE
The role of pyridoxine as a countermeasure for in-flight loss of lean body mass p 2796 N93-26068
PYROELECTRICITY
Research on lead titanate films for radiation detection
| AD-A261187 | p 2849 N93-25823
PYROLYSIS
A model of concurrent flow flame spread over a thin solid fuel
| NASA-CR-191111 | p 2663 N93-24946
The acute inhalation toxicity of pyrolysis products of halon 1301
| AD-A260874 | p 2795 N93-25629
Detection of atomic oxygen and hydrogen in solid propellant flames and pyrolysis gases using multiphoton laser-induced fluorescence p 2628 N93-26029
Development of a pyrolysis waste recovery model with designs, test plans, and applications for space-based habitats p 2803 N93-26076
PYROTECHNICS
Pyroshock: Bibliography
| DE93-007605 | p 2726 N93-25489
Molecular composition, structure, and sensitivity of explosives
| DE93-003850 | p 2662 N93-26493

Q

Q FACTORS
Long term drift and gamma-irradiation effect p 2833 N93-24992
Q SWITCHED LASERS
Generation of acoustic waves by focused infrared neodymium-laser radiation p 2714 N93-25761
QUADRATIC PROGRAMMING
Methods of optimization under uncertainty
| AD-A261487 | p 2873 N93-26342
QUADRUPOLES
Structure of sodium 4-(1'-heptylnonyl) benzenesulfonate adsorbed on alumina using H-2 NMR
| AD-A261224 | p 2645 N93-26300
QUALITATIVE ANALYSIS
A study of mapping exogenous knowledge representations into CONFIG p 2827 N93-26072
QUALITY CONTROL
Health and environmental chemistry: Analytical techniques, data management, and quality assurance
| DE93-002853 | p 2760 N93-24674
What procedure to choose while designing a fuzzy control? Towards mathematical foundations of fuzzy control
| NASA-TM-108719 | p 2820 N93-25459
Quality control: Variability in protocols
| PB93-157790 | p 2766 N93-25876
Rendezvous, proximity operations and capture quality function deployment report
| NASA-TM-108752 | p 2614 N93-25952
Implementation of quality improvement techniques for management and technical processes in the ACRV project p 2723 N93-26074
Exploring the link between intrinsic motivation and quality
| AD-A261722 | p 2722 N93-26246
NDT standards from the perspective of the Department of Defense
| MTL-TR-92-68 | p 2722 N93-26434
Designing and implementing a state quality award
| PB93-154458 | p 2722 N93-26546
QUANTUM EFFICIENCY
Studies of avalanche photodiodes for scintillating fibre tracking readout
| DE93-008370 | p 2689 N93-25491
QUANTUM ELECTRODYNAMICS
Notes on radial drift for dalitz detection
| DE93-006971 | p 2846 N93-24959
QUANTUM ELECTRONICS
Joint services electronics program
| AD-A261801 | p 2692 N93-26539
QUANTUM MECHANICS
Theoretical calculations on the electron absorption spectra of selected Polycyclic Aromatic Hydrocarbons (PAH) and derivatives
| NASA-CR-192762 | p 2892 N93-25200
Correlated wavefunction quantum Monte Carlo approach to solids
| DE93-007730 | p 2863 N93-25367
Bimolecular reaction dynamics from photoelectron spectroscopy of negative ions
| DE93-007669 | p 2647 N93-26599
QUANTUM OPTICS
Experimental studies of fundamental problems in quantum optics
| AD-A261183 | p 2853 N93-25822
QUANTUM THEORY
Twistor diagrams and a quantum field theory p 2871 N93-25423
Fundamental aspects of metal joining: The study of strong interfaces
| AD-A261293 | p 2653 N93-26304
Interferometric measurement with squeezed light
| AD-A260910 | p 2856 N93-26457
Low temperature Hall and Shubnikov-de Haas effects
| AD-A261871 | p 2869 N93-26540
QUANTUM WELLS
Electric field effects on quantum-confined semiconductor structures p 2865 N93-25703
Time resolved studies of in-well and cross-well carrier transport in MQW semiconductor structures
| AD-A261170 | p 2714 N93-25774
Resonant tunneling through chemisorbed halogen atoms on Ag(111)
| AD-A261794 | p 2868 N93-26254
QUARK MODELS
High-energy pion-nucleus scattering at LAMPF
| DE93-007364 | p 2852 N93-25380
QUARKS
Results from the NA36 on strangeness production in 200 GeV/c per nucleon S + Pb and p - Pb reactions
| DE93-007711 | p 2848 N93-25364
Detection of fragments arising from greater than 10 GeV electron-nucleus collisions
| DE93-007725 | p 2848 N93-25366
QUARTZ
Comparison of energy trapping resonators and filters using the AT cut of quartz, berlinite and gallium phosphate p 2836 N93-25013
QUARTZ CRYSTALS
Long term drift and gamma-irradiation effect p 2833 N93-24992
Weak magnetic field sensitivity of quartz crystal oscillators p 2833 N93-24993
Improved PI-network measurement of all quartz crystal parameters by appropriate modelling of the test fixture p 2833 N93-24995
The measurement of the resonant frequency of quartz crystal units: An ongoing saga p 2833 N93-24996
Monolithic quartz vibrating beam accelerometer p 2711 N93-25011
Surface Transverse Wave (STW) quartz resonators in the GHz range p 2836 N93-25012
Dedicated oscillator for immersed crystal sensor p 2837 N93-25020
Radiation effects in germanium doped quartz p 2837 N93-25021
Trapped energy quartz crystal resonator on wedge-shaped plate p 2837 N93-25022
Quartz crystal twinning under mechanical stress: Finite element analysis p 2839 N93-25032
Very wide bandwidth HF crystal filters p 2693 N93-25039
Thermionic current measurement in quartz p 2840 N93-25045
The third-order permittivity of quartz obtained by different methods p 2840 N93-25046
Thermoelasticity in quartz p 2841 N93-25047
Quartz oscillators, frequency synthesizers, and timing systems for geodesy and radio science applications p 2693 N93-25052
Space radiation susceptibility of ultra stable crystal oscillators p 2693 N93-25053
QUASARS
Propagation of radiation in astrophysical media: Gravitational lenses and astrophysical masers p 2892 N93-24949
QUASI-STEADY STATES
Flame response in oscillatory solid propellant combustion p 2630 N93-26041
QUATERNIONS
Attitude analysis in Flatland: The plane truth p 2603 N93-24712
Quaternion normalization in spacecraft attitude determination p 2606 N93-24730

QUERY LANGUAGES
The StarView intelligent query mechanism
p 2826 N93-25984

R

RADAR
Selected results from LLNL-Hughes RAR for West Coast Scotland Experiment 1991
| DE93-006972 | p 2788 N93-24960
RADAR ASTRONOMY
Goldstone solar system radar signal processing
p 2680 N93-26130
RADAR BEAMS
Orbital parameter estimation using an extended Kalman filter
| AD-A260618 | p 2608 N93-25636
RADAR CROSS SECTIONS
DSN observations of Titan p 2680 N93-26129
RADAR DATA
DSN acquisition of Magellan high-rate telemetry data
p 2614 N93-26124
Goldstone solar system radar signal processing
p 2680 N93-26130
Study of auroral dynamics with combined spacecraft and incoherent-scatter radar data
| NASA-CR-192224 | p 2775 N93-26159
Status of the Olympus experiment at CRC
p 2685 N93-26480
Technical operating report on the Data Integration and Collection Environment (DICE) instrumentation system design
| AD-A261105 | p 2591 N93-26572
RADAR DETECTION
Discrete range clustering using Monte Carlo methods
| NASA-TM-104004 | p 2584 N93-24914
RADAR EQUIPMENT
OTH-B radar system: System summary
| AD-A261727 | p 2681 N93-26247
RADAR GEOLOGY
Revealing the face of Venus: Magellan
| NASA-CR-192922 | p 2898 N93-26517
Proceedings of the Government Users Workshop on Ground Penetrating Radar Applications and Equipment
| AD-A261873 | p 2686 N93-26541
RADAR IMAGERY
Land cover monitoring in the Netherlands applying satellite remote sensing p 2740 N93-24789
The use of polarimetric radar remote sensing data for application in forestry p 2749 N93-24845
DSN observations of Titan p 2680 N93-26129
V-GRAM: Magellan bulletin about Venus and the radar mapping mission
| NASA-CR-192923 | p 2898 N93-26424
RADAR MAPS
V-GRAM: Magellan bulletin about Venus and the radar mapping mission
| NASA-CR-192923 | p 2898 N93-26424
Proceedings of the Government Users Workshop on Ground Penetrating Radar Applications and Equipment
| AD-A261873 | p 2686 N93-26541
RADAR MEASUREMENT
Lightning precursor signatures from dual-polarization radar measurements of storms p 2777 N93-24877
Radar backscatter measurements from Arctic sea ice during the fall freeze-up
| NASA-CR-193100 | p 2790 N93-26050
Radar sensing of petroleum seepage gases
| AD-A261431 | p 2682 N93-26455
RADAR NAVIGATION
Discrete range clustering using Monte Carlo methods
| NASA-TM-104004 | p 2584 N93-24914
RADAR RANGE
Discrete range clustering using Monte Carlo methods
| NASA-TM-104004 | p 2584 N93-24914
RADAR RECEIVERS
Frequency diversity sidelobe canceller
| AD-D015647 | p 2674 N93-25332
Distortion measurements on bandpass filters with powdered iron toroidal inductors
| AD-A260790 | p 2675 N93-25689
RADAR SCATTERING
Theoretical study of topside ionospheric clutter
| AD-A260982 | p 2774 N93-25852
RADAR TRACKING
Initialization of a modeled convective storm using Doppler radar-derived fields p 2782 N93-25294
OTH-B radar system: System summary
| AD-A261727 | p 2681 N93-26247
RADAR TRANSMISSION
Frequency diversity sidelobe canceller
| AD-D015647 | p 2674 N93-25332
RADIAL DISTRIBUTION
Proton Monte Carlo transport program PTRAN
| PB93-158673 | p 2850 N93-26314
RADIAL FLOW
Design and performance of nozzle-less volute casings for inward flow radial turbines p 2593 N93-25471
RADIAL VELOCITY
Origin and evolution of cataclysmic variables
p 2893 N93-25245
Radial velocity studies of the secondary in cataclysmic variables p 2888 N93-25286
Radial velocity measurements of carbon stars
p 2895 N93-25713
RADIANCE
Measuring the intensity of nitrogen fertilization of grassland by means of remote sensing
p 2751 N93-24859
Neural networks for atmospheric retrievals
p 2824 N93-25975
RADIANT HEATING
An experimental and analytical study of the unsteady combustion of homogeneous energetic solids using the laser-recoil method p 2630 N93-26042
RADIATION BELTS
Analysis of reentry into the White Sands Missile Range (WSMR) for the LifeSat mission p 2603 N93-24717
RADIATION DAMAGE
AFRRI research, fiscal year 1991
| AD-A260933 | p 2911 N93-25710
Temperature dependence of radiation damage and its annealing in silicon detectors
| DE93-003854 | p 2869 N93-26494
RADIATION DETECTORS
Study of atmospheric electrical events above complex terrain p 2780 N93-24897
Interferometric fiber-optic radiation sensor
| DE93-003841 | p 2852 N93-25127
Cosmic ray composition investigations using ICE/ISEE-3
| NASA-CR-192808 | p 2900 N93-25241
RADIATION DISTRIBUTION
Fractal determination of parameters in lightning and ESD model p 2686 N93-24893
Spectra of stable sonoluminescence
| AD-A260621 | p 2844 N93-25637
RADIATION DOSAGE
Radiation effects in germanium doped quartz
p 2837 N93-25021
Detailed component design for a Compact Environmental Anomaly Sensor (CEASE)
| AD-A261729 | p 2620 N93-26248
Effects of space radiation on humoral and cellular immunity in rhesus monkeys
| AD-A261808 | p 2793 N93-26259
RADIATION EFFECTS
Momentum accumulation due to solar radiation torque, and reaction wheel sizing, with configuration optimization
p 2600 N93-24695
Analysis of reentry into the White Sands Missile Range (WSMR) for the LifeSat mission p 2603 N93-24717
Solar array thermal snap and the characteristics of its effect on UARS p 2607 N93-24734
Radiation and temperature effects on electronic components investigated under the CSTI high capacity power project
| NASA-TM-106096 | p 2687 N93-24746
Long term drift and gamma-irradiation effect
p 2833 N93-24992
Radiation effects in germanium doped quartz
p 2837 N93-25021
Mechanical properties of martensitic alloy AISI 422
| DE93-006563 | p 2649 N93-25255
Progress in imaging microscopy with x ray lasers at LLNL
| DE93-007508 | p 2712 N93-25363
Environmental test program for superconducting materials and devices
| DE93-003646 | p 2864 N93-25506
CRRES: Combined release and radiation effects satellite program summary
| NASA-CR-192469 | p 2774 N93-25886
Utilization of an electronic circuit simulator in CMOS latch-up studies
| AD-A260877 | p 2690 N93-25935
Thermal radiation in non-metalized solid rocket motors: Effect on burning rate and temperature sensitivity
p 2626 N93-26020
Composite materials for the extravehicular mobility unit p 2642 N93-26060
Modeling and analysis tools p 2897 N93-26397
RADIATION HARDENING
Radiation-hardened control system
| DE93-007248 | p 2688 N93-25377
Utilization of an electronic circuit simulator in CMOS latch-up studies
| AD-A260877 | p 2690 N93-25935
RADIATION HAZARDS
HERO resistant semiconductor bridge igniter
p 2627 N93-26024
RADIATION MEASUREMENT
Aerospace techniques in radiation and ecological monitoring of the Republic Belarus
p 2741 N93-24793
SRB environment evaluation and analysis. Volume 3: ASRB plume induced environments
| NASA-CR-192519 | p 2631 N93-26054
RADIATION PRESSURE
Momentum accumulation due to solar radiation torque, and reaction wheel sizing, with configuration optimization
p 2600 N93-24695
Orbit determination error analysis and comparison of station-keeping costs for Lissajous and halo-type libration point orbits and sensitivity analysis using experimental design techniques p 2604 N93-24721
RADIATION PROTECTION
AFRRI research, fiscal year 1991
| AD-A260933 | p 2911 N93-25710
Use of Taguchi design of experiments to optimize and increase robustness of preliminary designs
p 2670 N93-26063
Nuclear safety policy working group recommendations on nuclear propulsion safety for the space exploration initiative
| NASA-TM-105705 | p 2632 N93-26200
RADIATION SHIELDING
A heat transfer analysis of a mobile vehicle radiation-shielded operator compartment
| DE93-007428 | p 2800 N93-25318
RADIATION THERAPY
Measuring the metastatic potential of cancer cells
p 2794 N93-25566
RADIATION TOLERANCE
Quartz oscillators, frequency synthesizers, and timing systems for geodesy and radio science applications
p 2693 N93-25052
Space radiation susceptibility of ultra stable crystal oscillators p 2693 N93-25053
RADIATIVE HEAT TRANSFER
A correlated K-distribution model of the heating rates for H2O and a molecular mixture in the 0-2500 cm(exp -1) wavelength region in the atmosphere between 0 and 60 km
| DE93-005741 | p 2762 N93-25147
A heat transfer analysis of a mobile vehicle radiation-shielded operator compartment
| DE93-007428 | p 2800 N93-25318
RADIATIVE TRANSFER
Propagation of radiation in astrophysical media: Gravitational lenses and astrophysical masers
p 2892 N93-24949
The role of multiple scattering in twilight zenith sky observations of atmospheric absorbers: Diurnal photochemistry and airmass factors
p 2772 N93-25535
Thermal infrared radiation transfer in the planetary boundary layer p 2772 N93-25688
Vector radiative transfer model: Application to rainfall retrieval with microwave radiometric data
p 2784 N93-25743
Further analysis of ECOM-721 data
| AD-A260863 | p 2774 N93-25790
RADII
A nanoradian differential VLBI tracking demonstration
p 2677 N93-26108
RADIO ANTENNAS
Orbiter-orbiter and orbiter-lander tracking using same-beam interferometry p 2677 N93-26110
RADIO ASTRONOMY
The Telecommunications and Data Acquisition Report
| NASA-CR-192804 | p 2676 N93-26105
DSS-13 26-meter antenna upgraded radiometer system p 2679 N93-26122
RADIO BEACONS
The Virginia Tech OLYMPUS propagation experiment
p 2685 N93-26479
Status of the Olympus experiment at CRC
p 2685 N93-26480
RADIO COMMUNICATION
Statistics of sampled Rician fading
| AD-A261397 | p 2681 N93-26289
WARC 92 and some thoughts as to its impact on the NASA propagation program p 2684 N93-26475
Allocations by the 1992 World Administrative Radio Conference p 2684 N93-26476
ESA's planning and coordination of the OLYMPUS propagation experiment p 2684 N93-26477
Observations on the NASA Propagation Program
p 2685 N93-26482
ACTS propagation terminal update
p 2685 N93-26484
RADIO DIRECTION FINDERS
Discrete range clustering using Monte Carlo methods
| NASA-TM-104004 | p 2584 N93-24914

Geolocation of an electromagnetic emitter using a cyclostationary time difference of arrival technique
| AD-A261781 | p 2686 N93-26603

RADIO EQUIPMENT
A Biphase Shift Keying (BPSK), direct sequence, spread spectrum modem for Petite Amateur Navy Satellite (PANSAT)
| AD-A261301 | p 2618 N93-26295
A channel simulation processor for the multi-node tactical network simulator
| AD-A261810 | p 2776 N93-26430

RADIO FREQUENCIES
HERO resistant semiconductor bridge igniter
p 2627 N93-26024
Step stress testing of receiver/transmitter units
| AD-A261286 | p 2730 N93-26279
RF vacuum microelectronics
| AD-A261343 | p 2691 N93-26311
Allocations by the 1992 World Administrative Radio Conference p 2684 N93-26476

RADIO FREQUENCY HEATING
Plasma heating in toroidal systems
| NIFS-208 | p 2858 N93-25092
An outgoing energy flux boundary condition for finite difference ICRP antenna models
| DE93-007788 | p 2674 N93-25300

RADIO FREQUENCY INTERFERENCE
Geolocation of an electromagnetic emitter using a cyclostationary time difference of arrival technique
| AD-A261781 | p 2686 N93-26603

RADIO NAVIGATION
The accuracy of SYLT- and RNS-based time scales at MTI and SNT during 1990-1991 p 2835 N93-25006

RADIO RECEIVERS
First experience with the ASN-16 GLONASS receiver
p 2693 N93-25033
Oscillators for mobile GPS receivers
p 2694 N93-25055
Step stress testing of receiver/transmitter units
| AD-A261286 | p 2730 N93-26279
Flight termination receiver catalog
| AD-A261558 | p 2682 N93-26460
The ACTS propagation program p 2683 N93-26465

RADIO TRANSMISSION
The accuracy of SYLT- and RNS-based time scales at MTI and SNT during 1990-1991 p 2835 N93-25006
High Frequency (HF) radiowave propagation
| AD-A261726 | p 2681 N93-26280
Statistics of sampled Rician fading
| AD-A261397 | p 2681 N93-26289
Proceedings of the 16th NASA Propagation Experimenters Meeting (NAPEX 16) and the Advanced Communications Technology Satellite (ACTS) Propagation Studies Miniworkshop
| NASA-CR-192800 | p 2682 N93-26463
Opening remarks p 2682 N93-26464
The ACTS propagation program p 2683 N93-26465
A database for propagation models
p 2684 N93-26472
ACTS propagation terminal update
p 2685 N93-26484

RADIO TRANSMITTERS
Improvements in X-band transmitter phase stability through Klystron body temperature regulation
p 2678 N93-26114
Step stress testing of receiver/transmitter units
| AD-A261286 | p 2730 N93-26279

RADIO WAVES
High Frequency (HF) radiowave propagation
| AD-A261726 | p 2681 N93-26280
Proceedings of the 16th NASA Propagation Experimenters Meeting (NAPEX 16) and the Advanced Communications Technology Satellite (ACTS) Propagation Studies Miniworkshop
| NASA-CR-192800 | p 2682 N93-26463

RADIOACTIVE DECAY
Topics in CP violation
| DE93-007615 | p 2847 N93-25323

RADIOACTIVE ISOTOPES
Health and environmental chemistry: Analytical techniques, data management, and quality assurance
| DE93-002853 | p 2760 N93-24674
Cosmic ray composition investigations using ICE/ISEE-3
| NASA-CR-192808 | p 2900 N93-25241
Reclamation with recovery of radionuclides and toxic metals from contaminated materials, soils, and wastes
p 2769 N93-25571
Development of resonance ionization spectroscopy for genome mapping and DNA sequencing using stable isotopes as DNA labels
| DE93-007815 | p 2793 N93-26587

RADIOACTIVE MATERIALS
A comparison of the WIND System atmospheric models and MATS data
| DE93-002687 | p 2760 N93-24673
Aerospace techniques in radiation and ecological monitoring of the Republic Belarus
p 2741 N93-24793

RADIOACTIVE WASTES
Human factors in environmental management: New directions from the Hanford site
| DE93-004337 | p 2767 N93-26495

RADIOBIOLOGY
AFRRI research, fiscal year 1991
| AD-A260933 | p 2911 N93-25710

RADIOCHEMISTRY
Health and environmental chemistry: Analytical techniques, data management, and quality assurance
| DE93-002853 | p 2760 N93-24674

RADIOGRAPHY
Analysis of shaped charge jet penetration experiments with Pen
| UCRL-LR-110773 | p 2730 N93-26177

RADIOISOTOPE BATTERIES
Solid-state isotopic power source for computer memory chips p 2694 N93-25596

RADIOLOGY
Automated system for early breast cancer detection in mammograms p 2796 N93-25568

RADIOMETERS
Analysis of LARI sensor system
| DE93-006334 | p 2761 N93-24977
Commercial applications multispectral sensor system
p 2758 N93-25615
Walsh function generator for the Electronically Scanned Thinned Array Radiometer (ESTAR) instrument
| NASA-TM-4449 | p 2689 N93-25618
The pressure modulation system in the Improved Stratospheric and Mesospheric Sounder
p 2773 N93-25739
DSS-13 26-meter antenna upgraded radiometer system p 2679 N93-26122
Opening remarks p 2682 N93-26464
The effects of cloud inhomogeneities upon radiative fluxes, and the supply of a cloud truth validation dataset
| NASA-CR-191711 | p 2787 N93-26492

RAILGUN ACCELERATORS
Energy and Technology Review, October - December 1992
| DE93-007784 | p 2674 N93-25299

RAIN
North-central Mexico blue grama rangeland biomass assessment at the end of the rainy season using NOAA-AVHRR-LAC p 2750 N93-24854
Rainfall frequency atlas of the Midwest
| PB93-164606 | p 2785 N93-25872
Satellite communications application to Pacific countries above Ku band p 2683 N93-26471
Rain compensation algorithm using adaptive linear prediction p 2685 N93-26485
More rain compensation results p 2686 N93-26486

RAIN FORESTS
World Forest Watch: A global forest monitoring test
p 2748 N93-24836
Tropical forest monitoring with high resolution satellite data p 2748 N93-24841

RAIN GAGES
Rain rate instrument for deployment at sea, phase 2
| NASA-CR-192442 | p 2786 N93-26156
Rain rate and modeled fade distributions at 20 GHz and 30 GHz derived from five years of network rain gauge measurements p 2683 N93-26468
A comparative assessment of R. M. Young and tipping bucket rain gauges p 2685 N93-26483

RAINDROPS
Rain rate instrument for deployment at sea, phase 2
| NASA-CR-192442 | p 2786 N93-26156

RAINSTORMS
Rainfall frequency atlas of the Midwest
| PB93-164606 | p 2785 N93-25872

RAMAN SPECTRA
Apparatus for imaging an object in or through a scattering medium using coherent anti-Stokes Raman scattering
| AD-D015642 | p 2852 N93-25358
Experimental studies of fundamental problems in quantum optics
| AD-A261183 | p 2853 N93-25822

RAMAN SPECTROSCOPY
Experimental studies of fundamental problems in quantum optics
| AD-A261183 | p 2853 N93-25822
Visible light emission from porous silicon examined by photoluminescence and Raman spectroscopy
| DE93-006780 | p 2646 N93-26502
Spectroscopic effects of disorder and vibrational localization in mixed-halide metal-halide chain solids
| DE93-007361 | p 2646 N93-26505

RANDOM ACCESS
Considerations for space and naval aviation applications of ferroelectric memory
| AD-A261300 | p 2807 N93-26294

RANDOM NOISE
Figure of merit for direct-detection optical channels
p 2678 N93-26117
New results in signal design for the AWGN channel
| AD-A261424 | p 2682 N93-26451

RANDOM PROCESSES
Determination of design and operation parameters for upper atmospheric research instrumentation to yield optimum resolution with deconvolution, appendix 4
| NASA-CR-192834 | p 2769 N93-24910
Considerations of the error variances of time-averaged estimators for correlated processes
| AD-A261796 | p 2830 N93-26255
Properties of readings of periodically correlated random processes
| AD-A261225 | p 2686 N93-26573

RANDOM VIBRATION
On the effect of acoustic coupling on random and harmonic plate vibrations
| NASA-TM-107740 | p 2844 N93-25189

RANGE AND RANGE RATE TRACKING
The application of the PRARE principle for precise two-way time transfer to space-based atomic clocks
p 2832 N93-24983

RANGE FINDERS
Real-time construction of three-dimensional occupancy maps
| DE93-001645 | p 2756 N93-25505
Uncertainty in object pose determination with three light-stripe range measurements
| AD-A261435 | p 2857 N93-26488

RANGEFINDING
Application of GPS tracking techniques to orbit determination for TDRS p 2601 N93-24702
Discrete range clustering using Monte Carlo methods
| NASA-TM-104004 | p 2584 N93-24914
The advances in F and T technology: Their benefits of and for space science and technology
p 2831 N93-24979
The application of the PRARE principle for precise two-way time transfer to space-based atomic clocks
p 2832 N93-24983
A new modem for microwave time synchronisation via geosynchronous telecommunication satellites
p 2686 N93-24999
Deep-space navigation with differenced data types. Part 3: An expanded information content and sensitivity analysis p 2614 N93-26109
Image-based ranging and guidance for rotorcraft
| NASA-CR-177608 | p 2586 N93-26549

RANGELANDS
North-central Mexico blue grama rangeland biomass assessment at the end of the rainy season using NOAA-AVHRR-LAC p 2750 N93-24854

RAPID QUENCHING (METALLURGY)
Solidification processing and phase transformations in ordered high temperature alloys
| AD-A261751 | p 2652 N93-26284

RARE GAS-HALIDE LASERS
Electron-beam-pumped recombination lasers
p 2712 N93-25344

RARE GASES
The physics of spin polarized gases
| AD-A261396 | p 2850 N93-26288
FALCON nuclear-reactor-pumped laser program and wireless power transmission
| DE93-007607 | p 2715 N93-26597

RATES (PER TIME)
A comparative assessment of R. M. Young and tipping bucket rain gauges p 2685 N93-26483

RATIONAL FUNCTIONS
Estimation of coefficients in a rational function from observed values
| AD-A261126 | p 2828 N93-25773

RATS
Progress in imaging microscopy with x ray lasers at LLNL
| DE93-007508 | p 2712 N93-25363
The acute inhalation toxicity of pyrolysis products of halon 1301
| AD-A260874 | p 2795 N93-25629

RAY TRACING
Digital Oblique Remote Ionospheric Sensing (DORIS) program development
| AD-A261750 | p 2776 N93-26283

RAYLEIGH SCATTERING
Data analysis and interpretation of lunar dust exosphere p 2898 N93-26059
Pulsed laser Rayleigh scattering diagnostic for hydrogen/oxygen rocket exit plane flowfield velocimetry
| NASA-TM-106098 | p 2631 N93-26149

RAYLEIGH WAVES
Structural acoustics: A general form of reciprocity principles in acoustics
| AD-A261515 | p 2846 N93-26376

RAYLEIGH-RITZ METHOD
Optimization techniques for contact stress analysis
| AD-A260846 | p 2729 N93-25911
RDX
Development of rate expressions for the thermal decomposition of RDX p 2629 N93-26034
Chemistry during the induction time in heated nitramines p 2629 N93-26035
Thermal decomposition of energetic materials. 4: Deuterium isotope effects and isotopic scrambling condensed-phased decomposition of 1,3,5-trinitrohexahydro-s-triazine
| AD-A261804 | p 2662 N93-26387
REACTING FLOW
Asymptotic studies of gravity-driven reacting coating flows and pultrusion processes p 2704 N93-25683
A new LU-SGS flow solver for calculating reentry flows p 2579 N93-25759
Visualization of a Mach 2 reacting flow using Planar Laser-Induced Fluorescence (PLIF) p 2598 N93-26006
Gasp 1.3 results for the transverse hydrogen reacting jet p 2625 N93-26011
Turbulence interacting with chemical kinetics in airbreathing combustion of ducted rockets p 2625 N93-26012
REACTION KINETICS
Coarsening of a quiescent electrorheological fluid I: Experiment
| DE93-006776 | p 2642 N93-24972
Studying the kinetics of magnetization in high Tc superconductors
| NASA-CR-192916 | p 2862 N93-25108
Design of a high activity and selectivity alcohol catalyst
| DE93-008103 | p 2659 N93-25112
Measurements of soot formation and hydroxyl concentration in near critical equivalence ratio premixed ethylene flame
| NASA-CR-191099 | p 2642 N93-25116
A novel process for methanol synthesis
| DE93-008037 | p 2659 N93-25118
Probe molecule studies: Active species in alcohol synthesis
| DE93-008097 | p 2659 N93-25119
Processing and properties of Ti5Si3
| DE93-007284 | p 2649 N93-25149
The structure of particle cloud premixed flames
| NASA-CR-192827 | p 2643 N93-25229
Electron-beam-pumped recombination lasers p 2712 N93-25344
Results from the NA36 on strangeness production in 200 GeV/c per nucleon S + Pb and p - Pb reactions
| DE93-007711 | p 2848 N93-25364
Temperature dependent sensor response caused by polymer-solvent interactions
| DE93-005368 | p 2655 N93-25444
Energy transfer properties and mechanisms
| DE93-008540 | p 2849 N93-25488
Chemical dynamics studies of high energy species
| AD-A260743 | p 2852 N93-25676
Luminescence probe studies of ionomers. 3: Distribution of decay rate constants for tris bipyridyl ruthenium(2) in Nafion membranes
| AD-A260764 | p 2645 N93-25916
Turbulence interacting with chemical kinetics in airbreathing combustion of ducted rockets p 2625 N93-26012
Hybrid rocket fuel combustion study p 2626 N93-26019
Flame structure studies of a lean, 20 torr H2/N2O/AR flame employing molecular beam mass spectrometry p 2627 N93-26025
Kinetic studies in gas-phase reaction mechanisms important to the combustion process of high energy density materials: The H2/NO2 reaction p 2628 N93-26027
Dark zone modeling of solid propellant flames p 2628 N93-26028
Condensed-phase processes during solid propellant combustion. Part 4: Chemical and microscopic examination of laser-irradiated propellant samples p 2628 N93-26032
Development of rate expressions for the thermal decomposition of RDX p 2629 N93-26034
Interactions of acoustic waves and combustion of homogeneous solid propellants in rocket motors p 2630 N93-26039
Mechanisms of decomposition and oxidation of borane compounds
| AD-A261137 | p 2645 N93-26045
Phosphorus-, nitrogen-, sulfur-, and chlorine-containing molecules on surfaces
| AD-A261265 | p 2657 N93-26303
Thermal decomposition of energetic materials. 4: Deuterium isotope effects and isotopic scrambling condensed-phased decomposition of 1,3,5-trinitrohexahydro-s-triazine
| AD-A261804 | p 2662 N93-26387
In-process cure monitoring of composites via fiber-optic fluorescence
| AD-A261712 | p 2641 N93-26580
REACTION PRODUCTS
Treatment of hazardous organic wastes using silent discharge plasmas
| DE93-003789 | p 2768 N93-26592
REACTION WHEELS
Momentum accumulation due to solar radiation torque, and reaction wheel sizing, with configuration optimization p 2600 N93-24695
Testing of the on-board attitude determination and control algorithms for SAMPEX p 2600 N93-24698
Accurate attitude determination of the LACE satellite p 2605 N93-24726
Attitude control of the LACE satellite: A gravity gradient stabilized spacecraft p 2605 N93-24727
REACTIVITY
Design and synthesis of reactive separation systems
| DE93-008764 | p 2642 N93-25115
Hazards of explosives dusts: Particle size effects
| DE93-009380 | p 2668 N93-25498
REACTOR DESIGN
Seismic buckling capacity of unstiffened, free-standing steel containments
| DE93-005325 | p 2723 N93-24957
REACTOR SAFETY
Human factors engineering: A key element of instrumentation and control system design
| DE93-006731 | p 2800 N93-25415
READ-ONLY MEMORY DEVICES
Lossless compression of image data products on th e FIFE CD-ROM series p 2804 N93-25929
READING
A framework for the design of usable electronic text p 2877 N93-25754
The adult literacy evaluator: An intelligent computer-aided training system for diagnosing adult illiterates p 2799 N93-26082
REAGENTS
Studies of the analyte-carrier interface in flow injection analysis
| DE93-008374 | p 2644 N93-25311
Effect of cytoskeletal reagents on stretch activated ion channels
| AD-A261089 | p 2793 N93-25764
REAL TIME OPERATION
A comparison of the WIND System atmospheric models and MATS data
| DE93-002687 | p 2760 N93-24673
TDRSS-user orbit determination using batch least-squares and sequential methods p 2601 N93-24703
Real-time attitude determination and gyro calibration p 2602 N93-24708
Computationally efficient algorithms for real-time attitude estimation p 2602 N93-24709
Accurate attitude determination of the LACE satellite p 2605 N93-24726
Use of remote sensing spacecrafts in real time support to disaster management: Interfaces with ground segment facilities and services p 2743 N93-24809
Lightning precursor signatures from dual-polarization radar measurements of storms p 2777 N93-24877
The role of ocean climate data in operational Naval oceanography p 2732 N93-24916
Global Temperature and Salinity Pilot Project p 2733 N93-24924
The use of remotely sensed data for operational fisheries oceanography p 2734 N93-24927
Automated in situ observations of upper ocean biogeochemistry, bio-optics, and physics and their potential use for global studies p 2736 N93-24939
A new method for infrared imaging of air currents in and around critical hazard fume hoods
| DE93-003009 | p 2761 N93-24956
Coarsening of a quiescent electrorheological fluid I: Experiment
| DE93-006776 | p 2642 N93-24972
Putting time into proof outlines
| NASA-CR-192978 | p 2809 N93-25152
An advanced data-acquisition system for wind energy projects
| DE93-000079 | p 2874 N93-25254
Concurrency control in real-time database systems p 2874 N93-25271
Dynamic error analysis of numerical methods for simulation of state-variable derivatives with discontinuities p 2819 N93-25278
Log-ratio signal-processing technique for beam position monitors
| DE93-007356 | p 2851 N93-25314
Numerical kinematic transformation calculations for a parallel link manipulator
| DE93-005778 | p 2718 N93-25449
Real-time construction of three-dimensional occupancy maps
| DE93-001645 | p 2756 N93-25505
Real-time construction and rendering of three-dimensional occupancy maps
| DE93-007818 | p 2756 N93-25516
Use of high performance networks and supercomputers for real-time flight simulation p 2598 N93-25574
Improved performance and safety for high energy batteries through use of hazard anticipation and capacity prediction p 2694 N93-25582
The Generic Spacecraft Analyst Assistant (GenSAA): A tool for developing graphical expert systems p 2814 N93-25589
MAC to VAX connectivity: Heartrate spectral analysis system p 2796 N93-25594
Adaptive liquid crystal TV based joint transform correlator as applied to real-time pattern recognition
| AD-A260724 | p 2864 N93-25655
Active control of NiTiNOL-reinforced structural composites
| AD-A261062 | p 2638 N93-25780
The Grid Analysis and Display System (GRADS): A practical tool for Earth science visualization p 2880 N93-25805
Multi-layer holographic bifurcative neural network system for real-time adaptive EOS data analysis p 2880 N93-25807
An optimal scheduling of pick-place operations of a robot-vision-tracking system by using neural networks and rule-based systems p 2821 N93-25880
Multi-rate, real time image compression for images dominated by point sources p 2805 N93-25932
The WorkPlace distributed processing environment p 2825 N93-25977
VETA x ray data acquisition and control system p 2854 N93-26186
Real-time value-driven monitoring and repair
| AD-A260959 | p 2811 N93-26221
Realtime control of multiple sensor systems
| AD-A261037 | p 2680 N93-26226
Advanced technology for portable personal visualization
| AD-A261294 | p 2807 N93-26293
Intelligent, real-time problem solving, phase 3
| AD-A261441 | p 2829 N93-26345
United States Army space experiment 601
| AD-A261460 | p 2798 N93-26353
Multivariable control for flexible IC processing
| AD-A261685 | p 2692 N93-26366
Managing real-time software projects: Problems and issues
| AD-A261428 | p 2813 N93-26453
RECEIVERS
GPS standardization for the needs of time transfer p 2836 N93-25016
Osciliators for mobile GPS receivers p 2694 N93-25055
Low-frequency room responses. Part 2: Calculation methods and experimental results
| BBC-RD-1992/9-PT-2 | p 2673 N93-25169
A superconducting tunnel junction receiver for submillimeter astronomy, and analysis of observations of post-AGB star molecular envelopes p 2889 N93-25440
Figure of merit for direct-detection optical channels p 2678 N93-26117
Cross-switched MICRAD seeker
| AD-D015676 | p 2691 N93-26142
Trellis coded CPFSK
| AD-A261788 | p 2682 N93-26441
RECESSES
Prediction of hydrogen entry and permeation in metals and alloys
| AD-A260580 | p 2651 N93-25903
RECIPROCATION
Prospects of two-way international time scale comparisons p 2832 N93-24988
RECIPROCITY THEOREM
Structural acoustics: A general form of reciprocity principles in acoustics
| AD-A261515 | p 2846 N93-26376
RECIRCULATIVE FLUID FLOW
Heterogeneous photocatalytic oxidation of atmospheric trace contaminants
| NASA-CR-192937 | p 2767 N93-26427
RECOIL ATOMS
Modeling of atom-diatom scattering
| AD-A261645 | p 2849 N93-26173

Progress in impulse approach research
| AD-A261728 | p 2850 N93-26281

RECOMMENDATIONS
Atomic time scales for dynamical astronomy
p 2832 N93-24984
The application of integrated knowledge-based systems for the Biomedical Risk Assessment Intelligent Network (BRAIN) p 2799 N93-25595
Automation and robotics human performance
| NASA-CR-193049 | p 2802 N93-26153

RECONSTRUCTION
Bayesian cross-entropy reconstruction of complex images
| AD-A261812 | p 2812 N93-26257

RECTANGULAR PLATES
Uniform roughness studies
| WL-TR-92-3041 | p 2706 N93-25951

RECTANGULAR WAVEGUIDES
Feasibility study of a Ka-/Ka-band dichroic plate with stepped rectangular apertures p 2671 N93-24660

RECYCLING
Application of remote sensing data for the investigation of environmental degradation sites in East Germany
p 2739 N93-24785
Low cost dewatering of waste slurries
p 2769 N93-25573

REDUCED GRAVITY
Analysis of reentry into the White Sands Missile Range (WSMR) for the LifeSat mission p 2603 N93-24717
Contributions of microgravity test results to the design of spacecraft fire safety systems
| NASA-TM-106093 | p 2614 N93-24755
Electrodeposition in low gravity p 2663 N93-24774
A model of concurrent flow flame spread over a thin solid fuel
| NASA-CR-191111 | p 2663 N93-24946
A simple and compact source of cold atoms for cesium fountains and microgravity clocks p 2831 N93-24981
The Columbus Metrology Science Team: Report on activities p 2670 N93-24987
NASA Microgravity Science and Applications Program
| NASA-TM-108775 | p 2663 N93-25194
Whisker growth studies under conditions which resemble those available on an orbiting space station
| NASA-CR-192701 | p 2664 N93-25218
On the generation and dispersion of Yanai waves with a spectral Chebyshev-collocation reduced-gravity ocean model p 2788 N93-25276
Modeling of bubble and drop formation in flowing liquids in terrestrial and microgravity environments
p 2664 N93-25390
Gas-Grain Simulation Facility (GGSF). Volume 1: Stage 1 facility definition studies
| NASA-CR-177606 | p 2887 N93-25442
Modelling of microgravity ignition phenomena
p 2664 N93-25465
Annular flow enhanced two-phase evaporative heat exchanger for space-based systems
p 2700 N93-25478
Numerical study of cavity natural convection flow with augmenting and counteracting effects by projection finite element method p 2701 N93-25540
Gravity-dependent transport phenomena in zeolite crystal growth p 2664 N93-25740
Investigation of the effects of Extra Vehicular Activity (EVA) and Launch and Entry (LES) gloves on performance p 2803 N93-26061
The role of pyridoxine as a countermeasure for in-flight loss of lean body mass p 2796 N93-26068
Conceptual design for the Space Station Freedom fluid physics/dynamics facility
| NASA-TM-103663 | p 2618 N93-26209

REDUCTION (CHEMISTRY)
Whisker growth studies under conditions which resemble those available on an orbiting space station
| NASA-CR-192701 | p 2664 N93-25218
Prediction of hydrogen entry and permeation in metals and alloys
| AD-A260580 | p 2651 N93-25903

REDUNDANCY
Algorithms for optimal redundancy allocation
| DE93-005709 | p 2827 N93-24973
Time and frequency reference for a trajectory measurement system p 2837 N93-25023

REDUNDANCY ENCODING
Computationally efficient algorithms for real-time attitude estimation p 2602 N93-24709

REED-SOLOMON CODES
A (72, 36; 15) box code p 2671 N93-24663
A low-complexity and high performance concatenated coding scheme for high-speed satellite communications
| NASA-CR-192715 | p 2673 N93-25198

REENTRY VEHICLES
Combined LAURA-UPS hypersonic solution procedure
| NASA-TM-107682 | p 2696 N93-25176
A new LU-SGS flow solver for calculating reentry flows p 2579 N93-25759

REFINING
INEL spray-forming research p 2658 N93-25562

REFLECTANCE
Analysis of LARI sensor system
| DE93-006334 | p 2761 N93-24977
Temperature dependent sensor response caused by polymer-solvent interactions
| DE93-005368 | p 2655 N93-25444
The x ray reflectivity of the AXAF VETA-I optics
p 2855 N93-26192

REFLECTION NEBULAE
Shells, outflows and star formation in the giant molecular cloud Monoceros R2 p 2893 N93-25555

REFLECTOR ANTENNAS
Ka-band feed arrays for spacecraft reflector antennas with limited scan capability: An overview
p 2680 N93-26128

REFLECTORS
DSN observations of Titan p 2680 N93-26129

REFRACTED WAVES
Proceedings of the 5th International Symposium on Long Range Sound Propagation
| AD-A260666 | p 2845 N93-25643

REFRACTIVITY
Condensation on cooled surfaces of optical devices at the cosmic conditions p 2753 N93-24869
Interferometric fiber-optic radiation sensor
| DE93-003841 | p 2852 N93-25127
Optical and scratch resistant properties of diamondlike carbon films deposited with single and dual ion beams
p 2658 N93-25564

REFRACTORY COATINGS
Control of crystallite size in diamond film chemical vapor deposition
| AD-D015660 | p 2867 N93-26090

REFRACTORY MATERIALS
Evaluation of a candidate material for a coal-fired magnetohydrodynamic (MHD) high temperature recuperative air heater
| DE93-006630 | p 2858 N93-24968
Development of thin film thermocouples on ceramic materials for advanced propulsion system applications
| NASA-TM-106017 | p 2709 N93-25173
Properties of extruded PS-212 type self-lubricating materials p 2659 N93-25565
Computer modelling of cyclic deformation of high-temperature materials
| AD-A260978 | p 2639 N93-25936

REFRIGERANTS
An assessment of alternatives and technologies for replacing ozone-depleting substances at DOE facilities
| DE93-002862 | p 2760 N93-24675
Compressor calorimeter performance of refrigerant blends: Comparative methods and results for a refrigerator/freezer application
| DE93-006734 | p 2667 N93-24970
Experimental and theoretical studies of dense fluid mixtures
| DE93-006070 | p 2695 N93-24976
Malone refrigeration
| DE93-005439 | p 2668 N93-25447

REFRIGERATING
Malone refrigeration
| DE93-005439 | p 2668 N93-25447

REFRIGERATORS
Compressor calorimeter performance of refrigerant blends: Comparative methods and results for a refrigerator/freezer application
| DE93-006734 | p 2667 N93-24970
Malone refrigeration
| DE93-005439 | p 2668 N93-25447
Basic research thermoacoustic heat transport
| AD-A261334 | p 2759 N93-26310
Low temperature Hall and Shubnikov-de Haas effects
| AD-A261871 | p 2869 N93-26540

REFUELING
Military standardization handbook: Aircraft refueling handbook
| AD-A261755 | p 2662 N93-26600

REGENERATION (ENGINEERING)
A survey of life support system automation and control
| NASA-TM-103977 | p 2667 N93-25085

REGIONAL PLANNING
The regional planning and control using the satellite data p 2740 N93-24788
Monitoring and analysis of urban trends using multitemporal satellite-imagery (case-study: Greater Cairo) p 2740 N93-24790
Use of remote sensing and GIS for the environmental planning proposal of the Sarno River Valley (Campania, southern Italy) p 2741 N93-24797

REGOLITH
Lunar regolith and structure mechanics
p 2670 N93-26412
Indigenous lunar construction materials
p 2670 N93-26413

REGRESSION ANALYSIS
Interpretation and segmentation of changed forest stands from difference imagery based on regression functions p 2748 N93-24839

REGULATIONS
Regulatory impact analysis of the Part 503 sewage sludge regulation
| PB93-110625 | p 2768 N93-26567

REINFORCING FIBERS
International Workshop on Advances in Inorganic Fibre Technology
| AD-A260719 | p 2639 N93-25908
Electrostatic fiber spreader
| AD-D015677 | p 2640 N93-26143
Effects of moisture and other contaminants in friction composites
| AD-A261226 | p 2640 N93-26301

RELATIVISTIC EFFECTS
The advances in F and T technology: Their benefits of and for space science and technology
p 2831 N93-24979
Relativistic effects for low Earth orbit satellites using GPS p 2608 N93-24986
Prospects of two-way international time scale comparisons p 2832 N93-24988

RELATIVITY
Atomic time scales for dynamical astronomy
p 2832 N93-24984
Relativistic effects for low Earth orbit satellites using GPS p 2608 N93-24986

RELAY SATELLITES
Frequency generation and synthesis in the DRSS
p 2693 N93-25054

RELIABILITY
Time and frequency reference for a trajectory measurement system p 2837 N93-25023
Expert system for UNIX system reliability and availability enhancement p 2723 N93-25588

RELIABILITY ANALYSIS
Statistical modelling of software reliability
| NASA-CR-192985 | p 2809 N93-25257
Stress and reliability analyses of multilayered composite cylinder under thermal and mechanical loads
p 2726 N93-25533

RELIABILITY ENGINEERING
Reliability assessment at airline inspection facilities. Volume 1: A generic protocol for inspection reliability experiments
| DOT/FAA/CT-92/12-VOL-1 | p 2582 N93-25110

RELIEF MAPS
A ground track control algorithm for the Topographic Mapping Laser Altimeter (TMLA) p 2602 N93-24707

REMOTE CONTROL
Experimental modal survey of the probe mass mock-up
| DE93-008846 | p 2617 N93-25494
Digital filter control of remotely operated flexible robotic structures
| DE93-007587 | p 2827 N93-26596

REMOTE HANDLING
Initial experiments with a myoelectric-based muscle sensor
| DE92-016034 | p 2799 N93-25099
Detailed solution to a complex kinematics chain manipulator
| DE93-004619 | p 2725 N93-25357

REMOTE MANIPULATOR SYSTEM
Dynamics of on-orbit construction process
p 2669 N93-26406

REMOTE SENSING
Resolution of the COBE Earth sensor anomaly
p 2600 N93-24700
Orbit determination support of the Ocean Topography Experiment (TOPEX)/Poseidon operational orbit
p 2601 N93-24704
Environment Observation and Climate Modelling Through International Space Projects. Volume 2: Remote Sensing for Environmental Monitoring and Resource Management
| ESA-ISY-1-VOL-2 | p 2737 N93-24775
Use of airborne imaging spectrometry to the definition of optimised specifications for land applications with future spaceborne imaging spectrometers
p 2738 N93-24776
Remote sensed spectral signatures classification and recognition by neural networks: An approach to unsupervised techniques p 2738 N93-24779
Verification of a climate convention: Role and limitations of a space based remote sensing system
p 2738 N93-24781

Spectral remote sensing of anomalous mineralogy induced by hydrocarbon migration and uranium mineralization, San Rafael Swell, Utah, USA p 2739 N93-24783
Satellite remote sensing for environmental geology: The Bandung (West Java) experience p 2739 N93-24784
Application of remote sensing data for the investigation of environmental degradation sites in East Germany p 2739 N93-24785
Application of remote sensing to environmental monitoring in Poland p 2739 N93-24786
The regional planning and control using the satellite data p 2740 N93-24788
Land cover monitoring in the Netherlands applying satellite remote sensing p 2740 N93-24789
Detection of land use/land cover changes using remote sensing and GIS in Vietnam p 2740 N93-24791
Geologic and hydrogeologic mapping of Iceland with multisensor data (JERS-1, ERS-1, SPOT, Landsat and SEASAT) p 2740 N93-24792
Aerospace techniques in radiation and ecological monitoring of the Republic Belarus p 2741 N93-24793
Determination of environmental dynamics using NOAA satellite data and a water balance model for the Mediterranean landscape p 2741 N93-24794
Agroclimatological zonation by AVHRR data for vegetation monitoring p 2741 N93-24795
A knowledge-based approach to waste disposal sites detection through integration of Landsat-TM imagery and geographical context information p 2741 N93-24796
Use of remote sensing and GIS for the environmental planning proposal of the Sarno River Valley (Campania, southern Italy) p 2741 N93-24797
Complex investigation of a system industrial site-environment using remote sensing and landscape-geochemical methods p 2741 N93-24798
Archaeological, historical and geoelectrical data as ground truth for Landsat TM imagery application to coastal plain evolution studies p 2742 N93-24799
Demonstration of seasonal changes in the territory of Finland using multitemporal NOAA-AVHRR data p 2742 N93-24801
The use of remote sensing and GIS for the assessment of environmental degradation caused by fires, applied upon South-Euboia (central Greece) p 2742 N93-24802
Lithologic mapping with LANDSAT Thematic Mapper guided by laboratory spectral measurements, Air, Niger (Africa) p 2742 N93-24803
Natural disasters and their mitigation using space technology p 2742 N93-24804
Alternative strategies for the use of satellite data analysis systems for hazard monitoring and disaster mitigation p 2743 N93-24805
Satellite borne remote sensing data: A tool for natural disaster reduction p 2743 N93-24806
Application of multitemporal Landsat-MSS and -TM data for the development of an inundation-risk-map p 2743 N93-24807
Sustainable remote sensing: A major improvement for realtime resource management and disaster early warning in developing countries p 2743 N93-24808
Use of remote sensing spacecrafts in real time support to disaster management: Interfaces with ground segment facilities and services p 2743 N93-24809
A method for sequential image analysis of hazard areas p 2743 N93-24810
The use of SPOT data in natural disaster prevention and damage assessment p 2743 N93-24811
Aerospace monitoring for ecological hazard and disaster mitigation p 2744 N93-24812
The need for spaceborne observations for meteorology and climatology p 2744 N93-24813
Remote sensing of non-renewable resources p 2744 N93-24814
Remote sensing geology p 2744 N93-24815
Remote sensing in hydrology and water management p 2744 N93-24816
Potential operational use of remote sensing from space in forestry p 2745 N93-24817
Remote sensing applied to agriculture state of the art and new trends p 2745 N93-24818
Applications of remote sensing for tidal waters, coastal areas and inland waters p 2745 N93-24819
Supporting the Portuguese fisheries with satellites p 2745 N93-24821
Application of satellite imageries data to fisheries in Japan p 2745 N93-24822
Oil pollution and water quality mapping of Augusta Bay, Italy using remote sensing techniques p 2746 N93-24823
NORSMAP 1989: Norwegian remote sensing spectrometry for mapping and monitoring of algal blooms and pollution p 2746 N93-24824
SEOMAR: An Italian approach to the observation of the Mediterranean area p 2746 N93-24825
The extent and status of mangroves in Mombasa district, Kenya: A case study based on remote sensing p 2746 N93-24826
Remote sensing of coastal zone Sabkha deposits, Gulf of Sirt, Libya p 2746 N93-24827
Inherent optical properties of lakes as measured by Landsat 5 Thematic Mapper p 2746 N93-24828
Multi-date algorithms for predicting surface water quality parameters in estuarine and coastal waters using Landsat TM data
| ED-659-CP | p 2746 N93-24829
Remote sensing monitoring and hindcasting of the accident occurred to the tanker Haven in the Gulf of Genoa (Italy) p 2747 N93-24830
Algal blooms and gel production in Adriatic Sea observed by remote sensing techniques p 2747 N93-24831
Hel's peninsula coastal zone changes in the last 40 years on a base of remote sensing methods p 2747 N93-24832
Evaluation of nearshore suspended sediment concentration through Landsat TM data: First results p 2747 N93-24833
Monitoring and evaluation of morphohydrographical changes in the Danube Delta by remote-sensing p 2747 N93-24834
Coastal environmental mapping using Landsat data
| ED-658-CP | p 2747 N93-24835
World Forest Watch: A global forest monitoring test p 2748 N93-24836
The national parks of Bavarian Forest and Sumava: A Landsat TM perspective on the structure and dynamics of the largest woodland of Central Europe p 2748 N93-24837
Application of photographic remote sensing data from space for information about forests p 2748 N93-24838
Interpretation and segmentation of changed forest stands from difference imagery based on regression functions p 2748 N93-24839
The ESA ISY initiatives for forest inventory in Europe p 2748 N93-24840
Assessment of storm damage in forests using SPOT imagery p 2748 N93-24842
Mapping of windfall damage in the Hunsrueck plateau with Landsat TM-data p 2749 N93-24843
A prototype system for forest fire prevention and control p 2749 N93-24844
The use of polarimetric radar remote sensing data for application in forestry p 2749 N93-24845
Forest decline monitoring using Landsat TM, digital stand data and DEMs p 2749 N93-24846
Swedish forest information atlas p 2749 N93-24847
Observation of forest damages in the Harz mountains by means of satellite remote sensing p 2749 N93-24848
Toward a satellite based crop information system in Hungary p 2750 N93-24849
Remote sensing of land resource management in agriculture with regard to its influence on the environment p 2750 N93-24850
Assessment and forecasting of crop yield in Niger through NOAA NDVI data p 2750 N93-24851
Global drought monitoring from NOAA polar orbiting satellites p 2750 N93-24852
Interest of complementary data of coarse and high spatial resolution for agro-climatic crop monitoring p 2750 N93-24853
North-central Mexico blue grama rangeland biomass assessment at the end of the rainy season using NOAA-AVHRR-LAC p 2750 N93-24854
Registration of the use of agricultural fields and soil erosion using satellite remote sensing p 2751 N93-24856
Appliction of remote sensing to forestry mapping: Experience from the European collaborative programme for the less favoured areas p 2751 N93-24857
Biodiversity indication by Earth observation data p 2751 N93-24858
Measuring the intensity of nitrogen fertilization of grassland by means of remote sensing p 2751 N93-24859
Crop agroecological diagnostics by remote sensing technique p 2751 N93-24860
Combining spectral information with crop rotation knowledge for crop classifications p 2752 N93-24861
Atmospheric correction of Landsat/TM data over mountainous terrain for forestry applications p 2752 N93-24862
Standwise forest inventory and mapping for operational management planning p 2752 N93-24863
Forest damage detection and reflection of conifers: From micro to field level p 2752 N93-24864
Scale dependence in the reflectance of deciduous woodland: Evidence from a helicopter-mounted spectroradiometer p 2752 N93-24865
Operational use of MOMS-02 (P2) data p 2752 N93-24866
Influence due to antenna pattern change in brightness temperature estimation for a space-based microwave radiometer p 2753 N93-24868
Data processing and control in a transputer system for remote sensing of the Earth p 2753 N93-24870
EUROSTARS: A system for thematic analysis of remote sensed data p 2753 N93-24871
Earthquake vulnerability map of the Lake Constance area p 2753 N93-24872
Current trends in satellite data supply for environmental monitoring p 2754 N93-24874
The Global Ocean Observing System p 2733 N93-24923
The use of remotely sensed data for operational fisheries oceanography p 2734 N93-24927
Feasibility study of a long duration balloon flight with NASA/GSFC and Soviet Space Agency Gamma Ray Spectrometers
| NASA-CR-192934 | p 2573 N93-25077
Application of optical remote sensing to the study of surface fluxes related to cloud formation
| DE93-003783 | p 2781 N93-25125
An expert system shell for inferring vegetation characteristics: Inrerface for the addition of techniques (Task H)
| NASA-CR-192897 | p 2754 N93-25154
CEOS Committee on Earth Observations Satellites consolidated report, 1992
| NASA-TM-108776 | p 2615 N93-25217
Cloud properties as inferred from HIRS/2 multi-spectral data p 2782 N93-25293
Former Soviet Republic capabilities in space and science
| DE93-007613 | p 2598 N93-25322
JPRS report: Science and technology. Central Eurasia: Life sciences
| JPRS-ULS-92-020 | p 2793 N93-25406
Passive microwave remote sensing of snow-covered floating ice during spring conditions in the Arctic and Antarctic
| ISBN-0-315-70444-6 | p 2754 N93-25422
Integrating satellite imagery and digital elevation data for geobotanical mapping in Quetico Provincial Park, Ontario, Canada p 2754 N93-25430
Multi-temporal satellite image analysis for crop inventories in the Po River Valley (Italy) p 2755 N93-25434
Commercial applications multispectral sensor system p 2758 N93-25615
A high performance room-temperature near-infrared camera
| AD-A260602 | p 2709 N93-25634
Remote sensing of precipitation and electrification with a dual-polarization, coherent, wideband radar system
| AD-A260779 | p 2756 N93-25679
Detecting the scale and resolution effects in remote sensing and GIS p 2756 N93-25707
Geographic information system for fusion and analysis of high-resolution remote sensing and ground truth data p 2878 N93-25798
System of Experts for Intelligent Data Management (SEIDAM) p 2879 N93-25800
Advanced data visualization and sensor fusion: Conversion of techniques from medical imaging to Earth science p 2880 N93-25810
A Spatial Analysis and Modeling System (SAMS) for environment management p 2881 N93-25813
The probabilistic neural network architecture for high speed classification of remotely sensed imagery p 2824 N93-25972
Image analysis by integration of disparate information p 2824 N93-25973
Method and apparatus for deflection measurements using eddy current effects
| NASA-CASE-GSC-13506-1 | p 2710 N93-26103
Digital Oblique Remote Ionospheric Sensing (DORIS) program development
| AD-A261750 | p 2776 N93-26283
Coastal ocean processes: A science prospectus
| AD-A261702 | p 2790 N93-26384
Bibliography of remote sensing techniques used in wetland research
| AD-A261704 | p 2757 N93-26440
Radar sensing of petroleum seepage gases
| AD-A261431 | p 2682 N93-26455

REMOTE SENSORS
Resolution of the COBE Earth sensor anomaly p 2600 N93-24700
The constant current loop: A new paradigm for resistance signal conditioning
| NASA-TM-108744 | p 2673 N93-25181
Handbook of actuators and edge alignment sensors
| NASA-CR-193203 | p 2620 N93-25317

Rain rate instrument for deployment at sea, phase 2
| NASA-CR-192442 | p 2786 N93-26156

REMOTELY PILOTED VEHICLES
A mission concept for near term Lunar exploration
| DE93-007598 | p 2896 N93-25321

RENDEZVOUS SPACECRAFT
Optimal cooperative power-limited rendezvous
p 2607 N93-24904

REPLACING
AEW aircraft design
| AD-A261800 | p 2590 N93-26444

REPORTS
NASA Microgravity Science and Applications Program
| NASA-TM-108775 | p 2663 N93-25194
AFOSR technical report summaries
| AD-A261551 | p 2918 N93-26380

REQUIREMENTS
The SE role in establishing, verifying and controlling top-level program requirements p 2666 N93-24685
Optimization in the systems engineering process
p 2666 N93-24691
GPS standardization for the needs of time transfer
p 2836 N93-25016
Languages for requirements specifications
| RSRE-MEMO-4585 | p 2810 N93-25453
Determination of burn rate requirements from ASRM performance specifications p 2627 N93-26023
Distributed project scheduling at NASA: Requirements for manual protocols and computer-based support
p 2815 N93-26075
Advanced Launch System (ALS) test requirements
| MCR-91-5004 | p 2610 N93-26181

RESEARCH AND DEVELOPMENT
Remote sensing applied to agriculture state of the art and new trends p 2745 N93-24818
Viewgraph description of Penn State's Propulsion Engineering Research Center: Activity highlights and future plans
| NASA-CR-192317 | p 2622 N93-24943
R and D of transmission lines for ECH system
| NIFS-210 | p 2687 N93-24951
Technology Transfer 92/93
| DE93-003623 | p 2887 N93-24965
The development progresses of hydrogen masers at Shanghai Observatory p 2716 N93-25048
Current research activities: Applied and numerical mathematics, fluid mechanics, experiments in transition and turbulence and aerodynamics, and computer science
| NASA-CR-191408 | p 2803 N93-25084
Applied aerodynamics: Challenges and expectations
| NASA-TM-103963 | p 2575 N93-25091
Advanced energy systems and technologies - National R and D programme
| DE93-769943 | p 2758 N93-25097
JSC research and technology
| NASA-TM-104763 | p 2901 N93-25188
NASA Microgravity Science and Applications Program
| NASA-TM-108775 | p 2663 N93-25194
Science, technology, and national security
p 2886 N93-25232
SIHTI: The research and development program of energy and environmental technology
| DE93-769925 | p 2763 N93-25360
JPRS report: Science and technology. Central Eurasia: Earth sciences
| JPRS-UES-92-003 | p 2737 N93-25398
JPRS report: Science and technology. Central Eurasia: Life sciences
| JPRS-ULS-93-002 | p 2737 N93-25399
JPRS report: Science and technology. Central Eurasia: Earth sciences
| JPRS-UES-93-001 | p 2599 N93-25400
JPRS report: Science and technology. Central Eurasia: Earth sciences
| JPRS-UES-92-005 | p 2737 N93-25401
JPRS report: Science and technology. Central Eurasia: Physics and mathematics
| JPRS-UPM-92-004 | p 2844 N93-25402
JPRS report: Science and technology. Central Eurasia: Physics and mathematics
| JPRS-UPM-92-003 | p 2844 N93-25403
JPRS report: Science and technology. Central Eurasia: Physics and mathematics
| JPRS-UPM-93-001 | p 2844 N93-25404
JPRS report: Science and technology. Central Eurasia: Life sciences
| JPRS-ULS-92-025 | p 2793 N93-25405
JPRS report: Science and technology. Central Eurasia: Life sciences
| JPRS-ULS-92-020 | p 2793 N93-25406
JPRS report: Science and technology. Central Eurasia: Life sciences
| JPRS-ULS-92-022 | p 2795 N93-25407
JPRS report: Science and technology. Japan. 30th National Aerospace Laboratory Conference
| JPRS-JST-93-009 | p 2901 N93-25418
JPRS report: Science and technology. Central Eurasia: Earth sciences
| JPRS-UES-92-002 | p 2737 N93-25426
JPRS report: Science and technology. Central Eurasia: Engineering and equipment
| JPRS-UEQ-92-003 | p 2668 N93-25427
Air Force Office of Scientific Research
| AD-A260675 | p 2911 N93-25893
The 1993/1994 NASA Graduate Student Researchers Program
| NASA-EP-283 | p 2872 N93-26051
National Aeronautics and Space Administration (NASA)/American Society for Engineering Education (ASEE) Summer Faculty Fellowship Program, 1992, volume 1
| NASA-CR-188242-VOL-1 | p 2911 N93-26058
National Aeronautics and Space Administration (NASA)/American Society for Engineering Education (ASEE) Summer Faculty Fellowship Program, 1992, volume 2
| NASA-CR-188242-VOL-2 | p 2914 N93-26070
High performance computing and communications panel report p 2807 N93-26131
Engineering: Research development and technology
| UCRL-53868-91 | p 2917 N93-26326
Summary report of the Defense Sciences Research Council Summer Conference
| AD-A261375 | p 2917 N93-26359
Science, Technology, and Industrial Policy in the Former Soviet Union
| DE93-006528 | p 2887 N93-26499

RESEARCH FACILITIES
Space exploration initiative candidate nuclear propulsion test facilities
| NASA-TM-105710 | p 2622 N93-24753
Gas-Grain Simulation Facility (GGSF). Volume 1: Stage 1 facility definition studies
| NASA-CR-177606 | p 2887 N93-25442
Space research in Sweden, 1990-1991
p 2888 N93-25887
The state of computing at Los Alamos National Laboratory, FY 1991
| LA-12326-MS | p 2811 N93-25943

RESEARCH MANAGEMENT
Climate Monitoring and Diagnostics Laboratory
| PB93-156388 | p 2785 N93-25871
CRRES: Combined release and radiation effects satellite program summary
| NASA-CR-192469 | p 2774 N93-25886
Space research in Sweden, 1990-1991
p 2888 N93-25887
Technology for America's economic growth: A new direction to build economic strength
| AD-A261553 | p 2887 N93-26458

RESEARCH PROJECTS
Viewgraph description of Penn State's Propulsion Engineering Research Center: Activity highlights and future plans
| NASA-CR-192317 | p 2622 N93-24943
NASA Microgravity Science and Applications Program
| NASA-TM-108775 | p 2663 N93-25194
CRRES: Combined release and radiation effects satellite program summary
| NASA-CR-192469 | p 2774 N93-25886

RESIDUAL STRESS
Internal stresses and the cyclic deformation of an aluminum matrix composite p 2650 N93-25436
A three-dimensional model for the residual stresses in a unidirectional composite plate p 2728 N93-25825
Experimental studies of stress management by optical fluorescence
| AD-A261539 | p 2730 N93-26362
Failure considerations in composite systems based on 3D micromechanical stress fields, part A
| AD-A261698 | p 2641 N93-26382

RESIN MATRIX COMPOSITES
Inelastic behavior of thermoplastic composites
p 2636 N93-25674
Damage and failure analysis on continuous fiber-reinforced polymer composites
p 2637 N93-25716

RESINS
Improved composite fabrication process
| AD-D015679 | p 2640 N93-26145
Effects of moisture and other contaminants in friction composites
| AD-A261226 | p 2640 N93-26301

RESISTOJET ENGINES
Experimentation in the low-density plume of a simulated electrothermal thruster for computer code validation
| NASA-CR-191112 | p 2622 N93-24758

RESISTORS
Investigation into the common mode rejection ratio of the physiological signal conditioner circuit
p 2794 N93-26073

RESONANCE
Pressure dependence of conductivity
| DE93-008466 | p 2687 N93-25113
Nonlinear wave phenomena related to interactions in the ionosphere
| AD-A261450 | p 2776 N93-26348
Development of resonance ionization spectroscopy for genome mapping and DNA sequencing using stable isotopes as DNA labels
| DE93-007815 | p 2793 N93-26587

RESONANCE SCATTERING
Resonance electron scattering by O2 monolayers on graphites: Reinterpreted
| AD-A261851 | p 2850 N93-26287

RESONANT FREQUENCIES
The measurement of the resonant frequency of quartz crystal units: An ongoing saga p 2833 N93-24996
Surface Transverse Wave (STW) quartz resonators in the GHz range p 2836 N93-25012
Dedicated oscillator for immersed crystal sensor
p 2837 N93-25020
Trapped energy quartz crystal resonator on wedge-shaped plate p 2837 N93-25022
Stability of nonlinear phase motion from the study of oscillator mappings p 2693 N93-25034
Controlling an optical frequency by a single ion
p 2841 N93-25051
Identification and control of lightly damped, large space structures: An experimental evaluation
p 2616 N93-25351
Using input command pre-shaping to suppress multiple mode vibration p 2732 N93-25834

RESONANT TUNNELING
Resonant tunneling through chemisorbed halogen atoms on Ag(111)
| AD-A261794 | p 2868 N93-26254

RESONATORS
Microwave frequency discriminator with a cryogenic sapphire resonator for ultra-low phase noise
p 2693 N93-24982
Miniature optically-pumped cesium beam resonator
p 2833 N93-24990
Actual limits of fluorescence S/N ratio in an optically-pumped cesium beam resonator
p 2833 N93-24991
Long term drift and gamma-irradiation effect
p 2833 N93-24992
Weak magnetic field sensitivity of quartz crystal oscillators p 2833 N93-24993
Synchrotron radiation X ray topography study of lateral field resonators p 2833 N93-24994
Design of a low phase noise UHF oscillator using a partly metallized dielectric resonator p 2693 N93-25003
Surface Transverse Wave (STW) quartz resonators in the GHz range p 2836 N93-25012
Comparison of energy trapping resonators and filters using the AT cut of quartz, berlinite and gallium phosphate p 2836 N93-25013
Dedicated oscillator for immersed crystal sensor
p 2837 N93-25020
Controlled dissolution of a piezoelectric material berlinite (AlPO4) p 2840 N93-25043
Oscillators for mobile GPS receivers
p 2694 N93-25055
Microwave interrogation frequency noise and clock frequency stability: Experimental results
p 2842 N93-25056
Line inhomogeneity effects and power shift in miniaturized rubidium frequency standards
p 2694 N93-25066

RESOURCE ALLOCATION
Estimating spares requirements for Space Station Freedom using the M-SPARE model
| AD-A260878 | p 2617 N93-25630

RESOURCES MANAGEMENT
Environment Observation and Climate Modelling Through International Space Projects. Volume 2: Remote Sensing for Environmental Monitoring and Resource Management
| ESA-ISY-1-VOL-2 | p 2737 N93-24775
Sustainable remote sensing: A major improvement for realtime resource management and disaster early warning in developing countries p 2743 N93-24808
Use of remote sensing spacecrafts in real time support to disaster management: Interfaces with ground segment facilities and services p 2743 N93-24809
Remote sensing in hydrology and water management
p 2744 N93-24816
Use of the Environmental Resource Management and Analysis System at the Fernald Environmental Management Project
| DE93-002943 | p 2760 N93-24955

Aerial photographic sampling for statewide resource inventory p 2755 N93-25441
Department of Energy: Better information resources management needed to accomplish missions. Report to the Secretary of Energy
| GAO/IMTEC-92-53 | p 2882 N93-26096

RESPIRATION
The acute inhalation toxicity of pyrolysis products of halon 1301
| AD-A260874 | p 2795 N93-25629

RESPIRATORY SYSTEM
The acute inhalation toxicity of pyrolysis products of halon 1301
| AD-A260874 | p 2795 N93-25629

RETINA
JPRS report: Science and technology. Central Eurasia: Life sciences
| JPRS-ULS-92-025 | p 2793 N93-25405
Receptoral and neural aliasing
| AD-A261438 | p 2799 N93-26489

REVERBERATION
The design of a modular sound absorber for very low frequencies
| BBC-RD-1992/10 | p 2673 N93-25170
A modular wideband sound absorber
| BBC-RD-1992/11 | p 2673 N93-25171

RHENIUM
Fundamental aspects of metal joining: The study of strong interfaces
| AD-A261293 | p 2653 N93-26304

RHEOLOGY
Dynamic test apparatus for electro-rheological fluids
| AD-D015632 | p 2643 N93-25284
Rheology of YBa2Cu3O(7-x) precursors
| DE93-007285 | p 2863 N93-25362
Crustal deformation studies in subaerial parts of the world oceanic rift system: Iceland and Afar p 2789 N93-25558

RIBLETS
An experimental study of passive drag reduction in a turbulent boundary layer by a riblet surface p 2705 N93-25746
Flow control of low heat load turbine airfoils
| AD-A260941 | p 2595 N93-26219

RIGID STRUCTURES
Position and force control of a vehicle with two or more steerable drive wheels
| DE92-041301 | p 2717 N93-25100
Nonholonomic geometry, mechanics and control p 2724 N93-25270
Stability analysis and modeling of rotating flexible structures
| DE93-008493 | p 2844 N93-25520
Mullite whiskers and mullite-whisker felt p 2642 N93-25586
Conical Euler analysis and active roll suppression for unsteady vortical flows about rolling delta wings
| NASA-TP-3259 | p 2581 N93-26134
Investigation of liquid sloshing in spin-stabilized satellites
| AD-A261671 | p 2619 N93-26438

RING LASERS
An active solid state ring laser gyroscope p 2709 N93-25291
Injection seeded, diode-pumped, short pulse Nd:YAG ring laser for space-based laser ranging p 2713 N93-25389
Applications of inertial-sensor high-inheritance instruments to DSN precision antenna pointing p 2621 N93-26112

RING STRUCTURES
An in-depth probabilistic study of external tank attach ring
| NASA-TM-108403 | p 2624 N93-25671

RISK
An introductory guide to uncertainty analysis in environmental and health risk assessment
| DE93-002873 | p 2760 N93-24676
The use of remote sensing and GIS for the assessment of environmental degradation caused by fires, applied upon South-Euboia (central Greece) p 2742 N93-24802
Application of multitemporal Landsat-MSS and -TM data for the development of an inundation-risk-map p 2743 N93-24807
A prototype system for forest fire prevention and control p 2749 N93-24844
A procedure for defining lightning risk to air vehicles p 2583 N93-24885
Environmental risks and future generations: Criteria for public policy
| DE93-004691 | p 2764 N93-25443
The application of integrated knowledge-based systems for the Biomedical Risk Assessment Intelligent Network (BRAIN) p 2799 N93-25595
On the estimation of risk associated with an attenuation prediction p 2683 N93-26469

RIVERS
Use of remote sensing and GIS for the environmental planning proposal of the Sarno River Valley (Campania, southern Italy) p 2741 N93-24797
Interactive forecasting with the National Weather Service River Forecast System p 2788 N93-25616
Inorganic nitrogen and phosphorus dynamics in the water column of the Patuxent River
| PB93-172955 | p 2767 N93-26511

ROASTING
Production of ultrafine, high-purity ceramic powders using the US Bureau of Mines developed turbomill p 2659 N93-25585

ROBOT ARMS
A control structure for fault-tolerant operation of robotic manipulators
| DE93-005783 | p 2717 N93-25413
Parametric motion control of robotic arms: A biologically based approach using neural networks p 2822 N93-25964
Interaction dynamics and control for orbital assembly p 2669 N93-26407
Controls for orbital assembly of large space structures p 2620 N93-26408

ROBOT CONTROL
Using fuzzy behaviors for the outdoor navigation of a car with low-resolution sensors
| DE93-002428 | p 2584 N93-25120
A control structure for fault-tolerant operation of robotic manipulators
| DE93-005783 | p 2717 N93-25413
Numerical kinematic transformation calculations for a parallel link manipulator
| DE93-005778 | p 2718 N93-25449
Real-time construction and rendering of three-dimensional occupancy maps
| DE93-007818 | p 2756 N93-25516
Robotic Variable Polarity Plasma Arc (VPPA) welding p 2720 N93-25605
Biped control via nonlinear dynamics p 2718 N93-25697
Passivity motivated controller design for flexible structures
| AD-A261122 | p 2719 N93-25771
Parametric motion control of robotic arms: A biologically based approach using neural networks p 2822 N93-25964
Interaction dynamics and control for orbital assembly p 2669 N93-26407
Controls for orbital assembly of large space structures p 2620 N93-26408
Reinforcement learning for robots using neural networks
| AD-A261434 | p 2827 N93-26487

ROBOT DYNAMICS
Biped control via nonlinear dynamics p 2718 N93-25697
The induction of elastic fine motion in robotic grasps p 2718 N93-25727
A surface integral algorithm for the motion planning of nonholonomic mechanical systems
| AD-A261746 | p 2720 N93-26249

ROBOT SENSORS
Using fuzzy behaviors for the outdoor navigation of a car with low-resolution sensors
| DE93-002428 | p 2584 N93-25120

ROBOTICS
Probabilistic analysis of manipulation tasks: A research agenda
| DE93-000713 | p 2827 N93-25103
Nonholonomic geometry, mechanics and control p 2724 N93-25270
Prototype PC user interface
| DE93-008008 | p 2809 N93-25303
A control structure for fault-tolerant operation of robotic manipulators
| DE93-005783 | p 2717 N93-25413
Numerical kinematic transformation calculations for a parallel link manipulator
| DE93-005778 | p 2718 N93-25449
Robotic Variable Polarity Plasma Arc (VPPA) welding p 2720 N93-25605
A virtual environment for manufacturing systems
| AD-A260813 | p 2810 N93-25699
Analysis and design of a novel robotic finger-tip sensor for adaptive grasping p 2719 N93-25745
Passivity motivated controller design for flexible structures
| AD-A261122 | p 2719 N93-25771
Using input command pre-shaping to suppress multiple mode vibration p 2732 N93-25834
Knowledge-based control for robot self-localization p 2822 N93-25963
An autonomous satellite architecture integrating deliberative reasoning and behavioural intelligence p 2823 N93-25970
NASA Center for Intelligent Robotic Systems for Space Exploration
| NASA-CR-193208 | p 2826 N93-25986
Architecture of autonomous systems
| NASA-CR-192974 | p 2801 N93-26047
A vision architecture for the extravehicular activity retriever p 2827 N93-26071
Automation and robotics human performance
| NASA-CR-193049 | p 2802 N93-26153
Digital filter control of remotely operated flexible robotic structures
| DE93-007587 | p 2827 N93-26596

ROBOTS
Using neural networks and Dyna algorithm for integrated planning, reacting and learning in systems
| NASA-CR-193018 | p 2817 N93-24743
Initial experiments with a myoelectric-based muscle sensor
| DE92-016034 | p 2799 N93-25099
Position and force control of a vehicle with two or more steerable drive wheels
| DE92-041301 | p 2717 N93-25100
Probabilistic analysis of manipulation tasks: A research agenda
| DE93-000713 | p 2827 N93-25103
Real-time construction of three-dimensional occupancy maps
| DE93-001645 | p 2756 N93-25505
Robotic Variable Polarity Plasma Arc (VPPA) welding p 2720 N93-25605
An optimal scheduling of pick-place operations of a robot-vision-tracking system by using neural networks and rule-based systems p 2821 N93-25880
Knowledge-based control for robot self-localization p 2822 N93-25963
Parametric motion control of robotic arms: A biologically based approach using neural networks p 2822 N93-25964
Telerobotic rovers for extraterrestrial construction p 2670 N93-26416
Digital filter control of remotely operated flexible robotic structures
| DE93-007587 | p 2827 N93-26596

ROBUSTNESS (MATHEMATICS)
Robust controls with structured perturbations
| NASA-CR-192956 | p 2817 N93-24757
On the robustness of Herlihy's hierarchy
| NASA-CR-193002 | p 2808 N93-25107
How to control if even experts are not sure: Robust fuzzy control
| NASA-TM-108745 | p 2818 N93-25142
Robust nonlinear control of vectored thrust aircraft
| NASA-CR-192727 | p 2596 N93-25199
Parametric stability margin for multilinear interval control systems
| NASA-CR-192892 | p 2819 N93-25296
The WorkPlace distributed processing environment p 2825 N93-25977
Use of Taguchi design of experiments to optimize and increase robustness of preliminary designs p 2670 N93-26063
Develop margin philosophy to attain robustness
| MCR-92-5005 | p 2610 N93-26182

ROCKET ENGINE CONTROL
A neural network-based estimator for the mixture ratio of the Space Shuttle Main Engine
| NASA-TM-106070 | p 2622 N93-25089

ROCKET ENGINE DESIGN
Nuclear thermal propulsion technology: Results of an interagency panel in FY 1991
| NASA-TM-105711 | p 2621 N93-24740
Liquid Rocket Booster (LRB) for the Space Transportation System (STS) Systems Study. Amendment 13: Orientation meeting
| NASA-CR-192515 | p 2614 N93-26152

ROCKET ENGINES
Measurement of droplet vaporization rate enhancement caused by acoustic disturbances p 2626 N93-26015
Development and use of hydrogen-air torches in an altitude facility
| NASA-TM-106047 | p 2598 N93-26214

ROCKET EXHAUST
Generic hypersonic vehicle performance model
| NASA-CR-192953 | p 2587 N93-25162
An experimental study of under-expanded jets p 2577 N93-25467
Pulsed laser Rayleigh scattering diagnostic for hydrogen/oxygen rocket exit plane flowfield velocimetry
| NASA-TM-106098 | p 2631 N93-26149
Application of the Saha equation to high temperature (greater than or equal to) rocket exhaust
| AD-A261648 | p 2632 N93-26174
Molecular interactions and properties with many-body methods
| AD-A261688 | p 2850 N93-26367

Analysis of the IBSS spectra of Space Shuttle control engine exhaust
| AD-A261749 | p 2632 N93-26373

ROCKET NOZZLES
Remtech SSME nozzle design TPS
| NASA-CR-192516 | p 2631 N93-26056

ROCKET OXIDIZERS
A neural network-based estimator for the mixture ratio of the Space Shuttle Main Engine
| NASA-TM-106070 | p 2622 N93-25089

ROCKET PROPELLANTS
Near Earth object fuels (neo-fuels): Discovery, prospecting and use
| DE93-005185 | p 2892 N93-25164
Minutes of the Twenty-Fifth Explosives Safety Seminar, volume 4
| AD-A261116 | p 2660 N93-25769
Application of the Saha equation to high temperature (greater than or equal to) rocket exhaust
| AD-A261648 | p 2632 N93-26174

ROCKY MOUNTAINS (NORTH AMERICA)
Pressure torques and circulation changes in Rocky Mountain lee cyclones p 2783 N93-25724

RODS
Comparative performance of lightning air terminals under natural storm conditions p 2781 N93-24902
Design of flexible rods with embedded SMA actuators
| AD-A260742 | p 2729 N93-25846
Variational theory of motion of curved, twisted and extensible elastic rods
| AD-A261028 | p 2729 N93-25941
Deformations of active flexible rods with embedded line actuators
| AD-A261207 | p 2729 N93-25950

ROLL
Conical Euler analysis and active roll suppression for unsteady vortical flows about rolling delta wings
| NASA-TP-3259 | p 2581 N93-26134

ROLLER BEARINGS
Detection of bearing failure in mechanical devices using neural networks p 2822 N93-25965

ROOM TEMPERATURE
Room temperature fracture of FeCo
| DE93-008266 | p 2650 N93-25519
A high performance room-temperature near-infrared camera
| AD-A260602 | p 2709 N93-25634

ROOMS
Low-frequency room responses. Part 1: Background and qualitative considerations
| BBC-RD-1992/8-PT-1 | p 2673 N93-25168
Low-frequency room responses. Part 2: Calculation methods and experimental results
| BBC-RD-1992/9-PT-2 | p 2673 N93-25169

ROSAT MISSION
ROSAT investigation of flaring and activity on Prox Cen
| NASA-CR-192972 | p 2891 N93-26139

ROSIN
Aqueous cleaning of flux residue from solder joints
| KCP-613-4803 | p 2652 N93-26208

ROTARY WING AIRCRAFT
An aeroelastic model structure investigation for a manned real-time rotorcraft simulation p 2574 N93-24756
Design and analysis of curved composite components for rotorcraft fuselage frames p 2589 N93-25701
Image-based ranging and guidance for rotorcraft
| NASA-CR-177608 | p 2586 N93-26549

ROTARY WINGS
An aeroelastic model structure investigation for a manned real-time rotorcraft simulation p 2574 N93-24756
Rotor design optimization using a free wake analysis
| NASA-CR-177612 | p 2575 N93-25075
Application of finite-state inflow to flap-lag-torsion damping in hover p 2587 N93-25486
Aeroelastic response and aeromechanical stability of helicopters with elastically coupled composite rotor blades p 2588 N93-25530
An integrated finite-state model for rotor deformation, nonlinear airloads, inflow, and trim p 2588 N93-25538
Structural dynamic analysis of bearingless rotor blade p 2590 N93-25719
Unsteady airfoil flow solutions on moving zonal grids
| AD-A261925 | p 2582 N93-26198
Helicopter forced response vibration analysis method RTVIB20
| AD-A261809 | p 2597 N93-26260

ROTATING BODIES
Simulation study of MHD dynamo: Convection in a rotating spherical shell
| NIFS-207 | p 2860 N93-25356

ROTATING DISKS
Flow between finite rotating disks and its linear stability p 2705 N93-25747

ROTATING FLUIDS
Heat transfer in rotating serpentine passages with selected model orientation for smooth or skewed trip walls
| NASA-TM-106126 | p 2667 N93-25177

ROTATING STALLS
Active stabilization of aeromechanical systems
| AD-A261366 | p 2595 N93-26335

ROTATION
Turbine turbobrake systems p 2717 N93-25268
Stability analysis and modeling of rotating flexible structures
| DE93-008493 | p 2844 N93-25520
Variational theory of motion of curved, twisted and extensible elastic rods
| AD-A261028 | p 2729 N93-25941
Rotating rake design for unique measurement of fan-generated spinning acoustic modes
| NASA-TM-105946 | p 2595 N93-26161

ROTOR AERODYNAMICS
Rotor design optimization using a free wake analysis
| NASA-CR-177612 | p 2575 N93-25075
Far field rotor noise
| AD-A260703 | p 2845 N93-25651
Flow control of low heat load turbine airfoils
| AD-A260941 | p 2595 N93-26219
The blade curving effects in a turbine stator cascade with low aspect ratio
| AD-A261063 | p 2595 N93-26239

ROTOR BODY INTERACTIONS
Aeroelastic response and aeromechanical stability of helicopters with elastically coupled composite rotor blades p 2588 N93-25530

ROTOR DYNAMICS
Application of finite-state inflow to flap-lag-torsion damping in hover p 2587 N93-25486

ROTORS
Variable-speed generators with flux weakening p 2694 N93-25599
Far field rotor noise
| AD-A260703 | p 2845 N93-25651
Radial inflow turbine study
| AD-A260767 | p 2594 N93-25917
Helicopter forced response vibration analysis method RTVIB20
| AD-A261809 | p 2597 N93-26260

RUBBER
Elastomer compound developed for high wear applications p 2659 N93-25607
Dynamic hardness tester and cure meter p 2711 N93-25608

RUBIDIUM
Rubidium atomic frequency standards for GPS block 2R p 2836 N93-25014
TF-4020A: TFL's new compact military rubidium standard p 2838 N93-25026
Use of the TV-signal in stabilizing a local rubidium oscillator p 2693 N93-25029
Experiments on a diode-laser-pumped Rb-87 maser p 2716 N93-25030
High resolution digital synthesizer for a Rb frequency standard p 2694 N93-25057
Line inhomogeneity effects and power shift in miniaturized rubidium frequency standards p 2694 N93-25066
Fundamental characteristics of a laser-diode-pumped rubidium maser with an external feedback loop p 2716 N93-25068

RUN TIME (COMPUTERS)
Set based program analysis
| AD-A260979 | p 2806 N93-25841

RUNWAYS
ILS mathematical modeling study of an ILS glide slope proposed for runway 19L at the Meridian Naval Air Station, Mississippi
| DOT/FAA/CT-TN93/8 | p 2584 N93-24741
Runway Visual Range (RVR) Operational Test and Evaluation (OT&E) integration and OT&E operational test report
| DOT/FAA/CT-TN93/37 | p 2584 N93-25243
The dependent converging instrument approach procedure: An analysis of its safety and applicability
| DOE/FAA/RD-93/6 | p 2585 N93-25456
Expedient repair of structural facilities
| AD-A260727 | p 2598 N93-25656

RUTILE
Vickers indentation hardness of stoichiometric and reduced single crystal TiO2 (rutile) from 25 to 800 C
| NASA-TM-105959 | p 2633 N93-26204

S

SAFETY
Seismic buckling capacity of unstiffened, free-standing steel containments
| DE93-005325 | p 2723 N93-24957
Improved performance and safety for high energy batteries through use of hazard anticipation and capacity prediction p 2694 N93-25582
An in-depth probabilistic study of external tank attach ring
| NASA-TM-108403 | p 2624 N93-25671
Minutes of the Twenty-Fifth Explosives Safety Seminar, volume 4
| AD-A261116 | p 2660 N93-25769
Development of a concept for a national construction industry health and safety data base
| PB93-159325 | p 2884 N93-26568

SAFETY DEVICES
The 1992 International Aerospace and Ground Conference on Lightning and Static Electricity: Addendum
| DOT/FAA/CT-92/20-ADD-1 | p 2777 N93-24875
Launch pad lightning protection enhancement by induced streamers p 2609 N93-24876
Applications of triggered lightning to space vehicle operations p 2619 N93-24878
Zoning of aircraft: A review of the definitions p 2583 N93-24880
A system to measure lightning-induced transients on spacecraft umbilical lines p 2693 N93-24889
Comparison of the damage for various types of fibre reinforced composites due to different lightning test standards (MIL-STD-1757A, German military VG-standard 96903) p 2642 N93-24891
A single-point warning system for thunderstorms and electric fields p 2711 N93-24900

SAFETY FACTORS
The dependent converging instrument approach procedure: An analysis of its safety and applicability
| DOE/FAA/RD-93/6 | p 2585 N93-25456

SAGNAC EFFECT
Prospects of two-way international time scale comparisons p 2832 N93-24988

SAHA EQUATIONS
Application of the Saha equation to high temperature (greater than or equal to) rocket exhaust
| AD-A261648 | p 2632 N93-26174

SALINITY
Global Temperature and Salinity Pilot Project p 2733 N93-24924
Wrap-up session p 2737 N93-24940

SALT BEDS
Remote sensing of coastal zone Sabkha deposits, Gulf of Sirt, Libya p 2746 N93-24827

SAMPLED DATA SYSTEMS
Dynamics and robust control of a sampled data system for large space structures. Volume 2: The LQG/LTR methodology for the discrete-time system and the design of reduced order robust digital controller for orbiting flexible shallow spherical shell system
| AD-A260793 | p 2599 N93-25693

SAMPLING
Indian Ocean analyses p 2733 N93-24925
Automated in situ observations of upper ocean biogeochemistry, bio-optics, and physics and their potential use for global studies p 2736 N93-24939
Development and testing of the digital control system for the Archytas unmanned air vehicle
| AD-A261656 | p 2597 N93-26196
Statistics of sampled Rician fading
| AD-A261397 | p 2681 N93-26289

SAND CASTING
X-ray computed tomography for casting development
| AD-A261786 | p 2722 N93-26526

SANDS
Energy dissipation in inelastic flow of cohesionless granular media p 2703 N93-25662

SANDWICH STRUCTURES
Low-velocity impact of composite sandwich plate p 2637 N93-25695

SAPPHIRE
Microwave frequency discriminator with a cryogenic sapphire resonator for ultra-low phase noise p 2693 N93-24982

SATELLITE ALTIMETRY
Satellite altimetry p 2734 N93-24930
Injection seeded, diode-pumped, short pulse Nd:YAG ring laser for space-based laser ranging p 2713 N93-25389

SATELLITE ATMOSPHERES
Residual mean meridional circulation in titan's middle atmosphere
| PB93-162931 | p 2898 N93-26571

SATELLITE ATTITUDE CONTROL
Flight Mechanics/Estimation Theory Symposium, 1992 | NASA-CP-3186 | p 2599 N93-24694
Spacecraft detumbling through energy dissipation p 2600 N93-24696
The results of the in-flight attitude sensor calibration for the Arthur Holly Compton Gamma Ray Observatory p 2600 N93-24697
Testing of the on-board attitude determination and control algorithms for SAMPEX p 2600 N93-24698
Resolution of the COBE Earth sensor anomaly p 2600 N93-24700
Orbit determination and orbit control for the Earth Observing System (EOS) AM spacecraft p 2601 N93-24705
Real-time attitude determination and gyro calibration p 2602 N93-24708
Computationally efficient algorithms for real-time attitude estimation p 2602 N93-24709
Improvements in ERBS attitude determination without gyros p 2602 N93-24710
Rate determination from vector observations p 2603 N93-24713
A multimission three-axis stabilized spacecraft flight dynamics ground support system p 2603 N93-24714
Accurate attitude determination of the LACE satellite p 2605 N93-24726
Attitude control of the LACE satellite: A gravity gradient stabilized spacecraft p 2605 N93-24727
Upper Atmosphere Research Satellite (UARS) onboard attitude determination using a Kalman filter p 2606 N93-24732
Goddard Space Flight Center (GSFC) Flight Dynamics Facility (FDF) calibration of the Upper Atmosphere Research Satellite (UARS) sensors p 2606 N93-24733
Solar array thermal snap and the characteristics of its effect on UARS p 2607 N93-24734
Upper Atmosphere Research Satellite (UARS) attitude accuracy using coarse attitude sensors p 2607 N93-24735

SATELLITE COMMUNICATION
Federal Communications Commission (FCC) Transponder Loading Data Conversion Software. User's guide and software maintenance manual, version 1.2 | NASA-CR-191067 | p 2808 N93-24947
Prospects of two-way international time scale comparisons p 2832 N93-24988
A low-complexity and high performance concatenated coding scheme for high-speed satellite communications | NASA-CR-192715 | p 2673 N93-25198
An introduction to Doppler effect and fading in mobile communications | AD-A260976 | p 2676 N93-25866
Anomalous event diagnosis for environmental satellite systems p 2619 N93-25971
Trellis coded CPFSK | AD-A261788 | p 2682 N93-26441
Opening remarks p 2682 N93-26464
Large scale rainfall diversity and satellite propagation p 2683 N93-26466
ETS-5, ETS-6, and COMETS projects in Japan p 2683 N93-26470
Satellite communications application to Pacific countries above Ku band p 2683 N93-26471
Allocations by the 1992 World Administrative Radio Conference p 2684 N93-26476
ESA's planning and coordination of the OLYMPUS propagation experiment p 2684 N93-26477
Observations on the NASA Propagation Program p 2685 N93-26482
ACTS propagation terminal update p 2685 N93-26484
Rain compensation algorithm using adaptive linear prediction p 2685 N93-26485

SATELLITE CONTROL
The Generic Spacecraft Analyst Assistant (GenSAA): A tool for developing graphical expert systems p 2814 N93-25589

SATELLITE DESIGN
Aspects of the design of a satellite borne infra-red radiometer p 2620 N93-25474

SATELLITE DOPPLER POSITIONING
Precise Doppler tracking from the Medicina VLBI station p 2608 N93-24998

SATELLITE IMAGERY
Monitoring and analysis of urban trends using multitemporal satellite-imagery (case-study: Greater Cairo) p 2740 N93-24790
Agroclimatological zonation by AVHRR data for vegetation monitoring p 2741 N93-24795
Remote sensing geology p 2744 N93-24815
Potential operational use of remote sensing from space in forestry p 2745 N93-24817
Application of satellite imageries data to fisheries in Japan p 2745 N93-24822
Remote sensing of coastal zone Sabkha deposits, Gulf of Sirt, Libya p 2746 N93-24827
Remote sensing monitoring and hindcasting of the accident occurred to the tanker Haven in the Gulf of Genoa (Italy) p 2747 N93-24830
Evaluation of nearshore suspended sediment concentration through Landsat TM data: First results p 2747 N93-24833
Interpretation and segmentation of changed forest stands from difference imagery based on regression functions p 2748 N93-24839
Tropical forest monitoring with high resolution satellite data p 2748 N93-24841
Assessment of storm damage in forests using SPOT imagery p 2748 N93-24842
A prototype system for forest fire prevention and control p 2749 N93-24844
Toward a satellite based crop information system in Hungary p 2750 N93-24849
Remote sensing of land resource management in agriculture with regard to its influence on the environment p 2750 N93-24850
Cartography and statistics of crops under irrigation in the Donana area of Andalucia through the use of Landsat-TM imagery and its incorporation into a GIS p 2751 N93-24855
Registration of the use of agricultural fields and soil erosion using satellite remote sensing p 2751 N93-24856
Standwise forest inventory and mapping for operational management planning p 2752 N93-24863
EUROSTARS: A system for thematic analysis of remote sensed data p 2753 N93-24871
Earthquake vulnerability map of the Lake Constance area p 2753 N93-24872
The use of remotely sensed data for operational fisheries oceanography p 2734 N93-24927
Applications of wavelet-based compression to multidimensional earth science data | DE93-007348 | p 2762 N93-25166
Integrating satellite imagery and digital elevation data for geobotanical mapping in Quetico Provincial Park, Ontario, Canada p 2754 N93-25430
Multi-temporal satellite image analysis for crop inventories in the Po River Valley (Italy) p 2755 N93-25434
An analysis of mesoscale convective systems observed during the 1992 Tropical Cyclone Motion field experiment | AD-A260889 | p 2783 N93-25633
Detecting the scale and resolution effects in remote sensing and GIS p 2756 N93-25707
A land-surface testbed for EOSDIS p 2878 N93-25797
Relations between blue whiting biomass and satellite derived phytoplankton and temperature in the Norwegian Sea | AD-A261205 | p 2757 N93-25868
United States Army space experiment 601 | AD-A261460 | p 2798 N93-26353

SATELLITE INSTRUMENTS
Testing of the on-board attitude determination and control algorithms for SAMPEX p 2600 N93-24698
Rate determination from vector observations p 2603 N93-24713
DORIS precise orbit determination and location system performances of ultra stable oscillators p 2608 N93-24997
A system design for laser time synchronization via geodetic satellite Ajisai p 2716 N93-25005
CEOS Committee on Earth Observations Satellites consolidated report, 1992 | NASA-TM-108776 | p 2615 N93-25217
Lageos laser ranging earth rotation | AD-A261471 | p 2757 N93-26354

SATELLITE NAVIGATION SYSTEMS
Relativistic effects for low Earth orbit satellites using GPS p 2608 N93-24986
Mixed constellation synchronization of GPS time p 2836 N93-25015
Comparison of GLONASS and GPS time transfers p 2836 N93-25017
An experimental health monitoring unit for GPS and GLONASS p 2586 N93-25018
Collaboration in the UK on time transfer using the GLONASS system p 2837 N93-25019
First experience with the ASN-16 GLONASS receiver p 2693 N93-25033

SATELLITE NETWORKS
Mixed constellation synchronization of GPS time p 2836 N93-25015

SATELLITE OBSERVATION
WCRP surface radiation budget shortwave data product description, version 1.1 | NASA-TM-107747 | p 2777 N93-24742
Environment Observation and Climate Modelling Through International Space Projects. Volume 2: Remote Sensing for Environmental Monitoring and Resource Management | ESA-ISY-1-VOL-2 | p 2737 N93-24775
Satellite remote sensing for environmental geology: The Bandung (West Java) experience p 2739 N93-24784
The regional planning and control using the satellite data p 2740 N93-24788
Land cover monitoring in the Netherlands applying satellite remote sensing p 2740 N93-24789
Geologic and hydrogeologic mapping of Iceland with multisensor data (JERS-1, ERS-1, SPOT, Landsat and SEASAT) p 2740 N93-24792
Aerospace techniques in radiation and ecological monitoring of the Republic Belarus p 2741 N93-24793
Alternative strategies for the use of satellite data analysis systems for hazard monitoring and disaster mitigation p 2743 N93-24805
Satellite borne remote sensing data: A tool for natural disaster reduction p 2743 N93-24806
Sustainable remote sensing: A major improvement for realtime resource management and disaster early warning in developing countries p 2743 N93-24808
Use of remote sensing spacecrafts in real time support to disaster management: Interfaces with ground segment facilities and services p 2743 N93-24809
Potential operational use of remote sensing from space in forestry p 2745 N93-24817
Remote sensing applied to agriculture state of the art and new trends p 2745 N93-24818
Applications of remote sensing for tidal waters, coastal areas and inland waters p 2745 N93-24819
European applications of space-borne Earth observation for land cover mapping p 2745 N93-24820
Supporting the Portuguese fisheries with satellites p 2745 N93-24821
Oil pollution and water quality mapping of Augusta Bay, Italy using remote sensing techniques p 2746 N93-24823
SEOMAR: An Italian approach to the observation of the Mediterranean area p 2746 N93-24825
Algal blooms and gel production in Adriatic Sea observed by remote sensing techniques p 2747 N93-24831
World Forest Watch: A global forest monitoring test p 2748 N93-24836
Biodiversity indication by Earth observation data p 2751 N93-24858
Current trends in satellite data supply for environmental monitoring p 2754 N93-24874
The Global Ocean Observing System p 2733 N93-24923
Satellite monitoring of the global ocean surface during 1987-1989 p 2734 N93-24926
The use of remotely sensed data for operational fisheries oceanography p 2734 N93-24927
Satellite altimetry p 2734 N93-24930
Data management for JGOFS: Theory and design p 2735 N93-24935
Automated in situ observations of upper ocean biogeochemistry, bio-optics, and physics and their potential use for global studies p 2736 N93-24939
CEOS Committee on Earth Observations Satellites consolidated report, 1992 | NASA-TM-108776 | p 2615 N93-25217
JPRS report: Science and technology. Central Eurasia: Life sciences | JPRS-ULS-92-020 | p 2793 N93-25406
A high performance room-temperature near-infrared camera | AD-A260602 | p 2709 N93-25634
Tropical cyclone/upper-atmospheric interaction as inferred from satellite total ozone observations p 2784 N93-25741
Data fusion with artificial neural networks (ANN) for classification of earth surface from microwave satellite measurements p 2824 N93-25974

SATELLITE ORBITS
Orbit determination support of the Ocean Topography Experiment (TOPEX)/Poseidon operational orbit p 2601 N93-24704
Orbit determination and orbit control for the Earth Observing System (EOS) AM spacecraft p 2601 N93-24705
Generalized probability model for calculation of interference to the Deep Space Network due to circularly Earth-orbiting satellites p 2679 N93-26127

SATELLITE ORIENTATION
Space Station Freedom assembly and operation at a 51.6 degree inclination orbit | NASA-TM-107731 | p 2615 N93-25174

SATELLITE PERTURBATION
Mars: The dynamics of orbiting satellites and gravity model development p 2896 N93-25439

SATELLITE POWER TRANSMISSION
Laser beamed power: Satellite demonstration applications
| NASA-CR-190793 | p 2623 N93-25132
SATELLITE SOUNDING
The pressure modulation system in the Improved Stratospheric and Mesospheric Sounder
p 2773 N93-25739
SATELLITE TRACKING
TDRSS orbit determination using short baseline differenced carrier phase p 2601 N93-24701
The advances in F and T technology: Their benefits of and for space science and technology
p 2831 N93-24979
Precise Doppler tracking from the Medicina VLBI station p 2608 N93-24998
Synchronisation, acquisition and tracking for telemetry and data reception p 2614 N93-25000
SATELLITE TRANSMISSION
Large scale rainfall diversity and satellite propagation
p 2683 N93-26466
OLYMPUS/ACTS scintillation experiment at the Lewis Research Center p 2685 N93-26481
SATELLITE-BORNE INSTRUMENTS
SEOMAR: An Italian approach to the observation of the Mediterranean area p 2746 N93-24825
Commercial applications multispectral sensor system
p 2758 N93-25615
Determination of design and operation parameters for upper atmospheric research instrumentation to yield optimum resolution with deconvolution
| NASA-CR-192832 | p 2775 N93-26084
SATELLITE-BORNE PHOTOGRAPHY
Application of photographic remote sensing data from space for information about forests
p 2748 N93-24838
SATURN 5 LAUNCH VEHICLES
The initial flight anomalies of Skylab 1
p 2619 N93-24692
SCALARS
Scalar gain interpretation of large order filters
p 2606 N93-24729
Measurements of scalar power spectra in high Schmidt number turbulent jets
| AD-A261542 | p 2707 N93-26379
SCANNERS
Preliminary design of the BPM electronics memory scanner/dual boxcar averager for the advanced photon source
| DE93-007893 | p 2848 N93-25368
Ka-band feed arrays for spacecraft reflector antennas with limited scan capability: An overview
p 2680 N93-26128
SCANNING ELECTRON MICROSCOPY
Study of grain refinement in Al alloy 2519 using backscattering orientation-contrast mode in the scanning electron microscope
| AD-A260886 | p 2651 N93-25632
Condensed-phase processes during solid propellant combustion. Part 4: Chemical and microscopic examination of laser-irradiated propellant samples
p 2628 N93-26032
Single electron charging effects in mesoscopic systems
| AD-A261228 | p 2868 N93-26302
SCANNING TUNNELING MICROSCOPY
Prediction of hydrogen entry and permeation in metals and alloys
| AD-A260580 | p 2651 N93-25903
SCATHA SATELLITE
SCATHA mission termination report
p 2605 N93-24725
SCATTERING
Progress in impulse approach research
| AD-A261728 | p 2850 N93-26281
Dynamics of gas-surface interactions
| AD-A261402 | p 2646 N93-26402
SCATTERING CROSS SECTIONS
Strangeness production in S + Pb and p + Pb collisions at 200 GeV/c per nucleon nucleon
| DE93-007654 | p 2847 N93-25326
Progress in impulse approach research
| AD-A261728 | p 2850 N93-26281
SCENE ANALYSIS
Scene segmentation of natural images using texture measures and back-propagation
| NASA-TM-104003 | p 2803 N93-25235
Image-based ranging and guidance for rotorcraft
| NASA-CR-177608 | p 2586 N93-26549
SCHEDULES
Management issues in systems engineering
p 2665 N93-24682
The reuse of logistics carriers for the first lunar outpost alternative habitat study p 2671 N93-26083
SCHEDULING
Supercomputer Debugging Workshop 1992
| DE93-007322 | p 2805 N93-25165
Concurrency control in real-time database systems
p 2874 N93-25271
A genetic algorithm tool (splicer) for complex scheduling problems and the Space Station Freedom resupply problem p 2814 N93-25613
An optimal scheduling of pick-place operations of a robot-vision-tracking system by using neural networks and rule-based systems p 2821 N93-25880
Using AI/expert system technology to automate planning and replanning for the HST servicing missions
p 2822 N93-25962
Distributed project scheduling at NASA: Requirements for manual protocols and computer-based support
p 2815 N93-26075
Intelligent, real-time problem solving, phase 3
| AD-A261441 | p 2829 N93-26345
SCHMIDT NUMBER
Measurements of scalar power spectra in high Schmidt number turbulent jets
| AD-A261542 | p 2707 N93-26379
SCHOTTKY DIODES
Ultrafast measurements of 200 gigahertz Schottky photodiodes p 2688 N93-25392
SCHROEDINGER EQUATION
Molecular interactions and properties with many-body methods
| AD-A261688 | p 2850 N93-26367
SCIENCE
Science, Technology, and Industrial Policy in the Former Soviet Union
| DE93-006528 | p 2887 N93-26499
SCIENTIFIC SATELLITES
A multimission three-axis stabilized spacecraft flight dynamics ground support system p 2603 N93-24714
Analysis of reentry into the White Sands Missile Range (WSMR) for the LifeSat mission p 2603 N93-24717
CRRES: Combined release and radiation effects satellite program summary
| NASA-CR-192469 | p 2774 N93-25886
Bibliography of remote sensing techniques used in wetland research
| AD-A261704 | p 2757 N93-26440
SCINTILLATING FIBERS
Studies of avalanche photodiodes for scintillating fibre tracking readout
| DE93-008370 | p 2689 N93-25491
SCINTILLATION
Laser propagation through turbulence
| AD-A260712 | p 2714 N93-26217
OLYMPUS/ACTS scintillation experiment at the Lewis Research Center p 2685 N93-26481
SCINTILLATION COUNTERS
The sub 60 ps timing resolution using large area silicon avalanche diodes
| DE93-007723 | p 2688 N93-25365
Studies of avalanche photodiodes for scintillating fibre tracking readout
| DE93-008370 | p 2689 N93-25491
SCREWS
The design of mechanically compatible fasteners for human mandible reconstruction p 2796 N93-25569
SEA ICE
Passive microwave remote sensing of snow-covered floating ice during spring conditions in the Arctic and Antarctic
| ISBN-0-315-70444-6 | p 2754 N93-25422
Radar backscatter measurements from Arctic sea ice during the fall freeze-up
| NASA-CR-193100 | p 2790 N93-26050
The effects of cloud inhomogeneities upon radiative fluxes, and the supply of a cloud truth validation dataset
| NASA-CR-191711 | p 2787 N93-26492
SEA LEVEL
Sea level variation p 2734 N93-24929
Satellite altimetry p 2734 N93-24930
A coastal hazards data base for the US East Coast
| NASA-TM-108265 | p 2791 N93-26586
SEA SURFACE TEMPERATURE
Satellite monitoring of the global ocean surface during 1987-1989 p 2734 N93-24926
Simulation and prediction of tropical SST with a coupled ocean-atmosphere model p 2789 N93-25469
Relations between blue whiting biomass and satellite derived phytoplankton and temperature in the Norwegian Sea
| AD-A261205 | p 2757 N93-25868
An observational study of the local and remote response of the equatorial Pacific to westerly wind events during the 1991-92 El Nino
| AD-A261777 | p 2787 N93-26286
SEA WATER
Loss of temporal coherence of laser light propagated through simulated coastal waters
| AD-A261303 | p 2715 N93-26296
SEALS (STOPPERS)
Advanced bristle seals for gas turbine engines
| AD-A261296 | p 2720 N93-26564
SEASAT SATELLITES
Report of the Seasat Failure Review Board
p 2619 N93-24693
SEATS
Crashworthiness of composite seats for civil aircraft
p 2582 N93-24773
SECONDARY FLOW
Flow and heat transfer experiments in the turbine airfoil/endwall region p 2704 N93-25725
SECONDARY ION MASS SPECTROMETRY
State-selected studies of atoms and molecules ejected from ion bombarded surfaces
| AD-A261275 | p 2850 N93-26267
SECULAR VARIATIONS
Steady induction effects in geomagnetism. Part 1B: Geomagnetic estimation of steady surficial core motions: A non-linear inverse problem
| NASA-TP-3272-PT-1B | p 2776 N93-26421
SEDIMENTS
Evaluation of nearshore suspended sediment concentration through Landsat TM data: First results
p 2747 N93-24833
SEEPAGE
Radar sensing of petroleum seepage gases
| AD-A261431 | p 2682 N93-26455
SEISMOLOGY
A geological and geophysical information system for Eurasia
| AD-A261789 | p 2883 N93-26442
SEIZURES
Automatic detection of seizures with applications
p 2796 N93-25592
SELECTIVE DISSEMINATION OF INFORMATION
The SWORD multilevel secure DBMS
| RSRE-92005 | p 2811 N93-25942
SELECTIVITY
GPS standardization for the needs of time transfer
p 2836 N93-25016
SELENIDES
Laser Induced Phonons (LIPs) in MBE grown ZnSe
| RSRE-MEMO-4544 | p 2864 N93-25454
SELF CONSISTENT FIELDS
Implementation of cyclic spectral analysis methods
| AD-A261715 | p 2681 N93-26372
SELF LUBRICATING MATERIALS
Properties of extruded PS-212 type self-lubricating materials p 2659 N93-25565
SELF ORGANIZING SYSTEMS
Demonstration for novel self-organization theory by three-dimensional magnetohydrodynamic simulation
| NIFS-212 | p 2859 N93-25227
SELF OSCILLATION
Basic research thermoacoustic heat transport
| AD-A261334 | p 2759 N93-26310
SEMANTICS
Visualizing the semantic content of large text databases using text maps p 2826 N93-25982
Virtually-synchronous communication based on a weak failure suspector
| NASA-CR-193003 | p 2721 N93-26135
Towards a formalism for program generation
| AD-A261689 | p 2812 N93-26368
SEMICONDUCTOR DEVICES
Correlated wavefunction quantum Monte Carlo approach to solids
| DE93-007730 | p 2863 N93-25367
Electric field effects on quantum-confined semiconductor structures p 2865 N93-25703
Time resolved studies of in-well and cross-well carrier transport in MQW semiconductor structures
| AD-A261170 | p 2714 N93-25774
Experimental and theoretical studies of proximity effect and Coulomb blockade phenomena in Josephson junctions
| AD-A261652 | p 2867 N93-26194
RF vacuum microelectronics
| AD-A261343 | p 2691 N93-26311
1992 technical digest series volume 16. Conference edition: Summaries of papers presented at the Nonlinear Dynamics in Optical Systems Topical Meeting
| AD-A261915 | p 2857 N93-26544
Transition metal chelate-fulleride compounds: Electrocrystallization of semiconducting (Ru(bpy)s)(C60)2
| AD-A261549 | p 2869 N93-26577
SEMICONDUCTOR JUNCTIONS
An inverted AlGaAs/GaAs patterned-Ge tunnel junction cascade concentrator solar cell
| DE93-000073 | p 2759 N93-25102

SEMICONDUCTOR LASERS
Noise measurements in single-mode GaAlAs diode lasers p 2716 N93-25067
An active solid state ring laser gyroscope p 2709 N93-25291
Studies of avalanche photodiodes for scintillating fibre tracking readout
| DE93-008370 | p 2689 N93-25491
SEMICONDUCTORS (MATERIALS)
Radiation and temperature effects on electronic components investigated under the CSTI high capacity power project
| NASA-TM-106096 | p 2687 N93-24746
FNAS computational modeling
| NASA-CR-192512 | p 2863 N93-25225
JPRS report: Science and technology. Central Eurasia: Life sciences
| JPRS-ULS-93-002 | p 2737 N93-25399
The DX centers in three to five semiconductors under hydrostatic pressure
| DE93-007701 | p 2864 N93-25490
High speed solid state circuit breaker p 2694 N93-25598
Transmission electron microscopy investigation of ion implantation damage in GaAs and other semiconductors p 2865 N93-25715
Time resolved studies of in-well and cross-well carrier transport in MQW semiconductor structures
| AD-A261170 | p 2714 N93-25774
Monolithic integration of semiconductor and superconductor components
| AD-A260589 | p 2690 N93-25906
HERO resistant semiconductor bridge igniter p 2627 N93-26024
Gordon Conference on Point Defects, Line Defects and Interfaces in Semiconductors
| AD-A261485 | p 2868 N93-26357
Multivariable control for flexible IC processing
| AD-A261685 | p 2692 N93-26366
Electronics and Electrical Engineering Laboratory technical publication announcements covering laboratory programs, July to September 1992 with 1992/1993 EEEL events calendar
| PB93-158632 | p 2884 N93-26530
Joint services electronics program
| AD-A261801 | p 2692 N93-26539
Optical characterization of Ga(1-x)In(x)As(y)Sb(1-y)/GaSb alloy and device application
| AD-A261713 | p 2870 N93-26581
SENSITIVITY
Autonomic physiological data associated with simulator discomfort
| NASA-CR-177609 | p 2794 N93-24738
ANOVA method to estimate vegetation indices sensitivity assessing nitrogen fertilizing influence on spectral reflectance coefficients p 2739 N93-24782
Weak magnetic field sensitivity of quartz crystal oscillators p 2833 N93-24993
Elastic plate mode sensitivities to mass loading applications to gas sensors p 2711 N93-25009
A computational aerodynamic design optimization method using sensitivity analysis p 2589 N93-25552
Neural networks for atmospheric retrievals p 2824 N93-25975
Thermal radiation in non-metalized solid rocket motors: Effect on burning rate and temperature sensitivity p 2626 N93-26020
Task 5: Architecture sensitivity to STME performance
| MCR-92-5010 | p 2609 N93-26176
Molecular composition, structure, and sensitivity of explosives
| DE93-003850 | p 2662 N93-26493
SENSORIMOTOR PERFORMANCE
Coordinated action in 3-D space
| AD-A261418 | p 2799 N93-26449
SENSORS
Digitization of analog data from in-flight lightning strikes p 2778 N93-24884
A single-point warning system for thunderstorms and electric fields p 2711 N93-24900
A survey of life support system automation and control
| NASA-TM-103977 | p 2667 N93-25085
Realtime control of multiple sensor systems
| AD-A261037 | p 2680 N93-26226
SENSORY FEEDBACK
Modeling of a full vision system using combined Visual/Haptic search for remote object identification
| AD-A260977 | p 2801 N93-25867
SENSORY PERCEPTION
Biomagnetic localization from transient quasi-static events
| DE93-007328 | p 2794 N93-25186
Neuropsychological components of object identification
| AD-A261449 | p 2797 N93-26347
SEPARATED FLOW
Surface and flow field measurements in a symmetric crossing shock wave/turbulent boundary-layer interaction
| NASA-TM-106086 | p 2575 N93-24911
Numerical simulation of a shock wave/turbulent boundary layer interaction in a duct p 2699 N93-25342
Computational modelling of 3D flow in complex ducts and passages p 2704 N93-25698
SEPARATORS
Design and synthesis of reactive separation systems
| DE93-008764 | p 2642 N93-25115
Pyroshock: Bibliography
| DE93-007605 | p 2726 N93-25489
SEQUENCING
Development of resonance ionization spectroscopy for genome mapping and DNA sequencing using stable isotopes as DNA labels
| DE93-007815 | p 2793 N93-26587
SEQUENTIAL ANALYSIS
A method for sequential image analysis of hazard areas p 2743 N93-24810
SERIES EXPANSION
Asymptotic derivation of the simplified P(sub N) equations
| DE93-007342 | p 2828 N93-25151
SERVICE LIFE
Elastomer compound developed for high wear applications p 2659 N93-25607
Improved fatigue life for moorings
| PB93-161198 | p 2730 N93-26320
SERVICES
Factors associated with perceptions of productivity and usage of information technology in a service organization p 2875 N93-25421
SERVOMECHANISMS
Dynamic modeling of fluid transmission lines of the DSN 70-meter antennas by using a lumped parameter model p 2678 N93-26119
SERVOMOTORS
Development and testing of the digital control system for the Archytas unmanned air vehicle
| AD-A261656 | p 2597 N93-26196
SETTLING
Gravity-dependent transport phenomena in zeolite crystal growth p 2664 N93-25740
SEWAGE
Regulatory impact analysis of the Part 503 sewage sludge regulation
| PB93-110625 | p 2768 N93-26567
SEWAGE TREATMENT
Regulatory impact analysis of the Part 503 sewage sludge regulation
| PB93-110625 | p 2768 N93-26567
SH WAVES
Elastic plate mode sensitivities to mass loading applications to gas sensors p 2711 N93-25009
SHADOWGRAPH PHOTOGRAPHY
Generation of acoustic waves by focused infrared neodymium-laser radiation p 2714 N93-25761
SHAFTS (MACHINE ELEMENTS)
Radial spline assembly for antifriction bearings
| NASA-CASE-MFS-28629-1 | p 2719 N93-26001
SHAPE CONTROL
Design of flexible rods with embedded SMA actuators
| AD-A260742 | p 2729 N93-25846
SHAPE MEMORY ALLOYS
Design of flexible rods with embedded SMA actuators
| AD-A260742 | p 2729 N93-25846
Deformations of active flexible rods with embedded line actuators
| AD-A261207 | p 2729 N93-25950
SHAPED CHARGES
Analysis of shaped charge jet penetration experiments with Pen
| UCRL-LR-110773 | p 2730 N93-26177
Algorithms for the analysis of penetration by shaped charge jets
| UCRL-LR-109887 | p 2730 N93-26178
SHAPES
Hypervelocity impact study: The effect of impact angle on crater morphology
| NASA-CR-192711 | p 2724 N93-25260
Topography from shading and stereo p 2879 N93-25803
Thermomechanical response of shape memory composites
| AD-A260828 | p 2639 N93-25919
Deformations of active flexible rods with embedded line actuators
| AD-A261207 | p 2729 N93-25950
SHARP LEADING EDGES
Conical Euler analysis and active roll suppression for unsteady vortical flows about rolling delta wings
| NASA-TP-3259 | p 2581 N93-26134
SHEAR FLOW
An analysis of lift forces on aerosols in a wall bounded turbulent shear flow
| DE93-003362 | p 2695 N93-24963
Spatial simulation of transition in wall-bounded shear flows: Active control and effects of surface roughness p 2701 N93-25483
Particle dynamics modeling of boundary effects in granular Couette flow p 2705 N93-25738
Proceedings of the NUWC Division Newport Seminar Series on Turbulence and its Control
| NUWC-NPT-TM-922089 | p 2707 N93-26328
SHEAR LAYERS
Studies in air/air supersonic mixing layers p 2582 N93-26007
SHEAR PROPERTIES
On the stability of finite plastic deformations
| AD-A261526 | p 2730 N93-26361
European tri-service advanced materials workshop on compressive strength in rigid-rod polymers
| AD-A261517 | p 2658 N93-26576
SHEAR STRAIN
On existence of solutions and duality for a model of non-linear elastic plates with transverse shear deformations p 2726 N93-25437
High strain rate damage development and failure mechanisms in tungsten heavy alloys
| AD-A260856 | p 2651 N93-25788
Shear band formation in a W-Ni-Fe alloy under plate impact
| AD-A260702 | p 2651 N93-25907
SHEAR STRENGTH
Dynamic hardness tester and cure meter p 2711 N93-25608
SHEAR STRESS
Thermoelastic stresses in multi-layered media in non-uniform temperature fields
| AD-A260901 | p 2727 N93-25658
Gravity-dependent transport phenomena in zeolite crystal growth p 2664 N93-25740
An experimental study of passive drag reduction in a turbulent boundary layer by a riblet surface p 2705 N93-25746
Optimization techniques for contact stress analysis
| AD-A260846 | p 2729 N93-25911
Proceedings of the NUWC Division Newport Seminar Series on Turbulence and its Control
| NUWC-NPT-TM-922089 | p 2707 N93-26328
SHIPS
High-performance visualization applied to computational electromagnetics: Method-of-moments on a silicon graphics workstation
| AD-A260820 | p 2675 N93-25700
SHOCK LAYERS
Numerical simulation of a shock wave/turbulent boundary layer interaction in a duct p 2699 N93-25342
An experimental study of under-expanded jets p 2577 N93-25467
SHOCK SPECTRA
Pyroshock: Bibliography
| DE93-007605 | p 2726 N93-25489
SHOCK TUBES
Ignition and combustion of lunar propellants
| NASA-CR-192814 | p 2659 N93-24745
Shock tube application to the study of compressible turbulent boundary layer with mass injection p 2697 N93-25252
SHOCK WAVE INTERACTION
An experimental study of the sources of fluctuating pressure loads beneath swept shock/boundary-layer interactions
| NASA-CR-192918 | p 2698 N93-25266
Numerical simulation of a shock wave/turbulent boundary layer interaction in a duct p 2699 N93-25342
Navier-Stokes simulations of unsteady transonic flow phenomena p 2578 N93-25542
Heat transfer measurements in swept shock wave/turbulent boundary-layer interactions p 2704 N93-25705
SHOCK WAVE PROPAGATION
Surface and flow field measurements in a symmetric crossing shock wave/turbulent boundary-layer interaction
| NASA-TM-106086 | p 2575 N93-24911
SHOCK WAVES
Development and application of computational aerothermodynamics flowfield computer codes
| NASA-CR-192940 | p 2574 N93-24736
Observations and models of shock structures in Herbig-Haro objects p 2891 N93-24770

Fuel Injector: Air swirl characterization aerothermal modeling, phase 2, volume 2
| NASA-CR-189193 | p 2592 N93-25106
Alfven wave transport effects in the time evolution of parallel cosmic-ray modified shocks
| NASA-CR-192932 | p 2899 N93-25161
The modeling of complex continua: Fundamental obstacles and grand challenges
| DE93-006507 | p 2696 N93-25193
Shock tube application to the study of compressible turbulent boundary layer with mass injection
p 2697 N93-25252
Computation of transonic flow over a porous surface projectile p 2577 N93-25409
Pyroshock: Bibliography
| DE93-007605 | p 2726 N93-25489
Turbulence interacting with chemical kinetics in airbreathing combustion of ducted rockets
p 2625 N93-26012

SHORELINES
A coastal hazards data base for the US East Coast
| NASA-TM-108265 | p 2791 N93-26586

SHORT WAVE RADIO TRANSMISSION
WARC 92 and some thoughts as to its impact on the NASA propagation program p 2684 N93-26475

SHROUDED PROPELLERS
Rotating rake design for unique measurement of fan-generated spinning acoustic modes
| NASA-TM-105946 | p 2595 N93-26161

SIDELOBE REDUCTION
Frequency diversity sidelobe canceller
| AD-D015647 | p 2674 N93-25332

SIDEREAL TIME
The advances in F and T technology: Their benefits of and for space science and technology
p 2831 N93-24979

SIERRA NEVADA MOUNTAINS (CA)
Natural and augmented snowfall growth processes and their interactions with the natural and modified aerosol
| PB93-153096 | p 2786 N93-25874

SIGNAL ANALYSIS
Use of the TV-signal in stabilizing a local rubidium oscillator p 2693 N93-25029
Center for intelligent control systems
| AD-A260995 | p 2821 N93-25853
Recommendations for a Kalman filter to estimate and control freeze and sublime rates of gaseous diffusion plant freezer/sublimer systems
| ORNL/TM-12183 | p 2668 N93-25937

SIGNAL ANALYZERS
A channel simulation processor for the multi-node tactical network simulator
| AD-A261810 | p 2776 N93-26430

SIGNAL DETECTION
Implementation of cyclic spectral analysis methods
| AD-A261715 | p 2681 N93-26372
Geolocation of an electromagnetic emitter using a cyclostationary time difference of arrival technique
| AD-A261781 | p 2686 N93-26603

SIGNAL DETECTORS
Optical fiber for acoustic sensor applications
| AD-A261580 | p 2857 N93-26515

SIGNAL DISTORTION
Symbol signal-to-noise ratio loss in square-wave subcarrier downconversion p 2672 N93-24668

SIGNAL ENCODING
Experiments with the HIVITS HDTV contribution CODED
| BBC-RD-1992/12 | p 2674 N93-25391
Golay and other box codes p 2678 N93-26116

SIGNAL FADING
Propagation at microwave frequencies in the presence of tropospheric stratified layers p 2674 N93-25340
An SPW software simulation model of a dispersive fading multipath narrowband HF channel
| AD-A261101 | p 2675 N93-25767
An introduction to Doppler effect and fading in mobile communications
| AD-A260976 | p 2676 N93-25866
Statistics of sampled Rician fading
| AD-A261397 | p 2681 N93-26289
L- and K-band LMSS propagation measurements using MARECS-B, OLYMPUS, and ACTS
p 2683 N93-26467
Rain rate and modeled fade distributions at 20 GHz and 30 GHz derived from five years of network rain gauge measurements p 2683 N93-26468
Effect-specific analysis of propagation parameters
p 2684 N93-26478

SIGNAL GENERATORS
Adaptive control of nonlinear flexible systems
| AD-A261676 | p 2826 N93-26365
New results in signal design for the AWGN channel
| AD-A261424 | p 2682 N93-26451

SIGNAL PROCESSING
Determination of design and operation parameters for upper atmospheric research instrumentation to yield optimum resolution with deconvolution, appendix 4
| NASA-CR-192834 | p 2769 N93-24910
Synchronisation, acquisition and tracking for telemetry and data reception p 2614 N93-25000
Determination of design and operation parameters for upper atmospheric research instrumentation to yield optimum resolution with deconvolution, appendix 2
| NASA-CR-192833 | p 2770 N93-25088
The constant current loop: A new paradigm for resistance signal conditioning
| NASA-TM-108744 | p 2673 N93-25181
An example of a phase-segregated enhanced PAL broadcasting system
| BBC-RD-1992/6 | p 2674 N93-25239
Proceedings of the Second SISAL Users' Conference
| DE93-008019 | p 2815 N93-25304
Log-ratio signal-processing technique for beam position monitors
| DE93-007356 | p 2851 N93-25314
Beam position and total current monitor for heavy ion fusion beams
| DE93-007653 | p 2851 N93-25325
Very high-speed arithmetic processors (The Gauss Machine)
| AD-A260693 | p 2806 N93-25650
VLSI for high-speed digital signal processing
| AD-A260754 | p 2690 N93-25678
An SPW software simulation model of a dispersive fading multipath narrowband HF channel
| AD-A261101 | p 2675 N93-25767
Exploitation of cyclostationarity for signal-parameter estimation and system identification
| AD-A260833 | p 2728 N93-25784
Signal processing in impulsive electromagnetic interference
| AD-A260755 | p 2676 N93-25847
Design, fabrication, and testing of a three-dimensional acoustic orientation instrument (3-D AOI): Drawings, engineering and associated lists (conceptual and development design)
| AD-A260934 | p 2845 N93-25915
Phase discriminating capacitive array sensor system
| NASA-CASE-GSC-13460-1 | p 2691 N93-26104
Goldstone solar system radar signal processing
p 2680 N93-26130
Realtime control of multiple sensor systems
| AD-A261037 | p 2680 N93-26226
OTH-B radar system: System summary
| AD-A261727 | p 2681 N93-26247
Bayesian cross-entropy reconstruction of complex images
| AD-A261812 | p 2812 N93-26257
Digital Oblique Remote Ionospheric Sensing (DORIS) program development
| AD-A261750 | p 2776 N93-26283
A channel simulation processor for the multi-node tactical network simulator
| AD-A261810 | p 2776 N93-26430
Pseudo Wigner-Ville distribution, computer program, and its applications to time-frequency domain problems
| AD-A261839 | p 2813 N93-26431
New results in signal design for the AWGN channel
| AD-A261424 | p 2682 N93-26451
More rain compensation results p 2686 N93-26486
Electronics and Electrical Engineering Laboratory technical publication announcements covering laboratory programs, July to September 1992 with 1992/1993 EEEL events calendar
| PB93-158632 | p 2884 N93-26530
Geolocation of an electromagnetic emitter using a cyclostationary time difference of arrival technique
| AD-A261781 | p 2686 N93-26603

SIGNAL RECEPTION
Synchronisation, acquisition and tracking for telemetry and data reception p 2614 N93-25000
Bandwidth compression of noisy signals with square-wave subcarrier p 2678 N93-26120
DSN acquisition of Magellan high-rate telemetry data
p 2614 N93-26124

SIGNAL TO NOISE RATIOS
A functional description of the Buffered Telemetry Demodulator (BTD) p 2614 N93-24667
Symbol signal-to-noise ratio loss in square-wave subcarrier downconversion p 2672 N93-24668
Microwave frequency discriminator with a cryogenic sapphire resonator for ultra-low phase noise
p 2693 N93-24982
Actual limits of fluorescence S/N ratio in an optically-pumped cesium beam resonator
p 2833 N93-24991
Optimizing the G/T ratio of the DSS-13 34-meter beam-waveguide antenna p 2678 N93-26118
Bandwidth compression of noisy signals with square-wave subcarrier p 2678 N93-26120

SIGNAL TRANSMISSION
Timing and time signal distribution in digital communications networks p 2686 N93-25061
Statistics of sampled Rician fading
| AD-A261397 | p 2681 N93-26289

SIGNATURE ANALYSIS
The use of polarimetric radar remote sensing data for application in forestry p 2749 N93-24845

SIGNATURES
Lightning precursor signatures from dual-polarization radar measurements of storms p 2777 N93-24877
Pseudo Wigner-Ville distribution, computer program, and its applications to time-frequency domain problems
| AD-A261839 | p 2813 N93-26431

SIGNS AND SYMPTOMS
Anomalous event diagnosis for environmental satellite systems p 2619 N93-25971

SILICA GLASS
Surface preparation and characterization of a 400 micrometer diameter fused silica optical fiber for direct optical initiation (DOI) applications
| DE93-005485 | p 2852 N93-25182

SILICIDES
Processing and properties of Ti5Si3
| DE93-007284 | p 2649 N93-25149

SILICON
Photoluminescence of silicon nanostructures formed by ion beam implantation
| DE93-006777 | p 2862 N93-24958
Anisotropic etching of silicon in KOH solutions
p 2647 N93-25037
The sub 60 ps timing resolution using large area silicon avalanche diodes
| DE93-007723 | p 2688 N93-25365
Smart microsensors for high temperature applications
| AD-A260747 | p 2710 N93-25677
Monolithic integration of semiconductor and superconductor components
| AD-A260589 | p 2690 N93-25906
Optoelectronic III-V heterostructures on Si substrates
| AD-A261651 | p 2867 N93-26193
Visible light emission from porous silicon examined by photoluminescence and Raman spectroscopy
| DE93-006780 | p 2646 N93-26502

SILICON ALLOYS
Fundamental studies of defect generation in amorphous silicon alloys grown by remote plasma-enhanced chemical-vapor deposition (Remote PECVD)
| DE92-010560 | p 2862 N93-24953
Metastable SiC and SiGeC alloys by carbon implantation and solid phase epitaxy
| DE93-007594 | p 2863 N93-25387

SILICON CARBIDES
Metastable SiC and SiGeC alloys by carbon implantation and solid phase epitaxy
| DE93-007594 | p 2863 N93-25387
Processing and properties of silicon carbide reinforced reaction bonded silicon nitride composites
| AD-A260570 | p 2640 N93-26236
SiC microsensor with piezoresistive diamond sensing elements
| AD-A261346 | p 2868 N93-26312

SILICON NITRIDES
Research on lead titanate films for radiation detection
| AD-A261187 | p 2849 N93-25823
Processing and properties of silicon carbide reinforced reaction bonded silicon nitride composites
| AD-A260570 | p 2640 N93-26236

SILICON RADIATION DETECTORS
Temperature dependence of radiation damage and its annealing in silicon detectors
| DE93-003854 | p 2869 N93-26494
Large area, low capacitance Si(Li) detectors for high rate x ray applications
| DE93-007661 | p 2692 N93-26598

SILICONES
Characterization of the synthesis of M-61, a random equilibrium silicone terpolymer, using dry starting materials
| KCP-613-4985 | p 2657 N93-26213

SILOXANES
Characterization of the synthesis of M-61, a random equilibrium silicone terpolymer, using dry starting materials
| KCP-613-4985 | p 2657 N93-26213

SILVER COMPOUNDS
Colloid formation in implanted glasses
| DE93-006763 | p 2653 N93-24971

SILVER IODIDES
Investigation of winter mountain storms in Utah during the 1989 Utah/NOAA field program
| PB93-153021 | p 2785 N93-25849

Natural and augmented snowfall growth processes and their interactions with the natural and modified aerosol
| PB93-153096 | p 2786 N93-25874

SIMD (COMPUTERS)
Construction of a connectionist network supercomputer
| AD-A260929 | p 2820 N93-25648

SIMPLEX METHOD
New results in signal design for the AWGN channel
| AD-A261424 | p 2682 N93-26451

SIMULATED ANNEALING
Discrete range clustering using Monte Carlo methods
| NASA-TM-104004 | p 2584 N93-24914
New ground states in unconventional superconductors
p 2688 N93-25282
Digital Oblique Remote Ionospheric Sensing (DORIS) program development
| AD-A261750 | p 2776 N93-26283

SIMULATION
Optimal message log reclamation for independent checkpointing
| NASA-CR-192886 | p 2815 N93-24749
Striped tape arrays
| NASA-CR-192914 | p 2806 N93-25267
Multi-rate, real time image compression for images dominated by point sources p 2805 N93-25932
Studies in air/air supersonic mixing layers
p 2582 N93-26007
Imaging the magnetosphere in the extreme ultraviolet
| NASA-CR-192218 | p 2775 N93-26151
NLS operations concepts: Failure modes scenario simulation model analysis
| MCR-92-5013 | p 2609 N93-26175

SIMULATORS
Commercial Precipitation Static (P-static) test equipment p 2711 N93-24901
Data systems dynamic simulator p 2814 N93-25602
Utilization of an electronic circuit simulator in CMOS latch-up studies
| AD-A260877 | p 2690 N93-25935

SINE WAVES
Performance results of a 300-degree linear phase modulator for spaceborne communications applications
p 2672 N93-24670
Equipment testing with damped sinewaves between 1 and 50 MHz p 2692 N93-24881
New algorithms for the detection and elimination of sine waves and other narrow-band signals in the presence of broadband signals and noise
| AD-A261811 | p 2681 N93-26261
Monaural and binaural processing of complex waveforms
| AD-A261659 | p 2846 N93-26358

SINGLE CRYSTALS
Crack tip fields in ductile crystals and bicrystals
p 2866 N93-25749
Activation of methane by clean and chemically modified single crystal oxide surfaces
| PB93-157295 | p 2644 N93-25817
Fatigue in single crystal nickel superalloys
| AD-A260709 | p 2651 N93-25843
Vickers indentation hardness of stoichiometric and reduced single crystal TiO2 (rutile) from 25 to 800 C
| NASA-TM-105959 | p 2633 N93-26204
Fatigue in single crystal nickel superalloys
| AD-A261742 | p 2652 N93-26282
Dynamics of gas-surface interactions
| AD-A261402 | p 2646 N93-26402

SINGLE STAGE TO ORBIT VEHICLES
Aerospace-plane flights and stratospheric ozone: Review and preliminary assessment of the National Aerospace Plane (NASP) operations
| RAND/N-3464-AF | p 2767 N93-26327

SINGLE-PHASE FLOW
Predictive modeling of particle-laden, turbulent flows
| DE93-008208 | p 2698 N93-25309

SINGULARITY (MATHEMATICS)
Optimal thrust magnitude on a singular arc in atmospheric flight p 2819 N93-25410
Analysis of wing wake roll-up using a vortex-in-cell method p 2579 N93-25706

SINTERING
Densification of ceramics by gas overpressure sintering
| MTL-TR-92-45 | p 2657 N93-26432

SIS (SUPERCONDUCTORS)
A superconducting tunnel junction receiver for submillimeter astronomy, and analysis of observations of post-AGB star molecular envelopes
p 2889 N93-25440

SIZE (DIMENSIONS)
Assessing patterns of change in anthropometric dimensions: Secular trends of US Army females, 1946-1988
| AD-A260869 | p 2800 N93-25628

SIZE DISTRIBUTION
Volatiles in interplanetary dust particles: A comparison with CI and CM chondrites p 2896 N93-26062
Intensity distribution of the x ray source for the AXAF VETA-I mirror test p 2854 N93-26184
Particulate emissions from gas turbine engines
| AD-A261374 | p 2595 N93-26339

SKIN FRICTION
Uniform roughness studies
| WL-TR-92-3041 | p 2706 N93-25951

SKY SURVEYS (ASTRONOMY)
The ALEXIS data processing package: An update
| DE93-007374 | p 2899 N93-25185
Starburst Galaxies: Hard X-ray spectra and contribution to the diffuse background
| NASA-CR-192790 | p 2892 N93-25211
A study of the large-scale infrared emission from a selected dark cloud
| NASA-CR-192775 | p 2888 N93-25289
The structure of the nearby universe traced by theIRAS galaxies
| NASA-CR-192809 | p 2889 N93-25331
Cape Photographic Durchmusterung, volume 1
| NASA-RP-1300-VOL-1 | p 2890 N93-26002
Cape Photographic Durchmusterung, volume 2
| NASA-RP-1300-VOL-2 | p 2890 N93-26003
Cape Photographic Durchmusterung, volume 3
| NASA-RP-1300-VOL-3 | p 2890 N93-26004
ROSAT x ray survey observations of active chromospheric binary systems and other selected sources
| NASA-CR-192933 | p 2891 N93-26426

SKYLAB 1
The initial flight anomalies of Skylab 1
p 2619 N93-24692

SLABS
Minimization of heat slab nodes with higher order boundary conditions
| DE93-004238 | p 2695 N93-24966

SLENDER CONES
Combined LAURA-UPS hypersonic solution procedure
| NASA-TM-107682 | p 2696 N93-25176

SLIDING
A micromechanical viscoplastic stress-strain model with grain boundary sliding
| DE93-009109 | p 2649 N93-25095

SLIDING CONTACT
Three-dimensional boundary element analysis of contact and fracture problems p 2725 N93-25335

SLIDING FRICTION
Energy dissipation in inelastic flow of cohesionless granular media p 2703 N93-25662

SLOTS
A three-dimensional algebraic grid generation scheme for gas turbine combustors with inclined slots
| NASA-CR-191095 | p 2694 N93-24759
Shock tube application to the study of compressible turbulent boundary layer with mass injection
p 2697 N93-25252
Radial spline assembly for antifriction bearings
| NASA-CASE-MFS-28629-1 | p 2719 N93-26001

SLUDGE
Converting environmental wastes into valuable resources p 2759 N93-25572
Regulatory impact analysis of the Part 503 sewage sludge regulation
| PB93-110625 | p 2768 N93-26567

SLURRIES
Low cost dewatering of waste slurries
p 2769 N93-25573
Ultrasonic polishing p 2670 N93-25580
Particle size as a factor in agglomeration in slurry fuels p 2625 N93-26013

SLURRY PROPELLANTS
Atomization and combustion of a gelled, metallized slurry fuel
| AD-A261778 | p 2647 N93-26602

SMALL SCIENTIFIC SATELLITES
Satellite communications application to Pacific countries above Ku band p 2683 N93-26471

SMART STRUCTURES
Damage-survivable and damage-tolerant laminated composites with optimally placed piezoelectric layers
| AD-A260879 | p 2636 N93-25631
Design of flexible rods with embedded SMA actuators
| AD-A260742 | p 2729 N93-25846
Smart structural composites with piezoelectric micro-constituents
| AD-A260970 | p 2640 N93-26225
Investigation of coupled analysis techniques for adaptive material structural systems
| AD-A261359 | p 2868 N93-26332

SMOKE DETECTORS
Contributions of microgravity test results to the design of spacecraft fire safety systems
| NASA-TM-106093 | p 2614 N93-24755

SNOW
Alternative strategies for the use of satellite data analysis systems for hazard monitoring and disaster mitigation
p 2743 N93-24805
Natural and augmented snowfall growth processes and their interactions with the natural and modified aerosol
| PB93-153096 | p 2786 N93-25874

SNOW COVER
Passive microwave remote sensing of snow-covered floating ice during spring conditions in the Arctic and Antarctic
| ISBN-0-315-70444-6 | p 2754 N93-25422

SOBOLEV SPACE
Line formation and the Poynting-Robertson effect in accretion discs p 2847 N93-25355

SOCIAL FACTORS
Small business access to equity capital
| PB93-144582 | p 2872 N93-25735

SODIUM
Temperature-dependent electrical conductivity of soda-lime glass
| DE93-007872 | p 2654 N93-25359
Structure of sodium 4-(1'-heptylnonyl) benzenesulfonate adsorbed on alumina using H-2 NMR
| AD-A261224 | p 2645 N93-26300

SOFTWARE ENGINEERING
A multimission three-axis stabilized spacecraft flight dynamics ground support system p 2603 N93-24714
Analysis of large system black box verification test data
| NASA-CR-192885 | p 2815 N93-24748
The ALEXIS data processing package: An update
| DE93-007374 | p 2899 N93-25185
PCG: A software package for the iterative solution of linear systems on scalar, vector and parallel computers
| DE93-007366 | p 2809 N93-25315
FORTRAN M as a language for building earth system models
| DE93-007897 | p 2763 N93-25370
The database Query Support Processor (QSP)
p 2807 N93-25577
Software lifecycle support environment (SLCSE) knowledge-based enhancements
| AD-A261042 | p 2811 N93-25791
Multivariate statistical analysis software technologies for astrophysical research involving large data bases
p 2878 N93-25796
SAVS: A Space Analysis and Visualization System
p 2881 N93-25812
A Spatial Analysis and Modeling System (SAMS) for environment management p 2881 N93-25813
Model-based reasoning for system and software engineering: The Knowledge From Pictures (KFP) environment p 2825 N93-25978
In search of meta-knowledge p 2826 N93-25983
An OSI architecture for the Deep Space Network
p 2679 N93-26121
High performance computing and communications panel report p 2807 N93-26131
Research directions in software analysis, synthesis and certification
| AD-A261367 | p 2812 N93-26336
Towards a formalism for program generation
| AD-A261689 | p 2812 N93-26368
Test, Control and Monitor System (TCMS) operations plan
| NASA-CR-193098 | p 2873 N93-26419
Test, Control and Monitor System maintenance plan
| NASA-CR-193099 | p 2873 N93-26420
Managing real-time software projects: Problems and issues
| AD-A261428 | p 2813 N93-26453
IDEF6: A design rationale capture method concept paper
| AD-A261594 | p 2884 N93-26523

SOFTWARE RELIABILITY
Putting time into proof outlines
| NASA-CR-192978 | p 2809 N93-25152
Statistical modelling of software reliability
| NASA-CR-192985 | p 2809 N93-25257
Software testing initiative for strategic defense systems
| AD-A261350 | p 2831 N93-26330
Managing real-time software projects: Problems and issues
| AD-A261428 | p 2813 N93-26453

SOFTWARE REUSE
A multimission three-axis stabilized spacecraft flight dynamics ground support system p 2603 N93-24714
An application of machine learning to the organization of institutional software repositories
p 2825 N93-25981
The design and implementation of a reusable component library and a retrieval/integration system
| AD-A261827 | p 2812 N93-26271

Department of Defense technical architecture framework for information management. Volume 1: Implementation concept, version 1.1
| AD-A261911 | p 2884 N93-26531
Three view language: A graphics-based language for requirements definition, version 01.00.00
| AD-A261732 | p 2813 N93-26583

SOFTWARE TOOLS
Object-oriented tools for distributed computing p 2817 N93-25576
ASTROS-ID: Software for system identification using mathematical programming
| AD-A260867 | p 2810 N93-25627
High level design for distributed application instrumentation
| AD-A260812 | p 2710 N93-25696
Construction of an advanced software tool for planetary atmospheric modeling p 2815 N93-25799
A methodology and software environment for testing process model's sequential predictions with protocols
| AD-A260980 | p 2882 N93-25844
The design and implementation of a reusable component library and a retrieval/integration system
| AD-A261827 | p 2812 N93-26271
Research directions in software analysis, synthesis and certification
| AD-A261367 | p 2812 N93-26336

SOIL EROSION
Registration of the use of agricultural fields and soil erosion using satellite remote sensing p 2751 N93-24856

SOIL MECHANICS
Lunar regolith and structure mechanics p 2670 N93-26412

SOIL MOISTURE
Land surface processes and climate modeling p 2783 N93-25685
Development and testing of improved techniques for modeling the hydrologic cycle in a mesoscale weather prediction system
| AD-A261454 | p 2787 N93-26351

SOILS
Development of a cone penetrometer for measuring spectral characteristics of soils in situ p 2776 N93-25570
Reclamation with recovery of radionuclides and toxic metals from contaminated materials, soils, and wastes p 2769 N93-25571

SOL-GEL PROCESSES
Passive vibration damping materials: Piezoelectric ceramics composites for vibration damping applications
| AD-A260792 | p 2727 N93-25690

SOLAR ACTIVITY
Nonlinear techniques for forecasting solar activity directly from its time series p 2603 N93-24716
Further analysis of ECOM-721 data
| AD-A260863 | p 2774 N93-25790
Solar-geophysical data number 581, January 1993. Part 1: (Prompt reports). Data for December, November 1992, and late data
| PB93-161743 | p 2899 N93-26537
Solar-geophysical data number 581, January 1993. Part 2: (Comprehensive reports). Data for July 1992 and miscellaneous
| PB93-161750 | p 2899 N93-26538

SOLAR ACTIVITY EFFECTS
Bit hit/solar activity correlation study
| AD-A261381 | p 2896 N93-26340

SOLAR ARRAYS
Momentum accumulation due to solar radiation torque, and reaction wheel sizing, with configuration optimization p 2600 N93-24695
Optimizing the fine lock performance of the Hubble Space Telescope fine guidance sensors p 2604 N93-24723
Solar array thermal snap and the characteristics of its effect on UARS p 2607 N93-24734
Laser beamed power: Satellite demonstration applications
| NASA-CR-190793 | p 2623 N93-25132
UARS in-flight jitter study for EOS
| NASA-CR-191419 | p 2615 N93-25133
Structural load control during construction p 2669 N93-26409

SOLAR CELLS
New concepts for high efficiency energy conversion: The avalanche heterostructure and superlattice solar cells
| DE92-010592 | p 2758 N93-25098
An inverted AlGaAs/GaAs patterned-Ge tunnel junction cascade concentrator solar cell
| DE93-000073 | p 2759 N93-25102
Non-H2Se, ultra-thin CIS devices
| DE93-000078 | p 2759 N93-25253
Role of polycrystallinity in CdTe and CuInSe2 photovoltaic cells
| DE93-000045 | p 2759 N93-25504

SOLAR COLLECTORS
Computational and experimental studies on large scale solar heating
| DE93-769942 | p 2758 N93-25096
An inverted AlGaAs/GaAs patterned-Ge tunnel junction cascade concentrator solar cell
| DE93-000073 | p 2759 N93-25102

SOLAR ENERGY
Computational and experimental studies on large scale solar heating
| DE93-769942 | p 2758 N93-25096
Advanced energy systems and technologies - National R and D programme
| DE93-769943 | p 2758 N93-25097

SOLAR FLARES
Star tracker operation in a high density proton field p 2600 N93-24699
The generation of Langmuir waves by thick target electron beams in solar flares p 2861 N93-25730
Use of Taguchi design of experiments to optimize and increase robustness of preliminary designs p 2670 N93-26063
Solar-geophysical data number 581, January 1993. Part 1: (Prompt reports). Data for December, November 1992, and late data
| PB93-161743 | p 2899 N93-26537
Solar-geophysical data number 581, January 1993. Part 2: (Comprehensive reports). Data for July 1992 and miscellaneous
| PB93-161750 | p 2899 N93-26538

SOLAR FLUX
Further analysis of ECOM-721 data
| AD-A260863 | p 2774 N93-25790

SOLAR GRAVITATION
Analysis of the effects of mean local node-crossing time on the evolution of Sun-synchronous orbits p 2602 N93-24706

SOLAR HEATING
Computational and experimental studies on large scale solar heating
| DE93-769942 | p 2758 N93-25096

SOLAR INTERIOR
Inverse problem with continuous parameters for solar oscillations p 2895 N93-25728

SOLAR MAGNETIC FIELD
Beam position and total current monitor for heavy ion fusion beams
| DE93-007653 | p 2851 N93-25325
Solar-geophysical data number 581, January 1993. Part 1: (Prompt reports). Data for December, November 1992, and late data
| PB93-161743 | p 2899 N93-26537
Solar-geophysical data number 581, January 1993. Part 2: (Comprehensive reports). Data for July 1992 and miscellaneous
| PB93-161750 | p 2899 N93-26538

SOLAR NEUTRINOS
An investigation of neutrino properties through study of the sun, supernovae, the early universe and lab data p 2898 N93-25180
The Sudbury Neutrino Observatory
| DE93-007697 | p 2899 N93-25327

SOLAR ORBITS
Analysis of the effects of mean local node-crossing time on the evolution of Sun-synchronous orbits p 2602 N93-24706
A ground track control algorithm for the Topographic Mapping Laser Altimeter (TMLA) p 2602 N93-24707

SOLAR OSCILLATIONS
Inverse problem with continuous parameters for solar oscillations p 2895 N93-25728

SOLAR PHYSICS
Solar-geophysical data number 581, January 1993. Part 1: (Prompt reports). Data for December, November 1992, and late data
| PB93-161743 | p 2899 N93-26537
Solar-geophysical data number 581, January 1993. Part 2: (Comprehensive reports). Data for July 1992 and miscellaneous
| PB93-161750 | p 2899 N93-26538

SOLAR PROMINENCES
Solar-geophysical data number 581, January 1993. Part 2: (Comprehensive reports). Data for July 1992 and miscellaneous
| PB93-161750 | p 2899 N93-26538

SOLAR RADIATION
Momentum accumulation due to solar radiation torque, and reaction wheel sizing, with configuration optimization p 2600 N93-24695
Orbit determination error analysis and comparison of station-keeping costs for Lissajous and halo-type libration point orbits and sensitivity analysis using experimental design techniques p 2604 N93-24721
Solar array thermal snap and the characteristics of its effect on UARS p 2607 N93-24734
Analysis of LARI sensor system
| DE93-006334 | p 2761 N93-24977
Computational and experimental studies on large scale solar heating
| DE93-769942 | p 2758 N93-25096
Summary information and data sets for NREL's Solar Radiation Research Laboratory, 1981 - 1991
| DE93-000052 | p 2898 N93-25101
Comparison of high-resolution solar irradiance spectra and the solar luminosity in the period 1980-1989
| NASA-CR-192776 | p 2898 N93-25222
Further analysis of ECOM-721 data
| AD-A260863 | p 2774 N93-25790
ATMOS: Long term atmospheric measurements for mission to planet Earth
| NASA-TM-108720 | p 2757 N93-26429
Solar-geophysical data number 581, January 1993. Part 2: (Comprehensive reports). Data for July 1992 and miscellaneous
| PB93-161750 | p 2899 N93-26538

SOLAR RADIATION SHIELDING
New directions in phthalocyanine pigments
| NASA-CR-192443 | p 2656 N93-26155

SOLAR RADIO BURSTS
Solar-geophysical data number 581, January 1993. Part 2: (Comprehensive reports). Data for July 1992 and miscellaneous
| PB93-161750 | p 2899 N93-26538

SOLAR RADIO EMISSION
Solar-geophysical data number 581, January 1993. Part 1: (Prompt reports). Data for December, November 1992, and late data
| PB93-161743 | p 2899 N93-26537
Solar-geophysical data number 581, January 1993. Part 2: (Comprehensive reports). Data for July 1992 and miscellaneous
| PB93-161750 | p 2899 N93-26538

SOLAR SENSORS
The results of the in-flight attitude sensor calibration for the Arthur Holly Compton Gamma Ray Observatory p 2600 N93-24697
Testing of the on-board attitude determination and control algorithms for SAMPEX p 2600 N93-24698
Accurate attitude determination of the LACE satellite p 2605 N93-24726
Goddard Space Flight Center (GSFC) Flight Dynamics Facility (FDF) calibration of the Upper Atmosphere Research Satellite (UARS) sensors p 2606 N93-24733
Upper Atmosphere Research Satellite (UARS) attitude accuracy using coarse attitude sensors p 2607 N93-24735

SOLAR SPECTRA
Comparison of high-resolution solar irradiance spectra and the solar luminosity in the period 1980-1989
| NASA-CR-192776 | p 2898 N93-25222

SOLAR WIND
Anomalous aspects of magnetosheath flow and of the shape and oscillations of the magnetopause during an interval of strongly northward interplanetary magnetic field
| NASA-CR-192851 | p 2770 N93-25081
The upper atmosphere and ionosphere of Mars p 2897 N93-26393
Solar-geophysical data number 581, January 1993. Part 2: (Comprehensive reports). Data for July 1992 and miscellaneous
| PB93-161750 | p 2899 N93-26538

SOLAR X-RAYS
Solar-geophysical data number 581, January 1993. Part 2: (Comprehensive reports). Data for July 1992 and miscellaneous
| PB93-161750 | p 2899 N93-26538

SOLDERED JOINTS
Aqueous cleaning of flux residue from solder joints
| KCP-613-4803 | p 2652 N93-26208

SOLDERS
Automated inspection of solder joints for surface mount technology
| NASA-TM-104580 | p 2721 N93-26137

SOLENOIDS
Studies of several small seawater MHD thrusters using the high-field solenoid of MIT's Bitter Magnet Laboratory
| AD-A260645 | p 2860 N93-25641
Magnetic field source for bi-chambered electron beam devices
| AD-A261316 | p 2691 N93-26299

SOLID ELECTROLYTES
Thin rechargeable batteries for CMOS SRAM memory protection p 2694 N93-25583

SOLID LUBRICANTS
Properties of extruded PS-212 type self-lubricating materials p 2659 N93-25565
Vickers indentation hardness of stoichiometric and reduced single crystal TiO2 (rutile) from 25 to 800 C
| NASA-TM-105959 | p 2633 N93-26204

SOLID MECHANICS
Formulation and treatment of frictional contact problems using finite elements p 2717 N93-25412
Mechanics and control of multibody structural systems | AD-A261576 | p 2619 N93-26456
Use and analysis of finite element methods for problems of solid mechanics and fracture | AD-A261574 | p 2731 N93-26522
SOLID PHASES
Metastable SiC and SiGeC alloys by carbon implantation and solid phase epitaxy | DE93-007594 | p 2863 N93-25387
SOLID PROPELLANT COMBUSTION
A model of concurrent flow flame spread over a thin solid fuel | NASA-CR-191111 | p 2663 N93-24946
Modeling of H2/N2O flames p 2627 N93-26026
Dark zone modeling of solid propellant flames p 2628 N93-26028
Detection of atomic oxygen and hydrogen in solid propellant flames and pyrolysis gases using multiphoton laser-induced fluorescence p 2628 N93-26029
Infrared fiber optic diagnostic for solid propellant combustion p 2628 N93-26031
Condensed-phase processes during solid propellant combustion. Part 4: Chemical and microscopic examination of laser-irradiated propellant samples p 2628 N93-26032
Interactions of acoustic waves and combustion of homogeneous solid propellants in rocket motors p 2630 N93-26039
Flame response in oscillatory solid propellant combustion p 2630 N93-26041
SOLID PROPELLANT ROCKET ENGINES
An in-depth probabilistic study of external tank attach ring | NASA-TM-108403 | p 2624 N93-25671
Particle behavior in solid propellant rocket motors and plumes | AD-A260900 | p 2624 N93-25913
The 29th JANNAF Combustion Subcommittee Meeting, volume 2 | CPIA-PUBL-593-VOL-2 | p 2624 N93-26005
Thermal radiation in non-metalized solid rocket motors: Effect on burning rate and temperature sensitivity p 2626 N93-26020
Determination of burn rate requirements from ASRM performance specifications p 2627 N93-26023
Interactions of acoustic waves and combustion of homogeneous solid propellants in rocket motors p 2630 N93-26039
Experimental investigation of flow turning losses in unstable rocket motors p 2630 N93-26040
SRB environment evaluation and analysis. Volume 3: ASRB plume induced environments | NASA-CR-192519 | p 2631 N93-26054
SOLID PROPELLANTS
The 29th JANNAF Combustion Subcommittee Meeting, volume 2 | CPIA-PUBL-593-VOL-2 | p 2624 N93-26005
Improved burn rate determination techniques p 2627 N93-26021
Dark zone modeling of solid propellant flames p 2628 N93-26028
Detection of atomic oxygen and hydrogen in solid propellant flames and pyrolysis gases using multiphoton laser-induced fluorescence p 2628 N93-26029
SOLID STATE
Solid-state isotopic power source for computer memory chips p 2694 N93-25596
SOLID STATE DEVICES
High speed solid state circuit breaker p 2694 N93-25598
SOLID STATE LASERS
Advances in nonlinear optical materials and devices | NASA-CR-192681 | p 2852 N93-25281
An active solid state ring laser gyroscope p 2709 N93-25291
SOLID STATE PHYSICS
Proceedings of the 16th International Workshop on Condensed Matter Theories | AD-A261078 | p 2868 N93-26252
SOLID SURFACES
Structure of sodium 4-(1'-heptylnonyl) benzenesulfonate adsorbed on alumina using H-2 NMR | AD-A261224 | p 2645 N93-26300
SOLID SUSPENSIONS
Development of an expendable particle sensor | AD-A261127 | p 2710 N93-26044
SOLID WASTES
Reclamation with recovery of radionuclides and toxic metals from contaminated materials, soils, and wastes p 2769 N93-25571
SOLID-SOLID INTERFACES
Models of crack growth along polymer interfaces p 2728 N93-25750
Fundamental aspects of metal joining: The study of strong interfaces | AD-A261293 | p 2653 N93-26304
SOLIDIFICATION
A model for the filling of cold cavities with solidifying, semi-crystalline polymers | DE93-003817 | p 2655 N93-25507
Solidification processing and phase transformations in ordered high temperature alloys | AD-A261751 | p 2652 N93-26284
Phase-field models for anisotropic interfaces | PB93-164564 | p 2646 N93-26323
Computation of complex solidification morphologies using a phase-field model | PB93-156743 | p 2869 N93-26547
SOLIDS
Correlated wavefunction quantum Monte Carlo approach to solids | DE93-007730 | p 2863 N93-25367
Phosphorus-, nitrogen-, sulfur-, and chlorine-containing molecules on surfaces | AD-A261265 | p 2657 N93-26303
Liquid and solid ion plasmas | AD-A261888 | p 2862 N93-26528
SOLIDS FLOW
Particle dynamics modeling of boundary effects in granular Couette flow p 2705 N93-25738
SOLITARY WAVES
From fractals to wormholes via string theory p 2871 N93-25742
SOLUBILITY
Reclamation with recovery of radionuclides and toxic metals from contaminated materials, soils, and wastes p 2769 N93-25571
SOLVATION
Molecular/polymeric magnetism | DE93-008635 | p 2847 N93-25114
SOLVENTS
Femtosecond dynamics in hydrogen-bonding solvents: Formamides | DE93-003476 | p 2643 N93-25123
Temperature dependent sensor response caused by polymer-solvent interactions | DE93-005368 | p 2655 N93-25444
Converting environmental wastes into valuable resources p 2759 N93-25572
Effects of moisture and other contaminants in friction composites | AD-A261226 | p 2640 N93-26301
SONOLUMINESCENCE
Spectra of stable sonoluminescence | AD-A260621 | p 2844 N93-25637
SOOT
Measurements of soot formation and hydroxyl concentration in near critical equivalence ratio premixed ethylene flame | NASA-CR-191099 | p 2642 N93-25116
SORBENTS
An experimental study of particle-laden jet interactions with cocurrent flows p 2701 N93-25534
SORPTION
Novel approaches to the construction of miniaturized analytical instrumentation | NASA-CR-191988 | p 2709 N93-25345
Effects of moisture and other contaminants in friction composites | AD-A261226 | p 2640 N93-26301
SOUND FIELDS
Low-frequency room responses. Part 2: Calculation methods and experimental results | BBC-RD-1992/9-PT-2 | p 2673 N93-25169
Experimental investigation of flow turning losses in unstable rocket motors p 2630 N93-26040
SOUND PRESSURE
Low-frequency room responses. Part 2: Calculation methods and experimental results | BBC-RD-1992/9-PT-2 | p 2673 N93-25169
SOUND PROPAGATION
Low-frequency room responses. Part 1: Background and qualitative considerations | BBC-RD-1992/8-PT-1 | p 2673 N93-25168
Low-frequency room responses. Part 2: Calculation methods and experimental results | BBC-RD-1992/9-PT-2 | p 2673 N93-25169
Proceedings of the 5th International Symposium on Long Range Sound Propagation | AD-A260666 | p 2845 N93-25643
SOUND TRANSDUCERS
Optical fiber for acoustic sensor applications | AD-A261580 | p 2857 N93-26515
SOUND TRANSMISSION
The design of a modular sound absorber for very low frequencies | BBC-RD-1992/10 | p 2673 N93-25170
SOUND WAVES
Low-frequency room responses. Part 2: Calculation methods and experimental results | BBC-RD-1992/9-PT-2 | p 2673 N93-25169
A modular wideband sound absorber | BBC-RD-1992/11 | p 2673 N93-25171
Spectra of stable sonoluminescence | AD-A260621 | p 2844 N93-25637
Proceedings of the 5th International Symposium on Long Range Sound Propagation | AD-A260666 | p 2845 N93-25643
Far field rotor noise | AD-A260703 | p 2845 N93-25651
Generation of acoustic waves by focused infrared neodymium-laser radiation p 2714 N93-25761
Nonlinear wave phenomena related to interactions in the ionosphere | AD-A261450 | p 2776 N93-26348
Monaural and binaural processing of complex waveforms | AD-A261659 | p 2846 N93-26358
SPACE BASES
Systems engineering studies of on-orbit assembly operations p 2669 N93-26410
SPACE COMMERCIALIZATION
Space research in Sweden, 1990-1991 p 2888 N93-25887
Space business indicators p 2886 N93-26158
SPACE COMMUNICATION
The Telecommunications and Data Acquisition Report | NASA-CR-192887 | p 2671 N93-24659
Management of space networks p 2672 N93-24671
Hydrogen masers for space p 2716 N93-24980
The application of the PRARE principle for precise two-way time transfer to space-based atomic clocks p 2832 N93-24983
Deep Space Network information system architecture study p 2679 N93-26126
Ka-band feed arrays for spacecraft reflector antennas with limited scan capability: An overview p 2680 N93-26128
SPACE DEBRIS
Space environmental interactions for the space exploration initiative p 2897 N93-26396
SPACE ENVIRONMENT SIMULATION
Time dependent simulation of cosmic-ray shocks including Alfven transport | NASA-CR-192931 | p 2899 N93-24752
Numerical and experimental analyses of large composite skeletal satellite systems p 2616 N93-25463
SPACE EXPLORATION
An approach for finding long period elliptical orbits for precursor SEI missions p 2604 N93-24720
Summary and recommendations on nuclear electric propulsion technology for the space exploration initiative | NASA-TM-105707 | p 2622 N93-24744
Space Nuclear Thermal Propulsion Test Facilities Subpanel | NASA-TM-105708 | p 2622 N93-25105
JSC research and technology | NASA-TM-104763 | p 2901 N93-25188
Space transfer vehicle concepts and requirements study. Volume 1: Executive summary | NASA-CR-192524 | p 2610 N93-25479
NASA Center for Intelligent Robotic Systems for Space Exploration | NASA-CR-193208 | p 2826 N93-25986
Evaluating science return in space exploration initiative architectures | NASA-TP-3339 | p 2897 N93-26094
Nuclear safety policy working group recommendations on nuclear propulsion safety for the space exploration initiative | NASA-TM-105705 | p 2632 N93-26200
Electrical and Chemical Interactions at Mars Workshop. Part 2: Appendix | NASA-CP-10093-PT-2 | p 2897 N93-26392
Representative systems for space exploration p 2897 N93-26395
Space environmental interactions for the space exploration initiative p 2897 N93-26396
Modeling and analysis tools p 2897 N93-26397
Mars exploration planning p 2898 N93-26399
SPACE LOGISTICS
Space transfer vehicle concepts and requirements study. Volume 2, book 1: STV concept definition and evaluation | NASA-CR-192525 | p 2611 N93-25510
Space transfer vehicle concepts and requirements study. Volume 2, book 3: STV system interfaces | NASA-CR-192527 | p 2611 N93-25513
Dynamics of on-orbit construction process p 2669 N93-26406
SPACE MISSIONS
Systems engineering considerations for operational support systems p 2666 N93-24689

Precise Doppler tracking from the Medicina VLBI station p 2608 N93-24998
Parametric analysis of atmospheric processes
| NASA-CR-192523 | p 2770 N93-25086
NASA Microgravity Science and Applications Program
| NASA-TM-108775 | p 2663 N93-25194
An alternate approach to space missions involving a long tether p 2616 N93-25470
Space transfer vehicle concepts and requirements study. Volume 2, book 1: STV concept definition and evaluation
| NASA-CR-192525 | p 2611 N93-25510
Space life support technology applications to terrestrial environmental problems p 2803 N93-25617
Planetary data analysis and display system: A version of PC-McIDAS p 2880 N93-25806
STS-39 Space Shuttle mission report
| NASA-CR-193063 | p 2611 N93-25955
STS-37 Space Shuttle mission report
| NASA-CR-193062 | p 2612 N93-25956
STS-43 Space Shuttle mission report
| NASA-CR-193064 | p 2612 N93-25957
STS-40 Space Shuttle mission report
| NASA-TM-108737 | p 2612 N93-25958
STS-45 Space Shuttle mission report
| NASA-CR-193054 | p 2612 N93-25959
STS-47 Space Shuttle mission report
| NASA-CR-193056 | p 2612 N93-25960
An architecture for object-oriented intelligent control of power systems in space p 2823 N93-25968
STS-44 Space Shuttle mission report
| NASA-TM-108735 | p 2612 N93-25988
STS-42 Space Shuttle mission report
| NASA-CR-193059 | p 2613 N93-25989
STS-48 Space Shuttle mission report
| NASA-CR-193060 | p 2613 N93-25990
STS-46 Space Shuttle mission report
| NASA-CR-193058 | p 2613 N93-25991
STS-50 Space Shuttle mission report
| NASA-CR-193057 | p 2613 N93-25992
STS-52 Space Shuttle mission report
| NASA-CR-193061 | p 2613 N93-25993
Analysis of the lettuce data from the variable pressure growth chamber at NASA Johnson Space Center: A three-stage nested design model p 2794 N93-26069
Distributed project scheduling at NASA: Requirements for manual protocols and computer-based support p 2815 N93-26075
Nuclear safety policy working group recommendations on nuclear propulsion safety for the space exploration initiative
| NASA-TM-105705 | p 2632 N93-26200
Representative systems for space exploration p 2897 N93-26395
Mars exploration planning p 2898 N93-26399

SPACE NAVIGATION
An approach for finding long period elliptical orbits for precursor SEI missions p 2604 N93-24720
Frequency and Time Forum
| ESA-SP-340 | p 2831 N93-24978
Deep-space navigation with differenced data types. Part 3: An expanded information content and sensitivity analysis p 2614 N93-26109
Geometric distortion analysis of a wide-field astrograph p 2621 N93-26111

SPACE PERCEPTION
Neural basis of motion perception
| AD-A261452 | p 2798 N93-26349

SPACE PLASMAS
Anomalous aspects of magnetosheath flow and of the shape and oscillations of the magnetopause during an interval of strongly northward interplanetary magnetic field
| NASA-CR-192851 | p 2770 N93-25081

SPACE POWER REACTORS
Nuclear electric propulsion for planetary science missions: NASA technology program planning
| NASA-TM-106139 | p 2632 N93-26210
Representative systems for space exploration p 2897 N93-26395

SPACE PROCESSING
Gravity-dependent transport phenomena in zeolite crystal growth p 2664 N93-25740

SPACE PROGRAMS
Environment Observation and Climate Modelling Through International Space Projects. Volume 2: Remote Sensing for Environmental Monitoring and Resource Management
| ESA-ISY-1-VOL-2 | p 2737 N93-24775
Viewgraph description of Penn State's Propulsion Engineering Research Center: Activity highlights and future plans
| NASA-CR-192317 | p 2622 N93-24943
Space research in Sweden, 1990-1991 p 2888 N93-25887
A study of mapping exogenous knowledge representations into CONFIG p 2827 N93-26072
Space business indicators p 2886 N93-26158

SPACE RENDEZVOUS
Optimal cooperative power-limited rendezvous p 2607 N93-24904
Rendezvous, proximity operations and capture quality function deployment report
| NASA-TM-108752 | p 2614 N93-25952

SPACE SHUTTLE BOOSTERS
An in-depth probabilistic study of external tank attach ring
| NASA-TM-108403 | p 2624 N93-25671
SRB environment evaluation and analysis. Volume 1: Redesigned SRB flight heating evaluation
| NASA-CR-192517 | p 2631 N93-26053
SRB environment evaluation and analysis. Volume 2: RSRB joint filling test/analysis improvements
| NASA-CR-192518 | p 2631 N93-26057

SPACE SHUTTLE MAIN ENGINE
A neural network-based estimator for the mixture ratio of the Space Shuttle Main Engine
| NASA-TM-106070 | p 2622 N93-25089
Calculations of combustion response profiles and oscillations
| NASA-TM-106135 | p 2623 N93-25236
Detection of bearing failure in mechanical devices using neural networks p 2822 N93-25965
Remtech SSME nozzle design TPS
| NASA-CR-192516 | p 2631 N93-26056
On-line implementation of nonlinear parameter estimation for the Space Shuttle main engine
| NASA-TM-106097 | p 2632 N93-26211

SPACE SHUTTLE ORBITERS
Dynamics of on-orbit construction process p 2669 N93-26406
Controls for orbital assembly of large space structures p 2620 N93-26408
Structural load control during construction p 2669 N93-26409

SPACE SHUTTLE PAYLOADS
Tethered Satellite System Contingency Investigation Board
| NASA-TM-108704 | p 2616 N93-25231
Data analysis support for the Shuttle Potential and Return Electron Experiment (SPREE) on the Tethered Satellite System 1 (TSS-1) flight
| AD-A261646 | p 2618 N93-26232

SPACE SHUTTLES
Parametric analysis of atmospheric processes
| NASA-CR-192523 | p 2770 N93-25086
STS-39 Space Shuttle mission report
| NASA-CR-193063 | p 2611 N93-25955
STS-37 Space Shuttle mission report
| NASA-CR-193062 | p 2612 N93-25956
STS-43 Space Shuttle mission report
| NASA-CR-193064 | p 2612 N93-25957
STS-40 Space Shuttle mission report
| NASA-TM-108737 | p 2612 N93-25958
STS-45 Space Shuttle mission report
| NASA-CR-193054 | p 2612 N93-25959
STS-47 Space Shuttle mission report
| NASA-CR-193056 | p 2612 N93-25960
Multi-viewpoint clustering analysis p 2825 N93-25980
STS-44 Space Shuttle mission report
| NASA-TM-108735 | p 2612 N93-25988
STS-42 Space Shuttle mission report
| NASA-CR-193059 | p 2613 N93-25989
STS-48 Space Shuttle mission report
| NASA-CR-193060 | p 2613 N93-25990
STS-46 Space Shuttle mission report
| NASA-CR-193058 | p 2613 N93-25991
STS-50 Space Shuttle mission report
| NASA-CR-193057 | p 2613 N93-25992
STS-52 Space Shuttle mission report
| NASA-CR-193061 | p 2613 N93-25993
ASRM design philosophy and modelling challenges p 2627 N93-26022
External tank aerothermal design criteria verification
| NASA-CR-192514 | p 2618 N93-26055
A vision architecture for the extravehicular activity retriever p 2827 N93-26071
Liquid Rocket Booster (LRB) for the Space Transportation System (STS) Systems Study. Amendment 13: Orientation meeting
| NASA-CR-192515 | p 2614 N93-26152
Analysis of the IBSS spectra of Space Shuttle control engine exhaust
| AD-A261749 | p 2632 N93-26373

SPACE STATION FREEDOM
Space Nuclear Thermal Propulsion Test Facilities Subpanel
| NASA-TM-105708 | p 2622 N93-25105
Space Station Freedom assembly and operation at a 51.6 degree inclination orbit
| NASA-TM-107731 | p 2615 N93-25174
Space biology research development
| NASA-CR-192830 | p 2792 N93-25242
Gas-Grain Simulation Facility (GGSF). Volume 1: Stage 1 facility definition studies
| NASA-CR-177606 | p 2887 N93-25442
Space transfer vehicle concepts and requirements study. Volume 2, book 3: STV system interfaces
| NASA-CR-192527 | p 2611 N93-25513
Robotic Variable Polarity Plasma Arc (VPPA) welding p 2720 N93-25605
A genetic algorithm tool (splicer) for complex scheduling problems and the Space Station Freedom resupply problem p 2814 N93-25613
Estimating spares requirements for Space Station Freedom using the M-SPARE model
| AD-A260878 | p 2617 N93-25630
Advanced life support study. Modification 10: ECLSS logistical support analysis for Space Station Freedom
| NASA-CR-192481 | p 2801 N93-25888
The effects of video compression on acceptability of images for monitoring life sciences' experiments p 2805 N93-25930
Study of plate-fin heat exchanger and cold plate for the active thermal control system of Space Station p 2619 N93-26064
A prototype for simulation of the space-to-ground assembly/contingency system of Space Station Freedom p 2619 N93-26065
A vision architecture for the extravehicular activity retriever p 2827 N93-26071
Spacelab, Spacehab, and Space Station Freedom payload interface projects p 2620 N93-26080
Model reduction for Space Station Freedom p 2620 N93-26081
Knowledge-based decision support for Space Station assembly sequence planning
| NASA-CR-193048 | p 2599 N93-26095
Conceptual design for the Space Station Freedom fluid physics/dynamics facility
| NASA-TM-103663 | p 2618 N93-26209
Plasma current collection of Z-93 thermal control paint as measured in the Lewis Research Center's plasma interaction facility
| NASA-TM-106132 | p 2618 N93-26215
Assured crew return vehicle man-systems integration standards
| NASA-CR-193065 | p 2614 N93-26329

SPACE STATION PAYLOADS
Earth observing system. Output data products and input requirements, version 2.0. Volume 1: Instrument data product characteristics
| NASA-TM-108770 | p 2755 N93-25460
Earth observing system. Output data products and input requirements, version 2.0. Volume 2: Analysis of IDS input requirements
| NASA-TM-108771 | p 2755 N93-25461

SPACE STATION STRUCTURES
A prototype for simulation of the space-to-ground assembly/contingency system of Space Station Freedom p 2619 N93-26065

SPACE STATIONS
Whisker growth studies under conditions which resemble those available on an orbiting space station
| NASA-CR-192701 | p 2664 N93-25218
Two-phase/two-phase heat exchanger analysis
| NASA-CR-192783 | p 2697 N93-25221
Architecture of autonomous systems
| NASA-CR-192974 | p 2801 N93-26047
The role of pyridoxine as a countermeasure for in-flight loss of lean body mass p 2796 N93-26068
Conceptual design for the Space Station Freedom fluid physics/dynamics facility
| NASA-TM-103663 | p 2618 N93-26209
Center for Space Construction Third Annual Symposium
| NASA-CR-192688 | p 2669 N93-26405
Dynamics of on-orbit construction process p 2669 N93-26406
Interaction dynamics and control for orbital assembly p 2669 N93-26407
Controls for orbital assembly of large space structures p 2620 N93-26408
Structural load control during construction p 2669 N93-26409
Systems engineering studies of on-orbit assembly operations p 2669 N93-26410

SPACE TRANSPORTATION
Space transfer vehicle concepts and requirements study. Volume 2, book 4: Integrated advanced technology development
| NASA-CR-192528 | p 2611 N93-25512
Task 5: Architecture sensitivity to STME performance
| MCR-92-5010 | p 2609 N93-26176

SPACE TRANSPORTATION SYSTEM
Weather forecasting expert system study
| NASA-CR-192929 | p 2777 N93-24747
Space transfer vehicle concepts and requirements study. Volume 2, book 3: STV system interfaces
| NASA-CR-192527 | p 2611 N93-25513
Knowledge-based decision support for Space Station assembly sequence planning
| NASA-CR-193048 | p 2599 N93-26095
Liquid Rocket Booster (LRB) for the Space Transportation System (STS) Systems Study. Amendment 13: Orientation meeting
| NASA-CR-192515 | p 2614 N93-26152
Assured crew return vehicle man-systems integration standards
| NASA-CR-193065 | p 2614 N93-26329
SPACE TRANSPORTATION SYSTEM FLIGHTS
Parametric analysis of atmospheric processes
| NASA-CR-192523 | p 2770 N93-25086
A genetic algorithm tool (splicer) for complex scheduling problems and the Space Station Freedom resupply problem p 2814 N93-25613
STS-39 Space Shuttle mission report
| NASA-CR-193063 | p 2611 N93-25955
STS-37 Space Shuttle mission report
| NASA-CR-193062 | p 2612 N93-25956
STS-43 Space Shuttle mission report
| NASA-CR-193064 | p 2612 N93-25957
STS-40 Space Shuttle mission report
| NASA-TM-108737 | p 2612 N93-25958
STS-45 Space Shuttle mission report
| NASA-CR-193054 | p 2612 N93-25959
STS-47 Space Shuttle mission report
| NASA-CR-193056 | p 2612 N93-25960
STS-44 Space Shuttle mission report
| NASA-TM-108735 | p 2612 N93-25988
STS-42 Space Shuttle mission report
| NASA-CR-193059 | p 2613 N93-25989
STS-48 Space Shuttle mission report
| NASA-CR-193060 | p 2613 N93-25990
STS-46 Space Shuttle mission report
| NASA-CR-193058 | p 2613 N93-25991
STS-50 Space Shuttle mission report
| NASA-CR-193057 | p 2613 N93-25992
STS-52 Space Shuttle mission report
| NASA-CR-193061 | p 2613 N93-25993
Distributed project scheduling at NASA: Requirements for manual protocols and computer-based support p 2815 N93-26075
Utilization of the graded universal testing system to increase the efficiency for assessing aerobic and anaerobic capacity p 2794 N93-26077
SPACE-TIME FUNCTIONS
Propagation velocity and space-time correlation of perturbations in turbulent channel flow
| NASA-TM-103932 | p 2695 N93-25082
SPACEBORNE EXPERIMENTS
Analysis of reentry into the White Sands Missile Range (WSMR) for the LifeSat mission p 2603 N93-24717
The Columbus Metrology Science Team: Report on activities p 2670 N93-24987
An investigation of the degradation of Fluorinated Ethylene Propylene (FEP) copolymer thermal blanketing materials aboard LDEF in the laboratory
| NASA-CR-192824 | p 2653 N93-25078
Tethered Satellite System Contingency Investigation Board
| NASA-TM-108704 | p 2616 N93-25231
Laser ignition application in a space experiment
| NASA-TM-106133 | p 2664 N93-25337
MAC to VAX connectivity: Heartrate spectral analysis system p 2796 N93-25594
MIT Space Engineering Research Center
| NASA-CR-192879 | p 2821 N93-25833
STS-45 Space Shuttle mission report
| NASA-CR-193054 | p 2612 N93-25959
STS-42 Space Shuttle mission report
| NASA-CR-193059 | p 2613 N93-25989
STS-50 Space Shuttle mission report
| NASA-CR-193057 | p 2613 N93-25992
STS-52 Space Shuttle mission report
| NASA-CR-193061 | p 2613 N93-25993
Conceptual design for the Space Station Freedom fluid physics/dynamics facility
| NASA-TM-103663 | p 2618 N93-26209
Data analysis support for the Shuttle Potential and Return Electron Experiment (SPREE) on the Tethered Satellite System 1 (TSS-1) flight
| AD-A261646 | p 2618 N93-26232
United States Army space experiment 601
| AD-A261460 | p 2798 N93-26353
SPACEBORNE LASERS
Basic design of a spaceborne hydrogen maser p 2716 N93-25024
Injection seeded, diode-pumped, short pulse Nd:YAG ring laser for space-based laser ranging p 2713 N93-25389
SPACECRAFT
Readings in Systems Engineering
| NASA-SP-6102 | p 2665 N93-24678
SPACECRAFT ANTENNAS
Ka-band feed arrays for spacecraft reflector antennas with limited scan capability: An overview p 2680 N93-26128
SPACECRAFT CHARGING
SCATHA mission termination report p 2605 N93-24725
Plasma sheath effects on ion collection by a pinhole
| NASA-TM-106098 | p 2615 N93-25090
Data analysis support for the Shuttle Potential and Return Electron Experiment (SPREE) on the Tethered Satellite System 1 (TSS-1) flight
| AD-A261646 | p 2618 N93-26232
Detailed component design for a Compact Environmental Anomaly Sensor (CEASE)
| AD-A261729 | p 2620 N93-26248
Space environmental interactions for the space exploration initiative p 2897 N93-26396
SPACECRAFT COMMUNICATION
The Generic Spacecraft Analyst Assistant (GenSAA): A tool for developing graphical expert systems p 2814 N93-25589
SPACECRAFT CONFIGURATIONS
Space transfer vehicle concepts and requirements study. Volume 2, book 1: STV concept definition and evaluation
| NASA-CR-192525 | p 2611 N93-25510
SPACECRAFT CONSTRUCTION MATERIALS
An investigation of the degradation of Fluorinated Ethylene Propylene (FEP) copolymer thermal blanketing materials aboard LDEF in the laboratory
| NASA-CR-192824 | p 2653 N93-25078
Composite materials for the extravehicular mobility unit p 2642 N93-26060
Plasma current collection of Z-93 thermal control paint as measured in the Lewis Research Center's plasma interaction facility
| NASA-TM-106132 | p 2618 N93-26215
SPACECRAFT CONTAMINATION
Space environmental interactions for the space exploration initiative p 2897 N93-26396
Modeling and analysis tools p 2897 N93-26397
SPACECRAFT CONTROL
Flight Mechanics/Estimation Theory Symposium, 1992
| NASA-CP-3186 | p 2599 N93-24694
A ground track control algorithm for the Topographic Mapping Laser Altimeter (TMLA) p 2602 N93-24707
Analysis of the Command and Control Segment (CCS) attitude estimation algorithm p 2604 N93-24722
Optimal cooperative power-limited rendezvous p 2607 N93-24904
A survey of life support system automation and control
| NASA-TM-103977 | p 2667 N93-25085
Aerospace vehicle model simplification for feedback control p 2596 N93-25292
The Generic Spacecraft Analyst Assistant (GenSAA): A tool for developing graphical expert systems p 2814 N93-25589
An autonomous satellite architecture integrating deliberative reasoning and behavioural intelligence p 2823 N93-25970
Dynamics of on-orbit construction process p 2669 N93-26406
Controls for orbital assembly of large space structures p 2620 N93-26408
Structural load control during construction p 2669 N93-26409
Mechanics and control of multibody structural systems
| AD-A261576 | p 2619 N93-26456
SPACECRAFT DESIGN
A system to measure lightning-induced transients on spacecraft umbilical lines p 2693 N93-24889
Space Station Freedom assembly and operation at a 51.6 degree inclination orbit
| NASA-TM-107731 | p 2615 N93-25174
Space transfer vehicle concepts and requirements study. Volume 2, book 1: STV concept definition and evaluation
| NASA-CR-192525 | p 2611 N93-25510
Space transfer vehicle concepts and requirements study. Volume 2, book 2: System and program requirements trade studies
| NASA-CR-192526 | p 2611 N93-25511
Space transfer vehicle concepts and requirements study. Volume 2, book 4: Integrated advanced technology development
| NASA-CR-192528 | p 2611 N93-25512
Space transfer vehicle concepts and requirements study. Volume 2, book 3: STV system interfaces
| NASA-CR-192527 | p 2611 N93-25513
Space transfer vehicle concepts and requirements study. Volume 3, book 1: Program cost estimates
| NASA-CR-192529 | p 2611 N93-25514
Advanced life support study. Modification 10: ECLSS logistical support analysis for Space Station Freedom
| NASA-CR-192481 | p 2801 N93-25888
National Launch System. Task 4: System architecture options analysis
| MCR-92-5011 | p 2609 N93-26098
SPACECRAFT DOCKING
Rendezvous, proximity operations and capture quality function deployment report
| NASA-TM-108752 | p 2614 N93-25952
SPACECRAFT ELECTRONIC EQUIPMENT
A system to measure lightning-induced transients on spacecraft umbilical lines p 2693 N93-24889
Fractal determination of parameters in lightning and ESD model p 2686 N93-24893
Ultra stable oscillators for satellite applications p 2621 N93-25027
Preliminary results of a newly designed mini-OCXO oscillator especially dedicated to space applications p 2621 N93-25028
Microwave synthesizers in space p 2693 N93-25038
SPACECRAFT ENVIRONMENTS
EnviroNET p 2886 N93-26398
SPACECRAFT EQUIPMENT
Detailed component design for a Compact Environmental Anomaly Sensor (CEASE)
| AD-A261729 | p 2620 N93-26248
SPACECRAFT GUIDANCE
Computationally efficient algorithms for real-time attitude estimation p 2602 N93-24709
Optimizing the fine lock performance of the Hubble Space Telescope fine guidance sensors p 2604 N93-24723
The Hubble Space Telescope fine guidance system operating in the coarse track pointing control mode p 2605 N93-24724
Trajectory optimization for the National aerospace plane
| NASA-CR-192954 | p 2589 N93-25670
SPACECRAFT INSTRUMENTS
Earth observing system. Output data products and input requirements, version 2.0. Volume 1: Instrument data product characteristics
| NASA-TM-108770 | p 2755 N93-25460
Walsh function generator for the Electronically Scanned Thinned Array Radiometer (ESTAR) instrument
| NASA-TM-4449 | p 2689 N93-25618
SPACECRAFT LAUNCHING
What is a system? NASA's phased project description p 2665 N93-24681
Practical aspects of transfer from GTO to lunar orbit p 2604 N93-24719
The 1992 International Aerospace and Ground Conference on Lightning and Static Electricity: Addendum
| DOT/FAA/CT-92/20-ADD-1 | p 2777 N93-24875
Applications of triggered lightning to space vehicle operations p 2619 N93-24878
Development of models for predicting the triggering of lightning by launch vehicles p 2610 N93-24899
CRRES: Combined release and radiation effects satellite program summary
| NASA-CR-192469 | p 2774 N93-25886
Space research in Sweden, 1990-1991 p 2888 N93-25887
Inferring heuristic classification hierarchies from natural language input p 2825 N93-25979
National Launch System. Task 4: System architecture options analysis
| MCR-92-5011 | p 2609 N93-26098
SPACECRAFT MANEUVERS
SCATHA mission termination report p 2605 N93-24725
Attitude control of the LACE satellite: A gravity gradient stabilized spacecraft p 2605 N93-24727
External tank aerothermal design criteria verification
| NASA-CR-192514 | p 2618 N93-26055
SPACECRAFT MODELS
Rate determination from vector observations p 2603 N93-24713
What is the relationship between altitude and weight in a model rocket? p 2603 N93-24715
SPACECRAFT MODULES
Conceptual design for the Space Station Freedom fluid physics/dynamics facility
| NASA-TM-103663 | p 2618 N93-26209
SPACECRAFT MOTION
The dynamics and control of large flexible asymmetric spacecraft p 2617 N93-25525

Deep-space navigation with differenced data types. Part 3: An expanded information content and sensitivity analysis p 2614 N93-26109

SPACECRAFT ORBITS

Orbit determination error analysis and comparison of station-keeping costs for Lissajous and halo-type libration point orbits and sensitivity analysis using experimental design techniques p 2604 N93-24721

Mars: The dynamics of orbiting satellites and gravity model development p 2896 N93-25439

Minimum-fuel power-limited transfers between coplanar elliptic orbits p 2608 N93-25684

A determination of the radio-planetary frame tie from comparison of Earth orientation parameters p 2676 N93-26106

Orbiter-orbiter and orbiter-lander tracking using same-beam interferometry p 2677 N93-26110

SPACECRAFT POWER SUPPLIES

Radiation and temperature effects on electronic components investigated under the CSTI high capacity power project

| NASA-TM-106096 | p 2687 N93-24746

Laser beamed power: Satellite demonstration applications

| NASA-CR-190793 | p 2623 N93-25132

The interaction of high voltage systems with the environments of the Moon and Mars

| NASA-TM-106107 | p 2618 N93-26148

DC-DC power converter research for Orbiter/Station power exchange

| NASA-CR-192939 | p 2633 N93-26425

SPACECRAFT PROPULSION

Summary and recommendations on nuclear electric propulsion technology for the space exploration initiative

| NASA-TM-105707 | p 2622 N93-24744

Space exploration initiative candidate nuclear propulsion test facilities

| NASA-TM-105710 | p 2622 N93-24753

Viewgraph description of Penn State's Propulsion Engineering Research Center: Activity highlights and future plans

| NASA-CR-192317 | p 2622 N93-24943

Stationary plasma thruster evaluation in Russia

| NASA-CR-192823 | p 2859 N93-25206

Space transfer vehicle concepts and requirements study. Volume 2, book 4: Integrated advanced technology development

| NASA-CR-192528 | p 2611 N93-25512

The design of a propulsion system using vent gas from a liquid helium cryogenic system p 2623 N93-25539

Nuclear electric propulsion for planetary science missions: NASA technology program planning

| NASA-TM-106139 | p 2632 N93-26210

SPACECRAFT REENTRY

Analysis of reentry into the White Sands Missile Range (WSMR) for the LifeSat mission p 2603 N93-24717

Multi-viewpoint clustering analysis p 2825 N93-25980

A hybrid multigrid technique for computing steady-state solutions to supersonic flows p 2582 N93-26078

SPACECRAFT SHIELDING

An investigation of the degradation of Fluorinated Ethylene Propylene (FEP) copolymer thermal blanketing materials aboard LDEF in the laboratory

| NASA-CR-192824 | p 2653 N93-25078

SPACECRAFT STABILITY

Spacecraft detumbling through energy dissipation p 2600 N93-24696

Nonlinear stability analysis of the attitude motion of spin-stabilized thrusting spacecraft p 2617 N93-25527

SPACECRAFT STRUCTURES

Optimizing the fine lock performance of the Hubble Space Telescope fine guidance sensors p 2604 N93-24723

The MODE family of on-orbit experiments: The Middeck Active Control Experiment (MACE) p 2599 N93-25835

Model reduction for Space Station Freedom p 2620 N93-26081

Expert systems for assembly sequence evaluation p 2669 N93-26411

Mechanics and control of multibody structural systems

| AD-A261576 | p 2619 N93-26456

SPACECRAFT TRACKING

TDRSS-user orbit determination using batch least-squares and sequential methods p 2601 N93-24703

Orbit determination support of the Ocean Topography Experiment (TOPEX)/Poseidon operational orbit p 2601 N93-24704

Orbit determination error analysis and comparison of station-keeping costs for Lissajous and halo-type libration point orbits and sensitivity analysis using experimental design techniques p 2604 N93-24721

Orbiter-orbiter and orbiter-lander tracking using same-beam interferometry p 2677 N93-26110

Geometric distortion analysis of a wide-field astrograph p 2621 N93-26111

SPACECRAFT TRAJECTORIES

Tsien's method for generating non-Keplerian trajectories. Part 2: The question of thrust to orbit a sphere and the restricted three-body problem p 2603 N93-24718

An approach for finding long period elliptical orbits for precursor SEI missions p 2604 N93-24720

Orbit determination error analysis and comparison of station-keeping costs for Lissajous and halo-type libration point orbits and sensitivity analysis using experimental design techniques p 2604 N93-24721

Optimal cooperative power-limited rendezvous p 2607 N93-24904

Mars: The dynamics of orbiting satellites and gravity model development p 2896 N93-25439

External tank aerothermal design criteria verification

| NASA-CR-192514 | p 2618 N93-26055

Galileo early cruise, including Venus, First Earth, and Gaspra encounters p 2599 N93-26125

SPACECREWS

JPRS report: Science and technology. Central Eurasia: Life sciences

| JPRS-ULS-92-022 | p 2795 N93-25407

The application of integrated knowledge-based systems for the Biomedical Risk Assessment Intelligent Network (BRAIN) p 2799 N93-25595

Utilization of the graded universal testing system to increase the efficiency for assessing aerobic and anaerobic capacity p 2794 N93-26077

Automation and robotics human performance

| NASA-CR-193049 | p 2802 N93-26153

SPACELAB

Spacelab, Spacehab, and Space Station Freedom payload interface projects p 2620 N93-26080

SPACELAB PAYLOADS

STS-40 Space Shuttle mission report

| NASA-TM-108737 | p 2612 N93-25958

SPATIAL DISTRIBUTION

Cartography and statistics of crops under irrigation in the Donana area of Andalucia through the use of Landsat-TM imagery and its incorporation into a GIS p 2751 N93-24855

The effects of large-amplitude, low-frequency excitation on a three-dimensional jet p 2702 N93-25553

SPATIAL RESOLUTION

Interest of complementary data of coarse and high spatial resolution for agro-climatic crop monitoring p 2750 N93-24853

High speed x ray gating cameras for ICF imaging applications

| DE93-007500 | p 2709 N93-25515

Commercial applications multispectral sensor system p 2758 N93-25615

Detecting the scale and resolution effects in remote sensing and GIS p 2756 N93-25707

Intensity distribution of the x ray source for the AXAF VETA-I mirror test p 2854 N93-26184

SPECIES DIFFUSION

The extent and status of mangroves in Mombasa district, Kenya: A case study based on remote sensing p 2746 N93-24826

SPECIFICATIONS

Languages for requirements specifications

| RSRE-MEMO-4585 | p 2810 N93-25453

SPECTRA

An improved spectral load balancing method

| DE93-007582 | p 2810 N93-25386

Toward a parallel recursive spectral bisection mapping tool

| DE93-006632 | p 2816 N93-25414

Parallelizing the spectral transform method: A comparison of alternative parallel algorithms

| DE93-008664 | p 2816 N93-25521

Research support for the Laboratory for Lightwave Technology

| AD-A261488 | p 2856 N93-26343

Complex auditory signals

| AD-A261491 | p 2846 N93-26374

OLYMPUS/ACTS scintillation experiment at the Lewis Research Center p 2685 N93-26481

Bimolecular reaction dynamics from photoelectron spectroscopy of negative ions

| DE93-007669 | p 2647 N93-26599

SPECTRAL CORRELATION

Implementation of cyclic spectral analysis methods

| AD-A261715 | p 2681 N93-26372

SPECTRAL ENERGY DISTRIBUTION

Complex auditory signals

| AD-A261491 | p 2846 N93-26374

SPECTRAL LINE WIDTH

Noise measurements in single-mode GaAlAs diode lasers p 2716 N93-25067

SPECTRAL METHODS

Studies of the analyte-carrier interface in flow injection analysis

| DE93-008374 | p 2644 N93-25311

An improved spectral load balancing method

| DE93-007582 | p 2810 N93-25386

Incompressible spectral-element method: Derivation of equations

| NASA-TM-106109 | p 2708 N93-26554

SPECTRAL REFLECTANCE

ANOVA method to estimate vegetation indices sensitivity assessing nitrogen fertilizing influence on spectral reflectance coefficients p 2739 N93-24782

Spectral remote sensing of anomalous mineralogy induced by hydrocarbon migration and uranium mineralization, San Rafael Swell, Utah, USA p 2739 N93-24783

Lithologic mapping with LANDSAT Thematic Mapper guided by laboratory spectral measurements, Air, Niger (Africa) p 2742 N93-24803

Measuring the intensity of nitrogen fertilization of grassland by means of remote sensing p 2751 N93-24859

Crop agroecological diagnostics by remote sensing technique p 2751 N93-24860

Forest damage detection and reflection of conifers: From micro to field level p 2752 N93-24864

Scale dependence in the reflectance of deciduous woodland: Evidence from a helicopter-mounted spectroradiometer p 2752 N93-24865

Condensation on cooled surfaces of optical devices at the cosmic conditions p 2753 N93-24869

Development of a cone penetrometer for measuring spectral characteristics of soils in situ p 2776 N93-25570

SPECTRAL RESOLUTION

European applications of space-borne Earth observation for land cover mapping p 2745 N93-24820

SPECTRAL SIGNATURES

Use of airborne imaging spectrometry to the definition of optimised specifications for land applications with future spaceborne imaging spectrometers p 2738 N93-24776

Potential operational use of remote sensing from space in forestry p 2745 N93-24817

Observation of forest damages in the Harz mountains by means of satellite remote sensing p 2749 N93-24848

Measuring the intensity of nitrogen fertilization of grassland by means of remote sensing p 2751 N93-24859

Combining spectral information with crop rotation knowledge for crop classifications p 2752 N93-24861

SPECTRAL THEORY

On the generation and dispersion of Yanai waves with a spectral Chebyshev-collocation reduced-gravity ocean model p 2788 N93-25276

Prediction of global cloud cover with a very high resolution global spectral model

| AD-A261047 | p 2785 N93-25777

SPECTROMETERS

Condensation on cooled surfaces of optical devices at the cosmic conditions p 2753 N93-24869

Data processing and control in a transputer system for remote sensing of the Earth p 2753 N93-24870

Large area, low capacitance Si(Li) detectors for high rate x ray applications

| DE93-007661 | p 2692 N93-26598

SPECTROPHOTOMETRY

Observations and models of shock structures in Herbig-Haro objects p 2891 N93-24770

SPECTRORADIOMETERS

Remote sensing geology p 2744 N93-24815

SPECTROSCOPIC ANALYSIS

Measurements of density, temperature, and their fluctuations in turbulent supersonic flow using UV laser spectroscopy

| NASA-TM-103943 | p 2708 N93-25076

Development of resonance ionization spectroscopy for genome mapping and DNA sequencing using stable isotopes as DNA labels

| DE93-007815 | p 2793 N93-26587

SPECTROSCOPY

Scale dependence in the reflectance of deciduous woodland: Evidence from a helicopter-mounted spectroradiometer p 2752 N93-24865

Ion trap frequency standard research at PTB p 2841 N93-25050

Photomodulation spectroscopy of photocarrier dynamics, electronic defects and morphology of conducting polymers

| DE93-010140 | p 2655 N93-25524

Electrochemical and spectroscopic studies of molten halides

| AD-A261687 | p 2646 N93-26439

The surface characterization of a series of hydroxybenzenes on Ag(111): An EELS and TDS study
| DE93-007541 | p 2647 N93-26595

SPECTRUM ANALYSIS
Determination of design and operation parameters for upper atmospheric research instrumentation to yield optimum resolution with deconvolution, appendix 4
| NASA-CR-192834 | p 2769 N93-24910
Determination of design and operation parameters for upper atmospheric research instrumentation to yield optimum resolution with deconvolution, appendix 2
| NASA-CR-192833 | p 2770 N93-25088
Comparison of high-resolution solar irradiance spectra and the solar luminosity in the period 1980-1989
| NASA-CR-192776 | p 2898 N93-25222
Development of a cone penetrometer for measuring spectral characteristics of soils in situ
p 2776 N93-25570
MAC to VAX connectivity: Heartrate spectral analysis system p 2796 N93-25594
Estimation of coefficients in a rational function from observed values
| AD-A261126 | p 2828 N93-25773
Tomographic analysis of sight infrared spectra of low pressure flames p 2628 N93-26030
On the cross-stream spectral method for the Orr-Sommerfeld equation
| NASA-TM-107737 | p 2845 N93-26086
Implementation of cyclic spectral analysis methods
| AD-A261715 | p 2681 N93-26372
Analysis of the IBSS spectra of Space Shuttle control engine exhaust
| AD-A261749 | p 2632 N93-26373

SPECULAR REFLECTION
Enhanced backscattering from rough surfaces
| AD-A261000 | p 2676 N93-25855

SPEECH
Perception and the temporal properties of speech
| AD-A261439 | p 2686 N93-26490

SPEECH RECOGNITION
Speech research
| AD-A260643 | p 2675 N93-25639
The adult literacy evaluator: An intelligent computer-aided training system for diagnosing adult illiterates p 2799 N93-26082

SPERMATOZOA
Progress in imaging microscopy with x ray lasers at LLNL
| DE93-007508 | p 2712 N93-25363

SPHERICAL COORDINATES
Rapid exploration of curvilinear grids using direct volume rendering
| NASA-CR-192765 | p 2808 N93-24944

SPHERICAL SHELLS
Simulation study of MHD dynamo: Convection in a rotating spherical shell
| NIFS-207 | p 2860 N93-25356

SPHEROMAKS
Ion temperature measurements in the Maryland Spheromak p 2859 N93-25290

SPIN EXCHANGE
The physics of spin polarized gases
| AD-A261396 | p 2850 N93-26288

SPIN STABILIZATION
SCATHA mission termination report
p 2605 N93-24725
Attitude control of the LACE satellite: A gravity gradient stabilized spacecraft p 2605 N93-24727
Nonlinear stability analysis of the attitude motion of spin-stabilized thrusting spacecraft p 2617 N93-25527
Investigation of liquid sloshing in spin-stabilized satellites
| AD-A261671 | p 2619 N93-26438

SPIN-LATTICE RELAXATION
Deuteron and oxygen-17 NMR studies of molecular motion in methanol-saturated Nafion membranes
| AD-A261579 | p 2851 N93-26514

SPINNERS
Ultrasonic rate measurement of multiphase flow
| DE93-000112 | p 2695 N93-24954

SPIRAL GALAXIES
Numerical modeling of barred spiral galaxies
p 2893 N93-25537
Far-infrared emission, gas, and ultraluminous HII regions in M101
| NASA-CR-192791 | p 2890 N93-25755

SPLICING
Investigation of corrosion in aluminum/adhesive lap-splices using pulse-echo ultrasonic techniques
| DE93-008074 | p 2721 N93-25518

SPLINE FUNCTIONS
Elastic curves on the sphere
| AD-A261057 | p 2829 N93-26228

SPLINES
Radial spline assembly for antifriction bearings
| NASA-CASE-MFS-28629-1 | p 2719 N93-26001

SPLITTING
Phase differences of the fields in a Ramsey resonator for submillimetric frequency standards
p 2840 N93-25042

SPORADIC E LAYER
High Frequency (HF) radiowave propagation
| AD-A261726 | p 2681 N93-26280

SPORADIC METEOROIDS
The Taurid meteoroid complex p 2889 N93-25536

SPOT (FRENCH SATELLITE)
Satellite remote sensing for environmental geology: The Bandung (West Java) experience p 2739 N93-24784
The use of SPOT data in natural disaster prevention and damage assessment p 2743 N93-24811
Interest of complementary data of coarse and high spatial resolution for agro-climatic crop monitoring
p 2750 N93-24853

SPRAY NOZZLES
Narrow-body aircraft water spray optimization study
| DOT/FAA/CT-TN93/3 | p 2582 N93-25224

SPRAYERS
Fuel injector: Air swirl characterization aerothermal modeling, phase 2, volume 1
| NASA-CR-189193 | p 2592 N93-24754
INEL spray-forming research p 2658 N93-25562
Vision-aided monitoring and control of thermal spray, spray forming, and welding processes
p 2670 N93-25604
Fundamental studies of droplet interactions in dense sprays
| AD-A261165 | p 2661 N93-25948
Development of a second generation spray combustion code p 2626 N93-26016
Eulerian-Eulerian treatment of turbulent dense spray combustion in a bipropellant liquid rocket engine
p 2626 N93-26017

SPRAYING
INEL spray-forming research p 2658 N93-25562

SPREAD SPECTRUM TRANSMISSION
A new modem for microwave time synchronisation via geosynchronous telecommunication satellites
p 2686 N93-24999
A Biphase Shift Keying (BPSK), direct sequence, spread spectrum modem for Petite Amateur Navy Satellite (PANSAT)
| AD-A261301 | p 2618 N93-26295
Geolocation of an electromagnetic emitter using a cyclostationary time difference of arrival technique
| AD-A261781 | p 2686 N93-26603

SPREADING
Electrostatic fiber spreader
| AD-D015677 | p 2640 N93-26143

SPRING (SEASON)
Passive microwave remote sensing of snow-covered floating ice during spring conditions in the Arctic and Antarctic
| ISBN-0-315-70444-6 | p 2754 N93-25422

SPUTTERING
Sputter deposition of yttrium-oxides
| DE93-007499 | p 2654 N93-25382

SQUARE WAVES
Symbol signal-to-noise ratio loss in square-wave subcarrier downconversion p 2672 N93-24668
A frequency generating source: Frequency synthesizers p 2693 N93-25041
Bandwidth compression of noisy signals with square-wave subcarrier p 2678 N93-26120

SQUEEZED STATES (QUANTUM THEORY)
Interferometric measurement with squeezed light
| AD-A260910 | p 2856 N93-26457

STABILITY
How can millisecond pulsars improve the long term stability of atomic time scales? p 2832 N93-24985
High-order cyclo-difference techniques: An alternative to finite differences
| NASA-TM-107745 | p 2575 N93-25074
Transverse instabilities in a relativistic klystron two-beam accelerator
| DE93-007110 | p 2852 N93-25375
Stability analysis and modeling of rotating flexible structures
| DE93-008493 | p 2844 N93-25520
Spectra of stable sonoluminescence
| AD-A260621 | p 2844 N93-25637
Nonlinear vibrations, stability, and dynamics of structures and mechanisms
| AD-A260871 | p 2728 N93-25838
On the stability of finite plastic deformations
| AD-A261526 | p 2730 N93-26361
Theoretical treatment of spin-forbidden and electronically nonadiabatic processes. Methods and applications
| AD-A261596 | p 2851 N93-26525

STABILITY TESTS
Stability analysis and modeling of rotating flexible structures
| DE93-008493 | p 2844 N93-25520
Aeroelastic response and aeromechanical stability of helicopters with elastically coupled composite rotor blades p 2588 N93-25530
Performance of a 12-GHz fiber-optic system for beam-waveguide antenna stability testing
p 2677 N93-26113

STABILIZATION
Thermal decomposition and stabilization of ammonium dinitramide p 2630 N93-26038

STAGE SEPARATION
Space transfer vehicle concepts and requirements study. Volume 2, book 2: System and program requirements trade studies
| NASA-CR-192526 | p 2611 N93-25511

STAGNATION PRESSURE
Experimentation in the low-density plume of a simulated electrothermal thruster for computer code validation
| NASA-CR-191112 | p 2622 N93-24758
An experimental study of under-expanded jets
p 2577 N93-25467

STAGNATION TEMPERATURE
Experimentation in the low-density plume of a simulated electrothermal thruster for computer code validation
| NASA-CR-191112 | p 2622 N93-24758

STAINLESS STEELS
Macromolecules for inhibition of corrosion and wear
| AD-A261041 | p 2655 N93-25816
External stress-corrosion cracking of a 1.22-m-diameter type 316 stainless steel air valve
| NASA-TP-3190 | p 2652 N93-26201

STANDARD DEVIATION
General aviation aircraft: Normal acceleration data analysis and collection project
| DOT/FAA/CT-91/20 | p 2586 N93-24739

STANDARDIZATION
GPS standardization for the needs of time transfer
p 2836 N93-25016
Guidelines for evaluating and expressing the uncertainty of NIST measurements results
| PB93-159465 | p 2830 N93-26318
NDT standards from the perspective of the Department of Defense
| MTL-TR-92-68 | p 2722 N93-26434

STANDARDS
Zoning of aircraft: A review of the definitions
p 2583 N93-24880
Improved PI-network measurement of all quartz crystal parameters by appropriate modelling of the test fixture
p 2833 N93-24995
The measurement of the resonant frequency of quartz crystal units: An ongoing saga p 2833 N93-24996
Rubidium atomic frequency standards for GPS block 2R p 2836 N93-25014
Development of ASTM standards in support of advanced ceramics development
| DE93-003024 | p 2654 N93-25361
An OSI architecture for the Deep Space Network
p 2679 N93-26121
Proof of fault coverage for a formal protocol test procedure
| AD-A261612 | p 2680 N93-26166

STANDING WAVES
Basic research thermoacoustic heat transport
| AD-A261334 | p 2759 N93-26310

STAR CLUSTERS
A study of the large-scale infrared emission from a selected dark cloud
| NASA-CR-192775 | p 2888 N93-25289
30 Doradus in the Large Magellanic Cloud: The stellar content and initial mass function p 2894 N93-25559

STAR FORMATION
Structure and star forming activities of the cold massive molecular cloud G216-2.5 p 2893 N93-25477
Shells, outflows and star formation in the giant molecular cloud Monoceros R2 p 2893 N93-25555
30 Doradus in the Large Magellanic Cloud: The stellar content and initial mass function p 2894 N93-25559

STAR TRACKERS
The results of the in-flight attitude sensor calibration for the Arthur Holly Compton Gamma Ray Observatory
p 2600 N93-24697
Star tracker operation in a high density proton field
p 2600 N93-24699
The Hubble Space Telescope fine guidance system operating in the coarse track pointing control mode
p 2605 N93-24724
Miniature Optical Wide-Angle-Lens Startracker (Mini-OWLS) p 2606 N93-24728
Goddard Space Flight Center (GSFC) Flight Dynamics Facility (FDF) calibration of the Upper Atmosphere Research Satellite (UARS) sensors
p 2606 N93-24733

Upper Atmosphere Research Satellite (UARS) attitude accuracy using coarse attitude sensors p 2607 N93-24735

STARBURST GALAXIES
Starburst Galaxies: Hard X-ray spectra and contribution to the diffuse background
| NASA-CR-192790 | p 2892 N93-25211

STATE VECTORS
Sequential design of a linear quadratic controller for the Deep Space Network antennas p 2679 N93-26123
Generalized probability model for calculation of interference to the Deep Space Network due to circularly Earth-orbiting satellites p 2679 N93-26127

STATIC ELECTRICITY
The 1992 International Aerospace and Ground Conference on Lightning and Static Electricity: Addendum
| DOT/FAA/CT-92/20-ADD-1 | p 2777 N93-24875
Commercial Precipitation Static (P-static) test equipment p 2711 N93-24901

STATIC LOADS
An improved spectral load balancing method
| DE93-007582 | p 2810 N93-25386

STATIC PRESSURE
Surface and flow field measurements in a symmetric crossing shock wave/turbulent boundary-layer interaction
| NASA-TM-106086 | p 2575 N93-24911
The transient development of vortices over delta wings p 2576 N93-25269
Model fan passage flow simulation
| AD-A261613 | p 2707 N93-26167

STATIC TESTS
Commercial Precipitation Static (P-static) test equipment p 2711 N93-24901

STATIONKEEPING
TDRSS orbit determination using short baseline differenced carrier phase p 2601 N93-24701
Orbit determination error analysis and comparison of station-keeping costs for Lissajous and halo-type libration point orbits and sensitivity analysis using experimental design techniques p 2604 N93-24721

STATISTICAL ANALYSIS
Improvements in ERBS attitude determination without gyros p 2602 N93-24710
Upper Atmosphere Research Satellite (UARS) onboard attitude determination using a Kalman filter p 2606 N93-24732
Assessment and forecasting of crop yield in Niger through NOAA NDVI data p 2750 N93-24851
Global drought monitoring from NOAA polar orbiting satellites p 2750 N93-24852
Interest of complementary data of coarse and high spatial resolution for agro-climatic crop monitoring p 2750 N93-24853
Cartography and statistics of crops under irrigation in the Donana area of Andalucia through the use of Landsat-TM imagery and its incorporation into a GIS p 2751 N93-24855
The evaluation of technical models used for major-accident hazard installations. Report to Commission of the European Communities Directorate General 12
| CUED/A-AERO/TR-19 | p 2668 N93-25238
Statistical modelling of software reliability
| NASA-CR-192985 | p 2809 N93-25257
Multivariate statistical analysis software technologies for astrophysical research involving large data bases p 2878 N93-25796
Joint flexibility effects on the dynamic response of structures. Part 2: Stochastic analysis
| AD-A261003 | p 2729 N93-25938
Implementation of quality improvement techniques for management and technical processes in the ACRV project p 2723 N93-26074
On-line implementation of nonlinear parameter estimation for the Space Shuttle main engine
| NASA-TM-106097 | p 2632 N93-26211

STATISTICAL CORRELATION
Lightning precursor signatures from dual-polarization radar measurements of storms p 2777 N93-24877
Bit hit/solar activity correlation study
| AD-A261381 | p 2896 N93-26340
Implementation of cyclic spectral analysis methods
| AD-A261715 | p 2681 N93-26372

STATISTICAL DISTRIBUTIONS
Experimental studies of fundamental problems in quantum optics
| AD-A261183 | p 2853 N93-25822

STATISTICAL MECHANICS
Multilevel techniques in large scale computation
| AD-A261082 | p 2828 N93-25762

STATISTICAL WEATHER FORECASTING
Lightning precursor signatures from dual-polarization radar measurements of storms p 2777 N93-24877
The effects of sampling frequency on the climate statistics of the ECMWF general circulation model
| DE93-003338 | p 2761 N93-25145

STATOR BLADES
The blade curving effects in a turbine stator cascade with low aspect ratio
| AD-A261063 | p 2595 N93-26239

STATORS
The blade curving effects in a turbine stator cascade with low aspect ratio
| AD-A261063 | p 2595 N93-26239

STEADY FLOW
Steady induction effects in geomagnetism. Part 1B: Geomagnetic estimation of steady surficial core motions: A non-linear inverse problem
| NASA-TP-3272-PT-1B | p 2776 N93-26421

STEADY STATE
Two-phase/two-phase heat exchanger analysis
| NASA-CR-192783 | p 2697 N93-25221
Simultaneous determination of gain parameters in steady state lasers
| DE93-007389 | p 2713 N93-25381
A hybrid multigrid technique for computing steady-state solutions to supersonic flows p 2582 N93-26078
Dynamic modeling of fluid transmission lines of the DSN 70-meter antennas by using a lumped parameter model p 2678 N93-26119
Oblique MHD cosmic-ray modified shocks: Two-fluid numerical simulations
| NASA-CR-192930 | p 2900 N93-26132
Another look at the driven cavity problem
| AD-A261903 | p 2708 N93-26543

STEEL STRUCTURES
Photovoltaic power without batteries for continuous cathodic protection p 2759 N93-25597

STEELS
Seismic buckling capacity of unstiffened, free-standing steel containments
| DE93-005325 | p 2723 N93-24957
In situ surface studies of conversion coatings for steel and aluminum
| AD-A261016 | p 2655 N93-25861
Hydrogen-induced stress corrosion cracking susceptibility analysis of pitch links from the AH-64 Apache helicopter
| AD-A260692 | p 2651 N93-25895

STELLAR ATMOSPHERES
Steady-state numerical models of accreting neutron stars: The effect of atmospheric CNO depletion and diffusion p 2889 N93-25624
Radial velocity measurements of carbon stars p 2895 N93-25713

STELLAR CORONAS
ROSAT investigation of flaring and activity on Prox Cen
| NASA-CR-192972 | p 2891 N93-26139

STELLAR ENVELOPES
A superconducting tunnel junction receiver for submillimeter astronomy, and analysis of observations of post-AGB star molecular envelopes p 2889 N93-25440
The effects of rotation on the winds from hot stars p 2894 N93-25620

STELLAR EVOLUTION
Origin and evolution of cataclysmic variables p 2893 N93-25245
30 Doradus in the Large Magellanic Cloud: The stellar content and initial mass function p 2894 N93-25559

STELLAR FLARES
ROSAT investigation of flaring and activity on Prox Cen
| NASA-CR-192972 | p 2891 N93-26139

STELLAR LUMINOSITY
Comparison of high-resolution solar irradiance spectra and the solar luminosity in the period 1980-1989
| NASA-CR-192776 | p 2898 N93-25222

STELLAR MAGNETIC FIELDS
Chromospheric activity in algol binaries
| AD-A261440 | p 2896 N93-26508

STELLAR MAGNITUDE
Cape Photographic Durchmusterung, volume 1
| NASA-RP-1300-VOL-1 | p 2890 N93-26002
Cape Photographic Durchmusterung, volume 2
| NASA-RP-1300-VOL-2 | p 2890 N93-26003
Cape Photographic Durchmusterung, volume 3
| NASA-RP-1300-VOL-3 | p 2890 N93-26004

STELLAR MASS
Origin and evolution of cataclysmic variables p 2893 N93-25245
Structure and star forming activities of the cold massive molecular cloud G216-2.5 p 2893 N93-25477

STELLAR MASS ACCRETION
Steady-state numerical models of accreting neutron stars: The effect of atmospheric CNO depletion and diffusion p 2889 N93-25624

STELLAR MASS EJECTION
A revised and expanded catalogue of mass ejections observed by the Solar Maximum Mission coronagraph
| NASA-CR-193146 | p 2899 N93-26556

STELLAR MODELS
Steady-state numerical models of accreting neutron stars: The effect of atmospheric CNO depletion and diffusion p 2889 N93-25624

STELLAR OSCILLATIONS
Diskoseismology: Probing relativistic accretion disks p 2894 N93-25622

STELLAR ROTATION
The effects of rotation on the winds from hot stars p 2894 N93-25620

STELLAR SPECTRA
An atlas of selected calibrated stellar spectra
| NASA-CR-177604 | p 2888 N93-25135
Radial velocity studies of the secondary in cataclysmic variables p 2888 N93-25286
Photospheric abundance analysis of low-mass pre-main sequence stars p 2894 N93-25623
Radial velocity measurements of carbon stars p 2895 N93-25713

STELLAR STRUCTURE
Diskoseismology: Probing relativistic accretion disks p 2894 N93-25622

STELLAR SYSTEMS
Prograde anomalous orbits in triaxial gravitational potentials that rotate about the long axis: VLA neutral hydrogen observations and modeling of the inclined rings around the galaxies NGC 2685 and NGC 660 p 2607 N93-25396

STELLAR WINDS
Observations and models of shock structures in Herbig-Haro objects p 2891 N93-24770
The effects of rotation on the winds from hot stars p 2894 N93-25620

STELLARATORS
Assessment of torsatrons as reactors
| DE93-006721 | p 2858 N93-24969

STEREOPHONICS
Low-frequency room responses. Part 1: Background and qualitative considerations
| BBC-RD-1992/8-PT-1 | p 2673 N93-25168

STEREOPHOTOGRAPHY
High resolution stereo imaging and data compression p 2753 N93-24867

STEREOSCOPY
Experiments in multiple-baseline stereo
| AD-A261415 | p 2757 N93-26448

STIFFENING
Fatigue resistance of orthotropic plates with trapezoidal stiffeners
| TRL-TRANS-T3908 | p 2726 N93-25419

STIFFNESS
Determination of the elastic constants of composite materials from ultrasonic group velocity measurements p 2635 N93-25544
Joint flexibility effects on the dynamic response of structures. Part 2: Stochastic analysis
| AD-A261003 | p 2729 N93-25938
Damage detection and mitigation of composite structures using smart materials
| AD-A261121 | p 2639 N93-25945

STIFFNESS MATRIX
Using a multifrontal sparse solver in a high performance, finite element code
| NASA-CR-192718 | p 2828 N93-25223
Joint flexibility effects on the dynamic response of structures. Part 2: Stochastic analysis
| AD-A261003 | p 2729 N93-25938

STIMULATED EMISSION
Simultaneous determination of gain parameters in steady state lasers
| DE93-007389 | p 2713 N93-25381

STIMULATION
Mechanical stimulation of skeletal muscle mitigates glucocorticoid induced decreases in prostaglandin synthesis
| NASA-CR-193040 | p 2794 N93-24763

STIRLING CYCLE
Malone refrigeration
| DE93-005439 | p 2668 N93-25447

STIRLING ENGINES
Test results of a Stirling engine utilizing heat exchanger modules with an integral heat pipe
| NASA-TM-105883 | p 2759 N93-25136
Malone refrigeration
| DE93-005439 | p 2668 N93-25447

STOCHASTIC PROCESSES
Fuel injector: Air swirl characterization aerothermal modeling, phase 2, volume 1
| NASA-CR-189193 | p 2592 N93-24754
Fuel Injector: Air swirl characterization aerothermal modeling, phase 2, volume 2
| NASA-CR-189193 | p 2592 N93-25106

Stochastic and seismic design response of linear and nonlinear structures p 2726 N93-25484
Control of complex dynamic systems by neural networks p 2827 N93-25611
Time series analysis and multivariate analysis
| AD-A261014 | p 2830 N93-25860
Probability and statistics applied to the theory of algorithms
| AD-A261019 | p 2830 N93-25863
Joint flexibility effects on the dynamic response of structures. Part 2: Stochastic analysis
| AD-A261003 | p 2729 N93-25938
Substantiation of a stochastic model of rhythmic phenomena
| AD-A261232 | p 2830 N93-26262
Methods of optimization under uncertainty
| AD-A261487 | p 2873 N93-26342

STOICHIOMETRY
Hot corrosion of the B2 nickel aluminides
| NASA-CR-191082 | p 2649 N93-25128
Polyimides with improved compression moldability
| NASA-CASE-LAR-14457-1 | p 2656 N93-25997
Kinetic studies in gas-phase reaction mechanisms important to the combustion process of high energy density materials: The H2/NO2 reaction p 2628 N93-26027
Vickers indentation hardness of stoichiometric and reduced single crystal TiO2 (rutile) from 25 to 800 C
| NASA-TM-105959 | p 2633 N93-26204

STORAGE RINGS (PARTICLE ACCELERATORS)
Preliminary design of the BPM electronics memory scanner/dual boxcar averager for the advanced photon source
| DE93-007893 | p 2848 N93-25368

STORAGE TANKS
Tank issues: Design and placement of vapor monitoring wells
| PB93-161131 | p 2768 N93-26536

STORM DAMAGE
Assessment of storm damage in forests using SPOT imagery p 2748 N93-24842
Guide for conducting convective windstorm surveys
| PB93-148427 | p 2787 N93-26570
Tornado: An engineering-oriented perspective
| PB93-148435 | p 2788 N93-26584

STORM SURGES
Magnetotail processes associated with auroral surge formation
| ATR-90(7186)-1 | p 2895 N93-26147

STORMS
Investigation of winter mountain storms in Utah during the 1989 Utah/NOAA field program
| PB93-153021 | p 2785 N93-25849
A climatology of polar low occurrences in the Nordic Seas and an examination of katabatic winds as a triggering mechanism
| AD-A261719 | p 2786 N93-26245
An investigation into the causative mechanisms for explosive cyclone development over the Atlantic
| AD-A261831 | p 2786 N93-26273

STORMS (METEOROLOGY)
Positive cloud-to-ground flashes in severe storms p 2780 N93-24896
Initialization of a modeled convective storm using Doppler radar-derived fields p 2782 N93-25294
National Weather Service Winter Weather Workshop
| PB93-146785 | p 2785 N93-25775
The North Dakota thunderstorm project
| PB93-153039 | p 2785 N93-25776
Synoptic and Mesoscale Meteorology Instruction Workshop
| PB93-156347 | p 2785 N93-25870
Rainfall frequency atlas of the Midwest
| PB93-164606 | p 2785 N93-25872
Natural and augmented snowfall growth processes and their interactions with the natural and modified aerosol
| PB93-153096 | p 2786 N93-25874

STOVL AIRCRAFT
Jet-induced ground effects on a parametric flat-plate model in hover
| NASA-TM-104001 | p 2581 N93-26099

STRAIN DISTRIBUTION
Image correlation velocimetry
| AD-A261599 | p 2707 N93-26163
Failure considerations in composite systems based on 3D micromechanical stress fields, part A
| AD-A261698 | p 2641 N93-26382

STRAIN ENERGY RELEASE RATE
Numerical investigations on fracture behavior of ductile materials p 2725 N93-25411

STRAIN GAGES
The constant current loop: A new paradigm for resistance signal conditioning
| NASA-TM-108744 | p 2673 N93-25181
Magnetic multilayer strain gage
| AD-D015672 | p 2710 N93-26141

STRAIN MEASUREMENT
Internal strain analysis of ceramics using scanning laser acoustic microscopy
| NASA-CR-191118 | p 2721 N93-25451

STRAIN RATE
Approximate analysis on strain rate effects and behavior of stress and strain fields at the crack tip in Mode 2 in metallic materials, appendix no. 1
| AD-A260836 | p 2728 N93-25785
High strain rate damage development and failure mechanisms in tungsten heavy alloys
| AD-A260856 | p 2651 N93-25788

STRAKES
Helicopter low-speed yaw control
| NASA-CASE-LAR-14219-1 | p 2597 N93-25998

STRANDS
Thermal radiation in non-metalized solid rocket motors: Effect on burning rate and temperature sensitivity p 2626 N93-26020

STRANGE ATTRACTORS
Boundedness and asymptotics of the generalized theodorus iteration
| AD-A261427 | p 2829 N93-26452

STRANGENESS
Strangeness production in S + Pb and p + Pb collisions at 200 GeV/c per nucleon nucleon
| DE93-007654 | p 2847 N93-25326
Results from the NA36 on strangeness production in 200 GeV/c per nucleon S + Pb and p - Pb reactions
| DE93-007711 | p 2848 N93-25364

STRATA
Experiments on the physics of turbulent mixing in stably stratified ocean layers
| AD-A261312 | p 2790 N93-26298

STRATIFIED FLOW
Effects of surface thermal forcing on stratified flow past an isolated obstacle
| PB93-156776 | p 2776 N93-26548

STRATOCUMULUS CLOUDS
Summary by the cloud and aerosol research group for ASTEX
| AD-A261292 | p 2766 N93-26292

STRATOSPHERE
The atmospheric effects of stratospheric aircraft. Report of the 1992 Models and Measurements Workshop. Volume 1: Workshop objectives and summary
| NASA-RP-1292-VOL-1 | p 2762 N93-25157
The atmospheric effects of stratospheric aircraft. Report of the 1992 Models and Measurements Workshop. Volume 2: Comparisons with global atmospheric measurements
| NASA-RP-1292-VOL-2 | p 2762 N93-25158
The atmospheric effects of stratospheric aircraft. Report of the 1992 Models and Measurements Workshop. Volume 3: Special diagnostic studies
| NASA-RP-1292-VOL-3 | p 2762 N93-25159
Kelvin waves in total column ozone
| NASA-CR-192984 | p 2764 N93-25431
The pressure modulation system in the Improved Stratospheric and Mesospheric Sounder p 2773 N93-25739

STRESS ANALYSIS
Quartz crystal twinning under mechanical stress: Finite element analysis p 2839 N93-25032
Stress and reliability analyses of multilayered composite cylinder under thermal and mechanical loads p 2726 N93-25533
Reliable stress and fracture mechanics analysis of complex aircraft components using a h-p version of FEM
| AD-A260628 | p 2726 N93-25638
Computational gearing mechanics
| NASA-CR-191127 | p 2719 N93-25884
Optimization techniques for contact stress analysis
| AD-A260846 | p 2729 N93-25911
External stress-corrosion cracking of a 1.22-m-diameter type 316 stainless steel air valve
| NASA-TP-3190 | p 2652 N93-26201
Approximate techniques for predicting size effects on cleavage fracture toughness (J(sub c))
| AD-A261591 | p 2731 N93-26516
The influence of primary and secondary orientations on the elastic response of a nickel-base single-crystal superalloy
| NASA-TM-106125 | p 2731 N93-26550

STRESS CORROSION CRACKING
Hydrogen-induced stress corrosion cracking susceptibility analysis of pitch links from the AH-64 Apache helicopter
| AD-A260692 | p 2651 N93-25895
External stress-corrosion cracking of a 1.22-m-diameter type 316 stainless steel air valve
| NASA-TP-3190 | p 2652 N93-26201

STRESS DISTRIBUTION
Stress distribution in composite flatwise tension test specimens
| NASA-TM-106074 | p 2634 N93-25071
Stress and reliability analyses of multilayered composite cylinder under thermal and mechanical loads p 2726 N93-25533
Numerical simulation of damage and progressive failures in composite laminates using the layerwise plate theory p 2636 N93-25661
Low-velocity impact of composite sandwich plate p 2637 N93-25695
Design and analysis of curved composite components for rotorcraft fuselage frames p 2589 N93-25701
Structural dynamic analysis of bearingless rotor blade p 2590 N93-25719
Crack tip fields in ductile crystals and bicrystals p 2866 N93-25749
Failure considerations in composite systems based on 3D micromechanical stress fields, part A
| AD-A261698 | p 2641 N93-26382

STRESS INTENSITY FACTORS
Reliable stress and fracture mechanics analysis of complex aircraft components using a h-p version of FEM
| AD-A260628 | p 2726 N93-25638

STRESS MEASUREMENT
Micromechanics of fatigue
| AD-A260577 | p 2729 N93-25901
Experimental studies of stress management by optical fluorescence
| AD-A261539 | p 2730 N93-26362

STRESS RELAXATION
Internal strain analysis of ceramics using scanning laser acoustic microscopy
| NASA-CR-191118 | p 2721 N93-25451

STRESS-STRAIN RELATIONSHIPS
Effect of cytoskeletal reagents on stretch activated ion channels
| AD-A261089 | p 2793 N93-25764
Approximate analysis on strain rate effects and behavior of stress and strain fields at the crack tip in Mode 2 in metallic materials, appendix no. 1
| AD-A260836 | p 2728 N93-25785
Thermomechanical response of shape memory composites
| AD-A260828 | p 2639 N93-25919

STRETCHING
Deuteron and oxygen-17 NMR studies of molecular motion in methanol-saturated Nafion membranes
| AD-A261579 | p 2851 N93-26514

STRIATION
Trailing vortex/free-surface interaction
| AD-A261654 | p 2581 N93-26195

STRING THEORY
Cosmic string cosmology p 2891 N93-24907
From fractals to wormholes via string theory p 2871 N93-25742

STRONGLY COUPLED PLASMAS
Liquid and solid ion plasmas
| AD-A261888 | p 2862 N93-26528

STRONTIUM
Collisional recombination lasers p 2713 N93-25393

STROUHAL NUMBER
Vortex shedding in oscillatory flow p 2700 N93-25438

STRUCTURAL ANALYSIS
Evaluation of MARC for the analysis of rotating composite blades
| NASA-TM-4423 | p 2723 N93-24909
High temperature composite analyzer (HITCAN) user's manual, version 1.0
| NASA-TM-106002 | p 2724 N93-25070
Integrated aerodynamic-structural wing design optimization p 2587 N93-25279
Integration of design, thermal, structural, and optical analysis, including thermal animation p 2814 N93-25601

STRUCTURAL DESIGN
Grid sensitivity for aerodynamic optimization and flow analysis
| NASA-CR-192980 | p 2575 N93-25117
Integrated aerodynamic-structural wing design optimization p 2587 N93-25279
Reliable stress and fracture mechanics analysis of complex aircraft components using a h-p version of FEM
| AD-A260628 | p 2726 N93-25638
Design and analysis of curved composite components for rotorcraft fuselage frames p 2589 N93-25701
Development and application of an advanced ductile fracture mechanics methodology p 2727 N93-25718
Nonlinear vibrations, stability, and dynamics of structures and mechanisms
| AD-A260871 | p 2728 N93-25838
Deformation mechanisms of NiAl cyclicly deformed near the brittle-to-ductile transition temperature
| NASA-CR-191121 | p 2652 N93-26235
Design concepts for pressurized lunar shelters utilizing indigenous materials p 2670 N93-26414
Lunar surface structural concepts and construction studies p 2670 N93-26417

STRUCTURAL ENGINEERING
Tornado: An engineering-oriented perspective
| PB93-148435 | p 2788 N93-26584
STRUCTURAL FAILURE
Thermally induced stresses in a composite exposed to fire
| AD-A261714 | p 2641 N93-26371
J and CTOD estimation equations for shallow cracks in single edge notch bend specimens
| AD-A261679 | p 2731 N93-26390
STRUCTURAL PROPERTIES (GEOLOGY)
Earthquake vulnerability map of the Lake Constance area p 2753 N93-24872
Geologic structure and processes of the eastern Pacific margin: California and Costa Rica p 2771 N93-25424
STRUCTURAL RELIABILITY
An efficient technique for structural reliability with applications p 2727 N93-25681
STRUCTURAL STABILITY
Active control of NITINOL-reinforced structural composites
| AD-A261062 | p 2638 N93-25780
MIT's interferometer CST testbed
p 2609 N93-25836
Repair, evaluation, maintenance, and rehabilitation research program. Continuous Deformation Monitoring System (CDMS)
| AD-A261833 | p 2586 N93-26274
STRUCTURAL VIBRATION
Optimizing the fine lock performance of the Hubble Space Telescope fine guidance sensors
p 2604 N93-24723
Attitude control of the LACE satellite: A gravity gradient stabilized spacecraft p 2605 N93-24727
Global dynamic modeling of a transmission system
| NASA-CR-191117 | p 2716 N93-24751
UARS in-flight jitter study for EOS
| NASA-CR-191419 | p 2615 N93-25133
On the effective reflection properties of the randomly segmented elastic bar p 2724 N93-25328
Pyroshock: Bibliography
| DE93-007605 | p 2726 N93-25489
Using input command pre-shaping to suppress multiple mode vibration p 2732 N93-25834
Computational gearing mechanics
| NASA-CR-191127 | p 2719 N93-25884
Digital filter control of remotely operated flexible robotic structures
| DE93-007587 | p 2827 N93-26596
STRUTS
An in-depth probabilistic study of external tank attach ring
| NASA-TM-108403 | p 2624 N93-25671
MIT's interferometer CST testbed
p 2609 N93-25836
Structural load control during construction
p 2669 N93-26409
STUDENTS
MIT Space Engineering Research Center
| NASA-CR-192879 | p 2821 N93-25833
Performance-based testing and success in Naval advanced flight training
| AD-A260838 | p 2590 N93-25933
The 1993/1994 NASA Graduate Student Researchers Program
| NASA-EP-283 | p 2872 N93-26051
Contribution of personality to the prediction of success in initial air traffic control specialist training
| DOT/FAA/AM-93/4 | p 2797 N93-26138
SUBASSEMBLIES
Expert systems for assembly sequence evaluation
p 2669 N93-26411
SUBDUCTION (GEOLOGY)
Geologic structure and processes of the eastern Pacific margin: California and Costa Rica p 2771 N93-25424
SUBMARINES
Membrane technology: A search for membranes for submarine atmosphere control
| AD-A260581 | p 2801 N93-25904
SUBMILLIMETER WAVES
Phase differences of the fields in a Ramsey resonator for submillimetric frequency standards
p 2840 N93-25042
Solid state frequency synthesis up to 600 GHz: An application to the Mg frequency standard
p 2842 N93-25058
Theoretical and experimental investigation of electron beam acceleration and sub-millimeter wave generation
| AD-A261117 | p 2609 N93-25770
SUBROUTINE LIBRARIES (COMPUTERS)
NSWC library of mathematics subroutines
| AD-A261511 | p 2884 N93-26575
SUBROUTINES
Interactive interface for National Center for Atmospheric Research (NCAR) Graphics p 2878 N93-25794
SUBSONIC FLOW
Uniform roughness studies
| WL-TR-92-3041 | p 2706 N93-25951
Unsteady airfoil flow solutions on moving zonal grids
| AD-A261925 | p 2582 N93-26198
An extended Lagrangian method
| NASA-TM-106129 | p 2707 N93-26203
SUBSTRATES
Optoelectronic III-V heterostructures on Si substrates
| AD-A261651 | p 2867 N93-26193
Phosphorus-, nitrogen-, sulfur-, and chlorine-containing molecules on surfaces
| AD-A261265 | p 2657 N93-26303
Halogen adlayers on Ag(111)
| AD-A261792 | p 2850 N93-26443
SUCCESS PROJECT
Implementation of quality improvement techniques for management and technical processes in the ACRV project p 2723 N93-26074
SUCTION
Effect of cytoskeletal reagents on stretch activated ion channels
| AD-A261089 | p 2793 N93-25764
SUDDEN IONOSPHERIC DISTURBANCES
Solar-geophysical data number 581, January 1993. Part 1: (Prompt reports). Data for December, November 1992, and late data
| PB93-161743 | p 2899 N93-26537
Solar-geophysical data number 581, January 1993. Part 2: (Comprehensive reports). Data for July 1992 and miscellaneous
| PB93-161750 | p 2899 N93-26538
SULFUR
Results from the NA36 on strangeness production in 200 GeV/c per nucleon S + Pb and p - Pb reactions
| DE93-007711 | p 2848 N93-25364
SULFUR FLUORIDES
Redistribution of trace chemical species by a small convective cloud
| PB93-156164 | p 2765 N93-25873
SUMMER
Gordon Conference on Point Defects, Line Defects and Interfaces in Semiconductors
| AD-A261485 | p 2868 N93-26357
SUNSPOTS
Solar-geophysical data number 581, January 1993. Part 1: (Prompt reports). Data for December, November 1992, and late data
| PB93-161743 | p 2899 N93-26537
Solar-geophysical data number 581, January 1993. Part 2: (Comprehensive reports). Data for July 1992 and miscellaneous
| PB93-161750 | p 2899 N93-26538
SUPERCHARGERS
Radial inflow turbine study
| AD-A260767 | p 2594 N93-25917
SUPERCOMPUTERS
Supercomputer Debugging Workshop 1992
| DE93-007322 | p 2805 N93-25165
Wavelet transform-vector quantization compression of supercomputer ocean model simulation output
| DE93-005453 | p 2876 N93-25448
Use of high performance networks and supercomputers for real-time flight simulation p 2598 N93-25574
Construction of a connectionist network supercomputer
| AD-A260929 | p 2820 N93-25648
The state of computing at Los Alamos National Laboratory, FY 1991
| LA-12326-MS | p 2811 N93-25943
SUPERCONDUCTING DEVICES
Environmental test program for superconducting materials and devices
| DE93-003646 | p 2864 N93-25506
Published assessments bearing on the future use of ceramic superconductors by the electric power sector
| DE93-007737 | p 2658 N93-26588
SUPERCONDUCTING FILMS
Development of high Tc (greater than 100 K) Bi, Tl and Y-based materials as superconducting circuit elements
| NASA-CR-192344 | p 2863 N93-25219
Film fabrication technologies at NREL
p 2658 N93-25563
SUPERCONDUCTING MAGNETS
Low temperature Hall and Shubnikov-de Haas effects
| AD-A261871 | p 2869 N93-26540
SUPERCONDUCTING SUPER COLLIDER
Studies of avalanche photodiodes for scintillating fibre tracking readout
| DE93-008370 | p 2689 N93-25491
SUPERCONDUCTIVITY
Consequences of spontaneous and anomalous symmetry breaking for the orbital and mass flow hydrodynamics of He-3 - A p 2698 N93-25295
JPRS report: Science and technology. Central Eurasia: Physics and mathematics
| JPRS-UPM-92-004 | p 2844 N93-25402
JPRS report: Science and technology. Central Eurasia: Physics and mathematics
| JPRS-UPM-92-003 | p 2844 N93-25403
JPRS report: Science and technology. Central Eurasia: Physics and mathematics
| JPRS-UPM-93-001 | p 2844 N93-25404
Inelastic scattering in condensed matter with high intensity Moessbauer radiation
| DE93-008763 | p 2864 N93-25503
A novel method for characterization of superconductors: Physical measurements and modeling of thin films
p 2871 N93-25584
Developing and improving numerical algorithms to study intrinsically correlated electron systems
| AD-A261214 | p 2849 N93-25734
Advanced HTS S-N-S devices
| AD-A261552 | p 2869 N93-26381
Computational methods for flow problems: Parallel algorithms, flow control, and novel approaches
| AD-A261400 | p 2707 N93-26400
Transition metal chelate-fulleride compounds: Electrocrystallization of semiconducting (Ru(bpy)s)(C60)2
| AD-A261549 | p 2869 N93-26577
SUPERCONDUCTORS
A novel method for characterization of superconductors: Physical measurements and modeling of thin films
p 2871 N93-25584
Aerospace devices for magnetic replicas
| NASA-CR-192958 | p 2865 N93-25667
Monolithic integration of semiconductor and superconductor components
| AD-A260589 | p 2690 N93-25906
Experimental and theoretical studies of proximity effect and Coulomb blockade phenomena in Josephson junctions
| AD-A261652 | p 2867 N93-26194
Electronics and Electrical Engineering Laboratory technical publication announcements covering laboratory programs, July to September 1992 with 1992/1993 EEEL events calendar
| PB93-158632 | p 2884 N93-26530
SUPERCRITICAL FLOW
Influence of supercritical conditions on pre-combustion chemistry and transport behavior of jet fuels
| AD-A261813 | p 2661 N93-26268
SUPERCRITICAL PRESSURES
Fundamental studies of droplet interactions in dense sprays
| AD-A261165 | p 2661 N93-25948
SUPERFLUIDITY
Consequences of spontaneous and anomalous symmetry breaking for the orbital and mass flow hydrodynamics of He-3 - A p 2698 N93-25295
SUPERHIGH FREQUENCIES
Effect-specific analysis of propagation parameters
p 2684 N93-26478
The Virginia Tech OLYMPUS propagation experiment
p 2685 N93-26479
SUPERLATTICES
New concepts for high efficiency energy conversion: The avalanche heterostructure and superlattice solar cells
| DE92-010592 | p 2758 N93-25098
Magnetic excitations in antiferromagnetically coupled superlattices: Fe/Mo and Fe/Cr
| DE93-007894 | p 2863 N93-25369
Electric field effects on quantum-confined semiconductor structures p 2865 N93-25703
Measurement of optical properties of infrared bandgap superlattices
| AD-A260859 | p 2866 N93-25789
Short-period superlattice materials for heterojunction bipolar transistors
| AD-A260701 | p 2866 N93-25897
Optoelectronic III-V heterostructures on Si substrates
| AD-A261651 | p 2867 N93-26193
SUPERNOVAE
An investigation of neutrino properties through study of the sun, supernovae, the early universe and lab data
p 2898 N93-25180
SUPERPLASTICITY
Study of grain refinement in Al alloy 2519 using backscattering orientation-contrast mode in the scanning electron microscope
| AD-A260886 | p 2651 N93-25632
SUPERSONIC AIRCRAFT
Experimental performance of a ventral nozzle with pitch and yaw vectoring capability for SSTOVL aircraft
| NASA-TM-106054 | p 2592 N93-25129
Physiological indices of mental workload
| AD-A261692 | p 2798 N93-26391

SUPERSONIC COMBUSTION
Solid fuel supersonic combustion p 2625 N93-26010
Turbulence interacting with chemical kinetics in airbreathing combustion of ducted rockets p 2625 N93-26012
SUPERSONIC COMBUSTION RAMJET ENGINES
Generic hypersonic vehicle performance model | NASA-CR-192953 | p 2587 N93-25162
Optimized scramjet engine integration on a waverider airframe p 2593 N93-25480
Workshop Report: A validation study of Navier-Stokes codes for transverse injection into a Mach 2 flow p 2624 N93-26008
The effect of entrance radius and film injection on wall heating in scramjet nozzles p 2625 N93-26009
SUPERSONIC FLOW
Surface and flow field measurements in a symmetric crossing shock wave/turbulent boundary-layer interaction | NASA-TM-106086 | p 2575 N93-24911
Measurements of density, temperature, and their fluctuations in turbulent supersonic flow using UV laser spectroscopy | NASA-TM-103943 | p 2708 N93-25076
A contribution to the great Riemann solver debate | NASA-CR-191409 | p 2575 N93-25083
Nonlinear evolution of the first mode supersonic oblique waves in compressible boundary layers. Part 1: Heated/cooled walls | NASA-TM-106087 | p 2696 N93-25175
An investigation of laser velocimetry measurements within high speed, complex flows p 2697 N93-25237
Supersonic shock wave/vortex interaction | NASA-CR-192917 | p 2576 N93-25249
Experimental and computational investigation of helium injection into air at supersonic and hypersonic speeds p 2577 N93-25487
Studies in air/air supersonic mixing layers p 2582 N93-26007
Workshop Report: A validation study of Navier-Stokes codes for transverse injection into a Mach 2 flow p 2624 N93-26008
A hybrid multigrid technique for computing steady-state solutions to supersonic flows p 2582 N93-26078
An extended Lagrangian method | NASA-TM-106129 | p 2707 N93-26203
SUPERSONIC HEAT TRANSFER
Heat transfer measurements in swept shock wave/turbulent boundary-layer interactions p 2704 N93-25705
SUPERSONIC SPEED
Numerical simulation of a shock wave/turbulent boundary layer interaction in a duct p 2699 N93-25342
Visualization of a Mach 2 reacting flow using Planar Laser-Induced Fluorescence (PLIF) p 2598 N93-26006
The effect of entrance radius and film injection on wall heating in scramjet nozzles p 2625 N93-26009
Experimental effects of wing location on wing-body pressures at supersonic speeds | NASA-TM-4434 | p 2581 N93-26085
Supersonic aeroelastic instability results for a NASP-like wing model | NASA-TM-107739 | p 2591 N93-26553
Optically smart surfaces survivability testing at Mach 3 | AD-A261785 | p 2857 N93-26566
SUPERSONIC TRANSPORTS
Aerodynamic design and synthesis of the oblique flying wing supersonic transport p 2587 N93-24768
Screening studies of advanced control concepts for airbreathing engines | NASA-TM-106042 | p 2592 N93-25079
Bibliography on propulsion airframe integration technologies for high-speed civil transport applications, 1980-1991 | NASA-TM-105602 | p 2573 N93-26136
SUPERSONIC WIND TUNNELS
NASA Lewis 8- by 6-foot supersonic wind tunnel user manual | NASA-TM-105771 | p 2597 N93-25080
SUPPORT SYSTEMS
Systems engineering considerations for operational support systems p 2666 N93-24689
JSC research and technology | NASA-TM-104763 | p 2901 N93-25188
Adaptive decision support systems: Concepts, characterization, and an application p 2876 N93-25475
Department of Defense technical architecture framework for information management. Volume 3: Reference model and standards profile, version 1.3 | AD-A261913 | p 2882 N93-26230
Data analysis support for the Shuttle Potential and Return Electron Experiment (SPREE) on the Tethered Satellite System 1 (TSS-1) flight | AD-A261646 | p 2618 N93-26232
A hypertext framework for group support systems | AD-A261731 | p 2885 N93-26582
Task Type E report for National Launch Demonstration Center (NLDC) (Task 32) | MCR-91-5010 | p 2610 N93-26591
SUPPORTS
Automated inspection of solder joints for surface mount technology | NASA-TM-104580 | p 2721 N93-26137
SURFACE DEFECTS
Correlation of damage threshold and surface geometry of nodular defects in HR coatings as determined by in-situ atomic force microscopy | DE93-007509 | p 2654 N93-25384
Continuum and micromechanics treatment of constraint in fracture | AD-A260927 | p 2727 N93-25647
Defect initiation/growth and energy dissipation induced by deformation and fracture | AD-A261703 | p 2869 N93-26385
Modeling of electric-field enhancement at nodular defects in dielectric mirror coatings | DE93-007513 | p 2857 N93-26593
SURFACE DIFFUSION
Surface diffusion studies by optical diffraction techniques | DE93-007707 | p 2853 N93-25550
SURFACE ENERGY
Surface energy fluxes at Central Florida during the convection and precipitation electrification experiment | NASA-CR-192826 | p 2769 N93-24945
Theoretical predictions of platinum-rhodium bimetallic catalysts | DE93-007540 | p 2649 N93-25428
Phase-field models for anisotropic interfaces | PB93-164564 | p 2646 N93-26323
SURFACE FINISHING
Surface preparation and characterization of a 400 micrometer diameter fused silica optical fiber for direct optical initiation (DOI) applications | DE93-005485 | p 2852 N93-25182
Ultrasonic polishing p 2670 N93-25580
Surface finish quality of the outer AXAF mirror pair based on x ray measurements of the VETA-I p 2855 N93-26191
SURFACE GEOMETRY
On machine capacitance dimensional and surface profile measurement system p 2670 N93-25579
Computational gearing mechanics | NASA-CR-191127 | p 2719 N93-25884
SURFACE IONIZATION
Diagnostics of diamond film deposition plasmas | AD-A260866 | p 2860 N93-25626
SURFACE LAYERS
In situ surface studies of conversion coatings for steel and aluminum | AD-A261016 | p 2655 N93-25861
Experiments on the physics of turbulent mixing in stably stratified ocean layers | AD-A261312 | p 2790 N93-26298
SURFACE NAVIGATION
Using fuzzy behaviors for the outdoor navigation of a car with low-resolution sensors | DE93-002428 | p 2584 N93-25120
SURFACE PROPERTIES
Inherent optical properties of lakes as measured by Landsat 5 Thematic Mapper p 2746 N93-24828
Surface diffusion studies by optical diffraction techniques | DE93-007707 | p 2853 N93-25550
SURFACE REACTIONS
Theoretical studies of surface reactions on metals and electronic materials | DE93-009761 | p 2650 N93-25502
A numerical simulation of adsorption onto a crystalline surface | AD-A261079 | p 2866 N93-25781
Activation of methane by clean and chemically modified single crystal oxide surfaces | PB93-157295 | p 2644 N93-25817
Dynamics of gas-surface interactions | AD-A261402 | p 2646 N93-26402
SURFACE ROUGHNESS
Uniform roughness studies | WL-TR-92-3041 | p 2706 N93-25951
Isolation and analysis of key components of seafloor relief | AD-A261635 | p 2790 N93-26170
Interface engineering in oxide fiber/oxide matrix composites | AD-A261705 | p 2641 N93-26579
SURFACE TEMPERATURE
Winter warming from large volcanic eruptions | NASA-CR-192848 | p 2763 N93-25244
Errors caused by incompatible wind and buoyancy forcing in the ocean general circulation models | AD-A260894 | p 2789 N93-25657
Land surface processes and climate modeling p 2783 N93-25685
Neural networks for atmospheric retrievals p 2824 N93-25975
Effects of surface thermal forcing on stratified flow past an isolated obstacle | PB93-156776 | p 2776 N93-26548
SURFACE WAVES
The instability of a liquid jet in a compressible airstream p 2703 N93-25560
SURFACTANTS
Structure of sodium 4-(1'-heptylnonyl) benzenesulfonate adsorbed on alumina using H-2 NMR | AD-A261224 | p 2645 N93-26300
SURGES
A system to measure lightning-induced transients on spacecraft umbilical lines p 2693 N93-24889
Applications of stress envelope concepts to aircraft EMP and lightning survivability p 2584 N93-24898
Active stabilization of aeromechanical systems | AD-A261366 | p 2595 N93-26335
SURVEILLANCE
Rome Laboratory Journal, 1992 | AD-A260821 | p 2911 N93-25910
Algorithms for space-based infrared surveillance | AD-A261891 | p 2857 N93-26542
SURVEILLANCE RADAR
The ATC evaluation of the prototype Airport Surveillance Radar Wind Shear Processor (ASR-WSP) at Orlando International Airport | DOT/FAA/CT-TN92/48 | p 2673 N93-25210
SURVEYS
The JGOFS North Atlantic Bloom Experiment: An overview p 2735 N93-24934
Data management for JGOFS: Theory and design p 2735 N93-24935
The continuous plankton recorder survey: A long-term, basin-scale oceanic time series p 2736 N93-24937
Experimental modal survey of the probe mass mock-up | DE93-008846 | p 2617 N93-25494
Assessing patterns of change in anthropometric dimensions: Secular trends of US Army females, 1946-1988 | AD-A260869 | p 2800 N93-25628
Aircraft electrical and environmental systems, AFSCs 452x5, 454x5, and 454x6 | AD-A261213 | p 2590 N93-25733
Design Knowledge Management System (DKMS) Beta Test Report | AD-A261453 | p 2883 N93-26350
SWEDEN
Space research in Sweden, 1990-1991 p 2888 N93-25887
SWELLING
Temperature dependent sensor response caused by polymer-solvent interactions | DE93-005368 | p 2655 N93-25444
SWEPT WINGS
Stationary crossflow instability on an infinite swept wing p 2580 N93-25865
Conical Euler analysis and active roll suppression for unsteady vortical flows about rolling delta wings | NASA-TP-3259 | p 2581 N93-26134
Supersonic aeroelastic instability results for a NASP-like wing model | NASA-TM-107739 | p 2591 N93-26553
SWIRLING
Fuel Injector: Air swirl characterization aerothermal modeling, phase 2, volume 2 | NASA-CR-189193 | p 2592 N93-25106
SWITCHES
Radiation and temperature effects on electronic components investigated under the CSTI high capacity power project | NASA-TM-106096 | p 2687 N93-24746
Modeling of plasma flow switches at low, intermediate and high energies | DE93-007359 | p 2858 N93-25167
SYMBOLIC PROGRAMMING
Analysis of symbolic parameter models | AD-A261930 | p 2811 N93-26253
SYMBOLS
Symbol signal-to-noise ratio loss in square-wave subcarrier downconversion p 2672 N93-24668
Information transmission using CHAOS | AD-A261519 | p 2883 N93-26377

SYMMETRY
Hypervelocity impact study: The effect of impact angle on crater morphology
| NASA-CR-192711 | p 2724 N93-25260
New ground states in unconventional superconductors p 2688 N93-25282

SYNCHRONISM
Analysis of the effects of mean local node-crossing time on the evolution of Sun-synchronous orbits p 2602 N93-24706
Frequency and Time Forum
| ESA-SP-340 | p 2831 N93-24978
A new modem for microwave time synchronisation via geosynchronous telecommunication satellites p 2686 N93-24999
Synchronisation, acquisition and tracking for telemetry and data reception p 2614 N93-25000
A microcomputer compensated crystal oscillator MCXO p 2834 N93-25001
A system design for laser time synchronization via geodetic satellite Ajisai p 2716 N93-25005
Mixed constellation synchronization of GPS time p 2836 N93-25015
Time and frequency reference for a trajectory measurement system p 2837 N93-25023
Time generation and distribution system for a military national synchronization p 2842 N93-25060
Timing a national telecommunications network using GPS p 2687 N93-25062
Strategies for synchronisation in an evolving telecommunications network p 2687 N93-25063
Supercomputer Debugging Workshop 1992
| DE93-007322 | p 2805 N93-25165
A software development approach for parallel processing systems integrating object-oriented and functional paradigms p 2816 N93-25481
Virtually-synchronous communication based on a weak failure suspector
| NASA-CR-193003 | p 2721 N93-26135
Fast mutual exclusion for uniprocessors
| AD-A261663 | p 2883 N93-26389

SYNCHRONOUS SATELLITES
Analysis of the effects of mean local node-crossing time on the evolution of Sun-synchronous orbits p 2602 N93-24706
A ground track control algorithm for the Topographic Mapping Laser Altimeter (TMLA) p 2602 N93-24707
SCATHA mission termination report p 2605 N93-24725
Satellite communications application to Pacific countries above Ku band p 2683 N93-26471

SYNCHROTRON RADIATION
Synchrotron radiation X ray topography study of lateral field resonators p 2833 N93-24994
Poster session: Fifth Users Meeting for the Advanced Photon Source
| DE93-006019 | p 2598 N93-26498

SYNCHROTRONS
Preliminary design of the BPM electronics memory scanner/dual boxcar averager for the advanced photon source
| DE93-007893 | p 2848 N93-25368

SYNOPTIC METEOROLOGY
Synoptic and Mesoscale Meteorology Instruction Workshop
| PB93-156347 | p 2785 N93-25870
Rainfall frequency atlas of the Midwest
| PB93-164606 | p 2785 N93-25872

SYNTHESIS (CHEMISTRY)
Design of a high activity and selectivity alcohol catalyst
| DE93-008101 | p 2659 N93-25111
A novel process for methanol synthesis
| DE93-008037 | p 2659 N93-25118
Probe molecule studies: Active species in alcohol synthesis
| DE93-008097 | p 2659 N93-25119
New directions in phthalocyanine pigments
| NASA-CR-192443 | p 2656 N93-26155
Characterization of the synthesis of M-61, a random equilibrium silicone terpolymer, using dry starting materials
| KCP-613-4985 | p 2657 N93-26213
Electrochemical and spectroscopic studies of molten halides
| AD-A261687 | p 2646 N93-26439

SYNTHESIZERS
Design, fabrication, and testing of a three-dimensional acoustic orientation instrument (3-D AOI): Drawings, engineering and associated lists (conceptual and development design)
| AD-A260934 | p 2845 N93-25915
Step stress testing of receiver/transmitter units
| AD-A261286 | p 2730 N93-26279

SYNTHETIC APERTURE RADAR
The use of polarimetric multifrequency SAR for characterizing terrain classes p 2738 N93-24777
The scope of DLR's SAR calibration program p 2738 N93-24778
Registration of the use of agricultural fields and soil erosion using satellite remote sensing p 2751 N93-24856
Methods of evaluating the effects of coding on SAR data p 2804 N93-25926
SAR-related stress variability in the marine atmospheric boundary layer
| AD-A261129 | p 2775 N93-25946
DSN acquisition of Magellan high-rate telemetry data p 2614 N93-26124

SYNTHETIC RESINS
Extruded films from modified polypropylene resin: Dielectric and breakdown studies
| AD-A261382 | p 2657 N93-26341

SYSTEM EFFECTIVENESS
Analysis of large system black box verification test data
| NASA-CR-192885 | p 2815 N93-24748
Firmware development improves system efficiency p 2807 N93-25606

SYSTEM FAILURES
Expert system for UNIX system reliability and availability enhancement p 2723 N93-25588

SYSTEM IDENTIFICATION
The 32nd CDC: System identification using interval dynamic models
| NASA-CR-192895 | p 2818 N93-25155
Robust nonlinear control of vectored thrust aircraft
| NASA-CR-192727 | p 2596 N93-25199
ASTROS-ID: Software for system identification using mathematical programming
| AD-A260867 | p 2810 N93-25627
Exploitation of cyclostationarity for signal-parameter estimation and system identification
| AD-A260833 | p 2728 N93-25784

SYSTEMS ANALYSIS
Parametric analysis of atmospheric processes
| NASA-CR-192523 | p 2770 N93-25086
Space transfer vehicle concepts and requirements study. Volume 2, book 3: STV system interfaces
| NASA-CR-192527 | p 2611 N93-25513
A digital hardware test system analysis with test vector translation
| AD-A260849 | p 2810 N93-25786
System Concept of Operations Evaluator (SCOPE)
| AD-A261257 | p 2813 N93-26563
A hypertext framework for group support systems
| AD-A261731 | p 2885 N93-26582

SYSTEMS ENGINEERING
Readings in Systems Engineering
| NASA-SP-6102 | p 2665 N93-24678
The systems engineering overview and process (from the Systems Engineering Management Guide, 1990) p 2665 N93-24679
Systems engineering for very large systems p 2665 N93-24680
What is a system? NASA's phased project description p 2665 N93-24681
Management issues in systems engineering p 2665 N93-24682
Spacecraft systems engineering: An introduction to the process at GSFC p 2665 N93-24683
Systems engineering and integration and management for manned space flight programs p 2666 N93-24684
The SE role in establishing, verifying and controlling top-level program requirements p 2666 N93-24685
The importance of cost considerations in the systems engineering process p 2666 N93-24686
Systems engineering and the user: Incorporation of user requirements into the SE process p 2666 N93-24687
Systems engineering and integration processes involved with manned mission operations p 2666 N93-24688
Systems engineering considerations for operational support systems p 2666 N93-24689
Political and institutional factors affecting systems engineering p 2666 N93-24690
Optimization in the systems engineering process p 2666 N93-24691
A system design for laser time synchronization via geodetic satellite Ajisai p 2716 N93-25005
Ultra stable oscillators for satellite applications p 2621 N93-25027
First experience with the ASN-16 GLONASS receiver p 2693 N93-25033
Time generation and distribution system for a military national synchronization p 2842 N93-25060
Integrated Development Support Environment (IDSE)
| AD-A261088 | p 2877 N93-25763
Architecture of autonomous systems
| NASA-CR-192974 | p 2801 N93-26047
Advanced Launch System (ALS) test requirements
| MCR-91-5004 | p 2610 N93-26181
Develop margin philosophy to attain robustness
| MCR-92-5005 | p 2610 N93-26182
Advanced technology for portable personal visualization
| AD-A261294 | p 2807 N93-26293
Multivariable control for flexible IC processing
| AD-A261685 | p 2692 N93-26366
Proceedings of the complex systems engineering synthesis and assessment technology workshop
| AD-A261404 | p 2807 N93-26403
Systems engineering studies of on-orbit assembly operations p 2669 N93-26410
CALS-HSC data element dictionary
| AD-A261560 | p 2813 N93-26461
System Concept of Operations Evaluator (SCOPE)
| AD-A261257 | p 2813 N93-26563
Task Type E report for National Launch Demonstration Center (NLDC) (Task 32)
| MCR-91-5010 | p 2610 N93-26591

SYSTEMS INTEGRATION
Land cover, an essential component of the CORINE information system on the environment: GIS implications p 2740 N93-24787
A knowledge-based approach to waste disposal sites detection through integration of Landsat-TM imagery and geographical context information p 2741 N93-24796
Cartography and statistics of crops under irrigation in the Donana area of Andalucia through the use of Landsat-TM imagery and its incorporation into a GIS p 2751 N93-24855
Runway Visual Range (RVR) Operational Test and Evaluation (OT&E) integration and OT&E operational test report
| DOT/FAA/CT-TN93/37 | p 2584 N93-25243
Piloted simulation of an air-ground profile negotiation process in a time-based Air Traffic Control environment
| NASA-TM-107748 | p 2585 N93-26087
Bibliography on propulsion airframe integration technologies for high-speed civil transport applications, 1980-1991
| NASA-TM-105602 | p 2573 N93-26136
Methodology investigation: Global Positioning System integration (GPS)
| AD-A261054 | p 2586 N93-26237
CALS-HSC data element dictionary
| AD-A261560 | p 2813 N93-26461
Improved selective catalytic NOx control technology for compressor station reciprocating engines
| PB93-158566 | p 2768 N93-26529

SYSTEMS MANAGEMENT
Management issues in systems engineering p 2665 N93-24682
Spacecraft systems engineering: An introduction to the process at GSFC p 2665 N93-24683
Systems engineering and integration and management for manned space flight programs p 2666 N93-24684
The SE role in establishing, verifying and controlling top-level program requirements p 2666 N93-24685
Systems engineering and the user: Incorporation of user requirements into the SE process p 2666 N93-24687
Political and institutional factors affecting systems engineering p 2666 N93-24690
Optimization in the systems engineering process p 2666 N93-24691
System of Experts for Intelligent Data Management (SEIDAM) p 2879 N93-25800
Intelligent access to multiple relational database systems
| AD-A261198 | p 2881 N93-25824
Fast mutual exclusion for uniprocessors
| AD-A261663 | p 2883 N93-26389
Test, Control and Monitor System maintenance plan
| NASA-CR-193099 | p 2873 N93-26420

SYSTOLIC ARRAYS
Very high-speed arithmetic processors (The Gauss Machine)
| AD-A260693 | p 2806 N93-25650

T

T TAURI STARS
Structure and star forming activities of the cold massive molecular cloud G216-2.5 p 2893 N93-25477
Photospheric abundance analysis of low-mass pre-main sequence stars p 2894 N93-25623

TACTILE SENSORS (ROBOTICS)
Modeling of a full vision system using combined Visual/Haptic search for remote object identification
| AD-A260977 | p 2801 N93-25867

TAIWAN
Effects of Taiwan orography on the motion and structure of typhoons
| AD-A261819 | p 2786 N93-26270

TALC
Chromate-free corrosion resistant talc coatings for aluminum alloys
| DE93-005370 | p 2655 N93-25446
TANKS (COMBAT VEHICLES)
Elastomer compound developed for high wear applications p 2659 N93-25607
A Hierarchical Target Extraction, Recognition, and Tracking (HiTert) system
| AD-A260567 | p 2854 N93-25898
TARGET ACQUISITION
Algorithms for space-based infrared surveillance
| AD-A261891 | p 2857 N93-26542
TARGET RECOGNITION
Efficient generation of synthetic terrain imagery for automatic target recognition
| AD-A260705 | p 2756 N93-25653
A Hierarchical Target Extraction, Recognition, and Tracking (HiTert) system
| AD-A260567 | p 2854 N93-25898
Molecular interactions and properties with many-body methods
| AD-A261688 | p 2850 N93-26367
TARGETS
Sputter deposition of yttrium-oxides
| DE93-007499 | p 2654 N93-25382
TASK COMPLEXITY
Performance-based testing and success in Naval advanced flight training
| AD-A260838 | p 2590 N93-25933
TASKS
Tree classification software p 2814 N93-25591
Conversion of the CTA, Inc., en route operations concepts database into a formal sentence outline job task taxonomy
| AD-A261410 | p 2586 N93-26447
TAURID METEOROIDS
The Taurid meteoroid complex p 2889 N93-25536
TAXONOMY
Biodiversity indication by Earth observation data p 2751 N93-24858
TAYLOR SERIES
Image correlation velocimetry
| AD-A261599 | p 2707 N93-26163
TDR SATELLITES
TDRSS orbit determination using short baseline differenced carrier phase p 2601 N93-24701
Application of GPS tracking techniques to orbit determination for TDRS p 2601 N93-24702
TDRSS-user orbit determination using batch least-squares and sequential methods p 2601 N93-24703
Orbit determination support of the Ocean Topography Experiment (TOPEX)/Poseidon operational orbit p 2601 N93-24704
Orbit determination and orbit control for the Earth Observing System (EOS) AM spacecraft p 2601 N93-24705
A low-complexity and high performance concatenated coding scheme for high-speed satellite communications
| NASA-CR-192715 | p 2673 N93-25198
A prototype for simulation of the space-to-ground assembly/contingency system of Space Station Freedom p 2619 N93-26065
TECHNOLOGICAL FORECASTING
Using AI/expert system technology to automate planning and replanning for the HST servicing missions p 2822 N93-25962
TECHNOLOGIES
JPRS report: Science and technology. Central Eurasia: Life sciences
| JPRS-ULS-93-002 | p 2737 N93-25399
JPRS report: Science and technology. Central Eurasia: Earth sciences
| JPRS-UES-93-001 | p 2599 N93-25400
JPRS report: Science and technology. Central Eurasia: Earth sciences
| JPRS-UES-92-005 | p 2737 N93-25401
JPRS report: Science and technology. Central Eurasia: Physics and mathematics
| JPRS-UPM-92-004 | p 2844 N93-25402
JPRS report: Science and technology. Central Eurasia: Physics and mathematics
| JPRS-UPM-92-003 | p 2844 N93-25403
JPRS report: Science and technology. Central Eurasia: Physics and mathematics
| JPRS-UPM-93-001 | p 2844 N93-25404
JPRS report: Science and technology. Central Eurasia: Life sciences
| JPRS-ULS-92-025 | p 2793 N93-25405
JPRS report: Science and technology. Central Eurasia: Life sciences
| JPRS-ULS-92-020 | p 2793 N93-25406
JPRS report: Science and technology. Central Eurasia: Life sciences
| JPRS-ULS-92-022 | p 2795 N93-25407
JPRS report: Science and technology. Central Eurasia: Engineering and equipment
| JPRS-UEQ-92-003 | p 2668 N93-25427
Science, Technology, and Industrial Policy in the Former Soviet Union
| DE93-006528 | p 2887 N93-26499
TECHNOLOGY ASSESSMENT
An assessment of alternatives and technologies for replacing ozone-depleting substances at DOE facilities
| DE93-002862 | p 2760 N93-24675
Systems engineering for very large systems p 2665 N93-24680
Optimization of knowledge-based systems and expert system building tools
| NASA-CR-192763 | p 2874 N93-25288
Gas-Grain Simulation Facility (GGSF). Volume 1: Stage 1 facility definition studies
| NASA-CR-177606 | p 2887 N93-25442
Space transfer vehicle concepts and requirements study. Volume 2, book 4: Integrated advanced technology development
| NASA-CR-192528 | p 2611 N93-25512
Small satellites and RPA's in global-change research
| AD-A260762 | p 2765 N93-25837
Special technology area review on microwave packaging technology
| AD-A261852 | p 2681 N93-26276
Observations on the NASA Propagation Program p 2685 N93-26482
A comparative assessment of R. M. Young and tipping bucket rain gauges p 2685 N93-26483
Japanese Technology Evaluation Center Workshop on Advanced Manufacturing Technology for Polymer Composite Structures in Japan
| PB93-165249 | p 2641 N93-26589
TECHNOLOGY TRANSFER
EXCHANGE
| DE93-007227 | p 2808 N93-24962
Technology Transfer 92/93
| DE93-003623 | p 2887 N93-24965
Energy and Technology Review, August-September 1992
| DE93-005882 | p 2901 N93-24974
The evaluation of technical models used for major-accident hazard installations. Report to Commission of the European Communities Directorate General 12
| CUED/A-AERO/TR-19 | p 2668 N93-25238
Energy and Technology Review, October - December 1992
| DE93-007784 | p 2674 N93-25299
The PACSAT Communications Experiment (PCE)
| DE93-008185 | p 2674 N93-25308
Technology 2002: The Third National Technology Transfer Conference and Exposition, volume 1
| NASA-CP-3189-VOL-1 | p 2901 N93-25561
Film fabrication technologies at NREL p 2658 N93-25563
Technology for America's economic growth: A new direction to build economic strength
| AD-A261553 | p 2887 N93-26458
TECHNOLOGY UTILIZATION
Performance results of a 300-degree linear phase modulator for spaceborne communications applications p 2672 N93-24670
Natural disasters and their mitigation using space technology p 2742 N93-24804
Technology Transfer 92/93
| DE93-003623 | p 2887 N93-24965
The development progresses of hydrogen masers at Shanghai Observatory p 2716 N93-25048
JPRS report: Science and technology. Central Eurasia: Earth sciences
| JPRS-UES-92-003 | p 2737 N93-25398
JPRS report: Science and technology. Central Eurasia: Earth sciences
| JPRS-UES-92-002 | p 2737 N93-25426
The 1993 Goddard Conference on Space Applications of Artificial Intelligence
| NASA-CP-3200 | p 2822 N93-25961
High performance computing and communications panel report p 2807 N93-26131
Technology for America's economic growth: A new direction to build economic strength
| AD-A261553 | p 2887 N93-26458
TECTONICS
Earthquake vulnerability map of the Lake Constance area p 2753 N93-24872
Geologic structure and processes of the eastern Pacific margin: California and Costa Rica p 2771 N93-25424
Crustal deformation studies in subaerial parts of the world oceanic rift system: Iceland and Afar p 2789 N93-25558
TELECOMMUNICATION
The Telecommunications and Data Acquisition Report
| NASA-CR-192887 | p 2671 N93-24659
Synopsis of timing measurement techniques used in telecommunications p 2687 N93-25064
Rome Laboratory Journal, 1992
| AD-A260821 | p 2911 N93-25910
Anomalous event diagnosis for environmental satellite systems p 2619 N93-25971
The Telecommunications and Data Acquisition Report
| NASA-CR-192804 | p 2676 N93-26105
Advanced optical fiber communication systems
| AD-A261802 | p 2856 N93-26256
A channel simulation processor for the multi-node tactical network simulator
| AD-A261810 | p 2776 N93-26430
TELECONFERENCING
Gigabit network communications research
| AD-A260644 | p 2675 N93-25640
TELEMETRY
A functional description of the Buffered Telemetry Demodulator (BTD) p 2614 N93-24667
Resolution of the COBE Earth sensor anomaly p 2600 N93-24700
Solar array thermal snap and the characteristics of its effect on UARS p 2607 N93-24734
Synchronisation, acquisition and tracking for telemetry and data reception p 2614 N93-25000
An advanced data-acquisition system for wind energy projects
| DE93-000079 | p 2874 N93-25254
The Generic Spacecraft Analyst Assistant (GenSAA): A tool for developing graphical expert systems p 2814 N93-25589
Exploitation of cyclostationarity for signal-parameter estimation and system identification
| AD-A260833 | p 2728 N93-25784
DSN acquisition of Magellan high-rate telemetry data p 2614 N93-26124
Galileo early cruise, including Venus, First Earth, and Gaspra encounters p 2599 N93-26125
TELEOPERATORS
Telerobotic rovers for extraterrestrial construction p 2670 N93-26416
TELEROBOTICS
Modeling of a full vision system using combined Visual/Haptic search for remote object identification
| AD-A260977 | p 2801 N93-25867
Telerobotic rovers for extraterrestrial construction p 2670 N93-26416
TELESCOPES
Testing of the on-board attitude determination and control algorithms for SAMPEX p 2600 N93-24698
Miniature Optical Wide-Angle-Lens Startracker (Mini-OWLS) p 2606 N93-24728
Development of laser guide stars and adaptive optics for large astronomical telescopes
| DE93-007511 | p 2888 N93-25320
Development of a tool-set for simultaneous, multi-site observations of astronomical objects p 2878 N93-25795
Feasibility experiment for sodium-layer laser guide stars at the Lawrence Livermore National Laboratory
| DE93-007115 | p 2715 N93-26503
TELEVISION RECEPTION
An example of a phase-segregated enhanced PAL broadcasting system
| BBC-RD-1992/6 | p 2674 N93-25239
TELEVISION SYSTEMS
Experiments with the HIVITS HDTV contribution CODED
| BBC-RD-1992/12 | p 2674 N93-25391
Adaptive liquid crystal TV based joint transform correlator as applied to real-time pattern recognition
| AD-A260724 | p 2864 N93-25655
Emerging large-screen display technology
| AD-A261066 | p 2681 N93-26241
TELEVISION TRANSMISSION
Use of the TV-signal in stabilizing a local rubidium oscillator p 2693 N93-25029
An example of a phase-segregated enhanced PAL broadcasting system
| BBC-RD-1992/6 | p 2674 N93-25239
Experiments with the HIVITS HDTV contribution CODED
| BBC-RD-1992/12 | p 2674 N93-25391
TEMPERATE REGIONS
An analysis of mesoscale convective systems observed during the 1992 Tropical Cyclone Motion field experiment
| AD-A260889 | p 2783 N93-25633
TEMPERATURE COMPENSATION
A microcomputer compensated crystal oscillator MCXO p 2834 N93-25001
OSCCAR: Oscillator-compensated with a capacitance array p 2693 N93-25002
Noise-optimal control of HEMT LNA's for compensation of temperature deviations p 2678 N93-26115

TEMPERATURE CONTROL
Control of environmental and clock parameters in Time and Frequency Standards Laboratory p 2835 N93-25007
Study of plate-fin heat exchanger and cold plate for the active thermal control system of Space Station p 2619 N93-26064
The reuse of logistics carriers for the first lunar outpost alternative habitat study p 2671 N93-26083
Improvements in X-band transmitter phase stability through Klystron body temperature regulation p 2678 N93-26114
Plasma current collection of Z-93 thermal control paint as measured in the Lewis Research Center's plasma interaction facility
| NASA-TM-106132 | p 2618 N93-26215
Multivariable control for flexible IC processing
| AD-A261685 | p 2692 N93-26366

TEMPERATURE DEPENDENCE
Temperature-dependent electrical conductivity of soda-lime glass
| DE93-007872 | p 2654 N93-25359
Temperature dependent sensor response caused by polymer-solvent interactions
| DE93-005368 | p 2655 N93-25444
Temperature dependence of radiation damage and its annealing in silicon detectors
| DE93-003854 | p 2869 N93-26494

TEMPERATURE DISTRIBUTION
Indian Ocean analyses p 2733 N93-24925
The effects of large-amplitude, low-frequency excitation on a three-dimensional jet p 2702 N93-25553
Errors caused by incompatible wind and buoyancy forcing in the ocean general circulation models
| AD-A260894 | p 2789 N93-25657
Thermoelastic stresses in multi-layered media in non-uniform temperature fields
| AD-A260901 | p 2727 N93-25658
A new LU-SGS flow solver for calculating reentry flows p 2579 N93-25759

TEMPERATURE EFFECTS
Radiation and temperature effects on electronic components investigated under the CSTI high capacity power project
| NASA-TM-106096 | p 2687 N93-24746
Atomizing-gas temperature effect on cryogenic spray dropsize
| NASA-TM-106106 | p 2709 N93-25191
FNAS computational modeling
| NASA-CR-192512 | p 2863 N93-25225
Integration of design, thermal, structural, and optical analysis, including thermal animation p 2814 N93-25601
Active control of NITINOL-reinforced structural composites
| AD-A261062 | p 2638 N93-25780
Deformations of active flexible rods with embedded line actuators
| AD-A261207 | p 2729 N93-25950
Thermal radiation in non-metalized solid rocket motors: Effect on burning rate and temperature sensitivity p 2626 N93-26020
Deformation mechanisms of NiAl cyclicly deformed near the brittle-to-ductile transition temperature
| NASA-CR-191121 | p 2652 N93-26235
Thermally induced stresses in a composite exposed to fire
| AD-A261714 | p 2641 N93-26371

TEMPERATURE GRADIENTS
Crystal growth and physical characterizations of GaPO4 p 2840 N93-25044

TEMPERATURE MEASUREMENT
Thermoelasticity in quartz p 2841 N93-25047
Measurements of density, temperature, and their fluctuations in turbulent supersonic flow using UV laser spectroscopy
| NASA-TM-103943 | p 2708 N93-25076
Fibre optic sensors for heat transfer studies p 2853 N93-25748
Flame structure studies of a lean, 20 torr H2/N2O/AR flame employing molecular beam mass spectrometry p 2627 N93-26025
An experimental and analytical study of the unsteady combustion of homogeneous energetic solids using the laser-recoil method p 2630 N93-26042
Research support for the Laboratory for Lightwave Technology
| AD-A261488 | p 2856 N93-26343

TEMPERATURE PROFILES
The effects of large-amplitude, low-frequency excitation on a three-dimensional jet p 2702 N93-25553

TEMPERATURE RATIO
Optimizing the G/T ratio of the DSS-13 34-meter beam-waveguide antenna p 2678 N93-26118

TEMPERATURE SENSORS
SiC microsensor with piezoresistive diamond sensing elements
| AD-A261346 | p 2868 N93-26312

TEMPLATES
Template synthesis of electronically conductive polymers: A new route for achieving higher electronic conductivities
| AD-A261616 | p 2658 N93-26437

TEMPORAL DISTRIBUTION
The advances in F and T technology: Their benefits of and for space science and technology p 2831 N93-24979
Time generation and distribution system for a military national synchronization p 2842 N93-25060

TEMPORAL RESOLUTION
Correlation between NDVI values derived from NOAA AVHRR HRPT data and ground measurements of precipitation in the EFEDA study area (Spain) p 2738 N93-24780
Monitoring and analysis of urban trends using multitemporal satellite-imagery (case-study: Greater Cairo) p 2740 N93-24790
Geologic and hydrogeologic mapping of Iceland with multisensor data (JERS-1, ERS-1, SPOT, Landsat and SEASAT) p 2740 N93-24792
Application of multitemporal Landsat-MSS and -TM data for the development of an inundation-risk-map p 2743 N93-24807
European applications of space-borne Earth observation for land cover mapping p 2745 N93-24820
Atmospheric correction of Landsat/TM data over mountainous terrain for forestry applications p 2752 N93-24862
The sub 60 ps timing resolution using large area silicon avalanche diodes
| DE93-007723 | p 2688 N93-25365
High speed x ray gating cameras for ICF imaging applications
| DE93-007500 | p 2709 N93-25515

TENSILE PROPERTIES
Development of dispersion-strengthened XD (trademark) Cu alloys for high heat-flux applications
| NASA-CR-191124 | p 2653 N93-24761
Mechanical properties of martensitic alloy AISI 422
| DE93-006563 | p 2649 N93-25255
Processing and mechanical properties of laminated metal composites of Al/Al-25 vol. percent SiC and ultrahigh carbon steel/brass
| DE93-007504 | p 2635 N93-25383

TENSILE STRENGTH
High strain rate damage development and failure mechanisms in tungsten heavy alloys
| AD-A260856 | p 2651 N93-25788
Interface engineering in oxide fiber/oxide matrix composites
| AD-A261705 | p 2641 N93-26579

TENSILE TESTS
Stress distribution in composite flatwise tension test specimens
| NASA-TM-106074 | p 2634 N93-25071
Room temperature fracture of FeCo
| DE93-008266 | p 2650 N93-25519

TENSION
Effect of cytoskeletal reagents on stretch activated ion channels
| AD-A261089 | p 2793 N93-25764

TERMINAL BALLISTICS
Investigation and modeling of penetration process for composite laminates impacted by a blunt-ended projectile p 2637 N93-25675

TERMINAL GUIDANCE
Two neural network algorithms for designing optimal terminal controllers with open final time
| NASA-CR-177599 | p 2817 N93-25137

TERMINOLOGY
Agreement in naming objects and concepts for information retrieval p 2881 N93-25826

TERMS
Glossary of environmental terms and acronym list
| PB93-158004 | p 2765 N93-25851

TERNARY ALLOYS
Metal alloy and method of preparation thereof
| AD-D015670 | p 2652 N93-26234

TERRAIN
Use of the 1991 ASCOT field study data in a mesoscale model employing a four-dimensional data assimilation technique
| DE93-002683 | p 2769 N93-24672
ILS mathematical modeling study of an ILS glide slope proposed for runway 19L at the Meridian Naval Air Station, Mississippi
| DOT/FAA/CT-TN93/8 | p 2584 N93-24741
Use of airborne imaging spectrometry to the definition of optimised specifications for land applications with future spaceborne imaging spectrometers p 2738 N93-24776
The use of polarimetric multifrequency SAR for characterizing terrain classes p 2738 N93-24777
Study of atmospheric electrical events above complex terrain p 2780 N93-24897
Use of the Environmental Resource Management and Analysis System at the Fernald Environmental Management Project
| DE93-002943 | p 2760 N93-24955
Efficient generation of synthetic terrain imagery for automatic target recognition
| AD-A260705 | p 2756 N93-25653
Pressure torques and circulation changes in Rocky Mountain lee cyclones p 2783 N93-25724
Effects of Taiwan orography on the motion and structure of typhoons
| AD-A261819 | p 2786 N93-26270

TERRAIN ANALYSIS
Land cover, an essential component of the CORINE information system on the environment: GIS implications p 2740 N93-24787
The regional planning and control using the satellite data p 2740 N93-24788
Land cover monitoring in the Netherlands applying satellite remote sensing p 2740 N93-24789
Detection of land use/land cover changes using remote sensing and GIS in Vietnam p 2740 N93-24791
Complex investigation of a system industrial site-environment using remote sensing and landscape-geochemical methods p 2741 N93-24798
Swedish forest information atlas p 2749 N93-24847
Observation of forest damages in the Harz mountains by means of satellite remote sensing p 2749 N93-24848

TEST CHAMBERS
Ice thickness measurement system for the icing research tunnel calibration
| NASA-TM-106095 | p 2708 N93-24737
A feasibility study of using Langley 0.3-m transonic cryogenic tunnel sidewall boundary-layer removal system for heavy gas testing
| NASA-CR-191438 | p 2695 N93-25087
Hazards of explosives dusts: Particle size effects
| DE93-009380 | p 2668 N93-25498
Behavior of a steel-liner-and-bolts system under very high thermal and mechanical loading: The CONVEX Liner Add-On to DIAMOND FORTUNE
| DE93-007512 | p 2731 N93-26507

TEST EQUIPMENT
Commercial Precipitation Static (P-static) test equipment p 2711 N93-24901
Evaluation of a vibration diagnostic system for the detection of spur gear pitting failures
| NASA-TM-106103 | p 2718 N93-25672

TEST FACILITIES
Nuclear thermal propulsion technology: Results of an interagency panel in FY 1991
| NASA-TM-105711 | p 2621 N93-24740
Space exploration initiative candidate nuclear propulsion test facilities
| NASA-TM-105710 | p 2622 N93-24753
Space Nuclear Thermal Propulsion Test Facilities Subpanel
| NASA-TM-105708 | p 2622 N93-25105
Advanced Launch System (ALS) test requirements
| MCR-91-5004 | p 2610 N93-26181
Conceptual design for the Space Station Freedom fluid physics/dynamics facility
| NASA-TM-103663 | p 2618 N93-26209
Duct protection coating concept development and test: Test specimen fabrication, conditioning, and testing documentation.
| AD-A261250 | p 2657 N93-26278

TEST STANDS
A large hemi-anechoic enclosure for community-compatible aeroacoustic testing of aircraft propulsion systems
| NASA-TM-106015 | p 2846 N93-26551

TETHERED SATELLITES
Dynamics and control of maneuverable tethered flight vehicles p 2615 N93-24767
Tethered Satellite System Contingency Investigation Board
| NASA-TM-108704 | p 2616 N93-25231
An alternate approach to space missions involving a long tether p 2616 N93-25470
STS-46 Space Shuttle mission report
| NASA-CR-193058 | p 2613 N93-25991
Data analysis support for the Shuttle Potential and Return Electron Experiment (SPREE) on the Tethered Satellite System 1 (TSS-1) flight
| AD-A261646 | p 2618 N93-26232

TETHERING
Dynamics and control of maneuverable tethered flight vehicles p 2615 N93-24767
Tethered Satellite System Contingency Investigation Board
|NASA-TM-108704| p 2616 N93-25231
An alternate approach to space missions involving a long tether p 2616 N93-25470
TEXTS
Improving information search at the user interface: The impact of graphical innovation on query formulation and expression p 2873 N93-24905
Pyroshock: Bibliography
|DE93-007605| p 2726 N93-25489
Visualizing the semantic content of large text databases using text maps p 2826 N93-25982
THALLIUM COMPOUNDS
Development of high Tc (greater than 100 K) Bi, Tl and Y-based materials as superconducting circuit elements
|NASA-CR-192344| p 2863 N93-25219
THEMATIC MAPPERS (LANDSAT)
Spectral remote sensing of anomalous mineralogy induced by hydrocarbon migration and uranium mineralization, San Rafael Swell, Utah, USA p 2739 N93-24783
Lithologic mapping with LANDSAT Thematic Mapper guided by laboratory spectral measurements, Air, Niger (Africa) p 2742 N93-24803
Application of multitemporal Landsat-MSS and -TM data for the development of an inundation-risk-map p 2743 N93-24807
European applications of space-borne Earth observation for land cover mapping p 2745 N93-24820
Remote sensing of land resource management in agriculture with regard to its influence on the environment p 2750 N93-24850
Biodiversity indication by Earth observation data p 2751 N93-24858
Atmospheric correction of Landsat/TM data over mountainous terrain for forestry applications p 2752 N93-24862
Classifying multispectral data by neural networks p 2825 N93-25976
Bibliography of remote sensing techniques used in wetland research
|AD-A261704| p 2757 N93-26440
THEMATIC MAPPING
Spectral remote sensing of anomalous mineralogy induced by hydrocarbon migration and uranium mineralization, San Rafael Swell, Utah, USA p 2739 N93-24783
Complex investigation of a system industrial site-environment using remote sensing and landscape-geochemical methods p 2741 N93-24798
The use of remote sensing and GIS for the assessment of environmental degradation caused by fires, applied upon South-Euboia (central Greece) p 2742 N93-24802
Remote sensing of coastal zone Sabkha deposits, Gulf of Sirt, Libya p 2746 N93-24827
Inherent optical properties of lakes as measured by Landsat 5 Thematic Mapper p 2746 N93-24828
Multi-date algorithms for predicting surface water quality parameters in estuarine and coastal waters using Landsat TM data
|ED-659-CP| p 2746 N93-24829
Evaluation of nearshore suspended sediment concentration through Landsat TM data: First results p 2747 N93-24833
Monitoring and evaluation of morphohydrographical changes in the Danube Delta by remote-sensing p 2747 N93-24834
Coastal environmental mapping using Landsat data
|ED-658-CP| p 2747 N93-24835
The national parks of Bavarian Forest and Sumava: A Landsat TM perspective on the structure and dynamics of the largest woodland of Central Europe p 2748 N93-24837
Mapping of windfall damage in the Hunsrueck plateau with Landsat TM-data p 2749 N93-24843
Forest decline monitoring using Landsat TM, digital stand data and DEMs p 2749 N93-24846
Swedish forest information atlas p 2749 N93-24847
Observation of forest damages in the Harz mountains by means of satellite remote sensing p 2749 N93-24848
Toward a satellite based crop information system in Hungary p 2750 N93-24849
EUROSTARS: A system for thematic analysis of remote sensed data p 2753 N93-24871
Integrating satellite imagery and digital elevation data for geobotanical mapping in Quetico Provincial Park, Ontario, Canada p 2754 N93-25430
THEOREM PROVING
Use of fuzzy relational information retrieval technique for generating control strategies in resolution-based automated reasoning p 2874 N93-25258
THEOREMS
Monte Carlo approach to the approximation of invariant measures
|PB93-159069| p 2830 N93-26317
THEORETICAL PHYSICS
Topics in CP violation
|DE93-007615| p 2847 N93-25323
JPRS report: Science and technology. Central Eurasia: Physics and mathematics
|JPRS-UPM-92-004| p 2844 N93-25402
JPRS report: Science and technology. Central Eurasia: Physics and mathematics
|JPRS-UPM-92-003| p 2844 N93-25403
JPRS report: Science and technology. Central Eurasia: Physics and mathematics
|JPRS-UPM-93-001| p 2844 N93-25404
From fractals to wormholes via string theory p 2871 N93-25742
THERAPY
Automatic detection of seizures with applications p 2796 N93-25592
THERMAL ANALYSIS
A heat transfer analysis of a mobile vehicle radiation-shielded operator compartment
|DE93-007428| p 2800 N93-25318
The nature of the glass transition and its determination by thermal analysis
|DE93-006746| p 2654 N93-25374
Integration of design, thermal, structural, and optical analysis, including thermal animation p 2814 N93-25601
SRB environment evaluation and analysis. Volume 1: Redesigned SRB flight heating evaluation
|NASA-CR-192517| p 2631 N93-26053
Remtech SSME nozzle design TPS
|NASA-CR-192516| p 2631 N93-26056
THERMAL CONDUCTIVITY
Design and validation of optimal experiments for estimating thermal properties of composite materials p 2635 N93-25541
Deformation mechanisms of NiAl cyclicly deformed near the brittle-to-ductile transition temperature
|NASA-CR-191121| p 2652 N93-26235
Tables for the thermophysical properties of ethane
|PB93-160786| p 2646 N93-26319
THERMAL CYCLING TESTS
Development of thin film thermocouples on ceramic materials for advanced propulsion system applications
|NASA-TM-106017| p 2709 N93-25173
THERMAL DECOMPOSITION
Determination of the thermal stability of perfluoropolyalkyl ethers by tensimetry
|NASA-TM-106081| p 2654 N93-25093
Thermal decomposition of HMX, mononitroso-RDX, TNCHP and K6 in the liquid phase: Results from simultaneous thermogravimetry modulated beam mass spectrometry measurements p 2628 N93-26033
Development of rate expressions for the thermal decomposition of RDX p 2629 N93-26034
Chemistry during the induction time in heated nitramines p 2629 N93-26035
Thermal decomposition and stabilization of ammonium dinitramide p 2630 N93-26038
Thermal decomposition of energetic materials. 4: Deuterium isotope effects and isotopic scrambling condensed-phased decomposition of 1,3,5-trinitrohexahydro-s-triazine
|AD-A261804| p 2662 N93-26387
THERMAL EMISSION
The effects of cloud inhomogeneities upon radiative fluxes, and the supply of a cloud truth validation dataset
|NASA-CR-191711| p 2787 N93-26492
THERMAL ENERGY
Aquifer thermal energy (heat and chill) storage
|DE93-006446| p 2759 N93-25183
THERMAL EXPANSION
Thermoelasticity in quartz p 2841 N93-25047
Thermoelastic stresses in multi-layered media in non-uniform temperature fields
|AD-A260901| p 2727 N93-25658
Quantifying distributed damage in composites via the thermoelastic effect p 2637 N93-25691
A three-dimensional model for the residual stresses in a unidirectional composite plate p 2728 N93-25825
Characterization of aerospace grade resins and composites through pressurized volumetric dilatometry
|AD-A260794| p 2639 N93-25918
Thermal expansion measurements of polymer matrix composites and syntactics
|MTL-TR-92-27| p 2640 N93-25954
THERMAL FATIGUE
Fatigue in single crystal nickel superalloys
|AD-A261742| p 2652 N93-26282
THERMAL MAPPING
Image analysis by integration of disparate information p 2824 N93-25973
THERMAL PROTECTION
An investigation of the degradation of Fluorinated Ethylene Propylene (FEP) copolymer thermal blanketing materials aboard LDEF in the laboratory
|NASA-CR-192824| p 2653 N93-25078
Remtech SSME nozzle design TPS
|NASA-CR-192516| p 2631 N93-26056
THERMAL RADIATION
Thermal infrared radiation transfer in the planetary boundary layer p 2772 N93-25688
Thermal radiation in non-metalized solid rocket motors: Effect on burning rate and temperature sensitivity p 2626 N93-26020
THERMAL STABILITY
Determination of the thermal stability of perfluoropolyalkyl ethers by tensimetry
|NASA-TM-106081| p 2654 N93-25093
Characterization of ceramic capacitors for high-voltage pulse-discharge applications
|DE93-007601| p 2689 N93-25417
Design and validation of optimal experiments for estimating thermal properties of composite materials p 2635 N93-25541
Mullite whiskers and mullite-whisker felt p 2642 N93-25586
Effect of a metal deactivator fuel additive on fuel deposition in fuel atomizers at high temperature
|AD-A260915| p 2661 N93-25914
Thermal decomposition of HMX, mononitroso-RDX, TNCHP and K6 in the liquid phase: Results from simultaneous thermogravimetry modulated beam mass spectrometry measurements p 2628 N93-26033
Chemistry during the induction time in heated nitramines p 2629 N93-26035
THERMAL STRESSES
Stress and reliability analyses of multilayered composite cylinder under thermal and mechanical loads p 2726 N93-25533
THERMIONIC EMISSION
Photoexcitation of carbon fullerenes
|AD-A260739| p 2849 N93-25644
Time resolved studies of in-well and cross-well carrier transport in MQW semiconductor structures
|AD-A261170| p 2714 N93-25774
THERMIONICS
Thermionic current measurement in quartz p 2840 N93-25045
THERMOCHEMICAL PROPERTIES
Development and application of computational aerothermodynamics flowfield computer codes
|NASA-CR-192940| p 2574 N93-24736
THERMOCHEMISTRY
Development and application of computational aerothermodynamics flowfield computer codes
|NASA-CR-192940| p 2574 N93-24736
THERMOCLINES
Observations of an intrathermocline vortex p 2788 N93-24769
THERMOCOUPLE PYROMETERS
New pyro-optic techniques for imaging of long wavelength IR-Radiation (pyro-optic initiation program)
|AD-A260969| p 2856 N93-26224
THERMOCOUPLES
Development of thin film thermocouples on ceramic materials for advanced propulsion system applications
|NASA-TM-106017| p 2709 N93-25173
Physical and chemical processes governing the CO2 laser-induced deflagration of ammonium dinitramide (ADN) p 2629 N93-26037
THERMODYNAMIC PROPERTIES
Quartz crystal twinning under mechanical stress: Finite element analysis p 2839 N93-25032
Thermodynamic, kinetic, and structural properties of linear polyethylene crystallized from polymer-diluent mixture p 2864 N93-25528
Photoexcitation of carbon fullerenes
|AD-A260739| p 2849 N93-25644
Thermal decomposition and stabilization of ammonium dinitramide p 2630 N93-26038
Application of the Saha equation to high temperature (greater than or equal to) rocket exhaust
|AD-A261648| p 2632 N93-26174
Thermal decomposition of energetic materials. 4: Deuterium isotope effects and isotopic scrambling condensed-phased decomposition of 1,3,5-trinitrohexahydro-s-triazine
|AD-A261804| p 2662 N93-26387
Thermodynamic properties of natural gas mixtures
|PB93-167112| p 2872 N93-26509
Thermodynamic properties of natural gas mixtures
|PB93-156818| p 2872 N93-26558
THERMODYNAMICS
The nature of the glass transition and its determination by thermal analysis
|DE93-006746| p 2654 N93-25374

Measurements and computations of external heat transfer and film cooking in turbines
| RAE-TM-P-1223 | p 2592 N93-25455
Thermomechanical response of shape memory composites
| AD-A260828 | p 2639 N93-25919
Detection of atomic oxygen and hydrogen in solid propellant flames and pyrolysis gases using multiphoton laser-induced fluorescence p 2628 N93-26029

THERMOELASTICITY
Thermoelasticity in quartz p 2841 N93-25047
Thermoelastic stresses in multi-layered media in non-uniform temperature fields
| AD-A260901 | p 2727 N93-25658
Quantifying distributed damage in composites via the thermoelastic effect p 2637 N93-25691
Thermomechanical response of shape memory composites
| AD-A260828 | p 2639 N93-25919

THERMOELECTRICITY
Solid-state isotopic power source for computer memory chips p 2694 N93-25596

THERMOGRAPHY
In-situ ultrasonic C-scanner
| AD-A261113 | p 2638 N93-25768

THERMOGRAVIMETRY
Thermal decomposition of HMX, mononitroso-RDX, TNCHP and K6 in the liquid phase: Results from simultaneous thermogravimetry modulated beam mass spectrometry measurements p 2628 N93-26033

THERMOMECHANICAL TREATMENT
Study of grain refinement in Al alloy 2519 using backscattering orientation-contrast mode in the scanning electron microscope
| AD-A260886 | p 2651 N93-25632

THERMOPHYSICAL PROPERTIES
Tables for the thermophysical properties of ethane
| PB93-160786 | p 2646 N93-26319

THERMOPLASTIC RESINS
Effect of water immersion on fiber/matrix adhesion
| AD-A260704 | p 2636 N93-25652
Inelastic behavior of thermoplastic composites p 2636 N93-25674
Characterization of aerospace grade resins and composites through pressurized volumetric dilatometry
| AD-A260794 | p 2639 N93-25918

THERMOSPHERE
A study of vibrationally excited N2(+) ions in the daytime thermosphere p 2770 N93-25179
The Venus 130-nm dayglow as a diagnostic of thermospheric structure and dynamics p 2896 N93-25285
Polarizing Michelson interferometer for measuring thermospheric winds
| ISBN-0-315-70442-X | p 2784 N93-25731

THICK PLATES
Behavior of a steel-liner-and-bolts system under very high thermal and mechanical loading: The CONVEX Liner Add-On to DIAMOND FORTUNE
| DE93-007512 | p 2731 N93-26507

THICKNESS
Ice thickness measurement system for the icing research tunnel calibration
| NASA-TM-106095 | p 2708 N93-24737

THIN FILMS
Fundamental studies of defect generation in amorphous silicon alloys grown by remote plasma-enhanced chemical-vapor deposition (Remote PECVD)
| DE92-010560 | p 2862 N93-24953
An inverted AlGaAs/GaAs patterned-Ge tunnel junction cascade concentrator solar cell
| DE93-000073 | p 2759 N93-25102
Development of thin film thermocouples on ceramic materials for advanced propulsion system applications
| NASA-TM-106017 | p 2709 N93-25173
Novel approaches to the construction of miniaturized analytical instrumentation
| NASA-CR-191988 | p 2709 N93-25345
Analysis of pull-tests for determining the effects of ion implantation on the adhesion of iron films to sapphire substrates
| DE93-006732 | p 2725 N93-25373
Laser Induced Phonons (LIPs) in MBE grown ZnSe
| RSRE-MEMO-4544 | p 2864 N93-25454
High resolution interface nanochemistry and structure
| DE93-009750 | p 2635 N93-25501
Role of polycrystallinity in CdTe and CuInSe2 photovoltaic cells
| DE93-000045 | p 2759 N93-25504
Fast diagnostics of laser ablation used for pulsed laser deposition
| DE93-005155 | p 2713 N93-25508
Film fabrication technologies at NREL p 2658 N93-25563
Optical and scratch resistant properties of diamondlike carbon films deposited with single and dual ion beams p 2658 N93-25564
A novel method for characterization of superconductors: Physical measurements and modeling of thin films p 2871 N93-25584
Diagnostics of diamond film deposition plasmas
| AD-A260866 | p 2860 N93-25626
Research on lead titanate films for radiation detection
| AD-A261187 | p 2849 N93-25823
Extruded films from modified polypropylene resin: Dielectric and breakdown studies
| AD-A261382 | p 2657 N93-26341
RF vacuum microelectronics
| AD-A261784 | p 2692 N93-26565

THIN PLATES
Electroelastic equations for electroded thin plates subject to large driving voltages
| AD-A261123 | p 2675 N93-25772

THREE BODY PROBLEM
Tsien's method for generating non-Keplerian trajectories. Part 2: The question of thrust to orbit a sphere and the restricted three-body problem p 2603 N93-24718
Optimal transfers between libration-point orbits in the elliptic restricted three-body problem p 2608 N93-25758

THREE DIMENSIONAL FLOW
Implementation of the Turn Function Method in a three-dimensional, parallelized hydrodynamics code
| DE93-003744 | p 2696 N93-25124
Three-dimensional flow in radial turbomachinery and its impact on design
| NASA-CR-192957 | p 2593 N93-25668
Flow and heat transfer experiments in the turbine airfoil/endwall region p 2704 N93-25725

THREE DIMENSIONAL MODELS
Demonstration for novel self-organization theory by three-dimensional magnetohydrodynamic simulation
| NIFS-212 | p 2859 N93-25227
A method for transient, three-dimensional neutron transport calculations
| DE93-007243 | p 2847 N93-25256
Numerical simulation of a shock wave/turbulent boundary layer interaction in a duct p 2699 N93-25342
An alternate approach to space missions involving a long tether p 2616 N93-25470
A three-dimensional model for the residual stresses in a unidirectional composite plate p 2728 N93-25825
ADCIRC: An advanced three-dimensional circulation model for shelves, coasts, and estuaries. Report 1: Theory and methodology of ADCIRC-2DDI and ADCIRC-3DL
| AD-A261608 | p 2790 N93-26164

THREE DIMENSIONAL MOTION
Variational theory of motion of curved, twisted and extensible elastic rods
| AD-A261028 | p 2729 N93-25941

THROATS
Experimentation in the low-density plume of a simulated electrothermal thruster for computer code validation
| NASA-CR-191112 | p 2622 N93-24758

THRUST
Studies of several small seawater MHD thrusters using the high-field solenoid of MIT's Bitter Magnet Laboratory
| AD-A260645 | p 2860 N93-25641

THRUST CHAMBERS
Eulerian-Eulerian treatment of turbulent dense spray combustion in a bipropellant liquid rocket engine p 2626 N93-26017
Space transportation booster engine thrust chamber technology, large scale injector
| NASA-CR-192531 | p 2633 N93-26557

THRUST CONTROL
Optimal finite-thrust time-bounded direct-ascent interception p 2607 N93-25272

THRUST VECTOR CONTROL
Robust nonlinear control of vectored thrust aircraft
| NASA-CR-192727 | p 2596 N93-25199

THUNDERSTORMS
The 1992 International Aerospace and Ground Conference on Lightning and Static Electricity: Addendum
| DOT/FAA/CT-92/20-ADD-1 | p 2777 N93-24875
Lightning precursor signatures from dual-polarization radar measurements of storms p 2777 N93-24877
Study of atmospheric electrical events above complex terrain p 2780 N93-24897
A single-point warning system for thunderstorms and electric fields p 2711 N93-24900
Comparative performance of lightning air terminals under natural storm conditions p 2781 N93-24902
Parametric analysis of atmospheric processes
| NASA-CR-192523 | p 2770 N93-25086
The charge and size of precipitation particles inside thunderstorms and mesoscale convective systems on the Great Plains p 2781 N93-25275
The North Dakota thunderstorm project
| PB93-153039 | p 2785 N93-25776
The initiation of lightning and the growth of electric fields in thunderstorms
| AD-A261455 | p 2787 N93-26352
Guide for conducting convective windstorm surveys
| PB93-148427 | p 2787 N93-26570

THYRISTORS
High speed solid state circuit breaker p 2694 N93-25598
Investigations of the transient behavior of the cathode fall region in planar and hollow cathodes
| AD-A261636 | p 2691 N93-26171

TIDES
Sea level variation p 2734 N93-24929
A coastal hazards data base for the US East Coast
| NASA-TM-108265 | p 2791 N93-26586

TILT ROTOR AIRCRAFT
Screening studies of advanced control concepts for airbreathing engines
| NASA-TM-106042 | p 2592 N93-25079

TIMBER INVENTORY
Standwise forest inventory and mapping for operational management planning p 2752 N93-24863

TIME
Frequency and Time Forum
| ESA-SP-340 | p 2831 N93-24978
Hydrogen masers for space p 2716 N93-24980
The application of the PRARE principle for precise two-way time transfer to space-based atomic clocks p 2832 N93-24983
Atomic time scales for dynamical astronomy p 2832 N93-24984
How can millisecond pulsars improve the long term stability of atomic time scales? p 2832 N93-24985
Prospects of two-way international time scale comparisons p 2832 N93-24988
A new modem for microwave time synchronisation via geosynchronous telecommunication satellites p 2686 N93-24999
A system design for laser time synchronization via geodetic satellite Ajisai p 2716 N93-25005
Control of environmental and clock parameters in Time and Frequency Standards Laboratory p 2835 N93-25007
Mixed constellation synchronization of GPS time p 2836 N93-25015
GPS standardization for the needs of time transfer p 2836 N93-25016
Comparison of GLONASS and GPS time transfers p 2836 N93-25017
Collaboration in the UK on time transfer using the GLONASS system p 2837 N93-25019
Time and frequency reference for a trajectory measurement system p 2837 N93-25023

TIME DEPENDENCE
The WINCOF-I code: Detailed description
| NASA-CR-190779 | p 2573 N93-24760
BBU code development for high-power microwave generators
| DE93-007111 | p 2688 N93-25397
Numerical simulation of time-dependent thermocapillary convection in layered fluid systems p 2700 N93-25472
Energy transfer properties and mechanisms
| DE93-008540 | p 2849 N93-25488
Kinetic studies in gas-phase reaction mechanisms important to the combustion process of high energy density materials: The H2/NO2 reaction p 2628 N93-26027
Bimolecular reaction dynamics from photoelectron spectroscopy of negative ions
| DE93-007669 | p 2647 N93-26599

TIME DIVISION MULTIPLEXING
The Data Multiplexing Network (DMN) phase 3 Extended Distance Data Cable (EDDC) test and evaluation
| DOT/FAA/CT-TN93/11 | p 2680 N93-26160

TIME MARCHING
Numerical simulation of a shock wave/turbulent boundary layer interaction in a duct p 2699 N93-25342

TIME MEASUREMENT
Cosmic string cosmology p 2891 N93-24907
Frequency and Time Forum
| ESA-SP-340 | p 2831 N93-24978
Hydrogen masers for space p 2716 N93-24980
The application of the PRARE principle for precise two-way time transfer to space-based atomic clocks p 2832 N93-24983
Atomic time scales for dynamical astronomy p 2832 N93-24984
How can millisecond pulsars improve the long term stability of atomic time scales? p 2832 N93-24985

Relativistic effects for low Earth orbit satellites using GPS p 2608 N93-24986
Prospects of two-way international time scale comparisons p 2832 N93-24988
A new modem for microwave time synchronisation via geosynchronous telecommunication satellites p 2686 N93-24999
A system design for laser time synchronization via geodetic satellite Ajisai p 2716 N93-25005
The accuracy of SYLT- and RNS-based time scales at MTI and SNT during 1990-1991 p 2835 N93-25006
Analytical techniques for improved time transfer using common view of direct broadcasting satellites p 2835 N93-25008
Comparison of GLONASS and GPS time transfers p 2836 N93-25017
Collaboration in the UK on time transfer using the GLONASS system p 2837 N93-25019
Time and frequency reference for a trajectory measurement system p 2837 N93-25023
Time stability: An improvement of the multi-variance method for the oscillator noise analysis p 2839 N93-25036
The development progresses of hydrogen masers at Shanghai Observatory p 2716 N93-25048
Investigations of the frequency instability of CH1-75 hydrogen masers p 2716 N93-25049
Oscillators for mobile GPS receivers p 2694 N93-25055
Designing for frequency and time metrology at the 10 to the minus 18 power level p 2842 N93-25059
Time generation and distribution system for a military national synchronization p 2842 N93-25060
Timing and time signal distribution in digital communications networks p 2686 N93-25061
Timing a national telecommunications network using GPS p 2687 N93-25062
Strategies for synchronisation in an evolving telecommunications network p 2687 N93-25063
Synopsis of timing measurement techniques used in telecommunications p 2687 N93-25064

TIME SERIES ANALYSIS
Nonlinear techniques for forecasting solar activity directly from its time series p 2603 N93-24716
Observations of an intrathermocline vortex p 2788 N93-24769
The continuous plankton recorder survey: A long-term, basin-scale oceanic time series p 2736 N93-24937
Ocean time-series near Bermuda: Hydrostation S and the US JGOFS Bermuda Atlantic time-series study p 2736 N93-24938
Inverse sequential procedures for the monitoring of time series
|NASA-CR-192959| p 2765 N93-25666
Time series analysis and multivariate analysis
|AD-A261014| p 2830 N93-25860
Coastal ocean processes: A science prospectus
|AD-A261702| p 2790 N93-26384

TIME SIGNALS
Pseudo Wigner-Ville distribution, computer program, and its applications to time-frequency domain problems
|AD-A261839| p 2813 N93-26431

TIME TEMPERATURE PARAMETER
An evaluation of thermal energy storage options for precooling gas turbine inlet air
|DE93-005980| p 2758 N93-24975
Fundamental and applied aspects of defect engineering in GaAs
|AD-A260573| p 2867 N93-25899

TISSUES (BIOLOGY)
Cellular and tissue injury during nonfreezing cold injury and frostbite
|AD-A260574| p 2795 N93-25900

TITAN
DSN observations of Titan p 2680 N93-26129
Residual mean meridional circulation in titan's middle atmosphere
|PB93-162931| p 2898 N93-26571

TITANIUM
Monitoring damage growth in titanium matrix composites using acoustic emission
|NASA-TM-107742| p 2634 N93-25072

TITANIUM ALLOYS
Micromechanics of fatigue
|AD-A260577| p 2729 N93-25901
Thermal coatings for titanium-aluminum alloys
|NASA-TM-107760| p 2651 N93-26048
Solidification processing and phase transformations in ordered high temperature alloys
|AD-A261751| p 2652 N93-26284

TITANIUM COMPOUNDS
Processing and properties of Ti5Si3
|DE93-007284| p 2649 N93-25149

TITANIUM OXIDES
Vickers indentation hardness of stoichiometric and reduced single crystal TiO2 (rutile) from 25 to 800 C
|NASA-TM-105959| p 2633 N93-26204

TOBACCO
Using terrestrial plants in biomonitoring
|PB93-158780| p 2766 N93-26316

TOKAMAK DEVICES
Density dependence of line intensities and application to plasma diagnostics
|NIFS-209| p 2857 N93-24950
Plasma heating in toroidal systems
|NIFS-208| p 2858 N93-25092
Effect of continuous eigenvalue spectrum on plasma transport in toroidal systems
|NIFS-214| p 2859 N93-25215
TSC plasma halo simulation of a D3-D vertical displacement episode
|DE93-008688| p 2860 N93-25493

TOLERANCES (MECHANICS)
Ultrasonic polishing p 2670 N93-25580
Reliable stress and fracture mechanics analysis of complex aircraft components using a h-p version of FEM
|AD-A260628| p 2726 N93-25638

TOLLMIEN-SCHLICHTING WAVES
Numerical simulation of leading-edge receptivity to freestream vorticity p 2577 N93-25388

TOMOGRAPHY
Effect of cytoskeletal reagents on stretch activated ion channels
|AD-A261089| p 2793 N93-25764
Tomographic analysis of sight infrared spectra of low pressure flames p 2628 N93-26030
Inverse problems in nondestructive evaluations
|AD-A261370| p 2722 N93-26337

TOOLING
Special tooling disposition for aircraft entering post production support
|AD-A261614| p 2573 N93-26168

TOPEX
Star tracker operation in a high density proton field p 2600 N93-24699
Orbit determination support of the Ocean Topography Experiment (TOPEX)/Poseidon operational orbit p 2601 N93-24704

TOPOGRAPHY
Orbit determination support of the Ocean Topography Experiment (TOPEX)/Poseidon operational orbit p 2601 N93-24704
A ground track control algorithm for the Topographic Mapping Laser Altimeter (TMLA) p 2602 N93-24707
Synchrotron radiation X ray topography study of lateral field resonators p 2833 N93-24994
Crystal growth of berlinite: Methods for growing longer crystals and improving the quality p 2838 N93-25025
Crystal growth and physical characterizations of GaPO4 p 2840 N93-25044
Preliminary studies leading toward the development of a LIDAR bathymetry mapping instrument p 2711 N93-25614
Topography from shading and stereo p 2879 N93-25803
Isolation and analysis of key components of seafloor relief
|AD-A261635| p 2790 N93-26170
Interaction of an eddy with a continental slope
|AD-A261550| p 2791 N93-26578

TORCHES
Development and use of hydrogen-air torches in an altitude facility
|NASA-TM-106047| p 2598 N93-26214

TORNADOES
Positive cloud-to-ground flashes in severe storms p 2780 N93-24896
Initialization of a modeled convective storm using Doppler radar-derived fields p 2782 N93-25294
Guide for conducting convective windstorm surveys
|PB93-148427| p 2787 N93-26570
Tornado: An engineering-oriented perspective
|PB93-148435| p 2788 N93-26584

TOROIDAL PLASMAS
Density dependence of line intensities and application to plasma diagnostics
|NIFS-209| p 2857 N93-24950
R and D of transmission lines for ECH system
|NIFS-210| p 2687 N93-24951
Effect of continuous eigenvalue spectrum on plasma transport in toroidal systems
|NIFS-214| p 2859 N93-25215
Thermal and electric oscillation driven by orbit loss in helical systems
|NIFS-213| p 2860 N93-25346

TORQUE
Momentum accumulation due to solar radiation torque, and reaction wheel sizing, with configuration optimization p 2600 N93-24695
Pressure torques and circulation changes in Rocky Mountain lee cyclones p 2783 N93-25724

TORSION
Apparatus and methods for determining balance of a cylindrical vehicle
|AD-D015637| p 2717 N93-25228

TOTAL OZONE MAPPING SPECTROMETER
Kelvin waves in total column ozone
|NASA-CR-192984| p 2764 N93-25431
Rossby-gravity waves in tropical total ozone data
|NASA-CR-192983| p 2764 N93-25432

TOTAL QUALITY MANAGEMENT
Implementation of quality improvement techniques for management and technical processes in the ACRV project p 2723 N93-26074
Design and implementation of a pilot orientation program for new NASA engineering employees
|NASA-TM-105907| p 2872 N93-26205

TOUGHNESS
Mechanical properties of martensitic alloy AISI 422
|DE93-006563| p 2649 N93-25255
High temperature fracture toughness of Ni3Al alloy IC-396M
|DE93-008564| p 2650 N93-25492
High strain rate damage development and failure mechanisms in tungsten heavy alloys
|AD-A260856| p 2651 N93-25788

TOWED BODIES
Dynamics and control of maneuverable tethered flight vehicles p 2615 N93-24767
Experimental study of the effect of helical grooves on an infinite cylinder
|AD-A260890| p 2676 N93-25912

TOXIC HAZARDS
Reclamation with recovery of radionuclides and toxic metals from contaminated materials, soils, and wastes p 2769 N93-25571

TOXICITY
A comparison of the WIND System atmospheric models and MATS data
|DE93-002687| p 2760 N93-24673
Crop agroecological diagnostics by remote sensing technique p 2751 N93-24860
Application of non-thermal plasmas to pollution control
|DE93-007515| p 2763 N93-25385
The acute inhalation toxicity of pyrolysis products of halon 1301
|AD-A260874| p 2795 N93-25629

TOXINS AND ANTITOXINS
Immunoconjugates: Magic bullets for cancer therapy? p 2796 N93-25567

TRACE CONTAMINANTS
Heterogeneous photocatalytic oxidation of atmospheric trace contaminants
|NASA-CR-192937| p 2767 N93-26427

TRACE ELEMENTS
Redistribution of trace chemical species by a small convective cloud
|PB93-156164| p 2765 N93-25873

TRACKING (POSITION)
Optimizing the fine lock performance of the Hubble Space Telescope fine guidance sensors p 2604 N93-24723
Observation of radiation from lightning discharges by LPATS p 2779 N93-24888

TRACTORS
Transmission system for a transfer device gripping a double wheel
|CA-PATENT-APPL-SN-2024585| p 2597 N93-25178

TRADESCANTIA
Using terrestrial plants in biomonitoring
|PB93-158780| p 2766 N93-26316

TRAINING DEVICES
Design and implementation of a pilot orientation program for new NASA engineering employees
|NASA-TM-105907| p 2872 N93-26205

TRAINING EVALUATION
Contribution of personality to the prediction of success in initial air traffic control specialist training
|DOT/FAA/AM-93/4| p 2797 N93-26138

TRAINING SIMULATORS
Fidelity and validity in distributed interactive simulation: Questions and answers
|AD-A260971| p 2810 N93-25711

TRAJECTORIES
Modified point mass trajectory simulation for base-burn projectiles
|BRL-TR-3321| p 2609 N93-25985

TRAJECTORY ANALYSIS
Tsien's method for generating non-Keplerian trajectories. Part 2: The question of thrust to orbit a sphere and the restricted three-body problem p 2603 N93-24718
An approach for finding long period elliptical orbits for precursor SEI missions p 2604 N93-24720

Orbit determination error analysis and comparison of station-keeping costs for Lissajous and halo-type libration point orbits and sensitivity analysis using experimental design techniques p 2604 N93-24721

TRAJECTORY CONTROL

A ground track control algorithm for the Topographic Mapping Laser Altimeter (TMLA) p 2602 N93-24707

Optimal cooperative power-limited rendezvous p 2607 N93-24904

Two neural network algorithms for designing optimal terminal controllers with open final time | NASA-CR-177599 | p 2817 N93-25137

Nonholonomic geometry, mechanics and control p 2724 N93-25270

Control and optimization of aircraft trajectories p 2596 N93-25543

A surface integral algorithm for the motion planning of nonholonomic mechanical systems | AD-A261746 | p 2720 N93-26249

TRAJECTORY MEASUREMENT

Time and frequency reference for a trajectory measurement system p 2837 N93-25023

TRAJECTORY OPTIMIZATION

Optimal finite-thrust time-bounded direct-ascent interception p 2607 N93-25272

Optimal thrust magnitude on a singular arc in atmospheric flight p 2819 N93-25410

Control and optimization of aircraft trajectories p 2596 N93-25543

Trajectory optimization for the National aerospace plane | NASA-CR-192954 | p 2589 N93-25670

Minimum-fuel power-limited transfers between coplanar elliptic orbits p 2608 N93-25684

Optimal transfers between libration-point orbits in the elliptic restricted three-body problem p 2608 N93-25758

TRANSATMOSPHERIC VEHICLES

Information requirements analyses for transatmospheric vehicles | AD-A261189 | p 2590 N93-25949

TRANSCONTINENTAL SYSTEMS

Prospects of two-way international time scale comparisons p 2832 N93-24988

TRANSDUCERS

The constant current loop: A new paradigm for resistance signal conditioning | NASA-TM-108744 | p 2673 N93-25181

TRANSFER FUNCTIONS

The 32nd CDC: System identification using interval dynamic models | NASA-CR-192895 | p 2818 N93-25155

The 32nd CDC: Robust stabilizer synthesis for interval plants using Nevanlina-pick theory | NASA-CR-192894 | p 2818 N93-25156

TRANSFER ORBITS

Practical aspects of transfer from GTO to lunar orbit p 2604 N93-24719

Minimum-fuel power-limited transfers between coplanar elliptic orbits p 2608 N93-25684

Optimal transfers between libration-point orbits in the elliptic restricted three-body problem p 2608 N93-25758

Space transfer concepts and analyses for exploration missions. Technical directive 12: Beamed power systems study | NASA-CR-192532 | p 2599 N93-26146

TRANSFORMATIONS (MATHEMATICS)

Image coding by way of wavelets p 2671 N93-24665

Polar decomposition for attitude determination from vector observations p 2602 N93-24711

Combining spectral information with crop rotation knowledge for crop classifications p 2752 N93-24861

NSWC library of mathematics subroutines | AD-A261511 | p 2884 N93-26575

TRANSFORMERS

Nondestructive evaluation of ferrite c-cores | KCP-613-4677 | p 2721 N93-25939

TRANSIENT RESPONSE

Applications of stress envelope concepts to aircraft EMP and lightning survivability p 2584 N93-24898

TRANSISTOR AMPLIFIERS

Noise-optimal control of HEMT LNA's for compensation of temperature deviations p 2678 N93-26115

RF vacuum microelectronics | AD-A261784 | p 2692 N93-26565

TRANSISTOR CIRCUITS

Dedicated oscillator for immersed crystal sensor p 2837 N93-25020

TRANSISTORS

RF vacuum microelectronics | AD-A261784 | p 2692 N93-26565

TRANSIT TIME

Ultrasonic rate measurement of multiphase flow | DE93-000112 | p 2695 N93-24954

The third-order permittivity of quartz obtained by different methods p 2840 N93-25046

TRANSITION FLIGHT

Development and testing of the digital control system for the Archytas unmanned air vehicle | AD-A261656 | p 2597 N93-26196

TRANSITION FLOW

Dynamics of turbulent slugging in transitional pipe flow p 2702 N93-25548

TRANSITION METALS

Reclamation with recovery of radionuclides and toxic metals from contaminated materials, soils, and wastes p 2769 N93-25571

Transition metal chelate-fulleride compounds: Electrocrystallization of semiconducting (Ru(bpy)s)(C60)2 | AD-A261549 | p 2869 N93-26577

TRANSITION TEMPERATURE

Monolithic integration of semiconductor and superconductor components | AD-A260589 | p 2690 N93-25906

Deformation mechanisms of NiAl cyclicly deformed near the brittle-to-ductile transition temperature | NASA-CR-191121 | p 2652 N93-26235

TRANSLATING

A digital hardware test system analysis with test vector translation | AD-A260849 | p 2810 N93-25786

TRANSMISSION

The design and evaluation of transmit and receive antennas for an ionospheric communications probe system. B: Sloping-vee beams | AD-A261866 | p 2682 N93-26388

TRANSMISSION ELECTRON MICROSCOPY

Transmission electron microscopy investigation of ion implantation damage in GaAs and other semiconductors p 2865 N93-25715

TRANSMISSION LINES

R and D of transmission lines for ECH system | NIFS-210 | p 2687 N93-24951

Published assessments bearing on the future use of ceramic superconductors by the electric power sector | DE93-007737 | p 2658 N93-26588

TRANSMISSIONS (MACHINE ELEMENTS)

Global dynamic modeling of a transmission system | NASA-CR-191117 | p 2716 N93-24751

Transmission system for a transfer device gripping a double wheel | CA-PATENT-APPL-SN-2024585 | p 2597 N93-25178

Computational gearing mechanics | NASA-CR-191127 | p 2719 N93-25884

TRANSONIC FLOW

Prediction of unsteady flows in turbomachinery using the linearized Euler equations on deforming grids | NASA-CR-192919 | p 2696 N93-25109

Computation of transonic flow over a porous surface projectile p 2577 N93-25409

Navier-Stokes simulations of unsteady transonic flow phenomena p 2578 N93-25542

Model fan passage flow simulation | AD-A261613 | p 2707 N93-26167

Unsteady airfoil flow solutions on moving zonal grids | AD-A261925 | p 2582 N93-26198

TRANSONIC NOZZLES

Direct solutions of the Navier-Stokes equations with application to static aeroelasticity p 2697 N93-25259

TRANSONIC SPEED

A feasibility study of using Langley 0.3-m transonic cryogenic tunnel sidewall boundary-layer removal system for heavy gas testing | NASA-CR-191438 | p 2695 N93-25087

Shock tube application to the study of compressible turbulent boundary layer with mass injection p 2697 N93-25252

Visualization of a Mach 2 reacting flow using Planar Laser-Induced Fluorescence (PLIF) p 2598 N93-26006

TRANSONIC WIND TUNNELS

NASA Lewis 8- by 6-foot supersonic wind tunnel user manual | NASA-TM-105771 | p 2597 N93-25080

A feasibility study of using Langley 0.3-m transonic cryogenic tunnel sidewall boundary-layer removal system for heavy gas testing | NASA-CR-191438 | p 2695 N93-25087

TRANSPARENCE

Visual processing of object velocity and acceleration | AD-A261048 | p 2800 N93-25778

TRANSPONDERS

Performance results of a 300-degree linear phase modulator for spaceborne communications applications p 2672 N93-24670

TRANSPORT AIRCRAFT

An approach to configuration design synthesis of subsonic transport aircraft using artificial intelligence techniques p 2589 N93-25692

TRANSPORT PROPERTIES

Asymptotic derivation of the simplified P(sub N) equations | DE93-007342 | p 2828 N93-25151

Quantum conductance fluctuations in self-aligned, pinch-narrowed MOSFETs p 2863 N93-25265

TRANSPORT THEORY

Diabaticity of nuclear motion: Problems and perspectives | DE93-007252 | p 2847 N93-25148

Asymptotic derivation of the simplified P(sub N) equations | DE93-007342 | p 2828 N93-25151

TRANSPORTATION

Emissions from ethanol and LPG fueled vehicles | DE93-006410 | p 2660 N93-25192

Workshop on Diamond and Diamond-Like-Carbon Films for the Transportation Industry | DE93-007491 | p 2658 N93-26506

TRANSPUTERS

Data processing and control in a transputer system for remote sensing of the Earth p 2753 N93-24870

TRANSVERSE WAVES

Surface Transverse Wave (STW) quartz resonators in the GHz range p 2836 N93-25012

TRAPPED MAGNETIC FIELDS

Aerospace devices for magnetic replicas | NASA-CR-192958 | p 2865 N93-25667

TRAPPED PARTICLES

A simple and compact source of cold atoms for cesium fountains and microgravity clocks p 2831 N93-24981

Plasma heating in toroidal systems | NIFS-208 | p 2858 N93-25092

TRAPPED VORTICES

Interaction of an eddy with a continental slope | AD-A261550 | p 2791 N93-26578

TRAPPING

Ion trap frequency standard research at PTB p 2841 N93-25050

Controlling an optical frequency by a single ion p 2841 N93-25051

TRAVELING SALESMAN PROBLEM

Linear-programming tools in integer programming: The traveling salesman | AD-A261398 | p 2812 N93-26290

TRAVELING WAVE TUBES

Dynamic behavior of helix interaction circuits | AD-A261362 | p 2692 N93-26334

TRAVELING WAVES

Transverse instabilities in a relativistic klystron two-beam accelerator | DE93-007110 | p 2852 N93-25375

TREES

Entropy reduction via simplified image contourization p 2804 N93-25924

TREES (PLANTS)

Anomalous bioelectric potentials of silk trees in Naples zoo (Italy) prior to an earthquake in May, 1991 p 2753 N93-24873

TRELLIS CODING

A low-complexity and high performance concatenated coding scheme for high-speed satellite communications | NASA-CR-192715 | p 2673 N93-25198

TREND ANALYSIS

Aerospace monitoring for ecological hazard and disaster mitigation p 2744 N93-24812

TRENDS

Current trends in satellite data supply for environmental monitoring p 2754 N93-24874

Assessing patterns of change in anthropometric dimensions: Secular trends of US Army females, 1946-1988 | AD-A260869 | p 2800 N93-25628

TRIBOLOGY

Properties of extruded PS-212 type self-lubricating materials p 2659 N93-25565

TRIODES

RF vacuum microelectronics | AD-A261784 | p 2692 N93-26565

TROMBE WALLS

Laminar and turbulent natural convection heat transfer in Trombe wall channels p 2702 N93-25551

TROPICAL METEOROLOGY

Numerical simulation of the seasonal and interannual variability of the tropical Atlantic Ocean circulation during the 1980's p 2789 N93-25445

Climate data bases of the People's Republic of China, 1841-1988 | DE93-007907 | p 2764 N93-25517

On the vertical structure of seasonal, interannual and intraseasonal flows p 2782 N93-25557

Tropical cyclogenesis in the western North Pacific p 2783 N93-25714

Tropical cyclone/upper-atmospheric interaction as inferred from satellite total ozone observations p 2784 N93-25741

TROPICAL REGIONS
Tropical forest monitoring with high resolution satellite data p 2748 N93-24841
On the generation and dispersion of Yanai waves with a spectral Chebyshev-collocation reduced-gravity ocean model p 2788 N93-25276
Kelvin waves in total column ozone
|NASA-CR-192984| p 2764 N93-25431
An analysis of mesoscale convective systems observed during the 1992 Tropical Cyclone Motion field experiment
|AD-A260889| p 2783 N93-25633

TROPICAL STORMS
An analysis of mesoscale convective systems observed during the 1992 Tropical Cyclone Motion field experiment
|AD-A260889| p 2783 N93-25633
Tropical cyclogenesis in the western North Pacific p 2783 N93-25714
Tropical cyclone/upper-atmospheric interaction as inferred from satellite total ozone observations p 2784 N93-25741

TROPOSPHERE
Propagation at microwave frequencies in the presence of tropospheric stratified layers p 2674 N93-25340
Observed annual and interannual variations in tropospheric water vapor p 2782 N93-25549
Occultation of a compact radio source by Venus p 2676 N93-26107
A nanoradian differential VLBI tracking demonstration p 2677 N93-26108
Deep-space navigation with differenced data types. Part 3: An expanded information content and sensitivity analysis p 2614 N93-26109

TRUSSES
The MODE family of on-orbit experiments: The Middeck Active Control Experiment (MACE) p 2599 N93-25835
Interaction dynamics and control for orbital assembly p 2669 N93-26407
Controls for orbital assembly of large space structures p 2620 N93-26408
Structural load control during construction p 2669 N93-26409

TTL INTEGRATED CIRCUITS
TF-4020A: TFL's new compact military rubidium standard p 2838 N93-25026

TUMBLING MOTION
Spacecraft detumbling through energy dissipation p 2600 N93-24696

TUMORS
Measuring the metastatic potential of cancer cells p 2794 N93-25566
Immunoconjugates: Magic bullets for cancer therapy? p 2796 N93-25567

TUNABLE LASERS
Laser physics and laser techniques
|AD-A261595| p 2715 N93-26524

TUNGSTEN ALLOYS
High strain rate damage development and failure mechanisms in tungsten heavy alloys
|AD-A260856| p 2651 N93-25788
Shear band formation in a W-Ni-Fe alloy under plate impact
|AD-A260702| p 2651 N93-25907

TUNING
Investigations of the frequency instability of CH1-75 hydrogen masers p 2716 N93-25049
Synthetic-perturbation tuning of MIMD programs
|PB93-161339| p 2812 N93-26321

TURBINE BLADES
Heat transfer in rotating serpentine passages with selected model orientation for smooth or skewed trip walls
|NASA-TM-106126| p 2667 N93-25177
Turbine turbobrake systems p 2717 N93-25268
Three-dimensional flow in radial turbomachinery and its impact on design
|NASA-CR-192957| p 2593 N93-25668
Flow control of low heat load turbine airfoils
|AD-A260941| p 2595 N93-26219
The blade curving effects in a turbine stator cascade with low aspect ratio
|AD-A261063| p 2595 N93-26239

TURBINE ENGINES
Measurements and computations of external heat transfer and film cooling in turbines
|RAE-TM-P-1223| p 2592 N93-25455
Design and performance of nozzle-less volute casings for inward flow radial turbines p 2593 N93-25471
Effect of a metal deactivator fuel additive on fuel deposition in fuel atomizers at high temperature
|AD-A260915| p 2661 N93-25914

TURBINE PUMPS
On-line implementation of nonlinear parameter estimation for the Space Shuttle main engine
|NASA-TM-106097| p 2632 N93-26211

TURBINES
Turbine turbobrake systems p 2717 N93-25268
Estimating turbine limit load
|NASA-CR-191105| p 2580 N93-25883
Development of a method to determine the autoxidation of turbine fuels
|AD-A260578| p 2661 N93-25902
Radial inflow turbine study
|AD-A260767| p 2594 N93-25917

TURBOCOMPRESSORS
The effects of reaction on axial compressor performance p 2594 N93-25882
Radial inflow turbine study
|AD-A260767| p 2594 N93-25917
Active stabilization of aeromechanical systems
|AD-A261366| p 2595 N93-26335

TURBOFAN ENGINES
The WINCOF-I code: Detailed description
|NASA-CR-190779| p 2573 N93-24760
Transient performance of fan engine with water ingestion
|NASA-CR-190778| p 2573 N93-25134
Model fan passage flow simulation
|AD-A261613| p 2707 N93-26167

TURBOFANS
A computational method for the analysis of acoustic radiation from turbofan inlets p 2845 N93-25717

TURBOJET ENGINES
A preliminary sizing method for unmanned aircraft using multi-variate optimisation p 2587 N93-25408

TURBOMACHINE BLADES
Prediction of unsteady flows in turbomachinery using the linearized Euler equations on deforming grids
|NASA-CR-192919| p 2696 N93-25109
Three-dimensional flow in radial turbomachinery and its impact on design
|NASA-CR-192957| p 2593 N93-25668

TURBOMACHINERY
Three-dimensional flow in radial turbomachinery and its impact on design
|NASA-CR-192957| p 2593 N93-25668
Numerical modelling of viscous turbomachinery flows with a pressure correction method p 2594 N93-25702
Fibre optic sensors for heat transfer studies p 2853 N93-25748
Computation of broadband mixing noise from turbomachinery
|AD-A261611| p 2846 N93-26165

TURBULENCE
Flow visualizations of perpendicular blade vortex interactions
|NASA-CR-192725| p 2696 N93-25208
Studies in air/air supersonic mixing layers p 2582 N93-26007
Turbulence interacting with chemical kinetics in airbreathing combustion of ducted rockets p 2625 N93-26012
Measurements of scalar power spectra in high Schmidt number turbulent jets
|AD-A261542| p 2707 N93-26379
Chaos metrics for testing lagrangian particle models
|AD-A261429| p 2776 N93-26454

TURBULENCE EFFECTS
Numerical modelling of viscous turbomachinery flows with a pressure correction method p 2594 N93-25702
Flame-turbulence interactions
|AD-A260957| p 2645 N93-26220

TURBULENCE MODELS
Assessment of closure coefficients for compressible-flow turbulence models
|NASA-TM-103882| p 2697 N93-25247
Numerical simulation of a shock wave/turbulent boundary layer interaction in a duct p 2699 N93-25342
Proceedings of the NUWC Division Newport Seminar Series on Turbulence and its Control
|NUWC-NPT-TM-922089| p 2707 N93-26328

TURBULENT BOUNDARY LAYER
Surface and flow field measurements in a symmetric crossing shock wave/turbulent boundary-layer interaction
|NASA-TM-106086| p 2575 N93-24911
Shock tube application to the study of compressible turbulent boundary layer with mass injection p 2697 N93-25252
An experimental study of the sources of fluctuating pressure loads beneath swept shock/boundary-layer interactions
|NASA-CR-192918| p 2698 N93-25266
Numerical simulation of a shock wave/turbulent boundary layer interaction in a duct p 2699 N93-25342
Heat transfer measurements in swept shock wave/turbulent boundary-layer interactions p 2704 N93-25705
An experimental study of passive drag reduction in a turbulent boundary layer by a riblet surface p 2705 N93-25746
Large-eddy simulation of temporally developing boundary layers with embedded streamwise vortices p 2705 N93-25753
Correlations between organized turbulent structures and wall pressure fluctuations
|PB93-156479| p 2706 N93-25885
Uniform roughness studies
|WL-TR-92-3041| p 2706 N93-25951
Hybrid rocket fuel combustion study p 2626 N93-26019
Proceedings of the NUWC Division Newport Seminar Series on Turbulence and its Control
|NUWC-NPT-TM-922089| p 2707 N93-26328

TURBULENT COMBUSTION
A premixed laminar flame interacting with a vortex resulting in flame stretch and quenching p 2642 N93-24771
Eulerian-Eulerian treatment of turbulent dense spray combustion in a bipropellant liquid rocket engine p 2626 N93-26017

TURBULENT FLOW
An analysis of lift forces on aerosols in a wall bounded turbulent shear flow
|DE93-003362| p 2695 N93-24963
Measurements of density, temperature, and their fluctuations in turbulent supersonic flow using UV laser spectroscopy
|NASA-TM-103943| p 2708 N93-25076
Propagation velocity and space-time correlation of perturbations in turbulent channel flow
|NASA-TM-103932| p 2695 N93-25082
Assessment of closure coefficients for compressible-flow turbulence models
|NASA-TM-103882| p 2697 N93-25247
Predictive modeling of particle-laden, turbulent flows
|DE93-008208| p 2698 N93-25309
Numerical simulation of a shock wave/turbulent boundary layer interaction in a duct p 2699 N93-25342
Dynamics of turbulent slugging in transitional pipe flow p 2702 N93-25548
Laminar and turbulent natural convection heat transfer in Trombe wall channels p 2702 N93-25551
Computational modelling of 3D flow in complex ducts and passages p 2704 N93-25698
A basic research model of natural gas combustion in turbulent flow, phase 2
|PB93-158509| p 2644 N93-25819
Correlations between organized turbulent structures and wall pressure fluctuations
|PB93-156479| p 2706 N93-25885
Visualization of a Mach 2 reacting flow using Planar Laser-Induced Fluorescence (PLIF) p 2598 N93-26006
Image correlation velocimetry
|AD-A261599| p 2707 N93-26163
Trailing vortex/free-surface interaction
|AD-A261654| p 2581 N93-26195
Experiments on the physics of turbulent mixing in stably stratified ocean layers
|AD-A261312| p 2790 N93-26298
Interaction of vorticity with a free surface
|AD-A261524| p 2707 N93-26360
Measurements of scalar power spectra in high Schmidt number turbulent jets
|AD-A261542| p 2707 N93-26379

TURBULENT HEAT TRANSFER
Laminar and turbulent natural convection heat transfer in Trombe wall channels p 2702 N93-25551

TURBULENT JETS
An experimental study of under-expanded jets p 2577 N93-25467
Liquid surface breakup of nonturbulent and turbulent liquids p 2700 N93-25473
Measurements of scalar power spectra in high Schmidt number turbulent jets
|AD-A261542| p 2707 N93-26379
Oxides of nitrogen emissions from turbulent hydrocarbon/air jet diffusion flames, phase 2
|PB93-152478| p 2768 N93-26533

TURBULENT MIXING
An experimental study of under-expanded jets p 2577 N93-25467
An experimental study of particle-laden jet interactions with cocurrent flows p 2701 N93-25534
Image correlation velocimetry
|AD-A261599| p 2707 N93-26163
Computation of broadband mixing noise from turbomachinery
|AD-A261611| p 2846 N93-26165
Experiments on the physics of turbulent mixing in stably stratified ocean layers
|AD-A261312| p 2790 N93-26298

TWILIGHT GLOW
Anomalous aspects of magnetosheath flow and of the shape and oscillations of the magnetopause during an interval of strongly northward interplanetary magnetic field
| NASA-CR-192851 | p 2770 N93-25081

TWINNING
Quartz crystal twinning under mechanical stress: Finite element analysis p 2839 N93-25032

TWO DIMENSIONAL BOUNDARY LAYER
Nonlinear evolution of the first mode supersonic oblique waves in compressible boundary layers. Part 1: Heated/cooled walls
| NASA-TM-106087 | p 2696 N93-25175

TWO DIMENSIONAL MODELS
The rate form of equilibrium equation for problems of steady-state, elastic, viscous flows p 2704 N93-25708
Workshop Report: A validation study of Navier-Stokes codes for transverse injection into a Mach 2 flow p 2624 N93-26008
ADCIRC: An advanced three-dimensional circulation model for shelves, coasts, and estuaries. Report 1: Theory and methodology of ADCIRC-2DDI and ADCIRC-3DL
| AD-A261608 | p 2790 N93-26164
Model fan passage flow simulation
| AD-A261613 | p 2707 N93-26167

TWO PHASE FLOW
Fuel Injector: Air swirl characterization aerothermal modeling, phase 2, volume 2
| NASA-CR-189193 | p 2592 N93-25106
Atomizing-gas temperature effect on cryogenic spray dropsize
| NASA-TM-106106 | p 2709 N93-25191
The modeling of complex continua: Fundamental obstacles and grand challenges
| DE93-006507 | p 2696 N93-25193
Flow visualizations of perpendicular blade vortex interactions
| NASA-CR-192725 | p 2696 N93-25208
Two-phase/two-phase heat exchanger analysis
| NASA-CR-192783 | p 2697 N93-25221
Measurement of velocities in gas-liquid two-phase flow using laser Doppler velocimetry
| DE93-008083 | p 2698 N93-25306
Annular flow enhanced two-phase evaporative heat exchanger for space-based systems p 2700 N93-25478
Particle dynamics modeling of boundary effects in granular Couette flow p 2705 N93-25738

TWO STAGE TURBINES
Estimating turbine limit load
| NASA-CR-191105 | p 2580 N93-25883

TYPHOONS
Typhoon prediction (recurvature - 1990 experiment)
| AD-A260673 | p 2786 N93-25892
Effects of Taiwan orography on the motion and structure of typhoons
| AD-A261819 | p 2786 N93-26270

U

U.S.S.R.
Selected translated abstracts of Russian-language climate-change publications: 1. Surface energy budget
| DE93-003189 | p 2760 N93-24952
Digest of Russian Space Life Sciences, issue 33
| NASA-CR-3922(39) | p 2792 N93-25195
JPRS report: Central Eurasia. Aviation and cosmonautics, no. 9, September 1992
| JPRS-UAC-93-003 | p 2574 N93-26325
Science, Technology, and Industrial Policy in the Former Soviet Union
| DE93-006528 | p 2887 N93-26499

U.S.S.R. SPACE PROGRAM
First experience with the ASN-16 GLONASS receiver p 2693 N93-25033
Former Soviet Republic capabilities in space and science
| DE93-007613 | p 2598 N93-25322

UH-60A HELICOPTER
Techniques for designing rotorcraft control systems
| NASA-CR-192960 | p 2597 N93-26046
Helicopter forced response vibration analysis method RTVIB20
| AD-A261809 | p 2597 N93-26260

ULTRAHIGH FREQUENCIES
Design of a low phase noise UHF oscillator using a partly metallized dielectric resonator p 2693 N93-25003
Flight termination receiver catalog
| AD-A261558 | p 2682 N93-26460
L- and K-band LMSS propagation measurements using MARECS-B, OLYMPUS, and ACTS p 2683 N93-26467

ULTRASONIC CLEANING
Ultrasonic polishing p 2670 N93-25580
Development of a replacement for trichloroethylene in the two-stage cleaning process
| KCP-613-4941 | p 2669 N93-26207

ULTRASONIC MACHINING
Ultrasonic polishing p 2670 N93-25580

ULTRASONIC RADIATION
Methods of determining loads and fiber orientations in anisotropic non-crystalline materials using energy flux deviation
| NASA-CASE-LAR-14399-1 | p 2729 N93-26102

ULTRASONIC SCANNERS
In-situ ultrasonic C-scanner
| AD-A261113 | p 2638 N93-25768

ULTRASONIC TESTS
Investigation of corrosion in aluminum/adhesive lap-splices using pulse-echo ultrasonic techniques
| DE93-008074 | p 2721 N93-25518
Determination of the elastic constants of composite materials from ultrasonic group velocity measurements p 2635 N93-25544
In-situ ultrasonic C-scanner
| AD-A261113 | p 2638 N93-25768
Nondestructive evaluation of ferrite c-cores
| KCP-613-4677 | p 2721 N93-25939

ULTRAVIOLET LASERS
Ultraviolet waveguide lasers for phased array lidar
| AD-A261657 | p 2715 N93-26363

ULTRAVIOLET SPECTRA
Spectra of stable sonoluminescence
| AD-A260621 | p 2844 N93-25637

ULTRAVIOLET SPECTROMETERS
Further analysis of ECOM-721 data
| AD-A260863 | p 2774 N93-25790

ULTRAVIOLET SPECTROSCOPY
The interaction of HCN/DCN with Si(100)-2x1
| AD-A260837 | p 2645 N93-25920

UNDERGROUND STORAGE
Tank issues: Design and placement of vapor monitoring wells
| PB93-161131 | p 2768 N93-26536

UNDERWATER ACOUSTICS
Proceedings of the 5th International Symposium on Long Range Sound Propagation
| AD-A260666 | p 2845 N93-25643

UNITED STATES
Achieving the promise of the bioscience revolution: The role of the Federal Government
| PB93-139970 | p 2793 N93-25457

UNIVERSE
Cosmic string cosmology p 2891 N93-24907
Tully-Fisher distances and motions in the northern sky p 2889 N93-25621

UNIVERSITY PROGRAM
Viewgraph description of Penn State's Propulsion Engineering Research Center: Activity highlights and future plans
| NASA-CR-192317 | p 2622 N93-24943
The 1993/1994 NASA Graduate Student Researchers Program
| NASA-EP-283 | p 2872 N93-26051
Center for Advanced Propulsion Systems (fellowship)
| AD-A260571 | p 2632 N93-26216

UNIX (OPERATING SYSTEM)
An analysis of file migration in a UNIX supercomputing environment
| NASA-CR-192908 | p 2809 N93-25131
A trace-driven analysis of name and attribute caching in a distributed system
| NASA-CR-192899 | p 2815 N93-25251
Expert system for UNIX system reliability and availability enhancement p 2723 N93-25588
SAVS: A Space Analysis and Visualization System p 2881 N93-25812

UNSTEADY AERODYNAMICS
Aerodynamic foundations for use of unsteady aerodynamic effects in flight control p 2576 N93-25274
Application of finite-state inflow to flap-lag-torsion damping in hover p 2587 N93-25486

UNSTEADY FLOW
Prediction of unsteady flows in turbomachinery using the linearized Euler equations on deforming grids
| NASA-CR-192919 | p 2696 N93-25109
A simple, approximate model of parachute inflation
| DE93-002465 | p 2576 N93-25121
Navier-Stokes simulations of unsteady transonic flow phenomena p 2578 N93-25542
Conical Euler analysis and active roll suppression for unsteady vortical flows about rolling delta wings
| NASA-TP-3259 | p 2581 N93-26134
Unsteady airfoil flow solutions on moving zonal grids
| AD-A261925 | p 2582 N93-26198

UPLINKING
Feasibility study of a Ka-/Ka-band dichroic plate with stepped rectangular apertures p 2671 N93-24660
Improvements in X-band transmitter phase stability through Klystron body temperature regulation p 2678 N93-26114
More rain compensation results p 2686 N93-26486

UPPER ATMOSPHERE
Aspects of the design of a satellite borne infra-red radiometer p 2620 N93-25474
JARE data reports. No. 171 (upper atmosphere physics 9). Data, Syowa and Asuka Stations, 1989 p 2774 N93-25889
Determination of design and operation parameters for upper atmospheric research instrumentation to yield optimum resolution with deconvolution
| NASA-CR-192832 | p 2775 N93-26084

UPPER ATMOSPHERE RESEARCH SATELLITE (UARS)
Polar decomposition for attitude determination from vector observations p 2602 N93-24711
A multimission three-axis stabilized spacecraft flight dynamics ground support system p 2603 N93-24714
Upper Atmosphere Research Satellite (UARS) onboard attitude determination using a Kalman filter p 2606 N93-24732
Goddard Space Flight Center (GSFC) Flight Dynamics Facility (FDF) calibration of the Upper Atmosphere Research Satellite (UARS) sensors p 2606 N93-24733
Solar array thermal snap and the characteristics of its effect on UARS p 2607 N93-24734
Upper Atmosphere Research Satellite (UARS) attitude accuracy using coarse attitude sensors p 2607 N93-24735
UARS in-flight jitter study for EOS
| NASA-CR-191419 | p 2615 N93-25133
STS-48 Space Shuttle mission report
| NASA-CR-193060 | p 2613 N93-25990

UPWIND SCHEMES (MATHEMATICS)
Navier-Stokes simulations of unsteady transonic flow phenomena p 2578 N93-25542

URANIUM FLUORIDES
Recommendations for a Kalman filter to estimate and control freeze and sublime rates of gaseous diffusion plant freezer/sublimer systems
| ORNL/TM-12183 | p 2668 N93-25937

URBAN DEVELOPMENT
Satellite remote sensing for environmental geology: The Bandung (West Java) experience p 2739 N93-24784
Monitoring and analysis of urban trends using multitemporal satellite-imagery (case-study: Greater Cairo) p 2740 N93-24790
The photointerpretation of the area taken over from agriculture by intense urbanization at Villabate (Palermo, Italy) p 2742 N93-24800

URINE
Health and environmental chemistry: Analytical techniques, data management, and quality assurance
| DE93-002853 | p 2760 N93-24674

USER MANUALS (COMPUTER PROGRAMS)
Federal Communications Commission (FCC) Transponder Loading Data Conversion Software. User's guide and software maintenance manual, version 1.2
| NASA-CR-191067 | p 2808 N93-24947
High temperature composite analyzer (HITCAN) user's manual, version 1.0
| NASA-TM-106002 | p 2724 N93-25070
DSD Technology: A detonation reactive Huygens code
| LA-12235-MS | p 2706 N93-25987
Application of the Saha equation to high temperature (greater than or equal to) rocket exhaust
| AD-A261648 | p 2632 N93-26174
AMPHIB: A users manual
| AD-A261769 | p 2669 N93-26285
METal matrix composite ANalyzer (METCAN): Theoretical manual
| NASA-TM-106025 | p 2641 N93-26552

USER REQUIREMENTS
Systems engineering and the user: Incorporation of user requirements into the SE process p 2666 N93-24687
Factors associated with perceptions of productivity and usage of information technology in a service organization p 2875 N93-25421
A framework for the design of usable electronic text p 2877 N93-25754

UTILITIES
Published assessments bearing on the future use of ceramic superconductors by the electric power sector
| DE93-007737 | p 2658 N93-26588

V

V/STOL AIRCRAFT
Experimental performance of a ventral nozzle with pitch and yaw vectoring capability for SSTOVL aircraft
| NASA-TM-106054 | p 2592 N93-25129
ASTOVL combat aircraft design synthesis and optimization p 2589 N93-25704

Jet-induced ground effects on a parametric flat-plate model in hover
| NASA-TM-104001 | p 2581 N93-26099

VACANCIES (CRYSTAL DEFECTS)
Fundamental and applied aspects of defect engineering in GaAs
| AD-A260573 | p 2867 N93-25899

VACUUM
RF vacuum microelectronics
| AD-A261343 | p 2691 N93-26311

VACUUM APPARATUS
Vacuum powder injector and method of impregnating fiber with powder
| NASA-CASE-LAR-14179-1 | p 2668 N93-26101

VACUUM CHAMBERS
Control of crystallite size in diamond film chemical vapor deposition
| AD-D015660 | p 2867 N93-26090

VALENCE
Accurate determination of Auger line shape binding energies
| AD-A261803 | p 2868 N93-26258

VALLEYS
Use of remote sensing and GIS for the environmental planning proposal of the Sarno River Valley (Campania, southern Italy) p 2741 N93-24797

VALVES
External stress-corrosion cracking of a 1.22-m-diameter type 316 stainless steel air valve
| NASA-TP-3190 | p 2652 N93-26201

VANES
Three-dimensional flow in radial turbomachinery and its impact on design
| NASA-CR-192957 | p 2593 N93-25668

VAPOR DEPOSITION
Fundamental studies of defect generation in amorphous silicon alloys grown by remote plasma-enhanced chemical-vapor deposition (Remote PECVD)
| DE92-010560 | p 2862 N93-24953
Mechanistic studies of the CVD of silicon nitride from SiF4 and NH3
| DE93-004500 | p 2644 N93-25312
Novel approaches to the construction of miniaturized analytical instrumentation
| NASA-CR-191988 | p 2709 N93-25345
Diagnostics of diamond film deposition plasmas
| AD-A260866 | p 2860 N93-25626
Thermal coatings for titanium-aluminum alloys
| NASA-TM-107760 | p 2651 N93-26048
Control of crystallite size in diamond film chemical vapor deposition
| AD-D015660 | p 2867 N93-26090
Adhesion and corrosion behavior of Al-Zn and TiN/Ti/TiN coatings on a DU-0.75 wt. percent Ti alloy
| MTL-TR-92-56 | p 2658 N93-26433

VAPOR PHASE EPITAXY
An inverted AlGaAs/GaAs patterned-Ge tunnel junction cascade concentrator solar cell
| DE93-000073 | p 2759 N93-25102

VAPOR PHASES
The WINCOF-I code: Detailed description
| NASA-CR-190779 | p 2573 N93-24760
An experimental study of particle-laden jet interactions with cocurrent flows p 2701 N93-25534
Kinetic studies in gas-phase reaction mechanisms important to the combustion process of high energy density materials: The H2/NO2 reaction p 2628 N93-26027
Mechanisms of decomposition and oxidation of borane compounds
| AD-A261137 | p 2645 N93-26045

VAPORIZING
Atomizing-gas temperature effect on cryogenic spray dropsize
| NASA-TM-106106 | p 2709 N93-25191
Fundamental studies of droplet interactions in dense sprays
| AD-A261165 | p 2661 N93-25948

VAPORS
A new method for infrared imaging of air currents in and around critical hazard fume hoods
| DE93-003009 | p 2761 N93-24956
Temperature dependent sensor response caused by polymer-solvent interactions
| DE93-005368 | p 2655 N93-25444
Tank issues: Design and placement of vapor monitoring wells
| PB93-161131 | p 2768 N93-26536

VARACTOR DIODES
Performance results of a 300-degree linear phase modulator for spaceborne communications applications p 2672 N93-24670

VARIABILITY
Propagation of radiation in astrophysical media: Gravitational lenses and astrophysical masers p 2892 N93-24949
SAR-related stress variability in the marine atmospheric boundary layer
| AD-A261129 | p 2775 N93-25946

VARIANCE (STATISTICS)
Considerations of the error variances of time-averaged estimators for correlated processes
| AD-A261796 | p 2830 N93-26255

VARIATIONS
Data management for JGOFS: Theory and design p 2735 N93-24935

VAX COMPUTERS
Implementation of custom colors in the DECwindows environment
| AD-A261456 | p 2757 N93-26574

VECTOR ANALYSIS
Polar decomposition for attitude determination from vector observations p 2602 N93-24711
Rate determination from vector observations p 2603 N93-24713
Quaternion normalization in spacecraft attitude determination p 2606 N93-24730
Attitude determination using vector observations: A fast optimal matrix algorithm p 2606 N93-24731
Improved determination of vector lithospheric magnetic anomalies from MAGSAT data
| NASA-CR-192784 | p 2771 N93-25201

VECTOR PROCESSING (COMPUTERS)
Using a multifrontal sparse solver in a high performance, finite element code
| NASA-CR-192718 | p 2828 N93-25223

VECTOR QUANTIZATION
Wavelet transform-vector quantization compression of supercomputer ocean model simulation output
| DE93-005453 | p 2876 N93-25448

VEGETABLES
Analysis of the lettuce data from the variable pressure growth chamber at NASA Johnson Space Center: A three-stage nested design model p 2794 N93-26069

VEGETATION
Land cover monitoring in the Netherlands applying satellite remote sensing p 2740 N93-24789
Detection of land use/land cover changes using remote sensing and GIS in Vietnam p 2740 N93-24791
Determination of environmental dynamics using NOAA satellite data and a water balance model for the Mediterranean landscape p 2741 N93-24794
Agroclimatological zonation by AVHRR data for vegetation monitoring p 2741 N93-24795
Potential operational use of remote sensing from space in forestry p 2745 N93-24817
An expert system shell for inferring vegetation characteristics: Inrerface for the addition of techniques (Task H)
| NASA-CR-192897 | p 2754 N93-25154
Integrating satellite imagery and digital elevation data for geobotanical mapping in Quetico Provincial Park, Ontario, Canada p 2754 N93-25430
Evaluating climate-vegetation interactions at climate model sub-grid scales p 2764 N93-25476

VEGETATION GROWTH
North-central Mexico blue grama rangeland biomass assessment at the end of the rainy season using NOAA-AVHRR-LAC p 2750 N93-24854

VEGETATIVE INDEX
Correlation between NDVI values derived from NOAA AVHRR HRPT data and ground measurements of precipitation in the EFEDA study area (Spain) p 2738 N93-24780
ANOVA method to estimate vegetation indices sensitivity assessing nitrogen fertilizing influence on spectral reflectance coefficients p 2739 N93-24782
Agroclimatological zonation by AVHRR data for vegetation monitoring p 2741 N93-24795
Assessment and forecasting of crop yield in Niger through NOAA NDVI data p 2750 N93-24851
Global drought monitoring from NOAA polar orbiting satellites p 2750 N93-24852
Crop agroecological diagnostics by remote sensing technique p 2751 N93-24860

VEHICLES
Apparatus and methods for determining balance of a cylindrical vehicle
| AD-D015637 | p 2717 N93-25228

VELOCITY
Visual processing of object velocity and acceleration
| AD-A261048 | p 2800 N93-25778

VELOCITY DISTRIBUTION
The transient development of vortices over delta wings p 2576 N93-25269
The effects of large-amplitude, low-frequency excitation on a three-dimensional jet p 2702 N93-25553
Propagation of finite amplitude sound in a waveguide with a parabolic sound velocity profile
| ARL-TR-92-11 | p 2846 N93-26179
Tornado: An engineering-oriented perspective
| PB93-148435 | p 2788 N93-26584

VELOCITY ERRORS
Errors caused by incompatible wind and buoyancy forcing in the ocean general circulation models
| AD-A260894 | p 2789 N93-25657

VELOCITY MEASUREMENT
Ultrasonic rate measurement of multiphase flow
| DE93-000112 | p 2695 N93-24954
An investigation of laser velocimetry measurements within high speed, complex flows p 2697 N93-25237
The transient development of vortices over delta wings p 2576 N93-25269
Measurement of velocities in gas-liquid two-phase flow using laser Doppler velocimetry
| DE93-008083 | p 2698 N93-25306
The effects of large-amplitude, low-frequency excitation on a three-dimensional jet p 2702 N93-25553
An investigation on planar velocimetry by spatial cross-correlation p 2578 N93-25664
An investigation of photothermal velocimetry for application to transient, high-speed gas flows p 2579 N93-25720
Direct measurement of velocity space transport in a plasma p 2861 N93-25831
System for calibrating a gyro navigator
| AD-D015668 | p 2586 N93-26093
Pulsed laser Rayleigh scattering diagnostic for hydrogen/oxygen rocket exit plane flowfield velocimetry
| NASA-TM-106098 | p 2631 N93-26149
Image correlation velocimetry
| AD-A261599 | p 2707 N93-26163
Trailing vortex/free-surface interaction
| AD-A261654 | p 2581 N93-26195
Basic research thermoacoustic heat transport
| AD-A261334 | p 2759 N93-26310

VENUS (PLANET)
The Venus 130-nm dayglow as a diagnostic of thermospheric structure and dynamics p 2896 N93-25285
Occultation of a compact radio source by Venus p 2676 N93-26107
Galileo early cruise, including Venus, First Earth, and Gaspra encounters p 2599 N93-26125
Revealing the face of Venus: Magellan
| NASA-CR-192922 | p 2898 N93-26517

VENUS ATMOSPHERE
The Venus 130-nm dayglow as a diagnostic of thermospheric structure and dynamics p 2896 N93-25285
Occultation of a compact radio source by Venus p 2676 N93-26107

VERBAL COMMUNICATION
Spontaneous discovery and use of categorical structure
| AD-A261658 | p 2798 N93-26364

VERTICAL AIR CURRENTS
Redistribution of trace chemical species by a small convective cloud
| PB93-156164 | p 2765 N93-25873

VERTICAL DISTRIBUTION
On the vertical structure of seasonal, interannual and intraseasonal flows p 2782 N93-25557

VERTICAL TAKEOFF AIRCRAFT
Reduction in size and unsteadiness of a VTOL ground vortex by ground fences
| NASA-CR-192997 | p 2580 N93-26049

VERY LARGE SCALE INTEGRATION
Construction of a connectionist network supercomputer
| AD-A260929 | p 2820 N93-25648
Very high-speed arithmetic processors (The Gauss Machine)
| AD-A260693 | p 2806 N93-25650
VLSI for high-speed digital signal processing
| AD-A260754 | p 2690 N93-25678
The design and implementation of a read prediction buffer
| AD-A260902 | p 2806 N93-25934

VERY LONG BASE INTERFEROMETRY
The advances in F and T technology: Their benefits of and for space science and technology p 2831 N93-24979
Precise Doppler tracking from the Medicina VLBI station p 2608 N93-24998
The development progresses of hydrogen masers at Shanghai Observatory p 2716 N93-25048
A determination of the radio-planetary frame tie from comparison of Earth orientation parameters p 2676 N93-26106
A nanoradian differential VLBI tracking demonstration p 2677 N93-26108

VERY LOW FREQUENCIES
The design of a modular sound absorber for very low frequencies
| BBC-RD-1992/10 | p 2673 N93-25170
A modular wideband sound absorber
| BBC-RD-1992/11 | p 2673 N93-25171

Very low frequency signals and whistler-mode amplification in the magnetosphere and limit-cycle behavior in the CECAF infrared free electronic laser
| AD-A261776 | p 2716 N93-26601

VIBRATION
Vibration, buckling, and postbuckling of laminated composites with delaminations p 2723 N93-24765
Monolithic quartz vibrating beam accelerometer p 2711 N93-25011
A study of vibrationally excited N2(+) ions in the daytime thermosphere p 2770 N93-25179
Helmeted head and neck dynamics under whole-body vibration p 2800 N93-25531
ASTROS-ID: Software for system identification using mathematical programming
| AD-A260867 | p 2810 N93-25627
Evaluation of a vibration diagnostic system for the detection of spur gear pitting failures
| NASA-TM-106103 | p 2718 N93-25672
Nonlinear vibrations, stability, and dynamics of structures and mechanisms
| AD-A260871 | p 2728 N93-25838

VIBRATION DAMPING
Attitude control of the LACE satellite: A gravity gradient stabilized spacecraft p 2605 N93-24727
UARS in-flight jitter study for EOS
| NASA-CR-191419 | p 2615 N93-25133
Identification and control of lightly damped, large space structures: An experimental evaluation p 2616 N93-25351
Graphite/epoxy composite laminates with co-cured interlaminar damping layers p 2642 N93-25587
Passive vibration damping materials: Piezoelectric ceramics composites for vibration damping applications
| AD-A260792 | p 2727 N93-25690
Using input command pre-shaping to suppress multiple mode vibration p 2732 N93-25834
MIT's interferometer CST testbed p 2609 N93-25836
Mechanics and control of multibody structural systems
| AD-A261576 | p 2619 N93-26456
Digital filter control of remotely operated flexible robotic structures
| DE93-007587 | p 2827 N93-26596

VIBRATION MODE
Vibration, buckling, and postbuckling of laminated composites with delaminations p 2723 N93-24765
Joint flexibility effects on the dynamic response of structures. Part 2: Stochastic analysis
| AD-A261003 | p 2729 N93-25938

VIBRATIONAL SPECTRA
Molecular interactions and properties with many-body methods
| AD-A261688 | p 2850 N93-26367
Spectroscopic effects of disorder and vibrational localization in mixed-halide metal-halide chain solids
| DE93-007361 | p 2646 N93-26505

VIDEO COMMUNICATION
Video scan rate conversion method and apparatus for achieving same
| AD-D015661 | p 2854 N93-26091

VIDEO DATA
Data processing and control in a transputer system for remote sensing of the Earth p 2753 N93-24870
Evaluation of lens distortion errors in video-based motion analysis
| NASA-TP-3266 | p 2797 N93-25736

VIDEO EQUIPMENT
United States Army space experiment 601
| AD-A261460 | p 2798 N93-26353

VIDEO SIGNALS
Video scan rate conversion method and apparatus for achieving same
| AD-D015661 | p 2854 N93-26091

VIRTUAL REALITY
Autonomic physiological data associated with simulator discomfort
| NASA-CR-177609 | p 2794 N93-24738

VISCOELASTIC DAMPING
Graphite/epoxy composite laminates with co-cured interlaminar damping layers p 2642 N93-25587

VISCOELASTICITY
Use and analysis of finite element methods for problems of solid mechanics and fracture
| AD-A261574 | p 2731 N93-26522

VISCOPLASTICITY
A micromechanical viscoplastic stress-strain model with grain boundary sliding
| DE93-009109 | p 2649 N93-25095

VISCOSITY
Tables for the thermophysical properties of ethane
| PB93-160786 | p 2646 N93-26319
On the stability of finite plastic deformations
| AD-A261526 | p 2730 N93-26361

VISCOUS DAMPING
On the effect of acoustic coupling on random and harmonic plate vibrations
| NASA-TM-107740 | p 2844 N93-25189

VISCOUS FLOW
Prediction of forces and moments for hypersonic flight vehicle control effectors
| NASA-CR-193033 | p 2595 N93-24762
Computation of hypersonic viscous flowfields using the parabolized Navier-Stokes equations p 2694 N93-24766
An analysis of lift forces on aerosols in a wall bounded turbulent shear flow
| DE93-003362 | p 2695 N93-24963
The steady Navier-Stokes problem for low Reynolds number viscous jets p 2698 N93-25264
Numerical modelling of viscous turbomachinery flows with a pressure correction method p 2594 N93-25702
The rate form of equilibrium equation for problems of steady-state, elastic, viscous flows p 2704 N93-25708
Thermocapillary flow near a cold wall
| AD-A261050 | p 2706 N93-25779
Model fan passage flow simulation
| AD-A261613 | p 2707 N93-26167

VISIBILITY
Runway Visual Range (RVR) Operational Test and Evaluation (OT&E) integration and OT&E operational test report
| DOT/FAA/CT-TN93/37 | p 2584 N93-25243

VISION
The prevalence of artificial lens implants in the civil airman population
| DOT/FAA/AM-92/14 | p 2794 N93-25214
Receptoral and neural aliasing
| AD-A261438 | p 2799 N93-26489

VISUAL CONTROL
Robotic Variable Polarity Plasma Arc (VPPA) welding p 2720 N93-25605

VISUAL FIELDS
Visual perception of elevation
| AD-A261394 | p 2797 N93-26307
Neuropsychological components of object identification
| AD-A261449 | p 2797 N93-26347
Receptoral and neural aliasing
| AD-A261438 | p 2799 N93-26489

VISUAL FLIGHT
Visual approach data collection at St. Louis Lambert Field (STL)
| DOT/FAA/CT-TN93/2 | p 2584 N93-24948

VISUAL PERCEPTION
Visual processing of object velocity and acceleration
| AD-A261048 | p 2800 N93-25778
Perceptual factors that influence use of computer enhanced visual displays
| NASA-CR-192961 | p 2811 N93-26150
Visual perception of elevation
| AD-A261394 | p 2797 N93-26307
Neural basis of motion perception
| AD-A261452 | p 2798 N93-26349
Coordinated action in 3-D space
| AD-A261418 | p 2799 N93-26449

VISUAL STIMULI
Topography from shading and stereo p 2879 N93-25803

VISUAL TASKS
Duration of alpha suppression increases with angle in a mental rotation task
| AD-A261592 | p 2798 N93-26435

VITERBI DECODERS
A low-complexity and high performance concatenated coding scheme for high-speed satellite communications
| NASA-CR-192715 | p 2673 N93-25198

VLASOV EQUATIONS
Effect of continuous eigenvalue spectrum on plasma transport in toroidal systems
| NIFS-214 | p 2859 N93-25215

VOICE COMMUNICATION
Speech research
| AD-A260643 | p 2675 N93-25639
Admission control in integrated voice/data multihop radio networks
| AD-A261055 | p 2680 N93-26227

VOIDS
Improved composite fabrication process
| AD-D015679 | p 2640 N93-26145

VOLCANOES
Winter warming from large volcanic eruptions
| NASA-CR-192848 | p 2763 N93-25244

VOLTAGE CONVERTERS (DC TO DC)
DC-DC power converter research for Orbiter/Station power exchange
| NASA-CR-192939 | p 2633 N93-26425

VOLTAGE REGULATORS
A microcomputer compensated crystal oscillator MCXO p 2834 N93-25001

VORTEX BREAKDOWN
Supersonic shock wave/vortex interaction
| NASA-CR-192917 | p 2576 N93-25249
Simulation of vortex bursting p 2580 N93-25881

VORTEX GENERATORS
Vortex shedding in oscillatory flow p 2700 N93-25438

VORTEX SHEDDING
The transient development of vortices over delta wings p 2576 N93-25269
Vortex shedding in oscillatory flow p 2700 N93-25438

VORTEX SHEETS
Analysis of wing wake roll-up using a vortex-in-cell method p 2579 N93-25706

VORTICES
Observations of an intrathermocline vortex p 2788 N93-24769
A premixed laminar flame interacting with a vortex resulting in flame stretch and quenching p 2642 N93-24771
Computational study of the aerodynamics and control by blowing of asymmetric vortical flows over delta wings p 2574 N93-24772
The modeling of complex continua: Fundamental obstacles and grand challenges
| DE93-006507 | p 2696 N93-25193
Flow visualizations of perpendicular blade vortex interactions
| NASA-CR-192725 | p 2696 N93-25208
Supersonic shock wave/vortex interaction
| NASA-CR-192917 | p 2576 N93-25249
The transient development of vortices over delta wings p 2576 N93-25269
A dynamical theory for hurricane spiral bands p 2782 N93-25352
Dynamics of Gulf Stream meanders and frontal eddies in the South Atlantic Bight p 2788 N93-25354
The interaction of modulated vortex pairs with a free surface p 2701 N93-25485
Tangential fuselage blowing on an ogive cylinder p 2578 N93-25545
An analysis of mesoscale convective systems observed during the 1992 Tropical Cyclone Motion field experiment
| AD-A260889 | p 2783 N93-25633
Analysis of wing wake roll-up using a vortex-in-cell method p 2579 N93-25706
Initial streamwise vorticity formation in a two-stream mixing layer p 2579 N93-25752
Large-eddy simulation of temporally developing boundary layers with embedded streamwise vortices p 2705 N93-25753
Simulation of vortex bursting p 2580 N93-25881
Method of measuring cross-flow vortices by use of an array of hot-film sensors
| NASA-CASE-LAR-14824-1-SB | p 2706 N93-26000
Reduction in size and unsteadiness of a VTOL ground vortex by ground fences
| NASA-CR-192997 | p 2580 N93-26049
Conical Euler analysis and active roll suppression for unsteady vortical flows about rolling delta wings
| NASA-TP-3259 | p 2581 N93-26134
Trailing vortex/free-surface interaction
| AD-A261654 | p 2581 N93-26195
Flame-turbulence interactions
| AD-A260957 | p 2645 N93-26220
Interaction of vorticity with a free surface
| AD-A261524 | p 2707 N93-26360

VORTICITY
Nonlinear evolution of the first mode supersonic oblique waves in compressible boundary layers. Part 1: Heated/cooled walls
| NASA-TM-106087 | p 2696 N93-25175
The transient development of vortices over delta wings p 2576 N93-25269
A dynamical theory for hurricane spiral bands p 2782 N93-25352
Numerical simulation of leading-edge receptivity to freestream vorticity p 2577 N93-25388
Initial streamwise vorticity formation in a two-stream mixing layer p 2579 N93-25752
Interaction of vorticity with a free surface
| AD-A261524 | p 2707 N93-26360

VORTICITY EQUATIONS
Implementation of the Turn Function Method in a three-dimensional, parallelized hydrodynamics code
| DE93-003744 | p 2696 N93-25124

VULNERABILITY
Minutes of the Twenty-Fifth Explosives Safety Seminar, volume 4
| AD-A261116 | p 2660 N93-25769

W

WAFERS
Two- and three-dimensional high performance, patterned overlay multi-chip module technology p 2694 N93-25581
MOCVD process technology for affordable, high-yield, high-performance MESFET structures. Phase 3: MIMIC | AD-A261178 | p 2690 N93-25820
Fundamental and applied aspects of defect engineering in GaAs | AD-A260573 | p 2867 N93-25899

WAKES
Application of finite-state inflow to flap-lag-torsion damping in hover p 2587 N93-25486
Analysis of wing wake roll-up using a vortex-in-cell method p 2579 N93-25706

WALKING MACHINES
Biped control via nonlinear dynamics p 2718 N93-25697

WALL FLOW
An analysis of lift forces on aerosols in a wall bounded turbulent shear flow | DE93-003362 | p 2695 N93-24963
Assessment of closure coefficients for compressible-flow turbulence models | NASA-TM-103882 | p 2697 N93-25247
Particle dynamics modeling of boundary effects in granular Couette flow p 2705 N93-25738
Thermocapillary flow near a cold wall | AD-A261050 | p 2706 N93-25779

WALL JETS
Reduction in size and unsteadiness of a VTOL ground vortex by ground fences | NASA-CR-192997 | p 2580 N93-26049

WALL PRESSURE
An experimental study of the sources of fluctuating pressure loads beneath swept shock/boundary-layer interactions | NASA-CR-192918 | p 2698 N93-25266
A model for the filling of cold cavities with solidifying, semi-crystalline polymers | DE93-003817 | p 2655 N93-25507
Correlations between organized turbulent structures and wall pressure fluctuations | PB93-156479 | p 2706 N93-25885

WALLS
An analysis of lift forces on aerosols in a wall bounded turbulent shear flow | DE93-003362 | p 2695 N93-24963
The design of a modular sound absorber for very low frequencies | BBC-RD-1992/10 | p 2673 N93-25170
Nonlinear evolution of the first mode supersonic oblique waves in compressible boundary layers. Part 1: Heated/cooled walls | NASA-TM-106087 | p 2696 N93-25175
Laminar and turbulent natural convection heat transfer in Trombe wall channels p 2702 N93-25551
Radial spline assembly for antifriction bearings | NASA-CASE-MFS-28629-1 | p 2719 N93-26001

WALSH FUNCTION
Walsh function generator for the Electronically Scanned Thinned Array Radiometer (ESTAR) instrument | NASA-TM-4449 | p 2689 N93-25618

WAR GAMES
Fidelity and validity in distributed interactive simulation: Questions and answers | AD-A260971 | p 2810 N93-25711

WARFARE
Science, technology, and national security p 2886 N93-25232

WARNING SYSTEMS
A single-point warning system for thunderstorms and electric fields p 2711 N93-24900
PROAV Cable Warning System (CWS) - U.S. Army aircraft Integration assessment and OCONUS field evaluation | AD-A261233 | p 2583 N93-26263

WASTE DISPOSAL
Development of a cone penetrometer for measuring spectral characteristics of soils in situ p 2776 N93-25570
Development of a heuristic knowledge base for the selection of applicable or relevant and appropriate environmental requirements | AD-A261038 | p 2765 N93-25864
Human factors in environmental management: New directions from the Hanford site | DE93-004337 | p 2767 N93-26495

WASTE TREATMENT
Converting environmental wastes into valuable resources p 2759 N93-25572
Development of a pyrolysis waste recovery model with designs, test plans, and applications for space-based habitats p 2803 N93-26076
Human factors in environmental management: New directions from the Hanford site | DE93-004337 | p 2767 N93-26495
Treatment of hazardous organic wastes using silent discharge plasmas | DE93-003789 | p 2768 N93-26592

WASTE WATER
Health and environmental chemistry: Analytical techniques, data management, and quality assurance | DE93-002853 | p 2760 N93-24674
Low cost dewatering of waste slurries p 2769 N93-25573

WATER
The WINCOF-I code: Detailed description | NASA-CR-190779 | p 2573 N93-24760
Narrow-body aircraft water spray optimization study | DOT/FAA/CT-TN93/3 | p 2582 N93-25224
Effects of moisture and other contaminants in friction composites | AD-A261226 | p 2640 N93-26301

WATER BALANCE
Determination of environmental dynamics using NOAA satellite data and a water balance model for the Mediterranean landscape p 2741 N93-24794

WATER DEPTH
Preliminary studies leading toward the development of a LIDAR bathymetry mapping instrument p 2711 N93-25614

WATER IMMERSION
Effect of water immersion on fiber/matrix adhesion | AD-A260704 | p 2636 N93-25652

WATER MANAGEMENT
Remote sensing in hydrology and water management p 2744 N93-24816
Applications of remote sensing for tidal waters, coastal areas and inland waters p 2745 N93-24819

WATER POLLUTION
NORSMAP 1989: Norwegian remote sensing spectrometry for mapping and monitoring of algal blooms and pollution p 2746 N93-24824
Non-local description of pollution transport in random medium p 2763 N93-25329
Space life support technology applications to terrestrial environmental problems p 2803 N93-25617
Inorganic nitrogen and phosphorus dynamics in the water column of the Patuxent River | PB93-172955 | p 2767 N93-26511
Model for transport of floating debris in the ocean | PB93-172997 | p 2768 N93-26559

WATER QUALITY
Oil pollution and water quality mapping of Augusta Bay, Italy using remote sensing techniques p 2746 N93-24823
NORSMAP 1989: Norwegian remote sensing spectrometry for mapping and monitoring of algal blooms and pollution p 2746 N93-24824
Multi-date algorithms for predicting surface water quality parameters in estuarine and coastal waters using Landsat TM data | ED-659-CP | p 2746 N93-24829
Loss of temporal coherence of laser light propagated through simulated coastal waters | AD-A261303 | p 2715 N93-26296

WATER RECLAMATION
Low cost dewatering of waste slurries p 2769 N93-25573

WATER RESOURCES
Interactive forecasting with the National Weather Service River Forecast System p 2788 N93-25616

WATER RUNOFF
Remote sensing in hydrology and water management p 2744 N93-24816

WATER TABLES
Development and testing of improved techniques for modeling the hydrologic cycle in a mesoscale weather prediction system | AD-A261454 | p 2787 N93-26351

WATER TEMPERATURE
Neural networks for atmospheric retrievals p 2824 N93-25975

WATER TREATMENT
Treatment of hazardous organic wastes using silent discharge plasmas | DE93-003789 | p 2768 N93-26592

WATER VAPOR
The WINCOF-I code: Detailed description | NASA-CR-190779 | p 2573 N93-24760
Observed annual and interannual variations in tropospheric water vapor p 2782 N93-25549

WAVE ATTENUATION
Rain rate and modeled fade distributions at 20 GHz and 30 GHz derived from five years of network rain gauge measurements p 2683 N93-26468
On the estimation of risk associated with an attenuation prediction p 2683 N93-26469
Satellite communications application to Pacific countries above Ku band p 2683 N93-26471
Brightness temperature and attenuation diversity statistics at 20.6 and 31.65 GHz for the Colorado Research Network p 2684 N93-26473
ESA's planning and coordination of the OLYMPUS propagation experiment p 2684 N93-26477
Effect-specific analysis of propagation parameters p 2684 N93-26478
The Virginia Tech OLYMPUS propagation experiment p 2685 N93-26479
Status of the Olympus experiment at CRC p 2685 N93-26480
Rain compensation algorithm using adaptive linear prediction p 2685 N93-26485

WAVE EQUATIONS
Time dependent simulation of cosmic-ray shocks including Alfven transport | NASA-CR-192931 | p 2899 N93-24752
Elastic modeling and migration in Earth models p 2771 N93-25433

WAVE FRONT DEFORMATION
DSD Technology: A detonation reactive Huygens code | LA-12235-MS | p 2706 N93-25987

WAVE FUNCTIONS
Performance results of a 300-degree linear phase modulator for spaceborne communications applications p 2672 N93-24670
Correlated wavefunction quantum Monte Carlo approach to solids | DE93-007730 | p 2863 N93-25367

WAVE GENERATION
Theoretical and experimental investigation of electron beam acceleration and sub-millimeter wave generation | AD-A261117 | p 2609 N93-25770

WAVE INTERACTION
Interactions of acoustic waves and combustion of homogeneous solid propellants in rocket motors p 2630 N93-26039

WAVE PACKETS
On the generation and dispersion of Yanai waves with a spectral Chebyshev-collocation reduced-gravity ocean model p 2788 N93-25276
Bimolecular reaction dynamics from photoelectron spectroscopy of negative ions | DE93-007669 | p 2647 N93-26599

WAVE PROPAGATION
Tracking sharp interface of two fluids by the CIP (Cubic-Interpolated Propagation) scheme | NIFS-206 | p 2698 N93-25277
Propagation at microwave frequencies in the presence of tropospheric stratified layers p 2674 N93-25340
A dynamical theory for hurricane spiral bands p 2782 N93-25352
Determination of the elastic constants of composite materials from ultrasonic group velocity measurements p 2635 N93-25544
Proceedings of the 5th International Symposium on Long Range Sound Propagation | AD-A260666 | p 2845 N93-25643
Generation of acoustic waves by focused infrared neodymium-laser radiation p 2714 N93-25761
DSD Technology: A detonation reactive Huygens code | LA-12235-MS | p 2706 N93-25987
Propagation of finite amplitude sound in a waveguide with a parabolic sound velocity profile | ARL-TR-92-11 | p 2846 N93-26179
Laser propagation through turbulence | AD-A260712 | p 2714 N93-26217
High Frequency (HF) radiowave propagation | AD-A261726 | p 2681 N93-26280
Analysis of longitudinal impact on semi-infinite circular bars and tubes. Appendix no. 2 | AD-A261556 | p 2731 N93-26459
Proceedings of the 16th NASA Propagation Experimenters Meeting (NAPEX 16) and the Advanced Communications Technology Satellite (ACTS) Propagation Studies Miniworkshop | NASA-CR-192800 | p 2682 N93-26463
Opening remarks p 2682 N93-26464
The ACTS propagation program p 2683 N93-26465
L- and K-band LMSS propagation measurements using MARECS-B, OLYMPUS, and ACTS p 2683 N93-26467
A database for propagation models p 2684 N93-26472
Brightness temperature and attenuation diversity statistics at 20.6 and 31.65 GHz for the Colorado Research Network p 2684 N93-26473
WARC 92 and some thoughts as to its impact on the NASA propagation program p 2684 N93-26475
ESA's planning and coordination of the OLYMPUS propagation experiment p 2684 N93-26477

Effect-specific analysis of propagation parameters
p 2684 N93-26478
Status of the Olympus experiment at CRC
p 2685 N93-26480
Observations on the NASA Propagation Program
p 2685 N93-26482
ACTS propagation terminal update
p 2685 N93-26484
Rain compensation algorithm using adaptive linear prediction p 2685 N93-26485

WAVE REFLECTION
On the effective reflection properties of the randomly segmented elastic bar p 2724 N93-25328

WAVE SCATTERING
Enhanced backscattering from rough surfaces
| AD-A261000 | p 2676 N93-25855

WAVE-PARTICLE INTERACTIONS
Time dependent simulation of cosmic-ray shocks including Alfven transport
| NASA-CR-192931 | p 2899 N93-24752
Alfven wave transport effects in the time evolution of parallel cosmic-ray modified shocks
| NASA-CR-192932 | p 2899 N93-25161
Very low frequency signals and whistler-mode amplification in the magnetosphere and limit-cycle behavior in the CECAF infrared free electronic laser
| AD-A261776 | p 2716 N93-26601

WAVEFORMS
Monaural and binaural processing of complex waveforms
| AD-A261659 | p 2846 N93-26358

WAVEGUIDE ANTENNAS
Performance of a 12-GHz fiber-optic system for beam-waveguide antenna stability testing
p 2677 N93-26113
Optimizing the G/T ratio of the DSS-13 34-meter beam-waveguide antenna p 2678 N93-26118

WAVEGUIDE LASERS
Ultraviolet waveguide lasers for phased array lidar
| AD-A261657 | p 2715 N93-26363

WAVEGUIDES
Time resolved studies of in-well and cross-well carrier transport in MQW semiconductor structures
| AD-A261170 | p 2714 N93-25774
Propagation of finite amplitude sound in a waveguide with a parabolic sound velocity profile
| ARL-TR-92-11 | p 2846 N93-26179
Analysis of longitudinal impact on semi-infinite circular bars and tubes. Appendix no. 2
| AD-A261556 | p 2731 N93-26459

WAVERIDERS
Optimized scramjet engine integration on a waverider airframe p 2593 N93-25480

WEAPON SYSTEMS
The systems engineering overview and process (from the Systems Engineering Management Guide, 1990)
p 2665 N93-24679
Fidelity and validity in distributed interactive simulation: Questions and answers
| AD-A260971 | p 2810 N93-25711
CALS-HSC data element dictionary
| AD-A261560 | p 2813 N93-26461
Technical operating report on the Data Integration and Collection Environment (DICE) instrumentation system design
| AD-A261105 | p 2591 N93-26572

WEAR
Elastomer compound developed for high wear applications p 2659 N93-25607
Advanced bristle seals for gas turbine engines
| AD-A261296 | p 2720 N93-26564

WEAR RESISTANCE
Macromolecules for inhibition of corrosion and wear
| AD-A261041 | p 2655 N93-25816

WEATHER
A comparison of the WIND System atmospheric models and MATS data
| DE93-002687 | p 2760 N93-24673
Applications of triggered lightning to space vehicle operations p 2619 N93-24878

WEATHER FORECASTING
Weather forecasting expert system study
| NASA-CR-192929 | p 2777 N93-24747
The need for spaceborne observations for meteorology and climatology p 2744 N93-24813
A single-point warning system for thunderstorms and electric fields p 2711 N93-24900
Application of optical remote sensing to the study of surface fluxes related to cloud formation
| DE93-003783 | p 2781 N93-25125
The ATC evaluation of the prototype Airport Surveillance Radar Wind Shear Processor (ASR-WSP) at Orlando International Airport
| DOT/FAA/CT-TN92/48 | p 2673 N93-25210
A systematic satellite approach for estimating central pressures of mid-latitude oceanic storms
| NOAA-TR-NESDIS-63 | p 2781 N93-25220
Rossby-gravity waves in tropical total ozone data
| NASA-CR-192983 | p 2764 N93-25432
Numerical simulation of the seasonal and interannual variability of the tropical Atlantic Ocean circulation during the 1980's p 2789 N93-25445
Interactive forecasting with the National Weather Service River Forecast System p 2788 N93-25616
Computation of moisture flux from ocean to atmosphere using a synergy of SSM/I-derived precipitable water and ECMWF analyses p 2774 N93-25757
National Weather Service Winter Weather Workshop
| PB93-146785 | p 2785 N93-25775
Typhoon prediction (recurvature - 1990 experiment)
| AD-A260673 | p 2786 N93-25892
Development and testing of improved techniques for modeling the hydrologic cycle in a mesoscale weather prediction system
| AD-A261454 | p 2787 N93-26351

WEATHER MODIFICATION
Investigation of winter mountain storms in Utah during the 1989 Utah/NOAA field program
| PB93-153021 | p 2785 N93-25849

WEDGES
Combined LAURA-UPS hypersonic solution procedure
| NASA-TM-107682 | p 2696 N93-25176

WEIGHT (MASS)
What is the relationship between altitude and weight in a model rocket? p 2603 N93-24715

WEIGHTING FUNCTIONS
Computation and learning in neural networks with binary weights
| AD-A261182 | p 2821 N93-25821

WEIGHTLESSNESS
JPRS report: Science and technology. Central Eurasia: Life sciences
| JPRS-ULS-92-022 | p 2795 N93-25407
Numerical study of cavity natural convection flow with augmenting and counteracting effects by projection finite element method p 2701 N93-25540
MAC to VAX connectivity: Heartrate spectral analysis system p 2796 N93-25594
Conceptual design for the Space Station Freedom fluid physics/dynamics facility
| NASA-TM-103663 | p 2618 N93-26209

WELDED JOINTS
Fatigue resistance of orthotropic plates with trapezoidal stiffeners
| TRL-TRANS-T3908 | p 2726 N93-25419
Laser welding of selected aerospace alloys
p 2718 N93-25435
Robotic Variable Polarity Plasma Arc (VPPA) welding
p 2720 N93-25605
External stress-corrosion cracking of a 1.22-m-diameter type 316 stainless steel air valve
| NASA-TP-3190 | p 2652 N93-26201

WELDING
Vision-aided monitoring and control of thermal spray, spray forming, and welding processes
p 2670 N93-25604
Thermocapillary flow near a cold wall
| AD-A261050 | p 2706 N93-25779

WETLANDS
Bibliography of remote sensing techniques used in wetland research
| AD-A261704 | p 2757 N93-26440

WHEATSTONE BRIDGES
The constant current loop: A new paradigm for resistance signal conditioning
| NASA-TM-108744 | p 2673 N93-25181

WHEELS
Position and force control of a vehicle with two or more steerable drive wheels
| DE92-041301 | p 2717 N93-25100

WHISKER COMPOSITES
Mullite whiskers and mullite-whisker felt
p 2642 N93-25586

WHISKERS (CRYSTALS)
Whisker growth studies under conditions which resemble those available on an orbiting space station
| NASA-CR-192701 | p 2664 N93-25218

WHISPERING GALLERY MODES
R and D of transmission lines for ECH system
| NIFS-210 | p 2687 N93-24951
Microwave frequency discriminator with a cryogenic sapphire resonator for ultra-low phase noise
p 2693 N93-24982

WHITE NOISE
Frequency generation and synthesis in the DRSS
p 2693 N93-25054
Figure of merit for direct-detection optical channels
p 2678 N93-26117
New results in signal design for the AWGN channel
| AD-A261424 | p 2682 N93-26451

WIDE ANGLE LENSES
Miniature Optical Wide-Angle-Lens Startracker (Mini-OWLS) p 2606 N93-24728
High resolution stereo imaging and data compression
p 2753 N93-24867
Evaluation of lens distortion errors in video-based motion analysis
| NASA-TP-3266 | p 2797 N93-25736

WILDLIFE
Incorporating biodiversity considerations into environmental impact analysis under the National Environmental Policy Act
| PB93-139806 | p 2766 N93-25878

WIND (METEOROLOGY)
A climatology of polar low occurrences in the Nordic Seas and an examination of katabatic winds as a triggering mechanism
| AD-A261719 | p 2786 N93-26245
The Martian lower atmosphere p 2897 N93-26394

WIND EFFECTS
Mapping of windfall damage in the Hunsrueck plateau with Landsat TM-data p 2749 N93-24843
An observational study of the local and remote response of the equatorial Pacific to westerly wind events during the 1991-92 El Nino
| AD-A261777 | p 2787 N93-26286
Wind-driven coastal generation of annual mesoscale eddy activity in the California current
| AD-A261355 | p 2790 N93-26331
Model for transport of floating debris in the ocean
| PB93-172997 | p 2768 N93-26559
Guide for conducting convective windstorm surveys
| PB93-148427 | p 2787 N93-26570

WIND MEASUREMENT
Polarizing Michelson interferometer for measuring thermospheric winds
| ISBN-0-315-70442-X | p 2784 N93-25731

WIND PROFILES
Empirical wind model for the middle and lower atmosphere. Part 1: Local time average
| NASA-TM-104581 | p 2770 N93-25160

WIND SHEAR
The ATC evaluation of the prototype Airport Surveillance Radar Wind Shear Processor (ASR-WSP) at Orlando International Airport
| DOT/FAA/CT-TN92/48 | p 2673 N93-25210
Setting values for TDWR/LLWAS 3 integration parameters
| AD-A260740 | p 2783 N93-25645

WIND TUNNEL APPARATUS
NASA Lewis 8- by 6-foot supersonic wind tunnel user manual
| NASA-TM-105771 | p 2597 N93-25080
Nozzle diffuser for use with an open test section of a wind tunnel
| NASA-CASE-LAR-14424-1-SB | p 2598 N93-25996

WIND TUNNEL MODELS
Fabrication of composite propfan blades for a cruise missile wind tunnel model
| NASA-TM-105270 | p 2730 N93-26202
Optically smart surfaces survivability testing at Mach 3
| AD-A261785 | p 2857 N93-26566

WIND TUNNEL TESTS
Measurements of density, temperature, and their fluctuations in turbulent supersonic flow using UV laser spectroscopy
| NASA-TM-103943 | p 2708 N93-25076
A simple, approximate model of parachute inflation
| DE93-002465 | p 2576 N93-25121
Experimental study of the effect of helical grooves on an infinite cylinder
| AD-A260890 | p 2676 N93-25912
Fabrication of composite propfan blades for a cruise missile wind tunnel model
| NASA-TM-105270 | p 2730 N93-26202
Supersonic aeroelastic instability results for a NASP-like wing model
| NASA-TM-107739 | p 2591 N93-26553

WIND TUNNELS
Nozzle diffuser for use with an open test section of a wind tunnel
| NASA-CASE-LAR-14424-1-SB | p 2598 N93-25996

WIND TURBINES
An advanced data-acquisition system for wind energy projects
| DE93-000079 | p 2874 N93-25254

WIND VELOCITY
An analysis of mesoscale convective systems observed during the 1992 Tropical Cyclone Motion field experiment
| AD-A260889 | p 2783 N93-25633
Errors caused by incompatible wind and buoyancy forcing in the ocean general circulation models
| AD-A260894 | p 2789 N93-25657

Summary by the cloud and aerosol research group for ASTEX
| AD-A261292 | p 2766 N93-26292
Tornado: An engineering-oriented perspective
| PB93-148435 | p 2788 N93-26584
WINDPOWER UTILIZATION
An advanced data-acquisition system for wind energy projects
| DE93-000079 | p 2874 N93-25254
WINDS ALOFT
Polarizing Michelson interferometer for measuring thermospheric winds
| ISBN-0-315-70442-X | p 2784 N93-25731
WINGS
General aviation aircraft: Normal acceleration data analysis and collection project
| DOT/FAA/CT-91/20 | p 2586 N93-24739
Analysis of wing wake roll-up using a vortex-in-cell method p 2579 N93-25706
WINTER
Investigation of winter mountain storms in Utah during the 1989 Utah/NOAA field program
| PB93-153021 | p 2785 N93-25849
WIRE
PROAV Cable Warning System (CWS) - U.S. Army aircraft Integration assessment and OCONUS field evaluation
| AD-A261233 | p 2583 N93-26263
WIRE CLOTH
Reduction in size and unsteadiness of a VTOL ground vortex by ground fences
| NASA-CR-192997 | p 2580 N93-26049
WIRING
Report of the Seasat Failure Review Board p 2619 N93-24693
WORDS (LANGUAGE)
Facilitation and interference in identification of pictures and words
| AD-A261484 | p 2798 N93-26356
Perception and the temporal properties of speech
| AD-A261439 | p 2686 N93-26490
WORK HARDENING
Analysis of shaped charge jet penetration experiments with Pen
| UCRL-LR-110773 | p 2730 N93-26177
Use and analysis of finite element methods for problems of solid mechanics and fracture
| AD-A261574 | p 2731 N93-26522
WORK-REST CYCLE
Simulated sustained flight operations and performance. Part 1: Effects of fatigue
| AD-A261012 | p 2801 N93-25859
WORKING FLUIDS
Malone refrigeration
| DE93-005439 | p 2668 N93-25447
WORKLOADS (PSYCHOPHYSIOLOGY)
Physiological indices of mental workload
| AD-A261692 | p 2798 N93-26391
WORKSTATIONS
A trace-driven analysis of name and attribute caching in a distributed system
| NASA-CR-192899 | p 2815 N93-25251
Interfacing a high performance disk array file server to a Gigabit LAN
| NASA-CR-192898 | p 2816 N93-25458
Splash 2 p 2814 N93-25575

X

X RAY ANALYSIS
Crystal growth of berlinite: Methods for growing longer crystals and improving the quality p 2838 N93-25025
Crystal growth and physical characterizations of GaPO4 p 2840 N93-25044
VETA-I x ray test analysis
| NASA-CR-192321 | p 2854 N93-26183
X-ray computed tomography for casting development
| AD-A261786 | p 2722 N93-26526
X ray computed tomography for failure analysis
| AD-A261884 | p 2722 N93-26527
X RAY APPARATUS
Poster session: Fifth Users Meeting for the Advanced Photon Source
| DE93-006019 | p 2598 N93-26498
X RAY ASTRONOMY
Starburst Galaxies: Hard X-ray spectra and contribution to the diffuse background
| NASA-CR-192790 | p 2892 N93-25211
ROSAT x ray survey observations of active chromospheric binary systems and other selected sources
| NASA-CR-192933 | p 2891 N93-26426
X RAY ASTROPHYSICS FACILITY
Intensity distribution of the x ray source for the AXAF VETA-I mirror test p 2854 N93-26184
VETA-1 x ray detection system p 2854 N93-26185
VETA x ray data acquisition and control system p 2854 N93-26186
Correcting x ray spectra obtained from the AXAF VETA-I mirror calibration for pileup, continuum, background and deadtime p 2854 N93-26187
AXAF VETA-I mirror encircled energy measurements and data reduction p 2855 N93-26188
Precision of the calibration of the AXAF engineering test article (VETA) mirrors p 2855 N93-26189
Image analysis of the AXAF VETA-I x ray mirror p 2855 N93-26190
Surface finish quality of the outer AXAF mirror pair based on x ray measurements of the VETA-I p 2855 N93-26191
The x ray reflectivity of the AXAF VETA-I optics p 2855 N93-26192
X RAY BINARIES
ROSAT x ray survey observations of active chromospheric binary systems and other selected sources
| NASA-CR-192933 | p 2891 N93-26426
X RAY DETECTORS
VETA-1 x ray detection system p 2854 N93-26185
X RAY DIFFRACTION
Synchrotron radiation X ray topography study of lateral field resonators p 2833 N93-24994
Measurement results of the crystallographic orientation of the SC cut round plates p 2840 N93-25040
Probe molecule studies: Active species in alcohol synthesis
| DE93-008097 | p 2659 N93-25119
X RAY IMAGERY
High speed x ray gating cameras for ICF imaging applications
| DE93-007500 | p 2709 N93-25515
VETA-1 x ray detection system p 2854 N93-26185
X RAY LASERS
Progress in imaging microscopy with x ray lasers at LLNL
| DE93-007508 | p 2712 N93-25363
X RAY SOURCES
Steady-state numerical models of accreting neutron stars: The effect of atmospheric CNO depletion and diffusion p 2889 N93-25624
Intensity distribution of the x ray source for the AXAF VETA-I mirror test p 2854 N93-26184
Correcting x ray spectra obtained from the AXAF VETA-I mirror calibration for pileup, continuum, background and deadtime p 2854 N93-26187
Surface finish quality of the outer AXAF mirror pair based on x ray measurements of the VETA-I p 2855 N93-26191
The x ray reflectivity of the AXAF VETA-I optics p 2855 N93-26192
X RAY SPECTRA
Starburst Galaxies: Hard X-ray spectra and contribution to the diffuse background
| NASA-CR-192790 | p 2892 N93-25211
Correcting x ray spectra obtained from the AXAF VETA-I mirror calibration for pileup, continuum, background and deadtime p 2854 N93-26187
Large area, low capacitance Si(Li) detectors for high rate x ray applications
| DE93-007661 | p 2692 N93-26598
X RAY SPECTROSCOPY
The interaction of HCN/DCN with Si(100)-2x1
| AD-A260837 | p 2645 N93-25920
Interaction of O2 with the Fe(.84)Cr(.16) (001) surface studied by photoelectron spectroscopy
| AD-A261065 | p 2645 N93-26251
X RAY TELESCOPES
The ALEXIS data processing package: An update
| DE93-007374 | p 2899 N93-25185
The x ray reflectivity of the AXAF VETA-I optics p 2855 N93-26192
X RAYS
Large area, low capacitance Si(Li) detectors for high rate x ray applications
| DE93-007661 | p 2692 N93-26598
X-30 VEHICLE
Aerospace-plane flights and stratospheric ozone: Review and preliminary assessment of the National Aerospace Plane (NASP) operations
| RAND/N-3464-AF | p 2767 N93-26327
XENON CHLORIDE LASERS
Ultraviolet waveguide lasers for phased array lidar
| AD-A261657 | p 2715 N93-26363

Y

YAG LASERS
Injection seeded, diode-pumped, short pulse Nd:YAG ring laser for space-based laser ranging p 2713 N93-25389
YAW
Helicopter low-speed yaw control
| NASA-CASE-LAR-14219-1 | p 2597 N93-25998
YBCO SUPERCONDUCTORS
Studying the kinetics of magnetization in high Tc superconductors
| NASA-CR-192916 | p 2862 N93-25108
Rheology of YBa2Cu3O(7-x) precursors
| DE93-007285 | p 2863 N93-25362
Environmental test program for superconducting materials and devices
| DE93-003646 | p 2864 N93-25506
Aerospace devices for magnetic replicas
| NASA-CR-192958 | p 2865 N93-25667
Advanced HTS S-N-S devices
| AD-A261552 | p 2869 N93-26381
YEAST
Biological production of ethanol from coal
| DE93-008947 | p 2660 N93-25496
YTTERBIUM ISOTOPES
Ion trap frequency standard research at PTB p 2841 N93-25050
YTTRIUM OXIDES
Sputter deposition of yttrium-oxides
| DE93-007499 | p 2654 N93-25382

Z

ZEOLITES
Gravity-dependent transport phenomena in zeolite crystal growth p 2664 N93-25740
ZINC COATINGS
In situ surface studies of conversion coatings for steel and aluminum
| AD-A261016 | p 2655 N93-25861
ZINC OXIDES
Non-H2Se, ultra-thin CIS devices
| DE93-000078 | p 2759 N93-25253
ZINC SELENIDES
IR materials producibility
| AD-A261099 | p 2853 N93-25766
ZINC TELLURIDES
Study of surface behavior in function of temperature of the quaternary system (Hg, Cd, Zn)Te
| AD-A260968 | p 2867 N93-26223
ZIRCONIUM COMPOUNDS
Laser Induced Phonons (LIPs) in MBE grown ZnSe
| RSRE-MEMO-4544 | p 2864 N93-25454
ZIRCONIUM OXIDES
Transformation plasticity and fracture behavior of ceria-TZP/alumina composites p 2638 N93-25760
ZONAL FLOW (METEOROLOGY)
Kelvin waves in total column ozone
| NASA-CR-192984 | p 2764 N93-25431

Typical Personal Author Index Listing

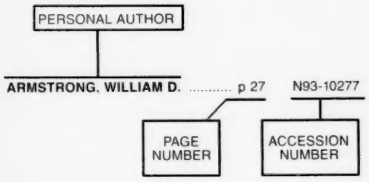

Listings in this index are arranged alphabetically by personal author. The page number helps you locate the citation in the abstract section. The accession number denotes the number by which the citation is identified.

A

ABARBANEL, H. ..... p 2762 N93-25184
ABATE, J. E. ..... p 2687 N93-25062
ABDUL-AZIZ, ALI ..... p 2731 N93-26550
ABI-AKAR, HIND MALAEB ..... p 2663 N93-24774
ABIODUN, ADIGUN ADE ..... p 2742 N93-24804
ABRAMOWICZ-REED, LINDA ..... p 2604 N93-24723
ABUL-FADL, A. ..... p 2870 N93-26581
ACKERSON, M. D. ..... p 2660 N93-25523
ADDIS, ROBERT P. ..... p 2760 N93-24673
ADLER, RICHARD M. ..... p 2817 N93-25576
ADRIAN, F. J. ..... p 2871 N93-25584
AGAPAKIS, JOHN E. ..... p 2670 N93-25604
AGARWAL, AVAL K. ..... p 2706 N93-26000
AGARWALA, VINOD S. ..... p 2655 N93-25816
AGINS, IRA A. ..... p 2811 N93-25943
AGRAWALA, ASHOK ..... p 2801 N93-26047
AHMAD, I. ..... p 2848 N93-25371
AIFANTIS, E. C. ..... p 2730 N93-26361
AKERLOF, CARL W. ..... p 2888 N93-25172
AKINC, M. ..... p 2649 N93-25149
AKINC, MUFIT ..... p 2863 N93-25362
AKINWANDE, A. I. ..... p 2692 N93-26565
AL-ASMI, KHALFAN ..... p 2700 N93-25438
ALBEE, ARDEN L. ..... p 2772 N93-25529
ALBEROTANZA, L. ..... p 2738 N93-24779
ALESSANDRO, V. ..... p 2742 N93-24799
ALEXANDER, D. J. ..... p 2650 N93-25492
ALEXANDER, M. JOAN ..... p 2896 N93-25285
ALEXANDER, M. L. ..... p 2712 N93-25150
ALEXANDER, S. ..... p 2669 N93-26406
ALFASATWI, Y. ..... p 2746 N93-24827
ALKEZWEENY, A. J. ..... p 2765 N93-25873
ALLEN, GEORGE C. ..... p 2622 N93-25105
ALLEN, JERRY M. ..... p 2581 N93-26085
ALLEN, M. ..... p 2628 N93-26027
ALLEN, MARK ..... p 2880 N93-25804
ALLER, ROBERT O. ..... p 2666 N93-24689
ALLEWIJN, ROELAND ..... p 2745 N93-24819
ALLNER, THOMAS ..... p 2751 N93-24858
ALLUISI, EARL A. ..... p 2810 N93-25711
p 2813 N93-26461
ALPERS, FREDERICK C. ..... p 2691 N93-26142
ALTMAN, BRAD STEWART ..... p 2634 N93-25234
AMBROSINI, R. ..... p 2608 N93-24998
AMES, TROY ..... p 2825 N93-25977
AMMER, U. ..... p 2749 N93-24845
AMUNDSEN, RUTH M. ..... p 2814 N93-25601
ANDERSEN, JERRY ..... p 2609 N93-26175
ANDERSON, DAVID J. ..... p 2573 N93-26136
ANDERSON, DAVID P. ..... p 2720 N93-26249
ANDERSON, E. ..... p 2712 N93-25363
ANDERSON, ERIC ..... p 2609 N93-25836
ANDERSON, G. K. ..... p 2768 N93-26592
ANDERSON, HUGH ..... p 2620 N93-26248
ANDERSON, KARL F. ..... p 2673 N93-25181
ANDERSON, MARK S. ..... p 2653 N93-25078
ANDERSON, R. E. ..... p 2692 N93-26501
ANDERSON, T. J. ..... p 2626 N93-26015
ANDERSON, TED L. ..... p 2727 N93-25647
ANDERSON, THEODORE W. ..... p 2830 N93-25860
ANDERSON, THOMAS E. ..... p 2805 N93-25130
ANDERSON, W. J. ..... p 2610 N93-26180
ANDERSON, W. R. ..... p 2627 N93-26026
p 2628 N93-26028
ANDERSSON, BORJE ..... p 2726 N93-25638
ANDERSSON, KAJ ..... p 2742 N93-24801
ANDREWS, GEORGE A., JR. ..... p 2898 N93-26059
ANDRISANI, DOMINICK, II ..... p 2854 N93-25898
ANGEL, JAMES R. ..... p 2785 N93-25872
ANGUS, W. J. ..... p 2625 N93-26010
ANHOLT, ROBERT R. ..... p 2795 N93-25944
ANLAS, GUNAY ..... p 2634 N93-25333
ANNIS, CHARLES ..... p 2651 N93-25843
ANSARI, RAFAT R. ..... p 2796 N93-25593
ANTOLOVICH, STEPHEN D. ..... p 2652 N93-26235
ANTONIAK, Z. I. ..... p 2758 N93-24975
ARAGON-SALAMANCA, ALFONSO
p 2890 N93-25712
ARAI, KOHEI ..... p 2753 N93-24868
ARBESSER-RASTBURG, B. ..... p 2684 N93-26477
ARCH, D. ..... p 2692 N93-26565
ARIYOSHI, HIDETOSHI ..... p 2774 N93-25889
ARLINGHAUS, H. F. ..... p 2793 N93-26587
ARNAUD, R. ..... p 2838 N93-25025
ARNOLD, G. W. ..... p 2653 N93-24971
ARNOLD, JEFFREY M. ..... p 2814 N93-25575
ARNONE, R. A. ..... p 2757 N93-25868
ARPE, KLAUS ..... p 2761 N93-25145
ARTHUR, TREY ..... p 2808 N93-25073
ASHBY, N. ..... p 2608 N93-24986
ASHER, D. J. ..... p 2889 N93-25536
ASHRAFI, S. ..... p 2603 N93-24716
ASTER, ROBERT ..... p 2665 N93-24682
ATAPINA, N. ..... p 2753 N93-24869
ATASSI, M. Z. ..... p 2794 N93-25566
ATCHLEY, ANTHONY A. ..... p 2759 N93-26310
ATCHOH, R. ..... p 2753 N93-24869
ATHERTON, L. J. ..... p 2870 N93-26594
ATKESON, CHRISTOPHER G. ..... p 2826 N93-26162
ATKINSON, D. J. ..... p 2679 N93-26126
ATWATER, TERRILL ..... p 2694 N93-25582
ATWOOD, CHRISTOPHER ALEXANDER
p 2578 N93-25542
AU, P. A. ..... p 2614 N93-26124
AUBRY, J. P. ..... p 2693 N93-25004
p 2840 N93-25045
p 2694 N93-25055
AUDOIN, C. ..... p 2833 N93-24990
p 2842 N93-25056
AUER, L. H. ..... p 2761 N93-25126
AULD, B. A. ..... p 2836 N93-25012
AUMILLER, D. L. ..... p 2860 N93-25641
AUSTON, DAVID H. ..... p 2856 N93-26306
AVERY, JIM ..... p 2670 N93-26416
AVERY, ROB ..... p 2687 N93-25063
AVERY, S. K. ..... p 2770 N93-25160
AVICOLA, K. ..... p 2888 N93-25320
p 2715 N93-26503
AYNIE, P. ..... p 2832 N93-24989
AZZARA, B. ..... p 2747 N93-24831

B

BABCOCK, S. M. ..... p 2725 N93-25357
BABULA, MARIA ..... p 2872 N93-26205
BABUSKA, IVO ..... p 2726 N93-25638
BACH, H. ..... p 2738 N93-24776
BACKHAUS, ROBERT ..... p 2751 N93-24858
BAE, DOO-HWAN ..... p 2816 N93-25481
BAE, Y. K. ..... p 2849 N93-25644
BAEK, MYUNG-JIN ..... p 2617 N93-25726
BAGNI, M. ..... p 2749 N93-24844
BAHADUR, HARISH ..... p 2837 N93-25021
BAILEY, MICHAEL ..... p 2880 N93-25804
BAILIN, SIDNEY ..... p 2825 N93-25981
BAILIN, SYDNEY ..... p 2825 N93-25978
BAINUM, PETER M. ..... p 2599 N93-25693
BAJKOVA, ANISA T. ..... p 2812 N93-26257
BAKER, G. K. ..... p 2657 N93-26213
BAKER, I. ..... p 2650 N93-25519
BAKER, N. R. ..... p 2625 N93-26009
BAKERIS, D. F. ..... p 2605 N93-24727
BAKUCKAS, J. G., JR. ..... p 2634 N93-25072
BALAKRISHNA, S. ..... p 2695 N93-25087
BALAS, MARK J. ..... p 2620 N93-26408
BALDWIN, DARRELL ..... p 2622 N93-24753
BALDWIN, R. E. ..... p 2692 N93-24881
p 2693 N93-24903
BALHORN, R. ..... p 2712 N93-25363
BALLA, R. JEFFREY ..... p 2598 N93-26006
BALLATO, A. ..... p 2841 N93-25047
BALOOCH, M. ..... p 2654 N93-25384
BALTEAS, N. ..... p 2693 N93-25033
BANCROFT, GORDON V. ..... p 2814 N93-25600
BANCROFT, STEVEN A. ..... p 2631 N93-26056
BANDARU, R. V. ..... p 2768 N93-26533
BANDYOPADHYAY, P. R. ..... p 2707 N93-26328
BANE, J. M. ..... p 2790 N93-26384
BANKMAN, ISAAC N. ..... p 2796 N93-25568
BANKS, BRUCE A. ..... p 2658 N93-25564
BANKS, P. ..... p 2765 N93-25837
BANKSTON, NATHANIEL G. ..... p 2583 N93-24880
BANNEROT, RICHARD B. ..... p 2911 N93-26058
p 2914 N93-26070
BANNERT, DIETRICH ..... p 2739 N93-24784
p 2744 N93-24815
BANSAL, NAROTTAM P. ..... p 2640 N93-26100
BAR-ITZHACK, ITZHACK Y. ..... p 2602 N93-24711
p 2606 N93-24730
BARAN, ROBERT H. ..... p 2827 N93-25610
BARAZANGI, MUAWIA ..... p 2883 N93-26442
BARBEE, T. W., JR. ..... p 2712 N93-25363
BARBERIS, E. ..... p 2869 N93-26494
BARDECHE, G. ..... p 2837 N93-25020
BARDSLEY, J. N. ..... p 2763 N93-25385
BARI, ROBERT A. ..... p 2632 N93-26200
BARILLET, R. ..... p 2842 N93-25056
BARKER, DAVID R. ..... p 2585 N93-25456
BARKER, J. R. ..... p 2849 N93-25488
BARKYOUMB, JOHN ..... p 2867 N93-26140
BARLOW, JEWEL ..... p 2597 N93-26046
BARNA, P. STEPHEN ..... p 2598 N93-25996
BARNBAUM, CECILIA SYFERT ..... p 2895 N93-25713
BARNES, FRANK ..... p 2670 N93-26412
BARNES, LESLIE A. ..... p 2848 N93-25450
BARNHART, CRAIG M. ..... p 2680 N93-26227
BARR, ALAN GEORGE ..... p 2772 N93-25556
BARRERA, ENRIQUE V. ..... p 2642 N93-26060
BARRETT, ERIC C. ..... p 2743 N93-24805
BARRETT, W. H. ..... p 2731 N93-26507
BARTLETT, RODNEY J. ..... p 2850 N93-26367
BARTOS, KAREN F. ..... p 2723 N93-24909
BARTOS, R. D. ..... p 2678 N93-26119
BARTZ, ROBERT ..... p 2710 N93-26044
BARWINSKI, K. ..... p 2752 N93-24866
BASARAB, DOUGLAS J. ..... p 2691 N93-26299
BASHKANSKY, MARK ..... p 2852 N93-25358
BASS, BARBARA F. ..... p 2766 N93-25875
BASTIAANS, GLENN J. ..... p 2709 N93-25345
BATCHELOR, D. B. ..... p 2674 N93-25300
BATEMAN, MONTE GENE ..... p 2781 N93-25275
BATINA, JOHN T. ..... p 2581 N93-26134
BATTAGLIN, G. ..... p 2653 N93-24971
BATTY, M. W. ..... p 2710 N93-25677
BAUCH, A. ..... p 2716 N93-25049
p 2841 N93-25050
BAUER, S. H. ..... p 2645 N93-26045
BAUHAHN, P. ..... p 2692 N93-26565
BAUMGARTEN, JOSEPH R. ..... p 2619 N93-26438
BAUTISTA, J. J. ..... p 2678 N93-26115
BAVA, E. ..... p 2840 N93-25042
BAZ, A. ..... p 2638 N93-25780
BDZIL, JOHN ..... p 2706 N93-25987
BEARD, RANDAL ..... p 2817 N93-24743
BEATTY, JOHN ..... p 2651 N93-25895
BEAUMONT, MICHAEL J. ..... p 2743 N93-24805
BEAVEN, S. ..... p 2790 N93-26050
BECHTOLD, L. A. ..... p 2768 N93-26592
BECK, GENE A. ..... p 2900 N93-25890
BEDFORD, C. D. ..... p 2630 N93-26038
BEDINGER, M. S. ..... p 2768 N93-26536

BEECROFT, TROY CANNON ..... p 2873 N93-24905
BEEMAN, DAVID ..... p 2583 N93-24885
BEHR, MAREK ANTONI ..... p 2703 N93-25663
BEHRENS, R., JR. ..... p 2629 N93-26034
BEHRENS, RICHARD, JR. ..... p 2628 N93-26033
p 2662 N93-26387
BELL, P. M. ..... p 2709 N93-25515
BELL, WAYNE E. ..... p 2680 N93-26160
BELTZ, MARK W. ..... p 2656 N93-25997
BENCH, MICHAEL WAYNE ..... p 2865 N93-25715
BENDER, R. L. ..... p 2631 N93-26054
BENDERSKY, LEONID A. ..... p 2652 N93-26284
BENEDEK, K. R. ..... p 2768 N93-26529
BENEDETTI, R. ..... p 2741 N93-24795
BENET, PH. ..... p 2848 N93-25371
BENNETT, BONNIE KATHLEEN HOLTE
p 2822 N93-25963
BENNETT, JOEL G. ..... p 2723 N93-24957
BENSEL, CAROLYN K. ..... p 2802 N93-26404
BENSON, C. E. ..... p 2768 N93-26529
BENSON, TIMOTHY A. ..... p 2686 N93-26603
BENTTI, E. RON ..... p 2609 N93-24876
BERDING, M. A. ..... p 2853 N93-25766
BERG, JOEL LEA ..... p 2616 N93-25351
BERGER, M. J. ..... p 2816 N93-25316
p 2850 N93-26314
BERLAD, A. L. ..... p 2643 N93-25229
BERMAN, A. L. ..... p 2614 N93-26124
BERMAN, STEPHEN ..... p 2760 N93-24673
BERNAT, ANDREW ..... p 2828 N93-25140
BERNERS, D. ..... p 2851 N93-25325
BERNHARD, MICHAEL A. ..... p 2872 N93-26250
BERNHOLC, J. ..... p 2862 N93-24953
BERNIER, L. G. ..... p 2716 N93-25024
BERNSTEIN, LESLIE R. ..... p 2846 N93-26358
BERRY, R. S. ..... p 2850 N93-26346
BERSHAD, BRIAN N. ..... p 2883 N93-26389
BERTHAUT, A. ..... p 2833 N93-24992
BERTHET, J. P. ..... p 2832 N93-24989
BERZINS, V. ..... p 2813 N93-26453
BEST, STEVE ..... p 2724 N93-25260
BESWICK, C. A. ..... p 2679 N93-26126
BETZ, JONATHAN ..... p 2603 N93-24715
BEYER, P. E. ..... p 2599 N93-26125
BEYER, R. A. ..... p 2628 N93-26032
BHALLA, A. S. ..... p 2856 N93-26224
BHATTACHARYA, SAIKAT ..... p 2818 N93-25156
BHATTACHARYYA, S. P. ..... p 2818 N93-25155
p 2818 N93-25156
p 2819 N93-25226
p 2819 N93-25296
BICKES, R. W., JR. ..... p 2627 N93-26024
BICOS, ANDY ..... p 2599 N93-25835
BIELSKI, WLODZIMIERZ ROBERT
p 2726 N93-25437
BIERMANN, PAUL J. ..... p 2796 N93-25569
BIGIO, I. J. ..... p 2713 N93-25379
BIGLER, E. ..... p 2836 N93-25012
BIHARI, TOM ..... p 2585 N93-25261
BILARDO, VINCENT ..... p 2665 N93-24682
BILBRO, J. ..... p 2855 N93-26190
BILLARDON, RENE ..... p 2729 N93-25901
BILLET, MICHAEL L. ..... p 2580 N93-26049
BILLINGSLEY, ARTHUR B. ..... p 2806 N93-25858
BINDER, MICHAEL ..... p 2657 N93-26341
BIRD, JOHN C. ..... p 2784 N93-25731
BIRK, RONALD J. ..... p 2758 N93-25615
BISHOP, A. R. ..... p 2646 N93-26505
BISHOP, JAMES K. B. ..... p 2735 N93-24935
BISHU, RAM R. ..... p 2803 N93-26061
BISSINGER, H. ..... p 2888 N93-25320
p 2715 N93-26503
BIXBY, ROBERT ..... p 2812 N93-26290
BJOERK, L. ..... p 2748 N93-24841
BJORKMAN, C. ..... p 2862 N93-24953
BJORKMAN, JON ERIC ..... p 2894 N93-25620
BLACKBURN, G. A. ..... p 2752 N93-24865
BLACKMOND, D. G. ..... p 2659 N93-25119
BLACKWOOD, GARY ..... p 2609 N93-25836
BLAES, V. ..... p 2602 N93-24706
p 2602 N93-24707
BLAHA, RICHARD J. ..... p 2681 N93-26241
BLAKE, CHERYL L. ..... p 2710 N93-25696
BLANKENSHIP, GILMER ..... p 2680 N93-26226
BLASK, S. G. ..... p 2756 N93-25653
BLATT, R. ..... p 2841 N93-25051
BLINN, THOMAS M. ..... p 2883 N93-26350
BLOCH, J. J. ..... p 2899 N93-25185
BLOCH, M. ..... p 2693 N93-25038
BLOM, RONALD ..... p 2880 N93-25804
BLOOM, BARD ..... p 2809 N93-25152
BLOWER, DAVID J. ..... p 2590 N93-25933
BLUM, FRANK D. ..... p 2645 N93-26300
p 2640 N93-26301
BLUM, L. ..... p 2866 N93-25781
p 2868 N93-26252
BLUME, LEO ..... p 2880 N93-25804
BOCK, O. ..... p 2822 N93-25964
BOCKELIE, MICHAEL J. ..... p 2808 N93-25073
BODECHTEL, J. ..... p 2738 N93-24776
p 2744 N93-24814
BODEN, THOMAS A. ..... p 2761 N93-25144
BOEHM-DAVIS, DEBBIE ..... p 2811 N93-26150
BOEHM, C. ..... p 2740 N93-24792
BOENIG, H. J. ..... p 2688 N93-25313
BOETTINGER, W. J. ..... p 2869 N93-26547
BOETTINGER, WILLIAM J. ..... p 2652 N93-26284
BOGDANSKI, MICHAEL S. ..... p 2658 N93-25564
BOGOVICH, L. ..... p 2822 N93-25962
BOHANDY, J. ..... p 2871 N93-25584
BOIME, G. ..... p 2837 N93-25023
BOISSEVAIN, J. G. ..... p 2869 N93-26494
BOLLINGER, J. J. ..... p 2862 N93-26528
BOLSTAD, JON ..... p 2670 N93-25604
BOLTZ, J. C. ..... p 2808 N93-24962
BOLVIN, D. T. ..... p 2601 N93-24704
BOND, VICTOR R. ..... p 2604 N93-24720
BONSIGNORI, R. ..... p 2746 N93-24825
BONTING, SJOERD L. ..... p 2792 N93-25242
BOONE, BRADLEY G. ..... p 2814 N93-25603
BOOTNIK, M. ..... p 2694 N93-25057
BORDER, J. S. ..... p 2677 N93-26110
BORG, SCOTT J. ..... p 2765 N93-25864
BORGONOVI, GIANCARLO ..... p 2582 N93-25110
BORMAN, G. L. ..... p 2632 N93-26216
BORNE, KIRK ..... p 2883 N93-26423
BORRETT, WALTER ..... p 2828 N93-25140
BORZELLI, G. ..... p 2747 N93-24831
BOSCHITSCH, ALEXANDER H. ..... p 2575 N93-25075
BOSCOLO-BOSCOLETTO, A. ..... p 2653 N93-24971
BOSS, W. ..... p 2858 N93-24968
BOSSI, RICHARD H. ..... p 2722 N93-26526
p 2722 N93-26527
BOUGIOUKOS, GEORGIOS T. ..... p 2682 N93-26388
BOUNOUA, LAHOUARI ..... p 2783 N93-25685
BOURQUIN, R. ..... p 2837 N93-25022
BOURRIAU, J. ..... p 2693 N93-25053
BOUTON, BRUCE ..... p 2611 N93-25511
BOUZID, S. ..... p 2832 N93-24989
BOWEN, CHARLES D. ..... p 2801 N93-25840
BOWER, GORDON H. ..... p 2798 N93-26364
BOWERS, R. L. ..... p 2858 N93-25167
BOWLEN, DON ..... p 2652 N93-26208
BOWLES, JEFFREY HENRY ..... p 2861 N93-25831
BOWMAN, KENNETH P. ..... p 2878 N93-25793
BOY, J. J. ..... p 2833 N93-24992
p 2839 N93-25032
BOYCHEVA, VALENTINA S. ..... p 2739 N93-24782
p 2751 N93-24860
BOYD, I. D. ..... p 2633 N93-26561
BOYD, JAMES G. ..... p 2639 N93-25919
BOYTCHEVA, VALENTINA ..... p 2753 N93-24870
BRAAMS, B. J. ..... p 2859 N93-25302
BRACE, LARRY H. ..... p 2897 N93-26393
BRACEWELL, B. L. ..... p 2687 N93-25113
BRADFORTH, S. E. ..... p 2647 N93-26599
BRADLEY, D. K. ..... p 2709 N93-25515
BRADLEY, J. N. ..... p 2762 N93-25166
p 2876 N93-25448
BRADLEY, JOHN P. ..... p 2757 N93-26369
BRADSHAW, P. ..... p 2697 N93-25247
BRAHIM-BOUNAB, A. ..... p 2647 N93-25037
BRANNING, D. A. ..... p 2713 N93-25381
BRASE, J. ..... p 2715 N93-26503
BRASE, J. M. ..... p 2888 N93-25320
BRAUN, R. J. ..... p 2646 N93-26323
BRAYMEN, STEVE D. ..... p 2709 N93-25345
BREAULT, ROBERT P. ..... p 2761 N93-24977
BREISACHER, KEVIN J. ..... p 2623 N93-25236
BRENDEL, R. ..... p 2833 N93-24993
BRENNER, WILLIAM E. ..... p 2584 N93-25243
BRETT, DANIEL J. ..... p 2608 N93-25636
BREWER, LAURA M. ..... p 2615 N93-25174
BREWSTER, M. Q. ..... p 2626 N93-26020
p 2630 N93-26042
p 2631 N93-26043
BRINK, K. H. ..... p 2790 N93-26384
BRINKMAN, C. R. ..... p 2654 N93-25361
BRINZA, DAVID E. ..... p 2653 N93-25078
BRISLAWN, C. M. ..... p 2762 N93-25166
p 2876 N93-25448
BRISSENDEN, R. J. V. ..... p 2854 N93-26183
BRISSENDEN, ROGER J. V. ..... p 2854 N93-26186
BRISTOW, WILLIAM ALBERT ..... p 2861 N93-25829
BRITT, J. ..... p 2759 N93-25253
BRITTER, R. E. ..... p 2668 N93-25238
BROACH, DANA ..... p 2797 N93-26138
BRODY, WILLIAM R. ..... p 2796 N93-25568
BROOK, MARX ..... p 2777 N93-24877
BROOKS, FREDERICK P., JR. ..... p 2807 N93-26293
BROOKS, R. A. ..... p 2689 N93-25416
BROPHY, JOHN R. ..... p 2859 N93-25206
BROST, R. C. ..... p 2827 N93-25103
BROWN, D. R. ..... p 2758 N93-24975
BROWN, DAVID H. ..... p 2882 N93-26231
BROWN, G. M. ..... p 2793 N93-26587
BROWN, I. G. ..... p 2859 N93-25324
BROWN, J. R. ..... p 2631 N93-26054
BROWN, J. S. ..... p 2805 N93-25165
BROWN, JEFFREY C. ..... p 2693 N93-24889
BROWN, KENNETH G. ..... p 2720 N93-25609
BROWN, PAUL M. ..... p 2694 N93-25596
BROWN, RICHARD ..... p 2651 N93-25895
BROWN, S. D. ..... p 2644 N93-25311
BROWN, TIMOTHY ..... p 2765 N93-25666
BROWNE, DAVID C. ..... p 2883 N93-26350
BROWNELL, J. ..... p 2861 N93-26512
BROWNELL, J. H. ..... p 2858 N93-25167
BRUCKER, J. ..... p 2713 N93-25379
BRUGHELLI, KEVIN ..... p 2609 N93-26175
BRUNET, M. ..... p 2608 N93-24997
p 2693 N93-25053
BRUNNETT, GUIDO ..... p 2829 N93-26228
BRUNO, D. ..... p 2691 N93-26171
BRUSK, KEVIN D. ..... p 2759 N93-25136
BRYANT, PAUL ..... p 2655 N93-25861
BRYKCZYNSKI, BILL ..... p 2831 N93-26330
BU, Y. ..... p 2645 N93-25920
BUCCHERI, A. ..... p 2746 N93-24825
BUCHHEIT, R. G. ..... p 2655 N93-25446
BUCKLAND, JULIA H. ..... p 2632 N93-26211
BUCKLEY, P. ..... p 2658 N93-26433
BUCKLEY, PAUL ..... p 2651 N93-25895
BUCKLEY, W. M. ..... p 2875 N93-25319
BUDDEN, NANCY ANN ..... p 2897 N93-26094
BUDGE, SCOTT E. ..... p 2805 N93-25932
BUEHLER, DAVID P. ..... p 2873 N93-26418
p 2873 N93-26420
BUEKER, C. ..... p 2751 N93-24859
BUELL, DUNCAN A. ..... p 2814 N93-25575
BUISSON, X. ..... p 2838 N93-25025
BULLOCK, ELLEN P. ..... p 2591 N93-26553
BULLOCK, THEODORE H. ..... p 2799 N93-26446
BULUSU, S. ..... p 2629 N93-26034
BULUSU, SURYANARAYANA ..... p 2628 N93-26033
p 2662 N93-26387
BUNNELL, L. ROY ..... p 2654 N93-25359
BUNTINE, WRAY ..... p 2814 N93-25591
BUNTING, W. F. ..... p 2787 N93-26570
BURGESS, DONALD W. ..... p 2780 N93-24896
BURKEPILE, J. T. ..... p 2899 N93-26556
BURKHARDT, C. ..... p 2822 N93-25962
BURNE, RICHARD A. ..... p 2822 N93-25965
BURNETT, STEVE ..... p 2730 N93-26279
BURNS, KAREN S. ..... p 2720 N93-25609
BURNS, STANLEY G. ..... p 2709 N93-25345
BURRIS, S. ..... p 2768 N93-26567
BURT, R. ..... p 2884 N93-26568
BURTIS, MARVEL D. ..... p 2760 N93-24952
BURTON, C. D. ..... p 2592 N93-25455
BURTON, RODNEY L. ..... p 2659 N93-24745
BURY, G. ..... p 2679 N93-26122
BUSCA, G. ..... p 2716 N93-24980
BUSS, R. J. ..... p 2644 N93-25312
BUSTIN, ROBERTA ..... p 2896 N93-26062
BUTER, THOMAS ALAN ..... p 2577 N93-25388
BUTLER, BARCLAY PHELPS ..... p 2800 N93-25531
BUTLER, DAVID W. ..... p 2807 N93-25606
BUTLER, DWAIN K. ..... p 2686 N93-26541
BUTLER, M. A. ..... p 2655 N93-25444
BUTTERLINE, E. W. ..... p 2687 N93-25062
BUZBEE, WILLIAM ..... p 2878 N93-25794
BUZZA, DAVID WAYNE ..... p 2650 N93-25464
BYER, ROBERT L. ..... p 2852 N93-25281
p 2715 N93-26297

C

CABE, JERRY L. ..... p 2720 N93-26564
CAIN, TERRENCE M. ..... p 2577 N93-25467
CALAHAN, DONALD ..... p 2707 N93-26269
CALDWELL, ROBERT REYNOLDS
p 2891 N93-24907
CALVEL, P. ..... p 2693 N93-25053
CAMBON, O. ..... p 2840 N93-25043
CAMPBELL, A. N. ..... p 2692 N93-26501
CAMPBELL, L. J. ..... p 2688 N93-25313
CAMPION, R. E. ..... p 2605 N93-24726
p 2605 N93-24727
CANAVAN, G. H. ..... p 2598 N93-25322
CANAVERO, F. ..... p 2686 N93-24893
CANDELIER, V. ..... p 2693 N93-25004
p 2694 N93-25055
CANRIGHT, DAVID ..... p 2706 N93-25779
CANTONE, M. ..... p 2753 N93-24871
CANTRELL, BEN H. ..... p 2674 N93-25332
CANZIAN, P. ..... p 2694 N93-25055

CAO, CHANGYONG p 2756 N93-25707
CAPELLE, B. p 2833 N93-24994
p 2836 N93-25013
p 2838 N93-25025
p 2840 N93-25044
CAPLINGER, MICHAEL p 2879 N93-25803
CAPONE, D. G. p 2767 N93-26511
CAPRIOTTI, D. P. p 2625 N93-26009
CAREY, G. F. p 2809 N93-25315
CARLIN, P. W. p 2694 N93-25599
CARLSON, J. B. p 2875 N93-25319
CARLSON, TOBY N. p 2787 N93-26351
CARNES, JAMES R. p 2823 N93-25966
CARO, A. p 2649 N93-25336
CARPENTER, M. P. p 2848 N93-25371
CARPENTER, MARK H. p 2575 N93-25074
CARRASCO, HECTOR R. p 2670 N93-26063
CARROLL, DAVID LEON p 2713 N93-25420
CARROLL, DOUGLAS LEE p 2847 N93-25355
CARTER, M. D. p 2674 N93-25300
CARTER, NANCY J. p 2681 N93-26372
CARTER, TYRONE R. p 2670 N93-26412
CARTIGLIA, N. p 2869 N93-26494
CARTY, THOMAS C. p 2584 N93-25243
CASARELLA, MARIO J. p 2706 N93-25885
CASE, K. p 2846 N93-26376
CASHDOLLAR, K. L. p 2668 N93-25498
CASTANEDA, JESSE A. p 2681 N93-26383
CASTNER, E. W., JR. p 2643 N93-25123
CATES, G. D. p 2850 N93-26288
CATTAFESTA, L. p 2576 N93-25249
CATTS, GLENN PAUL p 2755 N93-25441
CAUDLE, DARYL L. p 2716 N93-26601
CAVANAUGH, JOHN D. p 2817 N93-26277
CECAMORE, P. p 2747 N93-24830
p 2747 N93-24831
CEREZ, P. p 2833 N93-24990
p 2833 N93-24991
CEREZO, A. p 2653 N93-26500
CHAKRABARTI, SUPRIYA p 2774 N93-25790
p 2878 N93-25795
CHAKRABORTY, D. p 2683 N93-26465
CHALLA, M. p 2602 N93-24708
CHAMBERLAIN, ROBERT G. p 2665 N93-24682
CHAMIS, C. C. p 2641 N93-26552
CHAN, PAUL p 2881 N93-25813
CHAN, W. S. p 2636 N93-25631
CHAN, Y. D. p 2899 N93-25327
CHANA, K. S. p 2592 N93-25455
CHANDY, K. M. p 2816 N93-25522
CHANG, F. C. p 2658 N93-26433
CHANG, HUAKANG p 2698 N93-25264
CHANG, HYO DUCK p 2755 N93-25460
p 2755 N93-25461
p 2756 N93-25462
CHANG, R. P. H. p 2654 N93-25372
CHANG, SIN-CHUNG p 2829 N93-26560
CHANG, Y. L. p 2694 N93-24759
CHANG, YONG JOON p 2643 N93-25123
CHAPEL, JIM p 2669 N93-26407
CHAPPEL, SHERRY p 2585 N93-25330
CHAR, KOOKRIN p 2869 N93-26381
CHARLOCK, T. P. p 2777 N93-24742
CHARTAS, G. p 2854 N93-26183
p 2854 N93-26187
p 2855 N93-26189
p 2855 N93-26192
CHATTERJEE, ANINDYA p 2600 N93-24696
CHATTERJI, G. B. p 2584 N93-24914
CHATTERJI, GANO p 2803 N93-25235
CHAVEZ, FRANK R. p 2587 N93-25162
CHAWLA, K. K. p 2641 N93-26579
CHEN, C.-C. p 2678 N93-26117
CHEN, CHIN-TU p 2880 N93-25810
CHEN, FUH-SHENG p 2637 N93-25716
CHEN, J. C. p 2671 N93-24660
CHEN, L. L. p 2810 N93-25699
CHEN, P. M. p 2806 N93-25233
CHEN, R. p 2694 N93-24759
CHEN, R. S. p 2851 N93-26514
CHEN, SHENG-HSIEN p 2770 N93-25081
CHEN, TIEHAN p 2777 N93-24877
CHEN, TONY D. T. p 2702 N93-25551
CHENEY, ROBERT E. p 2734 N93-24930
CHEO, B. p 2691 N93-26171
CHERN, E. JAMES p 2807 N93-25606
CHERN, ENGMIN J. p 2710 N93-26103
CHERNG, JYH-SHIARN p 2638 N93-25760
CHERUKAT, P. p 2695 N93-24963
CHERVIN, R. p 2762 N93-25184
CHESBROUGH, RADM G. p 2732 N93-24916
CHETTRI, SAMIR R. p 2824 N93-25972
CHIANG, C. H. p 2661 N93-25948
CHIANG, WUYING p 2590 N93-25719
CHING, J. K. S. p 2765 N93-25873
CHINNAPALANIANDI, PERIASAMY p 2701 N93-25534
CHIOU, J. C. p 2669 N93-26406
CHIOU, Y. S. PETER p 2824 N93-25974
CHISHOLM, M. F. p 2653 N93-26500
CHIU, Y. T. p 2775 N93-26151
CHMURA, L. p 2813 N93-26453
CHOKR, BASSAM A. p 2874 N93-25139
CHOUDHURY, P. ROY p 2625 N93-26013
CHOY, F. K. p 2716 N93-24751
CHREN, WILLIAM A., JR. p 2689 N93-25618
CHRISTENS-BARRY, WILLIAM A. p 2796 N93-25568
CHRISTENSEN, C. P. p 2715 N93-26363
CHRISTIANSEN, A. D. p 2827 N93-25103
CHRISTY, STEVEN M. p 2722 N93-26246
CHROMIAK, JOSEPH A. p 2794 N93-24763
CHU, D. p 2602 N93-24708
p 2602 N93-24710
CHU, FA-DE JACK p 2635 N93-25532
CHUA, KIAT p 2575 N93-25075
CHUANG, SHERRY L. p 2805 N93-25930
CHUCKSA, RONALD J. p 2618 N93-26209
CHUN, FRANCIS KEOKI p 2773 N93-25709
CHUNG, ILSUP p 2636 N93-25674
CHUNG, JIN TAEK p 2704 N93-25725
CHUNG, JINTAI p 2725 N93-25394
CHUNG, T. J. p 2625 N93-26012
CHURCH, R. H. p 2769 N93-25573
CHURCH, T. M. p 2790 N93-26384
CHURGIN, JAMES p 2732 N93-24915
CHYU, MING-C. p 2619 N93-26064
CIAPPA, A. p 2747 N93-24830
p 2747 N93-24831
CIMBALA, JOHN M. p 2580 N93-26049
CISPER, M. E. p 2712 N93-25150
CLAIRON, A. p 2831 N93-24981
p 2832 N93-24989
CLAPP, KENNETH C. p 2815 N93-24748
CLAPPER, JOHN P. p 2798 N93-26364
CLARK, ARTHUR E. p 2710 N93-26141
CLARK, JOHN S. p 2621 N93-24740
p 2622 N93-24753
p 2622 N93-25105
CLARK, MELANA p 2814 N93-25602
CLARK, RONALD K. p 2651 N93-26048
CLARK, WILLIAM S. p 2696 N93-25109
CLARKE, DAVID R. p 2730 N93-26362
CLARKE, R. ALLYN p 2733 N93-24922
CLAUSEN, E. C. p 2660 N93-25523
CLEARY, M. P. p 2641 N93-26355
CLEMMONS, JAMES HART p 2773 N93-25732
CLEVELAND, JEFF I., II p 2598 N93-25574
CLEVERS, J. G. P. W. p 2751 N93-24859
CLIFTON, R. J. p 2651 N93-25907
CLINE, M. C. p 2694 N93-24759
CLINTON, WILLIAM J. p 2887 N93-26458
CLOEREN, J. M. p 2693 N93-25052
COAKLEY, T. J. p 2697 N93-25247
COENRADIE, B. p 2748 N93-24837
COFFEY, HELEN E. p 2899 N93-26537
p 2899 N93-26538
COHEN, A. p 2628 N93-26032
COHEN, MARSHALL J. p 2709 N93-25634
COHEN, MARTIN p 2888 N93-25135
COHEN, N. S. p 2626 N93-26019
COHEN, PAUL R. p 2829 N93-26345
COHN, MARTIN p 2881 N93-25811
COHN, ROBERT p 2813 N93-26378
COLDIRON, SHELLEY J. p 2709 N93-25345
COLE, BARRETT E. p 2849 N93-25823
COLE, E. I., JR. p 2692 N93-26501
COLE, RODNEY E. p 2783 N93-25645
COLE, STANLEY R. p 2591 N93-26553
COLELLA, P. p 2762 N93-25184
COLEMAN, SARAH L. p 2638 N93-25723
COLLANTES, LOURDES Y. p 2881 N93-25826
COLLET, P. p 2834 N93-25001
COLLINS, DONALD J. p 2879 N93-25801
COLLINS, WILLIAM E. p 2583 N93-25896
COLON, JORGE L. p 2645 N93-25916
COMBS, NATHAN p 2826 N93-25982
COMBS, VAUGHN T. p 2710 N93-25696
COMORETTO, G. p 2608 N93-24998
CONESE, C. p 2750 N93-24851
CONOVER, D. R. p 2760 N93-24675
CONRAUX, P. p 2839 N93-25032
CONROY, M. P. p 2873 N93-26419
CONSORTINI, ANNA p 2714 N93-26217
CONTE, ALFEO A., JR. p 2655 N93-25816
COOGAN, J. J. p 2768 N93-26592
COOK, L. M. p 2823 N93-25967
COOKE, DANIEL E. p 2812 N93-26368
COOLEY, J. p 2602 N93-24706
p 2602 N93-24707
p 2603 N93-24716
p 2603 N93-24717
COONS, L. W. p 2631 N93-26054
COOPER, BETH A. p 2846 N93-26551
COOPER, GRANT A., IV p 2787 N93-26286
COOPER, L. P. p 2679 N93-26126
COOPER, N. J. p 2851 N93-26518
CORIELL, S. R. p 2646 N93-26323
CORKER, KEVIN p 2585 N93-25330
CORNAERT, M.-H. p 2740 N93-24787
CORNUM, RHONDA L. p 2795 N93-26218
CORNWALL, J. p 2765 N93-25837
COSLO, M. J. p 2860 N93-25641
COTTON, A. D. R. p 2674 N93-25391
COUGHLAN, S. D. p 2756 N93-25694
COULTER, JOE E. p 2606 N93-24728
COURTEAU, STEPHANE p 2889 N93-25621
COURTNEY, THOMAS H. p 2652 N93-26264
COUSINEAU, K. L. p 2874 N93-25254
COVERSTONE-CARROLL, VICTORIA LYNN p 2607 N93-24904
COYLE, DONALD BARRY p 2713 N93-25389
COYLE, L. M. p 2716 N93-24980
CRAIG, KENNETH JOHN p 2574 N93-24772
CRAIG, KEVIN p 2639 N93-25945
CRAIG, KEVIN C. p 2729 N93-25846
CRAIN, WILLIAM K. p 2631 N93-26053
CRANE, R. K. p 2683 N93-26469
CRAWFORD, D. p 2659 N93-25607
CRAWFORD, GARY p 2724 N93-25260
CRAWLEY, EDWARD F. p 2821 N93-25833
p 2599 N93-25835
CREWS, ALAN R. p 2722 N93-26526
p 2722 N93-26527
CRICELLI, ANTONIO M. p 2582 N93-26198
CRISTION, JOHN A. p 2796 N93-25592
p 2827 N93-25611
CRIVELLI, LUIS A. p 2670 N93-26415
CROLL, M. G. p 2674 N93-25239
CROMP, ROBERT F. p 2824 N93-25972
CROMWELL, R. L. p 2756 N93-25653
CRONE, M. S. p 2823 N93-25967
CROSS, L. E. p 2856 N93-26224
CROUCH, PETER E. p 2829 N93-26228
CROUSE, DENNIS N. p 2694 N93-25583
CROWE, R. A. p 2679 N93-26126
CROWELL, CYNTHIA A. p 2597 N93-25998
CRUICKSHANK, ALEXANDER p 2868 N93-26357
CRUMPLER, MIKE p 2724 N93-25260
CSORNAI, GABOR p 2750 N93-24849
CULBERT, CHRIS p 2799 N93-25595
CULLERS, CHERYL L. p 2652 N93-26235
CULLEY, DENNIS E. p 2664 N93-25337
CULLINGFORD, HATICE S. p 2632 N93-26200
CUMMING, IAN p 2804 N93-25926
CUMMINS, K. L. p 2711 N93-24900
CUNNINGTON, GEORGE R. p 2651 N93-26048
CUOMO, DONNA L. p 2801 N93-25840
CURLISS, D. B. p 2639 N93-25918
CUTCHIS, PROTAGORAS N. p 2796 N93-25592
CZARNETZKI, ALAN C. p 2783 N93-25724
CZERANKA, MARION p 2740 N93-24790
CZUCHLEWSKI, S. J. p 2713 N93-25379

D

D'ELEUTERIO, G. M. T. p 2822 N93-25964
DAHM, WERNER J. A. p 2644 N93-25819
DAHMANI, B. p 2832 N93-24989
DAHOTRE, N. B. p 2858 N93-24968
DALY, P. p 2836 N93-25017
p 2837 N93-25019
DALY, P. J. p 2848 N93-25371
DAMANIA, BHAVESH p 2811 N93-25791
DAMBROSIO, BRUCE p 2811 N93-26221
DANA, ROGER A. p 2681 N93-26289
DANABASOGLU, GOKHAN p 2701 N93-25483
DANBERG, J. E. p 2609 N93-25985
DANG, A. L. p 2626 N93-26017
DANIAU, W. p 2693 N93-25002
DANIELS, R. C. p 2791 N93-26586
DANNERT, DAVID A. p 2695 N93-24954
DAOUD, YOUNIS SHARIF p 2596 N93-25543
DASILVA, L. B. p 2712 N93-25363
DAVARIAN, FARAMAZ p 2682 N93-26463
p 2682 N93-26464
p 2683 N93-26465
DAVENPORT, BILL p 2814 N93-25602
DAVENPORT, RONALD J. p 2801 N93-26088
DAVENPORT, WILLIAM J. p 2696 N93-25208
DAVIDSON, B. p 2862 N93-24953
DAVIDSON, J. L. p 2868 N93-26312
DAVIDSON, ROGER p 2620 N93-26408
DAVIS, D. O. p 2575 N93-24911
DAVIS, JOHN A. p 2835 N93-25008
DAVIS, ROBERT J. p 2856 N93-26306
DAVIS, V. A. p 2618 N93-26232

DAVIS, W. S. p 2600 N93-24697
DAYTON, D. C. p 2627 N93-26025
DEACETIS, LOUIS A. p 2619 N93-26065
DEADMORE, DANIEL L. p 2633 N93-26204
DEANDRADE, DONIZETI p 2587 N93-25486
DEANNA, RUSSELL G. p 2708 N93-26554
DEARBORN, A. p 2795 N93-26133
DEARMON, JOHN M. p 2708 N93-24737
DECHER, R. p 2716 N93-24980
DECLERCQ, E. p 2832 N93-24989
DEFLORE, THOMAS p 2586 N93-24739
DEFORD, J. F. p 2857 N93-26593
DEFUSCO, L. p 2749 N93-24844
DEINHAMMER, RANDALL S. p 2709 N93-25345
DEJOHN, C. A. p 2801 N93-25859
DEJONG, GERRIT p 2832 N93-24988
DELACRUZ, VANESSA A. p 2811 N93-25943
DELAHOY, A. E. p 2759 N93-25253
DELCUETO, J. p 2862 N93-25163
DELIANIDES, THEODORE PHILIP p 2579 N93-25720
DELLACORTE, CHRISTOPHER p 2633 N93-26204
DELUCA, DANIEL P. p 2651 N93-25843
p 2652 N93-26282
DELUIS, JAVIER p 2599 N93-25835
DEMARTINO, R. p 2856 N93-26309
DEMETRIADES-SHAH, T. D. p 2769 N93-24945
DEMIDOV, N. A. p 2716 N93-25049
DENINGER, WILLIAM D. p 2709 N93-25345
DENNIS, JOHN E. p 2829 N93-26344
DEPAULA, ABDON B. p 2676 N93-25866
DEPIFANIO, A. p 2741 N93-24794
DEROOVER, BOUDEWIJN P. p 2748 N93-24842
DETAINT, J. p 2833 N93-24994
p 2836 N93-25013
p 2838 N93-25025
p 2840 N93-25044
DETOMA, E. p 2694 N93-25057
DEUTSCHMANN, J. p 2606 N93-24730
DEVEREUX, R. WAYNE p 2711 N93-24901
DEVEREUX, WILLIAM S. p 2691 N93-26233
DEVLIEGHER, BEATA MARIA p 2742 N93-24802
DEVLIEGHERE, J. p 2693 N93-25054
DEWITT, K. J. p 2633 N93-26561
DEWULF, ROBERT R. p 2748 N93-24842
DEYOREO, J. J. p 2870 N93-26594
DEYZAC, F. p 2711 N93-25011
DHADWAL, HARBANS S. p 2796 N93-25593
DHANAK, MANHAR R. p 2576 N93-25153
DHARANI, L. D. p 2640 N93-26301
DIAZ, A. F. p 2644 N93-25500
DIAZDELARUBIA, T. p 2649 N93-25336
DIBB, JACK E. p 2763 N93-25287
DICK, G. JOHN p 2693 N93-24982
DICKERSON, GEORGE E. p 2656 N93-25995
DICKEY, TOMMY D. p 2736 N93-24939
DICKINSON, J. T. p 2869 N93-26385
DICKINSON, TAMARA L. p 2898 N93-26399
DIDZIULIS, STEPHEN V. p 2645 N93-26251
DIENERT, MICHAEL p 2686 N93-24999
DIEP, J. p 2880 N93-25807
DIKSHIT, PIYUSH p 2801 N93-26047
DILLON, ANDREW PATRICK p 2877 N93-25754
DIMARCO, N. p 2833 N93-24990
p 2833 N93-24991
DIMOTAKIS, P. E. p 2707 N93-26163
DIMOTAKIS, PAUL E. p 2707 N93-26379
DINTELMANN, F. p 2684 N93-26478
DIPASQUALE, R. C. p 2777 N93-24742
DIRE, J. R. p 2898 N93-26571
DISHMAN, GEORGE p 2611 N93-25511
DIXON, DAVID S. p 2634 N93-25283
DIXON, R. K. p 2767 N93-26510
DJORGOVSKI, STANISLAV p 2878 N93-25796
DOBSON, E. N. p 2722 N93-26546
DOCKTER, K. p 2750 N93-24850
DODD, B. A. p 2692 N93-26501
DODDS, H. L. p 2847 N93-25256
DODDS, R. H., JR. p 2727 N93-25647
DODDS, ROBERT H., JR. p 2811 N93-25845
p 2731 N93-26390
p 2731 N93-26516
DODGE, C. J. p 2769 N93-25571
DOHERTY, M. F. p 2642 N93-25115
DOHERTY, MICHAEL P. p 2622 N93-24744
p 2632 N93-26210
DOHRMANN, C. R. p 2844 N93-25520
DOKTYCZ, M. J. p 2793 N93-26587
DOLECEK, Q. E. p 2871 N93-25584
DOLL, C. E. p 2601 N93-24703
p 2601 N93-24704
DOMINIC, VINCENT G. p 2853 N93-25839
DOMON, WATARU p 2716 N93-25068
DONNET, G. p 2583 N93-24879
DOOLEY, HARRY D. p 2734 N93-24931
DORFMAN, GERALD A. p 2585 N93-25456
DORHOUT, PETER K. p 2869 N93-26577
DOTHE, H. p 2850 N93-26281
DOUGLAS, BRUCE C. p 2734 N93-24929
DOUGLAS, KENNETH p 2639 N93-25862
DOWNEY, JAMES REAGLE p 2607 N93-25272
DOYLE, B. L. p 2863 N93-25387
DOYLE, JOHN C. p 2596 N93-25199
DOYLE, RICHARD J. p 2879 N93-25801
DOZIER, JEFF p 2878 N93-25797
DRAGAN, YA P. p 2830 N93-26262
p 2686 N93-26573
DRAGUN, V. S. p 2741 N93-24793
DRAPEAU, A. L. p 2806 N93-25233
DRAPEAU, ANN L. p 2806 N93-25267
DRECHSLER, GENA K. p 2586 N93-26447
DREWERY, J. O. p 2674 N93-25239
DREWSEN, M. p 2831 N93-24981
DROBYSHEV, A. p 2753 N93-24869
DROST, M. K. p 2758 N93-24975
DRUMMOND, COLIN K. p 2593 N93-25673
DRYER, F. L. p 2628 N93-26027
DRYSDALE, S. L. T. p 2687 N93-25069
DSOUZA, G. p 2743 N93-24808
DU, PING p 2892 N93-25200
DUBOIS, PASCALE p 2878 N93-25798
DUCKLOW, HUGH W. p 2735 N93-24934
DUDASH, EDWARD J. p 2812 N93-26375
DUDLE, G. p 2716 N93-25065
DUESBERY, M. S. p 2639 N93-25936
DUFFEY, THOMAS A. p 2723 N93-24957
DUGUAY, L. p 2767 N93-26511
DUGUNDJI, JOHN p 2595 N93-26335
DULMET, B. p 2839 N93-25032
DUNCOMBE, R. L. p 2757 N93-26354
DUNLAP, JEFFREY R. p 2651 N93-25632
DURBIN, T. D. p 2645 N93-26251
DUTKIEWICZ, MELANIE p 2804 N93-25926
DUTREY, J. F. p 2693 N93-25053
DUVAL, LEONARD A. p 2759 N93-25572
DUXBURY, G. p 2687 N93-25069
DYSON, F. p 2762 N93-25184
p 2765 N93-25837

E

EAGAR, M. A. p 2627 N93-26022
EASTERBROOK, CALVIN C. p 2610 N93-24899
EASTERBROOK, J. E. p 2674 N93-25239
EATON, DAVID J. p 2604 N93-24723
EATON, PHILIP E. p 2662 N93-26308
EBADAN, GRACIE E. p 2718 N93-25435
EBERT, LEE G. p 2573 N93-26168
ECKARDT, ROBERT C. p 2715 N93-26297
ECKER, JOHN A. p 2796 N93-25569
ECKHARDT, CRAIG J. p 2866 N93-25854
EDELSTEIN, ALAN p 2640 N93-26143
EDER, D. p 2599 N93-26146
EDMONDS, J. p 2767 N93-26497
EDWARDS, B. C. p 2899 N93-25185
EDWARDS, C. D. p 2601 N93-24701
EDWARDS, W. J. p 2863 N93-25387
EHRLICH, DANIELE p 2755 N93-25434
EHSANI, M. p 2633 N93-26425
EIDEN, G. C. p 2712 N93-25150
EISSFELLER, B. p 2586 N93-25018
p 2693 N93-25033
EJIRI, MASAKI p 2774 N93-25889
EKIS, J. W. p 2721 N93-25939
EKLUND, DEAN R. p 2624 N93-26008
EKSTRAND, SAM p 2749 N93-24846
ELALAMI, M. p 2746 N93-24827
ELARADI, I. p 2746 N93-24827
ELBARAKA, MOHAMED p 2819 N93-25343
ELCHEIKH, R. E. p 2693 N93-25003
ELDER, R. L. p 2594 N93-25917
ELESHAKY, MOHAMED EL-AMIN p 2589 N93-25552
ELGHOBASHI, S. E. p 2661 N93-25948
ELLIOT, G. E. p 2610 N93-26591
ELLIOTT, C. M. p 2869 N93-26577
ELLIOTT, JAMES R. p 2778 N93-24884
ELLIS, DAVID L. p 2649 N93-25128
ELLIS, JOHN R. p 2883 N93-26389
ELSHAMY, M. p 2770 N93-25086
ELSNER, R. F. p 2855 N93-26192
ELSON, LEE p 2880 N93-25804
ELTSUFIN, E. p 2838 N93-25026
ELY, J. F. p 2646 N93-26319
EMERGY, MARK H. p 2715 N93-26445
EMERY, M. S. p 2688 N93-25377
EMERY, WILLIAM p 2878 N93-25797
EMSLIE, BETTY p 2828 N93-25773
ENDERS, V. p 2841 N93-25051
ENGEL, CARL D. p 2631 N93-26056
ENGLAND, HARVEY M., JR. p 2582 N93-25205
ENKE, G. M. p 2689 N93-25416
EPHREMIDES, ANTHONY p 2680 N93-26227
EPSTEIN, A. H. p 2595 N93-26219
EPSTEIN, ALAN H. p 2595 N93-26335
EPSTEIN, ARTHUR J. p 2657 N93-26401
ERICKSON, K. L. p 2629 N93-26034
ERICSSON, APRILLE J. p 2599 N93-25693
ERICSSON, JAN p 2748 N93-24839
ERJAVEC, J. L. p 2760 N93-24955
ERNST, D. E. p 2610 N93-26181
ERNST, MICHAEL A. p 2723 N93-24909
ESKER, BARBARA S. p 2592 N93-25129
ESMAILI, HOSSEIN p 2705 N93-25753
ESQUIVEL, M. S. p 2678 N93-26118
ESTEFAN, J. A. p 2614 N93-26109
EUDELL, A. H. p 2600 N93-24697
EURITT, M. p 2720 N93-26590
EURITT, M. A. p 2720 N93-26534
p 2720 N93-26585
EVANS, H. C. p 2899 N93-25327
EVANS, SARAH E. p 2766 N93-25875
EVENSON, KRAIG A. p 2670 N93-26412
EVERETT, HOBART R., JR. p 2719 N93-26244
EVERETT, RICHARD p 2640 N93-26143
EVERSON, J. p 2631 N93-26054
EWAN, G. T. p 2899 N93-25327
EZHOV, E. M. p 2716 N93-25049

F

FAIRALL, C. W. p 2790 N93-26384
FAIRFIELD, M. S. p 2696 N93-25124
FALCONER, J. L. p 2660 N93-25497
FALK, URBAN p 2726 N93-25638
FALLS, M. J. p 2684 N93-26473
FAN, J. C. p 2710 N93-25677
FAN, MARK S. p 2721 N93-26137
FANG, GUOR CHENG p 2763 N93-25263
FARDOUN, A. A. p 2694 N93-25599
FARMAKALIDES, C. D. p 2594 N93-25882
FARRAR, CHARLES R. p 2723 N93-24957
FARRINGTON, ROBERT BOIS p 2702 N93-25553
FARUQUE, MONAZER p 2796 N93-25594
FAST, JEROME D. p 2769 N93-24672
p 2760 N93-24673
FAUST, C. M. p 2627 N93-26026
FAWCETT, PHILIP ANDREW p 2578 N93-25664
FAXLANGER, EDWARD A., JR. p 2641 N93-26371
FEDDEMA, J. T. p 2827 N93-26596
FEESS, W. A. p 2836 N93-25015
FEGAN-MEYER, D. p 2795 N93-26133
FELCE, ANDREW GEORGE p 2871 N93-25742
FELDHEIM, DANIEL L. p 2869 N93-26577
FELIPPA, CARLOS p 2670 N93-26415
FELKER, FORT FRASER p 2697 N93-25259
FELTHAM, S. J. p 2716 N93-24980
FENG, KEQI p 2821 N93-25880
FENKER, H. p 2689 N93-25491
FENNEMAN, DAVID B. p 2687 N93-25212
FENNESSEY, RICHARD p 2605 N93-24725
FEO, J. T. p 2815 N93-25304
FEREBEE, ROBERT N. p 2794 N93-26066
FERGUSON, DALE C. p 2897 N93-26396
FERGUSON, ELDON E. p 2785 N93-25871
FERGUSON, SHEILA A. p 2766 N93-25875
FERIA, Y. p 2672 N93-24668
p 2678 N93-26120
FERKUL, PAUL V. p 2663 N93-24946
FERNANDEZ, P. B. p 2848 N93-25371
FERNANDEZPALACIOS, A. p 2751 N93-24855
FETHEROLF, B. L. p 2629 N93-26037
FEUER, H. p 2659 N93-25607
FEYOCK, STEFAN p 2823 N93-25969
FICKETT, WILDON p 2706 N93-25987
FIELD, STEPHEN W. p 2896 N93-26067
FIELDING, ERIC J. p 2883 N93-26442
FIFER, R. A. p 2628 N93-26032
FIFER, ROBERT A. p 2628 N93-26030
FILHOCUNHA, CARLOS ALVES p 2771 N93-25433
FILIATRE, C. p 2837 N93-25020
FILLA, O. p 2602 N93-24708
FINE, P. M. p 2692 N93-26598
FINGER, MARK HAROLD p 2676 N93-26106
FINLINSON, JERRY p 2630 N93-26041
FINN, CORY K. p 2667 N93-25085
FIONDA, E. p 2684 N93-26473
FIORITO, RALPH B. p 2711 N93-25608
FISCHER, B. p 2716 N93-25049
FISCHER, J. p 2712 N93-25378
FISCHER, W. p 2738 N93-24781
FISHER, DOUGLAS H. p 2828 N93-25262
p 2823 N93-25966
FITE, E. BRIAN p 2730 N93-26202
FITTING, DALE W. p 2729 N93-26102
FITZ-COY, NORMAN p 2600 N93-24696
FIUZA, ARMANDO F. G. p 2745 N93-24821
p 2734 N93-24927

FLANAGAN, D. p 2659 N93-25607
FLANAGAN, KATHY p 2854 N93-26187
FLANAGAN, KATHY A. p 2854 N93-26185
FLATLEY, THOMAS W. p 2600 N93-24698
FLATTE, S. p 2762 N93-25184
FLEMING, E. L. p 2770 N93-25160
FLETCHER, CHARLES p 2680 N93-26226
FLETCHER, DOUGLAS G. p 2708 N93-25076
FLETCHER, J. A. p 2673 N93-25170
FLIERL, GLENN R. p 2735 N93-24935
FLOCK, WARREN L. p 2684 N93-26475
FLORANCE, JAMES R. p 2591 N93-26553
FLUGRAD, DONALD R. p 2619 N93-26438
FLYNN, DAVID J. p 2600 N93-24699
FOCH, D. p 2607 N93-24735
FODOR, GEORGE E. p 2661 N93-25902
FOERSTER, B. p 2749 N93-24845
FOKAS, A. S. p 2776 N93-26348
FOLEY, H. C. p 2659 N93-25111
p 2659 N93-25112
FOLIAS, E. S. p 2641 N93-26382
FOLKNER, WILLIAM M. p 2676 N93-26106
p 2677 N93-26110
FOLLEN, GREGORY J. p 2593 N93-25673
FOLLSTAEDT, D. M. p 2862 N93-24958
p 2646 N93-26502
FOLTA, DAVID C. p 2601 N93-24705
FOLVING, STEN p 2751 N93-24857
FONT, GABRIEL IVAN p 2578 N93-25545
FORAN, D. A. p 2845 N93-25649
FORCH, B. E. p 2628 N93-26029
FORMAN, P. R. p 2852 N93-25127
FORSBERG, KEVIN p 2665 N93-24682
FORTSON, N. p 2765 N93-25837
FOSS, COLBY A., JR. p 2869 N93-26577
FOSTER, I. p 2763 N93-25370
p 2816 N93-25521
p 2816 N93-25522
p 2767 N93-26496
FOWLER, C. M. p 2861 N93-26512
FOX, PETER T. p 2796 N93-25654
FRAGOMENI, TONY p 2665 N93-24683
FRAIETTA, MICHAEL F. p 2604 N93-24720
FRANCIS, A. J. p 2769 N93-25571
FRANCO, M. M. p 2671 N93-24661
p 2677 N93-26113
FRANK, ADAM p 2900 N93-26132
FRANKE, S. J. p 2770 N93-25160
FRANZ, J. R. p 2863 N93-25225
FRASCA, ALBERT J. p 2687 N93-24746
FRAZIER, SAM p 2584 N93-24898
FREDGA, K. p 2888 N93-25887
FREEMAN, ANTHONY p 2878 N93-25798
FREEMAN, B. p 2861 N93-26512
FREEMAN, M. p 2762 N93-25184
FREEMAN, M. D. p 2854 N93-26183
FREEMAN, MARK D. p 2854 N93-26185
p 2855 N93-26188
p 2855 N93-26190
FREEMAN, W. R. p 2669 N93-26212
FRENDI, A. p 2844 N93-25189
FRERKING, C. p 2815 N93-25304
FRETTE, OEYVIND p 2746 N93-24824
FREY, MARKUS p 2693 N93-25010
FRICKE, ROBERT W. p 2611 N93-25955
p 2612 N93-25956
p 2612 N93-25957
p 2612 N93-25958
p 2612 N93-25959
p 2612 N93-25988
p 2613 N93-25989
p 2613 N93-25990
p 2613 N93-25991
p 2613 N93-25992
FRICKE, ROBERT W., JR. p 2612 N93-25960
p 2613 N93-25993
FRIEDEN, B. R. p 2812 N93-26257
FRIEDLAND, PETER p 2815 N93-25799
FRIEDMAN, H. p 2888 N93-25320
p 2715 N93-26503
FRIEDMAN, J. R. p 2760 N93-24675
FRIEDMAN, ROBERT p 2614 N93-24755
FRIEND, D. G. p 2646 N93-26319
FRIES, JOSEPH p 2597 N93-26260
FRITSCH, J. M. p 2787 N93-26351
FRITSCHE, K. p 2748 N93-24838
FRITZ, THOMAS M. p 2618 N93-26295
FROLOV, D. E. p 2744 N93-24812
FU, CONGBIN p 2764 N93-25517
FU, DONG p 2705 N93-25747
FUCHS, E. F. p 2694 N93-25599
FUCHS, HENRY p 2807 N93-26293
FUCHS, W. KENT p 2815 N93-24749
FUJITA, J. p 2860 N93-25347
FUJITA, SHIN p 2745 N93-24822
FUKIYAMA, N. p 2779 N93-24888
FULGHAM, DAN D. p 2591 N93-25783
p 2591 N93-25909
p 2845 N93-25915
FULLER, ERIC JAMES p 2577 N93-25487
FULLER, R. M. p 2745 N93-24820
FULLERTON, E. E. p 2863 N93-25369
FULTON, M. ANN p 2854 N93-26184
FULTON, M. S. p 2631 N93-26054
FUNG, KO p 2879 N93-25800
FURLONG, MIKE p 2611 N93-25511
FURMANCZYK, K. p 2747 N93-24832
FURNAS, RANDALL B. p 2872 N93-26205

G

GABELMANN, JEFFREY p 2845 N93-25915
GABRIEL, EDWARD A. p 2586 N93-24739
GADDY, J. L. p 2660 N93-25523
GAFFEN, DIAN JUDITH p 2782 N93-25549
GAITAN, FRANK PAUL p 2698 N93-25295
GAITO, STEVE p 2751 N93-24858
GAJJAR, J. S. B. p 2696 N93-25175
GALEA, S. C. p 2638 N93-25768
GALLIMORE, ALEC DAMIAN p 2623 N93-25665
GALLMAN, JOHN WALDEMAR p 2588 N93-25526
GALVEZ, JOSE p 2620 N93-26408
GAMBLE, JOHN C. p 2736 N93-24937
GAMPE, F. p 2748 N93-24840
GANG, P. O. p 2746 N93-24826
GANNAWAY, MARY T. p 2624 N93-26005
GARCIA-DAGUER, R. RENE p 2750 N93-24854
GARCIA, A. p 2899 N93-25327
GARDNER, WILLIAM A. p 2728 N93-25784
GARG, S. p 2698 N93-25266
GARIPOGLY, D. p 2753 N93-24869
GARLAND, JAMES W. p 2867 N93-26223
GARNEK, MIKE p 2615 N93-25133
GARNIER, VINCENT H. p 2595 N93-26335
GARRICK, J. p 2606 N93-24733
p 2607 N93-24734
p 2607 N93-24735
GARRICK, JOSEPH p 2606 N93-24732
GARRITY, CAREN p 2754 N93-25422
GARWIN, R. p 2765 N93-25837
GASTON, ROBERT J. p 2872 N93-25735
GAT, NAHUM p 2887 N93-25442
GATES, W. LAWRENCE p 2761 N93-25145
GATEWOOD, OLGA B. p 2796 N93-25568
GATTO, J. p 2628 N93-26027
GAUTHIER, BENOIT p 2640 N93-26145
GAUTIER, MARGARET A. p 2760 N93-24674
GAUVREAU, JEAN-LUC p 2859 N93-25290
GAVEL, D. p 2715 N93-26503
GAVEL, D. T. p 2888 N93-25320
GAVIGNET, E. p 2836 N93-25012
GAWRONSKI, W. p 2672 N93-24669
p 2679 N93-26123
GAY, M. p 2750 N93-24853
GAZZA, GEORGE E. p 2657 N93-26432
GEBO, NORMAN p 2683 N93-26468
GEBO, NORMAN E. p 2685 N93-26483
GEELEN, G. p 2795 N93-26133
GEERNAERT, G. L. p 2790 N93-26384
GEIB, STEVEN J. p 2851 N93-26518
GEOHEGAN, D. B. p 2713 N93-25508
GEORGE, E. P. p 2650 N93-25519
GEORGE, EUGENE G. p 2682 N93-26455
GEORGESON, GARY E. p 2722 N93-26526
p 2722 N93-26527
GEORGIEV, GEORGI p 2753 N93-24870
GERACE, G. C. p 2684 N93-26474
GERACI, ALBERTO L. p 2746 N93-24823
GERARD, A. H. p 2832 N93-24989
GERARD, EVELYNE p 2621 N93-25028
GERBSCH, REINHOLD ALFRED p 2694 N93-24766
GERWIN, RICHARD p 2633 N93-26555
GEVINS, ALAN p 2798 N93-26391
GHAFOOR, ABDUL p 2718 N93-25727
GHARIB, MORTEZA p 2707 N93-26360
GHOSH, M. p 2862 N93-25163
GIBSON, THERESA L. p 2708 N93-24737
GIBSON, WARREN C. p 2810 N93-25627
GIESE, R. F. p 2658 N93-26588
GILABERT, M. A. p 2750 N93-24851
GILBERT, J. B. p 2860 N93-25641
GILBERT, JOYCE A. p 2796 N93-26068
GILBERT, STEVEN REINO p 2782 N93-25557
GILMORE, C. M. p 2652 N93-26197
GILMORE, RANDY p 2670 N93-25580
GILMOUR, PHILLIP p 2863 N93-25219
GIORDANO, V. p 2833 N93-24990
p 2833 N93-24991
p 2842 N93-25056
GIORI, KATHY L. p 2583 N93-24887
GLASSMAN, ARTHUR J. p 2580 N93-25883
GLICKMAN, J. p 2602 N93-24710
GLITZ, R. p 2738 N93-24777
GLOVER, DANIEL p 2803 N93-25922
GLOVER, DAVID M. p 2735 N93-24935
GLYNN, MICHAEL S. p 2778 N93-24883
GODDARD, R. E. p 2621 N93-26112
GODDARD, R. G. p 2854 N93-26185
GODONE, A. p 2842 N93-25058
GOFORTH, H. W., JR. p 2802 N93-26229
GOGINENI, S. P. p 2790 N93-26050
GOIFFON, A. p 2840 N93-25043
p 2840 N93-25044
GOLDHIRSH, J. p 2683 N93-26467
GOLDHIRSH, JULIUS p 2683 N93-26468
p 2685 N93-26483
GOLDMAN, PEGGY A. p 2723 N93-24957
GOLDSTEIN, R. M. p 2680 N93-26129
GOLDSTEIN, STANLEY H. p 2911 N93-26058
p 2914 N93-26070
GOMEZ, FERNANDO p 2825 N93-25979
GONDOT, PASCAL p 2583 N93-24879
GONSALEZF., A. p 2751 N93-24855
GOOD, PHILIP p 2620 N93-26408
GOODENOUGH, DAVID G. p 2879 N93-25800
GOODISMAN, MICHAEL I. p 2717 N93-25268
GOODMAN, D. W. p 2644 N93-25817
GOODRICH, CHARLES C. p 2881 N93-25812
GOOSSENS, ROLAND E. p 2748 N93-24842
GOOYABADI, ALI A. p 2620 N93-26408
GORDON, CLAIRE C. p 2800 N93-25628
p 2802 N93-26404
GORDON, KAREN D. p 2883 N93-26313
GORDON, PETER C. p 2686 N93-26490
GORDON, STEVEN C. p 2604 N93-24721
GORE, ALBERT, JR. p 2887 N93-26458
GORMAN, R. PAUL p 2822 N93-25965
GORNITZ, V. M. p 2791 N93-26586
GOSLIN, JOSEPH J. p 2584 N93-25243
GOSLING, JACK T. p 2770 N93-25081
GOTOH, Y. p 2860 N93-25347
GOTSIS, P. p 2724 N93-25070
GOTSIS, P. K. p 2723 N93-24913
GOW, A. p 2790 N93-26050
GRABERT, GREGORY p 2863 N93-25219
GRAESSLE, D. p 2855 N93-26192
GRAHAM, GLENNA A. p 2794 N93-24738
GRAHAM, RONALD E. p 2872 N93-26205
GRAHAM, SCOTT R. p 2897 N93-26395
GRANATA, TIMOTHY C. p 2736 N93-24939
GRANT, KEITH p 2762 N93-25147
GRASSL, HARTMUT p 2746 N93-24828
GRASSO, CHRIS p 2670 N93-26416
GRATZNER, HOWARD p 2794 N93-25566
GRAY, GRANT p 2777 N93-24877
p 2756 N93-25679
GRAY, J. p 2712 N93-25363
GREBOGI, CELSO p 2883 N93-26377
GREEN, DAVID M. p 2846 N93-26374
GREEN, G. M. p 2668 N93-25498
GREEN, STEVEN M. p 2585 N93-26087
GREEN, TIMOTHY M. p 2863 N93-25362
GREENBAUM, E. p 2792 N93-25104
GREENBAUM, S. G. p 2851 N93-26514
GREENBAUM, STEVEN G. p 2655 N93-25642
GREENE, A. E. p 2858 N93-25167
GREENLEAF, J. E. p 2795 N93-26133
GREENWAY, D. p 2627 N93-26024
GREGG, M. p 2762 N93-25184
GREINER, D. E. p 2848 N93-25364
GREINER, THOMAS M. p 2800 N93-25628
GREITZER, EDWARD M. p 2595 N93-26335
GREKOV, D. L. p 2859 N93-25216
GREWE, L. L. p 2756 N93-25653
GRIFFIN, ANSELM C. p 2658 N93-26576
GRIFFIN, ROCK E. p 2873 N93-26418
GRIFFIOEN, K. A. p 2848 N93-25366
GRIFFITH, P. p 2802 N93-26229
GRIFFITH, PATRICIA A. p 2884 N93-26523
GRIMSDTICH, M. p 2863 N93-25369
GRIPSHOVER, RONALD J. p 2687 N93-25212
GRISIUS, MATTHEW A. p 2883 N93-26350
GRISON, D. p 2831 N93-24981
GRODSKI, J. J. p 2822 N93-25964
GRODY, NORMAN C. p 2824 N93-25974
GROSS, K. W. p 2626 N93-26017
GROSSMAN, ALLEN S. p 2762 N93-25146
p 2762 N93-25147
GROVES, KEITH M. p 2774 N93-25852
GRUBELICH, M. C. p 2627 N93-26024
GRUBER, DUANE E. p 2892 N93-25211
GRUMAZESCU, H. p 2747 N93-24834
GU, YEMING p 2895 N93-25728
GU, ZU-HAN p 2676 N93-25855
GUALTIERI, J. A. p 2824 N93-25975
GUALTIERI, J. G. p 2841 N93-25047
GUANGQIAN, XING p 2599 N93-25693

GUELL, D. C. p 2655 N93-25507
GUENETTE, G. R. p 2595 N93-26219
GUILINGER, T. p 2862 N93-24958
GUILINGER, T. R. p 2646 N93-26502
GUILMETTE, NEAL p 2595 N93-24762
GUIMARAES, KATIA p 2801 N93-26047
GUINAN, M. W. p 2649 N93-25336
GUINN, THOMAS ALAN p 2782 N93-25352
GUINOT, B. p 2832 N93-24984
GULEV, SERGEY K. p 2732 N93-24918
GUMLEY, J. R. p 2781 N93-24902
GUNZBURGER, MAX D. p 2707 N93-26400
GUO, T. H. p 2622 N93-25089
GUSTAFSSON, L.-E. p 2749 N93-24847
GUTMAN, SEMION p 2829 N93-26199
GUTOWSKI, MACIEJ p 2849 N93-25659
GUYENNE, T. DUC p 2737 N93-24775
GYSLING, DANIEL L. p 2595 N93-26335

H

HABERLE, ROBERT M. p 2897 N93-26394
HABLANI, HARI B. p 2600 N93-24695
HACKETT, MICHAEL p 2901 N93-25561
HAEFNER, H. p 2744 N93-24816
HAERTLING, GENE p 2863 N93-25219
HAGEN, JIM p 2611 N93-25511
HAGGERTY, JOHN S. p 2640 N93-26236
HAGNER, OLLE p 2752 N93-24863
HAIGH, STEPHEN J. p 2583 N93-24886
p 2693 N93-24903
HAINES, B. J. p 2601 N93-24702
HAINES, RICHARD F. p 2805 N93-25930
HAISCH, BERNHARD p 2891 N93-26139
HAISSIG, CHRISTINE MARIE p 2608 N93-25684
HAKIMI, M. p 2601 N93-24703
HALL, C. A. p 2689 N93-25416
p 2689 N93-25417
HALL, K. R. p 2872 N93-26558
HALL, KENNETH C. p 2696 N93-25109
HALL, KENNETH R. p 2872 N93-26509
HALL, MARK p 2699 N93-25348
HALLE, LINDA F. p 2867 N93-25947
HALLIN, A. p 2899 N93-25327
HALPERN, DAVID p 2734 N93-24926
HALSEY, THOMAS C. p 2642 N93-24972
HALT, DAVID W. p 2639 N93-25341
HAMETZ, M. p 2603 N93-24717
HAMID, S. p 2594 N93-25917
HAMILTON, M. L. p 2649 N93-25255
HAMMACK, JAMES H. p 2756 N93-25694
HAMMONDS, J. S. p 2760 N93-24676
HANDLEY, THOMAS H., JR. p 2879 N93-25801
HANGE, CRAIG E. p 2581 N93-26099
HANISCH, ROBERT J. p 2880 N93-25808
HANNA, ASHRAF E. p 2868 N93-26302
HANSEN, ELAINE R. p 2879 N93-25802
HANSEN, JAMES P. p 2682 N93-26455
HANSON-PARR, DONNA p 2629 N93-26036
p 2630 N93-26041
HANSON, D. p 2713 N93-25379
HANSON, DONALD B. p 2844 N93-25094
HAPPEL, JOHN AMIN p 2670 N93-26414
HARABAGLIA, PAOLO p 2771 N93-25202
HARASGAMA, S. P. p 2592 N93-25455
HARDING, KEVIN G. p 2711 N93-25578
HARDING, W. B. p 2669 N93-26207
HARDWICK, C. JOHN p 2692 N93-24881
p 2583 N93-24886
p 2642 N93-24890
p 2583 N93-24894
p 2693 N93-24903
HARDY, ALVA C. p 2632 N93-26200
HARMAN, R. R. p 2600 N93-24697
HARMAN, TODD B. p 2580 N93-26049
HARRIS, H. M. p 2758 N93-25098
HARRIS, JOHN C. p 2796 N93-25592
HARRIS, RICHARD W. p 2805 N93-25932
HARRISON, P. ANN p 2754 N93-25154
HART, DAVID M. p 2829 N93-26345
HART, MARY L. p 2896 N93-26340
HART, R. C. p 2601 N93-24703
HARTL, PH. p 2831 N93-24979
HARTMAN, J. K. p 2627 N93-26024
HARTMAN, JOHN H. p 2809 N93-25250
HARVIE, E. p 2602 N93-24710
HASHMALL, J. p 2606 N93-24733
HASSANI, S. p 2693 N93-25041
HATHAWAY, DAVID A. p 2813 N93-26563
HATHAWAY, KRISTL B. p 2710 N93-26141
HAUDEN, D. p 2711 N93-25009
HAUGER, A. p 2688 N93-25365
HAUGHT, DEBORAH A. p 2642 N93-25586
HAUNSCHILD, M. p 2586 N93-25018
HAUS, HERMANN A. p 2856 N93-26457
HAUSMANN, CLIFFORD R. p 2595 N93-26161
HAUTMAN, D. J. p 2625 N93-26014
HAVEL, JAN p 2740 N93-24788
HAVENHILL, J. W. p 2809 N93-25307
HAVENS, STEPHEN J. p 2656 N93-25997
HAWTHORNE, WILLIAM p 2593 N93-25668
HAYASAKA, KAZUHIRO p 2838 N93-25031
HAYES, DENNIS E. p 2790 N93-26170
HAYES, J. P. p 2654 N93-25382
HAYES, SCOTT p 2883 N93-26377
HAYES, WILLIAM A. p 2626 N93-26018
HAZELWOOD, JON p 2776 N93-26283
HE, J. W. p 2716 N93-25048
HEALY, BRIAN E. p 2811 N93-25845
HECK, H. G. p 2768 N93-26592
HECK, MICHAEL L. p 2615 N93-25174
HEDIN, A. E. p 2770 N93-25160
HEIKKILAE, OUTI p 2752 N93-24864
HEINTZE, NEVIN p 2806 N93-25841
HELLER, ADAM p 2690 N93-25782
HELM, H. p 2849 N93-25644
HELMICK, LARRY A. p 2654 N93-25093
HELMS, IRA p 2621 N93-24740
HEMBERGER, P. H. p 2712 N93-25150
HEMENWAY, DONALD F. p 2682 N93-26455
HENDERSON, SCOTT p 2825 N93-25977
p 2825 N93-25978
p 2825 N93-25981
HENDRICKSON, B. p 2810 N93-25386
HENDRICKSON, P. L. p 2760 N93-24675
HENINS, IVARS p 2633 N93-26555
HENRETTY, DEBRA A. p 2600 N93-24698
HERBENER, D. G. p 2610 N93-26182
HERBERG, JOSEPH R. p 2601 N93-24705
HERGENROTHER, PAUL M. p 2656 N93-25997
HERNANDO, J. A. p 2866 N93-25781
HERR, JOEL L. p 2615 N93-25090
HERTEL, D. p 2748 N93-24838
HERTZBERG, M. p 2668 N93-25498
HEUSER, W. R. p 2679 N93-26121
HEUZE, F. E. p 2731 N93-26507
HEYWARD, ANN O. p 2684 N93-26476
HICK, PETER T. p 2746 N93-24829
HIDAY, LISA ANN p 2608 N93-25758
HILDEBRANDT, G. p 2745 N93-24817
HILL, DAVID p 2724 N93-25260
HILL, JOHN p 2881 N93-25813
HILL, JOHN M. p 2711 N93-25614
HILL, L. R. p 2731 N93-26507
HILLARD, G. BARRY p 2618 N93-26148
p 2618 N93-26215
HILLER, K. p 2743 N93-24807
HINEDI, S. p 2614 N93-24667
HINGHOFER-SZALKAY, H. p 2795 N93-26133
HINGST, W. R. p 2575 N93-24911
HIRASAWA, TAKEO p 2774 N93-25889
HIRSCH, A. p 2688 N93-25365
HITES, M. H. p 2630 N93-26042
p 2631 N93-26043
HMAM, HATEM M. p 2718 N93-25697
HO, JOHN C. p 2621 N93-25027
HO, P. p 2644 N93-25312
HOANG, PHILLIP P. p 2680 N93-26160
HOBAN, FRANCIS T. p 2665 N93-24678
HOBBS, HERMAN H. p 2664 N93-25218
HOCHHEIMER, H. D. p 2687 N93-25113
HODGDON, M. L. p 2688 N93-25313
HODGE, JOHN D. p 2666 N93-24686
HODGE, STEVEN L. p 2845 N93-26086
HODGES, C. J. p 2687 N93-25069
HOFFMAN, F. O. p 2760 N93-24676
HOHMANN, NEIL p 2661 N93-25818
HOJO, JUNICHI p 2779 N93-24888
p 2779 N93-24892
HOLANDA, RAYMOND p 2709 N93-25173
HOLCOMB, ROBERT S. p 2622 N93-24744
HOLDEN, TINA p 2799 N93-25595
HOLLAND, GEOFFREY p 2737 N93-24940
p 2737 N93-24941
HOLLEY, E. R. p 2768 N93-26559
HOLMQUIST, SVEN G. p 2823 N93-25968
HOLSTE, J. C. p 2872 N93-26558
HOLSTE, JAMES C. p 2872 N93-26509
HOLZSCHEITER, K. p 2869 N93-26494
HONDA, OSAMU p 2745 N93-24822
HONIG, E. M. p 2713 N93-25379
HONMA, NORIYASU p 2779 N93-24892
HOOVER, MERVYN C. p 2691 N93-26142
HOPPER, PHILLIP L. p 2801 N93-25787
HORAK, DAN T. p 2822 N93-25965
HORN, BERTHOLD P. p 2879 N93-25803
HORNE, ROLAND N. p 2695 N93-24954
HORNING, ROBERT D. p 2849 N93-25823
HOSAKA, YASUO p 2859 N93-25227
HOSHIAI, TAKAO p 2774 N93-25889
HOSKING, CRAIG p 2611 N93-25511
HOSOKAWA, M. p 2687 N93-24951
HOSTETTER, CARL F. p 2822 N93-25961
HOUCK, T. L. p 2852 N93-25375
p 2688 N93-25397
HOUMMADY, M. p 2711 N93-25009
HOUTZ, JOHN p 2652 N93-26208
HOWARD, J. B. p 2644 N93-25500
HOWARTH, R. B. p 2764 N93-25443
HOWE, STEVEN p 2621 N93-24740
HOYER, JESSE L. p 2659 N93-25585
HRUSKA, CARL K. p 2840 N93-25046
HSIUNG, JIH-LAN p 2577 N93-25409
HSU, D. K. p 2721 N93-25518
HSU, LAN-SHENG p 2770 N93-25179
HSU, SU-YEN p 2637 N93-25680
HU, CHENMING p 2692 N93-26539
HU, W. L. p 2649 N93-25255
HUANG, BOHUA p 2789 N93-25445
HUANG, F. H. p 2649 N93-25255
HUANG, H. X. p 2716 N93-25048
HUANG, K. p 2880 N93-25807
HUANG, P. G. p 2697 N93-25247
HUANG, X. Z. p 2646 N93-26505
HUBER, A. KRIS p 2805 N93-25932
HUBER, ALAN C. p 2620 N93-26248
HUBER, CRAIG C. p 2761 N93-25143
HUBER, GARY T. p 2598 N93-26214
HUCH, DAVID p 2730 N93-26279
HUCKETT, S. C. p 2646 N93-26505
HUDSON, REGGIE L. p 2892 N93-25230
HUFF, FLOYD A. p 2785 N93-25872
HUGGINS, ARLEN W. p 2785 N93-25849
HUGHES, DECLAN p 2719 N93-25771
HUGHES, J. P. p 2854 N93-26183
HUGHES, JOHN P p 2855 N93-26190
HUGHES, JOHN P. p 2854 N93-26187
p 2855 N93-26188
p 2855 N93-26189
p 2855 N93-26191
p 2855 N93-26192
HUGHES, PETER M. p 2814 N93-25589
HUIE, R. p 2658 N93-26433
HUIJING, DONNA CHURYK p 2766 N93-25875
HULL, RICHARD p 2825 N93-25979
HUMPHRIES, T. T. p 2617 N93-25525
HUNT, F. Y. p 2830 N93-26317
HUNT, HAROLD G. p 2736 N93-24937
HUNT, JAMES J. p 2737 N93-24775
p 2831 N93-24978
HUSSAIN, FAZLE p 2695 N93-25082
HUSTON, RONALD L. p 2719 N93-25884
HUTSON, F. L. p 2868 N93-26258
HYDE, J. M. p 2653 N93-26500
HYDE, JAMES M. p 2732 N93-25834
HYDE, TUPPER p 2609 N93-25836

I

IBANEZ, A. p 2840 N93-25043
p 2840 N93-25044
IESS, L. p 2608 N93-24998
IIDA, TAKASHI p 2683 N93-26470
p 2683 N93-26471
IISAKA, JOJI p 2879 N93-25800
ILINCIC, N. p 2628 N93-26027
IMAJO, HIDETSUKA p 2838 N93-25031
IMAOKA, ATUSHI p 2686 N93-25061
IMATANI, TOSHIO p 2753 N93-24868
INBODY, MICHAEL ANDREW p 2642 N93-25116
INCEOGLU, ZAFER p 2682 N93-26441
INCROPERA, F. P. p 2644 N93-25495
INGEBO, ROBERT D. p 2709 N93-25191
INGHAM, H. p 2646 N93-26319
IOUP, GEORGE E. p 2769 N93-24910
p 2770 N93-25088
IOUP, JULIETTE W. p 2775 N93-26084
p 2769 N93-24910
p 2770 N93-25088
p 2775 N93-26084
ISACKS, BRYAN L. p 2883 N93-26442
ISHII, MASARU p 2779 N93-24888
p 2779 N93-24892
ISLAM, ABU S. p 2639 N93-25945
ISMAIL, IBRAHIM H. p 2594 N93-25751
ITOH, K. p 2860 N93-25346
ITOH, S. p 2860 N93-25347
ITOH, S.-I. p 2860 N93-25346
IVANOV, MIROSLAV p 2753 N93-24870
IVORY, J. E. p 2605 N93-24727
IYER, RAVISHANKAR KRISHNAN p 2815 N93-24748
IYER, S. p 2870 N93-26581

J

JACKSON, C. G. R. p 2795 N93-26133
JACOBS, E. L. p 2689 N93-25417
JACOBS, S. D. p 2714 N93-25869
JACOBSON, ALLAN S. p 2879 N93-25801
p 2880 N93-25804
JACOBSON, K. B. p 2793 N93-26587
JACOBUS, M. J. p 2689 N93-25429
JACOX, MICHAEL G. p 2892 N93-25164
JAFFERIS, WILLIAM p 2619 N93-24878
JAFFERY, WARIS S. p 2720 N93-25605
JAHNEN, WALTRAUD p 2746 N93-24828
JAKOBY, R. p 2684 N93-26478
JAMES, LARRY p 2730 N93-26279
JAMINET, PAUL ALOYSIUS p 2889 N93-25440
JAMNEJAD, V. p 2680 N93-26128
JANAJREH, IBRAHIM MUSTAFA p 2727 N93-25681
JANAWAY, G. A. p 2649 N93-25336
JANIAUD, D. p 2711 N93-25011
JANKE, DAVID E. p 2626 N93-26018
JANKOWSKI, A. F. p 2654 N93-25382
JANSCHE, A. p 2586 N93-25018
p 2693 N93-25033
JANSEN, BEN H. p 2823 N93-25968
JANSEN, J. F. p 2799 N93-25099
p 2725 N93-25357
JANSS, J. p 2726 N93-25419
JANSSENS, R. V. F. p 2848 N93-25371
JARDIN, S. C. p 2860 N93-25493
JASKE, ROBERT p 2881 N93-25813
JASKOLLA, F. p 2743 N93-24806
JASNOW, MONA p 2898 N93-26424
JAYAKODY, J. R. p 2851 N93-26514
JAYANTI, PRASAD p 2808 N93-25107
JAYARAM, PRAKASH p 2823 N93-25968
JEANDEL, G. p 2840 N93-25045
JEFFERIES, R. p 2837 N93-25019
JEFFRIES, JAY B. p 2860 N93-25626
JEMMA, F. p 2741 N93-24797
JENKINS, J. S. p 2679 N93-26126
JENKINSON, JOEL PATRICK p 2702 N93-25548
JENNE, E. A. p 2759 N93-25183
JENNINGS, NICHOLAS p 2642 N93-24890
JENSEN, C. C. p 2713 N93-25381
JENSEN, DANIEL DUANE p 2724 N93-25273
JEON, JAE-JIN p 2813 N93-26431
JERMSTAD, WAYNE p 2670 N93-26416
JERNIGAN, J. GARRETT p 2878 N93-25795
JEZEK, K. p 2790 N93-26050
JI, CHANGYUAN p 2752 N93-24861
JIANG, G. X. p 2716 N93-25048
JIMENEZ, C. p 2608 N93-24986
JING, Z. p 2862 N93-24953
JINGLI, MAO p 2574 N93-26238
JINQUAN, DENG p 2716 N93-25030
JIRSA, J. O. p 2598 N93-25656
JOHAN, ZDENEK p 2699 N93-25334
JOHANNESSEN, OLA M. p 2746 N93-24824
JOHANNESSON, BIRGIR p 2650 N93-25436
JOHNSON, B. V. p 2667 N93-25177
JOHNSON, BURGESS R. p 2690 N93-25906
JOHNSON, DERECK F. p 2652 N93-26201
JOHNSON, J p 2822 N93-25962
JOHNSON, LINDA F. p 2867 N93-26090
JOHNSON, P. M. p 2847 N93-25310
JOHNSON, W. S. p 2634 N93-25072
JOHNSTON, BROOKS p 2788 N93-24960
JOHNSTON, MARK D. p 2880 N93-25808
JOLLY, STEVE p 2669 N93-26411
JOLY, C. p 2836 N93-25013
JONES, J. P. p 2756 N93-25505
p 2756 N93-25516
JONES, MARK T. p 2854 N93-26186
JONES, PHILIP J. p 2781 N93-24902
JONES, T. L. p 2601 N93-24703
JONES, T. W. p 2899 N93-24752
p 2899 N93-25161
p 2900 N93-26132
JONES, WILLIAM R., JR. p 2654 N93-25093
JONGEWARD, G. A. p 2618 N93-26232
JONGEWARD, GARY p 2897 N93-26397
JORDAN, F. W. p 2627 N93-26021
p 2627 N93-26022
p 2627 N93-26023
JORDAN, P. p 2602 N93-24706
JOSHI, S. P. p 2636 N93-25631
JOSHI, YOGENDRA K. p 2669 N93-26285
JOUBERT, W. p 2809 N93-25315
JOY, M. p 2854 N93-26187
JOY, MARSHALL p 2855 N93-26188
JUE, TSWEN-CHYUAN p 2701 N93-25540
JUHOS, L. T. p 2795 N93-26133
JULICH, P. M. p 2823 N93-25967
JUNKINS, JOHN L. p 2619 N93-26456
JURGENS, R. F. p 2680 N93-26129
p 2680 N93-26130
JUSKA, THOMAS p 2636 N93-25652

K

KABACOFF, LAWRENCE T. p 2867 N93-26140
KABULI, M. G. p 2826 N93-26365
KACKER, R. p 2812 N93-26321
KADOKURA, AKIRA p 2774 N93-25889
KAGEYAMA, A. p 2860 N93-25356
KAILATH, THOMAS p 2692 N93-26366
KAISER, DALE p 2764 N93-25517
KAK, A. C. p 2756 N93-25653
KALLIOMAEKI, KALEVI p 2835 N93-25006
p 2835 N93-25007
p 2839 N93-25035
KALLURI, SREERAMESH p 2731 N93-26550
KAMADA, R. F. p 2776 N93-26454
KAMPUS, F. p 2862 N93-25163
KANADE, TAKEO p 2757 N93-26448
p 2857 N93-26488
KANCHEVA, RUMIANA H. p 2739 N93-24782
p 2751 N93-24860
KANE, M. p 2658 N93-26433
KANEMASU, E. T. p 2769 N93-24945
KANG, H. p 2756 N93-25653
KANG, HYUNG SUK p 2705 N93-25737
KANG, JA YOUNG p 2617 N93-25527
KANG, M. p 2768 N93-26592
KANTAK, ANIL V. p 2684 N93-26472
KAPER, H. p 2767 N93-26496
KAPUSTINSKY, J. S. p 2869 N93-26494
KARAMOUZIS, STAMOS T. p 2823 N93-25969
KARL, THOMAS p 2764 N93-25517
KARPENKO, V. P. p 2711 N93-24961
KARPUR, SHASHI RAO p 2875 N93-25421
KARR, C. L. p 2827 N93-25612
KASIF, SIMON p 2817 N93-26169
KATSCHER, R. p 2738 N93-24781
KATTAMIS, T. Z. p 2658 N93-26433
KATTENBORN, G. p 2752 N93-24862
KATTNER, URSULA R. p 2652 N93-26284
KATZ, I. p 2618 N93-26232
KATZ, R. H. p 2806 N93-25233
KATZ, R. NATHAN p 2657 N93-26432
KATZ, RANDY H. p 2805 N93-25130
p 2809 N93-25131
p 2806 N93-25267
p 2815 N93-25297
p 2816 N93-25458
KAUFMAN, L. p 2798 N93-26435
p 2799 N93-26521
KAUFMAN, LLOYD p 2798 N93-26436
KAUP, D. J. p 2776 N93-26348
KAZOVSKY, LEONID G. p 2856 N93-26256
KEANE, JOHN p 2882 N93-26230
p 2884 N93-26531
p 2884 N93-26532
KEAT, W. D. p 2641 N93-26355
KEBABIAN, P. L. p 2628 N93-26031
KEEL, L. H. p 2818 N93-25155
p 2818 N93-25156
p 2819 N93-25226
p 2819 N93-25296
KEEL, LEEHYUN p 2817 N93-24757
KEEN, ARTHUR A. p 2883 N93-26350
KEHAYAS, N. p 2589 N93-25704
KEIL, L. C. p 2795 N93-26133
KEIL, M. p 2748 N93-24837
KELAITA, PAUL G. p 2814 N93-25600
KELLEHER, MATTHEW D. p 2669 N93-26285
KELLER, RICHARD M. p 2815 N93-25799
KELLEY, HENRY L. p 2656 N93-25995
p 2597 N93-25998
KELLMAN, A. G. p 2860 N93-25493
KELLOGG, E. M. p 2854 N93-26183
KELLOGG, EDWIN M. p 2854 N93-26184
p 2854 N93-26185
p 2854 N93-26187
p 2855 N93-26188
p 2855 N93-26189
p 2855 N93-26192
KELLY, BRIAN GERARD JOSEPH p 2788 N93-25276
KELLY, M. p 2862 N93-24958
KELLY, M. J. p 2646 N93-26502
KEMMOTSU, KEIICHI p 2857 N93-26488
KENNEWEG, H. p 2749 N93-24848
KENNEY, J. D. P. p 2890 N93-25755
KENT, M. p 2884 N93-26568
KENT, RENEE M. p 2721 N93-25451
KENTLEY, ERIC p 2833 N93-24996
KERN, ALEXANDER W. p 2642 N93-24891
KERNS, THOMAS H. p 2882 N93-26242
KESTER, DANA p 2733 N93-24923
KEY, JAMES F. p 2658 N93-25562
KEYS, THERESA p 2661 N93-25857
KHOO, T. L. p 2848 N93-25371
KIANG, RICHARD K. p 2825 N93-25976
KICKBUSCH, W. p 2752 N93-24866
KIETZMANN, H. p 2738 N93-24778
KIHARA, MASAMI p 2686 N93-25061
KILGORE, W. ALLEN p 2695 N93-25087
KILKENNY, J. D. p 2709 N93-25515
KILLOUGH, S. M. p 2718 N93-25449
KIM, B. F. p 2871 N93-25584
KIM, DONG W. p 2796 N93-25568
KIM, ED p 2609 N93-25836
KIM, HYEONG-JIN p 2705 N93-25738
KIM, I. p 2661 N93-25948
KIM, IEE-HWAN p 2664 N93-25390
KIM, JOHN p 2695 N93-25082
KIM, RHYN H. p 2697 N93-25221
KIM, Y. p 2649 N93-25149
KIM, YONG-GI p 2874 N93-25258
KIMURA, KENICHI p 2774 N93-25889
KING, JAMES M. p 2802 N93-26265
KING, R. B. p 2845 N93-25649
KING, SCOTT D. p 2828 N93-25223
KINTER, JAMES L., III p 2880 N93-25805
KIRK, MARK T. p 2731 N93-26390
p 2731 N93-26516
KIRKPATRICK, R. C. p 2861 N93-26504
KIROUAC, G. J. p 2698 N93-25306
KISELEVSKII, L. I. p 2741 N93-24793
KISPERT, A. p 2822 N93-25962
KISS, Z. p 2759 N93-25253
KISSH, FRANK p 2600 N93-24699
KITHCART, M. p 2706 N93-25951
KIVELAE, REIJO p 2693 N93-25029
KIVELSON, MARGARET G. p 2770 N93-25081
KLEIN, DAVID L. p 2801 N93-25867
KLEINFELDER, WALTER J. p 2814 N93-25575
KLEMM, KARL A. p 2867 N93-26090
KLEMP, JOSEPH B. p 2879 N93-25802
KLEMP, MARJORIE K. p 2879 N93-25802
KLEPACZKO, J. R. p 2728 N93-25785
p 2731 N93-26459
KLETT, D. E. p 2706 N93-25951
KLIBANOV, MICHAEL V. p 2829 N93-26199
KLIMESOVA, DANA p 2740 N93-24788
KLINE, ROBERT C. p 2617 N93-25630
KLINGSPORN, P. E. p 2852 N93-25182
KLINK, KATHERINE MARGARET p 2764 N93-25476
KLUTE, GLENN K. p 2797 N93-25736
KNAP, ANTHONY H. p 2736 N93-24938
KNEE, H. E. p 2800 N93-25415
KNIGHT, D. J. E. p 2837 N93-25019
p 2687 N93-25069
KNOLL, GLENN p 2573 N93-25077
KNOX, E. C. p 2631 N93-26057
KO, HON-YIM p 2670 N93-26412
KOCH, B. p 2749 N93-24845
KOCH, J. A. p 2712 N93-25363
KOCH, STEVEN p 2881 N93-25814
KOELLING, ROGER p 2652 N93-26208
KOFSKY, IRVING L. p 2632 N93-26373
KOGAN, FELIX N. p 2750 N93-24852
KOHGUTI, TOSHIYUKI p 2745 N93-24822
KOKOTOVIC, PETAR V. p 2826 N93-26333
KOLECKI, JOSEPH C. p 2618 N93-26148
KOLESAR, RICHARD p 2611 N93-25511
KOLODZIEJCZAK, JEFFERY J. p 2855 N93-26188
KOLODZIEJEZAK, J. p 2854 N93-26187
KOMIYAMA, TAMOTSU p 2716 N93-25068
KOMURO, H. p 2779 N93-24892
KONDAS, DAVID A. p 2710 N93-25686
KONDOH, YOSHIOMI p 2859 N93-25227
KONNO, KEVIN E. p 2595 N93-26161
KOONIN, S. p 2762 N93-25184
KOPPES, W. M. p 2630 N93-26038
KOSHELYAEVSKY, N. B. p 2836 N93-25017
KOSINSKI, J. A. p 2841 N93-25047
KOSS, T. C. p 2760 N93-24675
KOSSLYN, STEPHEN M. p 2797 N93-26347
KOSTYUKEVICH, S. B. p 2741 N93-24793
KOSUT, ROBERT L. p 2826 N93-26365
KOTLAR, A. J. p 2628 N93-26028
KOTULSKI, ZBIGNIEW p 2724 N93-25328
p 2763 N93-25329
KOVALYOV, A. A. p 2741 N93-24793
KOYUNCU, HAYATI p 2739 N93-24783
KOZLOWSKI, M. R. p 2654 N93-25384
p 2857 N93-26593
KRABILL, WILLIAM p 2711 N93-25614
KRACK, K. p 2603 N93-24714
p 2607 N93-24735
KRAFT, CHRISTOPHER C. p 2666 N93-24688
KRAMER, WARNER p 2690 N93-25660
KRANZ, EUGENE F. p 2666 N93-24688

KRASNY, ROBERT p 2644 N93-25819
KREHBIEL, PAUL p 2777 N93-24877
KREHBIEL, PAUL R. p 2756 N93-25679
KREINOVICH, VLADIK p 2820 N93-25452
KREINOVICH, VLADIK YA. p 2818 N93-25138
p 2874 N93-25139
p 2828 N93-25140
p 2818 N93-25141
p 2818 N93-25142
p 2818 N93-25190
p 2818 N93-25196
p 2819 N93-25197
p 2820 N93-25425
p 2820 N93-25459
KRENEK, BRENDAN D. p 2711 N93-25614
KRESS, R. L. p 2725 N93-25357
KREZHOVA, DORA p 2753 N93-24870
KRICHEVSKY, VLADIMIR p 2683 N93-26468
KRIDER, E. PHILIP p 2711 N93-24900
KRIER, HERMAN p 2659 N93-24745
KRISHNAMURTI, T. N. p 2785 N93-25777
KRISHNAN, ANANTHA p 2661 N93-26268
KRIZ, RONALD D. p 2729 N93-26102
KRSKA, CAROL M. p 2652 N93-26208
KRULEWICH, D. A. p 2620 N93-25317
KRUMOV, ALEXANDAR H. p 2751 N93-24860
KRUPP, BRIAN p 2755 N93-25460
p 2755 N93-25461
p 2756 N93-25462
KRUSE, PAUL W. p 2849 N93-25823
p 2690 N93-25906
KUBO, S. p 2687 N93-24951
KUEHBAUCH, W. p 2750 N93-24850
p 2751 N93-24859
KUHN, RICHARD E. p 2581 N93-26099
KUIVINEN, DAVID E. p 2652 N93-26201
KUKLINSKI, WALTER p 2776 N93-26283
KULP, L. S. p 2600 N93-24697
KUMAR, K. SHARVAN p 2653 N93-24761
KUMAR, RAVINDAR p 2756 N93-25462
KUMAR, RAVINDRA p 2755 N93-25460
p 2755 N93-25461
KUMAR, RENJITH R. p 2615 N93-25174
KUMAR, S. p 2863 N93-25369
KUMAR, SUNDEEP p 2818 N93-25196
KUMAR, SURESH p 2689 N93-25619
KUNIMORI, HIROO p 2716 N93-25005
KUNZ, TERRY D. p 2711 N93-25614
KUO, YU-HENG p 2789 N93-25657
KUPERMAN, GILBERT G. p 2590 N93-25949
KURAMOCHI, NAIMU p 2716 N93-25068
KURDILA, ANDREW J. p 2619 N93-26456
KURIHARA, NORIYUKI p 2774 N93-25889
KURNIT, N. p 2713 N93-25379
KURODA, T. p 2687 N93-24951
KURTZ, A. D. p 2868 N93-26312
KURTZ, S. K. p 2727 N93-25690
KUSSMAUL, MICHAEL T. p 2658 N93-25564
KUYATT, C. E. p 2830 N93-26318
KWATRA, S. C. p 2803 N93-25922
KWON, YOUNG W. p 2727 N93-25658
KWONG, M. K. p 2767 N93-26496

L

LABATE, D. p 2686 N93-24893
LACKMAN, ROBERT L. p 2878 N93-25794
LACKNEY, J. J. p 2723 N93-24913
p 2724 N93-25070
LAGOUDAS, D. C. p 2729 N93-25950
LAGOUDAS, DIMITRIS C. p 2729 N93-25846
p 2639 N93-25919
p 2729 N93-25941
LAGOWSKI, JACEK p 2867 N93-25899
LAIKHTMAN, B. p 2867 N93-26194
LAKSHMINARAYAN, G. R. p 2658 N93-26433
LAMASTER, HUGH p 2809 N93-25246
LAMBERTSON, M. p 2607 N93-24734
p 2607 N93-24735
LAMKIN, STEPHEN L. p 2614 N93-25952
LAMPMAN, JANET L. p 2757 N93-26440
LANCASTER, JACK L. p 2796 N93-25654
LANCHBERY, J. F. p 2738 N93-24781
LAND, D. p 2811 N93-25943
LANDEN, O. p 2709 N93-25515
LANDIS, GEOFFREY A. p 2623 N93-25132
LANE, NORMAN E. p 2810 N93-25711
LANGSTON, J. p 2603 N93-24714
LANIGAN, CARL A. p 2586 N93-26274
LANKFORD, JAMES, JR. p 2651 N93-25788
LANTZ, E. p 2839 N93-25036
LAPORTE, J. B. p 2693 N93-25053
LAREDO, D. p 2625 N93-26010
LARIMER, F. W. p 2793 N93-26587
LAROSA, AGATINO p 2746 N93-24823
LARSEN, E. W. p 2828 N93-25151
LARSEN, RONALD L. p 2801 N93-26047
LARSON, M. C. p 2641 N93-26355
LASATER, SALLY W. p 2879 N93-25802
LASZLO, I. p 2777 N93-24742
LATHAM, JOHN p 2787 N93-26352
LATTIMORE, MORRIS R. p 2795 N93-26218
LAUE, ERIC G. p 2653 N93-25078
LAURENT, P. p 2831 N93-24981
LAURITSEN, T. p 2848 N93-25371
LAURSEN, TOD ALAN p 2717 N93-25412
LAVERY, P. p 2746 N93-24829
LAVIGNA, ANTHONY p 2680 N93-26226
LAWBAUGH, WILLIAM M. p 2665 N93-24678
LAWSON, DEL R. p 2656 N93-26172
p 2869 N93-26577
LAYMAN, LAURA D. p 2774 N93-25886
LAYTON, CHARLES p 2585 N93-25330
LAYTON, CHUCK p 2585 N93-25261
LAZARUS, ALLAN J. p 2770 N93-25081
LEA, ROBERT p 2818 N93-25138
p 2818 N93-25142
p 2820 N93-25459
LEADER, JEFFERY J. p 2829 N93-26370
LEADER, JEFFREY J. p 2829 N93-26452
LEAHY, R. M. p 2794 N93-25186
LEAR, WARREN L. p 2765 N93-25765
LEBERL, FRANZ p 2878 N93-25798
LECLERC, P. p 2832 N93-24989
LEE-RAUSCH, ELIZABETH M. p 2581 N93-26134
LEE, ALBERT W. p 2596 N93-25353
LEE, CHANGJIN p 2664 N93-25465
LEE, D. p 2862 N93-24953
LEE, E. K. p 2806 N93-25233
LEE, JAEHONG p 2723 N93-24765
LEE, JAMES H. p 2632 N93-26200
LEE, LANDRIS T., JR. p 2776 N93-25570
LEE, M. D. p 2669 N93-26212
LEE, M. GENE p 2801 N93-26088
LEE, MIN-CHANG p 2774 N93-25852
LEE, R. p 2614 N93-24667
LEE, S. R. p 2863 N93-25387
LEE, SAMKEUN p 2851 N93-26518
LEE, SHI-WEI RICKY p 2637 N93-25675
LEE, TZE-SAN p 2794 N93-26069
LEE, YEOL p 2704 N93-25705
LEE, YOUNGUNG p 2893 N93-25477
LEETE, C. A. p 2816 N93-25414
LEETMAA, ANTS p 2733 N93-24921
LEHMAN, SEAN K. p 2788 N93-24960
LEHMANN, MONTY R. p 2693 N93-24882
LEHNERT, BRUCE E. p 2795 N93-25629
LEITH, C. p 2762 N93-25184
LELAND, R. p 2810 N93-25386
LELAND, W. p 2713 N93-25379
LEMAITRE, JEAN p 2729 N93-25901
LEMMERMAN, LOREN A. p 2666 N93-24691
LEMOIGNE, JACQUELINE p 2824 N93-25973
LEMOINE, FRANK GEORGE RODRIGUE p 2896 N93-25439
LEMOS, P. J. p 2605 N93-24726
LENTZNER, HOWARD L. p 2873 N93-24677
LEONG, H. M. p 2798 N93-26391
LEONTSINIS, N. p 2627 N93-26021
LESCHIUTTA, S. p 2716 N93-24980
LESKO, K. T. p 2899 N93-25327
LESLIE, J. p 2869 N93-26494
LESSER, RONALD P. p 2796 N93-25592
LESSER, VICTOR R. p 2829 N93-26345
LESUER, D. R. p 2635 N93-25383
LEUPOLD, HERBERT A. p 2691 N93-26299
LEVI, B. p 2694 N93-25057
LEVINE, SEYMOUR p 2606 N93-24728
LEVINE, WILLIAM S. p 2597 N93-26046
LEVY, M. p 2658 N93-26433
LEVY, MILTON p 2651 N93-25895
LEW, J. S. p 2818 N93-25155
LEWANDOWSKI, W. p 2836 N93-25016
p 2836 N93-25017
LEWIS, M. A. p 2708 N93-26535
LEWIS, P. S. p 2794 N93-25186
LEWIS, SHARON R. p 2811 N93-25942
LEWIS, STEPHEN D. p 2844 N93-25637
LEWIS, WILLIAM DEAN p 2574 N93-24756
LEWKOWICZ, PAUL E. p 2665 N93-24680
LEYSEN, MARC M. p 2748 N93-24842
LI, HSI-SHANG p 2703 N93-25560
LI, SHANG-WU p 2787 N93-26545
LI, SHULONG p 2657 N93-26386
LIANG, JIA-LING p 2859 N93-25227
LIANG, PAK-YAN p 2626 N93-26016
LIANG, RANTY H. p 2653 N93-25078
LIANG, WENBIN p 2656 N93-26172
LIAW, JIUNN-YIH p 2697 N93-25252
LICHTEN, S. M. p 2601 N93-24702
LIDESSAU, KATHRYN p 2688 N93-25392
LIEBERMAN, MICHAEL A. p 2692 N93-26539
LIEBIG, V. p 2693 N93-25033
LIEN, FUE-SANG p 2704 N93-25698
LIESKE, R. F. p 2609 N93-25985
LIGI, R. p 2747 N93-24831
LIMA, PEDRO p 2817 N93-24743
LIMAYE, SANJAY S. p 2880 N93-25806
LIN, C. F. p 2716 N93-25048
LIN, CHUN C. p 2853 N93-25646
LIN, H. P. p 2683 N93-26466
LIN, LONG-JI p 2827 N93-26487
LIN, M. C. p 2645 N93-25920
LIN, RAY-SING p 2580 N93-25865
LIN, SHU p 2673 N93-25198
LIN, T. F. p 2860 N93-25641
LIN, YING p 2782 N93-25294
LINCE, JEFFREY R. p 2645 N93-26251
LIND, EDWARD N. p 2680 N93-26160
LINDEMUTH, I. R. p 2861 N93-26504
LINDH, ROLAND p 2848 N93-25450
LINDHOLM, JULIE M. p 2591 N93-26462
LINDLEY, CRAIG A. p 2823 N93-25970
LINDROSE, L. A. p 2600 N93-24697
LINFIELD, R. p 2676 N93-26107
LIOU, LARRY C. p 2664 N93-25337
LIOU, MENG-SING p 2707 N93-26203
LIPINSKI, R. J. p 2715 N93-26597
LIPITKAS, J. p 2822 N93-25964
LISHTVAN, I. I. p 2741 N93-24793
LITTLEFIELD, R. p 2822 N93-25962
LITTLETON, ERIC C. p 2583 N93-26263
LITTMAN, DAVID p 2811 N93-26150
LITZINGER, T. A. p 2629 N93-26037
LIU, BOWEN p 2848 N93-25450
LIU, HUA-KUANG p 2880 N93-25807
LIU, JIANHUI p 2728 N93-25825
LIU, MINZHU p 2725 N93-25335
LIU, NORLEY p 2804 N93-25928
LIU, S. K. p 2580 N93-25894
p 2767 N93-26327
LJUNGBERG, MALIN p 2854 N93-26186
LOCHTIE, GAIL D. p 2674 N93-25340
LOCKE, JAMES E. p 2586 N93-24739
LOCKLEDGE, JEFFREY C. p 2883 N93-26350
LOEBLEIN, JAMES T. p 2810 N93-25786
LOFTIN, KARIN C. p 2799 N93-25595
LOFTIN, R. B. p 2814 N93-25590
LOFTUS, P. J. p 2768 N93-26529
LOGUERCIO-POLOSA, R. p 2741 N93-24796
LOHR, U. p 2743 N93-24806
LONG, LYLE N. p 2595 N93-24762
LOOCHAN, FAREDOON K. p 2794 N93-25214
LOOMIS, H. H. p 2681 N93-26261
LOPEZ-BAEZA, E. p 2738 N93-24780
LOPEZ, ANTONIO M., JR. p 2826 N93-25983
LOPEZ, E. A. p 2688 N93-25313
LORENTS, D. C. p 2849 N93-25644
LORENZO, CARL F. p 2592 N93-25079
LOTTIG, ROY A. p 2598 N93-26214
LOU, GANG p 2699 N93-25349
LOUGHEED, M. J. p 2873 N93-26420
LOUIE, S. G. p 2863 N93-25367
LOUNIS, B. p 2831 N93-24981
LOURS, M. p 2832 N93-24989
LOVE, J. p 2767 N93-26511
LOVE, S. P. p 2646 N93-26505
LOVELAND, DAMIEN GERARD p 2713 N93-25393
LOWE, S. T. p 2677 N93-26108
LOWRY, ROY K. p 2736 N93-24936
LU, J. F. p 2716 N93-25048
LU, JUN p 2854 N93-25898
LU, LIDA p 2864 N93-25528
LU, PING p 2589 N93-25670
LU, YUN-CHI p 2755 N93-25460
p 2755 N93-25461
p 2756 N93-25462
LU, Z. L. p 2799 N93-26521
LUBLIN, LEONARD p 2609 N93-25836
LUCAS, ROBERT p 2828 N93-25223
LUCOVSKY, G. p 2862 N93-24953
LUETTICH, R. A., JR. p 2790 N93-26164
LUHMANN, N. C., JR. p 2609 N93-25770
LUMER, ERIK DANIEL p 2875 N93-25350
LUND, C. p 2861 N93-26512
LUND, P. D. p 2758 N93-25097
LUND, WALTER p 2670 N93-26416
LUO, W. H. p 2716 N93-25048
LUONG, PHAM TRUNG p 2740 N93-24791
LUQI, M. S. p 2813 N93-26453
LURE, Y. M. FLEMING p 2824 N93-25974
LUTES, G. F. p 2677 N93-26113
LUTZ, K. p 2806 N93-25233
LY, BEBE p 2799 N93-25595
LY, H. V. p 2814 N93-25590
LYKE, JAMES p 2694 N93-25581
LYON, G. p 2812 N93-26321

LYON, J. F. p 2858 N93-24969
LYONS, J. E. p 2644 N93-25499
LYONS, L. R. p 2895 N93-26147

M

MA, J. H. p 2828 N93-25905
MA, L. p 2645 N93-25920
MACCARLEY, C. p 2678 N93-26115
MACDIARMID, ALAN G. p 2657 N93-26240
MACDONALD, G. p 2762 N93-25184
MACFARLANE, C. K. p 2873 N93-26419
MACGORMAN, DONALD R. p 2780 N93-24896
MACGOWAN, B. J. p 2712 N93-25363
MACHA, J. M. p 2576 N93-25121
MACIEJEWSKI, WENDELL C. p 2643 N93-25284
MACKER, JOSEPH P. p 2776 N93-26430
MACOSKO, CHRISTOPHER W. p 2657 N93-26386
MADDALON, DAL V. p 2706 N93-26000
MADDEN, N. W. p 2692 N93-26598
MADI, FRANK J. p 2759 N93-25136
MADIGOSKY, WALTER M. p 2711 N93-25608
MAES, J. p 2740 N93-24787
MAGEE, MICHAEL p 2827 N93-26071
MAGIRL, C. S. p 2644 N93-25495
MAH, ROBERT W. p 2802 N93-26153
MAHMASSANI, H. p 2720 N93-26534
p 2720 N93-26585
p 2720 N93-26590
MAHON, MARY ELAINE p 2607 N93-25396
MAHONEY, BRIAN JOSEPH p 2637 N93-25691
MAHONEY, J. F. p 2669 N93-26212
MAI, YIU-WING p 2639 N93-25908
MALDONADO, GUSTAVO OMAR p 2726 N93-25484
MALIK, F. B. p 2868 N93-26252
MALINGREAU, JEAN PAUL p 2748 N93-24836
MALLA, R. P. p 2601 N93-24702
MALLASCH, PAUL G. p 2808 N93-24947
MALONE, PHILIP G. p 2776 N93-25570
MAMANTOV, GLEB p 2646 N93-26439
MAMMONE, ROBERT J. p 2657 N93-26341
MANDACHE, C. p 2716 N93-25067
MANDELL, M. J. p 2618 N93-26232
MANGALAM, SIVA M. p 2706 N93-26000
MANKOFSKY, ALAN p 2881 N93-25812
MANNERMAA, JARI p 2839 N93-25035
MANNING, P. A. p 2617 N93-25494
MANSFELD, FLORIAN p 2655 N93-25861
MANSON, A. H. p 2770 N93-25160
MANSTEN, TAPIO p 2835 N93-25006
p 2835 N93-25007
MAO, JIANPING p 2763 N93-25244
MAO, SHUDE p 2900 N93-25828
MARCH-LEUBA, S. p 2725 N93-25357
MARCHBANKS, R. D. p 2713 N93-25381
MAREK, KARL-HEINZ p 2739 N93-24785
MARGALIT, RUTH p 2793 N93-25994
MARIANNEAU, G. p 2693 N93-25002
MARICICH, PETER p 2611 N93-25511
MARION, W. p 2898 N93-25101
MARISCAL, YVONNE p 2828 N93-25140
MARKER, TIMOTHY R. p 2582 N93-25224
MARKLEY, F. L. p 2606 N93-24730
MARKLEY, F. LANDIS p 2600 N93-24698
p 2606 N93-24731
MARKLEY, R. W. p 2672 N93-24671
p 2679 N93-26126
MARSHALL, ALBERT C. p 2632 N93-26200
MARSHALL, HERMAN L. p 2878 N93-25795
MARSHALL, K. L. p 2714 N93-25869
MARTELLACCI, C. p 2741 N93-24794
p 2749 N93-24844
MARTIN, C. R. p 2869 N93-26577
MARTIN, CHARLES R. p 2645 N93-25916
p 2656 N93-26172
p 2658 N93-26437
MARTIN, ELIZABETH L. p 2591 N93-26462
MARTIN, J. S. p 2888 N93-25286
MARTIN, JAMES E. p 2642 N93-24972
MARTIN, LARRY K. p 2586 N93-26237
MARTIN, MICHAEL p 2880 N93-25806
MARTINELL, JOHN p 2622 N93-25105
MARTINEZ, RADAME p 2673 N93-25210
MARVIN, DEAN C. p 2867 N93-25947
MARZULLO, KEITH p 2809 N93-25152
MASAI, KUNIAKI p 2857 N93-24950
MASELLI, F. p 2742 N93-24799
p 2750 N93-24851
MASELLI, FABIO p 2747 N93-24833
MASI, JAMES V. p 2634 N93-25283
MASLINE, R. C. p 2679 N93-26126
MASON, PAUL A. C. p 2606 N93-24729
MASSEY, S. A. p 2730 N93-26320
MASTIN, C. WAYNE p 2810 N93-25669
MATHEU, ENRIQUE E. p 2729 N93-25938
MATHEWS, CHARLES W. p 2666 N93-24685
MATIN, LEONARD p 2797 N93-26307
MATTA, L. M. p 2630 N93-26040
MATTEUCIG, G. p 2753 N93-24873
MATTHEWS, D. L. p 2712 N93-25363
MATTHEWS, MIKE p 2670 N93-26416
MATTISON, E. M. p 2716 N93-24980
MATUSIK, KATHLEEN p 2766 N93-25875
MATYSIAK, S. J. p 2731 N93-26459
MAUGHMER, MARK D. p 2595 N93-24762
MAURICE, MARK S. p 2697 N93-25237
MAUSER, W. p 2738 N93-24776
MAX, C. p 2715 N93-26503
MAX, C. E. p 2888 N93-25320
MAXIMOV, S. p 2753 N93-24869
MAYER, J. W. p 2863 N93-25387
MAYER, RICHARD J. p 2877 N93-25763
p 2883 N93-26350
p 2884 N93-26523
MAYFIELD, BLAYNE E. p 2827 N93-26072
MAYO, ROBERT p 2633 N93-26555
MAZZOLDI, P. p 2653 N93-24971
MCARDLE, JACK G. p 2592 N93-25129
MCBREEN, JAMES p 2687 N93-24964
MCCABE, R. KEVIN p 2814 N93-25600
MCCAMPBELL, C. B. p 2627 N93-26024
MCCARTHY, J. p 2802 N93-26229
MCCAULEY, MICHAEL E. p 2794 N93-24738
MCCLEMENTS, KENNETH GEORGE p 2861 N93-25730
MCCLUNG, R. W. p 2654 N93-25361
MCCONNELL, DAVID E. p 2812 N93-26375
MCCONNELL, ROBERT D. p 2658 N93-25563
MCCORMICK, STEPHEN F. p 2828 N93-25762
MCCOWN, A. W. p 2713 N93-25379
MCCOY, C. ELAINE p 2585 N93-25330
MCCOY, ELAINE p 2585 N93-25261
MCCRARY, STEPHEN p 2777 N93-24877
MCCREARY, JAMES R. p 2761 N93-24956
MCCRORIE, JOHN D., II p 2624 N93-25913
MCCULLA, W. H. p 2768 N93-26592
MCCULLOCH, I. p 2856 N93-26309
MCCULLOCH, WILLIAM H. p 2632 N93-26200
MCCULLOUGH, JON D. p 2600 N93-24698
MCDANIEL, J. C. p 2624 N93-26008
MCDANIEL, PATRICK p 2621 N93-24740
MCDERMOTT, D. B. p 2609 N93-25770
MCDONALD, ERIC S. p 2729 N93-25911
MCDONALD, J. R. p 2788 N93-26584
MCDONELL, V. G. p 2592 N93-24754
p 2592 N93-25106
MCDOWALL, ROSEMARIE L. p 2778 N93-24883
MCELIECE, R. J. p 2671 N93-24664
MCEWAN, ANGUS p 2732 N93-24917
MCFADDEN, G. B. p 2646 N93-26323
p 2869 N93-26547
MCFARLANE, CRAIG p 2793 N93-25877
MCGARITY, JOHN O. p 2620 N93-26248
MCGAUGH, STACY SUTTON p 2895 N93-25832
MCGAW, MICHAEL A. p 2731 N93-26550
MCGHEE, J. M. p 2828 N93-25151
MCGLADE, JACQUELINE p 2751 N93-24858
MCHARGUE, C. J. p 2725 N93-25373
MCHUGH, KEVIN M. p 2658 N93-25562
MCINTOSH, KIRK DUNCAN p 2771 N93-25424
MCINTOSH, R. p 2602 N93-24707
MCKAY, CHRISTOPHER P. p 2815 N93-25799
MCKEE, SUZANNE p 2800 N93-25778
MCKELLAR, DONALD p 2874 N93-25288
MCKENZIE, R. L. p 2708 N93-25076
MCKINLEY, ERIC J. p 2783 N93-25633
MCLAIN, DOUGLAS R. p 2734 N93-24928
MCLARREN, WAYNE p 2652 N93-26208
MCLAUGHLIN, J. B. p 2695 N93-24963
MCLAUGHLIN, THOMAS EUGENE p 2576 N93-25274
MCLEAN, D. p 2822 N93-25962
MCLEAN, GARNET A. p 2582 N93-25205
MCLEOD, J. p 2713 N93-25379
MCLEOD, MALCOLM G. p 2775 N93-25891
MCMILLIN, LARRY p 2824 N93-25975
MCNALLY, JO-ANN p 2766 N93-25875
MCNESBY, KEVIN L. p 2628 N93-26030
MEDEPALLI, SUDHAKAR p 2819 N93-25410
MEDLEY, MICHAEL J. p 2675 N93-25767
MEESON, REGINALD N. p 2831 N93-26330
MEHL, H. p 2743 N93-24807
MEHROTRA, MALA p 2825 N93-25980
MEHTA, K. C. p 2788 N93-26584
MEISSNER, D. L. p 2633 N93-26561
MEISSNER, DANA L. p 2622 N93-24758
MELDAU, J. p 2687 N93-25069
MELDON, JERRY H. p 2706 N93-25953
MELIA, JOAQUIN p 2738 N93-24780
MELLSTROM, J. p 2672 N93-24666
MENG, J. C. S. p 2707 N93-26328
MENON, P. K. A. p 2586 N93-26549
MENON, V. p 2658 N93-26437
MENZEL, CHRISTOPHER P. p 2884 N93-26523
MERKLE, CHARLES L. p 2622 N93-24943
MERRILL, WALTER C. p 2592 N93-25079
MERRITT, FERGUS J. p 2814 N93-25600
MERZ, PAUL V. p 2597 N93-26196
MESSAGE, PHILIP p 2814 N93-25602
MESSER, RICHARD SCOTT p 2820 N93-25466
MESSERI, A. p 2608 N93-24998
METZGER, FERDINAND J., JR. p 2691 N93-26272
MEYER-ROUX, JEAN p 2745 N93-24818
MEYER, W. J. p 2627 N93-26024
MEYERS, GARY p 2733 N93-24925
MICHAELS, ANTHONY F. p 2736 N93-24938
MICHEL, C. M. p 2798 N93-26435
MICHELS, JAMES H. p 2830 N93-26255
MICOCCI, ANGELO p 2797 N93-25736
MIETTINEN, KRISTO p 2804 N93-25925
MIGLIN, M. F. p 2605 N93-24726
MIKHAILOV, NICKOLAI N. p 2735 N93-24932
MIKITEN, BRIAN p 2591 N93-25783
p 2591 N93-25909
MIKLUS, KENNETH J. p 2600 N93-24699
MIKULAS, M. p 2669 N93-26406
MIKULAS, MARTIN p 2669 N93-26409
p 2670 N93-26417
MILENOVA, L. p 2741 N93-24798
MILETI, G. p 2694 N93-25066
MILFORD, J. R. p 2743 N93-24808
MILLER, ALAN p 2714 N93-25774
MILLER, CATHERINE G. p 2766 N93-25875
MILLER, DAVID L. p 2866 N93-25897
MILLER, DAVID W. p 2821 N93-25833
p 2599 N93-25835
MILLER, DOUGLAS R. p 2809 N93-25257
MILLER, E. L. p 2806 N93-25233
MILLER, ETHAN L. p 2809 N93-25131
p 2815 N93-25297
MILLER, GEORGE P. p 2774 N93-25886
MILLER, GLENN E. p 2880 N93-25808
MILLER, JAMES C. p 2794 N93-24738
MILLER, JERRY L. p 2788 N93-25354
MILLER, K. B. p 2760 N93-24675
MILLER, K. M. p 2718 N93-25682
MILLER, MICHAEL L. p 2793 N93-26259
MILLER, P. J. p 2815 N93-25304
MILLER, PAUL L. p 2707 N93-26379
MILLER, RICK p 2606 N93-24728
MILLER, V. p 2767 N93-26511
MILLER, WARNER H. p 2804 N93-25928
MILLS, G. A. p 2659 N93-25111
p 2659 N93-25112
MILLS, GEORGE T. p 2854 N93-26091
MILTON, E. J. p 2752 N93-24865
MINOR, J. E. p 2788 N93-26584
MINTON, SUSAN S. p 2786 N93-26273
MINTON, TIMOTHY K. p 2653 N93-25078
MIRTICH, MICHAEL J. p 2658 N93-25564
MISTRETTA, G. D. p 2601 N93-24703
MITCHELL, WALTER E., JR. p 2898 N93-25222
MITTER, SANJOY K. p 2821 N93-25853
MIZIOLEK, A. W. p 2627 N93-26025
MIZUKAMI, MASASHI p 2573 N93-26136
MODESTINO, A. J. p 2644 N93-25500
MOEN, KENNETH J. p 2885 N93-26582
MOGIL, H. MICHAEL p 2781 N93-25220
MOHL, JAMES p 2620 N93-26408
MOLNAR, JOHN p 2615 N93-25133
MOLTZ, D. M. p 2848 N93-25366
MONGIA, H. C. p 2592 N93-24754
p 2592 N93-25106
MOODY, PAUL E. p 2719 N93-26144
MOOK, D. JOSEPH p 2606 N93-24729
MOOK, D. T. p 2728 N93-25838
MOORE, ALLAN S. p 2652 N93-26201
MOORE, DONNIE p 2852 N93-25182
MOORE, E. F. p 2848 N93-25371
MOORE, ELIZABETH MARY p 2893 N93-25537
MOORE, JERRY H. p 2719 N93-26001
MOORE, MARLA H. p 2892 N93-25230
MOORE, R. M. p 2761 N93-25212
MOORE, THOMAS J. p 2652 N93-26201
MOORE, W. E. p 2698 N93-25306
MOOREHEAD, T. W. p 2884 N93-26562
MOORES, D. K. p 2658 N93-26506
MOORJANI, K. p 2871 N93-25584
MOOZ, HAL p 2665 N93-24682
MORAN, MARK B. p 2867 N93-26090
MORAR, DORIN p 2718 N93-25682
MOREL, J. E. p 2828 N93-25151
MORENO, JOSE F. p 2738 N93-24780
MORGENSTERN, CAROLYN D. p 2780 N93-24896
MORGENTHALER, GEORGE W. p 2669 N93-26410
MORITA, NAOMI p 2583 N93-24885
MORLOT, G. p 2840 N93-25045

MORRIS, ALFRED H., JR. p 2884 N93-26575
MORRIS, C. L. p 2852 N93-25380
MORRIS, J. p 2715 N93-26503
MORRIS, J. R. p 2888 N93-25320
MORRIS, JOHN p 2596 N93-25199
MORRIS, OWEN p 2666 N93-24684
MORRIS, THERESA p 2852 N93-25182
MORRISON, DENNIS R. p 2794 N93-25566
MORSE, JON ARTHUR p 2891 N93-24770
MORSE, STEPHEN E. p 2802 N93-26265
MORSE, T. F. p 2856 N93-26343
MORTAZAVI, M. K. p 2719 N93-25745
MOSES, CLIFFORD A. p 2661 N93-25914
MOSHER, J. C. p 2794 N93-25186
MOSS, STEVEN C. p 2867 N93-25947
MOSSBERG, THOMAS W. p 2853 N93-25822
MOTOJIMA, O. p 2859 N93-25216
MOTTELER, HOWARD E. p 2824 N93-25975
MOURIER, V. p 2842 N93-25060
MROWKA, S. p 2712 N93-25363
MUDGWAY, D. J. p 2599 N93-26125
MUEHL, W. W., SR. p 2759 N93-25597
MUELLER, R. O. p 2672 N93-24670
MUELLER, STEPHEN p 2730 N93-26279
MUENZER, U. p 2740 N93-24792
MUIR, DOUGLAS C. p 2766 N93-25875
MUIR, WARREN R. p 2766 N93-25875
MUKUNDA, V. G. p 2634 N93-25338
MUKUTMONI, DEVADATTA p 2669 N93-26285
MULAC, WILLIAM A. p 2761 N93-24956
MULLER, S. p 2711 N93-25011
MULLICAN, A. p 2573 N93-24760
p 2573 N93-25134
MUNDRA, ANAND D. p 2585 N93-25456
MURAD, P. A. p 2603 N93-24718
MURAKAMI, SADAYOSHI p 2858 N93-25092
MURDOCCA, MILES p 2806 N93-25848
MURPHY, STEPHANIE p 2766 N93-25875
MURRAY, B. T. p 2869 N93-26547
MURRAY, FRANK p 2675 N93-25635
MURRAY, RICHARD p 2596 N93-25199
MURTHY, A. V. p 2695 N93-25087
MURTHY, P. L. N. p 2723 N93-24913
p 2724 N93-25070
p 2641 N93-26552
MURTHY, S. N. B. p 2573 N93-24760
p 2573 N93-25134
MUSGRAVE, J. p 2622 N93-25089
MUSGRAVE, JEFFREY L. p 2632 N93-26211
MUSIELAK, S. p 2747 N93-24832
MUTSCHLECNER, J. P. p 2761 N93-25126
MYERS, JENNIFER G. p 2796 N93-25213
MYRE, DAVID D. p 2707 N93-26167
MYRICK, STEPHANIE A. p 2757 N93-26574
MYSOOR, N. R. p 2672 N93-24670

N

NACHTRIEB, ROBERT T. p 2632 N93-26174
NADAL, JOSE L. p 2686 N93-26604
NADIR, A. p 2831 N93-24981
NAEGELI, DAVID W. p 2661 N93-25902
NAGELE, RAY p 2788 N93-24960
NAGURA, RIICHI p 2753 N93-24867
NAIR, SHANTI p 2640 N93-26236
NAKAGAWARA, VAN B. p 2794 N93-25214
NAKAHARA, TOMOHARU p 2757 N93-26448
NAKATANI, AKIFUMI p 2681 N93-26383
NANDI, S. p 2601 N93-24701
NANEVICZ, J. E. p 2583 N93-24887
NASH, P. T. p 2598 N93-25656
NATHAN, MARK P. p 2670 N93-26412
NATORI, M. C. p 2669 N93-26406
NAUGLE, JOHN E. p 2666 N93-24687
NAVAZ, H. K. p 2626 N93-26017
NAYFEH, A. H. p 2728 N93-25838
NAZAREWICZ, W. p 2847 N93-25148
NEALSON, KENNETH H. p 2803 N93-26157
NEALSON, MOLLY STONE p 2803 N93-26157
NEEDLEMAN, A. p 2651 N93-25907
NEIBERT, MICHAEL J. p 2727 N93-25658
NELSON, B. W. p 2766 N93-26243
NELSON, C. F. p 2689 N93-25429
NELSON, DONALD F. p 2866 N93-25789
NELSON, L. M. p 2842 N93-25059
NELSON, S. G. p 2766 N93-26243
NEMANICH, R. J. p 2862 N93-24953
NERI, D. F. p 2801 N93-25859
NERO, R. p 2757 N93-25868
NETZER, D. W. p 2625 N93-26010
NETZER, EHUD p 2616 N93-25470
NEUBERT, DONALD E., JR. p 2581 N93-26195
NEUBIG, B. p 2833 N93-24995
NEUBIG, BERND W. p 2693 N93-25010
NEUHAUSER, W. p 2841 N93-25051
NEUMANN, W. T. p 2711 N93-24900
NEWCOMER, JEFFREY A. p 2804 N93-25929
NEWLANDER, C. D. p 2656 N93-25940
p 2657 N93-26278
NEWMAN, BRETT ALAN p 2596 N93-25292
NEWROCK, R. S. p 2869 N93-26540
NEY, BOGDAN I. p 2739 N93-24786
NGUYEN, CUONG M. p 2807 N93-26403
NGUYEN, D. p 2854 N93-26187
NGUYEN, DAN T. p 2854 N93-26186
p 2855 N93-26188
NGUYEN, HUNG T. p 2818 N93-25138
p 2818 N93-25142
NIAL, JACK p 2693 N93-24882
NICHOLS, F. A. p 2658 N93-26506
NIE, D. p 2769 N93-24945
NIEDERAUER, GEORGE F. p 2632 N93-26200
NIEDRA, JANIS M. p 2687 N93-24746
NIELSEN, B. S. p 2647 N93-26595
NIEUWENHUIS, G. J. A. p 2740 N93-24789
NIKANPOUR, D. p 2700 N93-25478
NIKJOOY, M. p 2592 N93-24754
p 2592 N93-25106
NIKLASCH, N. p 2586 N93-25018
NIKOLOV, CHRISTO p 2753 N93-24870
NIU, LIN p 2635 N93-25544
NO, TAE SOO p 2615 N93-24767
NOBLE, R. D. p 2660 N93-25497
NOGAR, N. S. p 2712 N93-25150
NORMAN, E. B. p 2899 N93-25327
NORMAN, M. p 2711 N93-24961
NORRIS, CHARLES LESLIE p 2774 N93-25757
NORTHAM, G. B. p 2625 N93-26009
NORTHAM, G. BURTON p 2624 N93-26008
NORTON, J. R. p 2693 N93-25052
NORTON, T. J. p 2854 N93-26185
NORWOOD, R. p 2856 N93-26309
NOSSIN, JAN J. p 2743 N93-24810
NOVERO, C. p 2842 N93-25058
NOVIK, DMITRY A. p 2804 N93-25923
NOWAK, MICHAEL ALLEN p 2894 N93-25622
NOWICKI, GARY J. p 2806 N93-25934
NUGENT, DAVID M. p 2717 N93-25228
NURDEN, GLEN p 2633 N93-26555
NWANKPA, AMADI p 2819 N93-25278
NYSTROM, G. U. p 2716 N93-24980

O

OBARA, NORIAKI p 2683 N93-26470
OBRIEN, EDWARD M. p 2794 N93-26073
OCONNOR, R. C. p 2599 N93-26125
ODELL, S. L. p 2855 N93-26192
ODINEK, JUDY p 2642 N93-24972
ODONALD, LEWIS p 2871 N93-25423
OEFTERING, RICHARD C. p 2618 N93-26209
OERTEL, J. p 2709 N93-25515
OESTERLUND, H. p 2748 N93-24841
p 2749 N93-24847
OHARE, LEO PATRICK p 2615 N93-25207
OHKUBO, K. p 2687 N93-24951
OJO, S. O. p 2735 N93-24933
OKADA, NAOYUKI p 2703 N93-25662
OKADA, T. p 2859 N93-25248
OKAMOTO, MASAO p 2858 N93-25092
OKAMURA, HIROSHI p 2774 N93-25889
OKEEFE, LUCY MARGUERITE p 2788 N93-24769
OKUN, PAUL p 2620 N93-26248
OLEARY, DIANNE P. p 2828 N93-25687
OLIVER, J. H. p 2810 N93-25699
OLIVER, S. p 2715 N93-26503
OLIVIER, M. p 2693 N93-25003
OLIVIER, S. S. p 2888 N93-25320
OLLIS, DAVID F. p 2767 N93-26427
OLSEN, DALE E. p 2796 N93-25592
OLSEN, GREGORY H. p 2709 N93-25634
OLSEN, LOLA p 2737 N93-24942
OLSSON, HAAKAN p 2748 N93-24839
OLYNICK, DAVID RAMOS p 2579 N93-25759
OMALLEY, TERENCE F. p 2618 N93-26209
ONEILL, MARY KAE LOCKWOOD p 2593 N93-25480
ONSTOTT, JAMES R. p 2857 N93-26515
ONYSZCHUK, I. p 2671 N93-24664
ORASANU, JUDITH p 2585 N93-25330
ORIOL, R. A. p 2757 N93-25868
OROURKE, P. J. p 2696 N93-25124
ORR, JOHN L. p 2591 N93-25783
p 2591 N93-25909
ORTGIES, G. p 2684 N93-26478
ORTIZ, C. J. p 2814 N93-25590
OSAKABE, M. p 2860 N93-25347
OSTEEN, B. LANCE p 2769 N93-24672
OTOOLE, RONALD P. p 2709 N93-25345
OTOSHI, T. Y. p 2677 N93-26113
OTT, EDWARD p 2883 N93-26377
OTTO, JOHN C. p 2575 N93-25074
OUELLETTE, J. P. p 2854 N93-26185
OUKACI, R. p 2659 N93-25119
OURA, NOBUNORI p 2716 N93-25068
OUSTERHOUT, JOHN K. p 2805 N93-25130
p 2809 N93-25250
p 2815 N93-25251
OUZTS, PETER J. p 2592 N93-25079
OWARISH, HASSAM O. p 2593 N93-25471
OWEN, W. M., JR. p 2621 N93-26111
OZA, D. H. p 2601 N93-24703
OZDEMIR, DOGAN p 2812 N93-26271

P

PADDOCK, GREG p 2611 N93-25511
PADGETT, DEBORAH LYNNE p 2894 N93-25623
PAGANO, PETER p 2595 N93-24762
PAGE, B. p 2822 N93-25962
PAGE, DONNA p 2788 N93-25616
PAINTER, MICHAEL K. p 2877 N93-25763
PAINTER, S. L. p 2858 N93-24969
PALEN, A. C. p 2609 N93-26098
PALMER, EV p 2585 N93-25330
PALOUNEK, A. P. T. p 2869 N93-26494
PALUMBO, MARIO p 2688 N93-25282
PANTAZIS, JOHN A. p 2620 N93-26248
PAPATHANASIOU, T. D. p 2655 N93-25507
PARANJPE, SATISH p 2735 N93-24935
PARASKA, PETER J. p 2723 N93-24912
PARES-SIERRA, ALEJANDRO p 2790 N93-26331
PARFENOV, V. p 2753 N93-24869
PARHAM, KENNETH R. p 2802 N93-26404
PARK, HYUN SOO p 2721 N93-26137
PARK, K. C. p 2669 N93-26406
PARK, SEONG-RYONG p 2705 N93-25746
PARKER, JOEL WILLIAM p 2894 N93-25559
PARKINSON, B. A. p 2869 N93-26577
PARR, TIM p 2629 N93-26036
p 2630 N93-26041
PARTHASARATHY, R. p 2658 N93-26437
PARZYCH, DAVID J. p 2844 N93-25094
PASARIBU, H. M. p 2589 N93-25692
PASSERI, DANIEL R. p 2796 N93-25567
PATERRA, FRANK p 2825 N93-25978
PATTERSON, D. A. p 2806 N93-25233
PATTERSON, DAVID A. p 2805 N93-25130
PATTERSON, F. T. p 2641 N93-26355
PATTIARATCHI, CHARITHA p 2746 N93-24829
p 2747 N93-24835
PATTON, T. C. p 2721 N93-25518
PAVANATI, M. p 2738 N93-24779
PAVLICH, JANE p 2670 N93-26416
PAWEL, J. E. p 2725 N93-25373
PAXTON, A. T. p 2853 N93-25766
PAXTON, ANTHONY T. p 2653 N93-26304
PAYER, PAUL F. p 2822 N93-25965
PEARCE, PETER R. p 2835 N93-25008
PECCOUD, D. p 2750 N93-24853
PECK, ANN W. p 2589 N93-25701
PECKNOLD, DAVID A. p 2811 N93-25845
PEDROTTO, G. p 2694 N93-25057
PEFFLEY, AL F. p 2611 N93-25514
PELIZZARI, CHARLES p 2880 N93-25810
PELTIER, LEONARD JOEL p 2700 N93-25472
PELTOLA, S. p 2758 N93-25096
PELZ, E. p 2748 N93-24838
PENETRANTE, B. M. p 2763 N93-25385
PENG, Y. K. M. p 2860 N93-25493
PENKO, P. F. p 2633 N93-26561
PERALA, RODNEY A. p 2610 N93-24899
PEREIRA, J. MICHAEL p 2634 N93-25071
p 2642 N93-25587
PEREIRADACUNHA, ROBERTO p 2748 N93-24836
PEREZ, R. M. p 2678 N93-26114
PERITT, JONATHAN M. p 2640 N93-26143
PERKINS, DAVID p 2622 N93-25105
PERKINS, STEVE W. p 2670 N93-26412
PERLISKI, LORI MAC p 2772 N93-25535
PERNAMBUCO-WISE, P. p 2688 N93-25313
PERONI, P. p 2741 N93-24794
p 2749 N93-24844
PERRY, W. p 2884 N93-26568
PERUSINI, V. p 2747 N93-24830
PESCE-RODRIQUEZ, R. A. p 2628 N93-26032
PETERS, W. A. p 2644 N93-25500
PETERSON, D. L. p 2858 N93-25167
PETERSON, GARY L. p 2761 N93-24977
PETERSON, J. B. p 2769 N93-25573
PETERSON, VICTOR L. p 2575 N93-25091
PETIT, G. p 2832 N93-24985
p 2836 N93-25016
p 2836 N93-25017
PETIT, P. p 2833 N93-24990

PETKOV, DOINO p 2753 N93-24870
PETKOV, L. p 2750 N93-24851
PETTERSSON, LASSE H. p 2746 N93-24824
PEYTON, B. W. p 2816 N93-25414
PFAEFFLE, H. J. p 2729 N93-25846
PFEIFFER, B. p 2748 N93-24840
PFISTERER, RICHARD N. p 2761 N93-24977
PFLEEGER, T. G. p 2766 N93-26316
PFLEGER, S. p 2753 N93-24871
PHARAOH, K. I. p 2687 N93-25069
PHATAK, ANIL p 2803 N93-25235
PHILIPPOT, E. p 2836 N93-25013
p 2840 N93-25043
p 2840 N93-25044
PHILLIPS, T. E. p 2871 N93-25584
PHILLIPS, THOMAS J. p 2761 N93-25145
PICCINNI, C. p 2741 N93-24796
PICKARD, P. S. p 2715 N93-26597
PICKERING, HOWARD W. p 2651 N93-25903
PICRAUX, S. T. p 2863 N93-25387
PIERI, M. p 2742 N93-24799
PIETILA, SEPPO p 2763 N93-25360
PILI, P. p 2746 N93-24825
PIN, F. G. p 2584 N93-25120
PINKER, R. T. p 2777 N93-24742
PITSTICK, MARK E. p 2660 N93-25192
PITZL, D. p 2869 N93-26494
PIZZANO, FRANK p 2624 N93-25671
PLANAT, M. p 2693 N93-25034
PLEIM, J. E. p 2765 N93-25873
PLESSEL, TODD C. p 2814 N93-25600
PLETCHER, RICHARD H. p 2619 N93-26438
PLUMB, G. D. p 2673 N93-25171
PLUMER, EDWARD S. p 2817 N93-25137
PLUMER, J. ANDERSON p 2778 N93-24883
p 2780 N93-24895
PODGORSKI, W. A. p 2854 N93-26183
p 2854 N93-26185
PODLESAK, THOMAS F. p 2694 N93-25598
POIGNON, C. p 2840 N93-25045
POLASKI, LOU p 2665 N93-24682
POLINER, JEFFREY p 2797 N93-25736
POND, JOHN E. p 2631 N93-26056
PORCH, W. M. p 2781 N93-25125
PORILE, N. p 2688 N93-25365
PORTER, MARC D. p 2709 N93-25345
POSNER, E. C. p 2671 N93-24659
POSNER, EDWARD C. p 2676 N93-26105
POTENZIANI, ERNEST, II p 2691 N93-26299
POTTER, DOUGLAS p 2620 N93-26248
POTTER, W. p 2822 N93-25962
PRAHARAJ, SARAT C. p 2618 N93-26055
PRANZINI, E. p 2742 N93-24799
PRANZINI, ENZO p 2747 N93-24833
PRATHER, MICHAEL J. p 2762 N93-25157
p 2762 N93-25158
p 2762 N93-25159
PRATT, TIM p 2685 N93-26479
p 2685 N93-26484
PRIEM, RICHARD J. p 2623 N93-25236
PRINGLE, STEVEN R. p 2602 N93-24709
PRISCO, G. p 2608 N93-24986
PROFETI, GIULIANA p 2747 N93-24833
PROSSER, W. H. p 2634 N93-25072
PROSSER, WILLIAM H. p 2729 N93-26102
PRUSACZYK, W. K. p 2802 N93-26229
PSEINER, K. p 2748 N93-24840
PUETZ, GERALD B. p 2765 N93-25864
PURCELL, C. W. p 2760 N93-24675
PURVIS, J. W. p 2896 N93-25321
PUTCHA, C. S. p 2624 N93-25671
PUTOIS, G. p 2834 N93-25001
PUTT, CHARLES W. p 2593 N93-25673
PUYOU-LASCASSIES, PH. p 2750 N93-24853

Q

QI, QUAN p 2704 N93-25683
QIAN, W. p 2716 N93-24751
QUACKENBUSH, TODD R. p 2575 N93-25075
QUAN, RALPH p 2620 N93-26408
QUINN, G. D. p 2654 N93-25361
QUINN, H. R. p 2847 N93-25323
QUINN, J. W. p 2856 N93-26266
QUINTANA, CHRIS p 2819 N93-25197
p 2820 N93-25459
QUIRK, JAMES J. p 2575 N93-25083

R

RACCAH, PAUL M. p 2867 N93-26223
RADOK, UWE p 2765 N93-25666
RAEFSKY, ARTHUR p 2828 N93-25223
RAHIM, WADI p 2691 N93-26104
RAHMAN, HASAN H. p 2796 N93-25594
RAI, G. p 2688 N93-25365
RAIMAN, LAURA B. p 2723 N93-26074
RAIMONDI, SALVATORE p 2742 N93-24800
RAINER, F. p 2870 N93-26594
RAJPAL, SANDEEP p 2673 N93-25198
RALL, DAVID L. p 2632 N93-26373
RALL, H. p 2748 N93-24837
RAMACHANDRAN, V. S. p 2798 N93-26349
RAMAKER, D. E. p 2652 N93-26197
p 2868 N93-26258
RAMAKER, DAVID E. p 2850 N93-26287
RAMAMURTHY, MAYA p 2801 N93-26047
RAMANATHAN, VEERABHADRAN p 2880 N93-25810
RAMBONE, JAMES D. p 2584 N93-24741
RAMER, ARTHUR p 2818 N93-25141
RAMSAY, BRUCE H. p 2619 N93-25971
RAMSEY, LAWRENCE W. p 2891 N93-26426
RANDALL, MICHAEL A. p 2680 N93-26166
RANDELL, G. P. p 2810 N93-25453
RANDOLPH, H. p 2864 N93-25506
RANGARAO, K. V. p 2681 N93-26261
RAPOPORT, R. D. p 2760 N93-24675
RAPP, D. p 2888 N93-25320
RASCHKE, E. p 2744 N93-24813
RATSCH, H. C. p 2766 N93-26316
RAVAT, DHANANJAY p 2771 N93-25201
RAVIPRAKASH, G. K. p 2845 N93-25717
RAYMER, MICHAEL G. p 2853 N93-25822
RAYMOND, TERRY R. p 2813 N93-26563
REARDON, J. E. p 2631 N93-26054
RECKAMP, DOUGLAS E. p 2846 N93-26179
REDDY, YERUVA SATYANARAYANA p 2636 N93-25661
REDELL, DAVID D. p 2883 N93-26389
REDINIOTIS, OTHON KONS p 2576 N93-25269
REDMAN, D. A. p 2862 N93-24958
p 2646 N93-26502
REGINATO, L. L. p 2851 N93-25325
REINHART, M. J. p 2693 N93-25052
REINISCH, BODO W. p 2776 N93-26283
REINOVSKY, R. E. p 2861 N93-26504
REINTJES, JOHN F. p 2852 N93-25358
REISENAUER, BRIAN p 2620 N93-26408
REISNER, J. p 2776 N93-26548
REISTER, D. B. p 2717 N93-25100
REMP, KERRY p 2632 N93-26200
REMSBERG, ELLIS E. p 2762 N93-25158
p 2762 N93-25159
REMSBURG, ELLIS E. p 2762 N93-25157
RENDLEMAN, C. MATTHEW p 2661 N93-25818
RENO, T. J. p 2657 N93-26213
REPPERT, PETE p 2883 N93-26423
RESNICK, RALPH p 2670 N93-25579
RESS, D. B. p 2709 N93-25515
REUPKE, W. p 2603 N93-24714
REYHANOGLU, MAHMUT p 2596 N93-25729
RHEE, DOJUN p 2673 N93-25198
RHOADES, ROBERT LEWIS p 2712 N93-25344
RIBEIRO, RENATO SILVA p 2579 N93-25706
RICCIARDI, ALETA p 2721 N93-26135
RICE, C. K. p 2667 N93-24970
RICE, JOHN W. p 2632 N93-26200
RICE, ROBERT F. p 2804 N93-25928
RICHARDS, BILL p 2611 N93-25511
RICHARDS, J. B. p 2711 N93-24961
RICHARDS, MERCEDES T. p 2896 N93-26508
RICHARDS, STEPHEN F. p 2815 N93-26075
RICKEL, D. G. p 2688 N93-25313
RIFE, MICHAEL C. p 2696 N93-25208
RILEY, GARY p 2799 N93-25595
RILEY, WILLIAM K., JR. p 2836 N93-25014
RISHA, D. J. p 2582 N93-26007
RISON, WILLIAM p 2777 N93-24877
RITCHEY, N. A. p 2777 N93-24742
RITCHIE, R. H. p 2848 N93-25376
RITTER, FRANK E. p 2882 N93-25844
RITZ, E. p 2836 N93-25012
RIVEREAU, J. C. p 2743 N93-24811
ROACH, DENNIS p 2582 N93-25110
ROBBINS, FREDERICK W. p 2661 N93-25857
ROBERSON, BOBBY J. p 2803 N93-26076
ROBERSON, MARK p 2849 N93-25659
ROBERT, E. p 2833 N93-24993
ROBERTS, JACK C. p 2796 N93-25569
ROBERTS, TED A. p 2659 N93-24745
ROBERTS, WILLIAM LAFAYETTE p 2642 N93-24771
ROBERTSON, L. p 2620 N93-26408
ROBEY, HARRY p 2788 N93-24960
ROBINSON, GARY Y. p 2867 N93-26193
ROBINSON, J. H. p 2844 N93-25189
ROBINSON, JOHN C. p 2651 N93-26048
ROBINSON, STEPHEN M. p 2813 N93-26450
ROBOCK, ALAN p 2763 N93-25244
ROCCI, PETER J. p 2692 N93-26334
ROCHE, JAMES RICHARD p 2877 N93-25722
ROCHON, GILBERT p 2881 N93-25813
ROCKAFELLAR, R. T. p 2873 N93-26342
ROCKWAY, J. W. p 2675 N93-25700
RODERICK, N. p 2858 N93-25167
RODGERS, EDWARD BURTON p 2784 N93-25741
RODGERS, MARK D. p 2586 N93-26447
RODGERS, SANDRA L. p 2794 N93-26077
RODRIGUEZ, D. J. p 2761 N93-25122
RODRIGUEZ, G. p 2659 N93-25607
ROE, S. P. p 2801 N93-25904
ROGALLO, SARAH J. p 2809 N93-25246
ROGERS, BRADLEY A. p 2812 N93-26275
ROGERS, CRAIG A. p 2868 N93-26332
ROGERS, DAVE p 2787 N93-26513
ROGERS, DAVID V. p 2685 N93-26480
p 2685 N93-26482
ROGERS, J. D. p 2688 N93-25313
ROGERS, RALPH V. p 2585 N93-26052
ROGERS, WAYNE p 2670 N93-26413
ROHATGI, A. p 2758 N93-25098
ROHRBAUGH, D. p 2607 N93-24734
ROHRBAUGH, J. M. p 2884 N93-26530
ROLL, JOHN B., JR. p 2854 N93-26186
ROMPALLA, JOHN p 2619 N93-24878
ROSE, FRANK E. p 2724 N93-25260
ROSENGREN, M. p 2749 N93-24847
ROSOCHA, L. A. p 2768 N93-26592
ROSSI, F. p 2743 N93-24809
ROSSINGTON, C. S. p 2692 N93-26598
ROSSINI, P. p 2741 N93-24795
ROSSON, RITA M. p 2785 N93-25871
ROSZMAN, L. p 2602 N93-24706
p 2602 N93-24707
p 2603 N93-24716
p 2603 N93-24717
ROTAR, PAUL p 2878 N93-25797
ROTH, JAN-UWE p 2642 N93-24891
ROTHSTEIN, IRA ZIV p 2898 N93-25180
ROUFF, CHRISTOPHER p 2814 N93-25602
ROUMENINA, E. p 2741 N93-24798
ROUSSOPOULOS, N. p 2880 N93-25809
ROVERA, G. D. p 2832 N93-24989
ROVNAK, J. E. p 2601 N93-24704
ROWE, BILL p 2652 N93-26208
ROWE, JOSEPH p 2792 N93-25195
ROWLAND, J. R. p 2683 N93-26467
ROY, A. G. p 2854 N93-26185
RU, JON p 2849 N93-25659
RUDISILL, MARIANNE p 2799 N93-25595
RUDOLPH, TERENCE H. p 2610 N93-24899
RUECKER, F. p 2684 N93-26478
RUEEDI, I. p 2694 N93-25066
RUGGIER, C. J. p 2679 N93-26127
RUPPEL, F. R. p 2668 N93-25937
RUSSELL, J. D. p 2639 N93-25918
RUSSELL, L. C. p 2675 N93-25700
RUSSELL, T. P. p 2630 N93-26038
RYCKMAN, S. JAMES, JR. p 2761 N93-25143
RYSCHKEWITSCH, MICHAEL G. p 2665 N93-24683
RYU, DONGSU p 2900 N93-26132

S

SACHLEBEN, R. A. p 2793 N93-26587
SACHS, FREDERICK p 2793 N93-25764
SADREHAGHIGHI, I. p 2575 N93-25117
SAEEDVAFA, MARYAM p 2866 N93-25749
SAGISCHEWSKI, H. p 2749 N93-24848
SAGNA, N. p 2716 N93-25067
SAIC, STANISLAV p 2740 N93-24788
SAITO, T. p 2814 N93-25590
SAITOH, KATSUYA p 2745 N93-24822
SAKHAROV, B. A. p 2716 N93-25049
SAKREJDA, I. p 2847 N93-25326
SALADINO, ANTHONY J. p 2618 N93-26055
SALES, GARY S. p 2681 N93-26247
p 2681 N93-26280
SALINAS, DAVID p 2727 N93-25658
SALMON, J. T. p 2888 N93-25320
p 2715 N93-26503
SALO, TIMOTHY J. p 2817 N93-26277
SALOMON, C. p 2831 N93-24981
SALTZMAN, J. S. p 2816 N93-25316
SAMBE, HIDEO p 2850 N93-26287
SAMII, MINA V. p 2601 N93-24703
SAMPLER, JEFFREY LYNN p 2875 N93-25395
SAMUELSEN, G. S. p 2592 N93-24754
SAMUELSON, G. S. p 2592 N93-25106
SAN, JOSEPHINE K. p 2600 N93-24698
SANCHEZ, O. p 2680 N93-26130
SAND, J. R. p 2667 N93-24970
SANDERS, LES p 2883 N93-26350
SANDERS, R. S. p 2657 N93-26213

SANDERS, RICHARD ..... p 2582 N93-26078
SANDSTROM, TIMOTHY A. ..... p 2814 N93-25600
SANG, E. ..... p 2836 N93-25012
SANICANDRO, ROCCO ..... p 2619 N93-24878
SANTAVICCA, DOMENIC A. ..... p 2645 N93-26220
SANTIAGO, DAVID G. ..... p 2693 N93-24982
SANTINI, DANILO L. ..... p 2660 N93-25298
SANTOS, A. MIGUEL P. ..... p 2745 N93-24821
SANTOSA, FADIL ..... p 2722 N93-26337
SANUKI, H. ..... p 2860 N93-25346
SARGENT, NOEL B. ..... p 2693 N93-24889
SARTI, A. ..... p 2675 N93-25689
SASAO, M. ..... p 2860 N93-25347
SATIN, A. L. ..... p 2836 N93-25015
SATO, M. ..... p 2687 N93-24951
SATO, T. ..... p 2860 N93-25356
SATORIUS, E. ..... p 2680 N93-26130
SATORIUS, EDGAR ..... p 2685 N93-26485
SATULA, RAYMOND A. ..... p 2652 N93-26234
SAUMET, J.-L. ..... p 2795 N93-26133
SAUNDERS, D. S. ..... p 2638 N93-25768
SAUNDERS, R. S. ..... p 2880 N93-25806
SAUSA, R. C. ..... p 2627 N93-26025
SAVAGE, RICHARD C. ..... p 2880 N93-25810
SAVAGE, ROBERT M. ..... p 2721 N93-26137
SAVAGE, S. F. ..... p 2767 N93-26495
SAWADA, J. ..... p 2779 N93-24888
SAWYER, J. CHARLES, JR. ..... p 2632 N93-26200
SAXENA, A. ..... p 2646 N93-26505
SAYER, R. O. ..... p 2860 N93-25493
SCAPPATICCI, GERARDO ANGELO ..... p 2892 N93-24949
SCHAEFER, WOLFGANG ..... p 2832 N93-24983
SCHANZLE, A. F. ..... p 2601 N93-24704
SCHARDT, M. ..... p 2749 N93-24848
SCHARENBERG, R. ..... p 2688 N93-25365
SCHEFFNER, NORMAN W. ..... p 2790 N93-26164
SCHEINER, B. J. ..... p 2769 N93-25573
SCHELL, STEPHAN V. ..... p 2728 N93-25784
SCHEUER, JAY ..... p 2633 N93-26555
SCHILLIG, J. B. ..... p 2688 N93-25313
SCHIPER, ANDRE ..... p 2721 N93-26135
SCHLUETER, S. S. ..... p 2627 N93-26023
SCHMALZ, HENRY ..... p 2761 N93-24956
SCHMID, A. ..... p 2714 N93-25869
SCHMIDLIN, F. J. ..... p 2770 N93-25160
SCHMIDT, DAVID K. ..... p 2587 N93-25162
SCHMIDT, ERIC OTTO ..... p 2782 N93-25293
SCHMIDT, RAYMOND G. ..... p 2710 N93-26092
SCHNACKEL, J. A. ..... p 2609 N93-26176
SCHNEIDER-MUNTAU, H. J. ..... p 2688 N93-25313
SCHNEIDER, FRED B. ..... p 2809 N93-25152
SCHNEIDER, J. A. ..... p 2633 N93-26557
SCHNEIDER, J. W. ..... p 2657 N93-26213
SCHNIER, D. ..... p 2841 N93-25050
SCHOEB, A. M. ..... p 2649 N93-25428
SCHOENBERG, KURT ..... p 2633 N93-26555
SCHOTT, JOACHIM H. ..... p 2868 N93-26254
p 2850 N93-26443
SCHOTTEN, C. G. J. ..... p 2740 N93-24789
SCHRANK, M. G. ..... p 2668 N93-26206
p 2669 N93-26212
SCHRAWYER, L. R. ..... p 2654 N93-25382
SCHROEDER, DAVID J. ..... p 2797 N93-26138
SCHROEDER, M. A. ..... p 2628 N93-26032
SCHROEDER, R. ..... p 2841 N93-25050
SCHULZKE, L. ..... p 2833 N93-24995
SCHUMANN, A. H. ..... p 2744 N93-24816
SCHUPP, G. ..... p 2864 N93-25503
SCHURMAN, DON ..... p 2582 N93-25110
SCHUTZ, B. E. ..... p 2757 N93-26354
SCHWARTZ, D. A. ..... p 2854 N93-26183
p 2855 N93-26189
SCHWARTZ, DANIEL A. ..... p 2854 N93-26184
p 2854 N93-26185
p 2855 N93-26191
SCHWARTZEL, J. ..... p 2833 N93-24994
p 2836 N93-25013
p 2838 N93-25025
p 2840 N93-25044
SCHWARTZKOPF, STEVEN H. ..... p 2803 N93-25617
SCHWARZE, GENE E. ..... p 2687 N93-24746
SCHWEDA, H. ..... p 2694 N93-25066
SCHWING, JAMES L. ..... p 2808 N93-24750
SCIACOVELLI, N. ..... p 2741 N93-24796
SCOTT, B. ..... p 2646 N93-26505
SCOTT, CURTIS A. ..... p 2634 N93-25071
SCOTT, J. L. ..... p 2708 N93-26535
SCOUT, TERRA ..... p 2798 N93-26353
SCOVILLE, N. Z. ..... p 2890 N93-25755
SEARLE, BEN ..... p 2733 N93-24924
SEDLAK, J. ..... p 2602 N93-24708
SEDLER, J. ..... p 2600 N93-24700
SEERING, WARREN P. ..... p 2732 N93-25834
SEFCIK, J. A. ..... p 2674 N93-25299
SEFCIK, JOSEPH A. ..... p 2901 N93-24974
SEGARRA, D. ..... p 2738 N93-24780
SEKAR, B. ..... p 2582 N93-26007
SEKAR, BALU ..... p 2625 N93-26011
SEKERKA, R. F. ..... p 2646 N93-26323
SELIN, BENGT ..... p 2835 N93-25006
SELLIS, TIMOS ..... p 2880 N93-25809
SELVADURAY, GUNA ..... p 2643 N93-25240
SEMMEL, R. D. ..... p 2826 N93-25984
SENGUPTA, LOUISE C. ..... p 2640 N93-25954
SEPANSKI, ROBERT J. ..... p 2761 N93-25144
SERNICOLA, M. ..... p 2741 N93-24795
SESHADRI, K. ..... p 2643 N93-25229
SESHAN, S. ..... p 2806 N93-25233
SESHAN, SRINIVASAN ..... p 2816 N93-25458
SETNA, R. P. ..... p 2653 N93-26500
SETTLES, G. S. ..... p 2576 N93-25249
p 2698 N93-25266
SEVERE, GERALDA ..... p 2706 N93-25953
SEYMOUR, R. J. ..... p 2730 N93-26320
SGHIR, A. ..... p 2746 N93-24827
SHABANA, A. A. ..... p 2728 N93-25842
SHAFER, R. E. ..... p 2851 N93-25314
SHAH, B. ..... p 2614 N93-24667
SHAHSHAHANI, M. ..... p 2671 N93-24665
SHAIKH, NISAR ..... p 2640 N93-26225
SHAKLAN, S. B. ..... p 2621 N93-26111
SHANABLEH, M. ..... p 2790 N93-26050
SHANKS, HOWARD R. ..... p 2709 N93-25345
SHAO, YIBO ..... p 2854 N93-26184
SHAPPELL, S. A. ..... p 2801 N93-25859
SHARKEY, THOMAS J. ..... p 2794 N93-24738
SHARMA, S. K. ..... p 2769 N93-25573
SHARP, WILLIAM E. ..... p 2573 N93-25077
SHAW, MONTGOMERY T. ..... p 2645 N93-25879
SHAW, W. I. ..... p 2781 N93-25125
SHEEHEY, P. T. ..... p 2861 N93-26504
SHEPPARD, M. ..... p 2861 N93-26512
SHER, A. ..... p 2853 N93-25766
SHERBROOKE, CRAIG C. ..... p 2617 N93-25630
SHERBY, O. D. ..... p 2635 N93-25383
SHIER, HAMPTON N. ..... p 2775 N93-25946
SHIH, C. F. ..... p 2727 N93-25647
SHIMABUKU, R. A. ..... p 2766 N93-26316
SHIN, YOUNG S. ..... p 2813 N93-26431
SHING, BENSON ..... p 2670 N93-26414
SHIRATO, RYOTA ..... p 2716 N93-25068
SHIRRIFF, KEN W. ..... p 2815 N93-25251
SHISHKIN, A. A. ..... p 2859 N93-25216
SHISHKO, ROBERT ..... p 2665 N93-24682
SHOR, J. S. ..... p 2868 N93-26312
SHUH, D. K. ..... p 2645 N93-26251
SHUKLA, OODAYE B. ..... p 2814 N93-25603
SHUSTER, MALCOLM D. ..... p 2603 N93-24712
SIBENER, STEVEN J. ..... p 2646 N93-26402
SIEBENHUENER, MICHAEL ..... p 2739 N93-24784
SIEBERT, A. ..... p 2753 N93-24871
SIEGMAN, A. E. ..... p 2715 N93-26524
SIEKHAUS, W. J. ..... p 2654 N93-25384
SIEMERS, I. ..... p 2841 N93-25051
SIGMUNDSON, FREYSTEINN ..... p 2789 N93-25558
SILBERBERG, D. P. ..... p 2826 N93-25984
SILITONGA, P. H. ..... p 2739 N93-24784
SIMA, M. ..... p 2748 N93-24837
SIMES, G. Y. ..... p 2766 N93-25876
SIMMS, D. A. ..... p 2874 N93-25254
SIMON, RANDY W. ..... p 2869 N93-26381
SIMONS, JACK, II ..... p 2849 N93-25659
SIMONSON, S. CHRISTIAN, III ..... p 2730 N93-26177
p 2730 N93-26178
SIMS, J. R. ..... p 2688 N93-25313
SIMS, MICHAEL H. ..... p 2815 N93-25799
SINCLAIR, J. L. ..... p 2698 N93-25309
SINCOVEC, R. F. ..... p 2816 N93-25414
SINDONI, J. M. ..... p 2849 N93-26173
p 2850 N93-26281
SINDT, C. F. ..... p 2708 N93-26535
SINGHAL, S. N. ..... p 2724 N93-25070
SINHA, PRANAY G. ..... p 2853 N93-25748
SINKKONEN, MATTI ..... p 2597 N93-25178
SINNOTT, M. J. ..... p 2917 N93-26359
SIRIGNANO, W. A. ..... p 2661 N93-25948
SITES, J. R. ..... p 2759 N93-25504
SKJERVE, L. ..... p 2679 N93-26122
SKOWLUND, CHRISTOPHER T. ..... p 2648 N93-26079
SKUPINSKI, ROBERT C. ..... p 2759 N93-25136
SLEEPER, HOWARD L. ..... p 2803 N93-25617
SLIMMER, DAVID ALLEN ..... p 2863 N93-25265
SLINEY, H. E. ..... p 2659 N93-25565
SLOAN, ALAN D. ..... p 2804 N93-25927
SLOCOMB, C. ..... p 2811 N93-25943
SMIGIELSKI, FRANK J. ..... p 2781 N93-25220
SMIRNOVA, M. S. ..... p 2859 N93-25216
SMITH, A. R. ..... p 2899 N93-25327
SMITH, ALBERT E. ..... p 2761 N93-25143
SMITH, ARTHUR P., III ..... p 2585 N93-25456
SMITH, B. E. ..... p 2787 N93-26570
SMITH, B. W. ..... p 2899 N93-25185
SMITH, BRUCE LEE ..... p 2774 N93-25830
SMITH, CHARLES A. ..... p 2575 N93-25091
SMITH, CLIFF ..... p 2624 N93-26008
SMITH, DEAN LANCE ..... p 2620 N93-26080
SMITH, E. K. ..... p 2684 N93-26474
SMITH, EDWARD C. ..... p 2588 N93-25530
SMITH, ERNEST K. ..... p 2684 N93-26475
SMITH, G. D. W. ..... p 2653 N93-26500
SMITH, GEORGE F. ..... p 2788 N93-25616
SMITH, HOWARD W. ..... p 2586 N93-24739
SMITH, KENT F. ..... p 2583 N93-26263
SMITH, LINDA G. ..... p 2857 N93-26566
SMITH, PHILIP J. ..... p 2585 N93-25261
p 2585 N93-25330
SMITH, ROBERT A. ..... p 2799 N93-26489
SMITH, RON ..... p 2582 N93-25110
SMITH, S. F. ..... p 2688 N93-25377
SMITH, SEAN W. ..... p 2817 N93-26338
SMITH, W. H. ..... p 2668 N93-26206
SMOOKE, MITCHELL ..... p 2829 N93-26519
SMYTH, P. ..... p 2672 N93-24666
SNELICK, R. ..... p 2812 N93-26321
SNODGRASS, JOAN G. ..... p 2798 N93-26356
SNOW, F. ..... p 2603 N93-24717
SNYDER, DAVID B. ..... p 2615 N93-25090
SNYDER, GARY ..... p 2670 N93-26416
SNYDER, K. W. ..... p 2800 N93-25318
SOBCZYK, KAZIMIERZ ..... p 2763 N93-25329
SODERSTRAND, MICHAEL A. ..... p 2681 N93-26261
SOEDER, RONALD H. ..... p 2597 N93-25080
SOEDERLIND, E. ..... p 2645 N93-26300
SOLBERG, RUNE ..... p 2751 N93-24856
SOLBRIG, CHARLES W. ..... p 2695 N93-24966
SOLOMON, G. ..... p 2671 N93-24662
p 2671 N93-24663
p 2678 N93-26116
SOLTIS, R. F. ..... p 2659 N93-25565
SOMMER, S. ..... p 2738 N93-24776
SON, S. F. ..... p 2626 N93-26020
p 2630 N93-26042
p 2631 N93-26043
SONDHEIM, W. E. ..... p 2869 N93-26494
SONG, K. ..... p 2856 N93-26309
SOUNIK, J. ..... p 2856 N93-26309
SPACZER, M. ..... p 2649 N93-25336
SPAIN, CHARLES V. ..... p 2591 N93-26553
SPALL, JAMES C. ..... p 2827 N93-25611
SPALLICCI, A. ..... p 2608 N93-24986
SPALLICCI, A. D. A. M. ..... p 2670 N93-24987
SPARRY, D. A. C. ..... p 2616 N93-25463
SPECK, D. R. ..... p 2711 N93-24961
SPENCER, FLOYD ..... p 2582 N93-25110
SPENGLER, MICHAEL K. ..... p 2817 N93-26277
SPERRY, DAVID ..... p 2620 N93-26248
SPIEGEL, JACK ..... p 2796 N93-25567
SPIERING, BRUCE ..... p 2758 N93-25615
SPIRIDONOV, H. ..... p 2741 N93-24798
SPUDIS, PAUL D. ..... p 2897 N93-26094
SPURGEON, WILLIAM A. ..... p 2640 N93-25954
SRIDHAR, B. ..... p 2584 N93-24914
SRIDHAR, BANAVAR ..... p 2803 N93-25235
SRINIVASAN-RAO, T. ..... p 2712 N93-25378
SROMOVSKY, L. A. ..... p 2880 N93-25806
ST.CLAIR, TERRY L. ..... p 2656 N93-25999
ST.CYR, O. C. ..... p 2899 N93-26556
STAFFORD, MAX A. ..... p 2708 N93-26543
STAGGS, M. C. ..... p 2654 N93-25384
STAHMANN, JAMES R. ..... p 2609 N93-24876
STAKKESTAD, KJELL ..... p 2605 N93-24725
STALDER, KENNETH R. ..... p 2860 N93-25626
STAMBAUGH, JOHN S. ..... p 2586 N93-26093
STANCALIE, G. ..... p 2747 N93-24834
STANFORD, J. L. ..... p 2764 N93-25431
p 2764 N93-25432
STANLEY, MARLAND ..... p 2621 N93-24740
STARACE, A. F. ..... p 2849 N93-25509
STARKER, S. ..... p 2716 N93-24980
STATMAN, J. ..... p 2672 N93-24668
p 2678 N93-26120
STAYLOR, W. F. ..... p 2777 N93-24742
STEELE, J. M. ..... p 2830 N93-25863
STEELE, JIMMY W. ..... p 2786 N93-26156
STEFFEN, CHRIS ..... p 2670 N93-26416
STEIN, G. ..... p 2738 N93-24781
STEIN, H. S. ..... p 2863 N93-25387
STEINER, MICHAEL J. ..... p 2682 N93-26451
STEINMAN, ROBERT M. ..... p 2799 N93-26449
STELZRIED, C. T. ..... p 2679 N93-26122
STENGLE, THOMAS H. ..... p 2599 N93-24694
STENTOE, W. J. ..... p 2595 N93-26219
STEPHENS, V. M. ..... p 2582 N93-24773
STEPHENSON, J. ..... p 2743 N93-24808
STERN, A. ..... p 2838 N93-25026
p 2694 N93-25057
STERN, A. G. ..... p 2630 N93-26038

STERN, MIKAEL p 2754 N93-24874
STETINA, FRAN p 2711 N93-25614
p 2881 N93-25813
STEUBER, G. D. p 2667 N93-25177
STEWART, G. W. p 2828 N93-25687
STEWART, VEARL R. p 2581 N93-26099
STIEGMAN, A. E. p 2653 N93-25078
STINECIPHER, M. M. p 2629 N93-26035
STITH, J. L. p 2765 N93-25873
STOCKDALE, TIMOTHY N. p 2789 N93-25469
STOCKER, ALAN D. p 2857 N93-26542
STOCKHAM, L. W. p 2627 N93-26021
p 2627 N93-26022
p 2627 N93-26023
STOCKWELL, CATHERINE p 2604 N93-24722
STOKSTAD, R. G. p 2899 N93-25327
STOLOFF, M. J. p 2679 N93-26126
STONE, LYDIA RAZRAN p 2792 N93-25195
STONE, T. D. p 2595 N93-26219
STONE, WILLIAM H. p 2793 N93-26259
STONER, G. E. p 2655 N93-25446
STORER, JAMES A. p 2881 N93-25811
STOREY, R. p 2674 N93-25239
STORM, C. B. p 2662 N93-26493
STOSS, FREDERICK W. p 2761 N93-25144
STOUFFER, S. D. p 2625 N93-26009
STRAND, L. D. p 2626 N93-26019
STRANE, J. W. p 2863 N93-25387
STRAUSS, BERNARD p 2722 N93-26434
STREBEL, DONALD E. p 2804 N93-25929
STRINGFELLOW, B. C. p 2688 N93-25365
STROW, L. LARRABEE p 2824 N93-25975
STUCKEY, C. I. p 2631 N93-26054
STUMPF, WALTER MARTIN p 2588 N93-25538
STURE, STEIN p 2670 N93-26412
p 2670 N93-26413
STUTZMAN, WARREN p 2685 N93-26479
STUTZMAN, WARREN L. p 2685 N93-26484
SU, RENJENG p 2669 N93-26407
p 2670 N93-26416
SU, Y. C. p 2768 N93-26559
SUAREZ, LUIS E. p 2729 N93-25938
SUART, THOMAS D. p 2676 N93-25912
SUBRAMAMANIAM, N. p 2640 N93-26301
SUMMERS, C. J. p 2758 N93-25098
SUMMERS, L. G. p 2591 N93-24764
SUNG, C. S. p 2641 N93-26580
SUNG, N. H. p 2641 N93-26580
SUTER, J. J. p 2693 N93-25052
SUWITRA, KRISJANI S. p 2684 N93-26472
SWABEY, B. R. p 2837 N93-25019
SWANSON, B. I. p 2646 N93-26505
SWANSON, N. L. p 2715 N93-26296
SWAROOP, ANAND p 2755 N93-25460
p 2755 N93-25461
p 2756 N93-25462
SWIFT, G. W. p 2668 N93-25447
SWIFT, R. P. p 2731 N93-26507
SWORDER, D. D. p 2686 N93-26486
SYCHEV, YURI p 2735 N93-24932
SYN, C. K. p 2635 N93-25383
SZCZUR, MARTI R. p 2879 N93-25802
SZENTGYORGYI, ANDREW p 2855 N93-26191
SZU, HAROLD H. p 2825 N93-25976
SZUSZCZEWICZ, EDWARD P. p 2881 N93-25812

T

TADJBAKHSH, I. G. p 2729 N93-25950
TADJBAKHSH, IRADJ p 2729 N93-25846
p 2729 N93-25941
TAI, C. K. p 2790 N93-26331
TAKAHASHI, FUJINOBU p 2716 N93-25005
TAKITA, Y. p 2687 N93-24951
TAKTAK, RAMSIS p 2635 N93-25541
TALBOT, ROBERT W. p 2763 N93-25287
TALLANT, D. R. p 2646 N93-26502
TALMY, INNA G. p 2642 N93-25586
TAM, CHRISTOPHER p 2846 N93-26165
TAMAYO, J. p 2738 N93-24780
TAMEISHI, HIDEO p 2745 N93-24822
TAMM, C. p 2841 N93-25050
TAN, CHOON S. p 2593 N93-25668
TAN, JIAK-KWANG p 2580 N93-25881
TAO, SHIYAN p 2764 N93-25517
TAPIA, RICHARD A. p 2829 N93-26344
TAPLEY, B. D. p 2757 N93-26354
TAUPIER-LETAGE, ISABELLE p 2736 N93-24939
TAUSWORTHE, R. C. p 2679 N93-26126
TAVELLA, P. p 2832 N93-24985
p 2840 N93-25042
TAYLOR, B. N. p 2830 N93-26318
TAYLOR, D. p 2720 N93-26590
TAYLOR, D. B. p 2720 N93-26534
p 2720 N93-26585
TAYLOR, FRED J. p 2806 N93-25650
TAYLOR, GERALD R. p 2799 N93-25595
TAZAWA, H. p 2859 N93-25248
TEETER, RONALD p 2792 N93-25195
TEETS, A. p 2659 N93-25607
TELEGA, JOZEF JOACHIM p 2726 N93-25437
TELESMAN, JACK p 2652 N93-26201
TELFER, BRIAN A. p 2825 N93-25976
TELLIER, C. R. p 2647 N93-25037
TELLO, HECTOR M. p 2642 N93-26060
TENNANT, R. A. p 2768 N93-26592
TENORIO, M. F. p 2854 N93-25898
TERAMOTO, KENBU p 2753 N93-24868
TERAN, A. p 2598 N93-25656
TERRY, BECKY p 2681 N93-26276
TESAR, D. p 2717 N93-25413
THEILEN-WILLIGE, B. p 2753 N93-24872
THEOBALD, G. p 2833 N93-24990
p 2833 N93-24991
THEODOROPOULOS, PANAGIOTIS THEODOROS p 2714 N93-25721
THEOFYLAKTOS, NOULIE p 2685 N93-26481
THIEBAUD, D. p 2833 N93-24992
THOM, A. J. p 2649 N93-25149
THOMANN, P. p 2716 N93-25067
THOMANN, T. p 2716 N93-25065
THOMAS, C. p 2832 N93-24985
p 2836 N93-25016
p 2836 N93-25017
THOMAS, D. p 2893 N93-25245
THOMAS, G. A. p 2674 N93-25239
THOMAS, J. p 2689 N93-25491
THOMAS, J. L. p 2679 N93-26126
THOMAS, JAMES p 2584 N93-24948
THOMAS, JAMES H. p 2846 N93-24959
THOMASON, LEE B. p 2591 N93-26553
THOMPSON, DAVID E. p 2815 N93-25799
THOMPSON, DONALD L. p 2852 N93-25676
THOMPSON, RICHARD A. p 2696 N93-25176
THOMPSON, ROBERT L. p 2618 N93-26209
p 2851 N93-26518
THOMPSON, V. K. p 2583 N93-24894
THONNARD, J. p 2726 N93-25419
THUNNISSEN, H. A. M. p 2740 N93-24789
THURMAN, S. W. p 2614 N93-26109
THURSTON, R. S. p 2861 N93-26504
TIERNEY, J. W. p 2659 N93-25118
TIERSTEN, H. F. p 2675 N93-25772
TILAK, ANUP S. p 2691 N93-26299
TILLETT, JASON CLARK p 2889 N93-25624
TILTON, JAMES C. p 2803 N93-25921
p 2804 N93-25923
TIMOTEO, DOMINIC p 2584 N93-24948
TINCKNELL, M. p 2688 N93-25365
TING, YUNG p 2717 N93-25413
TIWARI, S. N. p 2575 N93-25117
TO, WAI-MING p 2829 N93-26560
TODD, RUSSELL F. p 2783 N93-25645
TOKUMARU, P. T. p 2707 N93-26163
TOLBERT, DANA p 2818 N93-25142
TONELLI, A. M. p 2741 N93-24796
TORABI, A. p 2758 N93-25098
TORIYAMA, H. p 2753 N93-24873
TORRENCE, G. W. p 2683 N93-26467
TORTORICIMONTAPERTO, A. p 2743 N93-24809
TOSCHEK, P. E. p 2841 N93-25051
TOSUNOGLU, S. p 2717 N93-25413
TOUCHET, P. p 2659 N93-25607
TOUDIC, T. p 2838 N93-25025
TOUDIC, Y. p 2836 N93-25013
TOURLIDAKIS, A. p 2594 N93-25702
TOWER, LEONARD K. p 2759 N93-25136
TOWNSEND, DENNIS P. p 2718 N93-25672
TRABOLD, T. A. p 2698 N93-25306
TRAHIOTIS, CONSTANTINE p 2846 N93-26358
TRAINOR, M. p 2811 N93-25943
TRAMONTIN, L. p 2653 N93-24971
TRAN, PEGGY p 2730 N93-26279
TRAN, T. p 2605 N93-24726
TRANSUE, AMY E. p 2584 N93-24948
TRAPP, S. p 2793 N93-25877
TRAVIS, J. R. p 2662 N93-26493
TREBES, J. E. p 2712 N93-25363
TREFOIS, P. p 2742 N93-24803
TREUHAFT, R. N. p 2677 N93-26108
TREW, ROBERT p 2709 N93-25634
TROCHET, PATRICK p 2583 N93-24879
TRONCOSO-LOZADA, OSCAR p 2780 N93-24897
TROUTMAN, PATRICK A. p 2615 N93-25174
TRUSZKOWSKI, WALT p 2825 N93-25978
p 2825 N93-25981
TRYGGVASON, GRETAR p 2644 N93-25819
TSAI, LUNG JOHN p 2704 N93-25708
TSANG, T. p 2712 N93-25378
TSCHANZ, JOHN p 2761 N93-25143
TSENG, I. S. p 2630 N93-26039
TSOU, H. p 2614 N93-24667
TUCHMAN, A. p 2822 N93-25962
TUCKER, W. p 2790 N93-26050
TUNG, CHAO-HUNG STEVE p 2579 N93-25752
TUPLEA, S. p 2747 N93-24834
TURCHI, P. p 2858 N93-25167
TURCHINSKAYA, MARINA p 2862 N93-25108
TURNBULL, A. p 2587 N93-25408
TURNER, MARTIN J. p 2804 N93-25924
TURNER, N. H. p 2868 N93-26258
TURNS, S. R. p 2768 N93-26533
TWOGOOD, RICHARD p 2788 N93-24960
TYGAR, J. D. p 2817 N93-26338
TYRRELL, DEBRA L. p 2918 N93-26380
TYSINGER, THOMAS LEE p 2702 N93-25546

U

UCHIDA, KUNIO p 2774 N93-25889
ULJANOV, B. A. p 2716 N93-25049
ULUSOY, OEZGUER p 2874 N93-25271
UNDERWOOD, S. p 2607 N93-24735
UNGER, ERIC ROBERT p 2587 N93-25279
UNSEREN, M. A. p 2717 N93-25100
UPCHURCH, BILLY T. p 2720 N93-25609
UPHOFF, CHAUNCEY p 2604 N93-24719
URABE, SHINJI p 2838 N93-25031
URBAN, DAVID L. p 2614 N93-24755
URBON, BRUCE C. p 2647 N93-26602

V

VAILAS, A. p 2802 N93-26229
VALDEZ, G. R. p 2842 N93-25059
VALENTIN, J.-P. p 2837 N93-25020
VALENZUELA-RENDON, MANUEL p 2814 N93-25613
VALLE, TIMOTHY JOSEPH p 2709 N93-25291
VANAMSTERDAM, J. D. p 2740 N93-24789
VANATTA, CHARLES W. p 2790 N93-26298
VANBIBBER, K. p 2848 N93-25366
VANDEMARK, MICHAEL R. p 2656 N93-26155
VANDENBELT, DAVID p 2670 N93-26415
VANDENBURGH, HERMAN H. p 2794 N93-24763
VANDENKIEBOOM, J. p 2827 N93-24973
VANDERHOFF, J. A. p 2628 N93-26028
VANDERMOLEN, R. I. p 2688 N93-25377
VANDERPLOEG, M. J. p 2810 N93-25699
VANDERVELDEN, ALEXANDER JACOBUS M. p 2587 N93-24768
VANDONINCK, A. p 2614 N93-25000
VANGELDER, ALLEN p 2808 N93-24944
VANLEHN, KURT p 2811 N93-26253
VANLOOCK, P. p 2693 N93-25054
VANSANT, TIM p 2886 N93-26398
VANSCHILFGAARDE, MARK p 2653 N93-26304
VANSPEYBROECK, L. p 2855 N93-26190
VANSPEYBROECK, LEON p 2855 N93-26191
p 2855 N93-26192
VANSTONE, D. A. p 2766 N93-26243
VANWONTERGFHEM, B. M. p 2711 N93-24961
VARDENY, Z. V. p 2655 N93-25524
VARFOLOMEYEV, I. V. p 2728 N93-25785
VARGA, L. p 2690 N93-25935
VARGAS, CAROLINA p 2671 N93-26083
VASSALLO, P. F. p 2698 N93-25306
VECCHI, GIUSEPPE p 2686 N93-24893
VELITCHKOV, ANTON p 2753 N93-24870
VENBRUX, JACK p 2804 N93-25928
VENKATAPATHY, ETHIRAJ p 2574 N93-24736
VENKATASUBRAMANIAN, R. p 2759 N93-25102
VENKATESH, SANTOSH S. p 2821 N93-25821
VENTERS, PETER p 2773 N93-25739
VEREBELYI, D. p 2864 N93-25506
VERLANDER, JAMES p 2799 N93-25595
VERMILLION, CHARLES H. p 2881 N93-25813
VERNOTTE, F. p 2839 N93-25036
VERTREES, T. H. p 2654 N93-25359
VERUTTIPONG, W. p 2671 N93-24661
VESSOT, R. F. C. p 2716 N93-24980
VETTER, THEODORE A. p 2807 N93-26294
VICTORIA, M. p 2649 N93-25336
VIENNET, J. p 2842 N93-25056
VIGIL, R. A. p 2689 N93-25429
VIGNAUD, F. p 2834 N93-25001
VIKRAM, CHANDRA S. p 2711 N93-26154
VILLA, ELSA p 2828 N93-25140
VINOGRADOV, B. V. p 2744 N93-24812
VITELLO, P. A. p 2763 N93-25385
VOGEL, CHRISTOPH ALEXANDER p 2773 N93-25756
VOGEL, W. J. p 2683 N93-26466
p 2683 N93-26467
VOGTLIN, G. E. p 2763 N93-25385

VOJAK, R. p 2686 N93-26486
VOLON, C. p 2742 N93-24803
VONPETERSDORFF, TOBIAS p 2726 N93-25638
VOORHIES, COERTE V. p 2776 N93-26421
VOTAW, A. J. p 2848 N93-25368
VRANISH, JOHN M. p 2691 N93-26104
VREDEVOOGD, LOREN p 2620 N93-26408
VRUDHULA, SARMA B. p 2690 N93-25856
VU, D. P. p 2710 N93-25677
VULCAN, A. p 2693 N93-25038

W

WACHSPRESS, DANIEL A. p 2575 N93-25075
WADDELL, M. W., JR. p 2847 N93-25256
WADE, RON p 2665 N93-24682
WADE, WILLIAM L., JR. p 2657 N93-26341
WAGNER, G. p 2693 N93-25004
WAGNER, GERARD p 2621 N93-25028
WAGNER, J. H. p 2667 N93-25177
WAGNER, MICHAEL J. p 2590 N93-26444
WAKANA, HIROMITSU p 2683 N93-26470
WALDMAN, MEL p 2599 N93-25835
WALKER, BRUCE K. p 2632 N93-26211
WALKER, K. P. p 2649 N93-25095
WALKER, R. p 2673 N93-25168
p 2673 N93-25169
WALKER, RAYMOND T. p 2770 N93-25081
WALKER, RUSSELL G. p 2888 N93-25135
WALL, PETER K. p 2693 N93-25039
WALLMAN, P. H. p 2763 N93-25385
WALLS, F. L. p 2842 N93-25059
WALSH, JOHN E. p 2878 N93-25793
WALTJEN, K. p 2715 N93-26503
WANG, C. p 2862 N93-24953
WANG, DAN L. p 2690 N93-25782
WANG, FREDERICK E. p 2652 N93-26234
WANG, J. p 2659 N93-25119
WANG, JIA Z. p 2798 N93-26436
WANG, LUI p 2814 N93-25613
WANG, QUANLU p 2660 N93-25298
WANG, TAO p 2760 N93-24908
WANG, WIE-CHYUNG p 2764 N93-25517
WANG, XIAOHUA p 2726 N93-25533
WANG, XIAOMING p 2791 N93-26578
WANG, YI-MIN p 2815 N93-24749
WANG, YONGDONG p 2876 N93-25554
WANJIN, HAN p 2595 N93-26239
WANTUCK, P. J. p 2768 N93-26592
WARBURTON, J. p 2786 N93-25874
WARD, BARRY p 2714 N93-25761
WARD, PAUL p 2813 N93-26583
WARDWELL, DOUGLAS A. p 2581 N93-26099
WARIN, A. p 2840 N93-25045
WARNER, THOMAS p 2787 N93-26351
WARNER, TIMOTHY ANDREW p 2754 N93-25430
WARNKE, LARRY L. p 2691 N93-26233
WARREN, JOHN W. p 2622 N93-25105
WATANABE, K. p 2860 N93-25356
WATANABE, K. Y. p 2859 N93-25216
WATANABE, MASAYOSHI p 2838 N93-25031
WATANABE, Y. p 2584 N93-25120
WATERMANN, JUERGEN p 2775 N93-26159
WATERS, W. J. p 2659 N93-25565
WATSON, CAROLYN B. p 2581 N93-26085
WATSON, J. V. p 2711 N93-26324
WATSON, T. J. p 2627 N93-26021
WATT, R. p 2709 N93-25515
WAY, JO BEA p 2878 N93-25798
WEBBER, W. ROBERT S. p 2796 N93-25592
WEBER, GARY A. p 2610 N93-25479
p 2611 N93-25510
p 2611 N93-25511
p 2611 N93-25512
p 2611 N93-25513
WEBSTER, FERRIS p 2732 N93-24919
WEBSTER, LAURIE p 2799 N93-25595
WEI, SHU-SHANG SAM p 2876 N93-25482
WEIGEL, HENRY S. p 2778 N93-24884
WEINBERG, IRVING N. p 2796 N93-25568
WEINSTEIN, ROY p 2865 N93-25667
WEISS, JEROLD L. p 2603 N93-24713
WEISS, K. p 2840 N93-25040
WEISSKOPF, M. p 2855 N93-26190
WEISSKOPF, M. C. p 2855 N93-26192
WELCH, RONALD M. p 2787 N93-26492
WELFORD, K. p 2864 N93-25454
WELLS, ANDREW T. p 2801 N93-25787
WELLS, BARRETT OTIS p 2865 N93-25744
WELLS, MARTHA S. p 2877 N93-25763
WELLS, N. D. p 2674 N93-25391
WELLS, VALANA L. p 2845 N93-25651
WEN, JOHN T. p 2719 N93-25771
WENDER, I. p 2659 N93-25118
p 2659 N93-25119
WENG, FUZHONG p 2784 N93-25743
WENG, TUNG-LI p 2725 N93-25411
WENZLER, CARL J. p 2693 N93-24889
WERRETT, STEPHEN T. R. p 2620 N93-25474
WESLEY, J. C. p 2860 N93-25493
WEST, JOHN T. p 2814 N93-25600
WESTENSKOW, G. A. p 2852 N93-25375
p 2688 N93-25397
WESTERFIELD, EDWIN E. p 2691 N93-26233
WESTERINK, J. J. p 2790 N93-26164
WESTERLUND, LARRY H. p 2623 N93-25132
WESTWATER, ED R. p 2684 N93-26473
WEYDAHL, DAN JOHAN p 2751 N93-24856
WHANG, WHAN-KYU p 2876 N93-25466
WHEELER, A. A. p 2646 N93-26323
p 2869 N93-26547
WHEELER, DAVID A. p 2831 N93-26330
WHELAN, DAVID p 2788 N93-24960
WHITAKER, MIKE p 2693 N93-24882
WHITE, C. W. p 2654 N93-25372
WHITE, HENRY S. p 2868 N93-26254
p 2657 N93-26386
p 2850 N93-26443
WHITE, HENRY W. p 2655 N93-25861
WHITE, J. M. p 2657 N93-26303
WHITE, RICHARD L. p 2805 N93-25931
WHITE, STEVEN R. p 2849 N93-25734
WHITE, T. W. p 2791 N93-26586
WHITE, WARREN B. p 2790 N93-26331
p 2787 N93-26513
WHITEMAN, J. R. p 2731 N93-26522
WHITLOCK, C. H. p 2777 N93-24742
WHITTAM, J. H. p 2795 N93-26133
WHITTEN, J. p 2862 N93-24953
WHITTEN, J. L. p 2650 N93-25502
WHITTLESEY, RICHARD p 2604 N93-24723
p 2605 N93-24724
WIECZOREK, JOHANNES p 2749 N93-24843
WIEDENBECK, MARK E. p 2900 N93-25241
WIEDMANN, JUERGEN p 2642 N93-24891
WIEDWALD, J. D. p 2709 N93-25515
WIEGAND, DONALD A. p 2675 N93-25635
WIESELTHIER, JEFFREY E. p 2680 N93-26227
WIESERMAN, WILLIAM R. p 2687 N93-24746
WIETING, MELVIN p 2788 N93-24960
WIKTOR, PETER J. p 2623 N93-25539
WILCOX, BRUCE C., JR. p 2582 N93-25205
WILCOX, R. B. p 2711 N93-24961
WILCZYNSKI, VINCENT p 2706 N93-25885
WILD, CHRIS p 2825 N93-25980
WILHELMS, JANE p 2808 N93-24944
WILHELMSON, ROBERT p 2881 N93-25814
WILHELMSON, ROBERT B. p 2878 N93-25793
WILLAM, KASPAR p 2670 N93-26414
WILLERT, CHRISTIAN ERNST p 2701 N93-25485
WILLIAMS, B. F. p 2672 N93-24671
WILLIAMS, DAVID H. p 2585 N93-26087
WILLIAMS, GLENN W. p 2857 N93-26566
WILLIAMS, J. B. p 2743 N93-24808
WILLIAMS, M. p 2862 N93-24953
WILLIAMS, TREVOR p 2620 N93-26081
WILLIAMSON, S. J. p 2798 N93-26435
p 2799 N93-26521
WILLIAMSON, SAMUEL J. p 2798 N93-26436
WILLIS, P. A. p 2678 N93-26115
WILLSON, ALAN N., JR. p 2690 N93-25678
WILMINGTON, ROBERT p 2797 N93-25736
WILSON, J. RON p 2733 N93-24920
WILSON, JOHN C. p 2597 N93-25998
WINELAND, D. J. p 2862 N93-26528
WINKLER, J. p 2858 N93-24968
WINOGRAD, NICHOLAS p 2850 N93-26267
WINTER, M. p 2626 N93-26015
WISCHOW, PERRY B. p 2757 N93-26574
WISE, J. A. p 2767 N93-26495
WISEMAN, ALAN GRAY p 2900 N93-25625
WISEMAN, SIMON R. p 2811 N93-25942
WITT, L. A. p 2796 N93-25203
p 2872 N93-25204
WITT, M. A. p 2625 N93-26010
WOEHRLE, T. G. p 2617 N93-25494
WOHLMAN, RICHARD p 2619 N93-24878
WOLF, E. L. p 2867 N93-26194
WOLFE, MICHAEL D. p 2885 N93-26582
WOLFS, F. L. H. p 2848 N93-25371
WOLK, J. A. p 2864 N93-25490
WOLSKY, A. M. p 2658 N93-26588
WOOD, ANDREW W. p 2811 N93-25942
WOOD, GEORGE M. p 2720 N93-25609
WOOD, KATHRYN J. p 2794 N93-25214
WOOD, WILLIAM A. p 2696 N93-25176
WOODRUFF, C. p 2607 N93-24735
WOODS, G. HAMILTON p 2631 N93-26057
WOOLSEY, C. p 2607 N93-24735
WORKING, DENNIS C. p 2668 N93-26101
WORL, L. A. p 2646 N93-26505
WORLEY, P. H. p 2816 N93-25521
WORMHOUDT, J. p 2628 N93-26031
WOS, KENNETH A. p 2786 N93-26245
WRIGHT, PEGGY p 2881 N93-25824
WU, CHUNG-LIN p 2637 N93-25695
WU, PEI-KUAN p 2700 N93-25473
WU, S. C. p 2601 N93-24701
p 2601 N93-24702
WUEBBLES, DONALD J. p 2762 N93-25146
WUN-FOGLE, MARILYN p 2710 N93-26141
WUNDERLICH, B. p 2654 N93-25374
WUU, TZYH-YUNG p 2690 N93-25856
WYATT, B. K. p 2745 N93-24820
WYCKOFF, J. J. p 2657 N93-26213
WYLLIE, A. p 2746 N93-24829
WYSOCKI, F. J. p 2861 N93-26504

X

XI, J. p 2862 N93-25163
XIA, LINXI p 2577 N93-25339
XIAO, F. p 2698 N93-25277
XIAO, X. D. p 2853 N93-25550
XIE, TAOLING p 2893 N93-25555
XIONG, FULIN p 2654 N93-25372
XIWEN, ZHU p 2716 N93-25030
XU, CATHERINE Q. p 2723 N93-25588
XU, DABEN p 2728 N93-25750

Y

YABE, T. p 2698 N93-25277
YADEN, DAVID B., JR. p 2799 N93-26082
YAHIL, AMOS p 2889 N93-25331
YAHYABEY, N. p 2693 N93-25041
YAMAGISHI, TOMEJIRO p 2859 N93-25215
YAMAMOTO, ATSUSHI p 2716 N93-25005
YAMAMOTO, T. p 2779 N93-24888
YAMAZAKI, K. p 2859 N93-25216
YAMNI, K. p 2833 N93-24992
YANEV, TONY K. p 2739 N93-24782
YANG, H. p 2652 N93-26197
YANG, HUNG-YU p 2681 N93-26383
YANG, RUI p 2724 N93-25270
YANG, S. L. p 2694 N93-24759
YANG, V. p 2630 N93-26039
YANG, WEI-LI p 2699 N93-25342
YARDLEY, JOHN F. p 2666 N93-24690
YARKONY, DAVID R. p 2851 N93-26525
YARMOFF, J. A. p 2645 N93-26251
YASUDA, PHYLLIS p 2874 N93-25288
YAU, STEPHEN S. p 2829 N93-26222
YEH, F. C. p 2667 N93-25177
YEH, H. Y. MICHAEL p 2824 N93-25974
YEH, PEN-SHU p 2804 N93-25928
YEH, TIEN C. p 2786 N93-26270
YELON, W. B. p 2864 N93-25503
YETTER, R. A. p 2628 N93-26027
YINGER, C. H. p 2836 N93-25015
YOKOSAWA, AKIHIKO p 2851 N93-25301
YONGFANG, TAN p 2716 N93-25030
YOO, BYUNGSU p 2865 N93-25703
YOON, W. S. p 2625 N93-26012
YORK, G. W. p 2713 N93-25379
YORK, THOMAS M. p 2862 N93-26520
YORKEY, THOMAS p 2788 N93-24960
YOSHIKAWA, SHOKO p 2727 N93-25690
YOUNG, ERICK T. p 2888 N93-25289
YOUNG, GEORGE S. p 2775 N93-25946
YOUNG, MICHAEL J. p 2797 N93-25815
YOUNG, WILLIE C. p 2797 N93-26138
YOUNGBLOOD, R. p 2827 N93-24973
YOUNGBLUT, CHRISTINE p 2831 N93-26330
YOUNGER, S. M. p 2858 N93-25187
YU, FRANCIS T. p 2864 N93-25655
YU, S. S. p 2852 N93-25375
p 2688 N93-25397
YUANHAI, XIANG p 2716 N93-25030
YUKIMATSU, AKIRA p 2774 N93-25889

Z

ZABIN, SERENA M. p 2676 N93-25847
ZADO, VICTORIA YOUSIP p 2874 N93-25209
ZAIMA, E. p 2779 N93-24888
ZAKRAJSEK, JAMES J. p 2718 N93-25672
ZAMPETTI, G. P. p 2687 N93-25062
p 2687 N93-25064
ZARBA, ROBERT p 2604 N93-24723
ZARKA, A. p 2833 N93-24994
p 2836 N93-25013
p 2838 N93-25025
p 2840 N93-25044
ZAVERI, JIGISH SHIRISH p 2876 N93-25475

ZBIB, H. M. ..... p 2730 N93-26361
ZDRAVEV, TOMAS ..... p 2753 N93-24870
ZEE, RALPH ..... p 2724 N93-25260
ZEHR, RAYMOND MILTON ..... p 2783 N93-25714
ZENG, ZHAOMEI ..... p 2764 N93-25517
ZHAI, Z. C. ..... p 2716 N93-25048
ZHANG, HAO ..... p 2664 N93-25740
ZHANG, QINGYUN ..... p 2764 N93-25517
ZHANG, QUAN ..... p 2712 N93-25280
ZHANG, SHENGPAN ..... p 2772 N93-25547
ZHAO, JING ..... p 2695 N93-24906
ZHAO, L. ..... p 2650 N93-25519
ZHAO, P. ..... p 2854 N93-26183
ZHAO, PING ..... p 2854 N93-26184
p 2855 N93-26188
p 2855 N93-26189
p 2855 N93-26191
p 2855 N93-26192
ZHAO, WENZHONG ..... p 2772 N93-25688
ZHENG, Y. ..... p 2833 N93-24994
p 2836 N93-25013
p 2838 N93-25025
ZHONGQI, WANG ..... p 2595 N93-26239
ZHOU, M. ..... p 2651 N93-25907
ZHOU, ZHEN ..... p 2727 N93-25718
ZICHELLA, V. ..... p 2742 N93-24799
ZIEMKE, J. R. ..... p 2764 N93-25431
p 2764 N93-25432
ZIMMERMAN, R. M. ..... p 2726 N93-25489
ZINN, B. T. ..... p 2630 N93-26040
ZIOCK, H. J. ..... p 2869 N93-26494
ZISHANG, LI ..... p 2574 N93-26238
ZLIMEN, I. ..... p 2899 N93-25327
ZOLOTUKHIN, A. V. ..... p 2859 N93-25216
ZOMBECK, M. ..... p 2854 N93-26187
ZORUMSKI, WILLIAM E. ..... p 2845 N93-26086
ZUPANC, FRANK J. ..... p 2631 N93-26149
ZUPPERO, ANTHONY C. ..... p 2892 N93-25164

Typical Corporate Source Index Listing

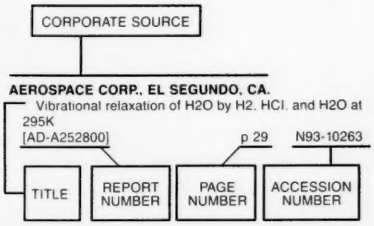

Listings in this index are arranged alphabetically by corporate source. The title of the document provides the user with a brief description of the subject matter. The report number helps to indicate the type of document cited (e.g., NASA report, translation, NASA contractor report). The accession number denotes the number by which the citation is identified. The page number helps you locate the citation in the abstract section. The titles are arranged under each corporate source in ascending accession number order.

A

ACADEMIA SINICA, WUHAN (CHINA).
Experiments on a diode-laser-pumped Rb-87 maser
p 2716 N93-25030

ACADEMY OF SCIENCES (USSR), ALMA-ATA.
Condensation on cooled surfaces of optical devices at the cosmic conditions p 2753 N93-24869

ACADEMY OF SCIENCES (USSR), MOSCOW.
Aerospace monitoring for ecological hazard and disaster mitigation p 2744 N93-24812

Data availability and data archeology from the former Soviet Union p 2735 N93-24932

ADVISORY GROUP FOR AEROSPACE RESEARCH AND DEVELOPMENT, NEUILLY-SUR-SEINE (FRANCE).
AGARD membership, 1993
| AGARD-MEMB-93 | p 2873 N93-26428

AERODYNE RESEARCH, INC., BILLERICA, MA.
Infrared fiber optic diagnostic for solid propellant combustion p 2628 N93-26031

AEROJET-GENERAL CORP., IUKA, MS.
Improved burn rate determination techniques
p 2627 N93-26021

ASRM design philosophy and modelling challenges
p 2627 N93-26022

Determination of burn rate requirements from ASRM performance specifications p 2627 N93-26023

AERONAUTICAL RADIO, INC., ANNAPOLIS, MD.
Expert system for UNIX system reliability and availability enhancement p 2723 N93-25588

AERONAUTICAL RESEARCH INST. OF SWEDEN, STOCKHOLM.
Reliable stress and fracture mechanics analysis of complex aircraft components using a h-p version of FEM
| AD-A260628 | p 2726 N93-25638

AERONAUTICAL RESEARCH LABS., MELBOURNE (AUSTRALIA).
In-flight evaluation of noise levels and assessment of active noise reduction systems in the Seahawk S-70B-2 helicopter
| AD-A260689 | p 2845 N93-25649

In-situ ultrasonic C-scanner
| AD-A261113 | p 2638 N93-25768

Estimation of coefficients in a rational function from observed values
| AD-A261126 | p 2828 N93-25773

AEROSPACE CORP., EL SEGUNDO, CA.
Mixed constellation synchronization of GPS time
p 2836 N93-25015

Analysis of transient photoluminescence measurements on GaAs and AlGaAs double heterostructures
| AD-A261154 | p 2867 N93-25947

Magnetotail processes associated with auroral surge formation
| ATR-90(7186)-1 | p 2895 N93-26147

Interaction of O2 with the Fe(.84)Cr(.16) (001) surface studied by photoelectron spectroscopy
| AD-A261065 | p 2645 N93-26251

AEROSPACE MEDICAL RESEARCH LABS., WRIGHT-PATTERSON AFB, OH.
Information requirements analyses for transatmospheric vehicles
| AD-A261189 | p 2590 N93-25949

AEROSPACE TECHNICAL INTELLIGENCE CENTER, WRIGHT-PATTERSON AFB, OH.
Substantiation of a stochastic model of rhythmic phenomena
| AD-A261232 | p 2830 N93-26262

AEROSPATIALE, SURESNES (FRANCE).
Numerical modelling of induced effects of lightning strike on an all composite helicopter p 2583 N93-24879

AIR FORCE ACADEMY, CO.
Orbit determination error analysis and comparison of station-keeping costs for Lissajous and halo-type libration point orbits and sensitivity analysis using experimental design techniques p 2604 N93-24721

Another look at the driven cavity problem
| AD-A261903 | p 2708 N93-26543

AIR FORCE ENVIRONMENTAL TECHNICAL APPLICATIONS CENTER, SCOTT AFB, IL.
Bit hit/solar activity correlation study
| AD-A261381 | p 2896 N93-26340

AIR FORCE HUMAN RESOURCES LAB., BROOKS AFB, TX.
Measuring hearing protection device performance using the metrosonics db-3100 sound level analyzer (dosimeter)
| AD-A260852 | p 2801 N93-25787

AIR FORCE HUMAN RESOURCES LAB., WRIGHT-PATTERSON AFB, OH.
A cognitive architecture for human performance process model research
| AD-A261040 | p 2797 N93-25815

AIR FORCE INST. OF TECH., WRIGHT-PATTERSON AFB, OH.
An environmental audit management plan for the Royal Australian Air Force
| AD-A261092 | p 2765 N93-25765

Development of a heuristic knowledge base for the selection of applicable or relevant and appropriate environmental requirements
| AD-A261038 | p 2765 N93-25864

An analysis of the reliability and maintainability of the Jian 6 and Jian 7 aircraft and ways to improve them
| AD-A261060 | p 2574 N93-26238

The blade curving effects in a turbine stator cascade with low aspect ratio
| AD-A261063 | p 2595 N93-26239

Properties of readings of periodically correlated random processes
| AD-A261225 | p 2686 N93-26573

AIR FORCE OCCUPATIONAL MEASUREMENT CENTER, RANDOLPH AFB, TX.
Aircraft electrical and environmental systems, AFSCs 452x5, 454x5, and 454x6
| AD-A261213 | p 2590 N93-25733

AIR FORCE OFFICE OF SCIENTIFIC RESEARCH, BOLLING AFB, WASHINGTON, DC.
Air Force Office of Scientific Research
| AD-A260675 | p 2911 N93-25893

AFOSR technical report summaries
| AD-A261551 | p 2918 N93-26380

AKADEMIE DER WISSENSCHAFTEN UND DER LITERATUR, MAINZ (GERMANY).
Mapping of windfall damage in the Hunsrueck plateau with Landsat TM-data p 2749 N93-24843

ALABAMA UNIV., HUNTSVILLE.
Electrodeposition in low gravity p 2663 N93-24774

Parametric analysis of atmospheric processes
| NASA-CR-192523 | p 2770 N93-25086

FNAS computational modeling
| NASA-CR-192512 | p 2863 N93-25225

CRRES: Combined release and radiation effects satellite program summary
| NASA-CR-192469 | p 2774 N93-25886

Turbulence interacting with chemical kinetics in airbreathing combustion of ducted rockets
p 2625 N93-26012

Advanced technology ` development multi-color holography
| NASA-CR-192451 | p 2711 N93-26154

ALASKA UNIV., FAIRBANKS.
The formation and characteristics of E-region thin ionization layers at high latitudes p 2861 N93-25829

ALCATEL BELL TELEPHONE, ANTWERP (BELGIUM).
Synchronisation, acquisition and tracking for telemetry and data reception p 2614 N93-25000

Frequency generation and synthesis in the DRSS
p 2693 N93-25054

ALLIED-SIGNAL AEROSPACE CO., COLUMBIA, MD.
Detection of bearing failure in mechanical devices using neural networks p 2822 N93-25965

ALLIED-SIGNAL AEROSPACE CO., KANSAS CITY, MO.
Surface preparation and characterization of a 400 micrometer diameter fused silica optical fiber for direct optical initiation (DOI) applications
| DE93-005485 | p 2852 N93-25182

CAD data exchange development
| DE93-008085 | p 2809 N93-25307

Finite element modeling of the hydroforming press
| KCP-613-4999 | p 2668 N93-26206

Development of a replacement for trichloroethylene in the two-stage cleaning process
| KCP-613-4941 | p 2669 N93-26207

Aqueous cleaning of flux residue from solder joints
| KCP-613-4803 | p 2652 N93-26208

Advanced engineering analysis
| KCP-613-4967 | p 2669 N93-26212

Characterization of the synthesis of M-61, a random equilibrium silicone terpolymer, using dry starting materials
| KCP-613-4985 | p 2657 N93-26213

ALLIED-SIGNAL CORP., KANSAS CITY, MO.
Nondestructive evaluation of ferrite c-cores
| KCP-613-4677 | p 2721 N93-25939

AMBASSADOR COLL., BIG SANDY, TX.
Distributed project scheduling at NASA: Requirements for manual protocols and computer-based support
p 2815 N93-26075

AMERICAN TELEPHONE AND TELEGRAPH CO., BEDMINSTER, NJ.
Timing a national telecommunications network using GPS p 2687 N93-25062

AMERICAN UNIV., WASHINGTON, DC.
Injection seeded, diode-pumped, short pulse Nd:YAG ring laser for space-based laser ranging
p 2713 N93-25389

AMES LAB., IA.
Processing and properties of Ti5Si3
| DE93-007284 | p 2649 N93-25149

Rheology of YBa2Cu3O(7-x) precursors
| DE93-007285 | p 2863 N93-25362

Theoretical predictions of platinum-rhodium bimetallic catalysts
| DE93-007540 | p 2649 N93-25428

The surface characterization of a series of hydroxybenzenes on Ag(111): An EELS and TDS study
| DE93-007541 | p 2647 N93-26595

AMPTEK, INC., BEDFORD, MA.
Detailed component design for a Compact Environmental Anomaly Sensor (CEASE)
| AD-A261729 | p 2620 N93-26248
ANALEX CORP., BROOK PARK, OH.
Federal Communications Commission (FCC) Transponder Loading Data Conversion Software. User's guide and software maintenance manual, version 1.2
| NASA-CR-191067 | p 2808 N93-24947
ANALYTIC SCIENCES CORP., READING, MA.
Visualizing the semantic content of large text databases using text maps p 2826 N93-25982
APPLIED ECONOMICS GROUP, INC., KNOXVILLE, TN.
Small business access to equity capital
| PB93-144582 | p 2372 N93-25735
ARGONNE NATIONAL LAB., IDAHO FALLS, ID.
Minimization of heat slab nodes with higher order boundary conditions
| DE93-004238 | p 2695 N93-24966
ARGONNE NATIONAL LAB., IL.
A new method for infrared imaging of air currents in and around critical hazard fume hoods
| DE93-003009 | p 2761 N93-24956
AQUIS: A PC-based air inventory and permit manager
| DE93-003006 | p 2761 N93-25143
Emissions from ethanol and LPG fueled vehicles
| DE93-006410 | p 2660 N93-25192
Magnitude and value of electric vehicle emissions reductions for six driving cycles in four US cities with varying air quality problems
| DE93-006417 | p 2660 N93-25298
Recent experiments on spin physics in high energy hadron interactions
| DE93-007900 | p 2851 N93-25301
Preliminary design of the BPM electronics memory scanner/dual boxcar averager for the advanced photon source
| DE93-007893 | p 2848 N93-25368
Magnetic excitations in antiferromagnetically coupled superlattices: Fe/Mo and Fe/Cr
| DE93-007894 | p 2863 N93-25369
FORTRAN M as a language for building earth system models
| DE93-007897 | p 2763 N93-25370
Feeding and decay of superdeformed states
| DE93-007899 | p 2848 N93-25371
Parallelizing the spectral transform method: A comparison of alternative parallel algorithms
| DE93-008664 | p 2816 N93-25521
Deterministic parallel FORTRAN
| DE93-008665 | p 2816 N93-25522
The Earth's climate as a dynamical system
| DE93-004666 | p 2767 N93-26496
Poster session: Fifth Users Meeting for the Advanced Photon Source
| DE93-006019 | p 2598 N93-26498
Workshop on Diamond and Diamond-Like-Carbon Films for the Transportation Industry
| DE93-007491 | p 2658 N93-26506
Published assessments bearing on the future use of ceramic superconductors by the electric power sector
| DE93-007737 | p 2658 N93-26588
ARIZONA STATE UNIV., TEMPE.
Generic hypersonic vehicle performance model
| NASA-CR-192953 | p 2587 N93-25162
Numerical simulation of leading-edge receptivity to freestream vorticity p 2577 N93-25388
High resolution interface nanochemistry and structure
| DE93-009750 | p 2635 N93-25501
Far field rotor noise
| AD-A260703 | p 2845 N93-25651
Stationary crossflow instability on an infinite swept wing p 2580 N93-25865
ARIZONA UNIV., TUCSON.
A study of the large-scale infrared emission from a selected dark cloud
| NASA-CR-192775 | p 2888 N93-25289
Inverse problem with continuous parameters for solar oscillations p 2895 N93-25728
Bayesian cross-entropy reconstruction of complex images
| AD-A261812 | p 2812 N93-26257
ARKANSAS COLL., BATESVILLE.
Volatiles in interplanetary dust particles: A comparison with CI and CM chondrites p 2896 N93-26062
ARKANSAS UNIV., FAYETTEVILLE.
Biological production of ethanol from coal
| DE93-008947 | p 2660 N93-25496
Biological conversion of synthesis gas
| DE93-009092 | p 2660 N93-25523
ARMED FORCES RADIOBIOLOGY RESEARCH INST., BETHESDA, MD.
AFRRI research, fiscal year 1991
| AD-A260933 | p 2911 N93-25710
ARMY AEROMEDICAL RESEARCH LAB., FORT RUCKER, AL.
The use of extended wear contact lenses in the aviation environment: An Army-wide study
| AD-A260938 | p 2795 N93-26218
Interpupillary and vertex distance effects on field-of-view and acuity with ANVIS
| AD-A261259 | p 2802 N93-26265
ARMY ARMAMENT RESEARCH, DEVELOPMENT AND ENGINEERING CENTER, PICATINNY ARSENAL, NJ.
Microwave absorption measurements and interference: Effects for a liquid fuel between 2.5 and 18 GHz
| AD-A260607 | p 2675 N93-25635
ARMY AVIATION APPLIED TECHNOLOGY DIRECTORATE, FORT EUSTIS, VA.
PROAV Cable Warning System (CWS) - U.S. Army aircraft Integration assessment and OCONUS field evaluation
| AD-A261233 | p 2583 N93-26263
ARMY AVIATION TECHNICAL TEST CENTER, FORT RUCKER, AL.
Methodology investigation: Global Positioning System integration (GPS)
| AD-A261054 | p 2586 N93-26237
ARMY BELVOIR RESEARCH AND DEVELOPMENT CENTER, FORT BELVOIR, VA.
Evaluation of the Migrating Combustion Chamber (MCC) engine
| AD-A260780 | p 2718 N93-25682
ARMY CHEMICAL RESEARCH AND DEVELOPMENT CENTER, ABERDEEN PROVING GROUND, MD.
Modified point mass trajectory simulation for base-burn projectiles
| BRL-TR-3321 | p 2609 N93-25985
ARMY ELECTRONICS TECHNOLOGY AND DEVICES LAB., FORT MONMOUTH, NJ.
Thermoelasticity in quartz p 2841 N93-25047
ARMY ENGINEER WATERWAYS EXPERIMENT STATION, VICKSBURG, MS.
Intelligent access to multiple relational database systems
| AD-A261198 | p 2881 N93-25824
Bibliography of remote sensing techniques used in wetland research
| AD-A261704 | p 2757 N93-26440
Proceedings of the Government Users Workshop on Ground Penetrating Radar Applications and Equipment
| AD-A261873 | p 2686 N93-26541
ARMY INTELLIGENCE CENTER AND SCHOOL, FORT HUACHUCA, AZ.
United States Army space experiment 601
| AD-A261460 | p 2798 N93-26353
ARMY LAB. COMMAND, FORT MONMOUTH, NJ.
Extruded films from modified polypropylene resin: Dielectric and breakdown studies
| AD-A261382 | p 2657 N93-26341
ARMY MATERIALS TECHNOLOGY LAB., WATERTOWN, MA.
Hydrogen-induced stress corrosion cracking susceptibility analysis of pitch links from the AH-64 Apache helicopter
| AD-A260692 | p 2651 N93-25895
Numerical simulation of permeation from deposited droplets: Model expansion
| MTL-TR-92-23 | p 2706 N93-25953
Thermal expansion measurements of polymer matrix composites and syntactics
| MTL-TR-92-27 | p 2640 N93-25954
Densification of ceramics by gas overpressure sintering
| MTL-TR-92-45 | p 2657 N93-26432
Adhesion and corrosion behavior of Al-Zn and TiN/Ti/TiN coatings on a DU-0.75 wt. percent Ti alloy
| MTL-TR-92-56 | p 2658 N93-26433
NDT standards from the perspective of the Department of Defense
| MTL-TR-92-68 | p 2722 N93-26434
ARMY NATICK RESEARCH AND DEVELOPMENT COMMAND, MA.
Assessing patterns of change in anthropometric dimensions: Secular trends of US Army females, 1946-1988
| AD-A260869 | p 2800 N93-25628
Anthropometry of the foot and lower leg of U.S. Army soldiers: Fort Jackson, SC
| AD-A261405 | p 2802 N93-26404
ARMY RESEARCH LAB., ABERDEEN PROVING GROUND, MD.
The burning rate behavior of pure nitrocellulose propellant samples
| AD-A261009 | p 2661 N93-25857
Flame structure studies of a lean, 20 torr H2/N2O/AR flame employing molecular beam mass spectrometry p 2627 N93-26025
Modeling of H2/N2O flames p 2627 N93-26026
Dark zone modeling of solid propellant flames p 2628 N93-26028
Detection of atomic oxygen and hydrogen in solid propellant flames and pyrolysis gases using multiphoton laser-induced fluorescence p 2628 N93-26029
Tomographic analysis of sight infrared spectra of low pressure flames p 2628 N93-26030
Condensed-phase processes during solid propellant combustion. Part 4: Chemical and microscopic examination of laser-irradiated propellant samples p 2628 N93-26032
Helicopter forced response vibration analysis method RTVIB20
| AD-A261809 | p 2597 N93-26260
ARMY RESEARCH LAB., ADELPHI, MD.
Information transmission using CHAOS
| AD-A261519 | p 2883 N93-26377
ARMY RESEARCH LAB., FORT BELVOIR, VA.
Elastomer compound developed for high wear applications p 2659 N93-25607
ARMY RESEARCH LAB., FORT MONMOUTH, NJ.
Improved performance and safety for high energy batteries through use of hazard anticipation and capacity prediction p 2694 N93-25582
High speed solid state circuit breaker p 2694 N93-25598
Magnetic field source for bi-chambered electron beam devices
| AD-A261316 | p 2691 N93-26299
ARMY TOPOGRAPHIC ENGINEERING CENTER, FORT BELVOIR, VA.
Repair, evaluation, maintenance, and rehabilitation research program. Continuous Deformation Monitoring System (CDMS)
| AD-A261833 | p 2586 N93-26274
US Army evaluation of the Electronic Map Data (EMD) prototype
| AD-A261693 | p 2757 N93-26369
ASSISTANT SECRETARY OF DEFENSE (INTELLIGENCE), WASHINGTON, DC.
Functional Economic Analysis Guidebook, version 1.1
| AD-A261390 | p 2886 N93-26305
AUBURN UNIV., AL.
Dynamics and control of maneuverable tethered flight vehicles p 2615 N93-24767
Hypervelocity impact study: The effect of impact angle on crater morphology
| NASA-CR-192711 | p 2724 N93-25260
Nonlinear stability analysis of the attitude motion of spin-stabilized thrusting spacecraft p 2617 N93-25527
AUSTRALIAN OCEANOGRAPHIC DATA CENTRE, NORTH SYDNEY.
Global Temperature and Salinity Pilot Project p 2733 N93-24924
AUTOMATIX, INC., BILLERICA, MA.
Vision-aided monitoring and control of thermal spray, spray forming, and welding processes p 2670 N93-25604

B

BALL CORP., BOULDER, CO.
Rate determination from vector observations p 2603 N93-24713
Practical aspects of transfer from GTO to lunar orbit p 2604 N93-24719
BARRIOS TECHNOLOGY, INC., HOUSTON, TX.
Accurate attitude determination of the LACE satellite p 2605 N93-24726
BATH UNIV. (ENGLAND).
The corrosion of metal matrix composites p 2638 N93-25723
BEDFORD INST. OF OCEANOGRAPHY, DARTMOUTH (NOVA SCOTIA).
World Ocean Circulation Experiment p 2733 N93-24922
BERMUDA BIOLOGICAL STATION FOR RESEARCH, INC., FERRY REACH.
Ocean time-series near Bermuda: Hydrostation S and the US JGOFS Bermuda Atlantic time-series study p 2736 N93-24938
BEVILL STATE COMMUNITY COLL., FAYETTE, AL.
Development of a pyrolysis waste recovery model with designs, test plans, and applications for space-based habitats p 2803 N93-26076
BOEING AEROSPACE AND ELECTRONICS CO., SEATTLE, WA.
Space transfer vehicle concepts and requirements study. Volume 1: Executive summary
| NASA-CR-192524 | p 2610 N93-25479
Space transfer vehicle concepts and requirements study. Volume 2, book 1: STV concept definition and evaluation
| NASA-CR-192525 | p 2611 N93-25510

Space transfer vehicle concepts and requirements study. Volume 2, book 2: System and program requirements trade studies
| NASA-CR-192526 | p 2611 N93-25511
Space transfer vehicle concepts and requirements study. Volume 2, book 4: Integrated advanced technology development
| NASA-CR-192528 | p 2611 N93-25512
Space transfer vehicle concepts and requirements study. Volume 2, book 3: STV system interfaces
| NASA-CR-192527 | p 2611 N93-25513
Space transfer vehicle concepts and requirements study. Volume 3, book 1: Program cost estimates
| NASA-CR-192529 | p 2611 N93-25514

BOEING DEFENSE AND SPACE GROUP, HUNTSVILLE, AL.

Robotic Variable Polarity Plasma Arc (VPPA) welding p 2720 N93-25605
Machine learning techniques for fault isolation and sensor placement p 2823 N93-25966
Space transfer concepts and analyses for exploration missions. Technical directive 12: Beamed power systems study
| NASA-CR-192532 | p 2599 N93-26146

BOEING DEFENSE AND SPACE GROUP, SEATTLE, WA.

X-ray computed tomography for casting development
| AD-A261786 | p 2722 N93-26526
X ray computed tomography for failure analysis
| AD-A261884 | p 2722 N93-26527

BONN UNIV. (GERMANY).

Remote sensing of land resource management in agriculture with regard to its influence on the environment p 2750 N93-24850

BRANDEIS UNIV., WALTHAM, MA.

High performance compression of science data p 2881 N93-25811

BRISTOL UNIV. (ENGLAND).

Alternative strategies for the use of satellite data analysis systems for hazard monitoring and disaster mitigation p 2743 N93-24805

BRITISH AEROSPACE PUBLIC LTD. CO., BRISTOL (ENGLAND).

A computational approach to predicting the extent of arc root damage in CFC panels p 2642 N93-24890

BRITISH BROADCASTING CORP., KINGSWOOD (ENGLAND).

Low-frequency room responses. Part 1: Background and qualitative considerations
| BBC-RD-1992/8-PT-1 | p 2673 N93-25168
Low-frequency room responses. Part 2: Calculation methods and experimental results
| BBC-RD-1992/9-PT-2 | p 2673 N93-25169
The design of a modular sound absorber for very low frequencies
| BBC-RD-1992/10 | p 2673 N93-25170
A modular wideband sound absorber
| BBC-RD-1992/11 | p 2673 N93-25171
An example of a phase-segregated enhanced PAL broadcasting system
| BBC-RD-1992/6 | p 2674 N93-25239
Experiments with the HIVITS HDTV contribution CODED
| BBC-RD-1992/12 | p 2674 N93-25391

BRITISH COLUMBIA UNIV., VANCOUVER.

The steady Navier-Stokes problem for low Reynolds number viscous jets p 2698 N93-25264

BROOKHAVEN NATIONAL LAB., UPTON, NY.

Characterization of electrochemical systems and batteries: Materials and systems
| DE93-003472 | p 2687 N93-24964
Algorithms for optimal redundancy allocation
| DE93-005709 | p 2827 N93-24973
Femtosecond dynamics in hydrogen-bonding solvents: Formamides
| DE93-003476 | p 2643 N93-25123
Laser field assisted photoemission using femtosecond laser pulses
| DE93-007277 | p 2712 N93-25378
Reclamation with recovery of radionuclides and toxic metals from contaminated materials, soils, and wastes p 2769 N93-25571

BROWN UNIV., PROVIDENCE, RI.

Mechanical stimulation of skeletal muscle mitigates glucocorticoid induced decreases in prostaglandin synthesis
| NASA-CR-193040 | p 2794 N93-24763
Shear band formation in a W-Ni-Fe alloy under plate impact
| AD-A260702 | p 2651 N93-25907
Research support for the Laboratory for Lightwave Technology
| AD-A261488 | p 2856 N93-26343

BRUNEL UNIV., UXBRIDGE (ENGLAND).

Use and analysis of finite element methods for problems of solid mechanics and fracture
| AD-A261574 | p 2731 N93-26522

BUERO FUER ANGEWANDTE GEOWISSENSCHAFTLICHE FERNERKUNDUNG, STOCKACH (GERMANY).

Earthquake vulnerability map of the Lake Constance area p 2753 N93-24872

BULGARIAN ACADEMY OF SCIENCES, SOFIA.

ANOVA method to estimate vegetation indices sensitivity assessing nitrogen fertilizing influence on spectral reflectance coefficients p 2739 N93-24782
Complex investigation of a system industrial site-environment using remote sensing and landscape-geochemical methods p 2741 N93-24798
Crop agroecological diagnostics by remote sensing technique p 2751 N93-24860
Data processing and control in a transputer system for remote sensing of the Earth p 2753 N93-24870

BUNDESANSTALT FUER GEOWISSENSCHAFTEN UND ROHSTOFFE, HANNOVER (GERMANY).

Satellite remote sensing for environmental geology: The Bandung (West Java) experience p 2739 N93-24784
Remote sensing geology p 2744 N93-24815

BUREAU INTERNATIONAL DES POIDS ET MESURES, SEVRES (FRANCE).

Atomic time scales for dynamical astronomy p 2832 N93-24984
How can millisecond pulsars improve the long term stability of atomic time scales? p 2832 N93-24985
GPS standardization for the needs of time transfer p 2836 N93-25016

BUREAU OF MINES, PITTSBURGH, PA.

Hazards of explosives dusts: Particle size effects
| DE93-009380 | p 2668 N93-25498

BUREAU OF MINES, TUSCALOOSA, AL.

Low cost dewatering of waste slurries p 2769 N93-25573
Production of ultrafine, high-purity ceramic powders using the US Bureau of Mines developed turbomill p 2659 N93-25585
Adaptive process control with fuzzy logic and genetic algorithms p 2827 N93-25612

BYELORUSSIAN SCIENTIFIC AND TECHNICAL CENTRE OF ENVIRONMENT REMOTE DIAGNOSTICS (BYELARUS).

Aerospace techniques in radiation and ecological monitoring of the Republic Belarus p 2741 N93-24793

C

CAELUM RESEARCH CORP., SILVER SPRING, MD.

Data fusion with artificial neural networks (ANN) for classification of earth surface from microwave satellite measurements p 2824 N93-25974

CALIFORNIA INST. OF TECH., PASADENA.

Management issues in systems engineering p 2665 N93-24682
Robust nonlinear control of vectored thrust aircraft
| NASA-CR-192727 | p 2596 N93-25199
Using a multifrontal sparse solver in a high performance, finite element code
| NASA-CR-192718 | p 2828 N93-25223
Intraplate deformation, stress in the lithosphere and the driving mechanism for plate motions
| NASA-CR-192782 | p 2772 N93-25529
Photospheric abundance analysis of low-mass pre-main sequence stars p 2894 N93-25623
Multivariate statistical analysis software technologies for astrophysical research involving large data bases p 2878 N93-25796
Image correlation velocimetry
| AD-A261599 | p 2707 N93-26163
Measurements of scalar power spectra in high Schmidt number turbulent jets
| AD-A261542 | p 2707 N93-26379

CALIFORNIA UNIV., BERKELEY.

Robo-line storage: Low latency, high capacity storage systems over geographically distributed networks
| NASA-CR-192910 | p 2805 N93-25130
An analysis of file migration in a UNIX supercomputing environment
| NASA-CR-192908 | p 2809 N93-25131
RAID-2: Design and implementation of a large scale disk array controller
| NASA-CR-192911 | p 2806 N93-25233
Zebra: A striped network file system
| NASA-CR-192912 | p 2809 N93-25250
A trace-driven analysis of name and attribute caching in a distributed system
| NASA-CR-192899 | p 2815 N93-25251
Striped tape arrays
| NASA-CR-192914 | p 2806 N93-25267
RAMA: A file system for massively parallel computers
| NASA-CR-192906 | p 2815 N93-25297
Control of nonlinear systems under input constraints with applications to flight control p 2596 N93-25353
A superconducting tunnel junction receiver for submillimeter astronomy, and analysis of observations of post-AGB star molecular envelopes p 2889 N93-25440
Interfacing a high performance disk array file server to a Gigabit LAN
| NASA-CR-192898 | p 2816 N93-25458
Performance studies of cache consistency and concurrency control algorithms in a distributed client/server DBMS architecture p 2876 N93-25554
Construction of a connectionist network supercomputer
| AD-A260929 | p 2820 N93-25648
Sounding rocket observations of precipitating ions in the morning auroral region p 2773 N93-25732
Further analysis of ECOM-721 data
| AD-A260863 | p 2774 N93-25790
Development of a tool-set for simultaneous, multi-site observations of astronomical objects p 2878 N93-25795
Joint services electronics program
| AD-A261801 | p 2692 N93-26539

CALIFORNIA UNIV., BERKELEY. LAWRENCE BERKELEY LAB.

Metal ion implantation for large scale surface modification
| DE93-007649 | p 2859 N93-25324
Beam position and total current monitor for heavy ion fusion beams
| DE93-007653 | p 2851 N93-25325
Strangeness production in S + Pb and p + Pb collisions at 200 GeV/c per nucleon nucleon
| DE93-007654 | p 2847 N93-25326
The Sudbury Neutrino Observatory
| DE93-007697 | p 2899 N93-25327
Results from the NA36 on strangeness production in 200 GeV/c per nucleon S + Pb and p - Pb reactions
| DE93-007711 | p 2848 N93-25364
The sub 60 ps timing resolution using large area silicon avalanche diodes
| DE93-007723 | p 2688 N93-25365
Detection of fragments arising from greater than 10 GeV electron-nucleus collisions
| DE93-007725 | p 2848 N93-25366
Correlated wavefunction quantum Monte Carlo approach to solids
| DE93-007730 | p 2863 N93-25367
Environmental risks and future generations: Criteria for public policy
| DE93-004691 | p 2764 N93-25443
The DX centers in three to five semiconductors under hydrostatic pressure
| DE93-007701 | p 2864 N93-25490
Surface diffusion studies by optical diffraction techniques
| DE93-007707 | p 2853 N93-25550
Large area, low capacitance Si(Li) detectors for high rate x ray applications
| DE93-007661 | p 2692 N93-26598
Bimolecular reaction dynamics from photoelectron spectroscopy of negative ions
| DE93-007669 | p 2647 N93-26599

CALIFORNIA UNIV., DAVIS.

Exploitation of cyclostationarity for signal-parameter estimation and system identification
| AD-A260833 | p 2728 N93-25784

CALIFORNIA UNIV. IRVINE.

Developing and improving numerical algorithms to study intrinsically correlated electron systems
| AD-A261214 | p 2849 N93-25734
Direct measurement of velocity space transport in a plasma p 2861 N93-25831
Fundamental studies of droplet interactions in dense sprays
| AD-A261165 | p 2661 N93-25948

CALIFORNIA UNIV., LOS ANGELES.

Anomalous aspects of magnetosheath flow and of the shape and oscillations of the magnetopause during an interval of strongly northward interplanetary magnetic field
| NASA-CR-192851 | p 2770 N93-25081
The instability of a liquid jet in a compressible airstream p 2703 N93-25560
VLSI for high-speed digital signal processing
| AD-A260754 | p 2690 N93-25678
A statistical study of field-aligned currents in the Earth's inner magnetosphere p 2773 N93-25709
Radial velocity measurements of carbon stars p 2895 N93-25713
Theoretical and experimental investigation of electron beam acceleration and sub-millimeter wave generation
| AD-A261117 | p 2609 N93-25770

CALIFORNIA UNIV., SAN DIEGO.

Dynamic deformations and analysis of a metal matrix composite p 2634 N93-25234

The interaction of modulated vortex pairs with a free surface p 2701 N93-25485
Energy dissipation in inelastic flow of cohesionless granular media p 2703 N93-25662

CALIFORNIA UNIV., SAN DIEGO, LA JOLLA.
Starburst Galaxies: Hard X-ray spectra and contribution to the diffuse background
| NASA-CR-192790 | p 2892 N93-25211
The structure of particle cloud premixed flames
| NASA-CR-192827 | p 2643 N93-25229
Experiments on the physics of turbulent mixing in stably stratified ocean layers
| AD-A261312 | p 2790 N93-26298
Neural basis of motion perception
| AD-A261452 | p 2798 N93-26349
Interaction of vorticity with a free surface
| AD-A261524 | p 2707 N93-26360
Comparative analytical study of evoked and event related potentials as correlates of cognitive processes
| AD-A261388 | p 2799 N93-26446
More rain compensation results p 2686 N93-26486

CALIFORNIA UNIV., SANTA BARBARA.
Multi-temporal satellite image analysis for crop inventories in the Po River Valley (Italy) p 2755 N93-25434
Nonlinear system design: Adaptive feedback linearization with unmodeled dynamics
| AD-A261360 | p 2826 N93-26333
Experimental studies of stress management by optical fluorescence
| AD-A261539 | p 2730 N93-26362

CALIFORNIA UNIV., SANTA CRUZ.
Rapid exploration of curvilinear grids using direct volume rendering
| NASA-CR-192765 | p 2808 N93-24944
Geologic structure and processes of the eastern Pacific margin: California and Costa Rica p 2771 N93-25424
Tully-Fisher distances and motions in the northern sky p 2889 N93-25621

CAMBRIDGE UNIV. (ENGLAND).
The evaluation of technical models used for major-accident hazard installations. Report to Commission of the European Communities Directorate General 12
| CUED/A-AERO/TR-19 | p 2668 N93-25238
Entropy reduction via simplified image contourization p 2804 N93-25924
European tri-service advanced materials workshop on compressive strength in rigid-rod polymers
| AD-A261517 | p 2658 N93-26576

CANADA CENTRE FOR REMOTE SENSING, OTTAWA (ONTARIO).
System of Experts for Intelligent Data Management (SEIDAM) p 2879 N93-25800

CARNEGIE COMMISSION ON SCIENCE, TECHNOLOGY, AND GOVERMENT, NEW YORK, NY.
Science, Technology, and Industrial Policy in the Former Soviet Union
| DE93-006528 | p 2887 N93-26499

CARNEGIE-MELLON UNIV., PITTSBURGH, PA.
Predictive modeling of particle-laden, turbulent flows
| DE93-008208 | p 2698 N93-25309
Set based program analysis
| AD-A260979 | p 2806 N93-25841
A methodology and software environment for testing process model's sequential predictions with protocols
| AD-A260980 | p 2882 N93-25844
Signed vector timestamps: A secure protocol for partial order time
| AD-A261371 | p 2817 N93-26338
Source-level debugging of automatically parallelized programs
| AD-A261520 | p 2813 N93-26378
Fast mutual exclusion for uniprocessors
| AD-A261663 | p 2883 N93-26389
Experiments in multiple-baseline stereo
| AD-A261415 | p 2757 N93-26448
Reinforcement learning for robots using neural networks
| AD-A261434 | p 2827 N93-26487
Uncertainty in object pose determination with three light-stripe range measurements
| AD-A261435 | p 2857 N93-26488

CASE WESTERN RESERVE UNIV., CLEVELAND, OH.
A model of concurrent flow flame spread over a thin solid fuel
| NASA-CR-191111 | p 2663 N93-24946
Hot corrosion of the B2 nickel aluminides
| NASA-CR-191082 | p 2649 N93-25128
Numerical simulation of a shock wave/turbulent boundary layer interaction in a duct p 2699 N93-25342
Modeling of bubble and drop formation in flowing liquids in terrestrial and microgravity environments p 2664 N93-25390
An experimental study of particle-laden jet interactions with cocurrent flows p 2701 N93-25534
Damage and failure analysis on continuous fiber-reinforced polymer composites p 2637 N93-25716
Gravity-dependent transport phenomena in zeolite crystal growth p 2664 N93-25740

CATANIA UNIV. (ITALY).
Oil pollution and water quality mapping of Augusta Bay, Italy using remote sensing techniques p 2746 N93-24823

CATHOLIC UNIV. OF AMERICA, WASHINGTON, DC.
Active control of NITINOL-reinforced structural composites
| AD-A261062 | p 2638 N93-25780

CENTRE NATIONAL D'ETUDES DES TELECOMMUNICATIONS, BAGNEUX (FRANCE).
Comparison of energy trapping resonators and filters using the AT cut of quartz, berlinite and gallium phosphate p 2836 N93-25013

CENTRE NATIONAL D'ETUDES SPATIALES, TOULOUSE (FRANCE).
DORIS precise orbit determination and location system performances of ultra stable oscillators p 2608 N93-24997
Space radiation susceptibility of ultra stable crystal oscillators p 2693 N93-25053

CENTRO STUDI ED APPLICAZIONI IN TECNOLOGIE AVANZATE, BARI (ITALY).
A knowledge-based approach to waste disposal sites detection through integration of Landsat-TM imagery and geographical context information p 2741 N93-24796

CESKOSLOVENSKA AKADEMIE VED, PRAGUE.
The regional planning and control using the satellite data p 2740 N93-24788

CFD RESEARCH CORP., HUNTSVILLE, AL.
Influence of supercritical conditions on pre-combustion chemistry and transport behavior of jet fuels
| AD-A261813 | p 2661 N93-26268

CHICAGO UNIV., IL.
Cosmic ray composition investigations using ICE/ISEE-3
| NASA-CR-192808 | p 2900 N93-25241
Energetic materials from cubane
| AD-A261317 | p 2662 N93-26308
Penning detachment: A new frontier
| AD-A261447 | p 2850 N93-26346
Dynamics of gas-surface interactions
| AD-A261402 | p 2646 N93-26402

CINCINNATI UNIV., OH.
Biped control via nonlinear dynamics p 2718 N93-25697
Computational gearing mechanics
| NASA-CR-191127 | p 2719 N93-25884
Model reduction for Space Station Freedom p 2620 N93-26081
Low temperature Hall and Shubnikov-de Haas effects
| AD-A261871 | p 2869 N93-26540

CITY UNIV. OF NEW YORK, BRONX.
A prototype for simulation of the space-to-ground assembly/contingency system of Space Station Freedom p 2619 N93-26065

CIVIL AEROMEDICAL INST., OKLAHOMA CITY, OK.
A review of civil aviation propeller-to-person accidents: 1980-1989
| AD-A260695 | p 2583 N93-25896
Contribution of personality to the prediction of success in initial air traffic control specialist training
| DOT/FAA/AM-93/4 | p 2797 N93-26138

CLARKSON UNIV., POTSDAM, NY.
An analysis of lift forces on aerosols in a wall bounded turbulent shear flow
| DE93-003362 | p 2695 N93-24963
Nonlinear wave phenomena related to interactions in the ionosphere
| AD-A261450 | p 2776 N93-26348

CLEMSON UNIV., SC.
Development of high Tc (greater than 100 K) Bi, Tl and Y-based materials as superconducting circuit elements
| NASA-CR-192344 | p 2863 N93-25219

CLIMATE ANALYSIS CENTER, WASHINGTON, DC.
Operational seasonal and interannual predictions of ocean conditions p 2733 N93-24921

COAST GUARD ACADEMY, NEW LONDON, CT.
Correlations between organized turbulent structures and wall pressure fluctuations
| PB93-156479 | p 2706 N93-25885
Residual mean meridional circulation in titan's middle atmosphere
| PB93-162931 | p 2898 N93-26571

COASTAL ENGINEERING RESEARCH CENTER, VICKSBURG, MS.
ADCIRC: An advanced three-dimensional circulation model for shelves, coasts, and estuaries. Report 1: Theory and methodology of ADCIRC-2DDI and ADCIRC-3DL
| AD-A261608 | p 2790 N93-26164

COLLEGE OF WILLIAM AND MARY, WILLIAMSBURG, VA.
The use of multiple models in case-based diagnosis p 2823 N93-25969

COLORADO SCHOOL OF MINES, GOLDEN.
Spectral remote sensing of anomalous mineralogy induced by hydrocarbon migration and uranium mineralization, San Rafael Swell, Utah, USA p 2739 N93-24783

COLORADO STATE UNIV., FORT COLLINS.
Pressure dependence of conductivity
| DE93-008466 | p 2687 N93-25113
A dynamical theory for hurricane spiral bands p 2782 N93-25352
Role of polycrystallinity in CdTe and CuInSe2 photovoltaic cells
| DE93-000045 | p 2759 N93-25504
The rate form of equilibrium equation for problems of steady-state, elastic, viscous flows p 2704 N93-25708
Tropical cyclogenesis in the western North Pacific p 2783 N93-25714
Tropical cyclone/upper-atmospheric interaction as inferred from satellite total ozone observations p 2784 N93-25741
Vector radiative transfer model: Application to rainfall retrieval with microwave radiometric data p 2784 N93-25743
Luminescence probe studies of ionomers. 3: Distribution of decay rate constants for tris bipyridyl ruthenium(2) in Nafion membranes
| AD-A260764 | p 2645 N93-25916
Inorganic and biological electron transfer across an electronically conductive composite polymer membrane
| AD-A261642 | p 2656 N93-26172
Optoelectronic III-V heterostructures on Si substrates
| AD-A261651 | p 2867 N93-26193
Template synthesis of electronically conductive polymers: A new route for achieving higher electronic conductivities
| AD-A261616 | p 2658 N93-26437
Transition metal chelate-fulleride compounds: Electrocrystallization of semiconducting (Ru(bpy)s)(C60)2
| AD-A261549 | p 2869 N93-26577

COLORADO UNIV., BOULDER.
Equilibrium constrained assumed natural coordinate strain finite elements for shell analysis p 2724 N93-25273
Aerodynamic foundations for use of unsteady aerodynamic effects in flight control p 2576 N93-25274
The Venus 130-nm dayglow as a diagnostic of thermospheric structure and dynamics p 2896 N93-25285
An active solid state ring laser gyroscope p 2709 N93-25291
Line formation and the Poynting-Robertson effect in accretion discs p 2847 N93-25355
Computation of transonic flow over a porous surface projectile p 2577 N93-25409
Mars: The dynamics of orbiting satellites and gravity model development p 2896 N93-25439
Numerical simulation of time-dependent thermocapillary convection in layered fluid systems p 2700 N93-25472
Spatial simulation of transition in wall-bounded shear flows: Active control and effects of surface roughness p 2701 N93-25483
Direct methane conversion to methanol
| DE93-009183 | p 2660 N93-25497
The role of multiple scattering in twilight zenith sky observations of atmospheric absorbers: Diurnal photochemistry and airmass factors p 2772 N93-25535
The effects of large-amplitude, low-frequency excitation on a three-dimensional jet p 2702 N93-25553
Crustal deformation studies in subaerial parts of the world oceanic rift system: Iceland and Afar p 2789 N93-25558
30 Doradus in the Large Magellanic Cloud: The stellar content and initial mass function p 2894 N93-25559
Variable-speed generators with flux weakening p 2694 N93-25599
Inverse sequential procedures for the monitoring of time series
| NASA-CR-192959 | p 2765 N93-25666
Computation of moisture flux from ocean to atmosphere using a synergy of SSM/I-derived precipitable water and ECMWF analyses p 2774 N93-25757
Applied Information Systems Research Program (AISRP). Workshop 2: Meeting Proceedings
| NASA-CR-193096 | p 2877 N93-25792
A land-surface testbed for EOSDIS p 2878 N93-25797
Experimenter's laboratory for visualized interactive science p 2879 N93-25802

Composite nanostructured material fabrication by electrochemical scanning probe microscopy
| AD-A261017 | p 2639 N93-25862
High-performance compression of astronomical images p 2805 N93-25931
Center for Space Construction Third Annual Symposium
| NASA-CR-192688 | p 2669 N93-26405
Dynamics of on-orbit construction process p 2669 N93-26406
Interaction dynamics and control for orbital assembly p 2669 N93-26407
Controls for orbital assembly of large space structures p 2620 N93-26408
Structural load control during construction p 2669 N93-26409
Systems engineering studies of on-orbit assembly operations p 2669 N93-26410
Expert systems for assembly sequence evaluation p 2669 N93-26411
Lunar regolith and structure mechanics p 2670 N93-26412
Indigenous lunar construction materials p 2670 N93-26413
Design concepts for pressurized lunar shelters utilizing indigenous materials p 2670 N93-26414
Configuration optimization of space structures p 2670 N93-26415
Telerobotic rovers for extraterrestrial construction p 2670 N93-26416
Lunar surface structural concepts and construction studies p 2670 N93-26417
Satellite communications application to Pacific countries above Ku band p 2683 N93-26471
Brightness temperature and attenuation diversity statistics at 20.6 and 31.65 GHz for the Colorado Research Network p 2684 N93-26473
A proposed study of multiple scattering through clouds up to 1 THz p 2684 N93-26474
WARC 92 and some thoughts as to its impact on the NASA propagation program p 2684 N93-26475

COLORADO UNIV., DENVER.
Multilevel techniques in large scale computation
| AD-A261082 | p 2828 N93-25762

COLUMBIA UNIV., NEW YORK, NY.
Multichip module high speed testing
| AD-A261391 | p 2856 N93-26306
Visual perception of elevation
| AD-A261394 | p 2797 N93-26307

COMMERCE DEPT., WASHINGTON, DC.
Space business indicators p 2886 N93-26158
Science, Technology, and Industrial Policy in the Former Soviet Union
| DE93-006528 | p 2887 N93-26499

COMMISSION OF THE EUROPEAN COMMUNITIES, BRUSSELS (BELGIUM).
Land cover, an essential component of the CORINE information system on the environment: GIS implications p 2740 N93-24787

COMMITTEE ON EARTH OBSERVATIONS SATELLITES, LONDON (ENGLAND).
CEOS Committee on Earth Observations Satellites consolidated report, 1992
| NASA-TM-108776 | p 2615 N93-25217

COMMONWEALTH SCIENTIFIC AND INDUSTRIAL RESEARCH ORGANIZATION, HOBART (AUSTRALIA).
International organisation of ocean programs: Making a virtue of necessity p 2732 N93-24917
Indian Ocean analyses p 2733 N93-24925

COMMUNICATIONS RESEARCH CENTRE, OTTAWA (ONTARIO).
Status of the Olympus experiment at CRC p 2685 N93-26480
Observations on the NASA Propagation Program p 2685 N93-26482

COMPAGNIA ITALIANA SERVIZI TECNICI, ROME.
Use of remote sensing spacecrafts in real time support to disaster management: Interfaces with ground segment facilities and services p 2743 N93-24809

COMPAGNIE D'ELECTRONIQUE ET DE PIEZO-ELECTRICITE, ARGENTEUIL (FRANCE).
Miniaturization and stability: A new generation of ovenised oscillators p 2693 N93-25004
Preliminary results of a newly designed mini-OCXO oscillator especially dedicated to space applications p 2621 N93-25028
Controlled dissolution of a piezoelectric material berlinite (AlPO4) p 2840 N93-25043
Oscillators for mobile GPS receivers p 2694 N93-25055

COMPOSANTS QUARTZ ET ELECTRONIQUE, PONT SAINTE MARIE (FRANCE).
A microcomputer compensated crystal oscillator MCXO p 2834 N93-25001

COMPUTER SCIENCES CORP., EL SEGUNDO, CA.
Resolution of the COBE Earth sensor anomaly p 2600 N93-24700

COMPUTER SCIENCES CORP., HAMPTON, VA.
A comparison using APPL and PVM for a parallel implementation of an unstructured grid generation program
| NASA-CR-191425 | p 2808 N93-25073

COMPUTER SCIENCES CORP., LANHAM, MD.
Real-time attitude determination and gyro calibration p 2602 N93-24708
Improvements in ERBS attitude determination without gyros p 2602 N93-24710
A multimission three-axis stabilized spacecraft flight dynamics ground support system p 2603 N93-24714

CONDUCTUS, INC., SUNNYVALE, CA.
Advanced HTS S-N-S devices
| AD-A261552 | p 2869 N93-26381

CONNECTICUT UNIV., FARMINGTON.
Monaural and binaural processing of complex waveforms
| AD-A261659 | p 2846 N93-26358

CONNECTICUT UNIV., STORRS.
Electrorheological fluids: A structural approach to mechanisms
| AD-A260563 | p 2645 N93-25879
In-process cure monitoring of composites via fiber-optic fluorescence
| AD-A261712 | p 2641 N93-26580

CONSIGLIO NAZIONALE DELLE RICERCHE, BOLOGNA (ITALY).
Precise Doppler tracking from the Medicina VLBI station p 2608 N93-24998

CONSIGLIO NAZIONALE DELLE RICERCHE, FLORENCE (ITALY).
Archaeological, historical and geoelectrical data as ground truth for Landsat TM imagery application to coastal plain evolution studies p 2742 N93-24799
Assessment and forecasting of crop yield in Niger through NOAA NDVI data p 2750 N93-24851

CONSIGLIO NAZIONALE DELLE RICERCHE, NAPLES (ITALY).
Use of remote sensing and GIS for the environmental planning proposal of the Sarno River Valley (Campania, southern Italy) p 2741 N93-24797

CONSIGLIO NAZIONALE DELLE RICERCHE, VENICE (ITALY).
Remote sensed spectral signatures classification and recognition by neural networks: An approach to unsupervised techniques p 2738 N93-24779

CONSOLIDATED SPACE TEST CENTER, ONIZUKA AFB, CA.
Analysis of the Command and Control Segment (CCS) attitude estimation algorithm p 2604 N93-24722
SCATHA mission termination report p 2605 N93-24725

CONTINUUM DYNAMICS, INC., PRINCETON, NJ.
Rotor design optimization using a free wake analysis
| NASA-CR-177612 | p 2575 N93-25075

CORNELL UNIV., ITHACA, NY.
Experimental and theoretical studies of dense fluid mixtures
| DE93-006070 | p 2695 N93-24976
On the robustness of Herlihy's hierarchy
| NASA-CR-193002 | p 2808 N93-25107
Putting time into proof outlines
| NASA-CR-192978 | p 2809 N93-25152
Determination of the elastic constants of composite materials from ultrasonic group velocity measurements p 2635 N93-25544
Implicit multigrid solution of the compressible Navier-Stokes equations with application to distributed parallel processing p 2702 N93-25546
Models of crack growth along polymer interfaces p 2728 N93-25750
Mechanisms of decomposition and oxidation of borane compounds
| AD-A261137 | p 2645 N93-26045
Virtually-synchronous communication based on a weak failure suspector
| NASA-CR-193003 | p 2721 N93-26135
A geological and geophysical information system for Eurasia
| AD-A261789 | p 2883 N93-26442

CORPS OF ENGINEERS, VICKSBURG, MS.
Development of a cone penetrometer for measuring spectral characteristics of soils in situ p 2776 N93-25570

CORVALLIS ENVIRONMENTAL RESEARCH LAB., OR.
Anatomy and physiology of plant conductive systems
| PB93-156032 | p 2793 N93-25877
Using terrestrial plants in biomonitoring
| PB93-158780 | p 2766 N93-26316
Response and feedbacks of forest ecosystems to global climate change
| PB93-167252 | p 2767 N93-26510

COUNCIL FOR NATIONAL ACADEMIC AWARDS (ENGLAND).
Design and performance of nozzle-less volute casings for inward flow radial turbines p 2593 N93-25471
Control and optimization of aircraft trajectories p 2596 N93-25543
Simulation of aircraft gas turbine engine p 2594 N93-25751

COUNCIL ON ENVIRONMENTAL QUALITY, WASHINGTON, DC.
Incorporating biodiversity considerations into environmental impact analysis under the National Environmental Policy Act
| PB93-139806 | p 2766 N93-25878

CRANFIELD INST. OF TECH., BEDFORD (ENGLAND).
Crashworthiness of composite seats for civil aircraft p 2582 N93-24773
North-central Mexico blue grama rangeland biomass assessment at the end of the rainy season using NOAA-AVHRR-LAC p 2750 N93-24854
Combining spectral information with crop rotation knowledge for crop classifications p 2752 N93-24861
A preliminary sizing method for unmanned aircraft using multi-variate optimisation p 2587 N93-25408
Annular flow enhanced two-phase evaporative heat exchanger for space-based systems p 2700 N93-25478
The dynamics and control of large flexible asymmetric spacecraft p 2617 N93-25525
An approach to configuration design synthesis of subsonic transport aircraft using artificial intelligence techniques p 2589 N93-25692
Numerical modelling of viscous turbomachinery flows with a pressure correction method p 2594 N93-25702
ASTOVL combat aircraft design synthesis and optimization p 2589 N93-25704
The effects of reaction on axial compressor performance p 2594 N93-25882
Radial inflow turbine study
| AD-A260767 | p 2594 N93-25917

CRYOLIFE, INC., MARIETTA, GA.
Cellular and tissue injury during nonfreezing cold injury and frostbite
| AD-A260574 | p 2795 N93-25900

CSA ENGINEERING, INC., PALO ALTO, CA.
ASTROS-ID: Software for system identification using mathematical programming
| AD-A260867 | p 2810 N93-25627

D

DAYTON UNIV., OH.
An investigation of laser velocimetry measurements within high speed, complex flows p 2697 N93-25237
Internal strain analysis of ceramics using scanning laser acoustic microscopy
| NASA-CR-191118 | p 2721 N93-25451
Effect of image update rate on moving-target identification range
| AD-A261562 | p 2591 N93-26462

DEFENCE RESEARCH AGENCY, MALVERN (ENGLAND).
Languages for requirements specifications
| RSRE-MEMO-4585 | p 2810 N93-25453
The SWORD multilevel secure DBMS
| RSRE-92005 | p 2811 N93-25942

DEFENCE RESEARCH ESTABLISHMENT, OTTAWA (ONTARIO).
Utilization of an electronic circuit simulator in CMOS latch-up studies
| AD-A260877 | p 2690 N93-25935

DEFENSE INFORMATION SYSTEMS AGENCY, ARLINGTON, VA.
Department of Defense technical architecture framework for information management. Volume 3: Reference model and standards profile, version 1.3
| AD-A261913 | p 2882 N93-26230
Human computer interface style guide, version 2.0
| AD-A261280 | p 2807 N93-26291
Department of Defense technical architecture framework for information management. Volume 1: Implementation concept, version 1.1
| AD-A261911 | p 2884 N93-26531
Department of Defense technical architecture framework for information management. Volume 2: Architecture guidance and design concepts, version 1.1
| AD-A261912 | p 2884 N93-26532

DEFENSE INTELLIGENCE AGENCY, WASHINGTON, DC.
Tsien's method for generating non-Keplerian trajectories. Part 2: The question of thrust to orbit a sphere and the restricted three-body problem p 2603 N93-24718

DEFENSE SYSTEMS MANAGEMENT SCHOOL, FORT BELVOIR, VA.
The systems engineering overview and process (from the Systems Engineering Management Guide, 1990) p 2665 N93-24679

DELAWARE UNIV., LEWES.
The role of the World Data Centers in handling ocean climate data p 2732 N93-24919

DELAWARE UNIV., NEWARK.
Design of a high activity and selectivity alcohol catalyst
| DE93-008101 | p 2659 N93-25111
Design of a high activity and selectivity alcohol catalyst
| DE93-008103 | p 2659 N93-25112
Studies of the analyte-carrier interface in flow injection analysis
| DE93-008374 | p 2644 N93-25311
Fracture of an elliptical inclusion and its implications for the properties of short fiber composites p 2634 N93-25333
Evaluating climate-vegetation interactions at climate model sub-grid scales p 2764 N93-25476
Steady-state numerical models of accreting neutron stars: The effect of atmospheric CNO depletion and diffusion p 2889 N93-25624
Inverse problems in nondestructive evaluations
| AD-A261370 | p 2722 N93-26337

DEPARTMENT OF DEFENSE EXPLOSIVES SAFETY BOARD, ALEXANDRIA, VA.
Minutes of the Twenty-Fifth Explosives Safety Seminar, volume 4
| AD-A261116 | p 2660 N93-25769

DEPARTMENT OF ENERGY, WASHINGTON, DC.
Technology Transfer 92/93
| DE93-003623 | p 2887 N93-24965

DEPARTMENT OF FISHERIES AND OCEANS, WINNIPEG (MANITOBA).
Wrap-up session p 2737 N93-24940
International ocean services: Is it time - will it ever be time? p 2737 N93-24941

DEPARTMENT OF RESOURCES, SURVEYS AND REMOTE SENSING, NAIROBI (KENYA).
The extent and status of mangroves in Mombasa district, Kenya: A case study based on remote sensing p 2746 N93-24826

DEPARTMENT OF THE NAVY, WASHINGTON, DC.
Liquid filled variable capacitor
| AD-D015639 | p 2687 N93-25212
Apparatus and methods for determining balance of a cylindrical vehicle
| AD-D015637 | p 2717 N93-25228
Method for providing EMI/EMP hardening and breakdown protection in composite materials
| AD-D015638 | p 2634 N93-25283
Dynamic test apparatus for electro-rheological fluids
| AD-D015632 | p 2643 N93-25284
Frequency diversity sidelobe canceller
| AD-D015647 | p 2674 N93-25332
Apparatus for imaging an object in or through a scattering medium using coherent anti-Stokes Raman scattering
| AD-D015642 | p 2852 N93-25358
Control of crystallite size in diamond film chemical vapor deposition
| AD-D015660 | p 2867 N93-26090
Video scan rate conversion method and apparatus for achieving same
| AD-D015661 | p 2854 N93-26091
Apparatus for determining the attitude of a vehicle
| AD-D015667 | p 2710 N93-26092
System for calibrating a gyro navigator
| AD-D015668 | p 2586 N93-26093
Method of joining diamond structures
| AD-D015671 | p 2867 N93-26140
Magnetic multilayer strain gage
| AD-D015672 | p 2710 N93-26141
Cross-switched MICRAD seeker
| AD-D015676 | p 2691 N93-26142
Electrostatic fiber spreader
| AD-D015677 | p 2640 N93-26143
Positive displacement rotary pump
| AD-D015678 | p 2719 N93-26144
Improved composite fabrication process
| AD-D015679 | p 2640 N93-26145
Variable pulse rate circuit
| AD-D015675 | p 2691 N93-26233
Metal alloy and method of preparation thereof
| AD-D015670 | p 2652 N93-26234
Pneumatic actuator with hydraulic control
| AD-D015652 | p 2719 N93-26244

DESERT RESEARCH INST., RENO, NV.
Investigation of winter mountain storms in Utah during the 1989 Utah/NOAA field program
| PB93-153021 | p 2785 N93-25849

DEUTSCHE FORSCHUNGSANSTALT FUER LUFT- UND RAUMFAHRT, COLOGNE (GERMANY).
Biodiversity indication by Earth observation data p 2751 N93-24858

DEUTSCHE FORSCHUNGSANSTALT FUER LUFT- UND RAUMFAHRT, OBERPFAFFENHOFEN (GERMANY).
The use of polarimetric multifrequency SAR for characterizing terrain classes p 2738 N93-24777
The scope of DLR's SAR calibration program p 2738 N93-24778
The national parks of Bavarian Forest and Sumava: A Landsat TM perspective on the structure and dynamics of the largest woodland of Central Europe p 2748 N93-24837

DORNIER LUFTFAHRT G.M.B.H., FRIEDRICHSHAFEN (GERMANY).
Comparison of the damage for various types of fibre reinforced composites due to different lightning test standards (MIL-STD-1757A, German military VG-standard 96903) p 2642 N93-24891

DORNIER SYSTEM G.M.B.H., FRIEDRICHSHAFEN (GERMANY).
Satellite borne remote sensing data: A tool for natural disaster reduction p 2743 N93-24806

DREXEL UNIV., PHILADELPHIA, PA.
Nonlinear dynamics and attitude control of articulated flexible space structures p 2617 N93-25726

DUKE UNIV., DURHAM, NC.
Prediction of unsteady flows in turbomachinery using the linearized Euler equations on deforming grids
| NASA-CR-192919 | p 2696 N93-25109
Primary events in olfactory reception
| AD-A260562 | p 2795 N93-25944

DURHAM UNIV. (ENGLAND).
Optical and infrared studies of distant galaxies p 2890 N93-25712

E

EAGLE-PICHER INDUSTRIES, INC., COLORADO SPRINGS, CO.
Introduction to lead salt infrared detectors
| AD-A260781 | p 2710 N93-25686

EASTERN RESEARCH GROUP, INC., LEXINGTON, MA.
Regulatory impact analysis of the Part 503 sewage sludge regulation
| PB93-110625 | p 2768 N93-26567

ECOLE NATIONALE SUPERIEURE DE MECANIQUE ET DES MICROTECHNIQUES, BESANCON (FRANCE).
Long term drift and gamma-irradiation effect p 2833 N93-24992
Dedicated oscillator for immersed crystal sensor p 2837 N93-25020
Trapped energy quartz crystal resonator on wedge-shaped plate p 2837 N93-25022
Quartz crystal twinning under mechanical stress: Finite element analysis p 2839 N93-25032
Anisotropic etching of silicon in KOH solutions p 2647 N93-25037

ECONOMIC RESEARCH SERVICE, WASHINGTON, DC.
Emerging technologies in ethanol production
| PB93-157014 | p 2661 N93-25818

EDGERTON, GERMESHAUSEN AND GRIER, INC., SALEM, MA.
Rubidium atomic frequency standards for GPS block 2R p 2836 N93-25014

EG AND G ENERGY MEASUREMENTS, INC., IDAHO FALLS.
EXCHANGE
| DE93-007227 | p 2808 N93-24962

EIC, INC., NORWOOD, MA.
Thin rechargeable batteries for CMOS SRAM memory protection p 2694 N93-25583

EKONO YMPAERISTOETEKNIIKKA, HELSINKI (FINLAND).
SIHTI: The research and development program of energy and environmental technology
| DE93-769925 | p 2763 N93-25360

ELECTRO MAGNETIC APPLICATIONS, INC., DENVER, CO.
Digitization of analog data from in-flight lightning strikes p 2778 N93-24884

ELECTRO MAGNETIC APPLICATIONS, INC., LAKEWOOD, CO.
Development of models for predicting the triggering of lightning by launch vehicles p 2610 N93-24899

ELORET CORP., PALO ALTO, CA.
The structure and energetics of Cr(CO)6 and Cr(CO)5
| NASA-CR-192889 | p 2848 N93-25450

ELORET CORP., SUNNYVALE, CA.
Development and application of computational aerothermodynamics flowfield computer codes
| NASA-CR-192940 | p 2574 N93-24736

EMORY UNIV., ATLANTA, GA.
The interaction of HCN/DCN with Si(100)-2x1
| AD-A260837 | p 2645 N93-25920

ENGINEERED DESIGNS, INC., CINCINNATI, OH.
Advanced bristle seals for gas turbine engines
| AD-A261296 | p 2720 N93-26564

ENGINEERING SCIENCE SOFTWARE, INC., SMITHFIELD, RI.
A micromechanical viscoplastic stress-strain model with grain boundary sliding
| DE93-009109 | p 2649 N93-25095

ENVIRONMENTAL AGENCY OF ANDALUCIA, SEVILLE (SPAIN).
Cartography and statistics of crops under irrigation in the Donana area of Andalucia through the use of Landsat-TM imagery and its incorporation into a GIS p 2751 N93-24855

ENVIRONMENTAL PROTECTION AGENCY, CINCINNATI, OH.
Quality control: Variability in protocols
| PB93-157790 | p 2766 N93-25876

ENVIRONMENTAL PROTECTION AGENCY, RESEARCH TRIANGLE PARK, NC.
National air pollutant emission estimates
| PB93-157808 | p 2765 N93-25850

ENVIRONMENTAL PROTECTION AGENCY, WASHINGTON, DC.
Glossary of environmental terms and acronym list
| PB93-158004 | p 2765 N93-25851

ENVIRONMENTAL QUALITY SYSTEMS, INC., WASHINGTON, DC.
Pollution prevention 1991: Progress on reducing industrial pollutants
| PB93-157725 | p 2766 N93-25875

ESSEX UNIV., COLCHESTER (ENGLAND).
Propagation at microwave frequencies in the presence of tropospheric stratified layers p 2674 N93-25340

EURIMAGE, ROME (ITALY).
Current trends in satellite data supply for environmental monitoring p 2754 N93-24874

EUROPEAN SPACE AGENCY, PARIS (FRANCE).
Environment Observation and Climate Modelling Through International Space Projects. Volume 2: Remote Sensing for Environmental Monitoring and Resource Management
| ESA-ISY-1-VOL-2 | p 2737 N93-24775
Frequency and Time Forum
| ESA-SP-340 | p 2831 N93-24978

EUROPEAN SPACE AGENCY. EUROPEAN SPACE RESEARCH AND TECHNOLOGY CENTER, ESTEC, NOORDWIJK (NETHERLANDS).
The ESA ISY initiatives for forest inventory in Europe p 2748 N93-24840
Relativistic effects for low Earth orbit satellites using GPS p 2608 N93-24986
The Columbus Metrology Science Team: Report on activities p 2670 N93-24987
ESA's planning and coordination of the OLYMPUS propagation experiment p 2684 N93-26477

EXECUTIVE OFFICE OF THE PRESIDENT, WASHINGTON, DC.
Technology for America's economic growth: A new direction to build economic strength
| AD-A261553 | p 2887 N93-26458

EXTRUDE HONE CORP., IRWIN, PA.
On machine capacitance dimensional and surface profile measurement system p 2670 N93-25579
Ultrasonic polishing p 2670 N93-25580

F

FAIRFAX MATERIALS RESEARCH, INC., ALEXANDRIA, VA.
Computer modelling of cyclic deformation of high-temperature materials
| AD-A260978 | p 2639 N93-25936

FEDERAL AVIATION ADMINISTRATION, ATLANTA, GA.
ILS mathematical modeling study of an ILS glide slope proposed for runway 19L at the Meridian Naval Air Station, Mississippi
| DOT/FAA/CT-TN93/8 | p 2584 N93-24741

FEDERAL AVIATION ADMINISTRATION, ATLANTIC CITY, NJ.
The 1992 International Aerospace and Ground Conference on Lightning and Static Electricity: Addendum
| DOT/FAA/CT-92/20-ADD-1 | p 2777 N93-24875
Visual approach data collection at St. Louis Lambert Field (STL)
| DOT/FAA/CT-TN93/2 | p 2584 N93-24948
The ATC evaluation of the prototype Airport Surveillance Radar Wind Shear Processor (ASR-WSP) at Orlando International Airport
| DOT/FAA/CT-TN92/48 | p 2673 N93-25210

Narrow-body aircraft water spray optimization study
| DOT/FAA/CT-TN93/3 | p 2582 N93-25224
Runway Visual Range (RVR) Operational Test and Evaluation (OT&E) integration and OT&E operational test report
| DOT/FAA/CT-TN93/37 | p 2584 N93-25243
The Data Multiplexing Network (DMN) phase 3 Extended Distance Data Cable (EDDC) test and evaluation
| DOT/FAA/CT-TN93/11 | p 2680 N93-26160

FEDERAL AVIATION ADMINISTRATION, OKLAHOMA CITY, OK.
Organizational politics, participation in decision-making, and job satisfaction
| DOT/FAA/AM-92/17 | p 2796 N93-25203
Procedural justice, occupational identification, and organizational commitment
| DOT/FAA/AM-92/21 | p 2872 N93-25204
Inward contaminant leakage tests of the S-Tron Corporation emergency escape breathing device. Phase 1: Tests of the original design. Phase 2: Tests with the redesigned neck seal
| DOT/FAA/AM-92/18 | p 2582 N93-25205
A longitudinal examination of applicants to the air traffic control supervisory identification and development program
| DOT/FAA/AM-92/16 | p 2796 N93-25213
The prevalence of artificial lens implants in the civil airman population
| DOT/FAA/AM-92/14 | p 2794 N93-25214
Conversion of the CTA, Inc., en route operations concepts database into a formal sentence outline job task taxonomy
| AD-A261410 | p 2586 N93-26447

FEDERAL EMERGENCY MANAGEMENT AGENCY, WASHINGTON, DC.
Handbook of chemical hazard analysis procedures
| PB93-158756 | p 2766 N93-26315

FERNERKUNDUNGSZENTRUM, POTSDAM (GERMANY).
Application of remote sensing data for the investigation of environmental degradation sites in East Germany p 2739 N93-24785

FINNISH METEOROLOGICAL INST., HELSINKI.
Forest damage detection and reflection of conifers: From micro to field level p 2752 N93-24864

FLORENCE UNIV. (ITALY).
Evaluation of nearshore suspended sediment concentration through Landsat TM data: First results p 2747 N93-24833
Laser propagation through turbulence
| AD-A260712 | p 2714 N93-26217

FLORIDA INTERNATIONAL UNIV., MIAMI.
Use of Taguchi design of experiments to optimize and increase robustness of preliminary designs p 2670 N93-26063
The reuse of logistics carriers for the first lunar outpost alternative habitat study p 2671 N93-26083

FLORIDA STATE UNIV., GAINESVILLE.
Thermodynamic, kinetic, and structural properties of linear polyethylene crystallized from polymer-diluent mixture p 2864 N93-25528
Prediction of global cloud cover with a very high resolution global spectral model
| AD-A261047 | p 2785 N93-25777

FLORIDA STATE UNIV., TALLAHASSEE.
Use of fuzzy relational information retrieval technique for generating control strategies in resolution-based automated reasoning p 2874 N93-25258
On the generation and dispersion of Yanai waves with a spectral Chebyshev-collocation reduced-gravity ocean model p 2788 N93-25276
Initialization of a modeled convective storm using Doppler radar-derived fields p 2782 N93-25294
Land surface processes and climate modeling p 2783 N93-25685
Typhoon prediction (recurvature - 1990 experiment)
| AD-A260673 | p 2786 N93-25892
Computation of broadband mixing noise from turbomachinery
| AD-A261611 | p 2846 N93-26165

FLORIDA UNIV., GAINESVILLE.
Spacecraft detumbling through energy dissipation p 2600 N93-24696
Prograde anomalous orbits in triaxial gravitational potentials that rotate about the long axis: VLA neutral hydrogen observations and modeling of the inclined rings around the galaxies NGC 2685 and NGC 660 p 2607 N93-25396
A logic-based approach to federated databases p 2876 N93-25466
A software development approach for parallel processing systems integrating object-oriented and functional paradigms p 2816 N93-25481
Numerical modeling of barred spiral galaxies p 2893 N93-25537
Very high-speed arithmetic processors (The Gauss Machine)
| AD-A260693 | p 2806 N93-25650
Molecular interactions and properties with many-body methods
| AD-A261688 | p 2850 N93-26367
Complex auditory signals
| AD-A261491 | p 2846 N93-26374

FOMI REMOTE SENSING CENTER, BUDAPEST (HUNGARY).
Toward a satellite based crop information system in Hungary p 2750 N93-24849

FOOTHILL-DE ANZA COMMUNITY COLL., LOS ALTOS HILLS, CA.
Optimization of knowledge-based systems and expert system building tools
| NASA-CR-192763 | p 2874 N93-25288

FORSCHUNGSINSTITUT DER DEUTSCHEN BUNDESPOST, DARMSTADT (GERMANY).
Effect-specific analysis of propagation parameters p 2684 N93-26478

FRANCHE-COMTE UNIV., BESANCON (FRANCE).
Weak magnetic field sensitivity of quartz crystal oscillators p 2833 N93-24993
OSCCAR: Oscillator-compensated with a capacitance array p 2693 N93-25002
Design of a low phase noise UHF oscillator using a partly metallized dielectric resonator p 2693 N93-25003
Elastic plate mode sensitivities to mass loading applications to gas sensors p 2711 N93-25009
Surface Transverse Wave (STW) quartz resonators in the GHz range p 2836 N93-25012
Stability of nonlinear phase motion from the study of oscillator mappings p 2693 N93-25034

FREIBURG UNIV. (GERMANY).
Potential operational use of remote sensing from space in forestry p 2745 N93-24817
Atmospheric correction of Landsat/TM data over mountainous terrain for forestry applications p 2752 N93-24862

FREQUENCY ELECTRONICS, INC., MITCHEL AFB, NY.
Ultra stable oscillators for satellite applications p 2621 N93-25027
Microwave synthesizers in space p 2693 N93-25038

FWG ASSOCIATES, INC., TULLAHOMA, TN.
Rain rate instrument for deployment at sea, phase 2
| NASA-CR-192442 | p 2786 N93-26156

G

GALAXY SCIENTIFIC CORP., PLEASANTVILLE, NJ.
Lightning data acquisition p 2778 N93-24883
Human Factors in Aviation Maintenance, phase 2
| DOT/FAA/AM-93/5 | p 2802 N93-26089

GAS RESEARCH INST., CHICAGO, IL.
Thermodynamic properties of natural gas mixtures
| PB93-156818 | p 2872 N93-26558

GENCORP AEROJET, SACRAMENTO, CA.
A new approach to cooled combustion chambers: The 40K formed platelet chamber p 2626 N93-26018
Space transportation booster engine thrust chamber technology, large scale injector
| NASA-CR-192531 | p 2633 N93-26557

GENERAL ACCOUNTING OFFICE, WASHINGTON, DC.
Department of Energy: Better information resources management needed to accomplish missions. Report to the Secretary of Energy
| GAO/IMTEC-92-53 | p 2882 N93-26096
Strategic information planning: Framework for designing and developing system architectures
| GAO/IMTEC-92-51 | p 2882 N93-26097

GENERAL ELECTRIC CO., HOUSTON, TX.
MAC to VAX connectivity: Heartrate spectral analysis system p 2796 N93-25594

GENERAL ELECTRIC CO., PHILADELPHIA, PA.
Compression of spectral meteorological imagery p 2804 N93-25925

GENERAL ELECTRIC CO., PRINCETON, NJ.
UARS in-flight jitter study for EOS
| NASA-CR-191419 | p 2615 N93-25133

GENERAL ELECTRIC CO., SCHENECTADY, NY.
Measurement of velocities in gas-liquid two-phase flow using laser Doppler velocimetry
| DE93-008083 | p 2698 N93-25306

GENERAL MOTORS CORP., INDIANAPOLIS, IN.
Fuel Injector: Air swirl characterization aerothermal modeling, phase 2, volume 2
| NASA-CR-189193 | p 2592 N93-25106

GEOLOGICAL SURVEY, RESTON, VA.
Model for transport of floating debris in the ocean
| PB93-172997 | p 2768 N93-26559

GEORGE MASON UNIV., FAIRFAX, VA.
Statistical modelling of software reliability
| NASA-CR-192985 | p 2809 N93-25257
Perceptual factors that influence use of computer enhanced visual displays
| NASA-CR-192961 | p 2811 N93-26150

GEORGE WASHINGTON UNIV., WASHINGTON, DC.
Whisker growth studies under conditions which resemble those available on an orbiting space station
| NASA-CR-192701 | p 2664 N93-25218
Accurate determination of Auger line shape binding energies
| AD-A261803 | p 2868 N93-26258
Resonance electron scattering by O2 monolayers on graphites: Reinterpreted
| AD-A261851 | p 2850 N93-26287

GEORGETOWN UNIV., WASHINGTON, DC.
Ir-Zr alloys as diffusion barriers between Cu and Si(100)
| AD-A261919 | p 2652 N93-26197

GEORGIA INST. OF TECH., ATLANTA.
An aeroelastic model structure investigation for a manned real-time rotorcraft simulation p 2574 N93-24756
Atmospheric reactive nitrogen oxides and their relationship with urban and rural ozone formation p 2760 N93-24908
Cloud properties as inferred from HIRS/2 multi-spectral data p 2782 N93-25293
Application of finite-state inflow to flap-lag-torsion damping in hover p 2587 N93-25486
An integrated finite-state model for rotor deformation, nonlinear airloads, inflow, and trim p 2588 N93-25538
An investigation on planar velocimetry by spatial cross-correlation p 2578 N93-25664
An investigation of the role of flux divergence in the turbulent kinetic energy balance of the atmospheric surface layer p 2773 N93-25756
Signal processing in impulsive electromagnetic interference
| AD-A260755 | p 2676 N93-25847
Experimental investigation of flow turning losses in unstable rocket motors p 2630 N93-26040
Deformation mechanisms of NiAl cyclicly deformed near the brittle-to-ductile transition temperature
| NASA-CR-191121 | p 2652 N93-26235
Image-based ranging and guidance for rotorcraft
| NASA-CR-177608 | p 2586 N93-26549

GEORGIA TECH RESEARCH INST., ATLANTA.
New concepts for high efficiency energy conversion: The avalanche heterostructure and superlattice solar cells
| DE92-010592 | p 2758 N93-25098

GEORGIA UNIV., GRIFFIN.
Surface energy fluxes at Central Florida during the convection and precipitation electrification experiment
| NASA-CR-192826 | p 2769 N93-24945

GHENT UNIV. (BELGIUM).
The use of remote sensing and GIS for the assessment of environmental degradation caused by fires, applied upon South-Euboia (central Greece) p 2742 N93-24802
Assessment of storm damage in forests using SPOT imagery p 2748 N93-24842

GKSS-FORSCHUNGSZENTRUM GEESTHACHT (GERMANY).
The need for spaceborne observations for meteorology and climatology p 2744 N93-24813

GLASGOW UNIV. (SCOTLAND).
The generation of Langmuir waves by thick target electron beams in solar flares p 2861 N93-25730

GORDON RESEARCH CONFERENCES, INC., KINGSTON, RI.
Gordon Conference on Point Defects, Line Defects and Interfaces in Semiconductors
| AD-A261485 | p 2868 N93-26357

GUELPH UNIV. (ONTARIO).
Local and regional estimates of sensible and latent heat flux densities from a patch-work surface
| ISBN-0-315-70882-4 | p 2772 N93-25556

H

HAMBURG UNIV. (GERMANY).
Controlling an optical frequency by a single ion p 2841 N93-25051

HARRIS CORP., MELBOURNE, FL.
Adaptive laser link reconfiguration using constraint propagation p 2823 N93-25967

HARVARD UNIV., CAMBRIDGE, MA.
Crack tip fields in ductile crystals and bicrystals p 2866 N93-25749
Single electron charging effects in mesoscopic systems
| AD-A261228 | p 2868 N93-26302
Neuropsychological components of object identification
| AD-A261449 | p 2797 N93-26347
Perception and the temporal properties of speech
| AD-A261439 | p 2686 N93-26490

HASKINS LABS., INC., NEW HAVEN, CT.
Speech research
| AD-A260643 | p 2675 N93-25639
HAUT COMMISSARIAT A LA RECHERCHE, ALGIERS (ALGERIA).
A frequency generating source: Frequency synthesizers p 2693 N93-25041
HAWAII UNIV., MANOA.
A low-complexity and high performance concatenated coding scheme for high-speed satellite communications
| NASA-CR-192715 | p 2673 N93-25198
HCC SCIENCE AND TECHNOLOGY CO., SUMMIT, NJ.
Development of organic nonlinear optical materials
| AD-A261332 | p 2856 N93-26309
HELSINKI UNIV. OF TECHNOLOGY, OTANIEMI (FINLAND).
Computational and experimental studies on large scale solar heating
| DE93-769942 | p 2758 N93-25096
Advanced energy systems and technologies - National R and D programme
| DE93-769943 | p 2758 N93-25097
HERIOT-WATT UNIV., EDINBURGH (SCOTLAND).
Fibre optic sensors for heat transfer studies p 2853 N93-25748
HONEYWELL, INC., BLOOMINGTON, MN.
Research on lead titanate films for radiation detection
| AD-A261187 | p 2849 N93-25823
Monolithic integration of semiconductor and superconductor components
| AD-A260589 | p 2690 N93-25906
RF vacuum microelectronics
| AD-A261784 | p 2692 N93-26565
HONEYWELL, INC., MINNEAPOLIS, MN.
Software lifecycle support environment (SLCSE) knowledge-based enhancements
| AD-A261042 | p 2811 N93-25791
Knowledge-based control for robot self-localization p 2822 N93-25963
HOUSTON UNIV., TX.
Dynamics of turbulent slugging in transitional pipe flow p 2702 N93-25548
Aerospace devices for magnetic replicas
| NASA-CR-192958 | p 2865 N93-25667
Initial streamwise vorticity formation in a two-stream mixing layer p 2579 N93-25752
An architecture for object-oriented intelligent control of power systems in space p 2823 N93-25968
National Aeronautics and Space Administration (NASA)/American Society for Engineering Education (ASEE) Summer Faculty Fellowship Program, 1992, volume 1
| NASA-CR-188242-VOL-1 | p 2911 N93-26058
Metabolic response of environmentally isolated microorganisms to industrial effluents: Use of a newly described cell culture assay p 2794 N93-26066
National Aeronautics and Space Administration (NASA)/American Society for Engineering Education (ASEE) Summer Faculty Fellowship Program, 1992, volume 2
| NASA-CR-188242-VOL-2 | p 2914 N93-26070
A hybrid multigrid technique for computing steady-state solutions to supersonic flows p 2582 N93-26078
The adult literacy evaluator: An intelligent computer-aided training system for diagnosing adult illiterates p 2799 N93-26082
HOWARD UNIV., WASHINGTON, DC.
Dynamics and robust control of a sampled data system for large space structures. Volume 2: The LQG/LTR methodology for the discrete-time system and the design of reduced order robust digital controller for orbiting flexible shallow spherical shell system
| AD-A260793 | p 2599 N93-25693
HUGHES AIRCRAFT CO., CULVER CITY, CA.
Advanced data visualization and sensor fusion: Conversion of techniques from medical imaging to Earth science p 2880 N93-25810
HUGHES AIRCRAFT CO., FULLERTON, CA.
Step stress testing of receiver/transmitter units
| AD-A261286 | p 2730 N93-26279
HUGHES AIRCRAFT CO., LOS ANGELES, CA.
Systems engineering for very large systems p 2665 N93-24680
HUGHES AIRCRAFT CO., TORRANCE, CA.
RF vacuum microelectronics
| AD-A261343 | p 2691 N93-26311
HUGHES DANBURY OPTICAL SYSTEMS, INC., CT.
Star tracker operation in a high density proton field p 2600 N93-24699
Optimizing the fine lock performance of the Hubble Space Telescope fine guidance sensors p 2604 N93-24723
The Hubble Space Telescope fine guidance system operating in the coarse track pointing control mode p 2605 N93-24724
HUGHES STX, INC., LANHAM, MD.
Lossless compression of image data products on th e FIFE CD-ROM series p 2804 N93-25929
HUNTER COLL., NEW YORK, NY.
NMR studies of ion mobility and association in polyether-based polymer electrolytes
| AD-A260662 | p 2655 N93-25642
Deuteron and oxygen-17 NMR studies of molecular motion in methanol-saturated Nafion membranes
| AD-A261579 | p 2851 N93-26514

I

IDAHO NATIONAL ENGINEERING LAB., IDAHO FALLS.
Near Earth object fuels (neo-fuels): Discovery, prospecting and use
| DE93-005185 | p 2892 N93-25164
INEL spray-forming research p 2658 N93-25562
ILLINOIS INST. OF TECH., CHICAGO.
A study of mass size distributions and particle deposition velocities in ambient air p 2763 N93-25263
ILLINOIS STATE WATER SURVEY, CHAMPAIGN.
Rainfall frequency atlas of the Midwest
| PB93-164606 | p 2785 N93-25872
ILLINOIS UNIV., CHICAGO.
Dynamics of deformable multibody systems using recursive projection methods
| AD-A260698 | p 2728 N93-25842
PDE: Differential, geometric and algebraic methods in nonlinear filtering
| AD-A260967 | p 2829 N93-26222
Study of surface behavior in function of temperature of the quaternary system (Hg, Cd, Zn)Te
| AD-A260968 | p 2867 N93-26223
ILLINOIS UNIV., URBANA.
Continuum and micromechanics treatment of constraint in fracture
| AD-A260927 | p 2727 N93-25647
An interactive environment for the analysis of large Earth observation and model data sets p 2878 N93-25793
A distributed analysis and visualization system for model and observational data p 2881 N93-25814
Applications of parallel and vector algorithms in nonlinear structural dynamics using the finite element method
| AD-A260716 | p 2811 N93-25845
Thermal radiation in non-metalized solid rocket motors: Effect on burning rate and temperature sensitivity p 2626 N93-26020
J and CTOD estimation equations for shallow cracks in single edge notch bend specimens
| AD-A261679 | p 2731 N93-26390
Approximate techniques for predicting size effects on cleavage fracture toughness (J(sub c))
| AD-A261591 | p 2731 N93-26516
ILLINOIS UNIV., URBANA-CHAMPAIGN.
Ignition and combustion of lunar propellants
| NASA-CR-192814 | p 2659 N93-24745
Analysis of large system black box verification test data
| NASA-CR-192885 | p 2815 N93-24748
Optimal message log reclamation for independent checkpointing
| NASA-CR-192886 | p 2815 N93-24749
Some new results for solving linear systems arising from computational fluid dynamics problems p 2699 N93-25349
An experimental and analytical study of the unsteady combustion of homogeneous energetic solids using the laser-recoil method p 2630 N93-26042
Dynamic burning rate measurements of metalized composite propellants using the laser-recoil technique p 2631 N93-26043
ILLINOIS UNIV. AT URBANA-CHAMPAIGN, SAVOY.
Optimal cooperative power-limited rendezvous p 2607 N93-24904
Propagation of radiation in astrophysical media: Gravitational lenses and astrophysical masers p 2892 N93-24949
Concurrency control in real-time database systems p 2874 N93-25271
Optimal finite-thrust time-bounded direct-ascent interception p 2607 N93-25272
Consequences of spontaneous and anomalous symmetry breaking for the orbital and mass flow hydrodynamics of He-3 - A p 2698 N93-25295
Electron-beam-pumped recombination lasers p 2712 N93-25344
Experimental and theoretical study of cw HF chemical laser overtone performance p 2713 N93-25420
Laser initiated corrosion pits on aluminum p 2650 N93-25464
Modelling of microgravity ignition phenomena p 2664 N93-25465
Asymptotic studies of gravity-driven reacting coating flows and pultrusion processes p 2704 N93-25683
Transmission electron microscopy investigation of ion implantation damage in GaAs and other semiconductors p 2865 N93-25715
Experimental and theoretical study of CW HF chemical laser residual fundamental gain p 2714 N93-25721
INDIANA UNIV., BLOOMINGTON.
A convergent finite difference scheme for the Navier-Stokes equations of nonisentropic compressible fluid flow p 2695 N93-24906
INDUSTRIAL TECHNOLOGY INST., ANN ARBOR, MI.
Application of an on-machine gage for diameter measurements p 2711 N93-25578
INSTITUTE FOR COMPUTER APPLICATIONS IN SCIENCE AND ENGINEERING, HAMPTON, VA.
A contribution to the great Riemann solver debate
| NASA-CR-191409 | p 2575 N93-25083
Current research activities: Applied and numerical mathematics, fluid mechanics, experiments in transition and turbulence and aerodynamics, and computer science
| NASA-CR-191408 | p 2803 N93-25084
Instability of flow in a streamwise corner
| NASA-CR-191410 | p 2576 N93-25153
INSTITUTE FOR DEFENSE ANALYSES, ALEXANDRIA, VA.
Fidelity and validity in distributed interactive simulation: Questions and answers
| AD-A260971 | p 2810 N93-25711
FY92 contributions to the Database Management System Interface Standards Working Group of the Navy Next Generation Computer Resources Program
| AD-A261348 | p 2883 N93-26313
Software testing initiative for strategic defense systems
| AD-A261350 | p 2831 N93-26330
CALS-HSC data element dictionary
| AD-A261560 | p 2813 N93-26461
INSTITUTE FOR SPACE AND TERRESTRIAL SCIENCE, YORK (ONTARIO).
Parametric motion control of robotic arms: A biologically based approach using neural networks p 2822 N93-25964
INSTITUTE OF GEODESY AND CARTOGRAPHY, WARSAW (POLAND).
Application of remote sensing to environmental monitoring in Poland p 2739 N93-24786
INSTITUTE OF METEOROLOGY AND HYDROLOGY, BUCHAREST (ROMANIA).
Monitoring and evaluation of morphohydrographical changes in the Danube Delta by remote-sensing p 2747 N93-24834
INSTITUTE OF TERRESTRIAL ECOLOGY, BANGOR (WALES).
European applications of space-borne Earth observation for land cover mapping p 2745 N93-24820
INSTITUTO DE PESQUISAS ESPACIAIS, SAO JOSE DOS CAMPOS (BRAZIL).
World Forest Watch: A global forest monitoring test p 2748 N93-24836
INTEGRATED SYSTEMS, INC., SANTA CLARA, CA.
Adaptive control of nonlinear flexible systems
| AD-A261676 | p 2826 N93-26365
INTERNATIONAL COUNCIL FOR THE EXPLORATION OF THE SEA, COPENHAGEN (DENMARK).
Data archaeology at ICES p 2734 N93-24931
INTERNATIONAL INST. FOR AEROSPACE SURVEY AND EARTH SCIENCES, ENSCHEDE (NETHERLANDS).
A method for sequential image analysis of hazard areas p 2743 N93-24810
INTERNATIONAL PROTECTION CONSULTANTS PROPRIETARY LTD., HOBART (AUSTRALIA).
Comparative performance of lightning air terminals under natural storm conditions p 2781 N93-24902
INTERNATIONAL TRADE ADMINISTRATION, WASHINGTON, DC.
Photographic industry and electronic imaging: The emergence of electronic still photography
| PB93-169399 | p 2711 N93-26324
IOWA STATE UNIV. OF SCIENCE AND TECHNOLOGY, AMES.
Novel approaches to the construction of miniaturized analytical instrumentation
| NASA-CR-191988 | p 2709 N93-25345
Kelvin waves in total column ozone
| NASA-CR-192984 | p 2764 N93-25431
Rossby-gravity waves in tropical total ozone data
| NASA-CR-192983 | p 2764 N93-25432
Investigation of corrosion in aluminum/adhesive lap-splices using pulse-echo ultrasonic techniques
| DE93-008074 | p 2721 N93-25518
Trajectory optimization for the National aerospace plane
| NASA-CR-192954 | p 2589 N93-25670

A virtual environment for manufacturing systems
[AD-A260813] p 2810 N93-25699
Investigation of liquid sloshing in spin-stabilized satellites
[AD-A261671] p 2619 N93-26438

ISOGEN RADIOISOTOPIC RESEARCH LAB., OREGON CITY, OR.
Solid-state isotopic power source for computer memory chips p 2694 N93-25596

ISTITUTO ELETTROTECNICO NAZIONALE (GALILEO FERRARIS), TURIN (ITLAY).
Solid state frequency synthesis up to 600 GHz: An application to the Mg frequency standard p 2842 N93-25058

ISX CORP., WESTLAKE VILLAGE, CA.
Knowledge-based decision support for Space Station assembly sequence planning
[NASA-CR-193048] p 2599 N93-26095

ITALIAN SPACE AGENCY, ROME.
A prototype system for forest fire prevention and control p 2749 N93-24844

ITERATED SYSTEMS, INC., NORCROSS, GA.
Fractal image compression: A resolution independent representation for imagery p 2804 N93-25927

J

JAMIESON SCIENCE AND ENGINEERING, INC., SCOTTS VALLEY, CA.
An atlas of selected calibrated stellar spectra
[NASA-CR-177604] p 2888 N93-25135

JAPAN FISHERIES INFORMATION SERVICE CENTER, TOKYO.
Application of satellite imageries data to fisheries in Japan p 2745 N93-24822

JET PROPULSION LAB., CALIFORNIA INST. OF TECH., PASADENA.
The Telecommunications and Data Acquisition Report
[NASA-CR-192887] p 2671 N93-24659
Feasibility study of a Ka-/Ka-band dichroic plate with stepped rectangular apertures p 2671 N93-24660
A technique for computation of noise temperature due to a beam waveguide shroud p 2671 N93-24661
Soft decoding a self-dual (48, 24; 12) code p 2671 N93-24662
A (72, 36; 15) box code p 2671 N93-24663
The analysis of convolutional codes via the extended Smith algorithm p 2671 N93-24664
Image coding by way of wavelets p 2671 N93-24665
Failure monitoring in dynamic systems: Model construction without fault training data p 2672 N93-24666
A functional description of the Buffered Telemetry Demodulator (BTD) p 2614 N93-24667
Symbol signal-to-noise ratio loss in square-wave subcarrier downconversion p 2672 N93-24668
Design of the reduced LQG compensator for the DSS-13 antenna p 2672 N93-24669
Performance results of a 300-degree linear phase modulator for spaceborne communications applications p 2672 N93-24670
Management of space networks p 2672 N93-24671
TDRSS orbit determination using short baseline differenced carrier phase p 2601 N93-24701
Application of GPS tracking techniques to orbit determination for TDRS p 2601 N93-24702
Satellite monitoring of the global ocean surface during 1987-1989 p 2734 N93-24926
Microwave frequency discriminator with a cryogenic sapphire resonator for ultra-low phase noise p 2693 N93-24982
An investigation of the degradation of Fluorinated Ethylene Propylene (FEP) copolymer thermal blanketing materials aboard LDEF in the laboratory
[NASA-CR-192824] p 2653 N93-25078
Stationary plasma thruster evaluation in Russia
[NASA-CR-192823] p 2859 N93-25206
Geographic information system for fusion and analysis of high-resolution remote sensing and ground truth data p 2878 N93-25798
Knowledge-based assistance for science visualization and analysis using large distributed databases p 2879 N93-25801
A distributed system for visualizing and analyzing multivariate and multidisciplinary data p 2880 N93-25804
Multi-layer holographic bifurcative neural network system for real-time adaptive EOS data analysis p 2880 N93-25807
Pseudomonas screening assay
[NASA-CASE-NPO-17653-1-CU] p 2793 N93-25994
Hybrid rocket fuel combustion study p 2626 N93-26019
The Telecommunications and Data Acquisition Report
[NASA-CR-192804] p 2676 N93-26105
A determination of the radio-planetary frame tie from comparison of Earth orientation parameters p 2676 N93-26106
Occultation of a compact radio source by Venus p 2676 N93-26107
A nanoradian differential VLBI tracking demonstration p 2677 N93-26108
Deep-space navigation with differenced data types. Part 3: An expanded information content and sensitivity analysis p 2614 N93-26109
Orbiter-orbiter and orbiter-lander tracking using same-beam interferometry p 2677 N93-26110
Geometric distortion analysis of a wide-field astrograph p 2621 N93-26111
Applications of inertial-sensor high-inheritance instruments to DSN precision antenna pointing p 2621 N93-26112
Performance of a 12-GHz fiber-optic system for beam-waveguide antenna stability testing p 2677 N93-26113
Improvements in X-band transmitter phase stability through Klystron body temperature regulation p 2678 N93-26114
Noise-optimal control of HEMT LNA's for compensation of temperature deviations p 2678 N93-26115
Figure of merit for direct-detection optical channels p 2678 N93-26117
Optimizing the G/T ratio of the DSS-13 34-meter beam-waveguide antenna p 2678 N93-26118
Dynamic modeling of fluid transmission lines of the DSN 70-meter antennas by using a lumped parameter model p 2678 N93-26119
Bandwidth compression of noisy signals with square-wave subcarrier p 2678 N93-26120
An OSI architecture for the Deep Space Network p 2679 N93-26121
DSS-13 26-meter antenna upgraded radiometer system p 2679 N93-26122
Sequential design of a linear quadratic controller for the Deep Space Network antennas p 2679 N93-26123
DSN acquisition of Magellan high-rate telemetry data p 2614 N93-26124
Galileo early cruise, including Venus, First Earth, and Gaspra encounters p 2599 N93-26125
Deep Space Network information system architecture study p 2679 N93-26126
Generalized probability model for calculation of interference to the Deep Space Network due to circularly Earth-orbiting satellites p 2679 N93-26127
Ka-band feed arrays for spacecraft reflector antennas with limited scan capability: An overview p 2680 N93-26128
DSN observations of Titan p 2680 N93-26129
Goldstone solar system radar signal processing p 2680 N93-26130
V-GRAM: Magellan bulletin about Venus and the radar mapping mission
[NASA-CR-192923] p 2898 N93-26424
Proceedings of the 16th NASA Propagation Experimenters Meeting (NAPEX 16) and the Advanced Communications Technology Satellite (ACTS) Propagation Studies Miniworkshop
[NASA-CR-192800] p 2682 N93-26463
Opening remarks p 2682 N93-26464
The ACTS propagation program p 2683 N93-26465
A database for propagation models p 2684 N93-26472
Rain compensation algorithm using adaptive linear prediction p 2685 N93-26485
Revealing the face of Venus: Magellan
[NASA-CR-192922] p 2898 N93-26517

JJM SYSTEMS, INC., IVYLAND, PA.
An expert system shell for inferring vegetation characteristics: Inrerface for the addition of techniques (Task H)
[NASA-CR-192897] p 2754 N93-25154

JOHNS HOPKINS UNIV., BALTIMORE, MD.
Complexity of connectionist and constraint-satisfaction networks
[AD-A261617] p 2817 N93-26169
Theoretical treatment of spin-forbidden and electronically nonadiabatic processes. Methods and applications
[AD-A261596] p 2851 N93-26525

JOHNS HOPKINS UNIV., COLUMBIA, MD.
The 29th JANNAF Combustion Subcommittee Meeting, volume 2
[CPIA-PUBL-593-VOL-2] p 2624 N93-26005

JOHNS HOPKINS UNIV., LAUREL, MD.
Attitude analysis in Flatland: The plane truth p 2603 N93-24712
Quartz oscillators, frequency synthesizers, and timing systems for geodesy and radio science applications p 2693 N93-25052
Automated system for early breast cancer detection in mammograms p 2796 N93-25568
The design of mechanically compatible fasteners for human mandible reconstruction p 2796 N93-25569
A novel method for characterization of superconductors: Physical measurements and modeling of thin films p 2871 N93-25584
Automatic detection of seizures with applications p 2796 N93-25592
A novel optical/digital processing system for pattern recognition p 2814 N93-25603
Control of complex dynamic systems by neural networks p 2827 N93-25611
The StarView intelligent query mechanism p 2826 N93-25984
Rain rate and modeled fade distributions at 20 GHz and 30 GHz derived from five years of network rain gauge measurements p 2683 N93-26468
A comparative assessment of R. M. Young and tipping bucket rain gauges p 2685 N93-26483

JOINT PUBLICATIONS RESEARCH SERVICE, ARLINGTON, VA.
JPRS report: Science and technology. Central Eurasia: Earth sciences
[JPRS-UES-92-003] p 2737 N93-25398
JPRS report: Science and technology. Central Eurasia: Life sciences
[JPRS-ULS-93-002] p 2737 N93-25399
JPRS report: Science and technology. Central Eurasia: Earth sciences
[JPRS-UES-93-001] p 2599 N93-25400
JPRS report: Science and technology. Central Eurasia: Earth sciences
[JPRS-UES-92-005] p 2737 N93-25401
JPRS report: Science and technology. Central Eurasia: Physics and mathematics
[JPRS-UPM-92-004] p 2844 N93-25402
JPRS report: Science and technology. Central Eurasia: Physics and mathematics
[JPRS-UPM-92-003] p 2844 N93-25403
JPRS report: Science and technology. Central Eurasia: Physics and mathematics
[JPRS-UPM-93-001] p 2844 N93-25404
JPRS report: Science and technology. Central Eurasia: Life sciences
[JPRS-ULS-92-025] p 2793 N93-25405
JPRS report: Science and technology. Central Eurasia: Life sciences
[JPRS-ULS-92-020] p 2793 N93-25406
JPRS report: Science and technology. Central Eurasia: Life sciences
[JPRS-ULS-92-022] p 2795 N93-25407
JPRS report: Science and technology. Japan. 30th National Aerospace Laboratory Conference
[JPRS-JST-93-009] p 2901 N93-25418
JPRS report: Science and technology. Central Eurasia: Earth sciences
[JPRS-UES-92-002] p 2737 N93-25426
JPRS report: Science and technology. Central Eurasia: Engineering and equipment
[JPRS-UEQ-92-003] p 2668 N93-25427

JOINT PUBLICATIONS RESEARCH SERVICE, WASHINGTON, DC.
JPRS report: Central Eurasia. Aviation and cosmonautics, no. 9, September 1992
[JPRS-UAC-93-003] p 2574 N93-26325

JOINT RESEARCH CENTRE OF THE EUROPEAN COMMUNITIES, ISPRA (ITALY).
Remote sensing applied to agriculture state of the art and new trends p 2745 N93-24818
Appliction of remote sensing to forestry mapping: Experience from the European collaborative programme for the less favoured areas p 2751 N93-24857

K

KANSAS UNIV., LAWRENCE.
General aviation aircraft: Normal acceleration data analysis and collection project
[DOT/FAA/CT-91/20] p 2586 N93-24739
Radar backscatter measurements from Arctic sea ice during the fall freeze-up
[NASA-CR-193100] p 2790 N93-26050

KAYSER THREDE G.M.B.H., MUNICH (GERMANY).
An experimental health monitoring unit for GPS and GLONASS p 2586 N93-25018
First experience with the ASN-16 GLONASS receiver p 2693 N93-25033

KENTUCKY UNIV., LEXINGTON.
Adaptive decision support systems: Concepts, characterization, and an application p 2876 N93-25475

KNOWLEDGE BASED SYSTEMS, INC. COLLEGE STATION, TX.
Design Knowledge Management System (DKMS) Beta Test Report
| AD-A261453 | p 2883 N93-26350
KOPIN CORP., TAUNTON, MA.
Smart microsensors for high temperature applications
| AD-A260747 | p 2710 N93-25677
KTECH CORP., LEXINGTON PARK, MD.
An integrated approach to 300 kV electrostatic discharge application during component testing that will satisfy MIL-STD-331B Appendix F p 2693 N93-24882
KULITE SEMI-CONDUCTOR PRODUCTS, INC., LEONIA, NJ.
SiC microsensor with piezoresistive diamond sensing elements
| AD-A261346 | p 2868 N93-26312
KVARZ, NISHNIJ NOVGOROD (RUSSIA).
Investigations of the frequency instability of CH1-75 hydrogen masers p 2716 N93-25049

L

LABORATOIRE DE L'HORLOGE ATOMIQUE, ORSAY (FRANCE).
Miniature optically-pumped cesium beam resonator p 2833 N93-24990
Actual limits of fluorescence S/N ratio in an optically-pumped cesium beam resonator p 2833 N93-24991
Microwave interrogation frequency noise and clock frequency stability: Experimental results p 2842 N93-25056
LABORATOIRE PRIMAIRE DU TEMPS ET DES FREQUENCES, PARIS (FRANCE).
A simple and compact source of cold atoms for cesium fountains and microgravity clocks p 2831 N93-24981
Preliminary results on an optically-pumped Cs beam frequency standard p 2832 N93-24989
LAGOS UNIV. (NIGERIA).
Ocean climate data for user community in West and Central Africa: Needs, opportunities, and challenges p 2735 N93-24933
LAWRENCE LIVERMORE NATIONAL LAB., CA.
Crossing the frontier between publishing and information service
| DE93-002894 | p 2873 N93-24677
Notes on radial drift for dalitz detection
| DE93-006971 | p 2846 N93-24959
Selected results from LLNL-Hughes RAR for West Coast Scotland Experiment 1991
| DE93-006972 | p 2788 N93-24960
A compact and versatile pulse generation and shaping subsystem for high energy laser systems
| DE93-007114 | p 2711 N93-24961
Energy and Technology Review, August-September 1992
| DE93-005882 | p 2901 N93-24974
The AFTAC model integration project
| DE93-003334 | p 2761 N93-25122
The effects of sampling frequency on the climate statistics of the ECMWF general circulation model
| DE93-003338 | p 2761 N93-25145
Global warming potential for CF4
| DE93-005740 | p 2762 N93-25146
A correlated K-distribution model of the heating rates for H2O and a molecular mixture in the 0-2500 cm(exp -1) wavelength region in the atmosphere between 0 and 60 km
| DE93-005741 | p 2762 N93-25147
Energy and Technology Review, October - December 1992
| DE93-007784 | p 2674 N93-25299
Proceedings of the Second SISAL Users' Conference
| DE93-008019 | p 2815 N93-25304
Handbook of actuators and edge alignment sensors
| NASA-CR-193203 | p 2620 N93-25317
A distributed heterogeneous client-server environment
| DE93-007496 | p 2875 N93-25319
Development of laser guide stars and adaptive optics for large astronomical telescopes
| DE93-007511 | p 2888 N93-25320
Radiation-induced disordering and defect production in CuAu and NiAl studied by molecular dynamics simulation
| DE93-007506 | p 2649 N93-25336
Progress in imaging microscopy with x ray lasers at LLNL
| DE93-007508 | p 2712 N93-25363
Transverse instabilities in a relativistic klystron two-beam accelerator
| DE93-007110 | p 2852 N93-25375
Sputter deposition of yttrium-oxides
| DE93-007499 | p 2654 N93-25382
Processing and mechanical properties of laminated metal composites of Al/Al-25 vol. percent SiC and ultrahigh carbon steel/brass
| DE93-007504 | p 2635 N93-25383
Correlation of damage threshold and surface geometry of nodular defects in HR coatings as determined by in-situ atomic force microscopy
| DE93-007509 | p 2654 N93-25384
Application of non-thermal plasmas to pollution control
| DE93-007515 | p 2763 N93-25385
BBU code development for high-power microwave generators
| DE93-007111 | p 2688 N93-25397
Experimental modal survey of the probe mass mock-up
| DE93-008846 | p 2617 N93-25494
High speed x ray gating cameras for ICF imaging applications
| DE93-007500 | p 2709 N93-25515
Analysis of shaped charge jet penetration experiments with Pen
| UCRL-LR-110773 | p 2730 N93-26177
Algorithms for the analysis of penetration by shaped charge jets
| UCRL-LR-109887 | p 2730 N93-26178
Engineering: Research development and technology
| UCRL-53868-91 | p 2917 N93-26326
Feasibility experiment for sodium-layer laser guide stars at the Lawrence Livermore National Laboratory
| DE93-007115 | p 2715 N93-26503
Behavior of a steel-liner-and-bolts system under very high thermal and mechanical loading: The CONVEX Liner Add-On to DIAMOND FORTUNE
| DE93-007512 | p 2731 N93-26507
Modeling of electric-field enhancement at nodular defects in dielectric mirror coatings
| DE93-007513 | p 2857 N93-26593
Laser damage to production- and research-grade KDP crystals
| DE93-007517 | p 2870 N93-26594
LEEDS UNIV. (ENGLAND).
Comparison of GLONASS and GPS time transfers p 2836 N93-25017
Collaboration in the UK on time transfer using the GLONASS system p 2837 N93-25019
LEHIGH UNIV., BETHLEHEM, PA.
Quantum conductance fluctuations in self-aligned, pinch-narrowed MOSFETs p 2863 N93-25265
LETOURNEAU COLL., LONGVIEW, TX.
Data analysis and interpretation of lunar dust exosphere p 2898 N93-26059
LIEGE UNIV. (BELGIUM).
Fatigue resistance of orthotropic plates with trapezoidal stiffeners
| TRL-TRANS-T3908 | p 2726 N93-25419
LIFE SYSTEMS, INC., CLEVELAND, OH.
Integrated oxygen recovery system
| NASA-CR-192982 | p 2801 N93-26088
LIGHTNING LOCATION AND PROTECTION, INC., TUCSON, AZ.
A single-point warning system for thunderstorms and electric fields p 2711 N93-24900
LIGHTNING TECHNOLOGIES, INC., PITTSFIELD, MA.
Lightning phenomenology bases for full threat return stroke occurrence following extended leader sweep at flight altitudes p 2780 N93-24895
LISBON UNIV. (PORTUGAL).
Supporting the Portuguese fisheries with satellites p 2745 N93-24821
The use of remotely sensed data for operational fisheries oceanography p 2734 N93-24927
LITTLE (ARTHUR D.), INC., CAMBRIDGE, MA.
Weather forecasting expert system study
| NASA-CR-192929 | p 2777 N93-24747
Improved selective catalytic NOx control technology for compressor station reciprocating engines
| PB93-158566 | p 2768 N93-26529
LOCKHEED ENGINEERING AND SCIENCES CO., HOUSTON, TX.
STS-39 Space Shuttle mission report
| NASA-CR-193063 | p 2611 N93-25955
STS-37 Space Shuttle mission report
| NASA-CR-193062 | p 2612 N93-25956
STS-43 Space Shuttle mission report
| NASA-CR-193064 | p 2612 N93-25957
STS-40 Space Shuttle mission report
| NASA-TM-108737 | p 2612 N93-25958
STS-45 Space Shuttle mission report
| NASA-CR-193054 | p 2612 N93-25959
STS-47 Space Shuttle mission report
| NASA-CR-193056 | p 2612 N93-25960
STS-44 Space Shuttle mission report
| NASA-TM-108735 | p 2612 N93-25988
STS-42 Space Shuttle mission report
| NASA-CR-193059 | p 2613 N93-25989
STS-48 Space Shuttle mission report
| NASA-CR-193060 | p 2613 N93-25990
STS-46 Space Shuttle mission report
| NASA-CR-193058 | p 2613 N93-25991
STS-50 Space Shuttle mission report
| NASA-CR-193057 | p 2613 N93-25992
STS-52 Space Shuttle mission report
| NASA-CR-193061 | p 2613 N93-25993
Assured crew return vehicle man-systems integration standards
| NASA-CR-193065 | p 2614 N93-26329
LOCKHEED ENGINEERING AND SCIENCES CO., WASHINGTON, DC.
Digest of Russian Space Life Sciences, issue 33
| NASA-CR-3922(39) | p 2792 N93-25195
LOCKHEED-GEORGIA CO., MARIETTA.
Optimization in the systems engineering process p 2666 N93-24691
LOCKHEED MISSILES AND SPACE CO., PALO ALTO, CA.
ROSAT investigation of flaring and activity on Prox Cen
| NASA-CR-192972 | p 2891 N93-26139
Imaging the magnetosphere in the extreme ultraviolet
| NASA-CR-192218 | p 2775 N93-26151
LOCKHEED MISSILES AND SPACE CO., SUNNYVALE, CA.
Space life support technology applications to terrestrial environmental problems p 2803 N93-25617
LOCKHEED TECHNICAL OPERATIONS CO., CROFTON, MD.
Analysis of the Command and Control Segment (CCS) attitude estimation algorithm p 2604 N93-24722
SCATHA mission termination report p 2605 N93-24725
LOGISTICS MANAGEMENT INST., BETHESDA, MD.
Estimating spares requirements for Space Station Freedom using the M-SPARE model
| AD-A260878 | p 2617 N93-25630
LOS ALAMOS NATIONAL LAB., NM.
Health and environmental chemistry: Analytical techniques, data management, and quality assurance
| DE93-002853 | p 2760 N93-24674
Seismic buckling capacity of unstiffened, free-standing steel containments
| DE93-005325 | p 2723 N93-24957
Surface discharge photoinitiation of pulsed chemical lasers
| DE93-006337 | p 2712 N93-24967
Analysis of LARI sensor system
| DE93-006334 | p 2761 N93-24977
Pressure dependence of conductivity
| DE93-008466 | p 2687 N93-25113
Implementation of the Turn Function Method in a three-dimensional, parallelized hydrodynamics code
| DE93-003744 | p 2696 N93-25124
Application of optical remote sensing to the study of surface fluxes related to cloud formation
| DE93-003783 | p 2781 N93-25125
Efficient inspection of network pollution data
| DE93-003810 | p 2761 N93-25126
Interferometric fiber-optic radiation sensor
| DE93-003841 | p 2852 N93-25127
Laser desorption in an ion trap mass spectrometer
| DE93-007330 | p 2712 N93-25150
Asymptotic derivation of the simplified P(sub N) equations
| DE93-007342 | p 2828 N93-25151
Supercomputer Debugging Workshop 1992
| DE93-007322 | p 2805 N93-25165
Applications of wavelet-based compression to multidimensional earth science data
| DE93-007348 | p 2762 N93-25166
Modeling of plasma flow switches at low, intermediate and high energies
| DE93-007359 | p 2858 N93-25167
The ALEXIS data processing package: An update
| DE93-007374 | p 2899 N93-25185
Biomagnetic localization from transient quasi-static events
| DE93-007328 | p 2794 N93-25186
Summary of progress in inertial confinement fusion
| DE93-007350 | p 2858 N93-25187
Prototype PC user interface
| DE93-008008 | p 2809 N93-25303
Poly-coil design for a 60 tesla quasi-stationary magnet
| DE93-007353 | p 2688 N93-25313
Log-ratio signal-processing technique for beam position monitors
| DE93-007356 | p 2851 N93-25314
PCG: A software package for the iterative solution of linear systems on scalar, vector and parallel computers
| DE93-007366 | p 2809 N93-25315
Structured adaptive mesh refinement on the connection machine
| DE93-007368 | p 2816 N93-25316

Former Soviet Republic capabilities in space and science
| DE93-007613 | p 2598 N93-25322
Mercury: The Los Alamos ICF KrF laser system
| DE93-007363 | p 2713 N93-25379
High-energy pion-nucleus scattering at LAMPF
| DE93-007364 | p 2852 N93-25380
Simultaneous determination of gain parameters in steady state lasers
| DE93-007389 | p 2713 N93-25381
Malone refrigeration
| DE93-005439 | p 2668 N93-25447
Wavelet transform-vector quantization compression of supercomputer ocean model simulation output
| DE93-005453 | p 2876 N93-25448
A model for the filling of cold cavities with solidifying, semi-crystalline polymers
| DE93-003817 | p 2655 N93-25507
The acute inhalation toxicity of pyrolysis products of halon 1301
| AD-A260874 | p 2795 N93-25629
The state of computing at Los Alamos National Laboratory, FY 1991
| LA-12326-MS | p 2811 N93-25943
DSD Technology: A detonation reactive Huygens code
| LA-12235-MS | p 2706 N93-25987
Chemistry during the induction time in heated nitramines p 2629 N93-26035
Molecular composition, structure, and sensitivity of explosives
| DE93-003850 | p 2662 N93-26493
Temperature dependence of radiation damage and its annealing in silicon detectors
| DE93-003854 | p 2869 N93-26494
Computational modeling of MAGO and other magnetized target fusion concepts
| DE93-007354 | p 2861 N93-26504
Spectroscopic effects of disorder and vibrational localization in mixed-halide metal-halide chain solids
| DE93-007361 | p 2646 N93-26505
Sensitivity of magnetic flux compression in cylindrical implosions to model parameters
| DE93-003819 | p 2861 N93-26512
Preliminary investigation of power flow and electrode phenomena in a multi-megawatt coaxial plasma thruster
| NASA-CR-191084 | p 2633 N93-26555
Treatment of hazardous organic wastes using silent discharge plasmas
| DE93-003789 | p 2768 N93-26592

LOUGHBOROUGH UNIV. OF TECHNOLOGY (ENGLAND).
Laser welding of selected aerospace alloys p 2718 N93-25435

LOUISIANA STATE UNIV., BATON ROUGE.
Detecting the scale and resolution effects in remote sensing and GIS p 2756 N93-25707

LOUISIANA TECH UNIV., RUSTON.
Utilization of the graded universal testing system to increase the efficiency for assessing aerobic and anaerobic capacity p 2794 N93-26077

LOYOLA COLL., BALTIMORE, MD.
Japanese Technology Evaluation Center Workshop on Advanced Manufacturing Technology for Polymer Composite Structures in Japan
| PB93-165249 | p 2641 N93-26589

LOYOLA UNIV., NEW ORLEANS, LA.
In search of meta-knowledge p 2826 N93-25983

LUDWIG-MAXIMILIANS-UNIV., MUNICH (GERMANY).
Use of airborne imaging spectrometry to the definition of optimised specifications for land applications with future spaceborne imaging spectrometers p 2738 N93-24776
Application of multitemporal Landsat-MSS and -TM data for the development of an inundation-risk-map p 2743 N93-24807
The use of polarimetric radar remote sensing data for application in forestry p 2749 N93-24845

M

MACAULAY-BROWN, INC., DAYTON, OH.
Inflight evaluation of an acoustic orientation instrument
| AD-A260752 | p 2591 N93-25909

MACAULAY-BROWN, INC., FAIRBORN, OH.
Development of a flight instrument package
| AD-A260830 | p 2591 N93-25783

MACDONALD, DETTWILER AND ASSOCIATES LTD., RICHMOND (BRITISH COLUMBIA).
Methods of evaluating the effects of coding on SAR data p 2804 N93-25926

MANCHESTER UNIV. (ENGLAND).
Computational modelling of 3D flow in complex ducts and passages p 2704 N93-25698
The initiation of lightning and the growth of electric fields in thunderstorms
| AD-A261455 | p 2787 N93-26352

MANUFACTURING AND TECHNOLGY CONVERSION INTERNATIONAL, INC., COLUMBIA, MD.
Production of low-cost hydrogen
| DE93-008070 | p 2643 N93-25305

MARTIN MARIETTA AEROSPACE, DENVER, CO.
NLS operations concepts: Failure modes scenario simulation model analysis
| MCR-92-5013 | p 2609 N93-26175
Task 5: Architecture sensitivity to STME performance
| MCR-92-5010 | p 2609 N93-26176
Task 2A: UNIS requirements and concepts
| MCR-92-5006-PT-A | p 2610 N93-26180
Advanced Launch System (ALS) test requirements
| MCR-91-5004 | p 2610 N93-26181
Develop margin philosophy to attain robustness
| MCR-92-5005 | p 2610 N93-26182
Task Type E report for National Launch Demonstration Center (NLDC) (Task 32)
| MCR-91-5010 | p 2610 N93-26591

MARTIN MARIETTA CORP., DENVER, CO.
National Launch System. Task 4: System architecture options analysis
| MCR-92-5011 | p 2609 N93-26098

MARTIN MARIETTA CORP., NEW ORLEANS, LA.
Liquid Rocket Booster (LRB) for the Space Transportation System (STS) Systems Study. Amendment 13: Orientation meeting
| NASA-CR-192515 | p 2614 N93-26152

MARTIN MARIETTA LABS., BALTIMORE, MD.
Development of dispersion-strengthened XD (trademark) Cu alloys for high heat-flux applications
| NASA-CR-191124 | p 2653 N93-24761

MARYLAND UNIV., CAMBRIDGE.
The JGOFS North Atlantic Bloom Experiment: An overview p 2735 N93-24934

MARYLAND UNIV., COLLEGE PARK.
Studying the kinetics of magnetization in high Tc superconductors
| NASA-CR-192916 | p 2862 N93-25108
An investigation of neutrino properties through study of the sun, supernovae, the early universe and lab data p 2898 N93-25180
Maneuvering a reentry body via magneto-gasdynamic forces p 2615 N93-25207
Winter warming from large volcanic eruptions
| NASA-CR-192848 | p 2763 N93-25244
Nonholonomic geometry, mechanics and control p 2724 N93-25270
Ion temperature measurements in the Maryland Spheromak p 2859 N93-25290
Optimal control of large space structures p 2819 N93-25343
Numerical simulation of the seasonal and interannual variability of the tropical Atlantic Ocean circulation during the 1980's p 2789 N93-25445
Optimized scramjet engine integration on a waverider airframe p 2593 N93-25480
Aeroelastic response and aeromechanical stability of helicopters with elastically coupled composite rotor blades p 2588 N93-25530
Observed annual and interannual variations in tropospheric water vapor p 2782 N93-25549
Parallel matrix computations
| AD-A260783 | p 2828 N93-25687
An experimental study of passive drag reduction in a turbulent boundary layer by a riblet surface p 2705 N93-25746
Large-eddy simulation of temporally developing boundary layers with embedded streamwise vortices p 2705 N93-25753
The Grid Analysis and Display System (GRADS): A practical tool for Earth science visualization p 2880 N93-25805
VIEWCACHE: An incremental pointer-based access method for autonomous interoperable databases p 2880 N93-25809
Techniques for designing rotorcraft control systems
| NASA-CR-192960 | p 2597 N93-26046
Architecture of autonomous systems
| NASA-CR-192974 | p 2801 N93-26047
Coordinated action in 3-D space
| AD-A261418 | p 2799 N93-26449

MARYLAND UNIV., SOLOMONS.
Inorganic nitrogen and phosphorus dynamics in the water column of the Patuxent River
| PB93-172955 | p 2767 N93-26511

MASSACHUSETTS INST. OF TECH., CAMBRIDGE.
Data management for JGOFS: Theory and design p 2735 N93-24935
Low-frequency source parameters of twelve large earthquakes
| NASA-CR-192806 | p 2771 N93-25202
Conversion of light hydrocarbon gases to metal carbides for production of liquid fuels and chemicals
| DE93-009707 | p 2644 N93-25500
Three-dimensional flow in radial turbomachinery and its impact on design
| NASA-CR-192957 | p 2593 N93-25668
Topography from shading and stereo p 2879 N93-25803
MIT Space Engineering Research Center
| NASA-CR-192879 | p 2821 N93-25833
Using input command pre-shaping to suppress multiple mode vibration p 2732 N93-25834
The MODE family of on-orbit experiments: The Middeck Active Control Experiment (MACE) p 2599 N93-25835
MIT's interferometer CST testbed p 2609 N93-25836
Theoretical study of topside ionospheric clutter
| AD-A260982 | p 2774 N93-25852
Center for intelligent control systems
| AD-A260995 | p 2821 N93-25853
Using modular neural networks with local representations to control dynamic systems
| AD-A261597 | p 2826 N93-26162
Flow control of low heat load turbine airfoils
| AD-A260941 | p 2595 N93-26219
Processing and properties of silicon carbide reinforced reaction bonded silicon nitride composites
| AD-A260570 | p 2640 N93-26236
Active stabilization of aeromechanical systems
| AD-A261366 | p 2595 N93-26335
Three-dimensional analysis and verification of fracture growth mechanisms in fiber-reinforced ceramic composites
| AD-A261483 | p 2641 N93-26355
Interferometric measurement with squeezed light
| AD-A260910 | p 2856 N93-26457

MASSACHUSETTS INST. OF TECH., LEXINGTON.
Setting values for TDWR/LLWAS 3 integration parameters
| AD-A260740 | p 2783 N93-25645

MASSACHUSETTS UNIV., AMHERST.
Design and synthesis of reactive separation systems
| DE93-008764 | p 2642 N93-25115
Intelligent, real-time problem solving, phase 3
| AD-A261441 | p 2829 N93-26345

MASSACHUSETTS UNIV., BOSTON.
Structure and star forming activities of the cold massive molecular cloud G216-2.5 p 2893 N93-25477
Shells, outflows and star formation in the giant molecular cloud Monoceros R2 p 2893 N93-25555

MASSACHUSETTS UNIV., LOWELL.
OTH-B radar system: System summary
| AD-A261727 | p 2681 N93-26247
High Frequency (HF) radiowave propagation
| AD-A261726 | p 2681 N93-26280
Digital Oblique Remote Ionospheric Sensing (DORIS) program development
| AD-A261750 | p 2776 N93-26283

MATERIALS RESEARCH LABS., ASCOT VALE (AUSTRALIA).
Membrane technology: A search for membranes for submarine atmosphere control
| AD-A260581 | p 2801 N93-25904

MAX-PLANCK-INST. FUER METEOROLOGIE, HAMBURG (GERMANY).
Inherent optical properties of lakes as measured by Landsat 5 Thematic Mapper p 2746 N93-24828

MCDONNELL-DOUGLAS SPACE SYSTEMS CO., COCOA BEACH, FL.
Test, Control and Monitor System (TCMS) operations plan
| NASA-CR-193098 | p 2873 N93-26419
Test, Control and Monitor System maintenance plan
| NASA-CR-193099 | p 2873 N93-26420

MCDONNELL-DOUGLAS SPACE SYSTEMS CO., HOUSTON, TX.
An approach for finding long period elliptical orbits for precursor SEI missions p 2604 N93-24720

MCDONNELL-DOUGLAS SPACE SYSTEMS CO., HUNTINGTON BEACH, CA.
Computationally efficient algorithms for real-time attitude estimation p 2602 N93-24709

MEMPHIS STATE UNIV., TN.
Spacelab, Spacehab, and Space Station Freedom payload interface projects p 2620 N93-26080

MERCER UNIV., MACON, GA.
Investigation into the common mode rejection ratio of the physiological signal conditioner circuit p 2794 N93-26073

MERIDIAN RESEARCH, INC., SILVER SPRING, MD.
Development of a concept for a national construction industry health and safety data base
| PB93-159325 | p 2884 N93-26568

METZ UNIV. (FRANCE).
Approximate analysis on strain rate effects and behavior of stress and strain fields at the crack tip in Mode 2 in metallic materials, appendix no. 1
| AD-A260836 | p 2728 N93-25785
Analysis of longitudinal impact on semi-infinite circular bars and tubes. Appendix no. 2
| AD-A261556 | p 2731 N93-26459

MIAMI UNIV., CORAL GABLES, FL.
Dynamics of Gulf Stream meanders and frontal eddies in the South Atlantic Bight p 2788 N93-25354

MICHIGAN STATE UNIV., EAST LANSING.
Design and validation of optimal experiments for estimating thermal properties of composite materials p 2635 N93-25541

MICHIGAN TECHNOLOGICAL UNIV., HOUGHTON.
On the stability of finite plastic deformations
| AD-A261526 | p 2730 N93-26361

MICHIGAN UNIV., ANN ARBOR.
A premixed laminar flame interacting with a vortex resulting in flame stretch and quenching p 2642 N93-24771
Feasibility study of a long duration balloon flight with NASA/GSFC and Soviet Space Agency Gamma Ray Spectrometers
| NASA-CR-192934 | p 2573 N93-25077
Correlative studies of astrophysical sources of very high and ultra high energy gamma-rays
| NASA-CR-192781 | p 2888 N93-25172
Dynamic error analysis of numerical methods for simulation of state-variable derivatives with discontinuities p 2819 N93-25278
Numerically dissipative time integration algorithms for structural dynamics p 2725 N93-25394
Optimal thrust magnitude on a singular arc in atmospheric flight p 2819 N93-25410
Liquid surface breakup of nonturbulent and turbulent liquids p 2700 N93-25473
Energy transfer properties and mechanisms
| DE93-008540 | p 2849 N93-25488
Helmeted head and neck dynamics under whole-body vibration p 2800 N93-25531
The damage, repair and design of fiber composite structural materials p 2635 N93-25532
Thermal infrared radiation transfer in the planetary boundary layer p 2772 N93-25688
Control and stabilization of nonholonomic dynamic systems p 2596 N93-25729
Transformation plasticity and fracture behavior of ceria-TZP/alumina composites p 2638 N93-25760
A basic research model of natural gas combustion in turbulent flow, phase 2
| PB93-158509 | p 2644 N93-25819
The physical properties of low surface brightness galaxies p 2895 N93-25832
Massively-parallel computational fluid dynamics
| AD-A261815 | p 2707 N93-26269
Summary report of the Defense Sciences Research Council Summer Conference
| AD-A261375 | p 2917 N93-26359
The upper atmosphere and ionosphere of Mars p 2897 N93-26393

MIDWEST RESEARCH INST., GOLDEN, CO.
Fundamental studies of defect generation in amorphous silicon alloys grown by remote plasma-enhanced chemical-vapor deposition (Remote PECVD)
| DE92-010560 | p 2862 N93-24953
New concepts for high efficiency energy conversion: The avalanche heterostructure and superlattice solar cells
| DE92-010592 | p 2758 N93-25098
Summary information and data sets for NREL's Solar Radiation Research Laboratory, 1981 - 1991
| DE93-000052 | p 2898 N93-25101
An inverted AlGaAs/GaAs patterned-Ge tunnel junction cascade concentrator solar cell
| DE93-000073 | p 2759 N93-25102
Research on stable, high-efficiency amorphous silicon multijunction modules
| DE93-000072 | p 2862 N93-25163
Non-H2Se, ultra-thin CIS devices
| DE93-000078 | p 2759 N93-25253
An advanced data-acquisition system for wind energy projects
| DE93-000079 | p 2874 N93-25254
Role of polycrystallinity in CdTe and CuInSe2 photovoltaic cells
| DE93-000045 | p 2759 N93-25504
Film fabrication technologies at NREL p 2658 N93-25563

MINISTRY OF POSTS AND TELECOMMUNICATIONS, KOBE (JAPAN).
Optical detection of laser-cooled ions in a Penning trap p 2838 N93-25031

MINISTRY OF POSTS AND TELECOMMUNICATIONS, TOKYO (JAPAN).
A system design for laser time synchronization via geodetic satellite Ajisai p 2716 N93-25005
ETS-5, ETS-6, and COMETS projects in Japan p 2683 N93-26470

MINISTRY OF THE ENVIRONMENT, OTTAWA (ONTARIO).
The Global Ocean Observing System: One perspective p 2733 N93-24920

MINNESOTA MINING AND MFG. CO., SAINT PAUL.
Optical fiber for acoustic sensor applications
| AD-A261580 | p 2857 N93-26515

MINNESOTA SUPERCOMPUTER CENTER, INC., MINNEAPOLIS.
Very high-speed report file system
| AD-A261068 | p 2817 N93-26277

MINNESOTA UNIV., MINNEAPOLIS.
Time dependent simulation of cosmic-ray shocks including Alfven transport
| NASA-CR-192931 | p 2899 N93-24752
Alfven wave transport effects in the time evolution of parallel cosmic-ray modified shocks
| NASA-CR-192932 | p 2899 N93-25161
A numerical and experimental studies of flow characteristics in centrifugal fans p 2577 N93-25339
Stabilized finite element methods for incompressible flows with emphasis on moving boundaries and interfaces p 2703 N93-25663
Flow and heat transfer experiments in the turbine airfoil/endwall region p 2704 N93-25725
Oblique MHD cosmic-ray modified shocks: Two-fluid numerical simulations
| NASA-CR-192930 | p 2900 N93-26132
Resonant tunneling through chemisorbed halogen atoms on Ag(111)
| AD-A261794 | p 2868 N93-26254
Electrochemical processing of electrically conductive polymer fibers
| AD-A261793 | p 2657 N93-26386
Halogen adlayers on Ag(111)
| AD-A261792 | p 2850 N93-26443

MISSION RESEARCH CORP., COSTA MESA, CA.
Duct protection coating concept development and test. Appendix D, volume 1: Test specimen fabrication, conditioning, and testing documentation
| AD-A261005 | p 2656 N93-25940
Duct protection coating concept development and test: Test specimen fabrication, conditioning, and testing documentation.
| AD-A261250 | p 2657 N93-26278

MISSION RESEARCH CORP., SANTA BARBARA, CA.
Statistics of sampled Rician fading
| AD-A261397 | p 2681 N93-26289

MISSISSIPPI STATE UNIV., MISSISSIPPI STATE.
Transformation of two and three-dimensional regions by elliptic systems
| NASA-CR-192955 | p 2810 N93-25669

MISSOURI UNIV., COLUMBIA.
Inelastic scattering in condensed matter with high intensity Moessbauer radiation
| DE93-008763 | p 2864 N93-25503
In situ surface studies of conversion coatings for steel and aluminum
| AD-A261016 | p 2655 N93-25861

MISSOURI UNIV., ROLLA.
Analysis of matrix damage in unidirectional composites p 2634 N93-25338
Two-dimensional fin analysis p 2705 N93-25737
New directions in phthalocyanine pigments
| NASA-CR-192443 | p 2656 N93-26155
Structure of sodium 4-(1'-heptylnonyl) benzenesulfonate adsorbed on alumina using H-2 NMR
| AD-A261224 | p 2645 N93-26300
Effects of moisture and other contaminants in friction composites
| AD-A261226 | p 2640 N93-26301

MITRE CORP., BEDFORD, MA.
Measures of user-system interface effectiveness: An encoding scheme and indicators for assessing the usability of graphical, direct-manipulation style user interfaces
| AD-A260606 | p 2801 N93-25840
Emerging large-screen display technology
| AD-A261066 | p 2681 N93-26241

MITRE CORP., MCLEAN, VA.
CHAMMP
| DE93-007290 | p 2762 N93-25184
The dependent converging instrument approach procedure: An analysis of its safety and applicability
| DOE/FAA/RD-93/6 | p 2585 N93-25456
Small satellites and RPA's in global-change research
| AD-A260762 | p 2765 N93-25837
Structural acoustics: A general form of reciprocity principles in acoustics
| AD-A261515 | p 2846 N93-26376

MOLECULAR RESEARCH INST., PALO ALTO, CA.
Theoretical calculations on the electron absorption spectra of selected Polycyclic Aromatic Hydrocarbons (PAH) and derivatives
| NASA-CR-192762 | p 2892 N93-25200

MONTEREY TECHNOLOGIES, INC., CARMEL, CA.
Autonomic physiological data associated with simulator discomfort
| NASA-CR-177609 | p 2794 N93-24738

MONTPELLIER UNIV. (FRANCE).
Crystal growth and physical characterizations of GaPO4 p 2840 N93-25044

MUSEE ROYAL DE L'AFRIQUE CENTRALE, TERVUREN (BELGIUM).
Lithologic mapping with LANDSAT Thematic Mapper guided by laboratory spectral measurements, Air, Niger (Africa) p 2742 N93-24803

MYSTECH ASSOCIATES, INC., MIDDLETOWN, RI.
System Concept of Operations Evaluator (SCOPE)
| AD-A261257 | p 2813 N93-26563

N

NANCY UNIV. (FRANCE).
Thermionic current measurement in quartz p 2840 N93-25045

NANSEN REMOTE SENSING CENTER, BERGEN (NORWAY).
NORSMAP 1989: Norwegian remote sensing spectrometry for mapping and monitoring of algal blooms and pollution p 2746 N93-24824

NAPLES UNIV. (ITALY).
Anomalous bioelectric potentials of silk trees in Naples zoo (Italy) prior to an earthquake in May, 1991 p 2753 N93-24873

NATIONAL AERONAUTICS AND SPACE ADMINISTRATION, WASHINGTON, DC.
Readings in Systems Engineering
| NASA-SP-6102 | p 2665 N93-24678
The SE role in establishing, verifying and controlling top-level program requirements p 2666 N93-24685
The importance of cost considerations in the systems engineering process p 2666 N93-24686
Systems engineering and the user: Incorporation of user requirements into the SE process p 2666 N93-24687
Systems engineering considerations for operational support systems p 2666 N93-24689
Political and institutional factors affecting systems engineering p 2666 N93-24690
The initial flight anomalies of Skylab 1 p 2619 N93-24692
Report of the Seasat Failure Review Board p 2619 N93-24693
The atmospheric effects of stratospheric aircraft. Report of the 1992 Models and Measurements Workshop. Volume 1: Workshop objectives and summary
| NASA-RP-1292-VOL-1 | p 2762 N93-25157
The atmospheric effects of stratospheric aircraft. Report of the 1992 Models and Measurements Workshop. Volume 2: Comparisons with global atmospheric measurements
| NASA-RP-1292-VOL-2 | p 2762 N93-25158
The atmospheric effects of stratospheric aircraft. Report of the 1992 Models and Measurements Workshop. Volume 3: Special diagnostic studies
| NASA-RP-1292-VOL-3 | p 2762 N93-25159
NASA Microgravity Science and Applications Program
| NASA-TM-108775 | p 2663 N93-25194
Tethered Satellite System Contingency Investigation Board
| NASA-TM-108704 | p 2616 N93-25231
Technology 2002: The Third National Technology Transfer Conference and Exposition, volume 1
| NASA-CP-3189-VOL-1 | p 2901 N93-25561
The 1993/1994 NASA Graduate Student Researchers Program
| NASA-EP-283 | p 2872 N93-26051
OSSA Information Systems Program
| NASA-TM-108774 | p 2882 N93-26231
Mars exploration planning p 2898 N93-26399
Aeronautics in NACA and NASA
| NASA-NP-156 | p 2574 N93-26422
ATMOS: Long term atmospheric measurements for mission to planet Earth
| NASA-TM-108720 | p 2757 N93-26429
OSSA Information Systems Program
| NASA-TM-108758 | p 2883 N93-26491

NATIONAL AERONAUTICS AND SPACE ADMINISTRATION. AMES RESEARCH CENTER, MOFFETT FIELD, CA.
Discrete range clustering using Monte Carlo methods
| NASA-TM-104004 | p 2584 N93-24914
Measurements of density, temperature, and their fluctuations in turbulent supersonic flow using UV laser spectroscopy
| NASA-TM-103943 | p 2708 N93-25076

Propagation velocity and space-time correlation of perturbations in turbulent channel flow
| NASA-TM-103932 | p 2695 N93-25082
A survey of life support system automation and control
| NASA-TM-103977 | p 2667 N93-25085
Applied aerodynamics: Challenges and expectations
| NASA-TM-103963 | p 2575 N93-25091
Scene segmentation of natural images using texture measures and back-propagation
| NASA-TM-104003 | p 2803 N93-25235
Space biology research development
| NASA-CR-192830 | p 2792 N93-25242
Using a Cray Y-MP as an array processor for a RISC Workstation
| NASA-TM-103961 | p 2809 N93-25246
Assessment of closure coefficients for compressible-flow turbulence models
| NASA-TM-103882 | p 2697 N93-25247
Construction of an advanced software tool for planetary atmospheric modeling p 2815 N93-25799
The effects of video compression on acceptability of images for monitoring life sciences' experiments p 2805 N93-25930
Jet-induced ground effects on a parametric flat-plate model in hover
| NASA-TM-104001 | p 2581 N93-26099
Vascular uptake of rehydration fluids in hypohydrated men at rest and exercise
| NASA-TM-103942 | p 2795 N93-26133
Automation and robotics human performance
| NASA-CR-193049 | p 2802 N93-26153
The Martian lower atmosphere p 2897 N93-26394

NATIONAL AERONAUTICS AND SPACE ADMINISTRATION. GODDARD INST. FOR SPACE STUDIES, NEW YORK, NY.

A coastal hazards data base for the US East Coast
| NASA-TM-108265 | p 2791 N93-26586

NATIONAL AERONAUTICS AND SPACE ADMINISTRATION. GODDARD SPACE FLIGHT CENTER, GREENBELT, MD.

Spacecraft systems engineering: An introduction to the process at GSFC p 2665 N93-24683
Flight Mechanics/Estimation Theory Symposium, 1992
| NASA-CP-3186 | p 2599 N93-24694
The results of the in-flight attitude sensor calibration for the Arthur Holly Compton Gamma Ray Observatory p 2600 N93-24697
Testing of the on-board attitude determination and control algorithms for SAMPEX p 2600 N93-24698
TDRSS-user orbit determination using batch least-squares and sequential methods p 2601 N93-24703
Orbit determination support of the Ocean Topography Experiment (TOPEX)/Poseidon operational orbit p 2601 N93-24704
Orbit determination and orbit control for the Earth Observing System (EOS) AM spacecraft p 2601 N93-24705
Analysis of the effects of mean local node-crossing time on the evolution of Sun-synchronous orbits p 2602 N93-24706
A ground track control algorithm for the Topographic Mapping Laser Altimeter (TMLA) p 2602 N93-24707
Polar decomposition for attitude determination from vector observations p 2602 N93-24711
Nonlinear techniques for forecasting solar activity directly from its time series p 2603 N93-24716
Analysis of reentry into the White Sands Missile Range (WSMR) for the LifeSat mission p 2603 N93-24717
Quaternion normalization in spacecraft attitude determination p 2606 N93-24730
Attitude determination using vector observations: A fast optimal matrix algorithm p 2606 N93-24731
Upper Atmosphere Research Satellite (UARS) onboard attitude determination using a Kalman filter p 2606 N93-24732
Goddard Space Flight Center (GSFC) Flight Dynamics Facility (FDF) calibration of the Upper Atmosphere Research Satellite (UARS) sensors p 2606 N93-24733
Solar array thermal snap and the characteristics of its effect on UARS p 2607 N93-24734
Upper Atmosphere Research Satellite (UARS) attitude accuracy using coarse attitude sensors p 2607 N93-24735
Proceedings of the Ocean Climate Data Workshop
| NASA-TM-108711 | p 2732 N93-24915
Computer systems p 2737 N93-24942
Empirical wind model for the middle and lower atmosphere. Part 1: Local time average
| NASA-TM-104581 | p 2770 N93-25160
Far infrared spectra of amorphous and crystalline water ice and changes in these phases as the result of proton irradiation
| NASA-CR-192849 | p 2892 N93-25230
Earth observing system. Output data products and input requirements, version 2.0. Volume 1: Instrument data product characteristics
| NASA-TM-108770 | p 2755 N93-25460
Earth observing system. Output data products and input requirements, version 2.0. Volume 2: Analysis of IDS input requirements
| NASA-TM-108771 | p 2755 N93-25461
Earth observing system. Output data products and input requirements, version 2.0. Volume 3: Algorithm summary tables and non-EOS data products
| NASA-TM-108769 | p 2756 N93-25462
The Generic Spacecraft Analyst Assistant (GenSAA): A tool for developing graphical expert systems p 2814 N93-25589
Data systems dynamic simulator p 2814 N93-25602
Firmware development improves system efficiency p 2807 N93-25606
Preliminary studies leading toward the development of a LIDAR bathymetry mapping instrument p 2711 N93-25614
Walsh function generator for the Electronically Scanned Thinned Array Radiometer (ESTAR) instrument
| NASA-TM-4449 | p 2689 N93-25618
A Spatial Analysis and Modeling System (SAMS) for environment management p 2881 N93-25813
Neutron energy determination with a high-purity germanium detector
| NASA-CR-192773 | p 2900 N93-25890
The Space and Earth Science Data Compression Workshop
| NASA-CP-3183 | p 2803 N93-25921
The implementation of a lossless data compression module in an advanced orbiting system: Analysis and development p 2804 N93-25928
The 1993 Goddard Conference on Space Applications of Artificial Intelligence
| NASA-CP-3200 | p 2822 N93-25961
Using AI/expert system technology to automate planning and replanning for the HST servicing missions p 2822 N93-25962
The probabilistic neural network architecture for high speed classification of remotely sensed imagery p 2824 N93-25972
Image analysis by integration of disparate information p 2824 N93-25973
Neural networks for atmospheric retrievals p 2824 N93-25975
Classifying multispectral data by neural networks p 2825 N93-25976
The WorkPlace distributed processing environment p 2825 N93-25977
Model-based reasoning for system and software engineering: The Knowledge From Pictures (KFP) environment p 2825 N93-25978
An application of machine learning to the organization of institutional software repositories p 2825 N93-25981
Cape Photographic Durchmusterung, volume 1
| NASA-RP-1300-VOL-1 | p 2890 N93-26002
Cape Photographic Durchmusterung, volume 2
| NASA-RP-1300-VOL-2 | p 2890 N93-26003
Cape Photographic Durchmusterung, volume 3
| NASA-RP-1300-VOL-3 | p 2890 N93-26004
Method and apparatus for deflection measurements using eddy current effects
| NASA-CASE-GSC-13506-1 | p 2710 N93-26103
Phase discriminating capacitive array sensor system
| NASA-CASE-GSC-13460-1 | p 2691 N93-26104
Automated inspection of solder joints for surface mount technology
| NASA-TM-104580 | p 2721 N93-26137
EnviroNET p 2886 N93-26398
Steady induction effects in geomagnetism. Part 1B: Geomagnetic estimation of steady surficial core motions: A non-linear inverse problem
| NASA-TP-3272-PT-1B | p 2776 N93-26421

NATIONAL AERONAUTICS AND SPACE ADMINISTRATION. HUGH L. DRYDEN FLIGHT RESEARCH FACILITY, EDWARDS, CA.

The constant current loop: A new paradigm for resistance signal conditioning
| NASA-TM-108744 | p 2673 N93-25181

NATIONAL AERONAUTICS AND SPACE ADMINISTRATION. JOHN C. STENNIS SPACE CENTER, BAY SAINT LOUIS, MS.

Commercial applications multispectral sensor system p 2758 N93-25615

NATIONAL AERONAUTICS AND SPACE ADMINISTRATION. JOHN F. KENNEDY SPACE CENTER, COCOA BEACH, FL.

Launch pad lightning protection enhancement by induced streamers p 2609 N93-24876
Applications of triggered lightning to space vehicle operations p 2619 N93-24878
TCMS operations and maintenance philosophy
| NASA-TM-108756 | p 2873 N93-26418

NATIONAL AERONAUTICS AND SPACE ADMINISTRATION. LYNDON B. JOHNSON SPACE CENTER, HOUSTON, TX.

Systems engineering and integration processes involved with manned mission operations p 2666 N93-24688
How to combine probabilistic and fuzzy uncertainties in fuzzy control
| NASA-TM-108746 | p 2818 N93-25138
How far we are from the complete knowledge: Complexity of knowledge acquisition in Dempster-Shafer approach
| NASA-CR-192944 | p 2874 N93-25139
Monte-Carlo methods make Dempster-Shafer formalism feasible
| NASA-CR-192945 | p 2828 N93-25140
Maximum entropy approach to fuzzy control
| NASA-CR-192949 | p 2818 N93-25141
How to control if even experts are not sure: Robust fuzzy control
| NASA-TM-108745 | p 2818 N93-25142
JSC research and technology
| NASA-TM-104763 | p 2901 N93-25188
Fast parallel algorithms that compute transitive closure of a fuzzy relation
| NASA-CR-192950 | p 2818 N93-25190
How to help intelligent systems with different uncertainty representations cooperate with each other
| NASA-CR-192947 | p 2818 N93-25196
Neural networks: What non-linearity to choose
| NASA-CR-192948 | p 2819 N93-25197
Strongly transitive fuzzy relations: A more adequate way to describe similarity
| NASA-CR-192951 | p 2820 N93-25425
What procedure to choose while designing a fuzzy control? Towards mathematical foundations of fuzzy control
| NASA-TM-108719 | p 2820 N93-25459
Measuring the metastatic potential of cancer cells p 2794 N93-25566
TARGET: Rapid capture of process knowledge p 2814 N93-25590
MAC to VAX connectivity: Heartrate spectral analysis system p 2796 N93-25594
The application of integrated knowledge-based systems for the Biomedical Risk Assessment Intelligent Network (BRAIN) p 2799 N93-25595
A genetic algorithm tool (splicer) for complex scheduling problems and the Space Station Freedom resupply problem p 2814 N93-25613
Evaluation of lens distortion errors in video-based motion analysis
| NASA-TP-3266 | p 2797 N93-25736
Rendezvous, proximity operations and capture quality function deployment report
| NASA-TM-108752 | p 2614 N93-25952
National Aeronautics and Space Administration (NASA)/American Society for Engineering Education (ASEE) Summer Faculty Fellowship Program, 1992, volume 1
| NASA-CR-188242-VOL-1 | p 2911 N93-26058
National Aeronautics and Space Administration (NASA)/American Society for Engineering Education (ASEE) Summer Faculty Fellowship Program, 1992, volume 2
| NASA-CR-188242-VOL-2 | p 2914 N93-26070
Evaluating science return in space exploration initiative architectures
| NASA-TP-3339 | p 2897 N93-26094

NATIONAL AERONAUTICS AND SPACE ADMINISTRATION. LANGLEY RESEARCH CENTER, HAMPTON, VA.

Systems engineering and integration and management for manned space flight programs p 2666 N93-24684
WCRP surface radiation budget shortwave data product description, version 1.1
| NASA-TM-107747 | p 2777 N93-24742
Evaluation of advanced displays for engine monitoring and control
| NASA-CR-191418 | p 2591 N93-24764
Monitoring damage growth in titanium matrix composites using acoustic emission
| NASA-TM-107742 | p 2634 N93-25072
High-order cyclo-difference techniques: An alternative to finite differences
| NASA-TM-107745 | p 2575 N93-25074
Space Station Freedom assembly and operation at a 51.6 degree inclination orbit
| NASA-TM-107731 | p 2615 N93-25174
Combined LAURA-UPS hypersonic solution procedure
| NASA-TM-107682 | p 2696 N93-25176
On the effect of acoustic coupling on random and harmonic plate vibrations
| NASA-TM-107740 | p 2844 N93-25189

Use of high performance networks and supercomputers for real-time flight simulation p 2598 N93-25574
Integration of design, thermal, structural, and optical analysis, including thermal animation p 2814 N93-25601
Instrumentation for measurement of gas permeability of polymeric membranes p 2720 N93-25609
Process for bonding elastomers to metals
| NASA-CASE-LAR-13645-1 | p 2656 N93-25995
Nozzle diffuser for use with an open test section of a wind tunnel
| NASA-CASE-LAR-14424-1-SB | p 2598 N93-25996
Polyimides with improved compression moldability
| NASA-CASE-LAR-14457-1 | p 2656 N93-25997
Helicopter low-speed yaw control
| NASA-CASE-LAR-14219-1 | p 2597 N93-25998
Polyimides containing the cyclobutene-3,4-dione moiety
| NASA-CASE-LAR-14753-1 | p 2656 N93-25999
Method of measuring cross-flow vortices by use of an array of hot-film sensors
| NASA-CASE-LAR-14824-1-SB | p 2706 N93-26000
Visualization of a Mach 2 reacting flow using Planar Laser-Induced Fluorescence (PLIF) p 2598 N93-26006
Workshop Report: A validation study of Navier-Stokes codes for transverse injection into a Mach 2 flow p 2624 N93-26008
The effect of entrance radius and film injection on wall heating in scramjet nozzles p 2625 N93-26009
Thermal coatings for titanium-aluminum alloys
| NASA-TM-107760 | p 2651 N93-26048
Experimental effects of wing location on wing-body pressures at supersonic speeds
| NASA-TM-4434 | p 2581 N93-26085
On the cross-stream spectral method for the Orr-Sommerfeld equation
| NASA-TM-107737 | p 2845 N93-26086
Piloted simulation of an air-ground profile negotiation process in a time-based Air Traffic Control environment
| NASA-TM-107748 | p 2585 N93-26087
Vacuum powder injector and method of impregnating fiber with powder
| NASA-CASE-LAR-14179-1 | p 2668 N93-26101
Methods of determining loads and fiber orientations in anisotropic non-crystalline materials using energy flux deviation
| NASA-CASE-LAR-14399-1 | p 2729 N93-26102
Conical Euler analysis and active roll suppression for unsteady vortical flows about rolling delta wings
| NASA-TP-3259 | p 2581 N93-26134
Supersonic aeroelastic instability results for a NASP-like wing model
| NASA-TM-107739 | p 2591 N93-26553

NATIONAL AERONAUTICS AND SPACE ADMINISTRATION. LEWIS RESEARCH CENTER, CLEVELAND, OH.

Ice thickness measurement system for the icing research tunnel calibration
| NASA-TM-106095 | p 2708 N93-24737
Nuclear thermal propulsion technology: Results of an interagency panel in FY 1991
| NASA-TM-105711 | p 2621 N93-24740
Summary and recommendations on nuclear electric propulsion technology for the space exploration initiative
| NASA-TM-105707 | p 2622 N93-24744
Radiation and temperature effects on electronic components investigated under the CSTI high capacity power project
| NASA-TM-106096 | p 2687 N93-24746
Global dynamic modeling of a transmission system
| NASA-CR-191117 | p 2716 N93-24751
Space exploration initiative candidate nuclear propulsion test facilities
| NASA-TM-105710 | p 2622 N93-24753
Fuel injector: Air swirl characterization aerothermal modeling, phase 2, volume 1
| NASA-CR-189193 | p 2592 N93-24754
Contributions of microgravity test results to the design of spacecraft fire safety systems
| NASA-TM-106093 | p 2614 N93-24755
Experimentation in the low-density plume of a simulated electrothermal thruster for computer code validation
| NASA-CR-191112 | p 2622 N93-24758
A three-dimensional algebraic grid generation scheme for gas turbine combustors with inclined slots
| NASA-CR-191095 | p 2694 N93-24759
A system to measure lightning-induced transients on spacecraft umbilical lines p 2693 N93-24889
Evaluation of MARC for the analysis of rotating composite blades
| NASA-TM-4423 | p 2723 N93-24909
Surface and flow field measurements in a symmetric crossing shock wave/turbulent boundary-layer interaction
| NASA-TM-106086 | p 2575 N93-24911
High Temperature Composite Analyzer (HITCAN) theoretical manual, version 1.0
| NASA-TM-106001 | p 2723 N93-24913
High temperature composite analyzer (HITCAN) user's manual, version 1.0
| NASA-TM-106002 | p 2724 N93-25070
Stress distribution in composite flatwise tension test specimens
| NASA-TM-106074 | p 2634 N93-25071
Screening studies of advanced control concepts for airbreathing engines
| NASA-TM-106042 | p 2592 N93-25079
NASA Lewis 8- by 6-foot supersonic wind tunnel user manual
| NASA-TM-105771 | p 2597 N93-25080
A neural network-based estimator for the mixture ratio of the Space Shuttle Main Engine
| NASA-TM-106070 | p 2622 N93-25089
Plasma sheath effects on ion collection by a pinhole
| NASA-TM-106098 | p 2615 N93-25090
Determination of the thermal stability of perfluoropolyalkyl ethers by tensimetry
| NASA-TM-106081 | p 2654 N93-25093
Space Nuclear Thermal Propulsion Test Facilities Subpanel
| NASA-TM-105708 | p 2622 N93-25105
Experimental performance of a ventral nozzle with pitch and yaw vectoring capability for SSTOVL aircraft
| NASA-TM-106054 | p 2592 N93-25129
Test results of a Stirling engine utilizing heat exchanger modules with an integral heat pipe
| NASA-TM-105883 | p 2759 N93-25136
Development of thin film thermocouples on ceramic materials for advanced propulsion system applications
| NASA-TM-106017 | p 2709 N93-25173
Nonlinear evolution of the first mode supersonic oblique waves in compressible boundary layers. Part 1: Heated/cooled walls
| NASA-TM-106087 | p 2696 N93-25175
Heat transfer in rotating serpentine passages with selected model orientation for smooth or skewed trip walls
| NASA-TM-106126 | p 2667 N93-25177
Atomizing-gas temperature effect on cryogenic spray dropsize
| NASA-TM-106106 | p 2709 N93-25191
Calculations of combustion response profiles and oscillations
| NASA-TM-106135 | p 2623 N93-25236
Laser ignition application in a space experiment
| NASA-TM-106133 | p 2664 N93-25337
Optical and scratch resistant properties of diamondlike carbon films deposited with single and dual ion beams p 2658 N93-25564
Properties of extruded PS-212 type self-lubricating materials p 2659 N93-25565
Graphite/epoxy composite laminates with co-cured interlaminar damping layers p 2642 N93-25587
A fiber optic probe for the detection of cataracts p 2796 N93-25593
Evaluation of a vibration diagnostic system for the detection of spur gear pitting failures
| NASA-TM-106103 | p 2718 N93-25672
Gas turbine system simulation: An object-oriented approach
| NASA-TM-106044 | p 2593 N93-25673
Subband coding for image data archiving p 2803 N93-25922
Ceramic fiber reinforced glass-ceramic matrix composite
| NASA-CASE-LEW-15262-1 | p 2640 N93-26100
Bibliography on propulsion airframe integration technologies for high-speed civil transport applications, 1980-1991
| NASA-TM-105602 | p 2573 N93-26136
The interaction of high voltage systems with the environments of the Moon and Mars
| NASA-TM-106107 | p 2618 N93-26148
Pulsed laser Rayleigh scattering diagnostic for hydrogen/oxygen rocket exit plane flowfield velocimetry
| NASA-TM-106098 | p 2631 N93-26149
Rotating rake design for unique measurement of fan-generated spinning acoustic modes
| NASA-TM-105946 | p 2595 N93-26161
Nuclear safety policy working group recommendations on nuclear propulsion safety for the space exploration initiative
| NASA-TM-105705 | p 2632 N93-26200
External stress-corrosion cracking of a 1.22-m-diameter type 316 stainless steel air valve
| NASA-TP-3190 | p 2652 N93-26201
Fabrication of composite propfan blades for a cruise missile wind tunnel model
| NASA-TM-105270 | p 2730 N93-26202
An extended Lagrangian method
| NASA-TM-106129 | p 2707 N93-26203
Vickers indentation hardness of stoichiometric and reduced single crystal TiO2 (rutile) from 25 to 800 C
| NASA-TM-105959 | p 2633 N93-26204
Design and implementation of a pilot orientation program for new NASA engineering employees
| NASA-TM-105907 | p 2872 N93-26205
Conceptual design for the Space Station Freedom fluid physics/dynamics facility
| NASA-TM-103663 | p 2618 N93-26209
Nuclear electric propulsion for planetary science missions: NASA technology program planning
| NASA-TM-106139 | p 2632 N93-26210
On-line implementation of nonlinear parameter estimation for the Space Shuttle main engine
| NASA-TM-106097 | p 2632 N93-26211
Development and use of hydrogen-air torches in an altitude facility
| NASA-TM-106047 | p 2598 N93-26214
Plasma current collection of Z-93 thermal control paint as measured in the Lewis Research Center's plasma interaction facility
| NASA-TM-106132 | p 2618 N93-26215
Electrical and Chemical Interactions at Mars Workshop. Part 2: Appendix
| NASA-CP-10093-PT-2 | p 2897 N93-26392
Representative systems for space exploration p 2897 N93-26395
Space environmental interactions for the space exploration initiative p 2897 N93-26396
Allocations by the 1992 World Administrative Radio Conference p 2684 N93-26476
OLYMPUS/ACTS scintillation experiment at the Lewis Research Center p 2685 N93-26481
The influence of primary and secondary orientations on the elastic response of a nickel-base single-crystal superalloy
| NASA-TM-106125 | p 2731 N93-26550
A large hemi-anechoic enclosure for community-compatible aeroacoustic testing of aircraft propulsion systems
| NASA-TM-106015 | p 2846 N93-26551
METal matrix composite ANalyzer (METCAN): Theoretical manual
| NASA-TM-106025 | p 2641 N93-26552
Incompressible spectral-element method: Derivation of equations
| NASA-TM-106109 | p 2708 N93-26554
A brief description of a new numerical framework for solving conservation laws: The method of space-time conservation element and solution element
| NASA-TM-105757 | p 2829 N93-26560
Measurement and analysis of a small nozzle plume in vacuum
| NASA-TM-106066 | p 2633 N93-26561

NATIONAL AERONAUTICS AND SPACE ADMINISTRATION. MARSHALL SPACE FLIGHT CENTER, HUNTSVILLE, AL.

What is a system? NASA's phased project description p 2665 N93-24681
Hydrogen masers for space p 2716 N93-24980
An in-depth probabilistic study of external tank attach ring
| NASA-TM-108403 | p 2624 N93-25671
Radial spline assembly for antifriction bearings
| NASA-CASE-MFS-28629-1 | p 2719 N93-26001
Eulerian-Eulerian treatment of turbulent dense spray combustion in a bipropellant liquid rocket engine p 2626 N93-26017
Space Science Laboratory Publications and Presentations
| NASA-TM-108402 | p 2884 N93-26562

NATIONAL AERONAUTICS AND SPACE ADMINISTRATION. PASADENA OFFICE, CA.

Pseudomonas screening assay
| NASA-CASE-NPO-17653-1-CU | p 2793 N93-25994

NATIONAL CENTER FOR ATMOSPHERIC RESEARCH, BOULDER, CO.

Interactive interface for National Center for Atmospheric Research (NCAR) Graphics p 2878 N93-25794
Synoptic and Mesoscale Meteorology Instruction Workshop
| PB93-156347 | p 2785 N93-25870
Effects of surface thermal forcing on stratified flow past an isolated obstacle
| PB93-156776 | p 2776 N93-26548
A revised and expanded catalogue of mass ejections observed by the Solar Maximum Mission coronagraph
| NASA-CR-193146 | p 2899 N93-26556

NATIONAL CENTER FOR SCIENTIFIC RESEARCH OF VIETNAM, HANOI.

Detection of land use/land cover changes using remote sensing and GIS in Vietnam p 2740 N93-24791

NATIONAL GEODETIC SURVEY, ROCKVILLE, MD.

Satellite altimetry p 2734 N93-24930

NATIONAL GEOPHYSICAL DATA CENTER, BOULDER, CO.
Solar-geophysical data number 581, January 1993. Part 1: (Prompt reports). Data for December, November 1992, and late data
|PB93-161743| p 2899 N93-26537
Solar-geophysical data number 581, January 1993. Part 2: (Comprehensive reports). Data for July 1992 and miscellaneous
|PB93-161750| p 2899 N93-26538

NATIONAL GOALS RESEARCH STAFF, WASHINGTON, DC.
Designing and implementing a state quality award
|PB93-154458| p 2722 N93-26546

NATIONAL INST. FOR FUSION SCIENCE, NAGOYA (JAPAN).
Density dependence of line intensities and application to plasma diagnostics
|NIFS-209| p 2857 N93-24950
R and D of transmission lines for ECH system
|NIFS-210| p 2687 N93-24951
Plasma heating in toroidal systems
|NIFS-208| p 2858 N93-25092
Effect of continuous eigenvalue spectrum on plasma transport in toroidal systems
|NIFS-214| p 2859 N93-25215
Some features of particle orbit behavior in LHD configurations
|NIFS-211| p 2859 N93-25216
Demonstration for novel self-organization theory by three-dimensional magnetohydrodynamic simulation
|NIFS-212| p 2859 N93-25227
Two-stream instability for a light ion beam-plasma system with external magnetic field
|NIFS-204| p 2859 N93-25248
Tracking sharp interface of two fluids by the CIP (Cubic-Interpolated Propagation) scheme
|NIFS-206| p 2698 N93-25277
Thermal and electric oscillation driven by orbit loss in helical systems
|NIFS-213| p 2860 N93-25346
A compact neutron counter telescope with thick radiator (Cotetra) for fusion experiment
|NIFS-205| p 2860 N93-25347
Simulation study of MHD dynamo: Convection in a rotating spherical shell
|NIFS-207| p 2860 N93-25356

NATIONAL INST. OF HEALTH, BETHESDA, MD.
Immunoconjugates: Magic bullets for cancer therapy? p 2796 N93-25567

NATIONAL INST. OF POLAR RESEARCH, TOKYO (JAPAN).
JARE data reports. No. 171 (upper atmosphere physics 9). Data, Syowa and Asuka Stations, 1989 p 2774 N93-25889

NATIONAL INST. OF STANDARDS AND TECHNOLOGY, BOULDER, CO.
Designing for frequency and time metrology at the 10 to the minus 18 power level p 2842 N93-25059
Tables for the thermophysical properties of ethane
|PB93-160786| p 2646 N93-26319
Liquid and solid ion plasmas
|AD-A261888| p 2862 N93-26528
Flow conditioner location effects in orifice flowmeters
|PB93-159457| p 2708 N93-26535

NATIONAL INST. OF STANDARDS AND TECHNOLOGY, GAITHERSBURG, MD.
Solidification processing and phase transformations in ordered high temperature alloys
|AD-A261751| p 2652 N93-26284
Proton Monte Carlo transport program PTRAN
|PB93-158673| p 2850 N93-26314
Monte Carlo approach to the approximation of invariant measures
|PB93-159069| p 2830 N93-26317
Guidelines for evaluating and expressing the uncertainty of NIST measurements results
|PB93-159465| p 2830 N93-26318
Synthetic-perturbation tuning of MIMD programs
|PB93-161339| p 2812 N93-26321
NIST reactor: Summary of activities, July 1991 through September 1992
|PB93-162873| p 2852 N93-26322
Phase-field models for anisotropic interfaces
|PB93-164564| p 2646 N93-26323
Electronics and Electrical Engineering Laboratory technical publication announcements covering laboratory programs, July to September 1992 with 1992/1993 EEEL events calendar
|PB93-158632| p 2884 N93-26530
Computation of complex solidification morphologies using a phase-field model
|PB93-156743| p 2869 N93-26547

NATIONAL OCEAN SERVICE, MONTEREY, CA.
OCEAN-PC and a distributed network for ocean data p 2734 N93-24928

NATIONAL OCEAN SERVICE, ROCKVILLE, MD.
Sea level variation p 2734 N93-24929

NATIONAL OCEANIC AND ATMOSPHERIC ADMINISTRATION, BOULDER, CO.
Climate Monitoring and Diagnostics Laboratory
|PB93-156388| p 2785 N93-25871

NATIONAL OCEANIC AND ATMOSPHERIC ADMINISTRATION, CAMP SPRINGS, MD.
Anomalous event diagnosis for environmental satellite systems p 2619 N93-25971

NATIONAL OCEANIC AND ATMOSPHERIC ADMINISTRATION, WASHINGTON, DC.
Global drought monitoring from NOAA polar orbiting satellites p 2750 N93-24852
Proceedings of the Ocean Climate Data Workshop
|NASA-TM-108711| p 2732 N93-24915
A systematic satellite approach for estimating central pressures of mid-lattitude oceanic storms
|NOAA-TR-NESDIS-63| p 2781 N93-25220

NATIONAL PHYSICAL LAB., NEW DELHI (INDIA).
Radiation effects in germanium doped quartz p 2837 N93-25021

NATIONAL PHYSICAL LAB., TEDDINGTON (ENGLAND).
Analytical techniques for improved time transfer using common view of direct broadcasting satellites p 2835 N93-25008
Progress towards laboratory frequency standards for the optical communication bands p 2687 N93-25069

NATIONAL SERVICE OF METROLOGY, DELFT (NETHERLANDS).
Prospects of two-way international time scale comparisons p 2832 N93-24988

NATIONAL SEVERE STORMS LAB., NORMAN, OK.
Positive cloud-to-ground flashes in severe storms p 2780 N93-24896

NATIONAL TECHNICAL INFORMATION SERVICE, SPRINGFIELD, VA.
Directory of US Government software for mainframes and microcomputers, 1993
|PB93-111565| p 2807 N93-26569

NATIONAL TRANSPORTATION SAFETY BOARD, WASHINGTON, DC.
Aircraft accident report: Tomy International, Inc., d/b/a Scenic Air Tours flight 22, Beech Model E18S, N342E in-flight collision with terrain, Mount Haleakala, Maui, Hawaii, 22 April 1992
|PB93-910401| p 2583 N93-25827

NATIONAL WEATHER SERVICE, FORT WORTH, TX.
Guide for conducting convective windstorm surveys
|PB93-148427| p 2787 N93-26570
Tornado: An engineering-oriented perspective
|PB93-148435| p 2788 N93-26584

NATIONAL WEATHER SERVICE, PORTLAND, OR.
National Weather Service Winter Weather Workshop
|PB93-146785| p 2785 N93-25775

NATIONAL WEATHER SERVICE, SILVER SPRING, MD.
Interactive forecasting with the National Weather Service River Forecast System p 2788 N93-25616

NATURAL RESOURCES INST., CHATHAM (ENGLAND).
Sustainable remote sensing: A major improvement for realtime resource management and disaster early warning in developing countries p 2743 N93-24808

NAVAL ACADEMY, ANNAPOLIS, MD.
An investigation into the causative mechanisms for explosive cyclone development over the Atlantic
|AD-A261831| p 2786 N93-26273

NAVAL AEROSPACE MEDICAL RESEARCH LAB., PENSACOLA, FL.
Simulated sustained flight operations and performance. Part 1: Effects of fatigue
|AD-A261012| p 2801 N93-25859
Performance-based testing and success in Naval advanced flight training
|AD-A260838| p 2590 N93-25933

NAVAL AIR REWORK FACILITY, NORTH ISLAND, CA.
Particulate emissions from gas turbine engines
|AD-A261374| p 2595 N93-26339

NAVAL AIR SYSTEMS COMMAND, WASHINGTON, DC.
Military standardization handbook: Aircraft refueling handbook
|AD-A261755| p 2662 N93-26600

NAVAL AIR WARFARE CENTER, CHINA LAKE, CA.
ADN propellant diffusion flame structure p 2629 N93-26036
Flame response in oscillatory solid propellant combustion p 2630 N93-26041

NAVAL AIR WARFARE CENTER, PATUXENT RIVER, MD.
Applications of stress envelope concepts to aircraft EMP and lightning survivability p 2584 N93-24898

NAVAL AIR WARFARE CENTER, WARMINSTER, PA.
Macromolecules for inhibition of corrosion and wear
|AD-A261041| p 2655 N93-25816

NAVAL COMMAND, CONTROL AND OCEAN SURVEILLANCE CENTER, SAN DIEGO, CA.
High-performance visualization applied to computational electromagnetics: Method-of-moments on a silicon graphics workstation
|AD-A260820| p 2675 N93-25700

NAVAL HEALTH RESEARCH CENTER, SAN DIEGO, CA.
Combined strength and endurance training: Functional and morphological adaptations to ten weeks of training
|AD-A261059| p 2802 N93-26229

NAVAL OBSERVATORY, WASHINGTON, DC.
The role of ocean climate data in operational Naval oceanography p 2732 N93-24916

NAVAL POSTGRADUATE SCHOOL, MONTEREY, CA.
Study of grain refinement in Al alloy 2519 using backscattering orientation-contrast mode in the scanning electron microscope
|AD-A260886| p 2651 N93-25632
An analysis of mesoscale convective systems observed during the 1992 Tropical Cyclone Motion field experiment
|AD-A260889| p 2783 N93-25633
Orbital parameter estimation using an extended Kalman filter
|AD-A260618| p 2608 N93-25636
Spectra of stable sonoluminescence
|AD-A260621| p 2844 N93-25637
Errors caused by incompatible wind and buoyancy forcing in the ocean general circulation models
|AD-A260894| p 2789 N93-25657
Thermoelastic stresses in multi-layered media in non-uniform temperature fields
|AD-A260901| p 2727 N93-25658
Thermocapillary flow near a cold wall
|AD-A261050| p 2706 N93-25779
A digital hardware test system analysis with test vector translation
|AD-A260849| p 2810 N93-25786
An investigation of memory latency reduction using an address prediction buffer
|AD-A261010| p 2806 N93-25858
An introduction to Doppler effect and fading in mobile communications
|AD-A260976| p 2676 N93-25866
Modeling of a full vision system using combined Visual/Haptic search for remote object identification
|AD-A260977| p 2801 N93-25867
Optimization techniques for contact stress analysis
|AD-A260846| p 2729 N93-25911
Experimental study of the effect of helical grooves on an infinite cylinder
|AD-A260890| p 2676 N93-25912
Particle behavior in solid propellant rocket motors and plumes
|AD-A260900| p 2624 N93-25913
The design and implementation of a read prediction buffer
|AD-A260902| p 2806 N93-25934
Solid fuel supersonic combustion p 2625 N93-26010
Proof of fault coverage for a formal protocol test procedure
|AD-A261612| p 2680 N93-26166
Model fan passage flow simulation
|AD-A261613| p 2707 N93-26167
Special tooling disposition for aircraft entering post production support
|AD-A261614| p 2573 N93-26168
Trailing vortex/free-surface interaction
|AD-A261654| p 2581 N93-26195
Development and testing of the digital control system for the Archytas unmanned air vehicle
|AD-A261656| p 2597 N93-26196
Unsteady airfoil flow solutions on moving zonal grids
|AD-A261925| p 2582 N93-26198
Elastic curves on the sphere
|AD-A261057| p 2829 N93-26228
A climatology of polar low occurrences in the Nordic Seas and an examination of katabatic winds as a triggering mechanism
|AD-A261719| p 2786 N93-26245
Exploring the link between intrinsic motivation and quality
|AD-A261722| p 2722 N93-26246
A surface integral algorithm for the motion planning of nonholonomic mechanical systems
|AD-A261746| p 2720 N93-26249
Introduction of chaotic dynamical systems
|AD-A261747| p 2872 N93-26250
New algorithms for the detection and elimination of sine waves and other narrow-band signals in the presence of broadband signals and noise
|AD-A261811| p 2681 N93-26261
Effects of Taiwan orography on the motion and structure of typhoons
|AD-A261819| p 2786 N93-26270

The design and implementation of a reusable component library and a retrieval/integration system
| AD-A261827 | p 2812 N93-26271
Investigation of a background suppression transimpedance amplifier for photovoltaic detectors
| AD-A261828 | p 2691 N93-26272
AMPHIB: A users manual
| AD-A261769 | p 2669 N93-26285
An observational study of the local and remote response of the equatorial Pacific to westerly wind events during the 1991-92 El Nino
| AD-A261777 | p 2787 N93-26286
Considerations for space and naval aviation applications of ferroelectric memory
| AD-A261300 | p 2807 N93-26294
A Biphase Shift Keying (BPSK), direct sequence, spread spectrum modem for Petite Amateur Navy Satellite (PANSAT)
| AD-A261301 | p 2618 N93-26295
Basic research thermoacoustic heat transport
| AD-A261334 | p 2759 N93-26310
Research directions in software analysis, synthesis and certification
| AD-A261367 | p 2812 N93-26336
Power iterations and the dominant eigenvalue problem
| AD-A261695 | p 2829 N93-26370
Thermally induced stresses in a composite exposed to fire
| AD-A261714 | p 2641 N93-26371
Implementation of cyclic spectral analysis methods
| AD-A261715 | p 2681 N93-26372
The design and evaluation of transmit and receive antennas for an ionospheric communications probe system. B: Sloping-vee beams
| AD-A261866 | p 2682 N93-26388
Pseudo Wigner-Ville distribution, computer program, and its applications to time-frequency domain problems
| AD-A261839 | p 2813 N93-26431
Trellis coded CPFSK
| AD-A261788 | p 2682 N93-26441
AEW aircraft design
| AD-A261800 | p 2590 N93-26444
Boundedness and asymptotics of the generalized theodorus iteration
| AD-A261427 | p 2829 N93-26452
Managing real-time software projects: Problems and issues
| AD-A261428 | p 2813 N93-26453
Chaos metrics for testing lagrangian particle models
| AD-A261429 | p 2776 N93-26454
A three-dimensional study of the influence of mountains on a front
| AD-A261927 | p 2787 N93-26545
Very low frequency signals and whistler-mode amplification in the magnetosphere and limit-cycle behavior in the CECAF infrared free electronic laser
| AD-A261776 | p 2716 N93-26601
Atomization and combustion of a gelled, metallized slurry fuel
| AD-A261778 | p 2647 N93-26602
Geolocation of an electromagnetic emitter using a cyclostationary time difference of arrival technique
| AD-A261781 | p 2686 N93-26603
A comparison of ionospheric propagation mode delay predictions from ADVANCED PROPHET 4.3 with measured data
| AD-A261782 | p 2686 N93-26604

NAVAL RESEARCH LAB., BAY SAINT LOUIS, MS.
Digital Nautical Chart
| AD-A260810 | p 2756 N93-25694
Relations between blue whiting biomass and satellite derived phytoplankton and temperature in the Norwegian Sea
| AD-A261205 | p 2757 N93-25868
A predicted geomagnetic field model for epoch 1990.0
| AD-A260669 | p 2775 N93-25891
Implementation of custom colors in the DECwindows environment
| AD-A261456 | p 2757 N93-26574

NAVAL RESEARCH LAB., WASHINGTON, DC.
Admission control in integrated voice/data multihop radio networks
| AD-A261055 | p 2680 N93-26227
A channel simulation processor for the multi-node tactical network simulator
| AD-A261810 | p 2776 N93-26430
Start-up imprinting and shock dynamics in laser-target interaction
| AD-A261384 | p 2715 N93-26445
New results in signal design for the AWGN channel
| AD-A261424 | p 2682 N93-26451
Radar sensing of petroleum seepage gases
| AD-A261431 | p 2682 N93-26455

NAVAL SEA SYSTEMS COMMAND, WASHINGTON, DC.
The Global Ocean Observing System
p 2733 N93-24923

NAVAL SURFACE WARFARE CENTER, BETHESDA, MD.
Axisymmetric deformations and stresses of unsymmetrically laminated composite cylinders in axial compression with thermally-induced preloading effects
| NASA-CR-192788 | p 2723 N93-24912
Effect of water immersion on fiber/matrix adhesion
| AD-A260704 | p 2636 N93-25652

NAVAL SURFACE WARFARE CENTER, DAHLGREN, VA.
AEGIS measures definition
| AD-A261494 | p 2812 N93-26375
Proceedings of the complex systems engineering synthesis and assessment technology workshop
| AD-A261404 | p 2807 N93-26403
NSWC library of mathematics subroutines
| AD-A261511 | p 2884 N93-26575

NAVAL SURFACE WARFARE CENTER, PANAMA CITY, FL.
Photovoltaic power without batteries for continuous cathodic protection p 2759 N93-25597
Loss of temporal coherence of laser light propagated through simulated coastal waters
| AD-A261303 | p 2715 N93-26296

NAVAL SURFACE WARFARE CENTER, SILVER SPRING, MD.
Mullite whiskers and mullite-whisker felt
p 2642 N93-25586
Dynamic hardness tester and cure meter
p 2711 N93-25608
A software package for neural network applications development p 2827 N93-25610
Thermal decomposition and stabilization of ammonium dinitramide p 2630 N93-26038

NAVAL UNDERSEA WARFARE CENTER, NEWPORT, RI.
Proceedings of the NUWC Division Newport Seminar Series on Turbulence and its Control
| NUWC-NPT-TM-922089 | p 2707 N93-26328

NEBRASKA UNIV., LINCOLN.
Dynamics of collision processes
| DE93-007143 | p 2849 N93-25509
Molecular devices based on new monolayer-forming systems
| AD-A260996 | p 2866 N93-25854
Investigation of the effects of Extra Vehicular Activity (EVA) and Launch and Entry (LES) gloves on performance p 2803 N93-26061
Smart structural composites with piezoelectric micro-constituents
| AD-A260970 | p 2640 N93-26225

NEVADA UNIV., LAS VEGAS.
Tank issues: Design and placement of vapor monitoring wells
| PB93-161131 | p 2768 N93-26536

NEVADA UNIV. SYSTEM, RENO.
Natural and augmented snowfall growth processes and their interactions with the natural and modified aerosol
| PB93-153096 | p 2786 N93-25874

NEW HAMPSHIRE UNIV., DURHAM.
Measurements of nitric acid, carboxylic acids, and selected aerosol species for the NASA/GTE Pacific Mission - West (PEM-WEST)
| NASA-CR-192976 | p 2763 N93-25287
Receptoral and neural aliasing
| AD-A261438 | p 2799 N93-26489

NEW JERSEY INST. OF TECH., NEWARK.
Particle dynamics modeling of boundary effects in granular Couette flow p 2705 N93-25738

NEW MEXICO INST. OF MINING AND TECHNOLOGY, SOCORRO.
Lightning precursor signatures from dual-polarization radar measurements of storms p 2777 N93-24877
Remote sensing of precipitation and electrification with a dual-polarization, coherent, wideband radar system
| AD-A260779 | p 2756 N93-25679
Interface engineering in oxide fiber/oxide matrix composites
| AD-A261705 | p 2641 N93-26579

NEW MEXICO STATE UNIV., LAS CRUCES.
Improving information search at the user interface: The impact of graphical innovation on query formulation and expression p 2873 N93-24905
Modeling of the WSTF frictional heating apparatus in high pressure systems p 2648 N93-26079

NEW ORLEANS UNIV., LA.
Determination of design and operation parameters for upper atmospheric research instrumentation to yield optimum resolution with deconvolution, appendix 4
| NASA-CR-192834 | p 2769 N93-24910
Determination of design and operation parameters for upper atmospheric research instrumentation to yield optimum resolution with deconvolution, appendix 2
| NASA-CR-192833 | p 2770 N93-25088
Determination of design and operation parameters for upper atmospheric research instrumentation to yield optimum resolution with deconvolution
| NASA-CR-192832 | p 2775 N93-26084

NEW SOUTH WALES UNIV., KENSINGTON (AUSTRALIA).
An autonomous satellite architecture integrating deliberative reasoning and behavioural intelligence
p 2823 N93-25970

NEW YORK UNIV., NEW YORK.
Boundary plasma modelling for ITER
| DE93-007963 | p 2859 N93-25302
Facilitation and interference in identification of pictures and words
| AD-A261484 | p 2798 N93-26356
Duration of alpha suppression increases with angle in a mental rotation task
| AD-A261592 | p 2798 N93-26435
Imaging regional changes in the spontaneous activity of the brain: An extension of the minimum-norm least-squares estimate
| AD-A261593 | p 2798 N93-26436
Neuromagnetic investigation of cortical regions underlying short-term memory
| AD-A261445 | p 2799 N93-26521

NIPPON ELECTRIC CO. LTD., YOKOHAMA (JAPAN).
High resolution stereo imaging and data compression
p 2753 N93-24867

NIPPON TELEGRAPH AND TELEPHONE PUBLIC CORP., YOKOSUKA (JAPAN).
Timing and time signal distribution in digital communications networks p 2686 N93-25061

NORTH CAROLINA AGRICULTURAL AND TECHNICAL STATE UNIV., GREENSBORO.
Uniform roughness studies
| WL-TR-92-3041 | p 2706 N93-25951
Optical characterization of Ga(1-x)In(x)As(y)Sb(1-y)/GaSb alloy and device application
| AD-A261713 | p 2870 N93-26581

NORTH CAROLINA STATE UNIV., RALEIGH.
Aerial photographic sampling for statewide resource inventory p 2755 N93-25441
Theoretical studies of surface reactions on metals and electronic materials
| DE93-009761 | p 2650 N93-25502
A new LU-SGS flow solver for calculating reentry flows p 2579 N93-25759
Heterogeneous photocatalytic oxidation of atmospheric trace contaminants
| NASA-CR-192937 | p 2767 N93-26427

NORTH CAROLINA UNIV., CHAPEL HILL.
Observations of an intrathermocline vortex
p 2788 N93-24769
Observations and models of shock structures in Herbig-Haro objects p 2891 N93-24770
Advanced technology for portable personal visualization
| AD-A261294 | p 2807 N93-26293

NORTH CAROLINA UNIV., CHARLOTTE.
Two-phase/two-phase heat exchanger analysis
| NASA-CR-192783 | p 2697 N93-25221
Activity report
| AD-A261933 | p 2829 N93-26199

NORTH DAKOTA ATMOSPHERIC RESOURCE BOARD, BISMARCK.
The North Dakota thunderstorm project
| PB93-153039 | p 2785 N93-25776

NORTH DAKOTA UNIV., GRAND FORKS.
Redistribution of trace chemical species by a small convective cloud
| PB93-156164 | p 2765 N93-25873

NORTHROP CORP., PICO RIVERA, CA.
A procedure for defining lightning risk to air vehicles
p 2583 N93-24885

NORWEGIAN DEFENCE RESEARCH ESTABLISHMENT, KJELLER.
Registration of the use of agricultural fields and soil erosion using satellite remote sensing
p 2751 N93-24856

O

OAK RIDGE NATIONAL LAB., TN.
An introductory guide to uncertainty analysis in environmental and health risk assessment
| DE93-002873 | p 2760 N93-24676
Selected translated abstracts of Russian-language climate-change publications: 1. Surface energy budget
| DE93-003189 | p 2760 N93-24952
Compressor calorimeter performance of refrigerant blends: Comparative methods and results for a refrigerator/freezer application
| DE93-006734 | p 2667 N93-24970

Initial experiments with a myoelectric-based muscle sensor
| DE92-016034 | p 2799 N93-25099
Position and force control of a vehicle with two or more steerable drive wheels
| DE92-041301 | p 2717 N93-25100
Kinetic studies of interfacial photocurrents in platinized chloroplasts
| DE93-002344 | p 2792 N93-25104
Using fuzzy behaviors for the outdoor navigation of a car with low-resolution sensors
| DE93-002428 | p 2584 N93-25120
Trends '91: A compendium of data on global change. Highlights
| DE93-003112 | p 2761 N93-25144
Diabaticity of nuclear motion: Problems and perspectives
| DE93-007252 | p 2847 N93-25148
An outgoing energy flux boundary condition for finite difference ICRP antenna models
| DE93-007788 | p 2674 N93-25300
Detailed solution to a complex kinematics chain manipulator
| DE93-004619 | p 2725 N93-25357
Development of ASTM standards in support of advanced ceramics development
| DE93-003024 | p 2654 N93-25361
Structure and properties of a-C: N films prepared by pulsed excimer laser deposition
| DE93-007908 | p 2654 N93-25372
Analysis of pull-tests for determining the effects of ion implantation on the adhesion of iron films to sapphire substrates
| DE93-006732 | p 2725 N93-25373
The nature of the glass transition and its determination by thermal analysis
| DE93-006746 | p 2654 N93-25374
The interaction of swift electrons with surface excitations
| DE93-007245 | p 2848 N93-25376
Radiation-hardened control system
| DE93-007248 | p 2688 N93-25377
Toward a parallel recursive spectral bisection mapping tool
| DE93-006632 | p 2816 N93-25414
Human factors engineering: A key element of instrumentation and control system design
| DE93-006731 | p 2800 N93-25415
Numerical kinematic transformation calculations for a parallel link manipulator
| DE93-005778 | p 2718 N93-25449
High temperature fracture toughness of Ni3Al alloy IC-396M
| DE93-008564 | p 2650 N93-25492
TSC plasma halo simulation of a D3-D vertical displacement episode
| DE93-008688 | p 2860 N93-25493
Real-time construction of three-dimensional occupancy maps
| DE93-001645 | p 2756 N93-25505
Fast diagnostics of laser ablation used for pulsed laser deposition
| DE93-005155 | p 2713 N93-25508
Real-time construction and rendering of three-dimensional occupancy maps
| DE93-007818 | p 2756 N93-25516
Climate data bases of the People's Republic of China, 1841-1988
| DE93-007907 | p 2764 N93-25517
Room temperature fracture of FeCo
| DE93-008266 | p 2650 N93-25519
Recommendations for a Kalman filter to estimate and control freeze and sublime rates of gaseous diffusion plant freezer/sublimer systems
| ORNL/TM-12183 | p 2668 N93-25937
Position sensitive atom probe study of the decomposition of a Cu-2.6 at. percent Co alloy
| DE93-006737 | p 2653 N93-26500
Development of resonance ionization spectroscopy for genome mapping and DNA sequencing using stable isotopes as DNA labels
| DE93-007815 | p 2793 N93-26587

OAK RIDGE Y-12 PLANT, TN.
A method for transient, three-dimensional neutron transport calculations
| DE93-007243 | p 2847 N93-25256

OBSERVATOIRE CANTONAL, NEUCHATEL (SWITZERLAND).
Basic design of a spaceborne hydrogen maser p 2716 N93-25024
A compact and high-performance reference cell for laser frequency stabilization p 2716 N93-25065
Line inhomogeneity effects and power shift in miniaturized rubidium frequency standards p 2694 N93-25066
Noise measurements in single-mode GaAlAs diode lasers p 2716 N93-25067

OBSERVATOIRE DE BESANCON (FRANCE).
Time stability: An improvement of the multi-variance method for the oscillator noise analysis p 2839 N93-25036

OFFICE NATIONAL D'ETUDES ET DE RECHERCHES AEROSPATIALES, PARIS (FRANCE).
Monolithic quartz vibrating beam accelerometer p 2711 N93-25011

OFFICE OF NAVAL RESEARCH, ARLINGTON, VA.
Isolation and analysis of key components of seafloor relief
| AD-A261635 | p 2790 N93-26170

OFFICINE GALILEO S.P.A., FLORENCE (ITALY).
SEOMAR: An Italian approach to the observation of the Mediterranean area p 2746 N93-24825

OHIO STATE UNIV., COLUMBUS.
Molecular/polymeric magnetism
| DE93-008635 | p 2847 N93-25114
Comparison of high-resolution solar irradiance spectra and the solar luminosity in the period 1980-1989
| NASA-CR-192776 | p 2898 N93-25222
Design concepts for the development of cooperative problem-solving systems
| NASA-CR-192708 | p 2585 N93-25261
Design of a cooperative problem-solving system for enroute flight planning: An empirical study of its use by airline dispatchers
| NASA-CR-192709 | p 2585 N93-25330
Design and analysis of algorithms for processing queries in database systems p 2876 N93-25482
Electrical conductivity of ion implanted ladder and semi-ladder polymers
| AD-A261401 | p 2657 N93-26401
IR and FIR laser diagnostics for plasma thrusters using a CW CO2 radiation source
| AD-A261399 | p 2862 N93-26520

OKLAHOMA STATE UNIV., STILLWATER.
Chemical dynamics studies of high energy species
| AD-A260743 | p 2852 N93-25676
An optimal scheduling of pick-place operations of a robot-vision-tracking system by using neural networks and rule-based systems p 2821 N93-25880
A study of mapping exogenous knowledge representations into CONFIG p 2827 N93-26072

OKLAHOMA UNIV., NORMAN.
The charge and size of precipitation particles inside thunderstorms and mesoscale convective systems on the Great Plains p 2781 N93-25275
On the estimation of risk associated with an attenuation prediction p 2683 N93-26469

OLD DOMINION UNIV., NORFOLK, VA.
Geometric modeling for computer aided design
| NASA-CR-192891 | p 2808 N93-24750
Grid sensitivity for aerodynamic optimization and flow analysis
| NASA-CR-192980 | p 2575 N93-25117
Laminar and turbulent natural convection heat transfer in Trombe wall channels p 2702 N93-25551
A computational aerodynamic design optimization method using sensitivity analysis p 2589 N93-25552

OPEN UNIV., MILTON (ENGLAND).
Proceedings of the 5th International Symposium on Long Range Sound Propagation
| AD-A260666 | p 2845 N93-25643

OPTICAL SOCIETY OF AMERICA, WASHINGTON, DC.
Optical computing, Volume 6: Organization of the Optical Society of America photonic science topical meeting series
| AD-A261267 | p 2856 N93-26266
1992 technical digest series volume 16. Conference edition: Summaries of papers presented at the Nonlinear Dynamics in Optical Systems Topical Meeting
| AD-A261915 | p 2857 N93-26544

OREGON STATE UNIV., CORVALLIS.
Real-time value-driven monitoring and repair
| AD-A260959 | p 2811 N93-26221

OREGON UNIV., EUGENE.
Experimental studies of fundamental problems in quantum optics
| AD-A261183 | p 2853 N93-25822

OSNABRUECK UNIV. (GERMANY).
Monitoring and analysis of urban trends using multitemporal satellite-imagery (case-study: Greater Cairo) p 2740 N93-24790

OULU UNIV. (FINLAND).
Control of environmental and clock parameters in Time and Frequency Standards Laboratory p 2835 N93-25007
Use of the TV-signal in stabilizing a local rubidium oscillator p 2693 N93-25029
Experimental results of the performance of the new phase and frequency controller p 2839 N93-25035

OXFORD UNIV. (ENGLAND).
Turbine turbobrake systems p 2717 N93-25268
Collisional recombination lasers p 2713 N93-25393
Twistor diagrams and a quantum field theory p 2871 N93-25423
An experimental study of under-expanded jets p 2577 N93-25467
Simulation and prediction of tropical SST with a coupled ocean-atmosphere model p 2789 N93-25469
Aspects of the design of a satellite borne infra-red radiometer p 2620 N93-25474
The Taurid meteoroid complex p 2889 N93-25536
The pressure modulation system in the Improved Stratospheric and Mesospheric Sounder p 2773 N93-25739

P

PACIFIC NORTHWEST LAB., RICHLAND, WA.
An assessment of alternatives and technologies for replacing ozone-depleting substances at DOE facilities
| DE93-002862 | p 2760 N93-24675
An evaluation of thermal energy storage options for precooling gas turbine inlet air
| DE93-005980 | p 2758 N93-24975
Aquifer thermal energy (heat and chill) storage
| DE93-006446 | p 2759 N93-25183
Temperature-dependent electrical conductivity of soda-lime glass
| DE93-007872 | p 2654 N93-25359
Human factors in environmental management: New directions from the Hanford site
| DE93-004337 | p 2767 N93-26495
Long term modeling of the links between economics, technical progress, and environment: Evolution of approaches and new trends
| DE93-005035 | p 2767 N93-26497

PALERMO UNIV. (ITALY).
The photointerpretation of the area taken over from agriculture by intense urbanization at Villabate (Palermo, Italy) p 2742 N93-24800

PALISADES INST. FOR RESEARCH SERVICES, INC., ARLINGTON, VA.
Microwave and millimeter wave monolithic integrated circuits (MIMIC) program. MIMIC briefs: Summaries of phase 3 technology support programs
| AD-A260914 | p 2690 N93-25660
Special technology area review on microwave packaging technology
| AD-A261852 | p 2681 N93-26276

PARIS VI UNIV. (FRANCE).
Synchrotron radiation X ray topography study of lateral field resonators p 2833 N93-24994
Micromechanics of fatigue
| AD-A260577 | p 2729 N93-25901

PENNSYLVANIA STATE UNIV., UNIVERSITY PARK.
Prediction of forces and moments for hypersonic flight vehicle control effectors
| NASA-CR-193033 | p 2595 N93-24762
Viewgraph description of Penn State's Propulsion Engineering Research Center: Activity highlights and future plans
| NASA-CR-192317 | p 2622 N93-24943
Supersonic shock wave/vortex interaction
| NASA-CR-192917 | p 2576 N93-25249
An experimental study of the sources of fluctuating pressure loads beneath swept shock/boundary-layer interactions
| NASA-CR-192918 | p 2698 N93-25266
Studies of several small seawater MHD thrusters using the high-field solenoid of MIT's Bitter Magnet Laboratory
| AD-A260645 | p 2860 N93-25641
Adaptive liquid crystal TV based joint transform correlator as applied to real-time pattern recognition
| AD-A260724 | p 2864 N93-25655
Passive vibration damping materials: Piezoelectric ceramics composites for vibration damping applications
| AD-A260792 | p 2727 N93-25690
Heat transfer measurements in swept shock wave/turbulent boundary-layer interactions p 2704 N93-25705
Short-period superlattice materials for heterojunction bipolar transistors
| AD-A260701 | p 2866 N93-25897
Prediction of hydrogen entry and permeation in metals and alloys
| AD-A260580 | p 2651 N93-25903
SAR-related stress variability in the marine atmospheric boundary layer
| AD-A261129 | p 2775 N93-25946
Physical and chemical processes governing the CO2 laser-induced deflagration of ammonium dinitramide (ADN) p 2629 N93-26037
Interactions of acoustic waves and combustion of homogeneous solid propellants in rocket motors p 2630 N93-26039

Reduction in size and unsteadiness of a VTOL ground vortex by ground fences
| NASA-CR-192997 | p 2580 N93-26049
The role of pyridoxine as a countermeasure for in-flight loss of lean body mass p 2796 N93-26068
Implementation of quality improvement techniques for management and technical processes in the ACRV project p 2723 N93-26074
Flame-turbulence interactions
| AD-A260957 | p 2645 N93-26220
New pyro-optic techniques for imaging of long wavelength IR-Radiation (pyro-optic initiation program)
| AD-A260969 | p 2656 N93-26224
State-selected studies of atoms and molecules ejected from ion bombarded surfaces
| AD-A261275 | p 2650 N93-26267
Development and testing of improved techniques for modeling the hydrologic cycle in a mesoscale weather prediction system
| AD-A261454 | p 2787 N93-26351
ROSAT x ray survey observations of active chromospheric binary systems and other selected sources
| NASA-CR-192933 | p 2891 N93-26426
Oxides of nitrogen emissions from turbulent hydrocarbon/air jet diffusion flames, phase 2
| PB93-152478 | p 2768 N93-26533

PENNSYLVANIA UNIV., PHILADELPHIA.
Computation and learning in neural networks with binary weights
| AD-A261182 | p 2821 N93-25821
Polymers by non-redox processes: Synthesis, physical studies, and application
| AD-A261064 | p 2657 N93-26240

PETROLEUM RESEARCH CENTRE, TRIPOLI (LIBYA).
Remote sensing of coastal zone Sabkha deposits, Gulf of Sirt, Libya p 2746 N93-24827

PHILLIPS LAB., EDWARDS AFB, CA.
Application of the Saha equation to high temperature (greater than or equal to) rocket exhaust
| AD-A261648 | p 2632 N93-26174

PHILLIPS LAB., KIRTLAND AFB, NM.
Two- and three-dimensional high performance, patterned overlay multi-chip module technology p 2694 N93-25581

PHOTOMETRICS, INC., WOBURN, MA.
Analysis of the IBSS spectra of Space Shuttle control engine exhaust
| AD-A261749 | p 2632 N93-26373

PHRAXOS RESEARCH AND DEVELOPMENT, INC., SANTA MONICA, CA.
Microstrip antennas on/in anisotropic material layers
| AD-A261700 | p 2681 N93-26383

PHYSIKALISCH-TECHNISCHE BUNDESANSTALT, BRUNSWICK (GERMANY).
Ion trap frequency standard research at PTB p 2841 N93-25050

PITTSBURGH UNIV., PA.
A novel process for methanol synthesis
| DE93-008037 | p 2659 N93-25118
Probe molecule studies: Active species in alcohol synthesis
| DE93-008097 | p 2659 N93-25119
A study of vibrationally excited N2(+) ions in the daytime thermosphere p 2770 N93-25179
An experimental examination of the effects of expertise and problem-solving cues on the identification of ideas for strategic information systems p 2875 N93-25395
Flow between finite rotating disks and its linear stability p 2705 N93-25747
Analysis of symbolic parameter models
| AD-A261930 | p 2811 N93-26253
Intramolecular bridge/terminal oxo exchange within (MoV2O3) (4+) complexes containing linear oxo bridges
| AD-A261230 | p 2851 N93-26518

PLYMOUTH MARINE LAB. (ENGLAND).
The continuous plankton recorder survey: A long-term, basin-scale oceanic time series p 2736 N93-24937

POLISH ACADEMY OF SCIENCES, WARSAW.
Measurement results of the crystallographic orientation of the SC cut round plates p 2840 N93-25040
On the effective reflection properties of the randomly segmented elastic bar p 2724 N93-25328
Non-local description of pollution transport in random medium p 2763 N93-25329
On existence of solutions and duality for a model of non-linear elastic plates with transverse shear deformations p 2726 N93-25437

POLITECNICO DI MILANO (ITALY).
Phase differences of the fields in a Ramsey resonator for submillimetric frequency standards p 2840 N93-25042

POLITECNICO DI TORINO (ITALY).
Fractal determination of parameters in lightning and ESD model p 2686 N93-24893

POLYTECHNIC UNIV., BROOKLYN, NY.
Experimental and theoretical studies of proximity effect and Coulomb blockade phenomena in Josephson junctions
| AD-A261652 | p 2867 N93-26194

POLYTECHNIC UNIV., FARMINGDALE, NY.
Investigations of the transient behavior of the cathode fall region in planar and hollow cathodes
| AD-A261636 | p 2691 N93-26171

POTOMAC PHOTONICS, INC., LANHAM, MD.
Ultraviolet waveguide lasers for phased array lidar
| AD-A261657 | p 2715 N93-26363

PRATT AND WHITNEY AIRCRAFT, WEST PALM BEACH, FL.
Fatigue in single crystal nickel superalloys
| AD-A260709 | p 2651 N93-25843

PRESIDENT'S COUNCIL OF ADVISORS ON SCIENCE AND TECHNOLOGY, WASHINGTON, DC.
Science, technology, and national security p 2886 N93-25232
Achieving the promise of the bioscience revolution: The role of the Federal Government
| PB93-139970 | p 2793 N93-25457
High performance computing and communications panel report p 2807 N93-26131

PRINCETON UNIV., NJ.
Tuned circuit electric levitation bearings for microactuators p 2689 N93-25619
Anode power deposition in coaxial MPD thrusters p 2623 N93-25665
Minimum-fuel power-limited transfers between coplanar elliptic orbits p 2608 N93-25684
From fractals to wormholes via string theory p 2871 N93-25742
Gravitational lensing and gamma ray bursts p 2900 N93-25828
Particle simulation of auroral double layers p 2774 N93-25830
Probability and statistics applied to the theory of algorithms
| AD-A261019 | p 2830 N93-25863
Kinetic studies in gas-phase reaction mechanisms important to the combustion process of high energy density materials: The H2/NO2 reaction p 2628 N93-26027
The physics of spin polarized gases
| AD-A261396 | p 2850 N93-26288

PROUDMAN OCEANOGRAPHIC LAB., BIRKENHEAD (ENGLAND).
Data management for community research projects: A JGOFS case study p 2736 N93-24936

PUERTO RICO UNIV., MAYAGUEZ.
Joint flexibility effects on the dynamic response of structures. Part 2: Stochastic analysis
| AD-A261003 | p 2729 N93-25938

PUERTO RICO UNIV., RIO PIEDRAS.
A numerical simulation of adsorption onto a crystalline surface
| AD-A261079 | p 2866 N93-25781
Proceedings of the 16th International Workshop on Condensed Matter Theories
| AD-A261078 | p 2868 N93-26252

PURDUE UNIV., WEST LAFAYETTE, IN.
The WINCOF-I code: Detailed description
| NASA-CR-190779 | p 2573 N93-24760
Measurements of soot formation and hydroxyl concentration in near critical equivalence ratio premixed ethylene flame
| NASA-CR-191099 | p 2642 N93-25116
Transient performance of fan engine with water ingestion
| NASA-CR-190778 | p 2573 N93-25134
New ground states in unconventional superconductors p 2688 N93-25282
Aerospace vehicle model simplification for feedback control p 2596 N93-25292
Three-dimensional boundary element analysis of contact and fracture problems p 2725 N93-25335
Numerical investigations on fracture behavior of ductile materials p 2725 N93-25411
Integrating satellite imagery and digital elevation data for geobotanical mapping in Quetico Provincial Park, Ontario, Canada p 2754 N93-25430
Flow and morphological conditions associated with the directional solidification of aqueous ammonium chloride
| DE93-008886 | p 2644 N93-25495
Efficient generation of synthetic terrain imagery for automatic target recognition
| AD-A260705 | p 2756 N93-25653
Inelastic behavior of thermoplastic composites p 2636 N93-25674
Investigation and modeling of penetration process for composite laminates impacted by a blunt-ended projectile p 2637 N93-25675
Low-velocity impact of composite sandwich plate p 2637 N93-25695
Optimal transfers between libration-point orbits in the elliptic restricted three-body problem p 2608 N93-25758
Simulation of vortex bursting p 2580 N93-25881
A Hierarchical Target Extraction, Recognition, and Tracking (HiTert) system
| AD-A260567 | p 2854 N93-25898

R

RAND CORP., SANTA MONICA, CA.
Numerical simulation of hypersonic aerodynamics and the computational needs for the design of an aerospace plane
| AD-A260681 | p 2580 N93-25894
Aerospace-plane flights and stratospheric ozone: Review and preliminary assessment of the National Aerospace Plane (NASP) operations
| RAND/N-3464-AF | p 2767 N93-26327

RANGE COMMANDERS COUNCIL, WHITE SANDS MISSILE RANGE, NM.
Flight termination receiver catalog
| AD-A261558 | p 2682 N93-26460

RECOTECH CORP., AURORA, OH.
Converting environmental wastes into valuable resources p 2759 N93-25572

REMTECH, INC., HUNTSVILLE, AL.
SRB environment evaluation and analysis. Volume 1: Redesigned SRB flight heating evaluation
| NASA-CR-192517 | p 2631 N93-26053
SRB environment evaluation and analysis. Volume 3: ASRB plume induced environments
| NASA-CR-192519 | p 2631 N93-26054
External tank aerothermal design criteria verification
| NASA-CR-192514 | p 2618 N93-26055
Remtech SSME nozzle design TPS
| NASA-CR-192516 | p 2631 N93-26056
SRB environment evaluation and analysis. Volume 2: RSRB joint filling test/analysis improvements
| NASA-CR-192518 | p 2631 N93-26057

RENSSELAER POLYTECHNIC INST., TROY, NY.
Using neural networks and Dyna algorithm for integrated planning, reacting and learning in systems
| NASA-CR-193018 | p 2817 N93-24743
Design and analysis of curved composite components for rotorcraft fuselage frames p 2589 N93-25701
Structural dynamic analysis of bearingless rotor blade p 2590 N93-25719
Passivity motivated controller design for flexible structures
| AD-A261122 | p 2719 N93-25771
Electroelastic equations for electroded thin plates subject to large driving voltages
| AD-A261123 | p 2675 N93-25772
Design of flexible rods with embedded SMA actuators
| AD-A260742 | p 2729 N93-25846
Thermomechanical response of shape memory composites
| AD-A260828 | p 2639 N93-25919
Variational theory of motion of curved, twisted and extensible elastic rods
| AD-A261028 | p 2729 N93-25941
Damage detection and mitigation of composite structures using smart materials
| AD-A261121 | p 2639 N93-25945
Deformations of active flexible rods with embedded line actuators
| AD-A261207 | p 2729 N93-25950
NASA Center for Intelligent Robotic Systems for Space Exploration
| NASA-CR-193208 | p 2826 N93-25986

RESEARCH INST. FOR ADVANCED COMPUTER SCIENCE, MOFFETT FIELD, CA.
Tree classification software p 2814 N93-25591

RESEARCH SUPPORT INSTRUMENTS, INC., ALEXANDRIA, VA.
Attitude control of the LACE satellite: A gravity gradient stabilized spacecraft p 2605 N93-24727

RESEARCH TRIANGLE INST., RESEARCH TRIANGLE PARK, NC.
An inverted AlGaAs/GaAs patterned-Ge tunnel junction cascade concentrator solar cell
| DE93-000073 | p 2759 N93-25102

RICE UNIV., HOUSTON, TX.
Combining particles and waves for fluid animation p 2699 N93-25348
Numerical study of cavity natural convection flow with augmenting and counteracting effects by projection finite element method p 2701 N93-25540
Composite materials for the extravehicular mobility unit p 2642 N93-26060
Linear-programming tools in integer programming: The traveling salesman
| AD-A261398 | p 2812 N93-26290

Integrated approaches to parallelism in optimization and the solution of inverse problems
| AD-A261490 | p 2829 N93-26344

RIJKSWATERSTAAT, DELFT (NETHERLANDS).
Applications of remote sensing for tidal waters, coastal areas and inland waters p 2745 N93-24819

ROCHESTER UNIV., NY.
Liquid crystals for laser applications
| AD-A261209 | p 2714 N93-25869

ROCKWELL INTERNATIONAL CORP., CANOGA PARK, CA.
Development of a second generation spray combustion code p 2626 N93-26016

ROCKWELL INTERNATIONAL CORP., DOWNEY, CA.
Zoning of aircraft: A review of the definitions p 2583 N93-24880

ROCKWELL INTERNATIONAL CORP., SEAL BEACH, CA.
Momentum accumulation due to solar radiation torque, and reaction wheel sizing, with configuration optimization p 2600 N93-24695

RODITI INTERNATIONAL CORP. LTD., LONDON (ENGLAND).
The measurement of the resonant frequency of quartz crystal units: An ongoing saga p 2833 N93-24996

ROME LAB., GRIFFISS AFB, NY.
The database Query Support Processor (QSP) p 2807 N93-25577
High level design for distributed application instrumentation
| AD-A260812 | p 2710 N93-25696
An SPW software simulation model of a dispersive fading multipath narrowband HF channel
| AD-A261101 | p 2675 N93-25767
Rome Laboratory Journal, 1992
| AD-A260821 | p 2911 N93-25910
Considerations of the error variances of time-averaged estimators for correlated processes
| AD-A261796 | p 2830 N93-26255
Dynamic behavior of helix interaction circuits
| AD-A261362 | p 2692 N93-26334

ROYAL AIRCRAFT ESTABLISHMENT, FARNBOROUGH (ENGLAND).
Measurements and computations of external heat transfer and film cooking in turbines
| RAE-TM-P-1223 | p 2592 N93-25455

ROYAL SIGNALS AND RADAR ESTABLISHMENT, MALVERN (ENGLAND).
Laser Induced Phonons (LIPs) in MBE grown ZnSe
| RSRE-MEMO-4544 | p 2864 N93-25454

RUTGERS - THE STATE UNIV., NEW BRUNSWICK, NJ.
Agreement in naming objects and concepts for information retrieval p 2881 N93-25826
Computer-aided design package for designers of digital optical computers
| AD-A260757 | p 2806 N93-25848

S

SAGA UNIV. (JAPAN).
Influence due to antenna pattern change in brightness temperature estimation for a space-based microwave radiometer p 2753 N93-24868

SAINT THOMAS COLL., SAINT PAUL, MN.
Knowledge-based control for robot self-localization p 2822 N93-25963

SALFORD UNIV. (ENGLAND).
The induction of elastic fine motion in robotic grasps p 2718 N93-25727
Analysis and design of a novel robotic finger-tip sensor for adaptive grasping p 2719 N93-25745

SAM TECHNOLOGY, INC., SAN FRANCISCO, CA.
Physiological indices of mental workload
| AD-A261692 | p 2798 N93-26391

SAN JOSE STATE UNIV., CA.
The properties of and analytical methods for detection of LiOH and Li2CO3
| NASA-CR-192771 | p 2643 N93-25240

SANDIA NATIONAL LABS., ALBUQUERQUE, NM.
Photoluminescence of silicon nanostructures formed by ion beam implantation
| DE93-006777 | p 2862 N93-24958
Colloid formation in implanted glasses
| DE93-006763 | p 2653 N93-24971
Coarsening of a quiescent electrorheological fluid I: Experiment
| DE93-006776 | p 2642 N93-24972
Probabilistic analysis of manipulation tasks: A research agenda
| DE93-000713 | p 2827 N93-25103
Reliability assessment at airline inspection facilities. Volume 1: A generic protocol for inspection reliability experiments
| DOT/FAA/CT-92/12-VOL-1 | p 2582 N93-25110
A simple, approximate model of parachute inflation
| DE93-002465 | p 2576 N93-25121
Mechanistic studies of the CVD of silicon nitride from SiF4 and NH3
| DE93-004500 | p 2644 N93-25312
A heat transfer analysis of a mobile vehicle radiation-shielded operator compartment
| DE93-007428 | p 2800 N93-25318
A mission concept for near term Lunar exploration
| DE93-007598 | p 2896 N93-25321
An improved spectral load balancing method
| DE93-007582 | p 2810 N93-25386
Metastable SiC and SiGeC alloys by carbon implantation and solid phase epitaxy
| DE93-007594 | p 2863 N93-25387
A comparison of moisture resistance with different types of end-terminations in ceramic capacitors
| DE93-007600 | p 2689 N93-25416
Characterization of ceramic capacitors for high-voltage pulse-discharge applications
| DE93-007601 | p 2689 N93-25417
Detecting damaged cables using a preionized gas technique
| DE93-007588 | p 2689 N93-25429
Temperature dependent sensor response caused by polymer-solvent interactions
| DE93-005368 | p 2655 N93-25444
Chromate-free corrosion resistant talc coatings for aluminum alloys
| DE93-005370 | p 2655 N93-25446
Pyroshock: Bibliography
| DE93-007605 | p 2726 N93-25489
Stability analysis and modeling of rotating flexible structures
| DE93-008493 | p 2844 N93-25520
HERO resistant semiconductor bridge igniter p 2627 N93-26024
Development of rate expressions for the thermal decomposition of RDX p 2629 N93-26034
Internal current probing of integrated circuits using magnetic force microscopy
| DE93-006752 | p 2692 N93-26501
Visible light emission from porous silicon examined by photoluminescence and Raman spectroscopy
| DE93-006780 | p 2646 N93-26502
Digital filter control of remotely operated flexible robotic structures
| DE93-007587 | p 2827 N93-26596
FALCON nuclear-reactor-pumped laser program and wireless power transmission
| DE93-007607 | p 2715 N93-26597

SANDIA NATIONAL LABS., LIVERMORE, CA.
Thermal decomposition of HMX, mononitroso-RDX, TNCHP and K6 in the liquid phase: Results from simultaneous thermogravimetry modulated beam mass spectrometry measurements p 2628 N93-26033
Thermal decomposition of energetic materials. 4: Deuterium isotope effects and isotopic scrambling condensed-phased decomposition of 1,3,5-trinitrohexahydro-s-triazine
| AD-A261804 | p 2662 N93-26387

SCHOOL OF AEROSPACE MEDICINE, BROOKS AFB, TX.
Proceedings of the 33rd Annual Military LibrariansWorkshop
| AD-A261071 | p 2882 N93-26242

SCIENCE APPLICATIONS, INC., MCLEAN, VA.
SAVS: A Space Analysis and Visualization System p 2881 N93-25812

SCRIPPS INSTITUTION OF OCEANOGRAPHY, LA JOLLA, CA.
Improved fatigue life for moorings
| PB93-161198 | p 2730 N93-26320
Wind-driven coastal generation of annual mesoscale eddy activity in the California current
| AD-A261355 | p 2790 N93-26331
Boundary layer coupling between an explosive cyclone and the Gulf Stream during ERICA
| AD-A261577 | p 2787 N93-26513

SEA TECH, INC., CORVALLIS, OR.
Development of an expendable particle sensor
| AD-A261127 | p 2710 N93-26044

SENSORS UNLTD., INC., PRINCETON, NJ.
A high performance room-temperature near-infrared camera
| AD-A260602 | p 2709 N93-25634

SEPA S.P.A., TURIN (ITALY).
High resolution digital synthesizer for a Rb frequency standard p 2694 N93-25057

SHANGHAI OBSERVATORY (CHINA).
The development progresses of hydrogen masers at Shanghai Observatory p 2716 N93-25048

SMITH-KETTLEWELL INST. OF VISUAL SCIENCES, SAN FRANCISCO, CA.
Visual processing of object velocity and acceleration
| AD-A261048 | p 2800 N93-25778

SMITHSONIAN ASTROPHYSICAL OBSERVATORY, CAMBRIDGE, MA.
VETA-I x ray test analysis
| NASA-CR-192321 | p 2854 N93-26183
Intensity distribution of the x ray source for the AXAF VETA-I mirror test p 2854 N93-26184
VETA-1 x ray detection system p 2854 N93-26185
VETA x ray data acquisition and control system p 2854 N93-26186
Correcting x ray spectra obtained from the AXAF VETA-I mirror calibration for pileup, continuum, background and deadtime p 2854 N93-26187
AXAF VETA-I mirror encircled energy measurements and data reduction p 2855 N93-26188
Precision of the calibration of the AXAF engineering test article (VETA) mirrors p 2855 N93-26189
Image analysis of the AXAF VETA-I x ray mirror p 2855 N93-26190
Surface finish quality of the outer AXAF mirror pair based on x ray measurements of the VETA-I p 2855 N93-26191
The x ray reflectivity of the AXAF VETA-I optics p 2855 N93-26192

SOCIETE INDUSTRIELLE DE COMBUSTIBLE NUCLEAIRE, ANNECY (FRANCE).
Crystal growth of berlinite: Methods for growing longer crystals and improving the quality p 2838 N93-25025

SOFTWARE PRODUCTIVITY CONSORTIUM, HERNDON, VA.
Three view language: A graphics-based language for requirements definition, version 01.00.00
| AD-A261732 | p 2813 N93-26583

SOLOMON (G.), PASADENA, CA.
Golay and other box codes p 2678 N93-26116

SORBENT TECHNOLOGIES CORP., TWINSBURG, OH.
Development and demonstration of a new filter system to control emissions during jet engine testing
| AD-A261203 | p 2766 N93-26243

SOUTH DAKOTA SCHOOL OF MINES AND TECHNOLOGY, RAPID CITY.
The effects of cloud inhomogeneities upon radiative fluxes, and the supply of a cloud truth validation dataset
| NASA-CR-191711 | p 2787 N93-26492

SOUTHAMPTON UNIV. (ENGLAND).
Scale dependence in the reflectance of deciduous woodland: Evidence from a helicopter-mounted spectroradiometer p 2752 N93-24865

SOUTHEASTERN CENTER FOR ELECTRICAL ENGINEERING EDUCATION, INC., SAINT CLOUD, FL.
Inflight evaluation of an acoustic orientation instrument
| AD-A260752 | p 2591 N93-25909
Design, fabrication, and testing of a three-dimensional acoustic orientation instrument (3-D AOI): Drawings, engineering and associated lists (conceptual and development design)
| AD-A260934 | p 2845 N93-25915

SOUTHWEST RESEARCH INST., SAN ANTONIO, TX.
High strain rate damage development and failure mechanisms in tungsten heavy alloys
| AD-A260856 | p 2651 N93-25788
Development of a method to determine the autoxidation of turbine fuels
| AD-A260578 | p 2661 N93-25902
Effect of a metal deactivator fuel additive on fuel deposition in fuel atomizers at high temperature
| AD-A260915 | p 2661 N93-25914

SPACE COMPUTER CORP., SANTA MONICA, CA.
Algorithms for space-based infrared surveillance
| AD-A261891 | p 2857 N93-26542

SPACE TELESCOPE SCIENCE INST., BALTIMORE, MD.
Development of an expert data reduction assistant p 2880 N93-25808
Hubble Space Telescope: The archived exposures catalog, version 2.0
| NASA-CR-192896 | p 2883 N93-26423

SPECTRA RESEARCH SYSTEMS, INC., HUNTSVILLE, AL.
Advanced life support study. Modification 10: ECLSS logistical support analysis for Space Station Freedom
| NASA-CR-192481 | p 2801 N93-25888

SPIRE CORP., BEDFORD, MA.
MOCVD process technology for affordable, high-yield, high-performance MESFET structures. Phase 3: MIMIC
| AD-A261178 | p 2690 N93-25820

SPOT IMAGE CORP., TOULOUSE (FRANCE).
The use of SPOT data in natural disaster prevention and damage assessment p 2743 N93-24811

SRI INTERNATIONAL CORP., MENLO PARK, CA.
Comparison of the electrical charging and discharging environments of multiple aircraft-borne electric-field measurement systems p 2583 N93-24887
Diagnostics of diamond film deposition plasmas
| AD-A260866 | p 2860 N93-25626
Photoexcitation of carbon fullerenes
| AD-A260739 | p 2849 N93-25644

IR materials producibility
| AD-A261099 | p 2853 N93-25766
Study of auroral dynamics with combined spacecraft and incoherent-scatter radar data
| NASA-CR-192224 | p 2775 N93-26159
Fundamental aspects of metal joining: The study of strong interfaces
| AD-A261293 | p 2653 N93-26304

STANFORD LINEAR ACCELERATOR CENTER, CA.
Topics in CP violation
| DE93-007615 | p 2847 N93-25323

STANFORD UNIV., CA.
Aerodynamic design and synthesis of the oblique flying wing supersonic transport p 2587 N93-24768
Computational study of the aerodynamics and control by blowing of asymmetric vortical flows over delta wings p 2574 N93-24772
Ultrasonic rate measurement of multiphase flow
| DE93-000112 | p 2695 N93-24954
Two neural network algorithms for designing optimal terminal controllers with open final time
| NASA-CR-177599 | p 2817 N93-25137
Shock tube application to the study of compressible turbulent boundary layer with mass injection p 2697 N93-25252
Direct solutions of the Navier-Stokes equations with application to static aeroelasticity p 2697 N93-25259
Advances in nonlinear optical materials and devices
| NASA-CR-192681 | p 2852 N93-25281
Data parallel finite element techniques for large-scale computational fluid dynamics p 2699 N93-25334
Hierarchical dynamics in distributed information processing p 2875 N93-25350
Ultrafast measurements of 200 gigahertz Schottky photodiodes p 2688 N93-25392
Formulation and treatment of frictional contact problems using finite elements p 2717 N93-25412
Elastic modeling and migration in Earth models p 2771 N93-25433
An alternate approach to space missions involving a long tether p 2616 N93-25470
Structural and aerodynamic optimization of joined-wing aircraft p 2588 N93-25526
The design of a propulsion system using vent gas from a liquid helium cryogenic system p 2623 N93-25539
Navier-Stokes simulations of unsteady transonic flow phenomena p 2578 N93-25542
Tangential fuselage blowing on an ogive cylinder p 2578 N93-25545
Diskoseismology: Probing relativistic accretion disks p 2894 N93-25622
Analysis of wing wake roll-up using a vortex-in-cell method p 2579 N93-25706
An investigation of photothermal velocimetry for application to transient, high-speed gas flows p 2579 N93-25720
Distributed information storage p 2877 N93-25722
Analysis of the gap in high-temperature superconductors using photoemission spectroscopy p 2865 N93-25744
Time series analysis and multivariate analysis
| AD-A261014 | p 2830 N93-25860
Advanced optical fiber communication systems
| AD-A261802 | p 2856 N93-26256
Efficient nonlinear optical conversion of 1.319-micron laser radiation
| AD-A261309 | p 2715 N93-26297
Spontaneous discovery and use of categorical structure
| AD-A261658 | p 2798 N93-26364
Multivariable control for flexible IC processing
| AD-A261685 | p 2692 N93-26366
Laser physics and laser techniques
| AD-A261595 | p 2715 N93-26524

STATE DEPT., WASHINGTON, DC.
Science, Technology, and Industrial Policy in the Former Soviet Union
| DE93-006528 | p 2887 N93-26499

STATE OCEANOGRAPHIC INST., MOSCOW (USSR).
Role of the ocean in climate changes p 2732 N93-24918

STATE UNIV. OF NEW YORK, ALBANY.
The modeling of complex continua: Fundamental obstacles and grand challenges
| DE93-006507 | p 2696 N93-25193

STATE UNIV. OF NEW YORK, BUFFALO.
Scalar gain interpretation of large order filters p 2606 N93-24729
Electric field effects on quantum-confined semiconductor structures p 2865 N93-25703
Effect of cytoskeletal reagents on stretch activated ion channels
| AD-A261089 | p 2793 N93-25764

STATE UNIV. OF NEW YORK, STONY BROOK.
Ionization probes of molecular structure and chemistry
| DE93-008211 | p 2847 N93-25310
The structure of the nearby universe traced by theIRAS galaxies
| NASA-CR-192809 | p 2889 N93-25331

STERLING SOFTWARE, MOFFETT FIELD, CA.
Scientific visualization using the Flow Analysis Software Toolkit (FAST) p 2814 N93-25600

STOCKTON STATE COLL., POMONA, NJ.
Geochemistry and petrology of primitive achondrite meteorites LEW 88280, MAC 88177, ALHA 81187, EET 84302, and LEW 88663 p 2896 N93-26067

STUTTGART UNIV. (GERMANY).
The advances in F and T technology: Their benefits of and for space science and technology p 2831 N93-24979
The application of the PRARE principle for precise two-way time transfer to space-based atomic clocks p 2832 N93-24983

SUN REFINING AND MARKETING CO., MARCUS HOOK, PA.
Catalytic conversion of light alkanes
| DE93-009646 | p 2644 N93-25499

SUPERCOMPUTER RESEARCH CENTER, BOWIE, MD.
Splash 2 p 2814 N93-25575

SUPERCONDUCTING SUPER COLLIDER LAB., DALLAS, TX.
Studies of avalanche photodiodes for scintillating fibre tracking readout
| DE93-008370 | p 2689 N93-25491

SURFACE OPTICS CORP., SAN DIEGO, CA.
Enhanced backscattering from rough surfaces
| AD-A261000 | p 2676 N93-25855

SURREY UNIV., GUILDFORD (ENGLAND).
Internal stresses and the cyclic deformation of an aluminum matrix composite p 2650 N93-25436
Vortex shedding in oscillatory flow p 2700 N93-25438
Numerical and experimental analyses of large composite skeletal satellite systems p 2616 N93-25463

SURVEILLANCE RESEARCH LAB., SALISBURY (AUSTRALIA).
Distortion measurements on bandpass filters with powdered iron toroidal inductors
| AD-A260790 | p 2675 N93-25689

SURVEYING AND MAPPING AGENCY OF NORTHRHINE-WESTFALIA, BONN-BAD GODESBERG (GERMANY).
Operational use of MOMS-02 (P2) data p 2752 N93-24866

SUSSEX UNIV., BRIGHTON (ENGLAND).
Origin and evolution of cataclysmic variables p 2893 N93-25245
Radial velocity studies of the secondary in cataclysmic variables p 2888 N93-25286

SVERDRUP TECHNOLOGY, INC., BROOK PARK, OH.
Laser beamed power: Satellite demonstration applications
| NASA-CR-190793 | p 2623 N93-25132

SVERIGES LANTBRUKSUNIV., UMEA.
Interpretation and segmentation of changed forest stands from difference imagery based on regression functions p 2748 N93-24839
Standwise forest inventory and mapping for operational management planning p 2752 N93-24863

SWEDISH BOARD FOR SPACE ACTIVITIES, STOCKHOLM.
Space research in Sweden, 1990-1991 p 2888 N93-25887

SWEDISH ENVIRONMENTAL PROTECTION BOARD, SKANE.
Forest decline monitoring using Landsat TM, digital stand data and DEMs p 2749 N93-24846

SWEDISH SPACE CORP., SOLNA.
Tropical forest monitoring with high resolution satellite data p 2748 N93-24841
Swedish forest information atlas p 2749 N93-24847

SYDNEY UNIV. (AUSTRALIA).
International Workshop on Advances in Inorganic Fibre Technology
| AD-A260719 | p 2639 N93-25908

SYMBIOTICS, INC., CAMBRIDGE, MA.
Object-oriented tools for distributed computing p 2817 N93-25576

SYNECTICS CORP., ROME, NY.
Arc Digital Raster Imagery (ADRI) development
| AD-A261850 | p 2812 N93-26275

SYSTEMS SCIENCE AND SOFTWARE, LA JOLLA, CA.
Data analysis support for the Shuttle Potential and Return Electron Experiment (SPREE) on the Tethered Satellite System 1 (TSS-1) flight
| AD-A261646 | p 2618 N93-26232

SYSTEMS SCIENCE AND SOFTWARE, SAN DIEGO, CA.
Modeling and analysis tools p 2897 N93-26397

SZCZECIN UNIV., LODZ (POLAND).
Hel's peninsula coastal zone changes in the last 40 years on a base of remote sensing methods p 2747 N93-24832

T

TANA-JYRA, KY (FINLAND).
Transmission system for a transfer device gripping a double wheel
| CA-PATENT-APPL-SN-2024585 | p 2597 N93-25178

TECHNICAL RESEARCH CENTRE OF FINLAND, ESPOO.
Demonstration of seasonal changes in the territory of Finland using multitemporal NOAA-AVHRR data p 2742 N93-24801
The accuracy of SYLT- and RNS-based time scales at MTI and SNT during 1990-1991 p 2835 N93-25006

TECHNISCHE UNIV., BERLIN (GERMANY).
Observation of forest damages in the Harz mountains by means of satellite remote sensing p 2749 N93-24848

TECHNISCHE UNIV., DRESDEN (GERMAN D.R.).
Application of photographic remote sensing data from space for information about forests p 2748 N93-24838

TECHNISCHE UNIV., MUNICH (GERMANY).
Geologic and hydrogeologic mapping of Iceland with multisensor data (JERS-1, ERS-1, SPOT, Landsat and SEASAT) p 2740 N93-24792
Remote sensing of non-renewable resources p 2744 N93-24814
EUROSTARS: A system for thematic analysis of remote sensed data p 2753 N93-24871

TECHNO-SCIENCES, INC., LANHAM, MD.
Realtime control of multiple sensor systems
| AD-A261037 | p 2680 N93-26226

TEKELEC-SYSTEMES, LES ULIS (FRANCE).
Time and frequency reference for a trajectory measurement system p 2837 N93-25023
Time generation and distribution system for a military national synchronization p 2842 N93-25060

TELE QUARTZ GROUP G.M.B.H., NECKARBISCHOFSHEIM (GERMANY).
Improved PI-network measurement of all quartz crystal parameters by appropriate modelling of the test fixture p 2833 N93-24995
A state-of-the-art crystal filter design package using Windows 3.0 techniques p 2693 N93-25010

TELECOM SOLUTIONS EUROPE LTD., LEATHERHEAD (ENGLAND).
Strategies for synchronisation in an evolving telecommunications network p 2687 N93-25063

TELECOM SOLUTIONS LTD., SAN JOSE, CA.
Synopsis of timing measurement techniques used in telecommunications p 2687 N93-25064

TELESPAZIO, S.P.A., ROME (ITALY).
Determination of environmental dynamics using NOAA satellite data and a water balance model for the Mediterranean landscape p 2741 N93-24794
Agroclimatological zonation by AVHRR data for vegetation monitoring p 2741 N93-24795
Remote sensing monitoring and hindcasting of the accident occurred to the tanker Haven in the Gulf of Genoa (Italy) p 2747 N93-24830
Algal blooms and gel production in Adriatic Sea observed by remote sensing techniques p 2747 N93-24831

TEMPLE UNIV., PHILADELPHIA, PA.
Factors associated with perceptions of productivity and usage of information technology in a service organization p 2875 N93-25421

TENNESSEE STATE UNIV., NASHVILLE.
Robust controls with structured perturbations
| NASA-CR-192956 | p 2817 N93-24757
The 32nd CDC: System identification using interval dynamic models
| NASA-CR-192895 | p 2818 N93-25155
Stability margins for multilinear interval systems by way of phase conditions: A unified approach
| NASA-CR-192893 | p 2819 N93-25226
Parametric stability margin for multilinear interval control systems
| NASA-CR-192892 | p 2819 N93-25296

TENNESSEE UNIV., KNOXVILLE.
Particle simulation for 10.6 micron picosecond laser-induced breakdown in gases p 2712 N93-25280
A computational method for the analysis of acoustic radiation from turbofan inlets p 2845 N93-25717
Development and application of an advanced ductile fracture mechanics methodology p 2727 N93-25718
Electrochemical and spectroscopic studies of molten halides
| AD-A261687 | p 2646 N93-26439

TENNESSEE UNIV. SPACE INST., TULLAHOMA.
Evaluation of a candidate material for a coal-fired magnetohydrodynamic (MHD) high temperature recuperative air heater
| DE93-006630 | p 2858 N93-24968
Assessment of torsatrons as reactors
| DE93-006721 | p 2858 N93-24969

TEXAS A&M UNIV., COLLEGE STATION.
The 32nd CDC: Robust stabilizer synthesis for interval plants using Nevanlina-pick theory
| NASA-CR-192894 | p 2818 N93-25156
Integrated Development Support Environment (IDSE)
| AD-A261088 | p 2877 N93-25763
Activation of methane by clean and chemically modified single crystal oxide surfaces
| PB93-157295 | p 2644 N93-25817
DC-DC power converter research for Orbiter/Station power exchange
| NASA-CR-192939 | p 2633 N93-26425
Mechanics and control of multibody structural systems
| AD-A261576 | p 2619 N93-26456
Thermodynamic properties of natural gas mixtures
| PB93-167112 | p 2872 N93-26509
IDEF6: A design rationale capture method concept paper
| AD-A261594 | p 2884 N93-26523

TEXAS TECHNOLOGICAL UNIV., LUBBOCK.
Study of plate-fin heat exchanger and cold plate for the active thermal control system of Space Station
p 2619 N93-26064

TEXAS UNIV., ARLINGTON.
Damage-survivable and damage-tolerant laminated composites with optimally placed piezoelectric layers
| AD-A260879 | p 2636 N93-25631

TEXAS UNIV., AUSTIN.
A control structure for fault-tolerant operation of robotic manipulators
| DE93-005783 | p 2717 N93-25413
Expedient repair of structural facilities
| AD-A260727 | p 2598 N93-25656
The 0.3 mm diameter flexible amperometric lactate probe
| AD-A260826 | p 2690 N93-25782
Propagation of finite amplitude sound in a waveguide with a parabolic sound velocity profile
| ARL-TR-92-11 | p 2846 N93-26179
Phosphorus-, nitrogen-, sulfur-, and chlorine-containing molecules on surfaces
| AD-A261265 | p 2657 N93-26303
Lageos laser ranging earth rotation
| AD-A261471 | p 2757 N93-26354
Large scale rainfall diversity and satellite propagation
p 2683 N93-26466
L- and K-band LMSS propagation measurements using MARECS-B, OLYMPUS, and ACTS
p 2683 N93-26467
Cost-effectiveness analysis of TxDOT CNG fleet conversion, volume 2
| PB93-159432 | p 2720 N93-26534
Cost-effectiveness analysis of TxDOT CNG fleet conversion, volume 1
| PB93-165603 | p 2720 N93-26585
Documentation for propane fleet conversion cost-effectiveness model
| PB93-165611 | p 2720 N93-26590

TEXAS UNIV., EL PASO.
Min and max are the only continuous ampersand-, V-operations for finite logics
| NASA-CR-192952 | p 2820 N93-25452
Towards a formalism for program generation
| AD-A261689 | p 2812 N93-26368

TEXAS UNIV., SAN ANTONIO.
Proceedings of Workshop 1: The Human Brainmap Database
| AD-A260720 | p 2796 N93-25654

THOMAS JEFFERSON HIGH SCHOOL, FALLS CHURCH, VA.
What is the relationship between altitude and weight in a model rocket? p 2603 N93-24715

TIME AND FREQUENCY LTD., HOLON (ISRAEL).
TF-4020A: TFL's new compact military rubidium standard p 2838 N93-25026

TIMETECH G.M.B.H., STUTTGART (GERMANY).
A new modem for microwave time synchronisation via geosynchronous telecommunication satellites
p 2686 N93-24999

TOHOKU ELECTRIC POWER CO., INC., SENDAI (JAPAN).
Lightning characteristics in the north-east part of Japan observed by a magnetic direction-finder network
p 2779 N93-24892

TOKYO INST. OF TECH., YOKAHAMA (JAPAN).
Fundamental characteristics of a laser-diode-pumped rubidium maser with an external feedback loop
p 2716 N93-25068

TOKYO UNIV. (JAPAN).
Observation of radiation from lightning discharges by LPATS p 2779 N93-24888

TOLEDO UNIV., OH.
Estimating turbine limit load
| NASA-CR-191105 | p 2580 N93-25883

TOULOUSE UNIV. (FRANCE).
Interest of complementary data of coarse and high spatial resolution for agro-climatic crop monitoring
p 2750 N93-24853

TRINITY UNIV., SAN ANTONIO, TX.
Effects of space radiation on humoral and cellular immunity in rhesus monkeys
| AD-A261808 | p 2793 N93-26259

TRW, INC., WARNER ROBINS, GA.
Technical operating report on the Data Integration and Collection Environment (DICE) instrumentation system design
| AD-A261105 | p 2591 N93-26572

TRW SPACE TECHNOLOGY LABS., REDONDO BEACH, CA.
Gas-Grain Simulation Facility (GGSF). Volume 1: Stage 1 facility definition studies
| NASA-CR-177606 | p 2887 N93-25442

TUFTS UNIV., MEDFORD, MA.
In-process cure monitoring of composites via fiber-optic fluorescence
| AD-A261712 | p 2641 N93-26580

U

UNITED KINGDOM ATOMIC ENERGY AUTHORITY, ABINGDON (ENGLAND).
Equipment testing with damped sinewaves between 1 and 50 MHz p 2692 N93-24881
Parameters influencing the hot-spot ignition of aviation fuel/air and ethylene/air mixtures p 2583 N93-24886
Zoning of aircraft by electric field modelling
p 2583 N93-24894
Alternative equipment test procedures for simultaneous current injection on multiple cable bundles
p 2693 N93-24903

UNITED NATIONS, NEW YORK, NY.
Natural disasters and their mitigation using space technology p 2742 N93-24804

UNITED TECHNOLOGIES CORP., WEST PALM BEACH, FL.
Fatigue in single crystal nickel superalloys
| AD-A261742 | p 2652 N93-26282

UNITED TECHNOLOGIES CORP., WINDSOR LOCKS, CT.
Theory for noise of propellers in angular inflow with parametric studies and experimental verification
| NASA-CR-4499 | p 2844 N93-25094

UNITED TECHNOLOGIES RESEARCH CENTER, EAST HARTFORD, CT.
A summary of the JANNAF workshop on liquid rocket atomization p 2625 N93-26014
Measurement of droplet vaporization rate enhancement caused by acoustic disturbances p 2626 N93-26015

UNIVERSIDAD NACIONAL AUTONOMA DE MEXICO, MEXICO CITY.
Study of atmospheric electrical events above complex terrain p 2780 N93-24897

UNIVERSITIES SPACE RESEARCH ASSOCIATION, GREENBELT, MD.
Adjustable lossless image compression based on a natural splitting of an image into drawing, shading, and fine-grained components p 2804 N93-25923

UNIVERSITY CORP. FOR ATMOSPHERIC RESEARCH, BOULDER, CO.
Synoptic and Mesoscale Meteorology Instruction Workshop
| PB93-156347 | p 2785 N93-25870

UNIVERSITY OF CENTRAL FLORIDA, ORLANDO.
Time resolved studies of in-well and cross-well carrier transport in MQW semiconductor structures
| AD-A261170 | p 2714 N93-25774
Inferring heuristic classification hierarchies from natural language input p 2825 N93-25979
Design of an air traffic computer simulation system to support investigation of civil tiltrotor aircraft operations
| NASA-CR-192920 | p 2585 N93-26052

UNIVERSITY OF SOUTH FLORIDA, TAMPA.
Fundamental and applied aspects of defect engineering in GaAs
| AD-A260573 | p 2867 N93-25899

UNIVERSITY OF SOUTHERN CALIFORNIA, LOS ANGELES.
Automated in situ observations of upper ocean biogeochemistry, bio-optics, and physics and their potential use for global studies p 2736 N93-24939
Second-harmonic generation in optical fibers and glass
| AD-A260592 | p 2853 N93-25839
Particle size as a factor in agglomeration in slurry fuels p 2625 N93-26013

UNIVERSITY OF SOUTHERN CALIFORNIA, MARINA DEL REY.
Gigabit network communications research
| AD-A260644 | p 2675 N93-25640
A design of a fast and area efficient multi-input Muller C-element
| AD-A261002 | p 2690 N93-25856

UNIVERSITY OF SOUTHERN ILLINOIS, CARBONDALE.
Improved determination of vector lithospheric magnetic anomalies from MAGSAT data
| NASA-CR-192784 | p 2771 N93-25201
Proceedings of the 16th International Workshop on Condensed Matter Theories
| AD-A261078 | p 2868 N93-26252

UNIVERSITY OF TECHNOLOGY, LOUGHBOROUGH (ENGLAND).
The General Information Programme (PGI) and developing countries: A case study of Iraq
p 2874 N93-25209
A framework for the design of usable electronic text
p 2877 N93-25754
Generation of acoustic waves by focused infrared neodymium-laser radiation p 2714 N93-25761

UNIVERSITY OF WESTERN AUSTRALIA, NEDLANDS.
Multi-date algorithms for predicting surface water quality parameters in estuarine and coastal waters using Landsat TM data
| ED-659-CP | p 2746 N93-24829
Coastal environmental mapping using Landsat data
| ED-658-CP | p 2747 N93-24835

UNIVERSITY OF WESTERN ILLINOIS, MACOMB.
Analysis of the lettuce data from the variable pressure growth chamber at NASA Johnson Space Center: A three-stage nested design model p 2794 N93-26069

UTAH STATE UNIV., LOGAN.
Multi-rate, real time image compression for images dominated by point sources p 2805 N93-25932

UTAH UNIV., SALT LAKE CITY.
Photomodulation spectroscopy of photocarrier dynamics, electronic defects and morphology of conducting polymers
| DE93-010140 | p 2655 N93-25524
On the vertical structure of seasonal, interannual and intraseasonal flows p 2782 N93-25557
Collisional energy transfer in biomolecular ion-molecule dynamics
| AD-A260911 | p 2849 N93-25659
A three-dimensional model for the residual stresses in a unidirectional composite plate p 2728 N93-25825
Failure considerations in composite systems based on 3D micromechanical stress fields, part A
| AD-A261698 | p 2641 N93-26382

V

VALENCIA UNIV., BURJASSOT (SPAIN).
Correlation between NDVI values derived from NOAA AVHRR HRPT data and ground measurements of precipitation in the EFEDA study area (Spain)
p 2738 N93-24780

VANDERBILT UNIV., NASHVILLE, TN.
Improving performance through concept formation and conceptual clustering
| NASA-CR-192726 | p 2828 N93-25262

VEDA, INC., LEXINGTON PARK, MD.
Commercial Precipitation Static (P-static) test equipment p 2711 N93-24901

VERTIC, LONDON (ENGLAND).
Verification of a climate convention: Role and limitations of a space based remote sensing system
p 2738 N93-24781

VIGYAN RESEARCH ASSOCIATES, INC., HAMPTON, VA.
A feasibility study of using Langley 0.3-m transonic cryogenic tunnel sidewall boundary-layer removal system for heavy gas testing
| NASA-CR-191438 | p 2695 N93-25087
Multi-viewpoint clustering analysis
p 2825 N93-25980

VIRGINIA POLYTECHNIC INST. AND STATE UNIV., BLACKSBURG.
Vibration, buckling, and postbuckling of laminated composites with delaminations p 2723 N93-24765
Flow visualizations of perpendicular blade vortex interactions
| NASA-CR-192725 | p 2696 N93-25208
The transient development of vortices over delta wings p 2576 N93-25269
Integrated aerodynamic-structural wing design optimization p 2587 N93-25279
Identification and control of lightly damped, large space structures: An experimental evaluation
p 2616 N93-25351
Analytical and experimental study of control effort associated with model reference adaptive control
p 2820 N93-25468
Stochastic and seismic design response of linear and nonlinear structures p 2726 N93-25484

Experimental and computational investigation of helium injection into air at supersonic and hypersonic speeds
p 2577 N93-25487
Stress and reliability analyses of multilayered composite cylinder under thermal and mechanical loads
p 2726 N93-25533
Numerical simulation of damage and progressive failures in composite laminates using the layerwise plate theory
p 2636 N93-25661
Finite element micromechanics modeling of inelastic deformation of unidirectionally fiber-reinforced composites p 2637 N93-25680
An efficient technique for structural reliability with applications p 2727 N93-25681
Nonlinear vibrations, stability, and dynamics of structures and mechanisms
| AD-A260871 | p 2728 N93-25838
Investigation of coupled analysis techniques for adaptive material structural systems
| AD-A261359 | p 2868 N93-26332
Computational methods for flow problems: Parallel algorithms, flow control, and novel approaches
| AD-A261400 | p 2707 N93-26400
The Virginia Tech OLYMPUS propagation experiment
p 2685 N93-26479
ACTS propagation terminal update
p 2685 N93-26484

VIRGINIA UNIV., CHARLOTTESVILLE.
Mechanical alloying processing and application to development of structural materials
| AD-A261251 | p 2652 N93-26264
Chromospheric activity in algol binaries
| AD-A261440 | p 2896 N93-26508

VOLUNTEERS IN TECHNICAL ASSISTANCE, INC., ARLINGTON, VA.
The PACSAT Communications Experiment (PCE)
| DE93-008185 | p 2674 N93-25308

W

WAGENINGEN AGRICULTURAL UNIV. (NETHERLANDS).
Measuring the intensity of nitrogen fertilization of grassland by means of remote sensing
p 2751 N93-24859

WALL (PETER K.) ELECTROACOUSTICS, PENRITH (ENGLAND).
Very wide bandwidth HF crystal filters
p 2693 N93-25039

WASHINGTON STATE UNIV., PULLMAN.
Defect initiation/growth and energy dissipation induced by deformation and fracture
| AD-A261703 | p 2869 N93-26385

WASHINGTON UNIV., SAINT LOUIS, MO.
Computation of hypersonic viscous flowfields using the parabolized Navier-Stokes equations
p 2694 N93-24766
A compact high-order Euler solver for unstructured grids p 2699 N93-25341

WASHINGTON UNIV., SEATTLE.
Gravitational radiation from coalescing binary star systems p 2900 N93-25625
Summary by the cloud and aerosol research group for ASTEX
| AD-A261292 | p 2766 N93-26292
Methods of optimization under uncertainty
| AD-A261487 | p 2873 N93-26342

WEST VIRGINIA UNIV., MORGANTOWN.
A hypertext framework for group support systems
| AD-A261731 | p 2885 N93-26582

WESTINGHOUSE ENVIRONMENTAL MANAGEMENT CO. OF OHIO, CINCINNATI.
Use of the Environmental Resource Management and Analysis System at the Fernald Environmental Management Project
| DE93-002943 | p 2760 N93-24955

WESTINGHOUSE HANFORD CO., RICHLAND, WA.
Mechanical properties of martensitic alloy AISI 422
| DE93-006563 | p 2649 N93-25255

WESTINGHOUSE SAVANNAH RIVER CO., AIKEN, SC.
Use of the 1991 ASCOT field study data in a mesoscale model employing a four-dimensional data assimilation technique
| DE93-002683 | p 2769 N93-24672
A comparison of the WIND System atmospheric models and MATS data
| DE93-002687 | p 2760 N93-24673
Environmental test program for superconducting materials and devices
| DE93-003646 | p 2864 N93-25506

WICHITA STATE UNIV., KS.
General aviation aircraft: Normal acceleration data analysis and collection project
| DOT/FAA/CT-91/20 | p 2586 N93-24739

WINAND STARING CENTRE, WAGENINGEN (NETHERLANDS).
Land cover monitoring in the Netherlands applying satellite remote sensing p 2740 N93-24789

WISCONSIN UNIV., MADISON.
The effects of rotation on the winds from hot stars
p 2894 N93-25620
Theoretical and experimental research in infrared technology
| AD-A260926 | p 2853 N93-25646
Quantifying distributed damage in composites via the thermoelastic effect p 2637 N93-25691
Pressure torques and circulation changes in Rocky Mountain lee cyclones p 2783 N93-25724
Planetary data analysis and display system: A version of PC-McIDAS p 2880 N93-25806
Center for Advanced Propulsion Systems (fellowship)
| AD-A260571 | p 2632 N93-26216
Computation and theory in large-scale optimization
| AD-A261419 | p 2813 N93-26450

WISCONSIN UNIV., MILWAUKEE.
Cosmic string cosmology p 2891 N93-24907
Planetary Biology and Microbial Ecology: Molecular Ecology and the Global Nitrogen cycle
| NASA-CR-4497 | p 2803 N93-26157

WOODS HOLE OCEANOGRAPHIC INST., MA.
Coastal ocean processes: A science prospectus
| AD-A261702 | p 2790 N93-26384
Interaction of an eddy with a continental slope
| AD-A261550 | p 2791 N93-26578

WORCESTER POLYTECHNIC INST., MA.
Measurement of optical properties of infrared bandgap superlattices
| AD-A260859 | p 2866 N93-25789

WRIGHT LAB., EGLIN AFB, FL.
Miniature Optical Wide-Angle-Lens Startracker (Mini-OWLS) p 2606 N93-24728

WRIGHT LAB., WRIGHT-PATTERSON AFB, OH.
Characterization of aerospace grade resins and composites through pressurized volumetric dilatometry
| AD-A260794 | p 2639 N93-25918
Studies in air/air supersonic mixing layers
p 2582 N93-26007
Gasp 1.3 results for the transverse hydrogen reacting jet p 2625 N93-26011
Optically smart surfaces survivability testing at Mach 3
| AD-A261785 | p 2857 N93-26566

WYOMING UNIV., LARAMIE.
A vision architecture for the extravehicular activity retriever p 2827 N93-26071

Y

YALE UNIV., NEW HAVEN, CT.
Far-infrared emission, gas, and ultraluminous HII regions in M101
| NASA-CR-192791 | p 2890 N93-25755
The rapid solution of the Laplace equation on regions with fractal boundaries
| AD-A260585 | p 2828 N93-25905
Solution of nonlinear boundary value problem on successively refined grids
| AD-A261395 | p 2829 N93-26519

YAP ANALYTICS, INC., LEXINGTON, MA.
Modeling of atom-diatom scattering
| AD-A261645 | p 2849 N93-26173
Progress in impulse approach research
| AD-A261728 | p 2850 N93-26281

YORK UNIV. (ONTARIO).
The third-order permittivity of quartz obtained by different methods p 2840 N93-25046
Passive microwave remote sensing of snow-covered floating ice during spring conditions in the Arctic and Antarctic
| ISBN-0-315-70444-6 | p 2754 N93-25422
Gravity waves from O2 airglow p 2772 N93-25547
Polarizing Michelson interferometer for measuring thermospheric winds
| ISBN-0-315-70442-X | p 2784 N93-25731

Z

ZURICH UNIV. (SWITZERLAND).
Remote sensing in hydrology and water management
p 2744 N93-24816

Typical Contract Number Index Listing

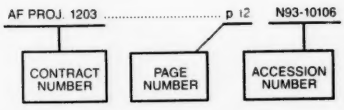

Listings in this index are arranged alphanumerically by contract number. Under each contract number the accession numbers denoting documents that have been produced as a result of research done under that contract are arranged in ascending order. The page number helps to locate the citation in the abstract section. The accession number denotes the number by which the citation is identified.

AF PROJ. 2104 ..... p 2598 N93-25656
AF PROJ. 2940 ..... p 2877 N93-25763
AF PROJ. 3153 ..... p 2722 N93-26526
AF PROJ. 4506 ..... p 2830 N93-26255
AF PROJ. 4519 ..... p 2675 N93-25767
AF PROJ. 5581 ..... p 2710 N93-25696
AF-AFOSR-0020-90 ..... p 2707 N93-26269
AF-AFOSR-0023-91 ..... p 2785 N93-25777
AF-AFOSR-0025-90 ..... p 2645 N93-26220
AF-AFOSR-0048-90 ..... p 2852 N93-25676
AF-AFOSR-0051-90 ..... p 2851 N93-26525
AF-AFOSR-0059-90 ..... p 2595 N93-26335
AF-AFOSR-0062-90 ..... p 2856 N93-26343
AF-AFOSR-0064-90 ..... p 2661 N93-25948
AF-AFOSR-0067-91 ..... p 2829 N93-26345
AF-AFOSR-0079-90 ..... p 2850 N93-26367
AF-AFOSR-0081-89 ..... p 2873 N93-26342
AF-AFOSR-0089-91 ..... p 2813 N93-26450
AF-AFOSR-0100-91 ..... p 2797 N93-26347
AF-AFOSR-0124-91 ..... p 2799 N93-26449
AF-AFOSR-0126-89 ..... p 2799 N93-26489
AF-AFOSR-0144-91 ..... p 2798 N93-26364
AF-AFOSR-0146-91 ..... p 2797 N93-26307
AF-AFOSR-0151-89 ..... p 2817 N93-26169
AF-AFOSR-0153-89 ..... p 2867 N93-26193
AF-AFOSR-0156-91 ..... p 2828 N93-25762
AF-AFOSR-0160-91 ..... p 2630 N93-26040
AF-AFOSR-0165-88 ..... p 2850 N93-26288
AF-AFOSR-0176-91 ..... p 2856 N93-26266
AF-AFOSR-0179-90 ..... p 2707 N93-26400
AF-AFOSR-0188-87 ..... p 2828 N93-25687
AF-AFOSR-0191-91 ..... p 2799 N93-26446
AF-AFOSR-0194-88 ..... p 2646 N93-26402
AF-AFOSR-0201-91 ..... p 2862 N93-26520
AF-AFOSR-0221-90 ..... p 2798 N93-26435
p 2798 N93-26436
AF-AFOSR-0256-89 ..... p 2850 N93-26346
AF-AFOSR-0307-88 ..... p 2646 N93-26439
AF-AFOSR-0329-89 ..... p 2729 N93-25901
AF-AFOSR-0338-89 ..... p 2867 N93-26194
AF-AFOSR-0348-90 ..... p 2811 N93-26221
AF-AFOSR-0351-90 ..... p 2641 N93-26382
AF-AFOSR-0360-91 ..... p 2722 N93-26337
AF-AFOSR-0401-91 ..... p 2798 N93-26436
p 2799 N93-26521
AF-AFOSR-0403-89 ..... p 2619 N93-26438
AF-AFOSR-0414-89 ..... p 2798 N93-26349
AF-AFOSR-0416-91 ..... p 2868 N93-26332
AF-AFOSR-0433-89 ..... p 2691 N93-26171
AF-AFOSR-0450-89 ..... p 2777 N93-24877
p 2756 N93-25679
AF-AFOSR-0461-89 ..... p 2686 N93-26490
AF-AFOSR-0500-89 ..... p 2826 N93-26162
AF-AFOSR-0510-89 ..... p 2776 N93-26348
AF-AFOSR-0523-89 ..... p 2821 N93-25821
ARPA ORDER 7330 ..... p 2813 N93-26378
p 2883 N93-26389
ARPA ORDER 7534 ..... p 2690 N93-25906
ARPA ORDER 7597 ..... p 2882 N93-25844
p 2827 N93-26487
p 2857 N93-26488
ARPA ORDER 8162 ..... p 2691 N93-26311
ARPA ORDER 8557 ..... p 2853 N93-25766
BD/123/90-IG ..... p 2745 N93-24821
BMFT-01-QS-154 ..... p 2832 N93-24983
CNES/CNRS-932-88-53-474-00 ... p 2833 N93-24993
DA PROJ. 1L1-61102-AH-45 ..... p 2708 N93-26554
DA PROJ. 1L1-61102-AH-47 ..... p 2691 N93-26299
DA PROJ. 1L1-62105-AH-84 ..... p 2706 N93-25953
p 2657 N93-26432
DA PROJ. 1L1-62211-A-47-A ..... p 2718 N93-25672
p 2719 N93-25884
DA PROJ. 1L1-62618-AH-80 ..... p 2661 N93-25857
p 2609 N93-25985
p 2597 N93-26260
DA PROJ. 3M1-62787-A-875 ..... p 2795 N93-25629
DA PROJ. 3M1-62787-A-879 ..... p 2802 N93-26265
DA PROJ. 3M1-62787-A-8879 ..... p 2795 N93-26218
DA PROJ. 8503Z ..... p 2846 N93-26376
DAAB10-87-C-0053 ..... p 2817 N93-25576
DAAJ02-92-C-0008 ..... p 2720 N93-26564
DAAK70-87-C-0043 ..... p 2661 N93-25914
DAAK70-92-C-0059 ..... p 2661 N93-25914
DAALO3-92-G-0123 ..... p 2639 N93-25945
DAAL02-89-K-0004 ..... p 2853 N93-25822
DAAL03-86-G-0200 ..... p 2632 N93-26216
DAAL03-86-K-0131 ..... p 2867 N93-26223
DAAL03-86-K-0171 ..... p 2821 N93-25853
DAAL03-88-K-0099 ..... p 2640 N93-26236
DAAL03-88-K-0187 ..... p 2645 N93-26045
DAAL03-88-K-0204 ..... p 2651 N93-25788
DAAL03-89-C-0036 ..... p 2676 N93-25855
DAAL03-89-G-0077 ..... p 2853 N93-25839
DAAL03-89-G-0080 ..... p 2645 N93-25879
DAAL03-89-G-0084 ..... p 2638 N93-25780
DAAL03-89-G-0086 ..... p 2640 N93-26225
DAAL03-89-G-0090 ..... p 2636 N93-25631
DAAL03-89-G-0092 ..... p 2830 N93-25863
DAAL03-89-G-0094 ..... p 2866 N93-25854
DAAL03-89-K-0030 ..... p 2866 N93-25789
DAAL03-89-K-0033 ..... p 2830 N93-25860
DAAL03-89-K-0057 ..... p 2774 N93-25790
DAAL03-89-K-0064 ..... p 2793 N93-25764
DAAL03-89-K-0081 ..... p 2641 N93-26580
DAAL03-89-K-0084 ..... p 2655 N93-25861
DAAL03-89-K-0086 ..... p 2854 N93-25898
DAAL03-89-K-0090 ..... p 2756 N93-25653
DAAL03-89-K-0093 ..... p 2866 N93-25897
DAAL03-89-K-0107 ..... p 2657 N93-26303
DAAL03-89-K-0123 ..... p 2829 N93-26222
DAAL03-89-K-0147 ..... p 2806 N93-25650
DAAL03-89-K-0155 ..... p 2715 N93-26297
DAAL03-89-K-0157 ..... p 2860 N93-25626
DAAL03-89-K-0178 ..... p 2795 N93-25944
DAAL03-90-C-0029 ..... p 2710 N93-25677
DAAL03-90-G-0007 ..... p 2728 N93-25842
DAAL03-90-G-0020 ..... p 2867 N93-25899
DAAL03-90-G-0151 ..... p 2730 N93-26361
DAAL03-90-G-0214 ..... p 2729 N93-25938
DAAL03-90-G-0221 ..... p 2845 N93-25651
DAAL03-91-C-0049 ..... p 2817 N93-26277
DAAL03-91-G-0025 ..... p 2651 N93-25907
DAAL03-91-G-0092 ..... p 2652 N93-26264
DAAL03-91-G-0112 ..... p 2864 N93-25655
DAAL03-91-G-0133 ..... p 2714 N93-25774
DAAL03-91-G-0190 ..... p 2609 N93-25770
DAAL03-91-K-0001 ..... p 2849 N93-25644
DAAL03-92-C-0025 ..... p 2680 N93-26226
DAAL03-92-C-0040 ..... p 2709 N93-25634
DAAL03-92-C-0043 ..... p 2868 N93-26312
DAAL03-92-G-0036 ..... p 2856 N93-26224
DAAL03-92-G-0085 ..... p 2639 N93-25862
DAAL03-92-G-0123 ..... p 2719 N93-25771
p 2675 N93-25772
p 2729 N93-25846
p 2639 N93-25919
p 2729 N93-25941
p 2729 N93-25950
DAAL03-92-G-0147 ..... p 2714 N93-25869
DAAL03-92-G-0211 ..... p 2728 N93-25838
DAAL03-92-G-0371 ..... p 2639 N93-25908
DABT63-91-C-0001 ..... p 2675 N93-25640
DAEA18-90-C-0044 ..... p 2807 N93-26293
DAJA45-89-C-0006 ..... p 2594 N93-25917
DAJA45-89-C-0023 ..... p 2731 N93-26522
DAJA45-90-C-0029 ..... p 2714 N93-26217
DAJA45-90-C-0052 ..... p 2728 N93-25785
p 2731 N93-26459
DAJA45-91-M-0345 ..... p 2845 N93-25643
DAJA45-92-M-0268 ..... p 2658 N93-26576
DARPA ORDER 7149 ..... p 2692 N93-26366
DARPA ORDER 7469 ..... p 2652 N93-26284
DARPA ORDER 8162 ..... p 2692 N93-26565
DARPA ORDER 8313 ..... p 2806 N93-25841
DE-AC-6-76RL-01830 ..... p 2760 N93-24675
DE-AC-9-89SR-18035 ..... p 2769 N93-24672
p 2760 N93-24673
DE-AC02-76CH-00016 ..... p 2687 N93-24964
p 2827 N93-24973
p 2643 N93-25123
p 2712 N93-25378
p 2769 N93-25571
DE-AC02-79ET-10815 ..... p 2858 N93-24968
DE-AC02-82CH-10093 ..... p 2862 N93-25163
DE-AC02-83CH-10093 ..... p 2862 N93-24953
p 2758 N93-25098
p 2898 N93-25101
p 2759 N93-25102
p 2759 N93-25253
p 2874 N93-25254
p 2759 N93-25504
DE-AC02-88ER-13895 ..... p 2649 N93-25095
DE-AC03-76SF-00098 ..... p 2859 N93-25324
p 2851 N93-25325
p 2847 N93-25326
p 2899 N93-25327
p 2848 N93-25364
p 2688 N93-25365
p 2848 N93-25366
p 2863 N93-25367
p 2764 N93-25443
p 2864 N93-25490
p 2853 N93-25550
p 2692 N93-26598
p 2647 N93-26599
DE-AC03-76SF-00515 ..... p 2847 N93-25323
DE-AC04-76DP-00613 ..... p 2852 N93-25182
p 2809 N93-25307
p 2721 N93-25939
p 2668 N93-26206
p 2669 N93-26207
p 2652 N93-26208
p 2669 N93-26212
p 2657 N93-26213
DE-AC04-76DP-00789 ..... p 2862 N93-24958
p 2653 N93-24971
p 2642 N93-24972
p 2827 N93-25103
p 2576 N93-25121
p 2644 N93-25312
p 2800 N93-25318
p 2896 N93-25321
p 2810 N93-25386
p 2863 N93-25387
p 2689 N93-25416
p 2689 N93-25417
p 2689 N93-25429
p 2655 N93-25444
p 2655 N93-25446
p 2726 N93-25489
p 2844 N93-25520
p 2627 N93-26024
p 2629 N93-26034
p 2692 N93-26501
p 2646 N93-26502
p 2731 N93-26507
p 2827 N93-26596
p 2715 N93-26597
DE-AC05-76OR-00001 ..... p 2760 N93-24676
DE-AC05-76OR-00033 ..... p 2725 N93-25373
p 2650 N93-25519
DE-AC05-84OR-21400 ..... p 2760 N93-24676
p 2760 N93-24952
p 2858 N93-24969
p 2667 N93-24970
p 2799 N93-25099
p 2717 N93-25100

DE-AC05-86OR-21600 ..... p 2760 N93-24955
DE-AC06-76RL-01830 ..... p 2758 N93-24975
p 2759 N93-25183
p 2654 N93-25359
p 2767 N93-26495
p 2767 N93-26497
DE-AC06-87RL-10930 ..... p 2649 N93-25255
DE-AC07-76ID-01570 ..... p 2808 N93-24962
p 2892 N93-25164
p 2658 N93-25562
DE-AC09-89SR-18035 ..... p 2864 N93-25506
DE-AC12-76SN-00052 ..... p 2698 N93-25306
DE-AC21-89MC-26367 ..... p 2643 N93-25305
DE-AC22-89PC-89876 ..... p 2660 N93-25496
DE-AC22-92PC-92111 ..... p 2644 N93-25500
DE-AC35-89ER-40486 ..... p 2689 N93-25491
DE-AI01-90EH-89084 ..... p 2668 N93-25498
DE-AI01-92IN-00554 ..... p 2887 N93-26499
DE-AI05-90ER-30174 ..... p 2762 N93-25184
DE-FC21-90MC-26029 ..... p 2644 N93-25499
DE-FG01-90CE-33017 ..... p 2674 N93-25308
DE-FG02-85ER-13442 ..... p 2849 N93-25488
DE-FG02-85ER-25001 ..... p 2811 N93-25845
DE-FG02-85ER-45200 ..... p 2864 N93-25503
DE-FG02-86ER-13542 ..... p 2644 N93-25311
DE-FG02-86ER-13590 ..... p 2847 N93-25310
DE-FG02-86ER-13623 ..... p 2695 N93-24976
DE-FG02-86ER-45271 ..... p 2847 N93-25114
DE-FG02-86NE-37966 ..... p 2717 N93-25413
DE-FG02-87ER-13759 ..... p 2644 N93-25495
DE-FG02-87ER-45305 ..... p 2635 N93-25501
DE-FG02-87ER-45311 ..... p 2650 N93-25519
DE-FG02-87ER-45314 ..... p 2654 N93-25372
DE-FG02-88ER-13919 ..... p 2695 N93-24963
DE-FG02-88ER-13946 ..... p 2642 N93-25115
DE-FG02-88ER-13955 ..... p 2849 N93-25509
DE-FG02-89ER-45409 ..... p 2655 N93-25524
DE-FG02-90ER-25084 ..... p 2696 N93-25193
DE-FG02-91ER-40652 ..... p 2848 N93-25364
DE-FG02-92ER-54165 ..... p 2859 N93-25302
DE-FG02-92ER-75709 ..... p 2828 N93-25151
DE-FG05-87ER-40361 ..... p 2847 N93-25148
DE-FG05-89ER-45384 ..... p 2687 N93-24964
DE-FG05-90ER-45436 ..... p 2650 N93-25502
DE-FG05-91ER-81235 ..... p 2793 N93-26587
DE-FG21-90MC-27115 ..... p 2660 N93-25497
DE-FG21-90MC-27225 ..... p 2660 N93-25523
DE-FG22-89PC-89786 ..... p 2659 N93-25118
DE-FG22-90BC-14600 ..... p 2695 N93-24954
DE-FG22-90PC-90291 ..... p 2659 N93-25111
p 2659 N93-25112
DE-FG22-90PC-90305 ..... p 2659 N93-25119
DE-FG22-92PC-92540 ..... p 2698 N93-25309
DI-14-08-0001-G1728 ..... p 2768 N93-26559
DI-14-08-0001-G1734 ..... p 2767 N93-26511
DNA001-89-C-0064 ..... p 2715 N93-26363
DNA001-91-C-0010 ..... p 2681 N93-26289
DTFA01-89-C-00001 ..... p 2585 N93-25456
DTFA01-89-Z-02033 ..... p 2783 N93-25645
DTFA03-83-A-00328 ..... p 2573 N93-24760
p 2573 N93-25134
DTFA03-86-C-00042 ..... p 2778 N93-24884
DTFA03-86-C-60027 ..... p 2778 N93-24884
EEC-SC1-CT91-0690 ..... p 2686 N93-24893
EPA-R-814701 ..... p 2768 N93-26536
EPA-68-CO-0080 ..... p 2768 N93-26567
ESA-9281/91/F/RD(SC) ..... p 2586 N93-25018
ESTEC-9099/90/NL/US(SC) ..... p 2716 N93-25065
p 2694 N93-25066
FAA PROJ. AM-A-91-PHY-144 ..... p 2794 N93-25214
FAA PROJ. AM-B-93-PHY-152 ..... p 2582 N93-25205
FAA PROJ. AM-C-92-HRR-122 ..... p 2796 N93-25203
p 2872 N93-25204
FAA PROJ. AM-C-92-HRR-125 ..... p 2796 N93-25213
FAA-F2006-G ..... p 2584 N93-24948
FAA-T0603-S ..... p 2584 N93-24741
FQ7624-90-00010 ..... p 2884 N93-26523
F04701-88-C-0089 ..... p 2867 N93-25947
p 2645 N93-26251
F04701-88-C-0109 ..... p 2609 N93-26098
p 2609 N93-26175
p 2609 N93-26176
p 2610 N93-26180
p 2610 N93-26181
p 2610 N93-26182
p 2610 N93-26591
F08635-90-C-0053 ..... p 2766 N93-26243
F19628-86-C-0076 ..... p 2853 N93-25646
F19628-88-C-0059 ..... p 2681 N93-26383
F19628-89-C-0001 ..... p 2681 N93-26241
F19628-89-C-0033 ..... p 2849 N93-26173
F19628-90-C-0002 ..... p 2783 N93-25645
F19628-90-C-0133 ..... p 2618 N93-26232
F19628-90-C-0159 ..... p 2620 N93-26248
F19628-90-K-0024 ..... p 2774 N93-25852
F19628-90-K-0029 ..... p 2681 N93-26247
p 2681 N93-26280
p 2776 N93-26283
F19628-91-C-0061 ..... p 2632 N93-26373
F19628-91-C-0142 ..... p 2850 N93-26281
F19628-91-C-0168 ..... p 2806 N93-25841
F29601-91-K-DB08 ..... p 2883 N93-26442
F30602-89-C-0130 ..... p 2824 N93-25974
F30602-89-C-0199 ..... p 2811 N93-25791
F30602-89-D-0096 ..... p 2823 N93-25967
F30602-89-D-0100 ..... p 2730 N93-26279
F30602-91-D-0003 ..... p 2812 N93-26275
F33615-C-87-3022 ..... p 2706 N93-25951
F33615-87-C-0534 ..... p 2591 N93-25783
p 2591 N93-25909
F33615-87-C-2729 ..... p 2595 N93-26219
F33615-87-D-0609 ..... p 2591 N93-25783
p 2591 N93-25909
p 2845 N93-25915
F33615-87-D-0626 ..... p 2793 N93-26259
F33615-88-C-5404 ..... p 2722 N93-26526
p 2722 N93-26527
F33615-89-C-0532 ..... p 2636 N93-25652
p 2590 N93-25949
F33615-89-C-3225 ..... p 2599 N93-25693
F33615-90-C-0005 ..... p 2591 N93-26462
F33615-90-C-0011 ..... p 2883 N93-26350
F33615-90-C-1465 ..... p 2882 N93-25844
p 2817 N93-26338
p 2757 N93-26448
p 2827 N93-26487
p 2857 N93-26488
F33615-90-C-3211 ..... p 2810 N93-25627
F33615-90-C-5958 ..... p 2869 N93-26540
F33615-91-C-5704 ..... p 2711 N93-25578
F33657-84-D-0165 ..... p 2595 N93-26239
F33657-88-D-2188 ..... p 2574 N93-26238
F40600-89-C-0002 ..... p 2656 N93-25940
p 2657 N93-26278
F44606-89-D-0040 ..... p 2591 N93-26572
F46920-89-C-0004 ..... p 2870 N93-26581
F49620-88-C-0096 ..... p 2829 N93-26519
F49620-89-C-0074 ..... p 2812 N93-26368
F49620-89-C-0084 ..... p 2619 N93-26456
F49620-89-C-0097 ..... p 2856 N93-26309
F49620-89-K-0004 ..... p 2715 N93-26524
F49620-90-C-0014 ..... p 2692 N93-26366
F49620-90-C-0029 ..... p 2692 N93-26539
F49620-90-C-00F4 ..... p 2826 N93-26365
F49620-90-C-0072 ..... p 2657 N93-26401
F49620-91-C-0003 ..... p 2580 N93-25894
p 2767 N93-26327
F49620-91-C-0093 ..... p 2869 N93-26385
F49620-92-C-0013 ..... p 2798 N93-26391
F49620-92-C-0030 ..... p 2661 N93-26268
F49620-92-C-0044 ..... p 2869 N93-26381
F49620-92-J-0004 ..... p 2826 N93-26333
F49620-92-J-0020 ..... p 2787 N93-26352
F49620-92-J-0024 ..... p 2896 N93-26508
F49620-92-J-0053 ..... p 2812 N93-26290
F49620-92-J-0062 ..... p 2846 N93-26358
F49620-92-J-0118 ..... p 2787 N93-26351
F49620-92-J-0119 ..... p 2798 N93-26356
F49620-92-J-0139 ..... p 2846 N93-26374
F49620-92-J-0156 ..... p 2800 N93-25778
F49620-92-J-0203 ..... p 2829 N93-26344
F49620-92-J-0220 ..... p 2641 N93-26355
F49620-92-J-0290 ..... p 2707 N93-26163
p 2707 N93-26379
F49620-92-J-0409 ..... p 2868 N93-26357
GRI PROJ. 5696 ..... p 2872 N93-26509
GRI-5086-260-1308 ..... p 2768 N93-26533
GRI-5087-260-1449 ..... p 2872 N93-26509
p 2872 N93-26558
GRI-5088-260-1692 ..... p 2644 N93-25819
GRI-5091-254-2235 ..... p 2768 N93-26529
GRI-5091-260-2182 ..... p 2644 N93-25817
JPL-957849 ..... p 2600 N93-24699
MDA903-89-C-0003 ..... p 2810 N93-25711
p 2883 N93-26313
p 2831 N93-26330
p 2813 N93-26461
MDA903-90-C-0006 ..... p 2617 N93-25630
MDA903-92-D-0020 ..... p 2690 N93-25856
MDA972-89-C-0087 ..... p 2690 N93-25660
MDA972-90-C-0035 ..... p 2813 N93-26378
p 2883 N93-26389
MDA972-91-C-0030 ..... p 2692 N93-26565
MDA972-92-C-0034 ..... p 2691 N93-26311
MDA972-92-C-0053 ..... p 2853 N93-25766
MDA972-92-J-1018 ..... p 2813 N93-26583
MIPR-FQ7624-90-00010 ..... p 2877 N93-25763
NAGW-1105 ..... p 2683 N93-26471
NAGW-1333 ..... p 2817 N93-24743
p 2826 N93-25986
NAGW-1334 ..... p 2669 N93-26405
NAGW-1335 ..... p 2821 N93-25833
p 2732 N93-25834
p 2609 N93-25836
NAGW-1356 ..... p 2622 N93-24943
NAGW-1406 ..... p 2804 N93-25928
NAGW-1905 ..... p 2771 N93-25202
NAGW-1984 ..... p 2790 N93-26050
NAGW-2166 ..... p 2805 N93-25931
NAGW-2436 ..... p 2803 N93-26157
NAGW-2548 ..... p 2899 N93-24752
p 2899 N93-25161
p 2900 N93-26132
NAGW-2706 ..... p 2765 N93-25666
NAGW-4561 ..... p 2882 N93-26231
NAG1-1070 ..... p 2698 N93-25266
NAG1-1108 ..... p 2863 N93-25219
NAG1-1119 ..... p 2696 N93-25208
NAG1-1233 ..... p 2763 N93-25287
NAG1-1241 ..... p 2809 N93-25257
NAG1-1255 ..... p 2589 N93-25670
NAG1-1329 ..... p 2724 N93-25260
NAG1-1341 ..... p 2587 N93-25162
NAG1-1425 ..... p 2811 N93-26150
NAG1-613 ..... p 2815 N93-24748
p 2815 N93-24749
NAG1-804 ..... p 2769 N93-24910
p 2770 N93-25088
p 2775 N93-26084
NAG1-849 ..... p 2595 N93-24762
NAG1-863 ..... p 2817 N93-24757
NAG1-901 ..... p 2723 N93-24912
NAG10-0058 ..... p 2825 N93-25979
NAG2-414 ..... p 2794 N93-24763
NAG2-484 ..... p 2580 N93-26049
NAG2-575 ..... p 2576 N93-25249
NAG2-591 ..... p 2805 N93-25130
p 2809 N93-25131
p 2806 N93-25233
p 2809 N93-25250
p 2815 N93-25251
p 2806 N93-25267
p 2815 N93-25297
p 2816 N93-25458
NAG2-593 ..... p 2808 N93-25107
p 2809 N93-25152
p 2721 N93-26135
NAG2-625 ..... p 2585 N93-26052
NAG2-684 ..... p 2767 N93-26427
NAG2-722 ..... p 2709 N93-25345
NAG2-792 ..... p 2596 N93-25199
NAG2-794 ..... p 2597 N93-26046
NAG3-1038 ..... p 2642 N93-25116
NAG3-1046 ..... p 2663 N93-24946
NAG3-1109 ..... p 2694 N93-24759
NAG3-1142 ..... p 2664 N93-25218
NAG3-1165 ..... p 2580 N93-25883
NAG3-1184 ..... p 2659 N93-24745
NAG3-1192 ..... p 2696 N93-25109
NAG3-1297 ..... p 2643 N93-25229
NAG3-481 ..... p 2573 N93-24760
p 2573 N93-25134
NAG3-577 ..... p 2622 N93-24758
NAG3-772 ..... p 2593 N93-25668
NAG3-900 ..... p 2716 N93-24751
NAG5-1132 ..... p 2828 N93-25223
NAG5-1158 ..... p 2573 N93-25077
NAG5-1221 ..... p 2888 N93-25289
NAG5-1228 ..... p 2889 N93-25331
NAG5-1273 ..... p 2900 N93-25890
NAG5-1326 ..... p 2898 N93-25222
NAG5-1385 ..... p 2892 N93-25211

NAG5-1435 ..... p 2891 N93-26426
NAG5-1503 ..... p 2697 N93-25221
NAG5-1519 ..... p 2764 N93-25431
p 2764 N93-25432
NAG5-1529 ..... p 2770 N93-25081
NAG5-1591 ..... p 2888 N93-25172
NAG5-1803 ..... p 2890 N93-25755
NAG5-1835 ..... p 2763 N93-25244
NAG5-1843 ..... p 2892 N93-25230
NAG5-1890 ..... p 2862 N93-25108
NAG5-1972 ..... p 2771 N93-25201
NAG5-2109 ..... p 2818 N93-25155
p 2818 N93-25156
p 2819 N93-25226
p 2819 N93-25296
NAG5-308 ..... p 2900 N93-25241
NAG5-549 ..... p 2771 N93-25202
NAG5-842 ..... p 2772 N93-25529
NAG5-931 ..... p 2673 N93-25198
NAG8-910 ..... p 2769 N93-24945
NAG9-431 ..... p 2633 N93-26425
NAG9-482 ..... p 2818 N93-25138
p 2874 N93-25139
p 2828 N93-25140
p 2818 N93-25141
p 2818 N93-25142
p 2818 N93-25190
p 2818 N93-25196
p 2819 N93-25197
p 2820 N93-25425
p 2820 N93-25452
p 2820 N93-25459
NAG9-562 ..... p 2799 N93-26082
NAG9-592 ..... p 2865 N93-25667
NASA ORDER S-04167-D ..... p 2899 N93-26556
NASW-4063 ..... p 2775 N93-26159
NASW-4292 ..... p 2792 N93-25195
NASW-4529 ..... p 2775 N93-26151
NASW-4561 ..... p 2883 N93-26491
NAS1-18028 ..... p 2591 N93-24764
NAS1-18585 ..... p 2695 N93-25087
NAS1-18605 ..... p 2575 N93-25083
p 2803 N93-25084
NAS1-19038 ..... p 2808 N93-25073
NAS1-19480 ..... p 2575 N93-25083
p 2803 N93-25084
p 2576 N93-25153
NAS10-11333 ..... p 2777 N93-24747
NAS10-11400 ..... p 2873 N93-26419
p 2873 N93-26420
NAS10-11606 ..... p 2817 N93-25576
NAS10-11882 ..... p 2817 N93-25576
NAS2-12927 ..... p 2794 N93-24738
NAS2-13092 ..... p 2575 N93-25075
NAS2-13296 ..... p 2599 N93-26095
NAS2-13327 ..... p 2888 N93-25135
NAS2-13408 ..... p 2887 N93-25442
NAS3-24222 ..... p 2844 N93-25094
NAS3-24350 ..... p 2592 N93-24754
p 2592 N93-25106
NAS3-25266 ..... p 2723 N93-24913
p 2623 N93-25132
NAS3-25776 ..... p 2808 N93-24947
NAS3-26474 ..... p 2653 N93-24761
NAS3-30065 ..... p 2633 N93-26555
NAS5-27772 ..... p 2822 N93-25962
NAS5-30127 ..... p 2754 N93-25154
NAS5-30960 ..... p 2890 N93-26002
p 2890 N93-26003
p 2890 N93-26004
NAS5-31500 ..... p 2600 N93-24697
p 2601 N93-24703
p 2601 N93-24704
p 2602 N93-24706
p 2602 N93-24707
p 2602 N93-24708
p 2602 N93-24710
p 2603 N93-24714
p 2603 N93-24716
p 2603 N93-24717
p 2606 N93-24733
p 2607 N93-24734
NAS5-31718 ..... p 2787 N93-26492
NAS5-31844 ..... p 2891 N93-26139
NAS5-31920 ..... p 2817 N93-25576
NAS5-32500 ..... p 2601 N93-24705
p 2615 N93-25133
NAS5-38494 ..... p 2605 N93-24724
NAS7-1000 ..... p 2671 N93-24659
NAS7-918 ..... p 2653 N93-25078
p 2859 N93-25206
p 2676 N93-26105
p 2682 N93-26463
NAS8-32700 ..... p 2604 N93-24723
NAS8-36123 ..... p 2854 N93-26183
NAS8-36151 ..... p 2631 N93-26056
NAS8-36955 ..... p 2770 N93-25086
NAS8-37136 ..... p 2614 N93-26152
NAS8-37470 ..... p 2633 N93-26557
NAS8-37855 ..... p 2610 N93-25479
p 2611 N93-25510
p 2611 N93-25511
p 2611 N93-25512
p 2611 N93-25513
p 2611 N93-25514
NAS8-37857 ..... p 2599 N93-26146
NAS8-37891 ..... p 2631 N93-26053
p 2631 N93-26054
p 2631 N93-26057
NAS8-38185 ..... p 2618 N93-26055
NAS8-38259 ..... p 2656 N93-26155
NAS8-38481 ..... p 2786 N93-26156
NAS8-38494 ..... p 2604 N93-24723
NAS8-38609 ..... p 2863 N93-25225
p 2774 N93-25886
p 2711 N93-26154
NAS8-38781 ..... p 2801 N93-25888
NAS8-39194 ..... p 2716 N93-24980
NAS8-39343 ..... p 2817 N93-25576
NAS8-39843 ..... p 2801 N93-26088
NAS8-50000 ..... p 2720 N93-25605
NAS9-17900 ..... p 2797 N93-25736
NAS9-18706 ..... p 2825 N93-25980
NA89AA-D-SG138 ..... p 2730 N93-26320
NA89RA-H-09087 ..... p 2786 N93-25874
NA89RA-H-09088 ..... p 2785 N93-25776
NA89RA-H-09090 ..... p 2785 N93-25849
NCC1-159 ..... p 2823 N93-25969
NCC1-68 ..... p 2575 N93-25117
NCC1-99 ..... p 2808 N93-24750
NCC2-342 ..... p 2874 N93-25288
NCC2-414 ..... p 2801 N93-26047
NCC2-420 ..... p 2574 N93-24736
NCC2-575 ..... p 2586 N93-26549
NCC2-614 ..... p 2792 N93-25242
NCC2-615 ..... p 2585 N93-25261
p 2585 N93-25330
NCC2-640 ..... p 2643 N93-25240
NCC2-645 ..... p 2828 N93-25262
NCC2-717 ..... p 2808 N93-24944
NCC2-733 ..... p 2892 N93-25200
NCC2-741 ..... p 2848 N93-25450
NCC3-233 ..... p 2696 N93-25175
NCC3-295 ..... p 2652 N93-26235
NCC3-81 ..... p 2721 N93-25451
NCC3-94 ..... p 2649 N93-25128
NCC9-16 ..... p 2814 N93-25613
NDARB-UND-NOAA91 ..... p 2765 N93-25873
NGT-44-001-800 ..... p 2582 N93-26078
NGT-44-005-803 ..... p 2911 N93-26058
p 2898 N93-26059
p 2642 N93-26060
p 2803 N93-26061
p 2896 N93-26062
p 2670 N93-26063
p 2619 N93-26064
p 2619 N93-26065
p 2896 N93-26067
p 2796 N93-26068
p 2794 N93-26069
p 2914 N93-26070
p 2827 N93-26071
p 2827 N93-26072
p 2794 N93-26073
p 2723 N93-26074
p 2815 N93-26075
p 2803 N93-26076
p 2794 N93-26077
p 2648 N93-26079
p 2620 N93-26080
p 2620 N93-26081
p 2671 N93-26083
NGT-50642 ..... p 2817 N93-25137
NIOSH-CDC-299-90-2847 ..... p 2884 N93-26568
NOAA NA-17RA021801 ..... p 2765 N93-25873
NR PROJ. M00-96 ..... p 2590 N93-25933
NR PROJ. 8068 ..... p 2715 N93-26445
NSF AST-91-00486 ..... p 2899 N93-24752
p 2899 N93-25161
p 2900 N93-26132
NSF ATM-88-00602 ..... p 2895 N93-26147
NSF BNS-88-20099 ..... p 2675 N93-25639
NSF BSR-90-18298 ..... p 2736 N93-24938
NSF CCR-87-01103 ..... p 2809 N93-25152
NSF CCR-88-09615 ..... p 2816 N93-25522
NSF CCR-88-58087 ..... p 2817 N93-26338
NSF CCR-89-00029 ..... p 2809 N93-25250
p 2815 N93-25251
NSF CCR-89-01780 ..... p 2808 N93-25107
NSF CCR-90-14363 ..... p 2809 N93-25152
NSF CCR-91-02231 ..... p 2808 N93-25107
NSF CDA-90-15006 ..... p 2818 N93-25138
NSF CES-88-00459 ..... p 2874 N93-25139
NSF DMS-90-12751 ..... p 2828 N93-25140
NSF EAR-86-18744 ..... p 2818 N93-25141
NSF IRI-91-96146 ..... p 2818 N93-25142
NSF MSS-89-07748 ..... p 2818 N93-25190
NSF MSS-89-20700 ..... p 2818 N93-25196
NSF OCE-86-13904 ..... p 2819 N93-25197
NSF OCE-88-01089 ..... p 2820 N93-25425
NSF OCE-90-13896 ..... p 2820 N93-25452
NSF OCE-90-16990 ..... p 2820 N93-25459
NSF OCE-90-17173 ..... p 2730 N93-26361
NSF OCE-91-08993 ..... p 2828 N93-25905
NSG-1577 ..... p 2828 N93-25223
NSG-3188 ..... p 2822 N93-25963
NSG-5172 ..... p 2730 N93-26361
N00014-82-K-0612 ..... p 2730 N93-26361
p 2736 N93-24938
p 2736 N93-24938
p 2736 N93-24939
p 2736 N93-24938
p 2736 N93-24938
p 2790 N93-26384
p 2810 N93-25669
p 2719 N93-25884
p 2892 N93-25230
p 2645 N93-25916
p 2656 N93-26172
p 2658 N93-26437
p 2869 N93-26577
N00014-84-K-0645 ..... p 2662 N93-26308
N00014-86-K-0685 ..... p 2732 N93-25834
N00014-86-K-0766 ..... p 2657 N93-26240
N00014-87-J-1217 ..... p 2917 N93-26359
N00014-87-K-2057 ..... p 2661 N93-25902
N00014-89-C-2011 ..... p 2605 N93-24727
N00014-89-C-2455 ..... p 2857 N93-26515
N00014-89-J-1023 ..... p 2868 N93-26302
N00014-89-J-1235 ..... p 2645 N93-25920
N00014-89-J-1238 ..... p 2629 N93-26037
N00014-89-J-1456 ..... p 2790 N93-26050
N00014-89-J-1459 ..... p 2641 N93-26579
N00014-89-J-1476 ..... p 2786 N93-25892
N00014-89-J-1497 ..... p 2849 N93-25659
N00014-89-J-1498 ..... p 2736 N93-24939
N00014-89-J-1527 ..... p 2828 N93-25905
N00014-89-J-1565 ..... p 2868 N93-26302
N00014-89-J-1693 ..... p 2860 N93-25641
N00014-89-J-1836 ..... p 2846 N93-26165
N00014-90-C-0123 ..... p 2710 N93-26044
N00014-90-C-0226 ..... p 2690 N93-25906
N00014-90-C-2183 ..... p 2857 N93-26542
N00014-90-J-1030 ..... p 2726 N93-25638
N00014-90-J-1263 ..... p 2868 N93-26252
N00014-90-J-1559 ..... p 2657 N93-26240
N00014-90-J-1716 ..... p 2787 N93-26513
N00014-90-J-1762 ..... p 2851 N93-26518
N00014-90-J-4012 ..... p 2775 N93-25946
N00014-90-J-4018 ..... p 2806 N93-25848
N00014-91-C-0001 ..... p 2624 N93-26005
N00014-91-C-0044 ..... p 2795 N93-25900
N00014-91-C-0067 ..... p 2639 N93-25936
N00014-91-C-0124 ..... p 2651 N93-25843
p 2652 N93-26282
N00014-91-C-2316 ..... p 2605 N93-24727
N00014-91-J-1116 ..... p 2815 N93-24748
N00014-91-J-1143 ..... p 2849 N93-25734
N00014-91-J-1189 ..... p 2651 N93-25903
N00014-91-J-1219 ..... p 2809 N93-25152
N00014-91-J-1274 ..... p 2645 N93-26300
p 2640 N93-26301
N00014-91-J-1278 ..... p 2790 N93-26331
N00014-91-J-1283 ..... p 2815 N93-24749
N00014-91-J-1334 ..... p 2676 N93-25847
N00014-91-J-1410 ..... p 2850 N93-26267
N00014-91-J-1529 ..... p 2811 N93-26253
N00014-91-J-1852 ..... p 2690 N93-25678
N00014-91-J-1857 ..... p 2856 N93-26256
N00014-91-J-1875 ..... p 2730 N93-26362
N00014-91-J-1896 ..... p 2652 N93-26197
p 2868 N93-26258
p 2850 N93-26287
N00014-91-J-1903 ..... p 2796 N93-25654
N00014-91-J-1927 ..... p 2868 N93-26254
p 2657 N93-26386
p 2850 N93-26443
N00014-91-J-1977 ..... p 2630 N93-26042
N00014-91-J-4045 ..... p 2856 N93-26306
N00014-91-J-4056 ..... p 2812 N93-26257
N00014-92-F-0038 ..... p 2862 N93-26528
N00014-92-J-0006 ..... p 2653 N93-26304
N00014-92-J-1008 ..... p 2829 N93-26199
N00014-92-J-1049 ..... p 2790 N93-26170
N00014-92-J-1121 ..... p 2790 N93-26298
N00014-92-J-1218 ..... p 2728 N93-25784
N00014-92-J-1302 ..... p 2856 N93-26457
N00014-92-J-1391 ..... p 2727 N93-25690

N00014-92-J-1587 ..... p 2766 N93-26292
N00014-92-J-1610 ..... p 2707 N93-26360
N00014-92-J-1617 ..... p 2820 N93-25648
N00014-92-J-1629 ..... p 2655 N93-25642
p 2851 N93-26514
N00014-92-J-4092 ..... p 2810 N93-25699
N00019-89-C-0152 ..... p 2690 N93-25820
N00039-91-C-0001 ..... p 2827 N93-25611
p 2683 N93-26468
p 2685 N93-26483
N00149-0-WX-24043 ..... p 2630 N93-26041
N00167-92-K-0038 ..... p 2727 N93-25647
N00600-91-C-0920 ..... p 2757 N93-26354
N61533-92-R-0030 ..... p 2727 N93-25647
p 2731 N93-26390
p 2731 N93-26516
N66604-90-D-0104 ..... p 2813 N93-26563
PROJ. NOAA-R/OE-14 ..... p 2730 N93-26320
PROJ. RR0-1509 ..... p 2680 N93-26227
RF PROJ. 768121/723186 ..... p 2898 N93-25222
RTOP 107-20-06 ..... p 2887 N93-25442
RTOP 144-10-10 ..... p 2808 N93-24947
RTOP 188-41-53 ..... p 2888 N93-25135
RTOP 196-41-73-02-00 ..... p 2680 N93-26129
p 2680 N93-26130
RTOP 199-18-12-07 ..... p 2795 N93-26133
RTOP 199-61-12 ..... p 2667 N93-25085
RTOP 310-10-60-50-00 ..... p 2676 N93-26106
RTOP 310-10-60-60-00 ..... p 2676 N93-26107
RTOP 310-10-60-86-02 ..... p 2677 N93-26108
RTOP 310-10-63-50-00 ..... p 2614 N93-26109
RTOP 310-10-63-88-01 ..... p 2677 N93-26110
RTOP 310-10-63-92-01 ..... p 2621 N93-26111
RTOP 310-20-64-22-00 ..... p 2678 N93-26114
RTOP 310-20-64-86-02 ..... p 2671 N93-24660
RTOP 310-20-65-67-00 ..... p 2621 N93-26112
RTOP 310-20-65-86-02 ..... p 2671 N93-24661
RTOP 310-20-65-91-00 ..... p 2672 N93-24666
RTOP 310-20-65-92-01 ..... p 2677 N93-26113
RTOP 310-20-66-09-01 ..... p 2678 N93-26115
RTOP 310-20-67-59-00 ..... p 2678 N93-26117
RTOP 310-30-42-10-87 ..... p 2678 N93-26119
RTOP 310-30-69-91-02 ..... p 2678 N93-26118
RTOP 310-30-71-83-02 ..... p 2671 N93-24662
p 2671 N93-24663
p 2671 N93-24664
p 2671 N93-24665
RTOP 310-30-71-92-02 ..... p 2678 N93-26116
RTOP 310-39-09-01-25 ..... p 2678 N93-26120
RTOP 310-40-73-89-01 ..... p 2721 N93-26137
RTOP 314-30-42-10-89 ..... p 2679 N93-26121
RTOP 314-30-55-30-01 ..... p 2672 N93-24668
RTOP 314-30-58-50-05 ..... p 2672 N93-24670
RTOP 314-30-61-02-02 ..... p 2679 N93-26126
RTOP 314-40-22-35-01 ..... p 2614 N93-24667
RTOP 314-40-22-37-01 ..... p 2614 N93-26124
RTOP 314-40-31-30-06 ..... p 2599 N93-26125
RTOP 314-40-41-10-15 ..... p 2679 N93-26122
p 2672 N93-24669
RTOP 315-20-50-00-06 ..... p 2679 N93-26123
RTOP 315-91-50-20-04 ..... p 2679 N93-26127
RTOP 316-30-19-41-04 ..... p 2680 N93-26128
RTOP 323-53-62 ..... p 2672 N93-24671
RTOP 462-61-14 ..... p 2614 N93-24755
RTOP 467-01-21 ..... p 2754 N93-25154
RTOP 476-14-15-01 ..... p 2687 N93-24746
RTOP 505-53-1A ..... p 2615 N93-25174
RTOP 505-59-00 ..... p 2654 N93-25093
p 2708 N93-25076
p 2809 N93-25246
RTOP 505-59-30-01 ..... p 2581 N93-26085
RTOP 505-59-36 ..... p 2575 N93-25075
RTOP 505-59-52 ..... p 2845 N93-26086
RTOP 505-59-53 ..... p 2697 N93-25247
RTOP 505-59-86-02 ..... p 2695 N93-25087
RTOP 505-60-00 ..... p 2695 N93-25082
RTOP 505-62-OK ..... p 2708 N93-26554
RTOP 505-62-10 ..... p 2716 N93-24751
p 2718 N93-25672
p 2719 N93-25884
RTOP 505-62-21 ..... p 2573 N93-24760
p 2573 N93-25134
p 2696 N93-25175
RTOP 505-62-50 ..... p 2592 N93-25079
RTOP 505-62-51 ..... p 2593 N93-25673
RTOP 505-62-52 ..... p 2592 N93-24754
p 2575 N93-24911
p 2592 N93-25106
p 2667 N93-25177
p 2709 N93-25191
p 2707 N93-26203
p 2829 N93-26560
RTOP 505-62-84 ..... p 2708 N93-24737
p 2597 N93-25080
p 2652 N93-26201
p 2598 N93-26214
RTOP 505-63-1A ..... p 2633 N93-26204
RTOP 505-63-1B ..... p 2634 N93-25071
RTOP 505-63-40 ..... p 2649 N93-25128
RTOP 505-63-5A ..... p 2652 N93-26235
RTOP 505-63-5B ..... p 2723 N93-24913
p 2724 N93-25070
RTOP 505-63-50-10 ..... p 2844 N93-25189
RTOP 505-63-50-12 ..... p 2581 N93-26134
RTOP 505-64-13-01 ..... p 2585 N93-26087
RTOP 505-64-13-12 ..... p 2591 N93-24764
RTOP 505-64-36 ..... p 2584 N93-24914
p 2803 N93-25235
RTOP 505-68-32 ..... p 2592 N93-25129
p 2581 N93-26099
RTOP 505-69-50 ..... p 2580 N93-25883
RTOP 505-70-62-06 ..... p 2575 N93-25074
RTOP 505-90-00 ..... p 2575 N93-25091
RTOP 505-90-52-01 ..... p 2575 N93-25083
p 2803 N93-25084
p 2576 N93-25153
RTOP 505-90-53-02 ..... p 2808 N93-25073
RTOP 506-40-91-01 ..... p 2696 N93-25176
RTOP 506-41-11 ..... p 2623 N93-25132
RTOP 506-41-41 ..... p 2615 N93-25090
p 2618 N93-26148
p 2618 N93-26215
p 2897 N93-26392
RTOP 506-42-31 ..... p 2622 N93-24758
p 2631 N93-26149
p 2633 N93-26555
p 2633 N93-26561
RTOP 506-73-43-01 ..... p 2651 N93-26048
RTOP 510-01-50 ..... p 2709 N93-25173
p 2721 N93-25451
p 2641 N93-26552
RTOP 535-03-01 ..... p 2595 N93-26161
RTOP 535-03-10 ..... p 2723 N93-24909
p 2844 N93-25094
p 2730 N93-26202
RTOP 537-02-20 ..... p 2694 N93-24759
p 2642 N93-25116
RTOP 537-02-22 ..... p 2846 N93-26551
RTOP 537-02-23 ..... p 2573 N93-26136
RTOP 550-00-00 ..... p 2599 N93-24694
RTOP 553-13-00 ..... p 2731 N93-26550
RTOP 578-12-23-70 ..... p 2777 N93-24742
RTOP 579-31-07 ..... p 2776 N93-26421
RTOP 582-01-11 ..... p 2622 N93-25089
RTOP 584-03-11 ..... p 2653 N93-24761
p 2632 N93-26211
RTOP 585-03-11-01 ..... p 2615 N93-25133
RTOP 590-13-11 ..... p 2759 N93-25136
RTOP 590-21-11 ..... p 2623 N93-25236
RTOP 590-32-14-01 ..... p 2803 N93-25921
RTOP 593-14-00 ..... p 2614 N93-25952
RTOP 593-71-00 ..... p 2621 N93-24740
p 2622 N93-24753
p 2622 N93-25105
p 2632 N93-26200
RTOP 593-72-00 ..... p 2622 N93-24744
p 2632 N93-26210
RTOP 633-00-00 ..... p 2890 N93-26002
p 2890 N93-26003
p 2890 N93-26004
RTOP 674-22-05 ..... p 2663 N93-24946
RTOP 676-40-02 ..... p 2776 N93-26421
RTOP 694-03-03 ..... p 2618 N93-26209
RTOP 694-03-08 ..... p 2664 N93-25337
RTOP 740-00-00 ..... p 2689 N93-25618
RTOP 763-23-41 ..... p 2591 N93-26553
RTOP 763-23-45-85 ..... p 2634 N93-25072
RTOP 910-00-00 ..... p 2770 N93-25160
SBA-5654-OA-90 ..... p 2872 N93-25735
SBIR-08.02-1982 ..... p 2786 N93-26156
SRI PROJ. 2781 ..... p 2775 N93-26159
SWRI PROJ. 12-2301 ..... p 2591 N93-25909
W-31-109-ENG-38 ..... p 2761 N93-24956
p 2695 N93-24966
p 2761 N93-25143
p 2660 N93-25192
p 2660 N93-25298
p 2851 N93-25301
p 2848 N93-25368
p 2863 N93-25369
p 2763 N93-25370
p 2848 N93-25371
p 2816 N93-25521
p 2816 N93-25522
p 2767 N93-26496
p 2598 N93-26498
p 2658 N93-26506
p 2658 N93-26588
W-7405-ENG-36 ..... p 2760 N93-24674
p 2723 N93-24957
p 2712 N93-24967
p 2761 N93-24977
p 2687 N93-25113
p 2696 N93-25124
p 2781 N93-25125
p 2761 N93-25126
p 2852 N93-25127
p 2712 N93-25150
p 2828 N93-25151
p 2805 N93-25165
p 2762 N93-25166
p 2858 N93-25167
p 2899 N93-25185
p 2794 N93-25186
p 2858 N93-25187
p 2809 N93-25303
p 2688 N93-25313
p 2851 N93-25314
p 2809 N93-25315
p 2816 N93-25316
p 2598 N93-25322
p 2713 N93-25379
p 2852 N93-25380
p 2713 N93-25381
p 2668 N93-25447
p 2876 N93-25448
p 2655 N93-25507
p 2629 N93-26035
p 2662 N93-26493
p 2869 N93-26494
p 2861 N93-26504
p 2646 N93-26505
p 2861 N93-26512
p 2768 N93-26592
W-7405-ENG-48 ..... p 2873 N93-24677
p 2846 N93-24959
p 2788 N93-24960
p 2711 N93-24961
p 2901 N93-24974
p 2761 N93-25122
p 2761 N93-25145
p 2762 N93-25146
p 2762 N93-25147
p 2674 N93-25299
p 2815 N93-25304
p 2620 N93-25317
p 2875 N93-25319
p 2888 N93-25320
p 2649 N93-25336
p 2712 N93-25363
p 2848 N93-25366
p 2852 N93-25375
p 2654 N93-25382
p 2635 N93-25383
p 2654 N93-25384
p 2763 N93-25385
p 2688 N93-25397
p 2617 N93-25494
p 2709 N93-25515
p 2730 N93-26177
p 2730 N93-26178
p 2917 N93-26326
p 2715 N93-26503
p 2731 N93-26507
p 2857 N93-26593
p 2870 N93-26594
W-7405-ENG-82 ..... p 2649 N93-25149
p 2863 N93-25362
p 2649 N93-25428
p 2721 N93-25518
WE10E3640N ..... p 2647 N93-26595
p 2627 N93-26021
p 2627 N93-26022
p 2627 N93-26023
W7711-0-7118 ..... p 2822 N93-25964

REPORT NUMBER INDEX

Typical Report Number Index Listing

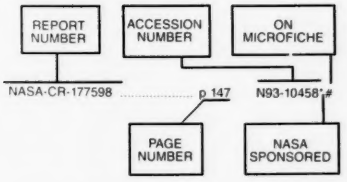

Listings in this index are arranged alphanumerically by report number. The accession number denotes the number by which the citation is identified. The page number helps to locate the citation in the abstract section. An asterisk (*) indicates that the item is a NASA report. A pound sign (#) indicates that the item is available on microfiche.

A-91212 ..... p 2697 N93-25247 * #
A-92088 ..... p 2695 N93-25082 * #
A-92113 ..... p 2795 N93-26133 * #
A-92120 ..... p 2708 N93-25076 * #
A-92158 ..... p 2809 N93-25246 * #
A-92160 ..... p 2575 N93-25091 * #
A-92191 ..... p 2667 N93-25085 * #
A-92194 ..... p 2817 N93-25137 * #
A-93022 ..... p 2888 N93-25135 * #
A-93026 ..... p 2794 N93-24738 * #
A-93040 ..... p 2581 N93-26099 * #
A-93043 ..... p 2803 N93-25235 * #
A-93044 ..... p 2584 N93-24914 * #
A-93050 ..... p 2575 N93-25075 * #
A-93055 ..... p 2887 N93-25442 * #
A-93061 ..... p 2586 N93-26549 * #

AAE-93-04 ..... p 2659 N93-24745 * #

AD-A2599994 ..... p 2575 N93-25083 * #
AD-A260562 ..... p 2795 N93-25944 #
AD-A260563 ..... p 2645 N93-25879 #
AD-A260567 ..... p 2854 N93-25898 #
AD-A260570 ..... p 2640 N93-26236 #
AD-A260571 ..... p 2632 N93-26216 #
AD-A260573 ..... p 2867 N93-25899 #
AD-A260574 ..... p 2795 N93-25900 #
AD-A260577 ..... p 2729 N93-25901 #
AD-A260578 ..... p 2661 N93-25902 #
AD-A260580 ..... p 2651 N93-25903 #
AD-A260581 ..... p 2801 N93-25904 #
AD-A260585 ..... p 2828 N93-25905 #
AD-A260589 ..... p 2690 N93-25906 #
AD-A260592 ..... p 2853 N93-25839 #
AD-A260602 ..... p 2709 N93-25634 #
AD-A260606 ..... p 2801 N93-25840 #
AD-A260607 ..... p 2675 N93-25635 #
AD-A260618 ..... p 2608 N93-25636 #
AD-A260621 ..... p 2844 N93-25637 #
AD-A260628 ..... p 2726 N93-25638 #
AD-A260643 ..... p 2675 N93-25639 #
AD-A260644 ..... p 2675 N93-25640 #
AD-A260645 ..... p 2860 N93-25641 #
AD-A260662 ..... p 2655 N93-25642 #
AD-A260666 ..... p 2845 N93-25643 #
AD-A260669 ..... p 2775 N93-25891 #
AD-A260673 ..... p 2786 N93-25892 #
AD-A260675 ..... p 2911 N93-25893 #
AD-A260681 ..... p 2580 N93-25894 #
AD-A260689 ..... p 2845 N93-25649 #
AD-A260692 ..... p 2651 N93-25895 #
AD-A260693 ..... p 2806 N93-25650 #
AD-A260695 ..... p 2583 N93-25896 #
AD-A260698 ..... p 2728 N93-25842 #
AD-A260701 ..... p 2866 N93-25897 #
AD-A260702 ..... p 2651 N93-25907 #
AD-A260703 ..... p 2845 N93-25651 #
AD-A260704 ..... p 2636 N93-25652 #
AD-A260705 ..... p 2756 N93-25653 #
AD-A260709 ..... p 2651 N93-25843 #
AD-A260712 ..... p 2714 N93-26217 #
AD-A260716 ..... p 2811 N93-25845 #
AD-A260719 ..... p 2639 N93-25908 #
AD-A260720 ..... p 2796 N93-25654 #
AD-A260724 ..... p 2864 N93-25655 #
AD-A260727 ..... p 2598 N93-25656 #
AD-A260739 ..... p 2849 N93-25644 #
AD-A260740 ..... p 2783 N93-25645 #
AD-A260742 ..... p 2729 N93-25846 #
AD-A260743 ..... p 2852 N93-25676 #
AD-A260747 ..... p 2710 N93-25677 #
AD-A260752 ..... p 2591 N93-25909 #
AD-A260754 ..... p 2690 N93-25678 #
AD-A260755 ..... p 2676 N93-25847 #
AD-A260757 ..... p 2806 N93-25848 #
AD-A260762 ..... p 2765 N93-25837 #
AD-A260764 ..... p 2645 N93-25916 #
AD-A260767 ..... p 2594 N93-25917 #
AD-A260779 ..... p 2756 N93-25679 #
AD-A260780 ..... p 2718 N93-25682 #
AD-A260781 ..... p 2710 N93-25686 #
AD-A260783 ..... p 2828 N93-25687 #
AD-A260790 ..... p 2675 N93-25689 #
AD-A260792 ..... p 2727 N93-25690 #
AD-A260793 ..... p 2599 N93-25693 #
AD-A260794 ..... p 2639 N93-25918 #
AD-A260810 ..... p 2756 N93-25694 #
AD-A260812 ..... p 2710 N93-25696 #
AD-A260813 ..... p 2810 N93-25699 #
AD-A260820 ..... p 2675 N93-25700 #
AD-A260821 ..... p 2911 N93-25910 #
AD-A260826 ..... p 2690 N93-25782 #
AD-A260828 ..... p 2639 N93-25919 #
AD-A260830 ..... p 2591 N93-25783 #
AD-A260833 ..... p 2728 N93-25784 #
AD-A260836 ..... p 2728 N93-25785 #
AD-A260837 ..... p 2645 N93-25920 #
AD-A260838 ..... p 2590 N93-25933 #
AD-A260846 ..... p 2729 N93-25911 #
AD-A260849 ..... p 2810 N93-25786 #
AD-A260852 ..... p 2801 N93-25787 #
AD-A260856 ..... p 2651 N93-25788 #
AD-A260859 ..... p 2866 N93-25789 #
AD-A260863 ..... p 2774 N93-25790 #
AD-A260866 ..... p 2860 N93-25626 #
AD-A260867 ..... p 2810 N93-25627 #
AD-A260869 ..... p 2800 N93-25628 #
AD-A260871 ..... p 2728 N93-25838 #
AD-A260874 ..... p 2795 N93-25629 #
AD-A260877 ..... p 2690 N93-25935 #
AD-A260878 ..... p 2617 N93-25630 #
AD-A260879 ..... p 2636 N93-25631 #
AD-A260886 ..... p 2651 N93-25632 #
AD-A260889 ..... p 2783 N93-25633 #
AD-A260890 ..... p 2676 N93-25912 #
AD-A260894 ..... p 2789 N93-25657 #
AD-A260900 ..... p 2624 N93-25913 #
AD-A260901 ..... p 2727 N93-25658 #
AD-A260902 ..... p 2806 N93-25934 #
AD-A260910 ..... p 2856 N93-26457 #
AD-A260911 ..... p 2849 N93-25659 #
AD-A260914 ..... p 2690 N93-25660 #
AD-A260915 ..... p 2661 N93-25914 #
AD-A260926 ..... p 2853 N93-25646 #
AD-A260927 ..... p 2727 N93-25647 #
AD-A260929 ..... p 2820 N93-25648 #
AD-A260933 ..... p 2911 N93-25710 #
AD-A260934 ..... p 2845 N93-25915 #
AD-A260938 ..... p 2795 N93-26218 #
AD-A260941 ..... p 2595 N93-26219 #
AD-A260957 ..... p 2645 N93-26220 #
AD-A260959 ..... p 2811 N93-26221 #
AD-A260967 ..... p 2829 N93-26222 #
AD-A260968 ..... p 2867 N93-26223 #
AD-A260969 ..... p 2856 N93-26224 #
AD-A260970 ..... p 2640 N93-26225 #
AD-A260971 ..... p 2810 N93-25711 #
AD-A260976 ..... p 2676 N93-25866 #
AD-A260977 ..... p 2801 N93-25867 #
AD-A260978 ..... p 2639 N93-25936 #
AD-A260979 ..... p 2806 N93-25841 #
AD-A260980 ..... p 2882 N93-25844 #
AD-A260982 ..... p 2774 N93-25852 #
AD-A260995 ..... p 2821 N93-25853 #
AD-A260996 ..... p 2866 N93-25854 #
AD-A261000 ..... p 2676 N93-25855 #
AD-A261002 ..... p 2690 N93-25856 #
AD-A261003 ..... p 2729 N93-25938 #
AD-A261005 ..... p 2656 N93-25940 #
AD-A261009 ..... p 2661 N93-25857 #
AD-A261010 ..... p 2806 N93-25858 #
AD-A261012 ..... p 2801 N93-25859 #
AD-A261014 ..... p 2830 N93-25860 #
AD-A261016 ..... p 2655 N93-25861 #
AD-A261017 ..... p 2639 N93-25862 #
AD-A261019 ..... p 2830 N93-25863 #
AD-A261028 ..... p 2729 N93-25941 #
AD-A261037 ..... p 2680 N93-26226 #
AD-A261038 ..... p 2765 N93-25864 #
AD-A261040 ..... p 2797 N93-25815 #
AD-A261041 ..... p 2655 N93-25816 #
AD-A261042 ..... p 2811 N93-25791 #
AD-A261047 ..... p 2785 N93-25777 #
AD-A261048 ..... p 2800 N93-25778 #
AD-A261050 ..... p 2706 N93-25779 #
AD-A261054 ..... p 2586 N93-26237 #
AD-A261055 ..... p 2680 N93-26227 #
AD-A261057 ..... p 2829 N93-26228 #
AD-A261059 ..... p 2802 N93-26229 #
AD-A261060 ..... p 2574 N93-26238 #
AD-A261062 ..... p 2638 N93-25780 #
AD-A261063 ..... p 2595 N93-26239 #
AD-A261064 ..... p 2657 N93-26240 #
AD-A261065 ..... p 2645 N93-26251 #
AD-A261066 ..... p 2681 N93-26241 #
AD-A261068 ..... p 2817 N93-26277 #
AD-A261071 ..... p 2882 N93-26242 #
AD-A261078 ..... p 2868 N93-26252 #
AD-A261079 ..... p 2866 N93-25781 #
AD-A261082 ..... p 2828 N93-25762 #
AD-A261088 ..... p 2877 N93-25763 #
AD-A261089 ..... p 2793 N93-25764 #
AD-A261092 ..... p 2765 N93-25765 #
AD-A261099 ..... p 2853 N93-25766 #
AD-A261101 ..... p 2675 N93-25767 #
AD-A261105 ..... p 2591 N93-26572 #
AD-A261113 ..... p 2638 N93-25768 #
AD-A261116 ..... p 2660 N93-25769 #
AD-A261117 ..... p 2609 N93-25770 #
AD-A261121 ..... p 2639 N93-25945 #
AD-A261122 ..... p 2719 N93-25771 #
AD-A261123 ..... p 2675 N93-25772 #
AD-A261126 ..... p 2828 N93-25773 #
AD-A261127 ..... p 2710 N93-26044 #
AD-A261129 ..... p 2775 N93-25946 #
AD-A261137 ..... p 2645 N93-26045 #
AD-A261154 ..... p 2867 N93-25947 #
AD-A261165 ..... p 2661 N93-25948 #
AD-A261170 ..... p 2714 N93-25774 #
AD-A261178 ..... p 2690 N93-25820 #
AD-A261182 ..... p 2821 N93-25821 #
AD-A261183 ..... p 2853 N93-25822 #
AD-A261187 ..... p 2849 N93-25823 #
AD-A261189 ..... p 2590 N93-25949 #
AD-A261198 ..... p 2881 N93-25824 #
AD-A261203 ..... p 2766 N93-26243 #
AD-A261205 ..... p 2757 N93-25868 #
AD-A261207 ..... p 2729 N93-25950 #
AD-A261209 ..... p 2714 N93-25869 #
AD-A261213 ..... p 2590 N93-25733 #
AD-A261214 ..... p 2849 N93-25734 #
AD-A261224 ..... p 2645 N93-26300 #
AD-A261225 ..... p 2686 N93-26573 #
AD-A261226 ..... p 2640 N93-26301 #
AD-A261228 ..... p 2868 N93-26302 #
AD-A261230 ..... p 2851 N93-26518 #
AD-A261232 ..... p 2830 N93-26262 #
AD-A261233 ..... p 2583 N93-26263 #
AD-A261250 ..... p 2657 N93-26278 #
AD-A261251 ..... p 2652 N93-26264 #
AD-A261257 ..... p 2813 N93-26563 #

REPORT

AD-A261259 ..... p 2802 N93-26265 #
AD-A261265 ..... p 2657 N93-26303 #
AD-A261267 ..... p 2856 N93-26266 #
AD-A261275 ..... p 2850 N93-26267 #
AD-A261280 ..... p 2807 N93-26291 #
AD-A261286 ..... p 2730 N93-26279 #
AD-A261292 ..... p 2766 N93-26292 #
AD-A261293 ..... p 2653 N93-26304 #
AD-A261294 ..... p 2807 N93-26293 #
AD-A261296 ..... p 2720 N93-26564 #
AD-A261300 ..... p 2807 N93-26294 #
AD-A261301 ..... p 2618 N93-26295 #
AD-A261303 ..... p 2715 N93-26296 #
AD-A261309 ..... p 2715 N93-26297 #
AD-A261312 ..... p 2790 N93-26298 #
AD-A261316 ..... p 2691 N93-26299 #
AD-A261317 ..... p 2662 N93-26308 #
AD-A261332 ..... p 2856 N93-26309 #
AD-A261334 ..... p 2759 N93-26310 #
AD-A261343 ..... p 2691 N93-26311 #
AD-A261346 ..... p 2868 N93-26312 #
AD-A261348 ..... p 2883 N93-26313 #
AD-A261350 ..... p 2831 N93-26330 #
AD-A261355 ..... p 2790 N93-26331 #
AD-A261359 ..... p 2868 N93-26332 #
AD-A261360 ..... p 2826 N93-26333 #
AD-A261362 ..... p 2692 N93-26334 #
AD-A261366 ..... p 2595 N93-26335 #
AD-A261367 ..... p 2812 N93-26336 #
AD-A261370 ..... p 2722 N93-26337 #
AD-A261371 ..... p 2817 N93-26338 #
AD-A261374 ..... p 2595 N93-26339 #
AD-A261375 ..... p 2917 N93-26359 #
AD-A261381 ..... p 2896 N93-26340 #
AD-A261382 ..... p 2657 N93-26341 #
AD-A261384 ..... p 2715 N93-26445 #
AD-A261388 ..... p 2799 N93-26446 #
AD-A261390 ..... p 2886 N93-26305 #
AD-A261391 ..... p 2856 N93-26306 #
AD-A261394 ..... p 2797 N93-26307 #
AD-A261395 ..... p 2829 N93-26519 #
AD-A261396 ..... p 2850 N93-26288 #
AD-A261397 ..... p 2681 N93-26289 #
AD-A261398 ..... p 2812 N93-26290 #
AD-A261399 ..... p 2862 N93-26520 #
AD-A261400 ..... p 2707 N93-26400 #
AD-A261401 ..... p 2657 N93-26401 #
AD-A261402 ..... p 2646 N93-26402 #
AD-A261404 ..... p 2807 N93-26403 #
AD-A261405 ..... p 2802 N93-26404 #
AD-A261410 ..... p 2586 N93-26447 #
AD-A261415 ..... p 2757 N93-26448 #
AD-A261418 ..... p 2799 N93-26449 #
AD-A261419 ..... p 2813 N93-26450 #
AD-A261424 ..... p 2682 N93-26451 #
AD-A261427 ..... p 2829 N93-26452 #
AD-A261428 ..... p 2813 N93-26453 #
AD-A261429 ..... p 2776 N93-26454 #
AD-A261431 ..... p 2682 N93-26455 #
AD-A261434 ..... p 2827 N93-26487 #
AD-A261435 ..... p 2857 N93-26488 #
AD-A261438 ..... p 2799 N93-26489 #
AD-A261439 ..... p 2686 N93-26490 #
AD-A261440 ..... p 2896 N93-26508 #
AD-A261441 ..... p 2829 N93-26345 #
AD-A261445 ..... p 2799 N93-26521 #
AD-A261447 ..... p 2850 N93-26346 #
AD-A261449 ..... p 2797 N93-26347 #
AD-A261450 ..... p 2776 N93-26348 #
AD-A261452 ..... p 2798 N93-26349 #
AD-A261453 ..... p 2883 N93-26350 #
AD-A261454 ..... p 2787 N93-26351 #
AD-A261455 ..... p 2787 N93-26352 #
AD-A261456 ..... p 2757 N93-26574 #
AD-A261460 ..... p 2798 N93-26353 #
AD-A261471 ..... p 2757 N93-26354 #
AD-A261483 ..... p 2641 N93-26355 #
AD-A261484 ..... p 2798 N93-26356 #
AD-A261485 ..... p 2868 N93-26357 #
AD-A261487 ..... p 2873 N93-26342 #
AD-A261488 ..... p 2856 N93-26343 #
AD-A261490 ..... p 2829 N93-26344 #
AD-A261491 ..... p 2846 N93-26374 #
AD-A261494 ..... p 2812 N93-26375 #
AD-A261511 ..... p 2884 N93-26575 #
AD-A261515 ..... p 2846 N93-26376 #
AD-A261517 ..... p 2658 N93-26576 #
AD-A261519 ..... p 2883 N93-26377 #
AD-A261520 ..... p 2813 N93-26378 #
AD-A261524 ..... p 2707 N93-26360 #
AD-A261526 ..... p 2730 N93-26361 #
AD-A261539 ..... p 2730 N93-26362 #
AD-A261542 ..... p 2707 N93-26379 #
AD-A261549 ..... p 2869 N93-26577 #
AD-A261550 ..... p 2791 N93-26578 #
AD-A261551 ..... p 2918 N93-26380 #
AD-A261552 ..... p 2869 N93-26381 #
AD-A261553 ..... p 2887 N93-26458 #
AD-A261556 ..... p 2731 N93-26459 #
AD-A261558 ..... p 2682 N93-26460 #
AD-A261560 ..... p 2813 N93-26461 #
AD-A261562 ..... p 2591 N93-26462 #
AD-A261574 ..... p 2731 N93-26522 #
AD-A261576 ..... p 2619 N93-26456 #
AD-A261577 ..... p 2787 N93-26513 #
AD-A261579 ..... p 2851 N93-26514 #
AD-A261580 ..... p 2857 N93-26515 #
AD-A261591 ..... p 2731 N93-26516 #
AD-A261592 ..... p 2798 N93-26435 #
AD-A261593 ..... p 2798 N93-26436 #
AD-A261594 ..... p 2884 N93-26523 #
AD-A261595 ..... p 2715 N93-26524 #
AD-A261596 ..... p 2851 N93-26525 #
AD-A261597 ..... p 2826 N93-26162 #
AD-A261599 ..... p 2707 N93-26163 #
AD-A261608 ..... p 2790 N93-26164 #
AD-A261611 ..... p 2846 N93-26165 #
AD-A261612 ..... p 2680 N93-26166 #
AD-A261613 ..... p 2707 N93-26167 #
AD-A261614 ..... p 2573 N93-26168 #
AD-A261616 ..... p 2658 N93-26437 #
AD-A261617 ..... p 2817 N93-26169 #
AD-A261635 ..... p 2790 N93-26170 #
AD-A261636 ..... p 2691 N93-26171 #
AD-A261642 ..... p 2656 N93-26172 #
AD-A261645 ..... p 2849 N93-26173 #
AD-A261646 ..... p 2618 N93-26232 #
AD-A261648 ..... p 2632 N93-26174 #
AD-A261651 ..... p 2867 N93-26193 #
AD-A261652 ..... p 2867 N93-26194 #
AD-A261654 ..... p 2581 N93-26195 #
AD-A261656 ..... p 2597 N93-26196 #
AD-A261657 ..... p 2715 N93-26363 #
AD-A261658 ..... p 2798 N93-26364 #
AD-A261659 ..... p 2846 N93-26358 #
AD-A261663 ..... p 2883 N93-26389 #
AD-A261671 ..... p 2619 N93-26438 #
AD-A261676 ..... p 2826 N93-26365 #
AD-A261679 ..... p 2731 N93-26390 #
AD-A261685 ..... p 2692 N93-26366 #
AD-A261687 ..... p 2646 N93-26439 #
AD-A261688 ..... p 2850 N93-26367 #
AD-A261689 ..... p 2812 N93-26368 #
AD-A261692 ..... p 2798 N93-26391 #
AD-A261693 ..... p 2757 N93-26369 #
AD-A261695 ..... p 2829 N93-26370 #
AD-A261698 ..... p 2641 N93-26382 #
AD-A261700 ..... p 2681 N93-26383 #
AD-A261702 ..... p 2790 N93-26384 #
AD-A261703 ..... p 2869 N93-26385 #
AD-A261704 ..... p 2757 N93-26440 #
AD-A261705 ..... p 2641 N93-26579 #
AD-A261712 ..... p 2641 N93-26580 #
AD-A261713 ..... p 2870 N93-26581 #
AD-A261714 ..... p 2641 N93-26371 #
AD-A261715 ..... p 2681 N93-26372 #
AD-A261719 ..... p 2786 N93-26245 #
AD-A261722 ..... p 2722 N93-26246 #
AD-A261726 ..... p 2681 N93-26280 #
AD-A261727 ..... p 2681 N93-26247 #
AD-A261728 ..... p 2850 N93-26281 #
AD-A261729 ..... p 2620 N93-26248 #
AD-A261731 ..... p 2885 N93-26582 #
AD-A261732 ..... p 2813 N93-26583 #
AD-A261742 ..... p 2652 N93-26282 #
AD-A261746 ..... p 2720 N93-26249 #
AD-A261747 ..... p 2872 N93-26250 #
AD-A261749 ..... p 2632 N93-26373 #
AD-A261750 ..... p 2776 N93-26283 #
AD-A261751 ..... p 2652 N93-26284 #
AD-A261755 ..... p 2662 N93-26600 #
AD-A261769 ..... p 2669 N93-26285 #
AD-A261776 ..... p 2716 N93-26601 #
AD-A261777 ..... p 2787 N93-26286 #
AD-A261778 ..... p 2647 N93-26602 #
AD-A261781 ..... p 2686 N93-26603 #
AD-A261782 ..... p 2686 N93-26604 #
AD-A261784 ..... p 2692 N93-26565 #
AD-A261785 ..... p 2857 N93-26566 #
AD-A261786 ..... p 2722 N93-26526 #
AD-A261788 ..... p 2682 N93-26441 #
AD-A261789 ..... p 2883 N93-26442 #
AD-A261792 ..... p 2850 N93-26443 #
AD-A261793 ..... p 2657 N93-26386 #
AD-A261794 ..... p 2868 N93-26254 #
AD-A261796 ..... p 2830 N93-26255 #
AD-A261800 ..... p 2590 N93-26444 #
AD-A261801 ..... p 2692 N93-26539 #
AD-A261802 ..... p 2856 N93-26256 #
AD-A261803 ..... p 2868 N93-26258 #
AD-A261804 ..... p 2662 N93-26387 #
AD-A261808 ..... p 2793 N93-26259 #
AD-A261809 ..... p 2597 N93-26260 #
AD-A261810 ..... p 2776 N93-26430 #
AD-A261811 ..... p 2681 N93-26261 #
AD-A261812 ..... p 2812 N93-26257 #
AD-A261813 ..... p 2661 N93-26268 #
AD-A261815 ..... p 2707 N93-26269 #
AD-A261819 ..... p 2786 N93-26270 #
AD-A261827 ..... p 2812 N93-26271 #
AD-A261828 ..... p 2691 N93-26272 #
AD-A261831 ..... p 2786 N93-26273 #
AD-A261833 ..... p 2586 N93-26274 #
AD-A261839 ..... p 2813 N93-26431 #
AD-A261843 ..... p 2790 N93-26050 * #
AD-A261850 ..... p 2812 N93-26275 #
AD-A261851 ..... p 2850 N93-26287 #
AD-A261852 ..... p 2681 N93-26276 #
AD-A261866 ..... p 2682 N93-26388 #
AD-A261871 ..... p 2869 N93-26540 #
AD-A261873 ..... p 2686 N93-26541 #
AD-A261884 ..... p 2722 N93-26527 #
AD-A261888 ..... p 2862 N93-26528 #
AD-A261891 ..... p 2857 N93-26542 #
AD-A261903 ..... p 2708 N93-26543 #
AD-A261911 ..... p 2884 N93-26531 #
AD-A261912 ..... p 2884 N93-26532 #
AD-A261913 ..... p 2882 N93-26230 #
AD-A261915 ..... p 2857 N93-26544 #
AD-A261919 ..... p 2652 N93-26197 #
AD-A261925 ..... p 2582 N93-26198 #
AD-A261927 ..... p 2787 N93-26545 #
AD-A261930 ..... p 2811 N93-26253 #
AD-A261933 ..... p 2829 N93-26199 #

AD-D015632 ..... p 2643 N93-25284
AD-D015637 ..... p 2717 N93-25228
AD-D015638 ..... p 2634 N93-25283
AD-D015639 ..... p 2687 N93-25212
AD-D015642 ..... p 2852 N93-25358 #
AD-D015647 ..... p 2674 N93-25332
AD-D015652 ..... p 2719 N93-26244
AD-D015660 ..... p 2867 N93-26090
AD-D015661 ..... p 2854 N93-26091
AD-D015667 ..... p 2710 N93-26092
AD-D015668 ..... p 2586 N93-26093
AD-D015670 ..... p 2652 N93-26234
AD-D015671 ..... p 2867 N93-26140
AD-D015672 ..... p 2710 N93-26141
AD-D015675 ..... p 2691 N93-26233
AD-D015676 ..... p 2691 N93-26142
AD-D015677 ..... p 2640 N93-26143 #
AD-D015678 ..... p 2719 N93-26144 #
AD-D015679 ..... p 2640 N93-26145 #

AD-E201405 ..... p 2849 N93-26173 #
AD-E201407 ..... p 2681 N93-26280 #
AD-E201408 ..... p 2681 N93-26247 #
AD-E201414 ..... p 2776 N93-26283 #
AD-E201418 ..... p 2632 N93-26373 #
AD-E201419 ..... p 2618 N93-26232 #
AD-E201422 ..... p 2850 N93-26281 #
AD-E201423 ..... p 2620 N93-26248 #
AD-E501629 ..... p 2813 N93-26461 #

AEDC-TR-92-23-APP-D-VOL-2 ..... p 2657 N93-26278 #

AESO-2-90-REV ..... p 2595 N93-26339 #

AFESC/ESL-TR-88-79 ..... p 2598 N93-25656 #

AFIT/GEE/CEC/92S-5 ..... p 2765 N93-25864 #

AFIT/GEE/CEV/92S-13 ..... p 2765 N93-25765 #

AFORS-TR-93-0014 ..... p 2828 N93-25687 #

AFOSR-TR-92-1010 ..... p 2911 N93-25893 #
AFOSR-TR-93-0051 ..... p 2918 N93-26380 #
AFOSR-TR-93-0073 ..... p 2661 N93-25948 #

AFOSR-92-0517TR ..... p 2856 N93-26266 #
AFOSR-92-1002TR ..... p 2756 N93-25679 #
AFOSR-93-0016TR ..... p 2729 N93-25901 #
AFOSR-93-0018TR ..... p 2852 N93-25676 #
AFOSR-93-0035TR ..... p 2657 N93-26401 #
AFOSR-93-0036TR ..... p 2856 N93-26309 #
AFOSR-93-0038TR ..... p 2646 N93-26402 #
AFOSR-93-0039TR ..... p 2850 N93-26346 #
AFOSR-93-0041TR ..... p 2707 N93-26400 #
AFOSR-93-0042TR ..... p 2686 N93-26490 #
AFOSR-93-0043TR ..... p 2799 N93-26446 #
AFOSR-93-0044TR ..... p 2896 N93-26508 #
AFOSR-93-0045TR ..... p 2787 N93-26351 #
AFOSR-93-0046TR ..... p 2787 N93-26352 #
AFOSR-93-0050TR ..... p 2798 N93-26349 #
AFOSR-93-0054TR ..... p 2798 N93-26436 #
AFOSR-93-0055TR ..... p 2798 N93-26435 #

AFOSR-93-0056TR ..... p 2799 N93-26521 #
AFOSR-93-0058TR ..... p 2869 N93-26381 #
AFOSR-93-0059TR ..... p 2715 N93-26524 #
AFOSR-93-0060TR ..... p 2799 N93-26489 #
AFOSR-93-0061TR ..... p 2851 N93-26525 #
AFOSR-93-0062TR ..... p 2826 N93-26162 #
AFOSR-93-0063TR ..... p 2829 N93-26345 #
AFOSR-93-0064TR ..... p 2776 N93-26348 #
AFOSR-93-0065TR ..... p 2828 N93-25762 #
AFOSR-93-0066TR ..... p 2821 N93-25821 #
AFOSR-93-0070TR ..... p 2797 N93-26347 #
AFOSR-93-0074TR ..... p 2817 N93-26169 #
AFOSR-93-0076TR-PT-A ..... p 2641 N93-26382 #
AFOSR-93-0077TR ..... p 2619 N93-26438 #
AFOSR-93-0078TR ..... p 2869 N93-26385 #
AFOSR-93-0079TR ..... p 2846 N93-26374 #
AFOSR-93-0080TR ..... p 2619 N93-26456 #
AFOSR-93-0081TR ..... p 2826 N93-26365 #
AFOSR-93-0082TR ..... p 2641 N93-26355 #
AFOSR-93-0083TR ..... p 2812 N93-26368 #
AFOSR-93-0084TR ..... p 2797 N93-26307 #
AFOSR-93-0085TR ..... p 2798 N93-26356 #
AFOSR-93-0086TR ..... p 2798 N93-26391 #
AFOSR-93-0089TR ..... p 2873 N93-26342 #
AFOSR-93-0090TR ..... p 2829 N93-26519 #
AFOSR-93-0091TR ..... p 2829 N93-26344 #
AFOSR-93-0092TR ..... p 2812 N93-26290 #
AFOSR-93-0093TR ..... p 2798 N93-26364 #
AFOSR-93-0094TR ..... p 2846 N93-26358 #
AFOSR-93-0096TR ..... p 2870 N93-26581 #
AFOSR-93-0098TR ..... p 2826 N93-26333 #
AFOSR-93-0099TR ..... p 2868 N93-26357 #
AFOSR-93-0101TR ..... p 2646 N93-26439 #
AFOSR-93-0102TR ..... p 2856 N93-26343 #
AFOSR-93-0103TR ..... p 2850 N93-26288 #
AFOSR-93-0104TR ..... p 2850 N93-26367 #
AFOSR-93-0105TR ..... p 2867 N93-26194 #
AFOSR-93-0106TR ..... p 2867 N93-26193 #
AFOSR-93-0107TR ..... p 2691 N93-26171 #
AFOSR-93-0108TR ..... p 2692 N93-26366 #
AFOSR-93-0132TR ..... p 2707 N93-26379 #
AFOSR-93-0133TR ..... p 2707 N93-26163 #
AFOSR-93-0134TR ..... p 2800 N93-25778 #
AFOSR-93-0135TR ..... p 2785 N93-25777 #
AFOSR-93-0136TR ..... p 2799 N93-26449 #
AFOSR-93-0137TR ..... p 2661 N93-26268 #
AFOSR-93-0138TR ..... p 2645 N93-26220 #
AFOSR-93-0139TR ..... p 2707 N93-26269 #
AFOSR-93-0141TR ..... p 2811 N93-26221 #
AFOSR-93-0142TR ..... p 2595 N93-26335 #
AFOSR-93-0144TR ..... p 2813 N93-26450 #
AFOSR-93-0146TR ..... p 2868 N93-26332 #

AGARD-MEMB-93 ..... p 2873 N93-26428 #

AIAA PAPER 92-2634 ..... p 2575 N93-24911 * #
AIAA PAPER 92-3108 ..... p 2633 N93-26561 * #
AIAA PAPER 93-0704 ..... p 2618 N93-26148 * #
AIAA PAPER 93-0805 ..... p 2631 N93-26149 * #
AIAA PAPER 93-1152 ..... p 2614 N93-24755 * #
AIAA PAPER 93-2176 ..... p 2598 N93-26214 * #
AIAA PAPER 93-2298 ..... p 2718 N93-25672 * #

AL-TP-1992-0043 ..... p 2883 N93-26350 #
AL-TP-1992-0050 ..... p 2884 N93-26523 #
AL-TP-1992-0052 ..... p 2877 N93-25763 #
AL-TP-1992-0054 ..... p 2797 N93-25815 #

AL-TR-1992-0082 ..... p 2590 N93-25949 #
AL-TR-1992-0101 ..... p 2793 N93-26259 #
AL-TR-1992-0132 ..... p 2801 N93-25787 #
AL-TR-1992-0154 ..... p 2845 N93-25915 #
AL-TR-1992-0160 ..... p 2591 N93-25909 #
AL-TR-1992-0161 ..... p 2813 N93-26563 #
AL-TR-1992-0165 ..... p 2885 N93-26582 #
AL-TR-1992-0172 ..... p 2591 N93-26462 #

AL/BROOKS-TR-1992-0155 ..... p 2591 N93-25783 #

ANL-HEP-CP-93-06 ..... p 2851 N93-25301 #

ANL-93007737 ..... p 2658 N93-26588 #

ANL/APS/TM-11 ..... p 2598 N93-26498 #

ANL/ASD/CP-77461 ..... p 2848 N93-25368 #

ANL/CHM/CP-75284 ..... p 2761 N93-24956 #

ANL/CP-76463 ..... p 2695 N93-24966 #

ANL/EAIS/CP-77721 ..... p 2761 N93-25143 #

ANL/ES/CP-77429 ..... p 2660 N93-25298 #
ANL/ES/CP-78570 ..... p 2660 N93-25192 #

ANL/MCS-TM-170 ..... p 2767 N93-26496 #

ANL/MCS/CP-78727 ..... p 2816 N93-25521 #
ANL/MCS/CP-78728 ..... p 2816 N93-25522 #
ANL/MCS/CP-78729 ..... p 2763 N93-25370 #

ANL/MSD/CP-78798 ..... p 2863 N93-25369 #

ANL/PHY/CP-78720 ..... p 2848 N93-25371 #

ARAED-SP-92004 ..... p 2662 N93-26387 #

ARAED-TR-92023 ..... p 2675 N93-25635 #

ARC-93-3 ..... p 2587 N93-25162 * #

ARFSD-TR-92024 ..... p 2710 N93-25686 #

ARL-CR-11 ..... p 2716 N93-24751 * #
ARL-CR-43 ..... p 2719 N93-25884 * #

ARL-TR-11 ..... p 2718 N93-25672 * #
ARL-TR-4 ..... p 2638 N93-25768 #
ARL-TR-75 ..... p 2597 N93-26260 #
ARL-TR-8 ..... p 2828 N93-25773 #
ARL-TR-92-11 ..... p 2846 N93-26179 #
ARL-TR-94 ..... p 2883 N93-26377 #
ARL-TR-9 ..... p 2845 N93-25649 #

ARO-23662.7-EL ..... p 2867 N93-26223 #
ARO-24625.1-EG-UIF ..... p 2632 N93-26216 #
ARO-24635.430-MA-UIR ..... p 2821 N93-25853 #
ARO-25202.1-MS ..... p 2640 N93-26236 #
ARO-25523.2-CH ..... p 2645 N93-26045 #
ARO-25546.16-PH ..... p 2853 N93-25822 #
ARO-26099.9-LS ..... p 2793 N93-25764 #
ARO-26158.24-MA ..... p 2830 N93-25863 #
ARO-26167.5-MS-A ..... p 2651 N93-25788 #
ARO-26188.4-EL ..... p 2866 N93-25789 #
ARO-26394.8-MA ..... p 2830 N93-25860 #
ARO-26400.7-MS ..... p 2655 N93-25861 #
ARO-26404.1-GS ..... p 2774 N93-25790 #
ARO-26444.4-EL ..... p 2866 N93-25897 #
ARO-26571.4-MS ..... p 2641 N93-26580 #
ARO-26674.6-MA ..... p 2829 N93-26222 #
ARO-26697.1-EL ..... p 2756 N93-25653 #
ARO-26735.1-EL ..... p 2806 N93-25650 #
ARO-26767.6-LS ..... p 2795 N93-25944 #
ARO-26791.2-EL ..... p 2849 N93-25823 #
ARO-26813.5-EL ..... p 2854 N93-25898 #
ARO-26822.12-CH ..... p 2657 N93-26303 #
ARO-26934.8-EG ..... p 2728 N93-25842 #
ARO-26959.5-PH ..... p 2860 N93-25626 #
ARO-27005.2-EL-F ..... p 2853 N93-25839 #
ARO-27031.22-GS-S ..... p 2676 N93-25855 #
ARO-27167.3-EG-SM ..... p 2636 N93-25631 #
ARO-27195.1-CH-SM ..... p 2866 N93-25854 #
ARO-27198.1-MS-SM ..... p 2640 N93-26225 #
ARO-27210.4-MS-SM ..... p 2645 N93-25879 #
ARO-27216.6-EG-SM ..... p 2638 N93-25780 #
ARO-27409.1-EG ..... p 2730 N93-26361 #
ARO-27418.4-PH ..... p 2715 N93-26297 #
ARO-27764.1-MS ..... p 2867 N93-25899 #
ARO-28002.1-EG ..... p 2845 N93-25651 #
ARO-28148.2-EL-SB2 ..... p 2710 N93-25677 #
ARO-28374.6-EG-H-PT-2 ..... p 2729 N93-25938 #
ARO-28396.1-PH ..... p 2609 N93-25770 #
ARO-28502.1-PH ..... p 2864 N93-25655 #
ARO-28575.1-MS ..... p 2651 N93-25907 #
ARO-28594.5-EL ..... p 2714 N93-25774 #
ARO-28639.2-MS ..... p 2652 N93-26264 #
ARO-28756.1-EG-CF ..... p 2728 N93-25838 #
ARO-28784.1-PH ..... p 2856 N93-26224 #
ARO-28955.1-PH ..... p 2849 N93-25644 #
ARO-29396.1-MA ..... p 2817 N93-26277 #
ARO-30367.2-PH-UIR ..... p 2714 N93-25869 #
ARO-30378.1-EG-URI ..... p 2719 N93-25771 #
ARO-30378.3-EG-URI ..... p 2675 N93-25772 #
ARO-30378.4-EG-URI ..... p 2639 N93-25919 #
ARO-30378.5-EG-URI ..... p 2729 N93-25846 #
ARO-30378.6-EG-URI ..... p 2729 N93-25941 #
ARO-30378.7-EG-URI ..... p 2639 N93-25945 #
ARO-30378.8-EG-URI ..... p 2729 N93-25950 #
ARO-30408.1-PH ..... p 2639 N93-25862 #
ARO-30479.1-EL-SBI ..... p 2709 N93-25634 #
ARO-30676.1-EL-SBI ..... p 2868 N93-26312 #
ARO-30744.1-MS-CF ..... p 2639 N93-25908 #

ARR-20 ..... p 2911 N93-25710 #

ASIAC-TR-92-2 ..... p 2810 N93-25627 #

ATR-90(7186)-1 ..... p 2895 N93-26147 #

AVSCOM-TR-92-C-022 ..... p 2708 N93-26554 * #

B-248529 ..... p 2882 N93-26096 #

BBC-RD-1992/10 ..... p 2673 N93-25170
BBC-RD-1992/11 ..... p 2673 N93-25171
BBC-RD-1992/12 ..... p 2674 N93-25391
BBC-RD-1992/6 ..... p 2674 N93-25239
BBC-RD-1992/8-PT-1 ..... p 2673 N93-25168
BBC-RD-1992/9-PT-2 ..... p 2673 N93-25169

BFLRF-280 ..... p 2661 N93-25902 #
BFLRF-281 ..... p 2661 N93-25914 #

BNL-48039 ..... p 2687 N93-24964 #
BNL-48196 ..... p 2643 N93-25123 #
BNL-48250 ..... p 2827 N93-24973 #
BNL-48308 ..... p 2712 N93-25378 #

BRDEC-2538 ..... p 2718 N93-25682 #

BRL-TR-3321 ..... p 2609 N93-25985 #

BR307779 ..... p 2864 N93-25454 #
BR310269 ..... p 2592 N93-25455 #
BR310395 ..... p 2810 N93-25453 #

CA-PATENT-APPL-SN-2024585 .. p 2597 N93-25178

CARDEROCKDIV-U-SSM-65-93/03 p 2723 N93-24912 * #

CDNSWC/SME-CR-17-92 ..... p 2731 N93-26390 #
CDNSWC/SME-CR-18-92 ..... p 2731 N93-26516 #

CDNSWC/SME-19-92 ..... p 2727 N93-25647 #
CDNSWC/SME-92/38 ..... p 2636 N93-25652 #

CDRL-A002 ..... p 2657 N93-26278 #

CDRL-103A-10 ..... p 2609 N93-26098 #
CDRL-103A10 ..... p 2609 N93-26175 #
CDRL-103A10 ..... p 2609 N93-26176 #
CDRL-103A10 ..... p 2610 N93-26180 #
CDRL-103A10 ..... p 2610 N93-26181 #
CDRL-103A10 ..... p 2610 N93-26182 #
CDRL-103A10 ..... p 2610 N93-26591 #

CEL-TR-92-49 ..... p 2766 N93-26243 #

CERC-TR-DRP-92-6 ..... p 2790 N93-26164 #

CFDRC-4240/2 ..... p 2661 N93-26268 #

CFL-93-002 ..... p 2818 N93-25190 * #

CIRSSE-122 ..... p 2817 N93-24743 * #

CIT/REF-06-769(E) ..... p 2594 N93-25917 #

CMU-CS-92-103 ..... p 2757 N93-26448 #
CMU-CS-92-183 ..... p 2883 N93-26389 #
CMU-CS-92-201 ..... p 2806 N93-25841 #
CMU-CS-92-204 ..... p 2813 N93-26378 #
CMU-CS-93-100 ..... p 2857 N93-26488 #
CMU-CS-93-101 ..... p 2882 N93-25844 #
CMU-CS-93-103 ..... p 2827 N93-26487 #
CMU-CS-93-116-REV ..... p 2817 N93-26338 #

CONF-920262 ..... p 2658 N93-26506 #
CONF-9203139-3 ..... p 2715 N93-26503 #
CONF-920401-1 ..... p 2888 N93-25320 #
CONF-9204225-SUMM ..... p 2887 N93-26499 #
CONF-9205138-3 ..... p 2875 N93-25319 #
CONF-920523-7 ..... p 2712 N93-25363 #
CONF-9206311-1 ..... p 2687 N93-24964 #
CONF-920673-16 ..... p 2649 N93-25255 #
CONF-9207169-3 ..... p 2848 N93-25364 #
CONF-920799-5 ..... p 2721 N93-25518 #
CONF-920801 ..... p 2759 N93-25183 #
CONF-9208109-75 ..... p 2688 N93-25397 #
CONF-9208109-76 ..... p 2852 N93-25375 #
CONF-9208154-2 ..... p 2892 N93-25164 #
CONF-9208205-1 ..... p 2653 N93-26500 #
CONF-920890-1 ..... p 2635 N93-25383 #
CONF-9209127-1 ..... p 2847 N93-25326 #
CONF-9209142-9 ..... p 2873 N93-24677 #
CONF-9209158-9 ..... p 2760 N93-24673 #
CONF-9209163-5 ..... p 2769 N93-24672 #
CONF-9209188-8 ..... p 2709 N93-25515 #
CONF-9209200-7 ..... p 2649 N93-25336 #
CONF-9209273-1 ..... p 2695 N93-24963 #
CONF-9209279-3 ..... p 2848 N93-25366 #
CONF-9209281 ..... p 2767 N93-26496 #
CONF-920967-1 ..... p 2768 N93-26592 #
CONF-921005-25 ..... p 2688 N93-25365 #
CONF-921005-26 ..... p 2692 N93-26598 #
CONF-921005-8 ..... p 2869 N93-26494 #
CONF-9210246-12 ..... p 2851 N93-25325 #

CONF-9210246-13 ..... p 2851 N93-25314 #
CONF-9210246-17 ..... p 2848 N93-25368 #
CONF-9210249-5 ..... p 2847 N93-25148 #
CONF-9210249-6 ..... p 2848 N93-25371 #
CONF-9210252-1 ..... p 2767 N93-26497 #
CONF-9210256-1 ..... p 2764 N93-25443 #
CONF-9210270 ..... p 2815 N93-25304 #
CONF-9210290-SUMM ..... p 2598 N93-26498 #
CONF-9210292-1 ..... p 2852 N93-25380 #
CONF-9210293 ..... p 2805 N93-25165 #
CONF-9210295-1 ..... p 2654 N93-25384 #
CONF-9210295-2 ..... p 2857 N93-26593 #
CONF-9210295-3 ..... p 2870 N93-26594 #
CONF-9210314-1 ..... p 2863 N93-25367 #
CONF-9210315-1 ..... p 2858 N93-25187 #
CONF-921048-7 ..... p 2767 N93-26495 #
CONF-921049-9 ..... p 2874 N93-25254 #
CONF-921058-1 ..... p 2760 N93-24955 #
CONF-921060-1 ..... p 2761 N93-25143 #
CONF-921095-2 ..... p 2761 N93-24956 #
CONF-921101-100 ..... p 2646 N93-26502 #
CONF-921101-14 ..... p 2662 N93-26493 #
CONF-921101-82 ..... p 2649 N93-25149 #
CONF-921101-86 ..... p 2862 N93-24958 #
CONF-921101-87 ..... p 2642 N93-24972 #
CONF-921101-89 ..... p 2863 N93-25387 #
CONF-921101-91 ..... p 2653 N93-24971 #
CONF-921101-94 ..... p 2654 N93-25372 #
CONF-921101-97 ..... p 2650 N93-25492 #
CONF-921102-48 ..... p 2695 N93-24966 #
CONF-9211127-3 ..... p 2650 N93-25519 #
CONF-9211178-2 ..... p 2654 N93-25359 #
CONF-9211188-1 ..... p 2899 N93-25185 #
CONF-9211189-1 ..... p 2863 N93-25362 #
CONF-9211193-1 ..... p 2848 N93-25376 #
CONF-9211193-2 ..... p 2863 N93-25369 #
CONF-9211198-1 ..... p 2763 N93-25370 #
CONF-9211222-42 ..... p 2899 N93-25327 #
CONF-921129-6 ..... p 2859 N93-25324 #
CONF-921129-7 ..... p 2654 N93-25382 #
CONF-921131-6 ..... p 2851 N93-25301 #
CONF-921133-15 ..... p 2688 N93-25313 #
CONF-921133-16 ..... p 2858 N93-25167 #
CONF-921133-18 ..... p 2861 N93-26504 #
CONF-921133-8 ..... p 2861 N93-26512 #
CONF-921256-1 ..... p 2713 N93-25381 #
CONF-921256-2 ..... p 2713 N93-25379 #
CONF-921257-1 ..... p 2725 N93-25373 #
CONF-921261-1 ..... p 2847 N93-25323 #
CONF-930116-30 ..... p 2827 N93-24973 #
CONF-930118-4 ..... p 2667 N93-24970 #
CONF-930120-3 ..... p 2660 N93-25298 #
CONF-930120-4 ..... p 2660 N93-25192 #
CONF-930159-11 ..... p 2646 N93-26505 #
CONF-930159-14 ..... p 2711 N93-24961 #
CONF-930159-16 ..... p 2793 N93-26587 #
CONF-930159-9 ..... p 2712 N93-25150 #
CONF-930164-8 ..... p 2858 N93-24968 #
CONF-930208-1 ..... p 2761 N93-25126 #
CONF-930254-2 ..... p 2689 N93-25429 #
CONF-930256-1 ..... p 2763 N93-25385 #
CONF-930258-1 ..... p 2715 N93-26597 #
CONF-9303102-1 ..... p 2731 N93-26507 #
CONF-930331-1 ..... p 2816 N93-25316 #
CONF-930331-2 ..... p 2809 N93-25315 #
CONF-930331-3 ..... p 2816 N93-25414 #
CONF-930331-4 ..... p 2810 N93-25386 #
CONF-930331-6 ..... p 2816 N93-25521 #
CONF-930331-7 ..... p 2816 N93-25522 #
CONF-930346-1 ..... p 2781 N93-25125 #
CONF-930354-2 ..... p 2692 N93-26501 #
CONF-930372-1 ..... p 2696 N93-25124 #
CONF-930390-1 ..... p 2876 N93-25448 #
CONF-930394-2 ..... p 2689 N93-25416 #
CONF-930394-3 ..... p 2689 N93-25417 #
CONF-930398-1 ..... p 2654 N93-25374 #
CONF-930403-16 ..... p 2688 N93-25377 #
CONF-930403-18 ..... p 2896 N93-25321 #
CONF-930403-19 ..... p 2827 N93-26596 #
CONF-930404-5 ..... p 2828 N93-25151 #
CONF-930489-1 ..... p 2794 N93-25186 #
CONF-930490-1 ..... p 2762 N93-25166 #
CONF-930493-1 ..... p 2756 N93-25516 #
CONF-930502-1 ..... p 2654 N93-25361 #
CONF-930519-1 ..... p 2799 N93-25099 #
CONF-930519-2 ..... p 2717 N93-25100 #
CONF-930519-3 ..... p 2827 N93-25103 #
CONF-930519-4 ..... p 2756 N93-25505 #
CONF-930519-5 ..... p 2584 N93-25120 #
CONF-930519-6 ..... p 2725 N93-25357 #
CONF-930519-7 ..... p 2717 N93-25413 #
CONF-930519-8 ..... p 2718 N93-25449 #
CONF-930525-1 ..... p 2668 N93-25447 #
CONF-930529-1 ..... p 2726 N93-25489 #
CONF-930561-1 ..... p 2800 N93-25415 #
CONF-930571-1 ..... p 2792 N93-25104 #
CONF-930571-3 ..... p 2644 N93-25312 #
CONF-930571-4 ..... p 2655 N93-25444 #
CONF-930571-5 ..... p 2655 N93-25446 #
CONF-930580-1 ..... p 2576 N93-25121 #
CONF-930584-1 ..... p 2655 N93-25507 #
CONF-930586-1 ..... p 2643 N93-25123 #
CONF-930586-2 ..... p 2713 N93-25508 #
CONF-930586-3 ..... p 2712 N93-25378 #
CONF-930588-1 ..... p 2852 N93-25127 #

CPIA-PUBL-593-VOL-2 ..... p 2624 N93-26005

CRHC-93-05 ..... p 2815 N93-24748 * #
CRHC-93-07 ..... p 2815 N93-24749 * #

CRWR-236 ..... p 2768 N93-26559 #

CSS-TM-627-92 ..... p 2715 N93-26296 #

CTN-93-60683 ..... p 2597 N93-25178

CTR-3-4-90/2-93-2/2-VOL-2 ..... p 2720 N93-26534 #
CTR-3-4-90/2-983-2/1-VOL-1 ..... p 2720 N93-26585 #
CTR-3-4-90/2-983-3 ..... p 2720 N93-26590 #

CU-TR-93-1332 ..... p 2808 N93-25107 * #
CU-TR-93-1333 ..... p 2809 N93-25152 * #
CU-TR-93-1339 ..... p 2721 N93-26135 * #

CUED/A-AERO/TR-19 ..... p 2668 N93-25238 #

C931021-U-2R07 ..... p 2754 N93-25154 * #

D-N01-92 ..... p 2813 N93-26563 #

DE92-010560 ..... p 2862 N93-24953 #
DE92-010592 ..... p 2758 N93-25098 #
DE92-016034 ..... p 2799 N93-25099 #
DE92-041301 ..... p 2717 N93-25100 #
DE93-000045 ..... p 2759 N93-25504 #
DE93-000052 ..... p 2898 N93-25101 #
DE93-000072 ..... p 2862 N93-25163 #
DE93-000073 ..... p 2759 N93-25102 #
DE93-000078 ..... p 2759 N93-25253 #
DE93-000079 ..... p 2874 N93-25254 #
DE93-000112 ..... p 2695 N93-24954 #
DE93-000713 ..... p 2827 N93-25103 #
DE93-001645 ..... p 2756 N93-25505 #
DE93-002344 ..... p 2792 N93-25104 #
DE93-002428 ..... p 2584 N93-25120 #
DE93-002465 ..... p 2576 N93-25121 #
DE93-002683 ..... p 2769 N93-24672 #
DE93-002687 ..... p 2760 N93-24673 #
DE93-002853 ..... p 2760 N93-24674 #
DE93-002862 ..... p 2760 N93-24675 #
DE93-002873 ..... p 2760 N93-24676 #
DE93-002894 ..... p 2873 N93-24677 #
DE93-002943 ..... p 2760 N93-24955 #
DE93-003006 ..... p 2761 N93-25143 #
DE93-003009 ..... p 2761 N93-24956 #
DE93-003024 ..... p 2654 N93-25361 #
DE93-003112 ..... p 2761 N93-25144 #
DE93-003189 ..... p 2760 N93-24952 #
DE93-003334 ..... p 2761 N93-25122 #
DE93-003338 ..... p 2761 N93-25145 #
DE93-003362 ..... p 2695 N93-24963 #
DE93-003472 ..... p 2687 N93-24964 #
DE93-003476 ..... p 2643 N93-25123 #
DE93-003623 ..... p 2887 N93-24965 #
DE93-003646 ..... p 2864 N93-25506 #
DE93-003678 ..... p 2791 N93-26586 * #
DE93-003744 ..... p 2696 N93-25124 #
DE93-003783 ..... p 2781 N93-25125 #
DE93-003789 ..... p 2768 N93-26592 #
DE93-003810 ..... p 2761 N93-25126 #
DE93-003817 ..... p 2655 N93-25507 #
DE93-003819 ..... p 2861 N93-26512 #
DE93-003841 ..... p 2852 N93-25127 #
DE93-003850 ..... p 2662 N93-26493 #
DE93-003854 ..... p 2869 N93-26494 #
DE93-004238 ..... p 2695 N93-24966 #
DE93-004337 ..... p 2767 N93-26495 #
DE93-004500 ..... p 2644 N93-25312 #
DE93-004619 ..... p 2725 N93-25357 #
DE93-004666 ..... p 2767 N93-26496 #
DE93-004691 ..... p 2764 N93-25443 #
DE93-005035 ..... p 2767 N93-26497 #
DE93-005155 ..... p 2713 N93-25508 #
DE93-005185 ..... p 2892 N93-25164 #
DE93-005325 ..... p 2723 N93-24957 #
DE93-005368 ..... p 2655 N93-25444 #
DE93-005370 ..... p 2655 N93-25446 #
DE93-005439 ..... p 2668 N93-25447 #
DE93-005453 ..... p 2876 N93-25448 #
DE93-005485 ..... p 2852 N93-25182 #
DE93-005709 ..... p 2827 N93-24973 #
DE93-005740 ..... p 2762 N93-25146 #
DE93-005741 ..... p 2762 N93-25147 #
DE93-005778 ..... p 2718 N93-25449 #
DE93-005783 ..... p 2717 N93-25413 #
DE93-005882 ..... p 2901 N93-24974 #
DE93-005980 ..... p 2758 N93-24975 #
DE93-006019 ..... p 2598 N93-26498 #
DE93-006070 ..... p 2695 N93-24976 #
DE93-006334 ..... p 2761 N93-24977 #
DE93-006337 ..... p 2712 N93-24967 #
DE93-006410 ..... p 2660 N93-25192 #
DE93-006417 ..... p 2660 N93-25298 #
DE93-006446 ..... p 2759 N93-25183 #
DE93-006507 ..... p 2696 N93-25193 #
DE93-006528 ..... p 2887 N93-26499 #
DE93-006563 ..... p 2649 N93-25255 #
DE93-006630 ..... p 2858 N93-24968 #
DE93-006632 ..... p 2816 N93-25414 #
DE93-006721 ..... p 2858 N93-24969 #
DE93-006731 ..... p 2800 N93-25415 #
DE93-006732 ..... p 2725 N93-25373 #
DE93-006734 ..... p 2667 N93-24970 #
DE93-006737 ..... p 2653 N93-26500 #
DE93-006746 ..... p 2654 N93-25374 #
DE93-006752 ..... p 2692 N93-26501 #
DE93-006763 ..... p 2653 N93-24971 #
DE93-006776 ..... p 2642 N93-24972 #
DE93-006777 ..... p 2862 N93-24958 #
DE93-006780 ..... p 2646 N93-26502 #
DE93-006971 ..... p 2846 N93-24959 #
DE93-006972 ..... p 2788 N93-24960 #
DE93-007110 ..... p 2852 N93-25375 #
DE93-007111 ..... p 2688 N93-25397 #
DE93-007114 ..... p 2711 N93-24961 #
DE93-007115 ..... p 2715 N93-26503 #
DE93-007143 ..... p 2849 N93-25509 #
DE93-007227 ..... p 2808 N93-24962 #
DE93-007243 ..... p 2847 N93-25256 #
DE93-007245 ..... p 2848 N93-25376 #
DE93-007248 ..... p 2688 N93-25377 #
DE93-007252 ..... p 2847 N93-25148 #
DE93-007277 ..... p 2712 N93-25378 #
DE93-007284 ..... p 2649 N93-25149 #
DE93-007285 ..... p 2863 N93-25362 #
DE93-007290 ..... p 2762 N93-25184 #
DE93-007322 ..... p 2805 N93-25165 #
DE93-007328 ..... p 2794 N93-25186 #
DE93-007330 ..... p 2712 N93-25150 #
DE93-007342 ..... p 2828 N93-25151 #
DE93-007348 ..... p 2762 N93-25166 #
DE93-007350 ..... p 2858 N93-25187 #
DE93-007353 ..... p 2688 N93-25313 #
DE93-007354 ..... p 2861 N93-26504 #
DE93-007356 ..... p 2851 N93-25314 #
DE93-007359 ..... p 2858 N93-25167 #
DE93-007361 ..... p 2646 N93-26505 #
DE93-007363 ..... p 2713 N93-25379 #
DE93-007364 ..... p 2852 N93-25380 #
DE93-007366 ..... p 2809 N93-25315 #
DE93-007368 ..... p 2816 N93-25316 #
DE93-007374 ..... p 2899 N93-25185 #
DE93-007387 ..... p 2620 N93-25317 * #
DE93-007389 ..... p 2713 N93-25381 #
DE93-007428 ..... p 2800 N93-25318 #
DE93-007491 ..... p 2658 N93-26506 #
DE93-007496 ..... p 2875 N93-25319 #
DE93-007499 ..... p 2654 N93-25382 #
DE93-007500 ..... p 2709 N93-25515 #
DE93-007504 ..... p 2635 N93-25383 #
DE93-007506 ..... p 2649 N93-25336 #
DE93-007508 ..... p 2712 N93-25363 #
DE93-007509 ..... p 2654 N93-25384 #
DE93-007511 ..... p 2888 N93-25320 #
DE93-007512 ..... p 2731 N93-26507 #
DE93-007513 ..... p 2857 N93-26593 #
DE93-007515 ..... p 2763 N93-25385 #
DE93-007517 ..... p 2870 N93-26594 #
DE93-007540 ..... p 2649 N93-25428 #
DE93-007541 ..... p 2647 N93-26595 #
DE93-007582 ..... p 2810 N93-25386 #
DE93-007587 ..... p 2827 N93-26596 #
DE93-007588 ..... p 2689 N93-25429 #
DE93-007594 ..... p 2863 N93-25387 #
DE93-007598 ..... p 2896 N93-25321 #
DE93-007600 ..... p 2689 N93-25416 #
DE93-007601 ..... p 2689 N93-25417 #
DE93-007605 ..... p 2726 N93-25489 #
DE93-007607 ..... p 2715 N93-26597 #
DE93-007613 ..... p 2598 N93-25322 #
DE93-007615 ..... p 2847 N93-25323 #
DE93-007649 ..... p 2859 N93-25324 #
DE93-007653 ..... p 2851 N93-25325 #
DE93-007654 ..... p 2847 N93-25326 #
DE93-007661 ..... p 2692 N93-26598 #
DE93-007669 ..... p 2647 N93-26599 #
DE93-007697 ..... p 2899 N93-25327 #

DE93-007701 ..... p 2864 N93-25490 #
DE93-007707 ..... p 2853 N93-25550 #
DE93-007711 ..... p 2848 N93-25364 #
DE93-007723 ..... p 2688 N93-25365 #
DE93-007725 ..... p 2848 N93-25366 #
DE93-007730 ..... p 2863 N93-25367 #
DE93-007737 ..... p 2658 N93-26588 #
DE93-007784 ..... p 2674 N93-25299 #
DE93-007788 ..... p 2674 N93-25300 #
DE93-007815 ..... p 2793 N93-26587 #
DE93-007818 ..... p 2756 N93-25516 #
DE93-007872 ..... p 2654 N93-25359 #
DE93-007893 ..... p 2848 N93-25368 #
DE93-007894 ..... p 2863 N93-25369 #
DE93-007897 ..... p 2763 N93-25370 #
DE93-007899 ..... p 2848 N93-25371 #
DE93-007900 ..... p 2851 N93-25301 #
DE93-007907 ..... p 2764 N93-25517 #
DE93-007908 ..... p 2654 N93-25372 #
DE93-007963 ..... p 2859 N93-25302 #
DE93-008008 ..... p 2809 N93-25303 #
DE93-008019 ..... p 2815 N93-25304 #
DE93-008037 ..... p 2659 N93-25118 #
DE93-008070 ..... p 2643 N93-25305 #
DE93-008074 ..... p 2721 N93-25518 #
DE93-008083 ..... p 2698 N93-25306 #
DE93-008085 ..... p 2809 N93-25307 #
DE93-008097 ..... p 2659 N93-25119 #
DE93-008101 ..... p 2659 N93-25111 #
DE93-008103 ..... p 2659 N93-25112 #
DE93-008185 ..... p 2674 N93-25308 #
DE93-008208 ..... p 2698 N93-25309 #
DE93-008211 ..... p 2847 N93-25310 #
DE93-008266 ..... p 2650 N93-25519 #
DE93-008370 ..... p 2689 N93-25491 #
DE93-008374 ..... p 2644 N93-25311 #
DE93-008466 ..... p 2687 N93-25113 #
DE93-008493 ..... p 2844 N93-25520 #
DE93-008540 ..... p 2849 N93-25488 #
DE93-008564 ..... p 2650 N93-25492 #
DE93-008635 ..... p 2847 N93-25114 #
DE93-008664 ..... p 2816 N93-25521 #
DE93-008665 ..... p 2816 N93-25522 #
DE93-008688 ..... p 2860 N93-25493 #
DE93-008763 ..... p 2864 N93-25503 #
DE93-008764 ..... p 2642 N93-25115 #
DE93-008846 ..... p 2617 N93-25494 #
DE93-008886 ..... p 2644 N93-25495 #
DE93-008947 ..... p 2660 N93-25496 #
DE93-009092 ..... p 2660 N93-25523 #
DE93-009109 ..... p 2649 N93-25095 #
DE93-009183 ..... p 2660 N93-25497 #
DE93-009380 ..... p 2668 N93-25498 #
DE93-009646 ..... p 2644 N93-25499 #
DE93-009707 ..... p 2644 N93-25500 #
DE93-009750 ..... p 2635 N93-25501 #
DE93-009761 ..... p 2650 N93-25502 #
DE93-010140 ..... p 2655 N93-25524 #
DE93-769925 ..... p 2763 N93-25360 #
DE93-769942 ..... p 2758 N93-25096 #
DE93-769943 ..... p 2758 N93-25097 #

DNA-TR-92-78 ..... p 2715 N93-26363 #
DNA-TR-92-98 ..... p 2681 N93-26289 #

DODA-AR-006-634 ..... p 2638 N93-25768 #
DODA-AR-006-752 ..... p 2675 N93-25689 #
DODA-AR-006-899 ..... p 2801 N93-25904 #
DODA-AR-007-077 ..... p 2845 N93-25649 #
DODA-AR-007-116 ..... p 2828 N93-25773 #

DOE/BC-14600/38 ..... p 2695 N93-24954 #

DOE/CE-33017/T1 ..... p 2674 N93-25308 #

DOE/EH-89084/T8 ..... p 2668 N93-25498 #

DOE/ER-13442/7 ..... p 2849 N93-25488 #
DOE/ER-13542/5 ..... p 2644 N93-25311 #
DOE/ER-13590/12 ..... p 2847 N93-25310 #
DOE/ER-13623/3 ..... p 2695 N93-24976 #
DOE/ER-13759/6 ..... p 2644 N93-25495 #
DOE/ER-13895/3 ..... p 2649 N93-25095 #
DOE/ER-13946/2 ..... p 2642 N93-25115 #
DOE/ER-13955/15 ..... p 2849 N93-25509 #
DOE/ER-45200/T2 ..... p 2864 N93-25503 #
DOE/ER-45271/T6 ..... p 2847 N93-25114 #
DOE/ER-45305/T2 ..... p 2635 N93-25501 #
DOE/ER-45409/3 ..... p 2655 N93-25524 #
DOE/ER-45436/4 ..... p 2650 N93-25502 #
DOE/ER-54165/1 ..... p 2859 N93-25302 #

DOE/ER/25084-3 ..... p 2696 N93-25193 #

DOE/ET-10815/203 ..... p 2858 N93-24968 #

DOE/FAA/RD-93/6 ..... p 2585 N93-25456 #

DOE/MC-26029/3273 ..... p 2644 N93-25499 #
DOE/MC-26367/3235 ..... p 2643 N93-25305 #
DOE/MC-27115/3280 ..... p 2660 N93-25497 #
DOE/MC-27225/3281 ..... p 2660 N93-25523 #

DOE/NBB-0091T ..... p 2784 N93-25517 #

DOE/NE-37966/2 ..... p 2717 N93-25413 #

DOE/PC-89786/T14 ..... p 2659 N93-25118 #
DOE/PC-89876/T17 ..... p 2660 N93-25496 #
DOE/PC-90291/T10 ..... p 2659 N93-25112 #
DOE/PC-90291/T8 ..... p 2659 N93-25111 #
DOE/PC-90305/T9 ..... p 2659 N93-25119 #
DOE/PC-92111/T1 ..... p 2644 N93-25500 #
DOE/PC-92540/T1 ..... p 2698 N93-25309 #

DOE/ST-0005P ..... p 2887 N93-24965 #

DOT/FAA/AM-92/14 ..... p 2794 N93-25214 #
DOT/FAA/AM-92/16 ..... p 2796 N93-25213 #
DOT/FAA/AM-92/17 ..... p 2796 N93-25203 #
DOT/FAA/AM-92/18 ..... p 2582 N93-25205 #
DOT/FAA/AM-92/21 ..... p 2872 N93-25204 #
DOT/FAA/AM-93/1 ..... p 2586 N93-26447 #
DOT/FAA/AM-93/2 ..... p 2583 N93-25896 #
DOT/FAA/AM-93/4 ..... p 2797 N93-26138 #
DOT/FAA/AM-93/5 ..... p 2802 N93-26089 #

DOT/FAA/CT-TN92-10 ..... p 2573 N93-24760 * #
DOT/FAA/CT-TN92/11 ..... p 2573 N93-25134 * #
DOT/FAA/CT-TN92/48 ..... p 2673 N93-25210 #
DOT/FAA/CT-TN93/11 ..... p 2680 N93-26160 #
DOT/FAA/CT-TN93/2 ..... p 2584 N93-24948 #
DOT/FAA/CT-TN93/37 ..... p 2584 N93-25243 #
DOT/FAA/CT-TN93/3 ..... p 2582 N93-25224 #
DOT/FAA/CT-TN93/8 ..... p 2584 N93-24741 #

DOT/FAA/CT-91/20 ..... p 2586 N93-24739 #
DOT/FAA/CT-92/12-VOL-1 ..... p 2582 N93-25110 #
DOT/FAA/CT-92/20-ADD-1 ..... p 2777 N93-24875 #

DOT/FAA/NR-92/12 ..... p 2783 N93-25645 #

DREO-1144 ..... p 2690 N93-25935 #

D180-32040-1-VOL-1 ..... p 2610 N93-25479 * #
D180-32040-2-VOL-2-BK-1 ..... p 2611 N93-25510 * #
D180-32040-2-VOL-2-BK-2 ..... p 2611 N93-25511 * #
D180-32040-2-VOL-2-BK-3 ..... p 2611 N93-25513 * #
D180-32040-2-VOL-2-BK-4 ..... p 2611 N93-25512 * #
D180-32040-3-VOL-3-BK-1 ..... p 2611 N93-25514 * #
D615-10050 ..... p 2599 N93-26146 * #

E-5868 ..... p 2618 N93-26209 * #
E-6810 ..... p 2652 N93-26201 * #
E-6938 ..... p 2573 N93-26136 * #
E-7016-2-PT-2 ..... p 2897 N93-26392 * #
E-7099 ..... p 2621 N93-24740 * #
E-7163 ..... p 2723 N93-24909 * #
E-7169 ..... p 2829 N93-26560 * #
E-7196 ..... p 2597 N93-25080 * #
E-7308 ..... p 2721 N93-25451 * #
E-7327 ..... p 2730 N93-26202 * #
E-7383 ..... p 2633 N93-26561 * #
E-7445 ..... p 2614 N93-24755 * #
E-7464 ..... p 2633 N93-26204 * #
E-7544 ..... p 2723 N93-24913 * #
E-7545 ..... p 2724 N93-25070 * #
E-7570 ..... p 2808 N93-24947 * #
E-7572-1 ..... p 2846 N93-26551 * #
E-7574 ..... p 2709 N93-25173 * #
E-7588 ..... p 2641 N93-26552 * #
E-7593 ..... p 2592 N93-24754 * #
E-7593 ..... p 2592 N93-25106 * #
E-7601 ..... p 2844 N93-25094 * #
E-7620 ..... p 2592 N93-25079 * #
E-7621 ..... p 2649 N93-25128 * #
E-7628 ..... p 2633 N93-26555 * #
E-7629 ..... p 2623 N93-25132 * #
E-7632 ..... p 2593 N93-25673 * #
E-7633 ..... p 2598 N93-26214 * #
E-7648 ..... p 2592 N93-25129 * #
E-7674 ..... p 2694 N93-24759 * #
E-7675 ..... p 2622 N93-25089 * #
E-7681 ..... p 2759 N93-25136 * #
E-7683 ..... p 2634 N93-25071 * #
E-7687 ..... p 2872 N93-26205 * #
E-7696 ..... p 2642 N93-25116 * #
E-7699 ..... p 2654 N93-25093 * #
E-7701 ..... p 2653 N93-24761 * #
E-7705 ..... p 2580 N93-25883 * #
E-7709 ..... p 2573 N93-25134 * #
E-7716 ..... p 2575 N93-24911 * #
E-7718 ..... p 2696 N93-25175 * #
E-7719 ..... p 2573 N93-24760 * #
E-7726 ..... p 2663 N93-24946 * #
E-7728 ..... p 2622 N93-24758 * #
E-7731 ..... p 2716 N93-24751 * #
E-7735 ..... p 2708 N93-24737 * #
E-7737 ..... p 2687 N93-24746 * #
E-7738 ..... p 2632 N93-26211 * #
E-7739 ..... p 2631 N93-26149 * #
E-7740 ..... p 2615 N93-25090 * #
E-7745 ..... p 2652 N93-26235 * #
E-7752 ..... p 2718 N93-25672 * #
E-7754 ..... p 2709 N93-25191 * #
E-7756 ..... p 2618 N93-26148 * #
E-7758 ..... p 2708 N93-26554 * #
E-7759 ..... p 2622 N93-24753 * #
E-7775 ..... p 2623 N93-25236 * #
E-7781 ..... p 2622 N93-25105 * #
E-7782 ..... p 2632 N93-26200 * #
E-7783 ..... p 2622 N93-24744 * #
E-7793 ..... p 2667 N93-25177 * #
E-7798 ..... p 2707 N93-26203 * #
E-7801 ..... p 2731 N93-26550 * #
E-7804 ..... p 2618 N93-26215 * #
E-7805 ..... p 2664 N93-25337 * #
E-7808 ..... p 2719 N93-25884 * #
E-7814 ..... p 2595 N93-26161 * #
E-7820 ..... p 2632 N93-26210 * #

ED-658-CP ..... p 2747 N93-24835 #
ED-659-CP ..... p 2746 N93-24829 #

EGG-CODP-10620(1-93) ..... p 2808 N93-24962 #

EGG-M-92057 ..... p 2892 N93-25164 #

EPA-19K-1002 ..... p 2765 N93-25851 #
EPA-21P-3003 ..... p 2766 N93-25875 #

EPA/454/R-92/013 ..... p 2765 N93-25850 #
EPA/600/A-93/017 ..... p 2793 N93-25877 #
EPA/600/A-93/025 ..... p 2765 N93-25873 #
EPA/600/A-93/029 ..... p 2766 N93-26316 #
EPA/600/A-93/049 ..... p 2767 N93-26510 #
EPA/600/9-90/044 ..... p 2768 N93-26536 #
EPA/600/9-91/034 ..... p 2766 N93-25876 #
EPA/821/R-93/006 ..... p 2768 N93-26567 #

ES/ER/TM-35 ..... p 2760 N93-24676 #

ESA-ISY-1-VOL-2 ..... p 2737 N93-24775 #

ESA-SP-340 ..... p 2831 N93-24978 #

ESD-TR-92-266 ..... p 2681 N93-26241 #

ESDP-3913 ..... p 2791 N93-26586 * #

ETN-93-93497 ..... p 2831 N93-24978 #
ETN-93-93503 ..... p 2737 N93-24775 #

FASTC-ID(RS)T-0312-92 ..... p 2595 N93-26239 #
FASTC-ID(RS)T-0561-92 ..... p 2686 N93-26573 #
FASTC-ID(RS)T-0562-92 ..... p 2830 N93-26262 #
FASTC-ID(RS)T-0628-92 ..... p 2574 N93-26238 #

FE-MIT-92111-1 ..... p 2644 N93-25500 #

FEMP/SUB-052 ..... p 2760 N93-24955 #

FFA-TN-1992-17 ..... p 2726 N93-25638 #

FHWA/TX-92 + 983-2-VOL-1 ..... p 2720 N93-26585 #
FHWA/TX-92 + 983-2-VOL-2 ..... p 2720 N93-26534 #
FHWA/TX-92 + 983-3 ..... p 2720 N93-26590 #

FR-10119 ..... p 2690 N93-25820 #

FRACTO-1992 ..... p 2869 N93-26385 #

FR21998-16 ..... p 2652 N93-26282 #
FR9201-01 ..... p 2720 N93-26564 #

GALCIT-FM92-1 ..... p 2707 N93-26163 #

GAO/IMTEC-92-51 ..... p 2882 N93-26097 #
GAO/IMTEC-92-53 ..... p 2882 N93-26096 #

GRI-92/0364 ..... p 2768 N93-26529 #
GRI-92/0421-PHASE-2 ..... p 2644 N93-25819 #
GRI-92/0470-PHASE-2 ..... p 2768 N93-26533 #
GRI-92/0486 ..... p 2644 N93-25817 #
GRI-93/0004 ..... p 2872 N93-26509 #
GRI-93/0005 ..... p 2872 N93-26558 #

IAF-92-0600 ..... p 2623 N93-25132 * #

ICASE-92-64 ..... p 2575 N93-25083 * #
ICASE-92-70 ..... p 2576 N93-25153 * #

ICOMP-93-08 ..... p 2696 N93-25175 * #

IDA-D-1066 ..... p 2810 N93-25711 #
IDA-D-1183 ..... p 2813 N93-26461 #
IDA-D-1244 ..... p 2883 N93-26313 #

IDA-P-2701 ..... p 2831 N93-26330 #

IDA/HQ-91-40476 ..... p 2810 N93-25711 #
IDA/HQ-92-41141 ..... p 2831 N93-26330 #
IDA/HQ-92-42001 ..... p 2813 N93-26461 #
IDA/HQ-92-42853 ..... p 2883 N93-26313 #

INT-PATENT-CLASS-B29C-45/16 p 2656 N93-25995 *
INT-PATENT-CLASS-B64C-27/00 p 2597 N93-25998 * #
INT-PATENT-CLASS-B64F-1/10 p 2597 N93-25178

INT-PATENT-CLASS-F16C-19/52 p 2719 N93-26001 *
INT-PATENT-CLASS-F16C-43/04 p 2719 N93-26001 *

INT-PATENT-CLASS-G01B-5/20 p 2710 N93-26103 *
INT-PATENT-CLASS-G01B-7/28 p 2710 N93-26103 *
INT-PATENT-CLASS-G01M-9/00 p 2598 N93-25996 *
INT-PATENT-CLASS-G01M-9/00 p 2706 N93-26000 *
INT-PATENT-CLASS-G01N-27/72 p 2710 N93-26103 *
INT-PATENT-CLASS-G01N-3/00 p 2729 N93-26102 *
INT-PATENT-CLASS-G01N-33/569 p 2793 N93-25994 *
INT-PATENT-CLASS-G01R-27/26 p 2691 N93-26104 *

IS-M-740 ..... p 2721 N93-25518 #
IS-M-743 ..... p 2649 N93-25149 #
IS-M-745 ..... p 2863 N93-25362 #

IS-T-1541 ..... p 2647 N93-26595 #
IS-T-1635 ..... p 2649 N93-25428 #

ISBN-0-16-042197-7 ..... p 2898 N93-26517 * #
ISBN-0-315-70442-X ..... p 2784 N93-25731
ISBN-0-315-70444-6 ..... p 2754 N93-25422
ISBN-0-315-70882-4 ..... p 2772 N93-25556
ISBN-0-934213-37-2 ..... p 2807 N93-26569 #
ISBN-92-9092-202-8 ..... p 2831 N93-24978 #

ISI-5878-2 ..... p 2826 N93-26365 #

ISI/RR-93-302 ..... p 2690 N93-25856 #

ISU-ERI-AMES-93113 ..... p 2619 N93-26438 #

ISWS/BUL-71 ..... p 2785 N93-25872 #

JPL-PUBL-91-10 ..... p 2653 N93-25078 * #
JPL-PUBL-92-16 ..... p 2682 N93-26463 * #
JPL-PUBL-92-4 ..... p 2859 N93-25206 * #

JPL-TDA-PR-42-109 ..... p 2676 N93-26105 * #
JPL-TDA-PR-42-112 ..... p 2671 N93-24659 * #

JPL-400-494 ..... p 2898 N93-26517 * #
JPL-410-11-20 ..... p 2898 N93-26424 * #

JPRS-JST-93-009 ..... p 2901 N93-25418 #

JPRS-UAC-93-003 ..... p 2574 N93-26325 #

JPRS-UEQ-92-003 ..... p 2668 N93-25427 #

JPRS-UES-92-002 ..... p 2737 N93-25426 #
JPRS-UES-92-003 ..... p 2737 N93-25398 #
JPRS-UES-92-005 ..... p 2737 N93-25401 #
JPRS-UES-93-001 ..... p 2599 N93-25400 #

JPRS-ULS-92-020 ..... p 2793 N93-25406 #
JPRS-ULS-92-022 ..... p 2795 N93-25407 #
JPRS-ULS-92-025 ..... p 2793 N93-25405 #
JPRS-ULS-93-002 ..... p 2737 N93-25399 #

JPRS-UPM-92-003 ..... p 2844 N93-25403 #
JPRS-UPM-92-004 ..... p 2844 N93-25402 #
JPRS-UPM-93-001 ..... p 2844 N93-25404 #

JSC-08249 ..... p 2612 N93-25956 * #
JSC-08250 ..... p 2611 N93-25955 * #
JSC-25458 ..... p 2614 N93-25952 * #

JSR-91-193 ..... p 2846 N93-26376 #
JSR-91-310 ..... p 2762 N93-25184 #
JSR-91-330 ..... p 2765 N93-25837 #

KAPL-4738 ..... p 2698 N93-25306 #

KCP-613-4677 ..... p 2721 N93-25939 #
KCP-613-4803 ..... p 2652 N93-26208 #
KCP-613-4864 ..... p 2809 N93-25307 #
KCP-613-4941 ..... p 2669 N93-26207 #
KCP-613-4967 ..... p 2669 N93-26212 #
KCP-613-4969 ..... p 2852 N93-25182 #
KCP-613-4985 ..... p 2657 N93-26213 #
KCP-613-4999 ..... p 2668 N93-26206 #

KU-FRL-926-1 ..... p 2586 N93-24739 #

L-17059 ..... p 2581 N93-26134 * #
L-17148 ..... p 2581 N93-26085 * #

LA-SUB-93-13 ..... p 2712 N93-24967 #
LA-SUB-93-29 ..... p 2809 N93-25303 #
LA-SUB-93-47 ..... p 2687 N93-25113 #
LA-SUB-93-4 ..... p 2761 N93-24977 #

LA-UR-92-3468 ..... p 2696 N93-25124 #
LA-UR-92-3500 ..... p 2781 N93-25125 #
LA-UR-92-3554 ..... p 2768 N93-26592 #
LA-UR-92-3655 ..... p 2761 N93-25126 #
LA-UR-92-3668 ..... p 2655 N93-25507 #
LA-UR-92-3712 ..... p 2861 N93-26512 #
LA-UR-92-3790 ..... p 2852 N93-25127 #
LA-UR-92-3823 ..... p 2662 N93-26493 #
LA-UR-92-3827 ..... p 2869 N93-26494 #
LA-UR-92-4002 ..... p 2876 N93-25448 #
LA-UR-92-4136 ..... p 2668 N93-25447 #
LA-UR-93-0004 ..... p 2646 N93-26505 #
LA-UR-93-0014 ..... p 2858 N93-25167 #
LA-UR-93-0045 ..... p 2861 N93-26504 #
LA-UR-93-0047 ..... p 2688 N93-25313 #
LA-UR-93-180 ..... p 2828 N93-25151 #
LA-UR-93-263 ..... p 2899 N93-25185 #
LA-UR-93-289 ..... p 2713 N93-25381 #
LA-UR-93-297 ..... p 2858 N93-25187 #
LA-UR-93-299 ..... p 2762 N93-25166 #
LA-UR-93-302 ..... p 2816 N93-25316 #
LA-UR-93-303 ..... p 2809 N93-25315 #
LA-UR-93-322 ..... p 2852 N93-25380 #
LA-UR-93-330 ..... p 2713 N93-25379 #
LA-UR-93-341 ..... p 2805 N93-25165 #
LA-UR-93-370 ..... p 2712 N93-25150 #
LA-UR-93-402 ..... p 2794 N93-25186 #
LA-UR-93-43 ..... p 2851 N93-25314 #

LA-10300-M-VOL-1 ..... p 2760 N93-24674 #
LA-12235-MS ..... p 2706 N93-25987 #
LA-12326-MS ..... p 2811 N93-25943 #
LA-12359-MS ..... p 2723 N93-24957 #
LA-12449-MS ..... p 2598 N93-25322 #

LBL-32203 ..... p 2859 N93-25324 #
LBL-32243 ..... p 2692 N93-26598 #
LBL-32289 ..... p 2688 N93-25365 #
LBL-32918 ..... p 2851 N93-25325 #
LBL-32993 ..... p 2764 N93-25443 #
LBL-33057 ..... p 2863 N93-25367 #
LBL-33145 ..... p 2847 N93-25326 #
LBL-33171 ..... p 2848 N93-25366 #
LBL-33248 ..... p 2853 N93-25550 #
LBL-33304 ..... p 2899 N93-25327 #
LBL-33328 ..... p 2647 N93-26599 #
LBL-33345 ..... p 2848 N93-25364 #
LBL-33379 ..... p 2864 N93-25490 #

LMI-NS101R1 ..... p 2617 N93-25630 #

M-92B0000010 ..... p 2681 N93-26241 #

MCC-RR-92-03 ..... p 2785 N93-25872 #

MCR-91-5004 ..... p 2610 N93-26181 #
MCR-91-5010 ..... p 2610 N93-26591 #
MCR-92-5005 ..... p 2610 N93-26182 #
MCR-92-5006-PT-A ..... p 2610 N93-26180 #
MCR-92-5010 ..... p 2609 N93-26176 #
MCR-92-5011 ..... p 2609 N93-26098 #
MCR-92-5013 ..... p 2609 N93-26175 #

MDC-92K0374 ..... p 2591 N93-24764 * #

MIL-HDBK-844(AS) ..... p 2662 N93-26600 #

MIT-SERC-17-90-R ..... p 2821 N93-25833 * #

MRC-COM-R-92-0315 ..... p 2657 N93-26278 #

MRC-R-1410 ..... p 2681 N93-26289 #

MRL-GD-0040 ..... p 2801 N93-25904 #

MT-161 ..... p 2726 N93-25419 #

MTCI-10039-11 ..... p 2643 N93-25305 #
MTL-TR-92-23 ..... p 2706 N93-25953 #
MTL-TR-92-27 ..... p 2640 N93-25954 #
MTL-TR-92-45 ..... p 2657 N93-26432 #
MTL-TR-92-56 ..... p 2658 N93-26433 #
MTL-TR-92-68 ..... p 2722 N93-26434 #

MTL/TR-92-69 ..... p 2651 N93-25895 #

MTR-92B0000047V3 ..... p 2801 N93-25840 #

NAMRL-1378 ..... p 2590 N93-25933 #

NAS 1.15:103663 ..... p 2618 N93-26209 * #
NAS 1.15:103882 ..... p 2697 N93-25247 * #
NAS 1.15:103932 ..... p 2695 N93-25082 * #
NAS 1.15:103942 ..... p 2795 N93-26133 * #
NAS 1.15:103943 ..... p 2708 N93-25076 * #
NAS 1.15:103961 ..... p 2809 N93-25246 * #
NAS 1.15:103963 ..... p 2575 N93-25091 * #
NAS 1.15:103977 ..... p 2667 N93-25085 * #
NAS 1.15:104001 ..... p 2581 N93-26099 * #
NAS 1.15:104003 ..... p 2803 N93-25235 * #
NAS 1.15:104004 ..... p 2584 N93-24914 * #
NAS 1.15:104580 ..... p 2721 N93-26137 * #
NAS 1.15:104581 ..... p 2770 N93-25160 * #
NAS 1.15:104763 ..... p 2901 N93-25188 * #
NAS 1.15:105270 ..... p 2730 N93-26202 * #
NAS 1.15:105602 ..... p 2573 N93-26136 * #
NAS 1.15:105705 ..... p 2632 N93-26200 * #
NAS 1.15:105707 ..... p 2622 N93-24744 * #
NAS 1.15:105708 ..... p 2622 N93-25105 * #
NAS 1.15:105710 ..... p 2622 N93-24753 * #
NAS 1.15:105711 ..... p 2621 N93-24740 * #
NAS 1.15:105771 ..... p 2597 N93-25080 * #
NAS 1.15:105883 ..... p 2759 N93-25136 * #
NAS 1.15:105907 ..... p 2872 N93-26205 * #
NAS 1.15:105946 ..... p 2595 N93-26161 * #
NAS 1.15:105959 ..... p 2633 N93-26204 * #
NAS 1.15:106001 ..... p 2723 N93-24913 * #
NAS 1.15:106002 ..... p 2724 N93-25070 * #
NAS 1.15:106015 ..... p 2846 N93-26551 * #
NAS 1.15:106017 ..... p 2709 N93-25173 * #
NAS 1.15:106025 ..... p 2641 N93-26552 * #
NAS 1.15:106042 ..... p 2592 N93-25079 * #
NAS 1.15:106044 ..... p 2593 N93-25673 * #
NAS 1.15:106047 ..... p 2598 N93-26214 * #
NAS 1.15:106054 ..... p 2592 N93-25129 * #
NAS 1.15:106070 ..... p 2622 N93-25089 * #
NAS 1.15:106074 ..... p 2634 N93-25071 * #
NAS 1.15:106081 ..... p 2654 N93-25093 * #
NAS 1.15:106086 ..... p 2575 N93-24911 * #
NAS 1.15:106087 ..... p 2696 N93-25175 * #
NAS 1.15:106093 ..... p 2614 N93-24755 * #
NAS 1.15:106095 ..... p 2708 N93-24737 * #
NAS 1.15:106096 ..... p 2687 N93-24746 * #
NAS 1.15:106097 ..... p 2632 N93-26211 * #
NAS 1.15:106098 ..... p 2615 N93-25090 * #
NAS 1.15:106098 ..... p 2631 N93-26149 * #
NAS 1.15:106103 ..... p 2718 N93-25672 * #
NAS 1.15:106106 ..... p 2709 N93-25191 * #
NAS 1.15:106107 ..... p 2618 N93-26148 * #
NAS 1.15:106109 ..... p 2708 N93-26554 * #
NAS 1.15:106125 ..... p 2731 N93-26550 * #
NAS 1.15:106126 ..... p 2667 N93-25177 * #
NAS 1.15:106129 ..... p 2707 N93-26203 * #
NAS 1.15:106132 ..... p 2618 N93-26215 * #
NAS 1.15:106133 ..... p 2664 N93-25337 * #
NAS 1.15:106135 ..... p 2623 N93-25236 * #
NAS 1.15:106139 ..... p 2632 N93-26210 * #
NAS 1.15:107682 ..... p 2696 N93-25176 * #
NAS 1.15:107731 ..... p 2615 N93-25174 * #
NAS 1.15:107737 ..... p 2845 N93-26086 * #
NAS 1.15:107739 ..... p 2591 N93-26553 * #
NAS 1.15:107740 ..... p 2844 N93-25189 * #
NAS 1.15:107742 ..... p 2634 N93-25072 * #
NAS 1.15:107745 ..... p 2575 N93-25074 * #
NAS 1.15:107747 ..... p 2777 N93-24742 * #
NAS 1.15:107748 ..... p 2585 N93-26087 * #
NAS 1.15:107760 ..... p 2651 N93-26048 * #
NAS 1.15:108265 ..... p 2791 N93-26586 * #
NAS 1.15:108402 ..... p 2884 N93-26562 * #
NAS 1.15:108403 ..... p 2624 N93-25671 * #
NAS 1.15:108704 ..... p 2616 N93-25231 * #
NAS 1.15:108711 ..... p 2732 N93-24915 * #
NAS 1.15:108719 ..... p 2820 N93-25459 * #
NAS 1.15:108720 ..... p 2757 N93-26429 * #
NAS 1.15:108735 ..... p 2612 N93-25988 * #
NAS 1.15:108737 ..... p 2612 N93-25958 * #
NAS 1.15:108744 ..... p 2673 N93-25181 * #
NAS 1.15:108745 ..... p 2818 N93-25142 * #
NAS 1.15:108746 ..... p 2818 N93-25138 * #
NAS 1.15:108752 ..... p 2614 N93-25952 * #
NAS 1.15:108756 ..... p 2873 N93-26418 * #
NAS 1.15:108758 ..... p 2883 N93-26491 * #
NAS 1.15:108769 ..... p 2756 N93-25462 * #
NAS 1.15:108770 ..... p 2755 N93-25460 * #

NAS 1.15:108771 ..... p 2755 N93-25461 * #
NAS 1.15:108774 ..... p 2882 N93-26231 * #
NAS 1.15:108775 ..... p 2663 N93-25194 * #
NAS 1.15:108776 ..... p 2615 N93-25217 * #
NAS 1.15:192469 ..... p 2774 N93-25886 * #
NAS 1.15:4423 ..... p 2723 N93-24909 * #
NAS 1.15:4434 ..... p 2581 N93-26085 * #
NAS 1.15:4449 ..... p 2689 N93-25618 * #
NAS 1.16:193003 ..... p 2721 N93-26135 * #
NAS 1.19:283 ..... p 2872 N93-26051 * #
NAS 1.21:6102 ..... p 2665 N93-24678 * #
NAS 1.26:105757 ..... p 2829 N93-26560 * #
NAS 1.26:106066 ..... p 2633 N93-26561 * #
NAS 1.26:177599 ..... p 2817 N93-25137 * #
NAS 1.26:177604 ..... p 2888 N93-25135 * #
NAS 1.26:177606 ..... p 2887 N93-25442 * #
NAS 1.26:177608 ..... p 2586 N93-26549 * #
NAS 1.26:177609 ..... p 2794 N93-24738 * #
NAS 1.26:177612 ..... p 2575 N93-25075 * #
NAS 1.26:188242-VOL-1 ..... p 2911 N93-26058 * #
NAS 1.26:188242-VOL-2 ..... p 2914 N93-26070 * #
NAS 1.26:189193 ..... p 2592 N93-24754 * #
NAS 1.26:189193 ..... p 2592 N93-25106 * #
NAS 1.26:190778 ..... p 2573 N93-25134 * #
NAS 1.26:190779 ..... p 2573 N93-24760 * #
NAS 1.26:190793 ..... p 2623 N93-25132 * #
NAS 1.26:191067 ..... p 2808 N93-24947 * #
NAS 1.26:191082 ..... p 2649 N93-25128 * #
NAS 1.26:191084 ..... p 2633 N93-26555 * #
NAS 1.26:191095 ..... p 2694 N93-24759 * #
NAS 1.26:191099 ..... p 2642 N93-25116 * #
NAS 1.26:191105 ..... p 2580 N93-25883 * #
NAS 1.26:191111 ..... p 2663 N93-24946 * #
NAS 1.26:191112 ..... p 2622 N93-24758 * #
NAS 1.26:191117 ..... p 2716 N93-24751 * #
NAS 1.26:191118 ..... p 2721 N93-25451 * #
NAS 1.26:191121 ..... p 2652 N93-26235 * #
NAS 1.26:191124 ..... p 2653 N93-24761 * #
NAS 1.26:191127 ..... p 2719 N93-25884 * #
NAS 1.26:191408 ..... p 2803 N93-25084 * #
NAS 1.26:191409 ..... p 2575 N93-25083 * #
NAS 1.26:191410 ..... p 2576 N93-25153 * #
NAS 1.26:191418 ..... p 2591 N93-24764 * #
NAS 1.26:191419 ..... p 2615 N93-25133 * #
NAS 1.26:191425 ..... p 2808 N93-25073 * #
NAS 1.26:191438 ..... p 2695 N93-25087 * #
NAS 1.26:191711 ..... p 2787 N93-26492 * #
NAS 1.26:191988 ..... p 2709 N93-25345 * #
NAS 1.26:192218 ..... p 2775 N93-26151 * #
NAS 1.26:192224 ..... p 2775 N93-26159 * #
NAS 1.26:192317 ..... p 2622 N93-24943 * #
NAS 1.26:192321 ..... p 2854 N93-26183 * #
NAS 1.26:192344 ..... p 2863 N93-25219 * #
NAS 1.26:192442 ..... p 2786 N93-26156 * #
NAS 1.26:192443 ..... p 2656 N93-26155 * #
NAS 1.26:192451 ..... p 2711 N93-26154 * #
NAS 1.26:192481 ..... p 2801 N93-25888 * #
NAS 1.26:192512 ..... p 2863 N93-25225 * #
NAS 1.26:192514 ..... p 2618 N93-26055 *
NAS 1.26:192515 ..... p 2614 N93-26152 * #
NAS 1.26:192516 ..... p 2631 N93-26056 * #
NAS 1.26:192517 ..... p 2631 N93-26053 * #
NAS 1.26:192518 ..... p 2631 N93-26057 * #
NAS 1.26:192519 ..... p 2631 N93-26054 * #
NAS 1.26:192523 ..... p 2770 N93-25086 * #
NAS 1.26:192524 ..... p 2610 N93-25479 * #
NAS 1.26:192525 ..... p 2611 N93-25510 * #
NAS 1.26:192526 ..... p 2611 N93-25511 * #
NAS 1.26:192527 ..... p 2611 N93-25513 * #
NAS 1.26:192528 ..... p 2611 N93-25512 * #
NAS 1.26:192529 ..... p 2611 N93-25514 * #
NAS 1.26:192531 ..... p 2633 N93-26557 * #
NAS 1.26:192532 ..... p 2599 N93-26146 * #
NAS 1.26:192681 ..... p 2852 N93-25281 * #
NAS 1.26:192688 ..... p 2669 N93-26405 * #
NAS 1.26:192701 ..... p 2664 N93-25218 * #
NAS 1.26:192708 ..... p 2585 N93-25261 * #
NAS 1.26:192709 ..... p 2585 N93-25330 * #
NAS 1.26:192711 ..... p 2724 N93-25260 * #
NAS 1.26:192715 ..... p 2673 N93-25198 * #
NAS 1.26:192718 ..... p 2828 N93-25223 * #
NAS 1.26:192725 ..... p 2696 N93-25208 * #
NAS 1.26:192726 ..... p 2828 N93-25262 * #
NAS 1.26:192727 ..... p 2596 N93-25199 * #
NAS 1.26:192762 ..... p 2892 N93-25200 * #
NAS 1.26:192763 ..... p 2874 N93-25288 * #
NAS 1.26:192765 ..... p 2808 N93-24944 * #
NAS 1.26:192771 ..... p 2643 N93-25240 * #
NAS 1.26:192773 ..... p 2900 N93-25890 * #
NAS 1.26:192775 ..... p 2888 N93-25289 * #
NAS 1.26:192776 ..... p 2898 N93-25222 * #
NAS 1.26:192781 ..... p 2888 N93-25172 * #
NAS 1.26:192782 ..... p 2772 N93-25529 * #
NAS 1.26:192783 ..... p 2697 N93-25221 * #
NAS 1.26:192784 ..... p 2771 N93-25201 * #
NAS 1.26:192788 ..... p 2723 N93-24912 * #
NAS 1.26:192790 ..... p 2892 N93-25211 * #
NAS 1.26:192791 ..... p 2890 N93-25755 * #
NAS 1.26:192800 ..... p 2682 N93-26463 * #
NAS 1.26:192804 ..... p 2676 N93-26105 * #
NAS 1.26:192806 ..... p 2771 N93-25202 * #
NAS 1.26:192808 ..... p 2900 N93-25241 * #
NAS 1.26:192809 ..... p 2889 N93-25331 * #
NAS 1.26:192814 ..... p 2659 N93-24745 * #
NAS 1.26:192823 ..... p 2859 N93-25206 * #
NAS 1.26:192824 ..... p 2653 N93-25078 * #
NAS 1.26:192826 ..... p 2769 N93-24945 * #
NAS 1.26:192827 ..... p 2643 N93-25229 * #
NAS 1.26:192830 ..... p 2792 N93-25242 * #
NAS 1.26:192832 ..... p 2775 N93-26084 * #
NAS 1.26:192833 ..... p 2770 N93-25088 * #
NAS 1.26:192834 ..... p 2769 N93-24910 * #
NAS 1.26:192848 ..... p 2763 N93-25244 * #
NAS 1.26:192849 ..... p 2892 N93-25230 * #
NAS 1.26:192851 ..... p 2770 N93-25081 * #
NAS 1.26:192879 ..... p 2821 N93-25833 * #
NAS 1.26:192885 ..... p 2815 N93-24748 * #
NAS 1.26:192886 ..... p 2815 N93-24749 * #
NAS 1.26:192887 ..... p 2671 N93-24659 * #
NAS 1.26:192889 ..... p 2848 N93-25450 * #
NAS 1.26:192891 ..... p 2808 N93-24750 * #
NAS 1.26:192892 ..... p 2819 N93-25296 * #
NAS 1.26:192893 ..... p 2819 N93-25226 * #
NAS 1.26:192894 ..... p 2818 N93-25156 * #
NAS 1.26:192895 ..... p 2818 N93-25155 * #
NAS 1.26:192896 ..... p 2883 N93-26423 * #
NAS 1.26:192897 ..... p 2754 N93-25154 * #
NAS 1.26:192898 ..... p 2816 N93-25458 * #
NAS 1.26:192899 ..... p 2815 N93-25251 * #
NAS 1.26:192906 ..... p 2815 N93-25297 * #
NAS 1.26:192908 ..... p 2809 N93-25131 * #
NAS 1.26:192910 ..... p 2805 N93-25130 * #
NAS 1.26:192911 ..... p 2806 N93-25233 * #
NAS 1.26:192912 ..... p 2809 N93-25250 * #
NAS 1.26:192914 ..... p 2806 N93-25267 * #
NAS 1.26:192916 ..... p 2862 N93-25108 * #
NAS 1.26:192917 ..... p 2576 N93-25249 * #
NAS 1.26:192918 ..... p 2698 N93-25266 * #
NAS 1.26:192919 ..... p 2696 N93-25109 * #
NAS 1.26:192920 ..... p 2585 N93-26052 * #
NAS 1.26:192922 ..... p 2898 N93-26517 * #
NAS 1.26:192923 ..... p 2898 N93-26424 * #
NAS 1.26:192929 ..... p 2777 N93-24747 * #
NAS 1.26:192930 ..... p 2900 N93-26132 * #
NAS 1.26:192931 ..... p 2899 N93-24752 * #
NAS 1.26:192932 ..... p 2899 N93-25161 * #
NAS 1.26:192933 ..... p 2891 N93-26426 * #
NAS 1.26:192934 ..... p 2573 N93-25077 * #
NAS 1.26:192937 ..... p 2767 N93-26427 * #
NAS 1.26:192939 ..... p 2633 N93-26425 * #
NAS 1.26:192940 ..... p 2574 N93-24736 * #
NAS 1.26:192944 ..... p 2874 N93-25139 * #
NAS 1.26:192945 ..... p 2828 N93-25140 * #
NAS 1.26:192947 ..... p 2818 N93-25196 * #
NAS 1.26:192948 ..... p 2819 N93-25197 * #
NAS 1.26:192949 ..... p 2818 N93-25141 * #
NAS 1.26:192950 ..... p 2818 N93-25190 * #
NAS 1.26:192951 ..... p 2820 N93-25425 * #
NAS 1.26:192952 ..... p 2820 N93-25452 * #
NAS 1.26:192953 ..... p 2587 N93-25162 * #
NAS 1.26:192954 ..... p 2589 N93-25670 * #
NAS 1.26:192955 ..... p 2810 N93-25669 * #
NAS 1.26:192956 ..... p 2817 N93-24757 * #
NAS 1.26:192957 ..... p 2593 N93-25668 * #
NAS 1.26:192958 ..... p 2865 N93-25667 * #
NAS 1.26:192959 ..... p 2765 N93-25666 * #
NAS 1.26:192960 ..... p 2597 N93-26046 * #
NAS 1.26:192961 ..... p 2811 N93-26150 * #
NAS 1.26:192972 ..... p 2891 N93-26139 * #
NAS 1.26:192974 ..... p 2801 N93-26047 * #
NAS 1.26:192976 ..... p 2763 N93-25287 * #
NAS 1.26:192978 ..... p 2809 N93-25152 * #
NAS 1.26:192980 ..... p 2575 N93-25117 * #
NAS 1.26:192982 ..... p 2801 N93-26088 * #
NAS 1.26:192983 ..... p 2764 N93-25432 * #
NAS 1.26:192984 ..... p 2764 N93-25431 * #
NAS 1.26:192985 ..... p 2809 N93-25257 * #
NAS 1.26:192997 ..... p 2580 N93-26049 * #
NAS 1.26:193002 ..... p 2808 N93-25107 * #
NAS 1.26:193018 ..... p 2817 N93-24743 * #
NAS 1.26:193033 ..... p 2595 N93-24762 * #
NAS 1.26:193040 ..... p 2794 N93-24763 * #
NAS 1.26:193048 ..... p 2599 N93-26095 * #
NAS 1.26:193049 ..... p 2802 N93-26153 * #
NAS 1.26:193054 ..... p 2612 N93-25959 * #
NAS 1.26:193056 ..... p 2612 N93-25960 * #
NAS 1.26:193057 ..... p 2613 N93-25992 * #
NAS 1.26:193058 ..... p 2613 N93-25991 * #
NAS 1.26:193059 ..... p 2613 N93-25989 * #
NAS 1.26:193060 ..... p 2613 N93-25990 * #
NAS 1.26:193061 ..... p 2613 N93-25993 * #
NAS 1.26:193062 ..... p 2612 N93-25956 * #
NAS 1.26:193063 ..... p 2611 N93-25955 * #
NAS 1.26:193064 ..... p 2612 N93-25957 * #
NAS 1.26:193065 ..... p 2614 N93-26329 * #
NAS 1.26:193096 ..... p 2877 N93-25792 * #
NAS 1.26:193098 ..... p 2873 N93-26419 * #
NAS 1.26:193099 ..... p 2873 N93-26420 * #
NAS 1.26:193100 ..... p 2790 N93-26050 * #
NAS 1.26:193146 ..... p 2899 N93-26556 * #
NAS 1.26:193203 ..... p 2620 N93-25317 * #
NAS 1.26:193208 ..... p 2826 N93-25986 * #
NAS 1.26:3922(39) ..... p 2792 N93-25195 *
NAS 1.26:4497 ..... p 2803 N93-26157 * #
NAS 1.26:4499 ..... p 2844 N93-25094 * #
NAS 1.55:10093-PT-2 ..... p 2897 N93-26392 * #
NAS 1.55:3183 ..... p 2803 N93-25921 * #
NAS 1.55:3186 ..... p 2599 N93-24694 * #
NAS 1.55:3189-VOL-1 ..... p 2901 N93-25561 * #
NAS 1.55:3200 ..... p 2822 N93-25961 * #
NAS 1.60:3190 ..... p 2652 N93-26201 * #
NAS 1.60:3259 ..... p 2581 N93-26134 * #
NAS 1.60:3266 ..... p 2797 N93-25736 * #
NAS 1.60:3272-PT-1B ..... p 2776 N93-26421 * #
NAS 1.60:3339 ..... p 2897 N93-26094 * #
NAS 1.61:1292-VOL-1 ..... p 2762 N93-25157 * #
NAS 1.61:1292-VOL-2 ..... p 2762 N93-25158 * #
NAS 1.61:1292-VOL-3 ..... p 2762 N93-25159 * #
NAS 1.61:1300-VOL-1 ..... p 2890 N93-26002 * #
NAS 1.61:1300-VOL-2 ..... p 2890 N93-26003 * #
NAS 1.61:1300-VOL-3 ..... p 2890 N93-26004 * #
NAS 1.83:156 ..... p 2574 N93-26422 * #

NASA-CASE-GSC-13460-1 ..... p 2691 N93-26104 *
NASA-CASE-GSC-13506-1 ..... p 2710 N93-26103 *

NASA-CASE-LAR-13645-1 ..... p 2656 N93-25995 *
NASA-CASE-LAR-14179-1 ..... p 2668 N93-26101 *
NASA-CASE-LAR-14219-1 ..... p 2597 N93-25998 * #
NASA-CASE-LAR-14399-1 ..... p 2729 N93-26102 *
NASA-CASE-LAR-14424-1-SB ..... p 2598 N93-25996 *
NASA-CASE-LAR-14457-1 ..... p 2656 N93-25997 * #
NASA-CASE-LAR-14753-1 ..... p 2656 N93-25999 *
NASA-CASE-LAR-14824-1-SB ..... p 2706 N93-26000 *

NASA-CASE-LEW-15262-1 ..... p 2640 N93-26100 *

NASA-CASE-MFS-28629-1 ..... p 2719 N93-26001 *

NASA-CASE-NPO-17653-1-CU ..... p 2793 N93-25994 *

NASA-CP-10093-PT-2 ..... p 2897 N93-26392 * #
NASA-CP-3183 ..... p 2803 N93-25921 * #
NASA-CP-3186 ..... p 2599 N93-24694 * #
NASA-CP-3189-VOL-1 ..... p 2901 N93-25561 * #
NASA-CP-3200 ..... p 2822 N93-25961 * #

NASA-CR-177599 ..... p 2817 N93-25137 * #
NASA-CR-177604 ..... p 2888 N93-25135 * #
NASA-CR-177606 ..... p 2887 N93-25442 * #
NASA-CR-177608 ..... p 2586 N93-26549 * #
NASA-CR-177609 ..... p 2794 N93-24738 * #
NASA-CR-177612 ..... p 2575 N93-25075 * #
NASA-CR-188242-VOL-1 ..... p 2911 N93-26058 * #
NASA-CR-188242-VOL-2 ..... p 2914 N93-26070 * #
NASA-CR-189193 ..... p 2592 N93-24754 * #
NASA-CR-189193 ..... p 2592 N93-25106 * #
NASA-CR-190778 ..... p 2573 N93-25134 * #
NASA-CR-190779 ..... p 2573 N93-24760 * #
NASA-CR-190793 ..... p 2623 N93-25132 * #
NASA-CR-191067 ..... p 2808 N93-24947 * #
NASA-CR-191082 ..... p 2649 N93-25128 * #
NASA-CR-191084 ..... p 2633 N93-26555 * #
NASA-CR-191095 ..... p 2694 N93-24759 * #
NASA-CR-191099 ..... p 2642 N93-25116 * #
NASA-CR-191105 ..... p 2580 N93-25883 * #
NASA-CR-191111 ..... p 2663 N93-24946 * #
NASA-CR-191112 ..... p 2622 N93-24758 * #
NASA-CR-191117 ..... p 2716 N93-24751 * #
NASA-CR-191118 ..... p 2721 N93-25451 * #
NASA-CR-191121 ..... p 2652 N93-26235 * #
NASA-CR-191124 ..... p 2653 N93-24761 * #
NASA-CR-191127 ..... p 2719 N93-25884 * #
NASA-CR-191408 ..... p 2803 N93-25084 * #
NASA-CR-191409 ..... p 2575 N93-25083 * #
NASA-CR-191410 ..... p 2576 N93-25153 * #
NASA-CR-191418 ..... p 2591 N93-24764 * #
NASA-CR-191419 ..... p 2615 N93-25133 * #
NASA-CR-191425 ..... p 2808 N93-25073 * #
NASA-CR-191438 ..... p 2695 N93-25087 * #
NASA-CR-191711 ..... p 2787 N93-26492 * #
NASA-CR-191988 ..... p 2709 N93-25345 * #
NASA-CR-192218 ..... p 2775 N93-26151 * #
NASA-CR-192224 ..... p 2775 N93-26159 * #
NASA-CR-192317 ..... p 2622 N93-24943 * #
NASA-CR-192321 ..... p 2854 N93-26183 * #
NASA-CR-192344 ..... p 2863 N93-25219 * #
NASA-CR-192442 ..... p 2786 N93-26156 * #

NASA-CR-192443 ..... p 2656 N93-26155 * #
NASA-CR-192451 ..... p 2711 N93-26154 * #
NASA-CR-192469 ..... p 2774 N93-25886 * #
NASA-CR-192481 ..... p 2801 N93-25888 * #
NASA-CR-192512 ..... p 2863 N93-25225 * #
NASA-CR-192514 ..... p 2618 N93-26055 *
NASA-CR-192515 ..... p 2614 N93-26152 * #
NASA-CR-192516 ..... p 2631 N93-26056 * #
NASA-CR-192517 ..... p 2631 N93-26053 * #
NASA-CR-192518 ..... p 2631 N93-26057 * #
NASA-CR-192519 ..... p 2631 N93-26054 * #
NASA-CR-192523 ..... p 2770 N93-25086 * #
NASA-CR-192524 ..... p 2610 N93-25479 * #
NASA-CR-192525 ..... p 2611 N93-25510 * #
NASA-CR-192526 ..... p 2611 N93-25511 * #
NASA-CR-192527 ..... p 2611 N93-25513 * #
NASA-CR-192528 ..... p 2611 N93-25512 * #
NASA-CR-192529 ..... p 2611 N93-25514 * #
NASA-CR-192531 ..... p 2633 N93-26557 * #
NASA-CR-192532 ..... p 2599 N93-26146 * #
NASA-CR-192681 ..... p 2852 N93-25281 * #
NASA-CR-192688 ..... p 2669 N93-26405 * #
NASA-CR-192701 ..... p 2664 N93-25218 * #
NASA-CR-192708 ..... p 2585 N93-25261 * #
NASA-CR-192709 ..... p 2585 N93-25330 * #
NASA-CR-192711 ..... p 2724 N93-25260 * #
NASA-CR-192715 ..... p 2673 N93-25198 * #
NASA-CR-192718 ..... p 2828 N93-25223 * #
NASA-CR-192725 ..... p 2696 N93-25208 * #
NASA-CR-192726 ..... p 2828 N93-25262 * #
NASA-CR-192727 ..... p 2596 N93-25199 * #
NASA-CR-192762 ..... p 2892 N93-25200 * #
NASA-CR-192763 ..... p 2874 N93-25288 * #
NASA-CR-192765 ..... p 2808 N93-24944 * #
NASA-CR-192771 ..... p 2643 N93-25240 * #
NASA-CR-192773 ..... p 2900 N93-25890 * #
NASA-CR-192775 ..... p 2888 N93-25289 * #
NASA-CR-192776 ..... p 2898 N93-25222 * #
NASA-CR-192781 ..... p 2888 N93-25172 * #
NASA-CR-192782 ..... p 2772 N93-25529 * #
NASA-CR-192783 ..... p 2697 N93-25221 * #
NASA-CR-192784 ..... p 2771 N93-25201 * #
NASA-CR-192788 ..... p 2723 N93-24912 * #
NASA-CR-192790 ..... p 2892 N93-25211 * #
NASA-CR-192791 ..... p 2890 N93-25755 * #
NASA-CR-192800 ..... p 2682 N93-26463 * #
NASA-CR-192804 ..... p 2676 N93-26105 * #
NASA-CR-192806 ..... p 2771 N93-25202 * #
NASA-CR-192808 ..... p 2900 N93-25241 * #
NASA-CR-192809 ..... p 2889 N93-25331 * #
NASA-CR-192814 ..... p 2659 N93-24745 * #
NASA-CR-192823 ..... p 2859 N93-25206 * #
NASA-CR-192824 ..... p 2653 N93-25078 * #
NASA-CR-192826 ..... p 2769 N93-24945 * #
NASA-CR-192827 ..... p 2643 N93-25229 * #
NASA-CR-192830 ..... p 2792 N93-25242 * #
NASA-CR-192832 ..... p 2775 N93-26084 * #
NASA-CR-192833 ..... p 2770 N93-25088 * #
NASA-CR-192834 ..... p 2769 N93-24910 * #
NASA-CR-192848 ..... p 2763 N93-25244 * #
NASA-CR-192849 ..... p 2892 N93-25230 * #
NASA-CR-192851 ..... p 2770 N93-25081 * #
NASA-CR-192879 ..... p 2821 N93-25833 * #
NASA-CR-192885 ..... p 2815 N93-24748 * #
NASA-CR-192886 ..... p 2815 N93-24749 * #
NASA-CR-192887 ..... p 2671 N93-24659 * #
NASA-CR-192889 ..... p 2848 N93-25450 * #
NASA-CR-192891 ..... p 2808 N93-24750 * #
NASA-CR-192892 ..... p 2819 N93-25296 * #
NASA-CR-192893 ..... p 2819 N93-25226 * #
NASA-CR-192894 ..... p 2818 N93-25156 * #
NASA-CR-192895 ..... p 2818 N93-25155 * #
NASA-CR-192896 ..... p 2883 N93-26423 * #
NASA-CR-192897 ..... p 2754 N93-25154 * #
NASA-CR-192898 ..... p 2816 N93-25458 * #
NASA-CR-192899 ..... p 2815 N93-25251 * #
NASA-CR-192906 ..... p 2815 N93-25297 * #
NASA-CR-192908 ..... p 2809 N93-25131 * #
NASA-CR-192910 ..... p 2805 N93-25130 * #
NASA-CR-192911 ..... p 2806 N93-25233 * #
NASA-CR-192912 ..... p 2809 N93-25250 * #
NASA-CR-192914 ..... p 2806 N93-25267 * #
NASA-CR-192916 ..... p 2862 N93-25108 * #
NASA-CR-192917 ..... p 2576 N93-25249 * #
NASA-CR-192918 ..... p 2698 N93-25266 * #
NASA-CR-192919 ..... p 2696 N93-25109 * #
NASA-CR-192920 ..... p 2585 N93-26052 * #
NASA-CR-192922 ..... p 2898 N93-26517 * #
NASA-CR-192923 ..... p 2898 N93-26424 * #
NASA-CR-192929 ..... p 2777 N93-24747 * #
NASA-CR-192930 ..... p 2900 N93-26132 * #
NASA-CR-192931 ..... p 2899 N93-24752 * #
NASA-CR-192932 ..... p 2899 N93-25161 * #
NASA-CR-192933 ..... p 2891 N93-26426 * #
NASA-CR-192934 ..... p 2573 N93-25077 * #
NASA-CR-192937 ..... p 2767 N93-26427 * #
NASA-CR-192939 ..... p 2633 N93-26425 * #
NASA-CR-192940 ..... p 2574 N93-24736 * #
NASA-CR-192944 ..... p 2874 N93-25139 * #
NASA-CR-192945 ..... p 2828 N93-25140 * #
NASA-CR-192947 ..... p 2818 N93-25196 * #
NASA-CR-192948 ..... p 2819 N93-25197 * #
NASA-CR-192949 ..... p 2818 N93-25141 * #
NASA-CR-192950 ..... p 2818 N93-25190 * #
NASA-CR-192951 ..... p 2820 N93-25425 * #
NASA-CR-192952 ..... p 2820 N93-25452 * #
NASA-CR-192953 ..... p 2587 N93-25162 * #
NASA-CR-192954 ..... p 2589 N93-25670 * #
NASA-CR-192955 ..... p 2810 N93-25669 * #
NASA-CR-192956 ..... p 2817 N93-24757 * #
NASA-CR-192957 ..... p 2593 N93-25668 * #
NASA-CR-192958 ..... p 2865 N93-25667 * #
NASA-CR-192959 ..... p 2765 N93-25666 * #
NASA-CR-192960 ..... p 2597 N93-26046 * #
NASA-CR-192961 ..... p 2811 N93-26150 * #
NASA-CR-192972 ..... p 2891 N93-26139 * #
NASA-CR-192974 ..... p 2801 N93-26047 * #
NASA-CR-192976 ..... p 2763 N93-25287 * #
NASA-CR-192978 ..... p 2809 N93-25152 * #
NASA-CR-192980 ..... p 2575 N93-25117 * #
NASA-CR-192982 ..... p 2801 N93-26088 * #
NASA-CR-192983 ..... p 2764 N93-25432 * #
NASA-CR-192984 ..... p 2764 N93-25431 * #
NASA-CR-192985 ..... p 2809 N93-25257 * #
NASA-CR-192997 ..... p 2580 N93-26049 * #
NASA-CR-193002 ..... p 2808 N93-25107 * #
NASA-CR-193003 ..... p 2721 N93-26135 * #
NASA-CR-193018 ..... p 2817 N93-24743 * #
NASA-CR-193033 ..... p 2595 N93-24762 * #
NASA-CR-193040 ..... p 2794 N93-24763 * #
NASA-CR-193048 ..... p 2599 N93-26095 * #
NASA-CR-193049 ..... p 2802 N93-26153 * #
NASA-CR-193054 ..... p 2612 N93-25959 * #
NASA-CR-193056 ..... p 2612 N93-25960 * #
NASA-CR-193057 ..... p 2613 N93-25992 * #
NASA-CR-193058 ..... p 2613 N93-25991 * #
NASA-CR-193059 ..... p 2613 N93-25989 * #
NASA-CR-193060 ..... p 2613 N93-25990 * #
NASA-CR-193061 ..... p 2613 N93-25993 * #
NASA-CR-193062 ..... p 2612 N93-25956 * #
NASA-CR-193063 ..... p 2611 N93-25955 * #
NASA-CR-193064 ..... p 2612 N93-25957 * #
NASA-CR-193065 ..... p 2614 N93-26329 * #
NASA-CR-193096 ..... p 2877 N93-25792 * #
NASA-CR-193098 ..... p 2873 N93-26419 * #
NASA-CR-193099 ..... p 2873 N93-26420 * #
NASA-CR-193100 ..... p 2790 N93-26050 * #
NASA-CR-193146 ..... p 2899 N93-26556 * #
NASA-CR-193203 ..... p 2620 N93-25317 * #
NASA-CR-193208 ..... p 2826 N93-25986 * #
NASA-CR-3922(39) ..... p 2792 N93-25195 *
NASA-CR-4497 ..... p 2803 N93-26157 * #
NASA-CR-4499 ..... p 2844 N93-25094 * #

NASA-EP-283 ..... p 2872 N93-26051 * #

NASA-NP-156 ..... p 2574 N93-26422 * #

NASA-RP-1292-VOL-1 ..... p 2762 N93-25157 * #
NASA-RP-1292-VOL-2 ..... p 2762 N93-25158 * #
NASA-RP-1292-VOL-3 ..... p 2762 N93-25159 * #
NASA-RP-1300-VOL-1 ..... p 2890 N93-26002 * #
NASA-RP-1300-VOL-2 ..... p 2890 N93-26003 * #
NASA-RP-1300-VOL-3 ..... p 2890 N93-26004 * #

NASA-SP-6102 ..... p 2665 N93-24678 * #

NASA-STD-3000-VOL-6 ..... p 2614 N93-26329 * #

NASA-TM-103663 ..... p 2618 N93-26209 * #
NASA-TM-103882 ..... p 2697 N93-25247 * #
NASA-TM-103932 ..... p 2695 N93-25082 * #
NASA-TM-103942 ..... p 2795 N93-26133 * #
NASA-TM-103943 ..... p 2708 N93-25076 * #
NASA-TM-103961 ..... p 2809 N93-25246 * #
NASA-TM-103963 ..... p 2575 N93-25091 * #
NASA-TM-103977 ..... p 2667 N93-25085 * #
NASA-TM-104001 ..... p 2581 N93-26099 * #
NASA-TM-104003 ..... p 2803 N93-25235 * #
NASA-TM-104004 ..... p 2584 N93-24914 * #
NASA-TM-104580 ..... p 2721 N93-26137 * #
NASA-TM-104581 ..... p 2770 N93-25160 * #
NASA-TM-104763 ..... p 2901 N93-25188 * #
NASA-TM-105270 ..... p 2730 N93-26202 * #
NASA-TM-105602 ..... p 2573 N93-26136 * #
NASA-TM-105705 ..... p 2632 N93-26200 * #
NASA-TM-105707 ..... p 2622 N93-24744 * #
NASA-TM-105708 ..... p 2622 N93-25105 * #
NASA-TM-105710 ..... p 2622 N93-24753 * #
NASA-TM-105711 ..... p 2621 N93-24740 * #
NASA-TM-105757 ..... p 2829 N93-26560 * #
NASA-TM-105771 ..... p 2597 N93-25080 * #
NASA-TM-105883 ..... p 2759 N93-25136 * #
NASA-TM-105907 ..... p 2872 N93-26205 * #
NASA-TM-105946 ..... p 2595 N93-26161 * #
NASA-TM-105959 ..... p 2633 N93-26204 * #
NASA-TM-106001 ..... p 2723 N93-24913 * #
NASA-TM-106002 ..... p 2724 N93-25070 * #
NASA-TM-106015 ..... p 2846 N93-26551 * #
NASA-TM-106017 ..... p 2709 N93-25173 * #
NASA-TM-106025 ..... p 2641 N93-26552 * #
NASA-TM-106042 ..... p 2592 N93-25079 * #
NASA-TM-106044 ..... p 2593 N93-25673 * #
NASA-TM-106047 ..... p 2598 N93-26214 * #
NASA-TM-106054 ..... p 2592 N93-25129 * #
NASA-TM-106066 ..... p 2633 N93-26561 * #
NASA-TM-106070 ..... p 2622 N93-25089 * #
NASA-TM-106074 ..... p 2634 N93-25071 * #
NASA-TM-106081 ..... p 2654 N93-25093 * #
NASA-TM-106086 ..... p 2575 N93-24911 * #
NASA-TM-106087 ..... p 2696 N93-25175 * #
NASA-TM-106093 ..... p 2614 N93-24755 * #
NASA-TM-106095 ..... p 2708 N93-24737 * #
NASA-TM-106096 ..... p 2687 N93-24746 * #
NASA-TM-106097 ..... p 2632 N93-26211 * #
NASA-TM-106098 ..... p 2615 N93-25090 * #
NASA-TM-106098 ..... p 2631 N93-26149 * #
NASA-TM-106103 ..... p 2718 N93-25672 * #
NASA-TM-106106 ..... p 2709 N93-25191 * #
NASA-TM-106107 ..... p 2618 N93-26148 * #
NASA-TM-106109 ..... p 2708 N93-26554 * #
NASA-TM-106125 ..... p 2731 N93-26550 * #
NASA-TM-106126 ..... p 2667 N93-25177 * #
NASA-TM-106129 ..... p 2707 N93-26203 * #
NASA-TM-106132 ..... p 2618 N93-26215 * #
NASA-TM-106133 ..... p 2664 N93-25337 * #
NASA-TM-106135 ..... p 2623 N93-25236 * #
NASA-TM-106139 ..... p 2632 N93-26210 * #
NASA-TM-107682 ..... p 2696 N93-25176 * #
NASA-TM-107731 ..... p 2615 N93-25174 * #
NASA-TM-107737 ..... p 2845 N93-26086 * #
NASA-TM-107739 ..... p 2591 N93-26553 * #
NASA-TM-107740 ..... p 2844 N93-25189 * #
NASA-TM-107742 ..... p 2634 N93-25072 * #
NASA-TM-107745 ..... p 2575 N93-25074 * #
NASA-TM-107747 ..... p 2777 N93-24742 * #
NASA-TM-107748 ..... p 2585 N93-26087 * #
NASA-TM-107760 ..... p 2651 N93-26048 * #
NASA-TM-108265 ..... p 2791 N93-26586 * #
NASA-TM-108402 ..... p 2884 N93-26562 * #
NASA-TM-108403 ..... p 2624 N93-25671 * #
NASA-TM-108704 ..... p 2616 N93-25231 * #
NASA-TM-108711 ..... p 2732 N93-24915 * #
NASA-TM-108719 ..... p 2820 N93-25459 * #
NASA-TM-108720 ..... p 2757 N93-26429 * #
NASA-TM-108735 ..... p 2612 N93-25988 * #
NASA-TM-108737 ..... p 2612 N93-25958 * #
NASA-TM-108744 ..... p 2673 N93-25181 * #
NASA-TM-108745 ..... p 2818 N93-25142 * #
NASA-TM-108746 ..... p 2818 N93-25138 * #
NASA-TM-108752 ..... p 2614 N93-25952 * #
NASA-TM-108756 ..... p 2873 N93-26418 * #
NASA-TM-108758 ..... p 2883 N93-26491 * #
NASA-TM-108769 ..... p 2756 N93-25462 * #
NASA-TM-108770 ..... p 2755 N93-25460 * #
NASA-TM-108771 ..... p 2755 N93-25461 * #
NASA-TM-108774 ..... p 2882 N93-26231 * #
NASA-TM-108775 ..... p 2663 N93-25194 * #
NASA-TM-108776 ..... p 2615 N93-25217 * #
NASA-TM-4423 ..... p 2723 N93-24909 * #
NASA-TM-4434 ..... p 2581 N93-26085 * #
NASA-TM-4449 ..... p 2689 N93-25618 * #

NASA-TP-3190 ..... p 2652 N93-26201 * #
NASA-TP-3259 ..... p 2581 N93-26134 * #
NASA-TP-3266 ..... p 2797 N93-25736 * #
NASA-TP-3272-PT-1B ..... p 2776 N93-26421 * #
NASA-TP-3339 ..... p 2897 N93-26094 * #

NATICK/TR-92/028 ..... p 2802 N93-26404 #
NATICK/TR-93/013 ..... p 2800 N93-25628 #

NAVY-CASE-74286 ..... p 2852 N93-25358 #

NAWCADWAR-92112-60 ..... p 2655 N93-25816 #

NCAR/CT-140 ..... p 2776 N93-26548 #

NCAR/TN-369+STR ..... p 2899 N93-26556 * #

NDP-043A ..... p 2791 N93-26586 * #

NEI-FI-179 ..... p 2763 N93-25360 #

NHRC-92-26 ..... p 2802 N93-26229 #

NIFS-204 ..... p 2859 N93-25248 #
NIFS-205 ..... p 2860 N93-25347 #

NIFS-206 ..... p 2698 N93-25277 #
NIFS-207 ..... p 2860 N93-25356 #
NIFS-208 ..... p 2858 N93-25092 #
NIFS-209 ..... p 2857 N93-24950 #
NIFS-210 ..... p 2687 N93-24951 #
NIFS-211 ..... p 2859 N93-25216 #
NIFS-212 ..... p 2859 N93-25227 #
NIFS-213 ..... p 2860 N93-25346 #
NIFS-214 ..... p 2859 N93-25215 #

NIST/GCR-92/620 ..... p 2722 N93-26546 #

NIST/TN-1297 ..... p 2830 N93-26318 #
NIST/TN-1346 ..... p 2646 N93-26319 #
NIST/TN-1356 ..... p 2708 N93-26535 #

NISTIR-4980 ..... p 2830 N93-26317 #
NISTIR-5113 ..... p 2850 N93-26314 #
NISTIR-5114 ..... p 2884 N93-26530 #
NISTIR-5120 ..... p 2852 N93-26322 #
NISTIR-5124 ..... p 2869 N93-26547 #
NISTIR-5130 ..... p 2646 N93-26323 #
NISTIR-5131 ..... p 2812 N93-26321 #

NOAA-TM-NWS-SR-146 ..... p 2787 N93-26570 #
NOAA-TM-NWS-SR-147 ..... p 2788 N93-26584 #

NOAA-TM-NWS-WR-218 ..... p 2785 N93-25775 #

NOAA-TR-NESDIS-63 ..... p 2781 N93-25220 #

NOARL-TN-153 ..... p 2757 N93-25868 #

NPS-CS-92-016 ..... p 2813 N93-26453 #

NPS-EC-93-005 ..... p 2681 N93-26261 #

NPS-MA-93-006 ..... p 2829 N93-26452 #
NPS-MA-93-007 ..... p 2829 N93-26370 #
NPS-MA-93-010 ..... p 2829 N93-26228 #
NPS-MA-93-011 ..... p 2706 N93-25779 #

NPS-ME-92-005 ..... p 2727 N93-25658 #
NPS-ME-93-001 ..... p 2669 N93-26285 #
NPS-ME-93-002 ..... p 2813 N93-26431 #

NPS-PH-93-006 ..... p 2759 N93-26310 #
NPS-PH-93-007 ..... p 2776 N93-26454 #

NPSCS-92-018 ..... p 2812 N93-26336 #

NRAD-TR-1564 ..... p 2675 N93-25700 #

NREL/TP-410-4960 ..... p 2758 N93-25098 #
NREL/TP-411-5289 ..... p 2759 N93-25102 #
NREL/TP-411-5327 ..... p 2862 N93-25163 #
NREL/TP-413-5334 ..... p 2759 N93-25253 #
NREL/TP-442-5102 ..... p 2874 N93-25254 #
NREL/TP-451-4852 ..... p 2862 N93-24953 #
NREL/TP-451-5190 ..... p 2759 N93-25504 #
NREL/TP-463-5217 ..... p 2898 N93-25101 #

NRL/FR/5341-93-9524 ..... p 2682 N93-26451 #
NRL/FR/7442-92-9414 ..... p 2775 N93-25891 #

NRL/MR/5300-93-7177 ..... p 2682 N93-26455 #
NRL/MR/5521-93-7196 ..... p 2680 N93-26227 #
NRL/MR/5523-93-7184 ..... p 2776 N93-26430 #
NRL/MR/6440-92-7174 ..... p 2715 N93-26445 #
NRL/MR/7240-92-7009 ..... p 2757 N93-25868 #
NRL/MR/7441-93-7011 ..... p 2756 N93-25694 #

NRLD-PR-92-085-351 ..... p 2757 N93-26574 #

NSTS-08251 ..... p 2612 N93-25958 * #
NSTS-08252 ..... p 2612 N93-25957 * #
NSTS-08254 ..... p 2613 N93-25990 * #
NSTS-08273 ..... p 2612 N93-25988 * #
NSTS-08274 ..... p 2613 N93-25989 * #
NSTS-08275 ..... p 2612 N93-25959 * #
NSTS-08277 ..... p 2613 N93-25992 * #
NSTS-08278 ..... p 2613 N93-25991 * #
NSTS-08279 ..... p 2612 N93-25960 * #
NSTS-08280 ..... p 2613 N93-25993 * #

NSWCDD/MP-92/304 ..... p 2807 N93-26403 #

NSWCDD/TR-92-425 ..... p 2884 N93-26575 #
NSWCDD/TR-92/119 ..... p 2812 N93-26375 #

NTSB/AAR-93/01 ..... p 2583 N93-25827 #

NUREG-CR-5669 ..... p 2731 N93-26390 #

NUREG/CR-5970 ..... p 2731 N93-26516 #

NUWC-NPT-TM-922089 ..... p 2707 N93-26328 #

ONR-TR-80 ..... p 2645 N93-25916 #
ONR-TR-81 ..... p 2656 N93-26172 #
ONR-TR-82 ..... p 2658 N93-26437 #
ONR-TR-83 ..... p 2869 N93-26577 #

ORNL/CDIAC-45 ..... p 2791 N93-26586 * #
ORNL/CDIAC-49 ..... p 2761 N93-25144 #
ORNL/CDIAC-57 ..... p 2760 N93-24952 #

ORNL/TM-12183 ..... p 2668 N93-25937 #
ORNL/TM-12189 ..... p 2858 N93-24969 #
ORNL/TM-12248 ..... p 2674 N93-25300 #
ORNL/TM-12281 ..... p 2860 N93-25493 #

OSU-CS-92-30-08 ..... p 2811 N93-26221 #

PB93-110625 ..... p 2768 N93-26567 #
PB93-111565 ..... p 2807 N93-26569 #
PB93-139806 ..... p 2766 N93-25878 #
PB93-139970 ..... p 2793 N93-25457 #
PB93-144582 ..... p 2872 N93-25735 #
PB93-146785 ..... p 2785 N93-25775 #
PB93-148427 ..... p 2787 N93-26570 #
PB93-148435 ..... p 2788 N93-26584 #
PB93-152478 ..... p 2768 N93-26533 #
PB93-153021 ..... p 2785 N93-25849 #
PB93-153039 ..... p 2785 N93-25776 #
PB93-153096 ..... p 2786 N93-25874 #
PB93-154458 ..... p 2722 N93-26546 #
PB93-156032 ..... p 2793 N93-25877 #
PB93-156164 ..... p 2765 N93-25873 #
PB93-156347 ..... p 2785 N93-25870 #
PB93-156388 ..... p 2785 N93-25871 #
PB93-156479 ..... p 2706 N93-25885 #
PB93-156743 ..... p 2869 N93-26547 #
PB93-156776 ..... p 2776 N93-26548 #
PB93-156818 ..... p 2872 N93-26558 #
PB93-156826 ..... p 2899 N93-26556 * #
PB93-157014 ..... p 2661 N93-25818 #
PB93-157295 ..... p 2644 N93-25817 #
PB93-157725 ..... p 2766 N93-25875 #
PB93-157790 ..... p 2766 N93-25876 #
PB93-157808 ..... p 2765 N93-25850 #
PB93-158004 ..... p 2765 N93-25851 #
PB93-158509 ..... p 2644 N93-25819 #
PB93-158566 ..... p 2768 N93-26529 #
PB93-158632 ..... p 2884 N93-26530 #
PB93-158673 ..... p 2850 N93-26314 #
PB93-158756 ..... p 2766 N93-26315 #
PB93-158780 ..... p 2766 N93-26316 #
PB93-159069 ..... p 2830 N93-26317 #
PB93-159325 ..... p 2884 N93-26568 #
PB93-159432 ..... p 2720 N93-26534 #
PB93-159457 ..... p 2708 N93-26535 #
PB93-159465 ..... p 2830 N93-26318 #
PB93-160786 ..... p 2646 N93-26319 #
PB93-161131 ..... p 2768 N93-26536 #
PB93-161198 ..... p 2730 N93-26320 #
PB93-161339 ..... p 2812 N93-26321 #
PB93-161743 ..... p 2899 N93-26537 #
PB93-161750 ..... p 2899 N93-26538 #
PB93-162873 ..... p 2852 N93-26322 #
PB93-162931 ..... p 2898 N93-26571 #
PB93-164564 ..... p 2646 N93-26323 #
PB93-164606 ..... p 2785 N93-25872 #
PB93-165249 ..... p 2641 N93-26589 #
PB93-165603 ..... p 2720 N93-26585 #
PB93-165611 ..... p 2720 N93-26590 #
PB93-167112 ..... p 2872 N93-26509 #
PB93-167252 ..... p 2767 N93-26510 #
PB93-169399 ..... p 2711 N93-26324 #
PB93-172955 ..... p 2767 N93-26511 #
PB93-172997 ..... p 2768 N93-26559 #
PB93-910401 ..... p 2583 N93-25827 #

PCMDI-5 ..... p 2761 N93-25145 #

PL-TR-92-2113 ..... p 2776 N93-26283 #
PL-TR-92-2123 ..... p 2681 N93-26280 #
PL-TR-92-2132 ..... p 2849 N93-26173 #
PL-TR-92-2134 ..... p 2681 N93-26247 #
PL-TR-92-2162 ..... p 2774 N93-25852 #
PL-TR-92-2174 ..... p 2632 N93-26373 #
PL-TR-92-2215 ..... p 2618 N93-26232 #
PL-TR-92-2252 ..... p 2853 N93-25646 #
PL-TR-92-2296 ..... p 2850 N93-26281 #
PL-TR-92-2307 ..... p 2620 N93-26248 #
PL-TR-92-3042 ..... p 2632 N93-26174 #

PNL-SA-21232 ..... p 2767 N93-26495 #
PNL-SA-21577 ..... p 2654 N93-25359 #
PNL-SA-21613 ..... p 2767 N93-26497 #

PNL-8222 ..... p 2760 N93-24675 #

PNL-8381 ..... p 2759 N93-25183 #
PNL-8427 ..... p 2758 N93-24975 #

PSGDL-R-92/93-0002 ..... p 2698 N93-25266 * #

PSU-ME-R-90/91-0005-PHASE-2 p 2768 N93-26533 #

PW/GESP-FR-21988-15 ..... p 2651 N93-25843 #

R/D-6458-EE-01 ..... p 2714 N93-26217 #
R/D-6792-EN-02 ..... p 2845 N93-25643 #

RAE-TM-P-1223 ..... p 2592 N93-25455 #

RAND/N-3253-AF ..... p 2580 N93-25894 #
RAND/N-3464-AF ..... p 2767 N93-26327 #

REPT-002 ..... p 2797 N93-26307 #
REPT-134 ..... p 2729 N93-25901 #
REPT-6078-MA-01 ..... p 2731 N93-26522 #
REPT-92-4 ..... p 2799 N93-26521 #
REPT-92-5 ..... p 2798 N93-26436 #
REPT-92-6 ..... p 2798 N93-26435 #
REPT-92B00100-PT-1B ..... p 2776 N93-26421 * #
REPT-93-001 ..... p 2673 N93-25198 * #
REPT-93B00012 ..... p 2599 N93-24694 * #
REPT-93B00030 ..... p 2689 N93-25618 * #
REPT-93B00035 ..... p 2721 N93-26137 * #
REPT-93B00049-VOL-1 ..... p 2890 N93-26002 * #
REPT-93B00049-VOL-2 ..... p 2890 N93-26003 * #
REPT-93B00049-VOL-3 ..... p 2890 N93-26004 * #
REPT-93B00069 ..... p 2770 N93-25160 * #

RF-6888 ..... p 2644 N93-25817 #

RL-TR-92-181 ..... p 2710 N93-25696 #
RL-TR-92-249 ..... p 2811 N93-25791 #
RL-TR-92-257 ..... p 2681 N93-26383 #
RL-TR-92-265 ..... p 2812 N93-26275 #
RL-TR-92-281 ..... p 2675 N93-25767 #
RL-TR-92-298 ..... p 2692 N93-26334 #
RL-TR-92-339 ..... p 2830 N93-26255 #
RL-TR-93-21-PT-2 ..... p 2730 N93-26279 #

RPT-91025 ..... p 2681 N93-26383 #

RSG-306-93 ..... p 2682 N93-26460 #

RSL-TR-8241-1 ..... p 2790 N93-26050 * #
RSL-TR-8243-1 ..... p 2790 N93-26050 * #

RSRE-MEMO-4544 ..... p 2864 N93-25454 #
RSRE-MEMO-4585 ..... p 2810 N93-25453 #

RSRE-92005 ..... p 2811 N93-25942 #

RTD-5824-AN-01 ..... p 2594 N93-25917 #

RTR-113-03 ..... p 2631 N93-26056 * #
RTR-213-01-VOL-1 ..... p 2631 N93-26053 * #
RTR-213-01-VOL-2 ..... p 2631 N93-26057 * #
RTR-213-01-VOL-3 ..... p 2631 N93-26054 * #
RTR-227-01 ..... p 2618 N93-26055 *

S-704 ..... p 2897 N93-26094 * #
S-713 ..... p 2901 N93-25188 * #
S-721 ..... p 2797 N93-25736 * #

SA-2 ..... p 2787 N93-26492 * #

SAND-92-1487C ..... p 2862 N93-24958 #
SAND-92-1560C ..... p 2646 N93-26502 #
SAND-92-1596C ..... p 2653 N93-24971 #
SAND-92-1617C ..... p 2863 N93-25387 #
SAND-92-1630C ..... p 2827 N93-26596 #
SAND-92-1973C ..... p 2715 N93-26597 #
SAND-92-2032C ..... p 2827 N93-25103 #
SAND-92-2067C ..... p 2692 N93-26501 #
SAND-92-2103C ..... p 2689 N93-25416 #
SAND-92-2120C ..... p 2689 N93-25417 #
SAND-92-2282C ..... p 2576 N93-25121 #
SAND-92-2378C ..... p 2655 N93-25444 #
SAND-92-2392 ..... p 2800 N93-25318 #
SAND-92-2396C ..... p 2655 N93-25446 #
SAND-92-2441C ..... p 2644 N93-25312 #
SAND-92-2537 ..... p 2844 N93-25520 #
SAND-92-2639C ..... p 2642 N93-24972 #
SAND-92-2917C ..... p 2689 N93-25429 #
SAND-93-0099C ..... p 2896 N93-25321 #
SAND-93-0164C ..... p 2810 N93-25386 #
SAND-93-0331C ..... p 2726 N93-25489 #

SAO-AXAF-DR-92-012 ..... p 2854 N93-26183 * #

SB92-A-02 ..... p 2869 N93-26381 #

SCC-R-181F ..... p 2857 N93-26542 #

SDAG-TN-86-01 ..... p 2801 N93-26047 * #

SGD-581-PT-1 ..... p 2899 N93-26537 #
SGD-581-PT-2 ..... p 2899 N93-26538 #

SIO-REF-92-33 ..... p 2730 N93-26320 #

SLCET-TR-91-11 ..... p 2691 N93-26299 #
SLCET-TR-91-29 ..... p 2657 N93-26341 #

SMC-TR-93-02 ..... p 2645 N93-26251 #
SMC-TR-93-03 ..... p 2867 N93-25947 #

SOC-R613-002-1292 ..... p 2676 N93-25855 #

SPC-PIRS-90-C-15 ..... p 2690 N93-25660 #

SPC-92114-CMC ..... p 2813 N93-26583 #

SR-109/110 ..... p 2675 N93-25639 #
SR-1 ..... p 2850 N93-26281 #
SR-1 ..... p 2632 N93-26373 #
SR-2 ..... p 2618 N93-26232 #
SR-3 ..... p 2849 N93-26173 #
SR-5 ..... p 2776 N93-26283 #
SR-6 ..... p 2681 N93-26280 #
SR-7 ..... p 2681 N93-26247 #

SRI-MP-257 ..... p 2860 N93-25626 #

SRL-0076-TM ..... p 2675 N93-25689 #

SRS-571 ..... p 2811 N93-25845 #

SRS/STG-PR93-5738/17 ..... p 2801 N93-25888 * #

SSCL-611 ..... p 2689 N93-25491 #

SSS-DTR-92-13437 ..... p 2618 N93-26232 #

SU-SLAC-PUB-6053 ..... p 2847 N93-25323 #

SUPRI-TR-89 ..... p 2695 N93-24954 #

SWRI-PN-06-2492 ..... p 2651 N93-25788 #
SWRI-PN-12-3384 ..... p 2845 N93-25915 #

TAO-60322 ..... p 2808 N93-25073 * #

TEC-0026 ..... p 2757 N93-26369 #

TKK-NEMO-19 ..... p 2758 N93-25096 #
TKK-NEMO-21 ..... p 2758 N93-25097 #

TR-003 ..... p 2690 N93-25782 #
TR-0091(6925-11)-2 ..... p 2867 N93-25947 #
TR-14 ..... p 2645 N93-25920 #
TR-1619-1-2 ..... p 2801 N93-26088 * #
TR-17 ..... p 2850 N93-26443 #
TR-18 ..... p 2868 N93-26254 #
TR-1 ..... p 2655 N93-25642 #
TR-21 ..... p 2868 N93-26252 #
TR-25 ..... p 2866 N93-25781 #
TR-25 ..... p 2657 N93-26386 #
TR-2 ..... p 2851 N93-26514 #
TR-30 ..... p 2849 N93-25659 #
TR-34 ..... p 2868 N93-26302 #
TR-3 ..... p 2870 N93-26581 #
TR-4 ..... p 2851 N93-26518 #
TR-61 ..... p 2850 N93-26267 #
TR-63 ..... p 2850 N93-26287 #
TR-64 ..... p 2868 N93-26258 #
TR-65 ..... p 2652 N93-26197 #
TR-80 ..... p 2645 N93-25916 #
TR-92(2935)-10 ..... p 2645 N93-26251 #

TRL-TRANS-T3908 ..... p 2726 N93-25419 #

TS-TCMS-92001 ..... p 2873 N93-26418 * #
TS-TCMS-92002 ..... p 2873 N93-26419 * #
TS-TCMS-92003 ..... p 2873 N93-26420 * #

TSI-ARO-93-1 ..... p 2680 N93-26226 #

UAH-5-32892 ..... p 2711 N93-26154 * #

UC-705 ..... p 2706 N93-25987 #
UC-741 ..... p 2706 N93-25987 #
UC-905 ..... p 2811 N93-25943 #

UCB/CSD-91/651 ..... p 2805 N93-25130 * #
UCB/CSD-92/683 ..... p 2809 N93-25250 * #
UCB/CSD-92/705 ..... p 2806 N93-25233 * #
UCB/CSD-92/712 ..... p 2809 N93-25131 * #

UCB/ERL-90/3 ..... p 2692 N93-26539 #

UCRL-ID-108226 ..... p 2761 N93-25145 #
UCRL-ID-111522 ..... p 2846 N93-24959 #
UCRL-ID-112129 ..... p 2761 N93-25122 #
UCRL-ID-112191 ..... p 2617 N93-25494 #
UCRL-ID-112295 ..... p 2762 N93-25146 #
UCRL-ID-112296 ..... p 2762 N93-25147 #
UCRL-ID-112606 ..... p 2620 N93-25317 * #
UCRL-ID-112755 ..... p 2788 N93-24960 #

UCRL-JC-107218 ..... p 2888 N93-25320 #
UCRL-JC-109178 ..... p 2875 N93-25319 #
UCRL-JC-109526 ..... p 2715 N93-26503 #
UCRL-JC-110195 ..... p 2852 N93-25375 #
UCRL-JC-110197 ..... p 2688 N93-25397 #
UCRL-JC-110346 ..... p 2654 N93-25382 #
UCRL-JC-111017 ..... p 2873 N93-24677 #
UCRL-JC-111215 ..... p 2635 N93-25383 #
UCRL-JC-111296 ..... p 2712 N93-25363 #
UCRL-JC-111452 ..... p 2711 N93-24961 #
UCRL-JC-111462 ..... p 2857 N93-26593 #
UCRL-JC-111463 ..... p 2870 N93-26594 #
UCRL-JC-111464 ..... p 2654 N93-25384 #
UCRL-JC-111660 ..... p 2649 N93-25336 #
UCRL-JC-112256 ..... p 2709 N93-25515 #
UCRL-JC-112455 ..... p 2731 N93-26507 #
UCRL-JC-112689 ..... p 2763 N93-25385 #

UCRL-LR-109887 ..... p 2730 N93-26178 #
UCRL-LR-110773 ..... p 2730 N93-26177 #

UCRL-52000-92-10-11-12 ..... p 2674 N93-25299 #
UCRL-52000-92-8/9 ..... p 2901 N93-24974 #
UCRL-53868-91 ..... p 2917 N93-26326 #

UCSC-CRL-93-02 ..... p 2808 N93-24944 * #

UILU-ENG-91-2013 ..... p 2731 N93-26390 #
UILU-ENG-92-2011 ..... p 2811 N93-25845 #
UILU-ENG-92-2014 ..... p 2727 N93-25647 #
UILU-ENG-92-2016 ..... p 2731 N93-26516 #
UILU-ENG-93-2212 ..... p 2815 N93-24748 * #
UILU-ENG-93-2213 ..... p 2815 N93-24749 * #

UIUL-93-0504 ..... p 2659 N93-24745 * #

UMR-FDB-28 ..... p 2640 N93-26301 #
UMR-FDB-29 ..... p 2645 N93-26300 #

US-PATENT-APPL-SN-149298 ..... p 2691 N93-26233
US-PATENT-APPL-SN-349381 ..... p 2586 N93-26093
US-PATENT-APPL-SN-363691 ..... p 2687 N93-25212
US-PATENT-APPL-SN-501908 ..... p 2793 N93-25994 *
US-PATENT-APPL-SN-520472 ..... p 2656 N93-25997 * #
US-PATENT-APPL-SN-544298 ..... p 2634 N93-25283
US-PATENT-APPL-SN-550097 ..... p 2674 N93-25332
US-PATENT-APPL-SN-575543 ..... p 2652 N93-26234
US-PATENT-APPL-SN-649501 ..... p 2691 N93-26142
US-PATENT-APPL-SN-702663 ..... p 2867 N93-26090
US-PATENT-APPL-SN-719436 ..... p 2719 N93-26244
US-PATENT-APPL-SN-721038 ..... p 2656 N93-25995 *
US-PATENT-APPL-SN-726483 ..... p 2867 N93-26140
US-PATENT-APPL-SN-740526 ..... p 2668 N93-26101 *
US-PATENT-APPL-SN-742235 ..... p 2854 N93-26091
US-PATENT-APPL-SN-743468 ..... p 2598 N93-25996 *
US-PATENT-APPL-SN-750998 ..... p 2717 N93-25228
US-PATENT-APPL-SN-762818 ..... p 2643 N93-25284
US-PATENT-APPL-SN-786641 ..... p 2710 N93-26141
US-PATENT-APPL-SN-788018 ..... p 2640 N93-26143 #
US-PATENT-APPL-SN-788908 ..... p 2597 N93-25998 * #
US-PATENT-APPL-SN-797507 ..... p 2729 N93-26102 *
US-PATENT-APPL-SN-804627 ..... p 2710 N93-26092
US-PATENT-APPL-SN-823805 ..... p 2706 N93-26000 *
US-PATENT-APPL-SN-845090 ..... p 2656 N93-25999 *
US-PATENT-APPL-SN-889577 ..... p 2691 N93-26104 *
US-PATENT-APPL-SN-892055 ..... p 2640 N93-26100 *
US-PATENT-APPL-SN-904308 ..... p 2710 N93-26103 *
US-PATENT-APPL-SN-917652 ..... p 2640 N93-26145 #
US-PATENT-APPL-SN-957128 ..... p 2719 N93-26001 *
US-PATENT-APPL-SN-970886 ..... p 2852 N93-25358 #
US-PATENT-APPL-SN-983957 ..... p 2719 N93-26144 #

US-PATENT-CLASS-118-308 ..... p 2668 N93-26101 *
US-PATENT-CLASS-118-325 ..... p 2668 N93-26101 *
US-PATENT-CLASS-156-245 ..... p 2656 N93-25995 *
US-PATENT-CLASS-244-17.11 ..... p 2597 N93-25998 * #
US-PATENT-CLASS-244-17.19 ..... p 2597 N93-25998 * #
US-PATENT-CLASS-244-75R ..... p 2597 N93-25998 * #
US-PATENT-CLASS-264-DIG.65 ..... p 2656 N93-25995 *
US-PATENT-CLASS-264-135 ..... p 2656 N93-25995 *
US-PATENT-CLASS-264-259 ..... p 2656 N93-25995 *
US-PATENT-CLASS-264-265 ..... p 2656 N93-25995 *
US-PATENT-CLASS-264-58 ..... p 2640 N93-26100 *
US-PATENT-CLASS-324-207.16 ..... p 2710 N93-26103 *
US-PATENT-CLASS-324-220 ..... p 2710 N93-26103 *
US-PATENT-CLASS-324-262 ..... p 2710 N93-26103 *
US-PATENT-CLASS-324-662 ..... p 2691 N93-26104 *
US-PATENT-CLASS-324-681 ..... p 2691 N93-26104 *
US-PATENT-CLASS-324-683 ..... p 2691 N93-26104 *
US-PATENT-CLASS-324-690 ..... p 2691 N93-26104 *
US-PATENT-CLASS-33-542 ..... p 2710 N93-26103 *
US-PATENT-CLASS-340-870.37 .. p 2691 N93-26104 *
US-PATENT-CLASS-342-351 ..... p 2691 N93-26142
US-PATENT-CLASS-358-140 ..... p 2854 N93-26091
US-PATENT-CLASS-364-453 ..... p 2710 N93-26092
US-PATENT-CLASS-364-453 ..... p 2586 N93-26093
US-PATENT-CLASS-375-96 ..... p 2691 N93-26233
US-PATENT-CLASS-384-493 ..... p 2719 N93-26001 *
US-PATENT-CLASS-384-537 ..... p 2719 N93-26001 *
US-PATENT-CLASS-384-585 ..... p 2719 N93-26001 *
US-PATENT-CLASS-427-180 ..... p 2668 N93-26101 *
US-PATENT-CLASS-427-195 ..... p 2668 N93-26101 *
US-PATENT-CLASS-427-294 ..... p 2668 N93-26101 *
US-PATENT-CLASS-427-295 ..... p 2668 N93-26101 *
US-PATENT-CLASS-427-296 ..... p 2668 N93-26101 *
US-PATENT-CLASS-428-428 ..... p 2640 N93-26100 *
US-PATENT-CLASS-428-698 ..... p 2640 N93-26100 *
US-PATENT-CLASS-435-7.32 ..... p 2793 N93-25994 *
US-PATENT-CLASS-435-7.92 ..... p 2793 N93-25994 *
US-PATENT-CLASS-435-874 ..... p 2793 N93-25994 *
US-PATENT-CLASS-436-518 ..... p 2793 N93-25994 *
US-PATENT-CLASS-501-32 ..... p 2640 N93-26100 *
US-PATENT-CLASS-501-89 ..... p 2640 N93-26100 *
US-PATENT-CLASS-501-8 ..... p 2640 N93-26100 *
US-PATENT-CLASS-501-95 ..... p 2640 N93-26100 *
US-PATENT-CLASS-528-125 ..... p 2656 N93-25997 * #
US-PATENT-CLASS-528-125 ..... p 2656 N93-25999 *
US-PATENT-CLASS-528-128 ..... p 2656 N93-25997 * #
US-PATENT-CLASS-528-128 ..... p 2656 N93-25999 *
US-PATENT-CLASS-528-170 ..... p 2656 N93-25997 * #
US-PATENT-CLASS-528-170 ..... p 2656 N93-25999 *
US-PATENT-CLASS-528-172 ..... p 2656 N93-25997 * #
US-PATENT-CLASS-528-172 ..... p 2656 N93-25999 *
US-PATENT-CLASS-528-173 ..... p 2656 N93-25997 * #
US-PATENT-CLASS-528-173 ..... p 2656 N93-25999 *
US-PATENT-CLASS-528-176 ..... p 2656 N93-25997 * #
US-PATENT-CLASS-528-176 ..... p 2656 N93-25999 *
US-PATENT-CLASS-528-183 ..... p 2656 N93-25997 * #
US-PATENT-CLASS-528-353 ..... p 2656 N93-25999 *
US-PATENT-CLASS-73-147 ..... p 2598 N93-25996 *
US-PATENT-CLASS-73-147 ..... p 2706 N93-26000 *
US-PATENT-CLASS-73-178R ..... p 2706 N93-26000 *
US-PATENT-CLASS-73-204.11 .... p 2706 N93-26000 *
US-PATENT-CLASS-73-641 ..... p 2729 N93-26102 *
US-PATENT-CLASS-73-779 ..... p 2710 N93-26141
US-PATENT-CLASS-73-788 ..... p 2729 N93-26102 *
US-PATENT-CLASS-91-42 ..... p 2719 N93-26244

US-PATENT-5,156,806 ..... p 2652 N93-26234
US-PATENT-5,157,695 ..... p 2691 N93-26233
US-PATENT-5,160,934 ..... p 2691 N93-26142
US-PATENT-5,161,449 ..... p 2719 N93-26244
US-PATENT-5,162,805 ..... p 2674 N93-25332
US-PATENT-5,162,972 ..... p 2687 N93-25212
US-PATENT-5,166,882 ..... p 2586 N93-26093
US-PATENT-5,168,359 ..... p 2854 N93-26091
US-PATENT-5,168,749 ..... p 2717 N93-25228
US-PATENT-5,168,760 ..... p 2710 N93-26141
US-PATENT-5,169,676 ..... p 2867 N93-26090
US-PATENT-5,172,323 ..... p 2710 N93-26092
US-PATENT-5,173,871 ..... p 2634 N93-25283
US-PATENT-5,176,788 ..... p 2867 N93-26140
US-PATENT-5,177,997 ..... p 2643 N93-25284
US-PATENT-5,209,111 ..... p 2706 N93-26000 *
US-PATENT-5,209,123 ..... p 2729 N93-26102 *
US-PATENT-5,209,430 ..... p 2597 N93-25998 * #
US-PATENT-5,210,019 ..... p 2793 N93-25994 *
US-PATENT-5,211,057 ..... p 2598 N93-25996 *
US-PATENT-5,211,489 ..... p 2719 N93-26001 *
US-PATENT-5,212,276 ..... p 2656 N93-25997 * #
US-PATENT-5,212,283 ..... p 2656 N93-25999 *
US-PATENT-5,213,739 ..... p 2656 N93-25995 *
US-PATENT-5,213,843 ..... p 2668 N93-26101 *
US-PATENT-5,214,004 ..... p 2640 N93-26100 *
US-PATENT-5,214,379 ..... p 2710 N93-26103 *
US-PATENT-5,214,388 ..... p 2691 N93-26104 *

USAARL-92-35 ..... p 2795 N93-26218 #
USAARL-93-9 ..... p 2802 N93-26265 #

USAATCOM-TR-92-A-001 ..... p 2794 N93-24738 * #
USAATCOM-TR-93-D-1 ..... p 2583 N93-26263 #

USAFA-TR-92-4 ..... p 2708 N93-26543 #

USAFETAC/PR-92/007 ..... p 2896 N93-26340 #

USAFSAM-PROC-89-29 ..... p 2882 N93-26242 #

USCGA-TR-11-92 ..... p 2706 N93-25885 #

USCGA-17-92 ..... p 2898 N93-26571 #

USDA/AIB-663 ..... p 2661 N93-25818 #

USNA-TSPR-191 ..... p 2786 N93-26273 #

UVA/525272/MSE93/101 ..... p 2652 N93-26264 #

WES/MP/GL-92-40 ..... p 2686 N93-26541 #

WES/TR/EL-WRP-SM-2 ..... p 2757 N93-26440 #

WES/TR/ITL-92-9 ..... p 2881 N93-25824 #

WES/TR/SL-REMR-CS-39 ..... p 2586 N93-26274 #

WHC-SA-1676 ..... p 2649 N93-25255 #

WHOI-92-18 ..... p 2790 N93-26384 #
WHOI-92-40 ..... p 2791 N93-26578 #

WJSA-R-92-B-012 ..... p 2712 N93-24967 #

WL-TM-93-300 ..... p 2857 N93-26566 #

WL-TR-91-2079 ..... p 2595 N93-26219 #
WL-TR-91-4102 ..... p 2722 N93-26527 #
WL-TR-92-3041 ..... p 2706 N93-25951 #
WL-TR-92-3089-VOL-2 ..... p 2599 N93-25693 #
WL-TR-92-3100 ..... p 2810 N93-25627 #
WL-TR-92-4032 ..... p 2722 N93-26526 #
WL-TR-92-4062 ..... p 2639 N93-25918 #
WL-TR-93-1001 ..... p 2591 N93-26572 #
WL-TR-93-4008 ..... p 2869 N93-26540 #

WSRC-MS-92-161 ..... p 2769 N93-24672 #
WSRC-MS-92-178 ..... p 2760 N93-24673 #

WSRC-TR-91-673 ..... p 2864 N93-25506 #

Y/DD-586 ..... p 2847 N93-25256 #

YAI-TR-106 ..... p 2849 N93-26173 #
YAI-TR-107 ..... p 2850 N93-26281 #

YALEU/DCS/RR-927 ..... p 2828 N93-25905 #

Appendix

NASA SCIENTIFIC AND TECHNICAL INFORMATION PROGRAM PRODUCTS AND SERVICES

The NASA Scientific and Technical Information (STI) Program provides for the collection and announcement of aerospace-related reports and literature obtained worldwide through agreements and exchanges. The result of the collection is the comprehensive NASA STI Database that covers aeronautics, space, and supporting disciplines.

The STI Database, documents generated or obtained by NASA, and products and services derived from or supporting the database are made available to the NASA research community and to the public. Descriptions and sources of these items are presented in the following pages.

Scientific and Technical Aerospace Reports (*STAR*) is an abstract journal, listing citations with abstracts for aerospace-related reports obtained from worldwide sources. *STAR* is issued on the first of each month, and announces current documents that have been entered into the NASA STI Database during the previous month. The reports are of the following types:

- NASA, NASA contractor, and NASA grantee reports;
- Reports issued by other U.S. Government agencies, domestic and foreign institutions, universities, and private firms;
- Translations in report form;
- NASA-owned patents and patent applications;
- Other U.S. Government agency and foreign patents and patent applications;
- Domestic and foreign dissertations and theses.

Journal, book, and conference literature, journal translations, and certain foreign dissertations having the same subject scope as *STAR* are announced in a companion journal, *International Aerospace Abstracts* (*IAA*). *IAA* is issued on the 1st and 15th of each month and is available from the American Institute of Aeronautics and Astronautics, Technical Information Service, 555 West 57th Street, 12th Floor, New York, NY 10019.

ELIGIBILITY AND REGISTRATION FOR NASA STI PRODUCTS AND SERVICES

Organizations of the type listed below that have registered with NASA can receive products and services.

- NASA offices and installations, contractors, subcontractors, grantees, and consultants;
- Other U.S. Government agencies and their contractors;
- Libraries in the United States that have arrangements with NASA to maintain collections of NASA documents for public reference;
- Other organizations in the United States having a need for NASA documents in work related to aeronautics and space research;
- Organizations abroad that have established reciprocal documents exchange arrangements with NASA.

The central service points — central points of document acquisition and control within qualified organizations — or individuals are eligible to register for NASA STI products and services. Domestic organizations or individuals may be eligible to receive various classes of NASA publications and services and should address their requests for registration or further information to:

ATTN: Registration Services
NASA Center for AeroSpace Information
800 Elkridge Landing Road
Linthicum Heights, MD 21090-2934
301-621-0390

Organizations abroad should direct requests to:

National Aeronautics and Space Administration
Scientific and Technical Information Program (JTT)
International STI Program
Washington, DC 20546-0001
USA
703-271-5640

SUBJECT SCOPE

The subject scope of *STAR* and *IAA* includes all aspects of aeronautics and space research and development, supporting basic and applied research, and applications. Aerospace aspects of Earth resources, energy development, conservation, oceanography, environmental protection, urban transportation, and other topics of high national priority are also covered.

HOW TO USE *STAR* SUBJECT CATEGORIES

Abstracts in *STAR* are categorized by 10 major subject divisions that are divided further into 76 specific subject categories. The subject divisions and categories are listed in the Table of Contents together with a note for each that defines its scope and provides any cross-references. For example:

16 SPACE TRANSPORTATION
Includes passenger and cargo space transportation, e.g., shuttle operations; and space rescue techniques. For related information see also *03 Air Transportation and Safety* and *18 Spacecraft Design, Testing and Performance*. For space suits see *54 Man/System Technology and Life Support*.

CROSS-REFERENCES

Individual *STAR* abstracts are not ordinarily cross-referenced, except for certain conference reports or book translations that have had separate abstracts written for their component papers or chapters. Citations and abstracts of the components follow immediately after those of the parent document. When the subject content of a component differs sufficiently from the general content of the parent, a cross-reference citation also is printed at the end of the category to which it normally would have been assigned if it were independent.

DOCUMENTS ON MICROFICHE

Documents available on microfiche are designated by a pound sign (#) following the accession number.

LIMITED REPRODUCIBILITY

A note of limited reproducibility appears in the citation, if there are factors affecting the reproducibility of more than 20% of the document. These factors include faint or broken type, color photographs, black and white photographs, foldouts, dot matrix print, or some other factor that limits the reproducibility of the document. This notation also appears on the microfiche header.

COLOR COPIES

An increasing number of NASA scientific and technical reports are being produced with color graphs, charts, illustrations, and photographs. An indication that a document has color pages follows the source and pricing (SAP) information in the *STAR* citation.

Registered users of the NASA Scientific and Technical Information Program will receive ordered documents with color at no additional cost, as long as stock copies of the document are available. Otherwise, an additional fee of $2.00 per color page will be charged. The NASA Center for AeroSpace Information staff will contact registered users to determine individual user's needs.

NASA PATENTS AND PATENT APPLICATIONS

Patents and patent applications owned by NASA are announced in *STAR* under appropriate subject categories and are referenced in the *STAR* indexes. In the Report/Accession Number Index, patents are indexed by the NASA Case Number, and the U.S. Patent Class. Patent applications are indexed by the NASA Case Number and the U.S. Patent Application Serial Number.

Printed copies of patents (which are not microfiched) are available for purchase from the U.S. Patent and Trademark Office.

When ordering patents, the U.S. Patent Number should be used, and payment must be remitted in advance, by money order or check payable to the Commissioner of Patents and Trademarks. Prepaid purchase coupons for ordering are also available from the U.S. Patent and Trademark Office.

NASA patent application specifications are sold in both paper copy and microfiche by the NASA Center for AeroSpace Information (CASI). The N accession number should be used in ordering either paper copy or microfiche from CASI.

The patents and patent applications announced in *STAR* are owned by NASA and are available for royalty-free licensing. Requests for licensing terms and further information should be addressed to:

National Aeronautics and Space Administration
Associate General Counsel for Intellectual Property
Code GP
Washington, DC 20546-0001

SOURCES FOR DOCUMENTS

One or more sources from which a document announced in *STAR* is available to the public is given in each citation. The most commonly indicated sources and their acronyms or abbreviations are listed below, and their addresses are listed on page A-6. If the publication is available from a source other than those listed, the publisher and address will be displayed on the availability line or in combination with the corporate source line.

Avail: CASI. Sold by the NASA Center for AeroSpace Information. Prices for hard copy (HC) and microfiche (MF) are indicated by a price code following the letters HC or MF in the *STAR* citation. Current values for the price codes are given in the tables on page A-7.

NOTE ON ORDERING DOCUMENTS: When ordering publications from CASI, use the N accession number or other report number. It is also advisable to cite the title and other bibliographic identification.

Avail: SOD (or GPO). Sold by the Superintendent of Documents, U.S. Government Printing Office, in hard copy.

Avail: BLL (formerly NLL): British Library Lending Division, Boston Spa, Wetherby, Yorkshire, England. Photocopies available from this organization at the price shown. (If none is given, address inquiry to the BLL.)

Avail: DOE Depository Libraries. Organizations in U.S. cities and abroad that maintain collections of Department of Energy reports, usually in microfiche form, are listed in *Energy Research Abstracts*. Services available from the DOE and its depositories are described in a booklet, *DOE Technical Information Center - Its Functions and Services* (TID-4660), which may be obtained without charge from the DOE Technical Information Center.

Avail: ESDU. Pricing information on specific data, computer programs, and details on Engineering Sciences Data Unit (ESDU) topic categories can be obtained from ESDU International Ltd. Requesters in North America should use the Virginia address while all other requesters should use the London address, both of which are on page A-6.

Avail: Fachinformationszentrum, Karlsruhe. Gesellschaft fur wissenschaftlich-technische Information mbH 7514 Eggenstein-Leopoldshafen 2, Germany.

Avail: HMSO. Publications of Her Majesty's Stationery Office are sold in the U.S. by Pendragon House, Inc. (PHI), Redwood City, CA. The U.S. price (including a service and mailing charge) is given, or a conversion table may be obtained from PHI.

Avail: Issuing Activity, or Corporate Author, or no indication of availability. Inquiries as to the availability of these documents should be addressed to the organization shown in the citation as the corporate author of the document.

Avail: NASA Public Document Rooms. Documents so indicated may be examined at or purchased from the National Aeronautics and Space Administration (JBD-4), Public Documents Room (Room 1H23), Washington, DC 20546-0001, or public document rooms located at NASA installations, and the NASA Pasadena Office at the Jet Propulsion Laboratory.

Avail: NTIS. Sold by the National Technical Information Service. Initially distributed microfiche under the NTIS SRIM (Selected Research in Microfiche) are available. For information concerning this service, consult the NTIS Subscription Section, Springfield, VA 22161.

Avail: Univ. Microfilms. Documents so indicated are dissertations selected from *Dissertation Abstracts* and are sold by University Microfilms as xerographic copy (HC) and microfilm. All requests should cite the author and the Order Number as they appear in the citation.

Avail: US Patent and Trademark Office. Sold by Commissioner of Patents and Trademarks, U.S. Patent and Trademark Office, at the standard price of $1.50 each, postage free. (See discussion of NASA patents and patent applications on page A-3.)

Avail: (US Sales Only). These foreign documents are available to users within the United States from the National Technical Information Service (NTIS). They are available to users outside the United States through the International Nuclear Information Service (INIS) representative in their country, or by applying directly to the issuing organization.

Avail: USGS. Originals of many reports from the U.S. Geological Survey, which may contain color illustrations, or otherwise may not have the quality of illustrations preserved in the microfiche or facsimile reproduction, may be examined by the public at the libraries of the USGS field offices whose addresses are listed on page A-6. The libraries may be queried concerning the availability of specific documents and the possible utilization of local copying services, such as color reproduction.

FEDERAL DEPOSITORY LIBRARIES: To provide the general public with greater access to U.S. Government publications, Congress established the Federal Depository Library Program under the Government Printing Office (GPO), with 53 regional depositories responsible for permanent retention of material, inter-library loan, and reference services. (These libraries are not sales outlets.) At least one copy of nearly every NASA and NASA-sponsored publication, either in printed or microfiche format, is received and retained by the 53 regional depositories. A list of the regional GPO libraries, appears on page A-8. A local library can contact a regional depository library to help locate specific reports, or direct contact may be made by an individual.

PUBLIC COLLECTION OF NASA DOCUMENTS

An extensive collection of NASA and NASA-sponsored publications is maintianed by the British Library Lending Divison, Boston Spa, Wetherby, Yorkshire, England, for public access. The British Library Lending Division also has available many of the non-NASA publications cited in *STAR*.

European requesters may purchase facsimile copy or microfiche of NASA and NASA-sponsored documents, those identified by both the symbols # and * from ESA—Information Retrieval Service, European Space Agency, 8-10 rue Mario-Nikis, 75738 Paris CEDEX 15, France.

SUBMITTING DOCUMENTS

All users of this abstract service are urged to forward reports to be considered for announcement in *STAR*. This will aid NASA in its efforts to provide the fullest possible coverage of all scientific and technical publications that might support aeronautics and space research and development. If you have prepared relevant reports (other than those you will transmit to NASA, DOD, or DOE through the usual contract- or grant-reporting channels), please send them for consideration to the NASA Center for AeroSpace Information, 800 Elkridge Landing Road, Linthicum Heights, MD 21090-2934.

Reprints of journal articles, book chapters, and conference papers are also welcome. These will be considered for announcement in *STAR*'s companion journal, *IAA*.

You may specify a particular source to be included in a report announcement if you wish; otherwise the report will be placed on a public sale at the NASA Center for AeroSpace Information. Copyrighted publications will be announced but not distributed or sold.

PURCHASE OF *STAR*

STAR is publicly available on annual subscription from the NASA Center for AeroSpace Information (CASI) at $94.00 domestic, $117.00 foreign. Single copy prices: $33/domestic, $41/foreign.

An annual, cumulative *STAR Index* is also available at $54/domestic and $65/foreign.

STAR is available to registered users on annual subscription from the NASA Center for AeroSpace Information, ATTN: Registration Services, 800 Elkridge Landing Road, Linthicum Heights, MD 21090-2934.

Microfiche of the abstract sections of *STAR* are available, on annual subscription, from CASI. Annual subscription rates are $216.00 North America; $432.00 foreign.

ADDRESSES OF ORGANIZATIONS

American Institute of Aeronautics and Astronautics
Technical Information Service
555 West 57th Street, 12th Floor
New York, New York 10019

British Library Lending Division,
Boston Spa, Wetherby, Yorkshire,
England

Commissioner of Patents and Trademarks
U.S. Patent and Trademark Office
Washington, DC 20231

Department of Energy
Technical Information Center
P.O. Box 62
Oak Ridge, Tennessee 37830

European Space Agency-Information Retrieval Service
ESRIN
Via Galileo Galilei
00044 Frascati (Rome) Italy

Engineering Sciences Data Unit International
P.O. Box 1633
Manassas, Virginia 22110

Engineering Sciences Data Unit International, Ltd.
251-259 Regent Street
London, W1R 7AD, England

Fachinformationszentrum Karlsruhe
Gesellschaft fur wissenschaftlich-technische
Information mbH
7514 Eggenstein-Leopoldshafen 2, Germany

Her Majesty's Stationery Office
P.O. Box 569, S.E. 1
London, England

NASA Center for AeroSpace Information
800 Elkridge Landing Road
Linthicum Heights, MD 21090-2934

National Aeronautics and Space Administration
Scientific and Technical Information Program (JTT)
Washington, DC 20546-0001

National Technical Information Service
5285 Port Royal Road
Springfield, Virginia 22161

Pendragon House, Inc.
899 Broadway Avenue
Redwood City, California 94063

Superintendent of Documents
U.S. Government Printing Office
Washington, DC 20402

University Microfilms
A Xerox Company
300 North Zeeb Road
Ann Arbor, Michigan 48106

University Microfilms, Ltd.
Tylers Green
London, England

U.S. Geological Survey Library National Center
MS 950
12201 Sunrise Valley Drive
Reston, Virginia 22092

U.S. Geological Survey Library
2255 North Gemini Drive
Flagstaff, Arizona 86001

U.S. Geological Survey
345 Middlefield Road
Menlo Park, California 94025

U.S. Geological Survey Library
Box 25046
Denver Federal Center, MS914
Denver, Colorado 80225

CASI PRICE TABLES

(Effective August 1, 1993)

STANDARD PRICE DOCUMENTS

PRICE CODE	NORTH AMERICAN PRICE	FOREIGN PRICE
A01	$ 9 00	$ 18.00
A02	12.50	25.00
A03	17.50	35.00
A04-A05	19.50	39.00
A06-A09	27.00	54.00
A10-A13	36.50	73.00
A14-A17	44.50	89.00
A18-A21	52.00	104.00
A22-A25	61.00	122.00
A99	CallForPrice	CallForPrice

MICROFICHE

PRICE CODE	NORTH AMERICAN PRICE	FOREIGN PRICE
A01	$ 9.00	$ 18.00
A02	12.50	25.00
A03	17.50	35.00
A04-A05	19.50	39.00
A06-A09	27.00	54.00
A10	36.50	73.00

IMPORTANT NOTICE

CASI Shipping and Handling Charges
U.S.—ADD $3.00 per TOTAL ORDER
Canada and Mexico—ADD $3.50 per TOTAL ORDER
All Other Countries—ADD $7.50 per TOTAL ORDER
Does NOT apply to orders
requesting CASI RUSH HANDLING.
CASI accepts charges to American Express, Diners Club, MasterCard and VISA.

FEDERAL REGIONAL DEPOSITORY LIBRARIES

ALABAMA

AUBURN UNIV. AT MONTGOMERY LIBRARY
Documents Dept.
7300 University Drive
Montgomery, AL 36117-3596
(205) 244-3650 FAX: (205) 244-0678

UNIV. OF ALABAMA
Amelia Gayle Gorgas Library
Govt. Documents
Box 870266
Tuscaloosa, AL 35487-0266
(205) 348-6046 FAX: (205) 348-8833

ARIZONA

DEPT. OF LIBRARY, ARCHIVES, AND PUBLIC RECORDS
Federal Documents
Third Floor State Capitol
1700 West Washington
Phoenix, AZ 85007
(602) 542-4121 FAX: (602) 542-4400; 542-4500

ARKANSAS

ARKANSAS STATE LIBRARY
State Library Services
One Capitol Mall
Little Rock, AR 72201
(501) 682-2869

CALIFORNIA

CALIFORNIA STATE LIBRARY
Govt. Publications Section
914 Capitol Mall - P.O. Box 942837
Sacramento, CA 94237-0001
(916) 322-4572 FAX: (916) 324-8120

COLORADO

UNIV. OF COLORADO - BOULDER
Norlin Library
Govt. Publications
Campus Box 184
Boulder, CO 80309-0184
(303) 492-8834 FAX: (303) 492-2185

DENVER PUBLIC LIBRARY
Govt. Publications Dept. BS/GPD
1357 Broadway
Denver, CO 80203
(303) 571-2135

CONNECTICUT

CONNECTICUT STATE LIBRARY
231 Capitol Avenue
Hartford, CT 06106
(203) 566-4971 FAX: (203) 566-3322

FLORIDA

UNIV. OF FLORIDA LIBRARIES
Documents Dept.
Library West
Gainesville, FL 32611-2048
(904) 392-0366 FAX: (904) 392-7251

GEORGIA

UNIV. OF GEORGIA LIBRARIES
Govt. Documents Dept.
Jackson Street
Athens, GA 30602
(404) 542-8949 FAX: (404) 542-6522

HAWAII

UNIV. OF HAWAII
Hamilton Library
Govt. Documents Collection
2550 The Mall
Honolulu, HI 96822
(808) 948-8230 FAX: (808) 956-5968

IDAHO

UNIV. OF IDAHO LIBRARY
Documents Section
Moscow, ID 83843
(208) 885-6344 FAX: (208) 885-6817

ILLINOIS

ILLINOIS STATE LIBRARY
Reference Dept.
300 South Second
Springfield, IL 62701-1796
(217) 782-7596 FAX: (217) 524-0041

INDIANA

INDIANA STATE LIBRARY
Serials/Documents Section
140 North Senate Avenue
Indianapolis, IN 46204
(317) 232-3678 FAX: (317) 232-3728

IOWA

UNIV. OF IOWA LIBRARIES
Govt. Publications Dept.
Washington & Madison Streets
Iowa City, IA 52242
(319) 335-5926 FAX: (319) 335-5830

KANSAS

UNIV. OF KANSAS
Govt. Documents & Map Library
6001 Malatt Hall
Lawrence, KS 66045-2800
(913) 864-4660 FAX: (913) 864-5380

KENTUCKY

UNIV. OF KENTUCKY LIBRARIES
Govt. Publications/Maps Dept.
Lexington, KY 40506-0039
(606) 257-3139 FAX: (606) 257-1563; 257-8379

LOUISIANA

LOUISIANA STATE UNIV.
Middleton Library
Govt. Documents Dept.
Baton Rouge, LA 70803
(504) 388-2570 FAX: (504) 388-6992

LOUISIANA TECHNICAL UNIV.
Prescott Memorial Library
Govt. Documents Dept.
305 Wisteria Street
Ruston, LA 71270-9985
(318) 257-4962 FAX: (318) 257-2447

MAINE

TRI-STATE DOCUMENTS DEPOSITORY
Raymond H. Fogler Library
Govt. Documents & Microforms Dept.
Univ. of Maine
Orono, ME 04469
(207) 581-1680

MARYLAND

UNIV. OF MARYLAND
Hornbake Library
Govt. Documents/Maps Unit
College Park, MD 20742
(301) 454-3034 FAX: (301) 454-4985

MASSACHUSETTS

BOSTON PUBLIC LIBRARY
Govt. Documents Dept.
666 Boylston Street
Boston, MA 02117
(617) 536-5400 ext. 226
FAX: (617) 267-8273; 267-8248

MICHIGAN

DETROIT PUBLIC LIBRARY
5201 Woodward Avenue
Detroit, MI 48202-4093
(313) 833-1440; 833-1409
FAX: (313) 833-5039

LIBRARY OF MICHIGAN
Govt. Documents Unit
P.O. Box 30007
Lansing, MI 48909
(517) 373-0640 FAX: (517) 373-3381

MINNESOTA

UNIV. OF MINNESOTA
Wilson Library
Govt. Publications Library
309 19th Avenue South
Minneapolis, MN 55455
(612) 624-5073 FAX: (612) 626-9353

MISSISSIPPI

UNIV. OF MISSISSIPPI
J.D. Williams Library
Federal Documents Dept.
106 Old Gym Bldg.
University, MS 38677
(601) 232-5857 FAX: (601) 232-5453

MISSOURI

UNIV. OF MISSOURI - COLUMBIA
Ellis Library
Govt. Documents
Columbia, MO 65201
(314) 882-6733 FAX: (314) 882-8044

MONTANA

UNIV. OF MONTANA
Maureen & Mike Mansfield Library
Documents Div.
Missoula, MT 59812-1195
(406) 243-6700 FAX: (406) 243-2060

NEBRASKA

UNIV. OF NEBRASKA - LINCOLN
D.L. Love Memorial Library
Documents Dept.
Lincoln, NE 68588
(402) 472-2562

NEVADA

UNIV. OF NEVADA
Reno Library
Govt. Publications Dept.
Reno, NV 89557
(702) 784-6579 FAX: (702) 784-1751

NEW JERSEY

NEWARK PUBLIC LIBRARY
U.S. Documents Div.
5 Washington Street - P.O. Box 630
Newark, NJ 07101-0630
(201) 733-7812 FAX: (201) 733-5648

NEW MEXICO

UNIV. OF NEW MEXICO
General Library
Govt. Publications Dept.
Albuquerque, NM 87131-1466
(505) 277-5441 FAX: (505) 277-6019

NEW MEXICO STATE LIBRARY
325 Don Gaspar Avenue
Santa Fe, NM 87503
(505) 827-3826 FAX: (505) 827-3820

NEW YORK

NEW YORK STATE LIBRARY
Documents/Gift & Exchange Section
Federal Depository Program
Cultural Education Center
Albany, NY 12230
(518) 474-5563 FAX: (518) 474-5786

NORTH CAROLINA

UNIV. OF NORTH CAROLINA - CHAPEL HILL
CB#3912, Davis Library
BA/SS Dept.—Documents
Chapel Hill, NC 27599
(919) 962-1151 FAX: (919) 962-0484

NORTH DAKOTA

NORTH DAKOTA STATE UNIV. LIBRARY
Documents Office
Fargo, ND 58105
(701) 237-8886 FAX: (701) 237-7138
In cooperation with Univ. of North Dakota, Chester Fritz Library
Grand Forks

OHIO

STATE LIBRARY OF OHIO
Documents Dept.
65 South Front Street
Columbus, OH 43266
(614) 644-7051 FAX: (614) 752-9178

OKLAHOMA

OKLAHOMA DEPT. OF LIBRARIES
U.S. Govt. Information Div.
200 NE 18th Street
Oklahoma City, OK 73105-3298
(405) 521-2502, ext. 252, 253
FAX: (405) 525-7804

OKLAHOMA STATE UNIV.
Edmon Low Library
Documents Dept.
Stillwater, OK 74078
(405) 744-6546 FAX: (405) 744-5183

OREGON

PORTLAND STATE UNIV.
Millar Library
934 SW Harrison - P.O. Box 1151
Portland, OR 97207
(503) 725-3673 FAX: (503) 725-4527

PENNSYLVANIA

STATE LIBRARY OF PENN.
Govt. Publications Section
Walnut St. & Commonwealth Ave. - P.O. Box 1601
Harrisburg, PA 17105
(717) 787-3752

SOUTH CAROLINA

CLEMSON UNIV.
Cooper Library
Public Documents Unit
Clemson, SC 29634-3001
(803) 656-5174 FAX: (803) 656-3025
In cooperation with Univ. of South Carolina, Thomas Cooper Library, Columbia

TENNESSEE

MEMPHIS STATE UNIV. LIBRARIES
Govt. Documents
Memphis, TN 38152
(901) 678-2586 FAX: (901) 678-2511

TEXAS

TEXAS STATE LIBRARY
United States Documents
P.O. Box 12927 - 1201 Brazos
Austin, TX 78711
(512) 463-5455 FAX: (512) 463-5436

TEXAS TECH. UNIV. LIBRARY
Documents Dept.
Lubbock, TX 79409
(806) 742-2268 FAX: (806) 742-1920

UTAH

UTAH STATE UNIV.
Merrill Library & Learning Resources Center, UMC-3000
Documents Dept.
Logan, UT 84322-3000
(801) 750-2684 FAX: (801) 750-2677

VIRGINIA

UNIV. OF VIRGINIA
Alderman Library
Govt. Documents
Charlottesville, VA 22903-2498
(804) 924-3133 FAX: (804) 924-4337

WASHINGTON

WASHINGTON STATE LIBRARY
Document Section
MS AJ-11
Olympia, WA 98504-0111
(206) 753-4027 FAX: (206) 753-3546

WEST VIRGINIA

WEST VIRGINIA UNIV. LIBRARY
Govt. Documents Section
P.O. Box 6069
Morgantown, WV 26506
(304) 293-3640

WISCONSIN

ST. HIST. SOC. OF WISCONSIN LIBRARY
Govt. Publications Section
816 State Street
Madison, WI 53706
(608) 262-2781 FAX: (608) 262-4711
In cooperation with Univ. of Wisconsin-Madison, Memorial Library

MILWAUKEE PUBLIC LIBRARY
Documents Div.
814 West Wisconsin Avenue
Milwaukee, WI 53233
(414) 278-2167 FAX: (414) 278-2137

National Aeronautics and
Space Administration
Code JTT
Washington, D.C.
20546-0001

Official Business
Penalty for Private Use, $300

SPECIAL FOURTH-CLASS RATE
POSTAGE & FEES PAID
NASA
PERMIT No. G27

NASA

POSTMASTER: If Undeliverable (Section 158
Postal Manual) Do Not Return

Please circulate this publication to other colleagues within your organization.